Virchows Arch (2003) 443:1–2 © Springer-Verlag 2003

SOCIETY NEWS

Invitation to the 19th European Congress of Pathology

On behalf of the European Society of Pathology (ESP) and the Organising Committee, we take great pleasure in inviting you to the 19th European Congress of Pathology, which will be held in Ljubljana, Slovenia, 6–11 September 2003.

Slovenia is not a large country, but at the hub of routes of trade and movement from east to west and north to south, it has always played a larger part in European events than its size would suggest. Slovenia is now an independent Central European state, on the sunny side of the Alps, bordering Italy, Austria, Hungary and Croatia. The landscape embraces rolling countryside leading to the Pannonian plain to the east, rugged Karst bordering the Adriatic Sea to the southwest, and the Alps to the north and west. The Slovenian nation of only two million today has survived mainly due to its culture, language and vitality. A bone flute, 30,000 years older than any other known in the world, and Europe's oldest bone needle, testify to the roots of culture here.

Its capital, Ljubljana, has a picturesque unity, composed of an architectural heritage spanning Roman Emona, through Renaissance and Baroque Ljubljana, to Secession Art Nouveau and Modern Ljubljana, so strongly marked by the influence of the world famous Slovenian architect, Jo e Plečnik. Ljubljana is an university city. The roots of the University go back to the seventeenth century with Academia Operosorum, the fourth Academy of Sciences in Europe. A Philharmonic Society dates back three centuries.

Ljubljana's congress tradition began in 1821, when the three emperors of the Holy Alliance met here to discuss the post-Napoleonic fate of Europe. These traditions have been brought together in the new Cultural and Congress Centre Cankarjev dom, with a capacity of 3,600, located in the heart of Ljubljana. Cankarjev dom is well equipped with all modern technical facilities and has an experienced in-house team to ensure the necessary high standards for scientific sessions and exhibitions. All Congress venues, and most hotels, are within walking distance of the centre of the city. Particular attention will be paid to stimulating the participation of trainees and young pathologists by securing as low a registration fee as possible, and inexpensive accommodations.

The European Society of Pathology has been succeeding in establishing its ever more continuous activity and influence. The old idea of a common programme of continuous education of pathologists has been realised through a number of courses organised each year by the European School of Pathology, at its headquarters in Turin and other centres throughout Europe. An increasing number of Working Groups within the European Society of Pathology, devoted to various fields, promote a continuous exchange of professional experiences and other information, the establishment of common diagnostic standards and collaboration on common research projects.

The biannual ESP Congresses retain a major role in fulfilling the main aims of the ESP in pathology education, exchange of the most recent research achievements and, particularly, in keeping together all branches of pathology, that otherwise tend to split according to organ systems, disease processes and the increasing number of techniques. The Congresses also keep together pathologists from the whole of Europe, irrespective of geographical and political borders.

We believe that the 19th European Congress of Pathology will continue the traditional approaches of previous Congresses and will serve to increase both links with European national and international pathology societies and intercontinental links, particularly with the International Academy of Pathology. The framework of the Congress Scientific Programme has been created with the strong impact and assistance of the ESP Working Groups, the ESP Executive/Scientific Committee and the Advisory Council as well as companion Societies. The programme covers all areas of pathology, provides information ranging from current diagnostic standards to recent advances in science and modern techniques, particularly those of molecular genetics, and includes a number of "hot" topics of today and tomorrow, which will be

presented by the best, internationally recognised experts at Keynote Lectures, Symposia, Special Presentations, Round Table Discussions, Short Courses and Slide Seminars. One evening is devoted to ESP Working Group Meetings, both business and scientific. Interesting Satellite Symposia will be organised by supporting companies, two by the main sponsor of the Congress Main Sponsor, Ventana Medical Systems S.A.

Furthermore, all practising pathologists and scientists are kindly invited to present their scientific achievements and exchange their professional experiences through Free Paper and Poster Sessions. The best Free Papers will be acknowledged by giving the authors the opportunity to present their achievements at the plenary session, at which the authors of the three best Poster Presentations will additionally receive special Awards.

All who are coming to Ljubljana are kindly invited to join us at two one-day Pre-Congress Meetings, prior to the Congress Opening Ceremony on Saturday: one on Pulmonary Pathology and the other devoted to non-neoplastic Nephropathology. There will also be a three-day Joint Meeting of the European and North American Society of Head and Neck Pathology. All Pre-Congress Meetings and a whole day Examination by the European Board of Pathology will be organised by using the facilities of the new building of the Faculty of Medicine, University of Ljubljana.

Culture kept the Slovenian national identity alive over the centuries and it still plays an important role in people's lives. The Congress will also highlight the traditional close connection between medicine and art. Some novel events are planned: an exhibition of the work of pathologists/painters and, especially, a Gala Concert on Monday evening in the main Gallus Concert Hall of the Congress Centre in Ljubljana, by pathologists/musicians from all over the world. A social programme is offered which reflects the warmth and hospitality of the Slovenian people.

The Second Millennium we have entered provides major challenges for all biomedical sciences, and the 19th European Congress of Pathology is a challenge for the Organisers. We sincerely hope that attendance at the Ljubljana Congress in 2003 will be a fruitful, enjoyable and memorable experience in every respect for all participants, and will give new impetus to our medical speciality in Slovenia.

We look forward to seeing you in September 2003 in Ljubljana.

Gianni Bussolati
President
European Society
of Pathology

Du an Ferluga
President
19th European Congress
of Pathology

Virchows Arch (2003) 443:3–16
DOI 10.1007/s00428-003-0834-y

REVIEW ARTICLE

Christoph Röcken · Knut Sletten

Amyloid in surgical pathology

Received: 10 March 2003 / Accepted: 5 May 2003 / Published online: 11 June 2003
© Springer-Verlag 2003

Abstract Amyloid is defined as a proteinaceous tissue deposit that shows a typical green birefringence in polarized light after staining with Congo red, the presence of non-branching linear fibrils of indefinite length with a mean diameter of 10 nm, and a distinct X-ray diffraction pattern consistent with Pauling's model of a cross β-fibril. Amyloid may deposit locally or may present as a systemic disease. The origin of amyloid is diverse: 25 different fibril proteins have been described so far. The precursor proteins differ from each other in their primary structures and functions. The only common denominator is the propensity to form anti-parallel cross β-fibrils under certain circumstances. Early diagnosis of amyloid is still a major challenge in surgical pathology. Histological proof can be obtained using Congo-red staining and polarization microscopy. However, small deposits may be difficult to discern, and sensitivity can be improved using fluorescence microscopy. Classification of amyloid is mandatory, since amyloid is treatable and different treatment regimens are applied to different amyloid diseases. This review focuses on the epidemiology, clinical features, pathology and diagnosis of amyloid in surgical pathology.

Keywords Amyloid · Surgical pathology

Introduction

In the past 20 years, considerable advancements have been made regarding the pathogenesis, diagnostics and treatment of amyloidoses. This is reflected by the constant increase in number of publications dealing with "amyloid", the founding of diverse national and international societies, an increasing number of congresses and symposia focussing on amyloid (International Symposium on Amyloidosis, International Symposium on Familial Amyloidotic Polyneuropathy and Other Transthyretin Related Disorders, International Workshop on Liver Transplantation in Familial Amyloid Polyneuropathy, Amyloidforum), an "Amyloidosis Support Network" (http://www.amyloidosis.org) and the publication of a journal in 1994 named "Amyloid. The Journal of Protein Folding Disorders". We have learnt that amyloid is not a single disease entity but rather a large group of diverse diseases, some of which are inherited.

C. Röcken (✉)
Department of Pathology, Otto-von-Guericke-University,
Leipziger Strasse 44, 39120 Magdeburg, Germany
e-mail: christoph.roecken@medizin.uni-magdeburg.de
Tel.: +49-391-6713179
Fax: +49-391-67190188

K. Sletten
Biotechnology Center of Oslo, University of Oslo, Norway

Definition

Amyloid is defined as an amorphous, eosinophilic proteinaceous deposit that shows a typical green birefringence in polarized light after staining with Congo red, the presence of non-branching linear fibrils of indefinite length with a mean diameter of 10 nm [14], and a distinct X-ray diffraction pattern consistent with Pauling's model of a cross β-fibril. The origin of amyloid is diverse and 25 different fibril proteins have been described so far (Table 1). The precursors of most fibril proteins differ from each other with respect to primary structure and function. The only feature common to all these proteins is their ability to form aggregates under specific circumstances, which leads to the formation and deposition of amyloid.

Epidemiology

Only limited epidemiological data are available about the incidences and prevalences of extracerebral amyloid deposits. Some hereditary amyloid syndromes show geographically increased frequencies (Table 2). Hereditary ATTR amyloidosis is most common in Portugal, northern Sweden and Japan, and ACys and AGel amyloidosis affects predominantly Icelanders and Finns.

Table 1 Amyloid fibril proteins and their precursors in human

Amyloid-protein	Precursor protein	Systemic or localized	Amyloidosis/underlying or associated disease
AL	Immunoglobulin light chain	S, L	Multiple myeloma, primary AL amyloidosis
AH	Immunoglobulin heavy chain	S, L	Multiple myeloma, primary AL amyloidosis
ATTR	Transthyretin	S	Familial amyloid polyneuropathie (Portugese type)
		S	Senile cardiovascular amyloidosis*
Aβ_2M	β2-microglobulin	S	Hemodialysis
		L?	Joints
AA	Serum amyloid A	S	Secondary, reactive
AApoAI	Apolipoprotein AI	S	Hereditary systemic amyloidosis
		L	Arteriosclerosis*
AApoAII	Apolipoprotein AII	S	Hereditary renal amyloidosis
AGel	Gelsolin	S	Familial amyloid polyneuropathy (Finnish type), Lattice corneal dystrophy
ALys	Lysozyme	S	Familial visceral amyloidosis
AFib	Fibrinogen α-chain	S	Hereditary systemic amyloidosis
ACys	Cystatin C	S	Familial amyloidosis (Icelandic type)
ABri	ABriPP (or Bri-L)**	S	Familial dementia (British type)
ADan	ADanPP (or Bri-D)**	L	Heredopathia ophthalmo-oto-encephalica (Danish type)
Aβ	Aβ precursor protein (AβPP)	L	Alzheimer's disease, Down syndrome, amyloidangiopathy; aging brain
APrP	Prion protein	L	Spongiform encephalopathy
ACal	(Pro)calcitonin	L	Medullary thyroid cancer
AIAPP	Islet amyloid polypeptide	L	Islets of Langerhans
		L	Insulinoma
AANF	Atrionatriuretic peptide	L	Cardiac atria, atrial fibrillation
APro	Prolactin	L	Pituitary
		L	Pituitary adenoma
AIns	Insulin	L	Iatrogenic
AMed	Lactadherin	L	Amyloid of the aortic media
AKer	Kerato-epithelin	L	Cornea
A(tbn)	tbn	L	Pindborg tumors
ALac	Lactoferrin	L	Cornea (Trichiasis)
ATau	Tau protein	L	Brain

*Non-hereditary amyloid with deposition of wild-type protein
**The fibril proteins originate from the same gene with different, kindred specific gene mutations generating fibril proteins, which differ in their 12 C-terminal amino acids

AA amyloidosis remains the most serious manifestation of Familial Mediterranean Fever (FMF) and is most common in sephardic Jews (37%) and Armenians (24%) living in Armenia. It affects less frequently Ashkenazi Jews (8%), Turks (12%) and Arabs (10%). Environmental factors contribute to the risk of amyloidosis in FMF, as AA amyloidosis is significantly less common in Armenians living in California. The incidence of secondary AA amyloidosis among patients who suffer from leprosy or tuberculosis may reach 17%. The prevalence of AA amyloidosis among ankylosing spondylitis, rheumatoid arthritis and Crohn's disease ranges from 0.5% to 13% [97]. As yet, no geographical or ethnic differences have been described for senile amyloidoses and systemic AL amyloidosis. In individuals over 85 years of age, senile amyloid reaches prevalences of up to 100%. The incidence of AL amyloidosis is 8 per 1,000,000 per year and has remained stable for the last 40 years [36].

Clinical features

Amyloid can effect both genders and occurs at any age, including childhood. The incidence of senile amyloid is, by definition, associated with age. Amyloidosis denotes the disease state that results from the deposition of amyloid. The clinical presentation and symptoms depend on the distribution pattern and amount of amyloid deposited. Although a particular combination of clinical symptoms may be highly indicative of amyloidosis in a given patient, the physical findings of different amyloid diseases can be variable and are generally unspecific and do not consistently raise suspicion of amyloidosis. Moreover, a single patient may suffer from different amyloid diseases simultaneously [21, 28, 52, 90]. The clinical significance of amyloid and amyloidosis can be anything between irrelevant to a life-threatening disease. On clinical presentation, nephrotic syndrome, renal failure, carpal tunnel syndrome, sensomotoric and autonomic neuropathy with and without postural hypotension, cardiac failure, arrhythmias, hepatosplenomegaly, diarrhea, ileus, infarction, macroglossia, malabsorption, ulcerations, lymphadenopathy, bruising, maculopapular skin lesions and purpura can be seen. Bleeding events may be related to factor II, V, VII, IX and/or X deficiency, capillary fragillity, dysfibrinogenemia and abnormal platelet aggregation [12, 24]. Amyloid may also be found in the absence of clinical symptoms.

Table 2 Hereditary systemic amyloidoses (modified according to [7])

Protein	Mutation	Clinical features	Geographic kindred(s)
Apolipoprotein AI	Gly26Arg	Peripheral neuropathy, nephropathy, peptic ulcer disease	Iowa (United States)
	Gly26Arg	Nephropathy, liver failure	Ireland, United States
	Leu60Arg	Nephropathy	England
	Trp50Arg	Nephropathy	England
	del60–71 insVal/Thr	Liver failure	Spain
	del70–72	Nephropathy	South Africa
	Leu90Pro	Cardiomyopathy, dermatopathy, larynx	France
	Arg173Pro	Cardiomyopathy, dermatopathy, larynx	United States
	Leu174Ser	Cardiomyopathy	Italy
	Leu178His	Cardiomyopathy, dermatopathy, larynx	France
Apolipoprotein AII	Stop78Gly	Nephropathy	United States
	Stop78Ser	Nephropathy	United States
ABriPP-277 (or Bri-L)	Stop267→Arg	Dementia	Great Britain
Cystatin C	Leu68Gln	Cerebral hemorrhage	Croatic-American, Iceland
Fibrinogen A α-chain	Arg554Leu	Nephropathy	African-American, France, Irish-American, Peruvian-Mexican, Polish-Canadian
	Glu526Val	Nephropathy	England, Irish-American
	Stop548Ile (4904delG)	Nephropathy	Caucasian-American
	Stop548Ile (4897delT)	Nephropathy	France
Gelsolin	Asp187Asn	Cranial neuropathy, dermatopathy, lattice corneal dystrophy	Finland, Japan, The Netherlands, United States
	Asp187Tyr	Cranial neuropathy, dermatopathy, lattice corneal dystrophy	Czech Republic, Denmark
Lysozyme	Ile56Thr	Nephropathy, dermal petechiae, gastrointestinal bleeding	England (?Scandinavian descent)
	Phe57Ile	Nephropathy	Italian-Canadian
	Trp64Arg	Nephropathy, ocular and oral sicca syndrome, gastrointestinal bleeding	France
	Trp64Arg	Gastrointestinal bleeding	Italy
	Asp67His	Nephropathy, hepatic and gastrointestinal bleeding	England
Transthyretin	More than 80	Peripheral neuropathy, cardiomyopathy, nephropathy, vitreous opacities	Worldwide, Portugal

Localization

Amyloid can affect any organ and tissue type. Deposits may be local or systemic. The distribution pattern of amyloid depends on the origin and type of the fibril protein (Table 1). Systemic amyloid is characterized by the ubiquitous deposition of a particular amyloid protein in different organs and tissues. Local amyloid may occur (Table 1) in the skin [75], tumors of the skin (e.g., basal cell carcinomas and seborrheic keratosis) [76], cornea, meningiomas [29], pituitary and their adenomas [92], odontogenic tumors [6], medullary cancer of the thyroid, neuroendocine tumors of the lung [1], cardiac atria [101], intima and media of arteries [46, 120], mesenteric and portal veins [95], islets of Langerhans [116], microcystic adenoma of the pancreas [113], gastroenteropancreatic endocrine tumors (i.e., insulinomas, vipomas, somatostatinomas) [16, 74, 119], renal angiomyolipoma [112], pheochromocytomas [107] and seminal vesicles [83]. Local deposits derived from immunoglobulin light chains (AL amyloid) have been found in various organ and tissue sites, often presenting as "amyloidoma". Luminal deposits (i.e., *corpora amylacea*) in the lung and prostate [94], and intracellular green birefringent deposits such as in the brain (ATau amyloid), choroid plexus [25] and adrenals [93], are also encountered as localized amyloid.

Macroscopy

Macroscopically, amyloid can be indistinct or be associated with a waxy cut surface. Advanced deposition of amyloid in the thyroid is known as "amyloid goitre". Amyloid in the gastrointestinal tract can lead to macroglossia, thickening of the gastric and intestinal walls, stiffness, hemorrhages and even necroses. Advanced local deposits may present as a tumor.

Histology

Amyloid is preferentially deposited in the interstitium and in vessel walls and, depending on the amount of amyloid, can lead to atrophy, ischemia and necrosis. On hematoxylin and eosin (H&E)-stained sections, amyloid appears as a monomorphous pale eosinophilic mass. However, the deposits may be indistinct and not apparent on routine H&E-stained sections. Amyloid does not stain with van Gieson's elastica stain or trichrome stains. Glycosaminoglycans are present in amyloid and can be identified by sulfonated Alcian blue stain. Macrophages and multinucleated histiocytic giant cells are commonly found adjacent to or within amyloid deposits (Fig. 1) [78, 99, 108]. A chronic inflammatory reaction is occasionally present [8]. An increased number of mast cells has also been described [17, 111]. Heterotopic ossifications and calcifications may be present occasionally [98].

Diagnosis

By definition, amyloid can only be diagnosed morphologically. No clinical, serological or radiological procedure has replaced the investigation of a tissue sample to provide definitive diagnostic proof.

Congo-red staining

Congo red was discovered in 1883 by Paul Böttiger. It was the first of many so-called direct dyes. In 1886, Congo red was used for the first time in histology, and in 1922 Bennhold published his observations that Congo red stains amyloid. The green birefringence was discovered by Divry in 1927 (for a review see [106]). Despite its age, Congo red remains the gold standard in the diagnosis of amyloid. In fact, any proteinaceous tissue deposit with affinity for the dye Congo red and a typical apple-green birefringence in polarized light is defined as amyloid. This also includes intracellular protein aggregates with amyloid properties [121]. Amyloid is considered a conformational disease. Several conformational diseases are characterized by intracellular protein aggregates, such as Parkinson's disease, Huntington's chorea, amyotrophic lateral sclerosis and α1-antitrypsin deficiency. Protein aggregates may be fibrillar (i.e., congophilic) and nonfibrillar in nature. Therefore, the notion that amyloid occurs only interstitially has been abolished [121].

Congo-red staining can be applied to tissue specimens fixed in Bouin's solution, ethanol, formalin, Helly's solution, *p*-formaldehyde, Zenker's solution, as well as to frozen sections and specimens obtained for cytology [11]. Fixation in Carnoy's solution has been reported to bear some risk of false-positive staining [11]. In general, fixation time has no significant effect on the staining. However, congophilia is reduced after extended periods of fixation. False-positive or false-negative results are usually related to (1) the staining technique, (2) the microscope equipment or (3) the presence of small amounts of amyloid:

1. Congo red dissolved in aqueous solvents (as it is when used in Bennhold's Congo-red technique) is unspecific and requires a differentiation step, which may lead to decoloration of amyloid, while collagen fibers and hyalin remain stained. Bennhold's technique does not yield reproducible results and should be avoided [86]. Specificity of Congo-red staining is significantly improved by extreme conditions with 50–80% ethanol, high salt and alkaline pH conditions, as was shown by Holde Puchtler [85]. Puchtler's Congo red should be applied accurately with aqueous hematoxylin counterstaining prior to Congo-red staining.
2. The green birefringence is specific for amyloid and a polarization facility is mandatory for diagnosing amyloid. Tension-free optics were recommended in the past. However, according to information provided by most companies and our own experience, modern objectives are of sufficient quality to provide a dark field in crossed polars. The light should be set at maximum, with all color filters out, and the pupils should be accommodated to the darkness. Rotation of the slide table within the horizontal plane can help to differentiate collagen from amyloid. Occasionally, in a particular position of the slide, collagen may show green birefringence with a typical periodic banding pattern. In contrast to collagen, amyloid retains it's birefringence continuously following horizontal rotation of the slide.
3. Puchtler's Congo red in conjunction with polarization microscopy is highly specific but of limited sensitivity. Small and tiny deposits can be missed. Cutting thicker sections (5–10 μm instead of 2–5 μm), and/or applying fluorescence microscopy, with a high pressure mercury burner and fluorescein isothiocyanate filter, on Congo-red stained sections increases sensitivity: amyloid yields a yellow–orange fluorescence (Fig. 1) [66]. However, fluorescence is not specific, and green birefringence should be sought in deposits identified by fluorescence microscopy. Double staining (Congo red + immunohistochemistry) has also been recommended to overcome low sensitivity [67]. The amyloid protein is stained using immunohistochemistry. Tiny immunoreactive deposits are sought in bright light and their amyloid nature is confirmed by green birefringence in polarized light. However, this procedure can only be applied, when the nature of the amyloid fibril protein is already known or when a battery of specific antibodies against various amyloid fibril proteins is available.

Electron microscopy

On electron microscopy, amyloid consists of rigid, nonbranching microfibrils of indefinite length, a mean

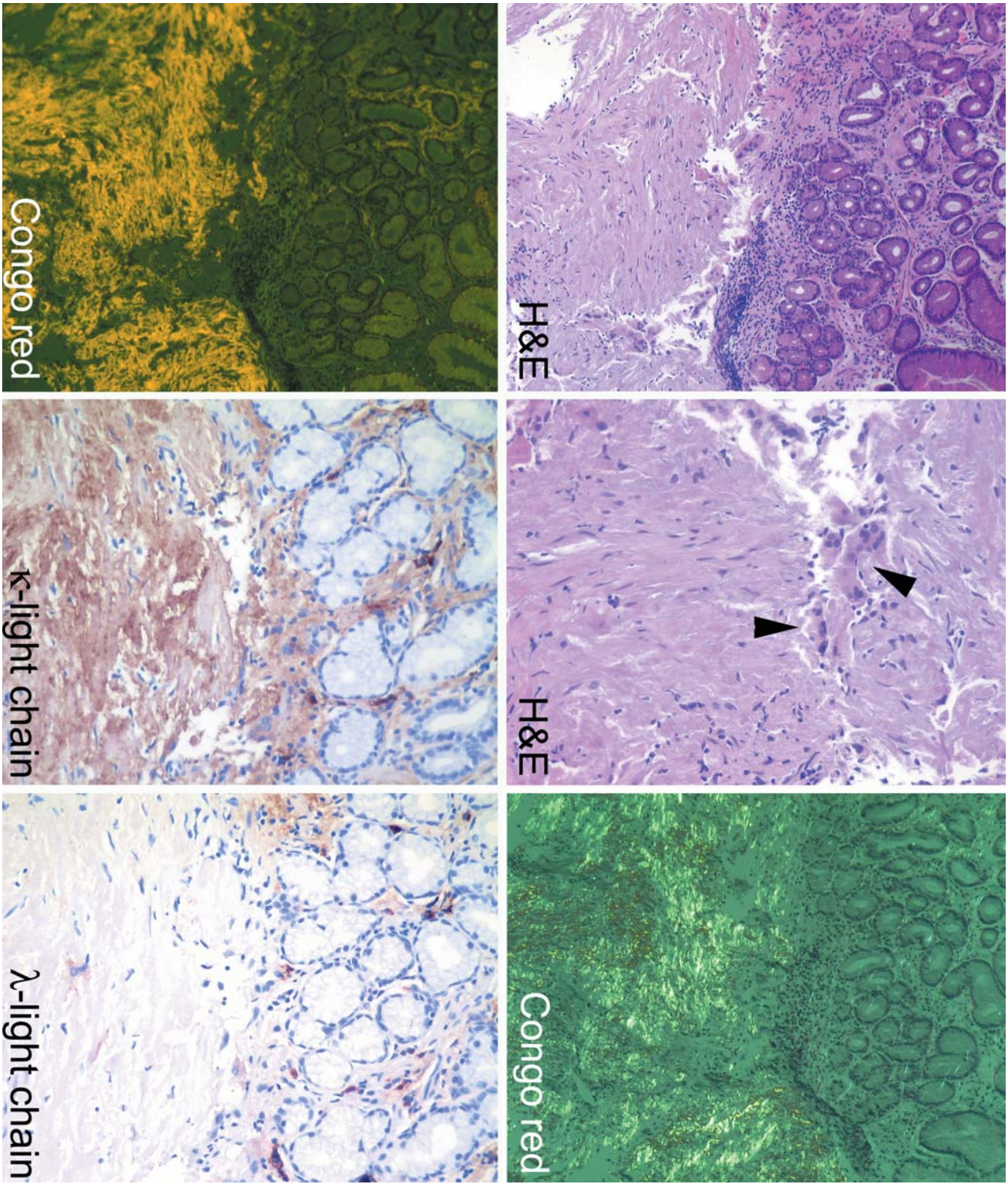

Fig. 1 A 57-year-old patient with extensive amyloid deposits in gastric biopsy specimens (hematoxylin and eosin; H&E). Multinulceated giant cells were found adjacent to the deposits (H&E; *arrow heads*). Congo-red staining showed green birefringence (Congo red, *upper right*) and polarized light and yellow-orange fluorescence in fluorescence microscopy (Congo red, *lower left*). Immunostaining with a polyclonal antibody directed against κ-light chain (κ-light chain) showed labeling of the deposits. λ-light chain was not present within the deposits (λ-light chain). This patient suffered from a plasmacytoma. Specimens were kindly provided by Prof. Dr. Jautzke, St. Gertrauden-Krankenhaus, Berlin

diameter of 10 nm and a central electron-lucent core. The presence of extracellular microfibrils is an ultrastructural observation that was initially thought to be diagnostic of amyloidosis. However, it is now known that many diseases may have biochemically diverse deposits of microfibrils [59], some sharing similarities "typical" for amyloid fibrils. Congo red staining and immunohistochemical detection of amyloid P component may help in separating amyloid from other, non-amyloidotic fibrillopathies [59].

Fat aspiration biopsy

Different organ and tissue sites are in use for biopsy confirmation of amyloid. In 1973, Per Westermark and Björn Stenkvist [117] introduced fat aspiration biopsy (FAB) for tissue confirmation of systemic amyloidosis, a procedure that has been validated subsequently by many different investigators (Table 3). Using a disposable syringe and a needle with an internal diameter of 0.7–1.2 mm, subcutaneous adipose tissue is aspirated and smeared onto a glass slide, air dried and stained with Congo red. Local anesthesia is unnecessary when thin needle biopsies are applied. Samples are most commonly obtained from the abdominal wall. FAB for confirmation of diagnosis is simple, does not require specific equipment, can be applied repeatedly and bears a negligible risk of complications. The incidence of amyloid in FAB ranges between 6% and 11% [3, 23, 33, 71], and therefore FAB is of little value as an independent or broadly applied screening test in a more general population [33, 60]. However, detection of amyloid in FABs has an excellent predictive value (almost 100%) for systemic amyloidosis and is the most important advantage. It can be performed in clinical situations where liver or kidney biopsies carry a high risk of complications, such as bleeding. FAB is less sensitive than kidney and rectal biopsies (Table 3). Studies with adequate control biopsies from distant organ and tissue sites reported sensitivities ranging from 35% to 84% (Table 3). However, sensitivity of FAB depends on the amount of fat tissue enclosed. It should not contain fat droplets only. Different types of amyloid have been diagnosed by FAB, including AA-, AApo AI-, AApoAII- [123], AFib- [114], AL-, ALys- [81] and ATTR amyloid (Table 3). Certain forms of systemic amyloidosis lack subcutaneous deposits including Aβ2 M amyloid associated with long-term hemodialysis [79, 115] and AA amyloidosis related to FMF [110]. Material obtained by FAB can be forwarded to electron and immunoelectron microscopy (IEM) [5], immunohistochemistry, immunodiffusion [118], enzyme-linked immunosorbent assays [47, 77, 79], gel electrophoresis and Western blotting [55]. The limited number of slides obtained is disadvantageous for immunohistochemical classification of amyloid (see below).

Biopsies from the oral cavity and gastrointestinal tract

Biopsies obtained from the oral cavity and gastrointestinal tract can also be used for confirmation of diagnosis. Sampling of gingiva [20, 61] and accessory salivary glands [19, 20, 26, 27] do not require special endoscopic equipment, while biopsies from the stomach (Fig. 1), duodenum, colon and rectum do. With regard to sensitivity, gastric, duodenal and rectal biopsies are superior to FAB and allow more extended immunohistochemical investigations [9, 27, 60]. Amyloid may be present as vascular and interstitial deposits and can effect all layers of the gastrointestinal wall. It is found more commonly in submucosa than muscularis mucosae and mucosa [96, 97, 122]. Advanced deposition of amyloid leads to atrophy and ulcers [122]. In specimens obtained from the large intestine, amyloid may be misinterpreted as collagenous colitis in H&E-stained sections. However, amyloid does not stain with van Gieson's elastica stain [32, 40, 96]. The amyloid fibril proteins originate most commonly from transthyretin [91, 124], serum amyloid A [58, 60] or immunoglobulin light chains [91, 122].

The rectal biopsy was introduced by Joseph Gafni and Ezra Sohar in 1960 [30] and has become a standard procedure for biopsy confirmation of amyloid. The sensitivity of rectal biopsy ranges between 69% and 97% and depends largely on the amount of tissue sampled [9, 27, 36, 57, 61]. False-negative results may be expected in as many as 60% of the cases, when submucosa is not enclosed [96]. Biopsies from the upper gastrointestinal tract became favorable with the advent of more sophisticated endoscopic tools: amyloid was found in gastric and duodenal biopsies of approximately 7–13.3% of the patients suffering from rheumatoid arthritis [58, 60].

Sural nerve and muscle biopsy

Sural nerve biopsy is frequently obtained for the investigation of peripheral neuropathies, including those related to amyloidosis. Amyloid deposits are present in approximately 1.2% of sural nerve biopsies obtained for a general investigation of peripheral neuropathy [87]. Amyloid is found in the vascular walls and interstitially in the endoneurium, perineurium and epineurium [49, 51, 87, 105]. It is associated with loss of myelinated axons, axonal degeneration and a chronic inflammatory response in one-third of the cases [51, 87]. The amyloid fibril proteins may originate from transthyretin, apolipoprotein AI or gelsolin in Familial Amyloid Polyneuropathies (Table 1), from serum amyloid A in AA amyloidosis [49], or from immunoglobulin light chains in primary systemic AL amyloidosis [49, 51]. Of patients with AL amyloidosis, 15–35% suffer from peripheral neuropathy and eventually show amyloid deposits in peripheral nerves. As yet, no systematic study has proven the sensitivity of sural nerve biopsy for amyloid poylneuropathy. Indeed, Simmons et al. [105] reported six cases with peripheral neuropathy related to amyloidosis without amyloid

Table 3 Fat aspiration and skin biopsy. *n.d.* data not given, *n.o.s* not otherwise specified

Reference	Needle size*	No. of patients studied	No. of patients with systemic amyloid	No. of fat aspirates/skin biopsies with amyloid	Type of amyloid					Controls	Sensitivity**
					AA amyloid	AL amyloid	Hereditary ATTR amyloid	Senile ATTR amyloid	Aβ2 M amyloid		
Westermark and Stenkvist [117]	0.7 mm	28	9	9	8	1	–	–	–	13 × rectal biopsy 2 × autopsy	100%
Rubinow and Cohen [102]	Punch or excisional biopsy	50	50	26	12	38	–	–	–	n.d.	52%
Libbey et al. [65]	19 gauge	32	32	28	6	19	7	–	–	32 × biopsy (various sites)	88%
Westermark et al. [118]	0.9 mm & 1.2 mm	150	150	150	114	31	4	1	–	n.d.	95%
Orfila et al. [80]	22 gauge	12	12	9	9	3	–	–	–	12 × biopsy (various sites)	75%
Maruyama et al. [70]	18 gauge	14	14	–	–	–	14	–	–	None	80%***
Duston et al. [23]	n.d.	443	83	96	21	75	13	–	–	98 × biopsy n.o.s or autopsy	84%
Klemi et al. [57]	0.8–0.9 mm	301	n.d.	106	n.d.	–	–	–	–	125 × oral biopsy 65 × rectal biopsy	82%
Varga et al. [115]	19 gauge	30	n.d.	0	–	–	–	–	n.d.	30 × patient records	–
Gertz et al. [34]	18 gauge	154	82	59	–	82	–	–	–	82 × biopsy (various sites)	72%
Tishler et al. [110]	19 gauge	20	20	4	15	5	–	–	–	18 × biopsy (various sites)	20%
Breedveld et al. [9]	Tru-Cut	44	26	14	26	–	–	–	–	44 × biopsy (various sites)	54%
Masouye [71]	0.8–0.9 mm	100	11	9	4	5	1	1	–	28 × biopsy (various sites) or autopsy	82%
Fatihi et al. [27	Biopsy n.o.s.	20	20	7	20	–	–	–	–	20 × renal biopsy 20 × rectal biopsy 20 × salivary gland	35%
Guy and Jones [43]	18 or 19 gauge	45	14	7	n.d.	n.d.	n.d.	n.d.	n.d.	18 × biopsy (various sites)	58%
Andrews et al. [3]	18 gauge	450	19	17	–	16	1	–	–	2 × biopsy n.o.s. 450 × patient records	n.d.
Kuroda et al. [60]	16 gauge	1006	71	11	71	–	–	–	–	1006 × upper gastrointestinal tract 33 × renal biopsy 21 × fat aspiration	52%

*As given by the author(s)
**When sensitivity was not given by the author(s) it was calculated as follows: number of fat aspirates with amyloid divided by the number of patients with amyloid deposits at other biopsy sites or at autopsy
***Sensitivity was calculated from the number of positive fat tissue fragments divided by the total number of fragments obtained per patient

deposits in the initial sural nerve biopsy, which was probably caused by a sampling error.

Amyloid can also be detected in muscle biopsies. Prayson found amyloid in 16 (0.004%) of 3937 muscle biopsy specimens [84]. Amyloid occurs in vessel walls, and the perimysial and endomysial interstitium. It is frequently associated with neurogenic atrophy, less commonly with scattered degenerating muscle fibers and chronic inflammation [84]. Concomitant detection of amyloid in skeletal muscle and peripheral nerve biopsies has been documented [84, 87].

Renal biopsy

Amyloid is also commonly diagnosed by renal biopsy. The incidence of amyloid in surgical biopsy specimens ranges from 0.002% to 8.4% [13, 27, 103, 111]. In non-diabetic adults with nephrotic syndrome, amyloid is found in 12% of renal biopsies [10]. Amyloid may be present as glomerular, tubulointerstitial and vascular deposits. The fibril protein may originate from any of the systemically occurring amyloid diseases and is also most sensitive in almost all hereditary non-neuropathic amyloid syndromes (Table 3). The majority of renal amyloid deposits are related to AA and AL amyloidosis. In systemic AA and AL amyloidosis, the kidney is almost always affected [36]. Among patients with rheumatoid arthritis and urinary abnormalities and/or renal dysfunction, renal deposits of AA amyloid were found in 19–30% of the cases [48, 73], while renal deposits of AA amyloid reached a prevalence of 0.86% in an unselected consecutive autopsy series [68]. Among the differential diagnoses are cryoglobulinemia, monoclonal gammopathy, systemic lupus erythematosus, immunotactoid glomerulopathy and diabetic fibrillosis [59]. Survival with renal AL amyloidosis depends on the concentration of serum creatinine at presentation. Patients with mean creatinine values of more than 1.3 mg/dl have a median survival of 14.9 months [36].

Cytology

Amyloid can also be diagnosed in specimens obtained for cytology [42]. On Diff-Quick stain, amyloid appears as amorphous, irregular outlined, basophilic to metachromatic clumps. In Papanicoulaou-stained specimens, it is cyanophilic to organophilic [44]. Congo-red staining is applicable to cytology specimens and green birefringence is required for diagnostic proof [41, 44]. However, like FAB, only limited immunohistochemical studies can be performed on specimens obtained for cytology. As yet, no systematic study has proven the sensitivity of cytology.

Others

Amyloid can be diagnosed and classified (see below) in any affected tissue sample. However, the surgical pathologist and the clinician eventually will have to clarify whether this is a local form or part of a systemic disease, which merits further diagnostic intervention and treatment. In the last 5 years, we found amyloid in the following biopsy or resection specimens submitted to our department (CR) of surgical pathology: aortic valve (16 patients), bladder (1), bone marrow biopsy (4), bronchial biopsy (4), breast specimens (3), cardiac ventricle (2), carotid endarterectomy specimens (16), cornea (2), fat aspiration biopsy (12), intervertebral disc (4), stomach (11) and duodenum (2), gall bladder (1), hip joint capsule (2), kidney (8), large intestine and rectum (23), liver (8), open lung biopsy (1), lymph node (5), meniscus (4), mitral valve (2), nasopharynx (3), parailiacal mass (1), portio (1), residual cyst of the mandibula (2), seminal vesicles (3), spleen (1), synovialis (3), thyroid gland (4), tongue (2), tonsil (1) and false cord (1); not all were later on proven to be clinically significant. As a rule, amyloid deposits in fat aspirates, biopsies of the gastrointestinal tract, peripheral nerve biopsies, endomyocardial biopsies of the cardiac ventricles, and from parenchymal organs (kidney, liver, lung, spleen) should be considered as part of a systemic disease until there is evidence to the contrary.

Classification

Following the diagnosis of amyloid, it is mandatory to classify the amyloid fibril protein (Table 1) [96]. This enables the identification of the underlying disease and the clinical significance. Amyloid and amyloidoses might be treatable and treatment schemes differ. There are no conclusive histological or morphological features that clearly distinguish among the different chemical forms. Historically, resistance to potassium permanganate treatment was used to differentiate between AA and AL amyloid deposits. However, this procedure is of limited use when it comes to separation of at least 13 different systemic forms of amyloidosis. Various, more specific procedures are currently available and in use for the classification of amyloid, such as immunohistochemistry, double immunodiffusion, Western blotting, enyzme-linked immunosorbent assay, and amino acid sequencing of purified amyloid fibril proteins.

Immunohistochemistry and immunoelectronmicroscopy

Many studies have confirmed the suitability and use of immunohistochemical classification of amyloid [96]. However, with an ever-increasing number of amyloid fibril proteins identified, one has to raise the issue of whether all these fibril proteins have to be considered in the "average" surgical pathology specimen. Many amy-

Table 4 Commercially available antibodies used for the classification of amyloid. We use additional, non-commercially available antibodies for the classification of AApoAI and AL amyloidosis. *EDTA* ethylenediaminetetraacetic acid, *MW* microwave

Antibody	Clonality	Dilution	Antigen retrieval	Distributor
AA Amyloid (clone mc1)	Monoclonal	1:600	–	Dako, Hamburg, Germany
Amyloid P component	Polyclonal	1:1600	EDTA, MW	"
Fibrinogen	Polyclonal	1:1000	–	"
Lysozyme	Polyclonal	1:5000	–	"
Prealbumin (TTR)	Polyclonal	1:600	EDTA, MW	"
β2-microglobulin	Polyclonal	1:2000	EDTA, MW	"
λ-light chain	Polyclonal	1:10000	–	"
κ-light chain	Polyclonal	1:10000	–	"

loid fibril proteins occur only as local amyloid deposits and hence do not necessitate investigation in a systemic disease or at distant organ and tissue sites. As an example, testing Aβ amyloid (as it is found in Alzheimer's disease) in extracerebral amyloid deposits is unnecessary. As a rule, we recommend testing the most common systemic amyloidoses, i.e., AA-, AApoAI, AFib, AL-, ALys, ATTR-, and Aβ2M-amyloid. We further use immunostaining with anti-amyloid P component, which may help to identify amyloid deposits in immunostained sections, differentiate light- and heavy-chain deposition disease from amyloid and tests general preservation and immunoreactivity of the tissue specimen. Immunohistochemical classification poses several problems and requires experience.

1. The amyloid fibril proteins of almost all systemic amyloid diseases are derived from serum proteins and are frequently detected in tissue specimens without any relationship to amyloid. This problem can, at least partly, be overcome by appropriate dilution of the primary antibody and the use of specific antibodies raised by immunizing specifically with amyloid fibril proteins or synthetic peptides derived from the amyloid fibril proteins. Still, it is recommended to use serial sections stained for Congo red. Immunostaining should demonstrate a spatial relationship to green birefringent deposits found in a Congo-red-stained serial section.
2. Many commercially available antibodies do not stain the amyloid fibril proteins. Several amyloid fibril proteins are cleavage products of the precursor protein with loss of epitopes or the tertiary structure of the amyloid proteins differ markedly from the tertiary structure of the precursor protein and hence abolishes immunoreactivity. This problem can only be bypassed by generating specific antibodies (see above).
3. Amyloid deposits often contain proteins that are not fibril proteins and no structural component of the amyloid fibril but give an intense and spatial signal in immunohistochemistry and are serious obstacles in classifying amyloid. Immunoglobulins are often present within amyloid deposits of non-immunoglobulin origin. An excellent example was described by Hamidi et al. [45]. Amyloid deposits in a patient, who was later on proven to suffer from hereditary renal amyloidosis of fibrinogen origin (AFib amyloidosis) stained with anti-IgM, and anti-immunoglobulin light chain antibodies (λ-light chain in the first patient of the kindred and κ-light chain in another patient of the same kindred) and were formerly interpreted and treated as AL amyloidosis [45].
4. Even antibodies generated using amyloid fibril proteins as immunogen may be misleading. We have shown in our own immunohistochemical studies that an antibody directed against λ-light chain amyloid deposits cross reacts "specifically" with amyloid of prolactin origin in pituitaries and pituitary adenomas [92].

However, some commercially available antibodies can be applied and have demonstrated their use in classifying amyloid deposits immunohistochemically, such as AA-, ATTR- (syn.: prealbumin), and Aβ2 M amyloidosis [89] (Table 4). Amyloid deposits can also be classified by IEM. The advantage of IEM is that labeling of the fibrils differentiates from "contaminating" proteins, not related to the amyloid fibrils, which is difficult to discern on light microscopic level [4].

Biochemistry

Unequivocal identification of the type of amyloid requires isolation of the fibril protein and determination of its primary structure. In most cases, a biochemical characterization will distinguish the type of amyloid, but even this method has its obstacles.

Amyloid fibrils are isolated from amyloidotic tissue in three principal ways: differential centrifugation after homogenization, a so-called "water-wash" procedure in which tissue is repeatedly homogenized in water, and by physical separation and recovery of amyloid proteins by extraction with denaturing solvents [54, 63, 72, 109]. The first two procedures can only be applied to unfixed amyloidotic tissue and generally require gram amounts of starting tissue. The physical separation and recovery of amyloid proteins by extraction with denaturing solvents can be applied to both unfixed and formalin-fixed tissue samples and requires relatively small amounts of amyloidotic tissue [54].

After the amyloid fibril proteins have been extracted from the tissue, they are separated by sodium dodecyl sulfate polyacrylamide gel electrophoresis (SDS-PAGE) or high-performance liquid chromatography (HPLC), and characterized by Western blotting, amino acid sequencing

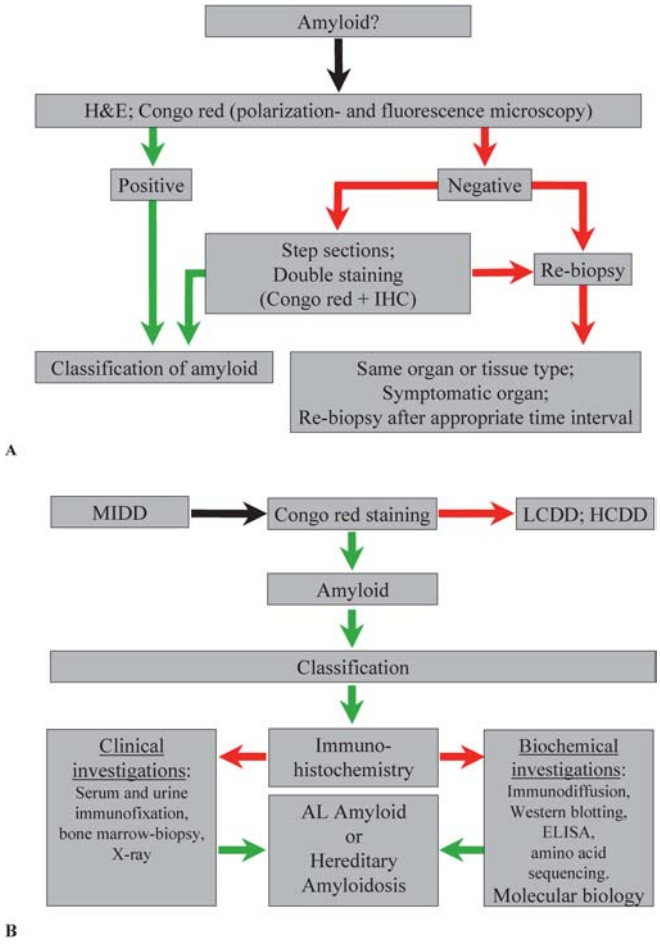

Fig. 2 Diagnostic algorithm for the identification and classification of amyloid in surgical pathology (**A**) and of AL amyloid (**B**). *IHC* immunohistochemistry, *MIDD* monoclonal immunoglobulin deposition disease, *LCDD* light-chain deposition disease, *HCDD* heavy chain deposition disease

or mass spectrometry. In most cases the amyloid fibril protein consists of proteolytic fragments derived from the precursor, or a mixture of the fragments and the precursor. Often the amyloid fibril proteins have a ragged N- and C-terminus, which in SDS-PAGE show up as multiple bands of different aggregated forms [88]. Electro-blotted bands to PVDF-membranes can be cut out and used for N-terminal analysis (Edman degradation). Interpretation of the data is sometimes rather difficult, as the amyloid protein may have a blocked or ragged N-terminus. However, this can in part be overcome if the same material is cleaved by cyanogenbromide or BNPS-skatole. In this case, there will be an increase in the yield, and if the polypeptide contains only one to two residues of either methionine or tryptophan, respectively, identification can be established based on the sequence data. The amyloid fibrils may also be dissolved in 8 mol/l containing 0.25 mol/l Tris (tri-hydroxymethyl amino-methane-hydrochloride) buffer, pH 8.0, with 3 mmol/l disodium-EDTA, reduced and alkylated as described [72]. The alkylated protein can then be purified on a reverse-phase column. Fractions from the different absorption peaks can be taken out for Edman degradation and protein identification. Amyloid components have also been isolated and purified according to a procedure outlined for aortic medial amyloid [46]. The amount of protein needed for N-terminal analysis is in the order of 10–50 pmol. We have applied these procedures successfully to characterize amyloid fibril proteins extracted from formalin-fixed and paraffin-embedded surgical specimens [39, 100]. However, some biopsy and autopsy cases escaped classification and illustrate that even biochemical characterization of amyloid from formalin-fixed specimens is not always successful. Figure 2 summarizes an algorithm for the diagnosis and classification of amyloid.

Differential diagnosis

AL amyloidosis

The diagnosis and classification of AL amyloid, which belongs to the family of monoclonal immunoglobulin deposition diseases (MIDDs), poses a particular problem in surgical pathology. MIDDs are a group of disorders which have in common the deposition of monoclonal proteins (M-protein) in organs and tissue. The proteins deposited are intact immunoglobulins or fragments thereof. The outcome of MIDD may depend on the site and number of M-proteins deposited that interfere with organ integrity. The deposits may be limited to certain organs, such as kidney in myeloma cast nephropathy or adult acquired Fanconi syndrome, or they may be more generalized as in AL and AH amyloidosis, light-chain deposition disease (LCDD), heavy-chain deposition disease (HCDD), and light- and heavy-chain deposition disease (LHCDD) [22, 69]. The tissue deposits in MIDD may take on a variety of morphological shapes, such as amorphous, granular, crystalline or fibrillar. Fibrils associated with MIDD can be amyloid in nature. Histopathologically, the type of MIDD can be separated by Congo-red staining and ultrastructural analysis as well as the presence of apolipoprotein E and amyloid P component [59]. Apolipoprotein E and amyloid P component are commonly found in amyloid deposits, but are absent in LCDD, HCDD and LHCDD [31]. Approximately 20% of patients with plasmacytoma suffer from secondary AL amyloidosis [2]. Tissue deposition of the M-protein may occur locally or systemically. Clinicopathological presentation of patients with AL amyloidosis depends on the extent and distribution of the disease as well as the cause. Specimens are frequently obtained from symptomatic organs, such as kidney in nephrotic syndrome and carpal ligament in carpal tunnel syndrome, or by resection of a mass lesion where there is no clinical suspicion of amyloidosis and the pathologist is the first to consider and diagnose amyloidosis and raises suspicion of a possible underlying disease [96]. Green birefringence after Congo-red staining is highly specific for amyloid, but often not very sensitive and can be misleading at times [66]: in

some cases, amyloidogenic and non-amyloidogenic deposits may be present simultaneously and green birefringence is weak and difficult to detect. Due to the deposition of the variable regions of light chains, AL amyloid stains approximately only in 40% of the cases with commercially available antibodies. Thus negative immunostaining does not exclude AL amyloid.

With all these obstacles in mind, AL amyloid should be diagnosed cautiously. The amyloid deposits need to be immunonegative for other systemically occurring amyloid proteins raising suspicion for AL amyloid. Clinical information should be sought. The presence of an underlying disease, e.g., plasmacytoma, or a monoclonal protein found in serum and/or urine strongly supports the diagnosis of AL amyloid. Systemic AL amyloidosis is a serious disease: patients with cardiac involvement survive 4–6 months, patients without cardiac involvement at the time of diagnosis have a median survival of 30 months [35]. If neither immunohistochemistry nor clinical history is informative, then preparation of the fibril protein and biochemical identification should be applied [54, 72, 98].

Hereditary systemic amyloidoses

A recent publication of Lachmann et al. [62] highlighted the issue of hereditary systemic amyloidoses, which have been misinterpreted as AL amyloid. Among 350 patients initially diagnosed as having AL amyloid, 18 (5.2%) were subsequently identified as hereditary AFib amyloidosis, 13 (3.7%) as ATTR-, 2 (0.6%) as AApoAI-, and 1 (0.3%) as ALys amyloidosis. The problem is further complicated by the fact that many hereditary systemic amyloidoses may mimic clinically AL amyloidosis by presenting with nephropathy (Table 2). To date, over 80 mutations in transthyretin, nine in apolipoprotein AI, four in fibrinogen α-chain, four in lysozyme, two in apolipoprotein AII, two in gelsolin, one in BRI-L and one in cystatin C have been identified as causative for hereditary systemic diseases (Table 2). Most patients with hereditary systemic amyloidosis are heterozygous for the mutation and show an autosomal dominant trait. The clinical amyloidosis syndromes that accompany the various mutations are diverse with respect to age of onset, mode of presentation, pattern of organ distribution, rate of progression and prognosis (Table 3). Different kindreds sharing the same gene mutation and having the same amyloid type may differ in their clinical presentation [53]. A hereditary amyloid syndrome can be identified by genetic counseling, sequencing amyloid fibril proteins purified from fresh or archival tissue specimens, and by means of molecular biology. However, molecular biological studies can only be successful, when the mutation leading to amyloidosis is known. It should also be considered that identification of a point mutation in it's own right is no proof of amyloid. There are several reports of patients with more than one amyloid disease. De Sousa et al. [21] described a patient who suffered from AApoAI- and ATTR amyloidosis. While AApoAI amyloidosis was related to gene mutation, transthyretin was found to be of wild-type origin and therefore a non-hereditary type [21]. A family history is important in the diagnosis of hereditary systemic amyloidosis, but genetic or environmental factors or both can modulate the clinical onset in this group of diseases.

Figure 2 summarizes an algorithm for the diagnosis and classification of amyloid in surgical pathology.

Therapy

Early diagnosis and classification of amyloid has become of paramount importance, since several different therapeutic schemes have been developed in the past decade. In AA amyloidosis, the underlying disease is treated vigorously. When AL amyloidosis is diagnosed and classified early, i.e., no cardiac involvement apparent, it can be treated with high-dose chemotherapy and autologous stem cell transplantation [15]. Hereditary amyloid diseases, such as ATTR-, AApoAI- and AFib amyloidosis, are treated with liver (as a form of "surgical gene therapy") or combined liver-kidney transplantation [18, 37, 38, 64, 104]. In addition, several laboratories in North America and Europe are developing drugs, which hopefully will prevent the formation and deposition of amyloid and support clearing of the deposits [50, 56, 82].

References

1. Abe Y, Utsunomiya H, Tsutsumi Y (1992) Atypical carcinoid tumor of the lung with amyloid stroma. Acta Pathol Jpn 42:286–292
2. Alexanian R, Weber D, Liu F (1999) Differential diagnosis of monoclonal gammopathies. Arch Pathol Lab Med 123:108–113
3. Andrews TR, Colon-Otero G, Calamia KT, Menke DM, Boylan KB, Kyle RA (2002) Utility of subcutaneous fat aspiration for diagnosing amyloidosis in patients with isolated peripheral neuropathy. Mayo Clin Proc 77:1287–1290
4. Arbustini E, Morbini P, Verga L, Concardi M, Porcu E, Pilotto A, Zorzoli I, Garini P, Anesi E, Merlini G (1997) Light and electron microscopy immunohistochemical characterization of amyloid deposits. Amyloid 4:157–170
5. Arbustini E, Verga L, Concardi M, Palladini G, Obici L, Merlini G (2002) Electron and immuno-electron microscopy of abdominal fat identifies and characterizes amyloid fibrils in suspected cardiac amyloidosis. Amyloid 9:108–114
6. Aviel-Ronen S, Liokumovich P, Rahima D, Polak-Charcon S, Goldberg I, Horowitz A (2000) The amyloid deposit in calcifying epithelial odontogenic tumor is immunoreactive for cytokeratins. Arch Pathol Lab Med 124:872–876
7. Benson MD, Liepnieks JJ, Yazaki M, Yamashita T, Asl KH, Guenther B, Kluve-Beckerman B (2001) A new human hereditary amyloidosis: the result of a stop-codon mutation in the apolipoprotein AII gene. Genomics 72:272–277
8. Bohle A, Wehrmann M, Eissele R, Gise Hv, Mackensen-Haen S, Müller C, Müller GA (1993) The long-term prognosis of AA and AL renal amlyoidosis and the pathogenesis of chronic renal failure in renal amyloidosis. Pathol Res Pract 189:316–331
9. Breedveld FC, Markusse HM, MacFarlane JD (1989) Subcutaneous fat biopsy in the diagnosis of amyloidosis secondary to chronic arthritis. Clin Exp Rheumatol 7:407–410
10. Cameron JS (1996) Nephrotic syndrome in the elderly. Semin Nephrol 16:319–329

11. Carson FL, Kingsley WB (1980) Nonamyloid green birefringence following Congo red staining. Arch Pathol Lab Med 104:333–335
12. Choufani EB, Sanchorawala V, Ernst T, Quillen K, Skinner M, Wright DG, Seldin DC (2001) Acquired factor X deficiency in patients with amyloid light-chain amyloidosis: incidence, bleeding manifestations, and response to high-dose chemotherapy. Blood 97:1885–1887
13. Chugh KS, Datta BN, Singhal PC, Jain SK, Sakhuja V, Dash SC (1981) Pattern of renal amyloidosis in Indian patients. Postgrad Med J 57:31–35
14. Cohen AS, Calkins E (1959) Electron microscopic observations on a fibrous component in amyloid of diverse origins. Nature 183:1202–1203
15. Comenzo RL, Gertz MA (2002) Autologous stem cell transplantation for primary systemic amyloidosis. Blood 99:4276–4282
16. Crowley PF, Slavin JL, Rode J (1996) Massive amyloid deposition in pancreatic vipoma: a case report. Pathology 28:377–379
17. Danilewicz M, Wagrowska-Danilewicz M (2002) Quantitative analysis of interstitial mast cells in AA and AL renal amyloidosis. Pathol Res Pract 198:413–419
18. de Carvalho M, Conceicao I, Bentes C, Luis ML (2002) Long-term quantitative evaluation of liver transplantation in familial amyloid polyneuropathy (in Portuguese). Amyloid 9:126–133
19. Delgado WA, Aranachavez VE (1997) Amyloid deposits in labial salivary glands identified by electron microscopy. J Oral Pathol Med 26:51–52
20. Delgado WA, Mosqueda A (1989) A highly sensitive method for diagnosis of secondary amyloidosis by labial salivary gland biopsy. J Oral Pathol Med 18:310–314
21. deSousa MM, Vital C, Ostler D, Fernandes R, PougetAbadie J, Carles D, Saraiva MJ (2000) Apolipoprotein Al and transthyretin as components of amyloid fibrils in a kindred with apoAl Leu178His amyloidosis. Am J Pathol 156:1911–1917
22. Dhodapkar MV, Merlini G, Solomon A (1997) Biology and therapy of immunoglobulin deposition diseases. Hematol Oncol Clin North Am 11:89–110
23. Duston M, Skinner M, Shirahama TS, Cohen AS (1987) Diagnosis of amyloidosis by abdominal fat aspiration. Analysis of four years' experience. Am J Med 82:412–414
24. Emori Y, Sakugawa M, Niiya K, Kiguchi T, Kojima K, Takenaka K, Shinagawa K, Ishimaru F, Ikeda K, Tanimoto M, Yamasaki R, Ohara N, Harada M (2002) Life-threatening bleeding and acquired factor V deficiency associated with primary systemic amyloidosis. Blood Coagul Fibrinolysis 13:555–559
25. Eriksson L, Westermark P (1986) Intracellular neurofibrillary tangle-like aggregations. A constantly present amyloid alteration in the aging choroid plexus. Am J Pathol 125:124–129
26. Fatihi E, Zahiri K, Hachim K, Fadel H, Benghanem GM, Sqalli S, Ramdani B, Zaid D (1999) Diagnostic value of accessory salivary gland biopsy in amyloidosis. Rev Med Interne 20:759–761
27. Fatihi E, Ramdani B, Fadel H, Hachim K, Zahiri K, Benghanem GM, Sqalli S, Zaid D (2000) Prevalence of subcutaneous, labial, and rectal amyloidosis in patients with renal amyloidosis. Nephrologie 21:19–21
28. Fernandez-Alonso J, Rios-Camacho C, Valenzuela-Castano A, Hernanz-Mediano W (1994) Mixed systemic amyloidosis in a patient receiving long term haemodialysis. J Clin Pathol 47:560–561
29. Foschini MP, Dadda T, Bordi C, Eusebi V (1993) Amyloid stroma in meningiomas. Virchows Arch 422:53–59
30. Gafni J, Sohar E (1960) Rectal biopsy for the diagnosis of amyloidosis. Am J Med Sci 240:332–336
31. Gallo G, Wisniewski T, Choi-Miura NH, Ghiso J, Frangione B (1994) Potential role of apolipoprotein-E in fibrillogenesis. Am J Pathol 145:526–530
32. Garciagonzalez R, Fernandez FA, Garijo MF, Valbernal JF (1998) Amyloidosis of the rectum mimicking collagenous colitis. Pathol Res Pract 194:731–735
33. Gertz MA (2002) Diagnosing primary amyloidosis. Mayo Clin Proc 77:1278–1279
34. Gertz MA, Li CY, Shirahama T, Kyle RA (1988) Utility of subcutaneous fat aspiration for the diagnosis of systemic amyloidosis (immunoglobulin light chain). Arch Intern Med 148:929–933
35. Gertz MA, Lacy MQ, Dispenzieri A (1999) Amyloidosis: recognition, confirmation, prognosis, and therapy. Mayo Clin Proc 74:490–494
36. Gertz MA, Lacy MQ, Dispenzieri A (2002) Immunoglobulin light chain amyloidosis and the kidney. Kidney Int 61:1–9
37. Gillmore JD, Booth DR, Rela M, Heaton ND, Rahman V, Stangou AJ, Pepys MB, Hawkins PN (2000) Curative hepatorenal transplantation in systemic amyloidosis caused by the Glu526Val fibrinogen α-chain variant in an English family. Q J Med 93:269–275
38. Gillmore JD, Stangou AJ, Tennent GA, Booth DR, O'Grady J, Rela M, Heaton ND, Wall CA, Keogh JA, Hawkins PN (2001) Clinical and biochemical outcome of hepatorenal transplantation for hereditary systemic amyloidosis associated with apolipoprotein AI Gly26Arg. Transplantation 71:986–992
39. Glasbrenner B, Güthner C, Röcken C, Mattfeld T, Hetzel W, Adler G (1999) 56jähriger Patient mit segmental florider Colitis und Colonamyloidose. Internist 40:668–672
40. Groisman GM, Lachter J, Vlodavsky E (1997) Amyloid colitis mimicking collagenous colitis. Histopathology 31:201–202
41. Gupta RK, Dowle CS (1996) Cytodiagnosis of amyloid deposition within the breast. Cytopathology 7:136–140
42. Gupta RK, Wakefield J, Halliwell T, Foo K, Lallu S, Naran S, Fauck R (2002) Aspiration cytodiagnosis of amyloid from vitreous fluid. Diagn Cytopathol 26:294–296
43. Guy CD, Jones CK (2001) Abdominal fat pad aspiration biopsy for tissue confirmation of systemic amyloidosis: specificity, positive predictive value, and diagnostic pitfalls. Diagn Cytopathol 24:181–185
44. Halliday BE, Silverman JF, Finley JL (1998) Fine-needle aspiration cytology of amyloid associated with nonneoplastic and malignant lesions. Diagn Cytopathol 18:270–275
45. Hamidi AL, Liepnieks JJ, Uemichi T, Rebibou JM, Justrabo E, Droz D, Mousson C, Chalopin JM, Benson MD, Delpech M, Grateau G (1997) Renal amyloidosis with a frame shift mutation in fibrinogen Aα- chain gene producing a novel amyloid protein. Blood 90:4799–4805
46. Häggqvist B, Naslund J, Sletten K, Westermark GT, Mucchiano G, Tjernberg LO, Nordstedt C, Engstrom U, Westermark P (1999) Medin: An integral fragment of aortic smooth muscle cell-produced lactadherin forms the most common human amyloid. Proc Natl Acad Sci U S A 96:8669–8674
47. Hazenberg BPC, Limburg PC, Bijzet J, Vanrijswijk MH (1999) A quantitative method for detecting deposits of amyloid A protein in aspirated fat tissue of patients with arthritis. Ann Rheum Dis 58:96–102
48. Helin HJ, Korpela MM, Mustonen JT, Pasternack AI (1995) Renal biopsy findings and clinicopathologic correlations in rheumatoid arthritis. Arthritis Rheum 38:242–247
49. Horn U, Goebel HH, Storkel S, Bohl J, Thomas E, Schlote W, Budzilovich G (1991) Immunohistochemistry of amyloid-related neuropathies. Clin Neuropathol 10:237–243
50. Hrncic R, Wall J, Wolfenbarger DA, Murphy CL, Schell M, Weiss DT, Solomon A (2000) Antibody-mediated resolution of light chain-associated amyloid deposits. Am J Pathol 157:1239–1246
51. Ii K, Kyle RA, Dyck PJ (1992) Immunohistochemical characterization of amyloid proteins in sural nerves and clinical associations in amyloid neuropathy. Am J Pathol 141:217–226
52. Isobe T, Matsushita T, Minakata T, Takahashi M, Hoshii Y, Ishiwara T, Uchino F (1996) Coexistence of AL and A beta 2 M amyloid in tissues of a patient with myeloma on hemodialysis. Amyloid 3:41–43

53. Jones LA, Harding JA, Cohen AS, Skinner M (1990) New USA family has apolipoprotein AI (Arg26) variant. In: Natvig JB, Forre O, Husby G, Husebekk A, Skogen B, Sletten K, Westermark P (eds) Amyloid and amyloidosis. Kluwer Academic, Dordrecht, Netherlands, pp 385–388
54. Kaplan B, Hrncic R, Murphy CL, Gallo G, Weiss DT, Solomon A (1999) Microextraction and purification techniques applicable to chemical characterization of amyloid proteins in minute amounts of tissue. Methods Enzymol 309:67–81
55. Kaplan B, Vidal R, Kumar A, Ghiso J, Gallo G (1999) Immunochemical microanalysis of amyloid proteins in fine-needle aspirates of abdominal fat. Am J Clin Pathol 112:403–407
56. Kisilevsky R, Lemieux LJ, Fraser PE, Kong X, Hultin PG, Szarek WA (1995) Arresting amyloidosis in vivo using small-molecule anionic sulphonates or sulphates: implications for Alzheimer's disease. Nat Med 1:143–148
57. Klemi PJ, Sorsa S, Happonen RP (1987) Fine-needle aspiration biopsy from subcutaneous fat. An easy way to diagnose secondary amyloidosis. Scand J Rheumatol 16:429–431
58. Kobayashi H, Tada S, Fuchigami T, Okuda Y, Takasugi K, Matsumoto T, Iida M, Aoyagi K, Iwashita A, Daimaru Y, Fujishima M (1996) Secondary amyloidosis in patients with rheumatoid arthritis: diagnostic and prognostic value of gastroduodenal biopsy. Br J Rheumatol 35:44–49
59. Korbet SM, Schwartz MM, Lewis EJ (1994) The fibrillary glomerulopathies. Am J Kidney Dis 23:751–765
60. Kuroda T, Tanabe N, Sakatsume M, Nozawa S, Mitsuka T, Ishikawa H, Tohyama CT, Nakazono K, Murasawa A, Nakano M, Gejyo F (2002) Comparison of gastroduodenal, renal and abdominal fat biopsies for diagnosing amyloidosis in rheumatoid arthritis. Clin Rheumatol 21:123–128
61. Kyle RA, Spencer RJ, Dahlin DC (1966) Value of rectal biopsy in the diagnosis of primary systemic amyloidosis. Am J Med Sci 251:501–506
62. Lachmann HJ, Booth DR, Booth SE, Bybee A, Gilbertson JA, Gillmore JD, Pepys MB, Hawkins PN (2002) Misdiagnosis of hereditary amyloidosis as AL (primary) amyloidosis. N Engl J Med 346:1786–1791
63. Layfield R, Bailey K, Lowe J, Allibone R, Mayer RJ, Landon M (1996) Extraction and protein sequencing of immunoglobulin light chain from formalin-fixed cerebrovascular amyloid deposits. J Pathol 180:455–459
64. Lewis WD (2002) Liver transplantation: an effective treatment for familial ATTR amyloidosis. Amyloid 9:201–202
65. Libbey CA, Skinner M, Cohen AS (1983) Use of abdominal fat tissue aspirate in the diagnosis of systemic amyloidosis. Arch Intern Med 143:1549–1552
66. Linke RP (2000) Highly sensitive diagnosis of amyloid and various amyloid syndromes using Congo red fluorescence. Virchows Arch 436:439–448
67. Linke RP, Gärtner HV, Michels H (1995) High-sensitivity diagnosis of AA amyloidosis using congo red and immunohistochemistry detects missed amyloid deposits. J Histochem Cytochem 43:863–869
68. Löfberg H, Grubb A, Thysell H, Nilsson E, Kjellander B, Moller C, Gruic V, Ljungquist A, Sternby NH (1987) The prevalence of renal amyloidosis of the AA-type in a series of 1.158 consecutive autopsies. Acta Pathol Microbiol Immunol Scand [A] 95:297–302
69. Maniatis A (1998) Pathophysiology of paraprotein production. Ren Fail 20:821–828
70. Maruyama K, Ikeda S, Yanagisawa N, Nakazato M (1987) Diagnostic value of abdominal fat tissue aspirate in familial amyloid polyneuropathy. J Neurol Sci 81:11–18
71. Masouye I (1997) Diagnostic screening of systemic amyloidosis by abdominal fat aspiration: an analysis of 100 cases. Am J Dermatopathol 19:41–45
72. Murphy CL, Eulitz M, Hrncic R, Sletten K, Westermark P, Williams T, Macy SD, Wooliver C, Wall J, Weiss DT, Solomon A (2001) Chemical typing of amyloid protein contained in formalin-fixed paraffin-embedded biopsy specimens. Am J Clin Pathol 116:135–142
73. Nakano M, Ueno M, Nishi S, Shimada H, Hasegawa H, Watanabe T, Kuroda T, Sato T, Maruyama Y, Arakawa M (1998) Analysis of renal pathology and drug history in 158 Japanese patients with rheumatoid arthritis. Clin Nephrol 50:154–160
74. Ohsawa H, Kanatsuka A, Tokuyama Y, Yamaguchi T, Makino H, Yoshida S, Horie H, Mikata A, Kohen Y (1991) Amyloid protein in somatostatinoma differs from islet amyloid polypeptide. Acta Endocrinol 124:45–53
75. Okuzono Y, Gondo T, Kawano H, Nagasawa T, Uchino F (1986) Histopathology of cutaneous amyloid: a comparitive study on 144 cases of localized cutaneous amyloidosis and 20 cases of systemic amyloidosis. In: Glenner GG, Osserman EF, Benditt EP, Calkins E, Cohen AS, Zucker-Franklin D (eds) Amyloidosis. Plenum Publishing Corporation, New York, pp 821–828
76. Olsen KE, Westermark P (1994) Amyloid in basal cell carcinoma and seborrheic keratosis. Acta Derm Venereol 74:273–275
77. Olsen KE, Sletten K, Westermark P (1998) Extended analysis of AL-amyloid protein from abdominal wall subcutaneous fat biopsy: kappa IV immunoglobulin light chain. Biochem Biophys Res Commun 245:713–716
78. Olsen KE, Sletten K, Sandgren O, Olsson H, Myrvold K, Westermark P (1999) What is the role of giant cells in AL-amyloidosis. Amyloid 6:89–97
79. Olsen KE, Sletten K, Westermark P (1999) The use of subcutaneous fat tissue for amyloid typing by enzyme-linked immunosorbent assay. Am J Clin Pathol 111:355–362
80. Orfila C, Giraud P, Modesto A, Suc JM (1986) Abdominal fat tissue aspirate in human amyloidosis: light, electron, and immunofluorescence microscopic studies. Hum Pathol 17:366–369
81. Pepys MB, Hawkins PN, Booth DR, Vigushin DM, Tennent GA, Soutar AK, Totty N, Nguyen O, Blake CCF, Terry CJ, Feest TG, Zalin AM, Hsuan JJ (1993) Human lysozyme gene mutations cause hereditary systemic amyloidosis. Nature 362:553–557
82. Pepys MB, Herbert J, Hutchinson WL, Tennent GA, Lachmann HJ, Gallimore JR, Lovat LB, Bartfai T, Alanine A, Hertel C, Hoffmann T, Jakob-Roetne R, Norcross RD, Kemp JA, Yamamura K, Suzuki M, Taylor GW, Murray S, Thompson D, Purvis A, Kolstoe S, Wood SP, Hawkins PN (2002) Targeted pharmacological depletion of serum amyloid P component for treatment of human amyloidosis. Nature 417:254–259
83. Pitkänen P, Westermark P, Cornwell GGI, Murdoch W (1983) Amyloid of the seminal vesicles. A distinctive and common localized form of senile amyloidosis. Am J Pathol 110:64–69
84. Prayson RA (1998) Amyloid myopathy: clinicopathologic study of 16 cases. Hum Pathol 29:463–468
85. Puchtler H, Sweat F, Levine M (1962) On the binding of Congo red by amyloid. J Histochem Cytochem 10:355–364
86. Puchtler H, Waldrop FS, Meloan SN (1985) A review of light, polarization and fluorescence microscopic methods for amyloid. Appl Pathol 3:5–17
87. Rajani B, Rajani V, Prayson RA (2000) Peripheral nerve amyloidosis in sural nerve biopsies—a clinicopathologic analysis of 13 cases. Arch Pathol Lab Med 124:114–118
88. Ramstad HM, Sletten K, Husby G (1995) The amino acid sequence and carbohydrate composition of an immunoglobulin kappa light chain amyloid fibril protein (AL) of variable subgroup I. Amyloid 2:223–228
89. Röcken C, Roessner A (1999) An evaluation of antigen retrieval procedures for immunoelectron microscopical classification of amyloid deposits. J Histochem Cytochem 47:1385–1394
90. Röcken C, Saeger W, Linke RP (1993) Mehrere unterschiedliche Amyloidtypen bei einer 93-jährigen Patientin: Kasuistik eines Sektionsfalles. Pathologe 14:42–46

91. Röcken C, Saeger W, Linke RP (1994) Gastrointestinal amyloid deposits in old age. Report on 110 consecutive autopsical patients and 98 retrospective bioptic specimens. Pathol Res Pract 190:641–649
92. Röcken C, Uhlig H, Saeger W, Linke RP, Fehr S (1995) Amyloid deposits in pituitaries and pituitary adenomas: immunohistochemistry and in situ hybridization. Endocr Pathol 6:135–143
93. Röcken C, Eick B, Saeger W (1996) Intracellular amyloid in pituitary and adrenal glands. Morphological and statistical investigations. Virchows Arch 429:293–299
94. Röcken C, Linke RP, Saeger W (1996) Corpora amylacea in the lung, prostate and uterus: a comparitive immunohistochemical study. Pathol Res Pract 192:998–1006
95. Röcken C, Saeger W, Linke RP (1996) Portal amyloid. Novel amyloid deposits in gastrointestinal veins? Arch Pathol Lab Med 120:1044–1051
96. Röcken C, Schwotzer E, Linke RP, Saeger W (1996) The classification of amyloid deposits in clinicopathological practice. Histopathology 29:325–335
97. Röcken C, Radun D, Glasbrenner B, Malfertheiner P, Roessner A (1999) Generalized AA-amyloidosis in a 58-year-old Caucasian woman with an 18-month history of gastrointestinal tuberculosis. Virchows Arch 434:95–100
98. Röcken C, Hegenbarth V, Schmitz M, Stix B, Schade G, Mohnert A, Roessner A (2000) Plasmacytoma of the tonsil with AL amyloidosis: evidence of post-fibrillogenic proteolysis of the fibril protein. Virchows Arch 436:336–344
99. Röcken C, Stix B, Brömme D, Ansorge S, Roessner A, Bühling F (2001) A putative role for cathepsin K in degradation of AA and AL amyloidosis. Am J Pathol 158:1029–1038
100. Röcken C, Kronsbein H, Sletten K, Roessner A, Bässler R (2002) Amyloidosis of the breast. Virchows Arch 440:527–535
101. Röcken C, Peters B, Juenemann G, Saeger W, Klein HU, Huth C, Roessner A, Goette A (2002) Atrial amyloidosis: an arrhythmogenic substrate for persistent atrial fibrillation. Circulation 106:2091–2097
102. Rubinow A, Cohen AS (1978) Skin involvement in generalized amyloidosis. A study of clinically involved and uninvolved skin in 50 patients with primary and secondary amyloidosis. Ann Intern Med 88:781–785
103. Schena FP, Pannarale G, Carbonara MC (1996) Clinical and therapeutic aspects of renal amyloidosis. Nephrol Dial Transplant 11[Suppl 9]:63–68
104. Shaz BH, Lewis WD, Skinner M, Khettry U (2001) Livers from patients with apolipoprotein A-I amyloidosis are not suitable as "domino" donors. Mod Pathol 14:577–580
105. Simmons Z, Blaivas M, Aguilera AJ, Feldman EL, Bromberg MB, Towfighi J (1993) Low diagnostic yield of sural nerve biopsy in patients with peripheral neuropathy and primary amyloidosis. J Neurol Sci 120:60–63
106. Steensma DP (2001) "Congo" red—out of Africa. Arch Pathol Lab Med 125:250–252
107. Steinhoff MM, Wells SAJ, DeSchryver Kecskemeti K (1992) Stromal amyloid in pheochromocytomas. Hum Pathol 23:33–36
108. Takahashi M, Yokota T, Kawano H, Gondo T, Ishihara T, Uchino F (1989) Ultrastructural evidence for intracellular formation of amyloid fibrils in macrophages. Virchows Arch 415:411–419
109. Tennent GA (1999) Isolation and characterization of amyloid fibrils from tissue. Methods Enzymol 309:26–47
110. Tishler M, Pras M, Yaron M (1988) Abdominal fat tissue aspirate in amyloidosis of familial Mediterranean fever. Clin Exp Rheumatol 6:395–397
111. Toth T, Toth-Jakatics R, Jimi S, Takebayashi S (2000) Increased density of interstitial mast cells in amyloid A renal amyloidosis. Mod Pathol 13:1020–1028
112. Toyoda M, Kudo M, Ebihara Y (1999) Amyloid deposition in renal angiomyolipoma. Pathol Int 49:180–184
113. Tripodi SA, Civitelli S, Schurfeld K, Cintorino M (2000) Microcystic adenoma of the pancreas (glycogen-rich cystadenoma) with stromal amyloid deposits. Histopathology 37:147–149
114. Uemichi T, Liepnieks JJ, Gertz MA, Benson MD (1998) Fibrinogen A α-chain Leu 554: an African-American kindred with late onset renal amyloidosis. Amyloid 5:188–192
115. Varga J, Idelson BA, Felson D, Skinner M, Cohen AS (1987) Lack of amyloid in abdominal fat aspirates from patients undergoing long-term hemodialysis. Arch Intern Med 147:1455–1457
116. Westermark P (1973) Fine structure of islets of Langerhans in insular amyloidosis. Virchows Arch 359:1–18
117. Westermark P, Stenkvist B (1973) A new method for the diagnosis of systemic amyloidosis. Arch Int Med 132:522–523
118. Westermark P, Benson L, Olofsson BO (1986) Fine needle aspiration biopsy of abdominal subcutaneous fat tissue for the diagnosis and typing of amyloidosis. In: Glenner GG, Osserman EF, Benditt EP, Calkins E, Cohen AS, Zucker-Franklin D (eds) Amyloidosis. Plenum Publishing Corporation, New York, pp 613–615
119. Westermark P, Wernstedt C, Wilander E, Hayden DW, O'Brien TD, Johnson KH (1987) Amyloid fibrils in human insulinoma and islets of Langerhans of the diabetic cat are derived from a neuropeptide-like protein also present in normal islet cells. Proc Natl Acad Sci U S A 84:3881–3885
120. Westermark P, Mucchiano G, Marthin T, Johnson KH, Sletten K (1995) Apolipoprotein A1-derived amyloid in human aortic atherosclerotic plaques. Am J Pathol 147:1186–1192
121. Westermark P, Benson MD, Buxbaum JN, Cohen AS, Frangione B, Ikeda S, Masters CL, Merlini G, Saraiva MJ, Sipe JD (2002) Amyloid fibril protein nomenclature—2002. Amyloid 9:197–200
122. Yamada M, Hatakeyama S, Tsukagoshi H (1985) Gastrointestinal amyloid deposition in AL (primary or myeloma-associated) and AA (secondary) amyloidosis: diagnostic value of gastric biopsy. Hum Pathol 16:1206–1211
123. Yazaki M, Liepnieks JJ, Yamashita T, Guenther B, Skinner M, Benson MD (2001) Renal amyloidosis caused by a novel stop-codon mutation in the apolipoprotein A-II gene. Kidney Int 60:1658–1665
124. Yoshimatsu SI, Ando Y, Terazaki H, Sakashita N, Tada S, Yamashita T, Suga M, Uchino M, Ando M (1998) Endoscopic and pathological manifestations of the gastrointestinal tract in familial amyloidotic polyneuropathy type I (Met30). J Intern Med 243:65–72

Virchows Arch (2003) 443:17–27
DOI 10.1007/s00428-003-0824-0

ORIGINAL ARTICLE

Hamdy Metwaly · Jun Cheng · Hiroko Ida-Yonemochi · Kazufumi Ohshiro · Kai Yu Jen · Ai Ru Liu · Takashi Saku

Vascular endothelial cell participation in formation of lymphoepithelial lesions (epi-myoepithelial islands) in lymphoepithelial sialadenitis (benign lymphoepithelial lesion)

Received: 7 January 2003 / Accepted: 7 April 2003 / Published online: 22 May 2003
© Springer-Verlag 2003

Abstract Lymphoepithelial lesions (LELs, or epi-myoepithelial islands) in lymphoepithelial sialadenitis (LESA, or benign lymphoepithelial lesion) of the salivary gland are known to be mainly composed of duct epithelial cells. However, other constituent cells are poorly characterized. Formalin-fixed paraffin sections obtained from six surgical specimens of LESA were examined using immunohistochemistry for cytoskeletal proteins, inflammatory cells, vascular endothelial cells, and extracellular matrix (ECM) molecules as well as by in situ hybridization for ECM molecules. In addition to keratin-immunopositive (+) duct-like epithelial cells, there were CD31/CD34+ vascular endothelial cells—which were either scattered in a singular fashion, in formed sheets, or in tubular structures—, CD20+ B lymphocytes, CD45RO+ T lymphocytes, and CD68 macrophages in the LELs. ECM molecules, such as heparan sulfate proteoglycan and tenascin, were immunolocalized in hyaline materials in the LELs. Their mRNAs were demonstrated mainly in endothelial cells and, to a lesser extent, in lymphomonocytic cells around hyaline materials, but were not as evident in epithelial constituent cells of LELs. The results indicate that endothelial cells as well as inflammatory cells are important constituents of the LELs, and the hyaline ECM cores mainly result from the intra-LEL angiogenesis by endothelial cells with the assistance of inflammatory cells. This intra-LEL vasculature seems to support regeneration and proliferation of salivary epithelial remnant cells.

Keywords Benign lymphoepithelial lesion · Endothelial cell · Epi-myoepithelial island · Lymphoepithelial lesion · Lymphoepithelial sialadenitis · Heparan sulfate proteoglycan

H. Metwaly · J. Cheng · H. Ida-Yonemochi · K. Ohshiro · K. Y. Jen · T. Saku (✉)
Division of Oral Pathology,
Department of Tissue Regeneration and Reconstruction,
Niigata University Graduate School
of Medical and Dental Sciences,
2-5274 Gakkocho-dori, 951-8514 Niigata, Japan
e-mail: tsaku@dent.niigata-u.ac.jp
Tel.: +81-25-2272832
Fax: +81-25-2270805

A. R. Liu
Department of Oral Pathology,
School of Stomatology, Shanghai Second Medical University,
China

Introduction

Lymphoepithelial sialadenitis (LESA [13], also referred to as benign lymphoepithelial lesion [2, 9, 40, 41], lymphoepithelial lesion [3, 5, 18, 27, 30], myoepithelial sialadenitis (MESA) [10, 11], Sögren-type sialadenitis [15], or autoimmune sialadenitis [21, 22, 32]) of the salivary glands is histologically characterized by an extensive infiltration of chronic inflammatory cells replacing the salivary parenchymal space, which is composed of acinar and ductal cells. In their full-grown stages, ductal cell remnants regenerate to form epi-myoepithelial islands (EMIs), which sometimes show minimal ductal lumina but ultimately show solid epithelial nests. EMIs were first investigated using electron microscopy (EM) in the 1960s [2, 5, 9, 11, 19, 28, 32, 35, 40, 41] and were shown to be composed of both duct epithelial and myoepithelial cells. However, immunohistochemical studies for cytoskeletal proteins were introduced in this lesion in the 1980s, which indicated that cells with duct epithelial characteristics are mainly responsible for the EMI formation [3, 15, 16, 21, 22, 26, 27, 32, 38]. In addition to the EM studies, these immunohistochemical studies have also indicated that the EMIs are composed of not only epithelial cells but also of other inflammatory cells, as not all of the constituent cells of EMIs are immunolabeled for epithelial cytoskeletal proteins. Because of the negligible contribution of myoepithelial cells to the island formation, the usage of the term EMIs has been questioned, and pathologists have

recently preferred the use of the term lymphoepithelial lesions (LELs) over EMI [15]. Thus, we use LELs hereafter in this paper, although the term LEL is still confused with the old terminology of BLEL, which has been used for the disease entity of this particular inflammatory condition for a long time. The term LEL was originally used for the structures produced by lymphocytes infiltrating the epithelium in normal mucosa-associated lymphoid tissue (MALT) or MALT lymphoma of organs other than salivary glands [17].

The presence of eosinophilic hyaline material is another characteristic histology of LELs. However, this characteristic material has not been fully substantiated [2, 5, 21, 27, 28, 35]. Recently, we have determined immunohistochemically that similar eosinophilic hyaline materials in adenomatoid odontogenic tumors (AOTs) are composed of enamel proteins as well as basement membrane (BM) molecules and that they might develop into the characteristic pseudocystic space formed by AOT cells with ameloblastic differentiation [25, 33]. Accordingly, we wanted to determine the constituent molecules in the eosinophilic hyaline materials in LELs, as their histological features resemble those in AOTs. In this trial, we found that eosinophilic materials contained BM-associated extracellular matrix (ECM) molecules. At the same time, the immunolocalization of the BM molecules indicated the presence of vascular elements within LELs.

In this study, therefore, we used the immunohistochemistry of vascular endothelial markers in addition to in situ hybridization for ECM molecules to examine the constituent cells of LELs. In addition, we determined the role that the constituent cells other than epithelial cells play in the formation of LELs with eosinophilic hyaline materials in the background of lymphoid cell infiltration.

Materials and methods

Surgical material

Six cases of LESA were selected from the surgical pathology files of the Division of Oral Pathology, the Department of Tissue Regeneration and Reconstruction, Niigata University Graduate School of Medical and Dental Sciences and the Department of Oral Pathology, School of Stomatology, Shanghai Second Medical University. The tissue specimens were all surgical materials and fixed in 10% formalin, routinely processed, and embedded in paraffin. Serial sections cut at 5 μm were stained with hematoxylin and eosin and immunohistochemically with the antibodies described below. Other sets of sections were used for in situ hybridization for perlecan and tenascin.

Antibodies

Antibodies against mouse BM-type heparan sulfate proteoglycan (HSPG, perlecan) core protein [31], fibronectin [7], and laminin [6] were raised in rabbits as described elsewhere. Rabbit polyclonal antibodies for tenascin were purchased from Chemicon International, Inc. (Temecula, CA, USA) and type-IV collagen from Cappel Laboratories (Cochranville, OH, USA). Rabbit antibodies against collagen types III, V, and VI were provided by Dr. H. Furthmayr of Stanford University [12]. Rabbit polyclonal antibodies to bovine brain S-100 protein and to human keratin (wide spectrum, pan-keratin) were purchased from Dako Ltd. (Copenhagen, Denmark). Monoclonal mouse antibodies to human keratin peptides 14 (clone CKB1, keratin 14) and human CD43 (clone DF-T1) were purchased from Sigma Chemical Co. (St. Louis, MO, USA). Mouse monoclonal antibodies to human CD31 (JC/70A), CD68 (PG-M1), CD20 (L26), CD45RO (UCHL1), and CD8 (C8/144B) and to bovine eye lens vimentin (Vim 3B4) were purchased from Dako. A mouse antibody to human CD34 (NU-4A1) was obtained from Nichirei Co. Ltd. (Tokyo, Japan). A mouse monoclonal antibody to human CD4 (4B12) was purchased from Novocastra Laboratories Ltd. (Newcastle upon Tyne, UK). A mouse monoclonal antibody to human MUC1 mucin (CA15-3, clone DF3) was purchased from Fujirebio Diagnostics, Inc. (Tokyo, Japan). The primary antibodies used in this study are summarized in Table 1.

Table 1 List of primary antibodies used in immunohistochemistry for lymphoepithelial sialadenitis

Antibody against	Immunogen		Clone	Dilution	Distributors
	Species	Tissues			
Keratin 14	Human	Callus keratin	CKB1	1:200	Sigma
CD31	Human	Spleen	JC/70A	1:50	Dako
CD34	Human	Myelocytic leukemia cells	NU-4A1	1:100	Nichirei
CD68	Human	Gaucher's cells	PG-M1	1:100	Dako
CD4	Human	Synthetic domain of CD4	4B12	1:20	Novocastra
CD8	Human	Synthetic domain of CD8	C8/144B	1:25	Dako
CD 20	Human	Tonsillar B cells	L26	1:20	Dako
CD43	Human	Myeloblastic cell line KG1	DF-T1	1:10	Sigma
CD45 RO	Human	IL-2-dependent T cells	UCHL1	1:75	Dako
MUC1	Human	Breast adenocarcinoma cells	DF3	Diluted	Fujirebio
Vimentin	Bovine	Eye lens	Vim 3B4	1:400	Dako
HSPG	Murine	EHS tumor perlecan	-	1:3000	[31]
Tenascin	Human	Purified tenascin	-	1:500	Chemicon
Laminin	Human	Placenta	-	1:500	[6]
Fibronectin	Human	ACC3 cells fibronectin	-	1:1000	[7]
Type-IV collagen	Human	Placenta	-	1:00	Cappel
Type-III collagen	Human	Embryo	-	1:300	[12]
Type-V collagen	Human	Amnion	-	1:200	[12]
Type-VI collagen	Human	Placenta	-	1:100	[12]
S-100 protein	Bovine	Brain	-	1:400	Dako
Pan-keratin	Human	Epidermis	-	1:1000	Dako

Immunohistochemistry

Serial sections of 5-μm-thick, paraffin-embedded tissues were used. For the primary rabbit antibodies, goat antibodies against rabbit immunoglobulin (Ig)Gs conjugated with peroxidase-labeled dextran polymers (EnVision+ peroxidase, rabbit; Dako) were used. For the primary mouse antibodies, goat antibodies against mouse IgGs conjugated with peroxidase-labeled dextran polymers (EnVision+ peroxidase, mouse; Dako) were used. Prior to immunostaining for HSPG, tenascin, laminin and type-IV collagen, sections were pretreated with 3 mg/ml hyaluronidase (bovine testicular origin, type I-S, 440 U/mg; Sigma) in phosphate-buffered saline (PBS) for 30 min at 37°C. For CD34, CD31, CD68, keratin 14, pan-keratin, CD43, MUC1 and S-100 protein, the sections were digested with 0.15% trypsin (Sigma) in 10 mM Tris-HCl (pH 7.6) for 10 min at 37°C. Endogenous peroxidase activity was blocked with 0.3% hydrogen peroxide in methanol. Visualization of the reaction products was developed with 0.02% 3, 3′-diaminobenzidine in 0.05 M Tris-HCl (pH 7.4) containing 0.005% hydrogen peroxide. The sections were counterstained with hematoxylin. For control studies on antibodies, the primary antibodies were replaced with normal mouse or rabbit IgGs.

RNA probes

HSPG RNA probes were prepared with digoxigenin (DIG) RNA labeling kits (Boehringer Mannheim GmbH, Mannheim, Germany) using T7/T3 RNA polymerase (Promega Corporation, Madison, WI, USA). A template of cDNA corresponding to a fragment of domain I of human HSPG (135–669) was amplified by reverse-transcription polymerase chain reaction (RT-PCR) using RNA samples of squamous epithelial cells of the oral mucosa and sense (5′-CTGCT GGCGG TGACC CATGG-3′) and antisense (5′-TTGGG AACTG GGGCA CTGTG-3′) primers, followed by nested PCR using sense (5′-CGGGA TCCGT GACCC ATGGG CTGAG GGC-3′) and antisense (5′-CCCAA GCTTG GGCAC TGTGC CCAGG CGTC-3′) primers. The PCR products (516 bp) were subcloned into a plasmid vector (pBluescript II, Promega) and were digested with *Bam*HI and *Hin*dIII. The linearized plasmids were used as templates to synthesize antisense probes by T7 RNA polymerase and sense probes by T3 RNA polymerase.

Tenascin RNA probes were also prepared with DIG RNA labeling kits (Boehringer) using SP6/T7 RNA polymerase (Boehringer). A template of cDNA corresponding to a fragment of EGF repeats of human tenascin (834–1037) was amplified using RT-PCR with RNA samples of squamous epithelial cells of the oral mucosa and sense (5′-CCCAA GCTTT GGAGT CTGCA-3′, including a *Hin*dIII site) and antisense (5′-GGAAT TCCAC ACGCA CTCAT-3′, including an *Eco*RI site) primers. The cDNA was digested with *Hin*dIII and *Eco*RI and the resultant 204-bp fragment was ligated into a pSPT18/19 vector (Boehringer). The vector plasmids were linearized with *Hin*dIII and then transcribed with SP6 RNA polymerase as antisense probes or were linearized with *Eco*RI and then transcribed with T7 RNA polymerase as sense probes.

In situ hybridization

In situ hybridization was performed as described previously [14]. In short, paraffin sections cut at 5 μm were used. After deparaffinization, they were washed in three changes of 2× standard saline citrate (SSC) and treated with 5 μg/ml proteinase K (Sigma) for 20 min at 37°C. They were then washed with 0.2% glycine in PBS, fixed with 4% paraformaldehyde in 0.1 M phosphate buffer (pH 7.5) for 30 min, dehydrated with a series of ethanol (70–100%), and air-dried. Hybridization was performed at 45°C for 16 h in a moist chamber. The hybridization solution contained 10 mM phosphate buffer (pH 7.4), 10% dextran sulfate, 1× Denhardt's solution, 100 μg/ml salmon sperm DNA, 125 μg/ml yeast tRNA, 3× SSC, 50% formamide, and 500 ng/ml probes. After hybridization, the sections were rinsed in 2× SSC, and then the hybridized probes were detected with DIG detection kits (alkaline phosphatase; Boehringer). The sections were counterstained with methyl green.

Results

Histopathology

In all six cases, the original salivary gland structures disappeared and the parenchymal spaces were replaced by diffuse infiltrations of mononuclear inflammatory cells, which were composed mostly of lymphocytes and macrophages. The lymphocytes were all small and mature but there were no obvious aggregates of monocytoid B cells. In the background of these lymphoid cells, LELs (which had been previously referred to as epi-myoepithelial islands) in various sizes and shapes were scattered. Under higher magnification, the major constituent cells of the LELs were revealed as polygonal cells with eosinophilic cytoplasm, indicating epithelial characteristics, but without any definite cellular alignments. The epithelial cells were apparently intermingled with non-epithelial cells, which were regarded as mononuclear inflammatory cells (Fig. 1a). In addition to such classic LELs, there were islands with apparent ductal structures or incomplete narrow luminal structures, although these islands contained solid epithelial sheets in other parts (Fig. 1b). LELs occasionally showed intercellular deposits of eosinophilic hyaline material that varied in size and shape. Some other LELs had strands of hyaline material in the periphery. These strands were apparently continuous with blood vessels (Fig. 1c). In places where the hyaline deposits were largely spread, round- or spindle-shaped cells seemed to be embedded in the hyaline matrices (Fig. 1d).

Immunohistochemistry

LELs were contrastively demonstrated using immunohistochemical staining with the antibodies against a wide spectrum of keratin species (pan-keratin). Most of the constituent cells were immunopositive for pan-keratin; however, there were a definite number of cells that were not positive for pan-keratin. Most of the intensive staining for pan-keratin tended to be localized along the periphery of the LELs (Fig. 2a), although this kind of peripheral enhancement of the staining was not always obtained. In the same way, MUC1, a duct epithelial cell marker, was immunolocalized in most of the keratin-positive cells (Fig. 2b). The elongated epithelial cells in the periphery of the LELs were also immunopositive for keratin 14 (Fig. 2c) and S-100 protein (Fig. 2d), which had already been recognized as markers for myoepithelial cells. The results indicated that cells in the periphery occasionally, but not always, attained myoepithelial differentiation. S-100 protein was also immunolocalized in irregular-shaped cells scattered within the LELs (Fig. 2d). These cells were considered to be dendritic macrophages, as some of them

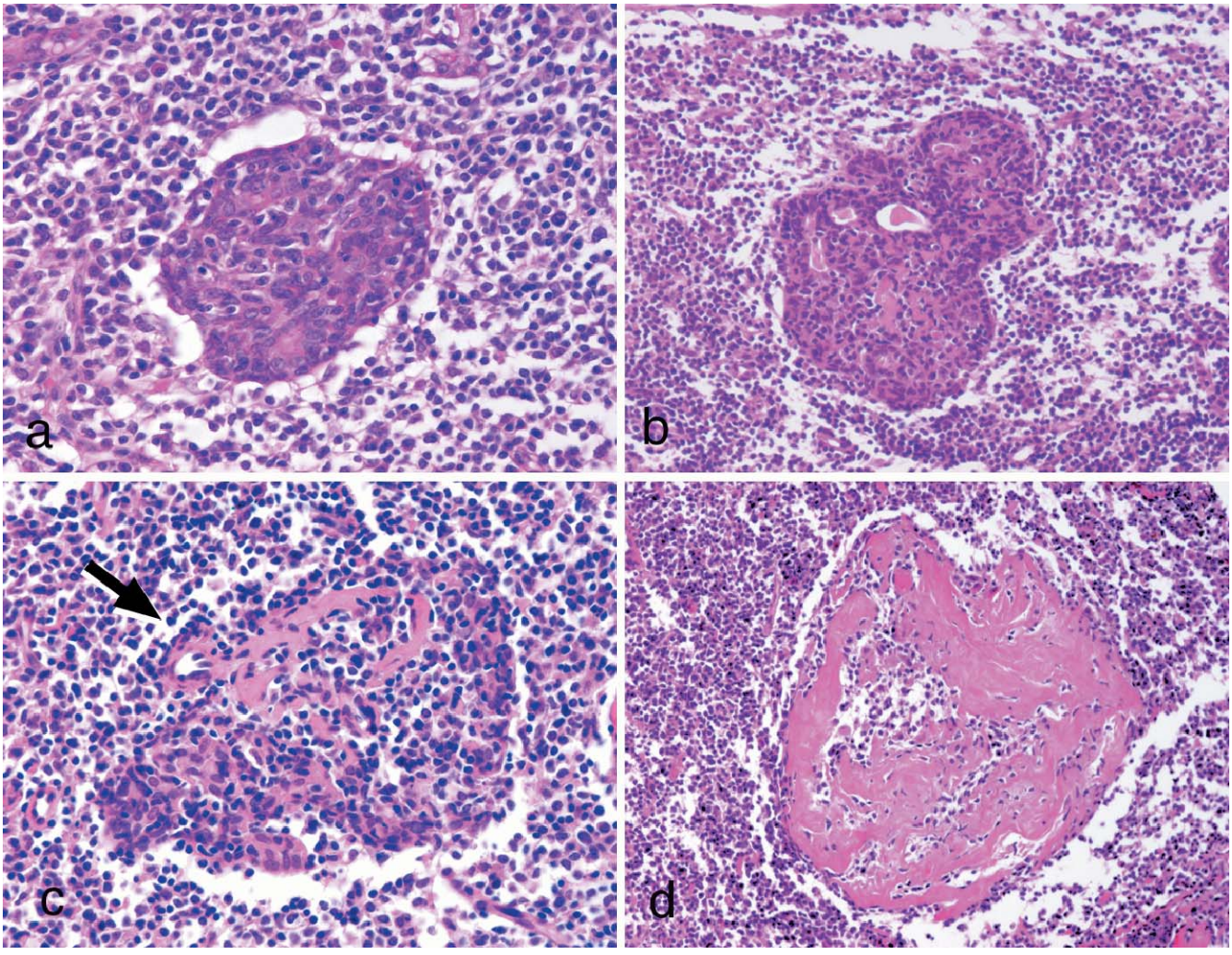

Fig. 1 Histological variations of lymphoepithelial lesions (LELs, also referred to as epi-myoepithelial islands) in lymphoepithelial sialadenitis (hematoxylin and eosin stain, **a**, **c** ×200; **b** ×150; **d** ×120). In the background of diffuse lymphoid cell infiltration, LELs were scattered. There were some variations in the architecture of the LELs, such as solid types (**a**), those with tubule formation (**b**), and those with eosinophilic hyaline deposits, which were apparently continuous with blood vessels at the periphery of the LELs (*arrow*; **c**). Some of the LELs were extensively occupied with eosinophilic hyaline deposits (**d**)

were simultaneously immunopositive for CD68 (Fig. 2e). CD68-immunopositive cells, i.e., macrophages, were instead more densely distributed in the lymphoid stroma.

In contrast to keratin, vimentin, another cytoskeletal protein, was predominantly immunolocalized in the lymphoid cells and vascular endothelial cells in the stroma. Within the LELs, many of the constituent cells, including epithelial cells, showed weakly positive reactions for vimentin, although enhanced staining for vimentin was obtained in the peripheral cells with myoepithelial differentiation as mentioned above as well as in non-epithelial cells located in the center, which were regarded as endothelial cells (Fig. 2f). When the antibodies against CD31 and CD34, vascular endothelial cell markers, were applied to the sections, all of the LELs without exception were shown to contain blood vessels or endothelial cells. CD34 was immunolocalized in the capillaries distributed over the stroma and within the LELs. The staining showed that the capillaries were more often located along the periphery of the LELs and also often penetrated the LELs. Only mature endothelial cells with tubule formation seemed to be positive for CD34 (Fig. 2g). In contrast, CD31-positive cells were more

Fig. 2 Lymphoepithelial lesions (LELs) in lymphoepithelial sialadenitis. Immunohistochemical localization for pan-keratin (**a**), MUC1 (**b**), keratin 14 (**c**), S-100 protein (**d**), CD68 (**e**), vimentin (**f**), CD34 (**g**), and CD31 (**h**) (immunoperoxidase, hematoxylin counterstain, **a**–**e**, **g**, ×150; **f**, **h**, ×200). Keratin and MUC1-positive epithelial cells are primary constituents of LELs. Keratin 14- and S-100 protein-positive (+) cells with myoepithelial or basal cell differentiation were located in the periphery of the LELs. Some of the S-100 protein+ cells showed similar distributions of CD68+ cells, suggesting the presence of macrophages or dendritic cells. Vimentin positivities were demonstrated in lymphoid cells and endothelial cells (*arrow*) within the LELs and stromal lymphocytes. CD34+ and CD31+ endothelial cells with formation of blood capillaries both within the LELs and in the stromata

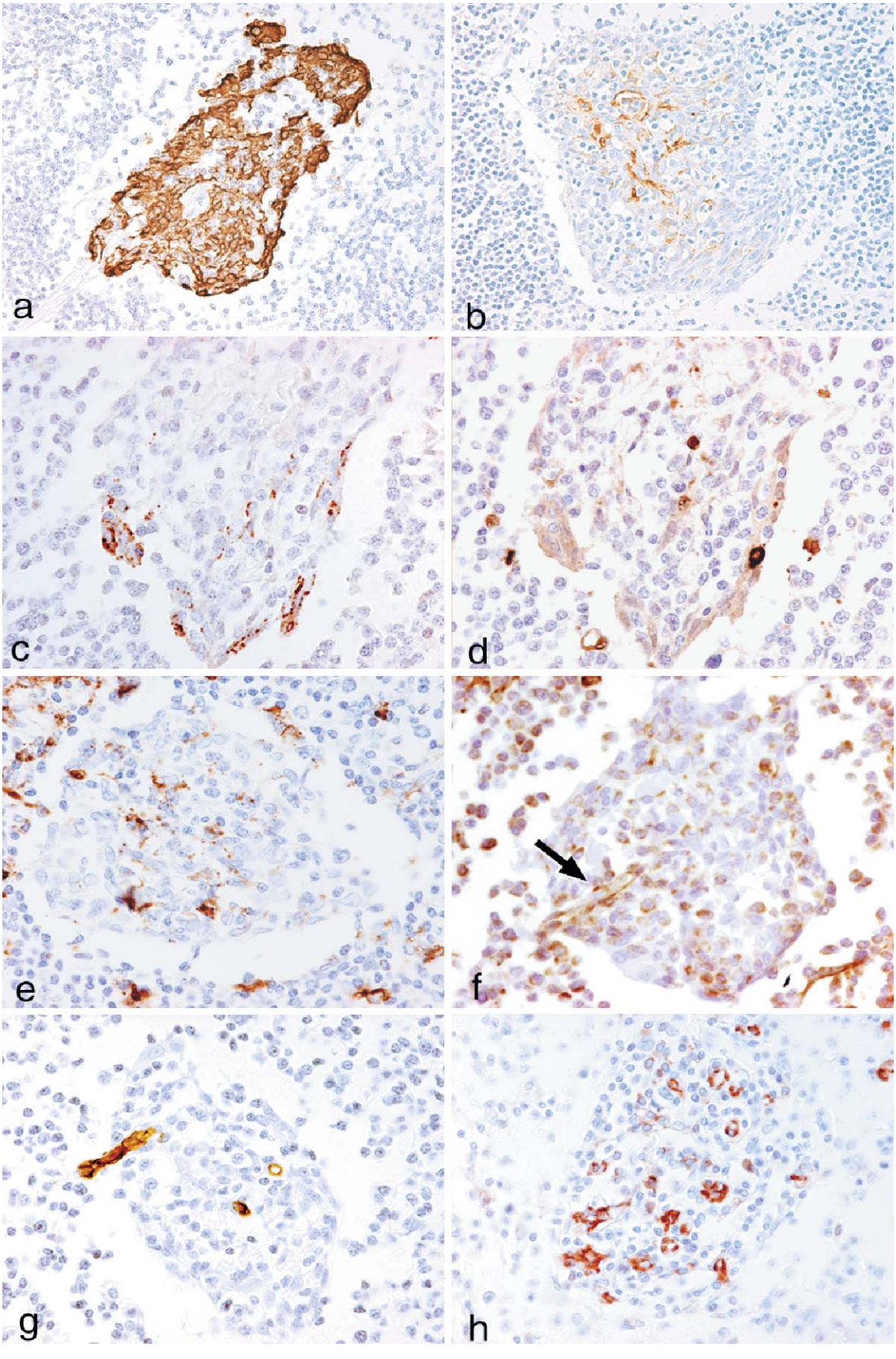
a
b
c
d
e
f
g
h

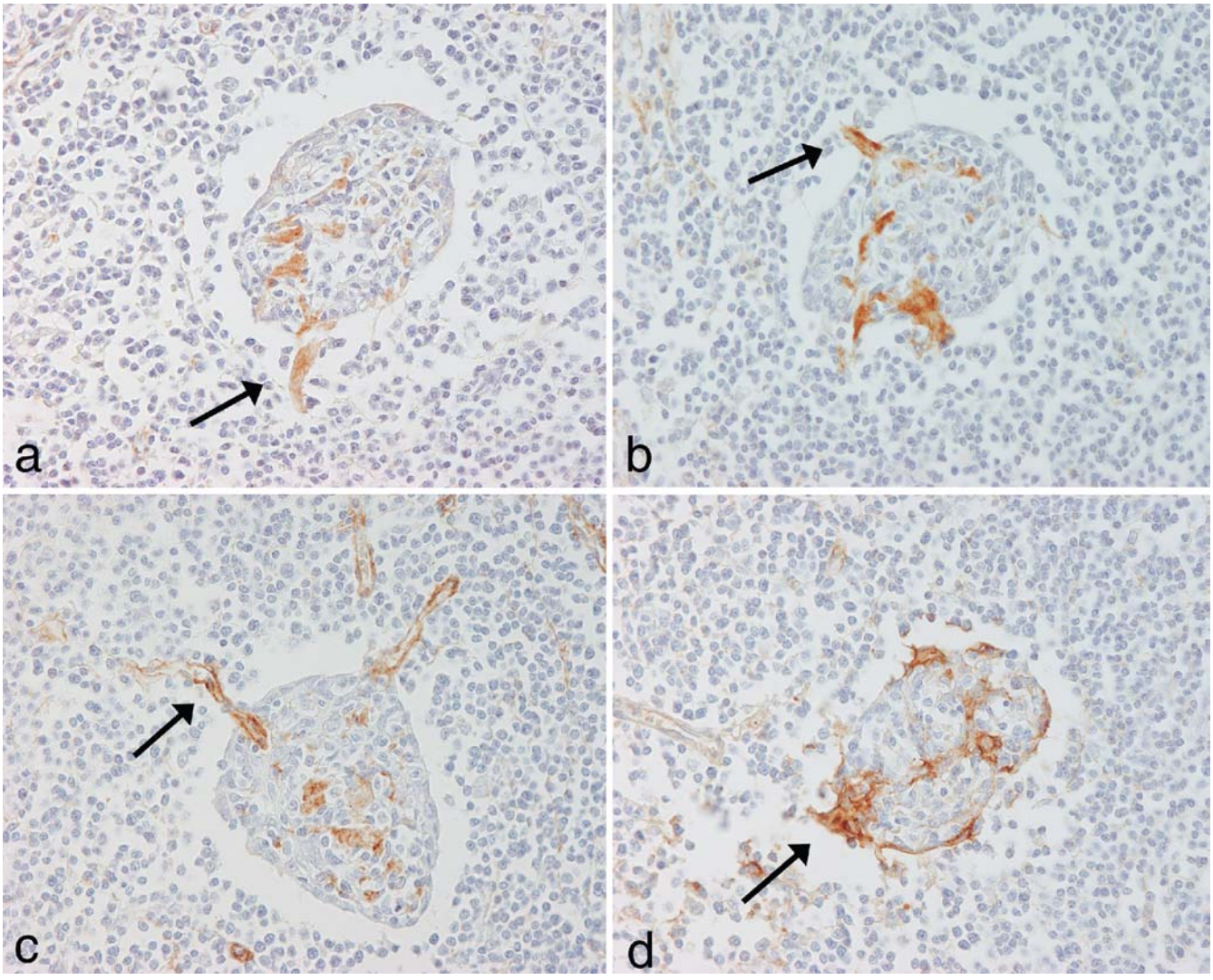

Fig. 3 Lymphoepithelial lesions (LELs) in lymphoepithelial sialadenitis. Immunohistochemical localization for extracellular matrix (ECM) molecules: (**a**) heparan sulfate proteoglycan, (**b**) tenascin, (**c**) type-IV collagen, and (**d**) laminin (immunoperoxidase, hematoxylin counterstain ×200). Characteristic deposits of eosinophilic hyaline material were immunopositive for ECM molecules examined. In addition to hyaline deposits, immunolocalization for basement membrane-associated ECM molecules indicated the presence of blood channels (*arrow*) within the LELs

widely distributed within the LELs in addition to both the immature and the mature vascular vessels in the lymphoid stroma. In the LELs, CD31 was demonstrated not only in mature endothelial cells but also in cells that did not consist of vascular channels. However, some of the cells seemed to be in the process of forming minimal tubule structures (Fig. 2h).

To characterize constituent molecules of eosinophilic hyaline deposits in the LELs, we performed immunohistochemical investigations for ECM molecules, in particular BM-associated molecules, such as laminin and type-IV collagen, HSPG, tenascin, fibronectin, and collagen types III, V, and VI. These molecules showed basically the same pattern of immunolocalization in the LELs. Hyaline deposits were strongly positive for these ECM molecules, especially HSPG (Fig. 3a), tenascin (Fig. 3b), and fibronectin. In addition to the hyaline deposits, the ECM molecules such as type-IV collagen (Fig. 3c), laminin (Fig. 3d), and collagen types III, V, and VI (data not shown) were immunolocalized in a spider-web-like fashion. Their staining patterns resembled stromal blood vessels, which were also revealed using the immunohistochemical stainings for the BM-associated molecules mentioned above.

Immunohistochemistry for lymphocytic markers demonstrated contrastive distribution of T- and B lymphocytes in the LESA. Larger parts of stromal lymphocytes were composed of CD20+ B lymphocytes (Fig. 4a), while CD45RO+ T lymphocytes were more sparsely packed (Fig. 4b). There were no foci of CD43+ monocytoid B cells among the lymphoid stroma in any of the six cases. B lymphocytes were also shown to be important con-

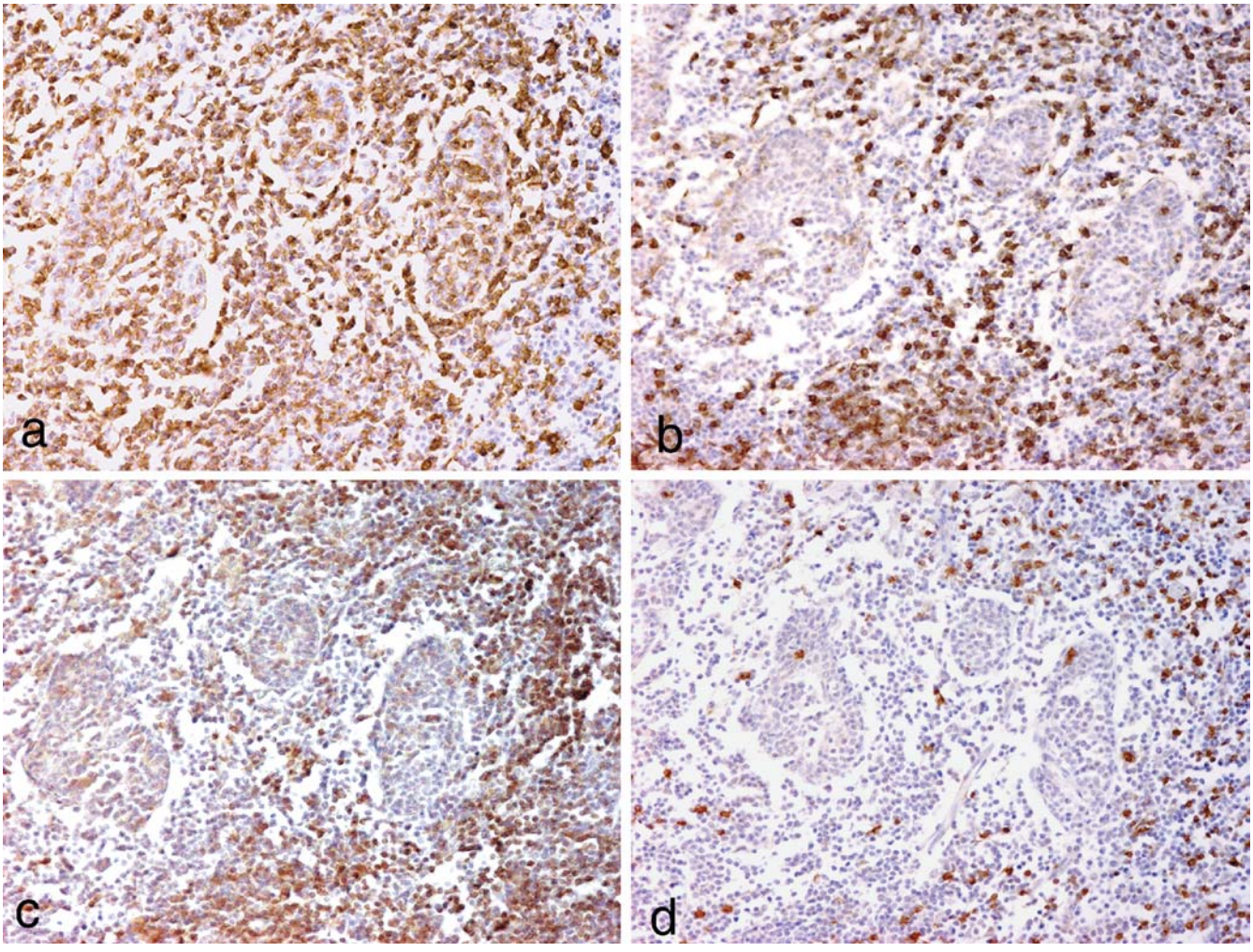

Fig. 4 Lymphoepithelial lesions (LELs) in lymphoepithelial sialadenitis. Immunohistochemical localization for lymphocytic markers: (**a**) CD20, (**b**) CD45RO, (**c**) CD4, and (**d**) CD8 (immunoperoxidase, hematoxylin counterstain, ×150). CD20+ B lymphocytes were more dense and diffused than CD45RO+ T lymphocytes in stroma as well as in LELs. Among T lymphocytes, CD4+ cells were more prominent than CD8+ cells in stromal space

stituent cells of the LELs, although only a small number of T lymphocytes were found within the LELs. Among the stromal T lymphocytes, CD4+ cells were definitely predominant (Fig. 4c), and CD8+ cells were fewer in number (Fig. 4d). The results obviously indicated that, in addition to epithelial cells, vascular endothelial cells, macrophages and B lymphocytes were constant constituents of the LELs.

In situ hybridization

mRNA signals for HSPG (Fig. 5a, b, d) and tenascin (Fig. 5f) were observed in some of the constituent cells of the LELs. The mRNA signal for HSPG was demonstrated in the cells around the ductal lumen both in the ducts (Fig. 5a) and in the cells surrounding the remnant tubules in some LELs (Fig. 5b), while it was observed in the central area of the fully formed LELs (Fig. 5d). HSPG and tenascin-positive cells were located around the hyaline deposits, which were immunopositive for HSPG (Fig. 5c) and tenascin (Fig. 5e), or they were sometimes aligned in a short row that contained immunopositivities. This kind of limited co-localization of mRNA and protein signals suggested that the hyaline deposits were not from epithelial cells that were distributed diffusely in the LELs but from cells that tended to align in a limited area within the LEL. In addition, cells in the periphery of the LELs showed mRNA signals for HSPG and tenascin, which was also similar to their protein localization revealed using immunohistochemistry. This suggests that HSPG and tenascin were localized not only in the BM of the LELs but also in the BM of vascular channels located within the LELs or along their periphery. In addition, mononuclear inflammatory cells, both lymphocytes and macrophages, within the LELs as well as in the stromal space showed mRNA signals for HSPG and tenascin. Since double stainings for lymphocytic markers and in situ hybridiza-

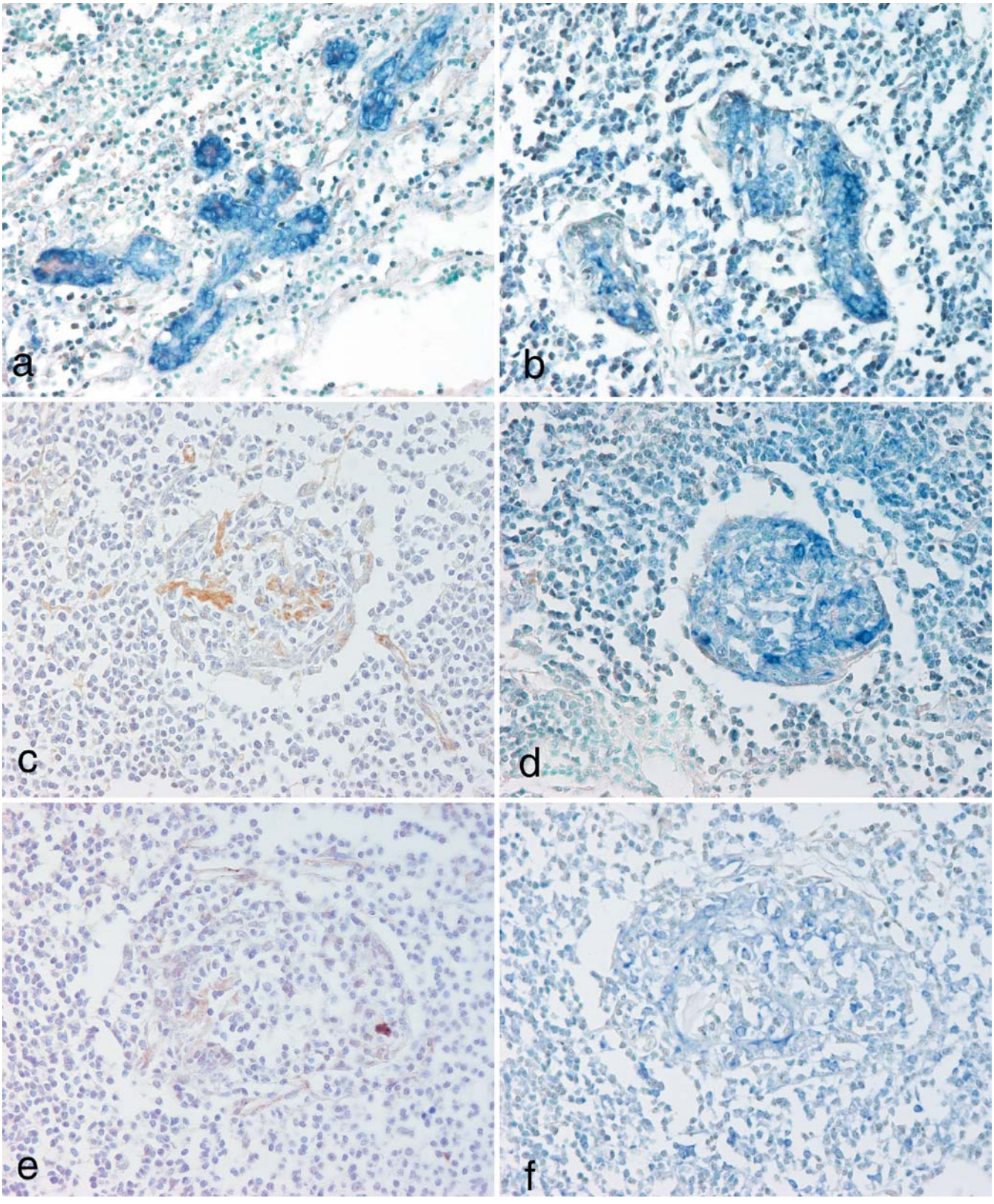

Fig. 5 Lymphoepithelial lesions (LELs) in lymphoepithelial sialadenitis. In situ hybridization for heparan sulfate proteoglycan (HSPG) (**a**, **b**, **d**) and tenascin mRNA (**f**) (immunoalkaline phosphatase with digoxygenin labeled RNA probes, methyl green counterstain, **a** ×150; **b**, **d** ×200; **f** ×250) and immunohistochemical localization for HSPG (**c**) and tenascin (**e**) (immunoperoxidase, hematoxylin counter stain, **c** ×200; **e** ×250). HSPG and tenascin mRNA signals were demonstrated in cells around deposits of eosinophilic hyaline material that was immunopositive for both HSPG and tenascin. HSPG mRNA signals were also observed in cells around lumen of the duct and of the remnant tubule within the LELs

tion were not possible, HSPG and tenascin mRNA-positive lymphocytes were not identified in terms of their subsets. These in situ hybridization results indicated that the ECM deposits within the LELs were not only produced by epithelial cells but rather mainly by vascular endothelial cells consisting, in part, of vascular channels as well as by macrophages and lymphocytes.

Discussion

In the present study, most of the constituent cells of LELs of LESA have at last been defined. These include epithelial cells, those with duct epithelial differentiation and those with myoepithelial differentiation, vascular endothelial cells, macrophages, and lymphocytes. The most striking finding in this study was the presence of a definite number of vascular endothelial cells in the LELs. These cells were sometimes in the process of forming vessel walls but at other times were not yet assembled into blood vessels. Although the duct epithelial nature of their constituent cells has been well investigated by ultrastructural [2, 5, 9, 11, 19, 28, 32, 35, 40, 41] and immunohistochemical [3, 15, 16, 21, 22, 26, 27, 32, 38] studies, there has been no postulation of endothelial cell participation in the formation of LELs. Only Qin et al. [29] reported von Willebrand factor-immunopositive capillaries in the inflammatory stroma, suggesting that an efficient blood supply elucidates regeneration and proliferation of epithelial cells in the formation of the LELs in a general sense. However, they did not intend to point out the direct role of endothelial cells in the process of the formation of the LELs, and they were, of course, not able to demonstrate conclusively the presence of immature endothelial cells within the LELs in the early 1990s. Our findings suggest that epithelial cell proliferation is supported not only by the presence of already-formed capillary vessels but also by in situ angiogenesis occurring at the same time within the LEL. The present immunohistochemical results for BM-associated ECM molecules also revealed abundant distribution of blood channels within the LELs. The mode of immunolocalization of ECM molecules, such as laminin and type-IV collagen, seemed to be identical to that for CD31; hence their immunolocalization may indicate a kind of blood supply network within the LEL. These findings suggest that vascular endothelial cells are essential for the formation of LELs. In other words, regeneration of epithelial cells that survived after the destruction of their original structures in the background of the severe lymphocytic infiltration could only have occurred along the core of vascular channels.

Another important finding from the present ECM study was the explanation for the formation of eosinophilic hyaline deposits, as the eosinophilic material was shown immunohistochemically to be deposits of at least the four BM-associated molecules, type-IV collagen, laminin, HSPG, and tenascin. The presence of type-IV collagen in eosinophilic hyaline deposits has already been demonstrated by Palmer et al. [27]. Ultrastructurally, hyaline materials were shown to have membranous or fibrillar structures with collagen characteristics [2, 35] or to have a close association with the BM [5, 19]. These hyaline materials were also considered to be immune complexes that originated from myoepithelial cells [28, 35]. However, the present intensive examination has confirmed that the hyaline material is composed of BM or BM-associated ECM molecules.

Which cells are responsible for deposition of such BM molecules in the LELs? The present results indicate that vascular endothelial cells and inflammatory cells are responsible for this production. Ultrastructurally, Takeda et al. [35] could not determine the cells responsible for the hyaline deposits because there were no secretory properties in the constituent cells, but instead they suggested some immune deposits. Since epithelial cells comprise the largest cell population in the LELs, their contribution to the production of the hyaline material in the process of deposition cannot be easily denied, because enhanced expression of laminin in minor salivary gland duct epithelial cells in Sjogren's syndrome has been demonstrated by Macarthur and his colleagues [23, 24]. Since we have also demonstrated the presence of mRNA signals for HSPG in myoepithelial cells of normal salivary ducts [20] and the in vitro biosynthesis of four BM molecules and fibronectin by salivary epithelial tumor cells [7], we had expected that epithelial cells would have taken part in the production more significantly. However, the endothelial cells and lymphocytes with mRNA signals for ECM molecules located around the hyaline deposits were most indicative of their production, at least at the time of the sampling of the tissues in which the hyaline material had already been deposited.

An unexpected finding in the present experiment was the presence of mRNA signals for ECM molecules in inflammatory cells, although infiltrations of lymphocytes and macrophage have been previously demonstrated by ultrastructural [2, 28] and immunohistochemical [21, 22] studies. However, such findings of the biosynthesis of ECM molecules by inflammatory cells have been infrequently recorded, although tenascin production by macrophages [37] and in vitro fibronectin synthesis by activated T lymphocytes have been recorded [36]. The results of immunohistochemistry and in situ hybridization experiments for elevated expression of laminin genes by Macarthur [23, 24] may be partially due to this phenomenon but not only by epithelial cells. Our in situ hybridization experiments showed that the mRNA signals were also present in lymphoid cells in the stroma and not only in inflammatory cells within LELs. Thus, it is not conceivable that lymphoid cells within the LELs are more responsible for the production of the hyaline materials than those in the stroma, because there were no hyaline deposits in the lymphoid stroma. However, it is more likely to consider that inflammatory cells may contribute to the formation of hyaline deposits to some extent in special circumstances in which epithelial cells are aggre-

gated but lymphoid cells simply need to produce ECM molecules for their migration [8].

The lymphocytic subpopulation among the infiltrating cells within the LELs has been analyzed immunohistochemically in the present study. B lymphocytes were more predominant than T lymphocytes in the full-grown stage of LESA as shown previously [18, 39]. Although other authors demonstrated an opposite finding of a fewer number of B lymphocytes in the lesion [4, 22], our present result should reasonably explain why this lesion could be one of the backgrounds for the secondary onset of MALT lymphomas [1, 13, 30, 34]. B-cell monoclonality has been demonstrated in 42% [30] to 68% [18] of LESA cases using PCR techniques for immunoglobulin heavy-chain gene rearrangements as well as discriminative antibodies against their gene products. However, Diss et al. [10] reported a totally opposite result, showing that no clonal B lymphocytes had been found in their nine cases of benign MESA. Thus, it is still controversial to determine whether differential diagnosis of MALT lymphomas from LESA is actually possible histopathologically, or if a precancerous status, which is not noticeable histologically, is included in conditions diagnosed as LESA. As far as the specimens of our series were concerned, there was no proliferation of monocytoid B cells in the stroma. The predominance of CD4+ cells to CD8+ cells in the stroma may be a natural proportion between helper and cytotoxic lymphocytes in the peripheral blood and in accordance with previous studies on the peripheral blood and salivary gland lymphocytes in patients with Sjögren's syndrome [4]. In addition, stromal CD4+ cells in LESA may play a role in favoring lymphomatous changes by stimulation of B lymphocytes [1]. The present study showed that not only T lymphocytes but also B lymphocytes were found within the LELs, although the question of which of them is responsible for the production of hyaline materials remains for further investigation.

Acknowledgements The authors thank Dr. H. Furthmayr, Stanford University School of Medicine, for his supply of the antibodies. This work was supported in part by Grants-in-Aid for Scientific Research from the Japan Society for the Promotion of Science.

References

1. Biasi D, Caramaschi P, Ambrosetti A, Carletto A, Mocella S, Randon M, Bambara LM (2001) Mucosa-associated lymphoid tissue lymphoma of the salivary glands occurring in patients affected by Sjogren's syndrome: report of 6 cases. Acta Haematol 105:83–88
2. Bouquist L, Kumilien A, Osberg Y (1970) Ultrastructural findings in a case of benign lymphoepithelial lesions (Sjogren's syndrome). Acta Otolaryngol 70:216–226
3. Caseltiz J, Osborn M, Wustrow J, Seifert G, Weber K (1986) Immunohistochemical investigations on the epi-myoepithelial islands in lymphoepithelial lesions. Use of monoclonal keratin antibodies. Lab Invest 55:427–432
4. Celenligil H, Kansu E, Ruacan S, Eratalay K, Irkec M (1990) Characterization of peripheral blood and salivary gland lymphocytes in Sjogren's syndrome. Oral Surg Oral Med Oral Pathol 69:572–577
5. Chaudhry A, Cutler L, Yamane G, Satchidanand S, Labay G, Sunderraj M (1986) Light and ultrastructural features of lymphoepithelial lesions of the salivary glands in Mikulicz's disease. J Pathol 146:239–250
6. Cheng J, Saku T, Okabe H, Furthmyr H (1992) Basement membrane in adenoid cystic carcinoma. Cancer 69:2631–2640
7. Cheng J, Irié T, Munakata R, Kimura S, Nakamura H, He RG, Lui AR, Saku T (1995) Biosynthesis of basement membrane molecules by salivary adenoid cystic carcinoma cells: an immunofluorescence and confocal microscopic study. Virchows Arch 426:577–586
8. Clark AR, Erickson PH, Springer AT (1997) Tenascin supports lymphocyte rolling. J Cell Biol 137:755–765
9. Dardick I, van Nostrand AWP, Rippstien P, Skimming L, Hoppe D, Dairkee SH (1988) Characterization of epi-myoepithelial islands in benign lymphoepithelial lesions of major salivary glands: an immunohistochemical and ultrastructural study. Head Neck Surg 10:168–178
10. Diss TC, Wotherspoon AC, Spieght P, Pan L, Isaacson PG (1995) The polymerase chain reaction detects B cell clonalities, Epstien Barr virus and t(14;18) in myoepithelial sialadinities and low-grade B-cell MALT lymphoma of the parotid gland. Am J Surg Pathol 19:531–564
11. Donath K, Seifert G. (1972) Ultrastructur und Pathogenese der myoepithelialen Sialadenitis. Virchows Arch 356:315–329
12. Furthmayr H (1981) Immunization procedures, isolation by affinity chromatography, and serological and immunochemical characterization of collagen specific antibodies. In: Furthmayr H (ed) Immunochemistry of the extracellular matrix, vol. 1. CRC Press, Boca Raton, pp 13–78
13. Harris LN (1999) Lymphoid proliferations of the salivary glands. Am J Clin Pathol 111:94–103
14. Ida-Yonemochi H, Ikarashi T, Nagata M, Hoshina H, Takagi R, Saku T (2002) The basement membrane-type heparan sulfate proteoglycan (perlecan) in ameloblastomas: its intercellular localization in stellate reticulum-like foci and biosynthesis by tumor cells in culture. Virchows Arch 441:165–173
15. Ihrler S, Zietz C, Sendelhofert A, Riederer A, Lohrs U (1999) Lymphoepithelial duct lesions in Sjogren-type sialadenitis. Virchows Arch 43:315–332
16. Ihrler S, Zietz C, Sendelhofert A, Menaure F, Blsenbeu-Vogt S, Lohrs U (2000) Zur Dfferenzial Diagnose Lymphoepithelialer Speicheldrusenlasionen. Mit Besonderer Berücksichtigung der Charakteristischen Speichelgangveränderungen. Pathologe 21:424–432
17. Isaacson P, Spencer J (1987) Malignant lymphoma of mucosa associated lymphoid tissue. Histopathology 11: 445–462
18. Jordan RC, Odell EW, Speight PM (1996) B-cell monoclonality in salivary lymphoepithelial lesions. Eur J Cancer B Oral Oncol 32:38–44
19. Khan LB (1979) Benign lymphoepithelial lesions (Mikulicz's disease) of the salivary glands: an ultrastructural study. Hum Pathol 10:99–104
20. Kimura S, Chen J, Ida H, Hao N, Fujimori Y, Saku T (2000) Perlecan (heparan sulfate proteoglycan) gene expression reflected in the characteristic histological architecture of salivary adenoid cystic carcinoma. Virchows Arch 437:122–128
21. Kjorell U, Ostberg Y (1984) Distribution of intermediate filaments and microfilaments in parotid autoimmune sialadenitis of Sjogren's syndrome. Histopathology 8:991–1011
22. Kjorell U, Ostberg Y, Virtanen I, Thornell LE (1988) Immunohistochemical analysis of autoimmune sialadenitis in man. J Oral Pathol 17:374–380
23. Macarthur CP, Fox NW, Kragel P (1993) Monoclonal antibody detection of laminin in minor salivary glands of patients with Sjogren's syndrome. J Autoimmun 6:649–661
24. Macarthur CP, Daniels PJ, Kragel P, Howard PF, Julian L (1997) Sjogren's syndrome salivary gland immunopathology: increased laminin expression precedes lymphocytic infiltration. J Autoimmun 10:59–65
25. Murata M, Cheng J, Horino K, Hara K, Shimokawa H, Saku T (2000) Enamel protein and extracellular matrix molecules are

colocalized in the pseudocystic stromal space of adenomatoid odontogenic tumor. J Oral Pathol Med 29:483–490
26. Nakai M, Tsukitani K, Tatemoto Y, Hikosaka N, Mori M (1985) Histochemical studies of obstructive adenitis in human submandibular salivary glands. II. Lectin binding and keratin distribution in the lesions. J Oral Pathol 14:671–679
27. Palmer R, Eveson J, Gusterson B (1986) Epimyoepithelial islands in lymphoepithelial lesions. An immunohistochemical study. Virchows Arch 408:603–609
28. Pirsig W, Donath K (1972) Zur Ultrastrukure der parotis beim Sjogren-Syndrome vor und nach immunosuppressiver Therapie. Arch Klin Exp Ohren Nasen Kehlkopfheilkd 20:309–323
29. Qin C, Pan Y, Hashimoto J, Takai Y, Yamada T, Mori M (1994) Destructive processes of salivary gland parenchyma and development of epimyoeoithelial islands assessed by immunohistochemistry. Arch Anat Cytol Pathol 42:16–25
30. Quintana GP, Kapaddia BS, Bahler WD, Johnson TJ, Swerdlow HT (1997) Salivary gland lymphoid infiltrates associated with lymphoepithelial lesions: a clinicopathologic, immunophynotypic, and genotypic study. Hum Pathol 28:850–861
31. Saku T, Furthmyr H (1989) Characterization of the major heparan sulfate proteoglycan secreted by bovine aortic endothelial cells in culture: homology to the large molecular weight molecule of basement membranes. J Biol Chem 264:3514–3523
32. Saku T, Okabe H (1984) Immunohistochemical and ultrastructural demonstration of keratin in epi-myoepithelial islands of autoimmune sialadenitis in man. Arch Oral Biol 29:687–689
33. Saku T, Okabe H, Shimokawa H (1992) Immunohistochemical demonstration of enamel proteins in odontogenic tumors. J Oral Pathol Med 21:113–119
34. Sutcliffe N, Smith C, Spieght PM, Isenberg DA (2000) Mucosa-associated lymphoid tissue lymphomas in two patients with rheumatoid arthritis on second-line agents, and secondary Sjogren's syndrome. Rheumatology 39:185–188
35. Takeda Y (1980) Histopathological studies of the labial salivary glands in patients with Sjogren's syndrome. Part II: Electron microscopic study. Bull Tokyo Med Dent Univ 27:27–42
36. Wagner C, Bürger A, Radsak M, Blum S, Hug F, Hänsch G (2000) Fibronectin synthesis by activated T lymphocytes: up-regulation of a surface-associated isoform with signaling function. Immunology 99:532–539
37. Wallner K, Li C, Shah PK, Fishbein MC, Forrester JS, Kaul S, Sharifi BG (1999) Tenascin-C is expressed in macrophage-rich human coronary atherosclerotic plaque. Circulation 99:1284–1289
38. Wilk C, Vigneswaran N, Heese A, Hornstien O, Naumann G (1990) Immunohistochemical characterization of epithelial cells in human lacrimal glands. II. Inflammatory and neoplastic lesions of lacrimal glands. Graefes Arch Clin Exp Ophthalmol 228:65–72
39. Yamamura Y, Onodera K, Ichinohasama R, Ooya K (2000) A histopathological study of lymphoepithelial island formation in labial salivary glands in patients with primary Sjogren's syndrome. J Oral Pathol Med 29:110–117
40. Yarington CT, Zagibe FT (1969) The ultrastructure of the benign lymphoepithelial lesion. J Laryngol Otol 83:361–365
41. Yoshihara T, Morita M, Ishii T (1995) Ultrastructure and three-dimensional imaging of epi-myoepithelial islands in benign lymphoepithelial lesions. Eur Arch Otorhinolaryngol 252:106–111

Virchows Arch (2003) 443:28–31
DOI 10.1007/s00428-003-0835-x

ORIGINAL ARTICLE

Lukas Hechelhammer · Stephan Störkel · Bernhard Odermatt · Philipp U. Heitz · Wolfram Jochum

Epidermal growth factor receptor is a marker for syncytiotrophoblastic cells in testicular germ cell tumors

Received: 23 January 2003 / Accepted: 28 April 2003 / Published online: 3 June 2003
© Springer-Verlag 2003

Abstract The epidermal growth factor receptor (EGFR) has been implicated in the pathogenesis, therapy and prognosis of various tumor types. The aim of this study was to investigate EGFR expression in a large series of testicular germ cell tumors (TGCTs). A total of 88 TGCTs (37 of pure type and 51 of mixed type) comprising a total of 44 seminoma, 49 embryonal carcinoma, 32 yolk sac tumor, 28 teratoma and 7 choriocarcinoma components were immunostained for EGFR. EGFR reactivity was observed in the stromal cells of embryonal carcinoma (29%) and in epithelial compartments of teratoma (71%). In addition, EGFR staining was consistently detected in syncytiotrophoblastic cells of choriocarcinoma, seminoma, embryonal carcinoma and yolk sac tumor components. EGFR staining, similar to β-human chorionic gonadotropin (HCG) immunohistochemistry, was efficiently able to identify syncytiotrophoblastic cells in TGCTs. This study shows that EGFR is expressed in a subset of testicular germ cell tumors and suggests that EGFR may be a useful marker for syncytiotrophoblastic cells.

Keywords Epidermal growth factor receptor (EGFR) · Testicular germ cell tumors · Syncytiotrophoblastic cells

Introduction

The epidermal growth factor receptor (EGFR) is a 170-kDa growth factor receptor tyrosine kinase [20]. Upon binding of its cognate ligands, which include EGF and transforming growth factor alpha (TGFα), it activates signal transduction cascades that contribute to the control of cell differentiation, proliferation, apoptosis, migration and adhesion [25]. The EGFR protein is frequently overexpressed in various types of cancer, and its overexpression has been correlated with poor prognosis in head and neck, ovarian, cervical, bladder and esophageal cancer [17, 19]. Novel treatment modalities that specifically inhibit EGFR-mediated signal transduction have recently become available [14]. This development provides a rationale for the systematic identification of tumor types that overexpress EGFR and therefore represent potential candidates for EGFR-targeted therapy.

Testicular germ cell tumors (TGCTs) are the most common type of cancer in young adult males. TGCTs can be classified as seminomas and non-seminomatous germ cell tumors, the latter group comprising embryonal carcinoma, yolk sac tumor, polyembryona, teratoma and chroriocarcinoma [6]. TGCTs occur either as tumors with one homogeneous histological pattern (pure types) or show more than one histological pattern (mixed types). The various histological forms of TGCT are clinically and biologically diverse despite sharing intratubular malignant germ cells as a common precursor [2, 3, 5]. Multiagent cisplatin-based chemotherapy has significantly improved the prognosis of patients with advanced TGCT. However, disease recurrence and progression still occur, indicating the need for additional treatment modalities [2].

The purpose of the present study was to analyze the expression of the EGFR protein in a large series of TGCT using immunohistochemistry.

L. Hechelhammer · B. Odermatt · P. U. Heitz · W. Jochum (✉)
Institute of Clinical Pathology,
Department of Pathology, University Hospital,
Schmelzbergstrasse 12, 8091 Zürich, Switzerland
e-mail: wolfram.jochum@usz.ch
Tel.: +41-1-2552512
Fax: +41-1-2554551

S. Störkel
Institute of Pathology, 42283 Wuppertal, Germany

Materials and methods

A total of 182 TGCTs were retrieved from the surgical pathology files of the Department of Pathology, University of Zürich, covering a period of 9 years (1993 to 2001). Tumors were classified according to the World Health Organization (WHO) classification of testis tumors [16]. Eighty-eight TGCTs were selected for EGFR immunohistochemistry. This group consisted of 37 pure-type and 51 mixed-type TGCTs comprising a total of 44 seminoma, 49 embryonal carcinoma, 32 yolk sac tumor, 28

Table 1 Epidermal growth factor receptor (EGFR) expression in testicular germ cell tumors according to histological tumor type

Histological tumor type	Number of tumor components	EGFR reactivity
Seminoma	44	0[a]
Embryonal carcinoma	49	14 (29%)[a]
Yolk sac tumor	32	0[a]
Teratoma	28	20 (71%)
Choriocarcinoma	7	7 (100%)

[a] EGFR expression was observed in syncytiotrophoblastic cells of 5 seminoma, 20 embryonal carcinoma and 10 yolk sac tumor components

teratoma and 7 choriocarcinoma components (Table 1). Immunostaining was performed on one to four representative tissue blocks for each tumor. Three-micron-thick sections of formalin-fixed, paraffin-embedded tissue samples were mounted on glass slides (SuperFrost Plus; Menzel, Braunschweig, Germany), dried for 20 min at 59°C, deparaffinized and rehydrated. Prior to incubation with primary antibody (EGFR, clone 31G7, dilution 1:30; Zymed Laboratories, San Francisco, USA), antigen retrieval was performed with the Ventana protease 1 reagent (Ventana Medical Systems, Tucson, Arizona, USA) for 2 min. Pretreatment of sections, antibody incubation and detection of primary antibody (Ventana Enhanced Alkaline Phosphatase Red Detection Kit) were performed on a Benchmark immunohistochemistry staining system (Ventana Medical Systems). EGFR immunoreactivity was scored separately for each histological component. Epidermis of normal human skin was used as a positive control, and primary antibody was omitted in negative controls.

For β-human chorionic gonadotropin (β-HCG) staining, antigen retrieval was performed with Ventana cell conditioning solution for 36 min at 100°C prior to incubation with primary antibody (β-HCG, clone h6, dilution 1:20.000; BMA Biomedicals, Augst, Switzerland). Pretreatment of sections, antibody incubation and detection of primary antibody (Ventana Basic DAB Detection Kit) were performed on a Benchmark immunohistochemistry staining system.

Results

EGFR staining was comparable in pure and mixed-type TGCTs. A strong membranous EGFR immunoreactivity was found in syncytiotrophoblastic cells of choriocarcinomas (100%; Fig. 1A). EGFR expression was also detected in the majority of teratomas (71%). Staining was found in squamous and columnar epithelia with predominant labeling of the basal cell layers (Fig. 1B, C), whereas cartilage and other non-epithelial (e.g. neural) tissues remained unstained. In 29% of embryonal carcinomas, EGFR immunostaining was observed in the stromal tumor cell compartment (Fig. 1D). EGFR immunoreactivity was absent in seminoma and yolk sac tumor cells. No EGFR staining was observed in intratubular malignant germ cells.

To study a potential role for EGFR as a marker for syncytiotrophoblastic cells, adjacent sections of 38 tumor samples with syncytiotrophoblasts were stained for EGFR and β-HCG [9]. In addtion to choriocarcinoma, syncytiotrophoblastic cells were found in 5 seminoma, 20 embryonal carcinoma and 10 yolk sac tumor components. In all tumors (100%), syncytiotrophoblastic cells identified by β-HCG immunohistochemistry also showed strong EGFR staining (Fig. 1E).

Discussion

In this study, we demonstrated EGFR expression in a subset of TGCTs, namely in the stromal compartment of embryonal carcinomas and in the squamous and columnar epithelia of teratomas. EGFR staining in the basal layers of squamous and columnar epithelia is consistent with the physiological functions of the EGFR in the proliferation and differentiation control of epithelial cells [25]. EGFR expression was also found in syncytiotrophoblastic cells, either as components of choriocarcinoma or scattered as single cells in other types of TGCT. This expression pattern corresponds to previous observations that EGFR is expressed in the implantation trophoblast, in the trophoblast of normal placenta and in gestational trophoblastic diseases [1, 7, 10, 11, 22].

TGCTs are often associated with elevated serum HCG levels, which can be due to the presence of either choriocarcinoma or single syncytiotrophoblasts. Differentiation between these possibilities is clinically important. Identification of choriocarcinoma in a mixed TGCT is associated with poor prognosis, whereas scattered syncytiotrophoblastic cells appear to exert no adverse effects on survival [21, 23, 24]. Immunohistochemical characterization of syncytiotrophoblastic cells has revealed expression of β-HCG [9], pregnancy-specific beta-1-glycoprotein [12], human placental lactogen [12], inhibin [13], epithelial membrane antigen [18], and cytokeratins 7, 8, 18 and 19 [4, 6]. Of these, β-HCG has been considered to be the most valuable marker for syncytiotrophoblastic cells. We found that EGFR immunolabelling was able to detect syncytiotrophoblasts with an efficiency comparable to that of β-HCG staining. This result suggests that the EGFR can be used as a marker for syncytiotrophoblastic cells instead of β-HCG or to resolve an equivocal β-HCG staining.

Two recent studies have also used immunohistochemistry to investigate EGFR expression in TGCTs [8, 15]. Our observation of EGFR expression in choriocarcinoma and single syncytiotrophoblastic cells confirms these previous results [8, 15]. In addition, we also found EGFR expression in embryonal carcinomas and teratomas, which had not been reported previously. These differences are most likely due to the larger size of our TGCT series and the more detailed histological analysis in our study.

Novel treatment modalities that specifically target EGFR signal transduction, such as anti-EGFR monoclonal antibodies and tyrosine kinase inhibitors, have

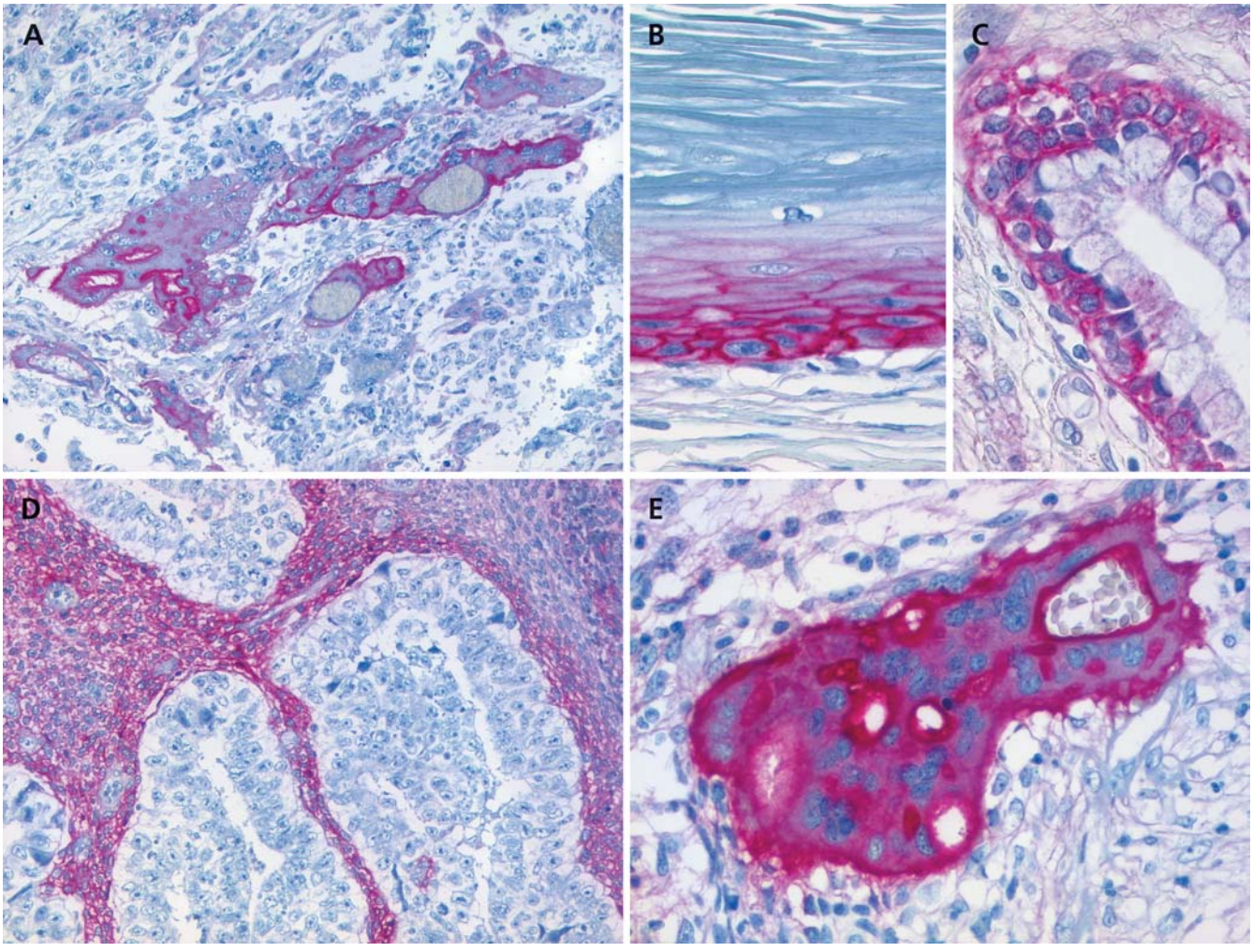

Fig. 1 Epidermal growth factor receptor (EGFR) expression in testicular germ cell tumors. EGFR immunoreactivity was detected in syncytiotrophoblastic cells of choriocarcinoma (**A**), squamous (**B**) and columnar (**C**) epithelia of teratoma, stromal cells of embryonal carcinoma (**D**) and in single syncytiotrophoblastic cells of teratoma (**E**)

recently become available [14]. Our result of a rather restricted EGFR expression pattern suggests that targeting EGFR signal transduction will be of limited value in the treatment of patients with TCGT.

References

1. Balaram P, John M, Rajalekshmy TN, Nair B, Schultz G, Nair K (1997) Expression of epidermal growth factor receptor in gestational trophoblastic diseases. J Cancer Res Clin Oncol 123:161–166
2. Bosl GJ, Motzer RJ (1997) Testicular germ-cell cancer. N Engl J Med 337:242–253
3. Chaganti RS, Houldsworth J (2000) Genetics and biology of adult human male germ cell tumors. Cancer Res 60:1475–1482
4. Damjanov I, Osborn M, Miettinen M (1990). Keratin 7 is a marker for a subset of trophoblastic cells in human germ cell tumors. Arch Pathol Lab Med 114:81–83
5. Dieckmann KP, Skakkebaek NE (1999) Carcinoma in situ of the testis: review of biological and clinical features. Int J Cancer 83:815–822
6. Fogel M, Lifschitz-Mercer B, Moll R, Kushnir I, Jacob N, Waldherr R, Livoff A, Franke WW, Czernobilsky B (1990) Heterogeneity of intermediate filament expression in human testicular seminomas. Differentiation 45:242–249
7. Hofmann GE, Drews MR, Scott RT, Navot D, Heller D, Deligdisch L (1992) Epidermal growth factor and its receptor in human implantation trophoblast: immunohistochemical evidence for autocrine/paracrine function. J Clin Endocrinol Metab 74:981–988
8. Kollmannsberger C, Mayer F, Pressler H, Koch S, Kanz L, Oosterhuis JW, Looijenga LH, Bokemeyer C (2002) Absence of c-KIT and members of the epidermal growth factor receptor family in refractory germ cell cancer. Cancer 95:301–308
9. Kurman RJ, Scardino PT, McIntire KR, Waldmann TA, Javadpour N (1977) Cellular localization of alpha-fetoprotein and human chorionic gonadotropin in germ cell tumors of the testis using direct and indirect immunoperoxidase technique. Cancer 40:2136–2151
10. Ladines-Llave CA, Maruo T, Manalo AS, Mochizuki M (1991) Cytologic localization of epidermal growth factor and its receptor in developing human placenta varies over the course of pregnancy. Am J Obstet Gynecol 165:1377–1382
11. Ladines-Llave CA, Maruo T, Manalo AM, Mochizuki M (1993) Decreased expression of epidermal growth factor and its

receptor in the malignant transformation of trophoblasts. Cancer 71:4118–4123
12. Manivel JC, Niehans G, Wick MR, Dehner LP (1987) Intermediate trophoblast in germ cell neoplasms. Am J Surg Pathol 11:693–701
13. McCluggage WG, Ashe P, McBride H, Maxwell P, Sloan JM (1998) Localization of the cellular expression of inhibin in trophoblastic tissue. Histopathology 32:252–625
14. Mendelsohn J (2002) Targeting the epidermal growth factor receptor for cancer therapy. J Clin Oncol 20:1S–13S
15. Moroni M, Veronese S, Schiavo R, Carminati O, Sorensen BS, Gambacorta M, Siena S (2001) Epidermal growth factor receptor expression and activation in nonseminomatous germ cell tumors. Clin Cancer Res 7:2770–2775
16. Mostofi FK, Sesterhenn IA (1998) Histological typing of testis tumours. Springer, Berlin Heidelberg New York
17. Nicholson RI, Gee JM, Harper ME (2001) EGFR and cancer prognosis. Eur J Cancer 37[Suppl 4]:S9–S15
18. Niehans GA, Manivel JC, Copland GT, Scheithauer BW, Wick MR (1988) Immunohistochemistry of germ cell and trophoblastic neoplasms. Cancer 62:1113–1123
19. Salomon DS, Brandt R, Ciardiello F, Normanno N (1995) Epidermal growth factor-related peptides and their receptors in human malignancies. Crit Rev Oncol Hematol 19:183–232
20. Schlessinger J (2002) Ligand-induced, receptor-mediated dimerization and activation of EGF receptor. Cell 110:669–672
21. Stoter G, Sylvester R, Sleijfer DT, ten Bokkel Huinink WW, Kaye SB, Jones WG, van Oosterom AT, Vendrik CP, Spaander P, de Pauw M (1988) A multivariate analysis of prognostic factors in disseminated non- seminomatous testicular cancer. Prog Clin Biol Res 269:381–393
22. Tuncer ZS, Vegh GL, Fulop V, Genest DR, Mok SC, Berkowitz RS (2000) Expression of epidermal growth factor receptor-related family products in gestational trophoblastic diseases and normal placenta and its relationship with development of postmolar tumor. Gynecol Oncol 77:389–393
23. Vaeth M, Schultz HP, Von Der Maase H, Engelholm SA, Krag Jacobsen G, Norgaard-Pedersen B (1984) Prognostic factors in testicular germ cell tumours. Experiences from 1058 consecutive cases. Acta Radiol Oncol 23:271–285
24. Von Hochstetter AR, Sigg C, Saremaslani P, Hedinger C (1985) The significance of giant cells in human testicular seminomas. A clinico-pathological study. Virchows Arch 407:309–322
25. Yarden Y, Sliwkowski MX (2001) Untangling the ErbB signalling network. Nat Rev Mol Cell Biol 2:127–137

Virchows Arch (2003) 443:32–37
DOI 10.1007/s00428-003-0812-4

ORIGINAL ARTICLE

Gabriela Aust · Jörg Hamann · Nicole Schilling · Manja Wobus

Detection of alternatively spliced EMR2 mRNAs in colorectal tumor cell lines but rare expression of the molecule in colorectal adenocarcinomas

Received: 4 October 2002 / Accepted: 20 March 2003 / Published online: 22 May 2003
© Springer-Verlag 2003

Abstract EMR2 and CD97, members of the epidermal growth factor (EGF)-TM7 family, show a very high homology. CD97, whose expression is closely related to clinical tumor stage in colorectal carcinomas, potentially functions as an adhesion molecule. Nothing is known about the presence of EMR2 in these tumors. We systematically examined the expression of EMR2 in colorectal carcinoma cell lines and adenocarcinomas. Of 18 cell lines, 10 were only slightly positive for EMR2 according to flow cytometry. Various EMR2 splice variants, including a new isoform, have been detected at the mRNA level. EMR2 expression did not correlate with in vitro migration or invasion capacity of the cell lines. Normal colorectal epithelial cells were EMR2 negative. In contrast to CD97, which is found in most colorectal adenocarcinomas, only 8 of 81 of these tumors expressed EMR2. No correlation was found between EMR2 expression and clinicopathological parameters of the tumors. In summary, a significant but low number of colorectal carcinomas are positive for EMR2, indicating different roles for this molecule and CD97 in these tumors.

Keywords Splice variant · EMR2 · CD97 · Colorectal carcinoma

Introduction

Epidermal growth factor (EGF)-TM7 receptors constitute a subfamily of class-B G-protein-coupled receptors (GPCRs) [1, 2]. Family members CD97 [3], EMR1 [4], EMR2 [5], EMR3 [6], EMR4 [7, 8], and ETL [9] possess an N-terminal with a variable number of EGF-like domains coupled to a seven span transmembrane (TM7) moiety via an extended stalk region. Structural variability in several EGF-TM7 molecules is created by extensive alternative splicing of exons encoding the EGF domains of the receptors [1].

Among members of the EGF-TM7 family, EMR2 and CD97 display a remarkable homology [5, 10, 11]. Both molecules are expressed as isoforms with three, four, or five EGF domains. The EGF domains are almost identical, with a common amino acid sequence identity ranging from 95% to 100% in the corresponding domains. Although small, this difference has been shown to alter ligand specificity [5, 12]. Whereas CD55/decay-accelerating factor has been identified as a cellular ligand of CD97 [13], EMR2 fails to interact with CD55. The significant amino acid sequence homology also extends to other regions in the two receptors. The EMR2 and CD97 genes are closely linked on human chromosome 19p13.1 and share a similar genomic organization of 20 exons, indicating that the genes are products of a recent duplication event [5].

Analysis of EMR2 expression on peripheral blood leukocytes, hematopoetic cell lines, and in situ revealed a myeloid-restricted profile [14]. In contrast to EMR2, CD97 is broadly distributed and can be found on hematopoetic and muscle cells as well as on various carcinomas [3, 15]. In thyroid carcinomas, CD97 expression correlates with tumor aggressiveness and lymph-node involvement [16, 17]. Recently, we demonstrated that colorectal carcinomas with more strongly CD97-stained, scattered tumor cells show a poorer clinical stage as well as increased lymph vessel invasion than cases with uniform CD97 staining [18].

The aim of this study was to examine the distribution pattern of EMR2 in normal colorectal tissues and carcinomas, and to evaluate whether EMR2 potentially might be involved in tumor development or progression. First, cancer cell lines were examined for EMR2 expres-

G. Aust (✉) · N. Schilling · M. Wobus
Institute of Anatomy,
University of Leipzig,
Ph.-Rosenthal-Strasse 55, 04103 Leipzig, Germany
e-mail: ausg@medizin.uni-leipzig.de
Tel.: +49-341-9722023
Fax: +49-341-9722029

J. Hamann
Laboratory for Experimental Immunology,
Academic Medical Center, University of Amsterdam,
The Netherlands

sion at the mRNA and protein levels using reverse-transcription polymerase chain reaction (RT-PCR) and flow cytometry. Second, malignant tumors and the corresponding normal tissues were screened by immunohistology to correlate EMR2 expression with pathomorphological criteria and clinical data of the patients.

Materials and methods

Cell lines

The human colorectal cancer cell lines Caco-2, Co115, Colo 201, Colo 205, DLD-1, HCT 116, HCT-15, HT-29, Lisp-1, LoVo, LS1034, LS174T, LS411 N, LS513, SW 1116, SW 480, SW 837, and WiDr were obtained from the American Type Culture Collection or European Collection of Cell Cultures.

Detection of the EMR2 isoform transcripts

Cellular RNA was isolated with the Qiagen total RNA isolation kit (Qiagen GmbH, Hilden, Germany). From the total RNA sample, 5 μg was taken to synthesize cDNA using a First-strand cDNA synthesis kit from Amersham Pharmacia Biotech (Freiburg, Germany). The primer pair PhEMR2s1 (5′-ccc ggt ggt gcc ctc agg act cc-3′)/r1 (5′-acg gga tcc tcc tcc tgc aca tcg tag tgg gcc-3′) spans 1515 bp from exon 3 to 14, encoding the alternatively spliced EGF domain region and the stalk region. The primer pair PhEMR2s2 (5′-agg tgc tct gtg tct tct ggg a-3′)/r2 (5′-ttc cac cgg caa aga ggg aag atc tta ttc-3′) amplifies 1077 bp from exon 13 to 20, encoding a part of the TM7 region. For the remaining exons, no alternative splicing was detected (data not shown). PCR products were cloned into the pGEM-T vector (Promega GmbH, Mannheim, Germany) and sequenced in both directions using a Big-Dye terminator kit on an ABI377 automated sequencer (PerkinElmer Instruments GmbH, Rodgau-Jügesheim, Germany).

Monoclonal antibodies (mAbs) and flow cytometry

Non-cross-reactive mAbs to the EMR2 and CD97 stalk region as used in this study were 2A1 [14] and CLB-CD97/3 [19], respectively. Cell lines were phenotyped with these mAbs by indirect immunofluorescence on a FACScan (Becton Dickinson, Mountain View, CA). A fluorescein isothiocyanate (FITC)-labeled $F(ab')_2$ fragment of goat anti-mouse Ig (Dako, Hamburg, Germany) was used as second-step reagent. Expression was depicted as mean fluorescence intensity of stained cells compared with cells stained with an isotype-matched but irrelevant mAb.

Migration and invasion assay

The migration and invasion capacity of colon carcinoma cell lines were measured using 24-transwell chambers (Costar, Bodenheim, Germany) or 6-well Matrigel pre-coated invasion chambers (BD Biosciences, Heidelberg, Germany) as described recently [18]. Briefly, cells were radiolabeled for 12 h using (methyl3H)-thymidine (0.1 µCi/ml, 7.4 MBq/mmol) and detached with 0.02% ethylenediaminetetra-acetic acid (EDTA). For the invasion assay, 8×10^5 cells per well were incubated on the reconstituted membrane for 72 h. For the migration assay, 1×10^5 cells per well were seeded onto the filter for 24 h. Cells passing the filters and attaching to the lower sites of uncoated or Matrigel-coated membranes were harvested using trypsin/EDTA. Cell-bound radioactivity was measured using a liquid scintillation counter. The percentages for migration and invasion were calculated on the number of migrating cells compared with the total number of cells. The correlation between percentage migration and invasion to mean fluorescence intensity of CD97 was calculated using Spearman's method.

Patients

The study comprised a series of 81 sporadic colorectal adenocarcinomas. From all patients, normal mucosal specimens were collected at least 5 cm away from the carcinoma lesions. Samples were cryopreserved in liquid nitrogen. No patient had been receiving chemotherapy or radiotherapy before surgery. Histological diagnosis and staging were performed following the TNM classification proposed by the UICC (International Union Against Cancer) according to standard criteria (stage I: n=10; stage II: n=21; stage III: n=27; stage IV: n=23). All tumors were further examined histologically: (i) for differentiation, according to the predominant growth pattern (well differentiated, grade I: n=3; moderately differentiated, grade II: n=59; poorly differentiated, grade III: n=19), and (ii) for the presence of blood and lymph vessel invasion [20].

The study was approved by the local committee of medical ethics and has therefore been performed in accordance with the ethical standards laid down in the 1964 Declaration of Helsinki. All patients gave their written consent prior to their inclusion in the study.

Immunohistology

Tissues were snap-frozen in liquid nitrogen. Serial frozen sections were cut at 5 µm, fixed in ice-cold methanol for 10 min followed by a short rinse in 0.2 M PBS, and then incubated with the primary mAb. In negative control sections, an irrelevant mAb was applied at the same concentration as the primary one in each case. Human skeletal muscle was taken as a negative staining control with the colorectal tissues. Unlike CD68, EMR2 is not a common antigen on all tissue macrophages; therefore, peripheral blood monocytes adhered to glass slides were used as the best positive staining control.

Following first-step incubation (4°C, overnight), bound mAbs were detected with a super-sensitive detection kit (BioGenex, San Ramon, CA) including biotinylated anti-mouse Ig and horseradish peroxidase-conjugated streptavidin.

Results

EMR2 in colorectal tumor cell lines

Eighteen colorectal tumor cell lines were tested by flow cytometry for cell surface expression of EMR2 (Table 1). We have only quoted those cell lines as positive where more than 5% of the cells were stained. EMR2 was detected at very low levels on 10 of 18 of these cell lines. This is in contrast with CD97, which we previously showed to be present on all of the cell lines examined [18]. There was no correlation between EMR2 and CD97 mean fluorescence intensity. Furthermore, EMR2 mean fluorescence intensity did not correlate with the in vitro migratory and invasive capacity of the cell lines (Fig. 1).

Analysis of EMR2 transcripts from all cell lines from RT-PCR products revealed highly variable splice patterns for exons encoding the EGF domains and the stalk region, but not for those encoding the TM7 region (Fig. 2). More than 25 RT-PCR products from seven cell lines were cloned and sequenced. The putative proteins deduced from the alternatively spliced mRNA molecules are

Table 1 Expression of EMR2 in colorectal tumor cell lines determined by flow cytometry (percentage of cells expressing the antigen and mean fluorescence intensity). We have only quoted those cell lines as slightly positive where more than 5% of the cells were stained by flow cytometry

Cell line	%	Intensity
Caco-2	5–50	1.8±1.3
Co115	5–50	0.6±0.4
Colo 201	0–5	0.1±0.1
Colo 205	0	0
DLD-1	0–5	1.2±1.5
HCT 116	50–90	3.0±0.6
HCT-15	50–90	2.1±1.6
HT29	0	0
Lisp-1	100	3.6±1.3
LoVo	0	0
LS1034	0–5	0.7±0.4
LS174T	50–90	1.9±0.6
LS411 N	0	0
LS513	100	4.7±0.4
SW 1116	100	4.3±0.2
SW 480	100	5.2±1.2
SW 837	50–90	2.0±0.1
WiDr	0	0

shown schematically in Fig. 3. In addition to full-length transcripts and six further isoforms described by Lin et al. [5], we detected two new alternative spliced transcripts lacking the amino acids encoded by exon 11. Due to alternative splicing of exon 11 and/or exon 12, different stop codons become functional, which is caused by a reading frame shift in the respective transcripts (Fig. 3). As these mRNA variants do not comprise the TM7-encoding exons, they are supposed to generate soluble gene products. This assumption was confirmed by data obtained from the cell line LOVO, which was found to be EMR2 negative in flow cytometry, but contained EMR2 mRNA. Analyzing transcripts from LOVO cells, splice variants were detected that encode soluble EMR2 isoforms. In other cell lines, such as SW1116 and SW480, mRNA variants were detected that encode both membrane-bound and soluble EMR2.

Sequencing the RT-PCR products revealed the existence of further splice variants missing partial exons. As characterizing these variants would exceed the aim of this study, they are not presented here. Apart from differential

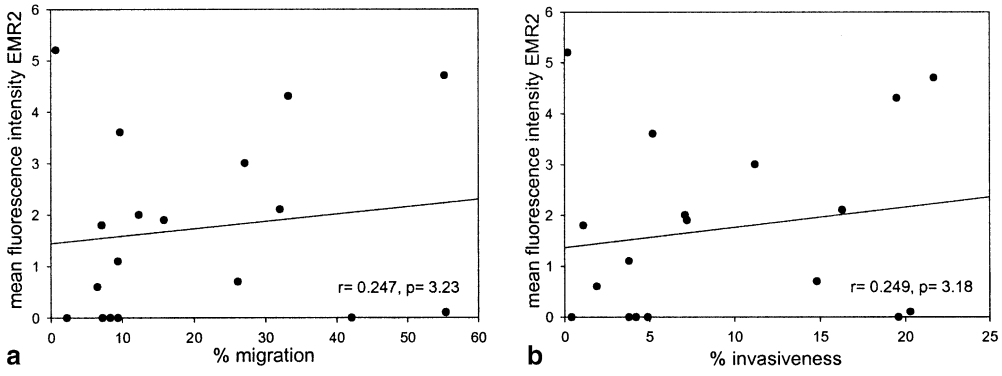

Fig. 1 EMR2 expression (see Table 1) does not correlate with in vitro migration (**a**) and invasion (**b**) capacity of colorectal carcinoma cell lines (n=18). Indicated is the mean percentage of migrating/invading cells relative to the total cell number (n=3)

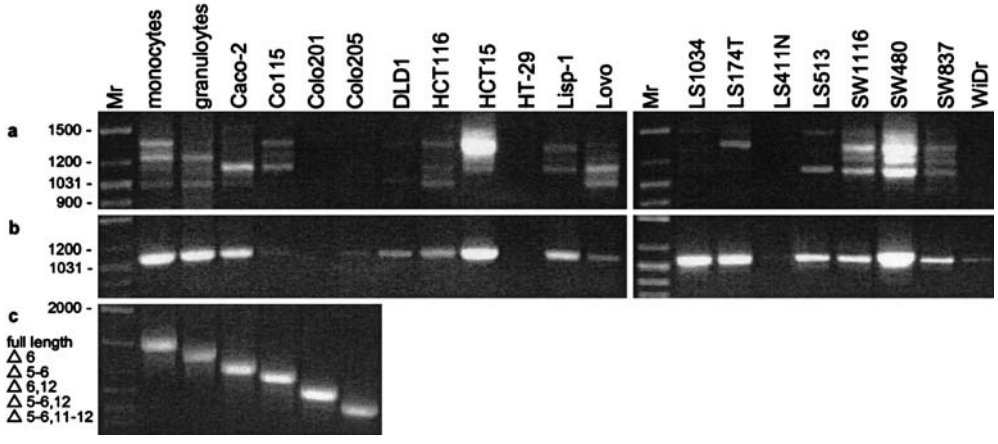

Fig. 2 Detection of EMR2 transcripts using reverse-transcription polymerase chain reaction (RT-PCR) in colorectal carcinoma cell lines. **a** The primer pair EMR2s1/r1 amplifies exons 3–14, encoding the epidermal growth factor (EGF) domains and the stalk region. Alternatively mRNA splicing results in PCR products of different size. **b** The primer pair EMR2s2/r2 amplifies exons 13–20, encoding the seven transmembrane (TM7) and the cytoplasmic region. **c** Re-amplification of some cloned EMR2 RT-PCR products (Fig. 3) with the primer pair EMR2s1/r1. cDNA from peripheral blood monocytes and granulocytes was used as positive control. Mr: 100 bp DNA ladder

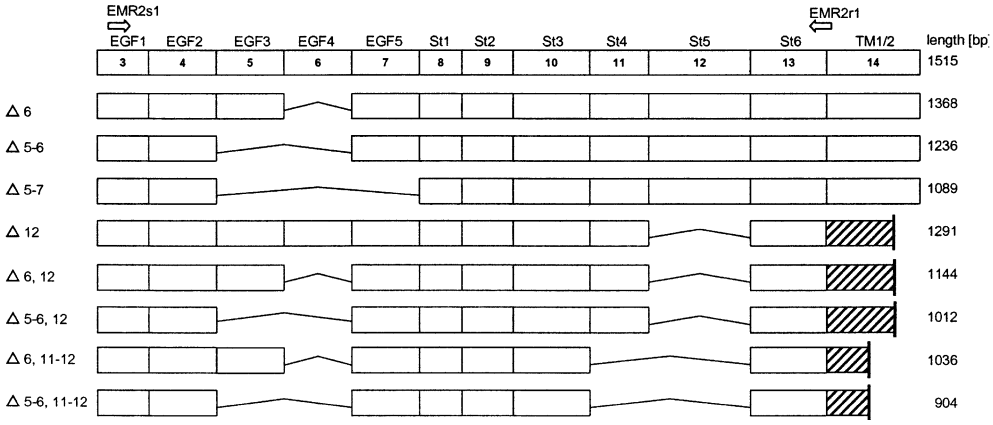

Fig. 3 Alternative spliced transcripts of EMR2 detected in colorectal carcinoma cell lines. Exon numbering refers to Lin et al. [5]. Variants without exon 11 and/or 12 encode putative soluble EMR2. Primer binding sites and the resulting polymerase chain reaction (PCR) products are indicated. *EGF* epidermal growth factor domain, *St* stalk region, *TM* transmembrane segment

splicing, no deviations from the published EMR2 sequence [5] were observed.

EMR2 expression in colorectal tissues

Normal epithelial cells and smooth muscle cells of colorectal tissues were EMR2 negative (Fig. 4a). A subpopulation of macrophages located within the lamina propria mucosae and scattered within other regions of the normal tissues were positive for EMR2 (Fig. 4a). In contrast, lymphocytes were EMR2 negative (Fig. 4c). We only found staining for EMR2 in 8 of 81 colorectal carcinomas (Fig. 4b, c, d), which is in clear contrast to the known high number of CD97-positive tumors. A subpopulation of tumor-infiltrating leukocytes strongly expressed EMR2 (Fig. 4e). Thus, EMR2 mRNA determination in EMR2-negative colorectal tissues to examine whether the tumor cells may be positive for soluble EMR2 variants is not useful. There were no statistically significant differences between EMR2-positive and EMR2-negative patient groups regarding the clinicopathological features examined such as tumor stage, differentiation, and the presence of blood or lymph vessel invasion (not shown).

Discussion

The observation that nearly all colorectal carcinomas express CD97 and the correlation found between the presence of scattered, strongly CD97-positive tumor cells at the tumor invasion front and tumor stage [18] raises the question whether EMR2, an EGF-TM7 receptor closely related to CD97, shows a comparable distribution pattern and clinical significance in these tumors. Here, we have demonstrated that a significant but low number of colorectal carcinomas are EMR2 positive. Recently, we showed that gastric, pancreatic, and esophageal carcinomas are EMR2 negative but CD97 positive [21], which indicates that EMR2 only has a restricted expression in tumors of the gastrointestinal tract. In contrast to CD97, expression of EMR2 on colorectal cell lines does not correlate with the in vitro invasive and migratory capacity of these cells. These observations, together with the previously reported differences with regard to cellular distribution, activation-dependent upregulation, and ligand binding of EMR2 and CD97 [5, 12, 14], further support the hypothesis that both molecules have different physiological and pathological functions despite their remarkable structural similarity. A better understanding of the role of EMR2 will accompany the identification of its physiological ligand(s).

EMR2 is expressed on a subpopulation of macrophages in normal and, as demonstrated here for the first time, in tumor tissues confirming the dominant myeloid expression pattern of the molecule [5, 14]. Only systematic screening would reveal whether the EMR2 staining pattern on macrophages/leukocytes indicates a role for EMR2 in stromal tumor interactions in a subset of the investigated colorectal carcinomas. The percentage of macrophages expressing EMR2 in normal, inflamed, and malignant tissues has to be determined in advance by double labeling with CD68 to obtain a first functional insight into the subpopulation of macrophages bearing EMR2. Moreover, this expression profile indicates that there is a closer relationship between EMR2 and the other EGF-TM7 molecules EMR1, EMR3, and EMR4 instead of to CD97 since the expression of these family members is also restricted to myeloid cells. No data have been published on the presence of these molecules on tumors.

The detection of slight EMR2 expression on colorectal tumor cell lines was the first indication of the presence of this molecule in some of the original carcinomas. In contrast, CD97 is expressed on all of these cell lines and shows considerably higher levels [18]. To confirm the flow cytometry results, EMR2 transcripts were analyzed. Surprisingly, RT-PCR and sequencing revealed multiple spliced forms of EMR2. The functional consequences of this observation, and especially the functional roles of the potential EMR2 products generated by these splicing events, are not known. Alternatively spliced mRNA molecules may be involved in the regulation of both protein expression and function [22, 23]. Many cancer-associated genes, such as CD44 and WT1, are alternatively spliced [24]. However, alternative splicing of

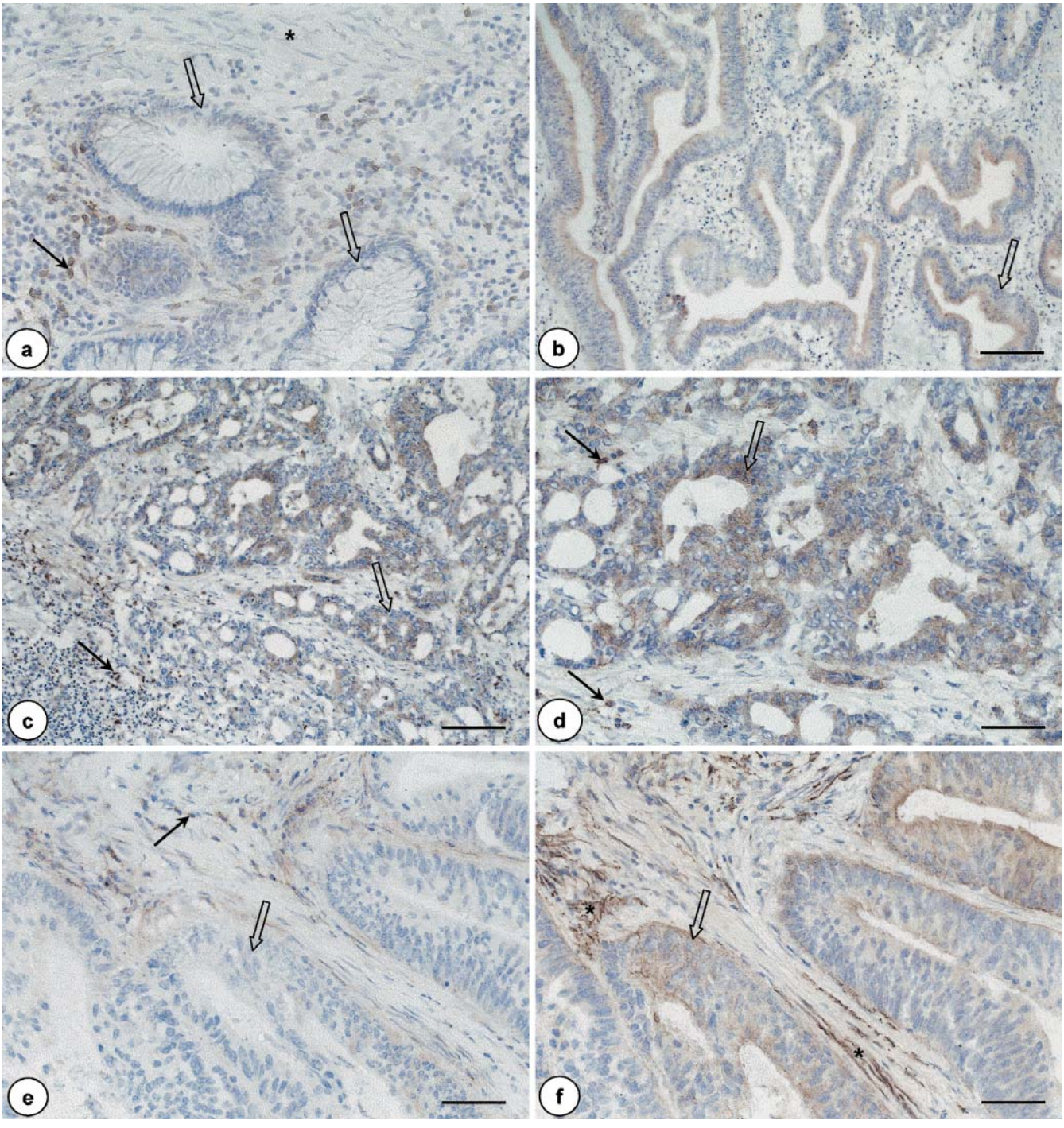

Fig. 4 Expression of EMR2 on cryosections of colorectal normal tissue and carcinoma. **a** Whereas normal epithelial cells (*open arrow*) and smooth muscle cells (*) are EMR2 negative, a subpopulation of leukocytes located within the lamina propria mucosae expresses the molecule (*arrows*). **b–d**: In an EMR2-positive colon adenocarcinoma, the tumor cells strongly express EMR2 (**c, d** *open arrows*). Lymphocytes located nearby the adenoid structures are EMR2 negative, whereas other leukocytes are EMR2 positive (*arrow*). **d** Part of **c** at higher magnification. In a few more patients, tumor cells slightly express EMR2 as seen by the faint staining at the adluminal side of the cells (**b**, *open arrow*). **e, f** In most colon adenocarcinomas, EMR2 is not expressed as demonstrated here in a typical example. Only a subset of tumor-infiltrating leukocytes (*arrow*) but not tumor cells (*open arrow*) express the molecule (**e**). In contrast, CD97 is present on the tumor cells (**f**, *serial sections*). Additionally, smooth muscle cells are labeled for CD97 (*)

EMR2 also still seems to be a common event in normal cells [5], suggesting that its high frequency may be intrinsic to the sequence of this gene. In contrast to the distinct distribution pattern of EMR2 transcripts demonstrated here, the splice pattern of CD97 in colorectal cell lines, but also in hematopoietic cells, is less diverse, generally being dominated by transcripts encoding the smallest isoform with three EGF domains [18, 25]. The mRNAs encoding the three known CD97 isoforms with three, four, and five EGF domains are always co-expressed.

EMR2 transcripts failing the transmembrane domain by loss of exon 11, as demonstrated here and not shown until now, and/or exon 12 [5] may result in soluble EMR2 molecules. Another possibility for forming soluble EGF-TM7 molecules seems to be a feature of all members of the family. Translated as a single polypeptide, cleavage of the molecules proximal to the first transmembrane domain in the GPCR proteolytic site results in the formation of a heterodimer consisting of an extracellular α-subunit non-covalently associated with the TM7 cytoplasmic β-subunit [2, 6, 8, 9, 11, 14]. For CD97, a soluble form that is probably identical to the α-subunit has been demonstrated [11, 26] whereas this evidence is still lacking for EMR2.

Taken together, EMR2 is rarely expressed on colorectal adenocarcinoma, indicating a different function than CD97 in these tumors.

Acknowledgements The study was supported by the Deutsche Krebshilfe, project 10–1530-Au I. We thank Dr. M. Steinert (Department of Surgery) and Dr. A. Schütz (Institute of Pathology; both University of Leipzig) for providing the colorectal tissues and Prof. C. Boltze (Institute of Pathology, University of Magdeburg) for performing the migration and invasion assays.

References

1. McKnight AJ, Gordon S (1998) The EGF-TM7 family: unusual structures at the leukocyte surface. J Leukoc Biol 63:271–280
2. Stacey M, Lin HH, Gordon S, McKnight AJ (2000) LNB-TM7, a group of seven-transmembrane proteins related to family-B G-protein-coupled receptors. Trends Biochem Sci 25:284–289
3. Eichler W, Aust G, Hamann D (1994) Characterization of the early activation-dependent antigen on lymphocytes defined by the monoclonal antibody BL-Ac(F2). Scand J Immunol 39:111–115
4. Baud V, Chissoe SL, Viegas-Pequignot E, Diriong S, N'Guyen VC, Roe BA, Lipinski M (1995) EMR1, an unusual member in the family of hormone receptors with seven transmembrane segments. Genomics 26:334–344
5. Lin HH, Stacey M, Hamann J, Gordon S, McKnight AJ (2000) Human EMR2, a novel EGF-TM7 molecule on chromosome 19p13.1, is closely related to CD97. Genomics 67:188–200
6. Stacey M, Lin HH, Hilyard KL, Gordon S, McKnight AJ (2001) Human epidermal growth factor (EGF) module-containing mucin-like hormone receptor 3 is a new member of the EGF-TM7 family that recognizes a ligand on human macrophages and activated neutrophils. J Biol Chem 276:18863–18870
7. Caminschi I, Lucas KM, O'Keeffe MA, Hochrein H, Laabi Y, Kontgen F, Lew AM, Shortman K, Wright MD (2001) Molecular cloning of F4/80-like-receptor, a seven-span membrane protein expressed differentially by dendritic cell and monocyte-macrophage subpopulations. J Immunol 167:3570–3576
8. Stacey M, Chang GW, Sanos SL, Chittenden LR, Stubbs L, Gordon S, Lin HH (2002) EMR4, a novel EGF-TM7 molecule up-regulated in activated mouse macrophages, binds to a putative cellular ligand on B lymphoma cell line, A20. J Biol Chem 277:29283–29293
9. Nechiporuk T, Urness LD, Keating MT (2001) ETL, a novel seven transmembrane receptor that is developmentally regulated in the heart. ETL is a member of the secretin family and belongs to the EGF-TM7 subfamily. J Biol Chem 276:4150–4157
10. Hamann J, Eichler W, Hamann D, Kerstens HM, Poddighe PJ, Hoovers JM, Hartmann E, Strauss M, van Lier RA (1995) Expression cloning and chromosomal mapping of the leukocyte activation antigen CD97, a new seven-span transmembrane molecule of the secretion receptor superfamily with an unusual extracellular domain. J Immunol 155:1942–1950
11. Gray JX, Haino M, Roth MJ, Maguire JE, Jensen PN, Yarme A, Stetler-Stevenson MA, Siebenlist U, Kelly K (1996) CD97 is a processed, seven-transmembrane, heterodimeric receptor associated with inflammation. J Immunol 157:5438–5447
12. Lin HH, Stacey M, Saxby C, Knott V, Chaudhry Y, Evans D, Gordon S, McKnight AJ, Handford P, Lea S (2001) Molecular analysis of the epidermal growth factor-like short consensus repeat domain-mediated protein-protein interactions: dissection of the CD97-CD55 complex. J Biol Chem 276:24160–24169
13. Hamann J, Vogel B, van Schijndel GM, van Lier RA (1996) The seven-span transmembrane receptor CD97 has a cellular ligand (CD55, DAF). J Exp Med 184:1185–1189
14. Kwakkenbos MJ, Chang GW, Lin HH, Pouwels W, de Jong EC, van Lier RA, Gordon S, Hamann J (2002) The human EGF-TM7 family member EMR2 is a heterodimeric receptor expressed on myeloid cells. J Leukoc Biol 71:854–862
15. Jaspars LH, Vos W, Aust G, van Lier RA, Hamann J (2001) Tissue distribution of the human CD97 EGF-TM7 receptor. Tissue Antigens 57:325–331
16. Aust G, Eichler W, Laue S, Lehmann I, Heldin N-E, Lotz O, Scherbaum WA, Dralle H, Hoang-Vu C (1997) CD97: a dedifferentiation marker in human thyroid carcinomas. Cancer Res 57:1798–1806
17. Hoang-Vu C, Bull K, Schwarz I, Krause G, Schmutzler C, Aust G, Köhrle J, Dralle H (1999) Regulation of CD97 protein in thyroid carcinoma. J Clin Endocrinol Metab 84:1104–1109
18. Steinert M, Wobus M, Boltze C, Schütz A, Wahlbuhl M, Hamann J, Aust G (2002) Expression and regulation of CD97 in colorectal carcinoma cell lines and tumor tissues. Am J Pathol 161:1657–1667
19. Kwakkenbos MJ, van Lier RA, Hamann J (2002) Characterization of EGF-TM7 family members by novel monoclonal antibodies. In: Mason D (ed) Leucocyte typing VII. White cell differentiation antigens. Oxford University Press, Oxford, pp 381–383
20. Minsky BD, Mies C, Recht A, Rich TA, Chaffey JT (1988) Resectable adenocarcinoma of the rectosigmoid and rectum. II. The influence of blood vessel invasion. Cancer 61:1417–1424
21. Aust G, Steinert M, Schütz A, Wahlbuhl M, Hamann J, Wobus M (2002) CD97, but not its closely related EGF-TM7 family member EMR2, is expressed on gastric, pancreatic and esophageal carcinomas. Am J Clin Pathol 118:699–707
22. Singh R (2002) RNA-protein interactions that regulate pre-mRNA splicing. Gene Expr 10:79–92
23. Nissim-Rafinia M, Kerem B (2002) Splicing regulation as a potential genetic modifier. Trends Genet 18:123–127
24. Caballero OL, De Souza SJ, Brentani RR, Simpson AJ (2001) Alternative spliced transcripts as cancer markers. Dis Markers 17:67–75
25. Eichler W (2000) CD97 isoform expression in leukocytes. J Leukoc Biol 68:561–567
26. Hamann J, Wishaupt JO, van Lier RA, Smeets TJ, Breedveld FC, Tak PP (1999) Expression of the activation antigen CD97 and its ligand CD55 in rheumatoid synovial tissue. Arthritis Rheum 42:650–658

Virchows Arch (2003) 443:38–43
DOI 10.1007/s00428-003-0813-3

ORIGINAL ARTICLE

Raffaèle Fauvet · Christophe Poncelet · Danièle Hugol · Anne Lavaur · Gérard Feldmann · Emile Daraï

Expression of apoptosis-related proteins in endometriomas and benign and malignant ovarian tumours

Received: 26 November 2002 / Accepted: 14 March 2003 / Published online: 20 May 2003
© Springer-Verlag 2003

Abstract Apoptosis is a physiological process by which multicellular organisms eliminate superfluous cells. Alterations in apoptosis play a key role in tumour development. The objective was to evaluate the immunohistochemical expression of p53, p21, bax, bak, fas, bcl-2 and bcl-x proteins in 10 endometriomas, 20 benign ovarian tumours (10 mucinous, 10 serous) and 30 malignant ovarian tumours (9 mucinous, 19 serous; 2 endometrioids). p53 positive cells (mean±SD) in endometriomas, and benign and malignant tumours were 1.9±3.2, 0 and 16.2±33.0, respectively. The difference was significant between benign tumours and endometriomas (P=0.003) but not between endometriomas and malignant tumours. P21 expression in endometriomas and benign and malignant tumours was 19.5±27.8, 1.7±6.7 and 4.1±8.6, respectively. Increased p21 expression was found in endometriomas compared with benign (P=0.001) and malignant (P=0.01) tumours. Bax expression was higher in endometriomas than in benign tumours (P=0.01), but no difference was found between endometriomas and malignant tumours. No difference in bak, fas, bcl-2 or bcl-x expression was observed among the groups. In endometriomas, a negative correlation was found between p53 and fas expression (P=0.04, r=0.66). Although endometriomas have histological features of benign ovarian tumours, endometriomas share with malignant ovarian tumours certain alterations in apoptosis-related proteins.

R. Fauvet · A. Lavaur · E. Daraï
Service de Gynécologie, Hôpital Hôtel-Dieu, AP-HP, France

R. Fauvet · C. Poncelet · G. Feldmann · E. Daraï
Laboratoire de biologie cellulaire,
INSERM U327, Faculté Bichat-Claude Bernard, France

E. Daraï (✉)
Service de Gynécologie-Obstétrique,
Hôpital Tenon, 4 rue de la Chine, 75020 Paris, France
e-mail: emile.darai@tnn.ap-hop-paris.fr
Tel.: +33-1-56017318, Fax: +33-1-56017317

D. Hugol
Service d'Anatomie Pathologie, Hôpital Hôtel-Dieu, AP-HP, France

Keywords Apoptosis · Endometriomas · Ovarian tumours · Ovarian cancer

Introduction

Endometriosis is defined by the presence of ectopic endometrial glands and stroma outside the uterus, and is a cause of pain and infertility. The main etiopathogenetic concepts forwarded to explain the development of endometriosis are the metaplasia and transplantation theories [33, 35]. The metaplasia theory, based on the concept that the peritoneum has the potential to differentiate into Muellerian-type epithelium, postulates that invasive mechanisms assist in the establishment of endometriotic lesions beneath the peritoneal surfaces. The transplantation theory implies that endometrial cells have the ability to detach from the endometrium, reattach after passive transport through the Fallopian tubes into the peritoneum and invade target tissues. The incidence of endometriosis in the general female population ranges from 5% to 15%, but reaches more than 50% in women with dysmenorrhea and/or infertility [34, 38, 40]. Clinically, one of the most frequent locations of endometriosis has been the ovary, with cysts called endometriomas [18]. The malignant transformation of ovarian endometriotic lesions varied from 0.6% to 1% [14].

Apoptosis, also called programmed cell death, was first discovered in 1842 by Vogt [41]. More than a century later, Kerr et al., rekindled apoptosis research [20]. This physiological process is involved in cellular homeostasis, maintaining a balance between cell proliferation and programmed cell death [16]. Apoptosis can be initiated by extracellular survival signals, mainly mediated by the bax/bcl-2 complex and also by intracellular death signals (genome instability) that increase the level of p53, and extracellular death signals involving membrane receptors such as the fas/fas-ligand system. Apoptosis-related protein expression in endometriotic lesions at different sites is controversial [19, 23, 30, 42]. Indeed, in glandular epithelial cells from ovarian endometriotic

tissue, McLaren et al. [26], contrary to Harada et al. [13], reported positive bcl-2 expression. Previous studies [13, 30, 38] showed lower bcl-2 expression in endometriotic cysts than in peritoneal endometriotic samples. In contrast to bcl-2 expression, few data have been reported on the expression of apoptosis-related proteins such as bax [27] and fas [13, 42], and no data are available on p21 expression in patients with endometriosis. The aims of this study were to evaluate the expression of pro-apoptotic proteins (p53, p21, bax, bak and fas) and anti-apoptotic proteins (bcl-2 and bcl-x) in endometriomas, in comparison with benign and malignant ovarian tumours.

Materials and methods

Materials

Between 1986 and 2000, tissue samples were obtained from 60 patients undergoing surgery in the Gynaecology Department of Hôtel-Dieu Hospital, Paris; the samples consisted of 10 endometriomas, 20 benign ovarian tumours (10 mucinous, and 10 serous) and 30 malignant ovarian tumours (9 mucinous, 19 serous; 2 endometrioids).

In the endometrioma group, the mean age of the patients was 34 years (range 23–43 years). All the patients were pre-menopausal, and none had received progestin or gonadotrophin releasing hormone (GnRH) analogues for at least 3 months before surgery. They underwent surgery during the proliferative phase of the menstrual cycle in five cases and during the secretory phase in five cases. All underwent cystectomy.

In the benign tumour group, the patients' mean age was 45 years (range 21–75 years). Eight women were post-menopausal (40%), and twelve (60%) were pre-menopausal. No medical treatment was given before surgery, but three post-menopausal women were on hormone replacement therapy (HRT). All the pre-menopausal patients underwent cystectomy during the proliferative phase. One post-menopausal woman underwent bilateral salpingo-oophorectomy.

In the malignant tumour group, the patients' mean age was 55 years (range 26–84 years). Twenty patients (66.6%) were post-menopausal, and ten (33.3%) were pre-menopausal. Five post-menopausal women (25%) were on HRT. The disease was staged according to the FIGO classification (Federation Internationale de Gynecologie et Obstetrique) [17]. Thirteen patients had stage-I, two stage-II, fourteen stage-III, and one stage-IV disease. No neo-adjuvant chemotherapy was used before surgery; the latter consisted of hysterectomy with bilateral salpingo-oophorectomy and omentectomy in all cases, and pelvic and para-aortic lymphadenectomy in 7 cases. Surgery was followed by chemotherapy.

The diagnosis was confirmed histologically on each tissue sample by reviewing hematoxylin/eosin-stained slides. None of the endometriomas contained clear nuclear atypia.

Methods

Antibodies

To evaluate pro-apoptotic protein expression, we used an anti-human-p53 mouse monoclonal antibody (Dako, Glostrup, Denmark), an anti-human-p21 mouse monoclonal antibody (Dako), an anti-human-bax mouse monoclonal antibody (Immunotech, Marseille, France), an anti-human-bak rabbit polyclonal antibody (Santa-Cruz Biotechnology, Santa-Cruz, CA, USA), and an anti-human-fas (CD 95) mouse monoclonal antibody (Immunotech). To evaluate anti-apoptotic protein expression, we used an anti-human-bcl-2 rabbit polyclonal antibody (Santa-Cruz Biotechnology), and an anti-human-bcl-x mouse monoclonal antibody (Transduction Laboratories, Lexington, KY, USA).

Immunohistochemical technique

In all cases, 5-µm-thick, paraffin-embedded sections of formalin-fixed tissues were used. Sections were deparaffinated in xylene and rehydrated through a graded series of ethanol solutions, followed by microwave antigen retrieval for 20 min in 0.01 M sodium citrate buffer. Endogenous peroxidase activity was inhibited with 0.3% hydrogen peroxide for 15 min. After washing in Tris buffer saline-Tween casein (TBS-TC), sections were incubated for 1 h with the primary antibody. The antibodies to p53, p21, bak, fas and bcl-2 were used at a dilution of 1/50. Anti-bax was diluted 1/200, and anti-bcl-x was diluted 1/75. After washing in TBS-TC, the sections were incubated with an anti-mouse or anti-rabbit peroxidase conjugate (Valbiotech, Paris, France) for 40 min. Binding was visualised by incubating sections with DAB (3,3′diaminobenzidine) (Dako) or AEC (3-amino-9-ethylcarbazol) (Beckman Coulter, Brea, CA, USA) and lightly counterstaining with hematoxylin.

Positive controls for p53, p21, bax, bak, fas, bcl-2 and bcl-x were sections obtained from colon carcinoma, tonsil, normal breast epithelium, normal breast epithelium, rhadomyosarcoma, lymph node and aortic endothelium, respectively. For negative controls, the primary antibody was replaced by the relevant IgG subtype (monoclonal antibodies) or with non-immune serum (polyclonal antibodies).

Analysis of immunohistochemical results

For qualitative analysis, samples were considered negative when no labelled cell was observed on the tissue section, and positive in all other cases.

For semi-quantitative analysis, positive cells were counted among 500 cells in the most characteristic areas, and the percentage of labelled cells was calculated by two independent observers in five consecutive high-power fields (0.1734 mm^2 per field) per section. Variations between the two observers were below 5%.

Statistical analysis

We used the Chi-square test for categorical variables, and the Kruskall-Wallis and Mann-Whitney tests for continuous variables. The Spearman correlation test was used to identify correlations between two quantitative variables. P values below 0.05 were considered significant.

Results

Qualitative expression of apoptosis-related proteins in endometriomas and benign and malignant ovarian tumours

P53 immunostaining was restricted to the nuclei (Fig. 1a). P53 expression differed among the three groups of tumours (P=0.01). The paired differences were significant between endometriomas and benign tumours (P=0.01), between benign and malignant tumours (P<0.001), but not between endometriomas and malignant ovarian tumours (Table 1).

P21 immunostaining was also restricted to the nuclei (Fig. 1b). P21 expression differed among the three groups of tumours (P=0.003). The difference was significant between endometriomas and benign tumours (P=0.003) and between endometriomas and malignant ovarian tumours (P=0.04).

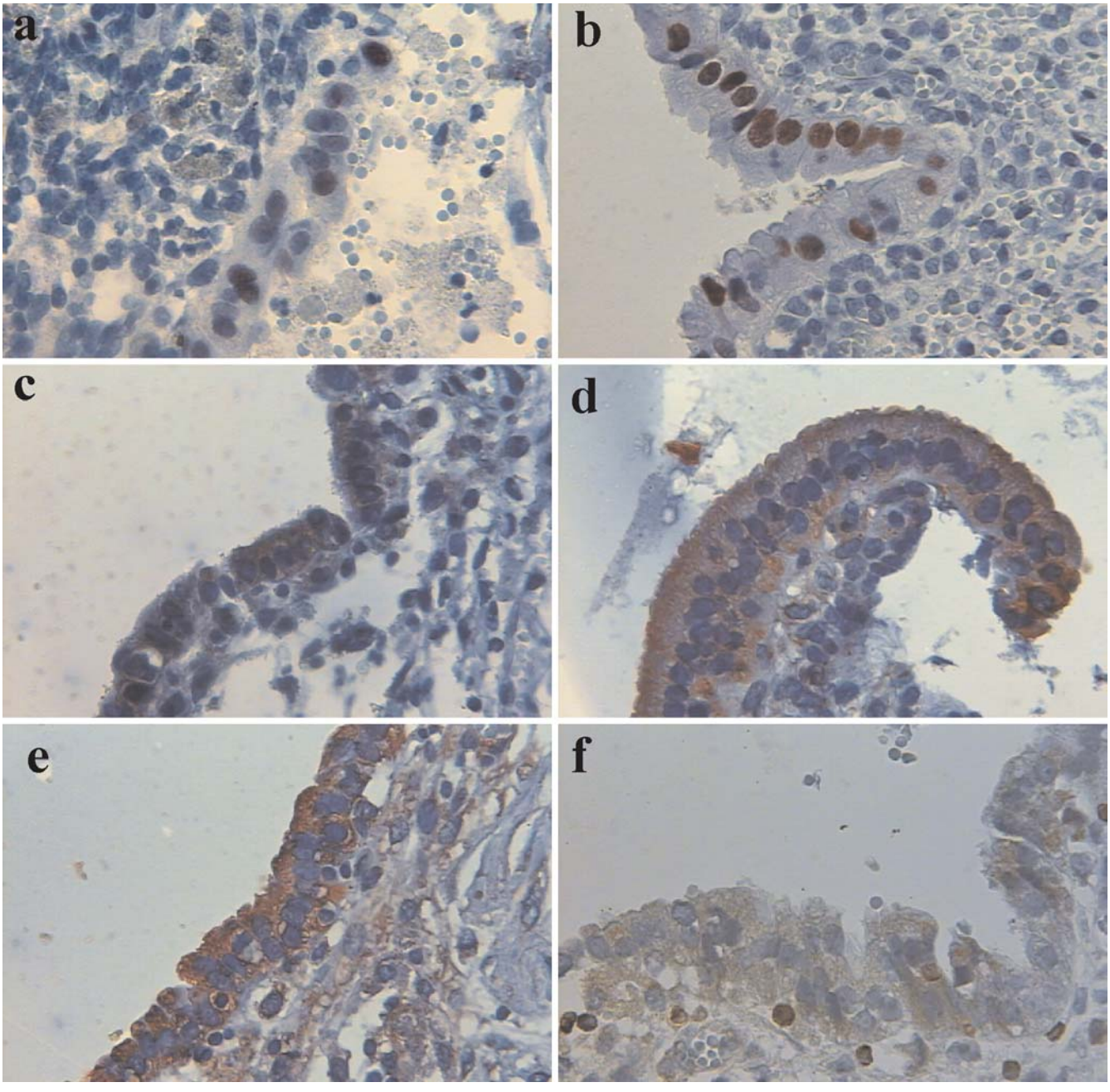

Fig. 1 Immunoperoxidase staining with 3-amino-9-ethylcarbazol (**a**–**e**) or diaminobenzidine (**f**) as chromogen, and nuclear counter-staining with Harris hematoxylin. Representative examples of p53 (**a**), p21 (**b**), bax (**c**), bak (**d**), fas (**e**) and bcl-2 (**f**) staining in endometriomas. p53 and p21 immunostaining was restricted to the nuclei. Bax, bak and bcl-2 immunostaining was detected in the cytoplasm. Fas labeling was observed in both the outer membrane and the cytoplasm

Table 1 Qualitative expression of apoptosis-related proteins in endometriomas and benign and malignant ovarian tumours. *NS* not significant

	Endometriomas (n=10)	Benign ovarian tumours (n=20)	Malignant ovarian tumours (n=30)	P value*
p53	4/10	0/20	9/30	0.01
P21	7/10	2/20	9/30	0.003
Bax	7/10	9/20	15/30	NS
Bak	10/10	20/20	30/30	NS
Fas	10/10	18/20	29/30	NS
Bcl-2	7/10	13/20	16/30	NS
Bcl-x	8/10	16/20	27/30	NS

* P value for the three groups using Chi square test

Table 2 Mean±SD percentages of cells positive for p53, p21, bax, bak, fas, bcl-2 and bcl-x in endometriomas and benign and malignant ovarian tumours. *NS* not significant

	Endometriomas (n=10)	Benign ovarian tumours (n=20)	Malignant ovarian tumours (n=30)	P value*
p53	1.9±3.2	0	16.2±33.0	0.02
p21	19.5±27.8	1.7±6.7	4.1±8.6	0.002
bax	30.5±29.3	6.5±12.7	18.6±26.2	0.04
bak	88.0±14.3	75.3±33.2	90.4±15.7	NS
fas	64.8±32.1	54.7±42.6	68.9±32.2	NS
bcl-2	37.6±40.6	38.0±38.6	35.4±40.0	NS
bcl-x	64.5±36.7	51.0±42.6	68.5±30.7	NS

* P value for the three groups using Kruskall Wallis test

Bax immunostaining (Fig. 1c) and bak immunostaining (Fig. 1d) was restricted to the cytoplasmic compartment. Fas immunostaining was observed on the outer cell membrane and in the cytoplasmic compartment (Fig. 1e). Bcl-2 and bcl-x immunostaining was restricted to the cytoplasmic compartment (Fig. 1f). No difference in bax, bak, fas, bcl-2 or bcl-x expression was observed among the three groups of tumours.

In endometriomas, no qualitative difference in immunostaining was found for p53, p21, bax, bak, fas, bcl-2 or bcl-x according to the phase of the menstrual cycle. In benign and malignant tumours, no difference in qualitative immunostaining was observed according to menopausal status.

Semi-quantitative expression of apoptosis-related proteins in endometriomas and benign and malignant ovarian tumours

A difference in p53 immunostaining was observed among the three groups of tumours (P=0.02). The difference was significant between endometriomas and benign tumours (P=0.003), and between benign and malignant tumours (P=0.008), but not between endometriomas and malignant tumours (Table 2).

A difference in p21 immunostaining was also found among the three groups of tumours (P=0.002). P21 expression was higher in endometriomas than in benign (P=0.001) or malignant ovarian tumours (P=0.01), but was not different between benign and malignant tumours.

A difference in Bax immunostaining was observed among the three groups of tumours (P=0.04). Bax expression was higher in endometriomas than in benign tumours (P=0.01), but no difference was noted between endometriomas and malignant ovarian tumours.

No difference in bak, fas, bcl-2 or bcl-x immunostaining was found among the three groups of ovarian tumours.

In endometriomas, no difference in semi-quantitative apoptosis-related protein expression was found according to the phase of the menstrual cycle. In benign and malignant tumours, no difference was observed according to menopausal status.

Correlations between the expression of individual apoptosis-related proteins in endometriomas

A negative correlation was found between p53 and fas expression (P=0.04, r=0.66). A trend towards a positive correlation was observed between p53 and p21 expression (P=0.06, r=0.62). No correlation was found between the other apoptosis-related proteins.

Discussion

Qualitative and semi-quantitative alterations in apoptosis-related protein expressions were observed in endometriomas relative to benign and/or malignant ovarian tumours. Although none of the endometriotic ovarian cysts presented features of nuclear atypia, four of the ten tissue samples showed positive nuclear staining for p53. These results contrast with those from previous reports showing no p53 expression in endometriomas without atypia, with atypia, or with reactive atypia, and positive staining in endometrioid carcinomas [3, 36]. Nevertheless, our results are in line with those from Nakayama et al. [29] showing focal p53 expression in endometriotic epithelial cells without nuclear atypia. Using fragment length polymorphism scanning and polymerase chain reaction DNA sequencing, these authors [29] found no mutations in *p53* exons 5–8. No loss of heterozygosity or microsatellite instability was detected either, suggesting that p53 expression by endometriotic cells could be due to overexpression of wild-type p53 protein [29]. Recently, Chang et al. [7] have reported that endometriosis is associated with p53 polymorphism and that heterozygotes and proline homozygotes have a higher risk for endometriosis.

P53 expression was increased in endometriomas compared with benign tumours, but no difference was observed between endometriomas and malignant ovarian lesions. Few data have been reported on p53 expression in endometriomas compared with that of benign or malignant ovarian tumours. In contrast to Nehzat et al. [31], in our experience, a positive p53 staining was found in 40% benign cystic endometriotic lesions. Moreover, these authors have shown that p53 expression was only found in benign endometriotic lesions next to endometrioid or clear cell carcinoma, suggesting a potential continuum from endometriosis to atypical endometriosis to carcinoma. The discrepancy of our results with those reported by

Nezhat et al. [31] could be in relation to the absence of a cut-off value taken in our study. However, this p53 overexpression found in our experience is reminiscent of previously reported data on cadherins, CD44 protein and ICAM-1, demonstrating that endometriomas share biological features with borderline and/or malignant ovarian tumours [8, 9].

We also observed p21 overexpression in endometriomas compared with benign and malignant ovarian tumours. Furthermore, despite the small number of endometriotic cysts included in this study, a trend towards a positive correlation was found between p53 and p21 expression. The p21 overexpression in endometriotic cysts partly contrasts with the lack of any association found by Hsieh et al. [15] between the p21 gene codon 31 arginine/serine polymorphism and endometriosis.

From the pathological point of view, overexpression of both p21 and p53 in endometriomas is in keeping with previous data [11], underlining the interaction of these apoptotic proteins. Indeed, the p53-inducible gene *p21* encodes an inhibitor of cyclin-dependent kinases involved in G1 arrest [2, 5, 10]. Moreover, these latter studies also showed that p21 was not necessarily required for p53-mediated apoptosis. Recently, in univariate analysis of a series of borderline ovarian tumours, Werness et al. [43] showed the prognostic relevance of p53 expression in the absence of p21 expression.

We observed increased bax protein expression in endometriomas compared with benign ovarian tumours. However, no difference in bax expression was observed between endometriomas and malignant ovarian tumours, probably owing to marked overlap of the relevant values. Few data have been reported on bax expression in endometriotic lesions. Goumenou et al. [12] reported similar bax expression in adenomyotic and endometriotic samples, and no variation according to the phase of the menstrual cycle. Furthermore, previous studies have shown no difference in endometrial bax expression between women with and without endometriosis [27] or between eutopic and ectopic endometrium [26], whereas bax expression was higher in endometrioid carcinomas than in normal and hyperplastic endometrium [22]. We found no correlation between p53 and bax expression. However, previous studies have shown that *bax* induction by p53 is necessary to inhibit tumour growth [44] and that the contribution of bax to p53-mediated apoptosis is cell-type dependent [21, 25].

The fas/fas-ligand system is a major pathway for the induction of apoptosis in cells and tissues [28]. It has been suggested that cellular fas ligand expression protects the host tissue from attack by T cells, which are killed through fas ligation. In the present study, despite higher fas expression in endometriomas than in benign tumours, the difference did not reach significance. However, a negative correlation was found between p53 and fas expression. This is in keeping with data showing that transcription of the death receptor CD95/fas/Apo1 is dependent on p53, through a p53-response element located within the first intron of the CD95 gene [32].

The B-cell lymphoma/leukaemia-2 gene (bcl-2) is a proto-oncogene that prevents apoptosis [39]. Using reverse-transcriptase polymerase chain reaction and Western blotting [24] or immunohistochemistry [6], a higher bcl-2 expression has been reported in normal compared with neoplastic ovarian tissues. We found no difference in bcl-2 expression among the three groups of tumours. This contrasts with a study from Ben-Hur et al. [4], Chan et al. [6] and Zusman et al. [45], showing a decrease in bcl-2 expression from benign to borderline and malignant ovarian tumours. However, bcl-2 expression is cell- and tissue dependent, and both p53 and bcl-2 expression are reduced in serous ovarian carcinomas [1]. Indeed, recently, Nezhat and Kalir [30] have demonstrated a qualitative underexpresssion of bcl-2 in cystic compared with non-cystic endometriotic lesions suggesting a differential expression pattern of bcl-2 according to endometriotic lesions. Moreover, Nezhat et al. [31] reported a less frequent bcl-2 expression in benign endometriotic cysts than endometrioid, clear cell and serous papillary carcinomas. These results suggest that bcl-2 pattern expression differs according to histological type of epithelial ovarian tumours.

We found no variation in apoptosis-related protein expression according to the phase of the menstrual cycle. This is in line with previous reports on bcl-2 [12, 13, 42], fas [42] and bax expression [12]. Watanabe et al. [42] suggested that the absence of cyclic changes in apoptosis-related proteins in ectopic endometrium points to a difference in the mechanisms of proliferation or differentiation between eutopic and ectopic endometrium. Furthermore, we found no difference in apoptosis-related proteins according to menopausal status in women with benign and malignant ovarian tumours.

The main limitation of this study is the small number of endometriotic cyst samples studied. This was partly due to the inclusion of tissue samples from women without previous medical treatment, at least for 3 months before surgery, and without cytologic atypia. Despite this limitation, in accordance with previous studies [11, 12, 27, 29], our data show that endometriomas share a similar pattern of apoptosis-related protein expression with malignant ovarian lesions.

In conclusion, our results point to a lack of cyclical regulation of apoptosis-related protein expression in endometriomas. Moreover, although endometriomas have histological features of benign ovarian tumours, their pattern of apoptotic protein expression was closer to that of malignant than benign ovarian lesions. From the pathological point of view, these data could suggest a role of defective apoptosis in endometriomas.

References

1. Athanassiadou P, Petrakakou E, Sakelariou V, Zerva C, Liossi A, Michalas S, Athanassiades P (1998) Expression of p53, bcl-2 and heat shock protein (hsp72) in malignant and benign ovarian tumours. Eur J Cancer Prev 7:225–231

2. Attardi LD, Lowe SW, Brugarolas J, Jacks T (1996) Transcriptional activation by p53, but not induction of the p21 gene, is essential for oncogene-mediated apoptosis. EMBO J 15:3693–3701
3. Bayramoglu H, Duzcan E (2001) Atypical epithelial changes and mutant p53 gene expression in ovarian endometriosis. Pathol Oncol Res 7:33–38
4. Ben-Hur H, Gurevich P, Huszar M, et al (1999) Apoptosis and apoptosis-related proteins in the epithelium of human ovarian tumors: immunohistochemical and morphometric studies. Eur J Gynaecol Oncol 20:249–253
5. Brugarolas J, Chandrasekaran C, Gordon JI, Beach D, Jacks T, Hannon GJ (1995) Radiation-induced cell cycle arrest compromised by p21 deficiency. Nature 377:552–557
6. Chan WY, Cheung KK, Schorge JO, et al (2000) Bcl-2 and p53 protein expression, apoptosis, and p53 mutation in human epithelial ovarian cancers. Am J Pathol 156:409–417
7. Chang CC, Hsieh YY, Tsai FJ, Tsai CH, Tsai HD, Lin CC (2002) The proline form of p53 codon 72 polymorphism is associated with endometriosis. Fertil Steril 77:43–45
8. Darai E, Bringuier AF, Walker-Combrouze F, Feldmann G, Madelenat P, Scoazec JY (1998) Soluble adhesion molecules in serum and cysts fluids from patients with cystic tumours of the ovary. Hum Reprod 13:2831–2835
9. Darai E, Leblanc M, Walker-Combrouze F, Bringuier AF, Madelenat P, Scoazec JY (1998) Expression of cadherins and CD44 isoforms in ovarian endometrial cysts. Hum Reprod 13:1346–1352
10. Deng C, Zhang P, Harper JW, Elledge SJ, Leder P (1995) Mice lacking p21CIP1/WAF1 undergo normal development, but are defective in G1 checkpoint control. Cell 82:675–684
11. Gottlieb TM, Oren M (1998) p53 and apoptosis. Semin Cancer Biol 8:359–368
12. Goumenou A, Panayiotides I, Matalliotakis I, Vlachonikolis I, Tzardi M, and Koumantakis E (2001) Bcl-2 and Bax expression in human endometriotic and adenomyotic tissues. Eur J Obstet Gynecol Reprod Biol 99:256–260
13. Harada M, Suganuma N, Furuhashi M, Nagasaka T, Nakashima N, Kikkawa F, Tomoda Y, Furui K (1996) Detection of apoptosis in human endometriotic tissues. Mol Hum Reprod 2:307–315
14. Heaps JM, Nieberg RK, Berek JS (1990) Malignant neoplasms arising in endometriosis. Obstet Gynecol 75:1023–1028
15. Hsieh YY, Tsai FJ, Chang CC, Chen WC, Tsai CH, Tsai HD, Lin CC (2001) p21 gene codon 31 arginine/serine polymorphism: non-association with endometriosis. J Clin Lab Anal 15:184–187
16. Hsu SY, Hsueh AJ (2000) Tissue-specific Bcl-2 protein partners in apoptosis: an ovarian paradigm. Physiol Rev 80:593–614
17. International Federation of Gynecology and Obstetrics (1971) Classification and staging of malignant tumours in the female pelvis. Acta Obstet Gynecol Scand 50:1–7
18. Jenkins S, Olive DL, Haney AF (1986) Endometriosis: pathogenetic implications of the anatomic distribution. Obstet Gynecol 67:335–338
19. Jones RK, Searle RF, Bulmer JN (1998) Apoptosis and bcl-2 expression in normal human endometrium, endometriosis and adenomyosis. Hum Reprod 13:3496–3502
20. Kerr JF, Wyllie AH, Currie AR (1972) Apoptosis: a basic biological phenomenon with wide-ranging implications in tissue kinetics. Br J Cancer 26:239–257
21. Knudson CM, Tung KS, Tourtellotte WG, Brown GA, Korsmeyer SJ (1995) Bax-deficient mice with lymphoid hyperplasia and male germ cell death. Science 270:96–99
22. Kokawa K, Shikone T, Otani T, et al (2001) Apoptosis and the expression of bax and bcl-2 in hyperplasia and adenocarcinoma of the uterine endometrium. Hum Reprod 16:2211–2218
23. Lebovic DI, Mueller MD, Taylor RN (2001) Immunobiology of endometriosis. Fertil Steril 75:1–10
24. Marone M, Scambia G, Mozzetti S, et al (1998) Bcl-2, bax, bcl-xl, and bcl-xs expression in normal and neoplastic ovarian tissues. Clin Cancer Res 4:517–524
25. McCurrach ME, Connor TM, Knudson CM, Korsmeyer SJ, Lowe SW (1997) Bax-deficiency promotes drug resistance and oncogenic transformation by attenuating p53-dependent apoptosis. Proc Natl Acad Sci U S A 94:2345–2349
26. McLaren J, Prentice A, Charnok-Jones DS, Sharkey AM, Smith SK (1997) Immunolocalization of the apoptosis regulating proteins bcl-2 and bax in human endometrium and isolated peritoneal fluid macrophages in endometriosis. Hum Reprod 12:146–152
27. Meresman GF, Vighi S, Buquet RA, Contreras-Ortiz O, Tesone M, Rumi LS (2000) Apoptosis and expression of Bcl-2 and Bax in eutopic endometrium from women with endometriosis. Fertil Steril 74:760–766
28. Nagata S (1994) Fas and Fas ligand: a death factor and its receptor. Adv Immunol 57:129–144
29. Nakayama K, Toki T, Zhai YL, Lu X, Horiuchi A, Nikaido T, Konishi I, Fujii S (2001) Demonstration of focal p53 expression without genetic alterations in endometriotic lesions. Int J Gynecol Pathol 20:227–231
30. Nezhat FR, Kalir T (2002) Comparative immunohistochemical studies of endometriosis lesions and endometriotic cysts. Fertil Steril 78:820–824
31. Nezhat F, Cohen C, Rahaman J, Gretz H, Cole P, Kalir T (2002) Comparative immunohistochemical studies of bcl-2 and p53 proteins in benign and malignant ovarian endometriotic cysts. Cancer 94:2935–2940
32. Owen-Schaub LB, Zhang W, Cusack JC, et al (1995) Wild-type human p53 and a temperature-sensitive mutant induce Fas/APO-1 expression. Mol Cell Biol 15:3032–3040
33. Ridley JH (1968) The histogenesis of endometriosis. A review of facts and fancies. Obstet Gynecol 23:1–35
34. Ryan IP, Taylor RN (1997) Endometriosis and infertility: new concepts. Obstet Gynecol Surv 52:365–371
35. Sampson JA (1927) Peritoneal endometriosis due to menstrual dissemination of endometrial tissue into the peritoneal cavity. Am J Obstet Gynecol 14:422–469
36. Schneider J, Jimenez E, Rodriguez F, del Tanago JG (1998) c-myc, c-erb-B2, nm23 and p53 expression in human endometriosis. Oncol Rep 5:49–52
37. Stovall DW, Bowser LM, Archer DF, Guzick DS (1997) Endometriosis-associated pelvic pain: evidence for an association between the stage of disease and a history of chronic pelvic pain. Fertil Steril 68:13–18
38. Suganuma N, Harada M, Furuhashi M, Nawa A, Kikkawa F (1997) Apoptosis in human endometrial and endometriotic tissues. Horm Res 48:42–47
39. Vaux Dl, Cory S, Adams JM (1988) Bcl-2 gene promotes haematopoetic cell survival and co-operates with c-myc to immortalize pre-B cells. Nature 335:440–442
40. Vercellini P, Trespidi L, De Giorgi O (1996) Endometriosis and pelvic pain: relation to disease stage and localization. Fertil Steril 65:299–304
41. Vogt J (1872) Untersuchungen uber die Entwicklungsgeschichte der Geburtshelferkroete (Alytes obstetricians). Jent & Gassman, Solothurn, Switzerland
42. Watanabe H, Kanzaki H, Narukawa S, Inoue T, Katsuragawa H, Kaneko Y, and Mori T (1997) Bcl-2 and Fas expression in eutopic and ectopic human endometrium during the menstrual cycle in relation to endometrial cell apoptosis. Am J Obstet Gynecol 176:360–368
43. Werness BA, Freedman AN, Piver MS, Romero-Gutierrez M, Petrow E (1999) Prognostic significance of p53 and p21(waf1/cip1) immunoreactivity in epithelial cancers of the ovary. Gynecol Oncol 75:413–418
44. Yin C, Knudson CM, Korsmeyer SJ, Van Dyke T (1997) Bax suppresses tumorigenesis and stimulates apoptosis in vivo. Nature 385:637–640
45. Zusman I, Gurevich P, Gurevich E, Ben-Hur H (2001) The immune system, apoptosis and apoptosis-related proteins in human ovarian tumors (a review). Int J Oncol 18:965–972

Virchows Arch (2003) 443:44–50
DOI 10.1007/s00428-003-0817-z

ORIGINAL ARTICLE

W. Reed · E. Hannisdal · E. Skovlund · S. Thoresen · P. Lilleng · J. M. Nesland

Pregnancy and breast cancer: a population-based study

Received: 17 September 2002 / Accepted: 9 March 2003 / Published online: 20 May 2003
© Springer-Verlag 2003

Abstract The incidence of pregnancy-associated breast cancer, i.e. during pregnancy and lactation, and of pregnancy subsequent to a breast-cancer diagnosis will increase as more women choose childbearing at a later age. Few larger series are published on pregnancy-associated breast cancer. In a population-based study, we evaluated the outcome and prognostic factors in 173 breast-cancer patients. One hundred and twenty-two patients had pregnancy-associated breast cancer (20 coincident with pregnancy and 102 during lactation) and 51 patients had pregnancy subsequent to breast cancer. The median follow-up time was 151 months. Histopathological parameters and immunoreactivity for oestrogen and progesterone receptors c-erbB-2 and c-erbB-4 were studied. All three groups had tumours with high histological grade, low frequency of hormone receptors and high expression of c-erbB-2. The pregnancy and lactation groups were near identical with regard to all histopathological parameters and outcome. In the two pregnancy-associated breast-cancer groups, tumours were significantly larger, with more extensive lymph-node involvement. For node-negative tumours the respective 5- and 10-year survival rates were 62% and 50% in the pregnancy group and 60% and 50% in the lactation group. For node-positive tumours, respective 5- and 10-year survival rates were 50% and 34% in the pregnancy group and 50% and 33% in the lactation group. In the subsequent group, overall survival was high in both node-negative and -positive groups, with 5- and 10-year survival rates of 80% and 73% and 86% and 76%, respectively. Tumour size, lymph-node status, histological grade, progesterone receptor, oestrogen receptor and c-erbB-2 were significant prognostic factors in the pregnancy-associated breast-cancer patients.

Keywords Pregnancy · Breast cancer · Hormone receptor · c-erbB-2 · c-erbB-4 · Prognostic factors

W. Reed (✉) · J. M. Nesland
Department of Pathology,
The Norwegian Radium Hospital, University of Oslo,
0310 Oslo, Norway
e-mail: wenchere@ulrik.uio.no
Tel.: +47-22-934136, Fax: +47-22-935426

E. Hannisdal
Health North, 8038 Bodø, Norway

E. Skovlund
Section of Medical Statistics, University of Oslo, Norway

S. Thoresen
The Norwegian Cancer Registry, Oslo, Norway

P. Lilleng
Institute of Gade, Haukeland Hospital, Bergen, Norway

Introduction

Approximately 25% of all breast-cancer patients are diagnosed in their childbearing years [16]. The reported incidence of pregnancy-associated (PA) breast cancer, usually defined as breast cancer diagnosed during pregnancy or within the first year post-partum (i.e. during lactation), is 0.2–3.8% [28, 44]. A higher prevalence of PA breast cancer is to be expected in the future. More women are becoming pregnant in their 30s and 40s, and the incidence of breast cancer is increasing in the younger age group. This rise in incidence will also result in more women choosing pregnancy subsequent to a breast-cancer diagnosis (subsequent group).

The prognosis of PA breast cancer is unfavourable [5, 40], although the reasons for this are still unsettled. Many reports argue that the poor prognosis is due to the patient's young age, being independent of the pregnancy [1, 8]. Other studies indicate that PA breast cancer is associated with more advanced disease at presentation. Matched for stage and age, no difference is seen with regard to survival between PA breast-cancer patients and non-pregnant patients [32, 45]. However, women with pregnancy subsequent to a breast carcinoma diagnosis seem to have a more favourable outcome than non-pregnant control groups [14].

Publications of larger series are few and the purpose of the present retrospective study was to evaluate the

outcome and possible prognostic factors in a population-based series of women with breast cancer during pregnancy and lactation and during pregnancy subsequent to breast cancer. Clinicopathological characteristics and immunohistochemical expression of oestrogen receptor (ER), progesterone receptor (PgR), c-erbB-2 (HER2/neu) and c-erbB-4 were analysed in all three groups. The follow-up was more than 10 years.

Materials and methods

The study population

The Norwegian Cancer Registry and the Medical Birth Registry have complete data from the Norwegian population from 1953 and 1968, respectively. Data from the Cancer Registry were matched with data from the Medical Birth Registry. The search was made during a 25-year period from 1968 to 1992. Eight thousand two hundred and twelve women aged 20–44 years were elicited with breast carcinoma verified histologically.

The patients excluded from the study were patients with a diagnosis before 1968 (24 patients), observation time less than 1 month due to emigration (22 patients), other primary cancers than carcinomas (5 patients), patients with unknown stage (1663 patients) and 2 patients with their diagnosis revised to benign lesions. This left a total study population of 6496 women. Number and date of the birth of children were obtained. The duration of pregnancy was set to 9 months where the gestation period was missing and the month/day for the breast-cancer diagnosis was missing.

Five patient groups were defined in relation to their pregnancies (Table 1).

1. Nullipara group
2. Early (birth) group, i.e. birth 13 months or more previous to breast-cancer diagnosis
3. Lactation group, i.e. birth 1–12 months before breast-cancer diagnosis
4. Pregnancy group, i.e. birth 0–9 months after breast-cancer diagnosis
5. Subsequent group, i.e. birth more than 9 months after breast-cancer diagnosis

Included in this work were the lactation, pregnancy and subsequent groups. Paraffin blocks of archival tissue were retrieved from 19 hospitals and one private laboratory.

Evaluated parameters

Clinical parameters obtained for all patients were clinical stage following the UICC recommendations [41], age at diagnosis and at death.

Table 1 Patient population with breast cancer in Norway 1967–1992

Age <50 years at diagnosis*		6496
Nullipara		3604
Previous	Diagnosis ≥13 months post-partum	2719
Lactation	Diagnosis 1–12 months post-partum	102
Pregnancy	Diagnosis 0–9 months pre-partum	20
Subsequent	Diagnosis ≥10 months pre-partum	51
Total for our study		173

* Of breast cancer

The histological parameters were not assessable for all the patients. In some cases, histopathological reports were incomplete and/or tumour tissue in the paraffin block was insufficient for the histopathological evaluation of certain parameters in a few of the cases.

Tumour tissue

The histological slides were reviewed by one of the authors (W.R.). The primary tumour characteristics included histological type (assessable for 94% of the patients) according to World Health Organization's (WHO's) recommendations. Histological grade (assessable for 99% of the patients) was evaluated using the modification by Elston and Ellis [12] of the method described by Bloom [3] on a scale from I to III, with I being well differentiated and III poorly differentiated. Microscopic lymph-node involvement was assessable for 86% of the patients.

Ductal carcinoma in situ (DCIS) within the invasive carcinoma (assessable for 97% of the patients) was evaluated as absent when no ducts within the tumour were involved, slight when comprising less than 25% of the tumour area, moderate when comprising 25–50% of the tumour area and marked when comprising more than 50% of the tumour area [35]. We registered whether DCIS was seen within the infiltrating margins of the tumour or outside the invasive component. All specimens were evaluated without knowledge of the clinical data.

Immunohistochemistry

ER, PgR, c-erbB-2 and c-erbB-4 were examined using immunohistochemistry (assessable for 92% of the patients). Formalin-fixed, paraffin-embedded material was used for immunostaining. The biotin-streptavidin-peroxidase method was applied. Primary antibodies used in this study were as follows: monoclonal antibody (mAb) for ER and PgR with a dilution of 1:50 (Novocastra Lab.NCL-6F11 and NCL-PGR), mAb for C-erbB-2 with a dilution of 1:100 (Novocastra Lab.NCL CB11) and mAb for c-erbB-4 with a dilution of 1:50 (Santa Cruz (C-18) Lab.SC-283). In all the immunohistochemical staining series, positive and negative controls were included. Nuclear reactivity in more than 10% of the tumour cells for ER and PgR was considered positive [30]. Protein expression in more than 10% of the cells was considered positive for c-erbB-2 and c-erbB-4, with only strong membranous c-erbB-2 staining products considered as positive [9, 33, 36]. Staining for c-erbB-4 was noted both in the cytoplasm and the membrane.

Statistics

Associations between categorical variables were assessed using Chi-square tests. Overall survival was defined as the time from diagnosis to death of any cause. Patients alive on 1 July 1999 were treated as censored. Overall survival was estimated using the Kaplan-Meier method and differences between survival curves compared with the log rank test. P values ≤ 0.05 were regarded as statistically significant. In Table 8, 95% confidence intervals are given in brackets. Data analysis was performed using SPSS software (version 10.1).

Results

Of a total of 6496 breast-cancer patients younger than 50 years at diagnosis, the prevalence of patients in the pregnancy and lactation groups was 1.9% and 0.8% for patients in the subsequent group (Table 1). The median observation time was 151 months (range 1–383 months). The median number of children born in all three groups

Table 2 Number of birth by groups of pregnancy, *n*

Pregnancy groups	1	2	3	4	5	6	7
Pregnancy	5	9	5	1			
Lactation	28	34	26	10	3		1
Subsequent	16	20	8	6	1		

Table 3 *P* values as a measure of associations of the histopathological parameters between the pregnancy, lactation and subsequent groups, *n*=173

Variables	Pregnancy *n*=20 (%)	Lactation *n*=102 (%)	Subsequent *n*=51 (%)	*P* value
Age (mean)	34	34	31	0.13
Tumour size				
≤20 mm (T1)	5(25)	32(31)	29(57)	
21–50 mm (T2)	11(55)	44(43)	13(26)	
>50 mm (T3+T4)	4(20)	26(26)	9(18)	0.02
Lymph-node status				
N-	8(50)	23(27)	26(67)	
1–3	5(31)	37(44)	9(23)	
≥4	3(19)	24(29)	4(10)	0.001
Histological grade				
I	2(10)	3(3)	5(13)	
II	8(40)	38(42)	16(40)	
III	10(50)	49(55)	19(48)	0.4
Histological type				
In situ	0	5 (5)	2 (5)	
Ductal	16 (80)	88 (92)	37 (86)	
Lobular	1 (5)	2 (2)	0	
Other	3 (15)	1 (1)	4 (9)	0.07
Stage				
0	0	5 (5)	2 (4)	
I	3 (15)	14 (14)	26 (51)	
II	12 (60)	62 (61)	21 (41)	
III	1 (5)	11 (11)	2 (4)	
IV	4 (20)	10 (9)	0	<0.001

was 2.0 (Table 2). The mean age of the patients was 34 years (SD 4.5 years) in the coincident and lactation groups versus 31±4.5 years in the subsequent group. In the group of patients with pregnancy subsequent to a breast-cancer diagnosis, the range of childbirth ranged from 10 months to 8 years after a breast-cancer diagnosis; the median value was 3.0 years. Of 51 patients, 33 (65%) underwent childbirth within 3 years of a breast-cancer diagnosis; 22% underwent childbirth within 1 year.

No statistically significant difference was found between the lactation group and the pregnancy group regarding any of the clinicopathological parameters studied (Table 3, Table 4, Table 5). We found a higher proportion of large tumours in the pregnancy and lactation groups versus the subsequent group (75% and 69% versus 43%, *P*=0.02). Thirty percent of the tumours in the PA group and fifty-seven percent in the subsequent group were ≤20 mm. Lymph-node involvement was more extensive in the PA group (*P*=0.001), with 67% node-negative tumours in the subsequent group versus 50% and 27% in the pregnancy and lactation groups, respectively. These differences were reflected in a higher clinical staging in the PA group, with 15% and 14% stage I in the coincident and lactation groups, respectively, versus 51% in the subsequent group (*P*<0.001). The distribution of the tumours with regard to histological grade was near identical in all three groups, with histological grade III in 50%, 55% and 48% of the cases in the pregnancy, lactation and subsequent groups, respectively. The majority of tumours were of ductal type, only 5% of lobular type in the pregnancy group, 2% in the lactation group and none in the subsequent group.

Table 4 *P* values as a measure of association of the presence and localisation of DCIS in the invasive carcinoma between the pregnancy, lactation and subsequent groups, *n*=152 (%)

DCIS	Pregnancy	Lactation	Subsequent	*P* value
None	10 (50)	31 (35)	15 (39)	
<25%	8 (40)	36 (41)	15 (38)	
25–50%	1 (5)	14 (16)	5 (13)	
>50%	1 (5)	7 (8)	4 (10)	0.8
Within	6 (60%)	20 (35)	8 (33)	
Outside	4 (40)	37 (65)	16 (67)	0.3

Table 5 *P* values as a measure of association of the tumour markers in the invasive carcinomas between the pregnancy, lactation and subsequent groups, *n*=152

Variables	Pregnancy *n*=20 (%)	Lactation *n*=91 (%)	Subsequent *n*=41 (%)	*P* value
ER				
−	14 (78)	53 (63)	21 (55)	
+	4 (22)	31 (37)	17 (44)	0.3
PgR				
−	12 (67)	65 (77)	22 (58)	
+	6 (33)	19 (23)	16 (42)	0.08
c-erbB-2				
−	10 (56)	47 (56)	26 (72)	
+	8 (44)	37 (44)	10 (28)	0.2
c-erbB-4				
−	9 (50)	48 (57)	17 (47)	
+	9 (50)	36 (42)	19 (53)	0.6

We analysed the component of DCIS in the infiltrating tumours (Table 4). No difference was seen between the lactation, pregnancy and the subsequent groups with regard to the amount of DCIS present in the infiltrating tumour or whether DCIS was localised within or outside the infiltrating part of the tumour.

The immunohistochemical staining results were evaluated in the invasive component (Table 5, Fig. 1). A high proportion of the tumours were negative for hormone receptors in all three groups, but fewer tumours were positive for PgR in the PA group than in the subsequent group (*P*=0.08). The percentage of c-erbB-2-positive tumours was high in all three groups (*P*=0.2), 44% in the pregnancy and lactation groups versus 28% in the subsequent group.

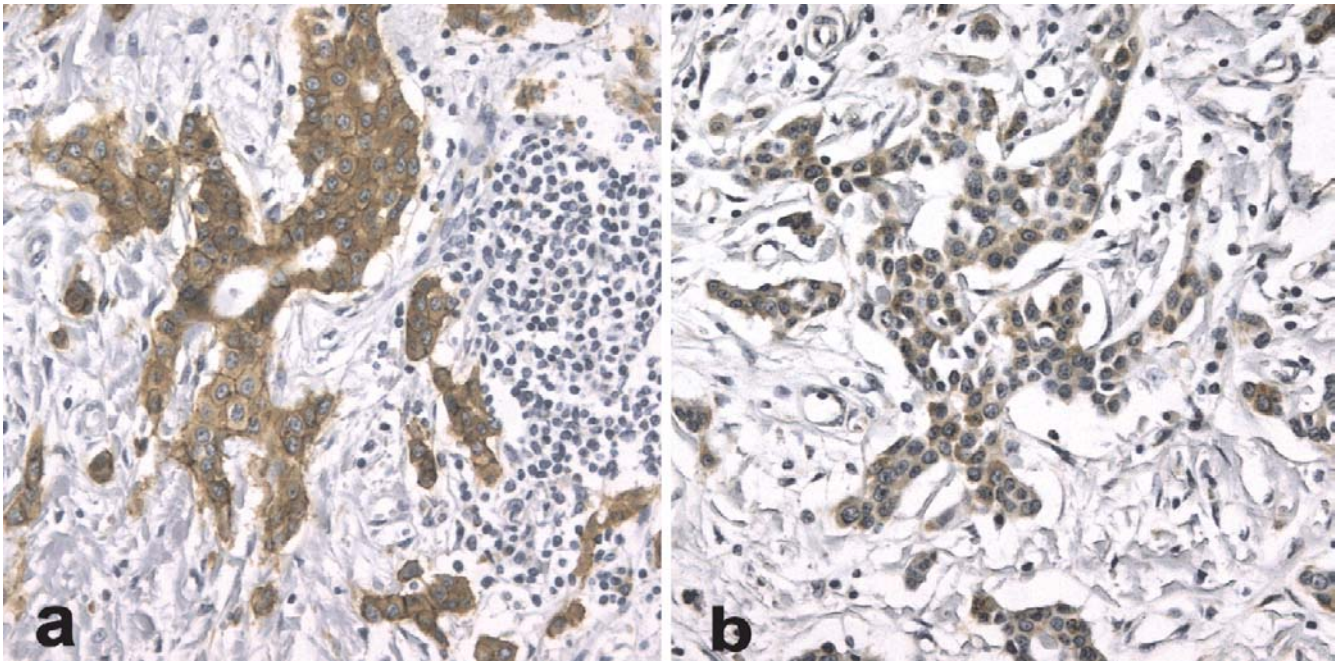

Fig. 1 Infiltrating ductal carcinoma in the lactation group with immunohistochemical staining for (**a**) c-erbB-2 with a positive expression in the cytoplasmic membrane and (**b**) c-erbB-4 with a nuclear and cytoplasmic expression

Table 6 Log-rank tests of different parameters for overall survival according to pregnancy, lactation and subsequent groups; significant values in bold

Parameter	Variables	Pregnancy		Lactation		Subsequent	
		χ^2	*P* value	χ^2	*P* value	χ^2	*P* value
Histological grade	I,II-III	2.27	0.13	2	0.2	0.3	0.6
Tumor size (mm)	≤20, 21–50*, >50*	4.6	0.1	8.2	**0.02**	0.4	0.8
Lymph node	N- vs 1–3* vs 4+*	4.7	0.2	26	**<0.001**	1.9	0.6
PgR	–*, +	3.6	0.06	4.7	**0.03**	1.2	0.3
ER	–*, +	0.01	0.9	7.6	**0.006**	0.00	1.0
c-erbB-2	–, +*	0.9	0.3	4.7	**0.03**	0.6	0.5
c-erbB-4	–, +	1.9	0.2	0.6	0.5	0.03	0.9

* Values with poor prognosis

Table 7 Log-rank test of different parameters for overall survival according to pregnancy-associated breast cancer, significant values in bold (*n*=122)

Variables	*P* value
Tumour size (T1 vs T2* vs T3+4*)	**<0.01**
Lymph node (N- vs 1–3* vs 4+*)	**<0.001**
Histological grade (I vs II–III*)	**0.04**
PgR (– *vs +)	**<0.01**
ER (– *vs +)	**0.02**
c-erbB-2 (– vs +*)	**0.02**
c-erbB-4 (– vs +)	1.0

* Values with poor prognosis

Prognostic factors for overall survival are shown in Table 6. Tumour size, lymph-node status, PgR, ER and c-erbB-2 status were significant prognostic factors in the lactation group in the univariate analysis. None of the parameters was a significant predictor of prognosis in the pregnancy and subsequent groups. When the lactation group and pregnancy group were pooled as one PA group (Table 7), tumour size, lymph-node status, histological grade, PgR, ER and c-erbB-2 were all significant prognostic factors. c-erbB-4 staining and the status of DCIS in the infiltrating tumour gave no prognostic information (data not shown). An age of 35 years or younger was an unfavourable prognostic factor in the univariate analysis, but only in the PA group (data not shown).

Five-year overall survival was 40% (95% CI 20–60) and 41% (95% CI 31–51) in the pregnancy and lactation groups, respectively, and 86% (95% CI 78–98) in the subsequent group (Table 8, Fig. 2). The three groups were subdivided into node-negative and node-positive groups, and the cumulative 5- and 10-year survival rates were analysed. Overall survival was high in both the node-negative and node-positive subsequent group. In the node-negative pregnancy group, the 5- and 10-year survival rates were 62% and 50%, in the node-negative lactation group, 60% and 50%, respectively. The difference in survival between the PA and subsequent group was

Table 8 Log-rank tests of lymph-node status for overall survival rate (95% CI) according to pregnancy, lactation and subsequent groups

Patient group	5 year	10 year
Pregnancy		
N–	62 (33–97)	50 (23–83)
N+	40 (20–60)	34 (14–54)
All	40 (20–60)	34 (14–54)
Lactation		
N–	60 (40–80)	50 (30–70)
N+	41 (33–49)	33 (25–41)
All	41 (33–49)	33 (23–43)
Subsequent		
N–	80 (66–94)	73 (57–89)
N+	86 (76–96)	76 (64–88)
All	86 (76–96)	76 (70–82)

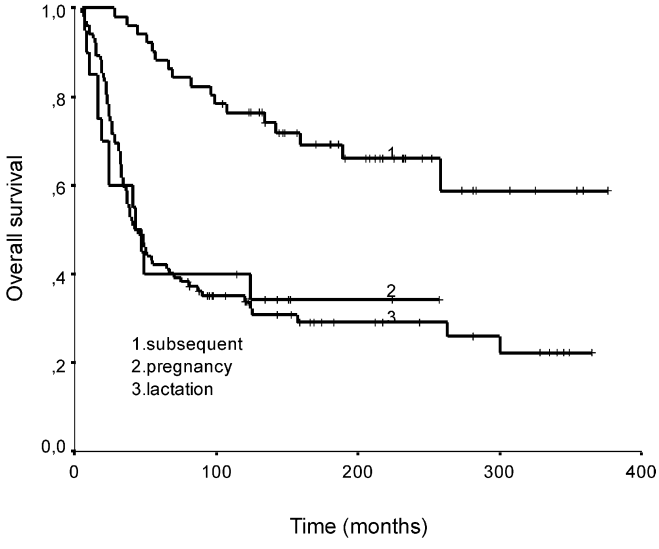

Fig. 2 Kaplan-Meier plot based on pregnancy, lactation and subsequent groups for overall survival (χ^2=25.3 and P<0.001)

significant at 5- and 10-year overall survival for both node-negative and node-positive tumour groups (P<0.001).

Discussion

PA breast cancer is usually defined as breast cancer diagnosed during pregnancy and/or up to 12 months post-partum. Some reports include pregnancy and 6 months post-partum [5], others pregnancy and 2 years post-partum [20], others again only pregnancy [11]. In the present population-based study, PA breast cancer included a pregnancy group and a lactation group, which was defined as up to 12 months after childbirth. PA breast cancer was compared with a subsequent breast-cancer group, defined as patients with pregnancy more than 9 months after a breast-cancer diagnosis. In women with breast cancer under 50 years of age, the prevalence of PA breast cancer and pregnancy subsequent to breast cancer was 1.9% and 0.8%, respectively.

Our data demonstrate that the lactation and pregnancy groups were very similar with regard to clinicopathological parameters, with large tumours, high histological grade, negative hormone receptor status and high c-erbB-2 positivity. Of the tumours, 50% had metastasised to axillary lymph nodes in the pregnancy group and 63% in the lactation group. This is a high frequency compared with all women diagnosed with breast cancer in Norway during the period 1991–1995 [17], where 41.5% of the tumours had metastasised. In our study, only 25% of the tumours were $\leq$20 mm in the pregnancy group and 31% in the lactation group, in contrast to 40% of the breast carcinomas diagnosed in Oslo during the period 1988–1995 [23]. Tumours with a high histological grade and a high occurrence of lymph-node metastases in PA breast cancer is in accordance with other studies [2, 28, 31]. In the subsequent group, we found that only 33% had metastasised and 57% of the tumours were $\leq$20 mm.

We found several similarities between the PA and the subsequent breast-cancer groups, which can be linked to the young age of the patients, as mean age was 34 years in the pregnancy and lactation groups and 31 years in the subsequent group. Approximately 50% of the tumours were of high histological grade. Only 5% and 2% of the tumours were lobular in the pregnancy and lactation groups, respectively, and none was in the subsequent group. c-erbB-2 protein expression was high and the expression of ER and PgR was low in all three groups. Aggressive tumour features are well known in breast carcinomas in young age groups [1, 4, 8, 19, 26]. The tumours are reported with high histological grade, often with vascular invasion [24], and with low occurrence of hormone receptor expression [4, 29]. Young age is also associated with a low frequency of infiltrating lobular carcinomas [24].

Age has been found to be a prognostic factor in some studies [1, 6, 10], but not in all [22]. In our study, age 35 years or younger was an unfavourable prognostic factor in the PA group only.

Even though a low expression of ER and PgR was seen in all three groups, fewer tumours were PgR positive in the pregnancy and lactation groups than in the subsequent group; 33% and 23% versus 42%. Low occurrence of hormone receptor-positive tumours in PA breast cancer is corroborated by others [5, 20].

We found c-erbB-2 expressed in 44% of the PA tumours and in 28% of the subsequent breast cancers. Few studies have looked at c-erbB-2 expression in PA breast cancer and none as far as we know in the subsequent group. Elledge and coworkers [11] found c-erbB-2 expression in 7 of 12 (58%) breast cancers in pregnant patients versus 10–25% of breast cancers overall. The very high expression of c-erbB-2 in pregnancy and lactation breast carcinoma may support a role for c-erbB-2 gene expression in the development of carcinoma in this selected group of patients. It suggests that immunotherapy with Herceptin could be a useful

adjuvant therapy in PA breast carcinoma patients and that the tumours should be tested for c-erbB-2 expression at an early stage of the disease.

c-erbB-4 expression was seen in 50% and 42% of the pregnancy and lactation groups and in 53% of the subsequent group. This is somewhat lower than reported by Suo et al. [37], who observed c-erbB-4 expression in 80% of the breast carcinomas. In their study, c-erbB-4 expression was lower in more aggressive breast cancer cell lines. Suo and coworkers [38] found c-erbB-4 expression to be a favourable prognostic factor in node-negative breast carcinomas. We could not corroborate their results as we did not find any significant association between c-erbB-4 expression and survival in the PA and subsequent breast carcinoma groups.

An extensive intraductal component (EIC) in the invasive carcinomas, defined as DCIS present in 25% or more of the total tumour, has been considered as a risk factor for local recurrence [18, 21, 35]. A high prevalence of EIC has been found in premenopausal women [21]. In our series, EIC was found in 10%, 24% and 23% in the pregnancy, lactation and subsequent groups, respectively. We did not find any association between the intratumoural burden of DCIS and patient outcome, in agreement with a recent study [7]. The risk of recurrence was not evaluated in our study. It has been suggested that the amount of DCIS surrounding the invasive carcinoma is a better indicator of survival and recurrence [7], but this was not confirmed in our study.

The outcome of PA breast-cancer patients is reported to be similar to that for non-pregnant women when adjusted for stage and age [45]. Ishida et al. [20] found a 5-year survival rate of 90% in node-negative versus 52% in the node-positive PA breast-cancer group. Petrek and coworkers [31] reported a 5-year survival rate of 82% in the node-negative and 47% in the node-positive PA group. In our series, 5-year survival rate was 62% and 60% in the node-negative pregnancy and lactation groups, respectively. Node-negative patients in the subsequent group had a 5-year survival rate of 80%. In the node-positive group, the survival rate was 40%, 41% and 86% for the pregnancy, lactation and subsequent groups, respectively. The same trend was seen for the 10-year survival rates. Even though the 95% CIs were large, we can surmise from our data that the pregnancy and lactation breast cancers were characterised by a poor survival in both the node-negative and the node-positive groups. This is in agreement with several publications [5, 15, 27]. In comparison, The Norwegian Cancer Registry [17] found, for the period 1988–1995, that 5-year relative survival for all women with breast cancer was 77% and 62% for the age group 30–34 years (Skare, The Norwegian Cancer Registry, personal communication). In a recent study of 113 breast-cancer patients aged 35 years and younger, 5-year overall survival was 64% [22]. The poor outcome seen in the pregnancy and lactation groups is possibly related to changes in immunological and hormonal status during pregnancy [13, 39], in addition to large metastasising tumours. The near identical outcome in the pregnancy and the lactation groups confirms the adequacy of including breast-cancer patients with recent previous pregnancy in the PA breast-cancer group. The shorter the time span between a breast-cancer diagnosis and a previous pregnancy, the greater is the risk of dying of the disease [15, 25].

Significant prognostic factors were only seen in the lactation group. We believe that the pregnancy group was too small to yield conclusive results in the univariate analysis. As the pregnancy and lactation groups were similar with regard to the histopathological parameters, they were pooled together for the analyses. Significant prognostic factors for the PA group were tumour size, lymph-node status, histological grade, ER, PgR and c-erbB-2 status.

Pregnancy subsequent to a breast-cancer diagnosis does not seem to adversely affect the prognosis of the patient. In several studies using matched comparisons, a survival advantage in the group with subsequent pregnancy has been found [42, 43]. The favourable prognosis in the subsequent group, with a majority of small, lymph-node negative tumours, demonstrated in the present study, illustrates the fact that women bearing children after a diagnosis of breast cancer is a highly selected group of women. Sankila et al. [34] studied 92 patients giving birth more than 10 months after a diagnosis of breast cancer. The 10-year survival rate was 92% versus 60% in their control group. They called this the “healthy mother effect”, arguing in favour of a selection bias, as only women feeling well have a wish to become pregnant. In our study, 61% of the patients underwent childbirth during the first 3 years after a breast-cancer diagnosis, in agreement with Gelber et al. [14], who found that 67% (63 of 94) of the patients underwent childbirth within 3 years. The superior survival seen in our study and in other series may merely reflect a healthy patient selection bias, although a possible anti-tumour effect of the pregnancy has been discussed [14].

In conclusion, breast cancer during pregnancy and lactation will increase as women choose childbirth at a later age. The prognosis is poor, but prognostic factors such as hormone receptors and c-erbB-2 may be of assistance in choosing treatment strategies. The prognosis of women with pregnancy subsequent to a breast-cancer diagnosis is very good, also after 10-year follow-up.

References

1. Adami HO, Malker B, Holmberg L, Persson I, Stone B (1986) The relation between survival and age at diagnosis in breast cancer. N Engl J Med 315:559–563
2. Anderson BO, Petrek JA, Byrd DR, Senie RT, Borgen PI (1996) Pregnancy influences breast cancer stage at diagnosis in women 30 years of age and younger. Ann Surg Oncol 3:204–211
3. Bloom HJG (1957) Histological grading and prognosis in breast cancer. Br J Cancer 11:359–373
4. Bonnier P, Romain S, Charpin C, Lejeune C, Tubiana N, Martin PM, et al (1995) Age as a prognostic factor in breast

cancer: relationship to pathologic and biologic features. Int J Cancer 62:138–144
5. Bonnier P, Romain S, Dilhuydy JM, Bonichon F, Julien JP, Charpin C, et al (1997) Influence of pregnancy on the outcome of breast cancer: a case- control study. Int J Cancer 72:720–727
6. Chung M, Chang HR, Bland KI, Wanebo HJ (1996) Younger women with breast carcinoma have a poorer prognosis than older women. Cancer 77:97–103
7. Crombie N, Rampaul RS, Pinder SE, Elston CW, Robertson JF, Ellis IO (2001) Extent of ductal carcinoma in situ within and surrounding invasive primary breast carcinoma. Br J Surg 88:1324–1329
8. de-la-Rochefordiere A, Asselain B, Campana F, Scholl SM, Fenton J, Vilcoq JR, et al (1993) Age as prognostic factor in premenopausal breast carcinoma. Lancet 341:1039–1043
9. De Potter CR, Quatacker J, Maertens G, Van Daele S, Pauwels C, Verhofstede C, et al (1989) The subcellular localization of the neu protein in human normal and neoplastic cells. Int J Cancer 44:969–974
10. Dubsky PC, Gnant MFX, Taucher S, Roka S, Kandioler D, Pichler-Gebhard B, et al (2002) Young age as an independent adverse prognostic factor in premenopausal patients with breast cancer. Clin Breast Cancer 3:65–72
11. Elledge RM, Ciocca DR, Langone G, McGuire WL (1993) Estrogen receptor, progesterone receptor, and HER-2/neu protein in breast cancers from pregnant patients. Cancer 71:2499–2506
12. Elston CW, Ellis I (1993) Method for grading breast cancer. J Clin Pathol 46:189–190
13. Ewan KB, Shyamala G, Ravani SA, Tang Y, Akhurst R, Wakefield L, et al (2002) Latent transforming growth factor-beta activation in mammary gland: regulation by ovarian hormones affects ductal and alveolar proliferation. Am J Pathol 160:2081–2093
14. Gelber S, Coates AS, Goldhirsch A, Castiglione-Gertsch M, Marini G, Lindtner J, et al (2001) Effect of pregnancy on overall survival after the diagnosis of early-stage breast cancer. J Clin Oncol 19:1671–1675
15. Guinee VF, Olsson H, Moller T, Hess KR, Taylor SH, Fahey T, et al (1994) Effect of pregnancy on prognosis for young women with breast cancer. Lancet 343:1587–1589
16. Hansen S, Naess A (1999) Cancer in Norway 1996. In: Cancer Registry Of Norway. Cancer Registry of Norway, Oslo
17. Hansen S, Langballe EM, Norstein J, Naess A (2002) Cancer in Norway 1999. In: Cancer Registry of Norway. Cancer Registry of Norway, Oslo
18. Holland R, Connolly JL, Gelman R, Mravunac M, Hendriks JH, Verbeek AL, et al (1990) The presence of an extensive intraductal component following a limited excision correlates with prominent residual disease in the remainder of the breast. J Clin Oncol 8:113–118
19. Host H, Lund E (1986) Age as a prognostic factor in breast cancer. Cancer 57:2217–2221
20. Ishida T, Yokoe T, Kasumi F, Sakamoto G, Makita M, Tominaga T, et al (1992) Clinicopathologic characteristics and prognosis of breast cancer patients associated with pregnancy and lactation: analysis of case-control study in Japan. Jpn J Cancer Res 83:1143–1149
21. Jacquemier J, Kurtz JM, Amalric R, Brandone H, Ayme Y, Spitalier JM (1990) An assessment of extensive intraductal component as a risk factor for local recurrence after breast-conserving therapy. Br J Cancer 61:873–876
22. Jmor S, Al-Sayer H, Heys S, Payne S, Miller I, Ah-See AK, et al (2002) Breast cancer in women aged 35 and under: prognosis and survival. J R Coll Surg Edinb 47:693–699
23. Karesen R, Jacobsen U, Sauer T, Skaane P (1999) A prospective registration of diagnosis and treatment of breast tumors at the Ulleval hospital 1988–1995 (in Norwegian). Tidsskr Nor Laegeforen 119:3562–3566
24. Kollias J, Elston CW, Ellis IO, Robertson JF, Blamey RW (1997) Early-onset breast cancer—histopathological and prognostic considerations. Br J Cancer 75:1318–1323
25. Kroman N, Wohlfahrt J, Andersen KW, Mouridsen HT, Westergaard T, Melbye M (1997) Time since childbirth and prognosis in primary breast cancer: population based study. BMJ 315:851–855
26. Kroman N, Jensen MB, Wohlfahrt J, Mouridsen HT, Andersen PK, Melbye M (2000) Factors influencing the effect of age on prognosis in breast cancer: population based study. BMJ 320:474–478
27. Kuerer HM, Cunningham JD, Brower ST, Tartter PI (1997) Breast carcinoma associated with pregnancy and lactation. Surg Oncol 6:93–98
28. Lethaby AE, O'Neill MA, Mason BH, Holdaway IM, Harvey VJ (1996) Overall survival from breast cancer in women pregnant or lactating at or after diagnosis. Auckland Breast Cancer Study Group. Int J Cancer 67:751–755
29. Nixon AJ, Neuberg D, Hayes DF, Gelman R, Connolly JL, Schnitt S, et al (1994) Relationship of patient age to pathologic features of the tumor and prognosis for patients with stage I or II breast cancer. J Clin Oncol 12:888–894
30. Pertschuk LP, Feldman JG, Kim YD, Braithwaite L, Schneider F, Braverman AS, et al (1996) Estrogen receptor immunocytochemistry in paraffin embedded tissues with ER1D5predicts breast cancer endocrine response more accurately than H222Spgamma in frozen sections or cytosol-based ligand-binding assays. Cancer 77:2514–2519
31. Petrek JA (1991) Pregnancy-associated breast cancer. Semin Surg Oncol 7:306–310
32. Petrek JA, Dukoff R, Rogatko A (1991) Prognosis of pregnancy-associated breast cancer. Cancer 67:869–872
33. Ridolfi RL, Jamehdor MR, Arber JM (2000) HER-2/neu testing in breast carcinoma: a combined immunohistochemical and fluorescence in situ hybridization approach. Mod Pathol 13:866–873
34. Sankila R, Heinavaara S, Hakulinen T (1994) Survival of breast cancer patients after subsequent term pregnancy: "healthy mother effect". Am J Obstet Gynecol 170:818–823
35. Schnitt SJ, Connolly JL, Harris JR, Hellman S, Cohen RB (1984) Pathologic predictors of early local recurrence in Stage I and II breast cancer treated by primary radiation therapy. Cancer 53:1049–1057
36. Styles JM, Harrison S, Gusterson BA, Dean CJ (1990) Rat monoclonal antibodies to the external domain of the product of the C-erbB-2 proto-oncogene. Int J Cancer 45:320–324
37. Suo Z, Emilsen E, Tveit KM, Nesland JM (1998) Type 1 protein tyrosine kinases in benign and malignant breast lesions. Histopathology 33:514–521
38. Suo Z, Yang H, Mei Q, Skovlund E, Cui J, Nesland JM (2001) Type 1 protein tyrosine kinases in Chinese breast carcinomas: a clinicopathologic study. Int J Surg Pathol 9:177–187
39. Torry DS, Faulk WP, McIntyre JA (1989) Regulation of immunity to extraembryonic antigens in human pregnancy. Am J Reprod Immunol 21:76–81
40. Tretli S, Kvalheim G, Thoresen S, Host H (1988) Survival of breast cancer patients diagnosed during pregnancy or lactation. Br J Cancer 58:382–384
41. UICC International Union Against Cancer (2002) In: Wittenkind SLH (ed) TNM Atlas, 6th edn. Wiley-Liss, New-York, pp 131–141
42. Velentgas P, Daling JR, Malone KE, Weiss NS, Williams MA, Self SG, et al (1999) Pregnancy after breast carcinoma: outcomes and influence on mortality. Cancer 85:2424–2432
43. Von-Schoultz E, Johansson H, Wilking N, Rutqvist LE (1995) Influence of prior and subsequent pregnancy on breast cancer prognosis. J Clin Oncol 13:430–434
44. Wallack CK, Wolf JA, Denes AE, Glasgow G, Kumar B (1983) Gestational carcinoma of the female breast. Curr Probl Cancer 7:1–58
45. Woo JC, Yu T, Hurd TC (2003) Breast cancer in pregnancy. A literature review. Arch Surg 138:91–98

Virchows Arch (2003) 443:51–56
DOI 10.1007/s00428-003-0771-9

ORIGINAL ARTICLE

W. O. F. Alazawi · L. S. Morris · M. A. Stanley · D. R. Garrod · N. Coleman

Altered expression of desmosomal components in high-grade squamous intraepithelial lesions of the cervix

Received: 13 January 2003 / Accepted: 13 January 2003 / Published online: 21 May 2003
© Springer-Verlag 2003

Abstract We have used immunohistochemistry to test the hypothesis that components of the desmosome are disrupted during neoplastic progression of squamous epithelial cells in the uterine cervix. Sections of normal cervix and squamous intraepithelial lesions (SILs) were immunostained for desmosomal proteins and glycoproteins, and results were assessed using a semi-quantitative grading system. No difference between normal cervix and low-grade SIL (LSIL) was found. A significant reduction in expression of desmogleins was seen between high-grade SIL (HSIL) and LSIL ($P<0.01$) and normal cervix ($P<0.001$). Desmocollin expression was not reduced significantly, although scores showed significantly greater variation in HSIL compared with LSIL ($P<0.05$) and normal cervix ($P<0.05$). There was no significant difference in desmoplakin expression among the three groups. The results suggest that there may be sequential disruption of desmosomal function during neoplastic progression of cervical squamous intraepithelial cells, with downregulation of desmogleins during the progression from LSIL to HSIL and loss of desmocollin expression occurring in some cases of established HSIL.

Keywords Cervix · Neoplasia · Desmosome · Desmoplakin · Desmoglein · Desmocollin

W. O. F. Alazawi · L. S. Morris · N. Coleman (✉)
Medical Research Council Cancer Cell Unit,
MRC/Hutchison Research Centre,
Hills Road, Cambridge, UK
e-mail: nc109@cam.ac.uk

M. A. Stanley
Department of Pathology,
University of Cambridge,
Tennis Court Road, Cambridge, CB2 1QP, UK

D. R. Garrod
School of Biological Sciences,
University of Manchester, 3.239 Stopford Building,
Oxford Road, Manchester, M13 9PT, UK

Introduction

Cell–cell adhesion interactions influence the position of each cell with respect to its neighbours and thereby contribute to tissue morphology. It is likely that in the progression towards the malignant phenotype, normal constraints that direct cell differentiation are lost, as a result of altered signalling from surrounding cells through intercellular adhesion molecules.

Desmosomes are strong intercellular adhesion complexes that are found in a range of tissues including most epithelia. They are formed of proteins and glycoproteins. The principal desmosomal proteins are desmoplakins I and II (DpI and II), plakoglobin and plakophilin. DpI and II are located between the dense plaque of the desmosomes and the region of attachment of intermediate filaments. These molecules are present in all desmosome-bearing tissues, although DpII is absent from cardiac muscle [6]. DpI is a dimer containing a central coiled-coil rod and globular end domains, while DpII—probably an alternatively spliced variant—has a substantially shorter rod [8, 12].

The major desmosomal glycoproteins are desmogleins 1, 2 and 3 and the desmocollins, all members of the cadherin family [5, 11]. Desmoglein 2 is ubiquitous in desmosome-bearing tissues, while desmogleins 1 and 3 are confined to stratified squamous epithelia including that of the cervix. The desmosomal glycoproteins bind to plakoglobin, an 82-kDa protein that shares almost complete sequence homology with β-catenin [6] and is believed to have an analogous role in the Wnt-1 signalling pathway.

Electron microscopic studies suggested that a reduction in desmosomal adhesion may correlate with invasive behaviour in squamous cell carcinoma (SCC) of the mouth [1] and cervix [7]. Immunohistochemistry has enabled a much more extensive analysis of expression of desmosomal components in normal and neoplastic tissue [10, 15] For example, studies have so far shown desmosomal protein downregulation in association with

invasion in transitional cell carcinoma of the bladder [3], and oral SCC [7].

The changes in expression of desmosomal components in pre-malignant conditions have received relatively scant attention. Cervical SCC is well suited to detailed studies of events involved in neoplastic progression as there are well-defined steps in the evolution of the disease, ranging from the non-invasive intraepithelial abnormalities, through microinvasive carcinomas to frankly malignant and metastatic disease. Premalignant conditions of the cervix may be classified as either low-grade or high-grade squamous intraepithelial lesions (LSIL and HSIL, respectively) [16]. LSIL generally reflects human papilloma virus (HPV) infection without neoplastic transformation, whereas HSIL generally represents an HPV-related neoplastic transformation of the cervical epithelium.

de Boer and colleagues have demonstrated reduced expression of desmogleins and desmoplakins in LSIL and HSIL, as compared with normal cervix [4]. In the current study, we have assessed the expression of a wider range of desmosomal proteins in normal cervix, LSIL and HSIL and developed a scoring system that allows changes in the distribution of desmosomal components to be quantified and subjected to statistical analysis.

We present quantitative immunohistochemical data suggesting that there is sequential disruption of desmosomal function during neoplastic progression of cervical squamous intraepithelial cells, with downregulation of desmogleins during the progression from LSIL to HSIL and loss of desmocollin expression occurring in some cases of established HSIL.

Materials and methods

Tissues

Normal cervix was obtained from hysterectomy specimens removed for disease unrelated to the cervix. Abnormal cervical tissue was obtained from colposcopy clinics in the East Anglia region. In all cases, tissue was obtained and used in accordance with ethical guidelines approved by the local research ethics committee. All tissue was immediately snap-frozen in liquid nitrogen and stored in liquid nitrogen until required. Lesions were assessed according to the Bethesda system as LSIL or HSIL. The histological diagnosis was made on frozen sections and from adjacent tissue that had been fixed in neutral buffered formalin and processed to paraffin. In all cases, sections from each side of the immunostained slides were stained with haematoxylin and eosin, in order to ensure that each lesion was of consistent grade. Due to limitations in the amount of available tissue, not all cases were stained with each antibody.

Immunoperoxidase

An indirect immunoperoxidase approach was used, employing an avidin-biotin detection system, as described previously [2] The primary mouse monoclonal antibodies have been described elsewhere [13, 15]. They were: 11–5F, mouse IgG1 versus DpI and II; 52–3D, mouse IgG1 versus desmocollins 1, 2 and 3; 32–32B, mouse IgG2a versus desmogleins 1 and 3; and 33–3D, mouse IgM versus desmoglein 2.

In preliminary experiments, it was determined that optimal staining with all four antibodies could be obtained by a 72-h 4°C incubation in Tris-buffered saline containing 1% bovine serum albumin. Control slides were incubated under the same conditions with 1:100 mouse IgG2a anti-epithelial membrane antigen as a positive control and with mouse IgG1 human melanoma-specific antibody (HMB-45) as a negative control.

Scoring

A grading system was devised in order to obtain a semi-quantitative evaluation of the distribution of each protein in the tissue sections. Scores were awarded as follows: 0, negative staining throughout the epithelium; 1, minimal membrane staining; 2, patchy non-pericellular membrane staining; 3, pericellular staining in any third of the epithelium; 4, pericellular staining in any two of the three-thirds of the epithelium; and 5, pericellular staining in all three-thirds of the epithelium.

Variation in staining patterns within individual lesions was seen only rarely; where this occurred the score awarded to the case was that of the most strongly staining region. The results for each group of sections were compared using the non-parametric Wilcoxon rank sum test. Analysis of variation of staining scores within a group of biopsies was undertaken using the variance ratio test. P values, where given, are two-sided.

Results

Desmoplakins

Normal cervix (n=9)

Staining for desmoplakins was restricted to the cell membranes of normal cervical keratinocytes (Fig. 1a; Table 1). All the cases showed full-thickness staining except one specimen in which the upper third of the epithelium was negative (Fig. 2a). The basal layer was negative in five cases, although in the other four cases basal layer cells stained positively, with predominant staining of the apical and lateral surfaces.

LSIL (n=13)

Twelve of thirteen specimens showed pericellular staining in at least two-thirds of the epithelium (Fig. 1b; Table 1). There was no significant difference between the scores for the LSIL cases and those for the cases of normal cervix (Fig. 2a).

HSIL (n=11)

Perimembranous staining was seen in the full thickness of the epithelium in 8 of 11 cases and in the lower two-thirds in two further cases (Fig. 1c; Table 1). There was no significant difference between staining scores for the HSIL group and the LSIL or normal cervix groups (Fig. 2a).

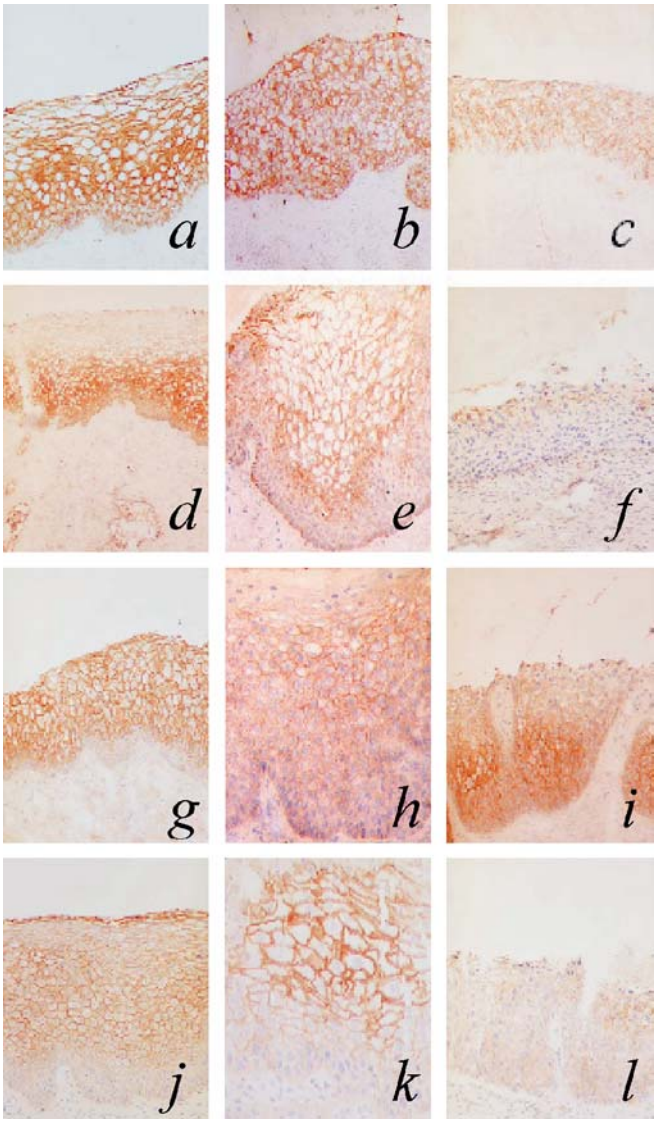

Fig. 1 Expression of desmoplakins (**a**, **b**, **c**); desmocollins 1, 2 & 3 (**d**, **e**,**f**); desmogleins 1 & 3 (**g**, **h**, **i**); and desmoglein 2 (**j**, **k**, **l**) in cervix. **a–j** Normal cervix; **b–k** low-grade squamous intraepithelial lesion (LSIL); **c–l** high-grade squamous intraepithelial lesion (HSIL). There was no significant difference in expression of desmoplakins. There was a significant reduction in expression of desmogleins in HSIL relative to LSIL and normal cervix. There was significantly greater variation in the expression of desmocollins in HSIL versus LSIL and normal cervix

Table 1 Table of semi-quantitative scores. Scores for each case are shown for each desmosomal component: desmoplakins I & II (Dp); desmocollins 1, 2 and 3 (Dsc); desmogleins 1 & 3 (Dg 1&3); and desmoglein 2 (Dg 2)

Case number	Dp	Dsc	Dg 1&3	Dg 2
N1	5	4	5	5
N2	5	5	5	5
N3	5	4	5	5
N4	5	3	5	3
N5	4	4	5	3
N6	5	3	5	3
N7	5	4	5	5
N8	5		5	5
N9	5	4	5	4
N10			5	4
L1	5		5	5
L2	5	5		
L3	4	4	4	3
L4	5	3		
L5	5			
L6	4	4		3
L7	5		4	4
L8	5	4	5	3
L9	5	4	4	
L10	3	3	5	
L11	4	3	4	4
L12	5			
L13	5	4		3
L14		2		
L15			5	5
L16			3	
H1	5	1	3	2
H2	5	5	3	
H3			0	1
H4	5	3		3
H5	5	3	2	2
H6			2	
H7			1	
H8	4			
H9	5		0	1
H10	5		1	0
H11		1	1	
H12		0		
H13	5	4	3	3
H14			3	
H15			2	
H16	2			1
H17				
H18	4	3		3
H19	5	4		2
H20			1	0
H21				2
H22				2
H23			1	

Desmocollins 1, 2 and 3

Normal cervix (n=8)

Only one case showed full thickness staining. In the other seven cases, staining was seen in one-third or two-thirds of the epithelium (Fig. 1d, Fig. 2b; Table 1), although there was variation in the level within the epithelium of the positively staining cells.

LSIL (n=10)

The pattern of staining in LSIL was similar to that seen in normal cervix; only one of ten cases showed full-thickness staining, while eight showed pericellular staining in one or two of the thirds of the epithelium (Fig. 1e; Table 1). There was no significant difference in staining scores between LSIL and normal cervix (Fig. 2b).

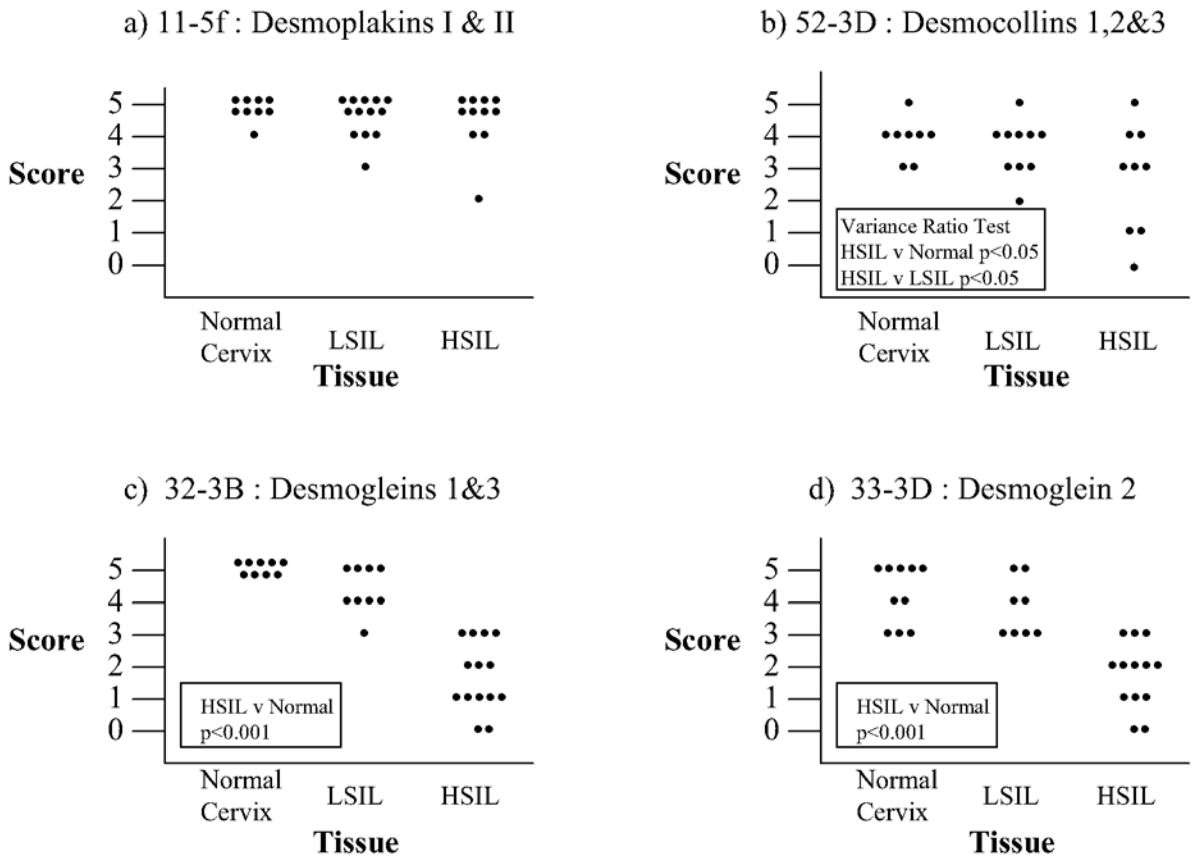

Fig. 2 Quantitative assessment of staining distribution in tissue biopsies. Distribution of desmosomal components in normal cervix, low-grade squamous intraepithelial lesion (LSIL) and high-grade squamous intraepithelial lesion (HSIL) as assessed by semi-quantitative scoring described in the text: desmoplakins (**a**); desmocollins (**b**); desmogleins 1 & 3 (**c**); and desmoglein 2 (**d**)

HSIL (n=9)

There was a wide variation in staining. Three of the nine cases examined showed either very little or no staining. Pericellular expression was seen in one-third of the epithelium in three cases, in two of the thirds in two cases and through the full thickness in one case. Variation was also seen within individual cases; one case, for example, showed patchy non-membranous staining in some areas and perimembranous staining in two-thirds of the epithelium in other regions (Fig. 1f; Table 1). There was no significant difference in the staining scores for HSIL versus LSIL and normal cervix by the Wilcoxon rank sum test. However, the variance ratio test using the F distribution showed that the spread of the scores in HSIL tissue was significantly greater than that in normal cervix ($P<0.05$) and LSIL ($P<0.05$) (Fig. 2b).

Desmogleins 1 and 3

Normal cervix (n=9)

All normal epithelia stained positively for desmogleins 1 and 3. Full-thickness perimembranous staining was seen in all nine cases (Fig. 1g, Fig. 2c; Table 1).

LSIL (n=9)

Full-thickness staining was seen in four of nine cases (Fig. 1h; Table 1). Where full-thickness expression was not observed, positive staining was seen in cells at varying levels in the epithelium; in some cases there was staining of the superficial layers, whereas in other cases there was staining of the parabasal cells. There was, however, no significant difference between staining scores for normal cervix and LSIL (Fig. 2c).

HSIL (n=14)

There was a marked decrease in desmoglein 1 and 3 staining, with 7 of 14 cases showing no staining or only

patchy membrane staining of an occasional cell (Fig. 1i; Table 1). The staining scores were significantly less than those for LSIL ($P<0.001$) and normal cervix ($P<0.001$) (Fig. 2c).

Desmoglein 2

Normal cervix (n=10)

All normal epithelia stained positively for desmoglein 2. Staining in at least two of three-thirds of the epithelium was seen in seven of ten cases (Fig. 1j, Fig. 2d; Table 1). Where full-thickness expression of desmoglein 2 was not observed, positive staining was seen at varying levels in the epithelium.

LSIL (n=8)

Patterns of expression were very similar to those for normal cervix, with no significant difference in staining scores between the two groups (Fig. 1k and Fig. 2d; Table 1).

HSIL (n=13)

Six of thirteen cases showed no expression of desmoglein 2 or a small amount of pericellular staining only (Fig. 1l; Table 1), with no case showing staining in more than one-third of the epithelium. There was a significant decrease in staining scores compared with normal cervix ($P<0.001$) and LSIL ($P<0.01$) (Fig. 2d).

Discussion

The work reported here has shown that the neoplastically transformed cells of cervical HSIL have different distributions of desmosomal proteins when compared with LSIL and normal ectocervix. Immunohistochemistry with all four antibodies used did not show a significant difference in staining between normal cervix and LSIL. In contrast, HSIL showed a marked reduction in expression of desmogleins 1 and 3 and desmoglein 2 compared with LSIL and normal cervix. Although there was no significant reduction in overall levels of expression of desmocollins in HSIL, there was a significantly greater variation in expression than in LSIL or normal cervix.

Our findings are consistent with observations that the expression of other adhesion molecules is altered in HSIL but not in LSIL. Our group has previously shown that ICAM-1 is upregulated in HSIL, whereas its expression in LSIL is the same as that in normal cervix [2]. However, this is not the case for other cell adhesion molecules. Reductions in the expression of molecules including E-cadherin [14] and α and β catenins [4] have been described in LSIL, suggesting that the cadherin–catenin system may be dysfunctional at an earlier stage of neoplastic progression in the cervix than are desmosomes.

We have seen no significant reduction in desmoplakin expression in cervical SIL. Interestingly, this data differs from the findings of de Boer et al. [4], who described a reduction in expression of desmoplakins in eight cases of LSIL and nine cases of HSIL. The antibody used was the same as that employed in our study, although the tissue was formalin fixed and paraffin embedded as opposed to the immediately snap frozen tissue that we were able to obtain. It is difficult to comment further on this discrepancy as no illustrations were provided in the earlier study. Our findings are consistent with those from studies of desmosomal components in oral SCC, in which desmoplakin expression is reduced predominantly in poorly differentiated carcinomas [7]. Our findings are perhaps not surprising given the role of desmoplakins in anchoring the intracellular intermediate filaments to the plasma membrane. Downregulation of desmoplakins may impair cellular structure and this may only be tolerated by cells that have accumulated a sufficient number of genetic mutations, as may occur in undifferentiated carcinomas.

Our evidence of reduced expression of desmogleins 1 and 3 and desmoglein 2 in HSIL is in agreement with the findings of de Boer et al. [4]. These authors also described a reduction in expression of desmoglein 3 in eight cases of LSIL, although the antibody used was different from the one used in our study and the tissue had been formalin fixed and paraffin embedded. Again, further comment is difficult, as illustrations of the expression of desmogleins in LSIL were not provided by de Boer and colleagues. Reduced expression of desmogleins 1 and 3 and desmoglein 2 would be expected to disrupt effective cell–cell contact, since it is the homotypic binding of these molecules in the intercellular space that mediates adhesion. Downregulation of desmogleins has also been demonstrated in neoplastic progression of epidermal keratinocytes. Expression is normal in keratocanthoma (generally regarded as a benign neoplasm), with reduced expression in actinic keratosis (the most common premalignant lesion of keratinocytes) and almost complete loss of expression in frank SCC [9].

Also involved in cell–cell binding are the desmocollins. Although the HSIL cases in this study did not show an overall decrease in expression of desmocollins, they did show a significantly greater spread of scores when assessed by our semi-quantitative grading system. One interpretation of this data is that downregulation of desmocollin expression occurs in some cases of established HSIL, perhaps as a result of clonal progression. This notion would be supported by our observation of variable desmocollin expression in different regions of individual HSIL lesions.

In summary, our observations suggest that there may be sequential disruption of desmosomal function in the progression of cervical intraepithelial neoplasia. The sequence may involve loss of desmoglein early in the development of HSIL and loss of desmocollins in at least some cases of established HSIL. Desmoplakins are still

present in HSIL cells, although, by analogy with data from other epithelia [7], there may be loss of expression in some cervical SCCs, particularly those that are poorly differentiated.

References

1. Burkhardt AB (1980) Oral cancer and pre-cancer: ultrastructural and immunopathological aspects. G. Fischer, Stuttgart
2. Coleman N, Greenfield IM, Hare J, Kruger-Gray H, Chain BM, Stanley MA (1993) Characterization and functional analysis of the expression of intercellular adhesion molecule-1 in human papillomavirus-related disease of cervical keratinocytes. Am J Pathol 143:355–367
3. Conn IG, Vilela MJ, Garrod DR, Crocker J, Wallace DM (1990) Immunohistochemical staining with monoclonal antibody 32–2B to desmosomal glycoprotein 1. Its role in the histological assessment of urothelial carcinomas. Br J Urol 65:176–180
4. de Boer CJ, van Dorst E, van Krieken H, Jansen-van Rhijn CM, Warnaar SO, Fleuren GJ, Litvinov SV (1999) Changing roles of cadherins and catenins during progression of squamous intraepithelial lesions in the uterine cervix. Am J Pathol 155:505–515
5. Garrod D, Chidgey M, North A (1996) Desmosomes: differentiation, development, dynamics and disease. Curr Opin Cell Biol 8:670–678
6. Garrod DR (1995) Desmosomes and cancer. In: Hart I, Hogg N (eds) Cell adhesion and cancer. Cancer Surv 24:97–111
7. Hiraki A, Shinohara M, Ikebe T, Nakamura S, Kurahara S, Garrod DR (1996) Immunohistochemical staining of desmosomal components in oral squamous cell carcinomas and its association with tumour behaviour. Br J Cancer 73:1491–1497
8. Kowalczyk AP, Stappenbeck TS, Parry DA, Palka HL, Virata ML, Bornslaeger EA, Nilles LA, Green KJ (1994) Structure and function of desmosomal transmembrane core and plaque molecules. Biophys Chem 50:97–112
9. Krunic AL, Garrod DR, Madani S, Buchanan MD, Clark RE (1998) Immunohistochemical staining for desmogleins 1 and 2 in keratinocytic neoplasms with squamous phenotype: actinic keratosis, keratoacanthoma and squamous cell carcinoma of the skin. Br J Cancer 77:1275–1279
10. Moll R, Cowin P, Kapprell HP, Franke WW (1986) Desmosomal proteins: new markers for identification and classification of tumors. Lab Invest 54:4–25
11. North AJ, Chidgey MA, Clarke JP, Bardsley WG, Garrod DR (1996) Distinct desmocollin isoforms occur in the same desmosomes and show reciprocally graded distributions in bovine nasal epidermis. Proc Natl Acad Sci USA 93:7701–7705
12. O'Keefe EJ, Erickson HP, Bennet V (1989) Desmoplakin I and desmoplakin II: purification and characterisation. J. Biol Chem 264:8310–8318
13. Parrish EP, Steart PV, Garrod DR, Weller RO (1987) Antidesmosomal monoclonal antibody in the diagnosis of intracranial tumours. J Pathol 153:265–273
14. Vessey CJ, Wilding J, Folarin N, Hirano S, Takeichi M, Soutter P, Stamp GW, Pignatelli M (1995) Altered expression and function of E-cadherin in cervical intraepithelial neoplasia and invasive squamous cell carcinoma. J Pathol 176:151–159
15. Vilela MJ, Parrish EP, Wright DH, Garrod DR (1987) Monoclonal antibody to desmosomal glycoprotein 1—a new epithelial marker for diagnostic pathology. J Pathol 153:365–375
16. Wright TC, Kurman RJ (1996) In: Lacey C (ed) Papillomavirus review: current research on papillomaviruses. Leeds Univ. Press, pp 215–225

Virchows Arch (2003) 443:57–66
DOI 10.1007/s00428-003-0818-y

ORIGINAL ARTICLE

Lars Morawietz · Thorsten Gehrke · Lars Frommelt · Petra Gratze · Andreas Bosio · Johannes Möller · Bernhard Gerstmayer · Veit Krenn

Differential gene expression in the periprosthetic membrane: lubricin as a new possible pathogenetic factor in prosthesis loosening

Received: 14 January 2003 / Accepted: 1 April 2003 / Published online: 29 May 2003
© Springer-Verlag 2003

Abstract About 10% of hip endoprostheses will loosen after 10 years. Prosthesis loosening is caused by two different pathomechanisms: aseptic loosening (AL) and septic loosening (SL). This study evaluated differences in gene expression in AL and SL. Eight hybridizations were performed on PIQOR cDNA arrays. Objects of the study were periprosthetic interface tissue samples from two patients with SL and three patients with AL. Tissue parts directly adjacent to the site of RNA isolation were analyzed immuno/histopathologically in order to overcome the problem of tissue heterogeneity. Thirty-three genes were found constantly differentially expressed, among which were cd11b, cd18, cd68, osteopontin and ferritin heavy-chain upregulated in AL and collagen types 1alpha-1, 3alpha-1, integrin alpha-1, thrombospondin2 and nidogen upregulated in SL. The most striking finding was the strong upregulation (from 20-fold to 323-fold) of megakaryocyte stimulating factor (*msf*) in all aseptic cases and one of the two septic cases, which was confirmed by real-time reverse transcription-polymerase chain reaction. In this study, *msf* is linked to prosthesis loosening for the first time. The upregulation in AL suggests an important pathogenetic role: the *msf* splice product lubricin is responsible for the lubrication of healthy joints, but its excellent lubrication ability may disturb the tight interaction between bone and prosthesis and thereby contribute to prosthesis loosening.

Keywords Aseptic prosthesis loosening · Septic prosthesis loosening · cDNA array · *msf* · Lubricin

Introduction

Because of joint destruction through inflammatory or degenerative diseases, 1.3 million total joint replacements are performed per year world wide. One major problem of total joint replacement is prosthesis loosening. About 10% of hip replacements need revision surgery after 10–15 years [2, 14]. At revision surgery, a periprosthetic membrane that has grown between prosthesis and bone is removed. This membrane is made responsible for prosthesis loosening [3]. It is generated by two different pathomechanisms, aseptic loosening (AL) and septic loosening (SL), which can be discriminated by their histomorphological characteristics and by microbiological detection/absence of bacteria [24, 27].

Constant movement of the prosthesis leads to shedding of polyethylene, metal and cement particles, if used. These wear particles provoke a foreign body reaction, which consists of mainly macrophages and multinucleated giant cells. Also, fibroblasts take part in the formation of periprosthetic interface tissue [12, 20, 39]. T-lymphocytes occur in a low quantity, but antigen specificity and oligoclonal expansion of T-cells were shown together with the transcription of interferon gamma, suggesting a key role of T-lymphocytes in the initiation and perpetuation of periprosthetic inflammation [38]. Osteoclasts and macrophages transformed into osteoclast-like cells on the membrane secrete bone-degrading enzymes [30]. As bone matrix is absorbed, the prosthesis no longer fits tightly and loosens.

In SL, a low quantity of bacteria induces a chronic inflammation characteristic of the presence of macrophages, activated fibroblasts, granulocytes and sprouting capillaries. There are case reports on different bacteria

Authors Lars Morawietz and Thorsten Gehrke contributed equally to this work.

L. Morawietz · P. Gratze · J. Möller · V. Krenn (✉)
Institute for Pathology, University Clinic Charité,
Charité University Hospital, Humboldt University of Berlin,
Schumannstrasse 20/21, 10117 Berlin, Germany
e-mail: veit.krenn@charite.de
Tel.: +49-30-450536134
Fax: +49-30-450536907

T. Gehrke · L. Frommelt
ENDO-Klinik Hamburg, Holstenstrasse 2,
22767 Hamburg, Germany

A. Bosio · B. Gerstmayer
Memorec Stoffel GMBH, Cologne, Germany

causing a prosthesis infection that suggest that bacteremia after a procedure, e.g., a dental extraction, could lead to bacterial aggregation in the periprosthetic tissue [17, 26]. Other factors contributing to this mechanism are not yet known, so there is no consistent explanation for SL.

Although both diseases have a different etiology, they display a similar histopathology, with macrophages as the predominant cell type. The mechanism of how the periprosthetic membranes of AL and SL are generated and which pathways are responsible for bone destruction is not understood.

cDNA array technology was introduced a few years ago; it has already given new insights into the pathogenesis of various diseases by means of whole tissue analysis [36] and has been applied to AL [11]. Using this approach, we expected to detect differentially expressed genes specific for AL and SL that have not yet been considered relevant to prosthesis loosening. A comparative hybridization with RNA from AL and SL was chosen because, in general, they have a similar morphology with macrophages as the predominant cell type, but, in particular, because genes contributing to their pathomechanisms should, in part, be different, as both mechanisms have different etiologies and their morphologies differ in detail. In septic cases, prosthesis loosening does not occur without infection. As it generates only few wear particles and a slight foreign body reaction, SL should thus have a low expression of genes linked to the pathomechanisms of AL. Therefore, regarding the initiation of AL, tissue from SL may be regarded as control tissue. However, tissue from AL shows no signs of infection and may be considered a control for SL. One should also consider that genes involved in both mechanisms might be upregulated in both AL and SL and, therefore, may not be found using this approach at all. This problem derives from the fact that there is no way to obtain periprosthetic tissue from prostheses that have not loosened. In closely fitting prostheses, there is hardly any periprosthetic membrane [13], and, since there is no need for surgery, this tissue could only be acquired at necropsy, which greatly reduces the RNA quality.

Materials and methods

Patients and tissue samples

The subjects of the study were five patients with total knee arthroplasty due to osteoarthritis. Tissue samples were derived from periprosthetic tissue at revision surgery of three patients with AL and two patients with SL. In all cases, the examined tissue came from the femoral part of the prostheses. The time between primary arthroplasty and revision surgery was 4 years on average (minimum 9 months, maximum 7 years). One patient was female, four patients were male, and the mean age at revision surgery was 70.2 years (minimum 66 years, maximum 80 years) (Table 1). At revision surgery, all cases showed radiographic osteolysis around the implants.

Some tissue samples were large enough to be divided into more than one segment. The sample from patient 92 was divided into nine segments, which still provided enough material for array hybridization. One part of each segment was directly used for bacterial culturing techniques (aerobe and anaerobe cultures), another part was fixed in phosphate-buffered formalin and embedded in paraffin for immunohistochemistry and routine microscopy. The main part of each segment was snap frozen for RNA isolation and hybridization.

Standard microbiological culturing was applied for the detection of bacteria to confirm the diagnosis of SL. Cultures were positive in two cases that also showed an infiltrate with neutrophil granulocytes in standard hemalaun-eosin staining, so that SL was diagnosed.

Histopathological diagnosis included the description of the inflammatory infiltrate in the periprosthetic membrane, the amount of fibroblast or fibrocytes, respectively, and the vascularization. Furthermore, detection of wear particles was performed. Polarized light microscopy was used in defining birefringent polyethylene particles, while metal particles were identified as very small black particles (about 1–2 μm) showing only a circumferential birefringence and were easily distinguishable from polyethylene particles because of their opaque appearance without polarization. Cement particles were detected without polarization as bizarre shaped particles of various sizes. The same microscope was used (Leitz DMRBE).

RNA isolation

RNA was isolated from snap-frozen full periprosthetic tissue by applying the guanidinium thiocyanate method [6] using TRI Reagent (Sigma-Aldrich, Munich, Germany) according to the supplier's manual: 1 ml TRI Reagentwas added per 50–100 mg of mechanically pulverized tissue. The preparation was homogenized and incubated at room temperature. Per 1 ml TRI Reagent, 0.2 ml $CHCl_3$ was added, incubated at room temperature and centrifuged for 15 min at 4°C. Isopropyl alcohol (0.5 ml) was adjoined to the aqueous phase to precipitate the RNA. After repeated incubation and centrifugation, the RNA pellet was washed with 75% EtOH. The RNA was solubilized in 100 μl H_2O per 200 mg original tissue.

RNA was isolated from 200–300 mg tissue from each sample. The amount of RNA ranged from 121 μg to 351 μg, and the concentration from 0.40 μg/μl to 1.25 μg/μl. The quality of the isolation process was controlled with electropherograms and calculation of the 28S/18S RNA ratio, which was, in all samples, at least 1.5.

Table 1 Patient data. *AL* aseptic loosening, *SL* septic loosening

Patient no.	Age	Sex	Time between primary and revision arthroplasty	Loosening type	Cemented
85	66 years	Male	4 years	AL	Yes
87	70 years	Female	2 years	AL	No
88	80 years	Male	6 years	SL	Yes
91	66 years	Male	7 years	AL	No
92	69 years	Male	9 months	SL	Yes

Labeling reaction and sample cleanup

Labeling was performed according to the PIQOR protocol (Memorec Stoffel GMBH, Cologne, Germany), which is in short: 8 μl 5x first strand buffer, 2 μl 10x hexanucleotide mix (Roche Diagnostics), 2 μl"low C dNTP" (10 mM dATP, 10 mM dGTP, 10 mM dTTP, 4 mM dCTP), 2 μl FluoroLink Cy3-dCTP (or Cy5-dCTP, respectively), 4 μl 0.1 M DTT, 1 μl RNasin (40 U), 2 μl of each control RNA 1 prior mRNA isolation and control RNA 2 prior reverse transcription and 15 μl of the isolated probe aRNA (2 μg) were combined in an RNase-free microcentrifuge tube. After vortexing, the solution was incubated at 65°C for 5 min and then cooled down to 42°C. SSII enzyme (1 μl; 200 U) was added, mixed and incubated at 42°C for 30 min. Another 2 μl of SSII enzyme was added, mixed and incubated at 42°C for 30 min. RNase H (0.5 µl) was added, and the solution was incubated at 37°C for 20 min.

For sample cleanup, we used QIAquick (Qiagen) according to the supplier's manual: labeled samples were combined with 400 μl buffer PB. The sample was applied to a QIAquick column inside a 2-ml collection tube and centrifuged for 30–60 s. After flow-through was discarded, the sample was washed with 0.75 ml buffer PE and centrifuged for 30–60 s, then the flow-through was discarded and the column again centrifuged for 1 min. DNA was eluted in a new 1.5-ml microfuge tube with 30 μl H_2O pH 8. After 1 min, it was centrifuged for 1 min. The eluate was diluted to a final volume of 55 μl and added to 55 μl of 2× hybridization solution. Finally, the sample was stored at room temperature in the dark until the array pre-hybridization procedure was finished.

Array selection

A variant of the commercially available PIQOR rheumatology array (Memorec Stoffel GMBH) containing 820 immunological relevant cDNAs and 6 cDNAs from housekeeping genes was chosen for hybridization. Each glass slide chip contains four piezoelectric spotted sets of 832 cDNAs, each consisting of those 826 being examined, four positive and two negative controls. Positive controls are four DNA fragments from E. coli. In vitro transcribed E. coli RNA is added to the target to control the hybridization process. One negative control is salmon sperm DNA, one is buffer.

The examined cDNA fragments were selected from a database research and computational based addition of cDNAs with relevant sequence motifs. The fragments were 200–400 bp long and fulfilled the following criteria: absence of repetitive elements, less than 85% sequence homology to other cDNAs, and the chosen fragment covered all known splice and polyadenylation variants.

Array hybridization and evaluation

Pre-hybridization solution was heated at 98°C for 2 min, then quick spun and cooled to 42°C. Of this solution, 110 μl was applied according to manufacturers guidelines (Memorec Stoffel GMBH) using a GeneTAC hybridization station (Perkin Elmer, Langen, Germany).

After prehybridization, 110 μl of the labeled probes were pipetted onto the fixed and prehybridized array within the Gene TAC hybridization station and the hybridization process was performed overnight. After washing, the array was dried by centrifugation at 500 *g* for 3 min, then stored in a dust-free cassette.

Eight comparative hybridizations were performed. One array compared two regions of SL from patient 92 (intraindividual control); another array compared two SL patients, 88 and 92 (intraspecific control). These arrays should control the variability of the gene expression in one disease. Four arrays compared different areas of the periprosthetic membrane from patient 91 (AL) with different areas of tissue from patient 92 (SL); one array compared patient 85 (AL) and one array patient 87 (AL) with patient 92 (SL).

Fluorescence signal intensity was measured with a laser scanner (ScanArray 3000, General Scanning Inc., Watertown, Mass., USA).

Data analysis

Calculation of intensities was performed using ImaGene 4.1 (BioDiscovery, Marina del Rey, Ca., USA) software. Genes were regarded as detected, when the signal intensity in either the Cy3 or the Cy5 probe was at least twice as high as the intensity of the negative controls (buffer and salmon sperm). After the Cy5/Cy3 quotients for the detected genes were calculated, these quotients were normalized over the median quotient of all genes on that chip. Then, for each gene, the mean quotient of all four hybridizations on one chip was calculated.

Two-dimensional hierarchical Cluster analysis was carried out using Gene Cluster and Tree View software [7].

Immunohistochemistry

Immunostaining was performed on microsections (1–2 µm) of paraffin-embedded periprosthetic tissue. Sections were deparaffinized with xylene and cooked for 5 min in 0.01 M citrate buffer for antigen retrieval.

For the detection of T-lymphocytes, we used rabbit anti-human CD3 antibodies, B-lymphocytes were stained with mouse anti-human CD20, dendritic cells were detected with mouse anti-human CD23, macrophages/giant cells were stained with mouse anti-human CD68, blood vessel endothelials were stained with mouse anti-human CD34 and proliferating cells were detected with mouse anti-human Ki67. Staining was performed according to the standard supplier's protocol. Immunohistochemical localization was carried out with the labeled Streptavidin Biotin method using the LSAB+ System (Dako, Denmark). Fuchsin+Substrate-Chromogen-System (Dako) was used as chromogene, giving a red staining. Counterstaining was performed using hemalaun.

Additionally Giemsa staining was performed for the detection of mast cells, elastica-van-Giesson staining was used for the differentiation of fibrin and collagen and Berlin blue staining for the detection of metal debris and hemosiderin.

Reverse transcription and real-time polymerase chain reaction

Of the same total RNAs used for the microarray hybridizations, 2 μg was reverse transcribed and 40 ng of the reverse-transcription reaction product was used as template for further analysis. Transcript levels were measured by real-time quantitative reverse-transcription polymerase chain reaction (RT-PCR) using ABI 7000 SDS (PE Applied Biosystems, USA). The sequences of megakaryocyte stimulating factor (*msf*) forward and reverse primers are identical to those used for the generation of the cDNA probe on the microarray. The *msf* cDNA probe fragment spans the region from position 3084 to 3482 of the mRNA, which corresponds to parts of exon 6 and 7 from *msf*. These exons are known to be a constituent of the *msf* splice product lubricin [15]. The following primer pairs were used: *msf* forward 5′-AAAAGC-CAACCAAAGCACC–3′ and reverse 5′-CAGTCCATCTACTG-GCTTACC-3′, Primer sequences for glyceraldehyde 3-phosphate dehydrogenase (GAPDH): Forward 5′-GAGCTGAACGGGAAG-CTCAC–3′ and reverse 5′-CACCACCCTGTTGCTGTAGC-3′. Real-time RT-PCR assays were performed in triplicate. Threshold cycle, which correlates inversely with the target mRNA levels, was measured as the cycle number at which the SYBRgreen emission increases above a threshold level. Microarray analysis indicated that transcript levels of GAPDH did not vary dramatically (less than twofold), therefore, GADPH was used to normalize real-time RT-PCR data. The following cycle conditions were used: 95°C for 10 min followed by 50 cycles of 95°C for 15 s and 60°C for 1 min. For each amplified product, melting curves were determined according to the supplier's guidelines (Applied Biosystems prism model 7000 SDS software) ensuring specific amplification of either *msf* or GAPDH in the tissues analyzed. mRNA transcript levels were expressed as fold differences between the indicated aseptic or septic tissues. For the determination of transcript levels, the

"relative quantification method", using a standard curve, was used as described in the manual (Abi Prism 7700 Sequence Detection System – User Bulletin, Perkin Elmer) [19].

Results

The periprosthetic tissue samples chosen for hybridization were clearly diagnosed as AL or SL. Samples from three patients with negative microbiological culturing exhibited the typical histopathology of AL (patients 85, 87 and 91), and samples from two patients with positive culturing showed the aspect of SL (patients 88 and 92).

Histopathology

Aseptic cases

The typical dense accumulation of CD68+ macrophages and multinucleated giant cells recognizing polyethylene particles, metal particles and cement particles could be observed (Fig. 1a, c) in all aseptic cases. Tissue from patient 87 contained fewer wear particles and macrophages than tissue from patients 85 and 91. Polyethylene particles were identified as highly birefringent fragments when viewed under polarized light. They were mainly found in the cytoplasm of multi-nucleated giant cells as well as in large sized macrophages. Abundant metal particles appeared as small black particles (about 1–2 μm) in hematoxylin and eosin staining and as dense blue areas in Berlin blue staining. They were found predominantly in large-sized macrophages. Few large-sized cement particles were found in the cemented cases. Aseptic cases also exhibited a low chronic inflammatory infiltrate with some CD3+ T-cells and CD20+ B-cells. This infiltrate was strongest in sample 85, in which some mast cells could also be found (Giemsa staining). Angioneogenesis, made visible through CD34+ endothelial cells, was low in AL. In all samples some fibrin and also hemosiderin deposits could be found. Tissue sample 87 was not as typical for aseptic loosening as the samples from patient 85 and 91, as it contained a lesser amount of CD68+ macrophages/giant cells but stronger angioneogenesis. However, no infiltrate of granulocytes could be found and no bacteria detected either by microscopy or by microbiological culturing in any of the tissues. Single Ki67+ proliferating cells occurred in all tissue samples.

Septic cases

The septic cases exhibited the characteristic pattern of chronic granulation with focal fibrosis, edema and abundant sprouting capillaries (CD34+). The moderate inflammatory infiltrate consisted mainly of neutrophil granulocytes, whereby septic loosening could be diagnosed. Microbiology found an infection with *Streptokokkus oralis* in sample 88 and an infection with *Enterococcus faecalis* in the samples from patient 92. The infiltrate of CD68+ macrophages was low and there were

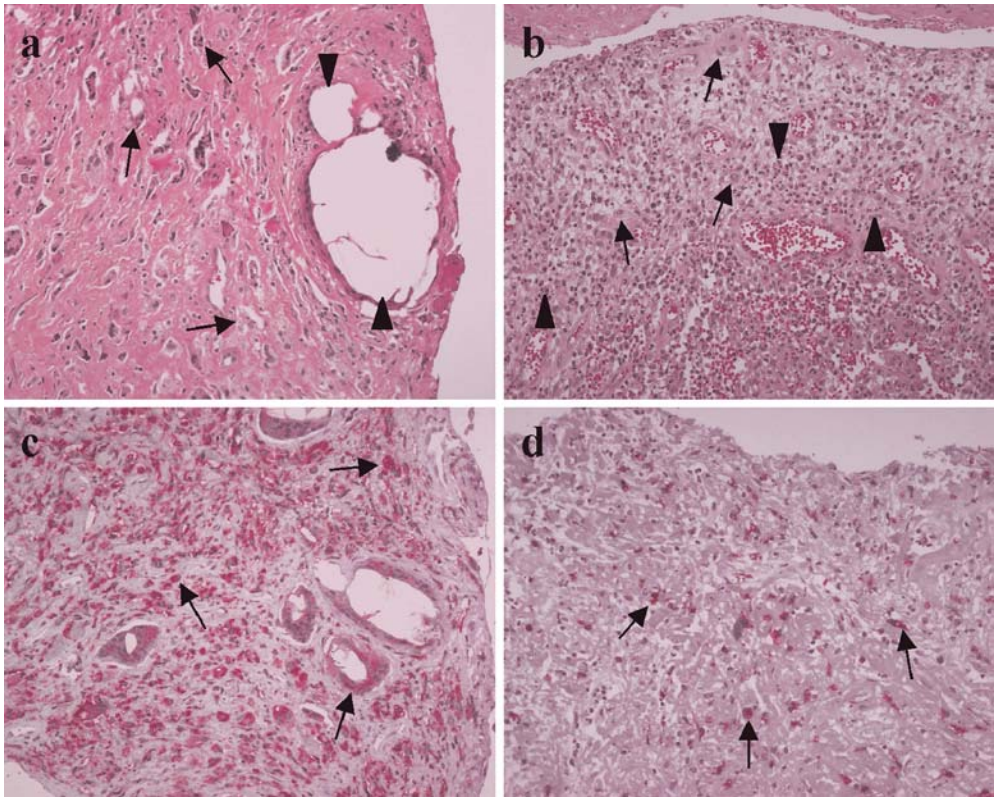

Fig. 1 a Histopathology of aseptic loosening (AL) (patient 91) with macrophages and multinucleated giant cells (*arrows*) containing different kinds of wear particles (*arrowheads* polyethylene particles; HE staining, ×200). **b** Histopathology of septic loosening (SL) (patient 92) with granulation tissue, macrophages (*arrows*) and infiltrate with granulocytes (*arrowheads*; HE staining, ×200). **c** Dense accumulation of CD68+ macrophages and multinucleated giant cells (*arrows*) in AL (CD68 immunohistochemistry, ×200). **d** Loose infiltrate with CD68+ macrophages (*arrows*) in SL (CD68 immunostaining, ×200)

Table 2 Number of detected and differentially expressed genes on eight arrays. *AL* aseptic loosening, *SL* septic loosening

Cy5-labeled target Cy3-labeled target	91 (AL) 92 (SL)	92 (SL) 92 (SL)	92 (SL) 88 (SL)	85 (AL) 92 (SL)	91 (AL) 92 (SL)	91 (AL) 92 (SL)	91 (AL) 92 (SL)	87 (AL) 92 (SL)	Mean
Number of cDNAs detected	441	510	426	354	426	290	424	420	411
>Two-fold differential	131	54	66	172	101	123	151	165	120
>Five-fold differential	21	6	5	53	24	30	22	43	26
Comment		Intrain-dividual control	Intra-septic control						

far fewer wear particles in the cytoplasm of these cells than in the aseptic tissues (Fig. 1b, d). Fibrin deposits of various sizes appeared throughout the tissue. Very few Ki67+ proliferating cells were found in all tissue samples.

Hybridization

From 826 genes examined on each array, 569 different genes were detected in at least one of the eight arrays. The number of detected genes per array ranged between 290 and 510 with a mean number of 411 genes. After normalization, a mean number of 120 genes (minimum 54, maximum 172) were at least twofold differentially expressed, meaning that the normalized, mean signal intensity of the four Cy3 targets was increased twofold in the Cy5 targets or vice versa. The differential expression was risen fivefold in a mean number of 26 genes per array (minimum 5, maximum 53) (Table 2).

The two control arrays showed by far the lowest number of twofold (54 and 66, respectively) and fivefold (6 and 5, respectively) differentially expressed genes. This is well in line with the fact that these arrays did not compare AL with SL but two different sites in one patient with SL (intraindividual control) or two patients both with SL (intraspecific control). The differential expression of these genes might either be due to the heterogeneity of the periprosthetic tissue or to artifacts.

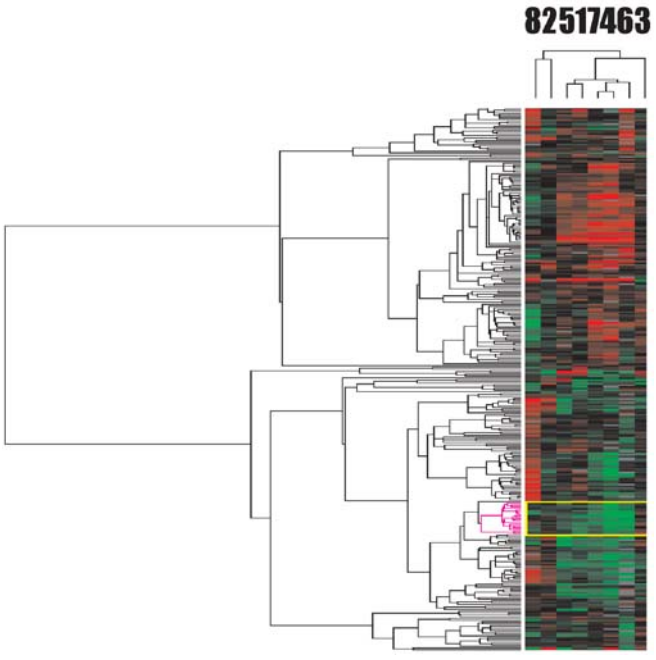

Fig. 2 Two-dimensional hierarchical clustering of genes detected in at least 60% of experiments (406 genes). *Rows* clustering of genes, *columns* clustering of arrays with array 2 (intraindividual control) and array 8 (aseptic patient 87 with untypical histomorphology) in one cluster and array 3 (intraspecific control) in a subcluster

Cluster analysis

In the two-dimensional computerized cluster analysis of all hybridization experiments, array 2 (intraindividual control) and array 8 were grouped together whereas the other arrays formed a main cluster with array 3 (intraspecific control) as a separate subcluster (Fig. 2). This is in good correlation with the histomorphological findings of the tissue used in these hybridizations. As array 2 and array 3 are a comparison among SL, it makes sense that they appear in a separate cluster or subcluster, respectively. It is somewhat surprising that clustering grouped together array 2 and array 8. However, the aseptic tissue sample from patient 87 used in array 8 is not typical for AL because it contained only few multinucleated foreign body cells but a strong angioneogenesis. This correlation between histomorphology and cluster analysis demonstrates that the array data go well in line with histological findings and that major artifacts concerning RNA isolation and hybridization, for example, can be excluded.

Differentially expressed genes

On at least one array, 388 of 826 genes were found at least twofold differentially expressed. In four or more arrays, 103 of these were found, among which were 33 genes that were differentially expressed in at least four of the six arrays comparing AL with SL, but not in the two control arrays. These 34 genes are of greatest interest, as a differential expression in the intraindividual or intraspecific control would rather be due to the heterogeneity of the tissue. A list of these genes is given in Table 3.

The strongest overexpression in AL showed *msf*. The Cy5/Cy3 ratios were 27.7, 87.8, 90.1, 142.9, 188.5 and 323.0. On the intraspecific control array, a ratio of 20.0 was found, indicating some variability of the *msf* expres-

Table 3 Genes at least two-fold differentially expressed on at least four arrays comparing AL with SL and less than two-fold differentially expressed on both control arrays. *AL* aseptic loosening, *SL*, septic loosening

Overexpressed in AL	On no. of arrays	Differential expression
BCL2-related protein A1	5	2.4–8.0
CD 11b	5	3.1–4.0
CD 18	4	2.5–5.7
CD 36	5	2.2–3.7
CD 37	4	2.4–5.1
CD 52	5	7.3–13.5
CD 53	4	2.3–4.6
CD 68	5	2.3–3.5
CD 74	4	2.1–5.0
CD 83	5	2.4–7.8
CD 86	4	2.1–4.8
Complement 3a receptor 1	4	2.0–3.6
Ferritin heavy-chain	4	2.1–4.3
Immunoglobulin gamma Fc receptor IIc	4	3.5–4.5
Lysosome-associated membrane glycoprotein 2	5	5.0–31.5
Proto-oncogene tyrosine-protein kinase	5	4.4–8.6
Small inducible cytokine B 16	4	2.3–3.7
Overexpressed in SL		
Collagen type 1 a2	4	2.6–14.3
Collagen type 3 a1	5	2.1–7.1
Collagen type 4 a1	4	2.3–4.8
Collagen type 4 a2	4	2.1–7.7
Collagen type 7 a1	4	4.0–7.1
Collagen type 8 a1	4	2.4–5.3
Collagen type 11 a1	6	3.9–50.0
Collagen type 12 a1	4	4.0–16.7
Collagen type 16 a1	4	2.7–12.5
Cadherin 5	4	2.0–2.6
Integrin alpha-1	4	2.0–5.0
Microfibril-associated glycoprotein	5	2.5–6.7
Nidogen	4	2.2–4.4
Platelet-derived growth factor receptor B	4	2.1–4.2
Regulator of G-protein signaling 3	4	3.3–9.1
Thrombospondin 2	4	2.0–4.6

sion. Yet the strong overexpression in aseptic tissue is striking. Therefore, the expression of *msr* was further investigated using real-time RT-PCR.

Real-time RT-PCR analysis of *msf* expression

In order to verify the strong induction (AL versus SL comparison) of *msf* using a different methodology, real-time RT-PCR analysis from six tissue samples from both AL and SL was performed (patient 85, AL; patient 87, AL; samples b, I and g from patient 92, SL; patient 88, SL), which corresponded to the samples used in three microarray experiments. Although the absolute values of *msf* ratios obtained by the two methodologies varied somewhat, overall a good correlation of whether *msf* gene transcripts were overexpressed or repressed could be observed (Fig. 3).

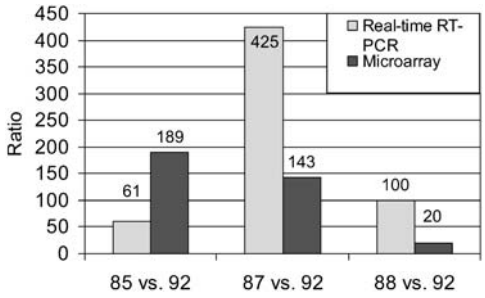

Fig. 3 Comparison of megakaryocyte stimulating factor ratios determined by microarray and real-time reverse-transcription polymerase chain reaction analysis. RNA from two aseptic loosening patients (85 and 87) and two septic loosening patients (92 and 88) were included for the comparative analysis

Discussion

On at least one array, 388 of 826 genes were at least twofold differentially expressed. As this is a high number of genes, it is possible that some expressions are only due to chance [23]. To find those genes that were consistently differentially expressed, we applied two criteria: as two arrays (intraindividual and intraspecific control) compare septic with aseptic tissues, the genes differentially expressed on those arrays seemed to resemble the heterogeneity of the process. So (with the exception of *msf*, which showed the strongest differential expression of all genes and therefore could not be ignored) we did not further investigate genes that appeared on any control array, even if they were also differentially expressed on some of the arrays comparing AL and SL. The second criterion was to investigate only genes that were differentially expressed on at least four of the six arrays comparing AL and SL. These genes are given in Table 3.

Lubricin

The strongest overexpression in aseptic cases of all genes showed *msf*. The differential expression showed ratios between 27.7 and 323.0. However, a ratio of 20.0 was found on the intraspecific control array. So we must assume that one SL patient expressed hardly any *msf*, whereas the other SL patient had a stronger expression. Examination of *msf* RNA levels in a large number of patients will show whether *msf* is suitable to differentiate between AL and SL. Only then might it be regarded as a marker gene. However, the strong overexpression in AL tissue is striking, suggesting an important pathogenetic function of *msf* protein for at least AL and perhaps for some SL patients. *msf* was first described in thrombocytopenic bone marrow transplant patients (Turner et al. 1991) and was found to have stimulating ability on megakaryocytes. It is composed of 12 exons encoding for 1404 amino acids [22]. However, the *msf* gene codes for two other products with possible relevance in joint pathology. Homologous to *msf* precursor protein is a

particular cartilage superficial zone protein, which is a proteoglycan synthesized by chondrocytes and synovial lining cells [10]. The other product of the *msf* gene is lubricin, which is secreted by synovial fibroblasts. Lubricin consists of at least *msf* exons 6 through 9 [15] and is a semi-rigid rod-shaped structure made of about 800 amino acids. It has a repetitive structure and extensive O-glycosylation which is most likely responsible for its lubricating ability [16, 34]. It is the one factor responsible for lubrication of joints [33]. In vitro tests showed that its lubricating ability is equal to that of unfractioned synovial fluid [16].

To further validate the differential *msf* expression in periprosthetic tissue with a microarray-independent approach, we performed real-time RT-PCR analysis of selected tissue samples. The same primers for RT-PCR analysis comprising parts of exon 6 and 7 were chosen as for the *msf* cDNA probes present on the array. The amplified RT-PCR product encodes for the lubricin protein. Overall a good match of *msf* ratios derived by microarray and real-time RT-PCR analysis could be observed. The differences in the absolute ratios might, at least in part, be explained by the different normalization procedures used. The real-time RT-PCR approach confirmed that mRNA coding for lubricin is present in both aseptic and septic periprosthetic tissues. However, the tissue samples derived from patient 92 seemed to lack significant *msf* expression. Here, all comparative approaches either with aseptic or septic samples indicated low expression of *msf* transcripts (Fig. 3). Still, all other tissues analyzed independently, whether they stemmed from aseptic or septic origin, expressed high amounts of *msf* transcripts.

The excellent lubricating ability of the encoded glycoprotein lubricin is essential for healthy joints. However, its synthesis in periprosthetic membranes does not seem desirable. Bone and prosthesis should interact so that the shaft is tightly held by the surrounding tissue. Lubrication of this tissue would reduce the adherence between bone and prosthesis and thereby cause prosthesis loosening. Future studies focusing on the analysis of lubricin protein levels and the site of lubricin secretion inside the periprosthetic membrane will reveal whether our above-mentioned working hypothesis holds true.

Alternatively, as *msf* can be isolated from urine [35], clinical examinations could focus on the urine *msf* level in prosthesis carriers to possibly have a tool for early and non-invasive diagnosis of prosthesis loosening.

Genes resembling the cellular composition of periprosthetic tissue

For this study, whole tissue samples were used and no cell separation was performed. Although arguments have been raised against this approach [9], it has been applied with great success in other fields [36]. Still, there are limits to this method. A high RNA level of certain genes is not necessarily due to an abundant transcription, but can also be explained by the abundant presence of a certain cell type that usually expresses this gene. Fortunately, this problem can be overcome by performing a detailed immuno/histopathological examination of tissue samples. The comparison of those genes with histomorphological and immunohistochemical findings will serve as plausibility control of cDNA array analysis. By applying histopathology and using immunostaining, we determined the different amounts of lymphocytes (CD3, CD20), macrophages (CD68), granulocytes, fibrocytes and endothelial cells (CD34) in aseptic and septic tissue so that we were able to explain the differential expression of a number of genes. Histopathology assured that those tissue sections used for the arrays were characteristic for AL or SL, respectively.

Overexpression in aseptic cases

In general, aseptic tissue contains more T- and B-lymphocytes, macrophages and giant cells, and this is reflected by an overexpression of a multitude of leukocyte surface markers. CD68 is overexpressed between 2.3-fold and 3.5-fold in all arrays except for one array, in which patient sample 87 did not have the typical aseptic appearance but showed fewer macrophages and wear particles and more angioneogenesis.

Other genes whose overexpression in AL can be explained by a higher number of lymphocytes, macrophages or giant cells are encoding CD 11b, CD18, CD36, CD37, CD52, CD53, CD74, CD83, CD107b, Bcl2-related protein A1, C-X-C chemokine receptor type 4, small inducible cytokine B16 (also known as CXCL16, which is a strong transmembrane chemoattractant) [21], low affinity immunoglobulin gamma Fc region receptor II-C and complement factor 3a receptor 1 (Table 3).

Not much is known about the tissue distribution of complement factor 3a receptor 1, which is present on macrophages, platelets, granulocytes and mast cells [25]. As the density of macrophages in AL is higher than that of granulocytes in SL, the complement factor 3a receptor 1 overexpression in AL is plausible; however, the involvement of the complement system in AL is surprising.

CD 11b and CD 18 together form the complement factor 3 receptor, which occurs not only on macrophages and granulocytes but is also a marker of natural killer (NK) cells. Little is known about their role in prosthesis loosening. Case et al. (2000) found a significant increase in the relative proportion of CD16-positive NK cells in the peripheral blood at revision arthroplasty compared with primary arthroplasty in a study of 83 patients [4], whereas Savarino et al. (1999) found a significant decrease of NK cells in the blood of patients with AL relative to patients without joint replacement [31]. Further investigation seems required for a better understanding of the role of NK cells in prosthesis loosening.

Osteopontin functions include macrophage and lymphocyte recruitment as part of a nonspecific immunolog-

ical response [28]. This fits the overexpression of osteopontin in AL. It is also one of the most abundant noncollagenous proteins in bone, and it plays an important role in bone formation and turnover [32]. Bone turnover occurs in both AL and SL. The overexpression of osteopontin in AL might indicate a pathogenetic contribution to AL, whereas SL might be osteopontin independent.

Very surprisingly, some expected genes with known contribution to chronic inflammation were not constantly differentially expressed, and some were not even detected. Among these were all interleukin subtypes 1 to 18, tumor necrosis factor (TNF) subtypes alpha and beta and interferon gamma. Interferon gamma was only detected on one array, TNFα and TNFβ were not detected on any array. Interleukin subtypes were detected, but not constantly differentially expressed. Regarding these data, one must say that interleukins, interferons and TNF have no key roles as mediators in prosthesis loosening.

According to this, it is surprising that ferritin heavy-chain (FTH) is overexpressed in AL. It has been shown that TNFα and interleukin 1 stimulate FTH synthesis [37], suggesting that FTH is involved in inflammatory processes. Its overexpression in AL might be explained by the fact that FTH was found to be expressed by T-helper 1 lymphocytes after stimulation with mycobacterial antigen [18]. Thus, it is possible that FTH is involved in the macrophage–T-cell interaction and the formation of multinucleated cells.

Proto-oncogene tyrosine-protein kinase, which is part of intracellular signaling pathways, is upregulated in AL, but its function is hard to interpret. Gentzsch et al. (2002) demonstrated an overexpression of nine cytokines (e.g., calgranulin A and B, interleukin 10, thymosin beta 10) in AL. None of these cytokines was found overexpressed in our present study. This can be explained by the use of a different reference tissue, which was skeletal muscle in the study of Gentzsch et al., by the use of different microarrays and by different evaluation algorithms [11].

Overexpression in septic cases

Except for the granulocytes, septic cases exhibit morphologically a lesser inflammatory infiltrate of CD68+ macrophages, but exhibit dense angioneogenesis and fibroblasts, which was proven by the immune and routine histopathological analysis. The overexpression of many different collagen transcripts resembles the fibroblast activity. This is especially true for array 4 (patient 85, AL vs patient 92, SL), in which genes encoding all collagens from 1 to 18 except for 2, 9 and 13 are overexpressed in SL. Collagen subtype genes overexpressed in at least four experiments are (alpha-1 or alpha-2 chain, respectively) *collagen 1a2, 3a1, 4a1, 4a2, 7a1, 8a1, 11a1, 12a1* and *16a1*. It is unclear why fibroblasts inside the periprosthetic membrane apparently produce different kinds of collagens that are normally not ubiquitously expressed. Interestingly, RNA for collagen type 2 was not detectable in the tissues analyzed. The absence of collagen type 2 was noticed before by Wooley et al. (1999) in an analysis of proteins bound to polyethylene components. They examined periprosthetic tissue of 42 explants and detected collagen type 1 and immunoglobulin in most specimens, aggrecan proteoglycans in some specimens, but collagen type 2 in no specimens [40].

The overexpression of integrin alpha-1 in SL can be explained by the higher density of mesenchymal cells (namely fibroblast). Integrins mediate cell adhesion to extracellular matrix components. A recent study of mice demonstrated the importance of collagen-integrin interaction in fracture healing [8], which is closely related to the conditions in the periprosthetic compartment where tissue damage and tissue regeneration occur permanently. Also microfibril-associated glycoprotein, which is a widespread product of mesenchymal/connective tissue cells [5], and thrombospondin 2, which has been shown to be produced by fibroblasts [1], are overexpressed in SL.

Beta platelet-derived growth factor receptor (also known as CD140b) is also overexpressed in SL. It is found in endothelial cells and can therefore be explained by the strong angioneogenesis in septic tissue [29]. The same is true for Nidogen, which is a basement membrane protein. Matrix metalloproteinase (MMP) 14, known equally as membrane-type 1 MMP, which has recently been shown to be involved in angioneogenesis [41], was also overexpressed in SL.

MMPs, enzymes responsible for extracellular matrix digestion, would be expected to be overexpressed in AL, as it is known that their secretion leads to bone loss and hence to prosthesis loosening [42]. However, no MMP subtype is consistently differentially expressed, although most appear also on the control arrays and most are, in fact, overexpressed in SL like MMP 13 (overexpressed on six arrays from 2.4-fold to 16.7-fold). This suggests a more important role for MMPs in SL than in AL.

Two genes of intracellular signaling pathway proteins are differentially expressed. However, their function regarding prosthesis loosening is hard to interpret. These genes are an encoding regulator of G-protein signaling and secreted frizzled-related sequence protein 4.

The complete list of differentially expressed genes can be downloaded from our homepage: http://www.charite.de/ch/patho/.

This study was undertaken to reveal genes relevant for the pathogenesis of prosthesis loosening. It is viewed as a preliminary search for potentially interesting genes. *msf* showed a strong expression in AL and one SL patient, suggesting an important pathogenetic role of lubricin. To prove definite pathomechanisms, further investigation of lubricin and other candidate genes by means of immunohistochemistry and other established methods is promising.

Acknowledgements We thank Prof. Reinhold Schäfer and Mrs. Claudia Campisi for their lectorship. The technical assistance of Mrs. Gabriele Fernahl and Mrs. Janine Karle is gratefully acknowledged. The present work was partially supported by the

SFB421 and by the Gemeinnütziger Verein ENDO-Klinik e.V., Hamburg (project W1/01, T.G., L.F., M.D., V.K.).

References

1. Armstrong LC, Bjorkblom B, Hankenson KD, Siadak AW, Stiles CE, Bornstein P (2002) Thrombospondin 2 inhibits microvascular endothelial cell proliferation by a caspase-independent mechanism. Mol Biol Cell 13:1893–1905
2. Berry DJ, Harmsen WS, Cabanela ME, Morrey BF (2002) Twenty-five-year survivorship of two thousand consecutive primary Charnley total hip replacements: factors affecting survivorship of acetabular and femoral components. J Bone Joint Surg Am 84:171–177
3. Boss JH, Shajrawi I, Mendes DG (1994) The nature of the bone-implant interface. Med Prog Technol 20:119–142
4. Case CP, Langkamer VG, Lock RJ, Perry MJ, Palmer MR, Kemp AJ (2000) Changes in the proportions of peripheral blood lymphocytes in patients with worn implants. J Bone Joint Surg Br 82:748–754
5. Chen Y, Faraco J, Yin W, Germiller J, Francke U, Bonadio J (1993) Structure, chromosomal localization, and expression pattern of the murine Magp gene. J Biol Chem 268:27381–27389
6. Chomczynski P (1993) A reagent for the single-step simultaneous isolation of RNA, DNA and proteins from cell and tissue samples. Biotechniques 15:532–537
7. Eisen MB, Spellman PT, Brown PO, Botstein D (1998) Cluster analysis and display of genomewide expression patterns. Proc Natl Acad Sci U S A 95:14863–14868
8. Ekholm E, Hankenson KD, Uusitalo H, Hiltunen A, Gardner H, Heino J, Penttinen R (2002) Diminished callus size and cartilage synthesis in alpha 1 beta 1 integrin-deficient mice during bone fracture healing. Am J Pathol 160:1779–1785
9. Firestein GS, Pisetsky DS (2002) DNA microarrays: boundless technology or bound by technology? Guidelines for studies using microarray technology. Arthritis Rheum 46:859–861
10. Flannery CR, Hughes CE, Schumacher BL, Tudor D, Aydelotte MB, Kuettner KE, Caterson B (1999) Articular cartilage superficial zone protein (SZP) is homologous to megakaryocyte stimulating factor precursor and is a multifunctional proteoglycan with potential growth-promoting, cytoprotective, and lubricating properties in cartilage metabolism. Biochem Biophys Res Commun 254:535–541
11. Gentzsch C, Kaiser E, Plutat J, Sellckau R, Wodtke J, Delling G (2002) CDNA array approach to cytokine expression profile of aseptic loosened hip arthroplasty. Pathologe 23:373–378
12. Goldring SR, Jasty M, Roelke MS, Rourke CM, Bringhurst FR, Harris WH (1986) Formation of a synovial-like membrane at the bone-cement interface. Its role in bone resorption and implant loosening after total hip replacement. Arthritis Rheum 29:836–842
13. Hahn M, Vogel M, Schultz C, Niecke M, Delling G (1992) Histologic reactions of the bone-implant zone and cortical bone area after long-term hip replacement (in German). Chirurg 63:958–963
14. Harvard Health Letter Authors (2002) Arthritis. Hip replacement. Harv Health Lett 27:4–5
15. Jay GD, Britt DE, Cha CJ (2000) Lubricin is a product of megakaryocyte stimulating factor gene expression by human synovial fibroblasts. J Rheumatol 27:594–600
16. Jay GD, Tantravahi U, Britt DE, Barrach HJ, Cha CJ (2001) Homology of lubricin and superficial zone protein (SZP): products of megakaryocyte stimulating factor (*msf*) gene expression by human synovial fibroblasts and articular chondrocytes localized to chromosome 1q25. J Orthop Res 19:677–687
17. Jellicoe PA, Cohen A, Campbell P (2002) Haemophilus parainfluenzae complicating total hip arthroplasty: a rapid failure. J Arthroplasty 17:114–116
18. Lim JS, Lee SH, Lee E, Kang Y, Kim JW, Kim JK, Kim HH, Lee C, Kim SJ, Bai GH, Lee HG, Kim KD, Chung TW, Choe YK (1997) Differential expression of ferritin heavy chain in THP-1 cells infected with Mycobacterium bovis BCG. Biochem Mol Biol Int 43:981–988
19. Livak KJ, Schmittgen TD (2001) Analysis of relative gene expression data using real-time quantitative PCR and the 2(-Delta Delta C(T)) method. Methods 25:402–408
20. Maloney WJ, Smith RL (1996) Periprosthetic osteolysis in total hip arthroplasty: the role of particulate wear debris. Instr Course Lect 45:171–182
21. Matloubian M, David A, Engel S, Ryan JE, Cyster JG (2000) A transmembrane CXC chemokine is a ligand for HIV-coreceptor Bonzo. Nat Immunol 1:298–304
22. Merberg DM, Fitz LJ, Temple P, Giannotti J, Murtha P, Fitzgerald M, Scaltreto J, Kelleher K, Preissner K, Kriz R, Jacobs K, Turner K (1993) A comparison of vitronectin and megakaryocyte stimulating factor. In: Preissner KT, Rosenblatt S, Kost C, Wegerhoff J, Mosher DF (eds) Biology of vitronectins and their receptors. Elsevier, New York, pp 45–52
23. Mills JC, Gordon JI (2001) A new approach for filtering noise from high-density oligonucleotide microarray datasets. Nucleic Acids Res 29:E72
24. Mirra JM, Amstutz HC, Matos M, Gold R (1976) The pathology of the joint tissues and its clinical relevance in prosthesis failure. Clin Orthop 117:221–240
25. Monsinjon T, Gasque P, Ischenko A, Fontaine M (2001) C3A binds to the seven transmembrane anaphylatoxin receptor expressed by epithelial cells and triggers the production of IL-8. FEBS Lett 487:339–346
26. Ortega-Andreu M, Rodriguez-Merchan EC, Aguera-Gavalda M (2002) Brucellosis as a cause of septic loosening of total hip arthroplasty. J Arthroplasty 17:384–387
27. Pandey R, Drakoulakis E, Athanasou NA (1999) An assessment of the histological criteria used to diagnose infection in hip revision arthroplasty tissues. J Clin Pathol 52:118–123
28. Patarca R, Saavedra RA, Cantor H (1993) Molecular and cellular basis of genetic resistance to bacterial infection: the role of the early T-lymphocyte activation-1/osteopontin gene. Crit Rev Immunol 13:225–246
29. Plate KH, Breier G, Farrell CL, Risau W (1992) Platelet-derived growth factor receptor-beta is induced during tumor development and upregulated during tumor progression in endothelial cells in human gliomas. Lab Invest 67:529–534
30. Santavirta S, Sorsa T, Konttinen YT, Saari H, Eskola AS, Eisen AZ (1993) Role of mesenchymal collagenase in the loosening of total hip prosthesis. Clin Orthop 290:206–215
31. Savarino L, Granchi D, Ciapetti G, Stea S, Donati ME, Zinghi G, Fontanesi G, Rotini R, Montanaro L (1999) Effects of metal ions on white blood cells of patients with failed total joint arthroplasties. J Biomed Mater Res 47:543–550
32. Sodek J, Ganss B, McKee MD (2000) Osteopontin. Crit Rev Oral Biol Med 11:279–303
33. Swann DA, Hendren RB, Radin EL, Sotman SL, Duda EA (1981) The lubricating activity of synovial fluids. Arthritis Rheum 24:22–30
34. Swann DA, Silver FH, Slayter HS, Stafford W (1985) The molecular structure and lubricating ability of lubricin isolated from bovine and human synovial fluids Biochem J 225:195–201
35. Turner KJ, Fitz LJ, Temple P, Jacobs K, Larson D, Leary AC, Kelleher K, Giannotti J, Calvetti J, Fitzgerald M, Kriz MJ, Ferenz C, Grobholz J, Fraser H, Bean K, Norton CR, Gesner T, Bhatia S, Kriz R, Hewick R, Clark SC (1991) Purification, biochemical characterization, and cloning of a novel megakaryocyte stimulating factor that has megakaryocyte colony stimulating activity (abstract). Blood 78:279
36. van 't Veer LJ, Dai H, van de Vijver MJ, He YD, Hart AA, Mao M, Peterse HL, van der Kooy K, Marton MJ, Witteveen AT, Schreiber GJ, Kerkhoven RM, Roberts C, Linsley PS, Bernards R, Friend SH (2002) Gene expression profiling predicts clinical outcome of breast cancer. Nature 415:530–536

37. Wei Y, Miller SC, Tsuji Y, Torti SV, Torti FM (1990) Interleukin 1 induces ferritin heavy chain in human muscle cells. Biochem Biophys Res Commun 169:289–296
38. Weyand CM, Geisler A, Brack A, Bolander ME, Goronzy JJ (1998) Oligoclonal T-cell proliferation and interferon-gamma production in periprosthetic inflammation. Lab Invest 78:677–685
39. Willert HG (1977) Reactions of the articular capsule to wear products of artificial joint prostheses. J Biomed Mater Res 11:157–164
40. Wooley PH, Fitzgerald RH, Song Z, Davis P, Whalen JD, Trumble S, Nasser S (1999) Proteins bound to polyethylene components in patients who have aseptic loosening after total joint arthroplasty. A preliminary report. J Bone Joint Surg Am 81:616–623
41. Yamaguchi S, Yamaguchi M, Yatsuyanagi E, Yun SS, Nakajima N, Madri JA, Sumpio BE (2002) Cyclic strain stimulates early growth response gene product 1-mediated expression of membrane type 1 matrix metalloproteinase in endothelium. Lab Invest 82:949–956
42. Yokohama Y, Matsumoto T, Hirakawa M, Kuroki Y, Fujimoto N, Imai K, Okada Y (1995) Production of matrix metalloproteinases at the bone-implant interface in loose total hip replacements. Lab Invest 73:899–911

Virchows Arch (2003) 443:67–77
DOI 10.1007/s00428-003-0827-x

ORIGINAL ARTICLE

Hirofumi Makino · Hitoshi Sugiyama · Yasushi Yamasaki · Yohei Maeshima · Jun Wada · Naoki Kashihara

Glomerular cell apoptosis in human lupus nephritis

Received: 27 January 2003 / Accepted: 10 April 2003 / Published online: 15 May 2003
© Springer-Verlag 2003

Abstract Disturbed apoptosis is proposed to be involved in the pathogenesis of systemic lupus erythematosus. However, the role of renal cell apoptosis in the pathogenesis and progression of human lupus nephritis is still controversial. We have investigated glomerular cell apoptosis and the clinicopathological relationship between apoptosis and immunoserological or histological findings in 22 patients with lupus nephritis using electron microscopy and the TdT-mediated dUTP-biotin nick end labeling (TUNEL) method. Resident glomerular cells as well as infiltrating neutrophils undergoing apoptosis were observed in 12 of 20 patients with lupus nephritis using electron microscopy. TUNEL-positive cells were recognized in 93% of patients with diffuse proliferative lupus nephritis (class IV) in contrast to the 20% of patients with class V. The number of TUNEL-positive cells in glomeruli significantly correlated with the level of immunoserological activity of lupus, such as anti-double-stranded DNA autoantibody and consumption of plasma complement. There was a positive correlation between glomerular cell apoptosis and the degree of proliferation in lupus nephritis. These data suggest that apoptosis is increased, but not decreased in glomeruli from patients with lupus nephritis. The signals that could induce glomerular cell apoptosis in lupus nephritis will need to be identified.

Keywords Apoptosis · Lupus nephritis · Mesangial cell · Electron microscopy · Anti-double-stranded DNA antibody

H. Makino (✉) · H. Sugiyama · Y. Yamasaki · Y. Maeshima · J. Wada
Department of Medicine and Clinical Science,
Okayama University Graduate School of Medicine and Dentistry,
2-5-1 Shikata-cho, 700-8558 Okayama, Japan
e-mail: makino@md.okayama-u.ac.jp
Tel.: +81-86-2357232, Fax: +81-86-2225214

N. Kashihara
Division of Nephrology,
Department of Internal Medicine, Kawasaki Medical School,
Kurashiki, Japan

Introduction

Lupus nephritis is one of the most severe forms of organ failure in systemic lupus erythematosus [7]. The condition progresses to end-stage renal failure that requires hemodialysis or kidney transplantation unless properly treated. The nephritis is histologically characterized by active lesions such as glomerular hypercellularity including leukocyte infiltration, nuclear karyorrhexis, fibrinoid necrosis, cellular crescents, subendothelial deposits, hematoxylin bodies, hyaline thrombi, vasculitis, interstitial mononuclear cell infiltrates, and edema. Another pathological characteristic is chronic lesions in the form of scarring or reparative processes such as glomerular sclerosis, fibrous crescents, adhesions, tubular atrophy, interstitial fibrosis, and arteriolosclerosis. These active and chronic lesions are of crucial importance in determining the prognosis and response to corticosteroid therapy for the affected patients [1, 2, 14, 15].

Apoptosis is a highly programmed form of cell death that plays a crucial role in physiological processes such as embryogenesis and normal cell turnover, as well as in some pathological conditions such as neurodegenerative disorders and tissue fibrosis [11, 30]. Defects of apoptosis are considered to be important in the development of human autoimmune disorders. Lack of this programmed cell death may cause a failure to delete self-reactive T cells during lymphocyte development [16, 17]. The unsuccessful clearance of apoptotic cells may result in the leakage of cytoplasmic contents and nucleosomes from dying cells and may trigger autoimmune responses [5] and exacerbate tissue injury around the cell [22]. Apoptosis of maturing T cells is involved in establishing and maintaining immune tolerance, and a disturbed apoptosis may cause a breakdown of tolerance [29].

It is, however, unclear whether renal cell apoptosis plays a role in human lupus nephritis. In this regard, several controversial studies have been reported. Soto et al. reported the decreased apoptosis in renal biopsies from 19 patients with lupus nephritis [World Health Organization (WHO) class IV; 11 cases, class V; 8 cases] [24].

They concluded that intense proliferation without apoptosis is a characteristic feature of lupus nephritis with chronic renal damage. The data are inconsistent with our previous study demonstrating the increased number of TUNEL-positive cells in the glomerulus of proliferative lupus nephritis (WHO class IV) [25]. Takemura et al. reported upregulation of glomerular Fas death receptor in diffuse proliferative lupus nephritis (WHO class IV) and the expression of Fas paralleled the number of fragmented DNA detected by TdT-mediated dUTP-biotin nick end labeling (TUNEL) in several proliferative glomerulonephritis, including purpura nephritis [27]. They studied a relatively low number of lupus nephritis (six) patients, and the study failed to demonstrate the precise relationship between the level of apoptosis and the degree of glomerular tissue injury in lupus nephritis or immunoserological activity of lupus. The report showed two electron micrographs of apoptotic cells in glomeruli of patients with lupus nephritis, but the precise morphology of glomerular cell apoptosis in lupus is still uncertain.

The most reliable evidence of apoptosis is ultrastructural morphology. To extend our previous study [25], we increased the number of patients, and extensive ultrastructural studies were performed focusing on lupus nephritis. Therefore, the purpose of our study is: (1) to demonstrate ultrastructural evidence of glomerular cell apoptosis in human lupus nephritis by electron microscopy (EM); (2) to investigate the role of apoptosis in tissue injury such as active or chronic glomerular lesions characteristic of human lupus nephritis; and (3) to examine the relationship between the level of glomerular cell apoptosis and immunoserological activity of lupus.

Materials and methods

Experimental design

The presence of apoptosis was assessed in renal biopsy specimens from 22 patients with lupus nephritis (Table 1). Renal biopsy specimens were studied using routine light and immunofluorescent microscopy. Since apoptosis is best confirmed with EM, extensive EM study was performed on renal biopsy specimens from 22 patients. In addition, DNA fragmentation associated with apoptosis was detected in situ using the TUNEL method as previously described [10, 25, 26]. In tissue specimens stained by the TUNEL method, the number of positive-staining nuclei per glomerulus was determined as the glomerular TUNEL score [25, 26]. Relationships between the TUNEL score and the histological index and clinical data were assessed.

Patients

Twenty-two patients with lupus nephritis who met the Classification of Systemic Lupus Erythematosus criteria established by the American Rheumatism Association [28] and underwent renal biopsy participated in this study with written informed consent (Table 1). Classification of lupus nephritis was according to the criteria defined by the WHO [8]. The diagnosis was confirmed on the basis of clinical symptoms, immunoserological findings, and routine light and immunofluorescence microscopy. Glomerular cell proliferation and glomerular sclerosis indices, and the activity and chronicity indices were determined as described [3, 14, 15]. Laboratory findings, including anti-double-stranded DNA autoantibody and plasma complement activity (CH50) as immunoserological indices of lupus, were examined at the time of renal biopsy. Other clinical data obtained from the patients included serum creatinine concentration, creatinine clearance, and daily urinary protein excretion (Table 1). Glucocorticoids were administered to 20 of 22 patients at the time of biopsy. There were two cases with different treatment regimens other than steroids, including cyclophosphamide. Informed consent was obtained from all patients prior to commencement of the study.

Light and immunofluorescent microscopic studies

Percutaneous renal biopsy was performed using a 16-gauge needle under ultrasound observation. The length of each biopsy specimen was approximately 15–20 mm, and two samples were taken from each patient. Renal biopsy specimens were divided into three portions, and a part of the specimen was fixed in 10% buffered formalin and embedded in paraffin. Sections 4 μm thick were stained with hematoxylin and eosin (HE), periodic acid-Schiff, Masson's trichrome, or periodic acid-silver methnamine stains. The number of apoptotic cells per glomerulus stained with HE was assessed as the glomerular HE apoptosis score [25, 26]. Tubulointerstitial injury was semi-quantified as follows: 0 none or trace, 1 mild, 2 moderate, and 3 severe. Another portion of the renal biopsy specimen was processed for immunofluorescent microscopy as described previously [12]. In brief, kidney specimens were immediately snap frozen and 4-μm-thick sections were prepared. The cryostat sections were stained with anti-human IgG, IgA, IgM, C3, C1q, and fibrinogen conjugated with fluorescein isothiocyanate (Cappel Co., West Chester, PA).

Table 1 Study population and clinical findings in patients with lupus nephritis

World Health Organization*	Cases (*n*)	Age (years)	Male/ female	Proteinuria (g/day)	Serum creatinine (mg/dl)	Creatinine clearance (ml/min)	Anti-DNA antibody (mg/dl)	CH50 (U/ml)
II	1	49	0/1	0.5	0.8	61	41	32
IV	15	32±9	4/11	2.6±3.0	1.2±1.0	63±31	116±136	23±8
a)	2	38±13	1/1	0.2±0.1	0.7±0.1	86±7	68±93	24±17
b)	9	29±7	3/6	3.2±3.4	0.9±0.3	65±30	142±165	20±6
c)	4	33±13	0/4	2.4±2.3	1.8±1.8	46±38	81±75	28±3
V	5	31±4	0/5	3.3±2.3	1.5±1.5	71±32	15±15	30±10
VI	1	67	1/0	0.4	3.7	17	5	17
Total	22	34±12	5/17	2.6±2.7	1.3±1.2	62±31	84±120	25±8

* World Health Organization classification of lupus nephritis [8]

EM studies

The rest of the renal biopsy specimen was processed for transmission EM as previously described [13]. The specimens were fixed with 2.5% glutaraldehyde in 0.1 M cacodylate buffer (pH 7.4) for 2 h, post-fixed with 1% osmium tetroxide, and embedded in Epon 812. Ultrathin sections were cut with a diamond knife (Diatome) using a Reichert-ultracut E microtome. After double staining with uranyl acetate and lead citrate, the sections were viewed with an electron microscope (Hitachi H-7000, Hitachi, Tokyo, Japan) with an accelerating voltage of 75 kV. Glomeruli were extensively studied by serial sections to detect apoptosis, and one to three glomeruli were observed in a total of 20 patients.

TUNEL method to detect DNA fragmentation in tissue sections

DNA fragmentation associated with apoptosis was detected in situ by the addition of biotinylated nucleotides to free 3′ hydroxyl groups in DNA according to the method of Gavrieli et al. [10, 25, 26]. The formalin-fixed, paraffin-embedded sections were incubated with proteinase K (20 μg/ml, Boehringer Mannheim/Yamanouchi, Tokyo, Japan). Endogenous peroxidase was inactivated by covering the sections with 2% H_2O_2. The sections were immersed in terminal deoxynucleotidyl transferase (TdT) buffer (Gibco, Gaithersburg, MD) and then incubated with TdT (0.3 e.u./μl, Gibco) and biotinylated dUTP (0.04 nmol/μl, Boehringer Mannheim/Yamanouchi) at 37°C for 90 min. The reaction was terminated by transferring the slides to TB buffer (30 mM sodium citrate, 300 mM sodium chloride) for 30 min at room temperature (RT). The sections were covered with 10% normal rabbit serum for 10 min to block non-specific protein adsorption. The slides were then incubated with peroxidase-labeled streptavidin (Seikagaku Corp., Tokyo, Japan) for 30 min, washed in phosphate buffered saline (PBS), and finally stained with 0.02% 3.3′-diaminobenzidine in 50 mM Tris-HCl buffer containing 0.02% H_2O_2 for 10 min at RT. The TUNEL-positive cells were counted in all glomeruli (3–14 glomeruli per specimen) in each biopsy. The mean number of positive-staining nuclei per glomerulus was determined as the glomerular TUNEL score [25, 26]. Each score was compared to the histological indices and clinical parameters. Serial sections used for TUNEL were stained with HE to examine the morphological changes of TUNEL-positive cells.

Statistical analysis

Statistical evaluation of the quantitative data was carried out by the Mann-Whitney U test and Spearman's rank coefficients. $P<0.05$ was accepted as statistically significant.

Results

Following extensive EM study, apoptosis was observed in the glomeruli of renal biopsy specimens from 12 of 20 patients (60%) with lupus nephritis. A high prevalence of apoptosis was observed in those with diffuse proliferative

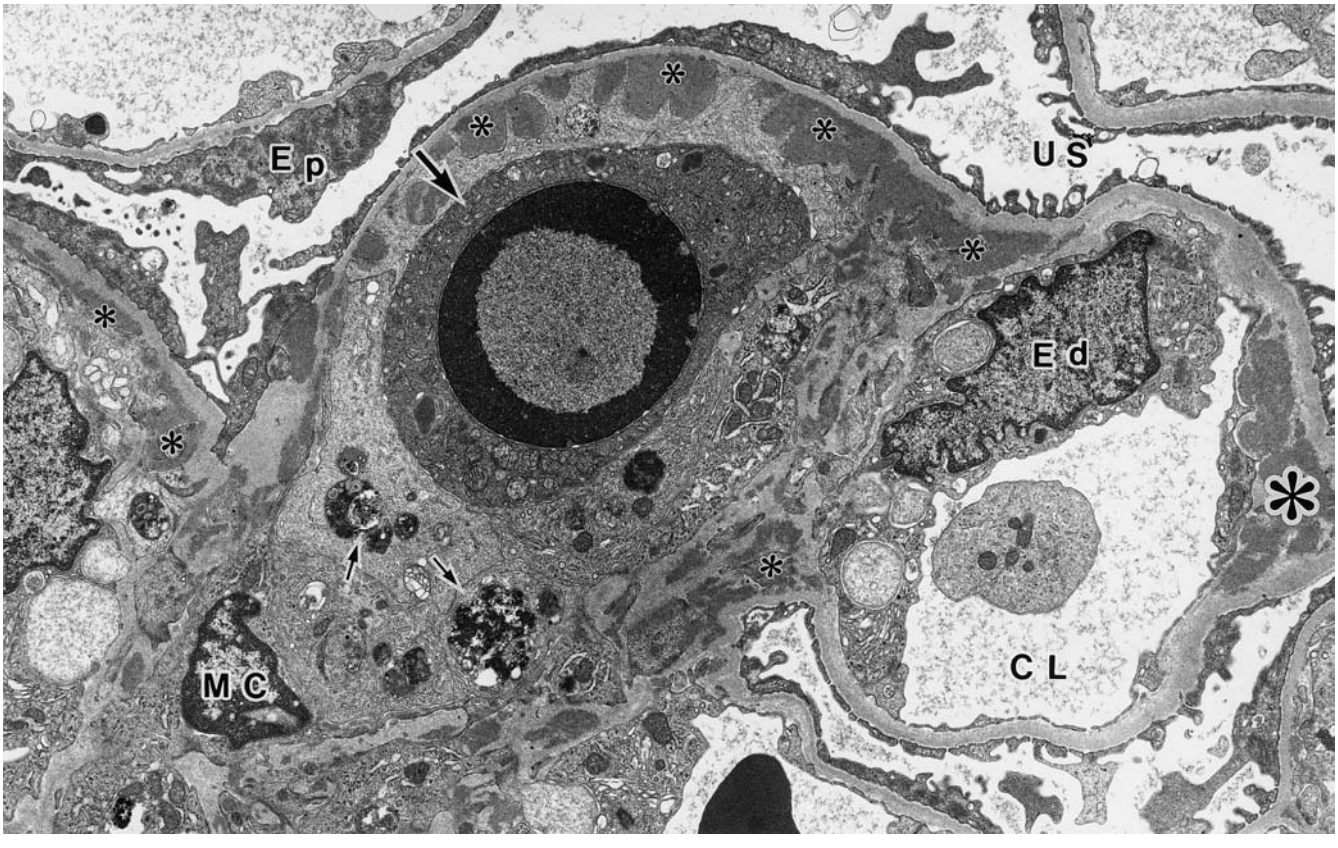

Fig. 1 Apoptosis in the glomerular mesangium. An electron micrograph of a renal biopsy specimen from a 33-year-old woman with diffuse proliferative lupus nephritis (World Health Organization class IVb) is shown. Note the characteristic condensed chromatin of the nucleus (*large arrow*) and the residual bodies (*small arrows*) in the mesangium accompanied by massive mesangial deposits (*small asterisk*). *US* urinary space, *Ep* epithelial cell, *Ed* endothelial cell, *MC* mesangial cell, *CL* capillary lumen, large asterisk (*right middle*), subendothelial deposit. *Magnification* ×7500

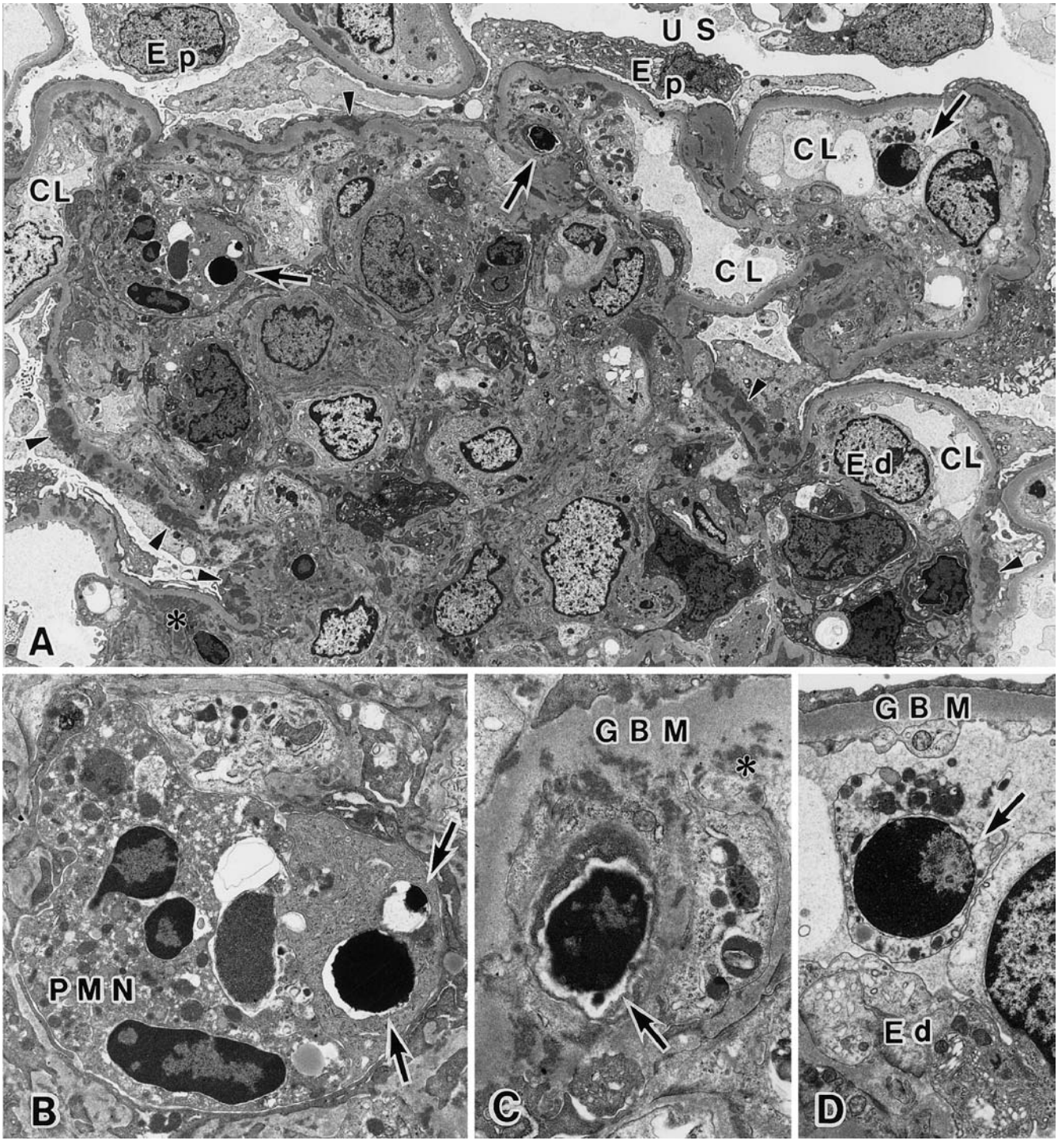

Fig. 2 Multiple apoptotic cells in the hypercellular lesion of glomerulus. Electron micrographs of a renal biopsy specimen from a 24-year-old woman with diffuse proliferative lupus nephritis (World Health Organization class IVc) are shown. **A** Lower magnification view showing apoptotic cells in the mesangial lesion (*left and center arrows*) and the capillary lumen (*right arrow*). *Arrowheads* indicate subepithelial deposits. An *asterisk* shows mesangial deposits (*left lower*). **B–D** Higher magnification of **A**. **B** An infiltrative neutrophil is ingesting two apoptotic bodies in the cytoplasm (*arrows*). **C** Nuclear condensation surrounded by a vacuole in the mesangial lesion (*arrow*). An *asterisk* indicates a mesangial deposit. **D** An infiltrating neutrophil is becoming apoptotic in the capillary lumen showing crescentic condensation of the nuclear chromatin. *US* urinary space, *Ep* epithelial cell, *Ed* endothelial cell, *PMN* polymorphonuclear leukocyte, *CL* capillary lumen, *GBM* glomerular basement membrane, *small asterisk*, mesangial deposit. *Magnification* **A** ×2500. **B** ×7500. **C** ×12,000. **D** ×7500

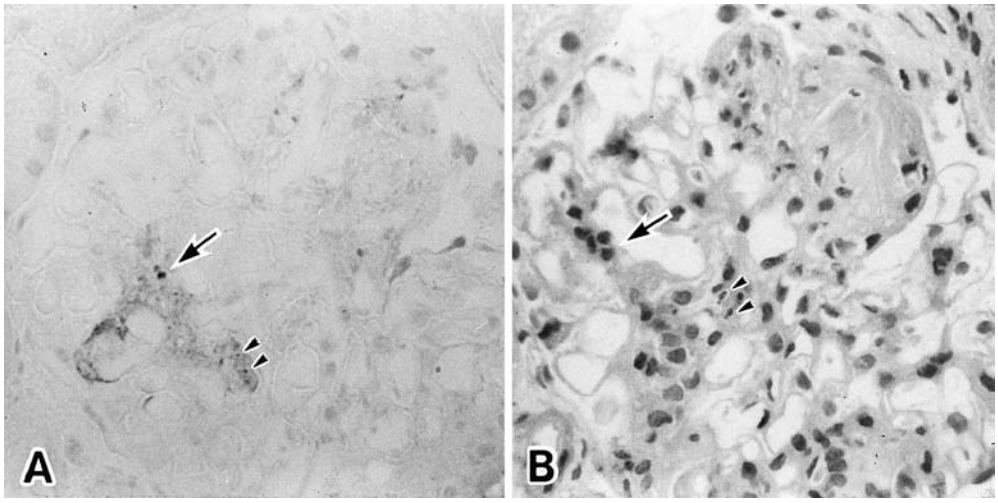

Fig. 3 TUNEL-positive cells in the active lesion of glomerulus. TdT-mediated DNA nick end-labeling (TUNEL) of glomerulus (**A**) and a serial section stained with hematoxylin and eosin (**B**) from a 23-year-old woman with diffuse proliferative lupus nephritis (World Health Organization class IVc) are shown. Note the TUNEL-positive cell in the proliferative lesion of glomerulus (*arrow*) and two apoptotic bodies surrounded by haloes (*arrowheads*) associated with karyorrhexis. *Magnification* ×400

lupus nephritis (WHO class IV) involving 10 of 13 patients (77%). Apoptosis was not observed in the glomeruli from six patients with IgA nephropathy.

Apoptosis in active lesions in diffuse proliferative lupus nephritis

One of the characteristic features in lupus nephritis is a severe form of glomerular cell proliferation and leukocyte infiltration in diffuse proliferative glomerulonephritis. Using light microscopy, it was occasionally difficult to distinguish apoptotic cells from infiltrated leukocytes or other cells. Using EM, a glomerular apoptotic cell characterized by margination of nuclear chromatin was observed in the mesangial lesions of class-IVb lupus nephritis with massive mesangial electron-dense deposits (Fig. 1). Infiltrating neutrophils undergoing apoptosis were observed in the glomerular capillary lumen in other patients with class-IVc lupus nephritis (Fig. 2A, D). Nuclear fragments with crescentic condensation of the chromatin within discrete, well-preserved cytoplasmic fragments characterized the early stage of apoptosis (Fig. 1 and Fig. 2D). In the advanced stage of apoptosis, apoptotic bodies were phagocytosed by polymorphonuclear leukocytes in the mesangial lesions (Fig. 2B, C). TUNEL technique stained a few nuclear fragments in the proliferative lesion of class-IVc lupus nephritis. Karyorrhexis defined by the presence of pyknotic and fragmented nuclei was stained using the TUNEL method (Fig. 3).

Apoptosis in chronic lesions in lupus nephritis

Apoptotic cells also were observed in glomerular sclerotic lesions by electron (Fig. 4) and light microscopy (data not shown), especially in those associated with segmental sclerosis. Serial thin sectioning revealed the various plane of an apoptotic cell, ranging from crescentic to diffuse condensation of the chromatin in class-IVc lupus nephritis (Fig. 4A–C). TUNEL-positive cells were identified in collapsing glomeruli with fibrous crescent formation (Fig. 5). Degradation of ingested apoptotic cells, most likely within the mesangial cells, was observed in chronic lesions of a patient with lupus nephritis (WHO class IVc) (Fig. 6). We observed crescents in 7 of 22 lupus patients in this study. Crescent formation is one of the pathways that lead to glomerular dysfunction and sclerosis. Crescents transform from cellular to fibrous. We observed apoptosis in fibrocellular crescents by EM. A pair of apoptotic cells was occasionally observed in a row (Fig. 7). Apoptosis may thus be related to the progression of crescents from a cellular to fibrous stage.

Frequency of DNA fragmentation in lupus nephritis

As only a few glomeruli were available for EM study and the identification of apoptotic cells was often difficult by light microscopy, the presence of apoptosis was also assessed utilizing the TUNEL method to detect DNA fragmentation in situ in human tissue sections. TUNEL-positive cells were identified in the glomeruli of 16 of 22 patients (73%) with lupus nephritis in total (Table 2). The glomeruli from 14 of 15 patients (93%) with diffuse proliferative lupus nephritis (WHO class IV) contained TUNEL-positive cells. In contrast, only one of the remaining five patients (20%) with lupus nephritis (WHO class V) had TUNEL-positive cells in glomeruli. The number of glomerular apoptotic cells (TUNEL score) was highest in patients with diffuse proliferative lupus nephritis, particularly WHO classes IVb (active "necro-

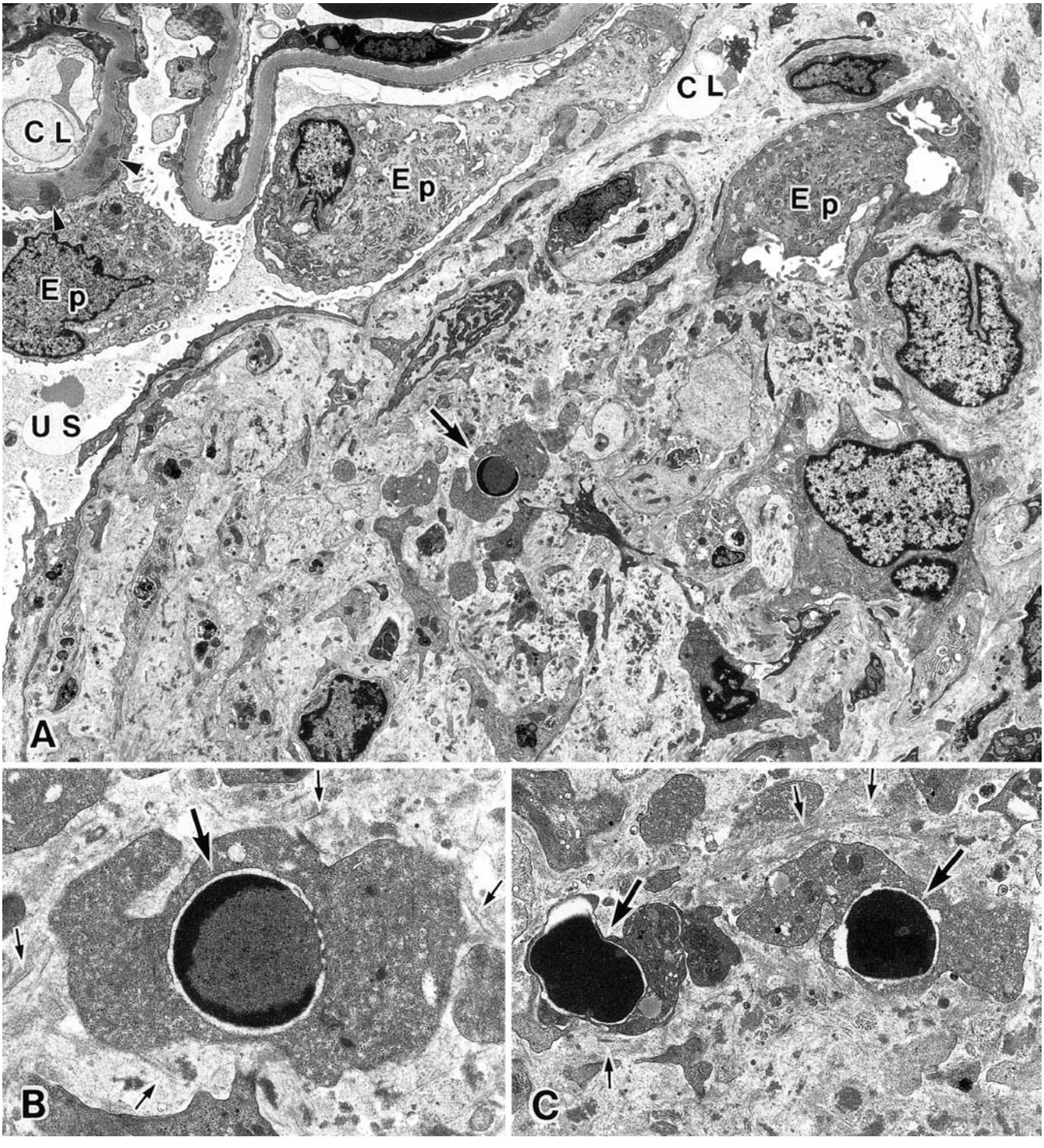

Fig. 4 Apoptosis in the sclerotic lesion of hypocellular glomerulus. Electron micrographs of a renal biopsy specimen from a 24-year-old woman with diffuse proliferative lupus nephritis (World Health Organization class IVc) are shown. **A** Lower magnification view. An *arrow* indicates a single apoptotic cell. **B**, **C** Higher magnification of **A**. **B** The cell has crescentic chromatin in the nucleus characteristic of apoptosis (*large arrow*). Note the collagen fibers around the apoptotic cell (*small arrows*). **C** A serial section of the lesion showing two apoptotic cells in a row (*large arrows*) and intervening collagen fibers (*small arrows*). *US* urinary space, *Ep* epithelial cell, *CL* capillary lumen, *arrowheads* subepithelial deposits. *Magnification* **A** ×4800. **B** ×14,400. **C** ×10,000

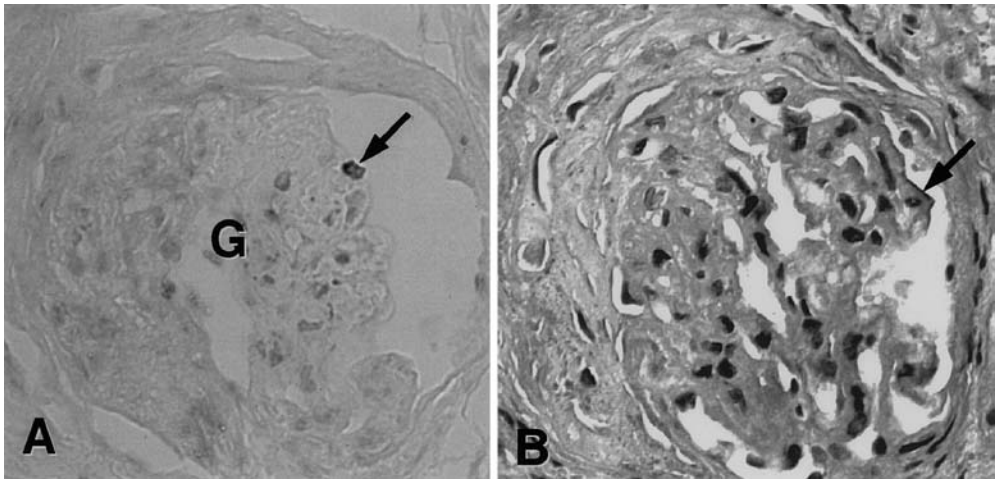

Fig. 5 TUNEL-positive cells in the chronic lesion of glomerular sclerosis. TdT-mediated DNA nick end-labeling (TUNEL) of glomerulus (**A**) and serial sections stained with hematoxylin and eosin (B) from a 51-year-old woman with diffuse proliferative lupus nephritis (World Health Organization class IVc). Note the TUNEL-positive cell in the sclerotic lesion of collapsing glomerulus (*arrow*). *G* glomerulus. *Magnification* ×400

Fig. 6 Late stage of apoptosis phagocytosed by mesangial cells in the glomerulus. An electron micrograph of a renal biopsy specimen from a 26-year-old woman with diffuse lupus nephritis (World Health Organization class IVc) is shown. Note two apoptotic bodies (*arrows*) ingested by a mesangial cell. *US* urinary space, *Ep* epithelial cell, *Ed* endothelial cell, *MC* mesangial cell, *CL* capillary lumen, *arrowheads* subepithelial deposits. *Magnification* ×6000

tizing" lesions) and IVc (active "sclerosing" lesions) (Table 2). The TUNEL score in class-IV lupus nephritis is significantly higher than that in the mild mesangial (0.05±0.08) (six cases), moderate mesangial (0.14±0.07) (six cases), or predominantly sclerosing group (0.38±0.32) (six cases) of IgA nephritis, as we reported previously [25]. The number of TUNEL-positive glomerular cells significantly correlated with the number of apoptotic cells identified in HE stain using light microscopy (Fig. 8). The average degree of tubulointerstitial damage was 1.91. We found much less apoptosis in tubulointerstitium than in glomerulus.

Correlation between apoptosis, histological and clinical parameters

The number of TUNEL-positive cells in glomeruli was compared with the clinical data of lupus and histological indices of nephritis. The glomerular TUNEL score correlated significantly with the immunoserological activities of lupus, such as anti-double-stranded DNA antibody (Fig. 9A) and plasma complement levels (Fig. 9B). There was no correlation between the glomerular TUNEL score and the daily volume of proteinuria or renal function as assessed by the serum creatinine concentration or 24-h creatinine clearance. Regarding renal histology, the glomerular TUNEL score correlated significantly with the glomerular proliferation index (Fig. 9C). There was no correlation between the glomerular TUNEL score and the sclerosis index as a whole, but in groups in which the sclerosis index was over 1.0, a significant correlation was noted (Fig. 9D).

Discussion

The role of glomerular cell apoptosis in human lupus nephritis has been unknown, but was important to determine due to of growing interest in molecular regulation of apoptosis as a therapeutic target in inflammatory disease [16, 18, 20, 30]. The present study showed the ultrastructure of glomerular cell apoptosis in mesangial cells as well as infiltrative neutrophils in human lupus nephritis. In contrast to a previous report by Soto et al. [24], glomerular cell apoptosis was increased not decreased in human lupus nephritis. Moreover, apoptosis in glomerular cells positively correlated with immunoserological activity of lupus, including the level of anti-

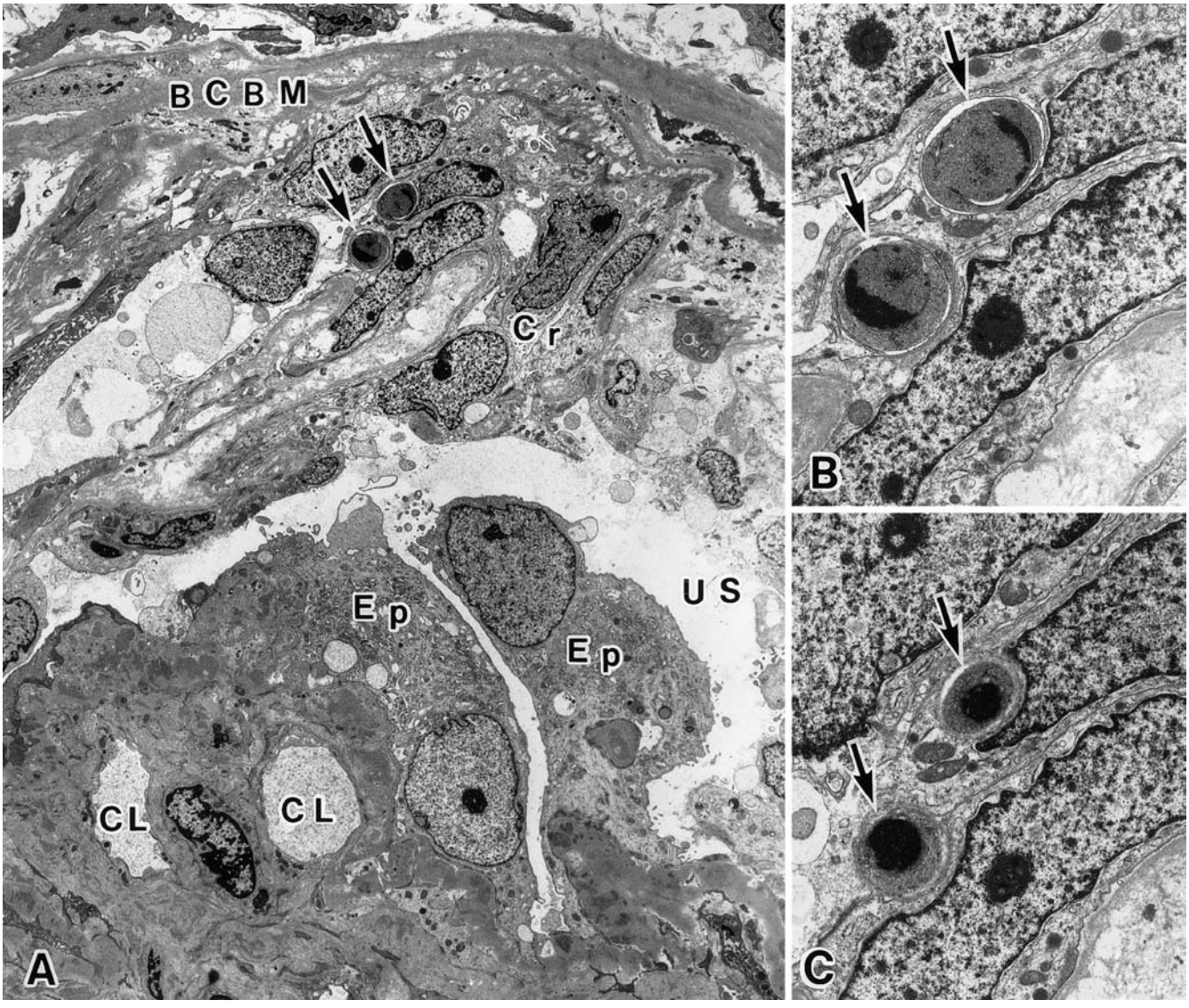

Fig. 7 Apoptosis in the fibrocellular crescent of glomerulus. Electron micrographs of a renal biopsy specimen from a 51-year-old woman with diffuse proliferative lupus nephritis (World Health Organization class IVc) are shown. **A** Lower magnification view. Two apoptotic cells are adjacent to the fibroblastic cells in fibrocellular crescent (*arrows*). **B**, **C** Higher magnification of **A**. **B** The apoptotic cells (*arrows*) are phagocytosed by neighboring cells. **C** A serial section of the lesion demonstrating another nuclear morphology in the same cells (*arrows*). *US* urinary space, *Ep* epithelial cell, *CL* capillary lumen, *Cr* crescent, *BCBM* Bowman's capsule basement membrane. *Magnification* **A** ×2400. **B** ×7200. **C** ×8000

double-stranded DNA antibody and consumption of plasma complement. The level of glomerular cell apoptosis significantly correlated with histopathological activity, such as the glomerular proliferation index. The data raise the intriguing concept that increased apoptosis of glomerular cells and infiltrative neutrophils may be involved in the progression of human lupus nephritis.

We speculate that both increase in apoptosis and defective clearance of dead cells [21] may explain the substantial number of cases of glomerular cell apoptosis in human lupus nephritis. The increase in apoptosis may result from: (1) high titer of circulating anti-double-stranded DNA antibody; (2) counterbalancing the hypercellularity in glomerulonephritis; and (3) local complement activation in the inflamed glomerulus. Anti-double-stranded DNA autoantibody purified from sera of patients with lupus can bind to the cell surface and induce apoptosis in cultured mesangial cells in vitro [31]. Highly significant correlation between the circulating level of anti-double-stranded DNA antibody and glomerular cell apoptosis in our patients with lupus nephritis ($P<0.0005$) supports the possibility that anti-double-stranded DNA antibody could directly induce apoptosis in mesangial cells in vivo. It is reported that nephritogenic anti-double-stranded DNA antibody did not modulate the gene expression of Fas, c-myc, p53, or bcl-2 in cultured mesangial cells [31]. Apoptosis in circulating neutrophils is increased and is associated with the level of serum anti-

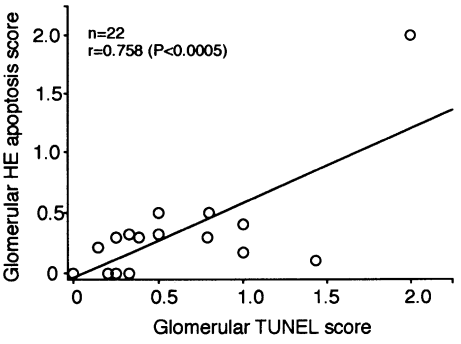

Fig. 8 The relationship between the number of glomerular apoptotic cells by light microscopy [glomerular hematoxylin and eosin (HE) apoptosis score] and the number of TUNEL-positive cells in the glomeruli [glomerular TdT-mediated DNA nick end-labeling (TUNEL) score]. The correlation between the glomerular TUNEL score and the glomerular HE apoptosis score is shown

double-stranded DNA antibody in patients with lupus [9]. The signal transduction of apoptosis in glomerular cells and neutrophils in human lupus nephritis needs to be further identified.

The cell number in tissue is determined by the balance between cell proliferation and cell death by apoptosis. Cell kinetic study in the Thy 1.1 mesangial proliferative glomerulonephritis in the rat has demonstrated that glomerular cell apoptosis and mitosis peaked at the same time point (day 5 after disease induction) [4]. This finding suggests that apoptosis may serve as a tax against mitosis and may limit an early increase in mesangial cell number by cell proliferation [20]. Mesangial cell proliferation and leukocyte influx are so severe in human lupus nephritis—in particular WHO class IV—that apoptosis observed in the mesangial lesion may be due to an attempt to counterbalance the glomerular hypercellularity. The acti-

Table 2 Histological data in patients with lupus nephritis. *TUNEL* TdT-mediated DNA nick end-labeling

World Health Organization*	Proliferation index**	Sclerosis index**	Activity index**	Chronicity index**	TUNEL-positive cases (%)	TUNEL score
II	0.2	0	3.0	1.0	0/1 (0)	0
IV	1.5±0.7	0.7±0.7	7.3±3.5	2.2±3.1	14/15 (93)	0.89±1.46
a)	0.8±0.2	0.5±0.7	2.5±0.7	2.0±1.4	1/2 (50)	0.10±0.14
b)	1.7±0.7	0.4±0.6	8.6±3.4	1.0±2.1	9/9 (100)	1.09±1.86
c)	1.3±0.6	1.3±0.6	7.0±2.8	5.0±4.0	4/4 (100)	0.83±0.48
V	0.4±0.4	0.2±0.3	2.6±2.2	1.0±1.2	1/5 (20)	0.16±1.35
VI	0	1.0	3.0	4.0	1/1 (100)	0.14
Total	1.1±0.8	0.5±0.6	5.9±3.8	2.0±2.6	16/22 (73)	0.65±1.26

* World Health Organization classification of lupus nephritis [8]
** Renal pathology scoring system of lupus nephritis according to Austin III HA et al. [2]

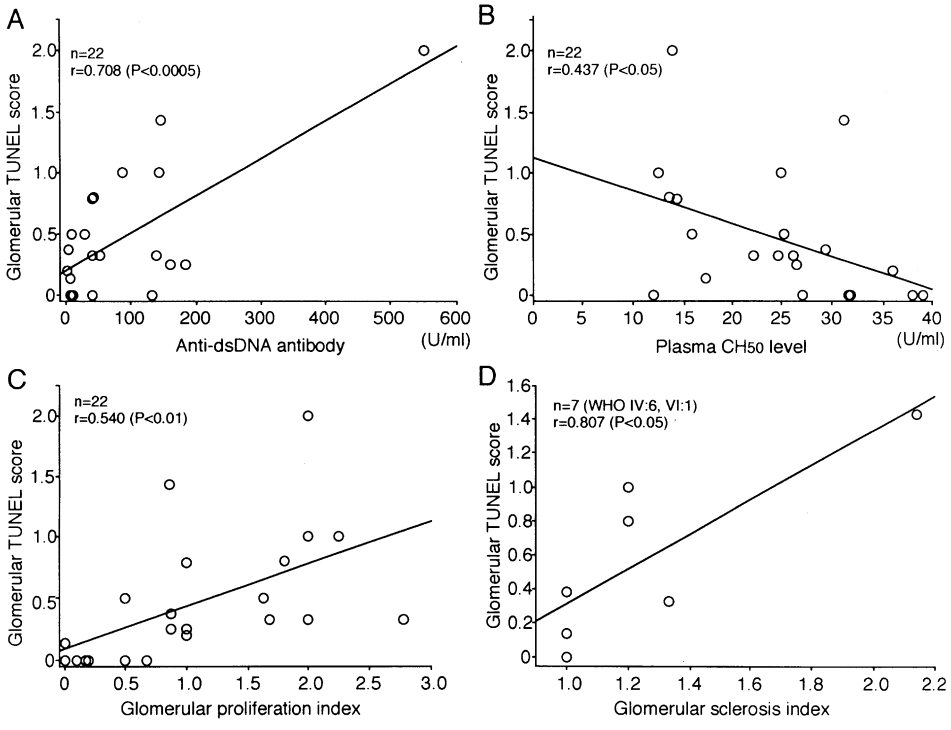

Fig. 9 The relationship between the number of TUNEL-positive cells in glomerulus [glomerular TdT-mediated DNA nick end-labeling (TUNEL) score] and clinical or histological indices in patients with lupus nephritis. The correlation between the glomerular TUNEL score and the level of anti-double stranded DNA antibody (**A**) plasma complement (**B**) glomerular proliferation index (**C**) or glomerular sclerosis index (**D**) are shown

vation of the complement system in lupus contributes to tissue injury. All of our patients with classes IV and V of lupus nephritis had deposition of complement components C3 and C1q in glomeruli detected using routine immunofluorescence microscopy. This finding indicates the local activation of a complement system in the inflamed glomeruli in human lupus nephritis. It has been reported that C1q can enhance apoptosis in cultured rat glomerular mesangial cells under certain circumstances [19]. It is possible that activation of a complement including C1q can amplify apoptosis in glomerular mesangial cells in lupus nephritis.

Apoptotic cells are rapidly phagocytosed by the neighboring cells in the tissue [11, 22]. However, if this did not occur properly, inflammation would be evoked around the cell [22]. Therefore, another mechanism of increased apoptosis in human lupus nephritis should be defective clearance of apoptotic cells by phagocytes. Resident glomerular mesangial cells as well as infiltrative macrophages into the glomerulus have phagocytic capacities as reported by Savill et al. [21]. Incomplete clearance of apoptosis may arise from: (1) overwhelming the phagocytic capacity in the glomerulus and (2) disturbed recognition of apoptotic cells by phagocytes. Neutrophil infiltration is one of the most characteristic features in human lupus nephritis. Karyorrhexis, defined by the presence of pyknotic and fragmented nuclei, is often observed in WHO class-IV lupus nephritis. This lesion is considered to be severe and active in glomerular abnormalities in lupus nephritis. From our study, it has become clear that apoptosis is involved in neutrophils in lupus nephritis. However, inflammation often appears to be uncontrolled in severe cases such as lupus nephritis, in that tissue injury is so severe that it leads to scarring or glomerulosclerosis. Leukocyte clearance by apoptosis may be perturbed in severe inflammatory lesions such as karyorrhexis of lupus nephritis, hence exacerbating rather than controlling inflammation.

The complement system plays a paradoxical role in the development of autoimmune disease. In contrast to the local activation and consumption of certain components of complement, inherited deficiency of a classical pathway, in particular C1q, is strongly associated with the pathogenesis of human lupus. Indeed, a recent report has demonstrated that C1q-deficient mice develop glomerulonephritis accompanied by multiple apoptotic bodies [6]. The phenomenon is probably due to the disturbed recognition of apoptotic cells via C1q by phagocytes. This possibility is unlikely in our study, because none of our patients had C1q deficiency in their sera at the time of biopsy.

To date, studies of the role of apoptosis in lupus nephritis have been restricted to animal models [16, 17, 18]. Schwarting et al. have recently reported an increase in renal cell apoptosis in MRL-Fas^{lpr} autoimmune mice, animal models for human lupus [23]. In contrast with the report by Soto et al. [24], the number cases of of glomerular cell apoptosis increased in human lupus nephritis in our study. The reasons for this discrepancy are obscure. The present study provides the ultrastructural evidence of glomerular cell apoptosis in human lupus nephritis. Glomerular cell apoptosis is increased rather than decreased in autoimmune lupus nephritis, in contrast to previous reports [24]. The glomerular cell apoptosis is involved in both active and chronic lesions of the nephritis. The mechanism of glomerular cell death in human lupus nephritis requires further study to gain new insights into the pathogenesis as well as the treatment of autoimmune lupus nephritis.

Acknowledgements This study was supported by Research Grants (to H.M. and to N.K.) for Scientific Research from the Ministry of Education, Science and Culture of Japan. We thank Ms. T. Hashimoto and Y. Saito for their technical assistance with the electron micrographs.

References

1. Appel GB, Cohen DJ, Pirani CL, Meltzer JI, Estes D (1987) Long-term follow-up of patients with lupus nephritis. A study based on the classification of the World Health Organization. Am J Med 83:877–885
2. Austin HA 3rd, Muenz LR, Joyce KM, Antonovych TA, Kullick ME, Klippel JH, Decker JL, Balow JE (1983) Prognostic factors in lupus nephritis. Contribution of renal histologic data. Am J Med 75:382–391
3. Austin HA 3rd, Muenz LR, Joyce KM, Antonovych TT, Balow JE (1984) Diffuse proliferative lupus nephritis: identification of specific pathologic features affecting renal outcome. Kidney Int 25:689–695
4. Baker AJ, Mooney A, Hughes J, Lombardi D, Johnson RJ,Savill J (1994) Mesangial cell apoptosis: the major mechanism for resolution of glomerular hypercellularity in experimental mesangial proliferative nephritis. J Clin Invest 94:2105–2116
5. Berden JH, Grootscholten C, Jurgen WC, van der Vlag J (2002) Lupus nephritis: a nucleosome waste disposal defect? J Nephrol 15:S1–S10
6. Botto M, Dell'Agnola C, Bygrave AE, Thompson EM, Cook HT, Petry F, Loos M, Pandolfi PP, Walport MJ (1998) Homozygous C1q deficiency causes glomerulonephritis associated with multiple apoptotic bodies. Nat Genet 19:56–59
7. Cameron JS, Turner DR, Ogg CS, Williams DG, Lessof MH, Chantler C, Leibowitz S (1979) Systemic lupus with nephritis: a long-term study. QJM 48:1–24
8. Churg J, Sobin LH (1982) Lupus nephritis. In: Churg J, LH Sobin (eds) Renal disease: classification and atlas of glomerular diseases. Igaku-Shoin, Tokyo, pp 127–149
9. Courtney PA, Crockard AD, Williamson K, Irvine AE, Kennedy RJ, Bell AL (1999) Increased apoptotic peripheral blood neutrophils in systemic lupus erythematosus: relations with disease activity, antibodies to double stranded DNA, and neutropenia. Ann Rheum Dis 58:309–314
10. Gavrieli Y, Sherman Y, Ben-Sasson SA (1992) Identification of programmed cell death in situ via specific labeling of nuclear DNA fragmentation. J Cell Biol 119:493–501
11. Kerr JF, Wyllie AH, Currie AR (1972) Apoptosis: a basic biological phenomenon with wide-ranging implications in tissue kinetics. Br J Cancer 26:239–257
12. Makino H, Gibbons JT, Reddy MK, Kanwar YS (1986) Nephritogenicity of antibodies to proteoglycans of the glomerular basement membrane—I. J Clin Invest 77:142–156
13. Makino H, Yamasaki Y, Haramoto T, Shikata K, Hironaka K, Ota Z, Kanwar YS (1993) Ultrastructural changes of extracellular matrices in diabetic nephropathy revealed by high resolution scanning and immunoelectron microscopy. Lab Invest 68:45–55

14. Makino H, Hayashi Y, Yamasaki Y, Shikata K, Kashihara N, Kira S, Ota Z (1994) Clinical significance of necrosis in lupus nephritis. Intern Med 33:461–465
15. Makino H, Yamasaki Y, Shikata K, Kashihara N, Sugiyama H, Ogura T, Ota Z (1995) Transition of morphologic features in lupus nephritis: does steroid therapy accelerate glomerulosclerosis? Intern Med 34:982–987
16. Nagata S (1997) Apoptosis by death factor. Cell 88:355–365
17. Nagata S, Golstein P (1995) The Fas death factor. Science 267:1449–1456
18. Nagata S, Suda T (1995) Fas and Fas ligand: lpr and gld mutations. Immunol Today 16:39–43
19. Sato T, van Dixhoorn MG, Heemskerk E, van Es LA, Daha MR (1997) C1q, a subunit of the first component of complement, enhances antibody-mediated apoptosis of cultured rat glomerular mesangial cells. Clin Exp Immunol 109:510–517
20. Savill J (1999) Regulation of glomerular cell number by apoptosis. Kidney Int 56:1216–1222
21. Savill J, Smith J, Sarraf C, Ren Y, Abbott F, Rees A (1992) Glomerular mesangial cells and inflammatory macrophages ingest neutrophils undergoing apoptosis. Kidney Int 42:924–936
22. Savill J, Fadok V, Henson P, Haslett C (1993) Phagocyte recognition of cells undergoing apoptosis. Immunol Today 14:131–136
23. Schwarting A, Wada T, Kinoshita K, Tesch G, Kelley VR (1998) IFN-gamma receptor signaling is essential for the initiation, acceleration, and destruction of autoimmune kidney disease in MRL-Fas(lpr) mice. J Immunol 161:494–503
24. Soto H, Mosquera J, Rodriguez-Iturbe B, Henriquez La Roche C, Pinto A (1997) Apoptosis in proliferative glomerulonephritis: decreased apoptosis expression in lupus nephritis. Nephrol Dial Transplant 12:273–280
25. Sugiyama H, Kashihara N, Makino H, Yamasaki Y, Ota A (1996) Apoptosis in glomerular sclerosis. Kidney Int 49:103–111
26. Sugiyama H, Kashihara N, Onbe T, Yamasaki Y, Wada J, Sekikawa T, Okamoto K, Kanao K, Maeshima Y, Makino H (1997) Bcl-2 expression and apoptosis in nephrotoxic nephritis. Exp Nephrol 5:481–489
27. Takemura T, Murakami K, Miyazato H, Yagi K, Yoshioka K (1995) Expression of Fas antigen and Bcl-2 in human glomerulonephritis. Kidney Int 48:1886–1892
28. Tan EM, Cohen AS, Fries JF, Masi AT, McShane DJ, Rothfield NF, Schaller JG, Talal N, Winchester RJ (1982) The 1982 revised criteria for the classification of systemic lupus erythematosus. Arthritis Rheum 25:1271–1277
29. Tax WJ, Kramers C, van Bruggen MC, Berden JH (1995) Apoptosis, nucleosomes, and nephritis in systemic lupus erythematosus. Kidney Int 48:666–673
30. Thompson CB (1995) Apoptosis in the pathogenesis and treatment of disease. Science 267:1456–1462
31. Yu CL, Huang MH, Tsai CY, Tsai YY, Tsai ST, Sun KH, Han SH, Yu HS (1998) The effect of human polyclonal anti-dsDNA autoantibodies on apoptotic gene expression in cultured rat glomerular mesangial cells. Scand J Rheumatol 27:54–60

Virchows Arch (2003) 443:78–86
DOI 10.1007/s00428-003-0804-4

ORIGINAL ARTICLE

Shuji Kawai · Hideaki Enzan · Yoshihiro Hayashi · Yu-Lan Jin · Li-Mei Guo · Eriko Miyazaki · Makoto Toi · Naoto Kuroda · Makoto Hiroi · Toshiji Saibara · Hirofumi Nakayama

Vinculin: a novel marker for quiescent and activated hepatic stellate cells in human and rat livers

Received: 11 September 2002 / Accepted: 11 February 2003 / Published online: 25 April 2003
© Springer-Verlag 2003

Abstract In liver injuries, the quiescent hepatic stellate cells (HSCs) promptly change to activated HSCs, which are easily identified by the intense immunoreactivity for α-smooth muscle actin. However, reproducible markers for quiescent HSCs in formalin-fixed, paraffin-embedded liver tissue sections have not yet been reported. We immunohistochemically examined the expression of vinculin, one major protein of dense plaques, on cultured LI90 cells and on HSCs in normal and diseased human and rat livers. In cultured LI90 cells, vinculin appeared as small linear patches. Although vinculin was consistently negative in the routine liver tissue sections, an antigen retrieval technique using microwave oven heating yielded excellent effects. Using this technique, the formalin-fixed, paraffin-embedded human and rat normal liver tissue sections showed the vinculin immunoreactivity along the sinusoidal wall. Immunoelectron microscopic observation of hepatic parenchyma demonstrated that the vinculin was exclusively expressed in quiescent HSCs. In fetal rat livers, vinculin-positive quiescent HSCs gradually increased in number with gestation. In diseased livers the activated HSCs showed more intense immunoreaction for vinculin. These results indicate that, using microwave pretreatment, vinculin is expressed in quiescent and activated HSCs in routinely processed liver tissue sections. It could allow us to evaluate the development and distribution of quiescent HSCs and to examine the relationship between quiescent and activated HSCs.

Keywords Hepatic stellate cell · Cell marker · Vinculin · Immunohistochemistry · Antigen retrieval

S. Kawai · H. Enzan (✉) · Y. Hayashi · Y.-L. Jin · L.-M. Guo · E. Miyazaki · M. Toi · N. Kuroda · M. Hiroi
First Department of Pathology,
Kochi Medical School,
Kohasu, Oko-cho, Nankoku City, 783-8505 Kochi, Japan
e-mail: enzanh@kochi-ms.ac.jp
Tel.: +81-88-8802329
Fax: +81-88-8802332

T. Saibara
First Department of Internal Medicine,
Kochi Medical School,
Kohasu, Oko-cho, Nankoku City, 783-8505 Kochi, Japan

H. Nakayama
Department of Molecular Pathology,
Graduate School of Biomedical Sciences, Hiroshima University,
1-2-3 Kasumi, Minami-ku, 734-8551 Hiroshima, Japan

Introduction

Hepatic stellate cells (HSCs) are located in the perisinusoidal space and interhepatocytic recessus of all vertebrate normal livers and play crucial roles in the storage of vitamin A, control of sinusoidal circulation, production and degradation of extracellular matrix components in the perisinusoidal space, and in maintaining the homeostasis of cellular networks consisting of liver cells and sinusoidal lining cells through cytokine production and cell-to-cell contact. When liver cell necrosis occurs, adjacent quiescent HSCs are immediately activated and transform their phenotype to myofibroblasts. If the injuries are continued, the activated HSCs synthesize and secrete excessive amounts of extracellular matrix components, resulting in liver fibrosis. In 1982, Knook et al. [24] reported a method for the isolation and purification of HSCs from rat livers. The subsequent improvement of the method and the introduction of molecular biology into this field brought dramatic progression in understanding the pathophysiology of HSCs. However, not only for in vivo but also in vitro studies on HSCs, it is a prerequisite to exactly identify HSCs in liver tissues. In addition to vitamin A autofluorescence and ultrastructural characteristic features of HSCs, many immunohistochemical markers for HSCs, such as desmin [2, 7, 39, 42, 44], glial fibrillary acidic protein (GFAP) [3, 4, 15, 30, 31], α-smooth muscle actin (α-SMA) [12, 34, 35], neural cell adhesion molecule (N-CAM) [23, 29], synaptophysin [8], class-VI intermediate filament protein (nestin) [32], low-affinity nerve growth factor receptor (p75) [41], prion [19, 22], and fibroblast activation protein (FAP) [26, 27], have been reported. However, except for α-SMA [12, 35] these

markers are restricted to use in frozen sections and acetone-fixed cultured cells. This is because the fresh frozen sections well preserve the antigenicity of such marker proteins in immunostaining, while the immunoreactivity does not survive routine fixation and embedding, mainly due to the masking effects of fixatives. On the contrary, the immunoreaction of α-SMA is demonstrated even in archival formalin-fixed, paraffin-embedded liver tissue sections and precisely shows the features of activated HSCs which are strongly positive for α-SMA [12]. Although limited to the use in rat livers, desmin staining has also been successfully performed in formalin-fixed, paraffin-embedded liver tissues, especially after microwave oven heating (MW), and revealed a strong positivity in activated HSCs [21]. However, quiescent HSCs were scarcely positive or negative for α-SMA and desmin [21]. It has caused difficulty in functional analysis of quiescent HSCs and also in simultaneous examination of both quiescent and activated HSCs in the diseased liver tissue sections.

Vinculin, one prominent component of focal adhesions [5, 6, 16, 17, 18], is a cytoskeletal protein of 116–130 kDa [1, 5, 6, 16, 17] involved in the membrane–cytoskeleton interactions [1, 5, 16, 17] and in the indirect binding of intracellular actin filaments to extracellular fibronectin [5, 6]. According to Geiger et al. (1980) [16], in several cell types, the immunolabeling for vinculin was concentrated close to the plasma membrane sites, where microfilament bundles terminate: at the zonula adherens in the junctional complex of the brush border of intestinal epithelial cells; at the membrane-associated dense plaques of smooth muscle cells and at the fascia adherens of the intercalated disk membranes of cardiac muscle cells. The localization of this cytoskeletal protein was also observed at the adhesion plaque of fibroblasts [5].

Because the HSCs have been assumed to be the liver-associated pericytes or adventitious connective tissue cells and contain dense plaques [12], which are distributed along the cell surface, we immunohistochemically examined the expression of vinculin protein in HSCs in normal and diseased human and rat livers, using an antigen retrieval technique based on MW treatment of tissue sections [9, 33, 36, 37, 38, 40, 43] and reported here, vinculin, as a novel immunohistochemical marker for quiescent and activated HSCs in formalin-fixed, paraffin-embedded liver tissue sections.

Materials and methods

Cultivation of human HSCs

Human HSC cell line, LI90 [28] was cultured in Dulbecco's modified Eagle's medium containing 10% heat-inactivated fetal bovine serum and antibiotics in a humidified atmosphere of 95% air and 5% CO_2 at 37°C. They were subcultured at a 1:3 split ratio (4×10^4 cells/ml) and used during the fourth to sixth passages.

Human liver tissues

Adult human liver tissues from 30 patients (20 men and 10 women with a mean age of 52 years, range 25–65 years) with acute and chronic liver diseases or no significant liver diseases were obtained from autopsied and biopsied cases at the Kochi Medical School Hospital.

Rat liver tissues

Five male Wistar strain rats (7–10 weeks old) were used for carbon tetrachloride (CCl_4; Wako, Tokyo, Japan)-induced acute liver injuries. Rats were given a single intraperitoneal injection of 1.0 ml/kg body weight CCl_4 as a 30% solution in corn oil. They were sacrificed at 48 h after injection. Five untreated and five saline-injected rats were used for normal controls. All animals were maintained under 12-h light/12-h dark cycles in a day with food and water available ad libitum. In addition, fetal rats on days 11–20 of gestation and early postnatal rats on days 1, 3, 5 and 7 after birth were sacrificed, three rats on each day. All animals were anesthetized with diethyl ether before sacrifice. Their livers were rapidly removed. This study was approved by the Animal Care and Use Committee of Kochi Medical School and followed the National Institutes of Health guidelines for humane care and use of animals.

Immunofluorescence staining and confocal microscopy of LI90 cells

The LI90 cells [28] grown on chamber slides (Nalge Nunc International, USA) were fixed in acetone at 4°C for 30 min. After washing in phosphate-buffered saline (PBS), the cells were incubated with a 1:50 dilution of monoclonal mouse anti-human vinculin antibody (V284, Novocastra, Newcastle, UK) for 1 h at room temperature. After a thorough rinse in PBS, the cells were incubated for 60 min at room temperature with a 1:200 dilution of biotinylated rabbit anti-mouse IgG $F(ab')^2$ fragment (Dako, Glostrup, Denmark) and then for 60 min with a 1:100 dilution of FITC (fluorescein isothiocyanate)-conjugated streptavidin (Dako). After counterstaining with propidium iodide, the cells were mounted in fluorescent mounting medium (Dako), and then observed using a confocal laser scanning microscope LSM-410 and LSM system soft version 3.70 (Carl Zeiss, Oberkochen, Germany).

Light microscopy and immunohistochemistry of human and rat liver tissues with or without antigen retrieval techniques

Human and rat liver tissues were fixed in 10% phosphate-buffered formalin for 24 h, and then embedded in paraffin. The formalin-fixed, paraffin-embedded liver tissue sections, about 4 μm in thickness, were dewaxed, rehydrated and stained with hematoxylin and eosin, for routine light microscopic observation. Before immunostaining procedures, the archival formalin-fixed, paraffin-embedded tissue sections were treated, using MW in 0.01 M citrate buffer solution (Na citrate-citric acid), pH 6.0, at 100°C for 15 min (5 min, three times), for retrieval of antigen masked by formalin fixation [36, 37, 38, 40]. After the MW treatment, sections were allowed to cool at room temperature for a minimum of 20 min. After rinsing with PBS, endogenous peroxidase was inhibited by 0.3% hydrogen peroxide in methanol for 10 min at room temperature and rinsed with 0.01 M PBS, pH 7.4 (5 min, three times), and incubated in 10% normal rabbit serum (Dako) for 10 min. Subsequently, the MW-pretreated sections were incubated overnight at 4°C with each monoclonal antibody for vinculin (1:50), desmin (D33, Dako, 1:50) and α-smooth muscle actin (α-SMA; 1A4, Dako, 1:50). However, the sections without any treatments for antigen retrieval were incubated overnight at 4°C with each monoclonal antibody for vinculin (1:50), α-SMA(1:50), and desmin (1:50). After rinsing with PBS, all sections with or

without MW pretreatments were incubated for 60 min at room temperature with a 1:200 dilution of biotinylated rabbit anti-mouse IgG $F(ab')^2$ fragment (Dako). After rinsing with PBS, these sections were incubated for 60 min at room temperature in an avidin-biotin-peroxidase complex solution (Vectastain, Vector, Burlingame, CA, USA). Finally, the sections were immersed in a substrate solution of 0.5% 3,3'-diaminobenzidine tetrahydrochloride (DAB; Sigma) and 0.1% hydrogen peroxide in 0.05 M Tris buffer, pH 8.0 for 3 min at room temperature. The sections were lightly washed, counterstained with hematoxylin, dehydrated in ethanol, and mounted with Eukitt (Kindler, Freiburg, Germany).

Confocal microscopy immunofluorescence localization of vinculin and desmin in normal adult and fetal rat livers

Dewaxed and rehydrated sections of formalin-fixed, paraffin-embedded normal adult and fetal rat livers were treated with MW as described above. For double labeling of the sections, we used monoclonal antibodies for vinculin (Novocastra) and desmin (Dako). The procedures of immunostaining were as follows: (1) incubation in 10% normal rabbit serum for 10 min, (2) incubation with the monoclonal anti-vinculin antibody (Novocastra) for 18 h at 4°C, washing in PBS, (3) incubation with biotinylated rabbit anti-mouse IgG $F(ab')^2$ fragment (Dako), for 1 h at room temperature, (4) incubation with FITC-conjugated streptavidin (Dako) for 1 h at room temperature, washing in PBS, (5) treatment with MW of the sections as described above, for antigen retrieval, inhibition of cross-reaction and reduction of nonspecific background staining, (6) incubation with the monoclonal anti-desmin antibody (Dako) for 18 h at 4°C, washing in PBS (7) incubation with biotinylated rabbit anti-mouse IgG $F(ab')^2$ fragment (Dako), for 1 h at room temperature, and (8) incubation with Texas Red-conjugated streptavidin (Vector), for 1 h at room temperature, washing in PBS. After fluorescence staining, the sections were mounted in fluorescent mounting medium (Dako), and then observed using a confocal laser scanning microscope as described above.

Immunoelectron microscopy

Small pieces of normal adult rat liver tissues were fixed in periodate-lysine-paraformaldehyde solution for 1 h at 4°C. For the pre-embedding method, the pieces were rinsed in 1 M PBS

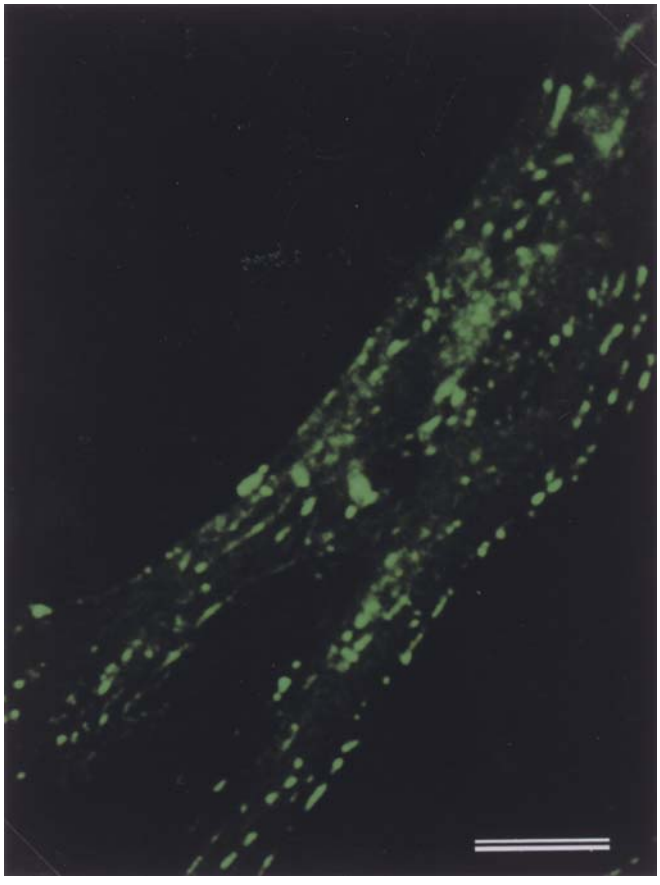

Fig. 1 Immunofluorescence localization of vinculin in a LI90 cell by confocal microscopy. The localization of vinculin is revealed with fluorescein isothiocyanate. Note the focal bright linear patches of fluorescence in the cell, predominantly along the cell surface. ×820, *bar* 20 μm

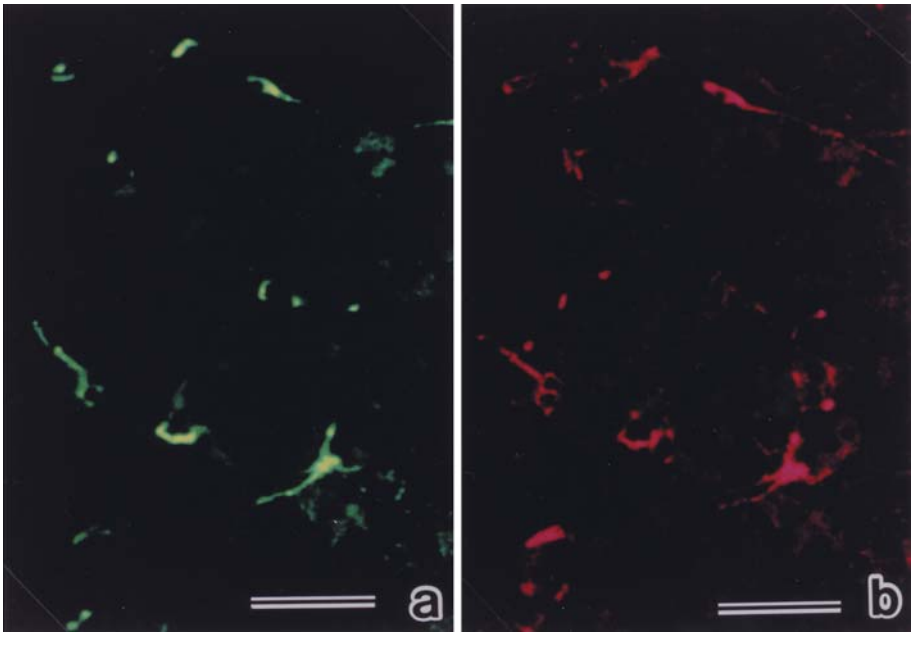

Fig. 2 Confocal microscopy immunofluorescence localization of vinculin and desmin in a 20-day-old fetal rat liver parenchyma. The localization of vinculin revealed with fluorescein isothiocyanate (**a**) is essentially the same as that of desmin revealed by Texas Red (**b**) in the same section. The formalin-fixed, paraffin-embedded liver tissue section has been treated with microwave oven heating before each fluorescence staining. ×370, *bar* 40 μm

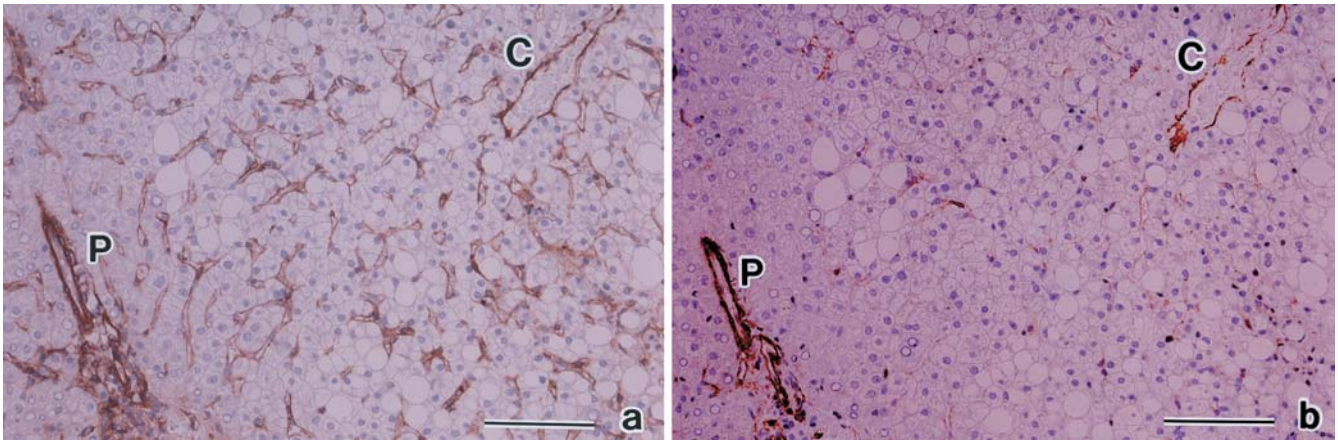

Fig. 3 Comparison of vinculin and α-smooth muscle actin (SMA) immunostaining in an adult human liver with mild fatty changes. **a** Vinculin is expressed along the sinusoidal wall throughout liver lobules. **b** However, the sinusoidal wall shows little or no staining for α-SMA. Vascular smooth muscle cells were positive for vinculin and α-SMA. **a**, **b** Formalin-fixed, paraffin-embedded, needle-biopsied liver tissue sections pretreated with the same microwave oven heating before immunostaining. *C* central vein, *P* portal tract. ×110, *bar* 100 μm

containing 10% sucrose, and embedded in OCT compound (Tissue-Tek, Sakura, Tokyo, Japan). They were cut into approximately 10 μm-thick sections on a cryostat and incubated with monoclonal anti-vinculin antibody (Novocastra) diluted at 1:50 in 0.01 M PBS overnight at 4°C. After rinsing in PBS, the sections were processed using routine methods for immunostaining, as described above, fixed in 1% glutaraldehyde in 0.1 M phosphate buffer for 10 min at room temperature, developed in a mixture of 0.05% DAB and 0.01% H_2O_2 in 0.05 M Tris-HCl buffer (pH 8.0), dehydrated in ethanol, and embedded in epoxy resin. Ultrathin sections were examined under an electron microscope (JEM-100S, JEOL, Tokyo, Japan).

As a negative control for these immunolabelings, the cultured LI90 cells and liver tissue sections were incubated in normal mouse serum at the same concentration as that of the primary antibodies used in this study.

Results

Localization and distribution of vinculin in cultured LI90 cells

In LI90 cells cultured on chamber slides, vinculin was widely distributed throughout the cytoplasm. The fluorescence for FITC-conjugated vinculin occurred in focal small linear patches, predominantly along the cell surface (Fig. 1).

Light microcopy of human and rat livers

In formalin-fixed, paraffin-embedded sections of human and rat livers, so long as the tissue sections were not pretreated using an antigen retrieval technique, the HSCs were consistently negative for vinculin and desmin. However, with the antigen retrieval technique using MW in citrate buffer, the immunostaining of vinculin and desmin was dramatically improved. The distribution of vinculin was essentially the same as that of desmin

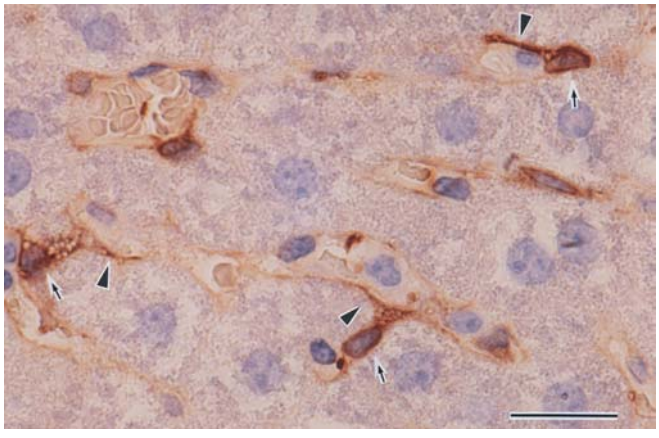

Fig. 4 Vinculin expression in a normal adult rat liver. Higher magnification shows vinculin-positive quiescent hepatic stellate cells (HSCs) containing small fat droplets (*arrows*). Subendothelial processes of the HSCs (*arrowheads*) are also positive for vinculin. Pretreatment of the tissue section with microwave oven heating before immunostaining. ×670, *bar* 20 μm

(Fig. 2). The cells showing co-expression of vinculin and desmin extended cytoplasmic processes along the sinusoidal wall. In the formalin-fixed, paraffin-embedded tissue sections of needle-biopsied adult human livers without significant morphological abnormalities except for mild fatty changes, following MW treatment, vinculin expression was observed along the sinusoidal wall throughout the liver lobules (Fig. 3a). However, the sinusoidal wall was usually negative for α-SMA and only a few positive portions were scattered along the sinusoidal wall in the consecutive tissue section, even if pretreated using the same antigen retrieval technique (Fig. 3b). In higher magnification, vinculin-positive quiescent HSCs of normal adult rat livers were easily identified by the presence of characteristic intracytoplasmic fat droplets

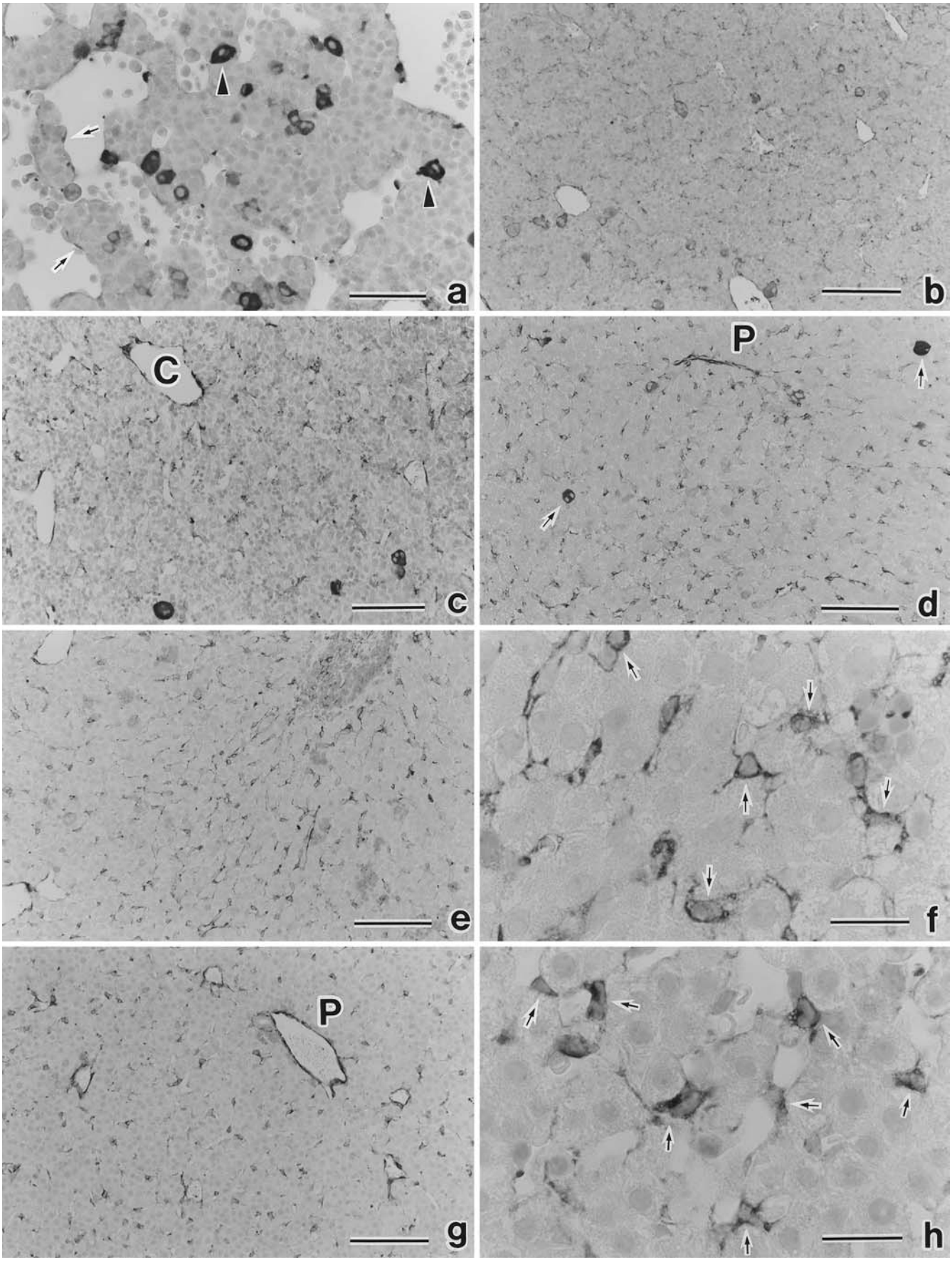
a
b
C
c
P
d
e
f
P
g
h

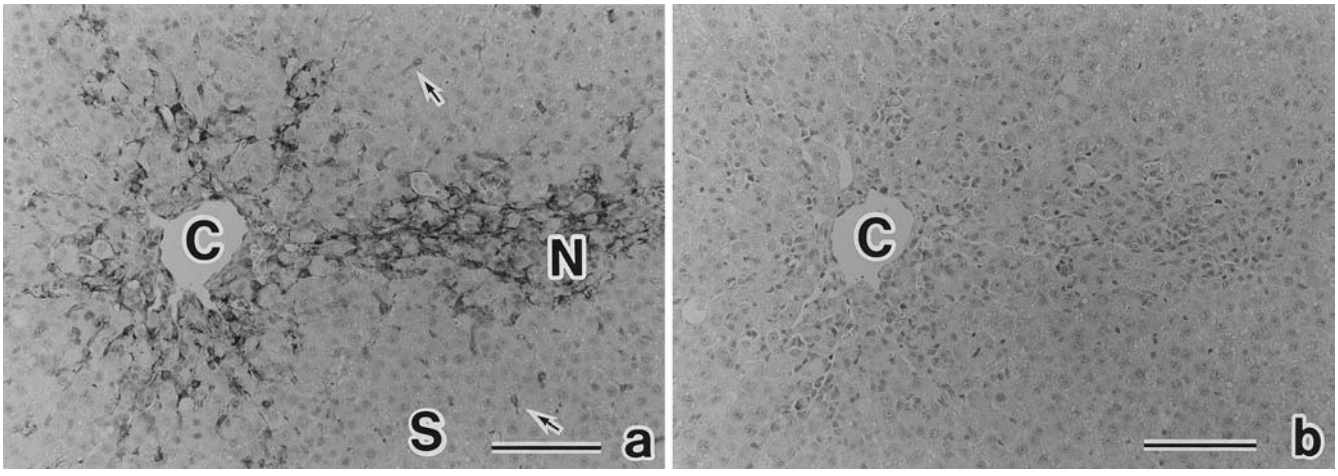

Fig. 6 Vinculin expression in carbon tetrachloride (CCl_4)-induced acute liver injury. **a** Not only activated hepatic stellate cells (HSCs) in necrotic areas (*N*), but also quiescent HSCs (*arrows*) in adjacent surviving liver parenchyma (*S*) are positive for vinculin. **b** No immunoreaction for vinculin in the consecutive tissue section. *C* central vein. **a** Pretreated with microwave oven heating of the tissue section before immunostaining. **b** No treatment for antigen retrieval. ×120, *bar* 100 μm

(Fig. 4). Within liver lobules, liver parenchymal cells and other types of sinusoidal lining cells were all negative for vinculin. Besides quiescent HSCs, vinculin-positive cells were also found in the portal tracts and perivenular areas, and around the hepatic veins. These vinculin-positive cells were vascular smooth muscle cells, serving as an internal positive control for vinculin. Endothelial cells of portal veins appeared to be focally reactive with vinculin antibodies. In biliary epithelial cells the apical border of their adjoining lateral membranes showed a dot-like positive reaction. Around bile capillaries, a similar dot-like immunostaining of vinculin was rarely encountered. In fetal and early postnatal rat livers, the number and distribution of vinculin-positive HSCs significantly varied during development (Fig. 5). On day 12 and day 13 of gestation, very small numbers of HSCs weakly positive for vinculin were scattered along the sinusoidal wall, while megakaryocytes strongly positive for vinculin frequently occurred in growing liver parenchyma (Fig. 5a). The vinculin-positive immature HSCs contained no or only a few fat droplets. With progression of gestation, vinculin-positive HSCs gradually increased in number (Fig. 5b, c). This contrasted with the decrease in number of vinculin-positive megakaryocytes. On day 1 after birth, almost all quiescent HSCs in liver lobules appeared positive for vinculin, while a few vinculin-positive megakaryocytes were as yet scattered in liver parenchyma (Fig. 5d). In the postnatal development, the vinculin-positive HSCs appeared to increase in cell size and extend subendothelial processes. The quiescent HSCs on day 5 and day 7 after birth showed almost the same vinculin expression (Fig. 5e–h) but contained less numerous fat droplets compared with those of normal adult rat livers. In the acute CCl_4-induced liver injuries at 48 h after an intraperitoneal injection of CCl_4, the hepatocytes in zones 2 and 3 showed severe degeneration and necrosis. The HSCs in this area were activated, swollen and became intensely stained with vinculin. Not only such activated HSCs, but also quiescent HSCs in the adjoining surviving liver parenchyma showed the positive immunoreaction for vinculin (Fig. 6a). However, if the sections were not pretreated with MW, all liver tissues including HSCs and vascular smooth muscle cells were negative for vinculin (Fig. 6b). In human autopsied livers showing focal necrosis, the distribution and intensity of vinculin expression in HSCs was almost similar to that in the CCl_4-induced rat liver injuries. In necrotic areas vinculin was strongly expressed in the activated HSCs which were swollen and extended thick cytoplasmic processes. In the perinecrotic areas, the quiescent HSCs were also positive for vinculin (Fig. 7).

Fig. 5 Increased expression for vinculin with development of fetal rat livers. **a** On day 13 of gestation, very little immunoreaction for vinculin along the sinusoidal wall is seen (*arrows*), while considerable numbers of vinculin-positive megakaryocytes (*arrowheads*) are present in growing liver parenchyma. **b** On day 16 of gestation, the vinculin immunoreaction along the sinusoidal wall is increased in intensity. **c** On day 20 of gestation; *C* central vein. **d** On 1 day after birth, almost all quiescent hepatic stellate cells (HSCs) in liver lobules are positive for vinculin, although very few megakaryocytes (*arrows*) are scattered. **e**, **f** On day 5 after birth (**f** higher magnification). **g**, **h** On day 7 after birth; *P* portal tract, (**h** higher magnification). In higher magnifications (**f** and **h**), quiescent HSCs containing small fat droplets (*arrows*) are positive for vinculin. All liver tissue sections have been pretreated with microwave oven heating before immunostaining. ×220 (**a**), ×110 (**b**–**e**, **g**), ×560 (**f**, **h**); *bar* 50 μm (**a**), 100 μm (**b**–**e**, **g**), 20 μm (**f**, **h**)

Immunoelectron microscopy of HSCs in normal adult rat livers

Immunoelectron microscopy clearly demonstrated that the vinculin-positive cells along the sinusoidal wall of

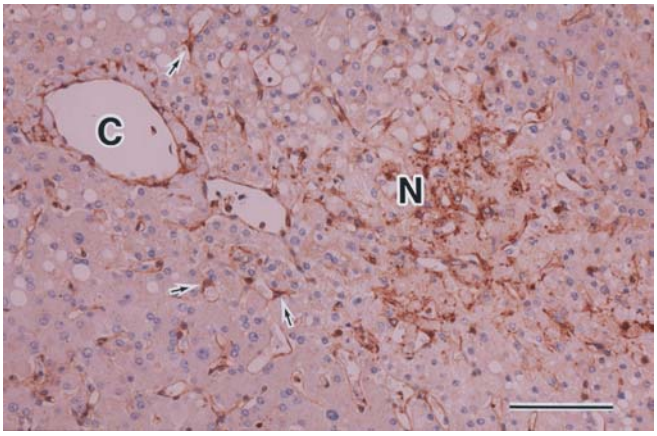

Fig. 7 Vinculin immunostaining in a formalin-fixed, paraffin-embedded autopsied human liver tissue section showing focal necrosis. Vinculin is positive not only for activated hepatic stellate cells (HSCs) in necrotic areas (*N*), but also for quiescent HSCs (*arrows*) in perinecrotic surviving areas. Pretreated with microwave oven heating of the tissue section before immunostaining. *C* central vein. ×130, *bar* 100 μm

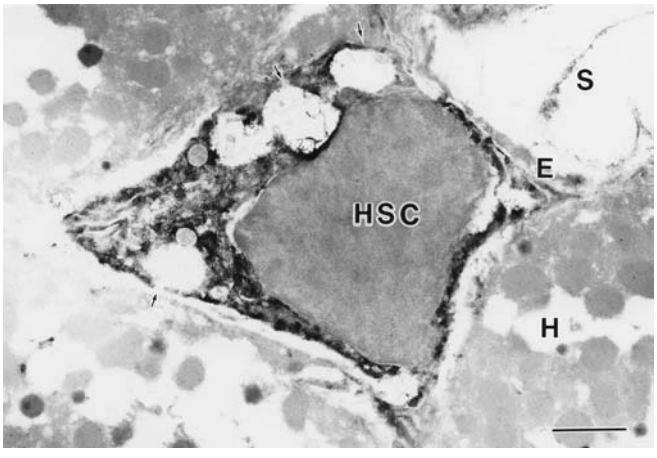

Fig. 8 Immunoelectron micrograph of a vinculin-positive quiescent hepatic stellate cell (*HSC*). A sinusoidal endothelial cell (*E*) is negative for vinculin. *H* liver cell, *S* sinusoid, *arrows* intracytoplasmic small fat droplets of HSC. ×4,540, *bar* 2 μm

normal adult rat livers were exclusively quiescent HSCs containing small fat droplets. Vinculin was expressed along the cell membrane and in the cytoplasm (Fig. 8).

Discussion

Cultured cells, including fibroblasts, epithelial cells, endothelial cells, and platelets, form the specialized structure on the cell surface known as focal adhesions, adhesion plaques, and focal contacts [17, 18]. Analogous structures to the focal adhesions seen in tissue culture are also found in vivo [6], including dense plaques in smooth muscle cells [17], myotendinous junctions in skeletal muscles [6], and fibronexus in myofibroblasts [14]. Vinculin is a permanent and major member of the protein complex that links actin filaments to the plasma membrane [5, 16, 17, 18]. The LI90 cells, exhibiting morphologic and functional features characteristic of HSCs [28], were established from a human hepatic mesenchymal tumor [28] and nowadays generally used as a human HSC cell line for in vitro studies on HSCs [20, 25]. In the cultured LI90 cells, the fluorescence of vinculin revealed with FITC occurred predominantly as small linear focal patches along the cell surface. As this staining pattern has been reported to be characteristic of focal contacts in cultured human dermal fibroblasts [17], the fluorescence of vinculin in LI90 cells may correspond to the site of dense plaques. According to Di Sario et al. (2002) [10], on cultured rat HSCs vinculin appeared evenly dispersed around the cell periphery. After the stimulation with platelet-derived growth factor, vinculin was arranged in dense clusters at the end of polarized extensions. Immunoelectron microscopy clearly demonstrated in this study that vinculin-positive cells along the sinusoidal wall in normal adult rat livers were exclusively quiescent HSCs containing small fat droplets. On a subcellular level, vinculin was expressed along the cell surface and in the cytoplasm of the HSCs and also in their subendothelial processes. In marked contrast to these findings of HSCs in culture and immunoelectron microscopy, HSCs were always negative for vinculin in archival formalin-fixed, paraffin-embedded tissue sections of human and rat livers. Formalin fixation has possibly masked or modified the antigenicity of vinculin protein in HSCs. Actually, in this study, the antigen retrieval technique on the archival liver tissue sections yielded excellent retrieval effects for vinculin antigenicity. This indicates that the modification of protein structure by formalin is reversible under high-temperature heating treatment [36, 38]. In the sections of normal rat liver tissues, the distribution and intensity of vinculin immunoreaction was essentially the same as those of desmin, one of the most reproducible and reliable immunohistochemical markers for rat HSCs [2, 7, 39, 44]. Quiescent HSCs clearly exhibited a coexpression of vinculin and desmin. Almost all the quiescent HSCs showed the positive staining for vinculin, with a good preservation of liver architecture and cellular details. Linear occurrence of immunoreaction for vinculin along the sinusoidal wall may exhibit the perisinusoidal cellular network of HSCs in normal adult livers. The HSCs are reported to be originated from the undifferentiated mesenchymal cells of the septum transversum which are incorporated into the tissue space between growing hepatoblasts and primitive sinusoids invading the septum transversum in early development of livers [13]. Although vinculin, like desmin [42], may actively participate both in the control of cellular interactions during early embryonic development and in cell differentiation [11], the expression of vinculin on HSCs was low in early organogenesis of rat livers. From the vinculin immunostaining of fetal rat livers in this study, the perisinusoidal cellular network of vinculin-positive HSCs in developing livers may be gradually formed from the early to late

gestational stages and extensively developed on day 1 after birth. However, the present study demonstrates that the vinculin antibody, by applying antigen retrieval technique on archival formalin-fixed liver tissue sections, can stain not only quiescent HSCs, but also activated HSCs in the same section. It would allow us to simultaneously examine both types of HSCs in various portions of diseased livers and postulate the mechanism of HSC activation from these in vivo findings. As the antigen retrieval technique based on MW in citrate buffer is a very simple and reproducible method [33, 36, 37, 38], the immunostaining of vinculin on routinely fixed/processed archival liver tissue sections may be useful for the better understanding of pathobiology of HSCs. According to previous studies [36, 40, 43], after the use of microwave pretreatment, certain antibodies that were typically unreactive with formalin-fixed tissues on a conventional immunostaining procedure gave an excellent immunostaining. The results of immunostaining on routinely processed tissue using antigen retrieval are usually equal to (and occasionally better than) the frozen tissue [37]. Furthermore, as the pretreatment of MW is a powerful tool also for broadening the use of antibodies for immunostaining [9, 43], various antibodies of previously reported immunohistochemical markers for HSCs, which are now restricted to use in frozen sections and acetone-fixed cultured cells, should be examined for immunoreactivity in formalin-fixed, paraffin-embedded liver tissue sections, by the appropriate use of MW pretreatment for retrieval of masked antigens.

In conclusion, in formalin-fixed, paraffin-embedded liver tissue sections, if pretreated with MW of the sections, the vinculin antibody clearly stains quiescent HSCs throughout normal liver lobules and simultaneously stains both the quiescent and activated HSCs in diseased human and rat livers.

Acknowledgements We would like to thank Mr. T. Tokaji, Ms. H. Yamasaki, and Ms. T. Kadota, First Department of Pathology, Mr. M. Shirota, Medical Research Laboratory, Kochi Medical School, for their excellent technical assistance. We are also grateful to Mr. D. Ribble, Department of English, Kochi Medical School, for English correction of our manuscript. This study was supported in part by a Grant-in-Aid for Scientific Research from the Ministry of Education, Culture, Sports, Science and Technology in Japan, grant C 13670176.

References

1. Asijee GM, Sturk A, Bruin T, Wilkinson JM, Ten Cate JW (1990) Vinculin is a permanent component of the membrane skeleton and is incorporated into the (re)organizing cytoskeleton upon platelet activation. Eur J Biochem 189:131–136
2. Ballardini G, Fallani M, Biagini G, Bianchi FB, Pisi E (1988) Desmin and actin in the identification of Ito cells and in monitoring their evolution to myofibroblasts in experimental liver fibrosis. Virchows Arch 56:45–49
3. Buniatian G, Gebhardt R, Schrenk D, Hamprecht B (1996) Colocalization of three types of intermediate filament proteins in perisinusoidal stellate cells: glial fibrillary acidic protein as a new cellular marker. Eur J Cell Biol 70:23–32
4. Buniatian G, Hamprecht B, Gebhardt R (1996) Glial fibrillary acidic protein as a marker of perisinusoidal stellate cells that can distinguish between the normal and myofibroblast-like phenotypes. Biol Cell 87:65–73
5. Burridge K, Feramisco JR (1980) Microinjection and localization of a 130 K protein in living fibroblasts: a relationship to actin and fibronectin. Cell 19:587–595
6. Burridge K, Fath K, Kelly T, Nuckolls G, Turner C (1988) Focal adhesions: transmembrane junctions between the extracellular matrix and the cytoskeleton. Ann Rev Cell Biol 4:487–525
7. Burt AD, Robertson JL, Heir J, MacSween RNM (1986) Desmin-containing stellate cells in rat liver; distribution in normal animals and response to experimental acute liver injury. J Pathol 150:29–35
8. Cassiman D, Van Pelt J, De Vos R, Van Lommel F, Desmet V, Yap S-H, Roskams T (1999) Short communication. Synaptophysin: a novel marker for human and rat hepatic stellate cells. Am J Pathol 155:1831–1839
9. Cattoretti G, Pileri S, Parravicini C, Becker MHG, Poggi S, Bifulco C, Key G, D'amato L, Sabattini E, Feudale E, Reynolds F, Gerdes J, Rilke F (1993) Antigen unmasking on formalin-fixed, paraffin-embedded tissue sections. J Pathol 171:83–98
10. Di Sario A, Bendia E, Svegliati-Baroni G, Marzioni M, Ridolfi F, Trozzi L, Ugili L, Saccomanno S, Jeqequel AM, Benedetti A (2002) Rearrangement of the cytoskeletal network induced by platelet-derived growth factor in rat hepatic stellate cell: role of different intracellular signaling pathways. J Hepatol 36:179–190
11. Duband J-L, Thiery JP (1990) Spatio-temporal distribution of the adherens junction-associated molecules vinculin and talin in the early avian embryo. Cell Differ Dev 30:55–76
12. Enzan H, Himeno H, Iwamura S, Saibara T, Onishi S, Yamamoto Y, Hara H (1994) Immunohistochemical identification of Ito cells and their myofibroblastic transformation in adult human liver. Virchows Arch 424:249–256
13. Enzan H, Himeno H, Hiroi M, Kiyoku H, Saibara T, Onishi S (1997) Development of hepatic sinusoidal structure with special reference to the Ito cells. Microsc Res Tech 39:336–349
14. Eyden BP (1993) Brief review of the fibronexus and its significance for myofibroblastic differentiation and tumor diagnosis. Ultrastruct Pathol 17:611–622
15. Gard AL, White FP, Dutton GR (1985) Extra-neural glial fibrillary acidic protein (GFAP) immunoreactivity in perisinusoidal stellate cells of rat liver. J Neuroimmunol 8:359–375
16. Geiger B, Tokuyasu KT, Dutton AH, Singer SJ (1980) Vinculin, an intracellular protein localized at specialized sites where microfilament bundles terminate at cell membranes. Proc Natl Acad Sci U S A 77:4127–4131
17. Grove BD, Pfeiffer DC, Allen S, Vogl AW (1990) Immunofluorescence localization of vinculin in ectoplasmic ("junctional") specializations of rat Sertoli cells. Am J Anat 188:44–56
18. Hemmings L, Barry ST, Critchley DR (1995) Cell-matrix adhesion: structure and regulation. Biochem Soc Trans 23:619–626
19. Ikeda K, Kawada N, Wang YQ, Kadoya H, Nakatani K, Sato M, Kaneda K (1998) Short communication. Expression of cellular prion protein in activated hepatic stellate cells. Am J Pathol 153:1695–1700
20. Imai K, Senoo H (1998) Morphology of sites of adhesion between hepatic stellate cells (vitamin A-storing cells) and a three-dimensional extracellular matrix. Anat Rec 250:430–437
21. Jin Y-L, Enzan H, Kuroda N, Hayashi Y, Nakayama H, Zhang Y-H, Toi M, Miyazaki E, Hiroi M, Guo L-M, Saibara T (2003) Tissue remodelling following submassive hemorrhagic necrosis in rat livers induced by an intraperitoneal injection of dimethylnitrosamine. Virchows Arch 442:39–47
22. Kitada T, Seki S, Ikeda K, Nakatani K, Sakaguchi H, Kawada N, Kadoya H, Kaneda K (2000) Clinicopathological characterization of prion: a novel marker of activated human hepatic stellate cells. J Hepatol 33:751–757

23. Knittel T, Aurisch S, Neubauer K, Eichhorst S, Ramadori G (1996) Cell-type-specific expression of neural cell adhesion molecule (N-CAM) in Ito cells of rat liver. Up-regulation during in vitro activation and in hepatic tissue repair. Am J Pathol 149:449–462
24. Knook DL, Seffelaar AM, de Leeuw AM (1982) Fat-storing cells of the rat livers, their isolation and purification. Exp Cell Res 139:468–471
25. Kojima N, Sato M, Imai K, Miura M, Matano Y, Senoo H (1998) Hepatic stellate cells (vitamin A-storing cells) change their cytoskeleton structure by extracellular matrix components through a signal transduction system. Histochem Cell Biol 110:121–128
26. Levy MT, McCaughan GW, Abbott CA, Park JE, Cunningham AM, Müller E, Rettig WJ, Gorrell MD (1999) Fibroblast activation protein: a cell surface dipeptidyl peptidase and gelatinase expressed by stellate cells at the tissue remodelling interface in human cirrhosis. Hepatology 29:1768–1778
27. Levy MT, McCaughan GW, Marinos G, Gorrrell MD (2002) Intrahepatic expression of the hepatic stellate cell marker fibroblast activation protein correlates with the degree of fibrosis in hepatitis C virus infection. Liver 22:93–101
28. Murakami K, Abe T, Miyazawa M, Yamaguchi M, Masuda T, Matsuura T, Nagamori S, Takeuchi K, Abe K, Kyogoku M (1995) Establishment of a new human cell line, LI90, exhibiting characteristics of hepatic Ito (fat-storing) cells. Lab Invest 72:731–739
29. Nakatani K, Seki S, Kawada N, Kobayashi K, Kaneda K (1996) Expression of neural cell adhesion molecule (N-CAM) in perisinusoidal stellate cells of the human liver. Cell Tissue Res 283:159–165
30. Neubauer K, Knittel T, Aurisch S, Fellmer P and Ramadori G (1996) Glial fibrillary acidic protein—a cell type specific marker for Ito cells in vivo and in vitro. J Hepatol 24:719–730
31. Niki T, De Bleser PJ, Xu G, Van Den Berg K, Wisse E, Geerts A (1996) Comparison of glial fibrillary acidic protein and desmin staining in normal and CCl_4-induced fibrotic rat livers. Hepatology 23:1538–1545
32. Niki T, Pekny M, Hellemans K, De Bleser P, Van Den Berg K, Vaeyens F, Quartier E, Schuit F, Geerts A (1999) Class VI intermediate filament protein nestin is induced during activation of rat hepatic stellate cells. Hepatology 29:520–527
33. Pileri SA, Roncador G, Ceccarelli C, Piccioli M, Briskomatis A, Sabattini E, Ascani S, Santini D, Piccaluga PP, Leone O, Damiani S, Ercolessi C, Sandri F, Pieri F, Leoncini L, Falini B (1997) Antigen retrieval techniques in immunohistochemistry: comparison of different methods. J Pathol 183:116–123
34. Ramadori G, Veit T, Schwögler S, Dienes HP, Knittel T, Rieder H, Meyer zum Büschenfelde K-H (1990) Expression of the gene of the α-smooth muscle-actin isoform in rat liver and in rat fat-storing (ITO) cells. Virchows Arch 59:349–357
35. Schmitt-Gräff A, Krüger S, Bochard F, Gabbiani G, Denk H (1991) Modulation of alpha smooth muscle actin and desmin expression in perisinusoidal cells of normal and diseased human livers. Am J Pathol 138:1233–1242
36. Shi S-R, Key ME, Kalra KL (1991) Antigen retrieval in formalin-fixed, paraffin-embedded tissues: an enhancement method for immunohistochemical staining based on microwave oven heating of tissue sections. J Histochem Cytochem 39:741–748
37. Shi S-R, Cote RJ, Taylor CR (1997) Antigen retrieval immunohistochemistry: past, present, and future. J Histochem Cytochem 45:327–343
38. Shi S-R, Cote RJ, Taylor CR (2001) Antigen retrieval techniques: current perspectives. J Histochem Cytochem 49:931–937
39. Takase S, Maria Leo MA, Nouchi T, Lieber CS (1988) Desmin distinguishes cultured fat-storing cells from myofibroblasts, smooth muscle cells and fibroblasts in the rat. J Hepatol 6:267–276
40. Taylor CR, Shi S-R, Cote RJ (1996) Review. Antigen retrieval for immunohistochemistry. Status and need for greater standardization. Appl Immunohistochem 4:144–166
41. Trim N, Morgan S, Evans M, Issa R, Fine D, Afford S, Wilkins B, Iredale J (2000) Hepatic stellate cells express the low affinity nerve growth factor receptor p75 and undergo apoptosis in response to nerve growth factor stimulation. Am J Pathol 156:1235–1243
42. Vassy J, Rigaut JP, Briane D, Kraemer M (1993) Confocal microscopy immunofluorescence localization of desmin and other intermediate filament proteins in fetal rat livers. Hepatology 17:293–300
43. Williamis JH, Mepham BL, Wright DH (1997) Tissue preparation for immunocytochemistry. J Clin Pathol 50:422–428
44. Yokoi Y, Namihisa T, Kuroda H, Komatsu I, Miyazaki A, Watanabe S, Usui K (1984) Immunocytochemical detection of desmin in fat-storing cells (Ito Cells). Hepatology 4:709–714

Virchows Arch (2003) 443:87–92
DOI 10.1007/s00428-003-0816-0

CASE REPORT

Marcos A. Rossi · Cláudio S. Santos

Sepsis-related microvascular myocardial damage with giant cell inflammation and calcification

Received: 7 March 2003 / Accepted: 1 April 2003 / Published online: 26 April 2003
© Springer-Verlag 2003

Abstract We report a case of a 27-year-old man who died suddenly 2 days after being discharged from the intensive care unit where he had resided for 25 days due to severe sepsis. On postmortem examination, the findings were restricted to the heart and characterized by microvascular myocardial damage with giant cell inflammation and calcification. The microcirculation seems to be involved in the mechanism of cell injury, very likely due to flow disturbances caused by septic shock. The dystrophic calcification occurred in myocytes showing myocytolysis. Lysozyme produced by macrophages and myocytes in areas of myocytolysis and giant cells appear to function cooperatively and/or synergistically to influence mineralization. In addition, the expression of inducible nitric oxide synthase by myocytes implies that nitric oxide could contribute to myocardial cell damage. Immunolabeling studies of the giant cells confirmed that they are derived from macrophages.

Keywords Sepsis · Heart · Microvascular myocardial damage · Nitric oxide · iNOS protein

Introduction

This report is about an autopsy case of microvascular myocardial damage with giant cell inflammation and calcification following long-term severe sepsis. The findings are arranged in an apparent sequence of events to explain the pathogenesis.

M. A. Rossi (✉) · C. S. Santos
Department of Pathology,
Faculty of Medicine, University of São Paulo,
14049–900 Ribeirão Preto SP, Brazil
e-mail: marossi@fmrp.usp.br
Tel.: +55-16-6023130
Fax: +55-16-6023130

Methods

Tissue specimens from both atria and the left and right ventricular walls were taken 6 h after death, fixed in buffered formaldehyde, and processed for routine light microscopic examination using hematoxylin and eosin, and von Kossa stains. Small cubes of tissue (3–8 mm) were embedded in glycolmetacrylate, sectioned at 2 μm, and stained with toluidine blue. Immunohistochemical stainings using the avidin-biotin-peroxidase complex method were performed with antibodies against macrophages (mouse anti-human macrophages; Dako, CD68, clone KP1; 1:1000), T lymphocytes (mouse anti-human T lymphocytes; Dako, CD45RO, UCHL1; 1:100), B lymphocytes (mouse anti-human B lymphocytes; Dako, CD20, L26; 1:200), desmin (mouse anti-human desmin; Dako, desmin, D33; 1:100), muramidase (mouse anti-human lysozyme; Dako; 1:1000), inducible nitric oxide synthase (iNOS) (mouse anti-human iNOS; BD Biosciences; 1:20), and endothelial nitric oxide synthase (eNOS) (mouse anti-human eNOS; BD Biosciences; 1:100).

Case report

A 27-year-old-man was admitted to the University Hospital due to worsening of a severe respiratory tract infection and septic shock. The patient had been treated in a basic unit of health with i.v. cephalosporin and catecholamines.

Physical examination revealed a fairly well-nourished man. His temperature was 37.2°C, pulse 144, and respiration 12. Blood pressure was 130 mmHg systolic, 60 mmHg diastolic (maintained with norepinephrine); without a vasopressor, the blood pressure dropped to 70 mmHg systolic, 40 mmHg diastolic. Examination of the chest revealed diffuse rales, mainly over the lower half of the right lung. The heart was not enlarged and no cardiac murmurs were heard. There was no swelling of the legs.

The urine gave a + test for bilirubin and ++ for protein; the sediment contained 10–15 white cells per high power field. The hemoglobin was 13.3, the hematocrit was 39%, and the white cell count was 2200, with 74% of neutrophils. The platelet count was 52,000. Blood culture was negative.

The patient was then placed on intensive cardiopulmonary support and treated with antibiotics (clarithromycin and ceftriaxone) and catecholamines. On the third hospital day, three episodes of supraventricular tachycardia occurred, successfully abolished with electrical cardioversion. Sinusitis caused by highly virulent *Pseudomonas spp.* and focal pneumonia by *Trychophyton bergelii* ensued during the following 3 weeks in the intensive care unit (ICU) and were successfully treated. Serum calcium concentrations and phosphate activities were normal, and no significant viral titers

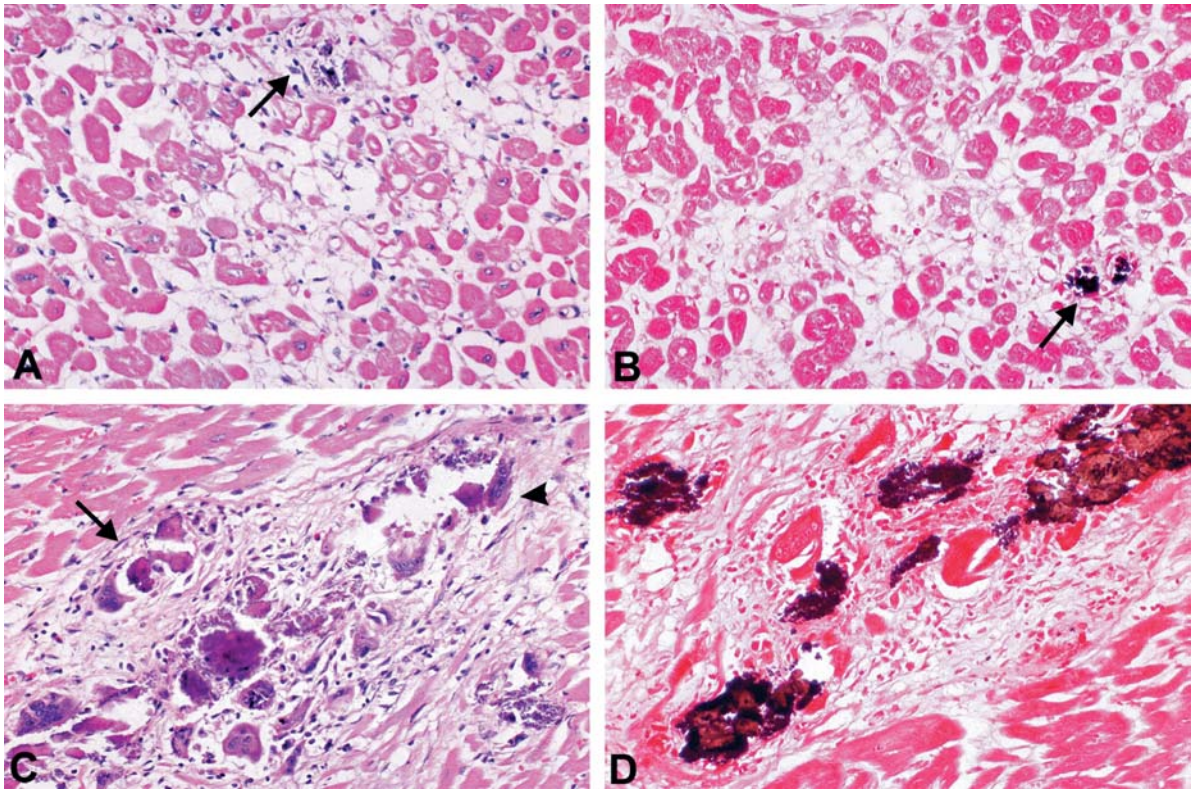

Fig. 1 A Focus of myocytolytic necrosis. Cytoplasmic calcification of myocytes (*arrow*); hematoxylin and eosin, ×535. **B** Calcium deposits in myocyte (*arrow*) in a focus of myocytolysis; von Kossa stain, ×535. **C** Typical myocardial lesion showing lymphomononuclear inflammatory infiltrate, multinucleated giant cells (*arrowheads*), and heavily and granularly calcified myocardial cells (*arrows*); hematoxylin and eosin, ×430. **D** Heavily calcified myocardial cells; von Kossa stain, ×430

were detected during the clinical course. Two echocardiographic examinations performed on day 21 and day 23 after admission showed no abnormalities. The patient gradually improved and was discharged from the ICU to the infirmary on day 25. On this day, X-rays of the chest showed moderate pulmonary congestion and a mild-to-moderately enlarged heart. Two days later the patient was found dead in his bed.

Autopsy findings

On postmortem examination, the significant findings were restricted to the heart, which weighed 470 g and was globally enlarged due to dilatation and hypertrophy, with flaccid ventricular walls. The cut surface of the myocardium showed interstitial fibrosis and chalky whitish punctate foci, particularly in the subepicardial areas, more pronounced in the diaphragmatic wall of the left ventricle. The coronary arteries were widely patent and the cardiac valves were normal. There was no evidence of myocardial infarction. The left and right lungs weighed 606 g and 785 g, respectively, and showed congestion and mild chronic interstitial disease characterized by inflammation and fibrosis in the alveolar walls. The liver and spleen were congested.

The histological examination of the myocardial tissue disclosed widespread interstitial perimysial fibrosis and foci of myocytolytic myocytes and calcified myocardial cells associated with inflammatory cells admixed with multinucleated giant cells. However, granulomas were absent. The findings can be arranged in an apparent sequence of events. In the first stage, foci of myocytolytic necrosis with cytoplasmic calcification are associated with mononuclear cells, mainly macrophages and T lymphocytes. The appearance of heavily calcified myocardial cells and multinucleated giant cells characterize the second stage (Fig. 1A, C). The von Kossa stain confirmed calcium deposits in the hematoxyphilic material (Fig. 1B, D). Organisms (bacteria, fungi, spirochetes, or viral mechanisms) could not be detected. The mononuclear cells reacted with antibodies against CD68 and muramidase (macrophages) and CD45RO (T lymphocytes) (Fig. 2A–C). Very few mononuclear cells reacted against CD20 (B lymphocytes). The giant cells reacted with antibodies against CD68 and muramidase (lysozyme) (Fig. 2B, D); none revealed any reactivity with the anti-desmin antibody (Fig. 2E). Calcified myocardial cells and many of those showing myocytolysis reacted with antibody against lysozyme (Fig. 2D). The normal myocytes displayed desmin expression; whereas, in the areas of myocytolysis, the desmin expression was more accentuated in the subsarcolemma (Fig. 2E, F). Practically all myocytes stained positively for iNOS protein by immunohistochemistry. However, in both first- and second-stage lesions, the myocardial cells showing lysis of

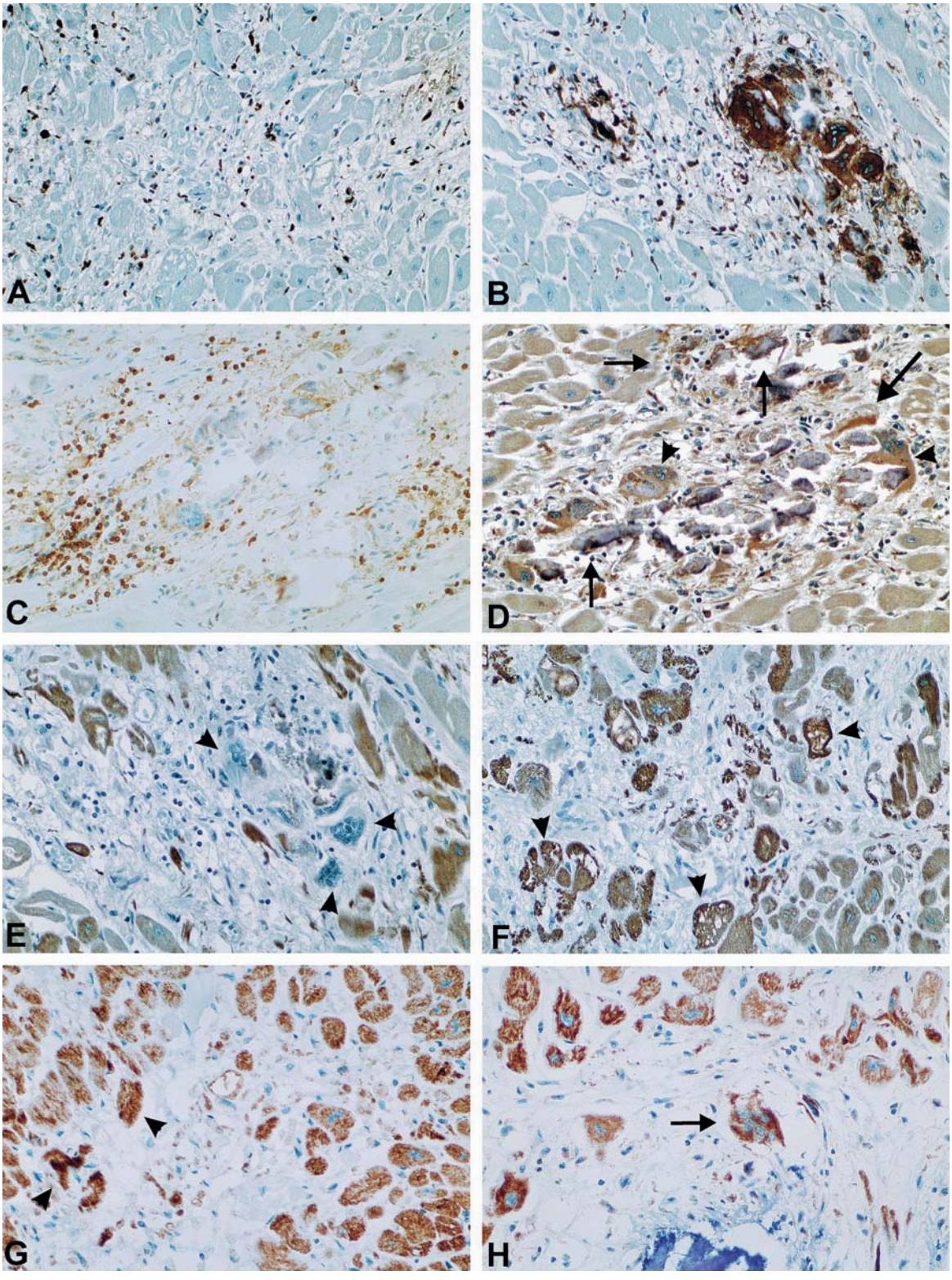

Fig. 2 A Focus of myocytolytic necrosis. Many mononuclear cells reacted with the antibody against CD68, the macrophage marker, ×430 . **B** Typical myocardial lesion. Giant cells and mononuclear cells reacted with the antibody against CD68, ×430. **C** Typical myocardial lesion. Many mononuclear cells reacted with the antibody against CD45RO, demonstrating that the lymphocytes of the inflammatory infiltrate are predominantly T cells, ×430. **D** Typical myocardial lesion. The multinucleated giant cells reacted with the antibody against muramidase (lysozyme; *arrowheads*). Calcified myocardial cells (*arrows*) and many of those showing myocytolysis (*thick arrow*) reacted with this antibody, ×535. **E** Typical myocardial lesion. The giant cells revealed no reactivity with the anti-desmin antibody (*arrowheads*). The desmin expression in cells showing myocytolysis is more accentuated in the subsarcolemma, ×535. **F** Focus of myocytolytic necrosis. The desmin expression is more intense in the cells showing myocytolysis (*arrowheads*), ×535. **G** Focus of myocytolytic necrosis. Myocytes and macrophages stained positively for iNOS protein by immunolabeling. Myocytolytic cells presented more intense immunolabeling (*arrowheads*), ×600. **H** Typical myocardial lesion. Giant cells (*arrow*), macrophages, and myocytes stained positively for iNOS protein by immunolabeling, ×600

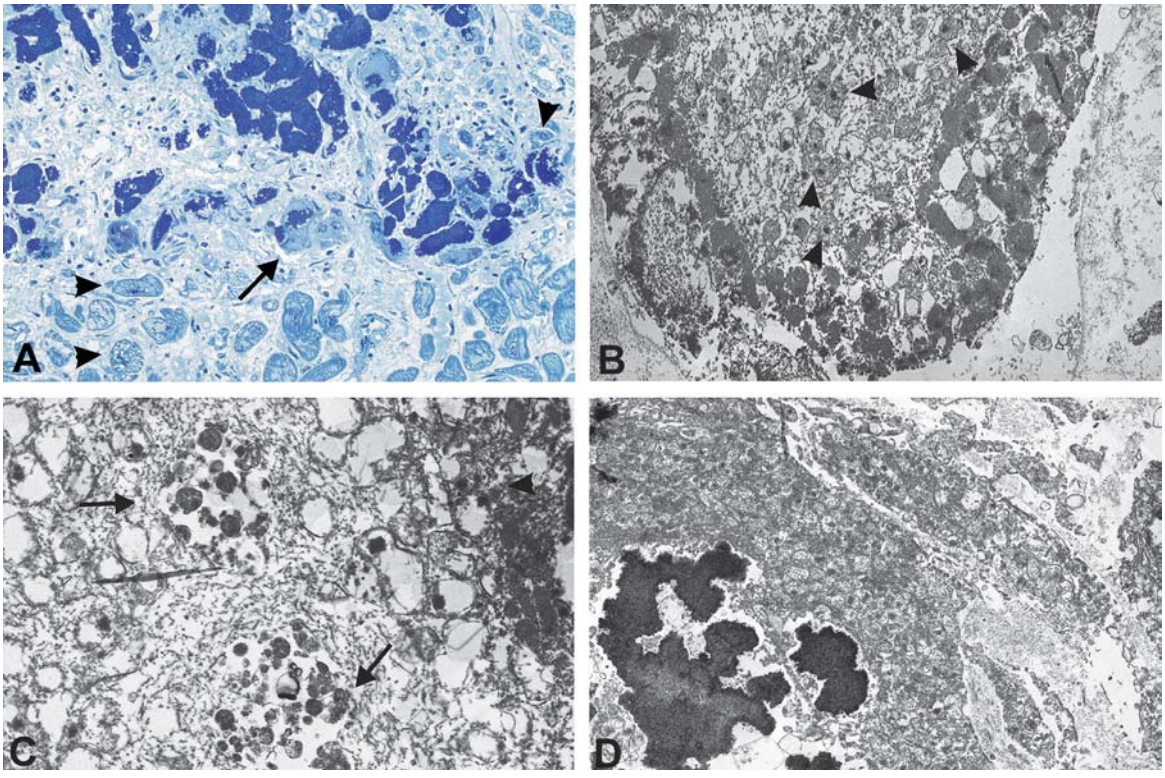

Fig. 3 **A** Typical myocardial lesion. Myocardial cells showing myocytolysis with granular calcification (*arrowheads*) strongly stained with toluidine blue. Multinucleated giant cells with phagocytosed calcium can be seen (*arrows*); toluidine blue, ×430. **B** Electron micrograph. Portion of a myocardial cell showing myocytolysis. Intramitochondrial calcareous granules increased in size and number can be seen (*arrowheads*), ×4400. **C** Electron micrograph. Portion of a myocardial cell showing myocytolysis. Enlarged intramitochondrial calcareous granules, ×7000. **D** Calcified masses within a myocardial cell, ×4400

myofilaments (myocytolysis) presented more intense immunolabeling for iNOS (Fig. 2G, H). Apparent iNOS immunolabeling was also seen in infiltrating macrophages (positive to CD68). Weak immunoreactivity to eNOS was seen in subendocardial ventricular myocytes and apparent immunolabeling was detected in the endothelium of intramyocardial vessels.

The glycol metacrylate embedded material disclosed details of the basic lesion, clearly demonstrating myocytolysis of peripheral myocardial cells, many of them with granular calcific deposits strongly stained with toluidine blue, progressive granular calcification of myocytes and multinucleated giant cells, many of them with phagocytosed calcium (Fig. 3A).

The ultrastructural study disclosed the mitochondrial localization of calcium in myocytolytic cells characterized by an increase in size and in the number of intramitochondrial calcareous granules. The fusion of these granules resulted in calcified mitochondria and, in turn, calcified masses within and/or outside the cells (Fig. 3B–D).

Discussion

This report is about an autopsy case of microvascular myocardial damage with giant cell inflammation and calcification following long-term severe sepsis.

A basic point needs elucidation concerning this very special myocardial injury: is this a case of sepsis-related microvascular myocardial damage with giant cell inflammation and calcification, a case of idiopathic giant cell myocarditis with unusual calcification, or a case of calcified myocardial necrosis after infectious myocarditis? The latter two possibilities are very unlikely. The histological findings in idiopathic giant cell myocarditis consist of widespread inflammatory infiltrate composed of lymphocytes, histiocytes, plasma cells and eosinophils admixed with giant cells, particularly at the margins of the necrotic zones of the myocardium. Moreover, calcific lesions are very uncommon in this type of myocarditis, with only one case of calcium overload reported previously [12]. Conversely, in the present case, the giant cells are always near the calcified areas and there is not much inflammation away from the areas of myocytolysis. However, although unusual in clinical presentation [1], myocardial calcification following viral myocarditis has been reported in experimental studies [3, 5, 21]. Viral myocarditis is most frequently characterized by an

interstitial mononuclear inflammatory infiltrate, predominantly lymphocytic, with damage to adjacent myocytes. In the present case, the sequence of events provides a clue to the pathogenesis of tissue injury: the myocyte damage, which takes the form of multifocal myocytolysis, occurs prior to the visible mononuclear cell accumulation, most of which are histiocytes. Additionally, the characteristics of the inflammatory process and the non-detection of organisms (bacteria, fungi, or spirochetes) make the possibility of a septic infection as an etiological factor very improbable.

The mechanism of cell injury in the present case could be ascribed to long-term severe sepsis. Although human and experimental studies argue against an ischemic origin of sepsis-induced cardiac injury [2, 13], the hallmark of septic shock is a dysfunctional microcirculation that produces regional flow disturbances and abnormal tissue oxygenation, which may cause relative ischemia in various organs, including the heart [6, 8]. The focal nature of the lesions suggests that the microcirculation could be involved, i.e., the primary site of disease could be at a level capable of causing focal myocytolysis of myocytes in discrete groups. A similar mechanism has been demonstrated in chronic chagasic cardiopathy [14, 15]. In addition, the expression of iNOS by myocardial cells, more intense in myocardial cells showing myocytolysis, could imply that enhanced production of nitric oxide (NO) by iNOS could contribute to hypotension and myocytolysis [17]. NO, directly or indirectly through formation of peroxynitrite, can induce cellular injury and death [4, 9, 22, 23]. One could argue that iNOS protein could be altered in heart samples taken 6 h postmortem. Therefore, control myocardial samples from normal (n=2), septic (n=6), and hypertensive (n=3) hearts were collected 6–10 h after death. Only weak or focal immunoreactivity to iNOS was seen in left ventricular myocytes from normal and hypertensive hearts, whereas diffuse immunolabeling was detected in all hearts from septic patients. (These data, not shown, are part of a study in progress). This finding is supported by previous observations demonstrating no alteration of iNOS protein expression, as evaluated by immunoblot analysis, in ventricular myocardium from non-failing hearts taken 8–64 h postmortem compared with those obtained immediately after transplantation [18]. Moreover, the immunoblotting revealed iNOS protein expression in septic hearts, although no iNOS expression was detected in dilated cardiomyopathy, ischemic cardiopathy, Becker muscular dystrophy, and mitoxantrone-induced toxic cardiopathy.

Cardiac calcification is nearly always dystrophic, i.e., due to deposition of calcium in previously degenerated, devitalized or dead tissue. Less commonly, calcification may be metastatic due to deposits of calcium in previously normal tissue. The former is associated with no generalized abnormality of calcium or phosphate metabolism, as in the present case. In the latter, the calcification is associated with elevated serum calcium concentrations. The pathogenesis of calcification is poorly understood. In dystrophic calcification, it is still debatable whether calcium is a phenomenon secondary to cell injury [16, 20] or one that affects viable cells and leads to irreversible damage [19]. The present case clearly shows that one is witnessing calcification of irreversibly damaged myocardial cells, as intramyocardial granular calcium deposition in and around mitochondria follows myocytolytic necrosis and appears to be a consequence. It is also tempting to suggest enhanced genetic susceptibility of cells to lethal injury and subsequent calcium deposition, similar to observations in certain inbred strains of mice that present a major gene-determining dystrophic cardiac calcification [10]. The loss of myofilamentous structure of myocytes showing myocytolysis led to collapse of intermyofibrillar desmin network and these fibers showed increased lysozyme labeling. Since lysozyme (muramidase) were depicted in macrophages and myocytes in areas of myocytolysis and in giant cells, macrophages and calcified myocardial cells in calcified foci, it is very likely that lysozyme functions cooperatively, and perhaps synergistically, to influence mineralization. It is known that cartilage lysozyme plays an important role in the regulation and initiation of calcification [11]. Also, shell matrix lysozyme may be a structural protein that in soluble form influences calcium carbonate deposition during avian eggshell mineralization [7].

The facts that the giant cells constantly showed strong positivity for lysozyme, predominantly present in histiocytes and myeloid-derived cells, and that the macrophage-associated antigen CD68 did not reveal any reactivity with the anti-desmin antibody clearly indicate that the giant cells are derived from macrophage, rather than myocyte, precursors.

In summary, this 27-year-old man died suddenly 2 days after being discharged from the ICU where he had resided for 25 days due to severe sepsis. On postmortem examination, the findings were restricted to the heart and characterized by microvascular myocardial damage with giant cell inflammation and calcification. The microcirculation seems to have been involved in the mechanism of cell injury, very likely due to flow disturbances caused by septic shock. The dystrophic calcification occurred in myocytes showing myocytolysis. Lysozyme produced by macrophages and myocytes in areas of myocytolysis and giant cells appeared to function cooperatively and/or synergistically, influencing mineralization. In addition, the expression of iNOS by myocytes implies that NO could have contributed to myocardial cell damage. Immunolabeling studies of the giant cells confirmed that they are derived from macrophages. Importantly, although this is an isolated case report, it supports the probable key role of ischemia and myocardial injury as a cause of cardiac depression in sepsis and septic shock.

Acknowledgements Supported by a grant from the Fundação de Amparo à Pesquisa do Estado de São Paulo (FAPESP 01/09879–8). Prof. Rossi is Senior Investigator (1A) of the Conselho Nacional de Desenvolvimento Científico e Tecnológico (CNPq–301109/79–6).

The authors would also like to thank Mônica A. Abreu and Maria Elena Riul for their excellent technical assistance.

References

1. Chow LTC, Chow WH (1992) Intracellular calcification: an unusual histological feature of acute myocarditis. Histopathology 21:385–387
2. Cunnion RE, Schaer GL, Parker MM, Natanson C, Parrillo JE (1986) The coronary circulation in human septic shock. Circulation 73:637–644
3. Deguchi H (1981) Ultrastructural alterations of the myocardium in coxsackie B-3 virus myocarditis in mice. Jpn Circ J 45:695–712
4. Eiserich JP, Patel RP, O'Donnell VB (1998) Pathophysiology of nitric oxide and related species: free radical reactions and modifications of biomolecules. Mol Aspects Med 19:221–357
5. Gwathmey JK, Nakao S, Come PC, Goad ME, Serur JR, Als AV, Abelmann WH (1992) An experimental model of acute and subacute myocarditis in the pig. J Am Coll Cardiol 19:864–869
6. Hersh M, Gnidee AA, Bersten AD, Trostel M. Ruthledge FS, Sibbald WJ (1990) Histologic and ultrastructural changes in non-pulmonary organs during early hemodynamic sepsis. Surgery 107:397–410
7. Hincke MT, Gautron J, Panheleux M, Garcia Ruiz J, McKee MD, Nys Y (2000) Identification and localization of lysozyme as a component of eggshell membranes and eggshell matrix. Matrix Biol 19:443–453
8. Hinshaw LB (1996) Sepsis/septic shock: participation of the microcirculation. Crit Care Med 24:1072–1078
9. Ishida H, Ichimori K, Hirota Y, Fukahori M, Nakazawa H (1996) Peroxynitrite-induced cardiac myocyte injury. Free Radic Biol Med 20:343–350
10. Ivandic BT, Qiao J-H, Machleder D, Liao F, Drake TA (1996) A locus of chromosome 7 determines myocardial cell necrosis and calcification (dystrophic cardiac calcinosis) in mice. Proc Natl Acad Sci U S A 93:5483–5488
11. Kuettner KE, Eisenstein R, Sorgente N (1975) Lysozyme in calcifying tissues. Clin Orthop 112:316–339
12. Olbricht HG, Hermann G, Vandesplassche G, Michaelis H, Schneider M, Krause E, Kober G (1990) Calcium overload in human giant cell myocarditis. J Clin Pathol 43:650–653
13. Piper RD, Lee FY, Myers ML, Sibbald WJ (1999) Effects of isoproterenol on myocardial structure and function in septic rats. J Appl Physiol 86:993–1001
14. Rossi MA (1990) Microvascular changes as a cause of chronic cardiomyopathy in Chagas' disease. Am Heart J 120:233–236
15. Rossi MA, Gonçalves S, Ribeiro-dos-Santos R (1984) Experimental *Trypanosoma cruzi* cardiomyopathy in BALB/c mice. The potential role of intravascular platelet aggregation in its genesis. Am J Pathol 114:209–216
16. Rossi MA, Braile DM, Teixeira MD, Carillo SV (1986) Calcific degeneration of pericardial valve xenografts implanted subcutaneously in rats. Int J Cardiol 12:331–339
17. Rubanyi GM (1998) Nitric oxide and circulation shock. Adv Exp Med Biol 454:165–172
18. Thoenes M, Förstermann U, Tracey WR, Bleese NM, Nüssler AK, Scholz H, Stein B (1996) Expression of inducible nitric oxide synthase in failing and non-failing human heart. J Mol Cell Cardiol 28:165–169
19. Trump BF, Berezevsky IK (1995) Calcium-mediated cell injury and cell death. FASEB J 9:219–228
20. Van Fleet JF, Ferrans VJ (1987) Ultrastructural changes in inherited cardiac calcinosis in DBA/2 mice. Am J Vet Res 48:255–261
21. Yanagawa B, Brad Spiller O, Choy J, Luo H, Cheung P, Zhang HM, Goodfellow IG, Evans DJ, Suarez A, Yang D, McMannus BM (2003) Coxsackie B3-associated myocardial pathology and viral load reduced by recombinant soluble human decay-accelerating factor in mice. Lab Invest 83:75–85
22. Yang X, Chowdbury N, Cai B, Brett J, Marboe C, Sciacca RR, Michler RE, Cannon PJ (1994) Induction of myocardial nitric oxide synthase by cardiac allograft rejection. J Clin Invest 94:714–721
23. Zingarelli B, O"Connor M, Wong H, Salzman AL, Szabó C (1996) Peroxynitrite-mediated DNA strand breakage activates poly-ADP ribosyl synthetase and causes cellular energy depletion in macrophages stimulated with lipopolysaccharide. J Immunol 156:350–358

Virchows Arch (2003) 443:93–97
DOI 10.1007/s00428-003-0829-8

CASE REPORT

M. A. den Bakker · S. J. Flood · M. Kliffen

CD31 staining in epithelioid sarcoma

Received: 22 November 2002 / Accepted: 31 March 2003 / Published online: 13 May 2003
© Springer-Verlag 2003

Abstract We report an unusual case of epithelioid sarcoma. The tumour occurred in the finger of a 27-year-old female. The clinical history, histology and the electron microscopy of the lesion were typical for epithelioid sarcoma. However, immunohistochemical analysis showed strong membranous CD31 staining, a finding hitherto not described. All other robust vascular markers, including factor-VIII-related antigen (FVIIIrag) were negative. The findings were compared with the available literature data, leading us to conclude that there is insufficient evidence for endothelial derivation of epithelioid sarcoma, but in the differential diagnosis with vascular tumours CD31 may stain and to rule out angiosarcoma FVIIIrag is a useful antibody.

Keywords Epithelioid sarcoma · CD31 · Immunohistochemistry

Introduction

Epithelioid sarcoma (ES) is a rare but distinctive soft tissue tumour, which most frequently arises in the extremities of young individuals [3, 5]. The classical type of ES often presents as a cutaneous lesion and may be mistaken for a benign process. Histologically, ES is composed of nodular aggregates of monomorphic intermediate sized cells often with eccentrically placed nuclei and deeply eosinophilic cytoplasm, imparting a rhabdoid appearance to the tumour cells. Epithelioid sarcoma tumour nodules frequently form granulomatous structures, which may have central necrosis. The differential diagnosis of ES includes carcinoma and epithelioid mesenchymal tumours. Cutaneous epithelioid angiosarcoma and the recently described tumour epithelioid sarcoma-like hemangioendothelioma (ES-H) are often considered on morphological grounds. In particular ES-H, which shares considerable morphological and immunohistochemical overlap with classical ES needs to be differentiated [2]. In ES, immunoreactivity for cytokeratin and epithelial membrane antigen (EMA) is almost invariably present. CD34 staining, present in most cases of ES, is valuable in ruling out carcinoma. The CD31 marker is often quoted as useful when distinguishing between epithelioid sarcoma and epithelioid angiosarcoma but is positive in ES-H. Although CD31 expression has been described in ES, it is reported as focal and non-membranous. We report a case of epithelioid sarcoma with typical clinical and morphological features but with unusual immunohistochemical findings.

M. A. den Bakker (✉) · M. Kliffen
Department of Pathology, Erasmus Medical Center,
PO Box 1738, 3000 DR Rotterdam, Netherlands
e-mail: m.denbakker@erasmusmc.nl
Tel.: +31-10-4087901, Fax: +31-10-4089487

S. J. Flood
Department of Plastic and Reconstructive Surgery,
Erasmus MC, Rotterdam, Netherlands

Clinical history

A 27-year-old female presented with an ill-defined mass in the soft tissue of the middle phalanx of the fourth finger of the right hand, which had slowly increased in size in a period of 3 years. The clinical impression raised the possibility of a giant cell tumour. An excisional biopsy was initially diagnosed as an inflammatory granulomatous lesion. However, the lesion recurred shortly after removal with ulceration of the skin. Histological review of the original specimen revealed histological findings in keeping with an ES. The finger was subsequently amputated in continuity with the metacarpal bone and submitted for pathological evaluation.

Materials and methods

The amputation specimen was submitted fresh; tumour tissue was reserved for frozen sections and small samples were placed in formalin—glutaraldehyde for electron microscopy (EM). Routine histological haematoxylin and eosin (H&E) stained sections from formalin-fixed paraffin-embedded tissue were prepared and, in

Table 1 Immunohistochemical reagents and staining results. Tissue: *P* paraffin, *F* frozen. Pre-treatment: *w* wet heat antigen retrieval, *pr* protease digestion. Result: ++ strong universal staining, + focal staining, variable intensity, – no staining, *m* membranous, *c* cytoplasmic, *n* nuclear

Antibody (clone)	Manufacturer	Tissue, pretreatment	Dilution	Result
Cytokeratin 8,18 (NCL5D3)	Biogenex, San Ramon, California, USA	P, pr	1:100	++ c
Pancytokeratin (AE1/AE3)	Biogenex	P, w	1:100	++ c
Cytokeratin 19 (RCK108)	Euro-diagnostica, Arnhem, Netherlands	P, w	1:20	++ c
EMA (E29)	Dako, Glostrup, Denmark	P,w	1:2000	++ c
Desmin (D33)	Dako	P, w	1:400	–
Muscle actin (HHF35)	Dako	P, w	1:400	+ c
Vimentin (V9)	Dako	P, w	1:3200	++ c
S100 (rabbit polyclonal)	Dako	P, –	1:2000	–
p53 (D-O7)	Dako	P, w	1:1000	+ n
CD99 (12E7)	Dako	P, w	1:100	++ m
CD31 (JC70A)	Dako	P, w	1:240	++ m
FVIIIrag (2C8)	Dako	P, pr	1:1000	–
CD34 (QBEnd10)	Dako	P, w	1:100	++ m
Fli-1 (polyclonal)	Santa Cruz Biotechnology Inc. Santa Cruz, California, USA	P, w	1:50	+n
EGF-R (H11)	Dako	F	1:80	++ m
VEGF-R1 (Flt-19)	Sigma, Saint Louis, Missouri, USA	F	1:80	–
VEGF-R2 (KDR-1)	Sigma	F	1:400	–
VEGF (JH121)	Oncogene Research Products, San Diego, California, USA	F	1:20	–
Thrombospondin (46.4)	Oncogene Research Products	F	1:320	–
CD146 (P1H12)	Chemicon International Inc. Temecula, California, USA	F	1:100	–
PAL-E	Monosan, Sanbio, Uden, Netherlands	F	1:80	–

addition, PAS and reticulin stains were prepared from selected blocks. Immunohistochemistochemistry was performed in an automated immunostainer on paraffin-embedded tissue and on acetone-fixed cryostat sections, using a polymer based system (Dako Envision, Dako, Glostrup, Denmark; Table 1)

Pathological findings

A nodular and ulcerated area was seen in soft tissues and skin of the middle phalanx, over an area of approximately 1.5×1 cm, extending over the dorsal, lateral and ventral regions (Fig. 1). Grey, shiny firm tissue was seen extending from the ulcerated surface down to the bone but without macroscopic invasion of the tendon or bone. The borders were ill defined; lesional tissue did not appear to involve the joint capsule.

The histology of the excisional biopsy and the amputation specimen were similar. A diffuse and nodular, focally granulomatous appearing lesion composed of intermediate sized cells was seen embedded in collagenous stroma and infiltrating diffusely in muscle and connective tissue. Angio-invasion was clearly present. The cells formed a monotonous population with many rhabdoid cells. Typical "granulomatous" structures with central necrosis were present (Fig. 2A). Fascicular areas were not observed and the cellular composition was exclusively epithelioid in nature.

Fig. 1 Amputation specimen with ulcero-nodular lesions over the mid-phalanx

Immunohistochemical staining

The immunohistochemical results are summarised in Table 1. The tumour cells showed intense staining with cytokeratin antibodies AE1/AE3, NCL5D3 (cytokeratins 8, 18) and cytokeratin 19 (Fig. 2B). Strong EMA staining was seen and the tumour cells expressed CD34 (Fig. 2C) and CD99 with a membranous pattern. Surprisingly, in the biopsy, all tumour cells stained strongly with CD31 antibodies. The staining pattern was membranous and consistent throughout the sample (Fig. 2D). In the amputation specimen, the staining was more variable. However, most tumour cells were positive again with membranous staining. Additional vascular markers were tested, including PAL-E, CD146, factor-VIII-related antigen (FVIIIrag), vascular endothelial growth factor (VEGF), VEGF receptors 1 and 2 and thrombomodulin, these were all negative. Nuclear staining of varying intensity was seen in Fli-1 immunostaining.

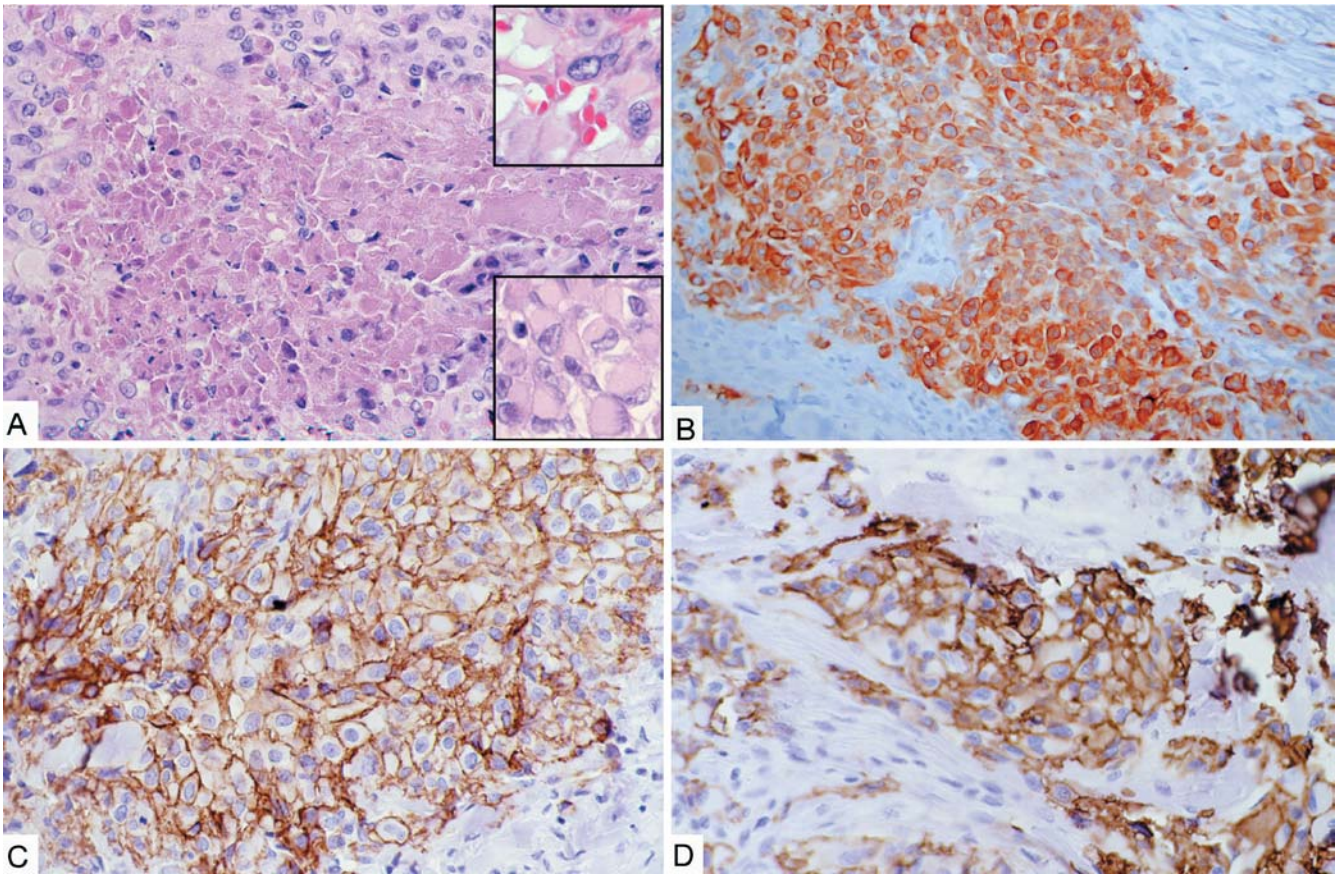

Fig 2 Light microscopy (amputation specimen). **A** Granulomatous structure with central necrosis formed by rhabdoid tumour cells (*lower inset*), occasionally with cytoplasmic vacuolisation (*upper inset*) (H&E staining, ×100, *insets* ×400 magnification). **B** Immunohistochemical staining for cytokeratin 19, cytoplasmic staining is seen (×100 magnification). **C** CD34 staining. Intense membranous staining is present (×100 magnification). **D** Immunohistochemical staining for CD31 shows distinct membranous staining (×100 magnification)

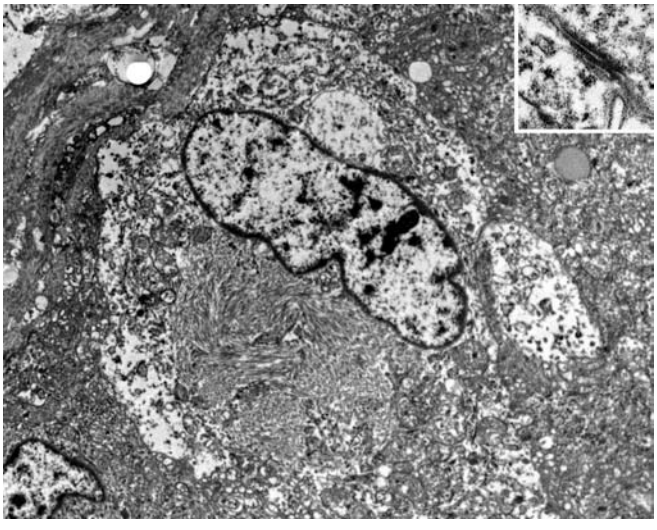

Fig. 3 Electron microscopy. Compact peri-nuclear whorls of intermediate filaments are seen. *Inset* Desmosomes were easily identified in the tumour

Electron microscopy

Compact perinuclear whorled aggregates of filaments were seen in many cells. Well-formed desmosomes were easily identified (Fig. 3). Weibel-Palade bodies were not observed.

Discussion

Epithelioid sarcoma is a unique soft tissue tumour of which the origin is not clear. Two distinct subtypes have been described. The classical form typically occurs in the superficial soft tissues of the distal parts of the extremities [3, 5]. A recently described second form, designated the proximal type of ES, tends to occur in deeper soft tissue of the limb girdles [9, 10]. The long-term prognosis of ES is poor, with local recurrences preceding distant metastases [3]. The typical histological appearance of ES consists of aggregates of monomorphic cells with well-defined cell boundaries and little nuclear pleomorphism. The cytoplasm is eosinophilic and often imparts a rhabdoid appearance to the cells, which on the ultrastruc-

tural level is caused by peri-nuclear aggregates of filaments. A characteristic feature of ES is areas mimicking granulomas, often with central necrosis. Cytoplasmic vacuoles and pseudo-vascular spaces may be seen in ES raising the differential diagnostic possibility of an (epithelioid) vascular lesion sometimes referred to as "angiomatoid ES" [3, 5, 9, 20, 21]. Immunohistochemical findings in ES include staining with epithelial markers such as EMA or cytokeratins and CD34. The latter marker is very useful to rule out metastatic carcinoma. However, in differentiating ES from angiosarcoma, CD34 staining cannot discriminate and, in addition, cytokeratin staining is well recognised in epithelioid angiosarcoma. Although EMA staining is unusual in angiosarcoma, this too has been described [7, 12]. Antibodies to the CD31 antigen PECAM (platelet endothelial cell adhesion molecule) are deemed to be highly specific vascular markers and are often used to mark endothelial derived tumours [4, 14]. In keeping with the nature of PECAM as an adhesion molecule, specific staining by CD31 is membranous. In the case we describe here, strong and consistent membranous CD31 staining was seen in the biopsy specimen and the resection specimen. Weak CD31 immunoreactivity was observed in five of 70 (7%) typical ESs and two of eight angiomatoid ESs in a large series by Miettinen et al. [15]. Other workers have also described positive CD31 staining in peripheral ES in a small percentage of cases [17, 18]. However, in the proximal type CD31 is reported as negative [9, 10]. In all published reports with positive CD31 staining in ES it has been focal and cytoplasmic, not membranous. Because of this unusual finding, we extended our panel of antibodies to include other recognised vascular markers (Table 1). With the exception of Fli-1, a recently described marker of vascular endothelium, no staining was observed [8]. In particular FVIIIrag staining was completely negative. This is consistent with data from the literature where FVIIIrag staining in ES has not been described [1, 3, 9, 11, 15, 18, 19, 21]. A close mimic of ES was recently described by Billings et al. [2]. These authors report on seven cases of a novel vascular tumour entity, which show markedly overlapping features with ES. Due to the absence of metastases indicating low-grade behaviour, it is suggested that this tumour is a new form of hemangioendothelioma for which the name epithelioid sarcoma-like hemangioendothelioma (ES-H) is coined. The clinical presentation and architecture of ES-H is similar to classical ES, although a fascicular and sheet-like growth pattern was also noted, which is not typical for ES. Although the authors note that the cells of ES-H have an epithelioid shape with prominent eosinophilic cytoplasm, they do not describe the typical rhabdoid inclusions, which characterise classical ES, caused by the perinuclear condensation of intermediate filaments. Similar to true vascular neoplasms, ES often has intracytoplasmic lumina, as we describe in the case presented here. In the cases of ES-H, this was an infrequent finding and may be a useful morphological clue when distinguishing these entities. Remarkably, all six cases of ES-H that were analysed immunohistochemically were positive for CD31 (membranous pattern) and for Fli-1 (nuclear) but did not stain for CD34. These observations support an endothelial derivation of this tumour and are similar to the results of the ES case presented here. The Fli-1 antibody is highly specific for Ewing sarcoma and in a single study was found to be a specific marker for endothelium-derived tumours. However, it also stains a small number of non-vascular tumours. At this time, there is not enough experience with this antibody to comment on its use in epithelioid sarcoma [8]. Although the initial series of ES-H is small, CD34 may still serve as a distinguishing immunostain as all cases of ES-H were negative. Unfortunately, EM was not performed on the ES-H cases. The presence of Weibel-Palade bodies and pinocytic vesicles would have strengthened the case for a vascular origin of ES-H. In our case presented here, electron microscopy did not reveal features suggesting endothelial differentiation and were otherwise consistent with ES with perinuclear whorls of intermediate filaments and desmosomes [6, 9, 13, 16]. It is noted that immunohistochemistry has a critical role in distinguishing ES- and ES-H and that CD31 and Fli-1 are important discriminators [2]. We thus conclude that the case of ES described here is highly unusual in its immunohistochemical profile and because of its distinctive CD31 staining and Fli-1 positivity could be mistaken for an angiosarcoma or for the newly described ES-H [2]. However, the morphological features, EM findings and CD34 positivity permit a confident diagnosis of ES. In cases where the differential diagnosis includes ES-H and angiosarcoma, careful attention should be paid to distinguishing morphological features. Addition of FVIIIrag to an immunohistochemical panel in cases where the differential diagnosis includes angiosarcoma is indicated.

Acknowledgements The authors wish to thank Prof. C.D.M. Fletcher, Brigham and Women's Hospital, Boston USA for his expert opinion in this case.

References

1. Arber DA, Kandalaft PL, Mehta P, Battifora H (1993) Vimentin-negative epithelioid sarcoma. The value of an immunohistochemical panel that includes CD34. Am J Surg Pathol 17:302–307
2. Billings SD, Folpe AL, Weiss SW (2003) Epithelioid sarcoma-like hemangioendothelioma. Am J Surg Pathol 27:48–57
3. Chase DR, Enzinger FM (1985) Epithelioid sarcoma. Diagnosis, prognostic indicators, and treatment. Am J Surg Pathol 9:241–263
4. DeYoung BR, Swanson PE, Argenyi ZB, Ritter JH, Fitzgibbon JF, Stahl DJ, Hoover W, Wick MR (1995) CD31 immunoreactivity in mesenchymal neoplasms of the skin and subcutis: report of 145 cases and review of putative immunohistologic markers of endothelial differentiation. J Cutan Pathol 22:215–222
5. Enzinger FM (1970) Epitheloid sarcoma. A sarcoma simulating a granuloma or a carcinoma. Cancer 26:1029–1041
6. Fisher C (1988) Epithelioid sarcoma: the spectrum of ultrastructural differentiation in seven immunohistochemically defined cases. Hum Pathol 19:265–275

7. Fletcher CD, Beham A, Bekir S, Clarke AM, Marley NJ (1991) Epithelioid angiosarcoma of deep soft tissue: a distinctive tumor readily mistaken for an epithelial neoplasm. Am J Surg Pathol 15:915–924
8. Folpe AL, Chand EM, Goldblum JR, Weiss SW (2001) Expression of Fli-1, a nuclear transcription factor, distinguishes vascular neoplasms from potential mimics. Am J Surg Pathol 25:1061–1066
9. Guillou L, Wadden C, Coindre JM, Krausz T, Fletcher CD (1997) "Proximal-type" epithelioid sarcoma, a distinctive aggressive neoplasm showing rhabdoid features. Clinicopathologic, immunohistochemical, and ultrastructural study of a series. Am J Surg Pathol 21:130–146
10. Hasegawa T, Matsuno Y, Shimoda T, Umeda T, Yokoyama R, Hirohashi S (2001) Proximal-type epithelioid sarcoma: a clinicopathologic study of 20 cases. Mod Pathol 14:655–663
11. Manivel JC, Wick MR, Dehner LP, Sibley RK (1987) Epithelioid sarcoma. An immunohistochemical study. Am J Clin Pathol 87:319–326
12. Miettinen M, Fetsch JF (2000) Distribution of keratins in normal endothelial cells and a spectrum of vascular tumors: implications in tumor diagnosis. Hum Pathol 31:1062–1067
13. Miettinen M, Lehto VP, Vartio T, Virtanen I (1982) Epithelioid sarcoma. Ultrastructural and immunohistologic features suggesting a synovial origin. Arch Pathol Lab Med 106:620–623
14. Miettinen M, Lindenmayer AE, Chaubal A (1994) Endothelial cell markers CD31, CD34, and BNH9 antibody to H- and Y-antigens—evaluation of their specificity and sensitivity in the diagnosis of vascular tumors and comparison with von Willebrand factor. Mod Pathol 7:82–90
15. Miettinen M, Fanburg-Smith JC, Virolainen M, Shmookler BM, Fetsch JF (1999) Epithelioid sarcoma: an immunohistochemical analysis of 112 classical and variant cases and a discussion of the differential diagnosis. Hum Pathol 30:934–942
16. Mukai M, Torikata C, Iri H, Hanaoka H, Kawai T, Yakumaru K, Shimoda T, Mikata A, Kageyama K (1985) Cellular differentiation of epithelioid sarcoma. An electron- microscopic, enzyme-histochemical, and immunohistochemical study. Am J Pathol 119:44–56
17. Quezado M (1996) Epithelioid sarcomas: prognostic factors and immunohistochemical profile (abstract). Mod Pathol 9:12
18. Smith ME, Brown JI, Fisher C (1998) Epithelioid sarcoma: presence of vascular-endothelial cadherin and lack of epithelial cadherin. Histopathology 33:425–431
19. von Hochstetter AR, Grant JW, Meyer VE, Honegger HP,Schreiber A (1990) Angiomatoid variant of epithelioid sarcoma. The value of immunohistochemistry in the differential diagnosis. Chir Organi Mov 75:158–162
20. von Hochstetter AR, Meyer VE, Grant JW, Honegger HP,Schreiber A (1991) Epithelioid sarcoma mimicking angiosarcoma: the value of immunohistochemistry in the differential diagnosis. Virchows Arch 418:271–278
21. Wick MR, Manivel JC (1987) Epithelioid sarcoma and epithelioid hemangioendothelioma: an immunocytochemical and lectin-histochemical comparison. Virchows Arch 410:309–316

Virchows Arch (2003) 443:98–103
DOI 10.1007/s00428-003-0831-1

CASE REPORT

Michael J. Schwerer · Jörg Hemmer · Klaus Kraft · Heinz Maier · Peter Möller · Thomas F. E. Barth

Endoreduplication in conjunction with tumor progression in an aneuploid laryngeal squamous cell carcinoma

Received: 11 April 2003 / Accepted: 11 April 2003 / Published online: 15 May 2003
© Springer-Verlag 2003

Abstract We report the case of a 58-year-old man who presented with a squamous cell carcinoma pT1a G2 of the left vocal cord. Six months after histologically verified complete resection, the patient experienced an endolaryngeal and extralaryngeal local recurrence pT4 pN2b G2. We applied DNA flow cytometry (FCM) and comparative genomic hybridization (CGH) on both primary and recurrent tumor. The primary tumor and the endolaryngeal compartment of the relapse was an aneuploid cell clone with a FCM DNA index of 1.42 and 1.44, respectively. The extralaryngeal compartment showed a shift featuring a DNA index of 2.78. In the primary tumor and in both compartments of the recurrence there was an identical pattern of complex chromosomal imbalances as detected in CGH (CGH karyotype: rev ish enh [8q24.2-q24.3, 10q26.1-q26.3, 11q24-q25, 12q24.2-q23.33,X], dim [4q, 13q14.3-q31], amp[1p36.1-p36.2]). Hence, the recurrence was not associated with further gains and losses of chromosomal material. However, in the anterior part of the recurrence, the aneuploid tumor cell genome had completely doubled, obviously due to endoreduplication. Immunohistochemical analysis of several cell-cycle regulators revealed altered expression of checkpoint proteins, pointing to a complex disturbance in cell-cycle regulation.

Keywords Endoreduplication · Aneuploidy · Complex karyotype · DNA flow cytometry · Comparative genomic hybridization

M. J. Schwerer · P. Möller · T. F. E. Barth (✉)
Department of Pathology, University of Ulm,
Albert Einstein Allee 11, 89081 Ulm, Germany
e-mail: thomas.barth@medizin.uni-ulm.de
Tel.: +49-731-50023300, Fax: +49-731-50023884

J. Hemmer
Division of Tumor Biology, University of Ulm, Germany

K. Kraft
Department of Pathology, Military Hospital Ulm, Germany

H. Maier
Department of Otorhinolaryngology,
Head and Neck Surgery, Military Hospital Ulm, Germany

Introduction

Emergence of aneuploidy in flow cytometrically diploid head and neck squamous cell carcinomas is associated with an increase in their malignant potential [6, 13, 14]. Most tumors develop a single aneuploid clone that remains stable during local recurrence and/or metastatic spread. Rarely, newly acquired chromosomal aberrations emerge in the aneuploid clone in the later clinical stages of tumor progression [13]. Recently, a wealth of data has been generated on the basic mechanisms of aneuploidy formation, including failures in mitotic spindle assembly as well as the presence of supernumerary centrosomes [4, 15, 20, 22]. In contrast, less is known about specialized forms of mitosis in tumor cells such as endomitosis and endoreduplication. We observed an aneuploid head and neck squamous cell carcinoma with complete endoreduplication of a complex tumor cell genome. This implies endoreduplication as a mechanism of tumor progression in a head and neck squamous cell carcinoma with an aneuploid cell clone and in the absence of newly acquired unbalanced chromosomal aberrations.

Case report

A 58-year-old man with a history of decades of smoking and recent development of hoarseness was referred to the Department of Otorhinolaryngology, Head and Neck Surgery, of the Military Hospital, Ulm. Laryngoscopy revealed an irregular protrusion in an area of leukoplakia on the anterior third of the left vocal cord. Biopsy revealed a moderately differentiated squamous cell carcinoma. Following clinical staging (T1), the tumor was curatively resected in left frontolateral hemilaryngectomy. Both in frozen sections and in routine histology after formalin fixation, all resection margins of the surgical specimen were free of tumor. No adjuvant therapy was administered in the postoperative period, and a clinical control was planned after 6 months. At this time the

patient presented with a tumor symmetrically destroying the anterior half of the glottis. The lesion was subtotally destroying the thyroid cartilage and the thyroid gland. The extralaryngeal compartment of the tumor deeply infiltrated the prelaryngeal tissues and extended into the skin of the anterior neck (Fig. 1A). Since complete resection of the primary tumor had been verified histologically, a local recurrence was diagnosed, although the possibility of a residual tumor cannot be completely excluded. Laryngectomy with bilateral neck dissection was carried out and yielded an advanced stage (pT4 pN2). Postoperative radiotherapy was performed. Forty-six months later, the patient is still free from disease.

Materials and methods

Tissue specimens

Fresh tumor tissue from the primary tumor as well as from both the endolaryngeal and the extralaryngeal compartment of the recurrent tumor was prepared for DNA flow cytometry (FCM). Specimens were formalin fixed and tumor tissue directly adjacent to the material used for FCM was paraffin embedded. Sections with a thickness of 5 μm were cut and stained with hematoxylin and eosin (H&E) for routine histology. Six additional sections of 5 μm thickness were prepared for immunohistochemistry. Thirty additional 10-μm serial sections were cut and every fifth section was stained with H&E for microscopic identification of tumor areas. Tumor tissue was microdissected from the non-stained slides for comparative genomic hybridization (CGH). In addition, sections from all lymph nodes were prepared for histological assessment of the nodular status of the tumor. However, the amounts of tumor tissue available from the metastatic lesions were too small to allow CGH analysis. Hence, CGH experiments on metastatic tumor tissue were not considered in the study concept.

DNA FCM

FCM was carried out as previously reported [14]. Briefly, the tissue samples were disaggregated with surgical scalpels in 0.9% NaCl. The nuclei were extracted by incubation in 0.5% (w/v) acid pepsin solution (pH 1.5) for 5 min, strained through a 50-μm nylon mesh, and fixed with 5 μM DAPI (4′, 6-diamidio-phenylindole; Sigma, St. Louis, MO, USA) solution containing 0.2 M trisodium dihydrate. FCM was carried out using a PAS III flow cytometer equipped with a high-pressure 100-W mercury lamp (Partec, Münster, Germany). The proportions of diploid and aneuploid cells and the DNA indices of the aneuploid peaks were calculated using the multi-cycle software package (Phoenix Flow Systems, San Diego, CA, USA).

Comparative genomic hybridization

CGH analysis was carried out according to a standardized protocol recently described [18]. Image analysis was carried out using an epifluorescence microscope (Axioscope, Zeiss, Jena, Germany) and the commercially available image analysis system ISIS (MetaSystems, Altlußheim, Germany). For each hybridization, at least ten metaphase cells were evaluated. Ratio values of 1.25 and 0.8 were used as upper and lower thresholds for the identification of chromosomal imbalances [1]. Overexpressions were considered as high-level amplifications when the fluorescein isothiocyanate (FITC) signal was restricted to strong, focal signals and the corresponding ratio profile was diagnostic for overrepresentation. The extension of imbalanced regions was assessed by comparing the fluorescence ratio profiles with the corresponding regions in chromosome ideograms. For confirmation of chromosomal gains and losses, particularly with regard to overexpressions in cytosine/guanine-rich regions of the genome resulting in false positivity, inverse CGH was carried out in an additional experiment, as recommended by Kallionemi et al. [17].

Immunohistochemistry

Immunohistochemistry was carried out as previously reported [27]. Investigation involved antibodies to the Ki-67 antigen (antibody MIB-1; Dako, Hamburg, Germany) as well as p53 protein (Anti-Human p53, clone DO-7; Dako) at 1:50 dilution, p21 protein (antibody NCL-Waf1; Novocastra, Newcastle-upon-Tyne, Great Britain) at 1:100 dilution, p16 protein (p16 F-12, clone sc-1661; Santa Cruz Biotechnology Inc, Heidelberg, Germany) at 1:500 dilution, Retinoblastoma gene product (pRb, Anti-Human pRb, clone Rb1; Dako) at 1:25 dilution and cyclin D1 (anti-human cyclin D1, clone DCS-6; Dako) at 1:50 dilution. Antigen retrieval was provided using microwave oven heating of tissue sections at 500 W (six times, 5 min each) in citrate buffer solution. For external positive controls, tissue sections were used from oral mucosa biopsy specimens with severe dysplasia and a squamous cell carcinoma previously known to express those antigens. Negative controls were carried out using normal horse serum at the same dilutions.

Pathological findings

Histopathology

The primary tumor was a squamous cell carcinoma of the left vocal cord with a maximum diameter of 1.4 cm. The tumor did not involve supraglottic or subglottic tissues and did not show fixation of the vocal cord to the underlying structures. The tumor cells showed moderate anisokaryosis with hyperchromatic nuclei. Nucleoli were inconstantly observed within the tumor cells. Keratinization of single or small clusters of tumor cells was found. Intercellular bridges were infrequently detected between the tumor cells. Hence, the tumor showed features of moderate differentiation. The local recurrence had a maximum diameter of 6 cm and comprised endolaryngeal and extralaryngeal compartments due to broad infiltration into the prelaryngeal tissues. Metastases were observed in 4 of 18 lymph nodes in the left neck dissection specimen. All metastatic foci were small in size and restricted to the lymph-node sinuses. Both the endo- and extralaryngeal tumor compartment was still a moderately differentiated squamous cell carcinoma (Fig. 1A). Particularly the nuclear size and morphology of the endolaryngeal and extralaryngeal compartments of the recurrent tumor closely resembled those of the primary tumor. Increased mitotic activity was comparably observed between the primary tumor and the recurrence. In the recurrent lesion, both the endophytic and the exophytic components showed increased mitotic activity. Especially in large, anaplastic nuclei of the flow-cytometrically hexaploid tumor cell clone, proliferative activity was indicated by abundant mitoses.

DNA FCM

In the primary tumor, an aneuploid tumor cell clone with an approximately triploid DNA content (DNA-index: 1.42) was observed. A clone with an almost identical triploid DNA content (DNA-index: 1.44) was present in the endolaryngeal compartment of the recurrent tumor. The extralaryngeal compartment of the recurrent tumor was characterized by the absence of triploid tumor cells but showed an aneuploid tumor cell population with an approximately hexaploid DNA content (DNA-index: 2.78, Fig. 1B).

Comparative genomic hybridization

In the primary tumor, a complex karyotype with gains of chromosomal material on the long arms of chromosomes 8, 10,

A)

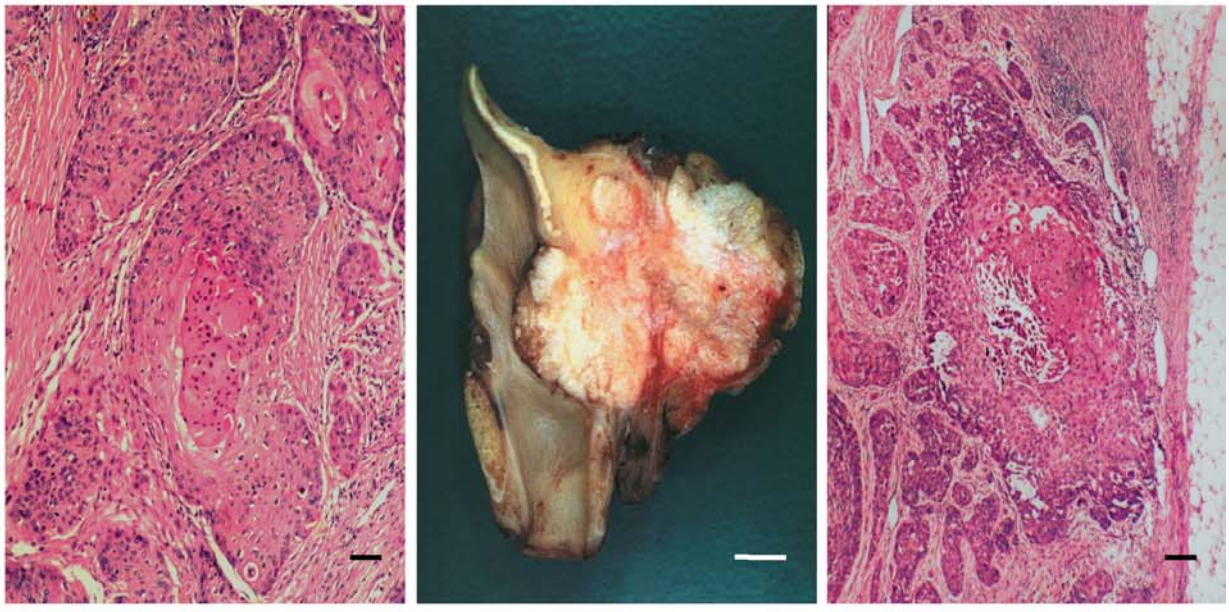

endolaryngeal component

extralaryngeal component

B)

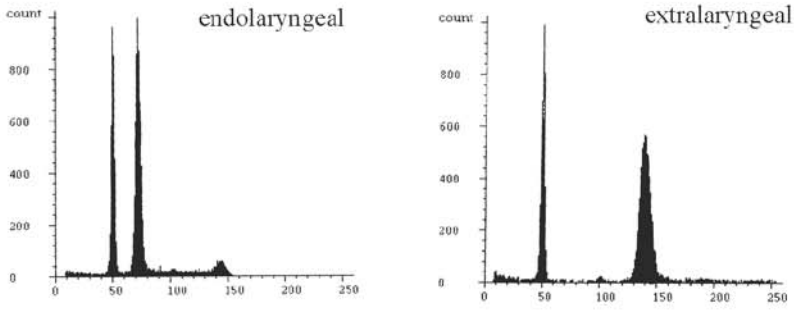

C)

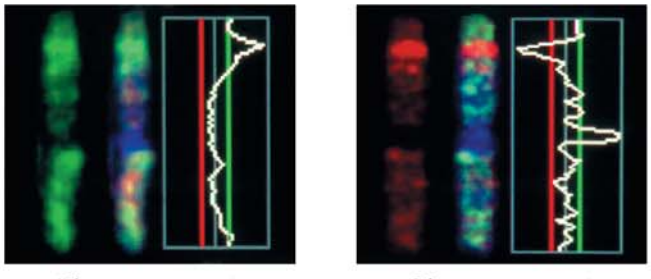

Chromosome 1 Chromosome 1

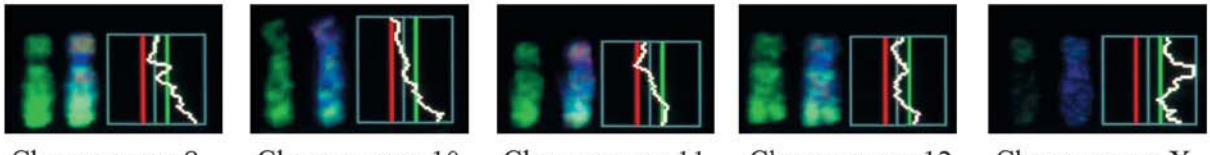

Chromosome 8 Chromosome 10 Chromosome 11 Chromosome 12 Chromosome X

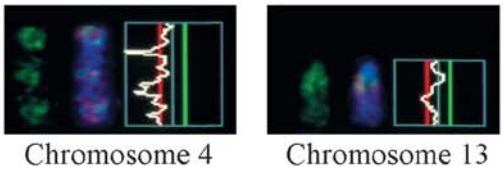

Chromosome 4 Chromosome 13

11, 12, and the whole axis of chromosome X was seen. Losses were detected on 4q and 13q. A high-level DNA amplification was found on chromosome band 1p36. In both the endolaryngeal and extralaryngeal compartments of the recurrent tumor the rev ish karyotypes exactly matched the chromosomal alterations found in the primary tumor (CGH karyotype: rev ish enh [8q24.2-q24.3, 10q26.1-q26.3, 11q24-q25, 12q24.2-q23.33,X], dim [4q, 13q14.3-q31], amp[1p36.1-p36.2]), (rev ish = reverse in situ hybridization; enh = enhanced; dim = diminished; amp = high level amplification; see hybridization examples Fig. 1C). The CGH experiment with the tumor DNA detected via rhodamine revealed an inversion of all gains and losses as per detection with FITC and, hence, confirmed the results.

Immunohistochemistry

Cell proliferation indicated by the expression of the Ki-67 antigen was approximately 30–40% in the primary tumor as well as in the endolaryngeal and the exolaryngeal compartment of the recurrence. No differences in the expression profiles of cell-cycle regulators were observed between the primary tumor and the recurrent lesion, either prior to or after endoreduplication: overexpression of p53 protein was observed with strong immunopositivity and weak immunostaining for p21 protein. Co-expression of pRb and p16 was found, together with strong immunopositivity for cyclin D1.

Fig. 1 **A** Macroscopy and histomorphology. The recurrent tumor represented a squamous cell carcinoma which was staged pT4 pN2b (*middle*, *bar* 1 cm). In both the endolaryngeal (*left*, *bar* 100 μm) and the extralaryngeal compartment (*right*, *bar* 100 μm) of the recurrent tumor, a moderately differentiated, partially keratinizing squamous cell carcinoma was observed. Nuclear size and morphology were very similar in the endolaryngeal and extralaryngeal tumor compartments. **B** DNA flow cytometry (FCM). Tissue directly adjacent to the material used for histopathology as shown in **A** was assessed in FCM. In the endolaryngeal tumor compartment (*left*), an aneuploid cell clone with a DNA index of 1.44 (second peak) was found compared with normal diploid cells (first peak, DNA index 1.00). The presence of normal diploid cells in the specimen represents inflammatory infiltration and stromal compartments. The extralaryngeal tumor compartment demonstrated only aneuploid tumor cells with a DNA index of 2.78 (second peak). Note the absence of an aneuploid peak with a DNA index of 1.44 in the extralaryngeal compartment. The presence of diploid cells (first peak) in this compartment was also due to stromal and inflammatory cells. **C** Comparative genomic hybridization (CGH). Hybridization examples from the endolaryngeal compartment are shown. The tumor DNA is detected via fluorescein isothiocyanate (*FITC*, *green signal*), the control DNA via rhodamine (*red signal*). The chromosomes are counterstained in blue with 4,6′-diamino-2-phenylindole (*DAPI*). In all images, the left chromosome shows only the tumor DNA signal (*green*), the right chromosome the combination of tumor DNA signal (*green*), control DNA signal (*red*) and DAPI counterstaining. On the right side of the chromosomes, the average ratio profiles of the FITC/ rhodamine fluorescence ratio are plotted. The *central line* indicates a ratio value of 1.0 (same DNA content in the tumor and the control); the line to the *left* indicates a value of 0.8 (diagnostic threshold for losses in the tumor DNA), the line to the *right* a value of 1.25 (diagnostic threshold for gains in the tumor DNA). An average of at least ten chromosomes was evaluated for each ratio profile. The first row shows a high level DNA amplification on chromosome 1p36.1-p36.2. Because 1p36 is a cytosine/guanine-rich region, probably leading to unspecific labeling with FITC resulting in false positivity; this finding was controlled by inverse labeling of tumor and control DNA in an additional hybridization experiment. The amplification and the other chromosomal gains and losses were confirmed by identical signals when the tumor DNA was labeled with rhodamine (*red signal*, *right picture*). The *second row* shows gains of chromosomal material on chromosomes 8, 10, 11, 12, and X. The *third row* indicates losses of chromosomal material on chromosomes 4 and 13

Discussion

In the vast majority of cases, tumor progression in aneuploid head and neck squamous cell carcinomas is characterized by the stability of the malignant aneuploid genotype [10, 12, 13]. Less frequently observed is the accumulation of newly acquired chromosomal aberrations in the tumor genome during disease progression [13]. In the present case, the aneuploid cell clone of the primary tumor proved stable during local recurrence and progression: FCM identified almost identical DNA indices of the tumor cells from the primary lesion and of the endolaryngeal compartment. The complex karyotype detected in CGH involved gains in the long arm on chromosomes 8 and 11 together with losses of chromosomal material on 4q and 13q. This pattern of chromosomal aberrations has repeatedly been detected in larger series of primary head and neck squamous cell carcinomas [3, 33]. Furthermore, gains on chromosome 11, 12, and X and a high level DNA amplification were observed on chromosome band 1p36 and confirmed by CGH with reverse labeling of tumor and control DNAs as recommended [17]. Local tumor progression in the recurrent carcinoma was associated with broad infiltration into the prelaryngeal tissues causing a lesion of about 6 cm in diameter within 6 months. In this anatomical site, complete doubling of the genomic material was detected, evidenced by a shift of the aneuploid DNA index in FCM from 1.44 in the endolaryngeal compartment to 2.78 in the extralaryngeal compartment. No additional chromosomal gains or losses were present. This was indicated by almost identical rev ish karyograms of the endolaryngeal and extralaryngeal tumor compartments in CGH. The complete doubling of genomic material in the cell is the consequence of endomitosis and endoreduplication [5, 23, 25, 26].

Endomitosis involves karyokinesis after the separation of sister chromatids leading to a single cell with two identical nuclei. The formation of multinucleated cells, e.g., in the trophoblast, neoplastic cells of Hodgkin's disease, and in cervical cancer might also result from endomitosis [23, 26, 30]. In contrast, endoreduplication implies the absence of karyokinesis after the segregation of the chromatids, leading to a single cell harboring one nucleus with exactly twice the chromosomal material of the nucleus of the parental cell. Endogenous polyploidization in late phases of megakaryocytopoiesis is currently attributed to endoreduplication [5, 25, 31]. A crucial role for cell-cycle regulators has been identified in this process [10, 24, 29, 31, 34]. In particular, it has been demonstrated that tumor cells deficient for the p21 protein enter endoreduplication [2, 28]. Induction of p21 protein expression executes downstream regulation of wild-type p53 protein-dependent growth control [8]. Expression of p21 protein in mutant-type p53 positive tumors is generally independent of the p53 protein pathway [7].

In the primary tumor, as well as in both the endolaryngeal and the exolaryngeal compartment of the recurrent tumor, strong overexpression of p53 protein was detected with the DO-7 antibody. Hence, mutant-type p53 protein expression can be postulated [19]. Extremely low levels of p21 protein expression were observed in all of these tumor samples. Low levels of p21 protein expression, induced independently from p53 protein regulation, must be assumed. Therefore, it can be hypothesized that endoreduplication has occurred resulting from p21 protein deficiency in conjunction with tumor progression from the endolaryngeal to the exolaryngeal compartment of the recurrence. However, the absence of endoreduplication from the primary tumor to the recurrent lesion regardless of p21 protein-deficiency indicates the effects of additional control mechanisms for DNA replication.

Recently, a low-level p21 protein-dosage-dependent control of endoreduplication has been described [28]. Furthermore, prevention of endoreduplication in p21-induced G2-arrested cells has been attributed to the presence of functional pRb [16, 20, 21]. In the primary lesion as well as in both compartments of the recurrent tumor, strong immunopositivity for pRb indicated the presence of functional pRb [11]. However, all tumor samples displayed a co-expression of p16 protein and pRb, but not a reverse downregulation of these proteins, which is commonly observed in head and neck squamous cell carcinomas [9]. In addition, a strong overexpression of cyclin D1 has been demonstrated in all tumor specimens. Accumulation of cyclin D1 in invasive head and neck squamous cell carcinomas is associated with deregulation of the pRb pathway of cell-cycle control [27]. Overexpression of cyclin D1 is associated with physiological polyploidization in megakaryocytes [29]. Hence, the emergence of p21-deficiency-related endoreduplication under coexisting epigenetic disturbances of pRb cell-cycle control can be hypothesized.

Recently, a strong prognostic significance has been attributed to the deregulation of these regulatory pathways in head and neck squamous cell carcinomas [12, 32]. The delineation of the role of endoreduplication due to dysregulated cell-cycle control may broaden our understanding of tumor progression in these lesions.

Acknowledgements This work was supported by a grant from the Deutsche Krebshilfe (70–2859-Ba2).

References

1. Barth TFE, Benner A, Bentz M, Döhner H, Möller P, Lichter P (2000) Risk of false positive results in comparative genomic hybridization. Genes Chromosomes Cancer 28:353–357
2. Bates S, Ryan KM, Phillips AC, Vousden KH (1998) Cell cycle arrest and DNA endoreduplication following p21 Waf1/Cip1 expression. Oncogene 17:1691–1703
3. Bockmühl U, Petersen S, Schmidt S, Wolf G, Jahnke V, Dietel M, Petersen I (1997) Patterns of chromosomal alterations in metastasizing and nonmetastasizing primary head and neck carcinomas. Cancer Res 57:5213–5216
4. Brinckley BR (2001) Managing the centrosome numbers game: from chaos to stability in cancer cell division. Trends Cell Biol 11:18–21
5. Carow CE, Fox NE, Kaushansky K (2001) Kinetics of endomitosis in primary murine megakaryocytes. J Cell Physiol 188:291–303
6. Chen RB, Suzuki K, Nomura T, Nakajima T (1993) Flow cytometric analysis of squamous cell carcinomas of the oral cavity in relation to lymph node metastasis. J Oral Maxillofac Surg 51:397–401
7. Datto MB, Li Y, Panus JF, Howe DJ, Xiong Y, Wang XF (1995) Transforming growth factor ß induces cyclin-dependent kinase inhibitor p21 through p53-independent mechanism. Proc Natl Acad Sci U S A 92:5545–5549
8. El-Deiry WS (1998) P21/ p53, cellular growth control and genomic integrity. Curr Top Microbiol Immunol 227:121–137
9. El-Naggar AK, Lai S, Clayman GL, Zhou JH, Tucker SA, Myers J, Luna MA, Benedict WF (1999) Expression of p16, Rb, and cyclin D1 gene products in oral and laryngeal squamous cell carcinoma: biological and clinical implications. Hum Pathol 30:1013–1018
10. Furukawa Y (1997) Cell cycle control during hematopoietic cell differentiation. Hum Cell 10:159–164
11. Gerardts J, Kratzke RA, Niehans GA, Lincoln CE (1995) Immunohistochemical detection of the cyclin-dependent kinase inhibitor 2/ multiple tumor suppressor gene 1 (CDKN2/ MTS1) product p16INK4A in archival human solid tumors. Correlation with retinoblastoma protein expression. Cancer Res 55:6006–6011
12. Gruner D, Sturm I, Hemmati P, Hermann S, Hauptmann S, Wurm R, Budach V, Dorken B, Lorenz M, Daniel PT (2003) Multiple analysis of Rb pathway and apoptosis control in esophageal squamous cell carcinoma identifies patients with good prognosis. Int J Cancer 103:445–454
13. Hemmer J, Kraft K (2001) Stability of aneuploid clones during oral squamous cell carcinoma metastasis. Anticancer Res 21:1459–1464
14. Hemmer J, Prinz W (1997) Comparison of DNA flow cytometry and fluorescence in situ hybridization with a set of 10 chromosome-specific DNA probes in four head and neck carcinomas. Cancer Genet Cytogenet 97:35–38
15. Honma M, Momose M, Sakamoto H, Sofuni T, Hayashi M (2001) Spindle poisons induce allelic loss in mouse lymphoma cells through mitotic non-disjunction. Mutat Res 493:101–114
16. Jiang Z, Liang P, Leng R, Guo Z, Liu Y, Liu X, Bubnic S, Keating A, Murray D, Goss P, Zacksenhaus E (2000) E2F1 and p53 are dispensable, whereas p21 (Waf1/Cip1) cooperates with Rb to restrict endoreduplication and apoptosis during skeletal myogenesis. Dev Biol 227:8–41
17. Kallionemi OP, Kallionemi A, Piper J, Isola J, Waldman FM, Gray JW, Pinkel D (1994) Optimizing comparative genomic hybridization for analysis of DNA sequence copy numbers in solid tumors. Genes Chromosomes Cancer 10:231–243
18. Lichter P, Bentz M, Joos S (1995) Detection of chromosomal aberrations by means of molecular cytogenetics: painting of chromosomes and chromosomal subregions and comparative genomic hybridization. Methods Enzymol 254:334–391
19. Linden MD, Nathanson SD, Zarbo RJ (1994) Evaluation of anti-p53 antibody staining: quality control and technical considerations. Appl Immunohistochem Mol Morphol 2:218–224
20. Marx A (2001) Cell biology. Do chromosome abnormalities lead to cancer? Science 292:426–429
21. Niculescu AB, Chen X, Smeets M, Hengst L, Prives C, Reed SI (1998) Effects of p21 (Cip1/Waf1) at both the G1/S and the G2/M cell cycle transitions: pRb is a critical determinant in blocking DNA replication and in preventing endoreduplication. Mol Cell Biol 18:629–643
22. Orr-Weaver TL, Weinberg RA (1998) A checkpoint on the road to cancer. Nature 392:223–224
23. Re D, Benenson E, Beyer M, Gresch O, Draube A, Diehl V, Wolf J (2001) Cell fusion is not involved in the generation of

giant cells in the Hodgkin-Reed Sternberg cell line L1236. Am J Hematol 67:6–9
24. Rooney RJ (2001) Cell cycle attenuation by p120E4F is accompanied by increased mitotic dysfunction. Cell Growth Differ 12:505–516
25. Roy L, Coullin P, Vitrat N, Hellio R, Debili N, Weinstein J, Bernheim A, Vainchenker W (2001) Asymmetrical segregation of chromosomes with a normal metaphase/ anaphase checkpoint in polyploid megakaryocytes. Blood 15:2238–2247
26. Sarto GE, Stubblefield PA, Therman E (1982) Endomitosis in the human trophoblast. Hum Genet 62:228–232
27. Schwerer MJ, Sailer A, Kraft K, Baczako K, Maier H (2003) Expression of retinoblastoma gene product in respiratory epithelium and sinonasal neoplasms: relationship with p16 and cyclin D1 expression. Histol Histopathol 18:143–151
28. Stewart ZA, Leach SD, Pietenpol JA (1999) p21 (Waf1/Cip1) inhibition of cyclin E/Cdk2 activity prevents endoreduplication after mitotic spindle disruption. Mol Cell Biol 19:205–215
29. Sun S, Zimmet JM, Toselli P, Thompson A, Jackson CW, Ravid K (2001) Overexpression of cyclin D1 moderately increases ploidy in megakaryocytes. Haematologica 96:17–23
30. Therman E, Buchler DA, Nieminen U, Timonen S (1984) Mitotic modifications and aberrations in human cervical cancer. Cancer Genet Cytogenet 11:185–197
31. Vitrat N, Cohen-Solal K, Pique C, Le Couedic JP, Norol F, Larsen AK, Katz A, Vainchenker W, Debili N (1998) Endomitosis of human megakaryocytes are due to abortive mitosis. Blood 91:3711–3723
32. Vora HH, Shah NG, Patel DD, Trivedi TI, Chikhlikar PR (2003) Prognostic significance of biomarkers in squamous cell carcinoma of the tongue. J Surg Oncol 82:34–50
33. Weber RG, Scheer M, Born IA, Joos S, Cobbers JMJL, Hofele C, Reifenberger G, Zöller JE, Lichter P (1998) Recurrent chromosomal imbalances detected in biopsy material from oral premalignant and malignant lesions by combined tissue microdissection, universal DNA amplification, and comparative genomic hybridization. Am J Pathol 153:295–303
34. Zimmet JM, Ladd D, Jackson CW, Stenberg PE, Ravid K (1997) A role for cyclin D3 in the endomitotic cell cycle. Mol Cell Biol 17:7248–7259

Virchows Arch (2003) 443:104–105
DOI 10.1007/s00428-003-0793-3

LETTER TO THE EDITOR

Marius John-Marc Ilario · Hach Vladimir Turyan · Constantine A. Axiotis

Glipizide treatment with short-term alcohol abuse resulting in subfulminant hepatic failure

Received: 17 January 2003 / Accepted: 10 February 2003 / Published online: 26 April 2003
© Springer-Verlag 2003

Sir,

A 50-year-old obese woman with a 3-month history of untreated, new-onset diabetes mellitus presented to the emergency room with complaints of polyuria, polydipsia, and dizziness. She had no signs or symptoms of icterus, ascites, or hepatic failure. Glucose was 238 mg/dl (65–109 mg/dl). She was prescribed 5 mg glipizide per os, once a day, and scheduled for further evaluation.

She missed her appointment and approximately 19 weeks later she presented to the emergency room with icterus and dark urine. Liver enzymes were abnormal with an aspartate aminotransferase of 2953 U/l, alanine aminotransferase of 2662 U/l, alkaline phosphatase of 232 U/l, and a total bilirubin of 10.2 mg/dl. A viral hepatitis profile was performed and found to be negative. The patient had no previous history of alcohol abuse; however, she claimed a recent history of binge drinking consisting of approximately a bottle of rum per day over the past 2 months because of extreme marital difficulties. The patient insisted on being discharged, and she was released with an additional prescription of 5 mg of glipizide per day.

Two weeks later she again presented to the emergency room with worsening icterus, dark urine, and tenderness to the right upper quadrant. She denied nausea or vomiting. Asterixis was not apparent. A diagnosis of non-viral hepatitis was made based on previous laboratory work. She was discharged with a prescription for ibuprofen 400 mg every 6 h for pain and told to come to the medical clinic in 2 weeks.

The patient returned 9 days later moderately obtunded with worsening abdominal pain and swelling. The liver enzymes continued to be elevated with an aspartate aminotransferase of 2708 U/l, alanine aminotransferase of 1840 U/l, alkaline phosphatase of 199 U/l, total bilirubin of 31.9 mg/dl, and a gamma-glutamyltransferase of 96 U/l. The prothrombin and partial thromobplastin times were 24.1 s and 53.1 s, respectively. Anti-smooth muscle antibody titer was 1:1280 (<1:20). Her acetaminophen level was less than 1 μg/ml. Anti-nuclear and anti-mitochondrial antibodies were negative. The patient was admitted with a diagnosis of liver failure and associated encephalopathy and coagulopathy of unknown etiology. Four days later, the patient was comatose and on day six the patient expired. There was no clinical evidence of hepatorenal syndrome [creatinine 2.9 mg/dl (0.6–1.5 mg/dl)] or significant azotemia, hypotension, or progressive oliguria.

A complete autopsy was performed. There was no evidence of cardiovascular or renal disease. The gall-bladder, pancreas, and extra-hepatic biliary system were unremarkable.

The liver weighed 1800 g and was focally necrotic. Histologically, the liver showed centriacinar necrosis and focal steatosis (Fig. 1). There was minimal fibrosis, centriacinar congestion and no inflammation. Perivenular collagen deposition was minimal (Fig. 2). Mallory bodies and megamitochondira were absent. The portal tracts were minimally fibrotic and cholestasis was not evident. Eosinophilia or lymphocytosis was not demonstrated. The bile ducts were adequate and there were no signs of regeneration or portal hypertension.

Grossly, the brain demonstrated minimal cerebral edema. Histologically, there was mild metabolic astrocystosis (alzheimer type 2) and scattered hypoxic neural degeneration in the cerebral cortex and Sommer's sector of the hippocampus.

The time interval between the development of icterus and the onset of hepatic failure in this patient, coupled with the lack of cerebral edema and the presence of moderate ascites, is characteristic of subfulminant hepatic failure [1]. The temporal sequence of clinical symptoms, concomitant elevations of hepatic enzymes, and the exclusion of alternate etiologies strongly incriminate

M. J.-M. Ilario · H. V. Turyan · C. A. Axiotis (✉)
Department of Pathology, State University of New York,
Health Science Center at Brooklyn,
450 Clarkson Avenue, Brooklyn, Box 25, NY 11203-2098, USA
e-mail: axiotismd@aol.com
Tel.: +1-718-2701293
Fax: +1-718-2704323

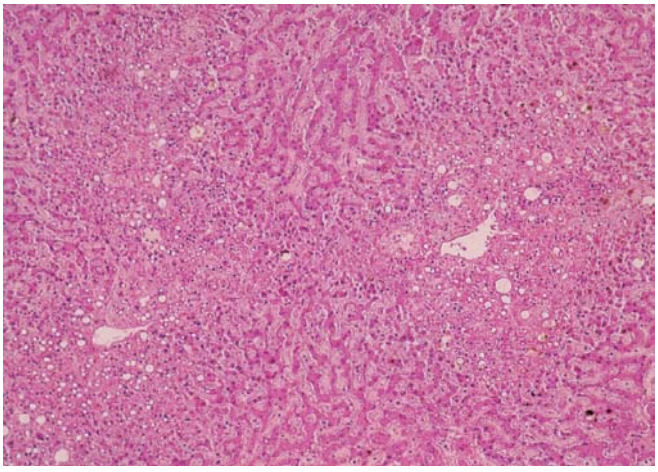

Fig. 1 Centriacinar necrosis and focal steatosis. (Hematoxylin and eosin, original magnification ×20)

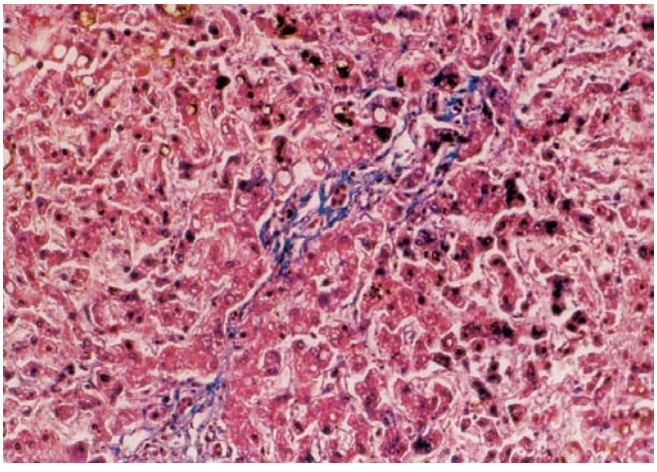

Fig. 2 Minimal perivenular collagen deposition. (Trichrome, original magnification ×20)

glipizide with associated short-term alcohol abuse. All other possible causes of hepatic failure were systematically excluded including viral hepatitis, cardiovascular disease, neoplasm, Wilson's disease, hyperthermia, illicit drug poisoning, Budd-Chiari syndrome, and alcoholic hepatitis. Though an Oil Red O stain was not performed, there was no clinical or strong pathological suspicion to suspect microvesicular steatosis.

A single case of fatal, toxic hepatitis linked with glipizide has been reported in the literature [2]. The patient was a diabetic 72-year-old female taking 2.5 mg twice a day. After 3.5 months, she developed signs and symptoms of liver failure. The liver demonstrated cholestasis, bile-duct proliferation, and panacinar necrosis consistent with a hypersensitivity drug reaction. Similar cases of non-fatal hepatitis consistent with a hypersensitivity reaction have been reported with glyburide [3] and gliclazide [4]. In all four cases, liver enzymes were only moderately elevated and only the patient treated with glipizide manifested hepatic failure.

In the current case, there were no signs of a hypersensitivity drug reaction and the liver enzymes were markedly elevated. In addition, the patient demonstrated sharply demarcated centriacinar zonal injury with markedly elevated anti-smooth muscle antibody. The chemical–chemical interactions between glipizide and alcohol represented both toxicokinetic and toxicodynamic components [5].

Short-term alcohol consumption may have interfered with the P_{450} enzymes necessary to hydroxylate and oxidize glipizide resulting in decreased drug metabolism. The consumption of glutathione by both glipizide and alcohol most probably resulted in the production of electrophilic metabolites. These excess electrophilic metabolites may have directly contributed to centracinar necrosis. In addition, the alcohol could have possibly induced the distinct liver cytochrome P_{450} 3a enzyme generating toxic metabolites and further aggravating liver toxicity. Furthermore, toxic metabolites may act indirectly as foreign haptens and induce immunological liver injury [6]. Covalent binding of these toxic metabolites may have resulted in metabolic activation of hepatic proteins and lipoproteins to produce haptens. This in turn results in autoimmune hepatitis in susceptible people [6]. A circulating anti-smooth muscle antibody was found in our patient and is the most frequent antibody in drug-induced hepatitis [7].

This unique case of subfulminant hepatic failure appears to follow exposure to glipizide potentiated by sub-acute alcohol consumption. A complete picture of autoimmune or alcoholic hepatitis was lacking both clinically and histologically. A mechanism of both toxic metabolic and toxic-induced immunologic injury is proposed. Vigilance should be assumed when prescribing glipizide with alcohol.

References

1. Bernuau J, Rueff B, Benhamou J-P (1986) Fulminant and subfulminant liver failure: definitions and causes. Semin Liver Dis 6:97–106
2. Clementsen P, Hansen CL, Hoegholm A (1986) Glipizide induced toxic hepatitis. Ugeskr Laeger 148:771–772
3. Goodman RC, Dean PJ, Radparvar A, Kitabachi A (1987) Glyburide-induced hepatitis. Ann Intern Med 106:837–839
4. Dourakis SP, Tzemanakis E, Sinani C, Kafri G, Hadziyannis SJ (2000) Gliclazide-induced acute hepatitis. Eur J Gastroenterol Hepatol 12:119–121
5. Ilario MJ-M, Ruiz JE, Axiotis CA (2000) Acute fulminant hepatic failure in a woman treated with phenytoin and trimethoprim-sulfamethoxazole. Arch Pathol Lab Med 214:1800–1803
6. Sherlock S (1986) The spectrum of hepatoxicity due to drugs. Lancet 23:440-444
7. Homeberg J-C, Abuaf N, Helmy-Khalil S, Biour M, Poupon R, Islam S, Darnis F, Levy VG, Opolon P, Beaugrand M (1985) Drug-induced hepatitis associated anticytoplasmic organelle autoantibodies. Hepatology 5:722–727

Virchows Arch (2003) 443:106–107
DOI 10.1007/s00428-003-0825-z

LETTER TO THE EDITOR

Elisabeth E. Türk · Michael Tsokos

Iliopsoas muscle bleeding as a complication of septic disseminated intravascular coagulation

Received: 18 March 2003 / Accepted: 1 April 2003 / Published online: 13 May 2003
© Springer-Verlag 2003

Keywords Psoas muscles · Haemorrhage

Sir,

We recently investigated a case of extensive bilateral psoas muscle haemorrhage as a complication of septic disseminated intravascular coagulation (DIC) in the sequel of polytrauma. The 35-year-old woman was admitted to hospital with several rib fractures and lung injuries after a suicide attempt by jumping out of the window of her fourth-floor flat under the influence of alcohol and bromazepam. In hospital she developed sepsis and died 9 days after admission under the clinical signs of septic multiple organ failure (MODS). External examination revealed sparse post-mortem lividity as a sign of internal blood loss and bruises in the upper trunk region. At medico-legal autopsy, several ventral rib fractures were seen, resulting from the sustained trauma. The impact site was stated as the upper thoracic region. In addition, signs of septic MODS, namely shock lungs and kidneys, soft tissue oedema and a yellow discoloration of the skin were present. The woman also had early signs of peritonitis. Furthermore, mucosal haemorrhages of the gastrointestinal tract and respiratory tract and extensive bleedings of both psoas muscles (Fig. 1) extending into the retroperitoneal cavity were seen, attributable to septic DIC. It could be excluded that the haemorrhage resulted from the initial trauma as there were no surrounding soft tissue or pelvic bleedings, and the major and minor blood vessels in the vicinity of the psoas muscles were unaffected. Based on the autopsy results, death was caused by a combination of septic MODS and internal blood loss.

E. E. Türk · M. Tsokos (✉)
Institute of Legal Medicine,
University of Hamburg,
Butenfeld 34, 22529 Hamburg, Germany
e-mail: mtsokos@web.de
Tel.: +49-40-428032748
Fax: +49-40-428033934

Extensive haemorrhages of the psoas muscles are a well-known complication of anticoagulant therapy [1, 3, 4], but have, to the best of our knowledge, not yet been described in septic DIC. The psoas muscles are considered as a relatively uncommon bleeding site in coagulation disorders [3], and, thus, haemorrhages in this body region are frequently overlooked in the clinical setting. Moreover, the wide range of symptoms in cases of psoas muscle bleeding, varying from mild pain to severe femoral neuropathy and haemorrhagic shock [1, 3, 4], can lead to additional problems in establishing the correct diagnosis. This is especially true if symptoms of the primary illness are more prominent, e.g., a high body temperature or signs of organ failure in sepsis. Moreover, in patients under anaesthetics, obvious symptoms might be weakened or completely absent [4]. However, the establishment of the correct diagnosis is essential, as psoas muscle haemorrhages may lead to life-threatening and sometimes even fatal internal blood loss [3, 4]. Our case demonstrates that in patients with septic DIC, the possibility of psoas muscle haemorrhage has to be considered. Abdominal ultrasonography or computed

Fig. 1 Autopsy specimen of iliopsoas muscle exhibiting extensive haemorrhage

tomography may assist in establishing the diagnosis [3]. If voluminous haematomas are diagnosed, percutaneous decompression should be performed, as surgery is critical in patients with sepsis and does not seem to have striking advantages [2].

References

1. Guivarćh M (1997) Hematoma of the iliac psoas muscle. 29 cases. J Chir 134:382–389
2. Merrick H, Zeis J, Woldenberg L (1991) Percutaneous decompression for femoral neuropathy secondary to heparin-induced retroperitoneal haematoma: case report and review of the literature. Am Surg 57:706–711
3. Qanadli SD, El Hajjam M, Mignon F, Bruckert F, Chagnon S, Lacombe P (1999) Life-threatening spontaneous psoas haematoma treated by transcatheter arterial embolization. Eur Radiol 9:1231–1234
4. Türk EE, Verhoff MA, Tsokos M (2002) Anticoagulant-related iliopsoas muscle bleeding leading to fatal exsanguination. Am J Forensic Med Pathol 23:342–344

Virchows Arch (2003) 443:108–110
DOI 10.1007/s00428-003-0830-2

LETTER TO THE EDITOR

Soledad Alonso · José Luis Rodríguez-Peralto · Claudio Ballestín · Pablo Ortiz

Metastatic malignant melanoma with Homer-Wright rosettes mimicking a neuroblastic tumor. An unusual morphological manifestation

Received: 10 December 2002 / Accepted: 11 April 2003 / Published online: 29 May 2003
© Springer-Verlag 2003

Sir, malignant melanoma is considered "the great histologic mimic" since it may exhibit a wide variety of histological patterns, mimicking any kind of tumor including sarcomas, carcinomas, lymphomas, plasmacytomas, and germinal tumors. Real ganglioneuroblastic differentiation is an exceptional event that has only been described in one case of malignant melanoma [3]. We report a case of lymph-node metastatic malignant melanoma with extensive areas of a neuroblastic-like morphology characterized by melanin pigmented Homer-Wright rosettes but without evidence of ganglionary differentiation. The patient, a 61-year-old man visited the dermatologist because of a 3-month history of a progressively enlarging 1.8-cm pigmented skin nodule on his abdominal wall that occasionally presented spontaneous bleeding. He had no other symptoms and denied fever or weight loss. Complete surgical resection was performed. The histopathological study identified a classic superficial spreading malignant melanoma level IV of Clark with a Breslow thickness of 4.8 mm (Fig. 1). The patient remained well with no recurrence until 4 years later, when he developed a progressively enlarging axillary mass. An axillary lymph-node resection was performed and four lymph nodes were taken. Microscopically, one of these was entirely replaced by a malignant tumor composed of sheets of spindle and epithelioid cells arranged in a typical Homer-Wright rosette pattern (Fig. 2). The tumoral cells had large nuclei with pseudoinclusions, coarse chromatin and eosinophilic cytoplasm. The presence in these rosettes of a subtle brown cytoplasmic pigment (Fig. 2, *inset*), along with the patient's previous history, led to the diagnosis of metastatic malignant melanoma. Moreover, the tumor was inmunohistochemically positive for specific melanocytic markers such as S-100 protein (polyclonal, Dako, UK, 1:2000), HMB-45 (HMB-45, Biogenex, 1:10) and melan A (A103, Dako, UK, 1:10) and negative for neural/neuroendocrine antibodies including: synapthophysin (SY38, Dako, UK, 1:10), chromogranin (LKZH10, Biogenex, 1:50), neurofilament (ZF11, DAKO, UK, 1:25) and glial fibrillary acid protein (Polyclonal, Dako, UK 1:3000). The antigen retrieval was performed in all cases by heat (pressure cooker) in citrate buffer 10 mM pH 6, except for S-100 protein where protease XIV (Sigma) was used. The patient was treated with chemotherapy and 4 months later he developed lung and liver metastases, was not biopsied, and died of metastatic disease 4 years and 5 months after the initial diagnosis of primary cutaneous malignant melanoma.

Rosettes are a main architectural feature in several tumors. Thus, Flexner-Wintersteiner rosettes, defined by cell processes surrounding a membrane-bound lumen, are characteristic of ependymoma, neuroepithelioma and retinoblastoma [13]; perivascular rosettes, characterized by cell processes surrounding a central vessel occur in astrocytomas, ependymomas, oligodendrogliomas, meningiomas [5] and rarely in sarcomas, carcinomas and melanomas [2]; while Homer-Wright rosettes, defined by a central tangle of fibrillary processes, are a typical feature of ganglioneuroblastoma, medulloblastoma and retinoblastoma [13], although they have also been described in small cell carcinomas and lymphomas [13]. Therefore, the presence of Homer-Wright rosettes in a metastatic malignant neoplasm initially raised the possible diagnosis of neuroblastic tumor.

Malignant melanoma can simulate any kind of tumor [2], including sarcomas [14], carcinomas, rhabdoid and neuroendocrine tumors [7], lymphomas [1], plasmacy-

S. Alonso
Pathology Program,
Centro Nacional de Investigaciones Oncológicas (CNIO),
Madrid, Spain

J. L. Rodríguez-Peralto (✉) · C. Ballestín
Department of Pathology,
"12 de Octubre" University Hospital,
Avenida de Cordoba, 28041, Madrid, Spain
e-mail: jrodriguezp.hdoc@salud.madrid.org
Tel.: +34-91-3908710

P. Ortiz
Department of Dermatology,
"12 de Octubre" University Hospital, Madrid, Spain

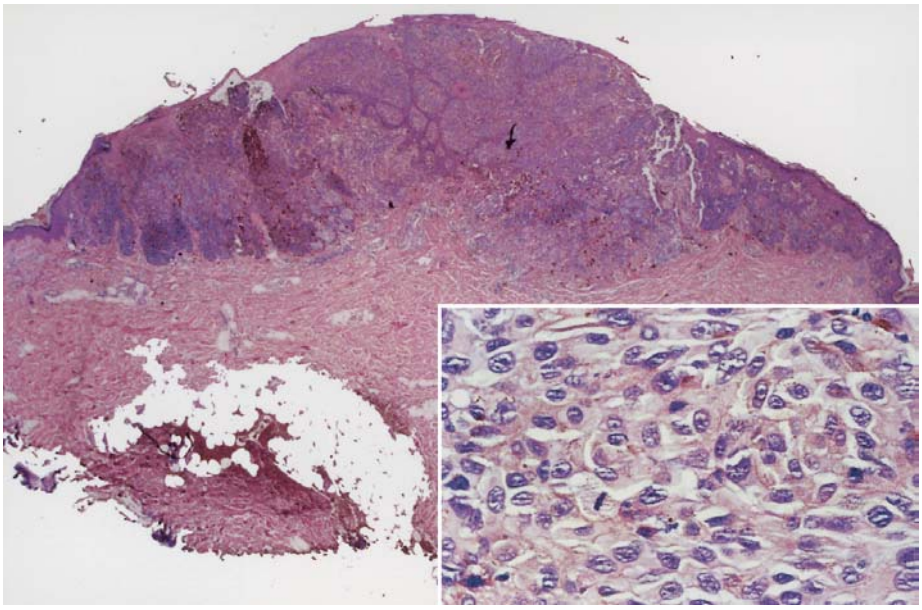

Fig. 1 Classic superficial spreading malignant melanoma composed of nest of ephitelioid atypical tumoral cells (×1.25). *Inset* Higher magnification of tumoral cells (×40)

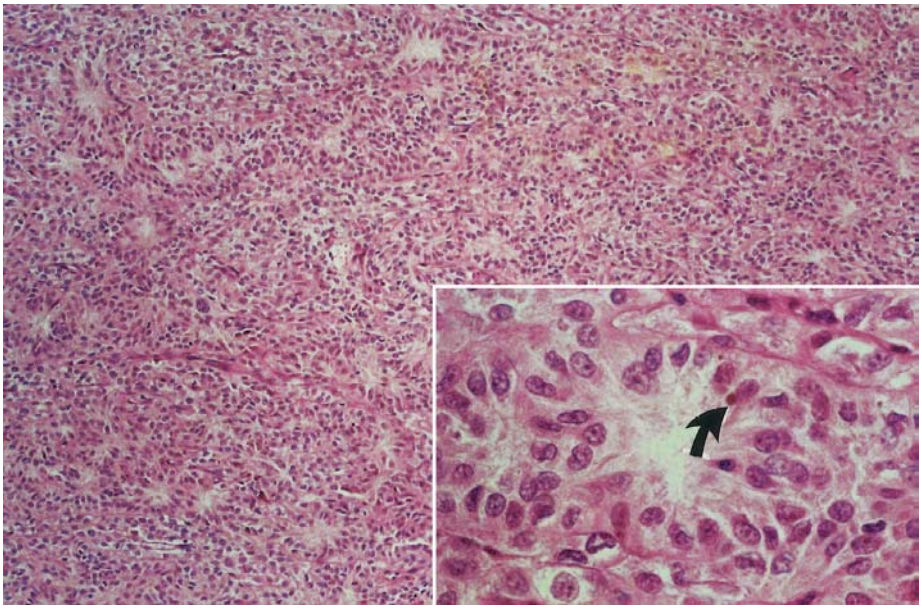

Fig. 2 Metastatic malignant melanoma located in a lymph node from the axillary region. The tumoral cells have grown in a prominent rosettoid pattern with abundant Homer-Wright rosettes. *Inset* Higher magnification of Homer-Wright rosettes in malignant melanoma (×10). No central lumen is observed. Note the presence of droplet (*arrows*) and diffuse brown cytoplasmic melanin pigment (×40)

tomas [2] and germinal tumors [2]. Moreover, melanoma cells can be small, pleomorphic, clear [6], signet-ring [9], rhabdoid [4], balloon, plasmacytoid [2] or spindle shaped [2]. In addition, malignant melanoma can also present any histopathological patterns including adenoid, pseudopapillary, pseudofollicular, fascicular, whorled, nested, trabecular, angiocentric and haemangiopericytomatoid [2].

Although extremely uncommon, Verocay bodies embedded in a fibrillary stroma simulating Schwannoid structures have also been reported in malignant melanoma [2, 8]. However, ganglioneuroblastic differentiation in malignant melanoma has only been described once by Banerjee et al. in 1999 [3]. In their case, they showed foci of ganglioneuroblastoma within an otherwise typical metastatic malignant melanoma. The ganglioneuroblastic population composed of islands of ganglion cells and spindle neuroblasts embedded in a fibrillary stroma with only sparse Homer-Wright rosettes differed from the classic malignant melanoma not only in its morphological appearance but also in its neuroblastic immunohistochemical phenotype [positivity for neurofilament protein (NFP), synaptophysin, chromogranin and glial fibrillary acid protein (GFAP)]. In our case, the striking neuroblastic appearance of the metastatic malignant melanoma with abundant rosettes, was only observed in the histological examination, since, in contrast with the Banerjee et al. case [3], we could not demonstrate immunohistochemical neuroblastic differentiation. Only melanin pigment and melanocytic markers (HMB-45, Melan A and S-100) were constantly positive.

Monteagudo et al. have recently reported [12] a peculiar primary nodular cutaneous malignant melanoma with psammoma bodies. Those authors show—in their figure 3c—focal rosette-like alveolar nest structures interpreted as pseudomeissner bodies. In our opinion, these structures display the characteristic morphological features of Homer-Wright rosettes and might be considered another case of malignant melanoma with neuroblastic morphology similar to the present one.

It is well known that melanocytes are neural crest-derived cells located in the basal layer of the epidermis, hair follicles, most squamous covered mucosal membranes and leptomeninges. The neuroectodermal origin of melanocytes was proposed many years ago by Masson [11] and has been proven by several techniques including cell culture [10], immunohistochemical stains and histopathological observations demonstrating the relationship between melanocytes and neural cells. Moreover, well-recognized conditions such as desmoplastic neurotropic melanoma, "neurotized" nevi and "neuronevi", melanotic neurofibromas and melanotic schwannomas support this observation. All these findings may support the neuroblastic morphology observed in the present case.

Differential diagnosis must be performed with those tumors mainly composed of Homer-Wright rosettes including ganglioneuroblastoma, neuroblastoma, medulloblastoma and retinoblastoma. A positive immunohistochemical staining for HMB-45 and Melan-A lead to the diagnosis of malignant melanoma. Melanotic schawnnoma should also be considered in the differential diagnosis; but, so far, the expression of Melan-A argues against a nerve sheath origin because, to the best of our knowledge, a melanocytic immunoreactivity lineage has never been reported in nerve sheath tumors.

In summary, we describe a case of metastatic malignant melanoma with prominent rosettoid appearance and extends the morphological spectrum of this tumor. We also consider that malignant melanoma with neuroblastic features must be included in the differential diagnosis of metastatic neuroblastic tumors.

Acknowledgements This work was supported by a grant from the Ministerio de Sanidad y Consumo (FIS 01/0037–03). S. Alonso is supported by a grant from the Ministerio de Sanidad y Consumo (FIS 01/9269) and the CNIO.

References

1. Attanoos R, Griffiths DFR (1992) Metastatic small cell melanoma to the stomach mimicking primary gastric lymphoma. Histopathology 21:173–175
2. Banerjee SS, Harris M (2000) Morphological and immunophenotypic variations in malignant melanoma. Histopathology 36:387–402
3. Banerjee SS, Menasce LP, Eyden BP, Brain AN (1999) Malignant melanoma showing ganglioneuroblastic differentiation. Report of a unique case. Am J Surg Pathol 23:582–588
4. Borek BT, McKee PH, Freeman JA, Maguire B, Brander WL, Calonje E (1998) Primary malignant melanoma with rhabdoid features: a histological and immunocytochemical study of three cases. Am J Dermatopathol 20:123–127
5. Chow CW, Brittingham J (1987) Perivascular pseudorosettes in childhood brain tumours: an ultrastructural and immunohistochemical study. Pathology 19:12–16
6. Ehara H, Takahashi Y, Saitoh A, Kawada Y, Shimokawa K, Kanemura T (1997) Clear cell melanoma of the renal pelvis presenting as a primary tumour. J Urol 157:634
7. House NS, Fedok F, Maloney ME, Helm KF (1994) Malignant melanoma with clinical and histologic features of Merkel carcinoma. J Am Acad Dermatol 31:839–842
8. King R, Busam K, Rosai J (1999) Metastatic malignant melanoma resembling malignant peripheral nerve sheath tumor: report of 16 cases. Am J Surg Pathol 23:1499–1505
9. Livolsi VA, Brooks JJ, Soslow R, Jonohnson BL, Elder DE (1992) Signet cell melanocytic lesions. Mod Pathol 5:515–520
10. Llombart-Bosch A, Carda C, Peydro-Olaya A, Noguera R, Boix J, Pellin A (1989) Pigmented esthesioneuroblastoma showing dual differentation following transplantation in nude mice. An immunohistochemical, electron microscopal and cytogenetic analysis. Virchows Arch 414:199–208
11. Masson P (1948) Pigment cells in man. In: Miner RW (ed) The biology of melanomas (special publication), vol 4. The New York Academy of Sciences, New York, pp 15–51
12. Monteagudo C, Ferrández A, González-Devesa M, Llombart-Bosch A (2001) Psammomatous malignant melanoma arising in an intradermal naevus. Histopathology 39:493–497
13. Rosai J (1989) Ackerman's Surgical Pathology, vol 2. Mosby, St. Louis, pp 1026–2501
14. Zelger BG, Steiner H, Wambacher B, Zelger B (1997) Malignant melanomas simulating various types of soft tissue tumors. Dermatol Surg 23:1047–1054

Virchows Arch (2003) 443:111
DOI 10.1007/s00428-003-0841-z

ERRATUM

Rodolfo Montironi · Roberta Mazzucchelli · Theodorus van der Kwast

Morphological assessment of radical prostatectomy specimens. A protocol with clinical relevance

Published online: 27 May 2003
© Springer-Verlag 2003

Virchows Arch (2003) 442:211–217

The formula in the published article (page 212) was:

$(\text{Width} \times \text{Height} \times \text{Length}) \times 0.532$

The correct formula is:

$(\text{Width} \times \text{Height} \times \text{Length}) \times 0.523$

The online version of the original article can be found at http://dx.doi.org/10.1007/s00428-002-0741-7

R. Montironi (✉) · R. Mazzucchelli
Institute of Pathological Anatomy,
University of Ancona School of Medicine,
Umberto 1° Hospital60020 Torrette, Ancona, Italy
e-mail: r.montironi@unian.it
Tel.: +39-071-5964830
Fax: +39-071-889985

T. van der Kwast
Department of Pathology, Josephine Nefkens Institute,
Erasmus MC, Rotterdam, The Netherlands

 © Springer-Verlag 2003

ANNOUNCEMENTS

6 September 2003
EUROPEAN BOARD OF PATHOLOGY
7th EXAMINATION 2003
Ljubljana, Slovenia

The Seventh Examination of the European Board of Pathology will be held in Ljubljana, Slovenia, Saturday September 6, 2003. This Examination precedes the 19th Congress of the ESP.

For information about the examination and application forms can be obtained from:
Prod. Dr. J.G. van den Tweel
(chairman of The Examination Board)
Utrecht University Medical Center
Department of Pathology, H 04.312
P.O. Box 85500
3508 GA Utrecht
Fax: ++31-30-2544990
Tel.: ++31-30-2506565
e-mail: j.vandentweel@lab.azu.nl *or*
W.vanBragt@lab.azu.nl (secretary)
The same information is also available from Internet:
http:www.uems.be/pathol.htm, see index 2 and 3

6–11 September 2003
19th European Congress of Pathology
Ljubljana, Slovenia

The largest congress of pathologists in Europe in 2003, covering basic diagnostic standards, update scientific achievements and recent technical advances in all areas of pathology at 4 keynote lectures, 30 symposia, 21 short courses, 21 slide seminars, 14 special presentations, 2 round table discussions and free paper and poster sessions. Internationally recognized invited speakers are from throughout Europe and the USA.

Updated information on the congress website: http://www.cd-cc.si

10–13 September 2003
Harvard Dermatopathology Update CME Course
(Fairmont Copley Plaza Hotel, Boston, MA)

The objective of this year's course is to provide an in-depth review and update on selected topics in dermatopathology focusing on non-neoplastic diseases and melanocytic lesions. The course has been redesigned, and is specifically aimed at practicing pathologists, dermatopathologists, and dermatologists. The program is also suitable for senior residents and fellows preparing for board certification examinations.

For further information please contact at
http://www.cme.hms.harvard.edu, at (617) 384-8600
or can be obtained by e-mail at hms-cme@hms.harvard.edu

13 October 2003
Continuing Medical Education

One day Multi-Disciplinary Update courses

Course fee: £95.00

For further information please contact:
Education Administrators
Nottingham International Breast Education Centre
City Hospital, Hucknall Road, Nottingham NG5 1PB
Tel.: 0115 969 1689; Fax: 0115 962 7707
E-mail: enquiries@nibec.co.uk; www.nibec.co.uk

17–19 November 2003
Multi-Disciplinary Courses on Breast Disease

Three day course. The first part is multi-disciplinary. Thereafter the different specialties meet to accommodate their own special requirements.

Course Tutors: Dr. I.O. Ellis, Dr. S.E. Pinder, Dr. A.H.S. Lee

Course fees:	NHS	£370.00
	Non-NHS	£415.00
	Overseas	£550.00

includes refreshments but not accommodation

For further information please contact:
Education Administrators
Nottingham International Breast Education Centre,
City Hospital, Hucknall Road, Nottingham NG5 1PB
Tel.: 0115 969 1689; Fax: 0115 962 7707
Email: enquiries@nibec.co.uk; www.nibec.co.uk

Virchows Arch (2003) 443:113–114
DOI 10.1007/s00428-003-0870-7
© Springer-Verlag 2003

SOCIETY NEWS

Invitation to the 19th European Congress of Pathology

On behalf of the European Society of Pathology (ESP) and the Organising Committee, we take great pleasure in inviting you to the 19th European Congress of Pathology, which will be held in Ljubljana, Slovenia, 6–11 September 2003.

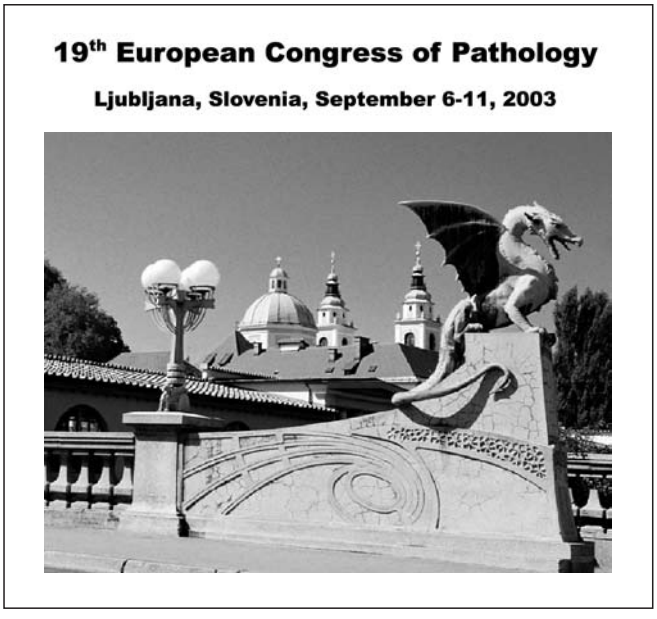

Slovenia is not a large country, but at the hub of routes of trade and movement from east to west and north to south, it has always played a larger part in European events than its size would suggest. Slovenia is now an independent Central European state, on the sunny side of the Alps, bordering Italy, Austria, Hungary and Croatia. The landscape embraces rolling countryside leading to the Pannonian plain to the east, rugged Karst bordering the Adriatic Sea to the southwest, and the Alps to the north and west. The Slovenian nation of only two million today has survived mainly due to its culture, language and vitality. A bone flute, 30,000 years older than any other known in the world, and Europe's oldest bone needle, testify to the roots of culture here.

Its capital, Ljubljana, has a picturesque unity, composed of an architectural heritage spanning Roman Emona, through Renaissance and Baroque Ljubljana, to Secession Art Nouveau and Modern Ljubljana, so strongly marked by the influence of the world famous Slovenian architect, Jo e Plečnik. Ljubljana is an university city. The roots of the University go back to the seventeenth century with Academia Operosorum, the fourth Academy of Sciences in Europe. A Philharmonic Society dates back three centuries.

Ljubljana's congress tradition began in 1821, when the three emperors of the Holy Alliance met here to discuss the post-Napoleonic fate of Europe. These traditions have been brought together in the new Cultural and Congress Centre Cankarjev dom, with a capacity of 3,600, located in the heart of Ljubljana. Cankarjev dom is well equipped with all modern technical facilities and has an experienced in-house team to ensure the necessary high standards for scientific sessions and exhibitions. All Congress venues, and most hotels, are within walking distance of the centre of the city. Particular attention will be paid to stimulating the participation of trainees and young pathologists by securing as low a registration fee as possible, and inexpensive accommodations.

The European Society of Pathology has been succeeding in establishing its ever more continuous activity and influence. The old idea of a common programme of continuous education of pathologists has been realised through a number of courses organised each year by the European School of Pathology, at its headquarters in Turin and other centres throughout Europe. An increasing number of Working Groups within the European Society of Pathology, devoted to various fields, promote a continuous exchange of professional experiences and other information, the establishment of common diagnostic standards and collaboration on common research projects.

The biannual ESP Congresses retain a major role in fulfilling the main aims of the ESP in pathology education, exchange of the most recent research achievements and, particularly, in keeping together all branches of pathology, that otherwise tend to split according to organ systems, disease processes and the increasing number of techniques. The Congresses also keep together pathologists from the whole of Europe, irrespective of geographical and political borders.

We believe that the 19th European Congress of Pathology will continue the traditional approaches of previous Congresses and will serve to increase both links with European national and international pathology societies and intercontinental links, particularly with the International Academy of Pathology. The framework of the Congress Scientific Programme has been created with the strong impact and assistance of the ESP Working Groups, the ESP Executive/Scientific Committee and the Advisory Council as well as companion Societies. The programme covers all areas of pathology, provides information ranging from current diagnostic standards to recent advances in science and modern techniques, particularly those of molecular genetics, and includes a number of "hot" topics of today and tomorrow, which will be presented by the best, internationally recognised experts at Keynote Lectures, Symposia, Special Presentations, Round Table Discussions, Short Courses and Slide Seminars. One evening is devoted to ESP Working Group Meetings, both business and scientific. Interesting Satellite Symposia will be organised by supporting companies, two by the main sponsor of the Congress Main Sponsor, Ventana Medical Systems S.A.

Furthermore, all practising pathologists and scientists are kindly invited to present their scientific achievements and exchange their professional experiences through Free Paper and Poster Sessions. The best Free Papers will be acknowledged by giving the authors the opportunity to present their achievements at the plenary session, at which the authors of the three best Poster Presentations will additionally receive special Awards.

All who are coming to Ljubljana are kindly invited to join us at two one-day Pre-Congress Meetings, prior to the Congress Opening Ceremony on Saturday: one on Pulmonary Pathology and the other devoted to non-neoplastic Nephropathology. There will also be a three-day Joint Meeting of the European and North American Society of Head and Neck Pathology. All Pre-Congress Meetings and a whole day Examination by the European Board of Pathology will be organised by using the facilities of the new building of the Faculty of Medicine, University of Ljubljana.

Culture kept the Slovenian national identity alive over the centuries and it still plays an important role in people's lives. The Congress will also highlight the traditional close connection between medicine and art. Some novel events are planned: an exhibition of the work of pathologists/painters and, especially, a Gala Concert on Monday evening in the main Gallus Concert Hall of the Congress Centre in Ljubljana, by pathologists/musicians from all over the world. A social programme is offered which reflects the warmth and hospitality of the Slovenian people.

The Second Millennium we have entered provides major challenges for all biomedical sciences, and the 19th European Congress of Pathology is a challenge for the Organisers. We sincerely hope that attendance at the Ljubljana Congress in 2003 will be a fruitful, enjoyable and memorable experience in every respect for all participants, and will give new impetus to our medical speciality in Slovenia.

Updated information about the 19th European Congress of Pathology available on Internet Congress website: <http://www.cd-cc.si/ecp>.

We look forward to seeing you in September 2003 in Ljubljana.

Gianni Bussolati
President
European Society
of Pathology

Du an Ferluga
President
19th European Congress
of Pathology

Virchows Arch (2003) 443:115–121
DOI 10.1007/s00428-003-0833-z

ORIGINAL ARTICLE

Florence Jourdan · Nicole Sebbagh · Eva Comperat · Najat Mourra · Antoine Flahault · Sylviane Olschwang · Alex Duval · Richard Hamelin · Jean-François Flejou

Tissue microarray technology: validation in colorectal carcinoma and analysis of p53, hMLH1, and hMSH2 immunohistochemical expression

Received: 1 November 2002 / Accepted: 23 April 2003 / Published online: 7 June 2003
© Springer-Verlag 2003

Abstract Tissue microarray technology enables the analysis of hundreds of specimens by arranging numerous 0.6-mm tissue core biopsy specimens into a single paraffin block. Validation studies are necessary to evaluate the representativeness of small disks taken from the original tissue. We validated the tissue microarray technology in colorectal carcinoma by analyzing the immunohistochemical expression of proteins involved in the two main pathways of colorectal carcinogenesis: p53 protein for loss of heterozygosity tumors, hMLH1 and hMSH2 proteins for microsatellite instability (MSI) tumors. We compared in 30 colorectal carcinomas (15 MSI^- and 15 MSI^+), 8 microarrays disks, and the whole section of the block from which they were derived. Tumoral tissue was present in 95.7% of the microarray disks. The analysis of three disks per case was comparable to the analysis of the whole section in 99.6% (p53), 98.8% (hMLH1), and 99.2% (hMSH2) of cases. In the second part we applied the tissue microarray technology to 263 consecutive cases of colorectal carcinoma, sampled by three cores. We showed that 48.5% overexpressed p53 and 8.7% lost hMLH1 or hMSH2. Tissue microarray technology, validated in colorectal carcinoma, appears as a useful research tool for rapid analysis of the clinical interest of molecular alterations.

F. Jourdan · N. Sebbagh · E. Comperat · N. Mourra · J.-F. Flejou (✉)
Department of Pathology, Hôpital Saint-Antoine, AP-HP, 184 rue du Faubourg Saint-Antoine, 75012 Paris, France
e-mail: jean-francois.flejou@sat.ap-hop-paris.fr
Tel.: +33-1-49282170
Fax: +33-1-49282878

F. Jourdan · N. Sebbagh · S. Olschwang · A. Duval · R. Hamelin · J.-F. Flejou
Unité INSERM 434, 10 rue Juliette Dodu, 75010 Paris, France

A. Flahault
Unité INSERM 444, Faculté de Médecine Saint-Antoine, 27 rue Chaligny, 75571 Paris cedex 12, France

Keywords Tissue microarray · Validation study · Colorectal carcinoma · Immunohistochemistry · Microsatellite instability

Introduction

Genome screening tools, such as cDNA microarrays, reveal different levels of expression of numerous genes within normal and pathological tissues. These potential markers need to be tested in hundreds of human specimens to confirm their clinical interest in diagnostic, prognostic or therapeutic fields. This is rapidly achieved by the tissue microarray (TMA), a high-throughput technique described in 1998 by Kononen et al. [21]. Studies combining cDNA microarray and TMA identify new markers with great efficiency [27, 30]. The TMA technique consists of arraying, in a paraffin block, up to 1,000 samples removed from selected areas of donor blocks. Parallel studies of morphology by standard histological staining, nucleic acids by in situ hybridization, and proteins by immunohistochemistry (IHC) can be carried out on serial sections of the array block. The limit of this technique may be the lack of representativeness of heterogeneous tissues by small disks (0.6 mm in diameter in most studies). Validation studies are necessary to compare microarrays disks and standard whole sections, and establish the number of cores required to adequately represent the expression of a marker. We evaluated the TMA in colorectal carcinoma (CRC) by the IHC pattern of three common markers of the two pathways of colorectal carcinogenesis [8, 22]. The loss of heterozygosity (LOH) pathway responsible for 85% of sporadic CRC and the familial adenomatous polyposis (FAP) [14] is characterized by losses of chromosomal segments bearing tumor suppressor genes. Mutation of the second allele leads to the inactivation of these genes, in the early stage of the tumor growth as *APC* (adenomatous polyposis coli) gene or later as *p53* gene. Most mutations in the *p53* gene result in a p53 protein with a long half-life and an ensuing nuclear accumulation detectable on IHC [17].

Immunohistochemistry can also be used in LOH tumors to show abnormal nuclear expression of β-catenin secondary to APC or β-catenin gene mutation [18]. However, a high rate of β-catenin nuclear expression has also been reported by some authors in tumors showing microsatellite instability (MSI) [11, 26]. The latter phenomenon of MSI is present in 15% of sporadic CRC and more than 90% of hereditary nonpolyposis colorectal cancers (HNPCC) [14]. This phenotype is due to a defective mismatch repair (MMR) system of which one gene, in most cases *hMLH1* or *hMSH2*, shows biallelic inactivation [20]. The diagnosis of MSI status is carried out by polymerase chain reaction (PCR) in accordance with the National Cancer Institute recommendations [4] but can also be effected on IHC by showing loss of expression of hMLH1 or hMSH2 proteins by tumoral cells [24].

After validation of the TMA in 30 CRC we applied this technique to 263 consecutive cases of CRC, by analyzing the IHC pattern of p53, hMLH1, and hMSH2 proteins.

Material and methods

Tumor samples

Cases of colorectal adenocarcinomas were retrieved retrospectively from the files of the Department of Pathology of the Hospital Saint Antoine (Paris, France). The specimens had been formalin-fixed, paraffin-embedded and the diagnosis made on hematoxylin and eosin (HE) sections. For the validation study we selected 30 CRC received between 1995 and 2000 and which were tested previously for MSI by PCR [31]. Fifteen CRC were classified MSI^+ in accordance with the National Cancer Institute recommendations [4]. Nine of these were associated with the HNPCC syndrome, and six were sporadic. Fifteen CRC were stable in PCR and classified MSI^-; nine were developed on FAP, and six were sporadic. In the second part of the study we included 263 consecutive cases of CRC received in our department in 2001.

Tissue microarray technique

A map of the receiver block was prepared with coordinates for each sample to correctly identify the tumors. Under a microscope areas of interest and nonnecrotic and rich in tumoral glands were marked out accurately with an indelible pen, on the HE whole section of each donor block. The tissue microarrayer, a custom-made precision instrument (Beecher Instruments, Woodland, USA) was used: cores of 0.6 mm diameter were punched from the donor blocks and positioned in a recipient paraffin array block, in smaller holes, of 0.4 mm for best adhesion of the samples to the array block. The cores were arranged 4 mm from the edges of the array block in an asymmetric way. The array blocks were then incubated 30 min at 37°C to improve adhesion between cores and paraffin of the recipient block. They were cut at room temperature with a standard microtome (Microm, Heidelberg, Germany).

Description of the array blocks of the study

For the validation study two blocks of 124 cores were made: each CRC was punched eight times. In ten cases it was possible to sample the edge (four cores) and the center (four cores) of the tumor. Four cores from a CRC already known as positive for p53, hMLH1, and hMSH2 were added as positive controls for IHC in each array block. Block I represented the 15 MSI^- CRC and block II the 15 MSI^+ CRC. In the second part of the study 263 CRC punched three times in accordance with the results of the validation study were allocated in three array blocks of 273 (block A) and 276 cores (blocks B and C). Twelve samples of normal colorectal mucosa were added in each block.

Immunohistochemistry

Sections of 5 µm from the five tissue arrays and 30 standard blocks were cut onto silane-treated Super Frost slides (CML, Nemours, France) and left to dry at 37°C overnight. The slides were deparaffinized in xylene and rehydrated in pure ethanol. Endogenous peroxidase was blocked using 3% hydrogen peroxide in methanol for 30 min. The slides were then placed in a microwave oven in citrate buffer (pH 6.0), for antigen retrieval, for 15 min at 750 W and 15 min at 150 W. All slides were processed using an automatic immunostainer (Optimax Plus 1.5, Biogenex, San Ramon, USA) with a supersensitive biotin-streptavidin-peroxidase technique (Super Sensitive Detection Kit, Biogenex). Mouse anti-human monoclonal antibodies to p53 (dilution 1:800, clone BP53-1, Biogenex), hMLH1 (dilution 1:100, clone G168-728, Pharmingen, San Diego Calif., USA) and hMSH2 (dilution 1:125, clone FE11, Calbiochem, Oncogene Research Products, Cambridge Mass., USA) were used. The slides were developed with amino-ethyl-carbazol, a red chromogen, and counterstained with Mayer's hemalun. Nuclear staining was interpreted for each antibody. A core was classified p53 positive when more than 50% of neoplastic cells showed a nuclear staining [3, 32]. For hMLH1 and hMSH2, a core was considered negative when there was a complete absence of nuclear staining of neoplastic cells in the presence of an internal positive control represented by normal epithelial cells, endothelial cells, fibroblasts, or lymphocytes [7]. In the validation study a case was classified p53 positive if at least one of eight cores was positive and was classified hMLH1 or hMSH2 negative if all the cores available were negative. Concerning the study of 263 consecutive CRC the same criteria were used for three cores per case. Whole sections of donor blocks and tissue array sections were read separately by two pathologists. Discordant cases were reviewed for consensus.

Statistical analysis

In the validation study, we calculated the percentage of cases correctly classified by the TMA, by comparing the cores to the whole section. We started from the theory that incorrectly classified cases (n) were independently arranged among the eight tissue cores, for each of the 30 tumors, according to Poisson distribution: percentage=$1-(n/30\times1/8)$. The percentage was calculated for each antibody according to the number of cores made by tumor, from one to eight. The 95% confidence interval was given by the Poisson distribution [13]. In the second part of the study differences between the IMC results recorded for CRC MSI^- and CRC MSI^+, were examined by χ^2 probability test [13]. Differences with P values less than or equal to 0.05 were regarded as statistically significant.

Results

Validation study

A disk was informative if at least 10% of the disk area contained tumoral glands (Figs. 1, 2): 94.5% for hMLH1, 96% for p53, and 96.7% for hMSH2. Eight disks per tumor could be interpreted in 78.8% of cases and seven in 90%. The lowest number of disks interpretable per case was four, only in one case. The loss of information was

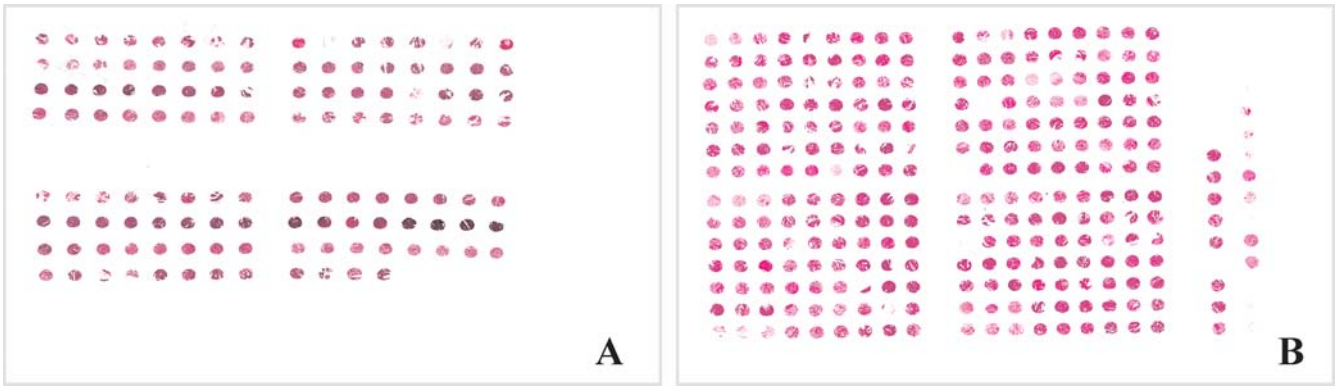

Fig. 1 Overview of hematoxylin and eosin stained sections of tissue array blocks of colorectal cancers; ×2.5. **A** Block I with 124 tissue cores. **B** Block A with 273 tissue cores

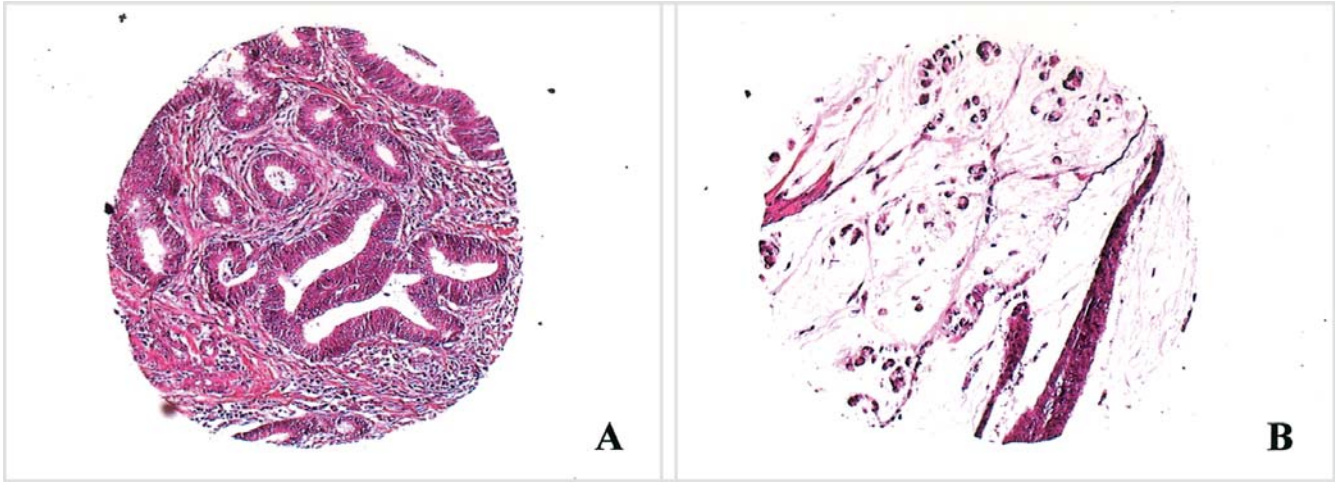

Fig. 2 Hematoxylin and eosin stained tissue microarray samples; ×100. **A** Well differentiated colorectal adenocarcinoma. **B** Mucinous colorectal adenocarcinoma

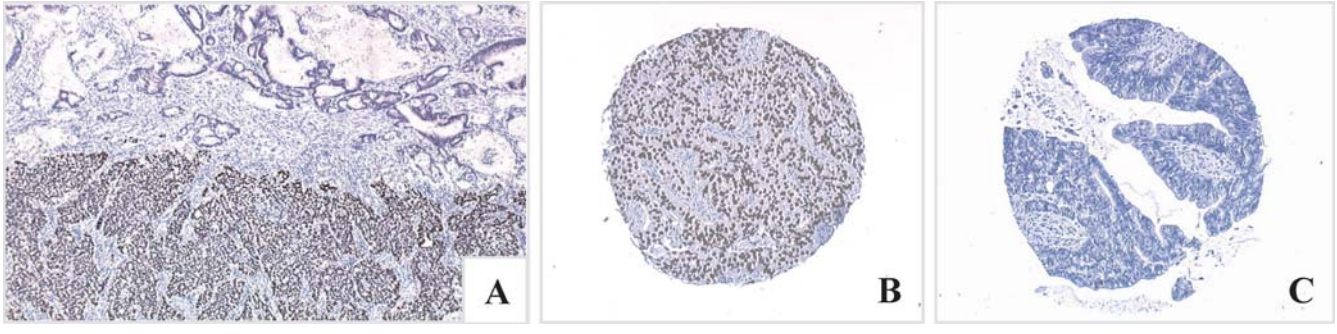

Fig. 3 **A** Heterogeneous immunohistochemical staining of p53 protein in a colorectal adenocarcinoma with varied differentiation patterns; ×50. **B** Tissue microarray sample of the p53 protein positive poorly differentiated area; ×100. **C** Tissue microarray sample of the p53 protein negative well differentiated area; ×100

due to the presence of normal tissue (muscle, connective tissue or mucosa) in 67.7% of cases, stroma without tumoral cells in 6.5% of cases and damaged disks in 25.8% of cases. An "interdisk" disagreement, that is, the presence of at least one disk classified differently from the other seven from the same tumor, was observed in 4.4% of cases. One case was due to varied differentiation patterns of the tumor, with overexpression of p53 limited to a poorly differentiated area (Fig. 3). In two cases for hMSH2 and one case for hMLH1, cores punched at the

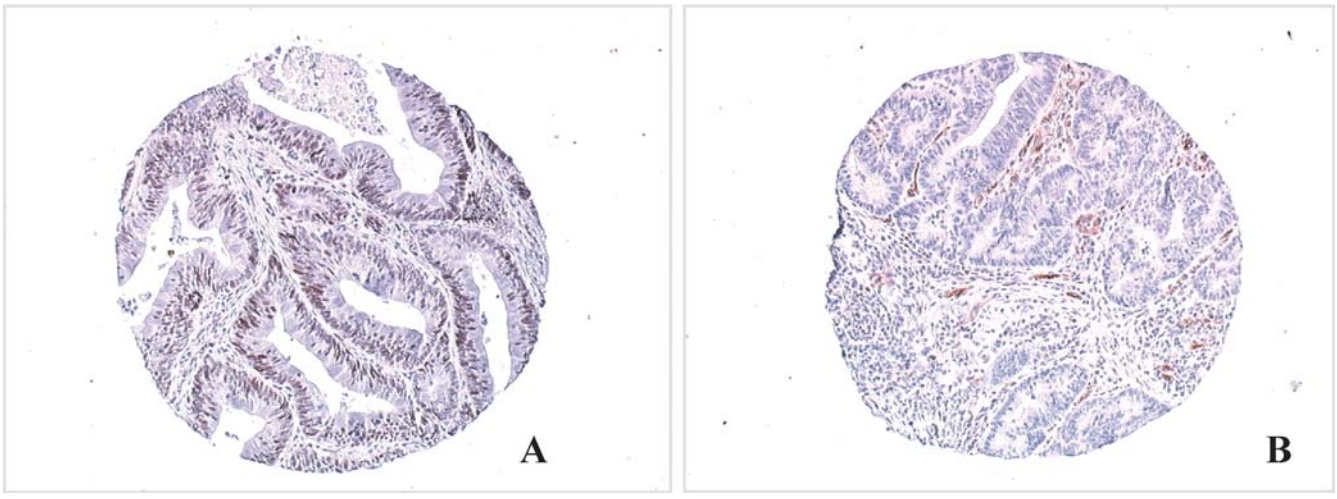

Fig. 4 hMLH1 immunohistochemical staining of tissue microarray samples; ×100. **A** hMLH1 positive colorectal adenocarcinoma. **B** hMLH1 negative colorectal adenocarcinoma with positive internal control represented by endothelial cells and lymphocytes of the stroma

Table 1 Immunohistochemical results of p53, hMLH1, and hMSH2 proteins expression in colorectal carcinoma (*CRC*) (*MSI* microsatellite instability)

	Overexpression of p53	Loss of expression of hMLH1	Loss of expression of hMSH2
Validation study of 30 CRC[a]			
15 MSI^-	5	0	0
15 MSI^+	1	8	7
Study of 263 consecutive CRC[b]	126	17	6

[a] Study of the whole section and eight tissue microarray cores
[b] Study of three tissue microarray cores

Table 2 Percentage of cases correctly classified on tissue microarray, in comparison with the whole section, in relation to the number of cores (*n*) analyzed by case (Poisson distribution)

Antibody	Number of cores punched by case							
	1	2	3	4	5	6	7	8
p53	97.1	97.9	99.6	99.6	100	100	100	100
hMLH1	96.7	98.3	98.8	99.2	100	100	100	100
hMSH2	96.7	98.4	99.2	99.6	100	100	100	100

surface of the tumor were positive while they were negative in deeper areas. The ten CRC sampled in the center (four cores) and edge (four cores) of the tumor had a perfect "interdisk" agreement. Overall the final result with eight disks was similar to the corresponding whole section in all cases (Table 1). Overexpression of p53 was observed in 33.3% of MSI^- cases and in 6.6% of MSI^+ cases. Loss of expression of hMLH1 or hMSH2 proteins was observed in 100% of MSI^+ cases and no MSI^- cases (Fig. 4). Then we established the number of cases correctly classified according to the number of cores made per case. For one core 96.7% of cases (hMLH1, hMSH2) and 97.1% (p53) were correctly evaluated. This concordance increased with the number of cores, reaching 98.8–99.6% for three cores and 100% for five cores and more (Table 2).

p53, hMLH1 and hMSH2 proteins expression in 263 consecutive CRC evaluated on TMA

According to the validation study, we applied the TMA technique in 263 consecutive CRC sampled by three cores. Three cases (1.1%) could not be interpreted for p53, the three disks being noninformative. In 8.7% of cases the expression of one MMR protein was lost, either hMLH1 (74%) or hMSH2 (26%). No case lost the expression of the two proteins. In 48.5% of cases there was overexpression of p53 protein; 17.4% of CRC losing an MMR protein and 51.5% of hMLH1/hMSH2 positive CRC overexpressed p53 ($P<0.005$; Table 3).

Table 3 Immunohistochemical results of p53, hMLH1, and hMSH2 proteins expression in 263[a] consecutive CRC ($P<0.005$)

p53	hMLH1 and hMSH2	
	Positive	One negative
Positive	122	4
Negative	115	19

[a] Three cases could not be interpreted because the three cores were noninformative

Discussion

The first concept of a multicore tissue block was described in 1986 by Battifora [2] to test new antibodies by IHC. A maximum of 100 samples of 1 mm thickness were tied up and embedded perpendicularly in a paraffin block. The TMA, described by Kononen et al. in 1998 [21], has many advantages on this technique. The tissue arrayer instrument enables to punch very small cores, of 0.6 mm diameter, and to array up to 1,000 samples into a single block. Moreover, specimens are arrayed in accordance with precise coordinates and are therefore correctly identified.

In our study, after a selection of donor blocks which is of great importance, it took 4 h to prepare a block of 273 cores. Moreover, as one section of one block enables the analysis of hundreds of cases with the amount of reagents usually used for one case, this technique allows a major reduction in cost. In our experience the interpretation of small areas of 0.6 mm was easier than for a whole section, which heterogeneity and staining artifacts at the borders can make it difficult to analyze. The latter phenomenon, frequently observed on large whole sections, was not encountered at the periphery of TMA blocks. Another advantage was that punches of 0.6 mm minimize tissue damage inflicted to the donor blocks. These blocks can still be used for other research studies or to test new markers of clinical interest for one patient.

Overall we attempted to answer the following question: are the small TMA samples representative of their potentially heterogeneous donor tumor? We conducted a validation study in CRC which is exceedingly common in most Western countries. We compared the IHC pattern of p53, hMLH1, and hMSH2 proteins between eight disks and the whole section of the block from which they were derived, in 15 MSI^- and 15 MSI^+ tumors. To our knowledge, we performed the first IHC study of hMLH1 and hMSH2 expression by the TMA technology. This technique was of great efficiency as only 4.3% of disks were not informative, a low rate in comparison with most validation studies [6, 10, 15, 19, 28, 29, 33] (Table 4). In our experience, the damage caused to a few disks was probably due to the IHC technique, especially to the antigen-retrieval step, as the corresponding cores were intact on HE-stained slides. The main reason for the loss of material was the absence of tumoral glands because of an abundant stroma or normal tissue. The selection of the donor blocks is crucial to minimize nonevaluable disks: large tumoral areas rich in glands must be selected. MSI^+ CRC are often mucinous, and it can be difficult to sample neoplastic cells in such cases. Moreover, the donor blocks must be chosen thick to obtain long cores that allow multiple studies on the same array block.

We analyzed eight cores per tumor and rare cases had some "interdisk" disagreement, showing that it is necessary to sample different areas in an heterogeneous tumor, as in one case, the expression of p53 protein depended on the tumor differentiation. If a marker is known to have an heterogeneous expression, it is crucial to sample the appropriate area, as the surface of the tumor for hMLH1 and hMSH2 proteins. On the other hand, we found no difference in expression of the three markers whether the cores were punched from the center or the edge of the tumor, contrary to the results obtained by Camp et al. [6] for hormonal receptors and Her2/neu in breast carcinoma. We then compared the results obtained with eight TMA disks to those obtained on the whole section: the results were similar in all cases. We statistically determined the minimal number of disks necessary to represent correctly the expression of the markers. One core enabled us to classify correctly 96.7–97.1% of cases, and more than four cores 100% of cases. We decided to make three cores in a large series to increase the concordance rate (98.8–99.6%) and decrease the risk of lost cases. Until now all TMA validation studies have confirmed the representa-

Table 4 Results of tissue microarray validation studies published in the literature and of the present study (*ER* estrogen receptor, *PR* progesterone receptor, NA not available)

Reference	Type of tumor	Number of cases	Number of disks by tumor	Number of array blocks	Immunohisto-chemical markers	Percentage of noninformative disks
Mucci et al. 2000 [28]	Prostate carcinoma	50	5–10	1 block of 458 disks	Synaptophysin, chromogranin A	27
Gillett et al. 2000 [15]	Breast carcinoma	157	23	10 blocks of 35 disks	ER, PR	11
Camp et al. 2000 [6]	Breast carcinoma	38	10	1 block of 380 disks	ER, PR, Her2/neu	NA
Torhost et al. 2001 [33]	Breast carcinoma	553	4	4 blocks of 553 disks	ER, PR, p53	23.5–29.7
Hoos et al. 2001 [19]	Fibroblastic tumors	59	3	1 block of 177 disks	Ki67, p53, pRb	10–20
Nocito et al. 2001 [29]	Bladder carcinoma	2317	4	NA	Ki67	11–14.6
Fernebro et al. 2002 [10]	Rectal carcinoma	20	3–6	1 block of 69 disks	Ki67, p53	17
Present study	Colorectal carcinoma	30	8	2 blocks of 124 disks	p53, hMLH1, hMSH2	4.3

tiveness of the technique and also suggested triplicate cores [6, 10, 15, 19]. However, it is important to realize that the TMA technology still remains a research tool. If a marker with a potential value is identified by this technique, for any given patient tests must be carried out on a large section. The IHC results of our validation study were similar to those obtained in previous studies: hMLH1 and hMSH2 antibodies enabled the diagnosis of MSI^+ CRC with a sensibility and specificity of 100% [24]; p53 overexpression was frequent in MSI^- CRC.

In the second part of the study we showed that TMA can be used efficiently to examine large series of tumors after a step of validation. In accordance with the results of our validation study we made three cores per case to study 263 consecutive CRC. We obtained the IHC pattern of the series of CRC for three markers of interest. There was a loss of expression of either hMLH1 or hMSH2 proteins in 8.7% of cases. Therefore we rapidly showed that almost 10% of the CRC operated on during 1 year in our center were MSI^+. As these tumors have a better prognosis [12, 16] and a better response to some chemotherapies [9], this result is potentially of great interest. In 17.4% of MSI^+ CRC and 51.5% of hMLH1/hMSH2 positive CRC there was overexpression of p53, corresponding to the inverse relationship between *p53* gene alterations and MSI [32]. The clinical significance of *p53* mutation and overexpression is controversial, with an influence on clinical outcome and therapeutic response still debated in the literature [1, 23, 25]. An interesting application of TMA would be the use of a "prognosis array block" containing CRC with available clinical follow-up data, to evaluate prognostic value of p53 and other prognostic markers.

In conclusion, we validated the TMA technology in CRC. The selection of donor blocks and sampling areas is a crucial step. The number of replicates must be adapted to the tissue type and the marker expression if it is known [5]. We confirmed by the rapid analysis of three IHC markers in 263 CRC that TMA is a high-throughput technology.

Acknowledgements F.J. was supported by a grant from the Association pour la Recherche sur le Cancer. We acknowledge the Association Charles Debray for its financial support.

References

1. Allegra CJ, Parr AL, Wold LE, Mahoney MR, Sargent DJ, Johnston P, Klein P, Behan K, O'Connell MJ, Levitt R, Kugler JW, Tirona MT, Goldberg RM (2002) Investigation of the prognostic and predictive value of thymidylate synthase, p53, and Ki-67 in patients with locally advanced colon cancer. J Clin Oncol 20:1735–1743
2. Battifora H (1986) Methods in laboratory investigation. Lab Invest 55:244–248
3. Bocker Edmonston T, Cuesta KH, Burkholder S, Barusevicius A, Rose D, Kovatich AJ, Boman B, Fry R, Fishel R, Palazzo JP (2000) Colorectal carcinomas with high microsatellite instability: defining a distinct immunologic and molecular entity with respect to prognostic markers. Hum Pathol 31:1506–1514
4. Boland RC, Thibodeau SN, Hamilton SR, Sidransky D, Eshleman JR, Burt RW, Meltzer SJ, Rodriguez-Bigas MA, Fodde R, Ranzani GN, Srivastava S (1998) A National Cancer Institute workshop on microsatellite instability for cancer detection and familial predisposition: development of international criteria for the determination of microsatellite instability in colorectal cancer. Cancer Res 58:5248–5257
5. Bubendorf L, Nocito A, Moch H, Sauter G (2001) Tissue microarray (TMA) technology: miniaturized pathology archives for high-throughput in situ studies. J Pathol 195:72–79
6. Camp RL, Charette LA, Rimm DL (2000) Validation of tissue microarray technology in breast carcinoma. Lab Invest 80:1943–1949
7. Chaves P, Cruz C, Lage P, Claro I, Cravo M, Leitão CN, Soares J (2000) Immunohistochemical detection of mismatch repair gene proteins as a useful tool for identification of colorectal carcinoma with the mutator phenotype. J Pathol 191:355–360
8. Chung DC (2000) The genetic basis of colorectal cancer: insights into critical pathways of tumorigenesis. Gastroenterology 119:854–865
9. Elsaleh H, Joseph D, Grieu F, Zeps N, Spry N, Iacopetta B (2000) Association of tumour site and sex with survival benefit from adjuvant chemotherapy in colorectal cancer. Lancet 355:1745–1750
10. Fernebro E, Dictor M, Bendahl PO, Fernö M, Nilbert M (2002) Evaluation of the Tissue Microarray technique for immunohistochemical analysis in rectal cancer. Arch Pathol Lab Med 126:702–705
11. Fukushima H, Yamamoto H, Itoh F, Horiuchi S, Min Y, Iku S, Imai K (2001) Frequent alterations of the β-catenin and TCF-4 genes, but not of the APC gene, in colon cancers with high-frequency microsatellite instability. J Exp Clin Cancer Res 20:533–559
12. Gafà R, Maestri I, Matteuzzi M, Santini A, Ferretti S, Gavazzini L, Lanza G (2000) Sporadic colorectal adenocarcinoma with high-frequency microsatellite instability: pathobiologic features, hMLH1 and hMSH2 expression and clinical outcome. Cancer 89:2025–2037
13. Gardner MJ, Altman DG (2000) Confidence interval and statistical guidelines. In: Statistics with confidence, 2nd edn. British Medical Journal, London, pp 116–118
14. Giardiello FM, Brensinger JD, Petersen GM (2001) AGA technical review on hereditary colorectal cancer and genetic testing. Gastroenterology 121:198–213
15. Gillett CE, Springall RJ, Barnes DM, Hanby AM (2000) Multiple tissue core arrays in histopathology research: a validation study. J Pathol 192:549–553
16. Gryfe R, Kim H, Hsieh E TK, Aronson MD, Holowaty EJ, Bull SB, Redston M, Gallinger S (2000) Tumor microsatellite instability and clinical outcome in young patients with colorectal cancer. N Engl J Med 342:69–77
17. Hamelin R, Laurent-Puig P (1997) p53 et cancers colorectaux. Pathol Biol (Paris) 45:876–881
18. Hao X, Frayling I, Willcocks T, Han W, Tomlinson I, Pignatelli M, Pretlow T, Talbot I (2002) β-Catenin expression and allelic loss at APC in sporadic colorectal carcinogenesis. Virchows Arch 440:362–366
19. Hoos A, Urist MJ, Stojadinovic A, Mastorides S, Dudas ME, Leung DH, Kuo D, Brennan MF, Lewis JJ, Cordon-Cardo C (2001) Validation of tissue microarrays for immunohistochemical profiling of cancer specimens using the example of human fibroblastic tumors. Am J Pathol 158:1245–1251
20. Jiricny J, Nyström-Lahti M (2000) Mismatch repair defects in cancer. Curr Opin Genet Dev 10:157–161
21. Kononen J, Bubendorf L, Kallioniemi A, Bärlund M, Schraml P, Leighton S, Torhorst J, Mihatsch MJ, Sauter G, Kallioniemi OP (1998) Tissue microarrays for high-throughput molecular profiling of tumor specimens. Nat Med 4:844–847
22. Laurent-Puig P, Blons H, Cugnenc P-H (1999) Sequence of molecular genetic events in colorectal tumorigenesis. Eur J Cancer Prev 8:S39–S47
23. Leahy DT, Salman R, Mulcahy H, Sheahan K, O'Donoghue DP, Parfrey NA (1996) Prognostic significance of p53 abnor-

malities in colorectal carcinoma detected by PCR-SSCP and immunohistochemical analysis. J Pathol 180:364–370
24. Lindor NM, Burgart LJ, Leontovich O, Goldberg RM, Cunningham JM, Sargent DJ, Walsh-Vockley C, Petersen GM, Walsh MD, Leggett BA, Young JP, Barker MA, Jass JR, Hopper J, Gallinger S, Bapat B, Redston M, Thibodeau SN (2002) Immunohistochemistry versus microsatellite instability testing in phenotyping colorectal tumors. J Clin Oncol 20:1043–1048
25. Manne U, Myers RB, Moron C, Poczatek RB, Dillard D, Weiss H, Brown D, Srivastava S, Grizzle WE (1997) Prognostic significance of Bcl-2 expression and p53 nuclear accumulation in colorectal adenocarcinoma. Int J Cancer 74:346–358
26. Miyaki M, Iijima T, Kimura J, Yasuno M, Mori T, Hayashi Y, Koike M, Shitara N, Iwama T, Kuroki T (1999) Frequent mutation of β-catenin and APC genes in primary colorectal tumors from patients with hereditary nonpolyposis colorectal cancer. Cancer Res 59:4506–4509
27. Moch H, Schraml P, Bubendorf L, Mirlacher M, Kononen J, Gasser T, Mihatsch MJ, Kallioniemi OP, Sauter G (1999) High-throughput tissue microarray analysis to evaluate genes uncovered by cDNA microarray screening in renal cell carcinoma. Am J Pathol 154:981–986
28. Mucci NR, Akdas G, Manely S, Rubin MA (2000) Neuroendocrine expression in metastatic prostate cancer: evaluation of high throughput tissue microarrays to detect heterogeneous protein expression. Hum Pathol 31:406–414
29. Nocito A, Bubendorf L, Tinner EM, Süess K, Wagner U, Forster T, Kononen J, Fijan A, Bruderer J, Schmid U, Ackermann D, Maurer R, Alund G, Knönagel H, Rist M, Anabitarte M, Hering F, Hardmeier T, Schoenenberger AJ, Flury R, Jäger P, Fehr JL, Schraml P, Moch H, Mihatsch MJ, Gasser T, Sauter G (2001) Microarrays of bladder cancer tissue are highly representative of proliferation index and histological grade. J Pathol 194:349–357
30. Otsuka M, Kato M, Yoshikawa T, Chen H, Brown EJ, Masuho Y, Omata M, Seki N (2001) Differential expression of the L-plastin gene in human colorectal cancer progression and metastasis. Biochem Biophys Res Commun 289:876–881
31. Rigau V, Sebbagh N, Olschwang S, Paraf F, Mourra N, Parc Y, Fléjou JF (2003) Microsatellite instability in colorectal carcinoma: the comparison of immunohistochemistry and molecular biology suggests the interest of hMLH6 immunostaining. Arch Pathol Lab Med 127:694–700
32. Samowitz WS, Holden JA, Curtin K, Edwards SL, Walker AR, Lin HA, Robertson MA, Nichols MF, Gruenthal KM, Lynch BJ, Leppert MF, Slattery ML (2001) Inverse relationship between microsatellite instability and K-ras and p53 gene alterations in colon cancer. Am J Pathol 158:1517–1524
33. Torhorst J, Bucher C, Kononen J, Hass P, Zuber M, Köchli O, Mross F, Dieterich H, Moch H, Mihatsch M, Kallioniemi OP, Sauter G (2001) Tissue microarrays for rapid linking of molecular changes to clinical endpoints. Am J Pathol 159:2249–2256

Virchows Arch (2003) 443:122–132
DOI 10.1007/s00428-003-0859-2

ORIGINAL ARTICLE

Jorge S. Reis-Filho · Pete T. Simpson · Albino Martins · Ana Preto · Fátima Gärtner · Fernando C. Schmitt

Distribution of p63, cytokeratins 5/6 and cytokeratin 14 in 51 normal and 400 neoplastic human tissue samples using TARP-4 multi-tumor tissue microarray

Received: 7 March 2003 / Accepted: 15 May 2003 / Published online: 16 July 2003
© Springer-Verlag 2003

Abstract p63, cytokeratin (CK) 5/6 and CK 14 have been employed in diagnostic pathology as markers of basal, squamous and myoepithelial differentiation in several types of human neoplasms; however, there is scant data on the concurrent expression of these markers in large series of human neoplasms. We analyzed the distribution of these three immunohistochemical markers in 51 normal human tissue samples, 350 carcinomas, 25 malignant melanomas (MMs), and 25 glioblastomas using three serial sections of tissue array research program (TARP)-4 multi-tumor tissue microarray. Also, we performed double immunostainings to characterize the differential distribution of p63/CK 5/6 and p63/CK 14 in normal breast, salivary gland and skin. p63, CK 5/6 and CK 14 were expressed in basal cells of the prostate and respiratory epithelia and in breast and bronchial myoepithelial cells. p63 was also expressed in cytotrophoblast cells of human placenta and in scattered cells of lymph node germinal center. CK 5/6 and CK 14 also stained the cytoplasm of basal cells of esophageal stratified squamous epithelium and transitional epithelial cells of the bladder. No mesenchymal, neural, endothelial, smooth muscle or adipose cells were stained by any of the markers. p63, CK 5/6, and CK 14 were respectively expressed in 92.6%, 75.0%, and 52.9% of the squamous cell carcinomas of the lung, 10.2%, 20.0%, and 7.4% of the ductal carcinomas of the breast, 12.9%, 34.4%, and 11.8% of the serous and 25.0%, 0%, and 0% of the endometrioid carcinomas of the ovary. Lung, prostate and colonic adenocarcinomas, as well as MMs and glioblastomas were only rarely decorated by one of the markers. Only matched samples of 16 squamous cell carcinomas and two ductal carcinomas of the breast co-expressed these three markers. In double immunostainings, p63-CK 5/6, as well as p63-CK 14 were co-expressed by basal/myoepithelial cells of the salivary glands and basal cells of the epidermis. Our results demonstrate that p63, CK 5/6 and CK 14 may be used together in immunohistochemical panels to characterize squamous differentiation in poorly differentiated carcinomas or carcinomas of unknown origin.

Keywords Tissue microarray · Immunohistochemisty · Double immunostaining · Squamous cell carcinoma · Myoepithelial cell

J. S. Reis-Filho · P. T. Simpson
The Breakthrough Toby Robins Breast Cancer Research Centre, Institute of Cancer Research, London, UK

J. S. Reis-Filho · A. Martins
Life and Health Sciences Research Institute, School of Health Sciences, University of Minho, Braga, Portugal

A. Preto · F. Gärtner · F. C. Schmitt (✉)
IPATIMUP – Institute of Molecular Pathology and Immunology, University of Porto, R. Roberto Frias, S/N, 4200 Porto, Portugal
e-mail: Fernando.Schmitt@ipatimup.pt

F. C. Schmitt
Medical Faculty, University of Porto, Porto, Portugal

Introduction

Cytokeratin (CK) is one of the three types of intermediate filaments that constitute the cytoskeleton of epithelial mammalian cells [7, 26]. At least 20 different keratin genes located either on chromosome 12 or 17 have been described [7, 38]. Each of these genes encodes specific keratin subunits, which may be classified as low- or high-molecular-weight CKs and as acidic or basic forms, based on their isoelectric points [7, 26]. Type-I CKs are small, acidic and encoded by genes located on chromosome 17, whereas type-II CKs are large, basic, and encoded by genes on chromosome 12 [7, 26, 38]. In epithelial cells, keratin filaments are composed of one type-I and one type-II CK [7, 26]. Different keratin isoforms are differentially expressed during development and differentiation and vary in different types of epithelia [2, 6, 7, 8, 9, 13, 28, 38, 40, 41, 42]. Several lines of evidence support that when an epithelial cell undergoes malignant transformation, it usually harbors a constant keratin

profile, and this profile might serve to recognize different types of carcinomas [2, 6, 7, 8, 9, 13, 28, 38, 40].

CK 5 and CK 14, also known as basal-type CKs, are consistently expressed in basal cells of multilayered epithelia, myoepithelial cells of the breast, salivary and sweat glands, Hassall's corpuscles of the thymus, parathyroid glands, hair follicle's outer root sheath, sebaceous glands and mesothelial cells [2, 6, 7, 8, 9, 13, 42]. CK 6 is a type-II CK expressed in filiform papillae of the tongue, oral and esophageal epithelia, the outer root sheath of the hair follicle and occasional glandular cells, but not in the breast [7]. CK 6 is only expressed in the epidermis of the palms and soles, or when it has undergone hyperplasia [7].

p63 is a nuclear transcription factor that harbors a high homology with p53 [10, 22, 32]. Its gene is located on 3q27 and encodes at least six different isoforms that may be classified in two discrete groups: transactivating p63 (TA-p63) isoforms, which may bind to p53-reporter genes and activate their transcription and dominant negative p63 (ΔN-p63) isoforms, which lack the transactivating N-terminal region and can bind to canonical DNA-binding sites but cannot transactivate these genes [10, 22, 32]. We [32, 33, 34, 35, 36, 37] and others [1, 5, 10, 11, 12, 19, 22, 24, 27, 29, 30, 31, 39, 43, 44, 46, 47] have described that p63 isoforms recognized by the antibody 4A4 are consistently expressed in the nuclei of basal cells of several types of multilayered epithelia and that ΔN-p63 isoforms are preferentially expressed in these cells. Dominant-negative p63 isoforms play an important role in the maintenance of basal cell populations, owing to their ability to overcome p53-driven cell cycle arrest and apoptosis [11, 19, 22, 24, 32, 47]. p63 is also consistently expressed by myoepithelial cells of the breast, salivary, bronchial and sweat glands [1, 5, 10, 11, 12, 19, 22, 24, 27, 30, 31, 32, 33, 34, 35, 36, 37]. Interestingly, p63 knockout mouse models have shown that the expression of p63 is of utmost importance for the correct differentiation of several types of multilayered epithelia [22, 27, 47] and that p63 may promote the transcription of genes associated with terminal epithelial differentiation [10, 22, 24, 47].

Multi-tumor tissue microarrays (TMAs) have proven to be very powerful tools for several purposes, including prognostic studies using immunohistochemical or in situ hybridization techniques, as well as the validation of results obtained from cDNA array experiments [3, 4, 11, 15, 16, 20, 25, 48]. However, there are limited data on TMAs for the evaluation of the distribution of antibodies that might be used as diagnostic markers in surgical pathology practice. As p63, CK 5/6 and CK 14 show a similar distribution in several types of tissues [2, 6, 8, 9, 11, 13, 19, 24, 28, 32, 33, 34, 35, 37, 38, 43, 47], our goals were: (i) to describe the expression of p63, CKs 5/6 and CK 14 in 51 normal tissue samples and in 350 epithelial neoplasms, 25 melanomas and 25 glioblastomas using three serial sections of tissue array research program (TARP)-4 multi-tumor TMA; (ii) to determine which types of human tumors co-express these markers; and (iii) to evaluate the impact of these markers in surgical pathology practice. We also performed double-immunostainings for p63/CKs 5/6 and p63/CK 14 to demonstrate the concurrent expression of these proteins in normal mammary and salivary gland myoepithelial cells, as well as in basal keratinocytes.

Materials and methods

Tissue microarray

TARP-4 multi-tumor TMA slides were obtained from the Cooperative Human Tissue Network under the TARP of The National Cancer Institute, The National Institutes of Health, Bethesda, MD, USA. Briefly, this multi-tumor TMA is composed of 0.6-mm samples of normal tissue [*n*=51: adrenal (*n*=2), bladder (*n*=2), bone marrow (*n*=1), breast (*n*=5), cerebellum (*n*=1), cerebrum (*n*=2), colon (*n*=2), esophagus (*n*=2), heart (*n*=1), kidney (1 cortex and 1 medulla), liver (*n*=3), lung (*n*=3), lymph node (*n*=2), mesothelium (*n*=2), muscle (*n*=1), ovary (*n*=2), pancreas (*n*=1), peripheral nerve (*n*=1), placenta (*n*=1), prostate (*n*=2), salivary gland (*n*=1), skin (*n*=2), small bowel (*n*=2), spleen (*n*=2), stomach (*n*=1), testis (*n*=1), thyroid (*n*=1), tongue (*n*=1), uterus (1 endometrium and 1 myometrium)], breast cancer (*n*=75), colon cancer (*n*=75), lung cancer (*n*=75), prostate cancer (*n*=75), ovarian cancer (*n*=50), lymphoma (*n*=50), glioblastoma (*n*=25), and melanoma (*n*=25). As the original TARP-4 database includes only scant data on the expression of immunomarkers expressed by the lymphomas included in the TMA block (http://resresources.nci.nih.gov/tarp/TARP4.xls) and does not include their final diagnosis, we decided to exclude these cases.

Immunohistochemistry

TMA sections were dried under a low-power ultraviolet light for 120 min. All sections were deparaffinized, rehydrated and subjected to heat-induced antigen retrieval in a water bath, using citrate buffer at pH 6.0 (CK 14 and p63) and pH 8.0 (CK 5/6) for 20 min. Immunohistochemistry according to the streptavidin-biotin-peroxidase complex technique with antibodies against all p63 isoforms (clone 4A4, 1:200; Neomarkers, Freemount, CA, USA), CK 5/6 (clone D5/16B4, 1:200; Zymed, South San Francisco, CA, USA), and CK 14 (clone MCA890H, 1:200; Serotec, 1:10, Oxford, UK) was performed as described elsewhere [37]. Positive (histological sections of a sclerosing papilloma with myoepithelial hyperplasia for p63 and skin for CK 5/6 and CK14) and negative (omission of primary and secondary antibodies) controls were included in each slide run. All controls gave appropriate results.

The distribution of p63, CK 5/6 and CK 14 was independently evaluated by two of the authors (JSRF and AM). All discordant results were resolved in a multi-head microscope. The differential expression of p63, CK 5/6 and CK 14 in normal tissue samples was recorded. p63, CK 5/6 and CK 14 expression in neoplastic samples on the TMA was quantitatively assessed and recorded as: (−) negative; (+) focally positive, up to 25% of neoplastic cells; or (++) positive, greater than 25% of the neoplastic cells. Briefly, all neoplastic cells of each TMA core were counted and a ratio between the number of positive cells ×100/number of negative cells was calculated.

For statistical analysis, cases were recorded either as (−) or as (+), without semiquantification of the positive cases.

Double immunostaining

One normal parotid, one minor salivary gland and one normal breast sample were subjected to double immunostaining, as described elsewhere [23], using p63 as first primary antibody and

either CK 5/6 or CK 14 as second primary antibody. Briefly, the sections were submitted to heat-induced antigen retrieval using a water bath with 10 mM citrate buffer (pH 6.0) before incubating for 2 h at room temperature with the first primary antibody. Then, the sections were sequentially incubated with biotin labeled secondary antibody for 30 min, avidin-biotin-peroxidase complex for 60 min and DAB for 5 min. Sections were then sequentially incubated with the second primary antibody for 2 h at room temperature, goat anti-mouse IgG for 30 min, alkaline phosphatase mouse anti-alkaline phosphatase for 60 min and fast-red for 45 min. Controls included (a) omission of the first primary antibody and (b) omission of the second primary antibody.

Statistical analysis

The statistical associations between the distribution of p63, CK 5/6 and CK 14 in different types of neoplasms were evaluated using the χ^2 test. We also evaluated whether matched samples of p63 positive (+) tumors also co-express CK 5/6 and CK 14 more frequently than p63 negative (−) tumors using Fisher's exact test. For statistical analysis, only carcinoma samples were evaluated. The ductal carcinoma in situ (DCIS) sample and the tubular adenoma samples (n=2) were excluded. All tests were two tailed. A 95% confidence interval was adopted for all tests.

Results

p63

Normal tissue samples

Table 1 summarizes the distribution of p63 immunoreactivity in normal tissue samples. Briefly, p63 decorated basal cells of the prostate and of the pseudostratified respiratory epithelium, myoepithelial cells of the bronchial glands and cytotrophoblasts of human placenta (Fig. 1A). Scattered lymphoid cells in the germinal centers were also stained with p63. No endothelial, smooth muscle, neural or adipocytic cells were stained with anti-p63 antibodies in any of the organs examined herein.

Neoplasms

In the present study, the distribution of p63 immunoreactivity was analyzed in 400 tumors (Table 2). Concerning carcinomas, p63 was consistently expressed in squamous cell carcinomas of the lung (92.6%) (Fig. 2A),

Table 1 Summary of p63, CK 5/6 and CK 14 distribution in 51 normal tissue samples using tissue array research program (TARP)-4 multi-tumor tissue microarrays. *CK* cytokeratin, *L/F* lost/fragmented, *NA* not available

Tissue	*n*	p63	L/F	Note	CK 5/6	L/F	Note	Ck 14	L/F	Note
Adrenal	2	-	0		+	0		-	0	
Bladder	2	-	0	No epithelial cells	+	1	Epithelial cells	1	1	Transitional cells
Bone marrow	1	-	0		NA	1		NA	1	
Breast	5	-	2	Only fat cells	1	4	Basal/myoepithelial cells	+	4	Basal cells
Cerebellum	1	-	0		-	0		-	0	
Cerebrum	2	-	0		-	0		-	0	
Colon	2	-	0		-	0		-	0	
Esophagus	2	NA	2	No epithelial cells	+	1	Epithelial cells	NA	2	
Heart	1	-	0		NA	1		-	0	
Kidney	2	-	0		-	1		-	1	
Liver	3	-	0		+	0	Focal	-	0	
Lung	3	+	0	Basal cells of respiratory epithelium	+	0	Basal cells of respiratory epithelium	+	2	Basal cells of respiratory epithelium
Lymph node	2	+	0	Germinal center cells	-	0		-	0	
Mesothelium	2	-	0		NA	2	No mesothelial cells	NA	2	No mesothelial cells
Muscle	1	-	0		-	0		-	0	
Ovary	2	-	0		-	0		-	0	
Pancreas	1	-	0		+	0	Scattered acinar cells	-	0	
Peripheral nerve	1	NA	1		-	0		-	0	
Placental	1	+	0	Cytotrophoblast cells	NA	1		NA	1	
Prostate	2	+	0	Basal cells	+	0	Basal cells of the acini	+	0	Basal cells of the acini
Salivary gland	1	-	1	Severely fragmented	+	0	Basal cells of acini and intercalated ducts	+	0	Basal cells of acini and intercalated ducts
Skin	2	-	0	No keratinocytes	NA	2		NA	2	
Small bowel	2	-	0		-	0		-	1	
Spleen	2	-	0		-	0		-	0	
Stomach	1	NA	1		+	0	Parietal cells	-	0	
Testis	1	-	0		-	0		-	0	
Thyroid	1	NA	1		NA	1		NA	1	
Tongue	1	NA	1		NA	1		NA	1	
Uterus	2	-	1	Rare endometrial cells	-	0		-	0	

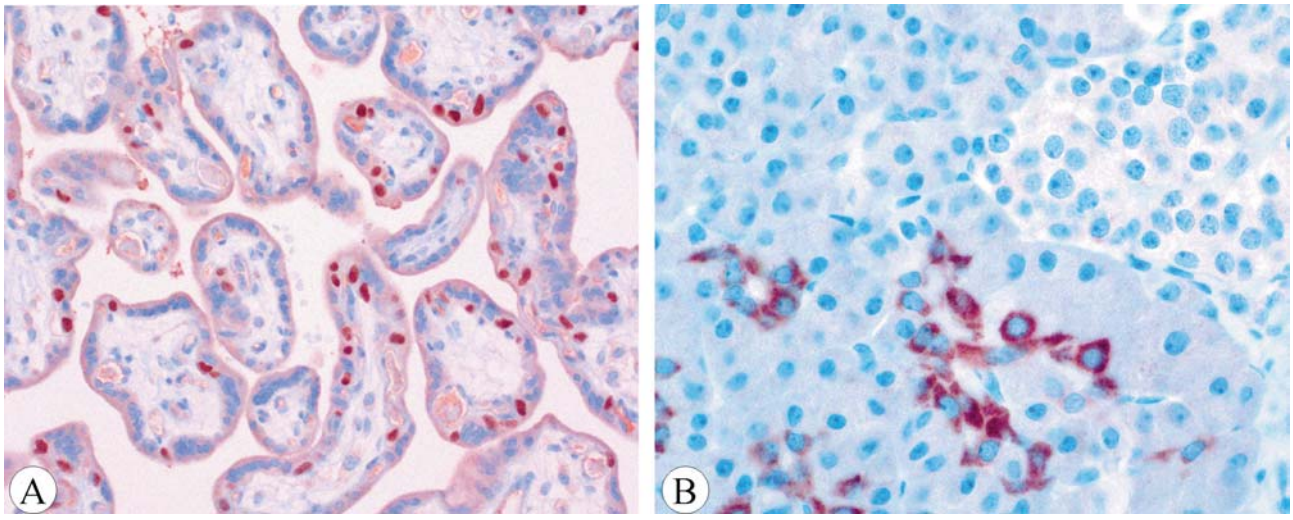

Fig. 1 **A** p63 expression in cytotrophoblasts of a placenta tissue core. **B** Medium-power magnification of pancreas tissue core: note the presence of scattered cytokeratin 5/6-positive cells. (Streptavidin-biotin-peroxidase/diaminobenzidine; original magnification ×200 **A**, **B**)

Table 2 Summary of p63, CK 5/6 and CK 14 distribution in 350 carcinomas, 25 malignant melanomas, and 25 glioblastomas using tissue array research program (TARP)-4 multi-tumor tissue microarrays. *Adenoca* adenocarcinoma, *CCC* clear cell carcinoma, *CK* cytokeratin, *CNS* central nervous system, *DCIS* ductal carcinoma in situ, *Endomet* endometrioid carcinoma, *IDC* invasive ductal carcinoma, *ILC* invasive lobular carcinoma, *L/F/N* lost/fragmented/necrotic, *Muc adenoca* mucinous adenocarcinoma, *N.A.* not available, *PDC* poorly differentiated carcinoma, *SCC* squamous cell carcinoma, *Serous pap* serous papillary carcinoma, *Tub adeno* tubular adenoma

Tumor samples	*n*	p63 (+)	p63 (++)	L/F/N	Total (%)	CK 5/6(+)	CK 5/6(++)	L/F/N	Total (%)	Ck 14(+)	Ck 14(++)	L/F/N	Total (%)
Breast	75	5	1	7	8.8	11	3	12	22.2	3	2	13	8.1
IDC	65	5	1	6	10.2	8	3	10	20.0	2	2	11	7.4
ILC	9	0	0	1	0.0	2	0	2	28.6	0	0	2	0.0
DCIS	1	0	0	0	0.0	1	0	0	100.0	1	0	0	100.0
Prostate	75	0	0	6	0.0	6	1	11	10.9	0	0	11	0.0
Adenoca	75	0	0	6	0.0	6	1	11	10.9	0	0	11	0.0
Lung	75	10	20	16	50.8	10	23	7	48.5	7	11	9	27.3
Adenoca	32	2	2	3	13.8	3	0	3	10.3	0	0	3	0.0
PDC	4	0	1	1	33.3	1	0	1	33.3	0	0	1	0.0
SCC	39	8	17	12	92.6	4	23	3	75.0	7	11	5	52.9
Colon	75	0	1	4	1.4	2	1	13	4.8	0	0	14	0.0
Adenoca	66	0	1	3	1.6	2	1	13	5.7	0	0	13	0.0
Liver met	1	0	0	0	0.0	0	0	0	0.0	0	0	0	0.0
Muc adenoca	6	0	0	1	0.0	0	0	0	0.0	0	0	0	0.0
Tub adeno	2	0	0	0	0.0	0	0	0	0.0	0	0	1	0.0
Ovary	50	5	0	5	11.1	6	6	6	27.3	4	0	5	8.9
CCC	8	0	0	1	0.0	0	1	1	14.3	0	0	1	0.0
Endomet	5	1	0	1	25.0	0	0	2	0.0	0	0	1	0.0
Muc adenoca	3	0	0	0	0.0	0	0	1	0.0	0	0	1	0.0
Serous pap	34	4	0	3	12.9	6	5	2	34.4	4	0	2	12.5
Melanoma	25	2	0	1	8.3	1	0	2	4.3	0	0	0	0.0
Primary	20	2	0	0	10.0	0	0	0	0.0	0	0	0	0.0
Metastatic	5	0	0	1	0.0	1	0	2	33.3	0	0	0	0.0
CNS	25	2	1	0	12.0	0	0	2	0.0	0	0	3	0.0
Glioblastoma	25	2	1	0	12.0	0	0	2	0.0	0	0	3	0.0
Total	400	24	23	39	13.0	36	34	53	20.2	14	13	55	7.8

and was occasionally expressed in ductal carcinomas of the breast (10.2%) (Fig. 2B), adenocarcinomas (13.8%) and poorly differentiated carcinomas of the lung (33.3%), adenocarcinoma of the colon (1.6%), serous (12.9%) and endometrioid (25.0%) carcinomas of the ovary. Of note, entrapped ducts and acini with p63 + basal cells amidst breast and prostate carcinomas were occasionally observed. p63 also stained 10% of primary malignant melanomas and 12% of glioblastomas.

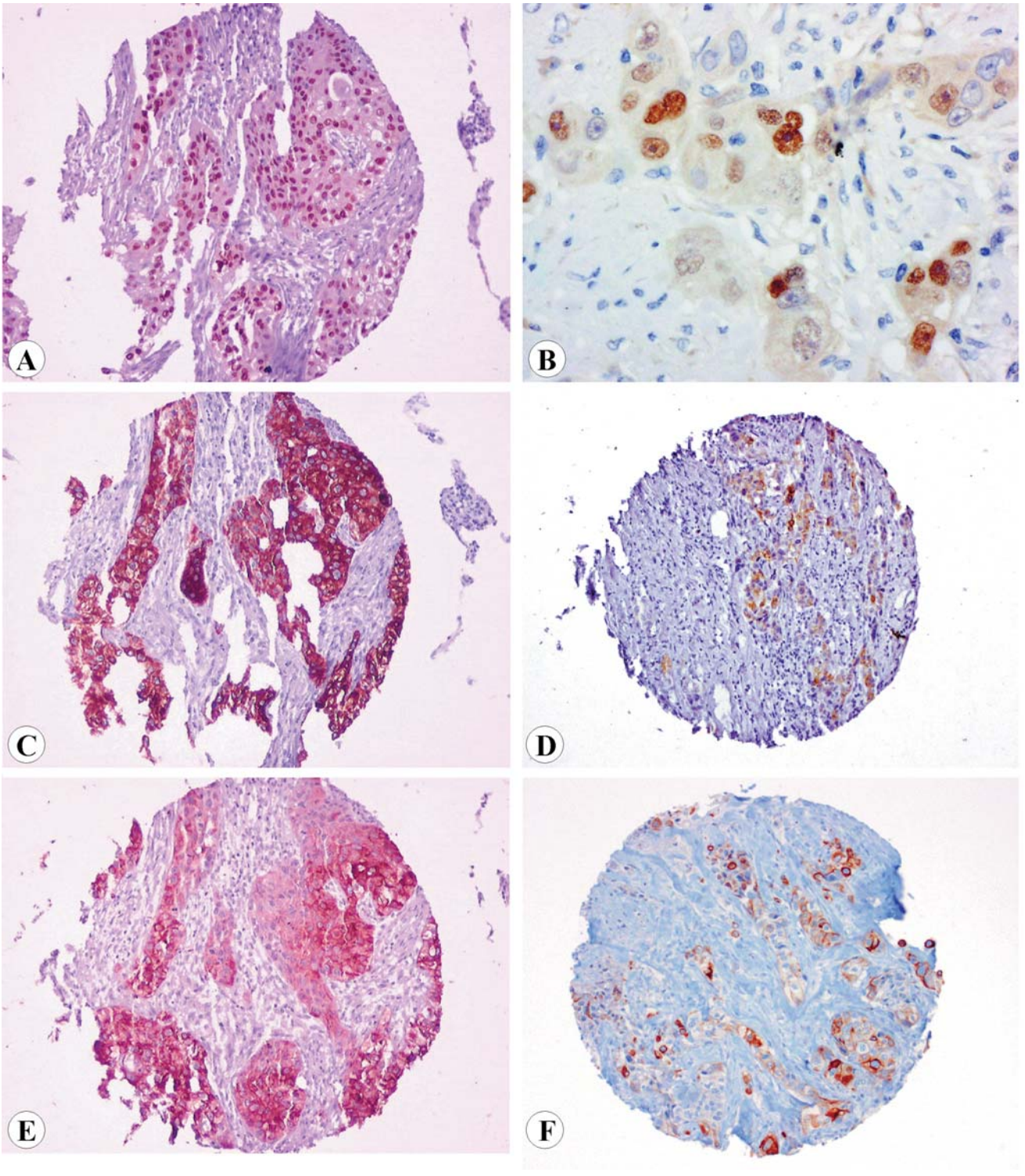

Fig. 2 Tissue microarray samples of a squamous cell carcinoma of the lung (**A**, **C**, **E**) and an invasive ductal carcinoma of the breast (**B**, **D**, **F**) showing expression of p63 (**A**, **B**), CK 5/6 (**C**, **D**) and CK 14 (**E**, **F**). (Streptavidin-biotin-peroxidase/diaminobenzidine; original magnification ×100 **A**, **C**, **D**, **E**, **F**; ×400 **B**)

Cytokeratin 5/6

Normal tissue samples

CK 5/6 was consistently expressed on the cytoplasm of basal cells of esophageal stratified squamous epithelium and pseudostratified bronchial epithelium; a variable proportion of transitional epithelial cells of the bladder was decorated as well. Myoepithelial cells of the breast and sweat glands, basal cells of prostate acini, and occasional cells lining pancreatic acini (Fig. 1B) showed consistent expression of CK 5/6. Noteworthy, no immunoreactivity was observed in luminal cells of these glands. A faint expression in hepatocytes, adrenocortical cells and gastric parietal cells was also observed. No other epithelial, mesenchymal, lymphoid or neural cell expressed these CKs (Table 1).

Neoplasms

CK 5/6 consistently decorated squamous cell carcinomas of the lung (75.0%, n=27) (Fig. 2C); conversely, only 10.3% of primary adenocarcinomas of the lung showed CK 5/6 positivity. In breast carcinoma samples, CK 5/6 expression was observed in 20.0% of ductal carcinomas (*n*=11) (Fig. 2D), 28.6% of lobular carcinomas (*n*=2), and in the DCIS analyzed herein. Ovarian tumors showed a differential expression of CK 5/6; whereas 34.4% of serous papillary carcinomas of the ovary (*n*=11) and 14.3% of clear cell carcinomas (*n*=1) expressed CKs 5/6, endometrioid (*n*=3) and mucinous (*n*=2) adenocarcinomas were negative. Up to 10% of prostatic carcinomas (*n*=7) and 5% of colonic carcinomas also showed CK 5/6 immunoreactivity. Tubular adenomas (*n*=2) showed no immunoreactivity for this marker. Interestingly, non-neoplastic breast ducts and prostate acini with CK 5/6 positive basal cells (admixed with breast and prostate carcinomas) were depicted (Table 2).

No non-epithelial neoplasm showed any immunoexpression of CK 5/6 except a case of metastatic malignant melanoma in which ~5% of the neoplastic cells showed a faint paranuclear staining.

Cytokeratin 14

Normal tissue samples

The distribution of CK 14 was very similar to CK 5/6 but for the lack of CK 14-positive cells in pancreatic acini evaluated herein (Table 1). No immunoreactivity in adrenocortical, hepatic or gastric epithelial cells was observed. No mesenchymal, lymphoid or neural cell stained with this antibody.

Neoplasms

CK 14 expression was observed in 52.9% of lung squamous cell carcinomas (*n*=18) (Fig. 2E) and in no lung adenocarcinomas. In the breast, 7.4% of invasive ductal carcinomas (*n*=4) (Fig. 2F) and the DCIS expressed CK 14, whereas all seven cases of lobular carcinomas were negative for this intermediate filament. CK 14 also decorated 12.5% of serous papillary carcinomas (*n*=4). All other adenocarcinomas were consistently negative. Normal breast ducts and prostate acini with CK 14 + cells (admixed with breast and prostate carcinomas) were observed. No CK 14 expression was detected in non-epithelial neoplasms (Table 2).

Double immunostaining results

In salivary glands, p63 consistently decorated basal cells of the excretory and striated ducts, as well as myoepithelial cells of intercalated ducts and serous acini. A slightly lower number of p63-positive cells was observed in seromucinous or mucinous acini. CK 5/6 and CK 14 were consistently expressed in myoepithelial cells of intercalated, striated and excretory ducts and in all types of acini. Noteworthy, some luminal cells showed immunoreactivity for both CK 5/6 and CK 14. Interestingly, basal cells of the ductal system (Fig. 3A and inset) and myoepithelial cells of the acini (Fig. 3B) frequently showed concurrent expression of p63/CK 5/6 and p63/CK 14.

In stratified squamous epithelia, we observed that p63 consistently stained basal cells and a variable proportion of suprabasal cells, but almost no granular or fully differentiated keratinocytes. CK 5/6 showed a similar distribution. CK 14 strongly decorated the basal cell layer, but was also expressed in suprabasal and fully differentiated keratinocytes. Double immunostainings demonstrated concurrent expression of p63/CK 5/6 and p63/CK 14 (Fig. 3C) in basal cells and in some suprabasal cells. Sebaceous glands showed a peculiar distribution of CK 14 and p63; while p63 decorated basal cells of the sebaceous glands, CK 14 preferentially stained fully differentiated sebocytes (Fig. 3C and inset). No sebaceous glands were observed in the sections double-stained for CK 5/6 and p63. In breast lobules, concurrent expression of CK 5/6 and p63 (Fig. 3D), as well as CK 14 and p63 was observed. Occasionally, scattered luminal cells of lobules and ducts were decorated by CK 5/6. No immunoreactivity for p63 or CK 14 was observed in luminal cells.

Statistical analysis

Squamous cell carcinomas expressed p63 ($P<0.001$), CK 5/6 ($P<0.001$) and CK 14 ($P<0.001$) more frequently than adenocarcinomas of any site. Also, co-expression of p63/CK 5/6, p63/CK 14, CK 5/6/CK 14, p63/CK 5/6/CK 14 in matched samples was also more frequently observed in squamous cell carcinomas than in adenocarcinomas

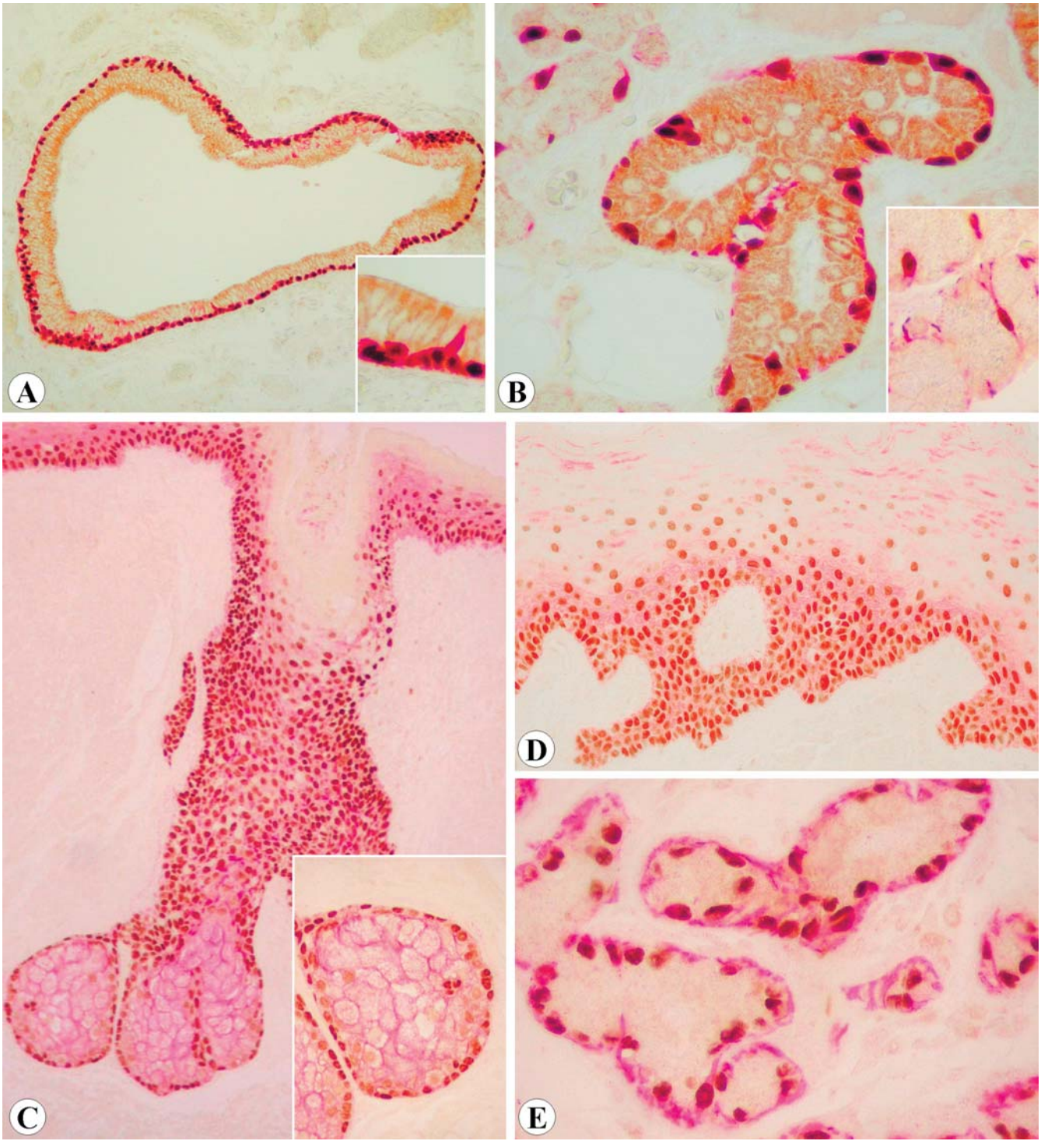

Fig. 3 **A** p63 (*dark-brown*)/CK 14 (*red*) double immunostaining showing concurrent expression of p63 and CK 14 in basal cells of excretory ducts. *Inset* High-power magnification of excretory duct epithelial cells. Note that only basal cells co-express p63 and CK 14. **B** Intercalated ducts and acini showing co-expression of p63 (*dark-brown*) and CK 5/6 (*red*) in basal and myoepithelial cells, respectively. *Inset* Myoepithelial cells of serous acini concurrently stained with p63 (*dark-brown*) and CK 14 (*red*). **C** Medium power magnification of the skin stained for p63 (*dark-brown*) and CK 14 (*red*). Note the co-expression of p63 and CK 14 in epidermal basal cells and the differential expression of these markers in basal cells of the sebaceous glands and mature sebocytes. *Inset* High-power magnification of a sebaceous gland. Note that p63 stained basal cells, whereas fully differentiated sebocytes were decorated by CK 14. **D** Breast lobule showing concurrent expression of p63 (*dark-brown*) and CK 5/6 (*red*) in basal/myoepithelial cells. [Streptavidin-biotin-peroxidase-diaminobenzidine (DAB)/alkaline phosphatase anti-alkaline phosphatase (APAAP)-fast red; original magnification ×100 **A**, **C**; ×400 **A** *inset*, **B**, **B** *inset*, **D**]

($P<0.001$, for all tests). Interestingly, p63 expression showed a statistically significant association with CKs 5/6 and CK 14 expression, irrespective of the histological type (squamous cell carcinoma or adenocarcinoma) of the neoplasm ($P<0.001$, for both tests).

In breast carcinomas, no statistical association between p63, CK 5/6 and CK 14 expression with the histological type (invasive ductal carcinoma vs invasive lobular carcinoma) was observed ($P>0.9999$, $P=0.6304$, and $P>0.9999$, respectively). Matched tumor samples that expressed p63 also expressed CK 5/6 ($P=0.0002$), all tumors that expressed CK 14 also expressed CK 5/6 ($P=0.0016$) and a significant correlation between p63 and CK 14 expression ($P=0.0463$) was found.

All cases of prostatic carcinomas were usual acinar carcinomas. As the Gleason grade of the whole section of these neoplasms was not provided in the TARP-4 database, we restricted the statistical analysis to the putative co-expression of p63, CK 5/6 and CK 14 in prostate adenocarcinoma matched samples. As no prostate carcinoma analyzed herein expressed p63 or CK 14, no statistical association was found in these neoplasms.

Concerning lung neoplasms, p63, CK 5/6 and CK 14 were more frequently expressed in squamous cell carcinomas than in adenocarcinomas or poorly differentiated carcinomas ($P<0.0001$, all tests). Also, a significant concordant expression of p63 and CK 5/6, p63 and CK 14, CK 5/6 and CK 14 in matched samples was found ($P<0.0001$, all tests). When squamous cell and poorly differentiated carcinomas were excluded, no statistical association between p63, CK 5/6 and CK 14 expression was found.

In colonic carcinomas, no statistical difference was observed between the expression of p63 ($P>0.9999$) and CKs 5/6 ($P>0.9999$) in glandular and mucinous adenocarcinomas. No colonic adenocarcinoma expressed CK 14. No statistical correlation was observed between the expression of p63 and CK 14 in matched samples of these neoplasms ($P>0.9999$).

In ovarian neoplasms, no association was found between the histological type and the expression of p63, CK 5/6 or CK 14 ($P=0.5455$, $P=0.3499$, $P=0.6185$). No statistical correlation was observed between the expression of p63 and CK 5/6 ($P=0.6077$), p63 and CK 14 ($P=0.3941$), and CK 5/6 and CK 14 ($P=0.2967$) in matched samples.

Discussion

Several studies have reported that ΔN-p63 isoforms are consistently expressed in the nuclei of basal cells of multilayered epithelia, including skin (epidermis and sebaceous glands), cervical and vaginal mucosa, urothelium, respiratory tract, and prostate, in myoepithelial and basal cells of the breast and sweat glands, as well as in cytotrophoblast of human placenta [1, 5, 10, 11, 12, 22, 24, 27, 30, 31, 32, 33, 34, 35, 36, 37, 39, 43, 47]. Analysis of p63−/− mice demonstrated that these mice present with truncated limbs and have no hair follicles, teeth, mammary, lachrymal or salivary glands [22, 24, 47]. Moreover, squamous epithelia of p63−/− mice (i.e., squamous epithelia of skin and tongue) failed to develop the spinosum, granulosum and stratum corneum and to correctly express CK 5 and CK 14 [22, 24, 47]. We demonstrated that in salivary glands, p63 has a preferential expression in basal/myoepithelial cells of the intercalated, striated and excretory ducts, as well as in myoepithelial cells of serous acini. A smaller proportion of p63 positive myoepithelial cells was observed in mucinous and seromucinous acini when compared with parotid gland serous acini.

It has been demonstrated that anti-p63 antibodies decorate the majority of squamous cell carcinomas [5, 11, 12, 19, 32, 36], basal cell carcinomas of the skin [11, 36], transitional cell carcinomas [11, 19, 32], and tumors with myoepithelial differentiation of the breast [32, 33, 38, 45] and lungs [30]. Our study confirmed and expanded the results of previously published studies that have demonstrated p63 expression in almost all squamous cell carcinomas [5, 11, 12, 14, 19, 30, 31, 43] and in a minor proportion of ductal carcinomas of breast (4.6–11%) [1, 27]. Also, we observed that some serous and endometrioid carcinomas of the ovary and rare adenocarcinomas of the colon express this marker.

Developmental analysis of p63 knockout mice has demonstrated that the expression of CK 5 and CK 14 is somehow controlled by p63 [22, 24, 47]. This is not striking, as in vitro studies using transformed human keratinocytes have shown that p63 is a nuclear transcription factor that triggers the expression of keratinocytic differentiation markers (i.e., involucrin and loricrin) [10, 22]. Conversely, when terminal differentiation is achieved or triggered by other mechanisms, such as high calcium exposure, there is a downregulation of all p63 isoforms [10]. These data are in accordance with previous publications showing that p63 is expressed in squamous cell carcinomas [5, 11, 12, 14, 19, 31]; however, terminally differentiated cells, such as those observed in the center of squamous pearls, are negative for this marker [36].

In the present study, we demonstrated a concurrent expression of p63, CK 5/6 and CK 14 in 6.54% of human carcinoma matched samples (18 of 275 carcinomas in which all three samples from each neoplasm could be unequivocally evaluated and none of them were necrotic, fragmented or lost during immunohistochemical staining). In adenocarcinomas, this triple concurrent expression in matched samples was only observed in two invasive ductal carcinomas of the breast. All the other 16 cases were lung squamous cell carcinomas (25 of the 39 squamous cell carcinoma samples were unequivocally evaluated for all markers and none of them were necrotic, fragmented or lost during immunohistochemical procedure). Our findings suggest that these markers may be reliably used for the diagnosis of squamous cell carcinomas and also indicate that some breast carcinomas co-express these markers.

Table 3 Summary of previously reported studies on p63, CK 5/6 and CK 14 distribution in large series of neoplasms (adenocarcinomas and squamous cell carcinomas) [1, 2, 5, 6, 7, 8, 9, 11, 12, 13, 14, 18, 19, 27, 28, 29, 31, 36, 42, 43, 44, 46] and in the present study using tissue array research program (TARP)-4 multi-tumor tissue microarray

Marker tumor	p63		CKs 5/6		CK 14	
	Previous studies (Range, mean %)	Current *n* (%)	Previous studies (Range, mean %)	Current *n* (%)	Previous study (Range, mean %)	Current *n* (%)
Breast*	14/337 (0–11, 4)	6/67 (8.9)	29/110(5–61, 26)	14/62 (22.6)	3/104 (0–4, 3)	5/62 (8.1)
Prostate	26/437 (0–13, 6)	0/69 (0)	0/46 (0–0, 0)	7/64 (10.9)	0/18 (0)	0/64 (0)
Lung**	21/156 (0–50, 13)	4/29 (13.8)	6/82 (0–33, 7)	3/29 (10.3)	2/11 (18.2)	0/29 (0)
Colon	1/22 (0–8, 4.5)	1/69 (1.4)	4/53(0–30, 7.5)	3/60 (5)	1/20 (5)	0/61 (0)
Ovary	3/32 (6–13, 9)	5/45 (11.1)	22/75(17–33, 29)	12/44(27.3)	3/24 (12.5)	4/45 (8.9)
Squamous cell carcinoma	221/247 (75–100, 89)	25/27 (92.6)	86/98 (84–100, 88)	27/36 (75)	13/15 (87)	18/34(53.0)

*Only usual types and usual variants of invasive breast carcinomas were included in this meta-analyses
**Adenocarcinomas and bronchioalveolar carcinomas were included in this category. Adenosquamous carcinomas were included in the squamous cell carcinoma, because p63 expression was restricted to those areas with squamous differentiation

It has been described that up to 18% of breast carcinomas may show a partial or complete basal/myoepithelial phenotype [17, 18, 21]. Our double immunohistochemical preparations demonstrated concurrent expression of p63 and CK 5/6, as well as p63 and CK 14 in a subset of basal cells of breast lobules and ducts. Also, we have already described a concurrent expression of p63, p-cadherin, maspin, alpha smooth muscle actin , and CK 14 in a subset of metaplastic carcinomas of the breast (tumors with putative basal/myoepithelial differentiation) [37]. In the present study, 2 of 56 (3.57%) invasive breast carcinomas samples that were unequivocally evaluated for p63, CK 5/6 and CK 14 co-expressed all of these markers, reiterating that a subset of breast carcinomas may show a basal/myoepithelial phenotype [17, 18, 21].

Multi-tumor TMAs have previously been used to screen different tumor types for molecular alterations of interest [3, 11, 15, 16, 20, 25, 41, 48]. We described herein another application of multi-tumor TMAs: to screen the distribution of immunohistochemical markers used for diagnostic purposes in a plethora of tumor types. The results of TMAs composed of a single 0.6-mm core of each tumor are disputable; while some authors have demonstrated that results from this sort of array have demonstrated 97–98% concordance with results observed in whole tissue sections for estrogen receptor, progesterone receptor and c-erbB-2 [48], others have claimed that arrays composed of a single 0.6 mm core would not cover and represent the heterogeneity of human neoplasms [16]. This issue is even more important regarding markers that are usually focally expressed in selected types of human neoplasms, such as p63 and basal keratins in breast carcinomas [1, 41]. Recently, validation studies of TMAs have demonstrated that even for heterogeneously expressed markers, one single core can match the staining pattern of an entire section more than 90% of the time and that full section cut-off values may also be applied when scoring TMAs [4, 15, 48]. Although we have not compared our TMA data with whole histological sections of the same tumors, our results are in accordance with previously reported series on p63 [1, 5, 12, 14, 18, 19, 27, 29, 31, 36, 43, 44, 47], CKs 5/6 [2, 6, 9, 13, 19, 28, 42] and CK 14 [7, 8, 13] distribution (Table 3).

In conclusion, we described the expression of p63, CKs 5/6 and CK 14 in 350 carcinomas, 25 malignant melanomas, and 25 glioblastomas using serial sections of TARP-4 multi-tumor TMA. Regardless of the small-sized samples included in the TMA, our results are in accordance with previous studies performed on whole histological sections [1, 2, 5, 6, 7, 8, 9, 12, 13, 14, 18, 19, 27, 28, 29, 31, 36, 42, 43, 44, 46] and showed only minor discrepancy with a similar study that was also performed on TMAs [11], suggesting that TMAs can be used to describe the distribution of antibodies that might be used as diagnostic markers. Moreover, our results also corroborate that p63, CKs 5/6 and CK 14 may be used as adjunct antibodies for the pathologic recognition of squamous cell carcinomas [6, 7, 8, 11, 19, 31, 47]. In addition, we also demonstrated that a subset of breast carcinomas express these markers [1, 17, 18, 32, 33, 37], and that this might reflect a basal or an intermediary phenotype [18, 21], despite their unremarkable morphology.

Acknowledgements This study was partially supported by a Ph.D. grant from the Portuguese Science and Technology Foundation [Fundação para a Ciência e a Tecnologia (FCT)—Ministério da Ciência e Tecnologia (MCT)—Portugal], reference SFRH/BD/5386/2001. Reis Filho J.S. is an FCT Ph.D. student and is the recipient of the Gordon Signy Foreign Fellowship Award, 2001, from the World Association of Societies of Pathology and Laboratory Medicine. The authors thank Dr. Andrew Folpe for his insightful comments on the manuscript and Mrs. Athely Guedes for preparing the manuscript for submission.

References

1. Barbareschi M, Pecciarini L, Cangi MG, Macri E, Rizzo A, Viale G, Doglioni C (2001) p63, a p53 homologue, is a selective nuclear marker of myoepithelial cells of the human breast. Am J Surg Pathol 25:1054–1060
2. Bocker W, Moll R, Poremba C, Holland R, Van Diest PJ, Dervan P, Burger H, Wai D, Ina Diallo R, Brandt B, Herbst H, Schmidt A, Lerch MM, Buchwallow IB (2002) Common adult stem cells in the human breast give rise to glandular and myoepithelial cell lineages: a new cell biological concept. Lab Invest 82:737–746

3. Bubendorf L, Nocito A, Moch H, Sauter G (2001) Tissue microarray (TMA) technology: miniaturized pathology archives for high-throughput in situ studies. J Pathol 195:72–79
4. Camp RL, Charette LA, Rimm DL (2000) Validation of tissue microarray technology in breast carcinoma. Lab Invest 80:1943–1999
5. Choi HR, Batsakis JG, Zhan F, Sturgis E, Luna MA, El-Naggar AK (2002) Differential expression of p53 gene family members p63 and p73 in head and neck squamous tumorigenesis. Hum Pathol 33:158–164
6. Chu PG, Weiss LM (2002) Expression of cytokeratin 5/6 in epithelial neoplasms: an immunohistochemical study of 509 cases. Mod Pathol 15:6–10
7. Chu PG, Weiss LM (2002) Keratin expression in human tissues and neoplasms. Histopathology 40:403–439
8. Chu PG, Lyda MH, Weiss LM (2001) Cytokeratin 14 expression in epithelial neoplasms: a survey of 435 cases with emphasis on its value in differentiating squamous cell carcinomas from other epithelial neoplasms. Histopathology 39:9–16
9. Cury PM, Butcher DN, Fisher C, Corrin B, Nicholson AG (2000) Value of the mesothelium-associated antibodies thrombomodulin, cytokeratin 5/6, calretinin, and cd44 h in distinguishing epithelioid pleural mesothelioma from adenocarcinoma metastatic to the pleura. Mod Pathol 13:107–112
10. De Laurenzi V, Rossi A, Terrinoni A, Barcaroli D, Levrero M, Costanzo A, Knight RA, Guerrieri P, Melino G (2000) p63 and p73 transactivate differentiation gene promoters in human keratinocytes. Biochem Biophys Res Commun 273:342–346
11. Di Como CJ, Urist MJ, Babayan I, Drobnjak M, Hedvat CV, Teruya-Feldstein J, Pohar K, Hoos A, Cordon-Cardo C (2002) p63 expression profiles in human normal and tumor tissues. Clin Cancer Res 8:494–501
12. Glickman JN, Yang A, Shahsafaei A, McKeon F, Odze RD (2001) Expression of p53-related protein p63 in the gastrointestinal tract and in esophageal metaplastic and neoplastic disorders. Hum Pathol 32:1157–1165
13. Heatley M, Maxwell P, Whiteside C, Toner P (1995) Cytokeratin intermediate filament expression in benign and malignant breast disease. J Clin Pathol 48:26–32
14. Hibi K, Trink B, Patturajan M, Westra WH, Caballero OL, Hill DE, Ratovitski EA, Jen J, Sidransky D (2000) AIS is an oncogene amplified in squamous cell carcinoma. Proc Natl Acad Sci U S A 97:5462–5467
15. Hoos A, Cordon-Cardo C (2001) Tissue microarray profiling of cancer specimens and cell lines: opportunities and limitations. Lab Invest 81:1331–1338
16. Hoos A, Urist MJ, Stojadinovic A, Mastorides S, Dudas ME, Leung DH, Kuo D, Brennan MF, Lewis JJ, Cordon-Cardo C (2001) Validation of tissue microarrays for immunohistochemical profiling of cancer specimens using the example of human fibroblastic tumors. Am J Pathol 158:1245–1251
17. Jones C, Foschini MP, Chaggar R, Lu YJ, Wells D, Shipley JM, Eusebi V, Lakhani SR (2000) Comparative genomic hybridization analysis of myoepithelial carcinoma of the breast. Lab Invest 80:831–836
18. Jones C, Nonni AV, Fulford L, Merrett S, Chaggar R, Eusebi V, Lakhani SR (2001) CGH analysis of ductal carcinoma of the breast with basaloid/myoepithelial cell differentiation. Br J Cancer 85:422–427
19. Kaufmann O, Fietze E, Mengs J, Dietel M (2001) Value of p63 and cytokeratin 5/6 as immunohistochemical markers for the differential diagnosis of poorly differentiated and undifferentiated carcinomas. Am J Clin Pathol 116:823–830
20. Lakhani SR, Ashworth A (2001) Microarray and histopathological analysis of tumours: the future and the past? Nat Rev Cancer 1:151–157
21. Lakhani SR, O'Hare MJ (2001) The mammary myoepithelial cell—Cinderella or ugly sister? Breast Cancer Res 3:1–4
22. Levrero M, De Laurenzi V, Costanzo A, Gong J, Wang JY, Melino G (2000) The p53/p63/p73 family of transcription factors: overlapping and distinct functions. J Cell Sci 113:1661–1670
23. Lopes JM, Nesland JM, Reis-Filho JS, Holm R (2002) Differential Ki67 and bcl-2 immunoexpression in solid-glandular and spindle cell components of biphasic synovial sarcoma: a double immunostaining assessment with cytokeratin and vimentin. Histopathology 40:464–471
24. Mills AA, Zheng B, Wang XJ, Vogel H, Roop DR, Bradley A (1999) p63 is a p53 homologue required for limb and epidermal morphogenesis. Nature 398:708–713
25. Moch H, Kononen J, Kallioniemi OP, Sauter G (2001) Tissue microarrays: what will they bring to molecular and anatomic pathology? Adv Anat Pathol 8:14–20
26. Moll R, Franke WW, Schiller DL, Geiger B, Krepler R (1982) The catalog of human cytokeratins: patterns of expression in normal epithelia, tumors and cultured cells. Cell 31:11–24
27. O'Connell JT, Mutter GL, Cviko A, Nucci M, Quade BJ, Kozakewich HP, Neffen E, Sun D, Yang A, McKeon FD, Crum CP (2001) Identification of a basal/reserve cell immunophenotype in benign and neoplastic endometrium: a study with the p53 homologue p63. Gynecol Oncol 80:30–36
28. Ordóñes NG (1998) Value of cytokeratin 5/6 immunostaining in distinguishing epithelial mesothelioma of the pleura from lung adenocarcinoma. Am J Surg Pathol 22:1215–1221
29. Parsons JK, Gage WR, Nelson WG, De Marzo AM (2001) p63 protein expression is rare in prostate adenocarcinoma: implications for cancer diagnosis and carcinogenesis. Urology 58:619–624
30. Pelosi G, Fraggetta F, Maffini F, Solli P, Cavallon A, Viale G (2001) Pulmonary epithelial-myoepithelial tumor of unproven malignant potential: report of a case and review of the literature. Mod Pathol 14:521–526
31. Pelosi G, Pasini F, Stenholm CO, Pastorino U, Maisonneuve P, Sonzogni A, Maffini F, Pruneri G, Fraggetta F, Cavallon A, Roz E, Iannucci A, Bresaola E, Viale G (2002) p63 immunoreactivity in lung cancer: yet another player in the development of squamous cell carcinomas? J Pathol 198:100–109
32. Reis-Filho JS, Schmitt FC (2002) Taking advantage of basic research: p63 is a reliable myoepithelial and stem cell marker. Adv Anat Pathol 9:280–289
33. Reis Filho JS, Schmitt FC (2003) p63 expression in sarcomatoid/metaplastic carcinomas of the breast. Histopathology 42:94–95
34. Reis Filho JS, Albergaria A, Milanezi F, Amendoeira I, Schmitt FC (2002) Naked nuclei revisited: p63 immunoexpression. Diagn Cytopathol 27:135–138
35. Reis Filho JS, Milanezi F, Albergaria A, Amendoeira I, Schmitt FC (2002) p63 staining of myoepithelial cells in breast fine needle aspirates: a study of its role in differentiating in situ from invasive ductal carcinomas of the breast. J Clin Pathol 55:936–939
36. Reis-Filho JS, Torio B, Albergaria A, Schmitt FC (2002) p63 expression in normal skin and usual skin carcinomas. J Cutan Pathol 29:517–523
37. Reis-Filho JS, Milanezi F, Paredes J, Silva P, Pereira EM, Maeda AS, de Carvalho LV, Schmitt FC (2003) Novel and classic myoepithelial/stem cell markers in metaplastic carcinomas of the breast. Appl Immunohistochem Mol Morphol 11:1–8
38. Romano V, Bosco P, Rocchi M, Costa G, Leube RE, Franke WW, Romeo G (1988) Chromosomal assignments of human type I and type II cytokeratin genes to different chromosomes. Cytogenet Cell Genet 48:148–151
39. Signoretti S, Waltregny D, Dilks J, Isaac B, Lin D, Garraway L, Yang A, Montironi R, McKeon F, Loda M (2000) p63 is a prostate basal cell marker and is required for prostate development. Am J Pathol 157:1769–1775
40. Tot T (2002) Cytokeratins 20 and 7 as biomarkers: usefulness in discriminating primary from metastatic adenocarcinoma. Eur J Cancer 38:758–763
41. van de Rijn M, Perou CM, Tibshirani R, Haas P, Kallioniemi O, Kononen J, Torhorst J, Sauter G, Zuber M, Kochli OR, Mross F, Dieterich H, Seitz R, Ross D, Botstein D, Brown P (2002) Expression of cytokeratins 17 and 5 identifies a group of breast

carcinomas with poor clinical outcome. Am J Pathol 161:1991–1996
42. Vlasoff DM, Baschinsky DY, Frankel WL (2002) Cytokeratin 5/6 immunostaining in hepatobiliary and pancreatic neoplasms. Appl Immunohistochem Mol Morphol 10:147–151
43. Wang BY, Gil J, Kaufman D, Gan L, Kohtz DS, Burstein DE (2002) p63 In pulmonary epithelium, pulmonary squamous neoplasms, and other pulmonary tumors. Hum Pathol 33:921–926
44. Wang TY, Chen BF, Yang YC, Chen H, Wang Y, Cviko A, Quade BJ, Sun D, Yang A, McKeon FD, Crum CP (2001) Histologic and immunophenotypic classification of cervical carcinomas by expression of the p53 homologue p63: a study of 250 cases. Hum Pathol 32:479–486
45. Wang X, Mori I, Tang W, Yang Q, Nakamura M, Nakamura Y, Sato M, Sakurai T, Kennichi K (2001) Metaplastic carcinoma of the breast: p53 analysis identified the same point mutation in the three histologic components. Mod Pathol 14:1183–1186
46. Weber A, Bellmann U, Bootz F, Wittekind C, Tannapfel A (2002) Expression of p53 and its homologues in primary and recurrent squamous cell carcinomas of the head and neck. Int J Cancer 99:22–28
47. Yang A, Schweitzer R, Sun D, Kaghad M, Walker N, Bronson RT, Tabin C, Sharpe A, Caput D, Crum C, McKeon F (1999) p63 is essential for regenerative proliferation in limb, craniofacial and epithelial development. Nature 398:714–718
48. Zhang D, Salto-Tellez M, Putti TC, Do E, Koay ES (2003) Reliability of tissue microarrays in detecting protein expression and gene amplification in breast cancer. Mod Pathol 16:79–85

Virchows Arch (2003) 443:133–138
DOI 10.1007/s00428-003-0858-3

ORIGINAL ARTICLE

Sebastian Leibl · Oleksiyy Tsybrovskyy · Helmut Denk

How many lymph nodes are necessary to stage early and advanced adenocarcinoma of the sigmoid colon and upper rectum?

Received: 27 November 2002 / Accepted: 2 June 2003 / Published online: 3 July 2003
© Springer-Verlag 2003

Abstract The lymph-node yields in specimens resected for colorectal adenocarcinoma show considerable variations, raising the question whether the minimum lymph-node number recommended by the UICC (International Union Against Cancer) for pN0 classification represents an appropriate quality standard for specimen work-up. The number of pericolic lymph nodes recovered from 568 archival surgical colorectal carcinoma specimens located in the sigmoid or upper rectum showed a highly statistically significant correlation with both the pT category and the presence of metastases ($P<0.0005$). The median lymph-node yield in standardized (i.e., resembling in size surgically removed cancer specimens) tumor-free specimens obtained during autopsies was 13 lymph nodes, compared with 20.5 when diverticula were present and more than 30 in specimens with chronic inflammation or from patients with systemic infections. In 48 pT2 and pT3 carcinoma specimens prospectively dissected in the same way, median numbers of 18 (pT2) and 23 (pT3) lymph nodes were detected (range between 8 and 39 nodes). The lymph-node numbers recommended in previous studies and by the UICC often seem to be too low to declare a specimen free of metastases. Although the great variation in lymph-node counts requires the recovery of all lymph nodes for pN0 classification, recommendations considering the pT status and additional factors like diverticula and inflammatory changes can be useful as a quality standard for specimen work up.

Keywords Colorectal adenocarcinoma · Lymph node yield · TNM classification · Quality standards

S. Leibl (✉) · O. Tsybrovskyy · H. Denk
Department of Pathology, University of Graz,
School of Medicine, Auenbruggerplatz 25, 8036 Graz, Austria
e-mail: sebastian.leibl@klinikum-graz.at
Tel.: +43-316-38581397
Fax: +43-316-384329

Introduction

A proper assessment of the lymph-node status of colorectal carcinoma specimens is essential to comply with the recommendations of the UICC [28] and also determines the application of adjuvant therapy in patients with positive lymph nodes. Immunohistochemical and molecular methods for the detection of micrometastases have been applied by pathologists [7, 19, 20] and surgeons [2] in the last few years, as tumor spread to locoregional lymph nodes is regarded as the most important prognostic factor [34]. However, little is known about the factors determining the number of lymph nodes under physiological and pathological conditions. Prior studies [3, 5, 8, 9, 10, 11, 12, 21, 22, 23, 24, 25, 30, 32, 33] that examined the issue of a minimum number of lymph nodes to be dissected and evaluated in colorectal resection specimens were associated with technical, sampling, and specimen-related flaws, which possibly substantially influenced the conclusions drawn by the authors. We evaluated factors contributing to the great variation in lymph-node counts and compared our results with the recommendations given in previous studies and by the UICC.

Materials and methods

From the files of the Department of Pathology, University of Graz, we selected 568 adenocarcinomas (including mucinous adenocarcinomas) located in the sigmoid or the upper rectum diagnosed between 1993 and 1997. This location was chosen because there is a higher variation in lymph-node counts than in right hemicolectomy specimens. The transition between the rectum and the sigmoid is anatomically defined (at the level of the third sacral vertebra), whereas the rectum is surgically divided into three levels, depending on the distance from the anocutaneous line (i.e., 8 cm ab ano, lower rectum; between 8 cm and 12 cm ab ano, middle; between 12 cm and 16 cm ab ano, upper rectum). In our study, carcinomas of the "upper rectum" were defined as adenocarcinomas of the upper two-thirds, which could be removed by anterior or deep anterior resection. Carcinomas of the "lower rectum" treated by complete rectum amputation were excluded since their lymphatic drainage differs from the former [26]. Cases with liver metastases (a fact that could have affected the pathologist's

diligence in dissecting lymph nodes) and multifocal carcinomas were also excluded. The pathology reports were reviewed for specimen length, patient's age, depth of tumor penetration (pT1-pT4), number of lymph nodes recovered, and number of lymph-node metastases.

With the help of three surgeons, 17 sigmoidorectal specimens resembling in size and resection technique specimens removed in cancer surgery were obtained during autopsies to assess the number of paracolic and intermediate lymph nodes present under normal tumor-free conditions (termed "pT0" specimens). Manual dissection after fixation was chosen since fat clearance techniques are expensive, laborious, and considered to cause an unacceptable delay in reporting [4, 16, 18, 25]. By dissecting the mesocolon into 1- to 2-mm slices under a strong light source, even aggregates of lymph follicles without a clearly visible fibrous capsule can be detected. In our study, an organized nodal structure or connections with lymphatic vessels were regarded as minimum requirements to qualify as a lymph node; lymphoid tissue lacking these features was not included in lymph-node counts. Embedding small lymph nodes together into small cassettes designed for biopsies helps to avoid loss of nodes during processing of the paraffin block.

Forty-eight pT2 and pT3 carcinoma specimens (termed "reference" specimens) were worked up prospectively under routine conditions by the same author (SL).

The obtained data were analyzed with a standard statistical software package (SPSS 10.0). Non-parametric statistics were preferred because they do not assume normal distribution of variables. Correlations among variables were assessed using the Spearman's correlation coefficient. Differences between median values were evaluated in the Kruskal-Wallis test; results were considered significant at $P<0.05$.

Results

Lymph-node recovery and lymph-node metastases

Of the 568 rectosigmoidal adenocarcinomas, 65 were classified as pT1, 200 as pT2, 191 as pT3, and 112 as pT4. The median specimen lengths in the pT1, pT2, pT3, and pT4 categories were 24 cm (range 15–47 cm), 25 cm (range 15–60 cm), 23 cm (range 15–45 cm) and 24 cm (15–55 cm), respectively.

The median numbers of lymph nodes detected per specimen consistently increased from 12 (range 2–36) in pT1 specimens to 23 (range 4–60) in pT4 specimens (Fig. 1). The percentage of lymph-node positive cases within each pT category showed the same trend, being only 9% in pT1 cases but 77% in pT4 cases (Fig. 2). The distribution of lymph nodes in different pT categories in the lymph-node positive cases is summarized in Table 1; both absolute and relative counts of positive lymph nodes increased from pT1 to pT4. The number of lymph nodes recovered per specimen showed a highly statistically significant association with both the pT category ($P<0.0005$) and the presence of metastases ($P<0.0005$). The correlation of the lymph-node yield with the specimen length was weak (Spearman's correlation coefficient=0.16); the patient's age did not correlate with the lymph-node yield (Spearman's correlation coefficient=–0.08).

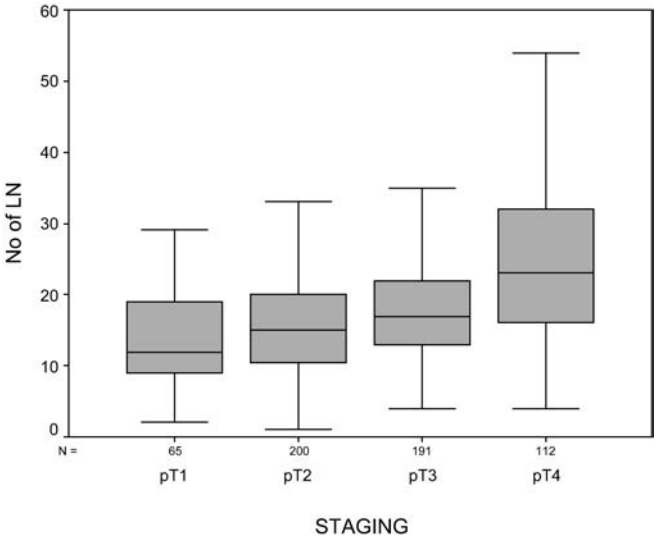

Fig. 1 Numbers of lymph nodes recovered per specimen in the different pT categories. The *shaded areas* comprise 50% of cases, the *horizontal bars* 95%. The increase of median values from pT1 to pT4 is significant at the level of $P<0.0005$

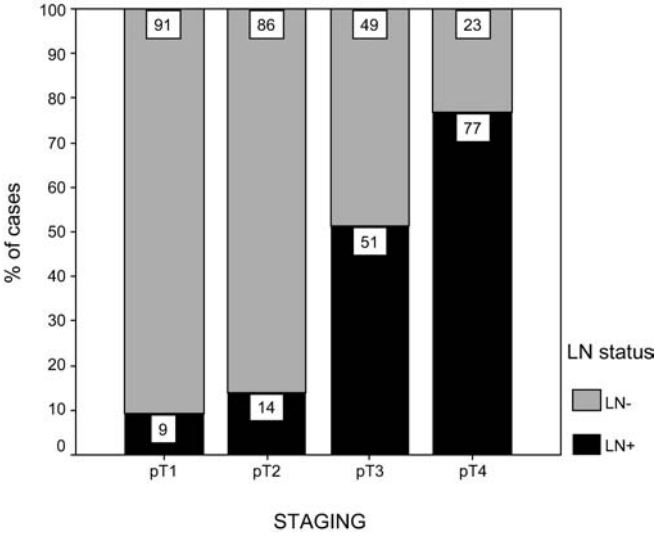

Fig. 2 Percentage of lymph node positive cases (*black columns*) per pT category

"pT0" specimens obtained during autopsies and pT2/3 ("reference") specimens worked up prospectively

Of the 17 tumor-free ("pT0") specimens obtained during autopsies, 4 had to be discarded because of systemic infections or chronic inflammatory bowel disease (under these circumstances the lymph-node count exceeded 30 per specimen). The remaining 13 specimens showed a median number of 15 pericolic lymph nodes (range 9–25) detected per specimen. However, subdivision of this group into specimens without diverticula (DIV–) and with diverticula (DIV+) led to a median number of 13 lymph

Table 1 Distribution of lymph nodes and lymph-node metastases in the different pT categories

n=568	Number of specimens	Median specimen lengths	Median number of lymph nodes per specimen	Number of specimens with lymph-node metastases	Median number. of metastases per lymph-node positive specimen	Percentage of positive lymph nodes of all lymph nodes recovered per positive specimen
pT1	65	24	12	6	1.5	6.6
pT2	200	25	15	28	1.5	8.7
pT3	191	23	17	98	3	16.0
pT4	112	24	23	86	5	27.9

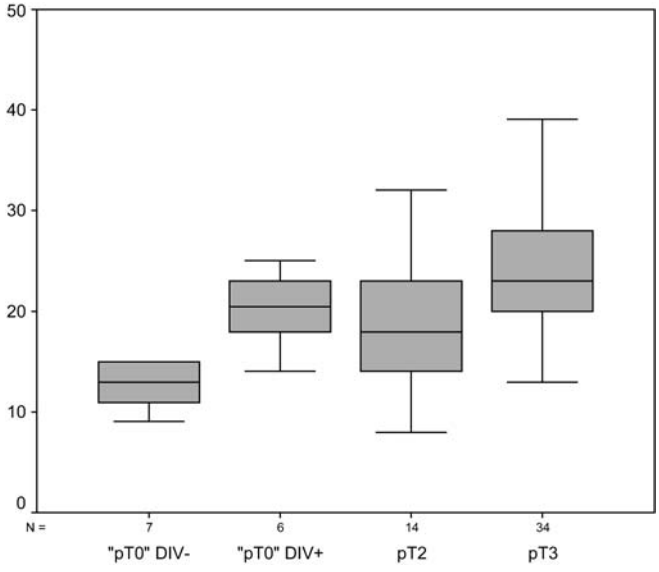

Fig. 3 Distribution of lymph nodes in the autopsy ("pT0") and pT2/pT3 "reference" specimens which were dissected in the same manual method

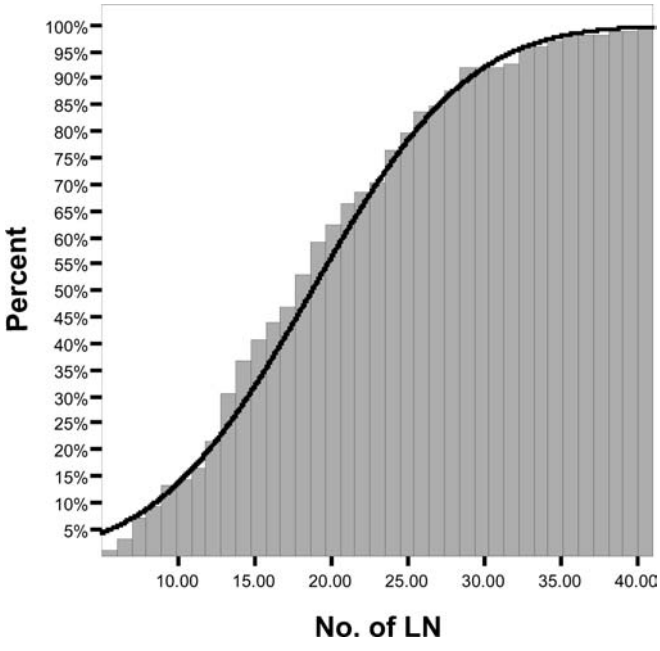

Fig. 4 Relationship between the cumulative percentage of all lymph node positive cases and the number of lymph nodes recovered from these specimens. The plateau of the graph begins between 90% and 95%, which correlates with a lymph-node yield of 30 to 32 nodes. The previously recommended yields of 12 and 17 lymph nodes, respectively, fall within the steep increase of the curve

nodes in the DIV− and 20.5 lymph nodes in the DIV+ group (Fig. 3)—the difference being highly statistically significant (P=0.002).

In the 48 "reference" specimens, dissected during routine work in the same way as the autopsy specimens, median numbers of 18 (range 8–32, pT2) and 23 (range 13–39, pT3) lymph nodes were detected (Fig. 3).

Recovery of a minimum number of lymph nodes

We adopted a graph presented by Goldstein et al. [10] that showed the relationship between the cumulative percentage of all pT3 cases with detectable metastases and the number of lymph nodes that were recovered from these specimens. In only 20% of our specimens with metastases, 12 (UICC recommendation) or fewer lymph nodes were recovered, while approximately 80% yielded 12 or more lymph nodes (Fig. 4). More than 17 lymph nodes (corresponding to the recommendation of Goldstein et al. [10]) were removed in 54%. The plateau phase of the graph began at approximately 30 lymph nodes per specimen.

Discussion

The lymph nodes of the colonic mesentery can be divided into epicolic (located at the base of appendices epiploicae or adjacent to the taenia), paracolic (along the marginal vascular arcades), intermediate (in the mid portion of the mesentery close to major bifurcations of the colic vessels), and central or principal nodes at the base of the mesentery [17, 26]. Although the paracolic nodes are by far the most important filters and seem to account for the great variation in lymph-node counts rather than the relatively small and inconsistent numbers of intermediate nodes, little is known about the number and distribution of the former under normal conditions. Based on our tumor-free autopsy ("pT0") specimens, the normal mesentery at a size usually removed during rectosigmoid cancer surgery contains a median of 13 pericolic lymph nodes (range 9–15). The great variation in lymph-node

counts (e.g., 4–60 in the pT4 category) can only partially be explained by a variation in the pathologist's diligence. It is rather the result of lymph-node neoformation following accumulation of lymphocytes around minute blood vessels or capillaries [29]. The importance of small lymph nodes is emphasized in several reports about the frequent occurrence of lymph-node metastases in nodes measuring less than 5 mm [1, 13, 14, 15]. One can only speculate about the factors involved in lymph-node formation, thus determining the number of nodes in the individual specimen. Lymph-node counts increase with tumor stage (Fig. 1) and the number of metastases (Fig. 2). This could be due to an immunological or non-specific inflammatory response to the carcinoma; the "pT0" specimens that were discarded because of local inflammation or systemic infections (with more than 30 lymph nodes) seem to support this assumption. Moreover, even the presence of few diverticula (in the absence of diverticulitis) raise lymph-node counts considerably to a median value of 20.5 (range14–25) (Fig. 3), suggesting a more complex interplay of local factors. However, neogenesis of lymph vessels [31] and nodes could be induced by the carcinoma itself (analogous to tumor angiogenesis), thus creating the ideal environment for metastatic spread.

Irrespective of the details of pericolic lymph-node development, it is important to be aware of the great variation in the lymph-node count among individual specimens resected for rectosigmoid adenocarcinoma. The generally higher lymph-node yield in right-sided hemicolectomy specimens [26] (which should be considered in the UICC recommendation) is caused by the numerous ileocolic intermediate nodes [26] that can be found in virtually every specimen of the ileocecal region, while the presence of intermediate lymph nodes is relatively inconstant in the mid and left colic drainage [26]. A report focusing on the lymph-node status of colorectal specimens should therefore examine right and left hemicolectomy specimens separately to avoid misleading statistical evaluation.

Goldstein et al. [10] reviewed 750 pT3 colon carcinomas for lymph-node counts and numbers of lymph-node metastases and displayed their results in a way adopted by Scott and Grace [24]. The latter authors stated that by examination of a minimum of 13 lymph nodes, 90% of their positive cases would have been detected. Goldstein et al. [10] concluded that almost 80% of the specimens with metastases had 17 or fewer lymph nodes recovered. On that basis, they recommended that at least 17 lymph nodes should be retrieved from colorectal specimens (a distinction between different locations was not made). However, neither study considered that the results in this type of analysis depended on how many lymph nodes were found by the pathologist. Therefore, their data can only be used for calculation of a minimum lymph-node count under the assumption that all lymph nodes were examined and no positive nodes missed. However, in the series of Goldstein et al. [10] only 93 (among 750) specimens with more than 17 lymph nodes were found. In addition, the fact that the maximum yield of lymph nodes considerably increased with time in the course of the study indicated a learning process and implies that specimens were not worked up as thoroughly in earlier years. Consequently, the deduced "gold standard" of 17 nodes just represents the standard achieved in the particular laboratory between 1955 and 1995 and does not reflect the situation in other laboratories. Using our data (derived from specimens worked up between 1993 and 1997 in our department), which provided higher lymph-node counts, the graph is altered drastically (Fig. 4), as 80% (cut-off chosen by Goldstein et al. [10]) of our specimens with metastases had 26 or fewer lymph nodes recovered (in contrast with 17 or fewer lymph nodes in the material reported by Goldstein et al. [10]), whereas, in our hands, in 54% more than 17 lymph nodes were recovered. In 2002, Goldstein published an additional report [9] presenting a new analysis of the data mentioned above supplemented by new data obtained between 1995 and 2000. He found a 50% increase in the number of recovered lymph nodes per specimen in the later series, which obviously indicates an improved specimen work-up and is consistent with our results.

In the editorial to a different report [8], a similar schematic figure was used to define a minimal threshold value of 15 lymph nodes to be recovered. In our figure (Fig. 4), the graph plateau is approached at approximately 90% of positive specimens, which correlates with a lymph-node yield of 30 or less. Interestingly, this result is consistent with the results of a logistical regression analysis performed by Goldstein [9] based on additional data. This author found that the chances of detecting a single metastasis in a hypothetical colorectal resection specimen are 80% only if 30 lymph nodes are recovered. His conclusion that all lymph nodes should be recovered is supported by another report [6] that examined 8574 colorectal specimens from a database. However, both statistical approaches do not reflect the individual situation, since the quality of specimen work up (on which the analyses depend) seems to vary considerably among different institutions, and the variation in lymph-node numbers in different locations and tumor stages were not taken into account. A French population-based study published in 1998 [22] concluded that there was no significant risk of misclassification above a number of eight retrieved lymph nodes; they recommended that between 9 and 15 lymph nodes should be examined. However, the report was based on an average of 7.7 lymph nodes examined per specimen and relied on the hypothesis that there was no misclassification of the reports reviewed in comparison with a reference group consisting of 91 pathology reports with more than 16 lymph nodes. Detailed information on the reference group was, however, not provided.

Interestingly, studies dealing with the prognostic importance of micrometastases showed no prognostic impact of micrometastases if the median lymph-node counts per specimen were low [7, 19], while studies with higher average counts [2, 20] detected a significantly

higher rate of micrometastic spread and suggested a better prognosis for the patients without micrometastases [2].

According to our results, the current UICC recommendation of 12 lymph nodes [28] is neither an appropriate tool to evaluate the lymph-node status of colorectal carcinomas nor does it provide a quality standard for specimen work up. Although an early adenocarcinoma of the sigmoid colon and upper rectum with little or no inflammatory changes or dicerticula could be well worked up and staged with 12 lymph nodes, a specimen with advanced cancer with accompanying colitis could be understaged and thus inadequately worked up by retrieving 17 of 50 possible lymph nodes. Of the 48 "reference" specimens (Fig. 3) worked up under routine conditions (with median numbers of 18 lymph nodes in the pT2 and 23 nodes in the pT3 category), six specimens had only one metastasis. If the pathologist had stopped after retrieving 12 lymph nodes or looked less carefully, the single metastasis might have been missed. However, some early stage colorectal adenocarcinomas do have low lymph-node counts like some of the non-neoplastic specimens we examined. In these cases, oncologists might be led to the false conclusion that the respective specimens were not worked up properly, because their lymph-node status was below the current UICC recommendation. Despite the clarification that the UICC recommendation was not intended to be a requirement for pN0 classification [27], such misunderstandings might result in pNx staging and unnecessary adjuvant chemotherapy. The increase of mean lymph-node counts in the prospectively worked up pT2 and pT3 specimens (18 and 23 compared with mean numbers of 15 and 17 nodes in the retrospectively reviewed pT2 and pT3 specimens of our archives) indicates that work up can be considerably improved using the methods explained above.

To avoid both extremes (i.e., understaging of advanced carcinomas or overtreatment of early stage carcinomas) a recommendation for the number of lymph nodes to be retrieved from colorectal specimens should deal with right and left hemicolectomy specimens separately, further grouping according to the pT status and facultative factors such as inflammatory changes or diverticula. Since statistical approaches for the evaluation of lymph-node counts bearing low risks of missed positive nodes are of limited value, median lymph-node counts should be determined by removing all lymph nodes in specimens of the respective category. The recommendation of these median numbers should be understood as a quality standard rather than a requirement for pN0 classification, as there may be still deviations in some individual cases due to unknown factors influencing the lymph-node status, and all lymph nodes should be removed. It is important to give both the pathologist and the surgeon/oncologist a clue for the number of lymph nodes they can expect in the average specimen rather than a recommendation that does not comply with the biology of the lymphatic system.

Acknowledgements The authors thank Drs. B. Grasser, T. Thalhammer and P. Bergmann from the Surgical Department of the University of Graz for the standard resection of several "pT0" sigmoidorectal specimens during autopsies and Prof. Dr. Firbas and Ms I. Klausnitzer from the Institute of Anatomy, University of Vienna, for valuable advice.

References

1. Andreola S, Leo E, Belli F, et al (1996) Manual dissection of adenocarcinoma of the lower third of the rectum specimens for detection of lymph node metastases smaller than 5 mm. Cancer 77:607–612
2. Arnold MW, Young DM, Hitchcock CL, et al (1998) Staging of colorectal cancer: biology vs. morphology. Dis Colon Rectum 41:1482–1487
3. Caplin S, Cerottini JP, Bosman FT, et al (1998) For patients with Dukes B (TNM Stage II) colorectal carcinoma, examination of six or fewer lymph nodes is related to poor prognosis. Cancer 83:666–672
4. Cawthorn SJ, Gibbs NM, Marks CG (1986) Clearance technique for the detection of lymph nodes in colorectal cancer. Br J Surg 73:58–60
5. Cianchi F, Palomba A, Boddi V, et al (2002) Lymph node recovery from colorectal tumor specimens: recommendation for a minimum number of lymph nodes to be examined. World J Surg 26:384–389
6. Cserny G, Vinh-Hung V, Burzykowski T (2002) Is there a minimum number of lymph nodes that should be histologically assessed for a reliable nodal staging of T3N0M0 colorectal carcinomas? J Surg Oncol 81:63–69
7. Davidson BR, Sams VR, Styles J, et al (1990) Detection of occult nodal metastases in patients with colorectal carcinoma. Cancer 65:967–970
8. Fielding LP (1999) Invited editorial. Dis Colon Rectum 42:154–158
9. Goldstein NS (2002) Lymph node recoveries from 2427 pT3 colorectal resection specimens spanning 45 years: recommendations for a minimum number of recovered lymph nodes based on predictive probabilities. Am J Surg Pathol 36:179–189
10. Goldstein NS, Sanford W, Coffey M, et al (1996) Lymph node recovery from colorectal resection specimens removed for adenocarcinoma: trends over time and a recommendation for a minimum number of lymph nodes to be recovered. Am J Clin Pathol 106:209–216
11. Hermanek P (1991) Onkologische Chirurgie/Pathologisch-anatomische Sicht. Langenbecks Arch Chir Suppl Kongressbd, pp 277–281
12. Hernanz F, Revuelta S, Redondo C, et al (1994) Colorectal adenocarcinoma: quality of the assessment of lymph node metastases. Dis Colon Rectum 37:373–377
13. Herrera L, Villarreal JR (1992) Incidence of metastases from rectal adenocarcinoma in small lymph nodes detected by a clearing technique. Dis Colon Rectum 35:783–788
14. Herrera-Ornelas L, Justiniano J, Castillo N, et al (1987) Metastases in small lymph nodes from colon cancer. Arch Surg 122:1253–1256
15. Hida J, Mori N, Kubo R, et al (1994) Metastases from carcinoma of the colon and rectum detected in small lymph nodes by the clearing method. J Am Coll Surg 178:223–228
16. Hyder JW, Talbott TM, Maycroft TC (1990) A critical review of chemical lymph node clearance and staging of colon and rectal cancer at Ferguson Hospital. Dis Colon Rectum 33:923–925
17. Jamieson JK, Dobson JF (1909) Lymphatics of colon with special reference to the operative treatment of cancer of colon. Ann Surg 1:1077
18. Jass JR, Miller K, Northover JMA (1986) Fat clearance method versus manual dissection of lymph nodes in specimens of rectal cancer. Int J Colorectal Dis 1:155–156

19. Jeffers MD, O'Dowd GM, Mulcahy H (1994) The prognostic significance of immunohistochemically detected lymph node micrometastases in colorectal carcinoma. J Pathol 172:183–187
20. Liefers GJ, Cleton-Jansen AM, van de Velde CJH, et al (1998) Micrometastases and survival in stage II colorectal cancer. N Engl J Med 339:223–228
21. Mainprize KS, Hewavisinthe J, Savage A, et al (1998) How many lymph nodes to stage colorectal carcinoma? J Clin Pathol 51:165–166
22. Maurel J, Launoy G, Grosclaude P, et al (1998) Lymph node harvest reporting in patients with carcinoma of the large bowel: a French population-based study. Cancer 82:1482–1486
23. Ratto C, Sofo L, Ippoliti M, et al (1999) Accurate lymph node detection in colorectal specimens resected for cancer is of prognostic significance. Dis Colon Rectum 42:143–154
24. Scott KW, Grace RH (1989) Detection of lymph node metastases in colorectal carcinoma before and after fat clearance. Br J Surg 76:1165–1167
25. Scott KW, Grace RH, Gibbons P (1994) Five year follow-up study of the fat clearance technique in colorectal carcinoma. Dis Colon Rectum 37:126–128
26. Slanetz CA, Herter FP (1972) The large intestine In: Haagensen CD (ed) The lymphatics in cancer. Saunders, Philadelphia, pp 489–513
27. Sobin LH, Greene FL (2001) TNM classification: clarification of number of regional lymph nodes. Cancer 92:452
28. Sobin LH, Wittekind C (eds) (2002) TNM classification of malignant tumors. In: International Union Against Cancer (UICC) (6th edn). Wiley-Liss, New York
29. Soderstrom N (1967) Post-capillary venules as basic structural units in the development of lymphogranular tissue. Scand J Haematol 4:411–429
30. Swanson RS, Compton CC, Stewart Ak, et al (2003) The prognosis of T3N0 colon cancer is dependent on the number of lymph nodes examined. Ann Surg Oncol 10:65–71
31. Swartz MA, Skobe M (2001) Lymphatic function, lymphangiogenesis, and cancer metastasis. Microsc Res Tech 55:92–99
32. Tepper JE, O'Connell MJ, Niedzwiecki D, et al (2001) Impact of number of nodes retrieved on outcome in patients with rectal cancer. J Clin Oncol 19:157–163
33. Wong JH, Severino R, Honnebier MB, et al (1999) Number of nodes examined and staging accuracy in colorectal carcinoma. J Clin Oncol 17:2896–2900
34. Wong JH, Bowles BJ, Bueno R, et al (2002) Impact of the number of negative nodes on disease-free survival in colorectal cancer patients. Dis Col Rectum 45:1341–1348

Virchows Arch (2003) 443:139–145
DOI 10.1007/s00428-003-0856-5

ORIGINAL ARTICLE

Gerrit Peters · Silvia Gongoll · Cord Langner · Michael Mengel · Pompiliu Piso · Jürgen Klempnauer · Josef Rüschoff · Hans Kreipe · Reinhard von Wasielewski

IGF-1R, IGF-1 and IGF-2 expression as potential prognostic and predictive markers in colorectal-cancer

Received: 6 March 2003 / Accepted: 23 May 2003 / Published online: 5 July 2003
© Springer-Verlag 2003

Abstract Insulin-like growth factors (IGF-1 and IGF-2) and the IGF-1 membrane receptor (IGF-1R) have been found to play a critical role in the carcinogenesis of several tumors, among them colorectal cancer (CRC). To study the prognostic impact of these molecules, a total number of 713 cases of CRC were examined for the expression of IGF-1, IGF-2, and IGF-1R. The results were correlated with other clinicopathological data and clinical follow-up. IGF-1 expression was noted in 53 (7.5%), IGF-2 in 88 (12.6%), and IGF-1R in 698 (99.6%) of the cases. There were significant associations between the two growth factors ($P<0.00001$), between IGF-1 and Ki-67 proliferation activity ($P<0.05$), and between IGF-2 and tumor stage ($P<0.005$). IGF-2 positivity was significantly correlated to a worse clinical outcome ($P<0.005$) only in univariate, but not in multivariate, survival analysis. A similar trend was obtained for patients with IGF-1-positive CRC, but reached statistical significance only in limited tumor stages (pT1/pT2; $P<0.01$). Although the synchronous expression of IGF-1, IGF-2, and IGF-1R in a subset of CRC is consistent with an auto-/paracrine loop of cancer cell autostimulation, the prognostic effect of IGF-1 and IGF-2 expression seems to be of limited value. However, the identification of IGF-positive CRC might be beneficial for predictive reasons, as new molecular therapeutic approaches are aimed at the IGF system and related pathways.

G. Peters · S. Gongoll · M. Mengel · P. Piso · J. Klempnauer · H. Kreipe · R. von Wasielewski (✉)
Hannover Medical School,
Department of Pathology and Department of Abdominal Surgery,
Carl-Neuberg-Strasse 1, 30625 Hannover, Germany
e-mail: Wasielewski.Reinhard.von@MH-Hannover.de
Tel.: +49-511-5324470

C. Langner
Karl-Franzenz-Universität Graz, Department of Pathology,
Auenbruggerplatz 25, 8036 Graz, Austria

J. Rüschoff
Klinikum Kassel, Department of Pathology,
Mönchebergstrasse 41–43, 34125 Kassel, Germany

Keywords Insulin-like growth factors · IGF-1 receptor · Colon · Cancer · Clinical correlation · Prognosis

Introduction

Colorectal cancer (CRC) is a leading cause of cancer death in the western world. Currently, the most effective treatment is surgical resection. Chemotherapy with or without additional radiotherapy can be used as a treatment approach for advanced disease or as an adjuvant or neoadjuvant therapy to surgery [19]. Fluorouracil (FU) has been the major agent with consistent clinical activity in CRC for nearly 40 years [6]. However, the response rate to FU does not exceed 40% [7, 21].

It thus seems to be of relevance to identify new therapeutic target molecules and to define patients likely to benefit from enhanced efficiency of chemotherapy or to respond to new therapeutic strategies. Cellular oncogenes, growth factors, and receptors have been implicated in the growth regulation and progression of CRC.

Among these, the insulin-like growth factor (IGF) system has emerged as a key regulator of mitogenesis and tumorigenicity [9, 26, 31, 36]. Members of the complex IGF system are its cell membrane receptors (IGF-1R and IGF-2R), the two polypeptide ligands (IGF-1 and IGF-2), and six binding proteins (IGFBP-1 through IGFBP-6). In addition, a large group of IGFBP proteases hydrolyzes IGFBPs [37].

The IGF-1R shares a 70% homology with the insulin receptor, it contains a cytoplasmic tyrosine kinase domain and binds both IGF-1 and IGF-2. There is much evidence to suggest that a functional IGF-1R is required for cellular growth and is essential for the onset and maintenance of transformed phenotypes of many cell types [15]. Overexpression of the IGF-1R occurs in several forms of cancer and has been reported for CRC in smaller studies [3, 11, 15, 20].

IGF-1 and IGF-2 bind to and activate the IGF-1R, inducing cellular proliferation and growth. It has been

suggested that IGF-2 may act as an auto-/paracrine growth factor by binding to IGF-1R in human CRC [17].

Both IGF-1 and IGF-2 are produced in many tissues in response to growth hormone (GH) and can be found in serum, either free (active form) or, more often, bound to the IGFBPs (>90%; inactive form) [10].

IGF-1 regulates vascular endothelial growth factor (VEGF) expression in human colon cancer cells by induction of transcription of the VEGF gene [2, 35]. IGFs also act as anti-apoptotic molecules that are involved in the regulation of cell proliferation and in renewing epithelial cell populations [5, 22, 24, 27, 34].

Recently, a study suggested IGF-2 to be among the most relevant biological markers in CRC. The authors concluded that high expression levels of three markers (including IGF-2) were strongly predictive for liver metastasis [4]. However, this study compared only two pre-selected groups of patients and lacked Kaplan-Meier survival analysis.

Here, we investigate the protein expression of IGF-IR, IGF-I, and IGF-2 in a large group of patients with CRC. We correlated these biological markers with various clinicopathological variables and scrutinized the prognostic value, if any, in this widespread carcinoma.

Patients and methods

For this study, all patients with primary CRC attending surgery between 1975 and 1995 in the surgical department of Hannover Medical School were reviewed (n=1057). Exclusion criteria were: no curative surgery or pathological assessment of tumor-positive resection margins (R1/R2 status: R1, 1% excluded; R2, 8% excluded), distant metastasis at time of diagnosis (pM1, 6% excluded), age at surgery >75 years (15% excluded), prior treatment with radiotherapy, postoperative lethality within 6 weeks (excluding patients who possibly died of surgical complications, 2% excluded), and no appropriate archival tissue available (1% excluded). Of the 713 remaining cases, each one was classified according to pT stage and nodal status [pTNM system, UICC (International Union Against Cancer)], histological tumor type (adenocarcinoma or other type), tumor differentiation (high, medium, or low tumor cell differentiation), tumor localization (right colon, left colon, rectum), and tumor size (less than 2 cm, 2–5 cm, more than 5 cm) (Table 1).

Table 1 Clinicopathological data of the 713 colorectal cancer patients

Variable	%
Age (mean) 62.3 years (range) 21–75 years	
<50 years	16.5
>50 years	83.5
Gender	
Male	58.3
Female	41.7
Tumor localization	
Right colon	17.4
Left colon	27.5
Rectum	55.1
Tumor histology	
Adenomatous	81.5
Mucinous	18.5
Tumor grade	
G1	24.8
G2	62.5
G3	12.7
Tumor stage	
pT_{1+2}	30.7
pT_{3+4}	69.3
Nodal stage	
N_0	69.5
N_1	28.8
N_2	1.7
Tumor size	
<2 cm	5.9
2–5 cm	62.0
>5 cm	32.1

Using a commercially available tissue microarray (System multiblock; Zytomed, Berlin, Germany; in US: MaxArray; Zymed, SanFrancisco, CA), all cases of paraffin-embedded CRC were placed into 12 tissue array blocks (60 cases each). This method requires tissue cores that are punched from the archival paraffin blocks after an adequate area of interest has been chosen. Finally, the tissue cores are melted together to form a homogeneous new paraffin block that can be cut as any standard paraffin block. For immunohistochemical analysis, four sets of the 12 slides (2 μm) were stained according to standard protocols. In brief, sections were deparaffined in xylene, rehydrated, and epitope retrieval was performed in a microwave oven, as described previously [33]. Endogenous peroxidase was blocked, and primary antibody was incubated at 4°C overnight. The following primary antibodies were used: IGF-1R (clone 3.G2.15D6; Roche, Basel, Switzerland) at 1:750, IGF-1 (clone I-5C9; Linaris, Bettingen, Germany) at 1:500, IGF-2 (W2-H1; Linaris, Bettingen, Germany) at 1:100, and Ki-67 (clone MIB-1; Dako, Hamburg, Germany) at 1:200. Detection was carried out using biotinylated rabbit-anti-mouse antibody, followed by incubation with peroxidase-linked avidin-biotin complex (Zytomed, Berlin, Germany). Diaminobenzidine (DAB) or 3-amino 9-ethylcarbazol (AEC) were used as chromogen; slides were counterstained with Meyer's hemalaun and mounted in immu-mount (Thermoshandon GmbH; Frankfurt/Main, Germany).

For all markers, six groups were evaluated on a percentage basis: 0–1%, 2–5%, 6–10%, 11–25%, 26–50% and over 50% of tumor cells showing specific positivity. Data analysis began with univariate Kaplan-Meier analyses of the effect on survival of each marker tested separately. By graphic inspection of the results, multi-category factors were converted into dichotomous factors by merging those categories showing similar overall survival. All further analysis was based on this dichotomous distribution if not otherwise specified. If the percentage of positive labeled tumor cells exceeded 50% for IGF-1R, the case was considered positive. The respective percentage values for IGF-1, IGF-2, and Ki-67 were 25, 5, and 25%. Assessment was made only in malignant tumor cells, and staining intensity was disregarded. The staining was interpreted by two investigators (G.P. and R.v.W) who were blind to the clinical and pathological data. A mean of 500 cells within at least four adjacent fields were analyzed for each case. Using the tissue microarray (TMA) technology, inter-observer agreement was improved, as both reviewers evaluated the same tissue area (tissue spot) of 1.4 mm^2. All slides were reviewed twice and resulting inter-observer disagreements (6.4%) were reviewed a third time, followed by a conclusive judgement. Intra-observer agreement was 98.6% when 10% of cases were reviewed 2 months later. In cases of disagreement, a final score was determined by consensus after re-examination on a multi-headed microscope.

To trace possible correlations between IGF-1, IGF-2, Ki-67 expression, and several clinico-pathological parameters, data were cross-tabulated and Fisher's exact test was performed. The

association of staining for IGF-1, IGF-2, and Ki-67 with patient survival was evaluated using life tables constructed from survival data with Kaplan-Meier plots. The end-point used in the present, retrospective investigation was overall survival, counting death from any cause as the event. Overall survival was measured from date of initial surgery until date of death or, if no event was documented, until date of last information (not counting as the event). For Kaplan-Meier, comparisons between groups were performed with the log-rank test.

A *P* value of less 0.05 was considered significant. All statistical analyses were performed using SPSS version 10.0.7 (SPSS Inc., IL/USA).

Results

IGF-1R, IGF-1, and IGF-2 expression was observed in the cytoplasm of the malignant cells. Staining mostly occurred as granules at the apical site of the tumor cell (Fig. 1A–D). Of all CRC evaluated, 53 (7.5%) showed positivity for IGF-1, 88 (12.6%) showed positivity for IGF-2, and 698 (99.6%) showed positivity for IGF-1R.

IGF-1 and IGF-2 expression were strongly associated with each other ($P<0.0001$). There was also a significant association between IGF-1 expression and proliferation activity (Ki-67; $P<0.05$) and between IGF-2 expression and tumor stage ($P<0.005$). All other factors showed no significant associations with IGF-1 or IGF-2 expression. Table 2 summarizes the associations between IGF-1 and IGF-2 immunostaining and clinicopathological characteristics, including sex, tumor localization, histology, grade, stage, nodal stage, tumor size, and proliferation.

Univariate survival analyses for IGF-1R revealed no relevant findings as almost all cases (99.6%) were positive for IGF-1R.

Kaplan-Meier plots stratified for IGF-1 and IGF-2 expression are demonstrated in Fig. 2A, B. Patients with IGF-1-positive CRC showed a trend toward a worse survival than with IGF-1-negative CRC, but this difference did not reach statistical significance (P=0.11) (Fig. 2A). The median postoperative 10-year-survival was 76 months versus 85 months for IGF-1-positive versus IGF-1-negative cases. A subanalysis regarding only those patients who presented with limited disease (pT1/T2) showed a significantly worse prognosis for the small group of IGF-1-positive cases ($P<0.02$). In ad-

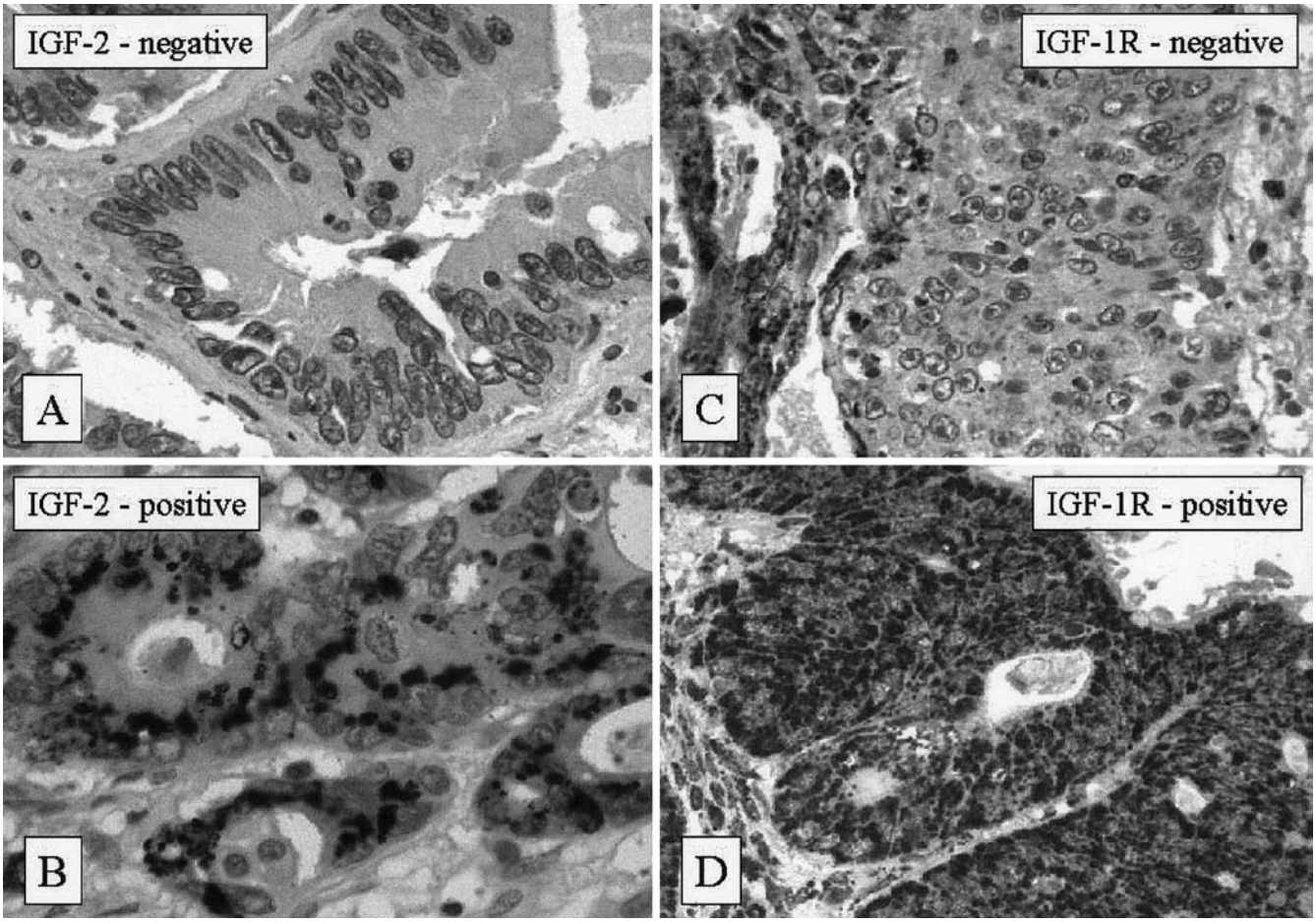

Fig. 1. A–B Representative examples of immunohistochemistry in primary colorectal cancer (CRC) with anti-insulin-like growth factor (IGF)-2 antibodies. In IGF-2-positive sections, the cytoplasm of the cell was stained. **C–D** Representative examples of immunohistochemistry in primary CRC with anti-IGF-1R antibodies. Note the apical intracellular staining reaction of the transmembrane IGF-1 receptor (**D**)

Table 2 Relationship between IGF-1/-2 expression and various clinicopathological data. *IGF* insulin-like growth factor

Variable	IGF-1		*P* value	IGF-2		*P* value
	Positive (7.5%)	Negative (92.5%)		Positive (12.6%)	Negative (87.4%)	
Gender						
Male	62.3%	57.9%	Not significant	63.6%	57.1%	Not significant
Female	37.7%	42.1%		36.4%	42.9%	
Tumor localization						
Right colon	13.2%	17.7%	Not significant	17.0%	17.6%	Not significant
Left colon	39.6%	26.7%		26.1%	27.5%	
Rectum	47.2%	55.6%		56.8%	54.9%	
Tumor histology						
Adenomatous	81.1%	81.9%	Not significant	83.0%	81.5%	Not significant
Mucinous	18.9%	18.1%		17.0%	18.5%	
Tumor grade						
G_1	28.3%	24.3%	Not significant	28.4%	24.3%	Not significant
G_2	60.4%	62.6%		60.2%	62.4%	
G_3	11.3%	13.1%		11.4%	13.3%	
Tumor stage						
pT_{1+2}	20.8%	31.6%	Not significant	17.0%	32.5%	<0.005
pT_{3+4}	79.2%	68.4%		83.0%	67.5%	
Nodal stage						
N0	73.6%	68.9%	Not significant	65.9%	70.0%	Not significant
N1	26.4%	29.4%		33.0%	28.2%	
N2	0%	1.7%		1.1%	1.8%	
Tumor size						
<2 cm	3.8%	5.7%	Not significant	1.1%	6.4%	Not significant
2–5 cm	67.3%	62.0%		65.5%	61.3%	
>5 cm	28.8%	32.3%		33.3%	32.3%	
Proliferation						
ki-67 negative	36.4%	22.6%	<0.05	28.8%	22.8%	Not significant
ki-67 positive	63.6%	77.4%		71.2%	77.2%	
IGF						
IGF-1-negative				6.4%	93.6%	<0.00001
IGF-1-positive				88.7%	11.3%	

vanced stages (pT3/T4), IGF-1 expression had no significant prognostic value ($P>0.2$).

IGF-2 expression was significantly associated with a worse clinical outcome ($P<0.005$) in all patients (Fig. 2B). The median postoperative 10-year-survival declined from 86 months in the IGF-2-negative cases to 73 months in the IGF-2-positive cases. In contrast to the effects observed for IGF-1, a further subanalysis of IGF-2 into limited (pT1/T2) versus advanced stages (pT3/T4) indicated no prognostic impact in the limited (pT1/T2) subgroup ($P>0.05$). In advanced stages (pT3/T4), IGF-2 expression reached borderline significance ($P=0.06$).

Ki-67 positivity (>25% of tumor cells) was observed in 60.9% of cases. Survival analysis revealed no significant differences between positive and negative cases, neither in all cases, limited stages (pT1/T2), nor in advanced stages (pT3/T4) ($P>0.2$).

Discussion

This study presents for the first time an analysis of IGF-1R and its ligands IGF-1/-2 in a large series of CRC with survival analysis. Although the role the IGF system plays in CRC is poorly understood, recent data suggest that the IGF-1R is required not only for the transformation of the mucosa of the colon, but also in other tissues [5, 14]. In colonic mucosa, a progressive increase in IGF-1R expression has been observed during the transition from normal to adenomatous and to carcinomatous tissue [3]. Overexpression of IGF-1R has been shown to inhibit apoptosis [5, 22, 24, 27, 34]. We found a strong expression of the IGF-1 receptor in nearly all CRC cases (>99%) investigated, a result supported by observations of previous smaller series [15]. Triggered upon binding of IGF-1 or IGF-2, an intracellular signaling cascade results in the activation of transcription factors involved in cell proliferation and transformation [16, 23, 29, 36].

IGF-1 can stimulate the expression of cyclin D1, which accelerates progression of the cell cycle from G1 to S phase [12]. This observation could explain our finding of

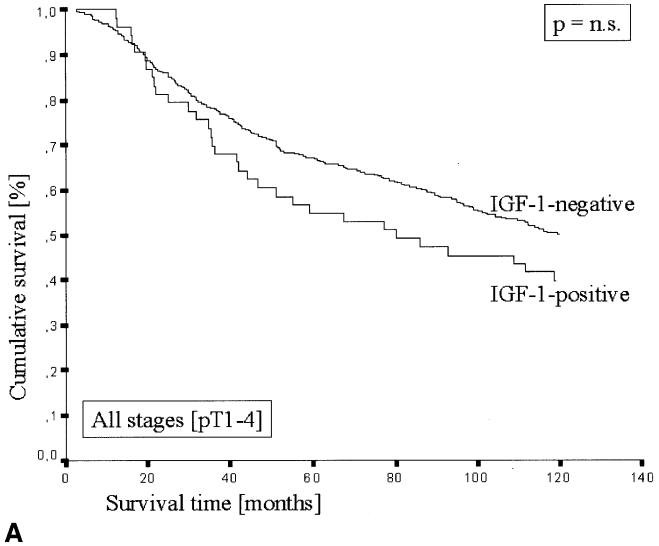

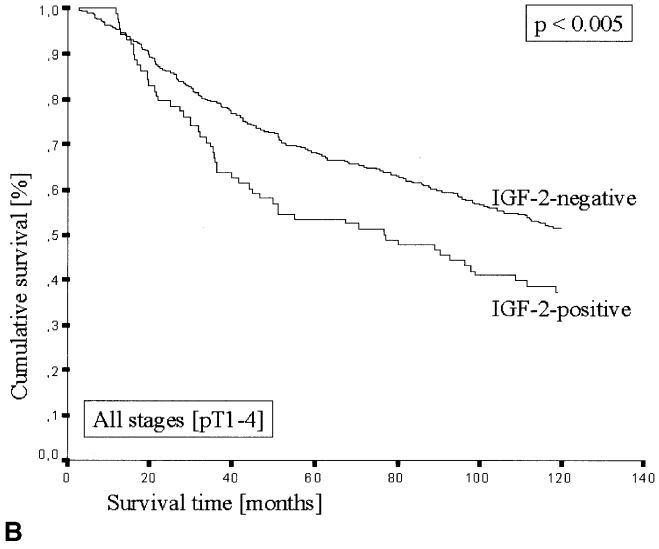

Fig. 2 Kaplan-Meier survival curves demonstrating the effects of insulin-like growth factor (IGF)-1 expression (**A**) and IGF-2 expression (**B**) on overall survival of colorectal cancer patients. **A** Positive expression of IGF-1 trends toward a worse prognosis. **B** IGF-2-positive cases were correlated with significantly shorter patient survival

a significant association of IGF-1 expression with the cell-cycle marker Ki-67 ($P<0.05$), indicating an increase in the proliferative activity of colorectal cancer cells. It is plausible to assume that there is an autocrine/paracrine acting loop in those CRC that express either IGF-1 or IGF-2 via self-stimulation of the IGF-1R. However, no associations between IGF-1 expression and tumor progression, including tumor stage, grade, and size, could be found in our study. In contrast, the expression of IGF-2 was highly associated with tumor stage ($P<0.005$). Among advanced tumor stages (pT3/T4), 83% of cases expressing IGF-2 were seen. This finding might be due to increased tumor growth and reduced apoptosis in response to autocrine IGF-2 production and IGF-R activation.

Univariate survival analysis of all cases using the Kaplan-Meier method revealed a trend toward a worse prognosis for IGF-1-positive cases ($P=0.11$) and a significantly worse prognosis for IGF-2-positive CRC ($P<0.005$). In concordance with the published literature, the proliferation fraction (Ki-67) proved not to be of any prognostic relevance in CRC, regardless of the stage of disease [18, 30]. Taken together, it seems obvious that the assessment of IGF-1 in CRC is of limited value for prognostic reasons.

In contrast, IGF-2 expression was significantly associated with a worse clinical outcome in univariate survival analysis. In our previous study, we identified S100A4 and p53 as the two most powerful prognostic markers for CRC [13]. To analyze the value of IGF-2 positivity in the context of these findings, an additional Cox regression analysis was performed. All clinical and immunohistochemical markers were included that had been shown to be of prognostic relevance, adding both factors IGF-1 and IGF-2. However, neither of the latter markers added any significant power to our model ($P>0.2$).

These findings clearly contrast the assumption of a recent paper by Barozzi et al. (2002), who reported that the expression of IGF-2 was among the three most relevant biological markers in CRC. However, this study was hampered by omitting a Kaplan-Meier survival analysis and comparing only preselected groups of patients with different clinical outcomes—one group of which already exhibited liver metastasis (palliative stage of disease). Moreover, S100A4 and p53 were not included in this investigation.

Besides its lack of multivariate prognostic relevance, the identification of IGF-1 and IGF-2 expressing carcinomas could be of particular importance as a predictive therapeutic target molecule for new therapies. In recent years, several approaches have been made to use the IGF system and its pathways for novel therapeutic strategies in CRC. For example, treatment with antagonists of GH-releasing hormone inhibits the growth of the colonic cell line HT-29 in vivo and in vitro, mediated by a reduced production and secretion of IGF-2 by the cells [32]. Therefore, the identification of IGF-2-positive tumors could help to select those patients most likely to benefit from such a novel therapeutic approach.

Another objective is the use of vitamin D-related compounds, aiming at the IGFBPs. These proteins physiologically regulate the bioavailability of IGF-1/-2 in serum and act as modulators of the biological effects of both—either inhibiting or enhancing their ability to bind to its receptor (depending on the specific IGFBP). Vitamin D-related compounds stimulate the production of IGFBP-5, thus suppressing effects of IGF-1/-2 in human cancer cell lines [28]. However, this intervention might turn out to be less effective in the subgroup of cases that are self-activated in an autocrine loop (IGF-1/-2 and

IGF-receptor expression). These tumors presumably are less affected by changing serum levels of active IGF-1/-2.

A similar mechanism could be of importance for the attempt to modulate IGF-1 concentrations via the use of somatostain-analogs, i.e., octreotide. It has been shown that octreotide is capable of lowering the IGF-1 concentration and slowing down the growth rate of tumor cells in vivo [8]. Although further studies are warranted to elucidate the detailed pathways of interaction, it seems important to differentiate between IGF-1 positive and negative tumors in those investigations for the reasons mentioned above.

The ubiquitous expression of IGF-1R in CRC also provides a novel target in anti-cancer treatment. Initial reports have already shown that the genetic blockade of IGF-1R in human colon cancer cell lines enhances the efficacy of chemotherapy by increasing the apoptosis rate [1]. Moreover, using IGF-1R antagonistic antibodies to block IGF-1R function increased the response rate of a combined treatment with 5-fluorouracil (5-FU) and external beam radiation in colon cancer cells [25].

In conclusion, synchronous expression of IGF-1, IGF-2, and IGF-1R in CRC is consistent with an auto-/paracrine loop of cancer cell stimulation, but the prognostic effect of IGF-1 and IGF-2 analysis seems to be of limited value if a multivariate survival analysis is performed. However, the identification of patients with IGF-positive CRC could turn out to be of clinical relevance as a predictive tumor marker for future molecular therapeutic strategies.

References

1. Adachi Y, Lee CT, Coffee K, Yamagata N, Ohm JE, Park KH, Dikov MM, Nadaf SR, Artega CL, Carbone DP (2002) Effects of genetic blockade of the insulin-like growth factor receptor in human colon cancer cell lines. Gastroenterology 123:1191–1204
2. Akagi Y, Liu W, Zebrowski B, Xie K, Ellis LM (1998) Regulation of vascular endothelial growth factor expression in human colon cancer by insulin-like growth factor-I. Cancer Res 58:4008–4014
3. Ardeshir H, Yeatman TJ, Lu L, Mora L, Marcet G, Santo VN, Karl RC, Coppola D (1999) Expression of insulin-like growth factor-I receptor in human colorectal cancer. Hum Pathol 10:1128–1133
4. Barozzi C, Ravaioli M, ÓErrico A, Grazi GL, Poggioli G, Cavrini G, Mazziotti A, Grigioni WF (2002) Relevance of biologic markers in colorectal carcinoma. Cancer 94:647–657
5. Baserga R (1995) The insulin-like growth factor I: a key to tumor growth? Cancer Res 55:249–252
6. Bleiberg H (1997) Colorectal cancer: is there an alternative to 5-FU? Eur J Cancer 33:536–541
7. Blijham G, Wagener T, Wils J, de Greve J, Buset M, Bleiberg H, Lacave A, Dalmark M, Selleslag J, Collette L, Sahmoud T (1996) Modulation of high dose infusional fluorouracil by low dose methotrexate in patients with advanced or metastatic colorectal cancer: final results of a randomized European Organization for Research and Treatment of Cancer Study. J Clin Oncol 14:2266–2273
8. Cascinu S, Del Ferro E, Grianti C, Ligi M, Ghiselli R, Foglietti G, Saba V, Lungarotti F, Catalano G (1997) Inhibition of tumor cell kinetics and serum insulin growth factor I levels by octreotide in colorectal cancer patients. Gastroenterology 113:767–772
9. Coppola D, Ferber A, Miura M, Sell C, D'Ambrosio C, Rubin R, Baserga R (1994) A functional IGF1 receptor is required for the mitogenic and transforming activities of the epidermal growth factor receptor. Mol Cell Biol 14:4588–4595
10. Ferry RJ, Katz LEL, Grimberg A, Cohen P, Weinzimer SA (1998) Cellular actions of insulin-like growth factor binding proteins. Horm Metab Res 31:192–202
11. Freier S, Weiss O, Flyvbjerg A, Dahan R, Nephesh I, Safra T, Shiloni E, Raz (1999) Expression of the insulin-like growth factors and their receptors in adenocarcinoma of the colon. Gut 44:704–708
12. Furlanetto RW, Harwell SE, Frick KK (1994) Insulin-like growth factor-1 induces cyclin D1 expression in MG63 human osteosarcoma cells in vitro. Mol Endocrinol 8:510–517
13. Gongoll S, Peters G, Mengel M, Piso P, Klempnauer J, Kreipe H, von Wasielewski R (2002) Prognostic significance of calcium-binding protein s100a4 in colorectal cancer. Gastroenterology 123:1478–1484
14. Grothey A, Voigt W, Schöber C, Müller T, Dempke W, Schmoll HJ (1999) The role of insulin-like growth factor I and its receptor in cell growth, transformation, apoptosis, and chemoresistance in solid tumors. J Cancer Res Clin Oncol 125:166–173
15. Guo YS, Narayan S, Yallampalli C, Singh P (1992) Characterization of insulin-like growth factor 1 receptors in human colon cancer. Gastroenterology 102:1101–1108
16. Kato H, Faria TN, Stannard B, Roberts CT Jr, LeRoith D. (1993) Role of tyrosine kinase activity in signal transduction by insulin-like growth factor 1 (IGF-1) receptor. J Biol Chem 1268:2655–2661
17. Kawamoto K, Ondera H, Imamura, et al (1998) Expression of insulin-like growth factor-2 can predict the prognosis of human colorectal cancer patients: correlation with tumor progression, proliferative activity and survival. Oncology 55:242–248
18. Kubota Y, Petras RE, Easley KA, Bauer TW, Tubbs RR, Fazio VW (1992) Ki-67-determined growth fraction versus standard staging and grading parameters in colorectal carcinoma. A multivariant analysis. Cancer 70:2602–2609
19. Labianca R, Pessi MA, Zamparelli G (1997) Treatment of colorectal cancer. Drugs 53:593–607
20. Lahm H, Suardet L, Laurent PL, Fischer JR, Ceyhan A, Givel JC, Odartchenko N (1992) Growth regulation and costimulation of human colorectal cancer cell lines by insulin-like growth factor 1, 2 and transforming growth factor. Br J Cancer 65:341–346
21. Leichman CG, Leichman L, Spears CP, Rosen PJ, Jeffers S, Groshen S (1993) Prolonged continuous infusion of fluorouracil with weekly bolus leucovorin: a phase II study in patients with disseminated colorectal cancer. J Natl Cancer Inst 85:41–44
22. Liu B, Fang M, Lu Y, Mendelsohn J, Fan Z (2001) Fibroblast growth factor and insulin-like growth factor differentially modulate the apoptosis and G1 arrest induced by anti-epidermal growth factor receptor monoclonal antibody. Oncogene 20:1913–1922
23. Myers MG, Sun XJ, Cheatham B, Jachna BR, Glasheen EM, Backer JM, White MF (1993) IRS-1 is a common element in insulin and insulin-like growth factor-1 signaling to the phosphatidylinositol 3′-kinase. Endocrinology 132:1421–1430
24. Parrizas M, Leroith D (1997) Insulin-like growth-factor-1 inhibition of apoptosis is associated with increased expression of the bcl-xL gene product. Endocrinology 138:1355–1358
25. Perer E, Madan A, Shurin A, Zakris E, Romeguera K, Pang Y, Beech D (2000) Insulin-like growth factor I receptor antagonism augments response to chemoradiation therapy in colon cancer cells. J Surg Res 94:1–5
26. Pietrzkowski Z, Lammers R, Carpenter G, Soderquist AM, Limardo M, Phillips PD, Ullrich A, Baserga R (1993) Constitutive expression of insulin-like growth factor 1 and insulin-like growth factor 1 receptor abrogates all requirements for exogenous growth factors. Cell Growth Differ 3:199–205

27. Remacle-Bonnet MM, Garrouste FL, Heller S, Andre F, Marvaldi JL, Pommier GJ (2000) Insulin-like growth factor-I protects colon cancer cells from death factor-induced apoptosis by potentiating tumor necrosis factor α-induced mitogen-activated protein kinase and nuclear factor κB signaling pathways. Cancer Res 60:2007–2017
28. Rozen F, Yang XF, Huynh H, Pollak M (1997) Antiproliferative action of vitamin D-related compounds and insulin-like growth factor-binding protein 5 accumulation. J Natl Cancer Inst 89:652–656
29. Rubin R, Baserga R (1995) Biology of disease: insulin-like growth factor 1 receptor. Its role in cell proliferation, apoptosis and tumorigenicity. Lab Invest 73:311–331
30. Sahin AA, Ro JY, Ayala AG (1994) Assessment of ki-67-derived tumor proliferative activity in colorectal adenocarcinomas. Mod Pathol 7:17–22
31. Sell C, Rubini M, Rubin R, Liu JP, Efstratiadis A, Baserga R (1993) Simian virus 40 large tumor antigen is unable to transform mouse embryonic fibroblast lacking type 1 insulin-like growth factor receptor. Proc Natl Acad Sci U S A 90:11217–11221
32. Szepeshazi K, Schally AV, Groot K, Armatis P, Halmos G, Hebert F, Szende B, Varga JL and Zarandi M (2000) Antagonists of growth hormone-releasing hormone (GH-RH) inhibit IGF-II production and growth of HT-29 human colon cancers. Br J Cancer 82:1724–1731
33. von Wasielewski R, Werner M, Nolte M, Wilkens L, Georgii A (1994) Effects of antigen retrieval by microwave heating in formalin-fixed tissue sections on a broad panel of antibodies. Histochemistry 102:165–172
34. Wang L, Ma W, Markovich R, Lee WL, Wang PH (1998) Insulin-like growth factor 1 modulates induction of apoptotic signalling in H9C2 cardiac muscle cells. Endocrinology 139:1354–1360
35. Warren RS, Yuan H, Matli MR, Ferrara N, Donner DB (1996) Induction of vascular endothelial growth factor by insulin-like growth factor 1 in colorectal carcinoma. J Biol Chem 271:29483–29488
36. White MF, Kahn CR (1994) The insulin signaling system. J Biol Chem 269:1–4
37. Yu H, Rohan T (2000) Role of the insulin-like growth factor family in cancer development and progression. J Natl Cancer Inst 18:1472–1489

Virchows Arch (2003) 443:146–151
DOI 10.1007/s00428-003-0845-8

ORIGINAL ARTICLE

Reiko Ito · Hirofumi Nakayama · Kazuhiro Yoshida · Kazuya Kuraoka · Junichi Motoshita · Noriko Oda · Naohide Oue · Wataru Yasui

Expression of osteoprotegerin correlates with aggressiveness and poor prognosis of gastric carcinoma

Received: 17 March 2003 / Accepted: 20 May 2003 / Published online: 28 June 2003
© Springer-Verlag 2003

Abstract Osteoprotegerin (OPG), identical with osteoclastogenesis inhibitory factor, is a member of a subgroup of the tumor necrosis factor (TNF)-receptor superfamily, which functions as a soluble decoy receptor. It has been reported that OPG expression is associated with bone metastasis of cancer of the breast and prostate. In the present study, we examined the expression of OPG in gastric carcinomas using immunohistochemistry and reverse-transcription polymerase chain reaction methods, and compared with clinicopathological parameters. The expression of OPG mRNA was confirmed in a gastric carcinoma cell line (MKN-7) and gastric carcinoma tissues. Immunohistochemically, strongly positive staining of OPG was found in 65% (67/103) of gastric carcinomas, whereas OPG protein was not detected in non-neoplastic mucosal epithelia. The expression of OPG protein in gastric carcinoma tissues correlates significantly with depth of tumor invasion, nodal metastases and advanced tumor stage. Furthermore, the prognosis of the cases with strong OPG expression was significantly worse than those with weak or no expression of OPG. These results suggest that OPG may participate in stomach carcinogenesis, invasion and metastasis, and may serve as a novel molecular marker for aggressive gastric cancer.

R. Ito · H. Nakayama · K. Kuraoka · J. Motoshita · N. Oue · W. Yasui (✉)
Department of Molecular Pathology,
Hiroshima University Graduate School of Biomedical Sciences, Japan
e-mail: wyasui@hiroshima-u.ac.jp
Fax: +81-82-2575149

K. Yoshida
Department of Surgery,
Research Institute for Nuclear Medicine and Biology,
Hiroshima University, 1-2-3 Kasumi, Minami-ku,
734-8551 Hiroshima, Japan

N. Oda
Department of Human Nutrition, Faculty of Human Sciences,
Hiroshima Bunkyo Women's University,
1-2-1 Kabe-higashi, Asakita-ku, 731-0295 Hiroshima, Japan

Keywords Osteoprotegerin · Aggressiveness · Gastric carcinoma

Introduction

Osteoprotegerin (OPG), identical with osteoclastogenesis inhibitory factor, is a member of a subgroup of the tumor necrosis factor (TNF)-receptor superfamily. It contains a cysteine-rich amino-terminal domain, a putative death domain and a COOH-terminal heparin-binding domain; but, unlike other members of the TNF-receptor superfamily, it does not contain a transmembrane domain [15]. It is, therefore, thought to function as a soluble decoy receptor. OPG has been found to be expressed in the bone, heart, lung, liver, placenta, artery, lymphocytes etc. [2]. Regulation of bone metabolism by OPG is the most studied in vivo process. OPG has a dramatic effect on both osteoclast differentiation and activation [8]. Addition of OPG to osteoclast precursor cultures inhibits their differentiation and fusion into multinucleated active osteoclasts as well as their survival. Much of the current interest in OPG in malignant neoplasms has been focused on its ability to inhibit osteoclastogenesis [9, 10, 18]. Furthermore, tight connection between OPG expression and bone metastasis has been found in certain tumors. Inhibitory effect of osteoclastogenesis by OPG prevents bone metastases of the breast cancer [11], while a high level of OPG expression is associated with bone metastases of the prostate cancer [1].

OPG has two known TNF family ligands: receptor activator of nuclear factor (NF)-κB ligand [17] and TNF-related apoptosis-inducing ligand (TRAIL) [3]. TRAIL in tumor, produced by monocytes in response to interferon (IFN)-γ or -α, is the principle mediator of acquired tumor killing activity of these cells [4]. TRAIL binds two classes of membrane-bound receptors carrying death domains (DR4 and DR5) and a decoy receptor, OPG. OPG competes for TRAIL binding to death-activating receptors, providing a mechanism for protection against apoptosis in the presence of TRAIL. Therefore, the

expression of OPG could be an appropriate strategy to avoid TRAIL-induced apoptosis, resulting in tumor development and progression. However, there are no analyses of the role of OPG in stomach carcinogenesis and its progression.

In the present study, we examined the expression of OPG in gastric carcinoma cell lines and primary gastric carcinomas using immunohistochemistry and reverse-transcription polymerase chain reaction (RT-PCR), and analyzed the correlation of OPG expression with clinicopathological characteristics such as tumor stage, depth of tumor invasion, lymph-node metastasis and patient's prognosis.

Materials and methods

Tissue samples

A total of 103 gastric adenocarcinoma cases (42 female and 61 male) were used. The median of patients' age was 67 years (range 24–89 years). The tumor tissues and corresponding non-neoplastic gastric mucosa were obtained by surgery at Hiroshima University Hospital and its affiliated hospitals. For laser capture microdissection (LCM) and RNA extraction, tissue samples obtained at the time of surgery were immediately embedded in O.C.T. compound (Sakura Finetechnical, Tokyo, Japan), frozen in liquid nitrogen and stored at −80°C until use. For immunohistochemistry, tissues were fixed in 10% buffered-formalin and embedded in paraffin.

We classified the gastric carcinomas according to the criteria of the Japanese Classification of Gastric Cancer [7]. Histological type was classified as follows: well-differentiated type (papillary adenocarcinoma and well-differentiated tubular adenocarcinoma), moderately differentiated type (moderately differentiated tubular adenocarcinoma) and poorly differentiated type (solid and non-solid type poorly differentiated adenocarcinoma, signet-ring cell carcinoma and mucinous adenocarcinoma). Classification of the quantity of stroma was made as follows: scirrhous type (sci), stroma is abundant and fibrous; medullary type (med), stroma is scanty; intermediate type (int), the quantity of stroma is intermediate between sci and med. Depth of carcinoma invasion was classified as follows: t1, mucosa (m) and submucosa (sm); t2, muscularis propria (mp) and subserosa (ss); t3, serosa-exposed (se); t4, serosa-infiltrating (si).

Cell line

Five human gastric carcinoma cell lines were studied. TMK-1 was established from a poorly differentiated adenocarcinoma in our laboratory [12]. Four cell lines of the MKN series (MKN-7, MKN-28 and MKN-74, well-differentiated adenocarcinoma; and MKN-45, poorly differentiated adenocarcinoma) were kindly provided by Dr. T. Suzuki (Fukushima Medical University, Fukushima, Japan). All cell lines were routinely maintained in RPMI 1640 (Nissui Pharmaceutical Co. Ltd., Tokyo, Japan) containing 10% fetal bovine serum (FBS) (Whittaker M. A. Bioproducts Inc., Walkersville, MD, USA) under conditions of 5% CO_2 in air at 37°C.

LCM

The tissues in frozen blocks were cut into 5-μm thick sections on a cryostat. The sections were fixed in 70% ethanol containing 5% acetic acid immediately after cutting, and counter stained with hematoxylin shortly thereafter. We used the system of LCM-220, PixCell II. LCM allows isolation of tissue fragments that are as small as the diameter of an area at which a laser beam focuses. The laser beam of this LCM system covers a circle of 30 μm or 60 μm diameter. About 100 circles were dissected from one section and used for RT-PCR. Through this step, we successfully collected carcinoma cells or non-neoplastic epithelia with minimal contamination of stromal components.

RNA extraction and RT-PCR

Total RNA was extracted from the micro-dissected tissue samples or cell lines using the Rneasy mini kit (Qiagen Inc., Santa Clarita, CA). Thereafter, the manufacturer's instructions were followed with the inclusion of 50 μg/ml carrier glycogen in all precipitation steps. Total RNA in 50-μl aliquots was stored at −80°C until use.

Each sample of total RNA was concentrated by vacuum evaporation for cDNA synthesis using the Super Script II (Gibco, Invitrogen Corp., Carlsbad, CA). The PCR reaction was performed with sense primer-1 [5′-GCCCCTTGCCCTGACCACTACTACAC-3′] and anti-sense primer [5′-GCTGTGTTGCCTTTTATCCTCTC-TA-3′] for detection of 548-bp OPG PCR product. The set of PCR reactions included a negative control with no template DNA. PCR conditions were 94°C for 5 min; 35 cycles of 94°C for 1 min, 55°C for 1 min and 72°C for 1 min and a final extension step of 72°C for 10 min. PCR products were visualized by ethidium bromide staining in agarose gels. RNA integrity was evaluated for each sample by amplification of 254-bp β-actin sequences using the test cDNA.

Immunohistochemistry

Consecutive 4-μm tissue sections were prepared from paraffin blocks and immunostained for OPG. Immunohistochemical staining was performed with the immunoperoxidase technique using a Histofine Simple Stain Kit (Nichirei Biosciences, Tokyo, Japan). Anti-OPG polyclonal antibody (Santa Cruz Biotechnology, CA) at a 1:100 dilution for OPG (N-20) was used as primary antibody, while negative control staining was made using nonspecific IgG in the primary reaction.

The stained slides were observed independently by two investigators (Ito R and Nakayama H) without clinicopathological information, and grade of staining was decided according to the definition as follows: ++, over 70% of tumor cells showed immunoreactivity; +, 30–70% of tumor cells showed immunoreactivity; ±, less than 30% of tumor cells showed immunoreactivity; −, no tumor cells showed immunoreactivity. In the analysis with clinicopathological parameters, grades ++ and + were regarded as strongly positive and grades ± and − were regarded as weakly positive or negative.

Statistical analysis

Statistical analyses were performed with non-parametric test and P values were shown. P values less than 0.05 were regarded as statistically significant.

Results

Expression of OPG mRNA in gastric carcinomas detected by RT-PCR

We first examined OPG mRNA expression in gastric carcinoma cell lines and microdissected gastric tumor and non-neoplastic epithelia by RT-PCR. The results of RT-PCR analysis for OPG are shown in Fig. 1. The expression of OPG mRNA was confirmed only in the MKN-7 cell line among five cell lines. In gastric tissues, OPG mRNA was expressed at various levels in all of the

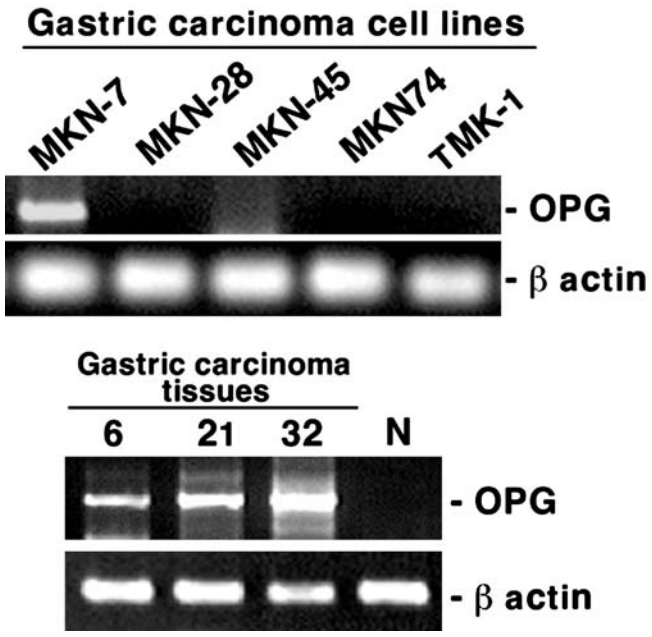

Fig. 1 Osteoprotegerin (OPG) mRNA expression in gastric carcinoma cell lines, gastric carcinoma tissues and non-neoplastic epithelia. Reverse-transcription polymerase chain reaction was performed as described in Materials and methods. The expression of OPG was found in MKN-7 out of five cell lines. In gastric tissues, OPG mRNA was expressed at various levels in all of the three carcinoma tissues, whereas it was not detected in non-neoplastic epithelia.*N* non-neoplastic epithelium

three carcinoma tissues examined, whereas it was not detected in non-neoplastic epithelia.

Immunohistochemical detection of OPG protein in gastric carcinoma tissue and non-neoplastic mucosa

We next examined the expression of OPG protein in 103 cases of gastric carcinomas and non-neoplastic mucosa by immunohistochemistry. Representative results of OPG staining are shown in Fig. 2. In non-neoplastic gastric mucosa, OPG protein was not detected in epithelial cells including foveolar epithelia and fundic glandular cells (Fig. 2A), which is consistent with the results of RT-PCR study. Figure 2B is a typical example that shows that a superficial carcinoma (t1) was negative for OPG while stromal cells such as lymphocytes and macrophages in both non-neoplastic mucosa and cancer lesions were positive for OPG, which was regarded as an internal positive control. In gastric carcinoma cases,

Table 1 Expression of osteoprotegerin (OPG) in gastric carcinomas. ++ over 70% of tumor cells showed immunoreactivity,+ 30–70% of tumor cells showed immunoreactivity, ± less than 30% of tumor cells showed immunoreactivity, – no tumor cells showed immunoreactivity

Case no.	OPG expression			
	(++)	(+)	(±)	(–)
103	28 (27%)	39 (38%)	24 (23%)	12 (12%)

Table 2 Expression of osteoprotegerin (OPG) in gastric carcinomas and its correlation with clinicopathological parameters

	Case no.	OPG expression[a]		*P* value[c]
		Strongly	Weakly or negative	
Gastric carcinomas	103	67 (65%)	36 (35%)	
Histology[b]				
Wel	29	19 (66%)	10 (34%)	
Mod	29	22 (76%)	7 (24%)	*P*=0.281
Por	45	26 (57%)	19 (42%)	
Med	46	27 (57%)	19 (41%)	
Sci and int	57	40 (70%)	17 (30%)	*P*=0.224
Depth of invasion[b]				
t1	34	9 (27%)	25 (73%)	
t2	46	37 (81%)	9 (19%)	*P*<0.001
t3	23	21 (91%)	2 (9%)	
Lymph-node metastasis[b]				
n0	44	16 (36%)	28 (64%) /	
n1	24	19 (79%)	5 (21%) /	
n2	25	24 (96%)	1(4%)*!*	*P*<0.001
n3	10	8 (80%)	2 (20%)*j*	
Stage[b]				
I and II	53	29 (55%)	24 (45%)	
III and IV	50	38 (76%)	12 (24%)	*P*=0.023

[a] Grades of OPG expression were classified as "strongly positive (++, +)" and "weakly positive or negative (±, -)", as described in Materials and methods
[b] According to the criteria of the Japanese Classification of Gastric Cancer
[c] Correlation was analyzed by non-parametric test and *P* values were shown. *P* values less than 0.05 were regarded as statistically significant

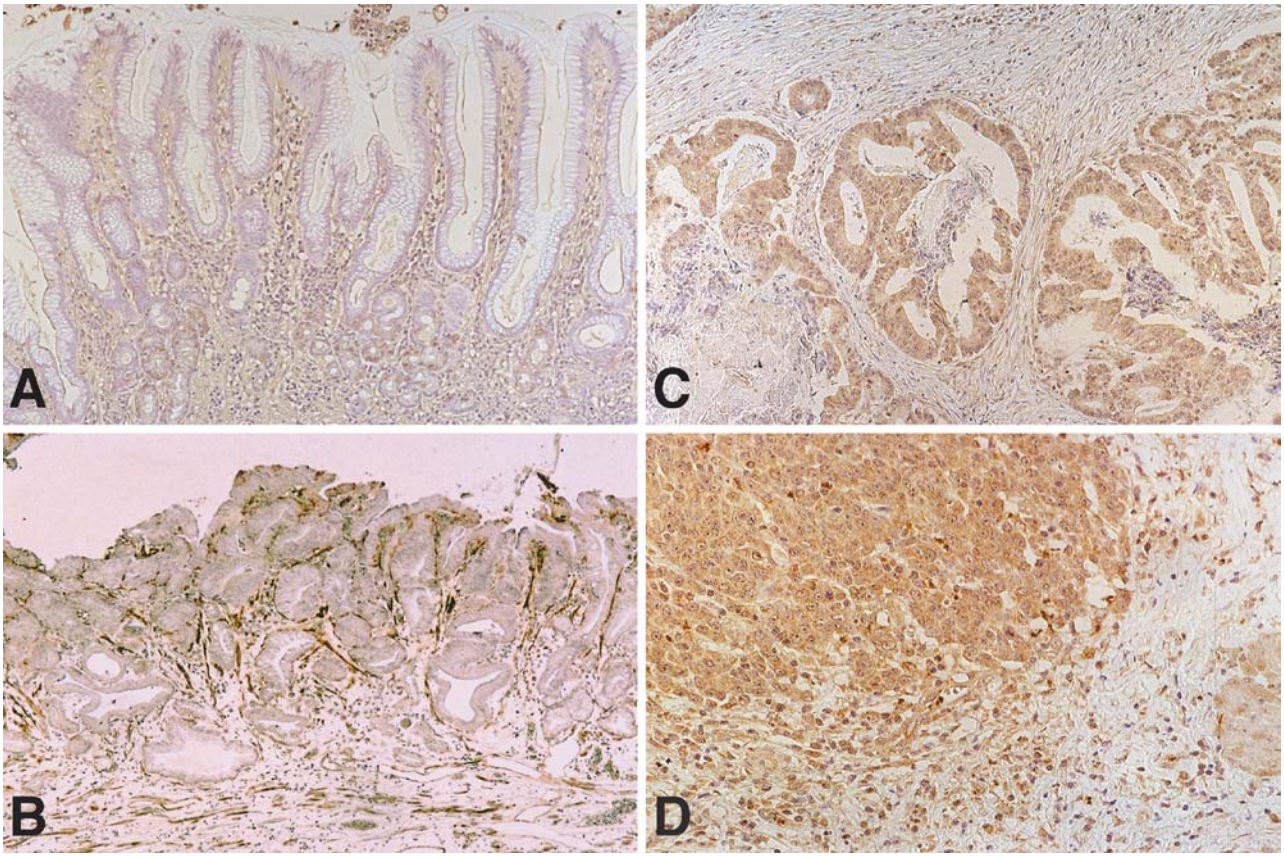

Fig. 2 A–D Immunostaining of osteoprotegerin (OPG) in gastric carcinoma tissues and gastric non-neoplastic mucosa. Non-neoplastic mucosa (**A**). OPG was not detected in epithelial cells including foveolar epithelia and fundic glandular cells, while OPG expression was found in many stromal cells such as lymphocytes and macrophages. Well-differentiated tubular adenocarcinoma (t1) (**B**). No tumor cells were positive for OPG (stain grade -, negative). Well-differentiated tubular adenocarcinoma (**C**) and solid type poorly differentiated adenocarcinoma (**D**). OPG protein was expressed in most of tumor cells in advanced cases (staining grade ++, strongly positive)

many tumor cells were also positive for OPG protein mainly in their cytoplasm (Fig. 2C and D). Strongly positive staining of OPG (sum of ++ and +, over 30% of tumor cells expressed OPG) was found in 65% (67/103) of gastric carcinomas (Table 1). Twelve percent (12/103) of cases showed completely negative expression. Stromal cells such as lymphocytes and macrophages in both non-neoplastic mucosa and cancer lesions were also positive to OPG. The rate of positive cells and intensity of the staining in the stroma were not different between non-neoplastic mucosa and tumor tissue.

Correlation between OPG expression and clinicopathological characteristics of gastric carcinoma

We then analyzed the relationship between the expression of OPG protein and clinicopathological parameters of gastric carcinoma. The results are summarized in Table 2. The expression of OPG in gastric cancer tissue was not correlated with histological type as well as the amount of stroma. However, significant correlation was detected between OPG expression and parameters that may influence prognosis, such as depth of tumor invasion, nodal metastases and tumor stage. Strongly positive staining of OPG was significantly associated with deep invasion of tumor cells in gastric wall ($P<0.001$) and high frequency of nodal metastasis ($P<0.001$). Furthermore, the cases with strong OPG expression were significantly more frequent in stages III and IV than in stages I and II ($P=0.023$).

Survival rate of gastric carcinoma cases with or without OPG expression

Finally, we examined the relationship between OPG expression in the tumor and the survival rate of patients after surgery. As shown in Fig. 3, the cases with strong OPG expression showed significantly worse prognosis than those with weak or negative expression of OPG ($P=0.008$).

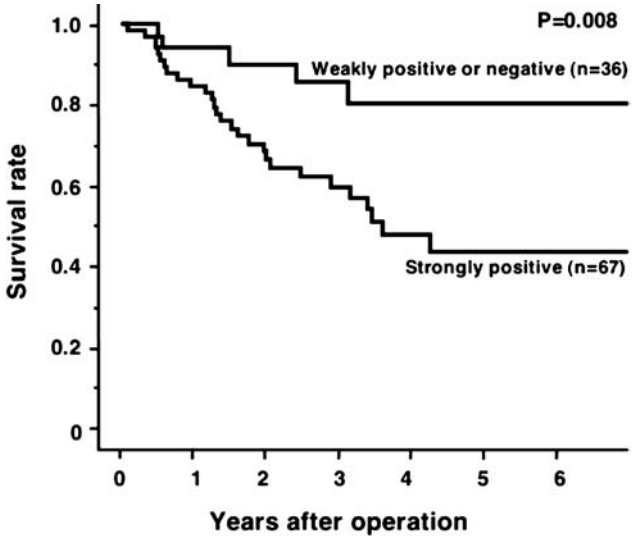

Fig. 3 Survival rate of the gastric carcinoma patients was compared with osteoprotegerin (OPG) expression. The cases with strong OPG expression showed a significantly worse prognosis than the cases with weak or negative expression (P=0.008)

Discussion

In the present study, we demonstrated the expression of OPG by gastric cancer cell line and primary carcinoma tissues using immunohistochemistry and RT-PCR. Strong expression of OPG protein was immunohistochemically detected in 65% (67/103) of the gastric cancer cases, whereas it was not detected in non-neoplastic gastric epithelia, which is consistent the results of RT-PCR study. Strong expression of OPG in gastric cancer tissue was closely associated with deep invasion, nodal metastases, advanced stage and poor prognosis. In order to determine the influence of OPG expression on survival, we performed a multivariate survival analysis including clinicopathological parameters (data not shown), and found that the factor which gave the strongest influence was not OPG expression but tumor stage. Therefore, we cannot completely deny a possibility that OPG expression may be epiphenomenon during tumor progression. We should certify the biological role of OPG in stomach carcinogenesis by analyzing more cases and also by using a model system.

OPG, unlike other members of TNF receptor superfamily, can act as a soluble factor in the regulation of bone mass and imply a utility for OPG in the treatment of osteoporosis associated with increased osteoclast activity [15]. However, another function of OPG, inhibition of apoptosis, may be important with regard to cancer biology. The potential involvement of OPG in suppression of apoptotic response to TRAIL seems to be of greater significance for the survival and progression of the prostate cancer than the bone-related effects of OPG [5]. Although TRAIL is highly expressed in the prostate, a function of TRAIL has yet to be established in this tissue [16]. In prostatic cancer cells, treatment of TRAIL induces OPG expression and expands survival of cancer cells [5]. Therefore, poor prognosis of gastric cancer patients with OPG expression found in the present study may be related to the inhibitory effect of OPG on apoptotic cell death. In addition, it has been reported in prostate cancer that expression of OPG is higher in metastatic tumors than in primary tumors [5]. To confirm whether this is also the case in gastric cancer, we should examine the expression of OPG in the primary tumors and metastases in the near future. However, Scatena and Giachelli [14] recently reported OPG involvement in endothelial cell survival. The effect of OPG on endothelial cells is affected by the level of TRAIL or a TRAIL-like death factor under the condition of serum starvation. The apoptosis inhibitory effect and survival extension of endothelial cells by OPG may stimulate neovascularization and establish suitable environment for proliferation and metastasis of tumor cells.

In the present data, OPG mRNA expression was observed in all the gastric carcinoma tissues examined and OPG protein was strongly positive in 65% of gastric carcinoma cases, although the expression was recognized in only the MKN-7 cell line among the five gastric carcinoma cell lines that we examined. OPG expression may be influenced by cancer–stromal interaction. Penno et al. [13] recently found that OPG secretion from prostate cancer cells is upregulated by IL-1 and TNFs. Therefore, it is possible also in gastric carcinoma tissues that IL-1 or TNFs, secreted by fibroblasts or the macrophages in the cancer stroma, interacts with tumor cells in a paracrine manner to induce OPG expression. However, among five gastric cancer cell lines used in this study, we have found that IL-1α is secreted into culture media by MKN-7 and TMK-1, while four cell lines expressed IL-1α mRNA in various levels [6]. Furthermore, the amount of OPG secretion is 20 times more by MKN-7 than by TMK-1. This evidence suggests that OPG expression by MKN-7 cells may be enhanced by IL-1α in an autocrine manner even without cancer-stromal interaction.

In conclusion, our results suggest that OPG may participate in stomach carcinogenesis, invasion and metastasis, possibly through inhibition of tumor cell apoptosis. OPG may serve as a novel molecular marker for aggressive gastric carcinoma.

Acknowledgements This work was supported, in part, by Grants-in-Aid from the Ministry of Education, Culture, Sports, and Technology of Japan, and the Ministry of Health, Labor, and Welfare of Japan. The authors thank Masayoshi Takatani and Mutsumi Ueda for their skillful technical assistance. The authors are also grateful to Noriko Sagawa for her secretarial assistance.

References

1. Brown JM, Corey E, Lee ZD, True LD, Yun TJ, Tondravi M, Vessella RL (2001) Osteoprotegerin and rank ligand expression in prostate cancer. Urology 57:611–616
2. Bucay N, Sarosi I, Dunstan CR, Morony S, Tarpley J, Capparelli C, Scully S, Tan HL, Xu W, Lacey DL, Boyle

WJ, Simonet WS (1998) Osteoprotegerin-deficient mice develop early onset osteoporosis and arterial calcification. Genes Dev 12:1260–1268
3. Emery JG, McDonnell P, Burke MB, Deen KC, Lyn S, Silverman C, Dul E, Appelbaum ER, Eichman C, DiPrinzio R, Dodds RA, James IE, Rosenberg M, Lee JC, Young PR (1998) Osteoprotegerin is a receptor for the cytotoxic ligand TRAIL. J Biol Chem 273:14363–14367
4. Griffith TS, Wiley SR, Kubin MZ, Sedger LM, Maliszewski CR, Fanger NA (1999) Monocyte-mediated tumoricidal activity via the tumor necrosis factor-related cytokine TRAIL. J Exp Med 189:1343–1354
5. Holen I, Croucher PI, Hamdy FC, Eaton CL (2002) Osteoprotegerin (OPG) is a survival factor for human prostate cancer cells. Cancer Res 62:1619–1623
6. Ito R, Kitadai Y, Kyo E, Yokozaki H, Yasui W, Yamashita U, Nikai H, Tahara E (1993) Interleukin 1 alpha acts as an autocrine growth stimulator for human gastric carcinoma cells. Cancer Res 53:4102–4106
7. Japanese Research Society for Gastric Cancer (ed) (1995) Japanese Classification of Gastric Carcinoma, 1st English edn. Kanehara & Co., Ltd, Tokyo, pp 38–65
8. Lacey DL, Timms E, Tan HL, Kelley MJ, Dunstan CR, Burgess T, Elliott R, Colombero A, Elliott G, Scully S, Hsu H, Sullivan J, Hawkins N, Davy E, Capparelli C, Eli A, Qian YX, Kaufman S, Sarosi I, Shalhoub V, Senaldi G, Guo J, Delaney J, Boyle WJ (1998) Osteoprotegerin ligand is a cytokine that regulates osteoclast differentiation and activation. Cell 93:165–176
9. Lin DL, Tarnowski CP, Zhang J, Dai J, Rohn E, Patel AH, Morris MD, Keller ET (2001) Bone metastatic LNCaP-derivative C4–2B prostate cancer cell line mineralizes in vitro. Prostate 47:212–221
10. Michigami T, Ihara-Watanabe M, Yamazaki M, Ozono K (2001) Receptor activator of nuclear factor kappaB ligand (RANKL) is a key molecule of osteoclast formation for bone metastasis in a newly developed model of human neuroblastoma. Cancer Res 61:1637–1644
11. Morony S, Capparelli C, Sarosi I, Lacey DL, Dunstan CR, Kostenuik PJ (2001) Osteoprotegerin inhibits osteolysis and decreases skeletal tumor burden in syngeneic and nude mouse models of experimental bone metastasis. Cancer Res 61:4432–4436
12. Ochiai A, Yasui W, Tahara E (1985) Establishment and characterization of human signet ring cell gastric carcinoma cell lines with amplification of the *c-myc* oncogene. Cancer Res 57:3669–3671
13. Penno H, Silfversward CJ, Frost A, Brandstrom H, Nilsson O, Ljunggren O (2002) Osteoprotegerin secretion from prostate cancer is stimulated by cytokines, in vitro. Biochem Biophys Res Commun 293:451–455
14. Scatena M, Giachelli C (2002) The alpha(v)beta3 integrin, NF-kappaB, osteoprotegerin endothelial cell survival pathway. Potential role in angiogenesis. Trends Cardiovasc Med 12:83–88
15. Simonet WS, Lacey DL, Dunstan CR, Kelley M, Chang MS, Luthy R, Nguyen HQ, Wooden S, Bennett L, Boone T, Shimamoto G, DeRose M, Elliott R, Colombero A, Tan HL, Trail G, Sullivan J, Davy E, Bucay N, Renshaw Gegg L, Hughes TM, Hill D, Pattison W, Campbell P, Boyle WJ et al (1997) Osteoprotegerin: a novel secreted protein involved in the regulation of bone density. Cell 89:309–319
16. Wiley SR, Schooley K, Smolak PJ, Din WS, Huang CP, Nicholl JK, Sutherland GR, Smith TD, Rauch C, Smith CA et al (1995) Identification and characterization of a new member of the TNF family that induces apoptosis. Immunity 3:673–682
17. Yasuda H, Shima N, Nakagawa N, Yamaguchi K, Kinosaki M, Mochizuki S, Tomoyasu A, Yano K, Goto M, Murakami A, Tsuda E, Morinaga T, Higashio K, Udagawa N, Takahashi N, Suda T (1998) Osteoclast differentiation factor is a ligand for osteoprotegerin/osteoclastogenesis-inhibitory factor and is identical to TRANCE/RANKL. Proc Natl Acad Sci USA 95:3597–3602
18. Zhang J, Dai J, Qi Y, Lin DL, Smith P, Strayhorn C, Mizokami A, Fu Z, Westman J, Keller ET (2001) Osteoprotegerin inhibits prostate cancer-induced osteoclastogenesis and prevents prostate tumor growth in the bone. J Clin Invest 107:1235–1244

Virchows Arch (2003) 443:152–158
DOI 10.1007/s00428-003-0844-9

ORIGINAL ARTICLE

A. Skalova · A. Cardesa · I. Leivo · M. Pfaltz · A. Ryska · R. Simpson · M. Michal

Sinonasal tubulopapillary low-grade adenocarcinoma. Histopathological, immunohistochemical and ultrastructural features of poorly recognised entity

Received: 6 February 2003 / Accepted: 14 April 2003 / Published online: 25 June 2003
© Springer-Verlag 2003

Abstract We present the clinicopathological, histological and immunohistochemical findings of six cases of primary tubulopapillary low-grade adenocarcinoma of the sinonasal tract with ultrastructural examination in one case. Due to its unique features, we believe that primary tubulopapillary low-grade adenocarcinoma of the sinonasal tract represents a tumour entity different from any tumours generally recognised in the sinonasal region. Our cases had an equal sex incidence, with an age range of 44–76 years. The tumour has a tendency to recur, but none of our six patients developed metastases. We feel that it is important to separate this tumour entity from other types of sinonasal adenocarcinomas that exhibit a papillary growth pattern, as they frequently pursue a much more aggressive clinical course than the tumours in this study.

Keywords Sinonasal · Tubulopapillary low-grade adenocarcinoma · Head and neck

A. Skalova · M. Michal (✉)
Sikl's Department of Pathology,
Laboratore Spec. Diagnostiky Medical Faculty Hospital,
Charles University,
Alej Svobody 80, 323 18 Plzen, Czech Republic
e-mail: michal@medima.cz
Tel.: +420-37-7104630
Fax: +420-37-7104650

A. Cardesa
Department of Pathology,
Hospital Clinic, University of Barcelona,
Barcelona, Spain

I. Leivo
Department of Pathology,
University of Helsinki,
Helsinki, Finland

M. Pfaltz
Institute of Clinical Pathology,
University Hospital of Zurich,
Switzerland

A. Ryska
Department of Pathology,
Medical Faculty, Charles University,
Hradec Kralove, Czech Republic

R. Simpson
Department of Histopathology,
Royal Devon and Exeter Hospital,
Exeter, UK

Introduction

Well-differentiated adenocarcinomas arising primarily within the sinonasal tract are uncommon, and only a few series have been published in the English language literature [3, 4, 10, 19]. Most of the reported nasopharyngeal adenocarcinomas arise from the seromucous glands [17], and they include distinctive salivary gland tumour types, such as adenoid cystic, mucoepidermoid and acinic cell carcinomas, in addition to mucous and papillary-cystic adenocarcinomas. The other reports describe neoplasms with apparent transition from normal surface epithelium of sinonasal mucosa [10, 19]. Histologically, these adenocarcinomas are characterised by papillary and glandular features and their histogenesis is most likely different from apparently similar neoplasms of salivary gland origin [10, 19]. The World Health Organization classification of sinonasal tumours recognises four major categories of primary adenocarcinomas: low-grade adenocarcinoma, papillary adenocarcinoma, intestinal type adenocarcinoma and polymorphous low-grade adenocarcinoma [16].

We have studied a series of six sinonasal tubulopapillary low-grade adenocarcinomas that do not conform to any of the above categories, but more closely resemble some of the cases Kleinsasser called "terminal tubulus adenocarcinoma" [11]. We believe the clinical, histological and ultrastructural features of our cases of sinonasal tubulopapillary low-grade adenocarcinomas are distinctive enough to allow differentiation from similar-appearing neoplasms, and that the tumours merit identification

as a new hitherto unrecognised subtype of a low-grade sinonasal adenocarcinoma category.

Materials and methods

Paraffin-embedded blocks were available in all cases. Sections were prepared in the conventional manner and stained with haematoxylin and eosin and by other methods, including Periodic Acid Schiff (PAS) with and without diastase digestion, mucicarmine, Alcian Blue (pH 2.5), and silver impregnation method according to Grimelius [2].

For immunohistochemical studies, 4-μm-thick sections were cut from paraffin blocks, mounted on slides coated with 3-aminopropyltriethoxy-silane (Sigma, St. Louis, MO), deparaffinized in xylene, and rehydrated in descending grades (100% to 70%) of ethanol. Sections were then subjected to heat-induced epitope retrieval by immersion in a 0.01 mol/l concentration of citrate buffer (pH 6.0) in microwave oven Micromed TTmega for 40 min. Endogenous peroxidase was blocked by a 5-min treatment with 3% hydrogen peroxide in absolute methanol. A panel of commercially available antibodies was applied to sections using the streptavidin-biotin-peroxidase technique, and appropriate positive and negative controls were employed. The sources and dilutions of the antibodies are listed in Table 1. The slides were incubated in an autostainer LabVision for 60 min at room temperature with primary antibodies. The bound antibodies were visualised using the supersensitive streptavidin-biotin-peroxidase complex (Novocastra, Newcastle upon Tyne, UK) and 3–3′-diaminobenzidine (Sigma) as chromogen. The slides were counterstained with Mayer's haematoxylin.

For electron microscopy, formalin-fixed wet tumour tissue samples of case 1 were washed in phosphate buffer, fixed briefly in 4% paraformaldehyde, postfixed in 1% osmium tetroxide, and embedded in epoxy resin (Durcupan-Epon). The sections were stained with uranyl acetate and lead citrate and examined using an electron microscope.

Clinical information was extracted from patient records. Follow-up data were obtained from the referring pathologists.

Results

Clinical findings

The clinical data are summarised in Table 2. There was an equal sex ratio, and the mean age at presentation was 59 years (range 44–76 years). All patients presented with nasal obstruction, and three complained of rhinitis or sinusitis. Patient 5 had recurrent headaches. Five tumours occurred in the nasal cavity and one in the left ethmoidal sinus. The size varied from 15 mm to 25 mm.

Treatment and follow-up

All tumours were removed surgically, mainly as small fragments. Patient 5 received post-operative radiotherapy. The initial pathological diagnosis in patient 1 was cylindrical cell adenoma of the nasal mucosa. He presented 8 months later with a slowly growing recurrent tumour filling the middle meatus of the nose and this was curetted. A second recurrence appeared 14 months later. Both recurrences were histologically identical to the primary tumour, and were later recognised as low-grade tubulopapillary adenocarcinoma arising from the nasal mucosa. At the time of the second recurrence, the patient underwent resection of the mandible for a histologically different and geographically separate moderately differentiated keratinising squamous cell carcinoma of usual type, which invaded bone and adjacent soft tissues. He died 7 months afterwards, due to cachexia and dissemination of the mandibular carcinoma, and residual tumour was noted within the nasal cavity. No autopsy was performed. Of the other patients, case 6 developed a recurrence after 2 years. This was excised and he remains free of disease after a further 2 years. Patients 2, 3, 4 and 5 were free of tumour after 12, 24, 24 and 14 months, respectively.

Table 1 Immunohistochemical findings*. *0* no significant staining, *F+* <5% cells show a definite reaction, + 5–25% cells positive, ++ 25–75% cells positive, +++ >75% cells positive. The figures are approximate, and where the percentage of positively staining cells overlaps two categories, the intensity of reaction is considered

Antiserum	Source	Dilution	Case 1	Case 2	Case 3	Case 4	Case 5
CAM5.2	Beckton-Dickinson	1:200	+++	+++	+++	+++	+++
AE1–3	Biotech	1:1000	+++	+++	+++	+++	+++
CK 14	NeoMarkers	1:1000	0	++	0	++	0
CK 19	Dako	1:100	+++	++	++	++	0
EMA	Dako	1:700	++	+	+	+	0
CEA	Dako	1:1000	0	0	+	0	0
GCDFP-15	Signet	1:200	0	0	0	0	0
MIA	Biogenex	1:800	F+	0	+	++	0
S-100	Dako	1:2500	++	+++	++	++	+
αSMA	Dako	1:1000	0	0	0	0	0
p63	Biotech	1:500	0	0	0	0	0
Calponin	Dako	1:50	0	0	0	0	0
GFAP	Biotech	1:100	0	0	0	10	0
CD10	Biotech	1:40	0	0	0	0	0
p53	Dako	1:50	F+	+	+	++	++
MIB1 (%)	Dako	1:1000	5	3	5	1	10
Leu-7 (CD57)	Biotech	1:150	0	0	0	0	0
Chromogranin A	Dako	1:400	0	0	0	0	0
HER2/neu	Novocastra	1:500	0	0	0	0	0

Table 2 Clinical data for six patients with sinonasal tubulopapillary low-grade adenocarcinoma. *RE* recurrence, *NED* no evidence of disease, *DOC* died of other causes

Case/age/sex	Size (cm)	Symptoms	Location/site	Treatment	Outcome
1/70/Male Plzen	2.5	Nasal obstruction, chronic hyperplastic rhinitis, 5 years	Nasal mucosa	Surgery only curettage of fragments	RE 8 months, RE 2 years, DOC with recurrent tumour, 2.5 years
2/44/Female Barcelona	1.5	Obstructed nose and "rhinitis",4 years	Left ethmoidal sinus	Surgery only with removal of the tumour in small fragments	NED 1 year
3/76/Female Helsinki	1.5	Nasal obstruction	Rear end of nasal cavity at the choana	Surgery only in small fragments	NED 2 years
4/54/Female Zurich	2.5	Nasal obstruction	Nasal mucosa	Surgery only, tumour sent in fragments	NED 2 years later lost for follow-up
5/57/Male Hradec Kralove	2.5	Obstructed nose, recurrent pansinusitis left side, 6 months	Nasal mucosa (middle concha) left	Surgical removal, postoperative actinotherapy	NED 14 months
6/53/Male Plzen	2 cm	Obstructed nose, recurrent	Posterior parts of nasal cavity	Surgical treatment	RE 2 years NED 2 years

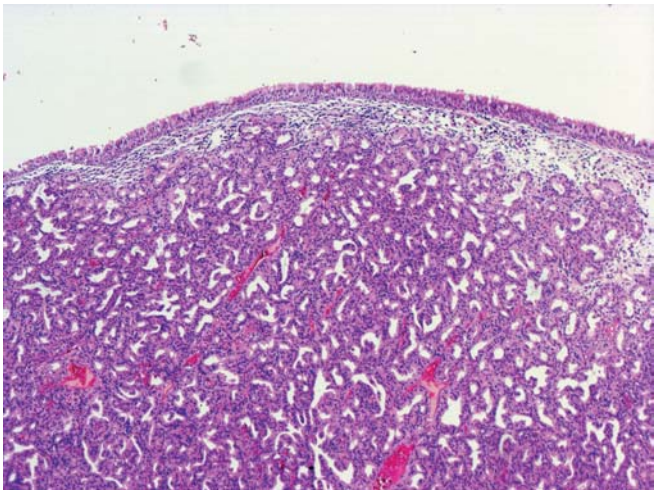

Fig. 1 Tumour consists of uniform small glands and tubular structures formed by a single row of cuboidal or columnar cells (haematoxylin and eosin, original magnification ×90)

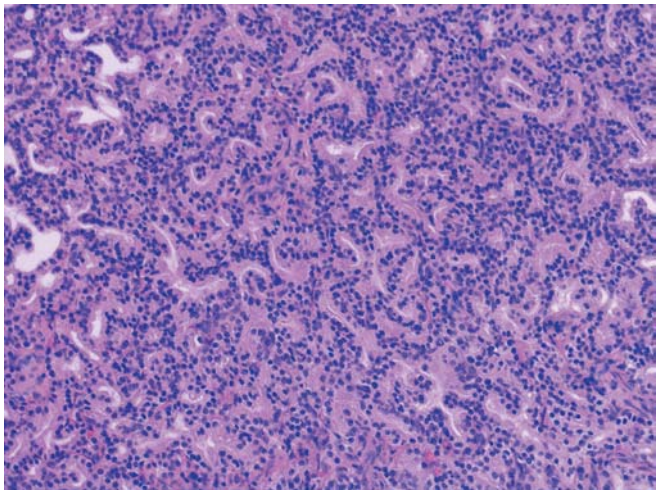

Fig. 2 Glands present crowded appearance with back-to-back pattern and little amount of intervening stroma (haematoxylin and eosin, original magnification ×180)

Histopathology

The original diagnosis was low-grade adenocarcinoma in three cases, once the diagnosis of cylindrical cell adenoma with oncocytic features was rendered, and in one case the contributing pathologist preferred diagnosis of acinic cell carcinoma arising in the minor salivary gland of nasal mucosa. In one case, the pathological diagnosis was a minor salivary gland adenoma.

All the tumours were histologically identical and consisted of uniform small glands and tubular structures formed by single row of cuboidal or columnar cells (Fig. 1). Glands showed crowded appearance with back-to-back pattern and little amount of intervening stroma (Fig. 2).

A distinctive portion of tumour tissue in each case showed a papillary growth pattern. Most papillae were simple and composed of a loose fibrovascular core and bland looking epithelium arranged in one row or in a bilayered pattern (Fig. 3). Some were more complex with a branching pattern (Fig. 4). Few papillae displayed a hyalinised stroma. Psammoma bodies and calcified foci were not seen. Scattered papillae in each case were covered by a distinctive bilayered epithelium composed of an inner eosinophilic layer and outer clear cells.

The cells lining both the glandular and papillary structures were bland, cuboidal or columnar with eosinophilic finely granular or clear cytoplasm, but no apical apocrine snouts were observed. The tumour cells were uniform, and nuclei were round with finely granular or optically clear looking chromatin (Fig. 5). Nucleoli were not conspicuous, and there was no significant nuclear polymorphism. Mitotic figures were extremely scanty. The tumours were devoid of cartilaginous differentiation.

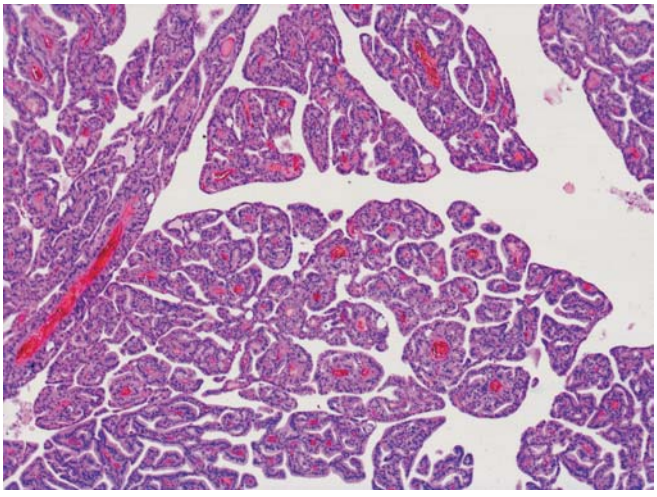

Fig. 3 Papillae composed of loose fibrovascular core and bland looking epithelium (haematoxylin and eosin, original magnification ×90)

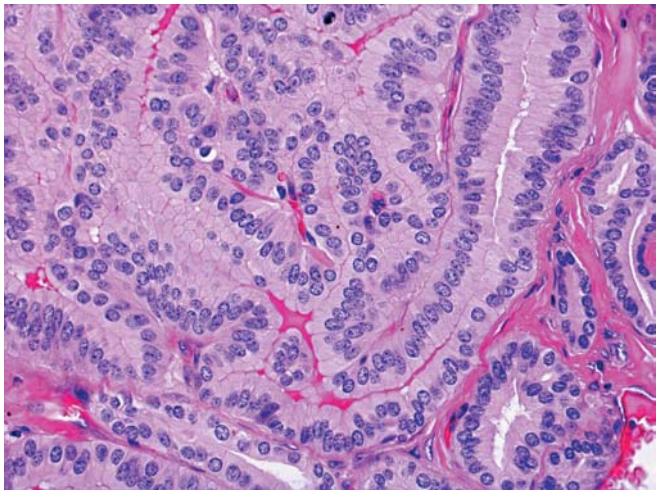

Fig. 5 The tumour cells are uniform with regular rounded nuclei with finely granular chromatin (haematoxylin and eosin, original magnification ×360)

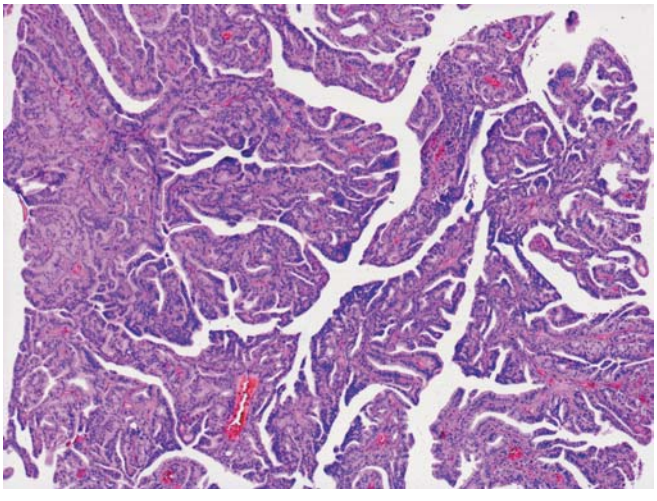

Fig. 4 Few papillae were more complex with branching growth pattern (haematoxylin and eosin, original magnification ×90)

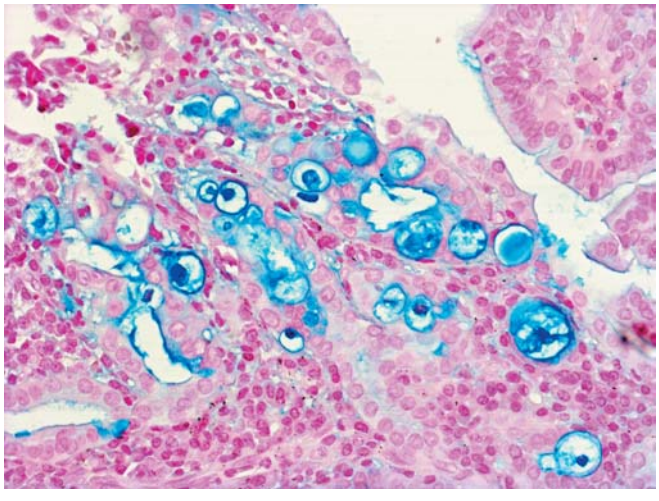

Fig. 6 Multiple intraepithelial mucin vacuoles (Alcian blue at pH 2.5, original magnification ×360)

One very distinctive feature was the presence of multiple tiny microcysts and vacuoles that looked as if they were located intracellularly. They stained with PAS (before and after diastase digestion), mucicarmine and alcian blue at pH 2.5 (Fig. 6). Mucicarmine and PAS stains were focally positive for intracytoplasmic and luminal mucin.

As the tumours were submitted in small fragments, full evaluation of the extent and pattern of invasion was not possible. However, there was no evidence of encapsulation, and some infiltration by the tumour margins into adjacent tissues could be identified, including the turbinate bone in case 5. No perineural and vascular invasion was seen in any case.

Immunohistochemistry

Sections from cases 1–5 were available for immunohistochemical study and the findings are summarised in Table 1. There was diffuse strong expression of broad-spectrum cytokeratins (AE1–3 and CAM5.2) in most cells in all cases. Staining for cytokeratins CK14 and CK19 was more restricted: CK14 was expressed in two cases in cells of the outer layer only of the tubular and papillary structures, while CK19 mostly decorated just the luminal cells. Reactivity for carcinoembryonic antigen (CEA) was seen only in one tumour in a minority of cells. Staining for S-100 protein was seen in most cells in all cases, but myoepithelial markers (smooth muscle actin αSMA, calponin, CD10, GFAP, and p63) were negative. There was no evidence of neuroendocrine differentiation, as chromogranin A and Leu-7 (CD57) were negative in all

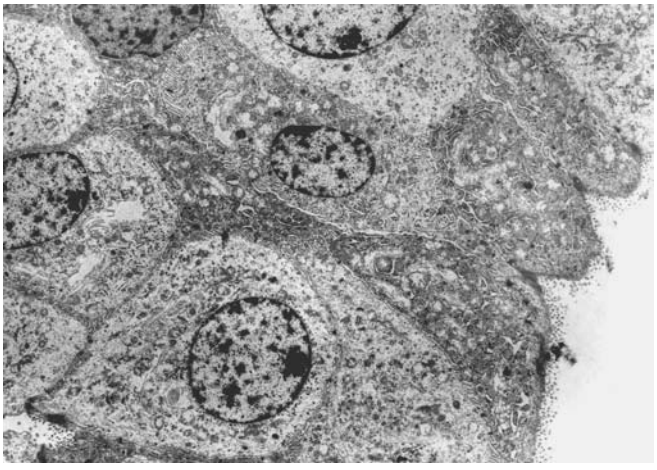

Fig. 7 Neoplastic cells have regular nuclei with finely dispersed chromatin and they possess numerous microvilli at their luminal surfaces (original magnification ×2000)

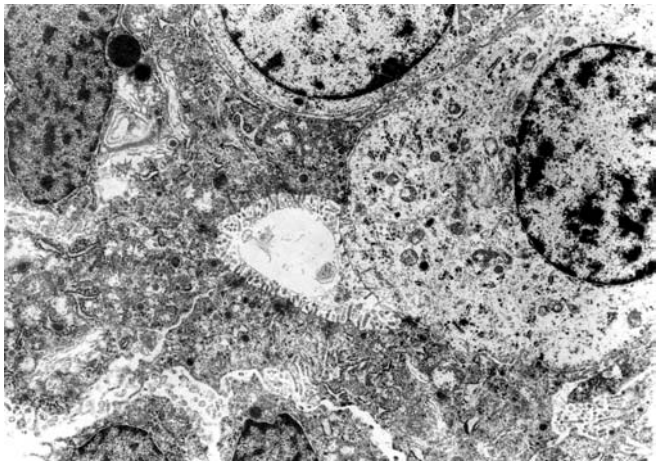

Fig. 9 Intercellular spaces are lined by microvilli. True gland contains junctional complexes and numerous microvilli projecting into the lumen (original magnification ×3200)

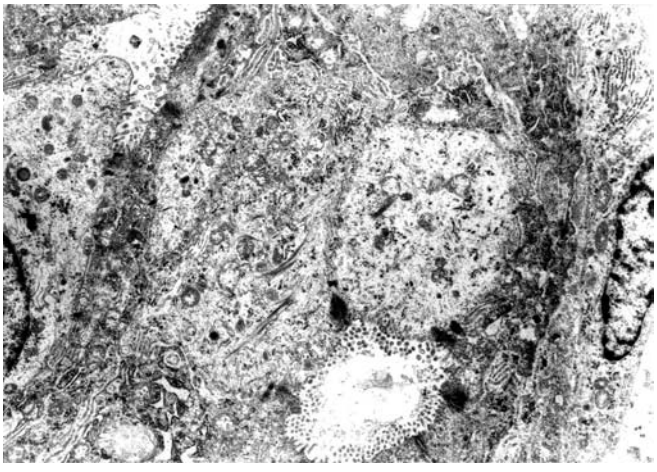

Fig. 8 The cells have numerous mitochondria and occasional randomly distributed keratin tonofilaments (original magnification ×3200)

cases. The neoplastic cells did not express HER-2/neu oncoprotein. Proliferative activity was low with a mean MIB1 index of 4.8% (range 1–10).

Ultrastructure

The neoplastic cells had regular nuclei with finely dispersed chromatin. The columnar epithelial cells possessed numerous microvilli at their luminal surfaces, and there were junctional complexes with desmosomes between adjacent cells (Fig. 7). Occasional randomly distributed keratin tonofilaments were seen, and few cells contained numerous mitochondria (Fig. 8). The multiple tiny microcysts and vacuoles thought to be intracellular using light microscopy were shown to be tiny true glandular lumina, and extracellular. Several adjacent cells participated in their formation and short, closely packed microvilli projected into the luminal spaces (Fig. 9).

Discussion

We have described a series of six tubulopapillary low-grade adenocarcinomas primarily arising from the sinonasal mucosa, which we believe represent a variant of low-grade sinonasal adenocarcinoma hitherto unrecognised in any classification. All six tumours were histologically identical, comprising a uniform population of cells lacking nuclear pleomorphism. The growth pattern was characteristic, being predominantly tubular with back-to-back glands, as well as focally papillary. There was also sparse mucus production with an unusual pattern.

A review of the literature disclosed only a few similar descriptions: in 1985, Kleinsasser reported seven tumours originating from the medial wall of the middle concha and ethmoidal sinus, calling them terminal tubulus adenocarcinoma [11]. The neoplastic cells were shown using light microscopy to have a striking similarity to the normal terminal tubules of seromucous glands, from which it was felt they arose [11]. In contrast, the tumours in the present study appear to originate from the surface epithelium, and, in cases 4 and 5, we could demonstrate a direct transition from the normal surface epithelium to the neoplasms. A surface origin from the mucosal epithelium has been previously proposed as the source for glandular neoplasms of the sinonasal tract [4, 10, 19]. Whereas some of the Kleinsasser tumours appear to be identical to our cases at the light microscopic level, his case 1 (as illustrated in Fig. 7, Fig. 8, Fig. 9, Fig. 10) seems to be different from the others and our cases, in that it shows a higher grade of malignancy. Furthermore, Fig. 5 and Fig. 6 show case 5 to have a cystadenomatous pattern with large

cystic spaces, neither of which was a feature of our cases [11].

One of the most characteristic and remarkable findings in tubulopapillary low-grade adenocarcinomas in our series was the presence of tiny intraepithelial spaces containing mucin stained by mucicarmine, PASD and alcian blue at pH 2.5, which by electron microscopy were seen to be intercellular microlumina. These have not been described before in terminal tubulus adenocarcinoma [11] and low-grade sinonasal adenocarcinomas [10, 19]. Similar mucinous intraepithelial microcysts are occasionally seen on a light microscopic level in columnar cell papillomas of the sinonasal tract [10, 16] and these tumours may be easily mistaken for tubulopapillary sinonasal low-grade adenocarcinoma. These intercellular spaces must be distinguished from true intracytoplasmic mucin filled vacuoles, which have been demonstrated, for example, in oncocytic (parietal cell) adenocarcinoma of the stomach [18] and in oncocytic papillary neoplasm of the pancreas [1]. In contrast to our cases, in the oncocytic tumours of gastrointestinal tract, electron microscopy clearly demonstrated intracytoplasmic location of those vacuoles (Fig. 9) [18].

Immunohistochemistry is not helpful in diagnosis with the exception of proliferative marker MIB1. All six tumours demonstrated very low proliferative activity in contrast to other types of glandular tumours of the sinonasal tract, such as intestinal-type adenocarcinoma [3]. The neoplastic cells expressed cytokeratins and S-100 protein in all cases, in contrast to which myoepithelial markers, including CD10 [14] were negative, thus supporting non-salivary origin for the tumour. Staining for epithelial membrane antigen and CEA (carcinoembryonic antigen) was variable.

The differential diagnoses of low-grade sinonasal tubulopapillary adenocarcinomas, which could be taken into consideration, are reflected in the original diagnoses from the submitting pathologists; this was low-grade adenocarcinoma in three cases and one each of cylindrical cell adenoma with oncocytic features, acinic cell carcinoma and “minor salivary gland adenoma”.

Sinonasal low-grade tubulopapillary adenocarcinoma is characterised by a general bland appearance. Thus, it must be distinguished from columnar cell papilloma [16]. Both tumour entities share several histological features, such as cytologically bland eosinophilic epithelium, mucin-containing intraepithelial lumina, regular simple papillary structures, absence of mitoses and nuclear uniformity. The distinguishing features of papilloma include stratified epithelium and lack of true glandular formation. Moreover, despite a very uniform bland appearance, sinonasal tubulopapillary low-grade adenocarcinomas display a true invasive growth pattern and they recur if treated inadequately.

The most important differential diagnoses are minor salivary gland neoplasms. Polymorphous low-grade adenocarcinoma of minor salivary glands of the oral cavity [5, 9] has been recently described in the sinonasal tract [12, 15, 20]. Polymorphous low-grade adenocarcinoma is characterised by histological blandness and cytological uniformity, but it differs from sinonasal tubulopapillary low-grade adenocarcinoma by its considerable morphological variability and frequent perineural invasion. The (probably related) low-grade papillary adenocarcinoma of minor salivary gland origin [13] is submucosal, does not secrete mucin and behaves more aggressively. The papillary-cystic variant of acinic cell carcinoma is only rarely seen in minor salivary glands, and it can be also confused with sinonasal tubulopapillary low-grade adenocarcinoma [6]. Both tumours have bland morphology, and they share S-100 protein positivity and presence of intraepithelial microcystic spaces. Acinic cell carcinoma, however, shows acinar cell differentiation (basophilic cytoplasm with PAS-positive diastase-resistant granules). Biologically, acinic cell carcinomas are more aggressive than sinonasal tubulopapillary low-grade adenocarcinoma [6].

Sinonasal tubulopapillary low-grade adenocarcinoma should be distinguished from more aggressive intestinal-type adenocarcinoma of nasal cavity [3, 8]. The papillary variant may be similar to the tumours of this study, but intestinal type adenocarcinoma is composed of columnar epithelium with goblet cells, it is more variable with mitotic figures, focal necrosis and nuclear polymorphism. These neoplasms show histological features reminiscent of colonic adenocarcinomas and generally pursue a much more aggressive clinical course [7].

In conclusion, we have described a new variant of low-grade sinonasal tubulopapillary adenocarcinoma that is characterised by a bland microscopic appearance and favourable clinical outcome. The authors have collectively seen many thousands of cases of tumours of the salivary glands and of the upper and lower respiratory tract, and no tumour outside of the sinonasal tract in their routine and consultation files showed similarity to the sinonasal tubulopapillary adenocarcinoma described here. The low-grade sinonasal tubulopapillary adenocarcinoma has a tendency to recur, but none of our patients showed metastatic disease. It is important to separate this tumour entity from other types of sinonasal adenocarcinomas with papillary growth pattern because they often pursue more aggressive behaviour.

Acknowledgements The authors are most grateful to Dr. Mukensnabl for preparing microphotographs. We also appreciate the technical assistance with the electron microscopy of Mr. Dostal.

References

1. Adsay NV, Adair CF, Heffess CS, Klimstra DS (1996) Intraductal oncocytic papillary neoplasms of the pancreas. Am J Surg Pathol 20:980–994
2. Bancroft JD, Cook HC (1994) Manual of histological techniques and their diagnostic application. Churchill Livingstone, New York, pp 229
3. Barnes L (1986) Intestinal-type adenocarcinoma of the nasal cavity and paranasal sinuses. Am J Surg Pathol 10:192–202
4. Batsakis JG (1970) Mucous gland tumors of the nose and paranasal sinuses. Ann Otol Rhinol Laryngol 79:557–562

5. Batsakis JG, Pinkston GR, Luna MA, Byers RM, Sciubba JJ, Tillery GW (1983) Adenocarcinoma of the oral cavity: a clinicopathologic study of terminal duct carcinomas J Laryngol Otol 97:825–835
6. Ellis GL, Corio RL (1983) Acinic cell carcinoma: a clinicopathologic analysis of 294 cases. Cancer 52:542–549
7. Franchi A, Gallo O, Santucci M (1999) Clinical relevance of the histological classification of sinonasal intestinal-type adenocarcinomas. Hum Pathol 30:1140–1145
8. Franquemont DW, Fechner RE, Mills SE (1991) Histologic classification of sinonasal intestinal-type adenocarcinoma. Am J Surg Pathol 15:368–375
9. Freedman PD, Lummerman H (1983) Lobular carcinoma of intraoral minor salivary glands. Oral Surg Oral Med Oral Pathol 56:157–165
10. Heffner DK, Hyams VJ, Hauck KW, Lingeman C (1982) Low-grade adenocarcinoma of the nasal cavity and paranasal sinuses. Cancer 50:312–322
11. Kleinsasser O (1985) Terminal tubulus adenocarcinoma of the nasal seromucous glands. A specific entity. Arch Otorhinolaryngol 241:183–193
12. Lloreta J, Serrano S, Coromunas JM, Ferres-Padro E (1995) Polymorphous low-grade adenocarcinoma arising in the nasal cavities with an associated undifferentiated carcinoma. Ultrastruct Pathol 19:365–370
13. Mills SE, Garland TA, Allen MS (1984) Low-grade papillary adenocarcinoma of palatal salivary gland origin. Am J Surg Pathol 8:367–374
14. Moritani S, Kushima R, Sugihara H, Bamba M, Kobayashi TK, Hattori T (2002) Availability of CD10 immunohistochemistry as a marker of breast myoepithelial cell on paraffin sections. Mod Pathol 15:397–405
15. Pittman CB, Zitsch RP (2002) Polymorphous low-grade adenocarcinoma of the tonsil: report of a case and review of the literature. Am J Otolaryngol 23:297–299
16. Shanmugaratnam K, Sobin L (1991) Histological typing tumours of the upper respiratory tract and ear, 2nd edn. World Health Organization, Geneva
17. Spiro RH, Koss LG, Hajdu SI, Strong EW (1973) Tumors of minor salivary gland origin: a clinicopathologic study of 492 cases. Cancer 31:117–129
18. Takubo K, Honma N, Sawabe M, Arai T, Izumiyama-Shimomura N, Kammori M, Sasajima K, Esaki Y (2002) Oncocytic adenocarcinoma of the stomach. Parietal cell carcinoma. Am J Surg Pathol 26:458–465
19. Wenig B, Hyams VJ, Heffner DK (1988) Nasopharyngeal papillary adenocarcinoma. A clinicopathologic study of a low-grade carcinoma. Am J Surg Pathol 12:946–953
20. Wenig BM, Harpaz N, DelBridge C (1989) Polymorphous low-grade adenocarcinoma of seromucous glands of the nasopharynx. A report of a case and a discussion of the morphologic and immunohistochemical features. Am J Clin Pathol 92:312–322

Virchows Arch (2003) 443:159–163
DOI 10.1007/s00428-003-0849-4

ORIGINAL ARTICLE

Umio Yamaguchi · Tadashi Hasegawa · Takanori Hirose · Kazunori Fugo · Tomoko Mitsuhashi · Michio Shimizu · Akira Kawai · Yasumasa Ito · Hirokazu Chuman · Yasuo Beppu

Sclerosing perineurioma: a clinicopathological study of five cases and diagnostic utility of immunohistochemical staining for GLUT1

Received: 5 February 2003 / Accepted: 21 April 2003 / Published online: 26 June 2003
© Springer-Verlag 2003

Abstract We reviewed five cases of sclerosing perineurial tumor of the hand. Four patients were male and one was female with ages ranging from 11 years to 49 years (mean 26 years). The predominant reason for consultation at the outpatient clinic was a slowly growing painless mass. The sites of involvement were the thumb in two cases, and the ring finger, middle finger and palm in one case each. The lesions were hard and firm, well-circumscribed white masses with a fibrous consistency ranging from 1.2 cm to 4.0 cm (mean 2.5 cm) in maximum dimension. Microscopically, all the tumors were composed of thick collagen and variable numbers of small, epithelioid cells exhibiting corded, trabecular and whorled growth patterns. Electron microscopy showed long cytoplasmic processes with a discontinuous basal lamina and occasional pinocytotic vesicles in the tumor cells. Immunohistochemically, most of the tumor cells were positive for epithelial membrane antigen, vimentin, collagen type IV and CD10, but not for S-100 protein, CD34, desmin and cytokeratin. We also observed that the tumor cells were positive for the human erythrocyte glucose transporter (GLUT1) antigen, suggesting that GLUT1 may be a useful marker for the identification of sclerosing perineurioma.

Keywords Sclerosing perineurioma · Epithelial membrane antigen · Human erythrocyte glucose transporter (GLUT1) · CD10

U. Yamaguchi · T. Hasegawa (✉) · K. Fugo · A. Kawai · Y. Ito · H. Chuman · Y. Beppu
Divisions of Orthopedic Oncology and Pathology,
National Cancer Center Hospital and Research Institute,
5-1-1 Tsukiji, Chuo-ku, 104-0045 Tokyo, Japan
e-mail: tdhasega@ncc.go.jp
Tel.: +81-3-35422511
Fax: +81-3-32482463

T. Hirose · T. Mitsuhashi · M. Shimizu
Department of Pathology,
Saitama Medical School,
Saitama, Japan

Introduction

Perineurial cells are normally found in the perineurium and are traditionally identified by their elongated bipolar cell processes upon light microscopic examination, lack of staining for S-100 protein immunohistochemically and ultrastructurally by a discontinuous basal lamina, occasional pinocytotic vesicles, moderate amounts of rough endoplasmic reticulum, scattered intermediate filaments, intercellular junctions and absence of interdigitating cell processes [3, 5, 13]. Identification of this cell type in histological materials is relatively easy because perineurium cells are immunoreactive for epithelial membrane antigen (EMA). Perineurioma is a rare soft tissue tumor composed of cells resembling those of the normal perineurium [1, 4, 8, 10, 12, 16, 19, 22]. Three distinct forms of perineurioma have been described: intraneural, extraneural and the recently reported sclerosing perineurioma [6]. Sclerosing perineurioma was first described by Fetsch and Miettinen in 1997 as a variant with distinctive clinical and histopathological features that shows a predilection for the hands of young adults [6]. Since this tumor is not a widely recognized entity, we report five new cases along with the results of immunohistochemical and ultrastructural studies to improve the definition of the clinicopathological features. In addition, we decided to use human erythrocyte glucose transporter (GLUT1) as a marker for this tumor because it is normally expressed in the perineurium of peripheral nerves and other tissues [24].

Materials and methods

Three of our five cases were retrieved from the pathology files of the National Cancer Center, Tokyo, and two from the Department of Pathology, Saitama Medical School, Saitama, Japan. All specimens were obtained by surgical excision, fixed in 10% (v/v) formalin and processed routinely for paraffin embedding. Five-micrometer-thick sections were stained with hematoxylin and eosin. Clinical details and follow-up information were obtained from hospital records. Case 5 has been reported previously [10] (Table 1).

Table 1 Clinical findings of five sclerosing perineuriomas

Case	Age (year)	Sex	Site	Symptom	Size (cm)	Follow-up	Recurrence ormetastasis
1	11	Female	Left palm	Mass	2.5×2.8×2.2	2 years 4 months	No
2	30	Male	Right thumb	Mass/slight pain	3.0×1.5×1.0	1 year 4 months	No
3	16	Male	Left ring finger	Mass	4.0×2.5	2 months	No
4	25	Male	Right middle finger	Mass	1.2×0.6×0.4	2.5 months	No
5	49	Male	Left thumb	Mass	1.7×1.7	3 years	No

Immunohistopathological studies were performed on paraffin sections using the avidin-biotin complex immunoperoxidase technique. We used monoclonal antibodies against EMA (E29, 1:100; Dako, Glostrup, Denmark), vimentin (V9, 1:200; Dako), desmin (D33, 1:100; Dako), alpha-smooth muscle actin (1A4, 1:100; Dako), CD34 (My10, 1:100; Becton Dickinson, San Jose, CA), CD10 (SS2/36, 1:200; Dako), muscle-specific actin (HHF35, 1:100; Enzo, New York, NY), Ki-67 (MIB-1, 1:100; Dako), collagen type IV (CIV22, 1:500; Dako) and cytokeratin (AE1/3, 1:100; Dako), and polyclonal antibodies against S-100 protein (1:2000; Dako) and human erythrocyte GLUT1 (1:200; Dako).

In one case (case 3), suboptimal material was available for electron microscopy. Small fresh fragments of tissue were fixed in 2% (v/v) glutaraldehyde, post-fixed in 1% (w/v) osmium tetroxide and embedded in epoxy resin. Thin sections were stained with uranyl acetate and lead citrate.

Results

Clinical features

The ages of the patients at the time of surgery ranged from 11 years to 49 years (mean 26 years; Table 1). Four patients were male and one was female. The preoperative duration ranged from 6 months to 120 months (mean 62 months). The predominant reason for consultation at the outpatient clinic was a slowly growing painless mass, although slight pain was present in one case (case 2). None of the patients had any signs of neurofibromatosis or a history of surgery. One patient had a local injury from a thorn (case 5). The sites of involvement were the thumb in two cases, and the ring finger, middle finger and palm in one case each. The tumors were firm, well-circumscribed and nodular or ovoid white masses with a fibrous consistency, ranging from 1.2 cm to 4.0 cm (mean 2.5 cm) in maximum dimension. The cut surfaces of these tumors were quite similar, showing a solid, whitish and homogeneous appearance. The average follow-up period was 17 months (range 2–36 months), and there was no evidence of recurrence or metastasis following simple local excision.

Light microscopy

Histologically, all the tumors were hypocellular and surrounded by a thin fibrous pseudocapsule (Fig. 1A). In an abundantly collagenous background, there were small, oval epithelioid or plump spindle cells scattered and arranged in a corded, whorled or trabecular pattern

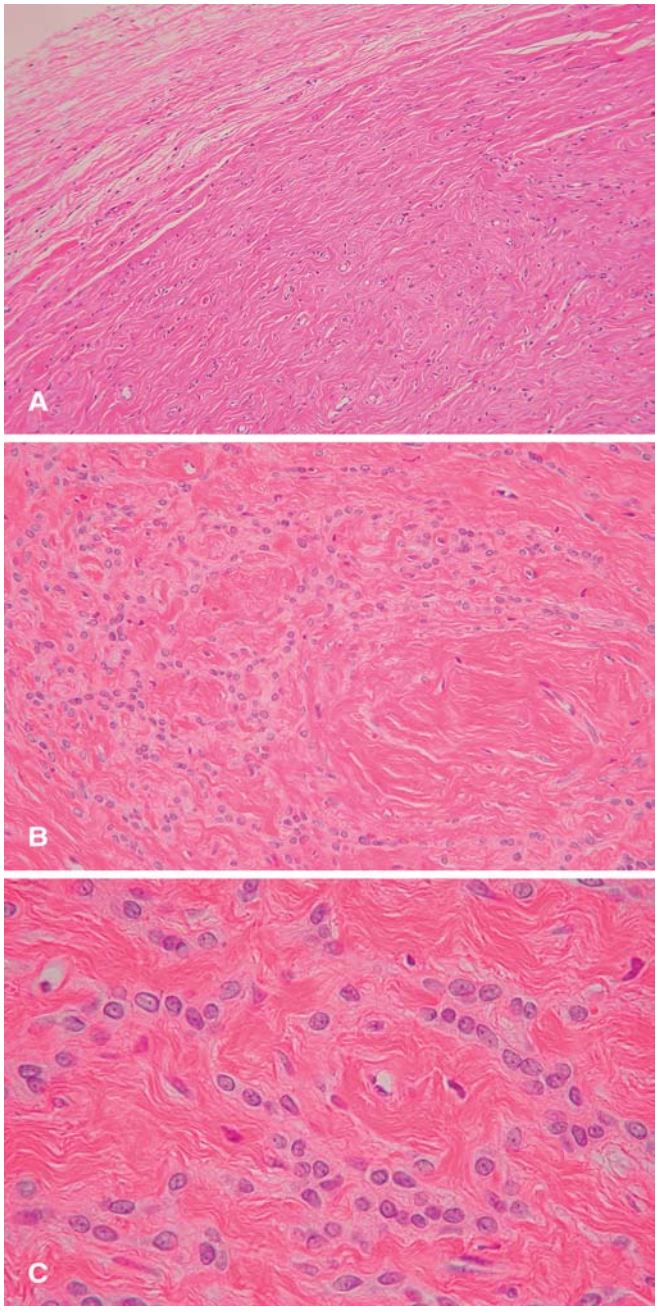

Fig. 1 Histology of sclerosing perineuriomas. **A** Tumor was sharply surrounded with a thin fibrous pseudocapsule. Original magnification, ×100. **B** Low-power view reveals whorls and cords of tumor cells within a dense stroma. Original magnification, ×200. **C** Tumor cells have oval nuclei, inconspicuous eosinophilic nucleoli and indistinct cytoplasmic borders. Original magnification, ×400

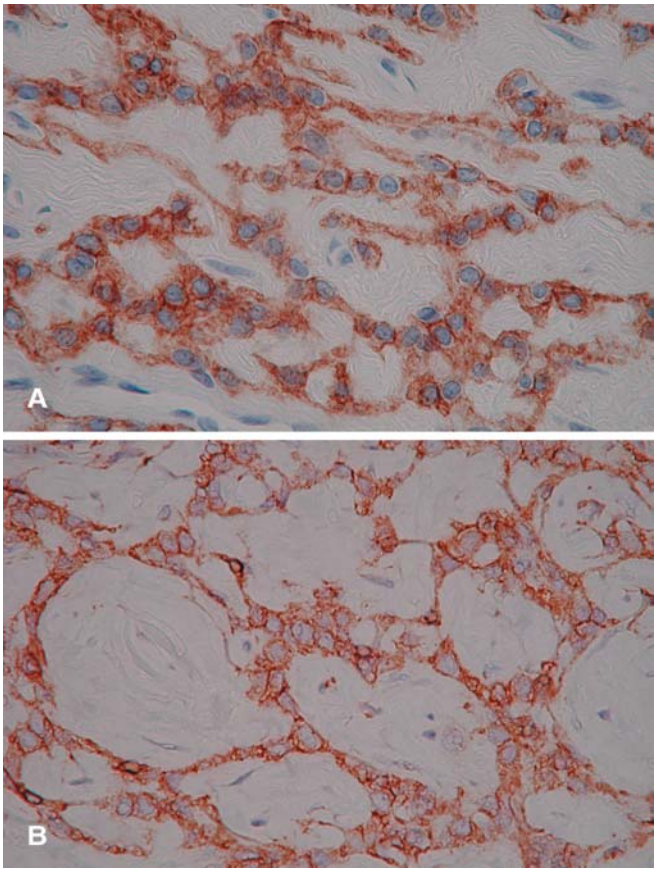

Fig. 2 Immunohistochemical staining of a sclerosing perineurioma. Original magnification, ×400. **A** Tumor cells show striking positivity for epithelial membrane antigen (EMA). **B** In this case, tumor cells also show diffuse, membranous staining for human erythrocyte glucose transporter (GLUT1). The intensity of GLUT1 expression is the same as that of EMA

(Fig. 1B). The small epithelioid and plump spindle cells had nuclei with a delicate chromatin pattern, an inconspicuous eosinophilic nucleolus and indistinct cell borders (Fig. 1C). Scattered small blood vessels were conspicuous among the tumor cells within the hyalinized stroma, but vascular proliferation was never prominent. Small foci of necrosis, that is, ischemic infarction—possibly as a result of thrombosis—were identified in one case (case 2). In two cases (cases 4 and 5), tiny nerve fibers with residual Schwann cells were seen outside the tumors but never inside the tumors. Nuclear pleomorphism or hyperchromasia was not evident.

Immunohistochemistry

All cases showed at least focal membranous positivity for EMA (Fig. 2A) and vimentin. The staining was strong in most cases. Membranous immunoreactivity for collagen type IV was noted around the cells in each case. CD10 was also positive in all cases. S-100 protein, desmin, CD34, Ki-67, muscle-specific actin, cytokeratin, alpha-smooth muscle actin and p53 were negative in all cases. Immunostaining for GLUT1 was positive in all five cases (Fig. 2B). Because erythrocytes always stain positively for GLUT1, they served as an internal positive control. In four of the five cases, the immunoreactivity was strong and diffuse, and in one case (case 5) it was weak and focal. The perineurial cells that formed sleeves around bundles of nerve fibers in the surrounding soft tissues were also GLUT1 positive (cases 4 and 5).

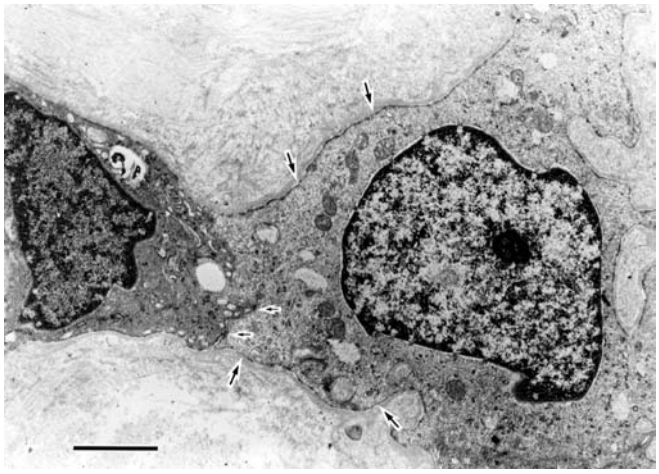

Fig. 3 Ultrastructure of a sclerosing perineurioma. Pinocytotic vesicles (*large arrows*) and an external basal lamina are observed on the cell surface. The cytoplasmic processes are joined by rudimentary cell junctions (*small arrows*). Original magnification, ×10,000. *Bar* 2 μm

Electron microscopy

Ultrastructurally, the tumor cells had a spindled or epithelioid morphology with long, straight or slightly curvilinear cytoplasmic processes surrounded by an abundant collagenous stroma (Fig. 3). The nuclei were elongated or ovoid, with abundant euchromatin with clumpy heterochromatin. The nucleoli were often inconspicuous, and the cytoplasm was relatively scant and contained scattered ribosomes, polyribosomes, rough endoplasmic reticulum, mitochondria and many intermediate filaments. The cell processes were joined by rudimentary cell junctions and bordered by a discontinuous external basal lamina. Electron-dense cell membrane plaques and pinocytotic vesicles were also noted.

Discussion

Sclerosing perineurioma is a distinctive clinicopathological entity that differs from the other two variants of perineurioma—intraneural and extraneural—and has a strong predilection for the digits and palms of young adults [6]. Microscopically, the tumor is hypocellular with an extensively collagenized stroma and contains small

epithelioid and plump spindle cells showing a characteristic corded or whorled growth pattern [6]. The tumor is EMA positive and S-100 protein negative. Ultrastructurally, there are long interdigitated cytoplasmic processes, pinocytotic vesicles, dense subplasmalemmal plaques, junction complexes and a discontinuous basal lamina [15]. Clonal chromosomal abnormalities of chromosome 10 and a cryptic deletion of the 5′BCR and NF2 gene loci on chromosome 22 have been observed in this tumor [21]. In the original series reported by Fetsch and Miettinen, residual Schwann cells and axons were not identified [6], and none was found in our five cases. The reason for this absence of axons and Schwann cells in sclerosing perineurioma is unclear, but could be related to the small size of the affected nerve segment, its susceptibility to degenerative change and/or a delay in presentation due to the limited nature of the sensory deficit [6]. Other authors, however, have documented the presence of axons and Schwann cells in the centers of perineuriomas [2, 12, 21]. Burgues et al. reported a case of a cutaneous form of perineurioma with combined features of the intraneural and sclerosing varieties and found evidence of Pacinian differentiation; they designated this form a "sclerosing Pacinian-like perineurioma" [2]. A patient who presented with multiple lesions has also been reported [12]. Reticular perineurioma, a further subgroup of soft-tissue perineurioma, which shows a predominantly reticular growth pattern, has been described recently [9].

To our knowledge, at least 27 cases of sclerosing perineurioma, including our new cases, have been reported in the English-language literature. In all of these cases, the tumors occurred in the fingers and palms of young adults. The reason for this tumor's strong predilection for the hands of young adults, particularly young males, is unknown. Further investigation is required to determine whether the tumor is a benign neoplasm or a secondary reactive change following trauma. It may reflect a traumatic etiology, since young males tend to be more prone to injuries and tolerant of minor, chronic disfigurement [10].

Since sclerosing perineurioma is poorly recognized, it tends to be misdiagnosed as other benign and low-grade soft tissue tumors with spindle-cell morphologies. The differential diagnoses have been discussed in detail by other authors [2, 6, 10, 12]. Peripheral nerve sheath tumors and fibrous tumors are the most important differential diagnoses; these include epithelioid neurofibroma [6], traumatic and Morton's neuroma, schwannoma [2], meningioma, neurothekeoma, nerve sheath myxoma [10], calcifying fibrous tumor [6], fibroma of the tendon sheath, sclerotic fibroma of Cowden's disease [6, 12], keloid and acquired digital fibrokeratoma [10]. Other conditions that need to be considered are epithelioid hemangioendothelioma, tenosynovial giant cell tumor, sclerosing adnexal tumor [6], glomus tumor [6, 12], nodular fasciitis, proliferative fasciitis and epithelioid sarcoma [10].

Human erythrocyte GLUT1 is a member of a family of six human epithelial glucose transporters [18] and has been shown to vary in expression according to epithelial type, growth rate, transformation and malignancy [24]. It is normally expressed in erythrocytes, the blood–brain barrier, the perineurium of peripheral nerves, renal tubules, the germinal centers of reactive lymphoid tissue and placenta [24]. It is also expressed in a significant number of carcinomas in a variety of organs and is not always detected in benign tumors by means of immunohistochemistry [24]. In our small series of sclerosing perineurioma, GLUT1 showed strong positive staining, with an intensity similar to that of erythrocytes in tissue sections, and in the perineurial cells that formed sleeves around bundles of nerve fibers outside the tumor lesions.

With regard to the expression of GLUT1 in other benign peripheral nerve sheath tumors, we have found that GLUT1 immunoreactivity is negative in neoplastic cells and localized only at normal perineurium-like structures in schwannomas and neurofibromas [11]. In addition, both tumors can be distinguished easily from sclerosing perineurioma by their EMA negativity and S-100 protein positivity. Meningiomas, which rarely arise in soft tissue of the extremities and show an EMA-positive and S-100 protein-negative immunophenotype [23], should be considered in the differential diagnosis. In this situation, GLUT1 immunostaining is helpful because meningiomas that we have examined have been consistently negative for GLUT1 (unpublished observation).

Likewise, a recent study showed that normal perineurial cells and perineuriomas were positive for claudin-1, a novel integral membrane protein that is localized at tight junctions [7]. Although the present study showed that CD10 was positive in all five cases, CD10 immunoreactivity has been found in a wide range of benign and malignant tumors [14, 17]. Thus, it seems that the CD10 antigen lacks specificity for the diagnosis of sclerosing perineurioma.

In summary, we have reported five cases of sclerosing perineurioma whose clinical outcomes were very satisfactory. No recurrence or metastasis was identified following conservative excision. Our study revealed that sclerosing perineurioma expresses GLUT1, suggesting that the antigen may be a useful marker for identification of this tumor.

References

1. Ariza A, Bilbao JM, Rosai J (1988) Immunohistochemical detection of epithelial membrane antigen in normal perineurial cells and perineurioma. Am J Surg Pathol 12:678–683
2. Burgues O, Monteagudo C, Noguera R, Robert A, Molina I, Llombart-Bosch A (2001) Cutaneous sclerosing Pacinian-like perineurioma. Histopathology 39:498–502
3. Erlandson RA (1985) Peripheral nerve sheath tumors. Ultrastruct Pathol 9:113–122
4. Erlandson RA (1991) The enigmatic perineurial cell and its participation in tumors and in tumorlike entities. Ultrastruct Pathol 15:335–351
5. Erlandson RA, Woodruff JM (1982) Peripheral nerve sheath tumors, an electron microscopic study of 43 cases. Cancer 49:273–287

6. Fetsch JF, Miettinen M (1997) Sclerosing perineurioma: a clinicopathologic study of 19 cases of a distinctive soft tissue lesion with a predilection for the fingers and palms of young adults. Am J Surg Pathol 21:1433–1442
7. Folpe AL, Billings SD, McKenney JK, Walsh SV, Nusrat A, Weiss SW (2002) Expression of claudin-1, a recently described tight junction-associated protein, distinguishes soft tissue perineurioma from potential mimics. Am J Surg Pathol 26:1620–1626
8. Giannini C, Scheithauer BW, Jenkins RB, Erlandson RA, Perry A, Borell TJ, Hoda RS, Woodruff JM (1997) Soft tissue perineurioma: evidence for an abnormality of chromosome 22, criteria for diagnosis, and review of the literature. Am J Surg Pathol 21:164–173
9. Graadt van Roggen JF, McMenamin ME, Belchis DA, Rosenberg AE, Fletcher CDM (2001) Reticular perineurioma: a distinctive variant of soft tissue perineurioma. Am J Surg Pathol 25:485–493
10. Hirose T, Scheithauer BW (1999) 'Sclerosing' perineurioma: a tumor variant? Int J Surg Pathol 7:133–140
11. Hirose T, Tani T, Shimada T, Ishizawa K, Shimada S, Sano T (2003) Immunohistochemical demonstration of EMA/Glut1-positive perineurial cells and CD34-positive fibroblastic cells in peripheral nerve sheath tumors. Mod Pathol 16:293–298
12. Huang HY, Sung MT (2002) Sclerosing perineuriomas affecting bilateral hands. Br J Dermatol 146:129–133
13. Johnson PC (1991) Peripheral nerve. In: Davis RL, Robertson DM (eds) Textbook of neuropathology, 2nd edn. Williams and Wilkins, Baltimore, pp 1004–1087
14. Kanitakis J, Bourchany D, Claudy A (2000) Expression of the CD10 antigen (neutral endopeptidase) by mesenchymal tumors of the skin. Anticancer Res 20:2539–3544
15. Lazarus S, Trombetta L (1978) Ultrastructural identification of a benign perineurial cell tumor. Cancer 41:1823–1829
16. Mentzel T, Dei Tos AP, Fletcher CDM (1994) Perineurioma (storiform perineurial fibroma): clinicopathologic analysis of four cases. Histopathology 25:261–267
17. Mikami Y, Hata S, Kiyokawa T, Manabe T (2001) Expression of CD10 in mullerian mixed tumors and adenosarcomas: an immunohistochemical study. Mod Pathol 15:923–930
18. Mueckler, M (1994) Facilitative glucose transporters. Eur J Biochem 219:713–725
19. Rank JP, Rostad SW (1998) Perineurioma with ossification: a case report with immunohistochemical and ultrastructural studies. Arch Pathol Lab Med 122:366–370
20. Robson AM, Calonje E (2000) Cuteneous perineurioma: a poorly recognized tumor often misdiagnosed as epithelioid histiocytoma. Histopathology 37:332–339
21. Sciot R, Dal Cin P, Hademeijer A, De Smet L, Van Damme B, Van den Berghe H (1999) Cutaneous sclerosing perineurioma with cryptic NF2 gene deletion. Am J Surg Pathol 23:849–853
22. Smith K, Skelton H (1998) Cutaneous fibrous perineurioma. J Cutan Pathol 25:333–337
23. Tomaru U, Hasegawa T, Hasegawa F, Kito M, Hirose T, Shimoda T (2000) Primary extracranial meningioma of the foot: a case report. Jpn J Clin Oncol 30:313–317
24. Younes M, Lechago LV, Somoano JR, Mosharaf M, Lechago J (1996) Wide expression of the human erythrocyte glucose transporter Glut1 in human cancers. Cancer Res 56:1164–116

Virchows Arch (2003) 443:164–169
DOI 10.1007/s00428-003-0836-9

ORIGINAL ARTICLE

Ronald Boonstra · Alice Koning · Mirjam Mastik · Anke van den Berg · Sibrand Poppema

Analysis of chromosomal copy number changes and oncoprotein expression in primary central nervous system lymphomas: frequent loss of chromosome arm 6q

Received: 13 December 2002 / Accepted: 14 April 2003 / Published online: 12 June 2003
© Springer-Verlag 2003

Abstract Primary central nervous system lymphoma (PCNSL) is a rare disease. A small number of cytogenetic studies of PCNSL have been conducted and several reports have been published on associated molecular and protein expression data. We combined these approaches in a series of eight PCNSL cases, analyzing the chromosomal abnormalities using comparative genomic hybridization (CGH), testing for Epstein Barr virus (EBV) involvement by in situ hybridization for EBER, assessing expression of p53, Bcl-2, Bcl-6 and CD10 by means of immunohistochemistry, and screening for mutations of the *TP53* gene by DGGE. *TP53* gene mutations and EBV expression were not detected. Most of the cases showed p53, Bcl-6 and Bcl-2 protein expression. CGH revealed DNA copy number changes in all eight cases. The most frequent changes were gains of chromosome 12 (63%), chromosome 18 (50%) and 20q (38%), and loss of chromosome arm 6q (75%). No correlation between protein expression and chromosomal abnormalities was found in these eight cases. Although gains of chromosome 12, 18 and 20q and loss of 6q have also been reported in systemic diffuse large B-cell lymphomas, the frequency of 6q deletion is clearly higher in PCNSL. This creates a similarity to primary lymphomas of the testes that also frequently have deletions of 6q. This suggests that suppressor genes located on chromosome 6q may play a role in the development of lymphomas at immunoprivileged sites, like the CNS.

Keywords CGH · PCNSL · del 6q · Oncoprotein

R. Boonstra · A. Koning · M. Mastik · A. van den Berg · S. Poppema
Department of Pathology and Laboratory Medicine,
Department of Genetics, University Medical Center Groningen,
The Netherlands

S. Poppema (✉)
Department of Pathology and Laboratory Medicine,
University Hospital Groningen, P.O. Box 30.001,
9700 RB Groningen, The Netherlands
e-mail: s.poppema@med.rug.nl
Tel.: +31-503-632881
Fax: +31-503-632510

Introduction

Primary central nervous system lymphoma (PCNSL) is a relatively rare neoplasm accounting for about 1% of all lymphomas [14]. During the last decades, the incidence of PCNSL has been increasing in both immunosuppressed and immunocompetent patients [6, 8, 21]. The majority of PCNSL is of B-cell origin and is usually of the diffuse large B-cell type [2, 14, 25].

The molecular pathology of PCNSL is still unclear. Only a few studies describe the expression of oncogenic molecules in PCNSL. PCNSL in immunocompromised as well as immunocompetent patients usually express Bcl-2, Bcl-6 and p53, although over-expression of Bcl-6 and p53 seems to occur more frequently in immunocompetent than in immunocompromised cases [3]. Epstein-Barr virus (EBV) infection is strongly associated with acquired immunodeficiency syndrome (AIDS)-related PCNSL and only rarely found in AIDS-unrelated PCNSL [4, 10, 18].

Thus far, only approximately 50 cases of PCNSL have been cytogenetically analyzed, using classical cytogenetics or CGH [11, 13, 28, 30, 32]. The findings suggest that chromosomal abnormalities like gain of chromosome 1, 12, or 18 and loss of 6q found in PCNSL are similar to those of systemic large B-cell lymphoma. In this study, we analyzed EBER, Bcl-2, Bcl-6, CD10 and p53 expression, the occurrence of *P53* mutations and the presence of chromosomal abnormalities by CGH.

Materials and methods

Patients

Eight cases of PCNSL from immunocompetent patients (7 male, 1 female) were selected from the frozen tissue bank at the University Medical Center Groningen. The diagnosis was confirmed by histological review and immunophenotyping, and the cases were reclassified according to the World Health Organization (WHO) classification. Tissue samples were obtained from tumor resection in three patients and from stereotactic biopsies in five patients. None of the patients received chemotherapy or radiation therapy before surgery (Table 1).

Table 1 Overview of clinical data in eight cases of primary central nervous system lymphoma (PCNSL). *DLBL* diffuse large B-cell lymphoma

Case	Biopsy location	WHO classification	Kiel classification	Sex	Age at diagnosis (years)
1	Intra spinal lumbar	DLBL	Immunoblastic	Male	62
2	Right temporal	DLBL	Polymorphic centroblastic	Female	63
3	Left frontal parietal	DLBL	Polymorphic centroblastic	Female	65
4	Deep left frontal basal	DLBL	Centroblastic	Male	54
5	Left cerebral hemisphere	DLBL	Immunoblastic	Male	59
6	Deep left hemisphere	DLBL	Polymorphic centroblastic	Male	50
7	Bifrontal	DLBL	Immunoblastic	Male	60
8	Left frontal/left parietal	DLBL	Immunoblastic	Male	59

EBER in situ hybridization

In situ hybridization (ISH) was performed to detect EBER 1–2 mRNAs using a fluorescein-conjugated EBV (EBER) peptide nucleic acid probe (Dako, Glostrup, Denmark) on paraffin tissue sections. Alkaline phosphatase conjugated anti-FITC sheep IgG Fab fragments (Roche, Mannheim, Germany) were used as a second step. The visualization was performed with 5-bromo-4-chloro-3-indolyl-phosphatase and 4-Nitrobluetetrazolium (Roche Corporation, Indianapolis, USA) and $MgCl_2$. Positive (EBV-positive Hodgkin lymphoma) and negative controls were performed and also two cases of PCNSL in human immunodefiency virus (HIV)-positive patients were included.

Immunohistochemistry

For immunohistochemical staining, a mouse anti-human p53 antibody (Bp53–12–1, Bio Genex, San Ramon, CA, USA), a mouse anti-human CD10 antibody (Novocastra Laboratories, Newcastle upon Tyne, United Kingdom), a mouse anti-human Bcl-2 antibody (Dako, Copenhagen, Denmark) and a mouse Bcl-6 monoclonal antibody PG-B6p [9] were used on paraffin sections following heat-induced antigen retrieval. Peroxidase-labeled rabbit anti-mouse followed by peroxidase-labeled goat anti-rabbit antibodies (Dako, Copenhagen) and peroxidase enzyme staining with diaminobenzidine and H_20_2 were used to visualize the p53 and CD10 protein-positive cells. Rabbit anti-mouse antibody followed by APAAP with two repeats and alkaline phosphatase staining with 5-bromo-4-chloro-3-indolyl-phosphatase and 4-nitrobluetetrazolium (Roche Corporation) were used to visualize the BCL-2 and BCL-6 protein.

The p53 protein staining was designated as + (weak), with a couple of scattered p53 protein positive tumor cells, ++ (moderate), with a substantial proportion of p53 protein positive tumor cells, varying in intensity or +++ (strong), with almost all the tumor cells strongly p53 protein positive. Bcl-2, Bcl-6 and CD10 protein were designated as + (positive), ± (weak positive) or − (negative). For Bcl-6, the total percentage of positive tumor cells was also estimated.

Laser micro dissection

Serial tissue sections (20 μM) from PCNSL were mounted on frame foil membranes (LDM-Foil 76×26 mm; Leica Microsystems Wetzlar Gmbh, Wetzlar, Germany) and stained with hematoxylin. Sections containing tumor cells were identified and microdissected with a Laser Microdissection System (LMD) according to the manufacturer's instructions (Leica Microsystems Wetzlar Gmbh). Cells were collected in 400 μl SE buffer containing 1% sodium dodecyl sulfate (SDS) and proteinase K (0.4 mg/ml) and digested overnight at 55°C. Genomic DNA was purified using standard chloroform/salt extraction.

From the PCNSL samples consisting of more than 70% of tumor cells, six serial tissue sections of 20 μM were cut and used for the isolation of genomic DNA using the same protocol. DNA was solved in TE at a concentration of 200 μg/ml

TP53 gene mutation screening

External and internal primer sequences used for the separate amplification of exons 5–8 of the *TP53* gene were derived from published data [12]. Mutation detection was carried out as previously described [20]. The PCR products were analyzed with denatured gradient gel electrophoreses (DGGE). From the cases that showed an aberrant four-banded pattern, the aberrant homoduplex band was excised, eluted in TE and re-amplified in a volume of 75 µl containing 0.2 mM dNTP, 2.5 U *Taq* polymerase (Amersham Pharmacia Biotech, Roosendaal, The Netherlands), reaction buffer and 375 ng of each primer (without GC-clamps) with a 5′ M13 sequence which allows direct sequencing of the PCR products (forward: 5′-cgacgttgtaaaacgacggccagt-3′ and reverse: 5′-tttcacacaggaaacagctatgac-3′). Sequence analysis was carried out as previously described [20].

Comparative genomic hybridization

Comparative genomic hybridization (CGH) was performed as described by Kallioniemi et al. with some minor adjustments [16]. Approximately 1 μg of test DNA and 1 μg of control DNA were labeled by nick translation with either Biotin-16-dUTP or digoxigenin-11-dUTP (Roche Molecular Biochemicals). Aliquots of 400 ng labeled test DNA and control DNA were ethanol precipitated with 50 μg unlabeled human Cot1 DNA (Life Technologies Breda, the Netherlands) and 10 μg of salmon sperm DNA (Sigma, Zwijndrecht, the Netherlands). The DNA mixture was dissolved in 15 μl hybridization mixture [50% deionized formamide, 2× sodium saline citrate (SSC), 10% dextran sulfate, pH 7.0] and applied to a normal male metaphase slide (Vysis, Downers Grove, IL).

The slide with the DNA hybridization mixture was denatured at 74°C for 3 min and hybridized at 37°C for 72 h. Post-hybridization washes three times in 4× SSC, and three times in 0.1× SSC at 60°C were performed before immunochemical detection. Immunochemical detection was performed using streptavidin-FITC (Roche Molecular Biochemicals) and l anti-DIG-TRITC (Roche Molecular Biochemicals) in 4× SSC, Tween-20 and 1% fat-free powder milk for 1 h to detect the biotin-labeled tumor DNA and digoxigenin-labeled normal DNA. The slides were mounted with anti-fading solution containing 4,6-diamidino-2-phenylindole (DAPI), used as a counter stain (Vectashield, Vector laboratories, Burlingame, CA).

The grayscale images of the three different fluorochromes were captured using a Leica DMRA fluorescence microscope equipped with DAPI, FITC and TRITC filters (Chroma, Brattleboro, VT), CCD camera (Cohu 4912 CCD camera, San Diego, Ca) and the image-capturing program QFISH (Leica, Cambridge, United Kingdom). The three captured images were combined and pseudocolor was applied matching the original colors of the fluorochromes. The ratio between the FITC (test) and TRITC (control)

fluorescence was calculated with use of the QCGH software program (Leica, Cambridge). For each case, the mean of the individual ratio profiles of 8–10 metaphase spreads was calculated.

Results

The results of immunohistochemistry, ISH, DGGE and CGH in the eight cases of PCNSL are summarized in Table 2. In none of the investigated cases was EBV detected using EBER ISH, while two cases of PCNSL in HIV-positive patients, that were investigated in parallel, had EBER-positive tumor cells. In five of eight patients, strong Bcl-2 protein expression and in one case weak Bcl-2 protein staining was observed in the tumor cells. Bcl-6 protein expression was found in seven of eight cases. In the seven positive cases, the protein expression varied in intensity and in amount of tumor cells stained. Cases six, seven and eight showed bcl-6 protein expression in less then 10% of the tumor cells, whereas the other four positive cases showed bcl-6 protein expression in 30–70% of the tumor cells. Five of eight cases showed CD10 protein expression. All CD10 positive cases also expressed bcl-6 protein. P53 protein expression was observed in all of the cases. In five cases, more than 90% of tumor cells were positive. In case three, we observed more than 90% positive tumor cells, although the intensity of the staining was weak. Examples of an

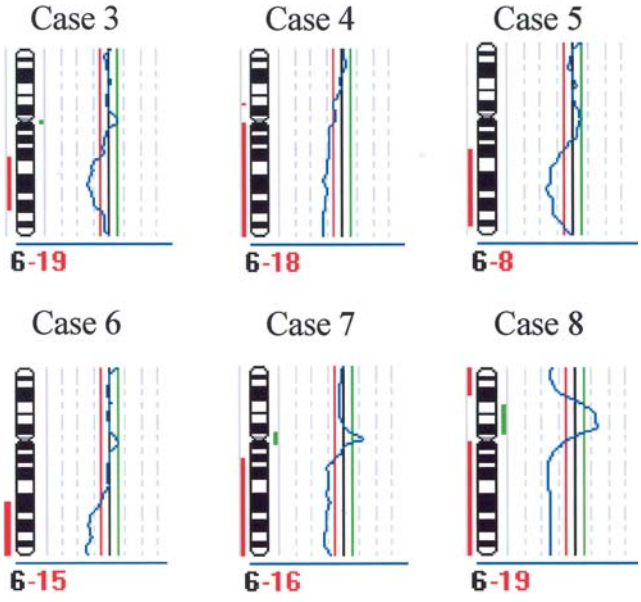

Fig. 1 Comparative genomic hybridization (CGH) ratio profiles illustrating loss of chromosome 6q in cases 3, 4, 5, 6, 7 and 8. The averaged CGH ratio profile shows primary central nervous system lymphoma (PCNSL) DNA versus normal control DNA (*blue line*). The *vertical red* and *green bars* right of the ideogram indicate the cutoff levels for gains (1.15>) and losses (0.85<)

Table 2 Overview of immunohistochemistry, in situ hybridization, denatured gradient gel electrophoreses (DGGE) and comparative genomic hybridization (CGH) data in eight cases of primary central nervous system lymphoma (PCNSL).*DLBL* diffuse large B-cell lymphoma, ± weak positive, + positive, +++ strong positive

Case	WHO class	In situ hybridization	DGGE	Immunohistochemistry				CGH
		EBER	P53 mutation	P53 protein (%)	Bcl-2	Bcl-6 (%)	CD10	Chromosomal gains and losses detected by CGH
1	DLBL	–	–	+++ (>90%)	–	+ (30%)*	+	Rev ish enh(18p13, 20q13.3, Xcent-q13, Xq21–21)
2	DLBL	–	–	++	–	+ (50%)	+	Rev ish enh(15,17p12-q21.1, 18p11.3, 19, 21, 22q13.3) Rev ish dim(9p21, 9q12–32, 20q12–13)
3	DLBL	–	–	+ (>90%)	±	+ (30%)	+	Rev ish enh(1q25, 7, 12pter-q15, 12q22-qter, 20q13) Rev ish dim(6q16-q24, X)
4	DLBL	–	–	+++ (>90%)	+	+ (>70%)	±	Rev ish enh(12p12-q21.3, 13, Xq28) Rev ish dim(6q, 9p22, 14q23, 15q21, 15q26)
5	DLBL	–	–	+++ (>90%)	+	+ (30%)	+	Rev ish enh(12, 13, 20q13, 21) Rev ish dim(6q22-qter, Xp21.3, Xq22.2, Xq24)
6	DLBL	–	–	+++ (>90%)	+	+ (10%)	–	Rev ish enh(18, 19p, Xp22.2, Xp11-q13, Xq22, Xq28) Rev ish dim(3p21.3, 6q16)
7	DLBL	–	–	+++ (>90%)	+	+ (<10%)	–	Rev ish enh(7p15, 7p14-q31.2, 12p12-q15, 12q21, 18p11.2, 19p13.1-qter, X) Rev ish dim(1p34.2, 4p16–16, 6q, 8p22, 8q24.2, 9q22, 14q24, 20q12, 20p12)
8	DLBL	–	–	++	+	–	–	Rev ish enh(1q32.1–32.1, 2p16, 6p11.1-p21.3, 11p11.2-qter, 12, 18q21, 19q13.2, 22q13.3) Rev ish dim(1p11–31.1, 3p21.3–14, 5q15–23, 6p22.3, 6q, 10q24, 17p12)

* Percentage of tumor cells expressing Bcl6 or p53 protein

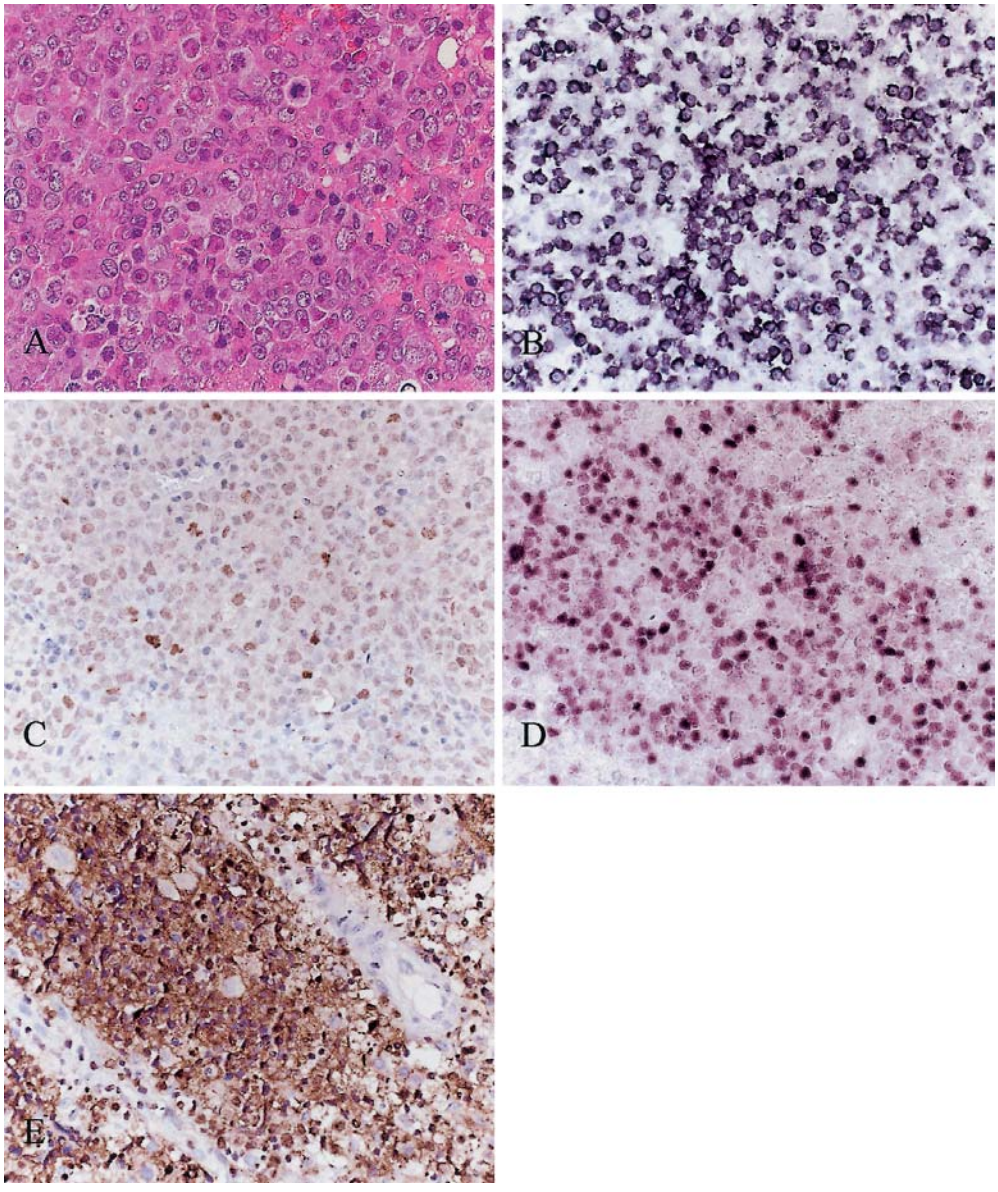

Fig. 2 Illustration of morphology and immunohistochemical staining for Bcl-2, Bcl-6, P53 and CD10 protein in primary central nervous system lymphoma (PCNSL). **A** Morphological illustration of immunoblastic PCNSL. **B** Bcl-2 protein staining. **C** P53 protein staining. **D** BCl-6 protein staining. **E** CD10 protein staining in PCNSL

immunoblastic PCNSL and immunohistochemical staining for Bcl-2, Bcl-6, P53 and CD10 protein in PCNSL are shown in Fig. 1. DGGE analysis of the *TP53* gene revealed no mutations in exons 5–9. CGH revealed DNA copy number changes in all eight cases. None of the cases showed a single chromosomal abnormality. In case seven, we detected 16 chromosomal abnormalities (Table 2). The most frequent changes found were gains of chromosome 19 (6 cases), 12 (5 cases), chromosome 18 (4 cases) and 20q (3 cases) and loss of chromosome 6q (6 cases, see Fig. 2). Overall, chromosomal gain (47×) was more frequently observed than chromosomal loss (31×). In none of the cases was a high level amplification detected. Strong overrepresentation (ratio >1.5) was only found in case seven for the chromosome arm 19q (see Table 2 for overview of all data).

Discussion

This is the first study to combine cytogenetic data obtained by CGH with protein expression data and *TP53* mutation analysis in a series of PCNSL in immunocompetent patients. Another important feature of this study is the employment of laser dissection microscopy to select pure tumor cells for the CGH analysis. The absence of EBV expression is consistent with other studies in immunocompetent PCNSL patients; in general, EBV is only associated with immunocompromised PCNSL patients [4, 10].

Co-expression of Bcl-6 and CD10 was detected in five cases, whereas in the three CD10-negative cases, Bcl-6 protein expression was present in less than 10% of the tumor cells or not at all. In general, Bcl-6 and CD10 are markers of germinal center B-cell derivation [7, 17], suggesting that the five cases with co-expression of CD10

and Bcl-6 are derived from germinal center B cells. Cases seven and eight, which were both CD10 and Bcl-6 negative or low, had immunoblastic morphology, a morphological feature thought to be associated with activated B cells and not with germinal center-derived cells.

One of the immunoblastic cases, case eight, was the only case with loss of material on 17p12, the region of the *TP53* gene. P53 protein was expressed in all cases, but no mutations were detected in exons 5–9 of the *TP53* gene. Mutations of the *TP53* gene are rare in PCNSL [5]. P53 protein expression in PCNSL does not differ from expression in other nodal and extranodal large B-cell lymphomas [3, 18, 27]. A combination of high bcl-2 and p53 expression has been reported to have a negative effect on patient survival in diffuse large B-cell lymphoma [26].

CGH revealed DNA copy number changes in all eight cases. This is most likely due to the laser microdissection that was applied to obtain pure tumor cells. The most frequent changes found were gains of chromosome 12 (5 cases), chromosome 18 (4 cases) and 20q (3 cases) and losses of 6q (6 cases) (Table 2). In general, these changes are similar to those found in systemic diffuse large B-cell lymphomas. However, the frequency of chromosome 6q loss in our series (75%) is higher than in systemic large B-cell lymphomas. This is in agreement with other cytogenetic studies on PCNSL that reported the frequency of 6q loss ranging from 47% to 62%, whereas the frequency in systemic diffuse large B-cell lymphomas is less than 35% [11, 28, 30]. This indicates a possible important role for one or more genes on 6q in the pathogenesis of PCNSL. In general, deletion of 6q is considered a secondary chromosomal abnormality in lymphoma [15]. Several studies have identified possible hotspots on chromosome arm 6q. Three minimal molecular deletion regions (RMD) were identified in NHL. RMD1, mapped to chromosome bands 6q25-q27, which was associated with intermediate grade NHL, RMD2 located at 6q21 was associated with high grade NHL; and RMD3 located at 6q23 was associated with low-grade NHL with and without t(14:18) [33]. All three RMD areas are suspected to harbor a tumor suppressor gene [24]. We found loss of the complete 6q arm in three cases, loss of 6q16–24, loss of 6q22-ter and loss of 6q16 each in one case (Fig. 2). In one previous study [28] on PCNSL, 6q16–21 was found to be a minimal common region of under-representation, whereas in another study 6q21–22 was commonly deleted [30]. In combination with our data it can be concluded that the region 6q16–22 indeed is the area where one or more suppressor genes involved in the pathogenesis of PCNSL may be localized. This is consistent with the RMD2 region that in general is frequently involved in high-grade lymphomas.

As indicated above, the frequency of 6q deletions is clearly higher in PCNSL than in systemic large B-cell lymphoma [1, 22]. Deletions of 6q are also quite frequent in testicular lymphoma. In 7 of 12 investigated cases of testicular lymphoma, a deletion of 6q was found (Bosga-Bouwer et al., unpublished observations). Genetic alterations of the HLA region on the short arm of chromosome 6 also arise more frequently in B-cell lymphomas in immunoprivileged sites, specifically testes and brain, than in DLBCL at other sites. Lack or abnormal expression of HLA may assist the lymphoma cells in their escape from an anti-tumor response [29]. The combination of loss of HLA expression and loss of a suppressor gene on 6q may contribute to the pathogenesis of diffuse large B-cell lymphomas of immunoprivileged sites in immunocompetent individuals.

Comparison of chromosomal abnormalities with the expression of the oncogenic proteins indicated no obvious relationships. Gain of chromosome 18 was present in four cases and, in two of these cases, specific gain of the q-arm of chromosome 18 was present. The Bcl-2 gene is located on chromosome 18q and was first described because of its participation in the translocation (14;18)(q32;q21). This translocation is found in approximately 30% of all diffuse large B-cell lymphomas [31]. No data are available on the occurrence of t(14;18)(q32;q21) in PCNSL. High Bcl-2 protein expression without the presence of the (14;18)(q32;q21) translocation has been described in diffuse large B-cell lymphomas, especially also in testicular lymphoma [19]. Monni et al. showed that amplification of the Bcl-2 gene is another important mechanism for Bcl-2 protein overexpression in DLBL [23]. We detected expression of Bcl-2 protein in six cases, including the two cases with gain of chromosome 18q. The other four Bcl-2-positive cases had no gain of chromosome 18. Of further interest is the finding that all Bcl-2-positive cases had deletion of chromosome arm 6q, whereas the only two cases without chromosome 6 imbalance also lacked Bcl-2 expression. There is no data in the literature suggesting a connection between 6q loss and Bcl-2 expression. P53 protein expression is probably not caused by gain of the *TP53* gene in these cases of PCNSL. We found p53 protein expression in all cases, whereas only in case six was loss of 17p12 detected, suggesting a potential breakpoint in the *TP53* gene region. Analysis of exons 5–9 did not reveal p53 gene mutations in any of these cases, including case six.

In conclusion, protein expression of CD10 and Bcl-6 was frequently detected in PCNSL, except for two cases with immunoblastic morphology. This suggests that most PCNSL in immunocompetent patients are of germinal center origin. The deletions and amplifications found by CGH in PCNSL are similar to those in systemic diffuse large B-cell lymphoma. However, the frequency of 6q deletions in our small series and in other series in the literature is higher than in the systemic cases and similar to that in testicular lymphoma. This suggests that one or more suppressor genes localized in the region 6q16–22 play a pathogenetically important role in the pathogenesis of primary lymphomas of immunoprivileged sites such as the CNS and testes in immunocompetent patients.

References

1. Barth TF, Dohner H, Werner CA, Stilgenbauer S, Schlotter M, Pawlita M, Lichter P, Moller,P, Bentz M (1998) Characteristic pattern of chromosomal gains and losses in primary large B-cell lymphomas of the gastrointestinal tract. Blood 91:4321–4330
2. Bataille B, Delwail V, Menet E, Vandermarcq P, Ingrand P, Wager M, Guy G, Lapierre F (2000) Primary intracerebral malignant lymphoma: report of 248 cases. J Neurosurg 92:261–266
3. Bergmann M, Blasius S, Bankfalvi A, Mellin W (1996) Primary non-Hodgkin lymphomas of the CNS-proliferation, oncoproteins and Epstein-Barr-virus. Gen Diagn Pathol 141:235–242
4. Chang KL, Flaris N, Hickey WF, Johnson RM, Meyer JS, Weiss LM (1993) Brain lymphomas of immunocompetent and immunocompromised patients: study of the association with Epstein-Barr virus. Mod Pathol 6:427–432
5. Cobbers JM, Wolter M, Reifenberger J, Ring GU, Jessen F, An HX, Niederacher D, Schmidt EE, Ichimura K, Floeth F, Kirsch L, Borchard F, Louis DN, Collins VP, Reifenberger G (1998) Frequent inactivation of CDKN2A and rare mutation of TP53 in PCNSL. Brain Pathol 8:263–276
6. Cote TR, Manns A, Hardy CR, Yellin FJ, Hartge P (1996) Epidemiology of brain lymphoma among people with or without acquired immunodeficiency syndrome. AIDS/Cancer Study Group. J Natl Cancer Inst 88:675–679
7. Dogan A, Bagdi E, Munson P, Isaacson PG (2000) CD10 and BCL-6 expression in paraffin sections of normal lymphoid tissue and B-cell lymphomas. Am J Surg Pathol 24:846–852
8. Eby NL, Grufferman S, Flannelly CM, Schold SC Jr, Vogel FS, Burger PC (1988) Increasing incidence of primary brain lymphoma in the US. Cancer 62:2461–2465
9. Flenghi L, Bigerna B, Fizzotti M, Venturi S, Pasqualucci L, Pileri, S, Ye BH, Gambacorta M, Pacini R, Baroni CD, Pescarmona E, Anagnostopoulos I, Stein H, Asdrubali G, Martelli MF, Pelicci PG, Dalla-Favera R, Falini B (1996) Monoclonal antibodies PG-B6a and PG-B6p recognize, respectively, a highly conserved and a formol-resistant epitope on the human BCL-6 protein amino-terminal region. Am J Pathol 148:1543-1555
10. Hamilton-Dutoit SJ, Raphael M, Audouin J, Diebold J, Lisse I, Pedersen C, Oksenhendler E, Marelle L, Pallesen G (1993) In situ demonstration of Epstein-Barr virus small RNAs (EBER 1) in acquired immunodeficiency syndrome-related lymphomas: correlation with tumor morphology and primary site. Blood 82:619–624
11. Harada K, Nishizaki T, Kubota H, Harada K, Suzuki M, Sasaki K (2001) Distinct primary central nervous system lymphoma defined by comparative genomic hybridization and laser scanning cytometry. Cancer Genet Cytogenet 125:147–150
12. Hayes VM, Bleeker W, Verlind E, Timmer T, Karrenbeld A, Plukker JT, Marx MP, Hofstra RM, Buys CH (1999) Comprehensive TP53-denaturing gradient gel electrophoresis mutation detection assay also applicable to archival paraffin-embedded tissue. Diagn Mol Pathol 8:2–10
13. Itoyama T, Sadamori N, Tsutsumi K, Tokunaga Y, Soda H, Tomonaga M, Yamamori S, Masuda Y, Oshima K, Kikuchi M (1994) Primary central nervous system lymphomas. Immunophenotypic, virologic, and cytogenetic findings of three patients without immune defects. Cancer 73:455–463
14. Jellinger KA, Paulus W (1992) Primary central nervous system lymphomas—an update. J Cancer Res Clin Oncol 119:7–27
15. Johansson B, Mertens F, Mitelman F (1995) Cytogenetic evolution patterns in non-Hodgkin's lymphoma. Blood 86:3905–3914
16. Kallioniemi A, Kallioniemi OP, Sudar D, Rutovitz D, Gray JW, Waldman F, Pinkel D (1992) Comparative genomic hybridization for molecular cytogenetic analysis of solid tumors. Science 258:818–821
17. King BE, Chen C, Locker J, Kant J, Okuyama K, Falini B, Swerdlow SH (2000) Immunophenotypic and genotypic markers of follicular center cell neoplasia in diffuse large B-cell lymphomas. Mod Pathol 13:1219–1231
18. Krogh JM, Johansen P, D'Amore F (1998) Primary central nervous system lymphomas in immunocompetent individuals: histology, Epstein-Barr virus genome, Ki-67 proliferation index, p53 and bcl-2 gene expression. Leuk Lymphoma 30:131–142
19. Lambrechts AC, Looijenga LH, van't Veer MB, van Echten J, Timens W, Oosterhuis JW (1995) Lymphomas with testicular localisation show a consistent BCL-2 expression without a translocation (14;18): a molecular and immunohistochemical study. Br J Cancer 71:73–77
20. Maggio EM, Stekelenburg E, van den Berg A, Poppema S (2001) TP53 gene mutations in Hodgkin lymphoma are infrequent and not associated with absence of Epstein-Barr virus. Int J Cancer 94:60–66
21. Miller DC, Hochberg FH, Harris NL, Gruber ML, Louis DN, Cohen H (1994) Pathology with clinical correlations of primary central nervous system non-Hodgkin's lymphoma. The Massachusetts General Hospital experience 1958–1989. Cancer 74:1383–1397
22. Monni O, Joensuu H, Franssila K, Knuutila S (1996) DNA copy number changes in diffuse large B-cell lymphoma—comparative genomic hybridization study. Blood 87:5269–5278
23. Monni O, Joensuu H, Franssila K, Klefstrom J, Alitalo K, Knuutila S (1997) BCL2 overexpression associated with chromosomal amplification in diffuse large B-cell lymphoma. Blood 90:1168–1174
24. Offit K, Parsa NZ, Gaidano G, Filippa DA, Louie D, Pan D, Jhanwar SC, Dalla-Favera R, Chaganti RS (1993) 6q deletions define distinct clinico-pathologic subsets of non-Hodgkin's lymphoma. Blood 82:2157–2162
25. Paulus W (1999) Classification, pathogenesis and molecular pathology of primary CNS lymphomas. J Neurooncol 43:203–208
26. Piris MA, Pezzella F, Martinez-Montero JC, Orradr JL, Villuendas R, Sanchez-Beato M, Cuena R, Cruz MA, Martinez B, Pezella F (1994) p53 and bcl-2 expression in high-grade B-cell lymphomas: correlation with survival time. Br J Cancer 69:337–341
27. Piris MA, Villuenda R, Martinez, JC, Sanchez-Beato M, Orradre JL, Mateo MS, Martinez P (1995) p53 expression in non-Hodgkin's lymphomas: a marker of p53 inactivation? Leuk Lymphoma 17:35–42
28. Rickert CH, Dockhorn-Dworniczak B, Simon R, Paulus W (1999) Chromosomal imbalances in primary lymphomas of the central nervous system. Am J Pathol 155:1445–1451
29. Riemersma SA, Jordanova ES, Schop RF, Philippo K, Looijenga LH, Schuuring E, Kluin PM (2000) Extensive genetic alterations of the HLA region, including homozygous deletions of HLA class II genes in B-cell lymphomas arising in immune-privileged sites. Blood 96:3569–3577
30. Weber T, Weber RG, Kaulich K, Actor B, Meyer-Puttlitz B, Lampel S, Buschges R, Weigel R, Deckert-Schluter M, Schmiedek P, Reifenberger G, Lichter P (2000) Characteristic chromosomal imbalances in primary central nervous system lymphomas of the diffuse large B-cell type. Brain Pathol 10:73–84
31. Weiss LM, Warnke RA, Sklar J, Cleary ML (1987) Molecular analysis of the t(14;18) chromosomal translocation in malignant lymphomas. N Engl J Med 317:1185–1189
32. Zattara CH, Horshowski N, Figarella BD, Dufour H, Grisoli F, Vagner CA (1996) Unusual chromosome abnormalities in primary central nervous system lymphoma. Leuk Lymphoma 21:515–517
33. Zhang Y, Weber MK, Siebert R, Matthiesen P, Schlegelberger B (1997) Frequent deletions of 6q23-24 in B-cell non-Hodgkin's lymphomas detected by fluorescence in situ hybridization. Genes Chromosomes Cancer 18:310–313

Virchows Arch (2003) 443:170–174
DOI 10.1007/s00428-003-0822-2

ORIGINAL ARTICLE

Yoshikazu Higami · Kazuo To · Hiroshi Ohtani · Kenta Masui · Keisuke Iwasaki · Daisuke Shiokawa · Sei-ichi Tanuma · Isao Shimokawa

Involvement of DNase γ in apoptotic DNA fragmentation in histiocytic necrotizing lymphadenitis

Received: 8 September 2002 / Accepted: 1 April 2003 / Published online: 12 June 2003
© Springer-Verlag 2003

Abstract DNA fragmentation induced by endonucleases is a hallmark of apoptotic process. One of the endonucleases responsible for apoptotic DNA fragmentation has been identified as DNase γ. It has been suggested that massive nuclear debris observed in histiocytic necrotizing lymphadenitis (HNL, Kikuchi disease) results mainly from apoptosis of T-lymphocytes rather than necrosis. To identify the role of DNase γ in apoptotic foci of HNL paraffin embedded tissue sections of HNL and lymphadenopathy with hyperplastic germinal centers and paracortex in the neck lymph nodes were immunohistochemically stained for DNase γ and the results compared with the reactivity of TdT-mediated dUTP nick end labeling (TUNEL). Immunoreactivity for DNase γ was detected in fragmented and condensed nuclei found abundantly in HNL as well as TUNEL reactivity. Moreover, the ratio of DNase γ immunoreactivity to TUNEL reactivity, which represents probability of apoptosis relevant to DNase γ, was higher in foci of nuclear debris in HNL than in the hyperplastic paracortex in lymphadenopathy including T-cell apoptosis. Our findings suggest that apoptosis detected in HNL depends more specifically upon DNase γ than apoptosis in the hyperplastic paracortex of lymphadenopathy, and that the dysregulation of DNase γ activation is involved in apoptosis in HNL

Y. Higami (✉) · K. To · H. Ohtani · K. Masui · I. Shimokawa
Department of Pathology and& Gerontology,
Nagasaki University Graduate School of Biomedical Science,
1-12-4 Sakamoto, 852-8523 Nagasaki, Japan
e-mail: higami@net.nagasaki-u.ac.jp
Tel.: +81-95-8497050
Fax: +81-95-8497052

K. Iwasaki
Division of Pathology, Department of Central Laboratory,
Sasebo City General Hospital, Sasebo, Japan

D. Shiokawa · S.-i. Tanuma
Department of Biochemistry, Faculty of Pharmaceutical Science,
Science University of Tokyo, Tokyo, Japan

Keywords DNase γ · Apoptosis · Histiocytic necrotizing lymphadenitis · Immunohistochemistry · Terminal deoxynucleotidyl transferase mediated deoxyuridine triphosphate mediated dUTP nick end labeling

Introduction

Apoptosis is involved in numerous physiological, adaptive, and pathological events including normal tissue turnover, immune selection, viral infection, and carcinogenesis [3]. Apoptosis is characterized by various morphological and biochemical changes such as cell shrinkage, nuclear fragmentation, chromatin condensation, formation of apoptotic bodies, phagocytosis, protein cleavage, and internucleosomal DNA fragmentation [3]. The latter, which is induced by endonucleases, is a critical event in the late apoptotic process [2, 14, 20]. Recently, several endonucleases, including DNase γ, which are considered responsible for DNA fragmentation in the apoptotic process have been identified and their biochemical properties and nucleotide sequences clarified [4, 10, 15, 16, 17, 19, 21]. DNase γ, which is a neutral 33-KDa endonuclease localized in the nucleus, is activated in the presence of both Ca^{2+} and Mg^{2+} and inhibited by Co^{2+}, Ni^{2+}, $Cu2^{+}$, and Zn^{2+}. DNase γ mRNA is found predominantly in the spleen, lymph nodes, thymus, and kidney, and to a lesser extent in the brain, heart, and pancreas. Activity of DNase γ is found during γ-ray irradiation and dexamethasone-induced apoptosis of thymocytes [15, 16, 17, 19]. Several investigators have suggested that certain human diseases are due to dysregulation of apoptosis; however, to our knowledge, no study has reported that the dysregulation of specific apoptotic endonucleases including DNase γ is responsible for the pathogenesis of human diseases.

Histiocytic necrotizing lymphadenitis (HNL), which was first described by Kikuchi [8] and is now well established as nonneoplastic disease, often involves the neck lymph nodes. The involved lymph nodes show proliferation of lymphocytes and histiocytes with massive

nuclear debris [8]. Ohshima et al. [11] reported that the majority of proliferating cells are CD8-positive T-cells. Moreover, the nuclear debris observed in large amounts in HNL results predominantly from apoptosis of T-lymphocytes rather than necrosis, suggesting that the main pathological feature of HNL is abnormal apoptosis and proliferation of T-lymphocytes, particularly cytotoxic T-cells [5, 9, 11, 12, 13, 18].

The aim of the present study was to define the role of DNase γ in apoptotic foci of HNL. For this purpose paraffin-embedded tissue sections of HNL and lymphadenopathy with hyperplastic germinal centers and paracortex in the neck lymph nodes were stained immunohistochemically for DNase γ. The immunoreactivity was compared with the reactivity of terminal deoxynucleotidyl transferase-mediated dUTP nick end labeling (TUNEL).

Materials and Methods

Samples

As shown in Table 1, 12 HNL cases of the neck lymph node which were diagnosed at Division of Pathology, Department of Central Laboratory, Sasebo City General Hospital, were examined in the present study. Ten cases of lymphadenopathy with hyperplastic germinal centers and paracortex were used as control. Lymph node samples fixed in formalin were processed using routine procedures and embedded in paraffin. The tissues were sectioned and stained with hematoxylin-eosin, periodic acid–Schiff and silver impregnation, immunohistochemistry for DNase γ, and TUNEL.

TdT-mediated dUTP-biotin nick end labeling

We used the TUNEL method as described previously [6, 7]. Briefly, tissue sections were incubated with 20 µg/ml proteinase K (Sigma, St. Louis, Mo., USA) for 20 min at 37°C after deparaffinization and hydration, and endogenous peroxidase was inactivated by 2% H_2O2 for 7 min. After washing and immersing in terminal deoxy-nucleotidyl transferase (TdT) buffer, the sections were reacted with TdT (Gibco BRL, Gaithersburg, Md., USA) and biotinylated uridine triphosphate (dUTP; Boehringer-Mannheim, Mannheim, Germany) in TdT buffer at 37°C for 90 min. The reaction was terminated in TB buffer (300 mM NaCl and 30 mM

Table 1 Quantitative analysis of DNase γ- and TUNEL-positive cells and the DNase γ/TUNEL ratio in each case (*GC* germinal center, *PC*paracortex, *HNL* histiocytic necrotizing lymphadenitis)

Case	Age (years)	Sex	Number of positive cells/area TUNEL	DNase γ	DNase γ to TUNEL ratio
GC					
1	64	F	207	153	0.74
2	66	F	246	87	0.355
3	23	F	241	155	0.643
4	57	M	307	114	0.372
5	43	F	305	83	0.271
6	57	M	432	118	0.273
7	41	F	274	213	0.777
8	79	F	363	75	0.205
9	64	M	242	36	0.148
10	17	M	309	144	0.465
Mean±SEM	–	–	–	–	0.425±0.071
PC					
1	64	F	85	28	0.329
2	66	F	84	13	0.155
3	23	F	104	42	0.404
4	57	M	125	22	0.176
5	43	F	146	28	0.192
6	57	M	114	49	0.43
7	41	F	109	17	0.156
8	79	F	81	10	0.123
9	64	M	102	16	0.157
10	17	M	94	12	0.128
Mean±SEM	–	–	–	–	0.225±0.037
HNL					
1	23	F	1636	548	0.335
2	16	F	1124	629	0.56
3	28	F	865	475	0.549
4	14	F	1268	738	0.582
5	27	F	921	403	0.438
6	26	M	2372	859	0.362
7	49	M	1167	574	0.492
8	41	F	1727	478	0.277
9	18	F	1476	574	0.389
10	36	M	2268	964	0.425
11	21	F	1501	398	0.265
12	25	M	1772	461	0.26
Mean±SEM	–	–	–	–	0.411±0.034

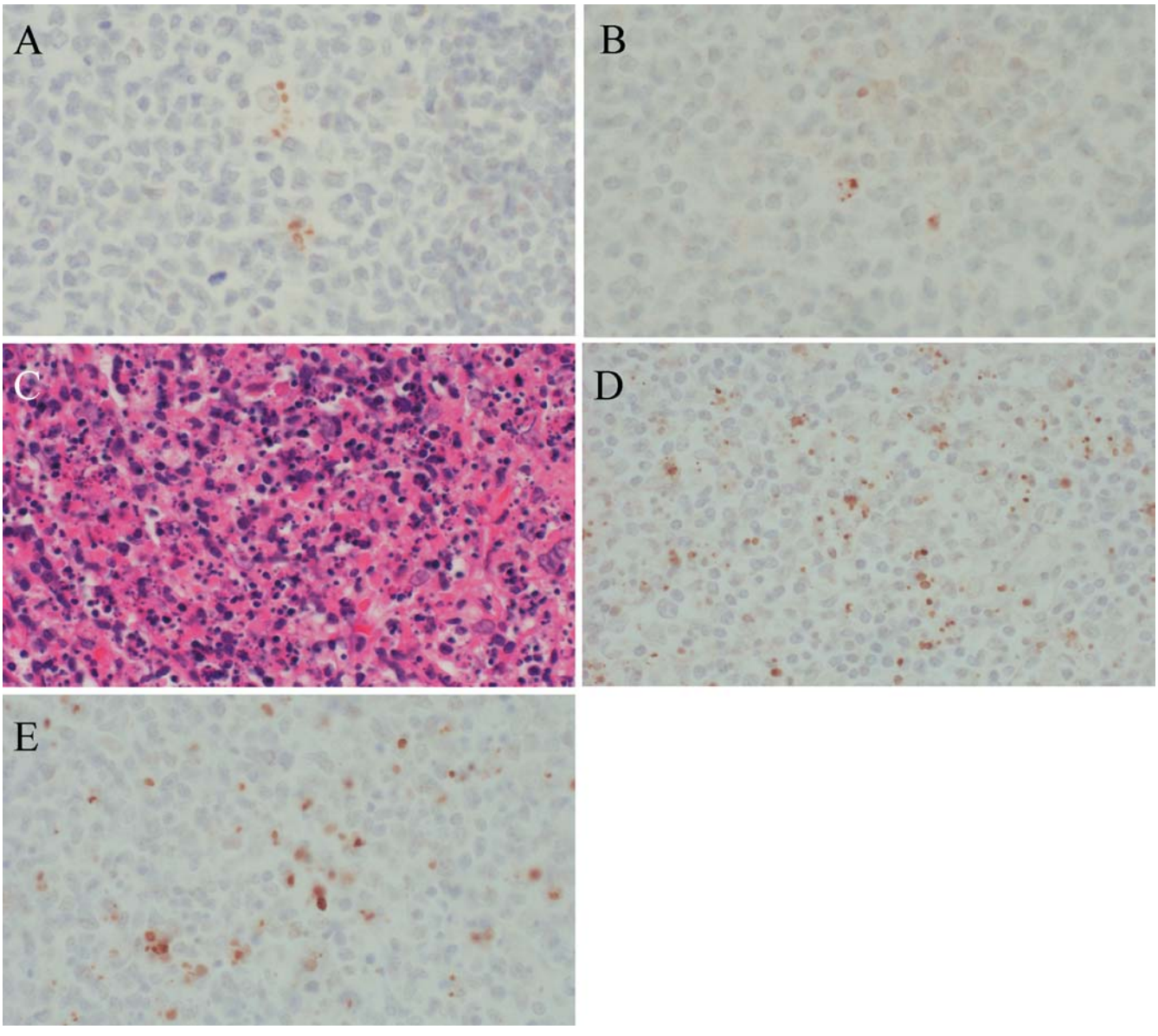

Fig. 1 **A** Immunohistochemistry for DNase γ in the hyperplastic germinal center of lymphadenopathy; ×600. **B** Immunohistochemistry for DNase γ in the hyperplastic paracortex of lymphadenopathy; ×600. **C** Foci containing several nuclear debris in histiocytic necrotizing lymphadenitis; hematoxylin-eosin staining, ×400. Note the presence of several and massive fragmented and condensed nuclei. **D** TUNEL on the serial section of **C**; ×400. Note the presence of positive reactivity in several fragmented and condensed nuclei and some intact cells morphologically. **E** Immunohistochemistry for DNase γ in serial sections of **C**; ×600. Note the presence of abundant positive immunoreactivity in several fragmented and condensed nuclei but not in morphologically intact cells. **A**, **B**, **D**, **E**: DAB with hematoxylin counterstaining

Na citrate) for 30 min. After washing, the sections were covered with 10% rabbit serum for 10 min and then reacted with avidin-biotin complex for 30 min at room temperature. Sections were rinsed and reacted in 3, 3′-diaminobenzidine tetrahydrochloride (DAB) solution as the chromogen.

Immunohistochemistry for DNase γ

The method of immunohistochemistry for DNase γ and the specificity of the antibody used for human DNase γ have been described previously [17]. Briefly, antigen retrieval was performed using an autoclave with 1 mM EDTA, pH 8.0, in 121°C for 20 min prior to immunohistochemistry. Endogenous peroxidase was inhibited by incubation with 3% H_2O_2 in absolute methanol for 15 min. Tissue sections were processed using mouse monoclonal IgG (clone 302, 1 μg/ml) and stained by the avidin-biotin peroxidase complex (Vectostain, CA, USA) method. DAB was used as the chromogen. The specificity of this antibody was confirmed by negative control using normal mouse IgG instead of the antibody, which showed no immunoreactivity. Hematoxylin counterstaining was performed.

Enumeration of TUNEL- and DNase γ-positive cells

The numbers of TUNEL- and DNase γ-positive cells were counted by one investigator using a light microscope with an eyepiece equipped with a square test grid. For evaluation of foci of nuclear debris in HNL, the numbers of TUNEL- and DNase γ-positive cells were counted in 50 microscopic fields in each sample using a ×40 objective lens. For evaluation of hyperplastic germinal centers and paracortex in lymphadenopathy, the numbers of TUNEL- and DNase γ-positive debris were counted in 50 microscopic fields in each sample using a ×20 objective lens.

Statistical analysis

The ratio of DNase γ-positive cells to TUNEL-positive cells (DNase γ/TUNEL) per area in each sample, which represents the probability of apoptosis relevant to DNase γ, was calculated, and data were expressed as mean ±SEM. Differences in this ratio among foci of nuclear debris in HNL, hyperplastic germinal centers, and paracortex of lymphadenopathy were examined by one-way analysis of variance using the SuperANOVA software (Abacus Concepts, CA, USA). The presence of significant difference among three lesions was examined by a post-hoc test (Games-Howell test). The presence of significant statistical differences was inferred with P values less than 0.05.

Results

Several cells with fragmented or condensed nuclei were observed in the hyperplastic germinal centers of lymphadenopathy. Most of the fragmented and condensed nuclei in these cells showed TUNEL reactivity and DNase γ immunoreactivity (Fig. 1A). In the hyperplastic paracortex of lymphadenopathy only a few cells had fragmented or condensed nuclei. Cells stained for TUNEL and DNase γ were also scarce (Fig. 1B). Nuclear debris together with fragmented and condensed nuclei were abundant in several foci in the lymph nodes with HNL (Fig. 1C). In addition, abundant TUNEL-positive and DNase γ-positive cells were evident in these foci (Fig. 1D, E). TUNEL reactivity was detected in the fragmented and condensed nuclei and morphologically intact cells, but DNase γ reactivity seemed to be limited to the fragmented and condensed nuclei (Fig. 1D, E).

Table 1 provides details of the TUNEL- and DNase γ-positive cell counts in each sample. Comparison of the DNase γ/TUNEL ratios of the three lesions showed a significantly higher ratio in the nuclear debris of HNL and germinal centers of lymphadenopathy than in the paracortex of lymphadenopathy (Fig. 2).

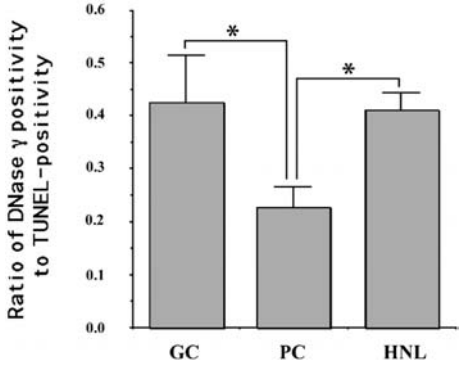

Fig. 2 The ratio of DNase γ positivity to TUNEL positivity, reflecting probability of apoptosis relevant to DNase γ in the germinal centers (*GC*) and paracortex (*PC*) of lymphadenopathy and foci of nuclear debris in histiocytic necrotizing lymphadenitis (*HNL*). Note the significantly higher probability of apoptosis induced by DNase γ in the germinal centers of lymphadenopathy and the foci of nuclear debris in HNL than in paracortex of lymphadenopathy. Data are mean ±SEM. *P<0.05, by Games-Howell test

Discussion

The antibody (clone 302) used in the present study recognized only a few DNase γ in normal thymocytes. However, strong immunoreactivity was noted in X-ray irradiated apoptotic thymocytes, particularly cells showing nuclear condensation and fragmentation [17]. Moreover, immunoreactivity for this antibody was not detected in living HeLa S3 cells transfected with DNase γ expression vector prior to apoptotic stimuli but was detected in cells undergoing apoptosis. These findings strongly suggest that the antibody (clone 302) used in our study specifically recognizes the activated form of DNase γ, as indicated previously by Shiokawa et al. [17]. In fact, as shown in Fig. 1C, the immunoreactivity was almost localized in cells with nuclear condensation and fragmentation but not in morphologically intact cells. Preliminary studies in our laboratories have also shown a positive immunoreactivity for DNase γ in fragmented nuclei of hepatocytes but not in morphologically intact hepatocytes in the liver after induction of apoptosis by an intravenous injection of cycloheximide (unpublished results).

Accumulation of nuclear debris is one of the main histopathological features of HNL [8]. These debris are considered to result mainly from abnormal apoptosis of proliferating CD8-positive lymphocytes [13]. Apoptosis observed in the germinal centers and paracortex of lymphadenopathy predominantly represents death of B-cells and T-cells, respectively. As shown in Fig. 2, the DNase γ/TUNEL ratio, which represents possible probability of apoptosis relevant to DNase γ, was significantly higher in the germinal centers of lymphadenopathy than in the paracortex, suggesting that the activated DNase γ participates more strongly in apoptotic DNA fragmentation of B-cells than that of T-cells. The DNase γ/TUNEL ratio was significantly higher in the nuclear debris derived from apoptosis of cytotoxic T-cells in HNL than in the hyperplastic paracortex of lymphadenopathy including predominantly T-cell apoptosis. This finding also suggests that apoptosis of cytotoxic T-cells in HNL is particularly more affected by the activation of DNase γ than that of T-cells in the hyperplastic paracortex of lymphadenopathy. Thus it seems that activation of DNase γ is involved in apoptotic DNA fragmentation observed in HNL.

Previous immunohistochemical studies demonstrated that CD8-positive cells in HNL express Fas ligand and Fas [12]. Moreover, immunoreactivities for perforin and granzyme, which are involved in other pathways involved in T-cell apoptosis, have also been detected in apoptotic cells in HNL [12, 18]. Therefore it is conceivable that apoptosis of CD8-positive cytotoxic T-cells in HNL depends on both Fas ligand/Fas and perforin/granzyme signalings as well as DNase γ activation. Since Fas ligand/Fas signaling allows caspase-activated DNase (CAD) to induce DNA fragmentation [4, 10], apoptotic DNA fragmentation observed in HNL might also result from CAD activation. Our preliminary data suggested that cycloheximide-induced apoptosis of hepatocytes, which probably involves DNase γ activation, is independent of Fas ligand/Fas signaling but is rather mediated by a sphingolipid metabolic pathway [1, 7]. Moreover, no activation of DNase γ is detected in Fas antibody-induced apoptosis of hepatocytes. Therefore it seems that activation of DNase γ observed in the lesion of HNL is probably involved in Fas-independent pathway of apoptosis. The exact subcellular mechanism of DNase γ activation in HNL is still unknown, but we suggest that activation of DNase γ, Fas ligand/Fas, and perforin/granzyme signalings are concomitantly involved in apoptotic DNA fragmentation of cytotoxic T-cells in HNL. This is the first report that suggests the involvement of dysregulation of specific apoptotic endonuclease, DNase γ, in human disease.

Acknowledgements The authors thank Akira Maeda and Toshihiro Ushio from the Division of Pathology, Department of Central Laboratory, Sasebo City General Hospital for their invaluable technical assistance. This work was conducted by K.M. as part of a thesis in Research Seminar, 4th grade program for undergraduate medical students at Nagasaki University School of Medicine.

References

1. Alessenko AV, Boikov PV, Filippova GN, Khrenov AV, Loginov AS, Makarieva ED (1997) Mechanisms of cycloheximide-induced apoptosis in liver cells. FEBS Lett 416:113–116
2. Arends MJ, Morris RG, Wyllie AH (1990) Apoptosis. The role of the endonuclease. Am J Pathol 136:593–608
3. Cotran RS, Kumar V, Collins T (1999) Cellular pathology I. Cell injury and cell death. In: Cotran RS, Kumar V, Collins T (eds) Robbins pathologic basis of disease, 6th edn. Saunders, Philadelphia, pp 1–29
4. Enari M, Sakahira H, Yokoyama H, Okawa K, Iwamatsu A, Nagata S (1998) A caspase-activated DNase that degrades DNA during apoptosis, and its inhibitor ICAD. Nature 391:43–50
5. Felgar RE, Furth EE, Wasik MA, Gluckman SJ, Salhany KE (1997) Histiocytic necrotizing lymphadenitis (Kikuchi's disease): in situ end-labeling, immunohistochemical, and serologic evidence supporting cytotoxic lymphocyte-mediated apoptotic cell death. Mod Pathol 10:231–241
6. Gavrieli Y, Sherman Y, Ben-Sasson SA (1992) Identification of programmed cell death in situ via specific labeling of nuclear DNA fragmentation. J Cell Biol 119:493–501
7. Higami Y, Tanaka K, Tsuchiya T, Shimokawa I (2000) Intravenous injection of cycloheximide induces apoptosis and up-regulates p53 and Fas receptor expression in the rat liver in vivo. Mutat Res 457:105–111
8. Kikuchi M (1972) Lymphadenitis showing focal reticulum cell hyperplasia with nuclear debris and phagocytes: a clinicopathological study (in Japanese). Acta Hematol Jpn 35:379–380
9. Liu Q, Ohshima K, Shinohara T, Kikuchi M (1995) Apoptosis in histiocytic necrotizing lymphadenitis. Pathol Int 45:729–734
10. Mukae N, Enari M, Sakahira H, Fukuda Y, Inazawa J, Toh H, Nagata S (1998) Molecular cloning and characterization of human caspase-activated DNase. Proc Natl Acad Sci U S A 95:9123–9128
11. Ohshima K, Kikuchi M, Sumiyoshi Y, Masuda Y, Mohtai H, Eguchi F, Takeshita M (1991) Proliferating cells in histiocytic necrotizing lymphadenitis. Virchows Arch B Cell Pathol 61:97–100
12. Ohshima K, Shimazaki K, Kume T, Suzumiya J, Kanda M, Kikuchi M (1998) Perforin and Fas pathways of cytotoxic T-cells in histiocytic necrotizing lymphadenitis. Histopathology 33:471–478
13. Ohshima K, Shimazaki K, Suzumiya J, Kanda M, Kumagawa M, Kikuchi M (1998) Apoptosis of cytotoxic T-cells in histiocytic necrotizing lymphadenitis. Virchows Arch 433:131–134
14. Peitsch MC, Polzar B, Stephan H, Crompton T, MacDonald HR, Mannherz HG, Tschopp J (1993) Characterization of the endogenous deoxyribonuclease involved in nuclear DNA degradation during apoptosis (programmed cell death). EMBO J 12:371–377
15. Shiokawa D, Tanuma S (1998) Molecular cloning and expression of a cDNA encoding an apoptotic endonuclease DNase gamma. Biochem J 332:713–720
16. Shiokawa D, Iwamatsu A, Tanuma S (1997) Purification, characterization, and amino acid sequencing of DNase gamma from rat spleen. Arch Biochem Biophys 346:15–20
17. Shiokawa D, Tanaka M, Kimura T, Hashizume K, Takasawa R, Ohyama H, Fujita K, Yamada T, Tanuma S (2000) Characterization of two DNase gamma-specific monoclonal antibodies and the in situ detection of DNase gamma in the nuclei of apoptotic rat thymocytes. Biochem Biophys Res Commun 275:343–349
18. Takakuwa T, Ohnuma S, Koike J, Hoshikawa M, Koizumi H (1996) Involvement of cell-mediated killing in apoptosis in histiocytic necrotizing lymphadenitis (Kikuchi-Fujimoto disease). Histopathology 28:41–48
19. Tanuma S, Shiokawa D (1994) Multiple forms of nuclear deoxyribonuclease in rat thymocytes. Biochem Biophys Res Commun 203:789–797
20. Wyllie AH (1980) Glucocorticoid-induced thymocyte apoptosis is associated with endogenous endonuclease activation. Nature 284:555–556
21. Zhao QL, Kondo T, Noda A, Fujiwara Y (1999) Mitochondrial and intracellular free-calcium regulation of radiation-induced apoptosis in human leukemic cells. Int J Radiat Biol 75:493–504

Virchows Arch (2003) 443:175–183
DOI 10.1007/s00428-003-0857-4

ORIGINAL ARTICLE

Marco Chilosi · Alberto Zamò · Antonietta Brighenti · Giorgio Malpeli · Licia Montagna · Paola Piccoli · Serena Pedron · Maurizio Lestani · Giorgio Inghirami · Aldo Scarpa · Claudio Doglioni · Fabio Menestrina

Constitutive expression of ΔN-p63α isoform in human thymus and thymic epithelial tumours

Received: 2 April 2003 / Accepted: 6 May 2003 / Published online: 8 July 2003
© Springer-Verlag 2003

Abstract p63, a member of the p53 family, is involved in the survival and differentiation of reserve/stem cells in different epithelia. To unveil the possible role of p63 in thymic physiology and pathology, we investigated the expression of p63 isoforms in normal thymus, thymomas and other mediastinal tumours. All samples were analysed using immunohistochemistry with three different antibodies: 4A4 antibody recognising all p63 isoforms, p40 antibody reacting only with truncated dominant-negative isoforms (ΔN-p63) and H-129 antibody recognising all alpha-isoforms. Reverse-transcription polymerase chain reaction (RT-PCR), and real-time PCR analyses were performed on RNA extracted from frozen samples of four thymomas and two primary-mediastinal large-B-cell lymphoma (PMLBCL). In normal thymus, ΔN-p63α was expressed in all cortical and medullary epithelial cells, with decreasing intensity in Hassall's corpuscles. This phenotype was conserved in neoplastic transformation since all 54 investigated thymomas (World Health Organization types A, AB, B1, B2, B3, C) expressed ΔN-p63α (virtually 100% cells). The predominance of ΔN-p63α isoform mRNA was confirmed by real-time PCR. Among other mediastinal tumours, ΔN-p63α was only expressed in those displaying either a stratified epithelial component (teratomas) or epidermoid differentiation (lung carcinoma). Among lymphomas, T-cell-precursor lymphomas did not express p63, whereas most PMLBCL expressed TA-p63α (7/8).

Keywords p63 · Thymus · Thymic tumours · Immunohistochemistry · Real-time PCR

M. Chilosi (✉) · A. Zamò · A. Brighenti · G. Malpeli · L. Montagna · P. Piccoli · S. Pedron · M. Lestani · A. Scarpa · F. Menestrina
Department of Pathology,
University of Verona, Policlinico G.B.Rossi,
Strada Le Grazie 8, 37134 Verona, Italy
e-mail: marco.chilosi@univr.it
Tel.: +39-045-8027616
Fax: +39-045-8027136

G. Inghirami
Department of Pathology,
New York University, New York, USA

C. Doglioni
Department of Pathology,
Belluno Hospital, Italy

Introduction

Although relatively rare, thymic epithelial tumours (TET) are clinically and pathologically heterogeneous, ranging from indolent thymomas to aggressive thymic carcinomas. The morphological heterogeneity of TET has been previously considered as evidence of divergent (ectodermal/endodermal) derivation of medullary and cortical thymic epithelial compartments [30, 43]. However, this view and the role of ectoderm in early thymic organogenesis have been challenged by recent experimental studies, suggesting that neural-crest mesenchyme is the only non-endoderm component necessary for thymic development [27] and that all thymic epithelial cell types derive from a common progenitor cell [2, 3, 17, 34]. The frequent occurrence of TET with overlapping morphological and immunophenotypic features is in line with this evolving view [7, 45]. TET heterogeneity could be, in part, determined by a diverse capacity of neoplastic epithelium to respond to microenvironmental signals, such as those provided by immature thymocytes often growing within thymoma tissue [7, 8, 45]. Nevertheless, the nature, morphology and location of putative thymic epithelial precursors are still unknown, and suitable molecular markers for their characterisation have not been so far described. Recently, p63 has been proposed as a specific marker of precursor/stem cells in many epithelial tissues [6, 18, 26, 32, 40, 46] and could represent a candidate marker for exploring thymic stem cells. Information regarding p63 expression in human thymus is scanty, and few data are available regarding TET [13, 46].

p63 is a member of the p53 tumour-suppressor gene family with structural homology to p53, but one that,

from a functional point of view, shows both similarities and differences from p53 [5, 39, 46, 47]. In fact, the p63 gene transcript undergoes multiple alternative splicing and, in addition, can be transcribed from two different promoters, resulting in the generation of a variety of p63 isoforms, including three transactivating (TA-p63, α–β–γ) and three amino terminal-truncated proteins (ΔN-p63, α–β–γ) [46, 47]. Interestingly, these different molecular species can exert contrasting effects on the same molecular targets, interfering with p53 functions. TA-p63 molecules (especially TA-p63γ) have functions similar to p53 in inducing cell-cycle arrest and apoptosis. However, the truncated proteins (especially the ΔN-p63α isoform) act as potent dominant-negative proteins, contrasting transactivation by p53 and p63 itself. When abnormally over-expressed as a result of gene amplification, these latter p63 isoforms behave as oncogenic molecules [11, 20, 21, 46, 47]. A complex network links p63 to the other members of the p53 family, as both TA-p63 and TA-p73 are required for p53-dependent apoptosis after DNA damage, and p53, in turn, has the ability to mediate ΔN-p63 degradation, thus balancing its oncogenic properties [15, 33]. The fine-tuning of different p63 isoforms in the basal and differentiating compartments is necessary to maintain the regenerative quality of epithelial stem cells, as well as the regulation of epidermal–mesenchyme interactions, replicative senescence, and angiogenesis [12, 14, 37]. All these functions render p63 essential during embryonic life for the correct development of limb, craniofacial and epithelial differentiation [29, 48].

Starting from these grounds, we have investigated the expression of p63 isoforms in normal thymic tissue and in a series of thymic and mediastinal tumours using immunohistochemistry and quantitative molecular analysis.

Materials and methods

Study population

The study group consisted of 14 normal thymic samples obtained from children undergoing heart surgery, and 54 previously untreated human TET, classified according to World Health Organization (WHO) criteria [35]. All tissue samples were fixed in buffered 4% formaldehyde and paraffin embedded following routine procedures. The TET series included: 4 type-A (medullary), 12 type-AB (mixed), 6 type-B1 (predominantly cortical), 15 type-B2 (cortical), 12 type-B3 (well-differentiated thymic carcinoma) and 5 type-C (4 epidermoid non-keratinising and 1 epidermoid keratinising thymic carcinomas).

Mediastinal tumour samples included six T-cell precursor lymphomas, eight primary large B-cell lymphomas of the mediastinum (PMLBCL), ten mediastinal germ cell malignancies (four seminoma, two embryonal cell carcinoma, one yolk-sac tumour, one mature teratoma, two malignant teratoma) and mediastinal metastases of pulmonary carcinomas (five small-cell and three squamous). Control tissues included three normal skin, ten reactive lymph node and four lung samples.

Immunohistochemical staining and antibodies

The antibody panel for characterising thymomas and lymphomas included anti-cytokeratin-5 (CK5, clone XM26; Novocastra, Newcastle, UK), anti-CD3 (clone PS1; Novocastra), anti-CD1a (clone 010; Immunotech, Marseille, France), anti-terminal-deoxynucleotidyl transferase (TdT, rabbit antibody; Dako, Glostrup, Denmark), anti-S100-protein (rabbit antibody; Dako), and anti-CD20 (clone L26; Dako) [6, 10, 32]. Anti-CD5 (clone 4C7; Novocastra) was used as a positive marker for type-C TET [22]. Tissue sections (4- to 5-μm thick) were cut and mounted on adhesive-treated glass-slides, rehydrated and treated for antigen retrieval (0.01 M, citrate buffer, pH 6, 5 min at 750 W, three times, 10 min at 600 W once). Immunostaining was performed using the avidin-streptavidin-peroxidase technique (Biogenex, San-Ramon, CA) in a semi-automated cell-staining system (GenoMx i6000, BioGenex, S.Ramon, CA). Consecutive sections were analysed using three different p63-specific antibodies. The first, 4A4, is a monoclonal antibody (clone-4A4, IgG2a; Santa Cruz Biotechnology, Santa Cruz, CA), raised against amino acids 1–205 of the transactivating form of the p63 gene, reacting broadly with all known variants of human p63. The second antibody, p40 (Oncogene Research Products, Boston, MA), is a polyclonal rabbit antiserum generated by immunising with a peptide corresponding to amino acids 5–17 of human p63, and recognising all truncated ΔN-p63 isoforms [10, 20]. The third antibody, H-129 (Santa Cruz Biotechnology), is a rabbit polyclonal antibody raised against a recombinant protein corresponding to

Fig. 1 TA-p63 and ΔN-p63 isoform expression in normal thymus and thymic epithelial tumours (TET). **a** Double-marker analysis of normal thymic cortex using p40 antibody (*brown*) and cytokeratin (CK5, *red immunostaining*). Both subcapsular and cortical epithelial cells express ΔN-p63. Subcapsular cells are characterised by intensely p63-reactive small, spindled nuclei, whereas cortical cells have larger, round nuclei with more variable p63 immunostaining. **b** Normal thymus immunostained with 4A4 antibody (*red*) and CD1a (*brown*). CD1a+ thymocytes are negative for all p63 isoforms. **c** Thymic medullary region immunostained with 4A4 antibody (*red*) and TdT (*brown*). The heterogeneous morphology of medullary epithelial cells expressing p63 is evidenced, including cells with large, vesicular nuclei at the cortico-medullary region (*arrow*), where immature TdT+ thymocytes stop growing. **d** A medullary area in the same section shown in **a**, immunostained for cytokeratin 5 (*red*) and ΔN-p63 (*brown*). A large cluster of medullary epithelial cells characterised by small, spindled nuclei that look identical to subcapsular cells (see **a**). Note the small Hassall's corpuscle containing p63-negative nuclei (*arrow*). **e** Normal thymic medulla immunostained with 4A4 antibody (*brown*) and CD20 (*red*). Medullary lymphoid B-cells lack nuclear p63. Note a large multinucleated epithelial cell characterised by intense p63 expression, which is leaned against a Hassall's corpuscle (*arrow*). **f** Double-marker analysis of normal thymic medulla (4A4 antibody *brown* and S100 *red*—immunostaining). S100+ dendritic cells do not express p63, whereas p63 expressing epithelial cells lack S100. **g** Type-A (medullary) thymoma. Most neoplastic cells are characterised by expression of p63 as shown by homogeneous nuclear immunostaining using 4A4 antibody. **h** Serial section of the same type-A thymoma showing similar immunoreactivity using p40 antibody. **i** The same case immunostained with H-129 antibody recognising all p63α isoforms. **l–m** Type-B1 (predominantly cortical) thymoma: neoplastic epithelial cells are very similar for morphology and location to those observed in normal thymus, and similarly react with 4A4 (**l**) and p40 antibodies(**m**). **n-o** Type-B2 (cortical) thymoma: many large, nucleolated epithelial cells are intermixed with CD1a+ thymocytes (**n**); ΔN-p63 nuclear expression is demonstrated in neoplastic cells characterised by heterogeneous nuclear size and atypia (**o**). **p–q** Type-B3 thymoma (well-differentiated thymic carcinoma). All neoplastic epithelial cells express nuclear ΔN-p63. The epithelial nature is confirmed by double staining with CK5 (**q**, *red* immunoreactivity)

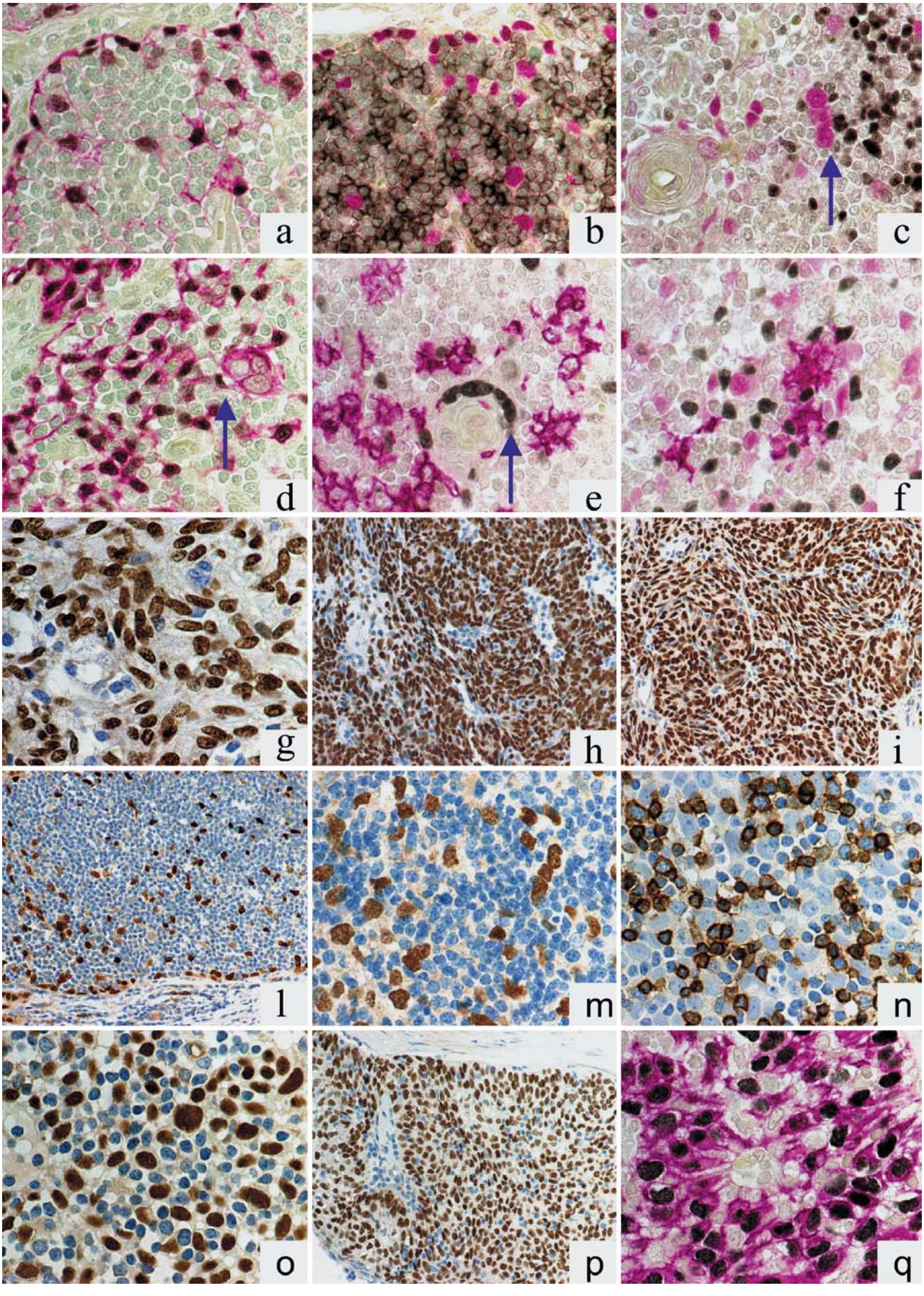
a
b
c
d
e
f
g
h
i
l
m
n
o
p
q

amino acids 513–641, mapping at the carboxy terminus of p63α of human origin.

Evaluation of immunohistochemical results

Only nuclear staining was interpreted as positive for p63 expression. To describe more precisely the complex distribution of p63 isoforms in a given cell population, we defined three immunoreactivity patterns: type-I, corresponding to prevalence of ΔN-p63, was assigned to cell populations reacting with both 4A4 and p40 antibodies at the same intensity; type-II, corresponding to TA-p63 expression, was assigned to cell populations reacting with 4A4, but negative on serial sections with p40; type-III, double negative, corresponding to cell populations not expressing p63 at the level of sensitivity of the immunohistochemical technique. As expected, immunoreactivity with p40 alone was never encountered.

The comparative expression of p63 isoforms was evaluated on serial sections. However, in selected cases, p63-expressing cells were further characterised by immunohistochemical double-marker analysis, performed using lineage-specific markers in combination with anti-p63 antibodies (including CD1a, TdT, S100 protein, CK5, and CD20) [8, 9, 10]. In double-marker analyses, p63 immunostaining was followed by alkaline-phosphatase immunostaining performed using the alkaline phosphatase-labelled polymer Envison (Dako).

RNA extraction and RT-PCR

Frozen tissue samples of TET (one each AB, B2, B3 and C-type) and two PMLBCL were obtained from the archive of Department of Pathology, Verona University. RNA extraction was performed according to the caesium chloride gradient method [19]. RNA (1 μg) was reverse transcribed by AMV (First Strand cDNA Synthesis, Roche, Mannheim, Germany) as recommended by manufacturer. The reverse transcription (RT) reaction (0.5 μl) was used as template. The polymerase chain reaction (PCR) mix contained PCR buffer type-II (Perkin-Elmer), 0.2 mM each dNTP, 1.5 mM $MgCl_2$, 0.32 μM forward and reverse primer, 0.5 U *Taq* polymerase in 25-μl volume. Primers used were: TAp63F: TGTTCAGTTCAGCCCATTGACT; TAp63R: AGTCCTGCATGCGGATACAGT; ΔNp63F: TGTACCTGGAAAACAATGCCCA; ΔNp63R: GACGAGGAGCCGTTCTGAATCT; p63αF: ATTGATGCTGTGCGATTCACC; p63αR: TGTTGCTTATTGCGGCGAG; p63βF: AACGCCCTCACTCCTACAAC; p63βR: GACTTGCCAGATCCTGACAATG; p63γF: GCAGCACCAGCACT-TACTTCA; p63γR: TGTTTTGGAGTTTCTCTCCGG. RT-PCR was performed on Gene-Amp 9700 (Perkin-Elmer) as follows: 95°C 5 min; 95°C 30 s, 58°C 30 s 72°C 45 s, for 35 cycles; 72°C 7 min. PCR products were sequenced using the di-deoxy method to confirm the identity of the amplicons.

Real-time quantification was performed by SYBR-Green I detection chemistry with 2× SYBR-Green PCR Master Mix (Applied-Biosystems, Warrington, UK) on ABI-PRISM 7000 Sequence Detection System (Applied-Biosystems). Each assay included a no-template control and 20 ng cDNA (in triplicate). Amplification mixture (25 μl) included 1× SYBR-Green Master Mix and 320 nM of each primer. Cycling conditions comprised 10 min at 95°C; 40 cycles at 95°C 20 s, 57°C 20 s, 72°C 30 s. At the end of each run, samples were checked by melting curve analysis and agarose gel electrophoresis. Beta-actin was amplified in parallel with that of p63 as internal control (not shown).

p63 absolute expression was evaluated using a standard curve-based method. Briefly, DNA template was obtained by PCR, run on agarose gel, cut out and extracted with a spin column (GenElute Agarose Spin Column, Sigma). The concentration of amplicons was calculated by spectrophotometric analysis and identity was determined by DNA sequencing. Standard curves were obtained by analysis of the amplification of known amount of template DNA (10, 2, 0.4, 0.08, 0.016 and 0.0032 fg, in quadruplicate). For each curve, a threshold cycle (Ct) value was chosen at the beginning of the geometric phase of amplification and a regression curve was obtained after plotting Ct values. The slopes of the standard curves, that reflect the efficiency of amplification, were −3.78, −3.61, −3.34, −3.80 and −3.32 cycles/log decade, for α, β, γ, ΔN- and TA-p63, respectively, while the correlation coefficients were >0.996. The Ct values of each sample were calculated and absolute amounts of each p63 isoform were determined by extrapolation from the appropriate standard curve (data not shown). Relative quantification, i.e. ΔN/TA and α/β and α/γ ratios, was performed by comparing absolute values.

Results

Immunohistochemistry

Control tissues

Nuclear p63 expression was confined to basal components of normal epidermis, and bronchial basal cells in lung. In these tissues, comparable intensity was observed using either 4A4 or p40 antibodies (immunoreactivity pattern type-I). In reactive lymph nodes, a few scattered p63-immunoreactive nuclei were observed within germinal centres using 4A4 antibody only.

Normal thymus

In adult and infant thymuses, p63 was expressed in the large majority of epithelial cells, including subcapsular, cortical and medullary elements (Fig. 1a–f). Within Hassall's corpuscles, peripherally located cells were p63 positive, whereas the more centrally located cells were mostly weakly reactive or negative (Fig. 1d–e, arrows), as observed in epidermis where p63 is progressively lost in maturing elements. Comparable immunoreactivity was evident in all thymic epithelial cells using either 4A4 or p40 antibodies (immunoreactivity pattern type-I, double positive), as well as using the H-129 antibody, recognising p63α isoforms. The epithelial nature of cells expressing p63 was demonstrated by double-marker analysis with p63 and CK5 (Fig. 1a, d). In medullary zones, all epithelial CK5-positive cells expressed p63, irrespective of their nuclear morphology. Among them, a large subset was characterised by small, spindle-shaped nuclei, similar to those located within the sub-capsular area (Fig. 1a, d). p63 expression was finally observed in an additional subset of epithelial cells located at cortico-medullary junctions, characterised by large, vesicular nuclei and occasionally forming giant cells (Fig. 1c, arrow).

Thymocytes, including sub-capsular, cortical and medullary types, were all negative for p63 (immunoreactivity pattern type-III), as confirmed on double-marker analysis combining p63 with anti-CD1a or anti-TdT antibodies (Fig. 1b, c). Medullary dendritic cells, recognised on p63/S100 double-staining preparations (Fig. 1f), were p63 negative, as were the large majority of medullary B-cells recognised on p63/CD20 preparations

Table 1 Immunohistochemical analysis of p63 isoform expression in normal thymus and thymic and mediastinal neoplasms. *TET* thymic epithelial tumours

	Number of cases	TA-p63*	ΔN-p63§	Pattern type#	Type of immunostaining and intensity score (#)
Normal thymic epithelium	14				
Cortex	14	14/14	14/14	I	Nuclear +
Medulla	14	14/14	14/14	I	Nuclear +
TET	54				
A	4	4/4	4/4	I	Nuclear +/++
AB	12	12/12	12/12	I	Nuclear +/++
B1	6	6/6	6/6	I	Nuclear +/++
B2	15	15/15	15/15	I	Nuclear +/++
B3	12	12/12	12/12	I	Nuclear +/++
C	5	5/5	5/5	I	Nuclear ++
Lymphomas	29				
T-cell lymphoblastic	6	0/6	0/6	III	–
Primary mediastinal large B-cell lymphoma	8	7/8	0/8	II	Nuclear –/+/++
Germ-cell tumours	10				
Seminoma	4	0/4	0/4	III	–
Embryonal carcinoma	2	0/2	0/2	III	–
Yolk sac tumour	1	0/1	0/1	III	–
Teratoma, benign	1	–/+	–/+	III	–/+**
Teratoma, malignant	2	–/+	–/+	III	–/+**
Mediastinal metastases	8				
Metastatic small cell carcinoma (lung)	5	0/3	0/3	III	–
Metastatic squamous carcinoma (lung)	3	2/2	2/2	I	Nuclear ++

* As revealed by 4A4 antibody nuclear immunoreactivity
** Nuclear (focal –/++)
§ As revealed by rabbit anti-p40 nuclear immunoreactivity
# See text (Materials and methods)

(Fig. 1e). Sparse medullary B cells showed nuclear p63 expression with the 4A4 antibody only.

Thymic epithelial tumours

All thymoma samples exhibited strong nuclear immunoreactivity using both p40 and 4A4 antibodies (type-I pattern) (Table 1 and Fig. 1). Homogeneous staining was seen in virtually all neoplastic epithelial cells. Comparable immunostaining was also observed using H-129 antibody (Fig. 1i). However, intermingled lymphocytes, when present, were all negative (Fig. 1g–q). In TET containing an exuberant lymphoid component, the distribution and density of immunoreactive nuclei allowed an easy determination of the corresponding percentages of the lymphoid and epithelial cells (Fig. 1l, m). The nuclear features, shape and size of neoplastic epithelial cells, as well as nuclear atypia were considerably simplified by p63 immunostaining (Fig. 1m, o, p).

All five cases of type-C TET were reactive for both p63 and p40 (pattern type I)(Table 1 and Fig. 2a–c).

Mediastinal lymphomas

All investigated T-cell precursor lymphomas were negative when investigated with both 4A4 and p40 antibodies (pattern type III; Table 1).

Seven of eight cases of PMLBCL exhibited nuclear reactivity with 4A4 and H-129 in a variable proportion of neoplastic cells (range 20–80%, Fig. 3a, c), whereas all cases were negative with p40 (pattern type-II; Table 1 and Fig. 3b).

Germ cell tumours

All mediastinal seminoma, embryonal carcinoma and yolk-sac tumours were negative using both 4A4 and p40 antibodies (pattern type-III). p63+ basal cells were only observed within foci of stratified epithelium in mature and immature teratomas (type-I pattern; Fig. 4a).

Mediastinal metastases of pulmonary carcinoma

All three cases of small-cell neuroendocrine carcinoma were negative with both 4A4 and p40 (type-III pattern; Fig. 4b, c). On the contrary, three mediastinal metastases of squamous pulmonary carcinoma were positive with both 4A4 and p40 (pattern type-I).

RT-PCR and real-time PCR

By standard RT-PCR, we were able to amplify only ΔN-p63 isoforms in two analysed thymoma samples, while the TA-mRNA was not detectable after 35 cycles of

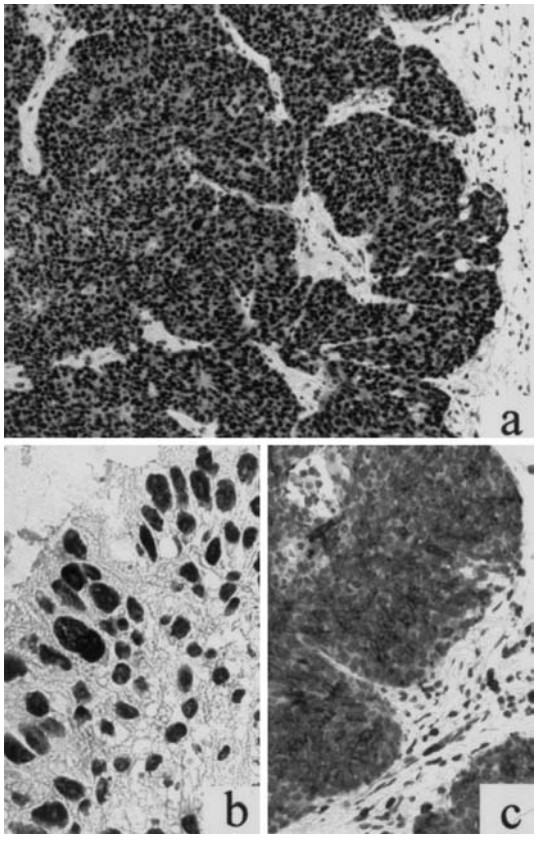

Fig. 2 Immunohistochemical demonstration of p63 proteins in type-C thymoma (thymic carcinoma, epidermoid non-keratinising). All neoplastic cells are immunoreactive with both 4A4 (**a**) and p40 (**b**) antibodies (immunoreactivity pattern type I). Diffuse immunoreactivity for CD5 is shown in (**c**)

Table 2 Relative abundance of p63 RNA isoforms in thymic epithelial tumours as determined by real-time polymerase chain reaction. (Case 1–3 thymomas type B3, B2 and AB, respectively; case 4: thymic carcinoma)

Case no.	ΔN/TA	α/β	α/γ
1	385.3	3.1	35.3
2	360.1	4.7	n.a. (γ=0)
3	228.6	99.8	148.4
4	59.5	5.8	136.7

amplification (Fig. 5a, b). As a positive control for TA-p63, we used two PMLBCL, which were positive at immunohistochemical analysis using 4A4 antibody and, as expected, showed a reliable signal after RT-PCR amplification (Fig. 5a). Among the differentially spliced p63 isoforms in thymomas, the alpha subtype was expressed at the highest level, while beta appeared to be present in one case only and gamma was not detectable (Fig. 5c).

Using real-time PCR, we found that both TA-p63 and ΔN-p63 isoforms were expressed in thymoma (three) and thymic carcinoma (one) samples, although at very different levels (Table 2 and Fig. 6). In thymomas, ΔN-p63 was the predominant form, with ΔN expressed at least 228-fold more than TA-p63. According to our data, the TA-isoforms are only 0.2–0.4% of total p63. Among α, β and γ isoforms, α was the most expressed, with α/β ratios variable from 3.1 to 99.8 and α/γ ratios between 35.3 and 148.4, but γ was not expressed at all in one case. In the thymic carcinoma, ΔN/TA ratio was 59.5, while α/β was 5.8 and α/γ was 136.7.

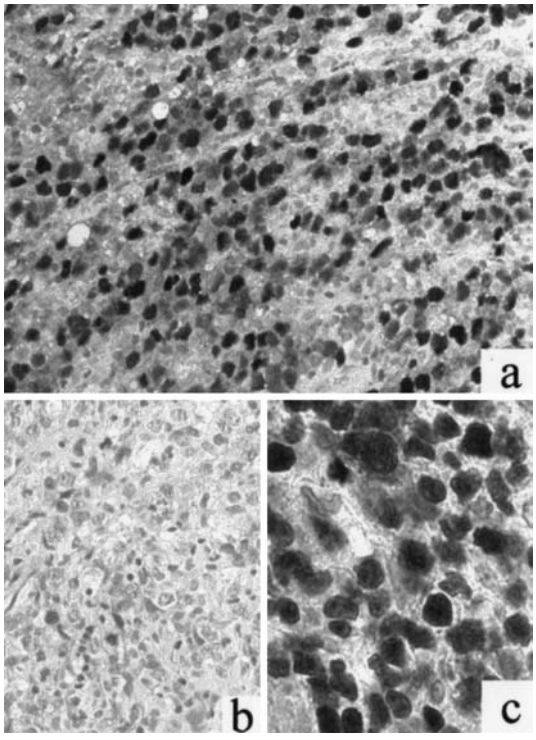

Fig. 3 Immunohistochemical demonstration of p63 isoforms in primary mediastinal large B-cell lymphoma: neoplastic cells exhibit nuclear expression of TA-p63, as defined by the immunoreactivity with 4A4 antibody (**a**) and lack of immunostaining with p40 antibody (**b**). p63α expression as shown in a section immunostained with H-129 antibody (**c**)

Discussion

In this study, we have provided new evidence on the constitutive expression of p63 in normal and neoplastic thymic epithelial cells. Since p63 encodes multiple products with either transactivating, cell death promoting or dominant negative activities [46, 47], we analysed the expression of p63 isoforms using three different antibodies. Using this screening approach, we were able to suggest that thymic epithelial cells preferentially express ΔN-p63 with consistent expression of the α-isoform. On these grounds, we turned to molecular analysis in order to verify the presence of p63 mRNA in TET samples. First, we performed a standard RT-PCR, which showed absence of TA-p63 in two thymomas, while ΔN-p63 was readily detectable after 35 amplification cycles. Moreover, while the α isoform was clearly detectable, β and γ were not.

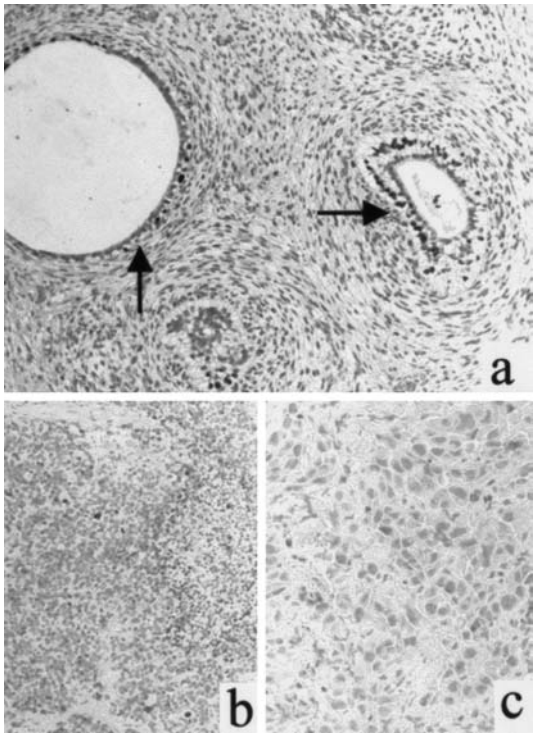

Fig. 4 a Mediastinal malignant teratoma. Basal cells of focal stratified gland-like structures express ΔN-p63. **b**, **c** Mediastinal metastasis of small-cell pulmonary carcinoma: all neoplastic cells are negative with both 4A4 and p40 antibodies

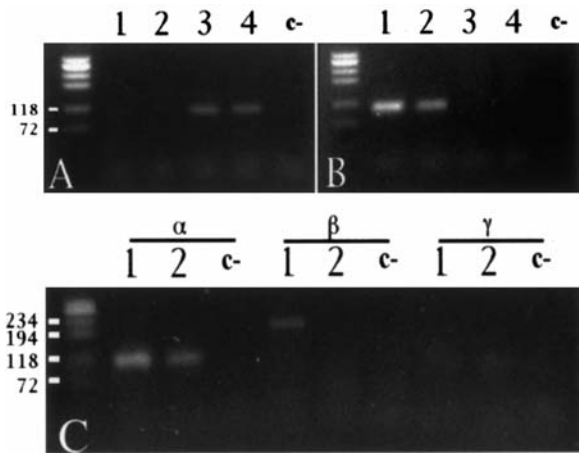

Fig. 5 Reverse-transcription polymerase chain reaction analysis of p63 isoforms in thymomas and primary-mediastinal large-B-cell lymphoma (PMLBCL). TA-p63 (**a**), ΔN-p63 (**b**) andα, β and γ p63 isoforms (**c**) in the two thymoma samples. *Lanes 1 and 2* are thymoma samples (one type AB and one type B2 thymoma), *lanes 3 and 4* are two PMLBCL samples; non-template control. ΔN–p63 isoforms are exclusively expressed by thymomas, whereas only TA-p63 is expressed by PMLBCL (**c**). In (**c**), among the differentially spliced p63 isoforms the α subtype is expressed at the highest level in thymomas, while β appears to be present in one case only, and γ is not detectable

The different intensity of our bands was probably due to the fact that after 35 cycles the reaction was still in the exponential phase. In order to quantify these differences more precisely, we turned to real-time PCR, which allows the precise quantification of signal intensity. According to our results, it was confirmed that ΔN-p63 isoforms are much more expressed than TA isoforms, with α being the most represented.

In our view, these data are relevant since the p53-antagonising ΔN-p63 isoforms are expressed in epithelial stem cells [46], and the ΔN-p63α isoform is the species with the strongest dominant-negative activity on p53 functions [39, 47]. Yang et al. [46] previously demonstrated p63 expression in mouse and human normal thymic tissues, but information regarding the type and location of cells expressing p63 was not provided. More recently, thymomas were described as p63-immunoreactive in a survey study on human tumours, but details on TET subtypes and discussion on the significance of this

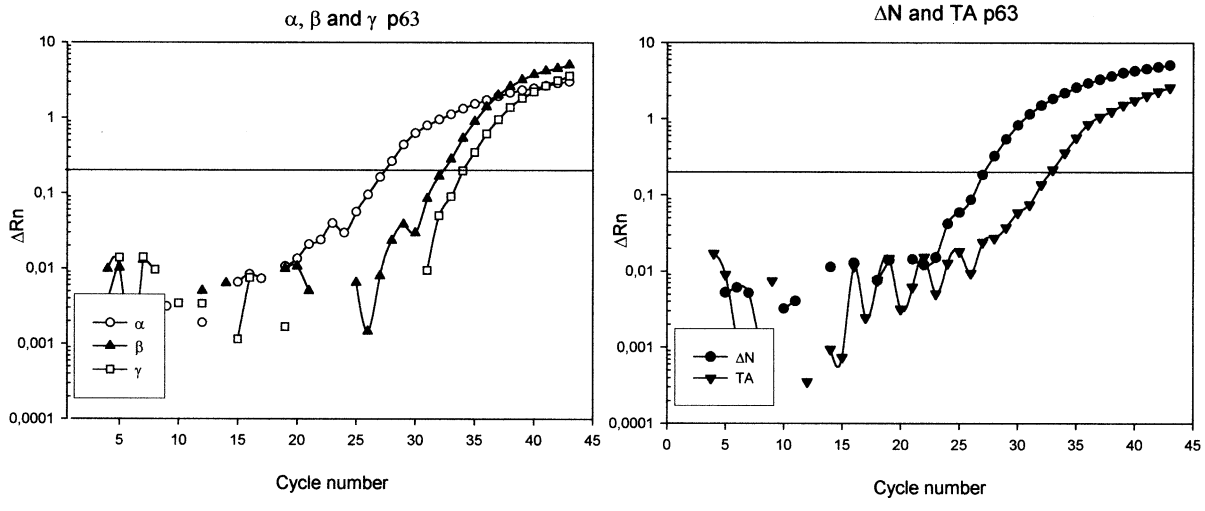

Fig. 6 Real-time polymerase chain reaction amplification plots of one exemplary case (B3 thymoma). For clarity purposes, only one curve for each amplification is shown; α, β, and γ isoforms (**a**), ΔN-p63 and TA-p63 (**b**)

finding were not provided [13]. At variance with that study, where all α, β and γ ΔN-p63 isoforms were found in thymomas by RT-PCR, we used a quantitative approach (real-time PCR), thus demonstrating an absolute predominance of the ΔN-p63α form. Little information is currently available on specific activities of different p63 C-terminal isoforms. One example in the same family is the specific preference for the Acquaporin 3 target gene by p73β rather than p73α [49]. The most represented isoform, p63α, contains a steric α-motif (SAM)-like sequence (small globular protein–protein-interaction modules usually involved in homo- and hetero-oligomerization with other SAM domains) and a post-SAM region with a transactivation inhibitory domain. The complexity of p63 functional heterogeneity is now being deciphered, and models explaining the transcriptional potential of homo-and heterotetramers formed by p63 isoforms and their effect on p53 have been recently proposed [16, 38].

Our immunohistochemical findings in normal infant and adult thymuses are somehow unexpected and intriguing. In fact, all thymic epithelial components, including subcapsular, cortical and medullary epithelial cells express nuclear ΔN-p63α. This peculiar distribution of p63 expression renders the thymus unique among human epithelial tissues so far investigated for p63 expression. In fact, in other tissues the cells that express p63 are strictly confined into discrete compartments in a basal position [6, 13, 26, 32, 40, 47], where epithelial cells are in close contact with extracellular matrix and stroma, in specialised niches where epithelial progenitors can find the proper microenvironment to exert their functions [44]. However, our findings clearly show that epithelial cells in all the three functional compartments of human thymus are able to maintain the "basal cell" phenotype, as defined by ΔN-p63α expression. It is possible to speculate that this peculiar phenotype could correspond to a unique renewal and/or differentiation strategy, centred on the presence and function of long-lived, poorly replicating cells, which are able to maintain the "basal/progenitor" phenotype still exploiting heterogeneous functional roles in providing specialised signals to thymocytes [1]. How thymic epithelial cells could avoid the asymmetric division fate that characterises all other progenitor cells in epithelia is not clear, nor is why end-stage differentiation only occurs within discrete foci in the medulla, corresponding to Hassall's corpuscles (the peculiar keratinising stratified structures representing the only morphologically differentiated component of thymic epithelium) [4]. Interestingly, recent convincing evidence has been provided suggesting that a common thymic epithelial progenitor exists, capable to fully reconstitute the complex thymic microenvironment [17, 34]. These findings are in line with previous data suggesting that early thymic organogenesis is determined, in discrete stages, by progressive interactions occurring between a single endodermal rudiment with neural crest derived mesenchyme in early organogenesis, and thymocytes in late stage organogenesis [23, 24, 27, 28, 36]. The peculiar expression of ΔN-p63 in thymic epithelium as demonstrated in this paper adds further complexity in this scenario, and manipulation of p63 expression could provide interesting new information regarding thymic epithelial cell differentiation. Another interesting finding to be discussed is the constitutive expression of ΔN-p63 proteins in 100% of cells in all types of thymic epithelial tumours. Different opinions exist on the histogenesis and classification of TET [25, 30, 31, 35, 41, 42]. The new data regarding the existence of common thymic epithelial progenitor cells, and the phenotypic changes characterising their differentiation and proliferative features (including data provided in this study regarding p63 isoform expression) could contribute to clarify the bio-pathologic issues of these tumours.

Acknowledgements Supported in part by: the Associazione Italiana Ricerca sul Cancro (AIRC, Milan, grant to M.C.), and Fondazione Cassa di Risparmio, Verona, Italy.

References

1. Anderson G, Jenkinson EJ (2001) Lymphostromal interactions in thymic development and function. Nat Rev Immunol 1:31–40
2. Bennett AR, Farley A, Blair NF, Gordon J, Sharp L, Blackburn CC (2002) Identification and characterization of thymic epithelial progenitor cells. Immunity 16:803–814
3. Blackburn CC, Manley NR, Palmer DB, Boyd RL, Anderson G, Ritter MA (2002) One for all and all for one: thymic epithelial stem cells and regeneration. Trends Immunol 23:391–395
4. Blau JN, Jones RN, Kennedy LA (1968) Hassall's corpuscles: a measure of activity in the thymus during involution and reconstitution. Immunology 15:561–570
5. Chen X (1999) The p53 family: same response, different signals? Mol Med Today 5:387–392
6. Chilosi M, Doglioni C (2001) Constitutive p63 expression in airway basal cells. A molecular target in diffuse lung diseases. Sarcoidosis Vasc Diffuse Lung Dis 18:23–26
7. Chilosi M, Iannucci AM, Pizzolo G, Menestrina F, Fiore-Donati L, Janossy G (1984) Immunohistochemical analysis of thymoma. Evidence for medullary origin of epithelial cells. Am J Surg Pathol 8:309–318
8. Chilosi M, Iannucci A, Menestrina F, et al (1987) Immunohistochemical evidence of active thymocyte proliferation in thymoma. Its possible role in the pathogenesis of autoimmune disease. Am J Pathol 128:464–470
9. Chilosi M, Castelli P, Martignoni G, et al (1992) Neoplastic epithelial cells in a subset of human thymomas express the B cell-associated CD20 antigen. Am J Surg Pathol 16:988–997
10. Chilosi M, Poletti V, Murer B, et al (2002) Abnormal re-epithelialization and lung remodeling in idiopathic pulmonary fibrosis: the role of deltaN-p63. Lab Invest 82:1335–1345
11. Crook T, Nicholls JM, Brooks L, O'Nions J, Allday MJ (2000) High level expression of ΔN-p63: a mechanism for the inactivation of p53 in undifferentiated nasopharyngeal carcinoma (NPC)? Oncogene 19:3439–3444
12. De Laurenzi V, Rossi A, Terrinoni A, et al (2000) p63 and p73 transactivate differentiation gene promoters in human keratinocytes. Biochem Biophys Res Commun 273:342–346
13. Di Como CJ, Urist MJ, Babayan I, et al (2002) p63 expression profiles in human normal and tumor tissues. Clin Cancer Res 8:494–501
14. Djelloul S, Tarunina M, Barnouin K, Mackay A, Jat PS (2002) Differential protein expression, DNA binding and interaction with SV40 large tumour antigen implicate the p63-family of proteins in replicative senescence. Oncogene 21:981–989

15. Flores ER, Tsai KY, Crowley D, et al (2002) p63 and p73 are required for p53-dependent apoptosis in response to DNA damage. Nature 416:560–564
16. Ghioni P, Bolognese F, Duijf PH, Van Bokhoven H, Mantovani R, Guerrini L (2002) Complex transcriptional effects of p63 isoforms: identification of novel activation and repression domains dagger. Mol Cell Biol 22:8659–8668
17. Gill J, Malin M, Hollander GA, Boyd R (2002) Generation of a complete thymic microenvironment by MTS24(+) thymic epithelial cells. Nat Immunol 3:635–642
18. Glickman JN, Yang A, Shahsafaei A, McKeon F, Odze RD (2001) Expression of p53-related protein p63 in the gastrointestinal tract and in esophageal metaplastic and neoplastic disorders. Hum Pathol 32:1157–1165
19. Glisin V, Crkvenjakov R, Byus C (1974) Ribonucleic acid isolated by cesium chloride centrifugation. Biochemistry 13:2633–2637
20. Hibi K, Trink B, Patturajan M, et al (2000) AIS is an oncogene amplified in squamous cell carcinoma. Proc Natl Acad Sci U S A 97:5462–5467
21. Hibi K, Nakayama H, Taguchi M, et al (2001) AIS overexpression in advanced esophageal cancer. Clin Cancer Res 7:469–472
22. Hishima T, Fukayama M, Fujisawa M, Hayashi Y, Arai K, Funata N, Koike M (1994) CD5 expression in thymic carcinoma. Am J Pathol 145:268–275
23. Janossy G, Bofill M, Trejdosiewicz LK, Willcox HN, Chilosi M (1986) Cellular differentiation of lymphoid subpopulations and their microenvironments in the human thymus. In: Muller-Hermelink HK (ed) The human thymus. Histopathology and pathology. Springer, Berlin Heidelberg New York, pp 89–125
24. Klug DB, Carter C, Crouch E, Roop D, Conti CJ, Richie ER (1998) Interdependence of cortical thymic epithelial cell differentiation and T-lineage commitment. Proc Natl Acad Sci U S A 95:11822–11827
25. Kornstein MJ (1999) Thymoma classification: my opinion. Am J Clin Pathol 112:304–307
26. Kurita T, Cunha GR (2001) Roles of p63 in differentiation of Mullerian duct epithelial cells. Ann N Y Acad Sci 948:9–12
27. Manley NR (2000) Thymus organogenesis and molecular mechanisms of thymic epithelial cell differentiation. Semin Immunol 12:421–428
28. Meilin A, Shoham J, Schreiber L, Sharabi Y (1995) The role of thymocytes in regulating thymic epithelial cell growth and function. Scand J Immunol 42:185–190
29. Mills AA, Zheng B, Wang XJ, Vogel H, Roop DR, Bradley A (1999) p63 is a p53 homologue required for limb and epidermal morphogenesis. Nature 398:708–713
30. Muller-Hermelink HK, Marino M, Palestro G (1986) Pathology of thymic epithelial tumors. In: Muller-Hermelink HK (ed) The human thymus. Histopathology and pathology. Springer, Berlin Heidelberg New York, pp 207–268
31. Okumura M, Miyoshi S, Fujii Y, et al (2001) Clinical and functional significance of WHO classification on human thymic epithelial neoplasms: a study of 146 consecutive tumors. Am J Surg Pathol 25:103–110
32. Pellegrini G, Dellambra E, Golisano O, et al (2001) p63 identifies keratinocyte stem cells. Proc Natl Acad Sci U S A 98:3156–3161
33. Ratovitski EA, Patturajan M, Hibi K, Trink B, Yamaguchi K, Sidransky D (2001) p53 associates with and targets Delta Np63 into a protein degradation pathway. Proc Natl Acad Sci U S A 98:1817–1822
34. Rodewald HR, Paul S, Haller C, Bluethmann H, Blum C (2001) Thymus medulla consisting of epithelial islets each derived from a single progenitor. Nature 414:763–768
35. Rosai J, Sobin LH (1999) Histological typing of tumors of the thymus. In: International Histologic Classification of Tumors, 2nd edn. Springer, New York, Berlin
36. Scupoli MT, Fiorini E, Marchisio PC, et al (2000) Lymphoid adhesion promotes human thymic epithelial cell survival via NF-(kappa)B activation. J Cell Sci 113:169–177
37. Senoo M, Matsumura Y, Habu S (2002) TAp63gamma (p51A) and ΔNp63alpha (p73L), two major isoforms of the p63 gene, exert opposite effects on the vascular endothelial growth factor (VEGF) gene expression. Oncogene 21:2455–2465
38. Serber Z, Lai HC, Yang A, et al (2002) A C-terminal inhibitory domain controls the activity of p63 by an intramolecular mechanism. Mol Cell Biol 22:8601–8611
39. Shimada A, Kato S, Enjo K, et al (1999) The transcriptional activities of p53 and its homologue p51/p63: similarities and differences. Cancer Res 59:2781–2786
40. Signoretti S, Waltregny D, Dilks J, et al (2000) p63 is a prostate basal cell marker and is required for prostate development. Am J Pathol 157:1769–1775
41. Suster S, Moran CA (1999) Thymoma, atypical thymoma, and thymic carcinoma. A novel conceptual approach to the classification of thymic epithelial neoplasms. Am J Clin Pathol 111:826–833
42. Suster S, Moran CA (1999) Thymoma classification. The ride of the valkyries? Am J Clin Pathol 112:308–310
43. Von Gaudecker B (1986) The development of the human thymus microenvironment. In: Muller-Hermelink HK (ed) The human thymus. Histopathology and pathology. Springer, Berlin Heidelberg New York, pp 2–41
44. Watt FM, Hogan BL (2000) Out of Eden: stem cells and their niches. Science 287:1427–1430
45. Willcox N, Schluep M, Ritter MA, Schuurman HJ, Newsom-Davis J, Christensson B (1987) Myasthenic and nonmyasthenic thymoma. An expansion of a minor cortical epithelial cell subset? Am J Pathol 127:447–460
46. Yang A, McKeon F (2000) P63 and P73: P53 mimics, menaces and more. Nat Rev Mol Cell Biol 1:199–207
47. Yang A, Kaghad M, Wang Y, et al (1998) p63, a p53 homolog at 3q27–29, encodes multiple products with transactivating, death-inducing, and dominant-negative activities. Mol Cell 2:305–316
48. Yang A, Schweitzer R, Sun D, et al (1999) p63 is essential for regenerative proliferation in limb, craniofacial and epithelial development. Nature 398:714–718
49. Zheng X, Chen X (2001) Aquaporin 3, a glycerol and water transporter, is regulated by p73 of the p53 family. FEBS Lett 489:4–7

Virchows Arch (2003) 443:184–193
DOI 10.1007/s00428-003-0776-4

ORIGINAL ARTICLE

Roberto Verdolini · Rino Cerio

Autoimmune subepidermal bullous skin diseases: the impact of recent findings for the dermatopathologist

Received: 14 January 2002 / Accepted: 21 January 2003 / Published online: 11 June 2003
© Springer-Verlag 2003

Abstract In recent years improved knowledge of the mechanisms of intercellular and cell-matrix adhesion has led to better understanding of the blistering process in many bullous dermatoses. The wide characterisation of adhesion molecules has partially changed some traditional views and invariably has made the routine work of the pathologist more complex. If understanding cell–cell cohesion structures such as desmosomes and adherens junctions is complex enough, the cell-matrix adhesion structures, such as hemidesmosomes and their structural analogues on the basement membrane and superficial dermis, are even more complex. Defects of such structures cause the subepidermal bullous diseases in which there has been most characterisation of the adhesion molecules and has also led to the discovery of new diseases (e.g. p200 pemphigoid). Most of the antigens are also the targets for mutations seen in patients with the inherited type of epidermolysis bullosa, a group of rare blistering genodermatoses. Another important aspect of bullous skin conditions is the more accurate definition of the role of the different inflammatory cells involved in triggering, development and maintenance of these diseases. Recent studies have outlined the important role of T-cell lymphocytes and their cytokines in their pathogenesis. All these studies, based mainly on highly sophisticated ultrastructural and molecular biology techniques, have updated our knowledge of the pathogenesis of blistering diseases. Nevertheless, the diagnostic characterisation of bullous diseases remains sometimes difficult, and some pathological features and mechanisms still represent an enigma. Diseases such as bullous pemphigoid and cicatricial pemphigoid, or anti-laminin cicatricial pemphigoid and acquired bullous epidermolysis share the same molecular target but have very different clinical manifestations. Explaining this phenomenon, probably linked to different expressions of MHC, is one of the challenges for the future.

Keywords Autoimmune bullous diseases · Blister · Adhesion molecules · Cytokines · Epidermolysis bullosa

R. Verdolini (✉) · R. Cerio
Department of Dermatology, Queen Mary-University of London,
The Royal London Hospital,
Whitechapel, London, E1 1BB, UK
e-mail: rverdolini@hotmail.com

Introduction

Vesciculobullous lesions represent a distinctive reaction pattern that morphologically characterises certain cutaneous diseases. Broadly, they result from the loss, either congenital or acquired, of keratinocyte cohesion. Vesicles or bullae can occur at any level within the epidermis from the stratum corneum to the dermoepidermal junction. The following review will focus particularly on subepidermal blister diseases. In recent years, much progress has been made in the comprehension of their pathophysiology. The most important discoveries concerned adhesion structures, the recruitment and the role of inflammatory cells and the role of their cytokines.

Adhesion molecules: new findings and new entities

Among autoimmune acquired diseases, our improved knowledge of the junctional structures and basement membrane components has enabled better definition and has sometimes also led to the discovery of new nosological entities. A good example is the recent discovery by several workers who have independently identified a novel subepidermal bullous disease associated with immunoglobulin G (IgG) autoantibodies to a 200-kDa dermal antigen (Ag) [12, 16, 19, 24]. Other new entities include forms of blistering diseases characterised by autoantibodies against a 105-kDa Ag [3, 4, 5] and against a 450-kDa Ag [13, 14] (p105 and p450 pemphigoid). Taking these new findings into consideration, autoimmune subepidermal blistering disorders include bullous pemphigoid, pemphigoid gestationis, lichen planus pemphigoides, dermatitis herpetiformis, linear IgA disease,

Table 1 Revised classification of congenital blistering diseases

Major epidermolysis bullosa type	Usual mode of transmission	Major epidermolysis bullosa sub-type	Protein/gene system involved	Localisation
Epidermolysis bullosa simplex (EBS) ("epidermolytic EB")	Autosomal dominant	EBS-Weber-Cockayne	Keratins 5 and 14	Cytoskeleton of basal cells
		EBS-Koebner	Keratins 5 and 14	Cytoskeleton of basal cells
		EBS-Dowling-Meara	Keratins 5 and 14	Cytoskeleton of basal cells
		EBS+muscle dystrophy	Plectin	Hemidesmosomal cytoplasmic plaque
Junctional epidermolysis bullosa (JEB)	Autosomal recessive	JEB Herlitz	Laminin-5	Anchoring filaments
		JEB non-Herlitz	Laminin-5	Anchoring filaments
			BPAg2 (180 kDa)	Transmembrane protein
		JEB+pyloric athresia	$\alpha 6\beta 4$ Integrin	Transmembrane protein
Dermolitic epidermolysis bullosa (DEB)	Autosomal dominant/ autosomal recessive	Dominant dystrophic EB	Type-VII collagen	Anchoring fibrils
		Recessive dystrophic EB-Hallopeau-Siemens	Type-VII collagen	Anchoring fibrils
		Recessive dystrophic EB non-Hallopeau-Siemens	Type-VII collagen	Anchoring fibrils

anti-p200, anti-p105, and anti-p450 pemphigoid, epidermolysis bullosa acquisita, cicatricial pemphigoid (now renamed mucous membrane pemphigoid), bullous systemic lupus erythematosus and paraneoplastic pemphigus [17].

Among the group of inherited bullous disorders encompassed by the term epidermolysis bullosa (EB) to date, at least 300 different mutations in ten different genes corresponding to various components of the basement membrane have been described, making new classification of these diseases necessary [10] (Table 1). This group of genodermatoses consists of distinct variants, such as EB simplex, EB with muscular dystrophy, EB with pyloric atresia, non-Herlitz EB (formerly called generalised atrophic benign EB), Herlitz junctional EB and dystrophic EB.

As shown in Table 2, frequently, congenital defects involve the adhesion molecules that also represent the targets of the autoimmune response in other acquired subepidermal diseases, such as 180-kDa (minor) bullous pemphigoid Ag.

The aforementioned molecule, for example, which is a transmembrane protein with an intracellular hemidesmosomal portion in basal keratinocyte and a long extracellular collagen-like component (identified as collagen XVII), is congenitally altered in the generalised atrophic benign EB. This protein, however, is one of the targets also in bullous pemphigoid (BP), linear IgA dermatosis and pemphigus gestationis.

The involvement of similar molecular targets also explains the presence of the morphological and biological overlap between different diseases such as BP and linear IgA dermatoses [25, 26]. In the latter disorder, IgA antibodies usually react with a 285-kDa Ag localised in the sublamina densa. In a sub-group, however, they can react with Ags of 97 kDa (LABD97) and 120 kDa (LAD-1), both of which appear in fact to be fragments of the extracellular domain of BP 180 Ag.

Further examples of different diseases that share the same target are: one of the forms of cicatricial pemphigoid, the lethal junctional form of EB and a subtype of EB acquisita. In all these conditions, the target is the laminin-5 (formerly recognised as epiligrine), a protein associated with the anchoring filaments at the junction between lamina lucida and lamina densa. Another example is one of the forms of paraneoplastic pemphigus and the rare p450 pemphigoid. In both these conditions, the targets belong to the group of desmoplakins. These molecules are important filament-binding proteins that connect with the tonofilaments of the cytoskeleton as keratins 5 and 14 and are components of the cytoplasmic plaque, the intracellular portion of the desmosome (Table 2).

Enrolment of inflammatory cells, chemokines and other molecules

The roles of T-cell lymphocytes (mostly of Th2 type) and their cytokines have recently been highlighted. The essential role of Th2 lymphocytes in the genesis of subepidermal blistering diseases has been recognised following studies on pemphigus vulgaris. As well as autoantibodies, an important part in triggering and maintaining this disease is in fact played by T cells, monocytes and activated resident cells such as mast cells [18, 28]. The traditional view that the granulocyte chemotaxis and subsequent dermoepidermal split following the complement cascade activated by the fixation of the antibodies to the basement membrane is today integrated in a complex molecular mechanism that includes molecules such as RANTES, interleukins, tumour necrosis factor (TNF)α, TNFβ, interferon (IFN)γ and more recently identified molecules such as eotaxin (Fig. 1, Fig. 2). Involvement of these molecules better explains the typical recruitment of inflammatory cells characteristic of autoimmune bullous disease [9].

The most recently identified chemokines have been shown to be essential in the recruitment of inflammatory infiltrate in BP [29] and in dermatitis herpetiformis [1], and their presence and functional activity also help to explain some steps in the final damage of the basement membrane zone, leading to blister formation. Excellent

Table 2 Subepidermal bullous diseases and their correlation to the principal molecular defects or target antigens recognised

Subepidermal blister disease	Target antigens–molecular defects	Localisation of antigen
With little inflammation		
Epidermolysis bullosa acquisita	Type-VII collagen	Anchoring fibrils
	Variants Uncein	Anchoring filament
	Laminin 5 (epiligrin)	
Bullous pemphigoid (cell-poor type)	BPAg1(230 kDa—major antigen)	Hemidesmosome
	BPAg2 (180 kDa—minor antigen)	Transmembrane protein
Porphyria cutanea tarda	–	–
Toxic epidermal necrolysis	–	–
Bullous variant of drug reaction	–	–
With lymphocytes		
Paraneoplastic pemphigus	Desmoplakin I (250 kDa)	Cytoplasmic plaque
	BPAg1 (230 kDa)	Hemidesmosome
	Desmoplakin II (210 kDa)	
	Periplakin (190 kDa)	
	Unidentified (170 kDa)	
Lichen planus pemphigoides	–	–
Bullous variant of erythema multiforme	–	–
Bullous variant of fixed drug reaction	–	–
Bullous variant polymorphous drug reaction	–	–
With eosinophils		
Bullous pemphigoid	BPAg1 (230 kDa—major antigen)	Hemidesmosome
	BPAg2 (180 kDa—minor antigen)	Transmembrane protein
Pemphigoid gestationis	BPAg2 (180 kDa—minor antigen)	Transmembrane protein
Bullous variant of drug reaction	–	–
p450 pemphigoid	450 kDa Ag	Cytoplasmic plaque
With neutrophils		
Dermatitis herpetiformis	?	?
Linear IgA bullous dermatosis	LABD97 (97 kDa)	Anchoring filament
	LAD-1 (120 kDa)	Anchoring filament
	285 kDa	Sublamina densa
Cicatricial (mucous membrane) pemphigoid	BPAg2 (180 kDa—minor antigen)	Transmembrane protein
	Variants: laminin 5 (epiligrin)	Anchoring filament
	β4 integrin	Transmembrane protein
Ocular cicatricial pemphigoid	45 kDa	Conjunctiva
	β4 Integrin	
Epidermolysis bullosa acquisita	Type-VII collagen	Anchoring fibrils
	Uncein	Anchoring filament
p105 pemphigoid	105 kDa Ag	Lower lamina lucida
p200 pemphigoid	200 kDa Ag	Lower lamina lucida
Bullous lupus erythematosus	Type-VII collagen	Anchoring fibrils
Erysipela	–	–

reviews about actions and mechanisms of every single cytokine have recently been published [7].

Mechanisms responsible for the split: final steps

The recruitment of granulocytes following the local release of cyto-chemokines also contributes to gain an understanding of the final process, which causes dermoepidermal splitting. Recent findings show that the final pathway, which leads to the formation of blisters, includes the release of granular protein with proteolytic activity by eosinophils [2, 6], collagenases [23, 27]—both by neutrophils and eosinophils—and neutrophilic elastase [22] by neutrophils. All have demonstrated the capacity to destroy proteic bindings.

Clues for classification

The introduction of molecular biology, immunoblotting and immunoelectron microscopy has resulted in a new understanding of pathological mechanisms, revolutionising sometimes the traditional approach, but bullous diseases of mucosae and skin are still classified on the basis of histological criteria.

The classification of this reaction pattern and microscopic diagnoses are usually made by the assessment of three main features: the anatomical level of the split, the pathogenetic mechanism responsible for the split (assessed by particular techniques: immunofluorescence, sodium chloride split skin, electron microscopy, immunoelectron microscopy) and the nature of the inflammatory infiltrate in the dermis or within the blisters. This latter feature is important for all the bullous diseases but is even more important for the differential diagnosis of subepidermal lesions.

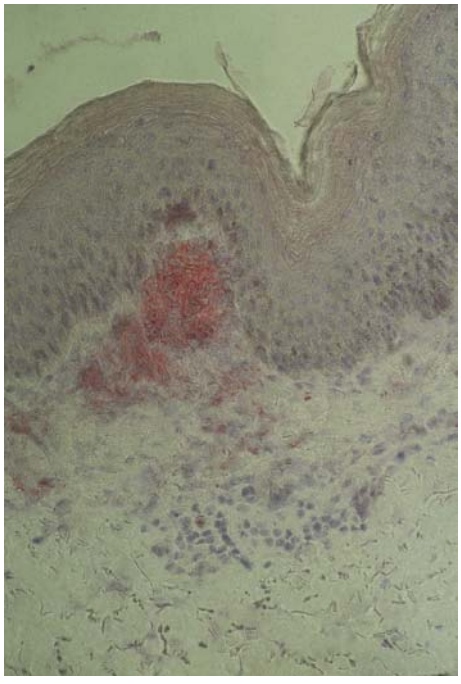

Fig. 1 Strong eotaxin positivity is seen in subepidermal microabscesses characterising dermatitis herpetiformis (immunostaining with Eotaxin, Streptavidin-biotin complex; frozen section)

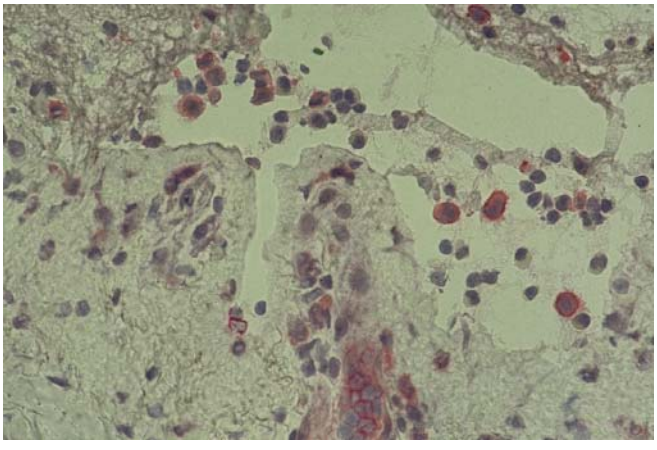

Fig. 2 Lymphomonocytic infiltrate within a bullous pemphigoid blister: clear cytoplasmic positivity for eotaxin (immunostaining with Eotaxin, Streptavidin-biotin complex; frozen section)

The anatomical level of the split may be subcorneal, in the stratum Malpighii, suprabasal or subepidermal. The mechanism of the vesciculation may be acantholysis (immunological or non-immunological, congenital or acquired), exaggerated spongiosis (aspecific breakdown of intercellular connection, as in eczema or contact dermatitis), and ballooning or intracellular oedema (e.g. Herpes viruses infections).

In subepidermal blisters, the different proportion of inflammatory cells, such as neutrophils or eosinophils within the lesion or in the adjacent dermis, provide another clue for diagnosis. Subtle clues for morphological assessment are summarised in Table 3. Nevertheless, morphological assessment alone is not always completely reliable for a definitive diagnosis and, in the case of subepidermal blistering disease, a supplementary study with immunofluorescence techniques is often essential. Therefore, fluorescence immunolabelling to detect basement membrane zone autoantibodies is widely used. This test has been used, traditionally, to detect the presence and eventually the type of immunoglobulins (mainly IgG or IgA) and the type of deposit (linear or granular). However, in the last decade, immunofluorescence microscopy has been updated by the chemically separated skin technique that now represents the test of choice to reach a more reliable diagnosis [15] (Table 4). This technique allows separation of the basal membrane at the middle lamina lucida using either 1 M NaCl or 20 mM Na-EDTA and can be applied in both direct and indirect immunofluorescence. Detection of autoantibody deposits at the epidermal roof of the salt split skin section indicates that the molecular target is located either in the hemidesmosome or in the upper lamina lucida. However, detection of autoantibodies in the dermal floor of the chemically separated skin indicates that the Ags are components either of the lower lamina lucida, the lamina densa or the sub-lamina densa (Table 4). Based on these findings, bullous diseases have been separated into two principal groups: one characterised by antibodies against hemidesmosomes/upper lamina lucida, such as BP and linear IgA dermatitis, the second group of diseases with autoantibodies against structures localised either at the lower lamina lucida (cicatricial pempigoid, anti-laminin cicatricial pemphigoid and the rare p105 pemphigoid) or in the lamina densa/sub-lamina densa as EB acquisita and anti-285 kDa Ag linear IgA dermatitis (Fig. 3, Fig. 4).

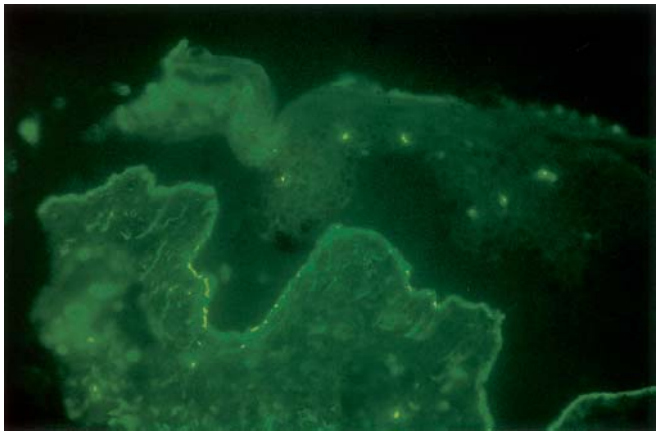

Fig. 3 Salt split skin. Linear deposition of anti IgG antibodies on the dermal side of the split: Epidermolysis bullosa acquisita

Table 3 Clues for diagnosis of autoimmune subepidermal bullous skin disease

Subepidermal blister disease	Diagnostic morphological clues
With little inflammation	
Epidermolysis bullosa acquisita (heterogeneous pattern, ranging from a form with little inflammation to a florid neutrophilic infiltrate[see below])	Sparse lymphocytic infiltrate around the vessels in the superficial dermis PAS stain: BM bisected and the most part of BM attached to the roof of the bulla
Bullous pemphigoid (cell-poor type)	Only few lymphocytes in the dermis, eosinophils usually detectable within the bulla
Porphyria cutanea tarda	Festooning (preservation of dermal papillae in the floor of the bullae) PASd positive material in the wall of superficial small vessels and BM
Toxic epidermal necrolysis	Confluent necrosis of the overlying epidermis
Bullous variant of drug reaction	Festooning, PASd material around the superficial vessel, few eosinophils
With lymphocytes	
Paraneoplastic pemphigus	Lichenoid tissue reaction pattern (heavy, band like dermal inflammatory infiltrate, exocytosis of lymphocytes, apoptotic keratinocytes, basal vacuolar changes) with suprabasal acantholisis and clefting. Focal epidermal spongiosis
Lichen planus pemphigoides	Civatte bodies usually present Few eosinophils and neutrophils beneath the blister
Bullous variant of erythema multiforme	Interface dermatitis at the borders of the split (obscuring of the junction), necrosis of keratinocytes in the upper layers
Bullous variant of fixed drug reaction	Interface dermatitis at the borders of the split with obscuring of the junction Melanin incontinence, extension of the infiltrate (deeper compared with the erythema multiforme)
Bullous variant polymorphous drug reaction	Dermal inflammatory infiltrates superficial and deep
With eosinophils	
Bullous pemphigoid	Unilocular subepidermal blister Eosinophilic infiltrate in dermis, along the BM, within the bulla, in the epidermis (eosinophilic spongiosis) Regeneration in old lesions Variants: pre-pemphigoid (also many years before): Oedema in the superficial dermis Superficial and mid-dermis perivascular infiltrate with numerous eosinophils
Pemphigoid gestationis	Early: oedema of papillary dermis, superficial and mid dermis perivascular infiltrate of lymphocytes and eosinophils. Focal spongiosis Late: eosinophils and lymphocytes within the bulla and in the dermis. Possible presence of eosinophilic microabscess at the tip of papillae
Bullous variant of drug reaction	Similar to bullous pemphigoid, but with less eosinophils
With neutrophils	
Dermatitis herpetiformis	Papillary microabscess with prominent fibrin, multilocular vesicles
Linear IgA bullous dermatitis	In many cases indistinguishable from dermatitis herpetiformis
Cicatricial (mucous membrane) pemphigoid	Early: neutrophilic microabscess similar to dermatitis herpetiformis Late: more eosinophils, tendency to produce scar (polarized light: bundle of collagen parallel to the surface) Mucosal lesion: predominance of plasma cells Variants: Localised cicatricial pemphigoid Ocular cicatricial pemphigoid
Epidermolysis bullosa acquisita	Heterogeneous pattern. Mixed infiltrate in the superficial dermis, with predominance of neutrophils, few eosinophils PAS stain shows the BM bisected and the most part of BM attached at the roof of the bulla
Bullous lupus erythematosus	Extensive liquefaction of the dermo-epidermal junction (mostly in anti-Ro [SS-A] positive patients) Microabscess with clefts at tips of dermal papillae
Erysipela	Massive oedema, extravasated erythrocytes

Morphological characterisation of subepidermal blistering diseases: features of the inflammatory infiltrate

Little inflammation

A wide and heterogeneous group of subepidermal diseases show only minimal inflammation, as the mechanism is not inflammatory. EB is a group of meccanobullous diseases characterised by a congenital defect of different adhesion molecules or of some structural components of keratinocytes, such as cytoskeletal molecules (Table 1). This group consists of distinct variants such as EB simplex, EB with muscular dystrophy, EB with pyloric atresia, generalised atrophic benign EB, Herlitz junctional EB and dystrophic EB.

Apart from this group of congenitally transmitted conditions, some acquired diseases may also show only minor inflammation. EB acquisita and bullous pemphig-

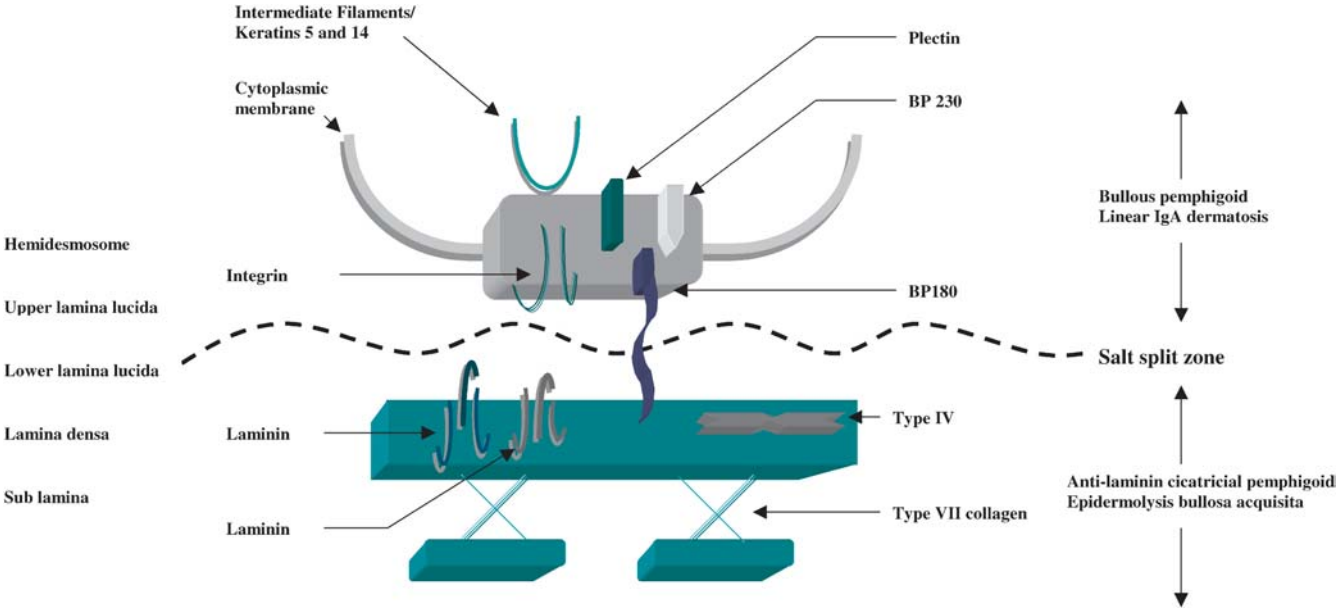

Fig. 4 Schematic diagram of basal membrane. The figure shows the relative location of known antigens in salt split skin

Table 4 Direct immunofluorescence in intact basement membrane preparations and in salt split skin.*BM* basement membrane

Subepidermal blister disease	Direct immunofluorescence			Salt split skin Results
	Immunoreactants	Pattern	Percentage of positivity	
With lymphocytes				
Paraneoplastic pemphigus	IgG, C3	Cell surface Linear band at BM	100% Occasional	Occasionally positive
Lichen planus pemphigoides	IgG, C3	Linear band at BM	>50%	
With eosinophils				
Bullous pemphigoid	C3 IgG IgA, IgM	Linear band at BM	100% 50–90% <30%	90% positive Epidermal
Pemphigoid gestationis	C3 IgG	Linear band at BM	100% 40%	Epidermal
With neutrophils				
Dermatitis herpetiformis	IgA	Granular deposition in dermal papillae	100%	Not applicable
Linear IgA bullous dermatosis	IgA	Linear band at BM	>90%	80–90% Epidermal or dermal
Cicatricial (mucous membrane) pemphigoid	IgG, C3 IgA	Linear band at BM	80–100% Occasional	50–80% Epidermal or dermal
Epidermolysis bullosa acquisita	IgG C3, IgA, IgM	Linear band at BM	100% Occasional	50–80% Dermal
Bullous lupus erythematosus	IgG C3 IgA IgM	Linear band at BM	100% 80–100% 60–70% 50%	Often positive Dermal

oid poor cell variant are paradigmatic for this group of disorders. In reality, EB acquisita often has a heterogeneous pattern, ranging from a form with minor inflammation to a form with a florid neutrophilic infiltrate. Also (though more rarely), BP, especially if the biopsy is taken from a bulla without erythematous base, may show a misleading histological appearance where the usually florid dermal infiltrate is absent. A careful search for eosinophils within the bulla may be the only feature that might lead to a correct diagnosis.

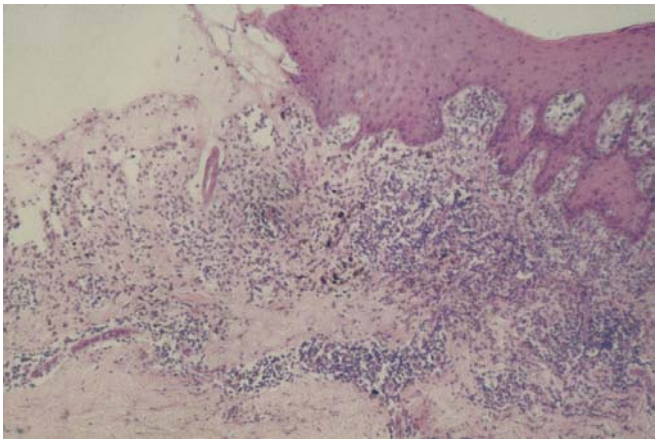

Fig. 5 Classic example of subepidermal blistering dermatoses characterised by wide infiltration of lymphocytes in lichen planus pemphigoides. In this case, low magnification shows the typical band-like lymphocytic infiltrate beneath the subepidermal split

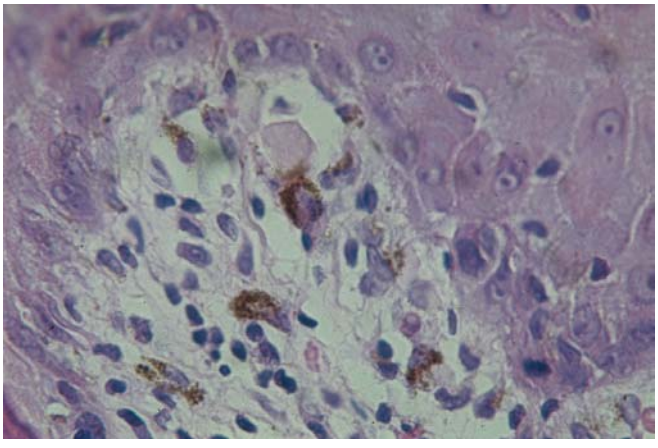

Fig. 6 Lichen planus pemphigoides: high magnification shows exocytoses of lymphocytes, pigment incontinence and the presence of Civatte bodies which are the basis for diagnosis

Lymphocytes

Blisters characterised by the wide infiltration of lymphocytes are present in the lichen planus pemphigoides (Fig. 5) and in the paraneoplastic pemphigus where autoantibodies are elicited against a complex of desmosomial Ags such as desmoplakin I (250 kDa) [17] and the BP 230 Ag (Table 2). In these cases the presence of features typical of lichenoid reactions, such as the band-like infiltrate reaction with exocytoses of lymphocytes and only occasional neutrophils and eosinophils, the presence of apoptotic keratinocytes are the basis for diagnosis. Direct immunofluorescence shows C3 and IgG intercellular and basal membrane positivity.

The diagnosis of bullous lichen planus pemphigoid requires the coexistence of features usually characterising the lichen planus, as Civatte bodies (Fig. 6) (Table 3).

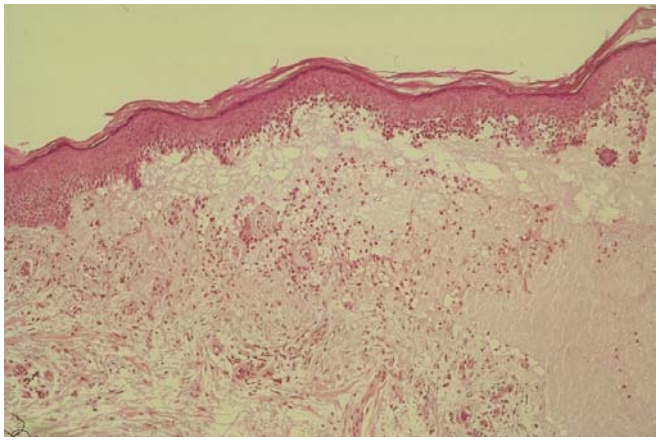

Fig. 7 Typical dermatosis with eosinophils is bullous pemphigoid. In this example, low magnification shows a unilocular subepidermal blister

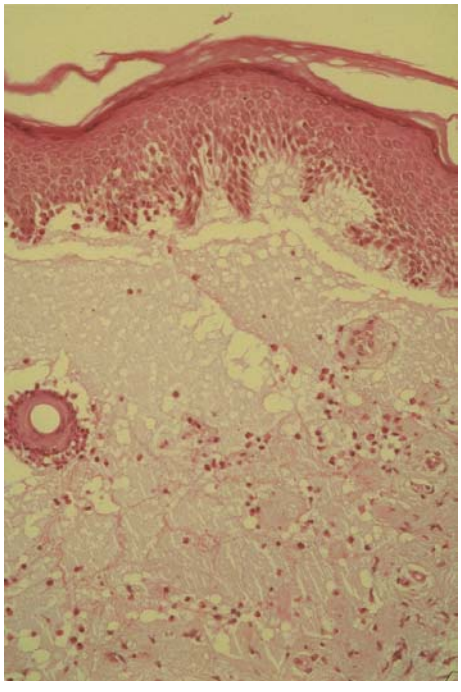

Fig. 8 Bullous pemphigoid: a florid eosinophilic infiltrate is widely present along the BM, within the bulla and in the epidermis (eosinophilic spongiosis)

Eosinophils

When the inflammatory infiltrate is mainly composed of eosinophils, the range of possible diagnoses is restricted to BP (Fig. 7, Fig. 8, Fig. 9) and pemphigoid gestationis. After 48 h, eosinophils may be the most represented cell type also in dermatitis herpetiformis.

As regards the pathogenesis of BP, studies have shown T-lymphocytes reacting against the 180 kDa ectodomain [21] and the subsequent recruitment of eosinophils by production of interleukin-5 and eotaxin (one of the most

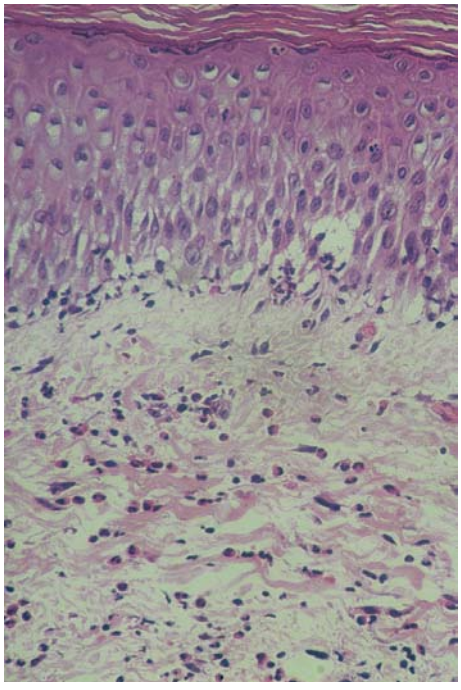

Fig. 9 This figure shows a variant of bullous pemphigoid: the pre-pemphigoid. It can also appear many years before the typical form of the disease develops and is histologically characterised by oedema in the superficial dermis and superficial and mid dermis infiltrate with numerous eosinophils

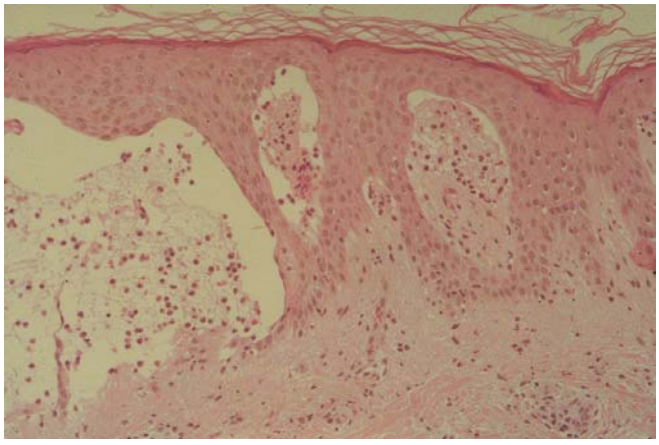

Fig. 10 Prototype of blistering dermatosis characterised by neutrophilic infiltrate is dermatitis herpetiformis. Papillary microabscess with prominent fibrin and multilocular vesicles are the main clues for diagnosis of dermatitis herpetiformis

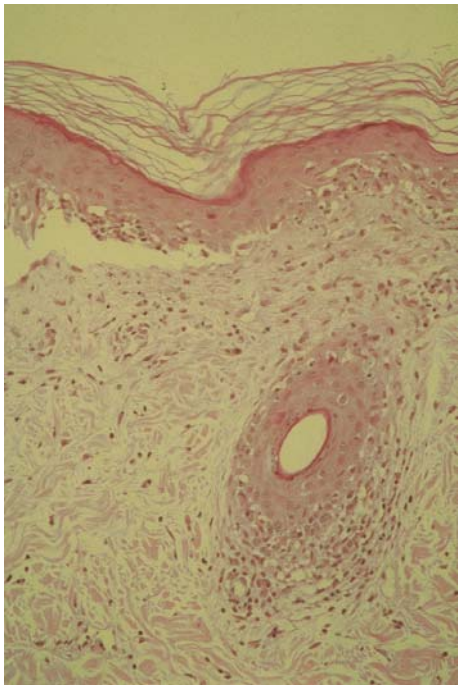

Fig. 11 Another example of dermatosis characterised by the presence of neutrophils is bullous lupus erythematosus. In this condition, involvement of adnexa and blood vessels is usual

powerful eosinophilic chemokines) [9]. Such new information now adds to the traditional view that eosinophil chemiotaxis follows the complement cascade activated by the fixation of antibodies (usually IgG) on the BP Ags. The importance of mast cells, myelo-monocytes, T lymphocytes and their products, such as cytokines, colony stimulating factors, TNFs and IFNs represent another milestone in the understanding of these diseases.

In bullous pemphigoid, direct immunofluorescence shows a linear deposit of IgG and C3 on the basement membrane (lamina lucida in electron microscopy). The same BP Ags, either 180 kDa or 230 kDa (extremely rare), could be involved in pemphigoid gestationis. In this disease, an IgG1 is easily identified in all the patients. This antibody, which is directed against a placental matrix Ag, cross reacts with the BP180 Ag [8] triggering the activation of the complement cascade and the following recruitment of eosinophils. C3 is almost always present at the direct immunofluorescence investigation; IgG in some cases only (electron microscopy: in lamina lucida, as in BP).

Neutrophils

When the inflammatory infiltrate is composed predominantly of neutrophils, possible diagnoses include dermatitis herpetiformis (Fig. 10), linear IgA bullous dermatosis, bullous lupus erythematosus (Fig. 11, Fig. 12) and cicatricial pemphigoid (also in the ocular and localised variants). In dermatitis herpetiformis, the disease is triggered by the fixation of autoantibodies (IgA class 1 or, rarely, class 2) to the basement membrane, characteristically on the tips of dermal papillae. The split seems to follow the same mechanism as the other diseases described above. The first mechanism ascertained was the recruitment of neutrophils following the activation of complement cascade as a result of the fixation of the IgA on the Ag. Local production of cytokines amplified the

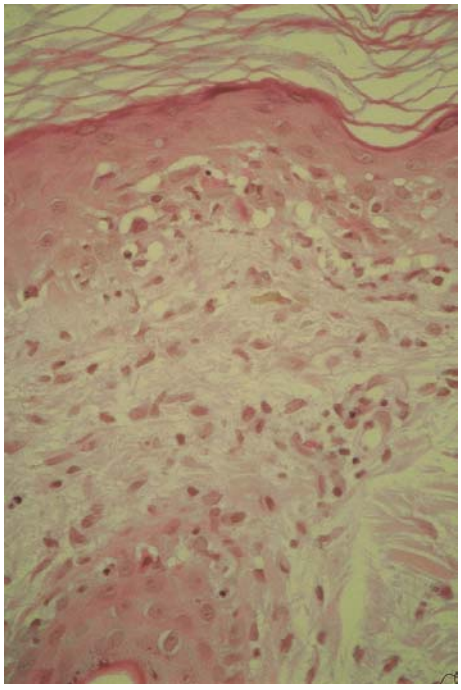

Fig. 12 Bullous lupus erythematosus: histology shows liquefaction of the dermo-epidermal junction and microabscess with clefts at tips of dermal papillae

recruitment of neutrophils and subsequently (36–48 h later) of eosinophils. Now a complex mechanism also involving lymphocytes and other inflammatory cells has been described [1]. Enzymes released by these cells destroyed the basement membrane with the split formation. Characteristic of this disease is the presence of microabscesses on the tips of oedematous dermal papillae that partially coalesce forming the typical multilocular vesicles (Fig. 10). Direct immunofluorescence shows the presence of granular deposits of IgA in the dermal papillae also in unaffected skin. The molecular target is still unknown, but recent studies suggest that at the base of the disease there is a congenital predisposition linked to alterations in BP230 and plectin/HD1, which may contribute or predispose to blister formation [20].

A disease histologically indistinguishable from dermatitis herpetiformis is linear IgA bullous dermatosis. In this disease (known in two variants, one in childhood and one in the adult), the main characteristic is the presence of a smooth deposit of IgA in the basement membrane. The autoimmune reaction is elicited either against anchoring filaments (97-kDa Ag or LABD97, and 120-kDa Ag or LAD-1) or molecules of the sublamina lucida region (285-kDa Ag). Another disease mediated by IgA autoantibodies is ocular pemphigoid. In reality, sometimes this condition also shows the presence of an IgG reaction. The autoimmune response is directed against a 45-kDa Ag present in the conjunctival basement membrane. Belonging to the same family of ocular cicatricial pemphigoid (this name reflects a traditional view, linked with the tendency of these lesions to scar) is the cicatricial pemphigoid (mainly affecting the mucous membranes and actually re-named mucous membrane pemphigoid) and the localised variant (affecting the skin without involvement of the mucous membrane) [11]. Not surprisingly, this last group of diseases also shows the involvement of BP 180 Ag. A minority of the cases examined had autoantibodies reacting against laminine-5 (or epiligrine), one of the anchoring filaments present at the junction between lamina lucida and lamina densa (Fig. 4). Direct immunofluorescence shows linear deposits of IgG and C3 along the basement membrane in the majority of cases (Table 4).

Summary

Recent advances in autoimmune vesiculobullous diseases of the skin and mucous membranes has led to a better understanding of their patho-physiology. They are now among the most studied dermatological conditions, and better understanding of them represents one of the most important successes of dermatological science in the last few years. Nevertheless, their diagnosis still sometimes presents a challenge for dermatopathologists. The very nature of these conditions, related to their complex pathogenic mechanisms and morphological overlapping, means that misdiagnoses often occur. Moreover, the reason why diseases with the same molecular target (such as cicatricial pemphigoid and BP or some forms of cicatricial pemphigoid and EB acquisita) have such different clinical expression is still not understood. This phenomenon has been attributed, in some cases, to the involvement of different antigenic targets located on the same Ags (as in BP and cicatricial pemphioid, where the antibody reaction involves two different portions of the BP 180 Ag). However, hypothetically, this phenomenon might also be linked to the different expression of MHC and opens up another extremely interesting field of research that would mesh the different expression of inflammatory reactions with the MHC asset.

Recent techniques such as sodium chloride split skin and “antigen mapping” with some newly developed immunohistochemical antibodies may, in time, become useful in differential diagnosis and complement the morphological approach, which still plays a pivotal role.

Acknowledgements We thank Dr Mirella Giangiacomi (Institute of Pathology, University of Ancona-Italy) and Edward Browning (Institute of Pathology, The Royal London Hospital, London, UK) for providing H&E and DIF microphotographs.

References

1. Amerio P, Verdolini R, Giangiacomi M, Proietto G, Feliciani C, Offidani A, Bossi G (2000) Expression of eotaxin, interleukin 13 and tumour necrosis factor-alpha in dermatitis herpetiformis. Br J Dermatol 143:974–978
2. Borrego L, Maynard B, Peterson EA, George T, Iglesias L, Peters MS, Newman W, Gleich GJ, Leiferman KM (1996) Deposition of eosinophil granule proteins precedes blister

formation in bullous pemphigoid. Comparison with neutrophil and mast cell granule proteins. Am J Pathol 148:897–909
3. Chan LS (1997) Human skin basement membrane in health and in autoimmune diseases Front Biosci 15;2:d343–352
4. Chan LS, Cooper KD (1994) A novel immune-mediated subepidermal bullous dermatosis characterized by IgG autoantibodies to a lower lamina lucida component. Arch Dermatol 130:343–347
5. Chan LS, Woodley DT(1996) The 105-kDa basement membrane autoantigen p105 is N-terminally homologous to a tumor-associated antigen. J Invest Dermatol 107:209–214
6. Czech W, Schaller J, Schopf E, Kapp A (1993) Granulocyte activation in bullous diseases: release of granular proteins in bullous pemphigoid and pemphigus vulgaris. J Am Acad Dermatol 29:210–215
7. D'Auria L, Cordiali Fei P, Ameglio F (1999) Cytokines and bullous pemphigoid. Eur Cytokine Netw 10:123–134
8. Engineer L, Bhol K, Ahmed AR (2000) Pemphigoid gestationis: a review. Am J Obstet Gynecol 183:483–491
9. Engineer L, Bhol K, Kumari S, Razzaque Ahmed A (2001) Bullous pemphigoid: interaction of interleukine 5, anti-basement membrane zone antibodies and eosinophil. A preliminary observation. Cytokine 13:32–38
10. Fine JD, Eady RA, Bauer EA, Briggaman RA, Bruckner-Tuderman L, Christiano A, Heagerty A, Hintner H, Jonkman MF, McGrath J, McGuire J, Moshell A, Shimizu H, Tadini G, Uitto J (2000) Revised classification system for inherited epidermolysis bullosa: report of the second international consensus meeting on diagnosis and classification of epidermolysis bullosa. J Am Acad Dermatol 42:1051–1066
11. Fleming TE, Korman NJ (2000) Cicatricial pemphigoid. J Am Acad Dermatol 43:571–594
12. Fujimoto W, Ohtsu T, Toi Y, Nakanishi G, Arata J (2000) Linear IgA disease with IgA antibodies directed against 200- and 280-kDa epidermal antigens. Br J Dermatol 142:1213–1218
13. Fujiwara S, Shinkai H, Takayasu S, Owaribe K, Tsukita S, Kageshita T (1992) A case of subepidermal blister disease associated with autoantibody against 450 kD protein. J Dermatol 19:610–613
14. Fujiwara S, Kohno K, Iwamatsu A, Shinkai H (1994) A new bullous pemphigoid antigen. Dermatology 189[Suppl 1]:120–122
15. Gammon WR, Fine JD, Forbes M, Briggaman RA (1992) Immunofluorescence on split skin for the detection and differentiation of basement membrane zone autoantibodies. J Am Acad Dermatol 27:79–87
16. Ghohestani RF, Hudson BG, Claudy A, Uitto J (2000) The alpha 5 chain of type IV collagen is the target of IgG autoantibodies in a novel autoimmune disease with subepidermal blisters and renal insufficiency. J Biol Chem 275:16002–16006
17. Hashimoto T, Amagai M, Watanabe K, Chorzelski TP, Bhogal BS, Black MM, Stevens HP, Boorsma DM, Korman NJ, Gamou S, et al (1995) Characterization of paraneoplastic pemphigus autoantigens by immunoblot analysis. J Invest Dermatol 104:829–834
18. Hertl M, Riechers R (1999) Analysis of the T cells that are potentially involved in autoantibody production in pemphigus vulgaris. J Dermatol 26:748–752
19. Kawahara Y, Zillikens D, Yancey KB, Marinkovich MP, Nie Z, Hashimoto T, Nishikawa T (2000) Subepidermal blistering disease with autoantibodies against a novel dermal 200-kDa antigen. J Dermatol Sci 23:93–102
20. Leivo T, Lohi J, Kariniemi AL, Molander G, Kiraly CL, Kotovirta ML, Owaribe K, Burgeson RE, Leivo I (1999) Hemidesmosomal molecular changes in dermatitis herpetiformis; decreased expression of BP230 and plectin/HD1 in uninvolved skin. Histochem J 31:109–116
21. Lin MS, Fu CL, Giudice GJ, Olague-Marchan M, Lazaro AM, Stastny P, Diaz LA (2000) Epitopes targeted by bullous pemphigoid t lymphocytes and autoantibodies map to the same sites on the bullous pemphigoid 180 ectodomain. J Invest Dermatol 115:955–961
22. Liu Z, Shapiro SD, Zhou X, Twining SS, Senior RM, Giudice GJ, Fairley JA, Diaz LA (2000) A critical role for neutrophil elastase in experimental bullous pemphigoid. J Clin Invest 105:113–123
23. Liu Z, Zhou X, Shapiro SD, Shipley JM, Twining SS, Diaz LA, Senior RM, Werb Z (2000) The serpin alpha1-proteinase inhibitor is a critical substrate for gelatinase B/MMP-9 in vivo. Cell 102:647–655
24. Mascaro JM Jr, Zillikens D, Giudice GJ, Caux F, Fleming MG, Katz HM, Diaz LA (2000) A subepidermal bullous eruption associated with IgG autoantibodies to a 200 kd dermal antigen: the first case report from the United States. J Am Acad Dermatol 42:309–315
25. Roh JY, Yee C, Lazarova Z, Hall RP, Yancey KB (2000) The 120-kDa soluble ectodomain of type XVII collagen is recognized by autoantibodies in patients with pemphigoid and linear IgA dermatosis. Br J Dermatol 143:104–111
26. Schumann H, Baetge J, Tasanen K, Wojnarowska F, Schacke H, Zillikens D, Bruckner-Tuderman L (2000) The shed ectodomain of collagen XVII/BP180 is targeted by autoantibodies in different blistering skin diseases. Am J Pathol 156:685–695
27. Stahle-Backdahl M, Inoue M, Guidice GJ, Parks WC (1994) 92-kD gelatinase is produced by eosinophils at the site of blister formation in bullous pemphigoid and cleaves the extracellular domain of recombinant 180-kD bullous pemphigoid autoantigen. J Clin Invest 93:2022–2030
28. Toto P, Feliciani C, Amerio P, Suzuki H, Wang B, Shivji GM, Woodley D, Sauder DN (2000) Immune modulation in pemphigus vulgaris: role of CD28 and IL-10. J Immunol 164:522–529
29. Wakugawa M, Nakamura K, Hino H, Toyama K, Hattori N, Okochi H, Yamada H, Hirai K, Tamaki K, Furue M (2000) Elevated levels of eotaxin and interleukin-5 in blister fluid of bullous pemphigoid: correlation with tissue eosinophilia. Br J Dermatol 143:112–116

Virchows Arch (2003) 443:194–205
DOI 10.1007/s00428-003-0846-7

ORIGINAL ARTICLE

Taiki Fujimoto · Yoshihide Fujigaki · Di Fei Sun · Akashi Togawa · Katsuhiko Yonemura · Akira Hishida

Important role for fibronectin-EIIIA during renal tubular repair and cellular recovery in uranyl acetate-induced acute renal failure of rats

Received: 2 April 2003 / Accepted: 20 May 2003 / Published online: 17 July 2003
© Springer-Verlag 2003

Abstract The present study was designed to identify the source and kinetics of an alternatively spliced "embryonic" cellular fibronectin EIIIA (cFn-EIIIA) in relation to regenerating renal tubules in uranyl acetate (UA)-induced acute renal failure (ARF) in rats. Damage of the proximal tubules was found as early as day 2 after induction of ARF, peaked at day 5, and was almost substituted by epithelial relining by day 7. Immunohistochemistry showed de novo deposition of cFn-EIIIA in peritubular regions as early as day 2, then on the tubular basement membrane (TBM) after day 4. β1 Integrin, the receptor for Fn, was mainly found at the basal side of tubules in the normal control and increased in the interstitium after induction of ARF, but the staining pattern gradually returned to the control after day 7. Immunoelectron microscopy revealed that cFn-EIIIA was produced initially by the peritubular endothelium and later by fibroblastic cells and was deposited to the TBM, on which regenerating tubules proliferated, probably with cFn-EIIIA production. β1 Integrin was expressed in cFn-EIIIA-producing cells, especially in regenerating tubular cells, suggesting that cFn-EIIIA signal transduction affects regenerating tubules. Transforming growth factor (TGF)-β1 was found in some damaged proximal tubules and interstitial cells after induction of ARF and later in the regenerating tubules. CFn-EIIIA and β1 integrin mRNA levels were upregulated as early as day 2. TGF-β1 mRNA level significantly increased after day 3, suggesting a modulatory role for TGF-β1 on cFn-EIIIA production, but not by day 2. Our data suggest that cFn-EIIIA production by the endothelium during the very early response to tubular injury and by fibroblastic cells and regenerating tubules may play an important role in the cellular recovery of UA-induced ARF in rats.

Keywords Cellular fibronectin · β1 Integrin · Acute renal failure · Proximal tubule · TGF-β1

T. Fujimoto · Y. Fujigaki (✉) · D. F. Sun · A. Togawa · A. Hishida
The First Department of Medicine,
Hamamatsu University School of Medicine,
1-20-1 Handayama, 431-3192 Hamamatsu, Japan
e-mail: yf0516@hama-med.ac.jp
Tel.: +81-53-4352261
Fax: +81-53-4349447

K. Yonemura
Hemodialysis Unit, Hamamatsu University School of Medicine,
431–3192 Hamamatsu, Japan

Introduction

The importance of extracellular matrix (ECM) deposition in wound healing is well known [12]. Fibronectin (Fn) deposition seems to be essential in ECM, because it influences various cellular processes, including cell migration, proliferation, and synthesis of ECM in remodeling after injury [1, 5, 33]. Integrins serve as Fn receptors at the cell surface, and the interaction of Fn and integrins is crucial for Fns to exhibit the aforementioned cellular activities [13, 20]. Thus, it is conceivable that Fn deposition and cells expressing Fn receptors may be closely involved in the wound-healing process.

Fns are dimeric glycoproteins present in the plasma (plasma fibronectin; pFn) [29] and in tissue ECMs (cellular fibronectin; cFn) [23]. Both forms of Fn are encoded by a single gene and arise from a primary transcript by alternative RNA splicing at three distinct regions termed EIIIA, EIIIB, and V in rats [25, 30]. The equivalent regions in humans are designated EDA, EDB, and IIICS, respectively [16, 21, 35]. EIIIA and EIIIB domains are either completely included or excluded within the mature molecule of cFn [7, 17]. PFn, which is produced only by hepatocytes and circulates as a soluble protein, lacks both domains [29]. Splice variants containing EIIIA are expressed during development but are minimally present in normal adult tissue [2]. CFn-EIIIA may reappear, however, in the setting of epithelial repair [7]. In fact, de novo expression of cFn-EIIIA has been reported to play an important role in epithelial repair of the skin, liver, and lung [14, 19, 26].

Barnes et al. [2] reported that the expression of cFn-EIIIA in the kidney parallels that of α-smooth muscle

actin (α-SMA, myofibroblast phenotype) in several settings of renal remodeling, including embryonic, maturation, and diseased kidney. Cellular recovery after acute renal failure (ARF) is a unique form of wound healing or tissue remodeling, and Fn expression was reported in this process in association with regeneration of proximal tubules (PT) in post-ischemic ARF [4, 34]. Recently, Zuk et al. [36] documented that both pFn and cFns containing the V95 and/or EIIIA regions may contribute to the pathogenesis of ARF and to the repair seen in the post-ischemic rat kidney. However, the source of cFns and their precise relationship to the regeneration of tubular cells are not clear at present. We recently reported that interstitial cellular response, including transient appearance of myofibroblasts and macrophage infiltration, might be important for regenerative repair of PT in uranyl acetate (UA)-induced ARF in rats [27, 28]. However, whether the interstitial cellular response, which is probably important for wound healing, is also associated with cFn-EIIIA deposition as in other disease conditions or wound healing remains to be confirmed.

In the present study, we investigated the expression and source of cFn-EIIIA as well as of β1 integrin (as Fn receptor) during renal tubular damage and repair in UA-induced ARF in rats.

Materials and methods

Induction of UA-induced ARF

Experiments were conducted on 45 male Sprague-Dawley rats weighing 220–280 g (SLC Co., Shizuoka, Japan). Rats had free access to standard rat chow and drinking water. They received a single intravenous injection of 5 mg/kg of UA via the dorsal penile vein, and five rats were sacrificed before and at 2, 3, 4, 5, 7, 9, 15, and 21 days after UA injection. Rats were anesthetized with intraperitoneal pentobarbital sodium (30 mg/kg) and a blood sample was collected through the abdominal aorta, then both kidneys were removed after flushing with phosphate-buffered saline (PBS). Serum creatinine level was measured by the enzymatic method (Mizuho Med., Saga, Japan).

Tissue processing

The harvested kidneys were bisected through the longitudinal axis and some were cut into smaller sections. They were fixed with 20% neutral-buffered formalin, 4% paraformaldehyde or methacarn solution, then embedded in paraffin. Portions of renal tissues were snap frozen in cold N-hexane and stored at −70°C for immunofluorescence (IF) studies. For pre-embedding for immunoelectron microscopy and immunohistochemistry, the renal tissues were fixed with 4% paraformaldehyde for 9 h and cryoprotected in 10%, 15% and 20% sucrose for 4 h each. The tissues were then placed in cryogenic embedding medium (OCT Compound, Sakura Finetechnical Co., Japan) and snap frozen in cooled N-hexane.

Histochemistry and immunohistochemistry

For histological examination, 4-μm-thick paraffin sections were stained with periodic acid-Schiff (PAS). To detect transforming growth factor (TGF)-β1, ED-1, as a marker of rat monocytes/macrophages, and α-SMA, as a phenotypic marker of myofibroblasts, paraffin sections were first incubated with normal serum matched to the species for secondary antibodies. To detect cFn-EIIIA, 4% paraformaldehyde-fixed cryostat sections were used. After incubation with the primary antibodies (rabbit polyclonal antibody against TGF-β1; anti-LC; a generous gift from Dr. K.C. Flanders, NIH, USA [8], mouse monoclonal anti-ED-1; Serotec, Oxford, UK, mouse monoclonal anti-human α-SMA; Dako, Carpinteria, CA, and mouse anti-cFn EDA, from human fibrosarcoma cells, this antibody cross-reacts with the rat EIIIA region; Chemicon International Inc., Temecula, CA), sections were reacted with biotin conjugated donkey anti-rabbit IgG (Chemicon) or donkey anti-mouse 1gG (Chemicon) for 30 min at room temperature. Then, streptavidin-conjugated peroxidase (Nichirei, Tokyo, Japan) was added for 30 min. After washing in PBS, the reaction products were visualized by incubation with diaminobenzidine detection kit (Nichirei). Histological controls were obtained by omitting the primary antibodies or replacing the primary antibodies with normal mouse or rabbit IgG at equivalent concentrations. No significant staining was observed in either normal control or experimental sections.

Cationic gold staining

Anionic sites (mainly representing sulfated glycosaminoglycans, the major constituents of the ECM) were visualized with a gold-conjugated poly-L-lysine probe [15]. Deparaffinized sections were rinsed in PBS (pH 2.0) for 10 min, then incubated on a drop of cationic (poly-L-lysine) colloidal gold (5 nm) (diluted 1:100 in PBS at pH 2.0; Biocell Rescarch Laboratories, Cardiff, UK) for 4 h at 37°C. The sections were washed in distilled water and developed with a silver enhancer (Biocell) for 10 min at room temperature.

Immunofluorescence studies

IF studies were performed on 4-μm-thick cryostat sections fixed in cold acetone. Indirect IF was performed with rabbit anti-rat pFn antibody (from rat plasma; Chemicon), mouse anti-cFn EDA antibody (Chemicon), rabbit anti-pan-laminin antibody (from EHS-mouse sarcoma; Sanbio, Netherlands), rabbit anti-collagen type-III antibody (from rat skin; Chemicon), rabbit anti-collagen type-IV antibody (from EHS-mouse sarcoma; LSL Co., Japan), or rabbit anti-β1 integrin antibody (a gift from Dr. K. Loester [18]), then followed by fluorescein isothiocyanate-Iabeled swine anti-mouse IgG (Dako) or swine anti-rabbit IgG (Dako). Liver tissues were also examined by IF for cFn-EIIIA.

Immunoelectron microscopy

For ultrastructural localization of cFn-EIIIA or β1 integrin, 4% paraformaldehyde-fixed 6- to 8-μm cryostat sections were rinsed in 10% sucrose in PBS and then incubated with 10% normal donkey serum for 20 min, followed by incubation with the primary antibodies (mouse anti-cFn EDA or rabbit anti-β1 integrin). Following extensive washing in 10% sucrose-PBS, the sections were incubated with biotinylated donkey anti-mouse IgG (Chemicon) or antirabbit IgG (Fab')2 (Chemicon) for 60 min. After the sections had been fixed in 2% glutaraldehyde for 10 min, reaction products were visualized by incubating with diaminobenzidine, then the sections were examined post-fixed in 1% osmium tetroxide for 1 h, dehydrated in graded ethanol series, and embedded in Epon 812. Ultrathin sections were stained with lead citrate for 1.5 min, and examined with a JEM-1220 electron microscope (JEOL, Tokyo).

Enumeration of PT cells and ED-1-positive monocyte/macrophages

To determine the number of PT cells, reflecting a balance of tubular cell death and tubular cell proliferation, we counted the number of epithelial cells in 100 cross-sections of the PT in the outer stripe of outer medulla (OSOM) using PAS-stained sections and calculated the number of cells per field at ×400 magnification. To minimize observer bias, morphometric examination was performed without the knowledge of the group from which the tissue was obtained.

The number of ED-1-positive cells was counted in 50 randomly selected fields in OSOM in each kidney at ×400 magnification. The mean number at each time point was displayed in histograms.

Semiquantitative reverse transcription-polymerase chain reaction for cFn EIIIA, β1 integrin, and TGF-β1 mRNAs

Total RNAs were isolated from frozen kidney tissues containing cortex and outer medulla by the acid guanidinium isothiocyanate-phenol-chloroform extraction method [6]. Reverse transcription (RT) of RNA was performed using a first-strand cDNA synthesis kit (Boehringer Mannheim Co., Indianapolis, IN) with 1 μg total RNA. After completion of cDNA synthesis, RT enzyme was heat inactivated for 5 min at 99°C. The polymerase chain reaction (PCR) reaction with Ampli *Taq* Gold (Applied Biosystems, Foster City, CA) was carried out for analysis of cFn-EIIIA, β1 integrin, and TGF-β1 mRNAs using primers described previously [11, 14, 31]. Primers for cFn-EIIIA were sense 5′-CTCCGAATTCAA-CATTGACCGCCCTAAAGGACTG-3′ and antisense 5′-CTC-CAAGCTTTGTGGACTGGACTCCAATCAGGGG-3′ with an amplified RT-PCR product of 280 bp. Primers for β1 integrin were sense 5′-AATGTTTCAGTGCAGAGCC-3′ and antisense 5′-TTGGGATGATGTCGGGAC-3′ with an amplified RT-PCR product of 260 bp. Primers for TGF-β1 were sense 5′-CAAAGACAT-CACACACAGTA-3′ and antisense 5′-GGCGTTGAGCCC TTTCCAGG-3′ with an amplified RT-PCR product of 440 bp. Primers for glyceraldehyde-3-phosphate dehydrogenase (GAPDH), a house keeping gene, were sense 5′-AATGCATCCTGCACCAC-CAA-3′ and antisense 5′-GTAGCCATATTCATTGTCATA-3′ with an amplified RT-PCR product of 515 bp. Cycles were: 1 min denaturation at 94°C, 30 s annealing at 45°C for cFn-EIIIA, 1 min annealing at 56°C for β1-integrin, 1 min annealing at 58°C for TGF-β1, 1 min annealing at 60°C for GAPDH and 1 min extension at 72°C using Zymoreactor II (ATTO Co., Tokyo). PCR products were electrophoresed and the density of each DNA band was measured with NIH Image (Bethesda, MD). The mRNA levels for cFn-EIIIA, β1 integrin, and TGF-β1 were expressed as a ratio of the optical density units relative to GAPDH. Each RNA aliquot was amplified in duplicate.

Statistical analysis

Data are expressed as mean ± standard error of the mean. Differences between data sets were determined using one-way analysis of variance followed by Fisher's *t*-test. A P level <0.05 was accepted as statistically significant. All statistical analyses were performed using StatView 4.02 software program for Macintosh.

Results

Serum creatinine

Serum creatinine increased significantly as early as day 3 after UA injection (P<0.01 vs baseline), reached a peak value at day 7 (P<0.01 vs baseline), then returned to normal level by day 15 (Fig. 1).

PT cell damage and recovery

Histological changes in PT were assessed in PAS stained sections. As described in our previous report [24, 27], the initial lesions of severe PT necrosis were predominantly located around the corticomedullary junction, where the denuded tubular basement membrane (TBM) was evident as early as day 2 (data not shown). Between day 4 and day 5, tubular necrosis was maximal and almost distributed in OSOM and cortex (Fig. 2A), and by day 7 denuded TBM was almost covered with regenerating cells of flattened cytoplasm (Fig. 2B). The number of PT cells per cross-section significantly decreased at day 2 and

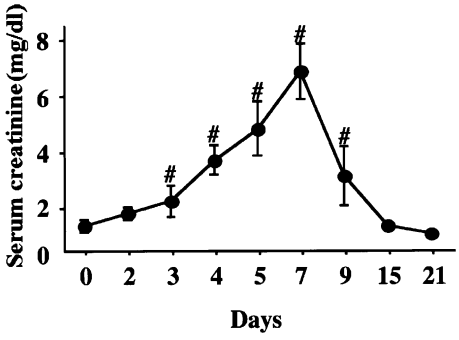

Fig. 1 Serial changes in serum creatinine before and after induction of uranyl acetate-induced acute renal failure. Data represent the mean ± standard error of the mean values of five animals. # P<0.01 versus baseline

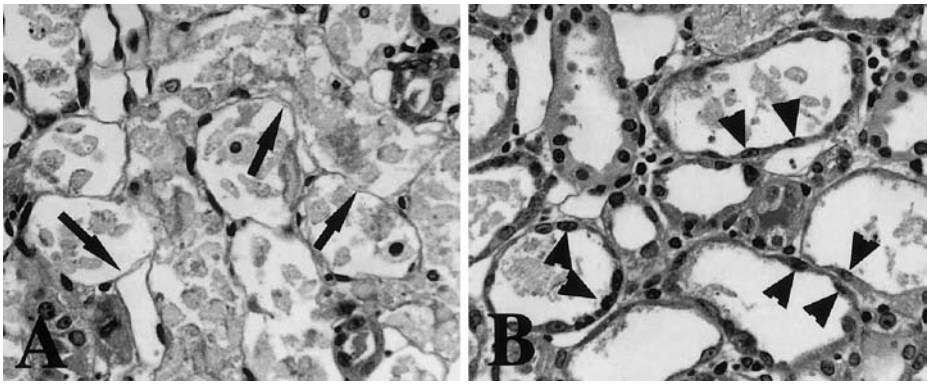

Fig. 2 Photomicrographs of periodic acid-Schiff stained sections, showing proximal tubular injury in the outer stripe of outer medulla (OSOM) at day 5 (**A**) and day 7 (**B**) after induction of acute renal failure. At day 5, tubular necrosis was distributed in OSOM where denuded tubular basement membrane (TBM) (**A**, *arrows*) was evident. At day 7, the TBM was almost covered with flattened, regenerating tubular cells (**B**, *arrowheads*)

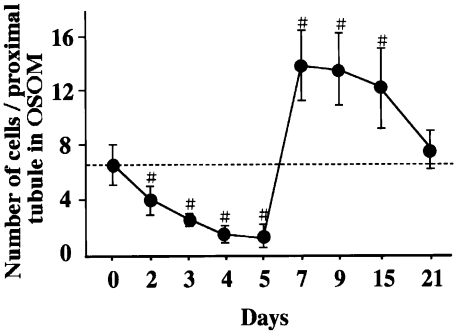

Fig. 3 Number of tubular epithelial cells per cross-section of proximal tubules in the outer stripe of outer medulla. *Dashed line* indicates baseline value. Data represent the mean ± standard error of mean values of five animals. $P<0.01$ versus before induction of acute renal failure

progressively decreased by day 5, then increased over the baseline level and reached a peak level at day 7, but gradually returned to the normal control level by day 21 (Fig. 3).

ECM components

Positive immunostaining of three major ECM components—type-IV collagen, pan-laminin, and sulfated proteoglycan—was detected along the TBM in normal rats. Immunostaining patterns of type-IV collagen and pan-laminin did not change after the induction of ARF except for moderate staining in the focally expanded interstitium and around the dilated tubules (Fig. 4A, B, C, D). However, strong staining for sulfated proteoglycan, as evaluated by colloidal gold stainable anionic sites, was

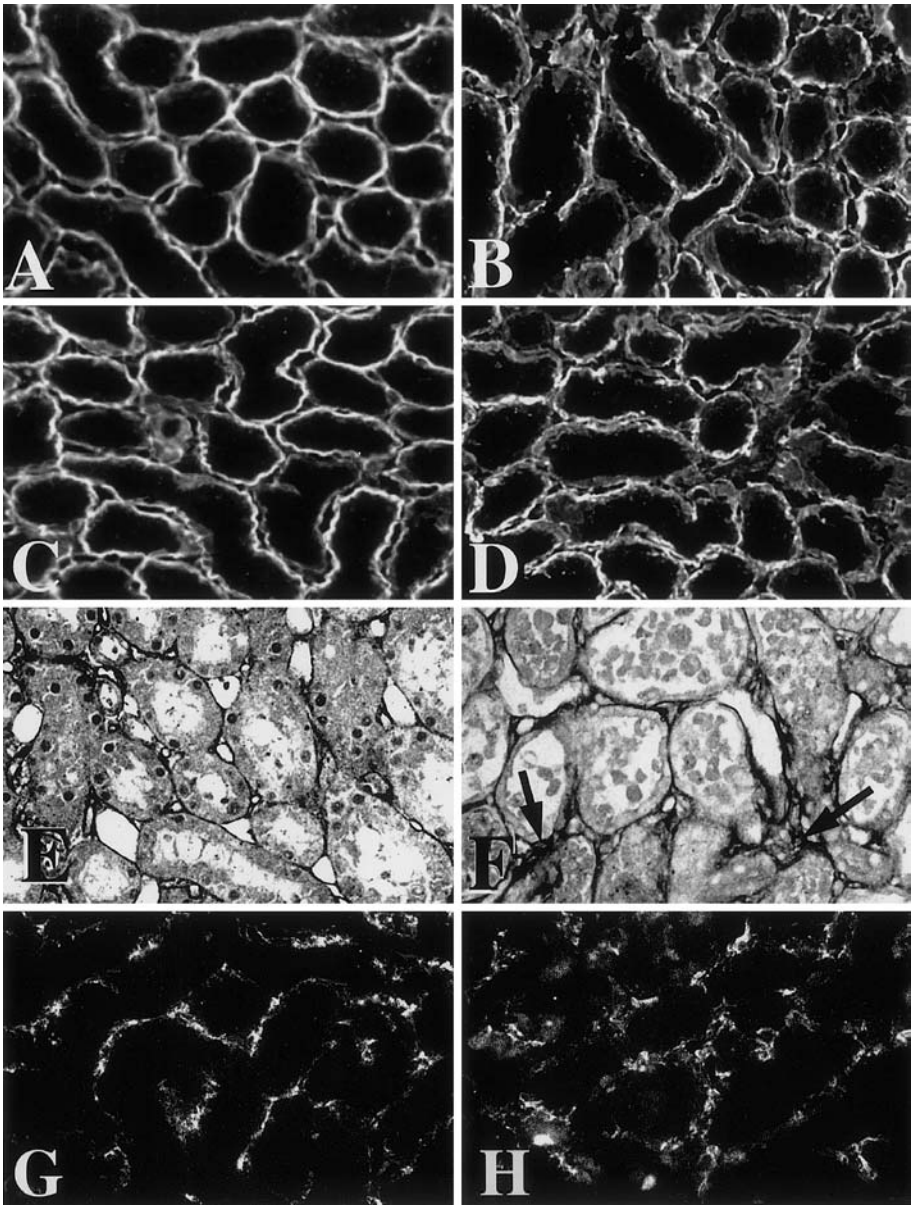

Fig. 4 Photomicrographs of immunostained section for collagen type IV (**A**, **B**), pan-laminin (**C**, **D**), sulfated proteoglycan (**E**, **F**) and collagen type III (**G**, **H**) in the outer stripe of outer medulla before (**A**, **C**, **E**, **G**) and day 7 (**B**, **D**, **F**, **H**) after induction of acute renal failure. Immunostaining patterns and intensities of collagen type IV, pan-laminin and collagen type III did not change at day 7 (**B**, **D**, **H**) compared with normal kidney (**A**, **C**, **G**). Staining intensity of sulfated proteoglycan judged by cationic gold staining in some peritubular areas (*arrows*) was stronger at day 7 (**F**) than that before induction of acute renal failure (**E**)

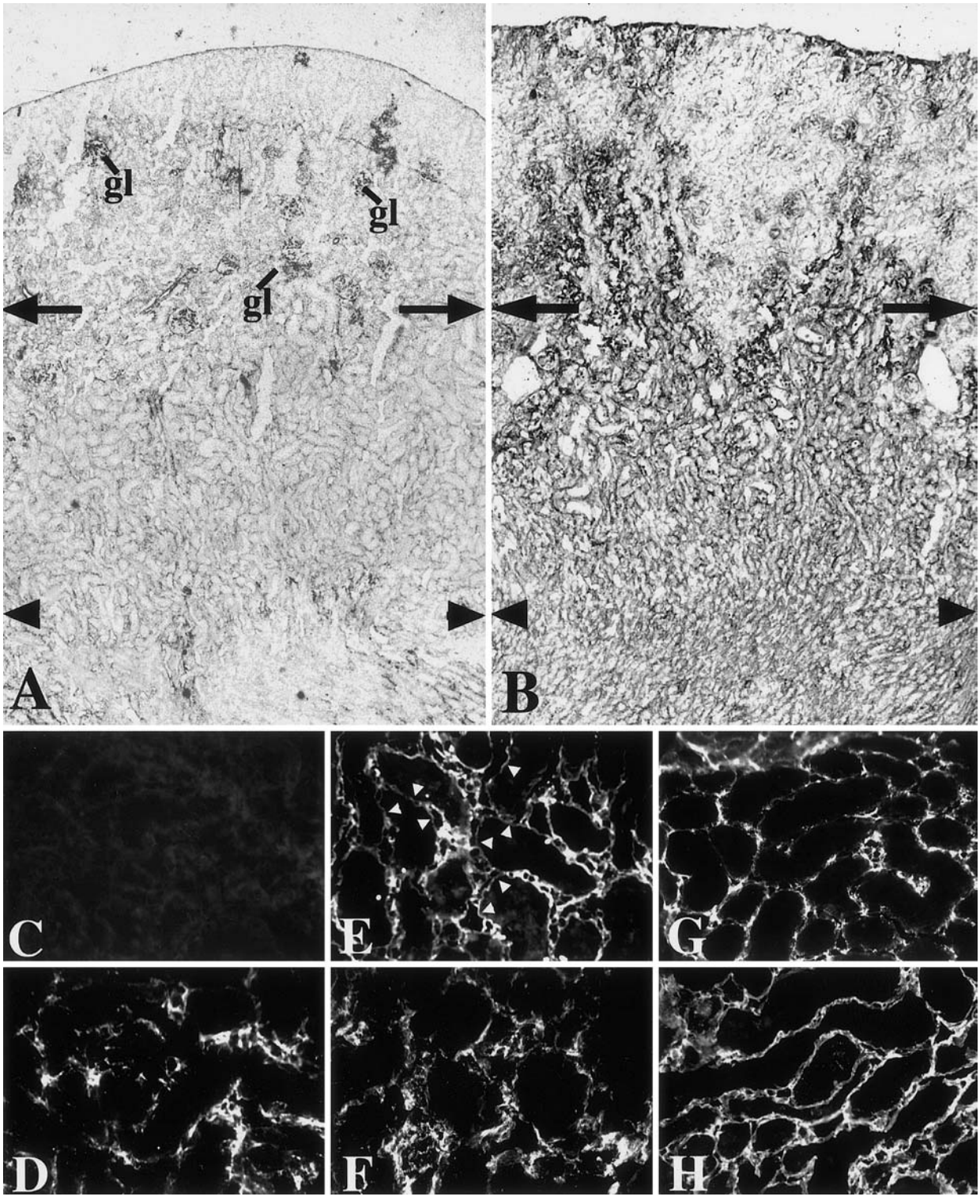

Fig. 5 Immunohistochemical (**A**, **B**) and immunofluorescent (**C**–**H**) staining of cellular fibronectin (cFn)-EIIIA (**A–F**) and plasma fibronectin (pFn) (**G**, **H**) on cryostat sections before (**A**, **C**, **G**), and at days 2 (**B**, **D**), 4 (**E**), 7 (**H**), and 15 (**F**) after induction of acute renal failure. In normal rat kidney (**A**, **C**) positive staining of cFn-EIIIA was absent in the interstitium but present in glomeruli (*gl*). At day 2 (**B**, **D**), cFn-EIIIA expressed in the peritubular regions throughout the outer stripe of outer medulla (OSOM) and inner stripe of outer medulla could be found. After day 4 (**E**), cFn-EIIIA staining on the tubular basement membrane (TBM) (*arrowheads*) was also noted and staining intensity was increased and was still present at day 15 (**F**). Immunostaining of pFn was weak along TBM and moderate in the peritubular regions in normal kidney (**G**), and the staining intensity was slightly increased at day 7 (**H**). **A**, **B** *Arrows*, border between cortex and OSOM; *arrowheads*, border between OSOM and inner stripe of outer medulla

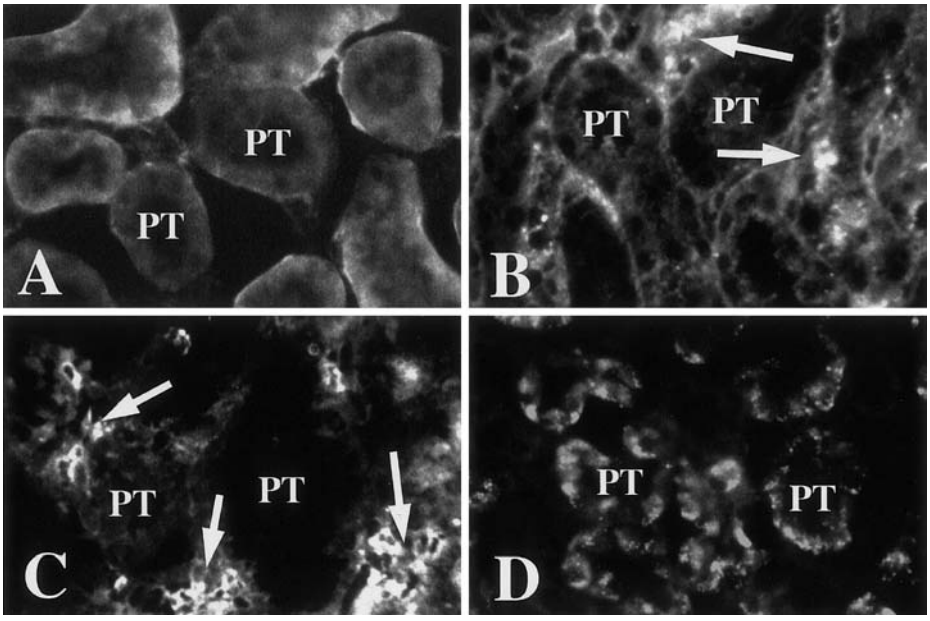

Fig. 6 Photomicrographs of immunofluorescent staining of β1 integrin on cryostat sections before (**A**), and at days 3 (**B**), 5 (**C**), and 7 (**D**) after induction of acute renal failure. In normal kidney (**A**), β1 integrin-positive staining is localized mainly to the basal side of proximal tubules and less extensively to the peritubular regions. β1 Integrin-positive staining increased in peritubular regions (*arrows*) at day 3 (**B**). The intensity of β1 integrin staining was further increased in the peritubular regions (*arrows*) at day 5 (**C**). Staining of β1 integrin began to return to the normal pattern after day 7 (**D**)

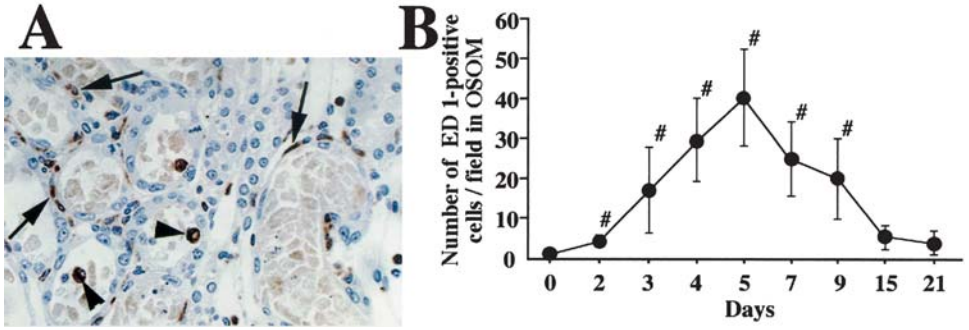

Fig. 7 **A** Photomicrographs of ED-1-positive monocyte/macrophages in the interstitial areas (*arrows*) and in the tubular lumen (*arrowheads*) at day 5 after induction of acute renal failure. Quantitative analysis of ED-1-positive cells in the interstitium in the outer stripe **B** of outer medulla. Data are mean ± standard error of mean. # $P<0.05$ versus before induction of acute renal failure

found in the peritubular areas after day 7 (Fig. 4E, F). Positive immunostaining of type-III collagen as one of the interstitial collagens was found slightly in the peritubular region in normal rats; however, it did not change after induction of ARF (Fig. 4G, H).

Immunoreactive cFn-EIIIA was not detected in the interstitium of normal rats except in glomeruli and vascular walls (Fig. 5A, C). However, immunoreactive cFn-EIIIA appeared mainly in the peritubular regions throughout the OSOM as early as day 2 (Fig. 5B, D), and both peritubular and TBM staining patterns could be seen after 4 days (Fig. 5E), suggesting that tubular epithelial cells may also produce cFn-EIIIA. The intensity of immunostaining of cFn-EIIIA was maintained until day 15, after then staining intensity on the TBM became weaker at day 21 (Fig. 5F). In contrast to cFn-EIIIA, weak immunoreactivity for pFn was found along the TBM and in the peritubular regions in normal rats, and the staining pattern of pFn did not change after induction of ARF, but the intensity of immunostaining increased transiently between day 3 and day 7 (Fig. 5G, H).

We also examined cFn-EIIIA in the liver tissues, but immunoreactive cFn-EIIIA could not be found in normal rats and in rats with UA-induced ARF (data not shown).

Immunostaining of β1 integrin

In normal control kidneys, positive staining for β1 integrin was observed mainly in the basal side of tubule and less extensively in the peritubular region (Fig. 6A). After induction of ARF, immunoreactive β1 integrin gradually increased in peritubular regions throughout the OSOM until day 5 (Fig. 6B, C). Positive staining of β1 integrin began to return to the normal pattern at day 7 (Fig. 6D).

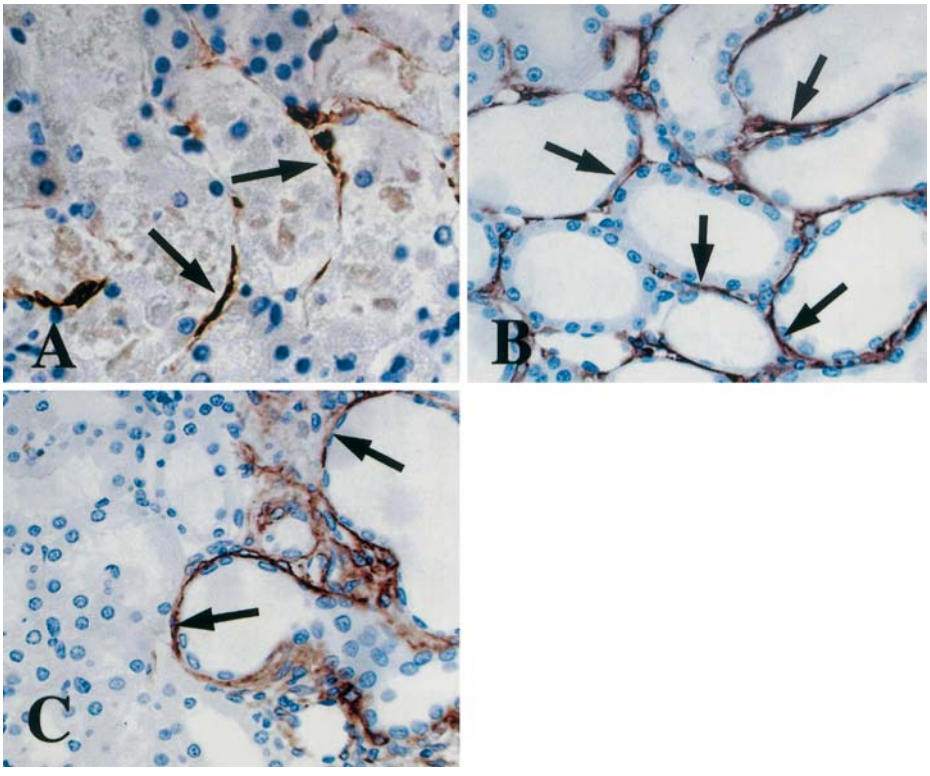

Fig. 8 Photomicrographs showing α-smooth muscle actin (SMA) immunostaining (*myofibroblasts*, *arrows*) in the outer stripe of outer medulla (OSOM) at days 2 (**A**), 7 (**B**), and 15 (**C**). α-SMA-positive staining is observed in peritubular interstitial cells around the damaged tubules at day 2 (**A**). At day 7, α-SMA-positive staining is found in the peritubular areas throughout OSOM (**B**). At day 15, α-SMA-positive cells are found mainly around the dilated tubules (**C**)

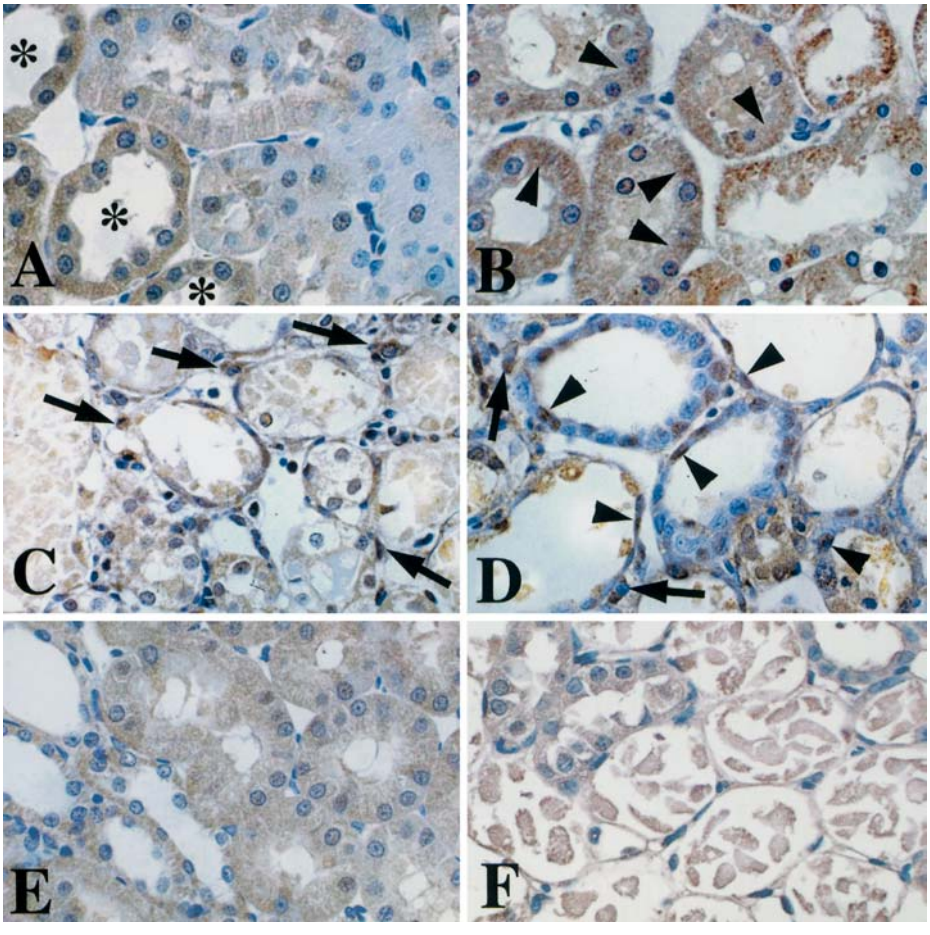

Fig. 9 Photomicrographs showing transforming growth factor (TGF)-β1 immunostaining in the outer stripe of outer medulla (OSOM) before (**A**) and at days 2 (**B**), 5 (**C**), and 7 (**D**) after induction of acute renal failure. In normal kidney, TGF-β1-positive staining is observed in the distal nephron in OSOM (**A**, *). At day 2, TGF-β1-positive staining is found in injured proximal tubules (PT) cells (**B**, *arrowheads*). At day 5, TGF-β1 staining is detected in interstitial cells around the denuded tubular basement membrane (**C**, *arrows*). At day 7, in addition to interstitial cells (*arrows*), regenerating PT cells show positive staining for TGF-β1 (**D**, *arrowheads*). When primary antibody was replaced with the corresponding animals normal IgG, no significant staining was observed before induction of acute renal failure (**E**) and at day 5 (**F**)

Infiltration of ED-1-positive interstitial macrophages

In kidneys of normal rats, ED-1-positive monocyte/macrophages were found only occasionally in the interstitium (data not shown). With the appearance of PT damage after induction of ARF, interstitial ED-1-positive cells increased in the region of injury, then gradually disappeared after PT regeneration had almost completed (Fig. 7A). Mainly at day 5 and day 7, ED-1-positive cells in the tubular lumen could be also found (Fig. 7A). Quantitative analysis revealed that interstitial ED-1-positive cells in OSOM increased significantly as early as day 2, reached a peak level at day 5, then gradually decreased in number (Fig. 7B).

Appearance of interstitial α-SMA-positive myofibroblasts

In normal control kidneys, α-SMA positive cells were not detected in the interstitial regions but were present on the vascular walls (data not shown). After induction of ARF, α-SMA positive myofibroblasts appeared exclusively around severely damaged tubules in OSOM as early as day 2 (Fig. 8A) and increased throughout OSOM with the progression of tubular necrosis by day 7 (Fig. 8B), then decreased after day 9. α-SMA positive cells remained in the interstitial regions around the dilated tubules after day 15, but the staining areas was small and limited to the focally expanded interstitium (Fig. 8C).

Immunostaining of TGF-β1

In normal control kidneys, positive staining of TGF-β1 was constitutively observed in the distal nephron (Fig. 9A). At day 2 after induction of ARF, TGF-β1 immunoreactivity was found in the injured PT cells (Fig. 9B) as well as in a small number of the interstitial cells around the damaged PT in OSOM. At day 5, positive staining of TGF-β1 was increasingly observed in the interstitial cells around the denuded TBM (Fig. 9C) and also appeared in the regenerating PT cells mainly after 7 days (Fig. 9D). By day 15, positive staining of TGF-β1 in regenerating PT cells was constantly found, but at day 21, staining intensity was reduced to that found in the normal control (data not shown). When the primary antibody against TGF-β1 was replaced with anti-rabbit IgG, no significant staining was observed before induction of ARF (Fig. 9E) and at day 5 or day 7 (Fig. 9F).

Ultrastructural localization of cFn-EIIIA and β1 integrin

In kidneys of normal rats, immunoelectron microscopy revealed the lack of cFn-EIIIA in the interstitium. At 2 days after induction of ARF, cFn-EIIIA was identified mainly in the basement membrane of endothelial cells of peritubular capillaries throughout OSOM and around a restricted area of fibroblast-like cells (Fig. 10A), indicat-

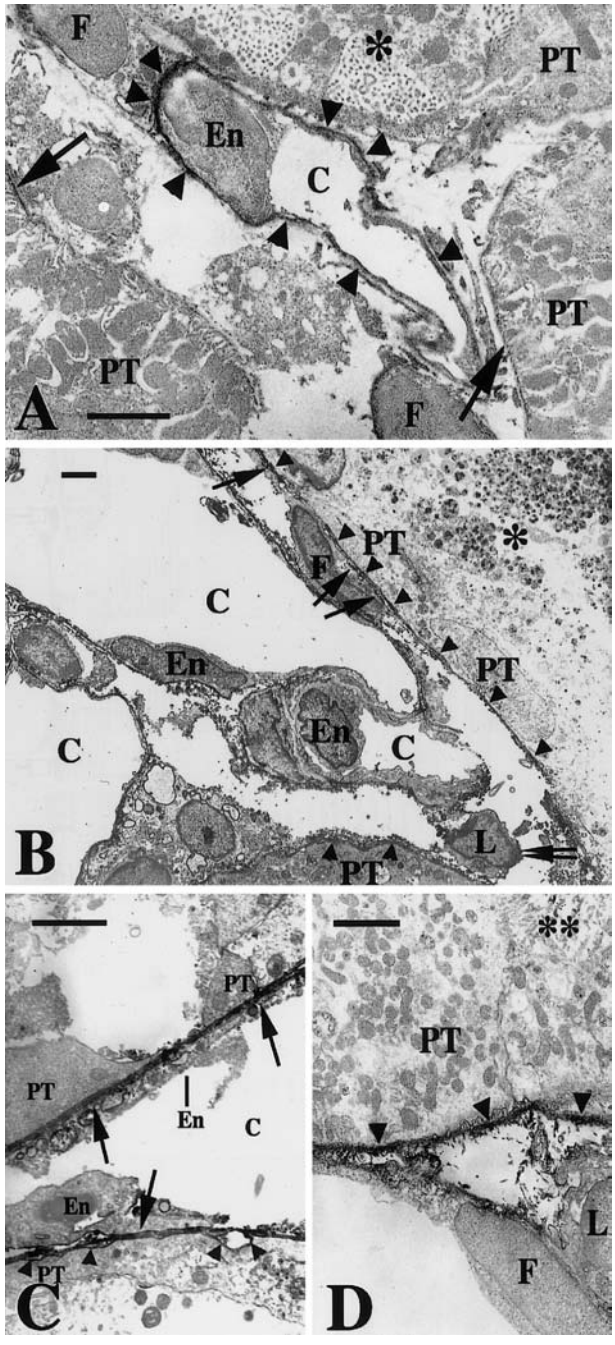

Fig. 10 Immunoelectron micrographs for cellular fibronectin (cFn)-EIIIA at days 2 (**A**), 5 (**B**, **C**) and 7 (**D**). **A** At day 2, reaction products indicative of cFn-EIIIA are found on the basement membrane of peritubular capillary (*arrowheads*), and very faintly on some tubular basement membrane (TBM) (*arrows*). **B** At day 5, cFn-EIIIA is found around the fibroblast-like cells (*arrows*) and less extensively around infiltrating leukocyte (*double arrow*) as well as on the TBM underneath the regenerating proximal tubules (PT) (*arrowheads*). **C** Note that cFn-EIIIA-positive peritubular capillary basement membrane and TBM are not distinguishable at some parts (*arrows*), and that cFn-EIIIA is found at the basal membrane of the regenerating PT (*arrowheads*). **D** At day 7, cFn-EIIIA is still present on the TBM underneath the relatively mature PT (*arrowheads*). * Necrotic PT, ** brush-border, *PT* proximal tubules, *En* endothelium, *F* fibroblast-like cells, *C* peritubular capillaries, *L* infiltrating leukocytes. *Scale bar* 2.0 μm

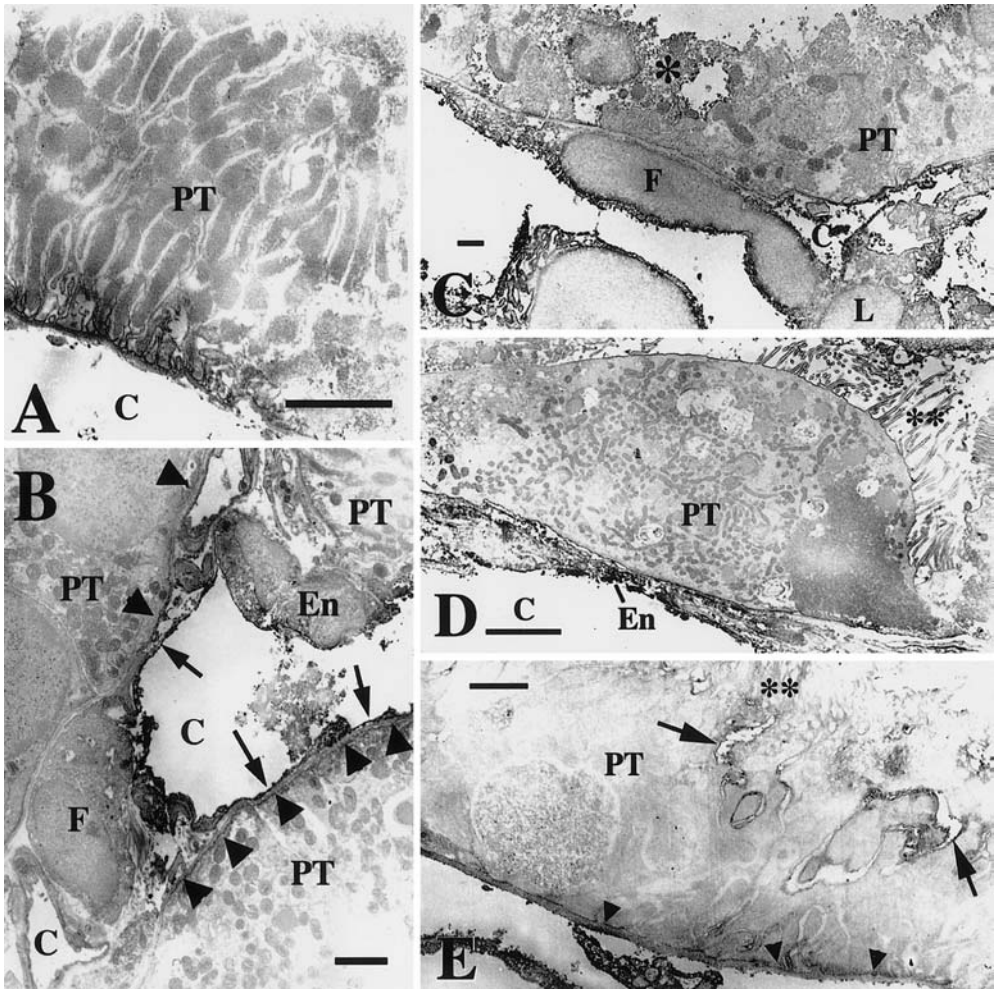

Fig. 11 Immunoelectron micrographs for β1 integrin before (**A**) and at days 2 (**B**), 4 (**C**), 5 (**D**), and 7 (**E**) after induction of acute renal failure. **A** In normal kidney, reaction products indicative of β1 integrin are found mainly at the basal fold of the proximal tubules (PT). **B** At day 2, β1 integrin is found at the cell surface of some peritubular endothelium (*arrows*) as well as at the basal membrane of the PT (*arrowheads*). **C** At day 4, β1 integrin is found at the cell surface of peritubular endothelium and fibroblast-like cell, but less extensively at the cell surface of leukocytes. **D** At day 5, staining for β1 integrin is weak around the whole surface of immature regenerating PT. **E** At day 7, staining for β1 integrin is almost restricted to the basal mernbrane and basal fold of the relatively matured PT with brush-border (*arrowheads*) and confined residually at the cell surface of the lateral and/or apical membrane (*arrows*). * necrotic PT, ** brush-border, *PT* proximal tubules, *En* endothelium, *F* fibroblast-like cells, *L* infiltratincy leukocyte. *Scale bar* 2.0 μm

ing that the initial source of cFn-EIIIA is mainly derived from peritubular vessel endothelium. Peritubular endothelial expression of cFn-EIIIA was persistently seen throughout the experiment. From day 4 to day 7, cFn-EIIIA was found around fibroblast-like cells, but in small amounts around infiltrating leukocytes (Fig. 10B). Some peritubular vessel endothelium as well as fibroblast like-cells, which attached firmly to the TBM, may supply cFn-EIIIA to the TBM (Fig. 10B, C). At day 5, cFN-EIIIA was found also along the TBM of regenerating PT and was clearly seen at the basal membrane of the regenerating PT (Fig. 10B, C), indicating that not only interstitial cells but also regenerating PT did produce cFn-EIIIA. After day 7, reaction products of cFn-EIIIA were still present along TBM covered with relatively maturated PT cells as well as around fibroblast-like cells (Fig. 10D).

A weak staining of reaction products for β1 integrin was found along the basal fold of PT as well as peritubular endothelial surface in normal rats (Fig. 11A). After 2 days, reaction products of β1 integrin were increasingly found at peritubular endothelium and basal side of PT as well as fibroblast-like cells (Fig. 11B, C). At day 5 and day 7, in addition to peritubular endothelial surface, reaction products of β1 integrin were weakly expressed throughout the entire surface of immature proliferating PT (Fig. 11D). At day 7, β1 integrin expression was relatively restricted to the basal fold of relatively maturate PT with brush border and was found occasionally at lateral and/or apical membrane of PT cells (Fig. 11E). After 9 days, expression of β1 integrin in PT cells was almost compatible with that in normal PT cells (data not shown).

Expression of cFn-EIIIA, β1 integrin and TGF-β1 mRNAs

At day 2, the expression of cFn-EIIIA mRNA was about 3.5-fold that in normal control, then it gradually increased reaching a peak level at day 9 and remained upregulated until day 21 (Fig. 12A, B). The expression of β1 integrin mRNA at day 2 was also about 1.6-fold that in normal control, reached a peak level at day 4 and tended to decrease by day 21 (Fig. 12A, C). The expression of TGF-β1 mRNA was first increased at day 3, continued to increase till day 15 and tended to decrease by day 21 (Fig. 12A, D).

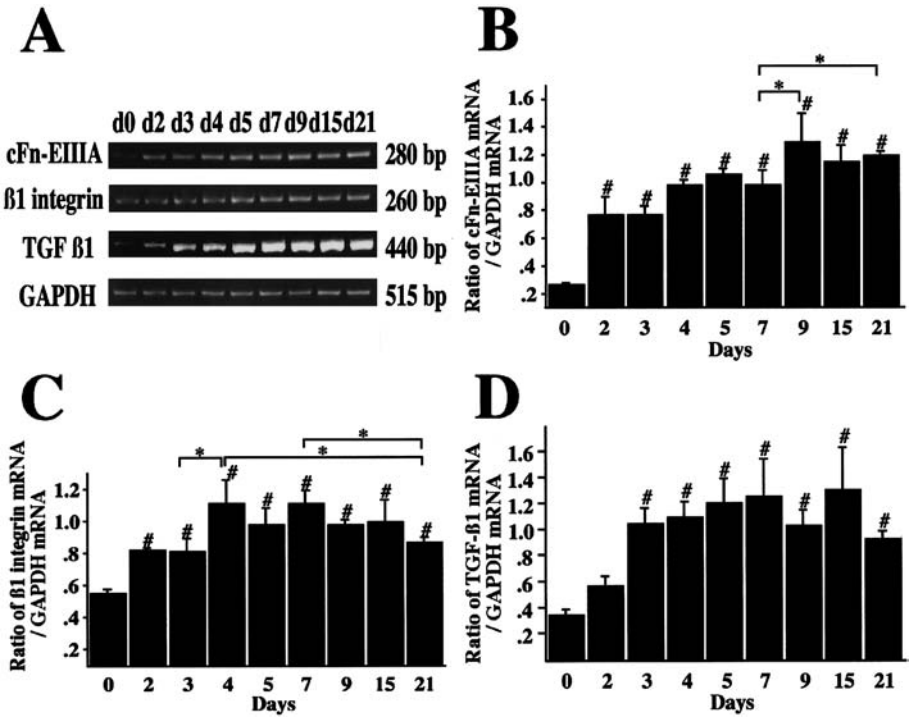

Fig. 12 Expression of cellular fibronectin (cFn)-EIIIA, β1 integrin, and transforming growth factor (TGF)-β1 mRNAs. Serial changes of reverse-transcription polymerase chain reaction products are shown (**A**). Relative abundance of cFn-EIIIA (**B**), β1 integrin (**C**), and TGF-β1 mRNA (**D**) against glyceraldehyde-3-phosphate dehydrogenase mRNA. Data are mean± SEM. # P<0.05 versus before induction of acute renal failure; * P<0.05

Discussion

The process of cellular recovery from ARF occurs through an orchestrated series of events, whereby dedifferentiated PT cells proliferate and/or migrate onto the denuded TBM to establish a new, differentiated epithelium [32]. To complete these processes of cellular recovery, synthesis of new ECM and reformation of cell–cell contacts must take place. In the present study, we found that of ECM components examined here, including pan-laminin, sulfated proteoglycan, collagen types III and IV, pFn, and cFn-EIIIA, only cFn-EIIIA newly appeared and then deposited in the peritubular regions before and during the PT regeneration.

As reported previously [27, 28] and here in this model, α-SMA-positive myofibroblasts transiently appeared just around the TBM of damaged PT and they often intervened between the basement membrane of the peritubular capillary and TBM until PT regeneration had completed. Interstitial myofibroblasts may be derived from the resident interstitial fibroblast-like cells [27]. In this model, cFn-EIIIA was mainly produced by the peritubular endothelium and the fibroblast-like cells (myofibroblasts) located very close to the TBM and may be furnished to the denuded TBM, on which the regenerating PT cells proliferated and/or migrated. In addition, we found cFn-EIIIA at the basal membrane of the regenerating PT cells, suggesting production of cFn-EIIIA by the regenerating PT.

Walker [34] demonstrated enhanced immunostaining of Fn during renal tubular regeneration after ischemic ARF in rats. Furthermore, Basile et al. [4] reported that the specific increase in cFn-EIIIA mRNA in regenerating PT correlated closely with the deposition of Fn-EIIIA protein in the TBM of regenerating PT. Recently, Zuk et al. [36] documented that both pFn and cFns containing V95 and/or EIIIA regions may contribute to the damage and repair in an ischemia model of ARF in rats. Though the ARF model is different, our data extended the findings of previous reports [4, 34, 36] by demonstrating the source and the location of cFn-EIIIA and its association with the regenerating PT cells.

CFn-EIIIA mRNA is abundantly expressed during embryogenesis and wound healing compared with normal adult tissue [2]. CFn-EIIIA may reappear, however, in the setting of epithelial repair and has been reported to play an important role in epithelial repair of the skin, liver, and lung [14, 19, 26]. Barnes et al. [2] reported that the expression of cFn-EIIIA in the kidney follows that of α-SMA (myofibroblast phenotype) in several settings of renal remodeling, including embryonic, maturation, and diseased kidney. Cellular recovery after ARF is a unique form of wound healing or tissue remodeling. Therefore, based on the known biological properties of cFn-EIIIA mentioned so far, our findings suggest that upregulation of cFn-EIIIA mRNA and deposition of cFn-EIIIA beneath the basal side of regenerating PT cells (on the TBM) before and during the cellular recovery after ARF may be necessary for proliferation, migration, and/or even differentiation of PT cells.

β1 Integrin, containing the non-covalently associated common β1 subunit and several types of α subunits, functions primarily as a cell surface receptor for ECM molecules such as Fn, collagen, laminin, and vitronectin and mainly mediates the interaction between cells and ECM. It also plays critical roles in ECM synthesis, ECM

assembly, proliferation, and differentiation of cells, thereby contributing to embryonic development, tissue homeostasis, and wound healing [13, 20, 22]. In the present study, β1 integrin mRNA was upregulated during damage and repair processes in rats with ARF, and β1 integrin protein increased in cells known to produce cFn-EIIIA, such as peritubular endothelial cells and interstitial cells, indicating that cFn is functional within these cells. Importantly, since the basal rnembrane of regenerating PT expressed β1 integrin, cFn-EIIIA on the TBM should affect cellular activity of the regenerating PT cells via paracrine and/or autocrine fashion and should contribute to cellular recovery from ARF.

The underlying pathomechanisms resulting in marked production of cFn-EIIIA by peritubular endothelium throughout OSOM during the early period of PT injury are poorly understood. We examined the source of TGF-β1 protein, which is one of the major cytokines that stimulate the production of cFn-EIIIA [10]. At day 2, when cFn-EIIIA was already expressed in the peritubular endothelium, TGF-β1 mRNA was not increased and TGF-β1 protein was found only in a few damaged PT cells but not in interstitial cells, suggesting that TGF-β 1 is probably not the initial stimulant of cFn-EIIIA expression in the peritubular endothelium. However, TGF-β1 might be released by platelets in the peritubular capillaries before day 2. Moreover, it is also possible that alterations of metabolic exchange between tubules and peritubular capillaries already exist, leading to the activation of peritubular endothelium to produce cFn-EIIIA. Since hepatic capillary endothelial cells did not express cFn-EIIIA during the experiment, it is unlikely that UA directly stimulated peritubular endothelium to produce cFn-EIIIA.

In our study, the expression of cFn-EIIIA in the peritubular endothelium preceded the appearance of peritubular myofibroblasts, suggesting that, in addition to TGF-β1 released by damaged PT, cFn-EIIIA might induce α-SMA expression (myofibroblastic phenotype) on fibroblast-like cells as reported by George et al. [10]. These investigators showed that hepatic stellate cells transdifferentiate to myofibroblast-like cells by cFn-EIIIA from sinusoidal endothelial cells following hepatic injury. In this model, the mechanisms of disappearance of myofibroblasts are not known and peritubular endothelium and regenerated PT may be the main sources of cFn-EIIIA after day 15, when almost all α-SMA-positive myofibroblasts disappear.

Basile et al. [3, 4] demonstrated a rapid and prolonged expression of TGF-β1 mRNA and peptide primarily in regenerating PT in ischemic ARF in rats [3] and the role of TGF-β1 in stimulating ECM synthesis, including cFn-EIIIA, during renal recovery [4]. In our study, we also found TGF-β1 protein in regenerating PT associated closely with cFn-EIIIA deposition on the proximal TBM. However, in contrast to the ischemia ARF model, TGF-β1 expression was also found in interstitial cells in our model. In the present study, the cells that produced TGF-β1 in the interstitium were not identified, but it is possible that both myofibroblasts and macrophages, as judged by the peritubular location of TGF-β1 stainable cells, can produce TGF-β1, resulting in stimulating cFn-EIIIA production among myofibroblasts, macrophages, and regenerating PT cells. While macrophages producing TGF-β1 may be one of the key elements in renal fibrosis [9], in our model, infiltration of macrophages was transient, so that the effect of TGF-β1 released by these macrophages on myofibroblasts must be limited, resulting in almost no production of interstitial collagen type III, a marker for renal fibrosis as shown in this study. Regulation of ECM production, deposition, and degradation in our model remain largely unknown.

In conclusion, the peritubular endothelium and fibroblast-like cells may furnish cFn-EIIIA on the denuded TBM, on which the regenerating PT cells proliferate and/or migrate, and regenerating PT cells per se also produce cFn-EIIIA, associated with expression of its receptor, β1 integrin, on the basal cell membrane. Based on the known biological properties of cFn-EIIIA, our data suggest that cFn-EIIIA may play an important role in the cellular recovery after UA-induced ARF in rats.

Acknowledgements This study was presented in part at the XXXVIlth Congress of the ERA-EDTA in Nice, France, 2000. We are grateful to Dr. K.C. Flanders (National Institutes of Health, USA) for providing anti-LC antibody and to Dr. K. Loester for anti-β1 integrin antibody. This work was supported by a Grant-In-Aid for scientific research (C; no. 13671107) from the Ministry of Education, Science, Sports and Culture, Japan.

References

1. Barnes JL, Torres ES, Mitchell RJ, Peters JH (1995) Expression of alternatively spliced fibronectin variants during remodeling in proliferative glomerulonephritis. Am J Pathol 147:1361–1371
2. Barnes VL, Musa J, Mitchell RJ, Barnes JL (1999) Expression of embryonic fibronectin isoform EIIIA parallel α-smooth muscle actin in maturing and diseased kidney. J Histochem Cytochem 47:787–797
3. Basile DP, Rovak JM, Martin RR, Hammerman MR (1996) Increased transforming growth factor-β1 expression in regenerating rat renal tubules following ischemic injury. Am J Physiol 270:F500–F17509
4. Basile DP, Martin DR, Hammerman MR (1998) Extracellular matrix-related genes in kidney after ischemic injury: potential role for TGF-β in repair. Am J Physiol 275:F894–F903
5. Brown LF, Dubin D, Lavigne L, Logan B, Dvorak HF, Van de Water L (1993) Macrophages and fibroblasts express embryonic fibronectins during cutaneous wound healing. Am J Pathol 142:793–801
6. Chomczynski P, Sacchi N (1987) Single-step method of RNA isolation by acid guanidinium isothiocynate-phenol-chloroform extraction. Anal Biochem 162:156–159
7. ffrench-Constant C (1995) Alternative splicing of fibronectin: many different proteins but few different functions. Exp Cell Res 221:261–271
8. Flanders KC, Thompson NL, Cissel DS, van Obberghen-Schilling E, Baker CC, Kass ME, Ellingsworth LR, Roberts AB, Sporn MB (1989) Transforming growth factor-beta 1: histochemical localization with antibodies to different epitopes. J Cell Biol 108:653–660

9. Fukuda K, Yoshitomi K, Yanagida T, Tokumoto M, Hirakata H (2001) Quantification of TGF-β1 mRNA along rat nephron in obstructive nephropathy. Am J Physiol 281: F513–F521
10. George J, Wang SS, Sevcsik AM, Sanicola M, Cate RL, Koteliansky VE, Bissell DM (2000) Transformin growth factor-β initiates wound repair in rat liver through induction of the EIIIA-fibronectin splice isoform. Am J Pathol 156:115–124
11. Ghassemifar MR, Tarnuzzer RW, Chegini N, Tarpila E, Schultz GS, Franzen LE (1997) Expression of alpha-smooth muscle actin, TGF-β and TGF-β type II receptor during connective tissue contraction. In Vitro Cell Dev Biol Anim 33:622–627
12. Hynes RO (1990) Fibronectins. Springer, Berlin, Heidelberg, New York
13. Hynes RO (1992) Integrins: versatility, modulation, and signaling in cell adhesion. Cell 69:11–25
14. Jarnagin WR, Rockey DC, Koteliansky VE, Wang SS, Bissell DM (1994) Expression of variant fibronectins in wound healing: cellular source and biological activity of the EIIIA segment in rat hepatic fibrogenesis. J Cell Biol 127:2037–2048
15. Klein NJ, Shennan Gl, Heyderman RS, Levin M (1993) Detection of glycosaminoglycans on the surface of human umbilical vein endothelial cells using gold-conjugated poly-L-lysine with silver enhancement. Histochem J 25:291–298
16. Kornblihtt AR, Umezwa K, Vibe-Petersen K, Baralle FE (1985) Primary structure of human fibronectin: differential splicing may generate at least 10 polypeptides from a single gene. EMBO J 4:1755–1759
17. Kornblihtt AR, Pesce CG, Alonso CR, Cramer P, Srebrow A, Werbajh S, Muro AF (1996) The fibronectin gene as a model for splicing and transcription studies. FASEB J 10:248–257
18. Loester K, Voigt S, Heidrich C, Hofmann W, Reutter W (1994) Cell-collagen adhesion is inhibited by monoclonal antibody 33.4 against the rat α1 -integrin subunit. Exp Cell Res 212:155–160
19. Maniscalco WM, Watkins RH, Chess PR, Sinkin RA, Horowitz S, Toia L (1998) Cell-specific expression of fibronectin and EIIIA and EIIIB splice variants after oxygen injury Am J Physiol 274:L599–L609
20. Norman JT, Fine LG (1999) Progressive renal disease: fibroblast, extracellular matrix, and integrins. Exp Nephrol 7:167–177
21. Owens RJ, Kornblihtt AR, Baralle FE (1986) Fibronectin, the generation of multiple polypeptides from a single gene. Oxf Surv Eukaryot Genes 3:141–160
22. Paller MS (1997) Integrins and repair after acute renal injury. Kidney Int 61[Suppl]:S52–S55
23. Paul JI, Schwarzbauer JE, Tamkun JW, Hynes RO (1986) Cell-type-specific fibronectin subunits generated by alternative splicing. J Biol Chem 261:12258–12265
24. Sano K, Fujigaki Y, Miyaji T, lkegaya N, Ohishi K, Yonemura K, Hishida A (2000) Role of apoptosis in uranyl acetate-induced acute renal failure and acquired resistance to uranyl acetate. Kidney Int 57:1560–1570
25. Schwarzbauer JE, Patel RS, Fonda D, Hynes RO (1987) Multiple sites of alternative splicing of the rat fibronectin gene transcript. EMBO J 6:2573–2580
26. Serini G, Bochaton-Piallat ML, Ropraz P, Geinoz A, Borsi L, Zardi L, Grabbiani G (1998) The fibronectin domain ED-A is crucial for myofibroblastic phenotype induction by transforming growth factor-β1. J Cell Biol 142:873–881
27. Sun DF, Fujigaki Y, Fujimoto T, Yonemura K, Hishida A (2000) Possible involvement of myofibroblasts in cellular recovery of uranyl acetate-induced acute renal failure in rats. Am J Pathol 157:1321–1335
28. Sun DF, Fujigaki Y, Fujimoto T, Goto T, Yonemura K, Hishida A (2002) Mycophenolate mofetil inhibits regenerative repair in uranyl acetate-induced acute renal failure by reduced interstitial cellular response. Am J Pathol 161:217–227
29. Tamkun JW, Hynes RO (1983) Plasma fibronectin is synthesized and secreted by hepatocytes. J Biol Chem 258:4641–4647
30. Tamkun JW, Schwarzbauer JE, Hynes RO (1984) A single rat fibronectin gene generates three different mRNAs by alternative splicing of a complex exon. Proc Natl Acad Sci U S A 81:5140–5144
31. Tarone G, Russo MA, Hirsch E, Odorrisio T, Altruda F, Silengo L, Siracusa G (1993) Expression of beta 1 integrin complexes on the surface of unfertilized mouse oocyte. Development 117:1369–1375
32. Toback G (1992) Regeneration after acute renal tubular necrosis. Kidney Int 41:226–246
33. Vartio T, Laitinen L, Narvanen O, Cutolo M, Thornell LE, Zardi L, Virtanen I (1987) Differential expression of the ED sequence-containing form of cellular fibronectin in embryonic and adult human tissues. J Cell Sci 88:419–430
34. Walker PD (1994) Alterations in renal tubular extracellular matrix components after ischemia-reperfusion injury to the kidney. Lab Invest 70:339–346
35. Zardi L, Carnemolla B, Siri A, Petersen TE, Paolella G, Sebastio G, Baralle FE (1987) Transformed human cells produce a new fibronectin isoform by preferential alternative splicing of a previously unobserved exon. EMBO J 6:2337–2342
36. Zuk A, Bonventre JV, Matlin KS (2001) Expression of fibronectin splice variants in the postischemic rat kidney. Am J Physiol 280:171037–171053

Virchows Arch (2003) 443:206–216
DOI 10.1007/s00428-003-0839-6

ORIGINAL ARTICLE

Yoshihide Fujigaki · Di Fei Sun · Tetsuo Goto · Akira Hishida

Temporary changes in macrophages and MHC class-II molecule-expressing cells in the tubulointerstitium in response to uranyl acetate-induced acute renal failure in rats

Received: 10 March 2003 / Accepted: 7 May 2003 / Published online: 13 June 2003
© Springer-Verlag 2003

Abstract The present study was designed to asses the dynamic changes in macrophages (Møs) with or without expression of major histocompatibility complex (MHC) class-II molecule in response to uranyl acetate-induced acute renal failure (ARF) in rats. ED1+ monocytes/Møs infiltrated into the interstitium as early as day 2, peaked in number on day 5 after uranyl acetate-induced ARF. ED1+ cells did not correlate with necrotic tubules but accumulated abundantly in the vicinity of the Ki67+ regenerating proximal tubules around days 4–5. Afterward, regeneration of proximal tubules was accelerated. After day 5, some ED1+ cells entered the tubular lumen, and became ED1+ giant cells, which had features of phagocytic Møs by immunoelectron microscopy, peaking in number on day 7. Most ED1+ cells did not incorporate [^{3}H]-thymidine, indicating lack of active proliferation. The number of OX6+ cells (directed to MHC class-II molecule) in the interstitium significantly increased on day 4 and peaked on day 5. Double staining revealed that ED1+OX6− cells entered the tubular lumen while ED1+OX6+ cells remained in the peritubular regions. Osteopontin (OPN) protein and mRNA were significantly upregulated. No specific relationship could be found between OPN+ regenerating proximal tubules and ED1+ cells, but most ED1+ giant cells were OPN+ and intermingled among OPN+ cell debris. Our findings suggest that ED1+ Møs are actively associated with regenerating proximal tubules and, thus, might promote proximal tubular regeneration. ED1+OX6− Møs may function as scavengers and phagocytose cellular debris in the tubular lumen, cleaning the wound site. OPN might be involved in this process. ED1+OX6+ Møs in the peritubular regions may act as outpost of the defense system to monitor incoming antigens. Our data indicate that Møs with or without expressing MHC class-II molecule contribute to the defense and repair of injured proximal tubules in this ARF.

Keywords Macrophages · MHC class-II molecule · Phagocytosis · Acute renal failure · Osteopontin

Y. Fujigaki (✉) · D. F. Sun · T. Goto · A. Hishida
First Department of Medicine,
Hamamatsu University School of Medicine,
1–20–1 Handayama, 431-3192 Hamamatsu, Japan
e-mail: yf0516@hama-med.ac.jp
Tel.: +81-53-4352261
Fax: +81-53-4349447

Introduction

It is generally accepted that activated macrophages (Møs) play important roles in promoting the repair of wound tissues [5, 14]. Møs are involved in removal of cellular debris and apoptotic cells by phagocytosis, thus contributing to tissue remodeling [1], antigen presentation in the defense reactions following the invasion of foreign elements from the wound site [29], and secretion of trophic agents necessary for wound healing [5].

Recovery of tubular epithelial cells after acute renal failure (ARF) is a unique form of wound healing or tissue remodeling where both Møs and myofibroblasts are important actively involved cellular elements [2, 21, 23]. In this respect, we reported that in uranyl acetate-induced ARF in rats, transient infiltration of ED1+ Møs and myofibroblasts in the interstitium occurred in association with the peak activity of tubular regeneration after acute tubular injury [27]. In this model [27], necrotic proximal tubules initially appeared around the corticomedullary junctions as early as day 2 after uranyl acetate injection, then almost maximally spread between day 4 and day 5. Regenerating proximal tubular cells appeared on day 2 and regenerating activity subsided on day 7 when the regenerating cells almost covered the denuded tubular basement membrane. Serum creatinine increased as early as day 3, reached a peak value on day 7, then returned to normal levels by day 15. Further studies from our laboratory [28] demonstrated that the regeneration of tubules was inhibited by the suppression of the interstitial cellular response by mycophenolate mofetil. Based on the findings, we concluded that infiltrating Møs in association with myofibroblasts may contribute like

wound Møs to cellular recovery in uranyl acetate-induced ARF.

Møs are heterogeneous groups of cells, and it is crucial to define the nature of Møs when assessing their role in disease. In addition to newly recruited monocyte-derived Møs, ED1 antibody recognizes tissue-fixed, resident Møs including dendritic cells, which are considered to be a subpopulation of resident Møs [7, 26]. Dendritic cells are professional antigen-presenting cells and are mobilized from bone marrow in response to injury [31]. They capture exogenous antigens and then move to lymphoid tissues to present their antigen peptide with major histocompatibility complex class II (MHC class II) to helper T cells [3]. Thus, it is likely that MHC class-II-expressing Møs are also involved in the ARF because the defense system against incoming antigen from bare tubular basement membrane should be operational after acute tubular injury. However, the amount of ED1 expression in a single cell correlates with the phagocytic activity of the respective cell type [4]. However, the dynamics of Møs that do and do not express MHC class-II molecule have not yet been examined in ARF.

Osteopontin (OPN) is a secreted, acidic glycosylated phosphoprotein with cell-adhesive and migratory properties [9]. The role of OPN in Mø accumulation in the tubulointerstitium has been immunohistochemically [6, 8, 20] and functionally proven [18, 19]. However, recent study could not show a specific relationship between OPN expression and accumulation of ED1+ Møs in gentamicin-induced ARF or, rather, suggested that OPN may contribute to the tubular regeneration [30].

In the present study, we hypothesized that Møs and MHC class-II molecule-expressing cells contribute to the defense and repair of the injured tubules. For this reason, we investigated the changes in density and distribution of these cells and how they respond in the renal interstitium of rats to uranyl acetate-induced ARF. We also examined the possible contribution of OPN to this process.

Materials and methods

Induction of uranyl acetate-induced ARF

A total of 42 male Sprague-Dawley rats weighing 230–300 g (SLC Co. Shizuoka, Japan) were used. They received a single intravenous injection of 5 mg/kg uranyl acetate, and four or five rats were sacrificed before and at 2, 3, 4, 5, 7, 9, 15, and 21 days after uranyl acetate injection. Another group of four rats received bolus intraperitoneal injections of [^{3}H]-thymidine (120 μCi/100 g body wt; Wako, Osaka, Japan) at 5 days (n=2) and 7 days (n=2) after uranyl acetate injection, and were sacrificed 90 min later for autoradiography. Urine was collected for 12 h before sacrifice. Rats were anesthetized intraperitoneally with pentobarbital sodium (30 mg/kg), a blood sample was collected through the abdominal aorta, then both kidneys were removed after flushing with phosphate-buffered saline (PBS). The right kidneys, except for the papilla and inner medulla, were snap-frozen in liquid nitrogen and stored at −70°C for RNA extraction. Serum creatinine level was measured using the enzymatic method (Mizuho Med. Saga, Japan).

Immunohistochemistry

The left kidneys were fixed with either 4% paraformaldehyde or methacarn solution (methanol:chloroform:acetic acid, 60:30:10 v/v) [24] and embedded in paraffin. As reported elsewhere [27], the standardized avidin-biotin-complex technique was applied using the antibodies listed in Table 1. Briefly, 4% paraformaldehyde (for Ki67 and OPN protein recognized by MPIIIB10) and methacarn (for ED1, OX6 and CD43) fixed sections were deparaffinized and dehydrated. Endogenous peroxidase was blocked by treatment with 3% H_2O_2, then the sections were incubated with 10% normal donkey serum, followed by incubation with primary antibodies overnight, and reacted with the biotinylated donkey polyclonal antibody against mouse IgG (Chemicon International Inc., Temecula, CA) for 30 min at room temperature. Then, avidin-conjugated peroxidase (Nichirei, Tokyo) was added for 30 min and reaction products were visualized by diaminobenzidine.

Double immunostaining for ED1 and OX6 was performed using the method by Lan et al. [13]. After staining the sections with ED1, sections were treated with microwave oven heating for 2 × 5 min in 0.01 M sodium citrate pH 6.0 at 800 W, then incubated with OX6 and with donkey polyclonal biotinylated antibody against mouse IgG. Then, Vectastain ABC-AP reagent (Vector Laboratories, Burlingame, CA) was added and the Vector Red alkaline Phosphatase Substrate Kit I (Vector Laboratories) was used as chromogen. For control sections, the first antibodies were omitted or replaced by the normal mouse IgG and signals in both control and experimental sections were negative or negligible.

Immunohistochemistry for ED1 and autoradiography

After staining the sections with ED1 as described above, slides were dehydrated, air dried, dipped in NTB2 emulsion (Eastman Kodak Co., Rochester, NY), and placed in light-tight boxes. Following a 4-week incubation at 4°C, slides were developed (D19; Eastman Kodak) and counterstained with hematoxylin and eosin.

Immunoelectron microscopy for ED1

Renal tissues were immersed in 2% paraformaldehyde-periodate-lysine for 9 h and cryoprotected in graded sucrose solution. Tissues were then embedded in OCT Compound (Miles Inc, Elkhart, IN) and snap-frozen in cooled N-hexane. Eight-micron cryostat sections were incubated with ED1 as described above. After the sections had been fixed in 2% glutaraldehyde for 10 min, reaction products were

Table 1 Antibodies used to detect specific antigens in paraffin-embedded kidney sections

Primary antibodies	Suppliers
Mouse monoclonal antibody against Ki67 as cell proliferation marker	Novocastra, Newcastle upon Tyne, UK
Mouse monoclonal antibody against ED1 for rat monocytes/macrophages	Serotec, Oxford, UK
Mouse monoclonal antibody against OX6 for MHC class-II antigen	Serotec
Mouse monoclonal antibody against CD43 for rat T lymphocytes (but not B lymphocyte), plasma cells, polymorphs, and stem cells	Cosmobio, Tokyo, Japan
Mouse monoclonal antibody, MPIIIB10 against rat OPN protein	Developmental Hybridoma Studies Institute, Iowa City, IA

visualized by incubating with diaminobenzidine, then the sections were postfixed in 1% OsO_4 for 2 h. Epon 812-embedded ultrathin sections were stained with lead citrate, and examined with a JEM-1220 electron microscope (JEOL, Tokyo).

Histochemical and immunohistochemical analysis of urinary sediments

Urinary sediments were obtained from 12-h urinary collection by centrifugation for 10 min at 1500 rpm and washed in PBS. The cells in 0.1 ml suspensions were deposited onto a slide by centrifugal force (500 rpm, 5 min) using Cytospin 3 (Shandon Scientific, Cheshier, UK). The slides were fixed by 4% paraformaldehyde for 5 min. Hematoxylin and eosin staining and staining for ED1 were performed as described above.

OPN mRNA

The methods for total RNA extraction and polymerase chain reaction (PCR) were reported elsewhere [28]. To quantify PCR products and confirm the integrity of RNAs, a housekeeping gene, glyceraldehyde-3-phosphate dehydrogenase (GAPDH) was co-amplified. We used the primers of OPN: 5′ TCCAAGGAG-TATAAGCAGAGGG-CCA 3′ (sense) and 5′ CTCTTAGGGTC-TAGGACTAG-CTTGT 3′ (antisense) to yield a 200-bp product [11] and of GAPDH: 5′-AATGCATCCTGCACCACCAA (sense) and 5′-GTAGCCATATTCATTGTCATA (antisense) to yield a 515-bp product [10]. PCR products were electrophoresed and the density of each DNA band was measured with NIH Image and the mRNA levels for OPN were expressed as a ratio of the optical density units relative to GAPDH.

Analysis of Ki67+, ED1+, OX6+, CD43+ cells and OPN+ tubules

The number of Ki67+ proximal tubular cells in the outer stripe of outer medulla (OSOM) and ED1+, OX6+ or CD43+ cells in the interstitium or tubular lumen were counted in 20 randomly selected fields of OSOM in each kidney at ×400 magnification. The mean number at each time point was displayed in histograms.

For double-staining sections with ED1 and OX6, the numbers of ED1+OX6+, ED1+OX6- and ED1-OX6+ cells in the interstitium were counted in 20 randomly selected fields of OSOM at ×400 magnification, and the mean percentage of ED1/OX6 double-positive cells among ED1+ cells and ED1/OX6 double-positive cells among OX6+ cells was calculated.

When immunostaining of ED1 with autoradiography was performed, the number of ED1+ cell labeled with [^{3}H]-thymidine (>5 nuclear grains) among ED1+ cells in the interstitium and in the tubular lumen was counted in 20 randomly selected fields of OSOM on day 5 and day 7 at ×400 magnification, and the mean percentage of ED1+ cell labeled with [^{3}H]-thymidine was calculated.

The number of proximal tubules in which OPN+ tubular epithelial cells were present was counted in 20 randomly selected fields of OSOM at ×400 magnification. To minimize observer bias, morphometric examination was performed without the knowledge of the group from which the tissue was obtained.

Statistical analysis

Data are expressed as mean ±SD. Differences between data sets were determined by performing one-way analysis of variance followed by Fisher test. A P level <0.05 was accepted as being statistically significant.

Results

Uranyl acetate-induced ARF

Serum creatinine level increased significantly as early as day 3 (baseline: 0.44±0.06, day 3: 1.87±0.22 mg/dl, P<0.01), reached a peak value (6.10±0.68 mg/dl, P<0.01) on day 7 and then returned to the basal values by day 15. Histological examination revealed extensive proximal tubular damage in OSOM by day 5. The number of Ki67+ regenerating proximal tubular cells in OSOM was increased significantly as early as day 3, reached a peak count on days 5–7, then decreased (Fig. 1 and Fig. 2). The denuded tubular basement membranes were almost covered with regenerating cells by day 7 (Fig. 1D).

Changes in density and distribution of ED1+ cells

ED1+ monocytes/Møs were found only occasionally in normal control kidneys. After induction of ARF, interstitial ED1+ cells increased in the region of injury mainly in the OSOM, then gradually decreased after regeneration of the tubules (Fig. 3A–E). Focal accumu-

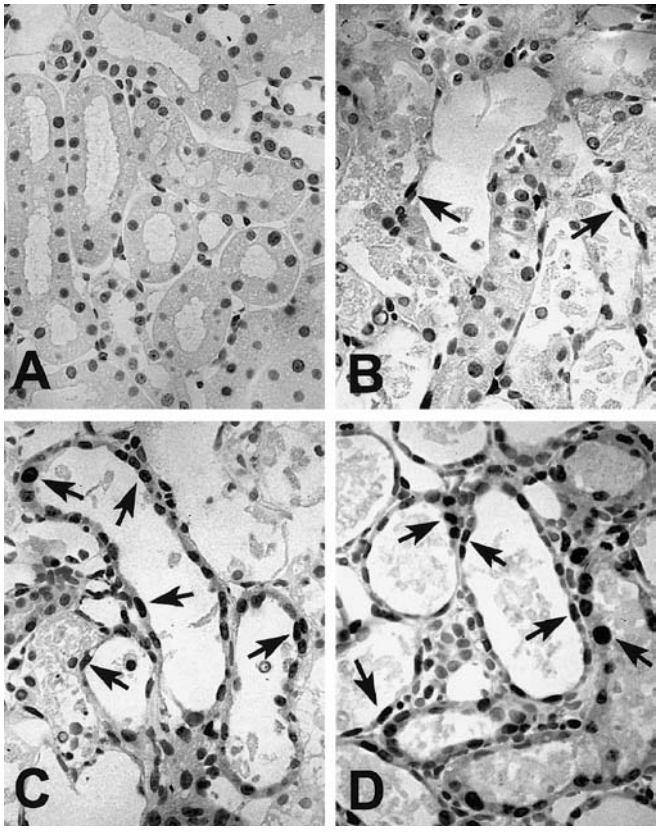

Fig. 1 Photomicrographs of immunostaining for Ki67 (*black color*) in outer stripe of outer medulla before (**A**) and on day 3 (**B**), day 5 (**C**) and day 7 (**D**) after induction of acute renal failure. *Arrows* immunoreactive proximal tubular cells. Original magnifications ×400

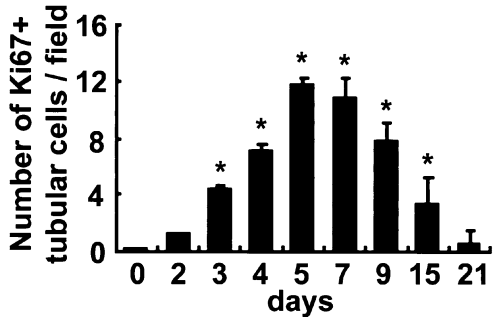

Fig. 2 Number of Ki67+ cells in the proximal tubules per field in outer stripe of outer medulla. Data represent the mean±SD values of four or five rats. *P<0.001 versus normal control (day 0)

lation of ED1+ cells was noted in and around the vascular bundles on day 2 (Fig. 3A). ED1+ cells adherent to the luminal surface of the vascular endothelial cells could be found from days 3–4 (Fig. 3F). Specific accumulation of ED1+ cells closely around the initially necrotic proximal tubules was not evident (Fig. 3A, B), whereas some ED1+ cells displaying pleomorphic morphology were apparently located in close proximity to the regenerating proximal tubules with flattened cytoplasm from days 4–7 (Fig. 3B,C and G). Mainly on day 5 and day 7, ED1+ cells between tubular epithelial cells and ED1+ giant cells in the tubular lumen (Fig. 3C, H) could be found. ED1+ giant cells formed clusters sometimes associated with cellular debris (Fig. 3J). There were clusters of degenerated ED1+ cells in the focal interstitium after day 9 (Fig. 3I).

Though urinary sediments showed many cellular elements but very few red blood cells from day 3 to day 9, ED1+ cells with cytoplasmic vacuoles, similar to ED1+ giant cells in the tubular lumen, were found only from day 5 (Fig. 3K).

Morphometric analysis revealed that the number of ED1+ cells in the interstitium significantly increased on day 2, and peaked on day 5 (Fig. 4A). The number of ED1+ cells in the tubular lumen significantly increased on day 5, peaked on day 7, then rapidly decreased (Fig. 4B). The proportion of [^{3}H]-thymidine radiolabeled ED1+ Møs in the interstitium was 3.4% on day 5 and 0.6% on day 7, and in the tubular lumen was 0.2% on day 5 and 0.2% on day 7 (Fig. 3J). These results indicated a low proliferation of local ED1+ Møs.

Immunoelectron microscopy revealed that pleomorphic cells around the regenerating proximal tubules showed labeling of multiple lysosomal compartments, characteristic of activated Møs (Fig. 5A, B). ED1+ Møs were often found to be located next to fibroblast-like cells around damaged and regenerating proximal tubules (Fig. 5B). ED1+ giant cells in the tubular lumen had features of phagocytic Møs (Fig. 5C, D). The tubular cells themselves were ED1 negative.

Changes in density and distribution of OX6+ cells

In control rats, a few OX6+ cells were found in the peritubular areas. After induction of ARF, pleomorphic OX6+ cells increased around the regenerating proximal tubules until day 7 (Fig. 6A), then OX6+ cells were mainly found in clusters in the interstitium after day 9 (Fig. 6B). Quantitative analysis revealed that the number of OX6+ cells in the interstitium significantly increased on day 4, peaked on day 5, and gradually decreased thereafter (Fig. 4C).

Double immunostaining showed that some ED1+ cells were also positive for OX6 (Fig. 6C), but the majority of ED1+ cells found in the tubular lumen were negative for OX6 (Fig. 6D). Quantitative analysis revealed that only 8.2% of OX6+ cells were ED1+ in the control kidney, but after induction of ARF, 58.6–88.7% of OX6+ cell were ED1+, though increment in the number of ED1-OX6+ cells in the interstitium was marginal (Fig. 7). However, ED1+OX6+ cells among ED1+ cells gradually increased in the interstitium after induction of ARF (Fig. 7). About 50% of ED1+ cells surrounding the proximal tubules were also OX6+ on day 5, and their proportion increased to about 90% after day 15 (Fig. 7), suggesting that ED1+OX6– cells mainly disappeared from the interstitium and ED1+OX6 cells were undiminished until day 21.

Changes in density and distribution of CD43+ cells

In control rats, a few CD43+ cells were found in the peritubular areas (Fig. 8A). Induction of ARF resulted in a slightly increased proportion of CD43+ cells (Fig. 8B). Since morphological evidence did not show the infiltration of neutrophils and plasma cells that can be recognized by the antibody used, most CD43 + cells in the interstitium may indicate T cells in this model.

Fig. 3 Serial changes in the distribution of ED1+ cells (*brown color*) in outer stripe of outer medulla (OSOM) on day 2 (**A**), day 4 (**B**), day 7 (**C**), day 9 (**D**), and day 15 (**E**) after induction of acute renal failure. *Arrows* border between cortex and OSOM, *arrowheads* border between OSOM and inner stripe of outer medulla, *G* glomeruli, *asterisks* necrotic tubules, *double arrow* vascular bundle. **F** ED1+ cells (*arrows*) are adherent on the luminal surface of the vascular endothelial cells on day 4. **G** ED1+ cells with pleomorphic profile (*arrows*) surround regenerating proximal tubules on day 5. H. An ED1+ cell located between regenerating proximal tubules (*arrowhead*) on day 7. ED1+ cells enter into the tubular lumen (*arrow*), and giant ED1+ cells are found in the tubular lumen. **I** Focal accumulation of degenerated ED1+ cells in the interstitium on day 15. **J** Autoradiograph of ED1 (*brown color*) stained section on day 7. Proliferating proximal tubular cells are identified by the presence of tritium (*black nuclear grains*), but most ED1+ cells in the interstitium and tubular lumen show lack of tritium. There is one proliferating ED1+ cell in the interstitium (*arrow*). **K** ED1 staining (*brown color*) in urinary sediments on day 7. Giant ED1+ cells (*arrow*) could be found among the ED1 sediments (*arrowheads*). Original magnification ×100 (**A**–**E**); ×300 (**F**); ×600 (**G**, **H** and **I**); ×1200 (**J**); ×800 (**K**)

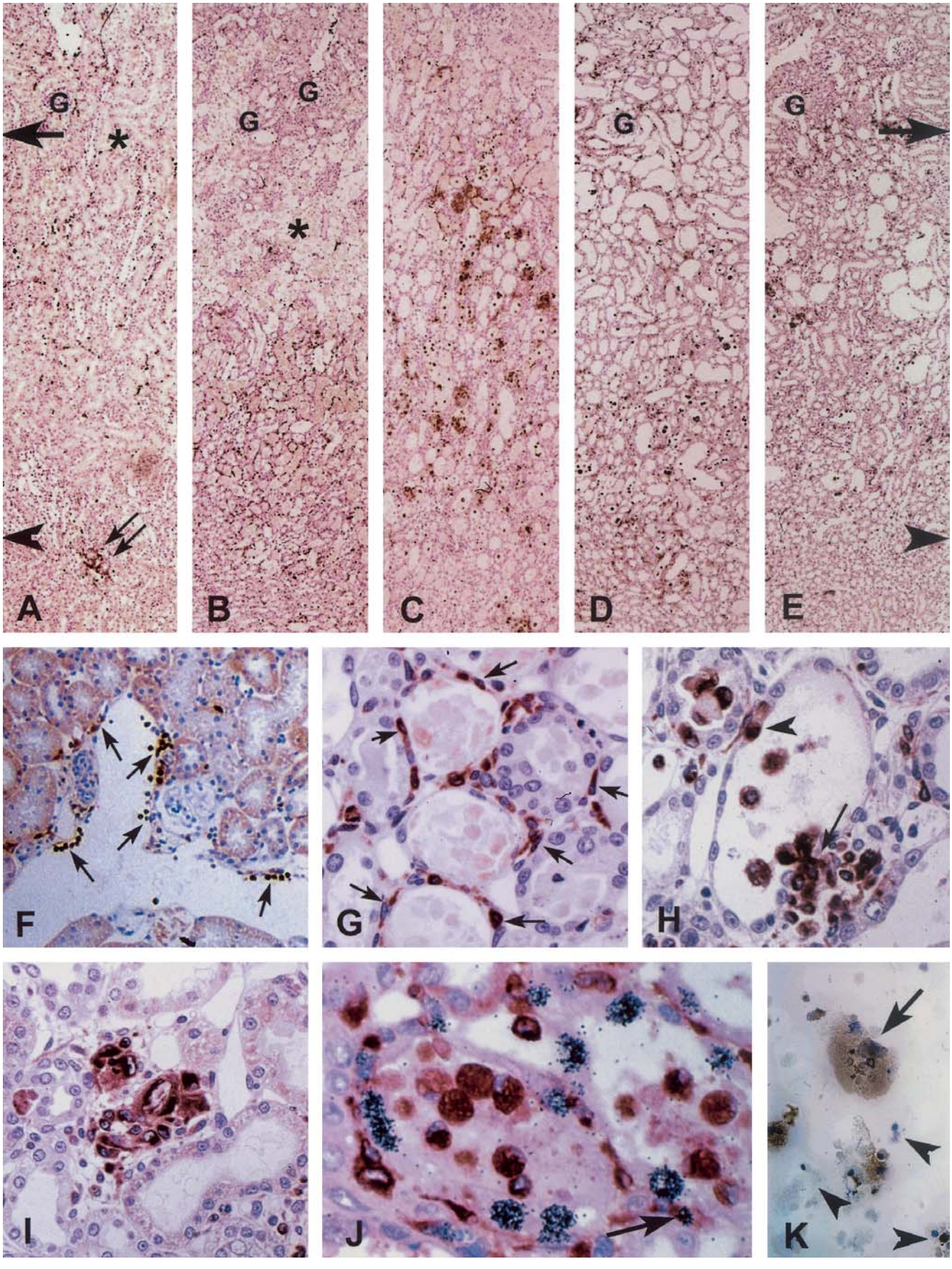

Fig. 3

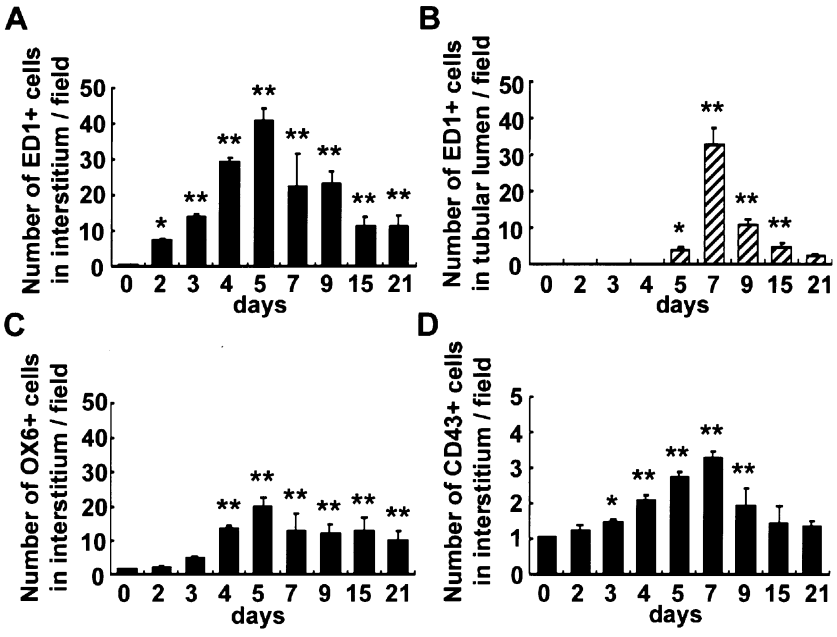

Fig. 4 Numbers of ED1+ cells in the interstitium (**A**), ED1+ cells in the tubular lumen (**B**), OX6+ cells in the interstitium (**C**) and CD43+ cells in the interstitium (**D**) per field in outer stripe of outer medulla. Data represent the mean±SD values of four or five rats. **P*<0.001 versus normal control (day 0)

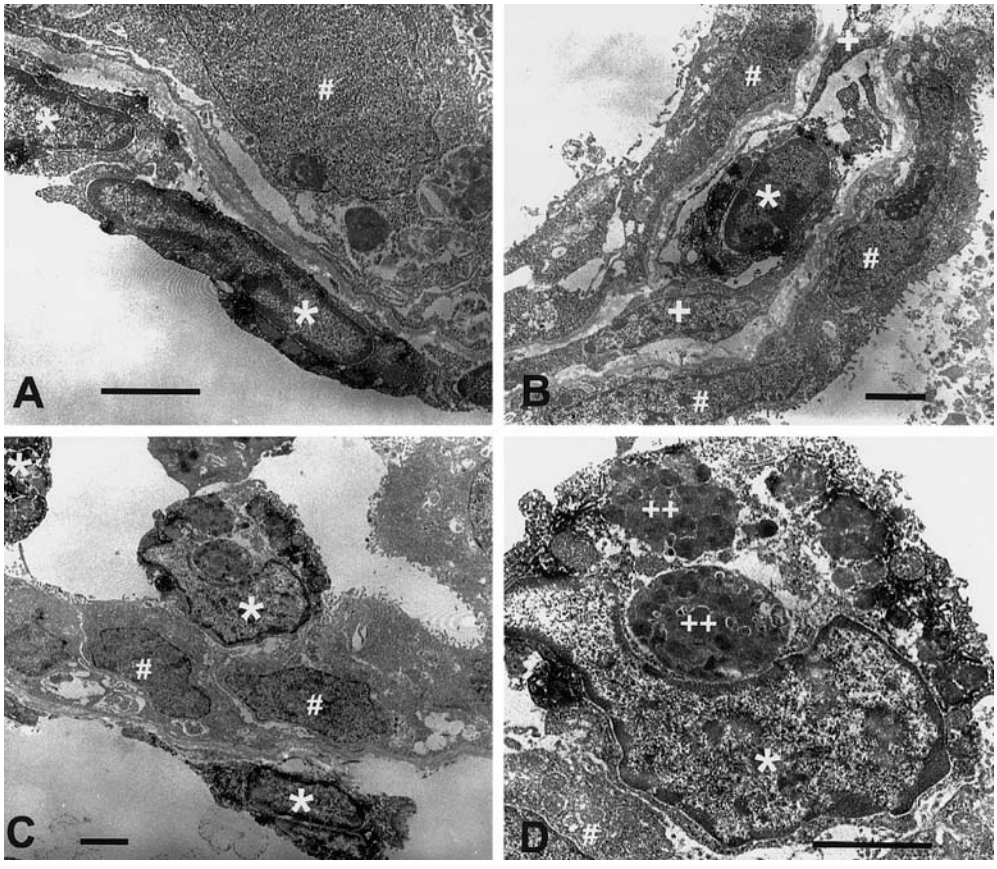

Fig. 5 Immunoelectron micrographs of immunoreactive cells on day 5 (**A**, **B**) and day 7 (**C**, **D**) after induction of acute renal failure. **A** On day 5, reaction products indicative of ED1 are found on the mononuclear cell with pleomorphic profile attached firmly to the tubular basement membrane, on which regenerating proximal tubules can be seen. **B** On day 5, ED1+ cell is found in association with the fibroblast-like cell (+) in the peritubular region. **C** On day 7, giant ED1+ mononuclear cells can be found in the tubular lumen. **D** An enlarged photograph of **C**. ED1+ cell showing characteristics of phagocytic macrophage with indented nucleus, multiple small protrusions, numerous lysosomes, well-developed Golgi apparatus, and secondary lysosomes, containing membranous materials (++). *Asterisks* ED1+ cells, # regenerating proximal tubular cells. *Scale bars* 2.0 μm

Quantitative analysis revealed that the number of CD43+ cells in the interstitium significantly increased from day 3 to day 9, reaching a peak value on day 7 (Fig. 4D).

OPN expression

In normal kidneys, OPN was almost exclusively located in the descending thin limb of the loop of Henle and papillary uroepithelium [12]. Newly expressed immuno-

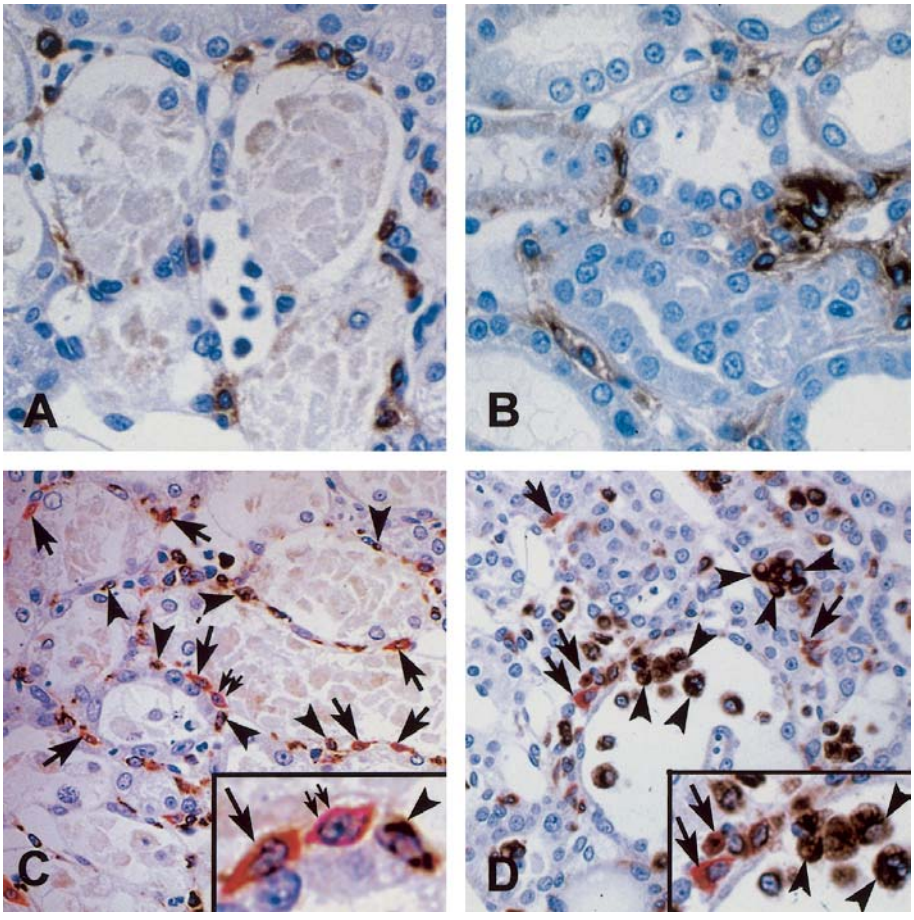

Fig. 6 Photomicrographs of immunostaining for OX6 (*brown color*) on day 5 (**A**) and day 9 (**B**) after induction of acute renal failure (ARF). Photomicrographs of double immunostaining for ED1 and OX6 on day 5 (**C**) and day 7 (**D**) after induction of ARF. *Arrows* ED1+OX6+ cells (*dark red color*), *arrowheads* cells ED1+OX6– (*brown color*), double arrow ED1-OX6+ cell (*pink color*). *Original magnifications* ×100 (**A**, **B**); ×600 (**C**, **D**); *insets* ×1200

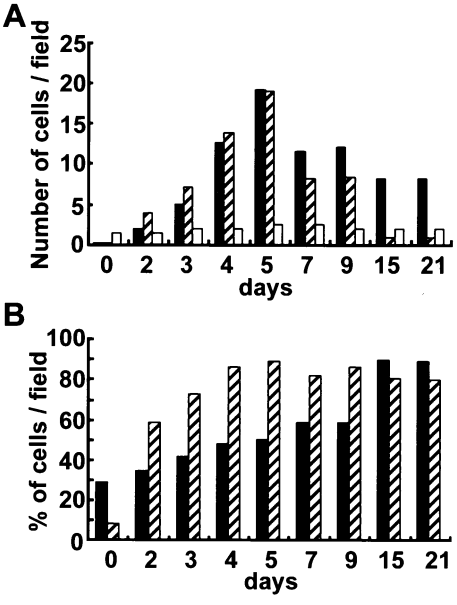

Fig. 7 Numbers of ED1+OX6+ (*solid bars*), ED1+OX6– (*hatched bars*) and ED1-OX6+ cells (*open bars*) per interstitial field of outer stripe of outer medulla (OSOM) (**A**), and mean percentage of ED1+OX6+ cells among ED1+ cells (*solid bars*) and ED1+OX6+ cells among OX6+ cells (*hatched bar*) in the interstitium of OSOM (**B**). Data represent the mean±SD values of three rats

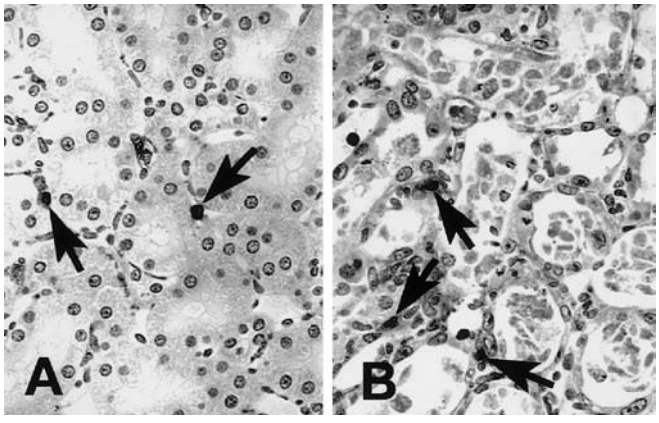

Fig. 8 Photomicrographs of immunostaining for CD43 (*black color*) in outer stripe of outer medulla before (**A**) and on day 7 (B) after induction of acute renal failure. *Arrows* immunoreactive cells. *Original magnifications* ×400

reactive OPN was found sporadically both in proximal tubules and the distal nephron in OSOM as early as day 2 after ARF (Fig. 9A). OPN immunostaining of proximal tubules in the OSOM was the strongest after 7–9 days (Fig. 9E). The subcellular OPN immunostaining showed a homogeneous pattern in proximal tubules with nuclear division (Fig. 9A, C), punctuated pattern in the perinu-

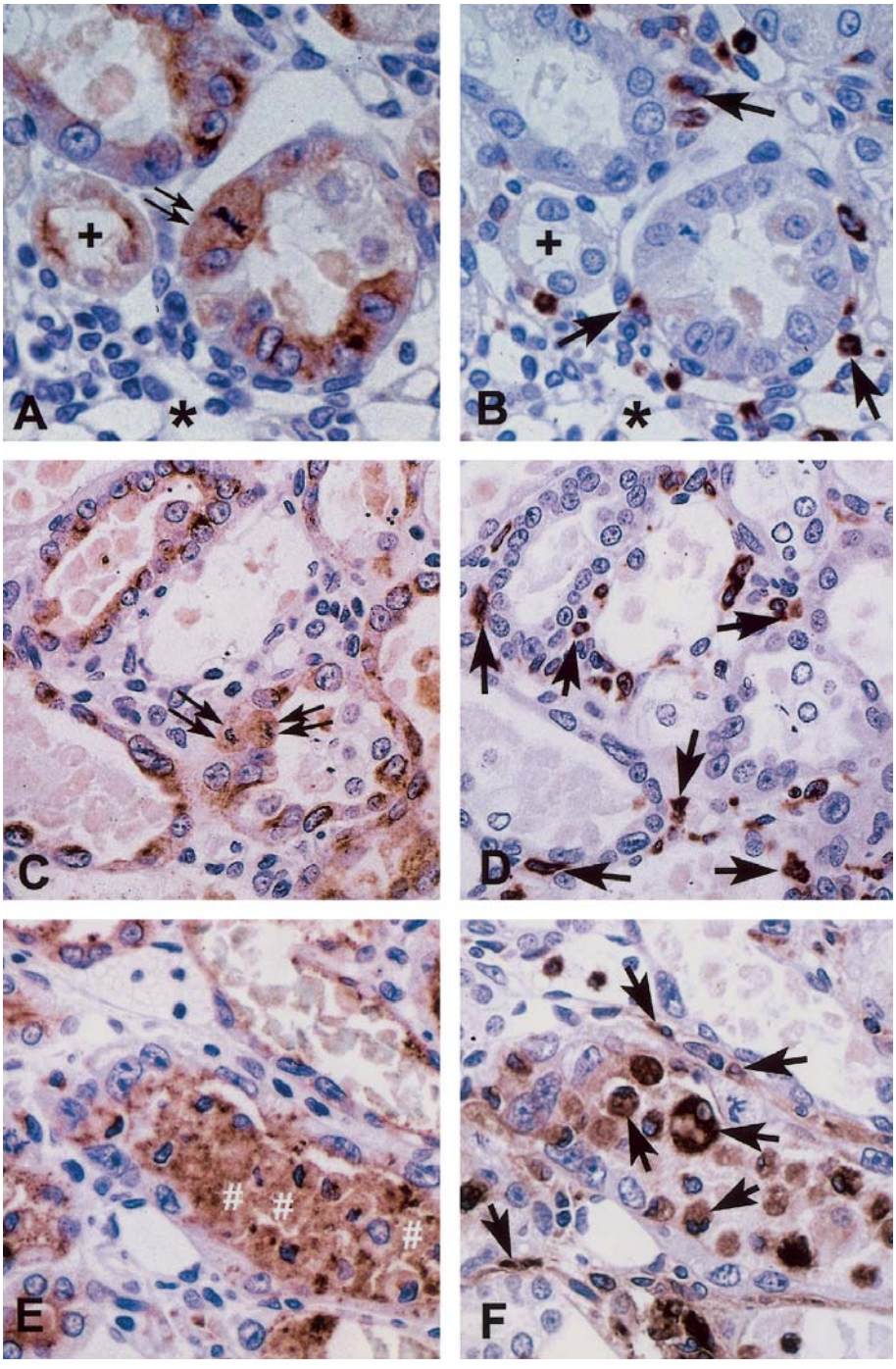

Fig. 9 Photomicrographs of immunostaining for osteopontin (OPN; **A**, **C** and **E**) and ED1 (**B**, **D** and **F**) in consecutive sections on day 2 (**A**, **B**), day 5 (**C**, **D**) and day 7 (**E**, **F**) after induction of acute renal failure. Note the presence of some ED1+ cells (*arrows*) in the vicinity of OPN+ proximal tubular cells (**A**–**D**). Most giant ED1+ cells (*arrowheads*) in the tubular lumen are OPN+ and are intermingled among OPN+ cell debris (#; **E**, **F**). *Asterisks* vascular bundle, + distal nephron, *double arrows* nuclear division. *Original magnifications* ×1200 (**A**, **B**); ×800 (**C**–**F**)

clear regions of the limited regenerating proximal tubules (Fig. 9A, C, D), and prominently subapical pattern in the distal nephron (Fig. 9A). Some ED1+ cells were located in the vicinity of OPN+ proximal tubular cells, but no specific relationship could be identified between OPN+ proximal tubular cells and ED1+ cells in the consecutive sections (Fig. 9A–D). Most ED1+ giant cells in the tubular lumen were OPN+ and intermingled among OPN+ cell debris (Fig. 9E, F). Quantitative analysis revealed that the number of OPN+ tubules significantly increased on day 2, and reached a peak number on day 9 (Fig. 10).

Compared with normal rats, OPN mRNA was significantly upregulated in the kidney on day 4, reached a peak level on day 7, and was still high by day 21 (Fig. 11).

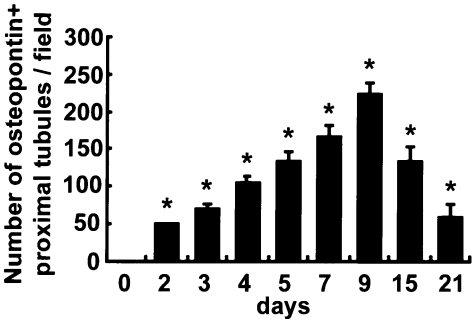

Fig. 10 Number of osteopontin (OPN+) proximal tubules per field in outer stripe of outer medulla. Data represent the mean±SD values of four or five rats. *P<0.001 versus normal control (day 0)

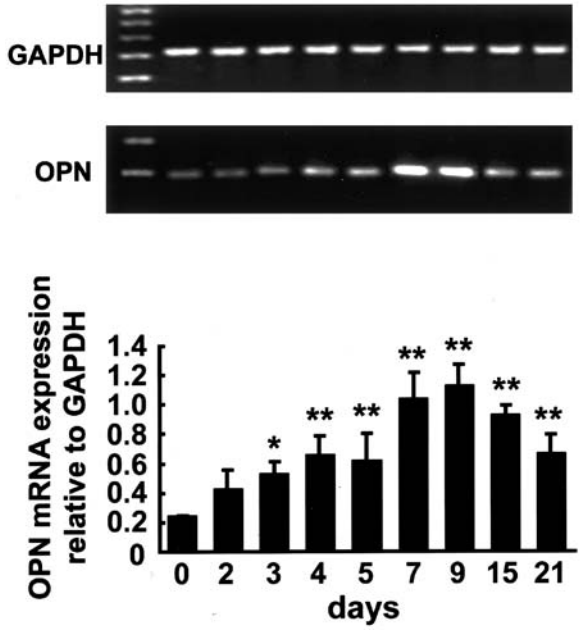

Fig. 11 Ratio of osteopontin to glyceraldehyde-3-phosphate dehydrogenase mRNA in the kidney. Data represent the mean±SD values of three to four rats per group. *P<0.05 versus normal control (day 0); **P<0.001 versus normal control

Discussion

It is generally recognized that activated Møs are major players in wound repair, with several studies suggesting a critical role for Møs throughout the wound-healing process [5, 14, 22, 25]. Studies from our laboratories [28] showed that suppression of interstitial infiltration of ED1+ Møs and myofibroblasts inhibited the regeneration of renal tubular epithelial cells in uranyl acetate-induced ARF in rats by using mycophenolate mofetil. These findings suggest that ED1+ Møs that infiltrate after the acute tubular injury may also contribute to cellular recovery in this model. Møs can possibly be involved in phagocytosing cellular debris and apoptotic tubular cells [1], thus contributing to tissue remodeling, antigen presentation in the defense reactions following the invasion of foreign elements [29] from damaged tubules, and secretion of trophic agents [5] necessary for proliferation of tubular cells. In the present study, not only MHC class-II molecule-expressing Møs but also Møs that did not express MHC class-II molecule showed massive accumulation in the vicinity of regenerating proximal tubules. In addition, a significant number of non-MHC class-II molecule-expressing Møs migrated into the tubular lumen. The aim of the present study was thus to assess the changes in density and distribution of each type of infiltrating Møs in response to the acute tubular injury.

In this model, only a small proportion of radiolabeled proliferating ED1+ Møs was found in the interstitium and the tubular lumen, indicating a lack of active proliferation of local ED1+ Møs. Pleomorphic morphology of ED1+ cells in the interstitium might also indicate newly recruited Møs from the blood. These kinetics of ED1+ Møs, the migratory figures of ED1+ Møs into the tubular lumen, and presence of mostly ED1+OX6– Møs in the tubular lumen, suggest that after the influx of ED1+ Møs with or without OX6 positivity around the proximal tubules, ED1+OX6– Møs mainly entered into the tubular lumen, then became giant cells with strong ED1-positivity and ultrastructural features of phagocytic Møs. ED1+ cells in the urinary sediments appeared only after day 5, when giant ED1+ cells were found in significant numbers in the tubular lumen. These findings also indicate that the origin of giant ED1+ cells in the tubular lumen is not proximal tubular cells, but rather ED1+OX6– Møs that accumulated around the proximal tubules. Since the amount of ED1 expression in a single cell correlates with the phagocytic activity of the respective cell type [4], it is likely that, in this model, the giant Møs with strong ED1-positivity act as scavengers of necrotic debris or apoptotic cells [1] in the tubular lumen to promote healing after tubular damage.

Dendritic cells are professional antigen-presenting cells and are considered to be mobilized from the bone marrow in response to injury [31]. They capture exogenous antigens and then move to lymphoid tissues to present their antigen peptide with MHC class-II molecule to helper T cells [3]. In this study, OX6+ cells (directed to MHC class-II molecule) significantly increased in the peritubular regions on day 4, reaching a peak number on day 5, then gradually decreased thereafter. However, the increment in ED1-OX6+ cells was marginal while the main increase was in ED1+OX6+ cells (Fig. 7). However, the proportion of OX6+ED1+ cells among ED1+ cells gradually increased after induction of ARF to become about 90% after day 15 (Fig. 7), indicating that ED1+OX6– cells disappeared from the interstitium more rapidly than ED1+OX6+ cells by day 15 mainly because of migration of ED1+OX6– cells into the tubular lumen. Thus, the number of ED1+OX6+ cells did not decrease after day 15. As the turnover rate of bone marrow-derived dendritic cells in the renal tissue was reported to be between 7 days and 10 days [15], it is possible that the turnover of ED1+OX6+ cells becomes active after day 15 in our model. Since increased expression of MHC class-II

molecules on Møs correlates well with an elevated immunoregulatory status [29], it is possible that MHC class-II molecule-expressing cells surrounding proximal tubules in our model contribute to the defense against incoming urinary noxious substances from bared tubular basement membrane and/or interspaces of proximal tubular cells with immature tight junction following acute proximal tubular injury.

Although the number of CD43+ lymphocytes (mostly T cells) in the interstitium significantly increased after day 3 and peaked on day 7, the increment was marginal and the peak value fell after completion of proximal tubular regeneration. Thus, any interaction among CD43+ cells, ED1+ cells with or without expressing MHC class II, and repair of proximal tubules is not apparent in this model.

OPN was examined in the present study as a representative potent chemoattractant for Møs. After induction of ARF, OPN protein and mRNA were upregulated and immunoreactive OPN was found in some damaged and regenerating proximal tubules. Møs accumulated around the regenerating tubules; however, only a limited number of regenerating proximal tubular cells expressed OPN. Though these findings do not strongly support that OPN functions as chemoattractant for Møs in this model, it cannot be excluded that OPN secreted into the interstitium could not be detected in the present system. However, giant ED1+OX6– cells found in the tubular lumen were OPN+ and intermingled among OPN+ cell debris. In support of this argument, Murry et al. [17] reported that OPN is synthesized by Møs during the repair of myocardial necrosis in rats and human, suggesting that OPN may be important in healing after tissue injury. Mckee et al. [16] reported that OPN secreted by Møs could serve as a Mø adhesion protein, and was concentrated on the surface of small particles, where it might act as an opsonin to facilitate cell adhesion and phagocytosis by Møs.

In conclusion, our findings suggest that ED1+ Møs are actively associated with regenerating proximal tubules and, thus, might promote proximal tubular regeneration. MHC class-II molecule non-expressing Møs may function as scavengers and phagocytose cellular debris in the tubular lumen, cleaning the wound site. MHC class-II molecule-expressing Møs in the peritubular regions might act as outpost of the defense system to monitor incoming antigens. Thus, Møs with or without expressing MHC class-II molecule possibly contribute to the defense and repair of injured proximal tubules in uranyl acetate-induced ARF in rats.

Acknowledgements This work was supported by research grant (no. 13671107) sponsored by The Ministry of Education Science, Sports and Culture in Japan.

References

1. Aderem A, Underhill DM (1999) Mechanisms of phagocytosis in macrophages. Annu Rev Immunol 17:593–623
2. Baird A, Mormende P, Bohlen P (1985) Immunoreactive fibroblast growth factor in cells of peritoneal exudate suggest its identity with macrophage-derived growth factor. Biochem Biophys Res Commun 126:359–364
3. Banchereau J, Steinman RM (1998) Dendritic cells and the control of immunity. Nature 392:245–252
4. Damoiseaux JG, Dopp EA, Calame W, Chao D, MacPherson GG, Dijkstra CD (1994) Rat macrophage lysosomal membrane antigen recognized by monoclonal antibody ED1. Immunology 83:140–147
5. Danon D, Kowatch MA, Roth GS (1989) Promotion of wound repair in old mice by local injection of macrophages. Proc Natl Acad Sci U S A 86:2018–2020
6. Diamond JR, Kees-Folts D, Ricardo SD, Pruznak A, Eufemio M (1995) Early and persistent up-regulated expression of renal cortical osteopontin in experimental hydronephrosis. Am J Pathol 146:1455–1466
7. Dijkstra CD, Dopp EA, Joling P, Kraal G (1985) The heterogeneity of mononuclear phagocytes in lymphoid organs: distinct macrophage subpopulations in the rat recognized by monoclonal antibodies ED1, ED2 and ED3. Immunology 54:589–599
8. Giachelli CM, Pichier R, Lombardi D, Denhardt DT, Alpers CE, Schwartz SM, Johnson RJ (1994) Osteopontin expression in antiostensin II induced tubulointerstitial nephritis. Kidney Int 45:515–524
9. Giachelli CM, Schwartz SM, Liaw L (1995) Molecular and cellular biology of osteopontin: potential role in cardiovascular disease. Trends Cardiovasc Med 5:88–95
10. Ishidoya S, Morrissey J, McCracken R, Reyes A, Klahr S (1995) Angiotensin II receptor antagonist ameliorates renal tubulointerstitial fibrosis caused by unilateral ureteral obstruction. Kidney Int 47:1285–1294
11. Kawashima R, Mochida S, Matsui A, YouLuTuZ Y, Ishikawa K, Toshima K, Yamanobe F, Inao M, Ikeda H, Ohno A, Nagoshi S, Uede T, Fujiwara K (1999) Expression of osteopontin in Kupffer cells and hepatic macrophages and Stellate cells in rat liver after carbon tetrachloride intoxication: a possible factor for macrophage migration into hepatic necrotic areas. Biochem Biophys Res Commun 256:527–351
12. Kleinman JG, Beshensky A, Worcester EM, Brown D (1995) Expression of osteopontin, a urinary inhibitor of stone mineral crystal growth, in rat kidney. Kidney Int 47:1585–1596
13. Lan HY, Mu W, Nikolic-Paterson DJ, Atkins RC (1995) A novel, simple, reliable, and sensitive method for multiple immunoenzyme staining: use of microwave oven heating to block antibody crossreactivity and retrieve antigens. J Histochem Cytochem 43:97–102
14. Leibovich SJ, Ross R (1975) The role of the macrophages in wound repair. A study with hydrocortisone and antimacrophage serum. Am J Pathol 78:71–100
15. Leszczynski D, Renkonen R, Hayry P (1985) Localization and turnover rate of rat renal 'dendritic' cells. Scand J Immunol 21:355–360
16. McKee MD, Nanci A (1996) Secretion of Osteopontin by macrophages and its accumulation at tissue surfaces during wound healing in mineralized tissues: a potential requirement for macrophage adhesion and phagocytosis. Anat Rec 245:394–409
17. Murry CE, Giachelli CM, Schwartz SM, Vracko R (1994) Macrophages express osteopontin during repair of myocardial necrosis. Am J Pathol 145:1450–1462
18. Okada H, Moriwaki K, Kalluri R, Takenaka T, Imai H, Ban S, Takahama M, Suzuki H (2000) Osteopontin expressed by renal tubular epithelium mediates interstitial monocyte infiltration in rats. Am J Physiol 278:F110–F121
19. Ophascharoensuk V, Giachelli CM, Gordon K, Hughes J, Pichler R, Brown P, Liaw L, Schhmidt r, Shankland SJ, Alpers

CE, Couser WG, Johnson RJ (1999) Obstructive uropathy in the mouse: role of osteopontin in interstitial fibrosis and apoptosis. Kidney Int 56:571–580
20. Pichler R, Giachelli CM, Lombardi D, Pippin J, Gordon K, Alpers CE, Schwartz SM, Johnson RJ (1994) Tubulointerstitial disease in glomerulonephritis: potential role of osteopontin (uropontin). Am J Pathol 144:915–926
21. Pierce GF, Mustoe TA, Lingelbach J, Masakowski VR, Griffin GL, Senior RM, Deuel TF (1989) Platelet-derived growth factor and transforming growth factor-beta enhance tissue repair activities by unique mechanisms. J Cell Biol 109:429–440
22. Pierce GF, Mustoe TA (1995) Pharmacologic enhancement of wound healing. Annu Rev Med 46:467–81
23. Powell DW, Mifflin RC, Valentich JD, Crowe SE, Saada JI, West AB (1999) Myofibroblasts. I. Paracrine cells important in health and disease. Am J Physiol 277:C1–C19
24. Puchtler H, Waldrop FS, Meloan SN, Terry MS, Conner HM(1970) Methacarn (methanol-Carnoy) fixation. Practical and theoretical considerations. Histochemie 21:97–116
25. Rappolee DA, Werb Z (1992) Macrophage-derived growth factors. Curr Top Microbiol Immunol 181:87–140
26. Spencer SC, Fabre JW (1990) Characterization of the tissue macrophage and the interstitial dendritic cell as distinct leukocytes normally resident in the connective tissue of rat heart. J Exp Med 171:1841–185
27. Sun DF, Fujigaki Y, Fujimoto T, Yonemura K, Hishida A (2000) Possible involvement of myofibroblasts in cellular recovery of uranyl acetate-induced acute renal failure in rats. Am J Pathol 157:1321–1335
28. Sun DF, Fujigaki Y, Fujimoto T, Goto T, Yonemura K, Hishida A (2002) Mycophenolate mofetil inhibits regenerative repair in uranyl acetate-induced acute renal failure by reduced interstitial cellular response. Am J Pathol 161:217–227
29. Unaue ER, Allen PM (1987) The basis for the immunoregulatory role of macrophages and other accessory cells. Science 236:551–556
30. Xie Y, Hishi S, Iguchi S, Imai N, Sakatsume M, Saito A, Ikegame M, Iino N, Shimada H, Ueno M, Kawashima H, Arakawa M, Gejyo F (2001) Expression of osteopontin in gentamicin-induced acute tubular necrosis and its recovery process. Kidney Int 59:959–974
31. Zhang J, Yu ZX, Fujita S, Yamaguchi ML, Ferrans VJ (1993) Interstitial dendritic cells of the rat heart. Quantitative and ultrastructural changes in experimental myocardial infarction. Circulation 87:909–920

Virchows Arch (2003) 443:217–219
DOI 10.1007/s00428-003-0852-9

CASE REPORT

Nicolaus Friedrichs · Roland Vorreuther · Hans-Peter Fischer · Otmar D. Wiestler · Reinhard Buettner

Neurocytoma arising in the pelvis

Received: 7 March 2003 / Accepted: 26 May 2003 / Published online: 3 July 2003
© Springer-Verlag 2003

Abstract Central neurocytoma represents a rare neoplasm of the central nervous system with advanced neurocytic and sometimes focal lipomatous differentiation, a low proliferative potential and a favorable prognosis depending on the efficiency of surgical resection. This entity has been described as an intraventricular tumor near the foramen Monroi. Here, we report a case of a 21-year-old male with peripheral neurocytoma. Using computed tomography, a tumor of unknown origin was located behind the bladder. After complete surgical resection of the tumor, histologically small uniform cells, zones of fibrillarity and neuropil-like islands were seen. Immunohistochemistry revealed positivity for the neuronal markers synaptophysin, neuron-specific enolase and neurofilaments. Vimentin, pan-keratin, desmin, chromogranin, CD-99 and glial fibrillary acidic protein were immuno-negative. A low proliferation rate (1–2%) was found. Several case reports described extraventricular central neurocytomas. A sole publication documented a peripheral neurocytoma arising within a mature cystic teratoma of the ovary. To our knowledge, this is the second reported case of a neurocytoma outside the central nervous system, indicating that this entity may also occur infrequently in peripheral tissues.

Keywords Neurocytoma · Extraventricular · Pelvis · Immunohistochemistry

N. Friedrichs · H.-P. Fischer · R. Buettner (✉)
Institute of Pathology, University of Bonn,
Sigmund-Freud-Strasse 25, 53127 Bonn, Germany
e-mail: Reinhard.Buettner@ukb.uni-bonn.de
Tel.: +49-228-2875375
Fax: +49-228-2875030

R. Vorreuther
Department of Urology, Evangelisches Waldkrankenhaus,
Waldstrasse 73, 53177 Bonn, Germany

O. D. Wiestler
Department of Neuropathology, University of Bonn,
Sigmund-Freud-Strasse 25, 53105 Bonn, Germany

Introduction

Neurocytoma is a tumor of the central nervous system usually located intraventricularly near the foramen of Monro. It was first described in 1982 by Hassoun et al. [6]. Young to middle aged patients are affected, showing symptoms such as headache and nausea. Clinical history is often short. There is no predominance of a certain gender. Radiological methods usually show a tumor mass with heterogeneous signals on computed tomography (CT), containing zones of calcification. Conventional therapy consists of tumor resection, often supported by radiotherapy. Clinical outcome depends on the amount of remaining tumor tissue, and the prognosis is excellent if the tumor can be excised completely.

Central neurocytomas are now well documented in the literature [4, 5, 6]. A neurocytoma can be classified as a central neurocytoma if localized intraventricularly or as an extraventricular central neurocytoma if arising outside lateral ventricles [1]. Unusual locations such as cerebellum [3, 9], cervical [13] and thoracal [10] segment of spinal cord or cauda equina [12] have also been described in various case reports. One case of a peripheral neurocytoma arising within a teratoma of the ovary has been documented [7].

Here, we report on a 21-year-old male patient with a tumor located in the pelvis, consisting of small uniform cells, zones of fibrillarity and neuropil-like islands, which was diagnosed as peripheral neurocytoma.

Clinical history

A 21-year-old male from Libya without significant previous medical history presented with a single and painless episode of macrohematuria. Physical examination was unremarkable and laboratory tests were normal. Sonography and CT scans revealed a large, inhomogeneous, well-circumscribed tumor in the pelvis located behind the bladder and the prostate (Fig. 1), but no signs of metastasis. Rectoscopy and cystoscopy showed that rectum and urinary bladder were not infiltrated. The prostate was slightly enlarged (30 ml) and prostate specific antigen was 4 ng/ml.

Fig. 1 Computed tomography scan revealing a pelvic tumor of 10.1×8.3 cm

Biopsies obtained by an explorative laparotomy in a hospital abroad did not lead to a definite diagnosis. Subsequently, a complete tumor excision was performed with partial resection of the bladder and left ureter followed by re-implantation of the ureter.

The patient has remained disease free 3 years after surgery, and CT scans did not reveal any signs of tumor recurrence.

Materials and methods

Surgical resection specimen was fixed in 10% buffered formalin and processed for further light microscopic evaluation. Conventional hematoxylin and eosin stain was applied followed by various immunohistochemical stainings.

Immunohistochemical stainings were performed using indirect immunoperoxidase as described in detail previously [2]. Antibodies, dilutions and the suppliers are listed in Table 1.

Table 1 Antibodies, suppliers and results of immunohistochemical staining

Antibody	Dilution	Supplier	Result
Neuron-specific enolase	1:500	Dako	+
Synaptophysin	1:10	Dako	+
Neurofilaments	1:50	Dako	+
Vimentin	1:1.500	Dako	–
Pan-keratin	1:1.000	Dako	–
Desmin	1:500	Dako	–
Chromogranin A	1:500	Dako	–
CD-99	1:50	Dako	–
Glial fibrillary acidic protein	1:500	Dako	–

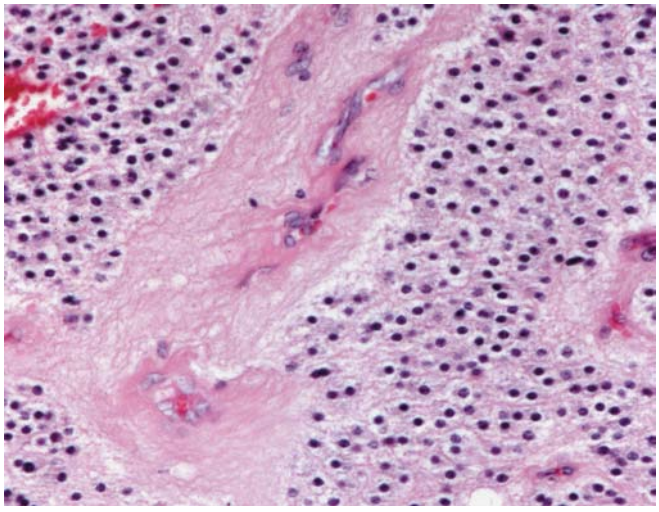

Fig. 2 Histological picture revealing small uniform cells without mitoses and with zones of fibrillarity and neuropil-like islands (×64)

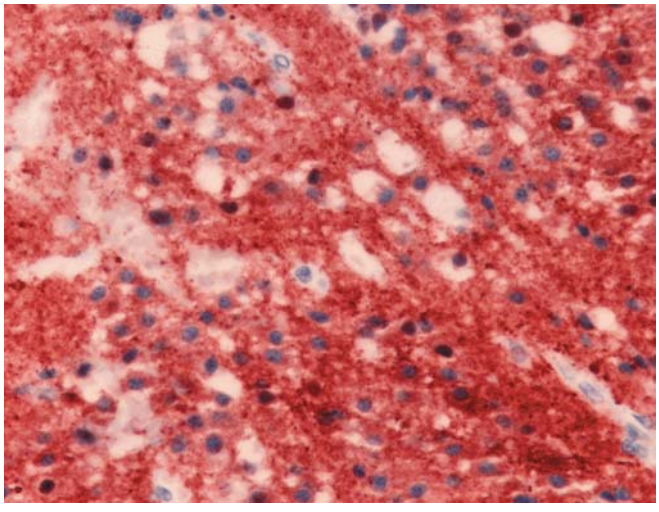

Fig. 3 Immunopositivity for synaptophysin (×64)

Results

A specimen of 10.1×8.3 cm with focal calcifications was examined macroscopically and found to contain microcystic areas.

Histologically, the tumor shows two components consisting of small uniform cells without mitoses as well as zones of fibrillarity and neuropil-like islands (Fig. 2). Tumor cells are immunoreactive for neuronal markers, including synaptophysin (Fig. 3) and neuron-specific enolase (NSE) and reveal a very low proliferative index (1–2%) as demonstrated by nuclear Ki67 staining. Zones of fibrillarity are immunoreactive for neurofilaments. Further immunoreactions against vimentin, pan-keratin, desmin, chromogranin, CD-99 and glial fibrillary acidic protein (GFAP) remain negative. Based on these results, our final diagnosis was peripheral neurocytoma of the

pelvis, which was confirmed by the German Brain Tumor Reference Center.

Discussion

Neurocytoma usually presents as a tumor of the central nervous system affecting young to middle aged adults [4]. Histologically, two characteristic components can be detected: small uniform cells with extremely scarce mitoses and fibrillary islands with a neuropil appearance. Occasionally areas of mature lipocytic differentiation are intermingled. Immunohistochemical features of central neurocytoma have been described in the literature previously [4, 5]. The tumor cells are characterized by reactivity for synaptophysin and NSE while GFAP and chromogranin are negative in most cases. Rarely, GFAP immunoreactivity of neurocytomas has been reported [1]. The proliferative index is usually low, indicating low malignancy and a favorable prognosis. In the literature, cases of extraventricular neurocytomas occurring in the central nervous system [3, 9] and also in unusual locations like the cauda equina [12] have been well documented. Hirschowitz et al. [7] described a neurocytoma arising within a mature cystic teratoma of the ovary.

Primarily due to the pelvic origin of the present case, the differential diagnostic exclusion of soft tissue tumors had to be performed to prove immunonegativity for vimentin and pan-keratin. As further differential diagnoses, we considered a paraganglion and a primitive neuroectodermal tumor (PNET)/neuroblastoma with advanced neuronal differentiation [11]. However, we did not find any evidence for a primitive tumor component and no immunoreactivity for CD-99. In addition, the clinical course and the low proliferative index are clearly inconsistent with the highly malignant features of PNET. A further differential diagnosis is a teratoma of the pelvis with neuroepithelial differentiation [7]. However, sacrococcygeal teratomas tend to manifest in infancy [8] and, in the present case, additional structures indicating a teratoma were not present. Therefore, we speculate that our case may have arisen from remnants of the caudal spinal cord.

In summary, our case represents the second report of a neurocytoma arising outside the central nervous system and, therefore, this entity needs to be included into the differential diagnosis of pelvic tumors.

References

1. Brat DJ, Scheithauer BW, Eberhart CG, Burger PC (2001) Extraventricular Neurocytomas. Am J Surg Pathol 25:1252–1260
2. Bosserhoff AK MM, Hein R, Landthaler M, Buettner R (1999) In situ expression patterns of melanoma-inhibiting activity (MIA) in melanomas and breast cancers. J Pathol 187:446–454
3. Enam SA, Rosenblum ML, Ho KL (1997) Neurocytoma of the cerebellum: case report. J Neurosurg 87:537–540
4. Figarella-Branger D, Söylemezoglu F, Kleihues P, Hassoun J (2000) Central neurocytoma. In: Kleihues P, Cavenee WK (eds) World Health Classification of Tumors, Pathology and genetics of tumors of the nervous system. IARC Press, Lyon, pp 107–109
5. George DH, Scheithauer BW (2001) Central liponeurocytoma. Am J Surg Pathol 25:1551–1555
6. Hassoun J, Gambarelli D, Grisoli F, Pellet W, Salamon G, Pelissier JF, Toga M (1982) Central neurocytoma. An electron-microscopic study of two cases. Acta Neuropathol 56:151–156
7. Hirschowitz L, Ansari A, Cahill DJ, Bamford DS, Love S (1997) Central neurocytoma arising within a mature cystic teratoma of the ovary. Int J Gynecol Pathol 16:176–179
8. Jung CK, Lee YS, Jung ES, Kang CS, Kim BK (2002) Oligodendroglioma arising in a sacrococcygeal immature teratoma. J Korean Med Sci 17:426–428
9. Kleihues P, Chimelli L, Giangaspero F (2000) Cerebellar liponeurocytoma. In: Kleihues P, Cavenee WK (eds) World Health Classification of Tumors, Pathology and genetics of tumors of the nervous system. IARC Press, Lyon, pp 110–111
10. Martin AJ, Sharr MM, Teddy PJ, Gardner BP, Robinson SFD (2002) Neurocytoma of the thoracic spinal cord. Acta Neurochir 144:823–828
11. Rorke LB, Hart MN, McLendon RE (2000) Supratentorial primitive neuroectodermal tumour (PNET). In: Kleihues P, Cavenee WK (eds) World Health Classification of Tumors, Pathology and genetics of tumors of the nervous system. IARC Press, Lyon, pp 141–144
12. Stephan CL, Kepes JJ, Arnold P, Green KD, Chamberlin F (1999) Neurocytoma of the cauda equina. Case report. J Neurosurg 90:247–251
13. Tatter SB, Borges LF, Louis DN (1994) Central neurocytomas of the cervical spinal cord: report of two cases. J Neurosurg 81:288–293

Virchows Arch (2003) 443:220–221
DOI 10.1007/s00428-003-0860-9

LETTER TO THE EDITOR

Ondrej Hes · Milan Hora · Tomas Vanecek · Radek Sima · Miroslav Sulc · Frantisek Havlicek · Milena Beranova · Michal Michal

Conventional renal cell carcinoma with granulomatous reaction: a report of three cases

Received: 10 February 2003 / Accepted: 12 May 2003 / Published online: 12 July 2003
© Springer-Verlag 2003

Keywords Conventional renal cell carcinoma · Granulomatous response · Non-caseating granulomas

Sir,
we report three cases of conventional renal cell carcinomas (CRCC) with granulomatous reaction occurring in the tumorous stroma. The patients were two women and one man aged from 73 years to 85 years (mean 78.3 years). All patients were treated only by nephrectomy. Tumours were well circumscribed, yellow to tan coloured with haemorrhagic foci. The size of the tumours ranged between 2.3 cm and 7.0 cm (mean 4.4 cm). Stage was pT1N0M0 in all cases according to the World Health Organization (WHO) 1998 staging system. Grossly, no features of necrosis were observed.

Histologically, all tumours were typical CRCC composed mainly of clear cells. All CRCCs were of Fuhrman 1. Granulomas were characterised by multinucleated giant cells without necrosis. They were irregularly dispersed within the tumorous stroma (Fig. 1). The amount of lymphoid admixture within granulomas varied from sparse (Fig. 2a) to heavy (Fig. 2b). In one case, we have found a small amount of granulomas within the normal kidney in the vicinity of the tumour. We have not found asteroid and Schaumann bodies and calcium oxalate crystals. No fungi or mycobacteria, respective acid fast bacilli were identified using Ziehl-Neelsen and Grocott stains within granulomas or within the tumour mass or the rest of normal kidney in any of the cases. No infection by *Mycobacterium spec.* and *Treponema pallidum* was proved using polymerase chain reaction (PCR) in any of our patients. Tuberculosis was excluded by thorough clinical check-up in all patients. No progression of the tumours or signs of any granulomatous process were observed from 6 months to 4 years of follow-up after nephrectomy.

Non-caseating granulomas (NCG) presented in local lymph nodes, which drain malignant neoplasms—especially carcinomas—are, in our experience, not a rare finding. Such granulomatous reaction has been reported in association with cervical and breast carcinomas [5, 9].

However, occurrence of NCG within tumourous stroma or within the parenchyma of the epithelial tumours is quite a rare phenomenon. NCG associated with carcinomas were documented in case reports from breast, liver, colon, stomach carcinoma and they are quite commonly

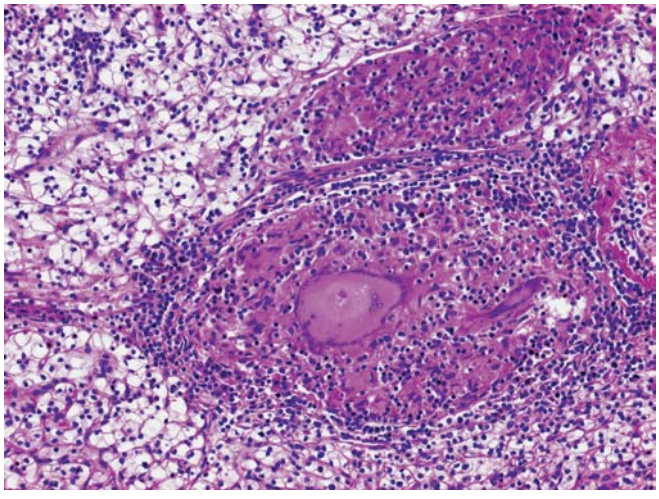

Fig. 1 Granulomas were irregularly dispersed within the conventional renal cell carcinomas, which had Fuhrman grade 1

O. Hes · T. Vanecek · R. Sima · F. Havlicek · M. Michal (✉)
Sikl's Department of Pathology, Laboratore Spec. Diagnostiky
Medical Faculty Hospital, Charles's University Hospital,
Alej Svobody 80, 30460 Pilsen, Czech Republic
e-mail: michal@medima.cz
Tel.: +420-37-7104630
Fax: +420-37-7104650

M. Hora
Department of Urology, Charles's University Hospital,
Pilsen, Czech Republic

M. Sulc
Regional Hospital, Chomutov, Czech Republic

M. Beranova
Department of Obstetrics and Gynecology,
Charles's University Hospital, Pilsen, Czech Republic

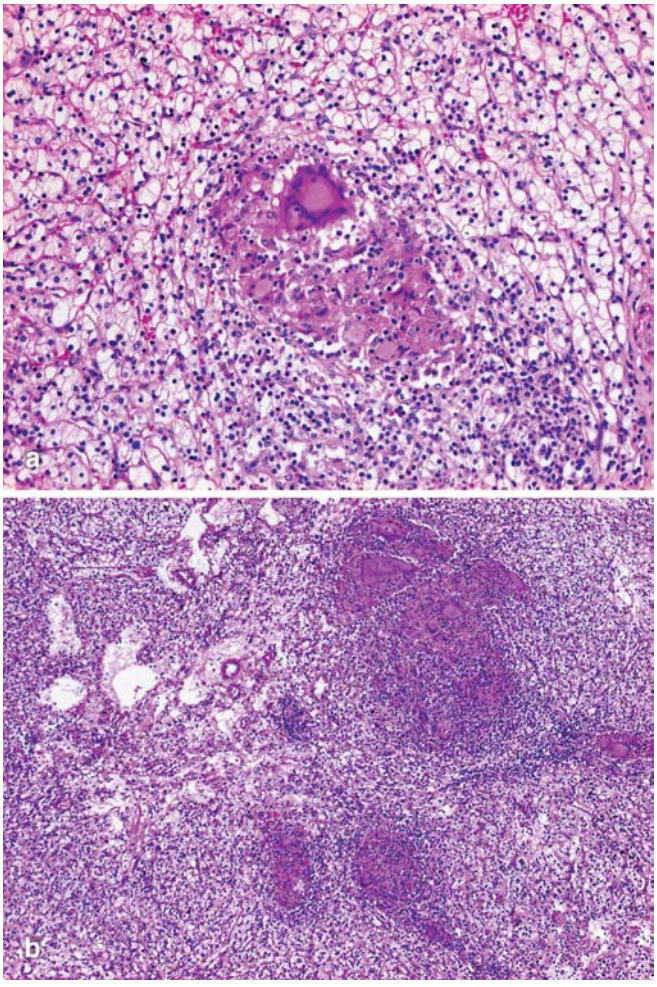

Fig. 2 The amount of lymphoid admixture within granulomas varied from sparse (**a**) to heavy (**b**)

seen in germ cell tumours especially seminomas [2, 3, 5, 8, 9, 11, 12]. A single case report dealing with granulomatous reaction within renal cell carcinoma was published by Campbell [1].

Granulomatous reaction was usually explained as a reactive response to necrotic material or immunological reaction to tumour-related antigens [1, 2, 11].

Coexistence of NCG and metastatic tumour in lymph node was documented in nasopharyngeal carcinoma, seminoma and malignant melanoma [4]. In our cases, we identified NCG within vital tumourous tissue without evidence of necrotic changes. Immunological response to soluble tumourous antigens seems to be the most likely explanation for the occurrence of the granulomas in our cases.

Differential diagnosis includes specific granulomatous infections, especially tuberculosis. Morphology of tuberculous granulomas is different from NCG. Typical tuberculous granulomas are composed of centrally located caseating necrosis, which is surrounded by histiocytes, giant multinuclear cells of Langhans' type and lymphocytes. No necrosis within the granulomas or widespread necrosis typical for tuberculosis was observed within the tumours or outside of the non-tumourous kidney tissue.

A case of generalized CRCC associated with sarcoidosis involving liver and peripancreatic lymph nodes was published by Moder [7]. No patient from our group had any history of sarcoidosis. Moreover the morphology of granulomas in our cases was not quite compatible with sarcoid granulomas. We have not identified any inclusions or Schaumann bodies within granulomatous areas, which are typically found in sarcoidosis [10]. A phenomenon similar to NCG can be observed in patients with renal cell carcinomas and history of preoperative artificial embolisation of the renal artery. Nowadays, it is seldom indicated as an alternative method to nephrectomy in patients with poor health having non-functioning kidneys who present with pain or bleeding [6]. All patients in our study were treated only with nephrectomy without preoperative embolisation. In addition, the morphology of granulomas occurring in tumours after embolisation is different from our case. Central parts of these granulomas are usually formed by necrotic tissue with features of ischaemic infarction. Necrosis is surrounded by multinucleated giant cells (foreign body type) and a dense rim of lymphocytes. Contrary to NCG, post-embolic granulomas have irregular flaggy edges. No Langhans' cells were identified within this type of granulomas.

Acknowledgements This study was supported by grant GA CR reg. no. 301/02/1232.

References

1. Campbell F, Douglas-Jones AG (1993) Sarcoid-like granulomas in primary renal cell carcinoma. Sarcoidosis 10:128–131
2. Coyne JD (2002) Colonic carcinoma with granulomatous (sarcoid) reaction. J Clin Pathol 55:708–709
3. Coyne JD, Haboubi NY (1992) Micro-invasive breast carcinoma with granulomatous stromal response. Histopathology 20:184–185
4. Coyne JD, Banerjee SS, Menasce LP, Mene A (1996) Granulomatous lymphadenitis associated with metastatic malignant melanoma. Histopathology 28:470–472
5. Gregori HB, Othersen HB, Moore M (1962) The significance of sarcoid-like reaction in association with malignant neoplasms. Am J Surg 104:577–586
6. Hom D, Eiley D, Lumerman JH, Siegel DN, Goldfischer ER, Smith AD (1999) Complete renal embolisation as an alternative to nephrectomy. J Urol 161:24–27
7. Moder KG, Litin SC, Gaffey TA (1990) Renal cell carcinoma associated with sarcoid-like tissue reaction. Mayo Clin Proc 65:1498–1501
8. Neville E, Piyasena KHG, James DG (1975) Granulomas of the liver. Postgrad Med J 51:361–365
9. Oberman HA (1987) Invasive carcinoma of the breast with granulomatous response. Am J Clin Pathol 88:718–721
10. Rosai J (1995) Ackerman's surgical pathology, 7th edn. Mosby, St. Louis, pp 1677–1680
11. Tomimatsu H, Kojiro M, Nakashima T (1982) Epithelioid granulomas associated with hepatocellular carcinoma. Arch Pathol Lab Med 106:538–539
12. Watterson J (1982) Epithelioid granulomas associated with hepatocellular carcinoma. Arch Pathol Lab Med 106:538–539

Virchows Arch (2003) 443:222–224
DOI 10.1007/s00428-003-0853-8

LETTER TO THE EDITOR

Ksenija Lučin · Elvira Mustać · Nives Jonjić

Breast sarcoma showing myofibroblastic differentiation

Received: 12 March 2002 / Accepted: 21 April 2003 / Published online: 3 July 2003
© Springer-Verlag 2003

Sir,
Myofibroblasts were originally described as a part of granulation tissue and healing wounds 30 years ago and were extensively studied in the past 20 years. However, the precise definition of myofibroblast as a distinctive cell type is still controversial as well as the concept of myofibroblast being neoplastic. Irrespective of that, it cannot be denied that tumors composed mainly of myofibroblasts do exist. Most of them are benign, i.e., myofibroblastomas [2, 4, 9], some with borderline biological course, i.e., inflammatory myofibroblastic tumor [1], and, rarely, they pursue a malignant biological behavior [2]. Among them, a distinctive form of low-grade myofibroblastic sarcoma was recognized [5, 7, 8], while high-grade lesions have not yet been well characterized. Here, we present the case of unusual high-grade breast sarcoma, which is showing myofibroblastic differentiation.

A 51-year-old woman presented with left-side breast enlargement of 3-months duration and hemorrhagic mammillar discharge. The ultrasound examination revealed a huge tumor replacing almost the entire breast tissue. During the surgery, an intraoperative biopsy was performed, showing malignant spindle-cell tumor. The patient underwent radical mastectomy, followed by chemo- and radiotherapy. Two years after the diagnosis she is still alive.

Macroscopically, the tumor tissue was grayish-white in color, mainly soft and gelatinous, with large foci of hemorrhage and necrosis. It was partially well demarcated from the surrounding breast tissue, but extended through and penetrated overlying skin (Fig. 1A), and measured 22×20×15 cm. On histological examination, the tumor was composed of spindle-shaped cells with poorly defined, pale cytoplasms and fusiform nuclei with small, inconspicuous nucleoli (Fig. 1B). Nuclei were mainly tapering and wavy; some became plumper, but with only mild nuclear atypia. The tumor showed various growth patterns; in most parts cells were arranged in a fascicular pattern (Fig. 1D) and set in a faintly fibrillar, partly mucoid stroma. In those parts, a striking nuclear palisading was the dominant feature (Fig. 1C). Somewhere, a storiform (Fig. 1E) or herringbone pattern (Fig. 1F) was seen. Cellularity varied from high to low in those parts where the stroma became more collagenized and hyalinized. Mitotic activity ranged from 8 to 35 per 10 HPF. Immunostaining showed strong and diffuse vimentin and α-smooth muscle actin (SMA) positivity (Fig. 1G), while stains for pan-cytokeratin, S-100 protein, CD34, desmin and h-caldesmon (Fig. 1H) were all negative. Axillary lymph nodes were negative for metastases.

Among various growth patterns, the most prominent was the fascicular pattern with marked nuclear palisading. This feature made the possibility of spindle cell sarcomatoid carcinoma—which, regarding the site of origin, would be the most likely diagnosis—much less probable. Indeed, tumor cells were negative for pan-cytokeratin, while positive for vimentin, and the surrounding breast tissue showed neither the signs of in situ or invasive carcinoma, nor the signs of epithelial proliferation. Among the malignant tumors described to contain nuclear palisading we considered MPNST, leiomyosarcoma, sinovial sarcoma and dermatofibrosarcoma protuberans. The results of immunostaining, i.e., strong and consistent positivity for SMA and negativity for all the other markers, narrowed our differential diagnosis to sarcomas with myoid differentiation. We included the h-caldesmon and desmin into the immunostaining panel and found tumor cells completely negative. H-caldesmon is a protein combined with actin and tropomyosin that regulates cellular contraction. It is a specific marker of both smooth-muscle cells and its neoplasms, while myofibroblasts and tumors with myofibroblastic differentiation are negative for this protein [10]. Thus, it can facilitate the differential diagnosis between leiomyosarcomas and other tumors with smooth-muscle cell-like differentiation,

K. Lučin (✉) · E. Mustać · N. Jonjić
Department of Pathology, Medical Faculty,
University of Rijeka,
Braće Branchetta 20, 51000 Rijeka, Croatia
e-mail: ksenijal@medri.hr
Fax: +385-51-325810

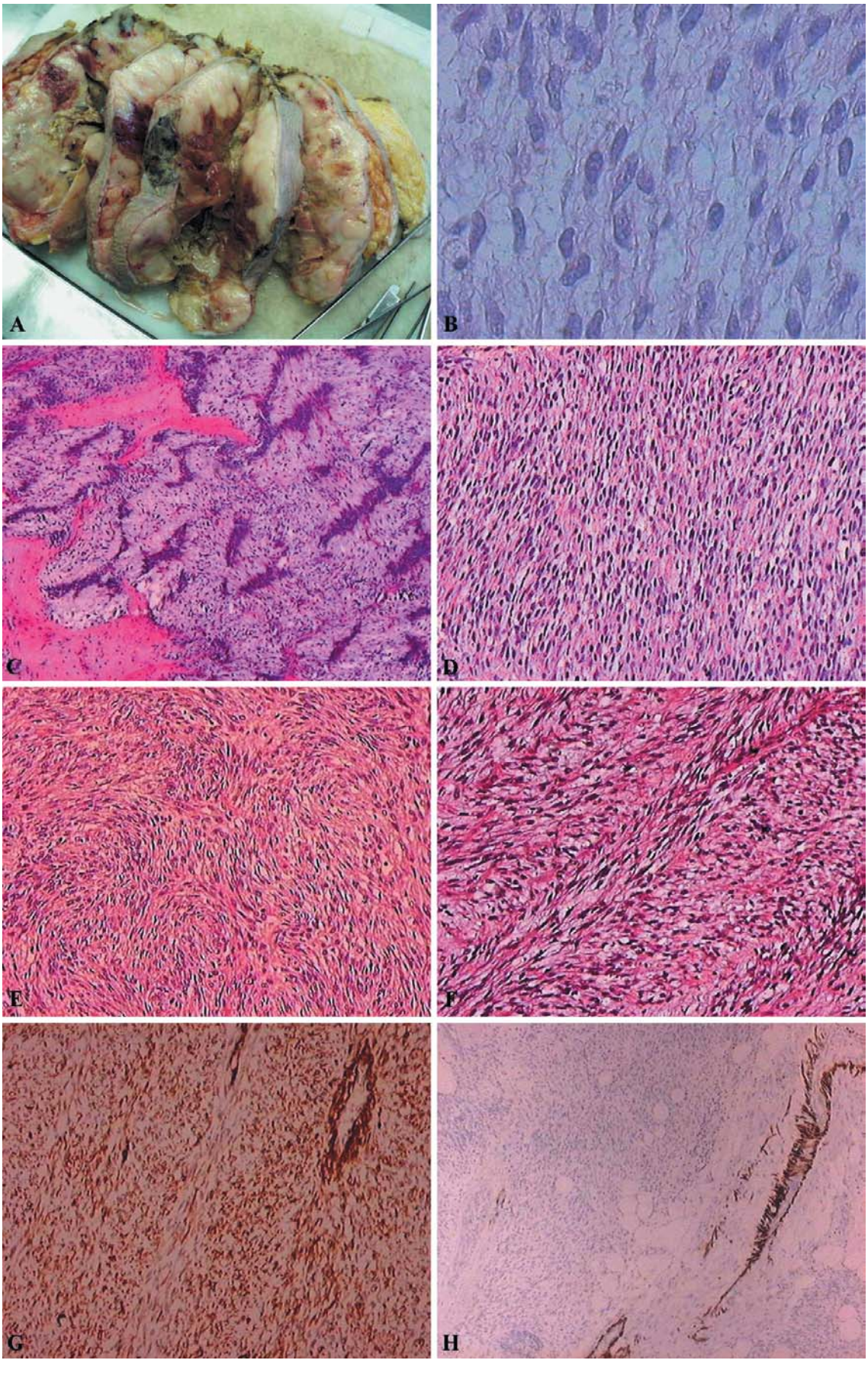
A
B
C
D
E
F
G
H

Fig. 1A–H The gross and histological features of breast sarcoma. **A** Tumor tissue is grayish-white with large foci of hemorrhage and necrosis. Cytological features in breast sarcoma: nuclei are tapering and wavy or vesicular with small nucleoli (**B**, ×400), and showing marked nuclear palisading (**C**, ×40). Growth patterns in breast sarcoma are either fascicular (**D**, ×100), storiform (**E**, ×100) or herring bone (**F**, ×100). The immunophenotype of breast sarcoma: tumor cells are strongly positive for SMA (**G**, ×100), while negative for h-caldesmon (**H**, ×100)

including myofibroblastic tumors. In some parts, mainly those with storiform architecture, the tumor closely resembled malignant fibrous histiocytoma (MFH). It is well known that myofibroblastic differentiation can be found in MFH. Montgomery et al. found the ultrastructural evidence of myofibroblastic differentiation in 29% of MFH [6]. Some of them expressed myoid markers on immunohistochemistry, but this expression was always focal, as well as in tumors without myofibroblastic ultrastructural morphology. The tumors they examined all had pleomorphic morphology, without recognizable myofibroblastic features. Our case demonstrated recognizable myofibroblastic morphology throughout the whole tumor, regardless of architectural pattern, as defined in low-grade myofibrosarcomas [8]. The tumor cells were not focal, but strongly and diffusely positive for SMA, while negative for caldesmon. If we consider these features as a signs of myofibroblastic differentiation, the diagnosis of high-grade myofibrosarcoma would be the most appropriate.

Although myofibrosarcoma has not yet been defined as a separate entity, a category of low-grade malignant myofibroblastic tumors were recently recognized and described in the article of Mentzel et al. [5]. The authors suggest the designation of this lesions as low-grade myofibroblastic sarcomas. Montgomery et al. also reported the series of soft-tissue sarcomas composed predominantly of myofibroblasts, which were of low- or intermediate-grade malignancy. The selection of their cases was based on recognizable and consistent morphology and was confirmed by immunohistochemical expression of myoid antigens, and, in some of the cases, with electron microscopy [7]. Our case demonstrates all these morphological and phenotypical features, except high-grade morphology expressed by high proliferative activity and broad areas of hemorrhage and necrosis.

The aim of this letter was to describe a type of breast sarcoma that needs further studies with a large number of cases to be better understood.

Acknowledgements We thank Professor Christofer D.M. Fletcher for his contribution in establishing the diagnosis.

References

1. Coffin CM, Dehner LP, Meis-Kindblom JM (1998) Inflammatory myofibroblastic tumor, inflammatory fibrosarcoma and related lesions: a historical overview with differential diagnostic considerations. Semin Diagn Pathol 15:102–110
2. Gocht A, Bosmuller HC, Bassler R, Tavassoli FA, Moinfar F, Katenkamp D, Schirrmacher K, Luders P, Saeger W (1999) Breast tumors with myofibroblastic differentiation: clinicopathological observations in myofibroblastoma and myofibrosarcoma. Path Res Pract 195:1–10
3. Gonzales-Palacios F, Enriquez JL, San Miguel P, Vazquez R, Carcia-Cosio M (1999) Myofibroblastic tumors of the breast: a histological spectrum with a case of recurrent male breast myofibrosarcoma. Int J Surg Pathol 7:11–17
4. Magro G, Bisceglia M, Michal M, Eusebi V (2002) Spindle cell lipoma-like tumor, solitary fibrous tumor and myofibroblastoma of the breast: a clinico-pathological analysis of 13 cases in favor of a unifying histogenetic concept. Virchows Arch 440:249–260
5. Mentzel T, Dry S, Katenkamp D, Fletcher CDM (1998) Low-grade myofibroblastic sarcoma. Am J Surg Pathol 22:1228–1238
6. Montgomery E, Fisher C (2001) Myofibroblastic differentiation in malignant fibrous histiocytoma (pleomorfic myofibrosarcoma): a clinicopathological study. Histopathology 38:499–509
7. Montgomery E, Goldblum JR, Fisher C (2001) Myofibrosarcoma. A Clinicopathologic study. Am J Surg Pathol 25:219–228
8. Taccagni G, Rovere E, Masullo M, Christensen L, Eyden B (1997) Myofibrosarcoma of the breast: review of the literature on myofibroblastic tumors and criteria for defining myofibroblastic differentiation. Am J Surg Pathol 21:489–496
9. Wargotz ES, Weiss SW, Norris HJ (1987) Myofibroblastoma of the breast: sixteen cases of a distinct benign mesenchymal tumor. Am J Surg Pathol 11:493–502
10. Watanabe K, Kusakabe T, Hoshi N, Saito A, Suzuki T (1999) h-Caldesmon in leiomyosarcoma and tumors with smooth muscle cell-like differentiation: its specific expression in the smooth muscle cell tumor. Hum Pathol 30:392–396

Virchows Arch (2003) 443:225
DOI 10.1007/s00428-003-0871-6
© Springer-Verlag 2003

ANNOUNCEMENTS

6 September 2003
EUROPEAN BOARD OF PATHOLOGY
7th EXAMINATION 2003
Ljubljana, Slovenia

The Seventh Examination of the European Board of Pathology will be held in Ljubljana, Slovenia, Saturday September 6, 2003. This Examination precedes the 19th Congress of the ESP.

For information about the examination and application forms can be obtained from:
Prod. Dr. J.G. van den Tweel
(chairman of The Examination Board)
Utrecht University Medical Center
Department of Pathology, H 04.312
P.O. Box 85500
3508 GA Utrecht
Fax: ++31-30-2544990
Tel.: ++31-30-2506565
e-mail: j.vandentweel@lab.azu.nl *or*
W.vanBragt@lab.azu.nl (secretary)
The same information is also available from Internet:
http:www.uems.be/pathol.htm, see index 2 and 3

6–11 September 2003
19th European Congress of Pathology
Ljubljana, Slovenia

The largest congress of pathologists in Europe in 2003, covering basic diagnostic standards, update scientific achievements and recent technical advances in all areas of pathology at 4 keynote lectures, 30 symposia, 21 short courses, 21 slide seminars, 14 special presentations, 2 round table discussions and free paper and poster sessions. Internationally recognized invited speakers are from throughout Europe and the USA.

Updated information on the congress website: http://www.cd-cc.si

10–13 September 2003
Harvard Dermatopathology Update CME Course
(Fairmont Copley Plaza Hotel, Boston, MA)

The objective of this year's course is to provide an in-depth review and update on selected topics in dermatopathology focusing on non-neoplastic diseases and melanocytic lesions. The course has been redesigned, and is specifically aimed at practicing pathologists, dermatopathologists, and dermatologists. The program is also suitable for senior residents and fellows preparing for board certification examinations.

For further information please contact at
http://www.cme.hms.harvard.edu, at (617) 384-8600
or can be obtained by e-mail at hms-cme@hms.harvard.edu

13 October 2003
Continuing Medical Education

One day Multi-Disciplinary Update courses

Course fee: £95.00

For further information please contact:
Education Administrators
Nottingham International Breast Education Centre
City Hospital, Hucknall Road, Nottingham NG5 1PB
Tel.: 0115 969 1689; Fax: 0115 962 7707
E-mail: enquiries@nibec.co.uk; www.nibec.co.uk

17–19 November 2003
Multi-Disciplinary Courses on Breast Disease

Three day course. The first part is multi-disciplinary. Thereafter the different specialties meet to accommodate their own special requirements.

Course Tutors: Dr. I.O. Ellis, Dr. S.E. Pinder, Dr. A.H.S. Lee

Course fees:	NHS	£370.00
	Non-NHS	£415.00
	Overseas	£550.00

includes refreshments but not accommodation

For further information please contact:
Education Administrators
Nottingham International Breast Education Centre,
City Hospital, Hucknall Road, Nottingham NG5 1PB
Tel.: 0115 969 1689; Fax: 0115 962 7707
Email: enquiries@nibec.co.uk; www.nibec.co.uk

1–11 June 2004
International course on Laboratory Animal Science
Utrecht, The Netherlands

A two week intensive course on laboratory animal science will be organized at the Department of Laboratory Animal Science – Utrecht, The Netherlands in June 2004. This course is organized once a year since 1993.

The objective of this course is to present basic facts and principles that are essential for the humane use and care of animals and for the quality of research.

The contents of the course are in line with recommendations of the Federation of European Laboratory Animal Science Associations (FELASA) regarding the training of the young scientist whose research involves the use of vertebrate animals.

The course may also be of interest for those who intend to set up a similar course at their location. For this purpose, during the course the acquisition of teaching materials can be discussed with the course committee.

For information and application forms please contact:
Prof. L.F.M. van Zutphen, PhD or
Mr. Stephan van Meulebrouck, MA
Department of Laboratory Animal Science
Faculty of Veterinary Medicine
P.O. Box 80.166
3508 TD Utrecht
The Netherlands
Tel.: ++31-30-2532033
Fax: ++31-30-2537997
E-mail: pdk@las.vet.uu.nl
Internet: http://las.vet.uu.nl (click on "Education and Training")

Virchows Arch (2003) 443:226–239
DOI 10.1007/s00428-003-0872-5

EUROPATH NEWS 3/2003

European Society
of
Pathology

Newsletter of the European Society of Pathology

Dear Colleagues,

We are very pleased to bring you the third 2003 issue of our ESP Newsletter.

This issue begins with a presidential address by Prof. Gianni Bussolati. It continues with the minutes from the Executive Committee meeting of the European Society of Pathology in Ljubljana and a report of the XIII EuroCellPath in Cagliari, written by the Secretary General of ESP Prof. Jahn Nesland, followed by a comment about the 15th and 16th IUCP. Also included are announcements of forthcoming conferences, seminars and tutorial courses. Furthermore, information about the formulated Working Groups is given. Do not hesitate to provide us with material on the activities of your department and even share with us, through *Europath News*, your problems. Last but not least, remember that we must increase the number of ESP members. This is vital for the continuity of our Society. You can easily sign up by using the application form for membership (which is included in each issue of *Europath News*) or visiting our new website (whose address is also included). At the same time, you could encourage the younger staff in your department to join us.

With warmest thanks
and regards,

Prof. Niki J. Agnantis
Chief Editor

Dr. Bjørn Risberg
Assistant Editor

Editors
Prof. Niki J. Agnantis
University Department of Pathology
Medical School of Ioannina
GR-45110 Ioannina, Greece
Tel.: +302-651-097795
Fax: +302-651-097858
e-mail: nagnanti@cc.uoi.gr

Dr. Bjørn Risberg
Department of Pathology
The Norwegian Radium Hospital
0310 Oslo, Norway
Tel.: +47-22934174
Fax: +47-22508554
e-mail: brisberg@labmed.uoi.no

The newsletter of the European Society of Pathology, EUROPATH NEWS, is sponsored by Leica Microsystems Nussloch GmbH

Report of the President of the European Society of Pathology, Gianni Bussolati (Torino, Italy)

Dear Members,

Two years after the Berlin Congress, it is time to consider the present status of the Society, its evolution and prospects.

Although we are not (have never been and never will be) politically oriented, we are still somewhat influenced by political processes, which in recent years saw a gradual expansion of the European Community. We shall become increasingly dependent on European grants for at least some of our activities, especially those related to our educational programmes, EuroCellPath and the European School of Pathology (EScoP) with its branches in Eastern countries. We have to thank the European headquarters for the support they have already given, and we hope that scientific and professional exchange programmes, mainly dedicated to young pathologists, will help us to continue and implement such exchanges.

The Society website was initially created thanks to the generous and dedicated work of Dr. Bjorn Risberg from Norway. Our site is constantly updated and is gradually becoming very important for the Society, enjoying a large number of visitors and several well-established links. We shall need to consider switching from a voluntary to a professional basis for our website, a transition that will require investment.

Very good news is the number of active Members, which has steadily increased and more than doubled in the 4 years since the Barcelona Congress. Many of these members are young pathologists, in part, I believe, because of our educational programmes. We are now „harvesting" the fruits of our labors.

Our Society has been steadily reinforcing its links with national Societies, through the Advisory Council, magisterially led by Antonio Llombart-Bosh. The Council and the national Societies contributed greatly to the success of the Ljubljana Congress. Institutional linkages and collaborations with IAP and with other international Societies have also been continued and expanded.

New Working Groups have been formed (on Electron Microscopy and on Skin Pathology) and, even more importantly, the already established ones have committed themselves to improving internal organization and have engaged in very productive scientific activity. A number of specific, organ-oriented meetings have been held, and contacts have been established with clinicians and basic scientists. The starting point for the Working Group activities was the Baveno Inter-Congress Meeting, but the Groups have also played a major role in setting the agenda and successfully implementing the Ljubljana Congress. Looking to the future, new Working Groups have been proposed and are awaiting official recognition from the Executive Committee of the Society. In addition, several Working Groups have been involved in the organization of the Iguazu Inter-Congress Meeting, planned for June 2004.

As the original organizer of the first Working Group in Endocrine Pathology, following the enlightened suggestion and enduring support of Prof. Manuel Sobrinho-Simões, then President of the ESP, I find the success of the Working Groups immensely gratifying. The Groups are really proving to be the „task forces" of our Society.

Educational activities have been carried out with great enthusiasm in the last few months and have been greatly appreciated. In May 2003 the EuroCellPath courses on Carcinogenesis, Genetic Disregulations, Metabolic Diseases were organized in Cagliari by Prof. Gavino Faa. Scientific seminars were a great success (on the very last day, the discussion had to be closed with 70 people still in the hall!) and Sardinian hospitality was superb.

In May and June 2003, EScoP courses on Lung Pathology (course leader: H.H. Popper) in Krachow and on Thyroid and Parathyroid Pathology (course leader: M. Sobrino-Simões) in Ankara were very well received by students. The course in Ankara was quite a novelty, benefited from the dedication of its local organizers and may initiate a new trend, whereas EScoP courses might not be linked to specific places, but follow the requests and needs of specific areas.

The Blue Book of the Society, comprehensive in its updated directory of Members, its historical notes (list of Congresses, Officers, and past Presidents) and its account of Society legislation (Statutes and By-Laws) has been reprinted, thanks to Christine and Urbain van Haelst, who have given careful attention to its publication. The system of regulations already underwent change in Berlin (2001) in order to establish definite rules for new activities such as the Intercongress Meetings and the Working Groups, to improve both efficiency and transparency and to promote the involvement of active Members in running the organizational life of the Society. Further developments, especially on topics related to Working Group Organization and the Nomination Process, are foreseen.

The close association between ESP and Virchows Archiv has been very successful and has been renewed for an additional 2 years. Moreover, different Working Groups might be in favour of special connections with scientific journals in their own field.

At the Ljubljana Congress I shall complete my term as ESP President, and I wish to extend my best wishes to Prof. Antonio Cardesa, who will lead the Society towards the Congress of Paris, in September 2005. I had a very intensive and smooth working relationship with Prof. Cardesa during my term, and I am fully confident in his experience and abilities.

Several other Officers will also be leaving the Executive Board:

– Fred Bosman, Efthimios Sivridis, Manfred Dietel and Pier Bedossa were very collaborative and helpful to the Society.
– Christine and Urbain van Haelst, after several years of dedicated support for the ESP activities, have asked to be replaced. We had no choice but to honour their request, but did so with deep sorrow and in fully awareness of how much we shall miss their warm and gentle efficiency.

Finally, I would like to express my gratitude to all of my colleagues, especially those on the Executive Committee, who have helped to solve problems and carry out various tasks in the best interest of our Society.

Gianni Bussolati

Gianni Bussolati
President of the European Society of Pathology

News from the ESP Executive Committee meeting in Ljubljana March 15, 2003

The congress organizers hosted the Executive Committee and arranged a very pleasant meeting for all of us. The congress centre in the middle of Ljubljana has all the necessary facilities and is within walking distance of the city's main sights.

European Congress of Pathology, Ljubljana, September 6–11, 2003

The President, Prof. Gianni Bussolati, discussed the work with the congress organizers. Although the global political situation and state of infectious diseases were not optimal, the interest expressed in the congress has been more than satisfactory. The organizers expect participation to be on the same level as previous congresses.

The President also mentioned the need for closer collaboration with the IAP and the need for setting regulations in this context.

Prof. Victor Swaen

Professor Victor Swaen, one of the founders of our society and honorary member, died in January this year. Professor Swaen's important contribution to the development of European pathology was highly appreciated.

Intercongress Meeting, Baveno, 2002

The very successful meeting arranged by the ESP President and his collaborators provided a very small but welcome financial surplus to be split between the Society and the organizers.

European School of Pathology

This year, courses in pancreatic pathology (Prof. G. Klöppel), and liver/bile tract pathology (Prof. P. Bedossa) will be held in **Torino** on 19–25 September.

Proposals for courses in 2004 include urology, testicular and gynaecological pathology.

The Krakow branch arranged a course in pulmonary pathology in 2003.

In **Moscow,** a course in head and neck pathology was held in May, 2003.

EuroCellPath

A very successful conference took place in Cagliari, Sardinia, in May this year (for further information see special report from the meeting).

The president of EuroCellPath, Prof. Fred Bosman, discussed the plans for next year's course to be held in **Girona, Spain,** on **9–12 May**. The local organizer is Prof. Josep Lloreta-Trull and the focus of the course will be on proteomics and genomics in pathology.

Conferences dealing with inflammation and degenerative diseases, cardiovascular disease, and cancer are also being planned.

Intercongress meeting 2006

A proposal from Prof. Niki Agnantis, Ioannina, to host the Intercongress meeting in 2006 was accepted. Plans were presented and a new conference centre in Ioannina University will be ready for this occasion.

Working groups

The society has several well-functioning working groups and is open to suggestions for more. A special request should be mailed to the Executive Committee together with the CVs of those submitting the proposal.

A proposal for guidelines for the working groups was presented by the

past president, Prof. Manuel Sobrinho-Simoes. Details will be presented in a business meeting with the leaders of the working groups.

Nominations for President-Elect and new members of the Executive Committee

After a discussion of the proposals and recommendations from the Nomination Committee, as well as a response from the members of the society and a ballot by mail among the members of the Executive Committee, the following nominations will be presented to the General Assembly for approval:

President-elect:
Prof. Niki Agnantis

Treasurer:
Prof. Van Krieken

New members of the Executive Committee:
Prof. Michael Wells,
Prof. Dilek Yilmazbayhan,
Prof. Veli-Pekka Lehto,
and Prof. Frederique Capron

Oslo, May 24, 2003

Jahn M. Nesland, Secretary ESP

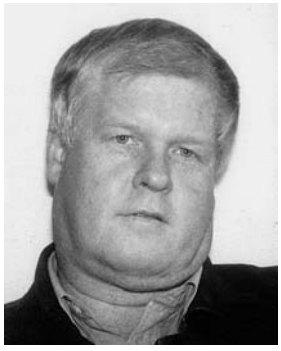

Jahn M. Nesland
Secretary ESP

Ioannina University Courses in Pathology (IUCP)

Between 27 and 31 May 2003, the 15th and 16th IUCP were held at the Institute of Pathology of the Ioannina University Medical School.

The topics of the courses were the kidneys and the urinary bladder, and updated tutorials and workshops were delivered by experienced Greek and British pathologists. Additionally, the participants had the opportunity to increase their knowledge in epidemiology, imaging and other therapeutic approaches.

There were 28 participants in the first topic and 38 in the second. They all left Ioannina satisfied from both a scientific and personal point of view.

Prof. Niki J. Agnantis,
Director and Coordinator

Dr. Lina Pappa, Secretary

The XIII EuroCellPath course

Carcinogenesis, genetic dysregulations and molecular diseases

In a perfect setting in Cagliari, Italy, Prof. **Gavino Faa and his collaborators** arranged the XIII EuroCellPath course which was held on 10–13 May, 2003. Just under 100 participants followed a high-quality scientific programme. The first day started with an interesting and reflective talk from the past-president of ESP, Prof. Manuel Sobrinho-Simoes, about mitochondrial DNA in human diseases: from neurodegenerative disorders to cancer.

The following day focussed on molecular mechanisms in **carcinogenesis**, where an update was given on the various fields, such as breast cancer, liver cancer, pancreatic cancer, gastric cancer, cancer development in inflammatory bowel disease, colon cancer and gastro-pancreatic endocrine tumours. Mechanisms of cancer development were outlined, showing the rapid development in our understanding of the disease. At the same time the difficulties of following developments outside one's own special interests became evident.

In the next session on the use of genetic markers in **diagnostic pathology**, the speakers provided important information about practical diagnostic work. The use of cytokeratins and molecular pathology in differential diagnosis of thyroid tumours was outlined. Furthermore, an important update of recent developments in the field of haematopathology was provided, along with a discussion of the present situation of sentinel lymph nodes and molecular mechanisms in the development of carcinoma in Barrett's oesophagus and in neuroendocrine tumours.

In the third part, the focus was on **metabolic diseases**. A presentation of the following subjects was given: the impact of metals in neurodegenerative disease, phosphaturic tumours and oncogenic osteomalacia, fibrosis in renal disorders, iron storage diseases, haemochromatosis, and alpha-1 antitrypsin deficiency. The impact of stromal elements, both in cancer and in metabolic diseases, was stressed.

The selected venue for the course was very interesting. Cagliari, the largest city in Sardinia, dates back to Phoenician and Punic periods. Unfortunately, the time did not allow us to explore Sardinia to any extent, but we got a taste of the place and were certainly tempted to return.

The very warm reception on the first day set the friendly atmosphere that we like to have in the EuroCellPath courses. Since the very beginning, the idea behind EuroCellPath courses has been to gather cell biologists and pathologists for discussions of disease mechanisms. This arena also provides young candidates with a place to present their latest data and discuss them in a positive way. Novel ideas are developed and new contacts and friendships are established. My compliments go to Prof. Gavino Faa and his staff for providing the ideal setting for the meeting.

The EuroCellPath courses aim to give high-quality reviews, and this course was no exception. This is the perfect meeting for those of us who need to be updated every now and then.. The next course will be held in Girona, Spain, on 9–12 May, 2004, and is in the hands of Prof. Josef Lloreta-Trull. I look forward to seeing you all again.

Oslo June 6, 2003

Jahn M. Nesland, Secretary ESP

ESCoP
European School of Pathology

Pathology of the Pancreas

Prof. G. Kloppel, Kiel

Pathology of the Liver & Biliary Tract

Prof. P. Bedossa, Paris

INSTITUTE FOR SCIENTIFIC INTERCHANGE FOUNDATION

2003 courses

September 19 - 25 Turin, Italy

AIM

Post-graduate residential course for young European pathologists based on workshops, slide seminars and few lectures to update and standardise participants' diagnostic ability.

FEE

- Registration is 300 Euro.
- Full board accomodation (to be paid upon departure) is 75 Euro/day/person.
- A limited number of EScoP scholarships (for ESP Members) is also available upon request

DATES

Pancreas Pathology
Sept. 19-20, 2003

Liver & Biliary Tract Pathology
Sept 21-25, 2002

PLACE & ORGANIZATION

Institute for Scientific Interchange (ISI)
Villa Gualino,
Viale S. Severo 65,
10133 Torino, Italy.

Phone Office
+39 011 6603090
Phone Residence
+39 011 6603555
E-mail: isi@isi36a.isi.it

PAST COURSES

1991 Liver & GI path (non neopl)
Ovarian pathology
Breast pathology
1992 Pulmonary pathology
Endocrine pathology
1993 Haematopathology
1994 Haematopathology
Uterine pathology
Breast pathology
1995 Quantitative pathology
Neuropathology
Head & Neck pathology
1996 Uropathology
Dermatopathology (neopl)
1997 Tumors of liver & pancreas
Tumors of GI tract
1998 Soft tissue tumors
Breast pathology
1999 Lung pathology
Cytopathology
2000 Ovarian pathology
GI pathology
2001 Hematopathology
2002 Head & Neck Pathology
Thyroid & parathyroid Path.

FUTURE COURSES

2004 Pathology of the Uterus
Pathology of the Bladder
Pathology of the Prostate

APPLY before April 30 to

European School of Pathology
c/o Dept Pathology, Univ Turin, Via Santena 7,
I-10126 Torino Italy Fax +39 011 6635267
E-mail mauro.papotti@unito.it
Note: By end June, a letter will confirm or reject the application. Do not send money now, please.

To EScoP

RE: Preliminary application

Surname: ..... Name: ..... Sex: .....
Date & place of birth: ..... Citizenship: .....
Full address.....
.....
Phone: ..... Fax: ..... E-mail: .....

- ☐ application for 2 courses ☐ application for 1 course ☐ Sept. 19-21 ☐ Sept. 21-25
- ☐ I apply for: ☐ EScoP scholarship ☐ EU grant, if available
- ☐ Member of ESP ☐ non member (I apply for 2003 ESP membership)
- ☐ I enclose a brief curriculum vitae stating my experience in pathology

Date.....

Signature: .....

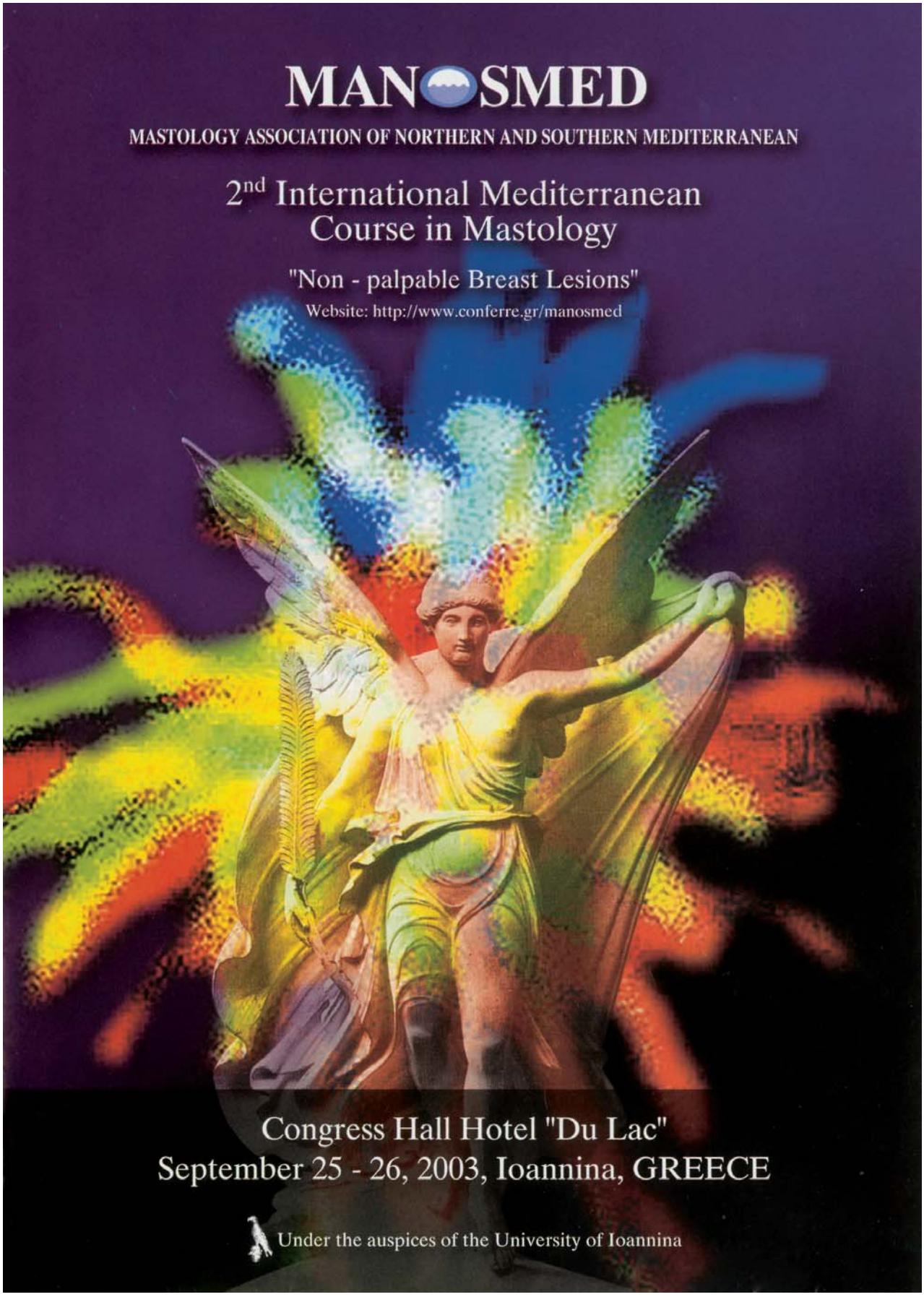
MANOSMED
MASTOLOGY ASSOCIATION OF NORTHERN AND SOUTHERN MEDITERRANEAN
2nd International Mediterranean Course in Mastology
"Non - palpable Breast Lesions"
Website: http://www.conferre.gr/manosmed
Congress Hall Hotel "Du Lac"
September 25 - 26, 2003, Ioannina, GREECE
Under the auspices of the University of Ioannina

First Announcement

XIV EuroCellPath Course

THE IMPACT OF PROTEOMICS AND GENOMICS IN PATHOLOGY

May 9-12, 2004 - Girona, Spain

PRELIMINARY PROGRAM

- DNA arrays: Methods and Goals
- Tissue Microarrays: A Tool for Rapid, Efficient Translational Research
- Proteomics: From Genes to Functions
- Tissue Procurement and Handling: Laser Capture Microdissection and Other Techniques
- Bioinformatic Tools for Array Data Mining
- Application of Array Genomics and Proteomics in Pathology
- Molecular Pathology of Genes and Proteins: What to Look For and When

Local Organiser:

Prof. Josep Lloreta-Trull
Department of Pathology,
Hospital del Mar-IMAS-IMIM
Universitat Pompeu Fabra
Passeig Marítim 25-29
08003-Barcelona, Spain
jlloreta@imas.imim.es
Phone +3493 248 30 31
Fax +3493 248 31 31

Helmut H. Popper, M.D., Prof. of Pathology
Laboratories for Molecular Genetics,
Environmental and Respiratory Pathology, Institute of Pathology
University of Graz
Auenbruggerplatz 25
Graz, A-8036, Austria
Tel.: +43-316-3804405
Fax: +43-316-384329
popper@uni-graz.at

Report of the Pulmonary Pathology Working Group

From October 2001 to September 2002 the working group was actively engaged in an EU-funded project on rare pulmonary diseases. We collected data of rare pulmonary and pleural diseases from around Europe, ending up with a collection of over 700 cases. Twenty-four pulmonary pathologists from the working group and beyond gathered in Graz in February and June 2002 to review these cases. In June, two clinicians for adult and paediatric pulmonary diseases joined us.

As a result we now have a collection set from each of these contributing pathologists (from Turkey to Portugal, Finland to Italy), which can be used for education purposes. A homepage for doctors and patients has been developed and will be hosted on the homepage of the contributing pathologists (details can be seen at: http://www.uni-graz.at/patwww/umweltpat/rarediseases.html).

The working group was actively engaged in the programme for the upcoming ESP congress in Ljubljana. A precongress meeting has been arranged with the help of the local organizers of the congress. This will focus on news and problems in pulmonary and pleural pathology. A postcongress meeting to be held in Golnik, north of Ljubljana, will focus on rare diseases. New entities and cases will be scoped out and discussed. During the congress, the group will actively take part in conferences, slide seminars and poster sessions.

The working group has already contributed in the programme discussion for the next Intercontinental Meeting to be held in Iguassu, Brazil. A presentation will also be given at the precongress meeting in Rio de Janeiro.

New officers for the working group, who will be responsible for preparing the ESP congress in Paris, will be elected in Ljubljana. As the central theme, the group decided to place the major emphasis on interstitial and other non-tumorous lung pathology.

With my best regards, yours sincerely,

Helmut H. Popper, MD

Working Group on Molecular Pathology

Foundation meeting: Baveno, Monday, 20 May, 2002

For further information use the following e-mail addresses:

For Prof. Dr. Heinz Hofler:
renate.hartmann@lrz.tu-muenchen.de
(his secretary's e-mail address)

For Prof. Generoso Bevilacqua:
g.bevilacqua@med.unipi.it

For information concerning ESP activities, please contact

ESP web-site: http://www.Europathology.org

Invitation to Pilot Project Group on the Status and Potentials of Pathology as an Epidemiological Tool on the European Level

Due to the current fall in autopsy rates with no improvement in sight, it becomes more necessary than ever to extract as much quality data as possible from the available material.

I have recently presented a proposal on this subject at the meeting of the Executive Board of the European Society of Pathology, held in Ljubljana on 15 March 2003. In response, the President encouraged me to present the plan at the upcoming ESP Congress (Ljubljana, 6–11 September 2003) in collaboration with qualified colleagues with similar interests.

The Danish Institute of Biological Age (DIBA) investigates and coordinates the relationship between clinical and postmortem pathology. A Danish baseline study of geriatric pathology was conducted in the late 1960s under DIBA's regimen, resulting in a unique set of data on the biology of the aged (70–100 years of age). For the pathology of the aged represents, after all, the culmination of a lifehistory of illnesses, trauma, and misfortunes.

The intention of the present project is to provide a comparable data set from the beginning of the twenty-first century and to extend the methods of the baseline study to all age groups. A study of the magnitude proposed will demand considerable resources, thus necessitating the involvement of many qualified professionals at a number of centers. The successful implementation of the proposed project depends upon two factors: scale and economy.

The Danish Institute of Biological Age is prepared to put its resources and experience at the disposal of this project, which, we are convinced, will become increasingly necessary with the passage of time.

Your suggestions and reservations at this early stage can be invaluable.

If you are interested in becoming involved at the ground-breaking stage or perhaps just curious about the details of the proposed project, please contact me for further information.

Claus Petri
Hillerød, 31 March 2003

Contact information:
Helenevangen 13
DK 3220
Tisvildeleje, Denmark
Tel.: +45-48-707667
e-mail: clauspetri@dadlnet.dk

Working Group of Pulmonary Pathology
by Helmut Popper

Address for information:
Helmut H. Popper, M.D.,
e-mail: ppopper@kfunigraz.ac.at
Fax: +43–316–380–9636
Laboratories for Molecular Cytogenetics, Environmental and Respiratory Tract Pathology,
Institute of Pathology,
University of Graz

Working Group on Head and Neck Pathology
by Antonio Cardesa

Information address:
Prof. Antonio Cardesa,
Dept. Anatomic Pathology,
Hospital Clinic, Villarroel 170,
08036 Barcelona, Spain
(Tel: +34 93 227 5450,
Fax: +34 93 227 5717,
e-mail: acardesa@clinic.ub.es)

New address:
Prof. Henrik B. Hellquist, Chairman,
Department of Laboratory Medicine and Pathology, Hamad Hospital,
P.O. Box 3050, Doha, Qatar

Working Group on Endocrine Pathology
by Gianni Bussolati

E.C.E.P
The European Club of Endocrine Pathology

The European Club of Endocrine Patholgoy
Via Santena 7, Torino 10126, Italy
Tel.: +39-11-6706505, Fax: +39-11-6635267
e-mail: fassina@uxl.unipd.it

All infomation, graphics and materials contained in this site are © 1997 by European Club of Endocrine Pathology Prof. Ambrogio Fassina
© All right reserved

Working Group of Uropathology
by Gregor Mikuz

Addresses for information:
Gregor Mikuz M.D.,
FRCPath (Chairman),
Institute of Pathology University
Innsbruck, Muellerstrasse 44,
6020 Innsbruck, Austria
(gregor.mikuz@uibk.ac.at)

Ferran Algaba M.D.,(Vice-chairman),
Fundacion Puigvert,
C/Cartagena 340 –350,
08025 Barcelona, Spain
(19612itp@comb.es)

Antonio Lopez-Beltran M.D.,
(Secretary),
Unit of Anatomical Pathology,
Faculty of Medicine,
14004 Cordoba, Spain
(Em1lobea@uco.es)

Margaret Constance Parkinson BSc,
M.D. (Secretary),
(HP) Fourth Floor Rockefeller Building,
University Street, London WC1E6JJ,
UK (Rmkdhmp@ucl.ac.uk)

Rodolfo Montironi M.D.,
FRCPath (Treasurer),
Institute of Pathology,
University of Ancona,
60020 Torrette / Ancona, Italy
(r.montironi@popcsi.unian.it)

Michael J Mihatsch MD
(Nephropathology),
Institute of Pathology,
University Basel,
4003 Basel, Switzerland
(Mihatschmj@uhbs.ch)

Important message to all ESP members who want to send material for publication in the *Europath News,* which will appear four times a year (February, May, August, November) incorporated in *Virchows Archiv*: the material should be sent to one of the editors 2 months ahead of time by e-mail:

nagnanti@cc.uoi.gr **brisberg@labmed.vio.no**

Slide seminar in the Internet

Diagnostic histopathology cases presented at the European School of Pathology courses in Turin are going to be shown via Internet.

You are kindly invited to visit the site at http://www.isi.it/pathology/index.htm.

A message from the Editors to the Chairpersons of the formulated ESP Working Groups

Dear Colleagues,
If you are interested in presenting your activities to the EUROPATH NEWS, please send your material by e-mail 2 months ahead of publication.

PLEASE NOTE:
Due to the restricted number of pages in each issue, texts will appear on a "first come, first served" basis.

Working Group of Cytopathology
by Fernando Schmitt

Address for information:
Prof Fernando Schmitt, IPATIMUP,
Rua Roberto Frias S/N,
4200 Porto, Portugal
(e-mail: fernando.schmitt@ipatimup.pt,
Fax: +351–225570799)

Working Group of Gynaecology
by Manfred Dietel

Addresses for information:
e-mail: manfred.dietel@charite.de

Working Group on Molecular Pathology

Foundation meeting:
Baveno Monday, 20 May 2002

For further information use the following e-mail addresses:

For Prof. Dr. Heinz Hofler:
renate.hartmann@lrz.tu-muenchen.de
(his secretary's e-mail address)

For Prof. Generoso Bevilacqua:
g.bevilacqua@med.unipi.it

Electron Microscopy Working Group:

Address for information:
Dr. Brian Eyden (PhD), Head of
Diagnostic Electron Microscopy,
Christie Hospital NHS Trust,
Manchester M20 4BX,
United Kingdom
Tel.: +44 161 446 3292
Fax: +44 161 446 3300
e-mail:
Brian.Eyden@christie-tr.nwest.nhs.uk

The European Society of Pathology

Dear Colleague,

It will surely not have escaped your attention that *Virchows Archiv* is now the Official Journal of the European Society of Pathology.

But did you realise what benefits membership in the society offer you?

- A subscription to the journal *Virchows Archiv* at no extra charge – this is automatically sent to every member every month.
- Access to the journal online (take a look at http://link.springer.de). If you are already a member of ESP but have not yet registered for your free electronic access, you will find the necessary form to complete online here too.
- A discount of 20% on most titles published by Springer. To take advantage of this, simply send your order directly to the publisher, with details of your membership.
- Attendance at the Society's conferences at a reduced fee.

If you have not yet joined the European Society of Pathology, why not do so now?
Simply complete and return the form enclosed. If you are already a member, please wait for our renewal letter for 2003.

We look forward to welcoming you as a member in 2003

Yours sincerely

G. Bussolati
President
European Society of Pathology

U. van Haelst
Treasurer
European Society of Pathology

G. Klöppel
Managing Editor
Virchows Archiv

Application for Membership of the
EUROPEAN SOCIETY OF PATHOLOGY (E.S.P.)

Please, type or use block letters to fill in this form!

FAMILY NAME: .....

First Name(s): .....

Male ❑ Female ❑

Place and date of birth: .....

Title/Present Position: Prof. ❑ Dr. ❑ Resident ❑

Other: .....

Please, clearly indicate which one of rhe following addresses should be used for subsequent correspondence, mailings, and listing in the Members Handbook

❑ PRIVATE ADDRESS:

Name: .....

Street: .....

Postcode: .....

City: .....

Country: .....

❑ INSTITUTE / OFFICE ADDRESS:

(This address will be used for subsequent correspondence and listing in Membership Directory)

Name of Institute: .....

Department: .....

Street: .....

Postcode: .....

City: .....

Country: .....

Tel.: .....

Fax: .....

E-mail: .....

FIELDS OF INTEREST: .....

.....

Date: .....

Signature of Applicant: .....
only applicable if sent back by fax.

Please e-mail or fax the completed application form to:

E.S.P. - OFFICE OF THE TREASURER,
Prof. Dr. U. VAN HAELST,
van Cranenborchstraat 6,
NL – 6525 BN Nijmegen
The Netherlands.

Tel: +31-24-3231950
Fax: +31-24-3222304
E-mail: Treasurer.ESP@vanHaelst.100.nl

Your acceptance as a member of E.S.P. will be confirmed in due time.

Membership fee for 2003:

including subscription to the combined printed and electronic version of the Society's journal *Virchows Archiv*: 95.00 EUR

including subscription to the electronic version only of *Virchows Archiv*: 75.00 EUR

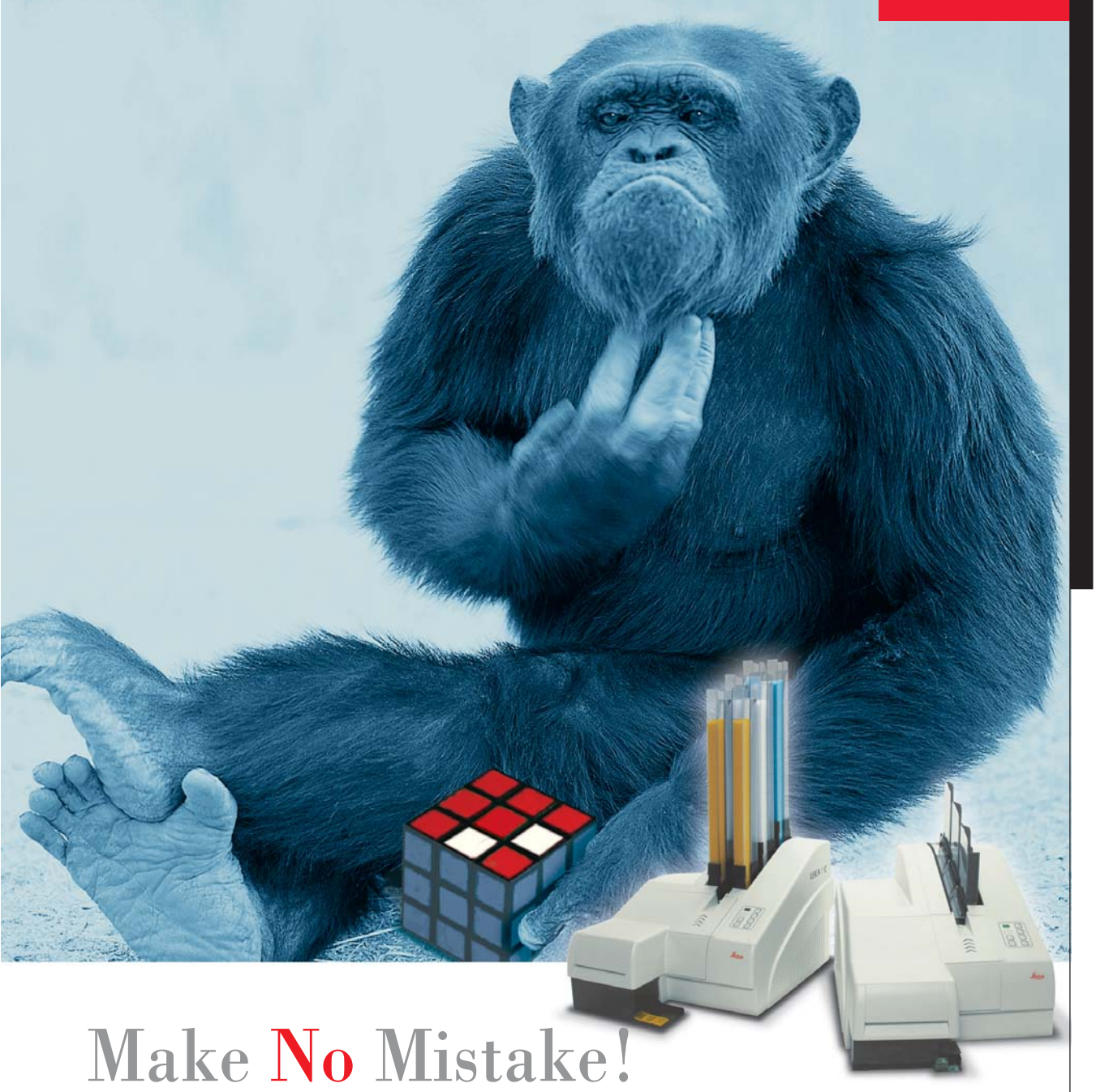

Make No Mistake!

Leica IP C and Leica IP S: Reduce Errors in Your Laboratory

With the new printing systems Leica IP C and Leica IP S for histology cassettes and slides you can easily minimize common marking problems such as illegible writing or incorrect labeling. Costly mistakes can also be avoided with:

- Durability: the chemically and mechanically resistant ink remains legible under adverse conditions
- Flexibility: the Leica IP C and Leica IP S can print bar and data-matrix codes, logos, alphanumeric characters and photos
- Versatility: most commonly used slides and cassettes, even those with lids, can be handled
- Simplicity: data entry is customized to the specific requirements of your laboratory

Make no mistake(s), call for more information today!
Leica Microsystems. Different to the Rest.

Leica Microsystems Nussloch GmbH
Heidelberger Strasse 17-19
D-69226 Nussloch

Phone: (6224) 143-0
Fax: (6224) 143-200
e-mail: histo_info@leica-microsystems.com
www.leica-microsystems.com

Leica
MICROSYSTEMS

19th European Congress of Pathology

Ljubljana, Slovenia, September 6-11, 2003

Abstracts

Abstract Review Board

M. Bračko, A. Cerar, A. Cör, V. Ferlan-Marolt, D. Ferluga, S. Frković-Grazio, N. Gale, D. Glavač, R. Golouh, A. Hvala, J. Jančar, V. Jurčić, I. Kern, V. Kloboves-Prevodnik, J. Lamovec, B. Luzar, L. Michaels, A. Mašera, Z. Ovčak, M. Poljak, Ž. Pohar-Marinšek, M. Popović, T. Rott, A. Vizjak, A. Zidar

Contents

Oral Presentations

Paediatric Pathology	O-001 – O-009
Molecular Pathology	O-010 – O-018
Nephropathology	O-019 – O-030
Cytopathology	O-031 – O-034
Miscelaneous	O-035 – O-039
Head and Neck Pathology	O-040 – O-057
Breast pathology	O-058 – O-067
Gynaecological Pathology	O-068 – O-076
Ultrastructural Pathology	O-077 – O-078
Uropathology	O-079 – O-087
Haematopathology	O-088 – O-096
Liver Pathology	O-097 – O-104
Digestive Tract Pathology	O-105 – O-117
Dermatopathology	O-118 – O-125
Infectious Disease Pathology	O-126 – O-130
Neuropathology	O-131 – O-135
Pulmonary Pathology	O-136 – O-143
Endocrine Pathology	O-144 – O-147
Cardiopathology	O-148 – O-155
Transplantation Pathology	O-156

Poster Presentations

Breast Pathology	P-001 – P-048
Gynaecological Pathology	P-049 – P-094
Soft Tissue, Joint and Bone Pathology	P-095 – P-117
Pulmonary Pathology	P-118 – P-147
Head and Neck Pathology	P-148 – P-187
Molecular Pathology	P-188 – P-218
Neuropathology	P-219 – P-242
Dermatopathology	P-243 – P-257
Nephropathology	P-258 – P-269
Transplantation and Immunopathology	P-270 – P-278
Digestive Tract Pathology	P-279 – P-346
Haematopathology	P-347 – P-390
Hepatopathology	P-391 – P-406
Infectious Disease Pathology	P-407 – P-416
Ultrastructural Pathology	P-417 – P-422
Urogenital Pathology	P-423 – P-477
Endocrine Pathology	P-478 – P-502
Cytopathology	P-503 – P-518
Cardiovascular Pathology	P-519 – P-539
Paediatric Pathology	P-540 – P-555
Miscelaneous	P-556 – P-569

Virchows Arch (2003) 443:245-475 © Springer-Verlag 2003

Prologue

Seven hundred and twenty one abstracts from 62 countries have been reviewed and accepted for 16 oral presentation and 40 poster presentation sessions at the 19th European Congress of Pathology in Ljubljana, Slovenia, September 6-11, 2003. This important contribution, mostly by younger pathologists and scientists, provides an excellent complementary programme to the 104 congress sessions and to the plenary keynote lectures prepared with invited speakers, internationally recognised experts in more than 20 different areas of our medical discipline.

The Abstract Review Board, chaired by R. Golouh and J. Lamovec, accepted most of the abstracts in the form submitted, with minor mostly linguistic changes being made in some cases. The preferences of authors for oral or poster type of presentation have been respected whenever possible. The high quality of most of the abstracts expresses the vitality, richness and prominence of our branch's contribution to biomedical science and the medical care of patients. The final selection of the best six of 23 pre-selected abstracts, for oral presentation at the plenary award session, was made by the Selection Committee, A. Llombart-Bosch, M. Sobrinho-Simões, and G. Bussolati, based on their scientific quality and originality of contribution. Furthermore, from 20 preselected best poster abstracts, the three best will be honoured by Congress Awards that will be presented at the same plenary session of the closing day of the Congress. Additionally, the best free paper contribution in the field of liver and digestive tract pathology will be selected by the Selection Committee complemented by D.G. Tiniakos and will be given the special, George Tiniakos Award.

It has become obvious that, for both scientific and professional reasons, our discipline requires organ and technique oriented sub-specialisation. However, congresses covering all areas of current pathology by means of invited lectures and free paper presentations, play an important role in establishing an appropriate balance between the need for sub-specialisation and the harmful effects of a complete splitting of our discipline.

Another important aim of the European Society of Pathology from its inception has been to keep together pathologists from all European countries, irrespective of their geographical and political borders, to promote professional and scientific exchange and to contribute to harmonisation among countries in relation to our discipline. There is no doubt that the collapse of the Iron Curtain has been a crucial turning point. In that sense, the significantly increasing number and quality of submitted free paper abstracts, with a concomitant increase in attendance at congresses, of pathologists from countries of the former Warsaw Pact, contributes to exchange and harmonisation within our medical branch and, to some extent, may represent a step towards the forthcoming European unity.

Finally, the Congress organisers would like to express our sincere gratitude to the Congress main sponsor, Ventana Medical Systems, for its financial support of this publication, and to the publishing house Springer-Verlag and the editor, G. Klöppel, for making it possible for all abstracts to be published in the September 2003 issue of the European Society of Pathology official, highly respected journal, Virchows Archiv.

Gianni Bussolati
President
European Society
of Pathology

Du an Ferluga
President
19th European Congress
of Pathology

O-001

Congenital tumours at foetal and neonatal autopsies during 17-years period

M Kos, L Hlupić, D Babić, S Jukić
Department of Gynaecological and Perinatal Pathology, KBC Rebro, Zagreb, Croatia

Introduction Nowadays, congenital tumours can be successfully diagnosed antenatally by means of ultrasound. Some of them may be an ultrasonic marker of foetal chromosomopathy. Depending upon their morphology and volume, some can be treated surgically immediately after birth, but in many cases the outcome is poor. The aim of this study was to assess the frequency and types of congenital tumours at autopsy of aborted foetuses, stillbirths and neonates that died within 28 days after birth.
Material and methods Autopsy protocols from the period 1986 to 2002. were analysed retrospectively, and the tumour tissue samples were retrieved from the archive (when available) and re-examined.
Results In the 17-years period 5139 autopsy of foetuses, stillbirths and neonates were performed. Congenital tumours were diagnosed in 65 cases (1.26%). Most frequent, in 45 cases (69.2%) were those considered to be hamartomas: cavernous lymphangiomas or cystic hygromas (43) and haemangiomas (2). Teratomas were next in frequency, with 13 cases (20%); 8 cases (61.5%)were sacrococcygeal; 3 cases (23.1%) originated from the skull base and 2 cases (15.4%) from the anterior mediastinum (one of them contained a relatively well formed foetus). Neuroblastoma and (lipo)fibromas were diagnosed in 2 cases (3.3%) each. Mesoblastic nephroma, rhabdomyoma of the heart and leukaemia were diagnosed in 1 case (1.6%), each. Congenital malformations were diagnosed in 23 cases (37.7%): in 24 cases (39.3%) generalized foetal hydrops was present.
Conclusions Congenital tumours are rare. The most frequent are hamartomas, which was confirmed also in this study. Oncogenesis and teratogenesis seem to be closely connected during embryonal development as can be presumed by frequent concurrent appearance of congenital tumours and malformations.

O-002

Potential prognostic value of the expression of P-glycoprotein in chosen solid tumours of childhood

J Kobos[1], K Taran[2]
[1]Department of Pathology Medical University of Lodz, Poland
[2]Laboratory of Pathology Institute of Paediatry Medical University of Lodz, Poland

Solid tumours in children are diagnostically and prognostically a very difficult group for both: clinicians and pathologists. Still we have to use complicated procedures to predict the clinical course of neoplasmatic disease. Current studies indicate that P-gp is one of the most important factors of multidrug resistance in some of malignant neoplasms. P-gp is a mdr1 gene product localized on the long arm of 7th chromosome. 95 formalin-fixed and paraffin-embedded tissue sections from cases diagnosed in the Laboratory of Pathology Institute of Pediatry, Medical University of Lodz (48 cases of nephroblastoma and 37 cases of neuroblastoma, 5 cases of rhabdomyosarcoma and 5 cases of EWS/pPNET) were selected for our study. In our research we used mouse anti-human P-glycoprotein (P-gp) (CHEMICON International, Inc.). We found the positive correlation with the expression of P-gp protein and poor clinical course in children with nephroblastomas, but we did not observe such a coincidence in children with neuroblastomas and PNETs.

O-003

C-kit protein expression as a poor prognostic factor in human neuroblastoma

S Uccini[1], U Pauser[3], T Andreano[1], S Bosco[1], R Boldrini[4], P Natali[5], HP McDowell[6], G Kokai[7], A Clerico[2], C Dominici[2]
[1]Department of Experimental Medicine And Pathology, University La Sapienza, Rome, Italy
[2]Department of Pediatrics, University La Sapienza, Rome Italy
[3]Department of Pathology, University of Kiel, Germany
[4]Bambino Gesu' Children Hospital, Rome, Italy
[5]Regina Elena Cancer Institute, Rome, Italy
[6]Division of Oncology, RLC NSH Trust Alder Hey, Liverpool, UK
[7]Division of Pathology, RLC NSH Trust Alder Hey, Liverpool, UK

Introduction Neuroblastic tumours (NTs) are childhood embryonal neoplasms of neuroectodermal cells of neural crest origin. The NTs are quite heterogeneous. In a subset of NTs, regression and maturation of neoplastic cells are widely documented. Other NTs are highly malignant and poorly responsive to therapeutic schemes. Aims: The recent development of specific small molecules that block the activity of tyrosine kinases suggested to investigate the prognostic relevance of the c kit oncogene expression in NTs.
Materials and methods One hundred and sixty eight NTs were investigated for expression of c kit protein and its ligand stem cell factor (SCF) using immunohistochemistry and Northern blot analysis. Mutations in exon 11 of the c kit gene were studied by PCR.
Results c kit protein expression was detected in 21 out of 168 NTs (13%). Immunostaining was observed in neuroblasts either diffuse in the cytoplasm and at cell membrane. Twenty out of 21 c kit positive cases were poorly differentiated neuroblastomas with high mitosis/karyorrhexis index. Nineteen out of 21 (90%) presented at III-IV advanced clinical stage, 17 out of 21 (81%) showed MYCN amplification and 1p36 deletions. Co-expression of c kit protein and SCF was documented by double immunostaining. These results were also confirmed by Northern blot analysis. Nine c kit positive cases were investigated for the presence of activating mutations in exon 11 of the c kit gene. In none deletion mutations were revealed.
Conclusions Our results show that c kit protein expression identifies a subset of NTs with unfavourable clinical and molecular parameters.

O-004

Congenital hepatic fibrosis with liver failure in an infant

E Wichrzycka-Lancaster[1], JA Targonski[2], KM Gaire[2], IBJ Targonska[3]
[1]University Of Transkei, Dept. Anatomical Pathology, South Africa
[2]Umtata General Hospital/UNITRA Dept. Pediatrics, South Africa
[3]Umtata General Hospital/UNITRA Dept. Radiology, South Africa

Introduction Congenital hepatic fibrosis (CHF) is rare developmental disorder, which is usually diagnosed in older children presenting hepatomegaly, normal liver functions and portal hypertension. It is defined as a ductal plate malformation. CHF is usually

associated with polycystic disease of the kidneys. It may be either sporadic or hereditary. We are reporting a very rare case of CHF in an infant who died of liver failure.
Case report A 2-month-old girl was admitted to the hospital because of fever, cough, jaundice, irritability and poor feeding. The physical examination revealed a jaundiced infant with hepatomegaly. Laboratory tests revealed an elevated WBC, low haemoglobin and normal platelets, prolonged PT and PTT. Bilirubin, ALP, GGT and LDH were all elevated and albumins were very low. Ultrasound showed an enlarged and diffusely echogenic liver, size and echo of both kidneys were normal. Ascites was present. Despite treatment the child's condition deteriorated and she died on the ninth day of admission. Clinical diagnosis was: Hepatitis? Cirrhosis? with secondary coagulopathy. Postmortem examination: hepatosplenomeagaly, ascites, hydropericardium, jaundice. Poorly aerated lungs with focal haemorrhages, PDA. In histology: ductal plate malformation-namely CHF, hemorrhagic necrosis of the liver and haemorrhages in different organs.
Conclusions 1. The early presentation of CHF at 2 months of age with fatal liver failure is unusual. Mortality affects older children and is related to variceal bleeding, cholangitis and/or kidney disease. 2. Our case was sporadic and associated with PDA, but not with Caroli's disease or kidney pathology.

O-005

Neurologic disorders in children patients with scoliosis

O Dmitrikova, SM Maximova
Donetsk Medical State University, Makeevka, Ukraine

Aims The purpose of our work was to study neurologic disorders in children at a scoliosis.
Materials and methods It is surveyed in 25 patients with a scoliosis 1-2 degrees in the age of 10-14 years. To all children was carried out general clinical research, including the general analysis of blood, urine, electrocardiogramm (ECCG), roentgenography of organs of chest and a backbone, and also instrumental research of parameters of haemodynamics by a method of rheoencephalography (REG).
Results Among surveyed children in 13 is diagnosed left-hand scoliosis (52%), right-hand scoliosis and disturbance of bearing in 12 children (48%). In all patients with a scoliosis of children is diagnosed vegetative vascular dystonia. Neurologic disorder in all patients were characterized: complaints to headaches, nausea, vomiting, the common weakness, fatigue, memory impairment disorder of the dream, raised perspiration, paresthesia, emotional instability, fears, cardialgia. In the neurologic status prevailed: easy asymmetry of nasolabial fold, weakness of convergence is more often from both sides, distal heperrhirosis, red proof dermographism, hernias. On electroencephalogram in 56% surveyed children are revealed moderate diffuse changes and decrease of a threshold of proximal readiness. On ultrasonic doplerography in 30% patients is revealed asymmetry of blood flow on supratrochlear arteries, acceleration of blood flow on common carotid artery, internal carotid and iliac arteries. On REG in surveyed children is revealed dystonia type REG-in 24% patients, hypotonic type-in 12%, hypertonic type – 24%, hypertonic REG due to increase of a tonus of arterial and venule – in 28% children, that is whom or specific deviations REG is not found in these patients.
Conclusions Thus, long displacement of position of a vertebral column at a scoliosis in children results in infringement of blood circulation in spinal cord and cerebrum already at early stages of a scoliosis that is revealed with the help of instrumental researches. With a deepening of gravity of current of a scoliosis are formed various functional disorders of the central and vegetative system.

O-006

Integrated optical density and nuclear volume in Down syndrome

D Mihailovic, Z Mijovic, B Djordjevic
Institute of Pathology, University of Nis, Nis, Serbia and Montenegro

Introduction Down syndrome (trisomy 21) is the most common numeric aberration of autosomal chromosomes in man; the incidence in newborn is about 1 in 700. Intrauterine growth retardation and endocrine disorders are a consistent finding in infants with Down's syndrome. The aim of this study was to estimate nuclear size and integrated optical density of parenchymal cells of various organs in patient with Down's syndrome and control group.
Material and methods During the years 1988 to 2000 fourteen cases of Down's syndrome were found (8 male and 6 female). Ten babies without congenital anomalies, died with respiratory distress syndrome, were analysed as a control group. Five nuclear variables were estimated: area, equivalent diameter, volume of equivalent sphere, roundness, and integrated optical density (IOD).
Results The mean nuclear volume and IOD of thyroid follicular cells were significantly lower in patient with Down's syndrome (65.46±15.31 mm^3, and 234.58±32.85) than in control group (43.82±8.95 mm^3, and 173.81±32.85, respectively) ($p<0.01$). The mean hepatocyte nuclear volume and IOD were significantly higher in control group (165.54±55.42 mm^3, and 220.84±51.75) than in trisomy 21 (110.39±32.97 mm^3, and 176.58±28.53, respectively) ($p<0.05$).
Conclusion The present results suggest altered gene expression in excessive genetic material, especially in thyroid follicular cells.

O-007

Comparison of Giemsa staining and immunohistochemical staining for the detection of Helicobacter pylori infection in gastric biopsies of urea breath test negative and positive paediatric patients

D Orhan, A Bulun, M Çadlar
Hacettepe University, Medical School, Department of Paediatric Pathology, Ankara, Turkey

Introduction Helicobacter pylori (HP) is a common cause of gastritis in both children and adults, and its incidence increases every year. Aim of the study was to evaluate the immunohistochemical and Giemsa stain of paediatric gastric biopsy specimens for the detection of HP infection from Urea Breath Test (UBT) negative and positive patients.
Materials and methods Eighty-two patients with positive UBT and thirty-eight patients with negative UBT were included to the study. Gastric biopsy specimens were evaluated histopathologically and graded according to the Sydney system. Giemsa staining immunohistochemical staining for HP were performed for the identification of HP.
Results With Giemsa staining, 7/38 (18%) UBT negative biopsies were HP positive. Biopsies from 79/82 (90%) UBT positive patients were HP positive with Giemsa staining. Immunohistochemical staining ratios of these cases were compared statistically.

Conclusion The results of this study suggested that, UBT may cause false positive HP infection diagnosis because of HP-like organisms. We conclude that Giemsa staining and immunohistochemical staining on gastric biopsy materials must be performed for the detection of HP infection.

O-008

Neuronal intestinal malformations in children - A review of 288 biopsy cases

M Skender-Gazibara, D Cvetkovic-Dozic, S Dozic
Institute of Pathology, Medical Faculty, University of Belgrade, Belgrade, Serbia and Montenegro

Introduction Neuronal intestinal malformations (NIM) encompass classical aganglionosis or Hirschsprung's disease (HD) and allied disorders (intestinal neuronal dysplasia - IND, hypoganglionosis, immaturity of ganglion cells, not classifiable dysganglionosis). According to histological and histochemical analyses of rectal biopsy, these entities may well be differentiated from HD. However, the diagnosis of IND remains controversial with a wide variation in the frequency in different series. The aim of this study was to determine the frequency of NIM in our series of children biopsied because of primary constipation.
Material and methods The morphological differentiation of NIM in rectal (suction or full thickness) biopsy or resected surgical specimens from 452 patients was performed using histological, specific histochemical and in some cases immunohistochemical methods.
Results Of the 452-biopsy cases, 288 or 63.72% had a form of NIM. Male/female ratio was 3:1, and age in ranged from 3 days to 18 years. Hirschsprung's disease was the most frequent, presented in 135 cases (46.88%). Twenty-nine of them were associated with IND proximal to the aganglionic zone. Isolated intestinal neuronal dysplasia type B (IND B) has been diagnosed in 66 cases (22.92%); not classifiable dysganglionosis in 42 (14.58%); hypoganglionosis in 30 (10.42%) and immaturity of ganglion cells in 17 cases (5.90%). In 164 cases (36.28%), the histology was reported to be normal.
Conclusion Rectal biopsy of children with primary constipation shows the spectrum of abnormalities. Some of them had to be specified. According to recent obligatory diagnostic criteria for NID it is easier to recognize this entity.

O-009

Placental villi maldevelopment and intrauterine hypoxia

I Voloshchuk, Y Gorbatcheva, N Buchulaeva, E Lukyanova
Moscow Medical Academy, Moscow, Russian Federation

Introduction Formation of terminal villi with syncytiocapillar membranes is necessary for optimal maternal-foetal exchange and especially for oxygen diffusion. Immature placentas with little number of syncytiocapillar membranes may worse foetal nutrition and gas exchange. The aim of this study was to estimate the role of villous tree immaturity in the development of intrauterine hypoxia.
Materials and methods 337 placentas from singleton pregnancies were investigated. According to ultrasound and doppler velocimetry data, Apgar score, placentas were divided into groups with chronic hypoxia (132), IUGR (70), acute intrauterine hypoxia (64), from normal pregnancies (71). Estimation of the degree of maturity according to gestational age was made on routine histological slides. Vascular endothelial growth factor (VEGF) and placental growth factor (PlGF) concentration in placental tissue homogenates were investigated by ELISA method in 40 placentas.
Results The frequency of placental immaturity was 2-fold higher in placentas with hypoxia in compare with control group. Preterm maturation of placental tree accompany with severe foetal hypoxia, a very high mortality and morbidity. Concentration of VEGF in placental tissue was elevated in placentas with terminal villi deficiency, and concentration of PlGF was elevated in placentas with synchronous immaturity.
Conclusion Due to importance of the placental maldevelopment it is necessary to devise methods of its early diagnostics and investigate mechanisms of villous tree development. Determining of VEGF and PlGF may be useful for this purpose.

O-010

SAGE profile and MLH1/MSH2 expression in colorectal adenocarcinomas: correlation with the tumor phenotype

SJ Diaz-Cano[1,2], JJ Jimenez-Martin[1], JJ Sanchez-Carrillo[1], B Cabra[1], MT Miranda[1], A Blanes[1]
[1]Barts and London School of Medicine, University of Londone, UK
[2]Univerity of Malaga School of Medicine, Malaga, Spain

Background The role of DNA mismatch proteins on tumor cell kinetic in sporadic colo-rectal adenocarcinomas (CRC) by topographic compartments remains unknown.
Design We selected 90 consecutive sporadic CRC (73 low-grade, 17 high-grade; 48 stage I, 18 stage II, and 24 stage III). Necrosis, inflammatory response, and growth pattern were evaluated. Mitotic figure counting, Ki-67 index, G2+M phase fraction, in situ end labeling (ISEL) of DNA fragments (scored by compartments, above muscularis propria vs muscularis propria) were studied regarding topographic mlh-1/msh-2 expression (positivity threshold 15%) and considered statistically significant if $P<0.05$. Oligo(dT)-primed double strand cDNA was produced from total RNA and libraries were produced from 3 normal colon specimens and 18 CRC. Sequential analysis of gene expression (SAGE) data was correlated with mlh-1 and msh-2 expression.
Results mlh-1/msh-2-negative CRC showed non-polypoid growth, necrosis, and inflammatory response, but no correlation with differentiation and stage. Superficial mlh1/msh2 expression showed direct correlation with mitotic figure counting, Ki-67 index, and G2+M phase fraction and inverse with ISEL index. Deep mlh1/msh2 expression showed direct correlation with Ki-67 and inverse with mitotic figure counting and G2+M phase fraction. MLH1/MSH2 SAGE revealed significant positive correlation with RAS homolog gene, and PI3P phosphatase, and negative correlation with Trefoil factor 3, Caspase recruitment domain (member 9), and Meprin A.
Conclusions mlh1/msh2-positive sporadic CRC show down-regulated apoptosis (Caspase 9), inflammation (Trefoil factor 3), and stromal degradation (Meprin A), and up-regulated proliferation (RAS homolog and MAPK activation by PI3P phosphatase). This gene profile explains both tumor phenotype and cell kinetic (↑proliferation, ↓apoptosis).

O-011

Molecular analysis of hereditary hemochromatosis

G Weirich, R Langer, H Nina, N Jörg, H Hoefler
Institute of Pathology Technische Universität München, Munich, Germany

Hereditary hemochromatosis (HH) is an autosomal recessive disorder, common in individuals of Northern European descent (prevalence close to 1:400). HH is characterized by increased iron absorption and iron deposits in various organs. HH patients may develop liver and pancreas cirrhosis, primary liver cancer, diabetes mellitus, and cardiomyopathy. In the majority of cases, HH is caused by mutations of the HFE-gene on chromosome 6p. HFE encodes an MHC class-I gene, a putative negative regulator of iron uptake. Three HFE mutation are common, C282Y, H63D and S65C. Patients with a homozygous C282Y genotype most often endure a severe clinical course, whereas homozygotes for H63D may develop mild forms of the disease. Heterozygotes are usually symptom-free, but show elevated serum ferritin levels. It has been speculated that secondary iron overload (heavy alcohol, chronic hepatitis, ?-thalassemia) may be a critical co-factor in those heterozygotes that develop symptoms of HH. HH not associated with HFE mutations is much less common. Within this heterogeneous group of non-HFE HH, three subtypes have been attributed to genetic alterations. Juvenile hemochromatosis (HFE2) is a rare but severe disorder mapped to chromosome 1q. HFE3 has recently been mapped to the transferring receptor 2 gene (TfR2) on chromosome 7q22. HFE4 follows an autosomal dominant trait and is associated with mutations of the ferroportin 1 gene (SLC11A3) on chromosome 2. Except for juvenile hemochromatosis, HFE, HFE3 and HFE4 are amenable to mutation analysis. The advent of modern high throughput technologies such as denaturing high performance liquid chromatography (DHPLC) has sparked clinical mutation screening programs, which also include screening of patients suspected to be affected by HH. In addition, DHPLC-based mutation screening can also be performed using archival formalin-fixed, paraffin embedded tissues (FFPE). We present here results from HFE-analyses of FFPE from autopsy cases using DHPLC and direct sequencing.

O-012

p63 expression pattern in squamous cell carcinoma of the oral cavity

A Gaiba[1], A Pession[1], R Cocchi[2], MG Pennesi[2], GP Frezza[1], MP Foschini
[1]Dept. of Pathology University of Bologna, Bologna, Italy
[2]Dept. of Maxillo-Facial Surgery, Bologna, Italy

Introduction p63/p73L/p51/p40/KET is highly expressed in basal cells of the epithelium. P63 generates two main splice variants the TAp63/p51 and DeltaNp63/p73L. TAp63/p51 is responsible for squamous cell differentiation; DeltaNp63/p73L is a self-renewal agent. Recently Senoo et al. (Br J Canc 2001, 84: 1235-1241) described a new isoform called DeltaNp73L that correspond to the DeltaNp63/p73L lacking exon 4. This novel splice variant has been found only in cell lines of neoplastic squamous cells and in SCC. The aim of the study was to define the expression pattern of TAp63/p51, DeltaNp63/p73L and DeltaNp73L in 33 cases of squamous cell carcinoma (SCC) of the oral cavity compared with non-neoplastic keratinocytes.
Material and methods Immunohistochemistry was performed in order to analyse p63 tissue distribution in all the 33 samples. P63 expression was studied, by RT-PCR and nested-PCR. Controls were obtained by non-neoplastic gingival mucosa and skin.
Results In invasive SCC a strong nuclear positivity for TP63 antibody in all the cases studied was found. The DeltaNp73L isoform was more frequent in metastasising tumours (18/20, 65%) compared with tumours without metastases (5/13, 38.5%). Analysing the TAp63 expression a band about 250bp shorter than the TA isoform was seen. The sequence of this new mRNA form was identical to TAp63/p51 lacking exon 4, thus we named this variant DeltaNp51 for homology with DeltaNp73L. DeltaNp51 was more frequent in metastasising tumours (9/20, 45%) rather than non metastasising (4/13, 30.7%).
Conclusions DeltaNp73L seems to be associated with higher metastatic potential of SCC. More experiments are needed to clarify DeltaNp51 function.

O-013

The synthetic ligand of peroxisome proliferator-activated receptor gamma ciglitazone affects viability, proliferation and apoptosis in human glioblastoma cell lines

N Vavrusova, J Ehrmann, Z Kolar
Institute of Pathology and Laboratory of Molecular Pathology, Faculty of Medicine, Palacky University, Olomouc, Czech Republic

Introduction Peroxisome proliferator-activated receptors (PPARs) are transcription factors, members of nuclear receptors superfamily, playing an important role in carcinogenesis, inflammation, atherosclerosis, lipid metabolism and diabetes. There is evidence that activation of PPARs by specific ligands inhibits the growth of different malignancies. The aim of our study was to determine whether ciglitazone, the synthetic ligand of PPAR gamma, affects proliferation, differentiation, apoptosis and expression of some cell cycle related proteins in glial tumor cell lines.
Material and methods The study was performed on U-87 MG, A172, T98G, and U-118 MG human glioblastoma cell lines. The lines U-87 MG, A172 and U-118 with inactive form of PTEN were transiently transfected with cDNA of wild type PTEN. MTT, flow cytometry, TUNEL assay and immunoblotting were used for detection of changes of the cell viability, proliferation, differentiation and apoptosis.
Results We have found that ciglitazone inhibited cell growth in studied glial tumor cell lines. The effect is accompanied by decreased expression of pRb protein, cyclin D1 and increased expression of c-myc and p27 after 12/24 hours of treatment by IC50 of ciglitazone. The flow cytometry confirmed the arrest in the G1 phase of cell cycle. We did not find any significant changes in expression of Bcl-2 family proteins and flow cytometry did not revealed any significant sub-G1 fraction. However, we have confirmed a degradation of PARP protein, caspase 3 and TUNEL staining showed an increase of the number of cells with DNA breaks. The level of GFAP, the marker of astrocytic differentiation, remained without change in U-87 MG and A172 cell lines. The effect of ciglitazone on cell lines transfected with functional PTEN is also discussed.
Conclusions We conclude that PPAR ligands may be potentially used in anticancer treatment. Supported by grants NC 6726-3/2001 and MSM 151100001.

O-014

Evaluation of real-time quantitative RT-PCR as diagnostic tool for the detection of carcinoma cells in routinely paraffin-embedded sentinel lymph nodes from various cancer patients

CJ Haas[1], H Starz[2], T Wagner[1], F Wawroschek[3], H Arnholdt[1]
[1]Department of Pathology, Klinikum Augsburg, Augsburg, Germany
[2]Department of Dermatology and Allergology, Klinikum Augsburg, Augsburg, Germany
[3]Department of Urology, Klinikum Augsburg, Augsburg, Germany

Introduction A prerequisite for the use of quantitative RT-PCR (qRT-PCR) in routine pathological evaluation of sentinel lymph nodes (SLNs) is its application to paraffin-embedded tissue. Its reliability has to be proved by direct correlation with (immuno)-histochemistry. The aims of the study were development of reliable protocols for the expression analysis of tumor markers in paraffin sections of SLNs, determination of their sensitivity and specificity for detection of micrometastases of diverse cancer types, and correlation between qRT-PCR results and micromorphometrically obtained data.
Methods RNA was extracted from 8 µm sections of routinely paraffin-embedded SLNs taken from prostate cancer, breast cancer, and melanoma patients. For several tumor markers qRT-PCR was performed and results were correlated with the (immuno)histochemical and micromorphometric data of adjacent tissue sections. When available, clinical follow up was included in the analysis.
Results Amplifyable RNA could be isolated from all analyzed specimens. Tyrosinase qRT-PCR was performed with 306 SLNs from melanoma patients with good correlation with S-classification. For detection of prostate cancer micrometastases qRT-PCR for PSA and PSM was performed on 108 SLNs. The obtained values for PSA expression correlated well with the micromorphometric data. From breast cancer patients 50 SLNs were analyzed for expression of mammaglobin and maspin. The detection rate of (micro)metastases increased significantly when both tumor markers were used.
Conclusions Quantitative RT-PCR on paraffin sections enables a further improvement of sensitivity for the detection of micrometastases in SLNs without impediment of the histomorphological diagnosis. The determination of expression thresholds for certain tumor markers can be of prognostic value.

O-015

Human Papillomavirus (HPV) and cervical carcinoma: Physical state of HPV DNA and HPV oncogenic expression

AK Lie[1], I Kraus[2], T Molden[2], H Skomedal[2], G Kristensen[3], R Holm[1]
[1]Department Of Pathology, Norwegian Radium Hospital, Oslo, Norway
[2]Norchip AS, Klokkarstua, Norway
[3]Gynecologic Oncology, Norwegian Radium Hospital, Oslo, Norway

Introduction HPV is a necessary cause of cervical carcinoma. Persistent high-risk HPV infection, integration, and E6/E7 oncogenic expression are required for development and maintenance of a malignant phenotype. The aims of this study were to compare DNA and RNA based methods for detection of HPV, to study the physical state of HPV DNA and the incidence of E6/E7 oncogenic expression in squamous cell carcinoma of the cervix.
Material and methods DNA and RNA were extracted from 204 squamous cell carcinomas. The HPV DNA prevalence was investigated using the L1 Gp5+/6+ consensus primers and E6/E7 type specific primers for HPV 16, 18, 31, 33, and 45. PreTect HPV-Proofer (NorChip AS, Norway) was used to study the presence of HPV E6/E7 mRNA, detecting HPV 16, 18, 31, 33, and 45. The physical state of HPV DNA was tested by in situ hybridization (ISH) for HPV type 16, 18, 31, and 33 using a cloned HPV DNA probe labeled with biotin. The ISH was carried out with an alkaline phosphatase anti-alkaline phosphatase detection system.
Results The HPV prevalence was 97%, as detected by consensus PCR, type-specific PCR, and PreTect HPV-Proofer. HPV 16 was the predominant type (65%), followed by HPV 18 (11%), 45 (10%), 33 (6%) and 31 (5%). ISH analyses revealed that 166 cases tested positive. All cases had punctate signals indicating integrated virus DNA, whereas 48% contained both punctate and diffuse signals indicating both integrated and episomal virus DNA.
Conclusions This study documents the presence of HPV E6/E7 transcripts from a limited number of high-risk HPV types in cervical carcinomas. HPV seems to be integrated in the human genome in the majority of cervical carcinomas.

O-016

A comprehensive human disease bank for functional genomics

D Zauner, K Zatloukal, H Denk
Institute of Pathology Graz, Graz, Austria

Introduction Diseased tissues contain all the information on the genetic and epigenetic changes that caused the disease and determine its outcome (prognosis). Recent developments in genome and proteome research offer the opportunity to unravel this information and provide new insight into the molecular pathogenesis of diseases. Aims: We are establishing a unique human tissue resource for genome research based on a collection actually comprising 2.5 Mio paraffin-embedded and 28 000 frozen tissue samples stored at the temperature of liquid nitrogen.
Materials and methods This collection is being expanded by national and international interdisciplinary cooperations. Blood samples, patient history, laboratory parameters, treatment and outcome information are included in addition to tissues. Special emphasis is placed on quality control and compliance with ethical and legal criteria. All protocols follow established standard operating procedures in accordance with guidelines of the FDA and recommendations of European countries. Informed consent is obtained from patients and appropriate security measures guarantee patient confidentiality.
Results To make this resource available to a wider scientific community, we generate disease-specific gene libraries and produce tissue micro arrays. Well defined expandable cell lines and nude mice xenografts are established for characterization of gene function.
Conclusion Proper access to collections of diseased human tissues is currently a major limiting factor for genome research in medicine. There is an urgent need of tissue banks that meet highest quality and legal criteria.

O-017
Withdrawn

O-018

Male microchimerism in fetal, infantile and female liver: role of pregnancy in hepatocyte microchimerism

C Guettier[1], S Mylene[1], F Dominique[2], G Michele[1], OS Martine[2], K Rachid[3], R Michel[1], S Didier[1], F Cyrille Feray[3]
[1]Hopital Paul Brousse, Paris, France
[2]Hopital Bicetre, Paris, France
[3]Inserm EPI 9941, Paris, France

Introduction Feto-maternal microchimerism has been described for many years. Besides an hypothetical role in the pathogenesis of autoimmune diseases, these fetal cells should provide stem cells which can participate to repair of damaged tissues. Their capacity to differentiate into hepatocytes is largely unknown. Our aim was to evaluate the frequency of male microchimerism in normal or diseased female livers, the nature of chimeric cells and the influence of a current pregnancy.
Material and methods 46 female liver specimens obtained from 29 women (chronic hepatitis C: 10; fulminant hepatitis: 4; acute liver disease during male-bearing pregnancy: 6; normal controls: 9) were studied for the detection of Y chromosome by combining fluorescent in situ hybridization (FISH) and 2 distinct PCR assays. Real-time PCR for quantification of Y chromosome was normalized on X chromosome. 11 fetal and 6 infant female livers were used as putative negative controls, 5 male livers (4 adult and 1 fetal) were used as positive controls.
Results Y chromosome was detected by at least one technique in 19/29 adult women but also in 6/6 children and in 7/11 fetuses. The two PCR assays were highly concordant and more sensitive than FISH. Mean Y/X ratio was 0.01 ±0.014 and was correlated to FISH
Results Hepatocyte microchimerism was observed only in 4/6 women with acute liver disease during pregnancy and in 4/9 fetuses while non-hepatocyte microchimerism was observed in all the groups (adult, children, fetuses) for normal and diseased livers.
Conclusion Male cells are frequently present within female livers from the fetal to the adult age. In case of children or fetuses, this demonstrates the transplacental transmission of fetal (male) cells preexisting in the mother, phenomenon we propose to call feto-fetal microchimerism. Their differentiation into hepatocytes was only observed in female fetuses and pregnant women.

O-019

The role of proximal tubular cells in macrophage migration and crescent formation

L Grcevska[1], G Petrusevska[2], M Polenakovic[1], S Dzikova[1]
[1]Department of Nephrology, University Clinical Center, Skopje, Republic of Macedonia
[2]Institute of Pathology, Faculty of Medicine University of Skopje, Skopje, Republic of Macedonia

Introduction Recent studies confirmed that proximal tubular cells played an important role in local macrophage proliferation. Locally produced macrophage inflammatory protein may be involved in development of cellular crescents.
Material and methods We analyzed 573 glomeruli of renal biopsy specimens of 40 patients with crescentic glomerulonephritis. Glomeruli with both segmental and circumferential crescents and cross section of urinary pole were studied. Macrophages were confirmed with CD 68 monoclonal antibodies.
Results 158/573 glomeruli presented both crescents and urinary pole at the same time. Segmental crescents affected urinary pole in 96.5% glomeruli and circumferential in 100%. Positive CD 68 cells were noted: 1) in cellular crescents, 2) surrounding proximal tubules close to urinary poles and 3) scanty positive proximal tubular cells.
Conclusion There are two possibilities: 1) crescents tend to migrate towards urinary pole, or 2) macrophages, originated from de-differentiated proximal tubular cells migrate to the nearest position.

O-020

NCAM expression on renal interstitial cells: a marker for renal progenitors?

J Markovic-Lipkovski[1], C Müller[2], G Klein[2], T Klatt[2], H Wessels[3], S Blaschke[3], G Müller[3]
[1]Institute of Pathology, Medical Faculty, University of Belgrade, Belgrade, Serbia and Montenegro
[2]University Medical Clinic, Section for Transplantation Immunology, University of Tübingen
[3]Center of Internal Medicine, Department of Nephrology, University of Göttingen

Introduction Neural cell adhesion molecule (NCAM) is highly expressed on cells of the murine metanephrogenic mesenchyme at early stages of kidney development. During further development, NCAM can still be detected on epithelial cells of comma and S-shaped bodies as well as on interstitial mesenchymal cells. During maturation of the fetal kidney NCAM gradually disappears from all epithelial structures and is confined to small areas of interstitial medullary cells. In the adult murine kidney NCAM expression is virtually absent.
Materials and methods In the present study NCAM expression was analyzed by immunohistochemistry and Western blots in adult human kidneys, including healthy kidneys and kidneys with different glomerular diseases associated with incipient interstitial fibrosis (IF). NCAM positive cells were characterized by triple immunofluorescence staining using antibodies against human NCAM combined with a panel of antibodies against neurofilaments, a smooth muscle actin (aSMA), HLA class II, CD133 and CD34, and DAPI for nuclei staining. Digital pictures from every fluorescence channel were taken and superimposed for the specific staining using the Analysis DOKUTM software from Soft Imaging Systems.
Results In adult human kidneys, NCAM expression was restricted to rare interstitial cells with a dendritic morphology, long cytoplasmatic extensions and elongated nuclei, which were localized predominantly in the outer medulla. In comparison to healthy kidneys, the number of NCAM-positive interstitial cells increased in the initial phases of IF in different forms of glomerulonephritis. Western blot analysis of renal tissues with incipient IF showed the exclusive expression of the 140 kDa isoform of NCAM; other isoforms were not detectable. Staining with antibodies against neurofilaments clearly differentiated nerve cells from NCAM-positive interstitial cells, which are neurofilament negative. They are also aSMA negative, though the number of the aSMA+ cells increased at the early stages of IF. However, some of the NCAM-positive cells clearly express the stem cell markers CD133 and CD34.
Conclusion These data indicate that a subpopulation of NCAM-positive interstitial cells may be renal progenitor cells, which can participate in the initial phases of IF.

O-021

Development of intrinsic innervation in human fetal kidney

D Tiniakos[1], S Stavrakis[1], V Anagnostou[1], D Karandrea[1], E Agapitos[2], C Kittas[1]
[1]Laboratory of Histology & Embryology, Medical School University of Athens, Athens, Greece
[2]Laboratory of Anatomic Pathology, Medical School University of Athens, Athens, Greece

Introduction We aimed to define, for the first time, the ontogeny of intrarenal innervation and to assess the distribution and nature of nerves in human fetal kidney.
Material and methods We studied routinely-processed tissue sections from 17 human fetuses (20-24 gestational weeks-gw n=6, 25-40 gw n=11) and 3 adults using immunohistochemistry and antibodies to pan-neural markers S100, neuron specific enolase (NSE), neurofilaments (NF), PGP9.5 and the adrenergic marker tyrosine hydroxylase (TH).
Results NSE-, NF-, S100-, PGP9.5-positive nerves, associated with arterial and venous vasculature, were identified in renal medulla and cortex at 20gw onwards and their density appeared to increase with gestation reaching adult levels at 28 gw. Nerve fibres extended from the cortico-medullary region to the outer cortex, reaching the renal capsule in the 3rd trimester. In renal medulla, S100-, PGP9.5- and TH-positive nerves were detected around tubular cells as early as 20 gw. However, their density gradually decreased during the 3rd trimester. Most of the intrarenal nerves were TH-positive. In detail, NSE-, NF-, S100-, PGP9.5- and TH-immunoreactive fibres were observed in close apposition to renal artery and its branches, occasionally reaching the afferent and efferent arteriole (3rd trimester). Nerve fibres were detected in close apposition to the juxtaglomerular apparatus in 2nd and 3rd trimester.
Conclusions Human kidney appears richly innervated during the 2nd and 3rd trimester. There is progressive increase in the density of parenchymal nerve fibres towards term from the cortico-medullary region to the cortex. Most intrarenal nerves are adrenergic and have a predominant perivascular distribution, implying that renal innervation plays an important functional role in intrauterine life.

O-022

Analysis of chimerism in human renal transplant biopsies by fluorescent in-situ hybridisation (FISH) and laser-microdissection based RT-PCR (LM - RT-PCR)

JWU Fries[1], A Awlakpui[1], T Roth[1], HP Dienes[1], M Weber[2], W Arns[2]
[1]Dept. of Pathology, University of Koeln, Cologne, Germany
[2]Med. Clinic1, Koeln-Merheim, Cologne, Germany

Introduction Cell migration from the host to the transplanted organ results in chimerism (1), and seems to be associated with chronic transplant rejection (2,3). However, early detection of recipient cells might provide an important clue for anti-rejection therapy.
Materials and methods 15 cases from sex-mismatched renal transplants (male kidney into female receiver) with 3 consecutive biopsies (one, six, and twelve months) were analysed by FISH and immunohistology (c-kit and smooth muscle actin). In 10 additional cases of renal transplants each at day 0 and twelve months after transplantation, glomeruli were microdissected and a RT-PCR for c-kit and ß-actin was performed. Umbilical vein endothelial cells served as positive control.
Results Glomeruli: Transplant glomerulopathy shows increasing numbers of y-positive cells with progression of the sclerosing lesion. By LM - RT-PCR, increased c-kit transcription is observed compared to controls, while immunohistology is negative. Arteries: Recognition of vascular lesions as chronic transplant vasculopathy was easily possibly by FISH, but not by light microscopy. Tubuli/interstitium: Infiltrates of acute interstitial rejection change sizes from focal/large to disseminated/small over time. Chimeric cells are seen in tubulitis but also in tubular epithelium with ischemic damage.
Conclusion Transplant glomerulopathy is a lesion of chronic rejection associated with the appearance of c-kit positive, recipient cells. Chimeric cells can be demonstrated in transplant vasculopathy and in damaged tubular epithelium, possibly homing to ischemic lesions as part of a repair process.
1. Lancet 1992; 339:1579; 2. Liver Transp 2000; 6:686; 3. Transfusion 2001; 41:419

O-023

Unique congenital glomerulopathy in a child with suspected Ehlers-Danlos syndrome

J Stejskal[1], K Vondrak[2], Z Vančíková[2], E Seemanová[3]
[1]Dept. of Pathology, Charles University, 2nd Medical Faculty, Prague, Czech Republic
[2]Dept. of Pediatrics, Charles University, 2nd Medical Faculty, Prague, Czech Republic
[3]Dept. of Biology and Medical Genetics, Charles University, 2nd Medical Faculty, Prague, Czech Republic

Introduction The aim of our demonstration is to call attention to a unique pediatric case with as yet unknown ultrastructural changes in the glomerular basement membrane (GBM).
Case report The full-term female patient – 3100 g/49 cm – has been developing well with the exception of early (intrauterine?) unilateral intraocular hemorrhage, which necessitated the enucleation of the bulbus at the age of 1 month. Nine months later, varicose enlargement of the left saphena vein was observed, and microscopic hematuria was detected. Later selective proteinuria and mild hypertension was found. At the age of 1 year an open renal biopsy was performed. Light microscopy showed thick-walled and dilated capillaries of glomerular tufts. Collagen IV staining demonstrated corrugated positivity in the GBM, also seen in COL IV alpha 1 chain. Chains alpha 3 and 5 appeared normal. Immunofluorescence gave only strong global IgM positivity. Electron microscopy showed peculiar mostly circular splitting of the GBM lamina densa with inclusions of small amorphous densities as well as of some remnants of cellular organelles. Analogous changes were observed in adjacent arterioles. At present, the 6 year-old child with signs of somatic underdevelopment is being treated for mild hyperazotemia, anemia and renal hypertension. Her body shows some asymmetry, the skin is thin, pink, but no areas of hyperextensibility are seen as well as any hypermobility of joints. NMR investigation of the brain disclosed a slowly growing mass in the left thalamus.
Conclusion The classification of the case among connective tissue disorders is difficult, type IV of Ehlers-Danlos syndrome seems to be the closest.

O-024

Chronic renal thrombotic microangiopathy (TMA) following radiation: study of 5 cases

S Guymar[1], J Lebleu[2], JM Trawale[3], D Droz[1]
[1]Hôpital Saint-Louis, France
[2]Cabinet de medecine interne et de néphrologie, Maubeuge, France
[3]Centre hospitalier de Versailles, Versailles, France

Introduction Renal TMA may develop in various etiological conditions including infections, drug toxicity, immune disorders and radiation.
Case reports We described 5 cases of chronic TMA associated with radiation injury. Patients 1, 2 and 3 underwent bone marrow transplantation (BMT) together with intensive chemotherapy and total body irradiation of 10 to 12 Gy without renal shielding. Two patients had received cyclosporin (CsA) and 1 aziathioprine for graft versus host reaction prevention. Three to 5 years later these 3 patients developed moderate proteinuria associated with slowly progressive renal failure in one, and hypertension in two. Biological signs of hemolytic anemia were no detected in all. Renal biopsy was performed. Patient 4 had been treated by chemotherapy and abdominal irradiation (20 Gy then surimposition of 20 Gy on the left lombo-aortic region) for splenic lymphoma. At this time carcinoma in the left kidney was discovered. The renal function was normal and no proteinuria was found; left kidney was removed 1 year later and pathologic study was performed. Three months after surgery the renal function remained normal and no proteinuria was noted. Patient 5 had a renal biopsy for discrete chronic renal failure and hypertension without proteinuria. She has been successfully treated, 26 years ago, by abdominal irradiation for sub-diaphragmatic lymphoma. In all patients the renal lesions were similar and associated glomerular chronic TMA with subendothelial expansion, mesangiolysis, aneurysmal dilatations and diffuse severe arteriolar lesions with hyalin obstruction. The glomerular lesions were focal in patient 5 and diffuse in the others. No immune deposits were found by immunofluorescence.
Conclusion This study shows that chronic severe lesions of TMA develop following renal radiation associated or not with BMT. These lesions may be clinically and biologically silent over long period of time and are probably underestimated. Although the role of irradiation seems pivotal, chemotherapy and cyclosporine may add deleterious effects in BMT patients.

O-025

Expression of cyclin-dependent kinase inhibitors (CDKI) in human mesangioproliferative glomerulonephritis: their role in mesangial cell proliferation (morphometric study)

A Wozniak, E Kaczmarek, W Salwa-Zurawska, J Zurawski
Chair and Department of Clinical Pathomorphology, Poznan, Poland

Introduction There is evidence for roles of the Cip/Kip family of CDKI (p21, p27) in mediating growth arrest in glomerular cells. Mature podocytes, highly specialized cells with a complex cellular structure (interdigitating foot processes) leave cell cycle and may undergo nuclear division, but not cytokinesis, because this would involve the breakdown of the actin cytoskeleton. It has been recognized that mesangial cells proliferate and accumulate matrix in response to certain forms of injury. The aim of the current study was to elucidate the role of CDKI expression in human glomerular diseases.
Material and methods The analysis was performed on 4 groups of renal biopsies (every consisting of 10 cases): minimal change disease (MCD), membranous glomerulonephritis (MGN), mesangioproliferative proliferative glomerulonephritis: IgA (IgAN) and IgM nephropathy (IgMN). We examined the expression of p27, p21, Ki 67 and PCNA by immunohistochemistry. Adult nephrectomy specimens (N=5) without evidence of glomerular disease served as controls. Morphometric analysis was additionally done in MCD, IgAN and IgMN cases. Color sampling was performed to extract "brown" nuclei stained for p27 and all nuclei of glomerular cells. Then the number of segmented "brown" nuclei was calculated per area of glomerular profiles and related to the number of all nuclei.
Results Immunostaining for p27 was abundant in normal podocytes and some mesangial cells. There was no evidence of p21 and proliferation markers Ki 67 and PCNA in normal glomeruli. In MCD and MGN expression did not change. In contrast there was a marked decrease in staining intensity for p27 in mesangial cells in patients with IgAN and IgMN. The ratio of stained for p27 nuclei was 56.1% and 39.1% for MCD and IgAN, IgMN group, respectively (p=0.03). Interestingly also podocytes focally - in sclerotic portions of glomeruli - revealed a marked decrease of p27. This loss of immunostaining occurred predominantly in mesangial cells and podocytes expressing Ki 67 and PCNA. This was accompanied by the de novo nuclear immunostaining for p21.
Conclusion The decrease in p27 level is required to induce podocyte and mesangial cell proliferation. Also the increase of p21 was observed. Thus changes in cell cycle regulatory molecules play central role in determining the renal response to injury and may underlie the development of progressive glomerulosclerosis. Understanding mechanisms regulating cell proliferation may target future therapies on these molecules.

O-026

Thin-basement-membrane nephropathy (TBMNP): global and segmental types

B Iványi[1], R Pap[1], Z Ondrik[1], G Abraham[2], S Sonkodi[2], E Kemeny[1]
[1]Department of Pathology, University of Szeged, Szeged, Hungary
[2]Clinics of Internal Medicine, University of Szeged, Szeged, Hungary

Aim Characterization of the clinico-pathologic spectrum of TBMNP.
Methods Retrospective determination of the harmonic mean GBM thickness (nm + SD) in a consecutive series of 33 adult patients whose GBM had been classified as "thin" during the original evaluation, who had no IgA nephritis or familial haematuria, and for whom at least 2 glomerular profiles were available for measurements. Controls: 5 living kidney donors and 5 patients with minimal change NP.
Results Three cohorts were distinguished. The first cohort, involving TBMNP consisted of 22 patients with microhaematuria (proteinuria in 15 patients), no glomerular immune complexes, histologically normal glomeruli, and an attenuated GBM. The attenuation was global in 14 patients, and segmental in 8. The second cohort, involving coexisting TBMNP and an established glomerular disease (4 focal sclerosis, 2 focal proliferative GN, 1 minimal change, 1 membranous, and 1 hypertensive arteriolosclerosis)

comprised 9 microhaematuric patients. The thinning was global in 5 patients, and segmental in 4. The third cohort contained 2 non-haematuric patients who had a globally thinned GBM and focal proliferative lupus GN or minimal change NP, respectively. In summary, 19 cases of global TBMNP (234 + 19 nm; controls: 334 + 43 nm; p<.0000), and 12 cases of segmental TBMNP (299 + 21 nm; p=0.02) were verified.
Conclusion TBMNP manifests with either a globally or a segmentally thinned GBM. TBMNP is not infrequently associated with other glomerular diseases. The clinical and morphologic data should be considered simultaneously when the diagnosis of TBMNP is made. Supported by OTKA T-038271(Budapest, Hungary) grant to I.B.

O-027

Simultaneous quantitative gene expression analysis in human renal biopsies in patients with lupus nephritis (LGN)

J Jeruc[1], D Ferluga[1], A Vizjak[1], T Roth[2], B Rozman[3], HP Dienes[2], JWU Fries[2]
[1]Institute of Pathology, Faculty of Medicine University of Ljubljana, Ljubljana, Slovenia
[2]Deptartment of Pathology, University of Koeln, Koeln, Germany
[3]Department of Rheumathology, University Medical Centre, Ljubljana, Slovenia

Introduction Inflammatory flares, enhanced proliferation and delayed apoptosis are important pathomechanisms in LGN. These are associated with increased expression of genes previously studied by semi-quantitative immunohistologic detection of an individual gene product. The aim of this study was to perform a simultaneous quantitative comparison of expression of genes tentatively relevant to pathogenesis of LGN.
Material and methods Renal tissue samples, fresh frozen (18) and formalin-fixed (8), obtained by percutaneous biopsy of 18 patients with LGN (WHO class II, III and IV) were used. Formalin-fixed zero transplant biopsies served as controls. From 5 µm thick sections, 25 glomeruli were laser-microdissected, RNA was extracted and transcribed. A real-time, quantitative PCR analysis was performed using VCAM-1, fractalkine as markers of inflammation, IL-6, PDGF-ßR as markers of proliferation, Bax, Fas ligand and TNF-R1 as regulators of apoptosis and ß-actin as housekeeping gene.
Results Frozen biopsies allowed detection of all genes; formalin-fixed only of some.
There was no correlation between levels of gene expression and age, sex, proteinuria or activity/chronicity indexes. WHO class II cases showed increased levels of VCAM-1, PDGF-ßR and Bax but not fractalkine as compared to controls. WHO class III and IV cases showed higher expression of fractalkine, IL-6 and PDGF- ßR than WHO class II cases. In WHO class III cases, IL-6, and fractalkine levels were clearly, while Bax levels were slightly higher than in WHO class IV cases.
Conclusions 1. Real-time quantitative PCR is useful for a simultaneous analysis of gene expression in frozen samples of human renal biopsies. 2. In this limited study, class II lesions, as expected, showed lower expression of genes in comparison with classes III and IV. However, class III lesions seemed to exhibit higher expression levels of genes involved in proliferation, inflammatory cell infiltration and apoptosis regulation compared to class IV, possibly relating to a different pathogenesis of those two classes.

O-028

Haemorrhagic glomerulonephritis (GN) and massive pulmonary haemorrhage in Goodpasture syndrome - unique case report

TM Perković[1], V Gorjup[2], A Vizjak[1], D Ferluga[1]
[1]Institute of Pathology, Faculty of Medicine University of Ljubljana, Ljubljana, Slovenia
[2]Centre for Intensive Internal Medicine, Clinic for Internal Medicine, Universitiy Clinical Centre, Ljubljana, Slovenia

Aim We present the autopsy study of an unique case of Goodpasture syndrome with a rapidly progressive fatal course.
Case report A 38-year-old previously healthy woman was admitted to hospital with a brief history of fever, chest pain and haemoptysis. She was anemic, dyspnoic with a blood oxygen saturation of 47% and WBC count of 17.7 x 103/µL. Chest x-ray showed pulmonary alveolar densities. Despite negative haemocultures for bacteria, broad spectrum antibiotics were introduced. Anti-GBM antibodies were positive by indirect immunofluorescence, while ELISA for α3(IV) chain was negative and she additionally received prednisone. She expired 3 days after admission due to rapidly progressive respiratory and renal failure. The autopsy study revealed massive intraalveolar pulmonary haemorrhage, leukocytoclastic alveolar capillaritis and linear immunofluorescence of IgG and C3. Kidney autopsy samples showed a significant glomerular influx of neutrophils (10-20 per glomerulus), diffuse effusion of blood in the Bowman's space and tubular lumen accompanied by linear IgG and C3 deposits along the glomerular and tubular basement membrane.
Discussion and conclusion Our patient fulfills diagnostic criteria for Goodpasture syndrome. Pulmonary haemorrhage associated with alveolar capillaritis and linear deposits of IgG is a characteristic finding which can be fatal when massive. However, renal involvement in Goodpasture syndrome is characterized by anti-GBM diffuse necrotising and extracapillary crescentic GN. To the best of our knowledge, this is the first reported case of Goodpasture syndrome with GN, which we have termed haemorrhagic due to similarities with lung pathology. It might be hypothesised that this unique renal involvement is related to the finding of atypical anti-GBM antibodies in our case, obviously not directed against the Goodpasture epitope on α3 chain of type IV collagen, but probably against another antigen.

O-029

Progressive diffuse proliferative and crescentic recurrent IgA glomerulonephritis (GN) in transplanted kidney

V Jurčić[1], A Vizjak[1], S Kaplan-Pavlovčič[2], D Ferluga[1]
[1]Institute of Pathology, Faculty of Medicine University of Ljubljana, Slovenia
[1]Department of Nephrology, University Clinical Centre Ljubljana, Slovenia

Introduction Recurrent IgA GN in renal transplant has been reported in 40-50% of patients, and it is even less frequently progressive than in the native kidney, probably due to immunosuppressive therapy. We present two patients with a severe form of recurrent progressive IgA GN.

Case reports A 53-year-old man with chronic mesangiopro-liferative GN developed terminal renal failure 7 years after the onset of the disease. The patient almost certainly had IgA GN according to the clinical and laboratory findings, histologic picture and confirmed IgA GN in his son, although immunofluorescence was not done on his native kidney biopsy. His first kidney allograft was lost due to surgical complications. The second allograft functioned well for 10 years, when decreased renal function, hypertension, nephrotic syndrome and erythrocyturia were observed. In addition, IgA ANCA was positive 1:1280. Renal biopsy revealed an IgA GN, severe diffuse proliferative with 25% crescents.
A 39-year-old man with advanced diffuse proliferative and crescentic (15%) sclerosing (38%) IgA GN received a cadaveric renal allograft. Six years later, decreased renal function, hypertension, proteinuria and erythrocyturia were found. Renal transplant biopsy disclosed severe diffuse IgA GN with 70% crescents.
Conclusions Only 4 cases of recurrent rapidly progressive crescentic IgA GN in transplant have been reported so far. In our first patient, severe IgA GN was probably causally related to capillary wall immune deposits accompanying mesangial deposits, and the occurrence of ANCA after transplantation. A peculiar immune process resulting in a severe progressive and crescentic IgA GN in the native and transplanted kidney could be hypothesised in our second patient. Arterial hypertension, established as the most frequent risk factor of non-immune progression of IgA GN, did not play a significant role in our patients.

O-030

Collapsing variant of FSGS associated with interferon-α treatment for hepatitis B infection

B Cizman, JE Tomaszewski
Renal Electrolyte and Hypertension Division, Department of Medicine and Department of Pathology, University of Pennsylvania School of Medicine, Philadelphia, USA

Introduction Use of recombinant interferon-α (IFN-α) has been associated with protean kidney manifestations, including episode of acute renal failure (ARF) secondary to ATN, nephrotic syndrome due to either FSGS or minimal change disease and chronic interstitial nephritis.
Patient and methods 45 year old African American male with long-standing hypertension, on diuretic and ACEI and normal kidney function, who initiated treatment for hepatitis B with IFN-α developed proteinuria and lower extremity edema. Laboratory testing revealed creatinine (Cr) 5.1 mg/dL (449 μmol/L), albumin 1.7 mg/dL and abnormal urine sediment. Proteinuria was estimated at 10 gm/d. All serologies were either normal or negative. US guided kidney biopsy was performed about three months after the initiation of IFN-α treatment.
Results Thirteen glomeruli were available for review, two were globally sclerotic. All glomeruli showed various degree of mesangial sclerosis, diffuse mild mesangial hypercellularity and variable degree of glomerular collapse. Four glomeruli had segmental scars. Interstitium showed diffuse moderate interstitial fibrosis and tubular atrophy with mild to moderate lymphoplasmocytic infiltrate. IF studies were nonspecific. EM revelaed hyperplastic visceral epithelial cells and diffuse effacement of the foot processes. Kidney function did not improve after the discontinuation of IFN-α treatment, however four months of prednisone was effective with partial remission of proteinuria to 1.5 gm/d and decrease in Cr to 3.0 mg/dL (264 μmol/L). Due to elevated liver enzymes prednisone was discontinued. Kidney function and proteinuria remained stable over the next 6 months.
Conclusion IFN-α should be included on growing list of medications associated with collapsing FSGS. It seems that discontinuation of IFN-α treatment and steroids may prevent rapid progression to advanced kidney disease. Further studies are needed to delineate the extent of this association and the potential mechanism of injury.

O-031

Use of TTF-1 in diagnosis of metastatic pulmonary adenocarcinoma in FNAB samples

M Strojan Fležar, I Srebotnik Kirbiš, J Lavrenčak
Institute of Oncology, Ljubljana, Slovenia

Introduction Diagnostic use of TTF-1 as an organ specific marker for thyroid and lung origin of carcinomas was documented mostly in tissue sections, while the information on TTF-1 in cytology samples is still insufficient. The aim of the study was to analyze the expression of TTF-1 by immunocytochemical detection in cytology samples.
Materials and methods We obtained material by fine needle aspiration biopsies (FNAB) of primary and metastatic neoplasms (104 cases). First, methodological approach with TTF-1 was tested in thyroid tissue (16 goiters, 4 adenomas, 13 carcinomas). Afterwards, we analyzed 3 primary and 18 metastatic lung adenocarcinomas, 5 primary and 13 metastatic extrapulmonary adenocarcinomas, 3 primary lung tumors and 11 metastatic lung carcinomas of other types and 10 metastatic carcinomas of different types. Additionally, 3 metastatic malignant melanomas were also included in the study. Finally, we tested 5 metastatic tumors of unknown origin.
Results All primary and 12/18 metastatic lung adenocarcinomas stained positive with TTF-1. Two of 5 metastatic tumors of unknown origin stained positive, however primary tumor was not found. Except for thyroid samples, normal lung, 3 metastatic microcellular and 1 macrocellular carcinoma of lung origin, none of other primary or metastatic tumors stained positive for TTF-1.
Conclusion In FNAB specimens, TTF-1 can confirm thyroid origin of carcinoma and more importantly, determine the lung origin of metastatic or primary adenocarcinoma. Therefore, TTF-1 could be used for early identification of primary site (pulmonary vs. extrapulmonary) in FNAB of metastatic adenocarcinomas skipping further expensive investigations.

O-032

Immunoprofile of adenocarcinomas in effusions: a retrospective study of 102 cases

M Smit Cordeiro, L Martins, M Mendes de Almeida
Serviço de Anatomia Patológica. Hospital de Santa Maria, Lisboa, Portugal

Introduction Adenocarcinoma is the most common metastatic neoplasia among malignant serous effusions. An effusion is often the initial presentation of a malignancy. The aim of the study was to assess the validity of immunocytochemical reactivity patterns in determining the origin of metastatic adenocarcinomas in serous effusions.
Material and methods We reviewed 102 non-consecutive specimens of serous effusions, containing adenocarcinomas, obtained from our department files. Of these, 100 had prior or posterior histological confirmation of the primary tumour. A battery of

monoclonal antibodies was applied (Ck7, Ck20, TTF-1, CA19.9, CA125, CA15.3 and HMFG-1) to Papanicolaou stained smears.
Results Positivity ratios for Ck7 in lung, breast, stomach, ovary, pancreas, colon and endometrial adenocarcinomas were 18/19, 19/20, 19/21, 20/20, 6/6, 0/6 and 6/6 respectively. The same ratios for Ck20 were 3/19, 4/20, 11/21, 3/20, 2/6, 6/6 and 1/6 respectively. We obtained positive immunoreactivity for TTF-1 in 15 of the 19 lung adenocarcinomas and in none of the other tumours. The positivity ratio for CA19.9 in stomach, pancreas and gallbladder adenocarcinomas were 18/21, 4/6, and 1/1 respectively. CA125 was positive in 18/20 of ovarian carcinomas. Of the 20 breast carcinomas, 13 were positive for HMFG-1 and 11 for CA15.3.
Conclusion The Ck immunoprofile was the single most important determinant in the assignment of the primary tumour. In some cases the Ck pattern was confirmatory in combination with additional immunostains (TTF-1, CA125, CA19.9, CA15.3 and HMFG-1). TTF-1 proved to be sensitive and highly specific in metastatic lung adenocarcinomas.

O-033

Interlaboratory quality control (QC) of PAP smear cytology as a part of the multi-centre trial comparing six optional screening tools in Latin America (The LAMS Study*)

M Branca[1], M Eržen[2], M Alderisio, A Longatto-Filho, K Syrjänen
[1]Istituto Superiore di Sanitá (ISS), Rome, Italy
[2]SIZE Diagnostic Center, Ljubljana, Slovenia

Aims As part of the external quality control (QC) programme incorporated in controlling all the diagnostic tests in the LAMS study, the reproducibility of the cytological diagnosis is being controlled using an inter-laboratory QC approach.
Study design Four sets of slides (20 in each), containing in different proportions 1) inadequate smears, 2) negative for SIL, 3) ASC, ASC-US, AGC, LSIL, 4) HSIL or CIN2, 5) HSIL or CIN3, and 6) invasive cancer, have been compiled, with consensus diagnoses by three cytopathologists as the gold standard. The reproducibility (inter-laboratory- and laboratory/consensus diagnosis) will be tested using both non-weighted and weighted kappa (ICC, intra-class correlation coefficient), as well as calculating three indexes measuring variability: A) between CIN1 and CIN2; B) between CIN2 and CIN3, and C) CIN1 versus CIN2, CIN3, invasive cancer.
Results The overall agreement with the laboratory- and the consensus diagnosis in two slide sets is substantial using non-weighted k=0.712 (95%CI 0.548-0.876) and almost perfect with weighted kappa ICC=0.963 (95%CI 0.929-0.980). The non-weighted k=0.873 (95%CI 0.705-1.00) for set 1 and k=0.608 (95%CI 0.350-0.866) for set 2. Using weighted kappa, ICC is almost perfect: ICC=0.989 (95%CI 0.977-0.996) and 0.940 (95%CI 0.836-0.977) for set 1 and 2, respectively. Further details will be presented in the conference.
Expected outcome measures This study design provides valuable data on the quality standards of individual laboratories and helps pinpointing the possible problem areas in their performance, where continuous quality improvement (CQI) could be helpful. *(LAMS: Latin American Screening Study, funded by EC, INCO-DEV Contract # ICA4-CT-2001-10013).

O-034

Similar MAC signals in buccal mucosa of breast and lung cancer patients

M Us-Krašovec[1], M Strojan Fležar[1], J Eržen[2], M Žganec[1], J Lavrenčak[1], A Doudkine[3], D Garner[3], B Palcic[3]
[1]Institute of Oncology, Ljubljana, Slovenia
[2]University Medical Centre, Ljubljana, Slovenia
[3]British Columbia Cancer Agency, Vancouver, Canada

Background Malignancy associated changes (MAC) were found in normal cells of patients with different types of cancer. It has been suggested that they could be used as a test for detection of early cancers. Any diffrences in MAC expression among different cancers remain to be determined. The aim of the study was to compare MAC signals detected in buccal mucosa of breast and lung cancer patients as measured by image cytometry.
Materials and methods 106 patients with lung cancer and 89 control subjects, and 100 breast cancer patients and 93 control subjects were included in the study. Scrapings of buccal mucosa were suspended in transport medium. Monolayer filter preparations were stained by Feulgen-Thionin method. Image cytometric analysis was performed by Cyto-Savant. Classifier, using nuclear texture features (NTF), was trained on lung cancer patients and corresponding controls and tested on breast cancer patients and their controls and vice versa.
Results When trained on lung cancer samples, the classifier with optimal combination of three NTF representing MAC recognized correctly 74% of breast cancers, while the correct recognition of lung cancer was 87% with the same classifier. When the classifier was trained on breast cancer samples, 78% of lung cancers were correctly classified, while 81% of breast cancers were correctly recognized with the same classifier.
Conclusions Our results indicate that MAC signals in buccal mucosa of breast and lung cancer patients are very similar. Therefore we now postulate that different cancers (at least of the epithelial origin) induce similar MAC changes, which would allow more universal test for detection of early cancers.

O-035

Rhabdomyosarcoma development in mice lacking p53 and Fos: tumor suppression by the Fos proto-oncogene

W Jochum[1], A Fleischmann[2], R Eferl[2], E Wagner[2]
[1]Institute of Clinical Pathology, University Hospital, CH-8091 Zurich, Switzerland
[2]Research Institute of Molecular Pathology (IMP), A-1030 Vienna, Austria

Introduction Rhabdomyosarcoma (RMS) is the most common soft-tissue sarcoma of childhood. Animal models of RMS are rare and the application of available models is limited due to low tumor incidence and long latency periods. The Fos protein, a major component of the AP-1 transcription factor, acts as an oncogene, mediates transforming signals, and controls invasive growth and angiogenesis during tumor progession.
Methods To investigate a potential genetic interaction between the p53 and Fos pathways, p53/Fos double knock-out mice were generated.
Results In contrast to p53 and Fos single mutant mice, these mice specifically develop RMS of the facial and orbital regions with more than 90% penetrance at 6 months of age. In cell lines established

from these tumors, re-expression of Fos is associated with enhanced apoptosis and reduced Pax-7 expression, whereas cell proliferation and the expression of other AP-1 components are not altered.
Conclusions Our results suggest that Fos acts as a tumor suppressor during RMS tumorigenesis and that p53/Fos mutant mice may be a suitable animal model for human RMS.

O-036

Long-term effect of neonatal monosodium glutamate (MSG) treatment on hypothalamus-pituitary-adrenal-thymus axis of rats

S Cekic, M Filipovic, M Nesic, O Dimitrijevic, M Pavlovic, S Brankovic, M Ciric
Instute of Physiology, Faculty of Medicine, University of Nis, Nis, Serbia and Montenegro

Introduction The study aimed at determining effects of MSG, introduced in the perinatal period, on hypothalamus-pituitary-adrenal-thymus (HPAT) axis of Wistar rats.
Material and methods In days 2, 4, 6, 8, 10 the newborn rats received s.c. injections of MSG (4mg/g body weight). The rats were killed at 10 months of age. The paraffin sections of investigated organs were stained with HE, PAS and Van Gieson methods.
Results Macroscopically, the treated rats showed: stunted skeletal development, Cushing's obesity of "buffalo" type, both pituitary and adrenal hypertrophy. Microscopically the hypothalamic arcuate nuclei were completely destroyed along with neuronal constituents in the median eminence. Gliosis, the most important histopathologic indicator of CNS injury, was found instead of these tissues. Astrocytes were hypertrophic and hyperplastic, with small and dark nuclei, located in a dense net of glial fibrils. Multifocal small loci of microglial nodules, associated with neuronophagia, were also observed. Basophile cells of pituitary gland were hyperplasic, with foamy aspect and infiltrating neurohypophysis. Cortical cells of the adrenal gland, symmetrically, were also hyperplasic. The adrenal fasciculate zone was disturbed by increased number of cells and obviously dilated sinusoids. The thymus atrophied and lymphocytes proliferation was apparently decreased.
Conclusion This study supports the idea that the disturbance of hypothalamus-pituitary-adrenal (HPA) axis is accompanied with cell-mediated immunodeficiency.

O-037

Development and routine evaluation of the digital histology laboratory

P Gombas[1], B Molnar[2], S Varga[2], A Tagscherer[2], G Csendes[2], V Kamaras[2], T Virag[3]
[1]MI Central Hospital, Department of Pathology, Budapest, Hungary
[2]Cell Analysis Laboratory, 2nd Department of Medicine, Semmelweis University, Budapest, Hungary
[3]3DHistech Ltd. Budapest, Hungary

Background Comparable to the digital radiology, recent significant developments in the microscopic slide scanning, data storage technology can contribute to the development of digital histology laboratory techniques. The aim of the study is to evaluate this technology in a routine setting.
Methods In the daily routine in a university pathology department 100 to 300 slides were prepared from 50 to 150 cases in a day. From the usual paraffin blocks 5 µm sections were prepared and processed. The bar-coded slides were digitized and stored on a digital slide server. Commercial short and long term storage may be used. The evaluation of the slides was done in local and remote access. For specific tissue types (colon, gastric) automated tissue component segmentation and analysis modules were developed. For the 3D reconstruction of serial sections a dedicated program was developed.
Results The daily prepared slides (100-200 pcs) could be scanned in the night. The virtual microscopy analysis yielded concordant results with the optical microscopy analysis. Teleconsultation based on digital slides and virtual microscopy was applicable in selected cases. The automated algorithms could classify gastric biopsy specimen cases with high accuracy (95%). 3D reconstruction yielded a more detailed insight and diagnosis. Reports including the low resolution digital slide image, high resolution selected field of views, alphabetical report were sent in e-mail to the referring specialists in higher safety and speed as compared to the traditional way.
Conclusions The digital histology laboratory technology improves the specialisation in pathology allowing remote access to selected tissue types, the reporting process' safety and efficiency.

O-038

Experiences in the production of digital slides by an automated high-resolution scanner system after automated slide preparation

B Molnar[1], V Varga[1], T Virag[2], A Tagscherer[1]
[1]II. Dept.of Medicine, Budapest, Hungary
[2]3DHistech Ltd, Budapest, Hungary

Background Automated slide preparation systems are available for histological routine use. We recently developed and installed the Hi-Scope slide scanner system in a routine environment. The aim of the present work was the evaluation of Hi-Scope for everyday applications.
Methods Hi-Scope and a digital storage environment were installed in the biopsy specimen laboratory. 5 µm sections from gastrointestinal and surgical pathology material were prepared as usual. The slides were deparaffined, stained and coverslipped using automated systems (Medite Inc., Germany). The barcode labeled slides were placed into the Slide-Scope cassette and scanned by the Hi-Scope system (3DHISTECH Ltd, Hungary) automatically. A day 100 to 200 slides were scanned. Hi-Scope is an autoloader, autoscanner, and auto focusing slide scanner. Slides were stored on dedicated slide server computers equipped with fast short term and slow long-term storage components.
Results In the experiment 4000 slides were scanned altogether and 6 cassettes were reused continuously. From the 80 cassette loading cycle the cassette stuck once. From the three type of slides used the machine could not load 3% of the cheap, low-quality no name slides, 0.5% of the Superfrost slide with square edges and corners and 0.1% percent of the Starfrost slide with grounded edges end corners. A slide load/unload cycle is 10 seconds. Slides were identified using 6 decimal digit barcodes. The resolution was 0.16µm / pixel. The scanning speed of the system was 2.5 images / second including auto focusing. With this resolution 1 mm^2 was scanned in 20 seconds and resulted 20 Mbyte digital data using 1:5 JPEG compression.
Conclusions Hi-Scope can be used in the routine for slide digitization and archiving.

O-039

Cytogenetical findings in a case of non-ossifying fibroma

RG Forsyth[1], B Poppe[2], K Verstraete[3], B Poffijn[4], D Uyttendaele[4], M Praet[1], F Speleman
[1]N. Goormaghtigh Institute of Pathology, Ghent, Belgium
[2]Center for Medical Genetics, Ghent, Belgium
[3]Department of Medical Imaging, Ghent, Belgium
[4]Department of Orthopaedic Surgery, Ghent, Belgium

Introduction Non-ossifying fibroma (NOF) is a benign osseous lesion with favourite localisations in the metaphyses of the tibia and distal femur. NOF is mostly asymptomatic and is therefore usually incidentally identified on radiographs. Most lesions stabilize at puberty and shows signs of healing by peripheral sclerosis or solid opacification. Only a few cases have been analysed cytogenetically.
Case report Clinical history: A 21-year old female presented with a lesion in the methaphysis of the tibia, which produces an eccentric cortical-based lesion with distinct sclerotic margins and ground glass aspect on radiographic imaging. A fracture line is observed. Surgical curettage is performed. Histopathology: This lesion is composed of short fascicles of benign appearing oval to spindle-shaped cells. The fascicles are arranged in a storiform pattern. In this stroma few multinucleated giant cells and some xanthomatous cells are present. In several stromal cells a substantial amount of hemosiderin pigment is clearly visible. Small numbers of mononuclear inflammatory cells are noticed. No atypical mitoses are found. Cytogenetics: G-banding analysis revealed following karyotype: 46, XX, der(2)t(2;?)(q22;?),-22, +mar[4]/46, XX[15].
Discussion and conclusion NOF is a benign osseous lesion confined to the metaphyses of the long tubular bones of skeletally immature patients. Most lesions stabilize at puberty. Malignant transformation is extremely rare and some individual cases of associated fibrosarcoma and osteosarcoma are described. These molecular findings together with earlier reported cytogenetical data are remarkable as NOF is generally considered to have frequently a spontaneous resolution indicating a self-limiting process which is most likely related to incomplete ossification. Further studies are needed to clarify the contribution of these clonal changes in these lesions.

O-040

Ret/PTC and p53 expression in normal, benign and malignant thyroid lesions

N Othman, E Omar
University Sains Malaysia, Kota Bharu, Malaysia

Introduction This study aims to investigate the expression of ret/PTC and p53 in the local normal, benign and malignant thyroid lesions in order to shed light on the pathogenesis of papillary carcinoma and explain the high prevalence of this condition among the nodular hyperplasia (multinodular goiter) cases in the local population.
Materials and methods Archival blocks from 50 follicular adenomas, 66 nodular hyperplasia and 53 papillary carcinoma cases were retrieved from HUSM pathology department files. They were studied by immunohistochemistry for the presence of ret/PTC and p53 mutant protein. Normal tissues from 74 cases served as controls.
Results 5.4% normal thyroid tissue, 18% follicular adenomas, 22.7% nodular hyperplasia cases and 71.7% papillary carcinomas expressed ret/PTC mutation. Ret/PTC expression in papillary carcinoma was not associated with coexistence of nodular hyperplasia lesion. P53 is expressed by 17% of papillary carcinoma. No association was found between p53 expression of nodular hyperplasia with or without coexisting papillary carcinoma. p53, not ret/PTC was an excellent predictor of tumour lymph node metastasis and capsular invasion. It is also a significant prognosticator of survival outcome.
Conclusion Ret/PTC mutation is highly prevalent in local papillary carcinoma, indicating a significant role in the pathogenesis of this tumour; with no apparent role in tumour behaviour and survival outcome. P53 on the other hand appear to be a significant factor in the latter events. The two genes appear to act in two different pathways; the former being the initiator, and the later perpetuator of papillary carcinoma.

O-041

Vascular invasion in pleomorphic adenoma of salivary gland: a possible consequence of FNA biopsy

S Di Palma[1], MG Cook[2], TK Mellor[3]
[1]Queen Alexandra Hospital, Portsmouth, UK
[2]Royal Surrey County Hospital, Portsmouth, UK
[3]Queen Alexandra Hospital, Portsmouth, UK

Introduction Benign intravascular invasion in association with pleomorphic adenoma (PA) of salivary glands is uncommon. In none of the reported cases has it been associated with subsequent development of metastases. It may cause a diagnostic and therapeutic dilemma in salivary glands, which appears otherwise benign. No explanation of the etiopathogenesis has been offered in previously reported cases. Aim: We suggest that pre-operative procedures undertaken such as fine needle aspiration (FNA) of the salivary gland may cause iatrogenic seeding of tumour cells.
Materials and methods Two cases of PA of the parotid gland showed vascular invasion. Both presented with a palpable nodule in the parotid gland. One patient had two FNAs the other one prior to surgery. Both underwent superficial parotidectomy.
Results Histologically both tumours were PAS positive with little chondromyxoid component but both were rich in myoepithelial cells. Clusters of myoepithelial and epithelial cells were seen within muscular and thin walled blood vessels, both outside the capsule and within the tumour. In spite of genuine vascular invasion there was no cytological evidence of atypia or malignancy. Our speculation is that the previous FNAs may have caused spillage of PA cells within vessels giving an impression of a potentially malignant tumour.
Conclusion We recorded two cases of PA with associated vascular invasion. We speculate that preceding operative procedures such as FNA may be relevant to the pathogenesis.

O-042

Extra-cellular signal-regulated ERK-1/ERK-2 pathway activation in human salivary gland mucoepidermoid carcinoma: association to aggressive tumor behaviour and tumor cell proliferation

A Handra-Luca, A Lesot, JC Bertrand, P Fouret
Université Paris VI UFR Pitié-Salpętrire, Paris, France

Information on oncogenetic events in salivary gland mucoepidermoid carcinoma is so far limited. Activation of extracellular signal-regulated kinases ERK-1 and ERK-2 is strongly correlated to cancer. Using an antibody specific for phosphorylated (active) ERK-1/ERK-2, we examined human salivary gland mucoepidermoid carcinoma samples by immunohistochemistry. The comparison in paired tumor and normal tissue samples showed that phosphorylated ERK-1/ERK-2 expression was higher in tumor cells as compared to surrounding normal salivary parenchyma. Using a threshold below which > 95% of normal samples expressed phosphorylated ERK-1/ERK-2, we showed that ~39 % of mucoepidermoid carcinomas expressed high levels of phosphorylated ERK-1/ERK-2. Those tumours where ERK-1/ERK-2 pathway was activated had a more aggressive tumor behaviour as compared to the group where this pathway was inactive. The association of ERK-1/ERK-2 phosphorylation to a worse prognosis was independent of histological grade. ERK-1/ERK-2 phosphorylation was associated with an increased tumor cell proliferative index. There was no relationship between ERK-1/ERK-2 phosphorylation and HER-2/neu expression. In conclusion, ERK-1/ERK-2 pathway is active in salivary gland mucoepidermoid carcinoma and this activation is associated to a more aggressive tumor behaviour and a higher proliferative activity. These data suggest that deregulation of ERK-1/ERK-2 pathway contributes to mucoepidermoid carcinoma phenotype and, possibly, represent a target for new anticancer drugs.

O-043

Sinonasal acinic cell carcinoma: what do we know about this rare entity?

A Neto[1], K Pineda-Daboin[2], M Luna[3]
[1]University Of Texas Medical School - Houston, Texas, USA
[2]Military Hospital 'Carlos Arvelo' - Caracas, Venezuela
[3]University of Texas MD Anderson Cancer Center - Houston, Texas, USA

Introduction Acinic cell carcinoma(ACC) is a low-grade salivary gland carcinoma with a predilection for the parotid gland. ACC originating in the sinonasal tract has rarely been reported. Four cases of ACC involving the sinonasal tract were identified in the Pathology files of M.D. Anderson Cancer Center from 1984 to 2002. The clinicopathologic information was reviewed.
Results There were 2 males and 2 females, aged 45 to 65 years, mean 58. The patients presented with unilateral nasal obstruction. All tumours were confined to the nasal cavity. Histologically, they were composed of round to ovoid cells with clear and/or granular basophilic cytoplasm and round, hyperchromatic, small, eccentrically located nuclei. The growth pattern was lobular, solid, and follicular. Histochemically, PAS diastase resistant cytoplasmic granules were demonstrated in all cases. Immunohistochemical stains were non-specific. Surgical resection was the treatment of choice. All patients are alive and well from 4 to 17 years.
Conclusion Sinonasal acinic cell carcinoma is a distinct low-grade carcinoma, which can be distinguished from any other neoplasm by light microscopy and histochemical stains. Pathologists should be aware of the occurrence of this salivary gland carcinoma in the sinonasal tract.

O-044

Aetiological correlates in Nigerian laryngeal cancers

O Ogunbiyi[1], G Nwaorgu[2]
[1]University College Hospital, Department of Pathology, Ibadan, Nigeria
[2]University College Hospital, Department of Otorhinolaryngology, Ibadan, Nigeria

Introduction A recent review of cancer data from the cancer registry of the University College Hospital Ibadan, showed an increase in the relative ratio frequency of carcinoma of larynx (CaL) in the last decade. An increase of appearance was found especially among adult males. The aims of the study were to characterise the epidemiology of laryngeal carcinoma and to compared with nasopharyngeal carcinomas, both representing upper airway lesions with some common environmental aetiological associations. The objective was to assess, if possible, the role of purported aetiological correlates with CaL.
Materials and methods Data from the cancer registry of University College Hospital, Ibadan was reviewed for cases with carcinoma of larynx and nasopharyngeal carcinoma over a 15-year period, 1986-2000. Information of the age, sex and histological type of tumours were recorded and analysed. Clinical information regarding social habits was sought from the histology request cards. Data was subjected to statistical analysis.
Results A total of 17,132 cases of cancer occurred in that period (7,283 in males and 9,849 in females). There were 256 laryngeal cancers (1.5%) with mean ages of 53.8 years for males and 58.8 years for females and male: female ratio of 6: 1, while there were 332 cases of nasopharyngeal carcinoma (1.9%) with mean ages of 42.8 and 37.5 and a male: female ratio of 2.7: 1. Amongst male cancers carcinoma of larynx constituted 3% while NPC constituted 3.3% of cases, compared with 0.38% and 0.9% respectively in females. Quinquenial analysis showed no increase in the number of cases of CaL while cases of NPC increased consistently during this period.
Conclusions Prevalence of the male population in Nigerian CaL suggest that additional hormone receptor studies might help to elucidate aetiopathogenesis of laryngeal cancer.

O-045

Immunohistochemical characterisation of adenocarcinoma of the nose and paranasal sinuses in woodworkers

A Sandison[1], A Lale[2], J Capper[2], D Peston[1], L Michaels[3]
[1]Charing Cross Hospital, London, UK
[2]Wycombe Hospital, Wycombe, UK
[3]UCLMS, London, UK

Introduction Adenocarcinoma of the nose and paranasal sinuses is rare but has been shown to occur with increased frequency in workers exposed to wood dust. Histologically the tumours resemble adenocarcinoma of the GI tract and show the same spectrum of

histological types and differentiation. Therefore tumours at this site may present a diagnostic problem in distinguishing between primary and metastatic disease. Immunostaining has shown colonic adenocarcinomas to express cytokeratin CK20 and carcinoembryonic antigen (CEA) but not cytokeratin CK7. Lung and squamous carcinomas of the head and neck are usually CK7 positive and CK20 negative. This prompted assessment of the immunohistochemical expression of CK7, CK20 and CEA in a retrospective series of primary nasal adenocarcinomas. The aims of the study were to establish the pattern of expression of CK7 CK20 and CEA in primary sinonasal adenocarcinoma and to compare it with that seen in colonic adenocarcinoma.
Materials and methods 22 cases of primary sinonasal adenocarcinoma were available from archival files. These were reviewed and classified into 4 histological subtypes including papillary, tubular, mucinous and signet ring. Representative paraffin sections were immunostained for CK7, CK20 and CEA.
Results Normal respiratory epithelium included in the sections was positive for CK7 and negative for CK20 and CEA. 13/22 (59%)of tumours expressed CK7. All of the tumours expressed CK20 and all but one of the tumours expressed CEA, with 3 showing only focal positivity. There were 7 tumours designated mucinous or signet ring type only one of which expressed CK7.
Conclusion Primary sinonasal adenocarcinomas express CK20 and CEA. There is variable expression of CK7, which may help to distinguish between primary sinonasal adenocarcinoma, which are positive, and metastatic colonic adenocarcinoma of papillary and tubular subtype, which are negative. Poorly differentiated mucinous tumours are indistinguishable by immunohistochemistry alone.

O-046

Provisional extracellular matrix – indicator of oral squamous cell carcinoma (OSCC) progression and target for therapy

H Kosmehl[1], A Berndt[2], D Neri[3], L Zardi[4]
[1]HELIOS Clinic Erfurt, Institute of Pathology, Erfurt, Germany
[2]Institute of Pathology, University of Jena, Germany
[3]Institute of Pharmaceutical Sciences, Swiss Federal Institute of Technology, Zürich, Switzerland
[4]Istituto Nazionale per la Ricerca sul Cancro, Genoa, Italy

Introduction Progression of OSCC embraces carcinoma cell invasion into the stroma but also includes invasion of blood vessels and stromal cells into the tumour. Both processes share a provisional matrix. The aims of the study were review of provisional matrix synthesis, distribution and co-localisation, demonstration of suitability of ED-B fibronectin for OSCC targeting and experimental tumour therapy.
Material and methods OSCC shock frozen tissue, cell lines; confocal microscopy; ISH or immunohistochemistry for ED-B fibronectin (ED-B Fn), high molecular weight tenascin (Tn-CL), and gamma2-chain of laminin-5 (Ln-gamma2), molecular engineered recombinant ED-B Fn antibody, experimental tumour therapy with fusion protein, recombinant ED-B Fn antibody - tissue factor, in mice.
Results OSCC progression is associated with ED-B Fn, Tn-CL and Ln-gamma2 synthesis and arrangement in strand-like matrix structures at the deep invasive OSCC edges. The strand-like organisation of ED-B Fn by stromal fibroblasts is the pre-condition for the formation of the multiprotein complexes. Additionally, ED-B Fn and Tn-CL are synthesised and deposited by/in newly formed blood vessels. At deep invasive OSCC edges Ln-gamma2 may be translocalised to newly formed blood vessels. The provisional ED-B Fn matrix is highly restricted in normal tissue. Fusion proteins, recombinant ED-B Fn antibody - tissue factor, are able to target mice tumours and to selectively induce thrombosis in tumour blood vessels.
Conclusions OSCC and angioneogenesis may use ED-B+Fn-Tn-CL matrix for invasion. The translocalisation of the invasion factor Ln-gamma2 to blood vessels of invasive front may contribute to angioinvasion. ED-D Fn is presented as ideal antigen for angioneogenesis-related therapy strategies.

O-047

On the application of the Ljubljana classification in the diagnosis of epithelial hyperplasic lesions of the oral mucosa. Pilot study

J Kobos[1], E Sienko[2]
[1]Department of Pathology Medical University of Lodz, Lodz, Poland
[2]Laboratory of Pathology Institute of Pediatry Medical University of Lodz, Lodz, Poland

The currently used systems of classification of the hyperplastic lesions of the oral mucosa are not strictly relevant to the picture and clinical data. In these systems a three step classification describing the lesions as 1st, 2nd and 3rd degree of epithelial changes is proposed. In our research we applied the specimens from 40 patients obtained from the Clinic of Periodontology Medical University of Lodz. Leukoplacic lesions with no or weak respond to the standard treatment were observed in most patients. Suspicion for carcinoma was another reason for biopsy. What we found microscopically was very useful for the description of the biopsed material, which was histologically classified according to the Ljubljana classification. Such terms as “simple hyperplasia”, as well as “abnormal hyperplasia” were strictly relevant to the histopathological picture and were by definition not related to malignant transformation. For some materials term “atypical hyperplasia-risky epithelium” was better accepted by clinicians than, for example, 3rd degree of dysplasia. In conclusion we found the Ljubljana classification to be a very useful tool for the diagnosis of epithelial hyperplastic lesions of oral mucosa, which is better than currently used other systems.

O-048

Gene expression profiling of squamous cell carcinomas of the head and neck - Fak-1 a potential predictive marker for loco-regional metastasis

A Weber[1], C Wittekind[2], A Tannapfel[2]
[1]Department of Oto-Rhino-Laryngology, Head And Neck Surgery, University Of Leipzig, Leipzig, Germany
[2]Institute of Pathology University of Leipzig, Leipzig, Germany

Introduction Despite numerous studies about possible molecular mechanisms leading to squamous cell carcinoma of the head and neck (HNSCC), specific markers indicating tumour stage or prognosis have not been elucidated yet. The new technology of microarray analysis allows the simultaneous examination of a broad spectrum of genes to assess a carcinoma-specific gene profile with the aim to reveal possible prognostic markers.
Methods We examined fresh frozen material of 25 patients with squamous cell carcinoma of the oropharynx (15 patients) and lar-

ynx (10 patients). A selective tumour cell sampling was achieved by laser capture microdissection. The expression profiles obtained by the cDNA PiquorTM Arrays (Immuno-Onco, Biozym) were compared with the pooled array data of normal mucosa taken at the resection margins. Controls were performed by immunohistochemical analyses, in-situ hybridisation on tissue microarrays and Western blot.

Results The analysis revealed 52 differentially expressed genes, 37 up- and 15 downregulated. As in previous studies, factors of proliferation, growth, apoptosis and differentiation were differentially expressed. Not reported yet is the differential regulation of several members of the caspases as well as the SOCS family. Upregulation of FAK-1 (focal adhesion kinase) was significantly correlated with the presence of lymph node metastasis.

Conclusion FAK-1 was elucidated as a potential predictive marker for lymph node metastases in HNSCC. Furthermore, the deregulation of signalling pathways controlled by SOCS and caspases, to date not associated with HNSCC, have been identified.

O-049

Correlation between cytogenetical and histopathological findings in 61 pleomorphic adenomas of the parotid gland

MA Chrestian[1], J Paris[2], M Zanaret[2]
[1]Pathology department, Pr Pellisssier, CHU La Timone, Marseille, France
[2]Head and Neck Surgery department, CHU La Timone, Marseille, France

Introduction Pleomorphic adenoma is the most common tumour of the parotid gland. Histomorphologic features and peculiarly tumour capsule play a major role in recurrences of parotid pleomorphic adenomas. Cytogenetically, pleomorphic adenomas are characterized by recurrent chromosome rearrangements. The aim of this study was to correlate cytogenetics and histopathology features in pleomorphic adenomas in order to define cytogenetical characteristics of tumours with high risk of recurrence.

Material and methods Histological and cytogenetical studies were performed in 61 patients with pleomorphic adenomas of the parotid gland treated in our institution during the period may 1992 – November 2002. Structural and numerical chromosomal abnormalities were: rearrangement of chromosome 12 (breakpoint at 12q13-15), rearrangement of chromosome 8 (breakpoint at 8q12), translocation between chromosome 3 and 8: t(3;8)(q21;q12), hyperdiploidy.

Results The studied population was distributed into 3 histological subtypes according to Seifert classification. Hypocellular (stroma rich) pleomorphic adenoma was reported in 61%, hypercellular pleomorphic adenoma was reported in 26% and "classic" in 13%. Thirty patients (49%) had normal karyotype while 31 (51%) had clonal chromosomal abnormalities. Chromosome 12 rearrangement tumours and hyperdiploid ones tend to be hypocellular. Tumours showing chromosome 8 abnormality tend to be hypercellular.

Conclusions As recurrences most likely appear in hypocellular tumours, patients with hyperdiploidy and chromosome 12 abnormalities could have a greater risk of recurrence because of their histomorphological characteristics. Because of the lack of patients, not sufficient statistical significance was demonstrated.

O-050

Histomorphological study of pleomorphic adenoma: Preliminary study for long term follow-up of recurrence

MA Chrestian[1], J Paris[2], M Zanaret[2]
[1]Pathology department, Pr Pellissier, CHU La Timone, Marseille, France
[2]Head and Neck surgery department, CHU La Timone, Marseille, France

Introduction Pleomorphic adenoma is the most common tumour of the parotid gland. The main issue of pleomorphic adenoma surgery is postoperative recurrence. Histomorphologic features and peculiarly tumour capsule play a major role in recurrences of parotid pleomorphic adenomas. The aim of this retrospective study was to define histomorphological characteristics of pleomorphic adenoma for better understanding of recurrence processes. This work corresponds to the preliminary prospective study of a long term follow-up for detection of recurrence.

Material and methods Histological study was performed after reviewing of slides originating from 100 patients with pleomorphic adenomas of the parotid gland. These randomly selected patients underwent parotid surgery in our institution during the period may 1992 – November 2002.

Results The studied population was distributed into 3 histological subtypes according to Seifert classification for better analysis. Hypocellular (stroma rich) pleomorphic adenoma was reported in 56%, hypercellular pleomorphic adenoma was reported in 29% and "classic" in 15%. Thinness of capsule was significantly related to hypocellularity. Pseudopodias and satellite nodules were reported in 72% of this series.

Conclusions Due to capsular characteristics, surgical exerecise should avoid dissection in the vicinity of the tumour to minimize the risk of surgical induced recurrence. According to these findings, enucleation surgery on a pleomorphic adenoma should not be performed anymore. These tumours should now be followed up in order to detect and define risk factors of recurrence.

O-051

Trend of nasopharyngeal cancer at the Ibadan Cancer Registry (1981-2000)

O Ogunbiyi[1], G Nwaorgu[2]
[1]University College Hospital, Department of Pathology, Ibadan, Nigeria
[2]University College Hospital, department of Otorhinolaryngology, Ibadan, Nigeria

Introduction Only two comprehnsive reports on nasopharyngeal carcinoma (NPC) are available from this large centre covering the periods from 1961 to1966, and from 1966 to 1980.

Objective This study describes the trend and pattern of nasopharyngeal cancer at the Ibadan Cancer Registry and shows that there have been some significant changes.

Method This is a retrospective review of all histologically confirmed cases of nasopharyngeal cancer accumulated in the Ibadan Cancer Registry from 1981-2000.

Results 223 cases were recorded; 156(70%) males and 67(30%) females with a male: female ratio of 2.3:1. It constitutes 2% of all cancers, 1% of female and 3.5% of male cancers. There is a steady

increase in the incidence of NPC over the last here decades. Overall, the mean age was 41.1 years (age range 10 to 81 years). The females had a mean age of 36.1years (age range 11-80 years) while the mean age for the males was 43.2 years (range 10-81 years). The peak age group of incidence for the females was 20-29 while in the males it was the 50-59 age group with an almost an equal incidence in the preceding three decades. The ratio of Regaud to Schmincke type cancer reversed with increasing age amongst the females with the Schmincke type being more common in the first decade but this was not reproduced in the males.

Conclusions There is a steady rise in the incidence of nasopharyngeal cancer over the last three decades. The two main histological types showed differential variation between the sexes suggesting a biological effect in manifestation of this disease. There is a need for health education and increased physician awareness at all levels of health care to stem this trend and especially to detect a role of Epstein Barr virus infection in aetiopathogenesis of the nasopharyngeal cancer.

O-052

Lactate dehydrogenase (LDH) in peripheral blood lymphocytes (PBL) of patients with solid head and neck tumours

B Jakovljevic[1], V Jurisic[2], J Bubalo[1], S Matkovic[1], N Baletic
[1]Military Medical Academy, ENT Department, Belgrade, Serbia and Montenegro
[2]Medical faculty Kragujevac, Institute for Pathophysiology, Kragujevac, Serbia and Montenegro

Lactate dehydrogenase(LDH)is intracellular enzyme, which take part in process of anaerobic glycolyse. It is located in all cells, but in higher amount in the stromal cells. LDH activity increased in the malignant cells, as well as in the peripheral blood lymphocytes (PBL) of patients suffered from head and neck tumours. The authors present results of their investigations in activity of intracellular LDH in PBL, spontaneous LDH releasing from PBL and correlation between spontaneous releasing of LDH and increasing of intracellular level of LDH in patients with solid head and neck tumours. Spontaneous releasing of LDH in all the patients with solid head and neck tumours were 2 to 4 times higher then in the health controlling group. There are correlation between clinical stage of the tumours and spontaneous releasing of LDH. The authors concluded that measuring of level of spontaneous released LDH from PBL, can prove the presence of head and neck tumours in the very early stage.

O-053

Protein expression profiles of cell cycle and apoptosis factors in head and neck cancer using tissue microarrays

SM Rodríguez-Pinilla[1], JL Rodríguez-Peralto[1], C Ballestín[1], F Sancho Poch[2], F Fernandez[3], F Alameda[4], M Niveiro[5], M Mayorga[3], R Hitt[1], M Sánchez-Céspedes[6]
[1]12 De Octubre, Madrid, Spain
[2]Hospital Sant Pau, Barcerlona, Spain
[3]Hospital de Valdecilla, Santander, Spain
[4]Hospital del Mar, Barcelona, Spain
[5]Hospital de Alicante, Spain
[6]Spanish National Cancer Center (CNIO), Spain

Introduction Squamous cell carcinoma (SCC) constitutes more than 90% of the malignancies from the head and neck. Thereafter, the survival of patients in stage III-IV is between 33%-11% at 5 years. As most stromal types, head and neck squamous cell carcinomas (HNSCC) harbour deregulation in the expression levels of many proteins that participate in critical biological pathways leading to cancer development. The aim of the study was to evaluate the correlation between several molecules implicated in cell cycle and apoptosis in an attempt to define their importance as prognostic indicators in HNSCC.

Material and methods 110 HNSCC specimens from stage III-IV patients were collected prior to chemotherapy. We constructed a tissue-microarray with paraffin-embedded tumours to analyse, by inmunohistochemistry, the expression levels of 18 proteins implicated in cell cycle arrest and apoptosis (P53, cyclin-D1, cyclin-A, RB, HDM2, topoisomerase, chk2, cdc2, Survivin, BCL-2, CDK-2, CDK-6, cyclin D3, cyclin E, cyclin B1, P21, P27 and P16).

Results Alterations in the expression levels of proteins that participate in the G1/S checkpoint were frequent. RB and P16 proteins were absent in 15% and 15% of the tumours, respectively, whereas high expression of cyclin D1, CDK-4 and CDK-2 was observed in 42%, 8% and 13% of the cases, respectively. On the other hand, des-regulation of markers implicated in the apoptosis were also evident as shown by over-expression of BCL-2 protein in 23% of the tumours. This last observation seems to be related to bad prognosis.

Conclusions Definitive conclusions from our results concerning expression levels of each marker isolately, according to tumour location and in relation to survival are still being evaluated.

O-054

p53 and MIB1 expression in basaloid squamous cell carcinoma of the larynx inversely correlates with p27 expression

D Di Vizio[1], L Insabato[1], G Salerno[2], E Mezza[1], S Staibano[1], G Mansueto[1], G Mottola[2], M Nardone[2], V Galli[2], G De Rosa[1]
[1]Dpt of Anatomic Pathology, Faculty of Medicine, Federico II University of Naples, Naples, Italy
[2]Dpt of Otolaryngology, Faculty of Medicine, Federico II University of Naples, Naples, Italy

Introduction Cell cycle regulators play a crucial role in cancer and their functional alteration may play an important role in the clinical progression of basaloid squamous cell carcinoma (BSCC) of the larynx. BSCC is a biologically aggressive tumour with high proliferative activity and a propensity to destructive local growth and early regional and distant metastases.

Methods Herein we report nine cases of BSCC of the larynx, selected from January 1987 to January 1999 by a review of all laryngo-hypopharyngeal cancers collected from our files. Clinical follow-up was obtained for all patients. The potential prognostic value of DNA ploidy status and immunohistochemical expression of Ki-67, p53, and p27 kip1 were analysed.

Results Histologically, all tumours were composed of squamous cell carcinoma with an intimately associated basaloid component, showing an irregular lobular pattern of growth. p53 expression was demonstrated in 8 cases, while Ki-67 (MIB-1) resulted positive in 7 of them. The positivity range scored from moderate (++ = <60%) to intense (+++ = >60%). p27 was expressed in 5 cases, two of them showing a moderate staining (++ = >60%), the others showing a weak staining (+ = <30%). It was either absent or weakly expressed in 7 cases, 5 of which with both p53 and Ki67 overexpression accompanied by a very poor outcome. Of the three alive

patients, two showed an inverse correlation between p53 and Ki-67 expression and p27 expression.
Conclusion An inverse correlation between p27 and Ki-67 and p27 and p53 was demonstrated in 7 cases. Image analysis of DNAc showed aneuploidy in all cases. The present study shows that over-expression of p53, and Ki-67, together with a down-regulation of p27 kip1 correlates with biological aggressiveness and consequent shortened survival in BSCC of the larynx. The DNA status doesn't correlate with any of the analysed parameters since all tumours in our series displayed an aneuploid pattern.

O-055

Human telomerase catalytic subunit (hTERT) gene re-expression is an early event in oral carcinogenesis

B Luzar[1], M Poljak[2], I Marin[2], N Gale[1]
[1]Institute of Pathology, Medical Faculty University of Ljubljana, Korytkova 2, 1000 Ljubljana, Slovenia
[2]Institute of Microbiology and Immunology, Medical Faculty, University of Ljubljana, Korytkova 2, 1000 Ljubljana, Slovenia

Introduction The exact role and timing of telomerase re-activation, a key enzyme implicated in cellular immortalisation and transformation in the multistep process of oral carcinogenesis is still unknown. The aims of the study were to determine whether a.) quantitative differences exist in the levels of telomerase catalytic subunit (hTERT) mRNA expression among different grades of oral epithelial abnormalities classified according to the Ljubljana classification; b.) telomerase re-activation is an important, most probably early event in oral carcinogenesis; and c.) to analyse whether the relative quantity of hTERT mRNA can be used as a molecular biomarker in the early detection of precancerous lesions.
Material and methods The relative quantity of hTERT mRNA was analysed in 45 frozen oral epithelia representing different morphological stages of oral carcinogenesis and in 37 oral squamous cell carcinomas (OC) by using a commercially available LightCycler Telo TAGGG hTERT Quantification kit (Roche Diagnostics, Branchburg, NY).
Results hTERT mRNA was not detected in normal and reactive hyperplastic oral epithelia, but was present in 43% of atypical hyperplasias (precancerous lesion), 60% of intraepithelial carcinomas and 68% of OCs. Statistical analysis revealed two groups of oral epithelial changes with significant differences in the levels of hTERT mRNA expression: 1. normal and reactive hyperplastic oral epithelium (simple and abnormal hyperplasia), and 2. atypical hyperplasia, intraepithelial and OCs.
Conclusions Telomerase re-activation is an early event in oral carcinogenesis, detectable already at the stage of precancerous oral epithelial changes. We believe that measurement of hTERT mRNA in oral tissue specimens may increase the sensitivity of standard microscopical analysis in early detection of those epithelial abnormalities associated with increased risk of progression towards OC.

O-056

Survivin is a negative prognostic marker in laryngeal squamous cell carcinoma and is associated with p53 accumulation

J Pižem[1], A Cör[2], N Gale[1]
[1]Institute of Pathology and [2]Institute for Histology and Embryology, Faculty of Medicine, Ljubljana, Slovenia

Introduction Survivin, a novel inhibitor of apoptosis, is expressed in cancer cells but not in normal tissues. The cancer-specific expression of survivin, coupled with its importance in inhibiting cell death and regulating cell division, makes it a useful diagnostic marker of cancer. Since both over-expression of survivin and loss of wild-type p53 are associated with cancer development, we investigated a possible connection between these two events in laryngeal squamous cell carcinoma (LSCC). The aim of our study was also to evaluate the prognostic value of survivin expression and its relation to apoptotic activity.
Methods The expression of survivin, p53 and apoptotic index were evaluated by immunohistochemistry on biopsy specimens of 68 patients with LSCC. An antibody against cleaved caspase 3 was used to detect apoptotic cells.
Results Overall, 98.5% of LSCC were positive for survivin. The proportion of survivin positive tumour cells varied from 8.2% to 100%, its localisation was nuclear and/or cytoplasmatic. The number of survivin positive cells was significantly higher in the p53 positive group. A positive correlation between survivin expression and the apoptotic index was found. In multivariate analysis, high level of survivin expression was an independent adverse prognostic factor in LSCC.
Conclusions Survivin is expressed in a varying proportion of tumour cells in virtually all cases of LSCC. A high level of its expression predicts poor survival. Loos of wild-type p53 could be responsible for survivin upregulation. The importance of survivin in inhibiting apoptosis remains unclear, as its expression is related to a higher apoptotic activity. Understanding the role of survivin in LSCC development and progression could give rise to improved therapeutic strategies.

O-057

Morphology, p53, Bcl2 and Bax spectrum of 125 surgically removed parathyroid lesions

B Szende[1], P Farid[1], L Kopper[1], G Végso[2], F Perner[2]
[1]Department of Pathology and Experimental Cancer Research and Research Group of Molecular Pathology, Hungarian Academy of Sciences and Semmelweis University, Budapest, Hungary
[2]Department of Transplantation and Surgery, Semmelweis University, Budapest, Hungary

Altogether 125 patients were operated on at the Department of Transplantation and Surgery of the Semmelweis University in the past four years, because of clinical symptoms of hyperparathyroidism. Chronically impaired renal function was found in 60 cases. The removed parathyroid glands showed histologically hyperplasia in 62, adenoma in 60 and carcinoma in 3 cases. The oxyphil/chief cell ratio and occasional mitotic and apoptotic figures were determined. The oxyphil component predominated both the hyperplastic and tumorous lesions. Apoptosis and mitosis were rarely seen in hyperplasias (0-2%) more frequently in adenomas (2-5%) whereas in carcinomas 3-5% of the tumor cells showed signs of mitosis and 3-5% were apoptotic. Immunohistochemical detection of p53, bcl2 and bax revealed diversity between the various lesions. Cytoplasmic p53 positivity could be observed in the majority of adenomas and in some of the oxyphil cells of the hyperplasias. The carcinomas and about one sixth of the adenomas showed nuclear p53 positivity. Bcl2 was detected in the cytoplasm of the tumor cells of adenomas and in lower extent in the oxyphil cells of hyperplasias. Co-localistion of bcl2 and bax was found randomly in all types of lesions. No significant differences in the p53, bcl2 and bax

spectrum were found regarding the primary and secondary (i.e. renal failure) parathyroid alterations. The very low incidence of carcinomas, the low mitotic and apoptotic ratio in adenomas and hyperplasias point to the potent antiproliferative defense mechanism in the parathyroid cell-population. This may be also reflected in the cytoplasmic co-localisation of various gene products which regulate cell death and cell proliferation.

O-058

Factors influencing the presence of sentinel lymph node metastasis in patients with breast carcinoma

Z Gatalica[1], S Sanati[2], S Soundararajan[1]
[1]Creighton University Medical Center, Omaha, USA
[2]The University of Texas Medical Branch at Galveston, USA

Introduction Primary tumor phenotypic characteristics influencing development of the SLN metastasis are not known. Loss of SYK tyrosine kinase expression and over-expression of CXCR4 chemokine receptor were recently described as important characteristics in establishment of mammary carcinoma metastasis in the lymph nodes in experimental models.
Material and methods 173 mastectomies with sentinel lymph node dissections from 172 female patients were included in the study. Radiolabeled sulfur colloid technique with or without blue dye was used to identify the SLN(s). Entirely submitted SLNs were formalin fixed, and stained with H&E for evaluation. Expression of SYK and CXCR4 was evaluated with standard immunohistochemical (IHC) procedures.
Results 45 patients had positive SLN as examined with H&E alone (26%). Cytokeratin IHC identified two more cases, yielding an overall total of 47 positive patient (27.2%). Both of these cases were invasive lobular carcinomas. 100 SLN biopsies were followed by completion axillary dissection. Predictive value of negative test was 0.98. No in-situ or pT1a carcinomas were associated with SLN metastasis. pT1b was associated with 17% SLN positivity, pT1c with 20%, pT2 with 53% and pT3 with 67% SLN positivity. No difference in SYK expression between SLN positive and negative cases was observed (1.9±0.8 vs. 2.0±0.72), and no difference in CXCR4 expression between these two groups was observed (1.13±0.68 vs. 1.18±0.56)
Conclusions False negative SLN was rare (2%), while overall predictive value was high, which supports the value of this treatment in low stage breast carcinomas. The frequency of SLN positivity is directly proportional to the size of the primary tumor. No evidence to support the role of SYK and CXCR4 expression in establishment of lymph node metastasis was found in this group of patients.

O-059

Prognostic importance of occult metastases in early breast cancer

B Susnik[1], S Frkovic-Grazio[2], M Bracko[2]
[1]Medical College of Wisconsin, Milwaukee, USA
[2]Oncology Institute, Ljubljana, Slovenia

Introduction At present the significance of occult axillary lymph node metastasis (OM) in early breast cancer patients is not known. The aim of the study was to evaluate the prognostic role of OM in stage I breast cancer.
Materials and methods We studied 96 patients with T1 breast carcinoma who underwent axillary dissection and originally had negative lymph nodes by routine microscopic examination. 48 patients who developed distant metastases within 15 years after surgery (M group) were compared to 48 age-matched patients who were disease free for 15 years (NM group). We examined 1539 lymph nodes by three deeper H&E levels and one section stained with immunohistochemistry for keratin.
Results We detected OM in 21/96 patients. All 21 had micro-metastases (<2.0 mm). OM was identified in 16 patients (34%) in the M group and in 5 (11%) in the NM group (P=0.007). Micrometastases larger than 0.2 mm were 10x more common in the M group (10/48 vs. 1/48, P=0.004). Tumors in the M group were significantly more often of higher grade, had a higher mitotic index (MI) and showed lymphovascular invasion. The two groups did not differ in size, histologic type, estrogen receptor status or type of treatment. In multiple logistic regression, only high MI and presence of micrometastases larger than 0.2 mm showed an independent significant correlation with the occurrence of distant metastases.
Conclusion Axillary micrometastases are associated with occurrence of distant metastases and are important prognostic factor in T1 breast cancer patients. This was not significant for OM smaller than 0.2 mm.

O-060

Immunohistochemical study of the pathological response of neoadjuvant chemotherapy and radiotherapy in invasive breast carcinoma

LG Cozma[1], F Zugun[2], C Diaconu[2], E Bild[2], G Dobrescu[2], E Carasevici[2]
[1]Institute of Public Health, Iasi, Romania
[2]Gr. T. Popa " University of Medicine and Pharmacy, Iasi, Romania

Introduction Current therapeutic protocols stratify patients to regimens of chemotherapy or associated chemo- and radiotherapy in locally advanced breast cancer. The aims of this study were to compare immunohistochemical breast evaluation after neoadjuvant chemotherapy and / or radiotherapy and to analyse post systemic and regional irradiation therapy prognostic markers, usefull for further treatment procedures.
Materials and methods 120 locally advanced breast cancer patients with preoperative chemotherapy, or combined chemo- and radiotherapy were semiquantitatively immunohistochemically assessed for the expression of ER, PR, pS2, c-erbB2 (DAKO – HercepTest), PCNA and CD34 (DAKO, LSAB2).
Discussion and conclusions Systemic therapy altered tumor cells retain immunohistochemical reactivity; ER, PR positive cases correlate with important decrease in tumor cellularity, difficulties in grading assessment, reduced rate of proliferation (20-25%). Single chemotherapy in negative ER, PR tumours correlates better with c-erbB2 expression ($p<0.02$). Complete histopathologic response for 12% cases (no residual tumor cells) was found after chemo and radiotherapy. The patients who express besides G3 tumor grading, an immunohistochemical pattern of negative ER, PR, 40-65% proliferating rate, could be included in a chemo and radiotherapy non responding group.

O-061

Reliability of HER-2/neu immunohistochemistry in Austria

A Reiner[1], P Regitnig[2], HP Dinges[3], G Höfler[2], S Lax[2], E Müller-Holzner[4], P Obrist[4], M Rudas[5]
[1]Pathology Department, Donauspital Vienna, Vienna, Austria
[2]Pathology Department, University Graz, Graz, Austria
[3]Pathology Department, Klagenfurt, Austria
[4]Pathology Department, University Innsbruck, Innsbruck, Austria
[5]Pathology Department, University Vienna, Vienna, Austria

Introduction Practice and accuracy of immunohistochemistry in different laboratories is known to vary highly. Since the introduction of targeted therapy in breast cancer patients reliability of immunohistochemistry has become crucial. The aim of the study was to assess reliability of HER-2/neu immunohistochemistry in Austrian pathology laboratories and to provide data for benchmarking with respect to quality improvement.
Material and methods The trial consisted of six cases of invasive ductal breast carcinoma. Presence / absence of gene amplification was determined by FISH to be used as a gold standard. Laboratories were asked to stain and assess slides using their routine immunohisto-chemical staining protocol. Participation was voluntary.
Results Participation rate was 75% of all pathology departments in public hospitals. Overall sensitivity and specificity was 96 %. Positive and negative predictive value were 92% and 98%, respectively. False positive and false negative results occurred in either 4%. Analysis of the laboratory method revealed that all false negative cases (9%) were due to staining methods other than Hercep-Test. False positive results occurred in 3,8 % using Hercep-Test and 4,5% using other staining protocols. Thus sensitivity was lower in staining protocols other than Hercep-Test (90% versus 100%). Specificity was 96% for Hercep-Test and 95% for other protocols.
Conclusion Participation rate was high.
Results were highly reliable when using Hercep-Test. Using other staining protocols the main problem were false negative immunohistochemical results, neglecting a possible therapy option for these patients.

O-062

Immunohistochemically defined myoepithelial cells in the diagnosis of benign and malignant papillary breast lesions

M Jovicic Milentijevic, V Zivkovic, R Ilic, L Kesic
Institute of Pathology, Medical School of Nis, Nis, Serbia and Montenegro

Introduction The presence or absence of myoepithelial (ME) cells has been considered as an important feature in the differential diagnosis of papillary breast lesions. The aim of this study was to evaluate the usefulness of monoclonal antibodies: alpha-actin (smooth muscle actin) and S-100 protein, which are known as good markers of ME cells in breast tissue.
Material and methods The distribution of ME cells in formalin-fixed paraffin-embedded tissue sections of 15 intraductal papillomas and 10 papillary carcinomas were immunohistochemicaly stained by ABC method.
Results Alpha-actin reacted strongly and consistently with the ME cells in all papillomas. In papillary carcinomas there were no alpha-actin reactive ME cells. Rare isolated ME cells were present in two cases, but they were inconspicuous and these reactions were also considered negative. The ME cells failed to express S-100 protein in four papillomas, while majority were weak positive. All the papillary carcinomas were S-100 protein negative.
Conclusions Consistency and uniformity of ME cells reaction is important because benign and malignant papillary lesions often coexist in the same tissue section. Although vascular smooth muscle in the papillary fronds and stromal myofibroblasts may mimic ME cells, the number of alpha-actin immunoreactive cells is much smaller and their distribution more irregular. S-100 protein has broad spectrum reactivity and it is of little value in the differential diagnosis of papillary breast lesions. Alpha-actin is more specific marker than S-100 protein for recognition of ME cells in breast tissue.

O-063

Prognostic significance of regional TIMP-2 mRNA expression in invasive breast carcinomas

A Kapranou[1], L Nakopoulou[1], E Panayotopoulou[1], I Giannopoulou[1], H Gakiopoulou[1], N Givalos[1], M Perdiki[1], S Markaki[2], A Keramopoulos[3]
[1]Department of Pathology, Medical School, The National and Kapodistrian University of Athens, Athens, Greece
[2]Department of Pathology, 'Alexandra' Hospital, Athens, Greece
[3]Department of Gynaecology and Obstetrics, Medical School, The National and Kapodistrian University of Athens, Athens, Greece

Introduction Despite wide agreement about TIMP-2 involvement in the progression of malignancy, there is uncertainty as to its precise role in the biology of cancer development. Aims: In order to elucidate the clinical significance of TIMP-2 in invasive breast cancer, TIMP-2 mRNA expression was investigated in 118 tissue samples in relation with clinicopathological parameters, overall and disease-free patients' survival, as well as c-erbB-2 and MMP-11 protein expression.
Materials and methods TIMP-2 mRNA transcripts were detected using non-radioisotopic mRNA in situ hybridization with a digoxigenin-labeled RNA probe. Immunohistochemistry (ABC-HRP) was performed for the detection of c-erbB-2 and MMP-11 proteins. Statistical analysis was univariate and multivariate.
Results TIMP-2 mRNA was detected in fibroblasts located within the tumor area in 57.6% of cases and at the tumor margin in 43% of cases. Intratumoral TIMP-2 mRNA expression demonstrated no significant correlations with the co-estimated parameters. On the other hand, TIMP-2 mRNA expression at the marginal portion associated significantly with the presence of lymph node metastases ($p=0.036$), c-erbB-2 overexpression ($p=0.022$) and MMP-11 (ST3) protein expression ($p=0.012$). In univariate analysis, TIMP-2 mRNA expression at the tumor margin, associated significantly with decreased recurrence-free survival ($p=0.019$). In multivariate analysis, TIMP-2 mRNA localization at the tumor margin, demonstrated a significant independent correlation with shortened overall patients' survival ($p=0.016$).
Conclusion TIMP-2 mRNA detection at the marginal portion of invasive breast carcinomas associates with lymph node metastases, c-erbB-2 overexpression and MMP-11 protein expression. Moreover, TIMP-2 mRNA detection at the marginal portion of tumors is associated with poor patients' outcome and may be a useful prognostic factor in invasive breast cancer.

O-064

Population screening for immunohistochemically evaluated HER2 status of breast carcinomas in Poland

W Olszewski, W Olszewski, A Mrozkowiak
Department of Pathology, Institute of Oncology, Warsaw, Poland

Introduction Aim of the study was so-called population screening for HER2 status of breast carcinomas in Poland and standardization of the immunohistochemical technique and reporting results**.**
Material and methods Study was done in 16 medical centers in Poland and during the period of 10 months 5088 breast cancers were diagnosed and evaluated. Histologic type and grade as well as the menopausal status were recorded. Number of patients evaluated in particular centers ranges from 85 to 1025. Immunohistochemical status of HER2 receptor was evaluated using Herceptest (DAKO) which is standardized kit for immunohistochemiacal evaluation. Four-tier classification proposed by Dako (0, +1,+2,+3) were used for describing strengths of the stain.
Results Among 5088 cases of breast carcinomas strongly positive results +3 was found in 1001 cases (19.7 %), +2 in 776 cases (15.3%), weakly positive in 1311 (25.8 %) and negative in 2000 cases (39.3%). There were no difference in the percentage of each group between premenopausal and postmenopausal women. Considering histopathologic type of tumor, ductal carcinoma (2993 patients) was HER2 positive in 21% (+3) and 16.7% (+2), while lobular carcinoma (541 patients) was HER2 positive in 7.6% (+3) and 13.5% (+2). Strong correlation was found between histologic grade of ductal carcinoma and HER2 expression, e.g. in G1 ductal carcinoma 3.3% were strongly positive (+3) while in G3 ductal carcinoma 28.1 % were strongly positive (+3).The striking feature in the results were differences in percentage of each group among the centers participating in the program. Percentage of HER2 +2 cases ranges from 4.1 to 27.1% and HER2+3 from 10.6 to 30.3%. Distribution of particular staining reaction were similar among the centers with largest number of cases
Conclusion Percentage HER2 positive breast cancer cases in our material corresponds with data from literature. To evaluate properly immunohistochemical stain certain experience is required.
*Representatives of 16 centers participating in the program. HER2 - population screening project was supported by Roche -Polska

O-065

Accuracy of the intraoperative sentinel lymph node examination by imprint cytology in breast cancer patients

A Pogačnik, U Klopčič, S Grazio-Frković, J Žgajnar
Institute of Oncology, Ljubljana, Slovenia

Introduction The utilization of lymphatic mapping for breast carcinoma has made intraoperative evaluation of sentinel lymph node (SLN) attractive, because axillary lymph node dissection can be performed during the initial surgery if SLN is positive. The aim of our study was to evaluate the accuracy of intraoperative SLN examination by imprint cytology (IC).
Material and methods 459 SLNs from 225 women were examined. For intraoperative cytological examination, touch imprints from bisected SLNs were prepared, air dried and stained with quick staining method (Hemacolor-Merck). SLNs were than formalin-fixed and embedded in paraffin. Histological sections were evaluated with 5 H&E stained levels and cytokeratin immunohistochemistry (CK-IHC).
Results Histological examination of the SLN revealed 84 (37,3%) cases with metastatic deposits: 41 (18.2%) macrometastases, 32 (14.2%) micrometastases and 11 (4.9%) cases with isolated tumor cells or clusters (ITC) detected by immunohistochemistry. Sensitivity and specificity of intraoperative IC was 41% and 99%, respectively. IC was significantly more sensitive for detection of macrometastasis: they were detected in 34 out of 41 cases (83%). IC generally failed to detect micrometastases or ITC: only one case of micrometatasis was cytologically suspicious for malignancy. Out of 141 histologically negative SLNs, one IC diagnosis was false positive.
Conclusions IC is a simple and quick method of intraoperative screening for the presence of SLN macrometastases in patients with breast cancer. If SLN micrometastases and ITC are used to determine the need for further lymphadenectomy, more sensitive intraoperative methods, such as rapid CK-IHC on touch preparations, will be needed to avoid second operation.

O-066

Comparison of fine-needle aspiration cytology and core biopsies of breast lesions

A Berner, E Sigstad, W Reed, B Risberg, B Davidson
Department of Pathology, The Norwegian Radium Hospital, Oslo, Norway

Introduction Fine-needle aspiration cytology (FNA) is an established, highly accurate method for diagnosing breast lesions. However, in recent years there has been increased use of core biopsy (CB) as a diagnostic alternative. This study aimed at comparing the value of FNA and CB in palpable and non palpable breast lesions.
Materials and methods The material consisted of 4367 FNA samples performed in our institution between 1999 and 2001. Correspoding histology results from 1275 lesions including 463 CB were available for comparison. Quality assessment parameters were calculated using metodology detailed in the National Health Service Breast Screening Programme guidelines.
Results High specificity (100%) and sensitivity (92%) and low inadequacy rates were found for CB. FNA showed high sensitivity (87%). Low specificity (49%) for FNA due to inclusion of many cell-poor lesions was particularly seen in the submitted material sampled by physicians lacking experience with FNA procedures.
Conclusion CB may be an alternative method for preoperative diagnosis when experienced cytopathologists are not available. CB is superior to FNA in fibrotic and collagenous lesions such as lobular carcinoma and radial scar. FNA is most accurate when immediate assessment by cytopathologist is performed for evaluation of material adequacy so that additional aspirations can be performed if necessary.

O-067

Atypical ductal hyperplasia (ADH): practical relevance in diagnostics and therapy

T Decker[1], M Ruhnke[1], U Kettritz[2], E Keil[3], G Morack[3]
[1]Dpt. of Pathology, The Breast Unit, HELIOS Medical Center Berlin, Berlin, Germany
[2]Dpt. for Diagnostic Radiology, The Breast Unit, HELIOS Medical Center Berlin, Berlin, Germany
[3]Dpt. of Gynaecology, The Breast Unit, HELIOS Medical Center Berlin, Berlin, Germany

Introduction In contrast to ductal hyperplasias, ADH belongs to intraductal neoplasias. ADH can be distinguished from non-high grade DCIS (among other criteria) by its size. Therefore, a question that is asked quite frequently is whether such small findings can be removed with sufficient security by minimal invasive biopsy (MIB). We prospectively investigated: 1. relative frequency of ADH without associated intraductal or invasive carcinoma 2. relevance of such small findings in MIB specimens.
Materials and methods Between 1998 and 2002, 2825 breast-lesions could be clarified by means of MIB in the interdisciplinary team. Excisions were carried out in all invasive carcinomas and all DCIS as well as in all cases with minimal parts of intraductal non-high grade neoplasias (with the differential diagnosis ADH vs. DCIS). Additional ADHs were diagnosed in excision specimens as incidental findings associated with other targets (except for DCIS and invasive carcinomas). The MIB- and operation specimens have been examined prospectively by two team pathologists according to the criteria of Page and Tavassoli.
Results We diagnosed altogether 25 ADHs and 138 DCIS. The proportion of ADH in all operated intraductal neoplasias (ADH+DCIS) was 1.56% (25/163). Findings with the differential diagnosis of ADH vs. DCIS could be found in 25 cases of 2825 MIBs (0,88%).The following excision specimens showed in 16 of 25 cases (64%) non-high grade DCIS and in 9 of 25 cases ADH (36%). The other 16 ADH were coincidental findings in excision specimen of benign lesions.
Conclusions ADH is a very rare finding. In ADH-like findings in MIB specimens even specialised breast-pathologists cannot exclude a non-high grade DCIS with sufficient security when applying strictly the most common morphological definitions. The high rate of 64% of DCIS in the specimen of the following operation highlights the indication for clarifying by excision (according to the European Guidelines for Quality Assurance in Mammography Screening).

O-068

Multifocal stromal invasion in microinvasive squamous cell carcinoma of the cervix - how to measure and stage these lesions

O Reich, H Pickel
Dpt. Obstet/Gynecol, University of Graz, Graz, Austria

Objectives About 12% of microinvasive squamous cell carcinomas of the cervix have more than one invasive focus at time they first break through into the cervical stroma. It is unclear how the lateral extent of lesions with multiple invasive foci should be measured to distinguish FIGO stage 1A1 and 1A2 carcinomas from clinically occult stage IB disease.
Methods and results We believe that three presentations of multiple invasive foci should be distinguished. Type I shows plump and coherent infiltration of the cervical stroma at different sites in one ore more step-serial sections. They originate from the squamous epithelium outside the transformation zone or from metaplastic cervical gland epithelium. All foci are contiguous with the epithelium. In this case, the largest lateral spread of each individual invasive focus should be measured. These measurements are added up to determine the total of horizontal spread. The normal tissue separating the different early invasive foci is not measured. In type II the origin of invasion cannot be seen in all early invasive foci but the greatest lateral extension can be seen in one of the step-serial sections. Lateral extension is defined as the maximum distance from one most lateral point of the border between the invasion and the adjacent tissue to the other. The lateral extension of type II includes the normal tissue separating the early invasive foci. Type III shows the same pattern as type II, but the maximum horizontal spread cannot be measured in a single step-serial section. In such lesions the width needs to be measured across all the step-serial sections involved and the second dimension must be calculated by knowing the distances between the sections.
Conclusions These growth pattern of stromal invasion should be considered when measuring the width of early invasive squamous cell carcinomas with multiple invasive foci. Lesions with multiple invasive foci taken together measuring more than 7 mm in lateral extension should be classified as stage IB.

O-069

Expression of cyclooxygenase-2 (COX-2) in gynecologic tumors

C Denkert[1], BM Müller[1], A Fürstenberg[1], S Pest[2], KJ Winzer[3], W Weichert[1], G Kristiansen[1], H Guski[1], M Dietel[1], S Hauptmann[1]
[1]Institute of Pathology, Charité Hospital, Berlin, Germany
[2]Department of Public Health, TU Berlin, Germany
[3]Department of Surgery, Charité Hospital, Berlin, Germany

Introduction Cyclooxygenases regulate the production of prostaglandins and play a role in tumor development and progression. The aim of this study was to investigate the prognostic impact of expression of the cyclooxygenase isoforms, COX-1 and COX-2 in 221 primary breast carcinomas as well as in 86 primary ovarian carcinomas.
Materials and methods COX isoform expression was determined by immunohistochemistry.
Results Expression of COX-2 was detected in 42% of 86 ovarian carcinomas and was associated with reduced overall survival in univariate analysis ($p=0.04$) as well as multivariate analysis (0.004). There was no correlation with other tumor parameters such as grade, stage or type. In contrast, COX-1 was no prognostic parameter in ovarian carcinoma. Expression of COX-2 was detected in 36% of breast carcinomas and was significantly associated with several clinicopathological parameters, such as positive nodal status ($p<0.0005$), larger tumor size ($p<0.0005$), poor differentiation ($p<0.0005$), vascular invasion ($p=0.003$) and negative estrogen receptor status ($p=0.04$). In univariate survival analysis a significant association between elevated COX-2 expression and decreased disease-free survival ($p=0.0007$) as well as decreased overall survival ($p=0.02$) was observed. In multivariate analysis expression of COX-2 was of borderline significance for disease-free survival (RR(95%CI) 1.90 (1.00-3.59)).
Conclusions Our data suggest that increased expression of COX-2 may play a role in progression of primary breast carcinomas as well as ovarian carcinoma. It remains to be investigated if treatment with selective inhibitors of COX-2 may be an additional therapeutic option for patients with gynecological tumors.

O-070

Simple endometrial hyperplasia: Bcl-2, HLDF expression and clinical behavior

II Babichenko[1], ON Lysenko[2], SM Dranitsyna[3], IA Kostanyan[3]
[1]Peoples' Friendship University of Russia, Moscow, Russian Federation
[2]Medical State University of Russia, Moscow, Russian Federation
[3]M.M.Shemyakin and U.A.Ovchinnikovs' Institute of Bioorganic Chemistry, Moscow, Russian Federation

The endometrial hyperplastic processes is characterized by major variety of clinical outcomes. The main feature of "spontaneous endometrial hyperplasia" is complete normalization after total curettage (Lindahl B., Willen R. 1994); there is also proof of recurring hyperplasia. The purpose of present research was to carry out clinical and morphological correlations between various types of endometrial hyperplasia and expression of pro- (HLDF) and antiapoptotic (BCL-2) proteins. Human leukemia cell differentiation factor (HLDF) with molecular mass 8.2 kd, having DNA/RNA hydrolyzing activity, was originally allocated from HL-60 cell line of promyelocyte leukemia medium, processed by retinoid acid or C2–ceramid (Kostanyan I.A. et al., 1994). Previously we have shown that HLDF is a useful tool for apoptosis visualization in prostate (Babichenko I.I. et al., 2001). We performed analysis of 139 patients with histologically documented simple endometrial hyperplasia without atypia: 74 women (53 %) had spontaneous recovery after total curettage, in 42 (30 %) patients endometrium recovered after gestagen treatment and in 23 (17 %) cases persistent recurring hyperplasic process was observed during 2-5 years. Immunohistochemical research showed that in samples of recurring hyperplasia HLDF was expressed in cytoplasm of glandular epithelium, while in sections with spontaneous or after-treatment recovery, HLDF was revealed as a thin line on the surface of glandular cells. BCL-2 protein was found only in the cytoplasm of glandular cells in all investigated groups. Thus expression of the HLDF factor in cytoplasm of glandular cells in endometrium allows revealing the disturbance of apoptotic processes in cells and predicting the subsequent recurrence of simple hyperplasia.

O-071

Surface epithelial changes in endometrial adenocarcinoma

B Djordjevic, D Mihailovic, D Dimov, L Velickovic, V Zivkovic, Z Mijovic
Institute of Pathology, University Of Nis, Nis, Serbia and Montenegro

Introduction Epithelial changes on the surface of endometrial adenocarcinoma (EAC) show greater maturation and better differentiation than the underlying adenocarcinoma. These changes are relatively common and can be misdiagnosed as benign surface changes on curettings, including endometrial metaplasias (EM), papillary syncytial change (PSC), or microglandular hyperplasia (MGH). The aim of this study was to investigate surface epithelial changes in EAC.
Material and methods 122 cases with EAC (96 endometrioid, 10 serous, 4 clear cell and 12 mixed types) were studied.
Results 48 (39%) of the EAC showed surface epithelial changes: four with microglandular pattern simulating MGH; 16 with syncytial aggregates of eosinophilic cell, frequently with papillary or squamoid appearance, simulating EM or PSC; and 28 with mixed patterns. Surface epithelial change often demonstrated focal conjunction with a frankly malignant gland or a fibrovascular core and ranged from rare foci to diffuse surface involvement. Cytologic atypia was less pronounced than that of the underlying EAC and varied from mild to moderate. Mitoses were very rare. In some scanty curetting specimens, distinguishing these surface epithelial changes from benign changes was difficult, as was a diagnosis of EAC.
Conclusion In postmenopausal women with curettings showing features of EM, MGH, or PSC, caution should be exercised in making that diagnosis, particularly PSC, in the absence of evidence of benign shedding, and any associated cytologic atypicality should raise the possibility of the underlying EAC.

O-072

Pap smear cytology, visual inspection (VIA), cervicography, colposcopy and HPV testing by hybrid capture II as optional screening tools in Latin America*

K Syrjänen[1], P Naud[2], S Derchain[3], C Roteli-Martins[4], A Longatto-Filho[5], S Tatti[6], M Branca[7], M Eržen[8], A Lörincz[9], S Syrjänen[10]
[1]National Institute of Health (ISS), Rome, Italy
[2]Hospital de Clinicas de Porto Alegre, Brazil
[3]Universidade Estadual de Campinas
[4]Hospital Leonor M De Barros, Sao Paulo, Brazil
[5]Instituto Adolfo Lutz, Sao Paulo, Brazil
[6]Gynecology Hosp. de Clinicas. Buenos Aires, Argentina
[7]National Institute of Health (ISS), Rome, Italy
[8]SIZE Diagnostic Center, Ljubljana, Slovenia
[9]Digene Corporation, Maryland, USA
[10]Department of Oral Pathology, University of Turku, Finland

Objectives The performance of conventional diagnostic techniques (PAP smear cytology, screening colposcopy) is compared with 1) two optional screening tools (VIA, cervicography) and with 2) Hybrid Capture II test for Human papillomavirus (HPV), from a) conventional samples and b) using self-sampling, in women at different risk for cervical cancer in Brazil and Argentina.
Study design In this cross-sectional- and prospective cohort study, consecutive women attending the clinics during the first 12 months (expected n=12.000) are screened using the six (quality controlled) diagnostic tools, and women with biopsy-confirmed low-grade CIN are enrolled in the follow-up cohort. Data on the risk factors are collected, and cervical biopsies are analysed for biological prognostic markers using molecular detection techniques; PCR, IHC.
Results Until now, over 10.000 women have been examined by the clinics, randomised according to the 6 diagnostic arms. Significant differences are evident in the key demographics of the patients enrolled in the different clinics as are in their clinical findings and HPV detection data.
Expected outcome measures Apart from elaborating the information on the performance of the 6 diagnostic tools (necessary for designing cost-effective prevention strategies for cervical cancer in Latin America) this prospective follow-up of women in different regions permits the analysis of whether variations in cervical cancer incidence in these regions are due to a) different natural history of the precursor lesions, or b) due to different level of exposure to the known risk factors, e.g. HPV. *the LAMS Study supported by European Commission, INCO-DEV Programme: Contract # ICA4-CT-2001-10013.

O-073

Prevalence of cervical neoplastic lesions in Egypt: a national cervical cancer screening project. Final report

H Abd El All[1], A Refaat [2], K Dandash[2]
[1]Suez Canal University, Dept Pathology, Faculty Of Medicine, Ismailia, Egypt
[2]Suez Canal University, Dept Community Medicine, Faculty of Medicine, Ismailia, Egypt

Introduction Reducing morbidity and mortality is one of the main objectives of the health and population policies in Egypt. However, data from Egyptian studies provide widely varying estimates of the prevalence of pre-malignant and malignant cervical lesions. The main goal was (1) to define the prevalence of pre invasive and invasive cervical cancer among Egyptian women, and (2) to identify risk factors including HPVs and associated co-factors, as bacterial vaginosis, HSV, CMV, Chlamydia, schistosomiasis.
Methods and results The study was a community based full-scale cross sectional, household survey that included 5658 women aged between 35 and 60 years conducted between 2000 and 2002. However, 5453 women with complete data were included in the study (96%). The Bethesda classification was used for cervical cytology. Three percent of cases were unsatisfactory. Normal, metaplastic, infectious, and neoplastic lesions represented 28.9%, 0.06%, 63.3% and 7.8%, respectively. The most common type of infection was bacterial (48.98%). Neoplastic conditions, were categorized into ASCUS and AGCUS (3.1%), ASCUS (34.4%), AGCUC (15.3%), LGSL5.44% (41.0%), HSIL (5.2%) invasive squamous and invasive adenocarcinoma (0. 5% for each). Colposcopic-guided biopsy was performed on 274 cases representing 66.51% of the epithelial abnormalities. For standardization, a score of ten points including koilocytic atypia (4), binucleation (2), papillomatosis, dyskeratosis, acanthosis and basal cell hyperplasia (1 point for each), was applied to qualify a lesion as HPV-related (6points out of ten). Unsatisfactory biopsies were encountered in 13.86 %. Normal biopsies including inflammatory and metaplastic changes and atypical metaplasia represented 13.1% and 19.7%repectively. Cervical intraepithelial lesions (CIN) (53.7%), further categorized as CIN I (45.5%), CIN II (5.3%), CIN III/CIS (2.9%) were identified. Endocervical lesions represented 5.3% and were divided into endocervical glandular dysplasia (EGD) (4.9%) and adenocarcinoma in situ (AIS) (0.4%). Combined dysplasia was found in 7.8%, while invasive squamous cell carcinoma (SqCC) and lymphoma accounted for 0.4%of the biopsies. On histological basis, HPV was found in association with CIN I, CIN II, CIN III/CIS and SqCC in 93.6%, 92.3%, 85.7% and 100% respectively. Neither EGD nor AIS showed evidence of HPVs. In situ hybridization (ISH) using the broad spectrum HPV probe recognizing HPVs 6, 11, 16, 18, 30, 31, 35, 45, 51 and 52 was tested on 217 biopsy specimens starting from the atypical metaplastic changes and was found to be positive among 66.8%, negative in 28.6% and non significant in 4.6%. Interestingly, 16.7% of atypical metaplastic changes were positive. Further subtyping with probes 6/11, 16/18 and 31/33 revealed positivity in 11.5%, 31.33%, and 18.4% of cases respectively. Noteworthy, multiple infections with HPV 6/11 and 31/33 (4cases) and HPV 16/18 and 31/33 (7 cases) were identified. To examine the main determinants of cervical cancer, multiple regression analysis was conducted using high-grade lesions as the dependant variable and risk factors as independent variables. This showed that the only determinant was HPV infection. When the regression analysis was conducted without HPV as one of independent variables, history of treatment from schistosomiasis was found to have OR of 2.4 (95%CI 1.1-5.5) but the model was not statistically significant.
Conclusion In the Egyptian population, the prevalence of the precursor lesions of the invasive carcinoma is 3% while invasive lesions account for 0.8% of the population. The prevalence of HPV histologically is 2.2% and by ISH 2.6%. However, detection of HPVs by ISH in this study cannot be precise due to technical limitations and limited number of probes used. Evaluation of HPVs using PCR technology will be subject to another study.

O-074

Clinico-morphological characteristics of leiomyosarcomas of the cervix and uterine body

C Amalinei, D Radulescu, R Balan, A Badescu, C Cotutiu
University of Medicine and Pharmacy, Iasi, Romania

Introduction Leiomyosarcomas represent mesenchymal tumors that are relatively frequent in the uterine body, but extremely rare in the cervix. Aims: We report 9 cases of leiomyosarcomas of the uterus: 2 of the cervix and 6 of the body. The macroscopical examination revealed fleshy tumoral masses of 3-6.5 cm in diameter (larger inside the uterine body).
Materials and methods The surgical specimens were routinely processed, stained with HE, PAS, Masson, silver impregnation and immunohistochemically for vimentin, actin, and desmin.
Results The microscopical examination revealed fascicles of smooth muscle fibers with anaplastic aspects, dyskariosis, and frequent mitoses. Leiomyosarcomas of the cervix did not extend to the body but were associated with leiomyomas of the uterine body. Leiomyosarcomas of the uterine body did not extend to the cervix. We analysed the following parameters: number of mitoses per microscopic field, size of cells and nuclei, degree of pleomorphism, level of nuclear hyperchromasia, intratumoral necrosis quantum, rate cellularity/connective matrix, and vascular invasion. The morphologic and immunophenotyping aspects confirmed the diagnosis of leiomyosarcomas stage I (5 cases of leiomyosarcomas of the uterine body), stage II (4 cases, 2 of the uterine body and 2 of the cervix).
Conclusion Although rare, beside leiomyosarcomas of the uterine body, leiomyosarcomas of the cervix may be diagnosed by pathologists, as separate unique location, even in the absence of clinical and cervico-vaginal cytological presumption of malignancy, as the surface epithelium remains intact. Both locations share morphologic, immunophenotypic and prognostic similarities, without evidence of extension to the neighboring counterpart.

O-075

Interferon Regulatory Factor 1 (IRF-1) suppression and derepression in endometrial carcinomas

A Giatromanolaki, E Sivridis, M Koukourakis, C Ritis,
C Mimidis, G Kartalis
Departments of Pathology, Internal Medicine and Radiotherapy, Democritus University of Thrace, Alexandroupolis, Greece

Interferon regulatory factor-1 (IRF-1) is a tumour supressor gene presumed to be involved in the control of cellular proliferation and transformation. Given that the IRF-1 is consistently expressed in the normally cycling endometrium, the question was raised of the

possible role of IRF-1 in the genesis of endometrial adenocarcinoma. A series of 86 such tumours was investigated using immunohistochemical techniques. Relatioships were sought with thymidine phosphorylase (TP), conventional histological features and prognosis. Malignant endometria were, by and large, deprived of IRF-1, as 81 of the 86 cases (94.2%) were negative for this antigen. Only 5 of the 86 cases were expressing IRF-1 in inner tumour areas. At the invading tumor front, however, IRF-1 was depressed in tumour cells in 35% of cases. This phenomenon was independent of the extent of lymphocytic response, but it was a strongly associated with TP expression. TP up-regulation and host's lymphocytic response in the area were directly associated. IRF-1 derepression by invading tumor cells was associated with poor prognosis. This prognostic parameter was independent of stage. It is concluded that down-regulation of IRF-1 is a constant finding in endometrial tumorigenesis. However, derepression of IRF-1 may occur in a subset of tumours, and this event is associated with TP up-regulation and aggressive tumor behaviour.

O-076

Morphometric study of GnRH analogue/ HMG/HCG effects on ultrastructure of human endometrial epithelium in the early luteal phase

M Ghaffari Novin[1], J Solimani[2], F Mehraein[2], SA Sarani[3], L Farzadi[2], A Ghasemzadeh[2]
[1]Avesina Research Center, Tehran, Islamic Republic of Iran
[2]Tabriz University of Medical Sciences, Islamic Republic of Iran
[3]Zahedan University of Medical Sciences, Islamic Republic of Iran

Introduction There is a little information about the effects of ovulation induction drugs on morphometry of human endometrium especially at electron microscopic level. The aim of the present study was to determine the effects of long protocol (GnRH analogue/HMG/HCG) on the ultrastructure of human endometrial epithelium at LH+4.
Material and methods Endometrial biopsies were obtained from fertile women (n=6) as well as infertile women (n=10) who had undergone this protocol at LH+4. Quantitative and qualitative studies on endometrial epithelium were performed by transmission electron microscopy (TEM) and morphometry and the results were statistically compared between the two groups.
Results Qualitative results revealed presence of nuclear channel system (NCS), sub vacuole of glycogen and giant mitochondria (GM) in both groups. Similarly, in quantitative analyses, the volume fractions (Vv) of glycogen, mitochondria and rough endoplasmic reticulum to cell and the also the Vv of euchromatin to nucleus were statistically not different between two groups ($P>0.05$).
Conclusion These results suggest that ovulation induction by long protocol is not associated with retarded or advanced endometrial epithelial development.

O-077

Is electron microscopy useful in the diagnosis of mitochondrial encephalomyopathies?

K Kyriacou, M Trikoupi, A Zenios, T Kyriakides
The Cyprus Institute of Neurology And Genetics, Nycosia, Cyprus

Introduction Historically the diagnosis of mitochondrial encephalomyopathies relied, on the presence of ragged red fibres (RRF) as well as finding ultrastructural abnormalities in mitochondria. Currently accurate diagnosis requires a multidisciplinary approach but the usefulness of electron microscopy has been questioned. The aim of this study was to define the diagnostic role of electron microscopy in comparison to histology and histochemistry.
Patients and methods Thirty-five patients who fulfilled a clinical phenotype for mitochondrial encephalomyopathies, were separated into two groups. The paediatric group, which included 21 cases, with an age range of 6 days to 18 years old and the adult group which included 14 cases, with an age range of 19 to 75 years old. All patients underwent a muscle biopsy which was examined by histology, histochemistry and electron microscopy.
Results In the paediatric group, 4 cases exhibited RRFs, 8 cases showed RRFe and 16 cases had COX abnormalities. Electron microscopy revealed the presence of mitochondrial abnormalities in 10 cases and mitochondrial aggregates in 7 others. In 4 cases light microscopy was normal, but in 2 of these electron microscopy was abnormal. In the adult group all 14 patients, showed COX abnormalities, 12 cases had RRFe and 7 others had RRFs. Electron microscopy revealed the presence of mitochondrial aggregates in 12 cases and structural abnormalities in 7 cases.
Conclusions Electron microscopy examination is a useful independent diagnostic tool in the investigation of mitochondrial encephalomyopathies. It is particularly helpful, in the paediatric cases, where the classic light microscopical findings are often not well developed.

O-078

Eosinophil-tumour cell interaction in advanced gastric carcinomas: an ultrastructural study

RA Caruso, G Basile, A Ieni, V Cavallari, C Inferrera
Department of Human Pathology, Messina, Italy

Introduction Tumour-associated tissue eosinophils (TATE) have been observed in human tumours and experimental tumour models, but the mechanism by which eosinophils induce tumour cell damage remains poorly understood. Aims: Electron microscopy is an essential technique in evaluating sublethal and lethal cellular injuries. Therefore, gastric carcinomas were studied by light and electron microscopy, focusing on the relationship between eosinophils and tumour cells and on the nature of tumour cell death.
Material and methods Fresh tumour tissue was obtained in the operating room for immediate fixation and processed for both light and electron microscopy examination from 1992 until 2002.
Results A light microscopy review of 107 cases of resected gastric carcinomas identified 5 cases (3 of intestinal-type and 2 of diffuse-type) with a massive TATE. In 3 cases of intestinal-type adenocarcinomas, eosinophils formed varied-sized aggregates in the tumour stroma. Some were seen passing through the neoplastic epithelium, and others were found lying within neoplastic tubules. In 2 cases of diffuse-type carcinoma, eosinophil clusters were seen to surround single tumour cells. With electron microscopy, performed in these 5 cases, tumour cells in intimate contact with eosinophils revealed sublethal and lethal cellular injuries. In particular, sublethal injuries, such as cytoplasmic vacuoles and indiscernible cell membrane, occurred at the contact region. Eosinophil “satellitosis” was associated with lethal damage of tumour cells including brush border disorganization, dilation of nuclear envelope, rough endoplasmic reticulum and Golgi apparatus forming empty spaces or vacuoles, small condensed chromatin particles, irregular distribution of nuclear pores. These

lethal injuries were compatible with non-apoptotic (non-lysosomal vesiculate) cell death. The adenocarcinoma cells, not contacted by eosinophils remained morphologically well preserved.
Conclusions These morphological data suggest the hypothesis of a direct relationship between eosinophil infiltration and induction of non-apoptotic tumour cell death in some cases of gastric adenocarcinoma. A deeper insight into the molecular mechanisms acting as cytokines that stimulate specific eosinophil functions may assist in the development of novel therapies to better treat human malignancies

O-079

Expression of p53 and c-erbB-2 oncoproteins in chronic schistosomal urinary bladder lesions

O Hammam, H EL Baz, M Wishahi
Theodor Bilharz Research Institute, Giza, Egypt

This study was conducted in a trial to better understand the genetic mechanisms underlying the proliferative, premalignant and malignant changes frequently displayed in chronic schistosomal cystitis (Ch.Sch.C.) and schistosomal associated transitional cell carcinoma (Sch.TCC) of the bladder. Tissue exepression of P53 (tumor suppressor gene) and c-erbB-2 (oncogene) was assesed immunohistochemically in bladder urothelial specimens of a well characterized cohort of 55 male Egyptian patients (25 Ch.Sch.C; 20 Sch.TCC and 10 normal urothelial specimens as controls). Both P53 and c-erbB-2 oncoproteins were not expressed neither in morphologically normal nor in the hyperplastic epithelium. Overexpression of nuclear P53 and membranous c-erbB-2 was detected in 20% of Ch.Sch.C cases in whom premalignant changes (metaplasia and dysplasia) were displayed. While, in the Sch.TCC cases they were detected in 80% and 70% of cases respectively. On stratifying these patients according to the well recognized prognostic parameters (histopathological grade, stage, tumor size, multifocality and growth pattern) P53 was positively correlated with all the forementioned parameters. In contrast c-erbB-2 was only correlated with tumor size and growth pattern. In conclusion, the results of the current study may suggest the early involvement of both P53 and c-erbB-2 in the initiation of the premalignant changes occuring with Ch.Sch.C and the progression of these changes to malignancy. Moreover, the high incidence of P53 and c-erbB-2 expression among Sch.TCC cases with poor prognostic parameters (higher grade, stage; bigger tumor size; tumor multifocality and nonpapillary growth pattern) may point out to the possibility of using these biomarkers as early predictive markers in Ch.Sch.Cyst. cases displaying premalignant lesions and as poor prognostic indicators for Sch.TCC.

O-080

CD10 expression in a subset of chromophobe renal cell carcinoma

G Martignoni[1], M Pea[2], M Brunelli[2], M Chilosi[2], M Bertaso[2], JN Eble[3], G Mikuz[4], V Ficarra[5], G Novella[5], F Bonetti[2]
[1]Anatomia Patologica, Universitá di Sassari, Sassari, Italy
[2]Anatomia Patologica, Universitá di Verona, Verona, Italy
[3]Department of Pathology, Indiana University, USA
[4]Department of Pathology, Insbruck University, Insbruck, Austria
[5]Urologia, Universitá di Verona, Verona, Italy

Introduction CD10 is a neutral endopeptidase which participates in the peptide hidrolysis in the renal proximal tubules. Its immunohistochemical detection has been considered useful in the differential diagnosis of renal carcinomas because of its expression in 93-100% of clear cell renal and papillary renal cell carcinomas and its absence in chromophobe renal cell carcinoma (ChRCC), a histotype positive for parvalbumin, a protein of the distal nephron.
Material and methods We studied immunohistochemically 26 ChRCCs including four with aggressive features (two with sarcomatoid transformation, one with renal vein involvement and one with pancreatic metastasis), for CD10 and parvalbumin developing the reactions with different methods (ABC, Envision peroxidase detection and labeled polymer-AP Dako Envision systems) to prevent false-positive staining due to endogeneous biotin. Western blotting was done to confirm the results. As control we stained 75 clear renal cell carcinomas with both antibodies.
Results CD10 immunoreactivity was observed in 5 (20%) primary ChRCCs, three with aggressive features, using all the developing systems. All ChRCCs were positive for parvalbumin, but not the sarcomatoid areas. Western blotting confirmed the specificity of the immunoreactivities.
Conclusions 1) About 20 % of ChRCC express CD10 2) CD10 is not specific for clear cell and papillary carcinomas of the kidney; 3) A panel including both CD10 and parvalbumin is useful in the differential diagnosis between ChRCC and clear renal cell carcinoma; 3) Three out of four tumors with aggressive features stained for CD10, but further studies are needed to highligh the prognostic significance of CD10 in ChRCC.

O-081

Expression of tenascin in superficial and invasive bladder cancer

AE Brunner, H Rogatsch, C Ensinger, G Mikuz
Institute of Pathology, University of Insbruck, Insbruck, Austria

Introduction Tenascin (TN) is an extracellular matrix glycoprotein, which is expressed during embryogenesis at the epithelial-stromal interface. TN is decreased in normal adult tissue but reexpressed in inflammatory, reparative and neoplastic processes. TN seems to be involved in neoangiogenesis, promotion of invasion and metastasis of malignant tumors. The aim of the study was to investigate the expression of TN in carcinoma in situ (CIS), invasive and superficial papillary bladder cancer.
Material and methods 33 cases of bladder cancer were selected (8 WHO grade I, 11 grade II, 9 grade III tumors, 5 CIS). We investigated the different staining patterns of TN by immunohisto-chemistry using a monoclonal antibody against TN (T2H5).
Results Immunhistochemical evaluation revealed stromal and cytoplasmic staining. Stromal staining was found at the borders of invasive tumors and in the lamina propria of most CIS. TN staining of blood vessels was located at the tips of the papillae or in invasive tumor. Cytoplasmic TN expression was present in all bladder cancer specimens. In CIS positive cells were present in all cell layers or distributed in a pagetoid pattern while adjacent normal urothelium showed staining of superficial cells. In WHO grade I papillary tumors TN staining was located in superficial cells, in grade II tumors scattered positive intermediate cells were present, while in grade III tumors TN was expressed focally in all cell layers. Most invasive tumor cell nests showed extensive TN staining.
Conclusion Expression of TN in bladder cancer seems to be associated with dedifferentiation and invasive potential.

O-082

Prognostic significance of cytokeratin 20, CD44v6, Bcl-2 and c-erb-b2 in stage T1, grade 3 urothelial carcinoma of the bladder (T1G3)

RJ Luque[1], A Lopez-Beltran[2], A Quintero[3], F Merlo[3], MF Lara[3]
[1]Dept. Pathology. Hospital Neurotraumatológico. Complejo Hospitalario de Jaén, Jaen, Spain
[2]Dept. Pathology. School of Medicine and 'Reina Sofía' University Hospital, Córdoba, Spain
[3]Research Unit. 'Reina Sofía' University Hospital, Córdoba, Spain

Introduction Stage T1 Grade 3 (T1G3) urothelial carcinoma is a heterogeneous group of aggressive bladder tumours at higher risk of progression and death. Several prognostic factors including depth of invasion, DNA ploidy and cell-cycle protein status have been previously tested, but additional prognostic factors are needed. The aim of the study was to test the ability of cytokeratins (7, 20 and high molecular weight), CD44v6, c-erb-B2, LEA.135 and bcl-2 in predicting tumor behaviour in T1G3 tumors.
Material and methods Clinical and pathological data (age, gender, tumour size and associated carcinoma 'in situ') and the immunohistochemical expression of cytokeratins (7, 20 and high molecular weight), CD44v6, c-erb-B2, LEA.135 and bcl-2 were tested in order of determine their prognostic significance. Univariate and multivariate analysis of overall, disease-free and progression-free survival were done.
Results Tumour size, expression of cytokeratin 20, CD44v6 and bcl-2 were associated with a decreased overall ($p=0.0087$, 0.0001, 0.0002 and 0.0320) and progression-free survival ($p>0.0001$, $p=0.0059$, $p=0.0290$ and $p=0.0432$). Tumour size and c-erb-B2 expression were associated to decrease in disease-free survival ($p<0.0001$ and $p=0.0021$). Cox regression analysis selected cytokeratin 20, c-erb-B2 and CD44v6 as independent predictor of overall survival, cytokeratin 20, c-erb-B2 and CD44v6 for progression-free survival and c-erb-B2 for disease-free survival.
Conclusion The immunohistochemical expression of cytokeratin 20 and c-erb-B2, CD44v6 and bcl-2 may add some prognostic information in stage T1 grade 3 bladder cancer patients.

O-083

Second primary malignant tumors in patients with primary renal cell carcinoma

I Novosel[1], M Turčić[2], A Znaor[3], A Reljić[4], M Strnad[3], M Belicza[2], B Krušlin[2]
[1]Department of Pathology, County Hospital 'Dr. Ivo Pedišić', Sisak, Croatia
[2]Ljudevit Jurak Clinical Department of Pathology, Sestre milosrdnice University Hospital, Zagreb, Croatia
[3]Croatian National Cancer Registry, Croatian National Institute of Public Health, Zagreb, Croatia
[4]Department of Urology, Sestre milosrdnice University Hospital, Zagreb, Croatia

Introduction Synchronous, antecedent or subsequent appearance of secondary primary malignancy (SPM) in patient with primary renal cell carcinoma (PRCC) is yet considered to be extremely rare. Recent surveys tend to confirm at least their higher if not even significant incidence. This study was performed to determine the incidence of SPM in the patients with PRCC as well as its localization and time of appearance in relation to PRCC.
Material and methods Of 447 patients who underwent surgery for renal malignancies at Department of Urology, Sestre milosrdnice University Hospital during the period from 1992 to 2000, data of 310 were available in Croatian National Cancer Registry. There were 297 patients with PRCC (193 males and 104 female patients) ranging in age from 24-91 years (median 59.9 years).
Results and conclusion In our series there were 24 (8.1%) patients with SPM. Secondary malignancies in descending order of frequency were cancer of prostate (2.1%), colon (1.0%), lungs (1.0%), bladder (1,0%) and skin (0.7%). There were 42.3% antecedent, 26.9% synchronous and 30,8% subsequent SPM. Only one patient had more than one synchronous second malignancy (urinary bladder, prostate and colon). SPM in patients with PRCC are of great importance for both the clinician and pathologist. Therefore, the clinician should maintain lifetime high-technique follow–up of the patients with PRCC. The knowledge of such an existence should raise an interest in pathologist for elucidating etiologic factors. Namely, it seems that the frequency of SPM in patients with PRCC is much higher that previously expected.

O-084

DNA damage repair in bladder urothelium after the Chernobyl accident in Ukraine

A Romanenko[1], A Vozianov[1], S Fukushima[2]
[1]Institute of Urology A.M.S. of Ukraine, Kiev, Ukraine
[2]Osaka City University Medical School, Osaka, Japan

Introduction In our recent studies we showed increased oxidative stress with p53 gene alterations in urinary bladder lesions in people living in radio-contaminated areas of Ukraine, after the Chernobyl accident. The aim of the study was to examined whether base and nucleotide excision repair is activated in bladder urothelium by chronic low doses of ionizing radiation in male patients with benign prostate hyperplasia and females with chronic cystitis living more than 17 years in 137Cs contaminated areas.
Materials and methods Bladder biopsies from 204 patients were submitted for histological examination and biopsies from 35 patients – for immunohistochemical study of 8-hydroxy-2'deoxyguanosine (8OHdG), 8-oxoguanine-DNA-glycosylase (OGG1-8), apurinic-apyrimidinic endonuclease (APE1) and xeroderma pigmentosum A (XPA).
Results Chronic proliferative atypical cystitis with multiple areas of dysplasia and carcinoma in situ was observed in 89% of patients from radio-contaminated areas with greatly elevated levels of 8OHdG, OGG1-8, APE1 and XPA in bladder urothelium.
Conclusion These findings support the hypothesis that significant activation of DNA damage repair (base and nucleotide excision repair) is induced by long-term low dose of ionizing radiation. The levels of DNA oxidative adducts pointing to mutagenic and carcinogenic potential were in line with the histopatologically diagnosed urothelial lesions.

O-085

Validation of combined use of Thin Prep monolayer preparation and multiprobe UroVysion FISH test for enchanced sensitivity of urinary cytology in detection of bladder cancer

L Baron, M Postiglione, A Cesarano, P Beltotti, F Quarto
U.O. Di Anatomia Ed Istologia Patologica E Citopatologia P.O.S. Leonardo, Castellamare, Italy

Introduction Urinary cytology (UC) and cystoscopy remain the standard methods for initial diagnosis and monitoring of recurrences in urothelial tumors. Low sensivity of UC and invasiveness of cystoscopy led to develop different ancillary methods to improve sensitivity of UC. Specific genetic alterations occurr in bladder cancers (BC), represented by aneuploidia of chromosome 3, 7, 17 and loss of chromosome 9. The aim of the study was to evaluate the use of thin layer techniques applied to UC diagnosis associated with multicolour interphase fluorescence in situ hybridization (FISH) for early identification of initial BC and recurrences.
Methods A total of 50 voided urine specimens were collected, 20 before resection of bladder cancer, 20 from patient with previous BC and 10 flogistic control patient. The samples were processed with Thin Prep (TP) monolayer technique and cytospin preparation (CS) and in cases with morphological alterations, was performed FISH UroVysion (Vysis) assay, consisting of four probes (3, 7, 17 and 9p21). Cytomorphology.
Results In general TP technique was better for cytomorphology, cleaner background little overlapping, with difficulties when only few urotelial cells are present and in cases of contamination with squamous cells. F I SH technique was positive in all carcinomas, with multiple gain of chromosomes 3, 7, 17, while none of negative controls was aneusomic. Only five cases in group of patients in follow-up with minimal atipia, showed FISH positity, with prevalence of loss of chromosome 9 (70%) compared to gain of chromosomes (30%).
Conclusions These preliminary findings suggest that the association of TP preparation with FISH anlysis can improve the efficience of UC to detect BC and predict its recurrence.

O-086

Chromophobe renal cell carcinoma: the variant with the best outcome?

S Rotman[1], P Jichlinski[2], L Guillou[1]
[1]Insitute of Pathology, University Hospital, Lausanne, Switzerland
[2]Depatment of Urology, University Hospital, Lausanne, Switzerland

Introduction Few large series comparing conventional, papillary and chromophobe renal cell carcinomas (RCC) have been published. Most have been heterogeneous, including RCC subgroups of different stage and/or grade. The purpose of this study was to examine the clinico-pathologic features of a series of chromophobe RCCs comparing their outcome with that of conventional and papillary RCCs in a grade and stage matched fashion.
Materials and methods The clinico-pathologic features of 41 chromophobe RCCs, 40 papillary and 153 conventional RCCs were examined, focussing on the following parameters: patient age and sex, tumor size, stage (1997 pTNM), Fuhrman grade, and histology. Survival was analyzed using the Kaplan Meier method. The most important prognostic factors were identified using the Cox model.
Results For patients with localized disease at diagnosis; median, 5-year, and 10-year Disease Specific Survivals (DSS) were similar for chromophobe (120 mths, 5 and 10-yr DSS: 80%) and papillary (120 mths, 5 and 10-yr DSS: 79.5%) tumors. Conventional RCC patients had a significantly worse outcome (84 mths, 5-yr DSS: 55.8%; 10-yr DSS: 46.5%). The best outcome in low grade (G1+G2), low stage (pT1+pT2) tumors was observed in chromophobe RCCs. In multivariate analysis, conventional (nonpapillary) RCC histology was the major independent adverse prognostic factor whether or not stage and grade were included in the Cox models.
Conclusion Chromophobe RCC is a rare RCC variant of good prognosis. This favorable prognosis is maintained when low grade (G1+G2) / low stage (pT1+pT2) tumors are specifically examined.

O-087

C-kit expression in fetal, normal adult and neoplastic renal tissues

D Miliaras[1,2], F Karasavidou[2]
[1]Laboratory of Histology & Embryology, Medical Faculty, Aristotle University of Thessaloniki, Greece
[2]Pathology Department, General Clinic of Thessaloniki, Greece

Introduction C-kit is a transmembrane tyrosine kinase receptor, expressed at high levels in hematopoetic stem cells, mast cells, melanocytic cells, germ cells and the interstitial cells of Cajal. Recently, it has been shown that for certain tumors (especially gastrointestinal stromal tumors and mast cell diseases) c-kit mutation or activation is a major pathogenetic event. Only one previous study has been published regarding c-kit expression in normal renal tissue, and none regarding renal neoplasms. In this preliminary report of an ongoing study, we investigated the expression of c-kit protein via immunohistochemistry in various normal and neoplastic renal tissues.
Material and methods Our material included eight fetal kidneys (16-28 weeks of gestation), seven normal adult kidneys, two cases of renal dysplasia, and 20 renal tumors: 13 renal cell carcinomas, two nephroblastomas, three oncocytomas, one mesoblastic nephroma and one angiomyolipoma. Staining intensity was recorded in a three-grade scale.
Results All fetal kidneys showed cytoplasmic staining of proximal tubules (++). Henle loops were also positive (++), especially in older embryos. Cytoplasmic and membrane staining (++) of renal tubules was also observed in all normal adult kidneys. The two cases of renal dysplasia studied, had c-kit expression in their normal but not in their aberrant tubules. Of the renal cell carcinomas, all conventional type cases (n=9), one sarcomatoid and one papillary type case were negative, while one chromophobe and one granular type were positive (++ and + respectively). All oncocytomas were positive (+++ to ++), and quite interestingly the mesoblastic nephroma was also positive. The angiomyolipoma and the two nephroblastomas were negative.
Conclusion We conclude that c-kit is expressed in normal fetal and adult renal tubules, as well as in a subset of renal tumors. The expression of c-kit in the latter group may prove to have diagnostic significance and therapeutic implications.

O-088

Expression of B-cell markers in classical Hodgkin lymphoma: a tissue microarray analysis of 330 cases

A Tzankov[1], A Zimpfer[1,2], AC Pehrs[1,2], A Lugli[2], P Went[2], R Maurer[3], S Pileri[4], S Dirnhofer[3]
[1]Institute of Pathology, University of Insbruck, Insbruck, Austria
[2]Institute of Pathology, University of Basel, Basel, Switzerland
[3]Institute of Pathology, Triemli Hospital, Zurich, Switzerland
[4]Chair of Pathologic Anatomy & Lymphoma Unit, Institute of Hematology and Clinical Oncology "L. & A. Seragnoli", University of Bologna, Bologna, Italy

Introduction Hodgkin and Reed-Sternberg cells (HRSC) of classical Hodgkin lymphoma (cHL) arise from B-lymphocytes. However, classical markers of the B-cell phenotype, such as CD20, are present only in about 25% of the cases. The aim of the present study was to assess expression of the B-cell related antigens CD20, CD79a and CD138 in cHL using a tissue microarray (TMA) consisting of 330 cHL cases.
Materials and methods Expression of CD15, CD20, CD30, CD79a, CD138 and LMP1 of EBV was assessed by immunohistochemistry, and the methodology was validated by direct comparison of CD20 expression on the TMA cores with corresponding large sections. The influence of the number of arrayed sample cores on the obtained expression levels of CD20 was analyzed by comparing the results from single, duplicate and triplicate cores.
Results Two-hundred fifty-three (77%) of the 330 cases were morphologically representative. CD20 was expressed in 84 cases (33%), CD79a in 26 (10%) and CD138 in 2 (0.8%), respectively. CD20 and CD79a were co-expressed in 16 cases ($p<0.005$), and expression of CD20 correlated inversely with CD15 ($p<0.01$). Comparing the TMA results with those from conventional sections for expression of CD20 yielded a concordance of 94% (63/67). Examining 1, 2 and 3 cores from individual cases revealed positivity for CD20 at 24.1% (61/253), 32.4% (82/253), and 33.2% (84/253), respectively.
Conclusions We conclude that B-cell markers are expressed in 38% of cHL in the following rank order: CD20>CD79a>>CD138. The use of 2 cores per tissue sample renders the TMA technology effectively representative, and thus very useful for high-throughput evaluation of heterogeneously-expressed markers in cHL.

O-089

Increased proliferation due to enhanced activation of the RAF/MEK/ERK pathway in relapsed and refractory acute myeloid leukemia

P Staber[1,2], W Linkesch[2], D Zauner[1], C Beham-Schmid[1], C Guelly[1], S Schauer[1], H Sill[2], G Hoefler[1]
[1]Department of Pathology, University of Graz, Graz, Austria
[2]Division of Hematology, Department of Internal Medicine, University of Graz, Graz, Austria

Background Relapsed/refractory acute myeloid leukemia (AML) is characterized by a deteriorating clinical course and resistance to therapy. Biological mechanisms responsible for resistance remain unclear, since consistent molecular characteristics of AML at relapse and refractory disease have not yet been reported.
Methods We explored paired bone marrow biopsy specimens of 18 patients (at diagnosis and relapsed/refractory AML after high dose chemotherapy) in an immunohistochemical study using Anti Human Ki-67 Antigen (MIB-1) antibody to determine the proliferation fraction of leukemic blasts. Gene expression was analyzed in a different sample set (15 at diagnosis and 11 relapsed/ refractory AML) using a "relapse specific" cDNA microarray covering 4128 genes, selected by literature and suppression subtractive hybridization. Microarray results were validated using quantitative real time PCR, immunohistochemistry and immunoblotting.
Results Recurrent and refractory AML blasts demonstrate a highly significantly increased ($P<0.0001$) proliferation fraction compared to primary diagnosis. mRNA levels of proliferation markers CD71 and PCNA were elevated 4.3-fold and 1.9-fold, respectively, in relapsed and refractory AML compared to diagnosis. Enhanced activation of the RAF/MEK/ERK mitogen-activated protein kinase cascade was indicated by increased mRNAs of B-RAF (1.7-fold), cyclin D1 (2.7-fold), MKP-1 (2.8-fold), c-fos (4-fold), and Egr-1 (5.6-fold). Additional immunohistochemical and immunoblotting analyses demonstrated an elevation of biphosphorylated ERK1/2 protein in recurrent AML, confirming enhanced activation of the RAF/MEK/ERK pathway.
Conclusion Our results provide for the first time evidence that high dose chemotherapy selects or induces leukemic blasts with increased proliferative potential via enhanced activation of RAF/MEK/ERK cascade.

O-090

Expression of VEGF, BFGF and VEGF receptors in diffuse large B cell lymphoma

FJ Bot, EV Meulemans, AW Griffioen, JWJ Bergs, M Roestenberg
Dept. of Pathology, University Hospital Maastricht, Maastricht, The Netherlands

Introduction Diffuse large B-cell lymphoma (DLBCL) is the most common of the Non-Hodgkin's lymphomas (NHL), comprising approximately 35% of newly diagnosed cases. In order to define the role of angiogenesis in DLBCL, mRNA and protein expression of the two most important angiogenic growth factors, VEGF and bFGF, and two VEGF receptors, VEGFR-1/flt-1 and VEGFR-2/KDR were evaluated by real time quantitative PCR (RTQ-PCR) and immunohistochemistry in DLBCL.
Methods We analyzed 27 DLBCL cases, 3 low-grade follicle center lymphomas (FLS) and 2 cases with chronic lymphocytic leukemia (CLL) for expression of VEGF-A, bFGF, VEGFR-1/flt-1 and VEGFR-2/KDR. We used a real-time reverse transcription-polymerase chain reaction (qRT-PCR) method to quantify mRNA levels of these angiogenic markers using an ABI 7000 qRT-PCR system. Protein expression of these angiogenic markers was assessed by immunohistochemical staining.
Results and discussion The results of the current study show that both the mRNA and protein expression of VEGF and bFGF varied considerably among 27 DLBCL patients, which do not correlate to the microvessel density. VEGF mRNA expression showed significant correlation with bFGF mRNA expression. The VEGFR-2/KDR mRNA expression was higher than VEGFR-1/flt-1 mRNA expression in DLBCL but their expressions were strongly correlated. Histological staining of both VEGF receptors in DLBCL sections showed strong staining of both receptors on the microvessel endothelial cells but not on the tumor cells. Our data suggest that VEGF plays a role in the pathophysiology of DLBCL however autocrine/paracrine stimulation by VEGF does not seem to be relevant in DLBCL. The expression of VEGF and its receptors raises the possibility of using angiogenesis inhibitors as a novel therapeutic strategy.

O-091

Analysis of provisional extracellular matrix in lymph nodes - loss of the laminin gamma2-chain indicates follicular lymphoma

K Hertel[1], R Dahse[1], K Scheibner[1], A Berndt[2], L Zardi[3], H Kosmehl[1]
[1]HELIOS Clinic Erfurt, Institute of Pathology, Erfurt, Germany
[2]Institute of Pathology, University of Jena, Germany
[3]Istituto Nazionale per la Ricerca sul Cancro Genoa, Genoa, Italy

Introduction ECM regulates cellular differentiation, life span, migration and contributes to lymph node compartmentalisation. The aim of this study was analysis of occurrence and distribution of embryonal fibronectin (Fn), tenascin (Tn) isoforms and laminin chains (Ln) in reactive lymph nodes (RLN) and follicular lymphoma (FL).
Material and methods Shock frozen tissue of 10 RLN and routine material of 10 FL and RLN. Primary antibodies: all Fn variants (IST-4), ED-A Fn (IST 9), (BC-1), all Tn-C variants (BC-4), Tn-CL (BC-2), Ln-alpha2- (5H2), Ln-alpha3- (BM 165), Ln-alpha5- (4C7), Ln-beta1- (4E10), Ln-beta2- (C4), Ln-gamma1- (2E8), Ln-gamma2-chain (GB3 and D4B5). APAAP-technique.
Results RLN: all Fn's, ED-A Fn and Tn-CL were demonstrated in lymphatic / blood vessels and as reticular depositions in the stroma; spot-like depositions in the follicle center and ribbon-like at the border follicle centre / mantle zone. Ln-alpha3, -alpha5, -beta1, -beta2 and -gamma1-chains were positive mainly in lymphatic and blood vessels with depositions in the stroma. Ln-gamma2-chain was restricted to follicular dendritic cells and ribbon-like co-deposited with Tn-CL at the border follicle centre / mantle zone. FL: in contrast to normal follicles, a total loss of Ln-gamma2-chain is regular observed in neoplastic follicles.
Conclusions 1. A provisional ED-B Fn / Tn-CL / Ln-gamma2-chain matrix membrane controls the traffic follicle centre/mantle zone. 2. In analogy to thymic T cell maturation, a role of Ln-gamma2-chain (Ln-5) can be assumed for B cell maturation mediated by Ln-gamma2-chain (Ln-5) positive follicular reticulum cells. 3. The loss of Ln-gamma2-chain indicates neoplastic follicular structures in follicular lymphoma.

O-092

Follicular lymphoma grading by Mann and Berard are predictive of overall survival and time to treatment failure, however, only grade 1 has favorable OS and TTF

N Bilalovic[1], R Golouh[2], JM Nesland[3], I Selak[1], E Torlakovic[3]
[1]Department of Pathology, Sarajevo University Hospital, Sarajevo, Bosnia and Herzegovina
[2]Department of Pathology, Ljubljana Institute of Oncology, Slovenia
[3]Department of Pathology, The Norwegian Radium Hospital, Norway
[4]Department of Pathology, Sarajevo University Hospital, Bosnia and Herzegovina
[5]Department of Pathology, The Norwegian Radium Hospital, Norway

Follicular lymphomas (FL) are a heterogeneous group of tumors, varying in clinical features, immunophenotype, and cytogenetics. WHO recommends grading of FLs by using the method of Mann and Berard, which recognizes three grades. The aim of this study was to examine whether Mann and Berard's grading has prognostic significance in patients with follicular lymphoma who were not uniformly treated. Samples from 73 patients with follicular lymphoma with follow up ranging from 7–223 months (median 59 months) were included in the study. Forty-three patients (59%) achieved a complete response (CR), 19 (26%) partial response (PR), while 11 (15%) were considered non-responders during the follow up period of 223 months. Twenty-seven (37%) patients died, 11 patients (15 %) from dissemination, 11 from transformation to other lymphoma type and 5 (6, 8%) patients died from non-lymphoma related causes. OS rate was significantly worse in patients with Ann Arbor stage IV than patients Ann Arbor stage I-III (p=0.07). Patients with lower IPI score did significantly better than those with a higher IPI score for OS (p<0.0001) and TTF (p<0.0001). Grade 1 FL patients had longer OS (p=0.02) than grade 2 and 3 patients. A trend for longer TTF was also found (p=0.05). Cox regression analysis showed that these results were independent of stage, but were not independent of IPI score. Higher grade was also associated with the presence of B symptoms (p=0.04) and larger size of the primary tumor (p=0.03).

O-093

BCL-6 and CD10 protein expressions are prognostic factors of overall survival and time to treatment failure in follicular lymphoma

N Bilalovic[1], R Golouh[2], JM Nesland[3], I Selak[1], E Torlakovic[3]
[1]Department of Pathology, Sarajevo University Hospital, Bosnia and Herzegovina
[2]Department of Pathology, Ljubljana Institute of Oncology, Slovenia
[3]Department of Pathology, The Norwegian Radium Hospital, Norway

Follicular lymphomas (FL) are a heterogeneous group of tumors, varying in clinical features, immunophenotype, and cytogenetics. The aim of this study was to examine interrelationship and prognostic significance of BCL6 and CD10 protein expression for overall survival (OS), and time to treatment failure (TTF). Samples from 73 patients with follicular lymphoma were evaluated by immunohistochemistry. Bcl-6 and CD10 expression levels were determined semiquantitatively. Since almost all cases expressed Bcl-6, FLs were designated either "low expression level-group" (LLG 0 and 1+, 29 patients) or "high expression level group" (HLG, 2+ and 3+, 44 patients). Based on CD10 expression, FLs were designated either "negative" (13 patients) or "positive" (58 patients). 44 patients with high levels of Bcl-6 expression had favorable overall survival (OS) (p=0.005) and TTF (p=0.01) compared to 29 patients with low levels of Bcl-6 expression. Cox regression analysis showed that the results for OS, but not TTF were independent of IPI score. Patients with CD10-negative follicular lymphomas also had worse OS (p=0.01) and TTF (0.005). Our results suggest that expression of CD10 and strong expression of Bcl-6 protein could be indicators of well-differentiated follicular lymphoma since such cases were associated with lower histological grade and better clinical outcome.

O-094

CD30+ primary cutaneous lymphoproliferative disorders (PCLDs): TCR-gamma gene analysis by PCR on DNA extracted from CD30+ microdissected cells

R Riboni, E Boveri, M Lucioni, P Incardona, A Viglio, M Paulli
Istituto Di Anatomia Patologica, IRCCS Policlinico San Matteo - University Di Pavia, Pavia, Italy

Introduction CD30+ PCLDs spectrum includes lymphomatoid papulosis (LyP), anaplastic large cell lymphoma (ALCL) and

"borderline lesions" with clinicopathologic features in between LyP and ALCLs. LyP nature (neoplastic vs reactive) is matter of debate because of its benign clinical course and variable molecular findings (T-cellular clonality in less than 50% of cases). Borderline lesions have a favourable outcome similar to LyP but, due to their rarity, limited data are available on their biologic features and clonal status. The aim of this study was to compare possible divergences in the search for clonality in the same individual skin lesions using respectively DNA extracted from laser microdissected CD30+ cells and DNA from whole paraffin sections.
Materials and methods 4 LyP and 2 borderline skin lesional biopsies were tested for TCR-gamma rearrangements by means of PCR on DNA extracted respectively from whole-tissue and a pool (50-100 cells) of CD30+ cells microdissected using the ZEISS-PALM Robot-MicroBeam System.
Results and conclusions PCR analysis of whole-tissue DNA documented TCR-gamma monoclonal rearrangement in 2/6 cases (2/2 borderline, 0/4 LyP); TCR analysis on DNA extracted from microdissected CD30+ cells showed monoclonal rearrangement in 5/6 cases (2/2 borderline, 3/4 LyP). We confirm that PCR analyses on DNA extracted by microdissected CD30+ cells enhance the rate of monoclonality detection mainly in LyP lesions, in which the limited number of atypical CD30+ cells and predominant reactive cellular background may be responsible for negative or ambiguous signalling when DNA extracted by the whole lesion is tested.

O-095

Malignant testicular lymphoma accompanied with complete AV block – case report

M Mocko[1], P Budakov[1], D Donat[2], M Štajnic[3], D Petrović[2], B Stojiljković[2], S Štajnic[1]
[1]Institute of Pathology and Histology, Clinical Center of Novi Sad, Novi Sad, Serbia and Montenegro
[2]Institute for Oncology, Sremska Kamenica, Serbia and Montenegro
[3]Institute for Cardiovascular Diseases, Sremska Kamenica, Serbia and Montenegro

A 43-year-old male patient was admitted, with the signs of complete AV block and bradycardia accompanied by syncopes. A complete lab examination with US, CT and MRI was done which all confirmed a massive tumorous infiltration into the root of mesenterium, presence of lymphadenomegaly around it, as well as nonhomogeneous and unclearly demarcated infiltrative lesion of myocardial septum. The patient completed his anamnesis by imparting that his right testicle was slightly enlarged and periodically painful. Semicastration was indicated and the removed tissue was prepared for pathohistologic analysis. The testicle had only peripherally preserved normal tissue, whereas the tumor was clearly demarcated, 4.5 cm in diameter. Five-micrometre-thick tissue sections from the paraffin-embedded tissue were stained with H&E. The cells were quite variable in their morpholoric features and size. The nuclei were generally hypochromatic, with irregular chromatin distribution. The nuclear morphologic properties varied and included pleomorphic mono- and multinucleated giant tumour cells with multiple nuclear lobulations. Nucleoli were conspicuous. Also, numerous benign-appearing lymphocytes and plasmacytoid elements were scattered throughout the background. This histologic picture could correspond either to spermatocytic seminoma or lymphoma. Since the patient needed an urgent therapy, histochemically (PAS-) and immunohistochemically (LCA +, CD3 +, CD20 +), the diagnosis of lymphoma was confirmed. The patient received CT (CHOP protocol), which resulted in a satisfactory clinical response. In this case, it is interesting to point to the most probable infiltration of the myocardium by the diagnosed lymphoma which elicited the cardiologic symptoms and from which the diagnosing of the patient's disease was to start.

O-096

Diffuse large B-cell lymphoma of bone: an analysis of differentiation-associated antigens with clinical correlation

L de Leval*, K Braaten, M Ancukiewicz, E Kiggundu, T Delaney, H Mankin, N Lee Harris
* Department of Pathology, University of Liège, Belgium, Massachusetts General Hospital, Boston, MA

Twenty-nine patients with diffuse large B-cell lymphomas (DLBCL) presenting with bone involvement, including 18 localized primary bone lymphomas (group I), 2 multifocal primary bone lymphomas (group II) and 9 patients with extraskeletal disease at diagnosis (group III) were studied. The tumors were subclassified according to the criteria of the WHO classification and evaluated by immunohistochemistry for expression of antigens associated with germinal center (GC) and non-GC stages of B-cell differentiation (bcl-6, CD10, MUM-1, VS38c, CD138, bcl-2 and CD44). The presence of a BCL-2/IgH gene rearrangement was investigated by PCR. All cases were characterized by similar clinicopathologic and morphologic features, and had similarly good overall outcome. The patients (23 M, 6F, median 44 y) had tumors in long bones (14), axial skeleton (8), and limb girdles (3) and multiple sites (4). Most tumors (24) were centroblastic, with multilobated cells in 12 cases. Almost half of the tumors (14/29, 48%) were bcl-6+CD10+ («GC-like»), 9/29 cases (31%) were bcl-6+CD10- («indeterminate» phenotype) and 6/29 cases (21%) were CD10-bcl-6- («post-GC like»). The «indeterminate» phenotype was seen only in primary bone lymphoma. MUM-1 was frequently expressed in GC-like and non-GC-like categories. We found no evidence of plasmacytic differentiation by CD138 and VS38c immunoreactivity was distinctly rare (2/29 cases). CD44 was detected in 6 tumors, all CD10-. Bcl-2 was expressed by 70% of the tumors but only 1/23 cases tested had a Bcl-2/JH rearrangement by PCR. A survival analysis showed that GC-like tumors had a longer overall survival duration compared to non-GC-like tumors (p=0.0046).
In conclusion, a "GC-like" immunophenotype, characterizes roughly half of large B-cell lymphomas of bone and is associated with an improved survival.

O-097

Ultrastructural characteristics of liver-associated lymphocytes in chronic delta hepatitis

B Aliev, S Khodjaev
Institute of Virology, Tashkent, Uzbekistan

Liver sinusoids contain a heterogenous population of lymphocytes including 'pit cells' discovered by Wisse in 1970. However, ultrastructural patterns of liver-associated lymphocytes (LAL) in delta hepatitis are still not well identified. In present work we investigated LAL in chronic delta hepatitis (CHD) with electron microscopy. Liver biopsies from 16 with CHD were fixed in 2,5% glutar aldehyde, postfixed with 1% osmium teroxide and embedded in Epon. Ultrathin sections were stained with uranyl acetate and lead

citrate. Ultrastructural study revealed migration of lymphocytes between hepatocytes in CHD. They have heterogenous population of lymphocytes varying in morphology. Some of them were large granular lymphocytes and could be natural killer cells. Some of LAL could correspond to a T lymphocyte. In electron microscopic study of LAL we also observed presence of plasma cells and the pattern of intracellular membrane systems common to cells that secrete protein: well developed granular endoplasmic reticulum, large juxtanuclear Golgi complex. A centriole occupies a position just marginal to the Golgi. The chromatin in the nucleus of these cells is characteristically condensed into large masses just within the envelope. Our results demonstrate a heterogenity of LAL in chronic delta hepatitis including the presence of B cells.

O-098

Hepatic steatosis in relation to serum apolipoprotein level in egyptian patients with HCV and HCV- associated HCC: histopathological, biochemical and clinico-sonographic study

T Aboushousha[1], N Assaly[2], A El-Ray[3]
[1]Pathology Department, Theodor Bilharz Research Institute, Cairo, Egypt
[2]Clinical Chemistry Department, Theodor Bilharz Research Institute, Cairo, Egypt
[3]Gastroenterology and Hepatology Department, Theodor Bilharz Research Institute, Cairo, Egypt

Chronic hepatitis C is a known risk factor for cirrhosis and hepatocellular carcinoma (HCC). Liver steatosis is common in HCV patients suggesting that specific mechanisms might be involved. The aim of our study was to assess variability in serum apolipoproteins in relation to hepatic steatosis in HCV patients of genotype 4 with or without HCC. Material included 73 Egyptian subjects; 25 (HCV), 25 (HCV-associated HCC), and 23 controls. Clinical examination for stigmata of chronic hepatic affection and ultrasonography for assessment of liver size, surface, echogenicity and the presence or absence of a focal lesion were done. Histopathological examination of liver biopsies was done for assessment of hepatitis activity index (HAI) and stage as well as the grade of hepatocytic steatosis (HS). Biochemical study included liver function tests, lipid profile and assessment of apolipoproteins. Results showed a significant decline in apo-A, apo-B, apo-CII, apo-CIII and apo–E lipoprotein in HCV and HCV-associated HCC groups compared to the control group. Analysis of HAI in HCV patients showed significant association of HS with periportal necrosis, but not portal inflammation or lobular degeneration. In patients with HCV associated HCC, HS was significantly associated with portal inflammation and lobular degeneration, suggesting a correlation between virus activity and hepatocytic neoplastic changes. We concluded that steatosis should be searched for in patients with chronic HCV, being an important cofactor in accelerating the development of hepatic fibrosis and in increasing necroinflammatory activity. A correct therapeutic approach to steatosis would slow down the evolution of chronic hepatitis.

O-099

Steatohepatitis – shortcut to diagnosis

J Gligorijevic[1], K Katic[1], V Zivkovic[1], S Ciric[2], V Katic[1]
[1]Institute of Patology, Medical Faculty of Nis, Nis, Serbia and Montenegro
[2]Military Hospital Nis, Nis, Serbia and Montenegro

Introduction Nonalcoholic fatty liver disease (NAFLD) is defined as a constellation of clinical conditions characterized by predominantly macro vesicular steatosis. It can be extremely difficult to reach the diagnosis of NASH in the absence of correct clinical data. Exclusion of excess alcohol intake is notoriously difficult and requires a desialylated transferin (the method rarely present in laboratories). Aim: Histomorphologic investigation of liver biopsies from patients with mild laboratory test abnormalities and steatosis complicated by necroinflamatory changes. A pilot study of morphometric characteristics of lipid droplets in NASH and alcoholic hepatitis were also performed.
Material and methods Forty liver biopsies with steatosis and inflammation were examined using the method of Dixon. Ten of these biopsies were morphometrically analysed regarding the lipid droplet features. Following morphometric parameters were estimated: 1) diameter, 2) perimeter and 3) area. We used Olympus Micro Image- Image Analysis Software v.3.0.1.
Results The presence and distribution of Mallory hyaline was the most variable parameter. Morphometric analyses confirm a statistically significant differences for all parameters tested in NASH and alcoholic hepatitis, and were more pronounced in NASH.
Conclusion In the cases of fatty change with necro-inflammatory changes and pericellular fibrosis in liver biopsy and presence or absence of Mallory hyaline, morphometric analysis of lipid droplets can help in reaching the diagnosis of NASH, if testing of desialilated transferring is not possible.

O-100

Mutations of the BRAF gene in cholangiocarcinoma, but not in hepatocellular carcinoma

A Tannapfel[1], F Sommerer[1], J Hauss[2], C Wittekind[1]
[1]Institute of Pathology University of Leipzig, Leipzig, Germany
[2]Department of Surgery University of Leipzig, Leipzig, Germany

Introduction The Raf/MEK/ERK (MAPK) signal transduction cascade is an important mediator of a number of cellular fates including growth, proliferation and survival. The BRAF gene, one of the human isoforms of RAF, is activated by oncogenic Ras, leading to cooperative effects in cells responding to growth factor signals. This study was performed to elucidate a possible function of BRAF in liver tumours.
Methods Mutations of BRAF and KRAS were evaluated in 25 hepatocellular carcinomas (HCC) and in 69 cholangiocarcinomas (CC) by direct DNA sequencing analyses after microdissection. The presence of active intermediates of the MAPK pathway was assessed immunohistochemically. The results obtained were correlated with histopathological variables and patient survival.
Results Activating BRAF missense mutations were identified in 15/69 CC (22%) and in one case of tumour surrounding liver. KRAS mutations were found in 31 out of 69 (45%) CC examined and in two cases of tumour-surrounding non-neoplastic liver tissue. In HCC, neither BRAF nor KRAS mutations were detected. All 31 CC with KRAS mutations had an intact BRAF gene. We failed to observe a correlation between BRAF or KRAS mutations and histopathological factors or prognosis of the patients.
Conclusions Our data indicate, that BRAF gene mutations are a relatively common event in CC, but not in HCC. Disruption of the Raf/MEK/ERK (MAPK) kinase pathway - either by RAS or BRAF mutation - was detected in about 65% of all CC and is therefore one of the most frequent defects in cholangiocellular carcinogenesis.

O-101

Prognosis and treatment of cholangitis after cholecystectomy

N Akhtar, AE Kuzmenko, VV Khatsko, GA Grintsov, AM Dudin, YG Kolkin
Donetsk Medical State University, Donetsk, Ukraine

Introduction The purpose of our research was to study prognostic tests of cholangitis after cholecystectomy (CE) for prophylaxis and optimal treatment.
Materials and methods For 10 years 134 patients with so called "Postcholecystectomic Syndrome" (PCES) were treated, 39 (29%) had a clinical picture of acute cholangitis (AC), which was shown by pains in the right hypochondrium, yellowness of skin and scleras, shivering, high hyperthermia and leukocytosis. Patients (25 women and 14 men) were 42-76 years old, 12 of them more than 60 years. Initial operation (CE) was made in various hospitals in terms from 4 months to 2 years ago. The diagnosis was verified by: clinical, laboratory and immunological researches, peroxidation of lipids (POL), ultrasonic research, computerized tomography, fibrogastroduodenoscopy, endoscopic retrograde pancreatocholangiography, transdermic and transhepatic cholangiography, fibrocholangiograpgy, bacteriological researches of bile and blood.
Results According to investigations, in 21 patients the reason of infringement of bile flow was choledocholithiasis (in a combination with stenosis of big duodenal papilla (BDP) or without it, in 10-stenosis of BDP, in 6-cicatricial stricture of hepatocholedochus, in 2 extended stenosis of BDP and a terminal part of the common bile duct (CBD). Laboratory prognostic tests (risk factor) AC concern: hyperbilirubinemia, increase of activity of alanine transpeptidase, aspartate transpeptidase, hypoproteinemia, dysproteinemia, decrease of a level of protrombin lower than 70%, leukocytosis, anemia, increase of the contents of urea in blood, bacteriocholia, concentration of molecule of average weight were higher than 0.6 unit, decrease of level of vitamin E, high contents of immunoglobulin M on a background of a low parameter immunoglobulin G.
Conclusions At the presence of 4 risk factors prognosis was frequently in contrary to expectations and mortality reached to 50-80%. All patients with acute cholangitis after cholecystectomy represented a complicated problem and demanded a complex approach. Revealed prognostic tests of the development of acute cholangitis are necessary for taking into account for its prophylaxis and optimum treatment.

O-102

Study of c-myc oncogene in hepatocellular carcinoma

S Abdel Salam[1], NM Moustafa[2], A Amer[1], M El Moufty[1], A Abdel Aziz[3], S Zaki[4]
[1]Faculty of Medicine, Microbiology Depart., Alexandria University, Alexandria, Egypt
[2]Faculty of Medicine, Pathology Depart., Alexandria University, Alexandria, Egypt
[3]Faculty of Medicine, Clinical Oncology Depart., Alexandria Unversity, Alexandria, Egypt
[4]Faculty of Medicine, Internal Medicine Depart., Alexandria University, Alexandria, Egypt

Structural alterations in c-myc oncogene, copy number and expression have been implicated in the pathogenesis and progression of several human neoplastic diseases. However, the biologic significance of c-myc gene in human hepatocellular carcinoma (HCC) is unconfirmed. In the present study we correlated c-myc gene amplification and protein expression with the clinicopathologic features. In 20 HCC cases c-myc amplification in tumour tissue was determined using a differential PCR, a procedure for evaluation of gene amplification in comparison with a dopamine D2 receptor gene. The c-myc gene was amplified in 6 out of 20 tumor specimens (30%). Amplification of c-myc was more frequent in younger male patients with HBV infection and in less differentiated tumors. All cases demonstrated positive staining using anti-c-myc monoclonal antibody with increasing percentage of immunoreactive cells in less differentiated tumors. However, the high protein expression was not statistically correlated with c-myc amplification.

O-103

Histological sectioning of brush bristles allows improved diagnosis of biliary tract and bronchial lesions

G Bussolati, G Accinelli, L Macri
Dept. Biomedical Science And Human Oncology, Turin, Italy

Brushing of thin ducts such as those of the biliary tract, pancreas and bronchial tree is often used by endoscopists in order to obtain diagnostic material proving the nature of related lesion. The material is spread on slides. Cytological examination folows. Preservation of the material so obtained is often sub-obtimal, partly because of the presence of fluids such as bile affecting cell preservation, partly because spreading of delicate cells may result in crushing artifacts. To circumvent such problems, we devised an original procedure, where brushes were not smeared, but instead immediately embedded in immersed Methanol. Then the tube with alcool and brush was sent to the laboratory. In order to induce formation of a glue surrounding the brush, this was immersed while wet into egg albumen (a mixture 1:1 of egg albumen and glycerol), then returned to methanol. For paraffin embedding, the metal handling was cut away and the brush was introduced as such into a cassette. Sections parallel to the long axis were cut until the metal wire was almost reached, then the block was rotated and new section was obtained from the opposite side. Sections were stained in Haematoxilin-Eosin and with the Papanicolau procedure. Small fragments of the mucosa, of inflammatory cell aggregates or of related carcinomas were observed. These resulted optimally fixed and allowed a definite histological diagnosis which proved mandatory for proper therapy. Advantages and prospects of this novel procedure will be illustrated and discussed.

O-104

Is telomerase catalytic subunit gene re-expression an early event in gallbladder carcinogenesis?

B Luzar[1], M Poljak[2], A Coer[3], U Klopčič[4], V Ferlan-Marolt[1]
[1]Institute of Pathology, Medical Faculty, University of Ljubljana, Ljubljana, Slovenia
[2]Institute of Microbiology and Immunology, Medical Faculty, University of Ljubljana, Ljubljana, Slovenia
[3]Institute of Histology and Embryology, Medical Faculty, University of Ljubljana, Ljubljana, Slovenia
[4]Department of Cytopathology, Institute of Oncology, Ljubljana, Slovenia

Introduction Telomerase catalytic subunit (hTERT) is a rate limiting step for telomerase activity, a key enzyme implicated in cellular immortalisation and transformation. The aims of this study

were to determine whether a.) differences in the levels of hTERT exist among different grades of gallbladder epithelial abnormalities, and b.) hTERT gene re-expression has any role in gallbladder carcinogenesis.
Material and methods The expression of hTERT was analysed in 89 gallbladder tissue samples: 16 normal epithelia, 14 reactive hyperplasias, 15 low grade dysplasias, 16 high grade dysplasias and in 28 adenocarcinomas by immunohistochemistry. At least 200 nuclei were quantified per slide and the number of positive signals per nucleus was expressed as a hTERT index.
Results The mean hTERT index increased progressively with the degree of gallbladder epithelial abnormalities: from 0.03 (standard deviation=0.05) in normal epithelia, 0.04 (SD=0.05) in hyperplastic epithelia, 0.25 (SD=0.14) in low grade dysplasia, 0.82 (SD=0.20) in high grade dysplasia to 0.93 (SD=0.27) in adenocarcinoma. According to the hTERT expression, three groups of gallbladder epithelial changes were found: 1.) normal and hyperplastic gallbladder mucosa, 2. low grade dysplasia, and 3.) high grade dysplasia and adenocarcinoma of the gallbladder. The differences between the groups were statistically significant ($p<0.001$).
Conclusions We believe that occasional presence of hTERT in normal and reactively hyperplastic gallbladder mucosa merely reflects its regenerative capacity. Nevertheless, significantly higher hTERT indices in low grade as well as high grade dysplastic epithelium and gallbladder adenocarcinoma are most probably the consequence of hTERT re-expression - an early event in the multistep process of gallbladder carcinogenesis.

O-105

Spontaneous intestinal perforation vs. necrotizing enterocolitis: 2 different entities clinically and pathologically

G De Hertogh, P Van Eyken, M Miserez, H Devlieger, K Geboes
K U Leuven, Leuven, Belgium

Introduction Necrotizing enterocolitis (NEC) is the most common neonatal surgical emergency. However, during recent years an increasing number of laparotomies has been performed for spontaneous intestinal perforation (SIP) in premature infants. The aims of this study were to compare the clinical and pathological features of SIP and NEC and to identify parameters useful to make the differential diagnosis.
Materials and methods We reviewed the clinical files and biopsies from 40 infants indexed as “necrotizing enterocolitis” or “intestinal perforation” between 1991 and 2002.
Results Twenty-six patients had SIP and 14 had NEC. Patients with SIP had lower gestational age and birth weight. They presented early with abdominal distension. Frequent radiological signs were dilatation of bowel loops and pneumoperitoneum. Perforation was in the small bowel in all cases. 77 % survived. Patients with NEC presented later with more systemic symptoms. Pneumatosis intestinalis was present in more than half. The colon was involved more frequently than the small bowel. 50 % survived. Cases of NEC were characterized by necrosis, inflammation and reparative tissue changes with or without pneumatosis intestinalis. In contrast, the bowel in cases of SIP was not necrotic and showed little inflammation. Its most distinguishing characteristic was the presence of one or more defects in the internal layer of the muscularis propia. The myenteric nerve plexus and interstitial cells of Cajal had developed normally.
Conclusions Spontaneous intestinal perforation and necrotizing enterocolitis differ in their clinical and histopathological characteristics. In our cases, SIP was always associated with segmental absence of the intestinal musculature.

O-106

Impact of epitope retrieval in detection of CD117 (c-kit) in gastrointestinal stromal tumors (GISTs) using manual and automated immunohistochemical (IHC) procedures

H Winther, HG Wendelboe, B Crillesen, A Larsen, T Knoll, D Chenoweth, R Welcher, J Askaa
Department of Immunohistochemistry, DakoCytomation A/S, Glostrup, Denmark

Introduction Gastrointestinal stromal tumours are solid tumours associated with c-kit and PDGF-R expressions. The recent introduction of Gleevec/Glivec, an effective inhibitor of the activated c-kit and PDGF-R has stimulated interest in standardizing the immunohistochemical detection of c-kit in GIST-tissues, assuring an appropriate selection of patients for therapy with Gleevec. Aims: The DakoCytomation anti-Human c-kit antibody, code A 4502, was investigated in four different set-ups: 1) without heat-induced epitope-retrieval (HIER), 2) with HIER, 3) preabsorbing the primary antibody with the synthetic peptide used for generation of the primary antibody and 4) testing on fresh versus archival tissue sections.
Materials and methods Tissue sections were obtained from 35 different cases of GIST, confirmed by morphology and IHC-characterisation (c-kit, CD34, S100, SMA, desmin). The IHC was performed manually as well as on automated platforms including the TechMate™ and the Autostainer instruments.
Results The use of HIER consistently displayed a stronger and more uniform staining pattern as compared to an IHC protocol without HIER. In few cases the expression of CD117 was found faintly positive in IHC without HIER. Automated and manual IHC methods displayed similar staining patterns. The specificity of detecting CD117 in a protocol using HIER was confirmed by preabsorption of the primary antibody with immunogen. Storing of fresh cut sections for more than 10 months demonstrated a decrease in IHC CD117 staining intensity.
Conclusion Epitope retrieval enhances the CD117 staining intensity in GIST-tissue. The specificity of the CD117 detection in GIST’s can be confirmed by complete blocking of the positive staining in a parallel set-up, using preabsorption of the antibody by a synthetic c-kit peptide.

O-107

Loss of heterozygosity and microsatellite instability in early onset gastric carcinomas

AAN Milne, R Carvalho, BP van Rees, E Caspers, GJA Offerhaus, MAJ Weterman
Academic Medical Centre, Amsterdam, The Netherlands

Introduction 5-16% of gastric cancer patients worldwide are under 45 and the clinicopathological features are different from the older age group. Here we characterise some of the genetic changes in 40 cases of early onset gastric cancer (EOGC).
Methods Using DNA isolated from microdissected material, a panel of 19 polymorphic microsatellite markers near known or presumed tumour suppresser genes was used to evaluate loss of

heterozygosity (LOH). Microsatellite instability (MSI) status was ascertained using 3 polymorphic microsatellite markers in 40 cases of EOGC and in an additional 24 biopsy cases. Corresponding immunohistochemistry was performed for p53, SMAD4, E-cadherin, MLH1, MSH2 and MSH6. EBV status of the carcinomas was determined using EBER1-mRNA in-situ hybridisation.
Results The most common losses were at loci adjacent to CDH1(17%), TP53(15-23%), RUNX3(22-29%) and SMAD4/DPC4(14-17%). Less frequently, losses were detected at 3p21, 14q24, and loci adjacent to APC, p16INK4a, PTEN, and TFF. No MSI was detected in the 64 cases examined. Immunohistochemistry revealed abnormalities for E-Cadherin in 55% and p53 in 34%. All tumours examined were EBV negative.
Conclusion Common events in EOCG are genetic alterations in CDH1, TP53 and RUNX3 whereas other LOH findings were infrequent. Protein abnormalities of E-Cadherin and p53 were commoner than losses near the corresponding gene. In contrast to gastric cancer in older patients, MSI does not appear to occur in young patients. These findings confirm that unique genetic alterations lead to gastric cancer in the young and highlight the need for further investigation to elucidate the mechanisms by which they occur.

O-108

A place of foveolar hyperplasia in benign epithelial gastric polyps development and classification: Ki-67 LI analysis

J Orlowska[1], A Cerar[2], E Kraszewska[3], J Pachlewski[1], E Butruk[1], J Kupryjanczyk[4]
[1]Dept. of Gastroenterology, Medical Ctr. Postgrad. Educ., Institute of Oncology, Warsaw, Poland
[2]Institute of Pathology, Medical Faculty of Ljubljana, Ljubljana, Slovenia
[3]Dept of Biostatistics, Institute of Oncology, Warsaw, Poland
[4]Dept. of Molecular Pathology, Institute of Oncology, Warsaw, Poland

Introduction A place of Foveolar Hyperplasia (FH) in benign epithelial gastric polyps (BEGP) classification, as well as its role in a development of Hyperplastic Polyps (HP) is still a matter of controversy. Aims: Two questions are to be studied: 1. does FH, HP, Adenoma (A) and Carcinoma (Ca) represent a continuum in terms of Ki-67 proliferative activity ? 2. are there any differences of the means of Ki-67 labelling index (LI) in hyperplastic areas of HP when comparison is made between HPs without other lesions (HP-NOS) and with HPs with different focal lesions such as intestinal metaplasia (HP-IM), dysplasia (HP-D) and/or carcinoma (HP-Ca)?
Materials and methods 135 BEGP from 110 patients were selected to perform Ki-67 immunohistochemical analysis. There were 40 FH, 72 HP (including 21 HP–NOS and 51 HP-IM, HP-D and/or HP-Ca) and 23 A. As controls 16 cases of normal mucosa (N), 9 cases of regenerative FH (FH-R) and 7 cases of Ca were used. Paraffin sections were studied immunohistochemically for Ki-67 LI with application of MIB-1 antibody. The data were analysed using one-way ANOVA models.
Results It has been found that the means of Ki-67 LI between all the groups studied differed significantly ($p<0.001$). Ki-67 LI for FH was high (38.8) and did not differ significantly from FH-R (47.6), A (43.3), and areas of low grade dysplasia in HP-D (42.5), but was significantly higher from N (24.4) and HP (22.8).
Conclusions 1.We hypothesize that FH may probably represent an early event in BEGP formation. 2.There were no significant differences of Ki-67 LI results for hyperplastic areas in HP (19.2) independently if there were focal IM, D and/or Ca simultaneously, or not.

O-109

Histopathological and immunohistochemical evaluation of gastric carcinoma investigated by endobiopsy

MS Mihailovici[1], M Danciu[1], S Teleman[1], L Ivan[2], C Stanciu[1], M Stan[1], G Balan[1], A Potoroaca
[1]University of Medicine And Pharmacy 'Gr. T. Popa', Iasi, Romania
[2]Armed Forces Hospital Iasi, Iasi, Romania

Introduction Among the malignant tumors that occur in stomach, carcinoma is overwhelmingly the most important and common (90-95%). The aims of this study were to report how we histologically evaluate gastric carcinoma (GC) on endobiopsies, using WHO and Lauren classifications. Additionally, we tried to detect the rhabdoid features in specimens with diffuse GC.
Material and methods The study included 2424 gastric endobiopsies, GC being diagnosed in 451 cases (19%), mostly in men (311 cases – 69%). Endobiopsies, routinely embedded, were stained by hematoxylin-eosin, Giemsa, PAS and Alcian blue (pH 2.5). Immunohistochemical studies were performed using vimentin and cytokeratin antibodies for detection of rhabdoid features.
Results and conclusions The highest incidence of GC was in 60-69-year-old aged patients (34%). Using Lauren classification, 279 cases were categorised as diffuse type (62%), 167 intestinal type (37%) and 5 (1%) mixed type GC. Each of these three types were also histologically analyzed according to WHO classification: intestinal type GC (formed by recognizable well/moderately differentiated glands) and diffuse type GC (consisting in poorly cohesive cells diffusely infiltrating the gastric wall with little or no gland formation). In diffuse type GC with rhabdoid features we evidentiated vimentin and cytokeratin in cells with an eccentric nucleus and a paranuclear inclusion. Finally, we pointed out that is very easy to diagnose GC by Lauren and WHO classifications, but is difficult to evidence the mixed type GC due to reduced size of endobiopsies. Recognition of the rhabdoid phenotype in diffuse type GC is important because this feature is associated with poor prognosis and unresponsiveness to conventional therapy.

O-110

Von Recklinghausen's disease: gastrointestinal manifestations of type 1 neurofibromatosis

C Kutlesic, B Stamenkovic, V Katic, L Velickovic, K Katic, M Krstic, M Mitrovic
Institute of Pathology, Medical Faculty of Nis University, Nis, Serbia and Montenegro

Introduction Gastrointestinal involvement in von Recklinghausen's disease occurs in three forms: hyperplasia of the submucous and myenteric nerve plexuses which leads to disordered gut motility; GISTomas showing varying degrees of neural or smooth differentiation; and a distinctive glandular somatostatinoma of the duodenum. This relatively uncommon disorder and late autopsy, diagnosis, are the reasons for this report.
Materials and methods A 42-year-old man reffered to Surgical Clinic for menagement of the profuse bleeding from the upper

gastrointestinal tract. The patient had a 4-year history of dyspepsia, diarrhorea, mild diabetes mellitus and cholelithiasis. One hour after the admission, he died in hypovolemic shock. Taken tissues from all organs were fixed in 10% formaldehyde and embedded in paraffin. Laboratory sections were stained with: HE, AB-PAS, Van Gieson, Grimelius, Masson's argentaffine reaction and BSP methods, using antibody to somatostatin.

Results Cafe au lait spots, multiple skin neurofibromas, mental retardation, skeletal deformities and a variety of tumours arising in the brain (Craniopharyngioma), follicular thyroid adenoma and duodenal somatostatinoma, were found during autopsy. Duodenal bleeding ulcer of gigantic size, was covered with coagula. In the bottom of the duodenal ulcer was discovered duodenal carcinoid of the glandular architecture, intermingled with solid acinar and trabecular growth pattern; its cells contained somatostatin. Marked increase in number and thickness of nerve fibres also was seen, leading to disordered motility and to striking hypertrophy of the muscularis propria.

Conclusion having in mind that the patient has the sister, and that this disease has hereditary character, we will invite the sister as soon as possible and she will be in the future the target of our investigation.

O-111

Increased expression of muc1 and muc6 and decreased expression of muc2 in colorectal adenoma-carcinoma spectrum: A tissue array study

I Kuzu[1], S Ozturk[1], G Kaygusuz[1], A Ensari[1], EO Kirimker[2], A Kuzu[3]
[1]Ankara University School of Medicine, Department of Pathology, Ankara, Turkey
[2]Ankara University School of Medicine, Fourth Grade Clinical Medical Student, Ankara, Turkey
[3]Ankara University School of Medicine, Department of General Surgery, Ankara, Turkey

Introduction Mucin-type glycoproteins are widely expressed in the gastrointestinal tract. Little is known concerning the relationship of altered mucin antigens in colorectal polyps. The aims of this study were to determine the different patterns of mucin distribution of MUC1, MUC2, MUC5AC and MUC6 and compare their patterns of expression with respect to histopathologic criteria of malignant potential in colorectal carcinogenesis by tissue array using immunohistochemistry.

Materials and methods Core tissue biopsies of 4 mm in diameter taken from paraffin-embedded tissue blocks of 97 colorectal adenomas [19 tubular, 40 tubulovillous, 38 villous] among which 16 contain intramucosal carcinoma (P-IMC) were examined for MUC1, MUC2, MUC5AC and MUC6 expression. MUC expression was defined as “markedly reduced expression (MRE)”, “reduced expression (RE)” and “strong expression (SE)”.

Results MUC1 expression significantly increased in P-IMC when compared with adenomas with mild (MRE: 75% vs 100%; RE: 25% vs no adenoma) and moderate dysplasia (MRE: 75% vs 96.7%; RE: 25% vs 3.3%). MUC6 expression increased as lesions proceeded from mild to moderate to severe to IMC. When the polyps were categorized as benign and malignant; MUC1 (MRE: 75% vs 96.2%; RE: 25% vs 3.8%) and MUC6 (MRE: 87.5% vs 98.8%; RE: 12.5% vs 1.3%) expression increased in malignant group compared with benign group. However MUC2 expression (MRE: 22.5% vs 43.8%; RE: 28.7% vs 31.3%; SE: 48.8% vs 25%) increased in benign adenomas compared with malignant ones.

Conclusion Increased expression of MUC1 and MUC6 and decreased expression of MUC2 play a role in the progression of colorectal adenomatous change.

O-112

Immunophenotypic analysis of submesothelial fibroblasts during peritoneal dialysis-related fibrosis

J Jimenez-Heffernan[1,2], A Perez-Campos[2], C Perna[1], MA Bajo[3], G del Peso[3], P Gonzalez-Peramato[1], A Aguilera[4], C Gamallo[4], M Lopez-Cabrera[4], R Selgas[4]
[1]University Hospital, Guadalajara, Spain
[2]Hospital La Zarzuela, Madrid, Spain
[3]University Hospital La Paz, Madrid, Spain
[4]University Hospital La Princesa, Madrid, Spain

Introduction Peritoneal dialysis (PD) is an alternative to hemodialysis for the treatment of end-stage renal disease. The long term exposure to dialysis solutions causes progressive peritoneal fibrosis and functional decline of the peritoneum. The pathologic process that leads to fibrosis is not well understood and most studies have focused on mesothelial cells, probably because they are easy to obtain from peritoneal effluents. The aims of this study were to establish diagnostic markers of peritoneal fibrosis and pathogenic clues to explain the fibrogenic process. The study was focused on submesothelial fibroblasts from normal controls and PD patients.

Materials and methods Parietal peritoneal biopsies were collected from three patient groups: normal controls (n=15), non-PD uremic patients (n=17) and uremic patients on PD (n=27). In order to study myofibroblastic differentiation and mesothelial-to-mesenchymal transition, alpha-smooth muscle actin, desmin, cytokeratins, and E-cadherin were analyzed. We also evaluated CD34 expression by submesothelial fibroblasts.

Results Fibroblasts from normal controls and non-PD, uremic patients showed no myofibroblastic nor mesothelial markers, but an intense expression of CD34. The opposite immunophenotypic pattern was present during PD-related fibrosis. Expression of mesothelial markers (cytokeratins and E-cadherin) by fibroblast-like cells and alpha-smooth muscle actin by mesothelial and modified mesothelial cells are evidence that mesothelial-to-mesenchymal transition occurs during PD. Loss of CD34 expression was another helpful indicator of fibrosis.

Conclusion The immunophenotype of submesothelial fibroblasts varies depending on the existence of a fibrogenic condition. This information results useful for the differentiation between quiescent and activated fibroblasts. In addition, it shows interesting information regarding the origin of this cell population.

O-113

Immunohistochemical and genetic high-throughput analysis of gastrointestinal stromal tumors

D Di Vizio[1], L Insabato[1], G Pettinato[1], A Boscaino[3], R Russo[4], E Carafa[2], G Duchini[2], A Di Blasi[3], L Terracciano[1], L Tornillo[2]
[1]Dpt of Anatomic Pathology, Federico II University of Naples, Naples, Italy
[2]Dpt of pathology, University of Basel, Basel, Switzerland
[3]Antonio Cardarelli Hospital, Naples, Italy
[4]S. Giovanni Di Dio and Ruggi d'Aragona Hospital, Salerno, Italy

Introduction Gastrointestinal stromal tumors (GIST) are among the most common primary mesenchymal tumors of gastrointestinal

tract. They are characterized by diffuse immunohistochemical positivity for c-KIT protein (CD117). The aims of this study were to assess the immunohistochemical and genotypic features of a large series of GIST using tissue microarray technique.
Methods 100 GIST were retrieved from the files of Dpt of Pathology of our Institutions and a tissue microarray (TMA) was built. Immunohistochemistry for CD117, Actin, Desmin, S100, NSE, Mib1 was performed. Interfase FISH analysis was carried out for the following genes: mdm2, EGFR, C-myc, CCD1 and Her-2.
Results 84% of the tumors resulted positive for CD34, 7% for Desmin, 48% for Actin, 10% for S100, 51% for NSE, 25% for Mib1. A significant difference between gastric and non-gastric GIST was observed for CD34, Desmin and S100. Age, size, necrosis and NSE positivity significantly correlated with aggressive behavior of the tumors. Moreover, an amplification of c-myc, mdm2, EGFR, CCD1 in 19 tumors was found. The tumors were all but two borderline or high risk tumors. Cases of co-amplification were also detected in clinically malignant or histologically high risk tumors.
Conclusion Useful parameters for prognostic evaluation of GIST are age, size and necrosis. Furthermore, the observed amplification of c-myc, mdm2, EGFR suggests a role of Rb-CCD1 pathway in the acquisition of malignant phenotype in a subset of GIST.

O-114

Digital slide and virtual microscopy based routine and telepathology evaluation of routine gastrointestinal biopsy specimen

L Berczi[1], C Diczhazy[1], V Varga[2], A Tagscherer[2], B Molnar[2], B Szende[1], Z Tulassay[2], L Kopper[1]
[1]I.Dept.of Pathology And Experimental Oncology, Budapest, Hungary
[2]II. Dept. of Medicine, Budapest, Hungary

Introduction The aim of the study was the evaluation of a recently developed digital slide and virtual microscope system, its comparison with optical microscopy on routine gastric biopsy specimen in local and remote access mode.
Materials and methods H/E stained routine gastric, duodenal and colon (altogether 61) biopsy specimen were selected, scanned and evaluated by two specialists on an optical (OM) and virtual microscope (VM).
Results The overall concordance of VM to a consensus diagnosis (CON) was 95.1% and 97% of the OM to CON. The clinically important concordance was 100% and 100% respectively. The two methods showed concordance in 92% and clinically important concordance in 94.1%. The reasons of the discordance was image quality (one case), interpretation difference (3 cases). The overall hard disc place for a gastric biopsy was between 30 to 50 megabytes. The scanning time was between 20 to 40 minutes on a commercial microscope (Axioplan 2, Carl Zeiss, Germany) and 2 to 5 minutes on an automated slide scanner (Hi-Scope, 3DHISTECH Ltd., Budapest)
Conclusions Remote evaluation of the digital slides through Internet shows the advantages of the previously used static and dinamic telepathology methods. The digital slide and the virtual microscope are real alternative techniques in the computerization of the histology laboratory and in teleconsultation services.

O-115

MUC4 neoexpression in intraductal papillary mucinous carcinomas and pancreatic ductal adenocarcinomas

J Lüttges, K Richter, L Schminke, C Heinitz, G Klöppel
Department of Pathology, University of Kiel, Kiel, Germany

Introduction The expression pattern of the MUC glycoproteins MUC1, MUC2 and MUC5AC may be useful in classifying the various types of intraductal pancreatic neoplasms (IPMNs). Recent studies have revealed that MUC4 is expressed in ductal pancreatic carcinomas (PDAC) only. This study investigates whether MUC4 is expressed in IPMNs and in particular in those with invasive components. In addition, MUC4 reactivity was studied in PanINs of both IPMN and PDAC.
Methods Paraffin blocks from resection specimens from 20 PDACs and 9 IPMNs (6 invasive) were investigated immunohistochemically ([IHC] antibody clone IG8) and by in-situ hybridization ([ISH] digoxigenin labeled 48 oligomer nucleotide specific for sequences corresponding to repeat domains of MUC4).
Results The normal pancreas is MUC4 negative. 17 of 20 PDACs were positive for MUC4 in both IHC and ISH. Only 3 IPMNs were MUC4 positive, and these cases were of the oncocytic type. Invasive IPMN components of the DAC type (3/3) and one of muconodular type (1/3) showed MUC4 expression at both the protein and the RNA level. In IPMNs associated PanIN lesions of all grades were negative, whereas in PDACs a few PanIN3 lesions were positive.
Conclusions MUC4 neoexpression in the pancreas seems to be a feature of invasive ductal neoplasms (IPMN, PDAC), with the exception of oncocytic IPMNs. The aberrant expression, in particular the shift from the negative intraductal to the positive invasive component in IPMNs, is so far unexplained, but it may be related to the genetic alterations known in IPMNs and PDACs.

O-116

Hypermethylation of hMLH1 and HPP1 in adenocarcinomas of the upper gastrointestinal tract

M Sarbia[1], H Geddert[1], S Kiel[1], E Iskender[1], A Florl[2], T Krieg[1], S Vossen[3], H Gabbert[1]
[1]Institute of Pathology, Heinrich Heine University, Dusseldorf, Germany
[2]Department of Urology, Heinrich Heine University, Dusseldorf, Germany
[3]Department of Surgery, Heinrich Heine University, Dusseldorf, Germany

Introduction Hypermethylation of CpG islands represents an important epigenetic mechanism for silencing of tumor suppressor genes during carcinogenesis. In this investigation, the prevalence of hypermethylation of the DNA mismatch repair gene hMLH1 and of the recently identified HPP1 gene was investigated in adenocarcinomas of the upper gastrointestinal tract.
Materials and methods Using methylation-specific real-time PCR and fluorescence-labeled DNA-probes, hypermethylation of hMLH1 and HPP1 was investigated in 50 Barrett's-esophagus-associated adenocarcinomas, 50 cardiac carcinomas and in 50 gastric carcinomas. Additionally, hMLH1 protein expression was investigated by means of immunohistochemistry. In a subset of cases the presence of DNA-microsatellite instability was tested.

Results Hypermethylation of hMLH1 was found in 14% of Barrett's carcinomas, 28% of cardiac carcinomas and in 32% of gastric carcinomas, whereas hypermethylation of HPP1 was found more frequently in all 3 tumor types (64% vs. 38% vs. 54%). In gastric cancer, HPP1 hypermethylation was found more frequently in tumors with concomitant hMLH1 hypermethylation (81%), than in those without hMLH1 hypermethylation (41%, p=0.008). Complete loss of hMLH1 protein expression which was present in 10 carcinomas (5 cardiac and 5 gastric) was invariably correlated with hMLH1 hypermethylation and with microsatellite instability.
Conclusion Our data indicate that microsatellite instability and loss of the mismatch repair protein hMLH1, which is mainly caused by hMLH1 gene hypermethylation, is more prevalent in the carcinogenesis of the stomach and the cardia than in the esophagus. Moreover, in gastric cancer hMLH1 hypermethylation is correlated with hypermethylation of the HPP1 gene.

O-117

Antral G-cells in sporadic fundic gland polyps patients: an immunohistochemical study

P Declich[1], E Tavani[1], L Pastori[1], A Prada[2], E Giannini[1], S Belone[1], M Buono[2], C Gozzini[2], M Porcellati[1], A Bortoli[2]
[1]Service of Pathology, Rho Hospital, Rho, Italy
[2]Division of Gastroenterology, Rho Hospital, Rho, Italy

Introduction Fundic gland polyps (FGPs) are tiny (2-5mm), often multiple polyps of the acid secreting gastric mucosa, described in a sporadic form prevalently in middle-aged females or in association with Familiar Adenomatous Polyposis (FAP) and attenuated (AFAP) variants, and recently in association with Zollinger-Ellison syndrome. This recently described association prompted us to evaluate the antral G-cell population in a case series of sporadic FGPs.
Materials and methods We studied prospectively a group of 26 patients with sporadic FGPs who had an antral biopsy available. Prior therapy with PPI was taken in account. The 26 antral samples, fixed in Bouin's fluid, were stained with hematoxylin-eosin, Giemsa and Alcian blue (pH2.5)-PAS and anti-gastrin polyclonal antiserum (Dako, Dakopatts, Denmark), diluted 1:300 for 30' at room temperature, using a standard ABC method. Four antral normal biopsies were used as controls. The results were scored as follows: normal: 1-2 G-cells per-gland or foveola, with uneven distribution; simple hyperplasia: more than four-five G-cells per gland; linear hyperplasia: continuous lining of G-cells.
Results All samples showed a normal appearing antrum, with slight hyperemia, but without significant inflammation, intestinal metaplasia and Helicobacter pylori (Hp) colonization. Two out of 26 samples showed a normal G-cell population (rare positive cells with uneven distribution) whereas 10 samples showed a simple, 14 a linear hyperplasia. Only 5 patients (1 with normal G-cell population, 4 with hyperplasia) had a previous long-term treatment with PPI.
Conclusions Our preliminary study of 26 sporadic FGPs with available antral biopsies, showed that morphologically normal, Hp-free antral mucosa harboured in fact a significant G-cell hyperplasia (24/26). This hyperplasia was correlated with an assumption of PPI in only 4 patients, being apparently primitive in 20 patients. The present results raise the possibility that primary antral G-cell hyperplasia may have a role in the genesis of sporadic FGPs, in close similarity with the occurrence of FGPs in the Zollinger-Ellison syndrome.

O-118

Activation of caspases could contribute to degradation of AP-2a and c-kit during melanoma progression

C Woenckhaus[1], J Giebel[1], K Failing[2], I Fenic[2], T Dittberner[3], M Poetsch[1]
[1]University of Greifswald, Greifswald, Germany
[2]University of Gießen
[3]Consultant Comitee of the Health Insurance

Introduction Malignant melanoma is an increasing neoplasm in the western world. Advanced tumors gain metastatic potential and are responsible for high mortality rates. During tumor progression a downregulation of the transcription factor AP-2a and the receptor thyrosine kinase c-kit was observed. However, mechanisms leading to a loss of both proteins are unknown. Besides genetic changes post-transcriptional downregulation by caspase-6 and -3 is recently discussed. Aims were: i) to investigate malignant melanoma for AP-2a and c-kit genetically and by protein expression, ii) to study the implication of activated caspases.
Methods 10 SSMs, 10 NMs and 30 metastases were analyzed by direct sequencing analysis for all exons of AP-2a and c-kit genes and by immunohistochemistry for the respective proteins and cleaved (activated) caspase-6 and -3.
Results Four tumors showed point mutations in the activation motif of AP-2a (exon 2). No genetic alterations were detected in the c-kit sequence. Immunohistochemistry revealed a progressive loss of dermal AP-2a and c-kit expression when comparing SSMs with NMs and Ms which was paralleled by a strong expression of caspase-6 in the primary melanomas and Ms, the later were also characterized by caspase-3 expression.
Conclusion Tumor progression in melanoma is characterized by a loss of AP-2a and c-kit. Caspase-6 probably contributes to this down-regulation, as it was recently shown in vitro. The activation of caspases in melanoma might not only induce apoptosis but could be substantial for tumor growth.

O-119

VEGF-A induced micronodular transformation as a novel mechanism of melanoma metastasis

B Kusters, RMW de Waal, P Wesseling, C Maass, K Verrijp, DJ Ruiter, WPJ Leenders
Department of Pathology, Nijmegen, The Netherlands

Introduction In cancer patients, tumor-expression of the angiogenic factor Vascular Endothelial Growth Factor-A (VEGF-A) correlates with high tumor vascularity and increased metastatis, but how these latter two relate is unclear. We investigated the mechanisms of VEGF-A –enhanced metastasis of the human melanoma cell line Mel57.
Methods Stably transfected Mel57 cells, expressing VEGF-A or EGFP, were injected into the internal carotid artery or tail vein of nude mice to establish brain or lung metastases (colonization models). Subcutaneous tumors were grown to examine spontaneous metastasis to lung. Tumors and metastases were examined by (immuno)-histochemistry.
Results In colonization models, VEGF-A expression did not give tumor cells a colonization advantage. Metastases originated predominantly by clonal expansion of single cells. In contrast, spontaneous metastasis from subcutaneous tumors was enhanced in

tumors with VEGF-A expression, this enhanced metastatic potential was induced by a distinct architectural transformation of the s.c. tumors: while Mel57-EGFP and parental Mel57 tumors showed extensive necrosis, Mel57-VEGF-A tumors presented a micronodular growth pattern, with nodules protruding into sinusoidal dilated vasculature. These micronodules proved to be polyclonal, had tissue characteristics and caused metastatic embolism in the pulmonary artery with subsequent metastatic outgrowth.

Conclusion VEGF-A may enhance spontaneous metastasis not simply by increased single cell shedding into the circulation by an increased tumor vascularity but by induction of a micronodular transformation of a tumor resulting in enhanced shedding of (polyclonal)tissue fragments into the circulation. This step of tumorintravasation is probably a rate limiting factor in development of metastasis.

O-120

Correction of cytogenetic disturbances in patients with relapsing genital herpes

LA Lebedinskya, OP Abaza
Donetsk Medical State University, Donetsk, Ukraine

Introduction Serious forms of relapses of genital herpes (GH) are accompanied by disturbances of chromosomal apparatus of lymphoid cells (L.A. Lebedinskya, 2001). Correction of the given infringements is the important problem of practical public health service. The aim of our research was development of a complex method of correction of cytogenetic infringements in patients with GH.

Materials and methods We had investigated and treated 45 patients (complex treatment) with GH in the age of 18-50 years, with frequency of relapses of one time in 1.5-2 months. The control group was made by 30 healthy persons, same age group. Cytogenetic disturbances in T-lymphocytes of peripheral blood surveyed determined by metaphase method. Complex method of treatment of patients with GH included acyclovir 200 mg 5 times per day before clinical recovery and Phytopreparation “Bacplan”, received by an original way from Quercus cortex. Phytopreparation “Bacplan” shows immunomodulation, anti-inflammatory and antimutagen properties. Preparation “Bacplan” appointed per Os 1.0 g per day within 20 days. External –2% solution of Bacplan in the form of lotion on affected body parts 5 time in day.

Results Average frequency of cells with aberrations of chromosomes (AC) in T-lymphocytes of peripheral blood of patients with GH before treatment were much higher in comparison with parameters of control group (accordingly 2.3±0.13 and 1.47±0.14% $P<0.05$). In patients were marked disturbance of chromosomal and chrmotoid types. In 51.8% cases aberration of chromosomes were registered in 1-5 chromosome pairs. After complex treatment of average frequency of cells with AC in patients has decreases to 20 days to1.6±0.11% ($P<0.05$) and practically come nearer to control parameter (1.47±0.14%).

Conclusions Thus, use of viral specific preparation acyclovir in combination with phytopreparation “Bacplan” reduces frequency of structural infringements of chromosomes in T-lymphocytes of patients with GH.

O-121

Different expression patterns of S-100 versus S-100B in primary skin melanoma

J Timar, N Udvarhelyi, Z Orosz
National Institute of Oncology, Budapest, Hungary

Differential diagnosis of melanoma involves immunohisto-chemistry where S-100 is a traditional marker which is recently completed by gp100/HMB45, MART-1 and tyrosinase. The S-100 family of Ca-binding proteins comprises the A (1-6) and B isoforms. Recent microarray analysis identified S-100B as the melanocyte lineage marker. In this work we have compared the expression patterns of S-100 proteins using antibody recognizing both isoforms versus that which is specific for S-100B in 68 human skin primary melanoma samples. There were 3 expression patterns observed: focal, herogenous and diffuse for both antibodies. The most frequent expression pattern was the diffuse one (36-45%) while the least frequent was the focal pattern (10-14%) in case of both antibodies. When the individual cases have been analysed for the expression patterns for the two antibody we found 49% discrepancy. In about half of these cases (22%) the discrepancy was minor (heterogenous versus diffuse staining pattern), but in almost a third of the cases (27%) it was found to be considerable (focal pattern versus heterogenous or diffuse). We have concluded that the expression patterns of S-100 and S-100B proteins in human melanoma are frequently different. Since gene expression studies identified S-100B as linage marker, it is highly recommended to use monospecific antibody for routine diagnosis. Furthermore, S-100B is validated as sensitive serum marker for melanoma progression accordingly it is another indication for the use of anti-S-100B antibody in the routine diagnosis.

O-122

Primary cutaneous diffuse large B-cell lymphoma

D Radulescu[1], S Stolnicu[2], C Amalinei[1], C Ardeleanu[3], S Mocan[4], G Dobrescu[1], A Stanciu[1]
[1]University of Medicine and Pharmacy, Iasi, Romania
[2]University of Medicine, Targu-Mures, Romania
[3]'V. Babes' Institute, Bucharest, Romania
[4]Municipality Hospital, Targu-Mures, Romania

Introduction Primary cutaneous B-cell lymphomas represent subtypes of extranodal B-cell lymphomas with distinct clinico-pathologic features. They account for approximately 25% of primary cutaneous lymphomas. The most common forms include follicle cell lymphoma, marginal zone lymphoma, immunocytoma, and diffuse large B-cell lymphoma. We report 2 cases of primary cutaneous diffuse large B-cell lymphomas, one in the left gluteal region (4/5 cm in diameter), and the other in the left leg (5/3 cm in diameter), both appearing clinically ulcerated.

Materials and methods Routine paraffin embedding and usual stainings, followed by immunohistochemistry were used.

Results Microscopy evidentiated in the papillary and reticular dermis a diffuse pattern of growth of cells with a moderate degree of morphologic variation, with moderate, slightly basophilic cytoplasm and round-ovalar nuclei, with vesicular aspect owing to

margination of chromatin at the nuclear membrane, 1-2 nucleoli, and frequent mitoses. Gomory staining revealed a network of reticulin with reduced intervening spaces. Immunohistochemistry evidentiated a diffuse positivity of vimentin and CD20 (L26), S100 positivity in few cells, desmin negativity, MIC 2 negativity, CD30 (BERH2/Ki-1) negativity, actin negativity in tumor, but positivity in vessels, EMA negativity and PCNA positivity in almost 50% of the cells.

Conclusion Final diagnoses of primary cutaneous diffuse large B-cell lymphomas were considered correlating the clinical, morphologic, and immunophenotyping features. Although prognosis of most primary cutaneous B-cell lymphomas is favorable, with 5-year survival rates over 90%, diffuse large B-cell lymphoma is more aggressive. We appreciated an unfavorable prognosis of both cases, but especially in the patient where the lymphoma occurred in the lower leg, as this location is associated with a more aggressive behaviour.

O-123

In malignant melanoma CD10 protein expression is associated with metastatic tumors, higher Clark levels and tumor thickness according to Breslow

N Bilalovic[1], R Golouh[2], JM Nesland[3], I Selak[1], E Torlakovic[3]
[1]Department of Pathology, Sarajevo University Hospital, Sarajevo, Bosnia and Hezegovina
[2]Department of Pathology, Ljubljana Institute of Oncology, Slovenia
[3]Department of Pathology, The Norwegian Radium Hospital, Norway

CD10 antigen is a 100 kD a cell surface zinc metalloendopeptidase and is expressed by a variety of normal and neoplastic lymphoid and non-lymphoid tissue including melanomas. Kanitakis et al. (Melanoma Res 2002;12:241-244) have recently demonstrated that CD10 expression is significantly more common in metastatic than primary melanomas. We have evaluated biopsies from 70 patients with primary and 27 patients with metastatic melanoma. Formalin-fixed/paraffin-embedded tissues were studied by immunohistochemistry using mAb 56C6 from NovoCastra Laboratories and EnVision+® from DakoCytomation. Overall, CD10 was expressed in 34/97 samples, but the percentage of CD10-positive cell was significantly higher in metastatic tumors (p=0.002) and also in primary tumors with higher Clark level (p=0.01) and tumor thickness according to Breslow (p=0.008). Even though the intensity of expression was associated with depth of invasion (Clack levels p=0.007, Breslow p=0.03), there was no definitive difference between primary and metastatic tumors (p=0.058). We conclude that CD10 expression in malignant melanoma is associated with tumor progression.

O-124

Sclerosing adenosis of the skin

G Collina[1], L Di Tommaso[1], M Reggiani[2]
[1]Section of Anatomic Pathology, Department of Oncology, Bellaria Hospital, University of Bologna, Bologna, Italy
[2]Dermatology Unit, Bellaria Hospital

Sclerosing adenosis is a lesion that occurs in the breast; rare cases have also been reported in other organs such as prostate and skin. We report a case of sclerosing adenosis of the skin incidentally found at the periphery of a basal cell carcinoma. A 72-year-old man had a polypoid lesion of the scalp measuring 3.5 cm in diameter. The lesion was surgically removed and, at histology, it was composed of a nodular basal cell carcinoma. Below the basal cell carcinoma, there was a well circumscribed but not encapsulated lesion constituted by small, packed glands separated by cellular stroma, reminiscent of sclerosing adenosis of the breast. Some glands showed open lumina bordered by cells with eosinophilic, granular cytoplasm while other glands were arranged in solid clusters or elongated cords. Two distinct layers of cells were seen bordering the glands: a luminal layer of cuboidal cells and an outer layer of basal cells with scanty cytoplasm and spindle nuclei. At immunohistochemistry the outer cell layer was positive for actin, calponin, caldesmon and keratin 14 antibodies showing therefore myoepithelial cell differentiation. The luminal layer was positive with low weight keratin; moreover luminal cells were decorated by GCDFP-15 antibody, a marker of apocrine differentiation. To the best of our knowledge this is the first case of sclerosing adenosis of the skin showing apocrine metaplasia of luminal cells. The case here reported is an additional example of the existence of occasional similar lesions between skin and mammary gland.

O-125

Immunolocalization of human sperm protein 17 in skin cancer

B Franceschini[1], F Grizzi[1], PL Hermonat[2], M Monti[1], N Dioguardi[1], M Chiriva-Internati[3]
[1]Istituto Clinico Humanitas, Milan, Italy
[2]University of Arkansas Medical Sciences, Little Rock, Arkansas, USA
[3]Texas Tech University Health Science Center, Amarillo, Texas, USA

Introduction A variety of cancer\testis (C\T) antigens has been found to be expressed in healthy testis and in a wide range of human malignancies, including melanoma. The effectiveness of these antigens as target for active specific immunotherapy has been largely demonstrated. Recently a new human C\T, called sperm protein 17 (HSp17) has been investigated in multiple myeloma and ovarian cancer. The aim of this study was to investigate the expression of HSp17 in healthy skin and melanocytic skin lesions, in order to evaluate the usefulness of this antigen to develop effective specific immunotherapeutic procedures.

Methods The authors assessed the immunolocalization of HSp17 in paraffin embedded formalin fixed specimens of healthy skin (n=3) and tissues representing cutaneous melanocytic lesions [common nevi (n=15), Spitz nevi (n=5), blue nevi (n=7), atypical nevi (n=5) and melanomas (n=19)].

Results HSp17 was not detected in healthy skin. It was recognized with a high frequency in cutaneous melanocytic lesions in some cells of the dermal stroma, often containing melanin, compatible with melanophages. A higher expression of HSp17 was observed in hyperpigmented nevi.

Conclusion The emergent complex function of HSp17 suggests the necessity of further studies to investigate the relation between melanophages and HSp17. Although HSp17 was not detected in healthy skin, its limited detection in resident melanophages recognized in cutaneous lesions, and not in tumoral cells precludes its applicability as target in skin cancer immunotherapy.

O-126

Histopathological findings in autopsy tissues of Crimean Congo haemorrhagic fever - a case report

J Dimitrijevic[1], S Zaki[2], G Brajuskovic[1], S Usaj Knezevic[1], S Cerovic[1], I Tufegdzic[1]
[1]Institute of Pathology, Military Medical Academy, Belgrade, Serbia and Montenegro
[2]Centres for Disease Control and Prevention, Atlanta, USA

Introduction Crimean Congo haemorrhagic fever (CCHF) is endemic in many countries in Asia, Africa and Europe. The virus, which causes CCHF, is a Nirovirus from the Bunyaviridae family. Although primarily a zoonosis, sporadic cases and outbraces of CCHF affect humans.
Case report A 43-year-old female patient was hospitalized due to sudden onset of fever, headache, vomiting and abdominal pain. During the next days, her condition became worse, she was unconscious, anuric, cyanotic with multiple edema on extremities, large vaginal coagulums and with appearance of haemorrhagic secretion in aspired fluid from the respiratory tract. Three days after admission, due to sudden onset of cardiac arrest, patient died. Pathologic findings: severe bleeding from the mucous membranes and internal organs were found, particularly emphasized in the liver, kidneys, heart, brain and other organs. Widespread hepatocellular necrosis with focal microvesicular steatosis and multiple intracytoplasmatic microvesicular inclusions were the most striking morphological findings. Diffuse necrosis of renal tissue was also found. Recent haemorrhages in lungs, cardiac muscle, suprarenal gland, spleen, and gastric mucosa were found. Lymphoid depletion was detected in lymph nodes. The RT- PCR method for detection CCHF virus has been applied in analysing serum and tissue samples. Serological testing and testing from paraffin embedded tissue were positive.
Conclusion Autopsy pathologic findings of CCHF include widespread haemorrhages of the skin, mucous membranes, pleura, peritoneum. Necrosis is frequent in all organs and tissues, often of ishaemic nature. Autopsy results of our patient showed similar pathologic findings and by PCR method we confirmed etiopathogenesis of this disease.

O-127

The modern morphological characteristic of placenta in syphilis

Z Parpiev[1], G Reymnazarova[2], B Magrupov[2]
[1]Dermatology and Venerology, Tashkent, Uzbekistan
[2]First Tashkent Medical Institute, Tashkent, Uzbekistan

Material and methods We investigated the placentas in three cases of intrauterine death caused by inherited syphilis. Grossly, they were small and medium lobular, showed a marked sclerosis of large vessels and they looked white-muddy. The umbilical cord was also sclerotic and showed obliteration of vessels. Their weight corresponded to term of gestation, whereas their area was smaller and their thickness greater than in normally proceeding pregnancy, but these differences were not significant ($p>0.05$).
Results Light microscopic investigation revealed avascularized stroma and sclerotic villi with vessels showing obliterating angiopathy. These changes were combined with processes of compensatory character, such as sharply extended subsyntitially located capillaries and large number of small vesels.
Conclusion In the morphological study of placenta, the attributes of damaged placental tissue and development of compensatory reactions directed towards the maintenance of necessary balance in the mother-placenta-fetus system were revealed. In placenta, contrary to the descriptions of the last years, we found no significant increase of its weight and change in this connection fetus-placenta of factor. The basic changes in placenta were characterized by the development of productive vasculitis with obliteration of the vascular lumina and presence of avascularized terminal villi. The thickening of vessel walls of the main villi as a result of proliferative endarteriitis can be considered as a characteristic attribute for syphilitic infection.

O-128

Immunohistochemical detection of deleted LMP1 in EBV associated lesions

J Nicholls[1], F Grasser[2], E Kremmer[3]
[1]Department of Pathology, University of Hong Kong, Hong Kong
[2]Institute for Microbiology, University of Saarlandes, Hamburg, Germany
[3]GSF-Institute for Immunology and Haematology, Munich, Germany

Introduction The latent membrane protein 1 (LMP1) of Epstein-Barr virus is one of two postulated viral oncogenic proteins. Previous reports have suggested that sequence variations, and in particular a 30 base pair deletion variant called CAO, may define different disease populations.
Material and methods We developed a cocktail of rat monoclonal antibodies that were specific for the non-wild type LMP1 and compared the presence of the antibody staining with LMP1 DNA sequence analysis on clinical samples of nasopharyngeal carcinoma, peripheral T-cell lymphoma, Hodgkin's disease and lymphoblastoid cell lines from normal volunteers and patients with NPC.
Results and conclusion Our results demonstrate specificity of the monoclonal cocktail for detecting the wild-type LMP1 and the ability to sub-differentiate between the Mediterranean type of LMP1 and the CAO-LMP1.

O-129

Visceral leishmaniasis primarily diagnosed in duodenal biopsy: report of three cases

F Pardal, A Silva, V Velasco, M Teixeira
Serviço De Anatomia Patológica, Braga, Portugal

Introduction Visceral leishmaniasis (kala-azar) is a zoonosis caused by a flagellate protozoan, of the genus Leishmania, which is transmitted to man from reservoir animals (like a dog), by a vector of the genus Phlebotomus. Generally it affects the mononuclear phagocytic system of the bone marrow, liver and spleen. The gastrointestinal system is rarely involved. Diagnosis of the infection depends on microscopic identification of leishmanias amastigotes in tissues or blood cultures or by serologic means. Aims: Visceral leishmaniasis is a rare disease in patients without immunodeficiency, the authors report three cases diagnosed primarily in duodenal and gastric biopsy from immunocompetent patients.
Materials and methods From the files of Pathology Department of S. Marcos Hospital five cases of visceral leishmaniasis have been collected in a 12 years period, all from immunocompetent patients, namely without HIV infections. The authors describe three of the five cases, which were primarily diagnosed by gastro-duodenal biopsy. Lately, was noted the presence of amastigotes in other tissues.

Results After histologic diagnosis resulted a full clinic diagnosis of systemic leishmaniasis with advanced stage of disease.
Conclusions Pathology Department files reveal a significant percentage of visceral leishmaniasis diagnosed by gastroduodenal biopsy, three of five cases. Thus, in no endemic countries for this opportunistic infection and in immunocompetent patients, gastrointestinal biopsy can, eventually be a rapid and sensitive method of diagnosis, since most of the patients present at an advanced stage of disease.

O-130

Impact of the Sudden Acute Respiratory Syndrome (SARS) on the pathology laboratory: a Singapore experience

AR Chang, A Wee, SM Chong, T Ming
Pathology Department, National University Hospital, National University of Singapore, Singapore

The sudden acute respiratory syndrome (SARS) is a new global health problem that has received unprecedented attention. The predominant route of infection is by droplets and close contact with an infected person poses the highest risk of being infected with the SARS virus. The majority of cases among health care workers have occurred in doctors and nurses who have cared for SARS patients. Pathologists and laboratory personnel are regarded as low risk for infection because they are infrequently in direct contact with patients. However, they receive specimens, including sputa, bronchiolo-alveolar lavage samples, excised tissues, blood and body fluids from infectious cases. Two further possible sources of infection are during autopsies and the onsite processing of fine needle aspiration specimens for immediate diagnosis. Not uncommonly, few clinical details are attached with a specimen to alert the laboratory so universal precaution must be in place and all specimens regarded as infectious. But with a new infection such as SARS where information on its natural history, infectiousness and mode of transmission are still evolving, greater vigilance and a pro-active approach are needed. During the period March - May 2003 Singapore was faced with a potentially serious SARS epidemic and to minimize the chance of personnel in the Pathology Department, National University Hospital being infected and thus compromise the diagnostic service a contingency plan was implemented. This report describes the impact of the plan on the department. SARS is a global disease and pathologists in countries who have not encountered it may find the information useful for preparing their laboratory for the eventual arrival of SARS.

O-131

Angiotropic large cell lymphoma of the central nervous system - report of four cases

D Cvetkovic Dozic, M Skender Gazibara, B Dozic, T Terzic, S Dozic
Institute of Pathology, Medical Faculty, Belgrade, Serbia and Montenegro

Introduction Angiotropic large cell lymphoma (ALCL), or intravascular lymphoma, is a rare form of high grade non-Hodgkin's lymphoma, predominantly of B-cell lineage. It is characterized by extensive proliferation of lymphoma cells within the lumina of small blood vessels particularly of the CNS and skin with tendency to disseminate into multiple organs. Because of nonspecific manifestations the clinical diagnosis of ALCL is difficult as well as the morphological diagnosis, which may be problematic and subtile.
Methods We studied four cases of ALCL with dominant neurologic symptoms in the form of vasculitis, dementia and cauda equina syndrome. The diagnosis was made by autopsy in three cases and by brain biopsy in one case. In one autopsy case, the ALCL was associated with AIDS in a 12-years old hemophilic boy.
Results Microscopically, in all cases, small blood vessels of the CNS were distended by collections of large atypical lymphoid cells which obstructed the vascular lumina. Tumor cells cytoplasm was amphophilic, the nuclei were large, irregular with prominent nucleoli. Mitoses were numerous. In the vicinity, there were small zones of spongy edema, reactive gliosis and foci of total or selective necrosis. In an autopsy case with diagnosis 'vasculitis' (female 52-years) there was dissemination into multiple organs. Immunohistochemistry shows strong positivity for CD45 and CD20, and the negative reaction for CD3, CD45RO and Factor VIII-related antigen. Based on the above findings the diagnosis of angiotropic large B-cell lymphoma was made.
Conclusion The antemortem diagnosis of ALCL of the CNS may be established by brain biopsy with application of immunohistochemistry.

O-132

Evaluation of cell death in animal model of brain contusion treated by hyperbaric oxygen therapy

E Vlodavsky, J Soustiel
Rambam Medical Center, Haifa, Israel

Cerebral contusion (CC) remains the most important consequence of traumatic brain injury and has unexplained unique evolving clinical course.The aim of this study was to evaluate the extent of apoptosis in perilesional area of CC and to examine the effects of hypoxia and hyperbaric oxygenation therapy (HBOT).The model of CC was based on the technique of cortical dynamic deformation (Shreiber et al.,1999) on Sprague-Dawley rats. One group of animals afterwards was placed in closed chamber and exposed to mild hypoxemia, simulating posttraumatic hypoxemia. Both groups of animals (hypoxia-exposed and non-exposed) were treated by HBOT. Brains were cut through produced lesion and paraffin sections were stained by TUNEL method and for active caspase-3. Apoptotic cells (AC) were counted in five successive perilesional layers of 0.5 mm each. It was shown that in the group of rats that were exposed to hypoxia, the width of perilesional area and the number of AC were significantly higher than in non-hypoxic animals, raising from 12.2% to 31.8% at 0.5 mm ($p<0.001$).One treatment by HBOT induced significant decrease both in the radius of perilesional area and the number of AC in both groups of animals (in hypoxia-exposed animals this effect was even more pronounced).The results of our study prove the role of perilesional area in the 'growth' of CC. Hypoxemia caused profound increase in cell death extension. HBOT shows marked positive effect in both hypoxic and nonhypoxic animals. We used quantative pathologic monitoring of number of AC to develop the optimal regimen of HBOT in animal model of CC.

O-133

Surgery for seizures. A pathological review between 1997 and 2003 at Jimenez Diaz foundation, Madrid, Spain

A Ruiz De La Parte[1], Y Bouhajeb[1], J Albisua[2], I Palma[2], JL Sarasa[1]
[1]Pathology Department. Jimenez Diaz Foundation, Madrid, Spain
[2]Neurosurgery Service. Jimenez Diaz Foundation, Madrid, Spain

Introduction Surgery for seizures consists of surgical procedures made in the central nervous system to treat drug-resistant epilepsy. Different lesions may be the cause. Aims: We review the cases diagnosed between the years 1997 and 2003 in our hospital.
Materials and methods The surgycal specimens were stained with hematoxilin-eosin and neural or glial immunostains after paraffin embeding.
Results The most frequent lesion is Mesial Temporal Sclerosis (47-70% of the cases). Other causes are tumors; Dysembrioplastic Neuroepithelial Tumor (DNT), neuronal tumors and glial tumors. Less frequent lesions are phacomatosis, malformative lesions like cortical dysplasias or vascular malformations, vascular or trauma lesions and inflammatory or unspecified lesions. Mesial Temporal Sclerosis consists of neuronal loss and gliosis in sectors CA1, CA3, CA4 and dentate gyrus. Between 1997 and 2003 we diagnosed 43 cases; 24 were women and 19 were males. DNT is a very infrequent, intracortical tumor composed of glia and neurons, usually associated with cortical dysplasia. In our experience we diagnosed 6 cases; 4 women and 2 men. We have found other tumors associated with epilepsy; 7 cases of ganglioglioma (3 women and 4 men), 3 cases of gangliocytoma (1women and 2 men), and astrocytic tumors (6 Protoplasmic Astrocytomas, 1 Mixed Astrocytoma and 2 Fibrillary Astrocytomas). We also diagnosed other processes associated with epilepsy: 2 cases of cortical dysplasia, 9 of glial scar, 7 of gliosis or unspecified changes and 2 cases of vascular malformation.
Conclusion Pathology associated with seizures is very diverse; a multidisciplinary and experienced team is needed.

O-134

Expression of sperm protein 17, a novel cancer-testis antigen in human nervous system tumours

F Grizzi[1], B Franceschini[1], P Gaetani[1], F Tancioni[1], R Rodriguez y Baena[1], N Dioguardi[1], M Chiriva-Internati[2]
[1]Istituto Clinico Humanitas, Rozzano, Milan, Italy
[2]Texas Tech University Health Science Center, Department of Internal Medicine, Amarillo, Texas, USA.

Introduction Human sperm protein 17 (HSp17) is a highly conserved protein originally isolated from a rabbit epididymal sperm membrane and testis membrane pellet. Recently, HSp17 has been included in the cancer/testis antigens (CT) family and showed to be expressed in multiple myeloma and ovarian cancer. The aim of the study was to investigate the immunolocalization of HSp17 in specimens of nervous system malignancies, in order to establish the usefulness of this antigen as target for tumour-vaccine strategies for nervous system tumours.
Methods The authors assessed the expression pattern of HSp17 in formalin-fixed and paraffin embedded surgical specimens of nervous system malignancies, including 25 neuroectodermal primary tumors (8 astrocytomas, 13 glioblastomas multiforme, 3 oligodendrogliomas, and 1 ependymoma); 19 meningeal tumours; and 5 peripheral nerve sheath tumours (4 schwannoma, and 1 neurofibroma), using a standardized immunohistochemical procedure.
Results HSp17 was found to be expressed in a low number of tumoral cases (nearly 14%), with a major expression in astrocytomas histological group (25%). No case among peripheral nerve sheath tumours was found to be immunopositive for HSp17. The expression pattern was found heterogeneous in all of the positive samples and it does not correlate with the degree of malignancy.
Conclusions The low frequency and the heterogeneous distribution of HSp17 suggest the useless of this antigen as unique target for immunotherapeutic strategies. However, the present study shows firstly the immunolocalization of HSp17 in some cells of nervous system tumors tissues. The emergent complex function of HSp17 renders necessary further studies to understand the link between positive-cells and this protein.

O-135

In vitro FDDNP labeling of pathological protein aggregates in the CNS of selected "conformational" disease cases

TD Vovko[1], LM Šmid[1], M Popović[2], M Bresjanac[1]
[1]University of Ljubljana, School of Medicine, Institute of Pathophysiology ond Prion Laboratory, Ljubljana, Slovenia
[2]University of Ljubljana, School of Medicine, Institute of Pathology, Ljubljana, Slovenia

Introduction A molecular imaging probe 2-(1-{6-[(2-fluoroethyl)(methyl)amino]-2-naphtyl}ethylidene)malononitrile (FDDNP), is a highly hydrophobic, fluorescent substance, known to label senile plaques and neurofibrillary tangles (NFT) in the brain of Alzheimer disease (AD) patients. The aims of this study were to evaluate in vitro FDDNP labeling of protein aggregates in selected "conformational diseases" of the brain and to determine if they fulfill the tinctorial and polarizing optics criteria for amyloid.
Material and methods Brain sections of patients with confirmed AD, variant AD (vAD), amyloid angiopathy (AA), sporadic Creutzfeldt-Jakob disease (CJD), variant CJD (vCJD), Gerstmann-Sträussler-Scheinker syndrome (GSS), Pick disease (PiD) and progressive supranuclear palsy (PSP) were labeled with FDDNP, Congo red (CR) and PAS. Analysis was performed using fluorescent microscope (FDDNP), and light microscope (CR and PAS) with polarizing optics (CR).
Results In addition to senile plaques and NFT in AD and vAD FDDNP reliably labeled: prion plaques in CJD, vCJD and GSS, Lewy bodies in vAD and vascular amyloid in AA. It did not label Pick bodies in PiD, and globoid NFT in PSP. With the exception of FDDNP positive Hirano bodies in AD and Lewy bodies in vAD, CR and PAS stained all the FDDNP positive deposits. All CR positive aggregates also showed birefringence.
Conclusion In our study, FDDNP labeled all protein aggregates that were shown to posses tinctorial and birefringent characteristics of amyloid, but also some that cannot be classified as amyloid. Aside from its potential for in vivo diagnostics of some neurodegenerative diseases, FDDNP may prove useful in labeling certain pathological protein aggregates in vitro. Work supported by MŠZŠ grants 0381-518 and L3-3435.

O-136

Remodelling in vascularization: an important step in the development of peripheral adenocarcinomas of lung?

G Kayser[1], TS Szöke[2], ZK Kosjerina[3], JO Nwoye[4], T Goldmann[5], E Vollmer[5], IT Trojan[2], MW Werner[1], K Kayser[4]
[1]Institute of Pathology, University Freiburg, Freiburg, Germany
[2]Department of Thoracic Surgery, University Szeged, Szeged, Hungary
[3]Institute of Pathology, University Novi Sad, Novi Sad, Serbia
[4]UICC-TPCC, Institute of Pathology, Humboldt University, Charite, Berlin, Germany
[5]Forschungszentrum Borstel, Borstel, Germany

Aim To investigate the development and clinical significance of vascularization in adenomatous alveolar hyperplasia (AAH) and peripherally located adenocarcinomas of the lung.
Material and methods Histological slides obtained from 70 patients with AAH, and from 190 patients with potentially curatively operated lung adenocarcinomas including normal lung parenchyma are immunohistochemically stained with an anti CD34 antibody, and subject to quantitative image analysis. Syntactic structure analysis measures the absolute and relative features of vessels including the vessel-associated cellular densities. These data are compared in between and associated with tumor volume, post surgical TNM stage, and the patients' survival.
Results AAH displays an increased level of vascularization characterized by regular size and increased number of newly formed vessels. Spatial agglutination (clusters formation) of vessels is common in AAH. The tumor vascularization (volume fraction Vv) amounts to 3% in AAH and to 7% in lung carcinomas, and increases in advanced tumor stages (pT4, pN3). AAH displays the lowest, advanced tumor stages the highest numerical vascular density. Minimum diameter and circumference of vessels maintain. The density of epithelial cells decreases with increasing distance from the vascular surface in both AAH and adenocarcinomas. It is the highest in advanced tumor stages. According to multivariate statistical analysis the patients' survival is closely associated with the pN-stage, tumor volume, cell type and the numerical density of tumor cells within a distance < 20m to the nearest neighboring vessel.
Conclusion AAH is characterized by probably non-reversible changes in vascular density and spatial vessel clustering. Vascularization of pulmonary adenocarcinomas becomes altered in advanced tumor stages. Of prognostic significance is the distribution of tumor cells in relation to the nearest neighboring vessel only. Changes in vascularization probably play an important role in genesis and development of pulmonary adenocarcinomas.

O-137

Cellular and connective elements between bronchial glands in sarcoidosis: a quantitative analysis

Z Kosjerina, V Kosjerina Ostric
Institute of Lung Diseases, Sremska Kamenica, Serbia and Montenegro

Objective Objective of the study was to quantify the inflammatory and connective cells, as well as connective fibres between the bronchial glands in pulmonary sarcoidosis (S).
Material The study included the bronchobiopsy samples obtained from 31 sarcoid patients. The control group (CG) included 25 young healthy subjects who lost their lives in an accident, having the bronchus sampled at autopsy. The quantity of inflammatory and connective cells was measured by the stereometric numerical density method and the quantity of the connective fibres by the volume density method.
Results In the examined group the total quantity of all cellular elements between the bronchial glands in S was estimated to range from 11.231/mm^3 to 101.739/mm^3 or 37.129/mm^3 on the average. In the CG, the quantity ranged from 10.653/mm^3 to 39.020/mm^3, or 24.205/mm^3 on the mean.

Table 1 reviews the mean quantities of certain cell types per mm^3.

Cells type	Sarcoidosis		Control group	
	No. cells	%	No. cells	%
Lymphocytes	26.909	72.5	15.417	63.7
Plasma cells	1.900	5.1	1954	8.1
Macrophages	227	0.6	25	0.1
Neutrophils	6	0.02	5	0.02
Fibroblasts	1.924	5.2	397	1.6
Fibrocytes	6.143	16.5	6.407	26.5

Besides cellular elements, connective fibres were also registered between the bronchial glands. In S, the connective fibres made 10% of the interstitium volume and only 5% of it in the CG. This difference is statistically significant.
Conclusion In sarcoidosis, the total quantity of all cellular elements between the bronchial glands exceeds their quantity in the CG for 1.5 times. The most numerous are lymphocytes in both groups, but in S their quantity is 1.7 times as high as their quantity in the CG. The quantity of the connective fibres is 2 times as high as their quantity in CG. These differences are statistically significant.

O-138

Cytogenetic variants of dysplastic epithelial lesions and their malignant potential in honeycomb lung in usual (UIP) and desquamative interstitial pneumonia (DIP)

E Kogan, N Paramonova, S Demoura, T Manuilova, V Denguine, B Kornev
Moscow Medical Academy, Moscow, Russian Federation

Introduction Honeycomb lung is characterized by the development of numerous dysplastic epithelial lesions: adenomatous hyperplasia, atypical adenomatous hyperplasia, goblet cell hyperplasia, squamous metaplasia and dysplasia. The aim of our study was to analyze morphology, cytogenesis and malignant potential of these lesions in accordance with clinical, functional, high resolution CT data in UIP and DIP patients at early and late stages of the disease.
Materials and methods 72 UIP patients were studied with open lung biopsy, which were performed by formal thoracotomy (47 cases), video-assisted thoracoscopy (6 cases), and transbronchial biopsy (19). Histologic classification was based on criteria for idiopathic interstitial pneumonias (Katzenstein A., Myers J., 1998). CD34, bTGF, FRF, IGF family proteins, p53, Ki-67, PCNA, bcl-2, c-myc were detected immunohistochemically in paraffin sections.
Results We obtained development of early interstitial sclerosis with honeycombing in UIP patients. Wide spectrum of epithelial changes was found, including new entities, such as atrophy of bronchial and alveolar epithelium and neuroendocrine hyperplasia in oval structures with background sclerosis.
Conclusion Obtained data may prove significant plasticity of bronchiolar stem cells in honeycomb lung. These morphological data correlates with predicted survival rate and progressive deterioration in lung function in patients with idiopathic interstitial

pneumonias. The dramatic progresion of UIP comparing with DIP is based on progressive interstitial fibrosis and prominent reconstr uction of pulmonary tissue.

O-139

Intrapulmonary lymph nodes in South African miners - An autopsy survey

K Honma[1], J Murray[2]
[1]Department of Pathology, Dokkyo University School of Medicine, Mibu, Tochigi, Japan
[2]National Centre for Occupational Health, and School of Public Health University of Witwatersrand, Johannesburg, South Africa

Introduction Progress in imaging technique has succeeded in visualizing intrapulmonary lymph nodes (IPLN), yielding a differential diagnostic challenge. There has been no systematic pathologic study on IPLN in the literature. The aim of this study was to describe the prevalence and histopathology of IPLN with special reference to dust-related lesions.
Materials and methods Histopathologic slides of lungs from 1984 consecutive autopsies of South African miners registered at National Centre for Occupational Health were reviewed to describe the pathology of IPLN. Special attention was paid to compare lung parenchyma and IPLN regarding dust-related lesions.
Results IPLN were seen in 73 of 1984 cases (3.7%). 9 cases (12.3%) had multiple IPLN. Silicotic nodules were seen in 28 cases (38.4%), of which only 2 (7.1%) cases showed co-existing parenchymal silicosis. In case of advanced IPLN silicosis, lymphoid tissue was almost totally replaced by confluent silicotic nodules, which contrasted with surrounding lung with no silicosis. Tuberculosis was not found in IPLN in 5 cases which had evidence of pulmonary tuberculosis. Metastatic deposits were seen in IPLN in 2 out of 4 cases which had both primary lung cancer and IPLN.
Discussion and conclusions Intrapulmonary lymph nodes (IPLN) are not rare. IPLN shares the general pathology of lymph nodes including metastatic malignancy. Silicotic nodules are commonly seen in IPLN in the absence of parenchymal silicosis in occupationally exposed individuals. IPLN that are completely replaced by silicotic fibrosis may mimick parenchymal disease, leading to an erroneous diagnosis of a pulmonary silicosis.

O-140

Karyometric analysis of small cell carcinoma and non-small cell lung carcinoma

Z Mijovic, D Mihailovic, D Dimov, V Zivkovic, B Djordjevic, M Krstic
Institute Of Pathology, University Of Nis, Nis, Serbia and Montenegro

Introduction Making a histologic distinction between small cell carcinoma (SCLC) and non-small cell carcinoma of the lung (NSCLC) on routine biopsies obtained via bronchoscopy sometimes presents diagnostic problem. In difficult cases additional classification methods may be helpful, particularly karyometry. The aim of this study was to estimate karyometric variables of SCLC and NSCLC.
Materials and methods At Institute of Pathology, University of Niš, formalin-fixed, paraffin-embedded bronchoscopic mucosal samples from 41 patients with SCLC and 83 patients with NSCLC were retrieved from pulmonary pathology archives. Serial histologic sections of 5 μm thickness were prepared for staining with hematoxilin and eosin and analyzed by image analyzer Lucia M 3.51 ab (Nikon, Tokio, Japan), using objective x40 (NA=0.65). The binary images were manually edited. Seven nuclear variables were estimated: nuclear area, equivalent diameter, volume of equivalent sphere, perimeter, mean chord, circularity and integrated optical density. In each case a hundred nuclei were measured. A statistical analysis was performed using Student's t-test.
Results All measured nuclear variables were found to be significantly different between these two major histological types of lung carcinoma. The values of nuclear variables (except circularity) of NSCLC were significantly larger than in SCLC, $p<0.001$.
Conclusions Histologic classification of lung cancer is subjective and often difficult to reproduce. Karyometric analysis, in which the morphology of the nucleus is described by a number of mathematical parameters, may be helpful in distinguishing SCLC from NSCLC.

O-141

Use of automated quantitative cytology sputum test for detection of early lung cancer

M Terčelj[1], A Aleš[1], B Turič[2], R Kemp[2], B Palčič[2,3], T Rott[4], N Zadravec[1], B Vrhnjak[1], J Eržen[5]
[1]Clinical Center, Center For Respiratory Diseases And Allergy, Ljubljana, Slovenia
[2]Perceptronix Medical Inc., Vancouver, Canada
[3]B.C. Cancer Research Center, Vancouver, Canada
[4]Institute of Pathology, Faculty of Medicine University, Ljubljana, Slovenia
[5]Clinic of Thoracic Surgery, Clinical Center, Ljubljana, Slovenia

We have been using a fully automated quantitative sputum test (Automated Quantitative Cytology sputum test, AQC sputum test) based on a fully automated, high resolution image cytometer, for detection of early lung cancer. The test involves measurements of several thousand cell nuclei per sputum sample, stained with a DNA specific and stoichiometric stain. The digital images of the nuclei are captured at the limit of optical (spatial and photometric) resolution with the cytometer, and over one hundred nuclear features are then calculated from each nucleus. Selected nuclear texture features are then used to calculate the probability of the presence or absence of lung cancer. In this study, a total of 382 sputum samples were collected of which 178 patients were subsequently confirmed by histopathology diagnoses of lung cancers. Approximately half of the lung cancers were of the early stage (stage 0 or stage I) and 204 subjects presents matching (high risk) population with no known malignancy. The results of the quantitative sputum test (sensitivity and specificity), as analyzed by AQC sputum test, were then compared to those derived by conventional cytology. The results of the AQC test from sputum cells show a several fold increase of sensitivity (35% -60% depending on the lung cancer stage and type vs. 1 - 25% by conventional cytology) at an acceptably reduced specificity (90% vs. 98%, for AQC and conventional cytology, respectively). The role of the AQC cytology test in a comprehensive approach to detection of early (non-invasive and minimally invasive) lung cancers will also be discussed.

O-142

Carcinogenesis in bronchial epithelium - an immunohistochemical evaluation of preneoplastic lesions

G Schlake, KM Müller
Institut für Pathologie, Bochum, Germany

Introduction Characterization of bronchial preneoplastic lesions is based upon cellular atypia and disturbed tissue architecture. Depending on the individual experience, the grading of such lesions varies considerably. We evaluated immunohistochemical staining for p53 and Mib-1 in regards of their value in routine diagnostics of bronchial biopsies.
Material and methods 40 bronchial biopsies ranging from normal bronchial epithelium to invasive squamous cell carcinoma have been stained with antibodies against p53 and Mib-1. The biopsies have been divided into 3 groups: squamous cell metaplasia with basal cell proliferation to low grade dysplasia, high grade dysplasia, and carcinoma in situ. For comparison, normal bronchial epithelium and invasive carcinoma have been included.
Results In normal epithelium 2% of the cells showed positivity for p53. With increasing degree of atypia, the number of posititive cells per 100 nuclei increased to 53% in carcinoma in situ. Almost linear progression has been found in the proliferation activity assessed by immunohistochemical staining with Mib-1. In normal epithelium the activity was <1.5%, and the number of positive cells increased to 42% in carcinoma in situ.
Discussion and conclusions In bronchial preneoplastic lesions an increasing accumulation of p53 and Mib-1 can be found in accordance to the degree of atypia. This provides additional and valuable information to facilitate differentiation between low grade and high grade lesions. In regards of an increase in less invasive diagnostic and therapeutic methods, immunohistochemical staining with p53 and Mib-1 adds valuable information for a correct grading of these lesions, and is therefore of considerable clinical importance.

O-143

Pitfalls in diagnosis and assessment of lymph node metastases in lung cancer - a morphometrical analysis of pulmonary and mediastinal lymphnodes

T Gumprich, K Junker, KM Müller
Institut für Pathologie, Bochum, Germany

Introduction Besides histological subtype and tumor size, metastatic spread in pulmonary and mediastinal lymphnodes in lung cancer is also an important factor concerning therapeutic strategies. Prior to resection of the primary tumor a thorough staging of pulmonary and mediastinal lymphnodes is performed using computer tomography – but lymphnodes will be judged by size only.
Material and methods In an autopsy study of ten cases with advanced lung cancer, 345 lymphnodes have been dissected. Lungs have been resected en bloc, and were cut in horizontal sections according to computer tomographic layers. Lymphnodes have been measured and histologically examined. Lymphnodes were judged as normal with a transversal diameter of not more than 10mm.
Results In the histological examination metastases were found in 45% of normal-sized lymphnodes, while 18% of enlarged lymphnodes presented as negative. Using other parameters did not yield better specifity or sensitivity. Discussion: There is a wide range of what maybe the normal size of a lymphnode which is influenced especially by the study collective. We found a variety of size-influencing factors (pneumoconioses, silicosis, previous infections). Furthermore, there are differences in size of lymphnodes in collectives from rural and industrial populations. The high number of metastases in normal-sized lymphnodes is explained by the highly advanced stage of disease in our study collective.
Conclusions For imaging diagnostics, sufficient size parameters for lymphnodes are not existing. We are convinced that pre-operative staging of lymphnode status is important. In many cases the radiological evaluation on the lymphnode stations is not sufficient to differentiate between reactive enlargement and metastatic involvement. Mediastinoscopy is still needed in pre-operative diagnostics, because it allows taking biopsies with following histological examination.

O-144

Expert system dedicated on diagnosis in thyroid pathology

DL Rotin[1], NN Petrovichev[1], AI Pavlovskaya[1], VG Nikitaev[2], EY Berdnickovich[2], DA Popov[2]
[1]N.N.Blokhin Cancer Research Center, Moscow, Russian Federation
[2]Moscow Engineer Physics Institute (State University), Moscow, Russian Federation

Introduction Encoutering diagnostically difficult cases, pathologists usually asks consultations from more experienced colleagues or uses materials in form of journal articles, textbooks, atlases etc. These sources can provide the information in a passive way. Usage of expert systems (special computer programs) let pathologists obtain the information in an interactive way and have more accuracy in the diagnosis. Our purpose was to create an expert system capable to improve histological diagnostics in area of thyroid tumors and tumor-like conditions.
Materials and methods Materials for our work consisted of more than 400 cases of thyroid tumors and tumor-like conditions (near 1200 pictures), representing 15 thyroid diseases. Every case was described by two experts according to 33 histologic features and then entered in PC data base.
Results Our computer program can act in two principal ways. These are 1) diagnostics – expert system propely, 2) learning – virtual textbook. 1) Using the expert system, pathologist enters new data in PC and marks so many features as he can. Then he obtains the information about all the possibilities of probable diagnosis and some other results. Entering more features can help to narrow the borders of probable diagnosis. 2) Applying our program as a virtual textbook, it is possible to learn better the known significance of pathological features, to take a look on the descriptions the experts made etc. The program can also function as a virtual trainer and examiner.
Conclusion Our computer program increases the diagnostic quality in the area of thyroid pathology by means of high capability of information integration and improving pathologist's qualification during his learning.

O-145

Vascular 3D features in normal and pathological thyroid tissue

L Di Tommaso[1], A Parmeggiani[2], L Castaldini[3], MP Foschini[1], V Eusebi[1]
[1]Servzio di Anatomia Patologica, Bologna, Italy
[2]Servizio di Otorinolaringoiatria, Bologna, Italy
[3]Servizio di Radiologia, Bologna, Italy

Introduction Neoangiogenesis has been demonstrated to be an important feature of numerous tumours. Three dimensional (3D) reconstruction has given important insights in breast neoplastic conditions. Purpose of the current study is to investigate the 3D features of vessels in normal and pathological thyroid tissue.
Materials and methods Twenty-three cases were considered: 6 post-mortem normal thyroid, 6 nodular goiter, 6 papillary carcinomas (4 classic, 1 follicular, 1 diffuse sclerosing), 3 follicular adenomas (1 oncocytic) 1 minimally invasive follicular carcinoma and 1 Basedow-Grave's disease. Two patients underwent preoperative eco-color-doppler (ECD) examination. Thin sections (thickness of 3 to 5 mm) were obtained from the surgical specimen, dehydrated for 3 D examination. Parallel sections were paraffin embedded for histology.
Results Normal tissue: thyroid follicles are surrounded by a network of small vessels which originate from main vessels located inside the capsule. Benign nodular lesions: show vascular pattern identical to that of normal thyroid tissue with an increased network at the periphery of the nodules. Vascular spots highlighted by ECD corresponded to these vessels. Carcinomas: in addition to the peripheral vessels, glomeruloid, anastomosing, small vessels were present within the lesion. No difference was seen between follicular and papillary tumours.
Conclusion The present data suggest that malignant thyroid lesions display a characteristic vascular pattern.

O-146

The peptide xenin: from the identification of the cellular source in neuroendocrine cells of the upper intestine to endocrine pathology

M Anlauf[1], G Hamscher[2], W Hartschuh[3], R Arnold[4], G Klöppel[1], GE Feurle[5], E Weihe[6]
[1]Institute of Pathology University of Kiel, Kiel, Germany
[2]Institute of Toxicology University of Hannover, Germany
[3]Department of Dermatology University of Heidelberg, Germany
[4]Department of Gastroenterology and Endocrinology University of Marburg, Germany
[5]DRK Hospital Neuwied, Germany
[6]Institute of Anatomy and Cell Biology University of Marburg, Germany

Introduction Xenin is a biologically active 25-amino-acid peptide extractable from the gastro-entero-pancreatic system. The aim of our study was to identify the unknown cellular source of xenin and to analyze the expression of xenin in neuroendocrine tumors.
Methods Normal tissue of humans, rhesus monkeys and dogs and a large series of 72 neuroendocrine foregut and midgut tumors were investigated by immunohistochemistry, confocal laser scanning microscopy, immuno-electronmicroscopy and high pressure liquid chromatography, assessed by radioimmunoassay.
Results In all three species, xenin was expressed in a subpopulation of gastric inhibitory (GIP)-cells of the upper intestine. Immuno-electronmicroscopy demonstrated presence of xenin in secretory granules (187±19 nm diameter). Xenin immunoreactivity and extractable xenin was found in 23 of 26 duodenal neuroendocrine tumors, including gastrinomas, somatostatinomas, non-functioning and enterochromaffin cell tumors. In contrast, xenin was absent from gastric, pancreatic, ileal and bronchial neuroendocrine tumors.
Conclusions The localization of xenin in ultrastructurally characterized secretory granules supports the concept that xenin represents a further endocrine regulatory peptide. The finding that xenin expression distinguishes between endocrine tumors arising in the duodenum from those of nonduodenal origin may be useful for topographical tumor classification and the differential diagnosis of neuroendocrine tumors of the upper gut. (Supported by DFG)

O-147

Tall cell variant is frequent in all types of papillary thyroid carcinomas in 405 investigated cases

C Ensinger[1], R Prommegger[2], R Kremser[1], K Schmid[3]
[1]Institute Of Pathology, University Of Innsbruck, Innsbruck, Austria
[2]Surgical Department, University of Innsbruck, Innsbruck, Austria
[3]Institute of Pathology, University of Essen, Essen, Germany

Introduction The tall-cell variant (TCV) is known as a rare but aggressive form of papillary thyroid carcinoma (PTC) with increased incidence of local recurrence and mortality. It is defined as papillary thyroid carcinoma with at least 30% of specific cellular changes within the tumor cells and occurs in 5-10% of all PTCs.
Materials and methods In our series of paraffin embedded and H&E stained tumor tissues, tall cell morphology was exactly defined for the first time and then 405 cases of PTCs, including all stages and variants, were investigated concerning tall cell morphology and associated changes within the tumors.
Results In contrast to previous reports, 163 cases (40,25%) were classified as TCV in our series. Taken together with minor tumor parts, 268 cases (66,17%) presented with TC morphology. These parts were in a high percentage associated with fibrosis and lymphocyte rich areas and showed a higher mitotic activity than usual PTCs.
Discussion The differences in the occurrence of TCV and TC-morphology between the presented series and previously reported cases might result from until now not clearly defined tall cell morphology as well as from similarities to PTCs, such as the oxyphilic variant, which is extremely rare in our series, and maybe also from often described squamous changes within PTCs. Due to these data it is not clear which tumor parts have relevance for prognosis and which tumors should be treated more aggressively than others. In accordance with previous reports concerning the prognostical impact of this variant, we think that the occurrence of TC morphology plays a major role in both development of extrathyroidal growth and metastatic disease.

O-148

Myocardial extensions around venae cavae as a potential substrate of atrial fibrillation

I Kholová[2], J Kautzner[3]
[1]A.I.Virtanen Institute For Molecular Sciences, Kuopio, Finland
[2]Fingerland Department of Pathology, Charles University Medical Faculty Hospital, Hradec Králové, Czech Republic
[3]Department of Cardiology, Institute for Clinical and Experimental Medicine, Prague, Czech Republic

Introduction Thoracic veins have been recognised as the important sites housing arrhythmogenic foci that trigger atrial fibrillation (AF). However, only limited data are available for the presence and characteristics of myocardial sleeves around venae cavae (VC). Aims: We studied VC to evaluate the presence, the length, the thickness, and the arrangement of myocardial fibres.
Materials and methods We studied microscopically 23 human autopsied hearts (13 males, age range 39-78 years, 6 subjects had a history of AF).
Results Myocardial extensions were found in 17 superior VC: the maximum length reached 47 mm, the average length was 17.5 mm. The maximum thickness was 4 mm, the average thickness was 1.5 mm in the whole group. In the AF group, the average length was 7.7 mm and the average thickness 1 mm. The most prevailed pattern was circular one. Myocardial sleeves in 19 inferior VC reached maximum length of 61 mm (the average length was 19.2 mm in the whole group and 21.8 mm in AF group). The maximum thickness was 4 mm (the average thickness was 1.5 mm in the whole group and 1.4 mm in AF group). The most prevailed pattern was circular one too.
Conclusions There is inter-individual variability in the presence, length, thickness, and pattern of myocardial fibres around VC. The results will have a clinical implication for the catheter ablation treatment of AF.

O-149

Altered endothelial permeability secondary to ischemia-reperfusion

E Stefanovic, V Kanjuh, N Tasic
Dedinje Cardiovascular Institute, Belgrade, Serbia and Montenegro

Introduction During open heart surgery some damages to myocardial capillary endothelium occur, with the consequence to the regarding structure and function of cardiomyocytes as well. Cardioplegia (CPL), long term hypoxia and reperfusion are strong contributing factors for these lesions. The aim of the study is to assess ultrastructural changes and permeability of endothelium of myocardial capillaries due to hypoxia and reperfusion during open heart surgery.
Patients and methods The study included 68 consecutive patients (pts) who underwent open heart surgery. 290 samples were taken from right ventricle anterior wall and apcal region. Biopsies were taken at the end of cardioplegic period, during ischemic period and during period of reperfusion. All patients were divided in two groups depending on duration of period of ischemia or cardioplegia-group 1 (CLP<65 min) and group 2 (CLP-66-120 min). All samples were analyzed by electron microscope using quantative stereological analysis. Volume fraction of the pinocyte vesicles (PV), mitochondria (M) and endoplasmatic reticulum (EPR) were calculated.
Results Endothelium ultrastructure analysis showed increase in permeability of the capillary wall. The worse damage was found after 65 min. of CPL usage: edema of the endothelial cells, widening of the cell junction and other degenerative changes of cardiomyocytes. Analyses of result confirmed that the more significant damages were found during reperfusion in group 2.
Conclusion Our study showed significant changes in endothelial permeability and function after ischemia and reperfusion. Disturbances of transendothelial transport may play certain role in the development of heart failure after open heart surgery.

O-150

Comparative clinico-pathological and immunohistochemical study of cases with postinfarction myocardial rupture

F Baranyay, K Bethlen
Department Of Pathology Nagykanizsa City Hospital H-8801, Nagykanizsa, Hungary

Introduction The authors compared the clinico-pathological and immunohistochemical features of 16 acute postinfarction cardiac rupture and 16 control (with near the same clinical age without rupture) cases.
Material and methods Cryostat sections of both groups from infarction/rupture and controls were stained with Oil red O, Sudan black B (BDH Chemicals) and were reacted to anti-C-reactive protein (CRP), to complement C5a and C5b-9 (Dakopatts).
Clinico-pathological findings Myocardial rupture occured in elder women with relative smaller weight of heart, thrombosis of one main coronary artery, location in the anterior wall at the first infarction within the first week. Microscopically the main observation is the large amount of granular lipid deposition in the area of myocardial rupture even in the cytoplasm of the necrotic myocardial fibers using Oil red O and Sudan black B staining. Immunohistochemistry: The anti-CRP and C5b-9 antibodies showed intense staining around the area of the rupture. The inflammatory cells were neutrophils in high numbers in both group. Eosinophils were represented in low percentage (below 10%).
Conclusion The postulation is, that the granular myocardial lipids in the area of infarction/rupture are phospholipids (mainly mitochondrial cardiolipin), which through binding CRP induce pathologic complement activation. In experimental heart infarctions complement target (recombinant etc.) molecules could reduce the neutrophil chemotaxis to the area of necrosis and the size of the infarction.

O-151

Nuclear factor-κB regulates apoptosis of intimal smooth muscle cells

A Orlandi[1], A Francesconi[1], M Marcellini[2], A Ciucci[1], LG Spagnoli[1]
[1]Anatomic Pathology - Dept. Biopathology - Tor Vergata University, Rome, Italy
[2]Sigma-Tau Research Laboratories, Pomezia, Rome, Italy

Introduction Apoptosis contributes to reduce intimal smooth muscle cell (SMC) hyperplasia following angioplasty or during atherogenesis. Nuclear factor (NF)-kB is involved in the regulation of many SMC functions. Aim of the work was to verify the role of NF-kB in bax-dependent SMC apoptotic cascade and its possible targeting for novel biologically based therapies of vascular hyperplasia.

Methods Apoptotic proteins were evaluated by immunohistochemistry and Western Blotting and NF-kB using a anti-p65 (RelA) antibody recognizing its active form. Apoptosis was induced in rat aortic neointimal SMCs after endothelial injury in vivo and in vitro by propyonil-l-carnitine (PLC).
Results In vivo, expression of constitutive NF-kB activity of SMCs of neointima was higher compared to underlying and normal media. Treatment with PLC associated to reduced neointimal relative volume and increased apoptotic rate of intimal SMCs compared to controls. Increased apoptotic rate associated to bax overexpression and RelA reduced immunopositivity. In vitro, PLC reduced G1 to S phase progression of intimal but not of medial SMCs. Hoechst staining, flow cytometry and ligation-mediated PCR showed increased apoptotic rate of intimal cells treated with PLC together with bax overexpression and the release of cytochrome c. SN50, an inhibitor of NF-kB nuclear translocation, induced an increase of apoptotic rate in intimal but not in medial SMC cultures, prevented the apoptotic effect of PLC and upregulated the cytoplasmic bax expression and the release of cytochrome c.
Conclusions Our studies with inhibitors of NF-kB strongly suggest that this nuclear factor plays a crucial role in the control of intimal SMC apoptosis.

O-152

Alpha-actin isoform distribution in normal and failing human heart: a morphological, morphometrical and biochemical study

A Orlandi[1], S Clément[2], AJH Suurmeijer[3], A Francesconi[1], A Angelini[4], LG Spagnoli[1], G Gabbiani[2]
[1]Anatomic Pathology - Dept. Biopathology - Tor Vergata University, Rome, Italy
[2]Department of Pathology-CMU, University of Geneva, Switzerland
[3]Dept.of Pathology, University Hospital Groningen, the Netherlands
[4]Anatomic Pathology, University of Padua, Italy

Introduction Two sarcomeric actins, α-cardiac (α-CA) and α-skeletal (α-SKA), are coexpressed in adult myocardium and represent the preponderant thin filament actin isoforms of cardiomyocyte contractile units. In the human heart, the relative amount of α-SKA mRNA increases steadily during development and after birth and becomes the predominant isoform in adults but data in the literature concerning hypertrophy and failure are scarce and controversial. Aim of the work was to determine how and where α-SKA isoform accumulates during heart development, ageing and with disease.
Methods By using monospecific antibodies, we investigated by immunohistochemistry and Western Blotting the distribution of α-SKA, α-CA and α-smooth muscle actin (α-SMA) isoforms.
Results At 20 weeks of fetal life, α-SKA was localized in a small proportion of subendocardial and papillary muscle cardiomyocytes, whereas a diffuse α-CA staining was observed, associated with a focal expression of α-SMA. In normal adult subjects, α-SKA positive cardiomyocytes were distributed in a transmural gradient with the highest proportion located subendocardially. In myocardial hypertrophy and cardiomyopathies, the amount of α-SKA was increased and a diffuse staining was seen in all layers of ventricular myocardium, with the exception of idiopathic dilated cardiomyopathies. Cardiomyocytes were always negative for α-SMA. As expected, fibroblasts in post-infarct scars expressed α-SMA and TGF-β1, but were negative for these proteins in interstitial fibrosis.
Conclusions Changes in the distribution of actin isoforms in hypertrophy and failure provide new insight into the mechanisms by which the heart adapts to work overload and help to define their role in these pathological situations.

O-153

Arrhythmogenic right ventricle dysplasia and sudden cardiac death. Controversial aspects

R H De Gouveia[1], A Becker[2]
[1]Hospital de Santa Cruz, Lisboa, Portugal
[2]Academic Medical Center, AMC, Amsterdam, The Netherlands

Introduction Arrhythmogenic right ventricular dysplasia (ARVD) has received much interest, since it may cause sudden cardiac death (SCD). Yet, pathogenesis remains controversial, not at least because adipose and fibroadipose types are considered different entities by some. The present study has looked into the histopathologic features of hearts with ARVD with a particular eye for a clue to pathogenesis.
Material and Methods Clinical history review and heart macroscopic/microscopic examination (with histochemical/immunohistochemical techniques) were performed on 29 patients dying suddenly with ARVD. Twenty-three, 15M/8F were young (13-35years) and 6, 4M/2F adults (37-73years).
Results 1)One young had family history of SCD. 2)One adult had cardiovascular antecedents. 3)Seven patients had died during exercise. 4)Both young and adults presented adipose (n=9vs4) and fibroadipose (n=14vs2) types, whilst each variant basically showed similar overall architectural arrangements. 5) Occasional inflammatory infiltrates were present in fibroadipose, but not in adipose type. 6) Left ventricular involvement occurred in 5 young and 1 adult heart. 7) Coexistent left ventricular pathology was occasionally identified.
Conclusions 1) ARVD can be manifest in young and older persons, either as adipose or fibroadipose variants. 2) Both types are morphologically identical, except that some may have additional fibrosis, occasionally accompanied by small inflammatory aggregates. Subtle differences hard to interpret as features distinguishing different entities. 3) Preferential and almost selective involvement of the right ventricular wall suggests a congenital nature of the disease, particularly since recent insights in right ventricular development have showed “regionalization” of genetic expression in the formation of cardiac chambers. Fatty/fibrofatty tissues may appear ab initium through an alternative mesenchymal pathway.

O-154

A new method of quantitative functional morphology for systemic examination of the cardiac muscle

T Ghevondyan[1], H Guski[2], G Avtandilov
[1]National Institute of Health, Yerevan, Armenia
[2]Medical Faculty of Humboldt University of Berlin, Berlin, Germany

Introduction Determination of the vital capacities of heart muscle has special importance for cardiac surgery. Morphological methods could be the most trustworthy in this respect. But it was not possible yet to extract this information from myocardial specimens.

The aim of this study was to elaborate a method, which will be able to determine the volume of vital reserve of myocardium taking into account all known morphological changes and alterations.

Material and methods The investigation was carried out on heart muscle tissue of healthy people, who died accidentally and of patients who died from myocardial infarction. The myocardium of white rats (normal, physically trained, during pancreonecrotic shock) was used.

Methods of histology, electron microscopy, cytoenzymochemistry, morphometry, micromechanography, statistics and mathematical modelling were used.

Results Most informative parameters were chosen for characterisation of the microcirculatory bed and of the paths of ultracirculation. The property of contractility has been taken as a system-forming criterion. A mathematical model was elaborated, which allows to unite the most important structural changes and alterations from tissue, cellular, ultracellular and macromolecular levels of the heart muscle. The basic variant of the model in a simplified version is the following:

$$fmcd.=K\bullet Vv_{1mfb.}\bullet N_{ATPI}\bullet\varphi= K\bullet Vv_{1mfb.}\bullet\{(1/Vv^{II}_{cap.}) + \\ +[1/(0{,}000625\bullet Sv^{II}_{cap.})] + (Vv^{II}_{int/}0{,}00550) + \\ +[1/(0{,}000219\bullet Sv^{II}_{mcl.})] + (Vv^{II}_{mcl./}0{,}04296) + \\ +[1/(Sv^{II}_{crst.}\bullet 0{,}0000245)] + [1/(Sv^{II}_{mit./mfb.}\bullet 0{,}0000551)] + \\ +(Vv^{II}_{spl./}0{,}00341) + [1/(\alpha\bullet Sv^{II}_{mfb./mit.}\bullet 0{,}0000551)] + \\ +(Vv^{II}_{mfb./}0{,}02299)\}^{-1}\bullet(\varphi\bullet vl).$$

The equation has a modular construction and an open architecture. All parameters are measurable. The indices (φ) and (v1) are considered as standard values.

Conclusion The examination of the contractility of myocardial specimens from same hearts by two different methods confirmed the functional adequacy and efficiency of the method of quantitative functional morphology. Supported by grant 0777 of RA.

O-155

The role of endomyocardial biopsy in end-stage heart failure

M Zorc[1], O Vraspir-Porenta[1], R Zorc-Pleskovič[1], N Radovanović[2], D Petrovič[1]
[1]Institute of Histology and Embryology, Medical Faculty, Ljubljana, Slovenia
[2]Clinique Cecil, Lausanne, Switzerland

Introduction Endomyocardial biopsy is considered to be an important diagnostic procedure for the evaluation of patients with end-stage heart failure. The aim of this retrospective study was to evaluate the role of apoptosis, proliferation markers, volume density of interstitium, and myofibril volume fraction for the prognosis in patients with end-stage dilated cardiomyopathy (DCM).

Methods Endomyocardial biopsy was performed during open-heart surgery in 56 pts with end-stage DCM. Patients were divided into 2 groups, one with shorter survival (24 ± 9 months, mean ± standard deviation) and another with survival of more than 7 years after operation. The TUNEL method was used for the detection of apoptosis, and immunohistochemical methods were used for the evaluation of inhibitor of apoptosis (bcl-2), and proliferation markers (PCNA, Ki-67).

Results The increased percentage of apoptotic myocytes, decreased expression of bcl-2, PCNA and Ki-67 antigen, but lower myofibril volume fraction and lower volume density of interstitium was found in the group with early mortality compared to that with longer survival.

Conclusion Morphometrical analysis of the endomyocardial specimens of the patients with terminal heart failure due to DCM may enable us to get access to crucial information about the status of the myocardium, which may help us to predict the prognosis and optimal treatment of patients with end-stage heart failure due to DCM.

O-156

Detection of GFP positive dendritic cells in tissues of bone marrow transplanted mice

S Schulz, C Schimmelpfennig, J Baker, R Negrin
Dept. of Medicine, Div. of Bone Marrow Transplantation, Stanford, USA

Introduction Trafficking studies in bone marrow transplantation (BMT) more often use fluorescent reporter molecules like the green fluorescent protein (GFP). Dendritic cells (DC) represent an interesting population for trafficking analysis, because they undergo steps of maturation, which seem to be related to their localization in the tissues. The aim of this study was detection of ex vivo expanded DCs, transduced to express GFP, in tissues of mice that had received an allogeneic BMT.

Material and methods Tissues of recipient mice were pretreated by fixation in 4% formalin followed by 20% sucrose, before embedding in OCT and freezing on dry ice. In addition tissues were also fresh frozen and exposed to formaldehyde vapor as cryostate sections. The GFP signals were validated using an anti GFP antibody. Additional markers investigated were CD11c, CD4, CD8, H-2Kb and H-2Kd.

Results Vapor fixation of slides showed equal properties in containing GFP in comparison with the immersion method. GFP+ DCs were detected in small bowel, lymph nodes, thymus and spleen for up to 42 days after i.v. injection. Many of these GFP+ cells were positive for CD11c. The GFP signals could be validated on fluorescence and light microscopic level using anti GFP antibodies.

Conclusions Allogeneic DCs survive in BMT recipients for up to 42 days. They migrate into small bowel, mesenterial lymph nodes, thymus and spleen without causing GvHD. The visualization of survival and migration in BMT settings will provide new insights into the immunological role of DCs in vivo and might contribute to the optimization of DC based treatment strategies.

P-001

Breast hamartoma: cytologic, pathologic and immunohistochemistry study of 36 cases

H Mehrdad[1], J Sandbank[1], S Mendlovic[1], G Hermann[1], P Liokumovich[2], S Zahavi[1], M Segal[1], M Schvimer[2]
[1]Department of Pathology, Assaf Harofeh Medical Center, Zerifin, Israel
[2]Megalab Institute of Pathology, Park Hameida, Rehovot, Israel

Introduction Breast hamartomas enter the differential diagnosis of breast masses, necessitating an accurate diagnosis. It is still not quite clear into which group of lesions these masses should be categorized. The aim of our study was to investigate the cytologic, histologic and immunohistochemical profile of breast hamartoma in order to obtain a detailed picture of this somewhat unusual lesion.
Materials and methods This study presents cytological, pathological and immunohistochemical analysis of 36 patients with breast hamartoma. The immunohistochemical panel included: estrogen and progesterone receptors, Her 2-neu protein, P-53, Ki-67, CKMNF116, vimentin, alpha-SMA.
Results The patients ranged in age between 16 and 69 years. All patients presented with a palpable unilateral mass. The aspirates contained sheets of both bland ductal cells and lobular units. Adipose tissue was present in varying amounts. Typical macroscopical and microscopical features were noted. Immuno-histochemical studies showed estrogen and progesterone receptor positivity in epithelial cells as well as in the stromal cells, in all 36 hamartomas. Her 2-neu protein over expression was noted, P-53 expression was not observed. Ki-67 showed a 2-3% positivity in epithelial cells in most cases.
Conclusions The finding of intact lobular units and a relative paucity of stroma in an aspirate from a well-circumscribed breast lesion, may suggest the diagnosis of hamartoma. Typical macroscopical and histological features of breast hamartoma were noted. The immunohistochemical profile appears to be similar to that of normal and fibrocystic breast tissue, raising the possibility of a spectrum of lesions.

P-002

Basal cell characteristics in breast carcinoma with medullary features (cmf)

PP Holck[1], P Christiansen[2], S Holck[2]
[1]Technical University of Denmark, Lyngby, Denmark
[2]Department of Pathology, Hilleroed Hospital, Denmark

Introduction CK-pattern in NOS breast carcinoma has been studied extensively, including high molecular weight types, such as CK-14, present in rare cases. Published data on CK-14-expression in less common subtypes of breast carcinoma are limited The aim of this study was to learn more about the immunohistochemical profile of CK-14 in cmf, a systematic analysis on CK-14-reaction in a consecutive series of this variant of breast carcinoma was undertaken, including correlation with some traditionally recorded tumor characteristics.
Materials and methods Forty-three consecutive cases of cmf were examined for CK-14. Extent of staining was assessed semiquantitatively and reported as a percentage; its correlation to tumor size and receptor status was calculated.
Results Sixteen (37,2%) of the 43 cases comprised CK-14-labelled tumor cells. Though CK-14+ tumors were less commonly receptor+ and tended to be larger than CK-14- cases, statistically significant differences were not obtained (p=0.14 and p=0.07, respectively).
Conclusion No specific immunohistochemical profile typifying cmf has been identified. Nevertheless, most cmf seem prone to exhibit immunophenotypic aberrations with higher incidence of vimentin+, c-erb-B2+, and P-53+, lower incidence of Her2+ and ER/PgR+. We here demonstrate that CK-14-expression can be added to this list. Though not statistically significant, a trend towards an inverse relation between basal cell characteristics and receptor expression and a positive correlation between CK-14+ and tumor size was demonstrated.

P-003

Evaluation of margin status in lumpectomy specimens and residual breast carcinoma

C Scopa, P Aroukatos, D Koumoundourou, C Aletra
University of Patras, Medical School, Patras, Greece

Introduction Residual disease leads to most local recurrences, especially in patients treated with breast conserving therapy. This study was undertaken to identify whether assessment of excisional biopsy margins accurately predicts the presence or absence of residual tumor in the lumpectomy bed.
Material and method The margin status of 166 consecutive lumpectomy specimens followed by re-excision, taken from an equal number of patients with primary breast carcinomas (148 infiltrating,18 in situ), were evaluated microscopically and classified as 'positive' if the tumor was found at the inked margin, 'negative' if the entire tumor was found in >0.1cm from the inked margins, 'close' if it was within 0.1cm of the inked margins, but did not transected them and 'indeterminate' if biopsy specimen was not inked or the tissue was fragmented. The tumor size and grade of the initial biopsy were also analyzed, as potential predictors for residual disease.
Results Residual tumor was found in 42% of the patients (69/166): in 16%(10/61) of the cases with negative, in 64%(41/64) with positive, in 32% (8/25) with close and in 62.5%(10/16) with indeterminate margin status. In 36%(23/64) of the 'positive margins' and in 68%(17/25) of the 'close margins' cases no tumor was found in re-excised specimens. In 23%(16/69) of the cases the residual disease was composed entirely of an in situ component of the same histologic type as the initial biopsy. No relationship was found between tumor size or grade and residual disease.
Conclusions For breast tumors histologically negative margins in biopsy specimens do not guarantee complete excision. 'Close' margins may be considered almost equal to 'positive' ones. Residual in situ carcinoma in the immediate vicinity of the previous biopsy site seems to represent the advanced edges of the tumor, apparently difficult to be excised completely and most likely responsible for the locally recurrent disease.

P-004

Syringomatous adenoma of the breast

S Stolnicu[1], S Mocan[1], D Radulescu[2], E Horvath[1], C Podoleanu[3], J Jung[1]
[1]Department of Pathology, University of Medicine Targu-Mures, Romania
[2]Department of Pathology, University of Medicine Iasi, Romania
[3]County Medical Hospital, University of Medicine Targu-Mures, Romania

Introduction Syringomatous adenoma of the breast is a benign lesion of the nipple, which may be confused with an infiltrating carcinoma. The presence of the myopithelial cells and the immunohistochemical profile is still controversy in the literature. We present the case of an 22 years old patient, with an left nipple mass.
Materials and methods After excision, the excised tissue was fixed and paraffin embedded and H-E stained. We performed also immunohistochemical staining: with cytokeratin, actin, ER, PR, p53.
Results The excised tumor measured 4 cm, had ill-defined margins and yellow color.Microscopically, the lesion consisted of tubules and strands, composed of small and uniform basophilic cells, diffusely infiltrating the stroma of the nipple. The tubules were lined by two layers of cells, had a comma-like appearance and their lumen was usually open and round. The tumor cells lack pleomorphism. Squamous differentiation resulted in keratotic cysts. Immunohistochemically, the luminal layer of epithelial tumor cells was cytokeratin-positive and the peripheral myoepithelial cells were actin-positive. The tumor cells were negative for ER, PR, p53.
Conclusion Syringomatous adenoma of the breast is a benign rare lesion. The pathologist must not confuse it with an tubular carcinoma or with an adenosquamous carcinoma. We demonstrated in this case the presence of the myoepithelial cells.

P-005

The role of smooth muscle myosin heavy chain in diagnosing sclerosing adenosis of the breast with an infiltrative pattern

J Richmond[1], D Weaver[1], B Beatty[2], K Cooper[1]
[1]Fletcher Allen Health Care - University Of Vermont, Burlington, VT, USA
[2]University of Vermont, Burlington, VT, USA

Introduction Sclerosing adenosis (SA) of the breast can produce an infiltrative pattern mimicking invasive carcinoma. Immunohistochemical markers for myoepithelial cells, such as smooth muscle myosin heavy chain (SMMHC), have been shown to stain basal myoepithelial cells in normal mammary glands and fibrocystic changes. Absence of myoepithelial cells is associated with invasive carcinoma; however, we have observed occasional attenuation of SMMHC staining in SA. Studies evaluating the role of SMMHC in sclerosing adenosis have not been performed. The intent of this study is to further evaluate the staining pattern of SMMHC in SA with an infiltrative pattern.
Materials and methods Twenty cases of SA with an infiltrative pattern were identified, H&E stained, and immunohistochemistry performed for SMMHC (M3558, Dako Corp), 4µg/ml, as primary antibody, using a polymer based Envision+ detection system (Dako Corp). Normal-breast tissue positive controls and negative isotype matched IgG1 controls were used. Cases were then classified into one of three categories: positive (staining >95% of myoepithelial cells), intermediate (51% – 94%), or attenuated (<50%).
Results Three of the first ten cases (30%) showed attenuated staining with SMMHC. The remaining seven cases demonstrated positive staining of myoepithelial cells. All cases exhibited positive staining within normal lobules, serving as an internal control for each case. Ten additional cases of SA have been identified and are being stained with SMMHC for evaluation.
Conclusions Preliminary findings show that SMMHC yields inconsistent results when applied to SA with an infiltrative pattern. Such lesions can have features similar to invasive carcinoma on H&E, and application of SMMHC could produce misleading results.

P-006

Co-expression of ErbB family members in human breast cancer: Her-2/neu is the preferred dimerization candidate in nodal-positive tumors

G Hudelist[1,2], C Singer[1], M Manavi[1], K Pischinger[3], E Kubista[1], K Czerwenka[3]
[1]Dept. OB/GYN, Division of Special Gynecology, University of Vienna, Vienna/Villach, Austria.
[2]Dept. OB/GYN, Landeskrankenhaus Villach, Carinthia, Austria.
[3]Dept. of Clinical Pathology, Division of Gynecopathology, University of Vienna, Austria

Introduction Overexpression of members of the ErbB receptor family has been asssociated with malignant transformation and the amplification of Her-2/neu in tumor tissue is now an established prognostic factor in breast cancer. In order to initiate signal transduction, ErbB receptor monomers need to form homo- or hetero- dimers. The composition of these dimers is thought to greatly influence both quality and quantity of downstream signalling pathways, and to ultimately determine the elicited biological response.
Material and methods The protein expression pattern of all four ErbB receptors EGF-R, Her-2/neu, Her-3 and Her-4, and expression of their putative ligands EGF, TGF-a and HRG was investigated in 74 women with invasive breast cancer by membrane isolation and Western blot analysis.
Results The co-expression of all four ErbB family members was detected in 79,7% of cases, and of all of the three investigated ligands in 82,4%. While we did not observe a correlation between EGFR and Her-2/neu or Her-4 protein expression, EGFR and Her-3 ($p=0.005$), and Her-3 and Her-4 ($p=0.05$) were clearly co-expressed. The strongest overall correlation, however, was found between Her-2/neu and Her-3 ($p=0.001$) and between Her-2/neu and Her-4 ($p=0.001$). This was particularly true in nodal-positive tumors ($p<0.001$ and $p=0.002$, respectively) whereas in nodal-negative tumors the co-expression was either less significant (Her-2/neu and Her-3: $p=0.01$) or not significant at all (Her-2/neu and Her-4). The co-expression of EGFR/Her-3 was associated with the expression of all three ligands, whereas the Her-2/neu/Her-3 was correlated with HRG ($p=0.002$), thereby indicating a functional relation between specific receptor-dimer combinations and putative ligands.

Conclusion Taken together, we have performed a comprehensive survey of ErbB system expression in breast cancer, and have demonstrated the presence of a co-regulated receptor/ligand system in vivo. Her-2/neu appears to function as the preferred co-expression partner in nodal-positive tumors, thus rendering him the most likely dimerization candidate in malignant breast tumors.

P-007

The role of the AP-1 family members c-Fos, FosB, Fra-1 and Fra-2 in the invasion process of breast cancer cells

K Milde-Langosch, B Aslan, T Löning, AA Bamberger
Institute of Pathology, University Clinics Hamburg-Eppendorf, Hamburg, Germany

Introduction Members of the AP-1 family of transcription factors (c-Jun, JunB, JunD, c-Fos, FosB, Fra-1 and Fra-2) are able to form Jun-Jun or Jun-Fos dimers which bind to the regulatory sequences of target genes. In a prior study on mammary carcinomas, we found that high Fra-1 and reduced FosB expression are associated with indicators of poor prognosis. As most of the proteases involved in degradation of the extracellular matrix and basal membrane (matrix-metalloproteinases, members of the uPA/PAI-system) are regulated by AP-1 complexes, we assumed that the expression of single AP-1 proteins might also be important for the process of invasion of breast cancer cells.
Method In order to analyze the influence of the single Fos family members (c-Fos, FosB, Fra-1 and Fra-2) on the invasive behavior of mammary cancer, we performed Western Blot analysis of MMP1 and MMP9 and of the members of the plasminogen activator system PAI-1, uPAR, and PAI-1-uPA-complexes in 75 breast cancer samples, and correlated the expression of these proteins with that of the AP-1 proteins.
Results Interestingly, c-Fos, Fra-1 (phosphorylated form), and Fra-2 correlated with MMP9 expression levels. High expression of Fra-2 was also significantly associated with that of PAI-1 and the SDS-insoluble uPA/PAI-1 complex. On the other hand, the expression of FosB was significantly associated with high levels of MMP1.
Conclusion Our results indicate that a shift in AP-1 protein expression, especially high expression of Fra-1 and Fra-2, might be involved in invasion of breast cancer cells. (supported by Deutsche Krebshilfe, No. 10-1867-Ba2)

P-008

Immunohistochemical study of estrogen receptors and progesteron receptors in primary breast carcinomas and their axillary lymph node metastases

NH Aksoy, HE Pestereli, S Karaveli
Akdeniz University School of Medicine, Department of Pathology, Antalya, Turkey

Estrogen receptors (ER) and progesteron receptors (PR) was investigated in 57 primary breast carcinomas and their axillary lymph node metastases to determine if the malignant cells retained or changed this phenotypic feature during the metastatic process. The data were also compared with the tumour size, histologic type, grade and age. Immunohistochemistry with the ER (DAKO-1D5-N1575) and PR (DAKO-PgR 636-N1630) on formalin-fixed paraffin embedded tissue was used. The ER status in primary tumours and lymph node metastases was concordant in 45 patients (78,9%) and discordant in 12 (21,1%). Six of these eleven patients had ER-positive primary tumours and ER-negative lymph node metastases. The PR status in primary and lymph node metastases was concordant in 43 patients (75,4%) and discordant in 14 patients (24,5%). Ten of these twenty-four patients had PR-negative primary tumours and PR-positive lymph node metastases. We observed higher PR positivity in axillary lymph node metastases. The parameters, tumour histology, grade and age showed no statistically significant relation with receptor status. There was a significant correlation between the tumour size and the number of axillary lymh node metastases. The discordance of hormone receptors status between the primary tumour and lymph node metastases might be due to the heterogenity of tumour cells or loss of the phenotypic features of metastatic cells.

P-009

Breast carcinoma in a cancer hospital

P Arapantoni - Dadioti[1], O Tzaida[1], V Leodara[1], G Sotiropoulou[1], E Trichia[1], PK Sotirakoglou[2]
[1]Pathology Department Metaxas Cancer Hospital of Piraeus, Piraeus, Greece
[2]Department of Mathematics and Statitics Agriculture University of Athens, Athens, Greece

A total of 1302 cases of infiltrating breast Ca, diagnosed in our hospital during the last decade, was studied. The material concerned mastectomies with ispilateral lymph nodes dissection specimens. The patients were classified according the TNM staging system, based upon the primary tumor size (T), the presence of regional axillary nodal involvement (N) and distant metastases (M). This categorization revealed a preponderance of patients with T2 tumors. The overall decade rate for T1, T2 and T3 tumors was 51, 0,1%±2,77%, 31,86%±2,58% and 17,13%± 1,9%, respectively. There was a statistically significant difference between the three groups ($p<0,0001$). The annual distribution of these groups revealed that since 1992 the mean group rate had a tendency to approach the corresponding decade rate, a finding suggesting some degree of stabilization of these proportions. On the other hand, the lymph node metastases were more common in the T3 tumors. The mean rate for T3N+, T2N+ and T1N+ was 76,53%±5,9%, 66,01%±3,01% and 42,09%±-4,88%, respectively; the difference is statistically significant for the T3N+ and T2N+ ($p<0,004$) as well as for T2N+ and T1N+ ($p<0,0001$). The annual overall rate of patients with lymph nodes metastases, independently of T (TN+) was 60,09%± 2,73%. In conclusion, there is no tendency of early patient presentation and a more careful intimate medical care. The infiltrating breast cancer in our material, is represented mainly by theT2 tumors and the great majority of patients come to the hospital in an advanced stage regarding the T and N.

P-010

Aberrant copies of chromosome 16 and X are related with an aggressive phenotype and impaired prognosis of invasive breast tumors

L Nakopoulou[1], E Panayotopoulou[1], I Giannopoulou[1], J Mavrommatis[1], A Kapranou[1], H Gakiopoulou[1], S Markaki[2], M Perdiki[1], A Keramopoulos[3]
[1]Department of Pathology, Medical School, The National and Kapodistrian University of Athens, Athens, Greece
[2]Department of Pathology, 'Alexandra' Hospital, Athens, Greece
[3]Department of Gynaecology and Obstetrics, Medical School, The National and Kapodistrian University of Athens, Athens, Greece

Introduction Breast cancer is a genetically complex disease, which involves the accumulation of various structural and numerical aberrations. In the present study, we assessed the numerical status of chromosomes 16 and X in 114 primary invasive breast carcinomas in relation to clinicopathological parameters, patients' overall survival, and indices of cell growth (c-erbB-2, topoisomerase IIa) and survival (caspase-3, bcl-2).
Material and methods The number of copies of both chromosomes was detected by interphase chromogenic in situ hybridization with pericentromeric probes on paraffin embedded sections. ER, PR, cerbB-2, topoIIa, caspase-3 and bcl-2 expression was immunohistochemically detected (ABC/HRP). The results were statistically assessed by univariate and multivariate analysis.
Results Polysomy of chromosomes 16 and X was detected as the predominant aberration (73.7% and 57.9% respectively). Gain of chromosome 16 copies was associated with high nuclear grade (p=0.009), increased tumor size (p=0.041), advanced stage (p=0.002), the expression of topoIIa proliferation index (p=0.005), and worse overall survival by multivariate analysis (p=0.0317). The levels of chromosome X polysomy were elevated in ductal carcinomas of high histological grade (p=0.008), in high nuclear grade tumors (p=0.001), and were associated with the expression of topoIIa (p=0.005) and loss of caspase-3 protein (p=0.036). In addition, gain of chromosome X copies was an independent predictor of impaired prognosis of ductal carcinomas (p=0.0414).
Conclusion Polysomy of chromosomes 16 and X was observed as the predominant alteration in phenotypically aggressive breast tumors, characterized by poor differentiation, increased growth potential and impaired prognosis, whereas gain of chromosome X in particular, is probably implicated in cell survival.

P-011

Expression of survivin, bcl-2, p53 and bax in breast carcinoma and ductal intraepithelial neoplasia (DIN 1a)

F Kayaselcuk[1], TZ Nursal[2], A Polat[3], T Noyan[2], S Yildirim[2], A Tarim[2], G Saydaoglu[4]
[1]Baskent University Department of Pathology, Faculty of Medicine, Adana Teaching and Medical Research Center, Adana, Turkey.
[2]Department of General Surgery, Faculty of Medicine, Adana Teaching and Medical Research Center, Adana, Turkey.
[3]Pathology Department, Mersin University, Mersin, Turkey
[4]Biostatistics Department Cukurova University, Adana, Turkey

Introduction Survivin is a recently discovered member of the family of proteins that inhibits apoptosis. This anti-apoptotic compound can be detected in most types of cancer and expression is associated with a poor prognosis. We immunohistochemically investigated the expression of survivin in breast carcinomas and intraductal epithelial neoplasia of breast to determine whether expression of this protein is associated with clinicopathological parameters such as grade, stage, mitotic rate.
Materials and methods The study involved 43 patients with invasive ductal carcinoma (IDC) and 62 patients with intraductal epithelial neoplasia with mild, moderate and severe, florid ductal epithelial cell hyperplasia. Survivin, bax, bcl-2, and p53 monoclonal antibodies were administered by immunohistochemical method. Findings were analyzed with statistical methods.
Results In 34 of 43 cases (79.1%) of breast carcinomas and 22 of 62 cases (35.4%) of intraductal epithelial neoplasia with mild, moderate and severe ductal epithelial cell hyperplasia stained positively for survivin. None of the histological parameters analyzed were significantly correlated with survivin expression in breast carcinomas. In the carcinoma cases, survivin expression was positively correlated expression of bcl-2, but was not correlated with expression of p53, bax, c-erbB-2 and estrogen, or progesterone receptors. Some of the intraductal epithelial neoplasia cases with moderate or severe ductal epithelial hyperplasia stained positively for both survivin and p53. The breast carcinomas exhibited significantly increased expression of survivin, p53, and bcl-2 than the breast with intraductal epithelial neoplasia.
Conclusion Survivin was not correlated with any of the clinicopathological parameters studied, however, it could be a useful tool in early carcinomas and florid, severe ductal epithelial hyperplasia.

P-012

Non malignant and pre malignant lesions in large needle core biopsy of the breast (LNCB)

FJ Andreu, A Sáez, LE Pons, O Balagué, S Fernández, C Dinares, MA Cabezuelo, M Rey
UDIAT- Centre Diagnostic S.A. - Corporació Parc Taulí, Sabadell, Spain

Introduction Certain non-malignant and pre-malignant lesions cause dilemmas for the most appropriate management following LNCB. The aim of this study was to determine the accuracy of LNCB in diagnosising the most frequent non-conclusive findings: benign papillary lesions (BPL), radial scars (RS), fibroepithelial lesions with stromal hypercellularity (FLSH), atypical ductal hyperplasia (ADH) and intraductal carcinoma (DCIS).
Material and methods In a retrospective review of 2,052 imaging guided LNCBs (1993-2001), we found: 19 (0.9%) BPL - 9 with surgical correlation (SC) and 10 with mammographic follow-up (MF); 21 RS (1%) with SC in 6 and MF in 15; 15 (0.7%) FLSH all with SC; 54 (2.6%) ADH - with SC in 40, and 174 (8.5%) DCIS - with SC in 118.
Results 1) BPL: 10 patients without changes in MF. At surgery: 5 BPL - 1 with ADH and 4 invasive carcinomas (3 with mammographic histologic discordance and 1 diagnosed 4 years post LNCB). 2) RS: 15 without mammographical changes and 6 RS (3 with ADH). 3) FLSH: at surgery, 3 fibroadenomas, 11 benign and 1 malignant phyllodes tumours. 4) ADH: at surgery, 19 (47.5%) ADH, 12 (30%) DCIS, 9 (22.5%) invasive carcinomas - 2 of which microinvasive. 5) DCIS: at surgery, 64 (54.2%) DCIS; 12 (10.1%) microinvasive, and 42 (35.6%) invasive carcinomas.
Conclusions 1) Diagnosis of BPL at LNCB seems accurate when

correlating with image findings. 2) RS at LNCB can be followed mammographically. 3) FLSH at LNCB always requires surgical excision. 4) ADH and DCIS diagnosed at LNCB need complete removal of lesion, due to frequent underdiagnosis.

P-013

Estrogen receptor beta protein expression in invasive breast cancer

K Pavlaki[1], A Lazaris[1], H Gakiopoulou[1], E Panayotopoulou[1], S Markaki[2], I Giannopoulou[1], J Mavrommatis[1], A Keramopoulos[3], L Nakopoulou[1]
[1]Department of Pathology, Medical School, The National And Kapodistrian University of Athens, Athens, Greece
[2]Department of Pathology, 'Alexandra' Hospital, Athens, Greece
[3]Department of Gynaecology and Obstetrics, Medical School, The National and Kapodistrian University of Athens, Athens, Greece

Introduction Estrogen receptor beta (ERb) is known to be present in breast tumors; its prognostic and pathophysiological roles, however, remain to be established. The aim of this study was to investigate ERb protein expression in a well documented series of 181 invasive breast carcinomas.
Materials and methods Standard immunohistochemistry with a specific monoclonal antibody (clone PPG5/10, Serotec) was performed on paraffin sections; 10% of strongly immunostained carcinoma cells was used as a cutoff point to classify tumors as ERb-positive. Statistical correlations were sought with clinico-pathological variables (including hormone receptor status) and patients' disease-free and overall survival. Cell proliferation was immunohistochemically assessed by topoisomerase IIa (topoIIa) index. Statistical analysis was univariate and multivariate.
Results ERb immunoreactivity was detected in the majority of specimens (71.2%)and was positively linked with ERa immunoreactivity ($p<0.001$) and increased topoIIa index ($p=0.045$). A significant favorable impact of ERb immunopositivity emerged with regard to disease-free and overall survival in both univariate ($p=0.0002$, $p=0.0002$, respectively) and multivariate ($p=0.001$ and $p=0.011$ respectively) statistical analysis; progesterone receptor expression was also found to exert an independent favorable influence on patient's survival with less statistical significance though ($p=0.045$ and $p=0.041$). On the contrary, patients' survival was not significantly impacted by ERa status.
Conclusions Because of the positive association between ERb immunoreactivity and topoIIa expression, the presence of ERb in breast cancer cells may be considered an indication of increased proliferation. Nevertheless, ERb immunoreactivity emerges as a valuable, independent indicator of favorable prognosis.

P-014

Large needle core biopsy (LNCB) in invasive lobular carcinoma of the breast (ILC) including immunohistochemical expression of E-cadherin (EC) and high molecular weight cytokeratin (CK34ssE12): analysis of results

A Sáez, FJ Andreu, LE Pons, O Balagué, S Fernández, C Dinares, MA Cabezuelo, M Rey
UDIAT- Centre Diagnostic S.A. - Corporació Parc Taulí, Sabadell, Spain

Aims To determine diagnostic value of LNCB in patients with ILC using EC and CK34ssE12.
Material and methods Retrospective review of 50 cases diagnosed as ILC either at LNCB or at surgical biopsy (SB), between 1990 and 2000. Immunohistochemical (IHQ) study with EC and CK34ssE12 was performed at both LNCB and SB. Three immunoprofiles were established: EC- CK34ssE12 + (IHQ of ILC); EC + CK34ssE12 - (IHQ of ductal carcinoma - IDC) and EC + CK34ssE12 + (IHQ of mixed ILC-IDC). Initial diagnosis at LNCB was correlated with final diagnosis (morphologically and immunoprofile). Discordant cases were analysed in order to determine usefulness of IHQ at LNCB.
Results In LNCBs initially diagnosed as: 1) ILC (19 patients), final diagnosis was ILC in 18 cases (EC- CK34ssE12+) and IDC in 1 case (EC+ CK34ssE12 -); 2) Invasive carcinoma probably lobular type (ILCp) (26 patients), final diagnosis was ILC in 20 cases (EC- CK34ssE12+), IDC in 4 (EC+ CK34ssE12 -) and mixed ILC-IDC in 2 (EC+ CK34ssE12+); 3) IDC (5 patients), final diagnosis was ILC in all cases (EC- CK34ssE12+), 3 of them ILC pleomorphic-type. In all discordant cases, immunoprofile at LNCB was concordant with final diagnosis
Conclusion 23% of patients diagnosed as ILCp at LNCB corresponded finally to IDC or mixed IDC-ILC. 11.6% of patients finally diagnosed as ILC were initially interpreted as IDC at LNCB. Our findings suggest that EC and CK34ssE12 are of great value to help characterise breast carcinomas at LNCB, and improve management of patients.

P-015

Recurrence of ductal carcinoma in situ of the breast (DCIS) in a series of 371 patients. A multiinstitutional study

S Fernández[1], FJ Andreu[1], A Sáez[1], LE Pons[1], V Marco[2], J Autonell[3], J Esquius[4], I Roig[5], T Soler[6], E López[7]
[1]UDIAT- Centre Diagnostic S.A. - Corporació Parc Taulí, Sabadell, Spain
[2]Hospital General de Catalunya, Spain
[3]Hospital General de Vic, Spain
[4]Fundació Asil Granollers, Spain
[5]Consorci Sanitari de Terrassa, Spain
[6]Consorci Sanitari de Mataró, Spain
[7]Hospital Universitari Josep Trueta, Spain

Aims To assess recurrence rate of DCIS, evaluating initial treatment and histological criteria.
Material and methods 371 patients with DCIS were identified between 1990-2001. DCIS type, nuclear grade, lesion size, margin clearance (Van Nuys Score), initial treatment and recurrence type (DCIS vs invasive carcinoma) were analysed. Median follow-up: 45 months (range 1-146).
Results 12 cases of recurrence appeared in 11 patients (3.2 %). 4.1% (6/146) after mastectomy and 2.7% (6/225) after breast-conserving surgery. Actuarial rate of 5-year recurrence was 5.2% (Kaplan-Meier). 4 cases (36%) recurred as invasive carcinoma or as metastasis.

1st treatment	Recurrence (months)	Grade	Size	Margins	Recurrence type
		(Van Nuys Score)			
T(1)- M+AD(2)	7 and 31	2	1	3	DCIS and DCIS
M	13	3	2	-	DCIS
T - M	15	3	2	-	Axillary MTX
T + RT	17	2	1	1	DCIS
T + AD + RT	21	3	1	1	DCIS
T – M + AD	22	1	2	-	Invasive carc.
M + AD	24	3	2	-	Invasive carc.
T + RT	47	3	2	3	DCIS
T + AD	51	1	2	3	DCIS
M + AD	58	3	3	-	DCIS
T – M + AD	66	2	1	-	Systemic MTX

(T: Tumorectomy / M: Mastectomy / AD: Axillary Dissection / RT: Radiotherapy / MTX: Metastasis)

Conclusions 1) In our series, higher recurrence occurred in patients treated with mastectomy. Recurrence may occur despite radical treatment. 2) No significant differences in grade, size or margin status were observed in patients with recurrence comparing to whole DCIS series.

P-016

HER2 status in breast cancer determined by IHC and FISH: comparison of the results

A Mrozkowiak, W Olszewski, W Olszewski
Department of Pathology, Institute of Oncology, Warsaw, Poland

Background HER-2 status became an important prognostic and predictive factor in breast carcinoma. There are two main techniques of evaluation HER2 status: immunohistochemistry (IHC) for the protein expression and fluorescence in situ hybridisation (FISH) for amplification of HER2 gene. The aim of the study was to compare the results obtained by IHC and FISH methods in determination of HER2 status in breast cancer.
Materials and methods Two hundred breast cancer specimens were examined. IHC and FISH were performed in every case. IHC was performed with DAKO HercepTest, FISH with Oncor-QBiogene reagents. IHC results were classed into 4 groups, accordingly to the intensity of membrane staining (0,1+, 2+, 3+). FISH results were divided into three main categories: NA - no amplification, LA - low amplification and HA - high amplification. The number of copies of chromosome 17 was also assessed.
Results Over 87% of cases described by IHC as 3+ exhibited also amplification of HER2/neu gene. Remaining cases were positive with IHC, but presented no gene amplification. This might be due to the subjective assessment of the membrane staining or to the procedure of material fixation. Another possibility is that overexpression of the protein was caused by mRNA stability or disorders in receptor circulation. The majority of cases classed by IHC as 2+ were also negative by FISH (over 75%). Nearly one fifth of IHC 2+ were found to exhibit gene amplification. Remaining cases showed no amplification of HER2/neu gene, combined with aneuploidy of chromosome 17. All cases described by IHC as 0/1+ showed no amplification.
Conclusions IHC is well-established method of assessing HER2 status in breast cancer. Nonetheless, group of cases described as 2+ should be additionally examined using FISH method because the results are more reliable. In order to improve accuracy and gain the highest quality of HER2 status evaluation, in those cases both methods should be applied.

P-017

DCIS of the breast with excessive cancerization of the lobules simulating invasive carcinoma

B Nielsen
Institute of Pathology, Randers, Denmark

A 33-years old woman had a right sided mastectomy with axillary dissection performed, because of suspicious mammografic microcalcifications and finding of malignant cells by fine needle aspiration. Grossly, an 9 cm large suspicious area with accentuaded consistency and multiple pale-yellow flecks, representing comedo-necrosis, were found. Multiple sections representing the suspicious area showed DCIS. The ducts were dilated and contained malignant cells and central necrosis. In areas classical cancerization of the lobules were present. Furthermore, in multiple microscopic areas the stroma of the lobules were oedematous and infiltrated by lymphocytes. The acini were slightly dilated and covered by one or two layers of malignant epithelial cells, but the central lumen was preserved. The morphology greatly simulated invasive ductal carcinoma. However, by immunohistochemistry the myoepithelial cells were showed to be preserved and the lobular unit were well demarcated with preserved circumscription. The axillary fat contained 13 lymph nodes all without metastasis. It was concluded that the alterations represented a variant of lobular cancerization, earlier described by Tavassoli (1992).

P-018

Spindle cell tumors of the breast; difficulties in the differential diagnosis

F Staniceanu[1], S Zurac[2], C Ardeleanu[3], E Gramada[2], G Micu[2], S Simion[4], F Ticmeanu[4]
[1]University of Medicine And Pharmacy, Colentina Hospital, Department of Pathology, Bucharest, Romania
[2]Colentina Hospital, Department of Pathology, Bucharest, Romania
[3]University of Medicine And Pharmacy, Victor Babes Institute, Department of Pathology, Bucharest, Romania
[4]University of Medicine And Pharmacy, Colentina Hospital, Department of Surgery, Bucharest, Romania

Spindle cell tumors of the breast are rare entities with difficult differential diagnosis. We report four spindle cell tumors: a metaplastic carcinoma, a fibromatosis, a malignant spindle cell myoepithelioma and an inflammatory pseudotumor. The metaplastic carcinoma occurred in a 66-year-old woman as a 2.5x2.2x2 cm nodule with scarce bland clear cells proliferation and very important desmoplastic reaction; immunohistochemical stains revealed positivity for cytokeratins (MNF116) and vimentin and negativity for actin and desmin. The fibromatosis occurred in a 36-year-old man as an 8x6x5 cm tumor with bland spindle cell morphology; very little atypia and rare mitoses were identified and immunohistochemical positivity for vimentin was demonstrated. The malignant spindle cell myoepithelioma occurred in a 52-year-old woman as 4x3x2 cm nodule with central necrosis; histopathologic examination revealed a malignant spindle cell proliferation with many mitoses and atypical cells; focal positivity for MNF 116, vimentin, actin and S 100 was identified. The inflammatory pseudotumor occurred in a 35-year-old woman as a highly cellular spindle cell proliferation with fascicular pattern admixed with myxoid areas and inflammatory cells – type I-II mammary inflammatory pseudotumor. One important criterion

which should be kept in mind in the process of evaluation of a spindle cell tumor of the breast is that these tumors may have deceptive histopathologic appearance – some of them have bland looking morphology despite of their biological behavior (our example of metaplastic carcinoma) and others with worrisome morphology were diagnosed as benign or intermediate malignancy entities (inflammatory pseudotumor).

P-019

Calcitonin receptor down-regulation in breast cancer. Quantitative analysis of gene expression with laser capture microdissection

X Wang[1], N Misa[1], I Mori[1], K Takeda[1], Y Nakamura[1], H Utsunomiya[1], G Yoshimura[2], T Sakurai[2], K Kakudo[1]
[1]Wakayama Medical University, Wakayama, Japan
[2]Affiliated Kihoku Hospital, Wakayama Medical University, Wakayama, Japan

Introduction Calcitonin receptor (CTR) belongs to the G protein-coupled receptors and it binds calcitonin (CT), which acts on bone and kidneys to maintain calcium homeostasis. However, both of CT and CTR have also been identified in a large number of tissue and cell, suggesting it might has any unrecognized roles. Although CTR expression has been found in several breast cancer cell lines and in primary breast cancer, quantitative analysis of CTR expression in matched normal breast tissue and primary breast cancer has not been explored up to date. Here we present the detection and quantitation of CTR gene expression in matched normal breast tissue and breast cancers, by using laser capture microdissection.
Materials and methods Fourteen breast cancers and matched normal epithelium from the same patient were laser capture microdissected to obtain pure cell groups and to submit to quantitative analysis by using one step real time RT-PCR.
Results Both normal breast epithelium and cancer cells expressed CTR. As compared with paired normal epithelium, decreased CTR expression was found in 9 of 14 cases breast cancer (64.28%) while increased CTR expression in 2 cases (14.29%) and no change in 3 cases (21.43%).
Conclusion Our investigation revealed that CTR expression was constantly expressed in normal breast tissue and breast cancers. To the best of our knowledge, this is the first report, which revealed that CTR RNA expressed in normal breast epithelium. Down-regulation of CTR is a common phenomenon in the breast cancer, suggesting that it may have important roles on the development of breast cancer.

P-020

Effect of neoadjuvant chemotherapy on HER 2 status in patients with breast carcinoma

S Popovska, T Betova
Medical University-Pleven, Pleven, Bulgaria

Introduction Neoadjuvant chemotherapy is the standard of care for patients with locally advanced breast cancer and is being evaluated in patients with earlier-stage operable disease. The effects of chemotherapy on biological markers such as an oncoprotein expression are not well known. The aim of the study was to determine whether Her 2 expression was modified by neoadjuvant chemotherapy.
Methods Forty-nine patients with T2-4N0-2M0 breast cancer were treated in a prospective trial utilizing FEC regimen. Matched pairs of pre and post-chemo therapy breast tissue were evaluated immunohistochemically for HER 2 status using HercepTest Kit (DAKO).
Results Her 2 overexpression was observed in 12/49 patients (24%). The Her 2 status of 41 (83.6%) patients was unchanged after chemotherapy. Modification was found in 6 cases- decreasing in 2, increasing in 3 and loss of expression in 1 patient. Her 2 status was not changed significantly following primary chemotherapy.
Conclusions Our results showed that, in most patients HER 2 status is stable parameter in patients with breast carcinoma after primary treatment with neoadjuvant chemotherapy.

P-021

The microvessel density in female breast cancer among younger and older age groups

Z Dobrosz, D Gołka, J Pająk, P Właszczulk, M Wilk
Dept. of Pathomorphology; Medical University of Silesia, Katowice, Poland

Introduction Breast cancer remains one of the most important oncologic problems worldwide. It seems that breast cancer first detected by the age of 20-40 years follows more aggressive clinical course than tumors developing later. Young females with breast cancer more frequently present with axillary lymph nodes metastases. Expression of the estrogene receptors is less frequent, and the histological grade is usually higher among this group. The main purpose of our study was the evaluation, quantification, and comparison of the angiogenesis in breast cancer among young women, below the age of 35 years and older patients, above 60 years.
Material and methods Tissue samples of breast cancer from patients aged 35 years and less (50 cases), and from patients older than 60 (20 cases) were studied. Ten specimens of non-neoplastic breast tissue from the normal breast in the tumor vicinity (younger patients) served as a control. Microvessels were visualized immunohistochemically with use of CD-34 antibody and counted within the areas of the highest density („hot spots"). Six separate high power fields (HPF), 0.216 mm2 each, were studied in each case.
Results and conclusion The average microvessels count per HPF in the breast cancer tissue in younger group was higher than in the older age group and non-neoplastic tissue. The differences were statistically significant. The increased density of proliferating microvessels seems to play a role in the aggressive clinical behavior.

P-022

Assessment of telepathological frozen section diagnosis of sentinel lymph node of breast cancer

I Mori[1], X Wang[1], T Suzuma[2], G Yoshimura[2], T Sakurai[2], K Kakudo[1]
[1]Department of Pathology, Wakayama Medical University, Wakayama, Japan
[2]Affiliated Kihoku Hospital, Wakayama Medical University, Wakayama, Japan

Introduction Telepathology has now become widely used in Japan. After we introduced telepathology equipment on November 2000,

total 178 frozen section diagnoses have been performed mainly on sentinel lymph node of the mammary gland.The aim of the study was to analyze our result, and estimate whether the telepathology is of practical use or not.
Material Total 178 cases including 244 lymph nodes diagnosed using telepathology.
Results and conclusion We failed to find carcinoma metastasis in 1 out of 244 sentinel lymph nodes of breast. It was very minute metastasis, and was not contained in the transmitted pictures. Our transmission speed is 64 Kb that takes about 8 seconds for each picture. There exists a limitation about the transmittable pictures within a restricted time. Improvement of transmission speed may solve this problem. In two cases, while telepathologically negative of sentinel node, we found metastasis in the other dissected nodes by permanent section examination. The method of sentinel node identification should be improved. There was a confounding of the specimens that occurred between two patients on the same day. It was a case that happened at the beginning of telepathology. Since the surgeon and the technicians are far away from the pathologist, and communication is done by the telephone, it is important for each party to keep in close contact with each other. Our result is fairly good considering the limitation of the telepathology. Although some issues are still remaining, we conclude that telepathology is now of practical use.

P-023

Pigmented mammary Paget disease in a 65 year old man- a case report

AR Monsef Esfahani
Hamedan University of Medical Sciences, Hamedan, Islamic Republic of Iran

Mammary Paget disease results from intraductal mammary Paget carcinoma that extends to the epidermis of the nipple and areola through a lactiferous duct or from invasive breast carcinoma that reaches the epidermis via direct extension from the dermis. Pigmented mammary Paget disease is a rare clinicopathologic variant of mammary Paget disease. It may mimic malignant melanoma clinically and histophatologically. It seems that involvement of the dermo-epidermal junction by neoplastic cells of the mammary Paget carcinoma seems to be a prerequisite for the development of the clinical pigmentation. We report a case of pigmented mammary Paget disease. The patient was a 65-year-old male who complained of an erythematous, pigmented scaly plaque around his right nipple measuring 8x6 cm with mild fissuring of two year duration. The histopathology revealed pagetoid spread of large cells in the epidermis with pigmentation of basal cells and melanocytes. The IHC confirmed the mammary Paget disease and excluded malignant melanoma and squamous cell carcinoma.

P-024

Frozen section evaluation of sentinel lymph nodes in breast cancer

B Stojiljkovic[1], A Golubovic[1], A Plzak[1], Z Radovanovic[1], A Opacic, B Guduric[1], M Breberina[1], M Kostov[2]
[1]Institute of Oncology Sremska Kamenica, Novi Sad, Serbia and Montenegro
[2]Military hospital Nis, Nis, Serbia and Montenegro

Introduction The use of Sentinel Concept as the newest approach in surgical treatment of breast cancer, apart from tumorectomy, means the extirpation and analysis of one or more regional lymph nodes which receives lymph drainage from primary tumor (guardian lymph nodes - sentinel nodes). The presence or the absence of secondary deposit in them is considered the most important predictor of the positive secondary deposit status of the other axillary lymph nodes. Depending on histological analysis of sentinel node, the operation is finished with or without the axillary lymph node dissection.
Materials and methods Sentinel concept in surgical treatment of the breast cancer is applied only in the cases where the largest dimension of the tumor is not more than 2cm (pT1). Marking of the sentinel node is conducted before the operation by a combined method, the usage of Patent Blau color and Technetium 99m as a radio marker. Sentinel lymph nodes identity, before sending to a pathohistological analysis, is checked by gamma detection probe. Two groups of prospective tests (A and B) were formed with 50 cases each. Sentinel lymph nodes from group A in the first stage of the testing were treated by pathohistological method (one hematoxylin and eosin preparation) and then microscoped. The cases in which secondary deposit was not noted, were subjected to a serial cutting and immunohistochemical staining by the EMA markers, specific for intraductal epithelium of a breast. Sentinel nodes from group B were submitted fresh for frozen section investigation, where they were approached with a series of cuttings and immunohistochemical analysis by the EMA markers. The nodes without secondary deposits were fixed in formalin, paraffin embedded and, with the application immunohistochemistry (EMA), submitted to serial cutting (similar to the second phase in group A) as a precaution.
Results In the first stage 50 paraffin samples (group A) were first examined by H&E method, and additionally with immunohistochemistry (using EMA). With this additional examination secondary deposits were found in 6 cases (12 %). This can only prove already known fact about statistically significant higher sensitivity and specifity of immunohistochemistry compared to H&E. In the second stage (group B) 50 new samples of SN, first investigated by frozen section investigation, were examined by immunohistochemichal method (using EMA). In addition, these samples were serially cut and treated like paraffin samples by immunohistochemistry method. The results of these two analysis were identical. Facts mentioned above show that sensitivity and specifity of the frozen section analysis using immunohistochemical method (EMA) is 100% (high percentage is probably the consequence of a relatively small number of samples).
Discussion Acquired data suggested that implementation of one of the used methods (serial frozen section analysis with immunohistochemistry) from the Sentinel Concept is an efficient histo-morphological method in the evaluation of sentinel lymph nodes that make valid intraoperative staging of breast carcinoma possible. The authors came to significant data in both groups of tests and determined sensitivity, particularity and the efficiency of the applied methods.
Conclusion Application of the suggested method would spare a considerable number of patients with pT1 breast cancer of subsequent axillary lymph node dissection and thus reduce the number of postoperative complications and long term morbidity.

P-025

Correlation of histologic prognostic factors in core biopsies and in surgical excisions of breast lesions.

MG Cattani[1], MC Cucchi[2], G Saguatti[3], G Baruzzi[1]
[1]U.O. Anatomia Patologica Ospedale Maggiore Azienda USL Citta' di Bologna, Bologna, Italy
[2]U.O. Chirurgia B Ospedale Maggiore Azienda USL Citta' di Bologna, Bologna, Italy
[3]Centro Diagnostica Senologica Azienda USL Citta' di Bologna, Bologna, Italy

Introduction Needle core biopsy (NCB) of palpable lesion and stereotactic biopsy (SMB) of non-palpable mass are the major preoperative methods of breast tumor diagnosis. The aim of this study was to evaluate methods accuracy and to emphasize the main detectable prognostic factors.
Materials and methods 809 core biopsies (398 NCBs and 411 SMBs) were performed between January 2000 and December 2002. In 483/510 cases, the correlation between biopsy results and subsequent surgical excision was available.
Results The lesion diameter was < 1 cm (in 45 % of the NCBs and 72 % of the SMBs). With SMB, the average number of tissue core obtained per lesion was 12. At histology, in 67 % of NCB and in 48% of SMB diagnosis of malignancy was given. The DCIS/IDC ratio was 46/219 for NCB and 93/78 for SMB, respectively. Grade and type of the invasive and in situ carcinoma were determined in both biopsy and definitive excision, and the results compared. The agreement for overall grade was in 82 % with SMB and in 66 % with NCB. At surgical excision, 26/139 DCIS showed foci of IDC. In 15 % of SMB cases no residual neoplastic tissue was found.
Conclusions The accuracy of both methods is very high. SMB shows highest reliability and accuracy, because of the increased quantity of tissue obtained. The possibility to assess tumour size is limited. The preoperative assessment of the other prognostic factors (type and grade, tumour markers) are key determinants in planning the optimal breast lesions management.

P-026

Expression of MCP-1 mRNA and macrophage infiltrates in invasive breast carcinoma

D Fučkar[1], T Valković[2], M Hasan[3], S Štifter, K Matušan, N Jonjić
[1]Department of Pathology, Medical Faculty, University of Rijeka, Rijeka, Croatia
[2]Department of Internal Medicine, Medical Faculty, University of Rijeka, Rijeka, Croatia
[3]Department of Histology and Embriology, Medical Faculty, University of Rijeka, Rijeka, Croatia

Introduction Monocyte Chemotactic Protein-1 (MCP-1) has been detected in many human tumors; however, its chemoattractant role for macrophages in breast carcinomas is still questionable. The aim of this study was to determine the possible correlation between tumor-associated macrophages (TAM) and the number of MCP-1 mRNA in the invasive breast carcinoma.
Material and methods Tissues obtained from 27 surgical specimens of invasive breast carcinomas and 8 cases of normal breast tissues were frozen in liquid nitrogen and kept at – 80 ^{o} C until they were used for quantification of MCP-1 mRNA by RT-PCR. The expression was calculated as a number of MCP-1 cDNA copies per 100 copies of G-6-PHD mRNA. Paraffin embedded sections from breast carcinomas were immunohistochemically processed for CD68 staining. Positively stained tumor associated macrophages (TAM) were counted on three “hot spots” (x 400) and mean value was calculated.
Results The result of RT-PCR showed that in all cases of breast carcinomas (27/27) and the majority of normal breast tissues (7/8) the number of detected MCP-1 cDNA copies was above the detection limit. Furthermore, carcinomas showed higher levels of MCP-1 mRNA (229.5 ± 275.6) then normal breast tissue (48.06 ± 69.5). The value of TAM within a single carcinoma was very inconsistent (48.3 ± 23.8). Statistical analysis did not find a significant correlation between MCP-1 expression and macrophage infiltrations (r= -0,19592).
Conclusion MCP-1 is an important factor in the recruitment of macrophages. However, the results indicate that MCP-1 is probably not the only and/or crucial factor involved in macrophage attraction to tumor locus in breast carcinomas.

P-027

Comparison of mitotic index, growth fraction (evaluated by Ki-67), ER, PR, cathepsin D, p53, and Bcl-2 status between primary breast cancer and corresponding axillary metastatic sites

B Dmitrovic[1], J Kristek[2], S Kurbel[3]
[1]Osijek Clinical Hospital, Department of Pathology, Osijek, Croatia
[2]Osijek Clinical Hospital, Department of Thoracic Surgery, Osijek, Croatia
[3]Osijek Clinical Hospital, Department of Oncology and Radiotherapy, Osijek, Croatia

Introduction It has been postulated that the equilibrium of different clones within a tumor is eventually overcome by a biologically dominant one with enhanced metastatic potential. Therefore, the metastatic tumor should be composed of more aggressive tumor cell clones than the primary one. We analyzed mitotic index, proliferation antigen Ki-67, estrogen receptors (ER), progesterone receptors (PR), cathepsin D activity, protein p53, and Bcl-2 oncoprotein status in order to explore the assumed differences in the clonal composition between the primary breast cancer and axillary metastasis.
Materials and methods ER, PR, p53, Bcl-2, Ki-67, and cathepsin D statuses in 60 patients with the primary ductal invasive carcinoma of the breast and at least one axillary metastatic lesion were analyzed by immunohistochemistry (IHC – DAKO LSAB2 System). Mitotic index was assessed by counting the number of mitoses in primary and metastatic lesions. Statistical analysis included t-test for dependent samples, linear correlation analysis, and ROC-curve based contingency table analysis.
Results We found higher mitotic index (p=0.018, r=0.51), higher growth fraction (Ki-67, p=0.045, r=0.71), and higher level of overexpression of Bcl-2 (p=0.014, r=0.86) in axillary metastatic lesion than in primary breast tumor. There were no significant differences in ER (p=0.16, r=0.98), PR (p=0.08, r=0.87), cathepsin D (p=0.92, r=-0.06), and p53 (p=0.36, r=0.87) status. Higher mitotic and Ki-67 rates were associated with lower ER and PR expression, whereas higher cathepsin D level was associated with lower Bcl-2 expression, both in primary tumor and metastasis.

Conclusion Between the paired primary tumor and axillary metastatic lesions, samples had concordant ER, PR, p53, and cathepsin D status when analyzed by IHC. Tumor clone with enhanced metastatic potential might be characterized with higher mitotic index and overexpression of both Ki-67 antigen and Bcl-2 oncoprotein.

P-028

Basaloid breast carcinoma with pleomorphic lipoblast-like giant cells and neuroendocrine differentiation

JS Reis-Filho[1,2], LG Fulford[1], SR Lakhani[1,3]
[1]The Breakthrough Toby Robins Breast Cancer Research Centre - Institute Of Cancer Research, London, UK
[2]Life and Health Sciences Research Institute, School of Health Sciences, University of Minho, Braga, Portugal
[3]Breast and Cytopathology Unit, Department of Pathology, The Royal Marsden Hospital, London, UK

Liposarcomatous differentiation in breast neoplasms is a rather infrequent phenomenon and so far restricted to rare cases of malignant phyllodes tumour and true liposarcomas of the breast. The terms lipid-rich and lipid-secreting breast carcinomas encompass breast tumours in which neoplastic cells accumulate or secret lipid; however, lipoblasts are not usually seen. Recently, we have observed a distinctive type of breast carcinoma in which pleomorphic lipoblast-like cells were seen admixed with the carcinomatous component. An 82-year-old female presented with a 5cm hard lump in the right breast with palpable nodes in the right axilla. Mammography and ultrasound disclosed two irregular dense central masses in the right breast, measuring 5cm in aggregate, and an enlarged axillary node measuring approximately 3cm. A diagnosis of breast carcinoma was made and the patient received neoadjuvant tamoxifen despite the lack of estrogen receptor (ER) in the primary tumour. Four months later, her disease had progressed and she underwent right mastectomy with axillary dissection.. Histologically, both the primary tumour and the 3/24 lymph node metastases were characterised by a high-grade carcinomatous component which imperceptibly merged with pleomorphic lipoblast-like cells. Immunohistochemistry demonstrated epithelial differentiation in the carcinomatous and liposarcomatous-like components (epithelial membrane antigen, cytokeratins 5/6, 8/18, 14, 19 and MNF116). Both components were also positive for vimentin, S-100 protein, and focally for chromogranin, GCDFP-15, and E-cadherin. Hormone receptors (estrogen, progesterone and androgen receptors), Her2/neu, p63, smooth muscle actin, desmin, synaptophysin were negative. Based on the histological and immunohistochemical profile, we believe that this case represents a breast carcinoma with basaloid phenotype and showing divergent differentiation (liposarcomatous and neuroendocrine), features that have to our knowledge not been documented to date.

P-029

Collagenous spherulosis arising in an adenomyoepithelioma of the breast: a hitherto unrecognised association

JS Reis-Filho[1,2], LG Fulforf[1], B Crebassa[3], S Charpentier[4], SR Lakhani[5]
[1]The Breakthrough Toby Robins Breast Cancer Research Centre - Institute Of Cancer Research, London, UK
[2]Life and Health Sciences Research Institute, School of Health Sciences, University of Minho, Braga, Portugal
[3]Cabinet Prado Pathologie, Marseille, France
[4]Marseille North University, Marseille, France
[5]Breast and Cytopathology Unit, Department of Pathology, The Royal Marsden Hospital, London, UK

Collagenous spherulosis (CS) is a benign epithelial and myoepithelial breast lesion characterised by the accumulation of basement membrane material in the form of eosinophilic or rarely basophilic spherules that exhibit concentric and radiating fibrillar patterns. CS is an incidental finding that usually occurs in association with benign proliferative and pre-invasive lesions. Adenomyoepithelioma is a biphasic neoplasm of the breast, composed of both luminal epithelial and myoepithelial cells. Despite the shared histogenesis, CS has never been described in association with adenomyoepithelioma. We report a case of a 48-year-old female who presented with CS of the breast arising in an adenomyoepithelioma. The differential diagnosis included adenoid cystic carcinoma. Immunohistochemistry with antibodies for cytokeratins (CKs) 19, 14 and 5/6, smooth muscle actin (SMA), calponin, smooth muscle myosin heavy chain (SMMHC), p63, collagen IV, oestrogen receptor (ER), progesterone receptor (PgR), Ki67, and c-kit was performed. Myoepithelial cells of the adenomyoepithelioma and the cells surrounding the collagen spherules of CS showed a similar profile (CKs 14 and 5/6, SMA, calponin, SMMHC, p63, and S100 reactivity), luminal cells of both lesions also showed overlapping immunophenotypes (Ck19, ER and PgR positivity). Collagen IV highlighted the spherules in CS. Ki67 labelling indices were similar in both lesions. C-kit expression was restricted to the adenomyoepithelioma and no expression was observed in the CS. The association is important to recognise as it could potentially lead the unwary to a misdiagnosis of adenoid cystic carcinoma, cribriform carcinoma or cylindroma of the breast.

P-030

Lymphoepithelioma-like carcinoma of the breast

EÜ Akyildiz[1], S Ilvan[2], Z Calay[2]
[1]Institute of Forensic Medicine, Istanbul, Turkey
[2]Istanbul University, Cerrahpa, Faculty of Medicine, Department of Pathology, Istanbul, Turkey

Introduction Lymphoepithelioma of the nasopharynx is an undifferentiated carcinoma with a prominent lymphoid infiltrate. Tumors, with histologic features similar to nasopharyngeal lymphoepithelioma in other locations are referred as lymphoepithelioma-like carcinoma.(LEC). In differential diagnosis of this lesions, medullary carcinoma and lymphoma must be considered. In this study, we report a case of LEC of the breast which is very rare tumor..

Material and method A 59-year-old female was noted to have a lesion of the right breast on mammography. An excisional biopsy was performed and sections revealed a well-demarcated elastic mass of 3 cm in diameter. Routine histologic examinations and immunohistochemical analysis were performed and compared with reported cases in literature.

Results Clinical features, macroscopic and microscopic findings, immunohistochemical analysis were consistent with LEC of the

breast. On immunostaining, the tumor cells showed strong staining for epithelial membrane antigen (EMA) and low weight cytokeratin (LCW).Lymphoid cells stained positively for leucocyte common antigen (LCA).The tumor cells showed no staining for CD30. Staining for UCHL -1 and L26 demonstrated that there were more T cells than B cells. The tumor cells were immunohistochemically negative for Epstein-Barr virus (EBV).

P-031

Comparative evaluation of DNA-ploidy and survival rate of patients with breast cancer

E Karbova[1], E Kanchev[1], P Kolova[1], M Bruckner[2], B Manevska[1]
[1]Dept. General And Clinical Pathology, Medical University, Varna, Bulgaria
[2]Regional Oncology Center, Varna-Bulgaria

Introduction This retrospective study was performed to investigate the role of DNA- ploidy and S-phase fraction in determining prognosis in advanced breast cancer.
Methods The study included 68 female patients with breast cancer, investigated for the period 1996-2002. The nuclear DNA-content has been measured by CAS-200 (Beckton Dickinson, Image analysis) on intraoperative cytologic samples of the tumour (imprints). The tumours have been divided into diploid, tetraploid, aneuploid and hyperdiploid.
Results 37 of all patients had aneuploid and multiploid histogram, whereas 75% of them had developed distant metastases. Lymph metastases have been registered in 15% of the cases with diploid histogram. S-phase has been considerably higher in patients with aneuploid than those with diploid histogram. The survival of 57 of all 68 patients has been analyzed as to the type of their histogram and as to the presence of metastases in lymph nodes and distant organs. The results showed that 9 breast cancer patients (15.7%) with aneuploid histogram and metastases in lymph nodes had a survival of less than 5 years, compared to the better survival rate of those patients with diploid histogram and no metastases in lymph nodes. The higher S-stage has correlated to the metastases in lymph nodes and distant locations.
Conclusion The analysis of all results proved that the DNA-morphometry could successfully be used as an independent criterion for evaluation of the biologic behaviour of breast cancer tumours and their prognosis.

P-032

Hypercholesterolemia impairs angiogenesis in patients with breast carcinoma and therefore lowers the risk of metastasis

BH Ozdemir[1], Z Akcah[2]
[1]Baskent University, Faculty of Medicine, Departments of Pathology, Ankara, Turkey
[2]Baskent University, Faculty of Medicine, Departments of Oncology, Ankara, Turkey

Introduction Angiogenesis plays a key role in tumor progression and it is also necessary for the development of distant metastasis. Previous experimental studies indicate that both diet-induced and genetic hypercholesterolemia (HCH) impairs angiogenesis. Our aim was to investigate the effect of HCH on angiogenesis induced by breast carcinoma and to elucidate the possible mechanisms by which it inhibits the progression of the cancer.
Material and method Fifty-one patients with invasive ductal carcinoma were included in the study. Of 51 cases 28 had HCH and 23 had no HCH. All patients were followed for a mean of 48 months after radical mastectomy. The intratumoral microvessel density (MVD) was evaluated immunohistochemically using anti-CD31 antibody and correlated with clinicopathologic parameters. Also the expression of bFGF and VEGF were examined immunohistochemically and graded semiquantitatively.
Results MVD was significantly correlated with tumor grade, VEGF and bFGF expression, recurrence, lymph node metastases (LNM), distant metastases (DM) and survival ($p<0.01$). Patients without HCH had significantly higher MVD (77.4 8.2) than those with HCH (54 5) ($p<0.05$). In addition the risk of LNM and DM were found higher in cases without HCH when compared to cases with HCH ($p<0.05$). Both bFGF and VEGF expression showed significant negative correlation with HCH ($p<0.05$).
Conclusion We suggest that, HCH impairs angiogenesis by suppressing bFGF and VEGF expression and therefore lowers the risk of metastases in cases with invasive breast carcinoma.

P-033

Use of CD10 antibody as a marker of myoepithelial cells in breast lesions

M Iglesias[1], JM Corominas, J Lloreta, V Baena, L Pijuan, A Munne, P Garcia, T Baro, S Serrano
[1]Hospital Del Mar. IMAS. UAB, Barcelona, Spain

Introduction The CD10 antibody (CALLA) is usually expressed in lymphoblastic acute leukemia and in follicular center cells of lymph nodes. It is also used in breast cancer cell culture to differentiate epithelial cells from myoepithelial cells. Usually the Smooth Muscle Actin (SMA) is used to identify myoepithelial cells in breast lesions, but this antibody is also positive in blood vessels. This study compares the expression of CD10 and SMA as a marker of myopepithelial cells in breast lesions.
Materials and methods We have compared 61 breast lesions, both benign and malignant (7 adenosis, 8 fibroadenomas, 5 intracystic papillomas, 1 hamartoma, 1 gynecomastia, 9 intraductal carcinomas, 11 invasive ductal carcinomas, 5 tubular carcinomas, 2 mucinous carcinomas, 6 invasive lobular carcinomas, 2 medullary carcinomas, 3 phyllodes tumors). The antibodies used have been CD10 (56C, 1:10, DAKO) and SMA (1A4, 1:200, BioGenex).
Results We observed CD10 expression in the cell membrane of myoepithelial cells and also in some stromal myofibroblastic cells. SMA expression was observed in the cytoplasm of myoepithelial cells, in some stromal myofibroblastic cells and also in smooth muscle cells. Proliferative breast lesions and benign tumors contain myoepithelial cells expressing CD10 and SMA. In malignant lesions the myoepithelial cell component is lost.
Conclusions The CD10 is a myoepithelial cell marker and yields a good, reproducible staining in the studied cases. We think that the use of CD10 combined with SMA is helpful in the differential diagnosis between benign and malignant lesions (epitheliosis vs intraductal carcinoma, tubular carcinoma vs atrophy, adenosis vs invasive ductal carcinoma, papilloma vs intracystic papillary carcinoma).

P-034

p63 expression in benign and malignant breast lesions

A Nonni, D Stefanou, A Batistatou, E Arkoumani, NJ Agnantis
Department of Pathology, University of Ioannina, Medical School, Ioannina, Greece

Introduction The identification of myoepithelial cells in breast lesions remains of diagnostic value for the discrimination between benign and malignant lesions. P63 is a p53 homologue, which is expressed in epithelial basal cells of different organs. The aim of the present study has been to investigate the immunohistochemical expression of p63 in breast lesions.
Materials and methods We examined immunohistochemically 266 formalin-fixed, paraffin-embedded, archival breast samples, which consisted of 140 benign lesions and 126 malignancies (30 in situ carcinomas, 62 invasive ductal carcinomas, NST and 34 invasive carcinomas special type). The monoclonal antibodies anti-p63 (Biocare Medical/Menarini), anti-a-smooth muscle actin (Biogenex) and anti-S-100 protein (Biogenex) were used.
Results In all cases, p63 expression was nuclear. In all benign lesions, there was an almost continuous basal rim surrounding the epithelial structures, whereas it was present but discontinuous in the in situ carcinomas. All invasive ductal carcinomas, NST, were devoided of p63 staining. P63 immunoreactivity was noted in a minor fraction of neoplastic cells in 15/24 (62.5%) in situ papillary carcinomas and in 9/27 (33.3%) invasive papillary carcinomas. The stromal cells were negative to p63. There were S-100 positive luminal epithelial cells in almost all cases, whereas many fibroblasts of the stroma were positive to smooth muscle actin.
Conclusion It appears that p63 is a more sensitive and specific myoepithelial marker than those currently used, with no staining of stromal myofibroblasts. The observed staining in scattered cells, only in papillary neoplasms, might be a clue to the speculated different histogenesis of this specific type of breast tumors.

P-035

Prediction of aggressive outcome in T1N0M0 breast cancer

P Kronqvist[1], T Kuopio[2], H Helenius[1], I Parvinen[3], L Kauhava[4], P Immonen-Räihä[1], L Pylkkänen[1], P Klemi[1]
[1]Department of Pathology, University of Turku, Turku, Finland
[2]Department of Pathology, Jyväskylä Central Hospital, Jyväskylä, Finland
[3]Finnish National Fund for Research and Development Sitra, Turku, Finland
[4]City of Turku, Turku, Finland

Introduction Small tumour size at the time of diagnosis is one of the most significant prognostic factor of favourable outcome in invasive breast cancer. However, unpredictable breast cancer recurrences and deaths also occur among the group of patients with T1N0M0 breast cancers. Aims: We set out to identify the clinically useful prognostic features predicting unfavourable outcome in patients with T1N0M0 invasive breast cancer.
Material and methods The study comprises 72 cases of invasive ductal or lobular carcinomas diagnosed and treated in Turku University Hospital and Jyväskylä Central Hospital during the years 1987-1997. Twenty-seven patients had an aggressive disease with a recurrence or death of breast cancer. The prognostic factors of each of the patients with aggressive disease were compared with control patients matched by tumour size, age at diagnosis and histological type of tumour. The follow up time was 4-14 years. The clinicopathological prognostic factors of the patients were surveyed.
Results The prognostic features indicating unfavourable outcome were immunohistochemically detected high Ki-67 expression, high p53 expression, low estrogen receptor expression and positive Her2/neu chromogen in-situ hybridization. The number of mitotic figures (Mitotic Activity Index, MAI), histological type of the tumour or number of studied axillary lymph nodes did not provide prognostic information.
Conclusion Our study summarizes the immunohistochemical features and criteria predicting unfavourable outcome in T1N0M0 invasive breast cancer.

P-036

Detection of overexpression of C-erbB2 through immunohistochemical and amplification of her2/neu established by fish in breast cancer. A comparative study

I Roig Quilis[1], I Jurado[1], C Rovira[1], M Culubret[1], F Rojo[2]
[1]Consorci Sanitari de Terrassa, Barcelona, Spain
[2]Hospitals Vall D'Hebrón, Barcelona, Spain

Introduction The prognostic and predictive implications of oncogene HER2/neu activation are very controversial, due to the extensive variation of results, mainly due to the different methods applied. Activation of HER2 in node positive patients as an independent prognostic factor has been established and correlated with tumour sensitivity to different therapeutic agents. The overexpression of this membrane receptor has converted it into a new therapeutic aim, requiring the application of a more suitable methodology for each case.
Objectives To evaluate the most suitable method (immunohistochemical vs. FISH) to determine HER2 activation and its correlation with other prognostic factors.
Material and methods A study of 42 cases of invasive breast carcinoma. Histological type: 90% infiltrating ductal carcinoma; age: 30-77, hormonal receptors: 61.9% (RH+), 23.8% (RH-); histological grade (Bloom-Richardson mod): 14.2% (G1), 28.5% (G2), and 47.6% (G3). Immunohistochemistry was performed in 20 patients with (Herceptest Dako), and 22 with anti C-erbB2 (Dako 1:200). 4 scores were used for evaluation: absence of membrane staining (0), faint and incomplete in > 10% of tumour cells (1+), weak to moderate in > 10% (2+), strong complete in > 10% (3+). FISH study was performed on paraffin sections through Path Vision system with evaluation of 60 nuclei.
Results A good correlation between immunohistochemical overexpression and amplification by FISH was observed, especially in cases evaluated as (3+) 7/7 (100%), and as (0) 6/6 (100%). No amplification by FISH occurred in 94.4% of (1+) 17/18 and in 81.8% of (2+) 9/11. 50% of negative hormonal receptor tumours showed amplification, while only 19.2% of positive receptor tumours amplified. None of the tumours classified as (G1) showed amplification.
Conclusions We emphasise the necessity to study gene amplification through FISH in cases with weak immunohistochemical over-expression (2+).

P-037

Expression of p53, p21waf1/cip1, p27kip1 and p34cdc2 in human breast cancers and its prognostic implications

DH Kim[1], CG Park[3], JH Baik[1], DW Kang[1], EK Kim[2], JE Joo[1], WM Lee[1], KH Kim[2], JH Kim[2], MJ Park[2]
[1]Department of Pathology, College of Medicine, Eulji University, Daejeon, Korea
[2]Department of Pathology, College of Medicine, Eulji University, Seoul, Korea
[3]Department of Pathology, College of Medicine, Hanyang University, Seoul, Korea

Introduction Cell cycle progression is governed by cell cycle regulators and inhibitors such as cyclin dependent kinases (cdks), p53, p21/WAF1 and p27/Kip1. The purpose of this study was to correlate the immunohistochemical expressions of p53, p21/WAF1, p27/Cip1 and p34cdc2, with its clinicopathologic prognostic parameters in human breast cancers.
Materials and methods Paraffin-embedded tissue sections from 102 patients with human breast carcinomas were examined for immunohistochemical staining. Primary antibodies used in immunohistochemical staining were mouse monoclonal antibody to human p53, p21/WAF1, p27/Cip1 and p34cdc2.
Results The expression rates of p53, p21/WAF1 and p34cdc2 were 49.1%, 40.2% and 29.3% in breast carcinomas, respectively. In normal breast tissues, p53, p21/WAF1 and p34cdc2 were not expressed. The expression rate of p27/Cip1 was 29.3% in breast carcinomas and 100% in normal breast tissues. The correlation between the expression of p53 and p21/WAF1 was noted($p=0.030$). The expression of p27/Cip1 was correlated with that of progesteron receptor(PR) ($p=0.035$). The expression of p21/WAF1 was correlated with that of estrogen receptor (ER) ($p=0.042$) and PR ($p=0.047$). No correlation was demonstrated between survival in patients and expression of p53, p21/WAF1, p34cdc2 and p27/Cip1.
Conclusion The loss of normal cell growth cycle by abnormal cyclin dependent kinases, inhibitors and steroid hormones may play an important role in human breast carcinogenesis. The p53 dependent p21 pathway, p27 gene loss and cdc2 overexpression were important in development and progression of human breast cancer.

P-038

Withdrawn

P-039

Interobserver variability in determination of HER2-protein overexpression by immunohistochemistry using Herceptest assay - 100 cases study

W Olszewski, A Mrozkowiak, W Olszewski
Center of Oncology, Warsaw, Poland

Background Since January 2002 until December 2002 in 5088 cases of breast cancers evaluation of HER2 protein was performed. Evaluation of immunohistochemical stains was accomplished in sixteen oncological centers in Poland. Comparison of results achieved by researchers from all participating oncologial centers was the aim of our study.
Material and method Among 5088 cases evaluated in population screening project total 100 cases from all centers were selected and presented to 16 representatives of those centers. The immunohistochemically stained slides came from all 16 laboratories. All IHCs were done using FDA-approved DAKO Herceptest. Evaluation was performed without knowledge of the original
Results The results from each researcher were coded. The study lasted 6 hours. The average concordance was nearly 70%, while the lowest concordance was 51 and the highest - 93%. This wide range of the results might be due to several things. Firstly, the experience in IHC evaluation varied among the participant of the study. Secondly, the quality of the stains differed significantly. Thirdly, the researchers worked under time pressure and the material was selected to include more cases considered 'difficult' (2+ according to DAKO HercepTest or technically inadequate).
Conclusions To achieve higher concordance among the obtained results, evaluation should be performed by the experienced pathologists. * - participants from: Bialystok, Bydgoszcz, Gdansk, Gliwice, Kielce, Krakow, Lublin, Lodz, Olsztyn, Poznan, Szczecin, Warsaw and Wroclaw. The population screening project study was supported by Roche-Polska.

P-040

A morphometric analysis of early invasive breast carcinoma using serial sectioning and 3D reconstruction technique

M Endoh[1], T Moriya[1], M Yang[2], M Oguma[1], C de la Cruz[1], K Sakamoto[1], M Watanabe[1], H Sasano
[1]Dept. of Pathol. Tohoku University Hospital, Sendai, Japan
[2]Dept. of Thoracic Surgery, The First Hospital of Jilin University

Introduction Mechanism of early invasion of breast ductal carcinoma has not been completely investigated not only from the genetic point of view but also morphologically. One of the reason is that starting sites of invasion from ductal carcinoma in situ (DCIS) might be extremely diminutive that routine histopathological examination should hardly reveal them usually. Thus, we examined a large number of complete serial sections from breast carcinomas so as to find out destroyed sites of duct wall from which carcinoma cells have started on invasion. Also we reconstructed 3D images from the sections so as to visualize the sites and to measure the size of those.
Materials and methods Used were three surgical specimens of breast cancer having extensive intraductal components with multiple invasive foci. After formalin fixed and paraffin embedded, six blocks from three cases were selected and sectioned serially in 3μm thickness. Total amount of the serial sections reached 724 sheets (mean 121/1block) indicating 2.172μm in actual thickness. After HE stained, invasive lesions connected with DCIS were searched and the lesions were reconstructed as 3D images with a computer-assisted-3D-reconstruction system.
Results Although numerous sections containing multiple invasive foci were examined, areas which connected with DCIS to invasive lesion through the destroyed site of duct wall were only three. The site were approximately 100μm, 150um and 50μm in diameter respectively, should be called as 'hole' of the duct wall. Invasive lesions were extended along the ducts with the holes.
Conclusion The holes, starting sites of invasion, were apparently smaller than surrounded invasive lesion.

P-041

Histological and immunohistochemical profile of invasive pleomorphic lobular carcinoma

Y Erhan[1], O Zekioglu[1], M Erkus[2], B Sarkik[1]
[1]Ege University Medical School Pathology Department, Izmir, Turkey
[2]Aydin Menderes University Medical School Pathology Department

Introduction Invasive pleomorphic lobular carcinoma (IPLC), a distinct subtype of invasive lobular carcinoma (ILC), shares the typical histologic patterns of classical ILC, but the nuclei are more pleomorphic and increased mitotic activity is a prominent feature.
Methods and results We reviewed 20 cases of IPLC and compared them with 40 cases of clssical ILC. Immunohistochemical analysis was performed in all cases for estrogen (ER) and progesterone receptors (PgR), p53, c-erbB-2, and Ki67. In this series, the average patient age was 54.9 years (age range, 37-76 years) for IPLC and 56.2 years (age range 33-82 years) for ILC. Tumor size ranged from 1 to 9.5 cm (mean size 3.09 cm) for IPLC and 0.9 to 6 cm (mean size 2.8 cm) for ILC. Axillary lymph node metastasis was detected in 75% of IPLC, and 35% of ILC. Fifty percent of IPLC and 15% of ILC cases had extranodal extensions ($p<0.01$). Tumor cells were large with eccentric pleomorphic nuclei and eosinophilic granular cytoplasms. High mitotic activity was observed. Immunohistochemically ER and PgR positivity in IPLC was 75% and 65%, and in ILC 75% and 70%, respectively. IPLC cases showed 50%, and ILC cases 15% p53 positivity ($p<0.01$). C-erbB-2 was detected in 55% of IPLC, and 45% of ILC. Ki67 mean rates were 26% and 12% for IPLC and ILC.
Conclusion IPLC exhibits distinct histologic fetures, higher expression of p53 protein and Ki67 rate in comparison with classical ILC. The aggressive clinical course of patients with IPLC is supported by higher rates of axillary lymph node metastasis and extranodal extensions.

P-042

Does breast phyllodes tumour harbour c-kit mutations?

S Carvalho[1], A Oliveira e Silva[2], F Milanezi, S Ricardo[1], D Leitao[1], I Amendoeira[2], F Schmitt
[1]Institute of Molecular Pathology and Immunology of the University of Porto - IPATIMUP, Porto, Portugal
[2]Sao Joao Hospital/ Medical Faculty of the University of Porto, Porto, Portugal
[3]School of Health and Science - University of Minho, Portugal
[4]Medical Faculty of the University of Port, Porto, Portugal

Introduction c-kit is a proto-oncogene that codes for a transmembrane tyrosine kinase receptor: CD117. Once activated, c-kit propagates signalling events throughout the cell via multiple signal transduction pathways. It was described an activating mutation in exon 11 of c-kit gene in gastrointestinal stromal tumours (GIST), which can be blocked by using a tyrosine kinase inhibitor (STI571). Phyllodes tumours (PT) are rare biphasic breast tumours that similarly to GISTs show a monoclonal stromal proliferation and high recurrence rates. Aims: To study the immunohistochemistry expression and prevalence of activating c-kit mutations in PT in order to explore whether this disease could be a potential target for treatment with STI571.
Materials and results We analysed 18 PT (12 benign and 6 malignant) by immunohistochemistry for c-kit expression and direct sequencing of exons 9, 11, 13 and 17 of c-kit gene for evaluate the mutational status. c-kit expression was detected in 10 out 18 cases (5/12 benign and 5/6 malignant). No mutations were found for exons 9, 11 and 13. In exon 17 we found the same silent alteration in 2 out of 18 cases.
Conclusions Although c-kit expression is a frequent finding in PT of the breast, we did not find activate mutations similar to those described in GISTs.

P-043

Expression of cyclin D1 in ductal breast carcinoma: relationship with histological parameters and estrogen receptors

E Mustać, G Dordević, N Jonjić, V Licul
Department of Pathology, Medical Faculty, University of Rijeka, Rijeka, Croatia

Introduction Recently, the role of cyclin D1 expression in breast cancer had received attention. It causes the activation of cyclin-dependent kinases in G1 phase and phosphorilation of the Retinoblastoma gene, required for entry of cell into S phase of the cell cycle. Recent investigations confer the role of cyclin D1 once again in G2 phase. The aim of this study was to analyse the expression of cyclin D1 in human breast cancer cells and to compare its value with the estrogen receptors and histological parameters.
Material and methods Immunohistochemical analysis for cyclin D1 and estrogen/progesteron receptors (ER/PR) was performed on 40 formalin-fixed infiltrating ductal breast carcinomas. Scoring was done using semiquantitative system. The stainining score was ranged from 0-3 (called cyclin D1-negative) and score larger or equal to 4 (called cyclin D1-positive).
Results According to the staining score 20% of the breast carcinomas were cyclin D1 positive, and those carcinomas were associated with higher nuclear and histological grade, while only 33% were ER-positive.
Conclusion These reslults suggest that higher expression of the cyclin D1 is related with poor prognostic parameters.

P-044

C-erb B2 overexpression in breast cancer with negative lymph nodes

C Ardeleanu[1], F Andrei[1], M Ceausu[2], D Terzea[1], V Comanescu[3], C Dobrea[1], M Neagu[1], C Iosif[1], M Mihai[4], F Halalau[1]
[1]'Victor Babes' National Institute, Bucharest, Romania
[2]'Carol Davila' University of Medicine and Pharmacy, Bucharest, Romania
[3]1st Clinical Hospital, Craiova, Romania
[4]Fundeni Clinical Hospital, Bucharest, Romania

Background It is known that c-erb B2 overexpression in advanced breast cancer represents a predictive factor of tumoral agressivity. The aim of this study was to assess the involvement of c-erb B2 and other prognostic factors expression (hormonal receptors, EGFR, PCNA) in breast cancer with negative lymph nodes.
Methods We investigated histopathologically and immunohistochemically 30 selected cases with G2 ductal invasive carcinoma and no lymph nodes involvement, from 200 breast cancers. We

used a monoclonal antibody panel (estrogen and progesteron receptors, EGFR, c-erb B2, PCNA) in formalin fixed paraffin embedded tissues.
Results We found a significant increased c-erbB2 overexpression associated with a low ER and PgR expression and minimal micro-angiogenesis as expressed by EGFR. The average of proliferative rate assessed by PCNA was 35.3%.
Conclusion Immunohistochemical c-erbB2 overexpression in negative lymph nodes breast cancer, may suggest an early amplification of its encoding gene, which can predict an aggressive biological behaviour (invasion and metastasis), so that this type of patients would benefit of humanized anti-her2/neu monoclonal antibody treatment.

P-045

Aspiration cytology of the breast with or without ultrasound guidance. Quality control

MA Chaves[1], A Nieto[1], A Torroba[1], A Giménez[1], R Guerao[1], J Aguilar[2], M Martínez[3]
[1]Pathology Service. J. M. Morales Meseguer Hospital, Murcia, Spain
[2]Surgery Service. J. M. Morales Meseguer Hospital, Murcia, Spain
[3]Radiology Service. J.M. Morales Meseguer Hospital, Murcia, Spain

Introduction Aspiration cytology of the breast is one of the three components of the triple test for breast cancer diagnosis. Ultrasound (US) guidance increases the complete sensitivity of this technique. The aim of this study was to compare the results between a group of mammary lesions aspirated with or without US using the European Quality Assurance Guidance.
Material and method We analyzed 206 mammary lesions by aspiration cytology with or without US guidance. One group was formed by 103 breast aspirates from women older than fifty years old, included in an screening programme, with palpable and non palpable lesions, using US guidance. Another group was formed by 103 breast aspirates from outpatients origin of all ages only with palpable lesions using no US guidance. We analysed and compare the results between both groups using using the European Quality Assurance Guidance for Breast Screening Pathology.
Results In both groups the positive predictive value of the C5 results were 100% (false positive rate=0%). The complete sensitivity of US guided aspirates were 91.1% and for the non guided aspirates were 83%. We compare the rest of values and analyze our deviations from the standards.
Conclusion The quality of our breast aspiration practice is between the margins of the standards in both techniques, with an increment in the sensitivity with US guidance and a light loose of specificity in the screening group (probably because of patients age characteristics).

P-046

Ultrastructural study of intercellular junctions in metastatic and non-metastatic breast cancer

MB Puchau, E Melo, J Lloreta, L Ferrer, L Pijuan, S Boluda, M Iglesias, JM Corominas, S Serrano
Departament de Ciencies Experimentals I de La Salut, Universitat Pompeu Fabra, Autonomous University Of Barcelona, Hospital Del Mar-IMAS-IMIM, Barcelona, Spain.

Introduction Functional and morphologic characteristics of intercellular junctions are involved in tumor dissemination. The purpose of this study was to investigate whether the number of intercellular junctions in breast cancer is predictive for the presence of lymph node metastases.
Materials and methods 76 infiltrating duct carcinomas were the subject of this study, 50 of them without (G1) and 26 with metastatic disease (G2) in axillary lymph nodes. The number of intercellular junctions was counted, and the length of the cell-to-cell contact surfaces was measured in randomly taken electron micrographs. The number of desmosomes/100µm of cell membrane apposition has been statistically compared between both groups.
Results Cell junctions in tumors with lymph node metastases were usually smaller and poorly developed. There were no statistically significant differences in the number of intercellular junctions between both groups [G1=14%, (10,75%; 25%). G2=12,5% (7,75%; 29%). p=0,546].
Conclusions Although intercellular junctions are more rudimentary in tumors that metastasize, their number is not significantly reduced. Therefore, it will be necessary to combine number, size and development of cell junctions in a single parameter to attempt prediction of tumor dissemination.
Supported in part by grant FIS 93/0394.

P-047

Analysis of the relation between presence of myoepithelial cells in tumour stroma and expression of prognostic indices in tumour cells of ductal breast cancer

P Surowiak[1], T Wysocka[1], P Dziegiel[1], A Wojnar[2], M Zabel[1,3]
[1]Chair and Department of Histology and Embryology, University School of Medicine, Wrocław, Poland
[2]Department of Pathomorphology, Lower Silesia Centre of Oncology, Wrocław, Poland
[3]Chair and Department of Histology and Embryology, University of Medical Sciences, Poznań, Poland

Introduction Numerous publications have been devoted to effects of myoepithelial cells on biology of breast cancer. The cells are thought to be able to inhibit invasion of neoplastic cells by production of inhibitors for serine proteases. Some authors suggest that, acting in a paracrine way, myoepithelium can affect breast cancer cells. Present study aimed at analysis of the relation between presence of myoepithelial cells (smooth muscle actin, SMA) in the structure of a ductal breast cancer and expression of the recognized prognostic factors (ER, PR, HER-2, TGF alpha, Ki67 and p53) in the cancer cells.
Materials and methods The studies were performed on samples of primary ductal breast cancers originating from 60 females, including 20 cases at G1, 20 cases at G2 and 20 cases at G3 grade. Immunocytochemical reactions were performed using antibodies directed to SMA, ER, PR, HER-2, TGF alpha, Ki67 and p53.
Results The study showed that the highest content of myoepithelial cells was noted in tumours of G1 grade while the lowest content of the cells was observed in tumours of G2 grade (Kruskal-Wallis ANOVA rank test, p=0.0018). In the entire group (G1-G3) a positive correlation was detected between the presence of myoepithelial cells and intensity of HER-2 expression (gamma correlation, p=0.0017) and a negative correlation with proliferation intensity measured by expression of Ki67 antigen (gamma correlation, p=0.00067). No relation was observed between manifestation of myoepithelium and expression of the other studied variables.

Conclusion Our studies confirmed the potential for paracrine communication between myoepithelial cells and cells of ductal breast cancer.

P-048

Immunohistochemical VEGF expression in breast carcinomas. Correlation with prognostic factors

A Matilla, L Vicioso, L Pérez, M Álvarez, I Ramírez
Dpto. Anat. Patológica. Universidad de Málaga, Malaga, Spain

Introduction VEGF (vascular endothelial growth factor) is considered as one of the most important angiogenic factors in breast cancer and its expression in tumor cells correlate with microvessel density. Several studies have proposed that VEGF may be a relevant prognostic factor. Aim: To study the immunohistochemical expression of VEGF in different histological types of breast cancer and its relation to established prognostic and predictive factors.
Material and methods We have analyzed 84 carcinomas (55 of invasive ductal type, 15 lobular, 5 mucinous, 2 papillary and 7 ductal in situ). Immunohistochemical staining was performed on formalin fixed, paraffin sections, using an avidin-biotin immunoperoxidase technique. A rabbit polyclonal antibody for human VEGF was used at a 1:100 dilution. Immunoreactivity was scored from 0 to 3+.
Results 44 (61,3%) of all invasive carcinomas showed VEGF expression (ductal: 61%, mucinous: 100%). All but 2 lobular carcinomas were negative or weakly positive. Both papillary carcinomas showed strong positivity. Staining in DCIS was generally absent or weak. VEGF positivity correlated inversely with nodal involvement (p=0.001) and RE status (p=0.05). There were no correlation of VEGF staining with tumor size, histological grade, p53 and c-erbB-2.
Conclusion Expression of VEGF is characteristically weak or absent in lobular carcinomas and them no relevant as a prognostic factor in this type of carcinomas. As VEGF staining correlate with absence of nodal involvement, its prognostic value may be mainly due to facilitate invasion of blood vessels, more than to lymphatic spread.

P-049

Clinical and histopathological parameters as predictors of clinical outcome for patients with vulvar carcinoma

A Blazanovic[1], S Dotlic[2], A Morovic, M Milosevic, H Munivrana, M Nola[2]
[1]General Hospital Vinkovci, Vinkovci, Croatia
[2]Clinical Hospital Centre Zagreb, Zagreb, Croatia

Introduction Squamous carcinoma accounts for approximately 90% of all primary vulvar carcinomas. Although the anatomic localization of this tumor allows early diagnosis and considerably easy surgical accessibility, the prognosis for these patients remains relatively grim. The explanation for this finding should be sought in the fact that most of the patients are diagnosed in the advanced clinical stage of the disease. Since radical vulvectomy (a complex and debilitating procedure) is often a therapy of choice, the recent studies have been focused on determining reliable prognostic parameters that would allow individualized, and hopefully simpler therapeutic modalities to be applied in a certain group of patients with the same effectiveness. The aim of this study was to determine the most important clinical and histopathological parameters that influence the prognosis and outcome of patients with invasive squamous carcinoma of the vulva in order to offer them the most suitable form of therapy. Moreover, it was designed to assess the clinical significance of DNA content analysis by flow cytometry.
Patients and methods 43 cases of squamous cell carcinoma of the vulva, diagnosed between 1978. and 1996. were selected. In order to assess the influence of the various prognostic factors on survival, the study included clinical and pathohistological parameters as well as the results of flow cytometric DNA analysis of paraffin-embedded tumor samples from all cases. Clinicopathological parameters focused on the age of patients, clinical stage of the disease, menstrual status, diameter and localization of the tumor, histological grade, nuclear grade, combined histological and nuclear grade, depth of tumor invasion, tumor growth pattern, presence of giant cells in the tumor and the form of therapy, while the flow cytometric DNA analysis comprised DNA ploidy, proliferative activity and DNA index.
Results Five-year survival of our selected population of patients was 62,3+/-7,8%. The results of univariate statistical analysis confirmed that statistically significant prognostic parameters included the age of patients (p=0,033), clinical stage of the disease (p=0,014), histological grade (p=0,047), nuclear grade (p<0,001) and the depth of invasion (p<0,001). On the other hand, the results of multivariate statistical analysis showed that only combined histological and nuclear grade (p=0,015) and the depth of tumor invasion (p<0,001) can be considered independent, statistically significant prognostic parameters.
Conclusion The age of patients at the time of diagnosis, clinical stage of the disease, histological grade and nuclear grade are considered to be the parameters of crucial relevance for the prognosis of patients with squamous cell carcinoma of the vulva. However, only combined histological and nuclear grade, as well as the depth of tumor invasion were proven to be independent statistically significant parameters relevant for the outcome of patients with this disease.

P-050

Can a pleomorphic vulvar leiomyoma be a tumor with local aggressive behavior? A case report

M Mrčela[1], Z Topolovec[2], D Habek[2], V Blažičević[1]
[1]Institute of Pathology and Forensic Medicine, Clinical Hospital Osijek, Croatia
[2]Department of Gynaecology and Obstetrition, Clinical Hospital Osijek, Croatia

Introduction Vulvar leiomyoma is uncommon and its pleomorphic or bizarre form is especially rare. Bizarre vaginal and vulvar (Bartholin's gland area) leiomyomas were reported in only few cases. This tumor is hard to differentiate from leiomyosarcoma. The main criterion to make a distinction between them is the mitotic activity, which is less than 3 per 10 HPF in the former.
Case report A 26-year-old female was referred to the clinic for the evaluation of paravaginal tumor in distal vaginal third and right vulvar area with a history of 6 month duration. She had no history of any earlier disease, and other examinations revealed normal findings. Macropathology: The tumor was a large solid mass measuring 10x7.5 cm in diameter. The tissue was yellow and seemed partly necrotic.

Micropathology Tumor consisted mostly of spindle cells arranged in bundles with round or oval nuclei and large prominent nucleoli or showed hyperchromatism in places where there were cells with giant nuclei. Cytoplasm was eosinophilic, elongated with small vacuole. There were areas where cells had two or more nuclei with the earlier mentioned polymorphism. Areas of hyaline or myxoid degeneration of the stroma were found. Mitoses were not found although the tumor was examined by three independent pathologists from different countries. The tumor margin looked infiltrative. The tumor was immunohistochemically positive for vimentin, smooth actin and desmin. Cytokeratin MNF 116, EMA, S-100, CD-34, and CD-117 were negative.
Conclusion We describe a vulvar smooth muscle tumor with marked polymorphism, without mitoses, with myxoid changes in the stroma and with infiltrative margins. Because of all these characteristics the tumor was considered biologically aggressive and additional surgery with resection of the tumor site and regional lymphadenectomy was performed. Three years after the last surgery the patient is alive and well.

P-051

Trophoblast apoptosis and proliferation in preeclamptic placentas

D Staribratova[1], Z Zaprianov[1], D Dikov[2], V Sarafian[1]
[1]Plovdiv Medical University, Plovdiv, Bulgaria
[2]Hospital Center Lagny

Introduction Preeclampsia is a specific disorder of pregnancy with an increased risk for both neonatal and maternal mortality rates. It is associated with shallow invasion of the placental cytotrophoblast within uterus developing decidual vasculopathy and results in dereased blood flow. The aim of the present report is to determine whether hypoxia influences the rates of apoptosis and proliferation and to compare them with those of normal controls.
Materials and methods Samples were taken from 20 liveborn, singleton preeclamptic pregnancies and 20 normal controls. We used routine light microscopy, immunohistochemical and quantitative studies for Bcl-2, and Bax (to assess apoptosis) and PCNA (to assess cellular proliferation). Bcl-2- and PCNA-positive trophoblast cells were counted in a minimum of 10 high-powered fields, of 3 consecutive sections free from any infarction of at least 3 paraffin blocks.
Results While increased apoptosis has been estimated in study groups, the rates of proliferation seems to be unaffected.

P-052

Placental pathologic features of preeclampsia

D Staribratova[1], Z Zaprianov[1]
[1]Plovdiv Medical University, Plovdiv, Bulgaria

Introduction The clinical and placental features of preeclampsia are subject of an extensive study. Clinical evidence suggests that this pregnancy specific disorder may be demographically heterogenous. Our purpose is to record the range of the most common pathologic features in placental specimens from a gypsy cohort and to compare them with those in nonethnic Bulgarian population.
Materials and methods Review of 20 preeclamptic placentas from liveborn singleton deliveries of gypsy mothers and 20 matching controls from Bulgarian population revealed histologic lesions that were considered as belonging to one of the following groups: (1) vascular lesions; (2) acute or chronic inflammation and (3) coagulation-related lesions. For each separate case, additional demographic and reproductive history was collected from the patients' charts. All placentas were studied by previously published standard protocols. Nonparametric statistical analysis was applied.
Results In gypsy preeclamptic group, lesions related to coagulation (52% vs 39%) and vascular lesions (26% vs 29%) were more frequent. Inflammatory features were equally distributed among the two groups (22%).

P-053

Versican in epithelial ovarian cancer; relation to hyaluronan, clinicopathological factors and prognosis

VM Kosma[1], K Voutilainen[2], S Sillanpää[2], R Tammi[3], M Tammi[3], S Saarikoski[4], M Anttila[2]
[1]Department of Pathology, University of Tampere and Tampere University Hospital, Tampere, Finland
[2]Department of Pathology and Forensic Medicine, University of Kuopio and Kuopio University Hospital, Kuopio, Finland
[3]Department of Anatomy, University of Kuopio, Kuopio, Finland
[4]Department of Obstetrics and Gynecology, Kuopio University Hospital, Kuopio, Finland

Introduction Versican is a chondroitin sulfate proteoglycan, which belongs to the aggrecan gene family. It has not been studied in epithelial ovarian cancer before. The aim of this study was to clarify the relation between versican and hyaluronan in epithelial ovarian cancer and to find out if versican expression affects prognosis in these patients.
Materials and methods Localization of versican was studied immunohistochemically in 299 primary epithelial ovarian cancers and their 43 metastases, as well as in 6 normal ovary specimens. The staining was scored according to the percentage area of strong versican signal of total peri- and intratumoural stroma as low or high. Epithelial staining of the tumours was scored as positive or negative.
Results Low and high levels of strong stromal versican staining were observed in 133 and 166 carcinomas, respectively. A low level of strong stromal versican was found to be a significant marker for early FIGO stage and mucinous histology. Stromal versican staining correlated significantly with stromal hyaluronan staining. Cancer cell-associated versican positivity was seen in 151 tumours and correlated with clear cell histology and early FIGO stage. The 5-year prognosis of patients decreased with increasing stromal versican levels for overall survival. The 5-year prognosis for recurrence-free survival was slightly better when cancer cells were positive for versican. In Cox's multivariate analysis neither stromal nor cancer cell-associated versican had any prognostic value.
Conclusion Enhanced stromal versican expression correlates with hyaluronan accumulation and is associated with unfavourable disease outcome, but it is not an independent prognostic marker in epithelial ovarian cancer.

P-054

Cytobrush-collected malignant cervical epithelial cells display a cancer-specific gene expression pattern in cDNA array analysis

G Hudelist[1,2], C Singer[1], M Manavi[1], K Pischinger[3], E Kubista[1], K Czerwenka[3]
[1]Dept. OB/GYN, Division of Special Gynecology, University of Vienna, Vienna/Villach, Austria
[2]Dept. OB/GYN, Landeskrankenhaus Villach, Carinthia, Austria.
[3]Dept. of Clinical Pathology, Division of Gynecopathology, University of Vienna, Vienna, Austria.

Introduction Although it is well known that persistent high-risk HPV infections are the principal causative agents of cervical cancer, the discrepancy between high infection rates and the relatively low rates of high-risk HPV positive women who actually develop carcinoma of the cervix suggest that development of cervical cancer is a multistep process involving additional factors and mutational events. Therefore, differentially expressed genes in normal and malignant cervical epithelial cells and the feasibility of gene expression profiling on cervical cells obtained by regular cervical swabs were investigated.
Material and methods Cervical epithelial cells obtained by regular cytobrushes from 3 women with high-risk HPV positive invasive cervical cancer and from 3 HPV negative women without suspicious PAP smears were pooled and subjected to cDNA array analysis. Dot blotting was then performed to detect the proteins which corresponded to the most highly up-regulated genes in the cDNA array analysis.
Results mRNA expression of c-erbB-2, C-kit, VEGFR-1, N-myc, K-ras, cyclin-dependent kinase inhibitor 4 (p16INK4A), cyclin D1, NM23-H1, NM23-H2, c-MET, KGF, KGFR, and STAT 1 was increased in malignant samples. Several genes associated with anti-apoptosis, such as bcl-2 like protein, cell structuring and/or cell attachment were also upregulated in tumoral cells. Conversely, decreased gene expression was observed for members of the transforming growth factor receptor superfamily (TGF-beta), interleukin 1 (IL-1), insulin-like growth factor binding proteins (IGFBPs) and for members of the integrin family.
Conclusions We identified a mRNA and protein expression pattern that might have an important role in the pathogenesis of invasive cervical carcinoma and appears to be specific for malignant cervical epithelium. We hypothesize that the presence of a cancer-specific gene-expression signature assessed by cDNA array analysis or immunohistochemical techniques could eventually turn out to become an additional tool to evaluate the dignity of routinely obtained cervical swabs.

P-055

Prognostic features and molecular markers in ovarian borderline tumors

E Nistor[1], AD Stanescu[1], CD Vrabie[2], E Ionica[3]
[1]Bucur Hospital, Bucharest, Romania
[2]V. Babes Institute, Bucharest, Romania
[3]University of Bucharest, Bucharest, Romania

Introduction Ovarian cancer represent the fourth most common cancer in women. Borderline ovarian serous tumors (BSOT) affect women of childbearig age and their prognosis is outstanding. The aims of this study were to characterize the group of patients with BSOT and evaluate the significance of various molecular markers expression versus serous papillary ovarian carcinomas (SPOC)
Material and methods We analyzed a total of 102 cases including: 64 cystadenoma, 10 borderline and 28 cystadenocarcinoma. For the BSOT the median age was 40 years. Eight women with BSOT underwent radical surgery and two fertility sparing surgery. The recurrence of disease appeared in one case with fertility sparing surgery. All the cases were analyzed on haematoxilin-eosin stained and immunohistochemistry (the indirect tristadial Streptavidin-Biotin method) for estrogen receptor (ER), progesteron receptor (PR), p53 protein (p53), proliferative activity (Ki67) and carcinoembrionic antigen (CEA).
Results The immunostaining demonstrated a significant increase in the expression of ER (90%) and a decrease for p53 (10%) and Ki67 (6%) in BSOT vs SPOC (ER-60%, p53-50% and Ki67-40%).
Conclusions The main differences between BSOT and SPOC was regarding the expression of p53 and Ki67. There was no significant correlation between Ki67 and the known histologic parameters of prognostic significance. Transvaginal ultrasound and CA 125 serum levels are the most effective diagnostic techniques for the follow up of patients treated conservatively for BSOT.

P-056

Gonadoblastoma and germ cell tumours of the ovary in childhood and adolescence

A Zuntova[1], S Vodickova[2], L Teslik[3], J Koutecky[2], D Sumerauer[2], M Bures[2]
[1]Department of Pathology and Molecular Medicine, Prague, Czech Republic
[2]Department of Paediatric Oncology, Prague, Czech Republic
[3]Department of Obstetrics and Gynaecology, Prague, Czech Republic

Introduction Gonadoblastoma with dysgerminoma or other germ cell tumor occurs almost exclusively in girls and young women with underlying gonadal disorder. The aim of this study was to review biopsy examinations of the tumours, stage, treatment strategy, follow up and outcome of five girls with gonadoblastoma and germ cell tumours.
Material and methods Retrospective review of 5 patients with gonadoblastoma and germ cell tumours was performed. The patients were 13,14, 14, 15 and 17 years old. The first 14-year-old girl (karyotype, 46 XX, normal ovary bilateral) with gonado-blastoma, dysgerminoma and choriocarcinoma had IIIc stage disease. She was treated by chemotherapy with cisplatinum and radiotherapy. Four patients had gonadoblastoma and dysger-minoma. The second 14-year-old girl (mixed gonadal dysgenesis, karyotype, 46, XY) had stage Ib and was treated by chemotherapy with cisplatinum. Two patients were treated with surgery only: 17-year-old girl (streak gonads, karyotype, 46, XY) - stage Ib and 15-year-old girl (karyotype 46, XX, der 22/ 45, XX, - 22) - stage Ia. The 13-year-old patient (karyotype, 46, XX, normal ovary bilateral) - stage Ia disease, had adnexotomy only, but because of recurrence (stage IIIc) 13 months after the original diagnosis, she was treated by chemotherapy.
Results Our review confirmed the original diagnosis of gonado-blastoma and dysgerminoma and in one case gonadoblastoma, dysgerminoma and choriocarcinoma. All patients were followed up for 42 to 170 months. Only one patient, who was initially treated with surgery only (stage Ia), had disease recurrence, but achieved

durable remission with chemotherapy and further surgery. The latest examinations revealed that all patients were in good health.
Conclusions Because the gonads are often replaced by a tumour, a diagnosis of the underlying abnormality may be impossible. Gonadoblastoma is regarded as in situ malignancy, and there is a high possibility for development of invasive germ cell tumour such as dysgerminoma. Young girls with unilateral encapsulated gonadoblastoma and dysgerminoma can be treated only by unilateral oophorectomy or salpingo-oophorectomy and subsequent careful follow up to prevent damage of contralateral ovary and preserve the fertility. The patients with gonadoblastoma and mixed germ cell tumor are treated in accordance with other tumour structures. The paper is sponsored by Ministry of Health of the Czech Republic (International Grant Agency) No 6511 – 3, CZ

P-057

Cadherin/catenin expression in squamous lesions of cervix

HE Pestereli[1], G Erdogan[1], T Simsek[2], H Gulkesen[3], S Karaveli[1]
[1]Akdeniz University, School of Medicine, Department of Pathology, Antalya, Turkey
[2]Akdeniz University, School of Medicine, Department of gynecology and Obstetrics, Antalya, Turkey
[3]Akdeniz University, School of Medicine, Department of Biostatistics, Antalya, Turkey

Introduction Cadherins and their associated cytoplasmic protein catenins are cell adhesion glycoproteins that are altered in tumor progression The aim of this study is to reveal the altered expression of E-cadherin, P-cadherin, α-catenin and β-catenin in cervical squamous cell carcinoma progression from dysplastic lesions (low grade squamous intraepithelial lesion-L-SIL, high grade squamous intraepithelial lesion-H-SIL) to invasive squamous cell carcinoma.
Material and method Immunohistochemical method was used in formalin-fixed, paraffin embedded representative tissue sections of 25 L-SIL (CIN I), 25 H-SIL (CIN II-III) and 30 invasive squamous cell carcinomas. The presence of immunostaining and the pattern of distribution of E-cadherin, P-cadherin, α-catenin and β-catenin were analyzed.
Results E-cadherin was detected in 91.7 %, 41.7 %, 6.9 % of L-SIL, H-SIL and invasive squamous cell carcinomas respectively. The difference was statistically significant (p=0.0001). The expression of P-cadherin and α-catenin was reduced significantly from L-SIL through invasive carcinoma (p=0.009 for P-cadherin, p= 0.0001 for α-catenin). β-catenin expression was revealed in all lesions with nearly the same frequency, 75.9 % L-SIL, 83.3 % H-SIL and 79.2 % invasive carcinomas.
Conclusion Loss of adhesion proteins, E-cadherin, P-cadherin and α-catenin is observed in cervical squamous cell carcinoma progression. The presence of β-catenin in H-SIL and invasive carcinomas might suggest its role in tumor progression by its effect in Wnt signaling pathway in cervical carcinomas.

P-058

Cadherin/Catenin alterations in squamous cell carcinoma of cervix. Correlation with clinicopathologic variables and Human papilloma virus (HPV) status

G Erdogan[1], HE Pestereli[1], T Simsek[2], G Zorlu[2], S Karaveli[1]
[1]Akdeniz University, School of Medicine, Deparment of Pathology, Antalya, Turkey
[2]Akdeniz University, School of Medicine, Deparment of Gynecology and Obstetrics, Antalya, Turkey

Introduction P, E- cadherin and their cytoplasmic domains alpha and beta-catenins are epithelial cell adhesion complexes. Their alteration is important in tumor progression. Beta catenin is also involved in Wnt signaling cascade which regulates cell proliferation. We investigated the altered pattern of cadherin/catenin complex in cervical squamous cell carcinomas. We also tried to find out if there was a correlation between adhesion proteins and clinico-pathologic variables (stage, depth of invasion, lymph node met-astases) and HPV status.
Material and methods E-cadherin, P-cadherin, alpha catenin and beta catenin expression in 15 squamous cell carcinomas were investigated by immunohistochemical method. The presence of HPV 16/18 infection was detected by in situ hybridization.
Results There were 11 large cell keratinizing, 3 nonkeratinizing and 1 small cell subtypes of squamous cell carcinoma. Lymph node metastases were found in 6 carcinomas. HPV 16/18 infection was detected in 8 of 15 carcinomas, all were large cell keratinizing except one. No correlation was found between the HPV status and cadherin and catenin expression of the tumors. E- cadherin was negative in 12 carcinomas, P- cadherin was positive in only 4 carcinomas. Strong cytoplasmic beta catenin positivity was revealed in 11 carcinomas. Alpha catenin reactivity was seen in 5 of 15 carcinomas. Neither cadherins nor catenins expressions were correlated with other clinicopathologic variables.
Conclusion Our results reveal that E-cadherin and P-cadherin expressions are lost in squamous cell carcinomas. However alpha and beta catenin immunopositivity in cervical squamous cell carcinomas might suggest catenins' role in tumor progression in a different way other than their activity in cell adhesion.

P-059

Prognostic significance of karyotype analysis in ovarian carcinomas

E Dainese[1], MG Tibiletti[2], B Bernasconi[1], D Micello[1], C Facco[2], N Donadello[3], C Riva[1], C Capella[1]
[1]Dept. of Clinical and Biological Sciences, University of Insubria, Varese, Italy
[2]Dept. of Pathology, Ospedale di Circolo, Varese, Italy
[3]Gynecology and Obstetric, Ospedale di Circolo, Varese, Italy

Introduction Traditional prognostic factors of ovarian carcinoma (OC) include disease stage, age, histologic grade and residual disease after surgery. At present it is quite difficult to predict the survival benefit of platinum analogues based chemotherapy. The aim of this study was to evaluate the clinicopathological / cytogenetic profile in a series of OCs and the reliability of karyotype in predicting benefit of chemotherapy and prognosis.
Materials and methods A series of 44 OCs (28 serous, 10 undifferentiated, 3 endometrioid, 2 mucinous and one mixed carcinomas) was investigated for grade (1/2:29% vs3/4: 71%), stage (I/II: 43% vs III/IV: 57%), residual disease after surgery (59%), chemotherapy (81%), remission (75%) vs progression (25%) after chemotherapy and follow-up (mean:56, range: 15-96 months). Cytogenetics were performed on direct preparations using the QFQ banding technique and describing abnormalities according to ISCN. Karyotypes were classified as diploid/near-diploid (41%)

and complex (hyperdiploid, multiple cell lines, fragmented chromosomes) (59%). Statistical analysis using chi-square and Fisher test was done.
Results Statistical analysis demonstrated that low stage (p=0.00005) and low grade (p=0.0004) were predictors of good prognosis, while residual disease correlated with a poor outcome (p=0.00001). Diploid/near-diploid karyotype correlated with a favourable prognosis (chi-square: 3.84). Complex karyotypes appeared much more frequently associated with chemoresistance (57% vs 7%).
Conclusion Our results confirm the correlation between grade, stage, residual disease and prognosis of OCs. In addition, these data suggest that a diploid/near-diploid karyotype might predict benefit of chemotherapy and favourable prognosis.

P-060

Behaviour of microinvasive (MIC) squamous- and adenocarcinoma of the uterine cervix in the light of world literature and experience from our clinic

M Eržen, S Rakar, M Čavič, J Šinkovec, D Kopač
Department of Obstetrics & Gynecology, University Medical Centre, Ljubljana, Slovenia

Introduction The aim of this study was to critically assess the progression- and recurrence rates of microinvasive (MIC) Stage IA cervical carcinoma, based on Medline search, and to compare these data with our own experience on these tumours in Ljubljana Medical Centre.
Materials and methods In the 25 published studies covering the years 1976-1999, a total of 4.311 squamous cell MICs were reported, including 2.967 stage IA1 lesions, 1.269 in stage IA2, and 75 cases of occult stage IB, classified according to FIGO or SGO classifications. Our experience in Ljubljana is based on the management of 400 stage IA squamous cell carcinomas (SCC), accumulated in the past 30 years and 33 early invasive adenocarcinomas (AC) collected in 5 years.
Results In the reported 4.311 SCC MIC cases, lymphatic space involvement was recorded in 342 (8%) cases, and in 53 of those, the disease recurred, and progressed to death in 15 patients. In 14 series, MICs were associated with 72 (1.7%) recurrences. In seven series, 20 (0.5%) cases of death due to cancer were reported. Lymph node metastases were found in 30 (0.7%) cases. Even when stage IA1 and IA2 carcinomas were treated with conservative surgical approach, very low risk of recurrence (1.7%), lymph node disease (0.7%), or death caused by cancer (0.5%) was reported by these studies. Most authors conclude that MIC with the depth of invasion <3 mm, without confluent growth or lymphatic invasion can be safely treated with conization. During 1966-1972 lymphadenectomy was included in 290 operations of MIC in Ljubljana. The pelvic LNs were invariably free of cancer. The 5-year survival was 97%, while 6 patients were lost to follow-up. In Medline search 1.170 cases of stage IA ACs were analysed in a 35-year period. Lymph node metastasis were found in 15 (1.3%) of 531 cases with lymphadenectomy, complicated with recurrent disease in 11 (2.1%) cases Compared to the SCC MIC, the risk of recurrence in AC was considerably higher, 3.4% and progression to death 1.4% (436 cases analysed by Östör, 2000). In our 33 AC patients diagnosed in stage IA there was no recurrence or death of disease.
Conclusions According to the world literature and our own experience, the prognosis of MIC of both squamous and glandular type is very favourable. This suggests that conservative management of stage IA cervical cancer is indicated and safe when strict evaluation of tumour extension and surgical margins of the cone are assured.

P-061

AgNOR counts, histological and immunohistochemical characteristics of placenta in preterm delivery with live and dead newborns

G Burkadze, G Turashvili, N Meckhvarishvili
Tbilisi State Medical University, Tbilisi, Georgia

Introduction The pathology of placenta constitutes one of the most poorly understood domains of general pathology. The significance of histological characteristics of preterm delivery is disputable. The aim of this study was to investigate histological and immunohistochemical characteristics and AgNOR counts of placenta in preterm delivery with alive and dead newborns.
Materials and methods We studied placental tissues in preterm deliveries of 19 live (first group) and 12 dead (second group) newborns (N1 Obstetrics Clinic of TSMU, 1999-2002). Paraffin sections were stained using H&E, AgNOR (Bio-Optica) and immunohistochemistry by Ki-67, CD68, CD31, bcl-2 (DAKO).
Results In the first group the number and area of chorionic villi was 2 times lower, the number and area of villous vessels 10.5 times higher, the number of villous lymphocytes is 4.1 times higher, neutrophils 1.27 times higher, Hofbauer cells 1.6 times lower, syncytiotrophoblasts 2.5 times lower (their area was the same), syncytial knots 2 times lower (their area is 2 times higher). The width of Nitabuch layer was 2 times greater, decidual tissue 2.2 times greater, the number of decidual cells was 3.3 times higher, decidual lymphocytes 1.2 times higher, neutrophils 1.4 times higher, macrophages 1.2 times lower, AgNOR(+) syncytiotrophoblastic cells 1.8 times lower, AgNOR granules did not differ, AgNOR(+) decidual cells 3 times higher, AgNOR granules 1.2 times higher, Ki-67(+) syncytiotrophoblasts and cytotrophoblasts 2 times higher.
Conclusion Preterm delivery shows incoordination between proliferation and involution of placental tissue. In death of newborns, morphological changes reflect non-efficacy of adaptative-compensative reactions of chorion-decidual system.

P-062

Tumor suppressive function of gelsolin in ovarian carcinoma

A Noske[1], H Schober[1], C Sers[1], B Zhumabayeva[2], M Dietel[1], K Wiechen[1]
[1]Institute of Pathology, Charité University Hospital, Berlin, Germany
[2]Clontech Laboratories Inc., Paolo Alto, California, USA

Introduction The ubiquitously expressed actin-binding protein gelsolin is known to play a role in modulation of the actin network and regulation of cell motility and cell growth. Decreased gelsolin expression occurs in transformed cells and in carcinomas of the colon, bladder, breast, lung and prostate.
Methods and results In the present study we analyzed expression of gelsolin in 241 matched human normal and tumor tissues using a Cancer Profiling Array.

Results We found a decreased expression of gelsolin in cancer tissue of female reproductive organs including ovary. Further we examined the expression of gelsolin in human benign and malignant ovarian tissues by immunohistochemistry, observing a diminished expression of gelsolin in borderline tumors and ovarian serous carcinomas compared to epithelium of normal ovaries and benign adenomas. In addition, low levels of gelsolin protein were observed in four of six ovarian carcinoma cell lines in contrast to immortalized ovarian surface epithelial cells. Re-expression of gelsolin in the ovarian carcinoma cell lines OAW42 and ES-2 resulted in a suppression of tumor cell survival in vitro. Finally, we showed an up-regulation of gelsolin in ovarian cancer cell lines after inhibition of both DNA methylation and histone deacetylation using 5-aza-2'deoxycytidine and Trichostatin A, respectively.
Conclusion Our results suggest that the gelsolin gene has a potential function as a class II tumor suppressor gene in human ovarian epithelium.

P-063

Steroid cell tumor of the ovary: presentation of two cases

I Lekka, O Tzaida, V Leodara, A Lountou, P Arapantoni-Dadioti, I Iakovidou
Pathology Department, Metaxas Cancer Hospital of Pireaus, Piraus, Greece

Two cases of steroid tumor of the ovary, diagnosed at our department during the last five years among a total of 254 ovarian tumors, are presented. Steroid cell tumors, previously classified as lipid or lipoid cell tumors are rare neoplasms of sex-cord-stromal origin derived in almost all cases from ovarian stromal lutein cells or from Leydig cells and rarely from adrenal rest cells. They have been subclassified as steroid cell tumors not otherwise specified (NOS), stromal luteomas and Leydig cell tumors. In our report we present two cases of the NOS subtype: one occurred in a 24-year-old woman and the other in a 72-year-old postmenopausal woman. Both patients presented with a pelvic mass and signs of virilization (resulting effect of elevated serum testosterone). Both tumors were composed of characteristic eosinophilic-granular or vacuolated (lipid rich) neoplastic cells lacking crystals of Reinke and expressing the appropriate immunohistochemical phenotype. Based on thorough pathological examination and evaluation of several findings such as tumor size, necrosis, haemorrhage, cellular atypia, mitotic activity, we classified the first case as a malignant and the second as a benign one. Various aspects of the clinical and pathological presentation, differential diagnosis and treatment of these tumors are discussed.

P-064

Choriocarcinoma following term pregnancy

L Alfaro[1], MJ Roca[2], A Froufe[1], M Rayon[1]
[1]Hospital 9 de Octubre, Valencia, Spain
[2]Hospital Lluys Alcanyis de Xativa, Valencia, Spain

Introduction Choriocarcinoma is the most malignant form of gestational trophoblastic disease. Most cases develop after an abnormal gestation mainly complete hydatidiform mole. Uncommonly choriocarcinoma follows a normal pregnancy. The aim of this study was to stress the importance of a correct and rapid diagnosis which will allow a high rate of success in therapy for this neoplasm.
Material and methods Histopathologic and immunohistochemical studies were performed to an endometrial curettage and a hysterectomy specimen.
Case report A 33–year-old female presented with uterine bleeding three months after a normal delivery from a term gestation in which placenta was not submitted for study. Endometrial curettage was performed, and it showed a dimorphic population of atypical cytotrophoblast and syncytiotrophoblast cells. Cytotrophoblast cells had pale cytoplasm with single nucleus, eosinophilic nucleoli and prominent mitotic figures. Syncytiotrophoblast appeared as large multinucleated cells with polygonal basophilic cytoplasm. Extensive necrotic and hemorrhagic areas were found. There was no presence of placental villi. Neoplastic cells expressed strongly ß-hCG and cytokeratin. With a diagnosis of choriocarcinoma, hysterectomy was performed and showed areas of normal proliferative endometrium, and hemorrhagic areas with nests of trophoblastic neoplastic cells infiltrating among myometrial muscle. There was no involvement of cervix or adnexa. Treatment was completed with chemotherapy, and one year after diagnosis the patient has not evidence of disease.
Conclusions The modern treatment with chemotherapeutic drugs is highly effective in complete cure of choriocarcinoma. Therefore a quick histological diagnosis has a very important role to reduce the risk of metastasis disease, even avoiding surgery to preserve reproductive function.

P-065

Role of angiogenesis in uterine leiomyomas treated with GnRH agonists

J Laforga[1], P López-Sánchez[1], I Aranda[2], J Aznar[1], E Ortega[2]
[1]Hospital Marina Alta, Denia, Spain
[2]Hospital General de Alicante, Denia, Spain

Introduction The mechanism of action and the histological features of uterine leiomyomas (UL) treated with GnRH are still a matter of debate. Recent reports suggest that neovascularization induced by specific angiogenic molecules may play a role in the response to GnRH. Also a reduced proliferative activity was observed and postulated as a possible histopathological feature of UL treated with GnRH. The aim of this study was to assess the possible role of angiogenesis and to quantify the percentage of proliferative cells in uterine leiomyomas in response to treatment with GnRH from premenopausic patients.
Material and methods A total of 60 patients were studied, with two groups comprising 30 samples each, including patients treated with GnRH and age-matched control patients. Clinical (age, length of treatment, assessment of response to treatment by ultrasonography) and histopathological dates (microvessel density (vessels/mm2) and cellular proliferation assesed by Ki-67 stain in 200 cells were studied.
Results The study group showed CD31= 59,28 vessels/mm2 (mean) and Ki-67= 4,38 (mean). The control group showed CD31= 38,95 vessels/mm2 (mean) and Ki-67= 9,3.
Conclusion The leiomyomas treated with GnRH showed a) high number of microvessel density, b) low proliferative activity and c) significant reduction in size compared with patients without treatment.

P-066

Potential prognostic significance of apoptosis related oncogenes: p53, bcl-2 and mdm-2 in early stage cervical carcinoma

I Prodanova, G Yashar, K Kubelka-Sabit, G Zogravski, N Basheska
Department of Histopathology And Clinical Cytology, Institute of Radiotherapy and Oncology, Medical Faculty, Skopje, Republic of Macedonia

Introduction Evaluations of expression of apoptosis related oncogenes are being increasingly called upon in an attempt to better understand the carcinogenesis of cervical carcinoma and to provide possible prognostic information. The aim of this study was to analyze the expression of bcl-2, p53 and mdm-2 oncoproteins and cellular proliferative marker Ki-67 in early stage cervical carcinoma, with an emphasis on their association with human papillomavirus (HPV) infection, recurrence rate and lymph node status.
Material and methods Using immunohistochemistry, 69 radical hysterectomy specimens with cervical carcinoma (pT1b1/pT1b2) were studied. Evaluation of expression of p53, bcl-2, mdm-2 and Ki-67 was performed in surface area, center and invasion front of the neoplasms. The HPV presence was determined by CARD in situ hybridization.
Results and conclusion In the invasion front bcl-2 was expressed in 31 (45%), p53 in 37 (53%) and mdm-2 in 33 (47%) cases. HPV infection was detected in 40 (58%) cases. Carcinomas with a higher Ki-67 labeling index were more frequently HPV positive than HPV negative (82.5% vs 17.5%, $p<0.01$). No association was found between p53, mdm-2 or Ki-67 and either lymph node status or recurrence rate. Negative staining for bcl-2 was associated only with the presence of lymph node metastasis (74% vs 26%, $p=0.05$), and not with the recurrence rate. Significant correlation among expression of bcl-2, p53, mdm-2 oncoprotein and Ki-67 values was also observed. These results suggest that further study of a larger series is needed to confirm whether bcl-2, either alone or in combined evaluation with other markers, could be a useful marker to identify more aggressive behavior in early stage cervical carcinoma.

P-067

Malignant potential of dysplastic endocervical epithelium assessed by ploidy status, S-phase fraction and c-myc expression

L Hlupic[1], S Jukic[2], M Kos[2], D Babic[2]
[1]Department of Pathology, Clinical Hospital Center, Zagreb, Croatia
[2]Department of Gynecological and Perinatal Pathology, Clinical Hospital Center, Zagreb, Croatia

Introduction During the past three decades, the incidence of cervical invasive primary adenocarcinoma (ACA) has increased. At the same time, incidence of squamous cell carcinomas of the cervix decreased, due to early detection of their well documented precursors lesions. The aim of this study was to determine if dysplastic endocervical cells (EC) have neoplastic potential as a precursor lesions of adenocarcinoma in situ (AIS) of the cervix. The malignant potential was determined by assessing the ploidy status, proliferative activity and c-myc expression in normal, dysplastic and malignant EC separately.
Patients and methods Serial sections from 49 patients with diagnosed AIS or primary invasive ACA were analyzed. One representative slide of cervix which showed normal, dysplastic and malignant endocervical glands simultaneously was chosen from each patient. Determination of ploidy status and S-phase by flow cytometry and expression of c-myc oncoprotein by immunohistochemistry in normal, dysplastic and malignant EC was done.
Results The morphologicaly normal EC were diploid, with normal proliferative activity and no expression of c-myc oncoprotein. The dysplastic and malignant EC had a significant proportion of cells with aneuploidy, higher proliferative activity and c-myc oncogene overexpression. The χ^2 test showed significant association of malignant EC with aneuploidy ($p=0.008$) and high proliferative activity ($p=0.042$). As one third of dysplastic EC are aneuploid, with high mitotic activity, they probably have malignant potential. Dysplastic endocervical cells had statistically significant association with c-myc oncogene expression ($p=0.028$).
Conclusion Our results support the existence of pre-malignant glandular lesions while the immunohistochemical detection of c-myc oncoproteine could be helpful in detection of EC with malignant potential even without dysplastic morphologic changes.

P-068

Immunohistochemical expression of c-erbB-2 in early stage cervical carcinoma: correlation with human papillomavirus infection and prognosis

N Basheska, G Yashar, K Kubelka-Sabit, I Prodanova, G Zografski
Department of Histopathology and Clinical Cytology, Institute of Radiotherapy and Oncology, Medical Faculty, Skopje, Republic of Macedonia

Introduction The attempts to determine the prognostic significance of c-erbB-2 oncoprotein expression (OPE) and its relation to human papillomavirus (HPV) infection in cervical cancer have yielded controversial**.** The aim of this study was to evaluate the patterns of c-erbB-2 OPE in early stage cervical carcinoma and to assess its prognostic value by exploring its relationships to various clinicopathological characteristics, HPV status and recurrence rate.
Materials and methods Radical hysterectomy specimens from 71 cervical carcinoma patients (pT1b1/1b2) were investigated immunohistochemically for c-erbB-2 presence. The c-erbB-2 score (range: 0-400) was determined in the surface area, center and invasion front of each carcinoma. CARD in situ hybridization was used for HPV detection.
Results and conclusion Strong c-erbB-2 OPE was detected in 21, 20, and 32 cases in the invasion front, center and surface area of the tumor, respectively. There was a significant difference in positive staining rate of c-erbB-2 between squamous cell, mixed carcinomas and adenocarcinomas (23%, 50% vs 83%, $p=0.005$). C-erbB-2 OPE was significantly higher in carcinomas with abundant than in tumors with less abundant peri-tumoral lymphocytic infiltration (36.5% vs 10.5%, $p=0.032$). In HPV positive carcinomas (41), c-erbB-2 was detected more frequently in type 31/33 versus type 16/18 lesions (75% vs 18.8%, $p=0.002$). No association was found between c-erbB-2 expression and recurrence rate, lymph node metastasis or any other clinicopathological variable investigated (age, tumor diameter, depth of invasion, grade, vascular invasion). Therefore, immunostaining for c-erbB-2 is unlikely to be of use as a prognostic indicator in early stage cervical carcinomas, while further study is warranted to examine relationships between HPV infection and c-erbB-2 OPE.

P-069

Determination of estrogen, progesterone receptor and Ki-67 immunoreactivity in early stage cervical carcinoma: association with human papillomavirus infection and prognosis

G Yashar, I Prodanova, K Kubelka-Sabit, G Zografski, N Basheska
Department of Histopathology and Clinical Cytology, Institute of Radiotherapy and Oncology, Medical Faculty, Skopje, Republic of Macedonia

Introduction The predictive values of estrogen (ER) and progesterone receptor (PgR) status and cell proliferation kinetics in cervical carcinomas are still unsettled. The purpose of this study was to clarify the associations among ER/PgR status and Ki-67 expression and to determine their relationship to human papillomavirus (HPV) infection, recurrence rate and other clinicopathologic parameters (age, tumor diameter, depth of invasion, histotype, grade, vascular involvement, inflammatory infiltrate, lymph node status) in early stage cervical carcinomas.
Materials and methods ER, PgR and Ki-67 immunostaining was performed in 72 cervical carcinoma radical hysterectomy specimens (pT1b1/pT1b2). ER/PgR staining was scored in a semiquantitative fashion, while to evaluate the cell proliferation, the Ki-67 labelling index (LI) was assessed in the surface area, center and invasion front of each tumor. HPV status was determined by CARD in situ hybridization.
Results and conclusion ER positivity was detected in 11 (15%), while PgR positivity in 14 (20%) carcinomas. ER/PgR values were in correlation with Ki-67 LI in all three tumors' compartments ($p<0.01$). In contrast to ER/PgR status, Ki-67 LI was strongly associated with HPV infection ($p<0.01$). No relationship was found between PgR or Ki-67 immunoreactivity and either recurrence rate or any other clinicopathological variable investigated. Nevertheless, reduced ER expression was significantly associated with larger tumor diameter ($p=0.04$) and poor differentiation ($p=0.03$), as well as lymphovascular involvement ($p=0.04$) and lymph node metastases ($p=0.02$). These results suggest that ER, PgR and Ki-67 expression are closely related to neoplastic cell proliferation, probably induced by HPV infection. Their determination may provide additional prognostic information in early stage cervical carcinomas.

P-070

Immunohistochemical assessment of heat shock protein 70 expression in epithelial ovarian carcinomas: Relationship with apoptotic markers as over-expression of bcl-2 and p53

F Aktepe[1], N Kapucuodlu[2], FH Dilek[3]
[1]Department of Pathology, University of Afyon Kocatepe, Faculty of Medicine, Afyon, Turkey
[2]Department of Pathology, University of Isparta Süleyman Demirel, Faculty of Medicine
[3]Department of Pathology, University of Afyon Kocatepe, Faculty of Medicine, Afyon, Turkey

Purpose Heat shock proteins (hsps) occupy a central role in the regulation of intracellular homeostasis and especially hsp70 and hsp27 are potent antiapoptotic proteins. Overexpression of hsp70 protects cells from stress-induced apoptosis. The aim of this study was to determine the distrubition pattern of hsp70-expression in ovarian carcinomas by immunohistochemistry and to evaluate its relationship with the prognostic parameters and over-expression of bcl-2 and p53 proteins.
Materials and methods Thirty-five patients with ovarian carcinoma were included in the present study. Expression of hsp70 was assessed by immunohistochemistry. The relationship between expression of these proteins and other prognostic markers such as stage was evaluated.
Results Hsp70 was expressed in all of ovarian cancer cells with different intensity. The staining was localized in the cytoplasm and/or nuclei. There was a negative correlation between stage and both intensity of hsp70 positivity and bcl-2 positivity (respectively: $r= -0,478$; $p<0.01$; $r= -0.386$, $p<0.05$). Intensity of hsp70 positivity was statistically associated with bcl-2 positivity ($r=0.435$, $p<0.01$). There were no significant associations between p53 positivity and bcl-2 positivity, intensity of hsp70 or stage of ovarian carcinoma.
Conclusions These data show that the intensity of hsp70 positivity was significantly stronger in early stage than in advanced stage ovarian carcinomas. Hsp70 expression detected by immunohistochemistry was correlated with bcl-2 expression but not with p53 protein expression.

P-071

Endometrial avb3 integrin expression and pinopode formation in women receiving hormone replacement therapy

M Garrido, J Ordi, M Creus, B Ferrer, F Fabregues, R Casamitjana, A Cardesa, J Balasch
Hospital Clinic de Barcelona, Barcelona, Spain

Background avb3 integrin and pinopodes have been proposed as new markers of endometrial receptivity. There is also a very limited experience on the responses of these markers to hormonal therapies. The aim of this study is to evaluate the effect different hormone replacement treatment on these markers.
Design We studied 12 fertile controls and 16 women with ovarian failure receiving hormone replacement therapy (estradiol valerate (EV) and vaginal progesterone (VP), group E+EP). Those women were divided randomly into two subgroups of 8 patients. Group E+P received EV for 14 days and VP alone for 14 days. Group E+P+EP was given E+EP therapy but including episodic VP on days 8 and 11. All women underwent two endometrial biopsies during a single menstrual cycle (days +7 to +8 and four days later). avb3 integrin was detected in frozen tissue using the EnVision system. Pinopode formation was evaluated in tissue fixed in glutaraldehide using a Zeiss DSM940A scanning electron microscopy. Both avb3 integrin and pinopode formation were semiquantitatively evaluated.
Results Patients in group E+P+EP showed markedly decidualized endometria in the midluteal biopsy and a significant increase of avb3 integrin expression ($p=0.01$ for both parameters). No significant changes in pinopode formation were observed in midluteal biopsies. No differences were observed in late luteal biopsies.
Conclusions avb3 integrin expression and pinopode formation are signs of endometrial maturation related to progesterone action but their significance in terms of endometrial receptivity in the clinical setting remains to be shown. Supported by grant PI020036 (Fondo de Investigaciones Sanitarias).

P-072

Gestational trophoblastic disease associated with ectopic pregnancy: a report of three cases

B Hadzi-Nicheva[1], I Prodanova[2], G Yashar[2], K Kubelka-Sabit[2], Z Grncharovska[1], N Basheska[2]
[1]Department of Obstetrics and Gynaecology, Medical Faculty, Skopje, Republic of Macedonia
[2]Department of Histopathology and Clinical Cytology, Institute of Radiotherapy and Oncology, Medical Faculty, Skopje, Republic of Macedonia

Introduction Gestational trophoblastic diseases (GTD) are extremely rare conditions, especially the ones associated with ectopic pregnancies (EP).
Case reports Only three cases (0.26%, 3/1133) of GTD associated with EP were diagnosed at the Department of Histopathology and Clinical Cytology in the last 14 years. The first patient, age 29 underwent salpingectomy for clinical suspicion of tubal pregnancy, whereas in the second, age 49 hysterectomy with bilateral salpingo-oophprectomy (HSOP) was performed for a clinical diagnosis of ovarian endometriosis. The third patient, age 42 underwent HSOP for malignant ovarian tumour which metastasised to lungs. Pathological findings: Chorionic villi were found in the tubal lumen of the first patient, showing marked hydropic degeneration, reduced/absent vascularisation and excessive trophoblastic cell growth. Diagnosis of partial hydatiform mole was established, and the patient remained under surveillance for the HCG level. Atypical trophoblastic cells, which penetrated the full thickness of the tubal wall and invaded the ovarian blood vessels of the second patient, led to the diagnosis of an invasive mole. The third patient was diagnosed with choriocarcinoma due to the presence of a tumour consisting of malignant trophoblastic cells that infiltrated the right ovary, tube and uterine cornu. The last two patients received chemotherapy and have been well for 15 and 118 months, respectively.
Conclusion Due to extremely low incidence of GTD associated with EP, these entities are rarely clinically recognised. Therefore, a careful histopathologic examination of the adnexal masses is essential for the establishment of the correct diagnosis and further treatment of the patients.

P-073

Advantages of liquid-based cytology in the diagnosis of atypia (ASCUS) - a follow-up study

DE Schledermann, D Ejersbo, B Hoelund
Odense University Hospital, Departement of Pathology, Odense, Denmark

Introduction In an organized screening programme for cervix cancer the diagnosis atypia (ASCUS) has always been a problem. The subsequent histological examination shows different diagnoses, such as negative, inflammation, CIN I-III (SIL) and carcinoma. In the County of Funen, a well-organized screening programme has existed since 1989.Using the cytological diagnosis of atypia, we distinguish between atypia 1 (ASC-US) probably inflammatory and atypia 2 (ASC-H) probably dysplasia. In previous studies on PAP-smears we have shown histological follow-up diagnoses for atypia 1(ASC-US): negative 84.3% and CIN I-III 15.7%, and for atypia 2 (ASC-H): negative 41.6%, CIN I-III 57% and carcinoma 1,4%. Since June 2001 we have implementated liquid-based cytology (LBC) ThinPrep, Cytyc. The aim of this investigation is to show the histological follow-up diagnoses of cytological atypia when using LBC-technique.
Materials and methods The total number of LBC-samples in 2002 were examined. The recommandations for atypia 1 are a repeated cervical sample, and for persistent atypia 1 or atypia 2 colposcopy, cervical biopsies and abrasion within 3 months.
Results In 2002 a total of 34,585 smears, including 30,060 LBC-samples, were examined. The diagnoses of the LBC-samples were: negative 92,9%, inadequate 2,8% (a reduction of 50% compared with PAP-smears), atypia 2,8 % and CIN I 4%. Preliminary histological follow-up diagnoses for atypia 1 and 2 were: negative 59% and CIN I-III 41%.
Conclusion ThinPrep shows two significant advantages: a markedly reduced number of cytological atypia diagnoses (40%) compared with PAP-smears and a higher diagnostic quality with fewer false positive diagnoses.

P-074

Ovarian Sertoli-Leydig cell tumor with heterologous elements of rhabdomyosarcoma: A case report

A Grove[1], V Vestergaard[2]
[1]Institute of Pathology, Aalborg Hospital, Aalborg, Denmark
[2]Institute of Pathology, Hjorring Hospital, Aalborg, Denmark

Introduction Ovarian Sertoli-Leydig cell tumors (SLCT) are very rare sex cord-stromal tumors and among them, tumors with heterologous sarcomatous elements are exceptional. Aims: A unilateral ovarian stage Ic SLCT with heterologous mesenchymal elements is presented.
Materials and methods A 29-year-old woman, para 1, was admitted to hospital with severe abdominal pain. At laparotomy, resection of a large right ovarian cyst was carried out. Histological examination revealed a SLCT, and subsequently surgical staging was performed. No adjuvant therapy was given. At 2 years follow-up she was well and without signs of recurrence. Routine staining of slides from 34 paraffin blocks and immunohistochemistry (IHC) were available.
Results Gross examination revealed a 18 x 14 x 11 cm large multilocular ovarian cyst with smooth interlocular septa and outer surface. Microscopy disclosed a SLCT of intermediate diff-erentiation with a very few Leydig cells. Major areas consisted of a hypocellular stroma with edema, hemorrhage and necrosis. In a few sections small foci of cartilage were seen. In a number of sections groups of small cells with indistinct cytoplasm and hyperchromatic nuclei were present. Mitotic and apoptotic figures were common. IHC revealed a positive reaction for desmin, myf4 and myogenin, indicating rhabdomyosarcoma of embryonal type.
Conclusion The most important prognostic factors of SLCT are stage and grade of differentiation. Variants of SLCT with immature skeletal muscle are often fatal. IHC with myf4 or myogenin with a high sensitivity and specificity for rhabdomyosarcoma, combined with inhibin is very important in differing immature Sertoli cells from rhabdomyoblasts, in order to diagnose the rhabdomyosarcoma and to grade the SLCT correctly.

P-075

Expression of the nerve growth factor (NGF) receptors TrkA and p75 shows biological diversity in ovarian, breast and mesothelial malignancy

B Davidson[1], R Reich[2], P Lazarovici[2], VA Florenes[1], M Skrede[1], B Risberg[1], C Bedrossian[3], JM Nesland[1]
[1]The Norwegian Radium Hospital, Oslo, Norway
[2]Department of Pharmacology, Hebrew University, Jerusalem. Israel
[3]Department of Pathology, Northwestern University, Chicago, IL, USA

Neurotrophins and their receptors are known to have a central role in biologic processes in the nervous system. However, recent studies have additionally highlighted the role of NGF and its receptors TrkA (inducer of proliferation) and p75 (inducer of apoptosis) in the development and progression of malignant tumors, including those of non-neural origin. We studied protein expression of p75 and activated phosphorylated TrkA (p-TrkA) in 145 serous ovarian carcinomas (80 effusions, 65 solid tumors), 107 breast carcinomas (42 effusions, 65 solid tumors) and 81 malignant mesotheliomas (MM) (24 effusions, 57 biopsies) using immuno-histochemistry and immunoblotting. p-TrkA was expressed in ovarian carcinoma cells in effusions in only 15/80 (19%) specimens, compared to 52/65 (80%) solid tumors, while the opposite was true for p75. In contrast, p-TrkA membrane expression was higher in effusions ($p=0.058$) of MM patients, while the opposite was true for p75 ($p=0.008$). In addition, p-TrkA (but not p75) expression was significantly higher in peritoneal MM compared to their pleural counterparts (20/20 vs. 46/61 positive tumors; $p=0.014$). In breast cancer, p-TrkA expression in effusions was significantly higher than in primary tumors ($p<0.001$) and lymph node metastases ($p=0.001$), while p75 expression was lower in both effusions ($p=0.019$) and primary tumors ($p=0.039$) compared to lymph node metastases. Our results provide the first evidence regarding the role of NFG receptors in tumor progression through site-specific changes in expression. Specifically, they may provide biologic evidence for the uniformly and rapidly fatal outcome of breast cancer patients with effusions and of MM patients.

P-076

The significance of mast cells in the differential diagnosis of uterine smooth muscle tumors

BH Ozdemir[1], AN Haberal[1], FP Uyar[1], A Sar[1], B Demirham[1], S Zergeroglu[2]
[1]Baskent University, Faculty of Medicine, Deparment of Pathology, Ankara, Turkey
[2]Zekai Tahir Burak Women Hospital, Deparment of Pathology, Ankara, Turkey

Aim To assess the role of the mean mast cell count in the differential diagnosis of uterine smooth muscle tumors.
Material and method Twenty-cases of ordinary leiomyoma, 6 cases of atypical leiomyoma, 6 cases of leiomyosarcoma, 8 cases of mitotically active leiomyoma and 38 cases of cellular leiomyoma were included in the study. The morphological features and clinical presentation was evaluated retrospectively. Toludine Blue stain was used to highlight the mast cells in the endometrium, myometrium and smooth muscle tumors. At least 40 high power fields were counted.
Results Considerable variation in mast cell numbers was found among smooth muscle tumors ($p<0.01$). The intratumoral mean mast cell count was found significantly higher in ordinary leiomyomas (82.7 14), when compared with other tumors, including atypical leiomyoma (68.4 18.4), mitotically active leiomyoma (45 10.3), cellular leiomyoma (34.2 5.9) and leiomyosarcoma (23.8 8.3) ($p<0.01$). No significant differences were found between these tumor groups in regards of the mean mast cell count of endometrium and myometrium adjacent to the tumor. In the endometrium, a drop in the number of mast cells has been demonstrated with advancing age, particularly after menopause ($p<0.05$). In addition 2 cases showed eosinophilia, 4 cases showed basophilia and 5 cases showed allergic reactions to different causes. A significant positive relationship was found between the intratumoral, myometrial mast cell number and basophilia.
Conclusion These data suggest that intratumoral mast cell quantitation may allow the differential diagnosis in uterine smooth muscle tumors.

P-077

Mutation analysis of proliferation genes in ovarian tumours by DHPLC

A Fassina[1], N Peloso[1], F Ganz[1], M Menegazzo[1], M Zoletto[1], E Pegoraro[2]
[1]Department of Pathology, University of Padova, Padova, Italy
[2]Neurological Sciences, University of Padova, Padova, Italy

Ovarian carcinoma is the most frequent cause of death in the world among gynaecologic malignancies. Diagnosis is usually late, and the biological behaviour is highly variable, depending on several factors such as the histopathological grading, the local and/or peritoneal spread and the proliferation rate. We choose a list of genes involved in cell growth and proliferation (IGF2, IGFBP3, CTNNBETA1, CDK-1C, FGFR4). Among these, so far, we analyzed IGFBP3 gene and studied loss of heterozygosity (LOH) in tumour tissue in order to identify potential relevant genes in ovarian cancer homeostasis. Twenty cases of formalin fixed, paraffin embedded ovarian carcinomas from the archives of the Department of Pathology of Padova University and five effusions (from peritoneal or pleural recurrences) of ovarian carcinomas, were selected for this study. Genomic DNA and tumour DNA for each case were extracted from blood cell, tumour or not-cancer surgery biopsy. LOH was searched using 2 published single nucleotide polymorphism (SNPs) in IGFBP3 gene. PCR product covering the SNPs from genomic and tumour DNA were DHPLC separated. Three of the twenty patients whose tumour DNA was obtained from paraffin material, were heterozygous at nucleotide 323 C/A (dbSNP ref. n. 2132570) and 1704 A/C (dbSNP ref. n. 2854744) of the IGFBP3 gene in genomic DNA. Analysis of tumour DNA failed to reveal LOH (preserved heterozygosity). In effusion cases, one of five patients showed heterozygosity at the same nucleotides. In these patients, LOH was also not identified. Our preliminary results suggest that DHPLC analysis for LOH is feasible, rapid and maybe of potential interest in the identification of genes involved in ovarian cancerogenesis.

P-078

Squamous intraepithelial lesions and Ki67

S Boluda, F Alameda, P Fusté, M Iglesias, M Jimeno, T Baró, L Marińoso, A Munné, R Carreras, S Serrano
Hospital Del Mar-IMAS-IMIM, Barcelona, Spain

Introduction The progression of low grade squamous intraepithelial lesion (L-SIL) to high grade squamous intraepithelial lesion (H-SIL) occurs in around 20% of cases. There are no morphologic changes to predict this progression. Aims: To study whether the Ki 67 immunostaining pattern and labeling present upon diagnosis of L-SIL is able to predict the regression or persistence/progression of the lesion to H-SIL of the cervix over a two year period following diagnosis.
Materials and methods 113 cervical biopsies from 113 patients diagnosed cytologically as cervical squamous intraepithelial lesion (SIL) were used. Biopsies were performed immediately after the cytological diagnosis resulting in 89 L-SIL and 24 H-SIL. Ki 67 immunostaining was performed on all cases and was classified as suprabasal immunostaining pattern (SBIP) for cases without Ki-67 immunoreactive cells in the upper two thirds of the epithelium thickness, or dispersed immunostaining pattern (DIP) for cases with Ki-67 immunoreactive cells in the upper two thirds of the epithelium thickness. 200 nuclei in 25 HPF including the total thickness of the epithelial layer of each sample were counted to determine the mean number of cells which reacted against Ki-67 antibody. In situ hybridization was used to demonstrate the presence of HPV and its typing. Chi Square Test, Fisher's Exact Test and Student T Test were used for statistical analysis with significance set at $p<0.05$.
Results Of the 113 biopsies performed 89 cases resulted in L-SIL (54 S-BIP and 34 DIP patterns) and 24 in H-SIL. 14% of the L-SIL cases that resulted in a S-BIP pattern showed persistence/progression of the lesions while 65% of the cases that resulted in a DIP pattern showed persistence/progression of the lesions. The difference between these values where statistically significative ($p<0.001$). Regarding Ki-67 labeling index (LI) in L-SIL cases, we found that 25% of the cases (15 out of 58) with a Ki-67 LI less than 28% persisted/progressed, while 51% of cases (16 out of 31) with Ki-67 LI over 28% persisted/progressed. In this case there was also a statistically significative difference ($p=0.015$). We found no statistical differences ($p=0.64$) regarding HPV "in situ" hybridization. 48% of the cases (14 out of 29) where HPV was detected by in situ hybridization persisted/progressed while 28% of the cases did not show HPV by hybridization.
Conclusions The L-SIL cases which showed DIP and high Ki-67 LI were significantly related with persistence or progression to H-SIL of these lesions, while L-SIL cases which showed SBIP and low Ki-67 were significantly related to regression of the lesions. Therefore, we conclude that Ki-67 immunostaining pattern may be of prognostic value to predict regression or persistence/progression of L-SIL.

P-079

Sclerosing stromal tumor of the ovary

EU Akyildiz[1], Z Calay[2], S Ilvan[2]
[1]Institute of Forensic Medicine, Istanbul, Turkey
[2]Istanbul Istanbul University, Cerrahpasa Faculty of Medicine, Department of Pathology, Istanbul, Turkey

Introduction Sclerosing stromal tumor (SST) of the ovary is a rare tumor. It was first described by Chalvardjan and Scully in 1973 as a distinct subtype in the thecoma-fibroma group. Most SSTs occur in young patients below the age of 30 years. The most common clinical symptom in patients is menstrual irregularity. In differential diagnosis, thecoma, fibroma, and hemangiopericytoma must be considered. Aim: In this report, 2 cases of SST of the ovary were described and compared with other ovarian tumors.
Material and methods Two cases of ovarian SST were examined. The first case occurred in a 28-year-old female. At operation, the patient was found to have the ovary replaced by a tumor mass measuring 5x4x2 cm. The second case occurred in a 24-year-old woman and the tumor mass measured 9x5x5 cm. The surgical material was fixed in 10% formaldehyde solution and prepared for paraffin sections. In addition to H&E staining, immunohistochemical analyses were performed.
Results The clinical features, gross features, light microscopic findings and immunohistochemical results were described and compared with literature. The findings were consistent with SST, which is a very rare tumor of the ovary. The tumor cells showed positive staining for vimentin and desmin. We discuss the results and differential diagnosis.

P-080

Unususal chorangioma of the placenta - A case report

W Pokieser[1], W Umek[2], R Jahn[1], W Ulrich[1]
[1]Institut of Pathology, Lainz Hospital, Vienna, Austria
[2]Institut of Pathology, Department of Obstetrics and Gynecology, University of Vienna, Austria

Chorangiomas (CA) are common lesions, occurring in 1 of 100 placentas. It is not clear whether CA are hyperplasias, hamartomas, or true neoplasms. Depending on their size and location, they may be devoid of symptoms or may cause difficulties for the infant and the mother. We describe a case of manual removal of the placenta in association with CA. On gross examination the tumor had a nodule-in-nodule appearance and was histologically composed of two well defined nodules. The larger, outer one had the appearance of an usual chorangioma; the inner nodule showed highly cellular vascular proliferation. This architecture might represent a morphological variant of the same disease. In the present case, the placenta had to be removed manually. It remains unclear if this was due to impaired contractility of the uterine wall or due to a lack of decidualisation, following a worse vascular support in the surrounding area of the CA. It can´t be excluded that placenta accreta was caused by strictures after Cesarian section which had been performed at the first delivery two years ago. On the other hand a placenta with a nodule form of CA could be less elastic than a placenta with regular architecture. However manual removal of the placenta may be regarded as a further complication of CA's larger than 4 cm in diameter.

P-081

Are MUC 2 and MUC 5AC reliable markers in the differential diagnosis of primary and metastatic ovarian carcinomas?

A Ensari[1], D Ergun[1], A Yorganci[3], A Sertcelik[1], F Ortac[2], N Kursun[4]
[1]Ankara University Medical School, Department of Pathology, Ankara, Turkey
[2]Ankara University Medical School, Department of Gynaecological Oncology, Ankara, Turkey
[3]Numune Hospital Gynaecology Department
[4]Ankara University Medical School, Department of Biostatistic, Ankara, Turkey

Introduction Aberrant expression of mucin glycoproteins has been observed during malignant transformation of human ovarian epithelium. However, there is limited information regarding the expression of these mucin proteins in primary and metastatic ovarian carcinomas. The aim of this study was to examine immuno-histochemical expression of MUC 2 and MUC 5AC mucin proteins in primary and metastatic carcinomas of the ovary in order to assess their value in the differential diagnosis.
Materials and methods Forty eight ovarian tumours comprising 37 surface epithelial carcinomas (8 endometrioid, 5 clear cell, 11 serous papillary and 13 mucinous type) and 11 metastatic carcinomas of gastrointestinal primaries were included in the study. The age of the patients, the histological type and grade of the tumours were evaluated in relation to the expression (percentage distribution and staining intensity) of MUC 2 and MUC 5AC studied immunohistochemically.
Results MUC 2 was expressed in 28 (75.7%) primary ovarian tumours while MUC 5AC was expressed in 27 (73%) primary tumours in comparison to 100% expression of MUC 2 and 82.3% expression of MUC 5AC in metastatic ovarian tumours. The differences in MUC 2 expression between non-mucinous (46.04 ± 38.11) and metastatic tumours (56.36 ± 41.72) and metastatic and mucinous tumours (28.46 ± 39.97) were statistically significant ($p< 0.01$). The difference in MUC 5AC expression was statistically significant ($p< 0.05$) between non-mucinous (27.92 ± 33.49) and mucinous tumours (51.54 ± 38.91).
Conclusion MUC 2 proves to be highly reliable in the differential diagnosis of primary and metastatic mucinous tumours of the ovary.

P-082

Deregulation of sFRP1 and sFRP4 RNA-expression in endometrial stromal sarcoma

A Hrzenjak, M Hiden, ML Kremser, B Strohmeier, D Neumeister, F Moinfar, S Lax, K Zatloukal, H Denk
Department of Pathology, Karl-Franzens University, Graz, Austria

Introduction Endometrial stromal sarcomas (ESS) are very rare uterine tumours. Whereas histology and immunohistochemistry of this tumour are well documented, little is known about molecular mechanisms involved. To characterize ESS-altered genes, we generated a genome-wide library by SSH-hybridisation and used it to produce cDNA arrays. Particular emphasis was also placed on data obtained from QRT-PCR analyses.
Materials and methods Using SSH-library a gene-bank with app. 4000 different clones was established. Total RNA was extracted from frozen tumour tissue and used for cDNA hybridisation. QRT-PCR analyses were performed both on frozen and paraffin-embedded tissue samples.
Results After cDNA-array analysis more than 300 genes were selected, sequenced and rearranged to different functional groups. Among the most strongly deregulated genes were secreted frizzled-related protein-1 (sFRP1) and sFRP4. These are putative genes that regulate wnt-signalling pathway and can influence different cell events including cell proliferation. Compared to post-menopausal endometrium the expression of sFRP1 and sFRP4 was increased in low-grade ESS, but decreased in aggressive ESS form. These results were additionally verified on paraffin embedded tissue probes by QRT-PCR analysis.
Conclusion Deregulation of sFRP1 and sFRP4 expression appears to be one of the crucial features of ESS. Whereas in low-grade ESS these two genes are up-regulated, their down-regulation could be associated with high-grade form of ESS. Therefore a sFRP1 and sFRP4 may not only represent useful markers for early ESS diagnosis but may also have prognostic impact and help to distinguish between low- and high-grade ESS. (This work was supported by LORE-SALDOW – Research Fund)

P-083

C-kit immunoreactivity in female genital tract carcinosarcoma (FGT-CS)

A Vidal-Bel[1], E Condom-Mundó[1], N Vidal-Sarró[1], M Carreras-Martínez[2], J Ponce-Sebastia[2], L Balagueró-Lladó[2]
[1]Department of Pathology. Institut Catala d'Oncologia. Hospital de Bellvitge, Barcelona, Spain
[2]Department of Gynecology.Hospital de Bellvitge, Barcelona, Spain

Introduction FGT-CS is a highly malignant neoplasm with poor response to current chemotherapy. The proto-oncogen c-kit encodes a transmembrane-tyrosine-kinase (t-k) receptor involved in cell diferentiation, that has been found to be expressed in certain solid tumors and may play a role in their tumorigenesis. A t-k inhibitor specific for c-kit (STI571) has been reported to have therapeutic effects in tumors expressing the aberrant forms or high quantities of target protein. Contradictory results are reported in the literature about the expression of c-kit in CS. The aim of this study was to investigate the immunoreactivity for c-kit in CS.
Materials and methods Immunostaining with anti-c-kit (CD117) polyclonal antibody (Dako) was evaluated in 34 CS (23 endometrial, 9 ovarian, 1 cervical and 1 tubal). Only cases with membrane staining were considered to be positive.
Results C-kit was expressed in 5 cases: in 3 cases only in the carcinomatous component (2 endometrial, 1 tubal), in 1 case only in the sarcomatous component (endometrial) and in 1 case in both components (ovarian). Positivity was focal and less than 5% of cells in all cases.
Conclusion CS of the female genital tract rarely express c-kit. It is unlikely that patients with these tumors will benefit from treatment with the currently avalaible t-k inhibitors.

P-084

Uterine heterologous sarcoma with the component of osteosarcoma on the base of lipoleiomyoma - a case report

P Tuzlali[1], E Sahan[1], A Igdem[1], S Tuzlali[2], N Erdogan[1]
[1]Taksim State Hospital Pathology Lab, Istanbul, Turkey
[2]Istanbul University, Istanbul Medical Faculty Pathology Lab, Istanbul, Turkey

Uterine homologous and heterologous sarcomas are rare neoplasms that are usually misdiagnosed as a component of malignant mixed Mullerian tumor (MMMT). We present a case of a 53-year-old woman who had a heterologous sarcoma with a component of osteosarcoma on the base of lipoleiomyoma, that can be differentiated from MMMT by the absence of epithelial component. In heterologous sarcomas, the other components of neoplasm are rhabdomyosarcoma, chondrosarcoma, osteosarcoma, liposarcoma and combined forms. These neoplasms are misdiagnosed as endometrial stromal sarcomas or as a component of MMMT. They are more agressive than MMMT.

P-085

Immunohistochemical detection of ER-β in ovarian sex cord-stromal tumors

E Kostopoulou[1], D Kaisaridou[2], A Nikolaidou[1], A Moulla[1], D Giakoustidis[1], M Zafrakas[1], M Leontsini[1]
[1]Hippokratio Hospital, Thessaloniki, Greece
[2]Theagenion Hospital, Thessaloniki, Greece

Introduction Since the discovery of a second subtype of estrogen receptor, ER-beta (ER-β), in 1996, approximately 10 years after the cloning of ER-α, several reports have been published regarding the tissue distribution of this receptor. In mammals so far studied ER-β predominates in the ovary. High expression of ER-β was observed by in situ hybridization or immunohistochemistry in granulosa cells of the ovarian follicles. The aim of the present study was to examine immunohistochemically the expression of ER-β in ovarian sex cord-stromal tumors.
Materials and methods Ten cases of ovarian granulosa-stromal cell tumors (five adult granulosa cell tumors, two juvenile granulosa cell tumors, and 3 sclerosing stromal tumors) and two cases of Sertoli-Leydig cell tumor were immunostained for ER-β (polyclonal ERb88, Biogenex). Representative sections from ten cases of ovarian carcinomas were immunostained for comparison.
Results Positivity for ER-β was observed in 50% to 80% of the nuclei in adult granulosa cell tumors and 40% to 75% of the nuclei in sclerosing stromal tumors. Only 10-15% of the nuclei from juvenile granulosa cell tumors were positive for ER-β. In Sertoli-Leydig cell tumors positivity was more extensive in areas of diffuse growth. Four cases of ovarian carcinomas exhibited positivity.
Conclusion Positivity for ER-β is a common finding in ovarian sex cord-stromal tumors. These findings might have therapeutic implications.

P-086

Adult fibrosarcoma of the vulva

OL Mejia Mejia
Instituto Nacional de Cancerología, Bucaramanga, Colombia

Introduction Sarcomas are rare and unusual lesions of the vulva. The aim of this study was to present a case with analysis of clinical, morphologic and immunohistochemical findings.
Materials and methods A 59-year-old female patient presented a rapidly growing of a mass in the pubis and left labium major of vulva of 17x16x10 cm associated with a second satellite lesion (2 months later) in the right inguinal area of 7x6x5 cm.
Results Histologic examination of both lesions disclosed a malignant neoplasm composed of uniform and orderly spindle cells with occasional epithelioid cells, oriented in curving or interlacing fascicles, forming a herringbone pattern with mitotic figures (8/10 HPF) and areas of necrosis and hemorrhage. The immunohistochemical profile showed strong reactivity for CD 34 and vimentin, and focal and weak reactivity for smooth muscle actin. Immunoexpression for S100, NSE, BCL-2, HMB-45, MelanA, AE1AE3 and desmin was lacking.
Discussion and conclusions We present a case of a malignant mesenchymal tumor of vulva. Due to histological features and behavior, pathologists must discard others spindle cell tumors, such as malignant melanoma, malignant peripheral nerve sheath tumor, monophasic synovial sarcoma or leiomyosarcoma. Fibrosarcoma is a diagnosis of exclusion and a wide immunohistochemical panel is useful to make differential diagnosis.

P-087

Serous tumor of borderline malignancy of the fallopian tube - a case report

M Krašević[1], T Stanković[2], O Petrović[2], S Behrem[1]
[1]Department of Pathology, Medical Faculty, University of Rijeka, Rijeka, Croatia
[2]Department of Obstetrics and Gynaecology, Clinical Hospital Center, Rijeka, Croatia

Introduction Serous tumors of borderline malignancy (STBM) of the fallopian tube are exceedingly rare. We report a case of STBM of fallopian tube in a 34-year woman.
Material and methods A 34-year old woman was found to have right adnexal mass on her routine gynaecologic examination. Serum CA-125 was not elevated. At laparoscopy a swollen fallopian tube was removed. During the operation a fine needle aspiration was performed. The cytological findings of the adequate Giemsa-stained smears were recorded. Haematoxylin and eosin-stained sections from the routinely fixed and paraffin embedded surgical material were histologically analysed.
Results A papillary tumor, with maximal diameter of 3 cm in the dilated part of the fallopian tube toward the fimbrial end, was found. Histologic features of the tumor were similar to the atypical proliferative serous tumor of the ovary. Two years after the operation the patient is well, without evidence of the disease.
Conclusion To the best of our knowledge only four cases of STBM of fallopian tube have been reported. Our case is unusual due to lack of any symptoms.

P-088

CDX2 immunoreactivity in primary and metastatic ovarian mucinous tumours

F Fraggetta[1], A Cafici[2], P Scollo[3], P Nuciforo[4], G Pelosi[5]
[1]Department of Pathology, Cannizzaro Hospital, Catania, Italy
[2]Experimental and Clinical Pharmacology University of Catania, Catania, Italy
[3]Department of Obstetric and Gynecology, Cannizzaro Hospital, Catania, Italy
[4]Molecular Pathology Unit, FIRC Institute of Molecular Oncology, Milan, Italy
[5]Department of Pathology and Laboratory Medicine, European Institute of Oncology, Milan, Italy

Introduction The caudal related homeobox transcription factor

CDX-2 regulates intestinal differentiation of the epithelial cells. Recent studies have suggested that in the setting of an unknown primary, CDX-2 immunostaining may be used in identifying a metastatic carcinoma as colonic in origin. Aim: We sought to evaluate the immunoreactivity of CDX2 in a series of primary and metastatic ovarian mucinous neoplasms.
Materials and methods 59 cases of mucinous tumour of the ovary, including 28 benign cystadenomas, 15 borderline mucinous tumours and 16 mucinous adenocarcinomas, were tested for CDX2 immunoreactivity. 25 cases of serous and endometrioid lesions as well as 5 cases of ovarian metastases from colonic adenocarcinoma were also evaluated.
Results CDX2 immunoreactivity was detected in 45/59 (76%) cases of primary ovarian mucinous tumour. Particularly, 20/28 (71,5%) cases of cystadenomas, 10/15 (66,5%) cases of borderline tumours and 15/16 (93,5%) cases of adenocarcinomas were immunostained. Immunoreactivity was usually related to an intestinal morphology. No immunoreactivity was observed in serous or endometrioid lesions whereas all five cases of ovarian metastases from colonic adenocarcinoma were immunoreactive for CDX2.
Conclusions CDX2 immunoreactivity may be detected in the majority of benign, borderline and malignant ovarian mucinous tumour whereas serous and endometrioid lesions are unstained for this marker. CDX2 immunoreactivity is not useful in distinguishing between primary and metastatic ovarian mucinous carcinomas whereas it may be useful in the distinction between endocervical and intestinal type of mucinous tumour of the ovary, which may have clinical relevance. An ovarian primary should be added to the list of CDX2 positive metastatic carcinoma in the setting of an unknown primary.

P-089

Expression of p16INK4A in serous lesions of the female genital tract

C Heffron[1], N Murphy[1], O Shiels, J O'Leary
[1]Coombe Women's Hospital, Dublin, Ireland
[2]Trinity College, Dublin, Ireland

Introduction A spectrum of serous lesions including benign, borderline and malignant tumours and endosalpingiosis commonly arise in tissues of the female genital tract. p16INK4A is a tumour suppressor protein which functions as a cyclin dependent kinase inhibitor and plays a vital role in the cell cycle control at the G1/S phase transition. Although well recognized as a discriminator of benign and potentially malignant squamous and glandular cervical lesions, the expression of p16 in ovarian lesions and their mimics is less well established. The aim of this study was to evaluate p16INK4A expression in serous lesions of the female genital tract and to investigate its potential diagnostic utility.
Methods Immunohistochemical analysis of p16INK4A (mouse monoclonal anti-p16 antibody) was performed on cases of serous epithelial lesions of the female genital tract (n=26) comprising endosalpingiosis, borderline serous cystadenomas of ovary and peritoneum, benign serous cystadenoma of ovary, serous adeno-carcinoma of ovary and peritoneum and normal fallopian tube epithelium.
Results All cases of endosalpingiosis were positive (definite cytoplasmic staining with occasional nuclear positivity) for p16INK4A expression, as were all normal fallopian tube epithelium samples. Varying degrees of p16INK4A expression were found in the serous neoplasms examined, with no clear pattern associated with any histological subtype.
Conclusion Diagnostic difficulties may arise in the distinction between benign serous glandular lesions and more sinister potentially malignant serous neoplasms. In this study the pattern and degree of expression of p16, although showing some differences, does not allow definitive classification of these lesions.

P-090

Epithelioid trophoblastic tumor of the lower uterine segment. An immunohistologic study

PA Nicotina, F Antico, G Basile, O Triolo, D Maisano, A Zangh
Messina, Italy

Introduction Epithelioid trophoblastic tumor [ETT] is an unfrequent gestational trophoblastic disease [GTD], whose epithelial-like cells derive from chorionic-type intermediate trophoblast. ETT mostly shows a benign behaviour, but metastases have also been reported, and pathologic prognosticators are not as yet recognized. The kinase-inhibitor p57KIP2 has been seen to be lacking in malignant GTDs, while different growth factors, such as the C-kit receptor, have been related to growing trophoblasts of p57-null embryos. Since C-kit is said to promote trophoblast growth and invasiveness, this study was aimed at immunolocalizing p57 and C-kit in ETT, as compared to a proliferation antigen.
Materials and methods - After a preterm birth of a living infant, a 37-year-old woman underwent hysterectomy for a postpartum metratonia. The patient had an antecedent miscarriage. A cervical ETT was found, and immunohistology was performed on paraffin sections, using C-kit, p57, and Ki67 antibodies, following a microwave antigen-unmasking. Positive reactions were recorded either as a focal or diffuse immunostaining.
Results and conclusions An escavated, hemorrhagic, endocervical lesion was found, which focally infiltrated the myometrium. Light microscopy showed poorly limited nodules of epithelial-like cells, arranged in cords and nests, with interposed hyaline material, extensive hemorrhages, and necrotic areas. Atypical mononucleate and syncytiotrophoblastic cells occasionally occurred. Immunohistology revealed a diffuse presence of C-kit-expressing tumor cells. The p57 nuclear staining was focally observed to be negative or weak, and Ki67 was totally unlabeled. In conclusion, this slowly-growing ETT is lacking in p57, but the C-kit over-expression substantiates trophoblastic survival and invasiveness.

P-091

Carcinosarcomas of the corpus uteri

R Balan, C Amalinei, C Cotutiu
Histology Department, University of Medicine and Pharmacy, Iasi, Romania

The aim of our study was to analyze the clinical and morphological characteristics of carcinosarcomas of the corpus uteri. 3 carcinosarcomas of the corpus uteri were studied in postmenopausal women. Paraffin-embedded material was stained with hematoxylin and eosin, trichromic, reticulin and PAS staining. Antibodies against EMA, cytokeratins, vimentin, desmin, and PCNA were also used. The size of tumor, depth of myometrial invasion, presence of vascular invasion, necroses, cellular atypia and differentiation, and mitotic activity were analyzed. All tumors were characterized by large size, foci of hemorrhage and necrosis.

Morphological and immunohistochemical analysis proved biphasic structure of the tumors. Epithelial component was represented by adenocarcinomas with high (2 cases) and moderate (1 case) degree of differentiation. All presented homologous pattern – leiomyosarcomas. No metastasis was encountered at the time of diagnosis. As EMA was intensely positive, both in malignant epithelium and in the majority of stromal component, we conclude that carcinosarcomas of the corpus uteri represent combination tumors with both elements originating from a single common stem cell. This conclusion was emphasized by the presence of PAS positive residues in both components.

P-092

Knowledge evaluation among Albanian women on risk factors of cervix cancer

K Kule[1], N Filipi[2]
[1]Institute of Public Health, Unit of Cancer, Department of Epidemiology, Tirana, Albania
[2]University Hospital 'Mother Tereza', Tirana, Albania

Aim This study evaluates the rate of awareness of women on risk factors and the preventive ways for the cervix cancer.
Methods The data were obtained through the questionnaire in a sample of 1660 women aged 20-60 years randomly selected throughout Albania (random cluster sample). The questionnaire included questions on: social-demography, sexual behavior, women health, and sources of the health information.
Results Only 20% of interviewed women were informed on PAP-test. In 60% of cases it was the doctor notified the women of the cluster for this screening as an examination of cervix cancer prevention. The PAP-test examination had been performed by only 12% of the women who had prior knowledge on PAP-test. In about 90% of cases the examination was performed for diagnostic reasons and not for prophylactic control reasons. In proportion to total only 2.5% had performed the test, which presents a very problematic situation. Among the women who performed PAP-test, 40% were aware of the need of periodical check-up every 1-2 year, but 50% of them never performed it. The reason for not doing periodical screening seemed to be the daily routine and fear of the unknown events. 80% of women who performed PAP-test were from the cities. Only 10% of women use contraceptive methods of the family planning. About 35% of women had undergone at least one abortion.
Conclusions The study supports the concept that information on health services as well as health education of women at risk plays an important role in early detection and prevention of cervix cancer.

P-093

Expression of checkpoint proteins p53, Hus-1 and Rad-9 and its relation with apoptosis in ovarian epithelial tumours

J De La Torre[1], R Freire[2], E Salido[2], A Gil[1], J Xercavins[1], S Ramón y Cajal[1], A Garcia[1]
[1]Department of Pathology and Gynecology Oncology Service. Vall d´Hebron Hospital, Barcelona, Spain
[2]Laboratory of Molecular Biology, Research Unit* of Universitary Hospital, Tenerife, Spain

Introduction Eukaryotic cells show surveillance mechanisms (checkpoints) of genomic integrity. An impaired checkpoint has been linked to genomic instability, and, in higher eukaryots has been associated to risk of cancer. The genes to be studied are involved in the mitotic checkpoint and DNA damage checkpoint (like p53, the tumour supressor gene frecuently mutated in human cancers). These proteins are also involved in the checkpoint responding to incomplete DNA replication (replication checkpoint) termed the Rad/Hus group of proteins. Failure of this checkpoint progress can result in genomic instability, and, in higher eukaryotes may lead to tumorigenesis or certain degenerative disease states.
Material and methods We have obtained antisera against recombinant hHus1 and hRad9. For this we will clone and overexpress in bacteria and immunize animals to obtain antisera. We will carry out extensive analysis of the expression levels of several proteins by Western blot analysis. We looked for possibles associations among Hus-1 and Rad-9 immunohistochemical expression and prognosis in ovarian carcinomas prior to chemotherapy. We studied, in addition to the levels of expression of the mentioned proteins, the localization and modifications of these proteins in 130 epithelial ovarian tumours (benign, borderline and carcinomas) in order to establish the probable relationship between these proteins and ovarian carcinogenesis.
Results Increased levels of checkpoint hus-1 protein was related to malignant transformation across all types of ovarian carcinomas ($p<0,05$). Similar results were observed with the expression of rad-9 protein, however was not statistically significant ($p>0,05$). In univariate survival analysis, the expression of hus-1 and rad-9 protein were not significantly correlated with shorter survival and shorter free period of illness ($p>0,05$). There were positive correlation between the apoptotic index, p53 and bax and the expression of checkpoint protein hus-1 ($p<0,05$), but none relation was detected with rad-9 expression ($p>0,05$).
Conclusions 1- The expression of hus-1 is higher in ovarian carcinomas and low in benign and borderline tumours. 2- The expression of hus-1 shows a positive correlation with the apoptotic index and with the pro-apoptotic factors (p53 and bax). 3- There was not statistical significant differences in the expression of Hus-1 and Rad-9 among the different histological types of ovarian tumours. 4- There was a positive correlation between the expression of Hus-1 protein with other prognostic factors such as the FIGO stages, and the histological grade.

P-094

Unilateral gonadoblastoma associated with 46, xy pure gonadal dysgenesis (Swyer's syndrome): a case report

M Velev[1], A Mihova[2], M Popova[3]
[1]City Hospital, 67 A Stoletov Blvd. Pathology Department, Sofia, Bulgaria
[2]National Medical Institution of Transportation, Department of Pathology, Sofia, Bulgaria
[3]City Hospital, 67 A Stoletov Blvd. Department of Oncological Gynecology, Sofia, Bulgaria

Gonadoblastoma develops almost exclusively in gonadal dysgenesis and is often associated with dysgerminoma. We report a 29-year-old female patient with Swyer's syndrome and gonadoblastoma in the right ovary. The patient was a phenotypic female with 46, XY karyotype. The external genitalia were female, the body structure was androgenic with virilization and primary amenorrhaea, with normal serum level of the testosterone. The dimensions of the gonadoblastoma were 2 cm x 2 cm x 1 cm, with proliferation of primitive germ cells, sex cord stromal cells and Sertoli cells organized into nests, separated by dense fibrous stroma

with numerous microcalcifications. The patient underwent bilateral salpingoophorectomy and total hysterectomy. The authors underline the importance of the correct diagnosis and the need of bilateral salpingoophorectomy for preventing the possible progression of the gonadoblastoma into malignant germinal cell tumor.

P-095

Histological and electron microscopic identification and analysis of uncommon particles in tissue after use of orthopaedic implants

M Huber[1], G Reinisch[2], F Lintner[1], K Zweymüller[3]
[1]Pathology & Bacteriology, SMZ Otto Wagner Hospital, Vienna, Austria
[2]Institute for Micro Technique and Precision Engineering, Vienna, Austria
[3]Orthopaedic Hospital Gersthof, Vienna, Austria

Introduction Deposits of solid products occur widely in tissue either from endogenous sources due to pathological changes, or from exogenous sources. After use of orthopaedic implants, particles produced by wear are commonly recognizable and identifiable in tissue by the surgical pathologist. Foreign body related tissue re actions may contribute to aseptic loosening of implants, which is regarded as one of the most significant complications in orthopaedic surgery. In the present study we report on very uncommon particles in periprosthetic tissue after aseptic loosening of metallic implants. Our study was performed to identify particles in periprosthetic tissue and to clarify whether they may contribute to the loss of implants.
Materials and methods Periprosthetic tissue including joint capsule, acetabular and femoral interface membranes of 62 cases of aseptic loosened cementless total hip replacements was histologically investigated. Four cases with present uncommon particles were selected for electron microscope investigation and dispersive x-ray analysis.
Results In four cases the histological investigation revealed uncommon green to yellow coloured foreign bodies. By the use of electron scanning microscopy and energy dispersive x-ray analysis, these particles were identified as deposits rich in chromium, phosphorus and oxygen. This detection indicates the presence of solid corrosion products derived from implant surfaces.
Conclusion Particles produced by wear and/or corrosion are associated with an alteration of the environment and the development of periprosthetic osteolysis which may result into the loss of the implant. The surgical pathologist should be aware that corrosion products may occur. Their identification is helpful to determine implant failures.

P-096

Paratesticular lipoleiomyosarcoma: a case report

L Kachko, R Shaco-Levy, I Sinelnikov, J Goldstein
Department of Diagnostic Pathology, Soroka Medical Center, Beer-Sheva, Israel

Introduction Leiomyomatous differentiation in liposarcoma is a rare phenomenon and may occur as a well differentiated liposarcoma with an intrinsic malignant smooth muscle component, so called " lipoleiomyosarcoma" or in the context of "dedifferentiated" liposarcoma.
Material and methods We have studied a paratesticular lipoleiomyosarcoma in a man 63 years old. Gross examination revealed 4 tumor nodules dispersed between identifiable testis and epididymis, the largest of which measured 13x7x4 cm. The specimen cut surface revealed smooth yellow tissue with distinct areas of gray myxomatous change. Microscopically the specimen consisted of a well differentiated lipoma-like, sclerosing liposarcoma with mature adipocytes and fibrous septa containing spindled and floret-like cells. The smooth muscle accounted for about 40% of the total tumor mass and consisted of fascicles and bundles of spindle cells with very little atypia or pleomorphism. Mitotic activity was moderate at most and focal in distribution. The cells colored well with immunohistochemical stain against SMA.
Results and conclusions An extraordinary rare combination-type tumor is presented. Only two previous examples of paratesticular lipoleiomyosarcoma have been published. The nature of combination-type tumors and dedifferentiated liposarcoma is addressed. The existence of two lines of tissue differentiation in the same tumor suggests the possibility of two separate tumors arising together or two lines of differentiation appearing from one pluripotent precursor cell. The differential diagnosis includes angiomyolipoma, which should be HMB45 positive.

P-097

Expression of estrogen receptor (ER) and progesterone receptors (PR) in renal angiomyolipoma

N Savelov, G Chemeris, I Sokolova
Cancer Research Center, Moscow, Russian Federation

Introduction Angoimyolipomas are the most common mesenchymal tumours of kidney. They are more common in female. Possibly estrogen and progesterone influence on tumours growth. We investigated the expression of estrogen receptors (ER) and progesterone receptors (PR) in renal angiomyolipomas.
Materials and methods 28 renal angiomyolipomas from 24 patients were tested. The expression of ER and PR was studied immunohistochemically. The expression of HMB-45, alpha-smooth-muscle actin and vimentin was also studied in all cases.
Results Most angiomyolipomas were of classic morphology with one exception. In that case, classical angiomyolipoma was combined with cystic hamartomatous lesions and involvement of regional lymph nodes. The vast majority of cells in the cases with typical morphology expressed alpha-smooth-muscle actin. Expression of HMB-45 was diffuse or focal. In the case with cystic hamartomatous lesions, an inverse correlation of expression of HMB-45 and alpha-smooth-muscle actin was observed in both renal and extrarenal components. Of the 28 tumours, two tumours were only ER positive and three tumours were ER and PR positive. In four cases, focal immunoreactivity for ER was mainly observed in the spindle shaped cells. In two cases, the immunoreactivity for PR was diffuse, but less than 5 percent of cells were positive. ER and PR positivity was diffuse, strong and widespread only in the case with cystic hamartomatous lesions.
Conclusion To our knowledge, estrogen and progesterone are not critical players in all angiomyolipoma growth, but only in the specific cases.

P-098

Proto-oncogene c-kit and c-myc expression in Kaposi sarcomas

P Ravazoula, A Tsamandas, S Sidira, P Aroukatos, D Koumoundourou, D Bonikos
Department of Pathology, University Hospital of Patras, Patras, Greece

Introduction c-kit proto-oncogene encodes a transmembrane receptor tyrosine kinase that has been shown to be structurally related to the platelet-derived growth factor receptor. c-kit gene mutation has been shown as a mechanism of c-kit oncogene activation in human mast cell disease and gastrointestinal stromal tumors. c-myc oncogene is believed to function as a sequence specific transcription factor regulating genes which control cell growth, differentiation and cell death. c-myc point mutation has been identified in Burkitt's lymphoma. The aim of our study is to identify the expression of c-kit and c-myc proteins in Kaposi sarcoma.
Materials and methods Tissue sections from 77 Kaposi sarcomas were stained immunohistochemically with anti-c-kit and anti-c-myc proto-oncogene protein product.
Results Only 31% of Kaposi sarcomas were positive for c-kit and the staining in these lesions was usually focal. The percentage of positive cells was 5% - 10%. c-myc expression was noticed in 36/77 (~47%) of Kaposi sarcomas. Staining was also observed in early Kaposi lesions.
Conclusions 1) c-kit and c-myc protein expression in Kaposi sarcomas suggest that these genes may play a role for tumor growth. 2) c-myc protein expression in early Kaposi lesions suggests that this gene may be implicated in the initiation of these tumors.

P-099

CD10 expression in malignant myofibroblastic and smooth muscle tumors

T Hirose[1], T Shimada[1], T Sano[2], T Hasegawa[3]
[1]Department of Pathology, Saitama Medical School, Saitama, Japan
[2]Department of Pathology, University of Tokushima School of Medicine, Japan
[3]Division of Pathology, National Cancer Center Research Institute, Japan

Introduction Myofibroblastic tumors are sometimes difficult to be distinguished from smooth muscle tumors. Recently, CD10, a cell surface metalloprotease, was shown to be present in myofibroblasts within the stroma of infiltrating cancers. To clarify the specificity of CD10 expression in myofibroblasts, we performed immunohistochemical studies on myofibroblastic and smooth muscle tumors.
Methods and materials consisted of 25 myofibroblastic and 22 smooth muscle lesions, ranging from reactive to benign and malignant tumors. All myofibroblastic lesions arose in soft tissue and smooth muscle tumors in soft tissue and organs. Using paraffin sections, immunohistochemical staining for CD10 (clone: 56C6, Serotec) was carried out by an automated stainer (BENCHMARK, Ventana).
Results Significant CD10-expression was demonstrated only in malignant or borderline lesions, including malignant fibrous histiocytoma (3 of 3 cases), low grade myofibroblastic sarcoma (4 of 7), inflammatory myofibroblastic tumor (3 of 3), and leiomyosarcoma (3 of 6). However, no positive reaction was seen in reactive lesions and benign tumors, such as scar (1 case), nodular fasciitis (4), superficial fibromatosis (3), desmoid (4), leiomyoma (7), vascular leiomyoma (3), angiomyolipoma (2), and glomus tumor (4). Furthermore, the intensity of staining was almost parallel to the microscopic anaplasia.
Conclusion The present study demonstrated that CD10 expression is not specific to myofibroblasts, but seems to be related to the biologic aggressiveness of myofibroblastic and smooth muscle tumors. Therefore, CD10 expression may be a potential predictor of malignancy in these tumors.

P-100

Correlation of metallothionein (MT) and antigen Ki-67 expressions with grade of malignancy (G) in some soft tissue sarcomas

P Dziegiel[1], P Surowiak[1], M Zabel[1,3], W Salwa-Zurawska[2], A Wojnar[4]
[1]Department of Histology and Embryology University School of Medicine, Wroclaw, Poland
[2]Chair and Department of Pathomorphology in Poznań, Poland
[3]Chair and Department of Histology and Embryology in Poznań, Poland
[4]Institute of Patomorphology, Lower Silesian Oncology Centre, Wroclaw, Poland

Introduction In soft tissue sarcomas the most significant prognostic criteria include grade of malignancy (G) and size of the tumour. Recently, metallothionein (MT) expression in cells of some malignant tumours has been shown to carry prognostic potential. Present study aimed at comparing expressions of MT and of Ki-67 antigen with G in selected sarcomas of soft tissues.
Materials and methods Immunocytochemical studies were performed on paraffin sections in 54 cases of malignant fibrous histiocytoma (MFH) and 18 cases of liposarcoma. Intensity of MT and Ki-67 expression was evaluated and the obtained results were compared to G grades.
Results Expression of MT was noted both in the cytoplasm and in cell nuclei in all studied sarcomas. Its intensity was high in 33% tumours, moderate in 35% tumours and in 32% it was low. In MFH and in liposarcoma a correlation was demonstrated between MT expression and G ($r = 0.7$; $r = 0.8$; $p < 0.05$), between MT expression and expression of Ki-67 ($r = 0.7$; $r = 0.75$; $p < 0.05$) as well as between Ki-67 expression and G ($r = 0.53$; $r = 0.74$; $p < 0.05$).
Conclusion Expression of MT in soft tissue sarcomas of MFH type and liposarcoma type strongly correlates with intensity of proliferation and with the grade of the tumour. Both markers may be helpful in determining the extent of malignancy of these tumours.

P-101

Occurrence of tumor-like lesions in pediatric orthopedics - 9 years of experience

M Antonic[1], R Brdar[2], J Sopta[3]
[1]The School of Medicine, Belgrade, Serbia and Montenegro
[2]The University Children's Clinic, Belgrade, Serbia and Montenegro
[3]The Institute for Pathologic Anatomy, Belgrade, Serbia and Montenegro

Introduction Tumor like lesions: solitary and aneurysmal bone cyst, non-ossifying fibroma, eosinophilic granuloma and fibrous

dysplasia may be found in the bones during the childhood and adolescence. They can cause pathologic fractures and deformities of involved bone. Rarely, some of them (fibrous dysplasia), undergo malignant transformation. The aim of this study is to analyse all the cases of tumor-like lesions of bones in children and adolescents, during the period time1993-2001.

Materials and methods The study was performed at the Institute for Pathologic Anatomy, School of Medicine Belgrade. The data source was The Bone and Joint Tumor Registry. The study was a retrospective analysis of 216 patients who had tumor-like lesion before the age of 18.

Results Solitary bone cyst was the most common lesion (64 patients). The median age was 9 years for fibrous dysplasia and solitary bone cyst, 16 years for aneurysmal bone cyst and eosinophilic granuloma, and 14 years for non-ossifying fibroma. Male to female ratio was 1:1.2 for fibrous dysplasia, 1:1.25 for aneurysmal bone cyst, 2.7:1 for solitary bone cyst, 2.3:1 for eosinophilic granuloma and 1:1 for non-ossifying fibroma. The most common sites were femur for fibrous dysplasia and aneurysmal bone cyst, humerus for solitary bone cyst, tibia for non-ossifying fibroma and bones of scull and vertebrae for eosinophilic granuloma. The most frequent symptoms and signs were pain, pathologic fractures and swellings.

Conclusion The results of our study mostly correspond to those of the current literature.

P-102

Extraspinal myxopapillary ependymoma. Case report and literature review

O Balague, R Orellana, LE Pons, M Rey
Corporació Parc Taulí, Sabadell, Spain

Introduction Ependymomas are glial tumors that on rare occasions occur in subcutaneous locations dorsal to the sacrum and coccyx.

Case report A 35-year-old woman presented with a soft tissues tumor in the intergluteal region. MRI revealed a 7cm large mass, with solid and cystic areas, located below the coccyx, without bone alteration. Surgical excision was performed.

Pathological features Grossly, the tumor was encapsulated and showed solid, spongy and myxoid areas with a peripheral hemorrhagic focus. Histologically it consisted of medium-sized cuboidal-columnar cells, with round-oval nuclei, granular cromatin and eosinophilic cytoplasm. Tumor cells showed myxopapillary and cystic-papillary growth pattern or were arranged on fibrovascular stalks, with a central hyalinized wall vessel, surrounded by a single layer of cuboidal cells. Tumoral necrosis and hemorrhage were observed. The peritumoral stroma was highly hyalinized. The immunohistochemical stains showed vimentin(+), S-100(+), GFAP(+) and keratins(-).

Discussion and conclusion Extraspinal ependymoma (EE) is a rare tumor usually localized subcutaneously in sacrococcygeal region of young adults; most are of myxopapillary type. EE may arise from normal remnants of the neural tube or from abnormal remnants resulting from embryologic malformations. EE has a greater propensity to metastasize than its intraspinal counterpart, because of easier accessibility to lymph channels. In a study of 32 cases, Elson found a metastases incidence of 20% and no clinical or histologic data was found to predict the biological behavior of the tumor. The differential diagnosis must be done with choroid plexus papilloma, myxoid chondrosarcoma, chordoma, meningioma, adenoid cystic carcinoma and paraganglioma.

P-103

Madura foot caused by Pseudoallescheria Boydii - a case report

J Sopta[1], S Popovic[2], L Markovic[3], M Atanackovic[1], V Raspopovic[4]
[1]Institute of Pathology, School of Medicine, Belgrade, Serbia and Montenegro
[2]2 Departmant of pathology and molecular medicine, McMaster University, Hamilton
[3]Institute of pathophysiology, School of medicine, Belgrade, Serbia and Montenegro
[4]Institute of orthopedics and traumathology “Banjica”, Belgrade, Serbia and Montenegro

Introduction Fungal infections of bone represent about 0,1-0,2% of all osteomyelitis cases. The disease most often affecting the feet - mycetoma pedis, is also known as Madura foot. In our geographic regions mycetoma is extremely rare. It is endemic in tropical and subtropical countries.

Case report We present a case of mycetoma pedis - Madura foot. The patient was a 50 years old woman. The clinical signs were pain, indurations and local redness with a long history of 10 years. The surgical material was routinely stained with hematoxylin-eosin (HE). Pathologically, a granulomatous inflammation of the bone was confirmed. All pathological characteristic pointed to fungal infection in the form of mycetona pedis. Special stains (PAS, Grocott's hexamine-silver and Giemsa) for fungi were performed: and the diagnosis of a mycetoma was confirmed. For the definitive microbiological analysis tissue inoculation on the Sabouraud dextrose agar laboratory media was done. Pseudoallesheria boydii - a sexual staging of Monosporium apiospermum was isolated. After microbiological verification of fungal infection the patient was treated surgically. Seven months after first operation the patient developed similar clinical signs again. The diagnostic procedure was repeated and mycetoma was confirmed again. The surgical therapy was performed as a therapy of choice because Pseudoallesheria boydii does not react to treatment with antimycotic drugs.

P-104

Pleomorphic variant of a spindle cell lipoma

F Staniceanu[1], S Zurac[2], C Ardeleanu[3], G Micu[2], E Gramada[2], O Popescu[4], I Boiangiu[4]
[1]University of Medicine and Pharmacy, Colentina Hospital, Department of Pathology, Bucharest, Romania
[2]Colentina Hospital, Department of Pathology
[3]University of Medicine and Pharmacy, Victor Babes Institute, Department of Pathology
[4]Reconstructive and Plastic Surgery Hospital, Department of Surgery

Spindle cell lipoma is a rare entity with an uncertain histogenesis; although the current classification includes this tumor in the lipomatous neoplasms, the immunohistochemical and electron microscopic data suggest a much closer link to the fibrous solitary tumor. We report the case of a 35 years woman with a 4/2/2/ cm nodule in the scapular area; the histopathologic examination revealed a tumor proliferation consisting mainly of giant cells, most of them multinucleated with floret-like appearance. The stroma consisted of an abundant collagen deposition with rope-like fascicles and prominent myxoid changes, most striking in the periphery of the tumor. The tumor proliferation was contiguous with nearby adipose tissue with no capsule in-between. Immuno-

histochemical tests revealed diffuse positivity for CD 34; PCNA was positive in 3 % of the cells. Smooth muscle actin, desmin and S100-protein were negative in tumor cells. The patient is well with no recurrence of the tumor one year after the resection. Despite the highly pleomorphic histopathologic appearance the tumor is benign with an uneventful clinical behaviuor.

P-105

Expression of p53 protein in GCT of bone with lung metastases

M Atanackovic[1], J Sopta[1], S Popovic[2], N Lujic[3]
[1]Institute of Pathology, School of Medicine, Belgrade, Serbia and Montenegro
[2]2 Departmant of pathology and molecular medicine, McMaster University, Hamilton
[3]Institute of orthopedics and traumathology "Banjica", Belgrade, Serbia and Montenegro

Introduction The giant cell tumor of bone (GCT) is a local osteolytic tumor with variable degrees of aggressiveness. In rare cases pulmonary metastases can be observed. The stromal cells are the neoplastic components of the GCT, and are probably responsible for biological behavior of the tumor.
Method and results In the last 10 years 2 cases of GCT with lung metastases were diagnosed at the Institute of pathology, School of medicine, Belgrade. Both tumors displayed characteristic histological appearance of GCT: a high number of osteoclast-like multinucleated giant cells and two mononuclear cell types. The first one resembles a monocyte, the second are fibroblast-like stromal cell. Mononuclear cells had benign cytological characteristics without polymorphism and mitosis. To elucidate the mechanism of metastasing, we searched for the molecular abnormalities of p53. We examined the expression of p53 in stromal cells immunohistochemically. Unexpectedly, both tumors were p53 negative and we could not show correlation between p53 expression and metastasing of GCT to the lung.
Conclusion Although p53 positivity in other tumors is closely associated with aggressive biological behavior we could not confirm this association for GCT.

P-106

Trichoblastic fibroma or primary soft tissue adamantinoma?

P Medley, EJ Raubenheimer
Medical University of South Africa, Pretoria, South Africa

Introduction Benign extragnathic tumors that may mimic the histological features of odontogenic ameloblastoma (and ameloblastic fibroma) include trichoblastic fibroma and primary osseous and soft tissue adamantinoma. Trichoblastic fibroma is a rare ectomesenchymal tumor of hair germ involving most often the dermis and subcutis of the head and neck. The mean age at presentation is 63,8 years.The youngest case reported was that of a shoulder tumor in a 49 year old female. Its occurrence in the soft tissue of the upper arm has not been documented. Primary soft tissue adamantinomas are extremely rare with isolated cases reported in the region of the jaw and the leg ie. close to sites where odontogenic and primary osseous adamantinomas occur, respectively. No cases involving the upper arm have been reported. We report a case of a benign appearing adamantinoid tumor involving the deep soft tissue of the upper arm.
Methods A 33 year old Black male presented with a slow growing mass involving the deep soft tissue of the left upper arm without associated cutaneous or osseous abnormalities.
Results The adamantinoid features in this benign appearing biphasic tumor included nests and acini of palisading columnar epithelium exhibiting reversed nuclear polarity, areas reminiscent of stellate reticulum and an intimately associated spindle cell proliferation.
Conclusion Our favored diagnosis was a trichoblastic fibroma but we discuss the complete differential diagnosis of all tumors with adamantinoid features with respect to clinical, morphological and immunohistochemical characteristics.

P-107

Intraosseous lipoma - a case report

V Janevska[1], L Spasevska[1], G Zafirovski[2], M Samardziski[2], J Zivadinovic[1]
[1]Institute of Pathology, Faculty of Medicine, Skopje, Republic of Macedonia
[2]Clinic for Orthopedic Surgery, Clinical Center, Skopje, Republic of Macedonia

Intraosseous lipoma is a rare benign tumor of mature adipocytes arising in the medullary canal, most often diagnosed incidentally. Most of these tumors occur in the long bones, with propensity for the proximal femur, fibula, and tibia. Ribs, calvarium, sacrum, metatarsus and calcaneus are other frequent sites. We report a case of a 49-yearold female with a histologically verified solitary intraosseous lipoma involving the distal part of the right fibula. Radiographically the tumor was a lytic benign-appearing lesion with sharply demarcated borders surrounded by a zone of sclerosis. Computed tomographic scan showed the lesion to have features of adipose tissue. The examination was made on surgically removed distal part of the right fibula. For histological verification of intraosseous lipoma, resected bone was decalcified, embedded in paraffin and stained with standard staining with hematoxilin-eosin. Histopathologic examination revealed mature adipose tissue with widely scattered trabeculae of bone and central calcifications. This case emphasizes the characteristics of intraosseous lipoma, and highlights the need for clinicopathologic and roentgenographic correlations.

P-108

FasL, C-ErbB2, Cyclin D1, p53 and TGFB3 expression in osteosarcomas: Evaluation of relationship with clinicopathologic parameters

G Gonlusen[1], A Uguz[1], F Bolat[1], M Ergin[1], S Ozbarlas[2]
[1]Cukurova University School of Medicine Dept. of Pathology, Adana, Turkey
[2]Cukurova University School of Medicine Dept. of Orthopedy, Adana, Turkey

Introduction FasL, c-erbB2, cyclin D1, p53 and TGFB3 are molecules which were shown to be related to prognosis of tumors. In this study expression of these molecules were evaluated in 36 osteosarcoma (Os) cases. The correlation between the expressions and age, gender of the patients, location, grade, and histologic subtype of tumors were investigated.
Material and method FasL, c-erbB2, cyclin D1, p53 and TGFB3 expressions were detected immunohistochemically.
Results Thirty-six Os cases (23 osteoblastic, 8 fibroblastic, five chondroblastic) were included in the study. Twenty-two were males

and 14 were females. Os were located in the extremities (25), jaw (6), pelvis (3), vertebra (2). Twenty-five of 36 were high grade and 11 were low grade tumors. FasL and p53 were detected in 41.7% of the cases, TGFB3 in 80.6%, c-erbB2 in 16.7%, and cyclin D1 in 8.3%. There were statistically significant correlations between FasL and tumor grade (p: 0.001), FasL and TGFB3 (p= 0.027), FasL and c-erbB2 (p= 0.003), p53 and TGFB3 (p= 0.027). No correlation was found among other parameters.
Conclusion Expression of these molecules and detection of correlation between some molecules show that pathogenesis of Os is a complex mechanism regulated by several molecular factors. Better insight into tumorigenesis may help to provide new therapeutic approaches and idntification of patients with better prognosis.

P-109

Does hemosiderin deposition have important role in accumulation of macrophages in total hip prostheses loosening?

A Rotter[1], S Kovac[2], V Pisot[2], R Trebse[2]
[1]Institute of Pathology, Medical Faculty, University of Ljubljana, Ljubljana, Slovenia
[2]Valdoltra Orthopedic Hospital, Ankaran, Slovenia

Introduction Granulation tissue with macrophages is usually found around loose total hip prosthesis (THP), usually explained with deposition of wear debris from THP. However, we often found a lot of hemosiderin (an insoluble form of storage iron) in macrophages. The aim of this study was to evaluate the amount of hemosiderin in granulation tissue around THP removed after relatively short period of duration, and compare it with an interface tissue around THP of very long duration.
Material and methods We assessed the interface tissue around the loosened THP of the longest duration described ever (Judet's THP was removed after 51 years) and compared it with the granulation tissue around THP of short duration (less than six years). At histology H&E, Giemsa, and Weigert-Van Gieson staining were used. For the demonstration of hemosiderin Perls' reaction and for macrophages CD68 were used. We compared the results of histologic evaluations performed according to modified Mirra's classification: semi quantitative assessment of neutrophils, mononuclear histiocytes, chronic inflammatory cells, giant-cells, metal particles, polymethacrylate globules, necrobiosis, bone chips, necrosis and necrotic debris. But, we also included the assessment of the intensity of hemosiderin deposition.
Results Comparison of granulation tissues of short duration THP to that of 51-year duration revealed a surprising difference in the amount of hemosiderin particles with intensive intracellular hemosiderin deposition in mononuclear macrophages and giant cells in the first group. In the 51-year-old THP there was predominantly hypocellular tissue with very little amount of mononuclear macrophages containing slight amount of intracellular hemosiderin deposition and no multinucleated giant cells at all.
Conclusions We don't know why hemosiderin deposition is more evident in early loosening of THP. Hemosiderin deposition may give rise to accumulation of macrophages, perhaps increasing the process of osteolysis and granulation tissue formation. But more 'aggressive' forms of loosening may also cause recurrent bleeding. Whether the higher level of hemosiderin is the cause or the result of the loosening of THP is to be determined.

P-110

The types of tumor and peritumor stroma and biological behavior of fibrohistiocytic tumors

L Zolotarevski[1], V Jacevic[2], S Ilic[1], S Cerovic[1], G Brajuskovic[1]
[1]Institute of Pathology, Military Medical Academy, Belgrade, Serbia and Montenegro
[2]National Poison Control Center, Military Medical Academy, Belgrade, Serbia and Montenegro

Introduction Tumor-host interaction induces different types of tumor and peritumor stroma which may reveal some aspects of tumor biology. The aim of this study was to establish a correlation between different types of tumor and peritumor stroma of fibrohistiocytic tumors (FH tumors) and their biological behavior.
Materials and methods The presence of colagenous-reticular (CR), myxoid (MYX) and mixed (MX) tumor and peritumor stroma was determineted on selected paraffin sections stained by Masson-trichrome, silver impregnation, alcian blue with and without hialuronidase pretretment and PAS reaction of 121 FH tumors: 69 benign (BFH), 14 dermatofibrosarcoma protuberans (DFSP) and 38 malignant (MFH), all graded in three degrees of malignancy. The collected data were statistically evaluated by means of Student T proportion test.
Results The difference in presence of MYX and MX tumor and peritumor stroma in relation to the CR type was statistically significant between MFH and BFH ($p<0,001$) or DFSP ($p<0,05$). With an increasing malignancy grade of MFH percentage of tumors with CR tumor stroma was decreasing and percentage of tumors with MYX and MX tumor stroma was increasing. However, MFH of G1 and G2 malignancy grade did not differ in distribution of peritumor stroma types, but 73,7% of MFHG3 had MYX and MX peritumor stroma.
Conclusion While MYX and MX types of tumor and peritumor stroma are associated with agressive, CR type of tumor and peritumor stroma is associated with benign and less agressive FH tumors.

P-111

Dynamic angiogenic models of human soft tissue tumors transplanted into immunodeficient nude mice

A Llombart Bosch, JA Lopez-Guerrero, C Carda-Batalla, A Peydró-Olaya
Depto. Patologia, Facultad de Medicina, Valencia, Spain

Introduction Animal models were used to study the vascular neogenesis of tumors. We undertook experiments using human sarcomas transplanted into the subcutaneous pad of immunodeficient nude mice. The aim of this study was analysis of: the microvasculature present within the tumor before the transplant; the early stages of the neovascularization; and the types of vascular connections established between the host and the tumor graft.
Material and methods Implants of 0.3-0.4cm in size of a Ewing's sarcoma (ES), an osteosarcoma (OS) and a fibrosarcoma (FS) were analyzed. The study was successively followed for 24, 48, 72 hours, one, two, three and four weeks. HE, PAS and immunohistochemistry for angiogenic factors were complemented with electron microscopy.

Results After 24-48 hours, the implants over-expressed several angiogenic factors. At this stage, the tumors initiated an active angiogenic remodeling in the surrounding stroma where capillary congestion and microhemorragies occurred. Endothelial sprouting of the host capillaries was seen. Vascular co-option between the endothelial cells, newly formed endothelial cells and the tumor cells was observed. No clear basal lamina was seen. Tumor-endothelial cell mosaics and vascular mimicry were detected only in the ES and OS.
Conclusions Vascular expression and neogenesis varies considerably from the fast ES to the FS while the OS reproduces patterns that are common in all three. Based upon present experience it seems evident that each tumor shows a different type of neovascularization. These models provide excellent examples of all the systems that are involved in the recapillarization of a sarcoma. This work has been supported by grants FIS 01/ 0673 and FIS 01/702 from the Ministry of Health, Madrid, Spain.

P-112

Prognostic significance of intratumoral neoangiogenesis in childhood osteosarcoma and Ewing sarcoma

D Mikulic[2], I Ilic[1], M Coric[1], L Batelja[1], J Stepan[2], S Seiwerth[1]
[1]Institute of Pathology Medical Faculty, Zagreb, Croatia
[2]Childrens Hospital, Zagreb, Croatia

Introduction Intratumoral neoangiogenesis quantified by microvessel density (MVD) has been shown to be a strong prognostic indicator in a number of malignant tumors, primarily carcinomas. Its association with prognosis in bone sarcomas has been subject to less extensive research. The aim of our study was to investigate clinical significance of neoangiogenesis in osteosarcoma and Ewing sarcoma.
Patients and methods A retrospective immunohistochemical study was performed. 39 patients with osteosarcoma and 27 patients with Ewing sarcoma were included. Sections from diagnostic biopsies were immunostained using factor VIII and CD 34 (DAKO) antibody and microvessels were counted at 400x magnification on three microscopic fields showing highest MVD per patient. MVD was correlated with overall and event-free survival by Kaplan-Meier and log-rank analysis. The difference between the mean microvessel counts in patients with or without metastasis and alive or dead was assessed by Mann-Whitney test.
Results In patients with osteosarcoma significant statistical difference was found as regards the death risk and risk of development of metastasis between patients with high (>31 vessels/field) and low (<31 vessels/field) microvessel counts (log-rank test p=0.0027 and p=0.0209, respectively). In patients with Ewing sarcoma a trend was noted for the patients with lower (<31.5 vessels/field) microvessel counts to have better outcomes than patients with higher vessel counts, however, the difference was not statistically significant.
Conclusion These findings strongly suggest that neoangiogenesis quantified by microvessel density is predictive of metastasis and poor prognosis in osteosarcoma. Valorization of its role in patients with Ewing sarcoma awaits further studies.

P-113

Epithelioid sarcoma - clinicopathological findings in 6 cases

M Demiryont[1], B Bilgic[1], T Özkan[2], H Özger[3], M Basaran[4]
[1]Istanbul Medical Faculty, Pathology, Istanbul, Turkey
[2]Istanbul Medical Faculty, Plastic and Reconstructive Surgery, Istanbul, Turkey
[3]Istanbul Medical Faculty, Orthopedic Surgery, Istanbul, Turkey
[4]Institute of Oncology, Medical Oncology, Istanbul, Turkey

Epithelioid sarcoma is a soft tissue sarcoma of unknown histogenesis with a predilection of young adults and hand/forearm location.The tumor is often multinodular showing central necrosis. Epithelioid sarcoma has a high potential of local recurrence and metastasis. Six cases were presented. Five patients were male with a mean age of 30. Tumor locations were finger, hand and forearm. Cytokeratin and vimentin were positive in all cases. Four cases showed positivity for CD34. Desmin and CD31 were negative. Ki-67(MIB-1)proliferation index was 12-15% in 4 cases. Initial surgery performed in all of the patients has been local excision with negative margins.Three patients received radiotherapy or chemotherapy after the primary excision.Except for one patient who was lost to follow-up, local recurrence was detected in all the patients in a period of 2 months to 2 years.Three patients died with distant metastasis. Epithelioid sarcoma can be easily identified with its typical features, but it can be confused with non-tumor lesions in patients having a long clinical history and a small tumor. Radical surgery and regional lymph node dissection may bring benefit; the incidence of the lymph node metastasis is high. Radiotherapy and chemotherapy can be added to therapy in the recurrent or metastatic state of the disease.

P-114

Intramuscular hemangioma of mixed type

D Tasic-Dimov[1], D Dimov[1], J Gligorijevic[1], L Velickovic[1], M Krstic[1], K Katic[1], I Dimov[2]
[1]Institute of Pathology Nis, Nis, Serbia and Montenegro
[2]Medical Faculty of Nis, Nis, Serbia and Montenegro

Introduction Intramuscular hemangiomas are relatively uncommon but significant lesions, and their unorthodox location and infiltrative pattern often raise the question of malignancy to clinician and pathologist. We present the histomorphological and immunohistochemical data of a hemangioma in a 20-year-old man who presented with an enlarging painful soft tissue mass of his right upper leg.
Methods The complete local excision of tumor arising in the quadriceps muscle was done. Sections of formalin-fixed, paraffin-embedded tissue material were stained with HE, Van Gieson, PAS, PTAH, Gomori's reticulin and trichrome, and immunohistochemically for detection of factor VIII-related antigen.
Results Grossly, the lesion (1x2,5 cm) was poorly circumscribed, reddish brown and partially haemorrhagic. Microscopically, it was composed both of small, capillary-sized and large, cavernous vessels lined by endothelial cells and surrounded by connective and mature adipose tissue. The adipocytic component wasn't prominent. Many cavernous spaces were separated by dense fibrous tissue and some of them were thrombosed. Foci of hemosiderin deposits and moderate lymphocytic infiltration were

also noted. The small vessels in some areas hadn't discernible lumina so that areas appeared solid. Mitotic figures and intraluminal papillary tufting were not seen, but infiltration of skeletal muscle bundles and rarely perineural spaces were present. The muscle fibres showed atrophy, degenerative changes and signs of regeneration. The cells lining both cavernous and capillary-sized vessels showed expression of factor VIII-related antigen.
Conclusions Presented case of tumor arising in the quadriceps muscle show histomorphological and immunohistochemical features of mixed type hemangioma with pronounced infiltrative pattern.

P-115

Alveolar soft part sarcoma: a review of 8 cases at National cancer institute from Colombia

OL Mejia Mejia
Instituto Nacional de Cancerología, Colombia, Bucaramanga, Columbia

Aims To review the histology and immunohistochemistry of alveolar soft part sarcoma with comparison of clinical features.
Material and methods Histology slides, paraffin blocks and files of patients were reviewed.
Results and discussion There were 8 patients retrospectively analysed, 5 female and 3 male, between 1 year and 39 years old. The initial symptom was mass. The most frequent location was thigh (25%), followed by the leg, orbit, chest wall, trunk, arm and forearm. Six patients had haematogenous metastases at the time of diagnosis (lung 4, brain 1, lung and bone 1). Histologically, all tumours were composed of nests of medium sized cells arranged in pseudo-alveolar or lobular patterns, separated by fibrovascular stroma. PAS & PAS diastase were positive in all cases, with rhomboid or rod-shaped crystals. Immunohistochemical staining for Myo D1 showed cytoplasmic positive in 8 cases (100%), desmin in 4 and smooth muscle actin in 2 cases.
Conclusion Alveolar soft part sarcoma is an uncommon neoplasm. The microscopic picture is a constant and typical feature of the lesion, and immunohistochemistry is a useful complementary method for diagnosis.

P-116

Malignant peripheral nerve sheath tumor with a t(X;18)

A Jiménez Sánchez, EM Huertas Valero, JA Ramos Ńíguez, R Baeza Guixot, P Sánchez Cańizares
Hospital Francesc de Borja de Gandia, Gandia, Spain

Introduction Malignant epithelioid schwannoma is a rare variant of malignant nerve sheath tumor (MPNST) that often causes differential diagnostic problems with other neoplasm.
Material and methods A 56-year-old woman presented with a palpable tumor located in the supraclavicular region. The lesion was partially resected. Grossly, the tumor was firm, gray to whitish and slighty nodular. Standard histological procedure and inmunohistochemical study was performed.
Results Microscopic examination revealed a solid proliferation of moderately large, rounded epithelioid cells, with pleomorphic nuclei, prominent nucleoli and atypical mitoses. In peripheral areas the tumor showed smaller cells with nuclei arranged in palisades and central necrosis. Immunohistochemical studies showed vimentine, S-100 protein, and cytokeratine positivity and HMB-45 negativity. The histopathology and the immunohistochemical results were consistent with MPNST, but a SSX2/SYT gene fusion was detected by molecular analysis, a characteristic chromosomal change of synovial sarcoma (SS).
Conclusions Spindle cell tumors with epithelioid areas can be difficult to diferentiate by histologic pattern alone. Cytogenetic analysis and molecular studies may reveal the diagnosis by demonstrating a characteristic chromosomal abnormality or molecular rearrangement. SSX/SYT gene fusion results from the t(X;18)(p11.2;q11.2). The translocation fuses the SYT gene from the chromosome 18 long arm to either of 2 highly homologous genes on the chromosome X short arm, SSX1 or SSX2. The translocation t(X;18) is currently regarded as a specific molecular marker of SS. Our case shows, that we might consider that SS may have a larger histologic spectrum than previously thought.

P-117

A case of idiopathic retroperitoneal fibrosis (Ormond's disease) and renal supracapsular liposarcoma

T Georgiev[1], E Nakov[2], R Gajdarski
[1]Department of Pathology, Faculty of Medicine, Sofia, Bulgaria
[2]Department of Pathology, Military Medical Academy, Sofia, Bulgaria

Background Idiopathic retroperitoneal fibrosis is an uncommon inflammatory disease characterized by proliferation and fibrosis of retroperitoneal tissue complicated by obstruction and encasement of retroperitoneal structures.
Case report We describe a 46-year-old female patient who underwent a gynecologic operation for left ovarian cyst in October 2001. A periaortic mass alongside with peritoneal nodules were biopsied which revealed endometriosis, necrotic xantomatous nodules and Ormond's disease. The last diagnosis was rejected and tumor misinterpreted as malignant fibrous histiocytoma. The course of the disease progressed and on computed tomography a left renal supracapsular tumor measuring 20/10/8cm together with a diffuse retroperitoneal fibrosis was demonstrated. In November 2002, a tumor localized in the adipose capsule of the left kidney was removed together with the kidney weighing 7,5kg. The kidney was markedly atrophic. A parallel excision of ten retroperitoneal tissue masses with a size up to 10/6/4cm was performed. Our final histological diagnosis was highly differentiated liposarcoma. Four months later the abdominal CT and the tumor markers were normal.
Conclusion The symptoms in our case were not specific for renoureteral obstruction and included abdominal pain and mass, weight loss and ascites during the year prior to second operation and finally urinary symptoms. We interpret our case as a slowly growing perirenal lipomatous tumor gradually compressing the kidney and causing slowly progressing retroperitoneal fibrosis.

P-118

A rare case of thoracic angiomatosis in an adult and review of the literature

N Lapidus, D Andrejev, A Arro
North-Estonian Regional Hospital, Tallinn, Estonia

Introduction Angiomatosis is a rare condition in which large segments of the body are involved by proliferating vessels. The

majority of angiomatoses present during childhood or infancy. A diffuse angiomatosis affecting thoracic organs is a rare, frequently fatal disorder. The origin of the lesion is unknown. The lesion consists of thin-walled sometimes bloodless capillary blood vessels. The definite diagnosis is usually made by open lung biopsy or autopsy. In our paper we are presenting the rare case of angiomatosis of pleura and lung in 37-years old woman and the review of the literature.

Materials and methods The patient was presented to the hospital with complaints to the pain in the right chest, dyspnea, weakness. The lesion manifested on chest radiographs and CT scans with unilateral pleural fluid and nodular pleural thickening. Thoracocenthesis was performed and 600 light brown fluid was drained. Cytologically the effusion contained erythrocytes and lymphocytes. Further 3000 ml more fluid was obtained. The open-lung biopsy revealed the extensive diffuse angiomatosis affecting visceral and parietal pleura and subpleural lung tissue. The lesion consisted of bloodless, thin walled, endothelium channels. Factor VIII-related antigen and CD31 were the most reliable immunocytochemical markers in highlighting the endothelia.

Results The palliative methods of treatment were not effective, and the patient was treated by total pleurectomy.

Conclusion Diagnosis is based exclusively on histologic finding as the only possibility of diagnosis. Open pleurectomy is the most succesful treatment in preventing reaccumulation of the effusion.

P-119

Immunolocalisation of cysteine proteinases and their inhibitors in asthma

I Kern[1], T Urbanc[1], P Meško Brguljan[1], N Cimerman[2]
[1]University Clinic of Respiratory and Allergic Diseases, Golnik, Slovenia
[2]Krka, Department of Biochemical Research and Drug Design, Ljubljana, Slovenia

Background Chronic inflammation with remodelling of the airway wall structures is an essential characteristic in asthma patients. Lysosomal proteinases are involved in extracellular proteolysis, which leads to matrix changes of subepithelial connective tissue in the airway wall. The aim of the study was to localise the expression of different cysteine proteinases and their endogenous inhibitors in lung tissue of asthma patients.

Material and methods We included ten specimens of bronchial biopsies of asthma patients and lung tissue specimens of fatal asthma case. Tissue specimens were fixed in formalin and embedded in paraffin. H&E slides were used for morphological examination. Immunohistochemistry was performed on an automated stainer (Benchmark, Ventana, Tuscon, AZ, USA). We used monoclonal antibodies to visualize cysteine proteinases (cathepsin B, H, L and S) and their inhibitors (stefin A and B, cystatin C) (Krka, Ljubljana, Slovenia).

Results Cathepsin B showed the most intense and wide distributed positive reaction. It was localized in the respiratory epithelium, macrophages, lymphocytes, mucous glands and smooth muscle cells. Cathepsin H showed intense reaction localized in the respiratory epithelium, macrophages, lymphocytes, mucous glands, but not in the smooth muscle cells. Cathepsins L and S showed positive reaction only in macrophages. The positive reaction of all three inhibitors was weaker compared to cysteine proteinases; it was observed in the respiratory epithelium, macrophages and mucous glands.

Conclusion These results suggest involvement of cysteine proteinases and their endogenous inhibitors in asthma, showing distinct immunoreactivity and different distributions in the lung tissue of asthma patients. Since the inhibitor expression is less intense we can speculate that remodelling of the extracellular matrix may be also a consequence of imbalance between cysteine proteinases and their inhibitors.

P-120

The correlation between aberrant connexin 43 mRNA expression induced by promoter methylation and nodal micrometastasis in non-small cell lung cancer

JT Chen[1], YW Cheng[2], WL Ho[1], H Lee[2]
[1]Department of Pathology, Taichung Veterans General Hospital, Taiwan, Republic of China
[2]Lung Cancer Research Center, Chung Shan Medical University, Taiwan, Republic of China

Introduction Reduced connexin (Cx) 43 gene expression has been shown in most of lung tumors and lung cancer cell lines. Although aberrant Cx43 gene expression was linked with lung tumorigenesis, our understanding to the mechanism was still limited. We hypothesized that the evidence of aberrant Cx43 gene expression was gradually intensified from adjacent normal lung tissues surrounding tumors towards to tumor tissues.

Materials and methods In this study, 90 lung tumors and adjacent normal tissues were collected to examine Cx43 mRNA expression by reverse transcription-polymerase chain reaction (RT-PCR).

Results Our data showed that Cx43 mRNA expression in adjacent normal lung tissue was significantly correlated with nodal involvement ($P = 0.03$), but the similar trend was not observed in tumor tissues. To verify whether lack of Cx43 mRNA expression was resulted from promoter methylation, PCR-based methylation assay was performed for Cx43 promoter methylation analysis. High frequency of promoter methylation was observed in Cx43 mRNA negative patients (21 of 33, 63.7%) compared with Cx43 mRNA positive patients (3 of 57, 5.3%, $P < 0.0001$). To elucidate whether aberrant Cx43 gene expression is originated from adjacent normal lung tissues, 25 lung tumors and each of five adjacent normal tissues with various distances from tumor tissues were collected to examine Cx43 mRNA and protein expression by RT-PCR and western blot, respectively. As the results shown, Cx43 mRNA and protein expressions were gradually decreased from adjacent normal lung tissues to tumor tissues with a positive correlation to the distance from tumor tissues. Gel shift assay data also revealed that shifted band binding with AP1 was only observed in adjacent normal tissues which were far from the tumor tissues.

Conclusion These results indicate that promoter methylation may interfere with AP1 binding to promoter to cause aberrant Cx43 gene expression. Thus, Cx43 mRNA in adjacent normal tissue surrounding lung tumor simply detected by RT-PCR may be act as a molecular marker of nodal micrometastasis in NSCLC.

P-121

Fhit, cell adhesion molecule and matrix metalloproteinase expression, and cell proliferative activity during peripheral lung adenocarcinogenesis

KM Kerr[1,3], S MacKenzie[1], S Ramasami[1], N Fyfe[1,3], AD Chapman[1], GI Murray[1], MC Nicolson[2,3], N Coleman[4], G King[1]
[1]Department of Pathology, Aberdeen University Medical School, Aberdeen, UK
[2]Department of Oncology, Aberdeen Royal Infirmary, Aberdeen, UK
[3]Aberdeen Lung Cancer Group, Aberdeen Royal Infirmary, Aberdeen, UK
[4]MRC Cancer Cell Unit, Hutchison/MRC Research Centre, Cambridge, UK

Introduction An adenoma-carcinoma sequence is recognised in peripheral lung. Atypical adenomatous hyperplasia (AAH) and bronchioloalveolar carcinoma (BAC) are the pre-invasive precursors of invasive adenocarcinoma, which frequently has a 'residual' peripheral BAC component. The biology of this neoplastic progression is poorly understood. The aim of this study was to examine the expression of the tumour suppressor gene FHIT, CD44v6, E-cadherin, beta-catenin, MMP-2, TIMP-2, and the cell cycle marker MCM2 at different stages in the proposed sequence.
Materials and methods Sections from formalin-fixed, wax-embedded tissue blocks of 118 AAH, 18 BAC and 133 invasive adenocarcinomas, stained immunohistochemically for the above molecules, were scored semiquantitatively. In invasive tumours, any BAC component was scored separately. For MCM2 a labelling index was determined as the ratio of immunopositive to total cells counted.
Results Fhit protein is abundant until the disease becomes stromally invasive ($P<0.0001$). CD44v6 levels are high in AAH and BAC, but fall in invasive disease ($P=0.007$). E-cadherin and beta-catenin levels rise between AAH and BAC ($P<0.001$), and remain well expressed thereafter. MMP-2 and TIMP-2 expression is relatively low in AAH, rises in BAC but falls when tumour becomes stromally invasive ($P<0.01$). The BAC component of invasive tumours expresses some molecules in a manner similar to pure BAC but mirrors expression in invasive tumour for others. MCM2 counts increase from 0.87%(low grade AAH) to 65.5% in invasive adenocarcinoma ($P=0.01$ or less)
Conclusion In peripheral adenocarcinogenesis, loss of Fhit is a relatively late event, while CD44v6 loss occurs earlier. Fhit loss has potential as a surrogate marker of invasion. E-cadherin and beta-catenin expression probably reflects changes in lesion architecture. MMP-2/TIMP-2 may be implicated in BAC but down-regulated as stromal invasion develops. Increasing cell cycle entry is consistent with neoplastic progression.

P-122

Immunohistochemical study of squamous and adenosquamous cancer of lungs

G Frank, L Zavalishina, J Andreeva
Hertsen Moscow Oncological Research Institute, Moscow, Russian Federation

Aims Expression of proliferation markers and factors of invasion in different forms of lung carcinomas.
Methods Using formalin-fixed and paraffin-embedded tissues, we examined by immunohistochemistry tenascine, collagen IV, CD44, MMP1, MMP9, TIMP1, TIMP2, CD95, Bcl2, p53, PCNA, Ki67, cyclin D1 in 30 cases of lung carcinoma - 15 squamous and 15 adenosquamous with (first group) and without (second group) metastases.
Results The positive staining with tenascine was observed in all cases of squamous and adenosquamous carcinoma, but the most strong expression was found in extracellular matrix and tumor cells of carcinomas of first group. The overexpression of MMP1 and MMP9 was found in cases with metastases in tumor cells and stromal cells. The reaction was localised on periferical zone of tumor complexes. At the same time reaction with TIMP1 was low in tumor of second group and very low – in first group, reaction with TIMP2 was moderate in metastatic tumor and low – in second group. Overexpression PCNA and Ki67 changed from 75% to 90% in 1 group and from 30% to 50% in 2 group. The increase expression of cyclin D1 was only in adenosquamous lung carcinoma. The overexpression of p53 was found only in metastatic tumors.
Conclusion There are some difference between squamous and adenosquamous lung carcinomas in expression of proliferation markers, and cyclin D1, but no difference in expression of metalloproteinases and their inhibitors. We found more prominent differences in groups of metastatic and nonmetastatic tumors.

P-123

Lack of Her-2/neu amplification or overexpression in malignant pleural mesothelioma (MPM)

S Orecchia, F Schillaci, M Salvio, R Libener, PG Betta
Pathology Unit - Dept. of Oncology - A.S.O., Alessandria, Italy

Introduction The Her-2/neu receptor, a member of the epidermal growth factor receptor (EGFR) family, represents a novel therapeutic target for the newly marketed recombinant anti-Her2 monoclonal antibody Herceptin®. MPM mortality continues to rise steeply (5% to 10% per year) with no known curative modality. Approximately 70% of MPMs have high levels of expression of EGFR. Two recent studies have reported expression of Her-2/neu in MPM but there was no analysis of overexpression or amplification. In this study, the amplification/overexpression of Her-2/neu gene has been evaluated in a series of 35 consecutive MPM biopsy specimens.
Materials and methods The tumour specimens had been formalin-fixed and paraffin-embedded. Immunohistochemistry (IHC) for Her-2/neu overexpression was performed using the Dako HercepTest kit. Only membrane staining intensity and pattern were evaluated using a 0 to 3+ scale with 2+ being the lower limit for a positive test. Amplification of the Her-2/neu gene was tested with the fluorescent in-situ hybridisation (FISH) method (Ventana INFORM Her-2/neu Probe) in 10 out of the 35 cases. Cases were considered as amplified by FISH when the mean number of fluorescent signals per nucleus was greater than four.
Results Of the 35 MPMs evaluated for the overexpression of the Her-2/neu receptor, all 35 scored 0 on the IHC test and all 10 cases additionally assayed by FISH were negative.
Conclusions Although the sample size was limited, these findings suggest that MPM do not overexpress or amplify Her-2/neu, which therefore should not be considered a prognostic and predictive marker in MPM. (This work was funded by the Alessandria branch of the Italian League against Cancer).

P-124

Morphological changes of bronchial glands at the localisation of preceding biopsy

R Gajanin[1], I Klem[2], Ä Eri[2], LJ Latinović[1], V Gajanin[3]
[1]Clinical Centre, Banja Luka, Department Of Pathology, Banja Luka, Bosnia and Herzegovina
[2]Institute for Pulmonary Diseases, Sremska Kamenica, Department of Pathology and Diagnostic Cytology, Serbia and Montenegro
[3]Medical faculty, Banja Luka, Department of Anatomy, Banja Luka, Bosnia and Herzegovina

Introduction At the location of preceding biopsy, in sero-mucous bronchial glands, there are certain changes of regenerative type. Hyper-plastic and meta-plastic squamous epithelia partially or wholly fills the acinus and duct of secretory glands. Aims: Regenerative atypical characteristics found in repeated materials can be misinterpreted as epidermoid or muco-epidermoid carcinoma.
Material and methods The research used 44 materials made by re-biopsy of bronchia, with regeneratory changes in bronchial glands. Presence of morphological parameters was examined semi-quantitatively, and then processed with methods of descriptive statistics.
Results In 59.09% lobular architectonics of the lesion was preserved; fibrin exudates were present in 90.91% cases; granulocytes in stroma were present in 68.18% cases; granulation tissue in 97.44% cases; planocellular metaplasia of duct and acinus was present in every single case. In 43.18% cases mucin-secreting cells were found in squamous epithelia. The squamous cells were diskeratotic in 35% cases; with polymorph nuclei in 27.73% cases; hyper-chromatic in 20%; multi-nuclear in 12.5%; with visible nucleolus in 72.5%, and with mitotic activity in 32.5% cases. In 61.36% cases the squamous cells were located in the fibrous tissue. Mucus in interstitium was present in 41.86% cases; cystoid formations were present in 23.25% cases.
Conclusions The changes are built of solid material, undifferentiated and/or squamous cells located in the granular tissue or in the fibrin. Infiltrates of granulocytes are found in fibrin, stroma, and squamous epithelia. Epithelial cells in regeneration show atypical cell characteristics in small percentage and therefore are hard to differentiate from carcinoma.

P-125

Immunohistochemical expression of Her-2/neu in patients with lung carcinoma

G Petrusevska[1], B Ilievska, S Banev, S Smickova
[1]Institute of Pathology, Skopje, Republic of Macedonia

The HER-2 protein or p185her2 is a membrane receptor with tyrosine kinase activity encoded by HE2/neu gene. Overexpression of HER-2/neu has been observed in many human cancer, including lung cancer. There are different reports about the expression of this protein in different lung cancer. The aim of the study is to determine the expression of HER-2 protein in the spectrum of lung cancer (adenocarcinoma, squamous cell carcinoma and small cell carcinoma). The study population consisted of two groups: 19 patients that have undergone to surgical treatment and 10 patients that have undergone to fiber-optic bronchoscopy and biopsy for primary diagnosis.Tissue specimens were neutral formaline fixed and paraffin embedded. Standard histochemical and immunohistochemical staining were used for diagnosis. Expression of Her-2/neu protein was determined by immunohistochemical staining with Hercep TestTM (DAKO). The results were graded 0-1 as negative and 2-3 as positive. Overall incidence of HER-2/neu overexpression was 34,4% (10 of 29). Higher incidence was found in patients with adenocarcinoma 45,4% (5of 11); squamous cell carcinoma 30,7% (4of 13) and small cell carcinoma 20% (1 of 5). No statistical significant difference was seen with age and gender. HER-2/neu overexpression was more relevant for patients with advanced tumor: all patients with squamous cell carcinoma were in stage 3b and 4, and 80% with adenocarcinoma were in stage 3a and 3b. These results are satisfactory and encourage us to continue this work in the follow-up study to evaluate HER-2/neu role as predictive and prognostic factor for patients with lung cancer.

P-126

The expression of the EGF-receptors (EGFR, ErbB-2, ErbB-3 and ErbB-4) in neuroendocrine tumors of the lung

L Ciocci, D Vitolo, S Spinelli, CD Baroni
Department of Experimental Medicine and Pathology, Roma, Italy

Introduction EGF and TGF-alfa play a major role in development of several human solid tumors. Hereby the expression of EGF receptors has been investigated to elucidate their role in tumor growth and progression. The aim of this study was to evaluate the expression and distribution of EGF receptors, EGFR, ErbB-2, ErbB-3 and ErbB-4 in neuroendocrine tumors of the lung, in order to relay them to histology, progression and prognosis of these tumors.
Material and methods We applied immunohistochemistry to paraffin sections of neuroendocrine tumors using MoAbs specific for EGFR, ErbB-2, ErbB-3 and ErbB-4.
Results In all cases of neuroendocrine carcinoma the majority of neoplastic cells displayed a nuclear and cytoplasmic positivity for ErbB-4. On the contrary in 75% of cases EGFR, ErbB-2 and ErbB-3 receptors were focally and randomly expressed in about a third of neoplastic cells. Carcinoid tumors displayed only a focal positivity for ErbB-4 in about two third of the cases, although they were all EGFR negative. Moreover about a third of carcinoids displayed a cytoplasmic and focal membrane positivity for ErbB-2 and ErbB-3.
Conclusions Our data suggest that ErbB-4 and EGFR may play a costant role in the pathogenesis of neuroendocrine lung carcinomas; moreover the modulation of expression of EGF receptors may contribute to elucidate the pathogenic relationship between neuroendocrine carcinomas and carcinoids of the lung.

P-127

Laminin alpha2 chain positive vessels and metastatic tendency in neuroendocrine lung carcinomas

D Vitolo, S Spinelli, L Ciocci, CD Baroni
Department of Experimental Medicine and Pathology, Roma, Italy

Introduction We previously demonstrated that laminin-α2-chain positive vessels are markers of early angiogenesis in tumors such as glioblastomas and supraglottis, breast and lung non small cell carcinomas. The aim of this study was to evaluate distribution of laminin-α2-chain positive vessels in lung neuroendocrine carcinomas to relay their number to metastatic tendency of these tumors.

Material and methods We applied immunohistochemistry on six neuroendocrine lung carcinomas using MoABs specific for extracellular matrix proteins and integrins; moreover transwell test migration assays evaluated the rate of transendothelial migration of AE-2 neuroendocrine carcinoma cell line throught a monolayer of EAHY endothelial cell line expressing laminin-α2-chain to establish wheather this protein may favour in vivo vascular invasion and metastasis.
Results 80%, 75%, 90%, 65%, 80% and 70% of vessels were respectivelly distributed within the parenchyma of these tumors. Studies on contignous sections demonstrated that parenchymal vessels were positive for all ECMPs, but laminin-α2-chain, which was respectively expressed in 100%, 30%, 80%, 30%, 60% and 100% of parenchymal and in 100%, 0%, 30%, 0%, 100% and 70% of stromal vessels of these tumors. In all cases about 25% of neoplastic cells were α6 positive. Preliminary results of transwell test migration assay indicate that the pretreatment of the AE-2 cell suspension with anti laminin-α2-chain and anti α6-integrin MoAbs reduced their migration through the EAHY monolayer.
Conclusions As known α6-integrin is a receptor of laminin-α2-chain, therefore the up-regulation of this protein in a large number of vessels during tumor angiogenesis may favour metastasis increasing neoplastic cell adhesiveness to newly formed vessels.

P-128

Brain death as a cause of primary lung graft disfunction in an isolated rabbit lung model

MA Cabezuelo[1], J López-Aguilar[2], G Murias[2], JR Hotchkiss[3], M Mignini[2], F Cicona[2], F Bernabé[2], A Vilagrá[2], PV Romero[4], L Blanch[2]
[1]UDIAT- Centre Diagnostic S.A. - Corporació Parc Taulí, Sabadell, Spain
[2]Centre de Crítics. Hospital de Sabadell - Corporació Parc Taulí, Sabadell, Spain
[3]Regions Hospital, St Paul, Minneapolis, Minnesota, USA
[4]Ciudad Sanitaria de Bellvitge. L´Hospitalet de Lobregat, Spain

Introduction early lung dysfunction observed after lung transplantation has been attributed to an increase of vascular permability. Factors involved in this mechanism are unknown. Our hypothesis was that brain death (BD) is a preconditioning factor that induces primary lung graft dysfunction.
Methods twenty-four rabbits were randomized to control (CRL) or induced BD (increasing intracraneal pressure above systolic pressure for 30 minutes) groups and were ventilated in volume controlled mode (tidal volume 10 ml/kg, positive end expiratory pressure (PEEP) 0 cmH2O and respiratory rate (RR) to obtain normocapnia) for 120 minutes. Isolated lungs were perfused with 300 ml/min (constant flow) and ventilated in pressure controlled mode (peack pressure 30 cmH2O, PEEP 5 cmH2O and RR 20) for 30 minutes. Pulmonary edema and lung injury were assessed by weight gain, change in ultrafiltration coefficient before and after ventilation; and extent of hemorrhage (scored by histology: intensity of alveolar hemorrhage, percentage of alveoli with hemorrhage and number of vessels with perivascular hemorrhage) Mean values (3 samples per lung) of the 3 indices of hemorrhage showed above were scored (0 to 5) and added to obtain a score of overall lung hemorrhage (range 0 to 15) for each lunch. Data are expressed as mean and 95% confidence interval and were compared with paired t test.

Results

	CRL	BD	p
Weight gain (g)	0.43(0.20-0.65)	0.92 (0.52-1.32)	0.031
Hist score (0-15)	5.4 (3.37-7.42)	8.80 (6.15-11.45)	0.036
Ultraf coeficient	0.00199	0.00315	
	(-0.00397-0.00165)	(-0.00402-0.00170)	0.404

Conclusions under these experimental conditions BD contributes to pulmonary edema and lung hemorrhage.

P-129

Expression of cyclooxygenase-2 in nonsmall cell lung carcinomas

N Akyürek[1], L Memis[1], N Köktürk[2], C Kirisoglu[2], C Öztürk[2]
[1]Gazi University Medical School, Department of Pathology, Ankara, Turkey
[2]Gazi University Medical School, Department of Pulmonary Medicine, Ankara, Turkey

Introduction Cyclooxygenase (COX) is an inducible enzyme that catalyses the conversion of arachidonic acid to prostaglandins and thromboxanes. COX-2 is induced by cytokines and growth factors and has been shown to be important in carcinogenesis. The aim of this study was to investigate the expression of COX-2 and clinicopathologic factors in nonsmall cell lung carcinomas (NSCLC) with regard to survival times.
Materials and methods Seventy-seven NSCLC specimens were evaluated for COX-2 expression by immunohistochemical method. Staining patterns were assessed semiquantitatively and correlated with tumor histologic type, TNM stage and prognosis. Chi-square and Kaplan-Meier survival analysis was performed.
Results COX-2 was not expressed in the normal bronchial epithelium. COX-2 expression was detected in 36 (46.8%) NSCLC. Expression of COX-2 was significantly higher in adenocarcinomas than in other histologic subtypes (p=0.018). There was no significant relationship found between COX-2 expression and age, gender, TNM stage, and prognosis.
Conclusion This study suggests that an increase in COX-2 expression may be associated with the development of adenocarcinomas. But, prognostic significance of COX-2 expression is controversial.

P-130

Prognostic significance of cyclin-dependent kinase inhibitor p27 and Bcl-2 protein in nonsmall cell lung cancer

G Ozbilim[1], I Kükrer[1], H Gülmez[1], L Dertsiz[2], S Karakaya[1]
[1]Akdeniz University School of Medicine Department of Pathology, Antalya, Turkey
[2]Akdeniz University School of Medicine Department of Thorasic Surgery, Antalya, Turkey

Introduction The expression of p27, which is known a cyclin-dependent kinase inhibitor, has considerable value for the prognosis of cancer patients. Bcl-2 gen product (Bcl-2 protein) is implicated in oncogenesis by its ability to prolong cell death through the inhibition of apoptosis. We studied the expresssion of p27 and bcl-2 protein to investigate their association between clinicopathologic factors and prognosis in nonsmall cell lung cancer (NSCLC)
Materials and methods Patients with NSCLC were included in our study.There were 30 patients(25 men,5 women), 15 patients

had adenocarcinoma (AC) and 15 had squamous cell carcinoma (SCC).Tumors were examined immunohistochemically with p27 and bcl-2 protein expression, using formalin-fixed, parafin-embedded tissue. For the evaluation of p27 expression, the number of nuclear staining was counted and showed as a percentage.Bcl-2 protein was primarily identified in the cytoplasm of tumor cells. Statistically, correlation between immunoreactivity and the clinicopathologic factors were evaluated.

Results P27 immunoreactivity was observed in 12(40%) of 30 cases. There were 9(60%) SCC, 3(20%) AC. Statistically, these findings were found significant (p=0,025). Percentage of p27 positive nuclei, the average being 25%. Positive bcl-2 immuno-staining was found in 8(26,6%) of 30 cases. 5 cases (33,3%) of 15 SCC and 3 (20%) of the 15 AC were positive. These findings were not found significant (p=0,68)

Conclusions There is no correlation between p27 and bcl-2 expression and clinical parameters, clinical stage, pathologic grade and prognosis. Our study suggest that p27 immunreactivity in NSCLC may provide prognostic information.

P-131

Pulmonary hamartoma – report of four cases

B Manevska, S Bojadjieva, A Kulova
Medical University of Varna, Varna, Bulgaria

Introduction Mesenchymal lesions of the lung encompass a wide variety of benign and malignant conditions. Pulmonary hamartoma (PH) is a bening mesenchymal tumor, usually described as a solitary pulmonary nodule, composed of fat, smooth muscle and respiratory epithelium. The diagnosis is based on clinical data, imaging methods (radiography, computed tomography), fine needle aspiration cytology (FNAC) and histomorphological study. Because of the tumor rarity we find just a few reports, concerning the cytologic characteristics. The aim of the present study is to describe the cytological features of PH and to compare them with the histological findings.

Materials and methods We have examined four cases of PH, who have undergone surgery, and we have used routine histological stains on paraffin sections for the diagnosis. FNAC is performed prior surgery in one patient, and in the other three offprints of the resected tumor are prepared.

Results The cytomorphological study show predominance of spindle cells, admixed with many stellate cells, and fibromyxoid material on a serosanquinous background as well. Postoperative histopathological study reveals spindle shaped smooth muscle cells, goblet cells, cystic spaces, covered with bronchiolar epithelium, cartilaginous or myxomatous tissue, thus confirming the diagnosis pulmonary hamartoma. In

Conclusion These rare tumors may be exactly diagnosed by correlating clinical and radiological data with cytological and histological findings.

P-132

A case of neuroblastoma in subpleural localisation in a 56-year-old man

P Mukenšnabl, D Havel, V Špidlen, R Bittenglová, Z Chudáček, M Pešek
Medical Faculty Hospital, Plzeň, Czech Republic

Introduction Neuroblastoma is a malignant tumor of early childhood and is very rare in adults, thus we report this case.

Case report We describe a case of a 56-year-old man, never before notably ill. Basic laboratory values were not significantly anomalous except of mild anaemia and high erythrocyte sedimentation rate. An X-ray scan showed a spherical opacity 4 cm in diameter in the top right pulmonary field paramediastinally. CT displayed a low-density tumor 5x3, 8x4,5 cm in the apex of the right hemithorax. The tumor was well circumscribed and seemed to be in a subpleural localisation. It was subsequently punctioned with Chiba and Core needle under CT control. Cytological and histological material did not contain any malignant cells. On MR scan there was a well encapsulated extrapulmonary tumor without destruction of ribs, probably of benign origin. Tumor extirpation was indicated. The lesion was growing out of spinal chord. It was completely removed. Grossly, the tumor looked like an old hematoma. Histologically, it had the typical appearance of neuroblastoma - malignant tumor which is found in more than 90% of cases in patients under 6 years of age. A scintigrafical examination and trephine biopsy showed massive bone marrow infiltration by neuroblastoma.

Conclusion A 56-year-old man was confirmed to have a typical early childhood tumor - neuroblastoma in a subpleural localisation. Despite the poor prognosis of this tumor in adults and a wide bone marrow infiltration, the patient is well and without signs of disease after surgical resection and two cycles of chemotherapy over 22 months after the initial diagnosis.

P-133

Measurements of DNA amount and nuclear size by image cytometry: are these two features sufficient for diagnosis of early lung cancer?

A Ales[1], M Tercelj[1], BMS Turic[2], S Goring[2], B Palcic, T Rott[4], S Vidmar[5], M Sok[5]
[1]Center for Pulmonary Disease and Allergy, Clinical Center, Ljubljana, Slovenia
[2]Center for Pulmonary Disease and Allergy, Clinical Center, Ljubljana, Slovenia
[3]Perceptronix Medical Inc., Vancouver, Canada
[4]B.C. Cancer Research Center, Vancouver, Canada
[5]Institute of Pathology, Faculty of Medicine University, Ljubljana, Slovenia
[6]Clinic of Thoracic surgery, Clinical Center, Ljubljana, Slovenia

Background Lung cancer represents 15% of all cancers, but is responsible for nearly 30% of cancer related deaths due to the fact that it is most often detected in a very late stage. It has been proposed that selected nuclear features could be used to assist lung cancer detection in an early, operable stage. It was shown that both DNA amount (DNA ploidy) and nuclear size are key features for positive diagnosis in oral, laryngeal, bronchial, and gastric epithelial tumors. We used image cytometry to assess the potential of this approach using nuclei of epithelial lung cells from sputum samples.

Experimental design Sputum samples were obtained by induction method, using hyperosmolar salinic solution, from 139 lung cancer patients and 148 high risk individuals. The cells were fixed and after breaking mucosa with mechanical and chemical treatment, they were cyto-centrifuged onto the microscopy slides. Cell nuclei were stained by a DNA specific and stoichiometric (Feulgen-Thionin) stain and DNA amount (ploidy) and nuclear size of 6000

(on average) cell nuclei from each sample were measured by a high resolution image cytometer.
Results The results showed that there were no statistical differences between the DNA ploidy values between control and cancer cases, as very few cancerous cells were found in the sputa of lung cancer patients. Interestingly, there was a measurable increase in the mean nuclear area of diploid cells from cancer patients in comparison to control cases.
Conclusions Despite the slight difference in the size distribution the nuclear size feature alone does not provide effective discrimination between the negative and positive populations.

P-134

Pulmonary blastoma: report of 10 cases

D Yilmazbayhan, MG Gulluoglu
Istanbul University, Istanbul Faculty of Medicine, Department of Pathology, Istanbul, Turkey

Introduction Pulmonary blastomas (PB) are rare lung tumors having unique histomorphological features. Although they were once regarded in the same group of lung neoplasms with well differentiated fetal adenocarcinomas, recently the two tumors were seperated from each other. We aim to discuss the morphological features and the changes of morphology on recurrences of pulmonary blastomas.
Materials and methods We present ten cases of PB, six of which were biphasic, two were pleuropulmonary, and two were cystic. Biphasic PB patients were five males and one female, with an age range of 29-70. Two female patients with pleuropulmonary blastoma were 6 and 22 years, and cystic PB patients were 3 and 4 years old female and male children, respectively.
Results One of our most striking histomorphological findings was that four of the biphasic PBs accommodate mature epithelium, not fetal epithelium. One of the other two cases presented with a fetal adenocarcinoma and the tumor recurred as a biphasic PB. One of the cystic PB, which arised in a background of congenital bullous emphysema, recurred with pleomorphic cells forming solid groups. The other cystic PB was diagnosed as congenital cystic adenomatoid malformation.
Conclusion Because of the changing morphological features and composition of epithelial component, classification of the pulmonary blastomas should be reviewed.

P-135

5-Lipoxygenase (5-LO) detection in pleural mesothelioma: an immunohistochemical study

D Villari[1], M Grosso[1], E Vitarelli[1], M Righi[1], A Procopio[2], M Falduto[3], G Calarco[3], M Romano[4]
[1]Dipartimento Di Patologia Umana, Policlinico Universitario Di Messina, Messina, Italy
[2]Istituto di Patologia Sperimentale, Universita di Ancona, Ancona, Italy
[3]Servizio di Anatomia Patologica, Ospedale Papardo, Messina, Italy
[4]Dipartimento di Scienze Biomediche, Universita 'G. D'annunzio' di Chieti, Italy

Introduction Evidence indicates that the 5-LO pathway is critical for malignant tumor cell growth. We have previously shown that human malignant pleural mesothelial (MM) cells, but not normal mesothelial cells, express a catalytically active 5-LO, which regulates MM cell proliferation and survival via a VEGF-related circuit (Romano et al., FASEB J. 15:20326,2001). Aim of our study was to investigate in vivo expression of 5-LO in human mesothelioma.
Materials and methods Immunohistochemical analyses were conducted in five micron sections from human pleural mesothelioma (9 epithelial, 2 biphasic and one fibrous type). 5-LO expression was evaluated using a 5-LO polyclonal antibody.
Results Immunohistochemical staining was observed in all cases. The staining pattern was cytoplasmic in 4 cases (2 epithelial, 1 biphasic and 1 fibrous type), both nuclear and membranous in one case of the epithelial type, both nuclear and cytoplasmic in 5 cases (4 epithelial and 1 biphasic type), nuclear, cytoplasmic and membranous in two cases of the epithelial type.
Conclusion These results are consistent with our in vitro data showing 5-LO expression in MM cells and strongly suggest that 5-LO may play a relevant role in the pathobiology of malignant pleural mesothelioma.

P-136

Expression of vascular endothelial growth factor (VEGF) and E-cadherin in human non-small cell lung cancer

D Stefanou, A Goussia, E Arkoumani, NJ Agnantis
Department of Pathology, University of Ioannina, Medical School, Ioannina, Greece

Introduction The present study is scheduled to analyze the intratumoral expression of vascular endothelial growth factor (VEGF) in human lung cancer and to determine the relation with microvessel density (MVD), E-cadherin expression and clinicopathological parameters.
Materials and methods Using immunohistochemical technique, the expression of VEGF (Neomarkers) and E-cadherin (Santa Cruz, Bioanalytica) was studied in 88 non-small cell lung cancer (NSCLC) specimens (48 squamous cell carcinomas, 30 adenocarcinomas and 10 large cell carcinomas). MVD was assessed by visual quantification of microvessels stained with anti-CD34 antibody.
Results A strong expression of VEGF (>25% of neoplastic cells) was observed in 77.27% of carcinomas (36/48 squamous cell carcinomas, 22/30 adenocarcinomas and 10/10 large cell carcinomas). VEGF expression was correlated with MVD and tumor cell differentiation ($p<0.001$). Absent or reduced E-cadherin expression (<50% of neoplastic cells) was noted in 61.36% of tumors. A higher percentage of undifferentiated carcinomas was observed in the reduced E-cadherin group than in the E-cadherin positive group ($p<0.0001$). The simultaneous strong expression of VEGF and reduced expression of E-cadherin was correlated with tumor dedifferentiation ($p<0.001$).
Conclusions The intratumoral VEGF expression correlates with tumor angiogenesis and histologic differentiation. E-cadherin expression is associated with tumor cell differentiation. Combined evaluation of VEGF and E-cadherin may provide evidence for a better understanding of the biological characteristics of NSCLC tumors, and it may appear useful in defining groups of patients with a poor prognosis.

P-137

A rare case of mucoepidermoid carcinoma of the thymus

E Arkoumani[1], A Goussia[1], E Sintou[1], Z Metafratzi[2], E Arkoumani[2], S Syminelakis[3], D Stefanou[1]
[1]Department of Pathology, University of Ioannina, Medical School, Ioannina, Greece
[2]Department of Radiology, University of Ioannina, Ioannina, Greece
[3]Department of Cardiothoracic Surgery, University of Ioannina, Ioannina, Greece

A 53-years old male presented with chest discomfort, dyspnea, weakness. Heart function tests were normal. CT examination revealed a well demarcated mass in the anterior-superior mediastinum as well as pleural and pericardial effusions. There was no clinical/radiographic evidence of tumor elsewhere. A surgical excision of the mass was performed. Grossly, the mass was round, well demarcated, measured 10x8.5x3 cm. The cut surface showed solid whitish or reddish with yellowish foci areas and cystic areas filled with mucinous fluid. Histologically, the tumor consisted of sheets and nests of atypical squamoid cells intermingled with gland-like lumens. Areas of clear cells were also present. In the tumor stroma, abundant amounts of mucin, foci of necrosis, lymphatic invasion, intense inflammation and cholesterol granulomas were observed. In some areas, the tumor cells were seen in contact to the lining of the cystic cavities. The latter were lined by a single layer of cuboidal or flattened or stratified epithelium with morphological features of squamous cells. At the periphery of the tumor, rare lymphoid follicles, residual thymic elements or degenerative Hassall's corpuscles were seen. These histologic features were more consistent with a mucoepidermoid carcinoma arising in association with a thymic cyst. The patient died two months after chemotherapy administration. Mucoepidermoid carcinoma of thymus is a rare entity and, to our knowledge, very few cases have been described in the International Literature. However, in case of absence of metastatic disease or other common primary tumors of thymus, the diagnosis of a mucoepidermoid carcinoma should be taken into consideration.

P-138

Tissue array for immunohistochemical profiling of intrathoracic localized fibrous tumors

S Ozturk[1], S Dizbay Sak[1], G Kaygusuz[1], A Cangir[2], D Kilic[2], A Sertcelik[1]
[1]Ankara University Medical School Department of Pathology, Ankara, Turkey
[2]Ankara University Medical School Department of Thoracic Surgery, Ankara, Turkey

Introduction Localized fibrous tumor (LFT) is a rare neoplasm generally presenting as a pleural-based mass. The aim of this study was to investigate expression of oncoproteins, prognostic markers, steroid receptors, antimesothelial markers, extracellular matrix proteins and a variety of other markers in LFTs by tissue array using immunohistochemistry.
Materials and methods Two core tissue biopsies (4 mm in diameter) were taken from the paraffin blocks of eight CD34 positive pleural tumors to represent both hypercellular and hypocellular areas. A tissue array block of 16 tissues were prepared and examined for 21 markers.
Results There were five female and three male patients (age range: 30-75). Six intrathoracic extrapulmonary pedinculated, two intrapulmonary non-pedinculated lesions measured 3 to19 cm. The tumor cells showed variable immunoreactivity with SMA, desmin, ER, PR, CD99, CD57, CD10, CD117, bcl-1, Ki-67 and laminin. Expression of bcl-2 and collagen type III was detected in all cases. None of the LFTs showed immunoreactivity for calretinin, mesothelin, S-100, CD5, CD31, c-erbB2 and p53. The diagnosis was changed as desmoid tumor in one case.
Conclusion No difference was detected between hypercellular and hypocellular areas of LFTs with respect to immunohistochemical profile. Collagen type III and bcl-2 could be used together with CD34 in the diagnosis of LFTs. Extracellular matrix proteins, CD10, CD57 and bcl-1 could be detected in LFTs. Overlapping immunoprofile of LFTs and gastrointestinal stromal tumors for CD117, CD34, bcl-2 and CD99 deserves further study. In ER, PR, SMA and desmin positive case, desmoid tumor should be considered in the differential diagnosis.

P-139

The value of intraoperative imprint cytology in mediastinal staging in non small cell lung cancer

A Ersev, A Orki, H Kiral, C Dudu, B Arman
Heybeliada Chest Disease and Thoracic Surgery Center, Istanbul, Turkey

Introduction Evaluation of lymph nodes is mandatory for the intraoperative staging of lung cancer. This evaluation can be done either by frozen section FS or imprint cytology IC. In this prospective study we compared the diagnostic accuracy of IC of mediastinal lymph nodes performed during the operation and permanent section.
Materials and methods One thousand and fifty mediastinal lymph nodes from two hundred and fiftyfive patients were evaluated. To obtain lymph node samples from various stations cervical medistinoscopy was performed in twohundred and thirtytwo patients. Twenty percent of the patients had anterior mediastinotomy and the rest videothoracoscopy. The average time for preparing an imprint slide was approximately two or two and a half minutes. For the final pathological diagnosis both imprint and permanent section slides were reviewed and the results compared.
Results There were five false positive and eight false negative results. The sensitivity of IC was ninetythree point one percent and the predictive value of a negative result was ninetynine percent.
Conclusion Reviewing the literature and comparing the diagnostic accuracy of FS in other studies we concluded that IC for the evaluation of mediastinal lymph nodes in lung cancer is an accurate reliable simple and less time consuming method.

P-140

Ultrastructure of bronchial mucosa in chronic obstructive bronchitis

N Zoirova, S Ariphkhanova
Uzbek Institute of Medical Rehabilitation and Physical Therapy, Tashkent, Uzbekistan

The purpose of this investigation was to determine ultrastructural peculiarity of bronchial mucosa in the patients with chronic obstructive bronchitis (COB). The study was performed in bronchial biopsy samples obtained from 30 patients with COB.

Material was fixed in 2,5% glutaraldehyde, postfixed with 1% osmium tetroxide and embedded in Epon. Ultrathin sections were stained with uranyl acetate and lead citrate. Morphological three types of COB have been reported, including chronic catarrhal, catarrhal sclerotic and sclerotic forms. Catarrhal COB was characterized with significant increasing of goblet cell count as compared to the bronchial mucosa in controls. Hyperplasia of endoplasmic reticulum and Golgi complex was observed. In the goblet cells, numerous secretory droplets were crowded together where they have been deposited from the surrounding cytoplasm. In ciliated cells, few cilia were seen in longitudinal section extending from the apical pole of epithelial cells, fragmentation of the endoplasmic reticulum and appearance of autophagosome were detected. In other types of COB, number of cell rows was decreased with different secretory activity of goblet cells. Interepithelial migration of lymphocytes with the damage of the basement membrane was described. Our findings demonstrated more aggressive changes of bronchial mucosa in sclerotic COB.

P-141

Chest trauma-induced rupture of benign mediastinal teratoma followed by a possible implantation of the tumor into the parietal pleura: a case report

B Salobir[1], M Turel[1], T Rott[2], M Dolenšek[3], J Eržen[4], M Terčelj-Zorman[1], A Aleš[1], T Bavčar-Vodovnik[3]
[1]Clinical Center Ljubljana, Department of Pulmonary Diseases And Allergy, Ljubljana, Slovenia
[2]Institute of Pathology, Medical Faculty, University Ljubljana, Ljubljana, Slovenia
[3]Clinical Center Ljubljana, Department of Radiology, Ljubljana, Slovenia
[4]Clinical Center Ljubljana, Department of Thoracic Surgery, Ljubljana, Slovenia

Introduction Mediastinal teratomas rarely rupture. An unusual case of chest trauma-induced rupture of benign mediastinal teratoma followed by a possible implantation of the tumor into the parietal pleura is reported.
Case presentation In a 26-year old woman, a pre-employment plain chest radiograph and CT of the chest revealed a large mediastinal tumor. Two smaller tumors were located on the left parietal pleura. On operation completely obliterated left pleural space and three well-encapsulated tumors were found. Microscope examination revealed three well-differentiated teratomas with no evidence of malignancy. Three years before the detection of the tumor the patient had a blunt chest trauma, with a left-sided chest pain and shortness of breath, which gradually disappeared. At the time the plain chest radiograph was analyzed as normal. Retrospectively an unusual mediastinal line, adjacent to the aortic arch, was disclosed. This line could be due to a small mass in the mediastinum. The left diaphragm was elevated, and a small left-sided pleural effusion could have been present. We suspect that teratomas located on the parietal pleura were caused by implantation of the tumor cells after the rupture of the mediastinal teratoma into the pleural space during blunt chest trauma.
Conclusion The chest trauma seen in presented case, could be at least a trigger, if not the only cause of the mediastinal teratoma rupture. The rupture was probably followed by both, obliteration of pleural cavity and possible implantation of benign tumor into the parietal pleura.

P-142

The Gorham - Stout Syndrome: presentation of a case with pleural effusion

A Ales[1], M Turel[1], M Jancar[2], M Tercelj-Zorman[1], B Salobir[1], V Pavlovcic[3]
[1]Clinical Center Ljubljana, Department of Pulmonary Diseases and Allergy, Ljubljana, Slovenia
[2]Institut of Oncology Ljubljana, Ljubljana, Slovenia
[3]Clinical Center Ljubljana, Clinic of Orthopedy, Ljubljana, Slovenia

Gorham - Stout syndrome is a rare disorder of unknown aetiology characterised by a nonmalignant proliferation of vascular structures originating in bone with progressive bone destruction and often extending into surrounding soft tissues. Pleural effusion is uncommon, but usually fatal complication of this condition. We present a 28 years old male patient admitted to our departement because of huge left - sided pleural effusion. 10 years ago his left humerus was injured in a motorcycle accident. One month later osteolysis of the left humerus was diagnosed. Histological examination of the lytic bone revealed Gorham - Stout syndrome. Until recently there were no symptoms, then dyspnea occured and the patient was admitted to our departement. A huge left pleural sterile haemorragic exudate was found. X ray revealed destruction of the left humerus, the left scapula, the left clavicle and the first two left ribs. CT scan revealed no mediastinal mass, nor any destructions of vertebrae. The pleural effusion was drained, thoracoscopy was performed, the histology of pleura revealed only fibrosis and inflammation, there was no angiomatous tissue. The patient received radiation therapy of 40 G of the left side of the chest and the left upper arm. He also received 30 mg of pamidronat. 4 month after this therapy the pleural effusion does not reappear and no new osteolytic lesions occured.

P-143

p27kip1 and MIB-1 immunoreactivity in pleural malignant mesothelioma

G Serio[1], A Scattone[1], E Mattioli[1], A Pennella[2], C Giardina[1], P Nazzaro[3], D Cavone[4], L Pollice[1], M Musti[4]
[1]Dpt. Pathologial Anatomy and Genetics, University of Bari, Bari, Italy
[2]University Service of Pathological Anatomy, University of Foggia, Foggia, Italy
[3]Dpt. Clinical Methodology and Medico-Surgical Technology, University of Bari. Bari, Italy
[4]Dpt. Internal Medicine and Public Medicine, Industrial Medicine, Universityof Bari, Bari, Italy

Introduction Malignant mesothelioma is an aggressive tumor with adverse prognosis (median survival 4-12 months) both in treated and untreated patients. In fact, only few patients survive more than two years. The identification of prognostic factors is critical to evaluate life-expectancy and crucial to approach novel therapeutical strategies. The study was performed to evaluate the use of MIB-1 and p27kip1 antigens as prognostic indicators of survival in malignant mesotheliomas.
Materials and methods A series of 122 surgical biopsies of patients with known follow-up were immunohistochemically examined. The results were compared with survival data and correlated with clinical and histological parameters. For immuno-

histochemistry, sections were stained for MIB-1 and p27kip1 antigens using ABC method. Number of positively stained nuclei was evaluated in consecutive high magnification fields (500 neoplastic cells were considered the minimum number to include the case in the study).
Results MIB-1, which is largely expressed in sarcomatoid MM ($p=0.02$), is more represented in patients with shorter (<12 months) then in subjects with medium ($12<\text{months}<24$, $p<0.05$) and longer (>24 months, $p<0.05$) survival. On the other hand, p27 is more expressed (52 ± 24.7) in patients with longer ($p<0.01$) then in subjects with shorter survival. Pearson's analysis showed no significant correlation between MIB-1 expression and p27, but this was predictive of survival in the entire population ($r=0.273$, $p<0.001$).
Conclusion The findings suggests that p27 and MIB-1 expression, although reliable attribute of MM, represent independent markers of prognosis in malignant mesothelioma.

P-144

Familial clustering of malignant mesothelioma without direct contact to asbestos. A genetic study

A Scattone[1], G Serio[1], M Gentile[2], L Pollice[1], L Bonadonna[2], D Cavone[3], P Nazzaro[4], M Bisconti[5], M Musti[3]
[1]Dpt. of Pathologial Anatomy and Genetics, University of Bari, Bari, Italy
[2]Medical Genetics 'DeBellis' Hospital-IRCCS, Castellana Grotte, Bari, Italy
[3]Dpt. Internal Medicine and Public Medicine, Industrial Medicine, University of Bari, Bari, Italy
[4]Dpt. Clinical Methodology and Medico-Surgical Technology, University of Bari, Bari, Italy
[5]Division of Pneumology- 'A. Galateo' Hospital, Lecce, Italy

Introduction Very few papers dealt with clustering of familial malignant mesothelioma (MM). Most of these, who developed mesotheliomas, presented work or domestic history of exposure to asbestos, but only in very few of them asbestos did not demonstrated any association. The aim of this study was to contribute to the hypothesis of a genetic predisposition in the pathogenesis of the mesothelioma.
Methods We report two cases of pleural malignant mesothelioma that affected two young sisters as part of a nine-member family with enviromental exposure to asbestos. They were affected by Marfan's syndrome and both developed pleural malignant deciduoid mesothelioma with long survival. We have performed comparative genomic hybridization (CGH) analyses of tumor samples to identify critical chromosomal regions involved in the onset of MM.
Results We found similar chromosomal changes in both cases and in particular we found losses at 6q12-q21 and 13q21.1-q22 chromosome.
Conclusions Early onset s. and same genetic impairments in the two sisters suggest that genetic factors may induce the onset of this cancer in those subjects who are exposed even to small environmental amounts of asbestos. However, the specific chromosomal changes we found might provide evidence for locations of relevant suppressor genes of familial MM.

P-145

Video assisted versus needle biopsy of the pleura in patients with pleural effusion

A Orki, M Keles, A Kosar, C Aydemir, A Ersev, B Arman
Heybeliada Chest Disease and Thoracic Surgery Center, Istanbul, Turkey

Introduction Pleural effusion is quite a frequent finding that should be thoroughly investigated and diagnosed. Besides cytological examination of the pleural fluid, second most frequently used method is biopsy. This study was planned to investigate if video assisted thoracoscopy is mandatory where the case is diagnosed as inflammation and fibrosis with biopsy or the biopsy is non diagnostic.
Materials and methods In a four year period needle biopsies and video assisted thoracoscopic VATS biopsies were performed at the same session on thirtythree patients with pleural effusion. The biopsy material was processed for routine haematoxilyn eosin stain. Histochemical stains PAS, Alcian blue mucicarmin and immunhistochemical methods cytokeratin, carcinoembryonic antigen, vimentin were performed on all material and the results compared.
Results The pathological diagnosis of needle biopsies Group I were chronic inflammation and fibrosis in twentythree, malignant mesothelioma in six and granulomatous inflamation in four patients. When compared with VATS biopsy results Group II in group I with chronic inflammation one patient was diagnosed as having malignant mesothelioma, one patient had a metastatic carcinoma, nine patients had granulomatous inflammation.
Conclusion In patients suspected to have malignancy who are diagnosed as having chronic inflammation and fibrosis with needle biopsy VATS biopsy should be performed.

P-146

Solitary fibrous tumor of the pleura

A Orki, Ţ Ürek, K Timurtekin, C Ţenol, A Ersev
Heybeliada Chest Disease and Thoracic Surgery Center, Istanbul, Turkey

Introduction Solitary fibrous tumor of the pleura is a rare tumour and frequently arises from visceral pleura with a pedincule. In this study three cases with histopathological diagnosis of solitary fibrous tumor is discussed in respect to clinical radiological and pathological aspects of differential diagnosis.
Materials and methods Three patients who had symptoms related to a thoracic pathology were investigated through chest x ray, computerized tomogrophy and magnetic resonance imaging. Cytologic examination of sputum bronchoscopy, fine nedle aspiration of the mass lesion and finally resection through thoracoscopy or thoracotomy were performed. Routine haematoksilyn eosin stains, histochemical stains such as PAS and Van Gieson and immuno-histochemically CK, EMA, Vimentin, Actin, S 100 and CD 34 were done.
Results All three resection material were diagnosed as Solitary fibrous tumor of pleura. CK, EMA, Actin, S 100 were negative. Vimentin and CD 34 were strongly positive. Van Gieson showed the collagenous nature of the tumor.
Conclusion Definite diagnosis mostly can be reached after total exision of the tumour and detailed pathological

P-147

The expression of p-53 in tracheal mucosa of patients with laryngeal squamous cell carcinomas

D Manestar, R Starcevic, D Kovac, N Jonjic
Clinical Hospital Centre of Rijeka, Medical Faculty, Rijeka, Croatia

Introduction Analysis of immunohistochemical markers as an indicator of development and progression in tobacco component–induced tumors in the respiratory tract. However, although the inhaled smoke is passing through laryngo-tracheo-bronchial tree, cancers of trachea are extremely rare. The role of p-53 in cell growth regulation and its frequent overexpresion in tumors has lead to studies investigating its involvement in cancer. Mutation of the p53 gene occurs in approximately 45% of human cancers. p-53 expression increased consistently during the formation of squamous cell carcinomas of the larynx, trachea, bronchi and lungs.
Materials and methods Samples of tracheal mucosa from patients with laryngeal carcinoma (No =91) or non-malignant diseases (controls, No =20) were embedded in paraffin and stained with HE. p-53 was immunohistochemical performed on 6 sections in the tissue samples. The immunohistochemical staining was carried out using monoclonal mouse anti-human p-53 protein (Clone Do-7). Scores were determined microscopically by independent pathologist. At least 200 cells at the tracheal mucosa front in at least five regions were counted. The final results was expressed as the percentage of positive nuclei per 200 cells.
Results Correlation was found between p-53-posivity tracheal mucosa and TNM classification system: p-53 index: Control group=38%, Group T2=46%, T3=56%, T4=54%.
Conclusion The opinion that the presence of p-53 oncoprotein reflects mutation of the p-53 gene is commonly accepted. Other data published evaluating the relationships between p-53 and TNM–stage, G-stage, tumor size and site, age and sex, did not reveal any dependencies, although some studies have suggested such correlations. Our analysis had shown a correlation between TNM stage and p-53 index of tracheal mucosa, but is significant only between control group and T3, and control group and T4. Authors expect such results that show the correlation between prognostic factors in laryngeal malignant epithelium and tracheal epithelium.

P-148

Undifferentiated nasopharyngeal carcinoma (lymphoepithelioma). Report of four cases

V Blažičević, M Mrčela, Ž Kotromanović
Clinical Hospital, Osijek, Croatia

Background Nonglandular nasopharyngeal carcinomas are much more common in some areas of the orient than the other parts of the world. They are subtyped as keratinizing squamous cell carcinoma (type 1), nonkeratinizing carcinoma (type 2) and undifferentiated carcinoma (Lymphoepithelioma). We present on four undifferentiated nasopharyngeal carcinomas and detail clinical and histopathological characterisation of these rare cases.
Methods All our patients were male, white and 47-75 years old. Initial complaints were various: hearing loss, epistaxis, headache, and dysphagia. Examination of the nasopharynx showed us entirely normal features, or fullness, surface granularity, or obvious carcinoma. But, all our patients had cervical lymph nodes metastases, two of them bilateral. Involved lymph nodes were typically posterior of the sternocleidomastoid at the level of the angle of the jaw.
Results Histologically, lesions show cytologically uniform cells with ovoid vesicular nuclei prominent nucleoli and indistinct cell borders resulting in a syncytial pattern. An inflammatory infiltrate rich in lymphocytes and occasionally containing prominent eosinophils is usually a component of lymphoepithelioma, but diagnosis is based solely on the nature of the neoplastic epithelial component. Neoplastic cells are negative for LCA, but positive for cytokeratin and EMA.
Conclusion Undifferentiated nasopharyngeal carcinoma (lymphoepithelioma) is very rare. About 50% to 80% of patients are initially seen with cervical lymph node metastases from an occult primary. Such lesions may be different or impossible to distinguish from lymphoma on haematoxylin and eosin stained sections, particularly when the lesion appears as a lymph node metastasis from an occult primary. Ancillary methods like immunohistochemistry and molecular techniques or detection of serum antibodies against viral proteins may be necessary.

P-149

"Atypical" pleomorphic adenoma of the parotid gland

S Mocan[1], S Stolnicu[1], D Radulescu[2], O Budisca[3], J Jung[1]
[1]Department of Pathology, University of Medicine, Targu - Mures, Romania
[2]Department of Pathology, University of Medicine, Iasi, Romania
[3]First Surgical Clinic, University of Medicine, Targu-Mures, Romania

Introduction Pleomorphic adenoma is a benign, epithelial tumor, composed of cells that demonstrate both epithelial and mesenchymal differentiation, with the absence of abnormal cytomorphologic features. We present the case of 31-years old white women, with a mass localized in the superficial, lower part of the right parotid gland.
Material and methods On clinical examination, the lesion was nodular, painless swelling, of smooth surface, measuring 40x30 mm in diameter. The tumour was excised, fixed in formaline, embedded in paraffin and the sections were stained with HE, PAS and ALCIAN blue.
Results The tumour was composed of both epithelial and mesenchymal-like tissue, with a complete capsule at the periphery. There was no neoplastic tissue within or extending through the fibrous capsule. On the other hand, the epithelial component expressed mild, limited, abnormal cytomorphologic features, such as enlarged, pleomorphic and hyperchromatic nuclei.
Conclusions Presence of prominent cytomorphologic atypias and capsular involvement in a pleomorphic adenoma causes concern about malignant transformation, but a lesion with mild or focally limited cytological atypias is designated as atypical pleomorphic adenoma and indicates an increase likelihood of malignant transformation if the tumor recurs.

P-150

Polymorphous low-grade adenocarcinoma of the minor salivary glands: immunohistochemical analysis and assessment of p53 expression and proliferative activity in two cases

Ö Tulunay[1], M Saatçi[2], EO Tulunay[2]
[1]Medical School of Ankara University, Department of Pathology, Ankara, Turkey
[2]Medical School of Ankara University, Department of Otorhinolaryngology, Ankara, Turkey

Introduction Polymorphous low-grade adenocarcinoma (PLGA) is a minor salivary gland carcinoma usually arising intraorally, primarily in the palate. These tumours may be confused histologically with cellular pleomorphic adenomas and adenoid cystic carcinomas. The aim of this study was to describe the immunohistologic features of PLGA, in comparison with those of PA and ACC.
Materials and methods This report describes the immunohistochemical distribution of epithelial membrane antigen (EMA), carcinoembryonic antigen (CEA), high-molecular-weight keratin (HMWCK), low-molecular-weight keratin (LMWCK), smooth muscle actin (SMA), vimentin (VIM) and glial fibrillary acidic protein (GFAP) in two cases of PLGA arising in the hard palate and the nasopharynx. Immunoprofile of a demonstrative case of PA and ACC were also evaluated. Immunoexpression of p53 oncoprotein and proliferative activity, measured by the expression of Ki-67 antigen and proliferating cell nuclear antigen (PCNA) were studied in all tumours, in aiding to distinguish benign from malignant lesions.
Results The tumor tissue in PLGA displayed diffuse and strong staining with HMWCK, LMWCK, VIM, and S-100. Cytoplasmic and luminal staining for CEA was seen in occasional cells. GFAP, SMA, and EMA displayed negative staining. Quantitative assessment revealed p53 positive staining in all tumor types. The percentage of tumor cells positive for PCNA staining was 80 % and Ki-67 antigen expression was 8.5 % in PLGA.
Conclusion PCNA and Ki-67 antigen, S-100, CEA and EMA immunoreactivity appears to be a potentially useful supplementary diagnostic tool in differentiating difficult cases of PLGA from ACC and PA.

P-151

Gene expression in major types of salivary gland carcinoma has similarities with gene expression in pancreatic and prostate carcinoma

KJ Jee[1], I Leivo[2], K Heikinheimo[3], N Balint[1], O Juha[4], K Sakari[1]
[1]Department of Medical Genetics, Helsinki, Finland
[2]Department of Pathology, Helsinki, Finland
[3]Department of Oral and Maxillofacial Surgery, Institute of Dentistry, Helsinki, Finland
[4]Department of Biosciences, Division of Biochemistry, Helsinki, Finland

Gene expression profiles were determined in fresh-frozen samples of mucoepidermoid carcinoma (MEC), acinic cell carcinoma (ACC), salivary duct carcinoma (SDC), and adenoid cystic carcinoma (AdCC), using cDNA microarrays containing cDNA fragments of 1176 cancer-related human genes. The validity of findings was checked by means of real-time reverse-transcript polymerase chain reaction studies. Seventy-five genes were found to be more than 2.5 times overexpressed and 87 less than 0.4 times underexpressed than in samples of normal parotid gland. Five genes, namely fibronectin 1 (FN1), tissue metalloproteinase inhibitor 1 (TIMP1), biglycan (BGN), tenascin-C (HXB), and insulin-like growth-factor-binding protein 5 (IGFBP5) were overexpressed in all of the types of carcinoma studied. Sixteen genes, including mothers against decapentaplegic homolog 4 (MADH4/SMAD4) and prostate-specific membrane antigen (PSM/PSA) were underexpressed in all types of carcinoma studied. Average-linkage hierarchical clustering undertaken in relation to selected genes showed that high- and low-grade MECs formed one group of tumours, ACC/SDC another. Significance analysis of microarray findings identified 33 genes related to the MEC group, 10 associated with the ACC/SDC group. Our results indicate genes that may be involved in carcinogenesis in the salivary glands. Gene expression in normal and malignant salivary tissues was also found to be similar in several respects to gene expression in normal and malignant pancreatic and prostate tissues.

P-152

Rare tumours in the sinonasal tract

P Nagy, F Salamon
National Medical Center, Dept. of Pathology, Budapest, Hungary

Introduction Sinonasal neoplasms include numerous groups of different histogenetic types. The epithelial tumours have the highest prevalence among them in the daily routine, but we can encounter such lesions, which may cause diagnostic difficulties. The purpose of this study is to determine the least frequent tumours in our sinonasal biopsy files. We collected those kinds of tumours which occurred only once in our series.
Material and methods We reviewed our archive material of a 10-year period (1993–2002) Five cases were selected. The histologic slides were re-examined. HE, special stains, immunohistochemistry and electronmicroscopy were applied.
Results The cases in the order of their occurrence: 1. Fibrous solitary tumour, we supported our original opinion by CD 34 immunostaining performed retrospectively. 2. Chordoma, in addition to the morphologic features the S100 and cytokeratin co expression were pathognomic. 3. PNET, in this problematic case finally the CD99 positivity proved to be diagnostic. 4. Intestinal-type adenocarcinoma, the mucocele-like appearance and the highly differentiated colonic type epithelial structures reminiscent of adenoma caused our dilemmas. 5. Meningeoma, the immunohistochemical results were not convincing. We established the diagnosis by means of electronmicroscopy.
Conclusions The incidence of sinonasal neoplasms is low. The recognition of the unusual lesions in this region is a challenge for the pathologist. Ancillary techniques may be necessary in the diagnostic process.

P-153

Squamous cell carcinoma: diagnostically problematic variants

F Salamon, P Nagy
National Medical Center, Dept. of Pathology, Budapest, Hungary

Introduction The diagnosis of squamous cell carcinoma (SCC) is seldom problematic. Although it may cause difficulties for the pathologist to verify its uncommon varieties. The aim of this study

was to distinguish the rare variants of SCC from the conventional ones in our laryngeal tumour file and to present the most instructive cases.
Material and methods We reviewed our archive material of a 5-year period (1998-2002). Four cases were selected. The histologic slides of the preoperative biopsies and the surgical specimens were re-examined as well. HE, special stains, immunohistochemistry and electronmicroscopy were applied.
Results 1. „ Carcinosarcoma" with rhabdomyosarcomatous differentiation. This case represents a unique example of the spindle cell carcinoma category. 2. Verrucous carcinoma with verrucous hyperplasia. The interpretation of the latter term is a complicated issue. By virtue of our patient's follow-up we encountered this dilemma. 3. Papillary squamous cell carcinoma (PSCC). This 13-year long case history is a well-documented instance of a papilloma-papilloma with dysplasia-carcinoma sequence. 4. Adenosquamous carcinoma. It was not easy to justify the clinical suspicion of malignancy preoperatively. Furthermore we faced a differential diagnostic problem when we evaluated the removed larynx.
Conclusions In all the cases we managed to establish the definite diagnosis only by the thorough examination of the surgical specimens. Additionally we found special features as far as the morphology and histogenesis are concerned. So we can confirm the subheading of the corresponding AFIP fascicle for this tumour group: diagnostically problematic variants.

P-154

Intraocular leiomyoma: case report

L Puńal-Vidal[1], J Suárez Peńaranda[1], MJ Blanco[2], A Pińeiro[2], C Capeáns[2], J Forteza Vila[1]
[1]Department of Pathology. University Hospital, Santiago de Compostela. Spain
[2]Department of Ophtalmology. University Hospital, Santiago de Compostela. Spain

Introduction Intraocular leiomyomas are rare tumours probably arising from the ciliary body smooth muscle. They represent a diagnostic dilemma and must be differentiated from neural tumours and, more importantly, from amelanotic melanoma. They occur more frequently in women, usually between the third and sixth decades of life.
Case report We report the case of a 44 year-old woman with gradual loss of vision in her right eye. Slit-lamp examination and binocular ophthalmoscopy showed a large and pigmented ciliary body mass located in the inferior quadrants. A and B ultrasound examination revealed a multicavitary tumor with low internal reflectivity measuring 19x13.8x10.9mm. Enucleation of the affected eye was decided. Histopathological examination showed a solid neoplasm composed of interlacing and tightly packet of spindle-shaped cells with little intervening collagen. Nuclei were oval with blunted ends with no significant atypia. Mitotic activity was negligible. Immunohistochemical stains for smooth muscle actin, HHF-35, vimentin and desmin were positive. No stain was noted for S-100 protein, AE1-AE3 cytokeratin, CAM 5.2 cytokeratin, HMB-45, glial fibrillary acid protein, neurofilaments, neuron-specific enolase and synaptophysin. Final diagnosis was leiomyoma and the patient is free of disease two years after surgery.
Conclusions Intraocular leiomyomas are of clinical concern since they are difficult to differentiate from more aggressive neoplasms, especially amelanotic melanoma. In this particular case, the situation was even more complicated because the lesion was clinically pigmented. Once removed, the diagnosis was not difficult and was based on conventional histopathological examination along with confirmatory immunohistochemistry.

P-155

Correlation of various histopathologic classifications of nasopharyngeal carcinoma (NPC) with clinical parameters

G Akyol[1], M Dodan[1], M Akmansu[2], D Yamaç[3]
[1]Gazi University Medical School, Department of Pathology, Ankara, Turkey
[2]Gazi University Medical School, Department of Radiation Oncology, Ankara, Turkey
[3]Gazi University Medical School, Department of Medical Oncology, Ankara, Turkey

Introduction The aim of this study was to show a possible impact of various histologic classification of NPC on survival and correlations with clinical parameters.
Materials and methods Biopsies belonging to 36 NPC cases were histologically reclassified according to WHO and Cologne classification, and classification proposed by Hsu. Age, sex therapy modality and survival of each case were analysed. Presence of Epstein-Barr virus (EBV) was verified immunohistochemically.
Results Twenty-six of cases were male and 10 were female. Follow-up was available for 26 cases and ranged between 2 to 66 months. Eight cases died and 3 had recurrences. The recurrent tumour histology changed from type 3 to 2 in 2 cases, remained unchanged in 1. None of the clinical parameters were correlated with the survival. The type of therapy seemed to have no impact on survival. According to WHO classification 2 cases were type 1, 8 were type 2 and 26 were type 3 and it showed correlation with survival (p=0.0058). Lymphocytic infiltration, which, was added to WHO system, were seen by Cologne classification in 24 of tumours, but did not have an impact on survival. Cellular morphology and atypia suggested by Hsu's classification had no significance as well, although most of the tumours were classified as type A (%69,4). EBV infection was found to be present in 11of 29 cases. However no correlation with other parameters was found.
Conclusion In accordance to literature we concluded that WHO classification is the only parameter that has an impact on survival in NPC.

P-156

Vascular endothelial growth factor expression and microvessel count in laryngeal squamous cell carcinoma

S Erdogan Cetin[1], G Özbilim[1], K Güney[2], S Karakaya[1]
[1]Akdeniz University School of Medicine Department of Pathology, Antalya, Turkey
[2]Akdeniz University School of Medicine Department of Otolaryngology, Antalya, Turkey

Introduction Vascular endothelial growth factor (VEGF) plays an important role in tumour growth and metastasis. The purpose of this study was to re-evaluate the prognostic value of VEGF and microvessel count (MVC) in laryngeal squamous cell carcinoma.
Materials and methods In this study, 27 patients were evaluated. Microvessel staining was performed with anti-factor VIII (F-VIII)

– related antigen. Paraffin embedded tumour specimens were stained with VEGF and F-VIII using immunohistochemical methods. VEGF staining was evaluated as negative (<%10 of tumour cells) or positive (>%10 of tumour cells). Staining intensity was graded mild, moderate and severe. For evaluation of F-VIII staining, average counts of the three most vascular areas on an x200 field were recorded. Statistically correlation between immunoreactivity and the clinicopathologic factors of laryngeal carcinomas was evaluated.

Results VEGF expression in the tumour cells was found positive in all cases (%100). Staining intensity was detected as severe of 9 cases, moderate of 11 cases, mild of 7 cases. In evaluation of F-VIII staining, average MVC of all cases was found 16,9. Statistically, no association was observed between the VEGF expression, F-VIII of carcinoma cells and histologic grade, TNM stage, tumour size and tumour site. Association was observed between the VEGF expression and MVC (P=0,007). In additional, significant correlation was observed between the VEGF percentage of positive tumour cells and staining intensity (P=0,000).

Conclusion Our data suggest that in laryngeal squamous cell carcinomas, VEGF expression and MVC of carcinoma cells are not prognostic markers.

P-157

Acinic cell adenocarcinoma: presentation of five cases

M Karampola, O Tzaida, V Leodara, G Sotiropoulou, G Vecchini, I Iakovidou
Pathology Department, Metaxas Cancer Hospital, Pireaus, Greece

Five cases of acinic cell adenocarcinoma, diagnosed in our laboratory during a period of 10 years, are presented. Four of them concerned salivary gland tumours of the parotid gland, the main site of their development, and the fifth was found as an endobronchial mass. The patients ranged from 28 to 76 years of age and the greatest stromal diameter varied from 0,6 to 1,5 cm. Microscopically all neoplasms had the typical morphological features consistent with acinic cell adenocarcinoma. This neoplasm has distinct clinicopathological features and a rather indolent biological course, in spite of its malignant potential, responsible for the prevalence of the term carcinoma instead of “stromal”. A broad histo- and immunohistochemical investigation was performed confirming the diagnosis. A review of the available reference is reported.

P-158

Relationship of p53 oncoprotein expression with histological grade and outcome of patients with oral squamous cell carcinoma

L Latinovic[1], R Gajanin[1], Z Eri[2], I Klem[2], D Janicic[3], V Gajanin[4], N Tanaskovic[2]
[1]Department of Pathology Clinical Center, Banja Luka, Bosnia and Herzegovina
[2]Institute of Pulmonary diseases, Sremska Kamenica, Department of pathology and diagnostic cytology, Sremska Kamenica, Serbia and Montenegro
[3]Department of thoracic surgery, Clinical center, Banja Luka, Bosnia and Herzegovina
[4]Department of anatomy, Medical faculty, Banja Luka, Bosnia and Herzegovina

Introduction An alteration in the p53 tumour suppressor gene is the most frequent genetic abnormality in human cancers.

Materials and methods Overexpression of the p53 oncoprotein and histological differentiation were investigated in 28 routinely formalin-fixed and paraffin embedded squamous cell carcinomas of the oral cavity. P53 oncoprotein was detected in all specimens with the monoclonal antibody DO-7. P53 oncoprotein expression was scored in the following way: score 0 <10%, score 1 10-50%, score 2 >50% positive cells.

Results and conclusions Using histological differentiation, all specimens are divided in three groups: group I - well-differentiated (6 cases), group II - moderately differentiated (12 cases) and group III - poorly differentiated carcinomas (10 cases). In the first group 33% specimens were negative, 67%highly positive for the p53 oncoprotein. In the second group, positive detection of the p53 oncoprotein was observed as low in 66,7% of cases, moderately in 25% and highly positive in 8,3%. In the third group 60% expressed low positivity for the p53 oncoprotein and 20% of the cases had moderate and high positivity respectively. Patients' survival was monitored for a five years. In the group with the highestp53 oncoprotein expression 7,14% of the patients survived 5 years or longer and 17,85% survived less than 5 years. Mutation in the p53 tumour suppressor gene is highest in the well-differentiated squamous cell carcinomas, and its expression decreases in poorly differentiated carcinomas.

P-159

Immunohistochemical prognostic factors in laryngeal squamous cell carcinoma

RN Kulagin[1], S Petrov[1,2], VV Savelyev[3], AR Utkuzov[2]
[1]Kazan Medical University, Kazan, Russian Federation
[2]Kazan Cancer Center, Kazan, Russian Federation
[3]Kazan Municipal Oncological Hospital, Kazan, Russian Federation

Introduction The molecular mechanisms of growth and progression of laryngeal carcinoma are not studied well. The aim of the present study was to investigate the prognostic significance of over expressions of p53 protein, cyclin D1, c-erbB2, and markers of cellular proliferation (Ki-67 and PCNA).

Materials and methods Primary tumours were studied on a series of 75 patients. All patients were treated between the years 1991 and 1998. The expression of p53 was analysed with monoclonal DO7 antibody, cyclin D1 (clone DCS-6), c-erbB2 (polyclonal antibody Hercep Test), proliferate activity with Ki-67 (clone MIB-1) and PCNA (clone PC10)

Results Overexpression of the p53 protein was found in 36% of patients, cyclin D1 in 47%, and c-erbB2- in 13% of patients with laryngeal squamous cell carcinomas. The reverse relationship of cyclin D1 with 5-year survival of patients ($p<0.05$) was revealed. Overexpression of the p53 protein was correlated with lymph node metastasis ($p<0.05$). The value of PCNA index in patients with metastasis is significantly higher than those in patients without metastasis ($p<0.05$). The PCNA index was correlated with the stages of the TNM. High level of the Ki-67 index and the PCNA index really decreases 5-year survival in patients. No significant correlations were found between positive p53, cyclin D1, c-erbB2, Ki-67 and PCNA immunostaining and anatomical localization and histological grade.

Conclusions Immunohistological examination of c-erbB2 is not a valuable prognostic factor in laryngeal carcinoma. High proliferation index (Ki-67 and PCNA) and expression of cyclin D1 correlate with worse prognosis of the disease. Overexpression of the p53 protein is correlated with progression of laryngeal cancer.

P-160

Gingival cell answer in patients with diabetes type I associated with parodonthal disease

L Kesic[1], G Jovanovic[2], R Zivkovic[1], M Jovicic[3]
[1]Medical Faculty, Dental Clinic, Department of Oral Medicine and Parodontology, Nis, Serbia and Montenegro
[2]Medical faculty, Dental Clinic, Department of Oral Surgery, Nis, Serbia and Montenegro
[3]Medical faculty, Institute for Pathological Anatomy, Nis, Serbia and Montenegro

Introduction Parodonthal disease associated with diabetes mellitus is a special entity present in a new classification of parodonthal diseases. The pathogenic mechanisms important for developing parodonthal disease in diabetics are the disturbances in the metabolism of collagen, changes of the gingival net of the microvascular elements and gingival basement membrane and disturbance in the function of the polymorphonuclear leukocytes. The aim of this investigation was to establish predominant cell type in gingiva of patients with diabetes type I and parodonthal disease.
Material and methods Out of 100 patients that were included in our study, 52 had diabetes type I and 48 were non-diabetics. Biopsies of gingival tissues were performed. The material was stained by HE, PAS, and van Gieson.
Results The gingival epithelium showed papillomatosis, acanthosis and necrobiosis. We identified infiltrates of lymphocytes, plasmacytes, fibroblasts as well as hyalinized collagen fibres.
Conclusions Gingival answer in patients with diabetes type I with parodonthal disease is imunodeficient and combined with deep disorders of metabolism in cells, vessels and epithelium.

P-161

Peripheral giant cell granulomas of the jaws - a clinico-pathological study of 91 cases

K Bodlovic[1], S Bojovic[1], J Sopta[2]
[1]Department for Oral pathology Faculty of Stomatology, Belgrade, Serbia and Montenegro
[2]Institute of pathology, School of medicine, Belgrade, Serbia and Montenegro

Introduction The peripheral giant cell granuloma (PGCG) is reactive lesion that is confined to alveolar and gingival mucosa. The aim of this study was to present epidemiological data and histopathological features of PGCG.
Material and methods All biopsies submitted from January 1994 to December 2000 at the Department for Oral pathology Faculty of Stomatology Belgrade were reviewed and the cases diagnosed as PGCG were included in this study. All section studied were stained with haematoxylin and eosin. Following parameters were analysed: sex and age distribution, epithelium condition, demarcation of the lesion, haemorrhage zones, distribution and types of giant cells and inflammatory infiltrate.
Results Females were found to be more commonly affected than males (1.22:1). All age groups were found to be affected, with a peak at 5th decade (female) and at 1st decade (male). Most of the lesions were clearly demarcated (84%). The covering epithelium was ulcerated (49%) and hyperplastic (26%), while intact epithelium was present in 9 lesions (25 %). Interstitial haemorrhage was found in all lesions, while hemosiderin deposits were found in 86 lesions. Giant cell arrangements were diffuse in 94.5% lesions, and focal in 5.5%. Inflammatory infiltration consisted of: lymphocytes, plasma cells, and polymorfonuclear leucocytes in 54 PGCG (59%).
Conclusions Giant cell lesions of the jaws are a diverse group of lesions, which are little understood. Fibrovascular stroma and multinucleated giant cells represent the most important but not pathognomonic elements for diagnosis. Key words: peripheral giant cell granuloma, histopathologic features

P-162

Vimentin and factor VIII: expression in benign lesions of the vocal folds

S Milenkovic[1], S Ivancevic[2], Z Milutinovic[3], J Vasiljevic[4]
[1]Department of Pathology, Clinical Hospital Center, Zemun, Serbia and Montenegro
[2]Health Home 'Zvezdara', Belgrade, Serbia and Montenegro
[3]Department of Otorhinolaryngology, Clinical Hospital Center, Zemun, Serbia and Montenegro
[4]Institute of Pathology, University of Belgrade, School of Medicine, Belgrade, Serbia and Montenegro

Object Precisely histopathologic diagnosis of benign lesions of the vocal fold is very important for therapy.
Material and methods 30 tissue samples benign lesions of the vocal folds were analysed by immunohistochemical methods with monoclonal antibodies for Vimentin and Factor VIII.
Results Using this specific monoclonal antibodies we concluded that the subepithelial tissue of vocal fold polyps contains vascular spaces lining with endothelial cells (Factor VIII positive). The subepithelial tissue of Reinke's oedema contains fissured space lining with cells, which are Vimentin positive.
Conclusion In this way, using immunohistochemistry for monoclonal antibodies, we can differentiated between Reinke's oedema and polys of the vocal folds.

P-163

Warthin's tumor with multiple granulomas: a search for the cause

SM Jung, C Hsueh, TT Kuo
Department of Pathology, Chang Gung Memorial Hospital, Taoyuan, Taiwan

Introduction Warthin's tumor (WT) is a well-recognized benign neoplasm of salivary gland. Granulomatous inflammation occurring in WT is a rare phenomenon. It has been suggested that prior fine needle aspiration (FNA) biopsy might be the triggering factor. Mycobacterial infection has also been reported as a cause of granulomatous change seen in WT. We report six cases of WT with granulomatous inflammation to analyse the possible relationship to prior FNA.
Materials and methods A computerized search of pathology file of Chang Gung Memorial Hospital yielded 382 cases of WT from 1983 to 2002. Granulomatous inflammation was described in six cases (1.6%). FNA cytology was performed in two cases before surgical excision. Clinical history, histology and cytology slides were reviewed. Ziel-Neelsen stain was performed.
Results All tumours occurred in parotid gland. There were 5 men and 1 women. Their age ranged from 54 to 82 yrs (mean 68) and the tumor size ranged from 2 to 5 cm (mean 3) in maximal dimen-

sion. All six cases showed typical features of WT accompanied by multiple granulomas composed of epitheloid histiocytes and multinucleated Langhans giant cells with or without necrosis. No acid-fast bacilli were found in any of these cases. History of prior FNA was identified in two cases. Both specimens also showed granulomas and features of WT.
Conclusions The pathogenesis of granulomatous inflammation in WT remains speculative. Prior FNA has been suggested to be the cause. However, this hypothesis cannot be supported by our observation of granulomas in the cytology specimens of two of our cases. It is most likely an immunologic reaction to the tumor, but a Ziehl-Neelsen stain should be performed to exclude the possibility of mycobacterial infection.

P-164

Malignant peripheral nerve sheath tumor masquerading as an allergic nasal polyp

P Medley
Medical University of South Africa, Pretoria, South Africa

Introduction Approximately 14% of all malignant peripheral nerve sheath tumours (MPNST'S) occur in the head and neck. Of these, 59% are sporadic. The mean age at presentation is 43 years. Sinonasal tumours are extremely rare and whilst they share the morphology of MPNST'S at other locations, they tend to be of low grade at this site. We describe a unique case of a high grade MPNST clinically simulating an allergic nasal polyp in an otherwise healthy child without identifiable risk factors.
Methods A 13 year old Black boy presented with an obstructive nasal mass, which was first felt 6 months earlier. The clinical diagnosis was an "allergic polyp" and the mass was excised without antecedent roentgenographic investigations.
Results The 7x4x3cm tumor was unencapsulated but circumscribed, lobulated and friable. Histologically, predominantly high-grade sarcomatoid and epithelioid areas were seen. However, differentiating features of peripheral nerve sheath tumor were also found. These included alternating hypercellular and hypocellular areas, palisading nuclei, perithelial accentuation of cells and serpentine, buckled nuclei. In low-grade areas, axons were demonstrated by silver staining. Of the broad panel of immunohistochemical stains done, only S100 protein positivity was observed. The latter was uncharacteristically prominent.
Conclusion The young age of the patient, the tumor location and clinical presentation as an allergic polyp, the predominantly high grade microscopic appearance and the strong S100 protein positivity of this MPNST are unusual and hence worthy of documentation.

P-165

Follicular dendritic sarcoma in a Black teenager – report of a South African case and literature review

P Medley[1], A Mahlobogona[1], A Fleming[2]
[1]Medical University of South Africa, Pretoria, South Africa
[2]SAIMR

Introduction The follicular dendritic cell (FDC) sarcoma is thought to differentiate towards the dendritic reticulum cell of the lymphoid follicle, possibly originating from a pluripotential stem cell. The mean age at presentation is 44years. Histologically the hallmark of the tumor is the intimate admix of a usually low-grade sarcomatoid proliferation with predominantly B-lymphocytes. A variety of architectural patterns may be observed in a single tumor thus simulating a variety of other fusocellular tumours. The use of diagnostic immunohistochemistry as well as electron microscopy, are often necessary. We describe the clinical and pathological features of a tonsillar follicular dendritic sarcoma, highlighting aspects that are particularly uncommon.
Methods An 18 year old Black male from a rural African village presented with a tonsillar mass that had evolved over a 12-month period.
Results At surgery, a pedunculated approximately 7 x 7 cm mass was excised in fragments. Histologically, the defining characteristics of FDC sarcoma were present. Unusual features included conspicuous "thymoma-like" lobulation, foci of epithelioid change as well as a prominent plasmacytic infiltrate. The immunohistochemical profile of the tumor confirmed the diagnosis.
Conclusion The race and young age of this patient as well as the presence of unusual histological features makes our case of FDC sarcoma, an already enigmatic entity, particularly fascinating reporting.

P-166

Natural killer cell immunohistochemical detection in laryngeal carcinoma

N Kavantzas[1], J Segas[2], E Patsouris[1], C Eftychiadis[1], A Lazaris[1], L Nakopoulou[1]
[1]Department of Pathology, School of Medicine, National and Capodistrian University of Athens, Athens, Greece
[2]Department of Otolaryngology, School of Medicine, National and Capodistrian University of Athens, Athens, Greece

Introduction Natural Killer (NK) cells may provide the first line of defence against many tumours. Cells bearing the NK phenotype along with CD8+ cells have been reported to be the most frequently encountered in laryngeal cancer, mainly within tumour mass. NK cells activity in peripheral blood samples of patients with laryngeal carcinoma seems to have a favourable prognostic effect on survival. We conducted this study to evaluate the distribution of NK cells in tissues of laryngeal carcinomas.
Material and methods The study included 30 males and 1 female with previously untreated epidermoid carcinoma of the larynx (mean age, 61.32 years; range, 42-75 years). After mean follow-up of 24.067 months (range, 4-36 months), 13 patients (41.9%) had relapsed. NK cells were identified by their immunohistochemical expression of monoclonal antibodies to CD16, CD56 and CD11b antigens on frozen tissue sections. NK cell presence was scored on a semiquantitave scale and possible associations were investigated between this presence and various clinicopathological variables including the expression of several immunohistochemical markers.
Results High CD16+ NK cell presence was detected in 7(22.6%) carcinomas while low and intermediate CD16+ NK cell presence was noticed in 7(22.6%) and 17(54.8%) tumours respectively. The majority of CD16+ cells expressed one or both of the other NK cell markers. NK cell presence was statistically unrelated to patients' age, tumour location, tumour maximum diameter, tumour stage, proliferation Ki-67 index and p53 accumulation in cancer cells. As far as the prognostic impact of NK cell tissue presence is concerned, using log rank test, this parameter was not related to patients' disease free survival. Interestingly, high NK cell presence was more often detected in poorly differentiated carcinomas by

comparison to well and moderately differentiated ones; this difference reached statistical significance (p=0.031).
Conclusion Poorly differentiated laryngeal cancer cells appear to be more capable of enhancing or altering the target antigens recognized by NK cells than well and moderately differentiated cancer cells.

P-167

Primary large cell neuroendocrine carcinoma of the larynx

L Greene, K Cooper, W Brundage
Fletcher Allen Health Care-MCHV Campus, Burlington, USA

Introduction The 1999 World Health Organization (WHO) classification of pulmonary neuroendocrine tumours recognizes typical carcinoid, atypical carcinoid, large cell neuroendocrine carcinoma (LCNEC), and small cell carcinoma. Recently, LCNEC has been reported in extrapulmonary sites such as the bladder, gallbladder, and the ampulla of Vater. Aims: Using the strict morphologic criteria for LCNEC set forth by the 1999 WHO classification, we report such a tumor in the larynx.
Materials and methods Chart review revealed a 74 y.o. male with a history of colon cancer who presented with otalgia. Direct laryngoscopy with biopsy revealed an invasive poorly differentiated carcinoma. Laryngectomy with bilateral modified neck dissections was performed. The tumor invaded the pre-epiglottic space with metastases to bilateral lymph nodes (AJCC T3N2c). Histologically, the tumor cells were large with a low nuclear:cytoplasmic ratio, vesicular chromatin, and prominent nucleoli. The cells were arranged in organoid and trabecular patterns in a background of extensive necrosis and mitotic figures. Ultrasound biopsy of the liver revealed metastatic disease. The patient died within weeks of surgery. The cause of death was unknown. No post-mortem examination was conducted. Immunohistochemical expression of anti-keratin AE1/AE3, chromogranin, and synaptophysin was evaluated. Electron microscopy was performed.
Results The tumor cells stained with anti-keratin AE1/AE3, chromogranin, and synaptophysin. Electron microscopy revealed dense core granules. These findings, along with the morphologic criteria, fit with a LCNEC.
Conclusion LCNEC is a rare tumor in the larynx. Recognition at this site is essential so that proper patient management can be initiated.

P-168

Analysis of blood serum lymphocytic phenotypes in chronic hepatitis C infected patients with advanced fibrosis and periodontium diseases

A Gabriel[1], B Mazur[2], A Ziolkowski[1], K Dabrowka[1], P Radlowski[1], A Dziambor[3], E Janczewska-Kazek[4]
[1]Chair and Department af Pathomorphology, Medical University of Silesia, Zabrze, Poland
[2]Chair of Pathophysiology and Endocrinology, Medical University of Silesia, Zabrze, Poland
[3]Clinical Ward of Contagious Diseases, Medical University of Silesia, Bytom, Poland
[4]Observation and Contagious Disease Ward of the Specialist Hospital, Chorzów, Poland

Introduction Few studies focus on periodontium diseases in the course of chronic viral hepatitis C. The aim of this study was analysis of the relationship between the stage of periodontium disease and a number of lymphocytic phenotypes in blood serum of patients infected with chronic hepatitis C and advanced fibrosis.
Materials and methods The study included 28 patients (mean age of 57,3 years), whose blood serum revealed the presence of HCV-RNA, demonstrated with RT-PCR method, while biopsies helped to reveal chronic hepatitis with septal fibrosis or cirrhosis. Periodontium inflammation was assessed according to the following criteria: inflammation limbus, swelling, gingival pocket depth, presence of supragingival and subgingival calculus and gomphiasis. Each criterion was assigned 0 or 1 point, cumulatively from 0 to 4 points. Flow cytometry analysis included monoclonal antibodies: CD3, CD4, CD8, CD3/CD16/CD56, CD19 provided by Becton-Dickinson. Analysis of morphological parameters and fluorescence was performed with CellQuest computer software.
Results All patients with advanced liver fibrosis were found to show signs of advanced periodontum diseases (mean cumulative value of 3,25 points). The diseases most frequently encountered included: bleeding and calculus (N= 28), deep gingival pockets (N=20) and gomphiasis (N=18). The degree of periodontal disease depended on the total number of T lymphocytes ($p<0,05$) and on the number of T helper lymphocytes ($p<0,01$). No significant dependencies were found between the degree of a periodontal disease and NK cells, B-lymphocytes or T suppressor.
Conclusion Degree of periodontum disease in patients infected with hepatitis C is dependent on low values of T and T helper lymphocytes in blood serum.

P-169

Adenomatous ductal proliferative foci accompanied the Warthin tumour in parotid gland

T Ohuchi[1,2], T Ikeda[2], S Kon[3], Y Konishi[3], M Satoh[2], T Kaku[1]
[1]Department of Oral Pathology, School of Dentistry, Health Sciences University, Hokkaido, Japan
[2]Department of Clinical Pathology, School of Medicine, Sapporo Medical University, Sapporo, Japan
[3]Department of Clinical Pathology, Muroran City Hospital, Japan

Adenomatous ductal proliferation (ADP) and intercalated duct hyperplasia (IDH) which are two new similar disease concepts in the field of salivary gland have been reported recently focusing on the relationship of precursor lesion to some salivary gland tumour, differential diagnosis, and possibility of dedifferentiated lesion. We report here a case of Warthin tumour accompanied by the foci of the adenomatous ductal proliferation in the parotid gland and these epithelial foci exhibited the histological and immunohistochemical findings resembling tubular type of basal cell adenoma. A 57-year-old female received the resection of Warthin tumour in the parotid gland, which was diagnosed as a benign parotid gland tumour. Macroscopically, this tumour showed two small legions in the parotid area, 13 X 7 mm and 7 x 3 mm in sizes respectively. The bigger legion was a typical Warthin tumour consisted of papillary epithelial projections into cystic spaces associated with variable number of lymphocytes. Papillary projections were lined by eosinophilic two cell layers having luminal columnar cells and basal polygonal to triangular shaped cells. On the other hand, histologically, the smaller legion resembled tubular type of basal cell adenoma. This lesion showed ductal proliferation with some admixed acinar cell complexes having a fibrous capsule in its half area.

Ductal proliferation consisted of bilayered structure (inner luminal cells were strongly positive for cytokeratin and weakly positive for S-100 protein). Some stromal areas around the ductal components appeared to be cellular with spindle shaped cells strongly positive for S-100 protein immunohistochemistry.

P-170

Malignant rhabdoid tumour (proximal epithelioid sarcoma) of the tongue: report of a case

C Tomasovic-Loncaric, S Lambasa, S Manojlovic
Department af Pathology, Clinical Hospital Dubrava, Zagreb, Croatia

Introduction Malignant rhabdoid tumour of the oral cavity is very rare. To our knowledge, there has been one reported case of malignant rhabdoid tumour of the tongue so far.
Patient and methods A case of an 18-year-old female with malignant rhabdoid tumour of the tongue is presented. A patient presented with the induration of the anterior third of the tongue of 16 months duration. The surface was bulging, berry-shaped and bleeding, suggestive of an animators lesion. The radial excision of the tongue was performed.
Results Histopathological analysis revealed a solid tumour measuring 1cm in the largest diameter. The tumour was composed of epithelioid, eosinophilic cells with "rhabdoid" features; some of these cells contained rounded eosinophilic cytoplasmic inclusions that displaced the nuclei to the periphery. Most of the cells showed strong diffusely distributed vimentin immunoreactivity and focal epithelial membrane antigen and keratin immunoreactivity. Angioinvasion was present at the periphery of the tumour. Following pathological report re-excision of the tongue was done and the patient received chemotherapy. Seven month after the diagnosis, respectively, the patient showed no signs of tumour recurrence or metastases.
Conclusion Although there has been a contradiction whether malignant rhabdoid tumour represents a distinctive clinicopathological entity or a phenotypic pattern shared by heterogeneous neoplasms, most of the authors support the diagnosis of "rhabdoid tumour" because the morphological pattern is attended by aggressive biological behaviour.

P-171

A case of sarcomatoid salivary duct carcinoma ex pleomorphic adenoma in buccal mucosal region

T Ohuchi[1,2], M Satoh[2], S Azuma[2], H Asanuma[2], T Kaku[1]
[1]Department of Oral Pathology, School of Dentistry, Health Sciences University of Hokkaido, Hokkaido, Japan
[2]Department of Clinical Pathology, School of Medicine, Sapporo Medical University, Sapporo, Japan

Salivary duct carcinoma (SDC) is an established aggressive salivary gland neoplasm resembling intraductal and infiltrative ductal carcinoma of breast. Diagnostic criteria and concept of SDC has been expanded along with subtype and new entity case reports such as low grade SDC and sarcomatoid SDC. Here we report a special case of sarcomatoid SDC ex pleomorphic adenoma (PA) arising from buccal mucosal region. A 32-year-old female noticed a painless swelling of 20 x 20 mm at left buccal mucosal area, which exhibited elastic hard lesion without surface ulceration. Prior to surgical operation, biopsy tissue revealed histological characteristics of typical PA without prominent cellular atypia. After operation, this stromal relapsed 3 times in 9 months. Although histologically greater part of primary tumor showed typical features of PA with two-cell layered ductal structures, a transition from ductal epithelia to atypical or malignant neoplastic epithelia was observed. These malignant neoplastic epithelia were arranged in intraductal infiltrative pattern with cribriform (Roman bridge-like) and/or solid nests of large polygonal eosinophilic cells and small central necrosis variably. Although a part of primary tumor showed sarcomatoid appearance characterized by pleomorphic and atypical spindle cells with few carcinomatous (ductal and solid) nests but all recurrent lesions exhibited atypical spindle and multinucleated giant cells without epithelial elements. Immunohistochemical findings for SDC component: cytokeratin (++), S-100 protein (-), smooth muscle actin (-), vimentin (-), PCNA (++), sarcomatoid area of primary tumor: cytokeratin (- to +), S-100 protein (-), vimentin (++), smooth muscle actin (-), PCNA (+++), a-antichymotripsine (+), recurrent sarcomatoid area: cytokeratin (-), S-100 protein (-), smooth muscle actin (-), vimentin (++).

172

Ameloblastic carcinoma with lymph node metastases

S Manojlović[1], Č Tomasović-Lončarić[1], V Uglešić[2], B Zupičić[2], D Müller[1], V Zubčić[2]
[1]Department af Pathology, University Hospital Dubrava, Zagreb, Croatia
[2]Clinic of Maxillofacial Surgery, University hospital Dubrava, Zagreb, Croatia

Background Malignant epithelial odontogenic tumours are extremely rare. Although locally aggressive and infiltrating, with high recurrence rate, ameloblastoma is a benign odontogenic tumour. Malignant form of ameloblastoma may present as ameloblastic carcinoma or malignant ameloblastoma. Ameloblastic carcinoma exhibits cytological features of frankly malignant epithelial cells along with recognizable ameloblastoma.
Patient and methods A case of a 47-year-old male with ameloblastic carcinoma of the mandible is presented. A year ago, presenting symptom was discomfort in the area of his left mandibular second premolar and first molar teeth. Nine months later physical examination revealed an expansion of the mandible and destruction of its lingual cortex, accompanied by marked exulcerated lesion of sublingual mucosa extending from medial line to the retromolar area. Panoramic radiograph revealed a large radiolucent lesion causing bony destruction of the mandible. A biopsy was done and the pathological report indicated a squamous cell carcinoma. Three months later patient presented at maxillofacial department with further local progression over the midline. Examination of the neck revealed no lymphadenopathy.
Results Patient underwent segmental mandibulectomy from right premolar region up to the left angular region and bilateral modified neck dissection. Pathological report indicated a ameloblastic carcinoma with positive neck nodes bilaterally.
Conclusions Ameloblastic carcinoma with metastasis is a rarity, and a case with lymph node metastases at the admission has not been found in the available literature. Further reporting of this highly aggressive neoplasm is encouraged.

P-173

Prognostic significance of cathepsin D intratumoral heterogeneity in laryngeal squamous cell carcinoma

M Coric[1], I Ilic[1], L Batelja[1], Z Bumber[2], M Bura[2], S Seiwerth[1]
[1]Institute of Pathology Medical Faculty, Zagreb, Croatia
[2]ENT Clinic, Zagreb, Croatia

Introduction Our previous investigations demonstrated prognostic significance for cathepsin D immunoreactivity in laryngeal squamous cell carcinoma (LSCC). We also demonstrated heterogeneity for AgNOR and DNA content in different areas of LSCC showing prognostic potential for DNA content of invasive tumour border. As this heterogeneity is a potential source of highly variable results we decided to investigate cathepsin D parameters in different microscopically defined tumour areas of LSCC.
Patients and methods 100 total laryngectomy specimen have been immunostained with anti-cathepsin D antibody (DAKO). Three distinct regions were analysed: transformation zone, invasive tumour margin and tumour center. Immunoreactivity in tumour and stromal cells was accessed by scoring (0 - 4) in at least 200 cells respectively. Tumour and stromal cell positivity was accessed in the most positive area of tumour staining of the respective tumour region.
Results and conclusion Significant difference of immunostaining was observed between tumour invasive margin and the other regions. In most cases the invasive margin was the most prominently stained region for tumour as well as for stromal cells. Most patients showed stronger staining of stromal than tumoral cells. Only patients with survival less than 30 months showed stronger tumour than stromal cell staining in invasive margin. From this we can conclude that the basis for cathepsin D prognostic value in laryngeal SCC lies in the stromal/stromal cell correlation of cathepsin D immunoreactivity of the invasive stromal margin.
Literature Seiwerth at al.: Immunohistochemical analysis and prognostic value of cathepsin D determination in laryngeal squamous cell carcinoma. J Chem Inf Comput Sci. 2000 May-Jun; 40(3):545-9.

P-174

Relationship between clinical and immunohistological properties of the middle ear cholesteatoma

N Milanovic, J Dimitrijevic, M Colic, M Jovic, M Djukic, V Jacimovic
Military Medical Academy, Belgrade, Serbia and Montenegro

Introduction Middle ear cholesteatoma is characterized by proliferation of the keratinised squamous epithelium and accumulation of keratin debris into the middle ear cleft and mastoid. By aggressive growth it leads to the destruction of the mucous membrane, middle ear ossicles and nearby bony structures. Various inflammatory and immunocompetent cells as well as cytokines are involved in activation of epidermis and subepithelial tissue and accumulation of keratin debris in cholesteatoma. In the matrix of cholesteatoma as well as in the epidermis of the skin, Langerhans and Merkel cells are identified. The aim of this study was to elucidate the role of Langerhans and Merkel cells in mechanisms of cholesteatoma growth.
Material and methods Pathohistological and immunohistochemical studies were performed in 26 cholesteatoma specimens compared to the ear canal and retroauricular skin. Mononuclear antibodies against cytokeratin 20, which label Merkel cells and CD1 molecule with expression on Langerhans cells, were studied immunohistochemically.
Results and conclusion Correlation of the presence of Merkel and Langerhans cells as well as the extent of mononuclear cellular infiltrate in the perimatrix according to the degree of ossicular defect and the destruction of the bony walls were made. We found that these cells are predominantly seen in the cholesteatoma with aggressive and destructive growth. They were seen in the less degree in the skin.

P-175

The role of high-resolution flow cytometry in the grading of mucoepidermoid carcinomas

W Van Heerden[1], L Dreyer[2], EJ Raubenheimer[3], H Coleman[4]
[1]Dept of Oral Pathology, University of Pretoria, Pretoria, South Africa
[2]Dept of Anatomical Pathology, University of Pretoria, Pretoria, South Africa
[3]Dept of Oral Pathology, MEDUNSA, Pretoria, South Africa
[4]Dept of Oral Pathology, University of the Witwatersrand, Pretoria, South Africa

Introduction The grading of mucoepidermoid carcinomas (MEC) is based on subjective microscopic evaluation of the prevalence of cell types as well as features of atypia and aggressiveness. A more objective, modified grading system based on the allocation of numerical scores to histological features was recently proposed by Brandwein et al 2001. Our study was aimed at evaluating the role of high-resolution DNA flow cytometry in the grading of MEC.
Material and methods Sixty-eight cases of intraoral- and major salivary gland tumours diagnosed as MEC were retrieved. The diagnosis of all cases was reviewed and the grading system proposed by Brandwein et al applied. Flow cytometry was performed on 50 μm sections of the formalin-fixed paraffin-embedded tumour blocks. The nuclei of the cell suspension were stained with DAPI solution (4`,6-diamidino-phenylindole) and at least 10 000 events from each case were analysed using a PAS III flow cytometer equipped with a high-pressure 100 W mercury lamp.
Results and conclusion Sixty-eight cases of MEC were retrieved and 44% were graded as high, 26% as intermediate and 30% as low. Ninety-four per cent of the high-grade MEC showed aneuploid DNA cell populations while 95% of the diploid tumours were graded as intermediate or low. Forty-four percent of our sample was graded as high, 26% as intermediate and 30% as low. Ninety-four per cent of the high-grade MEC showed aneuploid DNA cell populations while 95% of the diploid tumours were graded as intermediate or low. This study showed that high-resolution DNA flow cytometry of archival paraffin-embedded tissue is accurate in the grading of MEC.

P-176

Malignant melanoma of the head and neck mucosa: review and revision on six cases

H Harada[1], Y Toyozumi[1,2], N Arima[1]
[1]Department of Pathology, Kurume University School of Medicine, Kurume, Japan
[2]Department of Otorhinolaryngology, Kurume University School of Medicine, Kurume, Japan

Introduction Malignant melanoma is a well recognized cutaneous

malignancy with poor prognosis, but occasionally arises in the various mucosa of general site including nasal or paranasal sinuses and oral cavity. It shows wide variety in cellular morphology and histological architecture and, therefore, can be easily disregarded as other neoplasm in such instance above. We describe herein a series of malignant melanoma arising in the head and neck mucosa, which diagnosis was corrected in our review, and discuss its histological and immunohistochemical characteristic as well as important clues for diagnosis.
Materials and methods Six cases were selected from the pathology files of Kurume University Hospital. Histological sections were routinely processed, stained with H&E, and observed with a light microscope. Immunohistochemistry and special stains were done as needed. Among these, two arose in ethmoid sinus and the others in nasal cavity, inferior nasal choncha, tongue and palate, respectively. Age ranged between 62 and 88 years old (average 74.8).
Results and conclusion The tumours showed undifferentiated morphology with anaplastic or sarcomatoid appearance and cellular population included ovoid, polygonal and spindle cells, occasionally intermingled with those with rhabdoid or plasmacytoid features. Immunoreactivity for HMB45, Melan-A and CD63, know as melanoma-related markers, considerably varied for each case, while that for S100 protein was relatively stable and useful for initial screening. Melanin deposition was easily passed by, especially if it appeared in the stroma rather than neoplastic cells themselves, but quite important as well as intraepithelial spread of atypical melanocytes. If resected together, also mucosal tissue should be examined carefully.

P-177

Tenascin expression in salivary gland tumors: an immunohistochemical study in 33 cases

YS Gurbuz[1], C Ercin[1], Ö Aydin[2], A Almaç[2]
[1]Kocaeli University Medical Faculty Pathology Department, Kocaeli, Turkey
[2]Kocaeli University Medical Faculty Otolaryngology Department, Kocaeli, Turkey

Introduction Tenascin is an extracellular matrix glycoprotein, which interacts with other extracellular matrix proteins and cells. It is reported that tenascin expression is detected in different localizations of normal salivary gland tissue and in most of salivary gland tumours. It is accepted as an indicator of invading potential in a report. The aim of this study is to detect whether tenascin expression patterns relate with type and malignancy of salivary gland tumours.
Material and method 33 cases of salivary gland tumours: 8 Warthin's stromal, 18 mixed stromal, 1 myoepithelioma, 1 basal cell adenoma, 1 basal cell adenocarcinoma, 2 acinic cell carcinoma, 1 adenoid cystic carcinoma, 1 malign mixed stromal were included in our study. Antibody anti-tenascin was applied to the paraffin sections.
Results Tenascin expression was observed in all tumours. Most invasive expression was observed in mixed tumours, generally in extra cellular matrix localization and in the pattern of coarse clusters. Warthin's tumours demonstrated dominantly epithelial tenascin expression, sometimes in globular pattern. In malignant salivary gland tumours tenascin expression is relatively rare compared with benign ones.
Conclusion Our findings suggest that tenascin expression may show variations in patterns and localizations in different kind of salivary gland tumours. Tenascin expression is not a feature of invasive potential but may be responsible of epithelial mesenchymal interactions, stromal growth, cell differentiation and production of mixoid and chondroid matrix.

P-178

Links between nucleolar and extracellular matrix proteins: tenascin and Ki-67 in vocal cord biopsy

M Krstulja
Department of Pathology, Medical Faculty of Rijeka, Rijeka, Croatia

Introduction It is postulated that cancerogenesis goes through interchange of differentiation and proliferative processes. The aim of this study was to investigate morphogenesis and proliferation in the epithelial compartment of hyperplastic, dysplastic and neoplastic vocal cord mucosa with simultaneous expression of tenascin and Ki-67.
Materials and methods 48 vocal cord biopsies were analysed: 17 invasive squamous cell carcinomas, 10 in situ squamous cell carcinomas, 10 hyperkeratoses with low dysplastic change, 5 papillomas and 6 nodules with hyperkeratosis. Immunohistochemistry was performed for each marker separately as well as simultaneously for both markers.
Results Tenascin was expressed in differentiated and neoplastic tissues, decorating the membrane/cytoplasm of cells in carcinoma and dysplastic mucosa, but only the intercellular epithelial junctions in papilloma and hyperkeratosis. Ki-67, a nucleolar protein, decorated nuclei, nucleoli and chromosomes of cells engaged in mitosis in homotypic and heterotypic bioptic tissue. A double staining for tenascin and Ki-67 revealed synchronous decoration of cytoplasms and nuclei in invasive squamous cell carcinoma (17/17), in cells of in situ squamous cell carcinoma (6/10) and occasionally in cells of dysplastic hyperkeratosis (2/10). Simultaneous staining was not found in homotypic tissue. Neoplastic cells in mitosis had tenascin stained membranes/cytoplasms or were tenascin negative. In dysplastic hyperkeratosis basal cells in mitosis had rarely tenascin positive membranes (1 biopsy only).
Conclusion The observation that tenascin (a marker of morphogenesis) and Ki-67 (a marker of proliferation) express simultaneously in neoplastic epithelial cells makes a difference regarding homotypic proliferation.

P-179

RTPCR detection of ret/PTC 1 rearrangement in a case of osteoclastoma like anaplastic thyroid carcinoma

E O'Regan[1,2], P Smyth[2], S Finn[2], O Sheils[2], J O'Leary[1,2], M Toner[2]
[1]Dublin Dental Hospital, Lincoln Place, Dublin 2, Ireland
[2]University of Dublin, Trinity College

Introduction Anaplastic thyroid carcinoma with an osteoclastoma like component is a rare type of thyroid neoplasm. The origin of the osteoclastoma like element has been a source of controversy, with conflicting theories emerging from the literature, some supportive of an epithelial origin with others favouring macrophage/histiocytic lineage. Ret/PTC is a fusion transcript associated with papillary thyroid carcinoma but not previously described in a tumour of this type. Our aim was to examine more closely the osteoclastoma like component and assess the histogenesis of this tumour.
Materials and methods Electron microscopy, histochemistry and

a broad immunohistochemical panel were performed. In addition pure populations of each constituent cell type comprising the tumour were isolated using laser capture microdissection. After RNA extraction, each of these was examined by RTPCR for chimeric transcripts of ret/PTC-1 and ret/PTC-3.
Results Electron microscopy, histochemistry and immunohistochemistry were supportive of a macrophage origin for the osteoclastoma element. However, chimeric transcripts of ret/PTC were detected in the microdissected bland mononuclear cells of the osteoclastoma component. Ret/PTC could not be detected in the microdissected multinucleated giant cell component.
Conclusion We present a case of osteoclastoma-like anaplastic carcinoma of the thyroid and we demonstrate, for the first time, ret/PTC chimeric transcripts (ret/PTC-1) within the mononuclear cells of the osteoclastoma component thus shedding further light on the controversy regarding the histogenesis of this tumour.

P-180

Proliferative activity in oral peripheral and central giant cell lesions – immunohistohemical expression of p53, PCNA and Ki-67 - first report

TJ Mecik, H Fiegler-Mecik, D Sabat, A Ziolkowski
[1]Department of Pathomorphology, Medical University of Silesia, Zabrze, Poland

Introduction Aim of the study was to define a correlation between the index value of p53, PCNA and Ki-67 in several types of oral mucous epulides and to evaluate their proliferative activity.
Methods Histopathologic studies were performed in a group of 56 patients. Monoclonal antibodies p53 (DAKO) – clone DO-7, subclass Ig-2b Kappa, method ABC (code NPO 10) were applied in the immunohistologic analysis. Nuclear antigen of proliferating cells, PCNA, was marked thanked to monoclonal antibody PC10 (DAKO), subclass IgG2a Kappa. Nuclear antigen Ki-67 was marked with the use of mouse monoclonal antibody MIB-1 (DAKO), class Igg-1 Kappa, code N1633. The p53, PCNA and Ki-67 indices were defined as a percentage of positive reactions to 1000 cells in high power fields.
Results No expression of the protein coding gene, p53, which is present in a great number of neoplasms was observed. It can be a proof of their non-neoplastic origin. Analysing preparations with PCNA, one can observe great proliferative activity in the epulides of the studied types. In case of Ki-67, a small proliferative activity is observed. The average indices for women are: IEg 4.4, IEf 2.6, IEi 3.2. For men IEg 1.8, IEi 2.1. At this stage of our study, due to small differences in each epulis type, no far-reaching conclusions can be drawn. Further studies of CD68 and MDM-2 protein in the same group of patients seem to be justified since in the authors' opinion, they will explain biological behaviour of that type of tumours.
Conclusions Great proliferation activity of the cells in all types of epulides analysed with PCNA, with low Ki-67 and lack of p53 activity, was observed.

P-181

Adenoid cystic carcinoma and polimorphous low grade adenocarcinoma of salivary glands. A morphometric study

C Giardina[1], E Maiorano[1], C Rubini[2], M Carlucci[1], S Pentimella[1], T Valente[1], T Cipriani[1], T Lettini[1], G Serio[1], GF Favia[3]
[1]Dipartimento Anatomia Patologica e di Genetica, Universita di Bari, Bari, Italy
[2]Ist. di Anatomia Patologica, Universita di Ancona, Ancona, Italy
[3]Dip. Odontostomatologia E Chirurgia Generale, Universita di Bari, Bari, Italy

Introduction adenoid cystic carcinoma (ACC) and polymorphous low grade adenocarcinoma (PLGA) have a relatively high rate among salivary glands carcinomas. These tumours share several morphologic, histogenetic and cytogenetic features regarding their morphology. Nevertheless they present a different biological behaviour: PLGA is generally considered only a locally aggressive tumour whereas ACC, though in a long time, can cause recurrences and distant metastases. In this study five cases of ACC and four cases of PLGA are compared in order to identify morphological differences between epithelial cell nuclei useful for their discrimination.
Material and methods all the biopsies were formalin fixed, wax embedded and haematoxylin-eosin stained. 30 nuclei of PLGA and 30 of ACC were submitted to the SAM (Shape Analytical Morphometry) software system, which enables us to express numerically both dimensions (area, perimeter and diameter) and nuclear contour irregularities and shape distortions. Each selected nucleus was photographed at 1000X. For each nucleus 14 variables were obtained; all of them were submitted to univariant statistical comparisons by considering the total number of studied nuclei for the two lesions. Moreover, a multivariate test was performed.
Results nuclei of PLGA resulted significantly larger and with a more regular shape than nuclei of ACC. Multivariate analysis discriminated the 85% of nuclei by utilizing 3 variables: nuclear area and 2 variables obtained by the nuclear asymmetry evaluation.
Conclusion Morphocytological differences could have a discriminating power between PLGA and ACC, they seem to be more important than architectural differences and could be related to their different biological behaviour.

P-182

Oral synovial sarcoma – a report of two cases and a review of the literature

S Meer, H Coleman, M Altini
University of the Witwatersrand, Johannesburg, South Africa

Introduction The head and neck region constitutes the second most common site of involvement for synovial sarcomas, accounting for up to 9% of all cases. Intra-oral synovial sarcomas are rare, with only 29 cases having been reported. The aim of this study is to report 2 additional cases of intra-oral synovial sarcoma, which occurred in the floor of the mouth and retromolar areas respectively in middle-aged black males and to review the clinico-pathologic features of all previously reported intra-oral cases.

Materials and methods The current cases were immunohistochemically stained with EMA, CD99, bcl-2, vimentin, CAM5.2, MNF116, CK7, S-100 protein, HBA71, CD34 and calretenin; and subjected to ultrastructural studies. The literature was reviewed over a period of 40 years, examining a total of 31 cases of oral synovial sarcoma.
Results The intra-oral cases differ from lesions occurring in other sites only in respect of a more marked male predilection, and a generally painless presentation. This is the first report demonstrating calretinin immunopositivity in intra-oral synovial sarcomas. Even though in the oral cavity possible earlier detection, easy accessibility and small size renders them more amenable to surgical excision, their biological behaviour remains aggressive with a poor long-term prognosis.
Conclusion This study clearly demonstrates the histomorphologic, immunohistochemical and cytogenetic similarity of intra-oral synovial sarcomas to that of synovial sarcomas in general. The unusual intra-oral location often results in these lesions being misdiagnosed. These tumours should be considered, as both primary and metastatic tumours, in the differential diagnosis of intra-oral spindle cell malignancies.

P-183

Thirty nine years long follow up of the patient with dermatofibrosarcoma protuberans

S Vukelic-Markovic[1], S Ilic[2], N Jovic[1], J Dimitrijevic[2], M Brocic[1]
[1]Clinic for Maxillofacial Surgery, Military Medical Academy, Belgrade, Serbia and Montenegro
[2]Institute of Pathology, Military Medical Academy, Belgrade, Serbia and Montenegro

Background Dermatofibrosarcoma protuberans (DFSP) is an infiltrative, aggressive, nodular stromal with a great potential to relapse, that appears early in the life, in 15% of cases at the head and neck region. During last ten years there were five patients with the DFSP at the Clinic for Maxillofacial Surgery of the Military Medical Academy that makes 9.1% of all cases with mesenchimal malignancy. Here we present the most extreme case of the DFSP.
Case report S.S. was 8 years old when she injured a small subcutaneous stromal at the right side of her forehead. Ten years later it was 5 cm wide and excised for the first time, as well as two years later when the relapse of the same size, this time involving the bone, was removed and the patient went through radiation therapy. After four corrective operations in a meantime, at her age of 26 and 28 the relapse 6 cm wide from the right frontal region was removed. Three years later, at her age of 31, stromal sized 5 cm was excised from her right buccal mucosa. Two years later, at her age of 33, local relapse was widespread into the right parotid gland, superior eyelid and frontotemporoparietal region including dura. Two years after extensive ablative surgery and delicate reconstruction with scary compromised local cutaneous flaps, the relapse from the previously hardly mutilated right forehead region together with dura was removed. Six years later, at her age of 41, the right orbit was exenterated together with excision of adjacent temporoparietal tissues. One year later the local relapses from the right infraorbital and buccal region were removed. Two years after another stromal 5 cm sized from the periorbital region was removed. After two years, at her age of 46, the lesion from her cheek was removed. It has been her tenth, but obviously not the last surgery. Almost one year later there were no signs of local relapse or regional metastases at her routine postoperative check up.
Conclusion In spite of such a great mutilation of face and psychological disturbances connected with it, this is a case of successful surgical management of the DFSP. Few times some differential diagnostic dilemmas appeared, but careful and detailed revision of all specimens definitely confirmed the DFSP.

P-184

Multiple and multifocal malignancy - a case report

D Stefanovic[1], S Vukelic-Markovic[2], J Dimitrijevic[3]
[1]ENT and MFS Department, KBC Zvezdara - City Hospital, Beograd, Serbia and Montenegro
[2]Clinic for Maxillofacial Surgery, Military Medical Academy, Belgrade, Serbia and Montenegro
[3]Institute of Pathology, Military Medical Academy, Belgrade, Serbia and Montenegro

Background It is well known that one either benign or malignant stromal can appear multifocally, as well as the fact that histologically different tumours can exist coincidentally. There is just a few papers concerning on how many different concomitant tumours can appear in the human body. This is a case of 78 years old male with several tumours of different malignancy degree and morphologically benign or semimalignant cutaneous lesions.
Case report During previous 27 years three times he underwent surgical excision of epitheliomas of the scalp, body and limbs. The third one has been removal of the epithelioma of the right frontoparietal region. At his age of 78 because of the stromal sized 4 cm in the right parotid salivary gland, followed by paralysis of the frontal and paresis of buccal branches, along with laboratory finding of 22.48 leukocytes, right-sided radical parotidectomy and suprahyoid dissection of the neck has been performed. Pathohistologic analysis confirmed malignant mixed stromal of the parotid salivary gland. Postoperative irradiation therapy has been applied in 21 fraction and total dose of 45 Gy. Nine months later the patient has been operated again because of an exulcerated, 5 cm diameter cutaneous lesion of interscapular region, which has proved to be the infiltrative squamous carcinoma G-2 grade. At the same time the chronic lymphoproliferative disease in the form of chronic lymphocytic leucosis A grade has been diagnosed (although the reactivity following the neoplastic process could not be excluded), but specific haematological treatment has not been indicated. Nine months later nine cutaneous facial lesions have been removed: malignant mixed stromal of the left auricle, senile keratosis from the left temporoparietal region, chronic dermatitis from the forehead, squamous carcinoma G-2 and seborrhoic keratosis one inch inferiorly, two lesions, sebaceous adenomas from the right zygomatic region, corneal squamous carcinoma G-1 from the right parietal region, baseocellular carcinoma from the left one and adenoid type of baseocellular carcinoma from the right supraclavicular region. The patient has been operated without complications and came five times for monthly control in a good general condition, without relapse, regional or distant metastases. Later on we ascertained that the patient suddenly died during a sleep seven months after surgery.
Conclusion Pathohistologic examination of removed tissues and revision of the former specimens undoubtedly excluded the spreading of the one and same stromal in different regions, but proved multifocal appearance of tumours of the same embryologic – ectodermal origin in very different structures.

P-185

Melanoma of the oral cavity - a case report

S Vukelic-Markovic[1], S Ilic[2], D Stefanovic[3], S Stosic[1], S Loncarevic[1]
[1]Clinic For Maxillofacial Surgery, Military Medical Academy, Belgrade, Serbia and Montenegro
[2]Institute of Pathology, Military Medical Academy, Belgrade, Serbia and Montenegro
[3]ENT and MFS Department, KBC Zvezdara City Hospital, Beograd, Serbia and Montenegro

Background Melanoma is a capricious malignancy followed by reputation of aggressive growth and dissemination, able to originate from any tissue containing melanin. In less than 2% it appears at mucous membranes. Here we present a case of such localization.
Case report During last ten years there were 47 patients with primary cutaneous head and neck melanoma who underwent surgery because of secondary deposits at the neck, but only one patient, R.M., 52 years old (pale skin, dark hair and eyes, never working outside), who appeared four years ago with inoperable intraoral melanoma involving tongue, base of mouth, mucosa of the left cheek, retromolar region, tonsillar fossa and soft palate, including a single pendular mass from the left palatoglossal arc that almost completely narrowed his isthmus faucium. The first pigmentation he noticed eight months before his first admittance suffering of disturbed swallowing for few weeks. Although there was no sign of regional or distant metastases, only the last-mentioned mass has been removed and pathohistologically verified as melanoma. Patient was able to breathe normally, and continuing with his previous way of life. He received DTIC during the first four postoperative months. One year later, smaller mass from the same location has been removed again. Routine laboratory analyses, radiographic examination of the lungs, ultrasonographic examination of the neck and abdomen never revealed any changes. The third reduction under the same circumstances took place one year later and has been followed with minimal doses of adjuvant immunotherapy.
Conclusion This is a rare case of such a large, inoperable intraoral melanoma that has been three times reduced at the place of its exophytic growth into throat, otherwise demonstrating no signs of regional or distant spreading, as well as any disturbances in patient's general condition during last four years.

P-186

CD34, alfa-smooth muscle actin and TGFbeta1 expression in stromal cells in epithelial hyperplastic lesions and squamous carcinoma of the larynx

N Kojc, N Zidar, N Gale
Institute of Pathology, Medical Faculty, Ljubljana, Slovenia

Introduction Recent studies have shown that stromal reaction in cancer has an important diagnostic and prognostic significance. CD34-positive stromal cells and myofibroblasts may play an important role in host response to cancer. The aim of this study was to analyse the expression and significance of CD34, alfa-smooth muscle actin (SMA), and TGFbeta1 in epithelial hyperplastic lesions (EHL) and squamous carcinoma (SC) of the larynx, and tried to reveal the mechanism of myofibroblast formation in SC.
Materials and methods We investigated samples of 42 resected larynxes with SC, 12 laryngeal biopsies of EHL and SC, and 6 samples of normal laryngeal mucosa. Immunohistochemistry was performed with antibodies against SMA, CD34, CD31, TGFbeta1 and TGFbeta1 receptor. The expression of TGFbeta1 mRNA was detected by RNA in situ hybridisation.
Results Stroma of normal mucosa and EHL contained scattered CD34-positive cells, but there were no SMA-positive myofibroblasts. Stroma of SC contained SMA-positive myofibroblasts but there were no CD34-positive stromal cells. In normal mucosa and EHL, TGFbeta1 and its receptor were present in epithelial cells and scattered stromal and inflammatory cells. In SC, TGFbeta1, its receptor and TGFbeta1 mRNA were found in stromal cells, inflammatory cells and some stromal myofibroblasts.
Conclusions Disappearance of CD34-positive cells and appearance of SMA-positive myofibroblasts in the stroma is associated with transformation of laryngeal EHL to SC. This pattern of stromal reaction is limited to invasive carcinoma and should be regarded as an additional marker of invasion. Our results also support the hypothesis based on experimental studies that TGFbeta1 may be one of the mechanisms of transformation of stromal cells to myofibroblasts in SC.

P-187

FHIT gene alterations in squamous cell carcinoma of larynx and hypopharynx

M. Volavšek, D. Glavač, N. Gale
Institute of Pathology, Faculty of Medicine, Ljubljana, Slovenia

Introduction Loss of heterozygosity (LOH) on short arm of chromosome 3p is frequently found in squamous cell carcinoma of larynx and hypopharynx (LHSCC). This is a region where potential stromal suppressor gene, frequently changed in pulmonary cancer, the FHIT gene, is located. We wanted to determine whether there is presence of molecular and/or immunohistochemical changes in FHIT gene in 69 patients with LHSCC.
Materials and methods DNA was isolated from stromal and adjacent normal tissue using standard procedure. Non-isotopic LOH analysis was performed with micro satellite markers D3S1007, D3S1038, D3S1233, D3S1285, D3S1300. Formalin fixed tissue samples were stained immunohistochemically with antibody against FHIT protein and reactions scored according to % of nuclear positivity in stromal cells.
Results LOH at 3p was detected in 42 (60.9 %) and microsatellite instability (MSI) in 4 (5.8%) tumours, which were mostly moderately differentiated (60.9%). High expression of protein was found in 18, moderate in 14 and low in 18 tumours. Immune reaction was negative in 19 cases. There was no correlation between presence of LOH and/or MSI, results of immunohistochemistry and stromal grade.
Conclusion Our results show that alterations of FHIT gene are frequent in LHSCC. They are most commonly reflected by LOH, the most important mechanism in LHSCC cancerogenesis. The absence of correlation beween LOH and immunohistochemistry is probably caused by molecular changes, reflected in altered FHIT protein expression, which can not be detected with LOH analysis. Further studies are needed to determine the possible significance of FHIT gene in pathogenesis of LHSCC.

P-188

Two loci PCR test for prognosis of colorectal cancer

K Kashkin[1], A Nikolaev[2], D Turbin, A Perevoschikov
[1]Engelhardt Institute of Molecular Biology of RAS, Moscow, Russian Federation
[2]NN Blokhin Cancer Research Center of RAMS, Moscow, Russian Federation

Introduction Deletions of chromosomes 17p and 1p are usual in human colorectal cancer (CRC). Breakage of tumor suppressor genes located there is commonly considered as a cause of tumor progression. Loci YNZ22 (17p13.3) and Alu-VpA/MycL1 (1p34.3) may serve as markers of 17p and 1p loss. The aim of this study was to test whether lesions of named loci may be used as prognostic signs in CRC.
Materials and methods Losses of heterozygosity (LOH) of named loci in DNA isolated from 50 primary colorectal adenocarcinomas were tested by PCR.
Results YNZ22 LOH was found in 33% (13/39) of informative tumors and was 3 times more often in men than in women. This lesion was associated with moderate or low histological differentiation of tumors and ploidy >3n of tumor cells. Twenty two percent (11/50) of tumors showed Alu-VpA/MycL1 instability, and 14% (6/43 informative) lost Alu-VpA/MycL1 allele. LOH of this locus was associated with moderate or low differentiation. Instability of Alu-VpA/MycL1 was associated with proximal localization of tumors. By Kaplan-Meyer assessment, LOH of any one of the two loci correlates with development of CRC relapses or metastases (RM) in 30 months after tumor resection. In group of patients with any of the two LOH in tumor, 67% (8/12) had RM in this period, while in group whose tumors retained both loci heterozygous this index was 20%.
Conclusion We propose to make up group of CRC patients with RM risk in 30 months after surgery relying upon PCR test of loci YNZ22 and Alu-VpA/MycL1.

P-189

Age dependence of DNA preservation and retrieval relationship to fixative type

C Van Haaften, H Korporaal, G Kramer, M de Vries, D Meeuwisse, M Boon
LCPL Laboratories, Rooseveltstraat 4C, 2321 BM, Leiden, the Netherlands

Introduction Permeation of fixatives into tissue for optimal DNA preservation for molecular pathology studies is related to tissue type and fixative but also to glycosaminoglycan content of the ground substance. This may alter with age, warranting further study. The aim of this study was to assess nuclear DNA preservation related to age and fixation agent.
Materials and methods Fresh standardised testicular tissue samples from dogs 0 - 6 months (I), 6 months - 2 years (II) and 3 years and over (III) were used for immediate DNA extraction (T0), extraction after 24 hours (T1) and after 14 days (T14) of immersion in formaldehyde-based and formaldehyde-free, commercially available fixatives. DNA extraction used standard protocols, commercially available kits (QIAamp minikit, Qiagen, the Netherlands), standard primers for the betaglobin gene preserved between species (MYO9/MY11, Digene/Abbot, USA) and quantitative PCR (RealTime Light Cycler, Roche, 45 amplification cycles).
Results and conclusions In formaldehyde free fixatives, initial loss of extractable DNA in T1 samples of young (I) animals was 15% as compared to 20% in older (II+III) animals ($p<0.05$, student T-test). The same, with a significantly poorer result ($p<0.01$) was found in formaldehyde based fixation, with loss of 20% in young (I) as compared to 30% ($p<0.01$) in older (II+III) animals. At 14 days, further loss to 45% of T0 values occurred in all 3 age groups ($p<0.001$), with formaldehyde free fixatives retaining the proportional age associated difference. In formaldehyde based fixatives at T14, loss to 5% of T0 values was found ($p<0.001$), again without statistically significant differences between age groups.

P-190

The G870A polymorphism of CCND1 correlates with susceptibility and prognosis of breast cancer in Taiwan

CP Yu[1], J Ho[1], JC Yu[2]
[1]Department of Pathology, Tri-Service General Hospital, Taipei, Taiwan, Republic of China
[2]Division of General Surgery, Tri-Service General Hospital, Taipei, Taiwan, Republic of China

A frequent G870A polymorphism of CCND1 gene located on the splice donor site on exon 4-intron 4 boundary is implicated in influencing cyclin D1 mRNA splicing and production of two distinct mRNA transcripts. Although cyclin D1 is believed to perform an important role in cell cycle progression, this G870A single nucleotide polymorphism (SNP) seems to be a critical modulator of its functions. It has been reported that the prognostic significance and mRNA splicing regulatory effect of G870A varies with tumor type and ethnic diversity. To explore the association between the CCND1 G870A polymorphism and the breast cancer susceptibility as well as other prognostic parameters, we employed 103 infiltrating ductal carcinoma (IDC) cases and 215 native controls in this study. There is obviously correlation between the genotype distribution of these two groups ($p=0.038$), and the AA genotype reveals a higher association and risk than the AG+GG genotypes ($p=0.011$ with c2 test and OR 1.93, 95% CI 1.16-3.21, $p=0.012$). Moreover, there is no statistical significance found between genotype or allele frequencies and tumor stage, grade, nodal involvement, or patient'¡s age. However, the trend tests of CCND1 G870A genotype distribution or allele frequencies to the increasing of tumor grade or tumor stage are significantly different when comparing the A vs. G allele ($p=0.01$ in both tumor grade and stage) or AA vs. AG+GG genotype groups ($p=0.04$ and 0.05 in tumor grade and stage, respectively) but no significance when comparing GG vs. AG+AA or AG vs. AA+GG genotypes. These results suggest that CCND1 G870A polymorphism correlates with IDC susceptibility, and 870A allele reveals an increased risk in carcinogenesis of IDC and worse prognosis.

P-191

The new HOPE*-fixative as an enhancement in molecular pathology

E Vollmer[1], R Sen Gupta[1], J Galle[1], J Olert[2], KH Wiedorn[3], T Goldmann[1]
[1]Clin. & Exp. Pathology, Research Center Borstel, Borstel, Germany
[2]Childrens Pathology, Univ. Mainz, Mainz, Germany
[3]Pathology, Katharinenhospital Stuttgart, Stuttgart, Germany

During the last years the growing demand for the detection of

prognostic and diagnostic biomarkers has been slowed down to a large degree by the use of formalin and its influence onto antigenic structures and nucleic acids, although other reasons also exist. With regard to morphology a limitation in the possibilities, compared to frozen sections, takes place. With the introduction of the HOPE-fixation to date both has become possible; substantially enlarged possibilities concerning the detection of DNA, RNA and proteins together with a formalin-like morphology. This will be demonstrated by presenting several examples like preservation of nucleic acids (DNA, RNA), the detection of those by PCR and RT-PCR, in situ hybridization and the preservation and delectability of proteins by immunohistochemistry. We conclude that HOPE-fixation opens up new possibilities, especially within the growing number of diagnostic and prognostic biomarkers. *Hepes-glutamic-acid-buffer-Organic-solvent-Protection-Effect

P-192

Prognostic value of HPV viral load in cervical cancer evaluation of real-time PCR, conventional PCR and signal amplified in situ hybridization

K Biedermann[1,2], N Dandachi[1], M Trattner[3], K Peham[1,2], AH Graf[3], O Dietze[1], C Hauser-Kronberger[1]
[1]Institute of Pathology, Private Medical School, Salzburg, Austria
[2]Department of Genetics and General Biology, University of Salzburg, Austria
[3]Institute of Gynecology, Private Medical School Salzburg, Austria

Introduction High-risk human papillomaviruses (HPV) represent a major risk factor for the development of cervical cancer. Quantitative Real-Time PCR for viral load determination of HPV in archival cervical cancer specimens could be of clinical and prognostic relevance. The aim: We investigate the prognostic value of HPV status and viral load. Furthermore, we compared the applicability and sensitivity of three molecular HPV-detection methods.
Materials and methods All examinations were carried out from formalin-fixed, paraffin-embedded tissue of 164 cervical carcinomas. HPV status was detected by signal amplified chromogenic in situ hybridization (SA-CISH), conventional polymerase chain reaction (PCR), and detection and additional quantitation was performed using Real-Time PCR.
Results Patients with low viral load of HPV 16 in stage I carcinoma had a significantly better prognosis than HPV 16-negative patients (p=0.037). Additionally, high viral load of HPV 16 in patients indicating a higher stage carcinoma strongly tended to benefit prognosis compared to HPV-negative patients. Our evaluation of the molecular HPV-detection methods showed a higher sensitivity of Real-Time PCR and conventional PCR compared to SA-CISH.
Conclusion It appears that cervical cancer patients can be distinguished in a HPV 16-negative subgroup revealing a worse prognosis, and a lower-stage subgroup with low viral load, respectively a higher-stage subgroup with high viral load, both indicating a better survival, maybe due to an altered immune status caused by HPV-infection. These findings are crucial to accord each patient the individual therapy, and point out the importance of quantifying viral load and the necessity of Real Time-PCR in HPV-diagnosis.

P-193

Laser capture microdissection in 2-D coculture models as a novel tool to study tumor-stroma-interactions

R Dahse[1], A Berndt[2], H Kosmehl[1]
[1]HELIOS Clinic Erfurt, Institute of Pathology, Erfurt, Germany
[2]Institute of Pathology, Friedrich-Schiller-University Jena, Germany

Introduction Cellular adhesion, migration and invasion are essential processes in tumor progression and do include actions by malignant cells as well as by the stromal microenvironment. In vitro, these interactions can be studied in coculture models. In conventional coculture systems, the different cell types are grown together in glass-slide based chambers with medium. In situ analysis can be easily performed, however, for mutational or gene expression analyses the cell compartments have to be dissociated and sorted. We present a novel technique for co-culturing fibroblasts and carcinoma cells and separating them without cross-contamination.
Methods Our method is based on cell cocultivation on a 1.35 µm thin membrane followed by laser microdissection of tumor and stroma cells. For identifying the tumor cell compartment, immunolabeling for the laminin gamma 2 chain was performed, a marker that is expressed only in epithelial tumor cells. DNA and RNA was isolated from the microdissected cells. RNA quality was tested by RT-PCR for a housekeeping gene transcript and for the laminin gamma 2 chain gene transcript.
Results Co-cultivation on the membrane did not influence growth behaviour and cell morphology. The RNA quality from the microdissected co-cultured and immunostained cells could be successfully proved by RT-PCR. Laminin cDNA was amplificable only in tumor cells and not in the co-cultivated fibroblasts indicating no cell-cross-contamination during microdissection.
Conclusion Our technique provides a suitable tool to study tumor - stroma interactions at the DNA or RNA level for expression profiling and genetic analyses.

P-194

P53 expression in prostate cancer and its correlation with microvessel density

I Pavlenko, A Matsionis
Rostov Regional Bureau of Pathology, Rostov on Don, Russian Federation

Introduction Angiogenesis is important in the development and progression of all cancer types, including prostate adenocarcinoma (PCa). Increased vascularization may be influenced by p53 status. The aim of this study was to evaluate MVD in prostate cancer and its relationship with p53 nuclear accumulation.
Methods paraffin-embedded tissue from 61 patients with well-, moderately and poorly differentiated prostate carcinoma was examined immunohistochemically using monoclonal antibodies against CD31, VEGF and p53 (clone DO-7). A modified semiquantitative Weidner score and computerized image analysis was used to assess MVD.
Results expression of immunohistochemically detected p53 protein was found in 10 of 61 cases (16%). P53 nuclear accumulation was observed in two different groups of cancers – poorly differentiated PCa with high VEGF expression and high MVD, with high

level of serum PSA (6 cases) and moderately differentiated PCa without significant microvessels with low serum PSA (4 cases). We suppose p53 mutation in the first group of patients which leads to increased angiogenesis as the result of loss of wild-type p53-induced anti-angiogenic control. In our opinion p53 detection in the second group of p53+ patients is the result of overexpression due to stabilization but not mutation.
Conclusion p53 overexpression is observed due to either mutations or protein stabilization. Increased angiogenesis seems to be influenced by p53 mutations, while low MVD is observed in cancers with non-mutated p53. Immunohistochemistry alone is not able to detect p53 mutations, additional techniques are need for this purpose, especially in patients with p53 nuclear accumulation.

P-195

Malignancy-associated X chromosome LOH in foregut endocrine neoplasms: further evidences in lung tumors

T D'Adda[1], L Bottarelli[1], C Azzoni[1], S Pizzi[1], M Bongiovanni[2], M Papotti[2], G Pelosi[3], C Bordi[1]
[1]Dept. Pathology, University of Parma, Parma, Italy
[2]Dept. Pathology, University of Turin, Turin, Italy
[3]Dept. Pathology, European Institute of Oncology, University of Milan, Milan, Italy

Introduction association of X chromosome allelic losses (LOH) with tumor malignancy has been found in foregut-derived gastro-pancreatic endocrine neoplasms, but not in midgut carcinoids. Also lung endocrine tumors originate from the embryological foregut. They are classified into "typical" carcinoids (TC), "atypical" carcinoids (AC), large cell neuroendocrine carcinomas (LCNEC) and small cell lung carcinomas (SCLC), in order of increasing malignancy The aim of this study was to investigate X chromosome LOH and its association with malignancy in a series of endocrine tumors of the lung.
Materials and methods DNA extracted from 9 TCs, 17 ACs and 4 LCNECs from 30 female patients was PCR-amplified using fluorescently-labeled primers for 18 microsatellite markers spanning the whole X chromosome. For LOH evaluation, amplimers were analysed in an automatic DNA sequencer (CEQ2000, Beckman Coulter). All samples were formalin-fixed, paraffin-embedded and DNA from tumoral and non-tumoral adjacent tissue was available
Results allelic losses were absent in TCs, while LOH on X chromosome was found in 6 of 17 ACs (35%) and in 3 of 4 LCNECs (75%). Allelic losses were generally wide, involving all or most informative markers investigated
Conclusions allelic losses on X chromosome, absent in benign "typical" carcinoids, progressively increased their frequency from intermediate-grade "atypical" carcinoids to high-grade LCNECs. Therefore the observation that X chromosome LOH is associated with malignancy, already demonstrated in gastro-pancreatic endocrine tumors, is extended to another group of foregut-derived endocrine neoplasms, the lung endocrine tumors

P-196

Withdrawn

P-197

A new way of mycobacterial DNA-extraction for PCR targeting mycobacterial DNA in formalin-fixed, paraffin-embedded tissues

S Loeschke[1,2], T Goldmann[3], K Pueschel[4], J Caselitz[5], U Bonk[2], E Vollmer[3]
[1]Center for Human Genetics, University of Bremen, Leobener Strasse ZHG, D-28359 Bremen, Germay
[2]Department of Pathology, Central Hospital "Sankt Juergenstrasse", Am Schwarzen Meer 134-136, D-28205 Bremen, Germany
[3]Division of Clinical and Experimental Pathology, Forschungszetrum Borstel, Parkallee 1-40, D-23854 Borstel, Germany
[4]Institute for Legal Medicine, University Hospital Hamburg Eppendorf, Butenfeld 34. D-22529 Hamburg, Germany
[5]Department of Pathology, Akutkrankenhaus Altona, Paul-Ehrlich-Strasse 1, D-22763 Hamburg, Germany

Introduction Because of the withstanding mycobacterial cell-wall, DNA extraction for PCR-based detection testing is an obstacle in molecular diagnostics for mycobacteria. In formalin-fixed, paraffin-embedded (FFPE) tissues the DNA is fragmented by the fixation and embedding process. To get suitable DNA for PCR, the bacterial cell-wall has to be opened. Since currently used methods to open the bacterial wall might further increase DNA-fragmentation, we looked for a new, milder way to open up the mycobacterial cell-wall. Aims: As cut up mycobacteria in are regularly visible in Rhodamin-Auramin or Ziehl-Neelsen stained sections of FFPE tissue, we intended to open up the mycobacterial cell-wall by cutting very thin (1-2 µm) sections by microtome. In this mechanical opening there should be only little or no further fragmentation of DNA.
Materials and methods We investigated 28 formalin-fixed, paraffin-embedded tissue samples. From each paraffin-block four times 30 one to two µm sections in three steps and two 15µm sections were cut and put to 1.5 ml reactiontubes. One tube of the thin sections and the thick sections were exposed to heat/cold shock-treatment, one tube had a proteinase-K treatment for only three hours instead of overnight, and the thin cuts in another tube were treated with a Riboliser. DNA amount and purity measured by spectrophotometry after extraction. PCR was performed with routinely used 16SrDNA-Primers.
Results Over all we obtained best results with cutting up thin sections and proteinase-K treatment overnight. This tissue yielded the best purification, the highest DNA amounts and strongest bands in agarose gelelectrophoresis. Second best were thick and thin sections with heat/cold shock-treatment and proteinase-K treatment overnight.
Conclusion The mechanical opening of the mycobacterial wall using a standard microtome is a feasable way to obtain higher DNA-amounts –purity and -complexity resulting in stronger signals following PCR.

P-198

Impact of tumour suppressor gene PTEN on cell cycle and apoptosis in prostate cancer cell lines

A Hlobilkova[1], P Guldberg[2], M Svachova[1], J Knillova[1], A Pimrova[1], Z Kolar[1]
[1]Laboratory Of Molecular Pathology, Institute of Pathology, Faculty of Medicine, Palacky University, Olomouc, Czech Republic
[2]Danish Cancer Society

Introduction The tumour suppressor gene PTEN encodes a dual specifity phosphatase that recognizes lipid and protein substrates.

Aims: To study the influence of overexpressed PTEN on cell cycle progression and apoptosis.
Material and methods Prostate cancer cell lines DU-145 and PC-3 were transfected by PTENpxmyc and its mutation forms. Effect on the cell cycle was analysed by using bromdeoxyuridin (BrDU) incorporation and in situ immunocytochemistry.
Results The results are based on transient transfection of wt PTEN and its constructed point mutations with altered phosphatase activity in the prostate cancer cell lines DU-145 with mutated p53 and pRb and PC-3 with mutated p53 and wt pRb. Overexpression of the wt PTEN with intact phosphatase activity or its mutation G129E with altered lipid and functional protein phosphatase activity caused a block in G1-S transition in both tumour cell lines. Overexpression of the wt PTEN in DU-145 also led to an increase number of cells with nuclear changes which are characteristic for apoptosis.
Conclusion In tested prostate cancer cell lines PTEN blocked cell cycle by p53 and pRb independent manner. This result is not in agreement with already published mechanism in some breast cancer cells. Supported by grants IGA MZ CR NC/6779-3, GACR 204/01/0488 and MSM 151100001

P-199

Gene response to bicalutamide in prostate carcinoma cell lines LNCaP and DU-145 with respect to telomerase activity

J Bouchal[1], K Baumforth[2], M Svachova[1], J Knillova[1], P Murray[2], Z Kolar[1]
[1]Institute of Pathology and Laboratory of Molecular Pathology, Faculty of Medicine, Palacky University, Olomouc, Czech Republic
[2]CRC Institute for Cancer Studies & Department of Pathology, University of Birmingham, UK

Introduction The progression of prostate cancer from androgen-responsive to an androgen-unresponsive status remains the greatest problem in the treatment of this disease. Aims: To study the relationship between telomerase activity and gene expression after bicalutamide treatment in prostate cancer cells.
Material and methods Androgen-responsive (LNCaP) and androgen-unresponsive (DU-145) prostate cancer cell lines treated with 80 μM bicalutamide for 24 hours were analysed by Affymetrix HG-Focus Array Chips and their expression pofile was compared with control.
Results The decrease of telomerase activity which was associated with increase of p21waf1/cip1 and decrease of dyskerin and hsp90 were found in LNCaP cells only. DNA damage-responsive genes were upregulated in both cell lines. In LNCaP cells, the increase of p21waf1/cip1 was associated with induction of p53-dependent gene expression (GADD45α, bax, mdm-2 and TRAIL-R2). We have also found induced transcription of pro-apoptotic genes represented by BNIP3-like, Bcl-10, CBX4 and TRADD and the decrease of anti-apoptotic protein, survivin. In DU-145 cells, we observed an increase of mt p53, TRAIL-R2, GADD34, GADD45α expression together with a decrease in expression of survivin and the pro-apoptotic BNIP3 gene.
Conclusion The decrease of telomerase acivity in LNCaP cells after bicalutamide treatment could be explained by changes in expression of p21waf1/cip1, dyskerin and hsp90. Bicalutamide upregulates DNA-damage genes in androgen-responsive as well as androgen-unresponsive prostate cancer cell lines. This work was supported in part by MSM151100001 and NC/7497-3.

P-200

Involvement of Bcl-2 family proteins in induction of cell cycle arrest by bicalutamide in human prostate carcinoma cells

Z Kolar[1], J Bouchal[1], K Baumforth[2], J Knillova[1], N Vavrusova[1], M Svachova[1], P Murray[2]
[1]Institute of Pathology and Laboratory of Molecular Pathology, Faculty of Medicine, Palacky University, Olomouc, Czech Republic
[2]CRC Institute for Cancer Studies and Department of Pathology, University of Birmingham, UK.

Introduction Bicalutamide, an androgen antagonist used in the prostate cancer treatment, has a significant cytostatic effect on cancer cells. The aim of this study was to analyse the changes of Bcl-2 family members after bicalutamide treatment in androgen-responsive (LNCaP) and androgen-unresponsive (DU-145) prostate cancer cells.
Material and methods We examined mRNA and protein expression of the Bcl-2 family members by DNA-microarray (Affymetrix) and Western blotting.
Results Bcl-2 protein was expressed in LNCaP cells but not in DU-145 cells. Bax protein was present at similar levels in both cell lines. Bicalutamide induced decrease of Bcl-2 in LNCaP and slight increase of Bcl-2 in DU-145 cells, but the level of Bax decreased only in DU-145 cells. These changes were not accompanied by changes in levels of mRNA. Bcl-2 alpha mRNA and Bax mRNA were not detectable in both untreated cell lines. Following bicalutamide treatment, LNCaP cells showed increased transcription of Bax, Bcl-W, BNIP3, BNIP3L and BAG2, and a decreased transcription of Bik, Mcl-1 and Bid. DU-145 cells responded only by a decrease in BNIP3, BNIP3L and BAG4 mRNA levels. In addition, we have found induction of mt p53 transcription in DU-145 cells and transciptional activation of genes upregulated by p53 in both cell lines.
Conclusion Bicalutamide induces different levels of pro- and anti-apoptotic proteins of Bcl-2 family in these two cell lines. The effect of bicalutamide can be mediated by p53-driven pathway independently of hormone receptor status. This work was supported in part by MSM151100001, NC/6200-3 and NC/7497-3.

P-201

Comparing the toxicity and potential carcinogenicity of two antiestrogens. A short-term study with microarray analysis in female rat liver

P Hirsimäki[1], A Aaltonen[2], A Flores-Morales[3], L Kangas[2], G Norstedt[3]
[1]Department of Pathology, Turku University Central Hospital, BioCity, Tykistökatu 6.B.6, FIN-20520, Turku, Finland
[2]Hormos Medical Corp., PharmaCity, Itäinen Pitkäkatu 4, FIN-20520, Turku, Finland
[3]Dept. of Molecular Medicine and Cell and Molecular Biology, Karolinska Insitutet, 17176, Stockholm, Sweden

Introduction Tamoxifen and toremifene are triphynylethyle antiestrogens used in the treatment of breast cancer. Tamoxifen is genotoxic hepatocarcinogen in the rat, whereas toremifene is not. In humans, long-term tamoxifen treatment causes an increased risk of endometrial cancer. The major difference between the genotoxicity of the two drugs is the formation of liver DNA-adducts in

tamoxifen-treated rats. Differential gene expression in rat liver after administration of antiestrogens was studied by microarray analysis.
Materials and methods Equimolar doses of antiestrogens were given p.o. to six week old female Sprague-Dawley rats for 10 days. Total RNA was isolated using TRIzol Reagent. Equal amounts of total RNA from four animals in the same group was pooled and then purified from 1 mg total RNA using 35 mg oligo(dT)-cellulose. Our cDNA array contained approximately 4000 cDNA clones selected from the TIGR Rat Gene Index. The samples were hybridized to rat cDNA array scanned with a GMS 418 scanner (Afflymetrix). Image analysis was performed using the GenePix Pro software. Normalization was performed using Lowess normalization. The results from rat cDNA array were evaluated according to 'Significance Analysis of Microarrays' (SAM).
Results SAM plot for tamoxifen vs. control revealed 445 significant genes from which 183 were positive significant (up-regulated, red) q < 5 %, 165. Particularly the NADPH-cytochrome P450 oxidoreductase and microsomal epoxide hydrolase were upregulated genes which are apparently related to tamoxifen-induced carcinogenesis. SAM plot for toremifene vs. control revealed 443 significant genes from which 129 were positive significant q < 5 %, 35.
Conclusion Microarray technology gives important information of the toxicity as well as carcinogenicity of antiestrogens in experimental conditions.

P-202

Expression analysis of RET and its GDNF/GFRalpha1 ligand complex in normal gastrointestinal tract and derived tumors

J Gordillo-Chaves[1], J Moreno-Casado[1], M Jimenez-Almodovar[1], JM G-Pichel[2], C San Jose-Moreno[1]
[1]Department of Pathology and Laboratory of Investigation, Hospital de Mérida, Mérida, Spain.
[2]IBMCC/CSIC. Centro de Investigación del Cáncer, Salamanca, Spain.

Introduction The RET proto-oncogene tyrosine kinase receptor is activated by a ligand complex comprising glial cell line-derived neurotrophic factor (GDNF) and GDNF family receptor alpha-1 (GDFRalpha1). They are expressed in multiple organs during development and also in some types of human tumors in adults. The aim of this study is to investigate RET, GDNF and GDFRalpha1 expression in normal tissue and tumors derived from the gastrointestinal tract, circumstance that we have not found it published in the literature.
Material and methods RET, GDNF and GFRalpha1 expression was analyzed in samples of fresh frozen and formalin-fixed tissues from tumoral zone, and adjacent non-affected tissue of biopsies from 64 patients with gastrointestinal cancer using rt-PCR and immunohistochemical methods.
Results Presence of RET, GDNF and GFRalpha1 transcripts in most of normal tissues was confirmed by rt-PCR. Immunohistochemical study showed positive staining in citoplasms of glandular epithelium of the mucosa, ganglionar cells and muscular fibers (only GDNF) of esophagus, stomach, duodenum, colon and rectum but not in jejunum and ileum. Gastric oxyntic cells were negative. Sixty four gastrointestinal tumors (62 adenocarcinomas and 2 cases of GIST) were also studied. By immunohistochemistry, 90% of cases showed citoplasmic immunoreactivity for GDNF; 87% for RET and 96% for GFRalpha1. These findings were confirmed by rt-PCR. There was not association with microscopic type, size, grade or Duke stage.
Conclusions Our study shows RET, GDNF and GFRalpha1 positive protein and mRNA expression in normal tissues and in the majority of tumors derived from the gastrointestinal tract. There is no association with microscopic type, size, grade or lymph node metastasis. This expression gives no prognostic information in the clinical management after two years follow-up of our patients.

P-203

Expression analysis of RET and its GDNF/ GFRalpha1 ligand complex in breast cancer

J Moreno-Casado[1], C San Jose-Moreno[1], J Gordillo-Chaves[1], M Limon-Mora[1], JM G-Pichel[2]
[1]Department of Pathology and Laboratory of Investigation, Hospital de Mérida, Spain
[2]IBMCC/CSIC. Centro de Investigación del Cáncer, Salamanca, Spain

Introduction The RET proto-oncogene tyrosine kinase receptor is activated by a ligand complex comprising glial cell line-derived neurotrophic factor (GDNF) and GDNF family receptor alpha1 (GFRalpha1). They are expressed in multiple organs during development and also in some types of human tumors in adults. In this study we evaluated the expression of RET, GDNF and GFRalpha1 in normal mammary tissue and different types of breast cancer.
Material and methods RET, GDNF and GFRalpha1 expression was analyzed in samples of fresh frozen and formalin-fixed tissues from tumoral zone, and adjacent non-affected tissue of mastectomies from 31 patients with different types of breast cancer (24 DIC, 1 LIC, 3 medullary carcinoma, 1 mucinous carcimoma, 1 papillary carcinoma and 1 fibrosarcoma) using rt-PCR and immunohistochemical methods.
Results Normal breast ductal epithelium express RET, GDNF, and GFRalpha1. By immunohistochemistry, 54,8% of breast tumors showed citoplasmic immunoreactivity for RET, 83,8% for GDNF and 76,0% for GFRalpha1. rt-PCR confirmed mRNA expression in 88,4% of cases for GDNF, 42,3% for RET and 96,0% for GFRalpha1. By chi-square analysis, RET expression was associated with less tendency to the regional lymph nodes metastases ($p<0,001$) and low grade differentiation ($p<0,005$). There was not association with microscopic type, size or stage.
Conclusions We found that RET and its GDNF/GFRalpha1 ligand complex are expressed in normal breast tissues and in a high percentage of different types of breast tumors using immunohistochemistry and rt-PCR. Univariant analysis also revealed that only RET expression was associated with less tendency to the lymph nodes metastases and low grade DICs (highly differentiated tumors). The short time follow-up of our patients (less than two years) gave no information about clinical outcome.

P-204

Telomerase activity in chronic B-lymphocytic leukemia

R Jovanovic[1], D Efremov[2], G Petrusevska[1], V Janevska[1], A Stojanovic[2], M Pavkovic[2]
[1]Institute of Pathology, Faculty of Medicine, Skopje, Republic of Macedonia
[2]Clinic for Hematology, Clinical Center, Skopje, Republic of Macedonia

Telomerase, the enzyme that elongates telomeres, contains an RNA template complementary to TTAGGG repeats that permits de novo

synthesis of telomeric DNA onto chromosomal telomeric ends. Recent findings have suggested that activation of telomerase is one of the most common and fundamental steps in cancer genesis, although reactivation or telomerase up-regulation alone might be insufficient for cells to proliferate indefinitely. Telomerase expression seems to be concomitant with the attainment of immortality of cancer cells, but there are contradictory reports about telomerase activity in early and late B-CLL stages. In order to investigate the telomerase activity in patients with CLL and its correlation with the clinical stage, 47 frozen blood lymphocytes samples from patients with CLL (32 males, 15 females), and 47 age matched controls (32 males, 15 females) were investigated for telomerase activity using the 'Telomerase PCR ELISA-plus kit' from Roche, based on the Telomeric Repeat Amplification Protocol. Binet and Rai stages were evaluated at the time of sample collection, and re-evaluated after 14-16 months. Results were analyzed with a commercial statistic software package. The study showed that peripheral lymphocytes telomerase activity from B-CLL patients is significantly higher (3,9 times; $p<0,01$) compared to normal lymphocytes. The age and sex of patients does not influence the telomerase activity, while it is age dependent in healthy controls (Pearson Correlation – 0,543; $p<0,01$). The study also showed that telomerase activity is increased more significantly in advanced stages of the disease, and correlates with the disease course.

P-205

P63-driven nuclear accumulation of β–catenin is not a frequent event in human neoplasms

JS Reis-Filho[1,2], LG Fulford[1], PT Simpson[1], A Martins[2], FC Schmitt[3,4]
[1]The Breakthrough Toby Robins Breast Cancer Research Centre - Institute of Cancer Research, London, UK
[2]Life and Health Sciences Research Institute, School of Health Sciences, University of Minho, Braga, Portugal
[3]IPATIMUP - Institute of Molecular Pathology and Immunology, University of Porto, Porto, Portugal
[4]Medical Faculty, University of Porto, Porto, Portugal

Introduction DeltaN-p63 isoforms may act as oncogenes, owing to their ability to bind to p53-reporter genes without inciting their transcription, thus blocking the p53-driven cell cycle arrest and apoptosis. A novel mechanism, linking p63 and Wnt pathways has recently been proposed. Briefly, in vitro studies have suggested that deltaN-p63 may block the phosphorylation of beta-catenin, leading to its nuclear accumulation and triggering beta-catenin-responsive transcription of genes related with proliferation and oncogenic biological behaviour. To test this new mechanism, the authors evaluated the co-expression of deltaN-p63 and beta-catenin in a large cohort of human neoplasms.
Methods Two sections of TARP-4 multi-tumour tissue microarray, composed of 51 normal tissue cores and 400 human neoplasms (breast (n=75), colon (n=75), lung (n=75), prostate (n=75) and ovary (n=50) neoplasms, melanoma (n=25), and glioblastoma (n=25)) were subjected to immunohistochemistry with deltaN-p63 and beta-catenin monoclonal antibodies. p63 nuclear expression and b-catenin membranous, cytoplasmic, membranous+ cytoplasmic, and nuclear localisation were independently evaluated by three of the authors.
Results p63 expression and beta-catenin nuclear localisation were found in 92.6% and 0% of squamous cell carcinomas, 8.9% and 0% of breast carcinomas, 13.8% and 0% of lung adenocarcinomas, 1.4% and 23.2% colon adenocarcinomas, 0% and 4.8% of prostate adenocarcinomas, 11.1% and 5% of ovary carcinomas, 9.0% and 9.1% of malignant melanomas, and 12.5% and 40.0% of glioblastomas, respectively. No statistically significant association between p63 and nuclear beta-catenin expression was found for all tumours.
Conclusions At variance with squamous cell carcinoma cell lines, p63-driven nuclear accumulation of beta-catenin is an unusual phenomenon in human neoplasms. Caution should be exercised when translating the results of studies performed on cell lines to human neoplasms.

P-206

C-kit mutations in gastrointestinal stromal tumors from patients treated with STI- 571

X Matias-Guiu[1], L Catasús[2], E Casado[2], T Macarulla[2], R Nadal[2], JL Martínez[1], J Pallarés[1], A López-Pousa[2]
[1]Hospital Universitari Arnau De Vilanova, Barcelona, Spain
[2]Hospital de Sant Pau, Spain

Aims To evaluate c- Kit mutations in Exon 11 in 23 gastro-intestinal stromal tumors (GIST) from patients treatment with STI- 571 (Gleevec).
Material and methods DNA was extracted from 23 formalin-fixed, paraffin- embedded GIST samples. Mutations in Exon 11 of c- kit were analyzed by DNA sequencing. C- kit mutational status was correlated with the clinicalpathological findings and the response to STI- 571.
Results C-kit mutations in exon 11 were identified in 18 cases (78%) (delections in 14 cases, and missense mutations in 4 cases). Four GIST had no identificable KIT sequence alteration in exon 11. Mutations in c- kit seemed to be associated with favorable response to STI- 571 ($p= 0,078$).
Conclusion Kit mutations in exon 11 are common in diseminated gastrointestinal stromal tumors and appear to be associated with response to STI-571.

P-207

The use of macro-array to study the effect of intestinal trefoil factor on gene expression in caco-2 derived enterocytes

C Cuvelier[1], JA Van Huysse[1], D Laukens[1], P Demetter[1], K Vandenbroucke[1], EM Veys[1], M De Vos[1], E Remaut[1], L Steidler[2]
[1]UGhent, Belgium
[2]University College Cork

Intestinal trefoil factor (ITF) is a member of the trefoil family of peptides. It increases resistance to apoptosis, enhances mucosal healing and restitution in vivo and promotes migration of intestinal epithelial cells in vitro. The aim of this study was to investigate the influence of ITF on gene expression in intestinal epithelial cells. The human colon carcinoma cell line Caco-2 develops structural and functional characteristics of normal enterocytes when kept in culture. Enterocyte-like Caco-2 cells were treated with recombinant ITF during 2 hours. RNA was isolated and labelled cDNA was synthesised. The cDNA probe was hybridised to the Human Unigene Set 2 colony filters (RZPD). After several washing steps, the amount of signal was measured using a phospo-imager. Spot intensities were measured and signal quality was evaluated. Using a 2-fold increase or decrease as a cut off, comparison of the gene expression between un-stimulated Caco-2 cells and cells stimulated with ITF using the macro-array technique revealed a few hundred genes that were potentially differentially expressed. Our data show that the macro-array is a powerful technique to screen for differen-

tial gene expression as a result of trefoil administration, helping to study signalling cascades. However, it is necessary that the huge amount of data obtained is filtered through repeated hybridisations, only to retain the relevant changes and these data must be confirmed using other methods like quantitative Real-Time PCR and eventually studies at protein level.

P-208

BPC 157- related inhibition of cell growth in human melanoma cell line

S Radeljak[1], L Batelja[1], M Mirt[1], A Blagaic[2], P Sikiric[2], S Seiwerth[1]
[1]Institute of Pathology Medical Faculty, Zagreb, Croatia
[2]Institute of Pharmacology Medical Faculty, Zagreb, Croatia

Introduction Melanoma therapy still remains without notable success of any pharmacological agent. Gastric pentadecapeptide BPC 157 is a peptide with various pharmacological effects on different organ systems including wound healing and inflammation. Its possible effect on cell growth and differentiation was not investigated on human cancer cell lines.
Materials and methods Human melanoma cells were maintained in RPMI-1840 medium supplemented with 10% FBS and antibiotics. Cells were grown to confluency in humidified incubator (95% air atmosphere, 5%.CO2) at 37°C. Upon reaching confluency, cells were maintained in chemically defined medium (CDM). BPC157 was added in the culture medium in the various concentrations (2 pg. and 2ng, respectively) for a period of 48 hours. Cell morphology was observed daily under light microscope and the photomicrographs were taken. After harvesting cells were prepared in EtOH for flow cytometry analysis.
Results Microscopy did not reveal any changes upon treatment with BPC 157 after 48h comparing to controls. Flow cytometry showed 99% of cells ($p>0.01$) were in G0-G1 phase. Control cells had total S-phase fraction of 9.11%. However, upon introduction of BPC 157, in concentration of 2pg/ml, the percentage of cells in S-phase was decreased by 20% compared to controls. Moreover, the concentration of 2 ng/ml BPC 157 lowered total S-phase fraction by 55% comparing to controls and by 30% comparing to BPC 157 in picogram values ($p>0.01$).
Conclusion We assume that gastric pentadecapeptide BPC 157 could act as a inhibitory agent during G1-S transition state of cell cycle thereby preventing DNA synthesis and cell growth.

P-209

Profile of expression of histone genes differs in radioresistant and radiosensitive human glioma cell lines

J Slowinski[1], G Bierzynska-Macyszyn[2], U Mazurek[3], J Glogowska[3], M Latocha[3], M Widel[4], R Mrowka[1]
[1]Department of Neurosurgery and Neurotraumatology in Bytom, Medical University of Silesia, Bytom, Poland
[2]Deptartment of Pathology in Katowice, Medical University of Silesia, Poland
[3]Department of Molecular Biology in Sosnowiec, Medical University of Silesia, Poland
[4]Department of Radiobiology, Center of Oncology in Gliwice, Poland

Introduction Histones play an important role in the structural and functional properties of chromatin. Their protective role against radiation-induced damage of DNA is well established. The aim of this study was to evaluate relation between expression of histones genes and radiosensitivity of brain gliomas in vitro.
Materials and methods Five human glioma cell lines obtained from DSMZ (Germany) were irradiated with 2Gy and 10Gy doses (Co-60) and further grown for 3, 6 and 12 hrs. The expression of genes coding for histones H1, H2A, H2B, H3, H4 was measured with real-time quantitative RT-PCR assay (TaqMan). Radiosensitivity of the cell lines was assessed with cytokinesis-block micronucleus assay. Cell lines were regarded as radioresistant and radiosensitive at micronuclei per binucleate cell ratio (MN/BNC) <0.5, and > 1, respectively, as measured over a dose range of 0-10 Gy.
Results The global number of copies of histone mRNA did not differ in both groups. In radiosensitive cell lines (GAMG, 8-MG-BA) expression of H2B was highest in 2/2 cases, while in radioresistant (GOS-3, 42-MG-BA, U-138-MG) H4 predominated in 2/3 cases. In both groups significant decrease of global histone genes expression after 10Gy dose was found. Relative increase of H4 and H2B fractions after irradiation was observed.
Conclusion Overall expression of histone genes does not seem to influence radiosensitivity of glioma cells. Probably, more important is the profile of expression, e.g. differences between H4 and H2B genes. This profile may be a useful adjunctive criterion in the choice of treatment protocol for brain glioma.

P-210

Potential application of nested RT-PCR for human mammaglobin in the detection of micrometastasis in effusions

N Gorji[1], P Ferro[1], F Fais[2], PA Canessa[3], AM Carletti[3], P Pronzato[4], B Bacigalupo[1], F Fedeli[1], S Roncella[1]
[1]U.O. Anatomia Patologica, Ospedale Sant'Andrea, La Spezia, Italy
[2]Sezione di Anatomia Umana, Di.Me.S, Universita di Genova, Genova, Italy
[3]U.O. Pneumologia, Ospedale San Bartolomeo, Sarzana, Italy
[4]U.O. Oncologia, Ospedale Sant'Andrea, La Spezia, Italy

Introduction The detection of breast cancer (BC) micrometastasis in effusions is difficult since the malignant cells are rare and spread amongst the normal population. RT-PCR for human mammaglobin (hMAM) has been described as a new, sensitive method for use in BC cell research. Some authors have proposed using this assay for screening BC effusions for BC micrometastatic disease. The aim of this study was to investigate the possible application of RT-PCR for hMAM for assessing BC cells in effusions and compare this methodology with cytological examination.
Materials and methods The study was performed on 112 fluid specimens (19 BC, 52 other types of cancer and 41 without known carcinoma). The samples were analyzed by staining with EE, Papanicolau technique, and by nested RT-PCR for hMAM.
Results 16/19 (84%) cases of BC pathology were positive using nested RT-PCR for hMAM. All 9 cytology positives were also positive by nested RT-PCR. In contrast, 7 BC cases that were positive in the molecular test were negative according to the staining assay. hMAM was also detected in 19/52 (36%) specimens of other types of cancer and only 1/41 (2.4%) samples of non-neoplastic origin.
Conclusion Nested RT-PCR for hMAM was more sensitive than cytology in determining BC micrometastasis in effusions. Positivity was not restricted to samples from BC patients as specimens from other tumors and only 2.4% of patients without cancer were also positive. This test could be helpful in investigating neoplasticity in effusions.

P-211

Hepatic ischemia reperfusion injury in patients after liver segment resection

D Zauner[1], D Neumeister[1], B Heinz[2], HJ Mischinger[2], K Zatloukal[1]
[1]Institute of Pathology, Graz, Austria
[2]Dept. of Surgery, LKH Graz, Graz, Austria

Introduction Hepatic ischemia-reperfusion injury results from implementation of Pringle's manoeuvre to prevent blood losses in patients undergoing liver segment resection. Reoxygenation after the ischemic period leads to failure of hepatic microcirculation, leucocyte invasion and Kupffer-cell activation. Subsequent production of inflammatory cytokines and ROS (reactive oxidative species) are triggered, thus causing oxidative stress and damage of liver parenchyma. The goal of our study is to evaluate markers associated with the severity of this particular type of oxidative stress at the gene expression level.
Materials and methods We have analyzed liver tissue biopsies at 3 different timepoints obtained from 16 patients undergoing liver segment resection. In each case, the first sample is taken before clamping, the second sample is taken after 30 minutes of ischemia, and the third sample is taken after 30 minutes of ongoing reperfusion.
Results We compared mRNA levels of several genes (SQSTM1, HSPA1A, GPX1, SOD2, HMOX) in every set of samples by quantitative RT-PCR analysis. Significant elevation of HSPA1A at timepoint 3 was detected in 10 of 16 cases. This finding suggests that HSPA1A may represent a useful marker for oxidative injury of hepatic tissue. At the same time, we show that the detection of changes in gene expression within 30 minutes of reperfusion is possible by quantitative RT-PCR from a single biopsy.
Conclusion We hypothesize that individual differences in gene expression may reflect severity of the inflicted ischemia reperfusion injury as well as patient prognosis. The clinical significance of our preliminary results is currently under investigation.

P-212

Automated tissue microarray evaluation and normalization using a DNA scanner

W Haedicke[1], H Popper[2], C Buck[1], K Zatloukal[1,2]
[1]Oridis-Biomed GmbH, Graz, Austria
[2]Institute of Pathology, Graz, Austria

Introduction Tissue microarray (TMA) immunohistochemistry is gaining importance in drug target validation. Hundreds of tissue samples on a single slide enable simultaneous immunohistochemical assessment of protein expression. Correlation of expression levels of the target antigen with clinical parameters can facilitate determination of disease relevance and therapeutic potential. The aim of this study was to extend the scope of this technology, we developed a robot for automated TMA production. We further assessed the use of a DNA microarray two color laser scanner for automated analysis of TMA immunohistochemistry and the use of an internal reference antigen for standardization to the tissue content.
Materials and methods The TMA robot was developed in cooperation with an engineering company. A breast carcinoma TMA was stained with an estrogen receptor (ER) antibody. Lung carcinomas TMAs were double stained with combinations of rabbit and mouse antibodies. Immunoreactivity was detected with fluorescently labeled secondary antibodies. The slides were evaluated using a cDNA array scanner and software.
Results and conclusions Fluorescence intensity for ER IHC on a breast carcinoma TMA correlated positively with independent assessment of the diagnostic ER immunoreactivity score, suggesting that IHC quantitation can be achieved with the DNA array scanner. Double IHC on lung TMAs demonstrated that one antigen reference can normalize tumor marker IHC signals for the cellular content of TMA cores. IHC signal normalized in this fashion correlated with clinical parameters in agreement with published results.

P-213

Manifestation of metallothionein (MT) correlates rather with cell differentiation than with intensity of proliferation. Immunocytochemical analysis of expression of metallothionein (MT) and Ki67 in cells of ductal breast carcinoma, uterine cervix planoepithelial carcinoma and non-keratinising multilayer flat epithelium

P Surowiak[1], P Dziegiel[1], A Wojnar[2], M Zabel[1,3]
[1]Chair and Department of Histology and Embryology, University School of Medicine, Wroclaw, Poland
[2]Department of Pathomorphology, Lower Silesian Oncology Centre, Wroclaw, Poland
[3]Chair and Department of Histology and Embryology, University School of Medicine, Poznań, Poland

Introduction Metallothioneins (MT) are proteins which are supposed to play role in the cell cycle. Numerous publications describe positive correlation between intensity of MT expression and proliferative potential of cells. Our study aimed at examining the relationship between MT expression and intensity of proliferation, measured using Ki67 antigen.
Materials and methods The studies were performed on samples of ductal breast carcinomas of G1, G2 or G3 grade of differentiation as well as on samples of normal epithelium and planoepithelial carcinoma of uterine cervix. Paraffin sections of the examined cases served to perform immunocytochemical reactions using mouse monoclonal antibodies to MT and Ki67. Double staining reactions were also performed using the same antibodies.
Results The performed studies showed that MT expression in breast cancers of G1 grade was significantly lower than in cancers of G2 or G3 grades ($p=0.004$). In the case of Ki67, the least intense expression characterized cancers of G1 grade and the most intense reaction was noted in cancers of G3 grade ($p=0.00001$). No relation between MT and Ki67 expressions was observed in G1 and G3 groups of breast cancers ($p>0.05$) while in the G2 group as well as in the entire group of breast cancers (G1 to G3) a positive correlation between the two expressions was noted ($p<0.05$). Analysis of reactions in the non-keratinising stratified flat epithelium and in the planoepithelial cancers of uterine cervix showed no correlation between expressions of MT and Ki67. However, MT expression was detected only in the least differentiated cells of the epithelium.
Conclusion Our showed that MT expression tends to correlate more with cell differentiation extent than with proliferative potential of the cells.

P-214

Is the activation of Akt a prognostic parameter in colorectal cancer?

F Rojo[1], I de Torres[1], J de la Torre[1], J Tabernero[2], S Rodriguez-Muńoz[1], J Baselga[2], S Ramon y Cajal[1]
[1]Pathology Department. Vall D'hebron Hospital, Barcelona, Spain
[2]Oncology Department Vall D'hebron Hospital, Barcelona, Spain

Akt (protein-kinase B, PKB) is a serine-threonine kinase that is activated mainly by insulin, IGF-1 receptor and erbB family receptor signaling in a PI3-kinase dependent manner, and is implicated in tumor proliferation in breast, ovarian, pancreatic and gastrointestinal cancers. The phosphorylation of its substrate proteins result in increased growth and decreased susceptibility to apoptosis. The activation of the PI3K-Akt pathway is downregulated by PTEN phosphatase, and mutations or a loss of PTEN activity results in a high constitutive activation of the kinase. The aim of the present study is to investigate the levels of the activation of the PI3K-Akt pathway in a series of colorectal carcinomas and to evaluate its role on tumor resistance to chemotherapy. We achieved 46 surgical colorectal carcinoma specimens at pT3 stage. All patients received at least two chemotherapy lines based on platinum and CPT-11 after surgery. Levels of activation of Akt were tested by immunohistochemistry in primary tumors using a polyclonal antibody that recognizes the phosphorylated Akt at Ser473. In the series, 33 (71.74%) showed staining for phosphoAkt in tumor cells. PhosphoAkt was detected in tumor as clusters of cells related to necrotic foci and differentiated areas and correlated with less response to chemotherapy. These results point out that 1. Activated Akt is often overexpressed in human colorectal carcinomas and 2.Activated Akt can be a parameter of chemotherapy resistance in colorectal cancer.

P-215

Mutational analyses of the *RET* proto-oncogene in Slovenian MEN2 families

B Korošec[1], S Caserman[1], D Bergant[2], M Ravnik-Glavač[1], D Glavač[1]
[1]Department of Molecular Genetics, Institute of Pathology, Faculty of Medicine, Ljubljana, Slovenia; [2]Institute of Oncology, Ljubljana, Slovenia

Introduction Multiple endocrine neoplasia type 2 (MEN2) is an autosomal dominantly inherited cancer syndrome that appears in different subtypes MEN2A, MEN2B and FMTC. The loci for all three subtypes have been mapped to chromosome 10q11.2 which encompasses the RET proto-oncogene, a receptor-type tyrosine kinase. The key structural features include extracellular cadherin-like and cysteine rich domains, a transmembrane domain and an intracellular domain with a tyrosine kinase function. Aims: To study familial predisposition of MTC cancer in Slovenian population, 103 MTC patients were screened for germline mutations in the *RET* proto-oncogene.
Material and methods DNA was isolated from blood of patients with MTC from Slovenian registry at Institute of Oncology. The DNA samples were screened for mutations in *RET* proto-oncogene. Exons 10, 11, 12, 13, 14, 15 and 16 of *RET* proto-oncogene were amplified in PCR and analysed by single stranded conformational analyse (SSCA), direct sequencing and/or restriction digestion with endonucleases.
Results We determined typical germline *RET* mutations in 25 patients from 13 distinct families. We identified six MEN2A families, two MEN2B families and one FMTC family. In families in which the RET mutation is known, genetic testing identifies carriers with 100% specificity and 100% sensitivity.
Conclusions These findings demonstrate that molecular genetic analysis of blood derived DNA for RET point mutations is a reliable method to detect asymptomatic gene carriers of MEN2.

P-216

Mutations in *COL4A3*, *COL4A4* and *COL4A5* genes in relation to benign familial hematuria and Alport syndrome

M Šlajpah[1], A Meglič[2], A Vizjak[1], A Hvala[1], M Ravnik-Glavač[1], D Ferluga[1], D Glavač[1]
[1] Department of Molecular Genetics, Institute of Pathology, Medical faculty, Korytkova 2, Ljubljana, Slovenia
[2] Department of Pediatrics, University Medical Center Ljubljana, Slovenia

Introduction Alport syndrome (AS) is a progressive inherited nephropathy, characterized by irregular thinning, thickening and splitting of the glomerular basement membrane (GBM), associated with hearing loss and ocular symptoms. AS is caused by *COL4A5* mutations in its X-linked form and by *COL4A3* and *COL4A4* mutations in its autosomal recessive form. The mutations in *COL4A3* and *COL4A4* have been reported in familial benign hematuria (BFH). Aims: We screened *COL4A3*, *COL4A4* and *COL4A5* genes in 7 slovenian families with X-linked AS and in 31 slovenian families diagnosed with BFH to determine pathogenic mutations, to correlate them with clinical features and to confirm or provide precise diagnosis.
Materials and methods Genomic DNA was isolated from blood. Screening for mutation was done by the optimised SSCA after PCR amplification of each exon of *COL4A3*, *COL4A4* and *COL4A5* and changed samples were sequenced.
Results We found six different mutations in *COL4A5* gene in AS suspected patients. One of the mutations was present also in three families with BFH. In *COL4A3* gene three and in *COL4A4* four mutations, all in heterozygous state, were identified only in patients with BFH. Eleven of the mutations are new and private. Four rare variants of unknown pathogenesis and many polymorphisms were found in the *COL4A3* and *COL4A4* genes. A mutation was detected in 86% of AS patients and in 32% patients diagnosed with BFH
Conclusions Our study broadened the spectrum of mutations in *COL4A3*, *COL4A4* and *COL4A5* and demonstrated the involvement of the *COL4A3* and *COL4A4* genes in the pathogenesis of BFH.

P-217

Screening for genetic alterations in the *PRNP* gene

S Smerkolj, M Popovič, D Glavač
Department of Molecular Genetics, Institute of Pathology, Faculty of Medicine, University of Ljubljana, Ljubljana, Slovenia

Introduction Prion diseases are a group of fatal neurodegenerative disorders. The commonest human prion disease is Creutzfeldt-Jakob disease (CJD). Sporadic CJD is genetically characterized by a lack of pathogenic mutations in *PRNP* gene but methionine/ valine polymorphism at codon 129 determines the susceptibility to

sporadic and other non-genetic forms of CJD. Homozygosity for either methionine or valine increases the risk for acquiring CJD. Aims: We searched for changes in *PRNP* gene of healthy populations and sCJD cases and compared genotypes of codon 129 in order to prove differences among populations and non-familiar origin of sCJD cases and also to confirm the influence of codon 129 homozygosity on the disease development.
Material and methods Blood samples from six populations (Slovenian, Afro-American, PIMA Indian, Cheyenne Indian, Finnish, German) and brain or blood samples from sCJD Slovenian cases were collected and DNA was extracted. PCR-SSCA was performed and changed samples were sequenced.
Results Fourteen different nucleotide changes in coding sequence of *PRNP* gene were identified in control populations, one of them was also present in a sCJD patient. Slovenian and German genotypes of codon 129 are similar, other populations differ more significantly. Pimas lack the V/V genotype and Cheyennes show an increased V/V frequence. Proportions of codon 129 genotypes in sCJD patients show a different distribution: 90% are M/M and 10% are V/V.
Conclusions Codon 129 genotype frequencies proved to be population- and location-specific. Sporadic CJD cases do not contain any mutation, specific for familial form.

P-218

Molecular pathology of the *RASSF1* gene in colorectal cancer

M Stražišar, A Cerar, D Glavač
Department of Molecular Genetics, Institute of Pathology, Faculty of Medicine, University of Ljubljana, Ljubljana, Slovenia

Introduction Tumour suppressor gene RASSF1 encodes different isoforms, derived from alternative splicing and differential promoter usage. The major transcripts A and C are expressed in all normal tissues, but transcript A is missing all cancer tissues. Loss of expression is mainly corellated with methylation of the CpG island promoter sequences of *RASSF1A* but mutations in exons have also been found. We examined the status of promoter methylation and potential changes in the coding region of the *RASSF1A* gene in colon cancer tumours.
Materials and methods Isolated DNA from tumours of colon cancer was used for exon amplification of *RASSF1A* gene. For identification of mutations and polymorphisms SSCA was used. Abnormal patterns on SSCA plates were sequenced. For determination of methylation status of the CpG islands we used COBRA method.
Results COBRA analysis revealed the hypermethylation of CpG islands. Sequencing analysis of exons showed different nucleotide changes. We identified C>A mutation (R94S), G>C mutation (D116H), G>T mutation (A133S), G>A mutation (R200H), G>A mutation (R257Q) and C>A mutation (L305I). R94S, D116H, R200H and L305I mutations have not been published yet.
Conclusions These results indicate that hypermethylation of the promoter of *RASSF1A* gene in colon tumours and missense mutations in protein itself could be involved in tumorigenicity of colon cancer.

P-219

Expansive lesions in the pineal region: histological and immunohistochemical features of 24 cases

J Talan-Hranilović[1], M Vučić[1], T Rumboldt[1], T Sajko[2], V Lupret[2]
[1]"Ljudevit Jurak" University Department of Pathology and Department of Neurosurgery, Zagreb, Croatia
[2]"Sestre Milosrdnice" University Hospital, Zagreb, Croatia

Introduction Pineal lesions are rare and comprise 0,4-1% of all intracranial tumors. Various histological types of tumors arise in the pineal region. The aim of this study was to determinate histological types, immunohistochemical expression, age and sex distribution of lesions in pineal region.
Materials and methods Twenty-four expansive lesions in the pineal region, obtained between 1990 and 2002, were analyzed. Formalin-fixed, paraffin embedded surgical specimens were stained routinely and immunohistochemically for panel of antibodies; synaptophysin, neuron specific enolase, neurofilament, chromogranin A, glial fibrillary acid protein, cytokeratin, carcinoembrional antigen, β-HCG, human placental antigen, α-Fetoprotein and Ki-67.
Results Histology revealed six germinomas, seven pineocytomas, three pineoblastomas, five glial cysts and one ganglioglioma, pilocytic astrocytoma and epidermoid cyst. The study group consisted of 13 females (54,2%) and 11 males (45,8%) ranged from 4 to 66 years of age. All germinomas were in male patient while glial cysts were diagnosed in female patients. Slightly female predominance was observed in pineal parenchymal tumors. Immunoreactivity for neuron specific enolase, synaptophysin, neurofilament and for chromogranin A was positive in the pineocytomas, and partially expressed in pineoblastomas. The mean Ki-67 index in pineoblastomas and germinomas were significantly higher than in pineocytomas. Germinomas showed focal immunoreactivity for β-HCG, human placental antigen, α-Fetoprotein and low immunoreactivity for cytokeratin and carcinoembrional antigen.
Conclusion The most common tumors are pineal parenchymal tumors and germ cell tumors. Glial pineal cysts are also common. Occasionally other types of tumor are found. Immunohistochemistry is an important method in differential diagnosis of pineal tumors.

P-220

Immunohistochemical study of the metastatic brain tumors with accent of the role of thyroid-transcription factor-1

M Kamenova, N Sarbianova, P Danailova
Emergency Hospital N.I.Pirogov, Sofia, Bulgaria

Introduction The exact diagnosis of the metastatic brain tumors /MBT/ is challenge for the surgical pathologist especially in a case of unrecognized primary site. The aim of this study was to determine reliable immunohistochemical panel based on the histological features of the MBT.
Materials and methods Sixty five cases with solitary MBT operated in Neurosurgical department of the hospital were examined from the time period 1997- 2002; thirty nine were of unknown primary origin (60%). Immunohistochemical studies were performed using antibodies to CK-s, EMA, NSE, synaptophysin, PSA, vimentin, S-100 protein, HMB45, TTF-1 and GFAP.
Results Diagnosis of the MBT of unknown origin were as follow: squamous cell carcinoma - 5 cases from total 11, small-cell

undifferentiated - 4 from 6, large cell undifferentiated - 6 from 9, adenocarcinoma -14 from19, adenosquamous - 2 from 2, clear cell - 2 from 3, papillary carcinoma -1 from 3, tubular -1 from 7, spindle cell -1 from 1, unclassified - 3 from 3. The primary site of adenocarcinoma, undifferentiated small and large cell and clear cell carcinoma was established by using TTF-1 (positive in 27 from 41 lung cancer, 65.85%), neuroendocrine markers, CK-8 and PSA. After the investigation only three tumors were of unknown origin (7.69%). The origin of the rest unknown before studies of 36 MBT, confirmed with radiographic and endoscopic data were: lung - 27 from 41 total, breast - 2 from 7, kidney - 2 from 3, skin-2 from 4, thyroid gland - 1 from 2, stomach -1 from 1, prostate -1 from 1. The colon, testis and ovary, at one case each, were known before operation.

Conclusions Immunohistochemistry remains important and still very helpful method in determining primary origin of the MBT generally in undifferentiated neoplasmes and adenocarcinomas. Among the most reliable tumor markers should be included TTF-1, for its frequent expression in the lung cancer, predominant among MBT.

P-221

Brain calcification simulating brain tumour. A case report

A Shmeleva, S Romodanov
Neurosurgery Institute, Academy of Medical Science of Ukraine, Kiev, Ukraine

Objectives The aim of this study was to describe the plural calcifications in the brain.

Materials and methods The patient was a 32-year-old man. He had a severe headache and disorientation, he felt weakness in the left arm. The patient was mentally handicap. ST scan showed a tumour located in the deep parts of the right temporal lobe. With a working diagnosis of tumour, the patient underwent the operation. The surgical specimens were prepared by standard histological techiques.

Results Macroscopically, the lesion appeared as a stone. A histological examination demonstrated a massive deposits of calcium in the parenchyma of the brain. Calcification developed as small granules in the vessels and calcospherites of various dimensions were formed by confluence. There were zones of haemorrhage, neuronal loss, edema and proliferation of astrocytes.

Conclusions This patient is an interesting clinical case of dementia characterized pathologically by diffuse calcification.

P-222

Carcinoid tumour metastatic to the orbital muscle. A case report

O Casar Borota[1], R Kloster[2], V Isaksen[1], J Florholmen[3], R Bajic[4], S Lindal[1]
[1]University Hospital of Northern Norway, Department of Pathology, Tromso, Norway
[2]University Hospital of Northern Norway, Department of Neurosurgery, Tromso, Norway
[3]University Hospital of Northern Norway, Department of Gastroenterology, Tromso, Norway
[5]University Hospital of Northern Norway, Department of Radiology, Tromso, Norway

Introduction Ninety-three percent of symptomatic patients with small intestinal carcinoid tumours have metastases compared to 9% of tumours found incidentally. The most common sites of metastatic carcinoid tumours are lymph nodes and liver. Orbital metastasis from malignant carcinoid tumours have rarely been described and the majority of them involve the choroid rather than orbital structures. The aim of the study is to present an unusual case of ileal carcinoid tumor with metastasis to the orbital muscle.

Materials and methods We report a patient who developed a posterior left orbital mass eighteen months after the first operation for primary intestinal carcinoid tumour with hepatic metastases. Orbital involvement presented with proptosis, impairment of vision and reduced ocular motility on the left side. The patient was examined by CT and MR. Biopsy was taken and examined by imprint and frozen section. The tumor was removed. HE and staining for cytokeratin, chromogranin, NSE, serotonin, somatostatin and gastrin were performed.

Results CT and MR study revealed the orbital tumour mass infiltrated the inferior rectus muscle. Imprint and frozen section showed tumor consistent with metastatic carcinoid. The histological and immunohistochemical features of the tumour corresponded to those of the primary intestinal carcinoid tumour.

Conclusion Intramuscular orbital metastasis from carcinoid tumour is a rare occurrence. Diagnosis may be difficult especially where no evidence of primary carcinoid tumour is present. Although a rare event, metastatic orbital carcinoid should be suspected in patients with clinical history of carcinoid tumour who develop ocular complaints and mass lesion in the orbit.

P-223

Non-invasive photoacoustic tomography of brain: a novel functional neuroimaging with high contrast and high resolution

G Stoica, X Wang, Y Pang, G Ku, X Xie, L Wang
Texas A&M University, USA

Introduction Optical contrast is sensitive to monitor dynamic and functional changes, such as blood concentration, tissue oxygenation, and cellular swelling. Optical imaging has been widely employed in clinical applications including the investigations of functional neuroanatomy and neuroactivity. Due to the overwhelming scatter of light during the propagation inside biological tissues, past attempts to visualize brain architectures non-invasively with the optical contrast have been severely restricted by the unsatisfactory spatial resolution. The aim of this study was to investigate the feasibility of a novel non-invasive transcranial imaging of the structure and function of brain in vivo accomplished with laser-induced photoacoustic tomography (PAT).

Material and methods PAT visualized the tissue structures in rat/mouse brain based on the high sensitive intrinsic optical contrast while utilizing the diffraction-limited high spatial resolution of ultrasound.

Results Two-dimensional (or three-dimensional) rat (or mouse) brain structures, with and without lesions, were imaged clearly. In response to whisker stimulation, functional cerebral hemodynamic changes in cortical blood vessels around the whisker-barrel cortex were also mapped successfully. PAT imaged hyperoxia- and hypoxia-induced cerebral hemodynamic changes as well.

Conclusions This study demonstrates that (i) structural PAT of soft tissues lesions in the brain presents high intrinsic contrast, (ii)

functional PAT based on intrinsic optical signals can map the hemodynamic changes in the cerebral cortex and (iii) in contrast to other previously used optical methods, this technique enables completely non-invasive neuroimaging with high spatial resolution transcranially. This novel functional neuroimaging technique, will help to advance the research in neurophysiology, neuropathology, and neurotherapy significantly.

P-224

Microscopic disorders of cortical development of brain and the etiopathogenetic relevance of their detection in patients with temporal lobe epilepsy due to hippocampal sclerosis

J Zamecnik[1], P Krsek[2], P Marusic[3], R Druga[4], V Benes[5], M Tichy[6], V Komarek[2]
[1]Dept. of Pathology and Molecular Medicine, Charles University, 2nd Medical Faculty, Prague, Czech Republic
[2]Dept. of Pediatric Neurology, Charles University, 2nd Medical Faculty, Prague, Czech Republic
[3]Dept. of Neurology, Charles University, 2nd Medical Faculty, Prague, Czech Republic
[4]Inst. of Anatomy, Charles University, 2nd Medical Faculty, Prague. Czech Republic
[5]Dept. of Neurosurgery, Charles University, 1st Medical Faculty, Prague, Czech Republic
[6]Dept. of Neurosurgery, Charles University, 2nd Medical Faculty, Prague, Czech Republic

Introduction Hippocampal sclerosis (HS) represents a common structural basis of temporal lobe epilepsy (TLE). However, the etiological factors and mechanisms leading to its development still remain unexplained. The aim of this study was to identify the disturbed neuronal migration and differentiation (NMD) in the temporal lobe resected for HS and to evaluate its potential role in the individual pathogenesis of HS.
Materials and methods We present neuropathological findings in the resected hippocampus and the pole of the temporal lobe in 15 patients with hippocampal sclerosis with an attention paid to the histopathological identification of defects of NMD in the temporal lobe. The morphological findings were correlated with the results of clinical examinations and the patients´ histories.
Results 'Initial precipitating injuries' that are thought to cause the development of HS (febrile seizures in early childhood, head injury or meningoencephalitis) were present in the history of 12 patients. In the remaining 3 cases, no predisposing factors were found. Defects of NMD were observed in 7 cases; in three of these, no predisposing factors were identified in the patients´ histories. We suggest that in these cases, HS arises due to previously undetected disorders of cortical development. A latent neocortical malformation may also contribute to the development of HS in patients with an initial precipitating injury in anamnesis.
Conclusion Histopathological examination of resected epileptic brain tissue can provide insights into the individual pathogenesis of epileptic disorders, especially by the detection of microscopic disorders of cortical development.
Supported by: GACR 309/02/D076, VZ FNM 00000064203, VZ MSMT 111300004 and 111300003

P-225

Cerebellar liponeurocytoma: case report

S Dozic[1], D Cvetkovic[1], M Skender Gazibara[1], B Dozic[1], M Joksimovic[2]
[1]Institute of Pathology, Medical Faculty, University of Belgrade, Belgrade, Serbia and Montenegro
[2]Institute of Neurosurgery, CCS, Belgrade, Serbia and Montenegro

Introduction Cerebellar liponeurocytoma is a newly recognized rare clinicopathological entity of the posterior fossa, with advanced neuronal/neurocytic and lipomatous differentiation. The term 'cerebellar liponeurocytoma' was recently adopted by the WHO group to replace several other different terms used up to now. This tumour shows many morphological similarities to medulloblastoma and neurocytoma, but according to available literature has more favorable prognosis then typical medulloblastoma. We report a case of cerebellar liponeurocytoma in a 40-years-old woman who developed typical symptoms of a posterior fossa tumor. Computed tomography (CT) scan disclosed a heterogeneous tumor mass in the left cerebellar hemisphere. The lesion was totally resected.
Methods The surgical specimen was rinsed in saline solution and fixed in 4% paraformaldehyde in phosphate buffer at pH 7.35 for 24 hours, embedded in paraffin and prepared for histological and immunostaining.
Results Microscopically, the tumor was composed of small less differenerentiated, round or oval closely packed medulloblastoma-like cells and vacuolated cells with macrovesicular lipid accumulations giving in some large areas an appearance indistinguishable from mature fat cells. Glial and neuronal differentiation was histo-pathologically and immunohistochemically (GFAP, NSE, NF) noted. These cellular components were intermixed in different proportions without distinct separation. Many tumor cells of all types showed single or multiple smaller lipid vacuoles in their cytoplasm.
Conclusion Our case provides evidence that mature adipose-like tissue in these tumors appears as result of progressive lipidization of neuroectodermal tumour cells rather than as result of adipose metaplasia.

P-226

The expression of survivin and Ki-67 in meningiomas: correlation with grade and clinical outcome

S Zorludemir[1], F Kayaselcuk[2], S Erdogan[1], N Bal[2], B Erdogan[3], T Erman[4]
[1]Department of Pathology, Cukurova University Faculty of Medicine, Adana, Turkey
[2]Department of Pathology Baskent University Faculty of Medicine, Adana Teaching and Medical Research Center, Adana, Turkey
[3]Department of Neurosurgery Baskent University Faculty of Medicine, Adana Teaching and Medical Research Center, Adana, Turkey
[4]Department of Neurosurgery, Cukurova University Faculty of Medicine, Adana, Turkey

Introduction Determination of proteins taking place in the control of proliferation in normal cells helps a better understanding of cellular transformation and proliferation mechanisms. Measure-ment of proliferative activity is important in determining tumor grade, recurrence time and malignancy. PCNA and Ki-67 are two

of the nuclear markers used to demonstrate proliferative phase of cell cycle.

Material and methods In the presented study 26 meningiomas of various histological grade, which have been diagnosed in Baskent University and Çukurova University Medical Faculty, Department of Pathology, were graded according to WHO grading system and survivin and Ki-67 monoclonal antibodies were administered by immunohistochemical method. Findings were analyzed with statistical methods; distribution of survivin and Ki-67 LI values were determined for different grade meningiomas.

Results In meningiomas, the correlation between the increasing grades with survivin and Ki-67 LI values were statistically significant. In addition, we have found correlation between clinical outcome and survivin and Ki-67 LI.

Conclusion The results suggest that survivin, alone or in conjunction with Ki-67, is a significant prognostic marker of worse outcome in meningioma.

P-227

Progesterone receptors expression in benign meningiomas

S Milenkovic[1], D Cvetkovic-Dozic[2], I Berisavac[3], M Skender-Gazibara[2], V Lackovic[4], Z Milicevic[4], B Vukomanovic
[1]Department of Pathology, Clinical Hospital Center, Zemun, Serbia and Montenegro
[2]Institute of Pathology, University of Belgrade, School of Medicine, Serbia and Montenegro
[3]Department of Neurosurgery, Clinical Hospital Center Zemun, Serbia and Montenegro
[4]Institute of Histology and Embryology, University of Belgrade, School of Medicine, Belgrade, Serbia and Montenegro

Object Although they do not arise from a tissue normally thought to be a target tissue for progesterone, meningiomas show a number of epydemiologic and clinical features which suggest that females sex hormones can play a role in their development (higher incidence of meningiomas in woman, rapid progression of symptomas and icreasing in size during the pregnancy and during the luteal phase of the menstrual cycle, as well as significant association of meningiomas with obesity and breast carcinomas). The aim of our study was to investigate the progesterone receptor contents of 30 bening meningiomas (WHO gr. I), which is completly excised and evaluated possible relationship between receptor content and sex and age of the patients, histological tipe of meningiomas and localisation of tumor.

Material and methods Tissue samples, fixed in formalin, and embedded in paraffin were evaluated immunohistochemically for progesterone receptors using specific monoclinal antibodies.

Results and conclusion The correlation between number of positively nuclei and progesteron status was determined by the analitic statistical test Mann-Whitney. 57% of the 30 meningiomas tested were positive for progesterone receptors. Progesterone receptors in the benign meningiomas in the male patients was significantly higher when compared to the female patients ($p<0,05$).

P-228

Neonatal intractable seizures revealing diffuse and bilateral cortical dysplasia. A case report

S Bellefqih[1], C Rambaud[2], T Lacaze[2], JJ Hauw[1], G Lyon[1], D Seilhean[1]
[1]Groupe Hospitalier Pitié-Salpétrire, Paris, France
[2]Hôpital Antoine-Béclre, Paris, France

Cerebral cortical dysplasia is generally focal and sometimes related to tuberous sclerosis. It is believed to result from disrupted neuronal migration during cortical development. We report an unusual case of neonatal diffuse and bilateral cortical dysplasia revealed by refractory epilepsy. A male infant, born at 40 weeks' gestational age (GA) without familial history of neurologic disease, presented at birth a convulsive encephalopathy, associated with severe hypoxia with pulmonary hypertension and iterative hypoglycemia. A foetal goitre was attributed to hyperdose therapy for maternal Graves' disease between 20 and 30 GA. The patient died at 3 weeks of life from respiratory failure after intensive care. All the iso- and allocortical areas examined were normal at gross examination, but microscopically dysplastic. There was disorganization of the laminar architecture and presence of large multipolar neurones diffusely distributed over the cortex. They showed positive immunoreactivity with neurofilaments and synaptophysin, and were negative with GFAP and vimentin. Numerous ectopic neurons were found in the white matter. In addition, C shaped thickened inferior olive was noted. The cerebellum, including dentate nuclei, and other brain stem nuclei were normal. Focal cortical dysplasia lesions are localized malformation of the isocortex with positive GFAP and vimentin in dysplastic neurons. In this case, the dysplastic lesions were diffuse and astrocytes were normal. No genetic investigation was available, but the negative immunostaining of large cells by GFAP does not favour the diagnosis of tuberous sclerosis. The pathogenesis of this exceptional disease remains obscure but the responsibility of the foetal thyroid disorder cannot be excluded.

P-229

Structural genomic abnormalities of chromosomes 9 and 18 in myxopapillary ependymomas

B Mahler-Araujo[1], D Sanoudou[2], O Tingby[2], M Ferguson-Smith[3], N Coleman[2], K Ichimura[2], P Collins[2]
[1]Departamento de Anatomia Patologica, Hospital do Cancer A C Camargo, Sao Paulo, Brasil
[2]Department of Pathology, University of Cambridge, Cambridge, UK
[3]Department of Clinical Veterinary Medicine, University of Cambridge, Cambridge, UK

Myxopapillary ependymomas (MPE) are low-grade neuroepithelial tumors typically located in the cauda equina. They tend to grow slowly and may recur locally without progression. Very little is currently known about the genetic abnormalities involved in the development of MPE. In an attempt to clarify the chromosomal status of these tumors and identify commonly aberrant regions in the genome we have combined 3 molecular/cyto/genetic methods to study genomic abnormalities in 17 MPE. Comparative Genomic Hybridization analysis of 7/17 tumors identified concurrent gain on chromosomes 9 and 18 as the most frequent finding. The majority

of the 17 tumors were also studied using microsatellite analysis (14 markers for chromosome 9 and 8 markers for chromosomes 18) and interphase-FISH with centromeric probes for chromosomes 9 and 18. Our combined results were consistent with polysomy 9 and 18 in 7 cases, polysomy either 9 or 18 with partial gain in the other chromosome in 3 cases, tetrasomy or partial gain either 9 or 18 with complex rearrangement in the other chromosome in 3 cases. In the remaining 4 cases allelic imbalance alone of either chromosome 9 or 18 was identified. Other numerical abnormalities observed included gain of chromosomes 3, 4, 5, 7, 8, 11, 13, 17q, 20 and X and loss of chromosomes 10 and 22. The combination of gains of genetic material from chromosomes 9 and 18 seems to be common in MPE and may represent genomic events of importance in the development of the tumor.

P-230

Nonsymptomatic nontumor cysts of the pineal gland: frequency and morphological characteristics

B Manevska, V Dokov, P Ghenev, W Dokov
Medical University of Varna, Varna, Bulgaria

Introduction Nonsymptomatic nontumor cysts (NNC) of the pineal gland (PG) are considered as normal structures. The aim of the present study is to evaluate the frequency of NNC in random postmortem examinations and their influence upon surrounding parenchyma.
Materials and methods The study includes PG out of 101 random autopsy cases (73 men and 28 women, mean age 51.60±6.21). Gross investigation is performed prior to fixation; histological stains are applied on paraffin sections.
Results The frequency of NNC is 18.81% (17.80% in men, 21.42% in women). There isn't significant difference between genders in all age groups. The mean weight of PG with and without NNC is 175.41±49.37mg and 126.45±18.69 mg respectively. The analysis of PG dimensions reveals: mean length 9.80±1.75 mm versus 8.18±0.11mm and mean width 6.95±1.24 versus 6.13±0.59 mm in NNC versus cases without NNC. No significant difference is established for PG density (3.34±2.26 versus 3.30±1.08 kg/m3). PG parenchyma around NNC doesn't reveal particular changes.
Conclusion NNC frequency is not age and/or gender dependent; NNC presence increases PG weight and length without influence on PG width and density. These findings show that NNC eventual clinical significance may be due to comression of surrounding structures only, without effect on PG functional activity.

P-231

The effect of bcl-2 protein and Ki-67 expression on the prognosis of medulloblastomas

IE Gurer[1], G Yildirim Kupesiz[1], GA Gokhan[1], A Kupesiz[2], V Hazar[2]
[1]Akdeniz University School of Medicine Department of Pathology, Antalya, Turkey
[2]Akdeniz University School of Medicine Department of Pediatric Hematology-Oncology, Antalya, Turkey

Introduction Medulloblastoma is the most common primary central nervous system tumor in childhood and accounts 20-25 % of all intracranial neoplasms in children. Aim: In this study the correlation between the patients survival and prognostic factors (Ki-67 and bcl-2) and the tumor size in CT scan were evaluated.
Material and method 10 selected cases were analyzed. Immunohistochemical staining was applied as polyclonal antibody for Ki-67 (DAKO-A- 0047) and monoclonal antibody for bcl-2 (bcl-2/ 100/D5 Novo Castra) on paraffin blocks.Fisher's qhi-square, correlation and Mann-Whitney-U tests were used for the statistical analyses.
Results The ages of these patients were ranged between 1-29 (mean 8.6).The size of the tumoral mass varied between 3 to 6 centimeter. 6 patients were alive without illness.4 patients were lost due to tumor. We could not found a statistical revelance between neither immunohistochemical staining (bcl-2, Ki-67) nor tumor size on survival rates.
Conclusion Due to radiotherapy and chemotherapy following surgery, the survival rates of medulloblastoma has increased despite the agresiveness of the tumor. There are reports showing no correlation between expression of the bcl-2 with the outcome of patients. Further investigation about the correlation of the prognostic factors with the outcome is required.

P-232

Clinical analysis and histo-clinical correlations in recurrent astrocytic brain tumours

G Bierzynska - Macyszyn[1], J Slowinski[2], P Wlaszczuk[1], M Wojtacha[3], P Bazowski[3]
[1]Department of Pathology in Katowice, Medical University of Silesia, Katowice, Poland
[2]Department of Neurosurgery and Neurotraumatology in Bytom, Medical University of Silesia, Poland
[3]Department of Neurosurgery in Katowice, Medical University of Silesia, Katowice, Poland

Introduction Results of glioma treatment are still unsatisfactory. An accurate histopathological study supplemented with examination of tumour parameters, like proliferation potential and apoptosis may be invaluable in designing an individualised therapy. The aim of this study was to analyze clinical data and histo-clinical correlations in recurrent brain tumours of astrocytic origin.
Materials and methods One hundred surgically removed supratentorial gliomas were studied (mean age: 49.3yrs). Histological grade was determined according to WHO 2000 classification and the Daumas-Duport scale (St.Anne/Mayo). Proliferation activity was measured using the PCNA index and AgNOR count. The expression of BCL-2 protein was examined with immunohistochemistry.
Results and conclusion The initial symptoms of glioma were headaches and vomiting (41 %), paresis (35 %), epilepsy (33 %) and aphasia (18 %). The tumour location was predominantly in the left hemisphere, in the temporal (32 %), parietal (22 %) and frontal (20%) lobes. The PCNA index correlated with WHO grade (GII - index 4%, GIII - 10-20% and GIV - 40%). For grades I, II, III and IV progression free survival (PFS) was: 50.0, 39.0, 15.6 and 1.7 months respectively. The AgNOR count did not correlate with WHO grade, Daumas-Duport grade or PFS. BCL-2 expression was observed in single cells in GI and GII tumors, in 80 % and 40% of cells in GIII and GIV, respectively. The Daumas-Duport scale is simple and useful in prognosing. BCL-2 expression does not correlate in a linear manner with tumour grade. As gliomas are extremely heterogeneous, for better characterization of the clinico-pathologic correlations new prognostic factors are needed.

P-233

Schilder's type of multiple sclerosis in a mid-aged woman. A case report

K Žarković[1], G Miklec[1], G Jurić[1], D Sporiš[2], D Chudy[3]
[1]Department of Pathology, Clinical Hospital Center, Zagreb, Croatia
[2]Department of Neurology, Clinical Hospital Center, Zagreb, Croatia
[3]Department of Neurosurgery, Clinical Hospital Center, Zagreb, Croatia

Introduction Schilder's type of myelinoclastic sclerosis is rare variant of multiple sclerosis in children and young adults. Usually, brain lesions occur in the white matter like solitary, or less often multifocal, acute plaques ranged in diameter more then 3 cm.
Case report The 49-year-old female patient was referred to our hospital with progressive right-sided hemiparesis, motor dysphasia and frontal lobe syndrome. Symptoms started 14 days earlier with acute headache and no febrile state was reported. MRI of the head revealed two oval lesions with hyperintensity in T2 weighted images of left frontal and parietal lobe. The first diagnostic impression was of glioblastoma multiforme. Results from standard blood and urine tests, tumor markers and cytological analysis of bone marrow were normal. Analysis of CSF and culturing CSF and serum for bacterial, viral, protozoan and fungal infections were negative. Analysis of CSF revealed increased immunoglobulins, 3OCB and increased intratecal synthesis of IgG. A stereotactic biopsy was performed one month after first symptoms. Neuropathology findings. The biopsy after neurosurgical treatment yielded five needle cores of grayish cerebral tissue. Hematoxylin and eosin-stained sections of paraffin embedded tissue showed demyelinating white cerebral tissue with relatively sharply defined margins. Lesion was infiltrated by macrophages (CD68 immunopositive cells and Luxol fast blue negative) and large reactive astrocytes with Ki67 and PCNA nuclear positivity. Around blood vessels were scattered perivascular CD4 and CD20 lymphocyte. Silver impregnation and NF immunostaining showed that the axons within the plaque are attenuated but not destroyed.
Conclusion Clinical and pathological findings suggested a demyelinating disease destroyed huge parts of white matter in before health mid-aged women, without previous infection or vaccination. Accordingly we diagnosed Schilder's type of MS.

P-234

Stereotactically guided brain biopsy: six years' experience of pathologic interpretations from Turkey

E Erden[1], A Okcu Heper[1], A Savas[2]
[1]Ankara University, School of Medicine, Pathology Department, Ankara, Turkey
[2]Ankara University, School of Medicine, Neurosurgery Department, Ankara, Turkey

Introduction Stereotactic biopsy is a widely used procedure in brain lesions. The aim of this study was to analyse the reasons of the discordance between the results of the intraoperative crush preparations (ICP) and final permanent paraffine preparations (FPPP) of stereotactically guided brain biopsies (SGBB) in our hospital, and find out the clinical benefits of this procedure.
Material and method Total 134 CT and/or MRI guided brain biopsies performed between 1995-2003 were analysed retrospectively. ICP and FPPP preparations were evaluated and discordant cases were detected. Then we evaluated the reasons of discrepancies.
Results The correct diagnosis was achieved by stereotactic biopsy in 91.8 % of the patients. Of them 107 were diagnosed as neoplasia and 16 were diagnosed as non-neoplastic pathology. There was discordance between ICP results and FPPP diagnosis in 8.2 % of the stereotactically diagnosed patients. The patients diagnosed as neoplasia were treated by RT and/or KT and the non-neoplastic pathologies were taken in suitable treatment and follow-up scheme.
Conclusion To improve the diagnostic accuracy of the SGBB, the following items should be taken into consideration: The quality of the ICP with giemsa staining is very important. In the biopsies from the lesions, which are suspected as neoplasia having, microscopic features such as gliosis, edema, hemorrhage must be interpreted as non-diagnostic. The number of the biopsies must be increased in the presence of necrosis. Epitheloid and pleomorphic cellular groups can mimic benign and malignant pathologies. Interpretation of the ICP and the FPPP should be done by the same pathologist.

P-235

Intraneural capillary haemangioma of spinal nerve root. Case report

P Xirou[1], S Barbanis[1], I Efstratiou[1], P Sevastiadou[1], I Tsitouridis[2]
[1]Papageorgiou General Hospital, Department of Pathology, Thessaloniki, Greece
[2]Papageorgiou General Hospital, Department of Radiology, Thessaloniki, Greece

Intraneural haemangiomas of the spinal nerve roots are rare. The few cases reported in the literature are usually of the capillary and less often of the cavernous type. These lesions occur in adults, mainly males and the majority of them are located in the cauda equina. A case of intraneural capillary haemangioma involving one lumbar nerve root is reported. The patient, a 53 year old male, presented with a 1-year history of severe intermittent low back pain. Magnetic resonance imaging detected an intradural, extramedullar, space occupying mass at the level of L2-L3, causing displacement of cauda equina roots. Laminectomy and complete removal of the lesion were performed without neurological problems. On gross examination the resected specimen was a red-brown, well demarcated, lobular mass, measuring 1.8 cm in greatest diameter. Remnants of a nerve root were recognized at the periphery. Histological examination showed that the lesion was located within the endoneurium. It consisted of multiple small dilated capillaries, often showing incomplete lobular pattern, dispersed within normal nerve fascicles. The endothelial lining showed neither nuclear atypia nor mitotic activity. In the substrate mild edema and focal inflammatory lympocytic infiltrations were found. Haemangiomas of the spinal nerve roots often pose a challenging diagnostic problem, and knowledge of their existence is relevant since they can mimic other more frequent tumors of the region.

P-236

Macrocellular lung cancer with neuroendocrine differentiation associated with subacute sensorimotoric neuropathy/encephalomyelitis: an autopsy case

B Gazič[1], L Dolenc-Grošelj[2], V Švigelj[2], M Popovič[3]
[1]Department of Cytopathology, Institute of Oncology, Ljubljana, Slovenia
[2]Neurology Clinic, University Medical Center, Ljubljana, Slovenia
[3]Medical Faculty, Institute of Pathology, University of Ljubljana, Slovenia

Introduction Sensorimotoric polyneuropathy has rarely been reported as a presenting paraneoplastic neurological disorder associated with anti-Hu antibodies. Electrophysiological studies suggest a dysfunction of axon-Schwann cells, but the exact pathological mechanisms remain unclear.
Case report A 68-year old woman with short history of weight loss and parastesias in the legs was admitted to the hospital. Triparesis and dyspnea were found. MRI scan showed leukencephalopathy, EEG revealed diffuse encephalopathy. Sensorimotoric axonal polyneuropathy was present in EMG, and small lesion in the lung was found on the CT scan. Anti-Hu antibodies were present in the serum and in the cerebrspinal-fluid. Autopsy revealed macrocellular adenocarcinoma of the lung with neuroendocrine differentiation and sensorimotoric neuronopathy/ encephalomyelitis.
Methods The brain, spinal cord, sensory ganglia and a part of sural nerve were fixed in formalin, paraffin embedded and stained with H&E. Other part of sural nerve was prepared for immunofluorescence, semi-thin and ultra-thin sections.
Results Axonal degeneration without any inflammatory reaction and a very few signs of regeneration were found in the sural nerve. The inflammatory destruction of spinal ganglia neurons, axonal degeneration in dorsal columns and motor neurons inflammatory destruction in the spinal cord were found. Neuronal degeneration, glial proliferation, perivascular inflammatory infiltrates and some CD8+ lymphocytes surrounding single neurons were a common finding in the brain.
Conclusions This study shows that inflammatory destruction of the spinal ganglia neurons and motor neurons in the spinal cord was the main cause of clinically rapidly progressive sensorimotoric polyneuropathy in the anti-Hu positive patient with macro cellular lung carcinoma with neurendocrine differentiation.

P-237

Isolated extranodal spinal Rosai-Dorfman disease. A case report

AI Freitas RC Silva L Costa, V Velasco, P Monteiro, M Teixeira, F Pardal de Oliveira
Hospital de Sao Marcos-Serviço de Anatomia Patológica, Braga, Portugal

Introduction Sinus histiocytosis with massive lymphadenopathy was first described in 1969, by Rosai and Dorfman, as an idiopathic histiocytic disorder, which typically involves lymph nodes. Lately, involvement of many other organ systems has been documented, either alone or in association with nodal manifestations. Nowadays, Rosai-Dorfman disease is a well-recognised clinico-pathologic entity. Extranodal disease has been reported in 43% of the reported cases, occasionally representing the first and exclusive manifestation of the disease. Although central nervous system involvement has been well documented, the spinal canal is affected only exceptionally. We report a case of an isolated extranodal spinal Rosai-Dorfman disease with review of the literature.
Results The authors describe a 41 old woman with a history of spastic hemiparesis in which radiology disclosed a dural-based intramedullary spinal cord lesion at C1 level. The authors describe the histologic and immunohistologic features of the lesion and discuss the differential diagnosis.
Conclusion Isolated CNS Rosai-Dorfman disease without contemporary lymph node involvement can be a diagnostic challenge. Pathologists must be aware of this disease in order to make a correct diagnosis and avoid diagnosis of malignant histiocytic lesions.

P-238

Ezrin immunoreactivity: Is it a usefull marker for the prognosis and grading of astrocytoma?

IE Gurer[1], GA Gökhan[1], T Uçar[2]
[1]Akdeniz University Scholl Of Medicine Department of Pathology, Antalya, Turkey
[2]Akdeniz University Scholl Of Medicine Department of Neurosurgery, Antalya, Turkey

Introduction The actin- binding protein ezrin is supposed to increase the invasiveness of the malignant cells. In this study, the value of ezrin immunoreactivity (IR) was invastigated as a grading and prognostic parameter in astrocytomas.
Material and method Ezrin IR was studied in 13 low grade and 17 high grade astrocytomas. The mean age of the patients was 37.83 (4-75). Monoclonal ezrin antibody (MS-661-R7 Neomarkers) was applied on the sections of the paraffin-embedded tissues. Immunostaining intensity of ezrin was estimated as semi-quantitatively. When no staining was visible the score of 0, mild staining scored as 1, moderate 2, and severe staining scored as 3. Also positive stained areas were evaluated as percantage (25%, 25-50%, above 50% staining areas). Statistically Man-Whitney U, Kruskal Wallis and Spearman tests were used.
Results There was no correlation between prognosis and neither the grade nor the staining intensity of ezrin IR.
Conclusion There are controversial reports especially about the prognostic value of ezrin IR in different types of tumors. There is one report about the association of ezrin IR with the increasing malignancy of astrocytic tumors. Results of our study revealed no evidence of correlation between prognosis and ezrin IR for grading of astrocytomas. We conclude that ezrin is not a usefull factor for the prognosis and grading in astrocytomas.

P-239

Cystatin C depositon in blood vessels outside the central nervous system in hereditary cystatin C amyloid angiopathy

H Blöndal, F Thormodsson
Dept. of Anatomy University of Iceland, Reykjavik, Iceland

Introduction Hereditary Cystatin C Amyloid Angiopathy (HCCAA), an autosomal hereditary disease uniquely found in Iceland, usually leads to early death of young adults from CNS vascular complications

following a disease progress of several years. Histopathological characteristics are cystatin C amyloid deposits in meningocerebral blood vessels, narrowing, splitting of media, segmental fibrinoid necrosis and microaneurysms of small arteries and arterioles. Associated changes: hemorrhages, infarctions and reparative reactions depending on length of the disease course. This study is a part of an investigation mapping the distribution of cystatin C immunopositive deposits outside the CNS in HCCAA.

Material and methods Formalin fixed, paraffin embedded autopsy material from 16 patients, 10 females and 6 males, was studied by conventional light microscopy (HE, Congo red; Thioflavin S) and immunohistochemistry (Avidin-Biotin-Peroxidase) with cystatin C antibodies (ABC-complex kit from Vector). For electron microscopy and specific identification of cystatin C deposits specimens were fixed in MacDowell's fixative and embedded in L.R. White resin and immunogold labelled (colloidal gold labelled protein A. Sigma).

Results and conclusion Cystatin C immunoreactive deposits were found in most organ systems outside CNS. The deposits were primarily located in the adventitia and perivascular tissue of small blood and lymphatic vessels and vascular smooth muscle; in subepithelial connective tissue of intestinal surface epithelium and glandular epithelium; in peripheral nerves. Cystatin C immunoreactive blood vessels were not obviously damaged as those in the CNS possibly reflecting environmental factors different in these two separate locations not yet identified and characterized. Details of cystatin C deposition in the vascular walls will be demonstrated.

P-240

Mononeuritis multiplex due to vasculitis in a patient with antiphospholipid syndrome

J Jeruc[1], M Popović[1], A Vizjak[1], B Lestan[2], D Ferluga[1]
[1]Institute of Pathology, Faculty of Medicine, University of Ljubljana, Slovenia
[2]Department of Rheumathology, University Medical Centre, Ljubljana, Slovenia

Introduction Neurological disorders are among the most prominent clinical manifestations of antiphospholipid syndrome (APS). They are predominantly related to thrombo-occlusive vascular events in central nervous system, vasculitis playing little or no role.

Case report A 49-year-old female with a history of seven spontaneous abortions presented with sudden onset of pain and numbness in her right and later left foot followed by pruritic rash over her hands and back and livedo reticularis around knees. EMG showed signs of axson injury in multiple nerves. Laboratory tests showed lymphopenia and antiphospholipid antibodies of IgG class in medium titer at the begining and in low titer three months later. ANCA, ANA, ENA, anti-DNA were negative, platelet count, complement, lupus anticoagulant and tumor markers were normal. Sural nerve biopsy revealed active necrotizing arteritis of small epineural arteries. Intimal circular fibrinoid necrosis was accompanied by pyknosis, karyorexis and myofibroblast proliferation in media. Inflammatory infiltration by lymphocytes, macrophages, plasma cells and segmented leucocytes was present in intima, but was most prominent in adventitia. Thrombosis in organization was observed. Vasculitis was present also in arterioles and venules. Immunofluorescence showed scarce focal granular deposits of IgM, IgA class, and complement components C3 and C1q in media of small epineural arteries, together with abundant fibrin deposition.

Discussion and conclusion It has been suggested that APS can not be the cause of vasculitis and that vasculitis in APS is associated with an independent underlying disease, such as systemic lupus erythematosus. Except for suspected APS, our patient did not fulfill the criteria for any systemic autoimmune disease that could present with vasculitis.

P-241

Immunoautoradiographic characterization of serotonin transporter in human pineal gland

M Castagna[1], M Boldrini[2], I Nardi[3], A Giromella[2], F Becherini[1]
[1]Dip. Anatomia Patologica 3 University di Pisa, Pisa, Italy
[2]Dip. Psichiatria University di Firenze, Florence, Italy
[3]Dip. Biologia Cellulare Universita di Pisa, Pisa, Italy

The mechanism that regulates human pineal gland melatonin synthesis is not completely clear. In fact, several studies performed on animals demonstrated the possible role of serotonin and the involvement of its receptors 5-HT(2C) and 5-HT(1A) in the modulation of this process even if is not clear how it is realized. The aim of our study is to verify the presence of serotonin transporter (SERT) in the pinealocytes, a molecule involved in the reuptake of 5-HT from synaptic space, and to represent the action site of I.R.S. antidepressant drugs. We tested with immunoautoradiographic method (IARG) frozen slices conserved at –80 C^{o}, derived from twenty cadaveric epiphysis (11 men, 9 women) by utilizing a mouse monoclonal anti-SERT antibody followed by a secondary biotinilated anti-mouse IgG antibody, consecutively linked with an avidine/[3H]-biotine complex for a precise localization of the researched molecule. The tritium sensitive films were exposited to treated slices in special cassetes. After thirty days of exposure at – 80 C^{o}, the films have been developed and fixed to obtain auto radiographic images in which the radioactivity distribution followed a continuum pattern in sequential slices of each subject. It was the expression of SERT presence in epiphysis. This is the first study that demonstrate the presence of SERT in human epiphysis. We suppose that serotonin in human is not only a melatonin precursor synthesized in the pinealocytes but it is involved in the neuroendocrine regulatory mechanism of the gland.

P-242

Correlations of LOH on chromosome 10q and chosen clinico- morphological features in glioblastoma

E Izycka-Swieszewska[1], A Wozniak[2], J Limon[2], J Slowinski[3], W Kloc[4], K Jaskiewicz[1], R Rzepko[1], M Klimkowska[1]
[1]Dpt. of Pathology, Medical University of Gdansk, Gdansk, Poland
[2]Dpt. of Biology and Genetics, Medical University of Gdansk, Gdansk, Poland
[3]Dpt. of Neurosurgery and Neurotraumatology, Medical University of Silesia, Bytom, Poland
[4]Dpt. of Neurosurgery, Gdansk Hospital, Gdansk, Poland

Loss of heterozygosity (LOH) studies allow to identify sites harbouring tumor suppressor genes involved in tumor initiation and progression. This study was performed to establish the frequency of LOH on chromosome 10q in glioblastoma. 30 cases of glioblastoma were examined (13 women,17 men; age: 33-75 years). Two cases were secondary glioblastoma. In all cases the

representative neoplastic tissue and normal brain tissue were cut out with lancet from respective paraffin blocks. DNA was isolated with proteinase K with phenol/ chloroform extraction and isopropanol precipitation. Polymorphic markers were localized close to three supressor genes PTEN (D10S1765, D10S215), LGI1 (D10S1680), DMBT1 (D10S587) which are known to be lost or mutated in glioblastoma. The fith marker was D10S607 10q22.2. Fragments were PCR-amplified and analysed using automated sequencer ABI1310. Signals from neoplastic and normal tissue were calculated. Result under 0,6 was scored as LOH. In 14 cases at least one marker from chromosome 10q was lost. 11 cases with LOH were men, both secondary glioblastomas showed deletion in 10q. The mean patients' age with and without 10qLOH was similar. 5 cases showed LOH only in PTEN locus. In 9 cases deletions were stated in two or more loci, what might suggest loss of longer part of chromosome 10. Cases with LOH in 10q revealed additional changes in different chromosomes: LOH in 1p (2 cases), 2p (2), 2q (1), 3p (2), 7q (1), 13q (1), 15q (2), 17p (1). Our results are similar to the other studies, showing changes in 10q in about 50% of glioblastoma.

P-243

Histopathological changes of the skin in systemic lupus erythematosus

TA Vervekina, BA Magrupov, GSh Shamukhitdinova
Tashkent, Uzbekistan

Introduction Morphologic examination of the skin is of great importance for the diagnosis of various nosologic forms of rheumatic diseases. The aim of the present study was to evaluate histopathologic changes in skin biopsies of patients with systemic lupus erythematosus (SLE).
Material and methods Skin biopsies of 30 patients (22 women and 8 men; age range from 15 to 55 years) with preliminary diagnosis of SLE, based on clinical data and laboratory analyses, were studied with the purpose to specify the differential diagnosis. Biosy tissue specimens were fixed in 4% neutral formalin, embedded in paraffin, and serial sections were stained with haematoxilin-eosin, picrofuxin, and the combined Rhitter-Olesson staining. After treatment of the specimens with 0.1 % trypsin, direct immunofluorescence technique was carried out for detection of immunoglobulins G and M at the dermo-epidermal junction (lupus band-test).
Results Our study established the presence of hyperceratosis with formation of keratic clogs, epidermal atrophy with vacuolization of basal cells, vasculitis, eosinophilic degeneration of collagen and an atrophy of appendages. Specific immunostaining for immunoglobulins G and M at the dermo-epidermal junction was observed in all except in 7 cases. We did not observe inflammatory cell infiltrates in dermis in any case.
Conclusion The pathogenesis of skin histologic lesions in SLE is most likely associated with immunological reactions and therapy carried out earlier.

P-244

Structural peculiarities of different nevuses and their prognostic value

E Stupina
First Tashkent Medical Institute, Tashkent, Uzbekistan

For the time being the causes of skin melanoma have not been clearly understood. Development of skin melanoma was related to preceding pigment formations in 18% to 85% of patients. Among a variety of investigation methods histologic one is basic to establish the final diagnostic. Complex morphologic study was carried out on 343 skin biopsies with different types of pigment nevuses and melanomas. Of them 106 biopsies were selected for the thorough pathomorphologic investigation. Light microscopy, electron microscopy and morphometric method were used. Serial sections for light microscopy were stained with hemotoxylin and eosine, picrofuchsin-fuchselin by Van-Gizon, combined staining by Riter and Oleson. The findings have shown that the rate of pigment skin neoplasms of all the biopsy material of a specialized institution came to 1,12% among neoplastic and 11,9% among non-neoplastic skin lesions. Pigment nevuses more frequently occurred in females aged 21 to 50 years applied for medical aid, while melanoma in ones above 60 years. Intradermal nevus was diagnosed in 86,9% of cases, its proliferative activity was expressed in 55% of patients. In 66,3% of patients skin melanona was assigned to 3-4th grade of invasion according Clark's classification. Each form of pigment nevus had morphometric peculiarities, significantly differing in dimensions of the cell, nucleus and their ratio. The most reliable parameter of malignization was the length of the nucleus and cell axial section circle. Of frequently occurred nevuses intraepidermal (borderline) one was more predisposed to malignization which was evident from significant increase of all morphometric parameters.

P-245

Cutaneous ciliated cyst of the lower limb

MC Durán, JM Suárez Peñaranda, J Varela Durán, J Forteza Vila
Department of Pathology. University Hospital, Santiago de Compostela, Spain

Introduction Cutaneous ciliated cysts are a rare type of skin cyst, usually presenting themselves in women between the 2nd and 4th decades of life. Their origin is unknown and has been related to müllerian remnants based on similarities of the epithelium to the fallopian tube, but the occurrence of cases in men has given rise to the possibility of a sweat gland origin.
Case report A 31 year-old woman complained of an asymptomatic, longstanding, lesion located in the skin of the thigh. Once removed it was seen to correspond to cyst with clear fluid inside. Histopathological examination revealed a dermal cyst with ciliated cuboidal epithelium, usually double layered, but with some pseudostratified areas. Occasionally, papillary projections were seen in the lumen. There was no evidence of cellular atypia or mitotic activity. Immunohistochemical staining with oestrogen and progesterone receptors was strongly positive throughout the lesion.
Discussion and conclusions The clinical and histopathological findings fit in with the diagnosis of a typical cutaneous ciliated cyst of the lower limbs (cutaneous ciliated cyst). This is a rare cyst usually arising in the lower limbs of young women. Its origin is unknown and the demostration of sex-hormone receptors has been used to favour the müllerian origin. Nevertheless, some cases have been reported in men, which has diverted attention towards sweat glands as a possible origin of the cyst. The real incidence of the sex- hormone receptor if unknown, since it has not been clear in most published cases.

P-246

p53 and Ki-67 in non-neoplastic and neoplastic proliferative skin diseases

T Batinac[1], G Zamolo[2], N Jonjić[2], F Gruber[1], M Krašević[2]
[1]Department of dermatovenerology, Clinical Hospital Center, Rijeka, Croatia
[2]Department of pathology, Medical faculty, University of Rijeka, Croatia

Introduction p53 protein is essential for the regulation of cell proliferation and its aberrant accumulation is usually seen in malignant tumors but, also, occurs in squamous epithelium of inflammatory skin diseases characterized by hyperproliferation. The aim of this study is to elucidate the role of the p53 tumor-suppressor protein in the pathogenesis of different hyperproliferative, non-malignant and malignant skin diseases, and association between p53 overexpression and cell proliferation. We also investigated the influence of ageing on p53 and Ki-67 protein expression.
Material and methods Hundred and fifty skin specimens, consisting 30 cases of each, normal skin (NS), psoriatic skin (PS), keratoacanthomas (KA), basal cell carcinomas (BCC), squamous cell carcinomas (SCC) were examined immunohistochemicaly to assess p53 and Ki-67 protein expression.
Results p53 immunostaining of NS, PS, KA, BCC and SCC was positive in 39.0%, 46.7%, 66.7%, 80% and 86.7% cases, respectively. p53 and Ki-67 positive cells were present in basal (NS) and suprabasal layers (PS), and not only in cancer nests of KA, BCC and SCC, but also in dysplastic and even morphologically normal epidermis adjoining cancers. The positivity of p53 and Ki-67 protein differed significantly among the groups, with no differences in p53 expression between NS and PS, and in Ki-67 expression between PS and KA. Within all groups, there was a significant correlation between p53 and Ki-67 protein expression. Localisation and age were significantly related to p53 and Ki-67 expression in all groups, except for localisation in PS, and age in BCC.
Conclusions Our findings suggest that p53 overexpression occurs widely in neoplastic and non-neoplastic skin lesions. It is associated with the cell proliferation in normal, as well as, in changed epithelium. P53 accumulation is an age related process and significantly related to sun exposure, especially in NS and PS, as well as in KA and SCC. We also suggest that p53 overexpression begins in the early stage of carcinogenesis, before the appearance of malignancies in skin, and may be a useful predictor for the detection of nonmelanocytic skin cancer.

P-247

Maspin and beta catenin expression in relation to angiogenesis in basal cell carcinoma

L Seada[1], N Khafagy[2]
[1]Benha Faculty of Medicine, Pathology Department, Kairo, Egypt
[2]Ain Shams Faculty of Medicine, Dermatology Department, Kairo, Egypt

Background Maspin, a member of the serine proteinase inhibitor (serpin) family, has been recently pointed to as a tumor suppressor gene and angiogenic inhibitor. Objectives of this study were to investigate role of maspin and Beta-catenin in basal cell carcinoma (BCC).
Material and methods We studied immunohistochemically their expression in 30 basal cell carcinomas together with 5 trichoepitheliomas (TE) and 5 normal skin controls. Microvessel count (MVC) was also done using FVIII-related antigen. We examined the correlation of nuclear and/or cytoplasmic maspin expression with histological type, age, gender, invasion of safety margin, as well as stromal reaction (lymphocytic or fibroblastic. All primary antibodies (maspin, beta catenin and FVIII-related antigen) as well as detection Kit (ABC peroxidase/DAB Quick test), were purchased from Novocastra Labs.UK.
Results Maspin expression was strongly cytoplasmic and membranously expressed in TE and down-regulated in nodular BCC. Nuclear maspin expression was found in 43.3% of our cases. It was statistically positively correlated with invasion of safety margin ($p=0.014$) and with infiltrative type ($p=0.049$) and negatively correlated with a MVC >30 ($p= 0.046$). Cytoplasmic maspin was correlated to a strong fibroblastic stroma ($p=0.01$). Beta-catenin expression was found in both TE and BCC with the same intensity and was only correlated to younger age($p= 0.021$).
Conclusion Cytoplasmic maspin expression could differentiate between TE and nodular BCC Nuclear maspin expression could be related to aggressive behaviour of BCC and is realted to lower MVC (<30).

P-248

Trichilemmal carcinoma: report of two cases

M Kostov[1], S Ilic[2], N Djordjevic[3], G Lazarevic[3], B Stojiljkovic[4]
[1]Department of Pathoanatomy, Military Hospital of Nis, Serbia and Montenegro
[2]Institute of Pathology, Military Medical Academy of Belgrade, Serbia and Montenegro
[3]Department of Otorhinolaryngology, Military Hospital of Nis, Serbia and Montenegro
[4]Department of Pathology, Institute of Oncology, Sremska Kamenica, Serbia and Montenegro

Introduction Trichilemmal carcinoma (TC) is rare skin tumour occurring in the sun-exposed areas (largely on the face or ears) of the elderly. Clinically, it may be mistaken for a squamous cell carcinoma, basal cell carcinoma, nodular melanoma or keratoacanthoma. Although the histological picture suggests a high-grade malignant neoplasm, TC has an indolent course, and conservative surgical excision with clear margins is curative. Aim: Histological and histochemical examination of rare cases of TC of the skin.
Materials and methods We report two patients (males) with TC on the ears, presented as slow-growing nodules. Tumour biopsy specimens were routinely fixed and processed. Deparaffinized sections were stained by HE, PAS, PAS-D.
Results Histologically tumour cells showed a solid and a lobular growth patterns in continuity with the epidermis, with foci of pilar-type keratinisation and peripheral palisading. Tumour nests were mostly composed of large atypical cells with clear cytoplasm containing PAS-positive, and diastase sensitive materials. These cases were treated only with surgical excision, and there has been no evidence since of local recurrence or metastasis.
Conclusion We believe that careful histopathological examination of pillar appendage tumours will help to classify the wide range of clinically and histologically different tumours and to establish the exact diagnosis.

P-249

HMB-45 and melan-A positive pigmented epidermotropic breast carcinoma metastasis

D Brasanac, I Boricic, S Tatic
Institute of Pathology, School of Medicine, Belgrade, Serbia and Montenegro

Introduction Pigmented cutaneous metastases from breast carcinoma are uncommon and may simulate malignant melanoma both clinically and morphologically. We report a case of a 54-year-old female who developed multiple cutaneous pigmented metastases twelve years after radical mastectomy for left breast carcinoma.
Materials and methods Hematoxylin-eosin and immunohistochemically (streptavidin-biotin method) stained slides from three different regions of the chest skin and from the scalp plaque.
Results Numerous darkly pigmented plaques and nodules have been developed over a 8-month period on the back of the chest spreading anteriorly to the right subcostal region together with large, focally eroded scalp plaque. Histopathological examination revealed full thickness dermal infiltration and superficial subcutaneous fat involvement with cords and nests of neoplastic epithelial cells showing ductal structures and intracytoplasmic lumina in some areas. Irregular nests and single tumor cells at epidermodermal junction were accompanied with melanophages in papillary dermis. Immunohistochemically all tumor cells were cytokeratin 7 positive and cytokeratin 20 negative while epidermal and most superficial dermal nests showed HMB-45 and Melan-A reactivity as well. Scalp metastasis displayed less pronounced epidermotropism and only focal, single cell HMB-45 and Melan-A positivity.
Conclusion Epidermotropic breast carcinoma metastases may mimic malignant melanoma not just clinically and morphologically but also immunohistochemically and that might be related to the location of metastatic lesions.

P-250

Immunolocalization of lactoferrin in pigmented lesions of the skin

G Barresi, G Giuffre, F Fedele, M Grosso, V Barresi, G Tuccari
Department of Human Pathology, University of Messina, Messina, Italy

Lactoferrin (Lf) expression has been immunohistochemically investigated in 55 formalin-fixed paraffin-embedded bioptic skin samples (23 nevi, 12 melanomas, 10 vulgaris or seborrhoic pigmented warts, 10 pigmented basal cell carcinoma; 10 specimens of normal skin were utilized as control. On 3µm thick sections, depigmentation and antigen retrieval procedures were performed. Lf immunoreactivity was revealed by a rabbit anti-human lactoferrin (Dako, Denmark, 1:300), incubating all sections at 4 C overnight; successively, bridging antibody and PAP complex for 30 min at room temperature (RT) were applied. For the demonstration of peroxidase activity, the sections were incubated with 3-3' diaminobenzidine tetrahydrochloride-H_2O_2 substrate solution for 10 min at RT in darkness; slides were then slightly counterstained with Mayer's haematoxylin. Quantification of Lf immunoreactivity was performed using the intensity-distribution (ID) score based on both the percentage and the staining intensity of positive neoplastic cells. An evident cytoplasmic immunoreactivity for Lf was encountered in melanocytes, either in nevi or in melanomas; no appreciable differences were found among junctional, intradermic or compound nevi as well as between spindle or epitheliod cells melanoma. Basal cell carcinomas were always unstained, even if some degree of positivity was found in areas which showed squamous differentiation; sheets and whorls of keratin also exhibited a strong immunoreactivity, when encountered in warts. If the Lf immunoexpression could represent the result of an endogenous synthesis by cells in order to have greater availability of iron for their metabolism or to modulate an unspecific inflammatory or anti-oxidant response remains to be fully understood.

P-251

Immunohistochemical expression of vascular endothelial growth factor (VEGF), c-kit and c-erb-B2 in cutaneous melanocytic lesions

A Batistatou, A Zioga, E Arkoumani, D Stefanou
Department of Pathology, University of Ioannina, Medical School, Ioannina, Greece

Introduction VEGF is a glycoprotein involved in angiogenesis, that promotes progression in several malignant neoplasms. The c-kit gene encodes a transmembrane receptor with tyrosine kinase activity, which plays a role in melanogenesis. Overexpression of c-erb-B2 oncoprotein has been related with poor prognosis in several malignant neoplasms. The aim of the present study has been to investigate the immunohistochemical expression of VEGF, c-kit and c-erb-B2 in cutaneous melanocytic lesions.
Material and methods We examined immunohistochemically 41 formalin-fixed, paraffin-embedded melanocytic lesions. These included 11 compound nevi, 12 dysplastic nevi and 18 melanomas. The antibodies anti-VEGF (Neomarkers), anti-Human c-kit (DAKO) and anti-c-erbB2 (DAKO) were used.
Results All compound and dysplastic nevi showed no immunoreactivity for VEGF. Strong cytoplasmic staining for VEGF was observed in 13/18 (72%) of melanomas, with higher levels in vertical growth phase. The junctional component in all compound nevi and in 8/12 (66.6%) dysplastic nevi was positive for c-kit (cytoplasmic staining with membrane accentuation). The dermal component was positive in 6/11 (54.5%) compound nevi, and in 4/12 (33.3%) dysplastic nevi. In melanomas c-kit expression was higher in radial growth phase (44%). No specific staining with c-erb-B2 antibody was noted in any of the cases examined.
Conclusion Assessment of VEGF expression might aid in the differential diagnosis between dysplastic nevi and melanomas. c-kit expression is not of diagnostic importance in melanoma, however its loss might play a role in tumor progression. c-erb-B2 overexpression is not involved in the pathogenesis of melanoma, and thus has no value as a target for specific therapy.

P-252

Apoptosis in cutaneous malignant melanomas

M Costache[1], E Ionica[2], M Costache[2], CD Vrabie[1]
[1]Victor Babes' National Institute, Bucharest, Romania
[2]University of Bucharest, Romania

Introduction Cutaneous melanomas were detected at an increasing rate worldwide. Even thought many patients are diagnosed at an early stage, the death rate continues to rise due to the increasing incidence of more advanced lesions. The aim of this

study is to detect in 30 cases of malignant melanomas.
Materials and methods Analysis were performed in 30 paraffin-embedded cases of cutaneous malignant melanomas (10 cases in situ and 20 cases invasive melanomas). Apoptotic index (AI) was determined using the in situ end-labeling technique(TUNEL), who quantify apoptotic cell death at single cell level and tissues.
Discussion and conclusion AI was high in the cases of in situ melanomas, but in invasive melanomas (nodular melanomas, superficial spreading melanomas with vertical growth phases, acral lentiginous melanomas etc) AI was decreased in tumor cells. We considered that usually apoptotic cells represent ~ 10% of tumor cells. At cases of cutaneous malignant melanomas in which AI was high (27%), frequently at in situ melanomas, the prognostic is good, when in the others cases in which apoptosis is missing or is very rare in cells (34%), the prognostic is reserved. This nonmorphologic technique to evaluate the prognosis of melanoma must be regarded as investigational and cannot yet be recommended for routine application. All necessary pathologic data, such as tumor location, size, depth, ulceration, mitotic activity and growth phase, can be obtained by examination of standard microscopic preparations of malignant melanoma as stained with hematoxylin and eosin.

P-253

Morphological and immunohistochemical findings in systemic small vessel vasculitis

B Bogoeva[1], S Kostadinova[1], A Pusevski[2], M Ristovski[1]
[1]Institute of Pathology, Faculty of Medicine, Skopje, Republic of Macedonia
[2]Clinic of Rheumatology, Clinical Center, Skopje, Republic of Macedonia

Introduction Small vessel vasculitis is a group of disorders of unknown etiology, possibly associated with connective tissue disease (CTD). The aim of this study is to find correlation between clinical, morphological and immunological changes in the skin and muscle biopsies of the patients with CTD, where small vessel vasculitis is the main finding.
Methods and results We analyzed 90 skin and muscle biopsies from patients with CTD: 20 dermatomyositis, 32 systemic sclerosis, 18 syndroma Raynaud, 5 vasculitis, 4 SLE, 1 polyarteritis nodosa. 70 were females, and 20 males. The age of the patients was between 3-78. Standard histological and histochemical stainings (HE, PAS, Van Gieson-elastica) were done. Small vessel vasculitis was found throughout skin and muscle biopsies, characterized with thickening of the basal lamina, tiny fibrinoid necrosis (if present), swollen endothelial cells and perivascular edema with lymfocytes. The muscles were necrotic with regeneration and fibrosis and reduction in the intramuscular capillaries. The changes were positive on PAS and elastic tissue staining. Direct immunofluorescence technique was done with antihuman IgG, IgM and IgA antibodies. Granular or linear immunofluorescent deposits were found at the dermo-epidermal junction zone and in the vessel walls. Antinuclear antibodies were done by indirect immunofluorescence technique using serum from same patients of which 80% were positive. Lymphoid cells around the vessels and in healthy muscle fibers were positive for markers for T cells (CD45RO and CD8).
Conclusion There is correlation between morphological and immunohistochemical changes. The presence of immunologic deposits in the vessels suggests possible autoimmune etiology.

P-254

Cutaneous angiomyolipoma

H Cingil
Department of Pathology, Istanbul Naval Hospital, Istanbul, Turkey

Introduction Angiomyolipoma is a benign tumor almost exclusively seen in the kidney. Cutaneous Angiomyolipoma (AML) is a very rare benign vascular tumor that consists of a proliferation of blood vessels, smooth muscle bundles, and mature fat tissue. AML occurs more often in adult male patients and is often seen in acral locations.
Case report A 48-year-old man who had a 10-year history of a painless, solitary, noninvasive nodule on the right auricle lobule. The patient had no signs of tuberous sclerosis.
Material and methods The lesion was 3cm in diameter and clinically appeared to be a lipoma. The lesion was excised. Skin specimens was fixed in 10% buffered formalin, routinely processed, and embedded in paraffin. It was examined by routine light microscopy with histochemical and immunohistochemical stains.
Results On sections, the lesion was a well-circumscribed nodule in the dermis. There was fibrous pseudocapsule around it. The nodule was composed of an intimate mixture of mature adipose tissue, blood vessels, and bundles of smooth muscle cells. Combination of different types and sizes of vessels were particularly evident. Cellular pleomorphism, mitotic figures, and mucoid degeneration were absent. Reactivity for HMB-45 was negative. The histopathological diagnosis was angiomyolipoma.
Conclusion AMLs are very rare at extrarenal locations. In 1986, Argenyi presented the first report of cutaneous angiomyolipoma in the upper helix of the ear. The reported lesions were located at acral sites. As most cases of angiomyolipoma were long-standing lesions located at acral sites, and therefore exposed to external forces, some angiomyolipoma could be considered to be a degenerated with replacement by fatty tissues.

P-255

Primary cutaneus B-cell lymphoma. Experience in a comunity hospital

I Español, I Trias, U Gonzalez, R Pedragosa
Clínica Plató, Fundació Privada, Barcelona, Spain

Introduction The primary B-cell cutaneous lymphoma is a low frequent disease in a General Hospital. Its nodal equivalent has very different behaviour and prognosis. Aims: To study the incidence, behaviour and follow up of the B-cell cutaneous lymphomas in our hospital over a period of 9 years.
Material and methods In a total of 49116 cases between 1992 and 2002 we have 12 cases of B-cell cutaneous lymphoma. The skin biopsies were diagnosed acording EORTC classification. We did histological and immunohistochemistry studies. These included CD20, CD3, CD10, CD5, CD43, bcl-2 and Ki67.
Results Eith cases of 12 were SALT and 4 cases were folicular lymphomas. The ages are between 37 and 88 and is no sex predominance. SALT lymphomas were located two in the face and six in the trunk. All the cases of folicular lymphoma were in the face. The immunohistochemistry study in SALT lymphoma showed positivity for CD20 and CD43 and negative for CD3, CD5 and CD10. The expression of Ki67 was very low. The reactive foliculars centers were demostrated with the negativity of bcl-2.

The folicular lymphomas showed positivity for CD20 and CD10 and the number of positive cells for Ki67 was bigger.
Conclusions In a General Hospital in our country the incidence of B-cell cutaneous lymphoma is very low. The majority of the cases arrive with surgical excision, that is a good therapeutic approach. The general pathologist must be aware with reactive limphoid infiltrates because the majority of the cutaneous lymphomas are low grade neoplasies.

P-256

CD30 expression in inflammatory lymphoid cells in scabies

L Pijuan Andújar, C Barranco, F Gallardo, M Jimeno, E Díaz, A Munné, RM Pujol, S Serrano
Hospital Del Mar, Barcelona, Spain

Background CD30 expression is a distinct feature of both B and T cell activation. The presence of CD30+ large atypical lymphoma cells in a cutaneous infiltrate has been considered a characteristic feature of lymphomatoid papulosis/cutaneous CD30+. Recently, however, CD30 expression has also been described in some nonneoplastic infiltrates of de skin.
Design Twenty skin biopsy specimens from 20 patients with scabies were evaluated. Of these, the lesions had been present for more than 3 months in 12 cases. The diagnosis of scabies was based on the presence of characteristic clinical features and the demostrations of Sarcoptes scabiei mite. For each biopsy, a panel of histopathological and inmmunophenotypic features was independently assesed by two pathologists. CD3, CD20, CD8, CD30 and S-100 protein expression was evaluated in each case.
Results CD30+ cells, either in isolation or in small clusters, were seen in 12 biopsy specimens (12/20; 60%). CD30+ cell clusters were located in the papillary and superficial reticular dermis and tended to show a perivascular pattern. All 12 biopsy specimens obtained from long-standing (>3 months) scabies lesions demonstrated the presence of CD30+ cells. In contrast, no CD30 expression was observed in lesions of less than 2 months duration.
Conclusions CD30+ large cells can be detected in skin inflammatory lymphoid infiltrates associated with scabies, particularly in long-standing (>3 months) lesions. Cutaneous CD30 expresion, therefore, is not an exclusive feature of neoplastic lymphoid proliferations. Probably as the result of persistent antigenic stimulation, CD30 expression can also be detected in activated lymphoid cells of nonneoplastic infiltrates associated with insect bites, viral and bacterial infections and peculiar drug reactions.

P-257

Proliferative and apoptotic markers in cutaneous melanocytic lesions

G Zamolo[1], D Fučkar[1], N Jonjić[1], T Batinac[2], D Stojanović[3], V Mičović[3]
[1]Department of Pathology, Medical Faculty, University of Rijeka, Croatia
[2]Department of Dermatology, Medical Faculty, University of Rijeka, Croatia
[3]Department of Public Health, Medical Faculty, University of Rijeka, Croatia

Introduction Malignant transformation of melanocytes is a multistep process characterized by distinct histopathological stages. Differentiation between naevi, especially dysplastic naevi and melanoma, can sometimes be difficult to assess by conventional histopathological analysis. The aim of this study was to analyse the differences in proliferative activity and apoptosis between intradermal naevi (IN), dysplastic naevi (DN) and cutaneous melanoma (CM).
Materials and methods Fifteen IN, 15 DN and 15 CM (thickness less than 1.5 mm) were immunohistochemically stained for Ki-67 which was used as a proliferative marker, whereas bcl-2 and p53 were used, respectively, as an anti-apoptotic and apoptotic marker. The number of positive cells were counted on 200 melanocytes. Statistical analysis was done using the Spearman and the Chi-square test.
Results The mean value of Ki-67 positive cells in IN, DN and CM 7 was 7.6, 8.3, and 31.7, respectively. Bcl-2 was expressed in 120.6 IN, 148.0 DN, and 178.1 CM cells while p53 overexpression was present in 14.6 IN, 151.0 DN and 85.3 CM cells. Statistical analysis showed a signifficant difference in proliferative activity and the overexpression of p53 ($p < 0.05$), while observed differences in bcl-2 expression were not statistically significant between these three groups.
Conclusion Proliferative and antiapoptotic activity showed a progressive growth from benign to malignant melanocytic lesions. The strongest expression of p53 in DN suggests that its overexpression could be the first step in the loss of cell cycle regulation and possible malignant transformation of melanocytes.

P-258

Myofibroblastic transdifferentiation of mesangial and interstitial cells as prognostic criteria of glomerulonephritis in kidney biopsy analysis

SB Petrov, AP Kiasov, AE Homiacov, AS Hairullov
Kazan State Medical University, Kazan, Russian Federation

Introduction It is now known that myofibroblastic transdifferentiation in glomerulus takes place during mesangial activation.
Material and methods We analyzed functional disorders (filtration, concentration insufficiency) and kidney biopsies of 82 patients aged from 15 to 62 years with various forms of glomerulonephritis. We used standard histological, immunohistochemical, immunofluorescence methods as well as electron microscopy in our research. For studying myofibroblastic transdifferentiation we stained tissue immunohistochemically for alpha-smooth muscle actin (alpha-SMA) and then carried out a quantitative analysis of the results.
Results Seventy patients had myofibroblasts in kidneys. We found out that level of alpha-SMA expression correlates with decrease of glomerular filtration. While disorders of concentration a lot of myofibroblasts appear in kidney interstitium. But we have not found any correlation between clinical forms of glomerulonephritis and those cell growth we had seen. And we should mention that for 12 patients without glomerular or interstitial fibrosis we didn't reveal any changes in cells phenotype.
Conclusion So we conclude that myofibroblastic transdifferentiation must be considered as an early symptom of kidney sclerosis and can be used as a prognostic criterion.

P-259

Glomerular pathology in 100 school children with abnormal urinalysis detected by mass urine screen in Taiwan

CC Tsai[1], HC Hsu[2]
[1]Dept. of Pathology, Far Eastern Memorial Hospital, Taipei, Taiwan, Republic of China
[2]Dept. of Pathology, National Taiwan University Hospital, Taipei, Taiwan, Republic of China

Introduction To early detect renal and metabolic diseases, a mass urine screen in elementary and high school students was started in 1990 in Taiwan. We retrospectively reviewed the nephropathologic features to elucidate its value.
Materials and methods One hundred students, 43 boys and 57 girls, who were found to have hematuria and/or proteinuria by this urine screen program and received renal biopsy, formed the basis of this study. The glomerular pathology was divided according to disease severity into two groups.
Results Group I diseases (58%) showed minor histologic alterations, including minimal glomerular change in 40 cases and mesangial cell proliferation in 18. Among them, 42 children had electron microscopic examination, 24 (57%) had thin glomerular basement membrane (TGBM) disease. Group II diseases (42%) had more severe glomerular changes, including IgA nephropathy in 19 cases, membranous nephropathy (MN) in 12, lupus nephritis in 4, focal sclerosis in 2, chronic glomerulonephritis in 3, and type I and type II membranoproliferative glomerulonephritis in one case each. These findings confirm that glomerular diseases often progress silently. We found a high frequency (74%) of IgA nephropathy and MN in group II diseases and a close association of MN with hepatitis B virus infection.
Conclusion We conclude that mass urine screen in school children and renal biopsy are very useful for the early detection of the progressing glomerular diseases and provide great opportunity for early therapeutic intervention and long-term follow-up to better understand the natural courses of glomerular diseases, including TGBM disease.

P-260

Kidney biopsy study in patients with nephrotic syndrome

B Magrupov[1], B Allaberdiev[2]
[1]First Tashkent Medical Institute, Tashkent, Uzbekistan
[2]Bukhara Medical Institute, Tashkent, Uzbekistan

Introduction The purpose of the study was to establish a correlation between morphometric kidney biopsy parameters and routine laboratory findings in patients with nephrotic syndrome.
Material and methods 104 kidney biopsies of 58 patients with nephrotic syndrome were studied using standard techniques of paraffin sections stained with haematoxylin and eosin, picrofuxin van Gieson and PAS reaction. Direct immunofluorescence on snap frozen sections was performed using commercially available antibodies against IgA, IgM and IgG.
Results and conclusion Of the 58 patients, 31 (53.0%) were men and 27 (47.0%) women, with an average age of 24.9±5.2 years. Biopsy study revealed different types of chronic glomerulonephritis of various incidence: membranous GN (14), mesangioproliferative GN (11), mesangiocapillary GN (4), focal segmental glomerulosclerosis (2) and terminal sclerosing GN (4). Morphometric analysis using the semi-automatic image analyser »Integral-2MT« included cross-section surface areas of the glomeruli and glomerular capillaries, the numerical density of total number of cells per glomerulus, numerical density of mesangial cells, cross-section surface area and numerical cells density of the proximal and distal tubules and cross-section surface area of the peritubular capillaries. Routine clinical laboratory analysis included the level of proteinuria, serum creatinine and creatinine clearance, erythrocyturia, leukocyturia and cylinders in urine. A correlation of clinical laboratory parameters with mathematical morphometric models was established for each type of GN associated with nephrotic syndrome.

P-261

The role of proliferation, growth arrest and apoptosis in the carcinogenesis and prognosis of renal cell carcinoma

GA Gökhan[1], G Karpuzoglu[1], T Köksal[2]
[1]Akdeniz University School of Medicine Department of Pathology, Antalya, Turkey
[2]Akdeniz University School of Medicine Department of Urology, Antalya, Turkey

Introduction Nuclear grade and stage are insufficient to predict the clinical behaviour of renal cell carcinoma (RCC). Therefore additional prognostic factors are needed. In this study we investigated the role of proliferation, growth arrest and apoptosis in the carcinogenesis and prognosis of RCC using Ki67, Cyclin A, Bax, P53 and Bcl-2.
Material and methods Formalin-fixed paraffin embedded tissue blocks from 30 patients were studied. Cases were divided into low/high grade and low/high stage. Apoptotic index (AI) was evaluated as morphologically in H&E stained sections. Proliferation index (PI) was detected by using Ki67 and Cyclin A immunostaining. AI, PI, P53, Bcl-2 and Bax expressions in tumor tissue (TT) and in adjacent non-tumoral tissue (ANT) and associations with clinical and histopathological parameters were analysed statistically.
Results The mean indices for apoptosis, Ki67 and Cyclin A were: 5.10±3.86 (0-16), 15.47±17.78 (0-63) and 19.50±26.21 (0-108) in TT as well as 4.93±3.74 (0-15), 0 and 4.13±3.28 (0-12) in ANT, respectively. The number of cases in which the expression of P53, Bax and Bcl-2 were detected was: 14 (46.7%), 19 (63.3%), 13 (43,3%) in TT, and 0 (0%), 16 (53,3%), 18 (60%) in ANT, respectively. Statistically, there was a significant relationship between the values of TT and ANT for AI but not for the PI and the other parameters. Only AI and PI significantly correlated with the grade.
Conclusion In this study the role of PI as a prognostic indicator in RCC was again confirmed. Our observations suggest that apoptosis, Cyclin A, Bcl-2 and Bax may have roles in the carcinogenesis of RCC and that AI may be used as a prognostic indicator.

P-262

Immunophenotypisation of amyloid deposits in kidney biopsies - Our experience

S Kostadinova-Kunovska[1], G Petrusevska[1], L Grcevska[2], M Tolovska[1], B Bogoeva[1]
[1]Institute of Pathology, Faculty of Medicine, Skopje, Republic of Macedonia
[2]Clinic of Nephrology, Clinical Center, Skopje, Republic of Macedonia

Introduction During the renal biopsy analyses, the presence of amorphous eosinophilic material in the mesangium, along the glomerular basal membrane and Bowman membrane, interstitial peritubular tissue, and in the walls of the arterial blood vessels is recognized as amyloid. This picture requires a panel of further stainings, both histochemical and immunohistochemical to prove the existence and possibly determine the nature of the amyloid. The reason for that is the different chemical composition of the amyloid in different underlying diseases. We reviewed a total of 7 proven cases of renal amyloidosis during the last 18 months.
Material and methods The tissue specimens went through standard histological procedure for paraffin embedded tissue. The obtained serial cuts were stained with Haematoxylin-eosin, Trichrome Goldner, Silvermethenamine Jones, PAS and Congo red. Histochemical stainings for Congo red were viewed under polarized light, and when found positive, immunohistochemical stainings for AA amyloid, beta 2 microglobulin, kappa and lambda light chains were done. We used the LSAB immunoperoxidase technique.
Results and conclusion Due to the immunophenotypisation, we classified three of the cases as primary amyloidosis (light chain positivity of the amyloid deposits) and the rest four were positive for AA amyloid staining. The history of these four patients revealed collagenoses as underlying diseases in three cases. The most interesting and still unanswered remained the fourth case where the clinical history revealed existence of two possible underlying diseases: renal cell carcinoma and inflammatory bowel disease. Both are well known to be effective stimulators of amyloid deposition.

P-263

The role of matrix metalloproteinase-11 protein in various types of glomerulonephritis

C Eftychiadis, A Lazaris, I Boletis, S Michail, P Zeis, H Gakiopoulou, C Iatrou, C Stathakis, L Nakopoulou
Department of Pathology, Medical School, The National and Kapodistrian University of Athens, Greece

Introduction Matrix metalloproteinases (MMPs) have been implicated in a number of developmental and pathological processes such as inflammation. In human glomeruli, the mesangial matrix turnover is controlled by a dynamic equilibrium between synthesis and degradation to which MMPs are known to contribute. MMP-11 was originally discovered as a gene whose expression was associated with tissue remodelling. The aim of this study was to investigate whether MMP-11 protein is involved in the pathogenesis of various types of glomerulonephritis (GN).
Materials and methods Using standard immunohistochemistry, we analysed MMP-11 expression (clone 5ST-4A9) in renal biopsies from 95 patients with primary GN (n=44) and secondary, either lupus-associated GN (n=21) or GN due to active Wegener's granulomatosis (n=6) or pauci-immune, ANCA-associated GN due to small vessel vasculitis (n=24). The examined cases were divided in two groups (proliferative and non-proliferative).
Results The highest incidence of MMP-11 immunopositivity (26.3%) was noticed in GNs associated with microscopic polyangiitis and Wegener's granulomatosis. Generally, MMP-11 was often expressed in segmental areas of sclerosis, microadhesions, cellular and fibrocellular crescents. Fibrotic crescents and fibrotic glomeruli were constantly MMP-11-immunonegative.
Conclusions According to the above observations, MMP-11, as an inflammatory mediator, may exert a chemotactic influence on macrophages, which aggregate in the mesangium and induce early fibrosis while it may have a parallel mitogenic effect on epithelial cells, which, in association with macrophages, form cellular crescents. MMP-11 appears to have no antifibrotic role in GN.

P-264

Investigation of diffuse mesangial proliferative glomerulonephritis in children

M Ćorić[1], M Šćukanec-Špoljar[1], S Čužić[2], D Batinić[3], M Matković[3], D Batinić[3], L Grković[3]
[1]Department of Pathology, Clinical Hospital Center, Zagreb, Croatia
[2]Pliva Research d.o.o., Zagreb, Croatia
[3]Department of Pediatric Nephrology, Clinical Hospital Center, Zagreb, Croatia

Introduction Pure diffuse mesangial proliferative glomerulonephritis (MEPGN), although one of the basic light microscopic (LM) structural glomerular lesions, is morphologically highly nonspecific, and additional investigations are needed to reach the final diagnosis (dg) of disease. We studied the value of immunofluorescence (IF) and electron microscopy (EM) for dg, and which proportion of cases represents an idiopathic form of disease.
Material and methods We reviewed clinical picture, IF and EM findings in 154 children with MEPGN in LM.
Results 50 presented as nephrotic syndrome (NS), 67 as proteinuria and/or microhematuria (P/MH), 10 as recurrent hematuria (RH), 20 cases were clinically identified as purpura (P) and 7 as SLE. IF revealed 22 cases of Berger disease, while in 105 cases IF was negative or non-specific (46 NS, 55 P/MH, 4 RH). EM revealed 7 cases of thin basement membrane disease, all with MH, and 33 with GBM lesions consistent with Alport syndrome (29 P/MH, 2 RH, 2 NS). 21 patients showed EM features of resolving stage of acute GN, all with P/MH, while residual 93 showed MEPGN with or without mesangial deposits (42 NS, 22 P/MH, 2 RH, 20 P, 7 SLE).
Conclusion By means of clinical data, IF and EM, it was possible to reach definite dg in 110 (71.4 %) cases. Among residual 28,6 % with negative/non-specific IF and MEPGN in EM, there were 36 cases of NS belonging to idiopathic but clinically well-defined childhood nephrosis. So, only 8 cases represented a truly non-defined category of MEPGN (5.2 % of all cases).

P-265

Evaluation of the renal biopsy importance in isolated microhematuria in children

M Šćukanec-Špoljar[1], M Ćorić[1], D Batinić[2], S Čužić[3], M Matković[2], D Batinić[2], L Grković[2]
[1]Department of Pathology, Clinical Hospital Center, Zagreb, Croatia
[2]Department of Pediatric Nephrology, Clinical Hospital Center, Zagreb, Croatia
[3]Pliva Research d.o.o., Zagreb, Croatia

Introduction Isolated microscopic hematuria (IMH) in children always raises the question of the necessity of renal biopsy. Many authors consider IMH as minor abnormality where glomerular changes are not expected, but general agreement has not yet been achieved. The aim of this study was to evaluate contribution of renal biopsy to diagnosis of glomerular disease in IMH.
Material and methods Biopsy was performed in 54 children with IMH of proven glomerular origin. Mean duration of IMH prior to biopsy was 2.8 years. Biopsy specimens were examined by light (LM), immunofluorescence (IF) and electron microscopy (EM).
Results 43 patients (79.6%) were found to have glomerular abnormalities. On LM 18 patients had normal glomeruli (NG), 22 mesangial proliferative glomerulonephritis (MEPGN), 9 focal segmental glomerulosclerosis (FGS) 3 focal glomerulonephritis (FGN) and 2 membranoproliferative glomerulonephritis (MPGN). IF revealed 10 cases as IgA nephropathy. EM discovered GBM changes consistent with Alport syndrome in 21 patients and diffuse thinning of GBM in 10. In 5 children, subepithelial hump-like deposits were found and considered as the sign of acute postinfectious glomerulonephritis in resolution. One of 2 cases of MPGN showed to be type II (DDD). On follow-up, 6 of 21 children with Alport-like GBM changes developed full clinical picture of the syndrome. Further surveillance is needed to confirm the significance of EM findings in others.
Conclusion In children with IMH renal biopsy is justified and should always be analyzed by light, immunofluorescence and especially electron microscopy, because EM was decisive for final diagnosis in about 66% of all cases.

P-266

Mesoblastic nephroma of adult. Report of a case

S Vazquez Navarrete, J Pinzon Bohorquez, JM Romero Maturana, JM Conde Sanchez
Hospital SAS La Linea, Cádiz, Spain

Introduction Mesoblastic nephroma is a very uncommon tumor in adults, similar to the congenital mesoblastic nephroma of infancy, first described by Bolande et al. Microscopically the tumor consist in uniform spindle cells proliferations with numerous vascular spaces, nest of glomeruli, renal tubules that often cystic and dysplastic and lack of nuclear anaplasia or mitotic activity.
Case report A 69-year-old woman was admitted to the emergency services for acute abdominal pain in September 1995. She was diagnosed with acute pancreatitis. In CAT (without urologic symptoms) a solid mass in the upper pole of the right kidney was founded. With a clinical diagnosis of renal cell carcinoma a radical nefrectomy was performed. Follow-up was without event and had no recurrence 8 years afterwards. The right kidney weighed 228 grs. and was unremarkable except for a 3 cms-diameter circumscribed, yellow-tan, solid tumor in the upper pole. Microscopic examination revealed a tumor composed of spindle cells, mostly smooth-muscle cells and fibroblast, with numerous vascular structures and some areas of renal tubules with clear cytoplasm. In some places there was atrophic tubules. No mitotic figures were identified. Immunohistochemistry findings: The majority of spindle cells were positive for actin, desmin and smooth-muscle actin, and vimentin. And the tubular epithelium stain for EMA and keratins.
Conclusion A combination of histological and immunohistochemical findings is useful to distinguish mesoblastic nephroma from other tumor of the kidney with spindle cells.

P-267

Expression of cyclin D1 in secondary parathyroid hyperplasia

G Dordević[1], N Jonjić[1], D Matić-Glažar[2], V Licul[1]
[1]Department of Pathology, Medical Faculty, University of Rijeka, Rijeka, Croatia
[2]Department of Nephrology, Clinical Hospital Center, Rijeka, Croatia

Introduction Hyperparathyroidism occurs in patients with chronic renal failure and is usually associated with multiglandular parathyroid hyperplasia. Clonal analysis has suggested that in renal hyperparathyroidism glands initially grow diffusely and polyclonally. Mechanism of monoclonal proliferation observed with appearance of nodular hyperplasia is not well understood. It might be induced by certain genetic disorders such as overexpression of PRAD/cyclin D1 induced by DNA rearrangement of the parathyroid hormone gene. The aim of this study was to analyse the expression of cyclin D1 in normal and hyperplastic, diffuse and nodular parathyroid glands in order to ascertain the possible difference.
Materials and methods 140 hyperplastic parathyroid glands, from 46 uremic patients who underwent surgery during the period 1977-2003, were analysed. Immunohistochemistry for cyclin D1 protein was performed on 10 normal parathyroid glands and 47 selected hyperplastic, 14 of diffuse and 33 of nodular type. Overexpression of cyclin D1 was considered to be present if 40 % or more of the sample showed positive nuclear staining.
Results In normal glands, the mean value of nuclear positivity was 19.94%. Overexpression for cyclin D1 was present in 11/15 (78%) diffuse and 27/33 (82%) nodular hyperplastic glands. No significant difference was found.
Conclusion In comparison to normal, hyperplastic glands (nodular as well as diffuse) overexpress cyclin D1 protein. These results indicate that overexpression of cyclin D1 is not limited only to neoplastic proliferation, as the most studies showed, respectively this genetic abnormality is not the only responsible mechanism for the monoclonal proliferation.

P-268

Proteins of extracellluar matrix as predictors of glomerulonephritis outcome

S Čužić[1], M Šćukanec-Špoljar[2], B Jelaković[2], Z Sonicki[3], D Kuzmanić[2], M Laganović[2]
[1]Pliva Inc., Pharmaceutical Industry, Zagreb, Croatia
[2]Klinički bolnički centar "Zagreb", Croatia
[3]Škola narodnog zdravlja "Andrija Štampar", Zagreb, Croatia

Introduction Chronic renal insufficiency develops only in those cases of glomerulonephritis in which the lumina of postglomerular

capillaries in the renal cortex are narrowed due to expansion of the extracellular matrix (ECM). Aim of the study was to compare the composition of interstitial ECM proteins with clinical data in various forms of primary glomerulonephritis (GN).

Material and methods We examined renal biopsies from 55 GN patients, while normal renal tissue was obtained from nephrectomy due to small renal tumour. Specimens fixed in B5 and/or Dubosque fixative were analysed by immunohistochemistry (APPAP-method) using a monoclonal antibodies against tenascin (TN), fibronectin (FN), collagen I, III and IV (COI, COIII, COIV) (DAKO). The same fixatives were used for control renal tissue. Evaluation of fibrin was performed on frozen sections by immunofluorescence. Clinical data were: proteinuria and serum creatinine level, obtained by standard laboratory methods, immunotherapy and ACE-genotype.

Results Fifty patients had proteinuria at time of biopsy and 33 of them continued to have it during the follow-up period. Patients with persistent proteinuria had more often interstitial fibrosis with elevated content of COI and COIV. Only 10% of patients who responded well to immunotherapy had deposits of fibrin. There were 12 patients with elevated creatinine at biopsy with similar composition of ECM as patients with proteinuria. Majority of patients with interstitial fibrosis had ACE-genotype II although this genotype wasn't the most common in the cohort.

Conclusion Our study showed that persistent proteinuria could be linked to interstitial fibrosis and fibrin deposits. Patients with II ACE-genotype are more prone to develop interstitial fibrosis.

P-269

Haemorrhagic fever with renal syndrome in Slovenia from 1983 to 2002: clinical aspects and clinical-pathological correlations

[1]J Pajek, [1]K Grego, [2]T Avšič-Zupanc, [3]A Vizjak, [1]AF Bren, [3]D Ferluga
[1]Department of Nephropathology, University Clinical Centre Ljubljana
[2]Institute of Microbiology and Immunology, Faculty of Medicine University of Ljubljana
[3]Institute of Pathology, Faculty of Medicine University of Ljubljana, Ljubljana, Slovenia

Introduction Haemorrhagic fever with renal syndrome (HFRS) in Slovenia is caused by two hantavirus agents - Puumala and Dobrava serotypes. There is still a lack of clinical and pathological information, especially about the Dobrava virus associated disease. The aim of this study was to analyse and compare the clinical course, outcome and pathological features of HFRS caused by these two virus serotypes.

Material and methods The clinical course of 41 patients (6 women) aged 32±12 years (range 16-71) treated in the nephrological department for serologically confirmed hantavirus associated HFRS was analysed, a serological diagnosis was made using immunofluorescence test and enzyme-linked immunosorbent assay. Kidney biopsy specimens of 18 patients were analysed by light microscopy, immunofluorescence and electron microscopic techniques. A semiquantitative scale for gradation of cumulative tubulointerstitial lesions and interstitial haemorrhagic lesions was applied (scores 0-4).

Results Seventeen patients (41.5%) had Puumala and 24 (58.5%) Dobrava virus infection. All patients were febrile and had proteinuria, and other clinical features were: nausea and vomiting (85% of patients), oliguria (73%), abdominal pain (61%), headache (61%), haemorrhages (54%), myalgias (44%), diarrhea (41%), neurological and ophthalmological abnormalities (34%), hypotension (12%). Pancreatitis (12%) and elevated transaminases (7%) were observed only in patients with the Dobrava serotype. None of the patients in this study died and there was none with permanent haemodialysis dependence. Comparison of clinical and pathological features of Dobrava and Puumala diseases is given in the table.

Clinical and histopathologic features	Dobrava serotype (24 patients)	Puumala serotype (17 patients)	P
Age	34±13 years	31±10 years	0.34
Elevated creatinine at discharge	64%	47%	0.3
Haemodialysis needed	79%	29%	0.001
Oliguria	83%	59%	0.04
Hypotension	4.2%	24%	0.07
Haemorrhages	63%	41%	0.13
Proteinuria (semiquantitave)	2.6	2.5	0.86
Tubulointerstitial lesion score	2.9±0.9	3±0.5	0.78
Haemorrhagic interstitial score	2±1.4	2.5±1.2	0.44

A need for haemodialysis and the creatinine level at discharge were not associated with the age of patients. Those patients who needed haemodialysis, had clinical haemorrhages or had elevated creatinine at discharge, also had higher haemorrhagic and cumulative tubulointerstitial lesion scores, but differences were not significant. Elevated serum creatinine above basal levels was present at discharge in 22 patients (54%), range 83-554 μmol/L and some patients remained with chronic renal insufficiency.

Conclusion Our results show that Dobrava virus infection is associated not only with a significant mortality, comparable to Hantaan virus infection, but also with a worse clinical course of renal disease than Puumala. The histopathology of the kidney in Dobrava and Puumala is characterised by haemorrhagic necrotising tubulointerstitial nephritis involving particularly the outer medulla, with quantitative and not qualitative differences between these two infections.

P-270

Renal parenchymal malakoplakia after kidney-pancreas transplantation. Case report

E Honsova, T Havrdova, A Lodererova, L Voska, P Boucek
Institute for Clinical and Experimental Medicine (IKEM), Prague, Czech Republic

Introduction Malakoplakia is an unusual chronic inflammatory disease rarely involving parenchyma of the transplanted kidney. It represents an unusual host response, probably due to leucocyte bactericidal defects to an infecting agent, usually gram-negative organisms, of which Escherichia coli is the commonest. Malakoplakia in renal transplant is very rare (to date only six cases have been reported) and is associated with a high rate of graft loss and significant mortality.

Case report We report a 31-year-old female recipient of kidney-pancreas allografts immunosupressed with Tacrolimus (Prograf, 2x3mg) and Mycophenolate Mofetil (CellCept, 3x500mg). The patient had suffered from recurrent urinary tract infections. Three years after transplantation she was admitted to the hospital with decreased kidney graft function. Percutaneous kidney needle biopsy was performed and diagnosis of malakoplakia was established. Histologically, on the inflammatory background many Mi-

chaelis and Gutmann bodies were present and confirmed ultrastructurally. The patient was treated with antibiotics and simultaneously immunosuppression (Tacrolimus) was reduced. Gradually, her renal function improved (with serum creatinine of 105 umol/l). For the entire following year, the patient has been monitored regularly and her renal and pancreas function are stable and both her allografts remain in situ.

P-271

Morphometric study of transbronchial biopsies in pulmonary transplantation

E Caballero, R Vilallonga, M Ferran, J Majo
Hospital Vall D´Hebrón, Barcelona, Spain

Introduction The transbronchial lung biopsy (TBB) is considered as the 'gold standard' for diagnosis of acute rejection. It has been pointed out that diagnostic utility depends mainly on the number of fragments (NF), but no other biopsy parameters have been studied. Aims: Morphometric study of TBB in frequent pulmonary transplantation pathologies, to determine differences between diverse parameters of the biopsies to reach a diagnosis.
Material and methods From 1997 to 2002, 139 lung transplantations were carried out in our institution and 158 consecutive TBB were performed for clinical indication with histologic diagnosis of: 1) acute rejection (AR) (n=65) classified according to the Working Formulation, 2) infection or highly suggestive of infection (INF) (n=49) and 3) non-diagnostic biopsy (ND) (n=44). In these biopsies we measured five parameters. We counted the number of fragments (NF), number of fragments with alveolated parenchyma (NFAP) and number of vessels (NV) on the hematoxilin-eosin slides. The microscopic images of each case were digitalized and captured to the calculated total area (TA) and the alveolated area (AA) that are expressed in mm^2.
Results See table

	NF	NFAP	NV	TA	AA
AR	3.04±1.57	2.44±1.44*	7.96±4.75**	8.76±4.20	5.75±3.92**
INF	3.24±1.66	1.73±1.22	4.91±4.74	7.29±4.73	3.36±3.47
ND	2.81±1.14	1.79±1.13	4.75±3.97	5.95±4.22**	2.63±2.77

Levels of statistical significance: * $p<0.05$, ** $p<0.005$
Conclusion In our series of TBB for transplant pathology, the AA and NV are the most important morphometric parameters of the biopsy to reach the diagnosis of AR. Conversely, the NF does not show significant statistical difference between diagnostic biopsies and ND biopsies.

P-272

The importance of glomerular deposits of von Willebrand factor in human renal allografts

BH Ozdemir[1], B Demirhan[1], M Haberal[2]
[1]Department of Pathology, Baskent University, Faculty of Medicine, Ankara, Turkey
[2]Department of General Surgery, Baskent University, Faculty of Medicine, Ankara, Turkey

Aim To evaluate the role and prognostic importance of glomerular endothelial cell alteration in human renal allografts.
Material and methods We examined 72 patients with renal transplantation among whom 40 showed acute rejection (AR) and 32 chronic rejection (CR). Biopsies were immunostained for Von Willebrand factor (vWF), fibronectin (FN) and CD68. Glomerular staining for vWF and FN was graded in a semiquantitative manner using the 1-3+ scale.
Results In the CR group there was markedly increased expression of vWF and FN in the glomeruli, whereas only 8 of 40 AR cases showed intense (grade 3) glomerular vWF (GvWF). A significant difference was found between patients with AR and CR with regard to GvWF ($p<0.01$). A positive correlation between the degree of GvWF and early interstitial fibrosis was found in cases with AR in follow-up biopsies ($p<0.05$). The presence of transplant glomerulopathy was found significantly earlier in cases with grade 3 GvWF in AR group ($p<0.01$). We found strong correlation of both intraglomerular FN expression and macrophage infiltration with the degree of GvWF both in AR and CR groups ($p<0.05$). The outcome of grafts that showed intense (grade 3) GvWF was significantly worse than the outcome of those grafts with grade 1 and 2 glomerular vWF during the follow-up ($p<0.001$).
Conclusion Increased GvWF deposition in cases with AR is in risk of early transplant glomerulopathy, early interstitial fibrosis and early graft loss. In conclusion, it may be beneficial to use new therapeutic approaches such as anticoagulant medicine for the treatment of AR and CR in future.

P-273

The role of microvascular injury on steroid and OKT3 response in renal allograft rejection

BH Ozdemir[1], B Demirhan[1], M Haberal[2]
[1]Department of Pathology, Baskent University, Faculty of Medicine, Ankara, Turkey
[2] Department of General Surgery, Baskent University, Faculty of Medicine, Ankara, Turkey

Aim Our aim is to understand the influence of HLA-DR positive microvascular (MV-DR) injury on the steroid and OKT3 response in renal allografts with acute rejection (AR).
Material and methods We examined 94 biopsies of 40 patients. Of 40 cases, 20 showed steroid resistant AR (group 1) and received OKT3 treatment. Remaining 20 cases showed steroid respondent AR (group 2). Biopsies were immunostained with HLA-DR, fibronectin (FN), CD-68, CD-3 and Factor VIII-RA.
Results The degree of MV-DR expression was decreased with increasing AR grade ($p<0.01$). There was a negative correlation between MV-DR expression and the degree of interstitial mononuclear cell infiltration ($p<0.001$). As the severity of MV-DR destruction increased, the response to steroid and OKT3 therapy declined ($p<0.05$). In group 2 severe MV-DR injury was found only in 15% of cases (3/20 cases), whereas severe MV-DR injury was found in 55% of cases (11/20 cases) in group 1 ($p<0.01$). After OKT3 treatment 70 % of cases in group 1 responded to therapy. Remaining 6/20 cases (30%) that had no response to OKT3 showed severe MV injury. Only 45.5% (5/11 cases) of 11 cases with severe MV-DR injury showed response to OKT3 therapy. The follow-up biopsies of all cases with severe MV-DR injury showed significant interstitial fibrosis and FN expression ($p<0.01$). The mean time between transplantation and diffuse interstitial fibrosis was found to be significantly shorter in cases with severe MV injury ($p<0.01$).
Conclusion The destruction of MV-DR could contribute to severe inflammatory reactions and subsequently to poor steroid response, early interstitial fibrosis and graft dysfunction.

P-274

Acute rejection in renal allografts: possible role for hepatocyte growth factor

P Kaynak Aksoy[1], B Bilezikçi[1], B Demirhan[1], S Görür[2], A Aktas[3], M Haberal[2]
[1]Department of Pathology, Baskent University, Faculty of Medicine, Ankara, Turkey
[2]Department of General Surgery, Baskent University, Faculty of Medicine, Ankara, Turkey
[3]Department of Nuclear Medicine, Baskent University, Faculty of Medicine, Ankara, Turkey

Introduction Acute renal allograft rejection is the most important threat to graft survival, and must be diagnosed and treated as early as possible. Clinical, radiological and histopathological confirmation of the diagnosis is essential. Several factors are being investigated as potential diagnostic markers for acute rejection (AR), and one of these is the hepatocyte growth factor (HGF). The aim of this study was to investigate the presence/density of HGF in core needle biopsies from renal allografts with AR using immunohistochemical staining.
Material and methods The study involved 84 cases of kidney recipients whose allografts were investigated for an initial AR episode without any other pathology. All the patients received cyclosporine-A anti-rejection treatment. Each archived slide was re-examined according to the modified Banff 97 classification, and patients were categorized as type I AR (Group 1; n=66), type II AR (Group 2; n=16) and type III AR (Group 3; n=2). Normal histopathological findings in graft biopsies were obtained as controls (Group 0; n=15). The clinical findings of patients were reviewed from archived records. The sections were stained immunohistochemically with monoclonal anti-HGF antibody. The mesenchymal cells (interstitial macrophages and glomerular endothelium) that showed cytoplasmic positivity were then counted using ocular micrometer. The results were statistically analyzed using Mann-Whitney U test.
Results On analysis of the groups' mean cell count, the only significant finding was higher concentration of HGF in the AR patient group than in the control group ($p<0.001$). Concerning all other parameters studied, the only significant differences were higher blood urea nitrogen and creatinine levels in Group 2 compared to Group 1 ($p <0.0167$).
Conclusion Our results showed that presence/density of HGF increases in favor of acute rejection and accompanies the histopathological findings. Therefore we suggest that density of HGF, excreted in renal allograft tissue, may be a useful marker for supporting AR diagnosis.

P-275

Graft biopsies after renal transplantation in children: differences between FK506 and CyA immunosuppression

M Chadimova[1], E Simkova[2], P Rossmann[3], M Hladikova[4]
[1]Dept. of Pathology and Molecular Medicine, Charles University, 2nd School of Medicine, Prague, Czech Republic
[2]Dept. of Pediatrics, Faculty Hospital Motol, Prague, Czech Republic
[3]Inst. of Microbiology, Academy of Sciences, Prague, Czech Republic
[4]Dept. of Medical Informatics, Faculty Hospital Motol, Prague, Czech Republic

Introduction In 1997 – 2003 we performed 84 graft biopsies in 41 children aged 3 to 18 years, 7 of whom underwent repeated transplantations. Aims: Differences in the treatment of renal grafts.
Materials and methods 84 biopsies were examined. Besides light microscopy (LM) and electron microscopy (EM), IgG, IgA, IgM, fibrinogen, C3 and C4d were detected by immunofluorescence (IF). Immunohistochemistry (IHC) was performed using CD3, CD45RO, CD20, and CD68 antibodies to study the presence of different types of cells in acute rejection. Banff's classification was used to evaluate the samples.
Results Graft rejection was found in 64 (76.1%) biopsies - hyperacute rejection (HAR) 1 (1.2%), borderline changes (BCH) 9 (10.7%), acute rejection (AR) 37 (44%), and chronic rejection (CHR) 17 (20.2%). CyA and FK506 nefrotoxicity (TOX) was present in 28 (33.3%) biopsies. C4d (25 biopsies from 12 patients) showed linear positivity of peritubular and glomerular capillaries in 3 patients, with HAR and AR. These three grafts failed and the same pattern was seen in the excised grafts. In all AR cases, IHC proved the prevalence of CD45RO+ cells in rejection infiltrates, including tubulitis. The rejection infiltrate contained from 10% to 30% of monocytes-macrophages. EM showed disjunction and tubular epithelia regression in tubulitis. AR and TOX findings in patients receiving immunosuppression with FK506 were compared with a group given CyA.

Group	Number	TOX	AR
FK506	15 patients	8 (53.3%)	6 (40.0%)
FK506	23 biopsies	12 (52.2%)	6 (26.1%)
CyA	26 patients	12 (46.2%)	21 (80.8%)
CyA	61 biopsies	16 (26.2%)	31 (50.8%)

No significant differences in the rate of toxic manifestation were found between the groups of patients on FK506 and those on CyA. More frequent findings of toxicity were noted in FK506 patients´ biopsies ($p=0.024$). AR was found more frequently both in the patients ($p=0.008$), and in the biopsies ($p=0.042$) of CyA-treated subjects.
Conclusion FK506 seems to be more potent suppressant than CyA in spite of its persistent toxic effect.
The paper is sponsored by Ministry of Health of the Czech Republic (International Grant Agency) No: NE/6442-3.

P-276

BK-polyomavirus infection in a renal transplant recipient - Diagnosis with renal biopsy, urinary cytology and electron microscopy of the urine

I Kilicaslan[1], A Turkmen[2], S Alisir[2], S Solakoglu[3], H Ander[4], M Sever[2], V Uysal[1]
[1]Istanbul University, Istanbul Faculty of Medicine, Department of Pathology, Istanbul, Turkey
[2]Istanbul University, Istanbul Faculty of Medicine, Department of Internal Medicine Nephrology Unit, Istanbul, Turkey
[3]Istanbul University, Istanbul Faculty of Medicine, Department of Histology, Istanbul, Turkey
[4]Istanbul University, Istanbul Faculty of Medicine, Department of Urology, Istanbul, Turkey

Introduction BK polyomavirus causes a variety of infections in the urinary tract, involving transitional and renal tubular epithelium in immune suppressed patients, including transplant recipients. It can cause irreversible loss of graft function. We report a case of polyomavirus infection in a transplant recipient diagnosed by renal biopsy, urinary cytology and electron microscopy of the urine.
Patient and results A 19-year-old female patient underwent renal transplantation, and received immunosuppressive treatment with tacrolimus, MMF and prednisolone. Serum creatinine level increased

and hydronephrosis was observed in ultrasonography in the 3rd month. A renal biopsy was taken. No glomerular or vascular changes were observed. Some tubular epithelial cells displayed pleomorphism, hyperchromatism with chromatin irregularities and clumping, and intranuclear inclusion bodies. No immunostaining was detected with anti-CMV, HSV and EBV antibodies. Cytopathic tubular lesions in biopsy, many decoy cells in urinary cytology and intranuclear viral particles in electron microscopy of the urinary sediment proved the BK-polyomavirus infection. As the high serum creatinine levels persisted, despite alternative immunosupressive therapies, two more renal biopsies were taken, and acute rejection Banff grade Ib and IIa was diagnosed respectively. The patient is still under a novel antiviral treatment as the focal tubular cytopathic changes were present in the latter biopsy. Serum creatinine levels were still high, even though urinary cytology is normal.
Conclusion As we have seen in this case, the differential diagnosis between rejection and infection in renal transplant biopsies is critical and complicated for both clinicians and pathologists, as well as patients.

P-277

Vascular changes in donor kidneys may have an impact on late graft-dysfunction

E Kemeny[1], AN Fricska[1], E Szederkenyi[2], J Eller[3], Z Morvay[4], G Illyes[5], B Iványi[1], P Szenohradszky[2]
[1] Department of Pathology University of Szeged, Hungary
[2] Department of Surgery University of Szeged, Hungary
[3] Department of Medical Informatics University of Szeged, Hungary
[4] Department of Radiology University of Szeged, Hungary
[5] II. Department of Pathology Semmelweis University, Budapest, Hungary

Introduction Morphological studies of "zero-hour" kidney donor biopsies have produced controversial results as to what type of vascular changes, if any, are associated with late graft-dysfunction. Our aim was to assess this question.
Materials and methods 94 consecutive pretransplant "zero-hour" biopsies from cadaver kidney grafts were studied. We examined the frequency and severity of arteriolar hyalinisation, intimal fibrosis, tubular atrophy, interstitial fibrosis and glomerulosclerosis semiquantitatively. The wall thickness/lumen (W/L) ratio of each vessel was determined by morphometry. Groups were then differentiated according to their blood vessel size: G1: d<79µm, G2: d=80-149µm, G3: d=150-300µm. Statistical analyses were carried out to examine the clinico-pathological correlations.
Results Non-specific morphological changes were frequently seen: arteriolar hyalinisation: 84.0%, intimal fibrosis: 76.6% (moderate 26.6%), interstitial fibrosis: 25.5%, tubular atrophy: 71.3% and the mean proportion of sclerotic glomeruli was 5.01%±7.3%. Among the vascular changes studied only the moderate intimal fibrosis ($p<0.01$), and the elevated mean W/L ratios of arteries in the G3 group ($p<0.05$) revealed a significant association with the mean elevated serum creatinine level measured at 24 months after transplantation. A significant correlation was also found between the mean W/L ratios and the degree of intimal fibrosis ($p<0.01$). As for intimal fibrosis, there was a significant correlation (a) with the non-specific morphological lesions ($p<0.001$), and (b) with the frequency of intracranial hemorrhage as the cause of donor-death ($p<0.01$).
Conclusion Our findings suggest that donor kidneys with moderate intimal fibrosis do indeed have a higher risk of late graft-dysfunction.

P-278

Importance of the immunofluorescence morphology in autoimmunity

M Ristovski, V Janevska, L Spasevska, P Cvetkovski
Institute of Pathology, Faculty of Medicine, Skopje, Republic of Macedonia

Introduction The analyses of serums or tissue specimens from the patients with autoimmune diseases are dispersed between microplate reader ELISA techniques and immunofluorescence (IF) microscopy techniques. The number and the complexity of IF morphological parameters are becoming greater, as well as their association with some of the clinical conditions. The quantity of the morphological signs and the notice capability exceed the possibilities of the experts who are not morphologists. The aim of this paper is to present compilation of IF morphological slides and their association with the clinical conditions, indicating the real position of this kind of diagnostics.
Material and methods More than 2000 serums and 100 tissue specimens from different locations were used as study material. The methods used were indirect IIF microscopy with commercial and own antigens, microplate reader ELISA techniques (MPR-ELISA) and direct IF microscopy.
Results The study showed that the morphology of antinuclear and anticytoplasmic antibodies, using HEp-2 kits was easily examined, wider, and associations with some clinical conditions could be easily done. The antigens for MPR-ELISA techniques derived from recombinated genetic technology, unlike those produced from extraction showed better correlation with indirect IF microscopy. The own antigens originating from the domestic animals and human cadavers, used for indirect IF microscopy in bullous diseases, had the same value as the commercial ones.
Conclusion In order to emphasize the importance of this paper, we can conclude that, undeservingly, very few papers from this area are being presented in the pathological congresses and are left to other specialities.

P-279

Expression of p53 in gastrointestinal stromal tumors predicts biological behavior and survival. A multivariable study of 49 cases

J Nuncio[1], J Baquera[1], H Medina-Franco[1], MM Urist[2]
[1]Instituto Nacional de Ciencias Medicas y Nutricion Salvador Zubiran, Mexico City, Mexico
[2]University of Alabama at Birmingham, Birmingham AL, USA

The gastrointestinal stromal tumors (GIST) are rare tumors. There have been few factors identified that predict survival and biological behavior. This study analizes the experience in two university hospitals. Forty nine patients with GIST were identified from the tumor registry of both institutions. A retrospective review of patient clinic data, tumor and treatment variable was done. Expression of p53 and cellular proliferation antigens (ki67/PCNA) was also analyzed with overall survival as the main outcome variable. Statistical analysis was performed by log rank test and Cox regression model. Significance was defined: $P<0.05$. As results we found that median age was 53 years (range 16-82 years). Twenty-five patients were women (51%) and 24 were men (49%). Hispanics were predominant race with 22 patients (45%) followed by Caucasians with 18 patients (38%) and 9 African American

patients (1%). The stomach was the most common site of presentation (47%) followed by small bowel (37%). Mean tumor size was 8 cm (range 2-46 cm). Complete resection was performed in 38 patients (77.6%). Actuarial 3-year survival was 65.5% with a median follow-up of 35 months (4-204). Univariable analysis identified overexpresion of p53 (P=0.00001), cellular progression antigens (Ki67/PCNA) (P=0.0065), high grade (P=0.00001), tumor size bigger than 10 cm (P=0.0045), and incomplete resection (P=0.00001), as significant negative factors, Hispanic race (P=0.013) and good performance status (P=0.0002) were significantly associated with prolonged survival. On multivariable analysis, overexpression of p53 was the only independent negative factor. In conclusion, p53 is the most significant negative prognostic factor for survival in GIST.

P-280

Granulomas in gastric mucosa, with focus on microgranulomas (mg)

S Holck[1], M Schmidt[1], T Rannem[2]
[1]Department of Pathology, Lyngby, Denmark
[2]Department of Internal Medicine, Lyngby, Denmark

Introduction Granulomatous gastritis (gg) is a poorly understood entity, reportedly identified in less than 1% of all gastric biopsies. A precise definition of granulomas has rarely been given, in particular mg, well-described in intestinal disorders, have not been focused on in gastric lesions. Aims: We summarize our experience with gg, including mg, and record prevalence as well as associated background morphology.
Materials and methods Among gastric biopsies from 6.677 patients (7.837 gastroscopies), gg was diagnosed in 20 patients. Groups of histiocytes producing conspicuous alteration of gastric architecture were classified as well-defined granuloma (wdg); subtle collections of histiocytes failing to distort surrounding glands were labelled mg. The background morphology and presence of micro-organisms were recorded.
Results The distribution of types of granulomas were as follows: mg only 7 patients, mg and wdg 4 patients, wdg only 9 patients. The background morphology of cases with only mg/wdg with/ without mg included chronic gastritis (n=2/5); chronic active gastritis (n=2/7); ulcus (n=2/2); lymphocytic gastritis (n=1/1); carcinoma (n=0/1); otherwise normal morphology (n=1/1); H. pylori (n=1/4).
Conclusion In concert with previous reports, we identified gg in less than 1% of all gastric biopsies. Since the identification of mg requires assiduous histologic examination, such subtle features may be overlooked; hence our calculated prevalence of gg is a minimun value. The functional relation between mg and wdg is uncertain. However, their coexistence in a proportion of gg could support a precursor function of mg in the development of wdg. Additionally, the background pathology of biopsies with mg and wdg were comparable.

P-281

Intravascular signet ring-like cells CD68/lysozyme positive in gastric ulcer due to chronic use of NSAID, diagnostic implications in endoscopic biopsy and surgical management of an unusual invasive cancer mimicker

J Nuncio, J Arista-Nasr, B Martinez
Pathology Department, Instituto Nacional de Ciencias Medicas y Nutricion Salvador Zubiran, Mexico City, Mexico

A 83-year old man treated with naproxen during two years was admitted because of hypovolemia and peritoneal irritation. A panendoscopic study was performed and an ulcer localized at the large curvature of the stomach was disclosed. The microscopic examination of the endoscopic biopsy reveled invasive intravascular and stromal neoplastic signet-ring cells. Because of the subsequent poorly differentiated carcinoma diagnosis, a gastrectomy was performed. In the specimen the ulcer showed necrosis, edema, fibrosis, chronic inflammatory infiltrate with lymphocytes and plasma cells. Additionally atypical cells with irregular and hyperchromatic nuclei or vacuolated cytoplasm were seen in the lamina propia and infiltrating the muscular layers; isolated signet-ring-like cells were also seen. There was no involvement in regional lymph nodes. Histochemical study with periodic acid-Schiff, mucicarmin, and colloidal stains revealed mucosubstances in these cells. A poorly differentiated carcinoma was initially diagnosed. However the immunohistochemical studies were positive for histiocytic markers (CD-68, S-100 protein and lysozyme) and negative for epithelial markers (cytokeratin, and EMA). The positivity mucus stains in the histiocytes could be explained in this case by phagocytosis of mucous substances released from broken hyperplastic glands in the vicinity of the ulcer. To our knowledge, atypical histiocytic infiltration in gastric ulcers has not been previously described; thus, it should be included in the group of gastric carcinoma mimickers; with this basis, the pathologist must to be careful in the assessment of vascular permeation or stromal infiltration by neoplastic cells overall in endoscopic specimens.

P-282

Ileal mucosa changes after total colectomy in patients with juvenile polyposis and familial adenomatous polyposis

A Tertytchnyi[1], A Talalaev[1], D Sotnikov[2], V Lukin[2]
[1]Russian State Medical University, Moscow, Russian Federation
[2]Centre of Children's Health, Russian Academy of Medical Science, Moscow, Russian Federation

Introduction We studied follow-up ileal mucosa biopsies from 11 patients with juvenile polyposis and 4 patients with familial adenomatous polyposis who had been previously underwent total colectomy with mucosal proctoectomy with the creation of straight ileoanal anastomosis. Patients' age ranged from 9 to 36 years (mean 18.7 years). The follow-up ranged from 13 months to 15 years (mean 87.5 months). Aim of this study was to identify the long-term changes in ileal mucosa after total colectomy in patients with polyposis coli syndromes.
Methods The biopsy specimens have been taken from the posterior wall of terminal ileum. Paraffin sections were stained with H&E, van Gieson, periodic acid Schiff (PAS) and Gomori's aldehyde fuchsin - Alcian-blue (GAF-AB) stains. Six biopsies were subjected to electron microscopy analysis.
Results On histological examination ileal mucosa revealed focal shortening of villi and lengthened crypts. The villi were lined by increased number of goblet cells. Mucin histochemical studies demonstrated partial conversion of the epithelium to a colonic sulfomucin mucin profile by positive GAF-AB staining in cytoplasm of goblet cells. Only 2 out of 15 patients had increased number of mononuclear cells in lamina propria. The electron microscopy examination revealed shortening and rarification of microvilli of absorptive enterocytes.

Conclusion Follow-up biopsies show incomplete and focal neocolonic transformation of ileal mucosa. Nevertheless, in most of the cases ileal mucosa preserved its architectural and histochemical characteristics. We failed to identify evidences of chronic inflammation that made us suggest that chronic terminal ileitis is not a common long-term event in patients with polyposis coli syndromes after total colectomy.

P-283

Eosinophilic gastroenteritis with pleural outflow and ascites. A case report

M Mrčela[1], V Blažičević[1], M Pajtler[2], Z Hrgović[3]
[1]Institute of Pathology and Forensic Medicine, Clinical Hospital, Osijek, Croatia
[2]Department of Cytology, Clinical Hospital, Osijek, Croatia
[3]Department of Gynaecology, Clinical Hospital, Osijek, Croatia

Introduction In our region eosinophilic gastroenteritis is a very rare disease. Etiology is unknown.
Case report A 39-year-old female patient was admitted to the clinic due to slight cough, right side pleural outflow and ascites, without other symptoms. Gynaecological ultrasound, ultrasound of the upper abdomen, CT refer to ascites besides normal findings of abdominal and pelvic organs. Laboratory examinations were normal except peripheral blood eosinophilia and increased values of Ca 125. Cytological findings of pleural outflow and ascites revealed a great number of eosinophilic granulocytes but without malignant cells.
Patohistological findings During explorative laparotomy resected parts of both ovaries, a lymph node, a hyperplastic part of pylorus, a knot from a small bowel designated as a tumor, and an appendix were taken out for a patohistological examimation. Both ovaries reveal normal ovarial parenhima. A regional lymph node showed reactive changes with hyperplastic follicles and prominent germinative centers. The main histological finding reveals pyloric stromal edema and a dense infiltrate of eosinophilic granulocytes throughout the muscle layer as well as eosinophils situated in perivascular spaces which is accompanied with swelling of endothelium of capillary blood vessels. Eosinophilic granulocytes were found in the smooth muscle layer of intestine as well as in the subserosal tissue. Lumen of the appendix was obliterated and the muscle layer and the subserosal tissue contained eosinophils.
Conclusion From our review it is visible that eosinophilic gastroenteritis can represent a great diagnostic problem especially when it is accompanied with pleural outflow and ascites and increasing values of tumor markers. That can possibly mislead a diagnostic procedure to the neoplastic rather than the immunological or allergic disease. Three years after surgery the patient is well.

P-284

Expression of TNF-alpha and IL-4 in patients with chronic pancreatitis

N Shirinskaya[1], V Akhmedov[2]
[1]Emergency Hospital, Omsk, Russian Federation
[2]Omsk Medical Academy, Omsk, Russian Federation

Introduction To study the serial levels of TNF-alpha and IL-4 in patients with chronic alcoholic and chronic relapsing pancreatitis.
Methods 112 consecutive patients with chronic pancreatitis admitted to the Emergency Hospital (32 patients with alcoholic pancreatitis and 80 - with chronic relapsing pancreatitis) were studied. Serum levels of TNF-alpha and IL-4, were determined on 1 and 6 days after admission and in remission by immunoenzyme multiplied.
Results In group of the patients with chronic alcoholic pancreatitis on day one after admission the high levels of TNF-alpha (376,4 ± 91,4 pg/ml) and IL-4 (41,99±13,3 pg/ml) were marked with the subsequent consecutive decrease of these values for 6 days (TNF-alpha-18,1±5,96 pg/ml, IL-4-37,8±14,95 pg/ml) and in the period of remission (TNF-alpha-6,6±5,3 pg/ml, IL-4-9,8±1,90 pg/ml). In patients with chronic relapsing pancreatitis the low levels of cytokines on days one after admission (TNF-alpha-27,7±6,1 pg/ml, IL-4-59,85±21,2 pg/ml) were marked with the deferred peak of values on day 6 (TNF-alpha-271,6±42,2 pg/ml, IL-4-120,4±34,3 pg/ml), and decrease in the period of remission (TNF-alpha-54,5±8,4pg/ml, IL-4-19,9+-4,9 pg/ml).
Conclusion The deferred peak of cytokines levels (on 6 days) in patients with chronic relapsing pancreatitis can testify indirectly about more expressed cytokines disturbance.

P-285

Gastric glomus tumor: report of one case

H El Attar, J Lamia, S Saida, I Ahmed
Central Laboratory af Pathology Pavillon 41, Hopital Ibn Rochd, Casablanca, Morroco

Introduction The majority of glomus tumors are benign neoplasms that occur in the dermis of extremities. However, rare case have been reported in the visceral locations, most often in the stomach.
Case report The tumor occurred in a 34-year-old male who presented ulcer-like pain. CT scan diagnosed a submucosal tumor. There was no endoscopic biopsy specimen. A wedge resection of stomach was performed with a frozen section study that conclude to a carcinoid tumor Glomus tumor was confirmed by further study of multiple sections of a surgical specimen and by immunhistochemical study.
Conclusion Correct identification of this essentially benign, very rare gastric tumor can prevent unnecessary radical operative procedures.

P-286

Composite carcinoid-adenocarcinoma of the ileum associated with transitional cell carcinoma of the urinary bladder

I Venizelos[1], D Sioutopoulou[2], Z Tatsiou[3]
[1]Department of Histopathology, Athenes, Greece

It is well known that sometimes carcinoid tumor is associated with other tumors. Approximately 15% of carcinoid tumors in the small intestine are associated with non-carcinoid neoplasms, most frequently adenocarcinomas of the gastrointestinal tract. The concurrent occurrence of carcinoid and other tumors in various organs is extremely rare. Here, we present a case of a 74-year-old male who was admitted to our Hospital with a 3-month history of haematuria. On cystoscopy a large tumor of the urinary bladder has found. A total cystectomy was performed. During the operation, while exploring the abdomen, a tumor with maximum diameter 2 cm was found in the terminal ileum, from which a biopsy was taken. Microscopically, the bladder tumor was a papillary transitional cell carcinoma grade II and the tumor of the ileum fulfilled the criteria for a composite carcinoid adenocarcinoma. The carcinoid component

was positive for chromogranin and NSE and negative for EMA, CEA and CA 19-9 whereas the adenocarcinoma component was positive for EMA, CEA and CA 19-9 and negative for chromogranine and NSE. 18-months after the operation there is no metastasis radiologically and the patient is in a good condition. Due to the small number of tumors reported as composite carcinoid-adenocarcinoma there is need for larger number of similar cases as well as long term follow-up to determine their natural history and prognostic significance. We describe the first reported case of composite carcinoid-adenocarcinoma of the ileum associated with carcinoma of the urinary bladder.

P-287

Mutational analysis and expression of CDX1 homeobox gene in 20 cases of colorectal carcinomas

E Pilozzi, M Rapazzotti Onelli, C Fidler, V Ziparo, JS Wainscoat, L Ruco
Istopatologia Ospedale Sant'Andrea Facolta, Roma, Italy

Introduction CDX1 is a transcription factor specifically expressed in normal intestinal epithelium. It plays a role in the regulation of cell proliferation and differentiation. Experimental evidences suggest that it could have a pro-oncogenic effect since Cdx1 over-expression up-regulates Bcl-2 and reduces p21; it is up-regulated by ras activation and its ectopic expression has been reported in intestinal metaplasia, in carcinomas of the stomach and in Barrett's esophagus. Despite these observations the role of CDX1 in colorectal carcinogenesis is not yet fully understood. In fact it has been shown to be down-expressed in colon cancers at mRNA and protein level. The aim of the study was to investigate the presence of CDX1 gene mutations.
Materials and methods Twenty cases of sporadic colon carcinomas were collected. Total RNA and DNA from neoplastic and normal tissues were extracted. cDNA was synthesized and used as template in RT-PCR using oligonucleotide for CDX1 and â-actin. CDX1 three exons were PCR amplified and directly sequenced.
Results We found lower expression of CDX1 in tumour samples in four out of ten cases. Sequencing showed a transversion G>C (10/20 cases) of exon 1 and a T>C transition in exon 2 (4/20 cases) that, being present in the corresponding normal tissue, were regarded as polymorphisms. No base substitution was observed in exon three.
Conclusions Our results showed that CDX1 expression is reduced in colon carcinoma. However CDX1 was not found to be mutated suggesting that alterations, other than base substitution, may affect CDX1 gene in colon cancer. We are now looking at CpG islands methylation in the same cases since methylation could be a likely explanation of the low expression of CDX1.

P-288

The potential role of TGF-beta-1, TGF-beta-2 and TGF-beta-3 proteins expression in colorectal carcinomas and their possible correlation with classic histopathologic factors and patients survival

A Tsamandas[1], V Zolota[1], P Ravazoula[1], T Kourelis[2], C Kalogeropoulou[3], T Petsas[3], K Tepetes[4], D Kardamakis[3], D Bonikos[1], H Kalofonos[2]
[1]University of Patras School of Medicine Department of Pathology, Patras, Greece
[2]University of Patras School of Medicine Department of Internal Medicine/Oncology, Patras, Greece
[3]University of Patras School of Medicine Department of Radiology, Patras, Greece
[4]University of Patras School of Medicine Department of Surgery, Patras, Greece

Aim This study investigates TGFbeta1, TGFbeta2 and TGFbeta3 proteins expression in patients with colorectal carcinoma and evaluates their correlation with classic prognostic markers and patients' survival.
Design The study comprised 124 patients with colorectal carcinoma. According to Astler-Coller system, 42 tumors were of stage A, 42-B, 48-C and 20-D, whereas 106 tumors were low-grade and 18 high-grade of malignancy. On paraffin sections the streptavidin-biotin technique, using antibodies to TGFbeta1, TGFbeta2 and TGFbeta3 (SantaCruz, USA) was employed. Staining results followed morphometric analysis and were correlated with clinicopathologic parameters.
Results TGFbeta1 protein was expressed in 88/124 (71%) carcinomas whereas TGFbeta2 and TGFbeta3 proteins were detected in all tumors examined. Normal colonic mucosal epithelial cells expressed less TGFbeta2 ($p<0.01$ compared to neoplastic cells) and less TGFbeta3 ($p>0.05$ compared to neoplastic cells), but not at all TGFbeta1. Statistical analysis revealed higher expression of TGFbeta1 in low grade carcinomas ($p=0.009$) and higher TGFbeta2 presence in advanced stage tumors ($p=0.008$). TGFbeta1 expression was related with higher disease free survival and higher total survival ($p<0.05$ respectively). TGFbeta2 presence was correlated with worse prognosis ($p<0.05$). Cox analysis revealed that besides tumor grade and stage, TGFbeta1 expression constituted independent prognostic factor.
Conclusions This study shows that in cases of colon adenocarcinoma there is different expression of TGFbeta1, TGFbeta2 and TGFbeta3. TGFbeta1 may be implicated in the pathogenesis of these tumors since it is expressed only within neoplastic and not normal cells. TGFbeta1 is related with higher disease free survival, higher total survival and constitutes an independent prognostic factor. In the late stages, TGFbeta2 seems to be involved in tumor progression and it is related with worse prognosis.

P-289

CDX2 is useful in distinguishing primary colorectal adenocarcinoma form pulmonary, mammary and pancreatic adenocarcinomas metastatic to the colorectum

G Groisman, A Meir, M Amar
Hillel Yaffe Medical Center, Hadera, Israel

Background The large bowel may be the site of metastasis from a number of tumors including pulmonary, mammary and pancreatic adenocarcinomas. The histological distinction of primary colorectal adenocarcinoma from these metastatic lesions may be difficult. The aim of this study was to evaluate the utility of the intestinal marker CDX2 in distinguishing primary colorectal adenocarcinoma from pulmonary, mammary, and pancreatic adenocarcinomas metastatic to the large bowel.
Design Routinely processed mucosal biopsies of 30 adenocarcinomas involving the colorectum [15 primary, 15 metastatic (lung 5, breast 6, pancreas 4)] and 15 control cases of primary lung, breast, and lung adenocarcinomas were immunohistochemically stained for CDX2 (Biogenex, San Ramon, CA, USA). The intensity and extent of the staining were recorded semi-quantitatively.

Results CDX2 diffussely and strongly stained the normal colorectal epithelium as well as all cases of primary colorectal adenocarcinoma. In contrast, all cases of metastatic lung, breast and pancreas adenocarcinoma as well as all control cases were CDX2 negative.
Conclusions CDX2 immunostaining is useful in discriminating primary colorectal adenocarcinomas from pulmonary, mammary and pancreatic adenocarcinomas metastatic to the large bowel. We recommend its use as a component of any antibody panel put together to discriminate between primary and secondary colorectal tumors.

P-290

Infiltrative and proliferative activity in central versus peripheral parts of colorectal cancer

A Nalecz[1], R Rzepko[1], M Klimkowska[1], W Kruszewski[2], E Izycka-Swieszewska[1], K Jaskiewicz[1]
[1]Department of Pathology, Medical University of Gdansk, Poland
[2]Department of Surgical Oncology, Medical University of Gdansk, Poland

Introduction Cellular proliferation is a basic phenomenon in neoplasms. Infiltration and destruction of stroma are features of malignant tumour growth. In colorectal cancer stromal production and its invasion by neoplastic cells is encountered in peripheral and central parts of tumours. This study presents quantitative analysis of stromal infiltration and cellular proliferative activity in central and peripheral parts of primary colorectal cancer.
Materials and methods 33 cases of colorectal adenocarcinoma seated mainly in sigmoid and rectum were examined. Investigated group included 15 women and 18 men (aged 35-85 yrs). According to the TNM classification, grade II was assigned in 17 cases and grade III in 16 cases. In every case infiltrative (under x200) and proliferative activity (under x400) was assessed in 3 central and 3 peripheral tumour fields. Number of small isolated cancer cell clusters of cross section area under 1000 μm^2 was assessed as measure of stromal infiltrative activity.
Results In the studied group peripheral infiltrative activity was greater than in central parts of tumours. Median value of isolated cellular clusters was 20.3 and 6.8 per field in peripheral and central parts respectively ($p<0.01$). Proliferative activity was slightly higher in peripheral than in central areas. Mean Ki67 labelling index was 42% (+/-22%) and 37% (+/-21%) in peripheral and central parts respectively ($p=0.04$). No important correlation was found between calculated parameters ($R=0.14$).
Conclusions Stromal infiltrative activity is greater in peripheral parts of the tumour. This parameter does not correlate however with proliferative activity of neoplastic cells in examined group.

P-291

Angiogenesis in primary and metastatic foci of colorectal cancer

M Klimkowska[1], R Rzepko[1], A Nalecz[1], W Kruszewski[2], E Izycka-Swieszewska[1], K Jaskiewicz[1]
[1]Department of Pathology, Medical University of Gdansk, Poland
[2]Department of Oncologic Surgery, Medical University of Gdansk, Poland

Introduction Growth of primary and metastatic tumour is accompanied by formation of stroma composed of connective tissue and new blood vessels. Colorectal cancer is a malignancy characterised by marked desmoplastic reaction both in primary tumour and in its secondary foci (metastases). Presented report was aimed to describe quantitatively microvessel density in primary tumour and lymph node metastases from this neoplasm.
Materials and methods Study material included 36 cases of colorectal cancer with metastases to the regional lymph nodes. Investigated group comprised 20 women and 16 men (aged 33-85 yrs); 32 tumours were T3 and four were T4 according to TNM classification. Microvessels were highlighted using monoclonal anti-CD34 antibodies. Vessel counts were performed in five fields of each primary and metastatic focus (x200; 0.747 mm2). Numbers of blood vessels in colorectal tumour were counted in areas free from prominent necrotic foci and non-specific granulation tissue due to process of reparation. Vessel density in nodal metastases was determined in fields occupied by neoplastic cells forming their own connective tissue stroma.
Results In the primary tumour group mean vessel density was 74.5 vessel/mm2 (median value 73.3; range 44-152). In metastatic foci the same parameter was 78.1 vessel/mm2 (median value 77.5; range 41-117); no statistically significant difference was detected. Only slight correlation was found between the microvessel densities in primary and metastatic tumours ($R=0.39$; $p=0.1$).
Conclusion Presented results seem to prove the similar pattern of neovascularisation in both groups, whereas marked differences in this process can be observed between subsequent analysed cases.

P-292

Clonality analysis of mutant E-cadherin-positive, diffuse-type early gastric cancers

M Bamba, H Sugihara[1], KF Becker[2], I Becker[2], T Hattori[1], M Stolte[3], H Hoefler[2]
[1]Department of Pathology, Shiga University of Medical Science, Ohrsu-Shiga, Japan
[2]Institute of Pathology, Technical University Munich, Germany
[3]Institute of Pathology, Klinikum Bayreuth, Germany

Early diffuse-type gastric carcinoma, especially signet ring cell carcinoma, often shows the superficially spreading growth pattern, and one of the unsolved questions concerning the histogenesis of this type of carcinoma is whether it is monoclonal or multiclonal in origin. We have performed Human Androgen Receptor Gene Assay (HUMARA assay) based on the random inactivation phenomenon of X chromosomes in female and reported that most of this type of carcinomas were of monoclonal origin (8/9 cases). However, this method demonstrated only probability of monoclonality in each lesion. Recently, 50% of diffuse-type gastric carcinomas have revealed mutations of the E-cadherin gene at the early stage of their progression, and in-frame skipping of exon 9 has been seen frequently. Thus, we performed an immunohistochemical analysis of early signet ring cell carcinomas using E-cad delta 9-1, which is a specific antibody against a peptide spanning the fusion junction region between exons 8 and 10 of mutant E-cadherin. E-cad delta 9-1 specifically reacts with tumor cells expressing E-cadherin mRNA lacking exon 9. Seven of 44 cases were positive for this antibody. In each positive case, the paraffin blocks of the tissue slices that included the whole tumor were analyzed using E-cad delta 9-1. Although some signet ring cells with abundant mucin in the upper and/or lower layers of a layered structure did not react with this antibody, tumor cells were confirmed to express E-cadherin mRNA lacking exon-9 by reverse transcriptase-polymerase chain reaction with paraffin-embedded

formalin-fixed tissues. These findings suggest that they are of monoclonal origin (7/7 cases) and support our previous data using HUMARA assay.

P-293

Unusual types of Gastrointestinal Malignant Lymphomas (GIMLs)

E Tsikou-Papafragou[1], T Papadaki[2], M Tsamouri[1], E Nikolaou[1], C Barbatis[1]
[1]Korgialenion-Benakion Hospital, Athenes, Greece
[2]Evangelismos Hospital, Athenes, Greece

Introduction MALT lymphoma is the commonest primary GI lymphoid malignancy but for correct diagnosis and classification, immunohistochemical and molecular analysis have been proven necessary. The aim of this study was to demonstrate the value of current methodology for diagnosing GIMLs by presenting four unusual cases.
Materials Case 1. A 33 years old male with common variable immunodeficiency. An obstructive ileal tumor 3cms was resected and multiple biopsies were taken along the GI tract from nodular areas. Case 2. Female 50 years old with generalised lymphadenopathy, lung shadows, dyspepsia and duodenal nodularity. Case 3. Female age 74 underwent gastrectomy with initial diagnosis of high grade B lymphoma. Case 4. Female age 74, had gastrectomy/ splenectomy for relapsed gastric Lymhpoma which had been diagnosed as MALT type.
Methods Immunophenotypical analysis for detection of CD20, CD79a, CD10, bcl-6pr, bcl-2pr, CD5, Cyclin D1, CD23, CD43, CD45RO, CD3, Ki-67 and genotypic analysis for the clonal IgH, TCva genes (case 3) and the IgH/bcl-1 rearrangement (case 4).
Results per case: 1. Atypical Burkitt Lymphoma with diffuse lymphoid hyperplasia of the GI tract (CD10/20/79a+, bcl-6+/2-, Ki67 100%). 2. Generalised follicular B Lymphoma, Grade 1 according to the WHO classification with involvement of the Duodenum. 3. Diffuse large B cell lymphoma with aberrant CD45 RO expression. Rearrangement of the IgH genes and not of the TCva gene. 4. CD5- Mantle cell lymphoma with anaplastic foci in the spleen. Clonal rearrangements of the IgH and concomitant IgH/bcl-1 gene rearrangements involving tonsils, stomach, spleen and abdominal lymph nodes.
Conclusion All cases represent unusual types of GIMLs easily misclassified or graded without thorough immunophenotypic and molecular analysis.

P-294

Malignat gastrointestinal stromal tumor: morphological and immunohistochemical investigation

A Petrescu[1], G Berdan[1], C Ardeleanu[2], M Dan[3]
[1]Prof. Dr. Th. Burghele Hospital, Bucharest, Romania
[2]Victor Babes Institute
[3]Harper Hospital

Introduction We present two cases of a 72 years old man and 77 years old woman hospitalized for bulky abdominal mass demonstrated by clinical, echographical and CT examination.Adenopathy, liver and peritoneal metastases were present.First patient underwent the tumor ablation and the second only a biopsy.
Matherial and methods Fragments of the tumors were fixed in formaldehyde 10%, included in paraffin and the sections were stained with HE and VG.;indirect immunoperoxidase method with cytokeratine.VIM, ACT, Desmine, S100, CD34, CD 117 were performed.
Results The histological examination in both cases revealed a cellular spindle cell tumors fascicular pattern, rare mitoses and areas of necrosis(in first case)Immunohistochemical analysis:the cytokeratin profile(AE1, AE3), ACT, Desm, S100 were negative; VIM, CD 34 and CD 117 were positive.
Conclusions The diagnosis of GIST was based on morphology and on the strong diffuse positivity of the tumor cells with CD117.The classification as malignant was made on the size of the mass and the presence of metastases

P-295

Cardiac mucosa develops during pregnancy: an autopsy study in embryos, fetuses and infants

G De Hertogh, P Van Eyken, N Ectors, J Tack, K Geboes
K U Leuven, Leuven, Belgium

Introduction The incidence of gastric cardiac adenocarcinoma has increased in the last decades. Gaining insight in the pathogenesis of this lesion is hampered by the limited knowledge of the origin and histology of cardiac mucosa (CM). Currently, the location, extent and even the existence of CM are controversial. Aims: We studied the development of the gastro-oesophageal junction (GOJ) in embryos, fetuses and infants to clarify whether CM is a normal structure at birth and where it is located.
Materials and methods Twenty-one autopsy cases were evaluated. Age range: 13 weeks gestational age (GA) - 7 months. The distal oesophagus and proximal part of the stomach were embedded entirely. Serial sections were stained with haematoxylin-eosin and alcian blue/periodic acid-Schiff. The following parameters were measured: length of abdominal oesophagus; length of columnar-lined oesophagus; length of CM; distance from CM to angle of His.
Results CM was present in all evaluated sections. Its mean length varied throughout gestation. A maximum value was reached at a GA of 16 weeks (1,2 mm). After term delivery, it was very short (0,3 – 0,6mm). CM was proximal to, or straddled the angle of His in all cases. During gestation, the mucin staining pattern of the CM was to a high degree similar to that of the developing pyloric mucosa.
Conclusions CM develops during pregnancy and is present at birth as a normal structure. If the angle of His is taken as a landmark for the GOJ, CM is located in the distal oesophagus.

P-296

Gastric mucosa-associated lymphoid tissue (MALT) and non-MALT lymphomas: clinicopathological study of 32 cases

S Taban, A Dema, N Tudose
University of Medicine and Pharmacy, Timisoara, Romania

Introduction Histologic features of low-grade B-cell MALT lymphoma of the stomach have been well described in recent years, but its relationship with the more common large B-cell gastric lymphoma has not been clarified. The authors investigate clinico-pathological differences among low-grade and high-grade gastric lymphomas.

Methods Clinical and histopathological aspects of 32 consecutive gastric lymphoma cases found in gastrectomy specimens were studied: 14 cases of low-grade MALT lymphoma (LG MALT lymphoma), 10 cases of high-grade MALT lymphoma appearing in low-grade MALT lymphoma (HG/LG MALT lymphoma), 4 cases of high-grade MALT lymphoma (HG MALT lymphoma) and 4 cases of diffuse large cell lymphoma (DLCL).
Results Mean age were as follow: LG MALT lymphoma-36,5 years; HG/LG MALT lymphoma-44,5 years; HG MALT lymphoma-61,5 years; DLCL-54,3 years. There was a male predominance of MALT lymphoma patients (male to female ratio-18/10). Macroscopically, the most common pattern of LG MALT lymphomas was the superficial spreading type with or without ulceration, whereas HG MALT lymphomas and DLCL exhibited a solitary tumor-forming lesion. B-cell immunophenotype was confirmed in 31 cases, only one case of DLCL was a T-cell lymphoma.
Conclusions In our study, the prevalence of high-grade MALT and non-MALT lymphomas was 56,25%. Our results suggests that some gastric lymphomas with high malignancy can arise through blastic transformation of the LG MALT lymphomas, this process(change) seems to take about ten years at least.

P-297

MSI-L and MSI-H in colorectal serrated adenocarcinomas

M Mäkinen, K Tuppurainen, O Junttila, TJ Karttunen
Department of Pathology, University of Oulu, Oulu, Finland

Background The recently described serrated adenocarcinoma accounts at least 5.8 % of colorectal malignancy. It develops from serrated polyps. DNA microsatellite instability (MSI) is more common in serrated adenocarcinomas than in conventional adenocarcinomas, but the frequency of MSI-low and MSI-high in these tumours is unknown.
Materials and methods An unselected series of 23 serrated adenocarcinomas were included. MSI status was evaluated using panel of five markers (BAT-25, BAT-26, D2S123, D5S346 and D17S250). A tumour was considered to present MSI-high if two or more markers showed MSI, MSI-low with one marker, and MSS when none of the markers showed MSI.
Results DNA MSI was observed in 47.8 % (11/23) of serrated adenocarcinomas, 13.0 % (3/23) being MSI-high and 34.8 % (8/23) MSI-low. MSI status showed no association with gender, age, location, size, Dukes stage, grade or mucinocity. MSI-positive serrated adenocarcinomas tended to have better prognosis (5-year survival 74.1 %) than MSS cancers (5-year survival 41.1 %), but this was not statistically significant (P=0.272, Log-Rank).
Conclusions Serrated adenocarcinomas show prevalence of MSI-low higher than that reported for colorectal cancers (7 to 15%), supporting idea that serrated carcinomas are formed through a pathway differing from other carcinonomas. Absence of any association of MSI and clinicopathological features could be due to homogeneity of these neoplasms although a more extensive material is necessary to show more conlusively absence of any association. A trend for better prognosis in MSI -positive serrated adenocarcinomas probably reflects the biological behaviour of MSI observed earlier in colorectal carcinomas in general.

P-298

Thyroid hormone receptor beta-1 expression in colorectal cancer is associated with polypoid growth type and K-RAS mutations

T Hörkkö, TJ Karttunen, P Jernvall, MJ Mäkinen
Department of Pathology, University of Oulu, Finland

Background The action of thyroid hormones is mediated via their receptors (TRa1, TRa2, TRb1 and TRb2). TRb1 expression is abnormal in cancer cells in vitro and in some malignant neoplasms, but the role TRb1 in colorectal carcinogenesis is unknown.
Materials and methods TRb1 expression pattern was evaluated by immunohistochemistry in 115 operated colorectal cancers and correlated with K-RAS mutations and clinicopathological features.
Results In normal mucosa, cytoplasmic TRb1 immunoreactivity was seen mainly in the superficial parts, while nuclear reactivity was most prominent in the cryptal epithelium. In tumours, nuclear expression was observed in 67% of cases and cytoplasmic staining in 68%, both mostly co-existing. Cytoplasmic staining for TRb1 was more common in polypoid (88%; 21/24) than in flat carcinomas (41%; 9/17; p=0.029). K-RAS mutations were more common in tumours with cytoplasmic expression of TRb1 (27.5 %; 11/40) than in those without (0%; 0/14). In lymph node metastases, occurrence of nuclear staining of TRb1 was more pronounced than in the primary lesion (P=0.003, Wilcoxon).
Conclusions Expression of TRb1 is present in normal colorectal mucosa and is mostly retained in carcinomas, suggesting that thyroid hormones and their receptors may be involved in the physiological regulation of normal colorectal epithelium and in the pathogenesis of colorectal cancer. Association of expression with K-RAS mutations indicate occurrence of functional linkage between TRb1 and ras signaling. Observations of a high expression in lymph node metastases and in polypoid cancers offer new clues to factors affecting metastatic cascade and growth pattern of colorectal cancer.

P-299

Gastric mucosal calcinosis in chronic renal failure patients

AN Haberal[1], B Demirhan[1], G Künefeci[2], M Gürsoy[2], A Kut[3]
[1]Department of Pathology, Baskent University, Faculty of Medicine, Ankara, Turkey
[2]Department of Gastroenterology, Baskent University, Faculty of Medicine, Ankara, Turkey
[3]Department of Family Physician, Baskent University, Faculty of Medicine, Ankara, Turkey
[4]Baskent University of Medical School, Gastroenterology Department
[5]Baskent University of Medical School, Nephrology Department

Introduction Gastric mucosal calcinosis (GMC) is rare. Some reports indicate that GMC is associated with gastric cancer, chronic renal failure (CRF), and ingestion of sucralfate or aluminum-containing antacids (SACA) in organ transplant patients. The aim was to determine the incidence and investigate the etiology and pathogenesis of GMC in a large group of CRF patients at one transplant center.

Materials and methods A review of the records for 326 CRF patients who underwent endoscopic biopsy revealed 45 GMC (patient group) and 281 non-GMC (control group) cases. For each subject we recorded the number and sites of biopsies, and re-assessed for inflammatory activity, mucosal atrophy, intestinal metaplasia, lymphoid aggregates, Helicobacter pylori, amyloid deposition, and gastritis type. Age, sex, cause of renal failure, time from renal failure diagnosis to biopsy, type of dialysis, indications for endoscopy, SACA use, and serum levels of calcium, phosphorus, calciumXphosphorus product and parathyroid hormone were also recorded. The GMC cases were classified according to pattern of deposition (nodular, granular, mixed) and disease severity (mild, moderate, severe).
Results The incidence of GMC was 13.8%. In GMC group there was male preponderance (73%). Compared to the control group, the GMC group had a significantly higher number of corpus biopsies; a significantly lower number of antral biopsies; a significantly lower frequency of mucosal atrophy; and a significantly lower parathyroid hormone level ($p<0.05$ for all). None of the GMC patients had used SACA.
Conclusion Unlike previous reports, these results show that GMC is not linked with SACA use or female gender in CRF patients. There was also no correlation with mucosal injury. These findings suggest that GMC is probably a metastatic process, not a dystrophic one.

P-300

The value of histology in diagnosis of Inflammatory Bowel Disease (IBD)

V Tzioufa, G Karayannopoulou, I Venizelos, A Asimaki, E Vrettou, C Kalekou, T Kehaya, A Kriaka, E Nenopoulou, K Patsiaoura
Aristotle University of Thessaloniki, Greece

In patiens with colitis colorectal biopsy is helpful in the differential diagnosis between IBD and other forms of colitis and also between ulcerative colitis (UC) and Crohn's disease (CD). However the histological features in biopsy specimens are not always sufficient for a definitive diagnosis and there is need to establish more sensitive and specific criteria for the distinction between UC and CD. A retrospective blind evaluation of biopsy specimens from 102 patients with the endoscopical diagnosis of colitis was undertaken in order to assess the value of histology in the diagnosis of IBD and the degree of inter-observer agreement. Twelve experienced pathologists participated in the study. Twenty histopathological features according to a modified version of the British Society of Pathology guidelines for the evaluation of colorectal biopsies in suspected IBD were studied and the results were statistically analysed. The clinical diagnosis after follow up was UC in 57 cases, probably UC in 3 cases, IBD 2 cases, CD 3 cases and non-specific colitis 37 cases. Higher than 90% agreement (by all 12 or 11 participating pathologists) on the diagnosis of UC based only on histologic parameters was reached in 28 of the 57 cases for which clinical follow up proved the diagnosis of UC. Unanimous agreement on the diagnosis of non-specific colitis was reached in 22 of the 37 cases. Our results indicate that although detailed assessment of a combination of histopathological features and the experience of histopathologist are important for the diagnosis of IBD, the final diagnosis depends on combination of histopathology with the clinical and endoscopical evaluation.

P-301

Atypical multinucleated stromal cells in the polypoid tumor lesions of the gastrointestinal tract

S Taban, A Dema, N Tudose
University of Medicine and Pharmacy, Timisoara, Romania

Aim The authors presented two cases of polipoid tumor lesions (gastric and anal) with pseudomalignant changes.
Methods and results Multiple sections from the stomach and anal mucosa were analysed by light microscopic and immunohisto-chemical methods. In the gastric hyperplastic polyp, there was surface ulceration with granulation tissue and acute and chronic inflammation. Within the stroma were numerous atypical cells with bizarre cytomorphology and atypical mitoses. The second case was a fibroepithelial polyp of the anus with collagenous stroma covered by squamous epithelium. Stromal cells with two or more nuclei were found and showed atypical nuclear features. In both cases, mast cells were frequently observed and sometimes intimately related to the stromal cells. Immunohistochemical study revealed that the stromal cells stained positive for vimentine and negative for actine, desmin, cytokeratin, S-100 protein and leukocyte common antigen, so considered to be fibroblastic cells. Clinical follow-up was available. None of the patients followed developed metastases or recurrences.
Conclusions Atypical stromal cells should not be misinterpreted as neoplastic cells. Mast cells may play an important role in their morphogenesis.

P-302

Prognostic value of nm 23 and c-erbB-2 expression in colorectal cancer

V Delektorskaya, A Perevoschikov, NE Kushlinsky
Cancer Research Centre, Moscow, Russian Federation

Increased expression of genetic markers is observed in a variety of malignancies, including colorectal cancer (CRC). Overexpression of these markers in the primary tumor is known to predict outcome after colonic resection. In this study we aimed to evaluate the expression level of the nm 23 and c-erbB-2 proteins in CRC and its correlation to prognosis and liver metastasis. Protein expression was examined immunohistochemically in formalin-fixed, paraffin-embedded tissue from 64 colorectal patients. CRC showed a high level of nm 23 protein expression in 63% of primary tumors and 66% of liver metastasis. Expression of c-erbB-2 was observed in 59% of primary carcinomas and 57% of distant metastasis. The positive expression of protein markers in primary lesion was significantly higer in the cases with liver metastasis than in those without metastasis. No significant relationship was observed between nm 23 and c-erbB-2 expression and other clinico-pathological parameters. These results suggest that nm 23 and c-erbB-2 expression play an important role in the progression of CRC and could provide additional information for the development of liver secondaries.

P-303

Relationship between gastritis severity, Helicobacter pylori intensity and mast cell density in the antrum and corpus: An immunohistochemical study with mast cell tryptase

F Kayaselcuk[1], Y Gumurdulu[2], E Serin[2], FA Bolat[1], B Ozer[2], I Tuncer
[1]Department of Pathology, Baskent University Faculty of Medicine, Adana Teaching and Medical Research Center, Adana, Turkey
[2]Department of Gastroenterology, Baskent University Faculty of Medicine, Adana Teaching and Medical Research Center, Adana, Turkey

Introduction Helicobacter pylori (H. pylori) is the most frequent and significant factor in the etiology of chronic active gastritis. In most persons infected with H. pylori, there is an increased chronic inflammation in the lamina propria of the stomach, including lymphocytes, monocytes, eosinophils, and plasma cells. Mast cells originate from bone marrow, which plays a role in the onset and regulation of inflammation. The aim of this study was to investigate the relationship between mast cell density and H. pylori intensity, gastritis severity in the corpus and antrum mucosa.
Material and methods 43 H. pylori- positive and 27 H. pylori-negative patients were included in the study. All cases underwent endoscopy. All biopsies were evaluated according to Sydney system and mast cell density in both corpus and antrum mucosa was analyzed by anti-human mast cell tryptase. In lamina propria and epithelial mast cells in both corpus and antrum counted one by one.
Results Both in the antrum and the corpus, epithelial and submucosal mast cell density was significantly higher in the H. pylori -positive group than in the H. pylori-negative group. The higher mast cell distribution is correlated with high scores of inflammation, activity, and H. pylori density in the antrum and corpus. No relationship was found between mast cell distribution and intestinal metaplasia or atrophy.
Conclusion Both submucosal and epithelial mast cells may be important effector cells in the pathogenesis of gastritis. They assume similar role in different regions in the development of H. pylori gastritis.

P-304

Apoptosis and activated intraepithelial cytotoxic T lymphocytes in gastric carcinomas characterized for microsatellite instability and Eepstein Barr virus infection

M Feltri, AM Chiaravalli, E Bagnoli, D Furlan, R Cerutti, C Capella
Department of Clinical and Biological Sciences, University of Insubria, Varese, Italy

Introduction Sporadic gastric carcinomas (GCs) with high level microsatellite instability (MSI+) tend to be poorly differentiated adenocarcinomas with abundant lymphocytic infiltration and are associated with a relatively good prognosis. The aim of the study was to define whether the nature and the activation status of lymphocytes infiltrating neoplastic epithelial cells (IELs)of MSI+ Gcs could be involved in an increased apoptosis of tumor cells and could be consistent with a tumor-specific immune response.
Materials and methods Tumor cells apoptosis and immunophenotype of IELs were investigated by immunohistochemistry in 35 MSI+ GCs. For comparison, a series of 31 MSI- GCs with similar histological features was investigated, including 7 cases, which were positive for Epstein Barr Virus infection (EBV+).
Results MSI+ and MSI-/EBV+ GCs displayed a significant higher mean number of cytotoxic IELs than MSI-/EBV- tumors (CD3: 30.7 and 29.8 versus 9.9; CD8: 21.7 and 22.1 versus 6.4; TIA-1: 16.7 and 15.6 versus 5.2; $p<0.01$). In addition the activated IELs were more frequent in MSI+ than in MSI-/EBV- GCs (mean granzyme B immunoreactive IELs: 7.5 versus 0.8; perforin 5.9 versus 0.9; $p<0.01$). The percentage of apoptotic tumor cells, evaluated with the M30 CytoDeath antibody, was higher in both MSI+ and MSI-/EBV+ GCs than in MSI-/EBV- GCs (5.99% and 4.31% versus 2.5%; $p<0.01$).
Conclusion The lymphoid infiltration in MSI+ GCs was significantly higher than that of MSI- GCs (except for EBV+ GCs) and this might explain the increased apoptotic index and the relatively better prognosis of these tumors.

P-305

Goblet cell carcinoid of the appendix: A clinicopathologic study and MUC1, MUC2 and MUC5A Expression

SM Jung[1], PH Chu[2], TS Yeh[3]
[1]Department of Pathology, Chang Gung Memorial Hospital, Taoyuan, Taiwan, Republic of China
[2]First Cardiovascular Division, Department of Medicine, Chang Gung Memorial Hospital, Taoyuan, Taiwan, Republic of China
[3]Department of Surgery, Chang Gung Memorial Hospital, Taoyuan, Taiwan, Republic of China

Introduction Goblet cell carcinoid (GCC), also known as mucinous carcinoid or adenocarcinoid, is a rare tumor of appendix, which exhibits both endocrine and adenocarcinoma differentiation. Different mucin phenotypes are associated with neoplastic transformation in epithelial tissue in various organ systems. MUC2 apomucin is a mucin gene product specific to intestinal goblet cells. MUC1 is suggestive to inhibit cell-to cell adhesion. In the present study, we retrospectivelly studied the clinicopathological features and immunohistochemical expression of MUC1, MUC2 and MUC5A in GCC.
Materials and methods Three appendiceal GCC were retrieved from our pathology files from 1988 to 2002. Medical records and histologic slides were reviewed. The expression of MUC1, MUC2 and MUC5A was assessed by immunohistochemistry.
Results All three cases were males and the age ranged from 44, 52 and 85 yrs. Two patients presented with acute appendicitis. The other one had ruptured diverticulitis and renal cell carcinoma. Two patients had appendectomy, and one patient had right hemicolectomy and right radical nephrectomy. Histologic examination showed infiltrative small nests and glands of tumor cells with goblet cells and mucinous cytoplasm. Perineural invasion was noted in one case. The tumors had invaded through the appendiceal wall to subserosa in two cases and to adjacent cecum in one case. The tumor cells are positive staining for synaptophysin. There was strong and diffuse reactivity in the tumor cells with MUC1, MUC2 and MUC5A antibodies in all three cases. Follow-up ranged from 1 month, 9 months, and 13 months. All were alive and without recurrence.

Conclusions These observations suggest that there is no differential expression of MUC1, MUC2 and MUC5A in GCC and both MUC1 and MUC2 may play a role in cancer cell growth and invasion.

P-306

Gastric parietal cell carcinoma: report of three cases

ML Gomez-Dorronsoro, R Beloqui, I Amat, P De llano,
A Cordoba, B Larrinaga, E Borobio
Hospital de Navarra, Pamplona, Spain

Gastric parietal cell carcinoma is an infrequent newly recognised variant of gastric carcinoma with only 16 cases published in the literature. The present study describes the findings in three cases of gastric parietal cell carcinoma consisting of parietal cells. We have used light and electron microscopy, and histochemical stains. We have studied three cases, two men and one woman, aged between 57 and 86 years. The tumour size ranged from 2,5 to 6,5 cm. The surgical specimens were stained with hematoxylin-eosin, alcian blue and PTAH. Small pieces of formalin fixed tumor tissue were collected in one case, and fresh tissue fixed in glutaraldehyde in another both for electron microscopy. Involvement of the gastric wall was observed in all tumours. The tumour pattern was characterised by an arrangement of tumour cells in sheets, elongated cords or in diffuse poorly cohesive sheets interspersed with a lymphocytic infiltrate. Tubular differentiation was only focally present in one of the cases. All the cases were composed by a large number of parietal-like cells with abundant eosinophilic cytoplasm, with a mixture of signet ring cells population in one of the cases. Alcian blue stain was negative throughout the tumour, whilst PTAH stained many tumour cells. Ultrastructurally the tumour cells were characterised by abundant mitochondria, tubulovesicles, intracellular canaliculi and intercellular lumina filled with microvilli. The three tumours presented are primary gastric carcinoma with cytological and ultraestructural patterns of parietal cell differentiation. They represent a morphologically distinct type of carcinoma, which has been said to have a favourable prognosis.

P-307

Analysis of CD8 positive cells of gastric mucosa in cases of peptic ulcer and gastritis

R Kleina, V Ose
Riga Stradinsh University Dept. of Pathological Anatomy, Riga, Latvia
[2]Riga Stradinsh University Institute of Anthropology and Anatomy, Riga, Latvia

Aim The aim of study is to investigate do really CD8+ cells have cytotoxic or suppressor influence upon gastric epithelium.
Material and methods We have examined biopsies from 23 patients with peptic ulcer and 22 - with gastritis only. Samples were formalin fixed, paraffin-embedded, stained with H/E, toluidineblue, Gimsa stain, PAS reaction. Comparative immunohistochemical analysis of CD 8+ lymphocytes, proliferative markers: MIB-1 and PCNA were performed. We evaluated the amount of CD8+ cells in 1 mm^2 and the proliferative activity of epithelium per 1000 nuclei. 8 biopsies were examined electronmicroscopically for the detection of cell-to-cell interactions and subcellular alterations of gastric epithelium.
Results Distribution, amount and characteristics of CD8+ cells are different in mucosa around ulcer and in gastritis (G.) cases without ulcer. In active G. around ulcer CD8+ cell are 12, 4; without ulcer - 7, 7, but in inactive G.-4, 2. In Helicobacter pylori-infected subjects CD8+ are located in addition at the lymphatic follicles. We have not proved any rise of apoptosis, exfoliation or ultrastructural injuries of epithelial cells in the areas of collections of T-lymphocytes of this subtype. In sites of increased amount of CD 8+ cells there is high proliferation activity of epithelium (19,7- 29,4%) due to the broadening of labeled nuclei zone with MIB-1 antibody.
Conclusions The amount of CD 8+cells correlates with activity of gastritis as this 34 kD glycoprotein realize molecular reactions between mediators or against H.pylori, food and other antigens in lamina propria, but it has no external direct domain upon gastric epithelium, capillaries or glandulocytes.

P-308

Prognostic value of nuclear area and microvessel density in gastric cancer

D Kovač[1], M Jašić[2], A Eubranić[1], M Krašević[1], H Grbas[3], N Pavlović[4], A Šustić[5], C Rizzardi[6], M Melato[6], N Jonjić[1]
[1]Department of Pathology, University of Rijeka, Croatia
[2]Medical Faculty, Rijeka, Croatia
[3]Department of Digestive Surgery, University of Rijeka, Croatia
[4]Department of Radiology, University of Rijeka, Croatia
[5]Department of Intensive Care and Anestesiology, University of Rijeka, Croatia
[6]Department of Pathology, Medical Faculty, Trieste, Italy

The incidence of gastric cancer decreases worldwide. Despite declining (due to intestinal type), incidence still remains the second cause of death amongst all malignancies worldwide. Diffuse type of gastric cancer shows constant incidence. Therapy and prognosis directly correlate with extent of the disease and reliable prognostic factor is still lacking. The aim of the study is to establish a value of two morphometric methods - nuclear area and microvessel density and their influence to the survival of the patients with advanced gastric cancer. 113 patients who had undergone gastric resections for gastric cancer were analysed in this study. We estimate size of the tumor, histologic type (according to Lauren's classification), stage, nuclear area (median value of nuclear areas in 100 cancer cells measured with computerised nuclear morphometry) and microvessel density (median value of F VIII- positive microvessels in five X 200 power field) for each case. Statistical analysis was performed and p-values lower than 0,05 were considered significant. Nuclear area shows statistical significant correlation with size of the tumor, tumor stage, TNM classification and metastases in regional lymph nodes, microvessel density does not. In univariate analysis to survival, size of the tumor, tumor stage and TNM classification have $p<0,05$. Nuclear area only in intestinal type of gastric cancer correlates with survival ($p<0,05$). In multivariate analysis, size of the tumor, tumor stage and TNM classification have an influence on survival. Reliable prognostic factors in patients with gastric cancer are still stage and size of the tumor. Diffuse type of gastric cancer is still an enygma. Spreading and metastazing of intestinal type of gastric cancer could be predicted using a nuclear-area method as a support in therapy planning and prognosis. The role of microvessel density in prognosis is unreliable.

P-309

Immunoexpression of C-kit and Ki-67 in GISTs

F Iordanidis, E Vrettou, E Nenopoulou, P Hytiroglou, C Papadimitriou
Pathology Dept. Medical School. Aristotle Univ., Thessaloniki, Greece

Introduction The kit receptor normally becomes dimerized and its tyrosine kinase phosphorylated (activated) upon the ligand binding, then enabling it to phosphorylate other proteins in the signal transduction pathway that ultimately carry the proliferation signal into the nucleus. The aim of this study was the evaluation of Ki-67 (MIB-1), proliferative cell index, in correlation to c-kit stain intensity, histological grade and immunophenotype in GISTs.
Materials and methods We studied a series of 50 GISTs (c-kit positive) in correlation to age, anatomic location, size, morphological features, mitosis and necrosis. Also we stained with vimentin, CD-34, smooth muscle actin (SMA), S-100 protein and Ki-67 with ABC method on paraffin sections.
Results The average age of the patients was 62 years (ranging from 29 to 83), included 27 male and 23 female patients. 26 were located in the stomach, 20 in the small intestine, 3 in the colon and 1 in the esophagus. Microscopically the tumors showed a fusiform cytology and 12 of them showed a mixed fusiform-epitheloid cytology. The average tumor size was 6,5±4,3cm (range 1,5-20cm). We found necrosis in tumor with size>5cm. The tumor cells expressed vim 94%, CD34 68%, SMA 37%, S-100 20% and ki-67 ranging from 0-20%. The most GISTs showed c-kit positivity in 90% of tumor cells with a small minority showed more focal staining in as few as 5% to 20% of tumor cells. The stain intenisty was mild to moderate.
Conclusion In our study, the Ki-67 expression was associated with tumor size and not with c-kit staining profile, other immunophenotypic features or histological parameters.

P-310

Expression of PCNA and Ki-67 protein in colorectal carcinomas. Correlation with tumor grade

V Zivkovic, A Nagorni, V Katic, J Gligorijevic, B Djordjevic, M Milentijevic, Z Mijovic
Institute of Pathology, Medical School, Nis, Serbia and Montenegro

Introduction The prognostic significance of PCNA and Ki-67 proliferation markers in colorectal carcinomas is debatable. Therefore, we evaluated immunoreactivity of the tumor for PCNA and Ki-67 antigen in 45 colorectal carcinomas with different histological grades.
Methods The paraffin embedded tissues were immunostained for PCNA and Ki-67 antigen by employing Streptavidin-biotin(LSAB) method.
Results PCNA was positive in 96% of carcinomas and localized in the nuclei of malignant cells.Immnunoreaction for Ki-67 was demonstrated in all carcinomas and mainly and strongly expressed in the nucleoli.Positive staining for PCNA and Ki-67 correlated positively with increasing grade. The labelling index was significantly higher in the poorly differentiated carcinomas than in the well differentiated tumors.
Conclusion The expression of PCNA and Ki-67 proliferation markers clearly shows differences between colorectal carcinomas of varying differentiation grades and it is useful as a diagnostic and prognostic parametar.

P-311

Collision tumours at the gastro-oesophageal junction: do they exist?

AAN Milne, R Carvalho, BP van Rees, JJB Lanschott, MAJ Weterman, GJ Offerhaus
Academic Medical Centre, Amsterdam, The Netherlands

Introduction Collision tumours have been thought to arise from the accidental meeting and interpenetration of two independent tumours. Here we present three cases of gastroesophageal junction tumours that could fill these criteria. We employ molecular and genetic techniques to ascertain the clonality of these tumours in order to determine whether they represent true collision tumours.
Methods P53 immunohistochemistry was performed, and p53 sequence analysis was carried out on RT-PCR material derived from fresh frozen tissue. Mutations were subsequently confirmed in paraffin embedded material. Standard and laser microdissection techniques provided tumour-enriched samples from which DNA was isolated. Analysis of loss of heterozygosity was performed using the microsatellite markers D3S1478, D5S346, D9S171, D10S2491, D14S68, D16D2624, D18S64, TP53, P53Alu and Bat26.
Results p53 immunohistochemistry was positive for both tumours in each case. All three tumours possessed a p53 point mutation that was identical in both components. Polymorphic microsatellite analysis confirmed shared losses of heterozygosity with an identical pattern of retention and loss at six loci in each component. Genetic differences were also observed between tumour components.
Conclusion A comparison of immunohistochemistry, p53 sequence and the pattern of LOH for a spectrum of polymorphic microsatellite markers for three possible collision tumours suggests that both components are derived from a single precursor cell that undergoes divergent differentiation in the evolution of the tumour. The evidence presented here refutes the “collision hypothesis” and introduces a new histopathological entity of a cardia tumour with distinct diffuse signet ring cell and squamous components.

P-312

The histologic spectrum of Gastrointestinal Stromal Tumors (GISTs)

A Nasierowska-Guttmejer, W Michej
Department of Pathology, Cancer Centre, Warsaw, Poland

Introduction GISTs are the most common mesenchymal tumors of the gastrointestinal tract. They are histologically heterogenous group and a practical diagnostic criteria for GISTs is c-KIT (CD117) expression by immunohistochemistry. The aim of this study was to present morphological pattern of radically operated and disseminated GISTs.
Material and methods Material included 103 GISTs treated between 1999 and 2003 in Cancer Center, Warsaw. Thirty pts. had been radically operated of gastric GISTs and 10 pts. – intestinal GISTs. Fifty three pts. had peritoneal and liver dissemination. The histopathological diagnosis based on the type of cells, mitotic activity and tumor size. The immunohistochemical expression of

CD117 (DAKO), CD34 (DAKO), SMA (DAKO) and S100P (DAKO) were performed in each of the case.
Results 1. Microscopic spectrum. Majority (70%) of cases had heterogenous pattern-spindle and epithelioid cells with high mitotic activity-more than 5 mitoses per 50 HPF. The intestinal and disseminated tumors had generally spindle cell histology with variable myxoid matrix or extracellular collagen globules reffered to as skeinoid fibers. The majority of gastric GISTs were composed of epithelioid, polygonal cells with perinuclear vacuolization. 2.The immunohistochemical analysis revealed strong and diffuse CD117 expression in 99 of cases, whereas CD34 was expressed in 65 cases. Four cases were negative for CD117 and positive for CD34. A minority of the tumors expressed smooth muscle actin which was focal.
Conclusions The heterogenous histologic pattern of GISTs CD117 (+) correlated with dissemination, diameter over 5 cm and more than 5 mitoses per 50 HPF.

P-313

Carcinosarcoma of the esophagus: two cases of the unusual neoplasm

M Malinowska, A Nasierowska-Guttmejer
Department of Pathology, Institute of Oncology, Warsaw, Poland

Introduction Esophageal carcinosarcoma comprise approximately 1-2% of all esophageal tumors. This is the first published report in Poland of the unusual malignant neoplasm consisted of both carcinomatous and sarcomatous components.
Materials and methods Two patients with esophageal tumors were presented. They were analyzed using endoscopic, histological and immunohistochemical procedures. An endoscopic examination showed polypoid tumors in the lower esophagus. Esophagogatrectomy with lymph node dissection was performed. The resected specimens were fixed in 10% formalin and paraffin embedded tissue sections were stained with routine hematoxylin and eosin. Immunohistochemical analysis for vimentin, cytokeratin, p53 and MIB1 were performed.
Results Histologically, the neoplasms consisted of two components, squamous cell carcinoma and sarcomatous components. In case1, the sarcomatous component was with no specific differentiation and in case 2 resembled malignant fibrous histiocytoma. A gradual transition between two components was found. In case 1 regional lymph nodes were involved by metastases and demonstrated both elements. The spindle cells of the tumors were positive for vimentin and negative for cytokeratin. The squamous carcinoma cells were immunoreactive for cytokeratin and negative for vimentin. The tumor cells in the transitional zone between the carcinomatous and sarcomatous elements were positive for vimentin and cytokeratin. The lymph node metastases were positive for vimentin in spindle cell component and positive for cytokeratin in carcinoma component.
Conclusion In terms of histogenesis of carcinosarcoma of the esophagus, there has been controversy over whether the sarcomatous component consist of malignant non-epithelial cells or of a morphological variation of carcinoma cells. The immunohistochemical findings suggest that spindle cells component of the tumors are epithelial in orgin.

P-314

p21/WAF1/CIP1 expression in gastric carcinomas: relationship with p53 and prognosis

N Akyürek[1], A Dursun[1], D Yamaç[2], N Günel[2]
[1]Gazi University Medical School, Department of Pathology, Ankara, Turkey
[2]Gazi University Medical School, Department of Medical Oncology, Ankara, Turkey

Introduction The cyclin-dependent kinase inhibitor p21 is a critical downstream effector in the p53 pathway and this protein acts as tumor suppressor in a negative cell cycle regulation. Aims: We investigated the prognostic influence of p21WAF1/CIP1 reactivity in gastric carcinomas in relation to the p53 expression.
Materials and methods The expression of p21WAF1/CIP1 and p53 protein was revealed immunohistochemically in 50 gastric carcinomas. Staining patterns were assessed semiquantitatively and correlated with clinicopathologic variables and survival times. Median follow-up time was 33 months (range 2-113 months). Chi-square and Kaplan-Meier survival analysis were performed as statistical analysis.
Results The p21WAF1/CIP1 protein was detected in 21 (42%) and p53 protein in 34 (68%) of 50 cases. p21WAF1/CIP1 expression was significantly higher in stages I and II carcinomas than in stages III and IV carcinomas (p=0.01). In tumors without lymph node metastasis, p21WAF1/CIP1 expression was significantly more frequent in tumors with lymph node metastasis (p=0.007). Low p21WAF1/CIP1 expression significantly associated with p53 protein expression (p=0.002). The survival rate of patients with p21WAF1/CIP1-positive tumors was significantly better than those without p21WAF1/CIP1 expression (p=0.02). In patients with p53 positive tumors showed significantly poorer prognosis than in patients with p53 negative tumors.
Conclusion The status of p21WAF1/CIP1 expression may have prognostic value in gastric carcinomas and evaluation of the expression of both p53 and p21WAF1/CIP1 might provide more prognostic information.

P-315

Altered distribution and decrease of interstitial cells of Cajal in patients with colonic inertia

L Spasevska, V Janevska, M Ristovski, G Petrusevska,
S Kostadinova, R Jovanovic
Institute of Pathology, Faculty of Medicine, Skopje, Republic of Macedonia

Introduction The normal motility of the gastrointestinal tract depends on the enteric nervous system, the smooth muscle layers, and the interstitial cells of Cajal (ICCs). The aim of this study was to investigate both the distribution of interstitial cells of Cajal and the pathohistology of the enteric nervous system in colonic inertia.
Materials and methods Large bowels were obtained from 8 patients with colonic inertia. The patients have been treated surgically with total abdominal colectomy and ileorectal anastomosis. Control large bowel specimens were collected from 4 patients with non-obstructing neoplasia. Colonic specimens were investigated with monoclonal anti-neurofilament antibody and CD34 antibody and compared with those of control patients. The analysis of ICCs included registration of the number and process length of the myenteric and muscular ICCs.

Results In the patients with colonic inertia the myenteric plexus showed moderate or severe hypoganglionosis compared with the control group. The apparently normal axon bundles in the myenteric plexus stained markedly less than normal ones with monoclonal antibody. Myenteric ICCs were evident as single cells or cell clusters closely related to the small myentric ganglia. The ICCs did not form the typical networks seen in the normal bowel. Muscular ICCs were markedly reduced in number compared to the number seen in normal bowels and were mainly expressed at the innermost layer of the circular muscle layer.
Conclusion The enteric nervous system and ICCs are altered in colonic inertia and may play a crucial role in the pathophysiology of colorectal motility disorders.

P-316

Immunohistochemical detection of the hMLH1 and hMSH2 proteins in hereditary and sporadic colon cancer tissues

P Plevova[1,2], A Krepelova[3], M Papezova[3], E Sedlakova[1], R Curik[4], L Foretova[5], J Palas[6], J Novotny[7], J Nieslanik[8], Z Kolar[1]
[1]Institute of Pathology an Laboratory of Molecular Pathology, Palacky University, Olomouc, Czech Republic
[2]Department of Radiotherapy, University Hospital, Ostrava, Czech Republic
[3]Institute of Biology, Charles University, Prague, Czech Republic
[4]Institute of Pathology, University Hospital, Ostrava, Czech Republic
[5]Masaryk Institute of Oncology, Brno, Czech Republic
[6]Institute of Pathology, Opava, Czech Republic
[7]Department of Oncology, Charles University, Prague, Czech Republic
[8]Institute of Pathology, Municipal Hospital, Ostrava, Czech Republic

Introduction Germline mutations of hMLH1 and hMSH2 mismatch repair genes (MMR) are associated with hereditary non-polyposis colon cancer (HNPCC). Somatic impairment of these genes can be detected in sporadic colon cancers (CC). All these tumours are characterised by microsatellite instability (MSI). The aim of this study was to correlate the results of immunohisto-chemical detection of hMLH1 and hMSH2 protein with results of mutational and MSI analyses.
Patients and methods There were included: 21 CC samples from hMLH1/hMSH2 germline mutation carriers, 36 CC samples from non-carriers, and 16 CC samples from patients not subjected to mutational analysis. Immunohistochemistry was performed using mouse monoclonal antibodies (anti-hMLH1, clone G168-15; anti-hMSH2, clone G219-1129, Pharmingen, USA). MSI was analyzed at ABI Prism 310 Genetic Analyzer, mutational analysis by DNA sequencing.
Results Loss of nuclear protein expression was detected in all 21 tumours from mutation carriers, all of these exhibiting a high grade of MSI (MSI-H), and in 8 of 11 MSI-H tumours from the other patients. None of the 41 tumours with stable microsatellites or a low level of MSI exhibited a nuclear protein loss. Immunohisto-chemical analysis was able to detect MSI-H tumours with a 100% specificity and a 84% sensitivity.
Conclusion Immunohistochemical detection of hMLH1 and hMSH2 proteins is a specific method of detection of tumours with MMR gene inactivation and might be used as a screening method of HNPCC. The 3 MSI-H cases with retained nuclear protein expression might express non-functional protein or carry another MMR gene defect. Suppported by NC6741-3.

P-317

Study of mucin changes in colorectal adenoma-carcinoma sequence

M Danciu[1], MS Mihailovici[1], M Stan[2], A Trifan[2], C Sfarti[2], S Khder[2], AM Gruia[1]
[1]University of Medicine and Pharmacy, Iasi, Romania
[2]Institute of Gastroenterology and Hepathology, Iasi, Romania

Introduction Mucins are known to have a protective role for the colorectal epithelium against extrinsic noxious factors (including carcinogens), changes of its characteristics being an early process in the adenoma-carcinoma sequence. Aims: Quantitative and qualitative evaluation of mucin changes in hyperplastic polyps (HP), adenomatous polyps (AP) with different degrees of dysplasia and adenocarcinomas (AC) of colon.
Material and methods We selected 137 colorectal endobiopsies (22 HP, 42 AP and 67 AC). Thin serial sections were stained with hematoxylin-eozin, van Gieson and Alcian blue (AB) pH1 (for strongly sulphured mucins) and pH2.5 (for acid mucins: weakly sulphured mucins, hyaluronic acid and sialomucins). Observations were made only on intracellular mucins. Intensity of the stain was analyzed and compared with non-tumoral (normal) adjacent mucosa.
Results and discussions Normal mucosa and HP showed a preponderance of sulphomucins (AB pH1) comparing with sialic acid (AB pH2.5). In AP (especially in those harboring high-grade dysplasia) we detected sialomucins in 72.96% cases and the depletion of sulphomucins (56.22%). In AC sialomucins were identified in 61.34% cases, while sulphomucins only in 36.84% cases. Significant depletion of sulphomucins occurs in AP with moderate and severe dysplasia and in AC, but it was also observed in AP with mild dysplasia. This suggests the possibility that without a proper mucin secretion consisting mainly in strongly sulphured mucins, colorectal epithelium is more vulnerable to environmental carcinogens.

P-318

Histological and immunohistochemical analysis of gastrointestinal stromal tumors (GIST)

M Tolovska, S Duganovska, Z Boceska, B Stojmanovska
Institute of Pathology, Faculty of Medicine, Skopje, Republic of Macedonia

Introduction Gastrointestinal mesenchymal tumors are composed mostly of undifferentiated long spindle cells with fibrillar cytoplasm, with multidirectional differentiation. The term GIST was accepted.
Material and methods At the Institute of Pathology, Faculty of Medicine, Skopje, we analyzed 10 cases of GIST from 1998-2002. This study is a continuum of the analysis until 1997. We analyzed biopsy and operative materials from the stomach and small bowel. We used the following histochemical stainings: HE, Van Gieson, reticulin, as well as immunohistochemical stainings with the following antibodies: CKWS, LCA, S100, actin, desmin, NSE, chromogranin, synaptophysin, vimentin.
Results and conclusion The analyzed group of cases consists of patients of age between 21-84 years with male predominance (6:4). Four of the analyzed ten cases were located in the stomach and 6 in the small bowel. 7 cases were benign, histologically composed of bundles of spindle cells with slightly pleomorphic nuclei and eosinophilic granular cytoplasm, with hyalinised collagen between

the cells. The mitoses were either rare or absent. Immunohistochemical analyses were most frequently positive for S100, actin, desmin and synaptophysin. Three of the cases were ranked as malignant, using the following diagnostic criteria: size of the neoplasm, existence of metastases and histological appearance with anaplastic spindle cells arranged in bundles and whorls with high mitotic index (10 mitoses per 10 HPF) and marked positivity for actin, desmin and vimentin.

P-319

What is the relation of age, gender and histological types to the subsite location of colon carcinoma?

I Drandarska[1], A Mihova-Pancheva[2], H Kadian[3]
[1]NCIPD, Department of Immunomorphology, Sofia, Bulgaria
[2]NMTB" Zar Boris III", Department of Pathology, Sofia, Bulgaria
[3]"Zariza Joanna" University Hospital, Clinic of Gastroenterology, Sofia, Bulgaria

Introduction Characteristics that determinate the anatomic site within the colon where the carcinoma is most likely to occur would be very useful in choosing optimal factories for screening of colon cancer /CC/. Aims: To study any association of gender, age or histological types with CC in the left or in the right colon.
Materials and methods Retrospectivitaly are studied cases of CC in NMTB between 1994 and 2002.The age and the gender of patients were determined. Localization, histological type and TNM staging of the cancer are identified on the histological slides.
Results 302 cases of CC at the age between 18 -92 years old are diagnosed. Gender, age and histological type were independently significantly associated with the frequency of the development of right and left colon carcinoma. The gender distribution of CC is in benefit of male independently of sub site location as they are suffered of CC in the younger age in comparison with the female. Independently age, gender and localization prevails the histological type adenocarcinoma with different morphological and functional differentiation. One CC in the left colon is developed on the background of FAP. Solitary are the cases with congenital FAP and Lynch II. In the most cases CC was diagnosed in advanced stage. Solitary is the cases with Tis and T1.
Conclusion We consider: 1/CC is more frequently in the male colon; 2/in CC predominate histological type of adenocarcinoma; 3/CC is developed in the middle and in the age advanced in years; 4/ cases with multicentrical CC with metachronic carcinoma are solitary.

P-320

Cathepsin B and L expression in colorectal carcinomas: relationship with tumor progression and clinico-pathological parameters

C Iglesias, R Miquel, A Castells, A Nadal, E Campo, A Cardesa
Hospital Clinic de Barcelona, Spain

Introduction Cathepsin B (CB) and L (CL) are cysteine peptidases with capacity of degrading extracellular matrix. CB expression in colorectal cancer (CRC) has been related with tumor progression. There are no data about the CL immunohistochemical expression. The aim of this study was to analyse the expression of both CB/L in CRC and to relate these findings with clinico-pathological data.
Material and methods Epithelial and stromal immunohistochemical expression of CB and CL was studied in 97 and 57 samples respectively. CB was analysed in 15 adenomas. Global and local infiltrating edge data were recorded. Clinico-pathological parameters were correlated with the immunohistochemistry.
Results CB/L expression in normal epithelium was apical, with scarce macrophages in the lamina propria. An increase of both CB/L was observed in tumoral stroma, with higher CB at the infiltrating edge. The both global and deep stromal CB increased according to the T ($p<0,005$). Neoplastic epithelial CB revealed a basal stain whereas CL was occasional. Epithelial CB tended to show high expression in T1 (like high grade dysplasia) and low expression in T2 that increased progressively in T3-4 ($p=0,058$). No differences were evidenced either as a function of N state, gender, site, differentiation or histological type.
Conclusions CB/L immunoexpression in colon have a distinctive pattern which is altered in carcinoma. Whereas increased CB stromal expression ise related with local progression, epithelial positivity seems to play an important role in the first steps of carcinoma. High stromal CL isassociated with carcinoma but CL epithelial expression seems not to be contributory.

P-321

Concomitant presence of gastric signet ring and breast ductal carcinoma

M Krstic[1], M Visnjic[2], V Katic[1], L Velickovic[1], K Katic[1], M Andjelkovic-Matic[1]
[1]Institute of Pathology, Medical Faculty of Nis University, Nis, Serbia and Montenegro
[2]Surgical Clinic, Medical Faculty of Nis University, Nis, Serbia and Montenegro

Introduction New approach on estrogen and progesteron receptors of the gastric signet ring cell carcinoma explains its histogenesis and poor prognosis. The pointed out facts are the reason for this study.
Material and methods The material was obtained from surgically resected stomach, together with ovaries. After two months from gastrectomy right mastectomy has been done. The specimens were fixed in 10% formaldehyde and embedded in paraffin. The sections were stained with HE, PAS, HID-AB pH=2,5 methods and ABC using estrogen and progesteron antibodies (Dako).
Results Histologically, mucin-producing signet ring carcinoma that diffusely infiltrates the antral wall and the ovaries known as Krukenberg tumor, has been found. Histochemically, type B signet ring cell carcinoma was discovered: cells contained blue positive (sialo) mucin. Ductal type of breast carcinoma with lymph node metastases also was found. Immunocytochemically, estrogen and progesteron positive receptors were discovered in cancer cells of the stomach, breast and ovaries.
Conclusions 1.Concomitant presence of gastric signet ring and breast ductal carcinoma, as well as the presence of estrogen and progesteron receptors in both, signet ring cells and cancer cells of the breast, confirm the role of ovarian hormones in the pathogenesis of gastric signet ring cell carcinoma and, in the same time open the door for new adjuvant therapy. 2.Sialomucin, characteristic of B signet ring type carcinoma, is responsible for its poor prognosis.

P-322

Gastric MALT lymphoma: histological features before and after eradication therapy

V Katic[1], N Suzuki[2], A Nagorni[3], V Zivkovic[1], B Petrovic[2]
[1]Institute of Pathology, Medical Faculty of Nis University, Nis, Serbia and Montenegro
[2]Clinic of Gastroenterology, Medical Faculty of Nis University, Nis, Serbia and Montenegro
[3]Department of Pathology of Shiga University of Medical Science, Ohtsu, Japan

Introduction Primary gastric low-grade marginal zone B cell lymphoma of MALT type is a distinct disease entity with a characteristic histological presentation and clinical behavior. The development of gastric MALT lymphoma is dependent of H.pylori infection. Many reports have stated that the cure of H.pylori infection can induce a complete remission of low-grade gastric MALT lymphoma. We performed a prospective study to evaluate the outcome of patients with low-grade gastric MALT lymphoma and the histological characteristics before and after therapy.
Materials and methods We prospectively enrolled 20 patients with H. pylori positive low-grade gastric MALT lymphoma (Stage I 1e except one patient in Stage II 1e). Paraffin sections were stained with: HE, Giemsa, PAS and immunohistochemical LAB methods. The patients were examined by endoscopic ultrasound before and after eradication therapy.
Results Endoscopically, enlarged gastric folds, erosions or ulcerations, hyperaemia or intragastric nodularity, with preferential localization in the antrum, were described. Histologically, the neoplastic cells infiltrated between pre-existing lymphoid follicles, then colonized the lymphoid follicles. The resemblance of these cells to the centrocyte has led to the term “centrocyte-like (CCL)” cell-neoplastic component of MALT lymphoma. In some cases the cells had monocytoid appearance, but plasma cell differentiation also was prominent. Typical lesion for MALT lymphoma – “lymphoepithelial lesion”, was frequent, representing infiltration of the glandular epithelium by clusters of neoplastic lymphoid cells with associated destruction of gland architecture and morphological changes within the epithelial cells, including increased eosinophilia. After the eradication of H.pylori, the patients were regularly followed-up with endoscopic and histological assessment. 18 patients achieved complete remission within 8 weeks, one had partial gastrectomy induced by ulcer with severe dysplasia, but with regression of MALT lymphoma (within 16 weeks), but the remission of the patient with Stage II 1e was achieved within 12 months. Lamina propria appeared “empty” with gland loss. Scattered lymphocytes and plasma cells were seen within the lamina propria and there were nodular collections of small lymphocytes. Lymphoepithelial lesions were scanty or absent.
Conclusions The time taken for achieve remission of gastric MALT lymphoma in these patients varied from 2 to 12 months. The only significant prognostic variables were stage and tumor-grade.

P-323

Comparative evaluation of the prognostic value of MUC1 and MUC2 antigens in colorectal adenocarcinoma

K Katic[1], V Katic[1], T Hattori[2], R Kushima[2], D Tasic[1]
[1]Institute of Pathology, Medical Faculty of Nis University, Nis, Serbia and Montenegro
[2]Department of Pathology of Shiga University of Medical Science, Ohtsu, Japan

Introduction During the last decade, information accumulated regarding the experssion of human mucins. MUC1 belongs to the group of membrane bound mucins. It is assumed to play various roles in tumor immunology. MUC2 is marker of goblet cell or mucinous differentation of adenocarcinoma. The significance of MUC1 and MUC2 as prognostic markers in colorectal adeno-carcinoma with mucinous differentation and mucinous adeno-carcinomas was studied because previous investigations revealed inconsistent results.
Materials and methods Tissues from 20 operated patients with mucinous or mucinous differentiation of colorectal adenocarcinomas were investigated. All specimens were classified according to WHO and TNM classification, including lymph node status and distant metastases at the time of the surgical intervention. Formalin-fixed paraffin-embedded colorectal cancer tissues were cut (5μm) and deparaffinized acording to standard histological techniques. Classical HE, histochemical PAS and HID-AB pH=2,5 and immunohistochemical BSP techniques were applied. The obtained results were evaluated by the x^2 test.
Results The MUC1 immunoreactivity showed a strong correlation with tumours progression (as suggested by advancing TNM stages) and also de-differentiation (as reflected by tumorous grading). Localization and histological grading were also statistically signifficant. On the other hand, MUC2 did not show any association with the data concerning prognosis.
Conclusions According to our data, only MUC1 presents as an independent prognostic factor of colorectal adenocarcinoma. MUC1 should therefore be considered as a potential target of immunotherapeutic strategies.

P-324

Sporadic form of colon cancer of a 12-year-old boy

I Stojanovic, V Katic, J Gligorijevic, K Katic, M Andjelkovic-Matic
Institute of Pathology, Medical Faculty of Nis University, Nis, Serbia and Montenegro

Introduction Sporadic form of colon cancer is one of the most frequent cancers in adults, but very rare in children; thus we report this case.
Case report We describe the case of a 12-year-old boy who had the agressive sporadic coecal cancer, surrounded by nodular lymphoid hyperplasia.The boy underwent to partial colectomy cum omentectomy during the night with clinical diagnosis “acute abdomen”. The surgical-pathological stage was: Stage III (T3NlMo). The patient received postoperative therapy, but he died with liver metastases eight months from surgery.
Materials and methods Formalin-fixed paraffin-embedded coecal cancer and surrounding nodular tissue were cut and deparaffinized according to standard histological techniques. HE, PAS, HID-AB pH 2,5 and immunohistochemical LAB techniques were applied.
Results Fungous advanced carcinoma, 28 mm in diameter, induced stenosis and clinical symptoms of occlusion. Histologically, it was poorly differentiated adenocarcinoma with high mitotic index(high activity of Ki-67) and neuroendocrine differentiation; cancer cells were diffusely positive for p53 protein. Immunological reaction to MUC2, MUC5AB and MUC6, as well as to B lymphocytes, was negative. Microscopic examination of surrounding MALT showed

large, confluent lymphoid follicles without germinal centres within lamina propria, causing nodular appearance of the overlying mucosa. B lymphocytes were markedly depressed in this nonhereditary form of colon cancer.
Conclusions The authors have suggested that antibody deficiency, environmental, endocrine and genetic factors cooperated in the development of this nonhereditary coecal carcinoma.

P-325

The histological findings in the gastroesophageal junction of fetuses

Š Hadravská[1], A Chlumská[2], L Boudová[1], P Mukenšnabl[1], M Šulc[3]
[1]Dept. of Pathology, Medical Faculty Hospital, Plzen, Czech Republic
[2]Surgical Pathology Laboratory, Plzen, Czech Republic
[3]Surgical Pathology Laboratory, Chomutov, Czech Republic

Introduction The histopathological concept of the gastroesophageal junction has been changed by American pathologists providing the evidence that the gastric cardia is not a physiological structure. Instead, it develops through glandular metaplasia of the squamous epithelium of the distal esophagus due to gastroesophageal reflux.
Methods, results and conclusion The development of the esophageal and gastric mucosa in the gastroesophageal junction was studied in 61 fetuses of 13 – 41 weeks of the gestational age. During the 13th –15th week, the esophageal multilayered epithelium was covered by a continuous layer of columnar mucous ciliated cells which were present only focally till the 25th week and disappeared later. Before the 15th week, the gastric mucosa was formed by pits only. The glands started as proliferating tubules in the basal parts of the pits in the 15th week. Further, they differentiated into oxyntic glands. The mucosa of the corpus was fully developed in the 27th week. The cardiac mucosa was absent in all the 10 fetuses examined between the 27th and 41st week of gestation. This supports the view that the gastric cardiac mucosa is not a physiological structure but that it results from glandular metaplasia of the distal esophageal mucosa due to gastroesophageal reflux.

P-326

ABO and Rh blood groups distribution and correlation with pathologic stage of colon adenocarcinoma

MR Jalali Nadoushan[1], A Dievan Beigi[1], N Fallah[1], B Mofid[2]
[1]Shahed University, Tehran, Islamic Republic of Iran
[2]Shahid Beheshti University of Medical Sciences, Tehran, Islamic Republic of Iran

Introduction There is not enough studies about relationship between colon cancer and ABO and Rh blood groups in compare to gastric cancer. Therefore in this study we will examine ABO and Rh blood groups distribution and correlation of them with pathologic stage of colon adenocarcinoma.
Methods Data on age, sex, ABO and Rh blood types and pathologic stage (wall thickness involvement and involvement of lymph nodes) of the 232 patients with colon adenocarcinoma; were under surgical operation, were collected from three Tehran hospitals. And also data on ABO and Rh blood groups from 1500 healthy persons from above hospitals collected by randomized selecting as control group.
Results The distribution of ABO blood groups in patients was different from control group; However, blood group A in patients was 5.3% higher than the corresponding control. There was no significant association between ABO blood groups and pathologic stage of colon adenocarcinoma. The distribution of Rh in patients was likely equal with control group; Although, there was a significant relationship between Rh (+) and wall thickness involvement ($P<0.001$) and involvement of lymph nodes ($P<0.021$).
Conclusion 1- ABO blood group A is more common in patients with colon adenocarcinoma. 2- Rh(+) has correlation with poor prognosis in colon adenocarcinoma.

P-327

Vascular endothelial growth factor, microvessels count and overexpression of p53 protein in colorectal carcinomas

S Usaj[1], A Bogdanovic[2], M Perunicic[2], G Brajuskovic[1], S Cerovic[1], I Klem[3], Z Eri[3], M Panisic[4], D Tarabar[5], J Dimitrijevic[1]
[1]Institute of Pathology, Military Medical Academy, Belgrade, Serbia and Montenegro
[2]Clinic of Haemathology, Clinical Center of Serbia, Belgrade, Serbia and Montenegro
[3]Institute of Pathology, Sremska Kamenica, Serbia and Montenegro
[4]Clinic of Surgery, Military Medical Academy, Belgrade, Serbia and Montenegro
[5]Clinic of Gastroenterology, Military Medical Academy, Belgrade, Serbia and Montenegro

Introduction Vascular endothelial growth factor (VEGF) is a cytokine involved in tumor angiogenesis. Compelling data implicate that deregulation of p53 protein function may be associated with increased neovascularization and aggressive tumor growth. The aim was to investigate the prognostic significance of VEGF overexpression and microvessel count (MVC) at the deepest invasive site in colorectal carcinoma tissue as well as their relationship with p53 protein expression in tumor tissue.
Material and methods Surgical specimens of 81 operated colorectal carcinomas were studied by immunohistochemical methods for detection of VEGF and p53 protein in tumor tissue and CD31 positive microvessels. Median folow up was 31.4 month (range, 2-66 months).
Results VEGF expression and nuclear p53 protein overexpression were found in 66,7% and 58% of colorectal carcinoma. VEGF and p53 protein positive status was identical in 75.9% of tumors. The Dukes stage C and high MVC were significantly more frequent in VEGF positive tumors (53.7% and 64.8% respectively) comparing with VEGF negative tumors (25.9% for both Dukes stage C and high MVC). Hypervascularity significantly correlated with advanced Dukes stages, but not with the p53 protein expression. Survival analysis showed that VEGF and p53 protein expression as well as hypervascularity of colorectal carcinomas correlated with poor survival ($p= 0.01$).
Conclusion VEGF is an important angiogenic factor in colorectal carcinoma, and its expression being dependent on p53 protein expression. Our data suggest that combined analysis of VEGF, p53 protein and MVC may be useful for predicting the more aggressive biological behaviour of colorectal carcinoma.

P-328

Occult involvement of lymph nodes in the splenic hilus and along the splenic artery in patients with proximal gastric carcinoma

M Bjelovic[1], P Pesko[1], V Todorovic[2], M Micev[1,2], M Cosic-Micev[1]
[1]Clinical Centre of Serbia, Institute of Digestive Diseases, Belgrade, Serbia and Montenegro
[2]Institute for Medical Research, Belgrade, Serbia and Montenegro

Introduction The aim of this study was to find out the incidence of occult metastatic involvement in lymph nodes in the splenic hilus (lymph node group 10 according to JRSGC) and along the splenic artery (lymph node group 11 according to JRSGC) as well as to identify pathological features that might be prognostic factors associated with involvement of these lymph nodes in the patients with proximal gastric carcinoma.
Material and methods Total of 24 patients with advanced proximal gastric carcinoma and up to 6 positive perigastric lymph nodes (T2/T3 N1 category) have been studied in the period between 1996 and 1998. Histopathological features (tumor size, macroscopic and histologic type, grade of differentiation, depth of penetration, invasion of intramural lymphatics and veins) as well as lymph node involvement have been routinely examined according to TNM and JRSGC systems. Detection of microcarcinosis (occult lymph node involvement) in lymph nodes groups 10 and 11 has been performed by multiple serial sectioning and using immuno-histochemistry (monoclonal antibodies against cytokeratins 8 and 18, LSAB+ technique) and classified according to modified Kikuchi criteria.
Results Occult lymph node involvement in lymph node group 10 has been observed in 7 patients (29,2%). Three of them (12,5%) had only single cell micrometastases (G1 type of microcarcinosis) and 4 patients (16,7%) had micrometastatic deposits greater than 200 microns (G3 type of microcarcinosis). Occult lymph node involvement in lymph node group 11 has been observed in 2 patients (8,4%) expressing single cell micrometastases in one case and micrometastatic cell clustering (up to 200 microns in diameter) in another case.
Conclusion Occult involvement of lymph node groups 10 and 11 could be expected in lymph node positive patients with more than three positive perigastric lymph nodes. In the patients with advanced proximal gastric carcinoma examined pathological tumor characteristics could not be associated with the involvement of lymph node groups 10 and 11.

P-329

Lymph node micrometastases in patients with gastric carcinoma: immunohistochemical evaluation

M Cosic-Micev[1], M Micev[1,2], V Todorovic[2], M Bjelovic[1], P Pesko[1]
[1]Clinical Centre of Serbia, Institute of Digestive Diseases, Belgrade, Serbia and Montenegro
[2]Institute for Medical Research, Belgrade, Serbia and Montenegro

Introduction For patients who underwent curative resection for gastric carcinoma, lymph node status seems to be a major prognostic factor of disease recurrence. Contrary to histologically overt lymph node metastasis, the biological significance and prognostic relevance of micrometastatic lymph node involvement are still controversial.
Material and methods We examined frequency and distribution of micrometastases in 883 lymph nodes obtained from 27 patients with advanced gastric carcinoma (32,7 lymph nodes per patient) without primarily histologically overt lymph node metastases. Identification of lymph node micrometases was performed using multiple serial sectioning and immunohistochemical detection of cytokeratin 8 and 18 positive cells. The results were correlated to tumoral histological type, growth pattern, depth of penetration and vascular invasion.
Results The overall detection rate of micrometastases showed their occurence in more than half of examined patients (15/27 or 55,55%) and in 10,87% of examined lymph nodes (96/883). Most of them were so-called single cell micrometastases (6,34%), followed by cluster-type of micrometastases up to 200 microns (4,07%) and few greater than 200 microns (0,45%). The incidence of micrometastases was 59,09% (13/22) in Lauren`s diffuse type of carcinoma contrary to 40% (2/5) in Lauren`s intestinal type of carcinoma. In addition, there was no significant difference in occurence of micrometastases in cases with and without penetration of muscular layer, contrary to cases with serosal tumoral involvement and obvious vascular invasion.
Conclusion Detection of micrometastases might influence tumour stage migration to TNM stage III in further 10% of examined patients with primarily stage II determined diseases. The frequency of micrometastases seems to be closely correlated to poorly differentiated carcinomas, especially Lauren`s diffuse type of carcinoma and higher pT stages, including serosal involvement. However, possible independent prognostic significance is still to be elucidated after survival analysis of larger series of these patients` subgroups.

P-330

Gastrointestinal stromal tumors of the stomach

M Micev[1,2], M Cosic-Micev[1], V Todorovic[2], M Bjelovic[1], P Pesko[1]
[1]Clinical Centre of Serbia, Institute of Digestive Diseases, Belgrade, Serbia and Montenegro
[2]Institute for Medical Research, Belgrade, Serbia and Montenegro

Introduction Gastrointestinal stromal tumors (GISTs) are the most common mesenchymal tumors of the gastrointestinal tract with the stomach as the most common site. The term 'GIST' is preferentially used for the tumors that express CD34 and CD117/c-KIT and the latter has been suggested as a specific marker for GISTs. As GISTs constitute a group of phenotypically heterogenous mesenchymal neoplasms with uncertain biological behaviour, we reevaluated their histogenetic differentiation and proliferative status.
Material and methods We reexamined clinically, histologically and immunohistochemically 33 cases of paraffin-embedded GISTs noted in the Tumor Registry of Clinical Centre of Serbia between 1997 and 2001, and especially in regard to their proliferation, measured by mitotic index and immunohistochemically by Ki-67 and PCNA expression scores. In addition, evaluation of malignancy of GISTs was based on mitotic count greater than 5/50 HPF and/or tumor size greater than 10 cm and extra-gastrointestinal spread.
Results Most of gastric GISTs were composed of spindle cells (73%), epithelioid cells (20%) or both cell types (7%), and nearly 30% showed obvious clinical malignant behavior. Immunohisto-chemical examination showed strong CD117 expression in 93%, CD34 in 66,7% (two of cases exlusively CD34 positive) in non-myogenic and non-neurogenic tumors. In addition, in GISTs with CD117 expression, focal expression of S-100 was found in 26,6%,

focal SMA in 33% and desmin in 6,7% of cases. Ki-67 and PCNA indices were correlated to mitotic index and other criteria of malignancy.
Conclusion Phenotypic differentiation of GISTs toward smooth muscle were found to be correlated with proliferative indicators of poor prognosis more consistently than those toward partial/focal neurogenic differentitation or uncommited type.

P-331

Deep topographic compartments of colorectal adenocarcinomas: Down-regulation of mlh1/msh2 expression results in lack of physiologic cell kinetic balance

A Blanes[1], JJ Jimenez-Martin[1], JJ Sanchez-Carrillo[1], B Cabra[1], MT Miranda[1], SJ Diaz-Cano[1,2]
[1]University of Malaga School of Medicine, Malaga, Spain
[2]Barts and The London School of Medicine, Univ. of London, UK

Background Topographic tumor cell selection is not well characterized in colo-rectal adenocarcinomas (CRC). The contribution of mlh-1/msh-2 expression to cell kinetics by topographic compartments remains unknown in sporadic CRC.
Design We selected 90 (73 low-grade, 17 high-grade) consecutive sporadic CRC, including 48 stage I, 18 stage II, and 24 stage III. Mitotic figure counting, Ki-67 index, G2+M phase fraction, in situ end labeling (ISEL) of DNA fragments, and mlh-1/msh-2 immuno-expression were scored by topographic tumor compartment (above muscularis propria vs. muscularis propria). Statistical correlation between proliferation and apoptosis variables was performed in each topographic compartment. Variables were studied by topographic compartments and considered statistically significant if $P<0.05$.
Results Results by topographic compartments appear in the table.
Kinetic results by topographic compartments:

	Superficial	Deep	Significance
MF/50 HPF	117.08±84.92	67.62±56.10	0.0001
Ki-67 Index (%)	29.88±11.02	21.31±12.03	0.0001
ISEL Index (‰)	9.57±4.85	4.14±2.61	0.0001
G2+M (%)	11.67±7.54	10.98±6.43	NS
mlh1 (%)	18.04±15.55	6.95±8.12	0.0001
msh2 (%)	13.47±16.71	4.92±8.58	0.0001

Physiologic correlations were preserved only in the superficial compartment for mitotic figures, Ki-67 expression, ISEL index, and mlh1/msh2 expression. G2+M phase fraction correlated with mlh-1 expression only in superficial compartments ($P=0.002$) and msh-2 expression only in deep compartments ($P=0.047$).
Conclusions Superficial compartments of sporadic CRC are characterized by high cellular turnover and maintained cell kinetic balance. mlh-1 and msh-2 expression in sporadic CRC is inefficient (no G2+M phase fraction differences by topographic compart-ments) and is dissociated (only one gene product correlates with G2+M), eventually resulting in mutation accumulation and cell progression.

P-332

Gastro-Intestinal Stromal Tumors (GISTs) classifications and their predictive value

J Sandbank[1], I Rabin[2], M Maklakovsky[1], H Mehrdad[1], I Wasserman[2], G Hermann[1], A Halevi[2]
[1]Assaf-Harofeh Medical Center, Pathology Department, Zerifin, Israel
[2]Assaf-Harofeh Medical Center, Division of Surgery, Zerifin, Israel

The biologic behaviour of GISTs has been difficult to predict based on the original criteria proposed in the early 1990s. Many isolated histological features, such as site, size, extent of bowel-wall involvement, necrosis, cellularity, mitotic counts, atypia, etc., had to be evaluated and integrated into a single and reproducible result that had also to be as accurately predictive as possible. Therefore numerous studies have been performed in order to reach the ideal combination of factors that may predict these tumors correctly. 55 GISTs were diagnosed either originally or retrospectively after reviewing diagnoses of GIT spindle cell tumors, examined in our Pathology Department between the years 1988-2002. All tumors were defined as GISTs only when displaying c-KIT (CD117) immunopositivity. Additional immunohistochemistry was performed to corroborate the diagnosis. We reclassified the tumors according to different proposed classifications and correlated the results with the clinical followup available for these patients. The followup periods ranged between 2-100 months for gastric GISTs (mean-32.2 months, median-24.5 months) and 6-62 months for patients with small-bowel GISTs (mean-32.3 months, median-30 months). While the median disease-free survival was 27.6 months for patients with malignant gastric GISTs, it was only 5 months for patients with small-bowel malignant GISTs. The results of the study show that all classifications stratified the patients in a very similar manner although some were more accurate than the others and more user-friendly and therefore probably also more reproducible. The relative high rate of deaths occuring in the small-bowel GIST group (45%) as compared to the 15.4% death rate in the gastric GIST patients, strengthens the supporters of different criteria to be applied to the GISTs arising in these different sites. Another important issue that has imerged in our study was the much higher incidence (80%) of malignant GISTs developing in the younger age group (20-49years), compared to 26.3% malignant GISTs in the age group of above 70 years, making this feature to be probably of major significance. It should therefore be considered whether age should be a built-in criterion when evaluating the biological potential of a GIST.

P-333

Epithelial metaplasias circle gastric ulcer disease

B Vukomanovic[1], S Jancic[1], N Djurdjevic[2], J Sopta[3]
[1]Medical Faculty of Kragujevac, Serbia and Montenegro
[2]KBC Zvezdara, Serbia and Montenegro
[3]Medical Faculty of Belgrade, Serbia and Montenegro

Introduction Gastric ulcer disease is the most important disease of the digestive tract becouse this illnes have big frequecy and circle gastric ulcus presents many histologic features characteristics which may be precancerous lesions. Gastritis is lesion which is always associated with gastric ulcer. Epithelial metaplasias are transformation of one kind of epithelium to other type epithelium and circle gastric ulcus it is very frequency changes of epithelium. The aim of this study was to to find frequency of appearance epithelial metaplasias circle gastric ulcus, types of metaplasias and grade of gastritis. Also we searched changes of epithelial mucins. We had citochemistry examination endocrine G, EC and D cells and we wanted to describe immunohistochemicaly feature characteristics in different kinds of epithelial metaplasias.
Material and methods For examination we use biopsy material:surgery and endoscopic of 100 patients with gastric peptic ulcer. We use standard HE method for identification micromorpholic changes; AB-PAS (pH 2,5) and HID-AB method for illustration biochemistry alteration about mucins;Grimelius (1968) and Masson citochemistry methods; immunocytochemistry Avidin-biotin

peroxidasa (ABC) with antiserotonin, antigastrin, antisomatostatin.
Results We found 16 cases completly mature intestinal metaplasias (IM), 5 cases incompletly IM;1 case imature IM and 1 case imature IM with displasia. Also we detected composition completely and incompletly IM in 2 cases, composition incompletly and pyloric metaplasia in 1 cases.We find pyloric metaplasias in 9 cases, colons metaplasia in 2 cases. Composition colons and incompletly mature IM were detected in 2 cases;composition pyloric and incompletly mature IM in 1 case.Summary the bigest frequency of appearance metaplastic alteration were in older patients.Histologicaly claracteristics metaplasias were imitation some segments of digestive tract. Metaplasias include many biochemicaly alterations and it can be present with changes in secretion of mucins.Gastric metaplasia is dynamic process with changes both in epithelial and endocrine cells.
Conclusion Metaplasias in gastric mucosa circle gastric ulcer is sign very important alteration.Standardisation of research this alteration may be very important guider about prognosis for patients with gaster ulcer disease.

P-334

Choice of immunohistochemical method for detection of defect mismatch repair system

C Fenger, O Nielsen, TP Hansen
[1]Department of Pathology, Odense, Denmark

Introduction Defects in the Mismatch Repair (MMR) system is involved in the pathogenesis of Hereditary Non Polyposis Colorectal Cancer (HNPCC) and in 15% of sporadic colorectal cancers, and in the latter the defect is associated with a better prognosis but posssibly also a higher risk for metachronous cancer and a different response to adjuvant chemotherapy. Screening for such defects can be done by testing for microsatellite instability, but immunohistochemistry gives similar results with less costs. The aim of this study was to select the optimal antibodies and methods for immunhistochemical detection of proteins involved in the MMR system.
Material and methods Twelve antibodies (4 against hMLH1, 5 against hMSH2, 2 against hMSH6 and 1 against PMS2) were tested using different dilutions and HIER-techniques on a material consisting of paraffin embedded tumours from 21 patients with well defined mutations and from 7 controls. The results were evaluated semiquantitatively.
Results The following clones, dilutions and pretreatment regimens were selected:

MLH1 (G168-15, BD Pharmigen)	1:50	EDTA 1mM, pH 8
MSH2 (27, Transduction Lab.)	1:400	EDTA 1mM, pH 8
MSH6 (44, Transduction Lab.)	1:200	EDTA 1mM, pH 8
PMS2 (A16-4, BD Pharmigen)	1:100	EDTA 1mM, pH 8

Conclusion All chosen antibodies gave a specific and reproducible staining. There were no false positive or negative results. The panel can be recommended for screening for defects in the MMR-system.

P-335

Immunoexpression of MUC1 and MUC2 mucins in advanced gastric cancer

M Grosso, E Vitarelli, A Ieni, R Caruso, G Tuccari, G Barresi
Department of Human Pathology, University of Messina, Messina, Italy

Introduction Mucins are a group of glycoproteins having a central polypeptidic structure and O-linked carbohydrates. To date, 12 MUC genes have been described that encode secreted and/or membrane associated epithelial mucins. In the normal gastric mucosa, MUC1 has been detected in the superficial foveolar epithelium, while MUC2, a marker of intestinal differentiation, has been reported as absent. In gastric carcinomas, the presence of MUC1 as well as de novo expression of MUC2 has been described. Aim: The relationship between the immunoexpression of MUC1 and MUC2 and histopathologic subtypes of gastric carcinomas was investigated.
Materials and methods According to Lauren's classification, a series of 45 cases of gastric carcinomas (30 of intestinal type and 15 of diffuse type) was studied. The percentage of stained neoplastic cells was graded: (-) 0-5%; (+) 5-50%; (++) >50%. MUC1 and MUC2 were demonstrated using monoclonal antibodies (NCL-MUC1, clone Ma695, 1:100; NCL-MUC2, clone Ccp58, 1:200; Novocastra).
Results Staining for MUC1 was present in 25 of 45 cases (55.5%) gastric carcinomas. In addition, the expression of MUC1 was significantly higher in the intestinal type (21/30) than in the diffuse type (4/15) ($P<0.01$). On the contrary, MUC2, expressed in 20 of 45 (44.4%) gastric carcinomas, showed a significantly higher positivity in diffuse type (12/15) than in the intestinal type (8/30) ($P<0.01$). Moreover, the co-expression of MUC1 and MUC2 was observed in eight cases of the intestinal type gastric carcinoma.
Conclusions Our results indicate that diffuse gastric carcinomas have features consistent with intestinal differentiation as documented by MUC2 expression.

P-336

Colon's metaplasia of gastric mucosa circle ulcer disease

B Vukomanovic[1], S Jancic[1], N Djurdjevic[2], S Milenkovic[3], Z Tepavcevic[4]
[1]Medical Fakulty of Kragujevac, Serbia and Montenegro
[3]KBC Zvezdara, Serbia and Montenegro
[4]KBC Zemun, Serbia and Montenegro
[5]Faculty of dentistry, Belgrade, Serbia and Montenegro

Introduction Colon's metaplasia may be variant of intestinal metaplasia in the gastric mucosa circle gastric ulcer.It is important precancerous stadium because 80 % colon's metaplasias of gastric mucous membrane transverse in gastric carcinoma. Aims: We want to find frequency of appearance colon's metaplasia in gaster mucosa with ulcer disease.Also we want to describe histologicaly, histochemicaly and immunohistochemicaly feature characteristics colon's metaplasia in gastric mucosa.
Materials and methods For examination we use biopsy's matherial:surgery's and endoscopic of 100 patients with gastric peptic ulcer. We use standard HE method for identification micromorfologic changes; AB-PAS (pH 2,5) for illustration biochemistry alteration about mucins;Grimelius citochemistry method;Imunocytochemistry Avidin-biotin peroxydasa with antiserotonin, antigastrin and antistomatostatin.
Results We find two cases so-called colon's metaplasia gastric mucous membrane. It was males in VI decade of life.Both of them were detected near parts with intestinal metaplasia and atrophic gastritis. Histology's design metaplastic epithelium appear big changes than normal gastric mucosa watched on cellular and tissue level;it was alike epithelium of colon. There was winding and arborescent cryptas, and wasn't find villosity. Cells in cryptas were voluminous and they group. Predominant componentof cells were

goblet cells. Cylindric cells also was alike goblet cells. We didn't see Paneth's cells. Histochemycaly we detected sufficiently sulphomucins and less sialomucins. G cells and ECL cells were insufficient; EC cells were less multiplied.
Conclusions Colon's metaplasia is sign of big intracellular alteration and we can detect this with changes in secretion of mucin. Colon's metaplasia gastric epithelium is dynamic process with changes both in epithel and endocrine cells.

P-337

Upregulated expression of RELP, a REG-like protein, in inflammatory, metaplastic and neoplastic gastrointestinal mucosa

LC Andersson[1], M Kämäräinen[1], K Heiskala[1], P Lankila[1], M Heiskala[2]
[1]Dept.of Pathology, University of Helsinki and University Hospital, Helsinki, Finland
[2]The R.W. Johnson Pharmaceutical Research and Development, 3210 Merryfield Row, San Diego, California 92121, USA

Material and methods We screened expressed sequence tag (EST) databases to detect genes specifically expressed in the gastrointestinal tract.
Results We identified a gene, called RELP (regenerating protein (REG) family-related protein). The RELP cDNA encodes a 158-amino-acid preprotein with a 22-amino-acid signal peptide. The amino acid sequence of RELP is 30-40% identical and 40-46% similar to the previously characterized members of the REG protein family. The REG proteins, which all belong to the family of C-type lectins, have been implicated in cell proliferation, migration and differentiation in the gastro-intestinal tissues. The RELP gene spans 17.5 kilobases and maps to chromosome 1p12-13.1, whereas the genes of the previously known REG proteins cluster on chromosome 2. Dot-blot hybridisation revealed expression of RELP mRNA mainly in the gastrointestinal tract, but also in prostate, and testes. Immunohistochemical staining demonstrated expression of RELP in mucosal neuroendocrine cells of in the small intestine and in the parietal cells of normal gastric mucosa. Regenerating borders of gastric ulcera, the goblet cells of inflammatory mucosa in ulcerative colitis and Crohns disesase, showed a strongly upregulated expression of RELP. Areas of intestinal metaplasia in the stomach and esophagus also displayed a robust content of RELP. More-over, RELP was strongly expressed in mucocellular and mucinous tumors of the gastrointestinal tract. The orthologous gene for mouse RELP was also cloned.
Conclusions RELP represents a novel marker of inflammatory, metaplastic and neoplastic changes in the GI-tract.

P-338

Current approach to the biopsy diagnosis of gastrointestinal stromal tumors (GISTs) - is it possible to predict clinical behaviour?

P Szepe[1], P Ondrejovič[1], K Kajo[1], P Slavik[1], LA Sokol[2], L Plank[1]
[1]Dept. of Pathology, Comenius University, Jessenius Medical Faculty and Faculty Hospital, Martin, Slovakia
[2]Dept. of Pathology, Faculty Hospital, Kosice, Slovakia

Introduction GISTs are the most common GI mesenchymal tumors showing CD117 positivity. Although according to accepted criteria none of them are 'benign', their metastatic risk depends on the tumor size (TS) and mitotic count (MC). Aim: Reclassification of a series of GISTs using morphological and immunohisto-chemical analysis of paraffin-embedded material and evaluation of the relevant clinical data.
Material and methods 32 patients with GISTs fulfilled the criteria of Fletcher et al. (2002). In addition to histological stainings, primary antibodies against vimentin, desmin, actins, S-100 protein and CD117 (all DakoCytomation) and CD 34 (Immunotech) were used for the immunoanalysis.
Results Majority of the tumors was localized in the stomach (n=18) and small intestine (n=11), one in the colon and two were extragastrointestinal. In relation to the accepted MC and TS criterias, 16 of 32 cases were of low and one of very low risk category. 8 tumors belonged to intermediate risk category, mostly due to TS in contrast to low MC. The inclusion of 7 cases into high risk category was based predominantly on the MC (>5/50HPF and TS 5-10 cm /n=5/ and >10 cm /n=1/; in the last one it was >6-10/50HPF in contrast to TS <5 cm).
Conclusion A prediction of clinical behaviour of GISTs requires a correct histopatological analysis related to initial staging data. Although the categorisation of the GISTs into different risk categories uses both criteria of TS and MC, the significance of the mitotic activity evaluation in our set of cases seems to be higher.

P-339

Multiple gastric composite carcinomas (adenocarcinoma and endocrine carcinoma) with adenosquamous differentiation

Y Kapran[1], N Akbas[1], M Aksoy[2], F Dizdaroglu[1]
[1]University of Istanbul, Istanbul Medical Faculty, Pathology Department, Istanbul, Turkey
[2]University of Istanbul, Istanbul Medical Faculty, General Surgery Department, Istanbul, Turkey

A case of multiple gastric composite carcinomas composed of endocrine carcinoma and adenocarcinoma with adenosquamous differentiation is presented. Tumours showed a composite architecture both within the site of origin and in lymph node metastasis. A 44-year-old woman had a diagnostic upper gastrointestinal system endoscopic evaluation for her long term dyspeptic complaints. After determination of two concurrent tumours in the stomach she underwent total gastrectomy operation. Gross examination of the stomach revealed a polypoid lesion in the anterior wall and an ulcerous lesion in the posterior wall of the corpus. Also there were multiple minute nodular lesions both in the corpus and fundus. Histopathological examination of the polypoid tumour revealed a well-differentiated tubular adenocarcinoma admixed with an endocrine carcinoma proved immunohisto-chemically. Ulcerous lesion was composed of a poorly-differentiated adenocarcinoma showing adenosquamous differentiation admixed with an endocrine carcinoma. Other nodular lesions were composed of endocrine tumours having different levels of invasion in the wall of stomach. Non-tumourous mucosa harboured atrophic gastritis. This is a unique case of multiple composite carcinomas devoloped in the setting of atrophic gastritis worth to discuss.

P-340

Primary retroperitoneal malignant fibrous histiocytoma metastasing to the stomach

Y Kapran[1], O Mete[1], O Asoglu[2], I Kilicaslan[1], M Demiryont[1], F Dizdaroglu[1]
[1]University of Istanbul, Istanbul Medical Faculty, Department of Pathology, Istanbul, Turkey
[2]University of Istanbul, Istanbul Medical Faculty, Department of General Surgery, Istanbul, Turkey

Introduction One of the most common malignant soft tissue tumours in adults is malignant fibrous histiocytoma. These tumours are accepted as an aggressive tumour and mainly treated surgically. Primary and metastatic malignant fibrous histiocytomas of the gastrointestinal tract are rarily described.
Patients and results Our case is a 55-year-old woman who had a retroperitoneal malignant fibrous histiocytoma that had metastased to the lung after 10 months following an adequate initial treatment. Four months later, because of having recurrent attacks of vomiting and nausea, gastroscopic examination was performed. Multiple nodular lesions in her stomach were seen and microscopic examination of these lesions revealed spindle–shaped, pleomorphic tumour cells. The positive immunoreactivity for anti–vimentin and anti-CD 68 justified the diagnosis of malignant fibrous histiocytoma's metastases. Total gastrectomy was performed following that diagnosis and she died after 1 month due to renal failure.
Conclusions This case is presented because of the rarity of distant metastases of malignant fibrous histiocytoma to the stomach and to discuss the entities that should be considered in the differential diagnosis of these tumours.

P-341

Role of p16INK4a in gastrointestinal stromal tumours (GISTs)

R Ricci, V Arena, N Maggiano, F Castri, M Martini, A Rinelli, LM Larocca, FM Vecchio
Ist. Anatomia Patologica - Universita Cattolica Del Sacro Cuore, Roma, Italy

Introduction The classification based on c-KIT/CD117 expression reordered the formerly rather confuse category of GIST. p16INK4a (p16) is a tumour suppressor gene of the cyclin D-Cdk4, 6/INK4/Rb/E2F pathway, altered in >80% human neoplasms. It is located on chromosome 9p21, a region consistently involved in DNA losses found in malignant GISTs. Aims: We studied the role of p16 in GISTs.
Materials and methods CD117-immunoreactive mesenchymal tumours with morphological and clinical features consistent with GIST were studied, excluding smooth muscle (desmin+, CD117-) and schwannian (S-100+, CD117-) neoplasms. 21 cases (17 gastric, 3 small intestinal and 1 colorectal; 10 males, 11 females; age at diagnosis: 51-87 years; follow-up: 6-193 –mean: 60.3- months) were considered. Immunohistochemistry, RNA extraction with semiquantitative RT-PCR and methylation specific PCR (MSP) were used. Kaplan-Meier method followed by log-rank test, and univariate and multivariate analyses with a proportional hazards model were performed (malignancy criteria adopted for uncensored events: recurrence, invasion of adjacent organs, peritoneal dissemination, metastases and death of disease).
Results A tumoral cell fraction with low/absent p16 immunoreactivity >20% was associated with malignancy; semiquantitative RT-PCR confirmed this result. By MSP, 7 cases (all underexpressing p16, six malignant) showed p16 promoter methylation. Low/absent p16 immunoreactivity, together with size, cellularity, mitotic count and presence of coagulative necrosis resulted associated with malignancy by univariate analysis, with the former factor being the only prognostic one selected by multivariate analysis.
Conclusions p16 downregulation is implied in GIST progression; p16 promoter methylation is one of its causes; p16 assessment opens possible perspectives in GIST prognostication.

P-342

Investigation of glandular epithelium cells proliferative activity in chronic superficial and deep inflammations of gastric mucosa

W Kozlowski[1], C Jochymski[2], G Klupińska[2], A Dabek[1], J Patera[1]
[1]Military Medical Institute, Department of Clinical Pathology, Warsaw, Poland
[2]Medical University of Lodz, Department of Histopathology and Molecular Biology of the 5th Clinical Hospital, Lodz, Poland

Introduction Regenerative abilities of gastric mucosa glandular epithelium cells are the main mechanism which condition its right function both within the range of gastric mucosa integrity and normal activity of its epithelial cellular elements. The aim of the work was to evaluate dependence between proliferative activity of gastric mucosa glandular epithelium and sex, age, chronic inflammation type and Helicobacter colonization.
Material and methods The examinations were conducted on paraffin blocks from gastric oligobiopsies taken from 35 women (of average age-52) and 34 men (of average age-54).To the examinations were rated only cases where oligobiopsies were taken from at least two gastric prepyloric parts (antrum) and corpus with recognized unspecific chronic gastric mucosa inflammation. Chronic gastritis was graded according to modified Whitehead's classification. Helicobacter pylori (Hp) was evaluated according to the Sydney system. Examination of the cells with PCNA proliferative antigen expression were conducted separately for foveolar area glands and for glands below gastric mucosa foveolar area. All the measurements were performed separately for gastric mucosa prepyloric part and gastric corpus. In tissue sections, in which were carried out proper immunocytochemical reactions, measurements of the PCNA positive cells number in circular, oblique short, oblique long and oblong gastric glands sections were conducted five times. The statistic analysis also included age, presence of Hp colonization, gastric mucosa inflammation type and the area where an oligobiopsy section was collected.
Results No significant differences were found in proliferative activity depending on the place of collecting a section, age and Hp colonization, while a higher proliferative activity was found in superficial chronic gastritis, particularly in gastric mucosa prepyloric part.
Conclusions 1. Chronic superficial inflammation coexists with significantly higher proliferative activity of gastric mucosa glandular epithelium, particularly with connection to its prepyloric part. 2. Changes in gastric mucosa glandular epithelium proliferative activity do not depend on its age and histotopography and Hp colonization.

P-343

Chromogranin-A-plus and D cells in superficial and deep gastric mucosa inflammation

W Kozlowski[1], C Jochymski[2], G Klupinska[2], A Dabek[1], J Patera[1]
[1]Military Medical Institute, Department of Clinical Pathology, Warsaw, Poland
[2]Medical University of Lodz, Department of Histopathology and Molecular Biology of The 5th Clinical Hospital, Lodz, Poland

Introduction Chromogranin-A-plus (chA) and D cells exist almost in the whole alimentary canal and in pancreas. These cells have an influence on secretory functions and normal gastric mucosa histostructure. Up to now investigations confirmed participation of these cells in e.g HCl and gastrin secretion regulation and in some of the proliferative states of gastric mucosa. The aim of the study was to estimate participation of chA and D cells in microscopic superficial (gchs) and deep (gch) gastric mucosa inflammation's indices.
Material and methods Paraffin blocks from gastric oligobiopsies was the material which was collected from 35 women (of average age-52) and 34 men (of average age-54). To the examinations were classified only the cases where oligobiopsies were taken from at least two areas of gastric prepyloric part (antrum) and corpus, with diagnosed unspecific chronic gastric mucosa inflammation. Chronic inflammations were graded according to modified Whitehead's classification. Helicobacter pylori (Hp)was evaluated according to the Sydney system. Neuroendocrine cells of gastric pylori were counted after proper immunohistochemical identification in circular, oblique short, oblique long and oblong gastric glands sections. All measurements were conducted separately for gastric mucosa prepyloric part and gastric corpus. The results of quantitative researches were analysed with the use of statistic methods.
Results In gastric mucosa antrum there were twice more chA and D cells in comparison with corpus. Gastric mucosa inflammation type did not have a significant influence on cells localization in gastric mucosa. The number of chA cells diminished in gchs gastric antrum among patients who were over 50 years old, whereas the same number increased in corpus inflammations of this type. The increase of chA cells number was found in gchs gastric antrum with Hp colonization. In these cases D cells number diminished.
Conclusions 1. In gchs gastric antrum with Hp colonization chA cells number significantly increases while D cells number decreases. 2. Quantitative changes of chA and D cells run differently in gchs and gch both in prepyloric part and in gastric corpus.

P-344

Response to preoperative chemoradiation on rectal adenocarcinoma: histopathological effects and relationship with level of p53 and PCNA expression

P Ramos[1], M Diez[2], G Olmedilla[1], A Ruiz[1]
[1]Dpt. of Pathology, Principe de Asturias University Hospital, Alcala de Henares, Madrid, Spain
[2]Dpt. of General Surgery, Principe de Asturias University Hospital, Alcala de Henares, Madrid, Spain

Introduction Adjuvant chemoradiotherapy delivered before surgery has been used to improve control and to reduce the likelihood of local recurrence in selected patients with rectal cancer. Although the status of p53 gene and the expression of PCNA has been widely studied in these tumors, little is known about their value to predict the responsiveness of rectal cancer to chemoradiation. The aim of this study was to To assess effects of preoperative chemoradiation in advanced rectal adenocarcinoma.
Materials and methods We examined the histopathologic effects of chemoradiotherapy on 73 rectal tumors and correlated the efficacy of treatment with the level of p53 and PCNA proteins expression in pretreatment biopsies.
Results Three patients showed no primary tumor in the resection specimen. Another eight carcinomas showed a good response to chemoradiation with only small nests of viable tumor cells. Grouping these two categories, we considered that the tumor response had been total or subtotal in 11 cases (15%). Nuclear accumulation of p53 protein was detected in 53 (72%) specimens. Thirty five tumors showed a high PCNA index (48%). No obvious relationship seemed to exist between pretreatment, p53 immunostaining and response to chemoradiotherapy. Tumors with high PCNA index were more likely to respond to chemoradiation: 8/35 (72%) versus 3/38 (43%)(p=0.07).
Conclusion Knowledge of proliferative activity of rectal cancer, as determined by PCNA immunostaining, should be useful in predicting the likelihood of response to preoperative chemoradiation.

P-345

Value of the mitosis-related PHH3 antibody in the prognosis of gastrointestinal stromal tumors

M Jimeno Ramiro, M Iglesias Coma, N Pérez, R Orellana, J Lloreta, J Vila, T Ribalta, E Musulén, R Miquel, E Díaz
Hospital Del Mar-Imas, Barcelona, Spain

Introduction Mitotic count and tumor size are the main predictors of outcome in gastrointestinal stromal tumors (GIST). However, they are not always useful in individual cases. The aim of the present study has been to assess whether mitotic counts performed using phosphorylated histone 3 (PHH3) antibody, expressed from the early steps of mitosis, could improve the prediction of prognosis in these tumors.
Materials and methods Sections from 30 GIST were stained with PHH3 antibody (Upstate Biotechnology, Lake Placid, NY; 1:1,000 dilution). Mitoses were counted per 50 high power fields (40X, Olympus BX). In addition, the H&E-based mitotic counts and tumor size were obtained from the pathology reports. Patient outcome was recorded as the endpoint. Statistical analysis: non-parametric tests (Mann-Whitney, Wilcoxon, Spearman), Kappa and Cox regression.
Results There were 17 gastric and 13 intestinal tumors. Correlation coefficient with mitotic counts performed by both techniques was 0.459 (p=0.006), indicating a moderate correlation. The cut-off was 2 mit/50 HPF for H&E, with an odds ratio (OR) of 3.39 (0.83;13.82; p=0.08); 4 mit/50 HPF with PHH3 antibody counts, with an O.R of 6.16 (1.39;27.22; p=0.016), and 7 cm for tumor diameter, with an O.R. of 4.29 (0.86;21.31; p=0.07).
Conclusion In the present series, PHH3-based mitotic counts allow a better prediction of prognosis than H&E-based counts or tumor size. Thus, PHH3 antibody could be applied in the pathological classification and grading of these tumors, and in the more precise definition of cases with higher risk of progression.

P-346

Immunohistochemical expression of cyclooxygenase-2 (COX-2) in human colorectal cancer

F Patakiouta[1], D Tzilves[2], P Xirou[1], N Pasteli[1], M Papagianni[1], I Katsos[2], M Kalaitzi[3]
[1]Pathology Department, Thessaloniki, Greece
[2]Gastroenterology Department, Thessaloniki, Greece
[3]Technician, Thessaloniki, Greece

Introduction Recent studies have implicated metabolites of arachidonic acid, such as prostaglandin E(2) in colorectal carcinogenesis. COX-2, a key enzyme in arachidonic acid metabolism, is present in the majority of colorectal cancer (CRC). Its overexpression seems to be associated with worse prognosis. The aim of this study was to examine the relationship between the expression of COX-2 in human CRC and the clinicopathological characteristics of the tumor.
Materials and methods Paraffin embedded tissue samples from 35 patients (M:19, F:16, Median Age: 63 yrs) with CRC (TNM staging: I - IV), who underwent radical surgical treatment in Thessaloniki Cancer Hospital "Theagenio" from 1/1/1997 until 1/8/97, were evaluated. Tumor sections were stained for COX-2 using a rabbit polyclonal antibody against human COX-2 and the staining was graded on a scale 1 – 4, using mononuclear cells as reference.
Results COX-2 expression was found in tumor epithelial cells in 85.7% of CRC (30/35 cases) with diffuse mainly, cytoplasmic staining and in inflammatory cells, vascular endothelium and fibroblasts. Low COX-2 expression (grade 1-2) was found in 54.3%, high COX-2 expression (grade 3-4) in 31.4% of cases and the remaining were negative. There was no correlation between clinicopathological characteristics of patients and intensity of COX-2 expression, although there was a slightly better overall survival rate in low expression group of patients (p:NS).
Conclusions This small study shows that COX-2 protein is overexpressed in most cancer cells in colorectal carcinomas and may be related to overall survival.

P-347

The expression of Bcl 2 family proteins in B-chronic lymphocytic leukemia

G Brajuskovic[1], S Vukosavic[2], S Cerovic[1], S Knezevic Usaj[1], S Marjanovic[3], J Dimitrijevic[1], S Romac[2], A Skaro Milic[1]
[1]Institute of Pathology, Military Medical Academy, Belgrade, Serbia and Montenegro
[2]Facilty of Biology, University of Belgrade, Belgrade, Serbia and Montenegro
[3]Clinic of Hematology, Military Medical Academy, Belgrade, Serbia and Montenegro

Introduction B-chronic lymphocytic leukemia (B-CLL) is a neoplastic disease caused primarily by defects in the apoptosis mechanism. Apoptosis is the process of programmed cell death or cell suicide. The Bcl-2 proteins are a family of proteins involved in the response to apoptosis. Some of these proteins (such as Bcl-2 and Bcl-Xl) are anti-apoptotic, while others (such as Bad or Bax) are pro-apoptotic.
Materials and methods Our study includes peripheral blood specimens from 20 patients with B-CLL and 20 healthy individuals (as a control group). Using Western blot analysis, we examined the levels of Bcl-2, Bcl-Xl, Bax and Bad protein expression.
Results The level of Bcl 2 (p= 3,68 x 10-10), Bax (p= 0,019) and Bad (p= 0,073) proteins were significantly increased in all analyzed patients while the level of Bcl Xl protein (p=0,75) showed no difference between patients and healthy individuals. Differences between the levels of analysed protein expression in group of patients had no statistical significance.
Conclusion Increased level of expression Bcl 2, Bax and Bad protein represents the most striking feature of B – CLL cells. The variations in expression of only one protein of the Bcl 2 family can not represent the prognostic factorr in B-CLL.

P-348

Recurrent Kikuchi-Fujimoto desease during pregnancy

I Venizelos[1], D Sioutopoulou[2], Z Tatsiou[3], S Vakalopoulou[4], V Garipidou[5]
[1]Department of Histopathology, Athenes, Greece

Introduction Kikuchi - Fujimoto disease (KFD) is a distinctive type of necrotizing lymphadenitis with unknown cause, has a self-limited clinical course and affects usually the cervical lymph nodes of young women. Although KFD occurs most often in young women, only two cases have been reported during pregnancy. In one of these cases KFD developed initially 6 years before.
Case report We report a case of a 37-year-old pregnant woman on her 20th week of gestation who was admitted with a history of swelling in the right side of the neck and fever of 20 days duration. On physical examination a 2 cm cervical lymph node was palpable. Microscopically, the excised lymph node showed large areas of necrosis and extensive karyorrhexis. No neutrophils or plasma cells or eosinophils were identified. It was found an admixture of non-phagocytic histiocytes and T-lymphocytes in the necrotizing area. There was a predominance of CD8+ cells over CD4+ cells. The patient received no treatment and 2 months later had no symptoms. Later she delivered a healthy boy. Five years ago the patient presented similar clinical history and histological diagnosis of the excised cervical lymph node. We present the second reported case of recurrent KFD during pregnancy and the third case of KFD developing during pregnancy.
Conclusion From our case and the other two reported cases it seems that if KFD occurs in a pregnant woman there is no need to terminate the pregnancy as there was no effect on both mother and fetus.

P-349

Monitoring of patients with follicular lymphoma carrying t(14;18)(q32;q21) by real time quantitative PCR

M Mrhalova[1], M Kalinova[2], L Krskova[1], J Soukup[1], R Kodet[1]
[1]Department of Pathology, 2nd School of Medicine, Prague, Czech Republic
[2]2nd Department of Pediatrics, 2nd School of Medicine, Prague, Czech Republic

Introduction Follicular lymphomas (FL) are characterized by t(14;18)(q32;q21) in a majority of patients. The identification of the translocation is utilized to monitor the disease behavior, and,

specifically, to detect minimal residual disease (MRD). Qualitative PCR is routinely used but without specification of the tumor cell quantity. Real time quantitative PCR (RQ-PCR) may be employed to address this issue. Aims: RQ-PCR was introduced to monitor MRD in patients with FL bearing the t(14;18)(q32;q21).
Materials and methods Samples of primary tumors, bone marrow and peripheral blood (BM/PB) specimens were taken in the course of the disease and were used for the t(14;18)(q32;q21) assessment. For translocation screening, FISH on interphasic nuclei was applied. Qualitative PCR was used to detect the break in the major breakpoint region (mbr) of the BCL-2 gene (18q21). Relative quantity of cells bearing mbr t(14;18)(q32;q21) was performed by the RQ-PCR. Fifteen samples of primary tumors and BM/PB in duplicates were investigated with appropriate controls.
Results and conclusion The relative quantity of cells with t(14;18)(q32;q21) was significantly higher in the primary tumors than in the BM/PB samples. The changes of the BM/PB infiltration were found during the course of the disease and included shifts toward the tumor progression or disappearance of the tumor cells. RQ-PCR is a technique suitable for monitoring the disease response to the therapy or the disease progression and it is superior to morphology and immunohistochemistry. Supported by: IGA-MZCR-NC/6296-3, Research Project FN-Motol/6073.

P-350

Phosphatase activity dependent apoptotic effect of transforming growth factor beta1 in HT58 human lymphoma cells

L Kopper[1,2], A Sebestyén[1], G Barna[1], S Paku[2], R Mihalik[2]
[1]Ist Department Pathology and Experimental Cancer Research, Semmelweis University, Budapest, Hungary
[2]Molecular Pathology Research Group, Joint Organization of the Hungarian Academy of Sciences and Semmelweis University, Budapest, Hungary

Introduction Transforming growth factor beta1 (TGFb1), a multifunctional cytokine, has antiproliferative and/or proapoptotic effect on lymphoid cells. The continuously proliferating lymphoma cells could be resistant to the endogenously produced TGFb1. Aims: To study the responsiveness of lymphoma cells using exogenously activated TGFb1.
Materials and methods The apoptotic effect and depolarization of the mitochondria was detected by flow cytometry, the different gene expression was studied by RT-PCR. The amount, the activity (Western blot) and the localization (confocal microscopy) of the signal elements (Smads, phoshpo-Smad2, Erk1/2, JNK, p38MAPK) and other proapoptotic and survival proteins (Bcl-2, Blc-xL, Bid, Bax, Bad, NFkB, phospho-IkB) were also studied. The role of PP2A phosphatase, MEK1 kinase and caspase activity was estimated by different inhibitors (endhothal, okadaic acid, PD980559, Z-VAD-fmk, Z-IETD-fmk, Z-LEHD-fmk) in vitro.
Results HT58 B cell lymphoma cells lost their sensitivity to the antiproliferative action of exogenous TGFb1, but the cells were killed by apoptosis. Smad2 phosphorylation, nuclear localization and the increased expression of TGFb1 induced early gene (TIEG) proved the rapid activation of Smad signal. The role of PP2A phosphatase activation followed by decreased expression of active phospho-JNK and phospho-Erk1/2 was supported by the antiapoptotic effect of PP2A inhibitors and the proapoptotic effect of specific MEK1 inhibitor. The Apoptosis was induced primarily through the mitochondrial pathway. It seems that both main iniciator caspases (caspase 8 and 9) took part in the apoptotic response.
Conclusion These data suggest that exogenous TGFb1 had double but interrelated actions on HT58 cells: a) suppression the survival signals produced by protein kinases, which b) allowed the Smads to induce apoptosis. Therefore, it is possible that the lost sensitivity of malignant lymphoid cells to proapoptotic regulators (such as TGFb1) could be reactivated especially by lowering the survival threshold. The work was supported by OTKA (T034892), ETT (192/2000,193/2000), FKFP (0150/2001) and Békésy foundation (118/2001).

P-351

Clinicopathological study of chromosome 7 abnormality related hematological disorders

M Ito[1], R Ichihashi[1], K Kitamura[2], I Sugiura[3], H Kosugi[4]
[1]Department of Pathology, Nagoya University Hospital, Nagoya, Japan
[2]Department of Hematology, Ichinomiya Municipal Hospital, Nagoya, Japan
[3]Department of Hematology, Toyohashi Municipal Hospital, Nagoya, Japan
[4]Department of Hematology, Ohgaki Municipal Hospital, Nagoya, Japan

Introduction Cytogenetic abnormalities sometimes determine the subtype of hematological disorders and are common in myelodysplastic syndromes (MDS). Although chromosome 7 abnormality is frequently observed in MDS, the specific characters of this type are not determined. In this study, we examined the clinicopathological characters of hematological disorders associated with chromosome 7 abnormality. Aim of this study is to assess whether these disorders are classified in special subtype or not.
Materials and methods We selected 54 hematological disorder cases with chromosome 7 abnormality from the bone marrow files of the Department of Pathology, Nagoya University Hospital. Clot sections of aspirated bone marrow were examined histopathologically. Immunohistochemical study was performed using paraffin embedded tissues.
Results 27 patients, 40 males and 14 femals respectively, with monosomy 7, 11 with der (1;7) and 16 with other abnormalities were studied.The median age of the patients was 65.5 years (range, 16-82 years). Pancytopenia was observed in 28, bicytopenia in 7 and monocytopenia in 11 cases. Past history of aplastic anemia was in 7 cases. Histopathologically, they were 40 cases of MDS, 7 of AML, 2 in ALL and 5 of others. Hypoplastic MDS (<40% cellularity) were found in18 cases, 2 of RA, 9 of RAEB, 6 of RAEB-t and 1 case of MDS with fibrosis. All cases of acute leukemia had dysplastic multi-lineage features other than blasts. Histopathological characteristics were weak erythroid dysplasia, increased micromegakaryocytes and hypocellular tendency. These characteristcs were common in patients with monosomy 7 and other abnormalities.
Concusion Hematological disorders with chromosome 7 abnormalities share similar clinicopathological characteristics.

P-352

Expression of topoisomerase I and topoisomerase II alpha as an independent prognostic factor and evaluation of the overall survival in NHL

E Catalano
Cooper Hospital/University Medical Center, Camden, USA

Introduction Topoisomerase II Alpha and Topoisomerase I (Topo I and II alpha) are the key targets for some anti-cancerous drugs that inhibit these enzymes. The purpose of this paper is to examine the expression of Topo I and Topo II alpha in different types and stages of NHL's the response of treatment with the overall survival.
Materials and methods Immunohistochemistry techniques with anti-topo I and topo II alpha were used. The results were evaluated with a semi-quantitative method.
Results and conclusion 30 cases were studied with topo I and topo II alpha. We include 21% of follicular lymphomas, 61% diffuse, 16% follicular and diffuse and high grade 2%. The stage of these tumors were stage I, 16%; stage II, 8%; stage III 18%; stage IV, 22%. The results show a higher intensity expression of the topo II alpha, and topo I indices, in the higher grade NHL. There appears to be a similar expression between the intermedium and indolent NHL. The survival indicates that the large cell NHL's show a higher response rate and better survival than the mixed or small cell type. The expression of these two enzymes may be useful for selecting the appropriate chemotherapy in NHL. Our data, although small, suggests an excellent correlation in response to treatment and longer survival in the NHL that have a high expression of topo I and topo II alpha.

P-353

Mantle cell lymphoma (MCL): Ki-67 antigen and chromosome 12 ploidy in an estimate of the tumor progression

R Kodet[1], M Mrhalova[1], L Krskova[1], J Soukup[1], V Campr[1], P Szepe[2], L Plank[2], K Kubackova[3]
[1]Department of Pathology and Molecular Medicine, 2nd School of Medicine, Charles University, Prague, Czech Republic
[2]Department of Pathology, Jessenius Medical School, Komensky University, Martin, Slovak Republic
[3]Department of Oncology, 2nd School of Medicine, Charles University, Prague, Czech Republic

Introduction MCL belongs to prognostically unfavorable lymphomas. However, the behavior may vary and it is difficult to predict it. A more aggressive course tends to be associated with blastic and anaplastic subtypes. Numerical chromosomal changes and proliferative activity may be of importance to improve the prediction. Aims: Risk of the tumor progression with the assessment of Ki-67 antigen-positive cell count and ploidy status of chromosome 12.
Materials and methods 44 patients with MCL characterized by t(11;14)(q13;q32) and by overexpression of cyclin D1. The proliferative activity was evaluated immunohistochemically (IHC) by double staining for Ki-67 antigen and CD20 (to rule out counting admixed Ki-67 positive T-lymphocytes). Ploidy status of chromosome 12 was evaluated by interphasic FISH.
Results and conclusion Trisomy and polysomy of chromosome 12 (9 patients) was associated with blastic/anaplastic forms of MCL with the same frequency as with the common variant. A finding of >30% Ki-67 and CD20 positive cells was associated with the blastic variant of the disease – 7 patients. Of them 5 died of the disease progression, one of unrelated cause and one is alive with the disease. Of the remaining 23 patients in whom the follow up was available, 2 died of the tumor, and the proliferative activity, measured by counting the Ki-67 positive cells was <15%. The assessment of proliferative activity with immunohistochemical demonstration of Ki-67 antigen seems to be useful in prediction of clinical behavior of MCL
Supported by IGA-MZCR-NC/6296-3, Research Project FN-Motol/6073.

P-354

Morphological criteria for differentiation of lymphocyte predominance Hodgkin's lymphoma from lymphocyte-rich classical Hodgkin's lymphoma

A Kovrigina, N Probatova
Cancer Research Center, Moscow, Russian Federation

Aims To reveal morphological features of differential diagnosis between lymphocyte rich classical Hodgkin's lymphoma (LRCHL) and nodular lymphoid predominance (NLPHL).
Materials and methods Retrospective analysis of 20 lymph node biopsies (age 3-69) with histological diagnosis of "nodular paragranuloma" or "Hodgkin's disease, lymphocytic and histiocytic variant". Immunological data were available in all cases. All patients presented with the early stages of disease. We used the following morphological criteria: growth patterns (nodular, nodular-diffuse or diffuse), distribution and cytomorphology of tumor cells ("popcorn", lacunar, classical, mummified cells), cellular composition of reactive background, presence or absence of secondary and atrophic follicles. The results of morphological algorithm were compared with immunology data in every case.
Results Among 20 biopsies,4 cases (20%) were classified as NLPHL. 16 cases were attributed to LRCHL, including 3 cases which were characterized by interfollicular sheets of cells resembling lacunar cells ("cellular phase of nodular sclerosis"), 3 cases had rare classical cells within expanded mantle zone ("follicular variant" of Hodgkin's disease). All 16 cases LRCHL exhibited secondary follicles. There were no cases of LRCHL with "pure" diffuse growth type; both NLPHL and LRCHL had nodular or nodular and diffuse pattern. 20 cases corresponded morphologically to NLPHL or LRCHL and this division was confirmed with immunological analysis..
Conclusion We proposed the algorithm of morphological criteria for differentiation of NLPHL from LRCHL

P-355

Bone marrow sinusoids in acute lymphoblastic leukemia (ALL)

V Rugal
Russian Institute Hematology, St.Petersburg, Russian Federation

Introduction Bone marrow sinusoids regulate the development of hemopoietic precursors and migration of stem cells and mature blood cells in blood stream. The purpose of the investigation was to study endothelium of bone marrow sinusoids in disordered hemopoiesis in ALL.

Materials and methods Pretreatment bone marrow trephine biopsy sections from 30 patients with ALL were studied using morphometric and ultrastructural methods.
Results Development of myelosuppression in ALL was accompanied by considerable changes in the morpho-functional status of sinusoid endothelium. Most vessels became thinned, endothelial cells were flattened. In such vessels cells of endothelium came apart with formation of gaps between cells. The basement membrane was interrupted. However, blast migration continued to be transendothelial. There were vessels in which the structure of endothelial cells was identical to that of blast cells. There were no signs of endo- and exocytosis in such cells. Intranuclear virus-like inclusions were found in endothelial cells of sinusoids of patients with ALL.
Conclusion The above data suggest the involvement of endothelial cells in the disordered haemopoiesis in ALL. Defects of the bone marrow sinusoids in leukemia can be the cause of the early release of blasts into circulation. Blast transformation of endothelial cells does not contradict the suggestion about existence of a common cell precursors of the endothelial and hemopoietic cells.

P-356

Complex diagnosis of follicular lymphomas

E Toth, E Csernak, Z Melegh, N Udvarhelyi, T Schneider, A Rosta, Z Szentirmay
National Institute of Oncology, Budapest, Hungary

Introduction The second most common type of non-Hodgkin lymphomas is follicular lymphoma (FL). Moreover, follicular lymphomas are the most common type of the low grade lymphomas. In Hungary they comprise about 15-20% of all the lymphomas but its occurrence shows increasing tendency. Our aim was to survey and revise FLs diagnosed in the last 10 years in the National Institute of Oncology. We studied the diagnostic relevance of histology, immunohistochemistry and the detection of immunoglobulin heavy chain (IgH) and bcl-2 gene rearrangements.
Materials and methods We surveyed 52 cases which were diagnosed as follicular or centrocytic, centroblastic lymphoma before. After the histological re-examination immunohistochemistry (CD20, CD3, bcl-2, CD10, bcl-6, CD5, p53, cyclin D1 and Ki-67) was performed on each case. We studied the IgH and bcl-2 (MBR) gene rearrangement both with conventional and real-time PCR methods from the paraffin embedded blocks. The classification was made according to the new WHO classification.
Results After the revision of the 52 cases we found 36 follicular, 11 diffuse large B-cell, 1 mantle cell and 1 marginal zone lymphoma, 2 paragranulomas and 2 follicular hyperplasias. The grade of the FLs showed relation to the expression of different antigens. CD10 and bcl-2 expression decreased with the grade. p53 expression was very rare and occurred only in grade 3 cases. The proliferation index with Ki-67 showed good correlation with the grade of FLs. The IgH showed 3 types of pattern: monoclonal, polyclonal and a sharp line in a polyclonal background. Grade 3 and grade 1-2 FLs were monoclonal almost in the same ratio. We could detect bcl-2 gene rearrangement in 55% of the FLs (72% grade1-2, 30% grade3). All the grade 3 cases which showed bcl-2 gene rearrangement belonged to grade 3a group while all the grade 3b cases were negative.
Conclusion In agreement with others we found that grade 1, 2 and 3a FLs showed similar morphological, immunohistochemical and genetical features while gr3b FLs are more similar to diffuse large B-cell lymphomas. Considering the diagnostic relevance of the different methods we can conclude that histology alone is not sufficient. 84% of our cases were solvable with the help of immunohistochemistry and in 10% of the cases the diagnosis based on the molecular pathological results. In the remaining 6 % even with the help of all diagnostic tools no unambiguous diagnosis could be reached.

P-357

Prognostic significance of angiogenesis, apoptosis and proliferation in B cell lymphomas

E Ozel[1], B Kilicarslan Akkaya[1], H Bekoz[2], A Ugur[2], KH Gulkesen[3], S Karakaya[1], L Undar[2], G Karpuzoglu[1]
[1]Akdeniz University School of Medicine Department of Pathology, Antalya, Turkey
[2]Akdeniz University School of Medicine Department of Haematology, Antalya, Turkey
[3]Akdeniz University School of Medicine Department of Biostatistics, Antalya, Turkey

Introduction The bcl-2 and p53 oncoproteins play important roles in carcinogenesis. Mutation of the p53 gene is considered the most common genetic aberration in many cancers including hematologic malignancies. Ki-67, a proliferation antigen, evaluates the proliferative activity of a lesion. Angiogenesis is also critical for tumor proliferation and has a prognostic value. The vascular density of tumor directly correlates with poor outcome in many malignancies. The aim of this study was to investigate correlation between Ki-67, p53 and bcl-2 immunostaining in B cell lymphomas and to identify any relation between these markers and microvessel density (mvd) and histopathological parameters including stage and tumor grade.
Materials and methods 19 low grade and 35 high grade non-Hodgkin lymphomas (NHL) were immunohistocemically stained with p53, Ki-67, bcl-2 and Factor VIII. The results were analysed statistically.
Results There was no correlation between stage and Ki-67 LI, mvd, p53 and bcl-2 expression. The cases which showed immunoreactivity for bcl-2 had decreased mvd counts compared with the cases negative for bcl-2. p53 immunoreactivity was correlated with mvd. Microvessel counts were significantly higher in patients with high grade NHLs. Statistical analysis showed association between Ki-67 LI, p53, bcl-2 expression, mvd and histological grade.
Conclusions The levels of Ki-67, bcl-2 and p53 expression and microvessel counts were closely related with the grade of NHLs. Our findings suggest that apoptosis, angiogenesis and proliferative activity can be used as prognostic indicators in NHLs.

P-358

Diffuse large B-cell lymphoma of the maxillary sinus complicated with Blastomycotic leptomeningitis

G Petrusevska[1], A Stojanovic[2], L Hagi-Pecova[2]
[1]Institute of Pathology, Faculty of Medicine, Skopje, Republic of Macedonia
[2]Clinic for Hematology, Clinical Center, Skopje, Republic of Macedonia

Introduction Sometimes a Non-Hodgkin's lymphoma presents as an isolated mass in the fossa canina, just anterior to the maxillary

sinus; however such a lesion is more likely to arise from an infraorbital lymph node, part of the facial lymph node group.
Case presentation We present a patient with diagnosed diffuse large B cell lymphoma of the maxillary sinus as well as involvement of the infraorbital region, who suffered from infective complications. 39-years old male was admitted at the Clinic of hematology because of tumor mass in nasal cavity. CT-scan showed tumor mass filling right maxillary sinus. Surgical biopsy was done. Histochemical and immunohisto-chemical findings suggested a diagnosis of diffuse large B cell lymphoma. Other clinical investigations showed I-E clinical stage. Treatment with four cycles of CHOP and Mab-Thera followed. After that adjuvant radiotherapy was delivered. Because of increased body temperature and meningeal symptoms, this therapy was interrupted. Microbiological investigations showed positive hemoculture for Escherichia coli and Staphylococcus aureus, and positive finding of Blastomyces in cerebrospinal fluid, while serological analyses revealed positivity for CMV and EBV. Beside severe antibiotic, antimycotic and antiviral treatment, the patient suffered from sepsis with main features of suppurative leptomeningitis and acute hepatitis.
Conclusion This case implies the conclusion that the clinicians should have in mind the possible presence of immune disregulation in patients with NHL, that could complicate the administered chemotherapy and radiotherapy.

P-359

Non-Hodgkin's lymphomas of head and neck in Macedonia classified accordingly to the WHO classification of lymphoid neoplasms

G Petrusevska[1], A Stojanovic[2], L Hagi-Pecova[2], B Georgievski[2], P Cvetkovski[1], S Banev[1], M Tolovska[1], V Janevska[1], L Spasevska[1], S Duganovska[1]
[1]Institute of Pathology, Faculty of Medicine, Skopje, Republic of Macedonia
[2]Clinic for Hematology, Clinical Center, Skopje, Republic of Macedonia

Aim The aim of this study is to determine the most frequent pattern of involvement by NHL of head and neck and to correlate it with clinical outcome of the disease.
Material and methods A retrospective review was performed on 190 patients with NHL during five years period. Paraffin sections stained with standard histochemical and immunohistochemical stainings were histologically analyzed for classification of the NHL accordingly to the WHO classification of lymphoid neoplasms. Clinical histories were used for clinical follow-up.
Results In fifty cases out of 190 patients with NHL the disease was primary localized in the head and neck region. Male-female ratio was 1,5. Twenty four cases were primarily nodal, 22 primarily extranodal and 4 had extranodal/nodal expression of the disease. Diffuse large B cell lymphoma comprised 40% of the group: 8 nodal, 11 extranodal and 1 extranodal/nodal. Three of these cases were CD30+ and ALK-1 -. Six cases (12%) with B-CLL NHL had nodal manifestation. MALT-zone lymphoma (12%) showed extranodal involvement in 4 cases and extranodal/nodal in 2 cases. B-lymphoblastic lymphoma (12%) showed 4 cases with nodal, one extranodal and one extranodal/nodal involvement. Two cases with Burkitt's lymphoma (4) had typical mandibular localization. Follicular lymphoma comprised 8%, with two nodal and two extranodal involvement. T cell NHL-s comprised 10% of the group with three nodal, one extranodal and one extranodal/nodal involvement.
Conclusion There was no significant predilection for clinical expression of the NHL of head and neck, and no difference between the mean survival of the groups for these parameter.

P-360

Expression of the bcl-2 family proteins, caspase 3 (CPP32) and poly adp-ribose polymerase (PARP-1) in multiple myelomas

V Zolota[1], M Melachrinou[1], I Xagoraris[2], A Mouzaki[2], P Aroukatos[1], D Koumoundourou[1], DS Bonikos[1]
[1]Dept. Pathology, Univ. Patras Med. School, Patras, Greece
[2]Dept. Laboratory Hematology and Transfusion Medicine, Univ. Patras Med. School, Patras, Greece

Introduction Multiple myeloma (MM) is a malignancy of the bone marrow characterized by the clonal expansion of plasma cells with low proliferative activity. Aberrant expression of genes regulating apoptosis/survival seems to be essential in the development of multiple myeloma. The aim of this study was to investigate the immunohistochemical expression apoptosis-regulating proteins in bone marrow of patients with initially presented multiple myeloma.
Methods The expression of bcl-2, mcl-1, bak, bax, CPP32 and PARP was examined on paraffin sections of 36 bone marrow biopsies obtained from equal number of patients with newly diagnosed MM, using commercially available monoclonal and polyclonal antibodies and LSAB technique. Specimens containing >10% immunostained tumor cells were considered positive.
Results Bcl-2, bak and bax positive immunostaining was detected in 94%, 100% and 94% of cases respectively. Most positive tumors showed high percentage of tumor cells immunoreactive for the above proteins: >50% for bcl-2, >80% for bak and >60% for bax. The mean value for bcl-2/bax ratio was 1.66, and the mean bcl-2/bak ratio was 0.95. Mcl-1 expression was detected in a small percentage of tumors (17%). Cytoplasmic expression of CPP32 was observed in 8,3% of cases and the number of positive cells was low. Nuclear expression of PARP was seen in 44,5% of cases and no association was found with the other apoptosis-related antigens, bcl-2/bax or bcl-2/bak ratio.
Conclusion The above data demonstrate an overexpression of bcl-2, bax and bak in myeloma plasma cells and an increased bcl-2/bax ratio. CPP32 does not seem to mediate any apoptotic event in MMs. The role of overexpression of PARP remains to be elucidated.

P-361

Immunoexpression of bcl-2 family members, p53, caspase 3 (CPP32), and poly adp-ribose polymerase (PARP-1) in diffuse large B-cell lymphomas

M Melachrinou[1], V Zolota[1], P Matsouka[2], A Symeonidis[2], D Koumoundourou[1], P Aroukatos[1], DS Bonikos[1]
[1]Dept. Pathology, Univ. Patras Med. School, Patras, Greece
[2]Dept. Internal Medicine, Division of Hematology, Univ. Patras Med. School, Patras, Greece

Introduction Diffuse large B-cell lymphomas (DLBCL) represent a biologically and clinically heterogeneous group. Although these tumors are curable with chemotherapy, their response to treatment varies. Apoptosis-related proteins may play an important role in the

chemosensitivity or chemoresistance of tumors. The aim of this study was to investigate if the expression of apoptosis-regulating proteins in DLBCL could be indicative of tumor chemosensitivity.
Methods Formalin-fixed, paraffin-embedded tissue from 58 cases of DLBCL [29 nodal, 27 extranodal, 2 splenic (42 centroblastic, 2 immunoblastic, 2 Burkitt's-like, 2 anaplastic, 1 TCRBCL, 9 primary mediastinal)] were immunostained with monoclonal [bcl-2 (DAKO), mcl-1, CPP32 (Neomarkers), p53 (Biogenex)] and polyclonal [Bax, Bak (DAKO), PARP (Neomarkers)] antibodies using LSAB method. Specimens containing >10% immunostained tumor cells were considered positive. Clinical data were available for 44 cases (30 chemosensitive, 14 chemoresistant).
Results Bcl-2, mcl-1, bax, bak, p53, CPP32 and PARP positive immunostaining was detected in 68.9%, 85.9%, 84.2%, 100%, 75.8%, 57.8% and 89.4% of cases, respectively. Mcl-1, bax, bak and PARP were overexpressed in >80% of tumor cells in most cases. There was a significant association between the expression of bcl-2 and mcl-1 ($p = 0.004$). A higher immunoexpression of bcl-2 (78.5% vs 63.3%), mcl-1 (92.8% vs 80%), bax (92.8% vs 80%), p53 (92.8% vs 70%) and CPP32 (69.2% vs 60%) was observed in chemoresistant cases. PARR expression was higher in chemosensitive cases (93.3% vs 84.6%). In the p53-negative group of cases (14 cases) those with a strong (3+) PARP expression showed a significant better response to treatment ($p = 0.0016$). A significant chemosensitivity was also detected in the group (8 cases) with strong (3+) bax and weak (+) or negative (-) p53 immunostaining ($p = 0.028$).
Conclusion Apoptosis-related proteins, though overexpressed in DLBCL, were not associated with response to treatment. A p53(-)/PARP(3+) or p53(+ or -)/bax(3+) tumor status may reflect sensitivity to chemotherapy.

P-362

Bcl-2 expression and apoptosis in non Hodgkin lymphomas

S Stifter[1], A Duletić-Naeinović[2], M Sever-Prebilić[2], K Lućin[1], N Jonjić[1]
[1]Department of Pathology, Medical Faculty, Rijeka, Croatia
[2]Department of Internal medicine Hematology, Clinical Hospital Center of Rijeka, Croatia

Introduction Non-Hodgkin lymphomas (NHL) are a heterogenous group of lymphoid malignancies classified according to their morphological, immunophenotypical and genotypical characteristics as well as their clinical behaviour. However, the progression of these diseases may be influenced by various others factors such as apoptosis, proliferation and angiogenesis. Aim: A possible correlation between Bcl-2 expression, apoptosis, disease outcome and overall survival in patients with NHL was analysed.
Material and methods 72 NHL devided in low- (N=29) and high-grade (N=43) were immunohistochemicaly analysed for Bcl-2 expression, while 12 low- and 12 high-grade NHL were procesed for terminate TdT mediated dUTP nick end labeling (TUNEL) method in order to determine the apoptotic index of tumor cells. Results were obtained by image analyser and statistically processed.
Results The expression of Bcl-2 protein, as an antiapoptotic marker was significantly higher in low- compared to high-grade NHL, $p=0.024$, whereas the apoptotic index obtained with the TUNEL method demonstrated inverse results, $p<0.001$. In high-grade NHL, partial remission was observed in patients whose tumors expressed significantly higher values of Bcl-2, ($p=0.03$), while complete remission was observed in a group with a lower expression of Bcl-2. Furthermore, patients with lower Bcl-2 expression showed longer overall survival $p=0.02$, whereas patients with a higher apoptotic index showed shorter survival, $p<0.001$. In both low and high-grade groups of NHL, Bcl-2 has been found as an independent predictor of patients disease relaps, $p< 0.05$.
Conclusion The expression of Bcl-2 is a strong independent predictor of disease progression in NHL patients.

P-363

The heterogeneity of anaplastic large cell lymphomas (ALCL)

O Mederle, M Raica
Dept. of Histology and Cytology, University of Medicine and Pharmacy, Timisoara, Romania

Introduction The aim of this study was to investigate the expression of CD30 and the distribution of the reticular network on the ALCL.
Material and methods Twelve cases of lymphomas were analyzed using morphologic and immunophenotypic features.
Results The patients (7 male and 5 female) were from 5 to 50 years. Five patients presented with generalized lymphadenopathy and seven with involvement of extranodal sites. ALCL was composed of large cells that grow in a diffuse pattern and involve the lymph node sinuses. The tumor cells have an abundant eosinophilic or pale cytoplasm. The nuclei were irregular with indentation, multilobated, round to oval. Multinucleated cells with wreath-like configurated nuclei were commonly seen. ALCL cells may closely resemble cells of malignant histiocytosis. Additional features include Reed–Sternberg-like cells, reactive infiltrate, partial lymph node involvement with localization of tumor cells in the paracortical region resembling Hodgkin's diseases. Tumor cells are CD30 +. The regular expression of CD30 antigen in both carcinoma and ALCL (both are anaplastic large cell tumors) has important implication for the differential diagnosis of these tumors. Leukocyte common antigen (CD45) positivity excludes an embryonal or any other non-hematopoietic tumor, but its absence does not rule out ALCL (a significant portion of ALCL are CD45 negative). Antibodies to cytokeratin label embryonal carcinoma but not ALCL. Thus, if cytokeratin is expressed in an anaplastic large cell tumor simultaneously with CD30 antigen, it is most likely to be an embryonal carcinoma
Conclusion This study confirms the view that ALCL are heterogeneous group of lymphomas and the CD30 is a useful marker for the diagnosis.

P-364

Leiomyosarcoma of the Meckel's diverticulum. Synchronous occurence with B-chronic lymphocytic leukemia. A case report

R Jovanovic[1], G Petrusevska[1], A Stojanovich[2], G Damjanovski[3], K Vasilevska[4], M Nikolovski[1]
[1]Institute of Pathology, Faculty of Medicine, Skopje, Republic of Macedonia
[2]Clinic for Hematology, Clinical Center, Skopje, Republic of Macedonia
[3]Institute for Radiology, Clinical Center, Skopje, Republic of Macedonia
[4]Clinic for Surgery 'Sv. Naum Ohridski' General City Hospital, Skopje, Republic of Macedonia

We describe a 66-years-old male developing a well differentiated leiomyosarcoma of the Meckel's diverticulum synchronously with B-CLL. The patient suffering disuria and malaise was admitted at the Clinic for Surgery. Clinical examinations showed leucocytosis (14.1x109/L) with lymphocytosis (56%), anemia (Hgb = 113 g/L) and thrombocytosis (473x109/L). CT-scan found a tumor mass near the urinary bladder and enlarged spleen. The FNAB from the tumor mass revealed neoplastic tissue composed of ribbons of spindle-shaped cells with hyperchromic and pleomorphic nuclei and variable amount of cytoplasm, surrounded by a fine reticulin network. Mitoses were rare (4-5 on HPMF). Immunohistochemistry showed positivity for SM-actin and desmin. S-100, CD31 and CD34 were negative. A leiomyosarcoma was diagnosed. Three weeks after the biopsy a large tumor mass (880g) from the vicinity of the urinary bladder was extracted, together with incidental Meckel's diverticulum. At the same time a splenectomy was performed because of splenomegaly (500g). Pathohistologic examination of the tumor mass confirmed the previous diagnosis, and the PCNA proliferative index was estimated to 35-40%. The analysis of the Meckel's diverticulum revealed a disturbance of the muscular layer structure caused by a tumor proliferation with the same histological features, infiltrating into the serosa. The pathohistologic examination of the extracted spleen showed partially presence of B-CLL infiltration (monoclonal positivity for lambda-light chains, CD20, CD79, CD5, CD43). Follow-up shows that the patient is in Binet A stage, and still in a good shape without any further treatment. It remains unclear which of the neoplasms developed first.

P-365

Composite low grade B cell lymphomas: Report of three cases

C Romagosa, L Colomo, V Morente, M Garrido, D Colomer, A López-Guillermo, A Palacin, E Campo
Hematopathology Section, Hospital Clínic, Institut de Recerca Biomčdica August Pi i Sunyer (IDIBAPS), University de Barcelona, Barcelona, Spain.

Introduction Synchronous composite low grade B-cell lymphomas involving the same site is rare and few cases have been reported. We describe three cases of composite lymphoma.
Material and methods Histological, immunohistochemical and molecular study.
Results The three neoplasms showed different morphological and phenotypic areas: Case 1. 64 years-old female with large splenomegaly. The splenectomy showed a blastoid mantle cell lymphoma (MCL) with nodular pattern, positive to CD20, CD79a, CD5, CD43 and cyclin D1, and a splenic marginal zone B-cell lymphoma CD20, CD79a and IgD. The MCL progressed, with liver and bone marrow involvement, treatment failure and death 8 months after diagnosis. Case 2. 75 years-old female with cervical and inguinal lymphadenopathy. A nodular MCL CD20, CD5 and cyclin-D1 positive, p27 negative, was observed. The internodular areas demonstrated a small lymphocytic lymphoma (SLL) expressing CD20, CD79a, CD5, CD23, and p27. Progression to peripheral blood involvement of SLL, and gastric and nodal relapses of MCL two and four years after diagnosis. Case 3. 51 years-old female with nodal follicular lymphoma expressing CD20, CD10, Bcl-2, IgD-kappa restriction. The internodular areas showed a lymphocytic lymphoma with plasmacelular differentiation, CD20, CD79a, CD23, IgD, and bcl-2 positive. IgH showed a biallelic arrangement, and bcl-2/JH rearrangement was obtained, suggesting the presence of two different clones. Alive with disease after first chemotherapy cycle.
Conclusion Morphology and immunophenotypic profiles may allow the identification of each component in composite lymphoma. Molecular studies can recognize different clones originating the neoplastic compartments.

P-366

Malignant B-cell lymphomas non-associated with Epstein-Barr virus (EBV) infection in angioimmunoblastic T-cell lymphoma (AITL)

V Morente[1], L Colomo[1], C Romagosa[1], E Roselló[2], D Colomer[1], A Palacín[1], E Campo[1]
[1]Hospital Clinic de Barcelona, Spain
[2]Hospital Dr. Peset Valencia, Spain

Introduction AITL accounts for about 20% of peripheral T-cell lymphomas (PTCL), presents with advanced stages at diagnosis and follows aggressive clinical course. In 10-40% of cases oligoclonal or monoclonal B-cell populations are detected, usually associated with EBV infection. We describe three cases of AITL with clonal B-cell lymphoma non-related to EBV infection.
Material and methods Histological, immunophenotypical, including EBV (LMP-1, EBERs), and molecular study.
Results Three cases of AITL in three female, 66, 69 and 77 year-old patients were diagnosed. All of them showed atypical lymphocytes with aberrant T-cell phenotype (CD3/CD5+ with loss of CD7), associated with vascular and dendritic proliferation, the latter showing T-cells CD10+. In addition, a population of B-cells with plasmacelular differentiation and immunoglobulin light chain restriction (1 kappa/2 lambda) was identified. EBV was not demonstrated in these populations. TCRgamma and IgH clonality was observed in two cases. The first patient presented isolated nodal AITL involvement, and she is in complete remission after chemotherapy six months after diagnosis. The second patient presented nodal AITL and developed skin involvement two months after the diagnosis. The third patient presented with an atypical ganglionar T-cell proliferation, developing cutaneous PTCL with associated clonal B-cell proliferation one year later and ganglionar PTCL with AILT features two years after the first biopsy. The three biopsies showed identical TCRgamma gene rearrangements in this case.
Conclusion AITL can show different morphological patterns. Alternative mechanisms non-related to EBV infection may be involved in the development of B-cell lymphomas in AITL.

P-367

Pregranulomatous phase of sarcoidosis: immunohistochemical diagnosis?

K Jaskiewicz
Dept. of Pathology, Gdansk, Poland

Introduction Histopathological confirmation of clinical suspicion of sarcoidosis is based on finding of non-caseating granulomas in biopsy material, usually in prescalene lymph nodes. Reactive sinus histiocytosis seen in relation to various inflammatory and non-inflammatory diseases can mimic pregranulomatous phase of sarcoidosis. Differentiation of sinus histiocytosis based on histopathological features alone can be impossible. Aim of this study is immunohistochemical determination of lymph node cellular

response in granulomatous sarcoidosis, pregranulomatous phase of sarcoidosis and reactive sinus histiocytosis using panel of antibodies.
Materials and methods Patient groups under study, each contained 25 patients include those with clinical and histopathological picture of sarcoidosis; the group of patients with clinical picture of sarcoidosis and histologically detectable sinus histiocytosis without granuloma formation and finally, the group free of clinical suspicion of sarcoidosis with 'reactive' sinus histiocytois in lymph nodes. Lymph node biopsy tissue processed routinely and stained immunohistochemically using triple-layer APAAP protocol with purified antibodies SP 70 and SP90 from Mycobacterium tuberculosis and monoclonal antibodies CD22, CD4, CD8, CD56, CD68. Intensity of immunostaining assessed semiquantitatively by two independent observers using the scale from 0 to 4+
Results An increased CD4:CD8 ratio, moderate increase of immunopositivity of CD68 and slight decrease of immunopositivity of CD20, CD56, and SP90 noted in PSH when compared with RSH. The most notable difference between studied groups is the intensity of immunostaining with SP70 and CD4 antibodies.
Conclusion Both immunostainings were more intense in lymph nodes with sarcoid granulomas and pregranulomatous sinus histiocytosis and can be used in differentiation of these lesions.

P-368

Haemophagocytic syndrome followed by a large B-cell lymphoma showing only bone marrow involvement: Case report

S Barbanis[1], V Kaloutsi[1], E Katodritou[2], C Hadjileontis[1], E Panoussi[1], C Papadimitriou[1]
[1]Department of Pathology Aristotle University-Medical School, Thessaloniki, Greece
[2]Department of Haematology Papageorgiou Hospital, Thessaloniki, Greece

Haemophagocytic syndrome (HPS) is a rare disease characterized by generalized histiocytic proliferation showing phagocytosis of hematopoietic cells. It occurs mainly in adults associated either with an acute viral infection, or with non-Hodgkin's lymphomas. The latter are usually T- or NK-cell lymphomas. The present case concerns a patient with HPS followed by a large B-cell lymphoma showing only bone marrow involvement. This constellation is extremely rare in Western countries and has been reported mainly in Asia. The patient was a 60 year old male admitted for persistent fever. Peripheral blood examination showed pancytopenia. Bone marrow biopsy showed haemophagocytosis by proliferating macrophages often situated into dilated marrow sinusoids. No viral infection was detected. The patient was treated with haemopoietic growth factors and showed improvement. After 6 months his blood cell count began to fall again and a second bone marrow biopsy showed, apart from haemophagocytosis, a focal, mainly intra-sinusoidal, infiltration by large B-cell lymphoma cells immunopositive for CD20 and CD45RA. Epstein-Barr virus RNA was not detected. Dissemination of lymphoma to other sites was not apparent. The patient was treated with 6 cycles of CHOP and Mab-Thera and showed remission. Some authors believe that these rare cases represent a peculiar "Asian" variant of intravascular lymphoma characterized by HPS and early involvement of bone marrow without dissemination to other organs. This variant has a poor prognosis and might constitute a distinct biological and clinical disease entity which merits separate consideration because of the problems posed in the initial diagnosis and therapeutic approaches.

P-369

Nodular type of mycosis fungoides. A case report

L Macukanovic-Golubovic[1], V Katic[2], D Dimov[2], L Spalevic[3], M Paravina[3], M Krstic[2], M Milenovic[1], M Pavlovic[1], G Stoiljkovic[1], A Petrovic[4]
[1]Clinic of Hematology, Nis, Serbia and Montenegro
[2]Institute of Pathology, Nis, Serbia and Montenegro
[3]Clinic of Dermatovenerology, Nis, Serbia and Montenegro
[4]Institute of Histology and Embryology, Nis, Serbia and Montenegro

Introduction Mycosis fungoides is a mature T-cell lymphoma presenting in the skin and characterised by epidermal and dermal infiltration of small to medium size T-cell with cerebriform nuclei. It is a rare disease wich accounts for no more than 0,5% of all non Hodgkin lymphomas.
Case report A 82 year-old man was refered to the Clinic of hematology because of the nodular red dermal tumours on the trunk. These lesions persisted for one year. The blood and bone marrow had not been involved. Lymph nodes were normal. The patient had the so called d' emblee lesions, presenting with skin tumours to 2 cm of diameter. The initial diagnostic lesions were rare limited patches and plaques. Extracutaneous dissemination did not occur. Formaldehyde fixed and paraffin embedded histological sections, taken from 4 surgically resected skin tumours, were stained with HE, Giemsa, trichrome and immunohistochemical stains. Morphology: Epidermotropic infiltrates consisted of medium size cells with cerebriform nuclei. A minority of larger cells with similar nuceli and with many mitotic figures also were present. So called Pautrier microabscesses consisted of aggregates of cerebriform cells in the epidermis (highly caracteristic for Mycosis fungoides) were numerous. In the dermis, infiltrates were band like and diffuse, associated with inflammatory infiltrate consisting of small lymphocytes and eosinophils.
Conclusions In spite of the presence of bad prognostic factors (very old patients, extent of disease and tumorous form) he had a very indolent course of the disease. The role of the observed inflammatory small lymphocytes and eosinophils is probably very important for the excellent prognosis of mycosis fungoides in this patient.

P-370

Low expression of p27 protein combined with altered p53 and Rb/p16 expression status is associated with increased expression of cyclin A and cyclin B1 in diffuse large B-cell lymphomas

D Papachristou[1], E Tsanou[1], S Dimou[1], K Grepi[1], V Galani[2], S Stefanaki[1], P Kanavaros[2], N Agnantis[1], M Bai[1]
[1]University of Ioannina, School of Medicine, Department of Pathology, Ioannina, Greece
[2]University of Ioannina, School of Medicine, Department of Anatomy-Histology-Embryology, Ioannina, Greece

Introduction Reduced p27 expression combined with alterations in Rb or p53 status, may have cooperative effects resulting in uncontrolled tumor cell proliferation and aggressive malignancies in experimental mouse models and in humans. The aim of this study was to investigate p27 expression in relation to a) the expression status of p53, Rb, p16, and b) proliferation profile (Ki67, cyclin A, cyclin B1).

Materials and method Expression of cell cycle regulating proteins was investigated immunohistichemically, in 80 cases of de novo Diffuse Large B-cell Lymphomas (DLBCL).
Results P27 expression was low/null in large tumor cells in 58/80 and intermediate/high in 22/80 cases. Increased expression of p53 was observed in 39/80 cases. Decreased expression of Rb/p16 was found in 5/80 and 14/80 cases, respectively. Low/null p27 expression was correlated to increased p53 expression (p=0.018). There was a correlation between increased p53 and decreased Rb/p16 expression levels (p=0.050). These findings suggest a tendency for concurrent alterations of cell cycle regulators p27, p53 and Rb/p16 in DLBCL, which might result in impaired tumor growth control. Indeed, combined p27/p53/Rb/p16 expression status analysis, with respect to proliferation profile showed that: 1) three alterations in the combined p27/p53/Rb/p16 status were correlated with increased expression of cyclin B1 (p=0.005) and 2) two or three alterations were correlated with increased expression of cyclin A (p=0.014).
Conclusions These findings suggest combined impairment of a complex cell-cycle control network involving the CDK inhibitor p27, as well as P53 and Rb1 pathways, which exerts a cooperative effect resulting in enhanced tumor cell proliferation.

P-371

Expression of cyclin D3 and cyclin E and identification of distinct clusters of proliferation and apoptosis in diffuse large B-cell lymphomas

S Kamina[1], M Bai[1], D Papachristou[1], E Tsanou[1], K Zioga[1], A Skyrlas[1], A Batistatou[1], V Galani[2], P Kanavaros[2], N Agnantis[1]
[1]University of Ioannina, School of Medicine, Departmentv of Pathology, Ioannina, Greece
[2]University of Ioannina, School of Medicine, Department of Anatomy-Histology-Embryology, Ioannina, Greece

Introduction The aim of this study was to examine a) cyclins D3, E and D1 expression in relation to other proliferative features (Ki67, cyclin A and cyclin B1), apoptosis status and p53, Rb, p16, p27 expression and b) whether distinct clusters of proliferation and apoptosis could be identified in DLBCL.
Materials and method Immunohistochemical expression of cell cycle regulating proteins were studed in seventy-nine cases of de novo Diffuse Large B-cell Lymphomas (DLBCL).
Results Overexpression of cyclins D3, E was found in 35/79 (43%) and 18/79 (22%) cases, respectively, whereas cyclin D1 was not detected. In 39/46 cases, overexpression of cyclins D3 and E was mutually exclusive, proposing different underlying pathways that induce deregulated expression of these cyclins. In 29/35 cases, cyclin D3 overexpression was equally exclusive with Rb/p16 aberrant expression status, supporting an oncogenic role for cyclin D3 and suggesting that pathogenetic effect of cyclin D3 overexpression occurs through perturbation of Rb1 pathway. Combined alterations of P53 and Rb/p16/cyclin D3 expression profile were significantly correlated to higher mean values of cyclins A (p=0.023) and B1 (p=0.033) indicating that concurrent impairment of p53 and Rb1 pathways induces increased tumor cell proliferation. Cluster analysis of apoptosis and proliferation status permitted separation of DLBCL into distinct groups with low and high apoptotic activity, as well as into groups with low, intermediate and high proliferative activity.
Conclusions In the present study, identification of separate groups with respect to proliferation and apoptosis profile indicates that groups with discrete cellular kinetic properties can be defined in the DLBCL population.

P-372

Immunohistochemical expression of p53, p21/waf1, Rb, p16, cyclin D1, p27, Ki67, cyclin A, cyclin B1, bcl2, bax and bak proteins and apoptotic index in normal thymus

A Papoudou-Bai[2], D Papachristou[1], M Doukas[1], K Grepi[1], V Galani[2], P Stefanaki, D Rontogianni[3], M Bai[1], N Agnantis[1], P Kanavaros[2]
[1]University of Ioannina, School of Medicine, Department of Pathology, Ioannina, Greece
[2]University of Ioannina, School of Medicine, Department of Anatomy-Histology-Embryology, Ioannina, Greece
[3]Athens, Evangelismos Hospital, Department of Pathology, Ioannina, Greece

Introduction Immunotopographical distribution of protein networks involved in cell-cycle and/or apoptosis regulation is useful in thymic histophysiology understanding. The aim of this study was to examine a) p53 and Rb1 growth control pathways, b) proliferation, c) apoptosis in relation with age.
Materials and methods P53, p21, Rb, p16, Ki67, p27, bcl2, bax, bak, cyclin D1, cyclin A, and cyclin B1 expression, and apoptotic index (AI) were investigated in 8 adult, 3 adolescent, 5 infant and 4 newborn normal thymuses, with immunohistochemistry.
Results and conclusions Rb, Ki67, cyclins A and B1 expression was elevated in cortex with a decreased tendency toward medulla. Apoptotic cells were mainly detected in cortex/corticomedullary junction, but rarely in Hassall's corpuscles. Mean values of Ki67 and cyclins A, B1 immunoreactivity were 77.2 %, 32.2%, 21.4% (newborns), 62.4%, 33.7%, 18.5% (infants), 56.9%, 23.4%, 18.9% (adolescents), 38.7%, 21.7%, 14.6% (adults), respectively. Mean values of AI were 1.4 %, 2.9%, 2.7%, 3.8 %, respectively. Most of Hassall's corpuscles were p16-positive. P16 expression paralleled aging, suggesting a role of p16 in cellular senescence. P27 was detectable within medulla, but not in subcapsular thymocytes Expressions of Ki67, cyclin A and cyclin B1 were inversely related to p27. P21 and p53 showed primarily subcapsular cortical epithelial cell localization. Our findings suggest: a) thymocyte apoptosis is mainly p53-independent, b) p21 function as negative cell cycle regulator seems redundant to other negative regulators (p16/27), and c) p21 expression is chiefly p53-independent. Hassall's corpuscles were p21-positive. Bcl2 was principally detected in medullary thymocytes. Expression of Bax/bak was widely distributed, suggesting an advanced role in thymic apoptosis, compared to bcl2.

P-373

Blastic MDS and AML - bone marrow biopsy findings versus clinical manifestation

L Plank[1], P Szépe[1], K Poliaková[2], Z Kviatkovská[1], P Kuchťáková[1], M Ševčíková[1], M Adamkov[1]
[1]Department of Pathol., Comenius University Medical Faculty, Martin, Slovakia
[2]Department of Pathology, Faculty Hospital Prešov, Slovakia

Introduction MDS represents a group of clonal hematopoietic stem cell disorders, which may progress to AML. According to WHO classification, the treshold of 20% blasts is recommended for the distinction of AML from MDS. The aim of this study was analysis of biopsy cases showing blastic proliferation and MDS patterns diagnosed in 1999-2002 to verify the percentage of blasts and the disease´s course.

Material and methods Paraffin-embedded bone marrow biopsies of 107 patients were examined by a standard panel approach and evaluated semiquantitatively. The course of the disease was recognized by evaluation of instrumentalized questionnaires.
Results a/ MDS with less than 20% of blasts (n=32) /either of myelo- (n=14), megaloblastic (n=9) or bilinear profile (n=9)/ - AML evolution appeared in 7% of patients, b/ MDS with more than 20% of myeloblasts (n=75) - AML diagnosis was established in 47% of cases.
Conclusion Although the therapeutical AML managment requires 'clinical verification', the identification of the MDS blastic proliferation higher than 20% is of a great clinical importance. However, the clinical manifestation of AML may be influenced by a delay of the increase of blasts in the peripheral blood.

P-374

Increased expression of the bcl6 and CD10 proteins is associated with increased apoptosis and proliferation in diffuse large B-cell lymphomas

M Bai[1], D Papachristou[1], A Skyrlas[1], E Tsanou[1], S Kamina[1], V Galani[2], V Kordela[1], P Kanavaros[2], N Agnantis[1]
[1]University of Ioannina, School of Medicine, Department of Pathology, Ioannina, Greece
[2]University of Ioannina, School of Medicine, Department of Anatomy-Histology-Embryology, Ioannina, Greece

Introduction There is increasing evidence that bcl6 and CD10 expression may be related to apoptosis and cell cycle progression.
Materials and methods To examine immunohistochemically the expression profile of bcl6 and CD10 in 79 cases of de novo diffuse large B-cell lymphomas, in relation to a) the apoptotic index (AI) b) the proliferation-associated proteins Ki67, cyclins A and B1 c) the expression of bcl2, p53, Rb, p16, p27.
Results and conclusions Expression of bcl6, CD10 and bcl2 was detected in 54/79 (68%), 28/79 (35%) and 47/79 (63%) cases, respectively. The bcl6/CD10 patterns were as follows: bcl6+/CD10+ (26 cases, 32%), bcl6+/CD10- (28 cases, 33%), bcl6-/CD10- (23 cases, 31%) and bcl6-/CD10+ (2 cases, 4%). Significantly positive correlations were found between bcl6/Ki67 (r=0.328, p=0.003), bcl6/cyclin A (r=0.265, p=0.018), bcl6/AI (r=0.327, p=0.010), CD10/Ki67 (r=0.296, p=0.008) and CD10/AI (r=0.397, p=0.001). High expression of bcl6 was correlated with null/low bcl2 expression (Hi-square-test, p=0.002). These findings indicate that increased expression of bcl6 and CD10 is associated with increased apoptosis and proliferation in diffuse large B-cell lymphomas. Association between increased bcl6 expression and enhanced apoptosis might be due to null/low bcl2 immunoreactivity, since previous in vitro data revealed that bcl6 overexpression induces apoptosis accompanied by bcl2 and bcl-xl downregulation. Significant correlation was found between increased AI and bcl6+/CD10+ pattern (T-test: p=0.014, Mann-Whitney test: p=0.046). This result combined with positive correlation between AI and bcl6 and CD10 immunostaining may be in accordance to previous studies showing that expression of these proteins has favorable effects on the clinical outcome of these neoplasms.

P-375

Primary non-Hodgkin lymphomas of bone: morphologycal and immunohistocehmical aspects

V Cemerikic-Martinovic[1], M Perunicic[1], S Knezevic-Usaj[2], Z Bogdanovic[2], M Atanackovic[3], J Sopta[3], B Mihaljevic
[1]Institute of Hematology Clinical Center of Serbia, Belgrade, Serbia and Montenegro
[2]Histolab, Belgrade, Serbia and Montenegro
[3]Institute of Pathology, Medical Faculty, Belgrade, Serbia and Montenegro

Introduction Primary non-Hodgkin lymphoma (NHL) of bone (PLB) is a rare clinic-pathologic entity that accounts for approximately 3% of all malignant bone tumors and 4-5% of all extranodal NHL. We analyzed morphological and immunohistocemical aspects of 8 PLB presented as solitary localized bone tumor.
Methods Paraffin embedded biopsy specimens of all 8 patients were diagnosed by the histomorphology and by immunohistochemistry using a wide panel of monoclonal antibodies (EMA, LCA, NSE, TdT, CD34, HLA-DR, CD79a, CD20, CD10, surface and cytoplasmic Ig, CD3, CD5, CD43, CD99, CD30, CD30, CD138, BCL2, BCL6 and Ki-67).
Results The median age of our pts. was 40 (from 14 to 65) with slight female predominance. Various sites were involved: 4 tumors were in tubular long bones, 2 in pelvic bones and 2 in spine with infiltration of soft tissue and without bone marrow involvement. All 8 cases were classified as diffuse large B-cell lymphoma (DLBCL) according to morphology and immunophenotype. Patohistological analyses showed markedly polymorphous cellular infiltrate with large cells with complex nuclear contours and multilobated nuclei, together with centroblasts-like cells and immunoblasts. All tumors were associated with some degree of fibrosis. Immunologic studies showed strong expression of pan-B markers and HLA-DR, weak expression of CD10 and cIg (mostly IgM) in half of tumors. BCL2 was positive in all cases as well as BCL6. The plasmacytic differentiation was observed in 1/3 of cases. The proliferative fraction was high, >50% cells in all patients.
Conclusion Our analysis revealed that all PLB were of DLBCL type with characteristic morphology and immunophenotype. Further study will show the outcome of patients with PLB, as well as the validity of various prognostic parameters.

P-376

Peripheral T-cell lymphoma with perifollicular growth pattern expressing CD10

JM Kim[1], YH Ko[2]
[1]Department of Pathology, School of Medicine, Cancer Research Institude, Chungnam National University, Daejeon, Republic of Korea
[2]Department of Pathology, Samsung Medical Center, Sungkyunkwan University School of Medicine, Seoul, Korea

Peripheral T-cell lymphomas (PTCLs) may reveal a variety of morphologic patterns and usually grow in a diffuse pattern with

inflammatory cells. PTCLs with nodular or perifollicular growth patterns are very rare. Only 18 cases have been reported in the literature. We report an unusual case of PTCL showing perifollicular growth pattern with expression of CD10 and bcl-6. The patient was a 46-year-old male who presented with a generalized lymphadenopathy, fever, and weight loss. Hepatosplenomegaly and polyclonal gammopathy were not identified. Cervical lymph node biopsy was performed. The histology showed nodular effacement of nodal architecture with proliferation of atypical lymphoid cells which mainly infiltrate perifollicular area. Interfollicular area also showed proliferation of atypical lymphoid cells and high endothelial venules with a few immunoblasts and eosinophils. Neoplastic cells were medium-sized, with irregular nuclei and clear cytoplasm. Immunohistochemically, the neoplastic cells were CD3+CD4+CD5+CD8-CD10+CD30-CD57-bcl-2+bcl-6+, demonstrating helper/inducer T-cell origin. The CD10 was strongly expressed mainly in the perifollicular tumor cells, whereas the normal germinal center (GC) cells showed down-regulation of CD10. The distribution of CD10+ perifollicular tumor cells was closely related with CD21+ follicular dentritic cells (FDCs), suggesting CD10 up-regulation might be induced by the proliferating FDCs. TCR-gamma gene rearrangement using PCR-SSCP was monoclonal. This case could be classified as PTCL, unspecified, and should be discriminated from other lymphomas, including marginal zone B-cell lymphoma and follicular lymphoma. Further studies are necessary to clarify the distinction of this tumor from angioimmunoblastic T-cell lymphoma.

P-377

Primary bone CD30+ anaplastic large cell lymphoma. Clinico-pathologic analysis of 5 cases

E Boveri[1], P Incardona[1], U Gianelli[2], M Lucioni[1], R Riboni[1], M Zecca[3], F Locatelli[3], E Orlandi[4], U Magrini[1], M Paulli[1]
[1]Istituto di Anatomia Patologica, IRCCS Policlinico San Matteo - Universitá di Pavia, Pavia, Italy
[2]Istituto di Anatomia Patologica, Dipartimento di Chirurgia, Medicina e Odontoiatria, II Cattedra di Anatomia Patologica, Universita di Milano - Azienda Ospedaliera San Paolo - Milano
[3]Oncoematologia Pediatrica, IRCCS Policlinico San Matte, Pavia, Italy
[4]Istituto di Ematologia, IRCCS Policlinico San Matteo - Universitá di Pavia, Pavia, Italy

Introduction CD30+ anaplastic large cell lymphomas (ALCLs) frequently involve extranodal sites, mainly skin and gastrointestinal tract, but primary bone ALCLs are exceedingly rare. The aim of this study was to detail the morphofunctional features and outcome of 5 cases of primary bone CD30+ ALCLs.
Materials and methods all the patients (M:F 3:2, median age 17 years, range: 6-50), but 1 (with 2 simultaneous occurring skin lesions) presented with bone confined lymphoma (osteolytic lesions of jaw, rib, sternum, iliac and pelvic bones). Biopsies from all cases were analysed.
Results and conclusion according to the WHO lymphoma classification, all cases were CD30+ ALCLs (4/5 common type, 1/5 small cell predominant variant). Lymphoma population showed a T (2/5) or "null" (3/5) phenotype, expressed cytotoxic associated molecules (TIA1, granzyme B and/or perforin); CD246/ALK was positive in 4/5 cases, whereas 1/5 expressed CD56. TCR-gamma clonal rearrangement was detected in 3/5 cases. All patients received polychemotherapy; at last follow up they all are alive, in complete remission (mean: 35 months, range: 5-132). In our cases, the morphofunctional features of the lymphoma population were similar to their nodal counterparts, including CD246 expression in the younger patients. On such bases, the hypothesis must be considered that primary bone CD30+ ALCLs represent the first extranodal site of presentation of a systemic disease. In contrast with similar reported series, our patients run a favourable prognosis and in the single positive case, CD56 expression does not negatively influence outcome. However, larger series of similar cases must be analysed before definitive conclusions can be drawn.

P-378

Immunohistochemical detection of follicular dendritic cells in B-cell chronic lymphocytic leukaemia/small lymphocytic lymphoma

L Boudova, F Fakan, P Mukensnabl, A Skalova, M Michal
Lab. Spec. Diagnostiky, Dept. Of Pathology, Medical Faculty Hospital, Charles University, Plzen, Czech Republic

Introduction Follicular dendritic cells (FDC) form a meshwork in the lymphoid follicle and take part in the regulation of the germinal centre reactions. FDC also interact with the neoplastic lymphoid proliferations. In B-cell chronic lymphocytic leukaemia/small lymphocytic lymphoma (B-CLL/SLL), FDC structures are reduced. The aim of this study was to evaluate the presence and patterns of follicular dendritic cells B-CLL/SLL using several anti-FDC antibodies.
Materials and methods 50 formalin-fixed paraffin-embedded lymph nodes diagnosed as B-CLL/SLL according to the WHO criteria were studied using CD21, CD23, and CNA.42 antibodies after microwave oven antigen retrieval
Results In 17 cases (34%) FDC meshworks were identified in none of the reactions. In 15 specimens (30%), FDC meshworks were exceptionally rare as follicle remnants at the lymph node periphery or as small irregular clusters not reminding of the normal follicle meshwork. In 18 cases (36%) FDC formed either frequent small irregular clusters, or rings at the follicle periphery, or regular follicular meshworks. Reticular structures in a given case were most frequent in CNA.42 stain, scarcer in anti-CD21, and anti-CD23 stains. The majority of cases showing FDC was obtained by CNA.42 (33 cases), CD21 (22 cases) and CD23 (16 cases).
Conclusion FDC structures were absent or scarce in up to 64% of B-CLL/SLL cases which can be used as an auxilliary diagnostic criterion. The positive cases showed small irregular clusters, rings at the follicle periphery, or normal follicular meshworks. Best results were obtained with CNA.42 antibody. This may be due to better antigen preservation or to non-specifity.

P-379

Usefulness of CD34 immunoreactivity in classification of myelodysplastic syndromes

E Conde, J Salamanca, I Alemany, MA Martínez
Pathology Department, University Hospital ' Doce de Octubre ' Madrid, Spain

Introduction Myelodysplastic syndromes (MDS) are clonal haematopoietic stem diseases characterised by dysplasia and ineffective haematopoiesis. The dysplasia may be often associated with an increased number of myeloblasts in peripheral blood and

bone marrow, which represents an important prognostic factor. Immunohistochemical detection of blast cells in bone marrow histological sections using CD34 antigen and its correlation with smear blast count and MDS classification are not well established. We report a quantitative study of CD34 blast cells in MDS and acute myeloid leukaemia with multilineage dysplasia (AMLMD), and analyse the relationship with both cytologic smear and clinical diagnosis.
Materials and methods We have studied 15 bone marrow biopsies diagnosed of MDS (4 with refractory cytopenia with multilineage dysplasia (RCMD), 3 with refractory anemia with excess blast (RAEB) type I and 8 with RAEB type II) and 5 with AMLMD. We added 6 controls and calculated the CD34 blast cells mean per high power field (hpf). Cytologic smears were reviewed.
Results The results were: controls showed 4-20 blasts/10hpf, RCMD 6-38/10hpf, RAEB I 21-46/10hpf, RAEB II 44-440/10hpf and AMLMD 358-950/10hpf.
Conclusions -CD34+ blast cells density is a good parameter in the histological diagnosis of MDS and has a close correlation ($p<0,01$) with smear count
Results -CD34 does not distinguish between RCMD and RAEB I. -More than 50 blast cells/ 10 hpf raise the diagnosis of RAEB II. More than 50 blast cells/ 1 hpf raise the diagnosis of AMLMD. The extrapolation of these features to "dry tap" aspiration remains to be established.

P-380

Primary intestinal lymphoma: clinical and pathologic features of 16 patients

T Terzic[1], A Laban[1], Z Stojsic[1], I Boricic[1], V Todorovic[2], S Radojevic[1], G Basta-Jovanovic[1], D Cvetkovic[1]
[1]Institute of Pathology, School of Medicine, Belgrade, Serbia and Montenegro
[2]Institute for Medical Research, Belgrade, Serbia and Montenegro

Introduction Although the gastrointestinal tract is the most common site of extranodal lymphoma, primary intestinal lymphomas (PIL) are rare. We report a retrospective analysis of 16 patients with PIL, presenting clinical and pathologic features.
Patients and methods PIL was defined according to the criteria of Dawson. Sixteen patients (11 males and 5 females) with age range of 4-74 years were studied. The formalin-fixed and paraffin-embedded tissue was used for routine microscopic examination and immunohistochemical stainings.
Results The most frequent clinical presentations were ileus (7/16) and intestinal bleeding (6/16). Painful abdominal tumor (2/16) and perforation (1/16) were rare. The most frequent locations were ileocecal region (6/16) and ileum (5/16); 3/16 were located in duodenum and 2/16 involved colorectum. All children showed involvement of ileocecal valve. Three patients had associated other diseases: AIDS (1/16), Crohn's disease (1/16) and celiac disease (1/16). Intestinal T-cell lymphoma (associated with celiac disease) was diagnosed in one case. Among B-cell NHL there were 8/16 aggressive NHL (4 Burkitt's lymphomas, 3 diffuse large B-cell lymphomas and one Burkitt-like lymphoma) which were localized as follows: 5 in ileocecal region, 2 in ileum and one in duodenum. Among indolent lymphomas there were 5/16 MALT-omas and 2/16 follicular lymphomas with predilection to duodenum (2/16) and colon (2/16).
Conclusion PIL are rare malignancies with distinct clinical features, but with ileus as the most frequent clinical presentation and ileocecal region as the most frequent site of involvement. Burkitt's lymphoma was predominant histological type. Indolent and aggressive type of NHL were almost equally presented.

P-381

Bone marrow angiogenesis in hairy cell leukaemia - a morphometric study

A Androulaki[1], P Korkolopoulou[1], N Kavantzas[1], I Thymara[1], DA Gribabis[2], M Perdiki[1], C Eftychiadis[1], GA Pangalis[2], E Patsouris[1]
[1]Department of Pathology, School of Medicine, National and Capodistrian University of Athens, Greece
[2]Haematologic Section, First Department of Internal Medicine, School of Medicine, National and Capodistrian University of Athens, Greece

Inroduction Bone marrow angiogenesis has been recently implicated in the pathophysiology and course of various haematological malignancies. Little is known, however, about the significance of this phenomenon in hairy cell leukaemia (HCL).
Methods We evaluated various morphometric characteristics of microvessels, highlighted by means of anti-CD34 immunohisto-chemistry, in the bone marrow of 44 patients with typical HCL, before and after treatment with interferon-α. Overall 104 bone marrows from HCL patients and twenty control bone marrows were examined. Microvessel density (MVD) and several size- and shape-related parameters were quantitated in the region of most intense vascularization using image analysis.
Results MVD, size-related parameters and the percentage of branching microvessels were higher in HCL than in controls and in partial/non-responders in comparison to complete responders. Acvievement of complete response was accompanied by smaller calibre microvessels. Interferon-α induced a decrease in MVD and branching values in cases with diffuse marrow involvement. In univariate analysis, progression-free survival was adversely affected by MVD and branching. Multivariate analysis indicated that factors related to the size of the microvessels and MVD/ branching independently affected progression-free survival. MVD/ branching was also related to the likelihood of complete response.
Conclusions Our data suggest that the generation of bone marrow microvessels connotes an increased risk for progression and interferon-α treatment failure in HCL. Furthermore the prognostic significance of angiogenesis requires the concomitant assessment of MVD, the size of microvessels and the complexity of the microvascular network. Key words: Hairy cell leukaemia, bone marrow, angiogenesis, morphometry

P-382

Inflammatory pseudotumor of the spleen and its relationship to Epstein-Barr virus (EBV): Report of a case

EP Labropoulou[1], V Zolota[1], E Katsiki[2], D Karavias[1], C Labropoulou[1]
[1]University Hospital of Patras, Greece
[2]General Hospital of Messologhi 'Hatzicostas', Greece

Introduction Inflammatory pseudotumors are uncommon and enigmatic benign lesions which may develop at several anatomical sites and recent studies demonstrated the frequent presence of

Epstein-Barr virus (EBV) in them. The occurence of inflammatory pseudotumor in the spleen is rare. A case of inflammatory pseudotumor of the spleen is presented and its relationship to Epstein-Barr virus (EBV) is examined.
Material and method The case was a 62-year-old woman in whom a solitary splenic mass was discovered as part of the workup of idiopathic thrombocytopenic purpura. Splenectomy was performed.
Results Grossly, the removed spleen, weighing 140 g, contained a tan-white, circumscribed mass, measuring 4.5X4X4 cm. Microscopically, the mass was composed of a heterogeneous cellular population of acute and chronic inflammatory cells. Plasma cells predominated, but lymphocytes, neutrophils, eosinophils, interlacing fibroblast-like spindle cells and rare multinuclear giant cells were found. Amorphous, acidophilic material was present focally with the plasma cell proliferation. Plasma cells presented light chains polyclonality. Lymphoid cells were mature and mainly of T-lineage. Spindle cells exhibited histiocyte phenotype (CD68+++). Immunohistochemical stain for EBV was negative.
Conclusions Inflammatory pseudotumor of the spleen is a benign tumorous lesion that has been described in only a few cases in the world literature (<75 cases). Its etiology and pathogenesis is unknown and association EBV is not always present. Recognition of this rare entity is important, as the clinical manifestations and imaging features could be indistinguishable from a lympho-proliferative disorder or another malignancy of the spleen.

P-383

Histopathological and immunohistochemical patterns of nodal non-Hodgkin's lymphoma in Montenegro

F Vukmirovic
Clinical Center Of Montenegro, Podgorica, Serbia and Montenegro

Introduction The diagnosis of nodal non-Hodgkin's lymphoma (NHL) in Montenegro has been done only in Clinical Center of Montenegro - incidence of diagnosed NHL can be considered as the incidence in epidemiological sense.The use of monoclonal antibodies since 1997, has improved our ability to diagnose and to treat NHL. Aims: By revision of immunohistologically diagnosed cases of NHL between 1997-2003, we wanted to estimate (a) the frequency of particular clinico-pathological types of NHL, (b) hypothesis about geo-socio-economic influences on patterns of NHL, and (c) the influence of immunophenotypisation of NHL on speciffic chemo- and immunotherapy.
Materials and methods NHLs were diagnosed with the use of HE, Giemsa, MGP, PAS, Gomori, LCA, bcl2, TdT, CD3, CD43, CD20, CD79a, CD15, CD30, and EMA stained slides and classified according to the Working Formulation criteria.
Results Between '97 and '03 we diagnosed 116 NHL. Low, intermediate and high grade malignancy comprised 33,6 %, 50,9 % and 15,5 % respectively. The highest incidence was estimated in 1999:1,5/100000. The NHLs of FCC origin constitute 60,3% of all our NHLs. In 80% of patients (25) low grade malignant NHLs were highly CD20+. Nine patients recieved Mabthera+CHOP/or +COP therapy during the last three years.All patients have been in remision.
Conclusion The estimated pattern of NHL - the most frequent NHL derivated from FCC- is comparable with geographic and socio-economic description of Montenegro as "underdeveloped, ecological, farming European country".The high frequency of CD20+ and initial therapeutical results indicate future prospective patho-clinical studies of this issue.

P-384

Lack of CD 20 expression in herpesvirus 8 (HHV8) infected cells in multicentric Castleman's disease (MCD)

I Oehri, M Baumann, G Cathomas
Kantonales Institute for Pathology, Liestal, Switzerland

Background The multicentric Castleman's disease (MCD) is a lymphoproliferative disease with increased risk for non-Hodgkin lymphoma. In AIDS patients, MCD is usually associated with human herpesvirus 8 (HHV8), the infectious agent of Kaposi's sarcoma but in contrast to Kaposi's sarcoma, HHV8 infected cells in MCD show evidence of lytic viral infection. Similar to other immunosuppression-associated lymphoproliferative diseases it has been suggested that anti-CD20 antibodies may be useful in the therapy of these lesions. Aim of the present study was the analysis of CD 20 expression in HHV8 associated MCD and their association with lytic viral infection.
Material and methods Formalin fixed, paraffin embeded lymph nodes were analyzed by a double immunofluorescence assay using antibodies against viral proteins and CD20. HHV8 proteins which were analyzed include the latent viral protein LANA (ORF 73) and the viral interleukin 6 (vIL-6) and the ORF74, both associated with lytic HHV8 infection.
Results Eleven lymph nodes of seven HIV-infected patients with MCD were analyzed. In the mantle zone of the lymphoid follicle, 8,4%, 2,8% and 1% of cells show positivity for LANA, vIL-6 and ORF74, respectively ($p < 0,02$). By double immunofluorescence, 91% of HHV8 infected cells showed co-expression of LANA/vIL-6 and LANA/vORF74 and 96% showed co-expression of LANA/vIL-6, respectively. In addition, there was statistical significant correlation between vIL-6 and LANA as well as vIL-6 and vORF74 ($p < 0,01$). Of the HHV8 infected cells, 6,5% showed CD20 expression and no difference between the three viral proteins analyzed were observed (5,5%, 7,4%, 6,6% of LANA, vIL-6 and vORF 74, respectively).
Conclusion The present data support the concept that HHV8 runs, in contrast to Kaposi's sarcoma, through a lytic viral infection in lymph nodes of patients with MCD. However, only a small subset of infected cells show co-expression of CD20, independent of the state of viral replication. This small number of infected cells expressing CD20 indicate little effect of anti-CD20 therapy. Based on the evidence of lytic HHV8 infection, however, anti-viral drugs inhibiting HHV8 replication may be more efficient.

P-385

Anaplastic large cell lymphoma - pathological and immunohistochemicals aspects

C Dobrea[1], C Iosif[1], D Terzea[1], F Vasilescu[1], L Caban[2], F Andrei[1], M Ceausu[1], G Butur[1], C Ardeleanu[1], F Halalau[1]
[1]"V Babes' National Institute, Bucharest, Romania
[2]Dpt of Haematology, 'Fundeni Clinical Institute, Bucharest, Romania

The WHO Classification of NonHodgkin Lymphoma (NHL) included also the cathegory of T and null Anaplastic Large-Cell Lymphoma (ALCL). ALCL is a very rare NHL (about 5%), with the systemic-aggressive variant, and the cutaneous variant. The presence of the t(2;5) and the formation of ALK protein identified one subgroup of ALCL with a good prognosis. The aim of our

study is to analyze the histopathological and immunohistochemical characters of the ALCL diagnosed in our department in the last 2 years. 15 cases of T and null ALCL (M/F=12/3, more half of them younger of 30 years) were clinical and immunohistochemical analyzed (by ABC indirect methods, with a large panel of monoclonal antibodies). The pattern of lymph node infiltration was diffuse (9 cases), parafollicular (5 cases) and only with sinus infiltration - 1 case. The pathological subtypes were common (7 cases), lymphohistiocytic (4 cases), small cell variant (1 case), sarcomatous (1 case), eosinophils-rich (1 case) and neutrophil-rich (1 case). Immunohistochemically, the malignant cells presented with T-fenotype (7 cases) and null (7 cases); 1 case (M, 17 y) presents histiocyte markers (CD68+CD30+EMA+ALK+). All cases of ALCL were CD30+, but only 13 cases were EMA+ (2 cases were CD45RO+CD30+ALK-EMA-). 2/3 of cases were ALK+ (5-T and 5-null), with a nuclear and a membranous pattern. 5 cases were BNH9+ (4 cases ALK+). Only 1 case presented CD15 expression(CD30+EMA+ALK+BNH9+). 2 of the cases with T fenotype expressed CD4 markers (both were CD4+CD8-). The PCNA and Ki67 proliferation markers were positive in a very large percent of the malignant cells (between 30 and 80%). Numerous reactive T- lymphocytes presented a helper fenotype (CD4>CD8), and Leu-7+ cells were very rare. The null and T-cell ALCL pose numerous problems of differential diagnosis and immunohisto-chemicals methods are very useful for diagnosis and prognosis of these NHL.

P-386

Myeloid sarcoma -9 cases analysis

F Vasilescu[1], C Dobrea[1,2], E Niculescu-Mizil[2], A Colita[2], L Caban[2], R Stoia[2], D Ostroveanu[2], A Iofciulescu[2], D Terzea[1], C Iosif[1]
[1]'V Babes' National Institute, Bucharest, Romania
[2]Dpt of Haematology, 'Fundeni' Clinical Institute, Bucharest, Romania

Myeloid (granulocytic) Sarcoma (MS) – also known as “Chloroma”, is a localized tumor of primitive myeloid cells, that can present before, simultaneously with, or after the diagnosis of acute myeloid leukaemia (AML). Rarely, MS may represent the first sign of blastic transformation of myelodysplastic syndrome (MDS) or chronic myeloproliferative disorders (CMPD). The aim of this study is to present our experience in the diagnosis of MS. In the last 7 years, we diagnosed 9 cases of MS (M/F=4/5, between 18 and 66 year-old, with 50,2 years median). A large panel of monoclonal antibodies (lymphoid and myeloid cell markers) was used for the diagnosis of MS and for the differential diagnosis with NonHodgkin Lymphomas (NHL). The tumor localizations were: lymph nodes (5 cases, including a bulky inguinal tumor), lymph node and skin (1 case), paravertebral (2 cases), testis (1 case). In our cases, 2 patients presented with MS before the AML diagnosis (F, 26y, paravertebral MS, 10 months before AML-M3, and M, 57y, 15 years after NHL diagnosis, presented with an inguinal lymph node MS, 6 months before AML-M4). In 3 cases, MS was diagnosed simultaneously with AML (AML-M2; AML-M3; AML-M4), and in 2 cases after AML (m, 34y, MS with testis localization, 3 years after AML-M3; F, 66y, lymph node and skin MS, 6 years afterAML-M4). In one case (F, 66y), 6 years after successful treatment of an acute lymphoblastic leukaemia (ALL), the patient presented with a lymph node MS, considered as a blastic transformation of a chronic myelo-monocytic leukaemia (CMML). The diagnosis of MS may be very difficult if this tumor precedes the myeloid proliferative disorders, and the differential diagnosis with NHL may pose a lot of problems.

P-387

B-cell prolymphocytic “leukemia” (B-PLL): a heterogeneous disorder with a broad clinical and genetic spectrum

C Lome Maldonado, A Lazo-Langner, L Quintanilla-Martínez, B Martínez-Benítez, G Kelly, E Reyes, A Angeles-Angeles
Departments of Pathology and Hematology-Oncology, Instituto Nacional de Ciencias, Médicas Y Nutrición Salvador Zubirán, Mexico City, Mexico

Introduction B-PLL is an infrequent disease, considered by the WHO lymphoma classification as an aggressive condition and characterized by the presence of B symptoms, massive splenomegaly without significant lymphadenopaty and peripheral lymphocytosis with more than 55% prolymphocytes. Herein we report 2 cases of B-PLL to show the wide clinical and genotypic spectrum of this disease.
Case reports Patient 1. A 51-year old male with a history of petechiae and ecchymoses of 1 year evolution. A CBC showed significant lymphocytosis with >55% prolymphocytes. Physical examination revealed an enlarged cervical lymph node and splenomegaly. Lymph node biopsy was diagnosed as infiltration by B-PLL (CD20+, CD79a+, IgM+, CD5-, CD23-, CD43- and cyclin D1-). A bone marrow biopsy showed infiltration by B-PLL. Cytogenetic analysis of the bone marrow showed a Burkitt’s variant translocation t(2;8) (p12;q24) Molecular analysis of the lymph node showed IgH rearrangement and germline bcl-2 and bcl-1 by PCR. He was treated with four cycles of fludarabine (25 mg/m2) and rituximab (500 mg/m2) and is in clinical and cytogenetic remission at 1 year of follow-up. Patient 2. A 54-year old female with a 2 month history of multiple cervical lymph node enlargement and fever. Physical examination was normal and she had no lymphocytosis on the CBC. Lymph node biopsy showed infiltration by a non-Hodgkin’s lymphoma with a prolymphocytic morphology (CD20+, CD79a+, IgM+, CD5-, CD23-, CD43- and cyclin D1-). Bone marrow biopsy showed focal infiltration by B-PLL. Cytogenetic analysis of the bone marrow revealed a normal female cariotype and normal FISH patterns were found for the following probes: chormosome 8 centromere, 8q24 (c-myc), chromosome 12 centromere, 13q14 (D13S319), 14q32.33 (IgH) and 17p13.1 (p53). She was initially treated with CHOP and then switched to fludarabine having achieved a good clinical response after one cycle each. Discussion. The association between B-PLL and translocation t(2;8) (p12;q24) has been reported in very few cases, however direct involvement of c-myc alterations affecting specifically 8q24 has been proposed as an important factor in the pathogenesis of B-PLL. In patient 1, the observed genetic alterations could be of significance to define the genetic spectrum of B-PLL. Case 2 corresponds to a B-cell prolymphocytic lymphoproliferation with isolated lymph node involvement and no leukemic component. To our knowledge this presentation has not been reported previously and it is not considered in WHO classification. Morphological and immunohistochemical characteristics of this case are fully compatible with a B-PLL. Even though it has been considered that some cases of B-PLL could in fact represent a morphological variant of mantle cell lymphoma, in this case the negativity for CD5 and cyclin D1 partially rule out this possibility. B-cell prolymphocytic lymphoproliferations constitute an heterogeneous group of disorders in which c-myc rearrengement can be present. In this group of neoplasia therefore, the nodal involvement can be either predominant or the only clinical manifestation, thus we

propose to consider the term B-cell prolymphocytic lymphoma/ leukemia instead of B-PLL to denote these disorders.

P-388

EBV-positive anaplastic large cel lymphoma (ALCL) in Mexican patients

C Lome Maldonado, B Martínez-Benítez, S Valdés, A Lazo-Langner, A Angeles-Angeles
Instituto Nacional de Ciencias Médicas Y Nutrición Salvador Zubirán, Mexico City, Mexico

Background ALCL is a particular type of T-cell non-Hodgkin's lymphoma originally characterized by a peculiar morphology and the consistent expression of CD30. This entity is frequently associated with the translocation t(2;5) (p23;q35) or some of its variants resulting in the overexpression of the chimeric protein NPM/ALK (ALK+), even though in the current classification ALK-negative cases are also considered within this group. EBV is classically and constantly associated with certain specific types of lymphoma but its association with ALCL is not considered a characteristic feature of this disease. The aim of this study was to investigate the frequency of the ALCL-EBV association in a population of adult mexican patients.
Results Eighteen patients with a morphological and immunohistochemical diagnosis of ALCL with nodal involvement were included. Immunohistochemical and ISH analysis was performed for CD3, CD43, CD45RO, CD45RB, CD20, CD30, CD15, EMA, LMP-1, ALK.and EBER1. Mean age was 45 years and the male-to-female ratio was 1.2:1. Immunohistochemistry and in situ hybridization results are summarized in the next table. All the so considered EBV positive cases expressed LMP-1 and EBER 1.
Conclusion In contrast to the information available in the literature we found a high incidence of the ALCL-EBV association 10 /18 (55%). The high incidence of ALK-/EBV+ cases 9/18 (50%), with morphological and immunophenotypical characteristics of ALCL gives rise to the possibility that this is a different subset of T-cell lymphomas with anaplastic morphology in which EBV plays a pivotal roll in the oncogenesis and evolution. These disorders have been considered so far to be ALCL /ALK- lymphomas. The high incidence of EBV infection in Mexico leads to the development of peculiar lymphoid proliferations as well as associations (EBV/ALCL) different from those considered to be frequent in world literature.

P-389

CDK9/Cyclin T expression in reactive lymph nodes and malignant lymphomas

Lazzi S[1], Bellan C[1], De Falco G[1], Schuerfeld K[1], Micheli P[2], Bartolommei S[1], Pileri S[3], Leoncini L[1], Tosi P[1], Giordano A[4].
[1] Institute of Pathological Anatomy and Histology, University of Siena, Siena, Italy.
[2] Azienda Ospedaliera Cotugno, Napoli, Italy
[3] Institute of Hematology and Clinical Oncology "L. and A. Seràgnoli", University of Bologna, Bologna, Italy
[4] Temple University, Philadelphia, PA, USA.

CDK9 is a member of the CDC2-like family of kinases. Its cyclin partners are members of the family of Cyclin T (T1, T2a and T2b) and cyclin K. CDK9/Cyclin T1 complex is very important in the differentiation program of several cell types, controlling specific differentiative pathways. Limited data are available regarding the expression of CDK9/Cyclin T1 in haematopoietic and lymphoid tissues. The aim of this paper is to analyze the expression of CDK9/Cyclin T1 complex in lymphoid tissue, in order to assess its role in B and T cell differentiation and lymphomagenesis. In reactive lymph nodes CDK9/Cyclin T1 expression was found by immunohistochemistry in germinal center and in B and T cell blasts in interfollicular areas, suggesting a role for CDK9 in the activation and differentiation of B and T cells. The staining of CDK9 and cyclinT1 complex in malignant lymphomas seems to reflect their normal counterpart, as it is highly expressed in lymphomas derived from germinal center cells, such as follicular lymphomas and classical Hodgkin's lymphomas and from activated T cells, (i.e. anaplastic large cell lymphomas). Diffuse large B-cell and Burkitt's lymphomas showed a wide range of values. No expression of CDK9 and Cyclin T1 was detected in marginal zone and mantle cells lymphomas. However, at RNA level we found an imbalance in CDK9/Cyclin T1 ratio in follicular lymphoma and diffuse large B cell lymphomas with germinal center phenotype, and in the cell lines of classical Hodgkin's lymphomas, Burkitt's lymphomas and anaplastic large cell lymphoma, in comparison with reactive lymph nodes.
Here we report CDK9/Cyclin T1 complex deregulation in neoplastic conditions for the first time, representing a step towards better understanding of through which molecular mechanism CDK9/Cyclin T1 complex acts on the activation and differentiation program of lymphoid cells and the role of its deregulation in malignant transformation.

P-390

The value of tartrate resistant acid phosphatase (TRAP) immunoreactivity in diagnosis of hairy cell leukaemia

H Akkaya, O Dogan, G Dincol, M Agan
Antalya, Turkey

Introduction Hairy cell leukaemia (HCL) is a chronic lymphoproliferative disease characterized by the presence of neoplastic B cells with hairy cytoplasmic projections in spleen, bone marrow and peripheral blood. Complete or near-complete remission can be achieved by recent chemotherapy protocols. These treatment methods are quite different from the chemotherapy protocols used for the treatment of other lymphoproliferative diseases. An absolute and correct diagnosis, i.e. detection of HCL cells by specific methods, is necessary for the achievement of complete or near-complete remission by special chemotherapy programs. Detecting intracytoplasmic tartrate resistant acid phosphatase (TRAP) enzyme activity in the peripheral blood and bone marrow aspirates is a classical, simple, sensitive and quite specific method for the detection of HCL cells and in the diagnosis of HCL. However, this method is insufficient in some cases. For example, the most of the HCL patients are leukopenic and there are a few number of neoplastic cells in their peripheric blood. An adequate number of neoplastic cells cannot be obtained by bone marrow aspiration because of the increase in reticulin fibbers of the bone marrow. In such cases, bone marrow trephine biopsy is almost the only and the most important method in diagnosis and follow-up of this disease. Specific detection of TRAP enzyme activity in bone marrow trephine biopsy materials is not possible because of the effect of tissue fixation and processing on these materials. In conclusion, a new method for detecting TRAP enzyme activity in bone marrow trephine biopsy

materials and for conforming the diagnosis of HCL is needed. A recently developed anti-TRAP antibody has been started to be used as an immunohistechemical marker in the diagnosis of HCL. The aim of this study was to investigate the specificity and the sensitivity of anti-TRAP antibody immunoreactivity in bone marrow trephine biopsy materials in the diagnosis of HCL.

Material and methods We divided the cases into two groups; a study and control group. The study group included the cases diagnosed as HCL by clinical, haematological and histopathological investigations. The cases in the control group were the cases characterised by non-HCL neoplastic or reactive lymphoid infiltrations, which raised the suspicion of HCL in the differentia l diagnosis. Immunohistochemical staining techniques were applied to paraffin block sections of biopsy materials with anti-TRAP antibody.

Results and conclusion We found that there is a statistically highly significant difference between TRAP immunoreactivities of the study and the control groups, and HCL can be diagnosed by TRAP immunoreactivity in the bone marrow trephine biopsy materials with the specificity of 98,27 % and with the sensitivity of 100 %.

P-391

Cathepsin L participation in collagen degradation during the recovery from experimental hepatic fibrosis

V Ryvnyak[1], E Ryvnyak[1], R Tudos[2]
[1]State University of Medicine and Pharmacy, Kishinec, Republic of Moldova
[2]Center of Pathology, Academy of Sciences, Kishinev, Republic of Moldova

Introduction Cathepsin L is one of the most important lysosomale cysteine proteinase, indispensable for proteolitic processes. The enzyme is capable to degrade the main components of the intercellular matrix. Aims: 1. To determine the participation of cathepsin L in collagen degradation in liver and to reveal the intracellular and/or extracellular localization of the enzyme activity. 2. To determine which cells of fibrotic liver are sources of cathepsin L.

Methods Biochemically cathepsin L activity and hidroxyproline level was determined in normal, CCl4-induced fibrotic rat liver and at 7, 14, 21, 30, 60 days after discontinuation of treatment. The activity of cathepsin L in fibrotic rat liver at the 7th and 21st days was investigated electron-histochemically. CBZ-Phe-Arg-4MBNA (Bachem) served as the substratum.

Results Biochemically in fibrotic liver an increase of cathepsin L activity as compared with normal liver was revealed. During fibrosis regression the maximums of enzymatic activity at the 7th day (170%) and at the 21st day (155%) after cessation of CCl4-treatment were fixed. At the 14th day of recovery some diminution of cathepsin L activity was noted. At the 60th day after toxin abolition enzyme activity was close to control. A close correlation between cathepsin L activity and liver hidroxyproline level was found. Electron-histochemically reaction product was revealed in the Kupffer cells and fibroblast phagolysosomes containing fragments of collagen fibrils. We also found extracellular localization of cathepsin L in both terms of investigation. The reaction product was noted on the hepatocyte, Kupffer cell and fibroblast plasmalemma and on adjacent collagen fibrils.

Conclusions Cathepsin L is directly implicated in collagen resorbtion during liver fibrosis regression. Detected extracellular activity of cathepsin L suggests that in addition to the intracellular proteolysis, cathepsin L is secreted by hepatocytes, macrophages and fibroblasts in intercellular space and can take part in extracellular collagen degradation. Ryvnyak Victor Laboratory of Morphology "Nicolae Testemitanu" State University of Medicine and Pharmacy Bd. Stefan cel Mare, 165 Kishinev, MD-2004 Moldova victorrivneac@yahoo.com

P-392

Solitary necrotic nodule of the liver. A report of three cases

A Córdoba, ML Gómez, B Larrinaga, I Amat, R Beloqui
Hospital Of Navarra, Pamplona, Spain

Introduction The solitary necrotic nodule (NNS) of the liver is an uncommon lesion with a round appearance near the surface of the liver, with a dense collar of hyalinised collagen surrounding a necrotic core.

Case reports We present three cases of NNS. Two patients underwent surgery to remove liver metastasis. We suggest a relationship with the previous hepatic surgery and with the microwave tissue coagulator. The other case have an history of abdominal traumatism by a seizure. The radiological image of NNS was misinterpreted as a tumor and the diagnosis by FNAC or frozen section could not exclude a metastasis. The potential risk of a malignant secondary tumour existed, and that was why limited liver resection was recommended. Several pathogenetic mechanisms have been avocated (infection, parasitic, traumatic, ischaemic, post chirurgical, iatrogenic, etc.), all of them having an identical morfological appearance.

Conclusion NNS is a rare non-tumorous lesion that might be misinterpreted as a tumor. The correct diagnosis can only be histological. It is important to differentiate the NNS from metastases due to the great influence on the treatment.

P-393

The significance of morphometrical analysis in staging of fibrosis in liver biopsies from patients with chronic hepatitis C

A Matsionis[1], E Romanova[2], Y Kirichenko[1], Y Ambalov[2], P Povilaitite[1]
[1]Rostov Regional Bureau of Pathology, Rostov on Don, Russian Federation
[2]Rostov Central Hospital, Rostov on Don, Russian Federation

Introduction Prognosis of the course of chronic hepatitis C (CHC) depends on fibrosis stage and its progression temps in the liver. Semi quantitative methods are currently regarded as a routine diagnostic procedure. But it is obvious that these methods are subjective. Morphometrical analysis with calculation of fibrosis index (FI) is an alternative method of evaluation. The aim of the study was to compare data obtained after morphometrical analysis of collagen formation to semi quantitative methods results and find out accordance with fibrosis stage.

Materials and methods Liver biopsies from 42 CHC patients were used. We applied V.J.Desmet (1994) semi quantitative method and software SigmaScan Pro 5.0 for morphometrical analysis of sections. All sections were stained by Masson Trichrome method for the detection of collagen. Fibrosis index (FI) was calculated as collagen area divided all section area.

Results 54,5% of patients had clinically significant level of liver fibrosis (Desmet F2, F3, F4). F1 Desmet stage was corresponding FI 0,01-0,02, F2 Desmet (moderate fibrosis) - FI 0,03-0,06 and

high level of fibrosis (F2 and F3) - IF 0,07-0,3. 15/42 cases (35,7%) showed differences between semi quantitative and morphometrical results. Four patients (9,5%) without fibrosis by semi quantitative methods showed IF corresponding moderate fibrosis (F2).
Conclusion Our results suggest that morphometrical analysis is beneficial in the evaluation of fibrosis stage and should be used for prognosis and monitoring the course of chronic viral hepatitis.

P-394

Phenotypic comparison of hepatic mucinous cystadenomas with mesenchymal stroma and ovarian mucinous cystadenomas

KN Vandewalker[1], B Stabile[2], A Suriawinata[3], B Ruebner[1]
[1]University of California, Davis, Sacramento, USA
[2]Harbor-UCLA Medical Center, Los Angeles, USA
[3]Mt. Sinai Hospital, New York, USA

Introduction Hepatic mucinous cystadenomas with mesenchymal stroma have been recognized as rare neoplasms that occur only in females and have recently been postulated as being hormonally dependent. Because of the similarity of these neoplasms to ovarian mucinous cystadenomas, we compared the immunohistochemical profiles of these neoplasms arising in two different organs. The aim of this study was to establish whether these two tumors were phenotypically similar.
Materials and methods We employed the following immunohistochemical stains, Estrogen Receptor, Progesterone Receptor, Inhibin, CK7, CK20 and Alcian Blue/ Periodic Acid-Schiff, to 6 cases of ovarian mucinous cystadenomas and to 5 cases of hepatic mucinous cystadenomas with mesenchymal stroma.
Results Both the ovarian and hepatic neoplasms showed similar results with all of these stains.
Conclusions Phenotypically, we have been unable to establish any difference between these two neoplasms. There appear to be two possible explanations for the origins of these tumors: One is that of a displaced ovarian anlage in the developing liver and the other would be that some of the primitive hepatic stem cells are capable of acquiring ovarian characteristics

P-395

Assessment of periodontum condition in hepatitis C infected patients with rapid and slow dynamics of advanced fibrosis

P Radlowski[1], K Dabrowka[1], A Gabriel[1], A Dziambor[2], E Janczewska-Kazek[3]
[1]Chair and Department of Patomorphology, Medical University of Silesia, Zabrze, Poland
[2]Clinical Ward of Contagious Diseases, Medical University of Silesia, Bytom, Poland
[3]Observation and Contagious Disease Ward of the Specialist Hospital, Chorzów, Poland

Aim Analysis of the relationship between the stage of periodontium disease and the extent and dynamics of fibrosis in patients infected with chronic hepatitis C.
Material and methods The study included 28 patients whose blood serum revealed the presence of HCV-RNA via RT-PCR, while biopsies showed chronic inflammation and either septal fibrosis, or liver cirrhosis. Fibrosis was evaluated according to Scheuer's 4 point scale, with Azan- staining method and the authors' own modifications. Fibrosis dynamics (FU/Y) was evaluated as a quotient of the number of points assessing fibrosis and the number of years of the disease. Periodontitis was determined by the following criteria: inflammation limbus, gum swelling, gingival pockets depth, presence of supragingival and subgingival calculus and gomphiasis. Each criterion was assigned either 0 or 1 point within the cumulative scale of 0-4 points.
Results All patients with advanced liver fibrosis were found to show signs of periodontosis. The patients whose periodontium condition scored 4 points with the mean value of FU/Y amounting to 0,49, while those who scored 3 points showed mean values of FYU/Y equalling 0,79. The group of 19 patients with high values of periodontium disease showed significantly higher values of periodontum disease stage (most frequently assessed at 4 points) compared with the group of nine patients with low FU/Y values (mean value = $p < 0,05$). Periodontium score of the patients with cirrhosis and bridge fibrosis showed similar values.
Conclusion The degree of periodontal disease was found to be dependent on the pace of fibrosis dynamics.

P-396

Molecular evidence for a toxic memory effect in chronic liver disease

C Stumptner, K Wagner, H Denk, K Zatloukal
Institute of Pathology, University of Graz, Graz, Austria

Introduction Alcoholic liver disease shows a toxic memory effect: patients with a history of alcoholic hepatitis show even after prolonged withdrawal from alcohol rapid reappearance of alcoholic hepatitis upon reexposure to alcohol. This type of liver injury can be mimicked in a mouse model by feeding 3,5-diethoxycarbonyl-1,4-dihydrocollidine (DDC). After 2 months of DDC intoxication mouse livers revealed ballooned hepatocytes containing numerous Mallory bodies. Within four weeks of recovery from intoxication most Mallory bodies disappear but rapidly reappear within three days of reintoxication indicating the existence of a toxic memory effect. The aim of this study was to investigate the molecular basis of the toxic memory effect.
Materials and methods cDNA-libraries were generated from normal and DDC-intoxicated mouse livers by subtractive suppressive hybridization. These gene libraries were used to produce cDNA-arrays for expression profiling. RNA was isolated from mouse livers at different stages of intoxication, recovery and reintoxication and hybridized to the cDNA-arrays. Expression profiles were analysed by Genesight- and Imagene software.
Results and conclusion Results obtained demonstrated several groups of genes differently expressed in short-term intoxicated naive and reintoxicated mice. These genes comprised Cyp2A5 as well as genes involved in the cellular response to oxidative stress and methionine metabolism. The sustained elevated level of Cyp2A5 during recovery and the enhanced induction upon reintoxication could explain why certain drugs lead to enhanced liver toxicity upon repeated administration even after long drug-free intervals.

P-397

The role of keratin in toxic liver injury

K Zatloukal[1], C Stumptner[1], A Fuchsbichler[1], P Fickert[2], M Trauner[2], H Denk[1],
[1]Institute of Pathology, University of Graz, Graz, Austria
[2]Department of Medicine, University of Graz, Graz, Austria

Introduction Alcoholic (ASH) and non-alcoholic (NASH) steatohepatitis as well as certain chronic cholestatic liver diseases and copper toxicosis are associated with severe alterations of the hepatocytic intermediate filament cytoskeleton. Diseased livers reveal ballooned hepatocytes with a loss of cytoplasmic keratin filaments and the formation of keratin-containing cytoplasmic inclusions named Mallory bodies. These alterations can be reproduced in mice by chronic intoxication with 3,5-diethoxycarbonyl-1,4-dihydrocollidine (DDC). The aim of this study was to investigate the role of keratin alterations in toxic liver injury we compared the effect of DDC-intoxication in keratin 8 null mice (obtained from H. Baribault, La Jolla) as well as keratin 18 null mice (obtained from T. Magin, Bonn).
Materials and methods Both knock-out mice were crossed into the same genetic background and their responses to toxic injury monitored by gene expression profiling using cDNA-arrays containing liver-specific gene libraries.
Results and conclusion A much more pronounced toxicity of DDC was found in keratin 8 null mice whereas keratin 18 null mice behaved like wild-type mice. Keratin 8 null mice revealed increased expression of several genes particularly related to the oxidative stress response. The different toxicities in keratin 8 and keratin 18 null mice indicate that keratins fulfill in addition to their structural role non-skeletal functions and that keratin 8 acts as a modulator of toxic injury in hepatocytes.

P-398

Evaluation of FAS, FASL and TGF-beta1 molecules in hepatocellular carcinoma

K Pancaroglu, F Doran, A Uguz
Cukurova University School of Medicine Dept. of Pathology, Adana, Turkey

Introduction TGF-beta, FAS, FASL molecules take part in the regulation of apoptosis. FAS is a cell surface receptor present in most of the cells. FASL can be secreted from the surface of the cells and when it binds to FAS, they activate the caspases to trigger the apoptosis. Although the mechanism of TGF-beta is not clear yet, it plays a role in tumorigenesis. TGF-alpha may indicate inhibitory or stimulatory functions in conjunct with the stage of the tumors and cooperation with oncogenes and growth factors. We aimed to evaluate the correlation among the expressions of FAS, FASL, TGF-beta1 molecules in HCC.
Material and method In this study fifty cases diagnosed as hepatocellular carcinoma (HCC) between the 1992-2002 years were included. TGF-beta1, FAS, FASL expressions were evaluated immunohistochemically.
Results FAS, FASL expressions were observed together in 84% of tissue samples with HCC and 100% of the nontumoral liver tissue samples. It was noticed that FAS and FASL staining were more densely in the lymphocytes of the tumorous areas and neighboring normal tissues than the control group. There was no statistically significant correlation between FAS, FASL, TGF-B1 staining except the positive correlation between the TGF-beta1 and FAS. The poor differentiated cases weakly expressed FAS, FASL and TGF-beta1. Where as the majority of the cases stained cytoplasmic positive, some cases stained either cytoplasmic or membraneous positive.
Conclusion In HCC, tumor cells use variable pathways for apoptosis. The lymphocytes near the tumorous tissue have an important role in this process.

P-399

Dynamics of liver histology in patients with chronic hepatitis C after interferon-alpha and ribavirin therapy

B Manevska[1], I Ivanova[2], I Kotzev[2]
[1]Medical University of Varna, Department of Pathology, Varna, Bulgaria
[2]Medical University of Varna, Clinic of Hepatogastroenterology, Varna, Bulgaria

Introduction Interferon-alpha therapy for chronic hepatitis C improves hepatic inflammation and may change the evolution of disease to cirrhosis and hepatocellular carcinoma. Accurate assessment of liver fibrosis is necessary for morphologic diagnostics. The aim of this study was to evaluate the effect of Interferon-alpha and Ribavirin on liver histology; to compare the semi-quantitative (according to Ishak) and quantitative methods for evaluation of fibrosis.
Materials and methods Twenty-two patients (13 males, 9 females at mean age 40 years) with chronic hepatitis C were studied. Within 18 to 60 months from the pre-therapy biopsy and at least 6 months after the end of treatment patients were followed with second liver biopsy. Histological activity in paired liver specimens was assessed by Knodell modified score. Fibrosis was evaluated according to Ishak staging system. In addition, fibrosis was quantified in Masson trichrome stained sections using morphometric image analysis. Interferon-alpha (mean dose 495 ME) and Ribavirin were administered for 6 to 18 months. Patients were classified as complete sustained responders (n=8), relapsed after therapy cessation (n=3) and “non-responders” (n=11).
Results After treatment reduction of the histological activity score (at least one grade) was observed in 15 patients (68%). Lobular and periportal necroinflammatory lesions were decreased in both responders and non-responders ($p<0.01$). After therapy, dynamics the fibrosis degree and calculated fibrosis ratio were not significant. Fibrosis stage was improved in only 4 sustained responders (18%); remained unchanged in 7 patients, and progressed in 10 patients (45%).
Conclusions Improvement of liver histology after Interferon-alpha and Ribavirin treatment was constricted to the patients who achieved hepatitis C virus eradication. Morphometry was the informative method for evaluation of fibrosis dynamics in addition to fibrosis assessment with semi-quantitative classification systems.

P-400

Neonatal hepatitis and intrahepatic bile duct paucity: the value of quantitative analysis of histopathological parameters

A Okcu Heper[1], E Erden[1], T Doganci, Z Kuloglu[2], A Kansu[2], Y Genc[3]
[1]Ankara University, School of Medicine, Pathology Department, Ankara, Turkey
[2]Ankara University, School of Medicine, Paediatry Department, Ankara, Turkey
[3]Ankara University, School of Medicine, Biostatistic Department, Ankara, Turkey

Introduction Liver biopsy is one of the diagnostic procedures for Neonatal Hepatitis (NH)and Intrahepatic Bile Duct Paucity (IHBP). In this study we aimed to evaluate the prognostic benefits of quantitative analysis of histopathological changes in NH and IHBP.
Material and methods We studied 28 liver biopsies in which 18 were NH and 10 were IHBP. The relationships between histopathological and prognostic parameters were analyzed. Hepatic histopathological changes such as portal and periportal fibrosis, portal and lobular inflammation, bridging necrosis with fibrosis, pericellular fibrosis, giant cell transformation and extramedullary hematopoesis were evaluated and according to their absence (0) or presence (1) a histopathological score was assessed. The sum of these data was accepted as total pathological injury score. Clinical prognostic parameters consisted of the patients height, presence or absence of hepatosplenomegaly and ascites, serum levels of ALT, albumin, bilirubin, and the value of protrombine time. The sum of these data was accepted as the clinical score. The patiens were also divided into two groups whose clinical scores were <4 as good prognosis and ≥4 as bad prognosis. For statistical analysis Pearson's chi-square, Mann-Whitney-U and ROC curve tests were used.
Results We found a statistically significant negative relation between prognosis and total pathological injury score ($p=0.042$), so as pericellular fibrosis ($p=0.016$).
Conclusion During the interpretation of liver biopsies of NH and IHBP, scoring of histopathological changes should be done in order to assess the clinical prognostic outcome. Moreover, the presence of pericellular fibrosis should be evaluated and reported.

P-401

Immunohistochemical analysis of hepatocellular carcinoma and intrahepatic cholangiocellularcarcinoma using markers supposed to indicate respective levels of diffentiation of the hepatic cell lineage

K Ishida, M Endoh, J Takeyama, K Sakamoto, M Watanabe, T Moriya, H Sasano
Department of Pathology, Tohoku University Hospital, Sendai, Japan

It is widely recognized that there are diagnostically problematic cases among primary hepatic tumors. They cause difficulties in distinguishing between hepatocellular carcinoma (HCC) and intrahepatic cholangiocellularcarcinoma (CC). Meanwhile, recent progression of study on hepatocyte-diffrentiation has revealed that both mature hepatocyte and biliary epithelial cell should originate from the common cell lineage called as hepatic-progenitor-cell (HPC), bipolar-cell (BC) and/or intermediate-hepatocyte-like-cells. Thus, we performed immunohistochemical analysis for HCC and CC using markers supposed to indicate respective levels of differentiation of the hepatic cell lineage, in order to identify the origin of the tumors particular in the diagnostically problematic cases.
Materials and method Surgical specimens of 21 cases of HCC and 7 cases of CC were used. Ordinary immunohistochemical staining was performed with following antibodies; hepatocyte monoclonal antigen (Hep), c-kit, CK7, CK19 and CK20. The results were compared from the view of the histopathological findings and immunohistochemical reactions.
Results Rate of positive (>50%) and focal positive (>5%) were Hep; HCC 76%, CC 29%, c-kit; HCC 17%, CC 44% and CK19; HCC 23%, CC; 100%. CK7 and CK20 were similar as previously reported. In addition noteworthily, double positive for Hep and c-kit was observed on two cases of CC having apparent glandular formation.
Conclusions 1) HCC had a lower positive rate for Hep compared with previous reports. 2) CC with positivity for Hep might exist. 3) According to the c-kit staining pattern, we considered that there might be a peculiar variant of tumor cells in CC differentiating both hepatocyte and biliary epithelial cell.

P-402

Morphological consequences of starvation upon the liver

L Bizjak Mali[1], V Ferlan-Marolt[2], B Bulog[1]
[1]Department of Biology, Biotechnical Faculty, Univ. of Ljubljana, Slovenia
[2]Institute of Pathology, Faculty of Medicine, University of Ljubljana, Slovenia

Introduction Proteus anguinus, the sole species of the European Cave salamander and the remarkable cave dweller of underground waters in the Karst of Slovenia is well adapted to poor and discontinuous food supplies. Remarkable accumulation of lipid droplets and glycogen deposits in the liver beside slow metabolism allow Proteus to survive for long periods without food. The aim of this study was to establish morphological changes in the liver during starvation with particular emphasis on mobilization of the liver energy reserves.
Material and methods The liver was examined after food deprivation periods of one, four and eighteen months, respectively using light and transmission electron microscopy. Glycogen and proteins concentrations were determined spectrofotometrically. Total fat in the liver was estimated by Folch method.
Results Intense depletion of glycogen was present during first month of starvation. The glycogen wasn't formed in clumps typical for normal liver tissue. After eighteen months of fasting glycogen was re-synthesized, dense glycogen deposits appeared. Lipid droplets were less condensed. Numerous peroxisomes formed clusters with small and round mitochondria. Particular mitochondria increased in size and lost cristae. Lysosomes and autophagic vacuoles were numerous, too. Dilated intercellular space included electron dense granular material.
Conclusions Carbohydrate and lipid reserves in the liver of Proteus serve for metabolic needs during food deprivation. While in many other vertebrates fasting causes depletion of liver carbohydrates, these reserves are maintained in large amounts in Proteus. Results of our study confirm that a detailed morphological analysis of the liver could be a relevant informative method to prove metabolic adaptability of this organ.

P-403

Evaluation of T lymphocyte subpopulations in chronic hepatitis- relationship with histological lesions

CI Iosif, F Vasilescu, G Butur, DC Terzea, C Dobrea, F Andrei, C Ardeleanu
'Victor Babes' National Institute, Bucharest, Romania

Background Intrahepatic T lymphocytes are believed to be involved in immunopathogenesis of chronic viral hepatitis. The aim of this study was to assess the correlation between morphological lesions and T lymphocyte subpopulations in liver and peripheral blood (PB) of patients with chronic hepatitis.
Methods and results 51 liver biopsy specimens from patients serologically confirmed (15 HBV and 36 HCV) were studied by histopathological and immunohistochemical methods. T cell subtypes (CD4, CD8, CD57) were tested by using monoclonal antibodies on tissue samples and by flow cytometry in PB.
Results In PB, 80% of patients have T lymphocyte CD8+ decreased and 65% of them have augmented values of T lymphocytes CD4+. In liver biopsy the prevalent subpopulation were CD4+ cell, being approximately twice higher than CD8+ cells. The observed histological lesions were quantified by Ishak score as moderate\severe chronic hepatitis.
Conclusions Decreased subpopulation of CD8+ T lymphocyte might contribute to the severity of liver disease. Relatively more frequent cell type was CD4 positive T cell, having a significant association with a higher inflammatory activity in both types, B and C virus hepatitis.

P-404

The role of survivin in regulation of proliferative and apoptotic activity of hepatocellular carcinoma

C Joksimovic[1], J Pizem[2], B Luzar[2], V Ferlan-Marolt[2], A Coer[1]
[1]Institute of Histology and Embriology, Medical Faculty, Ljubljana, Slovenia
[2]Institute of Pathology, Medical faculty, Ljubljana, Slovenia

Introduction Imbalance between proliferation and apoptosis is an important factor in progression of hepatocellular carcinoma (HCC). Aims: The percentage of proliferative (PI) and apoptotic cells (AI) in HCC compared to non-tumor liver was investigated. The role of unprocessed as well as active form of caspase-3, which is an important apoptotic protein was of great interest for this study. Expression of survivin, an inhibitor of apoptosis was investigated, too.
Material and methods Twenty patients with HCC were included in the study. Two samples were obtained from each patient, one of HCC and one of the surrounding non-tumor liver. MIB-1 antibody was used to determine the proliferative activity. Immunohistochemical staining for the detection of active form of caspase-3 was used to determine the percentage of apoptotic cells and for detection of procaspase-3 and survivin expression, as well.
Results AI was higher in HCC (1,532 ± 1,05) compared to non-tumor liver (0,426 ± 0,62), but the proliferative activity in HCC was much higher than apoptotic activity. 75% of HCC showed positive staining for pro-caspase 3. Positive correlation between expression of pro-caspase 3 and active form of caspase 3 proved to be statistically significant. 70% of HCCs were survivin positive. Stronger expression of survivin was detected in HCC compared to non-tumor liver. Positive correlation between survivin expression and the grade of tumor diferentiatiation as well as a significant association between survivin expression and both AI and PI was also detected.
Conclusion Our results indicate that survivin promoting cell proliferation in HCC has an important role in HCC progression.

P-405

The histopathological effects of offloading on liver of rat embryo

A Khaki[1], AA Khaki[2], J Solimany Rad[2]
[1]Faculty of Veterinary Medicine of Tabriz Islamic Azad University, Tabriz, Islamic Republic of Iran
[2]Faculty of Medicine Science.Tabriz Medical Science University, Tabriz, Islamic Republic of Iran

Introduction Ofloxacin is an antibiotic from fluroqinolne with a wide range and widely used in various infection diseases. Since there is little information about ofloxacin side effect on liver of rat embryo. This preliminary study was planed to see what kind of changes occurs in development of liver in Rat embryo. The aim of present study was to determine the histopathological effects of offloading on liver of rat embryo.
Material and methods Fourty nine Wistar rats were selected and randomly divided into two groups; control (n=21) and test (n=28). The test group has been received 14mg/kg (PO) Ofloxacin daily during pregnancy. However, the control group just received plate. After delivery, liver tissue of neonatal in both groups were taken and prepared for light microscopy. Staining method was H&E.
Results Microscopic study of liver tissue specimens showed that in the test group hepatocytes were vesiculated. Degeneration and vacuolated pycnotic nuclei were seen when compared to control group. Weight of neonatal in test group was reduced when it was compared with the control group ($P<0.05$).
Conclusion Since Ofloxacin had side effects on liver of rat embryo, it is not suggested to be used during pregnancy in human.

P-406

Gene expression profiling of human hepatocellular carcinoma

JH Neumann[1], C Gülly[2], K Panzitt[1], CR Buck[2], H Strohmaier[2], H Denk[1], K Zatloukal[1]
[1]Institute of Pathology, University of Graz, Graz, Austria
[2]Oridis-Biomed, Research & Development, Graz, Austria

Introduction While the underlying etiology of HCC has been well characterized the molecular mechanisms of hepatocarcinogenesis are poorly understood. The extremely poor prognosis of HCC and the limited value of the current standard clinical markers underscore the need for improvent of diagnosis and treatment of this deadly disease. Aims: We performed gene expression profiling using cDNA microarrays in order to identify novel molecular markers and therapeutic targets for the treatment of HCC.
Material and methods We used the method of subtractive suppressive hybridization (SSH) to generate cDNA libraries that are highly enriched with clones representing genes both up- and downregulated in the diseased liver tissue. The expression pattern of 4600 clones representing ~ 4000 genes was analyzed in 26 surgically resected hepatocellular carcinomas, 4 focal nodular hyperplasias, one adenoma, and 6 cirrhotic livers by competetive

hybridization on custom made cDNA microarrays using a pool of non-neoplastic human liver as reference. The expression data were verified independently by quantitative RT-PCR (TaqMan).
Results We found 500 genes which were consistently deregulated in more than one third of the HCCs under investigation. Of these, 250 genes had been previously implicated in HCC, whereas 210 known genes as well as 40 novel genes (with unknown function) had not yet been linked with liver cancer.
Conclusions The present study revealed a number of genes specifically deregulated in hepatocelluar carcinoma. Future work will aim to evaluate the medical relevance of the encoded proteins which will ultimately help to identify potential new markers for better diagnosis/ prognosis of HCC and new targets for therapeutic intervention.

P-407

Actinomycosis: a report of 10 cases - an experience of the Anatomy and Pathology Laboratory of Casablanca Hospital

H El Attar, S Azzouzi, S Saida, I Ahmed
Central Laboratory of Pathology Pavillon 41, Hopital Ibn Rochd, Casablanca, Morroco

Introduction Actinomycosis is a suppurative and granulomatous chronic infectious disease caused by Actinomyces sp. and most commonly affecting the cervicofacial area. Aim: To study the clinical characteristics of patients with actinomycosis, with regard to clinical history, presentation, method of diagnosis and comparing to the literature.
Patients and methods From January 2000 to July 2002, a retrospective review was performed on all cases of histologically proven actinomycosis.
Results Ten patients were studied, 5 men and 5 women, 5-65 years old. Two patients had a history of surgical procedures and/or dental manipulations. Two patients had a long history of diabetes mellitus. Locations were the liver (patient n 1), the feet articulation (patient n 2), the lung (patient n 3), the jugular lymph node (patient n 4), the skin (patients n 5 and 6), mandibular (patient n 7), the psoas muscle (patient n 8), the appendix (patient n 9) and the large bowel (patient n 10). Three patients showed a tumoral presentation (patients n 3, 8 and 10) and two patients had a tuberculosis disease presentation (patients n 2 and n 4). The patient n 9 had a clinical presentation of an inflammatory large bowel disease. One patient was diagnosed by cultures positive to A. israelii on microbiologic study and the others patients by surgical biopsy and detection of an actinomycosic granuloma. Special stains were used in all cases. Three patients received the classic initial regimen of iv.
Conclusion Actinomycosis is an uncommon disease in our country. In these cases gastrointestinal locations were predominant. Two uncommon locations were present. There was no IUD associated infection. Tuberculosis endemic in our country can mislead the diagnosis.

P-408

Further autopsy hazards: Mycobacterium tuberculosis in the autopsy room

R Flavin, S O Briain
St. James Hospital/TCD, Dublin, Ireland

Introduction Tuberculosis has been the major occupationally acquired disease in the autopsy room. The risk of encountering tuberculosis at autopsy has fallen with the decreased incidence of the disease and greater emphasis has been placed recently on the hazards of viral diseases. However, tuberculosis may still be found at autopsy. The aim of this study was to assess the magnitude of exposure to Mycobacterium tuberculosis at autopsy in a large general hospital setting.
Methods Retrospective search of the autopsy records from 1991-2000. The patient record and histological slides were reviewed. The quantity of mycobacteria was assessed from the Ziehl-Neelson stains as scanty, moderate or abundant.
Results 13 cases of active Mycobacterium tuberculosis were identified in the 10-year period in which 3740 autopsies were performed (1 per 374 autopsies) of which 10 cases were unsuspected (77%). These included 7 cases of miliary tuberculosis and 2 with pulmonary infection. 3 cases contained abundant organisms. Patients tended to be middle aged and male with complex clinical histories. 3 patients were dead on arrival at hospital.
Conclusion The risk of unexpectedly encountering tuberculosis at autopsy continues and has implications for the health of autopsy room staff, autopsy room ventilation and design, protective equipment and for the involvement of the public health service.

P-409

Testing of the histological parameters for predicting the liver fibrosis in hepatitis C virus infection in drug abusers

J Gligorijevic[1], D Tasic - Dimov[1], D Dimov[1], M Milentijevic[1], M Kostov[2]
[1]Inst. of Patology, Medical Faculty of Nis, Nis, Serbia and Montenegro
[2]Military Hospital Nis, Nis, Serbia and Montenegro

Introduction The course of chronic hepatitis C virus infection is difficult to predict. Although the disease is frequently asymptomatic, the development of fibrosis and cirrhosis are the major complications. Among patients suffering from chronic hepatitis C (CHC), special group are young drug abusers. Immunological toxicity of narcotics modulates the total immunologic response to the viral infection with characteristic morphologic expression of this disease. The aim of this study was to asses which pathological features are associated with liver fibrogenesis and are predictive to fibrosis in CHC drug abusers.
Methods Eighty liver biopsies with CHC from drug abusers (43 actively consumers; 26 free from drugs 3-6 months before liver biopsy and 11 free for more than one year before performing liver biopsy) stained by HE, Trichrom Masson, Perls and reticulin were analyzed semi quantitatively using standard questioner for determination of patohistological features for histological activity index. Results of fibrosis were correlated to all of them.
Results The fibrosis was 0, 1 and 2 in this group of young patients (mean age 22, 3 years). There were no correlation between any of the patohistological parameters and fibrosis, even for lobular necrosis.
Conclusion Histomorphological changes and the extent of fibrosis are in correlation to the duration of drug consumption. Morphological expression of immune toxicity of narcotic drugs in CHC patients make this disease special entity to which it is not possible to apply standard histopatologic parameters, nor the parameters predicting liver fibrosis.

P-410

Clinical, parasitological and morphological features of amebiasis in Vilnius

A Barakauskiene[1], A Marcinkute[2]
[1]National Centre of Pathology of Vilnius, Lituania
[2]Vilnius University Hospital for Infectious Diseases, Lituania

Introduction Among the acute bowel infections there is tendency of increasing cases of unknown diarrhoea. The occurrence of this disease in Lithuania is presented by only a few confirmed cases per year, mostly imported by travellers from abroad. The most pathognomic clinical features of the disease are hemocolitis without severe tenesmus. Fresh feces microscopy has improved the diagnosis. Parasitological morphological data were very useful**.** The aim of this study was to define prevalence of amebiasis among acute infectious diarrhoeal patients. To provide commonest clinical symptoms and syndromes of amebiasis. To improve routine morphological diagnostics in suspicion of amebiasis in Vilnius.
Material and methods Diarrhoeal patients with confirmed amebiasis were analysed during the four-year period in VU Hospital for Infectious Diseases and statistical analysis of epidemiological and clinical data was performed. Morphological data of biopsies were analysed too.
Results Common manifestations of amebic enterocolitis diarrhoea such as blood in stool, abdominal pain or cramps, tenezmus, fever, and gastrointestinal symptoms were present in all patients. Asymptomatic patients were as cysts carriers. Systematic complications were observed in one patient with hepatic abscesses. One patient had sigmoid ameboma. All patients were males.
Conclusion Amebiasis is a rare parasitic infection and makes up to one percent of all bowel infections. Amebiasis can be suspected in cases with abdominal cramps and bloody diarrhoeal episodes without severe tenezmus and with travel history. Fresh faeces microscopy was the main diagnostic method. It is very important to recognize the E histolytica trophozoites from histiocytes in the biopsies.

P-411

Conjunctival epithelial neoplasia and HIV infection in Africa

G Stropahl[1], A Timm[2], C Sinzidi[3], C Fischer[4], E Herz[5], E Reisinge[6], H Nizze[1], R Guthoff[2]
[1]Institute of Pathology, University of Rostock, Germany
[2]Clinic of Ophthalmology, University of Rostock, Germany
[3]Clinic of Ophthalmology, University of Kinshasa, D.R. Congo
[4]Christoffel Blind Mission, Maswingo, Zimbabwe
[5]Christoffel Blind Mission, Bafoussam, Kamerun
[6]Clinic of Internal Medicine, University of Rostock, Germany

Introduction Epithelial tumors of the conjunctiva are rare diseases in Europe. In sub-Saharan countries, an increasing incidence was observed in connection with the HIV epidemic. The definite causes of these tumors are not known. Aims: Based on tumor material from Africa, we search for possible cancerogenic agents and its pathogenetical interaction in conjunctival carcinoma.
Materials and methods Conjunctival specimens of 68 patients from three African centers with the following histological lesions were examined: papilloma (1 case), pinguecula (5), conjunctival intraepithelial neoplasia (8 CIN I, 12 CIN II, 18 CIN III), squamous cell carcinoma (SCC, 24 cases). Immunohistological reactions for p53 and p16 were done. 23 of 38 tested patients were HIV positive.
Results and conclusion 39 of the 44 benign and precancerous lesions were associated with histological signs of a solar damage. 62 of the 68 cases showed immunohistologically an overexpression of p53, among them all SCC. This finding might indicate a p53 mutation as mostly seen in solar induced skin cancer too. 50% of the cases with CIN III and SCC had an overexpression of p16. Corresponding findings are known from transformed or neoplastic cervical epithelium in strong correlation with an active HPV (type 16,18) oncogene expression. No significant differences occurred between HIV positive and HIV negative cases in comparison to the frequency of different histological lesions as well as the p53 and p16 expression. The average manifestation age for CIN III and SCC in HIV positive cases (30 resp. 38 years) was 20 years lower than that of HIV negative cases (51 resp. 58 years). The results suggest a multifactorial tumorgenesis (UV radiation, oncogenic viruses, HIV infection) for the conjunctival carcinoma in Africa.

P-412

Craniofacial Botryomycosis: an unusual South African case

P Medley, N Ramlachan
Medical University of South Africa, Pretoria, South Africa

Introduction Botryomycosis is an enigmatic pyogranulomatous infection, which may be caused by a variety of non-filamentous bacteria including Staphylococcus aureus and Pseudomonas aeruginosa. While the exact pathogenesis remains elusive, it is acknowledged that the interrelationship of host and agent factors is fundamental. We describe the clinicopathological features of a rare and particularly mutilating case of delayed onset post traumatic craniofacial botryomycosis.
Methods An immunocompetent 57-year-old Black male presented with multiple sinuses draining granules involving the frontal, parietal, orbital and maxillary areas. Nodulo-fibrous thickening was also present. This had evolved over a three-year period. Apart from the history of a head injury requiring cranioplasty 27 years earlier, no other predisposing factors were found.
Results The diagnostic features of clumped bacteria (cloxacillin sensitive Staphylococcus aureus), Splendore-Hoeppli phenomenon, granulomata and intense fibrosis were confirmed histologically. There was no response to intravenous cloxacillin and the patient died before surgical debridement could be done.
Conclusion This case report serves to highlight several points. Firstly, it illustrates that when considering the diagnosis of post traumatic botryomycosis, the time interval between the traumatic event and the onset of clinical features may span decades. We submit that this is due either to the small size of the bacterial load or their low virulence. Secondly, it is our contention that the poor response to antibiotics is due to the severe, impenetrable fibrosis. Finally, the destructive nature of the disease underscores the urgency in diagnosis and treatment.

P-413

Tuberculous meningitis in adulthood

F Staniceanu[1,2], A Streinu-Cercel[1,3], S Zurac[2], A Oprisan[1]
[1]University of Medicine and Pharmacy, Bucharest, Romania
[2]Colentina Hospital, Department of Pathology, Bucharest, Romania
[3]Matei Bals Institute, Department of Infectious Diseases, Bucharest, Romania

Introduction Tuberculous meningitis is a very frequent clinical manifestation of postprimary tuberculosis in childhood as the result of hematogenous dissemination of a pulmonary lesion; in adult patients tuberculous meningitis occurs less frequently, mainly associated with extrapulmonary disease, consequent to the rupture of a subependymal tubercle.
Case reports We report 4 cases of tuberculous meningitis in adulthood diagnosed by autopsy examination – median age 38,25 yrs – in an autopsy series of 20 tuberculous patients in 10 years. All but one of the patients had disseminated disease (lung, lymph nodes, liver, spleen and kidneys). None of the patients presented subependymal tubercles. One patient had dual mycobacterial infection - miliary tuberculosis due to Mycobacterium tuberculosis in all the extracranial affected organs and tuberculous meningitis with Mycobacterium avium-intracellulare (MAC). Cerebrospinal fluid examination revealed high cellularity and high albumin concentration in all cases; glucose levels were low, except in one case with normal glucose content – the MAC infected patient. One patient had associated systemic lupus erythematosus (SLE) and low CD4+ cells count. The histopathologic appearance consisted of a granulomatous meningitis with giant cells and epithelioids in three cases and polymorphous inflammatory infiltrate including numerous positive bacilli in Ziehl-Neelsen stain in MAC infected patient.
Conclusion The overall appearance suggested a hematogenous spread of the infection, the immune status correlating with the occurrence of the meningeal disease; in our series we had an immunodepressed patient (SLE) and another patient with miliary tuberculosis and superimposed MAC infection. Also, MAC meningitis had a different clinical and histopathologic appearance.

P-414

Surgical extrapulmonary tuberculosis - 12 years of experience

SD Enache[1], IE Plesea[2], M Ghilusi[1], E Vollmer[3], T Goldmann[3], J Galle[3]
[1]Department of Pathology, No. 1 County Emergency Hospital, Craiova, Romania
[2]Department of Pathology, University of Medicine and Pharmacy, Craiova, Romania
[3]Department of Pathology, Forschungszentrum Borstel, Germany

Aim The authors reviewed 390 cases of surgical extrapulmonary lesions diagnosed as tuberculosis in No.1 County Emergency Hospital Department of Pathology from Craiova, Romania and assessed the diagnosis by means of new diagnostic tools.
Material and methods The samples were fixed in formalin, embedded in paraffin wax and stained with hematoxilin-eosin, van Gieson and Ziehl-Neelsen stains. Immunohistochemical staining with antibodies for CD3, CD20, CD68, LCA and S100 were used. PCR technique was used in 27 cases with controversial diagnosis.
Results The diagnosis was confirmed in 363 cases. The most frequent affected sites were the lymph nodes, followed by digestive system, urinary system and male genital system. Immunohistochemical stains cleared up the diagnosis in 38 cases. PCR was used in 27 cases with atypical granulomas, establishing the diagnosis of tuberculosis in 10 of them.
Conclusions Tuberculosis in extrapulmonary sites discovered in surgery departments is more and more frequent. In cases with controversial diagnosis of granulomatous lesions, immunohistochemistry and PCR techniques are required for clearing up the diagnosis.

P-415

Molecular analysis of caseous granulomas

A Fassina[1], M Menegazzo[1], R Provvedi[2], R Manganelli[2]
[1]Dpt of Pathology University of Padova, Italy
[2]Dpt of Microbiology University of Padova, Italy

Introduction Clinical presentation and lesion morphology are often suggestive, but not conclusive for Mycobacterial (MB) infections. Rapid and accurate specific diagnosis is mandatory since appropriate therapy can be chosen only on the basis of the precise identification of the causative agent. One of the most promising tools for rapid and sensitive identification of MB species is represented by amplification of specific sequences of the 16S rRNA MB specific gene on the fragmented DNA (max 200 bp) obtained from fixed tissues.
Methods DNA was extracted from 15 cases selected from the archives of the Department of Pathology, University of Padova, with histopathologic features of granulomas, caseous necrosis, and Langhans-type giant cells. Ziehl-Neelsen staining for acid-fast bacilli and PCR/direct sequencing of a 155 bp variable region of the MB 16S rRNA gene were performed. H37Rv genome was employed as positive control.
Results MB specific sequences have been identified in 12 of 15 samples analyzed (80%). In two DNA samples (13%) an inserted DNA product was detected and it is currently under sequencing, while in one sample (7%) no evidence of MB infection has been gained. Agreement with Ziehl-Neelsen was present in 8 cases (53%).
Conclusion Our study suggests that PCR is a rapid, sensitive method for the diagnosis of MB in routinely processed formalin-fixed, paraffin-embedded histological specimens and is highly recommendable in cases of chronic inflammation without definite evidence of granulomatous inflammation.

P-416

Cerebral abscesses caused by Cladosporium bantianum - A report of six cases

M Chaturved, A Shenoy, A Goel
Seth G.S. Medical College, K.E.M. Hospital, Mumbai, India

Introduction Cladosporium bantianum is a pigmented highly neurotropic fungus which can be identified easily in tissue sections due to their golden brown colour. Cerebral lesions caused by this fungus are rare.
Case reports We present six cases diagnosed at our institute over a period of 36 yrs. (1966-2002). There were 5 Males and 1 Female. All patients belonged to the second to fourth decade and had presented with symptoms of space occupying lesion. Radiological investigations revealed well circumscribed lesions with ring enhancement. The smallest lesion measured 0.1x0.1cm and largest measured 3x1.5x1 cm. Only two of the six cases had detectable predisposing debilitating illness. One 48 yr. old male had past history of Liver Tuberculosis and had taken anti-Tuberculosis treatment and a 26 yr. old female had systemic lupus erythematosus and was on immunosuppressants. We received four surgically excised specimens and two autopsy specimens of the entire brain. Histopathology revealed necrotic areas, micro-abscesses and mainly foreign body type of giant cells. Lying within the giant cells as well as

freely within the tissue were numerous golden brown to deep brown spherical forms of Cladosporium bantianum measuring 8-10 microns in diameter and their hyphal forms measuring 4-5 microns in diameter, 10-12 microns in length with septae and occasional branching. These were confirmed by Gomori's methenamine silver stain for fungus and species identification was carried out by culture studies. All the four patients with surgical excision showed recurrence within 3-4 months. Three succumbed to the disease and one is still alive.

Conclusion Cladosporium bantianum can affect both healthy as well as immunocompromised individuals. It has a fatal outcome. Cases are being presented because of the relative rarity.

P-417

Necrobiotic changes of skeletal muscle simulating myxoid sarcoma. Report of a case with immunohistochemical and electron microscopic studies

KW Min[1], IS Seo[2]
[1]Deaciness Hospital, Oklahoma City, USA
[2]Wishard Memorial Hospital, Oklahoma City, USA

Background Skeletal muscles are known to undergo bizarre reactive changes in response to traumatic injuries and may produce pseudosarcomatous lesions which may give diagnostic challenges to pathologists. Such lesions usually produce proliferative myositis in which atypical spindle cells of fibroblastic and myofibroblastic nature predominate and may simulate the appearance of fibrosarcomas and myofibrosarcomas. However with proper setting of previous trauma history, their true nature can be easily appreciated. We are reporting an unusual case of myxoid cellular lesion found in the abdominal rectus muscle involved in a post hysterectomy abdominal hernia which simulated the appearance of an extraskeletal myxoid chondrosarcoma (EMC). Its true reactive nature was recognized by electron microscopic (EM) study.

Design Light brownish gelatinous material aggregating 2.5x 2.5x1.0CM was found around the sheath of rectus abdominis muscle of a 48 year old female during a repair surgery of posthyterectomy ventral hernia. The tissue was fixed in buffered formalin and a representative portion of the tissue was fixed in phosphate buffered 2.5% glutaraldehyde and post fixed in osmium with en bloc staining with uranyl acetate. Epon embedded thin sections were stained with uranyl acetate and lead citrate. For immunochemistry, paraffin sections were stained for S100 protein, myosin, and actin by routine ABC-peroxidase techniques.

Results On routine examination, the lesion was characterized by loosely arranged spindly to epithelioid cells in bundles with abundant myxoid stroma. The lesional cells varied in size with frequent bizarre hyperchromatic nuclei. Mitosis was rare. The cells showed weakly positive diffuse cytoplasmic stain for all of above antibodies. With the initial impression of EMC, an expert opinion confirmed the diagnosis of grade II EMC. However, EM revealed the lesional cells to be consistent with skeletal muscle cells having of varying stages of degeneration and regeneration. No ultrastructural characteristics seen in the tumor cells in EMC were present. The attending physician was advised of careful follow-up and close observation without any additional treatment. The patient remains with no evidence of disease by 7 year follow-up in spite of incomplete excision of the lesion.

Discussion and conclusion The myxoid gelatinous material found in the abdominal rectus muscle presented herein showed histopathologic characteristics of EMC, however, electron microscopic studies revealed the lesion to be necrobiotic process of the rectus muscle. Evidence of no disease in 7 years of follow-up with incomplete excision supports the conclusion the lesion was not malignant as EM study indicated. This case exemplifies another variety of pseudosarcomatous reaction of skeletal muscles important in the differential diagnosis in the pathologic evaluation of cellular myxoid lesions.

P-418

Peritoneal psammocarcinoma. A case report with ultrastructural study

IS Seo[1], H Michael[1], M Goheen[2], KW Min[3]
[1]Wishard Hospital-Indiana University Medical Center, Indianapolis, USA
[2]IU Medical Center, Indianapolis, USA
[3]Deaconess Hospital, Indianapolis, USA

Background Psammocarcinoma (PC) is a very rare variant of low grade serous tumors that appears to arise from the peritoneum and ovaries. This tumor has been defined as a serous neoplasm displaying 1) destructive invasion, 2) no more than moderate nuclear atypia, 3) no areas of solid epithelial proliferation except for occasional nests no more than 15 cells in diameter, and 4) at least 75 % of papillae or nests are associated with or completely obscured by psammoma bodies. PC shares some clinicopathologic features with serous tumor of low grade malignant potential (LMP), but may have been under-recognized at surgery and gross examination. The present case was incidentally found during a routine hysterectomy procedure for leiomyomas. The PC involved the omentum, peritoneum and diaphragm. We report, to our best knowledge, the first electon microscopic (EM) findings of PC.

Design Tumor tissue was fixed in buffered formalin for routine examination. In addition, a representative tissue was fixed in phosphate buffered 2.5% glutaraldehyde and post fixed in osmium with en bloc staining with uranyl acetate for EM study.

Results This tumor met the diagnostic criteria of psammocarcinoma. There were numerous psammoma bodies with or without nests of epithelial proliferation with minimal nuclear atypia. More than 75% of papillae were either associated with or completely replaced by psammoma bodies. Multifocal involvement was noted on the surfaces of both ovaries and fallopian tubes. Ultrastructurally, the tumor cells showed markedly villous surfaces with abundant long slender villi. Their length/diameter ratio (LDR) was 4 with some variation of their diameter. The cytoplasm contained abundant cytoplasmic organelles and intermediate filaments. Intracytoplasmic lumens were absent. Decalcified psammoma bodies resembled cut surfaces of geode.

Discussion and conclusion Our case met the proposed criteria for this tumor that arose de novo in peritoneum. Ultrastructurally, this tumor shared some findings with serous tumors (junctional complexes, irregular microvilli), but differed by the lack of prominent desmosomes and frequent intercellular lumens. PC differed from mesothelioma in that significantly greater microvillus LDR, prominent desmosomes, tomofilaments, intracytoplasmic lumens, external lamina and glycogen were rountine findings in the latter. Our findings justify classification of PC in the group of serous epithelial tumors arising from the coelomic mesothelium.

P-419

Application of electron- and immunoelectron microscopy in the differential diagnosis of pituitary adenomas

M Maksymowicz, W Olszewski
Department of Pathology, Institute of Oncology, Warsaw, Poland

Aim Evaluation of practical implementation of electron microscopic techniques in diagnosis of pituitary adenomas. **Material and methods** Material consists of 203 consecutive cases of surgically resected pituitary tumors. In 184 pituitary adenomas diagnosed clinically, there were 68 patients with symptoms of acromegaly, 32 patients with hyperprolactinemia, 33 cases of Cushing's syndrome and 1 case of TSH hypersecretion. There were 50 clinically nonfunctioning tumors. All cases were diagnosed by histological examination and immunohistochemical identification of known pituitary hormones (growth hormone, prolactin, ACTH, TSH, FSH, LH and alpha-subunit). The cases evaluated at light microscopy level as pituitary adenomas were examined with electron microscopy and immunoelectron microscopy using a postembedding immunogold technique.
Results Immunohistochemical investigation showed that about 40,1% of specimens of pituitary adenomas contained more than one pituitary hormone. Additionally, immunopositivity was discovered in 29% of tumors from patients with clinical and biological signs of silent pituitary adenoma. Ultrastructural analysis provided proper diagnosis of selected cases, e.g. silent corticotroph adenoma or distinction between densely- and sparsely granulated growth hormone secreting adenomas. Double labeling immunoelectron microscopy using gold particles of two different sizes greatly facilitated the distinction among mixed growth hormone/ prolactin, mammosomatotroph and acidophil stem cell adenomas.
Conclusions Electron microscopy analysis was valuable to provide a useful informations regarding the diagnosis. Our results confirmed practical value of WHO recommendation for five-tier evaluation of pituitary adenomas (clinical, neuroimaging, histological, immunohistochemical and ultrastructural). On the basis of our results and the published data, diagnostic postoperative algorithm for proper pathologic management has been proposed.

P-420

Apoptosis, sarcomere disruption and myofibrilar degeneration in skeletal muscles of stable COPD patients: an ultrastructural study

MD Ferrer[1], M Orozco-Levi[2], J Lloreta Trull[1], E Diaz[3], S Boluda[3], L Pijuan[3], E Barreiro[4], S Serrano[5], J Gea[2]
[1]Pathology Department, Hospital del Mar, IMIM-UPF, Barcelona, Spain
[2]Muscle Research Unit and Pneumology Department, Hospital del Mar, IMIM- UPF, Barcelona, Spain
[3]Pathology Department, Hospital del Mar, Barcelona, Spain
[4]Muscle Research Unit, Hospital del Mar, IMIM- UPF, Barcelona, Spain
[5]Chairman of Pathology, Hospital del Mar, IMIM-UAB, Barcelona, Spain

Introduction In patients with chronic obstructive pulmonary disease (COPD), the diaphragm muscle shows signs of injury, even during clinical stability. In addition, these patients have a markedly increased susceptibility to additional diaphragm injury following inspiratory loading. We have hypothesized that, if sytemic factors play a role in diaphragm injury, limb muscles may also be affected. The purpose of this study is to investigate whether apoptosis occurs in the diaphragm and quadriceps of COPD patients, and to evaluate fiber injury in non-respiratory muscles.
Methods Samples from both diaphragm and quadriceps muscles were obtained in 22 patients undergoing thoracotomy for a low-stage lung neoplasm (LN) and stratified into two cohorts according to pulmonary function: LN+COPD (n=11) and non-COPD patients (LN+non-COPD, n=11). In addition, samples form quadriceps muscle in 7 healthy age-matched volunteers were also included (control group). All samples were processed for ultrastructural analysis. The proportion (%) of normal nuclei (NN) and those showing early (EAN) and advanced (AAN) signs of apoptosis were determined in all samples. Digital images of longitudinal fiber sections (1950x) were used to determine the area fraction (%) of abnormal myofibrilar structures (AAb).
Results The level of apoptotic signs in the diaphragm of both COPD and non-COPD groups was minimal and very similar to that of control limb muscle. In contrast, quadriceps muscle of both COPD and non-COPD groups showed a two- and three-fold increase respectively in the apoptotic nuclei when compared to controls, mainly due to EAN. Apoptotic bodies were not found. In control quadriceps AAb was 1,7±0,3%, mostly due to sarcomere disruption, while quadriceps in COPD patients was associated with an increased AAb (21±7%, $p<0,005$) including myofibrilar disorganization and degeneration.
Conclusions In patients with COPD, the diaphragm is not altered by apoptotic phenomena. Muscle remodeling through apoptotic mechanisms as well as through structural changes, such as sarcomere disruption and myofibrilar degeneration, seem to be enhanced in the quadriceps muscle of these patients, regardless of the severity of pulmonary function impairment, suggesting that additional factors such as the degree of physical inactivity either related to the disease or to the preoperative status could also be involved. (Supported in part by Grants BIOMED, FIS, FUCAP and ARMAR)

P-421

Differential CD68 expression in chromophylic (papillary) renal cell carcinoma and clear cell renal cell carcinoma: an immunohistochemical and ultrastructural study

E Díaz[1], J Lloreta[2], L Ferrer[1], T Baró[1], M Iglesias[1], V Baena[1], L Pijuan[1], L Magán[1], JM Corominas[3], S Serrano[3]
[1]Hospital del Mar-IMAS-IMIM, Barcelona, Spain
[2]Hospital del Mar-IMAS-IMIM, Universitat Pompeu Fabra, Barcelona, Spain
[3]Hospital del Mar-IMAS-IMIM, Universitat Autňnoma de Barcelona, Barcelona, Spain

Background Renal chromophylic (papillary) carcinoma (CPRC) has a propensity for storing hemosiderin in tumor cells. By transmission electron microscopy (TEM), some tumors show a prominent lysosomal component, while in other cases, cells contain mostly isometric lipid vacuoles. It has been proposed that the latter would merely represent a papillary variety of clear cell renal cell carcinoma (CCRC). The aim of this study has been to analyze the lysosomal content in chromophylic (papillary) renal cell carcinoma

by both immunohistochemical study of CD68 expression and TEM, and to compare these results with those of conventional CCRC.
Design Cases of CPRC (n=21) and CCRC (n=12) are the subject of the study. The presence and relative amount of lysosomes and isometric fat vacuoles was investigated by TEM (n=11). Immunostaining with CD68 antibody (PG-M1, Dako, Denmark) was performed in representative sections. The presence, distribution and percentage of CD68 staining in tumor cells was compared with TEM data.
Results Expression of CD68 was observed in all cases of CPRC. The mean percentage of positive cells was 63% (1-95%). Distribution of positive cells was diffuse in 67% of cases. Of the 11 TEM cases, 9 contained abundant fat vacuoles, but only 4 had extensive isometric vacuolation by light microscopy. Electron-dense lysosomes were less abundant than fat in 7 cases, 4 of which had massive CD68 expression. Detailed examination of fat vacuoles in these cases suggested they were membrane-bound and of probable lysosomal origin. CD68 expression was also observed in 11 cases of CCRC, all of them with focal distribution, involving a mean of 14% tumor cells (1-50%). These differences were statistically significant ($p<0.001$).
Conclusions Diffuse CD68 expression is typical of CPRC and may be a useful auxiliary diagnostic criterion. The isometric fat vacuoles in CPRC are often membrane-bound and of probable lysosomal origin. These findings support the notion that the lipid-containing, vacuolated variety of CPRC is different from CCRC.

P-422

Nucleolar features and prognosis of breast cancer: an ultrastructural morphometric study

M Arumi-Uria[1], M Iglesias[2], J Lloreta[3], J Vila[4], JM Corominas[5], S Serrano[5],
[1]Hospital Dos de Maig-CSI-Universitat Pompeu Fabra, Barcelona, Spain
[2]Hospital del Mar-IMIM, Barcelona, Spain
[3]Hospital del Mar-IMIM-Universitat Pompeu Fabra, Barcelona, Spain
[4]IMIM, Barcelona, Spain
[5]Hospital del Mar-IMIM-Autonomous University of Barcelona, Barcelona, Spain

Introduction Several cytological features are taken into account in infiltrating duct carcinoma of the breast. The aim of this study has been to assess the prognostic value of the nucleolar area by means of ultrastructural morphometry.
Materials and methods Forty-six cases of ductal carcinoma of the breast were included in the current study. All biopsies were processed for electron microscopy and electron micrographs were taken at x3,600 magnification. Nucleolar area measurements were done using SigmaScanPro software and statistical analyses were performed. Nucleolar area measures were categorized in terciles. A Kaplan-Meier estimation was performed to assess those measures related with disease-free interval. Measures that reached statistical significance were dichotomized at the cut point with maximum likehood in a Cox Regression model and then were included in a multivariate analysis.
Results Statistically significant differences were found in terciles per area ($p=0.019$) and per variation coefficient ($p=0.012$). In terms of nucleolar area measurements, any given nucleolar area with a standard deviation 3 1.5, showed a relative risk for recurrence of 4.05 (1.23-13.36) ($p=0.02$).
Conclusions Ultrastructural morphometry shows that nucleolar features, particularly those related to size heterogeneity, have a significant impact on prognosis.

P-423

Determination of ploidy in different lesions of prostate

A Ibraeva[1], M Alchinbaev[2], A Seitaliyeva[1]
[1]Scientific Center of Urology, Department of Pathology, Almaty, Kazahstan
[2]Scientific Center of Urology, Almaty, Kazahstan

Introduction Any lesion in prostate is followed by different proliferative activity of cells. One of the markers, which relate to proliferative activity, is ploidy. It can be determined by cytometry, morphometry or by other methods. Aims: Study of DNA ploidy status in different lesions of prostate by morphometry.
Materials and methods Samples from 80 patients with atrophy, benign prostatic hyperplasia (BPH), squamous cell metaplasia (SCM), atypical adenomatous hyperplasia (AAH), basal cell hyperplasia (BCH), prostatic intraepithelial neoplasia (PIN) and prostatic carcinoma were processed in formalin, dehydratated in graded alcohols, embedded in paraffin, stained by Feulgen-stain. Integral optical density was assessed by morphometry on image analysis system. Integral optical density of lymphocyte was counted as 2c ploidy. Integral optical density at different prostatic lesions was divided on 1c.
Results Average ploidy at atrophy was 2.0, BPH - 2.2, SCM – 2.4, BCH – 2.6, AAH - 2.8, low grade PIN was 4.2. Average ploidy at high grade PIN was 5.1, high grade carcinoma – 5.2, moderate grade carcinoma – 5.9, low grade carcinoma – 7.9.
Conclusion Increase of ploidy status from atrophy to BPH, SCM, BCH, AAH, PIN and to carcinoma was observed. Regarding to ploidy lesions may be divided in benign and neoplastic processes, with cutoff point between them as 4.5.

P-424

Pseudohyperplastic prostatic adenocarcinoma in transurethral resection of the prostate

J Arista-Nasr, B Martinez, J Nuncio
Instituto Nacional De Ciencias Medicas Y Nutricion Salvador Zubiran, Mexico City, Mexico

Background the pseudohyperplastic prostatic adenocarcinoma (PHPA) is a recently described variant of adenocarcinoma, studied in needle biopsies and prostatectomy specimens. PHPA is characterized by malignant glands that simulate benign hyperplastic glands of variable size with complex architecture, papillary enfolding, luminal undulations branching or cystic dilations, columnar cells with macronuclei and nucleoli enlargement. The aim of this study was to define the frequency and microscopic aspect of PHPA in specimens originated in transuretral prostatectomy (TUP).
Material and methods 250 specimens of transurethral prostatectomy were analized from the Surgical Pathology Department at INCMyNSZ. 150 cases were initially diagnosed as benign glandular hyperplasia (BGH) and 100 as conventional adenocarcinoma (CC)
Results 2 cases (1.3%) with PHPA were identified in specimens diagnosed as BHG. These specimens demonstrated PHPA in two

microscopic areas of 3 mm. Both patients are well and free of disease 2 and 4 years after diagnosis. The review of cases diagnosed as CC, three specimens had 2 microscopic segments of PHPA. In the outcome the patients developed early bone metastasis. The histopathology study revealed papillary projections, nuclear enlargement, crawled glands, macronucleoli (5/5); cystic glandular dilatation, straight luminal borders, pink amorphous secretions (4/5); nuclear hypercromasia and transition to small cell carcinoma (3/5). Other changes observed were corpora amylacea, double nucleoli and mitoses.
Conclusions the PHPA is a rare neoplasm observed in TUP specimens and is observed in only few areas. The false negative frequency in BGH is 1.3%, and 3% in usual adenocarcinoma. The outcome for these cases is related to the main conventional adenocarcinoma component.

P-425

Vascular Endothelial Growth Factor: An important angiogenic mediator in chronic urinary bladder lesions

O Hammam, H EL Baz, A El Baz
Theodor Bilharz Research Institute, Giza, Egypt

Vascular endothelial growth factor (VEGF) is an overriding growth factor mediating tumor anigogenesis. This study was performed to assess VEGF levels of expression in both serum and tissue in benign, premalignant and malignant urinary bladder lesions with or without schistosomal infestation in a trail to study the angiogenic phenotype of these lesions and to address any possible role of VEGF as a prognostic biologic marker of bladder cancer. Also the impact of schistosomal infestation on the VEGF level of expression was assessed.The study included 62 patients: 27 chronic cystitis cases (17 schistosomal and 10 non-schistosomal), 5 cases with schistosomal premalignant lesions (metaplasia, dysplasia and leukoplakia) and 30 cases with bladder carcinoma (5 schistosomal SqCC, 14 schistosomal TCC and 11 non-schistosomal TCC). Eight cases with normal urothelium served as controls. VEGF serum concentration was measured by the enzyme immunoassay (ELISA) while, its tissue expression was detected by immunohistochemical staining.. Significantly higher levels of VEGF where detected in the premalignant and malignant cases in tissue ($p< 0.01$ & $p< 0.001$ respectively) and in serum ($p< 0.01$) compared to controls. Also an aberrant increase in VEGF serum and tissue levels was recorded in malignant cases compared to those with chronic cystitis ($p< 0.001$ & 0.01 respectively). Schistosomal infestation was found to have a positive impact on VEGF tissue and serum levels. Tissue VEGF positive rates was 100% in all the premalignant and malignant schistosomal associated cases. On stratifying malignant cases according to their histopathological grade and stage, an evident stepladder increase in VEGF serum and tissue levels was recorded. VEGF serum levels were well correlated with their corresponding tissue level which may indicate that VEGF serum levels are reflecting intratumoral angiogenic status. Although both VEGF serum and tissue levels were positively correlated with tumor histopathological grade and stage, yet this correlation was more evident with the tissue expression ($r= 0.7$, $r= 0.6$, $p< 0.001$ in tissue, while $r= 0.5$, $r= 0.4$, $p<0.01$, $p=0.05$ in serum with grade and stage respectively). In conclusion, our data indicate that VEGF expression level in both serum and tissue may be used as a valuable angiogenic marker for prediction of prognosis. This may help in selecting patients for more intensive surgical or chemotherapeutic approaches. Serum VEGF concentration may be used as a non-invasive prognostic parameter especially in high risk patients who need continuous follow up.

P-426

Microvessel density in urothelial tumors of the upper urinary tract

M Raica[1], C Suciu[1], F Baderca[1], R Minciu[2]
[1]"Victor Babes' University of Medicine, Department of Histology&Cytology, Timsoara, Romania
[2]"Victor Babes' University of Medicine, Department of Urology, Timsoara, Romania

Background Angiogenesis in tumors of the urinary bladder is relatively well studied, in spite of some conflicting results and usually correlates with bad prognosis. Few data are available about microvessel density (MVD) in urothelial tumors of the upper urinary tract (UUT). Our purpose was to investigate the MVD in patients with urothelial tumors of the UUT and to check for its relationships with stage, grade, and survival.
Patients, material, and methods There were investigated 32 patients with urothelial carcinoma of the UUT. Routine-stained slides were reviewed by two independent pathologists for the final diagnosis, T stage, and grade. Only cases with invasive and mixed papillary-invasive tumors were included. Two cases had lymph node metastasis. Additional slides were stained for FVIII, CD31, and CD34. MVD was estimated using the hot-spot method and mean value, calculated on 10 consecutive fields from the tumor area and 10 from the deeper connective tissue (x200). All cases had a follow-up of minimum 5 years.
Results Best results were obtained with CD34 and CD31. In the tumor area, mean values of MVD were 9.7 for T1, 23.78 for T2, and 37 for T3. The hot-spot method consists of choosing the field with maximum density of blood vessels, and results showed 16 for T1, 34.16 for T2, and 49.66 for T3. The comparison between MVD and G showed a significant increase from G1 to G3 in the mean values and maximal density as well: 6.1/10 for G1, 23.76/36.5 for G2, and 33.07/41.75 for G3. No relationship was found between MVD and N positive cases. Nine patients with high MVD died within 5 years. The extra-tumor MVD had no prognostic significance.
Conclusions Our results show a strong correlation between tumor areas MVD, T, G, and survival. MVD had no value as a predictor of lymph node metastasis.

P-427

Is there any prognostic significance for HER2 protein in urothelial tumors of the upper urinary tract?

F Baderca[1], C Suciu[1], R Minciu[2], A Alexa[1], R Lighezan[1], M Raica[1]
[1]University of Medicine, Department of Histology and Cytology, Timsoara, Romania
[2]University of Medicine, Department of Urology, Timsoara, Romania

Introduction HER2 protein is overexpressed in about 20-30% of breast tumours and in 28% of bladder tumours. Until now, only two articles were published about the expression of HER2 in urothelial tumors of the upper urinary tract, and its signifiance is still uncertain. Our purpose was to investigate the incidence of the overexpression

of HER2 protein in urothelial tumours of the upper urinary tract, and its relationships with the stage and grade. The final purpose was to conclude on the prognostic value of HER2 protein in patients with tumours of upper urinary tract. Patients,

Material and methods There were investigated 26 cases with tumours of the upper urinary tract. Routine HE stained slides were reviewed for the pathologic diagnosis and grade. Additional slides were stained with Her-2/neu (Dako HercepTest). Interpretation of results was based on the score system (from 0 to +3) already used in breast cancer. Results obtained with Her-2/neu were compared with stage and grade.

Results Eight from 26 cases were positive for HER2 protein (30.7%). No relationship was found between HER2 overexpression and 'G'. All but one case with G3 had a +3 score for HercepTest.

Conclusions The overexpression of HER2 protein does not correlate with tumour stage, and has no predictive value for lymph nodes metastasis. It strongly correlates with 'G'.

P-428

Immunohistochemical correlation between pattern of postatrophic hyperplasia and carcinoma of the prostate

AR Botticelli[1], P Incardona[1], L Botticelli[2], G Stella[3], A Pitino[4], D Zaffe[5]
[1]Department of Human Pathology, University of Pavia, Italy
[2]Hospital Pathology Services of Carpi MO, Italy
[3]Hospital Pathology Services of Voghera PV, Italy
[4]Hospital Pathology Services of Biella BI, Italy
[5]Dept. of Anatomy and Histology, Univ. of Modena and Reggio Emilia, Italy

Introduction Some authors consider postatrophic hyperplasia (PAH), a glandular hyperplasia that mimics some patterns of prostate carcinoma (PCa), without any correlation with neoplastic and preneoplastic condition of the prostate. The association of PAH with PCa recently suggested (Mucci et al., 2001; Tsujimoto et al., 2002) induced us to analyze the role of PAH as precursor of PCa.

Material and methods Formalin fixed and paraffin embedded archival sections (60 selected patients undergoing radical prostatectomy - mean age = 66.8 yr) were studied. Twenty cases (10 with PAH and 10 without PAH) were selected for each group: A) BPH (Benign Prostatic Hyperplasia), B) PCa-GHS<7 (Gleason Histological Score) and C) PCa-GHS=>7. Slides were immuno-cytochemically treated with PSA, 34ßE12, CD99, vimentin, CD34, AR, NSE, chromogranin A, PGP9.5, p53, bcl2, Ki67/MiB1, incubated with streptavidin-biotin complex (SBC) and revealed by diaminobenzidine (DAB).

Results Immunohistochemical investigations revealed the presence of basal cells (34ßE12) only in PAH. The nuclear cell cycle proliferation (MIB1/Ki67) and p53 mutation were quite similar in number of positive nuclei between PAH and PCa-GHS<7. The Chromogranin A were positive in PAH, randomly in PCa-GHS<7, and in nests in PCa-GHS=>7. Vimentin stained nests in PAH, whereas were negative in PCa. The bcl2 were positive in PAH and negative in PCa-GHS<7.

Conclusion These findings suggest a strong overlapping of cell cycle nuclear proliferation and mutation markers, supporting a possible role of PAH as a precursor of PCa.

P-429

Eosinophilic cystitis: clinico-morphologic aspects

D Staribratova[1], D Staikov[1], D Dikov[2], V Belovejdov[1], D Staikov[1]
[1]Plovdiv Medical University, Plovdiv, Bulgaria
[2]Hopsital Centre - Lagny, Paris, France

Collaborative study called for review of archived urinary bladder biopsy specimens with inflammatory lesions for the period 1995-2002. Features consistent with the diagnosis of eosinophilic cystitis were identified in 15 cases, thus positioning it at 6th place with an incidence of 5,63% from all inflammatory lesions. The distribution of clinical signs manifested in these patients often deceptive of interstitial cystitis or tumor processes is as follows: polakisuria, hematuria, suprapubical pains are evident in 11/73,3%/ patients; 3/20,0%/ presented with acute obstructive pyelonephritis as a result of bladder wall remodeling and 1 case /6,66%/ revealed combined features of gastroeneteritis and cystitis. Inflammed bladder wall and reduced bladder volume is estimated in 13/86,6%/ cases, ulcerations in 2/13,3%/ papillomatous and solid pseudotumoral lesions are 5/33,3%/ and 4/26,6%/ respectively. As all clinical signs are nonspecific, the only way to set a proper diagnosis is through bladder biopsy. Morphologic confirmation is based on the standard protocols. Histochemical (positive Ziehl-Neelsen stain) and ultrastructural identification of Charcot-Leyden's crystals are evident in some cases.

P-430

Adenocarcinoma of the male urethra in association with nephrogenic metaplasia

F Hostalet[1], JE Hernández[1], JA Ruiz[1], A Romero[2]
[1]Department of Pathology, 'Vega Baja' Hospital, Orihuela, Spain.
[2]Department of Urology, 'Vega Baja' Hospital, Orihuela, Spain.

We describe a case of adenocarcinoma of the urethra associated with so-called nephrogenic metaplasia in a 75 year-old male patient that showed a polypoid tumor of the proximal penile urethra. Histopathology examination of the biopsy specimen revealed two distinct patterns. The first showed a tumor composed of papillary fronds and glands lined by columnar epithelial cells with eosinophilic and clear cytoplasm, and contained atypical nuclei with frequent mitotic figures. This tumor was interpreted as adenocarcinoma. The second pattern was different, it consisted of small tubules some with mild cystic changes lying in an edematous stroma. The tubules were lined by a single layer of flattened cells with faintly eosinophilic cytoplasm and bland nuclei, mitotic figures were not identified. This area was interpreted as nephrogenic metaplasia and showed a direct transition into the adenocarcinoma. The immunohistochemical study revealed the presence of low-molecular-weight and some high-molecular-weight keratins in both types of lesions. The adenocarcinoma cells also showed nuclear staining for p53, in contrast, the cells of nephrogenic metaplasia were negative. The nephrogenic metaplasia as well as the adenocarcinoma cells were not stained with PSA and PAP. The histogenesis of adenocarcinoma of the lower urinary tract remains unclear. The association and direct transition of the nephrogenic metaplasia into the adenocarcinoma in this case suggest the proposed histogenetic pathway that the urethral adenocarcinoma may arise by malignant transformation of nephrogenic metaplasia.

P-431

Correlations between usual molecular markers and apoptotic index in bladder cancer

E Ionica[1], CD Vrabie[2], E Nistor[3]
[1]University of Bucharest, Bucharest, Romania
[2]V. Babes Institute, Bucharest, Romania
[3]Bucur Hospital, Bucharest, Romania

Introduction Transitional cell carcinoma (TCC) is the second most common malignancy in the genito-urinary tract. The recurrence rate is particulary high after first presentation. Aims. Before treatment we assess to determine the p53protein (p53), bcl-2 oncoprotein (bcl-2) expression and apoptotic index (AI) in papillary non-invasive (Ta), papillary invasive (T1) and in situ carcinoma (TIS) in TCC.
Materials and methods We analyzed a total of 30 patients who underwent transurethral resection for primary TCC. The tumor stage (T1/Ta/TIS) and grade (G1/G2/G3) was determined after haematoxilin-eosin stained. Immunostaining was performed using the indirect tristadial Streptavidin-Biotin method for p53 and bcl-2.Apoptosis was detected by using APO-DIRECTTM TUNEL Assay kit.
Results Positive immunostaining for p53 was detected in Ta (48%), and TIS (67%); bcl-2 was present in Ta (4%) vs TIS (30%). According the grade the percentage of p53 positive cases increased from 52% (G1) to 80% (G2);in the same time the positivity of bcl-2 was lower in G1 (9%) than G3 (20%). An increased AI was found in G3 tumors.
Conclusions The majority of tumors was included in T1 (60%) and G1 (56%). The intensity and positivity of p53 and bcl-2 increased with grade of TCC. There is no significant correlation between frecquency of apoptosis and pathological stage of TCC, but our study reveals an obvious relation between AI, p53, bcl-2 expression vs grade of TCC.

P-432

Growth factor expression in cultured, human prostatic stromal cells with upregulated oestrogen receptors

PH Smith[1], NP Rhodes[2], Y Ke[1], CS Foster[1]
[1]Department of Pathology, University of Liverpool, UK
[2]Department of Clinical Engineering, University of Liverpool, UK

Introduction Benign prostatic hyperplasia (BPH) is associated with a shift in sex hormone balance towards an increase in the oestrogen:androgen ratio. This is accompanied by elevated levels of oestrogen receptor alpha (ER), predominantly in the stroma. Recently, we described a simple, in vitro model to create moderate upregulation of ER in human, prostatic stromal cells. The aim of this study was to investigate the hypothesis that in BPH upregulated ER and the action of androgens differentially regulate expression of several stromal growth factors.
Materials and methods Eight human, prostatic stromal cell strains were subjected to a procedure to upregulate ER alpha by exposing them to 1 micro mol beta-estradiol for 10 days, followed by passage and growth in the absence of steroids. Four cell strains received instead 100 n mol of dihydrotestosterone for 48 hr. Immunoexpressions of ER alpha, AR, and six growth factors (FGF-2, FGF-7, IGF-1, TGF-beta1, NGF and eNOS) were quantified by flow cytometry.
Results Expression of ER was significantly increased above control (6 out of 8 cell strains). Expressions of all six growth factors were elevated but not significantly so. However, there was a significant positive correlation between the change in ER (expressed as percentage of control) and the change in FGF-2 and FGF-7. Exposure of four cell strains to dihydrotestosterone reduced the expression of ER and all six growth factors in comparison with oestrogen-treated cells. This reduction was significant for ER and FGF-7.
Conclusion Upregulated ER in prostatic stroma have a greater modulating effect on synthesis of certain growth factors than the direct action of androgens and hence may play a major role in the development of BPH.

P-433

Periacinar retraction clefting in the prostatic needle core biopsies

B Krušlin[1], D Tomas[1], H Rogatsch[2], I Novosel[1], Hrvoje[1], M Belicza[1], G Mikuz[2]
[1]Ljudevit Jurak University Department of Pathology, Sestre Milosrdnice University Hospital, Zagreb, Croatia
[2]Institute of Pathology Leopold Franzens University of Innsbruck, Innsbruck, Austria

Introduction The diagnosis of prostatic adenocarcinoma in needle core biopsy is based on major and supportive criteria. One of the supportive criteria is the presence of retraction clefting around neoplastic glands. The aim of our study was to analyze needle core prostatic biopsies in order to determine the frequency of periacinar clefting spaces in tumors and non-tumorous prostatic tissue.
Materials and methods We analyzed a consecutive series of 137 prostatic cancer cases diagnosed by needle core biopsy to determine the frequency and extent of periacinar clefting. All tumors consisted of at least 30 neoplastic glands. Specimens were fixed in 10% buffered formaldehyde, embedded in paraffin, cut at 5µm thickness and routinely stained with hematoxylin and eosin. Clefting was analyzed on 10 neoplastic and 10 normal glands in three different high power fields.
Results One third or more of 30 analyzed glands with clefts affecting more than 50% of circumference were significantly more common in tumors (51.8%) than in benign glands (8%). More strict criterion that designated as positive cases with at least 50% of neoplastic glands (fifteen out of thirty) with clefts that affected more than 50% of circumference revealed clefts in the malignant cases only (15.3%) but not in benign cases (0%). Fifteen or more glands with clefts regardless of their extension were also more prominent in malignant cases (86.9%) than in benign cases (20.4%).
Conclusion We conclude that retraction clefting represents a reliable criterion for diagnosis of prostatic adenocarcinoma.

P-434

Unusual causes of ureteral obstruction

A Dema, N Tudose, S Taban, V Bucuras, M Botoca, R Bardan
University of Medicine and Pharmacy, Timisoara, Romania

Objective To report a series of cases of ureteral obstruction due to unusual pathological lesions, most of them being clinically and/or radiographically suspicious for malignant tumors.
Materials and methods A retrospective study was done to

analyze the causes of ureteral obstruction in a series of patients managed at the Department of Urology, Timisoara County Hospital between 1996 and 2002. There were selected only those particular cases of ureteral obstruction, others than cases with lithiasis, stenosis of the ureteropelvic junction and transitional cell carcinoma. An additional case was send for evaluation from another institution was also included in the study. For three of the selected cases we performed additional histochemical (Alcian-Blue-PAS) and immunohistochemical study (anti-CK, anti-PSA, anti-vimentin, anti-smooth muscle actin, ABC and LSAB system, visualization with DAB).

Results We identified 8 cases of ureteral obstruction due to unusual pathological lesions. They occurred in 5 men and 3 women. The mean age of the study group was 50 years (range 34 and 58 years). There were 3 malignant and 5 benign lesions that produced ureteral obstruction. In 5 cases, the compression was extrinsic and only in 3 cases the obstruction was intrinsec. The site of ureteral obstruction was in the lower ureter in 2 cases, in the lower and the middle ureter in 3 patients and in the upper ureter in 3 cases. The pathological lesions were: ureteritis cystica - 2 cases, nephrogenic adenoma of the ureter - 1 case, retroperitoneal fibrosis - 1 case, reproperitoneal sarcoma - 1 case, pelvic endometriosis -1 case, prostate cancer metastasis - 1 case, signet ring cell carcinoma of the colon invading the ureter - 1 case.

Conclusions After discarding the more common causes of extrinsic or intrinsic ureteral obstruction, the proliferative-metaplastic lesions of the urothelium, the retroperitoneal fibrosis and sarcoma, the endometriosis and metastatic/invasive carcinoma should be considered in the diagnosis.

P-435

Immunohistochemical study of androgen receptor and TGF alpha in human benign and malignant prostate

A Petrescu[1], G Berdan[1], C Ardeleanu[2], V Jinga[1], S Persu[1]
[1]Prof. Dr. Th. Burghele Hospital, Bucharest, Romania
[2]Victor Babes Institute, Bucharest, Romania

Aims That androgen receptor(AR)and TGF alpha might be prognostic of hormonal response and biological behaviour in prostate carcinoma.

Methods AR and TGF alpha were studied in paraffin sections from 50 men (35 treated for prostate cancer and 15 for BPH by open, transurethral prostatectomy or prostate biopsy) No patient had undergone previous treatment for the prostate disease. The sections were stained with HE to establish morphological characteristics (Gleason Score) and then were studied with indirect immunoperoxidase method applying monoclonal antibodies to AR(F 39.4.1 Biogenex) and antiTGF alpha (clone 88, Biogenex). Results were semiquantified using Histoscore.Nuclei were graded for intensity of AR staining (0-absent,1-weak,2-moderate or3-strong) and the percentage of these intensity levels and a total intensity score were determined. We compared the AR and TGF alpha characteristics of prostate cancer (PCa) with BPH.

Results Increasing Gleason grade was correlated with decreasing intensity score and greater heterogeneity of AR staining and increased (+++) TGF alpha immunoreactivity.

Conclusions Our data indicate that AR and TGF alpha content could be useful predictors of endocrine response and biologocal behaviour of prostate cancer.

P-436

Penile leiomyosarcoma-morphological and immunohistochemical study

G Berdan, A Petrescu, C Ardeleanu
Prof. Dr. Th.Burghele Hospital, Bucharest, Romania

Introduction Our case is about a 48 years old male patient who was admitted with the diagnosis of a penile tumor, reason why a total penectomy was performed.

Material and methods Fragments of the tumor and penile tissue were fixed in formalin 10%, embedded in paraffin and sections were stained with HE and VG. Immunohistochemical tests have been done: actin, vimentin, S100, AE1-AE3, HMB45, PCNA.

Results On macroscopic examination, the tumor was bulky, ulcerative nodular, occupying the glans and the distal part of the shaft; it was gray white coloured, with hemoragic areas. Microscopic examination revealed a tumorous proliferation of elongated cells with moderate nuclear pleomorphism and mitosis (typical and atypical), organised in a fascicular pattern, well vascularised; the tumor was superficially ulcerated and invaded the corpora cavernosa. The tumor was diffusely positive for actin and vimentin, focally positive for S100, negative for AE1-AE3 and HMB45, and PCNA was 70%.

Conclusions The morphological appearance and immunhistochemical results led us to the diagnosis of penile leiomyosarcoma, moderately differentiated.

P-437

Do human papillomaviruses infect proximal parts of the male genital tract?

A Švec[1], I Mikyšková[2], O Hes[3], M Urban[4], R Zachoval[4], R Tachezy[2]
[1]Dept Pathology, Faculty Hospital Královské Vinohrady and the Third Medical Faculty Czech Republic
[2]Dept Experimental Virology, Inst of Hematology and Blood Transfusion, Prague, Czech Republic
[3]dept Pathology, University Hospital, Charles University, Pilsen, Czech Republic
[4]Clinic of Urology, Faculty Hospital Královské Vinohrady and the Third Medical Faculty, Czech Republic

Introduction Human papillomaviruses (HPV) play an essential role in the pathogenesis of squamous cell carcinoma of the uterine cervix. The male urogenital tract is considered to be a reservoir of HPV infection. Our previous finding of HPV in the squamous metaplastic epithelium with dysplasia in the epididymis prompted us to start a study focused on the presence of HPV in the male genital tract. Aims: Verifying the presence of HPV in the epididymis, ductus deferens and seminal vesicles.

Materials and methods Samples from three groups (A, B, C) of patients were analysed by means of nested PCR for the presence of HPV DNA extracted from a paraffin-embedded tissue sections. Types of HPV were determined by DNA nucleotide sequencing of the PCR products. Group A consisted of 22 patients (mean age 61, age range 39-87, except for one patients 19 years old), group B consisted of 22 patients (mean age 73, age range 43-87, except for two patients 23 and 24 years old) and group C consisted of 44 patients (mean age 65, age range 50-82). Patients in group A were surgically treated for non-tuberculous epididymitis (41 epididymal

and 8 ductus deferens samples), patients in group B were orchiectomised for the diagnosis of prostate cancer, teratocarcinoma of the testis and/or epididymal cyst (normal 22 epididymal and 7 ductus deferens samples) and subjects in group C were treated by radical prostatectomy or cystectomy for prostate or urinary bladder cancer (44 samples of seminal vesicles without inflammatory changes).
Results HPV DNA was detected in 7(31%) of patients in group A(HPV types 6,16, 33, 35, 55, 73), in 1 (0.5%) patient in group B(at present unclassified type) and in 5 (11.4%) patients in group C(HPV types 16, 18 and 52).Neither koilocytes nor dysplastic changes were observed.
Conclusion Our data confirmed the presence of HPV, both low- and high-risk types, in the male genital tract. They support the idea of a male reservoir of HPV infection.

P-438

Spermatogenetic function of the testis in patients of different varicocele grades

É Magyar[1], E Erdei[2], I Lellei[1]
[1]National Medical Center, Pathology, Budapest, Hungary
[2]National Medical Center, Andrology, Budapest, Hungary

Introduction Varicocele is one of the main reasons of male infertility. Surgical repair may improve sperm quality. The aim of this study is to investigate a grading system of varicocele and its correlation with the histological appearance using a multiple biopsy method.
Materials and methods Bilateral double testicular biopsies of 53 young infertile grade 2-4 varicocele patients were examined histologically. Spermatozoa numbers counted in ten round shaped tubules, severity of atrophy and presence of maturation arrest was recorded. Distribution pattern of observed spermatozoa numbers was evaluated.
Results Grade 2 and 3 cases showed normal distribution. In grade 4 cases five peaks were found indicating group inhomogenity. Lower grade varicoceles presented with milder histological changes (mild atrophy or normal spermatogenesis) while in higher grade varicoceles more marked alterations (moderate-marked atrophy and/or maturation arrest) were seen.
Conclusion Grade 4 varicocele cases represent an inhomogeneous group, which should be divided into more categories. Modification of the grading system is required. Spermatogenetic activity of varicocelic patients cannot be predicted from clinico-radiological examinations so before ART a diagnostic testicular biopsy is recommended.

P-439

Synchronous double urogenital cancer – A case report

S Banev[1], S Kostadinova - Kunovska[1], B Bogoeva[1], B Ilievski[1], V Vasilev[2], S Ristovski[2]
[1]Institute of Pathology, Faculty of Medicine, Skopje, Republic of Macedonia
[2]Clinic for Surgery - General City Hospital, Skopje, Republic of Macedonia

We present a case of synchronous double urogenital cancer, comprised of invasive transitional cell carcinoma of the urinary bladder and adenocarcinoma of the prostate. Cystoprostatectomy was performed in a 68-year-old male patient with previous cytological diagnosis of transitional cell carcinoma of the urinary bladder and no evidence of prostatic malignancy on preoperative clinical investigations. Gross analysis of the urinary bladder revealed a cauliflower tumor mass filling the entire lumen and infiltrating the wall of the bladder. The size of the prostate was slightly increased. Histological analysis of the urinary bladder specimens showed poorly differentiated transitional cell carcinoma, with only a few foci of preserved papillary architecture, infiltrating deeply into the muscle layer of the bladder wall. The specimens taken from the prostate gland for the purpose of staging of the neoplasm excluded the existence of infiltration of the prostatic urethra with the previously described neoplasm, but foci of moderately differentiated adenocarcinoma (Gleason score 6) of the prostate were discovered in its vicinity. The subsequent extensive sampling of the prostate showed organ confined adenocarcinoma. The review of the literature showed that the reported prevalence of synchronous existence of double primary malignant neoplasms of the urinary tract (transitional cell carcinoma of the bladder and prostatic adenocarcinoma) varies between 27% and 33%. The prevalence is noted to rise with increasing age. This leads to a conclusion that during standard cystoprostatectomy analysis, extensive sampling of the prostate is needed, even in the absence of macroscopic changes and preoperative clinical data suggesting prostatic neoplasm.

P-440

Multiple synchronous renal cell tumors

D Passetchnik
[1]Rostov State Medical University, Rostov on Don, Russian Federation
[2]Rostov Regional Hospital 12, Rostov on Don, Russian Federation

Introduction The use of the nephron-sparing surgery demands detection of multiple renal cell tumors.
Materials We performed a retrospective analysis of nephrectomies and autopsies performed in our clinic.
Results Of 120 renal cell tumors 26 (21, 7%) were multifocal. Most of the patients were men. Twelve cases were present where the histological subtype of the largest tumor was clear cell. Satellite tumors were clear cell carcinoma (7), papillary adenoma (5), angiomyolipoma (3), renomedullary fibroma (2), Bellini duct carcinoma (1). Six multiple renal cell tumors were found in T1, two in T2, four in T3A stage of the primary tumors. Four patients had bilateral neoplasms. In thirteen cases only multiple papillary adenomas and carcinomas were found. Usually tumors were no more than 3 cm in diameter. In six cases multiple tumors originated on a background of nephrosclerosis of various genesis (chronic pyelonephritis, gouty nephropathy, amyloidosis).
Conclusion When conservative surgery of kidney cancer is performed, it should be remembered that 20% of patients with renal cell tumor have multiple neoplasms, which may cause local recurrence. The origin of multiple renal cell tumors may be bound up with hereditary predisposition or nephrosclerosis creating multifocal tumor field.

P-441

Loss of Parkin expression in prostate carcinoma

A Di Napoli[1], A Vecchione[1,2], C Rossano[2], L Ruco[1], A Stoppacciaro[1]
[1]University "La Sapienza", Ospedale Santo Andrea, Rome, Italy
[2]Kimmel Cancer Center, Thomas Jefferson University, Philadelphia, Pa19107, USA

Introduction Prostate cancer is a leading cause of cancer-related deaths in men and is the most common malignancy in American males. The heterogeneity of prostate cancer defines the current clinical challenges. One challenge is to identify in early, still potentially curable, stages of prostate cancer, molecular markers that predict aggressive or metastatic behavior. Prostate cancer is characterized, like many other cancers, by molecular and genetics aberrations involving chromosome 6. Parkin, mapped at the long arm of chromosome 6, is a 465 amino acid protein with a molecular mass of 52 kDa, an ubiquitin-like domain at its amino terminus and two RING finger motifs flanking a cysteine-rich region. Our aim was to investigated whether Parkin alterations play a role in development and progression of prostate carcinoma
Materials and methods We examined Parkin expression, by Western blot analysis in eight prostatic carcinomas derived cell lines as well as in normal prostate, and in three prostatic intraepithelial neoplasias (PIN) and in twenty primary prostatic carcinomas by immunohistochemistry.
Results Parkin protein was undetectable in six out of eight prostate cancer cell lines tested and barely detectable in the remaining two whereas normal prostate showed a substantial expression. Preliminary results using immunohistochemistry showed that Parkin expression was absent in PIN lesions, and in the prostatic carcinomas analyzed.
Conclusion Our findings suggest that Parkin might be a useful tool to detect early alteration in prostate cancer.

P-442

The KDR/Flk-1 receptor of vascular endothelial growth factor in urothelial bladder cancer: relation with clinicopathologic parameters and patients' survival

P Rafailidis[1], H Gakiopoulou[1], I Giannopoulou[1], J Mavrommatis[1], C Eftychiadis[1], A Zervas[2], C Couvaris[1], A Giannopoulos[2]
[1]Department of Pathology, Medical School, The National and Kapodistrian University of Athens, Greece
[2]Department of Urology, Medical School, The National and Kapodistrian University of Athens, Athens, Greece

Introduction The impact of different angiogenic inducers and inhibitors in the switch of angiogenesis in urothelial bladder cancer, is not clarified. KDR/flk-1 is a receptor-tyrosine kinase that binds specifically vascular endothelial growth factor (VEGF) on vascular endothelium, mediating its full biologic spectrum. Although KDR/flk-1 expression was at first reported to be restricted to the classic endothelium there is increasing evidence that KDR/flk-1 is also expressed by normal and tumor cells other than endothelial. Aims: As data about KDR/flk-1 protein in urothelial bladder cancer is very limited, we investigated its expression in a series of 114 urothelial carcinomas in relation with clinicopathologic parameters and patients' survival. Moreover, prompted by studies suggesting that KDR/flk-1 may have broader functions apart from angiogenesis we evaluated KDR/flk-1 expression in relation with markers of cellular proliferation and apoptosis (Ki-67, p53, bcl-2).
Materials and methods Immunohistochemistry (ABC-HRP) was performed for the detection of KDR/flk-1 (mouse/A-3, SC-6251, Santa Cruz), Ki-67, p53 and bcl-2 using monoclonal and polyclonal antibodies. Statistical analysis was univariate (Pearson's x2, Mann-Whitney test, Log-Rank test) and multivariate (Cox's model).
Results KDR/flk-1 expression was observed in the cytoplasm of cancerous cells in 78/114 cases. No significant associations were observed between KDR/flk-1 expression and clinicopathologic parameters, Ki-67, p53 and bcl-2 expressions. On the other hand, widespread KDR/flk-1 expression in more than 50% of cancerous cells, was associated with patients' increased survival, in univariate and multivariate analysis ($p=0.0119$, $p=0.042$, respectively).
Conclusion Although non endothelial KDR/flk-1 expression has not yet been elucidated, its association with better patients' survival may be related with the failure of non-endothelial KDR/flk-1 to mediate angiogenic and mitogenic effects, that has been reported in some previous in vitro studies.

P-443

TIMP-2 protein expression in relation with cellular proliferation, apoptosis and survival of urothelial bladder cancer patients

I Papadaki[1], H Gakiopoulou[1], A Siatelis[2], I Giannopoulou[1], E Panayotopoulou[1], C Couvaris[1], C Stravodimos[2], A Giannopoulos[2], L Nakopoulou[1]
[1]Department of Pathology, Medical School, The National and Kapodistrian University of Athens, Greece
[2]Department of Urology, Medical School, The National and Kapodistrian University of Athens, Athens, Greece

Introduction The role of tissue inhibitors of matrix metalloproteinase (TIMPs) in cancer progression remains a controversial matter since apart from the well established inhibitory action of TIMPs on MMPs, several new functions are now attributing to TIMPs such as growth promoting activity, involvement in apoptosis control and in angiogenesis. The aim of this study was to elucidate the role of TIMP-2 in urothelial bladder cancer, we investigated its expression in a series of 106 urothelial carcinomas in relation to clinicopathological parameters, patients' survival and the expression of the Ki-67 proliferation index.
Materials and methods Immunohistochemistry (ABC-HRP) was performed for the detection of TIMP-2 and Ki-67 proteins, using monoclonal and polyclonal antibodies. Statistical analysis was univariate and multivariate.
Results TIMP-2 stromal cell expression was observed in 28/106 cases and associated significantly with urothelial carcinomas of high histologic grade ($p<0.0001$) and advanced stage ($p=0.001$) as well as with poor patients' survival ($p=0.0002$). TIMP-2 expression in cancerous cells was found in 58/106 cases. TIMP-2 either stromal or cancerous cell expression correlated significantly with Ki-67 expression ($p=0.02$, $p=0.044$ respectively).
Conclusion The association of TIMP-2 with Ki-67 supports the growth promoting activity of TIMP-2. Moreover, TIMP-2 expression in stromal cells may be a valuable marker of adverse prognosis in urothelial cancer patients.

P-444

Investigation of telomerase protein subunits (hTEP-1 and hTERT) and RNA component (hTR) in relation with clinicopathological parameters and patients' survival in urothelial cell bladder carcinomas

J Mavrommatis[1], H Gakiopoulou[1], I Giannopoulou[1], C Eftychiadis[1], A Kapranou[1], A Zervas[2], C Stravodimos[2], A Giannopoulos[2], L Nakopoulou[1]
[1]Department of Pathology, Medical School, The National and Kapodistrian University of Athens, Greece
[2]Department of Urology, Medical School, The National and Kapodistrian University of Athens, Athens, Greece

Introduction Telomerase is a large ribonucleoprotein complex that stabilizes and extends telomeres of eukaryotic chromosomes regulating cell replicative potential and lifespan. Human telomerase is composed of an RNA subunit (hTR) and several protein components including the catalytic telomerase reverse transcriptase (hTERT) and telomerase-associated-protein-1 (hTEP-1). Aims: To clarify the role of telomerase in bladder cancer we investigated for the first time the expression of hTERT, hTEP-1 and hTR in 132 urothelial carcinomas, in relation with clinicopathological parameters, patients' survival and markers related with proliferation and apoptosis (Ki-67, bcl-2, caspase-3).
Materials and methods Immunohistochemistry (ABC-HRP) using monoclonal and polyclonal antibodies and RNA in situ hybridization were performed for the detection of hTEP-1, hTERT, Ki-67, bcl-2, caspase-3 proteins and hTR respectively. Statistical analysis was univariate and multivariate.
Results hTEP-1 positive cytoplasmic expression associated significantly with the lower grade of carcinomas (p=0.027). Cytoplasmic hTEP-1, nuclear hTERT, cytoplasmic hTERT and hTR correlated inversely with stage of the disease (p=0.003, p=0.018, p=0.0001 and p=0.06 respectively). Cytoplasmic TEP-1 and hTERT demonstrated inverse associations with p53 expression (p=0.001 and p=0.047 respectively). Cytoplasmic hTERT associated with caspase-3 expression (p=0.004). Cytoplasmic hTEP-1 and nuclear hTERT correlated significantly with increased patients' survival in univariate (p=0.04) and multivariate (p=0.007) analysis respectively.
Conclusions 1) Telomerase expression associates with early stage urothelial carcinomas. 2) The correlations between cytoplasmic TEP-1 or cytoplasmic hTERT and p53 are supported by in vitro studies implicating p53 in telomerase regulation. 3) Nuclear hTERT seems to carry a favorable impact on patients' survival. This may be due to the induction of genomic instability, telomere-telomere fusion, aneuploidy and prevalence of more aggressive clones, known to be associated with telomerase inhibition.

P-445

Gleason score and nodal metastases of prostate cancer

R Radosavljević, J Hadži-Dokić, S Mićić, C Tulić, M Djokić, M Aćimović, N Bojanić
Institute of Urology and Nephrology Clinical Center of Serbia, Belgrade, Serbia and Montenegro

Introduction Gleason score is important predictor for differentiation and biological potential of prostate cancer. Node – negative (p N0) prostate cancer is the best result after radical prostatectomy which is indicated in patients with localised prostate cancer. The aim of the study was to analyze Gleason score in patients with nodal metastases of prostate cancer (PC).
Material and methods We analyzed 49 cases of radical prostatectomies due to localised prostate cancer in the period 1996-2000 in Clinic of Urology in Clinical Centre of Serbia, Belgrade. Nodal metastases (stage of disease), average age of the patients, Grade and Gleason score of tumors and premalignant lesions were analysed. Immunohistochemical staining was performed and pathological analyzed. We used statistical analysis ANOVA and H^2 test.
Results The average age of the patients was 65.6 years (range 44-76, pick 61-70). Most cases 25 (51%, $p<0.001$) were in pT2a N0M0, in pT2b N1M0 9 (18.36%), in pT3bN0M0 10 (20.4%), in pT3bN1M0 3 (6.12%), in pT4aN0M0 2 (4.08%). Positive nodal status was present in 12 cases: 9 (18%) in pT2bN1M0 - iliac 3 (right 2, left 1), obturatory 6 (right l, left 5) and 3 cases in pT3bN1M0-iliac left 1 and obturatory 2 (1 right and 1 left). We found Gleason score 8 in 9 cases (18.36%) in pT2bN1M0 versus 7 cases (14.5%) without nodal metastases. Gleason score 9 was found in 3 cases (6.1%) in pT3bN1M0 versus one case without nodal metastases ($p>0.05$). Gleason score 3 was present in 6.1%, 4 in 12.2%, 5 in 8.1%, 6 in 16.3%, 7 in 24.5%. Grade 1 tumors were found in 9 cases (18%), grade 2 in 11 (22%), and grade 3 in 29 (60%). HG PIN was present in 18 cases (36.7%), LG PIN in 10 (20.4%).
Conclusion Gleason score differ, but not significantly in prostate cancer with nodal metastases. Pelvic lymphadenectomy is necessary for staging purposes in prostate cancer. Radical prostatectomy is the most adequate method in surgical treatment of localised prostate cancer.

P-446

Immunohistochemical and molecular evaluation of c-erbB2 gene amplification and c-erbB2 protein overexpression in prostate cancer

A Sasor[1], E Balcerczak[2], W Kozlowski[1], M Mirowski[2]
[1]Military Medical Institute, Department of Clinical Pathology, Warsaw, Poland
[2]Medical University of Lodz, Department of Pharmaceutical Biochemistry, Lodz, Poland

Introduction The amplification of oncogene c-erbB2 and overexpression of C-erbB2 protein found in some human cancers is associated with more aggressive development of tumor. The previous data suggested an independent role of c-erbB2 protein as a prognostic factor in human breast cancer. However, the role of c-erbB2 gene and its protein product in prostate cancer cells still remain unclear. The aim of our study is to show what is the role of c-erbB2 protein in prostate cancer and to examine association between c-erbB2 gene amplification and its protein product expression in the histologicaly graded prostate tumor.
Materials and methods We have analyzed c-erbB2 gene amplification by RT PCR and c-erbB2 protein expression by immunohistochemistry in 39 cases of paraffin embedded slides. The tumors were divided according to WHO by Mostofi classification: 13 cases of G1 - well differentiated cancer; 13 cases of G2 - moderately differentiated cancer; and 13 cases of G3 - poorly differentiate cancer. These groups are equivalent to 1-4, 5-7 and 8-10 Gleason classification respectively.
Results The correlation between c-erbB2 protein expression and

well, moderately and poorly differentiated cancer respectively existed ($p<0.05$). There was no significant correlation between c-erbB2 gene amplification and c-erbB2 protein expression in all examined groups.
Conclusion Our results suggest that the c-erbB2 protein expression is an independent factor on the c-erbB2 gene amplification in prostate cancer cells. It is possible that there are other ways, except gene amplification, for overexpression of c-erbB2 protein in prostate cancer.

P-447

Comparison of needle biopsy and surgical specimen in prostatic carcinoma

S Nordling, J Vasama
Department of Pathology, University of Helsinki, Helsinki, Finland

In Finland carcinoma of the prostate is the most common form of cancer in men. The number of radical prostatectomies is increasing in most countries. The radical prostatectomy is normally preceeded by a needle biopsy. At the university Central Hospital of Helsinki 599 radical prostatectomies were performed between 1988 and 2001. in 474 patients, the preoperative needle biopsy was available. In many cases the preoperative PSA value was also available. The mean PSA value dropped from 20 to less than 10 ng/ml. The percentage of seminal vesicle invasion dropped from 35 to 10. Except for the earlier years, the men Gleason score was about 1 point higher in the radical prostatectomy specimen than in the biopsy. The mean Gleason score has increased, while the stage and PSA values have decreased indicating that the criteria for the Gleason grading has changed ovewr the years. This makes the comparison of treatment results very difficult.

P-448

Immunohistochemical profiles as an aid in borderline prostatic lesions

M Ivanovic, A De las Morenas
Department of Pathology, Boston University Medical Center, Boston, USA

Introduction Distinguishing atypical adenomatous hyperplasia (AAH) from small foci of prostatic adenocarcinoma in needle biopsies of the prostate often presents as a challenge for pathologists. The aim of the study was to establish characteristic immunohistochemical patterns in benign and malignant prostatic lesions so they can be used to classify foci of AAH as benign or malignant.
Materials and methods Using immunohistochemistry, prostatic needle biopsies from forty-five patients were evaluated for cytokeratin 903, p63 and alpha-methylacyl-CoA Racemase (P504S). Twenty-five of these biopsies were benign and twenty contained prostatic adenocarcinoma.
Results 96% of the benign prostatic biopsies were positive for cytokeratin 903 and p63 and 96% were negative for P504S. Only one case of benign prostatic tissue was focally positive for P504S. When evaluating cases with adenocarcinoma 95% were positive for P504S and 100% were negative for cytokeratin 903 and p63. P504S immunostain showed consistently positive staining in areas of low and intermediate grade adenocarcinoma and areas with high grade PIN. High-grade prostatic adenocarcinoma was frequently negative for P504S. Sensitivity and specificity for cytokeratin 903/p63 were 96% and 100% while sensitivity and specificity for P504S were 95% and 96%.
Conclusion Cytokeratin 903 was as sensitive and as specific as p63 and can be used interchangeably in cases of AAH. The combination of the two antibodies did not improve sensitivity or specificity. A combination of negative cytokeratin 903 or p63 with positive P504S may be helpful in positively identifying prostatic carcinoma in cases of AAH.

P-449

Myofibroblastic stromal reaction in prostatic adenocarcinoma

D Tomas, H Eupić, M Vučić, S Kozlović, M Belicza, B Krušlin
Ljudevit Jurak University Department of Pathology, Sestre Milosrdnice University Hospital, Zagreb, Croatia

Introduction Reactive stromal changes that occur in different human cancers probably are involved in local tumor spreading and progression. It seems that myofibroblast plays very important role in stromal reaction to certain types of human cancer.
Material and methods We have analyzed 47 prostatic carcinomas in radical prostatectomy specimens to determine the proportion of myofibroblasts around normal and neoplastic acini. Myofibroblast showed positive staining for alpha-smooth muscle actin (SMA) and vimentin. Positive cells were counted in the hot spots areas under high power magnification (HPF). Results were expressed as negative (-) for no staining, (+) for positive staining in up to 10% of stromal cells, (++) in 10-25% of cells and (+++) for more than 25% of positive cells. Stromal blood vessels were counted in ten HPF. The degree of desmoplasia was also analyzed by Mallory staining and expressed semiquantitatively as weak, moderate and strong.
Results and conclusions Highly increased number of myofibroblast was observed around neoplastic acini in 16 (34.1%) cancer cases, moderate in 10 (21.2%) and sparse in 21 (44.7%) cases while there were occasional myofibroblastic cells adjacent to normal acini. There was a positive correlation between the degree of stromal desmoplasia and the proportion of SMA and vimentin positive cells in adjacent stroma. The number of vessels in the adjacent stroma was also significantly increased in comparison with normal glands ($p<0.05$). It seems that myofibroblasts are present in the stroma and may play a significant role in the desmoplastic stromal reaction in prostatic adenocarcinoma.

P-450

C-kit expression in sarcomatoid renal cell carcinoma. Potential treatment with imatinib (STI-571) for this ominous tumor

M Castillo[1], J Carreras[1], B Mellado[2], P Beardo[3], A Palacín[1], C Mallofré
[1]Dpt. of Pathology. Hospital Clínic De Barcelona, Barcelona, Spain
[2]Dpt. of Oncology. Hospital Clínic de Barcelona, Barcelona, Spain
[3]Dpt. of Urology. Hospital Clínic de Barcelona, Barcelona, Spain

Background Sarcomatoid renal cell carcinoma (SRCC) is an uncommon subtype of Renal Cell Carcinoma (RCC) with a poor prognosis. Currently, there is no specific useful treatment for it.

Few immunohistochemical studies on SRCC have been published, and c-Kit expression has not been reported yet.
Material and methods We reviewed 215 cases of RCC diagnosed at our Department from 1995 to 2002. Among them, 20 cases (9.3%) were SRCC. Formalin-fixed, paraffin-embedded material was available in 19 cases and we performed immunohistochemical staining against c-Kit (rabbit polyclonal antihuman antibody CD117, dil. 1:100, Dako) on them.
Results Among the 20 SRCC, 2 (10%) showed no epithelial differentiation, and in the other cases the epithelial component was conventional RCC in 10 cases (50%), papillary CCR in 5 (25%), and chromophobe RCC in 3 (15%). There was no sex predominance and the average patient age at the time of diagnose was 61 years. Sixteen cases (80%) presented an advanced stage at the time of diagnose, and 13 (65%) died of disease. The immunohistochemical study showed that 17 cases were positive for c-Kit (89.5%), 7 diffusely (>50% of the sarcomatoid cells positive), 6 moderately (10-50% of the cells), and 4 focally (<10% of the cells).
Conclusion The high expression of c-Kit in SRCC in our series and the existence of target therapy against cells expressing this marker (Imatinib (STI-571, Gleevec, Novartis, Basel, Switzerland) suggests its potential use in the clinical management of these patients in order to improve their prognosis, especially in disseminated cases.

P-451

Does HPV play a role in the development of bladder TCC? A comparison of PCR and immunohistochemical detection methods

S Youshya[1], K Purdie[1], J Breuer[1], C Proby[1], M Sheaff[2], T Oliver[3], S Baithun[2]
[1]Centre for Cutaneous Research, The Royal London Hospital, UK
[2]Department of Histopathology & Morbid Anatomy, The Royal London Hospital, UK
[3]Department of Oncology, The Royal London Hospital, UK

The role of human papilloma virus (HPV) in the development of bladder carcinomas remains controversial. Varying techniques have been used to identify this virus in transitional cell carcinoma (TCC). Here we used two different methods to detect the presence of mucosal HPV in 78 TCC samples. The first, immunohistochemistry, involved using a polyclonal antibody that reacts with the L1 capsid protein of most known papilloma viruses. The second method is used on a general primer-mediated polymerase chain reaction (PCR) assay. This involves using type-specific oligonucleotide probes to identify 22 different mucosal HPV genotypes from a 150bp PCR product from the L1 region of the HPV genome. The two methods produced contrasting results, 78% of the samples were positive for HPV antigen and 2% were positive for HPV DNA. The reason for such conflicting results is that polyclonal antibodies are not specific and are likely to cross react with other antigens. PCR is specific, more sensitive, and it is widely used to detect HPV in a variety of clinical samples. The results obtained in our study implies that HPV does not play a role in the development of bladder carcinoma, and PCR remains to be the best method to detect HPV in TCC.

P-452

Does TGF-α1 prevent carcinoma spreading?

O Gladskikh[1], A Kouznetsova[1], T Danilova[1], B Alexeev[2], Y Andreeva[2], A Ivanov[1], M Paltsev[1]
[1]Research Institute of Molecular Medicine at Moscow Medical Academy, Moscow, Russian Federation
[2]Hertzen's Research Institute of Oncology, Moscow, Russian Federation

Introduction Most human carcinomas including prostate cancer are associated with stromal reaction typified by changes in growth factor expression and over-accumulation of extracellular matrix. Our study deals with the differential TGF-α1 production in neoplastic focuses and in adjacent paraneoplastic stroma in prostate.
Materials and methods Tissue samples from radical prostatectomies were examined. To verify malignant material or benign the immunohistochemical staining against high molecular weight cytokeratin was performed on sections and in heterogeneous primary cultures of the same specimens. The immunohistochemical identification of TGF-α1 was also performed. The ELISA technique for quantitative analysis of TGF-α1 soluble form in culture supernatants was applied.
Results Majority of selected cancer cases were histologically estimated as small-sized glands with large desmoplastic fibro-muscular stroma. The immunohistochemical staining for TGF-α1 in malignant focuses was much more significant than in neigh-bouring benign areas on sections in contrast to, the cultures obtained from neoplastic or paraneoplastic portions of prostate tissue which stained positively for TGF-α1 without any difference. Considering that immunohistochemistry shows only latent TGF-α1 we evaluated its bioactive form in culture supernatans. We found dramatically high supernatant levels of active TGF-α1 in benign cultures compared to the cultures from the malignant areas.
Conclusion Our data demonstrate that desmoplastic alterations in benign areas adjacent to malignant glands was associated with elevated expression of TGF-α1 active form. So significant alteration in factor production and accompanied tissue remodeling can be considered as a protective reaction of surrounding stroma against tumor invasion.

P-453

Primitive neuroectodermal tumor of the kidney: A case report

S Erdogan[1], C Ersoz[1], G Gonlusen[1], A Tuganalp[2]
[1]Cukurova University, Medical Faculty, Department of Pathology, Adana, Turkey
[2]Adana Numune Hospital, Department of Urology, Adana, Turkey

Introduction Primitive neuroectodermal tumors (PNETs) represent a family of neoplasms, of presumed neuroectodermal origin, that mostly presenting as bone or soft tissue masses in the trunk or axial skeleton in adolescents and young adults. The aim of this study was to report a case of PNET arising from kidney which is a rare localization.
Methods A 32 year-old-man presented with abdominal pain and abdominal mass. The imaging methods revealed a mass nearly replacing the right kidney and he underwent a right nephrectomy.

Results On gross examination the tumor measured 16 cmx14 cm with cystic areas and necrosis. Microscopically, it was a highly cellular neoplasm of consisting sheets of small-round-to-oval cells with irregular nuclei. Immunohistochemical stains were positive for vimentin and CD99. Microscopic and immunohistochemical findings were compatible with PNET.
Conclusion Although rare, PNET must be included in the differential diagnosis of renal tumors especially in children and young adults. We present a case of renal PNET as an unusual case and discuss the differential diagnosis

P-454

Pathologic stage of urinary bladder cancer at presentation in a non-selected patient population in a high-incidence region of the United States

A Schned[1], L Schned[1], A Andrew[2], K Kelsey[3], M Karagas[2]
[1]Dartmouth Medical School, Department of Pathology, Hanover, NH, USA
[2]Dartmouth Medical School, Department of Community and Family Medicine, Hanover, NH, USA
[3]Harvard School of Public Health, Department of Cancer Cell Biology, Boston, MA, USA

Introduction Most studies of pathologic stage in bladder cancer (Ca) are retrospective, using selected, usually hospital-based, patient populations. The aim of this study was to determine the pathologic stage of bladder Ca at initial presentation in a non-selected patient population in a high-incidence region of the northeastern United States.
Materials and methods All patients newly presenting with bladder Ca in the state of New Hampshire (U.S.A.) from July 1998 to December 2001 were identified through the State Tumor Registry. Slides were classified according to WHO and ISUP criteria.
Results Of 265 cases, 15 were diagnosed as non-malignant or technically inevaluable, leaving 250 Ca cases. 14 (5.6%) were carcinoma-in-situ (stage Tis). 205 (82.0%) were papillary, of which 150 (73.2%) were low-grade and 55 (26.8%) high-grade. Of the low-grade cases, only 7 (4.7%) were invasive, all limited to lamina propria (stage T1). Of the high-grade cases, 19 (34.5%) were non-invasive (stage Ta), 31 (56.4%) invaded lamina propria (stage T1), and 5 (9.1%) invaded muscle (stage 2). 26 cases (10.4%) had no papillary component and all were invasive; 14 (53.8%) were stage T1 and 12 (46.2%) were stage T2. 5 cases (2.0%) were non-urothelial, including 2 squamous cell Ca, 2 small cell Ca, and 1 adenoCa; 2 of these presented as stage T1 and 3 as stage T2. Overall, 74 cases (31.4%) were invasive (at least T1) at the time of presentation.
Conclusions This population-based series establishes the distribution of bladder tumor stage at initial presentation and documents a smaller percentage of invasive cancers than most hospital-based series

P-455

The relationship between mitotic index and nucleolar organizer region with histologic grade in transitional cell carcinoma of urinary bladder

MR Jalali Nadoushan, T Rezaei Nour, N Fallah, SK Foroutan
Shahed University, Tehran Islamic Republic of Iran

Background and object Transitional cell carcinoma (TCC) of urinary bladder is the second most common cancer of the genitourinary tract, that the prognosis and treatment is related to several parameters such as proliferative cell markers. In this study relationship between two proliferative cell markers:1-Mitotic Index(MI)& 2-AgNOR and tumor grade were studied.
Methods and materials In a cross sectional descriptive study 75 paraffin blocks of patients with TCC of the urinary bladder in the period from 2000 to 2002 from pathology department of shahid Mostafa Khomeini hospital, were obtained and from each one 3 micron sections were provided. Tumor grade on basis of WHO/ISUP grading system, was determined and number of mitosis on 100 tumor cells were counted. In the other section, after one-step silver nitrate staining, the number of NOR also on 100 tumoral cells were counted and the mean of it in each cell were determined.
Results The high grade tumors possessed more AgNOR per nucleus than did the low grade ones. Significant relationship between tumor grade and MI (P=0.000, rs=0.801) and AgNOR (P=0.000, rs=0.731), and also between MI and AgNOR (P=0.000, rs=0.638) were found. The regression analysis revealed relationship between MI & AgNOR. (AgNOR=1.58+0.45 MI)
Conclusion The MI and AgNOR have direct relationship with bladder TCC's grade. As statistical results didn't show difference between MI and AgNOR to predict the grade, we prefer to use MI for this purpose.

P-456

HER2 in invasive urothelial carcinoma of the bladder

K Peham, G Hutarew, E Prokop, O Dietze, C Hauser-Kronberger
Institute of Pathology, PMU Salzburg, Salzburg, Austria

Introduction The human epidermal growth factor receptor 2 (HER2) is overexpressed not only in breast, but in a range of other tumor types including, ovarian, salivary gland, endometrial, pancreatic, non-small cell lung (NSCLC) and bladder cancer. However, non-standardisation in HER2 status evaluation or population selection has generated conflicting results among the incidences of HER2 expression in individual tumor types and bladder cancer. The aim of the present study was to evaluate HER2 overexpression and gene amplification with standardized routinely performed assays (DAKO HercepTest, FISH-Vysis, CISH) on a selected population of poorly differentiated urothelial carcinomas of the bladder.
Materials and methods We analyzed 55 formalin-fixed, paraffin embedded tissue samples of urothelial carcinomas of the bladder at G3/pT3-4 as well as 22 cases at G1/2 pTis (2)and pTa-1 (20) using HercepTest to verify the HER2-status. Staining and scoring was performed according to the manufacturers instructions. According to diagnosis of HER2, all HercepTest positive (2+) tissue samples were used for further evaluation with fluorescence in situ hybridisation (FISH; Vysis) and chromogenic in situ hybridisation (CISH) to approve the expected gene amplification. This procedure is in agreement with the standardized guidelines for breast cancer.
Results 30 (60%) cases were considered as HER2 positive (3+ and 2+) in the primary tumor and therefrom 16 cases (32%) 2+ positive and 14 cases (28%) 3 + positive. Out of the 16 cases with 2+ positivity, only two cases showed a FISH/CISH positivity. No polysomy for chromosome 17 was detected.
Conclusion Our results indicate that HER2 may not only be a useful prognostic parameter in poorly differentiated invasive

bladder cancer, but accurate determination of overexpression and verification of gene amplification may also have therapeutic importance.

P-457

The prognostic importance of tumor volume (TV), non-tumor volume (NTV), TV/NTV, fibronectin distribution, β-hCG and PSA expression in localized prostatic adenocarcinoma

BH Ozdemir, AN Sar, FP Uyar, B Demirhan, A Dirim
Baskent University, Faculty of Medicine, Departments of Pathology and Urology, Ankara, Turkey

Aim To assess the importance of fibronectin (FN) distribution, β-hCG and PSA expression in localized prostatic adenocarcinomas with regard to tumor volume (TV), non-tumoral volume (NTV), TV/NTV and with other clinicopathological prognostic parameters.
Material and method Fifty-one radical prostatectomies were whole mounted, serially sectioned and examined for TV, NTV, TV/NTV, capsular invasion, vascular invasion, seminal vesicle invasion and Gleason score. The FN distribution, β-hCG and PSA expression were examined immunohistochemically. A FN-positive staining was defined as a constant diffuse, or pericellular demarcation of FN-positive fibers surrounding tumor cells at the invasive border. In lack of such staining pattern, FN-negative staining was recorded.
Results Both TV and TV/NTV showed very strong positive correlation with grade, capsular invasion, vascular invasion, seminal vesicle invasion, β-hCG and PSA expression ($p<0.01$). β-hCG was detected only in 16 cases (31.4%). A significant relationship was found between β-hCG expression and grade, capsular invasion, vascular invasion, seminal vesicle invasion, PSA expression ($p<0.01$). The FN-positive staining reaction was significantly associated with lower incidence of capsular, and seminal vesicle invasion ($p<0.05$). TV and grade was found higher in tumors with negative FN staining ($p<0.05$). PSA expression showed significant relationship with grade, vascular and capsular invasion ($p<0.01$). NTV statistically showed no relationship with all parameters.
Conclusion These data suggest that, TV, TV/NTV, FN distribution, β-hCG and PSA expression in prostatic adenocarcinoma have strong prognostic importance irrespective of Gleason score. The FN distribution could be important for the invasion of the tumor cells during cancer progression. These may allow stratification of patients to type of treatment and may allow selection of expectant management for men with localized prostatic adenocarcinoma.

P-458

Neuroendocrine differentiation in prostate cancer: correlation with biochemical failure after radical prostatectomy

S Cerovic[1], G Brajuskovic[1], J Dimitrijevic[1], S Knezevic Usaj[1], L Popovic[1], V Vukotic Maletic[2], B Ajdinovic[3]
[1]Institute of Pathology, Military Medical Academy, Belgrade, Serbia and Montenegro
[2]CHC " Dragisa Misovic" Belgrade, Serbia and Montenegro
[3]Institute of Nuclear Medicine, Belgrade, Serbia and Montenegro

Introduction Focal neuroendocrine differenatiation (NED) is a commom feature of prostate cancer (PC), occuring in 50%-100% tumors studied. Published results of the evaluation of NED as a prognostic factor in PC after radical prostatectomy (RP) have been contradictory. The aim of this study was to correlate NED in PC in relation to biochemical failure after RP.
Materials and methods Radical prostatectomy specimens from 36 PC patients without preoperative hormonal or radiation therapy were followed for 13 to 73 months. Neuroendocrine (NE) cells were identified using a panel of immunohistochemical NE markers: chromogranin A, serotonin, and neuron-specific enolase. NED was scored as NE-negative (0 to 1+) or NE-positive (2 to 3+) per 10HPF. Biochemical progression (BP) was defined as a prostate-specific antigen (PSA) level greater than 0.2 ng/ml in two consecutive measurements. Kaplan-Meier method was used to estimate BP-free survival time for each risk group. The Cox proportional hazards regression analysis was the model for BP time using pathological and clinical variables.
Results The total of 23(64%) patients developed BP after RP. The average time for BP was 16 months. The preoperative PSA serum level range <10 ng/ml in 52% of the patients. Postoperative staging confirmed that 23 (64%) of patients had pT2 stage and 13 (36%) of patients had pT3 stage. NED demonstrated in the 14(61%) PC patient with BP. The average time for BP was 10 months. Tumor volume ($p<0.05$), pathological stage ($p <0.05$), tertiary Gleason grade ($p= 0.01$) and NEDF ($p<0.01$) significantly affect the level of postoperative PSA progression.
Conclusion The expression of NED in PC correlates with tumor volume and tertiary Gleason grade and represents an independent prognostic factor of BP after RP.

P-459

Expression of Vascular Endothelial Growth Factor (VEGF) and correlation with microvessel density in benign hyperplasia and prostate carcinoma

NJ Agnantis, S Kamina, E Arkoumani, D Stefanou
Department of Pathology, University of Ioannina, Medical School, Ioannina, Greece

Aim The present study is scheduled to evaluate the levels of VEGF expression in benign prostatic hyperplasia (BPH) and prostate carcinoma and to correlate them with angiogenesis.
Material and method Formalin-fixed, paraffin-embedded tissue sections from patients who underwent radical prostatectomy or transurethral resection of the prostate were studied. Our material consisted of 32 cases of BPH and 30 cases of prostate carcinoma. Microvessel density (MVD), as determined by CD31, and expression of VEGF were investigated by immunohistochemistry using the monoclonal antibodies CD31 (DAKO) and VEGF (Neomarkers), respectively.
Results Expression of VEGF was detected in 26/32 (81,25%) cases of BPH and in all (100%) invasive prostate carcinomas. Cytoplasmic immunoreactivity for VEGF was detected in epithelial and stromal cells. VEGF expression was stronger in carcinomas, when compared to BPH ($p<0.05$), while it was minimal to absent in normal adjacent prostate tissue. A positive correlation between VEGF expression and Gleason score was found ($p<0.05$). Microvessel density (MVD) was higher in BPH and prostate carcinomas, when compared to normal adjacent prostate tissue. A statistically significant association was noted between VEGF and MVD expression ($p<0.001$).

Conclusions Our results indicate that generation of new capillary blood vessels begins in BPH and keeps progressing in invasive prostate carcinoma. VEGF seems to be a key functional regulator of angiogenesis in the prostate gland.

P-460

Paratesticular solitary fibrous tumor

A Nikolaidou[1], S Pervana[1], A Papanikolaou[2], P Hasakiolis[1], K Sachinis[1]
[1]General Hospital of Kilkis, Kilkis, Greece
[2]Hippocration Hosp. Salonica Greece

Aim To describe an additional case of paratesticular solitary fibrous tumor.
Methods and results A 46-year- old man presented with a paratesticular mass. Histological examination showed a well-circumscribed lesion composed of spindle cells without atypia, arranged in a fascicular pattern, intimately intertwining with thick collagen fibers. Tumor cells were strongly positive for vimentin and CD-34. Diagnostic criteria, clinical features and treatment of this condition are discussed.
Conclusion Solitary fibrous tumors are spindle cell neoplasms originally described in the pleura, but may occur in many different sites. Intrascrotal solitary fibrous tumors are uncommon and few cases have been reported.

P-461

The relationship between histologic grade and ABO blood groups in transitional cell carcinoma of the urinary bladder

B Mofid[1], MR Jalali Nadoushan[2]
[1]Shahid Beheshti University of Medical Sciences, Tehran, Islamic Republic of Iran
[2]Shahed University, Tehran, Islamic Republic of Iran

Introduction According to the statistics of 1996, the urinary bladder cancer is the fifth common cancer in Iran. The majority of urinary bladder tumors are transitional cell carcinomas. Different factors are effective in the prognosis of these patients. One of these factors is the histologic grade. Another factor is to determine the ABO blood groups and the relationship of it with the histologic grade. Thus, this study is conducted to shed some lights on this issue.
Materials and methods A cross sectional study was conducted in 198 patients with urinary bladder transitional cell carcinoma during 1996 - 2000.
Results Of 198 patients, 43 were female (21.7%) and 155 were male(78.3%). The mean age of patients was 63.7+/-12. There was no significant statistical relationship between of histologic grade and ABO blood groups. There was no significant differences between the ABO blood groups frequency in patients with urinary bladder transitional cell carcinoma and general population.
Conclusion Although the existing differences between Asian, European and American studies might be due to racial effects, it is better to carry out more studies in this respect in order to comment in this area with more confidence and certainty.

P-462

Prostatic mucinous carcinoma with signet ring cells treated by radical prostatectomy

N Medic[1], S Cerovic[1], G Brajuskovic[1], S Knezevic Usaj[1], J Dimitrijevic[1], L Popovic[1], N Milovic[2], P Aleksic[2]
[1]Military Medical Academy, Institute of Pathology, Belgrade, Serbia and Montenegro
[2]Military Medical Academy, Clinic of Urology, Belgrade, Serbia and Montenegro

Introduction A variable degree of mucin secretion may be present in prostatic carcinoma (PC), but true mucinous tumors are rare. Prostatic mucinous carcinoma (PMC) is a variant of high-grade adenocarcinoma, with a 77.8% rate of prostate-specific antigen (PSA) elevation and a similar rate of response to endocrine therapy. The aim of this study was to report on a case of PMC with signet ring cells treated with radical prostatectomy (RP).
Materials and methods A 70-year-old man presented with acute urinary retention and long history of difficult voiding. The serum PSA was 8.9 ng/ml. The transperineal biopsy of the prostate gland was done and the histology showed a poorly differentiated PC with large lakes of extracellular mucins. Isotope bone scan was normal and a CT-scan did not show evidence of extracapsular spread of the tumour. Radical prostatectomy was performed. Patient died seven month after RP.
Results Histopathologically, over 70% of the prostate samples were infiltrated by a poorly differentiated PC with mucinous and signet ring patterns. Mucin secretion is evident as large pools of mucin and periodic-acid-Schiff-positive diastase-resistant intraluminal and citoplasmic globules. Immunohistochemical staining for PSA and prostate-specific-acid phosphatase was positive, and negative for carcinoembryonic antigen and cytokeratin 20.
Conclusion The diagnosis of PMC with signet ring cells requires exclusion of an extra-prostatic origin, mainly within digestive tract. Since only small number of MPC cases treated with RP have been reported, treatment and prognosis of this tumour remain unclear.

P-463

Expression of CD10 antigen in Testicular Germ Cell Tumors (TGCTs)

E Condom-Mundó[1], A Vidal-Bel[1], X Garcia del Muro[2], E Franco[3], JR Germa-Lluch[2]
[1]Dept. Pathology. Hospital Universitari de Bellvitge, Barcelona, Spain
[2]Dept. Oncology. Institut Catala d'Oncologia, Barcelona, Spain
[3]Dept. Urology. Hospital Universitari de Bellvitge, Barcelona, Spain

Introduction CD10 is a well-known marker for hematolymphoid neoplasms and is expressed as well in various nonhematopoietic tissues and solid tumors. A systematic study of CD10 expression in TGCTs, however, is lacking. The aim of this study was to investigate the immunoreactivity for CD10 in the different patterns of TGCTs.
Material and methods Immunostaining with Mab against CD10 (clone 56C6) in 59 unselected cases of primary (46 cases: 18 classical seminoma (CS); 9 pure embryonal carcinoma (EC); 18 mixed-non-seminomas; 1 spermatocytic seminoma (SS) and metastatic (13 cases) TGCTs. In mixed tumors, the different histological patterns were evaluated separately.
Results CD10 was expressed in 18 (78%) out of 23 cases in the CS component, in 15 (100%) of 15 teratomas, in 13 (93%) of 14

endodermal sinus tumors (EST), in 11 (100%) of 11 cases of choriocarcinoma (ChC) or syncytiotrophoblastic giant cells (STGC) and in 1 (4%) of 23 EC. CD10 was focally positive in 28 (80%) of 35 cases of intratubular germ cell neoplasia (ITGCN) and was negative in one SS.
Conclusions Except for EC and SS, CD10 is expressed in the majority of histological types of primary and metastatic TGCTs. CD10 is useful to highlight minute foci of EST, ChC or STGC in EC. A TGCT is to be taken into account in the differential diagnosis of a CD10 positive metastatic tumor of unknown origin. Further studies are needed to evaluate the eventual significance of CD10 as a prognostic factor or as a potential therapeutic target in TGCTs.

P-464

Morphological changes of stromal components of the aging testis from patients with prostatic carcinoma

IE Plesea[1], SD Enache[3], M Ghilusi[3], L Mogoanta[2], B Zaharia[1], V Comanescu[3], C Foarfa[1], F Bogdan[2]
[1]Department of Pathology, University of Medicine and Pharmacy, Craiova, Romania
[2]Department of Histology, University of Medicine and Pharmacy, Craiova, Romania
[3]Department of Pathology, No. 1 County Emergency Hospital, Craiova, Romania

Introduction The authors assesed the correlations between age and morphologic aspects of stromal components in testes from 28 cases with orchiectomy for prostate adenocarcinoma.
Material and methods The samples were fixed in Bouin's fluid, embedded in paraffin wax and stained with hematoxilin-eosin, Goldner and Gömöri stains. Immunohistochemical staining with antibodies for smooth muscle Actin, Vimentin, Collagen IV and CD34 Classs I were used.
Results The seminiferous tubules basement mebrane (BM) narrowed and became discontinuous with age and with the severity of tubular sclerosis. Lamina propria (LP) generally became more thick with a decrease of myoid cells number in the inner layers and an increase of the collagen fibers right under the tubular BM and of the fybroblasts number in the outmost layers. The amount of peritubular capillaries remained relatively constant but the number of intralaminar capillaries decreased with the severity of LP sclerosis. The amount of Leydig cells increased with age especially in areas with tubular sclerosis.
Conclusions The stromal components presented morphological changes related with age with a 'mosaic', focal distribution. The evolution toward sclerosis in the LP seems to be influenced rather by Leydig cells hyperplasia than by vascular changes.

P-465

The expression of CD44 molecule in renal cell carcinoma

K Lučin, K Matušan, G Dordević
Department of Pathology, Medical Faculty, Rijeka, Croatia

Introduction It is generally accepted that the prognosis of renal cell carcinoma (RCC) differs according to the histological type, and, whatever the histological type, the tumor stage and nuclear grade are considered the main prognostic factors. However, in many cases of conventional renal cell carcinomas (CRCC), these parameters are insufficient to predict the clinical behaviour of these tumors. Therefore, several studies have focused on the evaluation of new markers. The CD44 proteins form a broadly distributed family of cell surface adhesion molecules involved in cell-cell and cell-matrix interactions. De novo expression of CD44s and its variant isoforms has been associated with aggressive behaviour in various tumours. The aim of this study was to analyse the prognostic value of CD44s and CD44v6 in renal cell carcinoma.
Materials and methods The expression of CD44s and CD44v6 was immunohistochemically evaluated on 75 RCC: 62 were CRCC, 9 papillary, 3 cromophobe and 1 collecting duct carcinoma. The expression was compared to usual clinicopathological parameters.
Results In normal renal tissue no staining was observed. The CD44s molecule was upregulated in 18 CRCC (29%), 4 papillary, one cromophobe and collecting duct carcinoma. Only 5 tumors were focally CD44v6 positive. The statistical analysis showed the correlation between CD44s expression and Fuhrman nuclear grade ($p<0,0025$) as well as Ki67 proliferative index ($p<0,0003$).
Conclusion The expression of CD44s molecule appears to mediate a more agressive phenotype to RCC.

P-466

Amplification of CerbB2 expression in bone metastasis of prostatic cancer: A pilot immunohistochemical and cytogenetic study

V Baena Perez, J Lloreta, J Carles, M Salido, M Suárez, E Díaz, S Boluda, F Sole, S Serrano
Departments of Pathology and Oncology, Hospital del Mar-IMAS, Pompeu Fabra University and Autonomous University of Barcelona, Barcelona, Spain

Introduction Her-2-neu expression is reported to increase in androgen-independent prostatic cancer. Consequently, it has been suggested that Trastuzumab, an antibody targeting the extracellular domain of Her-2, could be used in this setting. The possibility of assessing Her-2 expression by immunohistochemistry could be used as a rationale for the treatment of advanced cases with this drug. The aim of this study was to assess whether Her-2 expression is increased in bone metastases of prostatic cancer compared to the respective primitive tumors, and to determine whether this overexpression could be related to gene amplification.
Materials and methods In this pilot study, primary tumor needle biopsies and bone metastases from 7 patients diagnosed with prostatic cancer were immunostained wit C-erb-B2 antibody (Dako, Glostrup, Denmark), and the results scored using a three-tiered system. In addition, in a bone marrow sample from one of the cases, HER2 gene amplification was investigated using FISH.
Results There was a significant increase in Her-2 expression in four cases, with the same level of expression in primary and metastatic tumors in the remaining three patients. In addition, FISH showed no amplification of HER2 gene.
Conclusion HER-2 overexpression is not a constant event in prostate cancer metastatic to bone. Preliminary evidence suggests that in cases with overexpression, it is not related to gene amplification. A larger study will be required, however, to definitively determine the real therapeutic meaning of these findings.

P-467

Sarcoid-like granulomas (SGs) in renal cell carcinoma (RCC)

RA Queralt-Escarré[1], A Vidal-Bel[1], MJ Gonzalez[1], J Mańá[2], MA Lopez-Costea[3], E Condom-Mundó[1]
[1]Department of Pathology.Hospital Universitari de Bellvitge, Barcelona, Spain
[2]Department of Internal Medicine. Hospital Universitari de Bellvitge
[3]Department of Urology. Hospital Universitari de Bellvitge

Introduction SGs are known to occur in association with a variety of hematologic and solid neoplasms. Concerning RCC-associated SGs, only isolated case reports have been published. The aim of this study was to disclose the prevalence and clinical significance of SGs in a series of RCCs from a single institution.
Material and methods Clinicopathologic review of 210 consecutive cases of RCC surgically treated at the HUB between January-1999 and March-2003. Immunohistochemical staining with CD68, panB and panT antibodies.
Results SGs were seen in 7 cases, both within the tumor and/or in the nontumor tissue nearby. Patients were 4 females and 3 males aged 55 to 76(median 68) years. Tumors were 5 conventional clear cell RCCs and 2 chromophobe RCCs. There were 5 pT1, one pT2 and one pT3b. Two tumors were Fuhrman grade 3 and 5 were grade 2. In each case, the lymphocytes in the SGs were predominantly T cells. One patient was already known to have a CREST syndrome. In another one sarcoidosis was subsequently diagnosed. In the remaining 5 no systemic disease has been found to date.
Conclusions SGs are found in about 3.5 % of RCCs. Morphology and immunohistochemistry allow no distinction between local sarcoid-like reactions and sarcoidosis. The clinical profile of the patients and the pathologic features of the tumors are not different from those of RCCs unassociated with SGs. The finding of tumor-associated SGs must be reported to the clinicians in order to rule out a systemic granulomatous disease, thus avoiding misinterpretation of clinical symptoms or overstaging of tumors.

P-468

Metanephric adenoma in the kidney coexistent with paraganglioma in the bladder: A case report

S Seckin, I Paker
Ankara Numune Teaching and Education Hospital, Department of Pathology, Ankara, Turkey

We report a case of metanephric adenoma in the kidney and paraganglioma in the bladder in a 32 year-old woman. The patient presented with hematuria. Abdominal USG and BT revealed a mass in the lower pole of the kidney and in the posterior wall of the bladder. Left nephrectomy and transurethral resection of the mass in the bladder were performed. The tumor in the kidney which measured 4x3x2 cm. had a yellow to white cut-surface and well-defined margin. Histological examination demonstrated a monomorphous population of small cells with bland cytology arranged generally in tubular and occasionally in papillary structures. No atypia and mitotic activity were present. Immuno-histochemically tumor was diffusely positive for EMA, focally positive for pancytokeratin and negative for vimentin. The tumor in the bladder was characterized by well-defined nests of cuboidal cells with granular cytoplasm which were seperated by highly vascularized fibrous septa. Sustentacular cells were demonstrated with anti-S100 protein immunohistochemically. We didn't encounter the coexistence of these two tumors in the literature. We think that it is a coinsidence.

P-469

Co-occurrence of extra-adrenal myelolipoma, renal cell carcinoma and thymoma – a case report

K Steplewska, D Sabat, W Zajecki
Department of Pathomorphology, Medical University of Silesia, Zabrze, Poland

A case of never reported in literature of co-occurrence of a very rare tumour – extra-adrenal myelolipoma (EAML) with two other neoplasms, was presented in the report. 72-year man after a short hospital stay due to heart ischaemic disease died with the symptoms of acute circulatory insufficiency. An autopsy, which confirmed clinical diagnosis, was performed. A tumour of the size 15x11x8 cm, which compressed the heart and aorta, was found during the mediastinum autopsy. The tumour was covered with a sack, lobular, gray and beige at the cross-section with blood extravasation, necrosis foci and calcifications (histopathologic result – medullary thymoma). The compressed heart was moved to the middle, right side of the chest. In the adipose capsule of the left kidney, near the lower pole, an encapsulated solid fatty tumour of the size 7x5x5 cm was found. The tumour was connected to the kidney. Histopathologic result – myelolipoma. The tumour was composed of fat cells with normal marrow hematopoietic elements including megakaryocytes. The third tumour, 2cm of diameter, was found on the front surface of the right kidney (histopathologic result – multilocular cystic clear cell, renal cell carcinoma). None of the tumours was diagnosed during the patient's life.

P-470

Signet ring cell carcinoma of the prostate: pathologic and immunohistochemical analysis of two cases

M Kowanski, T Zabkowski
Military Medical Instituite, Warsaw, Poland

Introduction Signet ring cell carcinoma of the prostate is extremely rare and was first described by Giltman in 1981. To date, there have been 39 cases reported in the literature.
Materials and methods We evaluated two cases formaline fixed paraffine embedded tissue by histochemical (mucicarmine, alcian blue) and immunohistochemical methods (PSA, PSAP) to confirm our histological diagnosis.
Results Both our cases were high grade adenocarcinomas Gleason score 9 (4+5) and were positive for PSA and PSAP. One case contain a small amount of acid mucin, but both were negative for neutral mucin. The combined results from our and from previously reported cases: PSA positive in 88.8% (32/36), mucicarmine stain positive in 41.9% (13/31) and alcian blue stain positive in 50.0% (18/36) of cases.
Conclusion Signet ring cell carcinoma is variant of high grade adenocarcinoma of the prostate but results of histochemical and immunohistochemical staining are variable.

P-471

Value of ISUP (1998) and WHO (1999) criteria in the prediction of prognosis in urothelial tumors

J Lloreta[1], L Ferrer[2], S Serrano[3], A Amoros[4], D Puente[4], A Tardon[4], R Garcia[4], C Serra[4], A Carrato[4], M Kogevinas[4], FX Real[4], N Malats[4]
[1]Hospital del Mar, Universitat Pompeu Fabra, Barcelona, Spain
[2]Hospital del Mar, Barcelona, Spain
[3]Hospital del Mar, Autonomous University of Barcelona, Barcelona, Spain
[4]IMIM, Universitat Pompeu Fabra, Barcelona, Spain

Introduction The 1998 ISUP classification of urothelial tumors was followed by a modified WHO classification in 1999. The purpose of this study has been to assess the value of both systems in the prediction of progression, in a large series of cases with detailed follow-up.
Material and methods 500 "superficial" (pTa + pT1) urinary bladder tumors are the subject of this work. All tumors were reassessed strictly adhering to published criteria. Progression (increased grade or stage) was used as the end-point.
Results With a relative risk (RR) of 1 for G1, progression RR for G2 was 2.98 (1.05-8.46) and for G3 10.09 (3.82-26.65) ($p<0.001$). With a risk of 1 for pTa, RR for pT1 was 5.64 (3.01-10.56) and for pT2 4.80 (1.13-20.38) ($p<0.001$). When combining grade and stage, RR for pTa (G2+3) was 2.60 (1.06-6.39) and for pT1 (G2+3) was 10.03 (4.16-24.20) ($p<0.001$).
Conclusions Strictly adhering to the 1999 WHO grading and staging criteria, both systems result in a very efficient prediction of progression of urothelial carcinoma. Grouping G2 and G3 into a single high grade category does not improve these results. "Superficial" infiltration (pT1) introduces a relevant risk of progression when restrictively identified, thus suggesting that pT1 should not be lumped with pTa for therapeutic purposes.

P-472

Neuroendocrine expression in prostate cancer

L Velickovic[1], V Katic[1], V Savic[1], B Djordjevic[1], S Zivkovic[2]
[1]Institute of Pathology, Nis, Serbia and Montenegro
[2]Military Hospital, Department of Surgery, Nis, Serbia and Montenegro

Introduction Presence of neuroendocrine (NE) cells that are suggested to be important regulators of cell growth and differentiation represents uncommon finding in benign and neoplastic prostate epithelium. In order to correlate cellular expression with histological differentiation in benign epithelium and primary prostate cancer, expression of chromogranin A (CgA) had been determined.
Materials and methods HE and immunohistochemical analysis with antibody against CgA was performed in order to determine the coexistence of NE differentiation in tissues of twelve patients with prostatic adenocarcinoma (PC).
Results NE differentiation was found in 8 (66,6 %) tumors. Among them, 5 (41,66%) had CgA positive cells scattered or focally distributed, 3 (25%) intermediated and intensive. There was a significant correlation between the extent of NE features and Gleason score ($p<0,05$).
Conclusion These data support the concept that NE differentiation in human prostate cancer has a positive correlation with histological differentiation, i.e. patients with Gleason score > 7 had higher cellular expression of CgA.

P-473

The p130 retinoblatoma gene protein and p53 expression in transitional cell tumors

S Ramón Y Cajal[1], C Corbacho[2], V Fernández, J Guinea, C Parada, R Sánchez
[1]Hospital Vall D´Hebron, Madrid, Spain
[2]Clínica puerta de Hierro. Madrid, Spain

Background The retinoblastoma family of proteins (p105, p107 and p130) are implicated in cell cycle regulation, differentiation and apoptosis. p105 (retinoblastoma supressor gene) alterations seem to be correlated with worse prognosis in urothelial neoplasms, and the status of the other two proteins has been less studied. p53 mutations are usually associated with intranuclear accumulation of p53 protein, and have also been correlated with worse prognosis in urothelial neoplasms.
Design Formalin-fixed, paraffin-embedded archival tissue from 18 low-grade and 17 high-grade transitional tumors was immunostained with polyclonal and monoclonal antibodies against the Retinoblastoma Family of Proteins, and with monoclonal antibody against p53 protein. The avidin-biotin-peroxidase (ABC) method was utilized with every antibody (Dako, clone Rb1 for p105; Santa Cruz, clone sc-318 for p107; Santa Cruz, clone sc-317 for p130 and Dako, clone DO-7 for p53). Immunostaining was scored quantitatively by 3 pathologists, following previously described criteria, to study p105, p107 and p53. Nuclear and/or cytoplasmic location was determined by 3 pathologists to study p130.
Results p130 expression: among 18 low-grade tumors, 12 (66.67%) showed nuclear positivity and 4 (22.22%) showed a granular cytoplasmic pattern of staining. Among 17 high-grade tumors, 1 (5.88%) showed nuclear expression and 13 (76.47%) showed a granular pattern of staining. p53 expression: among 18 low-grade tumors, 1 (5.55%) showed positivity and among 17 high-grade tumors, 14 (82.35%) stained positively. We found no stadistically significative differences regarding p107 and p105 immunohistochemical stainings.
Conclusion Due to granular cytoplasmic pattern of staining for p130 is more frequent among high-grade transitional neoplasms, we propose that p130 granular cytoplasmic immunohistochemical pattern of staining may be considered a marker of tumor progression in transitional cell tumors. The prognostic value of p130 cytoplasmic positivity among low grade cases, as well as the prognosis of tumors with p53 overexpression and p130 granular cytoplasmic pattern will be discussed.

P-474

Are there any relationship between Bellini duct carcinoma and urothelial cell carcinoma?

I Trias, I Español, A Orsola, C Raventós
Clinica Plató Fundació Privada, Barcelona, Spain

Introduction Two collecting duct carcinomas (CDC) and 1 renal papilla urothelial carcinoma (UC) with similar outcome. Aims. To study the common features of CDC and UC.

Methods CDC's underwent nephroureterectomy under suspicion of urinary tract neoplasm. UC had radical nephrectomy for uncontrolled acute pyelonephritis.
Results All were male. Mean age was 67 years.

CASES	SIZE&SITE	PT	CK903	Ulex Eur(UE)	AE1/AE 3	CK2 0	Vim
CDC-1	All Kidney	4	-	+++	+++	-	-
CDC-2	5 cm Medullary	3	+++	+++	+++	-	-
UC-3	1cm renal papilae	3	-	+/-	+	-	-

All had atypical cells in nearby collecting ducts. UC had carcinoma in situ in adjacent urothelium. Median survival was 5.6 months.
Discussion Aggressiveness of our 3 lesions and ambiguous immunohistochemistry results on case 3, made us consider that CDC and UC of the renal papilla may share biological features. Normal collecting duct and the urinary tract have the same mesonephric origin. LOH 1q characteristic of all distal nephron tumors, have been described in UC. Immunophenotype of CDC includes positivity to CK903 which is also positive in UC. This overlappings shows us that these tumors are difficult to categorize and we may be in front of a spectrum of lesions. This may explain that some CDC may behave like UC and share some aspects, incuding their response to therapy.
Conclusions CDC are aggressive tumors, and general pathologists should be able to recognize them. Immunohistochemistry is needed for diagnosis. Possible relationship between UC and CDC may have therapeutical implications.

P-475

Serous papillary cystic tumor of borderline malignancy arising in testis - Case report

E Sahan[1], A Iddem[1], N Erdodan[1], A Dengizmen[1], C Balci[2], I Hazar[2]
[1]Taksim State Hospital Pathology Lab, Istanbul, Turkey
[2]Taksim State Hospital Urology Department, Istanbul, Turkey

Primary adenocarcinoma is one of the rarest types of malignant testicular tumors. There is a small number of reported patients of testicular tumors of the serous or mucinous ovarian type. A 63 years old white man presented with painless scrotal swelling. He was given antibiotic therapy, no regression appeared. Left high inguinal orchiectomy was performed. On histopathological examination the diagnosis was serous papillary cystic tumor of borderline malignancy arising in testis. The prognosis is poor. In these patients who are not diagnosed and treated early. The histopathological features, treatment and prognosis of this unusual malignancy are reviewed.

P-476

Morphological specialties of prostate at tuberculosis of lungs

SI Arifhanova, RT Nigmanov
Since Research Institute of Pulmanology and Phthisiology, Tashkent, Uzbekistan

The aim of researching is appear to examine of ofteness of come across of specific prostatitis and it's morphological form in autopsy material at patients with tuberculosis of lungs. Morphological researches of prostate including layer cut macro and micro preparations section was made and was paint by hemotoxilin-eosin and by Van-Hison. In Since Research Institute of Pulmanology and Phthisiology in Tashkent city was died 25 man at the age 20-60 age from 2001 till 2002y. The average age was 36 years. From that patients on the autopsi material at 14 (56%) was discovered tuberculosis of prostate, at 11(44%) nonspecific defeat of prostate. At 14 died patients with tuberculosis of prostate was found different types of tuberculosis inflammation: (1) aexudative - at 7, productive - at 2, and mixed - at 5., from them (2) infiltrative - at 8 and destructive - at 6 patients, aexudative type of inflammation was also diagnosed at 11 patients with nonspecific defeat of prostata. Patomorfological data's not always can help in diagnostic of tuberculosis of prostate it ties with patomorfose of tuberculosis under influence of treatment.

P-477

Cancerogenesis in prostate: ploidometric differential diagnostics

Avtandilov GG, Gundorova LV, Zajratiants OV, Perov YL
Russian Medical Academy for Postgraduate Education, Moscow, Russian Federation

Background The problem of unification in diagnostics of various prostate tumours and tumour-like lesions has gained a special significance in the modern oncology. Aim: Use the ploidometry research for studying the epithelial cell clones in the prostate, forming the different stages of cancerogenesis.
Methods Computer ploidometry test was carried out for nuclei of epithelial cells in biopsy specimen of the prostate, taken from 80 patients in different stages of cancerogenesis. Histological preparations of 8 micron thickness, stained by Feulgen's technique, were subject of the research. Nuclei's ploidy was defined by means of the computer image analyzer "Imager-CH" ("Avtan-San" software version). The integral brightness of nuclei of 396 small lymphocytes, found in histological sections, was tested to define the "tissue ploidy standard" (2c), which, in its turn, was used for obtaining the data on ploidy of 1332 epithelial cell nuclei of the prostate gland. Inter-phase cell nuclei of clones with normal and hyperplastic prostate gland, areas of prostate intraepithelial neoplasia (PIN-I– low grade – and PIN-II– high grade) and adenocarcinoma in different stages of dedifferentiation (well, moderate, poorly) were the subjects of investigation. The research determined that while the cancerogenesis progressed, the proliferative activity (indirect type information) of prostate gland cells and the ploidy of nuclei naturally increased.
Results In comparison with the average ploidy value of the normal epithelial cells nuclei (2.8 c), the average ploidy index increases 1.07 times in hyperplasia, 1.32 times in PIN-I, 1.53 times in PIN-II, 1.92, 1.96 and 2.4 times correspondingly of well, – moderate, – poorly adenocarcinoma. Taking into account the requirements of the oncological practice, it is advisable to single out only the four main stages of cancerogenesis. These stages differ substantially in the characteristics of the average ploidy of nuclei and the type of their cell clones histograms: namely normal prostate tissue and its hyperplasia; benign stages – slight intra-epithelial neoplasia, low grade (PIN –I); marginal stage – non-invasive intra–epithelial neoplasia, high grade (PIN–2); malignant stages – infiltrating adenocarcinoma (with and without metastasis).
Conclusions Computer ploidometry, as the new line of patohistological investigations may be used in the differential diagnostics

of prostate tumor and tumor-like lesions. Use of ploidometry data, obtained by means of the computer analyzer opens up the new opportunities in specifying the differential morphological diagnostics of tumors with various localization (basis of quantipathology).

P-478

Glucagonoma in Mexico. Clinical study, histopathology, immunohistochemistry and electron microscopy of six cases

J Nuncio[1], J Arista-Nasr[1], I Alvarado-Cabrero[2], J Fernandez-Diez[2]
[1]Departamento de Pathologia, Instituto Nacional De Ciencias Medicas Y Nutricion Salvador, Zubiran, Mexico City, Mexico
[2]Departamento de Patologia, Hospital de Oncologia, Centro Medico Nacional Siglo, Mexico

Introduction Glucagonoma is an alpha-cell pancreatic neoplasm with incidence of one in 20 million; the malignancy rate is unknown. The clinical, pathologic, immunohistochemistry and electron microscopy characteristics are described in a Mexican cohort of patients.
Material and methods We reviewed the pathology archives of INCMyNSZ and HOCMNSXXI for pancreatic tumors with neuroendrocrine morphology and expression of immunohistochemistry markers for neuroendocrine and glucagon-related peptides. Complete clinical history and follow-up were achieved.
Results Six cases of glucagonoma were obtained. Electron microscopy was available in two cases. Three man and three women with median age of 61.16 years, were admitted with glucagonoma syndrome complaints. The tumor localization was: head of pancreas (3/6) and tail (2/6), with average size of 6.4 cm. Two cases showed hepatic metastasis. The histopathologic study was constant with contrasting architectural, cytologic and mitotic count in all the cases. Expression of neuroendocrine markers was observed in all 6 cases, with positive glucagon stain, and negative for secretion markers (insulin, PP, serotonin, calcitonin). In electron microscopy, dense core granules were identified in two cases.
Discussion There are 200 cases of glucagonoma described in English literature; no one is originated from Latin American population. In this series, the neoplasms have equal prevalence for female and male patients, all from elderly group. The morphologic feature extremely varies in each tumor, the malignancy criteria were correlated in two cases with vascular invasion and this coincides with metastasis. A peculiar finding are the only expression of glucagon in tumoral cells, and two malignant cases with liver metastasis.

P-479

Primary neurilemoma of the thyroid gland: A case report

H El Attar, E Farida, Z Soumia, S Saida, I Ahmed
[1]Central Laboratory of Pathology Pavillon 41, Hopital Ibn Rochd, Casablanca Morroco

Introduction Primary nonepithelial tumors of the thyroid gland are rare.
Case report We present the case of a neurilemoma of the right lobe of the thyroid gland in a 16-year-old female patient. The tumor was asymptomatic and measured 6.5x2.5 cm in size. Histologic examination was consistent with an Antoni A-type neurilemoma. The tumor cells were strongly positive for S-100 protein. A loboisthmectomy was done.
Conclusion Only 12 other cases of neurilemomas of the thyroid gland have been reported in the literature. The tumor can be sporadic or associated with type 1 neurofibromatosis. The diagnosis can be made cytologically and a large exision can be avoided. The diagnosis is based on pathology that rules out malignancy.

P-480

Withdrawn

P-481

The synergetic role of granulosa cells in Ham's F10 and follicular fluid in primary stages of human embryos growth and development

HR Sadeghipour Roudsari
Tehran University Of Medical Sciences, Tehran, Islamic Republic of Iran

In early stage of embryonic growth and development the exchange of metabolite in uterus is carried via granulosa and endometrial cells. Numerous investigations have been carried to prepare a normal medium for cultivation of embryonic cells. The cultured embryos with supportive and protective cells, such as granulosa cells are usually called co-culture, show many beneficial effects such as better cleavage and nutritional status. These techniques have obviated the existing developmental barrier in this respect. Some authors have suggested that the use of natural media which contain follicular fluid have shows a better and faster clavage of zygot and nutrition status. Therefore to obtain a better culture media we have investigated 5 media preparation: 1) follicular fluid, 2) Follicular fluid and granulosa cells, 3) Ham's F10 with 10% human albumine, 4) Ham's F10 with 10% human albumine and granulosa cells, and 5) synthetic serum substitute (3S). The secondary metaphasic oocytes of 27 patient were evaluated and fertilized by intracytoplasmic sperm injection technique (ICSI) (n= 117). The injected oocytes have been transfered to one of the above media. The oocytes developmental process were evaluated approximately 21 and 43 hours after ICSI steps for two pronuclei formation and cell cleavage episodes respectively. The results showed that harvested fertilized oocytes were more abundant in 3S and follicular fluid media than in the other. After 43 hours of ICSI 18% of embryos were in 2-cell stages (n=21), 41.9% were in 4-cell stages (n=49), 11.1% were in 8 – cell stages (n=13) and 29.1% of them (n= 34) did not undergo cell devision at all. The maximum and minimum of uncleaved oocytes have been observed in Ham's F10 and 3S media respectively. The Co-culture media revealed the highest 8 – Cell stage embryos. The number of embryos have been significantly higher in 3S media than in Ham's F10 (P=0.0088). The best quality of embryos was only observed in Hsm's F10 alone and together with granulosa cells co-cultured media. The above results suggest that co-culture of embryos with granulosa cells made higher cleavage of embryo with the best grade of embryo quality and growth in Ham's F10 media decreased cleavage meanwhile increased cell fragmentation of embryos.

P-482

Effect of calcitriol and of its analogues on expression of calcitonin gene in cultured cells of medullary thyroid carcinoma

M Zabel[1,2], K Flig[1], E Gebarowska[1]
[1]Chair of Histology and Embryology, Wroclaw, Poland
[2]Chair of Histology and Embryology, Poznan, Poland

Introduction Calcitriol and its analogues affect function of several normal and neoplastic cells, including cells of medullary thyroid carcinoma originating from parafollicular cells. In the cells expression of calcitonin gene takes place, yielding due to alternative splicing calcitonin (CT) and calcitonin gene related peptide (CGRP). The aim of this study was examination of effects of calcitriol and of its two analogues, PRI-1906 and PRI-2191 on proliferation of two cell lines in vitro and on expression of calcitonin gene.
Material and methods The studies were performed on MTC 6-23 (rat cell line) and TT (human cell line) cells originating from medullary thyroid carcinomas. The cells were cultured with calcitriol or its analogues at 10(-9) to 10(-6)M for 5 days. The estimated variables included: cell number, proliferation-associated antigens (Ki-67, PCNA), CT and CGRP levels in medium (RIA), amounts of the two hormones and of their mRNAs in the cells (immunocytochemistry or hydridocytochemistry accompanied by image analysis).
Results Calcitriol and its analogues exerted low antiproliferative effect, more evident in MTC than in TT cells. PRI-2191 affected production and secretion of the two hormones. Evident correlation was noted in TT cells, positive for CT and negative one for CGRP. In MTC cells, the effect was slightly less intense. PRI-1906 exerted a similar effect in the two cell lines but only at higher concentrations of the analogue. On the other hand, calcitriol manifested its activity only in MTC cells. Effects of studied substances were also examined on CGRP/CT ratio of secreted hormones, which reflected corresponding ratio of alternative splicing of CT gene transcript. In TT cells the ratio decreased in presence of either analogue and in MTC cells the effect was observed following culture with calcitriol and the two analogues.
Conclusions Calcitriol and its analogues exert a weak antiproliferative effect and an effect on alternative splicing of calcitonin gene.

P-483

Allelotyping analysis of GEP endocrine tumors

D Furlan, R Cerutti, A Genasetti, S Uccella, S La Rosa, C Capella
Department of Clinical and Biological Sciences, University of Insubria, Varese, Italy

Background The molecular pathogenesis of GEP endocrine tumors is still largely unknown and no specific prognostic molecular markers have been yet identified. The purpose of this work was to identify specific chromosome regions or putative tumor suppressor loci that may be involved in the malignant evolution of these tumors.
Materials and methods 24 well differentiated endocrine tumors (WDETs) (11 pancreatic, 3 gastric, 10 intestinal) and 14 poorly differentiated endocrine carcinomas (PDECs) (1 pancreatic, 6 gastric, 7 colorectal) were allelotyped with an automated DNA sequencer (Applied Biosystems 310) using 38 polymorphic microsatellite markers covering chromosomes 1, 3, 5q, 6, 11, 17 and 18.
Results Regardless of the primary site, a significantly higher percentage of allelic imbalances (AI) was observed in PDECs than in WDETs ($p= 0.012$) with the only exception for 3 out of 8 nonfunctioning pancreatic tumors exhibiting multiple AI on chromosomes 11, 6q and 3p. A strong positive correlation between AI percentage and the Ki-67 proliferation index was detected considering both all tumors and WDETs alone ($p=0.002$ and $p=0.001$, respectively). Moreover, AI at 17p was the most frequent alteration observed in PDECs (92% of PDECs versus 4.8% of WDETs; $p<0.01$) together with 6q and 3p AI in gastric and 5q AI in colorectal PDECs, respectively.
Conclusion These findings suggest the existence of two different molecular profiles associated with PDECs and WDETs. Since no specific molecular markers of malignancy can be defined with certainty, the ploidy status and the evaluation of the global level of chromosomal instability of the tumors appear to be the most informative genetic factors with prognostic significance.

P-484

Mixed medullary-papillary thyroid carcinoma

DC Terzea[1], D Ioachim[2], M Ionescu[2], C Vartolomei[2], M Ghemigean[2], B Stanescu[2], C Dobrea[1], C Iosif[1], F Andrei[1], C Ardeleanu[1]
[1]Victor Babes National Institute of Pathology, Bucharest, Romania
[2]I.C. Parhon National Institute of Endocrinology, Bucharest, Romania

Mixed medullary-papillary carcinomas are rare neoplasms and must be distinguished from medullary carcinoma with entrapped follicles, papillary variant of medullary carcinoma and solid growth pattern of sclerosing variant of papillary carcinoma. These mixed tumors could arise from uncommited stem cells; it is also possible that these neoplasms could be collision tumors. The aim of our study was to show that these mixed tumors have some particular features. We studied 250 cases of thyroid carcinoma and for diagnosis we used immunohistochemical analyses for thyroglobulin, calcitonin, CEA, chromogranin and cytokeratin 19. We found 3 cases of mixed medullary-papillary carcinoma. These mixed tumors are not so frequent but the admixture of papillary and medullary components confer a different prognosis and a potential response to radioactive iodine treatment.

P-485

Genomic imbalances of sporadic and hereditary thyroid carcinomas

R Hinze[1,2], H Lange[1], O Gimm[3], H Dralle[3], HJ Holzhausen[1], H Schmidt[1]
[1]Institute of Pathology, Hospital Schwerin, Germany
[2]Institute of Pathology, University of Halle-Wittenberg, Germany
[3]Department of General Surgery, University of Halle-Wittenberg, Germany

Introduction Medullary thyroid carcinomas (MTC) are rare tumours, which can occur in a sporadic and a hereditary setting as well.
Material and methods Comparative genomic hybridization (CGH) was used to analyse 53 medullary thyroid carcinomas from 44 patients. 25 of the 53 MTC were characterized as hereditary.

Results Only four hereditary (4/25) tumours showed genomic imbalances. 28 MTC appeared as sporadic forms. In 21 of the sporadic tumours we detected DNA sequence copy number changes (mean: 7 per tumour, range: 1-15). The minimal common regions for the most frequent gains were narrowed down to 1q24-q42, 5p14, and 11q14 (48 percent), 1q43-q44, 5p15, and 11q21 (43 percent), 5p12-p13, 6p11.2-p22, and 11q22 (38 percent), and 6p23-pter, 6q12-q22, and 7p11.2-p15 (33 percent). Eight high-level amplifications were observed in four samples. 5p was affected twice. The minimal common regions for the most frequent losses were observed for 3p (48 percent), and 3q (38 percent).
Conclusion Only limited genomic alterations could be detected by CGH for hereditary MTC, which share a germline mutation of the RET proto-oncogene as initial step of cancerization. Additional genetic alterations, which are responsible for the progression of these tumours, are not identified yet. In contrast, sporadic MTC revealed a recurrent pattern of genomic imbalances. Our data are in accordance in part with the few cytogenetic data, which are reported in the literature and can help to rule out parts of the genome on which further studies should focus on.

P-486

Immunohistochemical analysis of tumor infiltrating immunocytes in thyroid tumors

V Zolota, P Aroukatos, S Sidira, D Koumoundourou,
D Papachristou, CD Scopa
Dept. Pathology, Univ. Patras Med. School, Patras, Greece

Introduction The presence of host inflammatory cells within or at the periphery of human tumors has long been recognized and is commonly viewed as representing a host tumor immune response. In the thyroid gland, the occurrence of chronic lymphocytic thyroiditis (CLT) in thyroid cancers has been reported and considered by some authors as a favorable prognostic sign.
Materials and method The inflammatory cell population in 46 consecutive thyroid tumors (22 papillary, 6 occult, 2 follicular, 1 myeloid carcinomas and 15 follicular adenomas), accompanied with chronic non-specific thyroiditis, were characterized imunohistochemically, using a panel of monoclonal antibodies against T-cells (anti-CD3, anti-CD4, anti-CD8), B-cells (anti-CD20), macrophages (anti-CD68) and dendritic cells (anti-S-100). The extent of lymphocytic infiltration was graded as: +(subtle), ++(moderate) and +++(intense and diffuse lymphoid aggregates).
Results Papillary carcinomas showed denser infiltrates than the follicular tumors or occult carcinomas: of the papillary cancers 63% (14/22) showed +, 27% (6/22) ++ and 10% (2/22) +++ peri- and intratumoral lymphocytic infiltration, whereas all follicular tumors and occult carcinomas exhibited + lymphoid aggregates, mostly in the peritumoral tissue. Tumor infiltrating lymphocytes (TILs) consisted of both B and T cells. B-cells tended to cluster focally in the stroma, whereas T-cells (mainly T8) contacted closely with tumor cells. TILs occurred in the setting of CLT (80% of the cases). Tumor infiltrating macrophages were found in 93% of the cases. Follicular tumors showed only small numbers of large, granule rich macrophages within the lumen of the follicles, whereas in papillary carcinomas they were found in increased numbers in the papillae or in intratumoral stroma. A significant proportion (75%) of papillary carcinomas showed an increased number of S-100(+) dentritic cells, in close contact with neoplastic cells, whereas 18%(3/17) of the follicular tumors exhibited only scant number of intratumoral dentritic cells.
Conclusions TILs are associated more often with papillary carcinomas. The observed low immune reaction in follicular tumors may be due to the capsular barrier.

P-487

CK-19, galectin-3, involucrin, p27 and Mib-1 expression in thyroid cells obtained by fine-needle aspiration citology and their histological counterparts: a preliminary report

R Orellana[1], M Bella[1], G Giménez[2], G Marqués[3], J Simó[3], A Zidan[4], E Musulén[1], D Maurici[2], N Combalia[1], M Rey[1]
[1]Corporació Parc Taulí, Pathology Dep., Barcelona, Spain
[2]Corporació Parc Taulí, Endocrinology Dep., Barcelona, Spain
[3]Corporació Parc Taulí, Surgical Dep., Barcelona, Spain
[4]Corporació Parc Taulí, Radiodiagnosis Dep., Barcelona, Spain

Introduction Thyroid cancer is the most frequent endocrine malignancy and its preoperative diagnosis is sometimes difficult. We investigate whether ck-19, galectin-3, involucrin, p27 and MIB-1 could be potential markers for diagnosis of conventional cytology.
Material and methods A preliminary immunohistochemical analysis was performed on 22 thyroid specimens (5 nodular hiperplasia-NH-, 5 follicular adenomas-FA-, 4 follicular carcinomas-FC- and 7 papillary carcinoma-PC-) from selected patients with thyroid nodules and their preoperative cytologic samples. We analysed ck-19(b170), galectin-3(9C4), involucrin (SY5), p27(1B4) and MIB-1 expression in both cell block and their histological counterparts, semiquantitatively.
Results This table corresponds to histological specimens.

Diagnosis	involucrin	galectin-3	CK-19	p27	Mib-1	Total
NH	-	-	2 (++)	5*	5•	5
FA	-	1 (+)	3 (+)	41	5•	5
FC	-	-	1 (++)	4,	4•	4
PC	6	7 (++)	7 (+++)	63	7•	7

*4 cases score 3+,1 case 2+/ 14 cases score 2+,1 case 1+/ ˛ 2 cases score 2+,2 cases1+/3 4 cases score 1+,2 cases 2+,1 case 0+/ • all cases score 1+
Results were similar in cell block, although involucrine was negative in three PC. Expression of Mib-1 and p27 is variably detected in benign and malignant proliferative lesions. Interestingly, galectin-3, ck-19 and involucrin are invariably detected in papillary carcinomas, although heterogeneous positive expression was observed into the same lesion.
Conclusions Our findings show that galectin-3($p<0.001$), ck-19($p<0.006$) and involucrin($p<0.001$) are useful to identify papillary carcinoma from other thyroid lesions; however, heterogeneous positive pattern expression is not useful for preoperative diagnostic of conventional cytology.

P-488

VEGF-C, VEGF-D, and VEGFR-3 in pheochromocytomas

K Salmenkivi[1], J Arola[1], C Haglund[2], P Heikkilä[1]
[1]Haartman Institute, Department of Pathology, Helsinki, Finland
[2]Department of Surgery, Helsinki University Central Hospital

Introduction Pheochromocytomas are rare neuroendocrine tumors that are highly vascular. Their malignancy is extremely difficult to estimate on the basis of histopathological features. Vascular

endothelial growth factor receptor 3 (VEGFR-3) is a marker for lymphatic endothelium. Its ligands VEGF-C and VEGF-D are expressed in many neuroendocrine tissues. Our aim was to investigate the expression and the potential role of VEGF-C, VEGF-D, and VEGFR-3 in various pheochromocytomas.
Materials and methods Thirty-three pheochromocytomas, six of them metastasized, were studied using immunohistochemistry. Thirteen tumors exhibited histologically suspicious features, such as necrosis, mitosis count over 5/10 HPF, vascular or capsular invasion, but they not metastasized, and were thus called borderline tumors.
Results and conclusions VEGF-C immunohistochemical positivity was found in most pheochromocytomas. The expression of VEGF-C was heterogenous and varied also within different tumor groups (benign, borderline, and malignant tumors). However, it tended to be stronger in extraadrenally located tumors. VEGF-D positivity was also found in most tumors studied (10/18). Interestingly, all malignant tumors (n = 3) were totally negative for VEGF-D. VEGFR-3 expression was found in 15 out of 33 tumors, but the staining was mostly weak. The expression of VEGFR-3 did not seem to correlate with the expression of VEGF-C or VEGF-D.
In conclusion, VEGF-C, VEGF-D, and VEGFR-3 are expressed in various pheochromocytomas, however, the diagnostic value of these markers needs further investigations.

P-489

Mixed corticomedullary tumor of the adrenal gland. A case report

S Tatić, D Brasanac, V Bozić, A Diklić, I Paunović, S Ognjanović, S Nikolić, M Havelka
Institute of Pathology, University School of Medicine, Belgrade, Serbia and Montenegro

Corticomedullary mixed tumors of the adrenal gland are quite rare, with only seven well-documented cases reported in the literature. We report the light microscope and immunohistochemical features of one case of this rare tumor. The patient is a 28-year-old woman who presented with hypertension, hirsutism, gain weight and ammenorhoea of 6-month duration. The surgically resected specimen consisted of a well-circumscribed, single adrenal mass, weighing 22,6gr, and 30 mm in diameter, surrounded by a rim of uninvolved adrenal cortical tissue. Paraffin-embedded cut sections were stained by both hematoxylin-eosin and PAS.The expression of inhibin, melan A, chromogranin A, synaptophysin, S-100 protein and ACTH was examined using the PAP method, with appropriate antibodies being applied. The tumor was composed of cords and nodules of adrenal cortical cells intimately admixed with pheochromocytes. Immunohistochemical investigations highlighted these two cellular components. The adrenal cortical cells revealed inhibin and melan A immunopositivity, whereas the pheochromocytes were strongly reactive with chromogranin A, synaptophysin, and ACTH, and the sustentacular cells with S-100 protein. Thus, we report one additional case of mixed corticomedullary tumor of the adrenal gland.

P-490

Bcl-2 and Fas antigen expression - immunohistochemical and molecular studies in chronic thyroiditis

A Ziolkowski[1], A Fila[2], M Kucharzewski[3], J Waler[3], K Zwirska-Korczala[4], K Tomaszek[1], U Mazurek[2], T Wilczok[2]
[1]Chair And Department of Patomorphology, Medical University of Silesia, Zabrze, Poland
[2]Department of Molecular Biology and Genetics, Medical University of Silesia, Katowice, Poland
[3]Chair and Clinic of General Surgery, Medical University of Silesia, Katowice, Poland
[4]Chair of Physiology, Medical University of Silesia, Katowice, Poland

Introduction The study of apoptotic markers seems to be important in understanding the pathogenesis of chronic inflammatory processes of the thyroid gland. Aim: Intensity determinations of BCL-2 and FAS immunohistochemical reactions with the quantitative assessment of BCL-2 and FAS gene expressions in inflammatory affected thyroid glands.
Materials and methods The specimens were taken from 16 women aged 21 to 66. The type of inflammation and the intensity of lymphocytic infiltration were assessed according to the Mizukami and the Waterhouse and Doniach classifications, respectively. The expression of BCL-2 and FAS antigens was determined immunohistochemically. Moreover, BCL-2 and FAS genes were quantitatively analysed by RT-PCR assay using TaqMan technology.
Results Intensity of immunostaining for BCL-2 antigen in patients with chronic thyroiditis was stronger than in patients without lymphocytic infiltration. An increase in the intensity of lymphocytic infiltration did not affect BCL-2 mRNA levels. FAS antigen got stained in subjects with mixed inflammation; a presence of oxyphilic cells enhanced the stain reaction. In the case of oxyphilic thyroiditis, the changes in FAS antigen were accompanied by a concomitant increase of FAS mRNA levels. Small differences, between various samples of the same specimen, in BCL-2 and FAS mRNA and protein levels were found in patients with focal thyroiditis. These differences were related to the intensity of lymphocytic infiltration.
Conclusions The thyroid gland is characterised by a high degree of antiapoptotic activity. Each type of thyroiditis has its own characteristic pattern of BCL-2 and FAS expressed as mRNA and as protein.

P-491

The use of galectin-3 and cytokeratin 19 in differential diagnosis of thyroid tumors with follicular growth pattern

A Ryska[1], J Laco[1], J Cap[2]
[1]Dept. of Pathology, Charles University Medical Faculty Hospital, Hradec Králové, Czech Republic
[2]Department of Internal Medicine, Charles University Medical Faculty Hospital, Hradec Králové, Czech Republic

Aim To study the use of galectin-3 (Gal) and cytokeratin 19 (CK19) in differential diagnostics of thyroid tumors with follicular growth pattern.

Material and methods A series of 31 thyroid lesions (10 follicular adenomas (FA), 9 follicular carcinomas (FC), 12 follicular variants of papillary carcinoma (FVPC)) was studied retrospectively by immunohistochemistry using monoclonal antibodies.
Results The staining intensity of either antibody was evaluated as positive or negative using different thresholds (0, 25 and 50% of positive cells). Generally, the intensity of staining of Gal was much higher than that of CK19. Using 0% threshold, 8/10 FA showed positivity of Gal and none was positive in CK19. In FC, 8/9 tumors were Gal positive, 4/9 were also CK19 positive. Among FVPC, all 12 cases were Gal positive and 11/12 were also CK19 positive. Using 50% threshold, only 1/10 FA was Gal positive, none was CK 19 positive. Among FC, however, all tumors were both Gal and CK19 negative. On the other hand, 9/12 of FVPC were Gal positive and 4/12 were CK19 positive. The sensitivity, specificity, negative and positive predictive value of Gal were 0.95; 0.20; 0.71; 0.67 for 0% threshold and 0.43; 0.90; 0.90; 0.43 for 50% threshold, respectively. For CK19 it was 0.71; 1.00; 1.00; 0.63 for 0% threshold and 0.19; 1.00; 1.00; 0.37 for 50% threshold, respectively.
Conclusions The use of Gal and CK19 may be helpful in differentiating FVPC from benign lesions. However, the use of these markers in differential diagnostics of FC from FA is of little value. Moreover, due to low intensity of staining, its use in preoperative diagnostics (e.g. in FNAC cytoblock specimens) seems to be questionable.

P-492

Adrenal cortical adenoma in association with Cushing's syndrome - case report

S Manxhuka-Kerliu, F Hoxha, M Maxhuni, F Zeqiri, S Dobruna-Manxhuka, A Kërliu, V Sahatqiu-Meka
Institute of Pathology, Faculty of Medicine, University of Prishtina, Serbia and Montenegro

Introduction Morphological feature of adrenal cortical adenoma by itself doesn't allow reliable distinction between tumors associated with any particular endocrine syndrome. Without being aware of the clinical setting and/or endocrinological data, it may be impossible to distinguish them from an incidental nonhyper-functional macronodule. The aim of this investigation was to represent the only case of adrenal cortical adenoma in association with Cushing's syndrome in our material.
Material and methods We have analyzed the only case of adrenal cortical adenoma with Cushing's syndrome according to its morphological changes, laboratory data, CT-scan as well as MRI of adrenal gland.
Results Gross examination showed a small ovoid adenoma. On section, it appeared yellow to golden yellow with dark brown foci, blood and degenerative changes. Microscopically, tumor contained cells with pale, lipid-rich cytoplasm, compact eosinophilic cytoplasm, arranged in trabeculae, short blunt cords, as well as in rounded nests. Nuclei were somewhat vesicular with a single small dot-like darkly stained nucleolus.
Discussion and conclusion Our data indicate that being aware of characteristic histologic feature in terms of architectural pattern and cell type for cortical adenoma associated with Cushing's syndrome, this could be the purpose of more comprehensive discussion.

P-493

Correlation of histopathology and sequential analysis of gene expression in follicular thyroid neoplasms

SJ Diaz-Cano[1,2], S Arif[1], A Blanes[2]
[1]Barts And The London School of Medicine, University of London, UK
[2]University of Malaga School of Medicine, Malaga, Spain

Background The expression profile and diagnostic relevance of nuclear features, inflammation, and stromal changes have not been systematically evaluated in follicular thyroid carcinomas (FTC).
Design We selected 69 FT neoplasms (22 adenomas, 14 minimally invasive carcinomas, 22 widely invasive carcinomas, and 11 anaplastic carcinomas), classified using standard criteria. Histological variables including anisokaryosis, chromatin pattern, nucleolus, nuclear pleomorphism, nuclear/cytoplasmic ratio, necrosis, stromal changes, and tumor interstitial lymphocytes (TIL) were studied by histological diagnosis (significant if $P<0.05$). Oligo(dT)-primed double strand cDNA was produced from total RNA, and libraries were produced from 3 normal thyroids and 8 FTC. Sequential analysis of gene expression (SAGE) was performed (FTC/control expression factor$\geq$2, significance$\leq$0.01).
Results TIL were absent in 64/69 neoplasms. Minimally invasive carcinomas were distinguished from adenomas by conspicuous nucleolus, increased nuclear/cytoplasmic ratio, and coexistence of apoptosis and myxoid changes in adenomas. The most specific variables of high-grade carcinoma were coagulative necrosis, and nuclear hyperchromatism and pleomorphism. FTC SAGE showed ubiquitin C and sequestosome 1 down-regulation, and tumor protein translationally controlled 1 and malate dehydrogenase 1 up-regulation. This SAGE profile correlated negatively with proinflammatory molecules expression (Interleukin-1beta, chemokine XC-receptor 1, interferon-induced transmembrane protein 2, protein tyrosine phosphatase C), BRCA2, and protein phosphatase 4. The correlation was positive with proliferation markers (myb, mitogen-activated protein kinase 12, cyclin-dependent kinase 8, BRCA2/CDKN1A interacting protein, and RAS oncogene family).
Conclusions Proliferation up-regulation and apoptosis down-regulation results in prominent nucleolus and high nuclear/cytoplasmic ratio for low-grade carcinomas and hyperchromatism and nuclear pleomorphism for high-grade carcinomas. Tumor down-regulation of proinflammatory molecules explains TIL absence.

P-494

Papillary carcinoma of the thyroid with bone formation. A case report

G Kaygusuz, S Dizbay Sak, E Erden, S Ozturk, S Kocak
Ankara University, Ankara, Turkey

Introduction Papillary carcinoma is by far the most common type of thyroid malignancy. However, ossification in papillary carcinoma is very rare. A case of papillary carcinoma of the thyroid metastatic to cervical and supraclavicular lymph nodes with associated bone formation and extensive calcification is presented.
Case report A 67 year-old male with a history of gastric carcinoma was admitted to hospital presenting with lumbal pain. A computed tomography scan revealed a calcified nodule, measuring in 33 mm diameter in the thyroid. Total thyroidectomy and modified neck dissection were performed. The thyroidectomy

specimen showed a well circumscribed, calcified, rock-hard nodule measuring 4x3x2 cm. Histologic examination of the hard nodule after decalcification showed spicules of bone formation and papillary carcinoma. Foci of metastatic papillary carcinoma with bone formation were also seen in the cervical and supraclavicular lymph nodes. There was also bone marrow formation both in the thyroid nodule and in the metastatic lymph nodes. Immunohistochemically, the tumour cells were positive for thyroglobulin.
Conclusion Ossification in papillary carcinoma of the thyroid is an unusual finding. The mechanism of bone formation is not clear. The presence of ossification both in primary and metastatic tumoral masses suggests that ossification is not a dystrophic process in the preexisting benign thyroid tissue but somehow related to the papillary carcinoma in the present case.

P-495

Sex hormones receptors in human thymoma - clinicopathological analysis

H Ishibashi, T Suzuki[1], S Suzuki[2], M Sunamori[3], M Handa[4], T Kondo[2], H Sasano[1]
[1]Department of Pathology, Tohoku University School of Medicine, Sendai, Japan
[2]Department of Thoracic Surgery, Institute of Development, Aging and Cancer, Tohoku University, Japan
[3]Department of Pathology, Thoracic Cardiovascular Surgery, Graduate School, Tokyo Medical and Dental University, Tokyo, Japan
[4]Department of Surgery, Sendai Kousei Hospital

Estrogens regulate the development, maturation, and function of various organs, including the thymus. Therefore it is suggested that estrogens play important roles in the development of human thymoma. However there is no study about influences of sex steroids to human thymoma. In this study, we examined the immunohistochemical localization of sex steroid receptors for estrogen (ER)α and ERβ, progesterone (PR)-A and PR-B, and androgen (AR) in human thymoma (n=132), and correlated these findings with various clinicopathological parameters. We used reverse transcription polymerase chain reaction (RT-PCR) and real-time PCR to further study the expression of these receptors in 20 thymoma cases.
Results Immunoreactivity for all sex steroid receptors was detected in the nuclei of thymoma epithelial cells. The percentage of immuno-positive cases and H-score values for each receptor (mean±SD) were: ERα, 65.9% and 85.8±80.2; ERβ, 6.8% and 7.2±8.7; PR-A, 3.8% and 2.7±4.9; PR-B, 49.2% and 55.8±68.3, and AR, 15.2% and 14.1±11.7, respectively. Results of real-time PCR were consistent with those of immunohistochemistry especially results for ERα, PR-B, and AR. A significant positive correlation was detected between immunoreactivity for ERα and PR-B. ERα immunoreactivity was inversely correlated with tumor size, clinical stage, WHO classification and Ki-67 labeling index. In addition, the status of ERα immunoreactivity was significantly associated with a better clinical outcome in thymoma patients.
Conclusions Sex hormones receptors express in human thymoma, and especially ERα may be related to sex, clinical stage and pathological cell type.

P-496

Galectin-3 immunodetection using a biotin-free system in a series of 137 oxyphilic (Hurthle) cell tumors of the thyroid

M Volante[1], F Bozzalla[1], R Depompa[1], C Pecchioni[1], A Bartolazzi[2], M Papotti[1]
[1]Dept. Biomedical Science and Human Oncology University of Turin, Turin, Italy
[2]S. Andrea Hospital, University of Rome, Rome, Italy

Introduction Galectin-3 was reported to distinguish follicular and papillary carcinomas of the thyroid from adenomas, but controversial results were obtained in oxyphilic cell tumors, possibly related to endogenous biotin reactivity. The aim of this study was to assess the role of galectin-3 immunodetection in a large series of benign and malignant oxyphilic tumors.
Materials and methods Galectin-3 expression was retrospectively analysed in 137 thyroid oxyphilic (Hurthle) cell tumors, including 42 adenomas [OA], 66 carcinomas [OC], 29 oxyphilic variant of papillary carcinoma [OPTC] and in 28 control cases of goiter with oxyphilic changes and Hashimoto's thyroiditis. A purified Galectin-3 monoclonal antibody and a biotin-free immunoperoxidase procedure were used in paraffin embedded specimens.
Results 60 of 66 OCs were focally (11 cases) or diffusely (49 cases) positive. 28/29 OPTC were focally (7 cases) or diffusely (21 cases) reactive. Overall, malignant oxyphilic tumors were positive in 93% (88/95). OA had a focal reactivity in 24% (10/42) of cases, with a preferential subcapsular immunostaining. Sensitivity and specificity were 93% and 76%, respectively. Control oxyphilic goiters were negative (0/13), as opposed to Hashimoto's thyroiditis (oxyphilic cells positive in 14/15 cases).
Conclusion The role of Galectin-3 immunoreactivity in the differential diagnosis of benign and malignant follicular lesions is confirmed also in oxyphilic cell tumors. The focal immunoreactivity observed in adenomas may be probably related to a true expression of Galectin-3, as confirmed by mRNA expression by means of in situ hybridisation, and could be related to early malignant changes in tumors still lacking the currently accepted morphological signs of malignancy.

P-497

c-Kit protein expression in Merkel cell carcinoma of the skin and other extrapulmonary poorly differentiated neuroendocrine carcinomas

M Volante[1], E Allia[1], M Cerrato[1], L Ciuffreda[2], M Papotti[1]
[1]Dept. Biomedical Science and Human Oncology University of Turin, Turin, Italy
[2]Dept. of Oncology Molinette Hospital Turin, Turin, Italy

Introduction c-Kit gene encodes for a transmembrane tyrosine kinase receptor which is expressed in a variety of human normal tissues and malignancies, being small cell lung carcinoma one of the most frequent among the latter group. The search for c-kit expression in human tumors bears clinical implications since several tyrosine kinase inhibitors have been proposed in the treatment of c-kit positive tumors. The aim of our study was to investigate c-kit protein expression in a series of Merkel cell carcinomas (MCC) and of other extrapulmonary poorly differentiated neuroendocrine carcinomas (PDNECs).

Materials and methods A total of 39 samples, including 25 Merkel cell carcinomas (MCC) of the skin (from 24 patients, 17 of them with follow up information available), and 14 cases of extrapulmonary PDNECs from different sites (bladder - 5 cases, colon - 4 cases, gallbladder and pancreas - 2 cases, parotid - 1 case) were analyzed by means of immunohistochemistry for c-kit protein expression. Only a membranous staining was considered specific, and scored according to the percentage of positive cells.
Results c-Kit protein was demonstrated in 8/17 (47%) MCC, and in 11/14 (79%) of other PDNECs. In MCC, a correlation, slightly below statistical significance (p=0.08), was observed between the presence of c-kit expression and clinically aggressive behaviour.
Conclusion Our data indicate that c-kit expression may play a role in the growth regulation of extrapulmonary PDNECs. Therefore this group of tumors may be considered as a possible target for tyrosine kinase inhibitors therapy.

P-498

Carcinoid tumors in the thyroid gland. Primary or metastatic? Report of two cases

M Volante[1], M Bongiovanni[1], P Filosso[2], G Bussolati[1], M Papotti[1]
[1]Dept. Biomedical Science and Human Oncology University of Turin, Turin, Italy
[2]Dept. Thoracic Surgery University of Turin, Turin, Italy

Introduction The occurrence of well differentiated endocrine tumors (carcinoid) in the thyroid gland is unfrequent and may represent both a differential diagnostic problem with medullary carcinoma, and a potential pitfall in the searching for its primary or metastatic origin. Our aim was to determine the differential morphological and immunohistochemical profile of two cases of carcinoid tumors localized in the thyroid - one metastatic from the lung, and the other of unknown origin.
Materials and methods The first collected case had a clinical history of an atypical lung carcinoid diagnosed two years before, while the other lacked a clinical, instrumental and laboratory history suggestive of a possible primary carcinoid elsewhere. Paraffin embedded material was histologically reviewed and analyzed by immunohistochemistry for thyroglobulin, calcitonin, CEA, chromogranin A, S-100, TTF1, and Ki-67.
Results The first case (F/55) presented as multiple nodules in both lobes, composed of poligonal eosinophilic cells arranged in the typical organoid pattern. Foci of necrosis were present. The morphological features overlapped with those of the primary lung tumor. The second case (M/52) presented as a single nodule in the left lobe, morphologically resembling typical carcinoid without necrosis. Both cases were negative for thyroglobulin, calcitonin, S-100 and CEA, positive for chromogranin A and TTF1, and low proliferating (Ki-67 <10% in both).
Conclusion Our data suggest that, even in the absence of a clinically detected primary tumor, the occurrence of a carcinoid tumor in the thyroid gland should be firstly considered metastatic in origin, the lung being the major candidate for the primary localization (as determined by TTF1 immunostaining).

P-499

Telomerase expression and proliferation activity in gastroenteropancreatic tumours

S Vural, Y Kapran, M Gulluoglu, U Cevikbas, F Dizdaroglu
University of Istanbul, Istanbul Medical Faculty, Department of Pathology, Istanbul, Turkey

Intruduction Gastroenteropancreatic endocrine tumours have a variable prognosis and the prediction of biological behavior based on histopathology is not always possible. Telomerase is a reverse transcriptase that synthesis telomere DNA to stabilize telomere length.Telomerase activity is increased in different human cancers. The aim of this study was to determine whether the expression of telomerase (hTERT) correlates with the histological typing of endocrine tumours and Ki-67 proliferation index.
Material and methods Formalin-fixed, paraffin-embedded tissue sections from 40 gastroenteropancreatic endocrine tumours and 10 normal pancreas were stained immunohistochemically for human telomerase reverse transcriptase (hTERT) and Ki-67 antigen.
Results 11 cases were diagnosed as well-differentiated endocrine tumour, 26 were well-differentiated endocrine carcinoma and 3 were poorly-differentiated endocrine carcinoma according to WHO Classification of Endocrine Tumours. The percentage and intensity of positive neoplastic cells were assessed for each case. Expression of hTERT was observed in one well-differentiated endocrine tumour (9%), in 7 well-differentiated endocrine carcinomas (26.9%) and in 3 poorly-differentiated endocrine carcinomas (100%). There was a significant correlation between the expression of hTERT and histopathological diagnosis ($p<0.01$). Also the correlation of hTERT expression and Ki-67 index was statistically significant ($p<0.01$).
Conclusion Immunohistochemical detection of hTERT expression in gastroenteropancreatic endocrine tumours may be a helpful tool in addition to morphological findings and Ki-67 index in predicting the malignant potential of these tumours.

P-500

Proliferation, p53 expression and apoptosis in pituitary adenomas: relationship to tumor behaviour

C Tanase[1], E Codorean[1], C Ardeleanu[1], D Terzea[1], G Butur[1], G Manda[1], M Neagu[1], V Ciubotaru[2], I Ogrezean[2]
[1]'Victor Babes' National Institute of Pathology, Bucharest, Romania
[2]'D. Bagdasar' Hospital, Neurosurgery Department, Bucharest, Romania

Introduction Pituitary adenomas are known to vary considerably from the stand point of their intrinsic aggresiveness that might imply a different therapeutical approach. The aim of this study was to estimate the relationship between proliferative activity (Ki67), p53 expression, apoptosis and pituitary tumor behaviour.
Materials and methods Immunohistochemical analysis of Ki67 and p53 expression were performed in 50 paraffin-embeded pituitary adenomas: 28 functioning; 22 non-functioning; 34 invasive adenomas. Apoptotic index (AI) was determined in 24 adenomas by the in situ end-labeling technique (TUNEL).
Results Ki67 expression in all adenomas was 3.68% (significantly higher in functioning comparatively with non-functioning pituitary adenomas - 4.45±0.5% versus 2.62±0.47%). We noticed a positive correlation between the proliferative activity and the tumoral invasiveness (Ki67 labeling index 4.82±0.4% in invasive and 1.25±0.3% in non-invasive adenoma). p53 nuclear positivity was identified in 50% of the invasive adenomas and only in 5% non-invasive adenomas, with a positive correlation between p53 and proliferative activity (Ki67: 5.58±0.4 in p53 positive versus 2.60±0.47% in p53 negative tumors). Apoptosis was found in 60% of tumors, higher in some of the invasive ones, with a positive correlation between the proliferation rates and apoptotic indices (AI: 4.54±1.22 in total versus 5.42±1.46 in invasive pituitary adenomas). Also, some differences were recorded in functioning

and non-functioning adenomas (AI: 5.14±1.62 versus 3.70±1.92).
Conclusions The data suggest that the assessment of proliferation, p53 expression and apoptosis might be used to evaluate tumor behaviour and susceptibility of adenomas to therapy.

P-501

Differentially expression of NESP55 in Langerhans islets of the human pancreas and overexpression in endocrine pancreatic tumors

C Ensinger[1], R Prommegger[2], K Schmid[3], R Fischer-Colbrie[4]
[1]Institute of Pathology, University of Innsbruck, Austria
[2]Surgical Department, University of Innsbruck, Austria
[3]Institute of Pathology, University of Essen, Germany
[4]Institute of Pharmacology, University of Innsbruck, Austria

Introduction NESP55 is a novel member of the chromogranin family and is processed by endopeptides within the chromaffin granules in various rat and bovine endocrine and neuronal tissues, including adrenal glands, pituitary glands, some brain regions and intestine. Nothing is known about the distribution in human organs and tissues.
Materials and methods We investigated human pancreatic tissues as well as pancreas derived endocrine tumors. Therefore Langerhans islets of different pancreatic parts and 24 endocrine pancreatic tumors were immunohistochemically investigated. To compare the results with other endocrine tumors, eight intestinal carcinoid tumors were incubated too. Additionally RT-PCR was used to confirm our results.
Results In Langerhans islets, all different cell types presented with different amounts of NESP55, including insulin, glucagon, somatostatin and pancreatic polypeptide producing cells. All of the endocrine tumors derived from these cells showed an occurrence of NESP55. Interestingly, in no carcinoid tumor of the intestine reactivity with the NESP55 antibodies could be found.
Discussion and conclusion NESP55, as other chromogranins too, is an important marker for neuroendocrine tissues and tumors with a prognostically relevant impact by clearly differentiating endocrine from exocrine pancreatic neoplasms. Moreover, by use of NESP55, it seems to be possible to distinguish between pancreatic derived endocrine tumors and intestinal carcinoids, especially important for identifiing the primary tumor, when neuroendocrine liver metastases and clinically unspecific symptoms are found.

P-502

Clinical importance of vascular endothelial growth factor (VEGF) for papillary thyroid carcinomas

Kilicarslan A, Ogus M, Arici C, Pestereli H.E, Cakir M, Karpuzoglu G
Antalya, Turkey

Introduction Vascular endothelial growth factor (VEGF) is a major regulator of angiogenesis and may be produced by some cancer cells. Several recent reports have documented that increased expression of VEGF is associated with a risk of recurrence or decreased recurrence-free survival in papillary thyroid cancers (PTC). The aims of this study were to determine whether immunohistochemical expression of VEGF is related to local and distant recurrence of PTC and to evaluate the relationship between hypervascularization and VEGF expression in papillary thyroid carcinomas.
Material and methods VEGF expression was examined immunohistochemically in 48 papillary carcinomas. Ten normal thyroids were used as controls. Patients were followed for 61.7 months, (range, 24-143). Twelve of the patients had local and distant recurrences. VEGF immunostaining was evaluated semiquantitatively by two pathologists, blinded for clinicopathological data.
Results The difference between the recurrent (n=12) and nonrecurrent (n=36) carcinomas was statistically significant (p=0.001). VEGF expression was also stronger in papillary thyroid carcinomas than in normal thyroid tissues. The mean microvascular densities were significantly higher than those in normal thyroid tissues.
Conclusion These data indicate that VEGF staining is strongly associated with increased frequency of local and distant recurrence in PTC and that the immunohistochemical profile of the expression may be used as a marker for predicting which tumors may have metastatic potential. Key words: thyroid, VEGF, angiogenesis.

P-503

Bone mineral density and Pap smears

A Repše Fokter[1], SK Fokter[1], R Komadina[1], D Štiblar Martinčič[2]
[1]Celje General Hospital, Celje, Slovenia
[2]Institute of Histology and Embriology, Medical faculty, Ljubljana, Slovenia

Introduction Osteoporosis is an increasingly prevalent bone disease. The key to the treatment of osteoporosis lies in prevention and requires screening of non-symptomatic population, which may not be cost-effective. The present study attempted to find out possible correlation between morphologic characteristics in Pap smears, and bone mineral density (BMD) as measured by dual energy X-ray absorbtiometry (DEXA)
Materials and methods Four different lumbar spine and left hip regions were automatically scanned in 79 women whom Pap smears for routine cervical cancer screening were taken. The smears were grouped into atrophic and mature cell patterns, which can easily be recognised during routine screening. Using astereological analysis, the mean areas of squamous cells, their nuclei, cytoplasm and nuclear cytoplasmatic ratio were estimated.
Results The mean areas of cells and cytoplasm were significantly lower at lower T-scores ($p<0.01$), while the mean areas of nuclei were not ($p>0.5$). Nuclear cytoplasmatic ratio was higher at lower T-scores ($p<0.01$). T-scores of all hip and spine regions were significantly lower in atrophic cell pattern group. The study group indicated concurrently high sensitivity of 81% and specificity of 78%, with positive predictive value of 84%.
Conclusion Our results suggest that a significant number of women with low BMD could be identified parallel with the routine Pap test for cervical cancer screening without additional costs.

P-504

Value of repeat fine needle aspiration cytology in the management of thyroid nodules with an initial cytology result of benignity

S Razquin, C De Miguel, E Menéndez, E Urbiola, A López Cousillas, AM Puras
Hospital Virgen del Camino, Pamplona, Spain

Introduction Management of benign thyroid nodules is controversial. Some studies recommend to repeat FNA in all benign thyroid

nodules, while others recommend to do it only if clinical changes are present. This study was done to determinate the usefulness of systematic repetition of FNA in patients with benign cytology result in the initial FNA.
Materials and methods Data were collected from 208 patients referred to Endocrinology Service for evaluation of thyroid nodular disease between 1998 and 2001. All patients underwent repeated FNA of thyroid nodule. Age of patients was 46.9+23.8 years, 91.8% were females, 74% had uninodular goiters, nodule size was 2.6+1.1cm. Time elapsed between both FNA was 14.3+9.7 months.
Results At second FNA, 175 aspirations had benign cytology, 21 were non diagnostic, 10 suggestive of follicular neoplasm and 2 had malignant cytology results. Excluding non-diagnostic aspirations, we get 6% of discordant results. Uninodular goiters as compared to multinodular have a higher rate of discordant results. We did not find other variables between groups of concordant and discordant results. Twenty-two patients with benign cytology underwent thyroid surgery, without any histological malignant result.
Conclusion 1- Uninodular goiters with an initial benign cytology have a significant rate of discordant results after repetition of FNA. However, in 30% of these cases the first diagnosis was based on limited material. 2-Our results show that 5 cases of thyroid carcinoma out of 208 patients with nodular goiter were misdiagnosed by initial FNA cytology. Therefore we recommend systematic repetition of FNA cytology in all patients with uninodular goiter.

P-505

Immunocytochemistry in FNA biopsy material

B Szczesniak- Klusek, E Chmielik, D Lange, A Goraj-Zajac
Oncology Center, Maria Sklodowska-Curie Memorial Institute in Gliwice, Poland. Department of Patology Ul. Wybrzeże Armii Krajowej 15, 44-100 Gliwice, Poland

Objective Assessing diagnostic value of immunocytochemical methods in destained cytology smear specimens prepared from fine needle aspiration (FNA) biopsy material.
Material and methods Investigated material comprised 135 samples from FNA biopsies that were diagnosed in 1999-2001. Alcohol-fixed cytology smears were typically stained with hematoxylin-eosin. For immunocytochemical studies, preparations were first destained using alcohol series. Following this, chosen antibodies were used either separately, or as a panel CKMNF, EMA, LCA, TG, CT, HMB-45, S-100, CHR, NSE, ER, PR, CD 68 (Dako LSAB 2 System, Peroxidase).
Results Immunocytochemical staining was helpful in 83% of cases. Initial diagnosis was confirmed in 45 cases. Immuno-cytochemical staining was important particularly in confirming diagnosis of poorly differentiated neoplasms. It was also helpful in identifying the primary site of metastatic carcinoma in 20 FNA cases. In 23(17%) cases diagnosis based on the investigated method failed. Precise diagnosis was not possible either due to negative staining with single marker/panel or when only single cells were stained positive.
Conclusion Immunocytochemical methods in destained smears allow basic as well as discriminating diagnosis even in cases of poor availability of cytologic material.

P-506

Fine needle aspiration of lesions in the thyroid bed.

E Chmielik, B Szczesniak-Klusek, D Ponikiewska, E Stobiecka, D Lange
Oncology Center, Department of Pathology, Gliwice, Poland

Introduction Clinical suspition of recurrent thyroid carcinoma based on ultrasound examination of thyroid bed with correlation to increased thyreoglobulin level or calcitonin level and/or radiomarker uptake on scintigraphy can be supported or dismissed by fine needle aspiration biopsy (FNAB). The aim of this study was assesment of specificity and possitive predictive value of ultrasound- guided FNAB of the lesions in the thyroid bed after total thyroidectomy for diagnosis of recurrent thyroid carcinoma.
Material and methods Ultrasound guided FNAB of thyroid bed lesions of diameter 0.4-3.2 cm performed by pathologist in 93 patiens after thyroidectomy. Immunohistochemistry stain for calcitonin was performed using DAKO antibody in 4 cases.
Results The recurrent papillary carcinoma was diagnosed in 18 (19.5%) patients, the recurrent follicular carcinoma in 7 (7.6%) patients, Hürtle cell carcinoma in 2 (2.3%) patients and medullary carcinoma in 5 (5.5%) patients (immunocytochemistry stain for calcitonin confirmed diagnosis in 3 patients). Pathologic correlation was able in 24 cases: 22 postoperative examinations confirmed recurrent carcinoma, and 2 cytologic diagnoses were false-negative. In the remaining 38 patients granulation, purulent inflammation and benign lesions were diagnosed. In 23 (24.8%) cases material was nondiagnostic. Specifity of the method was 96.8%, possitive predictive value 91.6%.
Conclusions Ultrasound- guided fine needle aspiration biopsy performed by pathologist is valuable and specific method in the diagnosis of recurrent thyroid carcinoma in thyroid bed.

P-507

The use of FNA in the management of thyroid goiter

J Sopta[1], S Tatic[1], M Havelka[1], B Vukomanovic[1], K Bodlovic[1], R Jankovic[2]
[1]Institute of Pathology, School of Medicine, Belgrade, Serbia and Montenegro
[2]Institute of Endocrinology and metabolic diseases, Clinical center of Serbia, Belgrade, Serbia and Montenegro

Introduction Fine-needle aspiration (FNA) is one of the most useful methods in the diagnosis of benign goiter. In consideration of the goiter; it is the most frequent lesion in the thyroid tissue, significance of FNA as a diagnostic method become greater.
Material and methods In 414 cases diagnosed as goiter we analyzed: 1) sex distribution, 2) age distribution, 3) correlation between clinical and cytological diagnoses and 4) goiter classification in accordance with cytological characteristics.
Results Goiter was five times more frequent in females than males (348 women, 66 men). The majority of the patients were between 41 and 50. The youngest was 13, and the oldest 78 years old. Almost 84% of cytologically diagnosed goiters had the same clinical diagnosis, in only 1.5% of all patients tumor was suspected clinically. We confirmed high correlation between clinical and cytological diagnosis. According to the cytological characteristics

all goiters were classified in 2 categories: goiters with and without degenerative changes. Hi-square test confirmed statistically significant difference in the presentation of such goiters (Hi-square test=10.4; p<0.01).
Conclusion FNA permits a substantial reduction or even elimination of other diagnostic procedures, such as imaging, with consequent saving in time and money. Furthermore, benign cystic lesion may be cured by FNA (a diagnostic and unexpected therapeutic value).

P-508

Diagnostic guidelines for Hashimoto's thyroiditis in fine-needle aspirates

J Sopta[1], S Tatic[1], M Havelka[1], T Terzic[1], S Radojevic[1], B Vukomanovic[1], K Bodlovic[2]
[1]Institute of Pathology, School of Medicine, Belgrade, Serbia and Montenegro
[2]Institute of Pathology School of Stomathology Belgrade, Serbia and Montenegro

Introduction Fine-needle aspiration (FNA) is a very useful method for diagnosing various lesion in the thyroid gland, among them Hashimoto's thyroiditis (HT). Although many methods may be used, FNA is a necessary diagnostic procedure nowadays in order to confirm the diagnoisis of HT.
Material and methods Durind a period of 2 years citologically 600 aspirates were citologically analyzed, stained with HE and MGG. The main cytological guidelines in the diagnostic procedure were: 1. lymphocytic cellularity of smears, 2. oncocytic follicular cells, 3. a lot of cellular debris.
Results From 600 aspirates analyzed 35 (3,5%) were diagnosed as HT. There was a high statistical significance in sex and ages for the genesis of HT (χ^2=24,02; p=0,005). We analyzed correlation between clinical and cytological diagnosis: in 82 cases initial clinical diagnosis was "Thyroiditis", and among them 46 (56%) were cytologically confirmed. From 35 patients with an FNA diagnosis of HT the same diagnosis was susspected clinically in 23 cases (66%). Several authors noted a high incidence of thyroid carcinoma in patients with HT. We researched association of HT and thyroid tumors, and we did not confirm that HT is a premalignant lesion (χ^2=1,22, p<0,05).
Conclusion HT and its association with other lesions could be clearly diagnosed with FNA, and we recommend FNA as a first line investigation in HT.

P-509

Colposcopic and cytologic findings in HPV infection of the uterine cervix

R Zivadinovic, V Lilic, B Djordjevic, S Petric
Gak Nis, University Clinical Center, Nis, Serbia and Montenegro

Introduction Uterine cervical carcinoma is a sexually transmitted disease. HPV infection, especialy types 16, and 18 oncogene is directly associated with occurrence of preinvasive and invasive changes in the uterine cervix ranging from 36 - 79%. Cyto-pathologic effect of this virus presence in a cell is called koilocytosis and occurs by the effect of fragment E4 on cytokeratin building protein. Koss observed these changes back in 1956, describing them as irregular cavities in cell protoplasm, but only later these cytologic findings were related to HPV infection. In our retrospective study we analyzed colposcopic and cytologic findings of 34 examinees in which the diagnose of HPV infection was established by biopsy.
Material and methods The mean age of examinees was 30,8, and in regards to parity and menarche there was no statistically significant difference between experimental and control group, since coefficient t was lower than 1,90 p<00,5. Therefore we concluded that the sample was representative.
Results Sensitivity of cytology in detection of HPV infection of the uterine cervix was 53,1% and the specificity was 64%. Positive predictive value was 85% and negative 65%. The most frequent colposcopic findings in the uterine cervix in case of HPV infection were aceto-white epithel in 34% and mosaic in 37%. Other colposcopic findings were significantly lower (punctate 19%, leucoplakia 7,3%). In examinees with colposcopically diagnosed HPV infection in external genitalia, the infection was also present in the uterine cervix in 82,6% which was statistically significant for X2 =29,7597>(X2 (1;0,16)=6,635).
Conclusion Based on the results presented above, we concluded that sensitivity of cytology in the detection of HPV infection of the uterine cervix was low and that it was necessary to combine that method with colposcopy and directed biopsy. In case of colposcopically diagnosed condylomas of the external genitalia and presence of pathologic colposcopic findings of the uterine cervix (aceto-white epithel, mosaic), the presence of HPV infection in the uterine cervix can be expected with high probability.

P-510

Fine needle aspirate of papillary thyroid carcinomas in correlation with histological diagnosis

P Fotiadou, K Zachou, E Dionyssopoulou, M Labropoulou, I Tolparidou, G Goutzamanis, K Papadimitriou
Aristotle University of Thessalonik Dep. of Pathology Cytology, Thessaloniki, Greece

Material and methods 32 cases of thyroid aspirates were studied in correlation with histological findings. The patients were 9 – 89 years old (mean age 46,3). Cytological diagnosis was made according to morphological criteria such as arrangement of cells, nuclear atypia and special features (colloid, giant cells, psammoma bodies).
Results Cytological diagnosis was in agreement with the histological diagnosis in 29 cases (90,6%). 2 cases were follicular adenomas and one Hürthle cell tumor. In cases of disagreement between cytological and histological diagnosis the cytomorphological findings were analysed.
Conclusion Cytological evaluation of papillary thyroid carcinomas is of high diagnostic accuracy, although overlapping of cytological criteria between the various pathological entities may lead to false evaluation.

P-511

The value of universal short-term storage cell medium in processing FNAB samples for ancillary diagnostic methods

I Srebotnik Kirbiš, B Gazič, V Kloboves Prevodnik, Ž Pohar Marinšek, A Pogačnik
Institute of Oncology, Ljubljana, Slovenia

Introduction The application of ancillary methods to FNAB samples is mainly impaired by a limited quantity of cells in the

samples, furthermore it is difficult to predict at patient's bedside which ancillary methods, if any, will be necessary. The aim of this study was to demonstrate the value of a universal short-term storage cell medium in processing FNAB samples for different ancillary methods.

Materials and methods After diagnostic smear preparation, the needle and syringe were washed out with the short-term storage cell medium in 6535 FNAB samples, obtained from 1998 to 2002. Microscopic smear analysis determined the choice of ancillary method used. Cell suspensions were then processed as required for each individual ancillary method.

Results We used 3200 (49%) FNAB samples stored in the medium for ancillary methods, while 3335 samples (51%) were discarded due to the clear morphology-based diagnosis or sample inadequacy. Immunocytochemistry was performed on 2057 samples. For various membrane, cytoplasmic and nuclear antigens, adequate immunoreaction without background was obtained in samples stored in the medium overnight (1797) or over the weekend (260). Immunophenotyping by flow cytometry was performed in 1088 FNAB samples where up to 8 lymphoma antigens per sample were successfully determined when the samples were stored in the medium overnight. High quality flow cytometric DNA histograms were obtained from all 55 FNAB samples suspended in the short-term storage cell medium.

Conclusion The short-term storage cell medium that we have been using, allows effective and easy processing of FNAB samples for several ancillary diagnostic methods. It preserves cell morphology, various membrane, cytoplasmic and nuclear antigens as well as DNA content.

P-512

Fine needle aspiration cytology of ovarian lesions

A Uguz[1], C Ersoz[1], F Bolat[1], A Gökdemir[1], MA Vardar[2]
[1]Cukurova University School of Medicine Dept. of Pathology, Adana, Turkey
[2]Cukurova University School of Medicine Dept. of Gynecology and Obstetrics, Adana, Turkey

Introduction Fine needle aspiration cytology (FNAC) is an alternative method to surgery for evaluting the ovarian lesions. Despite some arguments for indications of FNAC, it can be used for diagnosis and management of ovarian masses. The aim of this study was to assess the diagnostic value of aspiration cytology in ovarian lesions.

Materials and methods Fine needle aspirations were performed in sixty-two ovarian masses between January 2000 and February 2003. Aspiration material was obtained from fresh tissues at the time of frozen section before dissection of specimens. The slides of aspirates were stained with May Grunwald-Giemsa and Papanicolaou. They were evaluated by a pathologist who was anaware of the gross findings and the histopathologic diagnosis. Cytologic diagnoses were classified as benign and malignant.

Results Only sufficient aspirates were included in the study. The average age of the women was 43 years (range 14-85 years). 62.9% of the cases were assessed as malignant and 30.6% of the cases were benign. Two serous neoplasms of low malignant potential were evaluated in malignant category. Two false positive and two false negative cases were determined. In our series the overall sensitivity and specifity were 90.4% and 95.1%, respectively. Beside this seven benign and 15 malignant lesions could be subclassified specifically.

Conclusion We studied on excised specimens but since ovarian masses are reachable by laparoscopy or ultrasonography guided aspiration can be performed safely, FNAC may be suitable for the diagnoses of these lesions. If multidisciplinary approach can be carried out for patients with ovarian lesions cytopathologic interpretation can provide optimum benefits.

P-513

Human papillomavirus detection in cytological material of cervix. Evaluation of hybrid capture hybridisation assay, PCR and PAP smear

C Hauser-Kronberger[1], A Vatcheva[1,2], K Biedermann[1], K Peham[1], G Haitzmann[3], L Mustafa[2], G Mustafa[2]
[1]Institute Of Pathology, Landeskliniken Salzburg, Austria
[2]Mustafa Laboratory
[3]Department of Gynecology and Obstetrics

Introduction An improved understanding of the pathogenesis of cervical HPV-induced lesions has significantly changed the approach to diagnosis and treatment. The Pap smear is still the most effective cervical cancer screening test. However, molecular testing for the presence of high risk HPV-DNA increases the ability to identify women with an increased risk for cancer and true cancer precursors. The aim of the present study was to evaluate high risk HPV-DNA test systems in cervical cytological material and the correlation with Pap smear cytology.

Materials and methods We analysed 40 routinely processed cytological cervical specimen. Material was taken consecutively for Pap smear cytology and for Hybrid Capture (HC) hybridisation assay (Digene). The cytological report showed mild to severe dysplasia (7 cases were scored as PAP I/II). After performing the HC-assay, DNA was extracted from the same sample. HPV-DNA detection with conventional PCR using consensus primer (MY9/MY11), followed by subtyping of HPV 16 and 18 was carried out.

Results From the specimens showing dysplasia (83.3%), koilocytosis has been observed in 69% of Pap smear cytology. HPV-high risk positivity with the HC hybridisation assay was detected in 73% and 80% showed positivity for HPV-DNA content with conventional PCR. Subtyping of HPV-positive cases resulted in HPV-16 positivity in 65%, 12.5 were positive for HPV 18 and 18.5% showed a coexistence of HPV 16 and 18.

Conclusion Our results indicate that HPV-detection with highly sensitive and widely used molecular methods show a good concordance with cytological findings.

P-514

Fine needle aspiration findings of two different types of gastrointestinal stromal tumor

MG Gulluoglu[1], D Yilmazbayhan[1], Y Kapran[1], K Acarli[2], F Dizdaroglu[1]
[1]Istanbul University, Faculty of Medicine, Department of Pathology, Istanbul, Turkey
[2]Istanbul University, Faculty of Medicine, Department of General Surgery, Istanbul, Turkey

Introduction Gastrointestinal stromal tumors (GIST) are the most common mesenchymal tumors of the gastrointestinal tract, derived

from interstitial cells of Cajal. The cytologic features of these neoplasms in fine needle aspiration (FNA) have been described in several articles. Aims: Cytologic and histologic features of two GIST cases one of which presented with liver metastasis and other with an intrathoracic mass mimicking lung carcinoma radiologically are presented comparatively.
Patients and results Sixty year-old male patient with a previous history of gastric GIST has had an FNA from a liver mass. In the cytologic examination, epithelioid cells with round-oval nuclei, large cytoplasms and indistint cytoplasmic borders, forming three dimentional groups with thin fibrovascular stroma were observed. The other patient was a seventy two year-old female who had an FNA from an intrathoracic mass. Branching fascicles of spindle cells with indistinct cytoplasmic borders in a necrotic background were observed in the cytologic examination. Mesenchymal origin was verified by vimentin immunopositivity. By detailed computerized tomographic evaluation, it was revealed that the mass originated from the gastroesophageal junction. Both tumors were resected and histologically examined. Cytologic and histologic findings correlated including immunocytochemical and immunohistochemical results which were positive CD117 and CD34, and negative S100 and smooth muscle aktin immunoreactions.
Conclusion As they share common histomorphological features with other types of mesenchymal tumors of the gastrointestinal tract, CD117 immunopositivity is the only diagnostic marker to differentiate these tumors from other tumors of mesenchymal origin. Cytologic diagnosis also requires detection of this marker in the neoplastic cells.

P-515

Peritoneal fluid cytology of sarcomas

K Zachou[1], E Tzartza[1], A Orologa[1], A Skenderi[1], K Patsiaoura[2], E Kostopoulou[2], K Boni[1]
[1]Hippokratio Hospital of Thessaloniki Dept. Cytopathology, Thessaloniki, Greece
[2]Hippokratio Hospital of Thessaloniki Dept. Pathology, Thessaloniki, Greece

Material and methods Peritoneal fluid smears of 1179 female patients of all ages, were studied.
Results 229 cases were cytologically diagnosed as malignant (19,4%), the majority of which was characterized as adenocarcinomas. Histological diagnosis was available for 139 cases. Sarcomatous component was reported in only 7 cases, 4 cases were malignant mixed Müllerian tumors (MMMT), one was leiomyosarcoma, one rhabdomyosarcoma and one liposarcoma. The cytological findings in the equivalent 7 cases were « abnormal» neoplastic cells in isolation, with enlarged and hyperchromatic nuclei. Adenocarcinoma cells were identified in peritoneal fluid smears of 3 patients with MMMT.
Conclusion Cytological diagnosis of sarcoma is rare. Even when these «abnormal» cells are found, it is very difficult to give a definite diagnosis of sarcoma, based directly on the cytomorphological characteristics of peritoneal smears. However, such a possibility should be kept in mind by the cytopathologist to avoid missing the diagnosis.

P-516

Accuracy of cytologic diagnosis of primary malignant bone tumors and metastases in the bones

R Bokun, Z Tatomirovic, V Skuletic
Institute of Pathology, Military Medical Academy, Belgrade, Serbia and Montenegro

Purpose The aim of this study was to show that imprint cytology is a valuable method in the evaluation of bone tumors as well as to determine its diagnostic accuracy in primary and secondary bone tumors.
Materials and methods From thirthy three surgical specimens of bone tumor imprints were made, air-dried and stained by May-Grunwald- Giemsa method. The cytologist gave detailed description of the smears, concluded whether the lesion was malignant and suggested a final diagnosis if it was possible. Results were compared with the corresponding histopathologic diagnoses.
Results Out of 19 cases with primary malignant bone tumors (chondrosarcoma 9, Ewing sarcoma 2, ameloblastoma 2, synoviosarcoma 2, malignant osteoclastoma 1, malignant fibrous histiocytoma 1, malignant schwannoma 1, leiomyosarcoma 1) the cytologist recognized malignancy in 18 of them and in 10 suggested the final diagnosis. In 14 patients with metastases (squamous cell carcinoma 11, anaplastic carcinoma 1, malignant melanoma 2), the cytologic and histopathologic diagnoses correlated in all cases.
Conclusion Cytologic analysis of the imprints of bone tumors is valuable as early orientation for the clinicians since the final histopathologic diagnosis needs time because of the decalcination procedure. The correlation of cytologic and histopathologic diagnoses was better for the secondary bone tumors because cytologist was more familiar with their morphology.

P-517

The value of combined fine needle aspiration and needle core biopsy in diagnostic assessment of pancreatic tumors

P Sevastiadou[1], P Xirou[2], S Barbanis[2], I Efstratiou[2], E Athanasiou[1], I Tsitouridis[3]
[1]Papageorgiou General Hospital, Department of Cytology, Thessaloniki, Greece-
[2]Papageorgiou General HospitalDepartment of Cytology, Thessaloniki, Greece
[3]Papageorgiou General Hospital, Department of Radiology, Thessaloniki, Greece

Introduction Due to the anatomical location of the pancreas, it is often difficult to obtain sufficient diagnostic material from pancreatic lesions. The aim of this study is to present the results and our experience from CT guided fine needle aspiration (FNA) and needle core biopsy (NCB) from pancreatic tumors.
Materials and methods FNA using 22 Gauge needles and NCB using 16 and 18 Gauge needles were performed in 27 patients with pancreatic tumors. Both procedures were done under computerized tomography guidance, without complications. Twenty one tumors involved the body and 6 the tail of the pancreas

Results The diagnosed cases were 18 adenocarcinomas, 2 neuroendocrine tumors, 1 lymphoma and 2 pseudocysts. Diagnosis was reached in 21 cases by both FNA and NCB and in 2 cases by NCB only. 2 other cases were "diagnosed" as suspicious for malignancy by FNA only. Finally in 2 cases no diagnosis was reached by both methods, due to insufficient material.
Conclusion According to our experience, we believe that the combination of fine needle aspiration with needle core biopsy of pancreatic tumors under CT guidance improves the diagnostic accuracy.

P-518

Value of fine needle aspiration cytology in subtyping mucinous breast carcinoma

U Klopcic[1], S Frkovic-Grazio[2], M Us-Krasovec[1]
[1]Department of Cytopathology, Institute of Oncology, Zaloška 2, 1000 Ljubljana, Slovenia
[2]Department of Pathology, Institute of Oncology, Zaloska 2, 1000 Ljubljana, Slovenia

Background Subtyping of mucinous breast carcinoma into pure and mixed type has prognostic implications. Aims of the study were to evaluate a) the usefulness of fine needle aspiration biopsy (FNAB) in differentiation between pure and mixed mucinous carcinomas, and b) to correlate key cytological features with survival.
Material and methods We reviewed FNAB of 98 women with mucinous breast carcinoma treated at the Institute of Oncology from 1983 to 1999. Key cytological features analysed were cellularity, amount of mucin, presence of capillaries, cell pattern, cytoplasmic characteristics and nuclear pleomorphism. Type of mucinous carcinoma was determined histologically after resection of the tumour. Association of cytological features with cancer specific survival was evaluated by univariate and multivariate analysis.
Results Histological analysis revealed 64 cases (65%) of pure and 34 cases of mixed mucinous carcinoma. Nuclear pleomorphism and amount of mucin in FNAB differed significantly between the two subtypes of mucinous carcinoma. Whereas cellularity of cytological samples, presence of capillaries, cell pattern and cytoplasmic characteristics were not related to prognosis, nuclear pleomorphism and absence of mucin in cytological samples were associated with poorer cancer specific survival. Furthermore, the absence of mucin in FNAB samples retained independent prognostic significance also in multivariate analysis.
Conclusions Higher grade of nuclear pleomorphism and small amount or even absence of mucin in FNAB favor the diagnosis of mixed mucinous cell carcinoma and are features associated with poorer prognosis.

P-519

Cardiac lipoma in a Mexican patient - multidisciplinary approach in a right atrium tumor

J Nuncio[1], G Najera-Hernandez[2], G Garcia-Ramos[2]
[1]Pathology Department, Instituto Nacional de Ciencias Medicas Y Nutricion Salvador Zubiran, Mexico City, Mexico
[2]Internal Medicine and Neurology departments, Fundacion Medica Sur, Mexico City Mexico

Primary tumors of the heart are rare. Lipomas account for approximately 10% of all neoplasms of the heart and represent 14% of benign cardiac tumors. Symptoms may be produced by large lipomas, but more often the patients are asymptomatic and the diagnosis is made by chance. Recently, the ready availability of high-definition noninvasive imaging, such as echocardiography, computed tomography, and magnetic resonance image, has allowed easier diagnosis. Therefore, more cases have been reported. To date up to 70 cases of lipoma have been described. This case describes the multidisciplinary approach to the diagnosis of this rare entity with the use of open heart biopsy from right atrium, to sustain the correct diagnosis. After exhaustive internet-based search, this is the first case reported in Latin-American literature, a condition not previously informed from in vivo patient in Mexico.

P-520

Type I and III collagen synthesis and composition in the valve matrix in aortic valve stenosis

Y Soini[1], H Eriksen[2], J Satta[3], M Veijola[4], J Risteli[2,5]
[1]Department of Pathology, University of Oulu, Finland
[2]Department of Clinical Chemistry, University of Oulu, Finland
[3]Department of Surgery, University of Oulu, Finland
[4]Department of Forensic Medicine, University of Oulu, Finland
[5]Department of Clinical Chemistry, Kuopio University Hospital, Finland

Introduction Changes in the collagenous matrix may participate in the pathogenesis and progression of human aortic valve stenosis (AS). We investigated the expression, localization, rate of synthesis and composition of type I and III collagens in AS.
Methods Type I and III collagen mRNA expression and the immunohistochemical localization of the collagen antigens were studied from 36 AS and 2 normal aortic valves. The concentrations of various type I (PINP, PICP, ICTP and synthetic peptide SP4) and III (PIIINP and IIINTP) collagen antigens were measured by radioimmnoassays in soluble tissue extracts and trypsin solubilized calcified and noncalcified matrices of 11 AS samples, and 24 healthy aortic valves of different ages.
Results The synthesis of type I collagen, localized in the myo-fibro-blasts adjacent to calcified nodules, was 2-3 –fold higher in AS compared to controls. The proportion of collagen in total protein fraction was 90 % in the healthy valves, 50 % in the noncalcified matrix and 10 % in the calcified matrix of AS valves. In calcified valves the ICTP content was 6-fold higher than in the age matched controls and 2-fold higher than the young control group. In the controls, ICTP ($r=-0.908$, $p<0.001$) and IIINTP ($r=-0.753$, $p<0.001$) decreased with age, whereas SP4/ICTP ratio increased ($r=0.538$, $p<0.01$).
Conclusions Type I collagen synthesis was increased in AS. Localization of this collagen adjacent to calcified nodules and the profile of the C-telopeptide cross-linking indicate that the ectopic aortic valve calcification may have similarities to bone matrix mineralization.

P-521

A case report of sudden death in a patient recently diagnosed with cardiac hydatid cyst

D Butcovan, C Borza, C Arsenescu, G Georgescu
University of Medicine and Pharmacy, Iasi, Romania

Introduction The cardiac hydatid cysts are rare cases, representing 0,5-2% from all human hydatid cysts. They are commonly located in the left or right ventricle and exceptionally in the interventricular septum. Because the symptoms and clinical signs of the cardiac hydatid cysts are non-specific, the diagnosis may be difficult.
Material and methods We report an intramyocardial hydatid cyst, diagnosed at Cardiology Center Iasi, with an early history of atypical chest pain, the death occuring through anaphylactic shock, secondary to the hydatid cyst endocavitary rupture. The study was made on necropsiy specimens, and the diagnosis was established by using routine morphological techniques.
Results The gross examination evidentiated an hydatid cyst of about 6 cm in diameter, communicating through a small orifice with the left ventricular cavity and through a slit-like fissure with the right ventricular chamber. The systemic embolism was revealed, only grossly, by the presence of small "hydatid daughters" at the level of the ascending aorta and the pulmonary embolism was confirmed only histologically, by the presence of anhiste membrane emboli in the peripheral pulmonary vessels.
Conclusions The study revealed the morphological aspect defining hydatid cyst, emphasising the necessity of an early diagnosis due to a high risk of death through complications.

P-522

A case report of arrhytmogenic right ventricular dysplasia – cause of sudden death

C Borza, D Butcovan, C Grigoriu, V Astarastoaie
University of Medicine and Pharmacy Iasi, Romania

Arrhytmogenic right ventricular dysplasia (ARVD) is a new form of cardiomyopathy probable more frequent than commonly reported. ARVD is a heart muscle disorder of unknown cause that is characterized clinically by an electrical instability associated with secondary ventricular arrhythmia and pathologically by fibro-fatty replacement of the right ventricular myocardium. It is a rare but important cause of sudden unexpected cardiac death in young, otherwise healthy persons, especially those that are exercise related. We report a case of cardiac sudden death in a 40 years old man without personal and familial cardiac history. The study was made on a necropsic biopsy specimens from the medico-legal laboratory. The diagnosis was made using routine histological techniques. Grossly, we revealed a fibro-fatty right and left ventricular wall myocardial replacement and a focal white thickening of the left ventricular endocardium. Histologically, we evidentiated a fibro-fatty myocardial replacement of the right and left ventricle suggesting an arrhythmogenic ventricular dysplasia of cardiomyopathic type and an endomyocardial fibrosis supported by the presence of a subendocardial fibrosis, affecting internal one third of the myocardium. There were no evidence of coronarian and valvular lesions and hypertensive cardiac changes, as well. The study revealed the morphological features defining a fibro-fatty myocardial replacement and an endomyocardial fibrosis evidentiating the case particular features, as well.

P-523

Assessment of diabetic micro- and macroangiopathies

V Anestiadis, VV Anestiadis, Z Anestiadis, I Tsiple
Centre for Pathobiology and Pathology, Academy of Sciences, Chisinau, Republic of Moldova

Introduction The objective of this study was to determine the potential value of digital thermography (DT) for the assessment of micro- and macroangiopathies of lower limbs in diabetes mellitus (DM).
Materials and methods We have studied 250 patients (pts) with DM (120 male). 100 pts had DM type I, 150 pts had DM type II, with age varying from 27 to 80 years. Thermograms were acquired using an original PC-interfaced thermograph, averaged and reformatted to 128x128 8-bit images. Analysis included filtering, background cutoff, obtaining x- and y-axis profiles and averaged temperature curves (ATC), determination of local maximums and minimums of the ATCs, definition of anatomic regions, building regions of interest (ROI).
Results Following thermogram patterns were found: 1. asymmetric unilateral hypothermia of 1st toe (in 35% of DM I cases; probably indicating microangiopathy); 2. bilateral symmetrical hypothermia of both feet at the level of distal phalanges (in 25% of DM I cases); 3. unilateral hypothermia of foot ('thermo-amputation'); 4. unilateral hyperthermia of foot and tibial region; 5. focal hyperthermic regions (diameter = 2..4cm; indicating potential subsequent ulceration). ATCs and symmetric left-right ROI comparisons helped distinguishing between macro- and microvascular disease, between neuro- and angiopathy in DM, evaluating therapy effectiveness. DT was most valuable in surgical cases, permitting (1) to locate the optimum level of amputation and (2) to detect early the inflammation.
Conclusion DT results correlate well with pathomorphology, and depend upon DM type, DM duration, and presence of local inflammation.

P-524

Immunomodulatory treatment improves myocardial histopathology and function in patients with biopsy-proven myocarditis

J Vasiljevic[1], S Lastic-Maletic[1], Z Popovic, D Babic[1], S Glumac[1], M Miric[2]
[1]Institute of Pathology, Medical School, Belgrade, Serbia and Montenegro
[2]Dedinje Cardiovascular Institute, Belgrade, Serbia and Montenegro.

Aim The aim of this study was to determine the impact of immunomodulatory treatment (interferon-α) on myocardial histo-pathology and contractility in patients with biopsy-proven myocarditis (MC).
Methods A total of 40 consecutive pts (24/40 male, mean age 40+10 years, baseline EF= 35.6+9.3%) underwent endomyocardial biopsy which established diagnosis (using modified Dallas classification) of MC (active MC in 15/40 pts, focal-active MC in 10/40 pts, borderline MC in 5/40 pts, and healing MC in 10/38 pts). All patients received interferon-α (SC application, 3 MIU, 3 time PW, for 3 months) on top of conventional triple therapy for heart failure. Rebiopsy was performed in all patients after the termination of interferon-α treatment, and both baseline EF and repeated biopsies were analyzed. Semiquantitatively we comapred the amount of cellular infiltrate, degenerative and/or necrotic changes, and interstitial fibrosis. Repeated biopsies were than classified as improved, no change and/or deteriorated, for each histopathological variable (by 2 pathologists, in a blinded manner).
Results By the end of interferon-α treatment EF improved significantly (40+11.9% vs. 35.6+9.3%), and no deaths were

registered. Repeated biopsy revealed ongoing MC in 3/40 pts, late-healing MC in 17/40 pts, focal-healing MC in 8/40 pts, healed MC in 5/40 pts, and dilated cardiomyopathy in 7/40 pts. Amount of cellular infiltrate, degenerative and/or necrotic changes, and fibrosis was reduced in 28, 23, and 1 pts, respectively, remained the same in 7, 8, and 18 pts, respectively, and increased in 5, 9, and 21 pts, respectively ($p<0.01$, between groups). The significant reduction was achived in the amount of cellular infiltrate and degenerative and/or necrotic changes, contrary to the amount of fibrosis. Applied immunomodulatory therapy made substancial reduction of inflammation with "relative" increase of fibrosis.
Conclusion Interferon-α, as main immunomodulatory agent, has favourable effects on myocardial histology and contractility in patients with biopsy-proven myocarditis.

P-525

Morphological changes in heart died of a heart attack of a myocardium

V Ubaydullaeva
The Centre of Emergency Medical Aid, Tashkent, Uzbekistan

Diseases CVS take conducting place among the most actual problems of modern medicine. From them it is possible to count the main thing IHD. IHD – the special form of pathology CVS including group of diseases which, according to definition the CART, are treated as follows: «Dysfunction sharp or chronic, arising owing to relative or absolute reduction of supply of a myocardium by arterial blood». Despite of significant number of the morphological researches devoted IHD, morphogenesis separate displays of it, in particular, AMI, and also mechanisms of indemnification and decompensation of hearts are investigated insufficiently. In connection with, the purpose of the present research definition morphofunctional conditions of various departments of heart was above-stated at diagnostics of an intimate ischemia.
Material and methods For achievement of an object in view researches of hearts died of a heart attack of a myocardium have been lead (have been carried out), and also have been investigated 32 morphometric parameters, such as: weight of a cardiac muscle, pure weight of heart, weight right and left ventricles, an index right and left ventricles, an index of blood supply of a myocardium. All received data have been processed statistically on personal computer with use of standard software package Windows Excel.
Results Summarizing macro- and the microscopic changes which have been found out by us in a cardiac muscle, it is possible to make the conclusion that the long reorganization occuring in a cardiac muscle in conditions increasing hypoxy, results in an exhaustion processes, to use of all possible resources cardiomyocytes and causes development decompensation.

P-526

The mucin genes in cardiac myxoma

PH Chu[1], TS Yeh[2], YS Lee[1], SM Jung[3]
[1]The Division of Cardiology, Department of Internal Medicine, Chang Gung Memorial Hospital and Chang Gung University, Taipei, Taiwan, Republic of China
[2]Department of Surgery, Chang Gung Memorial Hospital and Chang Gung University, Taipei, Taiwan, Republic of China
[3]Department of Pathology, Chang Gung Memorial Hospital and Chang Gung University, Taipei, Taiwan, Republic of China

Introduction Cardiac myxoma, the most common primary tumor of the heart, has a varying clinical presentation and immunohistochemical profile. An abundant mucopolysaccharidic matrix exists, including mucin, within the cardiac myxoma. This study elucidates the clinical presentation and expression of mucin genes in cardiac myxoma.
Materials and methods From December 1976 to February, 2003, the retrospective study included 89 consecutive patients with cardiac myxoma underwent surgical excision. Detailed clinical parameters were reviewed as well. Mucin genes, Additionally, MUC1, MUC2 and MUC5AC, have been studied by immuno-histochemical method. The expression was scored from 0 to 3.
Results 52 (60%) women and 37 (40%) men with a mean age of 38 +/- 21 years comprised the control group. The presentation included asymptomatic (41%), dyspnea (35%), stroke (23%), chest pain (7%), fever (6%), syncope (5%) and tricuspid regurgitation (70%). We divided these patients into two groups; group A contained the 78 myxoma located in the left atrium, group B included three (3%) recurrent myxomas and 8 (9%) myxomas other than in left atrium. They did not differ with respect to many pathological scores, such as vascular proliferation, inflammation, cellularity, and hyaline. However, although less calcification and thrombosis occurred, more congestion was found in group B ($P < 0.0001$). Moreover, MUC1/5AC had a higher expression than MUC2 ($P < 0.005$). Interestingly, the group A displayed a stronger mucin expression than group B did.
Conclusion Preliminary results demonstrate invaluable and different pathological patterns, including mucin genes, between the myxoma coming from the left atrium and the other sites.
Acknowledgement: Dr Chu is supported by NHRI-EX91-9108SC, NHRI-EX92-9108SC and BMRP456.

P-527

Morphometric analysis of atherosclerotic changes in human coronary arteries adventitia

B Manevska, P Ghenev, I Stankulov, A Tonchev, G Chaldakov
Medical University of Varna, Varna, Bulgaria

Introduction Nowadays understanding of atherogenesis, Russell Ross' response-to-injury paradigm, considers atherosclerotic lesions as "a protective, inflammatory-fibroproliferative response" to harmful stimuli. Among these stimuli are the major risk factors, which contribute for atherosclerotic cardiovascular complications. Arterial blood flow impairment is associated with the progression of intimal atherosclerotic lesions. That is why most of the research work is concentrated upon intima, while adventitia is neglected. Several lines of evidence clearly show that adventitia is not an innocent bystander in atherogenesis. The aim of the present study is to evaluate morphologically adventitial changes in atherosclerotic arteries.
Materials and methods The cellular components and adventitial thickness are followed in 118 postmortem human coronary arteries.
Results Mononuclear cellular infiltration (lymphocytes, mast cells), neoangiogenesis and collagen overproduction are established in this part of adventitia, that corresponds to atherosclerotic lesion. Morphometric analysis reveals increased adventitia/media thickness ratio. The adventitial thickening represents an example of negative vascular remodeling, because of hampering the compensatory enlargement of the affected artery. On the other hand the cellular processes involved in adventitial thickening could be responsible for atherosclerotic lesion initiation.

Conclusion We need further arguments into the cell biology of atherosclerosis, viewed as a vascular healing process, involving also the adventitia, to provide new insights into atherogenesis and alternative therapeutical strategies respectively.

P-528

Study on postmortal autolytic changes of the myocardial blood vessels. Experimental study

L Kostic-Banovic[1], V Katic[2], R Karadzic[1], J Stojanovic[1], G Ilic[1], M Zdravkovic[1], A Antovic[1]
[1]Department of Forensic Medicine Nis, Nis, Serbia and Montenegro
[2]Department of Pathology Nis, Nis, Serbia and Montenegro

Introduction Modern forensic medicine practice has not yet been given the methods of investigation that would enable answering with sufficient accuracy to the question of death occurrence time. Present work is an attempt to make contribution to that very complex and significant problem in forensic medicine.
Materials and methods The investigation has been done on 112 Wister rats. The sacrifice was exerted by strangling. To respond on questions how both temperature of microenvironment and passed time influence on coronary arteries, the experimental animals were divided into 3 groups: I (10 C), II (20 C) and III (30 C). Every group had 8 subgroups, depending of passed time from the sacrifice, beginning of 1 hour, through 2, 4, 6, 12, 24, and 36 up to 72 hours. Control animals were autopsied and myocardial sections were taken immediately after sacrificed animals. Formaldehyde fixed and paraffin embedded blocks were cut and stained by HE, Van Gieson and Gomori methods.
Results In groups II and III almost all blood vessels of heart muscle had fragmented walls in the animals examined upon 72 hours after sacrifice. The vessels were almost normal in the group I also up to 72 hours after sacrifice. Basal membranes of blood vessels were observed upon 72 hours after sacrifice at the temperature of 10 C. Fragmented basal membranes in II and III group were found, in the form of spider's web residues. Total hemolysis of erythrocytes was upon 1 hour after sacrifice in III temperature group. However, contours of erythrocytes could be recognized upon 48 hours after sacrifice in I experimental group.
Conclusion Autolysis of myocardial vessels is influenced by two factors: time interval from the death and micro environmental temperature. The temperature exerted more profound influence on autolysis than time interval. The observed autolytic changes could be used in the expertise of the time of death occurrence.

P-529

Expression of tumor necrosis factor (TNF)-alpha and TNF-alpha receptors in human viral myocarditis

E Carturan[1], F Calabrese[1], A Angelini[1], M Crosato[2], M Valente[1], GM Boffa[2], G Thiene[1]
[1]University of Padua Medical School, Institute of Pathological Anatomy, Padua, Italy
[2]University of Padua Medical School, Department of Cardiology, Padua, Italy

Introduction Tumor necrosis factor (TNF)-alpha has been recognized as important physio-pathogenic factor in the initiation and continuation of inflammatory cardiomyopathies. Experimental and preliminary human studies have demonstrated that TNF-alpha plays a crucial role in enteroviral-induced myocarditis. The aim of this study was to investigate the expression of TNF-alpha and both its receptors (TNFRI and TNFRII) in the endomyocardial biopsies of patients (pts) with viral and non-viral myocarditis. Myocardial expression of TNF-alpha was then correlated with different clinical and pathologic findings.
Material and methods TNF-alpha expression was investigated in endomyocardial biopsies obtained from 38 pts with myocarditis and from 10 control subjects by using reverse transcriptase (RT)-polymerase chain reaction (PCR) and immunohistochemistry. Viral etiology was diagnosed by PCR in 20 cases. Immunohistochemistry was also used to analyse both TNF-alpha receptors (RI and II). Score 0-3 was used to grade morphological findings.
Results TNF-alpha mRNA and TNF-alpha protein was significantly more present in viral myocarditis than in non-viral myocarditis (16/20 vs 3/18, p=0.001). Remarkable immunostaining was observed for both receptors, particularly for TNFRI. Histological analysis revealed that myocardial necrosis (score 1.89 vs 1.15 p=0.01) and cellular infiltration (score 2.26 vs 1.78 p=0.05) were more prominent in TNF-alpha positive cases. Among TNF-alpha positive cases, TNF-alpha mRNAs were greater in pts with more impaired cardiac function.
Conclusion Our findings indicate that the expression of TNF-alpha plays an important role in the pathogenesis of viral myocarditis of any etiology and may influence severity of cardiac dysfunction. Cytokine effects are more strictly linked to over-expression of TNFRI.

P-530

Recurrence of viral myocarditis after cardiac transplantation: A retrospective study in a pediatric population

F Calabrese[1], E Carturan[1], A Angelini[1], O Milanesi[2], M Valente[1], G Thiene[1]
[1]University of Padua Medical School, Institute of Pathological Anatomy, Padua, Italy
[2]University of Padua Medical School, Department of Pediatrics, Padua, Italy

Introduction Heart transplantation remains the only therapeutic option for pediatric patients (pts) with severe, end stage myocarditis. The aim of this study was to determine the presence of viral genome in native heart and the frequency of viral recurrence after heart transplant in pts with myocarditis.
Material and methods From March 1987 to November 2000, 36 heart transplants were performed in children (1 month to 18 years 24M/12F) at our Institution. Histology/immunohistochemistry was carried out in all native hearts; among inflammatory cardiomyopathy,4 cases were active myocarditis and 16 dilated cardiomyopathy/ chronic myocarditis. Foci of active myocarditis were also found in one case of hypertrophic/restrictive cardiomyopathy and one case of congenital heart disease respectively. Retrospective PCR (polymerase chain reaction) and sequencing analysis for detection of cardiotropic viral genomes was performed in 20 native hearts (55%) and in all serial post-transplant biopsies from viral PCR positive cases.
Results PCR amplified a viral product in 10 native hearts (50%). PCR analysis on postransplant serial biopsies disclosed the same viral infection in 5 of 10 (50%). Early enteroviral recurrent

myocarditis with identical genotype was demonstrated in 2 cases at 1 month after transplant. Fatal outcome occurred in 4/5 pts with viral recurrent myocarditis when prompt molecular diagnosis was not available; misdiagnosis of acute rejection in histological monitoring may have concurred in the fatal outcome.
Conclusion Viral myocarditis frequently relapses after heart transplantation in children and is a risk of fatal outcome. Molecular study in native hearts is mandatory to improve diagnostic accuracy allowing to a more strict surveillance after transplantation.

P-531

Sudden cardiac death induced by acute viral myocarditis

R Karadzic[1], L Kostic-Banovic[1], V Katic[2], I Burazor[3], L Velickovic[2]
[1]Department of Forensic Medicine Nis, Nis, Serbia and Montenegro
[2]Department of Pathology Nis, Nis, Serbia and Montenegro
[3]Clinic of Cardiology, Nis, Serbia and Montenegro

Introduction Most commonly the sudden cardiac death (SCD) is defined as unexpected death from cardiac causes early after of without the onset of symptoms. Data suggested that SCD is a multifactorial catastrophe involving in most instances myocardial lesions that we confirm by this report.
Materials and methods Five cases were autopsied in Institute for Forensic Medicine because they have died from SCD. The mean age was 29,4 years, including one boy (13 years) and one girl (14 years). All specimens were fixed in 10 % formalin. Paraffin sections were cut and stained by: HE, Van Gieson and AB-PAS, pH=2,5.
Results Clinical symptoms lasted short time: fatigue, dyspnea, palpitations and precordial discomfort, accompanied by fever. Macroscopically, the hearts were normal or enlarged, with dilatation of chambers. The ventricular myocardium was typically flabby and mottled by either pale foci or minute hemorrhagic lesions. Histological finding: myocarditis was characterized by an interstitial mononuclear predominantly lymphocytic inflammatory infiltrate and by injury of focal necrosis to myocytes adjacent to the inflammatory cells; focal aggregates of macrophages and microhaemorrhages, often surrounding the conduction system, were also observed. Scattered incipient fibrosis inside the areas with disappeared myocytes was one of the features of myocarditis.
Conclusions The ultimate mechanism of death in viral myocarditis was fatal arrhythmia induced by inflammatory mononuclear infiltrates of the conduction system.

P-532

Surgical pathology of primary cardiac and pericardial tumors in the paediatric age

C Basso[1], M Valente[1], G Stellin[2], O Milanesi[3], G Thiene[1]
[1]Institute of Pathology, Padua, Italy
[2]Institute of Cardiac Surgery, Padua, Italy
[3]Department of Paediatrics, Padua, Italy

Background Primary cardiac and pericardial tumors (CPT) are rare at all ages and even less common in infancy and adolescence. Aim of this study is to assess the prevalence and pathologic features of paediatric CPT consecutively examined in a single Institution.
Methods and results Among 170 surgically removed CPT collected at our Cardiovascular Pathology Unit in the time interval 1970-2002, 21 (12%) occurred in the paediatric age (<18 yrs). We retrospectively analysed them by histotype, age and clinical presentation, location, type of surgery and outcome. They were 11 male and 10 female pts, age ranging from 2 days to 18 years (median 4 months). The majority of CPT were diagnosed before the age of 1 year (76%), including 4 prenatal diagnosis by foetal echocardiography. In the remaining 17 pts, clinical presentation of CPT was congestive heart failure in 5, cardiac murmur in 5, systemic embolism in 2, and constitutional symptoms in 1, whereas four were completely asymptomatic and the mass was an incidental finding at echocardiography (3) or during cardiac surgery for congenital heart disease (1). PCT were located most frequently in the right ventricle (6), followed by right atrium (3), left atrium (4), left ventricle (3), tricuspid valve (2), pericardium (2) and ventricular septum (1). All had surgical resection except one who underwent cardiac transplantation. As far as histotype, myxoma was the most frequent (7), followed by rhabdomyoma (4), fibroma (3), angioma (3), pericardial teratoma (2) and hematic cyst (2). No recurrence was found at echo during follow-up and only one pt died three years after cardiac transplantation due to cerebral malignancy.
Conclusions With the improvement of cardiac imaging techniques, CPT have increasingly been detected even early during life. Despite the benign histotype, CPT carry the risk of heamodinamic, embolic and arrhythmic complications. Prompt surgical resection is indicated in all symptomatic pts and in those with tumour related obstruction. Among surgically resected primary CPT in the paediatric age rhabdomyoma is less frequent than expected since it often does not require surgical resection due to its potential spontaneous regression.

P-533

In vivo histologic diagnosis of primary malignant cardiac and pericardial tumors

C Basso, M Valente, G Thiene
Institute of Pathology, Padua, Italy

Background Primary cardiac and pericardial tumors (CPT) are rare and even less common are malignant ones. Aim of our study was to assess the prevalence and histotype of malignant forms among a consecutive series of primary CPT examined in a single Institution.
Methods and results In the time interval 1970-2002 among 170 consecutive pts who had an in vivo diagnosis of primary CPT, either by surgical pathology and/or endomyocardial biopsy investigation, 16 (9.5%) had a malignant form. They were 7 female and 9 male pts, age ranging from 36 to 80 yrs (mean 54±12). Besides gross and histologic examination, tumour histotype was defined by immunohistochemistry using a large panel of antibodies and by transmission electron microscopy. Primary malignant CPT comprised 6 extracardiac (3 pericardial mesothelioma and 3 pulmonary artery sarcoma) and 10 intracardiac masses. The latter group consisted of angiosarcoma of the right atrium +/-right ventricle (3), undifferentiated sarcoma of the left atrium (3), fibrosarcoma of the right atrium (1), malignant fibrous histiocytoma of the left atrium (1), B cell lymphoma of the right atrium (1) and leiomyosarcoma of the right ventricle (1). In four (40%) a preoperative histologic diagnosis was achieved by transvenous endomyocardial biopsy (all right-sided). Four malignant primary CPT, all located in the left atrium, had a preoperative misdiagnosis of myxoma. Surgical resection was

performed in all but two pts. All pts died with a maximum survival time of 24 months.
Conclusions Primary malignant CPT are rare and represent 9.5% of all primary CPT in our series. The prognosis is poor and generally measured in months independently from the tumour histotype and from surgical resection and chemotherapy. Endomyocardial biopsy is a safe procedure to achieve an in vivo diagnosis in the setting of right intracavitary masses.

P-534

Haemangioendothelioma retiforme. A case report

M Djukic[1], L Popovic[1], J Kozarski[2], J Jovanovic[1], A Salapura[1], N Balaban[1]
[1]Institute of Pathology, Military Medical Academy, Belgrade, Serbia and Montenegro
[2]Clinical of Plastical Surgery, Military Medical Academy, Belgrade, Serbia and Montenegro

Introduction Haemangioendethelioma retiforme is rare form of tumor which may have histological appearance and biological behavior of a low grade angiosarcoma. This is the reason why this form of tumor represents great diagnostic problem especially in small biopsies. We present the case of an 50- year old man with inherited gigantism and tumor masses in soft tissue at the right forearm and hand without changes on bone and joint tissue.
Materials and methods Gross and microscopic findings were noted. Histochemical stains with Masson trichrom, elastica, Perls` and PAS reaction and immunohistochemical analyses for CD 31, F VIII and a smooth muscle actine was performed in paraffin-embedded sections.
Discussion and conclusion Patient had several esthetic operations in last 20 years. Few of this subcutaneous lesions have undergone exulceration followed by bleeding in past 3 years, which was the reason for operation three times in a row. Diagnosis of retiform hemangioendothelioma was than established. One of the biopsies showed well differentiated angiosarcoma. Vascular malformations were evident in all biopsies. Inherited gigantism was probably the consequence of morphological changes in soft tissue related to the existence of vascular malformation. These were preexisting changes that led to the development of multiple focuses of retiform hemangio-endothelioma.

P-535

Primary intimal sarcoma of the aorta. Report of an autoptic case

G Serio[1], A Marzullo[1], F Silvestris[2], A Scattone[1], G Parisi[1], M Tucci[2], G Caruso[1]
[1]Dpt. Pathologial Anatomy And Genetics-University, Bari, Italy
[2]Dpt. Biomedical Science and Clinical Oncology-University, Bari, Italy

Introduction Primary sarcomas of the aorta are extremely rare neoplasms, described in occasional single case reports and antemortem diagnosis is difficult because of their polymorphous presentation. The tumours are classified into intimal and mural types according to their location and clinical behaviour. We describe a case of intimal sarcoma arisen in the thoracic aorta of a 62-years-old woman with multiple embolic abdominal metastases (spleen, kidney, adrenal).
Case report In november 2002 the patient was hospitalized for the embolic occlusion of the left popliteal artery. The recent clinical history revealed irritative cough, dispnea and fever. The laboratory tests reported anemia (hemoglobin: 8.3mg/dl) and the VES was 119. Electrolities, liver function tests and fibrinogen were within normal limits. The antiphospholipid antibody and lupus anticoagulant were negative. A CT-scan showed an intraluminal thrombus-like mass in the thoracic aorta and multiple geographic infarctions of the spleen suggestive for a primary aortic tumor. She died before undergoing to surgery, for left ventricular failure.
Results Post-mortem examination showed mild atherosclerosis and a mass with grayish-yellow, solid, rubbery and mixoid aspects, attached to the wall of the aorta, just after the origin of the left subclavian artery. Histologic sections disclosed a spindle-shaped sarcoma cells with pleomorphic nuclei in a myxoid stroma; necrosis was abundant. At immunohistochemistry tumor cells resulted positive for vimentin, actin and cytokeratins.
Conclusion The preoperative diagnosis of sarcoma of the aorta is possible but it should be supported with imaging techniques; the definitive diagnosis need to be confirmed histologically and immunohistochemically.

P-536

Arterial allografts cryopreservation antigenicity in pigs

M Santos[1], N Solanes[2], M Rigol[2], J Marimon[2], E Khabiri[3], E Agustí[2], M Roqué[2], F Perez-Villa[2], M Heras[2], J Ramirez[1]
[1]Anatomia Patologica. Hospital Clínic. U. B, Barcelona, Spain
[2]Cardiologia. Hospital Clínic. U.B, Barcelona, Spain.
[3]Cirugía Cardiovascular. Hospital Clínic,. U.B, Barcelona, Spain

Background Coronary surgery requires vascular grafts. Donor fresh arterial grafts are useless because of rejection vasculopathy. Cryopreservation can be a good way for banking purposes and may limit rejection. The aim of this study was to assess the utility of arterial cryopreservation in increasing the quality of grafts, in an animal model in pigs.
Material and methods Small arteries, less than 3mm in diameters were implanted in pigs. Three groups were done: Group1(n=5): fresh autograft (AU) and fresh allograft (AL) one in each side; group 2 (n=5): Cryopreservated AU and cryopreservated AL; group 3 (n=5): fresh AL and cryopreservated AL. All animals got aspirin for three months and group 3 also cyclosporine A. The implanted grafts were embedded in paraffin and microscopically studied with hematoxilin/eosin and elastic stains for morphology and morphometrics. A basic immunohistochemical study with CD3 and MAC387 was also performed.
Results The patency rate of cryopreservated AL and AU was 100%, as it was in the fresh AU. The inflammatory reaction, evaluated by CD3 and MAC387 was present in all AL arteries, and absent in AU cases. In group 3, the infiltration was lower in cryopreservated, than in the fresh ones.
Conclusions In our series of pig's arteries, cryopreservation increases vascular patency and the inflammatory response is lower than in fresh arteries. This fact is independent of the immuno-supressive therapy.

P-537

Cytokeratin profile and neuroendocrine cells in the glandular component of cardiac myxoma

A Pucci[1], G Bartoloni[2], E Tessitore[1], A Carney[3], M Papotti[4]
[1]Anatomia Patologica- Az. Osp. OIRM-S. Anna, Turin, Italy
[2]Anatomia Patologica- Catania University, Italy
[3]Surgical Pathology- Mayo Clinic, Rochester, USA
[4]Anatomia Patologica- Turin University, Italy

Introduction Glandular cardiac myxomas are very rare tumors of uncertain histogenesis, displaying glandular structures within otherwise typical myxomas. Origin of glands has been attributed to epithelial differentiation of a cardiomyogenic precursor cell or to entrapped embryonal rests. We studied four cases of glandular myxomas (3 sporadic and one familial) to define the immunophenotypic profile of the glandular elements.
Materials and methods Histology and immunohistochemistry were performed on serial sections. Broad spectrum cytokeratin, cytokeratin 7 (CK7), cytokeratin 20 (CK20), CEA, EMA, chromogranin A, calretinin, thyroid transcription factor-1 (TTF-1), Ki-67 and p53 were investigated.
Results Three patients were males, aged 55, 23, 57, respectively and the fourth a 45 y.o. woman. The glands were either scattered within myxomatous stroma (3 cases) or in groups. In the latter case the glands featured villous projections, irregular profile, active inflammation or focal low grade dysplasia, and showed expression of acidic and neutral mucins (mostly sialomucins). Cytokeratin 7 and 20 co-expression was found, similarly to foregut derivatives. There were scattered chromogranin-positive neuroendocrine cells in one case and Ki-67 immunostaining showed a very low proliferative activity. There was no reactivity for TTF-1, calretinin or p53. None of the patients had adenocarcinoma or other neoplasm, either at diagnosis or at 1-19 years follow-up.
Conclusions Our findings indicate that glandular component of cardiac myxoma is morphologically heterogenous. The isolated glands suggest a possible divergent (epithelial) differentiation of myxoma cells, but other findings point to the possibility of entrapped foregut rests with mature neuroendocrine and mucous cell populations. Work partially supported by grants from the Italian Ministry of Education (Rome, to MP) and the Associazione Italiana per la Ricerca sul Cancro (Milan).

P-538

Infection and immune inflammation peculiarities in atherosclerosis

I Zota, E Foca, E Melnic
Pathology Department, The State University of Medicine and Pharmacy N.Testemitanu, Chisinau, Republic of Moldova

Introduction During the last decade the basic postulate of atherosclerosis etiology and pathogenesis has changed. This review presents a spectrum of data regarding the link between infection and immune inflammation development in atherosclerosis.
Material and methods This study has been carried out on the human aorta, coronary heart vessels collected from 59 early performed autopsies and on the carotid arteries gathered during surgical vessels remodeling of 18 persons. The patients with cardiovascular insufficiency on atherosclerosis background from 31 to 59 years were taken into study group. Chlamydia Pneumoniae was detected by routine microscopy on Shtive fixed material, and by immunohistochemical reaction performed on cryophilic specimens marked with Fits antibodies. HSP-60 and TNF-α implication have been studied trough immunohistochemical reaction using monoclonal antibodies. This material was fixed in 4% formaldechyde solution.
Results Chlamydia Pneumoniae has been detected in endothelial cells, macrophages, smooth muscle cells of fatty streaks and fibrous plaques. Its detection incidence decreases in advanced arterial lesions. We also determined that Chlamydia Pneumoniae infection is capable to induce immune reaction against HSP-60 which can be considered like a target in autoimmune reaction. They produce an cytotoxic effect on the endothelial cells followed by permeability disturbances, faciliting the atherosclerotic lesions progress. Among the inflammation mediators in increased quantity TNF-α have been detected being localized on the surface and in depth of atherosclerotic plaque around the foam cells.
Conclusions Our outcomes demonstrate the toxic and infectious factors existence which can be considerated decisive in atherosclerosis pathogenesis. This data give us the reason to elaborate other diagnosis and treatment strategy.

P-539

Cardiac hemangioma

Z Dolenc - Stražar[1], B Geršak[2], M Koželj[3]
[1]Institute of Pathology, Medical Faculty, University of Ljubljana, Slovenia
[2]Department of Cardiovascular surgery, University Medical center, Ljubljana, Slovenia
[3]Department of Cardiology, University Medical center, Ljubljana, Slovenia

Introduction Primary tumours of the heart are rare, the majority are benign, myxomas representing 50-80%. Hemangiomas are extremely rare, with an incidence of 0.8%-1.6%. They usually occur in adults, mostly are an incidental finding. We present a man with asymptomatic cavernous hemangioma of the left atrium.
Case report Transthoracic echocardiogram of a 46-year-old man with arterial hypertension, otherwise healthy, with normal ECG and chest X-ray, revealed a wide based isoechogenic tumour, measuring 3.1 x 2.2 cm, located in the moderately enlarged left atrium, attached to interatrial septum and anterior wall, adjacent to mitral valve annulus, sparing oval fossa. It showed minimal mobility but did not cause any obstruction of the blood flow or mitral regurgitation. Macroscopically, surgically removed tissue was spongy, partly haemorrhagic. Microscopically, there were cavernous venous structures, filled with blood and focally thrombosed. Focally, a few smaller capillary channels were found. There was no endothelial atypia and no papillary hyperplasia.
Discussion and conclusion Histologically, hemangioma of the heart has two major differential diagnostic possibilities. In case of a myxoid background, it is possible to be misdiagnosed as myxoma, but in hemangioma there are no myxoma cells and no ring structures. Grossly, opposite to myxomas, hemangiomas are rarely attached to the oval fossa. Papillary hyperplasia, which is reactive endothelial proliferation in hemangioma, may lead to misdiagnosis of angiosarcoma. Angiosarcoma can be excluded only when the whole tumour is examined and no marked endothelial atypia, cellular areas of spindle cells with poorly formed vascular channels, and necrosis are found. Compression, obstruction, effusion and bleeding are responsible for clinical picture. Symptoms depend also on the location, size and invasiveness. The natural history is unpredictable, for this reason surgical intervention is mandatory.

P-540

Limb-body wall complex (LBWC) versus amniotic band syndrome (ABS): a new pathological hypothesis

E Petcu[1], J Kasznica[2]
[1]Boston Univ Medical Center, Boston, MA 02118, USA
[2]Brown University School of Medicine, Womens & Infants' Hospital, Providence, RI 02905, USA

Introduction The limb-body wall complex is a congenital syndrome, which includes limb defects, abdominoschisis associated with facial and neural tube malformations. Some authors believe that the limb-body wall disruption is separate from amniotic band syndrome. Others suggest that both belong to a wider spectrum, with a possible overlap between these two categories. In the present study, we describe a case of LBWC and based on our findings we suggest a new pathogenic mechanism.
Case report A 32 years-old Cap-Verdean female gave birth at 33 weeks to a pair of twins. One foetus showed multiple malformations incompatible with life. Physical examination showed partial lower extremity amputations. A large omphalocele was also noted. There was a large lumbosacral meningocele and the head showed micrognathia and high-arched palate. There was right hydronephrosis secondary to right ureteral obstruction and cloacal anomaly. The lungs were hypoplastic. The histology of the internal organs was characteristic for the developmental stage and cytogenetic testing revealed a normal male karyotype.
Discussion and conclusion We believe, that early amniotic bands may lead to vascular insults, proximally and distally by altered haemodynamics. The lower limbs were partly amputated as a result of the continued growth associated with altered vascular supply. The same mechanism may explain the other findings as well. Vascular disruption by virtue of altered haemodynamic state may give rise to thromboemboli, which may affect the growth of external/internal structures, distant from the site of disruption. However, this vascular lesion was masked by continued growth of the foetus. Therefore, the ABS may precede and may cause the LBWC.

P-541

Two cases of pleuropulmonary blastoma

K Vuopala[1], H Tuominen[2], R Jauhola[1], P Valmari[1], R Herva[2]
[1]Lapland Central Hospital, Rovaniemi, Finland
[2]Oulu University Hospital, Oulu, Finland

Pleuro-pulmonary blastoma (PPB) is a malignant tumour of childhood. The most common clinical sign is respiratory difficulty. PPB appears as a pulmonary and/or pleural-based mass and is characterized histologically by a primitive, variably mixed, blastematous and sarcomatous appearance. No metastases have been reported in neonatal cases. We describe two cases that presented PPB. The first was a term male infant of a G8P7 mother. The pregnancy was uneventful. After normal delivery, a male infant with severe respiratory distress was born. By ultrasound examination, a thoracic mass were identified. There was no response to the intensive care. The infant died at the age of 3.5 hours. At autopsy, a tumour of 212 g, measuring 10x8 cm was found in the left lung. In addition, there was a smaller mass, of 3 cm diameter in the mediastinum. Microscopically, the tumour masses consisted of PPB. The second case was a 3-year-old female with persistent fever and respiratory difficulties. In CT scan, the lower lobe of the left lung was replaced with a tumour mass. During operation, the tumour was seen to be infiltrating to the mediastinum and was partially resected, followed by intense chemotherapy. Histologically, the diagnosis of PPB was given. The child has shown no sign of the disease during follow-up of six months. The PPB is regarded as the pulmonary dysontogenetic analogue of Wilms' tumour, neuroblastoma, and hepatoblastoma. The first case showed its highly aggressive nature, with mediastinal metastases found at birth.

P-542

Causes of intrauterine foetal death associated with placental pathologic features

V Blažičević[1], V Štitić[2], M Mrčela[1]
[1]Clinical Hospital Osijek, Croatia
[2]General Hospital Karlovac, Croatia

Introduction Improvements in antenatal and intrapartum care have reduced perinatal mortality, but the rapid advances in intensive neonatal care have had a dramatic effect in reducing neonatal deaths so that stillbirths have become relatively more important. The aim of this study was to identify the relationship between placental lesions and stillbirth.
Materials and methods We analysed the causes of intrauterine foetal death after the 26th week of pregnancy during the years 1991-2002 at the Departments of obstetrics and gynaecology of the Clinical Hospital Osijek and General Hospital Karlovac. A complete autopsy was made on each stillborn, including investigation of the placenta, cord and foetal membranes. Histological specimens were studied from all internal organs of the foetus and from the placenta, cord and membranes. Haematoxylin and eosin stain is used in routine causes, PAS staining to assess thickening of the basement membrane and trichrome staining to assess stromal fibrosis of the villi when it was necessary.
Results There were 201 stillbirths who died before labour - 174 placentas of them were examined and 27 weren't. Abnormalities were found in 142 (81.61%) placentas and 'normal' placentas were 32 (18.39%). Autopsy findings in stillborn foetuses: asphixia 133 (66.17%), maceration only 57 (28.36%), major malformations 6 (2.99%), vitium cordis 2 (0.99%), anencephalia 2 (0.99%), others 1(0.50%). Placental pathologic findings: infections 26 (18.32%), single chronic and acute infarction 36 (25.35%), multiple chronic and acute infarctions 23 (16.20%), placental failure for other reasons 16 (11.27%), chronic ischemic change 12 (8.45%), infections associated with circulatory disturbances 13 (9.15%), retroplacental haematoma 9 (6.34%), massive subchorial thrombosis 2 (1.41%), chorangiosis 2 (1.41%), umbilical cord tumour 1 (0.70%), intervillous thrombus 1 (0.70%), chorionic cysts 1 (0.70%).
Conclusion The most of women with a stillborn infant were quite healthy and did not reveal any risk factors when assessed on clinical grounds. There were patients in whom evident foetal growth retardation had been overlooked at the maternal health centre before the death of the foetus. The importance of routine ultrasound screening for detection of unrecognised risk patients and placentas is emphasized.

P-543

T - lymphocyte subtypes in the diagnosis of celiac disease

M Sajin[1], M Craiu[2], M Iordachescu[2], A Stanescu[1]
[1]University of Medicine, Bucharest, Romania
[2]IOMC Alfred Russescu Paediatric Hospital Bucharest, Romania

Introduction The objectives of this study was tot verify comparatively clinical age reported antecedents and the morphological aspect of the intestinal mucosa in patients sensitive to gluten, hospitalised at IOMC (Alfred Russescu Hospital) in the last 7 years. Celiac disease is an inflammation most frequently affecting the proximal small intestine, depending on the presence of gluten in the diet, whose pathogenesis seems to be immunological in nature.
Methods 107 cases were divided in three groups following clinical manifestations types at hospitalisation time: typical digestive, untypical digestive and extra digestive manifestations. Intestinal biopsies, made with Crosby probe, in children aged between 1.3 and 8 years (one single case was diagnosed as late as at the age of 15), regardless of gender. Then we analysed morphologically (HE usual and PAS histochemical staining) and immunohistochemically (lymphocytes B, T with possible subtypes).
Results The lesions counted according to the Marsh score were at the first biopsy: - 42 Marsh I infiltrating lesions (normal mucosa architecture, villi epithelium infiltrated with lymphocytes; lymphocytosis score: 30 lymphocytes /100 enterocytes); - 15 Marsh II infiltrating lesions (almost normal villi, enlarged crypts with immature epithelium and infiltrated with lymphocytes); - 17 Marsh IIIa destructive lesions (partial villi atrophy (VA) shortened, flattened villi, slight infiltration with intraepithelial lymphocytes and hyperplasic crypts); - 18 Marsh IIIb destructive lesions (subtotal VA clearly atrophied villi, still recognizable, widened hyperplasic crypts containing immature epithelial cells with a higher growth rate and influx of inflammatory cells); - 25 Marsh IIIc hyperplasic lesions (total VA completely absent villi, with severe atrophy, atrophied, hyperplastic glands and infiltrating lesions). The immunohistochemical tests have indicated the prevalence of T lymphocytes (UCHL1, CD3, CD4, CD8, gama-delta) both in the luminal epithelium with various degrees of aggression in lamina propria and also spread in stroma. B lymphocytes (L26) are distributed prevalently nodular in stroma.
Conclusion In conclusion, it is CD4 T cells that are present in particular in the control of the gluten immune response in patients with Marsh I and Marsh III lesions.

P-544

Clinical morphological analysis of early forms of polyarteritis nodosa

H Mazur-Zielińska[1], D Sabat[2], R Zieliński[3], W Zajęcki[1], A Ziólkowski[1]
[1]Department of Pediatrics, Medical University of Silesia, Zabrze, Poland
[2]Department of Pathomorphology, Medical University of Silesia, Zabrze, Poland
[3]Gastrology Clinic for Outpatients of the Specialist Hospital No 2, Bytom, Poland

Introduction Polyarteritis nodosa is a necrotic vasculitis of small and medium size arteries of not fully recognized aetiology. However, it occurs mostly in adults, it can also occur in children. The cutaneous form is one of the types of polyarteritis nodosa. It occurs in children very rarely. Polyarteritis nodosa is diagnosed on the basis of histopathologic results and clinical criteria established by the America College of Rheumatology. The aim of the study was to present 3 cases of polyarteritis nodosa in children.
Case reports Three cases of cutaneous polyarteritis nodosa in 16-year old girls and 1 case of general form of p.n. in a 14-year old boy At the beginning a tumour of pancreas head was suggested in the latter case. The final diagnoses in all cases were defined on the basis of histopathologic
Results The morphologic studies showed: skin and subcutaneous tissue specimens of 10mm diameter and 15mm thick were evaluated. Epidermis and corium were of normal structure. Abundant inflammatory infiltration consisting of neutral and acidophilic granulocytes, lymphocytes and plasmatic cells were observed on the boarder of corium and subcutaneous tissue. The infiltration was situated mainly in arterial walls and surrounding fibrous and fatty connective tissue. Different degrees of change advancement were observed in the walls of the vessels. Some changes were characteristic for an early stage of a disease and were demonstrated as swelling of the vessel wall and surrounding tissues (degeneration stage). In the oedematous wall fibrin concrement and only a few inflammatory cells were present. Other cells included abundant transmural inflammatory infiltrations (inflammatory stage). Vessel endothelium underwent desquamation and thrombi begun to appear in the arterial lumen. Only in few vessels, the process of considerable advancement of changes was observed – a repair process with consecutive fibrosis and thickening of arterial wall with considerable narrowing of its lumen. The described children were treated successfully with corticosteroid therapy and antistreptococcal prophylaxis with long-term remission.

P-545

Comparative morphologic analysis of the small intestine mucosa in a course of coeliac disease

W Zajęcki[1], D Sabat[1], H Mazur-Zielińska[2], K Stęplewska[1], M Slimok[2], A Sikora[2], B Kalita[2], B Slaby[1]
[1]Department of Pathomorphology, Medical University of Silesia, Zabrze, Poland
[2]Department of Pediatrics, Medical University of Silesia, Zabrze, Poland

Introduction Microscopic diagnosis of oligobiopsy material taken during endoscopic examination plays an important role in diagnosing syndromes of absorption disorders, especially in case of celiac disease. The aim of the study was a morphologic evaluation of the small intestine mucosa and comparison of the used from many years Shiner/Shmerling classification with a new modified Marsh classification.
Materials and methods During the study, 500 bioptates if small intestine evaluated in the Chair and Department of Pathomorphology in Zabrze in the years 1998-2002 were analysed again. Out of the bioptates 344 were with I of villous atrophy, 88 with II, 64 with III and 4 with IV. Study material was from the paediatric hospitals in Zabrze and Bytom. During routine histopathologic diagnosing, villus atrophy was evaluated in the Shiner/ Shmerling scale. Presently, the Marsh scale is being introduced into histopathologic diagnosing. It takes into consideration not only features of villus atrophy and glandular crypts proliferation but also intraepithelial lymphocyte infiltrations. Another evaluation of villus atrophy was performed according to the modified Marsh classification.

Results The received results are presented in the modified Marsh classification: type 0 – 309 (61.8%), type 1 – 25 (5.0%), type 2 – 10 (2.0%), type 3a – 88 (17.6%), type 3b – 48 (9.6%) and type 3c – 20 (4.0%). Our study allowed to compare two classifications used in the evaluation of the atrophic and proliferous processes and to select from the Shiner/Shmerling degree I a group of cases (type 1 and 2 according to Marsh), which had no equivalents in the so far used scale. Moreover, it was shown that the sub-groups of the type 3 of destructive changes did not correspond fully with the so far used Shiner's degrees II-IV. It enables fast comparison of the atrophy degree with the results received before the introduction of the new modified classification. Moreover, a routine application of precise descriptions of histopathologic results of small intestine mucosa in syndromes of absorption disorders facilitates retrospective selection, from the so far used Shiner's degree I, of the cases corresponding with Marshal types 1 and 2.
Conclusions Application of the modified Marshal classification for an evaluation of the small intestine mucosa in celiac disease enables accurate presentation of atrophic and proliferous changes including selection of type 1 and 2, which have no equivalents in the so far used Shiner/Shmerling classification.

P-546

Embryonal rhabdomyosarcoma: a case report

S Kocmanovska - Petreska, B Ilievski, P Cvetkovski, L Spasevska, S Kostadinova - Kunovska, S Duganovska
Institute of Pathology, Faculty of Medicine, Skopje

Rhabdomyosarcoma is an aggressive malignant skeletal muscle neoplasm arising from embryonal mesenchyme. The head and neck region is the most common site for this tumour in children. Neonatal presentation of this tumour is rare. We present an autopsy case of a female newborn having a large tumour mass (11x9x7 cm) in the frontal region, covering the entire upper half of the face. Similar subcutaneous noduli with diameter 3,5 cm, 3 cm and 2 cm were found on the left cheek, and another 4 with diameter 3,5 cm, 2,5 cm, 2 cm and 2 cm on the right cheek. The histological examination showed a tumour composed of large spindle cells with myoblastic features and small round to elongated undifferentiated cells. Associated with the spindle cells is various numbers of large round or globular cells with hyperchromatic nuclei surrounded by acidophilic granular or homogeneous cytoplasm. Cross-striations were found in the spindle cells. Imunohistochemically tumour cells were positive for desmin and vimentin. The final diagnosis was embryonal rhabdomyosarcoma. Immunohistochemical staining helped to make a proper diagnosis.

P-547

Effects of Sildenafile on ipsilateral testis damage following testicular torsion in rats

G Kale[1], IH Gol[2], D Orhan[1], N Kale[2]
[1]Hacettepe University, Medical School, Ankara, Turkey
[2]Gazi University, Medical School, Ankara, Turkey

Introduction Testicular torsion results in damage of the gonad and it is a surgical emergency. Testicular torsion evokes infertility as a result of ischemia. The aims of this study were to determine the effects of a vasodilatator agent Sildenafile on the testicular damage following testicular torsion.
Materials and methods Forty-two rats included to the study were divided into 7 groups: group 1; control, group 2; Sham, group 3: torsion (detorsion is performed 2 hours after torsion and orchiectomy is done at the 4th hour), group 4; torsion, detorsion and Sildenafile (1 mg/kg), group 5; torsion and Sildenafile (2 mg/kg), group 6; Sildenafile (1 mg/kg) without torsion, group 7; Sildenafile (2 mg/kg) without torsion. Testicular specimens were examined histopathologically for Johnsen tubular score and tubular diameter. The differences of these parameters between groups were evaluated statistically.
Results Johnsen tubular score and tubular diameters were fond to be significantly different in control and torsion groups ($p<0.05$). Johnsen tubular score and tubular diameter were significantly higher in the torsion groups which were given Sildenafile, and these parameters were again higher in the group which have taken Sildenafile at a higher dose ($p<0.05$).
Conclusion It is concluded that, by inhibiting cyclic guanosin monophosphate specific phosphodiesterase and resulting in vasodialatation, Sildenafile reduces the testicular damage caused by torsion (ischemia).

P-548

Expression of Bcl-x (S/L) in Wilms tumour

G Basta-Jovanovic[1], K Radotic-Smiljanic[1], D Brasanac[1], S Glumac[1], M Savin[2], S Skodric[1]
[1]Institute of Pathology, Medical School University of Belgrade, Belgrade, Serbia and Montenegro
[2]Clinical Centre of Serbia, Belgrade, Serbia and Montenegro

Introduction Apoptotic cell death represents an important mechanism for the precise regulation of cell numbers in normal tissues. Various apoptosis-associated regulatory proteins may contribute to the rate of apoptosis in neoplasia. The present study analyses the inter-relationship between the expression of the pro-apoptotic Bcl-x (S/L) protein and histological type and stage of Wilms tumour.
Materials and methods Bcl-x (S/L) expression was investigated using an indirect immunoperoxidase technique, applying antibodies to Bcl-x (S/L) protein. Correlation of semi quantitatively scored Bcl-x (S/L) levels with histological type and tumour stage was performed for 28 cases of Wilms tumours (23 classical and 5 anaplastic).
Results The expression of Bcl-x (S/L) protein was present in most cases of Wilms tumour (71%). Generally, Bcl-x (S/L) was expressed in the blastemal and epithelial components of Wilms tumour. In most cases, the expression of Bcl-x (S/L) was moderate. Blastemal Bcl-x (S/L) expression decreased with tumour stage. There was no correlation between histological type and expression of Bcl-x (S/L) protein. Diffuse expression of Bcl-x (S/L) protein was observed in 2 cases of anaplastic Wilms tumour. These two cases were stage I and of unfavourable histology. In 3 cases of Wilms tumour, no immunohistochemical staining was observed. So, these results cannot indicate whether absence of Bcl-x (S/L) could play a role in the development of anaplasia.
Conclusion According to clinical follow-up, the results of our morphologic and immunohistochemical analysis suggest that decrease of the blastemal Bcl-x (S/L) protein could be associated with the capacity of Wilms tumour for local and distant spread.

P-549

Expression of alpha, beta and gama catenins in Wilms tumour

S Radojevic[1], S Djuricic[2], D Brasanac[1], T Terzic[1], M Nenadovic[1], J Sopta[1], S Skodric[1], G Bunjevacki[2], G Basta-Jovanovic[1]
[1]Institute of Pathology, Medical School University of Belgrade, Belgrade, Serbia and Montenegro
[2]Mother and Child health Institute of Serbia 'dr Vukan Cupic', Belgrade, Serbia and Montenegro

Background Loss of catenins is suggested to promote tumour invasion and distant metastasis in tumour development. The aim of this study was to determine the expression of catenins in Wilms tumour and their relationship with histological type and stage of Wilms tumour.
Materials and methods Catenins expression was investigated using an indirect immunoperoxidase technique, applying antibodies to alpha, beta and gama catenins. Correlation of semiquantitatively scored adhesion molecule levels with histological type and tumour stage was performed on 28 cases of Wilms tumours (23 classical and 5 anaplastic).
Results Beta and gama catenins were present in most cases (89% and 75% respectively) and were usually coexpressed. Anaplastic type of Wilms tumour displayed higher beta catenin and lower gama catenin level in comparison with other types. Nuclear positivity, in each case, was found to be very strong, but was usually present only in 5 % of tumour cells. Beta and gama catenin expression was not correlated with stage of Wilms tumour. Alpha catenin was present in 35% cases of Wilms tumour. Stage III displayed higher alpha-catenin levels than stage I/II, suggesting that impairment of their function might exist without actual loss from tumour cells.
Conclusion Our results suggest that the level of catenin expression is associated with histological type of Wilms tumour, regardless of tumour stage. Observed nuclear expression of beta catenin indicates that the activation of wnt-signaling pathway is crucial step in Wilms tumour genesis.

P-550

Comparison of apoptosis and Fas, Fas-L and Bcl-2 expression in Wilms' tumor

M Ergin, A Uguz, S Erdogan, G Gonlusen, N Tunali
Cukurova University School of Medicine Dept. of Pathology, Adana, Turkey

Background Apoptosis is a complex process involving many genes that play role as antiapoptotic or apoptotic factors. It controls normal homeostasis of tissues. Expression of these genes vary from one type of tumour to another type. The aim of this study is to evaluate the expression of Bcl-2, Fas and Fas-L and apoptosis in Wilms' tumour (WT).
Method Thirty paraffin embedded tissue specimens were included. Immunohistochemical study was performed for Bcl-2, Fas and Fas-L and in-situ end-labelling technique (ISEL) for apoptosis.
Results The expression of these proteins varied among the tumours. There was no statistically significant correlation between the expressions of Bcl-2, Fas, Fas-L and. apoptotic index.
Conclusion Apoptosis is an important mechanism in the growth of the tumours. We suggest that not only Bcl-2, Fas and Fas-L play role as regulators of apoptosis in WT but also other apoptotic and antiapoptotic genes involve this process. Further investigations are necessary to understand the molecular mechanism of the progression of WT.

P-551

Uncommon tumours of the neuraxis in childhood

J Vila-Torres
Hospital Universitari Sant Joan de Déu. Department of Pathology, Barcelona, Spain

Case 1 A 3 year-old girl presented with seizures and weakness in the left part of de body of 1-year duration. CT scan showed a mass that filled the right ventricle, with a strong mass effect, peritumoural oedema, midline shifting and slight ventricular enlargement. A partial excision was carried out and the pathological diagnosis was that of choroid plexus carcinoma. The patient died six months later due to adjuvant therapy side effects. In the last WHO classififcation of brain tumours, grade III choroid plexus carcinoma is defined as a choroid plexus tumour showing features of malignancy: nuclear pleomorphism, frequent mitosis, high nuclear/cytoplasmic ratio, increased cellular, density, blurring of the papillary pattern, poorly structured sheets of tumour cells, necrotic areas, and often diffuse brain invasion. All those tumours classically displaying a papillary pattern must be considered in the differential diagnosis.
Case 2 A 5 month-old child presented with respiratory distress since 3 months old. On RX and CT scan, a tumour in the left hemithorax was seen, with right shifting of the mediastinum. The tumour was partially removed. Pathological diagnosis was that of spinal canal invasion by a soft tissue lipoblastoma. Eight months after surgery the tumour relapsed, infiltrating the epidural spinal canal from C5 to D8. The tumour was fully excised by means of microsurgery techniques, without neurological deficits. This case is an example of invasion of the vertebral canal by a soft tissue tumour previously removed. Lipoblastoma is a rare fatty tumour occurring in children in the extremities or less commonly in the trunk or retroperitoneum. The tumour is benign but may recur. Grossly, lipoblastoma showed a distinct lobulated pattern of yellow-grey myxoid tissue, histologically composed of highly vascular fat in a myxoid stroma resembling embryonic white fat. Differential diagnosis, based on clinical-pathological grounds, include fibrolipoma and myxoid liposarcoma.
Case 3 A 8 year-old boy presented with partial complex seizures for 1 year duration. NMR showed a discrete hypodense cortical-subcortical lesion in the left frontal lobe. Neither oedema nor mass affect was detected on CT scan. The tumour was completely removed by surgery and the pathological diagnosis was that of dysembryoplastic neuroepithelial tumor. This is an intracortical grade I tumour composed of oligodendrocyte-like cells. Macroscopically, is a nodular outward expansion of the superficial cortex. Histologically, a low-power view of a perpendicular section of the cortical surface shows the characteristic pattern of multiple intracortical nodules and internodular tissue, both containing mucin. Also seen, is a specific glioneuronal component of vertical columns of neu-

rites transversing the cortex, sheathed by oligodendrocyte-like cells accompanied by mucin and with 'floating neurons' (cortical ganglion cells seen in individual small pools of mucin).
Case 4 A 14 year-old boy presented with diplopia and proptosis. The NMR showed a hypodense, diffuse lesion in the left temporal and parietal lobes that produced a slight collapse of the left lateral ventricle. Two weeks later the patient developed symptoms of time and space cognitive disturbances, language difficulty and seizures. A biopsy was done and the pathological diagnosis was that of gliomatosis cerebri. This is a rare primary brain tumour characterized by a diffuse proliferation of neoplastic glial cells that typically involve multiple brain areas with preservation of brain structures. The diagnosis depends on both histologic and radiologic features. On NMR there is a uni or bilateral diffuse involvement of the white matter extending to the cortex with poor mass effect. Microscopically, there is a proliferation of monomorphous astrocytes, grade II or III, infiltrating the brain parenchyma freely. Some undifferentiated cells show 'naked' nuclei while others look like 'rod' structures. In cases of low cellularity and cytologically bland astrocytes, it may be extremely difficult to make the differential diagnosis with reactive gliosis. GC is associated with a poor prognosis.

P-552

Spleen depletion in neonatal sepsis and chorioamnionitis

P Toti[1], C De Felice[2], R Occhini[1], M Stumpo[1], L Barbagli[1], S Bartolommei[1], G Buonocore[2]
[1]Dept. Human Pathology and Oncology, Siena, Italy
[2]Dept. Pediatrics, Obstetrics and Reproduction, Siena, Italy

Introduction autopsy studies in adult patients who had died of sepsis revealed a profound, progressive, apoptosis-induced loss of cells of the adaptive immune system (Hotchkiss et al, New Engl J Med, 2003; 348:138-150). In neonatal sepsis and chorioamnionitis, thymus modifications and shrinkage have been exhaustively described (Toti et al, Hum Pathology 2000; 31:1121-1128), while morphology of the spleen has not. The aim of this study was to describe the morphology of the spleen in neonates with early onset sepsis and with chorioamnionitis.
Material and methods the study population has been described previously (Toti et al, Hum Pathology 2000; 31:1121-1128). Ten preterm or full-term neonates who died because of proven sepsis within 48 hours after birth (mean gestational age±SD, 29.2±6.2 weeks); 20 foetuses spontaneously aborted (22±7.4 weeks) because of extensive ascending chorioamnionitis. Controls included 10 foetuses with induced termination of pregnancy (20±2.4 weeks) and 10 babies who died suddenly in the perinatal period, without evidence of chorioamnionitis. Spleen cell populations were studied by means of immunohistochemistry.
Results Early onset sepsis in the neonates occurred with severe spleen depletion, involving both B and T lymphocytes. In particular, CD20+, CD45R0+ and CD4+ cells were dramatically diminished in the spleen of neonates with sepsis, in comparison to controls. Foetuses with chorioamnionitis also showed spleen cell depletion.
Conclusion These results indicate that preterm and term neonates show an inflammatory reaction similar to that of adult patients, and that chorioamnionitis is associated with an unspecific inflammatory response comparable to that of sepsis.

P-553

Familial hemophagocytic lymphohistiocytosis with CNS involvement - autopsy case presentation

G Kalan[1], M Benedik Dolničar[2], M Popović[3]
[1]General Hospital Jesenice, Slovenia
[2]Medical Centre Ljubljana, University Children's Hospital, Unit of Hematooncology
[3]Institute of Pathology, Medical Faculty, University of Ljubljana, Slovenia

Introduction Hemophagocytic lymphohistiocytosis (HLH) is a disorder of an immunological disturbance with proliferation of cells of the mononuclear phagocyte system, with the histiocyte as a central cell. It includes two different conditions: primary or familial HLH, an autosomal recessive disorder in which most patients develop the disease very early in life, and secondary HLH associated with neoplastic, autoimmune and a variety of infectious diseases, occurring as sporadic cases throughout life period. Clinically the disease is characterised by the occurrence of a hemophagocytic syndrome of prolonged fever and splenomegaly with laboratory signs of cytopenias, lipid, coagulation and liver abnormalities. Hemophagocytosis is readily identified in bone marrow, spleen or involved lymph nodes. Central nervous system spread of the disease may be present early, but is frequently seen later during the course of the disease. The aim of this study was to presentat an autopsy case of a 13 months old boy.
Case report Signs of HLH were present right after birth. He was treated by the treatment protocol HLH-94. The disease later progressed with CNS involvement. A complementary bone marrow donor was not found in time.
Materials and methods Tissue samples collected at the autopsy were proceeded with standard histological and immunohistochemical methods.
Results Severe bleeding in the right lung with other signs of coagulopathy were found as the main cause of death. Hepatosplenomegaly was a prominent feature. We detected hemophagocytosis in the bone marrow, liver and central nervous system.
Conclusions The diagnosis of HLH must be based on clinical, laboratory and cyto/histological findings. The pathogenesis of familial HLH is still not completely understood.

P-554

Evaluation of goblet cells in small intestine epithelium in celiac disease in children

E Zembala-Nozynska, D Sabat, M Jedrzejczyk, M Kaszuba, A Mazur, J Zeckei
Department of Pathomorphology, Medical University of Silesia, Zabrze, Poland

Introduction A changeable number of goblet cells in intestine epithelium is rarely a matter of consideration among other morphological factors of small intestine mucous membrane atrophy in celiac disease. It is also not evaluated in the current classifications of goblet cell condition in celiac disease. The aim of the study was to evaluate a number of goblet cells in small intestine epithelium with reference to the degree of atrophy in celiac disease.

Material and method Morphological analysis of 80 bioptates of small intestine mucous membrane, taken for a routine histopathologic diagnosis from patients aged from 0 to 18 years, was performed. The patients were diagnosed and treated in paediatric university hospitals in Zabrze and Bytom in the years 2001-2002. Specimens were stained with haematoxylin and eosin (H.E.) and alcian blue-PAS (AB-PAS). Villous atrophy was evaluated according to the modified Marshal scale.
Results The following types were defined: type 0 – 33 cases, type 1 – 8 cases, type 2 – 6 cases, type 3a – 9 cases, type 3b – 21 cases, type 3c – 3 cases. Then, a number of goblet cells per 100 enterocytes of small intestine epithelium of each oligobioptate were calculated. The received results were evaluated statistically with U Mann-Whitney test. The average number of goblet cells in small intestine epithelium was calculated in relation to the degree of atrophy with the modified Marsh scale: type 0 –8.08 (+/- 3.79), type 1 – 9.41 (+/- 4.04), type 2 – 10.48 +/- 1.59), type 3a – 11.55 (+/- 2.94), type 3b – 13.20 (+/- 3.52), type 3c – 17.53 (+/- 0,92). The analysis used significant relations between an average number of goblet cells in small intestine epithelium and a degree of mucous membrane atrophy in celiac disease. Moreover, a correlation according to Rang Spearmann test showed a coefficient $R=0.5790$ for $p<0.001$.
Conclusions Significant relation between a number of goblet cells in epithelium and a degree of small intestine mucous atrophy in celiac disease. It allows an introduction of a new objective quantitive parameter in the evaluation of atrophic lesions.

P-555

Immunohistohemical evaluation of mast cells activity in small intestine mucosa in children in the course of celiac disease

D Sabat[1], W Zajecki[1], E Zembala-Nozynska[1], B Drozdzowska[1], K Steplewska[1], M Slimok[2], A Sikora[2], B Kalita[2], B Slaby[1]
[1]Department of Pathomorphology, Medical University of Silesia, Zabrze, Poland
[2]Department of Pediatrics, Medical University of Silesia, Bytom, Poland

Introduction Microscopic evaluation plays an important role in diagnosing small intestine inflammatory diseases. Defining a degree of villous and brush border atrophy, enterocytes changes, elongation of glandular crypts allows a correct evaluation of treatment clinical effects and child's body response to the applied selective diet. Development of immunomorphological studies contributed to confirmation of the autoimmunological basis of several diseases and of the influence of exogenous factors on their development. Due to the new approach, evaluation of the changeable character of inflammatory infiltrations including mast cells and marking activity of enteroendocrinal cells have become very important diagnostic elements. The aim of the study is to examine a changeable intensity of infiltrations from mast cells of small intestine mucosa in children in the course of celiac disease.
Material and method Oligobioptates of small intestine mucosa taken in endoscopy from 500 patients (age 0-18 years) at the Department of Pathomorphology in Zabrze in the years 1998-2002. The patients were diagnosed and/or hospitalised in paediatric university hospitals in Zabrze and Bytom. A degree of villus atrophy was evaluated according to the modified Marsh classification. Tissue material in paraffin cubes from the routine oligobiopsy of the patients with celiac disease was qualified for immunohistochemical study. Immunohistochemical reactions revealed a presence of brown dyed mass cells in intestine mucosa. The cells were evaluated by counting their number in 5 high power fields (magnification 400x) in each oligobioptate. The received results were calculated statistically with Mann-Whitney U test.
Results Mean number of mass cells in intestine mucosa was calculated in relation to the degree of villus atrophy according to the modified Marsh classification: type 0 (status normalis) – 7.55 (+/- 2.23), type 1 – 13.59 (+/-5.20), type 2 – 17.62 (+/-1.94), type 3a – 20.82 (+/-6.10), type 3b – 27.94 (+/-4.59), type 3c – 34.31 (+/- 3.61). The analysis showed significant relation between a number of mass cells and a degree of mucosa atrophy in a course of celiac disease. Moreover, a correlation after the Rang Spearman test showed a coefficient $R=0.8151$ for $p<0.000001$.
Conclusions Significant relation between a number of mass cells and a degree of small intestine mucosa atrophy in a course of celiac disease was shown. Defining (marking) a number of mass cells in small intestine mucosa in a course of celiac disease allows an introduction of quantitive method of atrophic changes evaluation as a new objective parameter, especially in cases difficult to diagnose.

P-556

Morphological analysis of tissue reactions in mandible after dental implants of the pressed COCrMo alloy

M Adwent[1], D Sabat[2], T Cieslik[1], Z Szczurek[2], W Zajęcki[2], JR Dabrowski[3]
[1]1st Department and Clinic of Maxillo-Facial Surgery, Medical University of Silesia, Zabrze, Poland
[2]Department of Pathomorphology, Medical University of Silesia, Zabrze, Poland
[3]Mechanical Faculty Technical University, Biaystok, Poland

Introduction Production of materials for dental implants is of great social importance and is related to the progress in material technology. Main directions of development in this discipline concern an accurate choice of implant material in order to fix an implant in a bone tissue firmly and to decrease tissue reactions. New direction of research on implant materials is powder metallurgy. In comparison with the so far used technologies, it has many advantages, such as homogenous fine grained material structure, possibility to make composites including biologically active implants, and also ability to overgrow the implant with bone tissue. Aim of the study was morphological analysis of healing of dental alveolus canals filled with metal implants. Evaluation of tissue reactions in bones and surrounding soft tissue from several types of metal implants.
Material and method The experimental study was performed on 56 mixed breed rabbits of 2600-3200g weight. After premedication with atropine with relanium, surgical procedure was performed in each animal. One of the incisors was extracted and after the canal was formed, metal implant was inserted. The first group (D1) consisted of animals whose dental alveolus canals were filled with cylinder of 6x3 mm made of pressed Co-Cr-Mo alloy covered with calcium triphosphate. The second group (D2) consisted of animals whose dental alveolus was filled with implants of cylindrical shape of a size 6x3 mm made of pressed Co-Cr-Mo alloy. The third group (D3) consisted of animals whose dental alveolus canal were filled with a titanium screw of a size 3x1 mm. The control group (K) consisted of animals whose dental alveolus canal was left only with blood clot. The postoperative wounds were sutured with dexon thread. The clinical and observations and histopathological

examinations were performed after 3, 7 and 21 days and 6, 12, 24 and 52 weeks.
Results Fibrous connective tissue reconstructing dental ligament system was found to be created around metal implant in the three experimental groups. A reconstruction process of the bone tissue and its maturation in the form of calcification around the implant was the fastest in the group D1 (Co-Cr-Mo + TCP), next in the group D2 around the implant with a pure pressed Co-Cr-Mo alloy and the group D3 with a titanium screw. However, deposition of calcium salt in the mature bone tissue occurred at the fastest in the group D2. The reactions caused by corrosion of the implants were not observed.
Conclusions The process of bone tissue reconstruction was the most active at the presence of CoCrMo alloy covered with calcium triphosphate (group D1). The fastest maturing of the bone tissue manifested as its mineralization was observed in groups D1 and D2. The metallic implants did not influence negatively the healing process of the post-operative wounds.

P-557

Morphological evaluation of bone defects filled with deproteinized bovine bone

A Cieslik-Bielecka[1], D Sabat[2], T Cieslik[1], Z Szczurek[2], T Bielecki[3]
[1]1st Department and Clinic of Maxillo-Facial Surgery, Medical University of Silesia, Zabrze, Poland
[2]Department of Pathomorphology, Medical University of Silesia, Zabrze, Poland
[3]Department of Orthopedics, Medical University of Silesia, Sosnowiec, Poland

Introduction Correct reconstruction of bone defects is a serious problem in orthopedics and in maxillo-facial surgery. Hence, numerous experiments and clinical studies on a usage of natural and artificial materials being a scaffold enhancing a reconstruction of bone tissue (i.e. carbon fibre, hydroxyapatyte granulate). Deproteinized bovine bone is a new material. It was elaborated in at the Mineralogy Faculty, Mining and Steel Academy in Kraków. The technology of natural animal bone tissue enables its use in filling bone defects, accelerates reconstruction of bone tissue and minimizes unfavorable tissue reactions through total immersion into the reconstructed bone. It gives no incorrect immunological response of the body to the implanted xenogenic tissue. The aim of the study is to evaluate healing processes of the defects made in rat femoral bones and filled with deproteinized bovine bone and to compared it with spontaneous healing.
Material and method The experiment was conducted on 84 Wistar rats divided into 2 groups (42 rats per group). The surgically made bone defects were filled with the study material. The animals, whose defects filled with blood clots spontaneously, made up a control group. The healing process in bone tissue was examined clinically and morphologically after 1, 3, 7, 14, 28 and 56 days after the experiment.
Results In histopathological estimation, the healing speed of the defect in femoral bone filled with blood clot (control group) was compared to the healing of the defect filled with deproteinized bovine bone (study group). No inflammatory reaction to the implant was observed. Moreover, acceleration of the healing of the defect filled with deproteinized bovine tissue was observed. Bovine bone was, in the study group, totally immersed in the body's bone tissue, i.e. was surrounded by the arisen on its surface sponge bone. In the last periods of the observation, on the borders of the observed synostoses no osteoblast cell activity was observed and normal bone marrow was found between osseous trabeculae.
Conclusions Osseous wounds filled with deproteinized bovine bone heal without any inflammatory complications. No negative systemic reactions proves that the applied material was properly prepared for implantation. Histopathologic studies showed that deproteinized bovine bone accelerates regeneration process of a damaged bone tissue.

P-558

Withdrawn

P-559

The effect of specific inhibitors of caspases on apoptosis of thymocytes induced with paclitaxel

T Kravic[1], M Rajkovic[2], B Djuricic[2], V Bumbasirevic
[1]Institute for Histology and Embryology, Medical Faculty Belgrade, Belgrade, Serbia and Montenegro
[2]Institute for Biochemistry, Medical Faculty Belgrade, Belgrade, Serbia and Montenegro

Although caspases are involved in molecular mechanisms of the execution phase of apoptosis, the precise mechanisms of their involvement in paclitaxel induced apoptosis are still not identified. The aim of this study was to investigate and compare the effects of inhibitors of caspases (50 mMol/L) on apoptosis of rat thymocytes induced by paclitaxel (10 mMol/L) and colchicine (2 mMol/L). The effect of z VAD and specific inhibitors of caspases (caspase 1, 3 and 9) after 4, 8 and 12 hours of incubation of thymocytes with paclitaxel and colchicine were analyzed. After incubation cells were fixed, processed for LM and EM, and the percentage of apoptotic cells (apoptotic index) was determined. General inhibitor of caspases zVAD and inhibitor of caspase 9 led to a significant decrease of apoptotic index after 8 hours of incubation with paclitaxel (from 29.03% to 19.76% and 14.23%). Inhibitor of caspase 3 and caspase 1 lowered the apoptotic index after 12 hours incubation with paclitaxel from 64.54% to 26.36% and 44.23% respectively. Inhibitor of caspase 1 did not affect the apoptotic index in controls, while the other used inhibitors reduced it. Inhibitors of caspase 1, 3 and 9 and zVAD had similar effects on apoptosis of thymocytes induced by colchicine. These results show that apoptosis induced by paclitaxel is caspase dependent, and that it, due to the effect of inhibitor of caspase 9, probably involves mitochondria. Caspase 1 activity might also be involved in mechanisms of induction of apoptosis of thymocytes by paclitaxel.

P-560

Effects of concurrent administration of lithium and gentamicin on the histoembryogenesis of rat fetus during the developing periods

H Noori Mugahii[1], B Minaii Zanghii[1], M Akbari[2]
[1]Tehran University of Mediacl Sciences, Department of Histology, Tehran University of Medical Science, Tehran, Islamic Republic of Iran
[2]Tehran University of Mediacl Sciences, Department of Anatomy, Tehran University of Medical Science, Tehran, Islamic Republic of Iran

This study was planned to investigate the effects of gentamicin and

littium on rat histoembryogenesis and to determine the effects, if any, of lithium as a potent gentamicin inhibitor. The rats were exposed subcutaneously to 110-mg/kg gentamicin on days 6-15 of gestation. Lithium administered orally at doses 1200 mg/l on days 6-15 of gestation. Fetuses were collected on day 21 and compared with those of the untreated, and saline treated control as well as with those of the gentamicin and lithium treated groups. All control and cases embryos groups were killed and their tissues were obtained. Then prepared for paraffin block, sectioning, H-E staining and light microscopic studies. We fond that gentamicin caused growth retardation versus lithium which dosn't did so. Lithium has a state like control but no wary exactly. Furthermore, concurrent administration of gentamicin and lithium caused regularity in histoembryogenesis cycle and the normal growth beside the lithium or gentamicin. Of course the recent result is not exactly comparable to those of controls.

P-561

Immunohistological and pharmacological studies of anti-inflammatory drugs in experimental Schistosomiasis

O Hammam, M Rabie
Theodor Bilharz Research Institute, Giza, Egypt

Introduction Schistosomiasis mansoni infection increases the level of prostaglandins and leukotrienes that are secreted mainly by macrophages within the granulomas. These mediators have a pronounced role in mediation and modulation of inflammation. Most non steroidal anti-inflammatory drugs (NSAIDs) act mainly by inhibiting the cyclooxygenase pathway of arachidonic acid metabolism, thereby diverting it towards the lipoxygenase pathway. These leukotrienes are important in maintenance of acute and chronic inflammatory condition.
Methods In present study, we used mofebutazone (cylcooxygenase and lipoxygenase inhibitor) and tenoxicam (cylcooxygenase inhibitor) either alone or in combination with praziquantel (antibilharzial drug) in mice infected with Schistosomiasis mansoni. We study their effects on liver pathology as PCNA (proliferating cell nuclear antigen), granuloma diameters, percent of degenerated ova and type of granuloma after 10&14 weeks after infection.
Results shown that infection increased the percent of positive nuclei in granuloma and in hepatocytes to be about 72% & 82% at 10 weeks and these percentages were reduced to be about 37% & 43% at 14 weeks after infection respectively. Treatment with mofebutazone and tenoxicam produced a reduction in PCNA to be about 33% & 40% in granuloma and 36% & 44% in hepatocytes at 8 weeks and more reduction occurred after 14 weeks after infection. Also, mofebutazone tended to produce more protection to isolated hepatocytes (% viability of hepatocyte) than tenoxicam in Schistosomiasis mansoni infected mice. Combined therapy with praziquantel produced more reduction in PCNA and more protection to hepatocytes. It is evident from the present study that, mofebutazone when combined with praziquantel has shown good tolerability more than tenoxicam which was associated with an improvement in PCNA, granuloma diameter, % viability of isolated hepatocytes, liver function tests, a fact that would seen to advocate the use of mofebutazone in bilharzial patient.

P-562

Patterns of injury in car and motorcycle accidents

JM Suárez Peñaranda, C Bellido, R Rico, MT Alvarez Iglesias, M Rodríguez Calvo, I Muñoz, L Concheiro
Institute of Legal Medicine, Santiago de Compostela, Spain

Introduction The role of the forensic pathologist in road-traffic accidents is to detect atypical injuries that could suggest an alternative cause of death, demonstrate natural diseases capable of creating sudden incapacity, and to collect samples for toxicological examinations. The main objective of this work is to study the different patterns of injuries in car and motorcycle fatalities.
Material and methods We have studied the autopsy reports of 34 deaths related to road traffic accidents (25 involving cars and 9 motorcycles). A complete autopsy was performed in every case including toxicological investigation.
Results The most common cause of death was head injury, responsible for 52% and 66.6% of deaths in car and motorcycle accidents, respectively. Cranial base fractures were more commonly found in passengers rather than in drivers, both for cars and motorcycles (40% vs. 30% and 33.3% vs. 50%, respectively). The distribution of cranial vault fractures was similar with percentages of 15 and 12.6 for car and motorcycle drivers, versus 40 and 50 per cent for the respective passengers. Nevertheless, brain injury was even more frequent in car accidents, accounting for 60% of the cases, and in motorcycle fatalities, where every single case showed some degree of brain injury.
Conclusion Our results confirm the importance of head injury in road-traffic accidents, especially when motorcycles are involved, being the most common cause of death. Although all motorcycle victims wore a helmet at the time of the accident, it did not seem to provide an effective protection, probably because of the high speeds involved. The incidence of cranial fractures and brain injury is higher for passengers than for drivers, probably due to the lack of attention to the traffic of these latter, and the fact that drivers are usually holding the handlebar or wheel at the moment of the accident.

P-563

Heat-induced epitope retrieval in immunohistochemistry

C Espersen, B Crillesen, B Jepsen, JW Hansen, TH Veie,
H Winther, J Askaa
Department of Immunohistochemistry, DakoCytomation A/S,
Glostrup, Denmark

Introduction Heat-induced epitope retrieval (HIER) has dramatically changed the applicability of immunohistochemistry in routine pathology. HIER has increased the number of primary antibodies useful on formalin-fixed paraffin-embedded material and in general improved the histochemical staining. The aim of this study was to compare various buffers for HIER on a broad range of primary antibodies.
Materials and methods HIER using four different buffers (citrate pH6; Tris/EDTA pH9; DakoCytomation Target Retrieval Solution, High pH, code No. S 3307 and DakoCytomation Target Retrieval Solution pH6, code No S 1700) for pre-treatment of formalin-fixed paraffin-embedded material has been compared using more than 120 different primary antibodies and the EnVision+TM visualisation system.

Results HIER with citrate buffer retrieve epitopes recognised by the majority of the tested antibodies. However, in several cases the epitopes could not be detected using this method but were retrieved using Tris/EDTA and/or Target Retrieval Solution, code No. S 1700. Also retrieval by means of the Target Retrieval Solution, High pH can be used however, the morphology quite often was partly destroyed. Furthermore, some antibodies could only be used after enzymatic pre-treatment whereas HIER abolished the histochemical staining.
Conclusion Although HIER using citrate pH6 buffer is a standardised and widely used technique, it is in numerous cases sub-optimal or even obliterate the immunohistochemical staining. In general more epitopes can be retrieved using Tris/EDTA pH9 or DakoCytomation Target Retrieval Solution.

P-564

Bone morphology and calcemia in ovariectomised (OVX) Wistar rats

L Markovic[1], J Sopta[2], M Atanackovic[2]
[1]Institute of pathophysiology, School of medicine, Belgrade, Serbia and Montenegro
[2]Institute of Pathology, School of Medicine, Belgrade, Serbia and Montenegro

Postmenopausal oestrogen deficiency results in bone loss (osteoporosis) in humans and experimental animals. Wistar rats provide a useful experimental model of post-menopausal osteoporosis. To demonstrate the histomorphometric and histological changes of bone 4 weeks after bilateral ovariectomy in rats and to investigate the impacts of 2 different hormone replacement therapies on the bone. Specimens of proximal femur were embedded undecacified for histomorphometric analysis and of distal femoral metaphysis were procured for pathologic examinations. Three weeks after OVX the femoral BMD, mean cortical thickness decreased significantly while the number of osteoclasts increased significantly as compared with sham group. The trabeculae became thinner and irregular which changed the bone microstructure in three dimensions. After treatment with 2 different preparations, the above parameters restored to various extents to the sham operation levels. Bilateral ovariectomy induced increased osteoclast activity and bone turnover, therefore caused accelerated bone loss. Treatment with combined sex hormones preparation could inhibit bone absorption and stimulate bone formation. This investigation was supported by MSTD of Srbia.

P-565

Vilnius pathological anatomy in the first half of the 19th century

D Sabat
Department of Pathomorphology, Medical University of Silesia, Zabrze, Poland

The beginnings of pathological anatomy as a separate medical subject were connected in the area of the Republic of Poland and Lithuania with the Vilnius University. The first post mortem was done in Vilnius by a priest, Stefan Bisio only in 1770 year. At the end of the 18th century, Jakub Briotet, a surgeon and anatomist, created a modest anatomical surgery (study). In 1804, Jan Piotr Frank and his son Józef arrived to Vilnius and became professors of the University. Jan Piotr Frank became the Head of the Teaching Hospital and Józef Frank the Head of the Chair of Pathology. In November 1804, he started lecturing for students, which he recalled in his "Memoirs": Several days after my father, I also started a course with a dissertation "De meliori pathologiam tradendi modo" In this speech I put the main stress on a significance of the explanations at the patient's bed-side and of a good knowledge of pathological anatomy… When in 1805, Józef Frank became the Head of the Teaching Hospital, he founded the first anatomo-pathological study (surgery). Most of the samples kept in spirit in the Frank's study were eaten by the starving French soldiers during the retreat of Napoleon's army. Besides Frank's study at the Vilnius University at the Chair of Anatomy, there still existed the study founded by Briotet. In 1808, the Emperor Alexander I destined the ruins of the Spaska's Orthodox Church for an anatomical theater. After seven-year redecorations, the building was opened in 1815. Besides the theatre itself, dissection room and Veterinary Institute, it also included a zoological, veterinary and anatomical museum. The growing anatomical museum had, in 1841, 2881 preparations including 1239 anatomo-pathological preparations. After closing down the Vilnius University and foundation of the Academy of Medicine and Surgery, pathological anatomy was made an individual subject of study. The first lecturer of pathological anatomy in Vilnius was Ludwik Siewruk. He held the classes till 1840 and then he took charge of the Chair of Anatomy at the Moscow University. His successor was Jan Leonow who continued his work until the tsar's authorities closed down the Academy of Medicine and Surgery in 1842. After the Academy had been closed down, all the exhibits of the Vilnius anatomical museum, including anatomopathological preparations were moved to the anatomical museum of Kiev University. Few of them remained in the Vilnius Medical Society.

P-566

Detection of cardiac mast cells in rats poisoned by T-toxin

V Jacevic[1], L Zolotarevski[2], K Jelic[2], J Dimitrijevic[2], V Kilibarda[1], MP Stojiljkovic[1]
[1]National Poison Control Centre, Military Medical Academy, Belgrade, Serbia and Montenegro
[2]2Insitute of Pathology and Forensic Medicine, Military Medical Academy, Belgrade, Serbia and Montenegro

Introduction T-2 toxin, a mycotoxin produced by Fusarium fungi, is a well-known cardiotoxin that cause myocardial injury, capillary damage, haemorrhage and focal polymorphonuclear cell infiltration. Mast cell (MC) is one of the the earliest multifunctional effector cells of the immune system and important constituent of microvasulature in the heart. Aim: We wanted to investigate appearance and localisation of mast cells in the heart of T-2 toxin-poisoned rats.
Materials and methods Adult female Wistar rats were poisoned with a single injection of 1 LD-50 of T-2 toxin (0.18 mg/kg sc). Rats were divided into two groups: (1) control group and (2) T-2 toxin group. T-2 toxin was produced in laboratory conditions from Fusarium sporotrichoides fungi. Animals were sacrificed after the end of the day 1, 3, 5 and 7 of the study. Cardiac MCs were counted in whole visual fields, magnified by 40-fold on paraffin section stained with haematoxylin and eosin (HE) and Giemsa methods.
Results In the heart of rats treated with T-2 toxin, blood vessels were congested with thickned walls, and a large number of mononuclear cells was present nearby. 24 hours after administration of

T-2 toxin, a solitary hypergranular MCs were situated on the external wall of blood vessels. However, on days 3, 5 and 7 the number of perivascular MCs was increased. More than 50 percent of these MCs showed degranulation.
Conclusion Our results suggest that perivascular localisation and later degranulation of MCs may play an importantant role during the acute reaction in the heart of rats poisoned by T-2 toxin.

P-567

Effects of bromadiolone on rodent liver: pathohistological findings

K Jelic[1], V Jacevic[2], V Dragojevic-Simic[2], ZA Milovanovic[2], S Dobric[2], D Bokonjic[2], J Dimitrijevic[1]
[1]Insitute of Pathology and Forensic Medicine, Military Medical Academy, Belgrade, Serbia and Montenegro
[2]National Poison Control Centre, Military Medical Academy, Belgrade, Serbia and Montenegro

Introduction Bromadiolone is one of the most commonly used rodenticides. This coumarin anticoagulant blocks multiple steps in the coagulation cascade. It is absorbed through the gastrointestinal tract and accumulated in the liver, mainly. The aim of this study was to investigate pathohistological alterations in the liver after oral application of bromadiolone in rodents.
Materials and methods Adult Wistar rats and Swiss mice, of both sexes, were fed with a ready-to-use baits of low bromadiolone concentration (0.005%), for first three consecutive days. Animals were sacrificed every day during the one week period, starting with 24h after the beginning of the experiment. Liver paraffin sections were stained by haematoxillin and eosin (HE) method.
Results The pathological alterations detected in all animals ranged from diffuse degeneration to a focal necrosis of hepatocytes and massive circulatory changes. Parenchymal degeneration, diffuse oedema and hyperemia were predominant in the liver of animals sacrificed on the first three days of experiment. Dissolution of cytoplasm with nuclear pleomorphism in round or ovoid hepatocytes were seen. Thickening of the blood vessels with necrosis of endothelial cells were particularly prominent from the fourth to seventh day of experiment. The most interesting finding is the presence of massive hemorrhages with a focal mononuclear cell infiltrations. The majority of hepatocytes were irregular, with macronodular fat transformation of cytoplasm. These changes were the most intensive in male mice on the day 7 of the study.
Conclusion Multiple oral ingestion of bromadiolone induced prominent pathohistological alterations in rodent liver, especially mice.

P-568

Mobile telepathology - a new intringuing tool

S Seiwerth, L Batelja
Institute of Pathology Medical Faculty, Zagreb, Croatia

The mobility of information, patient data and images introduced by telemedicine/ telepathology systems designated a completely new viewpoint in pathology. Mostly two areas of diagnostic work are so far covered by telepathology service - second opinion/expert consultation and frozen section diagnosis. Frozen section diagnosis, is still a very important issue. Smaller hospitals, with no sufficient material for a resident pathologist often could benefit by introduction of telepathology. As in many of these hospitals surgery requiring frozen section diagnosis is not performed on a daily basis the telepathology system is not in full use, producing an unfavorable cost-benefit ratio. Also establishing a fully equipped frozen-sections lab yields additional costs and personnel cutting frozen sections only occasionally often produce suboptimal. In this the introduction of a mobile telepathology unit could solve some very important problems. The unit should include a fully equipped mobile frozen sections lab including a macro stand and a microscope with CCD TV color camera and a notebook (laptop) computer. The telepathology software used must be stabile and versatile like the Pharos/ISSA system (VAMSTECH, Croatia) used by us. By such a system and synchronization of operation schedules hospitals in a radius of up to 200 km around the referral center could be covered without exceeding standard working hours. The ISSA-server based system option alerting the consultant and referring pathologist by SMS that a consultation case is in his mailbox at the server ads additional time effectiveness.

P-569

A novel high throughput marker validation tool

J Korbelik, J Matisic, C MacAulay
B.C. Cancer Agency, Vancouver, Canada

High throughput genetic and expression screening is generating many possible diagnostic markers and therapeutic targets for wide variety of clinical conditions. The rapid validation of these markers is a challenging process. Tissue microarrays can be used for the evaluation of many of these markers. However, they have drawbacks and unresolved issues, which are result of the sampling and sectioning problems. We introduce a novel microarray technique based on cell suspensions. Multiple slides can be made, all of which are equally representative of the initial samples. A manually operated mechanical device was designed that can deposit 60 distinct spots on the glass slide. Each spot of cells deposited in this manner may correspond to unique source. Controlling the number of cells per spot their uniformity and size can be achieved by modifying the viscosity of the cell solution or precisely regulating amount of fluid deposited. A fully automated analysis of quantitatively stained microarray samples has been performed to quantify the number of cells per spot, the size of spots, and how reproducible these parameters are. Cellular material used in the experimental arrays constructed to date has been acquired from cell lines and liquid prepared lung and cervical specimens. A variety of molecular markers can be evaluated, with minimal cost. FISH probes have been tested on cytology microarrays constructed from 20 different lung cell lines. Using cell suspensions generated by the dissociation of tissue would enable the creation of more representative samples for clinical marker/target validation or evaluation.

Author Index

The numbers are the abstract numbers; oral presentations (O), poster presentations (P)

Aaltonen A, P-201
Abaza OP, O-120
Abd El All H, O-073
Abdel Aziz A, O-102
Abdel Salam S, O-102
Aboushousha T, O-098
Abraham G, O-026
Acarli K, P-514
Accinelli G, O-103
Acimovic M, P-445
Adamkov M, P-373
Adwent M, P-556
Agan M, P-390
Agapitos E, O-021
Agnantis N, P-370, P-371, P-372, P-374
Agnantis NJ, P-034, P-136, P-459
Aguilar J, P-045
Aguilera A, O-112
Agustí E, P-536
Ahmed I, P-285, P-407, P-479
Ajdinovic B, P-458
Akbari M, P-560
Akbas N, P-339
Akcah Z, P-032
Akhmedov V, P-284
Akhtar N, O-101
Akkaya H, P-390
Akmansu M, P-155
Aksoy M, P-339
Aksoy NH, P-008
Aktas A, P-274
Aktepe F, P-070
Akyildiz EÜ, P-030
Akyol G, P-155
Akyürek N, P-129, P-314
Akyýldýz EÜ, P-079
Alameda F, O-053, P-078
Albisua J, O-133
Alchinbaev M, P-423
Alderisio M, O-033
Aleksic P, P-462
Alemany I, P-379
Ales A, O-141, P-133, P-141, P-142
Aletra C, P-003
Alexa A, P-427
Alexeev B, P-452
Alfaro L, P-064
Aliev B, O-097
Alisir S, P-276
Allaberdiev B, P-260
Allia E, P-497
Almac A, P-177
Altini M, P-182
Alvarado-Cabrero I, P-478
Alvarez Iglesias MT, P-562
Álvarez M, P-048
Amalinei C, O-074, O-122, P-091
Amar M, P-289
Amat I, P-306, P-392
Ambalov Y, P-393
Amendoeira I, P-042
Amer A, O-102
Amoros A, P-471
Anagnostou V, O-021
Ancukiewicz M, O-096
Ander H, P-276
Andersson LC, P-337
Andjelkovic-Matic M, P-321, P-324
Andreano T, O-003
Andreeva J, P-122
Andreeva Y, P-452
Andrei F, P-044, P-385, P-403, P-484
Andrejev D, P-118
Andreu FJ, P-012, P-014, P-015
Andrew A, P-454
Androulaki A, P-381
Anestiadis V, P-523
Anestiadis VV, P-523
Anestiadis Z, P-523
Angeles-Angeles A, P-387, P-388
Angelini A, O-152, P-529, P-530
Anlauf M, O-146
Ann S, O-045
Antico F, P-090
Antonic M, P-101
Antovic A, P-528
Anttila M, P-053
Aranda I, P-065
Arapantoni-Dadioti P, P-009, P-063
Ardeleanu C, O-122, P-018, P-044, P-104, P-294, P-385, P-403, P-435, P-436, P-484, P-500
Arena V, P-341
Arici C, P-502
Arif S, P-493
Arifhanova S.I., P-476
Arima N, P-176
Ariphkhanova S, P-140
Arista-Nasr J, P-281, P-424, P-478
Arkoumani E, P-034, P-136, P-137, P-251, P-459
Arman B, P-139, P-145
Arnholdt H, O-014
Arnold R, O-146
Arns W, O-022
Arola J, P-488
Aroukatos P, P-003, P-098, P-360, P-361, P-486
Arro A, P-118
Arsenescu C, P-521
Arumi-Uria M, P-422
Asanuma H, P-171
Asimaki A, P-300
Askaa J, O-106, P-563
Aslan B, P-007
Asoglu O, P-340
Assaly N, O-098
Astarastoaie V, P-522
Atanackovic M, P-103, P-105, P-375, P-564
Athanasiou E, P-517
Autonell J, P-015
Avtandilov G, O-154
Awlakpui A, O-022
Aydemir C, P-145
Aydýn Ö, P-177
Aznar J, P-065
Azuma S, P-171
Azzoni C, P-195
Azzouzi S, P-407
Babic D, O-001, P-067, P-524
Babichenko II, O-070
Bacigalupo B, P-210
Baderca F, P-426, P-427
Badescu A, O-074
Baena Perez V, P-466
Baena V, P-033, P-421
Baeza Guixot R, P-116
Bagnoli E, P-304
Bai M, P-370, P-371, P-372, P-374
Baik JH, P-037
Baithun S, P-451
Bajic R, P-222
Bajo MA, O-112
Baker J, O-156
Bal N, P-226
Balaban N, P-534
Balagué O, P-012, P-014, P-102
Balagueró-Lladó L, P-083
Balan G, O-109
Balan R, O-074, P-091
Balasch J, P-071
Balcerczak E, P-446
Balcý C, P-475
Baletic N, O-052
Balint N, P-151
Ballestín C, O-053
Bamba M, P-292
Bamberger A, P-007
Banev S, P-125, P-359, P-439
Baquera J, P-279
Barakauskiene A, P-410
Baranyay F, O-150
Barbagli L, P-552
Barbanis S, P-235, P-368, P-517
Barbatis C, P-293
Bardan R, P-434
Barna G, P-350
Baró T, P-033, P-078, P-421
Baron L, O-085
Baroni CD, P-126, P-127
Barranco C, P-256
Barreiro E, P-420
Barresi G, P-250, P-335
Barresi V, P-250
Bartolazzi A, P-496
Bartolommei S, P-389, P-552
Bartoloni G, P-537
Baruzzi G, P-025
Basaran M, P-113
Baselga J, P-214
Basheska N, P-066, P-068,

P-069, P-072
Basile G, O-078, P-090
Basso C, P-532, P-533
Basta-Jovanovic G, P-380, P-548, P-549
Batelja L, P-112, P-173, P-208, P-568
Batinac T, P-246, P-257
Batinic D, P-264, P-265
Batistatou A, P-34, P-251, P-371
Baumann M, P-384
Baumforth K, P-199, P-200
Bavcar-Vodovnik T, P-141
Bazowski P, P-232
Beardo P, P-450
Beatty B, P-005
Becherini F, P-241
Becker A, O-153
Becker I, P-292
Becker KF, P-292
Bedrossian C, P-075
Beham-Schmid C, O-089
Behrem S, P-087
Bekoz H, P-357
Belicza M, O-083, P-433, P-449
Bella M, P-487
Bellan C, P-389
Bellefqih S, P-228
Bellido C, P-562
Bellone S, O-117
Beloqui R, P-306, P-392
Belovejdov V, P-429
Beltotti P, O-085
Benedik Dolnicar M, P-553
Benes V, P-224
Berczi L, O-114
Berdan G, P-294, P-435, P-436
Berdnickovich EY, O-144
Bergant D, P-215
Bergs JWJ, O-090
Berisavac I, P-227
Bernabé F, P-128
Bernasconi B, P-059
Berndt A, O-046, O-091, P-193
Berner A, O-066
Bertaso M, O-080
Bertrand JC, O-042
Bethlen K, O-150
Betova T, P-020
Betta PG, P-123
Biedermann K, P-192, P-513
Bielecki T, P-557
Bierzynska-Macyszyn G, P-209
Bierzynska-Macyszyn G, P-232
Bilalovic N, O-092, O-093, O-123
Bild E, O-060
Bilezikçi B, P-274
Bilgic B, P-113
Bisconti M, P-144
Bittenglová R, P-132
Bizjak Mali L, P-402
Bjelovic M, P-328, P-329, P-330
Blagaic A, P-208
Blanch L, P-128
Blanco MJ, P-154
Blanes A, O-010, P-331, P-493
Blaschke S, O-020
Blazanovic A, P-049
Blazicevic V, P-050, P-148, P-283, P-542
Blöndal H, P-239
Boceska Z, P-318
Bodlovic K, P-161, P-507, P-508
Boffa GM, P-529
Bogdan F, P-464
Bogdanovic A, P-327
Bogdanovic Z, P-375
Bogoeva B, P-253, P-262, P-439
Boiangiu I, P-104
Bojadjieva S, P-131
Bojanic N, P-445
Bojovic S, P-161
Bokonjic D, P-567
Bokun R, P-516
Bolat F, P-108, P-512
Bolat FA, P-303
Boldrini M, P-241
Boldrini R, O-003
Boletis I, P-263
Boluda S, P-046, P-078, P-420, P-466
Bonadonna L, P-144
Bonetti F, O-080
Bongiovanni M, P-195, P-498
Boni K, P-515
Bonikos D, P-098, P-288
Bonikos DS, P-360, P-361
Bonk U, P-197
Boon M, P-188
Bordi C, P-195
Boricic I, P-249, P-380
Borobio E, P-306
Bortoli A, O-117
Borza C, P-521, P-522
Boscaino A, O-113
Bosco S, O-003
Bot FJ, O-090
Botoca M, P-434
Bottarelli L, P-195
Botticelli AR, P-428
Botticelli L, P-428
Boucek P, P-270
Bouchal J, P-199, P-200
Boudová L, P-325
Boudova L, P-378
Bouhajeb Y, O-133
Boveri E, O-094, P-377
Bozic V, P-489
Bozzalla F, P-496
Braaten K, O-096
Bracko M, O-059
Brajuskovic G, O-126, P-110, P-327, P-347, P-458, P-462
Branca M, O-033, O-072
Brankovic S, O-036
Brasanac D, P-249, P-489, 5, P-48, P-549
Brdar R, P-101
Breberina M, P-024
Bresjanac M, O-135
Breuer J, P-451
Brocic M, P-183
Bruckner M, P-031
Brundage W, P-167
Brunelli M, O-080
Brunner AE, O-081
Bubalo J, O-052
Buchulaeva N, O-009
Buck C, P-212
Buck CR, P-406
Bucuras V, P-434
Budakov P, O-095
Budisca O, P-149
Bulog B, P-402
Bulun A, O-007
Bumbasirevic V, P-559
Bumber Z, P-173
Bunjevacki G, P-549
Buono M, O-117
Buonocore G, P-552
Bura M, P-173
Burazor I, P-531
Bures M, P-056
Burkadze G, P-061
Bussolati G, O-103, P-498
Butcovan D, P-521, P-522
Butruk E, O-108
Butur G, P-385, P-403, P-500
Caballero E, P-271
Caban L, P-385, P-386
Cabezuelo MA, P-012, P-014, P-128
Cabra B, O-010, P-331
Çadlar M, O-007
Cafici A, P-088
Cakir M, P-502
Calabrese F, P-529, P-530
Calarco G, P-135
Calay Z, P-030, P-079
Campo E, P-320, P-365, P-366
Campr V, P-353
Canessa PA, P-210
Cangir A, P-138
Cap J, P-491
Capeáns C, P-154
Capella C, P-059, P-304, P-483
Capper J, O-045
Carafa E, O-113
Carasevici E, O-060
Carda-Batalla C, P-111
Cardesa A, P-071, P-320
Carles J, P-466
Carletti AM, P-210
Carlucci M, P-181
Carney A, P-537
Carrato A, P-471
Carreras J, P-450
Carreras R, P-078
Carreras-Martínez M, P-083
Carturan E, P-529, P-530
Caruso G, P-535
Caruso R, P-335
Caruso RA, O-078
Carvalho R, O-107, P-311
Carvalho S, P-042
Casado E, P-206
Casamitjana R, P-071
Casar Borota O, P-222
Caselitz J, P-197
Caserman S, P-215
Caspers E, O-107
Castagna M, P-241
Castaldini L, O-145
Castells A, P-320
Castillo M, P-450
Castri F, P-341
Catalano E, P-352
Catasús L, P-206
Cathomas G, P-384
Cattani MG, P-025

Cavallari V, O-078
Cavic M, P-060
Cavone D, P-143, P-144
Ceausu M, P-044, P-385
Cekic S, O-036
Cemerikic-Martinovic V, P-375
Cerar A, O-108, P-218
Cerovic S, O-126, P-110, P-327, P-347, P-458, P-462
Cerrato M, P-497
Cerutti R, P-304, P-483
Cesarano A, O-085
Cevikbas U, P-499
Chadimova M, P-275
Chaldakov G, P-527
Chang AR, O-130
Chapman AD, P-121
Charpentier S, P-029
Chaturved M, P-416
Chaves MA, P-045
Chemeris G, P-097
Chen JT, P-120
Cheng YW, P-120
Chenoweth D, O-106
Chiaravalli AM, P-304
Chilosi M, O-080
Chiriva-Internati M, O-125, O-134
Chlumská A, P-325
Chmielik E, P-505, P-506
Chong CM, O-130
Chrestian MA, O-049, O-050
Christiansen P, P-002
Chu PH, P-305, P-526
Chudácek Z, P-132
Chudy D, P-233
Cicona F, P-128
Cieslik T, P-556, P-557
Cieslik-Bielecka A, P-557
Cimerman N, P-119
Cingil H, P-254
Ciocci L, P-126, P-127
Cipriani T, P-181
Ciric M, O-036
Ciric S, O-099
Ciubotaru V, P-500
Ciucci A, O-151
Ciuffreda L, P-497
Cizman B, O-030
Clément S, O-152
Clerico A, O-003
Cocchi R, O-012
Codorean E, P-500
Coer A, O-104, P-404
Coleman H, P-175, P-182
Coleman N, P-121, P-229
Colic M, P-174
Colita A, P-386
Collina G, O-124
Collins P, P-229
Colomer D, P-365, P-366
Colomo L, P-365, P-366
Comanescu V, P-044, P-464
Combalia N, P-487
Concheiro L, P-562
Conde E, P-379
Conde Sanchez JM, P-266
Condom-Mundó E, P-083, P-463, P-467
Cook MG, O-041
Cooper K, P-00 5, P-167
Cör A, O-056
Corbacho C, P-473
Cordoba A, P-306
Córdoba A, P-392
Coric M, P-112, P-173, P-264, P-265
Corominas JM, P-033, P-046, P-421, P-422
Cosic-Micev M, P-328, P-329, P-330
Costache M, P-252
Cotutiu C, O-074, P-091
Couvaris C, P-442, P-443
Cozma LG, O-060
Craiu M, P-543
Crebassa B, P-029
Creus M, P-071
Crillesen B, O-106, P-563
Crosato M, P-529
Csendes G, O-037
Csernak E, P-356
Cucchi MC, P-025
Culubret M, P-036
Cupic H, P-449
Curik R, P-316
Cuvelier C, P-207
Cuzic S, P-264, P-265, P-268
Cvetkovic D, P-225, P-227, P-380
Cvetkovic Dozic D, O-131
Cvetkovski P, P-278, P-359, P-546
Cyrille Feray F, O-018
Czerwenka K, P-06, P-054
Dabek A, P-342, P-343
Dabrowka K, P-168, P-395
Dabrowski JR, P-556
D'Adda T, P-195
Dahse R, O-091, P-193
Dainese E, P-059
Damjanovski G, P-364
Dan M, P-294
Danailova P, P-220
Danciu M, O-109, P-317
Dandachi N, P-192
Dandash K, O-073
Danilova T, P-452
Davidson B, O-066, P-075
De Falco G, P-389
De Felice C, P-552
De Hertogh G, O-105, P-295
de la Cruz C, P-040
de la Torre J, P-093, P-214
De las Morenas A, P-448
De llano P, P-306
De Leval L, O-096
De Miguel C, P-504
De Rosa G, O-054
de Torres I, P-214
De Vos M, P-207
de Vries M, P-188
de Waal RMW, O-119
Decker T, O-067
Declich P, O-117
del Peso G, O-112
Delaney T, O-096
Delektorskaya V, P-302
Dema A, P-296, P-301, P-434
Demetter P, P-207
Demirhan B, P-076, P-272, P-273, P-274, P-299, P-457
Demiryont M, P-113, P-340
Demoura S, O-138
Dengizmen A, P-475
Denguine V, O-138
Denk H, O-016, P-082, P-396, P-397, P-406
Denkert C, O-069
Depompa R, P-496
Derchain S, O-072
Dertsiz L, P-130
Devlieger H, O-105
Di Blasi A, O-113
Di Napoli A, P-441
Di Palma S, O-041
Di Tommaso L, O-124, O-145
Di Vizio D, O-054, O-113
Diaconu C, O-060
Díaz E, P-256, P-345, P-420, P-421, P-466
Diaz-Cano SJ, O-010, P-331, P-493
Diczhazy C, O-114
Didier S, O-018
Dienes HP, O-022, O-027
Dietel M, O-069, P-062
Dietze O, P-192, P-456
Dievan Beigi A, P-326
Diez M, P-344
Diklic A, P-489
Dikov D, P-051, P-429
Dilek FH, P-070
Dimitrijevic J, O-126, P-174, P-183, P-184, P-327, P-347, P-458, P-462, P-566, P-567
Dimitrijevic O, O-036
Dimou S, P-370
Dimov D, O-071, O-140, P-114, P-369, P-409
Dimov I, P-114
Dinares C, P-012, P-014
Dincol G, P-390
Dinges HP, O-061
Dioguardi N, O-125, O-134
Dionyssopoulou E, P-510
Dirim A, P-457
Dirnhofer S, O-088
Dittberner T, O-118
Dizbay Sak S, P-138, P-494
Dizdaroglu F, P-339, P-340, P-499, P-514
Djokic M, P-445
Djordjevic B, O-006, O-071, O-140, P-310, P-472, P-509
Djordjevic N, P-248
Djukic M, P-174, P-534
Djurdjevic N, P-333, P-336
Djuricic B, P-559
Djuricic S, P-549
Dmitrikova O, O-005
Dmitrovic B, P-027
Dobrea C, P-044, P-385, P-386, P-403, P-484
Dobrescu G, O-060, O-122
Dobric S, P-567
Dobrosz Z, P-021
Dobruna-Manxhuka S, P-492
Dodan M, P-155
Dogan O, P-390
Doganci T, P-400
Dokov V, P-230
Dokov W, P-230
Dolenc-Groselj L, P-236

Dolenc-Strazar Z, P-539
Dolensek M, P-141
Dominici C, O-003
Dominique F, O-018
Donadello N, P-059
Donat D, O-095
Doran F, P-398
Dordevic G, P-043, P-267, P-465
Dotlic S, P-049
Doudkine A, O-034
Doukas M, P-372
Dozic B, O-131, P-225
Dozic S, O-008, O-131, P-225
Dragojevic-Simic V, P-567
Dralle H, P-485
Drandarska I, P-319
Dranitsyna SM, O-070
Dreyer L, P-175
Droz D, O-024
Drozdzowska B, P-555
Druga R, P-224
Duchini G, O-113
Dudin AM, O-101
Dudu C, P-139
Duganovska S, P-318, P-359, P-546
Duletic-Nacinovic A, P-362
Durán MC, P-245
Dursun A, P-314
Dziambor A, P-168, P-395
Dziegiel P, P-047, P-100, P-213
Dzikova S, O-019
Eble JN, O-080
Ectors N, P-295
Eferl R, O-035
Efremov D, P-204
Efstratiou I, P-235, P-517
Eftychiadis C, P-166, P-263, P-381, P-442, P-444
Ehrmann J, O-013
Ejersbo D, P-073
El Attar H, P-285, P-407, P-479
El Baz A, P-425
EL Baz H, O-079, P-425
El Moufty M, O-102
Eller J, P-277
El-Ray A, O-098
Enache SD, P-414, P-464
Endoh M, P-040, P-401
Ensari A, O-111, P-081
Ensinger C, O-081, O-147, P-501
Ercin C, P-177
Erdei E, P-438
Erden E, P-234, P-400, P-494
Erdodan N, P-475
Erdogan B, P-226
Erdogan Cetin S, P-156
Erdogan G, P-057, P-058
Erdogan N, P-084
Erdogan S, P-226, P-453, P-550
Ergin M, P-108, P-550
Ergun D, P-081
Erhan Y, P-041
Eri Ä, P-124
Eri Z, P-158, P-327
Eriksen H, P-520
Erkus M, P-041
Erman T, P-226
Ersev A, P-139, P-145, P-146
Ersoz C, P-453, P-512
Erzen J, O-034, O-141, P-141
Erzen M, O-033, O-072, P-060
Español I, P-255, P-474
Espersen C, P-563
Esquius J, P-015
Eubranic A, P-308
Eusebi V, O-145
Fabregues F, P-071
Facco C, P-059
Failing K, O-118
Fais F, P-210
Fakan F, P-378
Falduto M, P-135
Fallah N, P-326, P-455
Farid P, O-057
Farida E, P-479
Farzadi L, O-076
Fassina A, P-077, P-415
Favia GF, P-181
Fedele F, P-250
Fedeli F, P-210
Feltri M, P-304
Fenger C, P-334
Fenic I, O-118
Ferguson-Smith M, P-229
Ferlan-Marolt V, O-104, P-402, P-404
Ferluga D, O-027, O-028, O-029, P-216, P-240
Fernandez F, O-053
Fernández S, P-012, P-014, P-015
Fernández V, P-473
Fernandez-Diez J, P-478
Ferran M, P-271
Ferrer B, P-071
Ferrer L, P-046, P-421, P-471
Ferrer MD, P-420
Ferro P, P-210
Feurle GE, O-146
Ficarra V, O-080
Fickert P, P-397
Fidler C, P-287
Fiegler-Mecik H, P-180
Fila A, P-490
Filho O, O-033, O-072
Filipi N, P-092
Filipovic M, O-036
Filosso P, P-498
Finn S, P-179
Fischer C, P-411
Fischer-Colbrie R, P-501
Flavin R, P-408
Fleischmann A, O-035
Fleming A, P-165
Flig K, P-482
Florenes VA, P-075
Flores-Morales A, P-201
Florholmen J, P-222
Florl A, O-116
Foarfa C, P-464
Foca E, P-538
Fokter SK, P-503
Foretova L, P-316
Foroutan SK, P-455
Forsyth RG, O-039
Forteza Vila J, P-154, P-245
Foschini MP, O-012, O-145
Foster CS, P-432
Fotiadou P, P-510
Fouret P, O-042
Fraggetta F, P-088
Franceschini B, O-125, O-134
Francesconi A, O-151, O-152
Franco E, P-463
Frank G, P-122
Freire R, P-093
Frezza GP, O-012
Fricska AN, P-277
Fries JWU, O-022, O-027
Frkovic-Grazio S, O-059, O-065, P-518
Froufe A, P-064
Fuchsbichler A, P-397
Fuckar D, P-026, P-257
Fukushima S, O-084
Fulford LG, P-028, P-029, P-205
Fulforf LG,
Furlan D, P-304, P-483
Fürstenberg A, O-069
Fusté P, P-078
Fyfe N, P-121
Gabbert H, O-116
Gabbiani G, O-152
Gabriel A, P-168, P-395
Gaetani P, O-134
Gaiba A, O-012
Gaire KM, O-004
Gajanin R, P-124, P-158
Gajanin V, P-124, P-158
Gajdarski R, P-117
Gakiopoulou H, O-063, P-010, P-013, P-263, P-442, P-443, P-444
Galani V, P-370, P-371, P-372, P-374
Gale N, O-055, O-056, P-186, P-187
Gallardo F, P-256
Galle J, P-191, P-414
Galli V, O-054
Gamallo C, O-112
Ganz F, P-077
Garcia A, P-093
Garcia del Muro X, P-463
Garcia P, P-033
Garcia R, P-471
Garcia-Ramos G, P-519
Garipidou V, P-348
Garner D, O-034
Garrido M, P-071, P-365
Gatalica Z, O-058
Gazic B, P-236, P-511
Gea J, P-420
Gebarowska E, P-482
Geboes K, O-105, P-295
Geddert H, O-116
Genasetti A, P-483
Genc Y, P-400
Gentile M, P-144
Georgescu G, P-521
Georgiev T, P-117
Georgievski B, P-359
Germa-Lluch JR, P-463
Gersak B, P-539
Ghaffari Novin M, O-076
Ghasemzadeh A, O-076
Ghemigean M, P-484
Ghenev P, P-230, P-527
Ghevondyan T, O-154
Ghilusi M, P-414, P-464

Giakoustidis D, P-085
Gianelli U, P-377
Giannini E, O-117
Giannopoulos A, P-442, P-443, P-444
Giannopoulou I, O-063, P-010, P-013, P-442, P-443, P-444
Giardina C, P-143, P-181
Giatromanolaki A, O-075
Giebel J, O-118
Gil A, P-093
Giménez A, P-045
Giménez G, P-487
Gimm O, P-485
Giordano A, P-389
Giromella A, P-241
Giuffre G, P-250
Givalos N, O-063
Gladskikh O, P-452
Glavac D, P-187, P-215, P-216, P-217, P-218
Gligorijevic J, O-099, P-114, P-310, P-324, P-409
Glogowska J, P-209
Glumac S, P-524, P-548
Goel A, P-416
Goheen M, P-418
Gökdemir A, P-512
Gökhan GA, P-231, P-238, P-261
Gol IH, P-547
Goldmann T, O-136, P-191, P-197, P-414
Goldstein J, P-096
Gołka D, P-021
Golouh R, O-092, O-093, O-123
Golubovic A, P-024
Gombas P, O-037
Gómez ML, P-392
Gomez-Dorronsoro ML, P-306
Gonlusen G, P-108, P-453, P-550
Gonzalez MJ, P-467
Gonzalez U, P-255
Gonzalez-Peramato P, O-112
Goraj-Zajac A, P-505
Gorbatcheva Y, O-009
Gordillo-Chaves J, P-202, P-203
Goring S, P-133
Gorji N, P-210
Gorjup V, O-028
Görür S, P-274
Goussia A, P-136, P-137
Goutzamanis G, P-510
Gozzini C, O-117
Graf AH, P-192
Gramada E, P-018, P-104
Grasser F, O-128
Grazi S, O-065
Grbas H, P-308
Grcevska L, O-019, P-262
Greene L, P-167
Grepi K, P-370, P-372
Gribabis DA, P-381
Griffioen AW, O-090
Grigoriu C, P-522
Grintsov GA, O-101
Grizzi F, O-125, O-134
Grkovic L, P-264, P-265
Grncharovska Z, P-072
Groisman G, P-289
Grosso M, P-135, P-250, P-335
Grove A, P-074
Gruber F, P-246
Gruia AM, P-317
Guduric B, P-024
Guelly C, O-089
Guerao R, P-045
Guettier C, O-018
Guillou L, O-086
Guinea J, P-473
Guldberg P, P-198
Gulkesen H, P-057
Gulkesen KH, P-357
Gulluoglu M, P-499
Gulluoglu MG, P-134, P-514
Gülly C, P-406
Gülmez H, P-130
Gumprich T, O-143
Gumurdulu Y, P-303
Gundorova LV, P-477
Günel N, P-314
Güney K, P-156
Gurbuz YS, P-177
Gurer IE, P-231, P-238
Gürsoy M, P-299
Guski H, O-069, O-0154
Guthoff R, P-411
Guymar S, O-024
Haas CJ, O-014
Habek D, P-050
Haberal AN, P-076, P-299
Haberal M, P-272, P-273, P-274
Hadjileontis C, P-368
Hadravská S, P-325
Hadzi-Dokic J, P-445
Hadzi-Nicheva B, P-072
Haedicke W, P-212
Hagi-Pecova L, P-358, P-359
Haglund C, P-488
Hairullov AS, P-258
Haitzmann G, P-513
Halalau F, P-044, P-385
Halevi A, P-332
Hammam O, O-079, P-425, P-561
Hamscher G, O-146
Handa M, P-495
Handra-Luca A, O-042
Hansen JW, P-563
Hansen TP, P-334
Harada H, P-176
Harris Lee N, O-096
Hartschuh W, O-146
Hasakiolis P, P-460
Hasan M, P-026
Hasegawa T, P-099
Hattori T, P-292, P-323
Hauptmann S, O-069
Hauser-Kronberger C, P-192, P-456, P-513
Hauss J, O-100
Hauw JJ, P-228
Havel D, P-132
Havelka M, P-489, P-507, P-508
Havrdova T, P-270
Hazar V, P-231
Hazar Ý, P-475
Heffron C, P-089
Heikinheimo K, P-151
Heikkilä P, P-488
Heinitz C, O-115
Heinz B, P-211
Heiskala K, P-337
Heiskala M, P-337
Helenius H, P-035
Henriques De Gouveia R, O-153
Heras M, P-536
Hermann G, P-00 1, P-332
Hermonat PL, O-125
Hernández JE, P-430
Hertel K, O-091
Herva R, P-541
Herz E, P-411
Hes O, P-437
Hiden M, P-082
Hinze R, P-485
Hirose T, P-099
Hirsimäki P, P-201
Hitt R, O-053
Hladikova M, P-275
Hlobilkova A, P-198
Hlupic L, O-001, P-067
Ho J, P-190
Ho WL, P-120
Hoefler H, O-011, P-292
Hoelund B, P-073
Höfler G, O-061, O-089
Holck PP, P-002
Holck S, P-00 2, P-280
Holm R, O-015
Holzhausen HJ, P-485
Homiacov AE, P-258
Honma K, O-139
Honsova E, P-270
Hörkkö T, P-298
Horvath E, P-004
Hostalet F, P-430
Hotchkiss JR, P-128
Hoxha F, P-492
Hrgovic Z, P-283
Hrzenjak A, P-082
Hsu HC, P-259
Hsueh C, P-163
Huber M, P-095
Hudelist G, P-06, P-054
Huertas Valero EM, P-116
Hutarew G, P-456
Hvala A, P-216
Hytiroglou P, P-309
Iakovidou I, P-063, P-157
Iatrou C, P-263
Ibraeva A, P-423
Ichihashi R, P-351
Ichimura K, P-229
Ieni A, O-078, P-335
Igdem A, P-084
Iglesias C, P-320
Iglesias Coma M, P-345
Iglesias M, P-033, P-046, P-078, P-421, P-422
Ikeda T, P-169
Ilic G, P-528
Ilic I, P-112, P-173
Ilic R, O-062
Ilic S, P-110, P-183, P-185, P-248
Ilievska B, P-125
Ilievski B, P-439, P-546
Ilvan S, P-030, P-079
Illyes G, P-277
Immonen-Räihä P, P-035
Incardona P, O-094, P-377, P-428
Inferrera C, O-078
Insabato L, O-054, O-113

Ioachim D, P-484
Iofciulescu A, P-386
Ionescu M, P-484
Ionica E, P-055, P-252, P-431
Iordachescu M, P-543
Iordanidis F, P-309
Iosif C, P-044, P-385, P-386, P-484
Iosif CI, P-403
Isaksen V, P-222
Ishibashi H, P-495
Ishida K, P-401
Iskender E, O-116
Ito M, P-351
Ivan L, O-109
Ivancevic S, P-162
Ivanov A, P-452
Ivanova I, P-399
Ivanovic M, P-448
Iványi B, O-026, P-277
Izycka-Swieszewska E, P-242, P-290, P-291
Jacevic V, P-110, P-566, P-567
Jacimovic V, P-174
Jahn R, P-080
Jakovljevic B, O-052
Jalali Nadoushan MR, P-326, P-455, P-461
Jancar M, P-142
Jancic S, P-333, P-336
Janczewska-Kazek E, P-168, P-395
Janevska V, P-107, P-204, P-278, P-315, P-359
Janicic D, P-158
Jankovic R, P-507
Jasic M, P-308
Jaskiewicz K, P-242, P-290, P-291, P-367
Jauhola R, P-541
Jedrzejczyk M, P-554
Jee KJ, P-151
Jelakovic B, P-268
Jelic K, P-566, P-567
Jepsen B, P-563
Jernvall P, P-298
Jeruc J, O-027, P-240
Jichlinski P, O-086
Jiménez Sánchez A, P-116
Jimenez-Almodovar M, P-202
Jimenez-Heffernan J, O-112
Jimenez-Martin JJ, O-010, P-331
Jimeno M, P-078, P-256
Jimeno Ramiro M, P-345
Jinga V, P-435
Jochum W, O-035
Jochymski C, P-342, P-343
Joksimovic C, P-404
Joksimovic M, P-225
Jonjic N, P-026, P-043, P-147, P-246, P-257, P-267, P-308, P-362
Joo JE, P-037
Jörg N, O-011
Jovanovic G, P-160
Jovanovic J, P-534
Jovanovic R, P-204, P-315, P-364
Jovic M, P-174
Jovic N, P-183
Jovicic M, P-160
Jovicic Milentijevic M, O-062
Juha O, P-151
Jukic S, O-001, P-067
Jung J, P-00 4, P-149
Jung SM, P-163, P-305, P-526
Junker K, O-143
Junttila O, P-297
Jurado I, P-036
Jurcic V, O-029
Juric G, P-233
Jurisic V, O-052
Kachko L, P-096
Kaczmarek E, O-025
Kadian H, P-319
Kaisaridou D, P-085
Kajo K, P-338
Kaku T, P-169, P-171
Kakudo K, P-019, P-022
Kalaitzi M, P-346
Kalan G, P-553
Kale G, P-547
Kale N, P-547
Kalekou C, P-300
Kalinova M, P-349
Kalita B, P-545, P-555
Kalofonos H, P-288
Kalogeropoulou C, P-288
Kaloutsi V, P-368
Kämäräinen M, P-337
Kamaras V, O-037
Kamenova M, P-220
Kamina S, P-371, P-374, P-459
Kanavaros P, P-370, P-371, P-372, P-374
Kanchev E, P-031
Kang DW, P-037
Kangas L, P-201
Kanjuh V, O-149
Kansu A, P-400
Kaplan-Pavlovcic S, O-029
Kapran Y, P-339, P-340, P-499, P-514
Kapranou A, O-063, P-010, P-444
Kapucuodlu N, P-070
Karadzic R, P-528, P-531
Karagas M, P-454
Karakaya S, P-130, P-156, P-357
Karampola M, P-157
Karandrea D, O-021
Karasavidou F, O-087
Karaveli S, P-008, P-057, P-058
Karavias D, P-382
Karayannopoulou G, P-300
Karbova E, P-031
Kardamakis D, P-288
Karpuzoglu G, P-261, P-357, P-502
Kartalis G, O-075
Karttunen TJ, P-297, P-298
Kashkin K, P-189
Kasznica J, P-540
Kaszuba M, P-554
Katic K, O-099, O-110, P-114, P-321, P-323, P-324
Katic V, O-099, O-110, P-310, P-321, P-322, P-323, P-324, P-369, P-472, P-528, P-531
Katodritou E, P-368
Katsiki E, P-382
Katsos I, P-346
Kauhava L, P-035
Kautzner J, O-148
Kavantzas N, P-166, P-381
Kayaselcuk F, P-011, P-226, P-303
Kaygusuz G, O-111, P-138, P-494
Kaynak Aksoy P, P-274
Kayse K, O-136
Kayser G, O-136
Ke Y, P-432
Kehaya T, P-300
Keil E, O-067
Keles M, P-145
Kelly G, P-387
Kelsey K, P-454
Kemeny E, O-026, P-277
Kemp R, O-141
Keramopoulos A, O-063, P-010, P-013
Kërliu A, P-492
Kern I, P-119
Kerr KM, P-121
Kesic L, O-062, P-160
Kettritz U, O-067
Khabiri E, P-536
Khafagy N, P-247
Khaki A, P-405
Khaki AA, P-405
Khatsko VV, O-101
Khder S, P-317
Khodjaev S, O-097
Kholová I, O-148
Kiasov AP, P-258
Kiel S, O-116
Kiggundu E, O-096
Kilibarda V, P-566
Kilic D, P-138
Kilicarslan AB, P-502, P-357
Kilicaslan I, P-276, P-340
Kim DH, P-037
Kim EK, P-037
Kim JH, P-037
Kim JM, P-376
Kim KH, P-037
King G, P-121
Kiral H, P-139
Kirichenko Y, P-393
Kirimker EO, O-111
Kirisoglu C, P-129
Kitamura K, P-351
Kittas C, O-021
Klatt T, O-020
Klein G, O-020
Kleina R, P-307
Klem I, P-124, P-158, P-327
Klemi P, P-035
Klimkowska M, P-242, P-290, P-291
Kloboves Prevodnik V, P-511
Kloc W, P-242
Klopcic U, O-065, O-104, P-518
Klöppel G, O-115, O-146
Kloster R, P-222
Klupińska G, P-342, P-343
Knezevic Usaj S, P-347, P-375, P-458, P-462
Knillova J, P-198, P-199, P-200
Knoll T, O-106

Ko YH, P-376
Kobos J, O-002, O-047
Kocak S, P-494
Kocmanovska-Petreska S, P-546
Kodet R, P-349, P-353
Kogan E, O-138
Kogevinas M, P-471
Kojc N, P-186
Kokai G, O-003
Köksal T, P-261
Köktürk N, P-129
Kolar Z, O-013, P-198, P-199, P-200, P-316
Kolkin YG, O-101
Kolova P, P-031
Komadina R, P-503
Komarek V, P-224
Kon S, P-169
Kondo T, P-495
Konishi Y, P-169
Kopac D, P-060
Kopper L, O-057, O-114, P-350
Korbelik J, P-569
Kordela V, P-374
Korkolopoulou P, P-381
Kornev B, O-138
Korosec B, P-215
Korporaal H, P-188
Kos M, O-001, P-067, P-409
Kosar A, P-145
Kosjerina Ostric V, O-137
Kosjerina Z, O-137
Kosjerina ZK, O-136
Kosma VM, P-053
Kosmehl H, O-046, O-091, P-193
Kostadinova S, P-253, P-315, P-546
Kostadinova-Kunovska S, P-262, P-439, P-546
Kostanyan IA, O-070
Kostic-Banovic L, P-528, P-531
Kostopoulou E, P-085, P-515
Kostov M, P-024, P-248, P-409
Kosugi H, P-351
Kotromanovic Z, P-148
Kotzev I, P-399
Koukourakis M, O-075
Koumoundourou D, P-003, P-098, P-360, P-361, P-486
Kourelis T, P-288
Koutecky J, P-056
Kouznetsova A, P-452
Kovac D, P-147, P-308
Kovac S, P-109
Kovrigina A, P-354
Kowanski M, P-470
Kozarski J, P-534
Kozelj M, P-539
Kozlovic S, P-449
Kozlowski W, P-342, P-343, P-446
Kramer G, P-188
Krasevic M, P-087, P-246, P-308
Kraszewska E, O-108
Kraus I, O-015
Kravic T, P-559
Kremmer E, O-128
Kremser ML, P-082
Kremser R, O-147
Krepelova A, P-316
Kriaka A, P-300
Krieg T, O-116
Kristek J, P-027
Kristensen G, O-015
Kristiansen G, O-069
Kronqvist P, P-035
Krsek P, P-224
Krskova L, P-349, P-353
Krstic M, O-110, O-140, P-114, P-321, P-369
Krstulja M, P-178
Kruslin B, O-083, P-433, P-449
Kruszewski W, P-290, P-291
Ku G, P-223
Kubackova K, P-353
Kubelka-Sabit K, P-066, P-068, P-069, P-072
Kubista E, P-06, P-054
Kucharzewski M, P-490
Kuchťáková P, P-373
Kukrer Ý, P-130
Kulagin RN, P-159
Kule K, P-092
Kuloglu Z, P-400
Kulova A, P-131
Künefeci G, P-299
Kuo TT, P-163
Kuopio T, P-035
Kupesiz A, P-231
Kupryjanczyk J, O-108
Kurbel S, P-027
Kursun N, P-081
Kushima R, P-323
Kushlinsky NE, P-302
Kusters B, O-119
Kut A, P-299
Kutlesic C, O-110
Kuzmanic D, P-268
Kuzmenko AE, O-101
Kuzu A, O-111
Kuzu I, O-111
Kviatkovská Z, P-373
Kyriacou K, O-077
Kyriakides T, O-077
La Rosa S, P-483
Laban A, P-380
Labropoulou C, P-382
Labropoulou EP, P-382
Labropoulou M, P-510
Lacaze T, P-228
Lackovic V, P-227
Laco J, P-491
Laforga J, P-065
Laganovic M, P-268
Lakhani SR, P-028, 029
Lale A, O-045
Lambasa S, P-170
Lamia J, P-285
Lange D, P-505, P-506
Lange H, P-485
Langer R, O-011
Lankila P, P-337
Lanschott JJB, P-311
Lapidus N, P-118
Lara MF, O-082
Larocca LM, P-341
Larrinaga B, P-306, P-392
Larsen A, O-106
Lastic-Maletic S, P-524
Latinovic L, P-158
Latinovic LJ, P-124
Latocha M, P-209
Laukens D, P-207
Lavrencak J, O-031, O-034
Lax S, O-061, P-082
Lazarevic G, P-248
Lazaris A, P-013, P-166, P-263
Lazarovici P, P-075
Lazo-Langner A, P-387, P-388
Lazzi S, P-389
Lebedinskya LA, O-120
Lebleu J, O-024
Lee H, P-120
Lee WM, P-037
Lee YS, P-526
Leenders WPJ, O-119
Leitao D, P-042
Leivo I, P-151
Lekka I, P-063
Lellei I, P-438
Leodara V, P-00 9, P-063, P-157
Leoncini L, P-389
Leontsini M, P-085
Lesot A, O-042
Lestan B, P-240
Lettini T, P-181
Libener R, P-123
Licul V, P-043, P-267
Lie AK, O-015
Lighezan R, P-427
Lilic V, P-509
Limon J, P-242
Limon-Mora M, P-203
Lindal S, P-222
Linkesch W, O-089
Lintner F, P-095
Liokumovich P, P-001
Llombart Bosch A, P-111
Lloreta J, P-033, P-046, P-345, P-421, P-422, P-466, P-471
Lloreta Trull J, P-420
Locatelli F, P-377
Lodererova A, P-270
Loeschke S, P-197
Lome Maldonado C, P-387, P-388
Loncarevic S, P-185
Longatt A, O-033, O-072
Löning T, P-007
López Cousillas A, P-504
López E, P-015
López-Aguilar J, P-128
Lopez-Beltran A, O-082
Lopez-Cabrera M, O-112
Lopez-Costea MA, P-467
Lopez-Guerrero JA, P-111
López-Guillermo A, P-365
López-Pousa A, P-206
López-Sánchez P, P-065
Lörincz A, O-072
Lountou A, P-063
Lucin K, P-362, P-465
Lucioni M, O-094, P-377
Lugli A, O-088
Lujic N, P-105
Lukin V, P-282
Lukyanova E, O-009
Luna M, O-043
Lupret V, P-219
Luque RJ, O-082
Lüttges J, O-115
Luzar B, O-055, O-104, P-404

Lyon G, P-228
Lysenko ON, O-070
Maass C, O-119
Macarulla T, P-206
MacAulay C, P-569
MacKenzie S, P-121
Macri L, O-103
Macukanovic-Golubovic L, P-369
Magán L, P-421
Maggiano N, P-341
Magrini U, P-377
Magrupov B, O-127, P-260
Magyar É, P-438
Mahler-Araujo B, P-229
Mahlobogona A, P-165
Maiorano E, P-181
Maisano D, P-090
Majo J, P-271
Mäkinen M, P-297
Mäkinen MJ, P-298
Maklakovsky M, P-332
Maksymowicz M, P-419
Malats N, P-471
Malinowska M, P-313
Mallofré C, P-450
Mañá J, P-467
Manavi M, P-06, P-054
Manda G, P-500
Manestar D, P-147
Manevska B, P-031, P-131, P-230, P-399, P-527
Manganelli R, P-415
Mankin H, O-096
Manojlovic S, P-170, P-172
Mansueto G, O-054
Manuilova T, O-138
Manxhuka-Kerliu S, P-492
Marcellini M, O-151
Marcinkute A, P-410
Marco V, P-015
Marimon J, P-536
Marin IJ, O-055
Marińoso L, P-078
Marjanovic S, P-347
Markaki S, O-063, P-010, P-013
Markovic L, P-103, P-564
Markovic-Lipkovski J, O-020
Marqués G, P-487
Martignoni G, O-080
Martine OS, O-018
Martinez B, P-281, P-424
Martínez JL, P-206
Martínez M, P-045
Martínez MA, P-379
Martínez-Benítez B, P-387, P-388
Martini M, P-341
Martins A, P-205
Martins L, O-032
Marusic P, P-224
Marzullo A, P-535
Matias-Guiu X, P-206
Matic-Glazar D, P-267
Matilla A, P-048
Matisic J, P-569
Matkovic M, P-264, P-265
Matkovic S, O-052
Matsionis A, P-194, P-393
Matsouka P, P-361
Mattioli E, P-143
Matusan K, P-026, P-465
Maurer R, O-088
Maurici D, P-487
Mavrommatis J, P-010, P-013, P-442, P-444
Maxhuni M, P-492
Maximova SM, O-005
Mayorga M, O-053
Mazur A, P-554
Mazur B, P-168
Mazurek U, P-209, P-490
Mazur-Zielińska H, P-544, P-545
McDowell HP, O-003
Mecik TJ, P-180
Meckhvarishvili N, P-061
Mederle O, P-363
Medic N, P-462
Medina-Franco H, P-279
Medley P, P-106, P-164, P-165, P-412
Meer S, P-182
Meeuwisse D, P-188
Meglic A, P-216
Mehraein F, O-076
Mehrdad H, P-00 1, P-332
Meir A, P-289
Mejia Mejia OL, P-086, P-115
Melachrinou M, P-360, P-361
Melato M, P-308
Melegh Z, P-356
Mellado B, P-450
Mellor TK, O-041
Melnic E, P-538
Melo E, P-046
Memis L, P-129
Mendes de Almeida M, O-032
Mendlovic S, P-001
Menegazzo M, P-077, P-415
Menéndez E, P-504
Merlo F, O-082
Mesko Brguljan P, P-119
Metafratzi Z, P-137
Mete O, P-340
Meulemans EV, O-090
Mezza E, O-054
Micello D, P-059
Micev M, P-328, P-329, P-330
Michael H, P-418
Michael L, O-045
Michail S, P-263
Michal M, P-378
Michej W, P-312
Michel R, O-018
Michele G, O-018
Micheli P, P-389
Micic S, P-445
Micovic V, P-257
Micu G, P-018, P-104
Mignini M, P-128
Mihai M, P-044
Mihailovic D, O-006, O-071, O-140
Mihailovici MS, O-109, P-317
Mihalik R, P-350
Mihaljevic B, P-375
Mihova A, P-094
Mihova-Pancheva A, P-319
Mijovic Z, O-006, O-071, O-140, P-310
Miklec G, P-233
Mikulic D, P-112
Mikuz G, O-080, O-081, P-433
Mikysková I, P-437
Milanesi O, P-530, P-532
Milanezi F, P-042
Milanovic N, P-174
Milde-Langosch K, P-007
Milenkovic S, P-162, P-227, P-336
Milenovic M, P-369
Milentijevic M, P-310, P-409
Miliaras D, O-087
Milicevic Z, P-227
Milne AAN, O-107, P-311
Milosevic M, P-049
Milovanovic ZA, P-567
Milovic N, P-462
Milutinovic Z, P-162
Mimidis C, O-075
Min KW, P-417, P-418
Minaii Zanghii B, P-560
Minciu R, P-426, P-427
Ming T, O-130
Miquel R, P-320, P-345
Miranda MT, O-010, P-331
Miric M, P-524
Mirowski M, P-446
Mirt M, P-208
Misa N, P-019
Mischinger HJ, P-211
Miserez M, O-105
Mitrovic M, O-110
Mocan S, O-122, P-004, P-149
Mocko M, O-095
Mofid B, P-326, P-461
Mogoanta L, P-464
Moinfar F, P-082
Molden T, O-015
Molnar B, O-037, O-038, O-114
Monsef Esfahani AR, P-023
Monteiro P, P-237
Monti M, O-125
Morack G, O-067
Moreno-Casado J, P-202, P-203
Morente V, P-365, P-366
Mori I, P-019, P-022
Moriya T, P-040, P-401
Morovic A, P-049
Morvay Z, P-277
Mottola G, O-054
Moulla A, P-085
Moustafa NM, O-102
Mouzaki A, P-360
Mrcela M, P-050, P-148, P-283, P-542
Mrhalova M, P-349, P-353
Mrowka R, P-209
Mrozkowiak A, O-064, P-016, P-039
Mukensnabl P, P-132, P-325, P-378
Müller BM, O-069
Müller C, O-020
Müller D, P-172
Müller G, O-020
Müller KM, O-142, O-143
Müller-Holzner E, O-061
Munivrana H, P-049
Munné A, P-033, P-078, P-256
Muńoz I, P-562
Murias G, P-128

Murphy N, P-089
Murray GI, P-121
Murray J, O-139
Murray P, P-199, P-200
Mustac E, P-043
Mustafa G, P-513
Mustafa L, P-513
Musti M, P-143, P-144
Musulén E, P-345, P-487
Mylene S, O-018
Nadal A, P-320
Nadal R, P-206
Nagorni A, P-310, P-322
Nagy P, P-152, P-153
Najera-Hernandez G, P-519
Nakamura Y, P-019
Nakopoulou L, O-063, P-10, P-013, P-166, P-263, P-443, P-444
Nakov E, P-117
Nalecz A, P-290, P-291
Nardi I, P-241
Nardone M, O-054
Nasierowska-Guttmejer A, P-312, P-313
Natali P, O-003
Naud P, O-072
Nazzaro P, P-143, P-144
Neagu M, P-044, P-500
Negrin R, O-156
Nenadovic M, P-549
Nenopoulou E, P-300, P-309
Neri D, O-046
Nesic M, O-036
Nesland JM, O-092, O-093, O-123, P-075
Neto A, O-043
Neumann JH, P-406
Neumeister D, P-082, P-211
Nicholls J, O-128
Nicolson MC, P-121
Nicotina PA, P-090
Niculescu-Mizil E, P-386
Nielsen B, P-017
Nielsen O, P-334
Nieslanik J, P-316
Nieto A, P-045
Nigmanov RT, P-476
Nikitaev VG, O-144
Nikolaev A, P-189
Nikolaidou A, P-085, P-460
Nikolaou E, P-293
Nikolic S, P-489
Nikolovski M, P-364
Nina H, O-011
Nistor E, P-055, P-431
Niveiro M, O-053
Nizze H, P-411
Nola M, P-049
Nonni A, P-034
Noori Mugahii H, P-560
Nordling S, P-447
Norstedt G, P-201
Noske A, P-062
Novella G, O-080
Novosel I, O-083, P-433
Novotny J, P-316
Noyan T, P-011
Nuciforo P, P-088
Nuncio J, P-279, P-281, P-424, P-478, P-519
Nursal TZ, P-011
Nwaorgu G, O-044, O-051
Nwoye JO, O-136
O Briain S, P-408
Obrist P, O-061
Occhini R, P-552
Oehri I, P-384
Offerhaus GJ, P-311
Offerhaus GJA, O-107
Ognjanovic S, P-489
Ogrezean I, P-500
Oguma M, P-040
Ogunbiyi O, O-044, O-051
Ogus M, P-502
Ohuchi T, P-169, P-171
Okcu Heper A, P-234, P-400
O'Leary J, P-089, P-179
Olert J, P-191
Oliveira e Silva A, P-042
Oliver T, P-451
Olmedilla G, P-344
Olszewski Wl, O-064, P-016, P-039
Olszewski Wo, O-064, P-016, P-039
Omar E, O-040
Ondrejovic P, P-338
Ondrik Z, O-026
Opacic A, P-024
Oprisan A, P-413
Ordi J, P-071
Orecchia S, P-123
O'Regan E, P-179
Orellana R, P-102, P-345, P-487
Orhan D, O-007, P-547
Orký A, P-139, P-145, P-146
Orlandi A, O-151, O-152
Orlandi E, P-377
Orlowska J, O-108
Orologa A, P-515
Orosz Z, O-121
Orozco-Levi M, P-420
Orsola A, P-474
Ortac F, P-081
Ortega E, P-065
Ose V, P-307
Ostroveanu D, P-386
Othman N, O-040
Ozbarlas S, P-108
Özbilim G, P-130, P-156
Ozdemir BH, P-032, P-076, P-272, P-273, P-457
Ozel E, P-357
Ozer B, P-303
Özger H, P-113
Özkan T, P-113
Öztürk C, P-129
Ozturk S, O-111, P-138, P-494
Pachlewski J, O-108
Pająk J, P-021
Pajtler M, P-283
Paker Ý, P-468
Paku S, P-350
Palacin A, P-365
Palacín A, P-366, P-450
Palas J, P-316
Palcic B, O-034, O-141, P-133
Pallarés J, P-206
Palma I, O-133
Paltsev M, P-452
Panayotopoulou E, O-063, P-010, P-013, P-443
Pancaroglu K, P-398
Pang Y, P-223
Pangalis GA, P-381
Panisic M, P-327
Panoussi E, P-368
Panzitt K, P-406
Pap R, O-026
Papachristou D, P-370, P-371, P-372, P-374, P-486
Papadaki I, P-443
Papadaki T, P-293
Papadimitriou C, P-309, P-368
Papadimitriou K, P-510
Papagianni M, P-346
Papanikolaou A, P-460
Papezova M, P-316
Papotti M, P-195, P-496, P-497, P-498, P-537
Papoudou-Bai A, P-372
Parada C, P-473
Paramonova N, O-138
Paravina M, P-369
Pardal de Oliveira F, P-237
Pardal F, O-129, P-237
Paris J, O-049, O-050
Parisi G, P-535
Park CG, P-037
Park MJ, P-037
Parmeggiani A, O-145
Parpiev Z, O-127
Parvinen I, P-035
Passetchnik D, P-440
Pasteli N, P-346
Pastori L, O-117
Patakiouta F, P-346
Patera J, P-342, P-343
Patsiaoura K, P-300, P-515
Patsouris E, P-166, P-381
Paulli M, O-094, P-377
Paunovic I, P-489
Pauser U, O-003
Pavkovic M, P-204
Pavlaki K, P-013
Pavlenko I, P-194
Pavlovcic V, P-142
Pavlovic M, O-036, P-369
Pavlovic N, P-308
Pavlovskaya AI, O-144
Pea M, O-080
Pecchioni C, P-496
Pedragosa R, P-255
Pegoraro E, P-077
Peham K, P-192, P-456, P-513
Pehrs AC, O-088
Pelosi G, P-088, P-195
Peloso N, P-077
Pennella A, P-143
Pennesi MG, O-012
Pentimella S, P-181
Perdiki M, O-063, P-010, P-381
Perevoschikov A, P-189, P-302
Pérez L, P-048
Pérez N, P-345
Perez-Campos A, O-112
Perez-Villa F, P-536
Perkovic TM, O-028
Perna C, O-112
Perner F, O-057
Perov YU, P-477
Persu S, P-435
Perunicic M, P-327, P-375
Pervana S, P-460

Pesek M, P-132
Pesko P, P-328, P-329, P-330
Pession A, O-012
Pest S, O-069
Pestereli HE, P-008, P-057, P-058, P-502
Peston D, O-045
Petcu E, P-540
Petrescu A, P-294, P-435, P-436
Petric S, P-509
Petrov S, P-159
Petrov SB, P-258
Petrovic A, P-369
Petrovic B, P-322
Petrovic D, O-095, O-155
Petrovic O, P-087
Petrovichev NN, O-144
Petrusevska G, O-019, P-125, P-204, P-262, P-315, P-358, P-359, P-364
Petsas T, P-288
Pettinato G, O-113
Peydró-Olaya A, P-111
Pichel JMG, P-202, P-203
Pickel H, O-068
Pijuan Andújar L, P-256
Pijuan L, P-033, P-046, P-256, P-420, P-421
Pileri S, O-088, P-389
Pilozzi E, P-287
Pimrova A, P-198
Pineda-Daboin K, O-043
Pińeiro A, P-154
Pinzon Bohorquez J, P-266
Pischinger K, P-06, P-054
Pisot V, P-109
Pitino A, P-428
Pizem J, O-056, P-404
Pizzi S, P-195
Plank L, P-338, P-353, P-373
Plesea IE, P-414, P-464
Plevova P, P-316
Plzak A, P-024
Podoleanu C, P-004
Poetsch M, O-118
Poffijn B, O-039
Pogacnik A, O-065, P-511
Pohar Marinsek Z, P-511
Pokieser W, P-080
Polat A, P-011
Polenakovic M, O-019
Poliaková K, P-373
Poljak M, O-055, O-104
Pollice L, P-143, P-144
Ponce-Sebastiŕ J, P-083
Ponikiewska D, P-506
Pons LE, P-012, P-014, P-015, P-102
Popescu O, P-104
Popov DA, O-144
Popova M, P-094
Popovic L, P-458, P-462, P-534
Popovic M, O-135, P-217, P-236, P-240, P-553
Popovic S, P-103, P-105
Popovic Z, P-524
Popovska S, P-020
Poppe B, O-039
Popper H, P-212
Porcellati M, O-117
Postiglione M, O-085
Potoroaca A, O-109
Povilaitite P, P-393
Prada A, O-117
Praet M, O-039
Probatova N, P-354
Proby C, P-451
Procopio A, P-135
Prodanova I, P-066, P-068, P-069, P-072
Prokop E, P-456
Prommegger R, O-147, P-501
Pronzato P, P-210
Provvedi R, P-415
Pucci A, P-537
Puchau MB, P-046
Puente D, P-471
Pueschel K, P-197
Pujol RM, P-256
Puńal-Vidal L, P-154
Puras AM, P-504
Purdie K, P-451
Pusevski A, P-253
Pylkkänen L, P-035
Quarto F, O-085
Queralt-Escarré RA, P-467
Quintanilla-Martínez L, P-387
Quintero A, O-082
Rabie M, P-561
Rabin I, P-332
Rachid K, O-018
Radeljak S, P-208
Radlowski P, P-168, P-395
Radojevic S, P-380, P-508, P-549
Radosavljevic R, P-445
Radotic-Smiljanic K, P-548
Radovanovic NN, O-155
Radovanovic Z, P-024
Radulescu D, O-074, O-122, P-00 4, P-149
Rafailidis P, P-442
Raica M, P-363, P-426, P-427
Rajkovic M, P-559
Rakar S, P-060
Ramasami S, P-121
Rambaud C, P-228
Ramírez I, P-048
Ramirez J, P-536
Ramlachan N, P-412
Ramón y Cajal S, P-093, P-214, P-473
Ramos Ńíguez JA, P-116
Ramos P, P-344
Rannem T, P-280
Rapazzotti Onelli M, P-287
Raspopovic V, P-103
Raubenheimer EJ, P-106, P-175
Ravazoula P, P-098, P-288
Raventós C, P-474
Ravnik-Glavac M, P-215, P-216
Rayon M, P-064
Razquin S, P-504
Real FX, P-471
Reed W, O-066
Refaat A, O-073
Reggiani M, O-124
Regitnig P, O-061
Reich O, O-068
Reich R, P-075
Reiner A, O-061
Reinisch G, P-095
Reis-Filho JS, P-028, P-029, P-205
Reisinge E, P-411
Reljic A, O-083
Remaut E, P-207
Repse Fokter A, P-503
Rey M, P-12, P-014, P-102, P-487
Reyes E, P-387
Reymnazarova G, O-127
Rezaei Nour T, P-455
Rhodes NP, P-432
Ribalta T, P-345
Riboni R, O-094, P-377
Ricardo S, P-042
Ricci R, P-341
Richmond J, P-005
Richter K, O-115
Rico R, P-562
Righi M, P-135
Rigol M, P-536
Rinelli A, P-341
Risberg B, O-066, P-075
Risteli J, P-520
Ristovski M, P-253, P-278, P-315
Ristovski S, P-439
Ritis C, O-075
Riva C, P-059
Rizzardi C, P-308
Roca MJ, P-064
Rodríguez Calvo M, P-562
Rodriguez y Baena R, O-134
Rodriguez-Muńoz S, P-214
Rodríguez-Peralto JL, O-053
Rodríguez-Pinilla SM, O-053
Roestenberg M, O-090
Rogatsch H, O-081, P-433
Roig I, P-015, 036
Roig Quilis I, P-036
Rojo F, P-036, P-214
Romac S, P-347
Romagosa C, P-365, P-366
Romanenko A, O-084
Romano M, P-135
Romanova E, P-393
Romero A, P-430
Romero Maturana JM, P-266
Romero PV, P-128
Romodanov S, P-221
Roncella S, P-210
Rontogianni D, P-372
Roqué M, P-536
Roselló E, P-366
Rossano C, P-441
Rossmann P, P-275
Rosta A, P-356
Roteli-Martins C, O-072
Roth T, O-022
Rotin DL, O-144
Rotman S, O-086
Rott T, O-141, P-133, P-141
Rotter A, P-109
Rovira C, P-036
Rozman B, O-027
Rubini C, P-181
Ruco L, P-287, P-441
Rudas M, O-061
Ruebner B, P-394
Rugal V, P-355
Ruhnke M, O-067

Ruiter DJ, O-119
Ruiz A, P-344
Ruiz De La Parte A, O-133
Ruiz JA, P-430
Rumboldt T, P-219
Russo R, O-113
Ryska A, P-491
Ryvnyak E, P-391
Ryvnyak V, P-391
Rzepko R, P-242, P-290, P-291
Saarikoski S, P-053
Saatçi M, P-150
Sabat D, P-180, P-469, P-544, P-545, P-554, P-555, P-556, P-557, P-565
Sachinis K, P-460
Sadeghipour Roudsari HR, P-481
Sáez A, P-012, P-014, P-015
Saguatti G, P-025
Sahan E, P-084, P-475
Sahatqiu-Meka V, P-492
Saida S, P-285, P-407, P-479
Sajin M, P-543
Sajko T, P-219
Sakamoto K, P-040, P-401
Sakari K, P-151
Sakurai T, P-019, P-022
Salamanca J, P-379
Salamon F, P-152, P-153
Salapura A, P-534
Salerno G, O-054
Salido E, P-093
Salido M, P-466
Salmenkivi K, P-488
Salobir B, P-141, P-142
Salvio M, P-123
Salwa-Zurawska W, O-025, P-100
Samardziski M, P-107
San Jose-Moreno C, P-202, P-203
Sanati S, O-058
Sánchez Cañizares P, P-116
Sánchez R, P-473
Sanchez-Carrillo JJ, O-010, P-331
Sánchez-Céspedes M, O-053
Sancho Poch F, O-053
Sandbank J, P-001, P-332
Sano T, P-099
Sanoudou D, P-229
Santos M, P-536
Sar A, P-076
Sar AN, P-457
Sarafian V, P-051
Sarani SA, O-076
Sarasa JL, O-133
Sarbia M, O-116
Sarbianova N, P-220
Sarkik B, P-041
Sasano H, P-040, P-401, P-495
Sasor A, P-446
Satoh M, P-169, P-171
Satta J, P-520
Savas A, P-234
Savelov N, P-097
Savelyev VV, P-159
Savic V, P-472
Savin M, P-548
Saydaoglu G, P-011
Scattone A, P-143, P-144, P-535
Schauer S, O-089
Scheibner K, O-091
Schillaci F, P-123
Schimmelpfennig C, O-156
Schlake G, O-142
Schledermann DE, P-073
Schmid K, O-147, P-501
Schmidt H, P-485
Schmidt M, P-280
Schminke L, O-115
Schmitt F, P-042
Schmitt FC, P-205
Schned A, P-454
Schned L, P-454
Schneider T, P-356
Schober H, P-062
Schuerfeld K, P-389
Schulz S, O-156
Schvimer M, P-001
Scollo P, P-088
Scopa C, P-003
Scopa CD, P-486
Scukanec-Spoljar M, P-264, P-265, P-268
Seada L, P-247
Sebestyén A, P-350
Seckin S, P-468
Sedlakova E, P-316
Seemanová E, O-023
Segal M, P-001
Segas J, P-166
Seilhean D, P-228
Seitaliyeva A, P-423
Seiwerth S, P-112, P-173, P-208, P-568
Selak I, O-092, O-093, O-123
Selgas R, O-112
Sen Gupta R, P-191
Seo IS, P-417, P-418
Serin E, P-303
Serio G, P-143, P-144, P-181, P-535
Serra C, P-471
Serrano S, P-033, P-046, P-078, P-256, P-420, P-421, P-422, P-466, P-471
Sers C, P-062
Sertcelik A, P-081, P-138
Sevastiadou P, P-235, P-517
Sevcíková M, P-373
Sever M, P-276
Sever-Prebilic M, P-362
Sfarti C, P-317
Shaco-Levi R, P-096
Sheaff M, P-451
Sheils O, P-179
Shenoy A, P-416
Shiels O, P-089
Shimada T, P-099
Shirinskaya N, P-284
Shmeleva A, P-221
Siatelis A, P-443
Sidira S, P-098, P-486
Sienko E, O-047
Sigstad E, O-066
Sikiric P, P-208
Sikora A, P-545, P-555
Sill H, O-089
Sillanpää S, P-053
Silva A, O-129
Silva L Costa AIFRC, P-237
Silvestris F, P-535
Simion S, P-018
Simkova E, P-275
Simó J, P-487
Simpson PT, P-205
Simsek T, P-057, P-058
Sinelnikov I, P-096
Singer C, P-06, P-054
Sinkovec J, P-060
Sintou E, P-137
Sinzidi C, P-411
Sioutopoulou D, P-286, P-348
Sivridis E, O-075
Skalova A, P-378
Skaro Milic A, P-347
Skender Gazibara M, O-008, O-131, M, P-225, P-227
Skenderi A, P-515
Skodric S, P-548, P-549
Skomedal H, O-015
Skrede M, P-075
Skuletic V, P-516
Skyrlas A, P-371, P-374
Slaby B, P-545, P-555
Slajpah M, P-216
Slavik P, P-338
Slimok M, P-545, P-555
Slowinski J, P-209, P-232, P-242
Smerkolj S, P-217
Smickova S, P-125
Smid LM, O-135
Smit Cordeiro M, O-032
Smith PH, P-432
Smyth P, P-179
Soini Y, P-520
Sok M, P-133
Sokol LA, P-338
Sokolova I, P-097
Solakoglu S, P-276
Solanes N, P-536
Sole F, P-466
Soler T, P-015
Solimani J, O-076
Solimany Rad J, P-405
Sommerer F, O-100
Sonicki Z, P-268
Sonkodi S, O-026
Sopta J, P-101, P-103, P-105, P-161, P-333, P-375, P-507, P-508, P-549, P-564
Sotirakoglou PK, P-009
Sotiropoulou G, P-009, P-157
Sotnikov D, P-282
Soukup J, P-349, P-353
Soumia Z, P-479
Soundararajan S, O-058
Soustiel J, O-132
Spagnoli LG, O-151, O-152
Spalevic L, P-369
Spasevska L, P-107, P-278, P-315, P-359, P-546
Speleman F, O-039
Spidlen V, P-132
Spinelli S, P-126, P-127
Sporis D, P-233
Srebotnik Kirbis I, O-031, P-511
Staber P, O-089

Stabile B, P-394
Staibano S, O-054
Staikov D, P-429
Stajnic M, O-095
Stajnic S, O-095
Stamenkovic B, O-110
Stan M, O-109, P-317
Stanciu A, O-122
Stanciu C, O-109
Stanescu A, P-543
Stanescu AD, P-055
Stanescu B, P-484
Staniceanu F, P-018, P-104, P-413
Stankovic T, P-087
Stankulov I, P-527
Starcevic R, P-147
Staribratova D, P-051, P-052, P-429
Starz H, O-014
Stathakis C, P-263
Stavrakis S, O-021
Stefanaki P, P-372
Stefanaki S, P-370
Stefanou D, P-034, P-136, P-137, P-251, P-459
Stefanovic D, P-184, P-185
Stefanovic E, O-149
Steidler L, P-207
Stejskal J, O-023
Stella G, P-428
Stellin G, P-532
Stepan J, P-112
Stęplewska K, P-469, P-545, P-555
Stiblar Martincic D, P-503
Stifter S, P-026, P-362
Stitic V, P-542
Stobiecka E, P-506
Stoia R, P-386
Stoica G, P-223
Stoiljkovic G, P-369
Stojanovic A, P-204, P-358, P-359, P-364
Stojanovic D, P-257
Stojanovic I, P-324
Stojanovic J, P-528
Stojiljkovic B, O-095, P-024, P-248
Stojiljkovic MP, P-566
Stojmanovska B, P-318
Stojsic Z, P-380
Stolnicu S, O-122, P-004, P-149
Stolte M, P-292
Stoppacciaro A, P-441
Stosic S, P-185
Stravodimos C, P-443, P-444
Strazisar M, P-218
Streinu-Cercel A, P-413
Strnad M, O-083
Strohmaier H, P-406
Strohmeier B, P-082
Strojan Flezar M, O-031, O-034
Stropahl G, P-411
Stumpo M, P-552
Stumptner C, P-396, P-397
Stupina E, P-244
Suárez M, P-466
Suárez Peńaranda J, P-154
Suárez Peńaranda JM, P-245, P-562
Suciu C, P-426, P-427
Sugihara H, P-292
Sugiura I, P-351
Sulc M, P-325
Sumerauer D, P-056
Sunamori M, P-495
Suriawinata A, P-394
Surowiak P, P-047, P-100, P-213
Susnik B, O-059
Sustic A, P-308
Suurmeijer AJH, O-152
Suzuki N, P-322
Suzuki S, P-495
Suzuki T, P-495
Suzuma T, P-022
Svachova M, P-198, P-199, P-200
Svec A, P-437
Svigelj V, P-236
Symeonidis A, P-361
Syminelakis S, P-137
Syrjänen K, O-033, O-072
Syrjänen S, O-072
Szczesniak-Klusek B, P-505, P-506
Szczurek Z, P-556, P-557
Szederkenyi E, P-277
Szende B, O-057, O-114
Szenohradszky P, P-277
Szentirmay Z, P-356
Szepe P, P-338, P-353
Szépe P, P-373
Szöke TS, O-136
Taban S, P-296, P-301, P-434
Tabernero J, P-214
Tachezy R, P-437
Tack J, P-295
Tagscherer A, O-037, O-038, O-114
Takeda K, P-019
Takeyama J, P-401
Talalaev A, P-282
Talan-Hranilovic J, P-219
Tammi M, P-053
Tammi R, P-053
Tanase C, P-500
Tanaskovic N, P-158
Tancioni F, O-134
Tanja R, O-027
Tannapfel A, O-048, O-100
Tarabar D, P-327
Taran K, O-002
Tardon A, P-471
Targonska IBJ, O-004
Targonski JA, O-004
Tarim A, P-011
Tasic D, P-323
Tasic N, O-149
Tasic-Dimov D, P-114, P-409
Tatic S, P-249, P-489, P-507, P-508
Tatomirovic Z, P-516
Tatsiou Z, P-286, P-348
Tatti S, O-072
Tavani E, O-117
Teixeira M, O-129, P-237
Teleman S, O-109
Ţenol C, P-146
Tepavcevic Z, P-336
Tepetes K, P-288
Tercelj M, O-141, P-133
Tercelj-Zorman M, P-141, P-142
Terracciano L, O-113
Tertytchnyi A, P-282
Terzea D, P-044, P-385, P-386, P-500
Terzea DC, P-403, P-484
Terzic T, O-131, P-380, P-508, P-549
Teslik L, P-056
Tessitore E, P-537
Thiene G, P-529, P-530, P-532, P-533
Thormodsson F, P-239
Thymara I, P-381
Tibiletti MG, P-059
Tichy M, P-224
Ticmeanu F, P-018
Timar J, O-121
Timm A, P-411
Timurtekin K, P-146
Tingby O, P-229
Tiniakos D, O-021
Todorovic V, P-328, P-329, P-330, P-380
Tolovska M, P-262, P-318, P-359
Tolparidou I, P-510
Tomas D, P-433, P-449
Tomasovic-Loncaric C, P-170, P-172
Tomaszek K, P-490
Tomaszewski JE, O-030
Tonchev A, P-527
Toner M, P-179
Topolovec Z, P-050
Torlakovic E, O-092, O-093, O-123
Tornillo L, O-113
Torroba A, P-045
Tosi P, P-389
Toth E, P-356
Toti P, P-552
Toyozumi Y, P-176
Trattner M, P-192
Trauner M, P-397
Trawale JM, O-024
Trebse R, P-109
Trias I, P-255, P-474
Trichia E, P-009
Trifan A, P-317
Trikoupi M, O-077
Triolo O, P-090
Trojan IT, O-136
Tsai CC, P-259
Tsamandas A, P-098, P-288
Tsamouri M, P-293
Tsanou E, P-370, P-371, P-374
Tsikou-Papafragou E, P-293
Tsiple I, P-523
Tsitouridis I, P-235, P-517
Tuccari G, P-250, P-335
Tucci M, P-535
Tudos R, P-391
Tudose N, P-296, P-301, P-434
Tufegdzic I, O-126
Tuganalp A, P-453
Tulassay Z, O-114
Tulic C, P-445
Tulunay EO, P-150
Tulunay Ö, P-150
Tunali N, P-550
Tuncer I, P-303
Tuominen H, P-541
Tuppurainen K, P-297
Turashvili G, P-061
Turbin D, P-189

Turcic M, O-083
Turel M, P-141, P-142
Turic B, O-141, P-133
Turkmen A, P-276
Tuzlali P, P-084
Tuzlali S, P-084
Tzaida O, P-00 9, P-063, P-157
Tzankov A, O-088
Tzartza E, P-515
Tzilves D, P-346
Tzioufa V, P-300
Ubaydullaeva V, P-525
Uçar T, P-238
Uccella S, P-483
Uccini S, O-003
Udvarhelyi N, O-121, P-356
Uglesic V, P-172
Ugur A, P-357
Uguz A, P-108, P-398, P-512, P-550
Ulrich W, P-080
Umek W, P-080
Undar L, P-357
Urban M, P-437
Urbanc T, P-119
Urbiola E, P-504
Ürek Ţ, P-146
Urist MM, P-279
Usaj Knezevic S, O-126
Usaj S, P-327
Us-Krasovec M, O-034, P-518
Utkuzov AR, P-159
Utsunomiya H, P-019
Uyar FP, P-076, P-457
Uysal V, P-276
Uyttendaele D, O-039
Vakalopoulou S, P-348
Valdés S, P-388
Valente M, P-529, P-530, P-532, P-533
Valente T, P-181
Valkovic T, P-026
Valmari P, P-541
Van Eyken P, O-105, P-295
Van Haaften C, P-188
Van Heerden W, P-175
Van Huysse JA, P-207
van Rees BP, O-107, P-311
Vancíková Z, O-023
Vandenbroucke K, P-207
Vandewalker KN, P-394
Vardar MA, P-512
Varela Durán J, P-245
Varga S, O-037
Varga V, O-038, O-114
Vartolomei C, P-484
Vasama J, P-447
Vasilescu F, P-385, P-386, P-403
Vasilev V, P-439
Vasilevska K, P-364
Vasiljevic J, P-162, P-524
Vatcheva A, P-513
Vavrusova N, O-013, P-200
Vazquez Navarrete S, P-266
Vecchini G, P-157
Vecchio FM, P-341
Vecchione A, P-441
Végso G, O-057
Veie TH, P-563
Veijola M, P-520
Velasco V, O-129, P-237
Velev M, P-094
Velickovic L, O-071, O-110, P-114, P-321, P-472, P-531
Venizelos I, P-286, P-300, P-348
Verrijp K, O-119
Verstraete K, O-039
Vervekina T, P-243
Vestergaard V, P-074
Veys EM, P-207
Vicioso L, P-048
Vidal-Bel A, P-083, P-463, P-467
Vidal-Sarró N, P-083
Vidmar S, P-133
Viglio A, O-094
Vila J, P-345, P-422
Vilagrá A, P-128
Vilallonga R, P-271
Vila-Torres J, P-551
Villari D, P-135
Virag T, O-037, O-038
Visnjic M, P-321
Vitarelli E, P-135, P-335
Vitolo D, P-126, P-127
Vizjak A, O-027, O-028, O-029, P-216, P-240
Vlodavsky E, O-132
Vodickova S, P-056
Volante M, P-496, P-497, P-498
Volavsek M, P-187
Vollmer E, O-136, P-191, P-197, P-414
Voloshchuk I, O-009
Vondrak K, O-023
Voska L, P-270
Vossen S, O-116
Voutilainen K, P-053
Vovko TD, O-135
Vozianov A, O-084
Vrabie CD, P-055, P-252, P-431
Vraspir-Porenta O, O-155
Vrettou E, P-300, P-309
Vrhnjak B, O-141
Vucic M, P-219, P-449
Vukelic-Markovic S, P-183, P-184, P-185
Vukmirovic F, P-383
Vukomanovic B, P-227, P-333, P-336, P-507, P-508
Vukosavic S, P-347
Vukotic Maletic V, P-458
Vuopala K, P-541
Vural S, P-499
Wagner E, O-035
Wagner K, P-396
Wagner T, O-014
Wainscoat JS, P-287
Waler J, P-490
Wang L, P-223
Wang X, P-019, P-022, P-223
Wasserman I, P-332
Watanabe M, P-040, P-401
Wawroschek F, O-014
Weaver D, P-005
Weber A, O-048
Weber M, O-022
Wee A, O-130
Weichert W, O-069
Weihe E, O-146
Weirich G, O-011
Welcher R, O-106
Wendelboe HG, O-106
Went P, O-088
Werner MW, O-136
Wesseling P, O-119
Wessels H, O-020
Weterman MAJ, O-107, P-311
Wichrzycka-Lancaster E, O-004
Widel M, P-209
Wiechen K, P-062
Wiedorn KH, P-191
Wilczok T, P-490
Wilk M, P-021
Winther H, O-106, P-563
Winzer KJ, O-069
Wishahi M, O-079
Wittekind C, O-048, O-100
Właszczulk P, P-021, P-232
Woenckhaus C, O-118
Wojnar A, P-047, P-100, P-213
Wojtacha M, P-232
Wozniak A, O-025, P-242
Wysocka T, P-047
Xagoraris I, P-360
Xercavins J, P-093
Xie X, P-223
Xirou P, P-235, P-346, P-517
Yamaç D, P-155, P-314
Yang M, P-040
Yashar G, P-066, P-068, P-069, P-072
Ýddem A, P-475
Yeh TS, P-305, P-526
Yildirim Kupesiz G, P-231
Yildirim S, P-011
Yilmazbayhan D, P-134, P-514
Yorganci A, P-081
Yoshimura G, P-019, P-022
Youshya S, P-451
Yu CP, P-190
Yu JC, P-190
Zabel M, P-047, P-100, P-213, P-482
Zabkowski T, P-470
Zachou K, P-510, P-515
Zachoval R, P-437
Zadravec N, O-141
Zaffe D, P-428
Zafirovski G, P-107
Zafrakas M, P-085
Zaharia B, P-464
Zahavi S, P-001
Zajęcki W, P-469, P-544, P-545, P-555, P-556
Zajratians OV, P-477
Zaki S, O-102, O-126
Zamecnik J, P-224
Zamolo G, P-246, P-257
Zanaret M, O-049, O-050
Zangh A, P-090
Zaprianov Z, P-051, P-052
Zardi L, O-046, O-091
Zarkovic K, P-233
Zatloukal K, O-016, P-082, P-211, P-212, P-396, P-397, P-406
Zauner D, O-016, O-089, P-211
Zavalishina L, P-122
Zdravkovic M, P-528
Zecca M, P-377

Zeckei J, P-554
Zeis P, P-263
Zekioglu O, P-041
Zembala-Nozynska E, P-554, P-555
Zenios A, O-077
Zeqiri F, P-492
Zergeroglu S, P-076
Zervas A, P-442, P-444
Zgajnar J, O-065
Zganec M, O-034
Zhumabayeva B, P-062
Zidan A, P-487
Zidar N, P-186
Zieliński R, P-544
Zimpfer A, O-088
Zioga A, P-251
Zioga K, P-371
Ziólkowski A, P-168, P-544, P-180, P-490
Ziparo V, P-287
Zivadinovic J, P-107
Zivadinovic R, P-509
Zivkovic R, P-160
Zivkovic S, P-472
Zivkovic V, O-062, O-071, O-099, O-140, P-310, P-322
Znaor A, O-083
Zografski G, P-066, P-068, P-069
Zoirova N, P-140
Zoletto M, P-077
Zolota V, P-288, P-360, P-361, P-382, P-486
Zolotarevski L, P-110, P-566
Zorc M, O-155
Zorc-Pleskovic R, O-155
Zorlu G, P-058
Zorludemir S, P-226
Zota I, P-538
Zubcic V, P-172
Zugun F, O-060
Zuntova A, P-056
Zupicic B, P-172
Zurac S, P-018, P-104, P-413
Zurawski J, O-025
Zweymüller K, P-095
Zwirska-Korczala K, P-490

Virchows Arch (2003) 443:490
DOI 10.1007/s00428-003-0885-0
© Springer-Verlag 2003

ANNOUNCEMENTS

13 October 2003
Continuing Medical Education

One day Multi-Disciplinary Update courses

Course fee: £95.00

For further information please contact:
Education Administrators
Nottingham International Breast Education Centre
City Hospital, Hucknall Road, Nottingham NG5 1PB
Tel.: 0115 969 1689; Fax: 0115 962 7707
E-mail: enquiries@nibec.co.uk; www.nibec.co.uk

17–19 November 2003
Multi-Disciplinary Courses on Breast Disease

Three day course. The first part is multi-disciplinary. Thereafter the different specialties meet to accommodate their own special requirements.

Course Tutors: Dr. I.O. Ellis, Dr. S.E. Pinder, Dr. A.H.S. Lee

Course fees:	NHS	£370.00
	Non-NHS	£415.00
	Overseas	£550.00

includes refreshments but not accommodation

For further information please contact:
Education Administrators
Nottingham International Breast Education Centre,
City Hospital, Hucknall Road, Nottingham NG5 1PB
Tel.: 0115 969 1689; Fax: 0115 962 7707
Email: enquiries@nibec.co.uk; www.nibec.co.uk

1–11 June 2004
International course on Laboratory Animal Science
Utrecht, The Netherlands

A two week intensive course on laboratory animal science will be organized at the Department of Laboratory Animal Science – Utrecht, The Netherlands in June 2004. This course is organized once a year since 1993.

The objective of this course is to present basic facts and principles that are essential for the humane use and care of animals and for the quality of research.

The contents of the course are in line with recommendations of the Federation of European Laboratory Animal Science Associations (FELASA) regarding the training of the young scientist whose research involves the use of vertebrate animals.

The course may also be of interest for those who intend to set up a similar course at their location. For this purpose, during the course the acquisition of teaching materials can be discussed with the course committee.

For information and application forms please contact:
Prof. L.F.M. van Zutphen, PhD or
Mr. Stephan van Meulebrouck, MA
Department of Laboratory Animal Science
Faculty of Veterinary Medicine
P.O. Box 80.166
3508 TD Utrecht
The Netherlands
Tel.: ++31-30-2532033
Fax: ++31-30-2537997
E-mail: pdk@las.vet.uu.nl
Internet: http://las.vet.uu.nl (click on "Education and Training")

11–15 February 2004
Conference on "Clinical Oncology 2004/2005"

In cooperation with the National Oncology Societies, the Tumorzentrum Düsseldorf (Director: Prof. Dr. med. R. Haas) will be holding a five-day conference. The results will be published in a symposium volume for the conference. More than 800 experts, mainly from the field of oncology, are expected to attend. The workshop will be held in the MNR Clinic, Lecture Hall 13A. The following general topics have been scheduled:

Wednesday:
Pharynx, larynx, CUP syndrome, parotid gland, nasopharynx, skin tumors
Bier, Dummer, Ganzer, Roth, Ruzicka, Schmitt, Schulte, Stadler, Suter
Thursday:
Esophageal carcinoma, gastric carcinoma, colorectal carcinoma
Gabbert, Häussinger, Knöfel, Ramp, Röher, Röhrborn, Wettstein, Willich, Sauer
Friday:
Seminoma, urinary bladder carcinoma, prostatic carcinoma, renal cell carcinoma
Ackermann, Alberti, Alken, Bamberg, Fornara, Hartmann, Rübben, Vögeli, Wirth
Saturday:
NHL, Hodgkin's disease, ALL, AML, CML, multiple myeloma, bronchial carcinoma, thymona
Bentz, Böhner, Gattermann, Germing, Haas, Kobbe, Stilgenbauer, Schmitt
Sunday:
Mammary carcinoma: biology, new treatment standards
Bender, Dall, Gerber, Harbeck, Kaufmann, Mallmann, von Mickwitz, Nitz, Yarnold
Head of the organization team: Prof. Dr. Stephan Roth, Klinik für Strahlentherapie, Moorenstr. 5, Postfach 101007, 40001 Düsseldorf, Germany
The conference fee will be € 30 per day.
The symposium volume published for the conference can be purchased for € 20.

For further information, please contact:
Head of the organization team:
Prof. Dr. Stephan Roth
Klinik für Strahlentherapie
Heinrich-Heine-Universität
Moorenstr. 5
40225 Düsseldorf
Germany
Tel.: +49 (0)211 811 8989/7990
Fax: +49 (0)211 811 8051
e-mail: roth@med.uni-duesseldorf.de
www.uni-duessdorf.de/tumorzentrum

Virchows Arch (2003) 443:491–500
DOI 10.1007/s00428-003-0840-0

ORIGINAL ARTICLE

Kyoung-Mee Kim · Mee-Sun Kwon · Seung-Jin Hong · Ki-Oak Min · Eun-Joo Seo · Kyo-Young Lee · Sang-Wook Choi · Mun-Gan Rhyu

Genetic classification of intestinal-type and diffuse-type gastric cancers based on chromosomal loss and microsatellite instability

Received: 11 March 2003 / Accepted: 6 May 2003 / Published online: 15 August 2003
© Springer-Verlag 2003

Abstract The stage of gastrointestinal cancers has been correlated with the loss of heterozygosity (LOH) and the presence of microsatellite instability (MSI). This study delineated the category of the extent of LOH and the presence of MSI for the genetic classification of the intestinal-type and diffuse-type gastric cancers that frequently exhibited intralesional heterogeneity. A total of 390 tumor foci from 116 gastric cancers were screened using a panel of 40 microsatellite markers on chromosomes 3p, 4p, 5q, 8p, 9p, 13q, 17p, and 18q. One MSI-positive gastric cancer accompanying a LOH-positive focus and 19 gastric cancers with an intralesional LOH heterogeneity with a similar extent were identified. One hundred and sixteen gastric cancers were categorized based on the presence of MSI (16 cases) and the extent of LOH (100 cases) in a representative focus. A large fraction of MSI-positive cases was found in the intestinal-type (94%), late-onset (mean age 68 years), early-stage (75%) diseases ($P<0.05$). The diffuse-type gastric cancers with a baseline-level loss involving zero or one chromosome showed a correlation with the earlier onset (mean age 45 years), advanced-stage (81%) diseases ($P<0.0001$). In both the intestinal-type and diffuse-type gastric cancers, a low-level loss involving 0–3 chromosomes (2–3 chromosomes in the diffuse type) and a high-level loss involving 4–7 chromosomes were predominant in the early (69%) and advanced (86%) stages, respectively ($P<0.0001$), at similar mean ages of onset (61 years and 65 years). Gastric cancers were categorized into low-risk (MSI and low-level LOH) and high-risk (baseline-level and high-level LOH) genotypes displaying cell-type- and age-dependent oncogenicity.

Keywords Intratumoral heterogeneity · Chromosomal loss · Microsatellite instability

K.-M. Kim · M.-S. Kwon · K.-O. Min · E.-J. Seo · K.-Y. Lee
Department of Clinical Pathology,
College of Medicine, The Catholic University of Korea,
Seoul, Korea

S.-W. Choi
Department of Internal Medicine,
College of Medicine, The Catholic University of Korea,
Seoul, Korea

S.-J. Hong · M.-G. Rhyu
Department of Microbiology,
College of Medicine, The Catholic University of Korea,
Seoul, Korea

M.-G. Rhyu (✉)
Department of Microbiology,
College of Medicine, The Catholic University of Korea,
505 Banpo-dong, Socho-gu, 137-701 Seoul, Korea
e-mail: rhyumung@catholic.ac.kr
Fax: +82-2-5968969

Introduction

The genome of solid tumors, such as gastric and colorectal cancers, in the gastrointestinal tract undergoes complex alterations. These complex genomic changes have been categorized into loss of heterozygosity (LOH) and microsatellite instability (MSI) [19, 23], representing a unilateral chromosomal loss [16, 29] and increased microsatellite mutations [1, 11, 14, 28], respectively. Both the LOH and MSI have been screened using a panel of microsatellite markers selected from a subset of chromosomes that frequently suffer from LOH in gastrointestinal cancers [5, 6]. The resultant genetic data on gastrointestinal cancers has indicated that the extent of the LOHs, rather than the individual LOHs themselves, has a close correlation with the disease prognosis, whereas the MSI is uniquely associated with a favorable prognosis [5, 6]. Therefore, polymerase chain reaction (PCR)-based microsatellite analysis was expected to promote the genetic staging of gastrointestinal cancers with the availability of routine pathological samples.

In comparison with colorectal cancers, the diagnostic microsatellite analysis of gastric cancer is somewhat unjustified due to the heterogeneous histological features. Histologically, gastric cancers are classified into two types, intestinal and diffuse, according to the formation of

an intestinal gland [17]. A large proportion of gastric cancer patients display intralesional heterogeneity with the different histological types and varying degrees of differentiation [20, 27]. Therefore, the genotype of a heterogeneous gastric cancer is unlikely to be determined with only a tumor cell-rich area microdissected from the pathological tissue, i.e., a limited portion of the whole tumor.

This multifocal microsatellite analysis was carried out on histotopographically distinct lesions selected from a given gastric cancer in order to delineate the category of LOH extent and the MSI for the genetic staging of gastric cancer. A total of 397 tumor foci from 118 gastric cancers were screened using a panel of 40 microsatellite markers on 8 cancer-associated chromosomal arms that frequently suffered from a LOH in gastric and colorectal cancers [4, 6, 31]. This panel of microsatellite markers has been confirmed to reproduce the stable allelic signals with a minimum number of PCR artifacts in the analysis of formalin-fixed paraffin-embedded pathological archives [6, 13]. In this multifocal study, an intratumoral heterogeneity was frequently identified in the LOH from heterogeneous tumor foci of a given gastric cancer. Interestingly, a heterogeneous gastric cancer showed a similar extent of LOH or one of the LOH and MSI through multiple tumor foci. The extent of LOH and the presence of MSI in a representative tumor focus allowed this study to group the intestinal-type and diffuse-type gastric cancers into low-risk and high-risk genotypes.

Materials and methods

Histopathological examination and DNA preparation

This study was based on the formalin-fixed, paraffin-embedded surgical archives of gastric cancer patients with no family history of cancer, and who were treated at Our Lady of Mercy Hospital, Inchon and at St. Paul's Hospital, Seoul, Korea, from 1995 to 2000. The whole or extensive tumor tissues including the tumor border and the adjacent non-tumor tissues were embedded in paraffin after being fixed in formalin and stained with hematoxylin-eosin. The institutional review board authorized the use of the pathological tissues.

The microscopic slides from each case were reviewed and the histological type of gastric cancer was defined as intestinal (glandular, cohesive, or solid), diffuse, and mixed including varying differentiation [2, 3, 18]. The tumor locations considered were the proximal stomach including the cardia and body, and the distal stomach including the antrum. The clinicopathological staging followed the TNM criteria [12], and the samples were categorized into the early (I and II) and advanced (III and IV) stages, according to previous reports where the 5-year survival rate differed significantly between these subsets [22, 26]. For multifocal analysis, a total of 397 tumor foci from 118 gastric cancers were chosen from the superficial-peripheral and deep-central areas as well as from the histologically distinct areas. Two pathologists independently reviewed the microscopic slides according to unified criteria in order to cope with the different annotations on the histopathological classification, which might be a major source for the equivocal findings on the genotype–phenotype relationship.

Seven-micron-thick sections were stained with hematoxylin-eosin, and multiple tumor-rich areas representative of the intralesional heterogeneity, each of which was composed of a homogeneous cellular component, were then chosen by a microscopic examination. The normal cell contents such as the stromal tissues and lymphocytes were manually scraped from a non-cover-slipped slide using a surgical scalpel under stereomicroscopic guidance (Fig. 1). Because of the non-cohesive cells diffusely infiltrating the surrounding tissue, the diffuse-type cancers were relatively less pure than the intestinal-type cancers. All microdissected samples with a tumor cell content greater than 70% were used to analyze the allelic status. The size of the microdissected tumor tissues ranged from 3 mm to 5 mm in diameter. For each case, approximately 100 harvested cells were digested with 1 μl Tween 20–proteinase K lysis buffer. Tissue lysate from each tumor focus (100–200 μl) was used as a template DNA for PCR.

Analysis of microsatellite alleles

The MSI and LOH were scored using a panel of 40 microsatellite markers on eight chromosomal arms: 3p, 4p, 5q, 8p, 9p, 13q, 17p, and 18q (Table 1). Five microsatellite markers from the centromere to the telomere of each chromosomal arm were selected on the basis of the allelic frequency and the PCR product size retrieved from The Genome Database (http://www.gdb.org/). The use of the five microsatellite markers per chromosomal arm ensured a high yield of the informative markers for each chromosomal arm and good estimate of the true LOH extent in each patient. As a reference type of the microsatellite sequences, the dinucleotide repeat markers ranging from 100 bp to 190 bp in the amplified size and with a heterozygous frequency more than 50% were selected. These microsatellite markers were examined for the reproducible allelic bands with a minimum number of PCR artifacts in previous studies on frozen and formalin-fixed tissue [6, 13].

The radioisotope-labeled microsatellite sequences were visualized by repeated exposures of each autoradiograph using a radioluminographic scanner (BAS 2500, Fuji Photo Film Co. Ltd., Kanakawa, Japan). An optimal range of allelic intensities was selected for the densitometric analysis using TINA image software (raytest Isotopenmeßgeräte GmbH, Straubenhardt, Germany). The microsatellite sequences amplified by PCR variably produced the extra ladder bands in addition to the main allelic bands, referred to as the "shadow or stutter band". The diverse patterns of microsatellite sequences were converted into one-dimensional peaks to standardize the allelic ratio using the "Profile" option in the TINA image software [6, 13].

The resultant allelic bands of the 40 microsatellite sequences were initially analyzed for MSI at the homozygous markers, because the MSI obscured the allelic intensity in the majority of markers examined. The LOH was scored at the heterozygous markers in the cases without a MSI. In heterozygous cases with intimately neighboring two alleles, MSI and LOH were frequently indistinguishable because a signal reduction in one of two alleles might result from not only allelic loss but also allelic shift co-migrating with adjacent allele [10]. Thus, a high-level MSI was

Fig. 1 Representative examples of a manual microdissetion (*photomicrograph*) and the allelic migration pattern (*autoradiograph*) of mixed-type gastric cancers (cases 3 and 20). *Upper panel in photomicrograph*: mixed-type gastric cancers contained diffuse (T1) and intestinal (T2) dual lesions. *Lower panel in the photomicrograph*: after a manual microdissection, the remaining tissue containing a tumor cell content >70% was harvested and the genomic DNAs were extracted. *Autoradiograph*: normal DNA (N) and the corresponding diffuse-type and intestinal-type tumor DNAs are indicated above the lanes. Loss of heterozygosity (LOH) is indicated by *arrowhead*. In case 3, the primary LOHs on chromosome 18q are commonly shared in both the diffuse- and intestinal-type tumor sites. The secondary LOHs on chromosomes 5q, 9p, 13q, and 17p are restricted to the intestinal-type tumor sites. In case 20, the same alleles on chromosomes 5q, 8p, 17p, and 18q are lost in both histological types. The upper and lower opposite alleles on chromosome 13q are reciprocally lost in the diffuse and intestinal types. A diffuse-type tumor focus demonstrates LOH with incompletely diminished allelic intensity

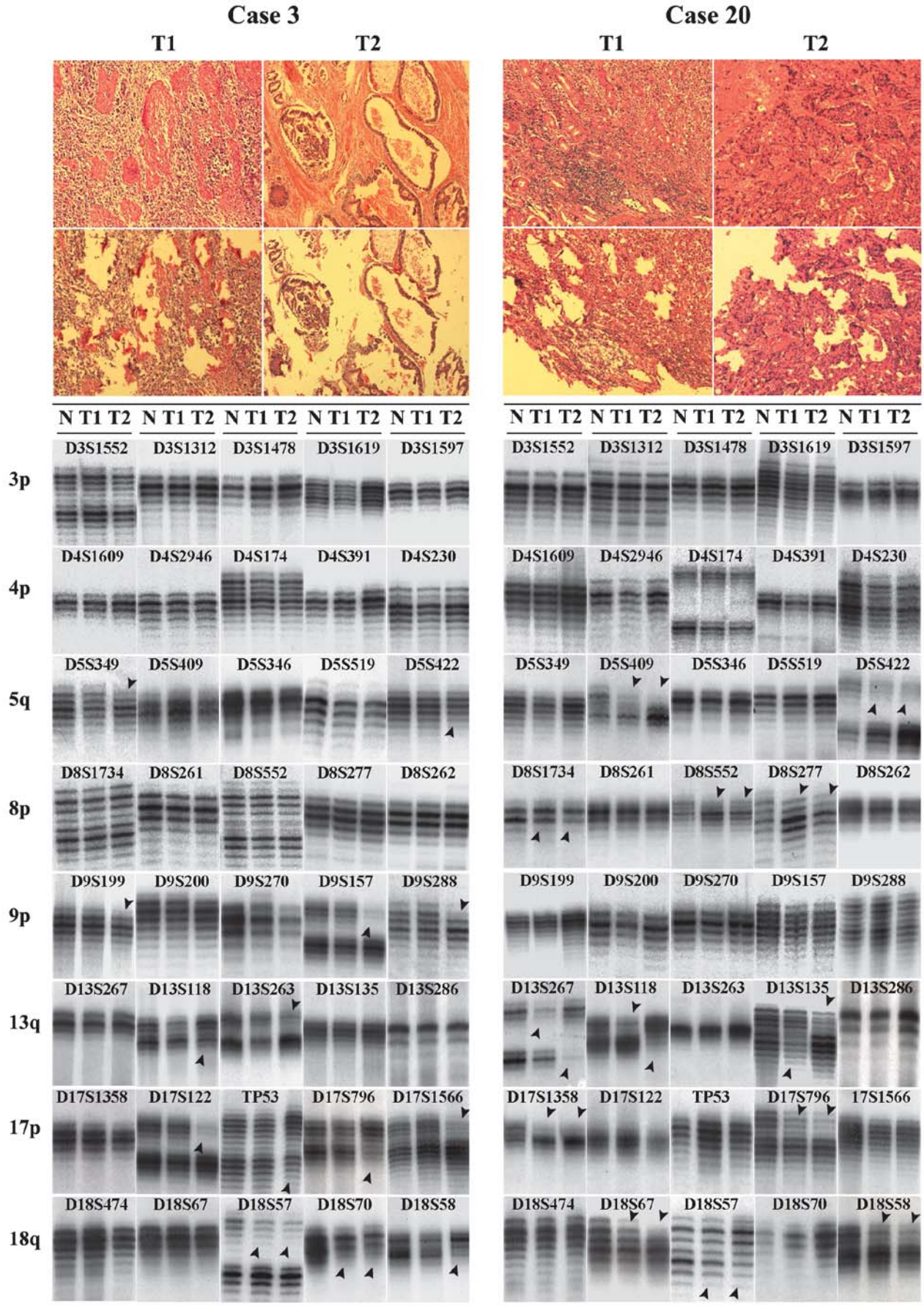
Case 3
T1
T2
Case 20
T1
T2
N T1 T2 N T1 T2 N T1 T2 N T1 T2 N T1 T2
N T1 T2 N T1 T2 N T1 T2 N T1 T2 N T1 T2
3p
D3S1552 D3S1312 D3S1478 D3S1619 D3S1597
D3S1552 D3S1312 D3S1478 D3S1619 D3S1597
4p
D4S1609 D4S2946 D4S174 D4S391 D4S230
D4S1609 D4S2946 D4S174 D4S391 D4S230
5q
D5S349 D5S409 D5S346 D5S519 D5S422
D5S349 D5S409 D5S346 D5S519 D5S422
8p
D8S1734 D8S261 D8S552 D8S277 D8S262
D8S1734 D8S261 D8S552 D8S277 D8S262
9p
D9S199 D9S200 D9S270 D9S157 D9S288
D9S199 D9S200 D9S270 D9S157 D9S288
13q
D13S267 D13S118 D13S263 D13S135 D13S286
D13S267 D13S118 D13S263 D13S135 D13S286
17p
D17S1358 D17S122 TP53 D17S796 D17S1566
D17S1358 D17S122 TP53 D17S796 17S1566
18q
D18S474 D18S67 D18S57 D18S70 D18S58
D18S474 D18S67 D18S57 D18S70 D18S58

Table 1 Microsatellite markers used for polymerase chain reaction (PCR)-based loss of heterozygosity (LOH) analysis on gastric cancers (n=100)

Marker	Chromosomal locus	Amplicon size (bp)	Number of cases with heterozygosity	Number of cases with LOH	LOH (%)
D3S1552	3p12.1–11.1	140–170	70	20	29
D3S1312	3p14.3–14.1	148–158	65	17	26
D3S1478	3p21.3–21.2	109–152	60	17	28
D3S1619	3p24.2–22	161–171	63	16	26
D3S1597	3p24.2	151–171	56	17	30
D4S1609	4p13	163–177	60	19	32
D4S174	4p11–13	134–154	70	21	30
D4S230	4p13	170–190	59	16	27
D4S391	4p15.1	165–185	69	23	33
D4S2946	4p15.2–15.3	104–126	64	17	26
D5S349	5q11.2–13.1	140–158	56	16	29
D5S409	5q14–15	138–154	55	17	31
D5S346	5q21–22	96–136	51	19	37
D5S519	5q32–33.2	114–128	64	21	33
D5S422	5q32–33	114–134	72	24	33
D8S1734	8p22–21.3	90–120	56	12	21
D8S261	8p22.3	100–124	48	11	23
D8S552	8p22	160–180	68	11	16
D8S503	8p23.1	107–120	60	11	18
D8S262	8p23.2–23.3	100–118	54	8	15
D9S200	9p13	107–127	56	15	27
D9S270	9p21	97–119	63	20	32
D9S157	9p22	113–149	66	20	30
D9S199	9p24	144–164	64	22	34
D9S288	9p24	124–140	71	19	27
D13S267	13q12.3	148–162	53	17	32
D13S118	13q14.1	160–174	52	13	25
D13S263	13q14	145–165	63	17	27
D13S135	13q14.3–22	168–184	67	17	25
D13S286	13q32	94–114	61	18	30
D17S1358	17p11.2	148–160	54	28	52
D17S122	17p12–11.2	159–162	57	32	57
TP53	17p13.1	103–135	73	44	60
D17S796	17p13.2	144–174	64	36	56
D17S1566	17p13.3	170–190	69	41	59
D18S474	18q12.3–21.1	119–139	60	22	37
D18S67	18q12.2–12.3	113–123	61	23	38
D18S57	18q12.2–12.3	88–110	59	25	43
D18S70	18q23	111–126	72	30	42
D18S58	18q22–23	144–160	67	25	37

scored if the tumor DNA exhibited novel alleles in more than 40% of the homozygous markers that were free of allelic loss noise. The LOH was scored as the allelic intensity ratio of the tumor DNA relative to the matched normal allelic ratio, which was calculated by dividing the allelic ratio of the tumor by the normal allelic ratio. In previous studies [6, 13], a cutoff point of a 1.5-fold relative allelic ratio was found to provide the best discrimination between the wild-type heterozygosity and the LOH. This cutoff point was applied to cases with a borderline LOH, and the majority of cases with a complete allelic loss greater than 2.0-fold were determined visually.

Statistical analysis

The statistical comparisons of the microsatellite alterations between the histological types and between the tumor stages were performed using a χ^2 test with SPSS 10 software. The Kruskal-Wallis non-parametric test was used to compare the clinicopathological parameters with microsatellite genotypes, and the Student's t-test was used between the MSI-negative and -positive cases. A P value <0.05 was considered significant in each statistical analysis.

Results

Histological heterogeneity

Of the 118 gastric cancers examined, 116 (98%) carried at least one heterozygous microsatellite marker in each chromosomal arm. The 116 gastric cancers, of which 47 (41%) were of the mixed type, were analyzed for the clinicopathological features and microsatellite alterations (Table 2). The 47 mixed-type cancers were classified into intestinal (28 cases) and diffuse (19 cases) types on the basis of their predominant histological components. The intestinal-type (76 cases including 28 mixed types) and the diffuse-type (40 cases including 19 mixed types) cancers were prevalent in the distal (56 cases, 74%) and the proximal (25 cases, 63%) stomachs, respectively (P<0.0001). There was a significant difference in the mean onset-age between the intestinal-type (64 years) and the diffuse-type (56 years) of gastric cancer (P=0.004)

Table 2 Clinicopathological features, loss of heterozygosity (LOH), and microsatellite instability (MSI) analyzed in gastric cancers

		Diffuse-type cancer			Intestinal-type cancer			*P* value
		Single lineage	Mixed	Total	Single lineage	Mixed	Total	
No. of patients	116	21	19	40	48	28	76	
Age (years)								0.004
Mean ±SD	61.02 ±12.71	53.14 ±16.52	58.49 ±13.06	55.85 ±14.93	62.30 ±10.76	66.21 ±9.89	63.76 ±10.55	
Sex								0.113
Male	69	15	13	28	27	14	41	
Female	47	6	6	12	21	14	35	
Site								<0.0001
Proximal	45	12	13	25	14	6	20	
Distal	71	9	6	15	34	22	56	
Stage								0.508
Early	54	5	10	15	25	14	39	
Advanced	62	16	9	25	23	14	37	
Genetic changes								
MSI	16 (1) [a]	0	1	1	3	12 (1)	15	
LOH	92 (19)	17 (1)	16 (7)	33 (8)	43 (1)	16 (10)	59 (11)	
No changes	8	4	2	6	2	0	2	

[a] No. of cases with heterogeneous genetic changes in a given tumor is indicated in parenthesis

Intralesional heterogeneity of MSI and LOH

Sixteen (14%) of the 116 gastric cancers examined were scored as having a MSI (Table 2). Of the 16 cases with a MSI, 12 were defined as being a mixed-type gastric cancer composed of a variably differentiated intestinal-type (11 cases) or diffuse-type (1 case) dominant admixture. Three cases manifested a homogeneous intestinal-type differentiation. Only one case (case 26 in Table 3) contained an intestinal-type lesion with a MSI accompanied by a diffuse-type lesion without a MSI.

Of 100 MSI-negative gastric cancers, 92 contained at least one chromosomal loss and 8 had no chromosomal losses (Table 2). Nineteen (21%) of the 92 LOH-positive gastric cancers had not only primary LOHs commonly shared by multiple tumor foci but also the secondary LOHs that were restricted to a part of tumor (Fig. 1, Table 3). The secondary LOHs were frequent in the histologically different foci of the mixed-type gastric cancers (53%, 17 of 32) and were rare in the topographically different foci of gastric cancers with a single cellular lineage (3%, 2 of 60). In 11 of the 19 cases, heterogeneous tumor foci carried the same number of the secondary LOHs involving the upper and lower opposite alleles on the same chromosomes (9 cases) or different chromosomes (2 cases). The losses of upper and lower alleles on the same chromosomal arm were reciprocally and randomly bifurcated into the intestinal and diffuse types. The remaining 8 cases harbored additional LOHs that were restricted to either an intestinal or diffuse component.

We analyzed 817 LOHs (Table 1) involving 297 chromosomes in a representative lesion of gastric cancer. 412 (51%) and 405 LOHs (49%) affected the upper and lower alleles, respectively. Of the 297 chromosomal arms containing LOH, 256 (86%) simultaneously lost all heterozygous alleles on a chromosomal arm (complete chromosomal losses) and the remaining 41 (14%) lost a part of the heterozygous alleles (incomplete chromosomal losses). The most frequent and infrequent LOHs were observed on chromosome 17p (61%) and 8p (19%), respectively. Other chromosomal losses were found with similar frequencies ranging from 31% (13q loss) to 44% (18q loss). When the extent of the LOH was scored as the number of chromosomes containing LOH, the gastric cancers yielded an overall mean value of 2.95, which is approximately three chromosomal losses. A mean value of three chromosomal losses was used as a cut-off point between the low and high levels of LOH.

Relationships between clinicopathological features and microsatellite genotypes

The relationships between the clinicopathological features and the individual chromosomal losses in gastric cancers were then analyzed (Table 4). Gastric cancers with either a 17p or 18q loss were associated with the late-onset and the intestinal-type histology and those with 5q loss or 18q loss were significantly more frequent in the distal stomach than in the proximal stomach ($P<0.05$). However, there were no significant differences in the frequencies of the 17p and 18q losses between the intestinal- and diffuse-type cancers in the distal stomach, and only a 13q loss showed a significant correlation with the advanced tumor stages ($P=0.049$).

The intestinal-type and diffuse-type gastric cancers were separately analyzed to determine the relationships of

Table 3 Intratumoral heterogeneity detected in 20 gastric cancers. Predominant histological type is capitalized. Losses of upper and lower alleles (U/L) on the same chromosomal arm were reciprocally and randomly bifurcated into the intestinal and diffuse types

Case	Histological type	Chromosomal loss	Level of LOH	Location	Tumor stage
77	INTESTINAL	4, 5, 9, 13, 17, 18 3(U/L)	High	Antrum	IV (T3N3 M0)
	Diffuse	4, 5, 9, 13, 17, 18 3(U/L)	High		
10	INTESTINAL	4, 5, 9, 13, 17 3(U/L)	High	Antrum	IV (T4N3M0)
	Diffuse	4, 5, 9, 13, 17 3(U/L)	High		
20	INTESTINAL	5, 8, 17, 18 13(U/L)	High	Antrum	IIIB (T3N2M0)
	Diffuse	5, 8, 17, 18 13(U/L)	High		
125	INTESTINAL	4, 17, 18 5(U/L)	High	Cardia	IIIA (T3N1M0)
	Diffuse	4, 17, 18 5(U/L)	High		
101	INTESTINAL	3, 8, 17 5(U/L)	High	Antrum	IIIA (T3N1M0)
	Diffuse	3, 8, 17 5(U/L)	High		
75	INTESTINAL	17 3(U/L), 18(U/L)	Low	Antrum	IIIA
	Diffuse	17 3(U/L), 18(U/L)	Low		(T3N1 M0)
41	DIFFUSE	4, 17 5(U/L)	Low	Body	IA (T1N0M0)
	Intestinal	4, 17 5(U/L)	Low		
72	DIFFUSE	8 3(U/L)	Low	Body	IA (T1N0M0)
	Intestinal	8 3(U/L)	Low		
126	DIFFUSE	9(U/L)	Baseline	Cardia	IV (T4N3M0)
	Diffuse	9(U/L)	Baseline		
27	DIFFUSE	9, 17, 18 3	High	Antrum	IB (T2bN0M0)
	Intestinal	9, 17, 18 5	High		
119	DIFFUSE	17, 18 4	Low	Body	II (T2aN1M0)
	Intestinal	17, 18 3	Low		
84	DIFFUSE	5, 18 4	Low	Cardia	II (T3N0M0)
	Intestinal	5, 18	Low		
29	DIFFUSE	18 5, 17	Low	Cardia	II (T3N0M0)
	Intestinal	18	Low		
95	INTESTINAL	18 3, 4	Low	Antrum	IA (T1N0M0)
	Intestinal	18	Low		
62	INTESTINAL	4, 5, 9, 17 3, 8, 18	High	Antrum	IV (T3N3M0)
	Diffuse	4, 5, 9, 17	High		
129	INTESTINAL	4, 5, 8 3, 17, 18	High	Antrum	IV (T3N3M0)
	Diffuse	4, 5, 8	Low		
3	INTESTINAL	18 5, 9, 13, 17	High	Body	IV (T4N3M0)
	Diffuse	18	Baseline		
17	INTESTINAL	4, 5, 13 3, 17	High	Antrum	IV (T4N2M0)
	Diffuse	4, 5, 13	Low		
109	DIFFUSE	9 4, 17, 18	High	Antrum	IIIA (T3N1M0)
	Intestinal	9	Low		
26	INTESTINAL	Microsatellite instability	MSI	Antrum	IB (T2aN0M0)
	Diffuse	8,13	Low		

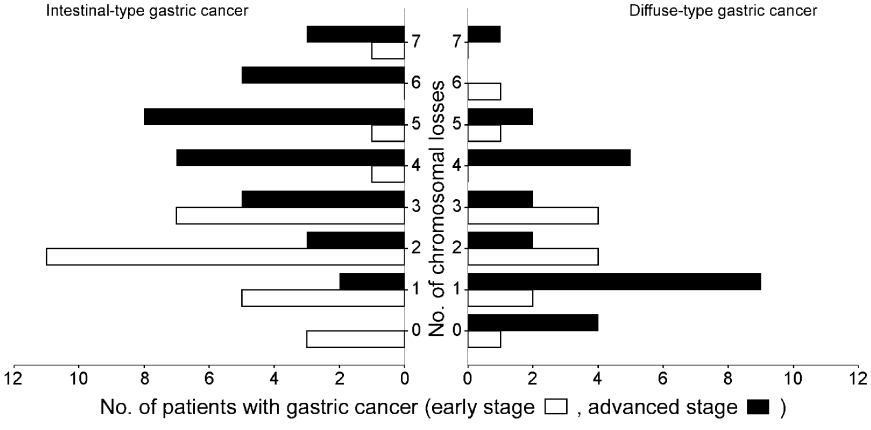

Fig. 2 Relationships between the number of chromosomal losses and the tumor stage separately analyzed in the intestinal-type and diffuse-type gastric cancers

the tumor stage with the number of chromosomal losses (Fig. 2). The intestinal-type cancers with the early and advanced stages demonstrated a unimodal LOH distribution clustering near two and five chromosomal losses, respectively. In the diffuse-type cancers, the advanced stages exhibited a bimodal LOH distribution clustering near one and four chromosomal losses and, the early stages exhibited a unimodal LOH distribution similar with the intestinal-type cancers. The diffuse- and intestinal-type gastric cancers with zero or one chromosomal loss

Table 4 Relationships between clinicopathological features and single chromosomal loss in gastric cancers

		3p	4p	5q	8p	9p	13q	17p	18q
No. of patients	100	33	35	36	19	37	30	61	44
Age (years)									
Mean	59.86	61.61	63.14	61.86	62.89	62.51	63.60	63.18	62.86
±SD	±12.79	±10.88	±10.66	±11.00	±8.61	±10.85	±9.65	±11.80	±11.54
P value		0.341	0.059	0.243	0.253	0.112	0.055	0.001*	0.037*
Sex									
Male	63	25	24	23	11	27	21	39	27
Female	37	8	11	13	8	10	9	22	17
P value		0.080	0.515	1.000	0.609	0.136	0.375	0.834	0.836
Tumor location									
Proximal	43	11	12	10	6	11	11	22	11
Distal	57	22	23	26	13	26	19	39	33
P value		0.201	0.212	0.035*	0.311	0.059	0.510	0.099	0.002*
Histological type									
Diffuse	38	9	11	11	8	11	11	17	11
Intestinal	62	24	24	25	11	26	19	44	33
P value		0.132	0.390	0.288	0.794	0.209	1.000	0.012*	0.023*
Location & histology									
Proximal	43	11	12	10	6	11	11	22	11
Diffuse	25	4	5	4	5	4	6	8	2
Intestinal	18	7	7	6	1	7	5	14	9
P value	57	0.156	0.301	0.275	0.375	0.156	1.000	0.005*	0.004*
Distal	13	22	23	26	13	26	19	39	33
Diffuse	44	5	6	7	3	7	5	9	9
Intestinal		17	17	19	10	19	14	30	24
P value		1.000	0.750	0.541	1.000	0.541	0.742	1.000	0.524
Tumor stage									
Early	42	11	12	12	6	12	8	21	15
Advanced	58	22	23	24	13	25	22	40	29
P value		0.282	0.283	0.211	0.439	0.149	0.049*	0.064	0.221

*P value <0.05

were different in the onset-age, tumor location, and tumor stage (Table 5). Therefore, a dual classification system of the LOH-extent, low (LOH-L, three or fewer losses) and high (LOH-H, four or more losses) levels for the intestinal-type and baseline (LOH-B, zero or one loss), low (LOH-L, two or three losses), and high (LOH-H, four or more losses) levels for the diffuse-type cancers, was designed. The divergent chromosomal losses detected in 19 cases were defined as having similar (15 cases) and dissimilar (4 cases) levels of chromosomal loss for a given gastric cancer (Table 3).

The gastric cancers examined were categorized into four microsatellite genotypes, which indicated the low-risk (MSI and LOH-L) and high-risk (LOH-H and diffuse-type-specific LOH-B) diseases (Table 5). The three LOH genotypes showed significant differences in terms of the onset age (P<0.0001), tumor location (P<0.0001), and tumor stage (P<0.0001). The average onset-age of the gastric cancers with a LOH-B (45 years) was significantly lower than that of the gastric cancers with a LOH-L (61 years) and LOH-H (65 years) (P<0.0001). The MSI was significantly more frequent in the late-onset disease (68 years) (P=0.005), early stages (P=0.014), intestinal type (P=0.012), and distal stomach (P=0.02) than the LOH. (Table 5).

Discussion

Many gastric cancer studies have reported a striking heterogeneity in the histological patterns and genetic alterations [8, 9, 15, 18, 21, 24]. The multifocal analysis results from this study using a panel of 40 microsatellite markers demonstrated that the heterogeneous tumor foci of a given gastric cancer had the same or a similar extent of chromosomal losses even if the primary and secondary LOHs coexisted (Table 3). This study also found that most (58 of 60) cases with a single cellular lineage shared the same chromosomal losses in the multiple lesions tested. Therefore, a gastric cancer with even heterogeneous intratumoral foci, was generally under the influence of a similar level of chromosomal losses.

Most divergent chromosomal losses were observed in the mixed-type gastric cancers, and there was no correlation between the extent of LOH and mixed-type cancer (Table 3). Therefore, it is believed that the secondary chromosomal losses stimulate the co-expansion of the

Table 5 Comparison of clinicopathological features among microsatellite genotypes in gastric cancers

Microsatellite genotype		Baseline-level chromosomal loss (%)	Low-level chromosomal loss (%)		High-level chromosomal loss (%)	*P* value[b]	Microsatellite instability (%)	*P* value[c]
No. of chromosomal loss		0–1[a]	0–1[a]	0–3[a]	4–8			
No. of patients	116	16 (14)		48 (41)	36 (31)		16 (14)	
Histological type								
Diffuse	39	16		12 (31)	10 (28)		1 (6)	
Intestinal	77		10	36 (69)	26 (72)		15 (94)	
						<0.0001		0.012
Age (years)								
Mean	61.01	45.44	57.30	61.15	64.56		68.25	
±SD	±12.71	±10.05	±12.29	±10.40	±10.65		±9.64	
						<0.0001		0.005
Sex								
Male	69 (59)	10 (63)	5 (50)	26 (54)	27 (75)		6 (38)	
Female	47 (41)	6 (37)	5 (50)	22 (46)	9 (25)		10 (62)	
						0.173		0.072
Tumor location								
Proximal	45 (39)	15 (94)	2 (20)	20 (42)	8 (22)		2 (13)	
Distal	71 (61)	1 (6)	8 (80)	28 (58)	28 (78)		14 (87)	
						<0.0001		0.020
Tumor stage								
Early	53 (46)	3 (19)	8 (80)	33 (69)	5 (14)		12 (75)	
Advanced	63 (54)	13 (81)	2 (20)	15 (31)	31 (86)		4 (25)	
						<0.0001		0.014

[a] Cases with zero or one chromosomal losses were differentially classified into baseline (diffuse type) and low (intestinal type) levels according to their histological types

[b] *P* values of Kruskal-Wallis test among baseline-level, low-level and high-level chromosomal losses

[c] *P* values of Student's *t*-test between MSI-negative vs MSI-positive cases

different clones, whereas multiple chromosomal losses themselves have little influence on the histological heterogeneity. A secondary functional loss of specific gene(s) on a chromosome is unlikely to play a role in the selection of a cellular lineage. This is because the upper and lower opposite allelic losses on the same chromosomes were reciprocally and randomly lost restricted to the histologically distinct foci within a mixed-type gastric cancer. A previous study on composite gastric cancers containing both glandular and neuroendocrine components also reported that different cellular lineages reciprocally shared the losses of the opposite alleles on the same chromosomes [15]. In addition, neither a direction of the diffuse-intestinal nor the intestinal-diffuse sequence was designated by the secondary chromosomal losses in the mixed-type gastric cancers. These findings suggest that other intrinsic genetic programs are stochastically stimulated by the secondary chromosomal losses, which directly contributed the co-expanding histological types.

Both the diffuse-type and intestinal-type cases burdened with more than one chromosomal loss harbored a greater extent of LOH in the advanced stages (LOH-H) than in the early stages (LOH-L) with similarities to colorectal cancers [6]. However, there was a bimodal LOH distribution in diffuse-type cancers with the advanced stage (Fig. 2), suggesting the presence of the diffuse-type-specific LOH-B type in addition to the LOH-H type. The diffuse-type gastric cancers with zero or one chromosomal loss (LOH-B) were uniquely related to the advanced stage and the early onset, whereas the intestinal-type gastric cancers with zero or one chromosomal loss revealed clinical features similar to the LOH-L cases (Table 5). Two or more chromosomal losses were considered to display similar dose-dependent effects on the epithelial cells through the gastrointestinal tract. Therefore, the diffuse-type gastric cancers, which are known to be associated with the early onset and poor survival [6, 17, 27], could be further delineated into the early- (LOH-B) and late- (LOH-H) onset high-risk and low-risk (LOH-L) diseases.

In a previous analysis of gastric cancers using 13 microsatellite markers from 5 chromosomal arms [5], the cases with neither LOH nor MSI were scored as being microsatellite stable (MSS), which were associated with the diffuse-type cancers with an advanced stage. When using 40 microsatellite markers, in the diffuse-type, early-onset, advanced gastric cancers, one chromosomal loss (9 cases) was more common than no chromosomal loss (4 cases). Therefore, the cases scored as being MSS or LOH-B appeared to contain a single chromosomal loss, which were increasingly detected as the number of chromosomal arms examined and microsatellite markers used per chromosomal arm increases. Furthermore, in intestinal-type cancers, independently of the tumor stage, there was

a unimodal distribution of the cases according to of the extent of LOH and, in diffuse-type cancers with the advanced stage, there was a bimodal distribution (Fig. 2). These data showed that diffuse-type gastric cancers with the advanced stage had two clearly distinct molecular events: a group of diploid cancers without a few LOH and two clearly of aneuploidy with high-level LOH. The DNA impurities of the diffuse-type gastric cancer are unlikely to be superimposed to infrequent chromosomal losses, because diffuse-type cancers also frequently demonstrate two or more chromosomal losses even with incompletely diminished allelic signals (Fig. 1).

The relationships between the single chromosomal losses and the tumor phenotype are unclear. For example, the 17p and 18q losses were significantly associated with the intestinal type in the proximal stomach but not in the distal stomach. In addition, none of the 17p and 18q losses showed a significant relationship with the degree of the tumor stage. A previous study also reported no significant relationship between an 18q loss and the disease prognosis [2]. The relationship of a single chromosomal loss with the biological behavior might originate from the genetic background against the LOH extent. The 17p and 18q losses, the two most frequent alterations, were the major components of the two opposite genotypes, LOH-L and LOH-H, thus making no statistical significance in the relationship with the tumor stage. In contrast, a 13q loss, which was preferentially detected in the LOH-B and LOH-H cases (data not shown), made a statistical significance (P=0.049) in the relationship with advanced tumor stages. Therefore, this study suggests that a single chromosomal loss plays a role in tumor progression as part of the concerted chromosomal function, which is in agreement with a previous colorectal cancer study [6].

Gastric cancers with a MSI have been reported to be preferentially located in the distal stomach and associated with intestinal-type histology and favorable clinical features [5, 8, 10, 25, 30]. The number of frame-shift mutations in multiple cancer-related genes varied from tumor area to tumor area, suggesting that the intralesional heterogeneity resulted from a complex set of successive mutations caused by the genetic instability [7, 8]. The clinicopathological characteristics of the MSI-positive gastric cancers were confirmed in this study. Most MSI genotypes were also found in the heterogeneous gastric cancers with varying degrees of intestinal differentiation (Table 2). Meanwhile, only one mixed-type case separately harbored a MSI and LOH in the histologically distinct tumor foci (Table 3). It is well known that LOH and MSI are inversely correlated and a given cancer contains one of the two genotypes [1, 8, 14]. The main stem of the genetic and clinical characteristics of MSI-positive gastric cancer is likely to be maintained during tumor progression even with successive MSI-associated frame-shift mutations.

It has always been a matter of controversy as to how a complex set of genetic alterations in gastric cancers influences the heterogeneous malignant phenotypes. In this multifocal study on gastric cancers, the extent of the LOH and MSI were categorized into four microsatellite genotypes displaying cell-type- and age-dependent oncogenicity. Cumulating data on the genetic staging of gastrointestinal cancers have consistently emphasized the extent of LOH and MSI as the universal determinant for tumor progression. The PCR-based microsatellite analysis using routine pathological samples is expected to promote the clinical utility of genetic staging.

Acknowledgements This study was supported by Ministry of the Health and Welfare grant 'HMP-99-M-03–0001' and Korea Science and Engineering Foundation grant '971–0710–090–2'.

References

1. Aaltonen LA, Peltomaki P, Leach FS, Sistonen P, Pylkkanen L, Mecklin JP, Jarvinen H, Powell SM, Jen J, Hamilton SR, Peterson GM, Kinzler KW, Vogelstein B, Chapelle A (1993) Clues to the pathogenesis of familial colorectal cancer. Science 260:812–816
2. Candusso ME, Luinetti O, Villani L, Alberizzi P, Klersy C, Fiocca R, Ranzani GN, Solcia E (2002) Loss of heterozygosity at 18q21 region in gastric cancer involves a number of cancer-related genes and correlates with stage and histology, but lacks independent prognostic value. J Pathol 197:44–50
3. Chiaravalli AM, Cornaggia M, Furlan D, Capella C, Fiocca R, Tagliabue G, Klersy C, Solcia E (2001) The role of histological investigation in prognostic evaluation of advanced gastric cancer. Analysis of histological structure and molecular changes compared with invasive pattern and stage. Virchows Arch 439:158–169
4. Choi S-W, Park S-W, Lee K-Y, Kim K-M, Chung Y-J, Rhyu M-G (1998) Fractional allelic loss in gastric carcinoma correlates with growth patterns. Oncogene 17:2655–2659
5. Choi S-W, Choi J-R, Chung Y-J, Kim K-M, Rhyu M-G (2000) Prognostic implications of microsatellite genotypes in gastric carcinoma. Int J Cancer 89:378–283
6. Choi S-W, Lee K-J, Bae Y-A, Min K-O, Kwon M-S, Kim K-M, Rhyu M-G (2002) Genetic classification of colorectal cancer based on chromosomal loss and microsatellite instability predicts survival. Clin Cancer Res 8:2311–2322
7. Chung Y-J, Park S-W, Song J-M, Lee K-Y, Seo E-J, Choi S-W, Rhyu M-G (1997) Evidence of genetic progression in human gastric carcinomas with microsatellite instability. Oncogene 15:1719–1726
8. Chung Y-J, Kim K-M, Choi J-R, Choi S-W, Rhyu M-G (1999) Relationship between intratumor histological heterogeneity and genetic abnormalities in gastric carcinoma with microsatellite instability. Int J Cancer 82:782–788
9. Chung Y-J, Choi J-R, Park S-W, Kim K-M, Rhyu M-G (2001) Evidence for two modes of allelic loss: multifocal analysis on both early and advanced gastric carcinomas. Virchows Arch 438:31–38
10. dos Santos NR, Seruca R, Constancia M, Seixas M, Sobrinho-Simoes M (1996) Microsatellite instability at multiple loci in gastric carcinoma: clinicopathologic implications and prognosis. Gastroenterology 110:38–44
11. Fishel R, Lescoe MK, Rao MR, Copeland NG, Jenkins NA, Garber J, Kane M, Kolodner R (1993) The human mutator gene homolog MSH2 and its association with hereditary nonpolyposis colon cancer. Cell 75:1027–1038
12. Greene FL, Page DL, Fleming ID, Fritz A, Balch CM, Haller DG, Morrow M (eds) (2002) AJCC cancer staging manual, 6th edn. Springer Verlag, Berlin Heidelberg New York
13. Hyun J-S, Jo B-K, Park C-J, Yi J-Y, Lee J-Y, Rhyu M-G (2002) Loss of heterozygosity and PCR artifacts in a microsatellite analysis of psoriasis and colorectal cancer. J Korean Med Sci 17:641–647

14. Ionov Y, Peinado MA, Malkhosyan S, Shibata D, Perucho M (1993) Ubiquitous somatic mutations in simple repeated sequences reveal a new mechanism for colonic carcinogenesis. Nature 363:558–561
15. Kim K-M, Kim M-J, Cho B-K, Choi S-W, Rhyu M-G (2000) Genetic evidence for the multi-step progression of mixed glandular-neuroendocrine gastric carcinomas. Virchows Arch 440:85–93
16. Lasko D, Cavenee W, and Nordenskjold M (1991) Loss of constitutional heterozygosity in human cancer. Annu Rev Genet 25:281–314
17. Lauren P (1965) The two histological main types of gastric carcinoma: diffuse and so-called intestinal-type carcinoma. Acta Pathol Microbiol Scand 64:31–49
18. Luinetti O, Fiocca R, Villani L, Alberizzi P, Ranzani GN, Solcia E (1998) Genetic pattern, histological structure, and cellular phenotype in early and advanced gastric cancers: evidence for structure-related genetic subsets and for loss of glandular structure during progression of some tumors. Hum Pathol 29:702–709
19. Martin L, Assem M, Piard F (1999) Are there several types of colorectal carcinomas? Correlations with genetic data. Eur J Cancer Prev 8:S13–S20
20. Ming SC (1977) Gastric carcinoma. A pathobiological classification. Cancer 39:2475–2485
21. Nagel S, Borisch B, Thein SL, Oestreicher M, Nothiger F, Birrer S, Tobler A, Fey MF (1995) Somatic mutations detected by mini- and microsatellite DNA markers reveal clonal intratumor heterogeneity in gastrointestinal cancers. Cancer Res 55:2866–2870
22. Nio Y, Tsubono M, Kawabata K, Masai Y, Hayashi H, Meyer C, Inoue K, Tobe T (1993) Comparison of survival curves of gastric cancer patients after surgery according to the UICC stage classification and the general rules for gastric cancer study by the Japanese Research Society for gastric cancer. Ann Surg 218:47–53
23. Rhyu M-G (1998) Genetic events underlying morphological complexity of gastric carcinoma. J Korean Med Sci 13:339–349
24. Sepulveda AR, Wu L, Ota H, Gutierrez O, Kim JG, Genta RM, Graham DY (2000) Molecular identification of main cellular lineages as a tool for the classification of gastric cancer. Hum Pathol 31:566–574
25. Shiao YH, Bovo D, Guido M, Capella C, Cassaro M, Busatto G, Russo V, Sidoni A, Parenti AR, Rugge M (1999) Microsatellite instability and/or loss of heterozygosity in young gastric cancer patients in Italy. Int J Cancer 82:59–62
26. Shiu MH, Perrotti M, Brennan MF (1989) Adenocarcinoma of the stomach: a multivariate analysis of clinical, pathologic and treatment factors. Hepatogastroenterology 36:7–12
27. Stemmermann GN, Brown C (1974) A survival study of intestinal and diffuse types of gastric carcinoma. Cancer 33:1190–1195
28. Thibodeau SN, Bren G, Schaid D (1993) Microsatellite instability in cancer of the proximal colon. Science 260:816–819
29. Weinberg RA (1991) Tumor suppressor genes. Science 254:1138–1146
30. Wu MS, Lee CW, Shun CT, Wang HP, Lee WJ, Sheu JC, Lin JT (1998) Clinicopathological significance of altered loci of replication error and microsatellite instability-associated mutations in gastric cancer. Cancer Res 58:1494–1497
31. Yustein AS, Harper JC, Petroni GR, Cummings OW, Moskaluk CA, Powell SM (1999) Allelotype of gastric adenocarcinoma. Cancer Res 59:1437–1441

Virchows Arch (2003) 443:501–507
DOI 10.1007/s00428-003-0863-6

ORIGINAL ARTICLE

Frauke Bataille · Frank Klebl · Petra Rümmele · Rainer H Straub · Peter Wild · Jürgen Schölmerich · Ferdinand Hofstädter

Histopathological parameters as predictors for the course of Crohn's disease

Received: 17 April 2003 / Accepted: 16 June 2003 / Published online: 24 July 2003
© Springer-Verlag 2003

Abstract *Background:* Recent classification systems discriminate penetrating Crohn's disease (CD) from stricturing and non-stricturing/non-penetrating CD. As yet, no easily detectable marker is known that can predict the course of CD. Individual, clinical course-specific new treatment schemes would be highly desirable for different potentially divergent pathophysiological pathways (e.g., fistula vs stenosis).*Methods:* Intestinal tissue biopsies from 63 CD patients with a disease follow-up of up to 7 years were studied retrospectively. In biopsy specimens, 34 histopathological features present prior to the onset of (a) strictures or (b) fistulas were evaluated and compared with biopsies from patients with non-stricturing/non-penetrating disease.*Results:* Five histomorphological parameters demonstrated significant associations to different disease courses when applying univariate analysis. In a multivariate logistic regression model (1) severe lymphocytic infiltration of the lamina propria, (2) presence of crypt atrophy, and (3) absence of lymphocytic infiltration of the epithelium are the best variables to predict an uncomplicated disease course (Nagelkerke R2=0.329; *P*=0.001). The combination of these parameters has a sensitivity of 67% and a specificity of 83% to predict non-stricturing/non-penetrating disease (positive predictive value=0.75).*Conclusion:* Histopathological parameters may help to predict complications of CD prior to their onset. The results of this study have to be confirmed prospectively.

Keywords Crohn's disease · Histological feature · Disease behavior

F. Bataille (✉) · P. Rümmele · P. Wild · F. Hofstädter
Department of Pathology, University of Regensburg,
93042 Regensburg, Germany
e-mail: frauke.bataille@klinik.uni-regensburg.de
Tel.: +49-941-9446634
Fax: +49-941-9446602

F. Klebl · R. H. Straub · J. Schölmerich
Department of Internal Medicine I, University of Regensburg,
93042 Regensburg, Germany

Introduction

Crohn's disease (CD) is a chronic inflammatory condition of the intestine that is characterized by a variable extent of periods of remission and episodes of clinical activity in individual patients. Clinical research of the last decade has suggested that it is a heterogeneous entity that requires individual approaches for management, as indicated, for example, by the wide variations of intestine affected and the different endoscopic expressions of involvement [11]. Main intestinal complications include stricture and fistula or abscess formation. To define more homogeneous subgroups of CD, the recently developed Vienna classification of CD [2] distinguishes a penetrating and a stricturing from a non-penetrating/non-stricturing disease. As yet, there is no laboratory test, clinical, endoscopical, or radiological feature known that can predict the development of these complications prior to their onset and, therefore, would enable an early decision on further disease course-specific management of individual patients.

CD itself has characteristic histopathological features that have been described in several studies [8, 19]. Usually, the correct histological diagnosis in resected specimens is easily made. In biopsy specimens, histological examination has been recognized as a helpful tool in differential diagnosis of CD versus ulcerative colitis and other entities.

During periods of active disease, the intestinal mucosa is infiltrated with inflammatory cells that contribute to the destruction of the extracellular matrix and formation of epithelial ulceration [10]. Resolution of inflammatory activity is associated with reparative processes that facilitate tissue remodeling. However, stricture formation frequently occurs in patients with CD [4] and is usually associated with persistent epithelial ulceration. Why a subgroup of CD patients is prone to the development of this complication is not understood, although patients with mutation in the CARD15/NOD2 gene present with a stricturing phenotype more frequently than those without this mutation [9]. There is not much information available

Table 1 Characteristics of 63 patients with Crohn's disease. The total numbers (*n*) of patients in each subgroup as well as mean age and duration of disease (range) in years are given. In addition, total numbers (*n*) of tissue biopsies studied and their location are included

	Fistula		Stenosis		Non-stricturing/non-penetrating
Total population	*n*=21		*n*=15		*n*=27
Age (years)	38 (24–52)		38 (28–48)		37 (22–49)
Female/male	11/10		6/9		14/13
Duration	3.4 (1.5–6.5)		3.7 (1.5–7.4)		3.3 (1.5–7.0)
Total tissue biopsies	286		215		672
Terminal Ileum	29*	18**	32*	4**	81
Colon	157*	82**	156*	23**	591

* Tissue biopsies taken 1–2 years prior to the onset of stenosis/fistula
** Tissue biopsies taken 3–9 months prior to the onset of stenosis/fistula

on various histological features of intestinal mucosa prior to the development of fistula or stenosis. The value of histological parameters, which directly describe the intestinal inflammation for the prediction of disease courses, has not been assessed.

The aim of this retrospective evaluation of biopsy specimens from patients with CD was to determine histological features that may distinguish patients with predominantly penetrating or stricturing CD in the later course from patients without these complications.

Materials and methods

Patients

This study was performed retrospectively. A total of 1173 intestinal tissue biopsies of ileum (*n*=164) and colorectum (*n*=1009) from 63 patients with CD were studied. The series were obtained from unselected consecutive files at the Department of Pathology of the University of Regensburg. Biopsies were taken between January 1992 and December 1999. All histopathological sections were evaluated by a single pathologist who was blinded to the clinical data of the patients except for the origin of the biopsy. In a population-based cohort of patients with known CD, 34 histological parameters were compared among CD with stricturing, penetrating, or uncomplicated disease course. "Stricturing disease" was defined as the occurrence of constant luminal narrowing demonstrated by radiological, endoscopical, or surgical examination combined with prestenotic dilatation and/or obstructive signs or symptoms without evidence of penetrating disease. "Penetrating disease" was defined as the occurrence of intra-abdominal or perianal fistulas, inflammatory masses, and/or abscesses at any time in the course of the disease [2]. The term "non-stricturing/non-penetrating disease" was reserved for uncomplicated inflammatory disease without evidence of stricturing or penetrating disease, but with repeatedly severe inflammation.

Patients had a disease follow-up of up to 7.4 years. The mean observation time of patients with stricturing or penetrating CD was 3.5 years (range 1.5–7.4 years). The observation period of patients without complications (non-stricturing/non-penetrating) was 3.3 years (range 1.5–7.0 years). Histopathological characteristics in biopsies taken 1–2 years and 3–9 months prior to the onset of strictures and fistulas, respectively, were compared with those in biopsies of patients with a non-complicated disease course. The diagnosis of CD was based on well-established clinical, endoscopical, and radiological parameters [2, 11] and on histological examination of resected specimens. Details on studied subgroups, localization of biopsies taken, and patient data are given in Table 1.

Biopsy preparation

Tissue specimens were fixed in 4% buffered formalin for at least 24 h and embedded in paraffin. Sections approximately 2–3 μm thick were cut from tissue blocks and stained with hematoxylin and eosin and periodic acid-Schiff according to standard protocols. At leastnine serial sections from each biopsy specimen were evaluated with calculation of mean values for each histological parameter.

Histopathological evaluation

All tissue specimens were studied using a standardized protocol, including 34 histological parameters (according to [19]; Table 2). This included evaluation of the epithelium (e.g., infiltration with neutrophils, eosinophils, lymphocytes, assessment of goblet cells, presence of atypical cells or paneth cell metaplasia), erosions and ulcers, infiltration of the lamina propria (neutrophils, eosinophils, lymphocytes), disturbance of the crypt structure, presence of fibrosis, fibrolamelar proliferation, edema, bleeding, and granuloma. All biopsies were evaluated by two pathologists (F.B., P.R.). Discussion to obtain consent was necessary very rarely. Main histopathological criteria are shown in Fig. 1.

The 34 histological attributes comprised: (a) 14 morphological features defined as present or absent and (b) 20 parameters whose distribution was documented—defined as focal versus diffuse. Definitions and expression of histological features are given in Table 2.

All histological features selected in this study can be recognized easily in daily pathology practice and do not require any special methods. Histiocytes and mast cells were not included in the list because their accurate recognition requires immunohistochemistry.

Statistics

Uni- and multivariate regression analysis was performed to determine predictors of clinical behavior. Cross-table analysis was initially undertaken in univariate fashion by chi-square testing or Fisher-exact test where appropriate. Multivariate logistic regression was then performed by Nagelkerke to adjust for potential confounders and determine the independent contribution

Fig. 1 Examples for the characteristics of the 34 histological parameters studied in all tissue specimens. **a** Crypt atrophy of colonic mucosa [hematoxylin and eosin (HE), ×200]. **b** Severe infiltration of the lamina propria by lymphocytes (*arrow*) (HE, ×400). **c** Excess of eosinophils in the lamina propria (*arrow*) (HE, ×400). **d** Excess of intraepithelial lymphocytes in colonic epithelium (*arrow*) (HE, ×400). **e** Excess of intraepithelial neutrophils in colonic epithelium (*arrow*) (HE, ×400). **f** Colonic epithelium with paneth cell metaplasia (*arrow*) (HE, ×400). **g** Fibrolamelar proliferation in the lamina propria (*arrow*) (HE, ×400)

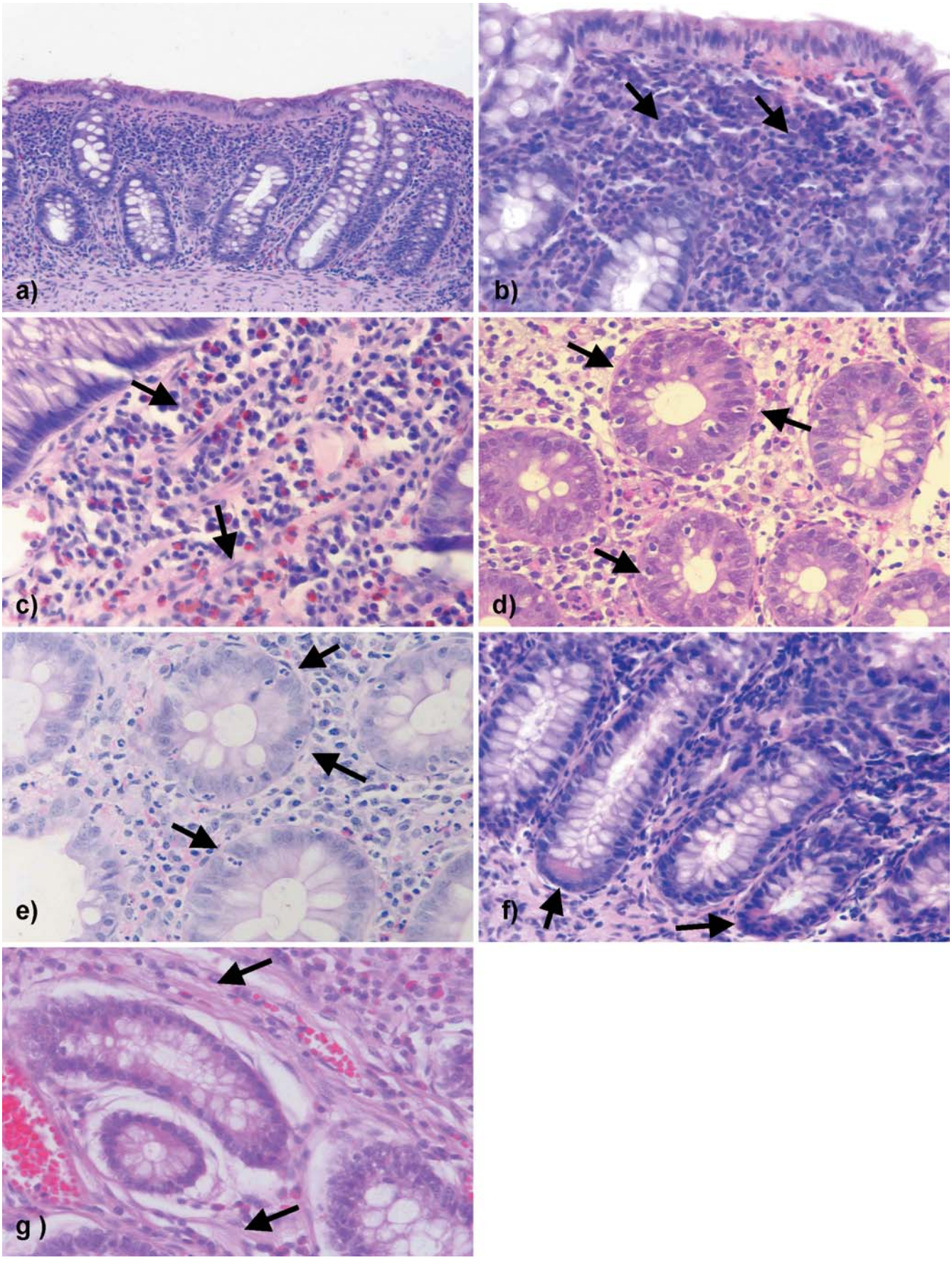
a)
b)
c)
d)
e)
f)
g)

Table 2 Histological features evaluated in ileocolonic biopsy specimens

Feature number	Description	Additional information
	Mucosal surface	
1	Mucosal surface (intact/segmental distribution)	
2	Excess of intraepithelial neutrophils	Features 2–4: excess of intraepithelial neutrophils, eosinophils, or lymphocytes was recorded as being present if more than 3 neutrophils and eosinophils, or more than 15 lymphocytes were observed within 100 surface epithelial cells [6, modified]
3	Excess of intraepithelial eosinophils	
4	Excess of intraepithelial lymphocytes	
	Mucus content	
5		Features 5–7: goblet cell reduction was divided into no or minimal (absent), or mild and severe. Goblet cell reduction was judged as "severe" when goblet cell mucin was almost completely exhausted in at least two crypts. "Focal" or "diffuse" described a change or no change in the pattern within a single biopsy specimen, respectively [19]
6		
7		
8	Dysplasia	Feature 8: "dysplasia" is reserved for epithelial changes that are unequivocally neoplastic, according to Riddell's classification [12]
9	Paneth cell metaplasia	Feature 9: paneth cell metaplasia was recorded as present only if it was found from the hepatic flexure to the rectum. In normal colon, paneth cells are occasionally found in the cecum and proximal ascending colon [19]
10	Pseudomembrane	
11	Pseudopolyp	
12	Inflammation with regenerative epithelium	
13	Focal erosion	Features 13–15: an erosion or ulceration was diagnosed if neutrophils were present in the base of an area with loss of the epithelial surface [7]
14	Segmental erosion	
15	Aphthoid ulceration	
	Lamina propria	
16	Lamina propria inflammation (focal/diffuse)	
17	Neutrophil infiltration in lamina propria (low/severe)	
18	Neutrophil infiltration deeper than 2/3 of the mucosal height	
19	Eosinophil infiltration in lamina propria (low/severe)	
20	Eosinophil infiltration deeper than 2/3 of the mucosal height	
21	Lymphoid infiltration in lamina propria (low/severe)	
22	Lymphoid infiltration deeper than 2/3 of the mucosal height	
23	Crypt architecture (normal/distorted)	Feature 23: crypt architecture was defined as being normal if the crypts were parallel, and the space between them was not excessive (see definition of "atrophy"). It was distorted if the crypts were dilatated, tortured, or branched within a well-orientated biopsy specimen [16, 18]
24	Crypt abscess	Feature 24: a crypt abscess was a chain of neutrophils extending from the lamina propria through the crypt epithelium into the lumen of the crypt [7]
25	Cryptitis	Feature 25: cryptitis was defined as a migration of inflammatory cells into the crypt epithelium combined with focal lysis of the epithelial cells [7]
26	Crypt distortion	
27	Crypt atrophy	Feature 27: crypt atrophy was diagnosed if the crypts were shortened and more widely spaced, and if there was a gap between the bottom of the crypts and the muscularis mucosa [7]
28	Lamina propria changes (focal/diffuse)	
29	Fibrosis	
30	Fibrolamelar proliferation	
31	Edema	
32	Hemorrhage	
33	Epithelioid granulomas	Feature 33: an epithelioid granuloma was an agglomeration of at least five epithelioid cells without caseating necrosis or foreign bodies [7]
34	Epithelioid granulomas with giant cells	Feature 34: giant cells contained multiple nuclei and homogeneous, fine, powdery cytoplasm without foreign bodies [7]

of each factor. Sensitivity, specificity, and positive predictive values of the multivariate logistic regression models were calculated to predict non-stricturing/non-penetrating, stricturing, and penetrating disease courses. Statistics were computed using SPSS software (SPSS, Inc.; Chicago, IL). All statistical tests were performed two-sided, with a P value of <0.05 considered statistically significant. Due to the explorative nature of this study, Bonferroni's adjustment for multiple comparisons was not used.

Results

Using univariate analysis, five histopathological parameters showed significant differences between subgroups of CD patients when comparing non-stricturing/non-penetrating CD with penetrating and stricturing CD 1–2 years and 3–9 months prior to the onset of complication. Uncomplicated disease was associated with a higher prevalence of extensive infiltration of the lamina propria with lymphocytes (P=0.012) and eosinophils (P=0.035) as well as crypt atrophy (P=0.027). Severe eosinophilic infiltration of the lamina propria was missing in all biopsies obtained 3–9 months prior to the development of a fistula or a stenosis. Excess of intraepithelial lymphocytes (P=0.010) and paneth cell metaplasia (P=0.034) was more frequently found in biopsies of patients with penetrating disease (Table 3).

Many other features (e.g., excess of intraepithelial eosinophils and neutrophils, presence of pseudopolyps, cryptitis, edema, hemorrhage, or epitheloid granuloma) did not show significant differences between the subgroups of patients when performing univariate analysis. In particular, the extent of fibrosis or fibrolamelar proliferation was not predictive for any clinical category.

By applying logistic regression analysis, best variables to predict an uncomplicated disease course were: (1) severe lymphocytic infiltration of the lamina propria, (2) presence of crypt atrophy, and (3) absence of lymphocytic infiltration of the epithelium (Table 4). In our series of patients, 18 of 27 patients with uncomplicated disease but only 3 of 21 patients with penetrating disease and 3 of 15 patients with stricturing disease would have fulfilled these

Table 3 Five histological parameters showed significant differences between subgroups of Crohn's disease in univariate analysis. Given are the number of patients and intestinal tissue biopsies of the colon that expressed the feature studied

Histological feature	Biopsy 1–2 years prior onset of stenosis/fistula		Biopsy 3–9 months prior onset of stenosis/fistula		Non-stricturing/ non-penetrating CD	P value
Patients (n)	12	12	3	9	27	
Tissue biopsies (n)(ileum/colon)	32/156	29/157	4/23	18/82	81/591	
Excess of eosinophils in lamina propria	3* 6/43**	3* 4/31**	0* 0/0**	0* 0/0**	10* 27/227**	0.035
Excess of lymphocytes in lamina propria	6* 20/75**	5* 12/61**	1* 2/9**	3* 6/23**	21* 67/502**	0.012
Presence of crypt atrophy	4* 8/56**	7* 15/105**	1* 2/9**	4* 9/52**	21* 65/483**	0.027
Excess of intraepithelial lymphocytes	0* 0/0**	1* 1/14**	0* 0/0**	3* 6/32**	0* 0/0**	0.010
Presence of paneth cell metaplasia	1* 4/8**	0* 0/0**	0* 0/0**	2* 5/22**	1* 4/29**	0.034

* Patients (n)
** Tissue biopses, ileum/colon (n)

Table 4 Histological characteristics for subgroups of Crohn's disease with different clinical course. Features were chosen depending on their impact in multivariate logistic regression analysis models

Histological feature	P value	
Prediction of uncomplicated clinical course		
Absence of intraepithelial lymphocytes	0.034	Nagelkerke R2=0.329 P=0.001
Severe lymphoid infiltration in lamina propria	0.035	
Presence of crypt atrophy	0.016	
Prediction of penetrating clinical course		
Presence of intraepithelial lymphocytes	0.001	Nagelkerke R2=0.271 P=0.001
Presence of fibrolamelar proliferation	0.037	
Prediction of stricturing clinical course		
Presence of intraepithelial neutrophils	0.015	Nagelkerke R2=0.457 P=0.001
Goblet cell reduction in crypts with surrounding neutrophils	0.006	
Presence of paneth cell metaplasia	0.051	
Excess of neutrophils in lamina propria	0.007	
Presence of crypt atrophy	0.001	
Presence of fibrosis	0.020	

criteria. Therefore, the combination of the three histological criteria would have yielded a sensitivity of 67%, a specificity of 83%, and a positive predictive value of 0.75 for non-stricturing/non-penetrating disease.

The best logistic regression model to predict penetrating disease contained two histopathological parameters: (1) presence of intraepithelial lymphocytes and (2) presence of fibrolamelar proliferation (Table 4). Only 2 of 21 patients with fistula formation would have been detected, reflecting a sensitivity of 10%. However, specificity was high with 100% (positive predictive value 1.00). Six histopathological parameters were included in the best model to predict stricturing disease: (1) presence of intraepithelial neutrophils, (2) goblet cell reduction in crypts with surrounding neutrophils, (3) presence of paneth cell metaplasia, (4) severe neutrophilic infiltration of the lamina propria, (5) presence of crypt atrophy, and (6) presence of fibrosis (Table 4). If in another model only four features were used (excess of intraepithelial neutrophils, goblet cell reduction in crypts with surrounding neutrophils, neutrophils in lamina propria, and crypt atrophy), only 2 of 15 patients with stricturing CD would be detected, corresponding to a sensitivity of 13% and a high specificity of 100% (positive predictive value 1.00, Nagelkerke R2=0.326).

Discussion

Prediction of disease development in CD is a difficult task. Most previous studies have focused on predicting disease activity (e.g., the lactulose/L-rhamnose ratio may be changed prior to a clinical relapse in CD [5,20,22] with the limitation that the ratio can only be used in CD patients with small bowel disease). Other studies have shown that the assessment of intestinal permeability has a fairly good predictive value for a flare up with a sensitivity of 84% and a specificity of 61% [17, 21]. Fecal calprotectin has been suggested as a marker of mucosal inflammatory activity in patients with inflammatory bowel disease and correlates well with histological and endoscopic disease activity [13, 14]. In addition, cytokines have been evaluated as predictors of disease activity [15]. Schreiber et al. reported that increased production of tumor necrosis factor α and interleukin-1β by intestinal lamina propria cells were associated with a relapse in patients who were in steroid-induced remission [15].

Less information is available on predictive markers of disease behavior. Differences in submucosal type-III collagen deposition may contribute to the formation of clinical stenosis rather than smooth-muscle cell proliferation [1]. Neomuscularization is not associated with the production of collagen [1]. Despite many diagnostic tools available, differential predictive diagnosis of subgroups of CD is not yet possible. No reliable marker with a sufficiently high predictive value for treatment failure has been identified. This might be due to the heterogeneity of CD with many clinical phenotypes, which requires subgroup analysis with high numbers of patients [3].

Previous studies on histopathological features have investigated factors discriminating chronic inflammatory bowel disease from non-chronic inflammatory bowel disease, and CD from ulcerative colitis. For example, Seldenrijk et al. [16] postulated three parameters with a high predictive value for the separation of CD from ulcerative colitis: an excess of histiocytes, in combination with a villous or irregular aspect of the mucosal surface, and granulomas.

The aim of this retrospective study was to identify histopathological factors predictive for disease behavior in CD. We demonstrate qualitative and quantitative differences in the inflammatory infiltrate and other histopathological parameters in non-stricturing/non-penetrating and later stricturing or penetrating disease. Mucosal histology considerably differs among patients belonging to these different groups long before the behavioral phenotype manifests clinically. Five histopathological features were observed to be significantly different in the univariate analysis: (1) excess of lymphocytes in lamina propria, (2) excess of eosinophils in lamina propria, (3) presence of crypt atrophy, (4) excess of intraepithelial lymphocytes, and (5) presence of paneth cell metaplasia. In a logistic regression model, severe lymphoid infiltration of the lamina propria in combination with crypt atrophy and absence of intraepithelial lymphoid infiltration were observed in 67% of patients with non-stricturing/non-penetrating disease. This combination of features was absent in 86% of patients with penetrating CD and 80% of those with stricturing CD. To our knowledge, the positive predictive value of 0.75 for an uncomplicated disease is the best published value in CD.

Histological examination of intestinal biopsy specimens provides information that compliments clinical and endoscopic findings when diagnosing CD. The results of this study suggest that it may also enable prediction of the further clinical course in a subset of patients. To our knowledge, no other study has examined associations of histopathological features and future complications in CD patients.

Of course, the findings of this study have to be confirmed in a prospective analysis in a larger cohort of patients. This study should also include intestinal biopsies of patients with complications that were taken just prior to the onset of strictures or fistulas and cases in which complications already had occurred. Such an evaluation was not possible in this study because of its retrospective design. Potentially, it will shed more light on the pathophysiology of fistula and stricture formation. If this is successful, simple histopathological scoring systems may be used to predict the clinical course of CD. Prediction of complications may lead to a more aggressive therapy of CD prior to the onset of fistulas and strictures. This may help to lower the incidence of these complications and to optimize individual care for CD patients.

Acknowledgement This work was supported by the Bundesministerium für Bildung und Forschung (BMBF) Competence network "Inflammatory Bowel Disease".

References

1. Borley NR, Mortensen NJ, Kettlewell M, George B, Jewell D, Warren B (2001) Connective tissue changes in ileal Crohn's disease: relationship to disease phenotype and ulcer-associated cell lineage. Dis Colon Rectum 44:388–396
2. Gasche C, Scholmerich J, Brynskov J, D'Haens G, Hanauer SB, Irvine EJ, Jewell DP, Rachmilewitz D, Sachar DB, Sandborn WJ, Sutherland LR (2000) A simple classification of Crohn's Disease: report of the Working Party for the World Congresses of Gastroenterology, Vienna 1998. Inflamm Bowel Dis 6:8–15
3. Gelbmann CM (2000) Prediction of treatment refractoriness in ulcerative colitis and Crohn's disease—do we have reliable markers? Inflamm Bowel Dis 6:123–131
4. Graham MF, Diegelmann RF, Elson CO, Lindblad WJ, Gotschalk N, Gay S, Gay R (1998) Collagen content and types in the intestinal strictures of Crohn's disease. Gastroenterology 94:257–265
5. Hilsden RJ, Meddings JB, Hardin J, Gall DG, Sutherland LR (1999) Intestinal permeability and postheparin plasma diamine oxidase activity in the prediction of Crohn's disease relapse. Inflamm Bowel Dis 5:85–91
6. Hirata I, Berrebi G, Austin LL, Keren DF, Dobbins WO (1986) Immunohistological characterization of intraepithelial and lamina propria lymphocytes in control ileum and colon and inflammatory bowel disease. Dig Dis Sci 31:593–603
7. Le Berre NL, Heresbach D, Kerbaol M, Caulet S, Bretagne JF, Chaperon J, Gosselin M, Ramée MP (1995) Histological discrimination of idiopathic inflammatory bowel disease from other types of colitis. J Clin Pathol 48:749–753
8. Lennard Jones JE (1989) Classification of inflammatory bowel disease. Scand J Gastroenterol 170[Suppl]:2–6
9. Lesage S, Zouali H, Cezard JP, Colombel JF, Belaiche J, Almer S, Tysk C, O'Morain C, Gassull M, Binder V, Finkel Y, Modigliani R, Gower-Rousseau C, Macry J, Merlin F, Chamaillard M, Jannot AS, Thomas G, Hugot JP (2002) CARD15/NOD2 mutational analysis and genotype-phenotype correlation in 612 patients with inflammatory bowel disease. Am J Hum Genet 70:845–857
10. McAlindon ME, Gray T, Galvin A, Sewell HF, Podolsky DK, Mahida YR (1998) Differential lamina propria cell migration via basement membrane pores of inflammatory bowel disease mucosa. Gastroenterology 115:841–848
11. Modigliani R and the GETAID group (1990) Clinical, biological and endoscopic picture of attacks of Crohn's disease. Gastroenterology 98:811–818
12. Riddell RH, Goldman H, Ransohoff DF, Appelman HD, Fenaglio CM, Haggitt RC, Ahren C, Correa P, Hamilton SR, Morson BC (1983) Dysplasia in inflammatory bowel disease: standardized classification with provisional clinical applications. Hum Pathol 14:931–968
13. Roseth AG, Aadland E, Jahnsen J, Raknerud N (1997) Assessment of disease activity in ulcerative colitis by faecal calprotectin, a novel granulocyte marker protein. Digestion 58:176–180
14. Roseth AG, Fagerhol MK, Aadland E, Schonsby H (1992) Assessment of the neutrophil dominating protein calprotectin in feces. A methodologic study. Scand J Gastroenterol 27:793–798
15. Schreiber S, Nikolaus S, Hampe J, Hamling J, Koop I, Groessner B, Lochs H, Raedler A (1999) Tumor necrosis factor alpha and interleukin 1 beta in relapse of Crohn's disease. Lancet 353:459–461
16. Seldenrijk CA, Morson BC, Meuwissen SG, Schipper NW, Lindeman J, Meijer CJ (1991) Histopathological evaluation of colonic mucosal biopsy specimens in chronic inflammatory bowel disease: diagnostic implications. Gut 32:1514–1520
17. Senju M, Wu KC, Mahida YR, Jewell DP (1990) Two color immunofluorescence and flow cytometric analysis of lamina propria lymphocyte subsets in ulcerative colitis and Crohn's disease. Dig Dis Sci 36:1453–1458
18. Surawicz CM, Belic L (1984) Rectal biopsy helps to distinguish acute self-limited colitis from idiopathic inflammatory bowel disease. Gastroenterology 86:104–113
19. Tanaka M, Riddell RH, Saito H, Soma Y, Hidaka H, Kudo H (1999) Morphologic criteria applicable to biopsy specimens for effective distinction of inflammatory bowel disease from other forms of colitis and of Crohn's disease from ulcerative colitis. Scand J Gastroenterol 34:55–67
20. Teahon K, Smethurst P, Levi A, Menzies IS, Bjarnason I (1992) Intestinal permeability in patients with Crohn's disease and their first degree relatives. Gut 33:320–323
21. Tibble JA, Sigthorsson G, Bridger S, Fagerhol MK, Bjarnason I (2000) Surrogate markers of intestinal inflammation are predictive of relapse in patients with inflammatory bowel disease. Gastroenterology 119:15–22
22. Wyatt J, Vogelsang H, Hubl W, Waldhoer T, Lochs H (1993) Intestinal permeability and the prediction of relapse in Crohn's disease. Lancet 341:1437–1439

Virchows Arch (2003) 443:508–517
DOI 10.1007/s00428-003-0884-1

ORIGINAL ARTICLE

Robert Grützmann · Melanie Foerder · Ingo Alldinger · Eike Staub · Thomas Brümmendorf · Stefan Röpcke · Xinzhong Li · Glen Kristiansen · Ralf Jesnowski · Bence Sipos · Matthias Löhr · Jutta Lüttges · Detlef Ockert · Günter Klöppel · Hans Detlev Saeger · Christian Pilarsky

Gene expression profiles of microdissected pancreatic ductal adenocarcinoma

Received: 30 April 2003 / Accepted: 10 June 2003 / Published online: 27 August 2003
© Springer-Verlag 2003

Abstract In a search for new molecular markers of pancreatic ductal adenocarcinoma (PDAC), we compared the gene expression profiles of seven pancreatic carcinomas and one carcinoma of the papilla Vateri with those of duct cells from three non-neoplastic pancreatic tissues. In addition, the human pancreatic duct cell line and five PDAC cell lines (AsPC-1, BxPC-3, Capan-1, Capan-2, HPAF) were examined. RNA was extracted from microdissected tissue or cultured cell lines and analysed using a custom-made Affymetrix Chip containing 3023 genes, of which 1000 were known to be tumour associated. Hierarchical clustering revealed 81 differentially expressed genes. Of all the genes, 26 were downregulated in PDAC and 14 were upregulated in PDAC. In PDAC cell lines versus normal pancreatic duct cells, 21 genes were downregulated and 20 were upregulated. Of these 81 differentially expressed genes, 15 represented human genes previously implicated in the tumourigenesis of PDAC. From the genes that were so far not known to be associated with PDAC tumorigenesis, we selected ADAM9 for further validation because of its distinct overexpression in tumour tissue. Using immunohistochemistry, the over-expressed gene, ADAM9, was present in 70% of the PDACs analysed. In conclusion, using microarray technology we were able to identify a set of genes whose aberrant expression was associated with PDAC and may be used to target the disease.

Keywords Pancreatic cancer · Expression profiling · Microarray hybridisation · Immunohistochemistry · Microdissection · ADAM9

R. Grützmann · M. Foerder · I. Alldinger · D. Ockert · H. D. Saeger · C. Pilarsky (✉)
Department of Visceral, Thoracic and Vascular Surgery,
University Hospital Carl Gustav Carus,
Technical University of Dresden,
Germany
e-mail: Christian.Pilarsky@mailbox.tu-dresden.de
Tel.: +49-351-4582742
Fax: +49-351-4584395

E. Staub · T. Brümmendorf · S. Röpcke · X. Li
metaGen Pharmaceuticals,
Berlin, Germany

G. Kristiansen
Department of Pathology,
Charité,
Berlin, Germany

R. Jesnowski · M. Löhr
Molecular Gastroenterology, II. Department of Internal Medicine,
Faculty of Clinical Medicine Mannheim, University of Heidelberg,
Germany

B. Sipos · J. Lüttges · G. Klöppel
Department of Pathology,
University of Kiel,
Germany

Introduction

Pancreatic ductal adenocarcinoma (PDAC) is an important cause of malignancy-related death. In the United States, it ranks fifth among the leading causes of cancer death, accounting for approximately 30,000 deaths annually [25]. Apart from surgery, there is no effective therapy and even resected patients usually die within 1 year of the operation. In the past years, several cancer-related genes have been identified in PDAC. Most frequently affected are K-ras, DPC4, p53 and p16 [19, 55], all of which appear to play a role in the development of PDAC. However, considering the complexity of the genome, it is most likely that most of the molecular changes causing PDAC still need to be elucidated [6].

Recently, DNA microarray technology has been applied to a number of tumours, e.g. breast [57], colon [1, 44, 60], prostate [37], oesophagus [51], stomach [18] and pancreas [10, 13, 22]. These studies generated large sets of new class-II cancer genes [49], revealing dysreg-

Table 1 Patients, their clinical and pathological data. *PDAC* pancreatic ductal adenocarcinoma

Code	Gender	Age[a]	Histology	T	N	M	Grading
PT10	Female	62 years	PDAC	3	1b	0	2
PT33	Female	73 years	PDAC	3	1b	0	3
PT35	Male	74 years	PDAC	2	0	0	3
PT39	Male	59 years	PDAC	2	0	0	2
PT44	Male	64 years	PDAC involving ampulla of Vateri	3	0	0	3
PT55	Male	66 years	PDAC with anaplastic component	3	1b	0	3
PT56	Female	71 years	PDAC	3	1a	0	3

[a] At time of operation

ulation at the level of gene expression. However, most of these studies were performed on either cell lines or whole tissue samples. In cell lines, in vitro conditions may induce changes in gene expression that are not present in vivo. When whole tissues are used in such studies, the expression profiles may represent both the tumour and the surrounding stromal tissue. Therefore, microdissection is the method of choice to generate a true picture of gene expression changes [35, 56]. In this study, we used microdissected tumour tissue and normal ductal epithelium. RNA extracted from these tissues were analysed using a cancer microarray containing 3023 genes. About 30% of these genes were included because of their association with various tumours. We identified genes whose expression levels differed significantly between malignant and benign pancreatic cells of ductal phenotype in order to generate a list of genes that may be used as diagnostic markers or as targets for new therapeutic approaches.

Materials and methods

Patients and tissues

Freshly frozen tissue samples of PDAC (n=7)—one involving the ampulla of Vateri—and of normal pancreas (n=3) were obtained from surgical specimens from patients who were operated on at the Department of Visceral, Thoracic and Vascular Surgery, University Hospital Carl Gustav Carus, Technical University of Dresden, between 1996 and 2001 (Table 1). The normal pancreatic tissue was from three patients who underwent pancreatic resection for malignancies unrelated to the pancreas. Prior to surgery, all had signed an informed consent form that had been approved by the local ethics committee. Immediately after surgical removal, the specimens were sectioned and microscopically evaluated. Suitable samples of tumour tissue or normal tissue were snap frozen in liquid nitrogen and stored at −80°C until further processing.

Cell culture

The established pancreatic cell lines AsPC-1 (CRL-1682), BxPC-3 (CRL-1687), Capan-1 (HTB-79), Capan-2 (HTB-80), and HPAF (CRL-1997) [54] were gifts from M. Schmitz, Department of Immunology, University of Dresden. They were cultured in RPMI 1640 (GIBCO) supplemented with 10% foetal bovine serum, 2 mM glutamine (GIBCO), non-essential amino acids (5 ml/l), penicillin (10,000 units/ml) and streptomycin (10 mg/ml) and passaged before they reached confluency.

The normal human pancreatic ductal cell line hPDC was prepared as follows [36]: non-neoplastic pancreatic tissue was obtained from patients undergoing surgery for chronic pancreatitis. The main pancreatic duct was dissected from the surrounding tissue and transferred to a tissue culture dish. The duct was then minced, and pieces of tissue were distributed evenly over the surface of the culture dish in a small volume of culture medium (500 μl/60 mm dish). Subsequently, an additional 2 ml of culture medium [Gibco Keratinocyte SFM supplemented with 5 ng/ml epidermal growth factor (EGF), 50 μg/ml BPE and 50 μg/ml Fungizone] were added. The pieces of tissue were cultured until colonies of outgrowing cells reached a diameter of about 10 mm. The tissue pieces were then removed and transferred to a new culture dish for a second round of outgrowth. In order to confirm that the cells were of epithelial origin, they were stained immunohistochemically for the epithelial marker cytokeratin 19.

Microdissection

Frozen tissue specimens were serially cut into 10-µm-thick sections and immediately fixed on slides in ice-cooled 70% ethanol. The sections were briefly stained with haematoxylin and eosin, dehydrated in ethanol and xylene and air-dried for 1.5 h. The first slide served as a template on which the areas with PDAC or normal duct segments were marked. On the consecutive slides, these areas were microdissected using a laser capture microdissection system (SL, Jena, Germany). For molecular analysis, 10,000 cells were pooled and collected in ice-cooled tubes containing 100–150 mM 98% GTC buffer and 2% beta-mercaptoethanol. Neoplastic duct-type cells and normal ductal cells were obtained from different blocks from each case. The normal tissue was preferably taken from areas at the resection margin, as these areas contained the main duct from which a sufficient amount of cells could be microdissected.

RNA preparation and array hybridisation

Poly A^+ RNA from the microdissected surgical specimens and cell cultures was prepared using the PolyATtract 1000 kit (Promega, Heidelberg, Germany) according to the manufacturer's recommendations. For each sample, the cDNA synthesis and repetitive in vitro transcription were performed three times according to the technique of Luo et al., with minor modifications [38]. All of the prepared mRNA from one sample was used. To synthesise cDNA from the cell lines, we started with 10 ng of the prepared poly A^+ RNA. First strand cDNA synthesis was initiated using the Affymetrix T7-oligo-dT promoter-primer combination 5′-GGCCAGTGAATTGTAATACGACTCACTATAGGGAGGCG-GT24–3′ at 0.1 mM. The second strand cDNA synthesis was generated with internal priming. In vitro transcription was performed using Ambion's Megascript kit (Ambion, Huntington, UK) as recommended by the manufacturer. From the generated aRNA, a new first strand synthesis was initiated using 0.025 mM of a random hexamer as primer. After completion, the second strand synthesis was performed using the Affymetrix T7-oligo-dT promoter-primer combination as primer at a concentration of 0.1 mM. A second in vitro transcription was performed and then the procedure was repeated one additional time. During the last in vitro transcription, biotin-labelled nucleotides were incorporated into the aRNA, as recommended by the Affymetrix protocol. Hybridisation

and detection of the labelled aRNA on the metg001A GeneChip were performed according to Affymetrix's instructions.

Chip design and bioinformatics analysis

Affymetrix GeneChips technology was used to identify genes that are expressed in one tissue type but not in another. The custom metg001A GeneChip utilised in this study consists of 6117 probe sets resembling 3023 cDNA fragments. The cDNA fragments were chosen from a data mining approach to characterise the expression of cancers by an electronic northern [15, 50]. In addition, we selected genes of signal transduction cascades like the Wnt cascade, which are implicated in cancer development and progression. For normalisation, we chose a combination of background subtraction and scaling to the median of all feature values. The background was computed as the mean of the 2% darkest feature intensities. Then, for each feature value, the background was subtracted and divided by the median of all values. We used the 75% quantile of the intensities from the 20 perfect-matching oligonucleotides to generate a representative expression value for each probe set in an approach similar to that of Irizarry et al. [23]. To distinguish signal from noise, we applied the Wilcoxon signed rank test to each probe set. The probe set was labelled as present if the result of the Wilcoxon signed rank was below 0.01.

For each group (benign, tumour and cell lines) a median expression value was calculated. Fold changes of these values were calculated and a gene was used for further analysis if the fold change was above two in one comparison. Then, differentially expressed genes were identified from this subset by calculating difference values for each gene among the three tissue types analysed. To perform these calculations, we used the difference between the maximal and minimal values of one gene. In this manner, we selected genes that are expressed only in one tissue type based on our present call (Table 2). Hierarchical clustering was applied to group the genes and samples. For clustering, expression values of genes called absent were floored to 0.1 before cluster analysis. Complete linkage clustering was done using the software "Cluster and TreeView" (http://rana.lbl.gov/EisenSoftware.htm).

Gene annotation

The most recent annotation for each of the 81 differentially expressed genes was obtained by BLASTN searches [2] of the DNA chip sequences versus current versions of the human Unigene and RefSeq mRNA sequence databases. The respective protein sequences of the identified mRNA sequences were either previously known or were derived by translation of open-reading frames. We searched the resulting peptides for the occurrence of known protein domains from the SMART [34] and PFAM [7] domain collections. Signal peptides and transmembrane helices were predicted using SIGNALP [42] and TMHMM [30]. The most probable cellular localisation of a protein was identified by scanning the available literature for the protein itself or its domains.

Immunohistochemistry

From formalin-fixed paraffin-embedded PDAC and normal pancreatic tissue, 4-μm sections were cut. The sections were mounted on superfrost slides (Menzel Gläser, Braunschweig, Germany), dewaxed with xylene and gradually hydrated. Antigen was exposed by heating the sections under high pressure in Tris-EDTA-citrate buffer. The primary goat polyclonal anti-mouse ADAM9 antibody (AF949, R&D Systems, Wiesbaden, Germany), which cross-reacts with human ADAM9, was diluted (15 μg/ml) in phosphate buffered saline containing 2% horse serum (Vector Laboratories, Burlingame, CA, USA). After incubation for 45 min, the reaction was detected with a biotinylated anti-goat antibody (5 μg/ml, Vector Laboratories) and avidin-biotin-peroxidase (ABC ELITE, Vector Laboratories). Diaminobenzidine served as chromogen. Afterwards, the slides were briefly counterstained with haematoxylin. The primary antibodies were omitted for the negative control. The staining intensity was evaluated semi-quantitatively as negative, weak, moderate or strong.

Results

Gene expression data and hierarchical clustering

Using laser capture microdissection, pure PDAC tissue from seven patients and pure normal ductal epithelium from three patients were obtained. Gene expression profiles of these tissues were compared with each other and with those of the normal human pancreatic duct cell line and the five PDAC cell lines using DNA microarray technology.

In a first step to identify differentially expressed genes, we selected genes with a fold change greater than two by means of their median expression levels. This resulted in the selection of 828 genes. Of these, 53 genes were over-expressed in tumour versus benign tissue, 221 were over-expressed in cell lines, 223 were under-expressed in tumour and 331 were under-expressed in cell lines versus benign tissue, respectively. This reflects the different sample number sizes of the tissue types analysed. Since Affymetrix GeneChip technology offers the possibility to identify differentially expressed genes not only by their expression value, but also by their significance of detection, we performed such an analysis. Genes were thought to be differentially expressed if they were called present in all samples of one tissue type but called absent in all samples of another tissue type. Altogether, 81 differentially expressed genes were found (Table 2). Of all the genes, 26 were downregulated and 14 were upregulated in PDAC. In PDAC cell lines versus normal pancreatic duct cells, 20 were upregulated and 20 downregulated. Hierarchical clustering of the samples revealed three distinct clusters of: (1) cell lines, (2) primary tumours and (3) benign tissue, including the primary ductal cell line (Fig. 1). The differentially expressed genes reflect a diversity of function, including but not limited to, cell cycle control (STK15) or tissue invasion (S100A14).

Meta-analysis of the expression data

To interpret our results in a general context, we analysed the data already published on the 81 genes. Of these, 15 were found to represent human genes known to be implicated in the tumourigenesis of PDAC. We also compared our data with those of other groups who had identified differentially expressed genes in PDAC by means of microarrays (Table 2). Moreover, the results of the virtual Northern analysis from the NCBI for pancreatic tissue were included (http://cgap.nci.nih.gov/Tissues/VirtualNorthern?TEXT=0&ORG=Hs&CID=2442). Most

Table 2 Differentially expressed genes with their Unigene Cluster ID, the cluster in which the gene was found to be upregulated, the description of the gene, the putative cellular localisation, the putative cellular function, citations of papers concerning the gene and pancreatic cancer/expression profiling in pancreatic ductal adenocarcinoma (PDAC) and statistical values. *C* cytoplasmic, *N* nuclear, *E/M* extracellular or cell membrane, *U* unknown, *Median FC T* the fold change of the expression values of seven microdissected PDAC against the median fold change of three microdissected normal pancreatic ductal tissues, *Median FC cell lines* fold change of the median of five established pancreatic tumour cell lines against the median fold changer of the three microdissected normal pancreatic ductal tissues, *T* upregulated in pancreatic tumour tissue (significance level of 0.05), *N* downregulated in pancreatic tumours (significance level of 0.05) [using virtual Northern from NCBI for each of the differentially expressed genes (62,520 EST clones 5262 normal pancreatic EST and 57,258 tumour EST)] and 277,243 SAGE tags (64,208 normal and 213,035 tumour tags). The classification of the significance of the virtual Northern data was obtained from the web site. *NA* not accessible since this gene was not expressed in a type of samples. *T/N* over-expression in tumour, *C/N* over-expression in cell lines, *N/T or N/C* over-expression in normal tissue

Unigene ID	Description	Putative cellular localisation	Putative cellular function	FC T/N	FC C/N	High in–VS	Reference PDAC/ array	Virtual Northern
Hs.2442	A disintegrin and metalloproteinase domain 9 (meltrin gamma) (ADAM9)	E/M	Extracellular protein degradation	2.43		T/N	-/[22]	ns
Hs.61311	cDNA, 5′ end /clone= IMAGE:4616903/clone_end=5′ /gb= BG483649	U	U	3.21		T/N		ns
Hs.288660	cDNA: FLJ22182 fis	U	U	2.52		T/N	-/[21]	T
Hs.278613	Interferon, alpha-inducible protein 27 (IFI27)	C	Immune system	5.29		T/N	[20]/-	T
Hs.288998	S100-type calcium binding protein A14 (LOC57402)	C	Signal transduction	3.30		T/N		T
Hs.251754	Secretory leukocyte protease inhibitor (antileukoproteinase) (SLPI)	E/M	Extracellular protein degradation	2.95		T/N	-/[22]	T
Hs.102482	Tracheobronchial mucin (MUC5)	E/M	Extracellular structure	2.63		T/N	[39]/-	T
Hs.3337	Similar to transmembrane 4 superfamily member 1	U	U	2.01		T/N	[41]/-	ns
Hs.153752	Cell division cycle 25B (CDC25B), transcript variant 4	C	Cell cycle	N/A		T/N	[4]/-	ns
Hs.146688	Clone PP102 unknown mRNA	C	Metabolism	N/A		T/N		ns
Hs.17409	Cysteine-rich protein 1 (intestinal) (CRIP1)	U	U	N/A		T/N		T
Hs.115907	Diacylglycerol kinase, delta (130kD) (DGKD)	C	Signal transduction	N/A		T/N		ns
Hs.2726	HMGI-C protein	N	Transcription regulation	N/A		T/N		ns
Hs.154036	Tumour suppressing subtransferable candidate 3 (TSSC3)	N	Transcription regulation	N/A		T/N		T
Hs.82425	Actin related protein 2/3 complex, subunit 5 (16 kDa) (ARPC5)	C	Cell structure maintenance		3.99	C/N	-/[22]	ns
Hs.78225	Annexin A1 (ANXA1)	C	Signal transduction		2.94	C/N	-/[16, 21, 22]	T
Hs.7476	ATPase, H+ transporting, lysosomal (vacuolar proton pump) 21kD (ATP6F)	C	Metabolism		2.84	C/N		ns
Hs.7771	B-cell associated protein (REA)	C	Signal transduction		3.33	C/N		N
Hs.83758	CDC28 protein kinase 2 (CKS2)	C	Cell cycle		11.48	C/N	-/[16]	ns
Hs.90107	Cell membrane glycoprotein, 110000 M(r) (surface antigen) (GP110)	E/M	Extracellular structure		3.01	C/N		ns
Hs.289271	Cytochrome c-1 (CYC1)	C	Apoptosis		5.18	C/N		T
Hs.77393	Farnesyl diphosphate synthase (farnesyl pyrophosphate synthetase, dimethylallyltranstransferase, geranyltranstransferase) (FDPS)	C	Signal transduction		2.79	C/N		T
Hs.159557	Karyopherin alpha 2 (RAG cohort 1, importin alpha 1) (KPNA2)	N	Protein synthesis and transport		2.04	C/N	-/[22]	ns
Hs.32916	Nascent-polypeptide-associated complex alpha polypeptide (NACA)	C	Protein synthesis and transport		3.60	C/N		N

Table 2 (continued)

Unigene ID	Description	Putative cellular localisation	Putative cellular function	FC T/N	FC C/N	High in–VS	Reference PDAC/ array	Virtual Northern
Hs.83848	Triosephosphate isomerase 1 (TPI1)	C	Metabolism		7.00	C/N	-/[22]	T
Hs.1600	Clone IMAGE:3543711	C	Cell structure maintenance		4.17	C/N	-/[22]	T
Hs.82906	CDC20 (cell division cycle 20, S. cerevisiae, homolog) (CDC20)	C	Cell cycle		N/A	C/N		ns
Hs.244367	cDNA, 5′ end /clone= IMAGE:4303454 /clone_end=5′ /gb=BF686037	U	U		N/A	C/N		ns
Hs.183650	Cellular retinoic acid-binding protein 2 (CRABP2)	N	Transcription regulation		N/A	C/N		T
Hs.71779	DNA from chromosome 19, cosmid F21856	U	U		N/A	C/N		ns
Hs.11042	Hypothetical protein (LOC51248); 37% similar to discs large (Drosophila)	C	Signal transduction		N/A	C/N		ns
Hs.145362	Immortalization-upregulated protein (IMUP)	N	U		N/A	C/N		ns
Hs.180655	Serine/threonine kinase 12 (STK12)	C	Cell cycle		N/A	C/N		ns
Hs.250822	Serine/threonine kinase 15 (STK15)	C	Cell cycle		N/A	C/N	-/[16, 22]	ns
Hs.298623	5-hydroxytryptamine (serotonin) receptor 2A (HTR2A)	E/M	Signal transduction	0.04		N/T		ns
Hs.33724	CGI-40 protein (LOC51092)	U	U	0.50		N/T		ns
Hs.273786	Chymotrypsinogen B1 (CTRB1)	E/M	Extracellular protein degradation	0.30		N/T		ns
Hs.74502	Chymotrypsinogen B1 (CTRB1)	E/M	Extracellular protein degradation	0.08		N/T	[32]/-	N
Hs.241363	Hyaluronan-binding protein 2 (HABP2)	E/M	Extracellular structure	0.25		N/T		ns
Hs.334409	Metallothionein 1G (MT1G)	C	Metal binding	0.09		N/T		ns
Hs.203936	Metallothionein-If gene (hMT-If)	C	Metal binding	0.23		N/T		ns
Hs.3164	Nucleobindin 2 (NUCB2)	N	Transcription regulation	0.34		N/T		ns
Hs.423	Pancreatitis-associated protein (PAP)	E/M	Signal transduction	0.09		N/T	[47]/-	ns
Hs.241561	Protease, serine, 2 (trypsin 2) (PRSS2)	E/M	Extracellular protein degradation	0.13		N/T		TN
Hs.4158	Regenerating islet-derived 1 beta (pancreatic stone protein, pancreatic thread protein) (REG1B)	E/M	Extracellular structure	0.04		N/T		N
Hs.181286	Serine protease inhibitor, Kazal type 1 (SPINK1)	E/M	Extracellular protein degradation	0.21		N/T		N
Hs.176658	Aquaporin 8 (AQP8)	E/M	Other functions	N/A		N/T		ns
Hs.80426	Brain and reproductive organ-expressed (TNFRSF1A modulator) (BRE)	C	Apoptosis	N/A		N/T		ns
Hs.2879	Carboxypeptidase A1 (pancreatic) (CPA1)	E/M	Extracellular protein degradation	N/A		N/T	[33]/-	N
Hs.192615	cDNA, 3′ end /clone=IMAGE:2382935 /clone_end=3′ /gb=AI76759	U	U	N/A		N/T		ns
Hs.124123	cDNA, 5′ end /clone=IMAGE:3950065 /clone_end=5′ /gb=BE969669	U	U	N/A		N/T		N
Hs.1340	Colipase, pancreatic (CLPS)	E/M	Metabolism	N/A		N/T		N
Hs.183864	Elastase 3B, pancreatic (ELA3B)	E/M	Extracellular protein degradation	N/A		N/T		N
Hs.123107	Kallikrein 1, renal/pancreas/salivary (KLK1)	E/M	Extracellular protein degradation	N/A		N/T	[59]/-	ns

Table 2 (continued)

Unigene ID	Description	Putative cellular localisation	Putative cellular function	FC T/N	FC C/N	High in–VS	Reference PDAC/ array	Virtual Northern
Hs.27373	cDNA DKFZp564O1763 (from clone DKFZp564O1763)	U	U	N/A		N/T		ns
Hs.992	Phospholipase A2, group IB (pancreas) (PLA2G1B)	C	Signal transduction	N/A		N/T	[28]/-	N
Hs.18910	Prostate cancer overexpressed gene 1 (POV1)	U	U	N/A		N/T	[27]/-	ns
Hs.306079	Protein transport protein SEC61 alpha subunit isoform 1 (SEC61A1)	C	Protein synthesis and transport	N/A		N/T		ns
Hs.303649	Small inducible cytokine A2 (monocyte chemotactic protein 1, homologous to mouse Sig-je) (SCYA2)	E/M	Immune system	N/A		N/T		ns
Hs.237356	Stromal cell-derived factor 1 (SDF1)	E/M	Immune system	N/A		N/T	[29]/-	ns
Hs.286124	CD24 antigen (small cell lung carcinoma cluster 4 antigen) (CD24)	E/M	Extracellular structure		0.24	N/C	-/[16]	T
Hs.327237	cDNA, 3′ end /clone= IMAGE:1992802 /clone_end=3′ /gb= AI289400	U	U		0.18	N/C		ns
Hs.317889	cDNA, 3′ end /clone=IMAGE:4053313 /clone_end=3′ /gb=BF128353	U	U		0.43	N/C		ns
Hs.184542	CGI-127 protein (LOC51646)	C	Metal binding		0.20	N/C		ns
Hs.78946	Cullin 3 (CUL3)	C	Cell cycle/intracellular protein degradation		0.39	N/C		ns
Hs.285115	Interleukin 13 receptor, alpha 1 (IL13RA1)	E/M	Signal transduction		0.40	N/C		ns
Hs.50651	Janus kinase 1 (a protein tyrosine kinase) (JAK1)	C	Signal transduction		0.26	N/C		ns
Hs.75140	Low density lipoprotein-related protein-associated protein 1 (alpha-2-macroglobulin receptor-associated protein 1) (LRPAP1)	E/M	Metabolism		0.18	N/C		N
Hs.76807	Major histocompatibility complex, class II, DR alpha (HLA-DRA)	E/M	Immune system		0.07	N/C		T
Hs.86386	Mcl-1 (MCL-1) and Mcl-1 delta S/TM (MCL-1) genes, alternative spliced forms	C	Apoptosis		0.35	N/C	[12]/-	N
Hs.3688	Cisplatin resistance-associated over-expressed protein	U	U		0.34	N/C		ns
Hs.273230	FLJ00064 protein	E/M	Extracellular protein degradation		0.21	N/C		ns
Hs.348412	Partial TCF-4 gene for T-cell transcription factor-4, exon 1 and joined CDS features	N	Transcription regulation		0.27	N/C		ns
Hs.75807	PDZ and LIM domain 1 (elfin) (PDLIM1)	C	Cell structure maintenance		0.30	N/C		T
Hs.75658	Phosphorylase, glycogen; brain (PYGB), N gene encoding mitochondrial protein	C	Metabolism		0.50	N/C		T
Hs.318885	Superoxide dismutase 2, mitochondrial (SOD2)	C	Metabolism		0.13	N/C		ns
Hs.179600	Tapasin (NGS-17)	C	Signal transduction		0.42	N/C	[52]/-	ns
Hs.273369	Unknown	U	U		0.28	N/C		ns
Hs.25647	V-fos FBJ murine osteosarcoma viral oncogene homolog (FOS)	N	Transcription regulation		0.27	N/C	-/[16]	T
Hs.297753	Vimentin (VIM)	E/M	Extracellular structure		0.05	N/C	[43]/[9]	T
Hs.184029	Clone MGC:2764 IMAGE:2958229	C	Intracellular protein degradation		0.34	N/C		ns

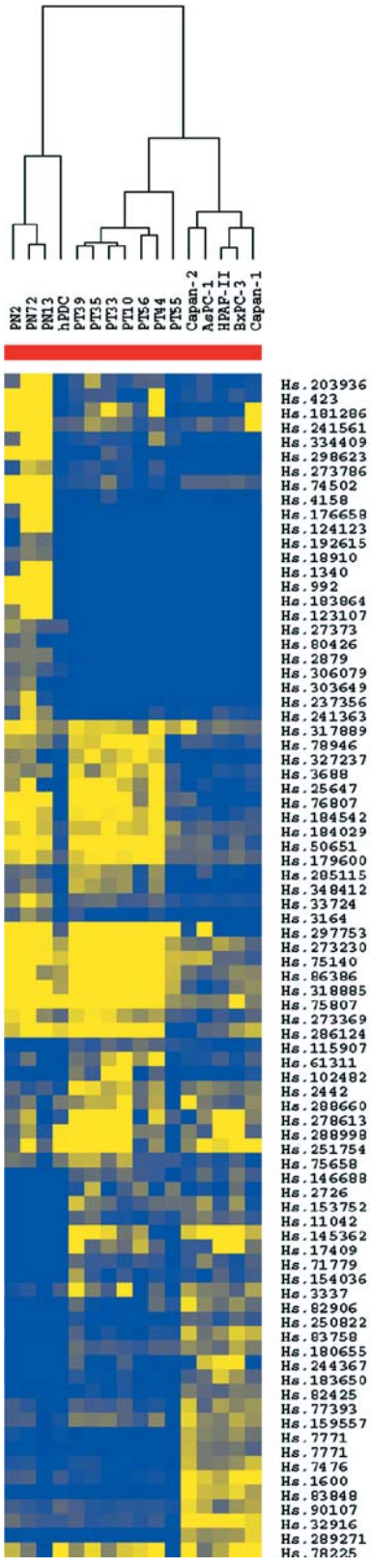

Fig. 1 Cluster analysis of microdissected pancreatic ductal adenocarcinoma, normal ductal cells, established pancreatic tumour cell lines, and one normal pancreatic duct cell line. Genes were subjected to a hierarchical clustering using a Euclidean distance metric and gene-expression families that were colour-coded for comparison. Genes that are upregulated appear in yellow, and those that are downregulated appear in blue, with the expression value reflected by the intensity of the colour

of the differentially expressed genes could not be validated statistically in the EST and SAGE databases. This is most likely due to the small number of tags in these databases.

Verification of the differential expression of ADAM9

The chip experiments showed ADAM9 to be overexpressed in PDAC tissue and cell lines when compared with normal ductal epithelium. Immunohistochemically, mild to moderate expression was seen in intralobular and interlobular ducts. Seven of ten PDACs exhibited strong membranous ADAM9 expression and three showed moderate expression in PDAC cells. The staining labelled the cell membrane with apical accentuation. Occasionally the staining was also cytoplasmatic, particularly in the poorly differentiated PDACs (Fig. 2).

Discussion

Using a custom-made oligonucleotide microarray based on Affymetrix technology, we identified the gene expression profiles of microdissected PDAC tissue and normal ductal epithelium of the pancreas and compared these profiles with each other as well as with the expression profiles of PDAC cell lines and a normal pancreatic ductal cell line. The analysis revealed 81 differentially expressed genes. We found 26 genes to be downregulated in PDAC, 14 to be upregulated in PDAC. In PDAC cell lines versus normal pancreatic duct cells, 21 were downregulated and 20 upregulated. A number of these genes were already reported by other groups that conducted global gene expression studies in PDAC [5, 9, 10, 13, 14, 15 16, 21, 22, 48]. However, we also identified additional genes that were not yet found to be differentially expressed in PDAC.

Since the stromal portion in PDACs often exceeds that of neoplastic cells, we carefully microdissected the tumour tissue, employing a laser capture device, and obtained highly homogeneous cell compartments. The same holds true for the microdissection of the normal pancreatic duct cells, which were selectively removed from large and medium-sized ducts. The fact that there is a need to distinguish neoplastic from non-neoplastic tissues is shown by studies on prostatic carcinomas, which compared the differential gene expression in microdissected and non-dissected tissue. Of the differential genes identified in microdissected tissues, only one-third was also found in bulk tissue [11]. Generally microdissection results in smaller amounts of poly A+ RNA. An unbiased amplification of this small amount of RNA material was therefore crucial for successful hybridisation of the gene chips. We tested several amplification protocols and found that with the use of a linear amplification protocol the bias introduced by the amplification was minimised, as already described by Wang et al. [45, 58].

In the four studies on array-based gene expression profiling in PDACs, only one used microdissection [10],

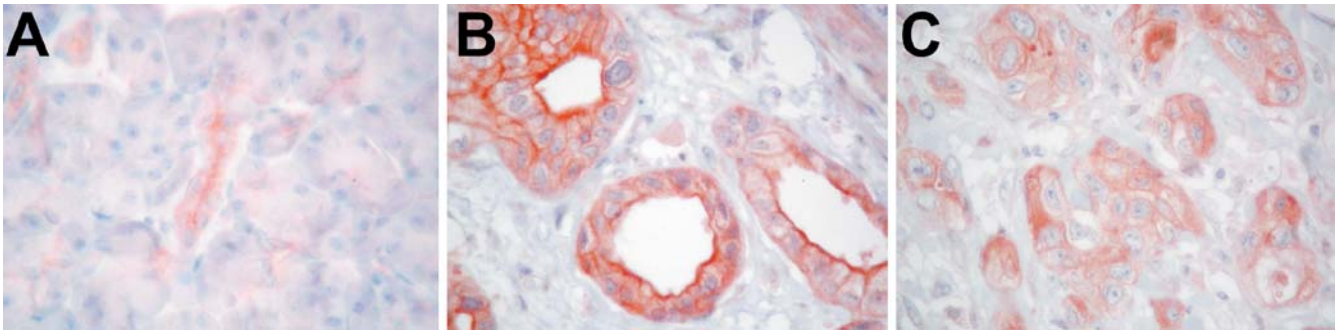

Fig. 2 ADAM9 expression in the normal pancreas and in pancreatic ductal adenocarcinoma (PDAC) **A** ADAM9 expression in a normal pancreatic duct. **B** ADAM9 expression in a well-differentiated PDAC; note the distinct apical and membrane staining. **C** ADAM9 expression in a poorly differentiated PDAC with predominant cytoplasmatic staining [peroxidase-based detection system with diaminobenzidine (DAB) as chromogen, ×500]

while the other three utilised bulk tissue [13, 21, 22]. Lemoine's group also used fine-needle aspiration to enrich the tumour cell population [9]. However, this method was unsuitable for obtaining sufficient amounts of normal duct cells and therefore was not used in this study for enrichment of normal ductal cells, which is based on a comparison between normal and neoplastic cell material.

Comparing our results with those of the above-mentioned studies, [9, 10, 13, 16, 22], we found that only a few genes were shown to be differentially expressed in more than one study. There are several potential reasons for the low concordance of these studies. First, the type, histology and number of samples used (i.e. established cell lines or PDAC cells) differed. This point could be even more of an issue for the type of normal tissue used (commercially available RNA, normal tissue from resected pancreatic tumours or donor organs). Second, microdissection was applied only by Crnogorac-Jurcevic et al. [10] and by our group. Third, different arrays and array technologies may lead to different gene expression results. As Kuo et al. [31] showed, there was a poor correlation when they used two types of DNA microarray technology (cDNA versus Affymetrix oligonucleotide microarrays) but the same cell culture samples. For these reasons, the results of expression profiling studies in PDAC are not yet comparable.

Of the 81 genes that were differentially expressed in PDAC, 15 represented human genes known to be implicated in the tumourigenesis of PDAC. These genes include: IFI27, MUC5B, Tapasin, PAP, SDF1 and POV1. Additionally, genes such as annexin A1 [17], STK15 [40], PTGES [61] and HMGI-C [53] are known from other neoplasms.

From the genes that were overexpressed in PDAC, we chose ADAM9 for evaluation of protein expression by immunohistochemistry, as other members of the ADAMs family have been implicated in the activation of growth factors and in the process of invasion [24, 26, 46]. Furthermore, the overexpression of ADAM9 was confirmed in a recent study, which identified ADAM9 by expression profiling of bulk samples of PDAC and verified its differential expression by reverse-transcription polymerase chain reaction [22]. ADAM9 is a member of the ADAMs protein family, which are membrane-anchored metalloproteases involved in modulating cell–cell and cell–matrix interactions [8]. Interestingly, it has been shown that ADAM9 is not inhibited by tissue inhibitors of metalloproteinases [3], enabling the tumour to activate growth factors without activating the urokinase pathway. It might also be involved in the ectodomain shedding of growth factors such as HB-EGF [24]. The expression of members of the ADAM gene family, like ADAM12, has been described as upregulated in many cancer cells [26]. This indicates that these proteins are critical for tumour development and invasion. The immunohistochemical analysis of ADAM9 in PDAC revealed that 70% of the analysed carcinomas overexpress ADAM9 compared with normal tissue. We also found a re-sorting of ADAM9 to the basal side of the cells. This might lead to enhanced release of growth factors and enhanced proliferation of the tumour cell.

In summary, the use of microarray analysis in combination with tissue microdissection is a powerful tool for identifying the changes in gene expression associated with tumour development and progression in PDAC. Because of the reduced heterogeneity of microdissected tissue, small changes in gene expression can be observed and used to generate new molecular markers and therapeutic targets. ADAM9 may be a molecular marker with prognostic significance, which has to be elucidated in a larger patient cohort.

Acknowledgements The authors would like to thank I. Klaman, E. Heiden and their colleagues at metaGen for their assistance, K. Dege and G. Faulmann for critical reading of the manuscript, as well as Alfred E. Neumann, whose comments were always appreciated. This paper was supported by Deutsche Krebshilfe (70–2937-SaI).

References

1. Alon U, Barkai N, Notterman DA, Gish K, Ybarra S, Mack D, Levine AJ (1999) Broad patterns of gene expression revealed by clustering analysis of tumor and normal colon tissues probed

by oligonucleotide arrays. Proc Natl Acad Sci U S A 96:6745–6750
2. Altschul SF, Madden TL, Schaffer AA, Zhang J, Zhang Z, Miller W, Lipman DJ (1997) Gapped BLAST and PSI-BLAST: a new generation of protein database search programs. Nucleic Acids Res 25:3389–3402
3. Amour A, Knight CG, English WR, Webster A, Slocombe PM, Knauper V, Docherty AJ, Becherer JD, Blobel CP, Murphy G (2002) The enzymatic activity of ADAM8 and ADAM9 is not regulated by TIMPs. FEBS Lett 524:154–158
4. Anderson KM, Alrefai WA, Bonomi P, Dudeja P, Ou D, Anderson C, Harris JE (1999) Altered oncogene, tumor suppressor and cell-cycle gene expression in PANC-1 cells cultured with the pleiotrophic 5-lipoxygenase inhibitor, MK886, assessed with a gene chip. Anticancer Res 19:3873–3887
5. Argani P, Rosty C, Reiter RE, Wilentz RE, Murugesan SR, Leach SD, Ryu B, Skinner HG, Goggins M, Jaffee EM, Yeo CJ, Cameron JL, Kern SE, Hruban RH (2001) Discovery of new markers of cancer through serial analysis of gene expression: prostate stem cell antigen is overexpressed in pancreatic adenocarcinoma. Cancer Res 61:4320–4324
6. Bardeesy N, DePinho RA (2002) Pancreatic cancer biology and genetics. Nat Rev Cancer 2:897–909
7. Bateman A, Birney E, Cerruti L, Durbin R, Etwiller L, Eddy SR, Griffiths-Jones S, Howe KL, Marshall M, Sonnhammer EL (2002) The Pfam protein families database. Nucleic Acids Res 30:276–280
8. Blobel CP (2000) Remarkable roles of proteolysis on and beyond the cell surface. Curr Opin Cell Biol 12:606–612
9. Crnogorac-Jurcevic T, Efthimiou E, Capelli P, Blaveri E, Baron A, Terris B, Jones M, Tyson K, Bassi C, Scarpa A, Lemoine NR (2001) Gene expression profiles of pancreatic cancer and stromal desmoplasia. Oncogene 20:7437–7446
10. Crnogorac-Jurcevic T, Efthimiou E, Nielsen T, Loader J, Terris B, Stamp G, Baron A, Scarpa A, Lemoine NR (2002) Expression profiling of microdissected pancreatic adenocarcinomas. Oncogene 21:4587–4594
11. Ernst T, Hergenhahn M, Kenzelmann M, Cohen CD, Bonrouhi M, Weninger A, Klaren R, Grone EF, Wiesel M, Gudemann C, Kuster J, Schott W, Staehler G, Kretzler M, Hollstein M, Grone HJ (2002) Decrease and gain of gene expression are equally discriminatory markers for prostate carcinoma: a gene expression analysis on total and microdissected prostate tissue. Am J Pathol 160:2169–2180
12. Evans JD, Cornford PA, Dodson A, Greenhalf W, Foster CS, Neoptolemos JP (2001) Detailed tissue expression of bcl-2, bax, bak and bcl-x in the normal human pancreas and in chronic pancreatitis, ampullary and pancreatic ductal adenocarcinomas. Pancreatology 1:254–262
13. Friess H, Ding J, Kleeff J, Liao Q, Berberat PO, Hammer J, Buchler MW (2001) Identification of disease-specific genes in chronic pancreatitis using DNA array technology. Ann Surg 234:769–779
14. Gress TM, Wallrapp C, Frohme M, Muller-Pillasch F, Lacher U, Friess H, Buchler M, Adler G, Hoheisel JD (1997) Identification of genes with specific expression in pancreatic cancer by cDNA representational difference analysis. Genes Chromosomes Cancer 19:97–103
15. Grutzmann R, Pilarsky C, Staub E, Schmitt AO, Foerder M, Specht T, Hinzmann B, Dahl E, Alldinger I, Rosenthal A, Ockert D, Saeger HD (2003) Systematic isolation of genes differentially expressed in normal and cancerous tissue of the pancreas. Pancreatology 3:169–178
16. Han H, Bearss DJ, Browne LW, Calaluce R, Nagle RB, Von Hoff DD (2002) Identification of differentially expressed genes in pancreatic cancer cells using cDNA microarray. Cancer Res 62:2890–2896
17. Hippo Y, Yashiro M, Ishii M, Taniguchi H, Tsutsumi S, Hirakawa K, Kodama T, Aburatani H (2001) Differential gene expression profiles of scirrhous gastric cancer cells with high metastatic potential to peritoneum or lymph nodes. Cancer Res 61:889–895
18. Hippo Y, Taniguchi H, Tsutsumi S, Machida N, Chong JM, Fukayama M, Kodama T, Aburatani H (2002) Global gene expression analysis of gastric cancer by oligonucleotide microarrays. Cancer Res 62:233–240
19. Hruban RH, Offerhaus GJ, Kern SE, Goggins M, Wilentz RE, Yeo CJ (1998) Tumor-suppressor genes in pancreatic cancer. J Hepatobiliary Pancreat Surg 5:383–391
20. Hu YX, Watanabe H, Li P, Wang Y, Ohtsubo K, Yamaguchi Y, Sawabu N (2000) An immunohistochemical analysis of p27 expression in human pancreatic carcinomas. Pancreas 21:226–230
21. Iacobuzio-Donahue CA, Maitra A, Shen-Ong GL, van Heek T, Ashfaq R, Meyer R, Walter K, Berg K, Hollingsworth MA, Cameron JL, Yeo CJ, Kern SE, Goggins M, Hruban RH (2002) Discovery of novel tumor markers of pancreatic cancer using global gene expression technology. Am J Pathol 160:1239–1249
22. Iacobuzio-Donahue CA, Maitra A, Olsen M, Lowe AW, Van Heek NT, Rosty C, Walter K, Sato N, Parker A, Ashfaq R, Jaffee E, Ryu B, Jones J, Eshleman JR, Yeo CJ, Cameron JL, Kern SE, Hruban RH, Brown PO, Goggins M (2003) Exploration of global gene expression patterns in pancreatic adenocarcinoma using cDNA microarrays. Am J Pathol 162:1151–1162
23. Irizarry RA, Bolstad BM, Collin F, Cope LM, Hobbs B, Speed TP (2003) Summaries of Affymetrix GeneChip probe level data. Nucleic Acids Res 31:e15
24. Izumi Y, Hirata M, Hasuwa H, Iwamoto R, Umata T, Miyado K, Tamai Y, Kurisaki T, Sehara-Fujisawa A, Ohno S, Mekada E (1998) A metalloprotease-disintegrin, MDC9/meltrin-gamma/ADAM9 and PKCdelta are involved in TPA-induced ectodomain shedding of membrane-anchored heparin-binding EGF-like growth factor. EMBO J 17:7260–7272
25. Jemal A, Murray T, Samuels A, Ghafoor A, Ward E, Thun MJ (2003) Cancer statistics, 2003. CA Cancer J Clin 53:5–26
26. Kang Q, Cao Y, Zolkiewska A (2000) Metalloprotease-disintegrin ADAM 12 binds to the SH3 domain of Src and activates Src tyrosine kinase in C2C12 cells. Biochem J 352:883–892
27. Kang S, Xu H, Duan X, Liu JJ, He Z, Yu F, Zhou S, Meng XQ, Cao M, Kennedy GC (2000) PCD1, a novel gene containing PDZ and LIM domains, is overexpressed in several human cancers. Cancer Res 60:5296–5302
28. Kashiwagi M, Friess H, Uhl W, Berberat P, Abou-Shady M, Martignoni M, Anghelacopoulos SE, Zimmermann A, Buchler MW (1999) Group II and IV phospholipase A(2) are produced in human pancreatic cancer cells and influence prognosis. Gut 45:605–612
29. Koshiba T, Hosotani R, Miyamoto Y, Ida J, Tsuji S, Nakajima S, Kawaguchi M, Kobayashi H, Doi R, Hori T, Fujii N, Imamura M (2000) Expression of stromal cell-derived factor 1 and CXCR4 ligand receptor system in pancreatic cancer: a possible role for tumor progression. Clin Cancer Res 6:3530–3535
30. Krogh A, Larsson B, von Heijne G, Sonnhammer EL (2001) Predicting transmembrane protein topology with a hidden Markov model: application to complete genomes. J Mol Biol 305:567–580
31. Kuo WP, Jenssen TK, Butte AJ, Ohno-Machado L, Kohane IS (2002) Analysis of matched mRNA measurements from two different microarray technologies. Bioinformatics 18:405–412
32. Kuroki T, Tomioka T, Tajima Y, Inoue K, Ikematsu Y, Ichinose K, Furui J, Kanematsu T (1999) Detection of the pancreas-specific gene in the peripheral blood of patients with pancreatic carcinoma. Br J Cancer 81:350–353
33. Laethem RM, Blumenkopf TA, Cory M, Elwell L, Moxham CP, Ray PH, Walton LM, Smith GK (1996) Expression and characterization of human pancreatic preprocarboxypeptidase A1 and preprocarboxypeptidase A2. Arch Biochem Biophys 332:8–18

34. Letunic I, Goodstadt L, Dickens NJ, Doerks T, Schultz J, Mott R, Ciccarelli F, Copley RR, Ponting CP, Bork P (2002) Recent improvements to the SMART domain-based sequence annotation resource. Nucleic Acids Res 30:242–244
35. Liotta L, Petricoin E (2000) Molecular profiling of human cancer. Nat Rev Genet 1:48–56
36. Lohr M, Muller P, Zauner I, Schmidt C, Trautmann B, Thevenod F, Capella G, Farre A, Liebe S, Jesnowski R (2001) Immortalized bovine pancreatic duct cells become tumorigenic after transfection with mutant k-ras. Virchows Arch 438:581–590
37. Luo J, Duggan DJ, Chen Y, Sauvageot J, Ewing CM, Bittner ML, Trent JM, Isaacs WB (2001) Human prostate cancer and benign prostatic hyperplasia: molecular dissection by gene expression profiling. Cancer Res 61:4683–4688
38. Luo L, Salunga RC, Guo H, Bittner A, Joy KC, Galindo JE, Xiao H, Rogers KE, Wan JS, Jackson MR, Erlander MG (1999) Gene expression profiles of laser-captured adjacent neuronal subtypes. Nat Med 5:117–122
39. Luttges J, Zamboni G, Longnecker D, Kloppel G (2001) The immunohistochemical mucin expression pattern distinguishes different types of intraductal papillary mucinous neoplasms of the pancreas and determines their relationship to mucinous noncystic carcinoma and ductal adenocarcinoma. Am J Surg Pathol 25:942–928
40. Miyoshi Y, Iwao K, Egawa C, Noguchi S (2001) Association of centrosomal kinase STK15/BTAK mRNA expression with chromosomal instability in human breast cancers. Int J Cancer 92:370–973
41. Muller-Pillasch F, Wallrapp C, Lacher U, Friess H, Buchler M, Adler G, Gress TM (1998) Identification of a new tumour-associated antigen TM4SF5 and its expression in human cancer. Gene 208:25–30
42. Nielsen H, Engelbrecht J, Brunak S, von Heijne G (1997) A neural network method for identification of prokaryotic and eukaryotic signal peptides and prediction of their cleavage sites. Int J Neural Syst 8:581–599
43. Notohara K, Hamazaki S, Tsukayama C, Nakamoto S, Kawabata K, Mizobuchi K, Sakamoto K, Okada S (2000) Solid-pseudopapillary tumor of the pancreas: immunohistochemical localization of neuroendocrine markers and CD10. Am J Surg Pathol 24:1361–1371
44. Notterman DA, Alon U, Sierk AJ, Levine AJ (2001) Transcriptional gene expression profiles of colorectal adenoma, adenocarcinoma, and normal tissue examined by oligonucleotide arrays. Cancer Res 61:3124–3130
45. Pilarsky CP, Schmitt AO, Dahl E, Rosenthal A (1999) Microarrays: chances and challenges. Curr Op Mol Ther 1:727–739
46. Prenzel N, Zwick E, Daub H, Leserer M, Abraham R, Wallasch C, Ullrich A (1999) EGF receptor transactivation by G-protein-coupled receptors requires metalloproteinase cleavage of pro-HB-EGF. Nature 402:884–888
47. Rosty C, Christa L, Kuzdzal S, Baldwin WM, Zahurak ML, Carnot F, Chan DW, Canto M, Lillemoe KD, Cameron JL, Yeo CJ, Hruban RH, Goggins M (2002) Identification of hepatocarcinoma-intestine-pancreas/pancreatitis-associated protein I as a biomarker for pancreatic ductal adenocarcinoma by protein biochip technology. Cancer Res 62:1868–1875
48. Ryu B, Jones J, Blades NJ, Parmigiani G, Hollingsworth MA, Hruban RH, Kern SE (2002) Relationships and differentially expressed genes among pancreatic cancers examined by large-scale serial analysis of gene expression. Cancer Res 62:819–826
49. Sager R (1997) Expression genetics in cancer: shifting the focus from DNA to RNA. Proc Natl Acad Sci U S A 94:952–955
50. Schmitt AO, Specht T, Beckmann G, Dahl E, Pilarsky CP, Hinzmann B, Rosenthal A (1999) Exhaustive mining of EST libraries for genes differentially expressed in normal and tumour tissues. Nucleic Acids Res 27:4251–4260
51. Selaru FM, Zou T, Xu Y, Shustova V, Yin J, Mori Y, Sato F, Wang S, Olaru A, Shibata D, Greenwald BD, Krasna MJ, Abraham JM, Meltzer SJ (2002) Global gene expression profiling in Barrett's esophagus and esophageal cancer: a comparative analysis using cDNA microarrays. Oncogene 21:475–478
52. Seliger B, Schreiber K, Delp K, Meissner M, Hammers S, Reichert T, Pawlischko K, Tampe R, Huber C (2001) Down-regulation of the constitutive tapasin expression in human tumor cells of distinct origin and its transcriptional upregulation by cytokines. Tissue Antigens 57:39–45
53. Sezer O, Langelotz C, Blohmer JU, Schmid P, Akrivakis K, Possinger K (2000) Detection of HMGI-C in the peripheral blood of breast cancer patients. Eur J Cancer 36:1944–1948
54. Sipos B, Möser S, Kalthoff H, Török V, Löhr M, Klöppel G (2003) A comprehensive characterization of pancreatic ductal carcinoma cell lines: towards the establishment of an in vitro research platform. Virchows Arch 442:444–452
55. Slebos RJ, Hoppin JA, Tolbert PE, Holly EA, Brock JW, Zhang RH, Bracci PM, Foley J, Stockton P, McGregor LM, Flake GP, Taylor JA (2000) K-ras and p53 in pancreatic cancer: association with medical history, histopathology, and environmental exposures in a population-based study. Cancer Epidemiol Biomarkers Prev 9:1223–1232
56. Sugiyama Y, Sugiyama K, Hirai Y, Akiyama F, Hasumi K (2002) Microdissection is essential for gene expression profiling of clinically resected cancer tissues. Am J Clin Pathol 117:109–116
57. van't Veer LJ, Dai H, van de Vijver MJ, He YD, Hart AA, Mao M, Peterse HL, van der Kooy K, Marton MJ, Witteveen AT, Schreiber GJ, Kerkhoven RM, Roberts C, Linsley PS, Bernards R, Friend SH (2002) Gene expression profiling predicts clinical outcome of breast cancer. Nature 415:530–536
58. Wang E, Miller LD, Ohnmacht GA, Liu ET, Marincola FM (2000) High-fidelity mRNA amplification for gene profiling. Nat Biotechnol 18:457–459
59. Wolf WC, Evans DM, Chao L, Chao J (2001) A synthetic tissue kallikrein inhibitor suppresses cancer cell invasiveness. Am J Pathol 159:1797–1805
60. Yanagawa R, Furukawa Y, Tsunoda T, Kitahara O, Kameyama M, Murata K, Ishikawa O, Nakamura Y (2001) Genome-wide screening of genes showing altered expression in liver metastases of human colorectal cancers by cDNA microarray. Neoplasia 3:395–401
61. Yoshimatsu K, Golijanin D, Paty PB, Soslow RA, Jakobsson PJ, DeLellis RA, Subbaramaiah K, Dannenberg AJ (2001) Inducible microsomal prostaglandin E synthase is overexpressed in colorectal adenomas and cancer. Clin Cancer Res 7:3971–3976

Virchows Arch (2003) 443:518–523
DOI 10.1007/s00428-003-0877-0

ORIGINAL ARTICLE

Shunji Matsumura · Naohide Oue · Reiko Ito · Hirofumi Nakayama · Yasuhiko Kitadai · Hiroshi Yokozaki · Kazuaki Chayama · Wataru Yasui

The promoter methylation status of the DNA repair gene *O*^{6}-methylguanine-DNA methyltransferase in ulcerative colitis

Received: 10 March 2003 / Accepted: 8 July 2003 / Published online: 15 August 2003
© Springer-Verlag 2003

Abstract Patients with long-standing and extensive ulcerative colitis (UC) have an increased incidence of colorectal cancer (CRC). It has been reported that a DNA repair gene, O^6-methylguanine-DNA methyltransferase (*MGMT*) is inactivated by promoter hypermethylation in sporadic CRCs. Hence, we investigated the promoter methylation status of *MGMT* by methylation specific polymerase chain reaction (PCR) in a total of 67 tissue samples (61 non-cancerous tissues and 6 cancer tissues) from 24 patients with UC. Promoter hypermethylation of *MGMT* was detected in one well-differentiated adenocarcinoma (16.7%) of 6 cancer samples and not detected in any of adenomas and dysplasias. In non-dysplastic tissues, promoter hypermethylation of *MGMT* was detected in 2 (3.7%, mucosa with mild inflammation) of 54 samples. The frequency of *MGMT* promoter hypermethylation in UC-associated CRCs found in this study (16.7%) is obviously lower than previously reported in sporadic CRCs (39.0–42.0%). We also confirmed that 42.9% (6/14) of sporadic CRCs showed the promoter methylation. These findings indicated that promoter hypermethylation of the *MGMT* gene is infrequent in patients with UC, and may not closely contribute to UC-associated colorectal tumorigenesis. A different genetic pathway for tumor progression may exist between sporadic CRC and UC-associated CRC.

Keywords DNA methylation · *MGMT* · Ulcerative colitis

S. Matsumura · N. Oue · R. Ito · H. Nakayama · W. Yasui (✉)
Department of Molecular Pathology,
Hiroshima University Graduate School of Biomedical Sciences,
1-2-3 Kasumi, Minami-ku, 734-8551 Hiroshima, Japan
e-mail: wyasui@hiroshima-u.ac.jp
Tel.: +81-82-257-5145
Fax: +81-82-257-5149

Y. Kitadai · K. Chayama
Department of Medicine and Molecular Science,
Hiroshima University Graduate School of Biomedical Sciences,
734-8551 Hiroshima, Japan

H. Yokozaki
Department of Biomedical Informatics,
Kobe University Graduate School of Medicine,
Faculty of Medical Sciences,
650-0017 Kobe, Japan

Introduction

Patients with long-standing and extensive ulcerative colitis (UC), a chronic inflammatory bowel disease (IBD), have an increased incidence of colorectal cancers (CRCs) [19, 20]. The inflammation causes epithelial damage, including multiple ulceration and hemorrhage. Furthermore, it has been believed that chronic inflammatory status predisposes to development of epithelial dysplasia and CRC [6, 25]. However, the frequency and timing of occurrence of the genetic and epigenetic alterations were reported to differ in UC-associated CRC and sporadic CRC [2]. *K-ras* mutation appears to be lower in UC-associated CRC than in sporadic CRC [3, 4, 5].

It has been reported that the promoter hypermethylation and reduced expression of O^6-methylguanine-DNA methyltransferase (*MGMT*), a DNA repair gene, occur in some primary human cancers, including brain tumors, lymphomas, sporadic CRCs, and gastric cancers [7, 12, 22, 23]. Inactivation of *MGMT* by promoter hypermethylation is associated with G to A mutations in *K-ras* gene in CRCs [9] and gastric carcinomas [24]. *MGMT* removes mutagenic and cytotoxic adducts from the O^6 position of guanine. If they are not removed, then the adducts mispair with T during DNA replication, resulting in G to A mutation [24]. However, the promoter methylation status of the *MGMT* gene has not been revealed in various colorectal lesions (i.e., inflammation, dysplasia, adenoma, cancer) in UC patients. Hence, we investigated it by means of methylation-specific polymerase chain reaction (PCR) and studied the relationship with the degree of inflammation, dysplasia, and cancer retrospectively.

Materials and methods

Samples and DNA extraction

We analyzed a total of 67 tissue specimens from 24 patients with UC retrospectively, who underwent surgical operation at Hiroshima University Hospital in 1995–2001. They were randomly selected for this study.

The clinico-pathological data of 24 patients with UC are shown in Table 1. Nineteen patients had pan-colitis and five had left-sided colitis. The length of their diseases ranged from 12 months to 309 months (median 74.6 months). Moreover, UC clinical activity was moderate to severe in 24 and mild in none. As a reference, 14 cases of sporadic CRC without IBD were analyzed using the same method. Colorectal tissues were surgically removed and fixed with 10% formaldehyde for 24 h and embedded in paraffin. The paraffin-embedded samples were divided into dysplasia, adenoma, cancer, and non-dysplastic mucosa by histological observation by authorized pathologists (Reiko Ito, Hiroshi Yokozaki, Wataru Yasui), who were unaware of patients' clinical and endoscopic data. In addition, the degree of the inflammation in non-neoplastic mucosa was classified according to the criteria of Matts [21]. An average of 22 samples were evaluated histologically in each case of colectomy, and one representative sample of each lesion (i.e., inflammation, dysplasia, adenoma, cancer) was used. If there were multiple areas of cancer or dysplasia, we selected the larger lesion to avoid the contamination of non-dysplastic mucosal epithelium. Moreover, non-dysplastic samples were taken far from (at least 5 cm) the areas of dysplasia or cancer.

Because written informed consent was not obtained, for strict privacy protection, we coded samples anonymously, which separated completely from subjects' ID to be unable to connect. This procedure follows the ethics guidelines for human genome/gene research enacted by the Japanese Government. The ethics review committee of the Hiroshima University School of Medicine approved the study.

Tissue sections were prepared, and deparaffinized in xylene before dehydration with 100% ethanol. Then, we microdissected and collected the selected areas of interest from the dysplastic and non-dysplastic mucosal epithelium with minimal contamination of stromal elements under the microscope with a wooden stick. Microdissected samples were mixed with low-temperature melting agarose beads that were preheated and melted. After the beads were treated with proteinase K and 3.5 M sodium bisulfite, they were sliced into several pieces and used as a template for PCR amplification [18].

Table 1 The clinicopathological features of tissue samples from 24 patients with ulcerative colitis (UC). Non-neoplastic mucosa was classified according to the criteria of Matts

Gender (n=24)	
Female	12
Male	12
Age (average, years)	36.2±16.8
Length of the disease (months, median)	12–309 (74.6)
Clinical activity of the disease (n=24)	
Mild	0
Moderate/severe	24
Clinical extent of the disease (n=24)	
Pan-colitis	19
Left-sided colitis	5
Histological type (n=67)	
Non-neoplastic mucosa (Degree of inflammation)	54
Mild	7
Moderate	24
Severe	23
Dysplasia	5
Adenoma	2
Cancer	6

Methylation-specific PCR

To determine the DNA methylation patterns in the promoter region of the *MGMT* gene, methylation-specific PCR (MSP) analysis [13] of *MGMT* was performed by M primer (methylated allele specific) and U primer (unmethylated allele specific) as previously described [11]. All PCRs were performed with positive controls for methylated alleles and no DNA control. The M primer sequence is: forward primer 5′-TTTCGACGTTCGTAGGTTTTCGC-3′; reverse primer 5′-GCACTCTTCCGAAAACGAAACG-3′. The U primer sequence is: forward primer 5′-TTTGTGTTTTGATGTTTGTAGGTTTTTGT-3′; reverse primer 5′-AACTCCACACTCTTCCAAAAACAAAACA-3′. The target sequence was amplified in a 20-μl reaction volume containing sliced beads which involved genomic DNA, 0.2 μM dNTP, 10 mM Tris-HCl (pH 8.3), 50 mM KCl, 2 mM $MgCl_2$, 0.3 μM each primer, and 0.75 U Ampli *Taq* Gold (Perkin-Elmer, Norwalk, CT). PCR amplification was carried out with 35 cycles of denaturation at 94°C for 30 s, annealing at 59°C (depending on the primer) for 30 s, and extension at 72°C for 30 s after the initial activation step of 94°C for 10 min.

Because we have confirmed that genomic DNA from MKN-28 cell lines was completely methylated at CpG sites of *MGMT* by the treatment of excess of SssI methyltransferase (New England Biolabs, Inc., Beverly, MA) [22], it was used as the positive control for methylated *MGMT* gene. Each PCR product was loaded onto 8% non-denaturing polyacrylamide gels, and then the gels were stained with ethidium bromide and visualized under UV light. This methylation assay detects methylation of the regions of primer sequences in the promoter.

Statistical analysis

Statistical analysis was performed with the use of Fisher's exact. $P<0.05$ was considered significant.

Results

We examined the promoter methylation status of *MGMT* in a total of 67 tissue samples from 24 patients with UC. Representative results are shown in Fig. 1A and the overall results are summarized in Table 2. Promoter hypermethylation of *MGMT* was found in 3 (12.5%: cases 2, 9 and 24) of 24 UC cases. In cancerous tissues, promoter hypermethylation of *MGMT* was detected in one (16.7%, case 2) of 6 samples. The promoter hypermethylation was not detected in any adenomas and dysplasias; whereas, in non-dysplastic tissues, promoter hypermethylation of *MGMT* was detected in 2 (3.7%, cases 9 and 24, non-dysplastic mucosa with mild inflammation) of 54 samples.

The details of each case with promoter hypermethylation are as follows: In case 2, the clinical activity was moderate to severe and the clinical extent of the disease was pan-colitis. The length of the disease was 292 months. The cancerous lesion (well-differentiated adenocarcinoma) was located in the ascending colon. Promoter hypermethylation of *MGMT* was detected in cancerous tissue (Fig. 1A, B—c), but not in non-dysplastic mucosa with mild, moderate, and severe inflammation or in

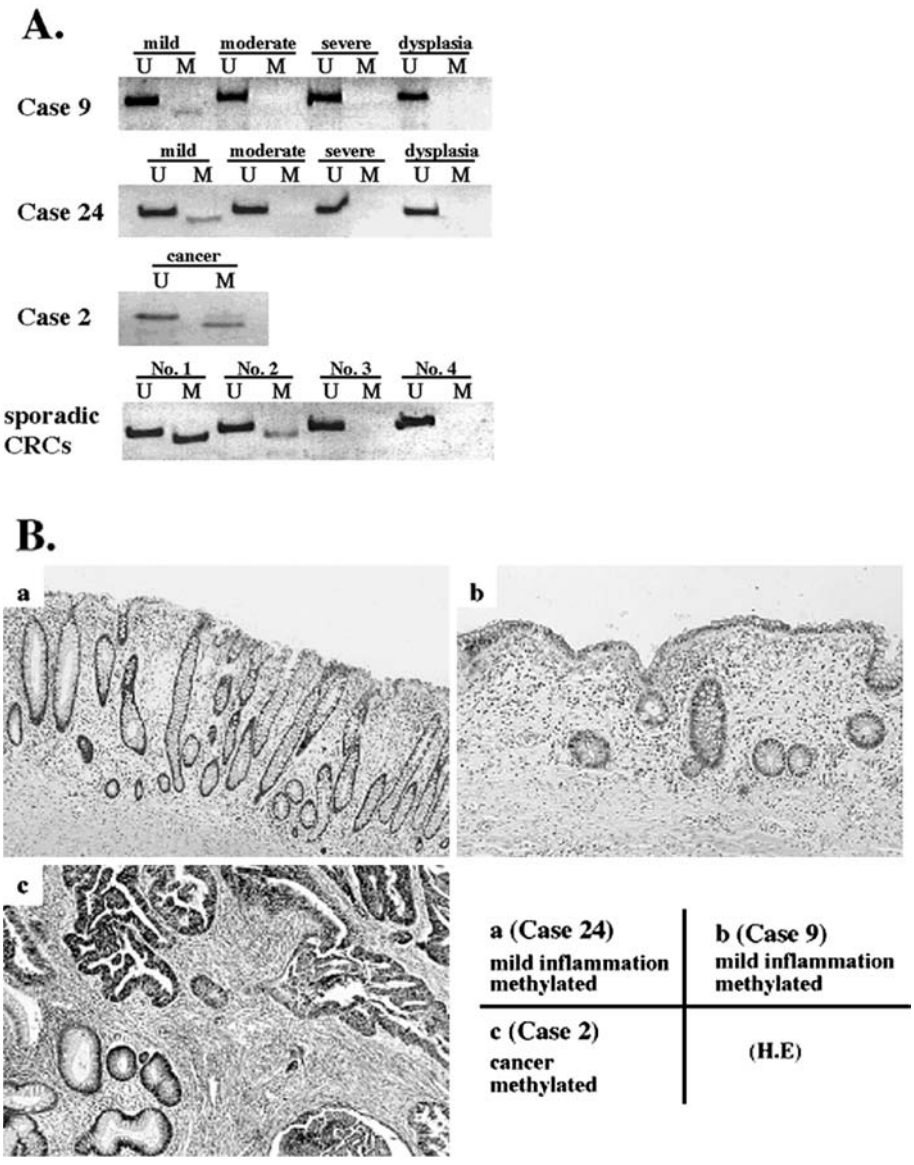

Fig. 1 **A** Methylation-specific polymerase chain reaction (PCR) analysis of *MGMT* in ulcerative colitis (UC)-associated colorectal cancer tissues and non-cancerous tissues. In UC-associated colorectal cancers, the methylated PCR product of MGMT was detected in only one case (case 2). The promoter hypermethylation of *MGMT* was detected in non-dysplastic mucosa with mild inflammation (cases 9 and 24). *M* methylated, *U* unmethylated PCR products. *mild* non-dysplastic mucosa with mild inflammation, *moderate* non-dysplastic mucosa with moderate inflammation, *severe* non-dysplastic mucosa with severe inflammation. Representative four cases of sporadic CRCs are shown in the bottom (*no. 1*, *2* methylated; *no. 3*, *4* unmethylated). **B** Histology of the samples with *MGMT* hypermethylation. Case 24 (*a*) and case 9 (*b*) were non-dysplastic mucosa with mild inflammation and case 2 (*c*) had well-differentiated adenocarcinoma

dysplasia and adenoma. In both cases 9 and 24, clinical activity was moderate to severe, and the clinical extent of the disease was pan-colitis. The length of the disease was 24 months and 33 months, respectively. The promoter hypermethylation of *MGMT* was detected in non-dysplastic tissues with mild inflammation (Fig. 1A, B—a and b), but not with moderate and severe inflammation or in dysplasia.

The frequency of *MGMT* promoter hypermethylation in UC-associated CRCs was lower than previously reported in sporadic CRCs (39–42%) [7, 9, 10, 29], although there was no significant difference between the two, possibly because of the small number of UC-associated CRCs analyzed (P=0.209–0.292; Table 3). We also analyzed 14 cases of sporadic CRC in our protocol (agarose-beads method) and found that six (42.9%) showed hypermethylation of *MGMT* promoter (Fig. 1A and Table 3).

Discussion

It has been believed that chronic inflammatory status such as UC predisposes to development of epithelial dysplasia and CRC [6, 25]. Issa et al. reported that age-related methylation of the several gene promoters was more frequent in the normal-appearing (non-dysplastic) epithelia from UC patients with dysplasia and/or UC-associated CRC than in non-UC controls [1, 16, 27]. An abnormality in age-related methylation is infrequent in UC patients without dysplasia. Chronic inflammation in UC may be associated with high levels of methylation and may predispose a colorectal neoplasia [17]. In fact, hypermethylation of the $p16^{INK4a}$ promoter region is detected in 12.7% of samples negative for dysplasia in UC, while 70.0% of samples with dysplasia and all of the samples with carcinomatous lesions reveal hypermethylation [14]. Moreover, $p14^{ARF}$ hypermethylation is found in 30% of

Table 2 The promoter methylation status of *MGMT* in ulcerative colitis (UC). *PC* pancolitis, *LSC* left-sided colitis

Case	Sex	Age (years)	Type	Non-dysplastic mucosa/ degree of inflammation			Dysplasia	Adenoma	Cancer
				Mild	Moderate	Severe			
1	Female	35	PC	U	U	U			
2	Female	32	PC	U	U	U	U	U	M
3	Female	21	LSC		U	U			
4	Female	42	PC		U	U			U
5	Female	35	PC		U	U			
6	Male	63	LSC	U	U				
7	Male	45	PC		U	U	U		U
8	Female	58	LSC		U	U			
9	Female	34	PC	M	U	U	U		
10	Male	45	LSC		U	U			
11	Male	17	PC		U	U			
12	Male	23	PC		U	U			
13	Male	41	PC	U	U	U			
14	Male	26	PC		U	U			
15	Male	20	LSC	U	U	U			
16	Female	26	PC		U	U	U	U	U
17	Male	76	PC		U	U			
18	Female	20	PC		U	U			
19	Male	32	PC		U	U			
20	Male	17	PC		U	U			
21	Female	20	PC		U	U			
22	Female	47	PC		U	U			U
23	Male	71	PC		U	U			U
24	Female	51	PC	M	U	U	U		
Hypermethylation (%)				2/7 (28.6) 2/54 (3.7)	0/24 (0)	0/23 (0)	0/5 (0) 0/7 (0)	0/2 (0)	1/6 (16.7) 1/6 (16.7)

M: Methylated
U: Unmethylated

Table 3 Correlation between the promoter methylation status of *MGMT* in the ulcerative colitis (UC)-associated colorectal cancer (CRC) and sporadic CRC. The frequencies of hypermethylation of *MGMT* in sporadic CRC are those reported. *CI* confidential interval

	Methylated (%)	Unmethylated (%)	*P* value[b]	OR (95%CI)[c]
UC-associated CRC	1 (16.7)	5 (83.3)		
Sporadic CRC				
Agarose-bead[a]	6 (42.9)	8 (57.1)	0.260	0.266 (0.024–2.914)
Ref. 1[d]	14 (38.9)	22 (61.1)	0.292	0.314 (0.030–2.768)
Ref. 2[e]	103 (42.2)	141 (57.8)	0.209	0.273 (0.031–2.372)
Ref. 3[f]	127 (39.3)	196 (60.7)	0.259	0.308 (0.034–2.553)
Ref. 4[g]	37 (41.1)	53 (58.9)	0.235	0.286 (0.032–2.549)

[a] The frequencies of hypermethylation of *MGMT* in sporadic CRC, analyzed using agarose-bead method
[b] Correlation was analyzed by Fisher's test. *P* values less than 0.05 were regarded as statistically significant
[c] Odds ratio of UC-associated CRC relative to sporadic CRC
[d] Esteller M, Hamilton SR et al. (Cancer Res 1999;59:793–7) [7]
[e] Esteller M, Toyota M et al. (Cancer Res 2000;60:2368–71) [9]
[f] Esteller M, Corn PG et al. (Cancer Res 2001;61:3225–9) [10]
[g] Whitehall VLJ, Walsh MD et al. (Cancer Res 2001;61:827–30) [29]

sporadic CRC and in none of normal colonic mucosa [8], whereas it was found in 60% of non-neoplastic inflamed UC mucosa [26]. Before the present study, no information of *MGMT* methylation was available in UC-related colorectal carcinogenesis. Here, we found *MGMT* hypermethylation in only 1 of 6 cases of CRC and 2 of 54 non-dysplastic mucosas with mild inflammation in UC patients.

In the meantime, it has been reported that inactivation of *MGMT* by promoter hypermethylation is associated with G to A mutations in *K-ras* gene in CRC [7] and the incidence of *K-ras* mutation is lower in UC-associated CRCs than in sporadic CRCs [3, 4, 5]. The frequency of *MGMT* promoter hypermethylation in UC-associated CRCs (16.7%) found in this study is obviously lower than previously reported in sporadic CRCs (39.0–42.0%) [7, 9, 10, 29]. We also confirmed that nearly the same proportion of sporadic CRCs (42.9%) showed *MGMT* methylation in our protocol (agarose-beads method). Therefore, in UC, promoter hypermethylation of *MGMT* is infrequent and may not lead to G to A mutations in the *K-ras* oncogene. *MGMT* methylation may not serve as a

maker to predict premalignant condition in non-neoplastic-looking mucosa in UC.

Some studies have reported the relationship between MSI status and UC-associated CRC [15, 28]. A high incidence of the MSI in long-standing UC with severe inflammation probably reflects genomic instability caused by repeated inflammation stress [15]. Furthermore, MSI is relatively common in UC-associated neoplasia and is present at the early stage of tumorigenesis [28]. MSI may be one of the pathways of the increased neoplastic risk in UC. Therefore, it is important to verify a relationship between *MGMT* methylation and a microsatellite instability (MSI) status of our cases. Further investigations are necessary to clarify the pathway of increasing cancer risk in UC as MSI status.

In conclusion, our results suggest that promoter hypermethylation of *MGMT* gene is infrequent in patients with UC, and may not deeply contribute to UC-associated colorectal tumorigenesis. A different genetic pathway for tumor progression may exist between sporadic CRC and UC-associated CRC. Furthermore, the retrospective use of formalin-fixed, paraffin-embedded pathological specimens for molecular biological analysis has become increasingly important. Our study revealed their usefulness as a source for analysis of methylation status.

References

1. Ahuja N, Li Q, Mohan AL, Baylin SB, Issa JP (1998) Aging and DNA methylation in colorectal mucosa and cancer. Cancer Res 58:5489–5494
2. Aust DE, Willenbucher RF, Terdiman JP, Ferrell LD, Chang CG, Moore DH II, Molinaro-Clark A, Baretton GB, Loehrs U, Waldman FM (2000) Chromosomal alterations in ulcerative colitis-related and sporadic colorectal cancers by comparative genomic hybridization. Hum Pathol 31:109–114
3. Bell SM, Kelly SA, Hoyle JA, Lewis FA, Taylor GR, Thompson H, Dixon MF, Quirke P (1991) c-Ki-ras gene mutations in dysplasia and carcinomas complicating ulcerative colitis. Br J Cancer 64:174–178
4. Burmer GC, Levine DS, Kulander BG, Haggitt RC, Rubin CE, Rabinovitch PS (1990) c-Ki-ras mutations in chronic ulcerative colitis and sporadic colon carcinoma. Gastroenterology 99:416–420
5. Chaubert P, Benhattar J, Sarage E, Costa J (1994) K-ras mutations and p53 alterations in neoplastic and nonneoplastic lesions associated with longstanding ulcerative colitis. Am J Pathol 144:767–775
6. Ekbom A (1998) Risk of cancer in ulcerative colitis. J Gastrointest Surg 2:312–313
7. Esteller M, Hamilton SR, Burger PC, Baylin SB, Herman JG (1999) Inactivation of the DNA repair gene O6-methylguanine-DNA methyltransferase by promoter hypermethylation is a common event in primary human neoplasia. Cancer Res 59:793–797
8. Esteller M, Tortola S, Toyota M, Capella G, Peinado MA, Baylin SB, Herman JG (2000) Hypermethylation-associated inactivation of p14(ARF) is independent of p16(INK4a) methylation and p53 mutational status. Cancer Res 60:129–133
9. Esteller M, Toyota M, Sanchez-Cespedes M, Capella G, Peinado MA, Watkins DN, Issa JP, Sidransky D, Baylin SB, Herman JG (2000) Inactivation of the DNA repair gene O6-methylguanine-DNA methyltransferase by promoter hypermethylation is associated with G to A mutations in K-ras in colorectal tumorigenesis. Cancer Res 60:2368–2371
10. Esteller M, Corn PG, Baylin SB, Herman JG (2001) A gene hypermethylation profile of human cancer. Cancer Res 61:3225–3229
11. Esteller M, Risques RA, Toyota M, Capella G, Moreno V, Peinado MA, Baylin SB, Herman JG (2001) Promoter hypermethylation of the DNA repair gene O(6)-methylguanine-DNA methyltransferase is associated with the presence of G:C to A:T transition mutations in p53 in human colorectal tumorigenesis. Cancer Res 61:4689–4692
12. Herfarth KK, Brent TP, Danam RP, Remack JS, Kodner IJ, Wells SA Jr, Goodfellow PJ (1999) A specific CpG methylation pattern of the MGMT promoter region associated with reduced MGMT expression in primary colorectal cancers. Mol Carcinog 24:90–98
13. Herman JG, Graff JR, Myohanen S, Nelkin BD, Baylin SB (1996) Methylation-specific PCR. A novel PCR assay for methylation status of CpG islands. Proc Natl Acad Sci U S A 93:9821–9826
14. Hsieh CJ, Klump B, Holzmann K, Borchard F, Gregor M, Porschen R (1998) Hypermethylation of the p16INK4a promoter in colectomy specimens of patients with long-standing and extensive ulcerative colitis. Cancer Res 58:3942–3945
15. Ishitsuka T, Kashiwagi H, Konishi F (2001) Microsatellite instability in inflamed and neoplastic epithelium in ulcerative colitis. J Clin Pathol 54:526–532
16. Issa JP, Ottaviano YL, Celano P, Hamilton SR, Davidson NE, Baylin SB (1994) Methylation of the oestrogen receptor CpG island links ageing and neoplasia in human colon. Nat Genet 7:536–540
17. Issa JP, Ahuja N, Toyota M, Bronner MP, Brentnall TA (2001) Accelerated age-related CpG island methylation in ulcerative colitis. Cancer Res 61:3573–3577
18. Kitazawa S, Kitazawa R, Maeda S (2000) Identification of methylated cytosine from archival formalin-fixed paraffin-embedded specimens. Lab Invest 80:275–276
19. Lennard JJE, Morson BC, Ritchie JK, Shove DC, Williams CB (1977) Cancer in colitis: assessment of the individual risk by clinical and histological criteria. Gastroenterology 73:1280–1289
20. Lashner BA, Silverstein MD, Hanauer SB (1989) Hazard rates for dysplasia and cancer in ulcerative colitis. Results from a surveillance program. Dig Dis Sci 34:1536–1541
21. Matts SGF (1961) The value of rectal biopsy in the diagnosis of ulcerative colitis. Quart J Med 30:393–407
22. Oue N, Shigeishi H, Kuniyasu H, Yokozaki H, Kuraoka K, Ito R, Yasui W (2001) Promoter hypermethylation of MGMT is associated with protein loss in gastric carcinoma. Int J Cancer 93:805–809
23. Pieper RO, Patel S, Ting SA, Futscher BW, Costello JF (1996) Methylation of CpG island transcription factor binding sites is unnecessary for aberrant silencing of the human MGMT gene. J Biol Chem 271:13916–13924
24. Park TJ, Han SU, Cho YK, Paik WK, Kim YB, Lim IK (2001) Methylation of O (6)-methylguanine-DNA methyltransferase gene is associated significantly with K-ras mutation, lymph node invasion, tumor staging, and disease free survival in patients with gastric carcinoma. Cancer 92:2760–2768
25. Riddell RH, Goldman H, Ransohoff DF, Appelman HD, Fenoglio CM, Haggitt RC, Ahren C, Correa P, Hamilton SR, Morson BC (1983) Dysplasia in inflammatory bowel disease: standardized classification with provisional clinical applications. Hum Pathol 14:931–968
26. Sato F, Harpaz N, Shibata D, Xu Y, Yin J, Mori Y, Zou TT, Wang S, Desai K, Leytin A, Selaru FM, Abraham JM, Meltzer SJ (2002) Hypermethylation of the p14(ARF) gene in ulcerative colitis-associated colorectal carcinogenesis. Cancer Res 62:1148–1151
27. Toyota M, Ho C, Ahuja N, Jair KW, Li Q, Ohe-Toyota M, Baylin SB, Issa JP (1999) Identification of differentially

methylated sequences in colorectal cancer by methylated CpG island amplification. Cancer Res 59:2307–2312
28. Umetani N, Sasaki S, Watanabe T, Shinozaki M, Matsuda K, Ishigami H, Ueda E, Muto T (1999) Genetic alterations in ulcerative colitis-associated neoplasia focusing on APC, K-ras gene and microsatellite instability. Jpn J Cancer Res 90:1081–1087
29. Whitehall VLJ, Walsh MD, Young J, Leggett BA, Jass JR (2001) Methylation of *O*-6-methylguanine DNA methyltransferase characterizes a subset of colorectal cancer with low-level DNA microsatellite instability. Cancer Res 61:827–830

Virchows Arch (2003) 443:524–527
DOI 10.1007/s00428-003-0862-7

ORIGINAL ARTICLE

Božo Krušlin · Davor Tomas · Hermann Rogatsch · Irena Novosel · Hrvoje Čupić · Mladen Belicza · Ognjen Kraus · Gregor Mikuz

Periacinar retraction clefting in the prostatic needle core biopsies: an important diagnostic criterion or a simple artifact?

Received: 17 April 2003 / Accepted: 16 June 2003 / Published online: 24 July 2003
© Springer-Verlag 2003

Abstract The diagnosis of prostatic adenocarcinoma in needle core biopsy is based on major and supportive criteria. One of the supportive criteria is the presence of retraction clefting around neoplastic glands. We analyzed a series of 137 prostatic cancer cases diagnosed by needle core biopsy to determine the frequency, extent and criteria for periacinar retraction clefting. Clefting was analyzed on ten neoplastic and ten normal glands in three different high power fields. One-third or more glands with clefts affecting more than 50% of circumference were significantly more common in tumors (51.8%) than in benign glands (8%) ($P<0.0001$). A stricter criterion that designated as positive the cases with at least 50% of neoplastic glands (15 of 30) with clefts that affected more than 50% of circumference revealed clefts in only 15.3% of the malignant cases but none in benign cases (0%) ($P<0.0001$). Regardless of their extension, 15 or more glands with clefts were also more prominent in malignant cases (86.9%) than in benign cases (20.4%) ($P<0.0001$). We conclude that periacinar retraction clefting represents a reliable criterion for diagnosis of the prostatic adenocarcinoma, especially in cases with clefts affecting more than 50% of circumference in at least 50% of suspicious glands.

B. Krušlin (✉) · D. Tomas · H. Čupić · M. Belicza
Ljudevit Jurak University Department of Pathology,
Sestre milosrdnice University Hospital,
Vinogradska 29, Zagreb, Croatia
e-mail: bkruslin@kbsm.hr
Tel.: +385-1-3787177
Fax: +385-1-3787244

I. Novosel
Department of Pathology,
Dr Ivo Pedišić, County Hospital Sisak, Croatia

H. Rogatsch · G. Mikuz
Department of Pathology, University of Innsbruck,
Muellerstrasse 44, Innsbruck, Austria

O. Kraus
Department of Urology, Sestre Milosrdnice University Hospital,
Vinogradska 29, Zagreb, Croatia

Keywords Prostate adenocarcinoma · Histological criteria · Retraction clefting · Needle core biopsy

Introduction

Prostatic adenocarcinoma is the most common non-cutaneous malignant neoplasm in humans, with an estimated prevalence—based on histological studies—of over 30% in males older than 50 years [12]. The diagnosis of prostatic carcinoma is complex and is based on a constellation of three major histological criteria: the infiltrative growth pattern, the absence of a basal cell layer and the presence of macronucleoli (nucleoli larger than 1 μm in diameter) [11, 12].

The valid clinical strategy of performing biopsies in patients with elevated serum prostate-specific antigen without suspicious digital rectal examination and the exchange of the traditional 14-gauge biopsy needle with an 18-gauge biopsy needle yield less tissue for examination and small foci of cancer, which are often presented with only few glands. Therefore, the histological diagnosis of prostatic adenocarcinoma becomes even more difficult [11]. Several supportive diagnostic criteria have been proposed, but only a minority of these supportive features is specific for tumor. Proposed additional criteria are: marginated nucleoli, multiple nucleoli, wispy, bluish mucinous secretions, intraluminal crystalloids, intraluminal amorphous eosinophilic material, collagenous micronodules, glomerulations, periacinar cleft-like spaces and others, but many of these supportive criteria may also be present in benign glands or in some non-neoplastic proliferative acinar conditions [1, 2, 4, 11, 12].

Few authors paid attention to the so-called periacinar halos, retraction clefting or cleft-like spaces within neoplastic tissue [3, 5, 6, 7, 11]. The neoplastic cells of prostatic cancer often appear pulled away from the surrounding stroma, leaving halos around the acini [5]. Only a limited number of reports have compared and validated retraction clefting as supportive diagnostic

features in needle core biopsies in tumor tissue and benign glands [3, 7, 11].

In this study, we analyzed the amount and frequency of retraction clefting in tumors and non-tumorous prostatic tissue in needle core biopsies to estimate diagnostic importance and to define the criteria for the determination of retraction clefting.

Materials and methods

The study group consisted of 137 patients who underwent prostatic needle core biopsy during the period from 1 January 2000 to 30 June 2002. Biopsy specimens (18-gauge prostate needle core) diagnosed as cancer from 100 patients at the Department of Pathology, Leopold Franzens University, Hospital Innsbruck, and 37 biopsy specimens diagnosed as a cancer at the Ljudevit Jurak University Department of Pathology, Sestre Milosrdnice University Hospital, were histologically analyzed. The diagnosis of adenocarcinoma was confirmed in all cases, and all tumors consisted of at least 30 or more neoplastic glands. The urologists of both hospitals pull needle core biopsies from different areas of the prostate into 6 to 16 parts, usually maintaining orientation of the side and the part of prostate where biopsies were taken. An improved pre-embedding method was applied in both institutions as recently described [8, 9]. We evaluated each case as a whole, without regard to separate parts. The age range of the patients was between 41 years and 87 years (median age 63.5 years). Level of prostate-specific antigen (PSA) in all patients varied from 0.9 ng/ml to 31.7 ng/ml. At the time of diagnosis, all patients were without lymph-node or distant metastases. Specimens from both hospitals were fixed overnight in 10% buffered formaldehyde, embedded in paraffin, and cut at 5-μm thickness and routinely stained with hematoxylin and eosin. In some cases the material was stained by high molecular weight cytokeratin, PSA (MSIP; Dako, Copenhagen, Denmark) and alcian-periodic acid-Schiff. All cancers were graded using the Gleason grading system. Periacinar retraction clefting were graded as a percentage of gland circumference separated from the stroma in the three categories: glands without clefts, glands with clefts up to 50% of circumference and glands with clefts which affected more than 50% of the circumference. Clefting at the edges of a biopsy and cleft-like spaces in glands with incomplete circumference were excluded from examination, as at least some of it was likely to be a consequence of sectioning. We examined ten neoplastic glands in three different fields in needle core biopsy specimens under high magnification (×400). We used the same material as a control group, examining ten non-neoplastic glands in three different fields under the same magnification, and compared number of glands with clefts. Cases with ten or more glands with clefts, which affected more than 50% of glands circumference, were considered as positive. After needle core biopsy, the patients underwent prostatectomy and the diagnosis of adenocarcinoma was confirmed by pathohistological analysis in all cases.

The difference between the two proportions was tested using test of proportion. For all analyses, type-I error of 5% was considered statistically significant.

Table 1 Distribution of Gleason score among 137 prostatic needle biopsies with prostatic adenocarcinoma

Gleason grades with scores	Number of cases	%
4 (2+2)	3	2.2
5 (2+3)	4	2.9
5 (3+2)	16	11.8
6 (2+4)	1	0.7
6 (3+3)	69	50.4
6 (4+2)	1	0.7
7 (3+4)	25	18.2
7 (4+3)	11	8.1
8 (3+5)	2	1.4
8 (4+4)	4	2.9
9 (5+4)	1	0.7
Total	137	100

Results

The Gleason score distribution is shown in Table 1. Of the tumors, 3 (2.2%) were well differentiated, 91 (66.5%) moderately differentiated (Gleason score 5–6) and 43 (31.3%) were poorly differentiated (Gleason score 7–9). However, there were 36 (26.3%) tumors with a Gleason score of 7 and 7 (5%) cases with a Gleason score of 8–9. The most common Gleason grade was 3. In 127 (92.7%) tumors, one or both grades were 3. Both Gleason grades of 3 were found in 69 (50.4%) cases.

The distribution of the various degrees of periacinar retraction clefting in the malignant and benign cases is shown in Table 2 and Fig. 1A, B and Fig. 2A, B.

Glands (10 or more) with clefts that affected more than 50% of circumference were significantly more common in tumors (51.8%) than in benign glands (8%) ($P<0.0001$). Glands (10 or more) with clefts, regardless of their extension, were also more frequent in malignant cases (93.4%) as opposed to benign cases (57.7%) ($P<0.0001$). A stricter criterion that designated as positive cases with at least 50% of glands (15 of 30) with clefts that affected more than 50% of circumference revealed clefts in the malignant cases only (15.3%) but not in benign cases (0%) ($P<0.0001$). Glands with clefts (15 or more), regardless of their extension, were also more

Table 2 Distribution of periacinar retraction clefting in the malignant and benign cases (n=137)

	Frequency in malignant cases	Frequency in benign cases	Statistical significance (test of proportion)
Glands (10/30 or more) with clefts that affected more than 50% of circumference	71 (51.8%)	11 (8%)	Yes ($P<0.0001$)
Glands (10/30 or more) with clefts regardless of their extension	128 (93.4%)	79 (57.7%)	Yes ($P<0.0001$)
Glands (15/30 or more) with clefts that affected more than 50% of circumference	21 (15.3%)	0	Yes ($P<0.0001$)
Glands (15/30 or more) with clefts regardless of their extension	119 (86.9%)	28 (20.4%)	Yes ($P<0.0001$)
Cases with clefts that affected more than 50% of circumference regardless of the number of positive glands	125 (91.2%)	113 (82.5%)	Yes ($P=0.034$)

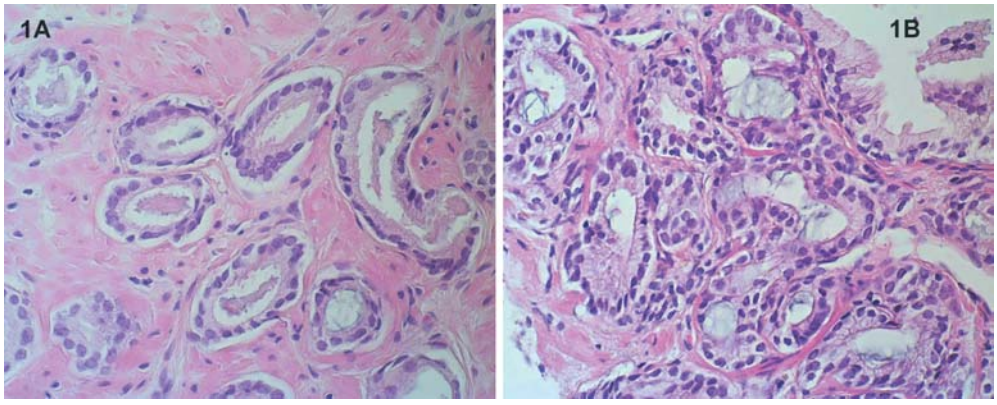

Fig. 1 **A** Periacinar retraction clefting affecting more than 50% of circumference of neoplastic acini in prostatic adenocarcinoma [hematoxylin and eosin (H&E) ×400]. **B** Neoplastic acini in prostatic adenocarcinoma without retraction clefting (H&E ×400)

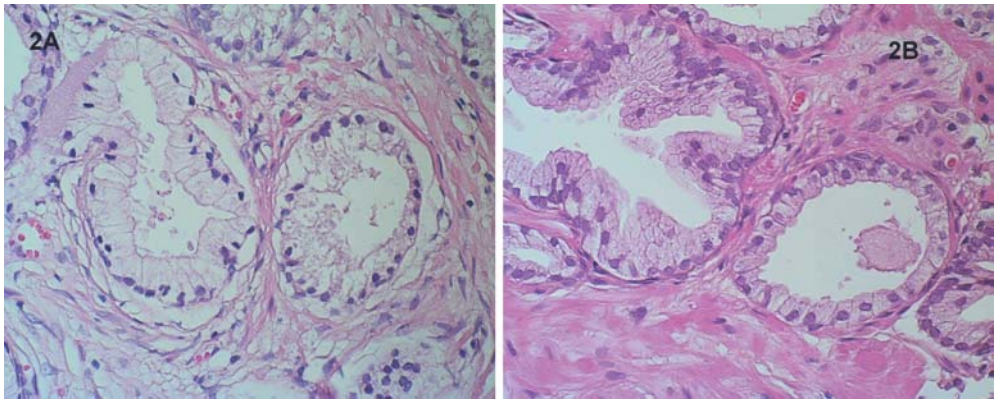

Fig. 2 **A** Periacinar retraction clefting affecting more than 50% of circumference of normal prostatic acini [hematoxylin and eosin (H&E) ×400]. **B** Normal prostatic acini without retraction clefting (H&E ×400)

prominent in malignant cases (86.9%) than in benign cases (20.4%) ($P<0.0001$). In all cases showing retraction clefting, at least one Gleason grade was 3. Comparison between malignant and benign cases with clefts which affected more than 50% of circumference regardless of the number of positive glands showed more frequent appearance of cleft in tumor (91.2%) than in non-tumor (82.5%) specimens ($P=0.034$). There was not a relationship between PSA value and the extent of retraction clefting.

Discussion

There are three histological criteria that are considered as diagnostic for prostatic adenocarcinoma on needle biopsy: perineural invasion, mucinous fibroplasias and glomerulations [1]. However, these features are very rarely seen. According to Baisden et al. [1], perineural invasion was observed in 9 of 1480 consult cases (0.6%), fibroplasias were observed in 0.1% of cases and glomerulations were not seen. Other authors reported perineural invasion in 2–3% of cases [4, 10]. Thorson et al. [10] reported the most common morphological features of minimal carcinomas (less than 1 mm) in needle biopsy to be nucleomegaly (96%), infiltrative growth pattern (88%), intraluminal mucinous secretions (78%) and prominent nucleoli (64%). Helpful diagnostic features reported by Epstein [4] were nuclear enlargement in 77%, prominent nucleoli in 76% and pink acellular luminal secretions in 53% of cases. Mean and median number of glands in Epstein's study were 31 and 20, respectively (range 2–300).

Many additional criteria for the diagnosis of prostatic carcinoma-like marginated nucleoli, multiple nucleoli, intraluminal crystalloids, intraluminal amorphous eosinophilic material, and others are used in routine diagnostic procedure [2, 11, 12]. One of the proposed additional criteria is a so-called retraction clefting, appearing more frequently about neoplastic glands in comparison with benign glands; but only few authors paid attention to this phenomenon [5, 6, 11]. Retraction clefting might also be observed in other tumor types, representing a well-known diagnostic criterion between basal cell carcinoma and adnexal skin tumors.

Halpert et co-workers were the first to briefly describe the clefts in prostatic adenocarcinoma [5, 6]. In their autopsy studies of prostatic adenocarcinoma, halos around neoplastic acini were observed. In a recent study by Amin and his group, retraction clefting was found in 38.6 cases of prostatic cancer diagnosed by needle core biopsy and in 7% of non-neoplastic glands [11]. They graded retraction clefting as a percentage of gland circumference separated from the stroma using a scale from 0 to 4. The same authors considered grades 3 (50–75%) and 4 (more than 75%) as positive. However, the authors did not specify the number of neoplastic glands showing clefting

that was regarded as positive. They also did not mention under which magnification the clefts were analyzed.

In the current study, we analyzed clefting under high magnification (×40 objective) counting ten glands in three different fields. Clefting could be observed under lower magnification but it is obvious that the same magnification should be used by different observers for the sake of comparison. Our results showed that clefting affecting more than 50% of circumference in more than 50% of analyzed glands was found in neoplastic glands only. Such strict criteria were fulfilled in 15.3% of all cancer cases and were not observed in normal glands, suggesting the potential use of this criterion in routine diagnostics. The application of less stringent criteria (one-third of glands with more than 50% of circumference) revealed positive clefting in 51.8% of carcinoma cases and 8% of non-neoplastic glands ($P<0.0001$).

The presence of clefting in prostatic needle core biopsy is usually attributed to the retraction artifact. Therefore, the quantity of clefting is considered as an indicator of quality of technicians and laboratory staff. In this study, we tried to quantify the extent of periacinar clefting. To minimize the influence of laboratory procedure, an improved pre-embedding method of prostatic needle core biopsy specimens was employed in both institutions as recently described by Rogatsch et al. [8, 9].

The origin of clefting in tumor specimens is unknown but may be related to an abnormality in the expression of collagenases or some other enzymes required for invasion. As it is known, malignant glands lack basal cells, and this also may be one of the reasons for appearance of clefts. The most prominent clefts were found in Gleason grade-3 prostatic carcinoma, especially in Gleason grade 3A, as was also observed in our study [7, 12].

Our criteria may be applied in a similar manner to carcinoma cases composed of few neoplastic glands. However, the cut-off value should be determined in the future studies. We propose that the presence of retraction clefting in at least one-third of glands affecting more than 50% of circumference along with one of other supportive criteria and/or clefting in at least 50% of glands with more than 50% of circumference should be considered as a criterion for the diagnosis of prostatic adenocarcinoma. Similar clefting changes should not be present in adjacent normal glands within the same specimens. Further studies regarding the determination of reliability of the proposed criterion and its refinement are certainly welcome.

References

1. Baisden BL, Kahane H, Epstein JI (1999) Perineural invasion, mucinous fibroplasia and glomerulations: diagnostic features on prostate needle biopsy. Am J Surg Pathol 23:918–924
2. Bostwick DG, Dundore PA. (1997) Biopsy pathology of the prostate. Chapmann & Hall Medical, London
3. Durham JR, Lee MW, Amin MB, Shulz DS, Stetler-Stevenson WG (1994) Clefting in adenocarcinoma of the prostate gland (abstract). Am J Clin Pathol 102:536
4. Epstein JI (1995) Diagnostic criteria of limited adenocarcinoma of the prostate on needle biopsy. Hum Pathol 26:223–229
5. Halpert B, Schmalhorst WR (1966) Carcinoma of the prostate in patients 70 to 79 years old. Cancer 19:695–698
6. Halpert B, Sheehan EA, Schmalhorst WR, Scott RJ (1963) Carcinoma of the prostate: a survey of 5000 autopsies. Cancer 16:736–742
7. Krušlin B, Novosel I, Reljić A, Čupić H, Spajić B, Belicza M (2002) Periacinar cleft-like spaces in prostatic needle core biopsies (abstract). Acta Clin Croat 41:175
8. Rogatsch H, Mairinger T, Horninger W, Gschwendtner A, Bartsch G, Mikuz G (2000) Optimized preembedding method improves the histologic yield of prostatic core needle biopsies. Prostate 42:124–129
9. Rogatsch H, Moser P, Volgger H, Horninger W, Bartsch G, Mikuz G, Mairinger T (2000) Diagnostic effect of an improved preembedding method of prostate needle biopsy specimens. Hum Pathol 31:1102–1107
10. Thorson P, Vollmer RT, Arcangeli C, Keetch DW, Humphrey PA (1998) Minimal carcinoma in prostate needle biopsy specimens: diagnostic features and radical prostatectomy follow-up. Mod Pathol 11:543–551
11. Varma M, Lee MW, Tamboli P, Zarbo RJ, Jimenez RE, Salles PGO, Amin MB (2002) Morphologic criteria for the diagnosis of prostatic adenocarcinoma in needle biopsy specimens. Arch Pathol Lab Med 126:554–561
12. Young RH, Srigley JR, Amin MB, Ulbright TM, Cubilla AL (1998) Atlas of tumor pathology. AFIP, Washington, D.C., pp 124–171

Virchows Arch (2003) 443:528–535
DOI 10.1007/s00428-003-0848-5

ORIGINAL ARTICLE

Tibor Glasz · Michael Frenken · Hans-Jürgen Knieriem · Arno Krian

Mechanisms of death in the early postoperative period following coronary artery bypass grafting for acquired heart disease. A clinicopathological study of 32 cases

Received: 21 May 2003 / Accepted: 21 May 2003 / Published online: 29 July 2003
© Springer-Verlag 2003

Abstract *Objectives:* A retrospective cardiopathological and clinical study was conducted in order to determine causes of perioperative death following coronary artery bypass grafting (CABG). *Experimental design:* Between January 1992 and June 1995, a total of 5749 CABG procedures were performed at the Heart Center Duisburg (Germany). Following the procedures, 218 patients died in hospital (mortality rate 3.8%). Fifty-eight were autopsied at the Institute of Pathology, Bethesda Hospital, Duisburg, and 32 autopsied cases were amenable to our study. Basis for selection was accessibility of clinical and morphological data and a postoperative death within 30 days. *Methods:* In each case, morphological analysis of the heart and an evaluation of surgical and clinical data were performed in order to draw a conclusion on the mechanism of death. *Results:* Using criteria defined by us, the following causes of death were determined: (1) surgical complications (43%); (2) severe coronary artery disease with incomplete revascularization (41%); (3) congestive heart failure (13%); (4) non-cardiac complications (3%). *Conclusion:* Criteria defined in this study may be useful in evaluations of causes of death after open heart surgery and may help to compare results in future series. Determination of the cause of death is important for the cardiac surgeon to reconsider indications and quality of surgical procedure.

Keywords Open heart surgery · Coronary artery bypass grafting · Clinicopathology · Causes of death

T. Glasz (✉)
2nd Department of Pathology,
Faculty of Medicine, Semmelweis University,
Üllői út 93, 1091 Budapest, Hungary
e-mail: gt@korb2.sote.hu
Tel.: +36-1-2157300
Fax: +36-1-2156921

M. Frenken
Department of Surgery, St. Joseph's Hospital,
Alte Schulstrasse 21–23, 40789 Monheim am Rhein, Germany

H.-J. Knieriem
Institute of Pathology, Bethesda Hospital,
Heerstraße 219, 47053 Duisburg, Germany

A. Krian
Department of Thoracic and Cardiovascular Surgery,
Heart Center Duisburg,
Gerrickstraße 21, 47137 Duisburg, Germany

Introduction

Since 1968, when Favaloro [7] and Green et al. [8] reported on a method of improving impaired blood flow to myocardium in severe coronary artery disease—either by use of a saphenous vein [7] or of an internal thoracic artery [8]—coronary artery bypass grafting (CABG) has gained wide acceptance. Morphological studies on changes after CABG have mainly been done on venous grafts [1, 2, 10, 14, 17, 18, 20, 23, 25, 27, 28, 29]. It has been noted that damage of the endothelium of the graft [14], placement of a disproportionate graft on a small coronary artery [28], or distal anastomosis on an arteriosclerotically stenosed coronary artery segment with subsequent decreased flow [9] may result in occlusive thrombosis. Poor run-off may be caused by kinking of a too long graft [4], or a graft trimmed too short, causing stretching and flattening of the grafting vessel [24], or spasm of a saphenous graft [10]. A further cause may be reduction of anastomotic circumference at both ends of the arteriotomy, resulting from the eversion and utilization of the arterial wall by the suture [9, 12]. Proximal (aortic) anastomoses have been described as relatively resistant to pathological changes [11], which are independent of the angle of the anastomosis [1]. Severe aortic sclerosis may, however, compromise the placement of a proximal anastomosis. In the myocardium, contraction band (reperfusion-type) necrosis generally occurs with a patent graft in the period of reflow after a transient ischemic phase [4], either explained by a dissolved thrombus [15] or by a brisk reperfusion damage after surgery [3, 11]. Coagula-

tion necrosis is seen in association with fixed obstructions of coronary blood flow [4].

In the present study, we performed a retrospective clinicopathological analysis of postmortem heart specimens of patients after CABG. This work was conducted in view of the fact that postmortem studies of patients after CABG are rather scarce, and even fewer of such studies are performed on a clinicopathological basis. The few publications evaluating causes of death in these patients often use poorly defined or inconsistent criteria, which limit comparison. Therefore, our aim was to propose criteria for categories of death and related entities, thus permitting comparison of results in future series.

Materials and methods

Population studied

Between January 1992 and June 1995, a total of 5749 coronary artery bypass grafting (CABG) procedures for acquired coronary heart disease were performed at the Heart Center of Duisburg (Germany). Of these patients, 218 died in hospital (mortality rate 3.8%). Fifty-eight cases underwent a postmortem evaluation at the Institute of Pathology, Bethesda Hospital in Duisburg. In a retrospective study, 32 of these cases were amenable to a detailed cardiopathological analysis in cooperation with a cardiac surgeon. The ages of the patients ranged from 45 years to 79 years, the male/female ratio was 21/11.

Materials and methods

At autopsy, the hearts were removed in a conventional way by transsection of the main arterial and venous trunks with preservation of the proximal anastomoses of the venous grafts. Internal mammary artery (IMA) grafts were transsected at the highest level possible. Before fixation, following prior X-raying of the native heart specimens, postmortem angiograms were made [4, 26]. To achieve this, barium-gelatin pigment was injected manually into each coronary artery and graft ostium, and separate X-ray pictures were taken to gradually document filling conditions of the vasculature. Postmortem angiograms were used later as means of orientation for a more accurate tissue sampling during gross examination. Every heart specimen was then fixed in a distended configuration at least for a week in 5% formalin. Initially, a detailed gross description of the specimen, including a statement of number and positions of grafts, was done with segmental transsection of all coronary arteries, anastomoses, and conduits at 5-mm intervals. Representative sections were embedded for routine histological processing from the pre- and postanastomotic coronary arteries, from the anastomoses, and from the grafts themselves. Standard tissue blocks from the myocardium of the anterior, lateral, posterior, and upper posterior wall, the mid- and upper septum, and the apex [4] were taken. Five-micron routine sections were prepared from each paraffin block for hematoxylin and eosin and for elastic-Van Gieson stains. In some instances other staining methods (periodic acid-Schiff, trichrome) were also used. The slides were then examined using the light microscope with special attention to presence, type, age, and degree of stenoses or occlusions of native coronary arteries, grafts, anastomoses, and myocardial damage. Coronary artery stenoses were evaluated by comparing the actual and original lumina, the latter being defined by the internal elastic lamina best demonstrated on elastic-Van Gieson stains. Only severe stenoses (over 75% luminal surface loss in any coronary artery or over 50% luminal surface loss in the main left coronary artery [4]) were taken into consideration. The degree of stenosis was estimated by diminution of the luminal diameter, an actual diameter equal to 50% of the original diameter in two planes corresponding to a 75% loss of the luminal surface [21]. The age of myocardial damage was classified according to established light microscopic criteria [4]: (1) "hyperacute" or "preterminal": substantially retained myocardial structure with formation of wavy fibers, hypereosinophilia, fine granulation or vacuolation of the sarcoplasm, focal or extensive loss of striation, corresponding to acute myocardial infarction a few hours before death; (2) "acute": structural damage to myocardium by degradation and rupture of myocytes, cytoplasmic hypereosinophilia, formation of contraction bands, appearance of leukocytic infiltration in necrotic areas, loss of nuclear staining, etc., corresponding to acute myocardial infarction about 12 hours to a few days before death; (3) "old" or "chronic": fibrotic area more than 1 cm in largest diameter corresponding to myocardial infarction several weeks to months/years before death. The above changes within circumscribed area(s) were named myocardial infarction; extensive myocardial involvement was termed subtotal/global myocardial ischemia not directly linked to disease of a single supplying coronary artery.

All organs other than the heart—with special respect to brain and lung—underwent dissection in all of the cases according to routine autopsy protocols. Morphological data for extracardiac organs were retrieved from the autopsy records.

Histological examination of the heart specimens was followed by a summary of gross and microscopic details of cardiac pathology, autopsy findings, and clinical data, the latter including clinical history, results of clinical examinations, report of operative procedure, clinical setting of death, etc., to achieve clinicopathological consensus on the mechanism of death.

Results

Clinical findings

Some characteristics and anamnestic data on conventional risk factors of patients who died after CABG procedure are summarized in Table 1 and Table 2.

Morphological findings

Coronary artery disease

According to our definitions on coronary artery disease (Table 3), distribution of the disease was central in 12 cases (38%) and diffuse in 20 cases (62%). No cases showed an exclusively peripheral distribution. A small-vessel disease was seen histologically in two cases (6%) without possible predisposing anamnestic factors for microangiopathy, such as hypertension and diabetes mellitus [13, 19].

Revascularization

In the 32 patients, 82 anastomoses were performed using 69 saphenous vein segments and 13 IMA grafts. According to our definitions on completeness of revascularization (Table 4), revascularization was found to be histomorphologically complete in n=12 patients (38%). Incomplete revascularization was revealed in n=20 patients (62%). Revascularization was found to be

Table 1 Patient characteristics

Characteristics	Patients treated by coronary artery bypass grafting procedures
No. of patients	32
Age (years; mean, range)	63 (45–79)
Sex ratio (male/female)	21/11
Death (*n*; %)	
On day of operation	11 (34%)
On postoperative days 1–7	15 (47%)
On postoperative days 8–30	6 (19%)
Pathological extent of coronary artery disease (*n*; %)	
Three-vessel disease	30 (94%)
Two-vessel disease	2 (6%)
One-vessel disease	–
Left main coronary artery disease	13 (41%)
Revascularization	
Grafts per patient	2.6
Arterial revascularization (*n*; %)	12 (38%)
Heart weight (g; mean, range)	557 (340–760)

Table 2 Anamnestic data on conventional risk factors in patients with early postoperative death following coronary artery bypass grafting procedure (*n*=32)

Hypertension	Diabetes	Excess body weight	Smoking	Hyperlipidemia	No risk factors noted
17 (53%)	8 (25%)	2 (6%)	1 (3%)	7 (22%)	11 (34%)

Table 3 Definitions on coronary artery disease (1)

1. Central	1.1. In vessels without revascularization Significant primary stenotic lesion(s) in a large epicardial coronary artery proximal to the most distal point at which grafting is still assumed to be technically possible 1.2. In revascularized vessels Arteriosclerotic lesion(s) in a large epicardial coronary artery with significant stenosis proximal to the most distal anastomosis on this vessel
2. Peripheral	2.1. In vessels without revascularization Significant primary stenotic lesion(s) in large epicardial coronary arteries distal to the most distal point where an anastomosis is still assumed to be technically possible 2.2. In revascularized vessels Arteriosclerosis with significant stenosis distal to the most distal anastomosis on a vessel
3. Diffuse	Significant primary stenotic lesions in both proximal and distal regions of a coronary artery as defined under (1) and (2)
4. Small vessel disease	Coronary arteriosclerotic remodelling of intramyocardial coronary artery branches with a diameter of less than 1 mm, as defined by the internal elastic membrane [13], resulting in a lumen narrowing more than 50% [19]

Table 4 Definitions on revascularization (2)

1. Complete revascularization	Revascularization of all major coronary arteries[1] with significant stenoses resulting in an effective blood supply of the corresponding myocardial areas[2]
2. Incomplete revascularization	Any case in which at least one of the three major coronary artery systems with significant stenotic lesion(s) has not been bypassed

[1] Major coronary arteries: left descendent, circumflex and right coronary arteries
[2] Revascularization of a side branch of a significantly stenotic major coronary artery without backward flow into the major coronary artery does not classify for complete revascularization; e.g., graft on diagonal branch and occlusion either of the proximal part of the diagonal artery or of the left descendent artery directly distal to the branching off

incomplete for two major reasons: first, due to coronary artery disease that was technically inaccessible for complete grafting (e.g., coronary artery disease of the diffuse type or central coronary artery disease coupled with distally vulnerable vessel anatomy) (*n*=17) and, second, because centrally positioned high-grade stenoses had not been detected preoperatively by angiography, as evidenced by retrospective analysis (*n*=3).

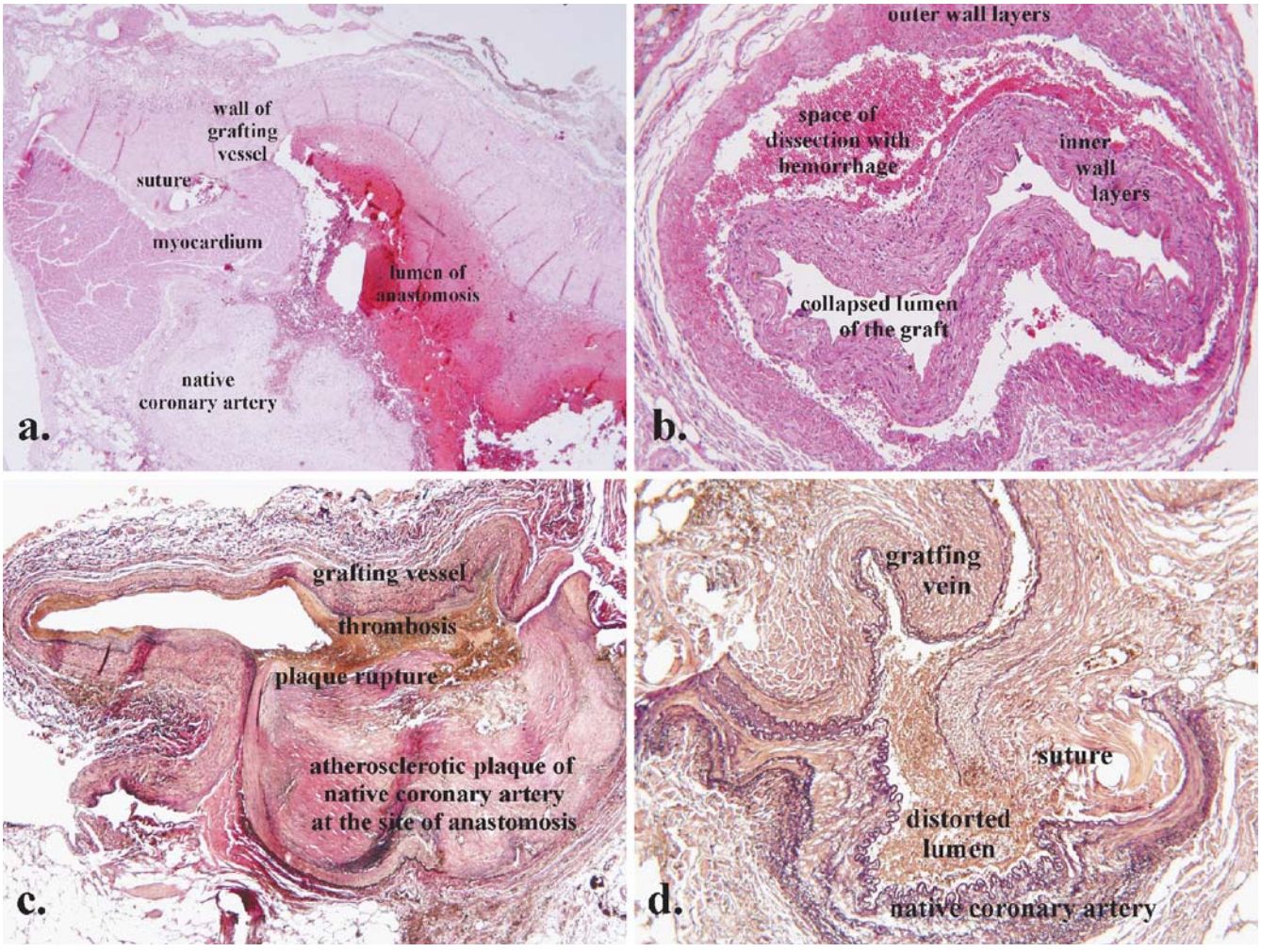

Fig. 1 Technical problems during coronary artery bypass grafting procedure. **a** Acute (thrombotic) occlusion of a saphenous vein graft anastomosis on the diagonal artery. Thrombogenic cascade was initiated by a piece of adjacent myocardium protruding into the anastomotic lumen. Hematoxylin and eosin; ×40. **b** Dissection and occlusion of an internal mammary artery graft to the left anterior descending artery. Hematoxylin and eosin; ×100. **c** Saphenous vein graft anastomosis on a primarily stenosed segment of the posterior descending artery with plaque rupture and lumen thrombosis. Elastic-van Gieson; ×40. **d** Anastomotic stenosis of the marginal artery by a too tightly placed suture. Note distorted anastomotic configuration and traces of suture. Elastic-van Gieson; ×100

Significant acute perianastomotic stenoses (i.e., within graft, distal to or at the anastomotic site) were histologically found in 39 (48%) of the 82 anastomoses (in 20 patients). In four instances (10%), acute perianastomotic stenoses were caused by dissection of the vessel wall, the rest (n=35, 90%) were thrombotic stenoses or occlusions. In 34 of 39 perianastomotic stenoses, it was the graft and/or the anastomotic site that was involved in the acute stenosis; of these grafts n=8 (24%) were arterial and n=26 (76%) were saphenous vein revascularizations. In five more instances (13%), grafts and anastomoses were patent and the stenoses were located in the native coronary artery distal to the anastomotic site. Of 39 significant acute perianastomotic stenoses, 33 (85%) were followed by acute myocardial infarction in the corresponding myocardial area. Contingency table analysis showed no statistical relationship between the type of revascularization (arterial vs saphenous vein) and the prevalence of significant acute graft stenosis alone or complicated by acute myocardial infarction. Non-revascularized coronary arteries revealed acute occlusions in 12 patients. Some histomorphologically demonstrated technical problems are shown on Fig. 1a–d.

Myocardium

Acute myocardial infarction could be detected histologically in 31 patients; one more patient died within 3 h postoperatively with incomplete revascularization and showed no myocardial infarction histologically, a period possibly too short to allow detectable myocardial changes with the light microscope. Histology and clinical data showed that four patients (13%) were operated on with preoperative acute myocardial infarction, 28 patients (88%) evolved a peri- or postoperative acute myocardial

Table 5 Definitions on causes of death (3)

1. CARDIAC causes	
1.1. Causes INTRINSIC to the heart	
1.1.1. Death due to coronary artery disease	1.1.1.1. Any case with evidence of a circumscribed early postoperative acute myocardial infarction in a myocardial area supplied by a coronary artery with distal or diffuse coronary artery disease where complete revascularization was not feasible 1.1.1.2. Also included are cases where despite central coronary artery disease an incomplete revascularization was done because (a) coronary artery disease was preoperatively undetected by angiography or (b) coronary artery configuration was intraoperatively evaluated as technically inoperable[1] or (c) excessive calcification in the ascending aorta (so-called porcelain aorta) allowing no placement of a proximal anastomosis was present with a circumscribed early postoperative acute myocardial infarction in the related area of a diseased but not grafted vessel 1.1.1.3. Death in cases operated on with a preoperative acute myocardial infarction is also classified to be due to coronary artery disease 1.1.1.4. Cases with a surgery-related complication or a non-cardiac cause of death are excluded
1.1.2. Death due to congestive heart failure	1.1.2.1. Any case with no coronary artery disease or with completely revascularized coronary artery disease and histological evidence of extensive myocardial damage with or without severely depressed left ventricular function preoperatively 1.1.2.2. Also included is a patient with a cor bovinum (heart weight >800 g) 1.1.2.3. There must be no evidence of surgery-related complications or of a non-cardiac cause of death
1.2. Causes NOT INTRINSIC to the heart	
1.2.1. Death due to surgery-related complications	1.2.1.1. Any case with acute myocardial infarction that occurred in the early postoperative period (according to clinical and/or histomorphological findings) in a patient with relatively good preoperative left ventricular function 1.2.1.2. One or more of the following criteria must also be fulfilled a) Acute myocardial infarction found in an area supplied by a grafted coronary vessel with a significant acute stenosis or occlusion either in the proximity of the anastomosis, or in the grafting vessel or in the native coronary artery distal to the anastomosis b) Acute myocardial infarction in an area supplied by a revascularized coronary artery showing significant primary stenosis at the anastomotic site c) Evidence of multiple acute thrombi of unknown origin in revascularized and/or non-revascularized coronary arteries without evidence of a non-cardiac cause of death d) Evidence of multiple acute myocardial infarctions in several myocardial areas without non-revascularized stenoses/occlusions of corresponding coronary arteries or stenosed/occluded grafts in a patient with an early postoperative low-output-syndrome, without evidence of death due to a non-cardiac cause
2. NON-CARDIAC causes	
2.1. Death due to non-cardiac complications	2.1.1. Any disease of extracardiac origin limiting vital functions[2]

[1] Technically inaccessible coronary artery anatomy (intramural position, vessel vulnerability, etc.); otherwise incorrect assumption of a diffuse type coronary disease with resignation to revascularize
[2] Pneumonia, cerebral or mesenteric infarction, etc

infarction, one patient had evidence for both pre- and postoperative acute myocardial infarctions. Widespread myocardial damage (acute myocardial infarction in at least two major myocardial areas) was evidenced in 24 patients (75%); two patients developed infarctions in the preoperative period. In 20 of the 28 patients (71%) with acute peri- or postoperative infarction, tissue damage was found in one or more of the revascularized myocardial areas with a patent corresponding graft and a non-occluding anastomosis [31 patent grafts (3 arterial, 28 saphenous vein grafts) and non-occluding anastomoses of the total of 57 revascularizations in the 20 patients; 54%].

In order to determine the primary cause of acute peri- or postoperative myocardial infarction, the cases (n=28) were analyzed according to the following settings:

1. Acute myocardial infarction caused by severe coronary artery disease (n=7 patients; 25%). All these patients had a diffuse type coronary artery disease; five were incompletely revascularized because of inaccessibility of coronary artery disease to complete revascularization.
2. Acute myocardial infarction with an acute event at the anastomotic site, within the graft or the native coronary artery (n=13 patients; 46%).
3. Acute myocardial infarction with histological evidence of a global myocardial ischemia (as a rule in a hyperacute or a preterminal situation) (n=8 patients; 29%).

Chronic infarctions in one or more myocardial areas were found in 28 of 32 patients (88%).

Causes of death

Based on the experience gained during case analyses, criteria shown in Table 3, Table 4 and Table 5 were determined. A detailed demonstration of the findings in every single patient enrolled in the present study is given

Table 6 Cumulative table on clinical and pathomorphological findings in patients no. 1–32. *Column labeling* (N.B.- in square brackets are references to Table 5): A: Emergency operation, B: preoperatively severely depressed left ventricular function [1.1.2.1.], C: preoperative instable angina pectoris, D: preoperative acute myocardial infarction [1.1.1.3.], E: porcelain aorta [1.1.1.2.], F: intraoperative graft flow control (0: no flow, 1: low, 2: moderate, 3: good; ND: no data), G: early postoperative low-output-syndrome [1.2.1.2./d.], H: postoperative intraaortic balloon pumping, I: postoperative respiration, J: reoperation (cause), K: extracardiac disease limiting vital functions [2.1.], L: incomplete revascularization [1.1.1.1.; 1.1.1.2.], M: early postoperative acute myocardial infarction [1.1.1.1.; 1.1.1.2.; 1.1.2.1.; 1.2.1.1.; 1.2.1.2.], N: no. of diseased coronary arteries, O: coronary artery disease of distal/diffuse type [1.1.1.1.], P: central coronary artery disease of a single coronary artery preoperatively undetected [1.1.1.2.], Q: significant primary stenosis of anastomotic site [1.2.1.2./b.], R: histologically evidenced extensive myocardial damage (acute myocardial infarction in at least two major myocardial areas) [1.1.2.1.; 1.2.1.2./d.], S: *cor bovinum* [1.1.2.2.], T: revascularization with significant acute stenosis or occlusion [1.2.1.2./a.], U: multiple acute thrombi in revascularized and/or non-revascularized coronary arteries [1.2.1.2./c.], V: data considered to be of special relevance for death evaluation in columns . . . W: clinicopathological consensus on cause of death. *CAD* death due to coronary artery disease, *CHF* death due to congestive heart failure, *SRC* death due to surgery related complication, *NCC* death due to non-cardiac complication, *ND* no data available, + yes, – no (with special respect to column 'L'; + incomplete revascularization, – complete revascularization; and column 'O'; + distal/diffuse-type coronary artery disease, – central-type coronary artery disease)

	Clinical data > *Clinicopathological data* < < < < < < < < < < < < < < < < < < < < < *Pathomorphologic data*																						
Pat. N°	***A:** Emerg. op.*	***B:** Preop.LVF↓*	***C:** Instable AP*	***D:** Preop.AMI*	***E:** Porcelain ao.*	***F:** Intraop. graft flow control*	***G:** Low-outp.-syn.*	***H:** Balloon pump*	***I:** Postop.respir.*	***J:** Cause of reoperation*	***K:** Severe extracardiac disease*	***L:** Incompl.revasc*	***M:** Postop. AMI*	***N:** N° of CAD*	***O:** Dist/diff. CAD*	***P:** Undetected central CAD of single coronary arteries*	***Q:** Prim.anast.sten.*	***R:** Extensive AMI*	***S:** Cor bovinum*	***T:** Revasc. with acute stenosis*	***U:** Multip. thrombi*	***V:** Data relevant for death evaluation in columns...*	***W:** Cause of death*	***Pat. N°***
1.	-	-	-	-	-	2-3	-	-	-	-	stroke	+	+	3	+	-	+	-	-	+	-	K	**NCC**	**1.**
2.	-	-	+	-	-	2-3	+	+	-	tamponade	-	-	+	3	-	-	-	+	-	+	-	G, M, R, T	**SRC**	**2.**
3.	-	+	+	-	-	3	+	-	+	-	-	+	+	3	-	-	+	-	-	+	-	M, Q, T	**SRC**	**3.**
4.	-	+	-	-	-	3	+	+	-	-	-	+	+	2	-	-	-	-	-	+	-	G, M, T	**SRC**	**4.**
5.	-	-	-	-	-	3	+	+	-	ventric. fibrill.	-	+	+	3	+	RCX	-	+	-	-	-	G, H, R	**SRC**	**5.**
6.	-	-	-	-	-	3	+	-	-	-	-	+	+	3	+	-	-	+	-	-	-	L, M, O	**CAD**	**6.**
7.	+	+	+	-	-	3	+	+	+	-	-	-	+	3	+	-	+	+	-	-	-	B, L, R	**CHF**	**7.**
8.	-	-	-	-	-	2-3	+	+	+	-	-	-	+	3	+	-	+	+	-	+	-	G, M, Q, R, T	**SRC**	**8.**
9.	+	-	+	-	-	3	+	+	-	low output	-	+	+	3	+	-	+	+	ND	-	-	A, C, L, M, O	**CAD**	**9.**
10.	-	-	-	-	-	3	+	-	+	-	-	+	+	3	-	-	-	+	-	+	+	G, M, R, T, U	**SRC**	**10.**
11.	-	+	+	-	-	3	-	-	-	-	-	+	+	3	-	RCA	-	+	-	-	-	B, R	**CHF**	**11.**
12.	-	-	+	-	-	ND	+	+	-	-	-	-	+	3	+	-	+	+	-	+	+	G, Q, R, T, U	**SRC**	**12.**
13.	+	-	+	-	-	ND	+	-	+	-	-	+	+	3	+	-	-	+	-	+	-	C, L, N, O, R	**CAD**	**13.**
14.	-	+	-	+	-	ND	+	-	-	-	-	+	-	3	+	-	-	-	-	-	-	D, L, M, O	**CAD**	**14.**
15.	-	+	-	-	+	3	+	-	-	-	-	+	+	3	-	-	-	+	-	+	+	M, T, U	**SRC**	**15.**
16.	-	-	-	-	-	3	+	-	-	-	-	+	+	3	+	-	-	-	-	-	-	L, M, N, O	**CAD**	**16.**
17.	-	+	-	-	-	2-3	+	-	-	-	-	-	+	3	+	-	+	+	-	+	-	M, N, O	**CAD**	**17.**
18.	-	+	-	-	-	2	+	-	+	bleeding	-	+	+	3	+	-	+	+	-	-	-	L, M, O	**CAD**	**18.**
19.	-	-	+	-	-	ND	+	-	+	-	-	+	+	3	+	RCX	-	+	-	+	-	L, M, O, P, R	**CAD**	**19.**
20.	-	+	-	+	-	2-3	+	+	-	-	-	+	-	3	+	-	+	+	-	-	-	D, L, M, N	**CAD**	**20.**
21.	-	-	-	-	-	3	+	+	+	-	-	+	+	3	-	-	+	+	-	+	+	Q, T, U	**SRC**	**21.**
22.	-	+	+	-	-	2-3	-	-	+	tamponade	-	-	+	3	+	-	-	+	-	+	+	J, M, T, U	**SRC**	**22.**
23.	-	+	-	-	-	2-3	+	+	+	-	-	-	+	2	-	-	-	+	-	+	-	B, L, O, R	**CHF**	**23.**
24.	-	-	-	-	-	1-3	+	+	-	postop. asystole	-	-	+	3	-	-	-	+	-	+	-	L, M, O, R, T	**SRC**	**24.**
25.	-	-	-	-	-	3	+	-	-	-	-	+	-	3	+	-	-	-	-	-	-	G, L, O	**CAD**	**25.**
26.	-	-	-	-	-	1-3	+	-	-	-	-	-	+	3	+	-	+	+	-	+	-	M, Q, T	**SRC**	**26.**
27.	+	-	+	-	-	3	-	-	-	-	-	-	+	3	-	-	-	+	-	+	+	M, O, R, T, U	**SRC**	**27.**
28.	+	+	+	+	-	3	+	+	+	-	-	-	-	3	+	-	+	+	-	-	-	D, L, M, R	**CAD**	**28.**
29.	-	-	-	-	-	3	+	-	-	-	-	+	+	3	+	-	-	-	-	+	-	M, T	**SRC**	**29.**
30.	-	+	-	+	-	ND	+	-	-	-	-	+	+	3	+	-	-	-	-	+	+	D, L, M, O	**CAD**	**30.**
31.	-	+	+	-	-	3	+	-	+	-	-	-	+	3	-	-	-	+	-	-	-	B, L, M, R	**CHF**	**31.**
32.	-	-	+	-	-	3	+	-	-	-	-	+	+	3	-	-	-	+	-	+	-	C, L, M, O	**CAD**	**32.**
Total	**5**	**14**	**13**	**4**	**1**	**-**	**28**	**12**	**12**	**6**	**1**	**20**	**28**	**-**	**20**	**3**	**12**	**24**	**0**	**20**	**7**	**-**	**-**	**Total**

Table 7 Causes of early post-operative death following coronary artery bypass grafting (CABG) procedure

Causes of death	Patients treated by CABG procedures (n=32)
Surgical complications	14 (43%)
Severe coronary artery disease	13 (41%)
Congestive heart failure	4 (13%)
Non-cardiac	1 (3%)[a]

[a] Non-cardiac death was caused by cerebral vascular accident

cumulatively in Table 6. Causes of death in the studied population as determined according to the definitions listed in Table 5 are presented in Table 7.

Discussion

The main goal of this study was to propose a system of definitions for mortality studies in patients who die after CABG procedures in the early postoperative period. Despite extensive investigations in this field since the introduction of CABG in the late 1960s, only relatively few clinicopathological studies on causes of death and complications have yet been reported [6, 16, 18, 29]. This may partly be explained by the fact that in the last decades the autopsy rate has shown continual declination in the western world. Still, postmortem examination is acknowledged as one of the most specific indicators of errors in diagnosis, management, judgment, and technique in surgery. Therefore, it is an invaluable means of quality assurance in clinical practice in general and especially in heart surgery [6]. A prospective study by Lee et al. [16] found cardiac failure to be the most common cause of death (52%), the preoperative acute myocardial infarction being the most important predisposing factor. Other causes of death were hemorrhage at operative sites, pulmonary embolism, and cerebral vascular accidents. A study by Rose [22] has shown surgery-linked technical problems to be a leading cause of death (30%). Cosgrove et al. [5] found that principal and persistent risk factors for surgical mortality were preoperative congestive heart failure, emergency operation, female gender, and advanced age. These authors found a gradual decrease of cardiac causes of death relative to non-cardiac (primarily neurological) causes. Also, incomplete revascularization was found to be an important risk factor.

In our population, a relatively large percentage (43%) of patients succumbed in the early postoperative period due to surgical complications. Yet, it is remarkable that severe diffuse coronary artery disease in a number of patients rendered revascularization incomplete, and this proved to be the cause of death in a similar number of cases (41%), a finding that is in line with those of Cosgrove et al. [5]. Our results, on the other hand, contradict these authors in that we found the frequency of non-cardiac causes to be low (3%), and, further, that congestive heart failure (13%) was not a leading cause of death. In our population, only four patients presented with an acute myocardial infarction histologically and clinically attributable to the preoperative period, which does not reflect the finding of Lee et al. [16]. This latter discrepancy is most probably due to an extreme selection in our series, as only 32 cases fit into our study out of the 5749 patients operated on in the selected period. In a recent publication on a clinicopathological evaluation of cardiac patients, Deiwick et al. [6] showed that the leading cause of death was cardiac pump failure (68.6%), followed in frequency by myocardial infarction (11.4%), arrhythmia, multi-organ-failure, sepsis, pneumonia, stroke, and bowel ischemia. Comparison of these results with our own is difficult, as this report considered a number of surgical modalities together (CABG, valve replacements, congenital heart disease, combined interventions, etc.).

The results of reports on causes of death show substantial discrepancies. Comparison is difficult, mainly because inconsistent terms are used, sometimes without unequivocal explanation of their meanings. The terms we propose (Table 5) along with their definitions are meant to clear up some obscurities. Instead of specifying a number of diverse diagnoses as causes of death, we propose to use a limited number of groups of alterations with similar or common characteristics. At this point, there is a simple division defining two major types of death causes developing in a cardiac patient after cardiac surgery: death due to cardiac origin (part 1; Table 5) and death due to a non-cardiac complication (part 2; Table 5). Non-cardiac complications are not further subdivided here; subgroups or remarks on exact entities/diagnoses may, however, be done while evaluating individual cases. More emphasis is laid on specifications of cardiac causes that may either arise in direct relation to the underlying cardiovascular abnormality (part 1.1.; Table 5) or be of external origin to the heart and linked therefore to the cardiosurgical procedure (part 1.2.; Table 5). A primary underlying cardiovascular abnormality as cause of death may further be specified and determined either at the coronary artery level (part 1.1.1.; Table 5) or at the myocardial level (part 1.1.2.; Table 5).

As can be seen from the descriptions in Table 5 and especially from the cumulatively presented data in Table 6, both clinical and pathological (postmortem) data are necessary in order to determine the cause of death. It is to be noted, however, that there are cases with multiplication of different pathological alterations not necessarily fitting in every detail into the complexity of a given case or, in fact, partly indicating a cause of death different from what we eventually concluded (e.g. 5P, 11P, 13T, 17T, 19T, 23T, 30TU, 32T in Table 6). Repeated controls of our files of these cases always

confirmed that a careful consideration of all relevant circumstances will help orientation. Namely, a thorough consideration of a case as a whole helped us to establish a hierarchy of findings, and rank lower the ones of lesser importance. To indicate this, we introduced 'column V' showing which parts of the large body of clinicopathological data reviewed were considered by us to be of special importance for death evaluation.

Conclusion

The value of clinicopathological studies in the evaluation of surgical treatment and quality assurance of a heart center is undisputed. Yet, comparison of the results in different series is difficult because of the lack of consistent criteria regarding terms of causes of death. The system of criteria proposed in this study may help to solve this problem. This system may be a first step toward standardization of the involved terms.

Acknowledgements The authors wish to thank Anna Kádár M.D., M.Sc., Géza Mózes M.D., Ph.D., Károly Balogh M.D., M.Sc. for their invaluable advice, Márta Hubay M.D. for her help preparing computed illustrations, and Ms. Susanne Dolle and Ms. Sylvia Katzke for their excellent technical assistance.

References

1. Breyer RH, Spray TL, Kastl DG, Roberts WC (1976) Histologic changes in saphenous vein aorta-coronary bypass grafts. The effect of the angle of the aortic anastomosis. J Thorac Cardiovasc Surg 72:916–924
2. Bulkley BH, Hutchins GM (1977) Accelerated "atherosclerosis". A morphologic study of 97 saphenous vein coronary artery bypass grafts. Circulation 55:163–168
3. Bulkley BH, Hutchins GM (1977) Myocardial consequences of coronary artery bypass graft surgery. The paradox of necrosis in areas of revascularization. Circulation 56:906–913
4. Bulkley BH, Hutchins GM (1978) Pathology of coronary artery bypass graft surgery. Arch Pathol Lab Med 102:273–280
5. Cosgrove DM, Loop FD, Lytle BW, Baillot R, Gill CC, Golding LA, Taylor PC, Goormastic M (1984) Primary myocardial revascularization. Trends in surgical mortality. J Thorac Cardiovasc Surg 88:673–684
6. Deiwick M, Löhrer A, Hoffmeier A, Baba HA, Böcker W, Scheld HH (1999) Postoperative death should be followed by autopsy—an analysis of the autopsy findings of the years 1990 and 1991 in a heart surgery center. Thorac Cardiovasc Surg 47:82–87
7. Favaloro RG (1968) Saphenous vein autograft replacement of severe segmental coronary artery occlusion. Operative technique. Ann Thorac Surg 5:334-339
8. Green GE, Paul RS, Walls E, Tice DA (1968) Coronary artery bypass grafting. Surg Forum 19:159–161
9. Griffith LSC, Bulkley BH, Hutchins GM, Brawley RK (1977) Occlusive changes at the coronary artery-bypass graft anastomosis. Morphologic study of 95 grafts. J Thorac Cardiovasc Surg 73:668–679
10. Heupler FA (1981) Aortocoronary vein graft spasm. A clinical entity? Chest 80:412–415
11. Hutchins GM (1980) Pathological changes in aortocoronary bypass grafts. Ann Rev Med 31:289–301
12. Hutchins GM, Bulkley BH (1977) Mechanisms of occlusion of saphenous vein-coronary artery "jump" grafts. J Thorac Cardiovasc Surg 73:660–667
13. James TN (1977) Small arteries of the heart. Circulation 56:2–14
14. Kennedy JH, Wieting DW, Hwang NH, Anderson MS, Bayardo RJ, Howel JF, De Bakey ME (1974) Hydraulic and morphologic study of fibrous intimal hyperplasia in autogenous saphenous vein bypass grafts. J Thorac Cardiovasc Surg 67:805–813
15. Kovacs CS, Sanfilippo AJ, Burggraf GW (1992) Anterior wall myocardial infarction in a 15-year-old diabetic female associated with spontaneously resolving coronary thrombosis. Can J Cardiol 8:733–736
16. Lee AH, Borek BT, Gallagher PJ, Saunders R, Lamb RK, Livesey SA, Tsang VT, Monro JL (1997) Prospective study of the value of necropsy examination in early death after cardiac surgery. Heart 78:34–38
17. Lie JT, Lawrie GM, Morris GC (1977) Aortocoronary bypass saphenous vein graft atherosclerosis. Anatomic study of 99 vein grafts from normal and hyperlipoproteinemic patients up to 75 months postoperatively. Am J Cardiol 40:906–914
18. Moore GW, Hutchins GM (1981) Coronary artery bypass grafts in 109 autopsied patients. Statistical analysis of graft and anastomosis patency and regional myocardial injury. JAMA 246:1785–1789
19. Rahlf G (1980) Intramyocardial microarteriopathy. Virchows Arch A 388:289–311
20. Roberts AJ, Hay DA, Mehta JL, Mehta P, Roy L, Faro RS, Knauf DG, Alexander JA (1984) Biochemical and ultrastructural integrity of the saphenous vein conduit during coronary artery bypass grafting. Preliminary results of the effect of papaverine. J Thorac Cardiovasc Surg 88:39–48
21. Roberts WC, Jones AA (1979) Quantitation of coronary arterial narrowing at necropsy in sudden coronary death. Analysis of 31 patients and comparison with 25 control subjects. Am J Cardiol 44:39–45
22. Rose AG (1985) State of vein grafts, native coronary arteries, and myocardium and principal cause of death in patients dying after aortocoronary bypass grafting. Thorax 40:940–947
23. Sellke FW, Stanford W, Rossi NP (1991) Failure of cryopreserved saphenous vein allografts following coronary artery bypass surgery. J Cardiovasc Surg 32:820–823
24. Spray TL, Roberts WC (1976) Tension on coronary bypass conduits. A neglected cause of real or potential obstruction of saphenous vein grafts. J Thorac Cardiovasc Surg 72:282–287
25. Spray TL, Roberts WC (1977) Changes in saphenous veins used as aortocoronary bypass grafts. Am Heart J 94:500–516
26. Thomas AC, Pazios S (1992) The postmortem detection of coronary artery lesions using coronary arteriography. Pathology 24:5–11
27. Tice DA, Zerbino VR, Isom OW, Cunningham JN, Engelman RM (1976) Coronary artery bypass with freeze-preserved saphenous vein allografts. J Thorac Cardiovasc Surg 71:378–382
28. Unni KK, Kottke BA, Titus JL, Frye RL, Wallace RB, Brown AL (1974) Pathologic changes in aortocoronary saphenous vein grafts. Am J Cardiol 34:526–532
29. Yamada T, Itoh T, Nakano S, Tokunaga O (1995) Time-dependent thickening of the intima in aortocoronary saphenous vein grafts: Clinicopathological analysis of 24 patients. Heart Vessels 10:41–45

Virchows Arch (2003) 443:536–540
DOI 10.1007/s00428-003-0855-6

ORIGINAL ARTICLE

Annette Ramaswamy · Roland Moll · Peter J. Barth

CD34+ fibrocytes in tubular carcinomas and radial scars of the breast

Received: 4 March 2003 / Accepted: 21 April 2003 / Published online: 29 July 2003
© Springer-Verlag 2003

Abstract The present study was undertaken to analyze whether and to what extent CD34+ fibrocytes and α-smooth muscle actin (α-SMA)-positive myofibroblasts occur in the stroma of radial scars and tubular carcinoma of the breast. We investigated a total of 24 radial scars obtained from 23 females and a total of 43 tubular carcinomas. All tubular carcinomas showed a virtually complete loss of CD34+ fibrocytes paralleled by a gain of α-SMA-positive myofibroblasts. The peripheral parts of radial scars harbored CD34+ fibrocytes comparable to normal breast tissue. In 23 of 24 radial scars, the central core was characterized by a loss of CD34+ fibrocytes accompanied by the presence of α-SMA-positive myofibroblasts in six cases, a pattern that up to now has only been described in malignant breast lesions. This finding underlines the close relationship between tubular carcinomas and radial scars. We conclude CD34- and α-SMA immunohistochemistry to be valuable adjunctive tools in distinguishing radial scars from tubular carcinomas. In the present study, the presence of CD34+ fibrocytes excluded malignancy. The absence of CD34+ fibrocytes paralleled by the presence of α-SMA myofibroblasts indicated malignancy in most cases, although it has to be carefully considered that in a minority of cases (6 of 24) the central core of radial scars may disclose this stromal composition.

Keywords Breast · Radial scar · Tubular carcinoma · Fibrocyte · Myofibroblast

Introduction

The normal mammary stroma as well as mesenchymal tumors of the breast, such as benign spindle cell stromal tumors [11, 12, 13], phyllodes tumor and fibroadenoma [14, 18], harbor huge numbers of CD34+ fibrocytes. To date, the histogenesis and function of this cell type is a matter of speculation and remains to be clarified [5, 6]. The broad expression of CD34 and bcl-2 in mesenchymal proliferations of the mammary gland led to the assumption that these lesions might derive from a single pluripotent mesenchymal fibroblast-like stem cell [14]. However, the occurrence of CD34+ fibrocytes is not restricted to the breast, as this cell type has also been detected in a multitude of organs, such as the pancreas [2], cervix uteri [4], stomach [16], skin [19] and colon [15]. In the aforementioned organs, stromal alterations associated with invasive carcinoma are characterized by a loss of CD34+ fibrocytes [2, 4, 15, 16, 19] and a gain of α-smooth muscle actin (α-SMA)-positive myofibroblasts [2, 4, 19]. The same is true for the breast; stromal alterations associated with invasive carcinoma are characterized by the loss of CD34+ fibrocytes [3]. Therefore, the immunohistochemical demonstration of the presence or absence, respectively, of CD34+ fibrocytes may constitute a valuable tool in distinguishing between benign and malignant lesions. Until now, it remained to be clarified whether CD34 immunohistochemistry might further improve the distinction of so-called pseudoinfiltrative lesions, such as radial scars from sclerosing adenosis and tubular carcinomas. Particularly, the distinction between radial scars—as defined by Hamperl [9] and Eusebi and coworkers [8]—and tubular carcinomas is not trivial and may indicate significant diagnostic problems [17, 21].

The present study was undertaken to elucidate whether immunohistochemical detection of CD34+ fibrocytes and α-SMA-positive myofibroblasts may facilitate the differential diagnosis of tubular carcinoma and radial scar.

A. Ramaswamy · R. Moll · P. J. Barth (✉)
Institute of Pathology,
Philipps-University Marburg,
Baldingerstrasse, 35033 Marburg, Germany
e-mail: barthp@med.uni-marburg.de
Tel.: +49-6421-2862465
Fax: +49-6421-2865640

Materials and methods

The present retrospective study comprises a total of 65 patients in whom the diagnosis of tubular carcinoma (*n*=43) or radial scar

(n=24 obtained from 23 patients) was rendered. All patients were females.

The diagnosis of radial scars was based on the criteria defined by Hamperl [9] and Eusebi et al. [8]. In brief, lesions with a central fibro-hyaline core and stromal elastosis surrounded by radiating ductal or acinar structures—called periphery in the context of this study—were diagnosed as radial scars. For quantitative evaluation, the central core and the periphery as defined above were assessed separately.

Patients with radial scars ranged in age between 38 years and 71 years with a median age of 52 years. The median diameter of the radial scars was 4 mm (range 2–17 mm). Patients with tubular carcinomas were older than those with radial scars ranging in age between 41 years and 81 years (median 67 years). pT stages were distributed as follows: pT1a: n=2, pT1b: n=21, pT1c: n=16, pT2: n=3 and pT3: n=1. Metastases to regional lymph nodes were observed in two cases, whereas the remaining 41 cases showed no nodal involvement. In all patients, normal or fibrocystic breast tissue was available for comparison.

Immunohistochemistry

Immunohistochemistry was performed by means of the standard avidin biotin complex (ABC)-peroxidase method (ABC Elite Kit; Vector, Burlingame, CA) and 3,3′-diaminobenzidine as chromogen. CD34 antigen was detected by means of a monoclonal antibody (QBEND10; Dako, Hamburg, Germany; dilution 1:50) after microwave pretreatment. Microwave pretreatment was performed by heating the deparaffinized and rehydrated sections, immersed in 10 mM sodium citrate buffer (pH 6.0), in a microwave oven at 600 W three times for 5 min. α-SMA was detected using a monoclonal antibody (ASM-1, Progen, Heidelberg, Germany; dilution 1:200) after tissue pretreatment with 0.1% trypsin for 15 min at 37°C.

Results

Normal breast

In the normal breast, CD34$^+$ fibrocytes were predominantly found in the intralobular parenchyma, encircling ductal and acinar structures. The muscularized arteries located in the extra- and intralobular parenchyma were also surrounded by CD34$^+$ fibrocytes. With rising distance to the aforementioned glandular and vascular structures, the density of CD34$^+$ fibrocytes decreased. Endothelia showed a strong reactivity with CD34; no CD34 reactivity was observed with epithelial cells. The stroma of the normal breast was free of α-SMA-positive

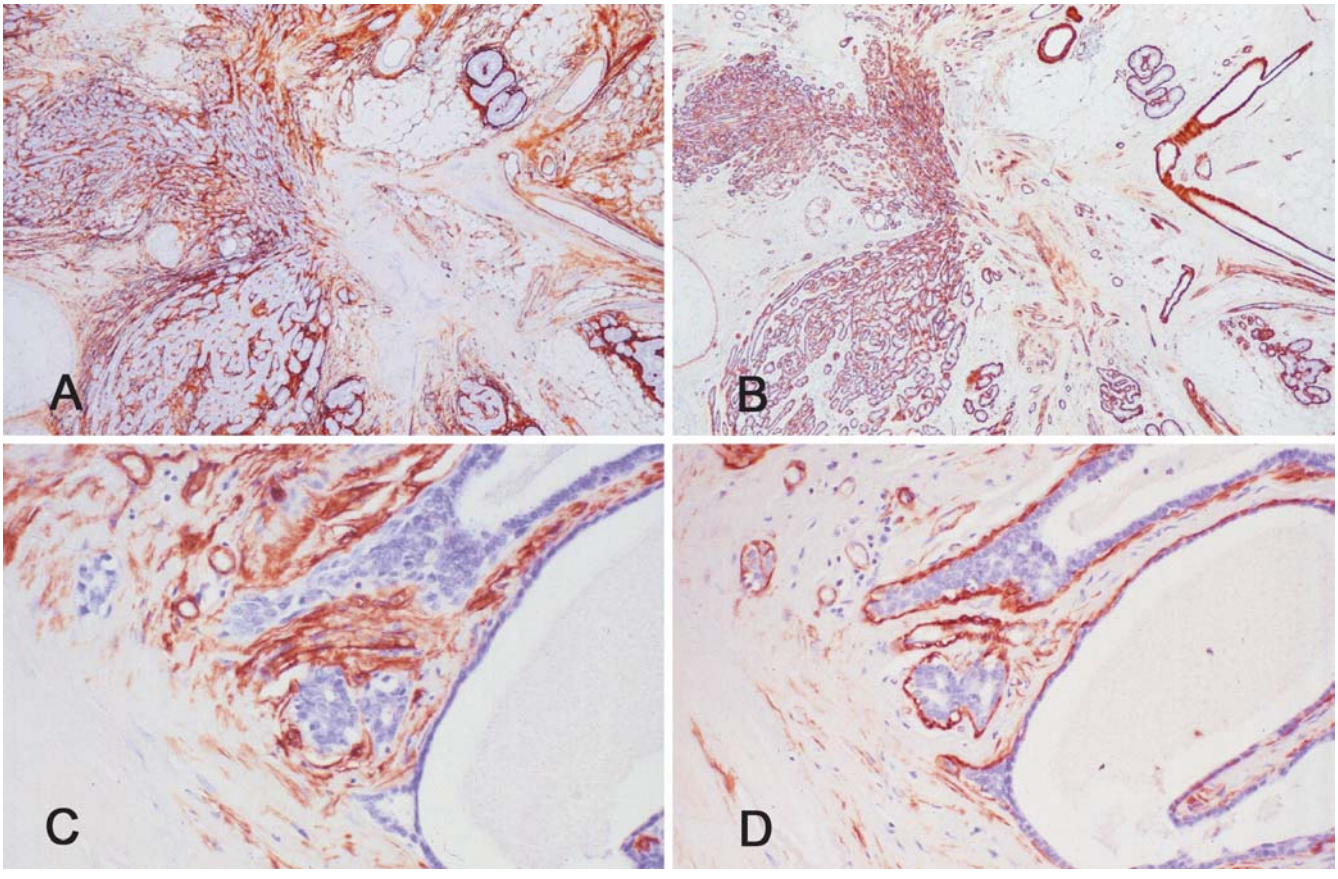

Fig. 1 CD34 immunohistochemistry (QBEND10; Dako) exhibits a normal population of CD34$^+$ fibrocytes surrounding the glandular structures forming the periphery of radial scars (**A**), the central core of radial scars (**C**, *lower left*) shows no CD34$^+$ fibrocytes. α-Smooth muscle actin (SMA) immunohistochemistry (ASM-1; Progen) discloses α-SMA-positive myothelia lining the ductal and acinar structures in the periphery of radial scars (**B**). The central core of this radial scar (**D**, *lower left*) is free of α-SMA-positive myofibroblasts

myofibroblasts, whereas myothelia and vascular smooth musculature disclosed a strong reactivity with α-SMA.

Radial scar

In contrast to the normal breast and tubular carcinomas, the radial scars investigated showed a more complex distribution of $CD34^+$ fibrocytes. The periphery of the lesions disclosed a population of $CD34^+$ fibrocytes similar to that observed in the normal breast tissue; the elongated ductal and acinar structures were encircled by densely packed $CD34^+$ fibrocytes (Fig. 1A, Table 1). In contrast, the central core of radial scars disclosed a complete loss of $CD34^+$ fibrocytes in 23 of 24 cases (Fig. 1C, Table 1).

In 16 of 24 cases, α-SMA-positive myofibroblasts were not detected in the periphery of radial scars (Table 2). The glandular structures comprising the periphery of radial scars were lined by α-SMA-positive myothelia as observed in normal breast tissue (Fig. 1B). The remaining eight cases showed small focal accumulations of few α-SMA-positive myofibroblasts intermingled with small foci of diffuse stromal staining that appeared not to be related to a certain cell population.

Table 1 Distribution of $CD34^+$ fibrocytes in the central core and periphery of radial scars and tubular carcinomas. o no $CD34^+$ fibrocytes detectable, + focal accumulations of $CD34^+$ fibrocytes, ++ diffusely scattered $CD34^+$ fibrocytes

Staining score	Radial scar Central core	Radial scar Periphery	Tubular carcinoma
0	23	1	43
+	1	15	0
++	0	8	0

The central core of radial scars was free of α-SMA-positive myofibroblasts in 18 of 24 cases (Fig. 1D, Table 2). In five cases, focal accumulations of α-SMA-positive myofibroblasts were seen together with faint staining with the α-SMA antibody, which was attributable to myothelia of atrophic ducts located in the sclerotic stroma. The central core of one radial scar showed diffusely scattered SMA-reactive myofibroblasts.

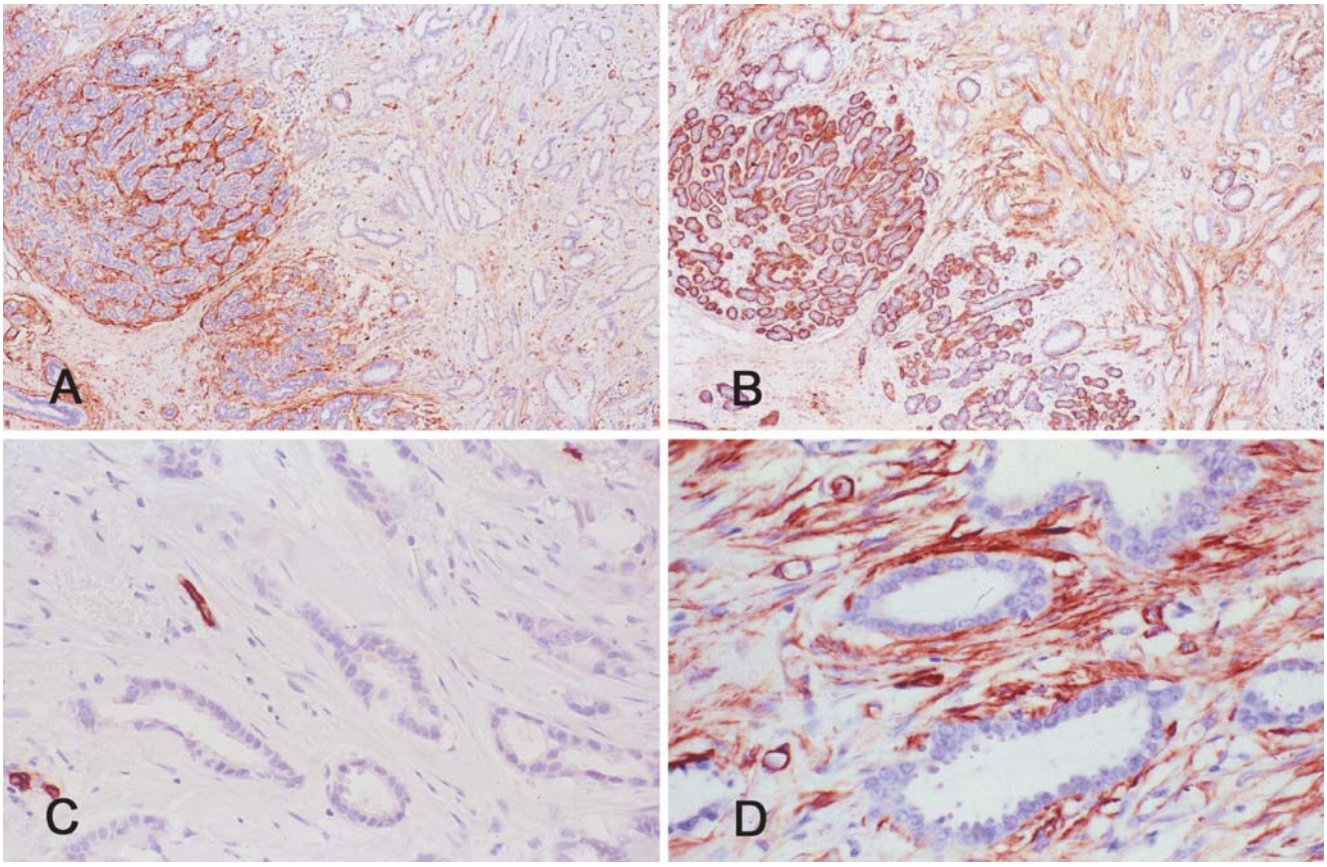

Fig. 2 In contrast to adjacent normal breast tissue (**A**, *left*) the stroma of tubular carcinomas (**A**, *right*) exhibits a loss of $CD34^+$ fibrocytes (**A**, QBEND10 immunohistochemistry) paralleled by a gain of stromal α-SMA-positive myofibroblasts (**B**, ASM-1 immunhistochemistry). The glandular structures of tumor-free tissue show α-SMA-positive myothelia (**B**). Endothelia of vessels located in the tumor show a normal CD34 reactivity (**C**). α-SMA-positive myofibroblasts found in the tumor-associated stroma show a plump spindled shape; immunohistochemistry discloses strong cytoplasmic α-SMA reactivity (**D**)

Table 2 Distribution of α-smooth muscle actin (SMA)-positive myofibroblasts in the central core and periphery of radial scars and tubular carcinomas. *0* no α-SMA-positive myofibroblasts detectable, + focal accumulations of α-SMA-positive myofibroblasts, ++ diffusely scattered α-SMA-positive myofibroblasts throughout the whole lesion

Staining score	Radial scar Central core	Radial scar Periphery	Tubular carcinoma
0	18	16	0
+	5	8	15
++	1	0	28

Tubular carcinoma

The interface between normal breast tissue and tubular carcinomas was characterized by an abrupt loss of stromal $CD34^+$ fibrocytes (Fig. 2A). In all tubular carcinomas, the stroma was virtually free of $CD34^+$ fibrocytes (Fig. 2C, Table 2). Endothelial cells of vessels located within the tumor exhibited a normal reactivity with the CD34 antibody (Fig. 2C). The normal breast tissue adjacent to tubular carcinomas showed no α-SMA-positive myofibroblasts; a strong α-SMA immunoreactivity was observed in myothelia lining ducts and acini (Fig. 2B). The stroma of all tubular carcinomas harbored various amounts of α-SMA-positive myofibroblasts. In 15 cases, focal accumulations of α-SMA-positive myofibroblasts were observed, 28 cases showed diffusely scattered α-SMA-positive myofibroblasts throughout the whole tumor (Table 2). α-SMA positive myofibroblasts found in the tumor-associated stroma showed a spindled outline, ill-defined cell borders and plump cigar-shaped nuclei; immunohistochemistry disclosed a characteristic tram tracking of cytoplasmic α-SMA-reactive fibers (Fig. 2D).

Discussion

$CD34^+$ fibrocytes constitute a population of stromal cells; the histogenesis and function of which remains to be elucidated [5, 6]. However, different studies have shown that the presence of this cell population or the absence of it, respectively, might be of a certain value in distinguishing benign from malignant lesions of the skin [19] and gastrointestinal tract [15, 16]. Recent studies also showed the loss of $CD34^+$ fibrocytes to be a feature of stromal alterations associated with invasive carcinomas of the breast [3]. This assumption is underlined by the findings of the present study. Tubular carcinomas disclosed a complete loss of stromal $CD34^+$ fibrocytes accompanied by a gain of stromal α-SMA expression. However, the presence of stromal $CD34^+$ fibrocytes is, as shown in the present and other studies, a feature of benign breast lesions [3, 7, 11, 12, 13,14, 18]. In this context, radial scars appear to merit special attention, as these lesions are the first benign mammary lesions reported to disclose a partial loss of $CD34^+$ fibrocytes. In the majority of cases investigated, the central sclerotic portion of the lesion disclosed a loss of $CD34^+$ fibrocytes, whereas the peripheral parts showed a well-preserved population of $CD34^+$ fibrocytes. Therefore, in order not to overdiagnose malignancy in radial scars solely on the basis of an absence of stromal $CD34^+$ fibrocytes, it has to be assured that the whole lesion has been excised and submitted to histological investigation.

The most important result of the present investigation is the finding that tubular carcinomas and radial scars of the breast can be distinguished by the detection of stromal $CD34^+$ fibrocytes and α-SMA-reactive myofibroblasts when some precautions and recommendations are met. The absence of $CD34^+$ fibrocytes paralleled by the presence of α-SMA-reactive myofibroblasts is a feature of tubular carcinoma and invasive ductal carcinomas [3]. However, the sole absence of $CD34^+$ fibrocytes without gain of α-SMA myofibroblasts in a questionable breast lesion does not justify the diagnosis of malignancy, as has been shown here for the core of radial scars. However, in 6 of 24 radial scars, the central core showed a loss of $CD34^+$ fibrocytes and a gain of α-SMA-positive myofibroblasts, a pattern that up to now has only been described in malignant breast lesions. This finding underlines the close relationship of tubular carcinomas and radial scars [10]. We conclude that CD34- and α-SMA immunohistochemistry is a valuable adjunctive tool in distinguishing radial scars from tubular carcinomas. In the present study, the presence of $CD34^+$ fibrocytes rendered malignancy unlikely. The absence of $CD34^+$ fibrocytes paralleled by the presence of α-SMA myofibroblasts indicated malignancy in most cases, although it has to be carefully considered that in a minority of cases (6 of 24) the central core of radial scars may disclose this stromal composition.

It has recently been pointed out that the stroma of invasive breast cancer and radial scars share some similarities concerning the expression of factors associated with stroma formation [10]. This is in keeping with our findings, as the central core of radial scars exhibits a loss of $CD34^+$ fibrocytes, which previously has mostly been observed in the stroma of invasive carcinomas. The mechanisms leading to a loss of $CD34^+$ fibrocytes in the stroma of carcinomas are far from understood. In a recent publication, it has been shown that medium conditioned by the breast cancer cell line MCF-7 induces SMA expression in stromal cells obtained from normal breast tissue [20]. Moreover, Abe and coworkers found that $CD34^+$ fibrocytes gain SMA expression when exposed to transforming growth factor-β [1]. The phenomenon of a stromal loss of CD34 expression in breast cancer might therefore be, at least in part, explained by these experimental findings.

References

1. Abe R, Donnelly SC, Peng T, Bucala R, Metz CN (2001) Peripheral blood fibrocytes: differentiation pathway and migration to wound sites. J Immunol 166:7556–7562

2. Barth PJ, Ebrahimsade S, Hellinger A, Moll R, Ramaswamy A (2002) $CD34^+$ fibrocytes in neoplastic and inflammatory pancreatic lesions. Virchows Arch 440:128–133
3. Barth PJ, Ebrahimsade S, Ramaswamy A, Moll R (2002) $CD34^+$ fibrocytes in invasive ductal carcinoma, ductal carcinoma in situ, and benign breast lesions. Virchows Arch 440:298–303
4. Barth PJ, Ramaswamy A, Moll R (2002) $CD34^+$ fibrocytes in normal cervical stroma, cervical intraepithelial neoplasia III, and invasive squamous cell carcinoma of the cervix uteri. Virchows Arch 441:564–568
5. Bucala R, Spiegel LA, Chesney J, Hogan M, Cerami A (1994) Circulating fibrocytes define a new leukocyte subpopulation that mediates tissue repair. Mol Med 1:71–81
6. Chesney J, Bacher M, Bender A, Bucala R (1997) The peripheral blood fibrocyte is a potent antigen-presenting cell capable of priming naive T cells in situ. Proc Natl Acad Sci U S A 94:6307–6312
7. Damiani S, Eusebi V (2001) Gynecomastia in type-1 neurofibromatosis with features of pseudoangiomatous stromal hyperplasia with giant cells. Report of two cases. Virchows Arch 438:513–516
8. Eusebi V, Grassigli A, Grosso F (1976) Lesioni focali sclero-elastiche mammarie simulanti il carcinoma infiltrante. Pathologica 68:507–518
9. Hamperl H (1975) Strahlige Narben und obliterierende Mastopathie. Virchows Arch 369:55–68
10. Jacobs TW, Schnitt SJ, Tan X, Brown LF (2002) Radial scars of the breast and breast carcinomas have similar alterations in expression of factors involved in vascular stroma formation. Hum Pathol 33:29–38
11. Magro G, Michal M, Vasquez E, Bisceglia M (2000) Lipomatous myofibroblastoma: a potential diagnostic pitfall in the spectrum of the spindle cell lesions of the breast. Virchows Arch 437:540–544
12. Magro G, Michal M, Bisceglia M (2001) Benign spindle cell tumors of the mammary stroma: diagnostic criteria, classification, and histogenesis. Pathol Res Pract 197:453–466
13. Magro G, Bisceglia M, Michal M, Eusebi V (2002) Spindle cell lipoma-like tumor, solitary fibrous tumor and myofibroblastoma of the breast: a clinico-pathological analysis of 13 cases in favor of a unifying histogenetic concept. Virchows Arch 440:249–260
14. Moore T, Lee AH (2001) Expression of CD34 and bcl-2 in phyllodes tumours, fibroadenomas and spindle cell lesions of the breast. Histopathology 38:62–67
15. Nakayama H, Enzan H, Miyazaki E, Kuroda N, Naruse K, Hiroi M (2000) Differential expression of CD34 in normal colorectal tissue, peritumoral inflammatory tissue, and tumour stroma. J Clin Pathol 53:626–629
16. Nakayama H, Enzan H, Miyazaki E, Kuroda N, Naruse K, Kiyoku H, Toi M, Hiroi M (2001) CD34 positive stromal cells in gastric adenocarcinomas. J Clin Pathol 54:846–848
17. Rosen PP (ed) (2001) Papilloma and related benign tumors. In: Rosen's breast pathology 2nd edn. Lippincott Williams & Wilkins, Philadelphia PA, pp 77–119
18. Silverman JS, Tamsen A (1996) Mammary fibroadenoma and some phyllodes tumour stroma are composed of CD34+ fibroblasts and factor XIIIa+ dendrophages. Histopathology 29:411–419
19. Swanson PE, Fitzpatrick MM, Ritter JH, Glusac EJ, Wick MR (1998) Immunohistologic differential diagnosis of basal cell carcinoma, squamous cell carcinoma, and trichoepithelioma in small cutaneous biopsy specimens. J Cutan Pathol 25:153–159
20. Valenti MT, Azzarello G, Balducci E, Sartore S, Sandri M, Manconi R, Sicari U, Bari M, Vinante O (2001) Conditioned medium from MCF-7 cell line induces myofibroblast differentiation, decreased cell proliferation, and increased apoptosis in cultured normal fibroblasts but not in fibroblasts from malignant breast tissue. Histochem J 33:499–509
21. Weidner N (ed) (1996) Breast diseases. In: The difficult diagnosis in surgical pathology. Saunders, Philadelphia, pp 625–679

Virchows Arch (2003) 443:541–548
DOI 10.1007/s00428-003-0861-8

ORIGINAL ARTICLE

Iris Bittmann · Adriana Bottino · Gustavo Bruno Baretton · Alexander Ludwig Gerbes · Reinhart Zachoval · Horst Günter Rau · Udo Löhrs

The role of graft-resident Kupffer cells and lymphocytes of donor type during the time course after liver transplantation—a clinico-pathological study

Received: 11 December 2002 / Accepted: 10 June 2003 / Published online: 23 July 2003
© Springer-Verlag 2003

Abstract Although graft-resident passenger leukocytes are known to mediate acute rejection by triggering direct allorecognition, they may also act in an immunomodulatory fashion and play an important role in tolerance induction. The present study evaluated by non-isotopic in situ hybridization and immunohistochemistry if and during which time period after transplantation Kupffer cells (KC) and lymphocytes of the liver were replaced by recipient cells and if there is any correlation with the occurrence of rejection episodes and the clinical course. A successive re-population of the liver by recipient lymphocytes and KC was observed after transplantation but a smaller portion of lymphocytes and KC with donor genotype was detectable during the whole time course studied. There was no correlation between the portion of recipient-derived KC and donor-derived lymphocytes and histopathological alterations of the liver tissue. The biopsy content of KC with recipient origin has had no prognostic significance for the probability of survival, but patients with a low portion of donor lymphocytes in the liver biopsy obtained during the first week after transplantation have had a better prognosis for survival. The present results indicate that graft-resident KC and lymphocytes are potentially not the main cell types involved in tolerance induction after liver transplantation.

Keywords Liver transplantation · Kupffer cell · Lymphocyte · Non-isotopic in situ hybridization · Chimerism

The study contains parts of the doctoral thesis of Adriana Bottino.

I. Bittmann (✉) · A. Bottino · G. B. Baretton · U. Löhrs
Institute of Pathology, Ludwig-Maximilians-University,
80337 Munich, Germany
e-mail: Iris.Bittmann@lrz.uni-muenchen.de
Tel.: +49-89-51604067
Fax: +49-89-51604043

A. L. Gerbes · R. Zachoval
Department of Internal Medicine II,
Klinikum of the University, Großhadern,
Marchioninistrasse 15, 81377 Munich, Germany

H. G. Rau
Department of Surgery, Klinikum of the University,
Großhadern,
Marchioninistrasse 15, 81377 Munich, Germany

Introduction

The development of immunological tolerance is an important feature after transplantation of solid organs. The emigration of passenger leukocytes from a transplanted organ results in a fortuitous decline in the allograft immunogenicity, similar to that which occurs in experiments when these cells are removed before organs are transplanted. These leukocytes, which include pluripotent stem cells, and dendritic cells are largely replaced in the graft by similar cells of the recipient, just like tissue macrophages [13, 21].

The question of whether the intragraft content of immunological competent donor and recipient cells influences the clinical course and the development and number of rejection episodes after liver transplantation has not been addressed. The aim of our study was to evaluate whether and during which time period after transplantation (ptx) Kupffer cells (KC) and lymphocytes (LC) of the liver were replaced by recipient cells and whether an influence on the clinical course was detectable.

The study was performed on paraffin-embedded liver tissue specimens by non-isotopic in situ hybridization (NISH) using digoxigenated centromer-specific DNA probes for the human Y and X chromosomes, respectively. To this end, liver tissue of male patients who had received organs from female donors was studied, allowing the discrimination of donor and recipient cells after sex mismatched organ transplantation. The various infiltrat-

Table 1 Survival time and cause of death of patients who died prior to June 1999. *PBC* primary biliary cirrhosis, *PSC* primary sclerosing cholangitis, *HCC* hepatocellular carcinoma, *HBV* hepatitis B virus, *HCV* hepatitis C virus

Patient ID	Initial disease	Cause of death	Survival time (months) after transplantation
9	Liver necrosis, HBV	Operative complications	–
14	PBC	Bleeding after liver biopsy	0.3
3	HCV	Fungal infection	1.0
24	HBV	Fungal infection	1.3
12	PSC	Bacterial peritonitis	1.8
4	HCV	Liver failure	3.0
10	Liver necrosis of unknown cause	Viral infection (CMV)	3.1
6	Acute liver failure of unknown cause	Sepsis	3.4
15	HCC/alcohol	Tumor recurrence + chronic rejection	6.0
26	HCC/alcohol	Multi-organ failure	12.0
27	HCV	Sepsis (pneumocystis carinii)	25.7
25	Oxalosis	Car accident	26.7
11	HBV	Unknown	Unknown

ing cell types were identified by immunohistochemistry (IHC).

Materials and methods

Patients

Liver tissue obtained ptx from 28 male patients who had received organs from sex mismatched (female) donors was studied. Four patients had to be re-transplanted due to chronic rejection (n=2) and arterial thrombosis (n=2). The transplantations were performed between 1 January 1991 and 31 December 1996, in the Department of Surgery, Klinikum of the University, Großhadern, Germany.

The initial diagnoses were hepatitis C virus-associated liver cirrhosis (n=6), hepatocellular carcinoma (n=5), acute liver failure (n=4), hepatitis B virus (HBV)-associated liver cirrhosis (n=3), alcohol abuse-associated liver cirrhosis (n=3), autoimmune hepatitis (n=2), primary biliary cirrhosis (n=1), primary sclerosing cholangitis (n=1), cirrhosis of uncertain origin (n=1), HBV/hepatitis D virus associated liver cirrhosis (n=1), and oxalosis (n=1). Age of organ recipients ranged from 16 years to 65 years (mean 46±12 years). Age of organ donors was between 13 years and 55 years (mean 39±11 years). Time of cold ischemia before transplantation ranged from 5.4 h to 18.3 h (mean 9±3.3 h). Survival of organ recipients was monitored until July 1999 (Table 1, Table 2). All patients received cyclosporin A as immunosuppressive regimen.

Materials

One hundred and eighty-five liver specimens (1 to 16 biopsy specimens per patient, mean 6) were evaluated. The biopsies were obtained from post transplantation day (PTD) 1 to PTD 2169 (mean 469 PTD±681). To study how the content of donor- and recipient-derived KC and LC developed during the course of time after transplantation, biopsies at a given time [$\leq$1 week ptx (A), 1–4 weeks ptx (B), 1–6 months ptx (C), 6–12 months ptx (D), $\geq$1 year ptx (E), only one biopsy for each time slice] were chosen for each patient. If several biopsies during a defined time slice (A–E) were available for one patient, the first biopsy obtained was picked out. In this way, a sample collective of 84 biopsy specimens (punch biopsies n=61, wedge biopsies n=15, liver explants n=6, autopsy cases n=2) was put together.

Table 2 Survival time of patients who were alive until June 1999. *HCC* hepatocellular carcinoma, *HBV* hepatitis B virus, *HCV* hepatitis C virus, *HDV* hepatitis D virus, *ptx* after transplantation

Patient ID	Initial disease	Survival time (months–ptx)
Patients without viral hepatitis		
13	HCC/alcohol	24
16	HCV	39
17	Cirrhosis/alcohol	46
20	Cirrhosis/unknown cause	61
18	Cirrhosis/alcohol	65
28	Autoimmune hepatitis	69
5	Cirrhosis/alcohol	86
22	Liver necrosis/virus hepatitis	88
Patients with chronic hepatitis		
1*	HCC/HCV	84
2*	HCV	74
7*	HBV	77
8*	HBV/HDV	87
19*	HCV	61
21[$]	HCC (fibrolamellar)	41
23[&]	Autoimmune hepatitis	88

* Recurrent viral hepatitis
[$] Hepatitis of unknown origin
[&] ptx acquired chronic hepatitis B

Tissue preparation

All liver biopsy specimens were routinely fixed in 4% buffered formalin, paraffin embedded and stained with hematoxylin and eosin, Elastic van Gieson and Prussian Blue according to standard procedures. The rejection reaction was graded according to the Banff Consensus Classification [19]. The following main histological alterations were found: acute and chronic rejection, reperfusion injury, recurrence of hepatitis, chronic hepatitis and non-specific alterations (Table 3).

Non-isotopic in situ hybridization

For NISH, commercial digoxigenated DNA probes (Appligene Oncor, Illkirch, France) binding to highly repetitive DNA located at the centromers of human chromosomes X (DXZ1) and Y (DYZ1/DYZ3) were used. NISH was performed according to the modified protocol of Hopman et al. [1], using the probes for the X and the Y

Table 3 Histological biopsy findings according to time after transplantation liver biopsies were obtained. *ptx* after transplantation

	A Until 1week ptx	B Until 1–4weeks ptx	C 1–6months ptx	D 6–12months ptx	E More than 1 year ptx	*n*
Acute rejection	13	15	10	4	–	42
Acute rejection + hepatitis	–	1	1	–	1	3
Suspicious of hepatitis	–	–	1	–	1	2
Dystrophy/viral hepatitis	–	–	1	–	–	1
Chronic hepatitis	–	–	–	1	5	6
Chronic rejection	–	–	–	2	–	2
Ischemic lesions	5	1	3	2	–	11
Non-specific	3	7	4	2	1	17
n	21	24	20	11	8	84

chromosome on consecutive serial sections. Briefly, 6-µm-thick sections were cut and mounted on SuperFrost/Plus slides (Menzel-Gläser, Germany). Sections were dried overnight at 56°C. After deparaffinizing in xylol, sections were rinsed in absolute methanol (10 min) and endogenous peroxidase activity was blocked in 1% hydrogen peroxide in methanol for 30 min. Sections were microwaved in Target Retrieval Solution 6.0 (Dako Corporation, Carpiteria, CA, USA) at 800 W for 15 min and digested with 0.05–0.4% protease E (Merck, Darmstadt, Germany) for 3 min at 37°C. After washing in phospate buffered saline (PBS, Sigma, Deisenhofen, Germany), slides were fixed in 4% paraformaldehyde for 10 min at 4°C, washed again in PBS, passed through a series of graded ethanol, air dried, and dried at 80°C for 30 min. Overnight hybridization at 37°C was performed 0.4 ng/µl DNA probe, 60% formamide 10%, 20× SSC (sodium chloride, NaCl, 30 mmol sodium citrate, pH 7), 5% dextran sulfate, and 1% herring sperm (Sigma, Deisenhofen, Germany). The hybridization reaction was visualized by means of a three-step immunoperoxidase technique.

Criteria for the evaluation of NISH signals were as follows [9]: (1) overlapping interphase nuclei were not counted; (2) signals within one nucleus had to have more or less the same size and intensity; (3) paired NISH spots (split spots) were counted as one signal. In all cases hybridization of the X and Y chromosome was performed.

Immunohistochemistry

IHC was performed using the alkaline phosphatase-anti-alkaline phosphatase technique, applying monoclonal antibodies. CD45 was used for the identification of LC (primary concentration 375 mg/l, dilution 1:90) and CD68 for macrophages (primary concentration 455 mg/l, dilution 1:100). Both antibodies were supplied by Dakopatts, Hamburg, Germany.

Combined IHC and NISH

To facilitate the typing of KC and LC, IHC and NISH was combined in nearly all tissue specimens. For KC, CD68 IHC and X- and Y-specific NISH were combined. In each biopsy, NISH signals of the X and Y probe of 100 non-overlapping nuclei of CD68+ KC were counted. CD68+/Y+ cells were assessed as recipient cells and CD68+/XX+ cells as donor cells. For LC, CD45 IHC and X-specific NISH were combined. In each biopsy, the NISH signals of 200 non-overlapping nuclei of CD45+ LC were counted. CD45+/XX+ LC were assessed as donor cells.

Data analysis and clinico-pathological correlation

Results are expressed as mean ± standard error of mean unless otherwise mentioned. The survival time of each patient and the content of recipient KC and donor LC in liver biopsies obtained 1 month (KC) and 1 week (LC), respectively, after transplantation were compared. The median number of KC and LC in all biopsies of this time slice was calculated and two groups formed: biopsies with portion of recipient KC and donor LC, respectively, lower or higher than the calculated median value. The end point of the study was death of the patient or June 1999. Analysis of the survival time was made by Kaplan Meier estimation.

To evaluate whether time of cold ischemia before transplantation influences the number of recipient KC, the median number of recipient KC within the first month after transplantation and the median time of cold ischemia before transplantation were calculated. Starting from the median value of KC count and of time of cold ischemia, two groups for each were formed (lower or higher than the median value) and compared by Pearsons $\chi 2$-test. $P<0.05$ was considered significant.

All data were analyzed utilizing SPSS (Superior Performance Software System Vers. 11.0 for Windows, Chicago, Il).

Results

Clinical course

Thirteen patients died between transplantation and June 1999 (Table 1). No patient of the study group died due to an acute rejection episode. Seven of the surviving patients (n=15) developed a chronic hepatitis with recurrence of viral hepatitis (n=5), hepatitis of unknown origin (n=1) and a ptx-acquired chronic hepatitis B (n=1) (Table 2). During the first 6 months ptx, acute rejection episodes were the main histopathological alterations. Later than 6 months after transplantation, recurrence of hepatitis with chronic hepatitis and chronic rejection was found (Table 3).

During the whole study, cells with detection of two signals of the X chromosome or one signal of the Y chromosome were assessed as donor- or recipient-derived cells, respectively. There was no evidence for another source from which the cells could derive than the recipient or the allograft itself. Since all patients received blood transfusions during transplantation or directly postoperative, the possibility that a blood transfusion could be partly the source of XX+ and Y+ leukocytes cannot be completely excluded for the early time period after transplantation. It seemed implausible that a blood transfusion dated back several years should be the source of XX+ and Y+ LC and KC, respectively, which were

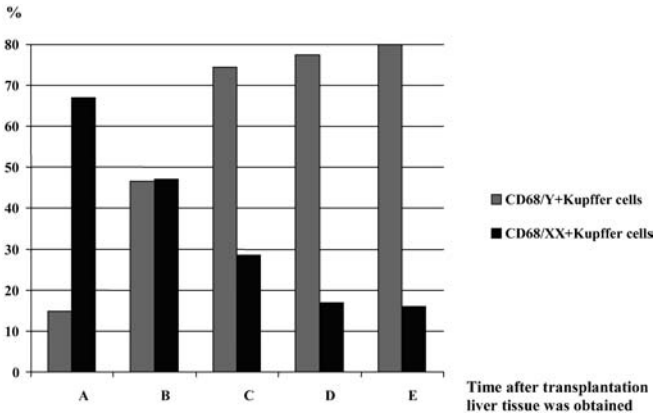

Fig. 1 Portion of donor (XX+) and recipient (Y+) Kupffer cells (KC) during the time course after transplantation (ptx); **A** first week ptx, **B** 1–4 weeks ptx, **C** 1–6 months ptx, **D** 6–12 months ptx, **E** later than 1 year ptx (CD68/Y+ KC recipient gender, CD68/XX+KC donor gender)

detected several years after transplantation in the liver tissue.

Kupffer cells

During the course of time after transplantation the portion of recipient (Y+) KC in liver biopsies increased, with a high variation during the first 6 months (Table 4, Fig. 1 and Fig. 2A). Simultaneously, the portion of donor (XX+) KC decreased over time (Fig. 2B). A small portion of donor (XX+) KC was detectable during the whole period studied (maximum 5 years and 344 days) (Table 4).

It was evaluated whether the time of cold ischemia before transplantation influenced the content of recipient (Y+)-derived KC. The portion of recipient (Y+)-derived KC within the first month ptx did not differ in liver tissues with cold ischemia time less than 9 h (n=13) and with cold ischemia time greater than 9 h (n=13).

No correlation was found between the portion of recipient (Y+) KC in the liver tissue and the different histopathological patterns, including episodes of acute rejection (Table 5). The varying portion of recipient (Y+)-derived KC of the different histopathological alterations was probably due to the time ptx that the biopsy specimens were obtained. Kaplan Meier analysis showed no prognostic significance of the portion of recipient (Y+)-derived KC for survival time.

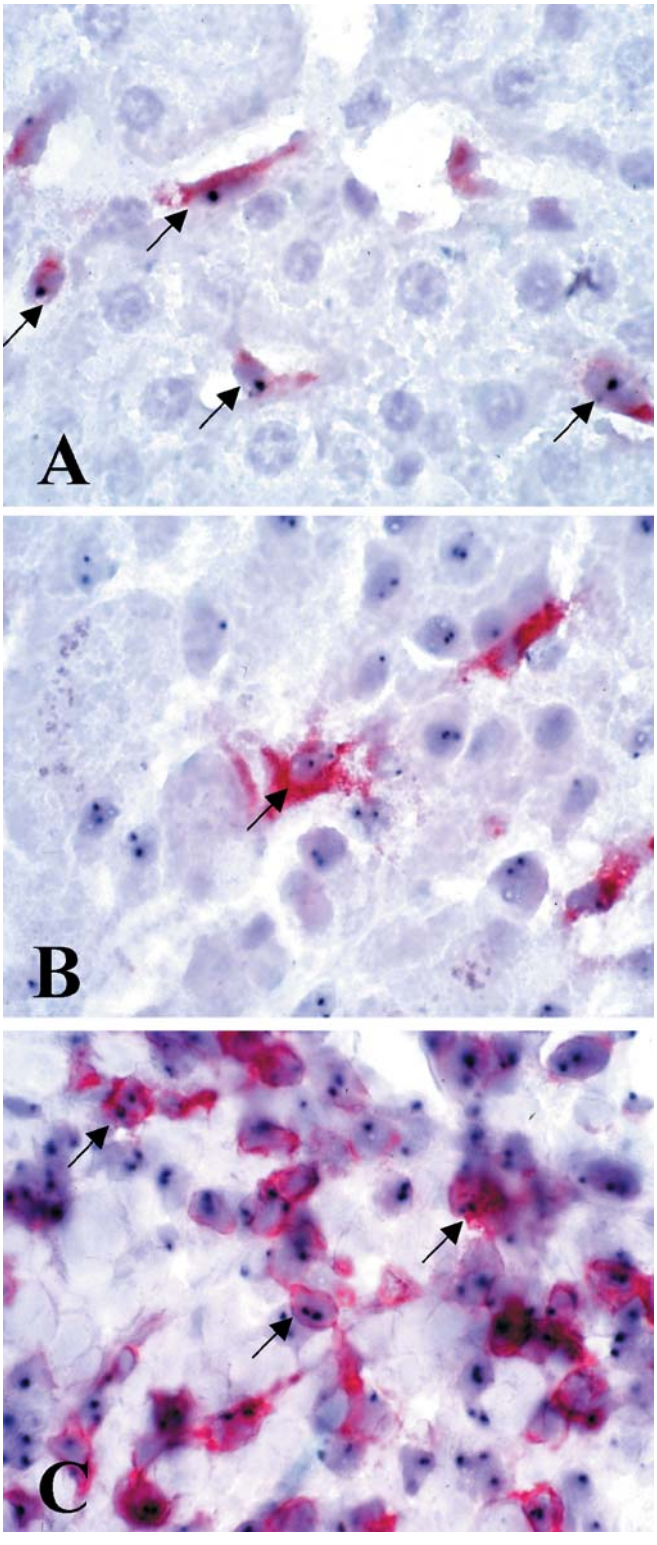

Fig. 2. A Punch biopsy nearly 5 years after transplantation (ptx). Recipient Kupffer cells (KC) with one nuclear signal of the Y chromosome, *arrows* (combination of Y/non-isotopic in situ hybridization and CD68/immunohistochemisty, original magnification ×1036). **B** Punch biopsy 7 days ptx. Donor-derived KC with two nuclear signals of the X chromosome (*arrow*) (combination of X/non-isotopic in situ hybridization and CD68/immunohistochemistry, original magnification ×1036). **C** Wedge biopsy 5 days ptx with ischemic lesions. Single donor lymphocytes with two nuclear signals of the X chromosome (*arrows*) in a subcapsular lymphocytic infiltrate (combination of X/non-isotopic in situ hybridization and CD45/immunohistochemisty, original magnification ×1036)

Table 4 Portion of recipient (Y+) and donor (XX+) derived Kupffer cells according to the time after transplantation liver biopsies were obtained

Time period after transplantation	A Up to 1 week	B 1–4 weeks	C 1–6 months	D 6–12 months	E >1 year
Portion of CD68/Y positive Kupffer cells of recipient origin (%) (*n*=71)					
Y positive	*n*=16	*n*=22	*n*=18	*n*=8	*n*=7
Minimal	8	15	37	63	70
Maximal	71	83	84	81	89
Median	15±18.78	46.5±21.81	74.5±12.08	77,5±6,88	80±5.52
Portion of CD68/XX positive Kupffer cells of donor origin (%) (*n*=83)					
XX positive	*n*=21	*n*=23	*n*=20	*n*=11	*n*=8
Minimal	24	10	9	6	6
Maximal	86	78	60	31	24
Median	67±15.82	47±20.92	28.5±13.00	17±6.46	16±5.18

Table 5 Correlation of histopathological findings and portion of recipient (Y+) derived Kupffer cells

Diagnosis (*n*=71)	Portion of CD68/Y+KC%			Time period after transplantation (days) Median
	Minimal	Maximal	Median	
Acute rejection (*n*=41)	8	83	53±25	20±91
Non-specific alterations (*n*=13)	14	82	52±25	25±54
Chronic hepatitis (*n*=5)	75	89	80±5	1653±543
Suspicious of hepatitis (*n*=2)	79	82	81±2	1164±1005
Acute rejection + hepatitis (*n*=3)	70	83	78±5	35±278
Ischemic lesions (*n*=5)	10	81	64±28	70±137
Chronic rejection (*n*=1)	–	–	79	206
Necrosis/viral hepatitis (*n*=1)	–	–	84	115

Table 6 Portion of donor (XX+) lymphocytes (%) according to time after transplantation liver biopsies were obtained. *ptx* after transplantation

Time	Ptx	A Up to 1 week	B 1–4 weeks	C 1–6 months	D 6–12 months	E >1 year
Biopsies (*n*=80)	Total	*n*=20	*n*=23	*n*=20	*n*=9	*n*=8
Minimal		1	0	0	1	0
Maximal		37	30	13	3	6
Median		10±10.2	4±7.5	2±5.8	2±1.6	2±2.6

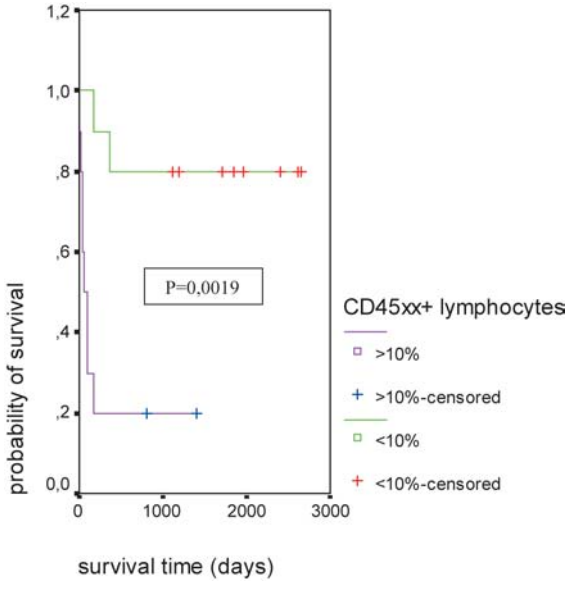

Fig. 3 Kaplan Meier analysis for the prognostic significance of the content of donor lymphocytes in liver tissue obtained during the first week after transplantation for survival time after transplantation

Lymphocytes

The portion of donor (XX+) LC decreased progressively during the follow-up ptx (Table 6). There was a significant decrease of donor (XX+) LC during the first month ptx (Fig. 2C). Single donor (XX+) LC were detectable more than 1 year ptx (maximum 4 years+340 days). A great number of these donor (XX+) LC were especially found in subcapsular liver tissue of wedge biopsies. No correlation was found between histopathological features, including episodes of acute rejection and portion of donor (XX+) LC (Table 7). Kaplan Meier analysis showed that patients with a low portion of donor (XX+) LC in the liver tissue obtained during the first week after transplantation have a longer survival than patients with high portion of donor LC (Fig. 3).

Discussion

Several theories have been proposed to explain the unique biological behavior of the liver after transplantation.

Table 7 Correlation of portion of donor (XX+) derived lymphocytes (%) and histopathological biopsy findings. *ptx* after transplantation

Diagnosis	Total number of evaluated biopsies		
	n=80	Portion of CD45/XX+ lymphocytes % median	Time ptx (days) median
Acute rejection	*n*=42	3.5±6.6	20±91
Non-specific	*n*=15	4±10.4	27±178
Ischemic lesions	*n*=10	9±9.9	23±113
Chronic hepatitis	*n*=6	3±2.8	1404±681
Suspicious of hepatitis	*n*=2	3±3	1164±1005
Acute rejection + hepatitis	*n*=3	5±2.6	35±69
Necrosis/viral hepatitis	*n*=1	1	115
Chronic rejection	*n*=1	2	206

Acceptance of the graft has been attributed to its relatively large parenchymal mass with the potential to shed a substantial amount of soluble major histocompatibility complex (MHC) class I [24], which can bind to soluble antigen, thus preventing them from damaging the graft. The demonstration that the elimination or substantial reduction of graft-resident bone marrow-derived passenger leukocytes breaks spontaneous acceptance of livers in a rat model seemingly challenged the dogma that these cells are primarily responsible for the vigor of acute rejection [23]. In fact, there exist several reports of prolonged allograft survival after elimination of graft-resident passenger leukocytes [15]. A theory that has been formulated to explain this intriguing observation in liver transplantation is clonal exhaustion of alloreactive T LC due to a relatively large number of passenger leukocytes that migrate from the liver to the host's lymphoid compartment [3]. A better understanding how hematopoietic cells contribute to allograft rejection and tolerance induction, respectively, may aid in the development of clinical strategies to achieve long-term allograft acceptance.

The aim of the present study was to evaluate whether and during which course of time after transplantation KC and LC of the liver were replaced by recipient cells and whether there is any correlation between the replacement of these immunologically competent donor cells of the graft and the occurrence of rejection episodes and the clinical course of the patients.

KC belong to the macrophage–monocyte system and are mainly derived from bone marrow cells. The bone marrow-derived monocytes circulate in the blood stream and are able to migrate into the liver where they stay and become tissue macrophages. The present study demonstrated that the KC of the allografted liver were increasingly replaced by recipient cells after transplantation beginning within the first week ptx. At the same time, the number of donor KC decreased during the same time period. Nevertheless, the persistence of donor KC could be proved during nearly 6 years ptx. Comparable observations have only been made in rats with detection of donor KC until 180 days ptx [12]. These results indicate that the majority of the KC population consists of maturing recipient monocytes originated from bone marrow, but a smaller part is derived from local cells of the liver.

After liver transplantation, KC play an important role during ischemia and reperfusion injury [2]. Together with endothelial cells, they become activated and release inflammatory mediators and oxygen radicals that change the surface of sinusoidal endothelial cells. These mechanisms lead to adhesion of leukocytes and thrombocytes and to hypercoagulability [4, 5, 11, 17]. We could not find any correlation between the number of recipient-derived KC during the first month ptx and time of cold ischemia before transplantation. Thus KC do not seem to be an important target of reperfusion injury. These data are in concordance with several studies that described a damage of endothelial cells, but only activation of KC by reperfusion injury [4, 5, 7, 16].

KC are able to express HLA-DR molecules to process antigens and to present them to T-LC. Several studies have demonstrated an increased re-population of KC during rejection episodes and infectious disease [6, 8, 22] as a result of a damage of donor-derived KC. These observations are in conflict with the fact that KC are not the main target of cellular rejection. We could not find any correlation between histopathological alterations of the liver tissue, including rejection episodes, and the number of recipient-derived KC, which, according to the data presented here, was only influenced by the time after transplantation that the liver tissue was studied. Likewise, no relationship between the content of recipient-derived KC and the survival time after transplantation could be observed, indicating that the portion of recipient-derived KC do not have any influence on the clinical course.

T-LC are the main cell type in allograft rejection. CD4+ helper cells and CD8+ cytotoxic cells recognize foreign class-II and I-antigen on different cell types and induce the alloreactive response. The re-population/infiltration of an allograft by LC of the recipient starts early after transplantation. Iwaki et al. [10] showed a complete re-population of the mucosa by recipient LC in the small intestine after 10–12 weeks ptx. In the present study, recipient LC were seen in the liver allograft starting in the first week after transplantation. Similar to the study of Iwaki, a decrease of donor-derived LC after transplantation was found over time with a significant decrease 1 month after transplantation. A small residual population of donor-derived LC, however, was present in nearly all biopsies obtained. Donor-derived LC could be demonstrated in the liver up to 5 years after transplantation.

They were mainly located in the subcapsular areas of the liver. To the best of our knowledge, our study is the first to report such a long time persistence of donor-derived LC in the transplanted liver. Schlitt et al. [20] found donor-derived LC only during the first weeks after transplantation. Possible sources of the residual donor lymphocyte population could be interstitial hematopoietic stem cells or the LC themselves, which might be able to proliferate.

No correlation was found between the number of donor-derived LC and the histopathological alterations. Analysis of the portion of donor LC in the liver during the first week after transplantation and survival time indicates that patients with a low portion of donor LC have a better prognosis to survive than those with a high portion of donor LC. These findings have to be interpreted cautiously due to the small number of patients studied. The findings support the former theory that the deletion of passenger leukocytes improves the graft acceptance.

In contrast, in an animal study, Meyer et al. [18] showed that the content of donor LC in the liver was low during rejection episodes and increased with development of immunological tolerance. The authors, however, could not explain conclusively these results, especially not if a higher portion of donor-derived LC leads to immunological tolerance or if they were only a side effect. Recent studies of Kreisel et al. [14] in a rat model demonstrated that the genotype of graft-resident hematopoietic cells could influence the tempo of acute rejection of liver allografts. Although their findings support previous observations that the presence of graft-resident bone marrow-derived cells is critical during the induction phase of graft acceptance, they showed that this immunological unresponsiveness is not dependent on the presence of antigen-presenting cells of donor type. These data suggested that tolerance induction could be conducted with the infusion of recipient or third-party hematopoietic cells that have been pulsed with soluble antigens of donor origin. The study left open the question of which graft-resident cells were responsible for the immunological acceptance after liver transplantation.

The present study indicates that neither graft-resident KC nor graft-resident LC were the cells that were mainly responsible for tolerance induction after transplantation.

Conclusions

The interaction of the allograft and its graft-resident hematopoietic cells and the recipient's immunological network seems to be essential for the development of graft acceptance after transplantation. A successive repopulation of the liver allograft by recipient LC and macrophages was observed after transplantation, but a smaller portion of LC and KC with donor genotype was detectable during the whole course of time studied. There was no correlation between the portion of recipient-derived KC and donor-derived LC and histopathological alterations of the biopsy specimens, including rejection episodes. The biopsy content of KC with recipient origin has had no prognostic significance for the probability of survival, but patients with a low portion of donor LC in the liver biopsy obtained during the first week after transplantation have had a better prognosis for survival than those with higher portion of donor LC. The interaction between graft-resident donor LC and the recipient's immunological network remains to be elucidated. The present results indicate that graft-resident KC and LC are potentially not the main cell types involved in tolerance induction after liver transplantation.

References

1. Baretton GB, Valina C, Vogt T, Schneiderbanger K, Diebold J, Lohrs U (1994) Interphase cytogenetic analysis of prostatic carcinomas by use of nonisotopic in situ hybridization. Cancer Res 54:4472–4480
2. Bilzer M, Gerbes AL (2000) Preservation injury of the liver: mechanisms and novel therapeutic strategies. J Hepatol 32:508–515
3. Bishop GA, Sun J, DeCruz DJ, Rokahr KL, Sedgwick JD, Sheil AG, Gallagher ND, McCaughan GW (1996) Tolerance to rat liver allografts. III. Donor cell migration and tolerance-associated cytokine production in peripheral lymphoid tissues. J Immunol 156:4925–4931
4. Carles J, Fawaz R, Hamoudi NE, Neaud V, Balabaud C, Bioulac-Sage P (1994) Preservation of human liver grafts in UW solution. Ultrastructural evidence for endothelial and Kupffer cell activation during cold ischemia and after ischemia-reperfusion. Liver 14:50–56
5. Clavien PA, Harvey PR, Strasberg SM (1992) Preservation and reperfusion injuries in liver allografts. An overview and synthesis of current studies. Transplantation 53:957–978
6. Gassel HJ, Engemann R, Thiede A, Hamelmann H (1987) Replacement of donor Kupffer cells by recipient cells after orthotopic rat liver transplantation. Transplant Proc 19:351–353
7. Goode HF, Webster NR, Howdle PD, Leek JP, Lodge JP, Sadek SA, Walker BE (1994) Reperfusion injury, antioxidants and hemodynamics during orthotopic liver transplantation. Hepatology 19:354–359
8. Gouw AS, Houthoff HJ, Huitema S, Beelen JM, Gips CH, Poppema S (1987) Expression of major histocompatibility complex antigens and replacement of donor cells by recipient ones in human liver grafts. Transplantation 43:291–296
9. Hopman AH, van Hooren E, van de Kaa CA, Vooijs PG, Ramaekers FC (1991) Detection of numerical chromosome aberrations using in situ hybridization in paraffin sections of routinely processed bladder cancers. Mod Pathol 4:503–513
10. Iwaki Y, Starzl TE, Yagihashi A, Taniwaki S, Abu-Elmagd K, Tzakis A, Fung J, Todo S (1991) Replacement of donor lymphoid tissue in small-bowel transplants. Lancet 337:818-819
11. Jaeschke H (1994) Pathophysiology of hepatic ischemia-reperfusion injury: the role of complement activation. Gastroenterology 107:583–586
12. Julie C, Astarcioglu I, Tricottet V, Fabiani B, Accordini C, Reynes M (1994) Expression of donor and recipient class I MHC antigens by Kupffer cells after orthotopic rat liver transplantation. An immunoelectron microscopic study. Transplantation 57:1525–1528
13. Kashiwagi N, Porter KA, Penn I, Brettschneider L, Starzl TE (1969) Studies of homograft sex and of gamma globulin phenotypes after orthotopic homotransplantation of the human liver. Surg Forum 20:374–376
14. Kreisel D, Petrowsky H, Krasinskas AM, Krupnick AS, Szeto WY, McLean AD, Popma SH, Gelman AE, Traum MK, Furth EE, Moore JS, Rosengard BR (2002) The role of passenger

leukocyte genotype in rejection and acceptance of rat liver allografts. Transplantation 73:1501–1507
15. Lechler RI, Batchelor JR (1982) Restoration of immunogenicity to passenger cell-depleted kidney allografts by the addition of donor strain dendritic cells. J Exp Med 155:31–41
16. Marzi I, Knee J, Buhren V, Menger M, Trentz O (1992) Reduction by superoxide dismutase of leukocyte-endothelial adherence after liver transplantation. Surgery 111:90–97
17. Marzi I, Walcher F, Buhren V (1993) Macrophage activation and leukocyte adhesion after liver transplantation. Am J Physiol 265:G172–G177
18. Meyer D, Loffeler S, Otto C, Gassel HJ, Timmermann W, Ulrichs K, Thiede A (1999) Donor cell population in the liver allograft reflects the recipient immune status. Transplant Proc 31:437
19. Racusen LC, Solez K, Colvin RB, et al (1997) Banff schema for grading liver allograft rejection: an international consensus document. Hepatology 25:658–663
20. Schlitt HJ, Kanehiro H, Raddatz G, Steinhoff G, Richter N, Nashan B, Ringe B, Wonigeit K, Pichlmayr R (1993) Persistence of donor lymphocytes in liver allograft recipients. Transplantation 56:1001–1007
21. Starzl TE, Zinkernagel RM (1998) Antigen localization and migration in immunity and tolerance. N Engl J Med 339:1905–1913
22. Steinhoff G (1990) Major histocompatibility complex antigens in human liver transplants. J Hepatol 11:9–15
23. Sun J, McCaughan GW, Gallagher ND, Sheil AG, Bishop GA (1995) Deletion of spontaneous rat liver allograft acceptance by donor irradiation. Transplantation 60:233–236
24. Sun J, Sheil AG, Wang C, Wang L, Rokahr K, Sharland A, Jung SE, Li L, McCaughan GW, Bishop GA (1996) Tolerance to rat liver allografts: IV. Acceptance depends on the quantity of donor tissue and on donor leukocytes. Transplantation 62:1725–1730

Virchows Arch (2003) 443:549–560
DOI 10.1007/s00428-003-0869-0

ORIGINAL ARTICLE

Dominik T. Schneider · Ute Jänig · Gabriele Calaminus · Ulrich Göbel · Dieter Harms

Ovarian sex cord–stromal tumors—a clinicopathological study of 72 cases from the Kiel Pediatric Tumor Registry

Received: 8 January 2003 / Accepted: 24 June 2003 / Published online: 9 August 2003
© Springer-Verlag 2003

Abstract We analyzed 72 patients with ovarian sex cord–stromal tumors (OSCST) registered at the German Pediatric Tumor Registry in Kiel over a 20-year period. Juvenile granulosa cell tumors (JGCT, n=48) were the most frequent histological subtype. In addition, there were 14 Sertoli-Leydig cell tumors, 5 sclerosing stromal tumors, 2 sex cord tumors with annular tubules, 2 thecomas and 1 steroid cell tumor. Stage according to FIGO (International Federation of Gynecologists and Obstetricians) was Ia in 39 patients, Ic in 17 patients, II in 3 patients and III in 1 patient (60 patients with complete data). Compared with adult granulosa cell tumors, JGCT showed pronounced mitotic activity [mean 9.8 mitoses/10 high power field (HPF)], which was significantly higher than in other histological subtypes (2.7/10 HPF, P=0.001). Immunohistochemical analysis revealed frequent coexpression of vimentin (positive in 52/52 examined tumors), cytokeratin (27/33), and inhibin (19/20). Of patients, 12 with Ic or higher stage tumors received adjuvant cisplatinum-based chemotherapy. Event-free survival at 10 years was 0.88±0.05 (38/43 patients with follow-up data). Outcome significantly correlated with stage and mitotic activity (<20 versus ≥20 mitoses/10 HPF: event-free survival 1.0 versus 0.48±0.05, P=0.0001). In conclusion, this analysis confirms that the majority of patients with OSCST present at low tumor stage and that prognosis in these patients is excellent. Refractory tumors are characterized by high proliferative activity. Therefore, histopathological evaluation substantially contributes to risk assessment in patients with OSCST and might be useful for therapy stratification in prospective therapeutic protocols.

Keywords Children · Adolescents · Sertoli-Leydig tumors · Granulosa cell tumors · Ovary

D. T. Schneider (✉) · G. Calaminus · U. Göbel
Clinic of Pediatric Oncology, Hematology and Immunology,
Children's Hospital,
University Hospital Düsseldorf, Heinrich-Heine-University,
Moorenstrasse 5, 40225 Düsseldorf, Germany
e-mail: dominik.schneider@uni-duesseldorf.de
Tel.: +49-211-8116491
Fax: +49-211-8116206

U. Jänig · D. Harms
Institute of Pediatric Pathology,
Christian-Albrechts-University,
Kiel, Germany

Introduction

Ovarian sex cord–stromal tumors (OSCST) constitute a heterogeneous group of rare tumors that develop from the gonadal non-germ cell component. Considering all age groups, OSCST amount to approximately 10% of all ovarian neoplasms with predominance of the thecoma–fibroma group [20]. Morphologically, they display at least some areas with unequivocal gonadal differentiation, such as granulosa, Sertoli, or Leydig cells. However, they may also show indifferent morphological features, such as fibroblastic differentiation. OSCST share some common biological features, such as steroid hormone production, that may give rise to characteristic clinical symptoms, such as isosexual precocity. Moreover, secretion of α-inhibin can be detected by immunohistochemical techniques or serologically and, therefore, may serve as a diagnostic marker [10, 18, 29]. These common characteristics allow the distinction of OSCST from the more frequent ovarian malignant germ cell tumors as well as from the rare but clinically important ovarian small cell carcinoma of the hypercalcaemic type, which is often associated with fatal outcome [18]. During the last three decades, considerable progress has been made in the histological classification of these tumors. In this context, the definition of juvenile granulosa cell tumors (JGCT) as a distinct clinical and pathological entity has been one important milestone. Histologically, JGCT show a characteristic growth pattern with focal follicle formation and often pronounced histological features of malignancy [30].

Unfortunately, the opportunity to establish an accurate diagnosis in these tumors has not yet translated into

standardized therapeutic strategies. Particularly, the treatment of advanced and poorly differentiated tumors still remains highly controversial, and a previous analysis of such patients registered at the German MAKEI (Maligne Keimzeiltumoren) studies has addressed this issue [21]. Several other investigators have also critically evaluated different therapeutic approaches in advanced OSCST [4, 7, 12, 14, 15, 16, 17, 26, 30]. Summarizing these studies, the conclusions derived from the first (and still largest) series of JGCT and Sertoli-Leydig cell tumors (SLCT) still hold true—that the vast majority of tumors present as localized disease confined to the ovary and that these tumors usually take a benign clinical course, even in spite of pronounced histopathological features of malignancy [30, 31]. However, patients that present with advanced disease or poorly differentiated SLCT have a poor prognosis. Previous analyses have demonstrated that adjuvant chemotherapy helps to achieve sustained complete clinical remissions [3, 14, 21]. Furthermore, poorly differentiated high-stage SLCT often take a malignant clinical course and, therefore, these are also considered prognostically poor [31].

The objective of this analysis of a large series of OSCST diagnosed or reviewed at the Kiel Pediatric Tumor Registry is to provide a morphological documentation and clinico-pathological evaluation of OSCST in children and adolescents. In addition, histopathological parameters should be evaluated with respect to their potential prognostic significance that may allow their use in the diagnostic evaluation of patients enrolled onto protocols that employ risk-stratified therapeutic strategies. Last, this evaluation should also reveal future directions for hopefully clinically relevant biological and genetic studies of OSCST.

Materials and methods

Patients and methods

The files of the Kiel Pediatric Tumor Registry were screened for all histological types of OSCST, and all patients younger than 20 years were included in this analysis. During the last three decades, an increasing number of patients with OSCST have been diagnosed or reviewed at the Kiel Pediatric Tumor Registry (Fig. 1). As it is evident from Fig. 1, the rise is predominantly due to the increasing numbers of JGCT diagnosed at the Kiel Registry. In total, 72 patients were registered until December 2000. For comparison, 331 cases of ovarian germ cell tumors were collected in the Registry during the same period of time. Thus, the relative frequency of OSCST relative to germ cell tumors is 1 to 4.6. Based on pretherapeutic samples, all tumors were classified according to the World Health Organization (WHO) classification of ovarian tumors [22, 23].

Data regarding the gross anatomy of the tumors were extracted from both the surgical protocols (n=41) and the pathological reports of the primary investigators. These data included site, size, and macroscopic appearance.

Slides were routinely stained with hematoxylin and eosin, Giemsa, Goldner, Bielschowsky (reticulin), and periodic acid-Schiff (PAS). Each slide was examined on several occasions, and, for this analysis, two observers (D.H., D.T.S.) re-analyzed all slides according to uniform standards.

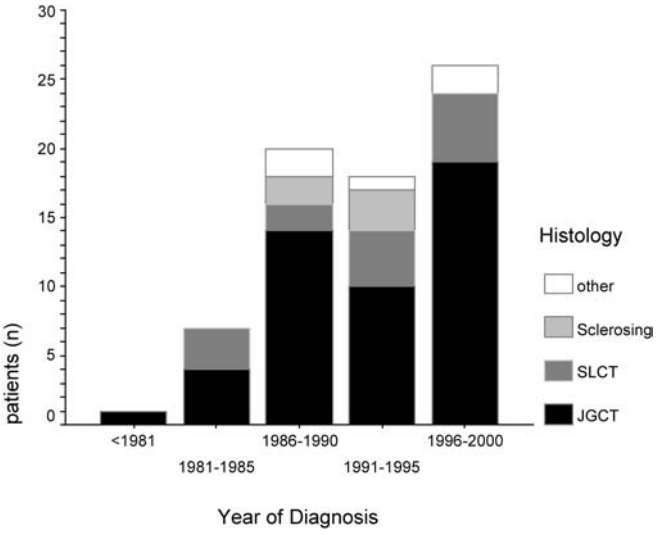

Fig. 1 Number of patients and distribution of histological subtypes of ovarian sex cord–stromal tumors diagnosed or reviewed at the Kiel Pediatric Tumor Registry during the last two decades

The general growth pattern, the grade of cellular atypia, presence of necrosis or hemorrhage as well as pronounced fibrosis were noted. In all patients, the mitotic rate was assessed by counting mitotic figures in at least 10 high power fields (HPF), evaluated at a ×400 magnification. Mitotic activity was categorized as low, intermediate or high, respectively, when less than 10, 10–19, or more than 19 mitoses per 10 HPF were counted. In 52 patients, paraffin blocks or additional sections were available, and the examination was expanded with immunohistochemical stainings using the alkaline phosphatase–anti alkaline phosphatase method, as described previously [9]. For this purpose, antibodies were used against inhibin (n=20), vimentin (n=52), cytokeratin (KL-1, n=33), Ki-67, and Ki-S5 (n=20) as well as other antibodies, e.g., against α-fetoprotein (AFP), and β-human chorionic gonadotrophin (HCG), which were used in single cases for diagnostic purposes, e.g., for distinguishing OSCST from malignant germ cell tumors. The types of antibodies applied in this study and the respective concentrations have been listed in a previous analysis of testicular Sertoli cell tumors and JGCT [9]. Additionally, a mouse anti-human inhibin-alpha subunit antibody (Oxford Bioinnovation Ltd., England) has been applied in a 1:10 dilution for inhibin detection.

This study also includes the clinical follow-up data of 43 patients prospectively enrolled as follow-up patients for the protocols for non-testicular germ cell tumors MAKEI of the German Society of Pediatric Oncology and Hematology. These patients or their parents gave informed consent to collection and evaluation of the clinical data. According to the MAKEI guidelines, initial assessment included diagnostic imaging with abdominal ultrasound and computerized tomography. Staging was performed according to the WHO and FIGO (International Federation of Gynecologists and Obstetricians) staging systems, and classification was based on both the surgical report and the pathological examination [1]. The MAKEI studies were approved by the responsible Ethics Committee at the Heinrich-Heine-University.

Statistical analysis

Statistical analysis was performed with the commercially available SPSS program (release 9.0. SPSS Inc., Chicago, IL, USA). For categorical data, the two-sided Pearson chi-square test was applied. Numerical data were calculated using the Mann-Whitney-U rank test. The overall and event-free survival (EFS) was estimated

Table 1 Synopsis of the clinical and therapeutic data. – zero patients

	Juvenile granulosa cell tumor	Sertoli Leydig cell tumor	Sclerosing stromal tumor	Sex cord tumor with annular tubules	Thecoma	Steroid cell tumor
Patients (*n*)	48	14	5	2	2	1
Age, median (range)	7.1 years (0.6–19.4)	13.9 years (0.5–17.6)	12.7 years (0.9–17.5)	9.8 years (8.5–10.9)	13.10 years (12.6–15.2)	8.2 years
Endocrinologic symptoms	61%	45%	50%	100%	50%	100%
Side (*n*)						
Right	27	4	4	–	1	–
Left	13	5	1	1	1	–
Bilateral	2	1		–	–	–
No data	6	4	–	1	–	1
Maximum diameter (median)	11.3 cm	10 cm	10 cm	14 cm	15.5 cm	No data
FIGO (International Federation of Gynecologists and Obstetricians) stage						
Ia	27	5	3	1	2	1
Ic	12	4	1	–	–	–
II	3	–	–	–	–	–
III	1	–	–	–	–	–
No data	5	5	1	1	–	–
Surgery						
Ovarectomy	13	2	1	–	–	–
Adnectomy	24	4	2	1	–	–
Hysterectomy	–	1	–	–	–	–
No data	11	7	2	1	2	1
Chemotherapy	9	3	–	–	–	–
Follow-up, median (range)	58.5 months (1–193)	35 months (7–90)	67 months (14–120)	47 months (1–193)	–	–
No evidence of disease	30	4	2	2	–	–
Recurrence/dead of disease	3*/3	2/2	–	–	–	–
No data	14	8	3	–	2	1

* Excluding one patient with a metachronous contralateral tumor 126 months after initial diagnosis

according to the method of Kaplan and Meier, and the influence of suspected prognostic factors was analyzed with the log-rank test. EFS was defined as the time from diagnosis to the first relapse or death (death of disease or death of therapy-related complication). The other patients were censored at the time of the last reported follow-up examination. Follow-up data until March 2002 have been included into this analysis. *P* values below 0.05 were considered significant.

Results

Clinical data

Until December 2000, 72 patients were registered. Median age was 9 years and 2 months (9;2 years) (mean 8;9 years; range 5 months to 19;4 years). There were 48 JGCT, 14 SLCT, 5 sclerosing stromal tumors, 2 sex cord tumors with annular tubules, 2 thecomas, and 1 steroid tumor. JGCT were diagnosed at a younger age than other histological subtypes. (P=0.035; Table 1). Symptoms due to endocrinological activity of the tumor (e.g., isosexual precocity, secondary amenorrhea) were presented in 30 patients. Endocrinological symptoms were most frequent among JGCT in young children. Abdominal pain was reported by 21 patients and, in 17 patients, the abdominal tumor was palpable on physical examination. There were neither patients with Ollier's disease, which can be associated with JGCT, nor patients with Peutz Jegher's syndrome, which is associated with sex cord tumors with annular tubules. However, one girl suffered from Zuelzer Wilson's syndrome, and her SLCT was diagnosed accidentally during laparatomy because of mechanical ileus due to peritoneal streaks after bowel resection and several previous laparotomies.

Macroscopic pathology

Among 60 tumors with complete data regarding the macroscopic pathology, 36 were right-sided and 21 left-sided. Of the tumors (2 JGCT and 1 SLCT), 3 occurred bilaterally. In addition, one patient with a JGCT developed a contralateral JGCT 126 months after initial diagnosis. This tumor was considered a metachronous contralateral tumor. Most tumors were large, and for the whole cohort, the median maximal tumor diameter was 11 cm, ranging from 5 cm to 30 cm. We found no significant difference in size between the different histological subentities. To a certain degree, the macroscopic appearance varied with respect to the histological subtypes. A cystic appearance (P=0.01) was seen in 30

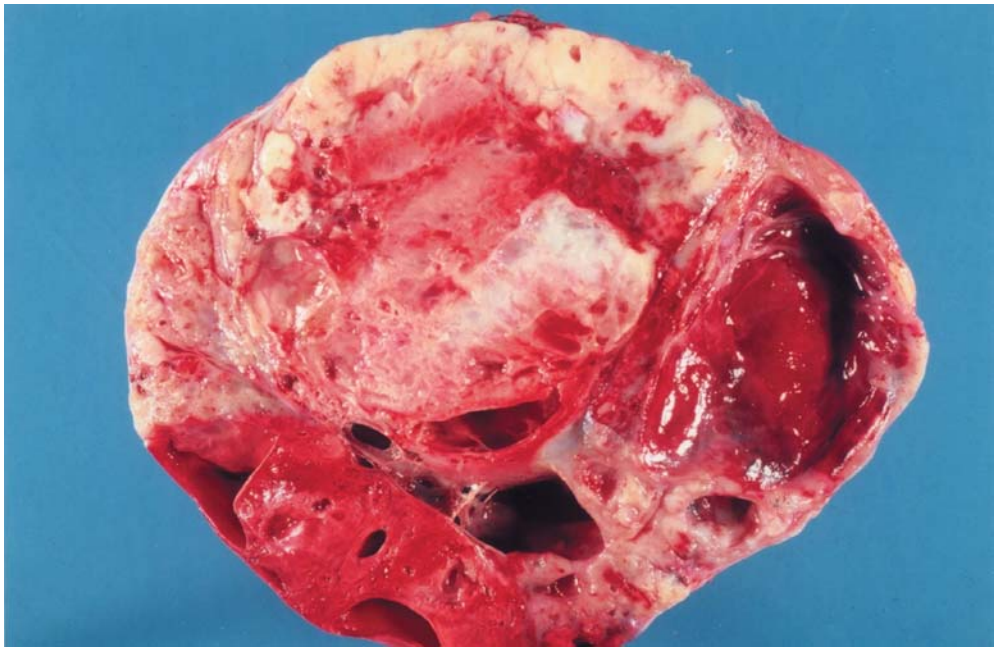

Fig. 2 Large juvenile granulosa cell tumor with pronounced regressive changes

JGCT and 5 SLCT but not in the other histological types, at least focally. In all tumor types, the cut surface most commonly appeared grayish-white to yellowish in color, and occasionally regressive changes with hemorrhage and necrosis were seen (Fig. 2).

Among the 60 patients with complete clinical and surgical data available for staging according to the WHO and FIGO staging system, there were 39 stage-Ia, 17 stage-Ic, 3 stage-II and 1 stage-III tumors. At diagnosis, no lymph node or distant hematogenous metastases were found.

Histopathology

Juvenile granulosa cell tumors

Microscopically, the majority of JGCT showed a predominantly solid, partly nodular growth pattern. The nodules were delineated indistinctly by strands of fibrous tissue. Most JGCT displayed follicle-like cavities of varying number and size (Fig. 3a). Generally, the cysts were small and their appearance was more immature than those in adult granulosa cell tumors. The follicles often contained a homogeneous eosinophilic material.

The granulosa cells were often intermediate in size and immature. The nuclei were round and non-grooved, and the nucleoli were small. Most tumor cells showed a moderate eosinophilic cytoplasm, but, in many tumors, cells with luteinized cytoplasm were also seen. Call-Exner bodies, characteristic for the adult variant of granulosa cell tumors, were detected only in one case.

The mean mitotic count was 9.8 mitoses per 10 HPF (median 6.5) and ranged from 1 to 47 per 10 HPF. Compared with all other histological types, mitotic activity was highest in JGCT (P=0.001, Table 2).

Varying degrees of nuclear atypia were seen focally in many tumors but only one case with fatal outcome presented with diffuse and high-grade nuclear atypia including atypical mitoses ("anaplastic" JGCT, Fig. 3b, c). In addition to granulosa cells, JGCT usually exhibited theca cells, which were admixed with granulosa cells or were arranged in larger cell complexes, predominantly around the tumor nodules (Fig. 3d).

Reticulin stains were helpful to distinguish between the almost reticulin fiber-free granulosa cell accumulations and the theca cell foci, which offered a dense reticulin fiber network encompassing either individual theca cells or small theca cell aggregates. Four tumors showed foci with Sertoli cell differentiation, which was usually distinguishable as cord-like streaks of tumor cells or as tubular structures (Fig. 3e). However, these foci did not contribute more than 10% to the examined tumor specimens.

Sertoli-Leydig cell tumors

The microscopic appearance of SLCT was variable with respect to the overall differentiation of the tumors. In well-differentiated SLCT (n=1) and in more differentiated areas of mostly undifferentiated tumors, tumor cells were lined in cord- or tubule-like structures (Fig. 4a). The tumor cells were elongated in shape, contained hyperchromatic nuclei with small nucleoli and usually PAS-negative cytoplasm. In addition, small or sometimes larger clusters of Leydig cells were also seen (Fig. 4b). SLCT with intermediate differentiation (n=8) sometimes contained foci that resembled sarcomatoid differentiation and were characterized by spindle-like cells and focally showed increased mitotic activity. Last, five tumors were

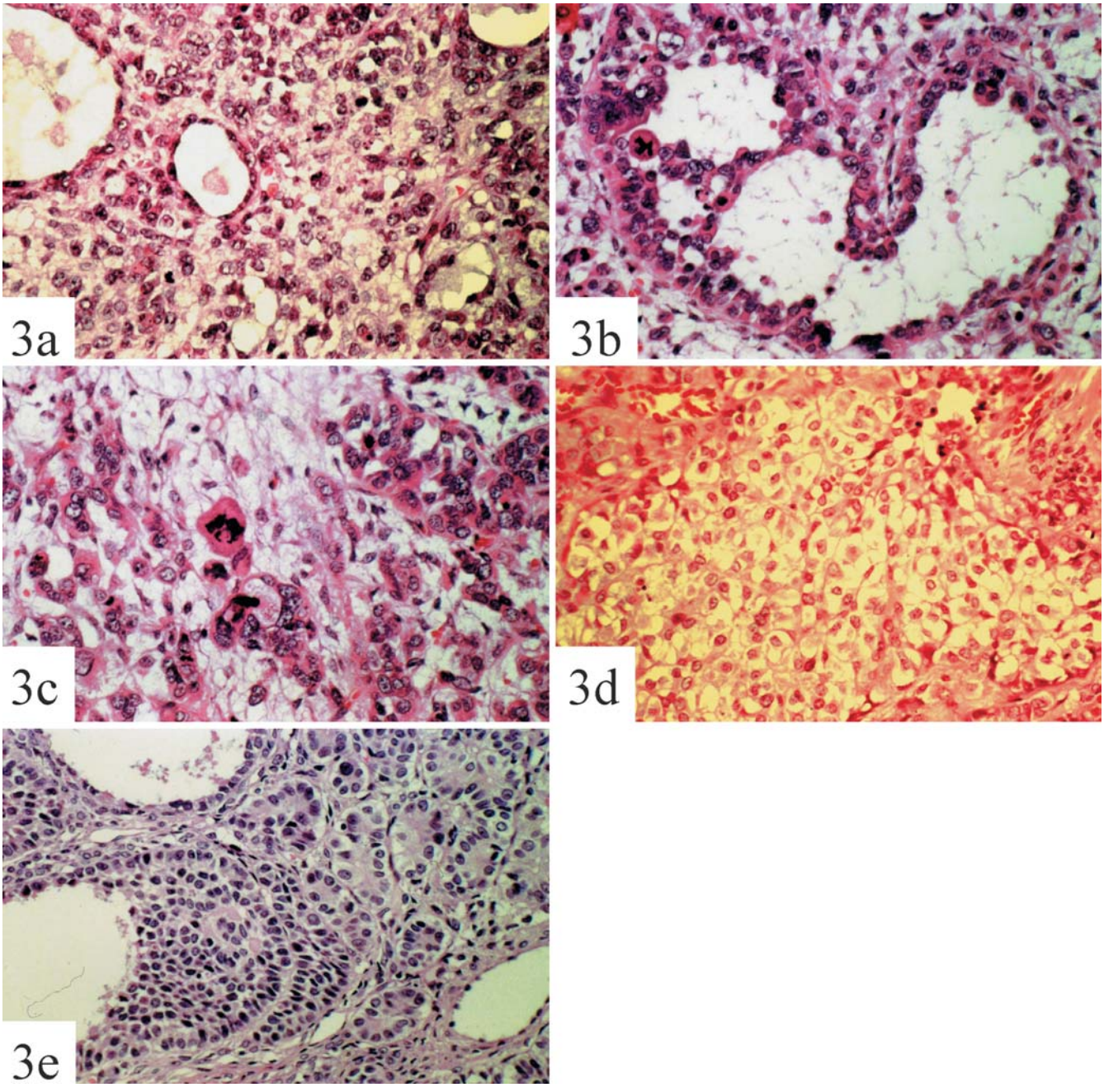

Fig. 3 Histological appearance of juvenile granulosa cell tumors (JGCT). **a** Small follicles surrounded by medium-sized granulosa cells with pale to weakly eosinophilic cytoplasm and round, slightly hyperchromatic nuclei. Scattered mitotic figures [hematoxylin and eosin (H&E), original magnification ×350]. **b** "Anaplastic" JGCT showing considerable nuclear atypia including atypical mitoses. Follicle-like cavity surrounded by atypical granulosa cells (H&E, original magnification ×280). **c** Solid area of the same tumor (H&E, original magnification ×280). **d** Focus of cells (presumably theca cells) with abundant clear cytoplasm (H&E, original magnification ×280). **e** JGCT (*left*) in combination with focal area of Sertoli-Leydig cell tumors (SLCT) differentiation (*right*). The SLCT component displays incompletely developed tubular structures (H&E, original magnification ×280

poorly differentiated (Fig. 4c), one of them with heterologous cartilagineous foci (Fig. 4d). A predominantly sarcomatoid differentiation (Fig. 4e) was shown by three tumors, and two exhibited an additional retiform growth pattern (Fig. 4f). One of the latter had initially been diagnosed as ovarian yolk sac tumor (serum AFP levels not obtained at diagnosis), but diagnosis was changed to retiform SLCT after central histopathological review. As in JGCT, the mitotic activity in SLCT was variable and ranged from 1 to 23 mitoses (mean 4.3) per 10 HPF. Comparing SLCT to JGCT, mitotic activity was less prominent than in JGCT (P=0.015) and only slightly higher than in the other histological subtypes (not significant) (Table 2).

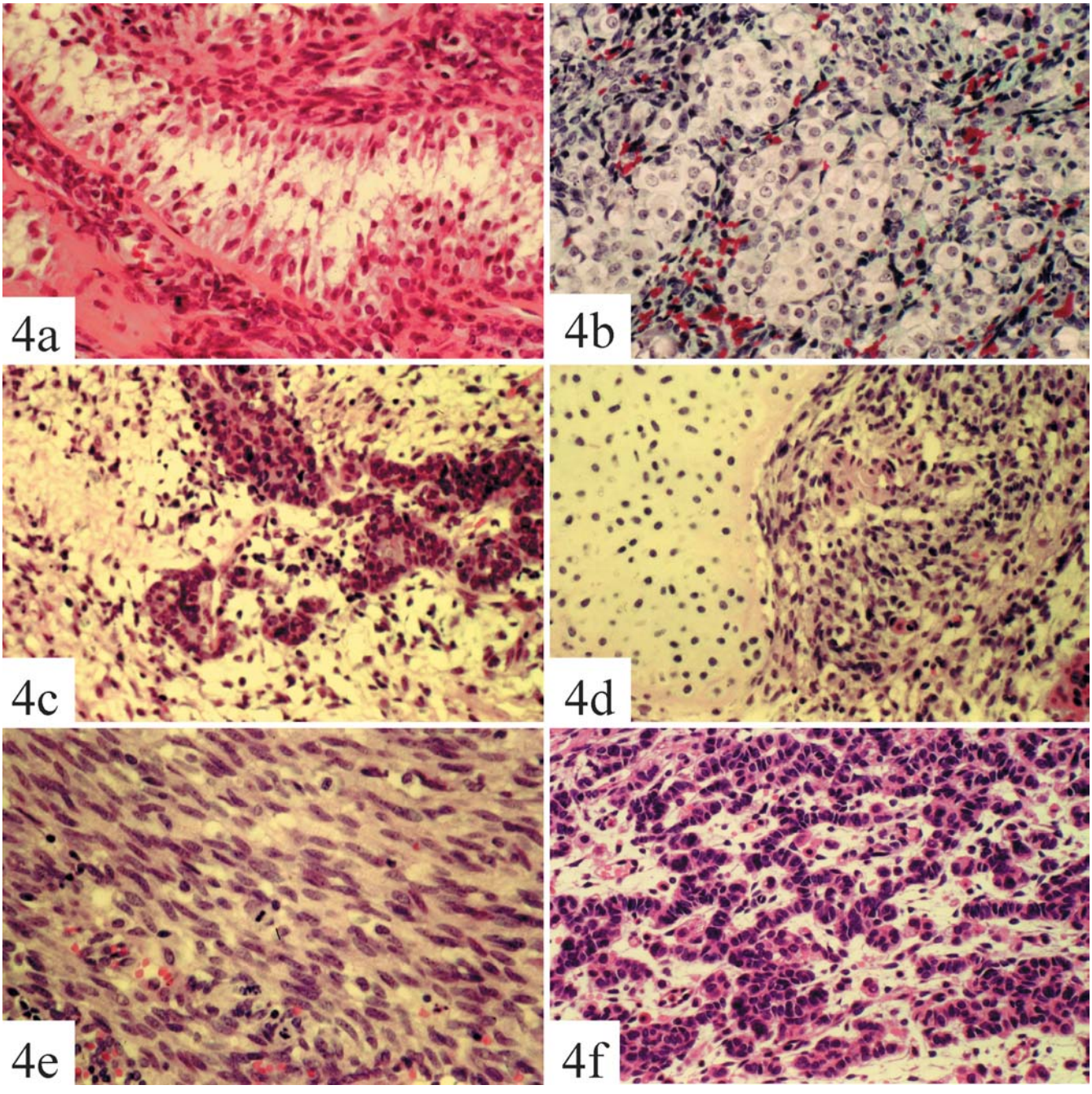

Fig. 4 Histological appearance of Sertoli-Leydig cell tumors (SLCT). **a** Well-differentiated SLCT showing tubular structures indistinguishable from ("Sertoli-only") testicular tubules [hematoxylin and eosin (H&E), original magnification ×280]. **b** Well-differentiated SLCT (same case as in **b**). Cluster of Leydig cells surrounded by indifferent gonadal stromal cells (H&E, original magnification ×280. **c** Poorly differentiated SLCT with small areas of incompletely tubular arranged Sertoli cells surrounded by dense accumulations of undifferentiated round- and spindle-shaped tumor cells (H&E, original magnification. ×280). **d** Poorly differentiated SLCT (same case as in **c**) showing heterologous cartilaginous islands (H&E, original magnification ×280). **e** Poorly differentiated SLCT (same case as in **c**, **d**) with highly cellular, fibrosarcoma-like areas composed of very immature, mitotically active spindle cells (H&E, original magnification ×350). **f** Poorly differentiated SLCT (same case as in **c**, **d**, **e**) focally showing a retiform pattern (H&E, original magnification ×280)

Rare subtypes and differential diagnosis

The sclerosing stromal tumors often showed a pseudolobular appearance with broad streaks of fibrous stroma separating the tumor nodules. Some of the nodules contained lipid-rich cells with clear cytoplasm (Fig. 5). In addition, they usually displayed a prominent vascular pattern that was characterized by ectatic thin-walled vessels, which in one case contained thrombi. Tumor cells were spindle shaped and showed a fibroblast-like appear-

Table 2 Synopsis of the pathological data. *HPF* high power field. *0* all cells negative, + 0–10% of tumor cells stained, ++ 10–50% of tumor cells stained, +++ >50% of tumor cells stained, – zero patients

	Juvenile granulosa cell tumor	Sertoli Leydig cell tumor	Sclerosing stromal tumor	Sex cord tumor with annular tubules	Thecoma	Steroid cell tumor
Patients (*n*)	48	14	5	2	2	1
Mitoses/10 HPF (mean, range)*	9.8, 1–47	4.2, 1–23	1.1, 0–3	0.5, 0–1	0.5, 0–1	1
Mitotic activity*						
<10/10 HPF	31	11	5	2	2	1
10–19/10 HPF	8	2	–	–	–	–
≥20/10 HPF	9	1	–	–	–	–
Inhibin (*n*=20)						
0	1	–	–	–	–	–
+	4	1	–	–	–	–
++	9	2	–	–	–	–
+++	2	–	–	1	–	–
Cytokeratin (KL–1, *n*=33)						
0	5	1	–	–	–	–
+	13	1	1	–	1	–
++	4	3	–	–	–	–
+++	3	1	–	–	–	–
Vimentin (*n*=52)						
0	–	–	–	–	–	–
+	12	6	3	1	2	1
++	10	2	–	–	–	–
+++	10	4	1	–	–	–

* Juvenile granulosa cell tumors show higher mean mitotic activity (9.8/10 HPF) than all other histological types (2.7/10 HPF, P=0.001)

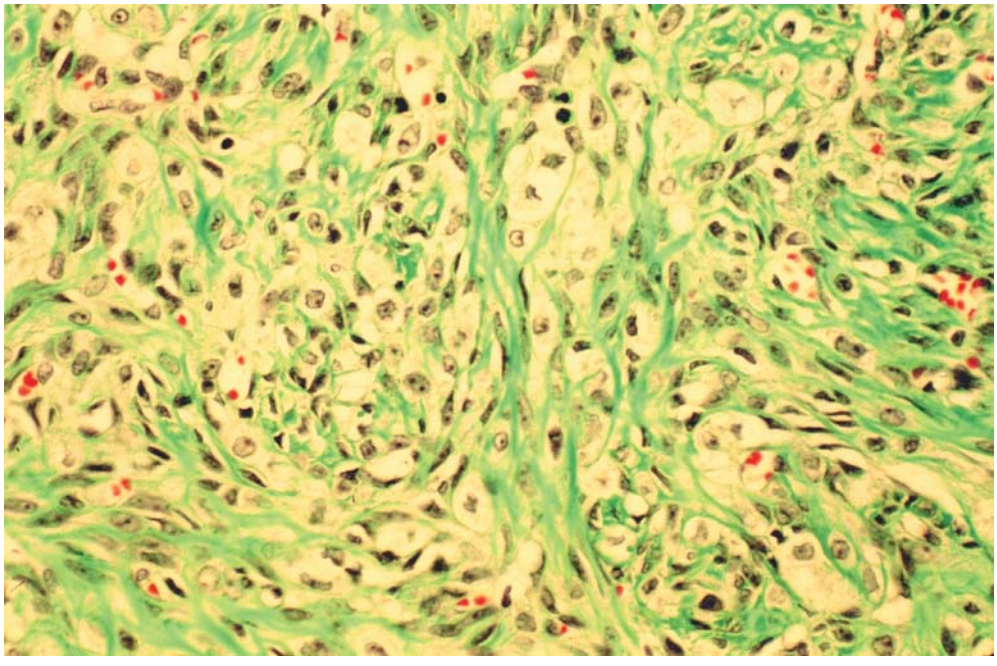

Fig. 5 Sclerosing stromal tumor. Spindle-shaped stromal cells with entrapped lipidized cells (Goldner, original magnification ×280)

ance. Focally, round cells with hyperchromatic nuclei were admixed. In all cases, mitotic activity was low (Table 2).

In some cases, the differential diagnosis between sclerosing stromal tumors and JGCT with pronounced stromal sclerosis was difficult. However, the characteristic vascular pattern and low mitotic activity were used in favor of sclerosing stromal tumor, whereas tumors with follicular structures, higher mitotic activity, and characteristic granulosa cell morphology were rather classified as JGCT.

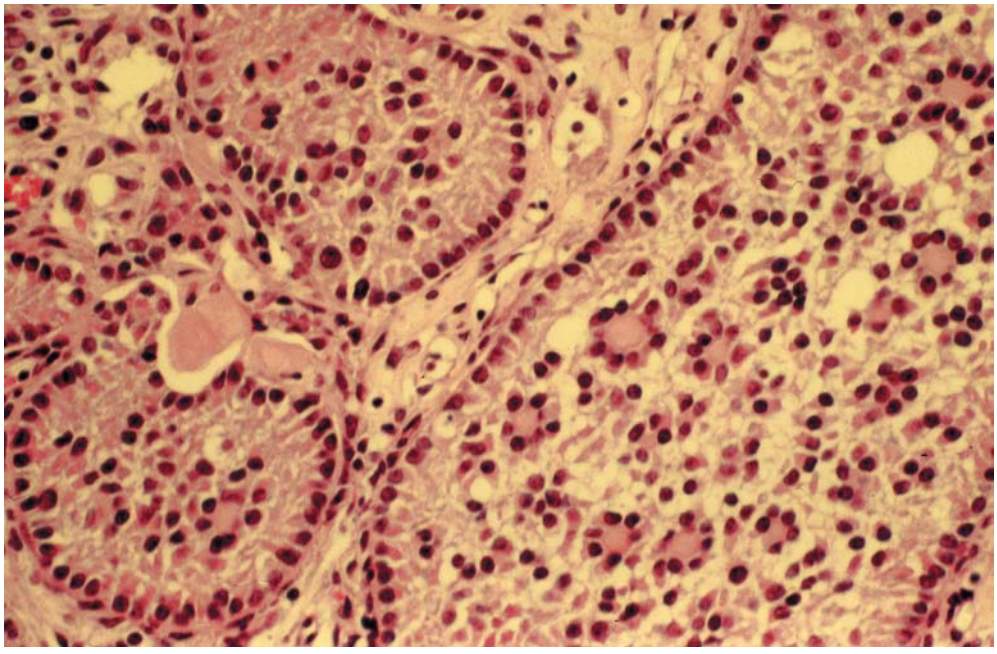

Fig. 6 Sex cord tumor with annular tubules. The tumor cell complexes are lined by cuboid gonadal stromal cells. In the center of the individual tumor cell complexes, small hyaline globules can be seen surrounded by small cells round and dark nuclei (hematoxylin and eosin, original magnification ×280)

Both sex cord tumors with annular tubules showed a cystic appearance and focally displayed the characteristic small tubules filled with homogeneous hyaline eosinophilic material (Fig. 6). In other areas, a cellular differentiation reflecting that of granulosa (in both cases) or Sertoli cells (one case) was noticed. Mitotic activity was low.

The two thecomas contained streaks of elongated cells with small oval nuclei and clear, sometimes vacuolated cytoplasm embedded in a fiber-rich stroma. Mitotic activity was generally low. The one steroid cell tumor contained small nests of cells with small round nuclei with well distinguishable nucleoli and clear cytoplasm. The tumor cell nodules were surrounded by a delicate fibrovascular stroma. Mitotic figures were also rare (1 per 10 HPF).

Immunohistochemistry

The immunohistochemical analysis of OSCST revealed expression of vimentin in all tumors (n=52; Fig. 7a), regardless of the histological subtype. In addition, the majority of OSCST co-expressed cytokeratin (27 of 33) (Fig. 7b). When comparing the intensity of vimentin and cytokeratin staining in individual cases as well as in the whole cohort, vimentin was generally stained more intensely and in a larger proportion of cells than cytokeratin, which was often expressed rather weakly and only in a minority of cells. Inhibin staining was most frequently performed in JGCT in order to distinguish these from malignant ovarian tumors of other types as well as from the ovarian small cell carcinoma of the hypercalcemic type. Inhibin expression was also evaluated in three poorly-differentiated SLCT and in one sex cord tumor with annular tubules. Overall, in 19 of 20 tumors, inhibin expression was found. However, inhibin expression was often limited to only a small proportion of cells (Fig. 7c). The most intensive inhibin expression was seen in one case of sex cord tumor with annular tubules (Fig. 7d).

In 12 tumors, additional immunohistochemical stainings have been performed, in most instances in order to exclude malignant germ cell tumors. However, all stainings for AFP (n=8), placenta-like alkaline phosphatase (n=5) and HCG (n=3) were negative. Additional examinations included smooth muscle antigen that was positive in all four cases examined, progesterone receptor (strongly positive in 2 of 2 cases) and estrogen receptors (positive in 1 of 1 case). Other antibodies, such as chromogranin, S100, neuron-specific enolase (each n=2) did not react.

In 20 cases, tumor proliferation was also assessed by staining with the antibody KiS5 (Fig. 7e), which stains positive in nuclei during the whole cell cycle. The number of nuclei stained positive was highly variable, ranging from 1% to 60% and correlated well with the mitotic activity assessed by counting mitotic figures per 10 HPF. Notably, in some tumors with an only moderate average proliferative activity, some foci with high proliferation up to 75% were seen.

Treatment and clinical outcome

Of patients, 16 underwent ovarectomy, 31 patients uni- (n=28) or bilateral (n=3) adnectomy, and 1 patient hysterectomy (Table 1). Of patients, 9 with JGCT and 3 with poorly differentiated SLCT additionally received adjuvant chemotherapy, which in 11 patients consisted of

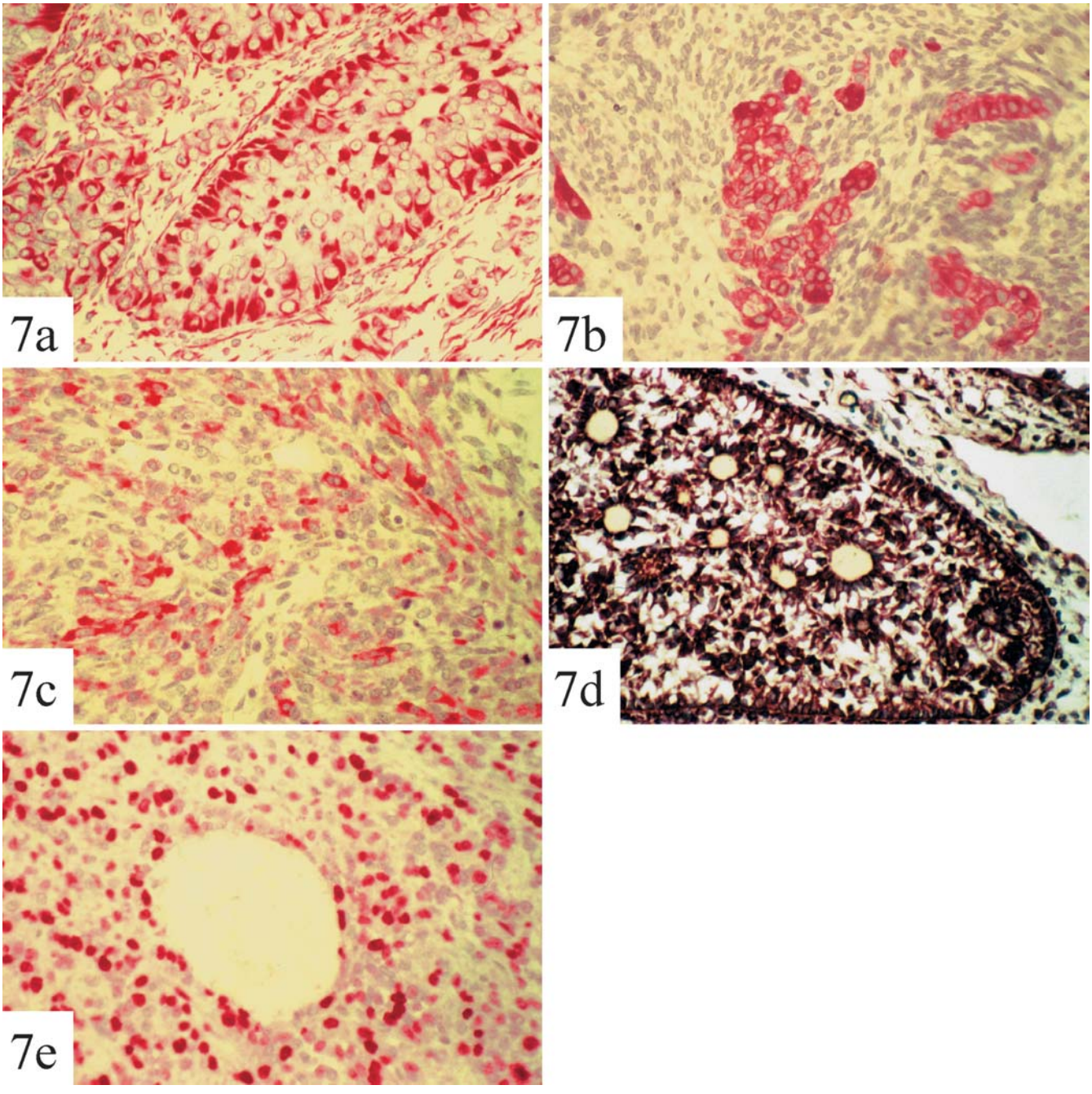

Fig. 7 Characteristic examples of the immunohistochemical investigations. **a** Small Sertoli cell tumor component in a juvenile granulosa cell tumor (JGCT). Strong expression of vimentin by many tumor cells (original magnification ×280). **b** Poorly differentiated Sertoli-Leydig cell tumors (SLCT) (same case as in **c**–**f**). The very immature Sertoli cells are arranged in primitive cords, which intensively stain positive for the monocloncal antibody KL1 against cytokeratin (original magnification ×280). **c** JGCT with scattered inhibin-positive tumors cells (original magnification ×280). **d** Sex cord tumor with annular tubules (same case as in Fig. 6). Most tumor cells are intensively inhibin-positive (original magnification ×280). **e** JGCT with high proliferative activity. Proliferating granulosa cells including cells lining the follicle show strong nuclear positivity for the monoclonal antibody KiS5 (original magnification ×280).

cisplatinum-based combination regimens analogous to the treatment of malignant germ cell tumors and resembled a soft tissue sarcoma-like regimen in 1 patient.

In 43 patients, follow-up data were reported to the MAKEI coordination center. In total, 6 patients suffered a tumor recurrence. Relapses were only seen among poorly-differentiated SLCT and JGCT. Among the latter group, there was 1 girl with a JGCT that developed a contralateral JGCT 126 months after initial diagnosis. This tumor was classified as a metachronous contralateral

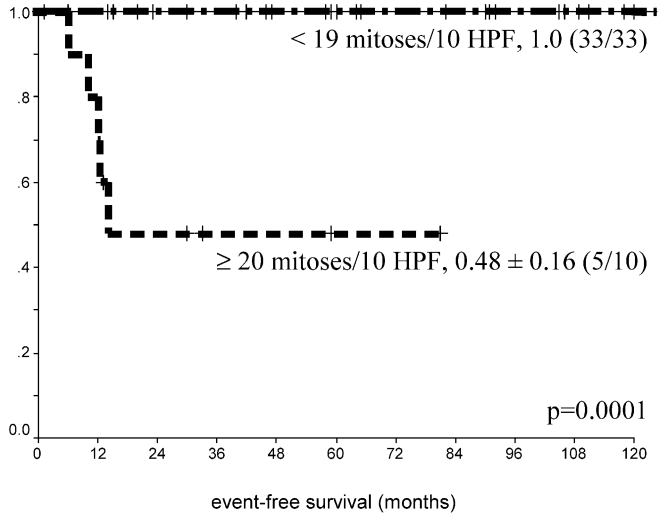

Fig. 8 Kaplan-Meier analysis of event-free survival of patients with ovarian sex cord–stromal tumors correlated with mitotic activity (P=0.0001, log-rank test)

tumor and is therefore not counted as an event in the Kaplan-Meier analysis. EFS at 10 years was 0.88±0.05 (38 of 43 patients). Survival significantly correlated with stage, as all five relapses were observed in patients with stage-Ic or higher tumors. Among the histopathological parameters, mitotic activity significantly correlated with prognosis; all events were seen in tumors that had more than 20 mitoses per 10 HPF at diagnosis. Thus, 5-year EFS for patients with low or moderate mitotic activity according to the criteria defined above was 1.0 (33 of 33 patients) and 0.48±0.16 (5 of 10 patients) for patients with high mitotic activity (P=0.0001) (Fig. 8). Since none of the 5 relapsed patients with high mitotic activity was salvaged with chemotherapy, overall survival of the high mitotic activity group was also low. This also holds true when JGCT and SLCT are analyzed as separate groups: JGCT, EFS 1.0 (26 of 26 patients) versus 0.6±0.18 (5 of 8 patients), P=0.0052; SLCT, EFS 1.0 (4 of 4 patients) versus 0.0 (0 of 2 patients), P=0.06. Other histological or immunohistochemical parameters such as histological subtyping, presence of necrosis, or grading of SLCT did not significantly correlate with outcome on statistical analysis. However, it has to be noted that the number of patients for the analysis of the influence of tumor grade on prognosis in SLCT was low.

Discussion

Sex-specific development of the external and internal genitalia as well as germ cell maturation and fertility heavily depend on fully differentiated and functional sex cord and stromal cells. The heterogeneity of the clinical and morphological appearance of sex cord–stromal tumors reflects the diverse differentiation patterns of gonadal stromal cells in both sexes. However, while the morphology of healthy testes and ovaries is absolutely diverse and characterized by a sex-specific pattern of terminally differentiated stromal cells, the appearance of sex cord–stromal cells in the testis and the ovary is strikingly similar. In fact, differentiation patterns can be seen in testicular sex cord–stromal tumors (TSCST) and OSCST that diverge from the sex-specific differentiation pathways. For instance, Sertoli-Leydig cell tumors can develop in the ovary, while granulosa cell tumors—especially their juvenile variant—may arise in the testis. These observations indicate a pluripotent and sex-ambivalent differentiation potential of the tumor cells. Conversely, other histological subtypes of OSCST show a clear sex association. While tumors of the thecoma–fibroma group rarely develop in the testis, typical examples of large-cell-calcifying Sertoli cell tumors (to the best of our knowledge) have not been reported in the ovarian location.

The homology between testicular and ovarian sex cord–stromal tumors, which has already been described by Teilum [25], as well as the finding that composite tumors (e.g., JGCT with focal Sertoli differentiation) may occur (Fig. 3e), suggests that OSCST and TSCST may develop from a yet undefined stromal stem cell with a broad differentiation potential. This hypothesis could be tested by genetic studies if such analyses find similar genetic patterns in the different histological subgroups. However, no such studies have been published to date.

In conclusion, the sex correlation suggests that—to a certain extent—physiological differentiation patterns might persist in the transformed stromal cell, whereas the age dependence may indicate an influence of the sex-specific "macro-environment", e.g., the hormone status, on the histological differentiation.

Sex cord–stromal tumors can be considered dysembryogenetic tumors. In this context, one has to remember that sex cord–stromal tumors may be associated with a broad range of developmental abnormalities, such as testicular maldescensus, constitutional sex chromosomal abnormalities, and intersexual genitalia [32]. This series adds the Zuelzer Wilson's syndrome to the list of syndromes associated with OSCST. Moreover, sex cord–stromal tumors can develop in patients who suffer from constitutional syndromes associated with an increased cancer risk, such as Ollier's disease [14], Peutz-Jegher's syndrome [28], and Carney complex [24]. This indicates that the gonadal stroma may be sensitive to pertubances in tumor suppressor pathways. However, further molecular genetic studies are necessary to elucidate the physiological and pathophysiological role of such pathways in gonadal stromal cells.

This and other immunohistochemical studies substantiate the interpretation of sex cord–stromal tumors as dysembryogenetic tumors. In this study and in our previous analysis of TSCST, we observed a high frequency of co-expression of vimentin and cytokeratins. Physiologically, vimentin is the basic intermediate filament of Sertoli cells, but co-expression of vimentin and cytokeratins is regularly seen in fetal testes [8, 19]. In

analogy, co-expression of vimentin and cytokeratins can be observed only in more immature granulosa cells of primordial follicles, while cytokeratin expression gets lost during granulosa cell development in mature follicles [2, 5]. Thus, SLCT and JGCT display immunological characteristics of immature Sertoli cells and granulosa cells, respectively.

Despite the clinical and morphological differences between TSCST and OSCST as well as between SCLT and JGCT, similar therapeutic strategies can be successfully applied in these tumors. In general, the vast majority of sex cord–stromal tumors present as localized tumors limited to the gonad [9, 30, 31]. In this situation, complete resection constitutes the therapy of choice, and there is no role for adjuvant chemotherapy [30, 31]. However, in OSCST there is a small group of tumors that presents at advanced stages, and in these tumors, adjuvant cisplatin-based chemotherapy may help to achieve long-lasting complete remissions [3, 21]. Therapeutic decisions can be made with regard to tumor stage and completeness of resection. Notably, this analysis reveals that histopathological features such as mitotic activity may provide additional information that may be helpful in risk-assessment of advanced tumors. Our data show that advanced tumors with high mitotic activity have a significantly higher risk of recurrence and fatal outcome than those with low mitotic activity (Fig. 8).

In adult granulosa cell tumors, the prognostic impact of mitotic activity and immunohistochemical proliferation markers such as KI67 have already been reported [6]. However, the cut-off level for prognostically unfavorable tumors was at about 4 mitoses per 10 HPF or 1.2% Ki67 positivity, respectively, which therefore was much lower than in our series [6, 11, 13]. In fact, such levels were well below average in our series of JGCT and SLCT, suggesting that these juvenile tumors have an overall higher proliferative activity than their adult counterparts, without per se affecting prognosis. In this context it is also important to note that in contrast to adult granulosa cell tumors, which usually show low proliferative activity, JGCT seem to show a lower risk of late recurrences [30]. In our series, we saw only one patient who developed a contralateral metachronous JGCT after more than 10 years follow-up. However, this tumor should be considered a true metachronous second tumor and not a late tumor relapse.

It must be pointed out that completely resected stage-Ia tumors should not be treated with adjuvant chemotherapy just in view of high proliferative activity. Our analysis suggests that the evaluation of the mitotic rate might help to define those patients with stage-Ic tumors who have a high risk of relapse. These patients could benefit from early implementation of adjuvant chemotherapy in situations with only microscopic tumor dissemination. In addition, the assessment of the mitotic activity also indicates those stage-II to -III patients with macroscopic metastases that respond poorly to adjuvant chemotherapy and may therefore be in need of alternative therapeutic strategies (e.g., locoregional hyperthermia [27]). Therefore, the evaluation of the mitotic activity may be an important tool in the risk assessment and therapeutic stratification of OSCST in future prospective protocols.

In summary, this and the previous analysis from the Kiel Pediatric Tumor Registry reveal both the common and divergent features of ovarian and testicular sex cord–stromal tumors. While testicular and ovarian sex cord–stromal tumors during childhood and adolescence show a striking homology, they must clearly be distinguished from those of the adult type, such as adult granulosa cell tumors, which show distinct clinical and biological characteristics. The homology of sex cord–stromal tumors in both sexes, the existence of composite tumors, and the immunohistochemical profiles support the hypothesis that these tumors develop from an immature gonadal stromal stem cells with a pluripotent differentiation potential. Further genetic studies are necessary to evaluate the molecular basis of malignant transformation as well as physiological and pathological differentiation of gonadal stromal cells. In addition, the biological relevance of the association of sex cord–stromal tumors with inherited disorders needs to be clarified. Last, this study outlines minimum diagnostic standards in the pathological evaluation of sex cord–stromal tumors. This should always include assessment of mitotic activity, as this parameter appears to be prognostically relevant and could be an important tool for the identification of high-risk patients in therapeutic protocols that use risk-adapted therapeutic strategies.

Acknowledgments The authors thank all pathologists that contributed samples to the Kiel Pediatric Tumor Registry. The authors also thank the Deutsche Krebshilfe e.V. for the support of the German Germ Cell Tumor program. The authors thank Irene Kiekbusch, Frantzel Rahlf, and Susanne Koch for secretarial work and data management. The authors wish to thank Dr. Martin Vogel, Institute of Paidopathology and Placentology, Rudolph-Virchow University Hospital, Berlin, for the photograph of the macroscopic aspect of a juvenile granulosa cell tumor. Last, the authors gratefully appreciate Dr. Aleksander Talerman, Thomas Jefferson University, Philadelphia, for critical review of ovarian neoplasms and inspiring discussions during his visit to the Kiel Pediatric Tumor Registry.

References

1. Benedet JL, Bender H, Jones H, III, Ngan HY, Pecorelli S (2000) FIGO staging classifications and clinical practice guidelines in the management of gynecologic cancers. FIGO Committee on Gynecologic Oncology. Int J Gynaecol Obstet 70:209–262
2. Benjamin E, Law S, Bobrow LG (1987) Intermediate filaments cytokeratin and vimentin in ovarian sex cord–stromal tumours with correlative studies in adult and fetal ovaries. J Pathol 152:253–263
3. Calaminus G, Wessalowski R, Harms D, Göbel U (1997) Juvenile granulosa cell tumors of the ovary in children and adolescents: results from 33 patients registered in a prospective cooperative study. Gynecol Oncol 65:447–452
4. Cronje HS, Niemand I, Bam RH, Woodruff JD (1998) Granulosa and theca cell tumors in children: a report of 17 cases and literature review. Obstet Gynecol Surv 53:240–247

5. Czernobilsky B, Moll R, Levy R, Franke WW (1985) Co-expression of cytokeratin and vimentin filaments in mesothelial, granulosa and rete ovarii cells of the human ovary. Eur J Cell Biol 37:175–190
6. Fujimoto T, Sakuragi N, Okuyama K, Fujino T, Yamashita K, Yamashiro S, Shimizu M, Fujimoto S (2001) Histopathological prognostic factors of adult granulosa cell tumors of the ovary. Acta Obstet Gynecol Scand 80:1069–1074
7. Gershenson DM, Morris M, Burke TW, Levenback C, Matthews CM, Wharton JT (1996) Treatment of poor-prognosis sex cord–stromal tumors of the ovary with the combination of bleomycin, etoposide, and cisplatin. Obstet Gynecol 87:527–531
8. Groisman GM, Dische MR, Fine EM, Unger PD (1993) Juvenile granulosa cell tumor of the testis: a comparative immunohistochemical study with normal infantile gonads. Pediatr Pathol 13:389–400
9. Harms D, Kock LR (1997) Testicular juvenile granulosa cell and Sertoli cell tumours: a clinicopathological study of 29 cases from the Kiel Paediatric Tumour Registry. Virchows Arch 430:301–309
10. Hussong J, Crussi FG, Chou PM (1997) Gonadoblastoma: immunohistochemical localization of Mullerian-inhibiting substance, inhibin, WT-1, and p53. Mod Pathol 10:1101–1105
11. Juric G, Zarkovic N, Nola M, Tillian M, Jukic S (2001) The value of cell proliferation and angiogenesis in the prognostic assessment of ovarian granulosa cell tumors. Tumori 87:47–53
12. Kudelka AP, Vasuratna A, Edwards CL, Augustine K, Benjapibal M, Verschraegen CF, Kavanagh JJ (1998) Gemcitabine after bone marrow transplantation for refractory juvenile granulosa cell tumor. Anticancer Drugs 9:621–623
13. Miller BE, Barron BA, Wan JY, Delmore JE, Silva EG, Gershenson DM (1997) Prognostic factors in adult granulosa cell tumor of the ovary. Cancer 79:1951–1955
14. Plantaz D, Flamant F, Vassal G, Chappuis JP, Baranzelli MC, Bouffet E, Dyon JF, Armari C, Bost M (1992) Granulosa cell tumors of the ovary in children and adolescents. Multicenter retrospective study in 40 patients aged 7 months to 22 years. Arch Fr Pediatr 49:793–798
15. Powell JL, Otis CN (1997) Management of advanced juvenile granulosa cell tumor of the ovary. Gynecol Oncol 64:282–284
16. Powell JL, Johnson NA, Bailey CL, Otis CN (1993) Management of advanced juvenile granulosa cell tumor of the ovary. Gynecol Oncol 48:119–123
17. Powell JL, Connor GP, Henderson GS (2001) Management of recurrent juvenile granulosa cell tumor of the ovary. Gynecol Oncol 81:113–116
18. Riopel MA, Perlman EJ, Seidman JD, Kurman RJ, Sherman ME (1998) Inhibin and epithelial membrane antigen immunohistochemistry assist in the diagnosis of sex cord–stromal tumors and provide clues to the histogenesis of hypercalcemic small cell carcinomas. Int J Gynecol Pathol 17:46–53
19. Rogatsch H, Jezek D, Hittmair A, Mikuz G, Feichtinger H (1996) Expression of vimentin, cytokeratin, and desmin in Sertoli cells of human fetal, cryptorchid, and tumour-adjacent testicular tissue. Virchows Arch. 427:497–502
20. Russell P, Robboy SJ, Anderson MC (2002) Ovarian tumors: classification and clinical perspectives. In: Robboy et al. S.J. (eds) Pathology of the female reproductive tract. Churchill Livingstone, London, pp 527–538
21. Schneider DT, Calaminus G, Wessalowski R, Pathmanathan R, Harms D, Göbel U (2002) Therapy of advanced ovarian juvenile granulosa cell tumors. Klin Pädiatr 214:173–178
22. Scully RE (1977) Sex cord–stromal tumors. In: Blaustein A (ed) Pathology of the female genital tract. Springer, Berlin Heidelberg New York
23. Scully RE (2002) Histological typing of ovarian tumours. Springer, Berlin Heidelberg New York
24. Stratakis CA, Kirschner LS, Carney JA (2001) Clinical and molecular features of the Carney complex: diagnostic criteria and recommendations for patient evaluation. J Clin Endocrinol Metab 86:4041–4046
25. Teilum G (1971) Special tumors of ovary and testis. Munksgaard, Copenhagen
26. Vassal G, Flamant F, Caillaud JM, Demeocq F, Nihoul-Fekete C, Lemerle J (1988) Juvenile granulosa cell tumor of the ovary in children: a clinical study of 15 cases. J Clin Oncol 6:990–995
27. Wessalowski R, Spaar HJ, Pape H, Willers R, Harms D, Göbel U (1995) Successful liver treatment of a juvenile granulosa cell tumor in a 4-year-old child by regional deep hyperthermia, systemic chemotherapy, and irradiation. Gynecol Oncol 57:417–422
28. Westerman AM, Wilson JH (1999) Peutz-Jeghers syndrome: risks of a hereditary condition. Scand J Gastroenterol Suppl 230:64–70
29. Yamashita K, Yamoto M, Shikone T, Minami S, Imai M, Nishimori K, Nakano R (1997) Production of inhibin A and inhibin B in human ovarian sex cord stromal tumors. Am J Obstet Gynecol 177:1450–1457
30. Young RH, Dickersin GR, Scully RE (1984) Juvenile granulosa cell tumor of the ovary. A clinicopathological analysis of 125 cases. Am J Surg Pathol 8:575–596
31. Young RH, Scully RE (1985) Ovarian Sertoli-Leydig cell tumors. A clinicopathological analysis of 207 cases. Am J Surg Pathol 9:543–569
32. Young RH, Lawrence WD, Scully RE (1985) Juvenile granulosa cell tumor–another neoplasm associated with abnormal chromosomes and ambiguous genitalia. A report of three cases. Am J Surg Pathol 9:737–743

Virchows Arch (2003) 443:561–564
DOI 10.1007/s00428-003-0874-3

ORIGINAL ARTICLE

Razvan Besleaga · Manuel Montesinos-Rongen · Jordi Perez-Tur · Reiner Siebert · Martina Deckert

Expression of the *LGI1* gene product in astrocytic gliomas: downregulation with malignant progression

Received: 2 February 2003 / Accepted: 26 June 2003 / Published online: 26 August 2003
© Springer-Verlag 2003

Abstract Loss of heterozygosity in the long arm of chromosome 10q is a frequent event in gliomas. It may involve the *LGI1/epitempin* gene, which is located in chromosomal region 10q23~24 and has been proposed to encode a tumor suppressor inactivated in the progression of brain tumors. Nevertheless, so far no data are available demonstrating that the reduced expression of the LGI1 transcript in high-grade astrocytic tumors indeed results in a decreased level of LGI1 protein in the tumor cells. Thus, the aim of the present study was to analyze the expression of the LGI1 protein in a series (ten of each) of pilocytic astrocytomas, astrocytomas [World Health Organization (WHO) grade II], anaplastic astrocytomas (WHO grade III), and glioblastoma multiforme (WHO grade IV). Immunohistochemistry demonstrated a strong expression of the LGI1 protein in normal brain tissue as well as in the majority of pilocytic astrocytomas and astrocytomas (WHO grade II). In anaplastic astrocytomas, the number of tumor cells expressing LGI1 decreased, while LGI1 expression was completely absent from the glioblastomas of this series. This highly significant reduction of LGI1 protein expression in the progression of astrocytic brain tumors lends further support to the hypothesized function of *LGI1* as a type-II tumor suppressor gene in glioma pathogenesis.

Keywords *LGI1* · Glioma · Pathogenesis · Tumor suppressor gene

R. Besleaga · M. Montesinos-Rongen · M. Deckert
Abteilung für Neuropathologie,
Universitätsklinikum Köln, Köln, Germany

J. Perez-Tur
Unitat de Genetica Molecular,
Instituto de Biomedicina de Valencia-CSIC, Valencia, Spain

R. Siebert
Institut für Humangenetik,
Universitätsklinikum Schleswig-Holstein Campus Kiel,
Kiel, Germany

M. Deckert (✉)
Abteilung für Neuropathologie,
Universitätsklinikum Köln,
Joseph-Stelzmann-Strasse 9, 50924 Köln, Germany
e-mail: neuropatho@uni-koeln.de
Tel.: +49-221-4785265
Fax: +49-221-4787237

Introduction

Genetic alterations of chromosome 10 play a major role in the development of glioblastoma, and deletions in 10q23~24, which may also affect genes distal to *PTEN*, can be detected in 80% of glioblastomas [4]. Thus, one may consider that inactivation of a tumor suppressor gene in this region may contribute to malignant progression of astrocytic tumors. In addition to the candidate tumor suppressor genes *PTEN/MMAC* and *DMBT* mapping to chromosomal bands 10q23 and 10q25, respectively, the leucine-rich repeat-glioma-inactivated (*LGI1*) gene was identified at 10q24 by means of breakpoint cloning in a glioblastoma cell line [1, 2, 10]. Subsequently, although the *LGI1/epitempin* gene was found to be only very infrequently rearranged or mutated in malignant brain tumors [2, 8], Northern blot and reverse-transcription polymerase chain reaction (RT-PCR) studies revealed reduced levels of LGI1 mRNA in glioma cell lines and malignant gliomas compared with normal brain tissue [2, 8]. However, information on the expression of the *LGI1* gene product is not yet available. To address this open question, which is crucial considering the reported poor correlation between transcript and protein levels of many genes, we have analyzed the expression of the LGI1 protein in a series of low-grade and high-grade astrocytic gliomas using immunohistochemistry and demonstrated a gradual downregulation of the *LGI1* gene product with increasing grade of malignancy. Thus, these data lend further support to the concept of *LGI1* as a tumor suppressor gene in gliomas.

Materials and methods

Ten pilocytic astrocytomas, ten astrocytomas [World Health Organization (WHO) grade II], ten anaplastic astrocytomas (WHO grade III), and ten cases of glioblastoma multiforme (WHO grade IV) were evaluated. Age, sex, and localization of the tumors are presented in Table 1.

Table 1 Median age, sex distribution, and localization of the gliomas studied. *PA* pilocytic astrocytoma, *AII* astrocytoma [World Health Organization (WHO grade II)], *AA* anaplastic astrocytomas (WHO grade III), *GB* glioblastoma multiforme

Case no.	Diagnosis	Sex	Age (years)	Localization
1	PA	Male	18	Medulla
2	PA	Male	6	Cerebellum
3	PA	Female	6	Thalamus
4	PA	Female	22	Hypothalamus
5	PA	Female	3	Cerebellum
6	PA	Male	40	Cerebellum
7	PA	Male	23	Optic nerve
8	PA	Male	6	Cerebellum
9	PA	Male	15	Thalamus
10	PA	Male	9	Cerebellum
11	AII	Female	34	Fronto-temporal lobe
12	AII	Female	59	Occipital lobe
13	AII	Male	34	Frontal lobe
14	AII	Female	34	Frontal lobe
15	AII	Female	27	Fronto-temporal lobe
16	AII	Male	23	Insular region
17	AII	Female	28	Parieto-occipital lobe
18	AII	Male	45	Fronto-temporal lobe
19	AII	Female	32	Temporo-parietal lobe
20	AII	Female	39	Parieto-occipital lobe
21	AA	Male	53	Fronto-lateral lobe
22	AA	Male	29	Frontal lobe
23	AA	Female	34	Temporal lobe
24	AA	Male	34	Frontal lobe
25	AA	Female	48	Frontal lobe
26	AA	Female	35	Fronto-temporal lobe
27	AA	Male	51	Frontal lobe
28	AA	Male	37	Occipital lobe
29	AA	Female	44	Frontal lobe
30	AA	Female	29	Frontal lobe
31	GB	Male	48	Fronto-temporal lobe
32	GB	Female	64	Temporo-occipital lobe
33	GB	Male	62	Temporal lobe
34	GB	Male	35	Temporal lobe
35	GB	Female	48	Temporal lobe
36	GB	Male	72	Fronto-temporal lobe
37	GB	Male	30	Temporal lobe
38	GB	Male	72	Temporal lobe
39	GB	Female	65	Parieto-occipital lobe
40	GB	Male	66	Parieto-occipital lobe

Immunohistochemistry to detect the LGI1 protein was performed on 4-μm paraffin sections using an avidin biotin complex protocol as described previously [3, 9]. P01C258 antiserum, obtained by immunization of rabbits with LGI1 N-terminal synthetic peptide (positions 201–220), EGPPEYKKRKINSLSSKDFD, was used as primary antibody [9]. The specificity of this serum has been previously shown [9]. In brain sections, the serum yields immunostainings comparable to those obtained with an antiserum directed to another epitope of LGI1 [9]. Normal brain tissue from the frontal and temporal lobes of autopsy cases served as control.

To assess LGI1 immunoreactivity, the following semi-quantitative grading system was employed: negative, <10% of tumor cells positive, 10–50% of tumor cells positive, >50–90% of tumor cells positive, and >90% of tumor cells positive for LGI1 protein, respectively (Table 2). Statistical comparisons between subgroups of tumors were performed using Kruskal-Wallis non-parametric test followed by Mann-Whitney U-test with Bonferroni correction as well as Fisher's Exact Test.

Results

In the normal brain, LGI1 protein was strongly expressed in cortical neurons, which is in agreement with data from Gu et al. [6], who identified pyramidal neurons of the cortex as a major cellular source of the LGI1 protein. Among the series of astrocytic gliomas, LGI1 was expressed in the highly differentiated tumors, and its expression declined with increasing grade of anaplasia (Fig. 1). Of pilocytic astrocytomas, 80% (eight of ten) expressed the LGI1 protein, and five of the eight LGI1-positive pilocytic astrocytomas contained more than 50% positive cells. In addition, 80% (eight of ten) of astrocytomas (WHO grade II) were positive for LGI1. Among eight LGI1-expressing tumors, seven had more than 50% of LGI1-positive tumor cells, and one of these tumors even exhibited more than 90% of LGI1-positive tumor cells. While 90% (nine of ten) of the anaplastic astrocytomas (WHO grade III) expressed the LGI1 protein, the fraction of tumor cells that showed a positive immunoreactivity for LGI1 had markedly decreased compared with pilocytic astrocytomas and astrocytomas (WHO grade II). In five of the nine anaplastic astrocytomas (WHO grade III) that expressed the LGI1 protein, the fraction of LGI1-positive tumor cells ranged from 10% to 50%, and in three of these nine tumors fewer than 10% of the tumor cells were LGI1 positive. In marked contrast, the LGI1 protein was not expressed in any of the ten glioblastomas analyzed (Fig. 1, Table 1). Based on these data, there is a highly significant difference in LGI1 expression among the histological subgroups, indicating a

Table 2 Semi-quantitative assessment of the expression of the *LGI1* gene product. In two different samples derived from the normal frontal and temporal lobe >90% of neurons expressed the LGI1 protein. *WHO* World Health Organization

Percentage of LGI1-expressing tumor cells	Pilocytic astrocytoma (WHO grade I)	Astrocytoma (WHO grade II)	Anaplastic astrocytoma (WHO grade III)	Glioblastoma multiforme (WHO grade IV)
>90%	0	1	0	0
>50–90%	5	6	1	0
10–50%	3	1	5	0
<10%	0	0	3	0
Negative	2	2	1	10

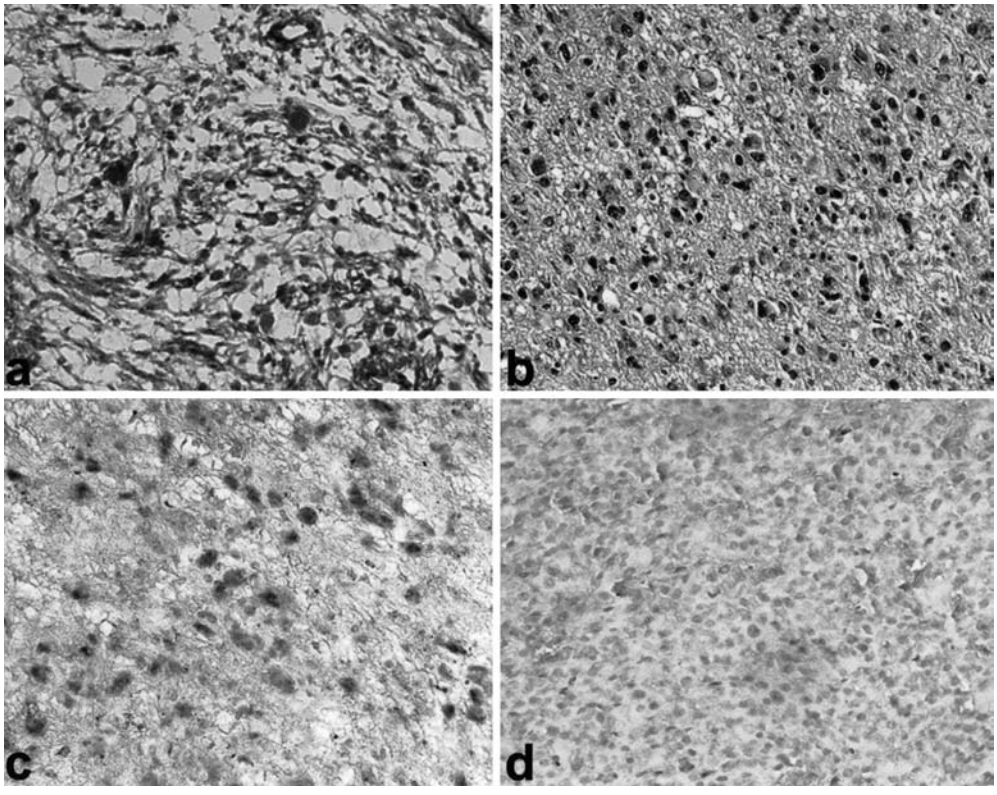

Fig. 1 Expression of the LGI1 protein in astrocytic gliomas. **a** Strong LGI1 expression in tumor cells of a pilocytic astrocytoma. **b** Marked LGI1 expression in a fibrillary astrocytoma (WHO grade II). **c** In contrast to well-differentiated astrocytomas (**a**, **b**), the number of LGI1-positive tumor cells in an anaplastic astrocytoma (WHO grade III) is low (<50%). **d** Absence of LGI1 immunoreactivity in glioblastoma multiforme. **a**–**d** Immunohistochemistry with rabbit anti-LGI1 antiserum detected using 3,3′-diaminobenzidine and H_2O_2 as co-substrate, slight counterstaining with hemalum; ×200

declining expression linked with malignant progression (P<0.001; Kruskal-Wallis test). According to the Mann-Whitney U-test, there was no overall significant difference in LGI1 expression among pilocytic astrocytomas, astrocytomas (WHO grade II), and anaplastic astrocytomas (WHO grade III). Nevertheless, the frequency of pilocytic astrocytomas and astrocytomas (WHO grade II) with more than 50% of LGI1-expressing tumor cells was significantly higher (12/20) than either anaplastic astrocytoma (1/10; P=0.011), glioblastoma (0/10; P=0.001), or higher malignant astrocytic tumors in general (1/20; P<0.001) by Fisher's exact test. Moreover, complete lack of LGI1 expression was significantly more frequent in glioblastoma (10/10) than in anaplastic astrocytoma (1/10; P<0.001) or lower malignant astrocytic tumors in general (5/30; P<0.001). This was also shown by Bonferroni corrected Mann-Whitney U-test, which revealed a highly reduced expression of LGI1 in glioblastoma multiforme compared with the other groups (P=0.002, P=0.002, and P<0.001 for pilocytic astrocytomas, astrocytomas (WHO grade II), and anaplastic astrocytomas, respectively.

Discussion

The present study demonstrates a highly significant gradual decline of the *LGI1* gene product expression in parallel with increasing malignancy in astrocytic gliomas. This was evidenced by a strong expression of the LGI1 protein in the vast majority of the tumor cells in pilocytic astrocytomas, astrocytomas (WHO grade II), as well as in a subset of tumor cells of anaplastic astrocytomas. In contrast, there was no evidence for any expression of the *LGI1* gene product in glioblastoma multiforme. These observations extend recent Northern blot and RT-PCR studies, which demonstrated low levels or complete absence of *LGI1* transcripts in 12 of 15 (80%) and 3 of 15 (20%) primary glioblastomas, respectively, as well as very low levels of transcription in 10 of 11 glioblastoma cell lines [2, 8]. In contrast, a heterogeneous group of low-grade gliomas, including pilocytic astrocytomas, astrocytomas (WHO grade II), and oligodendrogliomas (WHO grade II) had decreased, but clearly detectable, LGI1 mRNA levels as compared with the normal brain [2]. Taking the mRNA and protein studies together, there is a close correlation between mRNA and protein levels with a striking downregulation with increasing malignancy. Thus, these data favor the hypothesis of *LGI1* as a tumor suppressor gene, thereby possibly contributing to glioma pathogenesis. However, although the *LGI1* gene was found to be rearranged or translocated in some glioblastoma cell lines [2, 10], studies employing fluorescence in situ hybridization analysis and gene sequencing revealed that mutations or translocations of the *LGI1* gene were rare events in both glioblastoma cell lines and malignant gliomas [8]. Moreover, aberrant methylation of the LGI1 promoter was excluded as a mode of silencing of this gene [8]. Finally, the incidence of malignant tumors is not increased in individuals with hereditary germline mutations, which lead to a rare epilepsy disorder, i.e., the autosomal-dominant partial epilepsy

with auditory features [5, 6, 7, 9]. Taking these observations together, *LGI1* seems to act as a type-II tumor suppressor rather than a classical tumor suppressor. Considering the existence of several *LGI1*-related genes in other parts of the human genome proposed to harbor tumor suppressor genes, e.g., *LGI3* in 8p21 [11], future studies should attempt to unravel the hitherto unknown functions and precise mechanisms of *LGI1* inactivation in brain tumorigenesis.

Acknowledgements The authors wish to thank Drs. M. Plomann and J.I. Martin-Subero for help with antibody purification and with statistical analyses as well as H.U. Klatt for photographic help. The studies of R.S. on tumor suppressor genes in 10q24 and LGI1 changes in neurological diseases are supported by the Deutsche Krebshilfe and the Hensel-Stiftung Kiel, respectively. The work of J.P-T. is supported by the Ministerio de Ciencia y Technologia (grant SAF 2002-00060). J.P-T. and R.S. are members of the European Collaborative Consortium on the study of ADLTE. R.B., from the Colentina Clinical Hospital, Department of Neurology, Bucharest is a fellow of the EURON Ph.D. program.

References

1. Chernova O, Cowell JK (1998) Molecular definition of chromosome translocations involving 10q24 and 19q13 in human malignant glioma cells. Cancer Genet Cytogenet 105:60–68
2. Chernova OB, Somerville RP, Cowell JK (1998) A novel gene, LGI1, from 10q24 is rearranged and downregulated in malignant brain tumors. Oncogene 17:2873–2881
3. Deckert-Schlüter M, Rang A, Wiestler OD (1998) Apoptosis and apoptosis-related gene products in primary non-Hodgkin's lymphoma of the central nervous system. Acta Neuropathol (Berl) 96:157–162
4. Fujisawa H, Reis RM, Nakamura M, Colella S, Yonekawa Y, Kleihues P, Ohgaki H (2000) Loss of heterozygosity on chromosome 10 is more extensive in primary (de novo) than in secondary glioblastomas. Lab Invest 80:65–72
5. Gu W, Brodtkorb E, Steinlein OK (2002) LGI1 is mutated in familial temporal lobe epilepsy characterized by aphasic seizures. Ann Neurol 52:364–367
6. Gu W, Wevers A, Schröder H, Grzeschik KH, Derst C, Brodtkorb E, de Vos R, Steinlein OK (2002) The LGI1 gene involved in lateral temporal lobe epilepsy belongs to a new subfamily of leucine-rich repeat proteins. FEBS Lett 519:71–76
7. Kalachikov S, Evgrafov O, Ross B, Winawer M, Barker-Cummings C, Martinelli Boneschi F, Choi C, Morozov P, Das K, Teplitskaya E, Yu A, Cayanis E, Penchaszadeh G, Kottmann AH, Pedley TA, Hauser WA, Ottman R, Gilliam TC (2002) Mutations in LGI1 cause autosomal-dominant partial epilepsy with auditory features. Nat Genet 30:335–341
8. Krex D, Hauses M, Appelt H, Mohr B, Ehninger G, Schackert HK, Schackert G (2002) Physical and functional characterization of the human LGI1 gene and its possible role in glioma development. Acta Neuropathol (Berl) 103:255–266
9. Morante-Redolat JM, Gorostidi-Pagola A, Piquer-Sirerol S, Saenz A, Poza JJ, Galan J, Gesk S, Sarafidou T, Mautner VF, Binelli S, Staub E, Hinzmann B, French L, Prud'homme JF, Passarelli D, Scannapieco P, Tassinari CA, Avanzini G, Marti-Masso JF, Kluwe L, Deloukas P, Moschonas NK, Michelucci R, Siebert R, Nobile C, Perez-Tur J, Lopez de Munain A (2002) Mutations in the LGI1/Epitempin gene on 10q24 cause autosomal dominant lateral temporal epilepsy. Hum Mol Genet 11:1119–1128
10. Somerville RP, Chernova O, Liu S, Shoshan Y, Cowell JK (2000) Identification of the promoter, genomic structure, and mouse ortholog of LGI1. Mamm Genome 11:622–627
11. Staub E, Perez-Tur J, Siebert R, Nobile C, Moschonas NK, Deloukas P, Hinzmann B (2002) The novel EPTP repeat defines a superfamily of proteins implicated in epileptic disorders. Trends Biochem Sci 27:441–444

Virchows Arch (2003) 443:565–573
DOI 10.1007/s00428-003-0842-y

ORIGINAL ARTICLE

Manabu Nagata · Noriharu Shijubo · Andrew F Walls · Shingo Ichimiya · Shosaku Abe · Noriyuki Sato

Chymase-positive mast cells in small sized adenocarcinoma of the lung

Received: 3 February 2003 / Accepted: 20 May 2003 / Published online: 25 June 2003
© Springer-Verlag 2003

Abstract Mast cells accumulate in angiogenesis-dependent situations of lung adenocarcinoma. Human mast cells are divided into two major subsets: MC_T (mast cells with immunoreactivity for tryptase but not chymase) and MC_{TC} (reactive for tryptase and chymase). Chymase is an important mediator of tissue remodeling, but research into chymase-containing mast cell subpopulations has been hampered by the lack of reagents suitable for use with formalin-fixed tissue. We stained chymase using CC1 antibody in 66 cases of small sized lung adenocarcinoma as well as CD34 and tryptase. There were significant positive correlations of microvessel counts with MC_T-type and MC_{TC}-type mast cell counts in lung adenocarcinomas. When analyzed according to Noguchi's classification, MC_T-type and MC_{TC}-type mast cells were significantly increased in Noguchi type-C tumors [localized bronchioloalveolar carcinoma (LBAC) with active fibroblastic proliferation] compared with in Noguchi type-A (LBAC) plus type-B tumors (LBAC with alveolar collapse). Members in the high-count group of MC_{TC}-type but not MC_T-type mast cells showed a significantly worse outcome than those in the low-count group in LBACs. Counting chymase-positive (MC_{TC}-type) mast cells in tumor stroma may be a good prognosis predictor for LBACs, especially Noguchi type-C tumors.

Keywords Tissue remodeling · Non-small cell lung cancer · MC_{TC} · Microvessel counts · Tryptase · Chymase

M. Nagata · N. Shijubo · S. Abe
Third Department of Internal Medicine,
Sapporo Medical University School of Medicine,
South-1, West-16 Chuo-ku, 060-8543 Sapporo, Japan

S. Ichimiya · N. Sato
Department of Pathology,
Sapporo Medical University School of Medicine,
South-1, West-16 Chuo-ku, 060-8543 SapporoJapan

N. Shijubo (✉)
Department of Respiratory Medicine,
Sapporo Hospital, Hokkaido Railways Company,
North-3, East-1 Chuo-ku, 060-0033 Sapporo, Japan
e-mail: shijubo@jrsapporohosp.com
Tel.: +81-11-2414971
Fax: +81-11-2229260

A. F. Walls
Immunopharmacology Group,
University of Southampton, General Hospital,
Tremona Road, Southampton, S016 6YD, UK

Introduction

Mast cell accumulation is strongly associated with angiogenesis [21, 24, 26, 28]. Mast cells produce endopeptidases such as tryptase and chymase [3, 21, 28, 39], which show angiogenic activities [4, 13, 22]. Mast cells also produce angiogenic factors such as vascular endothelial growth factor (VEGF) [16] and basic fibroblast growth factor (bFGF) [19]. Increased numbers of mast cells detected with immunoreactivity for tryptase have been shown in malignant tumors, including non-small cell lung carcinoma (NSCLC) [17, 20, 32, 33]. Intratumoral tryptase-positive mast cells correlate with tumor angiogenesis assessed by microvessel counts (MVCs) in NSCLC [31], especially lung adenocarcinomas [17, 20, 33].

Using monoclonal antibodies to human tryptase and chymase, two major subsets of human mast cells distinguishable by protease immunoreactivity have been demonstrated [3, 21]. The predominant mast cell type found in skin and other connective tissues (e.g., gut submucosa) contains both chymase and tryptase, and the predominant mast cell type found in lung alveolar tissue and gut mucosa contains only tryptase. The mast cell subset having immunoreactivity for both proteases was labeled MC_{TC} to denote the presence of chymase and tryptase and the subset only showing immunoreactivity for tryptase was labeled MC_T.

Chymase, one of the major secretory products of MC_{TC} cells, can activate matrix metalloproteases (MMPs) without requiring other proteases or cofactors [10, 11, 27, 31]. Chymase can cleave and inactivate tissue inhibitor of metalloprotease-1 (TIMP-1) [13]. Data also show that

infiltration of premalignant lesions by mast cells activates MMP-9 via chymase processing, coincident with the activation of angiogenesis, thus demonstrating an in vivo role for chymase-dependent MMP activation in tissue remodeling [8]. In a hamster sponge implant model, chymase promotes angiogenesis through generating angiotensin II from angiotensin I [22]. Despite these key mediator actions, the studies of chymase and its tissue distribution have been hampered by the lack of reagents suitable for use with formalin-fixed tissue. Buckley et al. [6] have prepared a new monoclonal antibody CC1 against human chymase, which overcomes these major disadvantages.

Recently, Noguchi et al. subdivided small sized lung adenocarcinomas (i.e., 2 cm or less in diameter) into two groups using histological criteria [23]. In one of these subtypes, the tumor growth replaces the pulmonary alveolar structure (replacing growth type); whereas, in the other, the tumor growth is non-replacing and destructive. Replacing growth-type adenocarcinoma, which is the major histological subtype, including 75% of all small sized adenocarcinomas, can be further subdivided into three subgroups (type-A, -B and -C). Type-A, or localized bronchioloalveolar carcinoma (LBAC), is sometimes difficult to distinguish from the precancerous lesion, atypical adenomatous hyperplasia. Type-B comprises LBACs with foci of alveolar structural collapse. These two subgroups show no lymph-node metastasis and have a 5-year survival rate of 100%. However, 28% of type-C tumors (that is, LBACs with active fibroblastic proliferation) do show lymph-node metastasis, and their 5-year survival rate is 74.8%. These clinicopathological and biological findings suggest a sequential progression from type-A and -B to type-C tumors during the course of pulmonary adenocarcinogenesis.

The present study immunohistochemically assessed expression of tryptase, chymase and CD34 in small sized lung adenocarcinomas (2 cm or less across the greatest dimension). MC_{TC}-type and MC_T-type mast cell counts were analyzed according to Noguchi's classification of small sized lung adenocarcinomas [23] and compared with microvessel counts and clinical outcomes of patients with small sized lung adenocarcinoma.

Methods

Patients

The subjects consisted of consecutive patients with small sized lung adenocarcinoma (2 cm or less across the greatest dimension) who were treated only by surgery at Sapporo Medical University Hospital between January 1981 and December 1996. Lymph nodes were extensively sampled at thoracotomy. The present study excluded patients with atopic diseases, including asthma, atopic dermatitis and allergic rhinitis, to eliminate influence of atopy for mast cell counts. The patients who died of unrelated diseases were also excluded. The study consisted of 66 consecutive patients (40 men and 26 women). Fifty-eight patients had N0- (regional lymph nodes contain no metastases), four patients had N1- [metastasis to same-side peribronchial (around the bronchi) and/or hilar (pit in the lungs where vessels enter and exit) lymph nodes within the lungs that are involved by direct spread of the primary tumor] and four patients had N2 [metastais to same-side mediastinal and/or subcarinal (under the certain, or tracheal ridge) lymph nodes] tumors. These tumors included two cases of Noguchi type-A tumor (LBAC), five cases of Noguchi type-B (LBAC with alveolar collapse), 52 cases of Noguchi type-C (LBAC with active fibroblastic proliferation), three cases of Noguchi type-D (poorly differentiated adenocarcinoma), four cases of Noguchi type-E (tubular adenocarcinoma) and none of Noguchi type-F tumor (papillary adenocarcinoma with a compressive growth pattern) according to the previously described classification criteria [23]. Noguchi type-D, -E and -F tumors show compressive and expanding growth.

Postoperative follow-up comprised three or six monthly office visits with yearly re-staging or as indicated clinically. All reasonable attempts were made to confirm tumor recurrence/metastasis cytologically or histologically using radiologically guided or echo-guided fine needle aspiration or bronchoscopic biopsy. Of the patients, 19 had postoperative relapse and 47 were disease free and alive with a follow-up of 65–252 months (median, 155 months). Informed consent was obtained from the subjects.

Immunohistochemistry

Immunohistochemical analyses were performed on at least two paraffin blocks of resected lung tissue per patient. Details of the technique have been previously described for human mast cell tryptase [17] and chymase [6], and CD34 [17]. Tumor tissue specimens were fixed with 10% buffered formalin and embedded in paraffin. Five-micrometer-thick sections were mounted on silanized slides (Dako Japan, Kyoto, Japan) and deparaffinized with xylene and ethanol. To retrieve the antigen, sections were pretreated in 10 mM citrate buffer, pH 6.0, with autoclave for 15 min at 120°C before the immunohistochemical staining of tryptase and chymase. The sections were then washed three times with phosphate buffered solution (PBS) for 5 min. The sections were soaked in absolute methanol containing 0.3% hydrogen peroxide for 30 min at room temperature to remove endogenous peroxidase activity. To suppress nonspecific binding, the sections were incubated with 1.5% non-immune goat serum for 20 min. The sections were then incubated with mouse monoclonal antibody QBEND10 to CD34 (5 μg/ml; Immunotech, Cedex, France), with monoclonal antibody AA1 to human mast cell tryptase (1 μg/ml; Dako), or CC1 to human mast cell chymase (1 μg/ml) for 60 min at room temperature. The CC1 antibody can detect human chymase in formalin-fixed, paraffin-embedded tissue sections [6]. After being washed with PBS, the slides were subsequently incubated with biotin-conjugated goat anti-mouse IgG antibody for 30 min. Then, after being washed again with PBS, the sections were incubated with avidin-biotin-peroxidase complex (Vectastain Elite ABC kit, Vector Laboratories, Berlingame, CA) for 30 min, and washed once more with PBS. The sections were finally incubated with 0.03% hydrogen peroxide and 0.05% 3,3′-diaminobenzidine. The slides were then washed in running tap water, counterstained with hematoxylin and mounted in Canadian balsam. Non-immunized mouse IgG was used as a negative control. No significant immunohistochemical reaction occurred in the control sections.

We double labeled sections with anti-chymase plus anti-angiotensin II antibody (Phoenix Pharmaceutics Inc., Belmont, CA) or with anti-chymase plus anti-tryptase antibody using combined ABC-peroxidase and ABC-alkaline phosphatase methods (Vectastain-AP kit, Vector Laboratories). Diaminobenzidine was used as the substrate of horseradish peroxidase and 5-bromo-4-chloro-indolyl phosphate/nitroblue tetrazolium (Vector Laboratories) was applied to the alkaline phosphatase substrate. For this experiment, we used several controls: (1) anti-chymase antibody first and anti-angiotensin II or tryptase antibody later, (2) anti-angiotensin II or tryptase antibody first and anti-chymase antibody

later and (3) omission of the first antibody and/or secondary antibody.

Immunohistochemical reactivities for CD34, tryptase and chymase were evaluated. We assessed delineated CD34-positive cells as a microvessel and tryptase-positive cells as mast cells. We counted tryptase-positive and chymase-positive mast cells at the sites where they most intensively accumulated in a ×200 microscopic field (i.e., ×20 objective lens and ×10 ocular lens; 0.723 mm^2/field). We excluded perivascular, peribronchial and peribronchiolar regions within tumors for their evaluation. In the areas that were considered to be most active for neovascularization, stained vessels were counted in a ×200 microscopic field. The averages of tryptase-positive and chymase-positive mast cells and microvessels counted in five fields were calculated as described elsewhere [17]. The tryptase-positive and chymase-positive mast cell counts and MVCs were assessed without knowledge of patient outcome (the presence or absence of relapse or any other pertinent variable) by two investigators. We assessed total mast cell counts by counting tryptase-positive cells. The counts of tryptase-positive and chymase-positive mast cells (MC_{TC}-type mast cell counts) were evaluated by counting chymase-positive cells. The counts of chymase-negative and tryptase-positive mast cells (MC_T-type mast cell counts) were calculated by the subtraction of MC_{TC}-type mast cell counts from total mast cell counts in each case. Between two observers, there were good correlations of MVCs (r=0.876, P<0.0001) and total (r=0.924, P<0.0001), MC_{TC}-type (r=0.917, P<0.0001) and MC_T-type mast cell counts (r=0.931, P<0.0001).

Statistical analysis

Data are expressed as means ± standard deviation. The Mann-Whitney U test was used for analysis of two unpaired samples, and the Pearson's least squares linear regression analysis was used to determine correlations. Contingency tables were analyzed for trends with the chi-square test. Survivals were calculated from the day of operation using the Kaplan-Meier method and differences in the survivals were examined by the log-rank test. The level of critical significance was assigned at P<0.05.

Results

MVCs

The MVCs were assessed in the most intensive areas of neovascularization within tumors by an immunohistochemical survey of CD34. Delineated CD34-positive cells were counted as a microvessel. The mean MVC of small sized lung adenocarcinomas was 62.3±34.4 per ×200 microscopic field. There was no significant difference of MVCs in gender subgroups. The mean MVCs of Noguchi type-A plus type-B, type-C, type-D and type-E tumors were 33.7±21.5, 68.9±36.0, 58.0±6.08 and 68.3±21.8, respectively (Fig. 2A). The mean MVC of Noguchi type-C tumors was significantly higher than that of Noguchi type-A plus type-B tumors (P=0.006).

Total, MC_T-type and MC_{TC}-type mast cell counts

Tryptase-positive and chymase-positive cells were immunohistochemically evaluated in the control lung tissue and at the sites where mast cells most intensively accumulated within tumors in serial sections (Fig. 1A and B). In alveoli of the control lung tissue, the averages of total, MC_T-type and MC_{TC}-type mast cell counts were 9.03±2.76, 7.98±2.89 and 1.07±1.37 per ×200 microscopic field, respectively. Ratios of MC_{TC} type to total mast cell counts were 0.15±0.21. Total mast cell counts in cases of small sized lung adenocarcinoma (81.4±46.0) were significantly higher than those in the control lung (P<0.0001). There was no significant difference in intratumoral total mast cell counts in gender subgroups in adenocarcinomas. The averages of total mast cell counts of Noguchi type-A plus type-B, type-C, type-D and type-E tumors were 36.7±10.2, 87.8±48.4, 81.0±14.9 and 76.8±18.2, respectively (Fig. 2B). The average of total mast cell counts of Noguchi type-C tumors was significantly higher than that of Noguchi type-A plus type-B tumors (P=0.0002).

In serial sections, chymase-positive cells corresponded to a part of tryptase-positive cells. Double staining with anti-chymase plus with anti-tryptase antibody showed no evidence found for chymase in cells other than those that contained tryptase (Fig. 1C).

The averages of MC_T-type and MC_{TC}-type mast cell counts of small sized lung adenocarcinomas were 60.2±32.8 and 21.2±21.0, respectively. Ratios of MC_{TC}-type to total mast cell counts in adenocarcinomas (0.25±0.15) were significantly higher than those in alveoli in the control lung tissue (P=0.04). The averages of MC_{TC}-type mast cell counts of Noguchi type-A plus type-B, type-C, type-D and type-E tumors were 8.57±3.10, 23.52±22.75, 12.67±7.64 and 19.25±12.45, respectively (Fig. 2C). The average of MC_{TC}-type mast cell counts of Noguchi type-C tumors was significantly higher than that of Noguchi type-A plus type-B tumors (P=0.0142). The averages of MC_T-type mast cell counts of Noguchi type-A plus type-B, type-C, type-D and type-E tumors were 28.1±12.2, 64.2±34.0, 68.3±20.7, and 57.5±16.3, respectively (Fig. 2D). The average of MC_T-type mast cell counts of Noguchi type-C tumors was significantly higher than that of Noguchi type-A plus type-B tumors (P=0.0008). Ratios of MC_{TC} type to total mast cell counts of Noguchi type-A plus type-B, type-C, type-D and type-E tumors were 0.25±0.13, 0.25±0.15, 0.17±0.11 and 0.25±0.14, respectively, showing no significant differences.

Double staining of chymase and angiotensin II

Chymase is reported to convert angiotensin II from angiotensin I. To assess whether intratumoral MC_{TC}-type mast cells express angiotensin II, we double labeled sections with anti-angiotensin II plus with anti-chymase antibody (Fig. 1D). Angiotensin II expression was found in all chymase-positive mast cells in intratumoral stroma as well as immunoreactivity of angiotensin II of tumor cells.

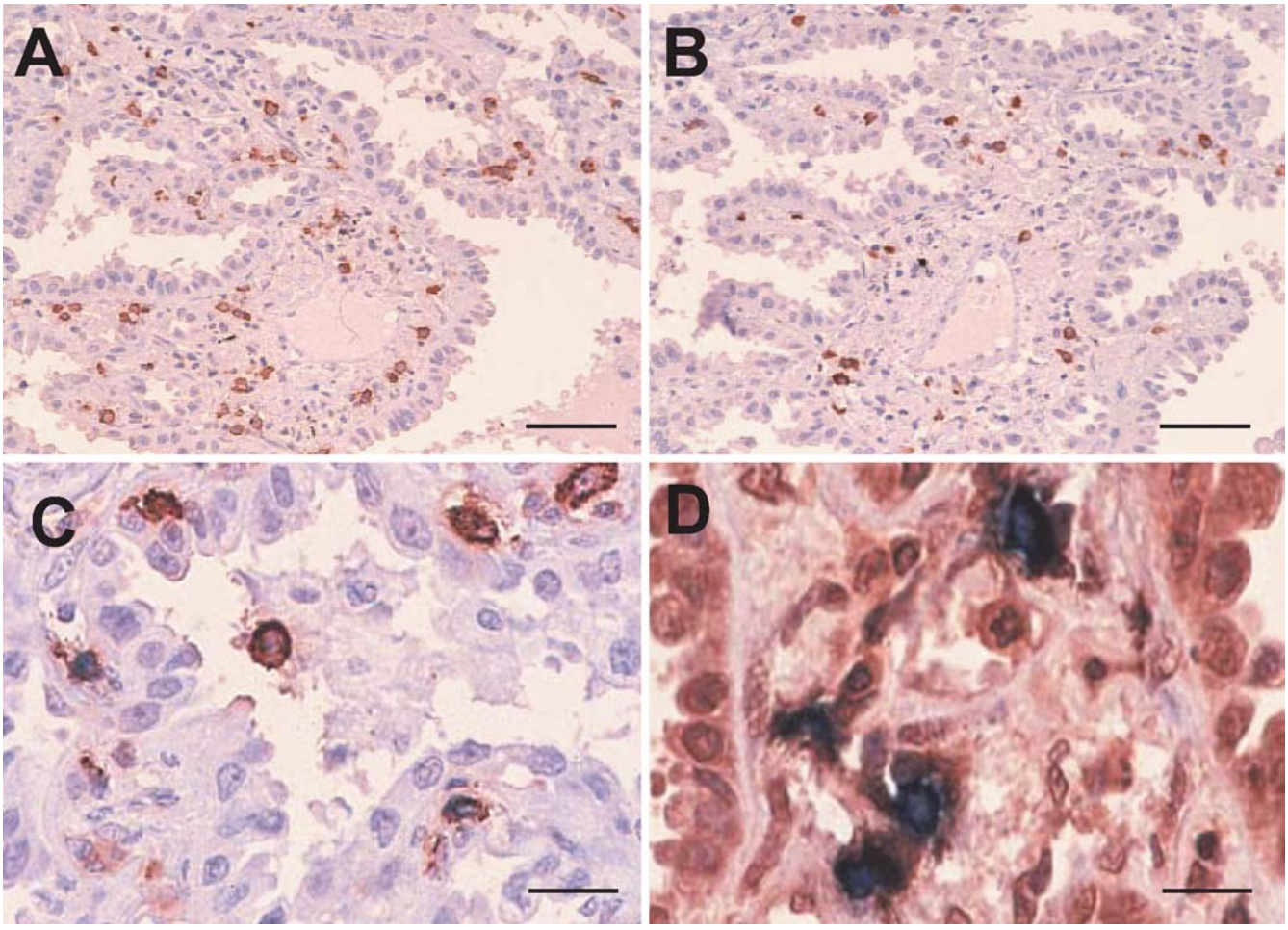

Fig. 1 Immunohistochemical study of tryptase (**A**) and chymase (**B**) and double staining of tryptase and chymase (**C**) and of chymase and angiotensin II (**D**) in small sized lung adenocarcinomas. Tryptase-positive cells are assessed as mast cells (**A**) and chymase-positive cells are assessed as MC_{TC}-type mast cells (immunoreactive for both tryptase and chymase). Tryptase (**C**) and angiotensin II (**D**) were visualized using diaminobentizine as brown and chymase (**C** and **D**) was visualized using 5-bromo-4-choro-indolyl phosphate/nitroblue tetrazolium as blue in double staining, respectively. There is no evidence found for chymase in cells other than those that contained tryptase (**C**). Angiotensin II expression is found in all chymase-positive mast cells in intratumoral stroma as well as immunoreactivity of angiotensin II of tumor cells (**D**). Internal scale *bars* are 25 μm (**A** and **B**) and 10 μm (**C** and **D**)

Correlations among MVCs and total, MC_{TC}-type and MC_T-type mast cell counts

In serial sections, the areas where tryptase-positive cells most intensively accumulated corresponded well to those where chymase-positive cells did so, and to those areas that MVCs most highly increased. We analyzed correlations among MVCs and total, MC_{TC}-type and MC_T-type mast cell counts. There were significant positive correlations of MVCs with total (r=0.776, P<0.0001; Fig. 3A), MC_{TC}-type (r=0.657, P<0.0001; Fig. 3B) and MC_T-type mast cell counts (r=0.669, P<0.0001; Fig. 3C). There were significant positive correlations of MC_{TC}-type mast cell counts with total (r=0.769, P<0.0001; Fig. 3D) and MC_T-type mast cell counts (r=0.440, P=0.0002; Fig. 3E).

Relationship of clinical outcome to mast cell counts

Using a cutoff value of means of mast-cell-related parameters (total, 81.4; MC_T-type, 60.2 and MC_{TC}-type mast cell counts, 20.2), the patients were separated into low- and high-count groups. In patients with small sized lung adenocarcinoma, the postoperative relapse rate in the high-count group of total mast cells (14/25, 56.0%) was significantly higher than that in the low-count group (5/41, 12.2%, P=0.0004). The postoperative relapse rate in the high-count group of MC_{TC}-type mast cells (16/23, 69.5%) was significantly higher than that in the low-count group (3/43, 6.9%, P<0.0001), whereas there was no significant difference in the low- (10/41, 24.4%) and high-count groups of MC_T-type mast cells (9/25, 36.0%). In patients with LBAC (the cut-off values of total, MC_T-type and MC_{TC}-type mast cell counts were 81.7, 59.9 and 21.7, respectively), the postoperative relapse rate in the high-count group of total mast cells (13/22, 59.1%) was

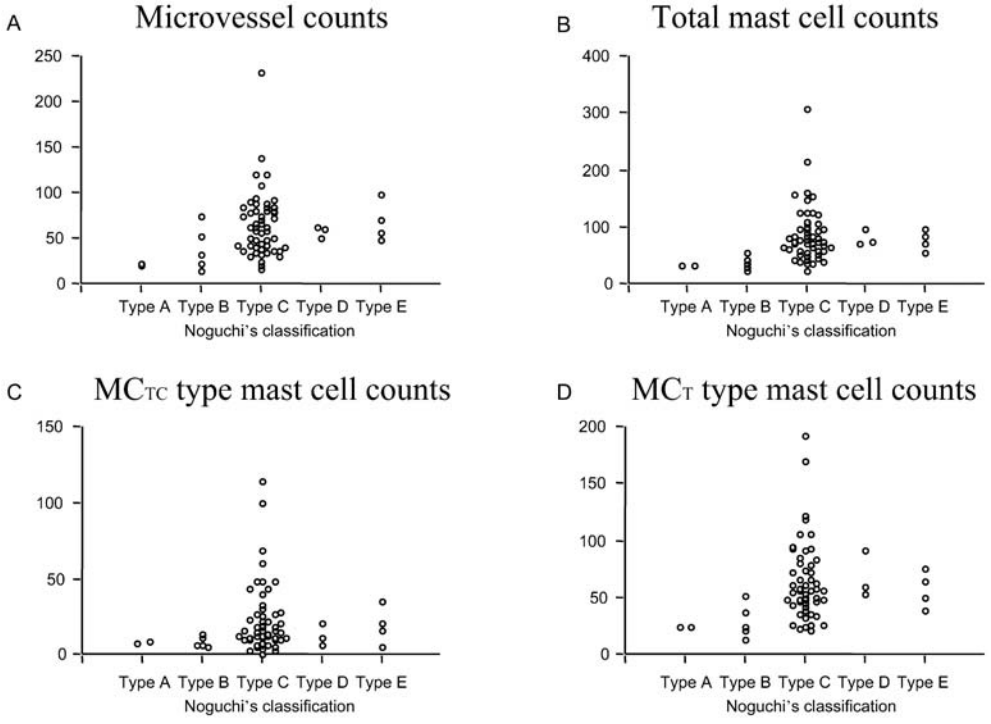

Fig. 2 Microvessel counts (MCVs, **A**), total mast cell counts (**B**), MC_{TC}-type mast cell counts (**C**) and MC_T-type mast cell counts (**D**) in small sized lung adenocracinomas according to Noguchi's classification. Total mast cell counts were assessed by counting tryptase-positive cells. The counts of tryptase-positive and chymase-positive mast cells (MC_{TC}-type mast cell counts) were evaluated by counting chymase-positive cells. The counts of chymase-negative and trypase-positive mast cells (MC_T-type mast cell counts) were calculated by the subtraction of MC_{TC}-type mast cell counts from total mast cell counts in each case. Noguchi type-C tumors have significantly higher MVCs (P=0.006), and total (P=0.0002), MC_{TC}-type (P=0.0142) and MC_T-type mast cell counts (P=0.0008) than Noguchi type-A plus type-B tumors

significantly higher than that in the low-count group (4/37, 10.1%, P=0.0002). The postoperative relapse rate in the high MC_{TC}-type mast cell count group (15/19, 78.9%) was significantly higher than that in the low-count group of MC_{TC}-type mast cells (2/40, 5.0%, P<0.0001), whereas there was no significant difference in the low- (8/37, 21.6%) and high-count groups of MC_T-type mast cells (9/22, 40.9%). In patients with type-C tumor, (the cut-off values of total, MC_T-type and MC_{TC}-type mast cell counts were 87.8, 64.2 and 23.5, respectively), the postoperative relapse rate in the high-count group of total mast cells (12/19, 63.1%) was significantly higher than that in the low-count group (3/33, 15.1%, P=0.001). The postoperative relapse rate in the high-count group of MC_{TC}-type mast cells (12/16, 75.0%) was significantly higher than that in the low-count group (5/36, 13.9%, P<0.0001), whereas there was no significant difference in the low- (8/33, 24.2%) and high-count groups (9/19, 47.4%).

Using the Kaplan-Meier survival estimates, we compared survivals. In patients with small sized lung adenocarcinoma, members in the high-count group of total mast cells had a significantly worse prognosis than those in the low-count group (P=0.001; Fig. 4A). Members in the high-count group of MC_{TC}-type mast cells had a significantly worse prognosis than those in the low-count group (P<0.0001; Fig. 4B), whereas members in the high-count group of MC_T-type mast cells did not (Fig. 4C).

In patients with LBAC, members in the high-count group of total mast cells had significantly worse prognosis than those in the low-count group (P<0.0008; Fig. 4D). Members in the high-count group of MC_{TC}-type mast cells had a significantly worse prognosis than those in the low-count group (P<0.0001; Fig. 4E), whereas members in the high-count group of MC_T-type mast cells did not (Fig. 4F). In patients with type-C tumor, members in the high-count group of total mast cells had a significantly worse prognosis than those in the low-count group (P=0.0007). Members in the high-count group of MC_{TC}-type mast cells had a significantly worse prognosis than those in the low-count group (P<0.0001), whereas members in the high-count group of MC_T-type mast cells did not (data not shown).

Discussion

Proteases are among the most abundant secretory products of mast cells. Two of these, tryptase and chymase, are attracting attention as key mediators of tissue remodeling and inflammation and have become valuable as specific biochemical markers for mast cells and their

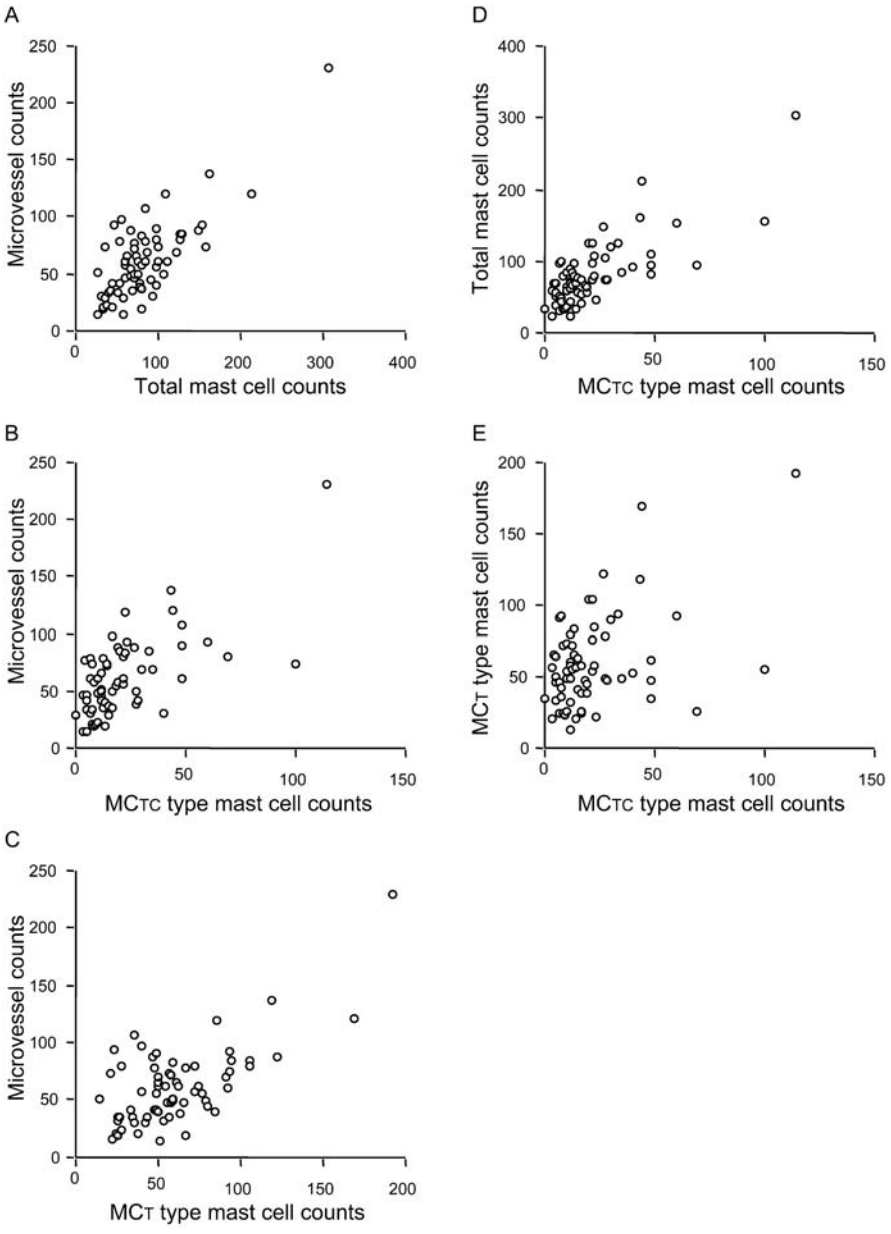

Fig. 3 Correlations among microvessel counts (MVCs) and total, MC_{TC}-type and MC_T-type mast cell counts in small sized lung adenocarcinomas. There were significant positive correlations of MVCs with total (r=0.776, P<0.0001; **A**), MC_{TC} type (r=0.657, P<0.0001; **B**) and MC_T-type mast cell counts (r=0.669, P<0.0001; **C**). There were significant positive correlations of MC_{TC}-type mast cell counts with total (r=0.769, P<0.0001; **D**), and MC_T-type mast cell counts (r=0.440, P=0.0002; **E**)

subsets [3, 21]. Human mast cells are separated into MC_T-type and MC_{TC}-type subsets. Despite the key mediator actions of chymase, the studies of its distribution in the normal tissue and in malignant lesions have been hampered by the lack of reagents suitable for use with formalin-fixed tissue. Buckley et al. [6] have prepared a new monoclonal antibody CC1 against human chymase, and the antibody can detect human chymase in formalin-fixed, paraffin-embedded tissue sections. In the present study, chymase-positive cells corresponded to a part of tryptase positive cells in serial sections. Double staining with anti-chymase plus with anti-tryptase antibody showed no evidence for chymase in cells other than those that contained tryptase. The present study demonstrates that by immunohistochemical survey with the CC1 antibody, 85% of mast cells are MC_T-type and 15% are MC_{TC}-type in alveoli of the control lung tissue. The results are in keeping with the results of the distribution of mast-cell subsets in alveoli of the lung [3, 6, 18, 38].

Angiogenesis has, in part, been related to mast cells because mast cells accumulate in a number of angiogenesis-dependent situations, including rheumatoid arthritis [14], wound healing [36] and malignant tumors [7, 17, 20, 32, 34]. Recent investigations [17, 20, 32, 33] have demonstrated that increased numbers of mast cells detected by immunohictochemical survey of tryptase correlate with angiogenesis assessed by MVCs and poor outcome in patients with NSCLC, especially lung adenocarcinoma. Mast cells have been shown to produce angiogenic factors, including VEGF [16] and bFGF [19]. Mast cells have been reported to express MMPs [9, 12, 36, 37], which are pivotal enzymes in matrix remodeling

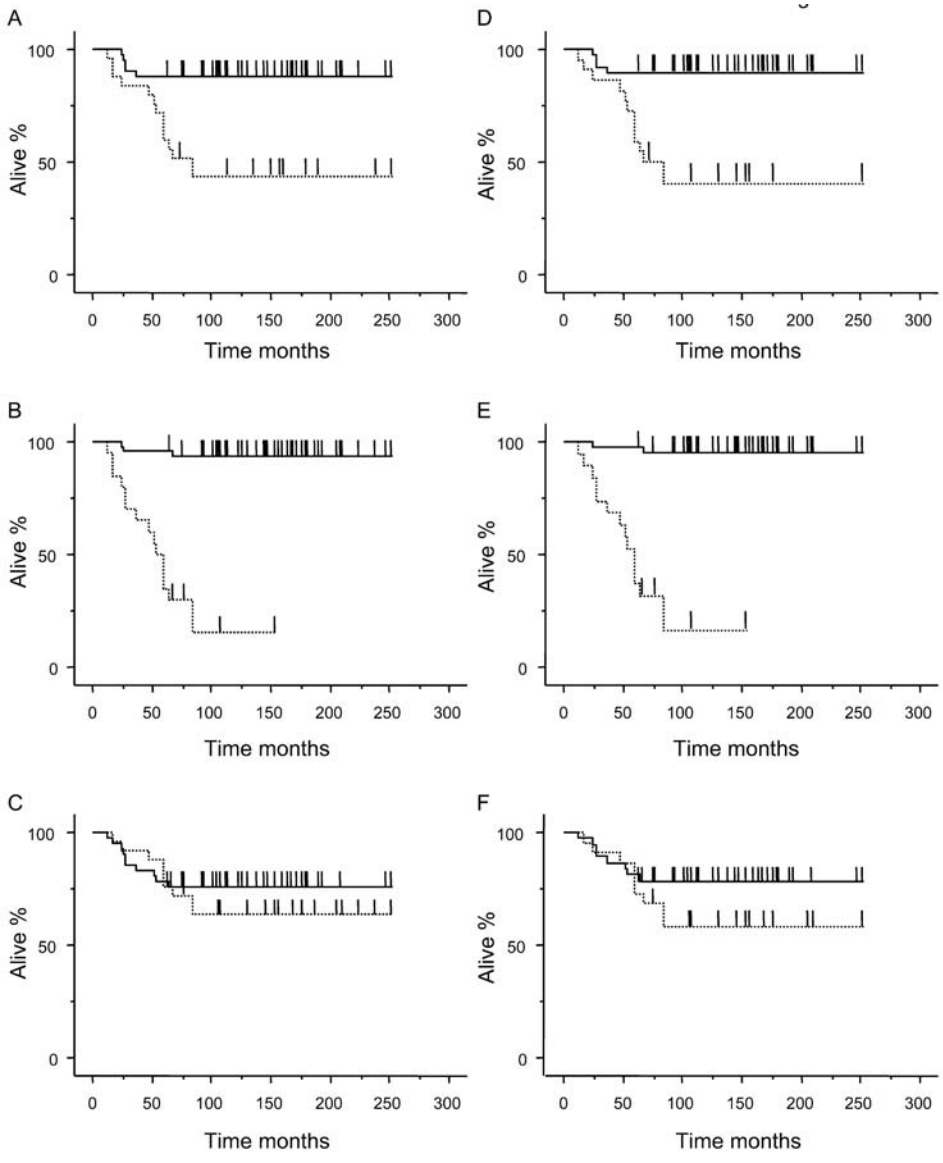

Fig. 4 Kaplan-Meier survival estimates stratified by total (**A** and **D**), MC_{TC}-type (**B** and **E**) and MC_T-type mast cell counts (**C** and **F**) in patients with small sized lung adenocarcinoma (**A**, **B** and **C**) and localized bronchioloalveolar carcinoma (*LBAC*, Noguchi type-A, -B and -C tumors) (**D**, **E** and **F**). The log rank test showed statistically significant differences between two groups [high- (*dotted line*) and low-count groups (*solid line*)] in patients with small sized lung adenocarcinoma stratified by total (P=0.001) and MC_{TC}-type mast cell counts (P<0.0001) but not by MC_T-type mast cell counts. In patients with LBAC, there were statistically significant differences between two groups stratified by total (P=0.0008) and MC_{TC}-type mast cell counts (P<0.0001), but not by MC_T-type mast cell counts

in the early stages of angiogenesis. Mast cell histamine induces angiogenesis [29], and heparin promotes new vessel formation in vivo [25]. Mast cell tryptase stimulates vascular tube formation and it can function as a mitogen for microvascular endothelial cells [2]. Tryptase also activates latent MMPs [15] and plasminogen activators [30]. However, mast cells produce TIMPs, which act in diverse biological processes via mechanisms that may be either dependent on or independent of their ability to inhibit active forms of MMPs.

The present study documents that accumulation of MC_{TC}-type mast cells correlates well with the poor outcome of patients with small sized lung adenocarcinoma, but not with accumulation of MC_T-type mast cells, although both MC_{TC}-type and MC_T-type mast cell counts significantly correlate with angiogenesis assessed by MVCs in small sized lung adenocarcinomas. In a hamster sponge implant model, chymase promotes angiogenesis through generating angiotensin II from angiotensin I [22]. The present study demonstrates that chymase-positive mast cells express angiotensin II. Several lines of evidence indicate that chymase is very important in matrix remodeling. Chymase cleaves and activates MMP-9 secreted from mast cells [12]. In addition to MMP-9, chymase also directly cleaves and activates MMP-1 and MMP-3 [27, 31]. Mast cells express these two MMPs plus MMP-2 [12], which shares in in vitro substrate specificity with MMP-9 [5, 12, 35]. A unique feature of the gelatinase class of MMPs is binding of the zymogens, MMP-2 and MMP-9, to TIMP-2 and TIMP-1, respectively. TIMP-1 not only inhibits activity of mature MMP-9, but also blocks activation of proenzyme. Chymase cleaves and inactivates TIMP-1 whether it exists free or bound in a complex with MMP-9 (a complex of MMP-9-TIMP-1 and neutrophil gelatinase-associated lipocalin) [13]. By cleaving TIMP-1 at exposed surface sites, chymase overcomes its inhibitory effects and coverts complexed MMP-9 to mature species with gelatinolytic

activity. Chymase from MC_{TC}-type mast cells cleaves TIMP-1 extracellularly and activates MMP-9. In this context, the accumulation of MC_{TC}-type mast cells, but not MC_T-type mast cells is very important in active tissue remodeling of cancerous stroma of NSCLC.

The present study documents that cases of Noguchi type-C tumor have intensive MC_{TC}-type mast cell accumulation in cancerous stroma. Noguchi type-C tumor is defined as having foci of active fibroblastic proliferation in cancerous stroma. Very recently, Aoyagi and coworkers [1] investigated allelic losses at eight loci on the eight chromosomes carrying the peripheral cancer-associated genes (FHIT, 3p; APC, 5q; p16, 9p; int-2, 11q; Rb, 13q; p53, 17p; Smad4, 18q; and Band M, 22q) in 66 replacing growth-type small sized lung adenocarcinomas (type-A, 12; type-B, 28 and type-C, 26). Allelic losses were shown in one or more regions in 16.7% of type-A tumors, 39.3% of type-B tumors and 96.2% of type-C tumors. Interestingly, the tumor cells in the central fibrotic areas exhibited more allelic losses than those in the peripheral bronchioloalveolar growths in type-C tumors that showed heterogeneous histological features. The present study documents extremely higher postoperative relapse rates and worse outcomes in members of the high MC_{TC} count group in patients with Noguchi type-C tumor. Counting chymase-positive (MC_{TC}-type) mast cells may be a good prognosis predictor in Noguchi type-C tumor (localized bronchioloalveolar carcinoma with active fibroblast proliferation), and the accumulation of MC_{TC}-type mast cells may indicate active tissue remodeling of cancerous stroma of NSCLC.

References

1. Aoyagi Y, Yokose T, Minami Y, et al (2001) Accumulation of losses of heterozygosity and multistep carcinogenesis in pulmonary adenocarcinoma. Cancer Res 61:7950–7954
2. Azizkhan RG, Azizkhan JC, Zetter BR, Folkman J (1980) Mast cell heparin stimulates migration of capillary endothelial cells in vitro. J Exp Med 152:931–944
3. Beil WJ, Pammer J (2001) In situ detection of the mast cell proteases chymase and tryptase in human lung tissue using light and electron microscopy. Histochem Cell Biol 116:483–493
4. Blair RJ, Meng H, Marchese MJ, Ren S, et al (1997) Human mast cells stimulate vascular tube formation: tryptase is a novel, potent angiogenic factor. J Clin Invest 99:2691–2700
5. Brownell E, Fiorentino L, Jolly G, Wolfe K, Kincaid S, Seperack P, Visco D (1995) Immunolocalization of stromelysin-related protein in murine mast cell granules. Int Arch Allergy Immunol 107:333–335
6. Buckley MG, McEuen AR, Walls AF (1999) The detection of mast cell subpopulations in formalin-fixed human tissues using a new monoclonal antibody specific for chymase. J Pathol 189:138–143
7. Cabanillas-Saez A, Schalper JA, Nicovani SM, Rudolph MI (2002) Characterization of mast cells according to their content of tryptase and chymase in normal and neoplastic human uterine cervix. Int J Gynecol Cancer 12:92–98
8. Coussens LM, Raymond WW, Bergers G, Laig-Webster M, Behrendtsen O, Werb Z, Caughey GH, Hanahan D (1999) Inflammatory mast cells up-regulate angiogenesis during squamous epithelial carcinogenesis. Genes Dev 13:1382–1397
9. Di Girolamo N, Wakefield D (2000) In vitro and in vivo expression of interstitial collagenase/MMP-1 by human mast cells. Dev Immunol 7:131–142
10. Fang KC, Raymond WW, Lazarus SC, Caughey GH (1996) Dog mastocytoma cells secrete a 92-kD gelatinase activated extracellularly by mast cell chymase. J Clin Invest 97:1589–1596
11. Fang KC, Raymond WW, Blount JL, Caughey GH (1997) Dog mast cell α-chymase activates progelatinase B by cleaving the Phe88-Gln89 and Phe91-Glu92 bonds of the catalytic domain. J Biol Chem 272:25628–25635
12. Fang KC, Wolters PJ, Steinhoff M, Bidgol A, Blount JL, Caughey GH (1999) Mast cell expression of gelatinases A and B is regulated by kit ligand and TGF-β. J Immunol 162:5528–5535
13. Frank BT, Rossall JC, Caughey GH, Fang KC (2001) Mast cell tissue inhibitor of metalloproteinase-1 is cleaved and inactivated extracellularly by α-chymase. J Immunol 166:2783–2792
14. Gotis-Graham I, McNeil HP (1997) Mast cell responses in rheumatoid synovium. Association of the MC_{TC} subset with matrix turnover and clinical progression. Arthritis Rheum 40:479–489
15. Gruber BL, Marchese MJ, Suzuki K, et al (1989) Synovial procollagenase activation by human mast cell tryptase dependence upon matrix metalloproteinase 3 activation. J Clin Invest 84:1657–1662
16. Grutzkau A, Kruger-Krasagakes S, Baumeister H, et al (1998) Synthesis, storage, and release of vascular endothelial growth factor/ vascular permeability factor (VEGF/VPF) by human mast cells: implications for the biological significance of VEGF206. Mol Biol Cell 9:875–884
17. Imada A, Shijubo N, Kojima H, Abe S (2000) Mast cells correlate with angiogenesis and poor outcome in stage I lung adenocarcinoma. Eur Respir J 15:1087–1093
18. Irani AM, Bradford TR, Kepley CL, Schechter NM, Schwartz LB (1989) Detection of MC_T and MC_{TC} types of human mast cells by immunohistochemistry using new monoclonal anti-tryptase and anti-chymase antibodies. J Histochem Cytochem 37:1509–1515
19. Kanbe N, Kurosawa M, Nagata H, Yamashita T, Kurimoto F, Miyachi Y (2000) Production of fibrogenic cytokines by cord blood-derived cultured human mast cells. J Allergy Clin Immunol 106:S85–S90
20. Kojima H, Shijubo N, Abe S (2002) Thymidine phosphorylase and vascular endothelial growth factor in patients with stage I lung adenocarcinoma. Cancer 94:1083–1093
21. Metcalfe DD, Baram D, Mekori YA (1997) Mast cells. Physiol Rev 77:1033–1079
22. Muramatsu M, Katada J, Hayashi I, Majima M (2000) Chymase as a proangiogenic factor. A possible involvement of chymase-angiotensin-dependent pathway in the hamster sponge angiogenesis model. J Biol Chem 275:5545–5552
23. Noguchi M, Morikawa A, Kawasaki M, et al (1995) Small sized adenocarcinoma of the lung. Histologic characteristics and prognosis. Cancer 75:2844–5282
24. Norrby K (2002) Mast cells and angiogenesis. APMIS 110:355–371
25. Norrby K, Sorbo J (1992) Heparin enhances angiogenesis by a systemic mode of action. Int J Exp Pathol 73:147–155
26. Ribatti D, Vacca A, Nico B, Crivellato E, Roncali L, Dammacco F (2001) The role of mast cells in tumour angiogenesis. Br J Haematol 115:514–521
27. Saarinen J, Kalkkinen N, Welgus HG, Kovanen PT (1994) Activation of human interstitial procollagenase through direct cleavage of the Leu83-Thr84 bond by mast cell chymase. J Biol Chem 269:18134–18140
28. Shijubo N, Kojima H, Nagata M, Ohchi T, Suzuki A, Abe S, Sato N (2003) Tumor angiogenesis of non-small cell lung cancer. Microsc Res Tech 60:186–198
29. Sorbo J, Jakobsson A, Norrby K (1994) Mast-cell histamine is angiogenic through receptors for histamine1 and histamine2. Int J Exp Pathol 75:43–50

30. Stack MS, Johnson DA (1994) Human mast cell tryptase activates single-chain urinary-type plasminogen activator (pro-urokinase). J Biol Chem 269:9416–9419
31. Suzuki K, Lees M, Newlands GF, Nagase H, Woolley DE (1995) Activation of precursors for matrix metalloproteinases 1 (interstitial collagenase) and 3 (stromelysin) by rat mast-cell proteinases I and II. Biochem J 305:301–306
32. Takanami I, Takeuchi K, Naruke M (2000) Mast cell density is associated with angiogenesis and poor prognosis in pulmonary adenocarcinoma. Cancer 88:2686–2692
33. Tomita M, Matsuzaki Y, Onitsuka T (2000) Effect of mast cells on tumor angiogenesis in lung cancer. Ann Thorac Surg 69:1686–1690
34. Toth-Jakatics R, Jimi S, Takebayashi S, Kawamoto N (2000) Cutaneous malignant melanoma: correlation between neovascularization and peritumor accumulation of mast cells overexpressing vascular endothelial growth factor. Hum Pathol 31:955–960
35. Tozzi CA, Thakker-Varia S, Yu SY, et al (1998) Mast cell collagenase correlates with regression of pulmonary vascular remodeling in the rat. Am J Respir Cell Mol Biol 18:497–510
36. Trabucchi E, Radaelli E, Marazzi M, et al (1988) The role of mast cells in wound healing. Int J Tissue React 10:367–372
37. Vincent AJ, Zhang J, Ostor A, et al (2000) Matrix metalloproteinase-1 and -3 and mast cells are present in the endometrium of women using progestin-only contraceptives. Hum Reprod 15:123–130
38. Weidner N, Austen KF (1993) Heterogeneity of mast cells at multiple body sites. Fluorescent determination of avidin binding and immunofluorescent determination of chymase, tryptase, and carboxypeptidase content. Pathol Res Pract 189:156–162
39. Welle M (1997) Development, significance, and heterogeneity of mast cells with particular regard to the mast cell-specific proteases chymase and tryptase. J Leukoc Biol 61:233–245

Virchows Arch (2003) 443:574–578
DOI 10.1007/s00428-003-0854-7

CASE REPORT

Alfredo Ribeiro-Silva · Daniel Chang · Frank Wagner Bisson · Luiz Orlando M Ré

Clinicopathological and immunohistochemical features of a sebaceous carcinoma arising within a benign dermoid cyst of the ovary

Received: 7 March 2003 / Accepted: 26 May 2003 / Published online: 27 June 2003
© Springer-Verlag 2003

Abstract Pure sebaceous neoplasms arising in dermoid cysts of the ovary are exceedingly rare. A 63-year-old female with abdominal swelling and pain underwent a right salpingo-oophorectomy that showed a unilocular cyst weighing 830 g and measuring 15×12×10 cm, filled with sebaceous material containing a few hair shafts. The cyst wall exhibited plaques protruding into the cavity of the cyst. Microscopy revealed a dermoid cyst with nests and lobules of atypical and infiltrating sebaceous cells surrounded by basaloid cells. The tumor cells stained diffusely for high-molecular-weight cytokeratins and focally for cytokeratin 7, cytokeratin 19, epithelial membrane antigen and carcinoembryonic antigen in the immunohistochemistry study. Low-molecular-weight cytokeratins, cytokeratin 20, vimentin, S100, p63, estrogen receptor, progesterone receptor, p53 and c-erbB-2 were negative in tumoral cells. The proliferative labeling index (Ki67 and proliferating cell nuclear antigen) was low. Basal cell carcinoma with sebaceous differentiation and sebaceoma must be considered in the differential diagnosis. However, the presence of obvious malignant sebaceous differentiation in nearly every tumor nest and lack of peripheral palisading and peri-tumoral myxoid stroma excluded these diagnoses. Some histogenetic concepts relevant to this case are discussed along with a brief review of this neoplasm. To our knowledge, this is the sixth case report of a sebaceous carcinoma arising in a mature cystic teratoma of the ovary.

Keywords Sebaceous carcinoma · Dermoid cyst · Teratoma · Ovary · Immunohistochemistry

A. Ribeiro-Silva (✉) · D. Chang
Department of Pathology, Hospital das Clínicas,
Faculdade de Medicina de Ribeirão Preto,
Campus Universitário Monte Alegre,
Avenida Bandeirantes s/n, Ribeirão Preto,
14048-900 São Paulo, Brazil
e-mail: ardsilva@rpa.fmrp.usp.br
Tel.: +55-16-6023240
Fax: +55-16-6330095

F. W. Bisson
Institute of Pathology and Cytology,
Sertãozinho, SP, Brazil

L. O. M. Ré
Hospital Santa Casa De Misericórdia,
Sertãozinho, SP, Brazil

Introduction

Mature cystic teratomas, also known as dermoid cysts, are the most common benign ovarian tumors [11]. They typically show adult-type tissues usually representative of one or more germ layers. Malignant change arising within one of the components of benign teratomas is very rare [2]. The most common secondary neoplasms arising in dermoid cysts are squamous cell carcinomas [15]. To the best of our knowledge, there are only five reports of sebaceous carcinomas arising within a benign teratoma of the ovary [5, 6, 9, 21, 29]. Along with a brief review of this neoplasm, we report the clinicopathological and immunohistochemical features of a new case of a pure sebaceous carcinoma arising in a dermoid cyst of the ovary.

Clinical history

A 63-year-old white female was admitted due to abdominal distension and lower abdominal pain for 5 months. Her previous medical history was unremarkable, with no prior surgery or other diseases. Ultrasonography revealed a heteroechogenic right adnexal mass. On exploratory laparotomy, a large tumor was found in the right ovary. The mass was restricted to the ovary and did not reach the uterus or infiltrate adjacent abdominal structures. The patient underwent a right salpingo-oophorectomy. The postoperative recovery was uneventful. No further therapy was given. She is doing well 4 months after surgery with no evidence of disease.

Materials and methods

The surgical specimen was fixed in 10% formalin. Sequential 3-mm sections were obtained throughout the specimen. Representative samples of the tumor were embedded in paraffin, and histological sections of 4 μm obtained from the paraffin-embedded blocks were stained with hematoxylin-eosin. For immunohistochemical staining, the paraffin-embedded blocks were cut at 3 μm, deparaffinized, and rehydrated. Using the standard avidin-biotin-peroxidase method, the following antibodies were used: high-molecular-weight cytokeratin (clone 34ßE12, 1:400; Dako), low-molecular-weight cytokeratin (clone 35ßH11, 1:400; Dako), cytokeratin 19 (CK19; clone BA17, 1:100; Dako), cytokeratin 20 (CK20; clone K_S20.8, 1:200; Dako), cytokeratin 7 (CK7; clone OV-TL 12/30, 1:750; Dako), epithelial membrane antigen (EMA; clone E29, 1:500; Dako), carcinoembryonic antigen (CEA; clone II-7, 1:6000; Dako), Ki67 (clone MM1, 1:150, Novocastra), proliferating cell nuclear antigen (PCNA; clone PC10, 1:1500; Dako), p63 (clone 4A4, 1:200; Santa Cruz), vimentin (clone 3B4, 1:1000; Dako), S100 (1:4000; Dako), estrogen receptor (ER; clone 1D5, 1:50; Dako), progesterone receptor (PR; clone PgR636, 1:50; Dako), p53 (clone DO7, 1:100; Novocastra), and c-erbB-2 (clone CB11, 1:300; Novocastra).

Results

Gross pathological examination showed a unilocular cyst weighing 830 g and measuring 15×12×10 cm. The smooth outer surface was glistening white. Upon opening, the cyst was filled with sebaceous material containing a few hair shafts. The inner surface was smooth except for multiple small plaques protruding into the cavity of the cyst (Fig. 1A). These plaques consisted of a solid white to yellow tissue, with friable areas. The cyst lining was sampled, including the aforementioned plaques, and submitted for microscopic evaluation.

At microscopy, most of the cyst was composed of mature ectodermal elements of epidermis, including benign squamous epithelium, hairs, and sweat glands. A clearly infiltrating neoplasm formed by nests and lobules of atypical vacuolated sebaceous cells constituted the plaques identifiable at the gross level (Fig. 1B). These nests exhibited an inconspicuous lumen with holocrine secretion (Fig. 1C). The sebaceous cells were large with uniformly round nuclei. Mitosis figures were frequent (Fig. 1D). The cytoplasm was abundant and vacuolated with clear boundaries. Basaloid cells surrounded the sebaceous cells, but peripheral palisading or cleft-like spaces between the lobules were not identified. Foci of necrosis, although present, were not extensive. Areas of malignant squamous differentiation were not found after extensive sampling.

The tumor cells stained strongly and diffusely for high-molecular-weight cytokeratins in the immunohistochemistry study (Fig. 1E). A focal positive reaction was observed for CK7, CK19 and EMA in neoplastic cells (Fig. 1F). Low-molecular-weight cytokeratins, CK20, CEA, vimentin, S100, and p63 were negative in tumoral cells. The neoplastic cells expressed no hormonal receptors (ER and PR negative). The proliferative labeling index was low (Ki67 and PCNA stained the nuclei in 10% and 15% of neoplastic cells, respectively). No overexpression of p53 or c-erbB-2 was observed.

Discussion

Mature cystic teratomas, also known as dermoid cysts, are the most common ovarian tumors, accounting for up to 44% of ovarian neoplasms. They represent up to 58% of benign ovarian tumors [11]. Dermoid cysts typically occur in young females (mean age 33 years), accounting for up to one-half of ovarian neoplasms in the first two decades. The major clinical symptom is abdominal pain, followed by a palpable abdominal mass. One-third of cases are asymptomatic. The tumors are bilateral in about 13% of cases and occasionally are multiple in the same ovary. The typical gross features include: a cyst measuring 6–10 cm in diameter, filled with yellow to brown sebaceous material with hair; a tissue resembling skin lining the cyst; and teeth present in one-third of the cases, occasionally within a rudimentary mandible or maxilla. In some cases, bone, cartilage, adipose tissue, thyroid tissue, and brain tissue may be seen grossly [4].

Microscopically, benign teratomas of the ovary show adult-type tissues usually representative of one or more germ layers. There is a predominance of ectodermal derivates in almost all cases, including keratinized epidermis, sebaceous and sweat glands, hair follicles, and neuroectodermal elements (glial and peripheral nervous tissue, cerebrum, cerebellum, and choroids plexus). Mesodermal derivatives include smooth muscle, bone, teeth, cartilage, and fat. Endodermal derivatives include respiratory and gastrointestinal epithelium and thyroid and salivary gland tissue. Rarely observed tissues are retina, pancreas, thymus, adrenal, pituitary, kidney, lung, breast, and prostate.

The morphological findings are usually characteristic enough to permit a precise diagnosis without any special techniques. Malignant change in a component of a mature teratoma is a rare event, occurring in less than 2% of cases [2]. It typically occurs in women who are between 40 years and 60 years of age. The clinical presentation depends on the extension and the histological type of the secondary tumor. In aggressive secondary tumors, such as squamous cell carcinomas, the neoplasm frequently has already spread throughout the abdomen at the time of diagnosis [7]. Teratomas with malignant changes are usually larger than the ordinary dermoid cysts, with more than 90% of them measuring 10–20 cm in maximal dimension. Gross examination may reveal cauliflower-like masses protruding into the cavity of the cyst, a mural nodule or plaque, or even a tumoral mass that obliterates the entire dermoid cyst. Foci of hemorrhage and necrosis within the malignant component are common. The most common secondary tumor is squamous cell carcinoma, corresponding to up to 80% of such neoplasms, but several malignancies have already been reported, including adenocarcinomas, adenosquamous carcinomas, undifferentiated carcinomas, sarcomas, carcinosarcomas, and

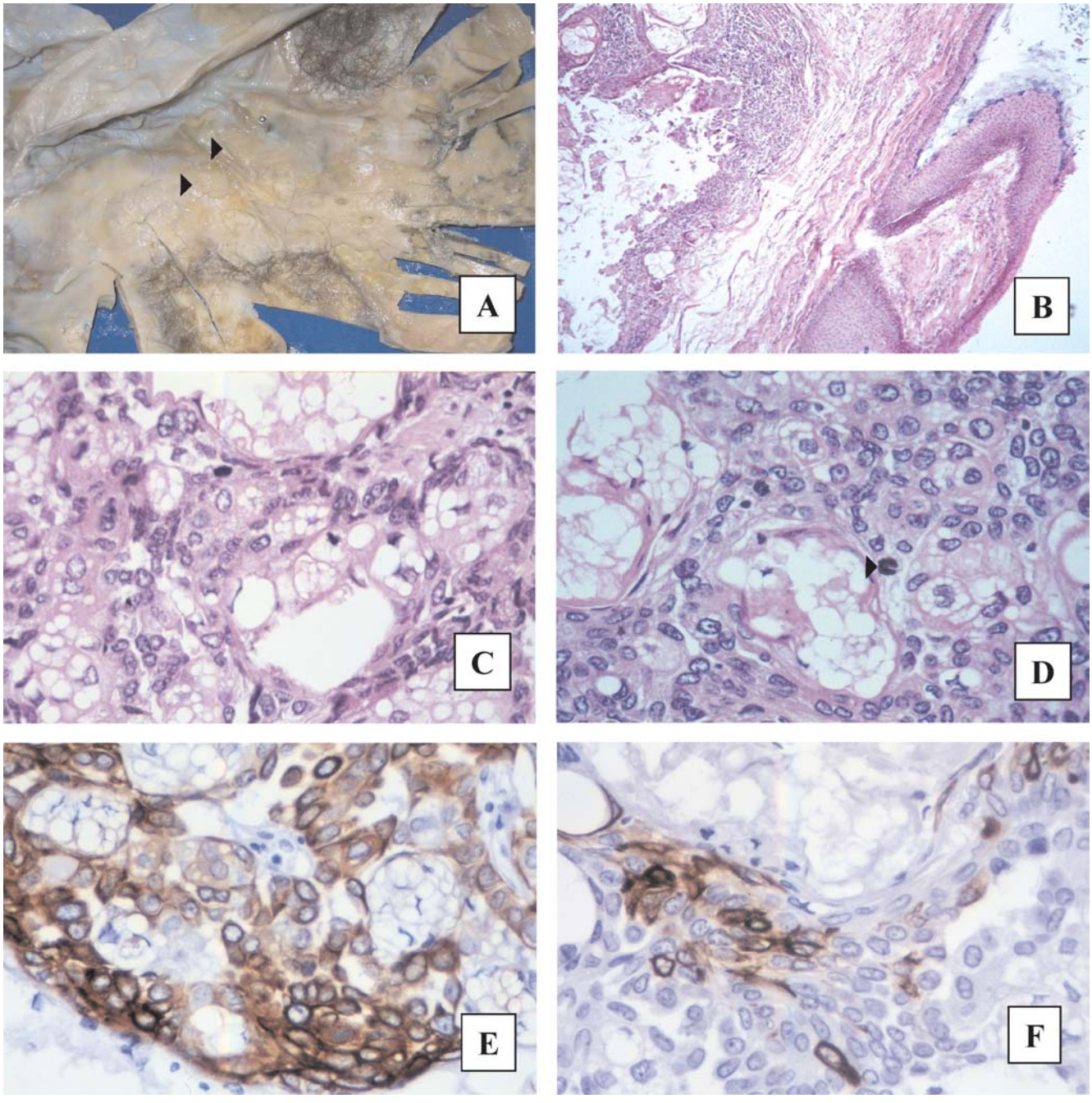

Fig. 1. A Grossly, yellow to white plaques (*arrowheads*) protruding into the lumen of an ovarian teratoma. **B** At low magnification, a sebaceous neoplasm arising within a benign dermoid cyst (hematoxylin-eosin, original magnification ×40). **C** Nest and lobules with inconspicuous lumen and holocrine secretion (hematoxylin-eosin, original magnification ×400). **D** Atypical vacuolated sebaceous cells. Note a mitosis (*arrowhead*; hematoxylin-eosin, original magnification ×400). **E** Diffuse positivity for high-molecular-weight cytokeratins in neoplastic cells (immunohistochemistry, 34βE12, original magnification ×400). **F** Focal positivity for cytokeratin 19 in neoplastic cells (immunohistochemistry, cytokeratin 19, original magnification ×400)

melanomas [1, 14, 16, 17, 24, 30]. Other neoplasms arising in teratomas include carcinoid tumors, thyroid-type tumors, and neuroectodermal tumors [3, 12, 22, 25]. There are only five undisputed reports of sebaceous carcinomas arising in benign teratomas of the ovary since the case reported by Tsuchiya et al. was reclassified by Chumas and Scully as "basal cell carcinoma with sebaceous differentiation" [5, 6, 9, 21, 26, 29].

Grossly and microscopically, sebaceous carcinomas arising in ovarian teratomas resemble their cutaneous counterparts [10]. However, the tumor cells are often large and may have a "squamoid" appearance. In addition, the cells may show basaloid differentiation with

only inconspicuous lipidization. In these cases, sebaceous carcinomas must be differentiated from basal cell carcinomas with sebaceous differentiation. Pure sebaceous carcinomas, however, do not show any area resembling typical basal cell carcinomas and the cells have a more eosinophilic cytoplasm and a higher degree of nuclear atypia, with greater invasiveness [20]. The sebaceous carcinomas must also be distinguished from sebaceomas. The differential diagnosis is based on architectural and cytological features. Sebaceomas are usually circumscribed and symmetrical, whereas carcinomas are larger, asymmetrical, poorly circumscribed, and may have areas of necrosis. The percentage of vacuolated cells is higher in sebaceomas, indicating that these neoplasms are more differentiated. Cytologically, sebaceomas lack striking nuclear atypia, usually present in the carcinomas. Mitoses are more frequent in carcinomas, but may be present in sebaceomas [19].

The immunoprofile of sebaceous carcinomas includes positivity for high-molecular-weight cytokeratins and EMA, and negativity for low-molecular-weight cytokeratins, vimentin, and S100 [28]. In sebaceous carcinoma arising in skin, CEA is usually negative, differing from the present case in which CEA was focally positive. Since expression of EMA is exceptional in basal cell carcinomas, focal EMA staining, as verified in the present report, is useful in distinguishing sebaceous carcinomas from basal cell carcinomas when the differential diagnosis is very difficult to make based only on morphological features [23].

The histogenesis of sebaceous carcinomas is still poorly understood. Some authors believe that these neoplasms originate from pluripotent stem cells destined to become sebaceous stem cells. This hypothesis is attractive since in very rare instances sebaceous carcinomas might arise without a concomitant cystic teratoma [18]. P63, a p53 homologue, stains the basal undifferentiated cells of several epithelia, including skin and its appendages, and is considered to be a progenitor stem cell marker of these tissues [27]. The present case was negative for p63. In addition, focal positivity for CK7 and CK19 may indicate differentiation toward apocrine structures. Taken together, these data may suggest that sebaceous carcinomas originate from more differentiated sebaceous cells usually present in dermoid cysts that undergo malignant change rather than from stem cells. Mutational inactivation of the p53 gene may be involved in the malignant change of sebaceous neoplasms [13, 31]. Curiously, the present case was p53 negative. Overexpression of the p53 gene product is an indicator of aggressiveness in most malignancies. The lack of p53 expression in association with the low proliferative rate assessed by PCNA and Ki67 may be related to the favorable outcome of the present patient. Overexpression of c-erbB-2 is found in 83% of sebaceous carcinomas, but is not associated with any specific pathological findings or clinical outcome [8]. Hormonal receptors are detectable in up to 22% of sebaceous carcinomas, suggesting a hormonal influence on these neoplasms [8]. In the current report, both c-erbB-2 and hormonal receptors were negative.

A sebaceous carcinoma that arises in skin may cause regional metastases, but visceral metastases resulting in death are very rare. None of the sebaceous carcinomas arising in the ovarian teratomas reported until now, including the present case, developed recurrence or metastasis, suggesting that this carcinoma has a favorable outcome. Due to its rarity, there is no consensus about the best therapy to be adopted. Our patient did not receive adjuvant therapy and is doing well 4 months after surgery.

Acknowledgements We acknowledge Ms. Ana Maria Anselmi Dorigan for excellent technical assistance.

References

1. Arora DS, Haldane S (1996) Carcinosarcoma arising in a dermoid cyst of the ovary. J Clin Pathol 49:519–521
2. Ayhan A, Bukulmez O, Genc C, Karamursel BS, Ayhan A (2000) Mature cystic teratomas of the ovary: case series from one institution over 34 years. Eur J Obstet Gynecol Reprod Biol 88:153–157
3. Azzena A, Zannol M, Bertezzolo M, Zen T, Chiarelli S (2002) Epidermoid cyst and primary trabecular carcinoid of the ovary: case report. Eur J Gynaecol Oncol 23:317–319
4. Benjapibal M, Boriboonhirunsarn D, Suphanit I, Sangkarat S (2000) Benign cystic teratoma of the ovary: a review of 608 patients. J Med Assoc Thai 83:1016–1020
5. Betta PG, Cosimi MF (1984) Sebaceous carcinoma arising in benign cystic teratoma of the ovary. Case report. Eur J Gynaecol Oncol 5:146–149
6. Changchien CC, Chen L, Eng HL (1994) Sebaceous carcinoma arising in a benign dermoid cyst of the ovary. Acta Obstet Gynecol Scand 73:355–358
7. Chen RJ, Huang PT, Lin MC, Huang SC, Chow SN, Hsieh CY (2001) Advanced stage squamous cell carcinoma arising from mature cystic teratoma of the ovary. Acta Obstet Gynecol Scand 80:84–86
8. Cho KJ, Khang SK, Koh JS, Chung JH, Lee SS (2000) Sebaceous carcinoma of the eyelids: frequent expression of c-erbB-2 oncoprotein. J Korean Med Sci 15:545–550
9. Chumas JC, Scully RE (1991) Sebaceous tumors arising in ovarian dermoid cysts. Int J Gynecol Pathol 10:356–363
10. Cicchini C, Larcinese A, Ricci F, Aurello P, Mingazzini PL, Indinnimeo M (2002) Monodermal highly specialized teratoma of the ovary: a sebaceous gland tumor. Eur J Gynaecol Oncol 23:442–444
11. Comerci JT Jr, Licciardi F, Bergh PA, et al (1994) Mature cystic teratoma: a clinicopathologic evaluation of 517 cases and review of the literature. Obstet Gynecol 84:22–28
12. den Boon J, van Dijk CM, Helfferich M, Peterse HL (1999) Glioblastoma multiforme in a dermoid cyst of the ovary. A case report. Eur J Gynaecol Oncol 20:187–188
13. Gonzalez-Fernandez F, Kaltreider SA, Patnaik BD, Retief JD, Bao Y, Newman S (1998) Sebaceous carcinoma: tumor progression through mutational inactivation of p53. Ophthalmology 105:497–506
14. Hsu CY, Yang CF, Chen WY, Chiang H (1996) Adenosquamous carcinoma and schneiderian papilloma-like lesion in a mature cystic teratoma of the ovary: a case report. Zhonghua Yi Xue Za Zhi (Taipei) 57:375–379
15. Kontogianni E, Koukoura E, Christopoulou E (2001) Squamous cell carcinoma arising in mature cystic teratoma of the ovary: a case report. Eur J Gynaecol Oncol 22:238–239

16. Kruger S, Schmidt H, Kupker W, Rath FW, Feller AC (2002) Fibrosarcoma associated with a benign cystic teratoma of the ovary. Gynecol Oncol 84:150–154
17. Lim SC, Choi SJ, Suh CH (1998) A case of small cell carcinoma arising in a mature cystic teratoma of the ovary. Pathol Int 48:834–839
18. Misago N, Narisawa Y (2001) Sebaceous carcinoma with apocrine differentiation. Am J Dermatopathol 23:50–57
19. Misago N, Mihara I, Ansai S, Narisawa Y (2002) Sebaceoma and related neoplasms with sebaceous differentiation: a clinicopathologic study of 30 cases. Am J Dermatopathol 24:294–304
20. Nakamura S, Nakayama K, Nishihara K, Imai T (1988) Sebaceous carcinoma with special reference to histopathologic differential diagnosis. J Dermatol 15:55–59
21. Papadopoulos AJ, Ahmed H, Pakarian FB, Caldwell CJ, McNicholas J, Raju KS (1995) Sebaceous carcinoma arising within an ovarian cystic mature teratoma. Int J Gynecol Cancer 5:76–79
22. Ribeiro-Silva A, Bezerra AM, Serafini LN (2002) Malignant struma ovarii: an autopsy report of a clinically unsuspected tumor. Gynecol Oncol 87:213–215
23. Sinard JH (1999) Immunohistochemical distinction of ocular sebaceous carcinoma from basal and squamous cell carcinoma. Arch Ophthalmol 117:776–783
24. Sumi T, Ishiko O, Maeda K, Haba T, Wakasa K, Ogita S (2002) Adenocarcinoma arising from respiratory ciliated epithelium in mature ovarian cystic teratoma. Arch Gynecol Obstet 267:107–109
25. Tanimoto A, Arima N, Hayashi R, Hamada T, Matsuki Y, Sasaguri Y (2001) Teratoid carcinosarcoma of the ovary with prominent neuroectodermal differentiation. Pathol Int 51:829–832
26. Tsuchiya K, Isumi M, Nagayame M, et al (1979) A case of sebaceous carcinoma originating in an ovarian cystic teratoma. J Clin Cancer 25:1448–1451
27. Tsujita-Kyutoku M, Kiuchi K, Danbara N, Yuri T, Senzaki H, Tsubura A (2003) P63 expression in normal epidermis and epidermal appendages and their tumors. J Cutan Pathol 30:11–17
28. Varga Z, Kolb SA, Flury R, Burkhard R, Caduff R (2000) Sebaceous carcinoma of the breast. Pathol Int 50:63–66
29. Vartanian RK, McRae B, Hessler RB (2002) Sebaceous carcinoma arising in a mature cystic teratoma of the ovary. Int J Gynecol Pathol 21:418–421
30. Vimla N, Kumar L, Thulkar S, Bal S, Dawar R (2001) Primary malignant melanoma in ovarian cystic teratoma. Gynecol Oncol 82:380–383
31. Yoshioka T, Tanaka T (1998) Immunohistochemical and molecular studies on malignant transformation in mature cystic teratoma of the ovary. J Obstet Gynaecol Res 24:83–90

Virchows Arch (2003) 443:579–582
DOI 10.1007/s00428-003-0893-0

CASE REPORT

Domenico Piscitelli · Giuseppe Ingravallo · Leonardo Resta · Maria G. Fiore · Eugenio Maiorano

Oncocytic adencarcinoma of the rectum with diffuse intra-luminal microcalcifications: the first reported case

Received: 7 April 2003 / Accepted: 6 July 2003 / Published online: 2 September 2003
© Springer-Verlag 2003

Abstract Several histological variants of colorectal carcinoma have been reported, some of them bearing prognostic significance, others only incidental findings showing unusual morphological features. The current report was aimed to describe the histological, immunohistochemical and ultrastructural features of an oncocytic adenocarcinoma of the rectum occurring in a 66-year-old woman. Histologically, it was a moderately differentiated adenocarcinoma composed by glandular structures lined by eosinophilic cells. The latter showed abundant granular cytoplasm and large nuclei with prominent nucleoli. Several glandular structures contained intraluminal, basophilic and non-birifrangent microcalcifications. The tumour cells displayed consistent anti-mitochondrial antigen, carcinoembryonic antigen, p53, CDX2 and cytokeratin 20 immunoreactivity. Ultrastructurally, more than 80% of the cytoplasmic area was occupied by abnormal mitochondria, while exocrine or endocrine granules were undetectable. The tumour infiltrated the intestinal wall through the subserosal tissue, but lymph node or distant metastases were absent. The patient is disease free 22 months after surgery. Based on the above features, this case could be appropriately named oncocytic adenocarcinoma with intraluminal microcalcifications. Like gastric neoplasms showing similar morphologic features, this tumour might have a better prognosis, and the presence of microcalcifcations could help its proper recognition at a pre-operative stage.

Keywords Colorectal carcinoma · Oncocytic tumour · Mitochondria · Microcalcification · Ultrastructure

D. Piscitelli · G. Ingravallo · L. Resta · M. Fiore · E. Maiorano
Department of Pathological Anatomy and Genetics,
University of Bari,
Bari, Italy

E. Maiorano (✉)
Department of Pathological Anatomy and Genetics,
Piazza G. Cesare 11, 70124 Bari, Italy
e-mail: emaiorano@anatopat.uniba.it
Tel.: +39-080-5478292
Fax: +39-080-5478263

Introduction

Malignant tumours of the bowel are frequently localised in the rectum, adenocarcinoma being the most common histotype at this site. However, several histological variants have been reported, including mucinous adenocarcinoma, signet-ring cell carcinoma, adenosquamous carcinoma, medullary carcinoma, undifferentiated carcinoma, spindle cell carcinoma and carcinosarcoma. Other rare histopathological variants of colorectal carcinoma include pleomorphic (giant cell), choriocarcinoma, pigmented, clear cell, hepatoid, stem cell and Paneth cell-rich (crypt cell) carcinoma. Some of these variants can bear better or worse prognoses than colorectal adenocarcinoma of the conventional type [8].

Although the occurrence of scattered oncocytic-like cells in otherwise conventional adenocarcinomas of the gastrointestinal tract has occasionally been observed [10], pure oncocytic carcinomas (i.e. malignant oncocytomas) have never been described in the large bowel. On the contrary, these neoplasms are relatively more common in other organs, such as salivary glands, breast, thyroid, parathyroids, pancreas, stomach, kidneys and respiratory tract [2, 3, 6, 10, 12, 13, 15].

The current report was aimed to describe the clinico–pathological, immunohistochemical and ultrastructural features of an oncocytic adenocarcinoma of the rectum arisen in a 66-year-old woman, which showed abundant intra-glandular microcalcifications that may allow proper identification of this tumour variant.

Case report

Clinical history

A 66-year-old woman was hospitalised for the evaluation of rectal bleeding during defecation for the previous 4 months. An ulcerative lesion of the rectum 2.3 cm in its largest diameter was found by total colonoscopy. Pre-operative total body computed tomography (CT)-scan showed local thickening of the rectal wall without infiltration of peri-rectal fat tissue. Lymph node and hepatic metastases were not detected. Following the diagnosis of adeno-

carcinoma with oncocytic features on colonoscopic biopsies, the patient underwent abdomino–perineal resection with sigmoidostomy and subsequent radio-therapy. The patient is in good health with no evidence of disease 22 months after therapy.

Materials and methods

The surgical specimen was fixed overnight in 10% neutral-buffered formalin, sampled and embedded in paraffin blocks, sectioned at 4-μm thickness and stained with haematoxylin-eosin (H&E) and phosphotungstic haematoxylin (PTAH). Additional sections, collected on poly-L-lysine-coated slides, were used for the immunohistochemical stains with the alkaline phosphatase-anti-alkaline phosphatase (APAAP) method. Antigen retrieval procedures were carried out in a pressure cooker for 1′30″, following immersion in 1 mM ethylene diamine tetra-acetic acid (EDTA), pH 8.0, with the exception of the sections to be incubated with anti-Ki67 and anti-p53 antibodies that were processed in a microwave oven, 4×5′ after immersion in 10 mM sodium citrate, pH 6.0. The sections were then incubated overnight at 4°C with the primary antibodies listed in Table 1. The APAAP method was preferred to avidin-biotin-based detection systems as mitochondria-rich tissues consistently show strong endogenous biotin and biotin-like activity (avidin-binding activity), thus possibly producing false-positive staining [4, 5]. Appropriate negative controls, obtained by substituting the primary antibodies with pre-immune serum, and positive controls, indicated in Table 1, were included in the procedure.

For electron microscopy, representative samples were retrieved from the paraffin blocks matched with the corresponding H&E stained section. They were dewaxed in xylene, rehydrated, post-fixed in 1% osmium tetroxide, dehydrated in ethanol and embedded in epon-araldite. Semi-thin sections were cut, stained with toluidine blue and examined by light microscopy to select representative areas. Ultra-thin sections, stained with uranyl acetate and lead citrate, were examined with a Philips CM10 transmission electron microscope.

Results

Histopathology

Overall, the architectural features of the tumour were those of a moderately differentiated adenocarcinoma ulcerating the surface epithelium and infiltrating the intestinal wall through the subserosal tissue (Fig. 1a). The neoplastic glands were lined by a single or double layer of plump epithelial cells showing abundant eosinophilic cytoplasm and large pleomorphic nuclei with prominent nucleoli (Fig. 1b). The cytoplasm of the tumour cells was eosinophilic and finely granular and stained dark blue with PTAH. Occasionally, the neoplastic cells were arranged in thin cords or dispersed as single cells. Mitotic figures were less than 1/10 high power field (HPF). At high power view, smaller cells were observed, with eosinophilic cytoplasm and small non-nucleolated nuclei, scattered among the granular tumour cells. Moreover, there seemed to be a transition from the former to the latter with progressive increasing of cytoplasmic granularity (Fig. 1c).

In addition, necrotic debris and clusters of amorphous calcified material filled the lumen of the neoplastic glands of larger dimension. Occasionally, foreign body multinucleated giant cells were associated with necrotic debris and microcalcifications. A prominent lympho-monocytic inflammatory response was evident in close association with the neoplastic glands and in the residual intestinal mucosa.

Immunohistochemistry

The tumour cells showed consistent intra-cytoplasmic immunoreactivity for cytokeratin 20 (Fig. 1d), carcino-embryonic antigen (CEA) and mitochondria antigen (Fig. 1e), along with nuclear immunoreactivity for p53 and CDX2 (Fig. 1f) in more than 50% of the neoplastic cells. Less than 1% tumour cells displayed nuclear anti-Ki 67 (MIB 1) positivity. No immunoreactivity for chromogranin A, cytokeratin 7, deleted in colon cancer antigen (DCC), neuron specific enolase (NSE) and synaptophysin was detected in tumour cells.

Ultrastructural study

The tumour cells were arranged in tubular structures and showed evident microvilli on their luminal surface, junctional complexes and desmosomes. Most neoplastic nuclei had a regular outline and prominent irregular nucleoli. In addition, numerous mitochondria, irregularly dispersed throughout the cytoplasm of the tumour cells, filled at least 80% of the total cytoplasmic area. These mitochondria showed elongated cristae and partial lamellar internal structure. Other organelles were scarce and, in

Table 1 Pertinent data of the monoclonal antibodies used to immuno-characterise oncocytic carcinoma of the rectum. *Ag* antigen, *CEA* carcinoembryonic antigen, *NSE* neuron specific enolase, *DCC* deleted in colon cancer

Antigen	Clone	Dilution	Source	Positive control
CDX2	CDX2–88	1/50	BioGenex, San Ramon, CA, USA	Colonic mucosa
CEA	II—7	1/90	Dako, Glostrup, Denmark	Colonic carcinoma
Chromogranin A	DAK—A3	1/1800	Dako	Carcinoid
Cytokeratin 7	OV-TL 12/30	1/250	Dako	Breast carcinoma
Cytokeratin 20	Ks 20.8	1/100	Novocastra, Newcastle upon Thine, UK	Colonic carcinoma
DCC	G 97–449	1/500	Pharmingen, Franklin Lakes, NJ, USA	Colonic mucosa
Ki 67	MIB–1	1/100	Dako	Breast carcinoma
Mitochondria Ag	113–1	1/300	BioGenex	Salivary oncocytoma
NSE	BSS/NC/VI-H14	1/400	Dako	Brain tissue
p53	DO7	1/50	Dako	Colonic carcinoma

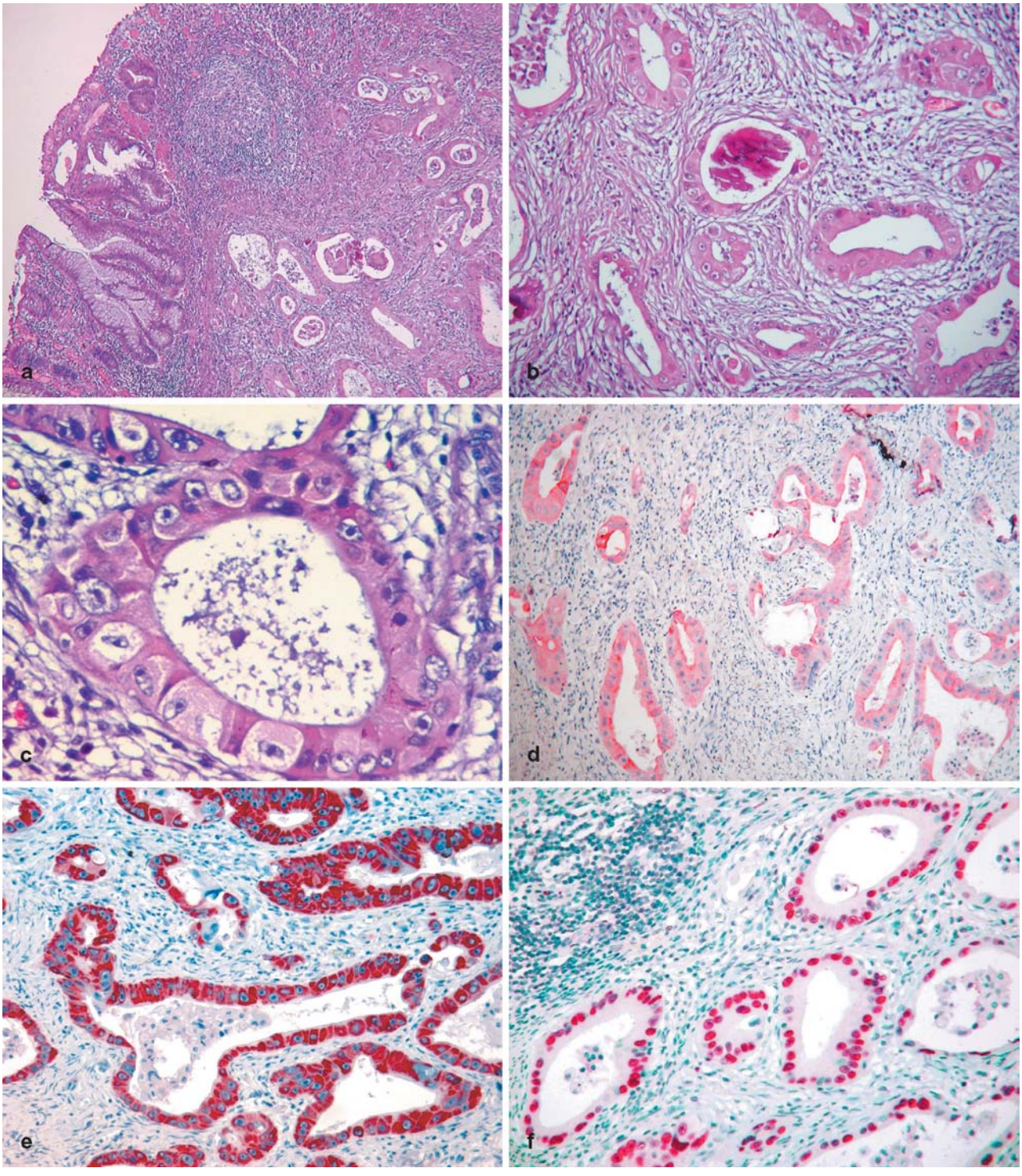

Fig. 1 The tumour is composed by haphazardly arranged glandular structures, resembling conventional adenocarcinoma of the colon, which infiltrate the rectal wall and ulcerate the surface [**a** haematoxylin-eosin (H&E), ×40]. The neoplastic glandular structures are lined by a single or double layer of strongly eosinophilic cells and occasionally contain intra-luminal calcifications and necrotic debris (**b** H&E, ×200). Most tumour cells show abundant cytoplasm with evident granularity and large pleomorphic nuclei with prominent nucleoli. Smaller eosinophilic cells with small nuclei are intermingled with the former, and transition between the two cell types, possibly due to progressive accumulation of cytoplasmic granules, is sometimes evident. The luminal cells also display apical cytoplasmic expansions suggestive of microvilli (**c** H&E, ×400). Most tumour cells display consistent cytokeratin 20 (**d** ×160), mitochondria antigen (**e** ×200) and CDX2 immunoreactivity (**f** ×200)

particular, no exocrine and endocrine granules were evident by electron microscopy.

Discussion

The neoplasm described herein was characterised by extensive infiltration of the rectal wall, glandular pattern of growth with a single layer of epithelial cells having a prominent eosinophilic cytoplasm and large nucleolated nuclei. Furthermore, the cytoplasm of the neoplastic cells was clearly granular and showed anti-mitochondria immunoreactivity. Ultrastructurally numerous and abnormal mitochondria filled the cytoplasm of these cells. This cumulative evidence points to an oncocytic differentiation of the tumour cells that also showed an antigenic profile (CDX2+ve, CEA+ve, cytokeratin 20+ve, DCC−ve, cytokeratin 7−ve) consistent with a primary colonic carcinoma. In addition, this particular tumour did not manifest endocrine differentiation, as supported by lack of chromogranin A, synaptophysin and NSE immunoreactivity and of endocrine granules at ultrastructural analysis.

Consistent with 40–60% of conventional colon cancer [1], the tumour cells displayed p53 nuclear positivity, although this tumour was not very active mitotically, as confirmed by the few mitotic figures and low (<1%) Ki 67 immunoreactivity. In addition, the tumour cells did not show DCC immunoreactivity, in contrast with normal epithelial cells in the same tissue sample, thus suggesting that this tumour variant shares the same genetic pathways (i.e. allelic loss of DCC on chromosome 18 and inactivation of p53) with more that 70% conventional colon cancers [14].

Tumours with eosinophilic and granular cells encompass a heterogeneous group of neoplasms of different lineages, such as granular cell tumours, oncocytomas and carcinoids. Intra-cytoplasmic granularity frequently derives from the accumulation of organelles. Consequently, secretory granules, either endocrine or exocrine in nature, as well as mithocondria, lysosomes and different types of vesicles may be responsible for the granular appearance of a cell cytoplasm [9]. In most instances, proper identification of the their nature necessitates ancillary techniques, such as histochemistry, immunohistochemistry or electron microscopy. Recently, a short series of gastric oncocytic carcinomas has been reported, mainly occurring in older patients and having a better prognosis, in comparison with conventional gastric carcinoma [15].

Although the current case exhibited unequivocal features of malignancy because of extensive infiltration of the intestinal wall, we have no definitive evidence to predict its aggressiveness—in comparison with conventional colonic adenocarcinoma—mainly because of limited follow-up. Nevertheless, this tumour showed very low proliferative activity and lack of lymph node metastases in the ten examined lymph nodes, notwithstanding its large size and depth of invasion through the rectal wall.

Interestingly, the tumour described herein also displayed prominent intra-luminal accumulations of calcified material within the neoplastic glands, which look very much like those encountered in several breast lesions (type-II microcalcifications) [7], both neoplastic and non-neoplastic, which are composed mainly of calcium phosphate and usually are associated with cellular degeneration or necrosis (so-called “dystrophic calcifications”) [11]. We are not aware whether or not these may be identified on colonic radiograms or CT scans as they can be on mammograms, but appropriate radiological studies on this issue may help to possibly identify this variant of colonic adenocarcinoma at a pre-operative stage.

Acknowledgments The authors wish to thank Mr. M. D’Elia, Mrs. G. Agazzino and Mr. P. Aldini for excellent technical assistance.

References

1. Allegra CJ, Paik S, Colangelo LH, Parr AL, Kirsch I, Kim G, Klein P, Johnston PG, Wolmark N, Wieand HS (2003) Prognostic value of thymidylate synthase, Ki-67, and p53 in patients with Dukes’ B and C colon cancer: a National Cancer Institute-National Surgical Adjuvant Breast and Bowel Project collaborative study. J Clin Oncol 21:241–250
2. Baloch ZW, LiVolsi VA (1999) Oncocytic lesions of the neuroendocrine system. Semin Diagn Pathol 16:190–199
3. Brandwein MS, Huvos AG (1991) Oncocytic tumours of major salivary gland: a study of 68 cases with follow-up of 44 patients. Am J Surg Pathol 15:514–528
4. Bussolati G, Gugliotta P, Volante M, Pace M, Papotti M (1997) Retrieved endogenous biotin: a novel marker and a potential pitfall in diagnostic immunohistochemistry. Histopathology 31:400–407
5. Chan JKC (2000) Advances in immunohistochemistry: impact on surgical pathology practice. Semin Diagn Pathol 17:170–177
6. Damiani S, Dina R, Eusebi V (1999) Eosinophilic and granular cell tumours of the breast. Semin Diagn Pathol 16:117–125
7. Gonzalez JE, Caldwell RG, Valaitis J (1991) Calcium oxalate crystals in the breast. Pathology and significance. Am J Surg Pathol 15:586–591
8. Hamilton SR, Vogelstein B, Kudo S, Riboli E, Nakamura S, Hainaut P, Rubio CA, Sobin LH, Fogt F, Winawer SJ, Goldgar DE, Jass JR (2000) Carcinoma of the colon and rectum. In: Hamilton SR, Aaltonen LA (ed) Pathology and genetics of tumours of the digestive system. World Health Organization classification of tumours. IARC Press, Lyon, pp 105–119
9. Nappi O, Ferrara G, Wick MR (1999) Neoplasms composed of eosinophilic polygonal cells: an overview with consideration of different cytomorphologic patterns. Semin Diagn Pathol 16:82–90
10. Papotti M, Cassoni P, Taraglio S, Bussolati G (1999) Oncocytic and oncocytoid tumours of the exocrine pancreas, liver, and gastrointestinal tract. Semin Diagn Pathol 16:126–134
11. Radi MJ (1989) Calcium oxalate crystals in breast biopsies. Arch Patol Lab Med 113:1367–1369
12. Reuter VE (1999) Renal tumors exhibiting granular cytoplasm. Semin Diagn Pathol 16:135–145
13. Ritter JH, Nappi O (1999) Oxyphilic proliferations of the respiratory tract and paranasal sinuses. Semin Diagn Pathol 16:105–116
14. Shibata D, Reale MA, Lavin P, Silverman M, Fearon ER, Steele G, Jessup JM, Loda M, Summerhayes IC (1996) The DCC protein and prognosis in colorectal cancer. N Engl J Med 335:1727–1732
15. Takubo K, Honma N, Sawabe M, Arai T, Izumiyama-Shimomura N, Kammori M, Sasajima K, Esaki Y (2002) Oncocytic adenocarcinoma of the stomach. Am J Surg Pathol 26:458–465

Virchows Arch (2003) 443:583–585
DOI 10.1007/s00428-003-0847-6

LETTER TO THE EDITOR

Tadashi Terada · Hiroaki Inatsuchi · Masanori Yasuda · Yoshiyuki Osamura

A kidney carcinoma with features of clear cell renal carcinoma and transitional cell carcinoma: a combined renal cell and transitional cell carcinoma?

Received: 22 April 2003 / Accepted: 2 May 2003 / Published online: 27 June 2003
© Springer-Verlag 2003

Keywords Kidney carcinoma · Clear cell renal carcinoma · Transitional cell carcinoma

Dear Editor,

Renal cell carcinoma (RCC) arises from kidney parenchyma, while transitional cell carcinoma (TCC) from the renal pelvis in the kidney. We report a kidney carcinoma with histological features of RCC and TCC.

A 72-year-old Japanese man presented with right lumbar pain and hematuria, and was admitted to our clinic. Imaging modalities showed a solid tumor in the upper half of the right kidney. RCC was suspected, and total nephrectomy was performed. Grossly, the tumor was solid and yellowish tan with a rather hard consistency. The tumor measured 5×6×5 cm and invaded into the pericapsular fat tissue and renal pelvis. Histologically, there were two populations of tumor cells. One component was composed of clear cells with hyperchromatic nuclei arranged in a trabecular pattern (Fig. 1A). This was interpreted as RCC of clear cell type. The other component consisted of stratified cells with hyperchromatic nuclei and dark cytoplasm (Fig. 1B). This was diagnosed as TCC. These two components were admixed in the tumor (Fig. 2A), and gradual transition between the two was recognized in places (Fig. 2B). The distribution of both components was even in the tumor. The renal pelvis and extracapsular invading front showed the same morphology. The RCC component comprised approximately 50% of the tumor, and the TCC component another 50%. Vascular and lymphatic invasion was recognized in some areas. The non-tumorous kidney showed no significant changes.

The tumor cells of both components were negative with periodic acid–Schiff base (PAS), alcian blue, and Grimelius stains. Immunohistochemically, the tumor cells of both components showed the same results. They were positive for low-molecular-weight cytokeratins (LMWCK) using antibodies (KL-1, MNF116, and CAM5.2) and epithelial membrane antigen, but were negative for high-molecular-weight CK (HMWCK) (AE1/AE3), vimentin, carcinogenic embryonic antigen (CEA), desmin, alpha-smooth muscle antigen, S-100 protein, chromogranin A, CD68, C-erbB2, p53, bcl-2, and placental alkaline phosphatase. CK profiling showed that both components of the tumor cells were positive for CK7, CK18 and CK19, while they were negative for CK8 and CK20. Ki-67 labeling was approximately 15%.

RCC and TCC are two major carcinomas occurring in the kidney. RCC may arise from proximal convoluted tubules, thus developing in the parenchyma of the kidney [5]. In contrast, TCC arises from urothelia of the renal pelvis and calices, thus occurring in the renal pelvis. Embryologically, both renal parenchyma and pelvis develop from mesodermal metanephros [5]. Renal parenchyma develops from metanephric tissue (nephrogenic blastema), and the renal pelvis from the ureteric bud. Thus, renal parenchyma and pelvis have common developmental origin.

Histologically, the present tumor was composed of RCC and TCC. Both elements were admixed in the tumor, and there were gradual transitions between the two. Therefore, we diagnosed the tumor as combined RCC and TCC. A search of the English literature failed to detect such a combined RCC and TCC, though there were several cases of RCC and TCC that were separately detected in the same kidney [2, 4]. Such an entity as the

T. Terada (✉)
Department of Pathology,
Shizuoka Municipal Shimizu Hospital,
Shimizu-Miyakami 1231, 424-8636 Shizuoka, Japan
e-mail: byouri@city.shimizu.shizuoka.jp
Fax: +81-543-361315

H. Inatsuchi
Department of Urology,
Shizuoka Municipal Shimizu Hospital, Japan

M. Yasuda · Y. Osamura
Department of Pathology,
Tokai University School of Medicine, Japan

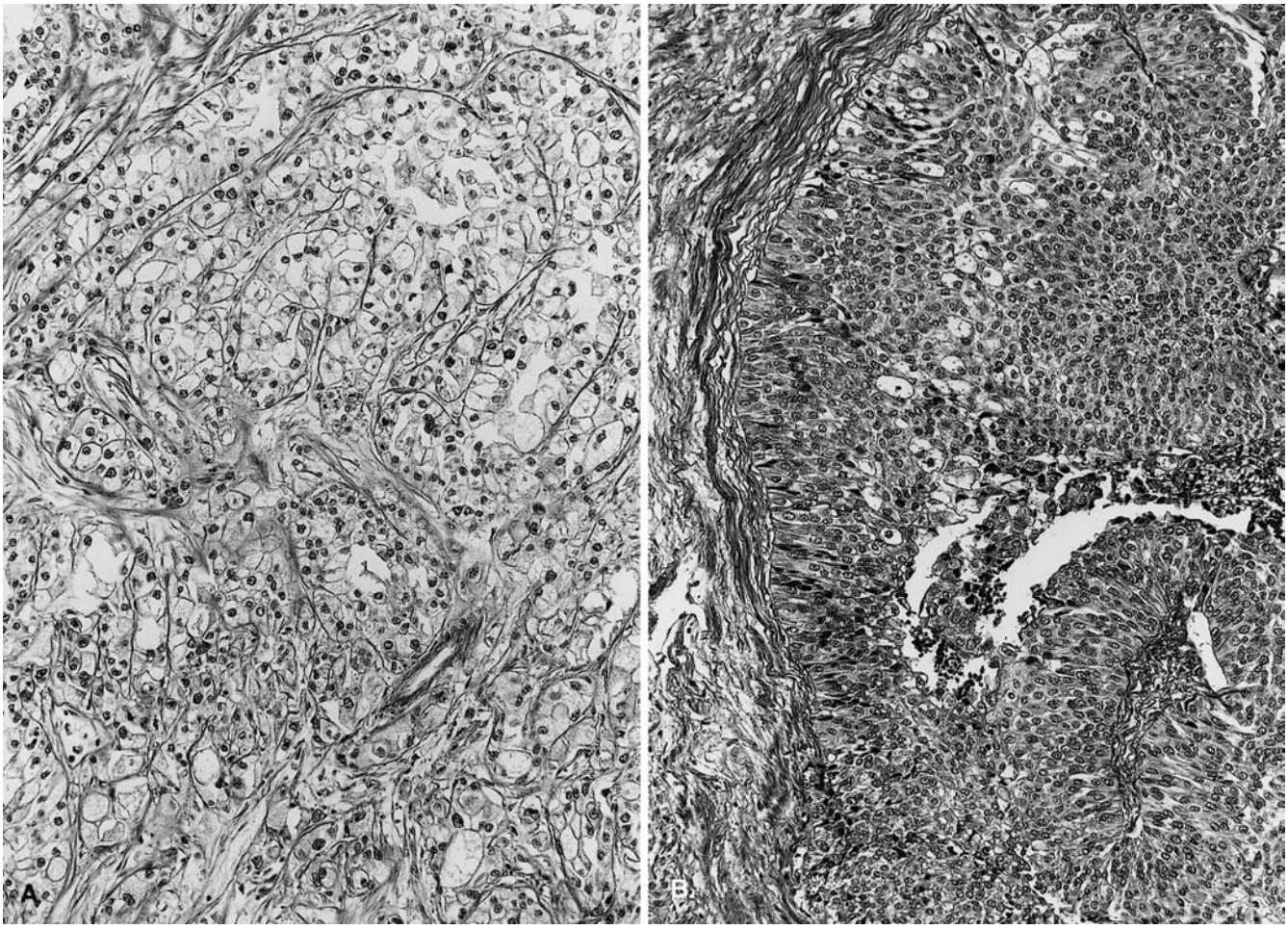

Fig. 1 Histology of the tumor. Some parts show clear cells with atypia arranged in a trabecular pattern, resembling renal clear cell carcinoma (A), while other parts show stratified dark cells with atypia, resembling transitional cell carcinoma (B). HE, A and B, x250

present case was not reported in Atlas of Tumor Pathology of AFIP [5].

Immunohistochemically, RCC of clear cell type usually expresses vimentin, bcl-2, CD10, LMWCK, and CK7, but is negative for CK8, CK19, CK20 and HMWCK. TCC, in contrast, is usually positive for LMWCK, CK7, CK8, CK19, CK20 and HMWCK, but negative for vimentin and CD10 [3]. The present case was positive for LMWCK, CK7, CK18 and CK19, but was negative for vimentin, CK8, CK20 and HMWCK. It is considered that reactivities of CK7, CK20 and HMWCK are useful in differential diagnosis of RCC and TCC. The present case is intermediate in the immunophenotypes between RCC and TCC. However, positive CK7 and negative CK20 and HMWCK may favor RCC in the present case.

The pathogenesis of our tumor is unclear. RCC is thought to arise from proximal convoluted tubules, while TCC of the kidney is considered to derive from renal pelvic urothelia [1]. Three hypotheses are conceivable in the present case. The first hypothesis is that the present case was at first RCC or TCC and later some parts of the tumor transformed into TCC and RCC, respectively. The second hypothesis is that RCC and TCC developed separately in a very near area and then fused with each other (collision cancer), thus creating the morphology of the present case. The third hypothesis is that the present tumor arose from renal stem cells which are capable of differentiating into RCC and TCC [1].

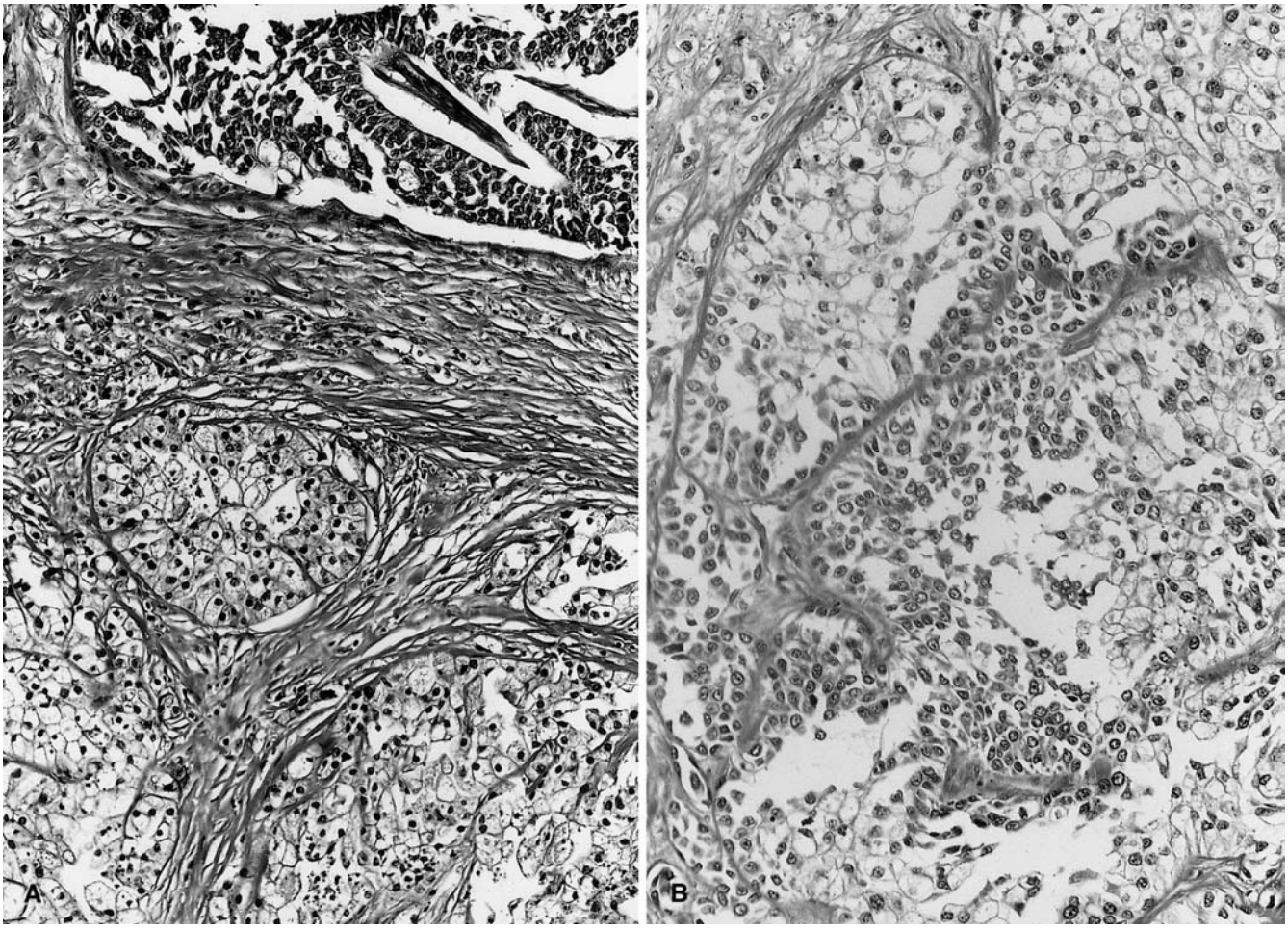

Fig. 2 Histology of the tumor. Transitional cell carcinoma-like area (upper) is admixed with renal clear cell carcinoma-like area (lower) (A). Gradual transition between dark transitional cell carcinoma-like cells and clear renal cell carcinoma-like cells are seen. HE, A, x250. B, x300

References

1. Fair WR, Heston WDW (1992) Overview of cancer biology and principles of oncology. In: Walsh PC, Retik AB, Stamey TA, Vaughan ED (eds) Campbells' urology, 6th edn, vol 2. Saunders, Philadelphia, pp1031–1047
2. Fallon B, Schellhammer PF (1975) Transitional cell carcinoma and renal cell carcinoma in single kidney. Urology 6:774–775
3. Kim MK, Kim S (2002) Immunohistochemical profile of common epithelial neoplasms arising in the kidney. Appl Immunohistochem Mol Morphol 10:332–338
4. Lundell C, Kadir S, Engel R, Nyberg LM (1982) Concurrent renal cell and transitional cell carcinoma in a single kidney: a case report. J Urol 127:761–763
5. Murphy WM, Beckwith JB, Farrow GM (1994) Atlas of tumor pathology. Tumors of the kidney, bladder, and related urinary structures. Third series. Fascicle 11. Armed Force Institute of Pathology, Washington, D.C.

Virchows Arch (2003) 443:586–588
DOI 10.1007/s00428-003-0823-1

LETTER TO THE EDITOR

Federico Roncaroli · Alessandro Consales · Christine Betts · Tshering Dorji · Fabio Calbucci · Vincenzo Eusebi

Schwannoma with small cell component

Received: 10 February 2003 / Accepted: 4 April 2003 / Published online: 28 June 2003
© Springer-Verlag 2003

We report a conventional schwannoma of the left trigeminal nerve featuring a small cell component. This 23-year-old male patient presented with a short history of headache and visual impairment to the left eye. Stigmata and family history of neurofibromatosis type 1 and type 2 were absent. Magnetic resonance imaging showed a "dumbbell-shaped" tumour of the cerebellopontine angle extending to the Meckel's cave. The left cavernous sinus was also invaded. On the T1-weighted sequences, the lesion was isointense with the grey matter and inhomogeneously enhanced after gadolinium administration (Fig. 1). The brain stem was shifted and the III ventricle compressed. On surgical inspection, the lesion was noted to dissociate the left trigeminal nerve bundles. Postoperative course was uneventful. Seventeen months after surgery, the patient was well with no neurological deficit. Histologically, the tumour was composed of interlacing bundles of bland spindle cells admixed with large sheets of small cells (Fig. 2A). The spindle cell component featured rare Verocay bodies, vessels with thickened and hyalinised wall, focal stromal myxoid changes and foamy macrophages. The small cells that were about 40% of the tumour had scanty cytoplasm and round, hyperchromatic nuclei. A minority of small cells also formed pseudorosettes lacking fibrillary core (Fig. 2B). In both components, mitoses were less than 1×50 high power fields (HPF) and necrosis was absent. Most tumour cells were immunoreactive for S-100 protein (Dako, Carpintera CA, USA; polyclonal 1:1500) (Fig. 2C), vimentin (Dako; monoclonal 1:50) and CD56 (Novocastra, Newcastle Upon Tyne UK; monoclonal 1:100). Collagen IV (Dako; monoclonal 1:100) surrounded the spindle cells and some, but not all, small cells. Some spindle cells surrounding blood vessels also expressed GFAP (Dako; polyclonal 1:1000). The Ki67 (Dako; polyclonal 1:50) labelling index was 1% in both components. No p53 (Dako; monoclonal 1:50) overexpression was present. Ultrastructurally, the spindle cells showed elongated cytoplasmic processes. Nuclei were ovoid with finely dispersed chromatin. Within cytoplasmic processes, occasional mitochondria were present. Cells were joint by rudimentary junctions. The free plasma membrane was coated by an external basal lamina. The small cells showed round

F. Roncaroli · T. Dorji · V. Eusebi (✉)
Department of Oncology,
Section of Anatomic and Cytopathology "Marcello Malpighi",
Bellaria Hospital, University of Bologna,
Via Altura 3, 40139 Bologna, Italy
e-mail: vincenzo.eusebi@ausl.bo.it

A. Consales · F. Calbucci
Division of Neurosurgery, Bellaria Hospital,
University of Bologna, Italy

C. Betts
Department of Experimental Pathology,
University of Bologna, Italy

Fig. 1 This T1-weighted axial magnetic resonance imaging sequence following gadolinium administration shows a contrast-enhanced "dumbbell-shaped" tumour of the cerebellopontine angle that extends to the Meckel's cave and cavernous sinus

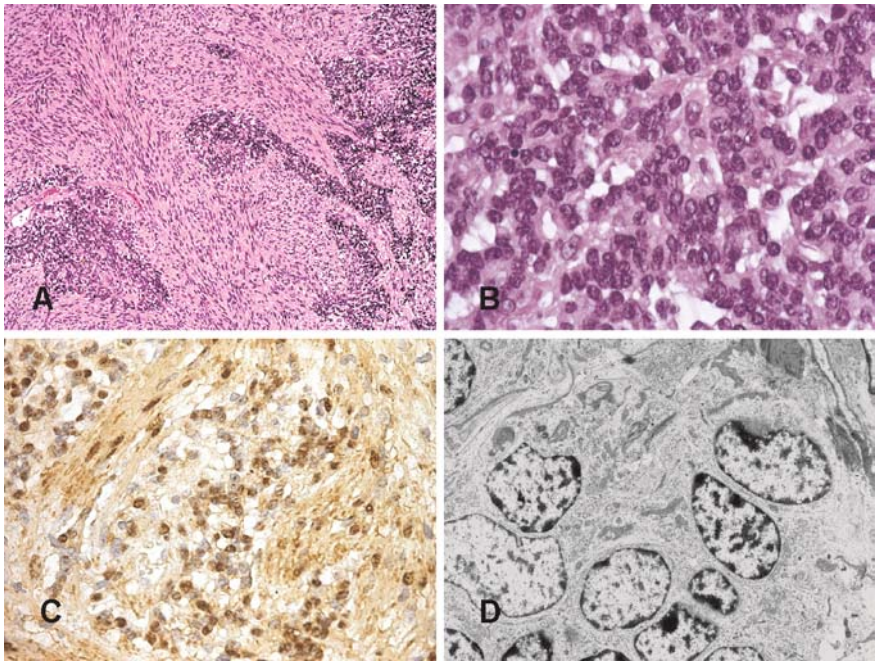

Fig. 2 The tumour features areas of conventional schwannoma admixed with small cells (**A**) [haematoxylin and eosin (HE), ×4]. The small cells are arranged in clusters lacking a fibrillary core (**B**) (HE, ×40). The neoplastic cells immunoreact for S-100 protein (**C**, ×25) (ABC/peroxidase). On electron microscopic examination, the small cells show a round nucleus with a prominent nucleolus; the cytoplasm contains mitochondria and rough endoplasmic reticulum; pericellular basal lamina is discontinuous (**D**, ×9.800)

Table 1 Clinicopathologic findings of schwannomas with small cell component. *n.r.* not reported, *NED* no evidence of disease, *DOD* died of disease, *NF 1* neurofibromatosis type 1

Case	Reference	Sex/age	NF1	Site	Schwannomatous component	Small cell component	Mitoses	Epithelioid cells	Follow-up
1	[8]	n.r.	n.r.	n.r.	Conventional	Sheets, lympocytic-like	n.r.	n.r.	n.r
2	[6]	Female/44	No	Neck	Conventional	Pervascular rosettes	1×50	No	NED 27 months
3	[6]	Male/32	No	Left palm	Conventional	Neuroblastic rosettes	n.r.	No	NED 12 months
4	[6]	Female/46	No	Right flank	Cellular	Neuroblastic rosettes	n.r.	No	NED 2 months
5	[5]	Female/24	No	Thigh	Conventional	Neuroblastic rosettes	n.r.	Yes	NED 9 months
6	[3]	Female/53	No	Left vulva	Plexiform	Neuroblastic rosettes	n.r.	Yes	NED 18 months
7	[3]	Female/35	No	Left knee	Conventional	Neuroblastic rosettes	n.r.	Yes	NED 24 months
8	Present	Male/23	No	Left trigeminum	Conventional	Sheets	1×50	No	NED 16 months
9*	[6]	Female/93	n.r.	Right thumb	Conventional	Sheets, few pseudorosettes	10×10	n.r.	n.r
10*	[7]	Female/48	No	Chest wall	Conventional	Sheets	30×10	Yes	DOD 16 months

*Cases 9 and 10 were malignant

nuclei with prominent nucleoli. In their cytoplasm, mitochondria and rough endoplasmic reticulum were present. Pericellular basal lamina was discontinuous (Fig. 2D). The immunoprofile together with ultrastructural features was consistent with the schwannian origin of the small cells.

Small cells have been reported in benign schwannomas [1, 2, 3, 4, 6] as well as in schwannomas with malignant transformation [2, 5] (Table 1). All patients were adults with no stigmata of neurofibromatosis. All tumours occurred in the soft tissue with no definite origin from a major nerve trunk. None involved the fifth cranial nerve. Sheets of small cells similar to those of the present tumour were seen in the two malignant examples [2, 5] and two benign lesions [3, 6], one of which also contained neuroblastic-like rosettes [3]. The small cells of the present lesion as well as the previously reported lesions showed no neuronal differentiation. Electron microscopic examination of the one benign tumour examined [4] showed that the small cells contained few organelles and, unlike the present lesion, were surrounded by continuous basal lamina. Malignant transformation in schwannomas is exceedingly uncommon [7]. Unlike patients with conventional malignant peripheral nerve sheath tumours, those with malignant schwannoma have a long-standing history of symptoms related to the tumour and lack stigmata of NF 1 (neurofibromatosis type 1). By definition, the underlying tumour has to be a conventional schwannoma [7]. Clinical outcome is poor.

The tumour described here originated from the common root of the fifth cranial nerve. Second in frequency to acoustic schwannomas, trigeminal schwannomas may originate from the common nerve root, gasserian ganglion or one of the three branches. Similar to the present

tumour, schwannomas extending to posterior and middle fossa are defined as "dumbbell-shaped" and, despite extension and displacement of the surrounding neurovascular structures, they are benign. No previously reported trigeminal schwannoma contained small cells. If criteria defining schwannoma with malignant transformation [7] are strictly applied, no malignant schwannoma of the fifth cranial nerve has previously been reported.

In conclusion, the small cells seen in the present tumour were benign and likely represented part of the morphologic spectrum of neoplastic Schwann cells. Overdiagnosis of malignancy has to be avoided.

Acknowledgements Mr Alessandro Busi for technical assistance in photographs.

References

1. Bhatnagar S, Banerjee SS, Mene AR, Prescott RJ, Eyden BP (1998) Schwannoma with features mimicking neuroblastoma: report of two cases with immunohistochemical and ultrastructural findings. J Clin Pathol 51:842–845
2. Casterns PHB, Schrodt GR (1969) Malignant transformation of a benign encapsulated neurilemoma. Am J Clin Pathol 51:144–149
3. Fisher C, Chappell ME, Weiss SW (1995) Neuroblastoma-like epithelioid schwannoma. Histopathology 26:193–194
4. Goldblum JR, Beals TF, Weiss SW (1994) Neuroblastoma-like neurilemoma. Am J Surg Pathol 18:266–277
5. Hanada M, Tanaka T, Kanayama S, Takami M, Kimura M (1982) Malignant transformation on intrathoracic ancient neurilemoma in a patient without von Recklinghausen's disease. Acta Pathol Jpn 32:527–536
6. Harkin JC, Reed RJ (eds) (1969) Solitary benign nerve sheath tumors. In: Tumors of the peripheral nervous system, 2nd series. Armed Forces Institute of Pathology, Washington DC, pp 29–65
7. Woodruff JM, Selig AM, Crowley K, Allen PW (1994) Schwannoma (neurilemoma) with malignant transformation. A rare, distinctive peripheral nerve tumor. Am J Surg Pathol 19:882–895

Virchows Arch (2003) 443:589–590
DOI 10.1007/s00428-003-0886-z

LETTER TO THE EDITOR

Michal Michal · Romuald Curik · Karel Matler · Zdenek Benes

Regarding the paper by Vieth et al. Virchows Archiv 442/4:317–321

Received: 28 May 2003 / Accepted: 13 June 2003 / Published online: 19 August 2003
© Springer-Verlag 2003

Sir, The article of Vieth et al. [5] about pyloric gland adenomas is a major contribution to the subject of gastrointestinal pathology due to the frequent extragastric locations of pyloric gland adenomas and because of their frequent association with dysplasias. In our opinion, many pathologists are not aware of this entity. We would like to add one case of pyloric gland adenomas. Our case supports the conclusions of Vieth et al. as it was extragastric in location and was associated with low-grade dysplasias. In addition, it is the first-ever reported example of pyloric gland adenomas occurring in the esophagus.

Case report

A 57-year-old female complained of dysphagia. She was found to have a tumor 18 cm distant from the incisors, located on the posterior wall of the esophagus. The tumor was bulging into the esophagus and it was 1.5 cm in diameter. Histologically, it was located under the normal squamous epithelium of the esophagus (Fig. 1). It was composed of pyloric-type glands (Fig. 2). Serous-type glands usually present in the submucosal glands of the esophagus were absent. Focally, we found low-grade dysplastic changes in the nuclei of the adenoma. Immunohistochemically, the tumor was devoid of serotonin- and chromogranin-positive cells. We found no infiltrative changes in the surrounding structures of the esophagus.

Pyloric-gland adenomas are important not only because of dysplastic changes often associated with them but because these lesions probably play roles thus far poorly understood in organs other than the stomach [1, 2, 3, 4, 6].

M. Michal
Department of Pathology,
Medical Faculty Hospital,
Plzen, Czech Republic

R. Curik
Department of Pathology,
Faculty Hospital,
Ostrava-Poruba, Czech Republic

K. Matler
ENT Department,
Faculty Hospital,
Ostrava-Poruba, Czech Republic

Z. Benes
Department of Hepatogastroenterology,
Medical Faculty Thomayer Hospital,
Prague, Czech Republic

M. Michal (✉)
Sikl's Department of Pathology,
Laboratore Spec. Diagnostiky Medical Faculty Hospital,
Alej Svobody 80, 323 18 Pilsen, Czech Republic
e-mail: michal@medima.cz
Tel.: +420-60-3886633
Fax: +420-37-7104650

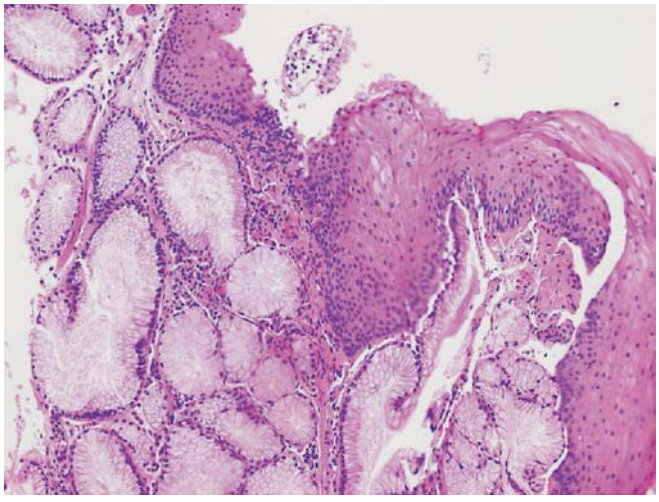

Fig. 1 Histologically, the adenoma was located under the normal squamous epithelium of the esophagus

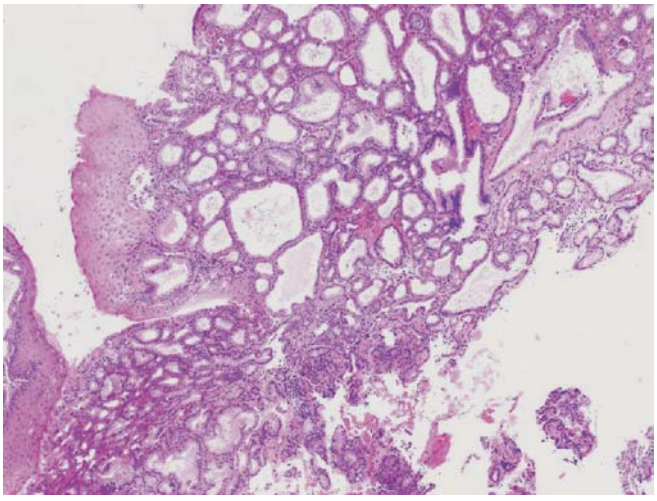

Fig. 2 The adenoma was composed of pyloric type glands

References

1. Kato N, Akiyama S, Motoyama T (2002) Pyloric gland-type tubular adenoma superimposed on intraductal papillary mucinous tumor of the pancreas. Pyloric gland adenoma of the pancreas. Virchows Arch 440:205–208
2. Kushima R, Remmele W, Stolte M, Borchard F (1996) Pyloric gland type adenoma of the gallbladder with squamoid spindle cell metaplasia. Pathol Res Pract 192:963–969
3. Kushima R, Ruthlein HJ, Stolte M, Bamba M, Hattori T, Borchard F (1999) "Pyloric gland-type adenoma" arising in heterotopic gastric mucosa of the duodenum, with dysplastic progression of the gastric type. Virchows Arch 435:452–457
4. Mikami Y, Hata S, Fujiwara K, Imajo Y, Kohno 1, Manabe T (1999) Florid endocervical glandular hyperplasia with intestinal and pyloric gland metaplasia: worrisome benign mimic of "adenoma malignum." Gynecol Oncol 74:504–511
5. Vieth M, Kushima R, Borchard F, Stolte M (2003) Pyloric gland adenoma: a clinicopathological analysis of 90 cases. Virchows Arch 442:317–321
6. Yoden E, Mikami Y, Fujiwara K, Kohno I, Imajo Y (2001) Florid endocervical glandular hyperplasia with pyloric gland metaplasia: a radiologic pitfall. J Comput Assist Tomogr 25:94–97

Virchows Arch (2003) 443:591–593
DOI 10.1007/s00428-003-0790-6

LETTER TO THE EDITOR

Ioannis Kostopoulos · Sotirios Barbanis · Haroula Kalekou · Stephanos Milias · Constantine S. Papadimitriou

Male breast carcinoma of the papillary solid variant with unique CD34 positivity

Received: 13 August 2002 / Accepted: 10 February 2003 / Published online: 19 June 2003
© Springer-Verlag 2003

Sirs, we have recently encountered an interesting case of an invasive male breast carcinoma of the solid papillary variant that displayed extensive and strong CD34 immunopositivity. We think that this finding makes this case unique in the literature since, to our knowledge, there is no reported case of male or female breast carcinoma (invasive or in situ) displaying CD34 positivity.

The patient was a 71-year-old man with a mass in his left breast measuring 2.3×2.0 cm in diameter. He had no family history of breast cancer, neither gynecomastia nor liver cirrhosis. He did not receive estrogenic medication and did not have a previous history of prostate cancer.

On gross examination, the excised tumor had a grayish-white cut surface and solid texture. It was located near the overlaying skin with a relatively smooth border. On microscopic examination, the tumor consisted of solid nodules of neoplastic cells with the presence of a rich delicate network of fibrovascular stroma distributed in an arborizing pattern throughout the tumor. Formation of fibrovascular cores was evident in some areas giving a solid papillary configuration (Fig. 1). Remnants of cystic areas were identified in peripheral locations. Tumor cells were relatively large and round with a moderate amount of cytoplasm and moderately polymorphic nuclei with one or more prominent nucleoli. Mitoses were focally moderate in number. Large areas of necrosis and hemorrhage were evident. Although the tumor nodules were relatively circumscribed, there were foci showing infiltration of the adjacent tissue. Immunohistochemically the absence of myoepithelial cells (SMA, monoclonal, 1:150; Dako) and basic membranes (laminin, monoclonal, 1:40, Novocastra) confirmed the invasive character of the tumor.

Tumor cells were diffusely positive for cytokeratins AE1/AE3 (monoclonal, 1:20; Novocastra), Cam 5,2 (monoclonal, 1:40; Novocastra), and cytokeratin 7 (monoclonal, 1:50; Dako) and focally positive for cytokeratin 20 (monoclonal, 1:20; Dako). They were also positive for estrogen receptors (ERs, monoclonal, 1:50; Novocastra), progesterone receptors (PRs, monoclonal,

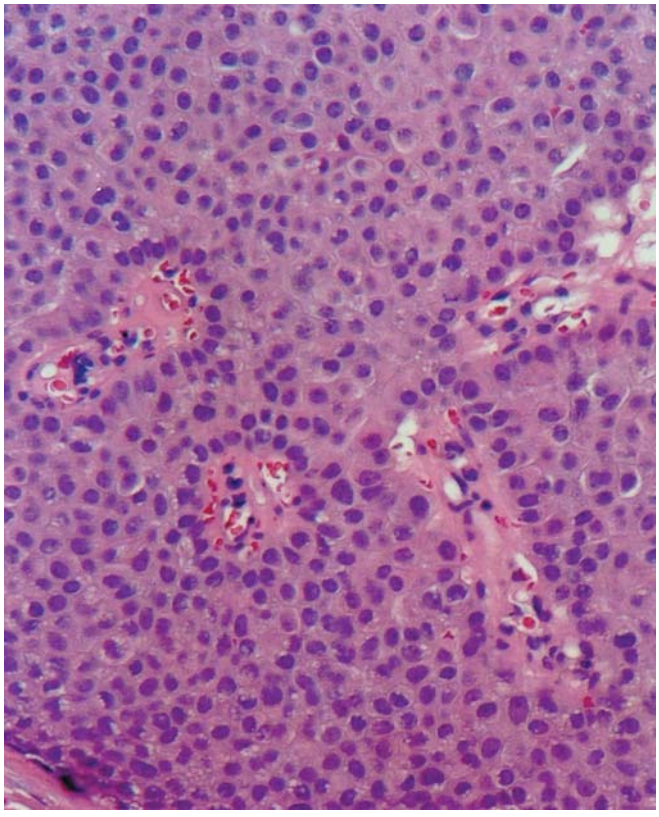

Fig. 1 Invasive breast carcinoma of solid papillary type. Hematoxylin and eosin, ×200

l. Kostopoulos (✉) · S. Barbanis · H. Kalekou · S. Milias
Department of Pathology,
Medical School, Aristotle University,
540 06 Thessaloniki, Greece
e-mail: Kostop@med.auth.gr
Tel.: +30-31-0820607
Fax: +30-31-2310999229

H. Kalekou
Department of Pathology,
St. Paul's Hospital,
Thessaloniki, Greece

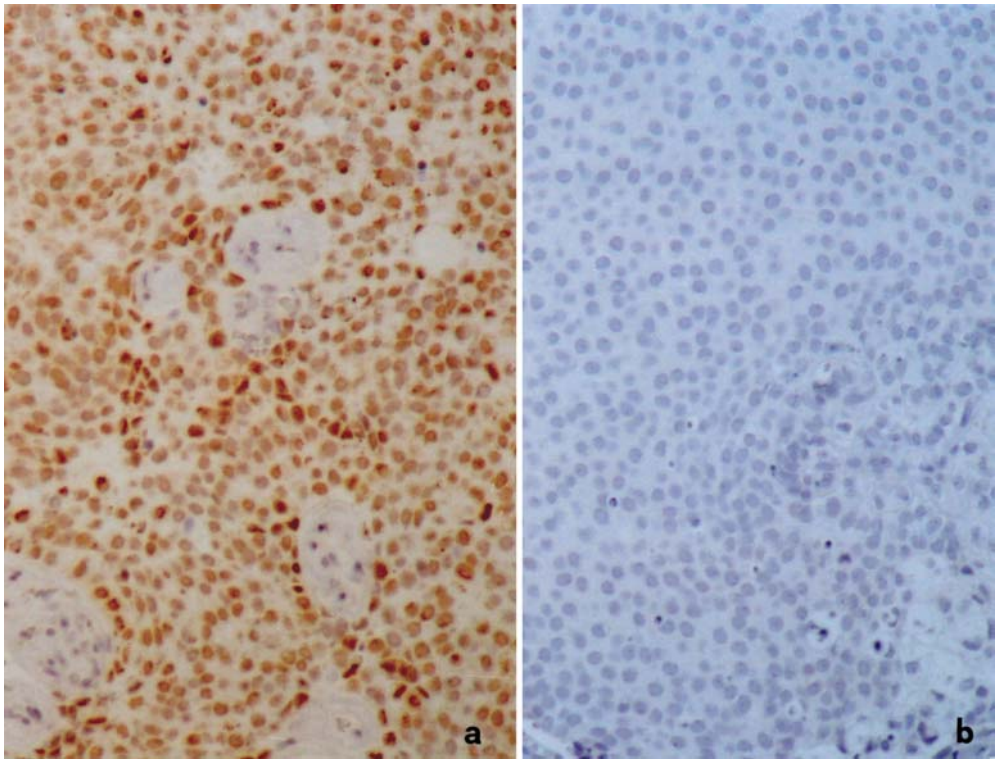

Fig. 2 **a** Intense immunostaining of tumor cells for androgen receptors, ×200. **b** Negativity of neoplastic cells to epidermal growth factor receptor, ×200

1:20; Novocastra) and androgen receptors (ARs, monoclonal, 1:40; Novocastra) (Fig. 2A) as well as for milk fat globules (HMFG-2, monoclonal, 1:10; Novocastra), GCDFP-15 (BRST-2, Monoclonal, 1:50; Signet), and e-cadherin (monoclonal, 1:50; Novocastra). The unique finding in the present case was the extensive and strong immunostaining of tumor cells to CD34 antigen (monoclonal, 1:40; Novocastra) (Fig. 3A). For evaluating the immunostaining, a gastrointestinal stromal tumor (GIST) was used as a positive control, and the primary antibody was omitted in one section serving as a negative control. The detection system used was streptavidin-biotin protocol.

On the contrary, tumor cells were negative for epidermal growth factor receptor (EGFR, monoclonal, 1:10; Novocastra) (Fig. 2B), chromogranin (monoclonal, 1:40; Dako) synaptophysin (monoclonal, 1:10; Dako), S100 protein (polyclonal, 1:120; Dako), vimentin (monoclonal, 1:15; Dako), prostate-specific antigen (PSA, monoclonal, 1:30), factor VIII (polyclonal, 1:300; Dako), CD31 (monoclonal, 1:25; Novocastra) (Fig. 3B), CD105 / endoglin (monoclonal, 1:40; Novocastra), CD117/c-Kit (monoclonal, 1:40; Novocastra), and Her-2/neu (polyclonal, 1:200; Dako).

Although tumor cells were positive for markers usually expressed by breast epithelia (GCFDP-15, milk fat globules, ERs and PRs), suggesting the mammary origin of the tumor, the same markers may also be observed in adnexal neoplasms of the skin such as eccrine/sweat gland tumors. These neoplasms do not express ARs and are usually positive for the EGFR. The positivity of tumor cells, in the present case, to ARs and their negativity for EGFR were more helpful in confirming the primary breast origin of the tumor.

Therefore, we believe that the present case is an infiltrating male breast carcinoma of ductal origin with features of the solid variant of the papillary carcinoma with extensive CD34 positivity of tumor cells, which makes this case especially interesting.

The human antigen CD34 is a single chain transmembrane glycoprotein with a molecular weight of 110 kDa. The CD34 protein (also known as Q BEND/10) is selectively expressed on the surface of cells with more primitive features such as progenitor or stem cells especially of hematolymphoid origin or some multipotent cells in fetal and adult nervous tissue [4]. CD34 antigen expression is highest in the most primitive stem cells and is gradually lost as lineage committed progenitors differentiate. Therefore, it is positive in acute myeloid and lymphoblastic leukemias which are believed to originate from multipotent hematolymphoid stem cells. It also stains normal and neoplastic endothelial cells as well as a variety of soft tissue neoplasms, such as dermatofibrosarcoma protuberans, solitary fibrous tumor, epithelioid sarcoma, spindle cell lipoma, GISTs, and a variety of peripheral nerve sheath tumors.

Natkunam et al. [4], using immunoblot analysis in a variety of CD34 positive tumors, showed that the observed CD34 immunohistological positivity with anti-CD34 antibodies is due to the expression of the same ~110-kDa CD34 protein and not to shared epitopes on unrelated proteins.

Myofibroblastoma, a rather rare benign mesenchymal neoplasm of the breast, is also CD-34 positive, and some

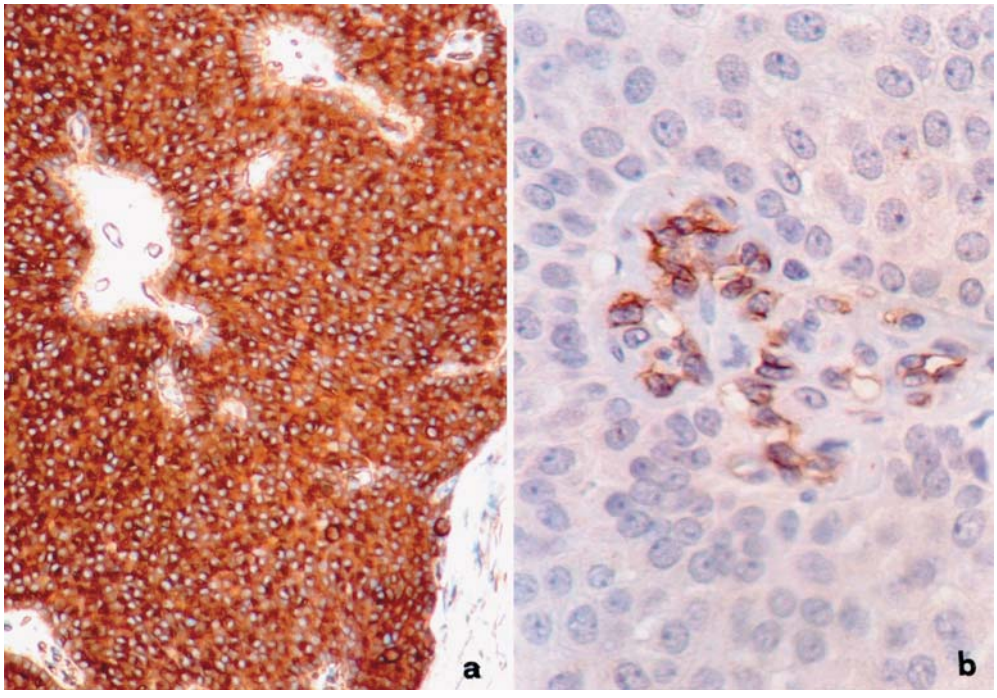

Fig. 3 **a** Prominent and extensive CD34 positivity of breast carcinoma, ×100. **b** CD31 negativity of tumor cells, ×400

investigators speculate that it originates from pluripotential undifferentiated mesenchymal cells of breast tissue stroma [1, 2]. Other more common spindle cell lesions of the breast, such as phylloides tumor and fibroadenoma, show inconsistent and patchy positivity for CD-34, suggesting a common origin with myofibroblastoma [3].

Apart from mesenchymal cells and tumors, CD34 positivity in epithelial cells has been observed in biliary epithelial progenitor cells, in hair outer root sheath cells and eccrine coil and in skin adnexal tumors showing trichilemmal differentiation, especially benign ones, such as trichilemmomas or of eccline coil origin such as cylindromas.

Epithelial breast neoplasms either benign or malignant (including spindle cell carcinomas) have never been reported to stain with monoclonal antibodies against CD34. As a matter of fact, large series of breast carcinomas have been studied using CD34 antibodies as well as other more-specific endothelial markers such as CD31, CD105 (endoglin) and factor VIII for the assessment of angiogenesis in these tumors. In these studies, cancer cells were always CD34 negative. Interestingly, in some cases, cancer cells showed positivity for CD31 [5]. In general, very few carcinomas (1%) and melanomas (0.5%) have been reported to express CD34, while Hodgkin's and non-Hodgkin's lymphomas, with the exception of lymphoblastic lymphomas, are CD34 negative [4].

The strong and extensive CD34 immunopositivity in the present case raises questions about the cellular origin of this solid papillary breast carcinoma. Endothelial/vascular differentiation (in the context of metaplastic breast carcinoma) is ruled out, since all other endothelial markers such as CD31, CD105 (endoglin), and factor VIII, as well as vimentin, were negative throughout the tumor.

We think that CD34 positivity in this case might be evaluated better under the concept of stem cell plasticity and totipotency as proposed for the myofibroblastoma category of breast stromal tumors [1]. To elucidate this matter further, CD34 expression should be evaluated in a wide range of papillary lesions of female and male breast.

References

1. Fukunaga M, Ushigome S (1997) Myofibroblastoma of the breast with diverse differentiations. Arch Pathol Lab Med 121:599–603
2. Magro G, Bisceglia M, Michal M, Eusebi V (2002) Spindle cell lipoma-like tumor, solitary fibrous tumor and myofibroblastoma of the breast : a clinico-pathological analysis of 13 cases in favor of a unifying histogenetic concept. Virchows Arch 440:249–260
3. Moore T, Lee AH (2001) Expression of CD34 and bcl-2 in phyllodes tumours, fibroadenomas and spindle cell lesions of the breast. Histopathology 38:62–67
4. Natkunam Y, Rouse RV, Zhu S, Fischer C, van De Rijn M (2000) Immunoblot analysis of CD34 expression in histologically diverse neoplasms. Am J Pathol 156:21–27
5. Sapino A, Bongiovanni M, Cassoni P, Righi L, Arisio R, Deaglio S, Malavasi F (2001) Expression of CD31 by cells of extensive ductal in situ and invasive carcinomas of the breast. 194:254–261

Virchows Arch (2003) 443:594
DOI 10.1007/s00428-003-0908-x
© Springer-Verlag 2003

ANNOUNCEMENTS

1–11 June 2004
International course on Laboratory Animal Science
Utrecht, The Netherlands

A two week intensive course on laboratory animal science will be organized at the Department of Laboratory Animal Science – Utrecht, The Netherlands in June 2004. This course is organized once a year since 1993.

The objective of this course is to present basic facts and principles that are essential for the humane use and care of animals and for the quality of research.

The contents of the course are in line with recommendations of the Federation of European Laboratory Animal Science Associations (FELASA) regarding the training of the young scientist whose research involves the use of vertebrate animals.

The course may also be of interest for those who intend to set up a similar course at their location. For this purpose, during the course the acquisition of teaching materials can be discussed with the course committee.

For information and application forms please contact:
Prof. L.F.M. van Zutphen, PhD or
Mr. Stephan van Meulebrouck, MA
Department of Laboratory Animal Science
Faculty of Veterinary Medicine
P.O. Box 80.166
3508 TD Utrecht
The Netherlands
Tel.: ++31-30-2532033
Fax: ++31-30-2537997
E-mail: pdk@las.vet.uu.nl
Internet: http://las.vet.uu.nl (click on "Education and Training")

11–15 February 2004
Conference on "Clinical Oncology 2004/2005"

In cooperation with the National Oncology Societies, the Tumorzentrum Düsseldorf (Director: Prof. Dr. med. R. Haas) will be holding a five-day conference. The results will be published in a symposium volume for the conference. More than 800 experts, mainly from the field of oncology, are expected to attend. The workshop will be held in the MNR Clinic, Lecture Hall 13A. The following general topics have been scheduled:

Wednesday:
Pharynx, larynx, CUP syndrome, parotid gland, nasopharynx, skin tumors
Bier, Dummer, Ganzer, Roth, Ruzicka, Schmitt, Schulte, Stadler, Suter
Thursday:
Esophageal carcinoma, gastric carcinoma, colorectal carcinoma
Gabbert, Häussinger, Knöfel, Ramp, Röher, Röhrborn, Wettstein, Willich, Sauer
Friday:
Seminoma, urinary bladder carcinoma, prostatic carcinoma, renal cell carcinoma
Ackermann, Alberti, Alken, Bamberg, Fornara, Hartmann, Rübben, Vögeli, Wirth
Saturday:
NHL, Hodgkin's disease, ALL, AML, CML, multiple myeloma, bronchial carcinoma, thymona
Bentz, Böhner, Gattermann, Germing, Haas, Kobbe, Stilgenbauer, Schmitt
Sunday:
Mammary carcinoma: biology, new treatment standards
Bender, Dall, Gerber, Harbeck, Kaufmann, Mallmann, von Mickwitz, Nitz, Yarnold
Head of the organization team: Prof. Dr. Stephan Roth, Klinik für Strahlentherapie, Moorenstr. 5, Postfach 101007, 40001 Düsseldorf, Germany
The conference fee will be € 30 per day.
The symposium volume published for the conference can be purchased for € 20.

For further information, please contact:
Head of the organization team:
Prof. Dr. Stephan Roth
Klinik für Strahlentherapie
Heinrich-Heine-Universität
Moorenstr. 5
40225 Düsseldorf
Germany
Tel.: +49 (0)211 811 8989/7990
Fax: +49 (0)211 811 8051
e-mail: roth@med.uni-duesseldorf.de
www.uni-duessdorf.de/tumorzentrum

Virchows Arch (2003) 443:595–596
DOI 10.1007/s00428-003-0915-y

EDITORIAL

G. Faller · M. Stolte

Barrett's oesophagus: time for consensus

Received: 24 September 2003 / Accepted: 24 September 2003 / Published online: 9 October 2003
© Springer-Verlag 2003

Barrett's oesophagus belongs to those issues in gastrointestinal pathology that in the last 50 years have undergone the most fundamental changes regarding the underlying pathogenic concepts, terminology, diagnosis and management.

In the beginning, Norman Barrett, who first described this lesion in 1950, believed that the columnar lining of the lower oesophagus was congenital in origin and represented a part of the stomach rather than of the oesophagus [2]. However, in the subsequent years it became evident that this condition truly belonged to the oesophagus and was acquired in nature. The key role of gastro-oesophageal reflux in the pathogenesis of Barrett's oesophagus was not recognized until the 1970s. The controversial discussions on gastric and/or intestinal subtypes of the columnar epithelium in Barrett's oesophagus continued until the late 1970s, when it finally became evident that only the intestinal type was premalignant. Clinically, difficulties in defining the border between the oesophagus and the stomach using early endoscopic methods led to the 3-cm rule in the definition of Barrett's oesophagus [3, 10]. Here, as in many other diseases, the implementation of size in the definition of biological entities reflects the uncertainties of the pathogenesis, clinical diagnosis and significance of Barrett's oesophagus. All the aforementioned changes and doubts are also echoed by the range of terms for Barrett's oesophagus, such as "CELLO", "endobrachyoesophagus" "Barrett's syndrome" or "specialised epithelium".

G. Faller (✉)
Institute of Pathology,
University of Erlangen-Nuremberg,
Krankenhausstrasse 8–10, 91054 Erlangen, Germany
e-mail: Gerhard.Faller@patho.imed.uni-erlangen.de
Tel.: +49-9131-8522524
Fax: +49-9131-8524745

M. Stolte
Institute of Pathology,
Clinic of Bayreuth,
Germany

It is possible that the long-lasting problems and controversies in Barrett's oesophagus are the main reason for the uncertainty in the histopathological diagnosis of Barrett's mucosa and its associated neoplasias. Be that as it may, due to the poor histopathological standardisation, significant variations in the diagnosis of Barrett's mucosa and its associated neoplasias are still widely prevalent among pathologists [1, 6]. This is of particular relevance as the histological diagnosis remains the gold standard in the diagnosis of Barrett's mucosa.

However, the pressure on pathologists to improve their diagnosis of Barrett's mucosa and associated lesions increased. In recent years, it became evident that the prevalence of Barrett's carcinoma raised rapidly [4]. Endoscopic methods in the diagnosis and treatment of gastrointestinal disorders considerably improved [8]. Finally, consensual guidelines for the clinical management of Barrett's mucosa and related neoplasias are created [9]. Therefore, the time for standardisation as a basis for improved histopathological diagnosis of Barrett's oesophagus and related neoplasias has come.

This issue of Virchows Archiv contains two consensus reports on the histopathological diagnosis of Barrett's mucosa and associated neoplasias. The Working Group for Gastrointestinal Pathology of the German Society of Pathology tried to work out criteria for the diagnosis of Barrett's mucosa and the different grades of associated neoplasias [5]. It also gives clear recommendations for the terminology, the usage of anxillary methods and the number of biopsies and, finally, suggests a "second opinion" in certain instances. The proposals of the Amsterdam Working Group on Barrett Oesophagus for the histological diagnosis of Barrett's mucosa [7] widely correspond to the report of the German group and to the results of a United States multi-institutional study [6]. Furthermore, valuable advice for the histological diagnosis on endomucosal resection specimens are given.

The hopes of the two study groups for a standardisation and improvement of the histological diagnosis by the criteria described are legitimate. However, the practical value of these consensus recommendations has still

to be evaluated. Furthermore, investigations on the molecular pathogenesis of Barrett's mucosa and of intraepithelial neoplasias will hopefully render new diagnostic tools, which are easy to apply in daily practice. Therefore, Barrett's oesophagus will remain in a state of flux, but possibly in more silent water than in the past.

References

1. Alikhan M, Rex D, Khan A, Rahmani E, Cummings O, Ulbright TM (1999) Variable pathologic interpretation of columnar lined esophagus by general pathologists in community practice. Gastrointest Endosc 50:23–26
2. Barrett N (1950) Chronic peptic ulcer of the oesophagus and "oesophagitis". Br J Surg 38:175–182
3. DeMeester SR, DeMeester TR (2000) Columnar mucosa and intestinal metaplasia of the esophagus. 50 years of Controversy. Ann Surg 231:303–321
4. DeVault KR (2000–2001) Epidemiology and significance of Barrett's esophagus Dig Dis 18:195–202
5. Faller G, Borchard F, Ell C, Seitz G, Stolte M, Walch A, Rueschoff J (2003) Histopathological diagnosis of Barrett mucosa and associated neoplasias: results of a consensus conference of the Working Group for Gastroenterological Pathology of the German Society for Pathology on 22 September 2001 in Erlangen. Virchows Arch 24:9–14
6. Montgomery E, Bronner MP, Goldblum JR, Greenson JK, Haber MM, Hart J, Lamps LW, Lauwers GY, Lazenby AJ, Lewin DN, Robert ME, Toledano AY, Shyr Y, Washington K (2001) Reproducibility of the diagnosis of dysplasia in Barrett esophagus: a reaffirmation. Hum Pathol 32:368–378
7. Offerhaus GJA, Correa P, van Eeden S, Geboes K, Drillenburg P, Vieth M, van Velthuysen ML, Watanabe H, Sipponen P, ten Kate FJW, Bosman FT, Bosma A, Ristimaki A, van Dekken H, Riddell R, Tytgat GNJ (2003) Report of an Amsterdam Working Group on Barrett esophagus. Virchows Arch 443:601–607
8. Pech O, Gossner L, May A and Ell C (2001) Management of Barrett's oesophagus, dysplasia and early adenocarcinoma. Best Pract Res Clin Gastroenterol 15:267–284
9. Sampliner RE (2002) Updated guidelines for the diagnosis, surveillance, and therapy of Barrett's esophagus. Am J Gastroenterol 97:1888–1895
10. Spechler SJ, Goyal RK (1996) The columnar-lined esophagus, intestinal metaplasia, and Norman Barrett. Gastroenterology 110:614–621

Virchows Arch (2003) 443:597–601
DOI 10.1007/s00428-003-0894-z

REVIEW ARTICLE

G. Faller · F. Borchard · C. Ell · G. Seitz · M. Stolte · A. Walch · J. Rüschoff

Histopathological diagnosis of Barrett's mucosa and associated neoplasias: results of a consensus conference of the Working Group for Gastroenterological Pathology of the German Society for Pathology on 22 September 2001 in Erlangen

Received: 25 June 2003 / Accepted: 4 August 2003 / Published online: 24 September 2003
© Springer-Verlag 2003

Abstract There are a number of difficulties regarding the diagnosis of Barrett's mucosa and the varying grades of neoplasia that may be associated with it. It was, therefore, the aim of a consensus conference of the Working Group for Gastroenterological Pathology within the German Society of Pathology to achieve standardisation regarding the following issues: definition and diagnostic criteria for Barrett's mucosa and its discrimination from intestinal metaplasia of the cardia, diagnostic criteria for intraepithelial neoplasia, number of biopsies necessary to establish the diagnosis, significance of additional immunohistochemical and/or molecular methods as well as importance of a second opinion in the diagnosis of intraepithelial neoplasia.

This manuscript was first published in "Der Pathologe" 2003 Feb;24(1):9–14.

G. Faller (✉)
Institute of Pathology, University of Erlangen-Nuremberg,
Krankenhausstrasse 8–10, 91054 Erlangen, Germany
e-mail: Gerhard.Faller@patho.imed.uni-erlangen.de
Tel.: +49-9131-8522524
Fax: +49-9131-8524745

F. Borchard
Institute of Pathology, Klinikum Aschaffenburg, Germany

C. Ell
Department of Internal Medicine II,
Dr.-Horst-Schmidt-Hospital, Wiesbaden, Germany

G. Seitz
Institute of Pathology, Clinic of Bamberg, Bamberg, Germany

M. Stolte
Institute of Pathology, Bayreuth Clinic, Bayreuth, Germany

A. Walch
Institute of Pathology, University of Freiburg, Germany

J. Rüschoff
Institute of Pathology, Clinic of Kassel, Kassel, Germany

Keywords Barrett's oesophagus · Consensus · Intraepthelial neoplasia

Introduction

The adenocarcinoma of the distal oesophagus (Barrett's carcinoma) belongs to those malignant tumours that, in the last 25 years, showed the highest increase in their prevalence. This increase is thought to be caused through the rise in gastro-oesophageal reflux disease [2]. Gastro-oesophageal reflux leads to metaplastic differentiation processes and, finally, to the development of a columnar epithelial layer in the lower oesophagus. It is well known that the occurrence of columnar epithelial-lined lower oesophagus represents a precancerous condition for the development of distal oesophageal adenocarcinoma. This is particularly true for the so-called "specialised" epithelium, which morphologically corresponds to incomplete intestinal metaplasia. In contrast, gastric cardia- or fundus-type mucosa in the distal oesophagus is not associated with a significant risk for developing adenocarcinoma [5]. This fact has led to a change in the terminology of metaplastic alterations within the oesophageal mucosa [5, 8]. Furthermore, the criteria for the different and clinically relevant grades of intraepithelial neoplasia (dysplasia) within the oesophageal mucosa are not exactly defined and are neither uniformly assessed nor consistently applied. This could explain the significant interobserver variability in the diagnosis of neoplastic alterations in Barrett's mucosa and has led to uncertainty and frustration for both pathologists and clinicians [4].

At a consensus conference of the Working Group for Gastroenterolological Pathology of the German Society for Pathology, which took place on 22 September 2001 in Erlangen, Germany, a standardisation of the histopathological diagnosis of Barrett's oesophagus and associated neoplasias was created in order to reduce diagnostic

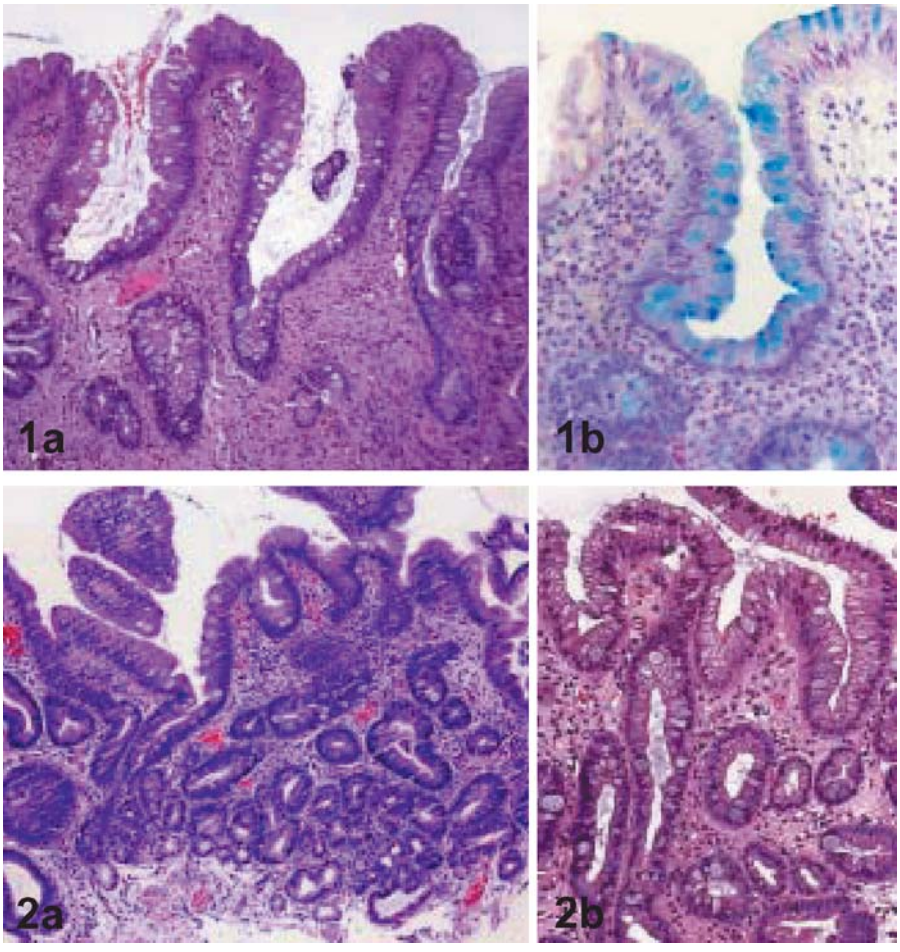

Fig. 1 Barrett's mucosa. Flat mucosa with epithelium corresponding to incomplete intestinal metaplasia with goblet cells (**a**). Detection of acid mucins in goblet cells by staining with astra-blue (**b**)

Fig. 2 Reactive changes in Barrett's mucosa. Slight architectural alterations and densely arranged crypts in the basal areas of the mucosa with increased nuclear size (**a**). Continuous surface maturation of regenerating epithelial cells and inconspicuous epithelial cells on the surface without any signs of intraepithelial neoplasia (**b**)

uncertainties and to facilitate the communication among pathologists and with clinicians.

Diagnosis and terminology of Barrett's mucosa

Barrett's mucosa is defined by the detection of metaplastic, intestinalised columnar epithelial cells in the mucosa of the distal oesophagus. Histologically, Barrett's mucosa is characterised by a relatively flat mucosa whose epithelium corresponds to incomplete intestinal metaplasia (type 2 or type 3; Fig. 1a). In rare cases, a combination with a focally occurring complete intestinal metaplasia (type 1) can be found. For the characteristic metaplasic changes, the term "Barrett's mucosa" should be used. Other terms, such as "specialised epithelium", "Barrett's syndrome", "Barrett's metaplasia" or "CELLO" are obsolete.

The histological detection of goblet cells is essential for the diagnosis of Barrett's mucosa ("no goblets, no Barretts"). In contrast to abundantly mucous-filled foveolar epithelial cells, the so-called pseudo-goblet cells, intestinal goblet cells, can be demonstrated through the staining of acid mucins with alcian-blue or astra-blue (Fig. 1b). The immunohistochemical analyses (e.g. with MUC-antibodies, with antibodies against cytokeratins 7 and 20 or with the antibody DAS-1) are not essential for the diagnosis of Barrett's mucosa.

The term "pre-goblet cells" characterises an epithelial cell type that can be often detected in Barrett's mucosa. However, detection of this cell type alone is not sufficient for the diagnosis of Barrett's mucosa.

A significant risk for the development of distal oesophageal adenocarcinoma exists only for Barrett's mucosa as defined above. Therefore, the application of the term "Barrett's mucosa" for any other type of metaplastic columnar epithelium in the distal oesophagus, in particular for gastric cardia- or fundic-type mucosa, is obsolete.

Discrimination of Barrett's mucosa from intestinal metaplasia of the cardia

In most cases, the discrimination of Barrett's mucosa from intestinal metaplasia of the gastric cardia is achievable on hematoxylin & eosin (H&E) sections and without any additional analysis [9]. Diagnostic key features of cardiac intestinal metaplasia (CIM) are as follows:

- Complete type of intestinal metaplasia (type 1)
- Higher mucosa constitution in CIM than in Barrett's mucosa

– Normal foveolar gastric epithelium with cardia- or fundus-type glands adjacent to CIM

Additional clinical information (e.g. endoscopic evaluation of the Z-line, length of the Barrett's segment, number of tongues and presence of reflux symptoms) as well as additional biopsies from the gastric antrum and corpus are recommended for the histological diagnosis of Barrett's mucosa. For example, the detection of complete intestinal metaplasia from the gastro-oesophageal junction in a patient without reflux symptoms but with *Helicobacter pylori* gastritis favours the diagnosis of CIM rather than Barrett's mucosa. In rare cases (e.g. incomplete intestinal metaplasia with reflux in a patient with normal Z-line and Helicobacter pylori gastritis), only a tentative diagnosis of Barrett's mucosa, including an adequate comment, is achievable.

Diagnosis of intraepithelial neoplasia

In Barrett's mucosa the term "dysplasia" is replaced by the new term "intraepithelial neoplasia". So the terminology is adapted to the proposals of the World Health Organization classification of tumours of the digestive system [11]. The grades of intraepithelial neoplasias in Barrett's mucosa are classified as follows:

– Negative for intraepithelial neoplasia
– Indefinite intraepithelial neoplasia or suspicious for intraepithelial neoplasia
– Low-grade intraepithelial neoplasia
– High-grade intraepithelial neoplasia

The usage of the term "moderate intraepithelial neoplasia" is obsolete.

Histologically, low-grade intraepithelial neoplasia (LGIN) is characterised through basically well-preserved architecture of the crypts. The crypts are mainly arranged in parallel. The epithelial cells in LGIN show basally localised nuclei, which are elongated and slightly hyperchromatic. Nuclear-to-cytoplasmic ratio is already increased. For the discrimination of LGIN from reactive changes in regenerating Barrett's mucosa, the missing maturation of abnormal epithelial cells along the crypts to the surface is very helpful because, in reactive alterations, continuous surface maturation of cells is well detectable. Furthermore, the transition from cells in LGIN to adjacent non-neoplastic cells is relatively abrupt, whereas in reactive changes this transition is more gradual. Slight alteration of crypt architecture might be present in reactive changes. However, this criterion must not be interpreted as neoplasia when other typical changes in regenerative mucosa (cell maturation, gradual transition to non-neoplastic epithelium) are present. Figure 2a, b shows Barrett's mucosa with regenerative changes. The histological alterations of LGIN are demonstrated in Fig. 3a, b. The histological criteria of LGIN are summarised in Table 1.

Table 1 Histological characteristics of low-grade intraepithelial neoplasia in Barrett's mucosa

Crypt architecture conserved or only slightly altered
Cell polarity maintained
Nuclear-to-cytoplasmic ratio increased
Nuclei elongated and hyperchromatic
No surface maturation
Abrupt transition between neoplastic and non-neoplastic epithelial cells

Table 2 Histological characteristics of high-grade intraepithelial neoplasia in Barrett's mucosa

Severely altered crypt architecture with budding and branching
Loss of cell polarity
Hyperchromasia of nuclei
Increased mitoses and atypical mitotic figures
Prominent nucleoli
No maturation of neoplastic cells to the surface

Table 3 Histological characteristics of invasive adenocarcinoma and differentiation from high grade intraepithelial neoplasia

Extreme branching of neoplastic glands
Dissociation of neoplastric cells
Infiltration into muscularis mucosae
Invasion into blood or lymph vessels

Cytologically, high-grade intraepithelial neoplasia (HGIN) shows similar alterations as LGIN; that is, increase in nuclear size, hyperchromasia and loss of goblet cells. However, the changes in HGIN are more marked than in LGIN. Polarity of neoplastic cells is often lost so that nuclei may also be localised at the apical pole of the cell. Furthermore, increased mitosis, including atypical mitotic figures and prominent nucleoli, can be found. The most important histological criterion for the diagnosis of HGIN, particularly for the discrimination from LGIN, is the severity of alterations of crypt architecture with branching and budding of neoplastic glands (Fig. 4a, b). The histological features of HGIN in Barrett's mucosa are summarised in Table 2.

For the discrimination of adenocarcinoma from HGIN, further architectural abnormalities with extreme branching and marked variation in the size of the glands are essential. Dissociation of neoplastic cells, infiltration into the muscularis mucosae or invasion into lymph or blood vessels also leads to the diagnosis of adenocarcinoma. However, it should be noted that Barrett's mucosa forms its own muscular layer, so that a double muscular layer might exist. Therefore, detection of neoplastic glands underneath the newly formed muscularis mucosae does not necessarily indicate submucosal invasion. In some cases, the diagnosis of invasive carcinoma might be very difficult, so that only the diagnosis "suspicious for invasion" might be established. The histological criteria of invasive adenocarcinoma are listed in Table 3. Well-differentiated invasive adenocarcinomas are demonstrated in Fig. 5a, b.

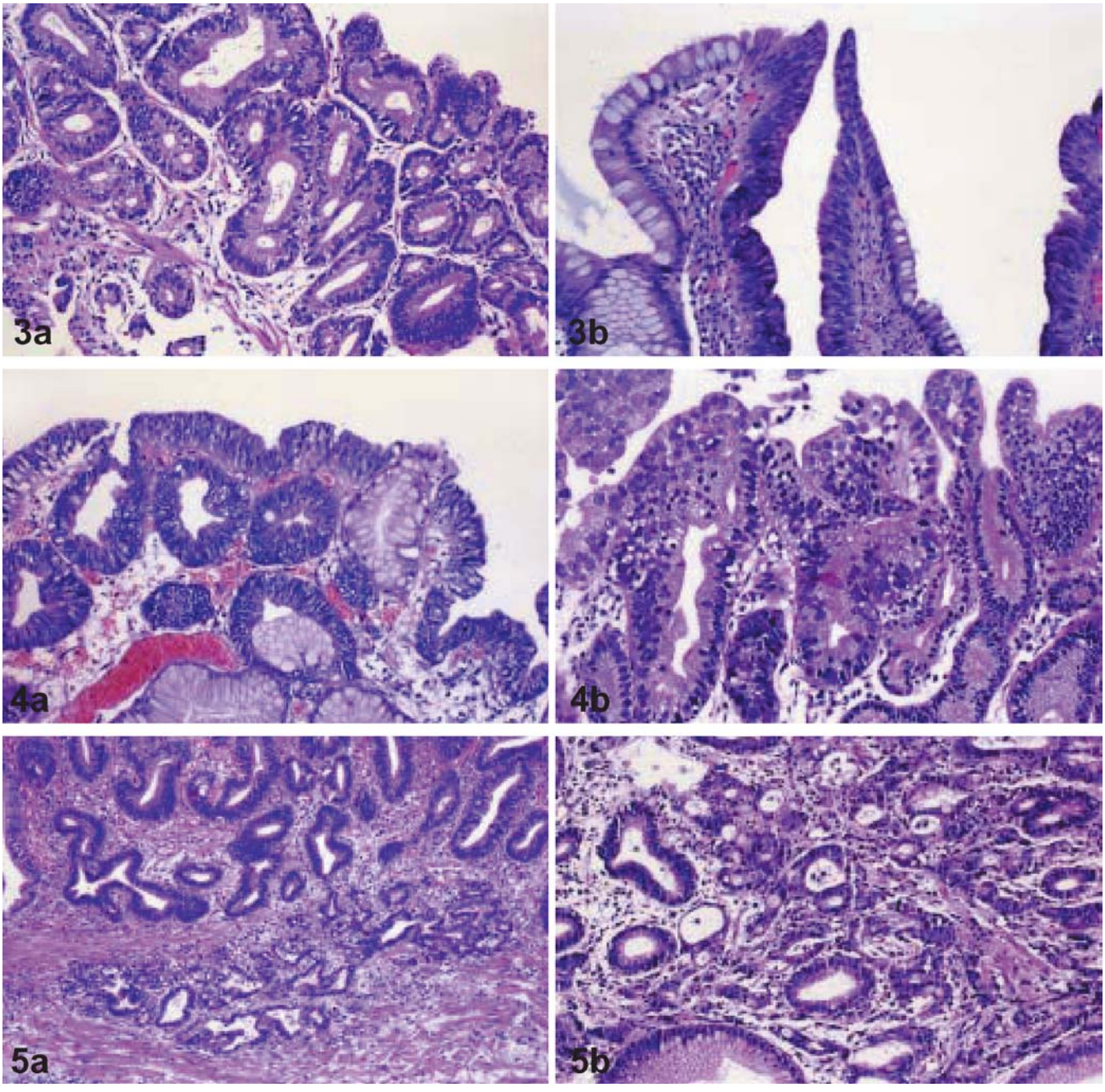

Fig. 3 Barrett's mucosa with low-grade intraepithelial neoplasia. Slight architectural changes of crypts and elongated nuclei in neoplastic epithelial cells with preserved cell polarity (**a**). Loss of surface maturation of neoplastic cells and abrupt transition to non-neoplastic epithelial cells (**b**)

Fig. 4 Barrett's mucosa with high-grade intraepithelial neoplasia. Pronounced architectural alterations of glands with budding and branching. Marked nuclear atypia and loss of cell polarity. No maturation and detection of neoplastic cells on the surface

Fig. 5 Barrett's carcinoma. **a** In the *upper half*, prominent architectural changes according to high-grade intraepithelial neoplasia. In the *lower half* of the figure, invasive formations of well-differentiated Barrett's carcinoma. **b** Shows highly distorted neoplastic glands and mucosa infiltration of well-differentiated Barrett's carcinoma

Number of biopsies

In cases with endoscopically conspicuous regions (e.g. verrucous surface, nodular lesions, areas with hyperaemia, erosions, polyps or surface depression), directed and extensive biopsies dependent on the size of the lesion are required. In inconspicuous Barrett's mucosa, at least two biopsies should be taken from lesions up to 5 mm and at least four biopsies from lesions up to 1 cm. From longer inconspicuous Barrett's mucosa, two biopsies for every

centimetre or, alternatively, quadrant biopsies for every 1–2 cm, are recommended.

Additional methods

The histopathological analysis represents the most appropriate method for grading intraepithelial neoplasias in Barrett's oesophagus [3, 9, 10]. Additional immunohistochemistry to investigate the accumulation of P53 or the number and distribution of proliferating Ki67/Mib-1-positive cells could support the morphological finding. However, the relative amount of positive cells and, in the case of P53 expression, the strength of the immunohistochemical staining must also be considered. For example, strong P53 expression in a high proportion of suspicious epithelial cells indicates intraepithelial neoplasia rather than reactive changes. However, negative immunohistochemical results do not exclude neoplastic alterations [9]. In any case, a second opinion by an independent and experienced histopathologist is more useful than additional immunohistochemical analysis. For a final estimation of intraepithelial neoplasias by means of immunohistochemical or/and molecular methods, more scientific investigations are needed. Markers that can be detected by immunohistochemical or molecular biological means and could allow a reliable assessment of the risk of the lesion do not exist [2].

"Second opinion"

The histopathological diagnosis of Barrett's carcinoma and particularly of its precursors is characterised by a significant intra- and interobserver variability. This is of clinical relevance as the histological diagnosis could have severe impact on the further clinical diagnostic procedures and therapy as well as on the patient's quality of life.

In systematic investigations concerning interobserver variability in the histological diagnosis of Barrett's oesophgus, the kappa values as marker for the variability of the diagnosis in Barrett's oesophagus are between 0.0 and 0.65. The categories of "indefinite for intraepithelial neoplasia" and "low-grade intraepithelial neoplasia" show the lowest kappa values and, thus, the highest variability. [1, 4, 6, 7]. Therefore, any histological diagnosis of low-grade and high-grade intraepithelial neoplasia should be confirmed by a second, independent and—at best—external pathologist with particular expertise in this field. Such a second opinion should also be requested in cases with difficult differentiation between high-grade neoplasia and invasive carcinoma. This applies accordingly if the category "indefinite for intraepithelial neoplasia" was diagnosed twice.

Acknowledgements Members of the consensus conference: R. Berndt (Ansbach), F. Borchard (Aschaffenburg), C. Ell, L. Gossner, A. May (Wiesbaden), G. Faller, T. Kirchner, S. Müller (Erlangen), K.-H. Fuchs (Würzburg), H. Geddert (Düsseldorf), T. Günther, M. Vieth (Magdeburg), H.-K. Koch, A. Walch (Freiburg), C. Langer (Graz, Austria), J. Lüttges (Kiel), G. Oberhuber (Überlingen), J Rüschoff (Kassel), G. Seitz, (Bamberg), M. Stolte (Bayreuth), A. Tannapfel (Leipzig).

References

1. Alikhan M, Rex D, Khan A, Rahmani E, Cummings O, Ulbright TM (1999) Variable pathologic interpretation of columnar lined esophagus by general pathologists in community practice. Gastrointest Endosc 50:23–26
2. Falk GW (2002) Barrett's esophagus. Gastroenterology 122:1569–1591
3. Geboes K, Van Eyken P (2000) The diagnosis of dysplasia and malignancy in Barrett's oesophagus. Histopathology 37:99–107
4. Montgomery E, Bronner MP, Goldblum JR, Greenson JK, Haber MM, Hart J, Lamps LW, Lauwers GY, Lazenby AJ, Lewin DN, Robert ME, Toledano AY, Shyr Y, Washington K (2001) Reproducibility of the diagnosis of dysplasia in Barrett esophagus: a reaffirmation. Hum Pathol 32:368–378
5. Reid BJ (1991) Barrett's esophagus and esophageal adenocarcinoma. Gastroenterol Clin North Am 20:817–834
6. Reid BJ, Haggitt RC, Rubin CE, Roth G, Surawicz CM, Van Belle G, Lewin K, Weinstein WM, Antonioli DA, Goldman H, et al (1988) Observer variation in the diagnosis of dysplasia in Barrett's esophagus. Hum Pathol 19:166–178
7. Skacel M, Petras RE, Gramlich TL, Sigel JE, Richter JE, Goldblum JR (2000) The diagnosis of low-grade dysplasia in Barrett's esophagus and its implications for disease progression. Am J Gastroenterol 95:3383–3387
8. Spechler SJ, Goyal RK (1996) The columnar-lined esophagus, intestinal metaplasia, and Norman Barrett. Gastroenterology 110:614–621
9. Vieth M, Seitz G (2001) 50 Jahre Barrett Ösophagus. Aktuelle diagnostische Möglichkeiten in der Pathologie. Pathologe 22:62–71
10. Werner M, Mueller J, Walch A, Hofler H (1999) The molecular pathology of Barrett's esophagus. Histol Histopathol 14:553–559
11. Werner M, Flejou JF, Hanaut P, Höfler H, Lambert R, Keller G, Stein HJ (2000) Adenocarcinoma of the oesophagus. In: Hamilton SR, Aaltonen LA (eds) Pathology and genetics of tumours of the digestive system. IARC Press, Lyon, pp 20–26

Virchows Arch (2003) 443:602–608
DOI 10.1007/s00428-003-0906-z

MEETING REPORT

G. J. A. Offerhaus · P. Correa · S. van Eeden · K. Geboes · P. Drillenburg · M. Vieth · M. L. van Velthuysen · H. Watanabe · P. Sipponen · F. J. W. ten Kate · F. T. Bosman · A. Bosma · A. Ristimaki · H. van Dekken · R. Riddell · G. N. J. Tytgat

Report of an Amsterdam Working Group on Barrett Esophagus

Received: 30 June 2003 / Accepted: 8 September 2003 / Published online: 27 September 2003
© Springer-Verlag 2003

G. J. A. Offerhaus · S. van Eeden · F. J. W. ten Kate · A. Bosma
Department of Pathology,
Academic Medical Center Amsterdam,
The Netherlands

G. J. A. Offerhaus (✉)
PO Box 22660, 1100DD Amsterdam,
The Netherlands
e-mail: g.j.offerhaus@amc.uva.nl
Tel.: +31-20-5665645
Fax: +31-20-6960389

P. Correa
Department of Pathology,
LSUMC, New Orleans, USA

K. Geboes
Department of Pathology,
KUL, Leuven, Belgium

P. Drillenburg
Department of Pathology,
OLVG, Amsterdam, The Netherlands

M. Vieth
Department of Pathology,
University of Magdeburg,
Germany

M. L. van Velthuysen
Department of Pathology,
NKI/AVL, Amsterdam, The Netherlands

H. Watanabe
Department of Pathology,
Niigata University,
Japan

P. Sipponen
Department of Pathology,
Jorvi Hospital,
Espoo, Finland

F. T. Bosman
Department of Pathology,
Lausanne University,
Switzerland

A. Ristimaki
Department of Pathology,
Helsinki University Central Hospital,
Finland

H. van Dekken
Department of Pathology,
Erasmus Medical Center Rotterdam,
The Netherlands

R. Riddell
Department of Pathology,
Mount Sinai Hospital,
Toronto, Canada

G. N. J. Tytgat
Department of Gastroenterology,
Academic Medical Center,
Amsterdam, The Netherlands

Keywords Barrett Esophagus · Peptic ulcer · Gastroesophageal reflux

Introduction

More than 50 years have passed since Barrett described a case of peptic ulcer disease of the esophagus and the condition that would carry his name [1]. It is now generally accepted that Barrett esophagus is the result of long-standing gastroesophageal reflux disease leading to replacement of the normal stratified squamous epithelial lining of the esophagus by glandular epithelium of various types [24, 32]. The importance of a diagnosis of Barrett esophagus is its association with the development of an esophageal adenocarcinoma. In contrast to what Norman Barrett originally thought, Barrett esophagus is a premalignant condition, and the incidence of Barrett carcinoma has increased dramatically since his publication in 1950 [12].

Barrett adenocarcinoma is preceded by a well-defined premalignant lesion, i.e., dysplasia (intraepithelial neo-

plasia—IEN—according to the recent WHO nomenclature) [9, 14]. IEN, as a dependable morphological marker for cancer risk, provides a potential opportunity for surveillance, early detection and secondary prevention of invasive Barrett carcinoma [13].

This is even more so now that new technical advances make it possible to treat preneoplastic noninvasive or early invasive lesions with local therapy. These new treatment modalities are accompanied by considerably fewer complications or morbidity than the so-called prophylactic surgery [5].

To prevent potentially lethal carcinomas, the clinician needs to make an accurate diagnosis of Barrett esophagus, and ensure appropriate surveillance and therapy. In this regard, a number of problems and uncertainties may cause confusion in the communication between pathologist and clinician when dealing with Barrett esophagus. Such miscommunication could potentially jeopardize the optimal treatment of the patient with Barrett esophagus.

In an effort to focus on the above issues and clarify some of the problems, a Working Group was convened on 15 December 2002, in Amsterdam, as part of the international 'From Gene to Cure' meeting at the Academic Medical Center. Sixteen international experts were invited and attended the Working Group. A set of hematoxylin and eosin (H&E) section slides of Barrett mucosa were distributed among the attending experts 1 month prior to the meeting and served as examples and illustrations of the issues that were discussed during the working group. Three distinctive areas were specified and discussed separately, led by two discussion leaders who had prepared for these issues in advance. The following issues were reviewed: 1. When is a diagnosis of Barrett mucosa justified? 2. What grading system needs to be used for IEN? 3. Which difficulties and problems can be expected when using local ablative or excision treatment modalities?

This report summarizes the discussions of the meeting of the Working Party and is a first attempt to reach consensus or otherwise define problematic areas that need to be clarified to advance our knowledge about Barrett mucosa.

When is a diagnosis of Barrett esophagus justified?

The normal esophagus is a tube that extends through the lower esophageal sphincter, a muscular structure that forms the most distal end of the esophagus. It marks the transition into the stomach, the so-called gastroesophageal junction. The esophagus is lined with stratified squamous cell epithelium and the stomach with glandular epithelium. Where these two epithelia meet, a grossly visible demarcation line is visible—the Z-line. This histologically defined transition is called the squamocolumnar junction. The gastroesophageal junction and the squamocolumnar junction may coincide, but also in normal individuals this is not necessarily the case, since a tiny segment (millimeters to one centimeter) of fundic- or cardiac-type mucosa in the distal tubular esophagus is common and part of the normal cardia endoscopically [4]. In Barrett esophagus, the squamous mucosa has been replaced by glandular mucosa that invariably includes cardiac or intestinalized mucosa, although sometimes parietal cells may be present. When only fundic and/or cardiac type mucosa are present in a biopsy, it is usually impossible morphologically to tell whether it comes from the (Barrett) esophagus or gastric cardia and, thus, the pathologist may not be able to make a definitive diagnosis of Barrett esophagus in that event. According to some, architectural distortion, inflammation, glandular atrophy and absence of neuroendocrine cells may make cardiac-type mucosa derived from the esophagus distinct [10], but these changes are subtle and not firmly established. The presence of squamous patches associated with the excretory duct of the submucosal esophageal glands is helpful in knowing that the biopsy originated in what was at one time squamous mucosa, as these do not occur in the cardia.

For the histological diagnosis of Barrett esophagus, the presence of specialized columnar epithelium, i.e., containing goblet cells, in a biopsy from the esophagus is accepted as the gold standard. Barrett mucosa harboring intestinal metaplasia carries an increased risk for cancer; conversely, carcinoma is extremely rare in other mucosal types associated with Barrett esophagus in the absence of intestinal metaplasia [15, 28]. However, a major problem is that intestinal metaplasia can also be encountered in the gastric cardia [30], and only when the biopsy with goblet cells comes from the esophagus that was previously squamous, is a diagnosis Barrett mucosa justified. This depends on the endoscopist identifying criteria indicative of this change. It is the combination of intestinal metaplasia in a biopsy originating in mucosa having endoscopic criteria of Barrett esophagus that allows the unequivocal diagnosis of Barrett esophagus. Whether or not intestinal metaplasia in the gastric cardia has the same significance, biology and clinical implications as in the esophagus is currently a matter of scientific debate [11], but until intestinal metaplasia is shown to have significant precancerous potential, it is important to distinguish the two.

Some ancillary methods have been suggested to help the pathologist to distinguish between Barrett mucosa and cardiac intestinal metaplasia. Intestinal metaplasia in Barrett mucosa is virtually always incomplete, whereas intestinal metaplasia of the cardia more often is of the complete type [26]. Therefore, mucin histochemistry could be of value [26, 30]. Also immunohistochemistry of cytokeratins 7 and 20 has been used to differentiate between cardiac and esophageal intestinal metaplasia: intestinal metaplasia in Barrett mucosa in theory shows superficial and deep CK7 staining, whereas there is only superficial CK20 staining, and in the gastric cardia there is superficial and deep CK20 immunoreactivity and only patchy or absent CK7 staining [19]. Technical differences between institutions can however account for differences in these cytokeratin patterns [37], and the data increas-

Fig. 1 Endoscopic picture of the longitudinal submucosal vessels characteristic for the distal esophagus. The figure was duplicated from: K. Takubo [34]; p 187, figure 12–38, with permission

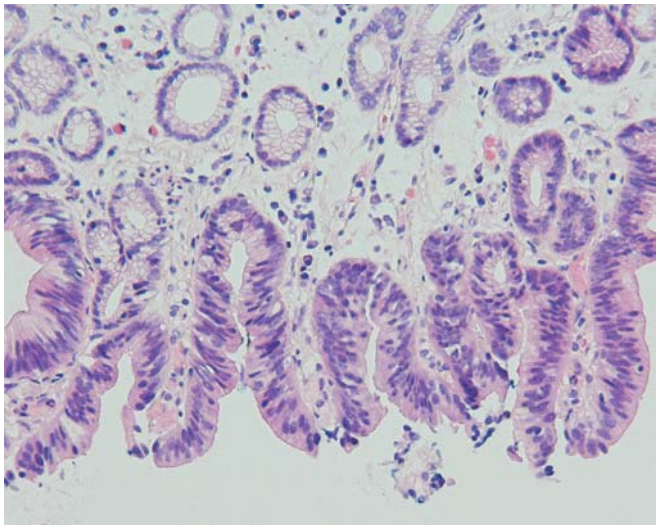

Fig. 2 Example of low-grade intraepithelial neoplasia

ingly suggest that it is of little value. Thus, neither one of these ancillary techniques per se is capable of differentiating the two with certainty.

In general, the endoscopist will be able to recognize whether or not a biopsy is obtained from the normal esophagus/z-line or from one in which Barrett esophagus is a consideration. This information needs to be communicated to the pathologist so that it is clear that intestinal metaplasia at this site will result in a diagnosis of Barrett esophagus.

When a hiatal hernia is present, and this is invariably the case in Barrett esophagus, the endoscopic picture can be more confusing because of the additional difficulty in identifying the true site of the gastroesophageal junction. The upper end of the gastric folds and the pattern of submucosal vessels are both valuable in establishing this. The proximal arborescent vessels pass into palisading vertical vessels in the distal 3–4 cm of the esophagus (Fig. 1). Where these vessels meet the proximal margin of the gastric folds can be recognized by endoscopy, and this forms the gastroesophageal junction [16]. Also, when there is inflammation, this pattern remains and a careful endoscopist will be able to trace the gastroesophageal junction.

In summary, there was agreement that the diagnosis of Barrett esophagus is made on the combination of an endoscopic appearance acceptable for Barrett esophagus which yields a biopsy containing goblet cells. This concurs with the definition provided by the Practice Parameters Committee of the American College of Gastroenterology [31].

Grading IEN

IEN is the premalignant lesion of Barrett mucosa that serves as a morphological marker for increased cancer risk. IEN refers to neoplastic change of the epithelium confined to the original glandular structures of the mucosa without invading into the lamina propria [9]. Clonality due to molecular genetic alterations providing growth advantage to the epithelial cells underlies IEN and is recognized microscopically through its architectural and cytonuclear features. Importantly, in Western countries, the architectural features, particularly poor maturation and excessive crowding are mostly taken into account to arrive at a diagnosis of IEN; whereas, in Japan, the cytonuclear features are predominant. When a diagnosis of IEN is considered it is advisable to request a second expert opinion [7].

Although the sequence of low-grade, high-grade IEN and cancer may be a morphological continuum that cannot be precisely subdivided into microscopically distinct grades of severity, it is important to attempt to grade in view of the clinical consequences. A two-tier system is recommended; i.e., low-grade and high-grade IEN (Fig. 2 and Fig. 3) [29]. The pathologist and the endoscopist should be aware of the heterogeneous nature of neoplastic lesions and, thus, a diagnosis of IEN relies on adequate sampling. This can be done following established guidelines [27]. If sampling is inadequate (i.e., fails to reach these guidelines), a repeat endoscopy with extensive sampling should be performed within 4–6 weeks in order to determine the follow-up strategy. When IEN is considered, but there are confounding factors such as inflammation that make the diagnosis of IEN problematic, a diagnosis of indefinite for IEN should be made. Repeat biopsy, ideally after a course of proton-pump inhibition, frequently helps to resolve the issue. When neoplastic cells invade into the lamina propria or anastomose to each other, then, by definition, an invasive carcinoma is present. When it is confined to the mucosal layer, a diagnosis of intramucosal carcinoma is justified (Fig. 4). In some biopsies when glands are tightly packed, it can be virtually impossible to be sure whether invasion

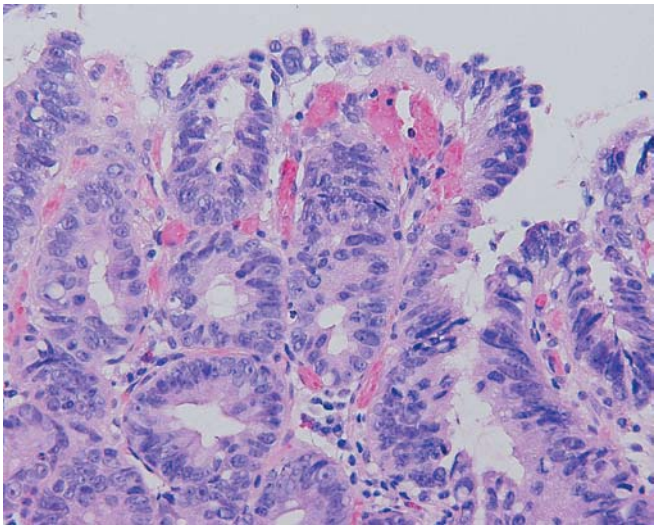

Fig. 3 Example of high-grade intraepithelial neoplasia

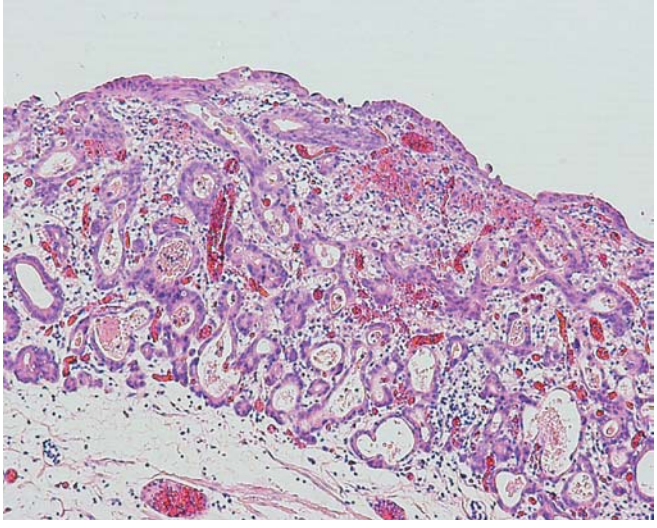

Fig. 4 Example of intramucosal carcinoma

of the lamina propria has or has not occurred; under these circumstances a term such as suspicious for invasion can be used. The above grading system hardly deviates from that used in Japan. Japanese pathologists are inclined to follow the Vienna system used for the stomach, when grading neoplastic epithelial change in Barrett mucosa [38]. This system uses negative for IEN, indefinite for IEN (follow-up), non-invasive low-grade IEN (follow-up or excision), non-invasive high-grade IEN including i high-grade IEN, ii carcinoma in situ, iii suspicious for invasive carcinoma (excision) and intramucosal carcinoma or beyond (excision).

There are no absolute, objective, firm and measurable microscopic criteria that can be applied to diagnose and grade IEN and intra- and interobserver variation remains a significant problem [25]. The morphological criteria recently described by Montgomery et al. are useful, but also these remain descriptive, subjective and semi-quantitative [21].

Morphometry can be a useful adjunct for a proper and consistent diagnosis of IEN, but can only be applied on selected areas or samples suitable for this methodology [36].

Molecular markers can provide additional information that contributes to an accurate diagnosis. Ki-67 is a marker that labels the proliferating cells. It visualizes the proliferative compartment and an upward shift and surface labeling of the proliferating cells as seen in IEN [17]. Immunohistochemical nuclear staining of the protein product of the tumor suppressor gene p53 is a surrogate marker for genetic change in this gene and, when positive, also supports a diagnosis of IEN [17]. DNA content measured by flowcytometry, expression of cyclin D1 or the cell adhesion molecule CD44-V6, or absence of expression of p16 are also used as markers [2, 3, 18, 28]. However, none of the above markers can replace the conventional microscopy and, thus, lightmicroscopy of the H&E section slide is still the mainstay and gold standard for the diagnosis and grading of IEN.

In summary, grading epithelial changes into no IEN, indefinite for IEN, low-grade, high-grade and invasive cancer is recommended. When the suspicious for invasion category is added, which is used from time to time by every pathologist, the system is very similar to the Vienna classification, preferred by the Japanese.

Local therapy

Local therapy to eradicate neoplastic changes in Barrett esophagus has enormous appeal and its use has gained a place in the gastroenterological armamentarium in recent years. The notion of endoscopic ablation, potentially for cure, without the need for thoracotomy and surgical resection is virtually first line therapy in many centers now. Follow-up data are still limited, but at several institutions the numbers are already sufficient to exchange experience and define areas that need particular attention. A variety of ablative techniques are available [20]. The main focus was on endoscopic mucosal resection with subsequent photodynamic therapy. It is important to emphasize that ablation therapy is still in an experimental stage and that long-term follow-up is needed to evaluate its value as treatment modality for early cancer or high-grade IEN. Endoscopic mucosal excision is an intervention that can also contribute to a more accurate diagnosis and it may result in reclassification of the diagnosis [22]. The optimal patient for local therapy is the older patient who is less fit for surgery and who has a visible and small neoplastic lesion limited to the mucosa.

When an endoscopic mucosal excision is performed, the pathologist is requested to provide an adequate diagnosis that leads to a sensible subsequent strategy and to judge radicality of treatment. When the specimen is received by the pathologist, he needs to stretch and orient it properly. A stereoscope maybe helpful and also

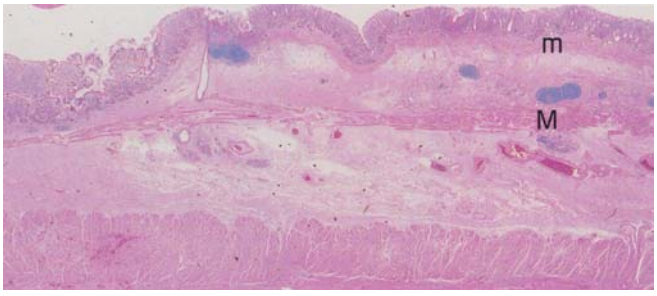

Fig. 5 Double layer of the muscularis mucosae underneath a segment of Barrett mucosa. The figure was duplicated from: K. Takubo [34]; p 184, figure 12–34, with permission

painting of the base and margins may be useful. Completeness of excision at the deep resection plane is more important than that at the lateral margins. Tumor extending to the deep margin is an indication for surgery. Re-excision or postoperative ablation by photodynamic therapy can be used for remnants of neoplastic epithelium at the lateral resection margins [5]. This is pertinent because particularly the lateral margins are often difficult to assess due to cautery artifact. Carcinomas in a mucosectomy specimen need to be graded because the presence of poorly differentiated adenocarcinoma is another indication for considering surgery. Staging is also part of an adequate histopathological diagnosis. Intramucosal carcinoma is a carcinoma that is confined to the mucosa and, by definition, does not extend beyond the muscularis mucosae. For intramucosal carcinoma, endoscopic mucosal excision can be sufficient if it is complete and it is not an undifferentiated carcinoma [5, 6]. However, one needs to be aware of the fact that Barrett mucosa often has a double layer of muscularis mucosae with disruption of the muscle fibers (Fig. 5). The most superficial layer is a newly formed layer directly underneath the Barrett epithelium. The deeper layer is the original muscularis mucosae and also continuous with the muscularis mucosae of other parts of the esophagus without Barrett mucosa [33]. This double layer of the muscularis mucosae complicates the picture, and only when the invasion extends beyond the deeper layer is a diagnosis of submucosal carcinoma (T1b) justified. Vasoinvasion and/or extension into the submucosa are accompanied by a risk of lymph-node metastasis and more extensive surgery with resection of the lymph nodes may then be indicated. Vessels can also be encountered in the mucosa and particularly between the two layers of the muscularis mucosae vasoinvasion could occur. It is at present unknown whether or not in that case also a risk of lymph node metastasis exists that would justify surgery. Review of all the operated Barrett carcinoma patients in the Academic Medical Center of Amsterdam since 1993 (n=367) showed no lymph-node metastasis in any of the 38 patients with carcinoma limited to the mucosa or superficial submucosa (upper one-third).

After local therapy close follow-up is crucial. Neoplastic epithelium may be left behind and subsequent development of metachronous carcinoma or recurrent high-grade IEN or cancer can be encountered [5, 35]. Surveillance after local therapy provides additional problems for the pathologist. Particularly when photodynamic therapy is applied, inflammatory changes and the epithelial regeneration may make the microscopic picture more difficult to interpret. Cytonuclear features and architectural distortion may mimic neoplastic change. Fibromuscular proliferation and disruption of muscle fibers with entrapment of glandular structures can even make it difficult to rule out invasiveness at times. In this regard, p53 immunostaining maybe of help, if it is known from the prior specimen that the neoplastic epithelium was p53 positive. Another phenomenon that needs attention and may blur the picture, are the so-called buried glands [23, 35]. Re-epithelialization after local excision or ablation takes place from the remaining squamous patches associated with the excretory ducts of the esophageal glands. The squamous re-epithelialization may overgrow the intestinalized glands and, in a biopsy, these glands lying beneath the neosquamous epithelium provide additional difficulties with the histopathological interpretation. Moreover, the significance and biology of these buried glands is at present uncertain but they may be the source of cancer growth [23, 35]. The cancer then could grow hidden beneath the neosquamous epithelium, and may also be undetectable by biopsy. This is particularly a concern since another sequela of the local ablative therapy that maybe encountered is an exuberant papillomatous overgrowth of the neosquamous epithelium (Fig. 6). This can be so prominent that one may start to wonder about the nature and biological properties of the neo-epithelium and neoplastic growth becomes a concern [8]. Also in this regard, follow-up data are limited and long-term results remain uncertain.

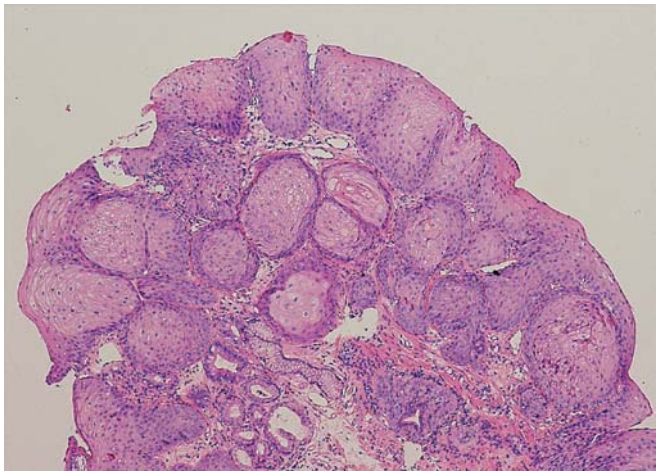

Fig. 6 Exuberant neosquamous epithelium with a papillomatous growth pattern after ablation therapy. Buried glands can be observed underneath the neosquamous mucosa

Thus, although local therapy became an exciting new option in the armamentarium of the modern gastroenterologist, its use is still experimental and long-term follow-

up is needed to resolve a number of specific issues associated with its application.

Conclusion

The premalignant lesion in Barrett mucosa is IEN and it is used as a morphological marker for cancer risk in surveillance of patients with Barrett esophagitis. The diagnosis of Barrett esophagus is contingent on finding goblet cells with an appropriate accompanying endoscopic change. The grading of IEN and intramucosal carcinoma should be along the lines suggested in the Vienna classification. Intra- and interobserver variation remain a problem, but as they occur primarily in the indefinite/low-grade IEN part of the spectrum, they tend to have less impact on therapeutic decision making. Also, a second opinion may minimize this problem. It is hoped that molecular markers will ultimately contribute to its clarification. Local ablative therapy for high-grade IEN and/or superficially growing adenocarcinoma is available in many centers now and increasingly used as first line therapy, which in turn causes problems in interpretation for the pathologist as the result of iatrogenic changes in endoscopic mucosal resections and follow-up biopsies.

Acknowledgements European Cancer Center for their assistance and support; Dr Anya Milne for critically reading the manuscript; Wilfried Meun for photography.

References

1. Barrett NR (1950) Chronic peptic ulcer of the oesophagus and 'oesophagitis'. Br J Surg 38:175–182
2. Bian YS, Osterheld MC, Fontolliet C, Bosman FT, Benhattar J (2002) P16 inactivation by methylation of the CDKN2A promoter occurs early during neoplastic progression in Barrett's esophagus. J Pathol 96:1113–1121
3. Coppola D, Falcone R, Livingston S, Karl R, Nicosia S, Cacho CM (1997) Cyclin D1 expression correlates with degrees of dysplasia in Barrett's esophagus. Lab Invest 76:298–302
4. De Hertogh G, Van Eyken P, Ectors N, Tack J, Geboes K (2003) On the existence and location of cardiac mucosa: an autopsy study in embryos, fetuses and infants. Gut 52:791–796
5. Ell C, May A, Gossner L et al. (2000) Endoscopic mucosal resection of early cancer and high-grade dysplasia in Barrett's esophagus. Gastroenterology 118:670–677
6. Falk GW (2002) Barrett's esophagus. Gastroenterology 122:1569–1591
7. Faller G (2003) Histopathologische Diagnostik der Barrett-Schleimhaut und ihrer neoplasien. Pathologe 24:9–14
8. Garewal H, Ramsey L, Sharma P, Kraus K, Sampliner R (1999) Biomarker studies in reversed Barrett's esophagus. Am J Gastroenterol 94:2829–2833
9. Geboes K, Van Eyken P (2000) The diagnosis of dysplasia and malignancy in Barrett"s oesophagus. Histopathology 37:99–107
10. Goldblum JR (2003) Barrett's esophagus and Barrett's related dysplasia. Mod Pathol 16:316–324
11. Goldstein NS (2000) Gastric cardia intestinal metaplasia: biopsy follow-up study of 85 patients. Mod Pathol 13:1072–1079
12. Haggitt RC (1992) Adenocarcinoma in Barrett's esophagus: a new epidemic? Hum Pathol 23:475–476
13. Hameeteman W, Tytgat GN, Houthoff HJ, Van Den Tweel JG (1989) Barrett's esophagus: development of dysplasia and adenocarcinoma. Gastroenterology 96:1249–1256
14. Hamilton SR, Aaltonen LA (2000) Pathology and genetics of tumours of the digestive system. WHO classification of tumours. IARC Press, Lyon
15. Hamilton SR, Smith RRL (1987) The relationship between columnar epithelial dysplasia and invasive adenocarcinoma arising in Barrett's esophagus. Am J Clin Pathol 87:301–312
16. Hoshihara Y, Kogure T, Fukuchi S, et al. (1986) Endoscopic observation of longitudinal vessels at the lower esophagus and its clinical significance (in Japanese with English abstract). Gastrenterol Endosc 28:941–946
17. Krishnadath KK, Tilanus HW, van Blankenstein M, et al. (1995) Accumulation of genetic abnormalities during neoplastic progression in Barrett's esophagus. Cancer Res 55:1971–1976
18. Lagorce Pages, Paraf F, Dubois S, Belghiti J, Flejou JF (1998) Expression of CD44 in premalignant and malignant Barrett's oesophagus. Histopathology 32:7–14
19. Latchford A, Eksteen B, Jankowski J (2001) The continuing story of cytokeratins in Barrett's mucosa: as you like it. Gut 49:746–749
20. May A, Gossner L, PechO, et al (2002) Local endoscopic therapy for intraepithelial high grade neoplasia and early adenocarcinoma in Barrett's oesophagus: acute phase and intermediate results of a new treatment approach. Eur J Gastroenterol Hep 14:1085–1091
21. Montgomery E, Bronner MP, Goldblum JR, et al. (2001) Reproducibility of the diagnosis of dysplasia in Barrett esophagus: a reaffirmation. Hum Pathol 32:368–378
22. Nijhawan PK, Wang KK (2000) Endoscopic mucosal resection for lesions with endoscopic features suggestive of malignancy and high grade dysplasia with Barrett's esophagus. Gastrointest Endosc 52:328–332
23. Overholt BF, Panjehpour M (1996) Photodynamic therapy for Barrett's esophagus: clinical update. Am J Gastroenterol 91:1719–1723
24. Paull A, Trier JS, Dalton MD, Camp RC, Loeb P, Goyal RK (1976) The histologic spectrum of Barrett's esophagus. N Engl J Med 295:476–480
25. Polkowski W, Baak JPA, van Lanschot JJB, et al. (1998) Clinical decision making in Barrett esophagus can be supported by computerized immunoquantitation and morphometry of features associated with proliferation and differentiation. J Pathol 184:161–168
26. Polkowski W, van Lanscot JJ, ten Kate FJ, et al. (2000) Intestinal and pancreatic metaplasia at the gastroesophageal junction in patients without Barrett's esophagus. Am J Gastroenterol 95:617–625
27. Reid BJ,Weinstein WM, Lewin KJ, Haggitt RC, VanDeventer G, Den Besten L, Rubin CE (1988) Endoscopic biopsies diagnose high grade dysplasia or early operable adencarcinoma in Barrett's esophagus without grossly recognizable neoplastic lesions. Gastroenterology 94:81–90
28. Reid BJ, Blount PL, Rubin CE, Levine DS, Haggitt RC, Rabinovitch PS (1992) Predictors of progression to malignancy in Barrett's esophagus: endoscopic, histologic, and flow-cytometric follow-up of a cohort. Gastroenterology 102:1212–1219
29. Riddell RH, Goldman H, Ransohoff DF, et al. (1983) Dysplasia in inflammatory bowel disease: standardized classification with provisional clinical implications. Hum Pathol 14:931–968
30. Riddell RH (1996) The biopsy diagnosis of gastroesophageal reflux disease, carditis, and Barrett's esophagus, and sequelea of therapy. Am J Surg Pathol 20[Suppl 1]:31–51
31. Sampliner RE (1998) Practice guidelines on the diagnosis, surveillance and therapy of Barrett's esophagus. Am J Gastroenterol 93:1028–1031
32. Spechler SJ, Goyal RK (1986) Barrett's esophagus. N Engl J Med 315:362–371

33. Takubo K, Sasajima K, Yamashita K, et al. (1991) Double muscularis mucosae in Barrett's esophagus. Hum Pathol 22:1158–1161
34. Takubo K (2000) Pathology of the Esophagus. Educa Inc, Tokyo
35. Van Laethem JL, Peny MO, Salmon I, Cremer M, Deviere J (2000) Intramucosal adenocarcinoma arising under squamous re-epithelialisation of Barrett's oesophagus. Gut 46:574–577
36. Van Sandick JW, Baak JPA, van Lanscot JJB, et al. (2000) Computerized quantitative pathology for the grading of dysplasia in surveillance biopsies of Barrett oesophagus. J Pathol 190:177–183
37. Van Sandick JW, van Lanschot JJB, van Felius L, et al. (2002) Intestinal metaplasia of the esophagus or esophagogastric junction. Evidence of distinct clinical, pathologic, and histochemical staining features. Am J Clin Pathol 117:117–125
38. Willis J, Riddell RH (2003) Biology versus terminology: east meets west in surgical pathology. Gastrointest Endosc 57:369–376

Virchows Arch (2003) 443:609–617
DOI 10.1007/s00428-003-0888-x

ORIGINAL ARTICLE

G. MacGrogan · F. A. Tavassoli

Central atypical papillomas of the breast: a clinicopathological study of 119 cases

Received: 5 September 2002 / Accepted: 6 July 2003 / Published online: 13 September 2003
© Springer-Verlag 2003

Abstract The clinicopathological features of central intraductal papillomas of the breast presenting with florid usual ductal hyperplasia or atypical ductal hyperplasia (ADH) were analyzed in a retrospective series of 119 patients, whose lesions were sent to the Armed Forces Institute of Pathology from 1976 to 1990. After histological review considering predefined morphological and quantitative criteria, the 119 central papillomas were classified into 22 papillomas with florid usual ductal hyperplasia (18%), 40 papillomas with focal atypia (34%), 24 atypical papillomas (20%) and 33 carcinomas arising in a papilloma (28%). After a median period of follow-up of 110 months, 16 recurrences (5 papillomas, 2 carcinomas arising in a papilloma, 4 ductal carcinomas in situ, 5 invasive carcinomas) occurred. No statistically significant difference was observed in relation to recurrence for the various categories of papillomas. The presence of epithelial hyperplasia, ADH or lobular neoplasia in the surrounding breast as well as infarction of the papilloma were significant predictive factors of recurrence (P=0.02 and P=0.005, respectively, log-rank test). The main reason for the observed low rate of significant recurrences in this series was that epithelial atypia (whether comprising 20% or 60% of the papillary lesion) was, in most of the cases, localized in a confined lesion that was completely excised.

G. MacGrogan (✉)
Department of Pathology,
Institut Bergonié,
229 Cours de l'Argonne, 33076 Bordeaux cedex, France
e-mail: macgrogan@bergonie.org
Tel.: +33-55-6330436
Fax: +33-55-6330438

F. A. Tavassoli
Department of Breast and Gynecology Pathologic,
Armed Forces Institute of Pathology,
Washington, DC, USA

Present address:
Yale University School of Medicine,
Department of Pathology,
New Haven, CT, USA

Keywords Breast papilloma · Epithelial atypia · Hyperplasia · Ductal carcinoma in situ · Invasive carcinoma

Introduction

The discovery of atypical epithelial hyperplasia or carcinoma within an intraductal papilloma remains a matter of concern for the pathologist. For atypical intraductal hyperplasia (ADH) or ductal carcinoma in situ (DCIS) found within the breast proper, the relative and/or absolute risk for subsequent development of invasive carcinoma has been determined in several studies [7, 15]. The risk represented by the occurrence of such abnormalities within a confined lesion, such as a fibroadenoma or an intraductal papilloma, is still not fully established. Papillomas have been separated into two risk categories for the development of carcinoma: the central/solitary type, for which the risk is low, and the peripheral/multiple type, which is more frequently associated with DCIS or invasive carcinoma [2, 4, 5, 6]. In some cases, the distinction between solitary and multiple lesions is clear cut. In others, however, the distinction between the two types can reasonably be made only by three-dimensional studies [5] and, in certain cases, any separation appears arbitrary on a routine breast biopsy.

Over the past 20 years, intraductal papillomas have been described by morphological and immunohistochemical criteria acknowledging a proliferation of luminal epithelial and subjacent myoepithelial cells overlying fibrovascular stalks within the lumen of the duct system. These criteria have helped distinguish benign intraductal papilloma from those papillary carcinomas characterized by a complete absence of myoepithelial cells [1, 9]. There are, however, papillary carcinomas that show focal retention of the myoepithelial cell layer [9]. The epithelial component of an otherwise benign papilloma can be subject to a spectrum of morphological changes ranging from metaplasia to hyperplasia, ADH and in situ carcinoma. Given the absence of any definitions or guidelines

in the literature concerning the amount of ADH within a papilloma that would qualify it as a papillary carcinoma, one of the authors of the present study had proposed assessment of the quantity of ADH within these papillary lesions and their separation under different designations [14]. By using the terms "atypical papilloma" and "carcinoma arising in a papilloma," this approach avoided the designation of papillary carcinoma for these lesions. Prior to this proposal, many pathologists diagnosed larger papillomas with such atypical foci as papillary carcinoma, and many women with such lesions had been managed by mastectomies. Using modifications of this quantitative approach, two separate studies have looked at the precancerous potential of proliferative atypia in papillary lesions [8, 10]. The presence of ADH within a papilloma and/or in the surrounding breast was associated with an increased risk of recurrence [10] or invasive carcinoma [8]. We undertook the present study to fully describe the morphological changes occurring within the epithelial component of central papillomas and to search for factors of prognostic significance concerning recurrence and progression.

Materials and methods

Patient selection

Retrieved from the files of the Armed Forces Institute of Pathology were 259 cases, coded as: solitary papilloma with focal atypia, atypical papilloma and carcinoma arising in a papilloma. These represented all the cases diagnosed as such over a 15-year period, from 1 January 1976 to 31 December 1990, and for which follow-up data was available. Patients' charts were reviewed for clinical information and gross description of their lesions. After the preliminary review of charts and histological analysis, 140 cases were excluded . The main causes of exclusion from the study were mastectomy and death of patient within 6 months of surgery. A mean number of 8.1 (1 to 135) hematoxylin-eosin (H&E)-stained sections were available per case. After histological analysis, additional cases showing the following features were discarded: sclerosing papilloma as defined by an adenomatous nodule made of small tubules confined to a duct lumen; peripheral papilloma consisting of a papillary lesion originating in a lobular unit or papillomatosis as defined by multiple small papillary lesions originating in different lobular units; nodular sclerosing adenosis as defined by a large conglomerate of small parallel tubules involving one or several lobular units with small secondary papillary structures; extensive myoepithelial hyperplasia, qualifying the lesion as adenomyoepithelioma; intraductal or infiltrating carcinoma in the surrounding breast parenchyma.

Histological definitions

A papilloma was defined as central or solitary if it was localized in a ductal space with no connection to the terminal lobular unit and complex if three or more duct transections involved by such a papillary proliferation were visible on a tissue section. The epithelial atypia observed in the central papillomas of our series was comparable to the atypia observed in low grade DCIS; we generally do not encounter high-grade DCIS patterns or cytology in this setting. Because there are no standardized criteria for classifying solitary papillomas presenting with epithelial atypia and due to their highly polymorphous nature, we arbitrarily defined four categories at the beginning of our study: papillomas with focal atypia, atypical papillomas, carcinoma arising in papilloma, papilloma with diffuse and extensive usual ductal hyperplasia. Classification into the first three categories was based on the presence of atypical cytological and architectural features and the extent of these features in the papilloma.

The atypical cytological and architectural features consisted of:

- An epithelial proliferation of ductal cell type, similar to atypical intraductal hyperplasia as defined by Tavassoli and Norris [15], e.g., an epithelial proliferation showing cytological atypia characterized by monotony and uniformity with either solid, cribriform (Fig. 1), micropapillary (Fig. 2) or stratified columnar cell (Fig. 3) architectural patterns.
- An epithelial proliferation of apocrine cell type, in patterns similar to what has been described by Tavassoli and Norris [16] as atypical apocrine metaplasia, e.g., apocrine cells with a three-fold variation in nuclear size and atypical apocrine hyperplasia, e.g., an apocrine cell population organized in a solid or cribriform pattern (Fig. 4d).
- An epithelial proliferation with cytological features intermediate between ductal cells and apocrine cells, coined apocrine-like cells, lacking one or more of the classic apocrine features [13], often presenting with an amphophilic granular cytoplasm and round nuclei and arranged in cribriform (Fig. 5), solid (Fig. 4b, c), micropapillary, stratified spindle cell patterns.

The central papilloma was designated papilloma with focal atypia if less than 10% of its entire surface in any given slide was involved by an atypical cell population as described in the preceding paragraph. If at least 10% but less than one-third of the papilloma's entire surface was involved by the same atypical population it was named atypical papilloma (Fig. 4). The term carcinoma arising in a papilloma was used if one of the following characteristics was present:

- If one-third up to 90% of its cross-section was involved by an atypical cell population as described for atypical papillomas.
- If tumoral necrosis, characterized by curdled eosinophilic material mixed with nuclear debris, was present in the atypical cell population, regardless of the quantity of the atypical cells relative to the surface of the papilloma involved.

With the exception of the immediately adjacent duct-extensions, abutting the wall of the papilloma, the surrounding breast parenchyma had to be devoid of intraductal carcinoma to qualify the lesion as carcinoma arising in a papilloma.

Papilloma with florid "sheet-like" hyperplasia

Even though this type of papilloma is not involved by atypia, we felt that it should be clearly defined and put in the differential diagnosis of the preceding categories because of its relative frequency and worrisome appearance to the inexperienced eye. At low power, this lesion had the appearance of a solid sheet of epithelial cells almost obscuring the lumen of a large duct, but at higher magnification, delicate fibrovascular stalks with overlying myoepithelial cells were apparent in the lesion. In the solid areas, the epithelial cells were arranged in streaming or whirling patterns; they were ovoid or spindle in shape with inconspicuous cytoplasmic margins, frequently overlapping bland nuclei (Fig. 6). Slit-like clear spaces punctuated the epithelial proliferation.

Additional features evaluated on H&E sections included: microcalcifications in the papilloma; a lymphoid infiltrate with germinal centers, if present in the vicinity of the papilloma; usual ductal hyperplasia, ADH or lobular neoplasia (LN) in the breast parenchyma surrounding the papilloma.

In 83 cases, paraffin-embedded tissue blocks were available. Immunostaining with smooth muscle actin antibody (SMA; Sigma Immunochemicals, St. Louis, Mo., 1/8000 po) was performed on all. Positivity was interpreted in reference to an adjacent control section in which normal rabbit serum was used as the secondary

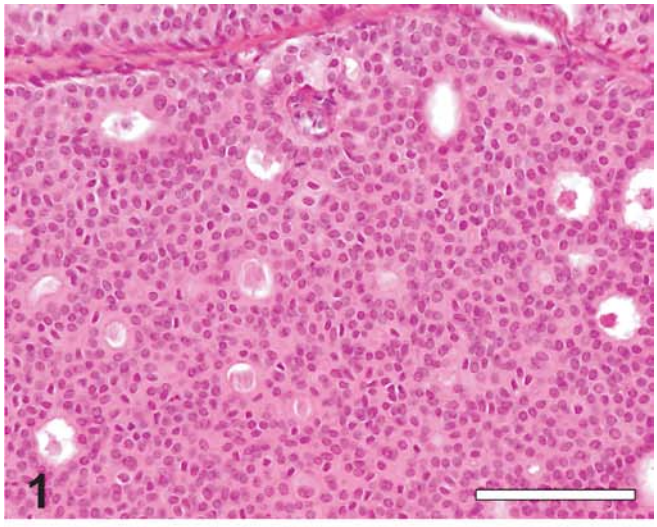

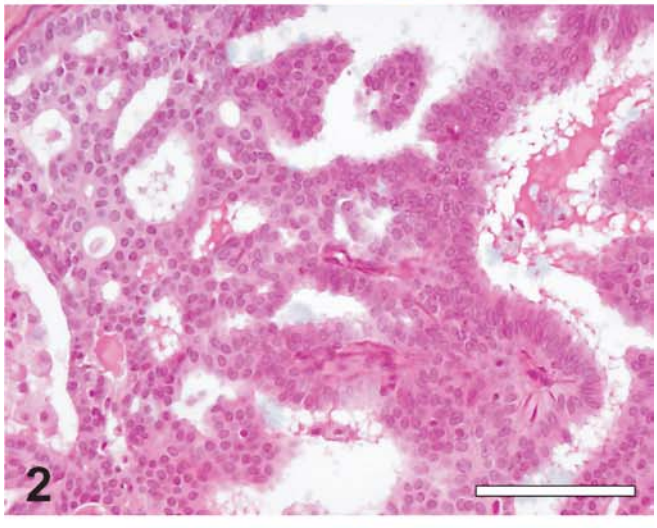

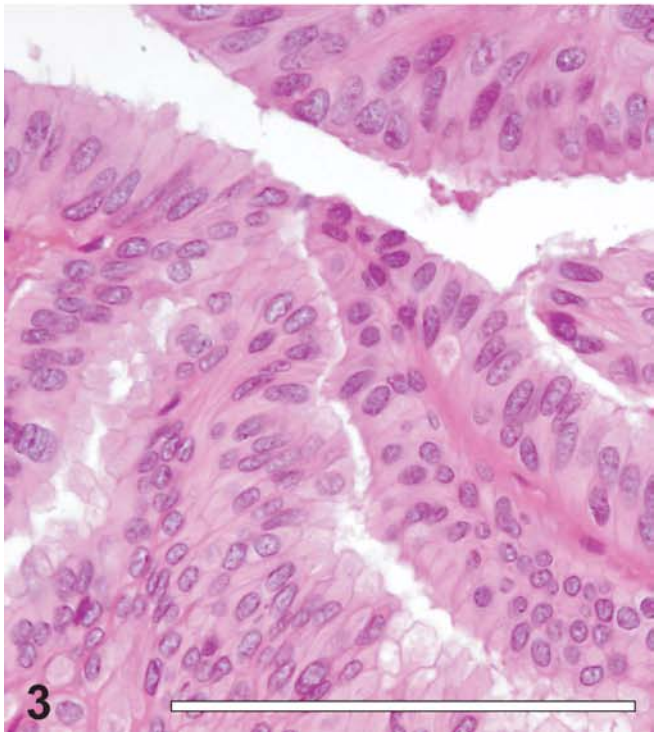

antibody, and positive controls were also examined for each case. Each case was reviewed on a double-headed microscope by both authors and a final diagnosis was made after reaching consensus.

Statistical analysis

Clinical follow-up was obtained for the 119 patients from the referring pathologist, the surgeon or the patient. The relationship between morphological features and clinical outcome was determined in a univariate analysis by the log-rank test using the Kaplan Meier method (BMDP software, program 1L). Local recurrences (in the same breast) were the events taken into account for the statistical analysis. These included: DCIS, carcinoma arising in a papilloma and invasive carcinoma. Subsequent ipsilateral or contralateral papillomas (five papillomas) as well as one contralateral carcinoma were not considered as significant events for the present statistical analysis.

Results

There were 119 women included in the study. The mean and median age was 56 years (19–83 years). For 77 patients, data on breast cancer history was available: a history of breast carcinoma involving first-degree relatives was present for 8 patients (10%). The right breast was preferentially involved and affected in 63 cases (57%), compared with 47 cases (43%) in the left breast. In a majority of cases, patients presented with a palpable mass [71 patients (60%)]. Other presenting symptoms included:

- Abnormal mammogram, 16 patients (13%)
- Nipple discharge, 6 patients (5%)
- Nipple discharge and lump, 12 patients (10%)
- Nipple discharge and abnormal mammogram, 2 patients

The size of the central papillomas ranged from 0.3 cm to 7 cm; mean size:1.5 cm, median size: 1.2 cm.

After histological review, the 119 central papillomas comprised: 40 papillomas with focal atypia (34%), 24 atypical papillomas (20%), 33 carcinomas arising in a papilloma (28%), 22 papillomas with florid hyperplasia (18%). The central papillomas were classified as localized in 81 cases (72%) and as complex in 32 cases (28%). Microcalcifications in the papillomas and lymphoid follicles surrounding the papillomas were present in 33 (28%) and 9 (8%) cases, respectively. Adjacent ducts and lobular units in the surrounding breast parenchyma were involved by usual ductal hyperplasia in 37 cases (31%), ADH in 19 cases (16%) and LN in 1 case (1%). The

Fig. 1 Focus of atypical ductal-type cells with monotonous small non-overlapping nuclei forming rosette-like structures within a papilloma. *Bar* 100 μm

Fig. 2 Focus of atypical ductal-type cells forming micropapillary and cribriform structures within a papilloma. *Space bar* 100 μm

Fig. 3 Focus of atypical ductal-type cells overlying papillary stalks arranged in a stratified columnar cell pattern. *Space bar* 100 μm

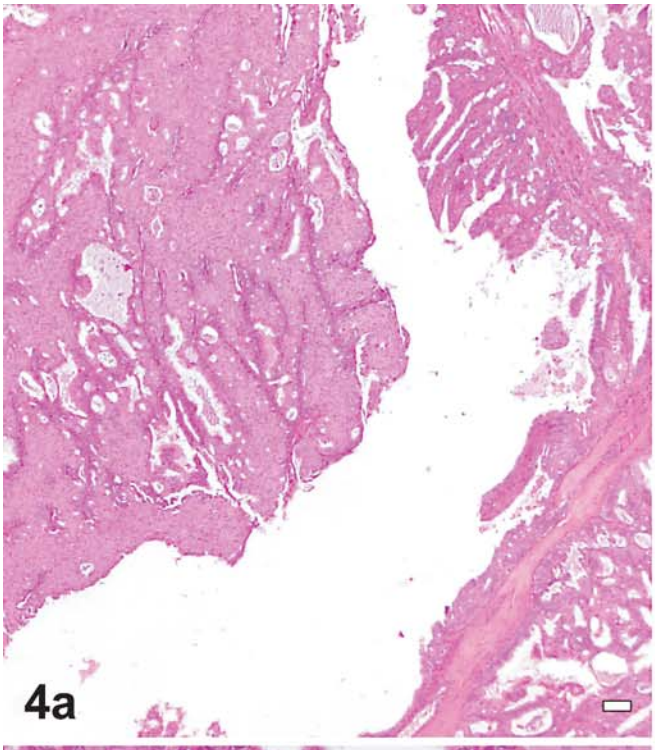
4a

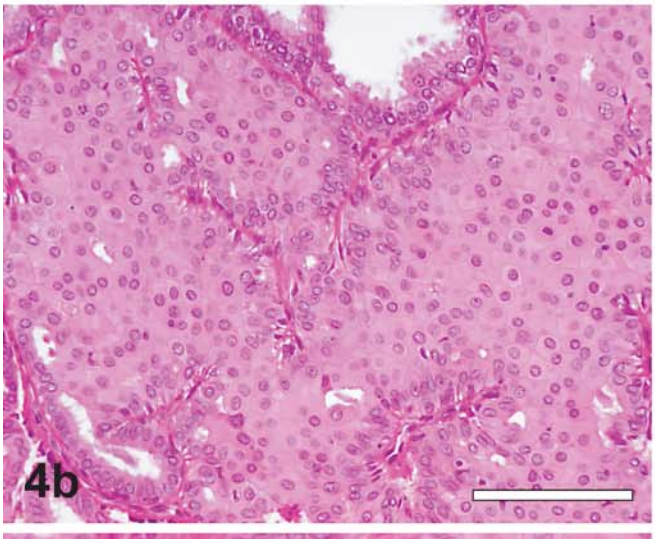
4b

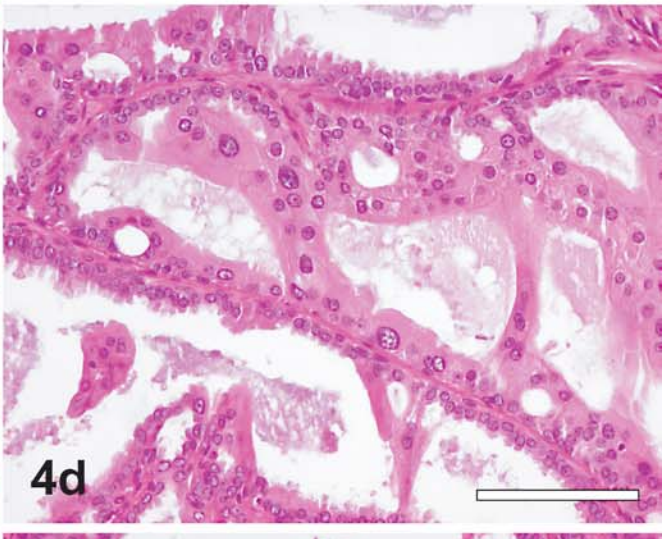
4d

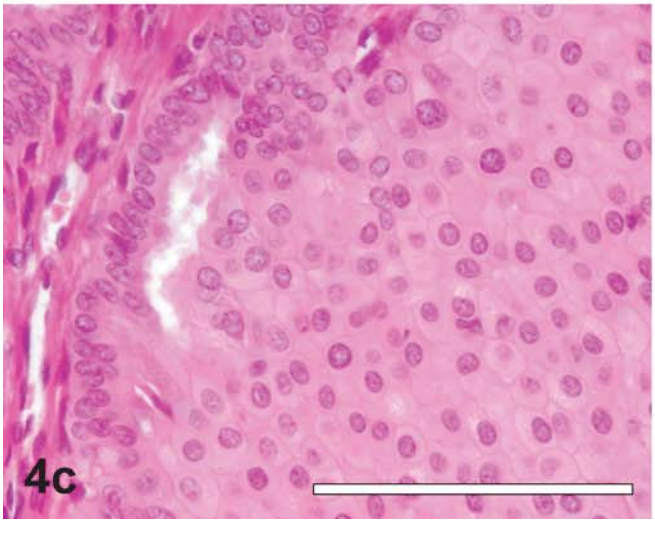
4c

4e

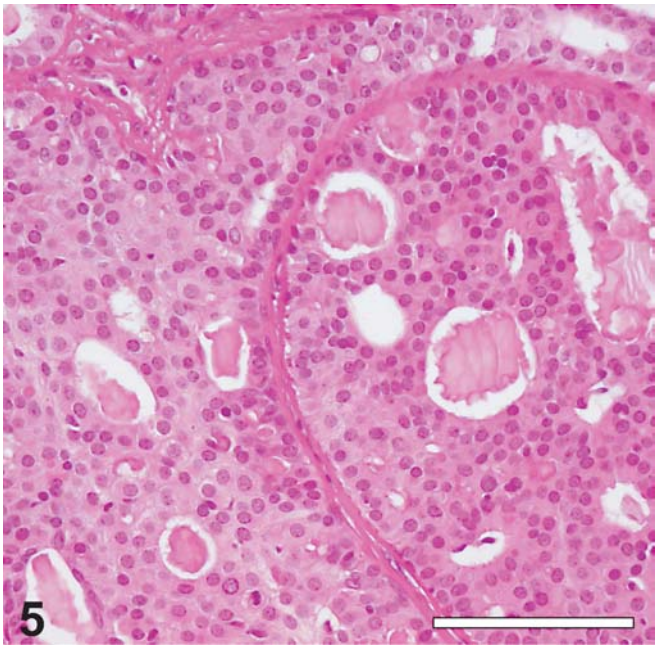

Fig. 5 Area of atypical apocrine-like cells with round monotonous non-overlapping nuclei organized around cribriform spaces containing eosinophilic secretions within a papilloma. *Space bar* 100 μm

adjacent ducts and lobules were devoid of any proliferative activity in 56 cases (47%).

The most common architectural patterns of atypical epithelial proliferation within the papillomas were: a cribriform pattern in 67 cases, a solid pattern in 52 cases, a stratified columnar cell pattern in 15 cases and an adenomatous pattern in 12 cases. Other patterns less frequently encountered were of the micropapillary type and a pagetoid diffusion of the atypical cells underneath the epithelium of adjacent papillary fronds. Apocrine cells and apocrine-like cells were the most frequently proliferating cell type encountered in the atypical areas (40 and 47 cases, respectively), followed by, native ductal-type cells (37 cases). Other cell types less frequently encountered were clear cells (8 cases), cells identical to those encountered in lobular neoplasia (1 case) and hypersecretory cells (1 case). Each of these cell types could either form the entire atypical population, or be associated with one another. Squamous changes were observed in 2 cases, in combination with the more usual atypical patterns. Foci of tumoral necrosis or infarction (Fig. 7) were respectively present in 24 and 12 papillomas. SMA immunostaining was positive in all cases analyzed and highlighted the presence of myoepithelial cells forming a continuous or discontinuous layer on the surface of the papillary stalks.

Fig. 4 Atypical central papilloma. **a** An atypical epithelial proliferation involving a portion of a central papilloma. **b** Same case, the atypical proliferation consists of apocrine-like cells arranged in solid sheets. **c** Same case, the apocrine-like cells show large eosinophilic cytoplasms, distinct cellular membranes and non-overlapping slightly irregular nuclei. **d** Same case, apocrine cells with a threefold variation in nuclear size organized in cribriform structures intermixed with apocrine-like cells. **e** Same case, non atypical epthelial and myoepithelial cells overlying papillary stalks in another area of the papilloma. *Space bars* 100 μm

Follow-up data

After a median period of 110 months 16 recurrences (five papillomas, two carcinomas arising in a papilloma, four DCIS, five invasive carcinomas) occurred. Nine recurrences were localized in the same area of the breast as the original papilloma, four recurrences in another area of the same breast and three recurrences in the other breast. At last follow-up, 103 patients were alive with no evidence of disease (87%), one patient died of ipsilateral invasive ductal carcinoma (1%), eight patients died of an unrelated cause (6%) and one patient died of an unknown cause (1%). Table 1 shows the characteristics of the central papillomas that recurred, the type of recurrence with the interval of time separating the original papilloma from the recurrence.

Table 2 shows the different categories of central papillomas with follow-up data and their corresponding recurrences, considering only recurrences with carcinomatous features. When comparing the different categories: papilloma with florid hyperplasia, papilloma with focal atypia, atypical papilloma and carcinoma arising in a papilloma, there was no statistically different trend observed with relation to recurrence (log-rank test). Other characteristics of these central papillomas were also studied for their pertinence in relation to recurrences: complexity of the papilloma, presence of lymphoid follicles in the adjacent breast parenchyma, presence of microcalcifications in the papilloma, presence of a cribriform or a stratified columnar cell pattern, presence of apocrine, apocrine-like or ductal-type cells and presence of foci of tumoral necrosis. No significant statistical trend was observed for any of these features. On the contrary, the presence of ordinary hyperplasia and/or ADH or LN in the breast parenchyma surrounding the papilloma was significantly associated with recurrences in the same breast (P=0.02, log-rank test) (Table 3). Interestingly, the presence of infarction in the original papilloma was also associated with a significant increase in recurrences (P=0.005, log-rank test) (Table 4). The presence of infarction in the original papilloma was more frequently observed in older patients (P=0.06, Wilcoxon test) and in larger papillomas (P=0.09, Wilcoxon test). When considering only invasive carcinomas as significant recurrences, five invasive carcinomas occurred in the series with follow-up (4%); two in the same area as the original papilloma, two in another area of the same breast and one in the contralateral breast. Again, there was no statistically significant trend observed when comparing the various categories of papillomas with relation to recurrence, nor the various morphological features ob-

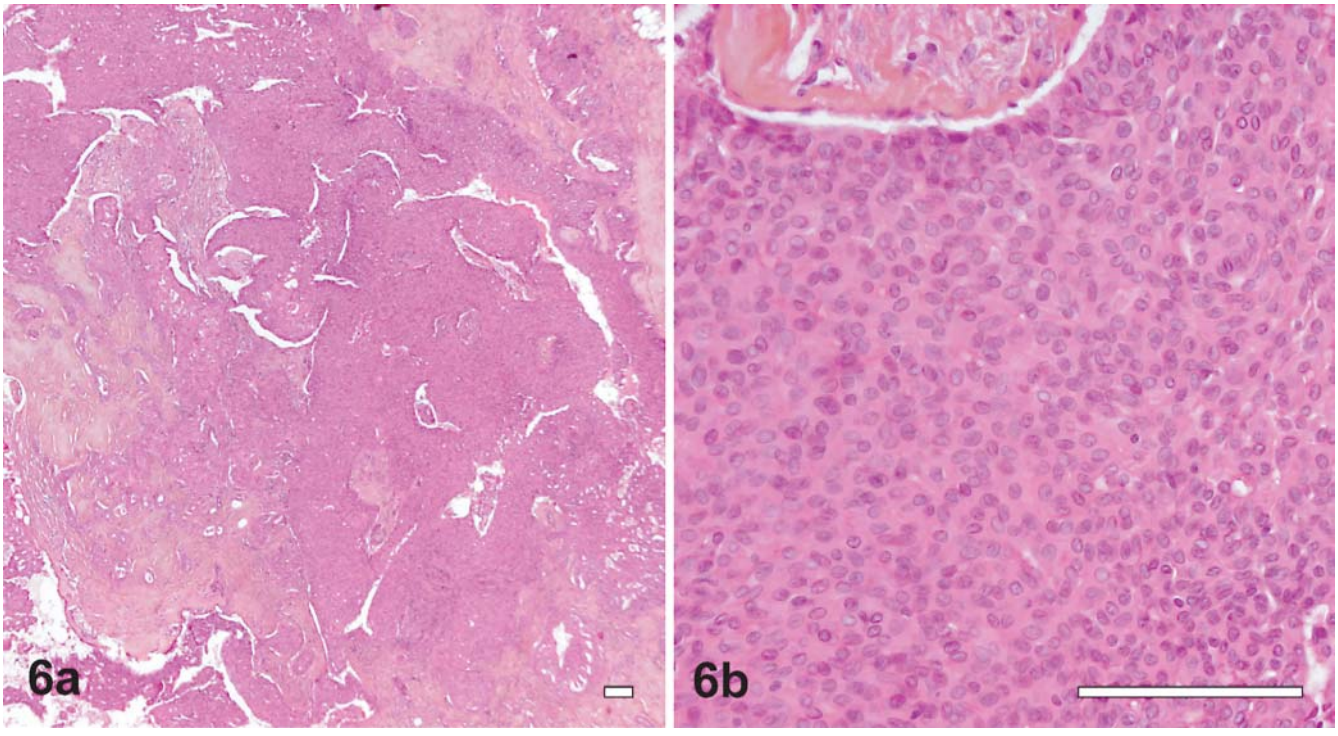

Fig. 6 a, b Central papilloma with florid usual ductal hyperplasia. The epithelial cells with overlapping coffee bean-shaped nuclei are arranged in swirling patterns. *Space bar* 100 μm

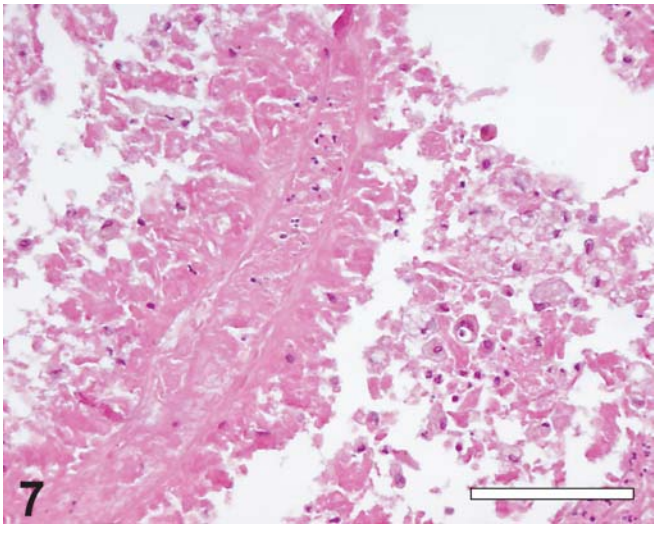

Fig. 7 Central papilloma with ischemic necrosis. *Space bar* 100 μm

served within the papillomas and in the surrounding breast parenchyma.

Discussion

The purpose of our study was to look for morphological features in papillomas that could serve as prognostic factors. The population studied retrospectively consisted of a series of papillomas sent to the Armed Forces Institute of Pathology because they presented with morphological features causing concern to the consulting pathologist. Among these papillomas, we distinguished four different categories. Our study did not show any statistically significant difference in terms of recurrence between these various categories, maybe because the number of recurrences was too small. Atypia occurring in papillomas appears to be a rare event, although no precise figure has been reported. Assembling a large group of such lesions is a difficult task, and, to our knowledge, this is the first large series of papillomas with atypia reported. The number of significant events that occurred after excluding patients who were treated by mastectomy, or patients with a personal history of breast cancer, was small: 11 events considering all lesions with carcinomatous features (both in situ and invasive) (8.4% ipsilateral, 0.8% contralateral) and 5 events considering only invasive carcinomas (3.3% ipsilateral, 0.8% contralateral). These rates are higher than those reported by Rosen in his review of the literature on 612 non-selected papillomas treated by excision only [11]. He found that recurrences, in the form of carcinoma, in situ or invasive, were reported in 23 of 612 cases (2% ipsilateral, 2% contralateral, 0.3% bilateral). Therefore, if we consider our population of papillomas with various types and patterns of epithelial proliferation as a whole, notwithstanding the degree or extent of atypical features within them, there appears to be an increased risk of subsequent develop-

Table 1 Characteristics of papillary lesions that recurred. *ADH* Atypical ductal hyperplasia, *DCIS* ductal carcinoma in situ

Case number	Age/side	Size	Type of papilloma	Necrosis	Surrounding breast	Recurrence	Location	Interval
1	59 years/left	19 mm	Papilloma with florid hyperplasia	None	Nothing	Papilloma	Other breast	96 months
2	63 years/left	10 mm	Papilloma with florid hyperplasia		Hyperplasia	Invasive carcinoma	Other area, same breast	104 months
3	61 years/right	6 mm	Papilloma with focal atypia	Infarction	Nothing	Invasive carcinoma	Same area, same breast	35 months
4	64 years/left	32 mm	Papilloma with focal atypia		Nothing	Papilloma	Other breast	38 months
5	34 years/right	11 mm	Papilloma with focal atypia	Infarction	Nothing	Invasive carcinoma	Other area, same breast	162 months
6	79 years/left	20 mm	Atypical papilloma	Infarction	ADH	DCIS	Same area, same breast	48 months
7	62 years/right	12 mm	Atypical papilloma	Infarction	Hyperplasia	Papilloma	Other area, same breast	217 months
8	55 years/right		Atypical papilloma		Hyperplasia	DCIS	Same area, same breast	145 months
9	73 years/left	15 mm	Atypical papilloma		Hyperplasia	Invasive carcinoma	Same area, same breast	28 months
10	40 years/right		Atypical papilloma		Hyperplasia	Papilloma	Same area, same breast	87 months
11	81 years/right	20 mm	Carcinoma arising in papilloma	Tumoral	Nothing	Papilloma	Same area, same breast	18 months
12	47 years/left	8 mm	Carcinoma arising in papilloma		Hyperplasia	DCIS	Same area, same breast	34 months
13	62 years/left		Carcinoma arising in papilloma	Tumoral	Hyperplasia	Carcinoma arising in papilloma	Same area, same breast	108 months
14	44 years/left	12 mm	Carcinoma arising in papilloma	Infarction	ADH	DCIS	Other area, same breast	55 months
15	48 years/right	15 mm	Carcinoma arising in papilloma	Infarction	ADH	Invasive carcinoma	Other breast	44 months
16	61 years	6 mm	Carcinoma arising in papilloma		Hyperplasia	Carcimona arising in papilloma	Same area, same breast	105 months

Table 2 Different categories of solitary papillomas among the patients with follow-up and the corresponding carcinomatous recurrences. *DCIS* ductal carcinoma in situ

Category of papilloma	Number of patients	Recurrences	Interval of time
Papilloma with florid hyperplasia	22	1 invasive carcinoma	104 months
Papilloma with focal atypia	40	2 invasive carcinomas	35 months, 162 months
Atypical papilloma	24	2 DCIS 1 invasive carcinoma	48 months, 145 months 28 months
Carcinoma arising in a papilloma	33	2 DCIS 2 carcinomas in papilloma 1 invasive carcinoma (contralat)	34 months, 55 months 105 months, 108 months 44 months

ment of invasive carcinoma among them when compared with papillomas in general. Raju and Vertes [10] compared 12 papillomas with ADH with 60 papillomas without ADH. Two contralateral invasive carcinomas subsequently occurred in the papilloma with ADH group compared with one ipsilateral and two contralateral invasive carcinomas in the non-atypical papilloma group. The authors concluded from these results that papillomas with atypia are more of a risk factor for subsequent development of invasive carcinoma in the contralateral breast. Page et al. [8] performed a nested case control study on 368 papillomas. Among these 368 benign

Table 3 Impact of proliferative breast disease (PBD) (hyperplasia and/or atypical ductal hyperplasia or lobular neoplasia) in surrounding breast on outcome of papillomas. *DCIS* ductal carcinoma in situ

Category of papilloma	Proliferative breast disease	Number of patients	Recurrences	Interval
Papilloma with florid hyperplasia	+PBD	8	1 Invasive carcinoma	104 months
	−PBD	12	1 Papilloma	96 months
Papilloma with focal atypia	+PBD	15	0	
	−PBD	22	1 Invasive carcinoma	35 months
			1 Invasive carcinoma	162 months
			1 Papilloma	38 months
Atypical papilloma	+PBD	17	1 DCIS	48 months
			1 DCIS	145 months
			1 Invasive carcinoma	28 months
			1 Papilloma	88 months
			1 Papilloma	217 months
	−PBD	7	0	
Carcinoma arising in papilloma	+PBD	17	1 Carcinoma in papilloma	105 months
			1 Carcinoma in papilloma	108 months
			1 DCIS	55 months
			1 DCIS	34 months
			1 Invasive carcinoma (contralat)	48 months
	−PBD	15	1 Papilloma	18 months

Table 4 Impact of infarction on outcome of papillomas. *DCIS* ductal carcinoma in situ

Category of papilloma	Infarction	Number of patients	Recurrences	Interval
Papilloma with florid hyperplasia	−Infarction	20	1 Invasive carcinoma	104 months
			1 Papilloma	96 months
	+Infarction	2	0	
Papilloma with focal atypia	−Infarction	35	1 Invasive carcinoma	162 months
			1 Papilloma	34 months
	+Infarction	5	1 Invasive carcinoma	35 months
Atypical papilloma	−Infarction	22	1 Papilloma	217 months
			1 Papilloma	88 months
			1 DCIS	145 months
			1 Invasive carcinoma	28 months
	+Infarction	2	1 DCIS	48 months
Carcinoma arising in papilloma	−Infarction	30	1 Carcinoma in papilloma	108 months
			1 Carcinoma in papilloma	105 months
			1 DCIS	34 months
			1 Papilloma	18 months
	+Infarction	2	1 DCIS	55 months
			1 Invasive carcinoma (contralat)	48 months

papilloma patients, 31 subsequently developed invasive carcinoma (8.4%). They found that the relative risk for invasive carcinoma for patients with papillomas containing atypical hyperplasia (AH) was nine and a half times that of patients without AH within their papillomas. Most of the invasive carcinomas in their study occurred in the same breast as the original papilloma, leading them to conclude that the risk represented by AH in papillomas was mainly local. Interestingly, the increased relative risk for subsequent development of invasive carcinoma observed in papillomas with AH appeared to be strongly linked to the presence of AH in the surrounding breast.

The risk of developing invasive carcinoma in the two previous studies was higher than that found in our own series [8, 10]. It is noteworthy that the criteria used to identify the atypical cell population observed in the papillomas of the three studies were similar. Judging from the information available in the three studies, the main reason for this discrepancy appears to be the number of cases and type of papillomas studied. While in rare cases the distinction was difficult, a vast majority of our cases were central, solitary papillomas of larger ducts of either simple (papillary projection into basically one distended space) or complex (multiple side branches involved) type. Both the mean and median size of our lesions exceeded 1 cm approaching 1.5 cm; the largest in the study of Page et al. [8] was 1.3 cm. More than half of the papillomas in that study were micropapillomas that measured 3 mm or less. Furthermore, in Raju and Verdes' study [10], of the 20 papillomas with atypical hyperplasia, 11 were of the solitary type and 9 were of the multiple type. Therefore, we believe that in the above-mentioned studies, there was

a significant proportion of multiple peripheral-type papillomas. Surgical margins were not truly assessed in these two studies, as in our own study, due to the absence of specific guidelines in the management of such lesions at the time of their excision. Incomplete excision of foci of atypical epithelial proliferation, especially for multiple peripheral-type papillomas, may partially explain the high rate of recurrences and subsequent development of cancer observed.

From both qualitative and quantitative standpoints, the atypical areas in a good proportion of our cases would have easily qualified as DCIS had they been found within the breast proper and out of the confines of a papilloma. The uneventful outcome for these patients can be explained by the complete excision of the atypical cell population localized within a confined lesion. Recurrences associated with carcinoma were usually developed within the same breast and were significantly associated with the presence of ductal cell hyperplasia and/or ADH, or LN in the surrounding breast. The study on the outcome of DCIS by the Van Nuys group [12], where no invasive recurrences occurred within the low-grade DCIS group of patients treated solely by complete excision with adequate margins, supports this explanation. The findings in the study of Carter et al. [3] on intracystic papillary carcinomas parallel ours. In the group of patients treated by excision alone in Carter et al.'s study, subsequent DCIS or invasive carcinomas were observed only in the subgroup of patients with associated DCIS in the surrounding breast while no recurrences were observed in the subgroup of patients presenting with fully developed intracystic papillary carcinoma alone but no evidence of DCIS in the surrounding breast tissues.

Surprisingly, a strongly significant morphological feature associated with recurrence in our series was the presence of areas of infarction within the original papilloma. We defined such areas as foci of coagulative necrosis involving the epithelial and myoepithelial cells as well as the underlying fibrovascular stalks. These areas retained their original architecture and "ghost" cells corresponding to the original epithelial cells were clearly visible. Such areas could be easily differentiated from tumoral necrosis, where only the epithelial cell compartment was involved and destroyed. Infarction tended to occur more often in older patients with larger papillomas. We have no clear hypothesis to explain this phenomenon. It could be the result of torsion secondary to dyssynchronous rapid growth of the epithelial, myoepithelial and stromal compartments of a papilloma, underlining its aggressive potential, or it may just reflect the physiological status of the patient.

The present study has demonstrated that, when confined to a central papilloma (simple or complex), the extent and quantity of epithelial atypia comparable to that of low-grade DCIS has no prognostic significance or impact on outcome for the patient. Recurrences, when they develop, appear to be related to the presence of proliferative breast lesions in the surrounding breast tissue. When atypia is encountered in a papilloma on an excisional biopsy, a rim of breast tissue surrounding the papilloma should be excised to allow assessment of the surrounding tissue for any evidence of atypical epithelial proliferations. Decisions on management of these lesions should be made in the context of the surrounding breast tissue and should be more conservative considering the findings of the present study. Assessment of the surrounding breast tissue for presence of an atypical epithelial proliferation is essential since follow-up would be particularly important in this group.

Acknowledgement We wish to thank Dr Carol Bodian for helpful and constructive discussion, Véronique Picot for statistical analysis and Isabelle Le Pollès for secretarial assistance. Gaëtan MacGrogan was supported by a "bourse d'aide à la mobilité de la Fondation De France et de la Fédération Nationale des Centres de Lutte Contre le Cancer."

References

1. Azzopardi J (1979) Papillary tumors. In: Azzopardi J (ed) Problems in breast pathology. Saunders, London, pp 150–166
2. Carter D (1977) Intraductal papillary tumors of the breast. A study of 78 cases. Cancer 39:1689–1692
3. Carter D, Orr SL, Merino MJ (1983) Intracystic papillary carcinoma of the breast. After mastectomy, radiotherapy or excisional biopsy alone. Cancer 52:14–19
4. Haagensen CD (1986) Solitary intraductal papilloma. In: Haagensen CD (ed) Diseases of the breast. Saunders, Philadelphia, pp 181–185
5. Ohuchi N, Abe R, Takahashi T, Tezuka F (1984) Origin and extension of intraductal papillomas of the breast: a three-dimensional reconstruction study. Br Cancer Res Treat 4:117–128
6. Ohuchi N, Abe Rikiya, Kasai M (1984) Possible cancerous change of intraductal papillomas of the breast. Cancer 54:605–611
7. Page DL, Dupont W, Rogers L, Rados M (1985) Atypical hyperplastic lesions of the female breast: a long-term follow-up study. Cancer 55:2698–2708
8. Page DL, Salhany KE, Jensen RA, Dupont WD (1996) Subsequent breast carcinoma risk after biopsy with atypia in a breast papilloma. Cancer 78:258–266
9. Papotti M, Gugliotta P, Eusebi V, Bussolati G (1983) Immunohistochemical analysis of benign and malignant papillary lesions of the breast. Am J Surg Pathol 7:451–461
10. Raju U, Vertes D (1996) Breast papillomas with atypical ductal hyperplasia: a clinicopathologic study. Hum Pathol 27:1231–1238
11. Rosen PP (1986) Arthur Purdy Stout and papilloma of the breast. Comments on the occasion of his 100th birthday. Am J Surg Pathol 10:100–107
12. Silverstein MJ, Lagios MD, Craig PH, Waisman JR, Lewinsky BS, Colburn W, Poller DN (1996) A prognostic index for ductal carcinoma in situ of the breast. Cancer 77:2267–2274
13. Tavassoli FA (1992) Benign lesions. In: Tavassoli FA (ed) Pathology of the breast. Appleton and Lange, Norwalk, pp 85
14. Tavassoli FA (1992) Papillary lesions. In Tavassoli FA (ed) Pathology of the breast. Appleton and Lange, Norwalk, pp 203–209
15. Tavassoli FA, Norris HJ (1990) A comparison of the results of long-term follow-up for atypical intraductal hyperplasia and intraductal hyperplasia of the breast. Cancer 65:518–529
16. Tavassoli FA, Norris HJ (1994) Intraductal apocrine carcinoma: a clinicopathologic study of 37 cases. Modern Pathol 7:813–818

Virchows Arch (2003) 443:618–624
DOI 10.1007/s00428-003-0882-3

ORIGINAL ARTICLE

Angela Pucci · Giovanni Bartoloni · Elena Tessitore · J. Aidan Carney · Mauro Papotti

Cytokeratin profile and neuroendocrine cells in the glandular component of cardiac myxoma

Received: 2 May 2003 / Accepted: 15 July 2003 / Published online: 13 September 2003
© Springer-Verlag 2003

Abstract Glandular cardiac myxomas are very rare tumors of uncertain histogenesis that display glandular structures within otherwise typical myxomatous tissue. The origin of the glands has been attributed to epithelial differentiation of a totipotent cardiomyogenic precursor cell or to entrapped embryonal rests in the tumor. We studied four cases of glandular myxomas (three sporadic and one familial) to define the immunophenotypic profile of the glandular elements. The glands were either single and located within the myxoma cell islands (three cases) or in groups embedded in the myxomatous matrix. In the latter case, the glands featured villous projections, irregular profile, active inflammation or focal reactive cellular atypia (case 3) and had acidic and neutral mucins (mostly sialomucins). The cytokeratin expression profile (cytokeratin 7 and 20 co-expression) was similar to that of foregut derivatives. Scattered chromogranin-positive neuroendocrine cells were observed in case 3. Our findings indicate that the glandular component in cardiac myxoma is morphologically heterogeneous. In some cases, the scattered glands may derive from a divergent (epithelial) differentiation of myxoma cells; in others, entrapment of embryonic gastrointestinal rests (with mature neuroendocrine and mucous cell populations) could be the case.

Keywords Glandular cardiac myxoma · Heart · Immunohistochemistry · Neuroendocrine differentiation · Cytokeratin

A. Pucci · E. Tessitore
Department of Pathology,
Regina Margherita Hospital,
Torino, Italy

G. Bartoloni
Department of Pathology,
University of Catania,
Catania, Italy

J. A. Carney
Department of Pathology,
Mayo Clinic,
Rochester, Minnesota, USA

M. Papotti
Department of Pathology,
University of Turin,
Torino, Italy

A. Pucci (✉)
Anatomia Patologica,
Ospedale Infantile Regina Margherita,
Piazza Polonia 94, 10126 Torino, Italy
e-mail: angelapucci@libero.it
Tel.: +39-11-3135410
Fax: +39-11-3135412

Introduction

Cardiac tumors are rare, and myxomas are the most common type in adults [4, 7, 23, 28, 47]. They are generally benign tumors, although exceptional cases of malignant myxomas have been reported [11, 12, 14, 15, 21, 27, 31, 35, 36, 37, 38, 42, 53]. The histogenesis of the tumor is poorly understood. Immunocytochemical studies have identified several differentiation patterns as shown by expression of endothelial, smooth muscle and epithelial markers [6, 11, 13, 19, 22, 25, 29, 30, 40, 46, 56]. Recently, cardiomyogenic differentiation [24] and calretinin expression [48] have been demonstrated in the tumor cells, suggesting an origin from a mesenchymal cardiomyocyte progenitor cell or a relationship to endocardial sensory nerve tissue, respectively.

Rarely, glandular structures have been described within benign [1, 6, 11, 13, 16, 17, 18, 22, 26, 34, 39, 50] and rarely malignant [12, 38] cardiac myxomas. The glands have been interpreted as entrapped foregut rests [22] and as glandular differentiation of myxoma cells [6]. The metastatic adenocarcinoma in a myxoma has also been considered as an explanation, but the absence of cytological atypia in the glandular cells is against such a hypothesis [26]. Immunohistochemical expression of epithelial membrane antigen (EMA), carcino-embryonic antigen (CEA), Ca19.9 and S-100 protein have been reported in glandular cardiac myxomas [1, 18, 26, 34], but

the histochemical [54] and immunophenotypic profile of the glandular elements have not been thoroughly investigated.

The aim of the present study was to investigate the histological and the immunohistochemical features of four cardiac myxomas with a glandular component. We found that the glandular component is variable in its amount and morphological features. The cytokeratin expression pattern of the glandular component is similar to that of upper gastrointestinal glands, and neuroendocrine cells may be occasionally found in the tumor.

Materials and methods

Among 103 consecutive, surgically resected cardiac myxomas filed in the Pathology Departments of the University of Turin (n=53, years 1980–1994) and Catania (n=50, years 1987–2002), respectively, 3 (2.8%) had a glandular component. Two of the three have been partially reported previously [34]. An additional case, also reported in part [9], was retrieved from the consultation file of one of us (J.A.C.). The histological diagnosis of the cases was based on previously described histological criteria [6, 34].

The tumors were fixed in formalin and blocks were embedded in paraffin for routine histology, histochemistry and immunohistochemistry. A mean of 7 (range 3–10) hematoxylin and eosin stained sections per tumor were examined, together with periodic acid-Schiff (PAS), Alcian blue and high-iron diamine (HID) stains for mucins [32]. The following immunohistochemical markers were investigated: broad spectrum cytokeratin, cytokeratin 7 (CK7), cytokeratin 20 (CK20), CEA, EMA, chromogranin A, synaptophysin, calretinin, thyroid transcription factor-1 (TTF-1), Ki-67 and p53. The type, source and dilution of the antibodies used for immunohistochemistry are listed in Table 1. Antigen retrieval was performed by heating the slides in citrate buffer (0.01 mol/l, pH 6.0) in a microwave oven (two 5-min passages at 650 W) for the following markers: CK7, CK20, synaptophysin, calretinin, TTF-1, Ki-67 and p53. The Dako EnVision System (DakoCytomation) was used to reveal the immune reaction. Briefly, slides were incubated for 30 min with the primary antisera (or non-immune serum for negative controls) after blocking endogenous peroxidase by H_2O_2 and performing, if required, antigen retrieval; immunoreactivity was revealed by application of Rabbit/Mouse EnVision reagent (30 min) and chromogen substrate (diaminobenzidine, 5 min); slides were counterstained by Harris' Hematoxylin. PAS-immunoperoxidase double staining was also performed in case 3 [20]. Immunohistochemical features were considered positive when at least 5% of the respective cells were positively stained.

Results

Clinical data

Three patients were males, aged 55, 23 and 57 years, and the fourth was a woman, aged 45 years. Three of the tumors arose in the fossa ovalis of the left atrium, the fourth in the right atrial septum. The mean diameter was 6 cm (range 3–9 cm). Follow-up information for periods ranging from 1.5 years to 19 years (mean 9.2 years) was available. The female patient died at age 46 years of cardiac failure, thought to be due to obstructive cardiomyopathy. In cases 1 and 2, constitutional, non-cardiac related symptoms, i.e., sweating and/or trembling, were present. In case 3, arrhythmias and fever were found at the time of diagnosis. One patient (case 4) was affected by Carney complex (multiple cardiac myxomas, cutaneous myxomas and primary pigmented nodular adrenocortical disease) [8]. None of the patients had adenocarcinoma at any site either at the time of detection of the cardiac myxoma or subsequently.

Morphological data

The cellularity of glandular cardiac myxomas varied from case to case and within different areas of the same tumor. Inflammatory cells (macrophages, lymphocytes, granulocytes and mast cells), hemorrhagic and fibrinous areas were variably present within a highly vascular myxoid stroma. Calcifications were also occasionally observed. Osseous metaplasia was prominent in case 3. The extent of glandular component among the cases was variable. In three cases, the glands represented 5–10% of the tumor area, whereas in case 3 they were approximately 15–20%. In all tumors, the glands were located near the tumor base, adjacent to myocardial fibers (Fig. 1a, b).

Two patterns of glandular distribution were recognized: (1) glands scattered in a loose myxoid stroma and (2) glands centrally located in islands of myxoma cells. In the former pattern, single glandular structures or glandular clusters were growing into the loose myxoid stroma, adjacent to the classical polygonal cell clusters of cardiac myxomas (Fig. 1c). This pattern was particularly promi-

Table 1 List of primary antibodies used. Antibody source: Dako Cytomation, Glostrup, Denmark; Immunotech, Marseille, France; Zymed, San Francisco, CA, USA; Biogenex, San Ramon, CA, USA; NeoMarkers, Fremont, CA, USA; Novocastra, Newcastle, UK

Marker	Species	Clone	Source	Dilution	Positive controls
Epithelial membrane antigen	Mouse	E29	DakoCytomation	1/50	Colon carcinoma
Carcinoembryonic antigen	Rabbit	–	DakoCytomation	1/1000	Colon carcinoma
Broad spectrum cytokeratin	Mouse	KL 1	Immunotech	1/100	Sqamous cell carcinoma
CK 7	Mouse	OV-TL 12/30	DakoCytomation	1/25	Lung
CK 20	Mouse	K_s20.8	DakoCytomation	1/25	Colon carcinoma
Calretinin	Rabbit	–	Zymed	1/100	Malignant pleural mesothelioma
Thyroid transcription factor-1	Mouse	8G7G3/1	DakoCytomation	1/25	Lung
Chromogranin A	Mouse	LK2H10	Biogenex	1/500	Pancreas
Synaptophysin	Rabbit	–	NeoMarkers	Prediluted	Pancreas
p53	Mouse	DO-7	Novocastra	1/100	Colon carcinoma
Ki-67	Mouse	MIB-1	DakoCytomation	1/10	Tonsil

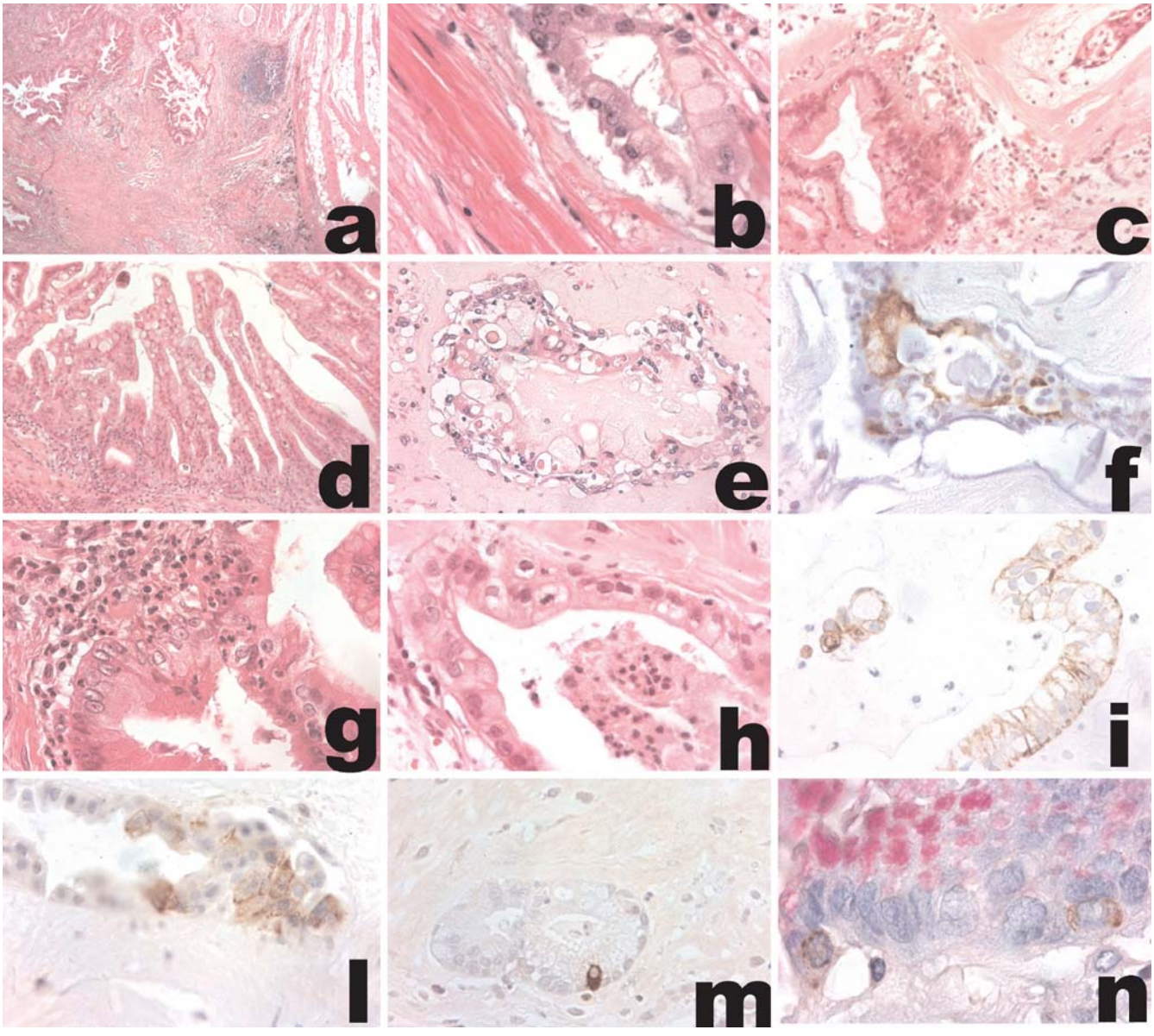

Fig. 1 Cardiac myxoma containing glandular structures. Two patterns are shown in **a–c** (pattern 1: glands separated from myxoma cell islands) and in **e–f** (pattern 2: glands within the myxoma cell islands). Numerous glandular structures are mainly located at the pedicle area (case 3) (**a**, ×25). The glands were lined by columnar mucinous cells (case 3) (**b**, ×400). The glands (*left*) were scattered in a loose myxoid stroma, independent from the myxoma cell islands (*top right*) (case 3) (**c**, ×200), and occasionally had villous-like projections (**d**, ×100). In other cases (pattern 2), the glands were centrally located in islands of myxoma cells, as seen with hematoxylin and eosin staining (case 4) (**e**, ×400), and cytokeratin immunostaining (case 2) (**f**, ×400). Foci of active inflammation (**g**, ×400) and of reactive cellular atypia (**h**, ×400) (case 3). Immunoreactivity for specific cytokeratin types 7 (**i**, case 3, ×400) and 20 (**l**, case 1, ×400) was found in the glandular elements. Chromogranin immunoreactivity was observed in single scattered neuroendocrine cells (**m**, ×400), basally located among mucus producing cells (**n**, double periodic acid-Schiff–immunoperoxidase staining, ×1000) (case 3)

nent in case 3, which showed dilated glands with villous-like projections. Columnar cells with maintained polarity covered the villi (Fig. 1d). Single epithelial cells were also detected in the stroma; they were highlighted by cytokeratin immunostaining (see below). The second pattern (predominant in cases 1, 2 and 4) was characterized by round or elongated glands usually centrally located in myxoma cell islands (Fig. 1e, f). The latter appearance suggested a progressive differentiation of the glandular structures from typical myxoma tissue. In case 2, the glands occasionally had a hyperplastic cuboidal epithelium, as seen in gastrointestinal hyperplastic polyps. An additional feature observed in case 3 was the presence of a chronic inflammatory infiltrate around and within the glands, with several intraepithelial granulocytes, similar to the active inflammation in the gastrointestinal mucosa

(Fig. 1g). Mild, reactive cellular atypia was shown in occasional glands of cases 1, 2 and 4. In case 3, glands were lined by tightly packed columnar cells, with hyperchromatic nuclei and rare mitoses (Fig. 1h).

Histochemical data

Many epithelial cells were mucin-secreting, as confirmed by positive PAS and Alcian blue stainings. HID stain showed that sialomucins were more common than sulphomucins within the glands.

Immunohistochemical data

The glandular cells were positive for EMA and CEA. A broad-spectrum cytokeratin antibody (clone KL1) and antibodies to gastrointestinal cytokeratin types (e.g., CK7) strongly stained all the glands (Fig. 1i). Colonic type CK20 was focally expressed in cases 1 and 2 (Fig. 1l), diffusely in case 3 and was negative in case 4. In case 3, scattered cells were strongly immunoreactive for the neuroendocrine marker chromogranin A. These cells were round or flask-shaped and basally located in the glands, admixed with the mucous cells (Fig. 1m, n). A very low proliferative activity (less than 2%) was detected in glandular cells of case 3 by means of Ki-67 immunostaining. There was no reactivity for TTF-1, calretinin or p53. Synaptophysin immunostaining was negative in cases 1, 2, 3; case 4 could not be investigated because no appropriate section was still available.

Discussion

In this study, we report the morphological features and the immunophenotypic profile of the glandular component in four cardiac myxomas. The gland arrangement showed a wide range of variability. In three cases, relatively small glands, apparently located within the myxoma cell islands, suggested a progression from myxoma elements to true glands, as proposed by Burke and Virmani [6]. In the fourth case, the glands were larger, arranged in clusters and showed irregular profile and villous-like projections. Other features of the glandular epithelium included the presence of sialomucins, occasional sulphomucin-containing mucous cells, areas of active inflammation, focal hyperplastic changes (similar to those seen in hyperplastic polyps) and also foci of reactive cellular atypia. These findings suggest that the origin of these glands may be different in different cases (see below).

Using immunohistochemistry, we confirmed that the glands were positive for broad-spectrum cytokeratins, CEA and EMA [6, 11, 13, 18, 34]. The cytokeratin subtypes co-expressed in the glandular component (types 7 and 20) are those expressed by the upper gastrointestinal mucosa (e.g., stomach) [10]. This finding suggests that the glands in cardiac myxomas may recapitulate foregut derivatives, such as the upper gastrointestinal glands, rather than colonic type epithelium (characterized by CK20 positivity only). Derivation from bronchial glands or alveolar cells of the lung is unlikely because these cells usually do not express CK20 and, in addition, are TTF-1-positive, which was absent in our cases. We could not confirm the recent report of the expression of the mesothelioma marker, calretinin, in cardiac myxomas [48]. To this purpose, appropriate positive (malignant pleural mesothelioma) as negative (squamous cell lung carcinoma) controls gave the expected results using the previously described immunohistochemical procedure, including antigen retrieval, to reveal calretinin immunoreactivity.

Scattered chromogranin-positive neuroendocrine cells were observed in the glandular structures in one of our cases. The cells were flask-shaped and basally located in the glands, as occurs in the gastrointestinal (and bronchial) mucosa [44]. The paucity of these cells in serial sections did not permit further characterization of the hormonal content of the cells. A previous study did not detect chromogranin-reactive cells in 11 cardiac myxomas, including 1 with glandular elements [11]. The presence of divergent (exocrine and endocrine) lines of differentiation in our case suggests that the glandular component of cardiac myxoma may feature more than one cell type (see below).

The reactive cellular atypia found in some cases and related findings deserve comment. First, the atypia indicates that the glandular component may exhibit the type of cytological abnormality seen in other sites and, therefore, may be subject to influences that affect glandular epithelium elsewhere in the body. Second, mild "reactive" atypia [1] has previously been described in a glandular cardiac myxoma. Third, carcinomas metastatic to the left atrium have been described [49]. Therefore, a metastatic adenocarcinoma must be excluded when glandular elements are found in a cardiac myxoma.

Glandular cardiac myxomas are very rare tumors; only 27 cases have been reported, to our knowledge (Table 2). Classical cardiac myxomas predominantly affect female patients in an older age group and show cardiac-related rather than constitutional symptoms [4, 7, 6, 47]. Our patients were relatively young (mean age 45 years), three of four were male and the fourth one was a female with Carney complex. This indicates that that the glandular component of myxoma may occur in both non-familial and familial clinical settings. Desphande and co-workers reported the occurrence of a glandular component in the recurrent myxoma of a patient with familial cardiac myxoma [13].

The clinical behavior of the presently described cases did not differ from that of previously reported non-glandular myxomas [5, 7, 9, 34]. There were no local recurrences or distant metastases after a mean follow-up period of 9.2 years. There have been only few cases of malignant glandular cardiac myxomas reported [12, 38]. Among these, it could be argued that the malignant behavior in at least some was the result of local

Table 2 Selected features in reported cases of glandular cardiac myxomas*. *na* not available, *LA* left atrium, *RA* right atrium, *H* histopathology, *IHC* immunohistochemistry, *US* ultrastructural analysis, *F8* factor VIII related antigen, *UEA* Ulex Europeus agglutinin, *NSE* neuron specific enolase, *AFP* alpha-feto-protein, *HID* high iron diamine stain. *CK* cytokeratin, *EMA* epithelial membrane antigen, *CEA* carcinoembryonic antigen, *TTF-1* thyroid transcription factor 1, *CGA* chromogranin A, *PAS* periodic acid Schiff, *GFAP* glial fibrillary acidicic protein, *AB* alcian blue

Case no.	Author, year (reference no.)	Reported cases	Sex	Age (years)	Location	Sporadic/ familial	Studies	Main markers
1	Anderson, 1946 [2]	1	Female	43	LA	na	H	
2	Vacek, 1963 [52]	1	Female	31	RA	na	H	Mucicarmin
3	Frishman, 1979 [17]	1	Female	59	RA	Sporadic	H, US	AB, PAS
4	Song, 1984 [45]	3	na	na	na	na	H	
5								
6								
7	Widder, 1985 [55]	2	Female	62	LA	na	H	
8			Female	43	RA			
9	Abenoza, 1986 [1]	1	Female	14	LA	Sporadic	H, IHC	F8, CK, EMA, UEA
10	Goldman, 1987 [18]	2	Female	65	RA	Sporadic	H, IHC, US	PAS, CEA, EMA, F8
11			Male	44	LA	Sporadic		
12	de Morais, 1988 [12]	1	Male	79	LA	Sporadic	H, IHC, US	F8, CEA
13	Johansson, 1989 [22]	1	na	na	LA	na	H, IHC	F8, CK, S-100
14	Toszegi, 1990 [51]	1	Female	49	LA	na	H	
15	Schultrich, 1990 [41]	1	Female	45	LA	na	H	
16	Curschellas, 1991 [11]	1	Female	44	LA	na	H, IHC	AB-PAS, CK, CEA, CGA, GFAP
17	Schmitt-Graff,1992 [39]	1	Male	55	LA	Sporadic	H, IHC	F8, CK, CEA, EMA, AFP
18	Burke, 1993 [7]	3	na	na	LA	Sporadic	H, IHC	CD34, F8, UEA, S100, CK
19					LA			
20					RA			
21	Thornton, 1993 [50]	2	Female	31	LA	Familial	H, IHC	Mucin stains, CEA, EMA,
22			na	na	na	Sporadic		CK
23	Wang, 1993 [54]	2	na	na	na	na	H, IHC	AB-PAS, HID, F8, S100,
24			na	na	na			CK, CEA, EMA
25	Deshpande, 1994 [13]	1	Female	55	RA?	Familial	H, IHC	F8, UEA, CK, S100
26	Sipos, 1995 [43]	1	Female	29	LA	na	H, IHC, US	PAS, F8, CK, EMA, CEA
27	Lindner, 1999 [26]	1	Female	78	LA	Sporadic	H, IHC	F8, CK,EMA,CEA,CA 19.9,CGA,NSE
28	Present cases	4	Male	55	LA	Sporadic	H, IHC	PAS, AB, HID, CK 7,
29			Male	23	LA	Sporadic		CK20, CGA, TTF-1
30			Male	57	LA	Sporadic		
31			Female	45	RA	Familial		

* Eight cases with glandular elements reported by Fine (1968) were excluded in the absence of individual case description.

recurrence of the tumor, tumor multifocality or embolic phenomena [3, 33].

The histogenesis of the glandular component could be related to a teratomatous or malformative process [22] or to divergent differentiation events in the tumor [6]. The morphological and immunophenotypic features of the glands in our cases do not exclude any of these mechanisms. In three cases (1, 2 and 4), the glandular elements were found within the myxoma cell islands, supporting the hypothesis of a progression from myxoma to glandular cells, as a result of divergent differentiation [6]. In case 3, however, most glands were independent of and separate from the myxoma cell clusters, suggesting the possibility that they represented entrapment of embryonic foregut rests. It seems unlikely that a totipotent cardiomyocyte progenitor cell could differentiate into highly specialized cell lineages of the gastrointestinal tract, including the neuroendocrine cell type. The glandular component of cardiac myxoma is usually located close to the tumor attachment at the atrial septum. In early embryogenesis, the foregut and the primitive cardiac tube (and particularly the septum transversum) lie close together in an area corresponding to the site of origin of myxomas. Glandular embryonic rests of foregut derivation could be entrapped in that area and subsequently grow into a myxoma. Such rests, however, have never been described in the normal atrial septum, although they could have been overlooked.

Myxomas with a glandular component do not have the attributes of true teratomas. Their atrial localization and morphological features, especially the lack of squamous epithelium (that is a regular component of teratomas), are against such a hypothesis. Moreover, no tissues other than glandular, osseous, fibrous connective, hemopoietic and thymic have been reported in cardiac myxomas. Thus, the origin of glandular elements in cardiac myxoma remains elusive. Molecular genetic analysis of the various tumor components using tissue microdissection could provide further information. We were unable to perform clonal analysis of the myxomatous and glandular cell populations in our cases because three of our patients were male and tissue for the study was not available in the fourth case.

In conclusion, we found that the glandular component in cardiac myxomas is heterogeneous and that its morphological and immunophenotypic (CK7 and CK20 and chromogranin expression) features are similar to those of the upper gastrointestinal tract mucosa. In some cases, the glands seem to evolve from myxoma cell islands, favoring a divergent differentiation histogenetic hypothesis. However, in other instances, the glands were independent from the myxoma cells and are consistent with entrapped embryonic rests.

Acknowledgement Work was partially supported by grants from the Italian Ministry of Education (Rome, to M.P.).

References

1. Abenoza P, Sibley RK (1986) Cardiac myxoma with gland-like structure: an immunohistochemical study. Arch Pathol Lab Med 110:736–739
2. Anderson WAD, Dmytryk ET (1946) Primary tumor of the heart containing epithelium-like elements. Am J Pathol 22:337–349
3. Attum AA, Johnson GS, Masri Z, Girardet R, Lansing AM (1987) Malignant clinical behavior of cardiac myxomas and "myxoid imitators". Ann Thorac Surg 44:217–222
4. Basso C, Valente M, Poletti A, Casarotto D, Thiene G (1997) Surgical pathology of primary cardiac and pericardial tumors. Eur J Cardiothorac Surg 12:730–737
5. Basson CT, Aretz HT (2002) Case records of the Massachussets General Hospital—a 27-year old woman with two intracardiac masses and a history of endocrinopathy. New Engl J Med 346:1152–1158
6. Burke A, Virmani R (1993) Cardiac myxoma. A clinicopathologic study. Am J Clin Pathol 100:671–680
7. Burke A, Virmani R (eds) (1996) Tumors of the heart and great vessels (Atlas of tumor pathology) Armed Force Institute of Pathology, Washington DC
8. Carney JA (1985) Differences between non-familial and familial cardiac myxoma. Am J Surg Pathol 9:53–55
9. Carney JA, Gordon H, Carpenter PC, Shenoy BV, Go VL (1985) The complex of myxomas, spotty pigmentation, and endocrine overactivity. Medicine 64:270–283
10. Chu PG, Weiss LM (2002) Keratin expression in human tissues and neoplasms. Histopathology 40:403–439
11. Curschellas E, Toia D, Borner M (1991) Cardiac myxomas: immunohistochemical study of benign and malignant variants. Virchows Arch 418:485–491
12. deMorais CF, Falzoni R, Ferreira Alves VA (1988) Myocardial infarct due to a unique atrial myxoma with epithelial-like cells and systemic metastases. Arch Pathol Lab Med 112:185–190
13. Deshpande A, Venugopal P, Sampath Kumar A (1996) Phenotypic characterization of cellular components of cardiac myxoma: a light microscopy and immunohistochemistry study. Hum Pathol 27:1056–1059
14. Desousa AL, Muller J, Campbell RL, Batnitzky S, Rankin L (1978) Atrial myxoma: a review of the neurological complications, metastases and recurrences. J Neurol Neurosurg Psychiatry 41:1119–1124
15. Diflo T, Cantelmo NL, Haudenschild CC, Watkins MT (1992) Atrial myxoma with remote metastases: case report and review of the literature. Surgery 111:352–356
16. Fine G, Morales A, Horn RC (1968) Cardiac myxoma. A morphologic and histogenetic appraisal. Cancer 22:1156–1162
17. Frishman W, Factor S, Jordan A (1979) Right atrial myxoma: unusual clinical presentation and atypical glandular histology. Circulation 59:1070–1075
18. Goldman BI, Frydman C, Harpaz N (1987) Glandular cardiac myxomas: histologic, immunohistochemical and ultrastructural evidence of epithelial differentiation. Cancer 59:1767–1775
19. Govoni E, Severi D, Cenacchi, Laschi R, Pileri S, Rivano MT, Alampi G (1988) Ultrastructural and immunohistochemical contribution to the histogenesis of human cardiac myxomas. Ultrastruct Pathol 12:221–233
20. Gugliotta P, Papotti M (1981) Colorazione associata acido periodico-Schiff e immunoperossidasi (PAS-IP). Basic Appl Histochem 25[Suppl]:62
21. Hannah H III, Eisemann G, Hiszezynskyj R, Winsky M, Cohen L (1982) Invasive atrial myxoma: documentation of malignant potential of cardiac myxomas. Am Heart J 104:881–883
22. Johansson L (1989) Histogenesis of cardiac myxomas: an immunohistochemical study of 19 cases, including one with glandular structures, and review of the literature. Arch Pathol Lab Med 113:735–741
23. Kieny R, deGeeter B, Kretz JG, Eisenmann B, Clovert JM, Buck P (1983) Cardiac tumors in infancy: recent aspects. Thorac Cardiovasc Surg 31:169–171
24. Kodama H, Hirotani T, Suzuki Y, Ogawa S, Yamazaki K (2002) Cardiomyogenic differentiation in cardiac myxoma expressing lineage-specific transcription factor. Am J Pathol 161:381–389
25. Landon G, Ordonez NG, Guarda LA (1986) Cardiac myxoma: an immunohistochemical study using endothelial, histiocytic and smooth muscle cell markers. Arch Pathol Lab Med 110:116–120
26. Lindner V, Edah-Tally S, Chafkè N, Onody T, Eisemann B, Walter P (1999) Cardiac myxoma with glandular component: case report and review of the literature. Pathol Res Pract 195:267–272
27. Markel ML, Amstrong WF, Waller BF, Mahomed Y (1986). Left atrial myxoma with multicentric recurrence and evidence of metastases. Am Heart J 111:409–413
28. McAllister HA Jr (1979) Primary tumors of the heart and pericardium. Pathol Annu 14:335–366
29. McComb RD (1984) Heterogeneous expression of factor VIII/von Willebrand factor by cardiac myxoma cells. Am J Surg Pathol 8:539–544
30. Morales AR, Fine G, Castro A, Nadij M (1981) Cardiac myxoma (endocardioma): an immunohistochemical assessment of histogenesis. Hum Pathol 12:896–899
31. Pastakia B (1979) Malignant atrial myxoma presenting as intracranial mass. Chest 75:531–532
32. Prophet EB, Mills B, Arrington JB, Sobin LH (eds) (1992) Laboratory methods in histotechnology. Armed Force Institute of Pathology, Washington DC
33. Pucci A, Gagliardotto P, Papandrea C, Di Rosa E, Morello M, di Summa M, Mollo F (1996) An unusual myxoid leiomyosarcoma of the heart. Arch Pathol Lab Med 120:583–586
34. Pucci A, Gagliardotto P, Zanini C, Pansini S, Di Summa M, Mollo F (2000) Histopathologic and clinical characterization of cardiac myxoma. Am Heart J 140:134–138
35. Rankin LI, DeSousa AL (1978) Metastatic atrial myxoma presenting as intracranial mass. Chest 74:451–452
36. Read RC, White HJ, Murphy ML, Williams D, Sun CN, Flanagan WH (1974) The malignant potentiality of left atrial myxoma. J Thorac Cardiovasc Surg 68:857–868
37. Rupp GM, Heyman RA, Martinez J, Shekhar LN, Jungreis CA (1989) The pathology of metastatic cardiac myxoma. Am J Clin Pathol 91:221–227
38. Scarpelli M, Montironi R, Ricciuti R (1997) Cardiac myxoma with glandular elements metastatic to the brain 12 years after the removal of the original tumor. Clin Neuropathol 16:190–194
39. Schmitt-Graff A, Borchard F (1992) Cardiac myxoma with a cytokeratin-immunoreactive glandular component. Pathol Res Pract 188:217–221
40. Schuger L, Ron N, Rosemann E (1987) Cardiac myxoma: a retrospective immunohistochemical study. Pathol Res Pract 182:63–66

41. Schultrich S (1990) Zur Histogenese des kardialen Myxoms anhand eines Myxoms mit drüsenartige Strukturen. Pathologe 11:220–223
42. Seo IS, Warner TFCS, Colyer RA, Winkler RF (1980) Metastasizing atrial myxoma. Am J Surg Pathol 4:391–399
43. Sipos B, Jaray B, Richter T (1995) Glandular myxoma of the heart. Orv Hetil 136:1333–1335
44. Solcia E, Capella C, Buffa R, Usellini L, Fiocca R, Sessa F (1987) Endocrine cells of the digestive system. In: Johnson LR (ed) Physiology of the gastro-intestinal tract. Raven Press, New York, pp 111–130
45. Song LF, Zhang ZQ, Huang WY (1982) Morphologic study of cardiac myxomas. Chin Med J 96:7–12
46. Tanimura A, Kitazono M, Nagayama K, Tanaka S, Kosuga K (1988) Cardiac myxoma. Morphologic, histochemical and tissue culture studies. Hum Pathol 19:316–322
47. Tazelaar HD, Locke TJ, McGregor CGA (1992) Pathology of surgically excised primary cardiac tumors. Mayo Clin Proc 67:957–965
48. Terracciano LM, Mhawech P, Suess K, D'Armiento M, Lehmann FS, Jundt G, Moch H, Sauter G, Mihatsch MJ (2000) Calretinin as a marker for cardiac myxoma. Diagnostic and histogenetic considerations. Am J Clin Pathol 114:754–759
49. Thomas AC, Mills PG, Gibbs NM, Davies MJ (1980) Secondary carcinoma of left atrium simulating myxoma. Br Heart J 44:541–544
50. Thornton CM, Walsh MY (1993) Glandular differentiation in cardiac myxomata. Ir J Med Sci 162:95–97
51. Toszegi A (1990) Morphology of cardiac myxomas. Morphol Igazsagugyi Orv Sz 30:43–50
52. Vacek R (1963) Das intracardiale Hamartoblastom. Zentralbl Allg Pathol 104:383–391
53. Wada A, Kanda T, Hayashi R, Imai S, Suzuki T, Murata K (1993) Cardiac myxoma metastasized to the brain: potential role of endogenous interleukin-6. Cardiology 83:208–211
54. Wang XY (1993) Immunohistochemcial study and evaluation of histogenesis of cardiac myxoma. Zhonghua Bing Li Xue Za Shi 22:262–264
55. Widder W, Schneider J, Schanz U (1985). Das Endokardmyxom mit drüsenartige Strukturen und seine Beziehungen zum AV-Knotentumor. Versuch einer histogenetischen Deutung. Pathologe 6:303–307
56. Wold LE, Lie JT (1980) Cardiac myxomas. A clinicopathologic profile. Am J Pathol 101:219–240

Virchows Arch (2003) 443:625–634
DOI 10.1007/s00428-003-0890-3

ORIGINAL ARTICLE

Yuzo Ogawa · Mitsunobu Kishino · Yukako Atsumi · Masaya Kimoto · Yasuo Fukuda · Takeshi Ishida · Naokuni Ijuhin

Plasmacytoid cells in salivary-gland pleomorphic adenomas: evidence of luminal cell differentiation

Received: 2 April 2003 / Accepted: 29 July 2003 / Published online: 28 August 2003
© Springer-Verlag 2003

Abstract To determine the cellular origin of plasmacytoid cells in salivary gland adenomas, immunohistochemistry was performed on sections from 12 pleomorphic adenomas rich in these cells. In normal salivary glands included in these sections, the myoepithelial cells (MECs) expressed α-smooth muscle actin (αSMA) and smooth muscle myosin heavy chain (SMMHC), whereas the duct luminal cells expressed keratins 19, 18 and 8. Some of the salivary duct basal cells expressed these keratins, and the acinar cells expressed keratins 18 and 8. The expression profile was similar in rat salivary glands not only after but also during development. The immature MECs never expressed the keratins nor did the immature duct cells express αSMA. In seven cases, up to 60% of the plasmacytoid cells expressed keratin 19. In three of these cases, about 10% of the plasmacytoid cells expressed keratin 18. No plasmacytoid cells expressed αSMA, SMMHC or keratin 8. These results indicate that plasmacytoid cells originate from luminal cells and not from MECs. Furthermore, in addition to the luminal tumor cells, the non-luminal cells could express keratins 19, 18 and 8. Therefore, it is necessary to re-evaluate the prevailing notion that non-luminal cells are modified MECs. Keratin 14, basic calponin, vimentin and p63 were bi-specific for the MECs and the duct cells. Therefore, expression of these proteins by significant numbers of the non-luminal tumor cells and the plasmacytoid cells never denied the above notion.

Keywords Plasmacytoid cell · Pleomorphic adenoma · Salivary gland · Immunohistochemistry · Cytoskeletal proteins

Y. Ogawa (✉) · M. Kishino · M. Kimoto · N. Ijuhin
Department of Oral Pathology,
Osaka University Graduate School of Dentistry,
1-8 Yamadaoka, Suita, 565-0871 Osaka, Japan
e-mail: ogawa@dent.osaka-u.ac.jp
Tel.: +81-6-68792892
Fax: +81-6-68792895

Y. Atsumi
Department of Oral Anatomy and Developmental Biology,
Osaka University Graduate School of Dentistry,
Osaka, Japan

Y. Fukuda · T. Ishida
Clinical Laboratory,
Osaka University Dental Hospital, Osaka, Japan

Introduction

Myoepithelial cells (MECs) are cellular components of various kinds of salivary gland tumor. There is strong evidence that they exert ameliorative effects in these tumors [4], as demonstrated, for example, in a series of recent studies by Barsky et al. [36, 46, 47, 48]. They have demonstrated that MECs (1) promote the differentiation of tumor cells, (2) synthesize basement-membrane and non-basement-membrane components, (3) secrete high amount of tumor-suppressor maspin and various proteinase inhibitors some of which accumulate within MEC-derived extracellular matrix and (4) inhibit invasion and angiogenesis [36, 46, 47, 48]. Therefore, exact identification of MECs is necessary to predict the biological behavior of the tumor.

Myoepithelioma is believed to be a rare kind of pleomorphic adenoma that is almost entirely composed of MECs [20]. Contrary to our expectation, the biological behavior of myoepithelioma is unpredictable and even erratic. In fact, some authors consider that myoepithelioma is more aggressive than pleomorphic adenoma [44]. The cellular components of myoepithelioma are spindle, plasmacytoid (hyaline), epithelioid and clear cells. It is surprising to know that, except for the spindle cells and some of the epithelioid cells, the nature of MECs has not been confirmed in these cells yet [20]. Therefore, it is conceivable that they did not originate from MECs and, thus, are related to the aggressiveness of myoepithelioma.

Keratins belong to the family of intermediate filaments and are associated with cellular differentiation and cytoskeleton organization. They are expressed by epithelial cells in a cell-specific and differentiation-specific

manner [30]. The MECs in salivary glands express keratins 5 and 14. These keratins, however, do not serve as specific markers for the MECs because they are also expressed by the basal cells of the ducts [18, 31, 37, 38]. On the other hand, the non-MECs express keratins 7, 8, 18 and 19. Keratins 8 and 18 are expressed by the acinar cells and duct cells, and keratins 7 and 19 by the duct cells [6, 18, 24, 28, 38]. Therefore, the presence of keratins 5 and 14 in combination with the absence of keratins 7, 8, 18 and 19 may serve as a reliable criterion for identification of salivary gland MECs.

The aim of the present study was to determine the cell of origin of plasmacytoid cells, the prototypic cells of unknown origin. They are oval to polygonal cells with an eccentrically placed nucleus and an eosinophilic hyaline cytoplasm. They are also the cellular constituents of pleomorphic adenoma [8, 20, 29]. Because previous studies have not observed the MEC character in plasmacytoid cells [13, 14, 21, 33, 38, 40], we decided to seek the non-MEC character in these cells. To this end, using antibodies specific for the non-MEC keratins, immunohistochemistry was performed on pleomorphic adenomas rich in plasmacytoid cells.

Table 1 Clinical features of pleomorphic adenomas rich in plasmacytoid cells

Case no.	Sex	Age	Site
1	Female	55	Palatine gland
2	Male	38	Palatine gland
3	Female	55	Palatine gland
4	Female	61	Upper labial gland
5	Male	48	Palatine gland
6	Female	66	Palatine gland
7	Female	52	Palatine gland
8	Male	30	Submandibular gland
9	Female	49	Palatine gland
10	Female	44	Palatine gland
11	Male	23	Parotid gland
12	Male	37	Palatine gland

Materials and methods

All experiments were reviewed and approved by the Intramural Ethics Committee and Animal Use and Care Committee of Osaka University Graduate School of Dentistry prior to the study. A total of 12 cases of pleomorphic adenoma were selected from the files of the Clinical Laboratory at the Osaka University Dental Hospital (Table 1). They included normal salivary glands that were used as the positive control for immunohistochemistry. The tissues were obtained during surgery, fixed in 10% neutral buffered formalin and embedded in paraffin. Rat major salivary glands were removed from pre- and post-natal animals (from 17 days in utero to 3 months after birth; three animals per each age group), fixed in methacarn and embedded in paraffin according to the method described previously [37]. Sections (about 4-μm thick) were cut and mounted on silane-coated glass slides. One section from each tissue block was stained with hematoxylin and eosin to assess the histology, and the others were used for immunohistochemistry.

For human materials, except for α-smooth muscle actin (αSMA), antigens were retrieved by treating the sections in a microwave oven [38]. Immunohistochemistry was performed by indirect immunoperoxidase method described previously [38]. The primary monoclonal antibodies, their dilutions and their sources are listed in Table 2. After immunostaining, the sections were incubated with 3, 3′-diaminobenzidine terahydrochlorode-H_2O_2 solution and counterstained briefly with Mayer's hematoxylin. Negative controls for immunostaining were performed by substituting the primary antibodies with 0.01 M phosphate-buffered saline (pH 7.2) and normal mouse IgG.

Table 2 Monoclonal antibodies used for immunohistochemistry. *αSMA* α-smooth muscle actin, *SMMHC* smooth muscle myosin heavy chain

Antibody	Specificity	Dilution	Source
C-51	Keratin 8 (Human)	1:60	Novocastra Laboratories Ltd., Newcastle upon Tyne, UK
LL002	Keratin 14 (Human and rat)	1:20 (rat) 1:100 (human)	Ylem, Roma, Italy
DC-10	Keratin 18 (Human)	1:40	Novocastra Laboratories Ltd.
Ks 18.04	Keratin 18 (Human and rat)	1:50	Progen Biotechnik GMBH, Heidelberg, Germany
A53-B/A2	Keratin 19 (Human)	1:500	Sigma Chemical Co., St. Louis, MO
CK-E3	Keratin 19 (Rat)	1:500	Sigma Chemical Co.
V9	Vimentin (Human and rat)	1:50 (rat) 1:500 (human)	Dako, Glostrup, Denmark
1A4	αSMA (Human and rat)	1:500 (rat) 1:1000 (human)	Dako
hSM-V	SMMHC (Human)	1:400	Sigma Chemical Co.
hCP	Basic calponin (Human and rat)	1:2000 (rat) 1:120000 (human)	Sigma Chemical Co.
4A4	p63 (Human and rat)	1:100 (rat) 1:200 (human)	Santa Cruz Biotechnology, Inc., Santa Cruz, CA

Results

Some clinical features of the 12 patients are shown in Table 1. Seven were women and five were men. The ages of the patients ranged from 23 years to 66 years (mean, 46.5 years). The tumors preferentially arose in the palatine gland (nine cases). All the patients presented with the primary complaint of a painless mass. At surgery, one case (case 1) expressed a tumor-bearing surgical margin. At present (after 6 years and 11 months), however, the patient does not show any signs of recurrence. All the other patients showed neither recurrence nor malignant transformation during follow-up period from 3 months (case 2) to 10 years (case 9).

Normal salivary glands

Immunohistochemistry was performed on nine palatine glands, one labial gland, one submandibular gland and one parotid gland (Table 1). In these glands, the MECs expressed immunoreactivity for αSMA, smooth muscle myosin heavy chain (SMMHC), basic calponin, vimentin, keratin 14 and p63 (Fig. 1A, B, C). In the MECs, αSMA, SMMHC, basic calponin, vimentin and keratin 14 were seen in the cytoplasm, whereas p63 was seen in the nucleus. Alpha-SMA, SMMHC, basic calponin and keratin 14 were broadly distributed in the cytoplasm, whereas vimentin was concentrated around the nucleus. In contrast to αSMA and SMMHC, which were selective for the MECs, immunoreactivity for vimentin, basic calponin, keratin 14 and p63 was observed in the duct cells (Fig. 1B, D) [5, 18, 31, 37, 38, 51]. Keratin 8, keratin 18 and keratin 19 were selective for the duct cells and, thus, never seen in the MECs (Fig. 1E, F). Keratin 8 and keratin 18 were seen in the same cell types: the serous and mucous acinar cells, the duct luminal cells and some of the duct basal cells (Fig. 1E). The keratin 18 immunoreactivity was generally more intense than the keratin 8 immunoreactivity. Any differences were not detected in the staining between two antibodies against keratin 18. Keratin 19 immunoreactivity was seen in the duct luminal cells, sometimes in the duct basal cells and occasionally in the acinar cells (Fig. 1F). Apart from these parenchymal stainings, the stromal vascular walls were stained by the antibodies to αSMA, SMMHC and basic calponin (Fig. 1A, B). The anti-basic calponin antibody occasionally stained the nerve fibers (Fig. 1B).

Except for keratin 8 and SMMHC, all the above proteins were detectable in rat tissues (Table 2). Cellular distribution of these proteins in adult rat (3-month-old) glands was basically the same as that in human glands (Fig. 2A, B, C). In the rat glands, however, keratin 19 was not seen in the intralobular striated ducts and its special form, the granular ducts in the submandibular glands (Fig. 2C). The duct cells and the nerve fibers were not stained by the anti-basic calponin antibody. To determine the expression of these proteins in the immature epithelial cells, immunohistochemistry was performed on the developing salivary glands.

After the early morphodifferentiation, each salivary gland primordium gives rise to an extensively branched system of cellular cords, each of which terminates in a spherical cellular mass—a terminal bud. Cellular cords develop into striated ducts and excretory ducts, and terminal buds develop into acini and intercalated ducts. The development of the striated duct/excretory duct precedes that of the acinus/intercalated duct, which starts at 18 days in utero in the submandibular and sublingual glands and immediately after birth in the parotid gland. The adult gland structures are established by 6 weeks after birth. The MECs first appear on the periphery of the terminal buds at the same time as the acinar development in the submandibular and sublingual glands, but slightly earlier than that in the parotid gland [39]. They showed immunoreactivity for αSMA, basic calponin, vimentin and p63 throughout the developmental period (Fig. 2E) [37]. In addition to the MECs, p63 was seen in the duct basal cells and vimentin in the terminal tubule and cellular cord cells and the nascent acinar and duct cells (Fig. 2E, F). Keratins were observed in the duct cells. Though keratin 14 was also observed in the MECs in the later developmental stage [37], the other keratins were never seen in the MECs (Fig. 2D). Keratin 19 appeared to occur in the duct cells earlier than keratin 18. At 18 days in utero when the submandibular and sublingual glands first expressed these keratins, keratin 19 is seen in more duct cells than is keratin 18. The immature serous acinar cells also expressed immunoreactivity for keratin 18, whereas the immature mucous cells in the sublingual glands were devoid of this protein.

Pleomorphic adenomas

Pleomorphic adenomas are composed of luminal tumor cells and non-luminal tumor cells. The former cells line neoplastic lumina and are surrounded by the latter cells. These cells make up solid proliferating structures and mesenchymal structures [20]. The luminal cells showed immunoreactivity for keratins 18 and 19 (Fig. 3A, B). They also sometimes expressed keratin 8, keratin 14 and basic calponin and occasionally vimentin (Fig. 3C) [38]. Many of the non-luminal cells expressed immunoreactivity for vimentin, keratin 14, basic calponin and p63 (Fig. 3C) [38]. They also sometimes expressed keratin 18, keratin 19 and αSMA and occasionally keratin 8 and SMMHC (Fig. 3A, B, D). The keratins 18-, 19- and 8-positive cells took both spindle (elongated) and non-spindle configurations, whereas the smooth muscle protein-positive cells were mostly spindle. The latter cells were usually observed on the periphery of the solid structure and occasionally in the mesenchymal structure (Fig. 3D).

Immunoreactivity of the plasmacytoid cells for various proteins was summarized in Table 3. In all cases, more than 90% of the plasmacytoid cells strongly expressed

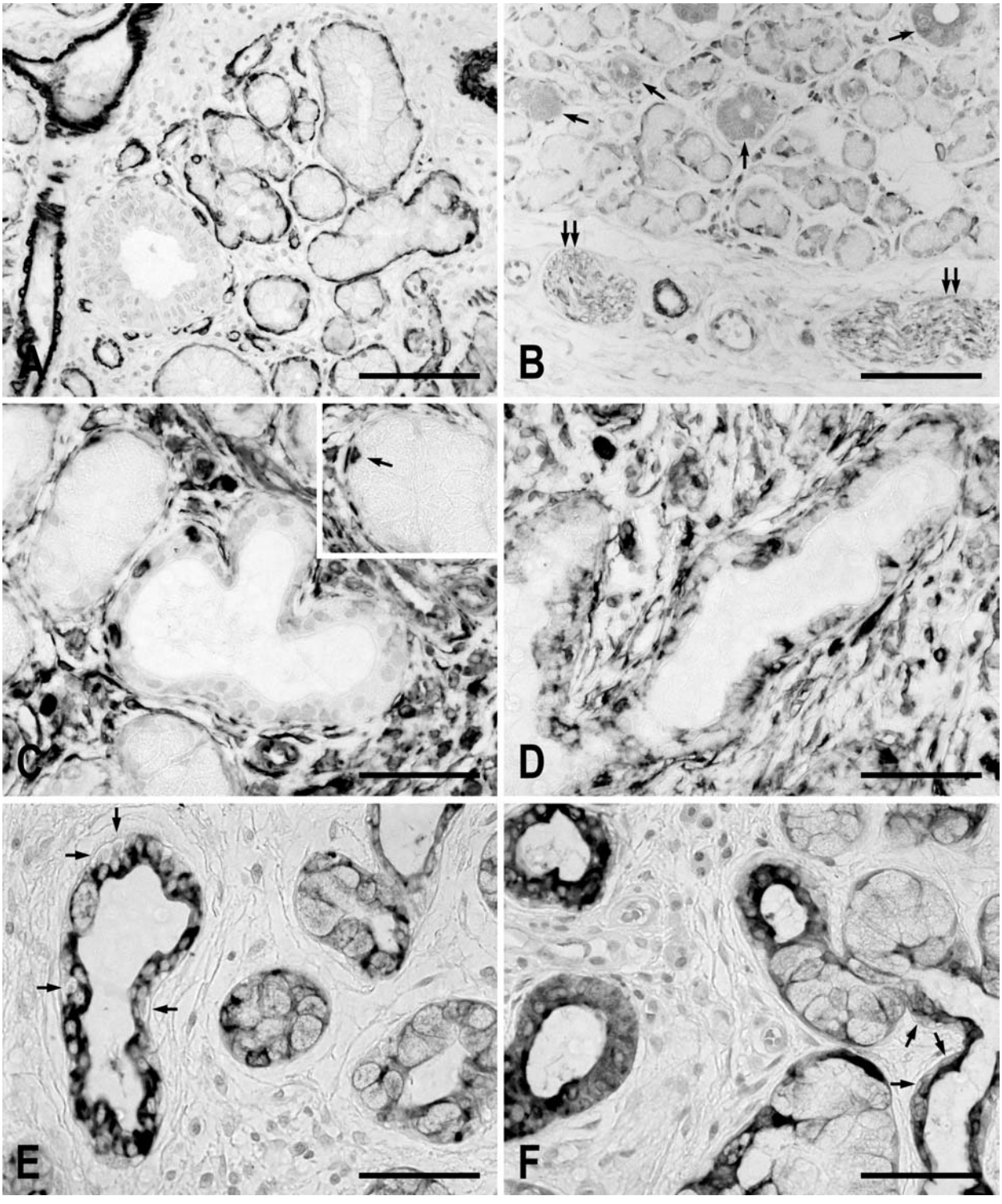

Fig. 1 Palatine (**A**, **C**–**F**) and parotid (**B**) glands. Alpha-smooth muscle actin is expressed by myoepithelial cells (MECs) around acini and intercalated ducts and smooth muscle cells in vascular walls (**A**). In addition to MECs and vascular walls, basic calponin is expressed by ducts (*arrows*) and nerve fibers (*double arrows*) (**B**). Vimentin is expressed by MECs around intercalated ducts (**C**) and acini (*arrow in inset* in **C**) and occasionally by duct cells (**D**). Ductal expression of vimentin is more frequent in inflamed glands. Keratin 18 (**E**) and keratin 19 (**F**) are expressed by duct cells. Keratin 18 (**E**) is also expressed by acinar cells. Note MECs around intercalated ducts are devoid of these keratins (*arrows* in **E** and **F**). *Bars* **A**, **B** 100 μm, ×200; **C**–**F** 50 μm, ×400

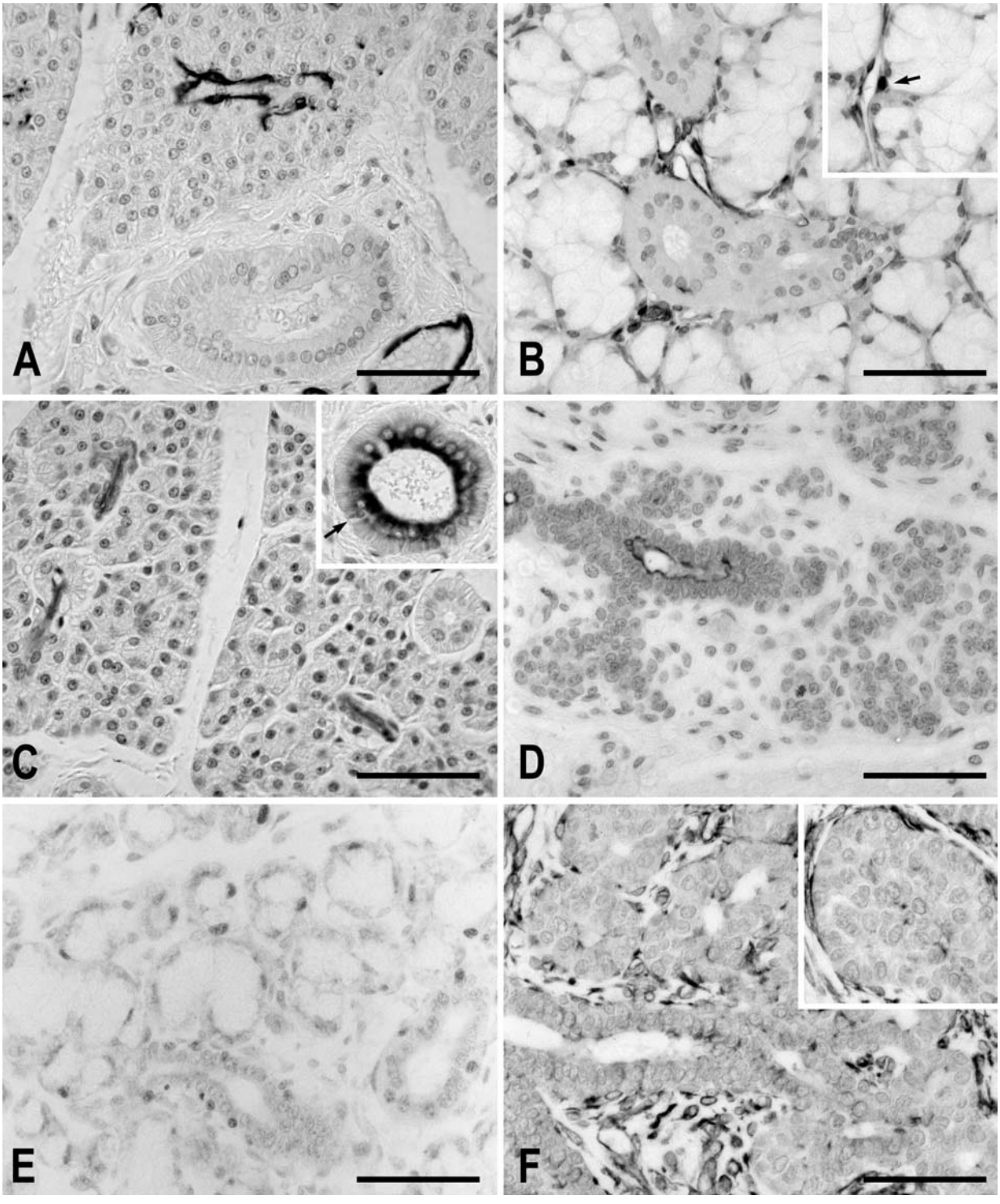

Fig. 2 Rat parotid (**A**, **C**, **D**), sublingual (**B**, **E**) and submandibular (**F**) glands. Mature glands (**A**–**C**) and immature glands: 1 day after birth (**D**, **E**), 18 days in utero (**F**) and 17 days in utero (*inset* in **F**). In mature glands, α-smooth muscle actin (αSMA) is expressed by myoepithelial cells (MECs) around intercalated ducts and smooth muscle cells in vascular walls (**A**). Acini of rat parotid glands are devoid of MECs. Besides interstitial mesenchymal cells, vimentin is expressed by MECs (*arrow in inset* in **B**) and occasionally by striated duct cells (*arrowhead* in **B**). Keratin 19 is expressed by intercalated duct cells and extralobular striated duct cells (*inset* in **C**). Intralobular striated duct cells and some duct basal cells (*arrow in inset* in **C**) do not express this keratin. In developing immature glands, αSMA is expressed only by MECs, whereas keratin 19 (**D**) only by duct cells. Nuclear staining of p63 is observed both in MECs and duct basal cells (**E**). Vimentin is expressed by terminal bud cells (*inset* in **F**), cellular cord cells, immature acinar cells (**F**) and immature duct cells (**F**). *Bars* 50 μm, ×400

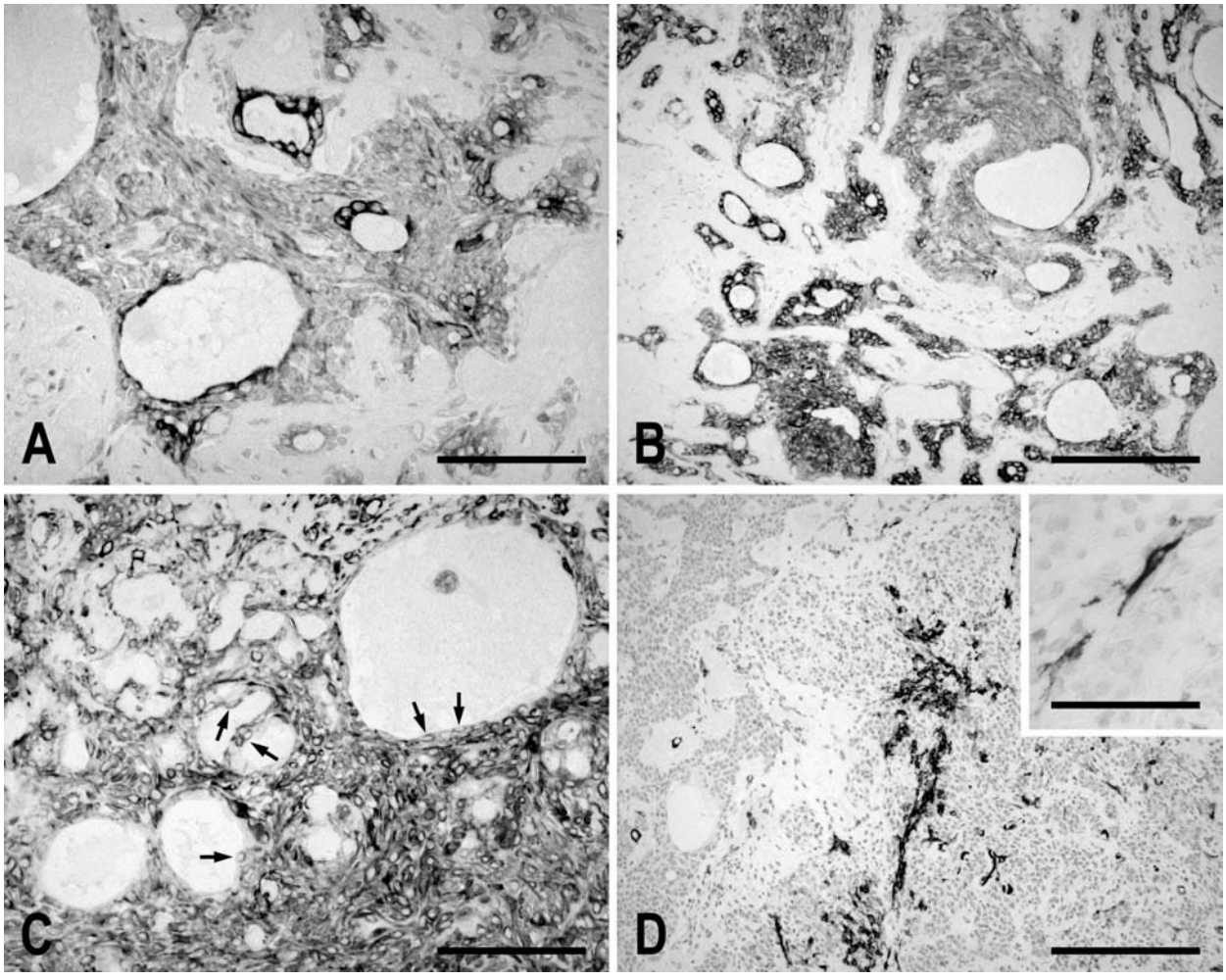

Fig. 3 Keratin 18 (**A**) and keratin 19 (**B**) are expressed by luminal tumor cells and sometimes by non-luminal tumor cells in pleomorphic adenomas. Vimentin is expressed by most non-luminal cells and occasional luminal cells (*arrows* in **C**). Alpha-smooth muscle actin is expressed by some non-luminal cells in solid epithelial sheets and by sporadic cells in mesenchymal structures (**D**). These cells usually have spindle appearance (*inset* in **D**). *Bars* **A**, **C** 100 μm, ×200; **B**, **D** 200 μm, ×100; *inset* in **D** 50 μm, ×400

Table 3 Immunoreactivity of plasmacytoid cells. Reactivity was scored as: −, no reactive cell; +, less than 30% reactive cells; ++, 30–60% reactive cells; +++, more than 60% reactive cells. *αSMA* α-smooth muscle actin, *SMMHC* smooth muscle myosin heavy chain

Case no.	Keratin 8	Keratin 14	Keratin 18	Keratin 19	Vimentin	αSMA	SMMHC	Basic calponin	p63
1	−	−	+	+	+++	−	−	+	+
2	−	−	+	++	+++	−	−	++	−
3	−	−	−	−	+++	−	−	−	−
4	−	++	−	−	+++	−	−	+	+
5	−	+	−	−	+++	−	−	++	−
6	−	−	−	+	+++	−	−	++	+
7	−	−	−	+	+++	−	−	+	−
8	−	+	−	−	+++	−	−	−	−
9	−	+	−	+	+++	−	−	+	+
10	−	+	−	+	+++	−	−	+	+
11	−	+	−	−	+++	−	−	+	+
12	−	−	+	++	+++	−	−	−	+

immunoreactivity for vimentin (Fig. 4A). The vimentin immunoreaction was usually diffuse in the cytoplasm and sometimes accentuated the thin rim surrounding the central globular structure. Next to vimentin, basic calponin distributed broadly over the plasmacytoid cells in nine cases (75%). In seven cases (58%), up to 60% of the plasmacytoid cells expressed keratin 19 (Fig. 4B). In three of these cases, about 10% of the plasmacytoid cells

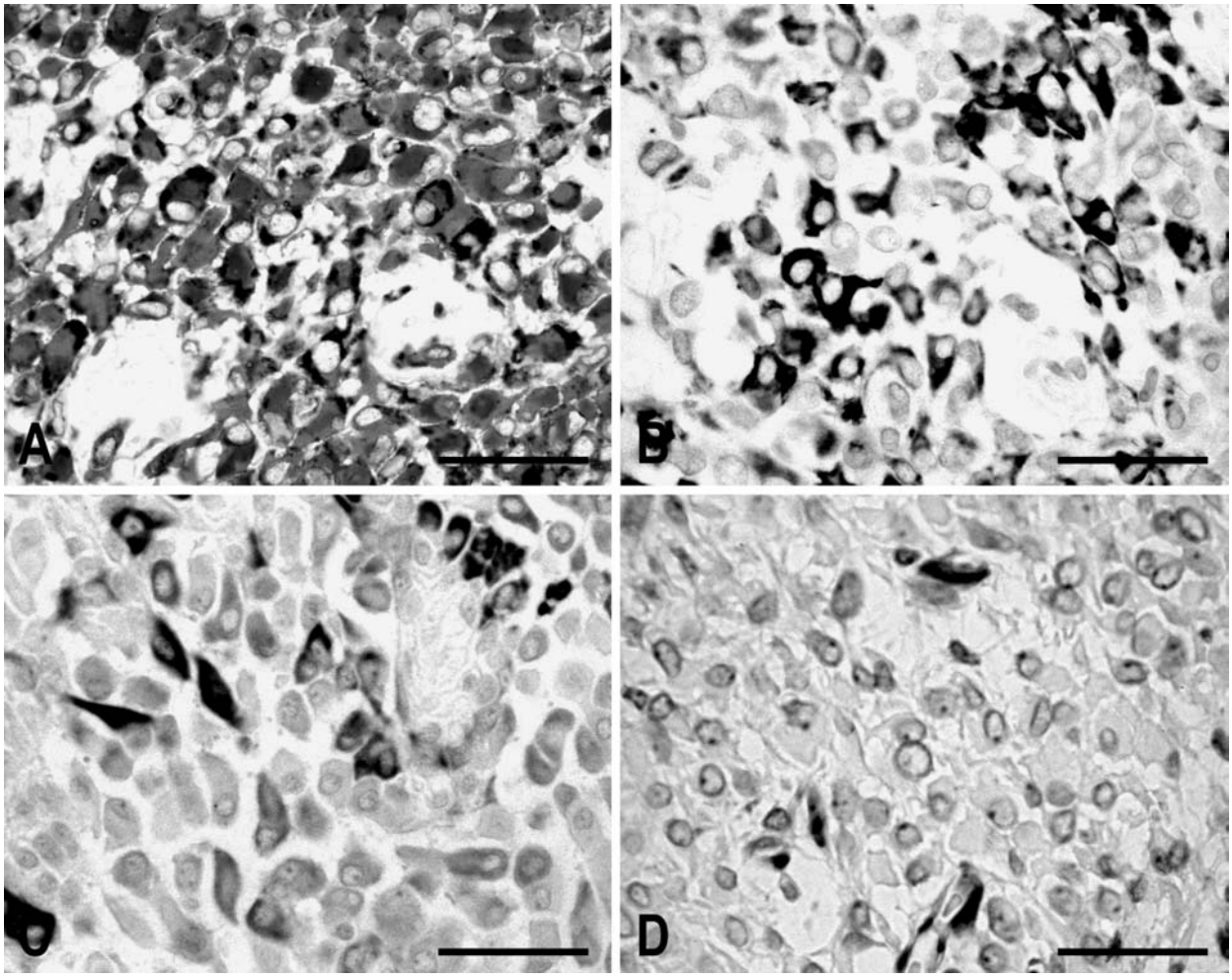

Fig. 4 Plasmacytoid cells usually express vimentin (**A**), sometimes keratin 19 (**B**) and occasionally keratin 18 (**C**). Though elongated cells with somewhat eccentrically placed nuclei are positive for α-smooth muscle actin (αSMA) and may represent a transitional form between plasmacytoid cells and spindle-shaped neoplastic myoepithelial cells, authentic plasmacytoid cells never express αSMA (**D**). *Bars* 25 μm, ×800

weakly expressed keratin 18 (Fig. 4C). The keratin 19 immunoreaction was often concentrated to the thin rim. Keratin 14 was expressed in six cases and p63 in seven cases. We could not find any plasmacytoid cells that were definitively positive for αSMA, SMMHC or keratin 8 (Fig. 4D).

Discussion

The present study has demonstrated that plasmacytoid cells are related to luminal cells but not MECs in pleomorphic adenomas. Small but definite number of the plasmacytoid cells expressed keratins 19 and 18, whereas none of them possessed αSMA and SMMHC. The number of the keratin 19-positive cells was larger than that of the keratin 18- and probably keratin 19-positive cells. Keratins 19 and 18 showed similar distribution in the normal salivary glands. They were expressed by the luminal cells and some of the basal cells in the ducts [18, 24, 26, 28, 38]. They also showed similar cellular distribution in the developing glands. The MECs never expressed these keratins either after or during development. Keratin 18, however, was constantly expressed by the acinar cells [18, 24, 26, 28]. During development, keratin 19 occurred in the duct cells earlier than keratin 18. These may indicate that keratin 19-positive tumor cells are more primitive than keratin 18-positive tumor cells.

A similar keratin profile has been found in pancreas, where keratin 18 is expressed by acinar and duct cells and keratin 19 by duct cells. During development, expression of keratin 18 by pancreatic cells is preceded by that of keratin 19. Pancreatic cancer cells with keratin 19 are thought to be less differentiated than those with keratins 18 and 19 [7]. Keratin 8 showed a cellular distribution similar to that of keratin 18 in the human salivary glands, suggesting that they make up a keratin-pair usually seen in simple epithelia [30]. Keratin 8, however, disappeared more frequently than keratin 18 after neoplastic transfor-

mation, and, thus, was not observed in the plasmacytoid cells.

Except for one study [45], previous immunohistochemistry could not demonstrate smooth muscle proteins in plasmacytoid cells [13, 14, 21, 33, 38, 40]. Many pleomorphic adenoma cells, including the plasmacytoid cells, however, were stained by an antibody to basic calponin, a putative regulatory protein in smooth muscle contraction [38, 40]. The anti-basic calponin antibody reacted not only with MECs and smooth muscle cells but also with duct cells, nerve fibers and keratinocytes [38]. Pleomorphic adenoma cells frequently possess tonofilaments and nerve proteins such as S100 protein and glial fibrillary acidic protein (GFAP) [1, 9, 10, 13, 14, 20, 34, 35, 52]. Therefore, these cells may have reacted with the antibody. S100 protein is not expressed by MECs but by duct cells [15, 34, 35]. MEC expression of GFAP is still a matter of controversy [1, 32, 34, 52].

Almost all the plasmacytoid cells expressed immunoreactivity for vimentin. It has been often difficult to identify vimentin immunostaining in MECs [18, 24, 33, 37], probably due to its restricted distribution in the cytoplasm [19, 23]. Despite this difficulty, the present and the previous [6, 24, 25] studies observed distinct vimentin staining in MECs. In this context, some authors have recommended this protein as a MEC marker [2, 3, 33]. The luminal tumor cells in the pleomorphic adenomas, however, occasionally expressed vimentin immunoreactivity. In the normal salivary glands, vimentin immunoreactivity was also observed in the duct cells [24]. Both the MECs and the duct cells expressed vimentin in the developing glands. Vimentin immunostaining in the terminal bud and cord cells strongly suggest that the precursors of these cells express this protein. Therefore, it can be concluded that vimentin expression does not necessarily mean the cell is derived from MEC. Vimentin expression is necessary for migration of epithelial cells in pathological and physiological processes [22]. Salivary cells migrate within and between each of the gland segments both during and after development [16, 39].

It has been hypothesized that MECs and duct basal cells make up a single cell lineage: MECs and duct basal cells are the proximal and the distal components, respectively, of a cellular continuum extending from acinus to distal most duct [11, 12]. However, the present observation of keratin 14 and p63 in both MECs and duct basal cells does not necessarily support the above hypothesis because keratin 14 was also expressed by the duct luminal cells, and keratins 8, 18 and 19 were observed in the duct basal cells [38]. Indeed, embryological studies of rodent salivary glands suggested that the MECs and the acinar/intercalated duct cells are derived from a common primordium, whereas the basal cells in the larger ducts and their luminal partners are derived from another primordium [39].

The characteristic hyaline cytoplasm of plasmacytoid cells is composed of haphazardly arranged filaments. Due to misinterpretation of these filaments as actin microfilaments, they were originally thought to be neoplastic MECs [27, 29, 42, 43, 50]. Though the filaments have been proved to be intermediate filaments, plasmacytoid cells are still considered neoplastic MECs because they are members of the non-luminal cells in pleomorphic adenomas [13]. According to these authors [9, 10], the luminal cells and the non-luminal cells in pleomorphic adenoma come from the luminal cells and the MECs in intercalated duct, respectively. During tumorigenesis, the MECs are modified to lose the smooth muscle nature and come to exhibit extensive morphological diversity (modified MECs). Our present and previous [38] studies have demonstrated that at least some of the modified MECs, irrespective of their cytomorphology, express the phenotype of the luminal cells. Though the notion that non-luminal cells are modified MECs has been adopted into many types of salivary gland tumors, it must be re-evaluated to predict their accurate biological behavior [38].

MECs, even after neoplastic transformation, possess anti-cancer properties and, consequently, MEC neoplasms have low-grade malignant nature [4, 46]. The atlas of salivary gland tumors published by the Armed Forces Institute of Pathology describes that myoepitheliomas are less likely to recur than pleomorphic adenomas [20], whereas the histological typing of salivary gland tumors by the World Health Organization says that myoepithelioma is characterized by more aggressive growth than pleomorphic adenoma and occasionally by transformation to malignancy [44]. By reviewing one Armed Forces Institute of Pathology case and 20 reported cases of malignant myoepitheliomas with follow-up information, Ellis and Auclair [20] referred to the high incidence of patients who died or were living with disease: six patients (29%) and seven patients (33%), respectively. The unpredictable and even erratic biological behavior of myoepitheliomas should relate to the fact that they are not composed of 100% neoplastic MECs. Indeed, luminal cells participate in many myoepitheliomas, as they often contain ductal structures [20]. In conclusion, we would like to propose that plasmacytoid cell tumors should not be considered a subtype of myoepithelioma but classified as plasmacytoid adenomas or adenocarcinomas [21]. In this context, it is noteworthy that malignant myoepitheliomas with predominant plasmacytoid cells exhibit more aggressive behavior than the other forms of these tumors [17, 49]. After the analysis of a large series of myoepithelial carcinomas, Savera et al. [41] concluded that the cell type and the prognosis did not show a statistically significant correlation. This conclusion, however, appears to be immature. There were only two cases of hyaline cell-rich myoepithelial carcinomas with available follow-up. One patient (case 12 of their study) died of the disease at 18 months after surgery. Another patient with cervical lymph node metastasis (case 1) is alive at 6 months, which is extremely shorter than the follow-up period of the other patients.

Acknowledgement The authors thank Dr. Ross T. Fernley for his critical reading of the manuscript.

References

1. Achstätter T, Moll R, Anderson A, Kuhn C, Pitz S, Schwechheimer K, Franke WW (1986) Expression of glial filament protein (GFP) in nerve sheaths and non-neural cells re-examined using monoclonal antibodies, with special emphasis on the co-expression of GFP and cytokeratins in epithelial cells of human salivary gland and pleomorphic adenomas. Differentiation 31:206–227
2. Araújo VC, Araújo NS (1990) Vimentin as a marker of myoepithelial cells in salivary gland tumors. Eur Arch Otorhinolaryngol 247:252–255
3. Araújo VC, Carvalho YR, Araújo NS (1994) Actin versus vimentin in myoepithelial cells of salivary gland tumors. A comparative study. Oral Surg Oral Med Oral Pathol 77:387–391
4. Batsakis JG, El-Naggar AK (1999) Myoepithelium in salivary and mammary neoplasms is host-friendly. Adv Anat Pathol 6:218–226
5. Bilal H, Handra-Luca A, Bertrand JC, Fouret PJ (2003) p63 is expressed in basal and myoepithelial cells of human normal and tumor salivary gland tissues. J Histochem Cytochem 51:133–139
6. Born IA, Schwechheimer K, Maier H, Otto HF (1987) Cytokeratin expression in normal salivary glands and in cystadenolymphomas demonstrated by monoclonal antibodies against selective cytokeratin polypeptides. Virchows Arch 411:583–589
7. Bouwens L (1998) Cytokeratins and cell differentiation in the pancreas. J Pathol 184:234–239
8. Buchner A, David R, Hansen LS (1981) "Hyaline cells" in pleomorphic adenoma of salivary gland origin. Oral Surg Oral Med Oral Pathol 52:506–512
9. Dardick I, van Nostrand AWP, Jeans MTD, Rippstein P, Edwards V (1983) Pleomorphic adenoma, I: ultrastructural organization of "epithelial" regions. Hum Pathol 14:780–797
10. Dardick I, van Nostrand AWP, Jeans MTD, Rippstein P, Edwards V (1983) Pleomorphic adenoma, II: ultrastructural organization of "stromal" regions. Hum Pathol 14:798–809
11. Dardick I, Rippstein P, Skimming L, Boivin M, Parks WR, Dairkee SH (1987) Immunohistochemistry and ultrastructure of myoepithelium and modified myoepithelium of the ducts of human major salivary glands: histogenetic implications for salivary gland tumors. Oral Surg Oral Med Oral Pathol 64:703–715
12. Dardick I, Parks WR, Little J, Brown DL (1988) Characterization of cytoskeletal proteins in basal cells of human parotid salivary gland ducts. Virchows Arch 412:525–532
13. Dardick I, Thomas MJ, van Nostrand AWP (1989) Myoepithelioma-new concepts of histology and classification: a light and electron microscopic study. Ultrastruct Pathol 13:187–224
14. Dardick I, Cavell S, Boivin M, Hoppe D, Parks WR, Stinson J, Yamada S, Burns BF (1989) Salivary gland myoepithelioma variants. Histological, ultrastructural, and immunocytological features. Virchows Arch 416:25–42
15. Dardick I, Stratis M, Parks WR, DeNardi FG, Kahn HJ (1991) S-100 protein antibodies do not label normal salivary gland myoepithelium. Histogenetic implications for salivary gland tumors. Am J Pathol 138:619–628
16. Denny PC, Ball WD, Redman RS. (1997) Salivary glands: a paradigm for diversity of gland development. Crit Rev Oral Biol Med 8:51–75
17. Di Palma S, Guzzo M (1998) Myoepithelial carcinoma with predominance of plasmacytoid cells arising in a pleomorphic adenoma of the parotid gland. Histopathology 33:485
18. Draeger A, Nathrath WBJ, Lane EB, Sundström BE, Stigbrand TI (1991) Cytokeratins, smooth muscle actin and vimentin in human normal salivary gland and pleomorphic adenomas. Immunohistochemical studies with particular reference to myoepithelial and basal cells. APMIS 99:405–415
19. Eckert F, de Viragh PA, Schmid U (1994) Coexpression of cytokeratin and vimentin intermediate filaments in benign and malignant sweat gland tumors. J Cutan Pathol 21:140–150
20. Ellis GL, Auclair PL (1996) Tumors of the salivary glands. Atlas of tumor pathology, 3rd series, fascicle 17. Armed Forces Institute of Pathology, Washington, DC
21. Franquemont DW, Mills SE (1993) Plasmacytoid monomorphic adenoma of salivary glands. Absence of myogenous differentiation and comparison to spindle cell myoepithelioma. Am J Surg Pathol 17:146–153
22. Gilles C, Polette M, Zahm JM, Tournier JM, Volders L, Foidart JM, Birembaut P (1999) Vimentin contributes to human mammary epithelial cell migration. J Cell Sci 112:4615–4625
23. Gould VE, Koukoulis GK, Jansson DS, Nagle RB, Franke WW, Moll R (1990) Coexpression patterns of vimentin and glial filament protein with cytokeratins in the normal, hyperplastic, and neoplastic breast. Am J Pathol 137:1143–1155
24. Gustafsson H, Kjörell U, Eriksson A, Virtanen I, Thornell L-E (1988) Distribution of intermediate filament proteins in developing and adult salivary glands in man. Anat Embryol 178:243–251
25. Hirano T, Gluckman JL, deVries EJ (1990) The expression of a vascular smooth-muscle actin in salivary gland tumors. Arch Otolaryngol Head Neck Surg 116:692–696
26. Ihrler S, Zietz C, Sendelhofert A, Lang S, Blasenbreu-Vogt S, Löhrs U (2002) A morphogenetic concept of salivary duct regeneration and metaplasia. Virchows Arch 440:519–526
27. Kahn LB, Schoub L (1973) Myoepithelioma of the palate. Histochemical and ultrastructural observations. Arch Pathol 95:209–212
28. Leoncini P, Cintorino M, Vindigni C, Leoncini L, Armellini D, Bugnoli M, Skalli O, Gabbiani G (1988) Distribution of cytoskeletal and contractile proteins in normal and tumour bearing salivary and lacrimal glands. Virchows Arch 412:329–337
29. Lomax-Smith JD, Azzopardi JG (1978) The hyaline cell: a distinctive feature of "mixed" salivary tumours. Histopathology 2:77–92
30. Moll R, Franke WW, Schiller DL, Geiger B, Krepler R (1982) The catalog of human cytokeratins: patterns of expression in normal epithelia, tumors and cultured cells. Cell 31:11–24
31. Moll R, Dhouailly D, Sun T-T (1989) Expression of keratin 5 as a distinctive feature of epithelial and biphasic mesotheliomas. An immunohistochemical study using monoclonal antibody AE14. Virchows Arch 58:129–145
32. Mori M, Ninomiya T, Okada Y, Tsukitani K (1989) Myoepitheliomas and myoepithelial adenomas of salivary gland origin. Immunohistochemical evaluation of filament proteins, S-100α and β, glial fibrillary acidic protein, neuron specific enolase, and lactoferrin. Pathol Res Pract 184:168–178
33. Morinaga S, Nakajima T, Shimosato Y (1987) Normal and neoplastic myoepithelial cells in salivary glands: an immunohistochemical study. Hum Pathol 18:1218–1226
34. Nakazato Y, Ishizeki J, Takahashi K, Yamaguchi H, Kamei T, Mori T (1982) Localization of S-100 protein and glial fibrillary acidic protein-related antigen in pleomorphic adenoma of the salivary glands. Lab Invest 46:621–626
35. Ninomiya T, Naito R, Okada Y, Kobayashi K, Mori M, Tsukitani K (1989) Immunohistochemical localization of the α and β subunits of S-100 protein in pleomorphic adenoma of the salivary glands. Virchows Arch 57:63–75
36. Nguyen M, Lee MC, Wang JL, Tomlinson JS, Shao Z-M, Alpaugh ML, Barsky SH (2000) The human myoepithelial cell displays a multifaceted anti-angiogenic phenotype. Oncogene 19:3449–3459
37. Ogawa Y, Yamauchi S, Ohnishi A, Ito R, Ijuhin N (1999) Immunohistochemistry of myoepithelial cells during development of the rat salivary glands. Anat Embryol 200:215–228
38. Ogawa Y, Toyosawa S, Ishida T, Ijuhin N (2000) Keratin 14 immunoreactive cells in pleomorphic adenomas and adenoid cystic carcinomas of salivary glands. Virchows Arch 437:58–68

39. Ogawa Y (2003) Immunocytochemistry of myoepithelial cells in the salivary glands. Prog Histochem Cytochem (in press)
40. Savera AT, Gown AM, Zarbo RJ (1997) Immunolocalization of three novel smooth muscle-specific proteins in salivary gland pleomorphic adenoma: assessment of the morphogenetic role of myoepithelium. Mod Pathol 10:1093–1100
41. Savera AT, Sloman A, Huvos AG, Klimstra DS (2000) Myoepithelial carcinoma of the salivary glands: a clinicopathologic study of 25 patients. Am J Surg Pathol 24:761–774
42. Sciubba JJ, Goldstein BH (1976) Myoepithelioma. Review of the literature and report of a case with ultrastructural confirmation. Oral Surg Oral Med Oral Pathol 42:328–338
43. Sciubba JJ, Brannon RB (1982) Myoepithelioma of salivary glands: report of 23 cases. Cancer 49:562–572
44. Seifert G, Sobin LH (1991) Histological typing of salivary gland tumors. World Health Organization international classification of tumors, 2nd ed. Springer Verlag, Berlin Heidelberg New York
45. Simpson RH, Jones H, Beasley P (1995) Benign myoepithelioma of the salivary glands: a true entity? Histopathology 27:1–9
46. Sternlicht MD, Barsky SH (1997) The myoepithelial defense: a host defense against cancer. Med Hypotheses 48:37–46
47. Sternlicht MD, Safarians S, Rivera SP, Barsky SH (1996) Characterizations of the extracellular matrix and proteinase inhibitor content of human myoepithelial tumors. Lab Invest 74:781–796
48. Sternlicht MD, Kedeshian P, Shao Z-M, Safarians S, Barsky SH (1997) The human myoepithelial cell is a natural tumor suppressor. Clin Cancer Res 3:1949–1958
49. Suzuki H, Inoue K, Fujioka Y, Ishikura H, Furuta Y, Fukuda S (1998) Myoepithelial carcinoma with predominance of plasmacytoid cells arising in a pleomorphic adenoma of the parotid gland. Histopathology 32:86–87
50. Wayne Stromeyer F, Haggitt RC, Nelson JF, Hardman JM (1975) Myoepithelioma of minor salivary gland origin. Light and electron microscopical study. Arch Pathol 99:242–245
51. Weber A, Langhanki L, Schutz A, Gerstner, A, Bootz F, Wittekind C, Tannapfel A (2002) Expression profiles of p53, p63, and p73 in benign salivary gland tumors. Virchows Arch 441:428–436
52. Zarbo RJ, Regezi JA, Hatfield JS, Maisel H, Trojanowski JQ, Batsakis JG, Crissman JD (1988) Immunoreactive glial fibrillary acidic protein in normal and neoplastic salivary glands: a combined immunohistochemical and immunoblot study. Surg Pathol 1:55–63

Virchows Arch (2003) 443:635–642
DOI 10.1007/s00428-003-0873-4

ORIGINAL ARTICLE

Mi-Seon Kwon · Seung-Jin Hong · Hyun-A Cho · Geung-Hwan Ahn · Seung-Sook Lee · Kyo-Young Lee · Mun-Gan Rhyu

Extensive and divergent chromosomal losses in squamous and spindle-cell components of esophageal sarcomatoid carcinoma

Received: 23 April 2003 / Accepted: 23 June 2003 / Published online: 20 August 2003
© Springer-Verlag 2003

Abstract Sarcomatoid carcinoma of the esophagus is an unusual type of squamous cell carcinoma (SCC) with a variable component of sarcomatoid spindle cells (SA). The loss of heterozygosity (LOH) involving multiple cancer-associated chromosomal arms has been reported to have a concerted, rather than an individual, effect on tumor progression. In order to delineate the role of LOH in the evolution of a biphasic tumor, the carcinoma in situ (CIS), invasive squamous cell carcinoma (ISCC), and SA components from a sarcomatoid carcinoma of the esophagus were compared for their clonality and extent of LOH. Forty microsatellite markers on the cancer-associated chromosomes, 3p, 4p, 5q, 8p, 9p, 13q, 17p, and 18q, were used for the polymerase chain reaction-based LOH analysis. All eight sarcomatoid carcinomas tested revealed extensive LOHs, involving an average of seven chromosomal arms. All CIS, ISCC, and SA components carried not only a high-level primary LOH (mean chromosomal involvement, 5.3) in common but also a low-level secondary LOH (mean chromosomal involvement, 1.8) in disparity. Interestingly, more secondary LOHs were always burdened in the CIS (four cases) rather than the matched ISCC. SA had a greater (four cases), equal (one case), or fewer (one case) number of secondary LOHs than ISCC. Given that excessive chromosomal losses may confer a disadvantage for tumor growth or a benefit for a metaplastic transformation, these results suggest that the multidirectional differentiation of a SCC precursor is stimulated by extensive and divergent LOHs acquired at the initial or early stages, and a precursor burdened with excessive LOH either remains in CIS or expands as a SA component.

Keywords Chromosomal loss · Cancer-associated chromosome · Loss of heterozygosity · Sarcomatoid carcinoma · Carcinoma in situ

M.-S. Kwon · S.-J. Hong · H.-A. Cho · M.-G. Rhyu
Department of Microbiology, College of Medicine,
Catholic University, Seoul, Korea

G.-H. Ahn
Department of Pathology, Samsung Medical Center,
Seoul, Korea

S.-S. Lee
Department of Pathology, Korea Cancer Center Hospital,
Seoul, Korea

K.-Y. Lee
Department of Pathology, College of Medicine,
Catholic University, Seoul, Korea

M.-G. Rhyu (✉)
Department of Microbiology, College of Medicine,
The Catholic University of Korea,
505 Banpo-dong, Socho-gu, 137–701 Seoul, Korea
e-mail: rhyumung@catholic.ac.kr
Tel.: +82-2-5901215
Fax: +82-2-5968969

Introduction

Sarcomatoid carcinoma of the esophagus is unusual [14, 15, 20, 21, 23] and is defined as a squamous cell carcinoma (SCC) with a variable sarcomatoid spindle cell (SA) component [6]. It is also known as a SCC with a spindle cell component, a spindle cell carcinoma, a pseudosarcomatous SCC, and a carcinosarcoma [6, 11, 12, 14, 20, 21, 25]. The major debate has centered on whether or not the two components evolved independently, due to the diverse combination of SCC and SA [20]. There is ample evidence supporting a shared epithelial lineage. Using light microscopy, a gradual transition between the carcinomatous and sarcomatous components has been observed in a majority of cases [6]. Immunohistochemical [7, 13, 24, 30] and electron microscopic [7, 24, 25] studies indicated that the SA component carried various degrees of epithelial differentiation. Limited genetic studies on sarcomatoid carcinomas have also found that the same genetic alterations are commonly shared in the SCC and SA components in the uterus, breast, lung, gastrointestinal tract, urinary bladder, pharynx, and the upper respiratory tract [1, 3, 28, 29]. However, although a great deal of progress in histogenetic

and genetic studies has been made toward unraveling the monoclonal origins of sarcomatoid carcinomas, few divergent genetic changes responsible for the biphasic differentiation have been identified. For example, a previous study on chromosomal losses in sarcomatoid carcinoma described the primary common chromosomal losses, but no secondary chromosomal losses were assigned for a SA component in support of a metaplastic transformation of a SCC [1].

During tumorigenesis, solid tumors of the digestive tract undergo complex alterations throughout the genome. The most common genetic alterations in esophageal cancers are unilateral chromosomal losses, which are detected as a loss of heterozygosity (LOH) [22]. Unilateral chromosomal losses give rise to the different extent and combinations of LOHs that are estimated using highly polymorphic microsatellite sequences dispersed throughout the genome [19, 33]. A single chromosomal loss has controversial biological effects on tumor growth, some of which were believed to coincidentally occur, or represent an indirect marker of a multi-factorial set of chromosomal losses [16, 32]. The amount of LOH has been estimated using a sufficient number of informative microsatellite markers on the cancer-associated chromosomal arms. The resulting LOH findings have demonstrated that the concerted effect of the chromosomal losses, rather than a single chromosomal loss, was closely correlated with tumor progression [5]. Given that chromosomal losses contribute to tumor progression through progressive or coincidental accumulation, there appear to be two possible genetic pathways for a given sarcomatoid carcinoma. One pathway may be composed of the primary chromosomal losses commonly shared in histologically different areas and the secondary losses restricted to a histological component. The other pathway may be composed of the different amount of common and/or different chromosomal losses that initially provide the selective growth advantage for a histological component.

In order to gain insight into the role of chromosomal loss in the evolution of biphasic tumor, the carcinoma in situ (CIS), invasive squamous carcinoma (ISCC), and SA components were microdissected from eight esophageal sarcomatoid carcinomas. Each microdissected component was examined for its extent and clonality of the LOH using a panel of 40 microsatellite markers on eight cancer-associated chromosomal arms: 3p, 4p, 5q, 8p, 9p, 13q, 17p, and 18q. This panel of microsatellite markers is known to reproduce the stable allelic signals with a minimum number of polymerase chain reaction (PCR) artifacts [5, 10]. All CIS, ISCC, and SA components demonstrated extensive chromosomal losses accompanied by the secondary divergent losses. Interestingly, more secondary LOHs were found in CIS and SA rather than ISCC. The LOH results suggest that a precursor burdened with excessive chromosomal losses remains in the CIS or is transformed into a SA component.

Materials and methods

Cases

Eight cases of sarcomatoid carcinoma of the esophagus surgically resected from 1996 to 2002 were retrieved from the files of the Pathology Department of Samsung Medical Center, Korea Cancer Center Hospital, and St. Mary's Hospital. The tissues had been routinely fixed in 10% buffered formalin and embedded in paraffin. The microscopic slides were reviewed, and paraffin blocks representative of each tumor were selected for the immunohistochemistry and LOH analysis. The clinicopathological data were collected by a review of the hospital records and the tumor stage was determined according to the TNM (tumor–node–metastasis) classification system [2].

Histological evaluation

The following features were recorded in all cases: mitosis, necrosis, pleomorphism, cellularity, and differentiation of the spindle cell component, the presence of a CIS and ISCC, and a gradual transition or sharp separation between the SCC and SA components (Fig. 1).

Immunohistochemical staining

Immunohistochemistry was performed for cytokeratin (AE1/AE3, 1:50; Zymed, San Francisco, CA) and vimentin (V-9, 1:50; Immunon, Pittsburgh, PA). After dewaxing and rehydration, the sections were incubated with the primary antibodies, biotinylated secondary antibody, streptavidin peroxidase, and chromogens (diaminobenzidine; amino-9-ethylcarbazole), which was followed by counterstaining with hematoxylin. The normal tissue adjacent to the tumor served as an internal control for each antibody.

Analysis of microsatellite alleles

Microsatellite markers

The dinucleotide repeat sequences with a heterozygous frequency of more than 50% were selected. The amplified DNAs ranging from 90 bp to 190 bp in size were confirmed to reproduce the stable ratios of the upper and lower alleles [5, 10]. A total of 40 microsatellite markers on chromosome 3p, 4p, 5q, 8p, 9p, 13q, 17p, and 18q, 5 markers per chromosomal arm, were used to increase the number of heterozygous cases.

Microdissection and DNA amplification

Tissue sections (7-μm thick) on the microscopic slides were briefly stained with hematoxylin and eosin and rinsed in 2% glycerol in a TE buffer (10 mM Tris-HCl, 1 mM EDTA, pH 8.0) for 2 min. Under a ×40 magnification in stereomicroscope, approximately 1000 tumor cells were dissected with a surgical scalpel and treated with 20 μl of a DNA extraction buffer (0.5% Tween-20, 1 mM EDTA pH 8.0, 50 mM Tris pH 8.0, 0.5 mg/ml proteinase K). For each tumor site, a 100- to 200-μl admixture of the microdissected tissue and DNA extraction buffer was incubated at 37 C for 24 h and used as template DNA for PCR analysis after the heat inactivation of proteinase K for 5 min. Of the genomic DNA, 1 μl was amplified and labeled with a radioisotope in 10 μl of the PCR mixture (0.5 μM of each primer, 1.5 mM $MgCl_2$, 0.2 mM of each deoxynucleotide triphosphate, 0.5 unit of *Taq* DNA polymerase, and 0.5 μl of [α-^{32}P]dCTP 10 μCi/ml). Each reaction mixture underwent 32 PCR cycles consisting of a denaturation step of 94 C for 1 min, an annealing step of 55 C–63 C for 1 min, and an elongation step of 72 C for 1 min. Of the PCR products, 2 μl was diluted with 5 μl of formamide-dye loading buffer, heated to 80 C

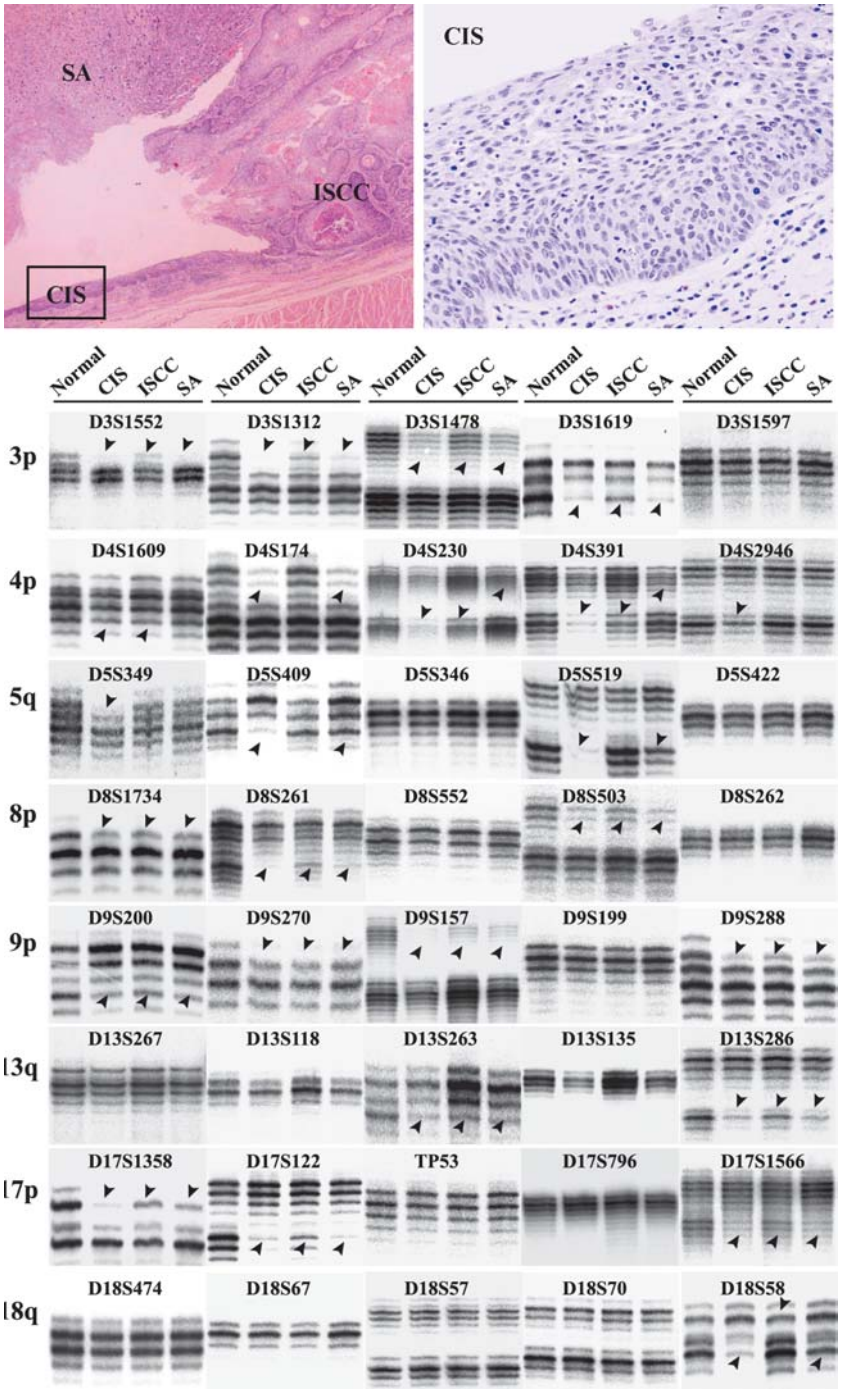

Fig. 1 Representative histological features (*photomicrograph*) and allelic migration (*autoradiograph*) of a sarcomatoid carcinoma (case 4). *Photomicrograph* squamous cell carcinoma in situ (*CIS*) in the *lower left* mucosa at the periphery, invasive squamous cell carcinoma (*ISCC*) at the *right side*, and a sarcomatoid spindle cell (*SA*) component in the *upper left* portion can be obviously distinguished with a sharp separation (magnification, ×15). *CIS* is shown at a higher magnification, ×200. *Autoradiograph* normal DNA and the corresponding tumor DNAs are indicated above the lanes. The loss of heterozygosity (LOH) was scored at a cutoff point of 1.5-fold relative allelic ratio, which was calculated by dividing the tumor allelic ratio by the normal allelic ratio. The *arrowhead* indicates the LOH

for 3 min, and electrophoresed on a 6% polyacrylamide gel containing 7 M urea. The radioisotope-labeled microsatellite bands were visualized by repeated exposures of each autoradiograph using a radioluminograph scanner (BAS 2500, Fuji Photo Film Co. Ltd., Kanakawa, Japan). An optimal range of allelic band intensities was selected for the densitometric analysis using the TINA image software package (raytest Isotopenmeβgeräte GmbH, Straubenhardt, Germany) (Fig. 1).

Analysis of microsatellite alleles

The allelic bands generated by PCR were converted into one-dimensional peaks using the "Profile" option of the TINA image software. The allelic status of the tumor DNA was scored as the relative allelic ratio, which was calculated by dividing the tumor allelic ratio by the normal allelic ratio. The LOH was defined at a cutoff point of a 1.5-fold relative allelic ratio that provided the best discrimination between the wild-type heterozygosity and the LOH in previous studies [5, 10]. The common loss of chromosome shared by all components in a given tumor is termed as a primary LOH whereas the divergent LOH uniquely restricted to a given component is termed as a secondary LOH.

Results

Clinicopathological analysis

The clinicopathological features of eight sarcomatoid carcinomas of the esophagus are summarized in Table 1. All the tumors occurred in men with a mean age of 62 years (range, 47–76 years), and all patients presented with dysphagia. The growth pattern of the tumors varied from polypoid to polypoid-ulceroinfiltrative. The tumor size ranged from 3.7 cm to 9.0 cm in the greatest dimension (mean, 6.2 cm). Microscopically, seven tumors were biphasic, with dual SCC and SA components, and one tumor showed only a SA component (Table 2). A gradual transition between the SCC and SA components was found in four cases and a sharp separation in three cases. The SCC element was present as a conventional ISCC and/or a CIS.

Immunohistochemical findings

The SCC components were diffusely and strongly positive for cytokeratin, and negative for vimentin in all cases. The SA components were diffusely and strongly positive for vimentin in all cases and focally positive for cytokeratin in five of eight cases. One case with only a spindle cell component revealed two distinct tumor foci with and without cytokeratin expression.

Analysis of chromosomal loss

All genomic DNAs from the eight sarcomatoid carcinomas tested were successfully amplified by all microsatellite markers used in PCR. All cases contained at least one heterozygous microsatellite marker in every chromosomal arm tested. A total of 20 tumor sites obtained separately from five CIS, six ISCC, and nine SA components revealed 441 LOHs, involving 141 chromosomal arms (Table 3). Of the 141 chromosomal losses, 128 (91%) simultaneously lost all heterozygous alleles on a chromosomal arm (complete chromosomal losses) and the remaining 13 (9%) lost part of the heterozygous alleles (incomplete chromosomal losses). All 9p and 17p losses were commonly present in all CIS, ISCC, and SA components, whereas the 4p (seven cases), 5q (five cases), and 18q (four cases) losses were frequently restricted to a CIS, an ISCC, or a SA component.

Table 1 Clinicopathological features of eight cases with esophageal sarcomatoid carcinoma

Case	Age/sex	Site	Gross	Size (cm)	Depth of invasion	Lymph-node metastasis	Stage
1	53/Male	Lower & mid	Polypoid	7.0	Adventitia	9/28	IVA (T3N1M1a)
2	67/Male	Lower & mid	Polypoid	6.0	Muscularis propria	0/35	IIA (T2N0M0)
3	63/Male	Lower & mid	Polypoid-ulcerative	9.0	Adventitia	8/47	IVA (T3N1M1a)
4	65/Male	Lower	Polypoid	3.7	Submucosa	2/37	IIB (T1N1M0)
5	63/Male	Lower	Polypoid	7.0	Adventitia	4/37	III (T3N1M0)
6	76/Male	Lower	Polypoid	4.5	Submucosa	0/25	I (T1N0M0)
7	47/Male	Lower & mid	Polypoid	8.1	Adventitia	4/38	IVA (T3N1M1)
8	63/Male	Lower	Elevated-ulcerative	4.5	Adventitia	3/25	III (T3N1M0)

Table 2 Histological findings of eight esophageal sarcomatoid carcinomas. *SA* sarcomatoid spindle cell component, *CIS* squamous cell carcinoma in situ, *ISCC* invasive squamous cell carcinoma, *HPF* high power fields

	Case 1	Case 2	Case 3	Case 4	Case 5	Case 6	Case 7	Case 8
Histological proportion								
CIS	0%	5%	5%	5%	1%	1%	1%	0%
ISCC	0%	0%	30%	20%	5%	15%	49%	90%
SA	100%	95%	65%	75%	94%	84%	50%	10%
Intratumoral border		Sharp separation	Gradual transition	Sharp separation	Gradual transition	Gradual transition	Gradual transition	Sharp Separation
Spindle cell component								
Cellularity	High	Moderate	Moderate	High	Moderate	High	High	High
Nuclear shape	Oval, spindle, multinucleated	Spindle, oval, multinucleated	Spindle, oval, multinucleated	Polygonal, oval, spindle	Oval, multinucleated	Oval, spindle	Oval, spindle, multinucleated	Oval
Nucleoli	Indistinct	Indistinct	Indistinct	Prominent	Occasionally prominent	Indistinct	Occasionally prominent	Prominent
Pleomorphism	Moderate	Mild	Moderate	Marked	Marked	Moderate	Marked	Moderate
Mitotic activity	60/10 HPF	2/50 HPF	9/10 HPF	30/10 HPF	25/10HPF	50/10HPF	25/10HPF	40/10HPF
Differentiation	–	–	Bone formation	–	–	–	–	–
Hemorrhage	–	–	–	–	–	+	–	–
Necrosis	–	–	–	–	–	–	–	–

Table 3 Loss of heterozygosity on eight cancer-associated chromosomal arms detected in eight esophageal sarcomatoid carcinomas. *SA* sarcomatoid spindle cell component, *CIS* squamous cell carcinoma in situ, *ISCC* invasive squamous cell carcinoma, *CK+ and CK−* cytokeratin positive and negative, *closed square* loss of heterozygosity, *open square* retention of heterozygosity, *N* noninformative marker, ■*L* and ■*U* loss of opposite (lower and upper) alleles on the same chromosome, *hatched square* secondary loss of heterozygosity

		Case 1		Case 2		Case 3			Case 4			Case 5			Case 6		Case 7			Case 8	
		SA CK+	SA CK-	CIS	SA	CIS	ISCC	SA	CIS	ISCC	SA	CIS	ISCC	SA	ISCC	SA	CIS	ISCC	SA	ISCC	SA
3p	D3S1552	N	N	□	■	■	■	■	■	■	■	N	N	N	N	N	■	■	■	■	■
	D3S1312	■	■	N	N	■	■	■	■	■	■	■	■	■	■	■	■	■	■	N	N
	D3S1478	■	■	□	■	■	■	■	■	■	■	■	■	■	■	■	■	■	■	■	■
	D3S1619	N	N	N	N	■	■	■	■	■	■	■	■	■	■	■	■	■	■	■	■
	D3S1597	■	■	N	N	■	■	■	N	N	N	N	N	N	■	■	■	■	■	N	N
4p	D4S1609	N	N	N	N	□	■	□	■	■	□	■	□	■	■	■	N	N	N	N	N
	D4S174	□	■	□	■	N	N	N	■	□	■	■	□	■	■	■	N	N	N	□	■
	D4S230	□	■	N	N	□	■	□	■L	■L	■U	■	□	■	■	■	■	□	■	□	■
	D4S391	□	■	□	■	■	■	□	■L	■L	■U	N	N	N	N	N	N	N	N	□	■
	D4S2946	□	■	□	■	□	■	□	■	□	□	■	□	■	N	N	■	□	■	N	N
5q	D5S349	N	N	□	□	■	□	■	■	□	□	■	■	□	■	■	□	□	■	■L	■U
	D5S409	■	■	N	N	N	N	N	■	□	■	N	N	N	N	N	□	□	■	N	N
	D5S346	N	N	□	□	N	N	N	N	N	N	■	■	□	N	N	N	N	N	■L	■U
	D5S519	■	■	N	N	■	□	■	■	□	■	■	■	□	■	■	□	□	■	N	N
	D5S422	N	N	□	□	N	N	N	N	N	N	■	■	□	■	■	□	□	■	N	N
8p	D8S1734	N	N	N	N	■	■	■	■	■	■	■	■	■	■	■	■	■	■	N	N
	D8S261	N	N	N	N	N	N	N	■	■	■	N	N	N	N	N	N	N	N	N	N
	D8S552	N	N	■	■	N	N	N	N	N	N	■	■	■	■	■	■	■	■	■U	■L
	D8S503	N	N	N	N	■	■	■	■	■	■	■	■	■	■	■	■	■	■	N	N
	D8S262	■	■	N	N	N	N	N	N	N	N	■	■	■	■	■	■	■	■	■U	■L
9p	D9S200	■	■	■	■	■	■	■	■	■	■	N	N	N	■	■	■	■	■	■	■
	D9S270	N	N	■	■	N	N	N	■	■	■	N	N	N	■	■	■	■	■	■	■
	D9S157	■	■	N	N	■	■	■	■	■	■	■	■	■	N	N	■	■	■	■	■
	D9S199	■	■	■	■	■	■	■	N	N	N	■	■	■	N	N	N	N	N	N	N
	D9S288	N	N	■	■	■	■	■	■	■	■	■	■	■	■	■	■	■	■	■	■
13q	D13S267	■	■	■	□	N	N	N	N	N	N	■	■	■	N	N	N	N	N	N	N
	D13S118	■	■	□	■	■	■	■	N	N	N	N	N	N	N	N	■	■	■	□	□
	D13S263	■	■	■	■	■	■	■	■	■	■	■	■	■	■	■	■	■	■	□	□
	D13S135	■	■	■	□	■	■	■	N	N	N	■	■	■	■	■	■	■	■	■L	■U
	D13S286	N	N	N	N	■	■	■	■	■	■	N	N	N	■	■	N	N	N	N	N
17p	D17S1358	N	N	N	N	■	■	■	■	■	■	N	N	N	■	■	N	N	N	N	N
	D17S122	■	■	N	N	■	■	■	■	■	■	■	■	■	■	■	■	■	■	N	N
	TP53	■	■	■	■	■	■	■	N	N	N	■	■	■	■	■	■	■	■	■	■
	D17S796	N	N	■	■	■	■	■	N	N	N	N	N	N	■	■	N	N	N	■	■
	D17S1566	■	■	■	■	■	■	■	■	■	■	■	■	■	■	■	■	■	■	■	■
18q	D18S474	□	□	N	N	■	□	■	□	□	□	■	■	■	N	N	N	N	N	■	■
	D18S67	■	□	N	N	■	□	■	N	N	N	N	N	N	□	□	N	N	N	N	N
	D18S57	N	N	N	N	■	□	■	□	□	□	N	N	N	■	□	■	■	■	■	■
	D18S70	■	□	□	□	N	N	N	□	□	□	N	N	N	□	□	■	■	■	■	■
	D18S58	□	□	□	□	■	□	■	■L	■U	■L	■	■	■	N	N	N	N	N	■	■

Table 4 The number of cancer-associated chromosomal arms containing a loss of heterozygosity (LOH) in squamous cell carcinoma in situ (CIS), invasive squamous cell carcinoma (ISCC), and a spindle cell component (SA)

Chromosomal loss (LOH)	CIS (*n*=5)	ISCC (*n*=6)	SA (*n*=9)	Total
Primary				
Mean±SD	5.0±1.2 (16.8±4.7)	5.5±1.1 (19.0±3.6)	5.3±1.2 (17.2±4.5)	5.3±1.1 (18.0±4.2)
Sum	25 (84)	33 (114)	48 (155)	106 (355)
Range	3–6 (9–20)	4–7 (14–25)	3–7 (9–25)	3–7 (9–25)
Secondary				
Mean±SD	2.0±1.0 (5.6±3.0)	1.3±1.0 (3.0±2.0)	1.9±1.2 (4.7±2.5)	1.8±1.1 (4.0±2.6)
Sum	10 (28)	8 (18)	17 (42)	35 (88)
Range	1–3 (2–8)	0–3 (0–5)	0–4 (0–8)	0–4 (0–8)
Total				
Mean±SD	7.0±1.7 (22.4±6.7)	6.8±0.8 (22.0±2.6)	7.2±0.6 (21.9±3.7)	7.1±1.0 (22.1±4.1)
Sum	35 (112)	41 (132)	65 (197)	141 (441)
Range	4–8 (11–27)	6–8 (19–26)	6–8 (15–27)	4–8 (11–27)

All eight esophageal sarcomatoid carcinomas showed extensive and divergent LOHs involving an average of seven chromosomal arms (Table 4). All CIS, ISCC, and SA components contained not only a high-level primary LOH (mean chromosomal involvement, 5.3) in common but also a low-level secondary LOH (mean chromosomal involvement, 1.8) in disparity. More secondary LOHs were observed in the CIS (5.6 LOHs per site) and SA (4.7 LOHs per site) than in the ISCC (3.0 LOHs per site).

Each case was analyzed for its clonality and extent of secondary LOHs between the matched CIS and ISCC components (four cases), the ISCC and SA components (six cases), and the CIS and SA components (five cases) (Fig. 2). All four cases (case 3, 4, 5, and 7) with CIS and ISCC contained more secondary LOHs in the CIS rather

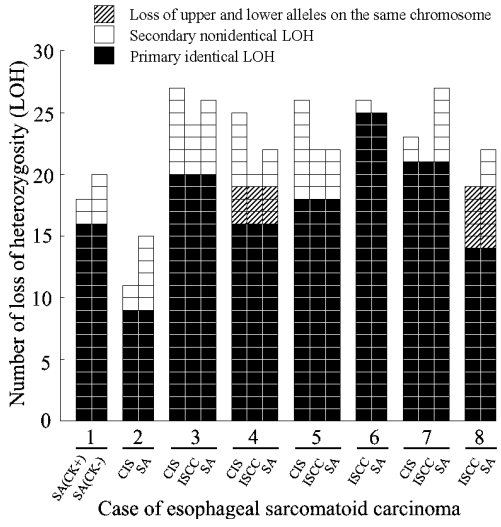

Fig. 2 Schematic diagram of the primary and secondary loss of heterozygosity (LOH) detected in eight cases with an esophageal sarcomatoid carcinoma. Squamous cell carcinoma in situ (CIS), invasive squamous cell carcinoma (ISCC), and the sarcomatoid spindle cell (SA) components in each case are compared for the number and clonality of the LOH. *CK+* and *CK−* cytokeratin positive and negative

than in the ISCC. Of the six cases with ISCC and SA, four (case 3, 4, 7, and 8), one (case 5), and one (case 6) had the greater, equal, and fewer numbers of secondary LOHs in a SA component, respectively. No ISCC had more secondary LOHs than the matched CIS. The ISCC in case 6 had excessive LOHs involving eight chromosomal arms, which were confined to the submucosa (stage I). The CIS had the greater (three cases) or fewer (two cases) number of secondary LOHs than with the SA. Two distinct SA foci with and without focal cytokeratin expression carried secondary LOHs on chromosome 18p and 4p, respectively (case 1).

Cases 4 and 8 harbored losses of upper and lower opposite alleles on the same chromosomes, which were reciprocally bifurcated into distinct cellular components (Fig. 1). None of the secondary LOHs were selectively distributed in a CIS, an ISCC, or a SA component.

Discussion

The presence of identical LOHs in different components is not always equivalent to monoclonality, as different genetic abnormalities may lead to allelic loss at the same locus. Nevertheless, in all eight cases examined, three different components commonly contained high-level LOHs involving the same alleles of multiple microsatellite markers, strongly suggesting the monoclonal origins of sarcomatoid carcinoma. More interestingly, all cases harbored extensive chromosomal losses when compared with a conventional SCC of the esophagus [4, 9, 26]. There were also considerable differences between colorectal cancers [5] and sarcomatoid carcinomas tested using the same microsatellite markers in terms of the frequency of the extensive chromosomal losses involving six (8% versus 15%), seven (6% versus 50%), and eight (1% versus 30%) chromosomal arms. In a previous study on colorectal cancers, the net level of chromosomal losses, rather than the individual chromosomal losses, was found to serve as the most important index of disease progression [5]. The present results on sarcomatoid carcinomas suggest that extensive chromosomal losses are essential for stimulating the pluripotency of a stem cell.

In colorectal cancers, the rarity of extensive chromosomal losses might be due to their deleterious effect over a growth advantage. Interestingly, the CIS tended to carry more secondary chromosomal losses than did the ISCC, suggesting that the excessively burdened losses provided few growth advantages. A SCC precursor with high-level primary LOH at the initial or early stage might remain in the CIS due to the addition of secondary losses to an excessive level of incompatibility with viability. Otherwise, a precursor acquiring no or relatively fewer secondary losses would progress to an ISCC.

With respect to the deleterious effect of excessive LOHs, it should be noted that all incomplete losses were found to contribute to the secondary losses (Table 3), which would be selected to alleviate the deleterious effect of the excessive losses. Losses of 4p (seven cases), 5q (five cases), and 18q (four cases) were frequently found as a secondary event. The preferential involvement of a secondary LOH for a certain chromosomal arm suggests a different harmful effect on viable cells among the individual chromosomal losses. It was believed that the losses of 4p were less harmful and had an advantage for acquiring extensive and divergent losses.

The secondary chromosomal losses in the SA component were likely to confer a benefit for the biphasic differentiation. However, none of the secondary LOHs were selectively confined to a spindle cell component. Similarly, divergent chromosomal losses, but no specific losses restricted to a histological type, were frequent in the intestinal and diffuse mixed-type gastric cancers [18]. Therefore, it is believed that the secondary chromosomal losses stimulate the co-expansion of the different clones indirectly or stochastically, rather than directly or specifically. Given that data on the previous studies of gastrointestinal cancers have consistently emphasized the extent of LOH as the universal determinant associated with diverse tumor phenotypes such as age of onset and tumor location, the unilateral chromosomal loss is thought to contribute to tumor progression through variable pathways stimulated stochastically according to the extent of LOHs, rather than inactivation of a single gene. The normal ontogeny of tumor cells is inherently stimulated by the intrinsic genetic programs, which lead to histologically heterogeneous cellular contents. The excessive chromosomal losses appear to stimulate the intrinsic program through which a squamous cell precursor is transformed into a spindle cell. On the other hand, esophageal sarcomatoid carcinomas have a peculiar

tendency to grow into the lumen rather than the wall and often remain at a low stage until they reach an enormous size. With respect to this, therefore, it has been suggested that esophageal sarcomatoid carcinomas have a better prognosis than a SCC of a comparable size [20]. The growth property of a SA may result from the unique role of the excessive chromosomal losses in mesenchymal cell proliferation, rather than invasion and metastasis.

There have been many individual false-positive and false-negative results reported in LOH studies. Formalin-fixed, paraffin-embedded tissue can result in the production of PCR artifacts due to the highly fragmented and cross-linked DNA extracted [8, 31]. The inherent instability of the microsatellite sequences caused by DNA slippage in the repeat units can lead to stochastic PCR artifacts in the LOH analysis using an increased number of microsatellite markers [10, 31]. In addition to methodological problems, the functional implication of the unilateral chromosomal losses defined by the LOH is unclear. Passenger chromosomal losses with little or no biological effects on tumor growth, which can be coincidentally accompanied with a functional loss of chromosomes [16, 32], can obscure the histogenetic implication of the LOH events. A panel of microsatellite markers used in this study on esophageal sarcomatoid carcinomas was selected from eight cancer-associated chromosomal arms that are frequently lost in esophageal cancers [4, 9, 26, 27]. The minimum number of PCR artifacts and passenger chromosomal losses has been confirmed in previous studies on colorectal cancers using the same set of chromosomal markers [5, 10].

The secondary LOHs restricted to a component of a sarcomoid carcinoma were likely to be identified due to the sufficient number of heterozygous markers per chromosomal arm. Because the secondary LOHs were relatively infrequent and were preferentially observed in chromosome 4p, they are unlikely to be detected accurately, even by a genome-wide microsatellite study using a limited number of microsatellite markers per chromosomal arm. However, the method of comparative genomic hybridization would identify neither the secondary LOH at the opposite alleles on the same chromosomal arm, i.e., cases 4 and 8 with multiple reciprocal losses of the upper and lower alleles, nor incomplete chromosomal losses involving a small part of the chromosomal arm. The SA component in case 4 demonstrated the secondary LOH with the incompletely diminished allelic intensity at D4S174, D4S230, D4S391, D5S409, D5S519, and D18S58 markers (Fig. 1). Because the allelic intensity of primary LOH was obviously diminished in the same SA component, the possibility of contamination by normal cells could be ruled out. The incomplete allelic diminution of pure tumor cell contents was also found in a previous study of composite gastric carcinoma [17], which was thought to reflect a genetically mixed population with and without additional LOHs to the initial multiple LOHs.

The metastatic rate of sarcomatoid carcinoma was found to be identical to that of conventional SCC with comparable depths of invasion [20]. In addition, the 5-year survival rate from sarcomatoid carcinoma and the conventional SCC was similar [14]. This suggests that the progression of esophageal sarcomatoid carcinoma is related to the biological properties of the SCC component. In this study, the ISCC was burdened with the relatively fewer chromosomal losses, whereas both the CIS and SA were burdened with excessive losses. Therefore, it is proposed that a high-level but not an excessive level of LOHs in ISCC are involved in driving the tumor progression, and that excessively added secondary LOHs confer a slight growth advantage to a CIS or a benefit for the metaplastic transformation of a SCC precursor.

References

1. Abeln EC, Smit VT, Wessels JW, de Leeuw WJ, Cornelisse CJ, Fleuren GJ (1997) Molecular genetic evidence for the conversion hypothesis of the origin of malignant mixed Mullerian tumours. J Pathol 183:424–431
2. American Joint Committee on Cancer (1998) AJCC cancer staging manual. (5th edn) Lippincott-Raven, Philadelphia, pp 65–69
3. Ansari-Lari MA, Hoque MO, Califano J, Westra WH (2002) Immunohistochemical p53 expression patterns in sarcomatoid carcinomas of the upper respiratory tract. Am J Surg Pathol 26:1024–1031
4. Aoki T, Mori T, Du X, Nisihira T, Matsubara T, Nakamura Y (1994) Allotype study of esophageal carcinoma. Genes Chromosomes Cancer 10:177–182
5. Choi SW, Lee KJ, Bae YA, Min KO, Kwon MS, Kim KM, Rhyu MG (2002) Genetic classification of colorectal cancer based on chromosomal loss and microsatellite instability predicts survival. Clin Cancer Res 8:2311–2322
6. Gabbert HE, Shimoda T, Hainaut P, Nakamura Y, Field JK, Inoue H (2000) Squamous cell carcinoma of the esophagus. In: Hamilton SR, Aaltonen LA (eds) World Health Organization classification of tumors: pathology & genetics of tumors of the digestive system. IARC, Lyon, pp 11–19
7. Hanada M, Nakano K, Ii Y, Yamashita H (1984) Carcinosarcoma of the esophagus with osseous and cartilagenous production: a combined study of keratin immunohistochemistry and electron microscopy. Acta Pathol Jpn 34:669–678
8. Heinoller E, Renke B, Beyser K, Dietmainer W, Langer C, Ruschoff J (2001) Pitfalls in diagnostic molecular pathology—significance of sampling error. Virchows Arch 439:504–511
9. Huang Y, Boynton RF, Blount PL, Silverstein RJ, Yin J, Tong Y, McDaniel TK, Newkirk C, Resau JH, Sridhara R, et al (1992) Loss of heterozygosity involves multiple tumor suppressor genes in human esophageal cancers. Cancer Res 52:6525–6530
10. Hyun JS, Jo BK, Park CJ, Yi JY, Lee JY, Rhyu MG (2002) Loss of heterozygosity and PCR artifacts in a microsatellite analysis of psoriasis and colorectal cancer. J Korean Med Sci 17:641–647
11. Iascone C, Barreca M (1999) Carcinosarcoma and pseudosarcoma of the esophagus: two names, one disease-comprehensive review of the literature. World J Surg 23:153–157
12. Ikura Y, Hosotani R, Aoyama H, Ogata M, Hayashi M, Takamine Y, Uchida H, Shirane H, Ishikawa T (1993) Carcinosarcoma of the esophagus: a report of two cases. Surg Today 23:562–567
13. Imada T, Yoneyama K, Suzuki Y, Nagano A, Hasuo K, Takahashi M, Rino Y, Ozawa Y, Amano T, Kondo J (1998) Carcinosarcoma of the esophagus: three cases with immunohistological examination. Hepatogastroenterol 45:2193–2196

14. Iyomasa S, Kato H, Tachimori Y, Watanabe H, Yamaguchi H, Itabashi M (1990) Carcinosarcoma of the esophagus: a twenty-case study. Jpn J Clin Oncol 20:99–106
15. Kashiwabara K, Sano T, Oyama T, Najahima T, Makita F, Hashimoto N, Iwanami K, Kawashima O, Matsumoto T, Matsuzaki Y (2001) A case of esophageal sarcomatoid carcinoma with molecular evidence of a monoclonal origin. Pathol Res Pract 197:41–46
16. Kern SE, Fearon ER, Tersmette KW, Enterline JP, Leppert M, Nakamura Y, White R, Vogelstein B, Hamilton SR (1989) Clinical and pathological associations with allelic loss in colorectal carcinoma. JAMA 261:3099–3103
17. Kim KM, Kim MJ, Cho BK, Choi SW, Rhyu MG (2002) Genetic evidence for the multi-step progression of mixed glandular–neuroendocrine gastric carcinomas. Virchows Arch 440:85–93
18. Kim KM, Kwon MS, Hong SJ, Min KO, Seo EJ, Lee KY, Choi SW, Rhyu MG (2003) Genetic classification of intestinal-type and diffuse-type gastric cancers based on chromosomal loss and microsatellite instability. Virchows Arch (in press)
19. Lasko D, Cavenee W, Nordenskjold M (1991) Loss of constitutional heterozygosity in human cancer. Annu Rev Genet 25:281–314
20. Lewin KJ, Appelman HD (1996) Squamous cell carcinoma. In: Rosai J, Sobin LH (eds) Atlas of tumor pathology: tumors of the esophagus and stomach (3rd edn). AFIP, Washington DC, pp 43–97
21. Matsusaka T, Watanabe H, Enjoji M (1976) Pseudosarcoma and carcinosarcoma of the esophagus. Cancer 37:1546–1555
22. Montesano R, Hollstein M, Hainaut P (1996) Genetic alterations in esophageal cancer and their relevance to etiology and pathogenesis: a review. Int J Cancer 69:225–235
23. Natsugoe S, Matsushita Y, Chuman Y, Kijima F, Haraguchi Y, Shimada M, Yoshinaka H, Baba M, Mueller J, Aikou T (1999) So-called carcinosarcoma of the esophagus: a clinicopathologic, immunohistochemical and DNA flow-cytometric analysis of 6 cases. Oncology 57:29–35
24. Ooi A, Kawahara E, Okada Y, Mizukami Y, Sugawara S, Noto Y, Fujita H (1986) Carcinosarcoma of the esophagus: an immunohistochemical and electron microscopic study. Acta Pathol Jpn 36:151–159
25. Osamura RY, Shimamura K, Hata J, Tamaoki N, Watanabe K, Kubota M, Yamazaki S, Mitomi T (1978) Polypoid carcinoma of the esophagus. A unifying term for "carcinosarcoma" and "pseudosarcoma". Am J Surg Pathol 2:201–208
26. Shibagaki I, Shimada Y, Wagata T, Ikenaga M, Imamura M, Ishizaki K (1994) Allelotype analysis of esophageal squamous cell carcinoma. Cancer Res 54:2996–3000
27. Sieben NL, ter Haar NT, Cornelisse CJ, Fleuren GJ, Cleton-Jansen AM (2000) PCR artifacts in LOH and MSI analysis of microdissected tumor cells. Hum Pathol 31:1414–1419
28. Thompson L, Chang B, Barsky SH (1996) Monoclonal origins of malignant mixed tumors (carcinosarcomas): evidence for a divergent histogenesis. Am J Surg Pathol 20:277–285
29. Torenbeek R, Hermsen MA, Meijer GA, Baak JP, Meijer CJ (1999) Analysis by comparative genomic hybridization of epithelial and spindle cell components in sarcomatoid carcinoma and carcinosarcoma: histogenetic aspects. J Pathol 189:338–343
30. Uchiyama S, Imai S, Hoshino A, Obara K, Yoshida K, Kodama H, Kamisago S (2000) Rapid-growing carcinosarcoma of the esophagus arising from intraepithelial squamous cell carcinoma: report of a case. Surg Today 30:173–176
31. Umetani N, Sasaki S, Watanabe T, Ishigami H, Ueda E, Nagawa H (2000) Diagnostic primer sets for microsatellite instability optimized for a minimal amount of damaged DNA from colorectal tissue samples. Ann Surg Oncol 7:276–280
32. Vogelstein B, Fearon ER, Kern SE, Hamilton SR, Preisinger AC, Nakamura Y, White R (1989) Allelotype of colorectal carcinomas. Science 244:207–211
33. Weinberg RA (1991) Tumor suppressor genes. Science 254:1138–1146

Virchows Arch (2003) 443:643–648
DOI 10.1007/s00428-003-0880-5

ORIGINAL ARTICLE

Timea P. Gurbity · Eniko Bagdi · Nicole A. Groen · Leo M. Budel · Mustaffa Abbou · Laszlo Krenacs · Winand N. M. Dinjens

Increased sensitivity of B-cell clonality analysis in formalin-fixed and paraffin-embedded B-cell lymphoma samples using an enzyme blend with both 5′→3′ DNA polymerase and 3′→5′ exonuclease activity

Received: 17 March 2003 / Accepted: 14 July 2003 / Published online: 21 August 2003
© Springer-Verlag 2003

Abstract Polymerase chain reaction (PCR)-based detection of immunoglobulin heavy chain (IgH) gene rearrangement for determination of B-cell clonality needs to be simple but optimally sensitive. Efficient IgH PCR analysis can be hampered by sequence variability in the template DNA, despite of the use of degenerative primers. To improve sensitivity of the B-cell clonality analysis in formalin-fixed and paraffin-embedded (FFPE) tissues, we have performed framework three-area (FR3)/joining gene (JH) IgH PCR utilizing an enzyme blend (r*Tth* DNA Polymerase, XL) providing both 5′→3′ polymerase and 3′→5′ exonuclease activities. The DNA samples were extracted from FFPE biopsies of 43 mature B-cell lymphoma cases of so-called germinal center and post-germinal center origin, including 6 nodal follicular lymphomas (FL), 15 gastric mucosa-associated lymphoid tissue (MALT) lymphomas, and 22 gastric diffuse large B-cell lymphomas (DLBCL). Of the cases, 31 (17 DLBCL and 14 MALT lymphoma) represented small endoscopic biopsies. Serial dilutions of target DNA were applied to avoid inconsistent bands that may be seen when the input amount of template is too low, which can be the case when DNA is extracted from FFPE endoscopic gastric biopsies. Using conventional *Taq* polymerase, consistent monoclonal product was found in 53% (23/43) of the cases (FL: 67%; MALT lymphoma: 47%; DLBCL: 55%). The r*Tth* polymerase showed reproducible monoclonal pattern in 72% (31/43) of the cases (FL: 67%; MALT lymphoma: 73%; DLBCL: 73%); the sensitivity is compatible with one that can be detected with conventional FR3/JH PCR in fresh/frozen tissues. In conclusion, the r*Tth* DNA polymerase greatly improves sensitivity of FR3/JH PCR in FFPE biopsies of mature B-cell lymphomas, most probably by increasing the primer matches during PCR amplification.

Keywords FR3 · PCR · B-cell lymphoma · Clonality · Paraffin

T. P. Gurbity
Hematology Unit,
2nd Department of Internal Medicine, University of Szeged,
Szeged, Hungary

E. Bagdi · L. Krenacs
Laboratory of Tumor Pathology and Molecular Diagnostics,
Institute for Biotechnology,
Bay Zoltan Foundation for Applied Research,
Szeged, Hungary

N. A. Groen · L. M. Budel · M. Abbou · W. N. M. Dinjens (✉)
Department of Pathology,
Josephine Nefkens Institute,
Erasmus Medical Center (Erasmus MC),
P.O. Box 1738, 3000 DR Rotterdam, The Netherlands
e-mail: w.dinjens@erasmusmc.nl
Tel.: +31-10-4088389
Fax: +31-10-4089487

Introduction

Discrimination between reactive and neoplastic B-cell proliferations is often difficult using morphological methods alone. In samples without immunohistochemically detectable immunoglobulin light chain restriction, application of molecular techniques can be inevitable.

During physiological B-cell maturation, immunoglobulin heavy chain (IgH) gene overcomes VDJ sequence recombination. After antigen contact, the rearranged IgH variable (IgV_H) gene sequences are further modified in germinal center reaction by means of somatic hypermutation mechanism. The rearranged IgH gene segments can be analyzed as clonal markers in distinction of polyclonal and monoclonal B-cell populations. The IgH gene rearrangement can be demonstrated by Southern blotting with high specificity, but this method is restricted by the requirement of a large amount (10–30 μg) of high-molecular-weight DNA, which can be obtained only from a substantial amount of fresh tissue. Polymerase chain reaction (PCR)-based detection of IgH gene rearrangement is an alternative, as this method has the advantages of high sensitivity, simplicity and cost effectiveness and

can be easily employed for routine diagnostic application [13, 15, 17]. Therefore, for detection of B-cell clonality in formalin-fixed and paraffin-embedded (FFPE) pathological samples, especially in smaller biopsies, the IgH PCR assay is the method of choice.

Several IgH PCR procedures have been published, including different DNA isolation methods, single, semi-nested and nested PCR protocols, different degenerative primers and the utilization of various DNA polymerases. Most studies have revealed that the highest monoclonality rate can be obtained with primers directed at the conserved framework three-area (FR3) and joining gene (JH) segments [1, 4, 7].

Efficient IgH PCR analysis can be hampered by primer mismatches, originating from random sequence variability in the template DNA due to somatic hypermutation and ongoing mutational activity [16, 19]. A mismatch at the 3′ terminus of the primer due to point mutation or single nucleotide deletion of the template DNA significantly influences the outcome of the PCR amplification. High-fidelity DNA polymerases or polymerases with proofreading (3′→5′ exonuclease) activity have the ability to correct any misincorporated nucleotides on the strand of DNA being synthesized, and, thus, to remove mismatched bases at the 3′ terminus of the primers, resulting in sufficient amplification [3, 8, 11, 12, 18]. High-fidelity PCR can be carried out either with a single high-fidelity polymerase or using an optimized polymerase mixture.

We conducted this study to increase the detection rate of IgH gene rearrangement achievable in FFPE samples of mature B-cell lymphomas of germinal center (GC) or postgerminal center (pGC) origin [10] and, in particular, in small endoscopic biopsies. Follicular lymphomas (FL), gastric extranodal marginal zone B-cell lymphomas of mucosa-associated lymphoid tissue (MALT lymphomas) and gastric diffuse large B-cell lymphomas (DLBCL) were included [2, 10, 9, 14]. GC/pGC lymphomas demonstrate random sequence alterations in the IgV_H regions related to somatic hypermutation and ongoing mutations [10], which result in a lower chance to amplify these gene segments using conventional PCR methods [11, 15, 16, 19]. In order to at least partly overcome this problem, we have utilized a DNA polymerase combination, providing both 5′→3′ polymerase and 3′→5′ exonuclease activities. Using this enzyme blend, we were able to significantly improve sensitivity of FR3/JH PCR clonality analysis in our FFPE GC/pGC B-cell lymphoma cases.

Materials and methods

Tissue specimens and controls

FFPE samples of 6 FL cases, 15 gastric MALT lymphoma cases and 22 gastric DLBCL cases were retrieved from the files of the Department of Pathology, Josephine Nefkens Institute, Erasmus Medical Center (Erasmus MC), Rotterdam, The Netherlands, and the Laboratory of Tumor Pathology and Molecular Diagnostics, Institute for Biotechnology, Bay Zoltan Foundation for Applied Research, Szeged, Hungary. Samples from 14 gastric MALT lymphoma cases and 17 gastric DLBCL cases were small endoscopic biopsies (Table 1). All cases included were histologically and immunophenotypically fully characterized at diagnosis. DNA samples from reactive tonsils and 2 nodal B-cell lymphoma cases with well-established clonal IgH rearrangement were employed as polyclonal and monoclonal controls, respectively. Two cloned and sequenced FR3 fragments from B-cell lymphomas (gift of Dr. van Belzen, Department of Hematology, Erasmus MC) were also used as controls in studying the effect of the 3′ end mismatch (Fig. 1). DNA from a human epithelial cell line (LNCap) was used as negative control. Water controls were included in all rounds to monitor contamination.

Table 1 Results of framework three area (FR3)/joining gene (JH) polymerase chain reaction with *Taq* and r*Tth* DNA polymerases. *M* monoclonal, *P* polyclonal, *OC* oligoclonal, *IC* inconsistent

	Specimen type	Tag FR3/JH	r*Tth* FR3/JH
Nodal follicular lymphoma			
1	Lymph node	M	M
2	Lymph node	M	M
3	Lymph node	M	M
4	Lymph node	M	M
5	Lymph node	IC	P
6	Lymph node	IC	IC
Gastric diffuse large B-cell lymphoma			
1	Endoscopic	M	M
2	Endoscopic	M	M
3	Endoscopic	M	M
4	Endoscopic	M	M
5	Endoscopic	M	M
6	Endoscopic	M	M
7	Endoscopic	M	M
8	Endoscopic	M	M
9	Endoscopic	M	M
10	Endoscopic	M	M
11	Endoscopic	P	M
12	Endoscopic	P	M
13	Endoscopic	P	P
14	Endoscopic	P	P
15	Endoscopic	P	P
16	Endoscopic	OC	OC
17	Endoscopic	IC	IC
18	Resection	M	M
19	Resection	M	M
20	Resection	P	M
21	Resection	P	M
22	Resection	IC	IC
Gastric mucosa-associated lymphoid tissue lymphoma			
1	Endoscopic	M	M
2	Endoscopic	M	M
3	Endoscopic	M	M
4	Endoscopic	M	M
5	Endoscopic	M	M
6	Endoscopic	M	M
7	Endoscopic	M	M
8	Endoscopic	P	M
9	Endoscopic	P	M
10	Endoscopic	P	M
11	Endoscopic	P	M
12	Endoscopic	P	P
13	Endoscopic	P	P
14	Endoscopic	IC	IC
15	Resection	P	P

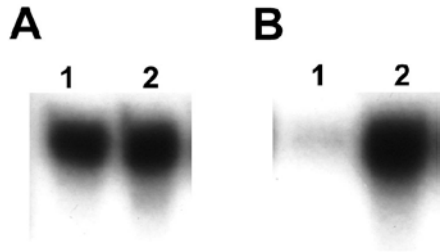

Fig. 1 Framework three-area (FR3)/joining genes (JH) amplification of two (**A, B**) cloned and sequenced FR3 fragments with *Taq* (*lanes 1*) and r*Tth* (*lanes 2*). *Sequences* FR3a primer: 5′ primer-ACTGT-3′. Fragment A: TGACA. FR3a primer: 5′primer-ACTGT-3′. Fragment B: TGACC. Note the primer 3′ end mismatch with fragment B, resulting in very minor amplification with *Taq* (*B1*) and strong amplification with r*Tth* (*B2*)

DNA extraction

Five paraffin sections of 5 μm from the selected samples were placed into Eppendorf vials, dewaxed and digested at 58°C in a lysis buffer (10 mM Tris-HCI, pH 8.0; 1 mM ethylene diamine tetraacetic acid (EDTA); 50 mM NaCl; 0.5% sodium dodecyl sulfate), containing 200 μg/ml proteinase K. Following an overnight digestion, an additional 10 μl proteinase K solution (20 mg/ml) was added to the same buffer, for a further 2 h at 58°C. Finally, the lysate was boiled for 10 min to inactivate the proteinase K, centrifuged at 14,000 rpm, and the supernatant was used for the study.

PCR amplification

For PCR amplification, a 15-μl reaction mixture was used, containing 1 μl target DNA, 0.2 mM of each dCTP, dGTP and dTTP, 0.02 mM dATP and 0.8 μCi α-^{32}P-dATP (Amersham, Buckinghamshire, UK) as well as 20 mM of each primer. FR3a (5′-ACA CGG CC/T G/C TGT ATT ACT GT-3′) [21] and JHC1 (5′-ACC TGA GGA GAC GGT GAC-3′) consensus primers were utilized. For conventional method, 0.4 U *Taq* polymerase (Promega, Madison, Wl, USA) was added with 1.5 mM concentration of $MgCl_2$. For the new method, 0.3 U r*Tth* polymerase, XL (GeneAmp XL Kit, Applied Biosystems, Foster City, CA, USA) enzyme was added with buffer XL and 1.5 mM $MgCl_2$. The primers and the cycling conditions were the same for both enzymes: 45 cycles of denaturation at 95°C for 30 s, annealing at 55°C for 45 s and extension at 72°C for 1 min. Reactions concluded with a final extension at 72°C for 10 min. The reaction was performed in a Biometra thermal cycler (Biometra, Göttingen, Germany). The expected product size was ~120 bp. In order to avoid "pseudo-monoclonal" band due to minute amount of B-cell DNA, we employed four serial dilutions of target DNA (neat; 1:10; 1:100; 1:1000) in each case.

Post-amplification steps and gel electrophoresis

For gel electrophoresis, 5 μl of the PCR amplification products were diluted immediately prior to analysis with 5 μl of loading buffer (95% formamide, 10 mM EDTA, 0.025% bromophenol blue, 0.025% xylene cyanol, pH 8.0). Then the PCR products were denatured at 95°C for 5 min and electrophoresed at 65 W for 1.5 h in a 6% denaturing polyacrylamide gel, containing 42% urea. Gels were dried and exposed to X-ray films at −80°C with intensifying screens. Because of large differences in signal intensities, multiple different exposures were made. Monoclonality was established if one or two consistent (identical sized) dominant bands were found in at least three different dilutions. An oligoclonal pattern was acknowledged if there were more than two consistent bands and a polyclonal product if a ladder was seen. An inconsistent result was seen to be accomplished if the dominant band(s) shifted by dilution.

Control experiments

To test the effect of the 3′→5′ exonuclease activity on the PCR result, two cloned and sequenced fragments were amplified with both polymerases. One fragment has a complete primer match while the other fragment has a 3′ end primer mismatch. In addition, from all eight cases with a monoclonal pattern with the r*Tth* enzyme and a polyclonal pattern with the *Taq* enzyme, the FR2 fragments were amplified with the r*Tth* enzyme in a semi-nested procedure. For the FR2 amplification, we used primers FR2 (5′-TGG A/GTC CGC/A CAG G/CCT/C T/CCN GG-3′) and JHCl in the first round and FR2 and VLJH (5′-GTG ACC AGG GTN CCT TGG CCC CAG-3′) in the second round. PCR products were purified and bidirectionally sequenced with FR2 and VLJH primers using Applied Biosystems Taq DyeDeoxy terminator cycle sequencing. The sensitivity of detection of a monoclonal population was determined by diluting DNA from a clear monoclonal sample with polyclonal tonsil DNA.

Results

Effect of r*Tth* polymerase on monoclonal and FR3 controls

The effect of the 3′→5′ exonuclease activity on the PCR result is shown in Fig. 1. The FR3/JH amplification of the cloned and sequenced fragment with complete primer match at the 3′ end resulted in identical strong product intensities using either *Taq* or r*Tth* polymerases (Fig. 1A). Whereas the fragment with a 3′ end primer mismatch was amplified far more efficiently with the r*Tth* than with *Taq*, the latter showed only a faint product (Fig. 1B). In one of the nodal B-cell lymphomas used as control, the *Taq* revealed a polyclonal FR3/JH pattern, whereas a clear dominant monoclonal band with a polyclonal background was observed using the r*Tth* DNA polymerase (Fig. 2). In eight cases, a polyclonal pattern was obtained with *Taq* and a monoclonal pattern with r*Tth* (Table 1). From these cases, FR2/JH fragments were amplified in a semi-nested procedure. PCR products were obtained from three cases (Table 1, gastric large B-cell lymphoma cases 20 and 21; gastric MALT lymphoma case 11). Lack of FR2 amplification in five cases is probably caused by the size of the FR2 fragment. After bidirectional direct sequencing, an unambiguous sequence was obtained from one case (Table 1, gastric large B-cell lymphoma case 20). This sequence revealed a FR3a primer 3′ end mismatch (AGG **ACA CGG CTG TGT ATT ACT G*C*** GCG). The two other cases had too many admixtures of polyclonal PCR products to get a clear sequence from the monoclonal population. No FR3/JH IgH PCR products were amplified from DNA samples from the epithelial tumor cell line LNCap (not shown).

FR3 monoclonal control DNA was diluted in polyclonal tonsil DNA and from these mixtures, FR3 was amplified both with *Taq* and r*Tth* enzymes. From 500–

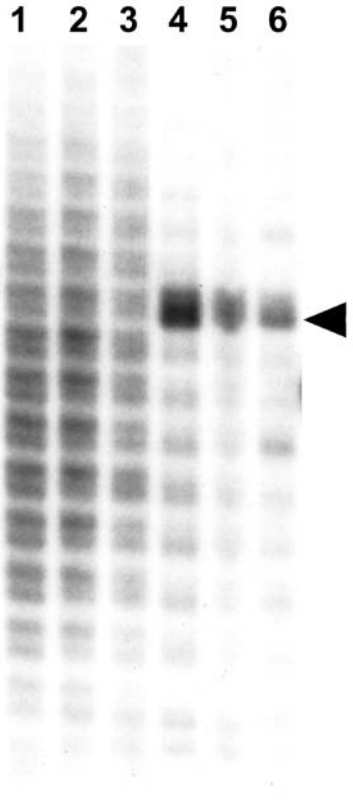

Fig. 2 The effect of the r*Tth* enzyme is shown on one of our nodal B-cell lymphoma cases used as control. One genomic DNA framework three-area (FR3)/joining gene (JH) sample amplified with *Taq* (*lanes 1–3*, undiluted, 1:10, 1:100) and r*Tth* polymerase (*lanes 4–6*, undiluted, 1:10, 1:100). In this case, the *Taq* revealed a polyclonal FR3/JH pattern, whereas a clear monoclonal pattern (*arrow*) in a polyclonal background was observed using the r*Tth* DNA polymerase

1000× dilutions of monoclonal genomic DNA in polyclonal DNA, the FR3 monoclonality can still be detected with both enzymes (results not shown).

Clonality analysis of lymphoma cases

The results are summarized in Table 1. Using conventional *Taq* polymerase, consistent monoclonal product was found in 53% (23/43) of the cases (FL: 67%; MALT lymphoma: 47%; DLBCL: 55%). The r*Tth* polymerase revealed reproducible monoclonal band in 73% (31/43) of the cases (FL: 67%; MALT lymphoma: 73%; DLBCL: 73%) (Fig. 3A). Oligoclonal pattern was ascertained in one gastric DLBCL case with both *Taq* and r*Tth*. An inconsistent result was seen in five cases with *Taq* polymerase and four (identical) cases with r*Tth* polymerase, as the size of the PCR products differed between different dilutions (Fig. 3B). Two of these inconsistent cases represented endoscopic biopsies (Table 1).

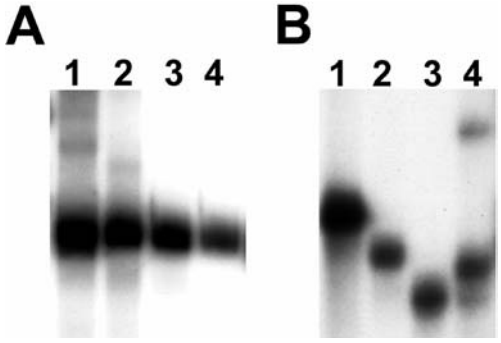

Fig. 3 Framework three-area (FR3)/joining gene (JH) amplification with r*Tth* of two gastric mucosa-associated lymphoid tissue lymphoma cases in four different serial dilutions. **A** A consistent clonal pattern is observed. **B** An inconsistent clonal pattern is observed

Discussion

In the present study, we optimized the IgH PCR assay for FR3/JH segment in FFPE mature B-cell lymphoma samples of GC/pGC origin, using r*Tth* DNA polymerase, an enzyme blend providing both 5→3′ polymerase and 3′→5′ exonuclease activities. The application of r*Tth* polymerase significantly increased the detection rate of monoclonal IgH rearrangements. The sensitivity for detection of a monoclonal population in a background of a polyclonal population was equal for *Taq* and the r*Tth* enzyme. In this study, B-cell clonality was determined by FR3/JH single PCR protocol, which amplifies small fragments; therefore, it can be easily employed on fragmented DNA retrieved from FFPE pathological specimens. The amplification of a FR3/JH segment is relatively simple and uses only one primer pair in a single PCR reaction [6, 13, 15, 16, 17]. We demonstrated that the sensitivity of the FR3/JH PCR method can be significantly improved by the use of the r*Tth* DNA polymerase, compared with the conventional *Taq* polymerase.

The sensitivity of a PCR-based assay for IgH gene rearrangements largely depends on lymphoma type and tissue fixation [4]. The GC/pGC lymphomas reveal signs of somatic hypermutation [2, 10, 9, 14], resulting in mutations and deletion in the IgV_H gene segments [10], which may cause false negativity due to primer mismatch during annealing [6, 11, 15, 19]. This fact can be at least partly overcome by application of degenerated primers as well as by using a DNA polymerase with proofreading activity, which has the ability to remove mismatched bases at the 3′ terminus of the primers and, thus, to increase the chance of amplification [8, 11, 12, 18]. According to this, a significantly increased sensitivity in FR3/JH PCR analysis has been reported by the use of *UlTma* DNA polymerase, a DNA polymerase with 3′→5′ exonuclease activity [11, 18]. We have tested the *UlTma* DNA polymerase in the Erasmus MC (Rotterdam, The Netherlands) with encouraging results, but the *UlTma* DNA polymerase is not more available. A survey for a

similar enzyme has led us to the r*Tth* DNA polymerase, XL (Applied Biosystems), an enzyme blend of *Thermus thermophilus* (*Tth*) and *Thermococcus litoralis* (*Tli*) DNA polymerases, combining both 5′→3′ polymerase and 3′→5′ exonuclease activities (information provided by the manufacturer). Thus, with the r*Tth* DNA polymerase, we were able to achieve the expected improvement provided by the 3′→5′ exonuclease activity in our polyacrylamide gel electrophoresis (PAGE) pattern analysis, using two cloned and sequenced FR3 fragments (Fig. 1). In addition, sequencing analysis revealed that the lack of amplification of the FR3 fragment from gastric large B-cell lymphoma case 20 (Table 1) with the *Taq* enzyme is probably caused by a FR3a primer 3′ end mismatch. In the targeted 43 FFPE mature B-cell lymphomas of GC/pGC origin, the r*Tth* DNA polymerase has markedly improved the sensitivity of the FR3/JH PCR method (from 53% to 73%), as compared with the conventional *Taq* polymerase. The most significant improvement was noticed in gastric MALT-type lymphoma cases (from 47% to 73%); however, all except one case represented small endoscopic biopsies. These figures concur with the monoclonality rate reported by others using the conventional FR3/JH PCR and DNA extracted from fresh/frozen tissues [4].

Another cornerstone of the accurate IgH PCR assays is the use of appropriate amounts of target DNA to ensure the correct assessment of clonality. Minute DNA amount may result in inconsistent size bands that can be misinterpreted as clonal rearrangement [5, 20], which is the case of endoscopic biopsies. In order to avoid these artificial bands, we employed a gradual target DNA dilution. We experienced inconsistent size bands in five cases with *Taq* polymerase and in four cases with r*Tth* polymerase. Nevertheless, only two of these cases were endoscopic gastric biopsies, suggesting that this phenomenon is not dependent purely on the size of the tissue and that the utilization of the r*Tth* polymerase has no significant influence on it. We believe that this can also occur due to the degraded template DNA, resulting in relative paucity of amplifiable B-cell DNA.

In our opinion, high resolution size separation for FR3 determinations is mandatory and superior to agarose gel electrophoresis with ethidium bromide or SYBR green staining. High-resolution size information is necessary to discriminate in the protocol with four DNA dilutions between inconsistent clonal patterns and true monoclonality. In addition, detection of FR3 monoclonality in a strong background of polyclonality is only possible reliable after high-resolution size separation.

We conclude that the utilization of r*Tth* DNA polymerase greatly improved sensitivity of PCR clonality analysis in the FR3/JH IgH gene segment, as applied in FFPE FL, gastric MALT lymphoma, and gastric DLBCL samples. Our method benefits from the 3′→5′ exonuclease activity, which appears to help in achieving superior fit of the primers to the rearranged IgH gene segments. The sensitivity of our assay seems to be similar to PCR methods that employ DNA from fresh/frozen tissues. In addition, the serial dilution of target DNA proved to be useful to avoid misinterpretation of inconsistent size bands that may be revealed due to the minute amount or poor quality of the B-cell DNA. The method we introduced here is optimally sensitive, fast and easy for diagnostic applications even in small routinely-processed paraffin-embedded tissue samples and can be easily adapted in any molecular pathology laboratory.

Acknowledgements This work was supported by a research grant of the Egészségügyi és Tudományos Tanács, Hungary (no. ETT 479 07/2000), by the Zoltan Magyary post-doctoral fellowship of the Foundation for Hungarian Higher Education and Research (Ministry of Education, Hungary) and by the Janos Bolyai Research Fellowship of the Hungarian Academy of Sciences. The authors thank Mr. Frank van der Panne for the photographic work.

References

1. Aiello A, Giardini R, Tondini C, Balzarotti M, Diss T, Peng H, Delia D, Pilotti S (1999) PCR-based clonality analysis: a reliable method for the diagnosis and follow-up monitoring of conservatively treated gastric B-cell MALT lymphomas? Histopathology 34:326–330
2. Bahler DW, Campbell MJ, Hart S, Miller RA, Levy S, Levy R (1991) Ig VH gene expression among human follicular lymphomas. Blood 78:1561–1568
3. Cheng S, Fockler C, Barnes WM, Higuchi R (1994) Effective amplification of long targets from cloned inserts and human genomic DNA. Proc Natl Acad Sci U S A 91:5695–5699
4. Derksen PWB, Langerak AW, Kerkhof E, Wolvers-Tettero ILM, Boor PPC, Mulder AH, Vrints LWMA, Coebergh JW, Van Krieken JHJM, Schuuring E, Kluin PM, Van Dongen JJM (1999) Comparison of different polymerase chain reaction-based approaches for clonality assessment of immunoglobulin heavy-chain gene rearrangements in B-cell neoplasia. Mod Pathol 12:794–805
5. Elenitoba-Johnson KS, Bohling SD, Mitchell RS, Brown MS, Robetorye RS (2000) PCR analysis of the immunoglobulin heavy chain gene in polyclonal processes can yield pseudoclonal bands as an artifact of low B cell number. J Mol Diagn 2:92–96
6. Gleissner B, Maurer J, Thiel E (2000) Detection of immunoglobulin heavy chain gene rearrangements in B-cell leukemias, lymphomas, multiple myelomas, monoclonal and polyclonal gammopathies. Leuk Lymphoma 39:151–155
7. Gong JZ, Zheng S, Chiarle R, De Wolf-Peeters C, Palestro G, Frizzera G, Inghirami G (1999) Detection of immunoglobulin κ light chain rearrangements by polymerase chain reaction. Am J Pathol 155:355–363
8. Holland PM, Abramson RD, Watson R, Gelfand DH (1991) Detection of specific polymerase chain reaction product by utilizing the 5′→3′ exonuclease activity of *Thermus aquaticus* DNA polymerase. Proc Natl Acad Sci U S A 88:7276–7280
9. Küppers R, Rajewsky K, Hansmann ML (1997) Diffuse large cell lymphomas derived from mature B cells carrying V region genes with a high load of somatic mutation and evidence of selection for antibody expression. Eur J Immunol 27:1398–1405
10. Küppers R, Klein U, Hansmann ML, Rajewsky K (1999) Cellular origin of human B-cell lymphomas. N Engl J Med 341:1520–1529
11. Linke B, Bolz I, Pott C, Hiddemann W, Kneba M (1995) Use of UITma DNA polymerase improves the PCR detection of rearranged immunoglobulin heavy chain CDR3 junctions. Leukemia 9:2133–2137
12. Luthra R, McBride JA, Cabanillas F, Sarris A (1998) Novel 5′ exonuclease-based real-time PCR assay for the detection of

t(14;18)(q32;q21) in patients with follicular lymphoma. Am J Pathol 153:63–68
13. McCarthy KP, Sloane JP, Wiedemann LM (1990) Rapid method for distinguishing clonal from polyclonal B cell populations in surgical biopsy specimens. J Clin Pathol 43:429–432
14. Qin Y, Greiner A, Trunk MJ, Schmausser B, Ott MM, Muller-Hermelink HK (1995) Somatic hypermutation in low-grade mucosa-associated lymphoid tissue-type B-cell lymphoma. Blood 86:3528–34
15. Ramasamy I, Brisco M, Morley A (1992) Improved PCR method for detecting monoclonal immunoglobulin heavy chain rearrangement in B cell neoplasms. J Clin Pathol 45:770–775
16. Segal GH, Jorgensen T, Scott M, Braylan RC (1994) Optimal primer selection for clonality assessment by polymerase chain reaction analysis: II. Follicular lymphomas. Hum Pathol 25:1276–1282
17. Slack DN, McCarthy KP, Wiedemann LM, Sloane JP (1993) Evaluation of sensitivity, specificity, and reproducibility of an optimised method for detecting clonal rearrangements of immunoglobulin and T-cell receptor genes in formalin-fixed, paraffin-embedded sections. Diagn Mol Pathol 2:223–232
18. Sninsky J, Gelfand D (1993) *UITma* DNA polymerase: the only proofreading enzyrne guaranteed for PCR. Amplifications 11:12–13
19. Stewart AK, Schwartz RS (1994) Immunoglobulin V regions and the B cell. Blood 83:1717–1730
20. Taylor JME, Spagnolo DV, Kay PH (1997) B-cell target DNA quantity is a critical factor in the interpretation of B-cell clonality by PCR. Pathology 29:309–312
21. Trainor KJ, Brisco MJ, Story CJ, Morley AA (1990) Monoclonality in B-lymphoproliferative disorders detected at the DNA level. Blood 75:2220–2222

Virchows Arch (2003) 443:649–654
DOI 10.1007/s00428-003-0892-1

ORIGINAL ARTICLE

Ana-Maria Bamberger · Antonis Makrigiannakis · Kerstin Röser · Jessica Radde · Tanja Carstens · Aljoscha M. Flohr · Christoph M. Bamberger · Jörn Bullerdiek · Thomas Löning

Expression of the high-mobility group protein HMGI(Y) in human trophoblast: potential role in trophoblast invasion of maternal tissue

Received: 10 March 2003 / Accepted: 31 July 2003 / Published online: 11 September 2003
© Springer-Verlag 2003

Abstract The high-mobility group protein HMGI(Y) is a member of a family of non-histone chromosomal proteins, which have been implicated in the regulation of inducible gene transcription, integration of retroviruses into chromosomes and induction of neoplastic transformation and metastatic progression in cancer cells. The human trophoblast is a tissue that shares proliferation capacity and invasiveness with neoplastic tissues, but in which these processes are tightly regulated. In the present study, we analyzed the expression of HMGI(Y) in the human placenta using immunohistochemistry. We found expression of HMGI(Y), with nuclear localization, in the villous cytotrophoblast (vCT), which is a highly proliferative cell type. In contrast, the majority of the nuclei of the villous syncytiotrophoblast, a terminally differentiated tissue, was negative. Interestingly, expression of HMGI(Y) was strongest in anchoring villi at the implantation site and in extravillous (intermediate) trophoblast (EVT) invading the maternal decidua. As vCT cells differentiate to become EVT, the HMGI(Y) protein appears to switch from a nuclear to a cytoplasmic localization. Expression of HMGI(Y) in isolated trophoblast populations in primary cell culture was also confirmed using Western-blot analysis. This study shows for the first time expression and localization of HMGI(Y) in the subpopulations of placental tissue.

Keywords High-mobility group protein · Human trophoblast · Trophoblast · Maternal tissue

A.-M. Bamberger · K. Röser · J. Radde · T. Carstens · T. Löning
Department of Gynecopathology,
Institute of Pathology University Hospital Eppendorf,
Hamburg, Germany

C. M. Bamberger
Department of Internal Medicine,
University Hospital Eppendorf, Hamburg, Germany

A. Makrigiannakis
Department of Obstetrics and Gynecology,
Medical School, University of Crete, Heraklion, Greece

A. M. Flohr · J. Bullerdiek
Center for Human Genetics,
University of Bremen, Bremen, Germany

A.-M. Bamberger (✉)
Institute of Pathology,
University Hospital Eppendorf,
Martinistrasse 52, 20246 Hamburg, Germany
e-mail: bamberger@uke.uni-hamburg.de
Tel.: +49-40-428033162
Fax: +49-40-428039252

Introduction

The high mobility group I (HMG I) proteins are a family of non-histone chromatin-associated proteins [5, 14, 22, 31]. HMGI and HMGY are isoforms derived from the same gene, HMG I(Y), located on chromosome 6 (6p21) and generated by alternative splicing of the pre-mRNA. They differ by 11 amino acids present in HMGI but deleted in HMGY [11, 15, 16]. Mammalian HMGI/Y proteins function as architectural transcription factors, which participate in multi-protein activating structures on target gene promoters and which have been shown to be implicated in various cellular processes, including regulation of inducible gene expression, integration of retroviruses into chromosomes and induction of neoplastic transformation and metastatic promotion of cancer cells [20, 26].

HMGI(Y) proteins are highly expressed during early stages of embryonic development, and their gene expression is either completely silent or markedly (approximately 200-fold) reduced in adult tissues [7, 27, 35]. As for neoplastic transformation, the first evidence for an oncogenic potential of HMGI(Y) proteins and their causal involvement in tumorigenesis came from the analysis of sporadic chromosomal translocations in human tumors [17], showing that HMGI(Y) is the target of 6p21.3 rearrangements in various benign mesenchymal tumors. Similarly, rearrangements on human chromosome 12q15, an event frequently found in benign solid tumors, were

shown to also involve a high-mobility group protein, HMGI-C [29].

The trophoblast is the first tissue to differentiate in the mammalian conceptus, and its normal development and specific properties are crucial for both implantation and further survival of the embryo. Furthermore, the placenta is unique in its ability to proliferate and invade another tissue in a fashion similar to malignant tumors, but is tightly controlled both spatially and temporally. It is, thus, a very interesting model for the study of molecular mechanisms involved in these processes and for differentiating them from those implicated in tumor progression.

During development of the human placenta, the cytotrophoblast (CT) proliferates and gives rise to the differentiated syncytiotrophoblast (ST) on the villous surface and to the extravillous (intermediate) trophoblast (EVT), which invades the maternal tissues and provides the anchoring of the placenta and the conceptus at the maternal–fetal interface [30].

The present study was designed to investigate the expression pattern of HMGI(Y) in the human placenta using immunohistochemistry. Furthermore, expression was investigated in isolated placental cells in primary culture using Western-blot analysis.

Materials and methods

Tissue collection

The tissue material was selected following histological review from the files of the Department of Gynecopathology, University Hospital Eppendorf, Hamburg. Only normal placentae were included in this study (for the second-trimester cases, these represented late abortions, i.e., for psychiatric indications. Cases with chromosomal abnormalities were not included). For immunohistochemistry, specimens that had been routinely fixed in 4% buffered formalin and embedded in paraffin were used. A total of 20 samples were analyzed, including 7 first-trimester, 6 second-trimester and 7 third-trimester samples.

Immunohistochemistry

Serial sections of 4–6 μm were cut from the paraffin blocks and mounted on 3-amino propyl tri-ethoxysilone (APES)-coated slides, deparaffinized in xylene and rehydrated in graded alcohol to TBS (Tris buffered saline; 50 mM Tris, 150 mM NaCl, pH 7.4). The slides were microwaved for 5×2 min in 10 mM citrate, pH 6.0. After cooling down for 20 min, the slides were washed in TBS, blocked for 20 min at room temperature with normal rabbit serum (Dako, Glostrup, Denmark), diluted 1:20 in TBS and incubated overnight at 4°C with HMGI(Y) affinity-purified goat polyclonal antibody (N-19; Santa Cruz Biotechnology) diluted 1:25–1:50. Omission of the first antibody was used for negative controls. Slides were reacted with biotin-labeled corresponding secondary antibody, incubated with preformed avidin biotinylated enzyme complex (ABC)-complex (Vectastain; Vector Laboratories, Burlingame, CA, USA) and detected with diaminobenzidine (DAB) kit (Vectastain; Vector Laboratories, Burlingame, CA, USA). The slides were counterstained with hemalaun and mounted with glycerin/gelatin.

Isolation of invasive and non-invasive trophoblast populations

Cultures of first-trimester invasive and non-invasive trophoblast populations were established and characterized as reported previously [1]. Briefly, eight to ten placentae (5–12 weeks) obtained after legal termination of pregnancy were washed in sterile phosphate buffer saline (s-PBS), and areas rich in chorionic villi were selected and minced between scalpel blades and were subjected to three sequential 10-min treatments with 0.125 % trypsin and 0.2 mg/ml DNAse I (Boehringer Mannheim, Germany) in s-PBS containing 5 mM $MgCl_2$. Cells released from each 10-min step were pooled and filtered through two layers of muslin, resuspended in 70% percoll (Pharmacia, Uppsala, Sweden) at a density of 2×10^5 cells/ml, and put under 20 ml of 25% percoll. Next, 10 ml s-PBS was put on top of the 25% percoll and a gradient was established by centrifuging for 20 min at 800×*g*. Cells from the middle band (density 1.048–1.062 g/ml) of the gradient were pooled, washed in s-PBS and seeded at a density of 1×10^6 cells/ml of keratinocyte growth medium (KGM) supplemented with 10% fetal calf serum (FCS).

Cells were identified as trophoblast using immunocytochemical staining with monoclonal antibodies to cytokeratin (Dako-CK, MNF 116 and 35BH11; 1:100). Their functional ability to produce hormones and the 92-kDa and 72-kDa gelatinases were described previously [1].

In vitro invasion assay

The invasive characteristics of the EVT cells were determined by an in vitro matrigel invasion assay as described [1] using transwells with a polycarbonate filter of 2.5 cm diameter and 8 μm pore size. The upper surface of the filter was coated with Matrigel (Collaborative Research, Bedford, MA; dilution 1:20 with KGM). The bottom chamber was filled with 3 ml of KGM containing 10% FCS. Trophoblast cells labeled for 72 h with 10 μci/ml H^3-thymidine in KGM were trypsinized, washed and resuspended at a density of 1.0×10^5 cells/ml KGM containing 10% FCS, and 2 ml of the labeled cell suspension was added to the upper well of the transwell chamber. After 72 h of incubation, the cells from the lower wells were harvested and used for Western-blot analysis.

Western-blot analysis of human placental tissue and trophoblast cells in primary culture

Extraction of proteins from endometrial tissue, HeLa cells (used as a positive control) and villous and EVT cells was carried out in PBS in the presence of 1% NP40 and protease inhibitors as previously described [2]. Sodium dodecyl sulfate–polyacrylamide gel electrophoresis (SDS-PAGE) was performed in a 7.5% polyacrylamid gel under reducing conditions, applying 50 μg of each sample of the concentrated protein extract. After electrophoretic transfer to nitrocellulose and blocking in TBS containing 5% bovine serum albumin (BSA) for 2 h, the anti-HMGI(Y) antibody (same as used for immunohistochemistry) was added (dilution 1:1000) and incubated overnight at 4 C. Detection was carried out with peroxidase.

Results

Immunohistochemical localization of HMGI(Y) in the human placenta

Representative results of immunohistochemical detection of HMGI(Y) in placental structures are shown in Fig. 1. As can be observed, HMGI(Y) is expressed in the villous CT (panels A–D), where it has a nuclear localization. The

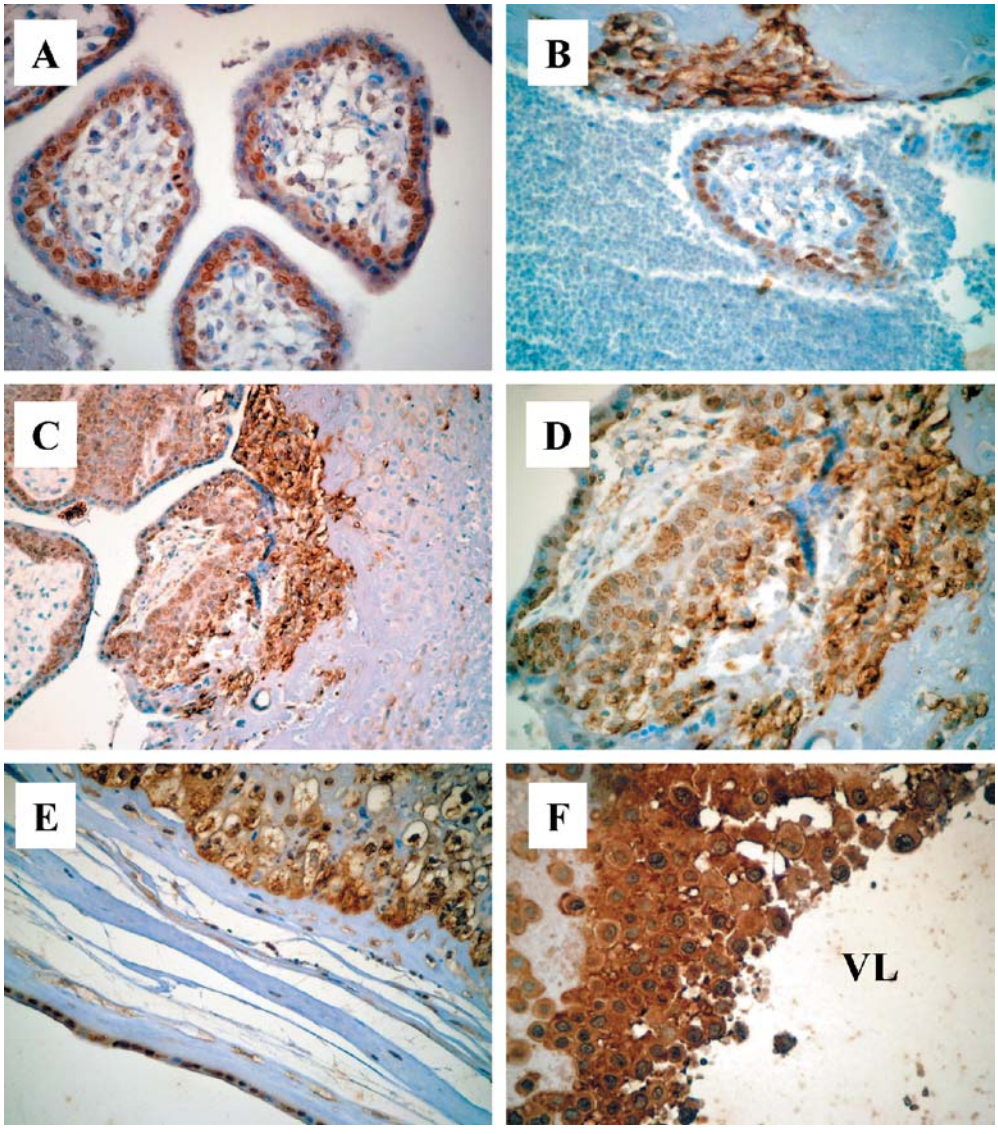

Fig. 1 Immunohistochemical localization of high-mobility group protein [HMGI(Y)] in the human placenta. **A** Chorionic villi showing nuclear expression of HMGI(Y) in cells of the villous cytotrophoblast. In contrast, most nuclei of the syncytiotrophoblast are HMGI(Y)-negative (×400). **B** Nuclear expression in the villous cytotrophoblast and almost absent expression in the villous syncytiotrophoblast. Additionally, strong, predominantly cytoplasmic/membranous expression pattern in the extravillous trophoblast invading the maternal decidua (×400). **C** Anchoring villus showing nuclear expression of HMGI(Y) in the cytotrophoblast and mostly membranous/cytoplasmatic expression in the emerging extravillous trophoblast invading the maternal decidua (×200). **D** Higher magnification of **C** showing a predominantly nuclear expression of HMGI(Y) in the proximal extravillous trophoblast and mostly cytoplasmatic/membranous expression in the deeper (interstitial) extravillous trophoblast invading the maternal decidua and maternal vessels (×400). **E** Both nuclear and cytoplasmatic/membranous expression of HMGI(Y) in extravillous trophoblast of the chorion laeve (×400). **F** Predominantly cytoplasmatic/membranous expression of HMGI(Y) in the endovascular extravillous trophoblast (×400). *VL* vascular lumen

nuclei of the terminally differentiated villous ST, however, were mostly HMGI(Y) negative. Also, expression of HMGI(Y) can be observed in some nuclei of villous core cells. As can be seen in panels B, C and D, expression of HMGI(Y) is strongest in anchoring villi at the implantation site and, specifically, in EVT invading the maternal decidua. Interestingly, in these cells, expression appears to switch from the nuclear pattern observed for CT (also the CT of the anchoring villi show this nuclear pattern) to a cytoplasmic localization. This pattern of expression is consistently observed in placenta samples from the first and second trimesters.

Expression of HMGI(Y) is also seen in the EVT of the chorion laeve (panel E) and in the amniotic epithelial cells. Cytoplasmic expression of HMGI(Y) is also observed in cells of the decidualized endometrium and in endometrial glands of pregnancy endometrium as well as in glandular epithelium of normal non-pregnant endometrium (not shown).

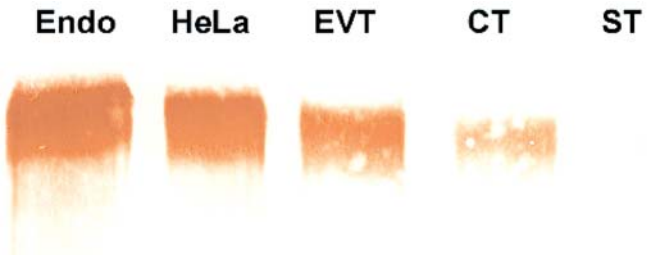

Fig. 2 Western-blot analysis of placental tissue (*panel A*) and isolated trophoblast cells in primary culture (*panel B*) showing a band of approximately 20 kDa corresponding to high-mobility group protein

Western-blot analysis of human trophoblast cells in primary culture

As can be seen in Fig. 2, Western-blot analysis with the same anti-HMGI(Y) antibody as has been employed for immunohistochemistry shows strong HMGI(Y) expression in the positive controls (Endo=endometrium and HeLa cells). From the trophoblast cell populations in primary culture, the invasive trophoblast (EVT) shows strong expression, followed by villous CT. Very weak/absent detection is observed in villous ST, corresponding to the observations made by analyzing the immunohistochemistry data, where expression was also strongest in EVT, while villous ST was frequently negative.

Discussion

In the present study, we used immunohistochemistry to investigate the expression pattern of the high-mobility group protein HMGI(Y) in the human placenta. In addition, HMGI(Y) expression was analyzed using Western blot on placental tissue and isolated placental cells in primary culture.

As shown in Fig. 1, HMGI(Y) is strongly expressed in the human placenta in both villous and extravillous trophoblast, with different subcellular localization patterns. In the villous cytotrophoblast (vCT), expression is strictly nuclear, with a granular appearance, indicating association with chromatin. The CT is a highly proliferative tissue, in which HMGI(Y) could be implicated in regulating proliferation, as has been shown to be the case for other rapidly dividing cells [20]. In the terminally differentiated villous syncytiotrophoblast (vST), the majority of nuclei were negative, indicating that HMGI(Y) expression is probably shut down during differentiation of CT into ST, similar to later embryonic developmental stages [7, 27, 35]. Aside from differentiating into ST, the CT also differentiates into EVT. The EVT can be further divided into proximal EVT originating from the anchoring villi, deep interstitial EVT invading the decidual stroma and the myometrium, endovascular trophoblast, which assumes endothelium-like characteristics, and "intermediate-like" EVT of the chorion laeve [6, 8, 36]. Interestingly, we observed very strong expression of HMGI(Y) in the EVT. Cytoplasmatic expression of HMGI(Y) was also found in the deeper (interstitial) EVT invading the maternal decidua, and the maternal vessels (endovascular trophoblast), as well as in the EVT of the chorion laeve. As found by others (A. Flohr, personal communication) and confirmed in this study, cytoplasmatic HMGI(Y) expression is also found in glandular epithelia of both cycling and pregnant endometrium and in decidual cells.

Regarding the possible roles of HMGI(Y) in the human placenta, these could obviously include regulation of cell proliferation in the CT and proliferation stop correlated with differentiation in the ST. In a previous study, we demonstrated that the proliferative CT expressed the cell cycle promoter cyclin E but not the cell cycle inhibitor p27, while ST showed an inverse expression pattern [3]. While expression of p27 is regulated mostly at the post-transcriptional level, expression of cyclin E is transcriptionally regulated and might be influenced by HMGI(Y). One could speculate that this could also be the case for the EVT, where expression of both proliferation-inducing molecules, such as cyclin E [3], adhesion molecules, such as CEACAM1 [4], or of invasion-promoting enzymes, such as matrix-metallo proteinase 9 (MMP-9) could be influenced by HMGI(Y). In this line of thought, one should notice that HMGI(Y) was shown to modulate expression of adhesion molecules, such as E-selectin [19, 34], which can function as a ligand for CEACAM1 [18], which is specifically expressed by EVT [4]. Also, junB and fra-1, members of the AP-1 transcription factor family, have been shown to be positively regulated by HMGI(Y) [33], and the MMP-9 promoter has been shown to carry AP-1 responsive and be regulated by AP-1 transcription factors [12, 28]. Furthermore, in invasive breast cancer cells (MDA-MB 231), which highly express HMGI(Y), treatment with an inhibitor of MMP-9 resulted in a reduction of both invasive capability of the cells in vitro and reduced expression of HMGI(Y), indicating the existence of a link among invasiveness, expression of HMGI(Y) and MMP-9 [21]. Since EVT cells invading the maternal decidua also use MMP-9 as a main matrix-degrading enzyme [25], this observation might apply to EVT as well. Furthermore, in mice lacking junB, lethality due to defects in placental development was observed, along with a downregulation of MMP-9 expression [13], and, as mentioned, junB has, in another context, been shown to be under the influence of HMGI(Y) [33].

However, the cytoplasmatic localization of HMGI(Y) in the deeper EVT indicates that it might also play roles different from those previously described. It is thus possible that it might be associated with proteins localized to the cytoplasm, or that it might be secreted and act as an extracellular ligand, as has recently been shown to be the case for HMGB1 [23]. HMG-B1 (also called amphoterin) has been shown to be secreted by neurons and be retained associated with their plasma membranes at the leading edge of migration [10] and with promoter cell migration

of vascular smooth muscle cells and fibroblasts [9, 23]. It is possible that HMGI(Y) might play a similar role, for instance, in the migration of EVTs, yet data supporting this hypothesis are lacking to date. Furthermore, HMGB1 appears to play a role in the activation of extracellular proteases, which are important for tissue invasion. It has been shown to bind to several components of the plasminogen activation system and enhance activation of tissue plasminogen activator [24] and also to activate MMP-2 and MMP-9 [23, 32], which play an important role in trophoblast invasion.

The present study shows, to our knowledge, for the first time the expression pattern of HMGI(Y) in the cellular populations of the human placenta and its nuclear localization in villous cytotrophoblast and cytoplasmatic localization in EVT cells. Further studies will now be necessary to investigate the new possible functions of this molecule in both the process of trophoblast proliferation, differentiation and invasion and in the related process of tumor invasion and metastasis.

References

1. Aboagye-Mathiesen G, Zdravkovic M, Toth FD, Ebbesen P (1997) Effects of human trophoblast-induced interferons on the expression of c-fms/CSF-1R, EGF-R and c-erbB2 in invasive and non-invasive trophoblast. Placenta 18:155–161
2. Bamberger AM, Riethdorf L, Nollau P, Naumann M, Erdmann I, Götze J, Brümmer J, Schulte HM, Wagener C, Löning T (1998) Dysregulated expression of CD66a (BGP, C-CAM), an adhesion molecule of the CEA family, in endometrial cancer. Am J Pathol 152:1401–1406
3. Bamberger AM, Sudahl S, Bamberger CM, Schulte HM, Löning T (1999) Expression pattern of the cell cycle inhibitor p27 and the cell-cycle promoter cyclin E in the human placenta throughout gestation: Implications for the control of proliferation. Placenta 20:401–406
4. Bamberger AM, Sudahl S, Löning T, Wagener C, Bamberger CM, Drakakis P, Coutifaris C, Makrigiannakis A (2000) The adhesion molecule CEACAM1 (CD66a, C-CAM, BGP) is specifically expressed by the extravillous intermediate trophoblast. Am J Pathol 156:1165–1170
5. Bewley CA, Gronenborn AM, Clore GM (1998) Minor groove-binding architectural proteins: structure, function and DNA recognition. Annu Rev Biopys Biomol Struct 27:105–131
6. Burrows TD, King A, Loke YW (1996) Trophoblast migration during human placental implantation. Hum Reprod Update 2:307–321
7. Chiappetta G, Bandiera A, Berlingieri MT (1995) The expression of the high mobility group HMGI(Y) proteins correlates with the malignan phenotype of human thyroid neoplasias. Oncogene 10:1307–1314
8. Damsky CH, Librach C, Lim KH, Fitzgerald ML, McMaster MT, Janatpour M, Zhou Y, Logan SK, Fisher SJ (1994) Integrin switching regulates normal trophoblast invasion. Development 120:3657–3677
9. Degryse B, Bonaldi T, Scaffidi P, Müller S, Resnati M, Sanvito F, Arrigoni G, Bianchi ME (2001) The High Mobility Group Boxes of the nuclear protein HMG1 induce chemotaxis and cytoskeleton organization in rat smooth muscle cells. J Cell Biol 152:1197–2006
10. Fages C, Nolo R, Huttunen HJ, Eskelinen E, Rauvala H (2000) Regulation of cell migration by amphoterin. J Cell Sci 113:611–620
11. Friedmann M, Holth LT, Zoghbi HY, Reeves R (1993) Organization, inducible-expression and chromosome localization of the human HMG-I(Y) nonhistone protein gene. Nucleic Acids Res 21:4259–4267
12. Huhtala P, Tuuttila A, Chow LT, Lohi J, Keski-Oja J, Tryggvason K (1991) Complete structure of the human gene for 92-kDa type IV collagenase: divergent regulation of expression for the 92- and 72- kilodalton enzyme genes in HT-1080 cells. J Biol Chem 266:16485–16490
13. Jochum W, Passegue E, Wagner EF (2001) AP-1 in mouse development and tumorigenesis. Oncogene 20:2401–2412
14. Johns EW (1982) History, definitions and problems. The HMG proteins. Academic Press, London, pp 1–7
15. Johnson KR, Lehn DA, Elton TS, Barr PJ, Reeves R (1988) Complete murine cDNA sequence, genomic structure, and tissue expression of the high mobility group protein HMGI(Y). J Biol Chem 263:18338–18342
16. Johnson KR, Lehn DA, Reeves R (1989) Alternative processing of mRNAs encoding mammalian chromosomal hig-mobility-group proteins HMG-I and HMG-Y. Mol Cell Biol 9:2114–2123
17. Kazmierczak B, Dal Cin P, Wanschura S, Borrmann L, Fusco A, Van den Berghe H, Bullerdiek J (1998) HMGIY is the target of 6p21.3 rearrangements in various benign mesenchymal tumors. Genes Chromosomes Cancer 23:279–285
18. Kuijpers TW, Hoogerwerf M, Van der Laan LJ, Nagel G, Van der Schoot CE, Grunert F, Roos D (1992) CD66 nonspecific cross-reacting antigens are involved in neutrophil adherence to cytokine-activated endothelial cells. J Cell Biol 118:457–466
19. Lewis H, Kaszubska W, DeLamarter JF, Whelan J (1994) Cooperativity between two NF-kappa B complexes, mediated by high-mobility-group protein I(Y), is essential for cytokine-induced expression of the E-selectin promoter. Mol Cell Biol 14:5701–5709
20. Liu F, Cahu K, Arlotta P, Ono SJ (2001) The HMG I Proteins: dynamic roles in gene activation, development and tumorigenesis. Immunol Res 23:35–51
21. Liu WM, Guerra-Vladusic FK, Kurakata S, Lupu R, Kohwi-Shigematsu T (1999) HMG-I(Y) recognizes base-unpairing regions of matrix attachment sequences and its increased expression is directly linked to metastatic breast cancer phenotype. Cancer Res 59:5695–5703
22. Lund T, Hotlund J, Fredriksen M, Laland SG (1983) On the presence of two new high mobility group-like proteins in HeLa cells. FEBS Lett 152:163–167
23. Müller S, Scaffidi P, Degryse B, Bonaldi T, Ronfani L, Agresti A, Beltrame M, Bianchi ME (2001) The double life of HMGB1 chromatin protein: architectural factor and extacellular signal. EMBO J 20:4337–4340
24. Parkinen J, Rauvala H (1991) Interactions of plasminogen and tissue plasminogen activator (t-PA) with amphoterin. Enhancement of t-PA-catalyzed plasminogen activation by amphoterin. J Biol Chem 266:16730–16735
25. Polette M, Nawrocki B, Pintiaux A, Massenat C, Maquoi E, Volders L, Schaapa JP, Birembaut P, Foidart JM (1994) Expression of gelatinases A and B and their tissue inhibitors by cells of early and term human placenta and gestational endometrium. Lab Invest 71:838–846
26. Reeves R, Beckerbauer L (2001) HMGI/Y proteins: flexible regulators of transcription and chromatin structure. Biochem Biophys Acta 1519:13–29
27. Rogalla P, Drechsler K, Frey G, Henning Y, Helmke B, Bonk U, Bullerdiek J (1996) HMGI-C expression patterns in human tissues. Implications for the genesis of frequent mesenchymal tumors. Am J Pathol 149:775–779
28. Sato H, Seiki M (1994) Regulatory mechanism of 92 kDa type IV collagenase gene expression which is associated with invasiveness of tumor cells. Oncogene 8:395–405
29. Schoenmakers EF, Wanschura S, Mols R, Bullerdiek J, Van den Berghe H, Van de Ven WJ (1995) Recurrent rearrangements in the high mobility group protein gene, HMGI-C, in benign mesenchymal tumours. Nat Genet 10:436–444
30. Shih I-M, Kurman RJ (1997) New concepts in trophoblastic growth and differentiation with practical application for the

diagnosis of gestational trophoblastic disease. Verh Dtsch Ges Pathol 81:266–272
31. Strauss F, Varhavsky A (1984) A protein binds to a satellite DA repeat at three specific sites that would be brought into mutual proximity by DNA folding in the nucleosome. Cell 37:889–901
32. Taguchi A, Blood DC, del Toro G, Canet A, Lee DC, Qu W, Tanji N, Lu Y, Lalla E, Fu C, Hofmann MA, Kislinger T, Ingram M, Lu A, Tanaka H, Hori O, Ogawa S, Stern DM, Schmidt AM (2000) Blockage of RAGE-amphoterin signalling suppresses tumour growth and metastasis. Nature 405:345–360
33. Vallone D, Battista S, Pierantoni GM, Fedele M, Casalino L, Santoro M, Viglietto G, Fusco A, Verde P (1997) Neoplastic transformation of rat thyroid cells requires the junB and fra-1 gene induction which is dependent on the HMGI-C gene product. EMBO J 16:5310–5321
34. Whitley MZ, Thanos D, Read MA, Maniatis T, Collins T (1994) A striking similarity in the organization of the E-selectin and the beta-interferon gene promoters. Mol Cell Biol 14:6464–6475
35. Zhou X, Benson KF, Ashar HR, Chada K (1995) Mutation responsible for the mouse pygmy phenotype in the developmentally regulated factor HMGI-C. Nature 376:771–774
36. Zhou Y, Fisher SJ, Janatpour M, Genbacev O, Dejana E, Wheelock M, Damsky CH (1997) Human cytotrophoblasts adopt a vascular phenotype as they differentiate. A strategy for successful endovascular invasion? J Clin Invest 99:2139–2151

Virchows Arch (2003) 443:655–663
DOI 10.1007/s00428-003-0843-x

ORIGINAL ARTICLE

Hiroshi Hano · Satoshi Takasaki

Three-dimensional observations on the alterations of lobular architecture in chronic hepatitis with special reference to its angioarchitecture for a better understanding of the formal pathogenesis of liver cirrhosis

Received: 6 March 2003 / Accepted: 30 April 2003 / Published online: 19 July 2003
© Springer-Verlag 2003

Abstract For a better understanding of the formal pathogenesis of liver cirrhosis, the angioarchitecture of the liver lobule in chronic viral hepatitis was investigated three dimensionally. The histological reconstruction method, using serial histological sections, was adopted for the three-dimensional observation. Histology of the case showed chronic active hepatitis with occasional fibrous bridging of the portal to portal tract or hepatic vein. Graphic reconstructions revealed various degrees of altered angioarchitecture from place to place. While the conducting portion of the portal vein was almost preserved, the pathological changes mostly began at the parenchymal portion, especially second step or subsequent branches of the portal vein. In general, portal vein branches showed damage such as stenoses, disappearance, an increase and decrease in number and distorted spatial arrangements. Even in less damaged portal tracts, portal veins showed such changes to some extent. In severely damaged places with bridging fibrosis, a normal lobular angioarchitecture was completely lost; instead, portal veins, arteries and hepatic veins were tangled with each other. Parenchymal nutrition was suggested to be dependent on the remaining third-step portal branches or newly formed ones. However, the hepatic vein system had a tendency to be preserved and distributed fluently in the parenchyma. The distortion of these portal vessels indicated various degrees of loss of the lobular architecture. In conclusion, it is suggested that an early histological sign of cirrhosis develops in the course of chronic hepatitis.

H. Hano (✉) · S. Takasaki
Department of Pathology,
Jikei University School of Medicine,
3-25-8 Nishi-Shinbashi, Minato-ku, 105-8461 Tokyo, Japan
e-mail: hhano@jikei.ac.jp
Tel.: +81-3-34331111
Fax: +81-3-54720700

Keywords Lobular architecture · Lobular disorganization · Chronic hepatitis · Liver cirrhosis · Histologic reconstruction

Introduction

Liver cirrhosis is ultimately caused by diffuse and persistent injury to the liver. Although liver cirrhosis is pathologically defined briefly by regenerative nodules surrounded by diffuse fibrosis, the nodules show a variety of morphological features according to the cause and length of the diseased period. Instead of the morphological variety, it is indicated that there is essentially a common pathway to liver cirrhosis. The pathway is nothing but the process of breakup and rebuilding, namely restructuring, of the liver lobules [1, 9, 10, 16, 17, 22]. However, the precise formal pathogenesis of liver cirrhosis has remained unsolved.

Hence, we tried to clarify the three-dimensional alteration of the liver lobule with special reference to its angioarchitecture in chronic viral hepatitis in order to determine the formal pathogenesis regarding the transformation from chronic hepatitis to liver cirrhosis.

Materials and methods

A liver tissue with chronic viral hepatitis (C type) accompanied with liver cell carcinoma was used. The liver tissue of a 46-year-old Japanese male was resected surgically to remove the tumor. Tissue blocks were taken from the portion sufficiently apart from the tumor. A normal liver of an autopsied case of a 39-year-old Japanese male with cerebral bleeding was used as control. Tissue blocks were embedded in paraffin in the usual manner. Serial sections were cut 3.5 μm in thickness and stained with modified Masson's trichrome. The fundamental structures were outlined serially by free hand on sheets of tracing paper. The drawing on the sheets was facilitated by the use of a projection apparatus attached to a microscope. Completion of reconstruction was made step-by-step by overlapping the outlines.

Although we focused mainly on the portal system in this study, the arterial and biliary systems were also depicted in the drawings in as much detail as possible.

Results

A normal liver

The angioarchitectural reconstruction of the parenchymal portion of the normal liver is shown in Fig. 1 and Fig. 2. The former was 520 μm and the latter 120 μm in thickness. Hereafter, we use the terminology and conception defined by Matsumoto et al. [14, 15] with reference to the angioarchitecture of a normal liver. The portal system is divided into the conducting and parenchymal portions. The main function of the former is the transportation of blood, while the latter provides the angioarchitectural framework of the liver lobule in addition to blood transportation. The portal veins of the parenchymal portion are distinguished by three steps; the first, second and third step branches (Fig. 1). The first step branches arise directly from the terminal conducting portion. The second step branches are given off mainly nearly at a right angle from the first step ones and correspond to the portal veins in the portal tracts located in the periphery of the hexagonal classic lobule. These first and second steps are regularly distributed. The third branches show two main branching modes. One mode is that the third step branches occur nearly at a right angle from the second step ones and run with little connective tissue sheath along the boundary zone of adjacent lobules like the veins of a leaf. The other is a fork-like branching mode at the terminal of the parenchymal portion (Fig. 2). A group of adjoining third step branches formed the basic framework of a sickle-shaped sinusoidal bed (sickle zone) (Fig. 1). The sickle zone is distinguished by a high potential area of blood flow. Several sickle zones cover almost the entire surface of the classic lobule. The portion corresponding to the edge of the sickle zones forms a surface-like inflow front from which blood pours into the sinusoids. It is worth pointing out that the surface-like inflow front shows a systemic continuity throughout the liver (see Matsumoto et al. [14, 15]).

A three-dimensional holistic view of the angioarchitecture of the liver with chronic hepatitis by histological reconstruction under a low magnification

The light microscopic features of the case showed enlarged portal tracts with inflammatory cell infiltration and fibrosis, occasional fibrous bridging between the portal tracts or between the portal tract and central vein and scattered focal necrosis and interface hepatitis (Fig. 3). Although the bridging fibrosis suggested the local disorganization of the lobules, the basic structure of the lobules seemed to have a tendency to be maintained on the whole throughout the liver. The complexity of the

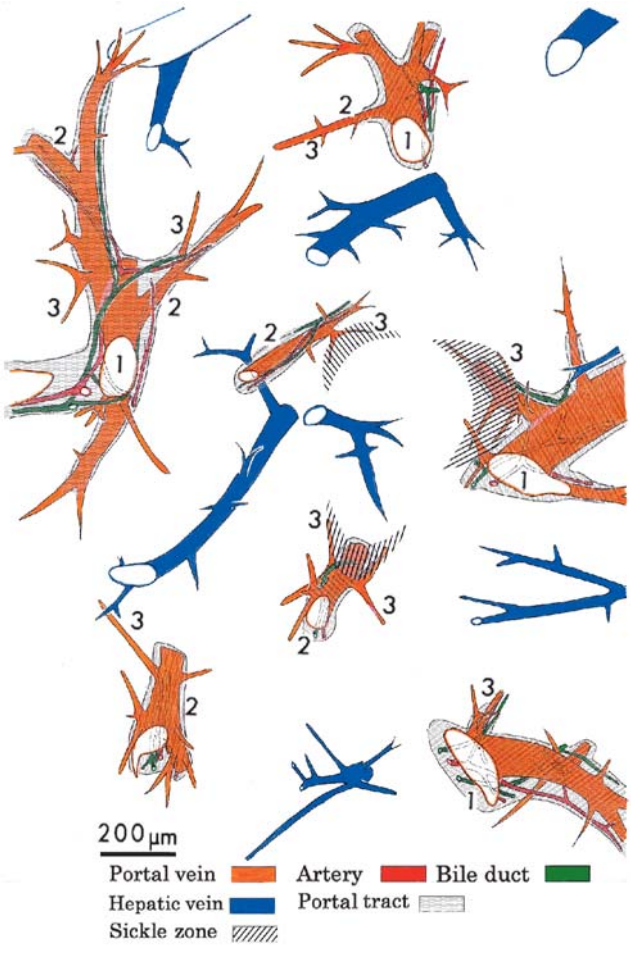

Fig. 1 Histological reconstruction of the normal liver at moderate magnification. The figure covers the parenchymal portion of the portal system composed of three step branches. Note the alternating arrangement of portal and hepatic veins and regular manner of ramification in the portal system. The third step branches form a basic structure of the liver lobule. Adjoining third step branches form a sickle zone with high potential blood flow (*hatched line area*). *1*: First step branch; *2*: second step branch; *3*: third step branch

vasculature was indicated by the increasing number of cut surfaces of blood vessels in the portal tracts.

The reconstruction was 480 μm in thickness and covered the range from the terminal trees of the conducting portion mainly to the second step branches of the portal vein and partly to the third steps (Fig. 4). Fibrous adhesions of the portal to portal tracts or to hepatic veins occasionally occurred and are indicated by arrows in the figure. In general, the first step branches of the portal vein and the corresponding hepatic veins showed a tendency to remain in the normal spatial relationship in that they were equally distributed in number (compare with Fig. 1). However, conspicuous changes in the angioarchitecture began at the second step, or subsequent branches, which showed a loss of regular distribution because they partly decreased and partly increased in number, were branched at various angles, ran

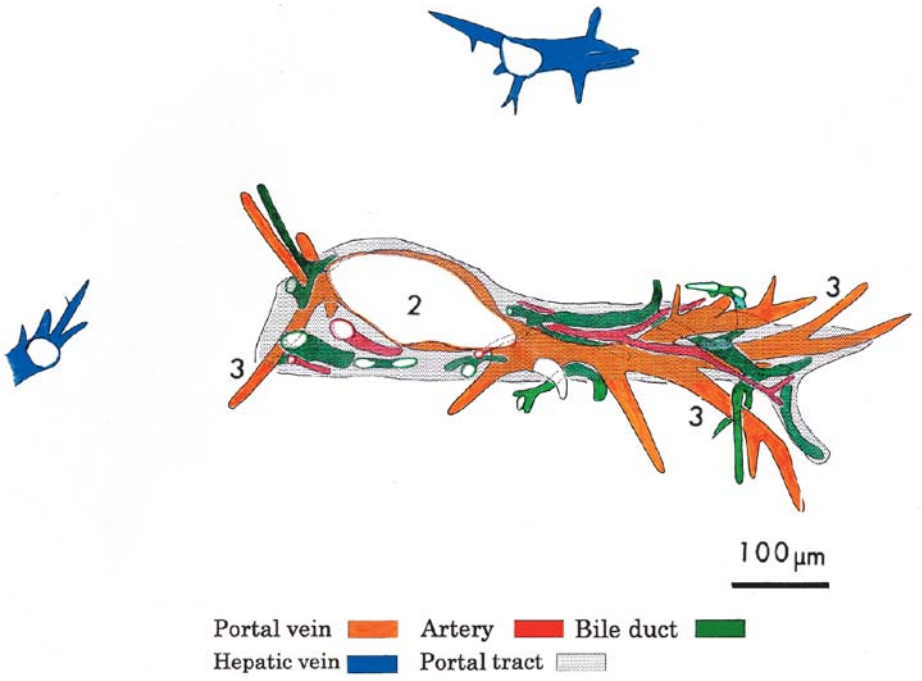

Fig. 2 Histological reconstruction of the normal liver at high magnification. Third step branches are given off nearly at a right angle in the left half of the figure and fork-like branching mode is shown at the terminal of the portal parenchymal portion in the right half. *2*: Second step branches; *3*: third step branches

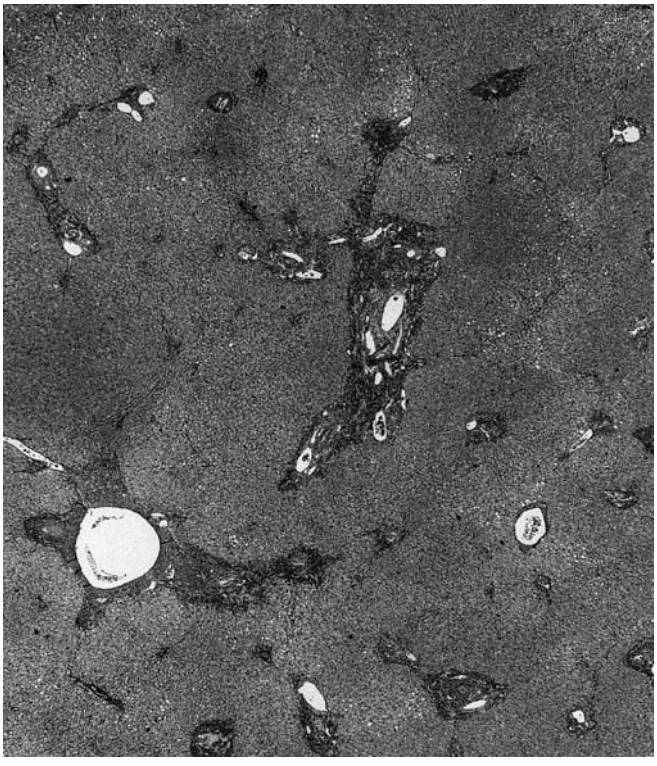

Fig. 3 Photomicrograph at low magnification. Portal areas are enlarged with lymphocyte infiltration and fibrosis. Fibrous bridging occasionally develops between portal-to-portal tract or hepatic vein. However, basic structures of the liver seem to be preserved in general

in close proximity to each other and were bent sharply. These features resulted in the loss of a regular pattern and complicated appearance of the angioarchitecture. However, the hepatic vein system tended to maintain a basic constellation except for some adherent lesions to the portal tracts.

These findings of the altered constellation of blood vessels appear to indicate the early phase of the loss of the basic framework of the lobular angioarchitecture, which was difficult to demonstrate in a histological plane section.

The reconstruction of the portal area corresponding to the parenchymal portion with relatively less damage

Common features in this case were the enlarged portal tracts accompanied by inflammation and fibrosis without fibrous bridging (Fig. 5). The reconstruction of this area was 280 μm in thickness and covered the terminal branch of the conducting portion and all the step branches of the parenchymal portion (Fig. 6). The second step branch b was a distal branch of a. Although the angioarchitecture seemed to remain normal as a rule, a precise examination revealed that branching of b portal vein was severely distorted. It gave off many more branches, corresponding to third step ones, than are normal (arrowheads in Fig. 6; compare with Fig. 2). This suggested that these branches contained not only preexisting branches, but also newly formed ones. Additionally, they were arranged in a disorderly fashion. Nearly half of them could not be traced because they were stenosed and buried in the connective tissue (arrows in Fig. 6). The remainder ran

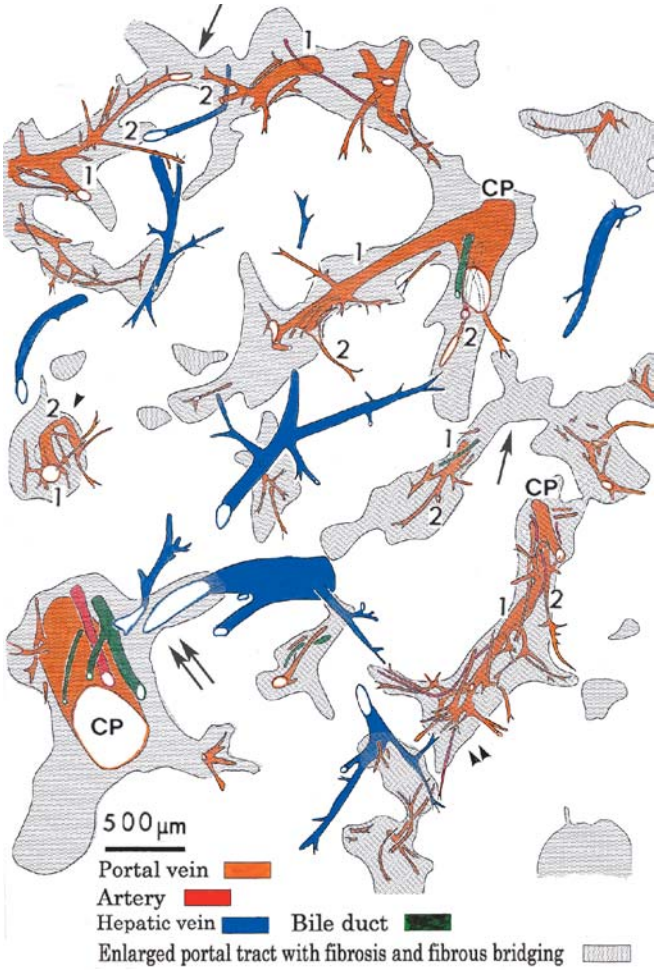

Fig. 4 Histological reconstruction of chronic hepatitis at low magnification. Spatial arrangement of the distal conducting portion and the first step branches of the parenchymal portion of the portal system are preserved as a rule. Irregular manner of ramification begins roughly at the second step or subsequent branches of the portal vein. Fibrous bridging lesions are found between the portal to portal tracts (*arrows*) or hepatic veins (*double arrows*). Area with an increase in the number of branches is indicated by *double arrowheads*. A single *arrowhead* shows an abnormal bend of the portal vein. *CP* conducting portion, *1*: first step branch; *2*: second step branch; *3*: third step branch

into the sinusoid to perfuse the parenchyma (asterisks in Fig. 6).

The reconstructions of the angioarchitecture in the fibrous bridging lesions under a high magnification

The portal-central (p-c) fibrous bridging lesions in the parenchymal portion

A representative light microscopic picture of the lesions is shown in Fig. 7. The reconstruction of the angioarchitecture was 420 μm in thickness and mainly included the parenchymal portion of the portal vein (Fig. 8). The enlarged portal tracts b, c and d were connected with

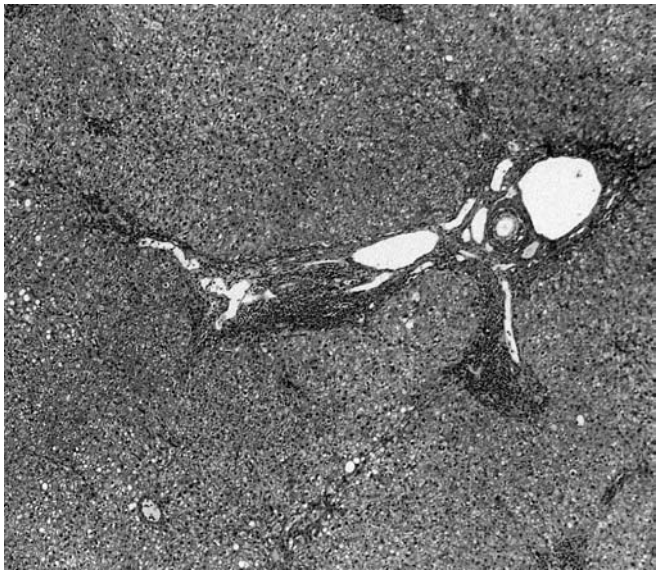

Fig. 5 Photomicrograph of histology of the reconstructed area demonstrated in Fig. 6. The portal area is inflamed and enlarged by fibrosis. Note the complexity of vasculature. Original magnification ×13

hepatic veins equivalent to the first step and its distal branches by irregular fibrous bands. Initially, the blood vessel arrangement appeared to be apparently unlike that of a normal liver in each area. In area b, it was not easy to identify the order of the portal branches. The portal veins, which were speculated to be the second step and its distal branches, ran in the fibrosed area. They gave off only a small number of branches on their course, resulting in a decrease of branches. Some branches were stenosed and buried in fibrosed tissue (arrows in Fig. 8), while the remainder reached the inside of the lobule (asterisks in Fig. 8). In area c, it was evident that the second step and its distal branches ran relatively randomly. Two portal veins were found to have run rather a long distance without effectively branching to the parenchyma and they finally disappeared with stenosis in the connective tissue (arrowheads in Fig. 8). Although area a seems to have a tendency to maintain the normal ramification pattern of portal veins, the first and second step branches became thicker and took tortuous courses. In more detail, while the branches equivalent to the third step branches were frequently found in parts, the portal vein ran simply without ramification in other parts as seen in area c (arrowhead in Fig. 8). The hepatic veins showed a distortion of their course and an increase in thickness; however, their terminal trees expanded in the lobule to drain sinusoidal flow. Thus, the drainage system was less damaged than the portal system.

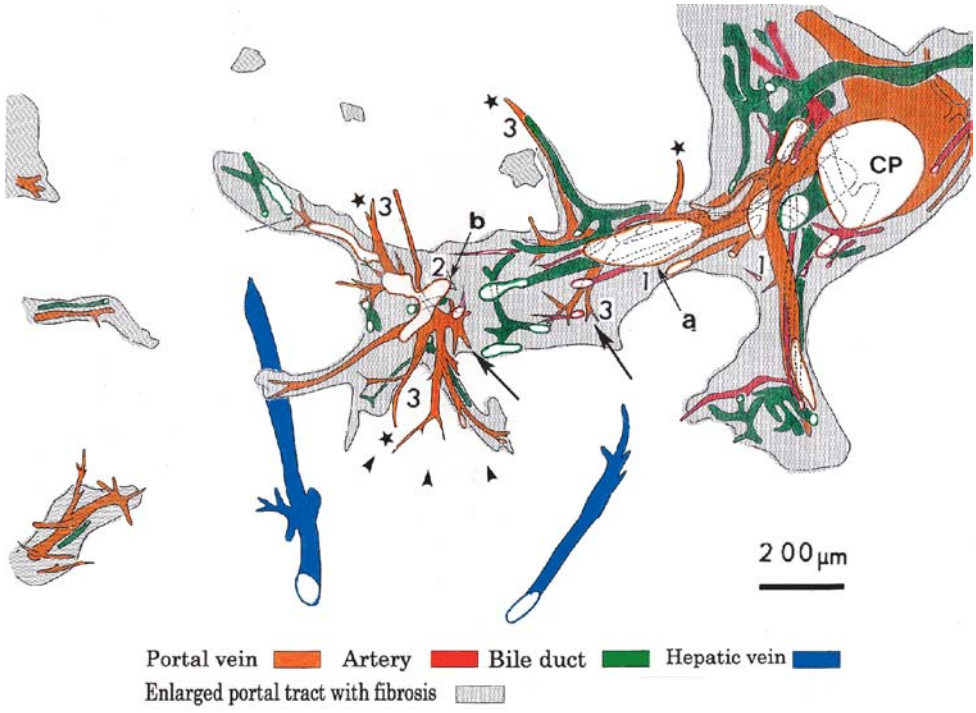

Fig. 6 Reconstruction of chronic hepatitis at moderate magnification. Angioarchitecture seems to be maintained as a rule. The number of third step corresponding branches increases and they run randomly (a part is indicated by *arrowheads*). While some of the third step branches are buried and disappear (*thick arrows*), the remaining ones reached the parenchyma to perfuse the cells (*asterisks*). Compare with Fig. 1. Branch *b* is a distal branch of *a*. *CP*: conducting portion; *1*: first step; *2*: second step; *3*: third step

The fibrous bridging lesion of the portal area to the hepatic vein corresponding to the conducting portion

A photomicrograph of the lesion and figure of its reconstruction are shown in Fig. 9 and Fig. 10. The latter was 670 μm thick. In the reconstructed area, roughly four fibrosed lesions (a, b, c and d) were observed to adhere to a thick hepatic vein corresponding to the conducting portion. Areas a and b were rich in vasculature, while the remainder showed a paucity of blood vessels. Areas a, b and d were identified as altered portal tracts because of the presence of portal veins that appeared most likely to be second step and their distal branches. Area c was also speculated to be fibrosed portal tract. The portal veins, arteries and hepatic veins were tangled with each other like ivy in area a. The portal veins showed abnormalities such as parallel running of two portal veins of the same order, slight tortuosity and paucity of branching. A few branches reached the edge of the parenchyma to nourish the cells (asterisk in Fig. 10). In the same area, hepatic veins were also found twisting their way through the other vessels. A normal angioarchitecture was not found. The intermingling of various vessels in the fibrous area resembled liver cirrhosis. These features indicated almost complete loss of lobular architecture. In area b, portal veins showed a ramification pattern similar to a normal ramification pattern to some extent. Nearly half of the branches equivalent to the third step ran into the parenchymal region (asterisks in Fig. 10). In both portal areas a and b, the development of arteries was conspicuous. The arteries sometimes ran over a long distance. However it was difficult to find branches that terminated clearly in the parenchyma to nourish the liver cells. Areas

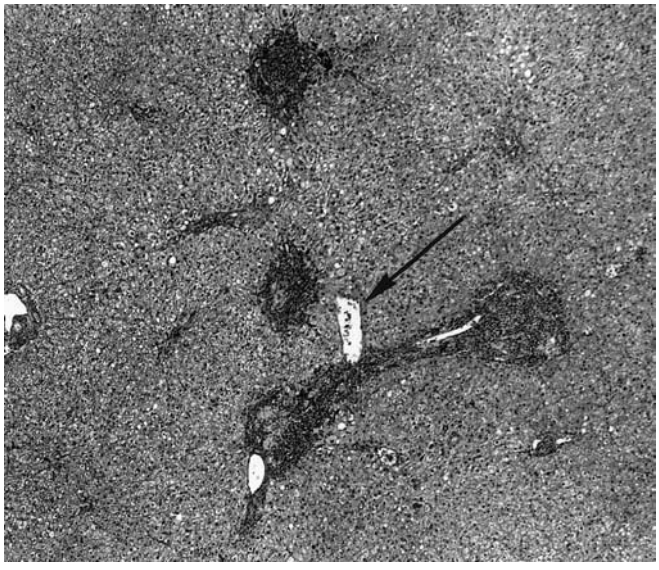

Fig. 7 Photomicrograph of the reconstructed area demonstrated in Fig. 8. Portal areas are inflamed and enlarged by fibrosis. Portal areas are connected by fibrosis with the hepatic vein (*arrow*). Paucity of vessels is conspicuous in the fibrosed areas. Original magnification ×12

c and d with prominent fibrosis were speculated to be brought about by severe damage to the parenchyma containing the small portal tracts and replacement by fibrosis, although portal veins were seldom seen. Although the hepatic vein of the conducting portion showed slight irregularity of caliber and distortion of running course by the fibrous adhesion in part, the distal branches spread abundantly in the lobule to drain blood.

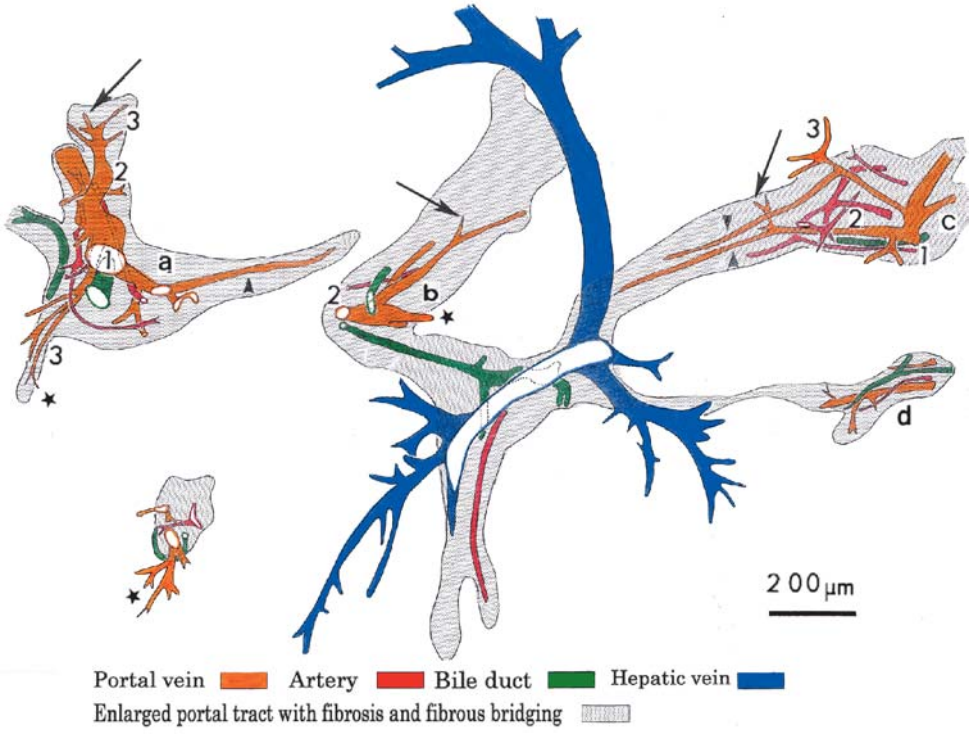

Fig. 8 Reconstruction of the lesion with p-c bridging fibrosis. Portal areas *b*, *c* and *d* are connected with the hepatic vein. Preservation of the portal tree varies from place to place. Portal area *b* connected with the hepatic vein shows a distal portal branch giving off only a small number of branches, one of which run into the parenchyma (*asterisk*) and the other of which disappears in the fibrosed area (*arrow*). Other *asterisks* and *arrows* indicate the same things in other areas. In portal areas *a* and *c*, a few portal branches are found to run for a relatively long distance without giving off effective branches to the parenchyma (*arrowheads*). Contrary to the portal system the hepatic vein extends out abundantly in the parenchyma. *1*: first step; *2*: second step; *3*: third step

Fig. 9 Photomicrograph of the reconstructed area demonstrated in Fig. 10. Portal tracts and conducting portion of the hepatic vein (*arrows*) are fused together. Portal areas are inflamed and poor in vasculature. Original magnification ×14

In the range of this histological reconstruction, the angioarchitecture was severely altered in general in comparison with the previous reconstructed area. The normal lobular angioarchitecture almost disappeared, especially in the fibrosed area around the large vein with a few exceptions.

The portal-portal (p-p) fibrous bridging lesions

As indicated by the histological reconstruction mentioned above, it is usual for diseased portal areas to be connected to each other by fibrous tissue with a paucity of vasculature. Paucity of vasculature or absence of thick portal veins indicates that the fibrous bridging area involved mainly distal portal tracts which were accompanied by the disappearance or marked decrease of the portal branches and parenchyma caused by necroinflammatory reaction. In comparison to p-c bridging lesions, the severity of the loss of parenchyma was thought to be less in p-p lesions.

Discussion

The aim of this report was to clarify the exact alteration of the lobular architecture in chronic hepatitis as much as possible to determine the formal pathogenesis of cirrhotic liver. The lobule is an essential concept concerning structure and indicates unitary parenchymal mass. Until now, three representative concepts of the liver lobule have been proposed [7]. They are “classic lobule” by Kiernan

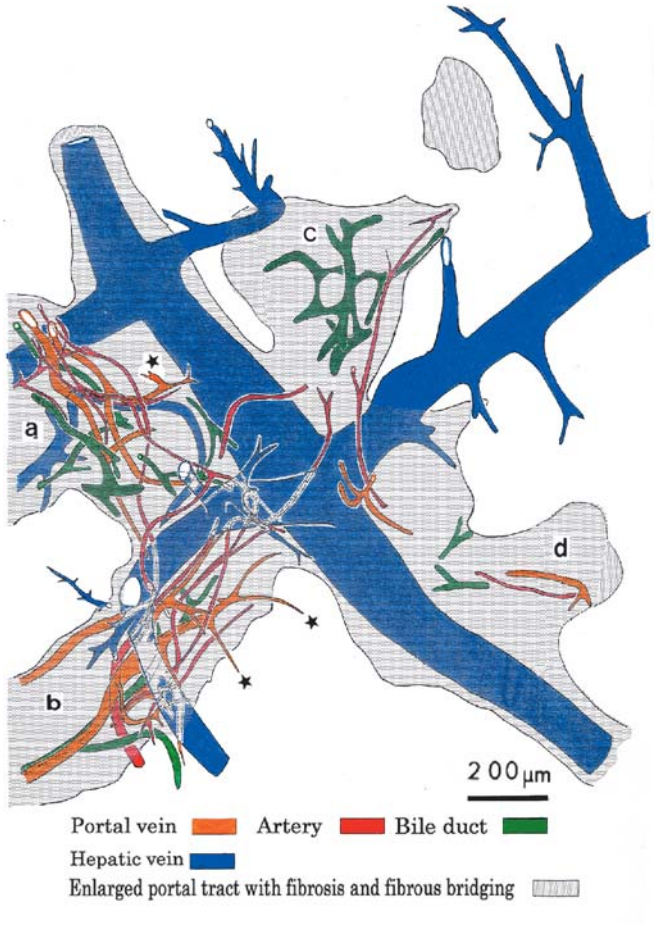

Fig. 10 Reconstruction of the severely damaged lesion with p-c bridging fibrosis. Four fibrosing areas (*a*, *b*, *c* and *d*) are observed to be adherent to the hepatic vein corresponding to the conducting portion. Areas *a* and *b* are rich in vascularity and show intermingling of portal veins, arteries and hepatic veins. Although complete loss of lobular angioarchitecture is indicated in areas *a* and *b*, some branches reach into parenchyma (*asterisks*). Areas *c* and *d* are poor in vasculature. Proliferation of bile ductules is seen

[8], the portal lobule by Mall [12] and the liver acinus by Rappaport [24]. With regard to this, Matsumoto's concept has already been described as a subitem of a normal structure.

We adopted the concept of the hexogonal classic lobule in this study because the concept is more reasonable for explaining the pathological changes, for example, the circulatory disturbances of the liver.

The angioarchitecture of the cirrhotic liver has been investigated by many researchers using the injection technique since the early twentieth century. Kretz [10], McIndoe [17], Popper et al. [23], Mann et al. [13], Nakamura et al. [20] and others showed the distortion of the angioarchitecture and anastomoses between portal and hepatic veins in cirrhotic livers with blood vessels treated with the injection cast technique. Mitra [18] reported a similar distorted angioarchitecture, however, failed to find anastomoses. In addition, Moschcowitz [19] also discussed the process of fibrosis in Lannec liver cirrhosis.

On the basis of pathological findings, the structural alterations of liver cirrhosis were variously described such as "Umbau", rebuilding, by Kretz [9], distortion of the lobule by Moschcowitz [19], altered reconstruction of the lobular pattern by Popper [22], abnormal reconstruction of the preexisting lobular architecture by Popper [21] and disorganization of the lobular architecture by Anthoney et al. [1]. Needless to say, these expressions meant the development of the newly formed parenchymal mass (regenerative nodules) was replacing the normal lobules. However, the precise process of the lobular architecture, rebuilding, has remained as yet unsolved.

We are now facing the problem that Popper et al. [22] stated in 1955—that the most acceptable description of cirrhosis is that of an altered reconstruction of the lobular pattern. Some Japanese literatures with English abstracts have reported the altered angioarchitecture of cirrhotic livers by histological reconstruction methods using serial tissue sections [5, 6, 11]. The results of these studies were briefly summarized as follows. Cirrhotic liver showed the complete loss of the normal lobular angioarchitecture due to severe damage to portal trees. This meant the loss of continuity of the surface-like inflow-front throughout the liver. Therefore, new blood supply and a venous draining system developed in regenerative nodules. Namely, inflow sources changed to point-like ones from which blood irrigated regenerative nodules. Draining veins corresponding to point-like inflow sources were distributed in the same nodules. As a result, regenerative nodules demonstrated conspicuous complexity concerning blood supply and venous draining system. These findings conflict with the view on the pathogenesis of cirrhosis by Rapport et al.—that nodules are remnants of acini of various orders that had their zonal damage replaced by scar tissue [25].

We will primarily discuss the distortion of the lobular architecture based on altered angioarchitecture of our case with chronic hepatitis, taking into account the problem of rebuilding of lobules.

The initial damage of preexisting portal veins themselves on microscopic examination was stenosis and disappearance with the consequence of complexity of vasculature partly due to new formation of distal portal veins. The damage was considered to be caused by the involvement of portal veins in inflammation. In addition, the persistence of inflammation and fibrosis following necroinflammatory lesion [2, 3, 4] in parenchyma containing portal tracts was deemed to induce subsequent new formation of portal veins, abnormal running course such as sharp bends and close apposition of portal veins of the same order. These changes resulted in spatial disarrangement of portal veins and hepatic veins. The severity of these changes is presumed to depend on the duration, intensity and deterioration of inflammation.

As mentioned above, various types of damage to the angioarchitecture were revealed by histological reconstruction. There is no doubt that the alteration of blood

vessels, especially portal veins of the parenchymal portion, more or less affects the angioarchitectural skeleton of normal lobules. This results in the alteration of the lobular structure. Although the severity varied from place to place, the distortion began mostly from the second step or subsequent branches. The mild distortion is shown in Fig. 6, while the severely damaged areas are demonstrated in Fig. 8 and Fig. 10. In the former, the possibility of the lobular angioarchitectural framework partially remaining was indicated. However, in the latter, especially in Fig. 10, conspicuous spatial derangement of blood vessels apparently suggests its complete loss. It is worth pointing out that the coexistence of portal and hepatic veins in the same fibrous septa usually seen in liver cirrhosis had already developed in the advanced lesions of chronic hepatitis. In other words, this indicates an early histological sign of cirrhosis. In this manner, the lobular architecture is considered to be altered step-by-step with the destruction of angioarchitecture and to be completely lost ultimately throughout the liver as the disease progresses. This process of destruction of the lobular angioarchitecture is conceived to be common pathway to liver cirrhosis regardless of its cause.

How was the blood supply to parenchymal cells achieved in the areas with the distortion of angioarchitecture? It is well known that the liver depends mainly on portal blood. It was also pointed out by Mitra that the parenchymal cells of cirrhotic liver were supported by portal blood [18]. Our study suggested that the same could be applied to chronic hepatitis. Namely, it was conceivable that only the remaining third step branches or newly formed ones supplied portal blood to the parenchymal area. Then, inflow source has inevitably changed from a surface-like to point-like inflow source in part in the damaged areas. The important thing is that these remaining portal veins containing point-like inflow sources provide a new nutritional basis for liver cells to regenerate. This is also one of the initial conditions of the development of liver cirrhosis. Although the marked development of arteries was observed, especially in the severely damaged lesions, they were considered to make far less of a contribution to maintaining the parenchyma in comparison to portal vessels—contrary to the opinions by Kretz [10] and McIndoe [17].

Although we failed to find anastomosis between portal and hepatic veins in this case, there is a possibility of its presence in the bridging fibrosed areas.

Why did the liver of this case still remain in the state of chronic hepatitis, but not liver cirrhosis, despite diffuse damage to the microcirculation? The principal reason is considered to be that damage to the parenchyma is uneven, and mild to moderate damage dominates throughout the liver, although severely damaged parenchyma is sometimes found. It is also possible that the areas with a tendency to retain the basic lobular angioarchitecture prevailed, although not completely, in this case. This point of chronic hepatitis is a great difference from a cirrhotic liver, which shows a complete replacement of the liver parenchyma by regenerative nodules and almost complete loss of a normal lobular angioarchitecture.

We have observed the changes in the lobular angioarchitecture in chronic hepatitis compared with a normal liver. It is evident that chronic hepatitis is situated in the process toward cirrhosis and already contains early signs of liver cirrhosis. It is relatively easy to presume that chronic hepatitis finally progresses to liver cirrhosis as a result of the persistence of inflammation, fibrosis and regeneration over a long period. However, we only clarified a part of the wide spectrum of the process. Further investigation is needed to elucidate the formal pathogenesis of liver cirrhosis.

References

1. Anthoney PP, Ishak KG, Nayak NC, Poulsen HE, Scheuer PJ Sobin LH (1978) The morphology cirrhosis. J Clin Pathol 31:395–414
2. Baggenstoss AH, Solway RD, Summerskill WHJ, Elveback LR, Schoenfield LJ (1972) Chronic active liver disease Hum Pathol 3:183–198
3. Chen TJ, Liaw YF (1988) The prognostic significance of bridging hepatic necrosis in chronic type B hepatitis: a histopathologic study. Liver 8:10–16
4. Cooksley WGE, Bradbear RA, Robinson W, Harrison M, Halliday JW, Powell LW, Ng HS, Seah C-S, Okuda K, Scheuer PJ, Sherlock S (1986) The prognosis of chronic active hepatitis without cirrhosis in relation to bridging necrosis. Hepatology 6:345–348
5. Hano H (1979) Three-dimensional approach to the angioarchitecture in a cirrhotic liver of alcoholic origin. Jikeikai Med J 94:1–12
6. Hayashi H (1989) Angioarchitectural changes in a mixed nodular cirrhotic liver. Acta Hepatologica Japonica 30:1687–1697
7. Jones AL, Spring-Mill E (1983) The liver and gall bladder. In: Weiss L (ed) Histology, 5th edn. McMillan, New York, pp 707–748
8. Kiernan F (1833) The Anatomy and physiology of the liver. Philos Trans R Soc Lond B Biol Sci 123:711–770
9. Kretz R (1900) Ueber Lebercirrhose. Wien Klin Wochenschr 13:271–276
10. Kretz R (1905) Cirrhosis of the liver. Int Clin 3:289–297
11. Magara T (1986) Three-dimensional characteristic of B' type cirrhosis, with special reference to its angioarchitecture. Jikeikai Med J 101:579–602
12. Mall FP (1906) A study of the structural unit of the liver. Am J Anat 5:227–308
13. Mann JD, Wakim KG, Baggenstoss AH (1953) Alterations in the vasculature of the diseased liver Gastroenterology 25:540–546
14. Matsumoto T, Kawakami M (1982) The unit concept of hepatic parenchyma- a reexamination based on angioarchitectural studies. Acta Pathol Jpn 32:285–314
15. Matsumoto T, Komori R, Magara T, Ui T, Kawakami M, Tokuda T, Takasaki S, Hayashi H, Jo K, Hano H, Fujino H, Tanaka H (1979) A study on the normal structure of the human liver, with special reference to angioarchitecture. Jikeikai Med J 26:1–40
16. McCallum WG (ed) (1940) A textbook of Pathology, 7th edn. W.B. Saunders Company, Philadelphia, pp 298–322
17. McIndoe AH (1946) Vascular lesions of portal cirrhosis. Arch Pathol Lab Med 5:23–42
18. Mitra SK (1966) Hepatic vascular changes in human and experimental cirrhosis. J Pathol Bacteriol 92:405–414

19. Moschcowitz E (1948) Lannec cirrhosis: its histogenesis with special reference to the role of angiogenesis. Arch Pathol 45:187–215
20. Nakamura T, Nakamura S, Suzuki T (1961) Study on cirrhosis of the liver: structure of shunted blood vessel in the autopsied cirrhotic liver. Tohoku J Exp Med 75:1–9
21. Popper H (1977) Pathologic aspects of cirrhosis: a review. Am J Pathol 87:228–264
22. Popper H, Elias H (1955) Histogenesis of hepatic cirrhosis studied by the three-dimentional approach. Am J Pathol 31:405–441
23. Popper H, Elias H, Petty DE (1952) Vascular pattern of the cirrhotic liver. Am J Clin Pathol 22:717–729
24. Rappaport AM, Borowy ZJ, Longheed WM, Lotto WN (1954) Subdivision of hexagonal liver lobules into a structural and functional unit. Anat Rec 119:11–33
25. Rappaport AM, MacPhee PJ, Fisher MM, Phillips MJ (1983) The scarring of the liver acini (Cirrhosis). Tridimentional and microcirculatory considerations. Virchows Arch 402:107–137

Virchows Arch (2003) 443:664–671
DOI 10.1007/s00428-003-0865-4

ORIGINAL ARTICLE

Laura Verga · Monica Concardi · Andrea Pilotto · Ornella Bellini · Michele Pasotti · Alessandra Repetto · Luigi Tavazzi · Eloisa Arbustini

Loss of lamin A/C expression revealed by immuno-electron microscopy in dilated cardiomyopathy with atrioventricular block caused by *LMNA* gene defects

Received: 14 February 2003 / Accepted: 17 June 2003 / Published online: 26 July 2003
© Springer-Verlag 2003

Abstract Mutations of the *LMNA* gene encoding the lamin A and C nuclear envelope proteins cause an autosomal dominant form of dilated cardiomyopathy (DCM) with atrioventricular block (AVB). The aim of this study was to investigate ultrastructural nuclear membrane changes by conventional electron microscopy and protein expression by immuno-electron microscopy in the heart of patients with DCM and AVB due to *LMNA* gene mutations. Four immunohistochemical techniques were used: pre-embedding and post-embedding in Epon-Araldite resin and London Resin White (LRW), with and without silver enhancement. Parallel light microscopy immunohistochemistry studies were performed. Conventional electron microscopy showed a loss of integrity of the myocyte nuclei with blebs of the nuclear membrane, herniations and delamination of the nuclear lamina and nuclear pore clustering. Post-embedding LRW was the most informative technique for morphology and immuno-labelling. Immuno-labelling was almost absent in the nuclear envelope of patients with *LMNA* gene mutations, but intensely present in controls. The loss of labelling selectively affected myocyte nuclei; the endothelial cell nuclei were immunostained in patients and controls. Light immunohistochemistry confirmed the results. These findings confirm the hypothesis that *LMNA* gene defects are associated with a loss of protein expression in the selective compartment of non-cycling myocyte nuclei.

Keywords Lamin A/C · Dilated cardiomyopathy · Immuno-electron microscopy · Atrioventricular block

L. Verga · M. Concardi · A. Pilotto · O. Bellini · E. Arbustini (✉)
Molecular Diagnostic Laboratory, Transplant Research Area,
I.R.C.C.S. Policlinico San Matteo,
Via Forlanini 16, 27100 Pavia, Italy
e-mail: e.arbustini@smatteo.pv.it
Tel.: +39-038-2501206
Fax: +39-038-2525866

M. Pasotti · A. Repetto · L. Tavazzi
Cardiology Division,
IRCCS Policlinico San Matteo, Pavia, Italy

Introduction

Dilated cardiomyopathy is inherited in approximately 25% of cases; the most common form of inheritance is autosomal dominant, but autosomal recessive, X-linked and mitochondrial inheritance may also occur [13]. It has been shown that mutations of the *LMNA* gene (1p1-q21), which encodes nuclear lamins A and C, cause an autosomal-dominant variant of dilated cardiomyopathy (DCM) with atrio-ventricular block (AVB) [10, 19]. Lamins A and C are intermediate filament proteins that polymerise at the inner surface of the nuclear membrane, maintaining its integrity. Together with other nuclear lamins, they are major components of the nuclear lamina, closely related to the cytoplasmic intermediate filaments. Lamins cooperate with emerin in maintaining cell cycle timing [9, 16, 17]. *LMNA* gene defects cause several inherited disorders: autosomal dominant DCM with and without AVB [2, 4, 10, 14], the autosomal dominant form of Emery-Dreifuss muscular dystrophy (EDMD) [3], limb girdle muscular dystrophy [19], the autosomal dominant partial lipodystrophy [6, 24, 25], the mandibuloacral dysplasia reported in an Italian family [20], autosomal recessive Charcot-Marie-Tooth disease type 2 [8], multi-system dystrophic syndrome [12], a new phenotype characterised by acquired generalised lipoatrophy with metabolic alterations, massive liver steatosis, distinctive cutaneous manifestations and cardiac abnormalities involving both endocardium and myocardium [7]. *LMNA* gene defects are associated with ultrastructural damage of the nuclear envelope, such as focal herniations [27], changes in the assembly properties of lamins A and C [22], bleb formation and nuclear pore clustering [2].

The aim of this study was to investigate nuclear membrane changes and the immunocytochemical expression of lamin A/C in patients with DCM due to *LMNA* mutations.

Materials and methods

We used electron microscopy, light microscopy immunostain and immuno-electron microscopy to investigate morphological changes and lamin A/C expression in myocardial samples of nine patients with a diagnosis of DCM associated with AVB causally linked to *LMNA* gene defects. All patients gave their informed consent prior to their inclusion in the study.

Immuno-electron microscopy for lamin A/C expression was performed using pre-embedding and post-embedding techniques (with and without silver enhancement) in order to establish the optimal method of investigation.

The study considered endomyocardial biopsies of nine patients with familial DCM and at least first-degree AVB (six males and three females; mean age 48.1 years), and the hearts excised at transplantation from five of them (three males and two females; mean age 49.2 years) (Table 1). Left ventricular specimens from the extracted hearts of three patients with DCM but without *LMNA* defects were used as negative controls, as were two endomyocardial biopsy specimens taken from normal hearts of donors before transplantation.

All patients gave their informed consent to the study. The protocol was approved by the Ethics Committee of the IRCCS San Matteo Hospital (project RC/2000–2003 Familial Cardiomyopathies and project Lamin A/C defects in familial DCM with AVB, RC 2001).

Conventional electron microscopy

The specimens were fixed in 0.5% Karnowsky's solution (0.5% glutaraldehyde, 2% paraformaldehyde in 0.2 M cacodylate buffer, pH 7.3) for 2 h, and post-fixed in 1.5% osmium tetroxide in the same buffer. They were then dehydrated and embedded in Epon-Araldite resin, as previously described [1]. Ultra-thin sections were stained with uranyl acetate 5% and lead citrate (Reynold's solution) and scanned using a Zeiss 902 electron microscope.

Light microscopy immunostain

Specimens of formalin-fixed paraffin-embedded hearts of patients with DCM due to *LMNA* gene defects and of controls were reacted with an antibody against lamin A/C (mouse anti-human lamin A+C monoclonal Ab, dilution 1:100; Chemicon International, Inc., CA, USA) using the avidin-biotin method, as previously reported [2]; nuclear staining was performed with 4′6 diamidino-2-phenylindole [2]. The anti-lamin antibody binds to a 464–572 amino acid sequence shared by both lamin A and C.

Post-embedding immunohistochemistry

The specimens were embedded in Epon-Araldite resin as described above, or in London Resin White (LRW), an acrylic resin that does not require total tissue dehydration, polymerises at 50°C, and allows better preservation of antigenicity than Epon-Araldite. The specimens were embedded in accordance with the manufacturer's recommendations.

Immuno-electron microscopy of the specimens embedded in Epon-Araldite was carried out on ultra-thin sections mounted on parlodion-coated nickel grids. The sections were etched with 3% H_2O_2 for 10 min, treated with 5% sodium metaperyodate for 10 min at room temperature, enzymatically pre-digested with 0.5% trypsin in Tris buffer with 0.05% $CaCl_2$ (10 min, 37°C), and then rinsed in 0.05 M TRIS/HCl buffer, pH 7.4, and incubated in the same buffer with 1:20 normal goat serum for 30 min at room temperature. The grids were incubated overnight at 4°C with a primary antibody (mouse anti-human lamin A+C monoclonal Ab, dilution 1:10; Chemicon International, Inc., CA, USA), rinsed in Tris buffer, re-incubated with a secondary antibody conjugated to 15-nm colloidal gold particles (British Biocell International, UK) and stained with uranyl acetate and lead citrate. The specificity of the immunoreactions was checked using normal serum as the primary antibody.

For the post-embedding immunohistochemical study of specimens embedded in LRW, ultra-thin sections mounted on parlodion-coated nickel grids were processed as follows. The sections were etched with 3% H_2O_2 for 10 min, treated with 5% sodium metaperiodate for 10 min at room temperature, enzymatically predigested with 0.5% trypsin in Tris buffer with 0.05% $CaCl_2$ (37°C, 15 min), and incubated for 1 min in a microwave oven at medium power. They were then rinsed in 0.05 M Tris/HCl buffer, pH 7.3, and incubated with 1:20 normal goat serum or 1% ovalbumin for 60 min at room temperature and then incubated with the primary antibody as described above. After being rinsed in the same buffer, they were then incubated with the secondary antibody (goat anti-mouse immunoglobulin, diluted 1:20 in the same buffer) or protein-A, both of which were conjugated to 15-nm colloidal gold particles (British Biocell International, UK). Finally, the sections were stained with uranyl acetate 5% and Reynold's solution. The specificity of the immunoreactions was checked using normal serum as the primary antibody.

Silver enhancement of immunogold-labelled specimens

This enhancement was used on sections treated by means of the above post-embedding technique and is based on the reduction of silver in the presence of a developer due to the gold particles attached to the secondary antibody on the tissue. After immunolabelling with the primary and secondary antibody conjugated to 5-nm gold particles (British Biocell International, UK), a drop of each of the two solutions from the commercial kit was mixed, and the sections floated on the surface for 20 min in the dark at room temperature. The grids were then thoroughly washed in distilled water, stained as described above and examined by means of electron microscopy.

Pre-embedding immunohistochemistry

The specimens were fixed by immersion in 4% paraformaldehyde (12 h, 4°C), and then washed in Tris buffer for 2 h at room temperature. A vibratome was used to obtain 50-μm sections, which were then immersed in 0.05% Triton X 100 for 20 min, washed in Tris buffer, and incubated in 10% normal goat serum for 30 min. They were then immersed in the primary antibody diluted 1:10 (48 h, 4°C). After careful washing in Tris buffer (ten times 10 min), the sections were incubated with the secondary antibody conjugated to 5-nm gold particles (48 h, 4°C), and then washed in Tris buffer (ten times 10 min), fixed in 2% glutaraldehyde (1 h, 4°C), post-fixed in 1% osmium tetroxide (1 h, room temperature), washed in Tris buffer and dehydrated in a graded series of ethyl alcohols. The specimens were subsequently cut into sections with a smaller surface area, embedded in Epon-Araldite and left to polymerise overnight at 60°C. The following day, ultra-thin sections were obtained, stained with uranyl acetate 5% and Reynold's solution and then scanned using a Zeiss 902 electron microscope.

Mutation detection

LMNA gene mutations were identified by means of polymerase chain reaction (PCR) on peripheral blood-derived genomic DNA and automated DNA sequencing of the amplicons as previously reported [2]. Briefly, the 12 exons of the *LMNA* gene were amplified by PCR; the fragments were analysed by means of denaturing high-performance liquid chromatography (Transgenomic, San Jose, California) using the Wave DNA Fragment

Table 1 Patients with dilated cardiomyopathy due to lamin A/C gene mutations. *M* male, *F* female, *pt* patient, *AVB* atrio-ventricular block, *LBBB* left bundle branch block, *PM* pacemaker, *NYHA* New York Heart Association, *LAFB* left anterior fascicular block

Patient	Age/Sex	Exon	Mutation	Clinical Findings
1	67/M	6	Gly317Lys 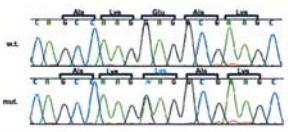	Onset 44y III° AVB+LBBB→PM 64y Actual NYHA class II
2	28/M	1	Arg89Leu 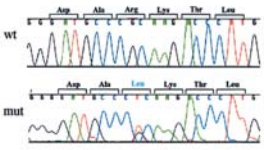	Onset 24y III° AVB→PM 27 y Cardiac Transplantation 28y
3	59/M	1	Glu111tt 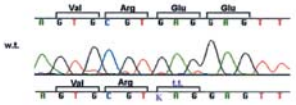	Onset 43y III° AVB→PM 53y Cardiac Transplantation 57y
4	58/M Brother of pt #3	1	Glu111tt	Onset 43y III° AVB→PM 47y Cardiac Transplantation 56y
5	35/F	1	Lys97Glu 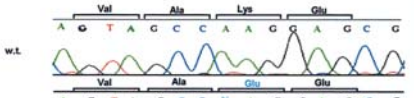	Onset 30y III°AVB+LBBB→PM 31y Cardiac Transplantation 32y
6	28/M Brother of pt #5	1	Lys97Glu	Onset 27y I°AVB+LBBB Awaiting for Cardiac Transplantation
7	44/M	3	Arg190Trp 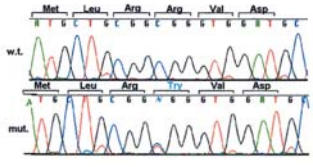	Onset 31y I°AVB+LAFB+RBBB+ Actual NYHA class II
8	66/F	9	Ins1713CTGC 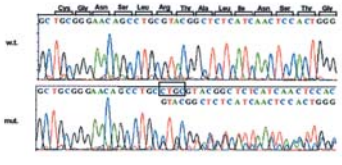	Onset 33y II°AVB+LBBB→PM 56y Cardiac Transplantation 58y
9	35/F	1	165delC 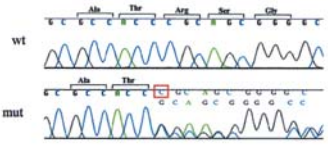	Onset 34y Paroxistical II°AVB Actual NYHA class II

Analysis System. The fragments with a heteroduplex conformation were purified (QIAquick Kit, Qiagen, Santa Clarita, California) and sequenced using a BigDye-terminator cycle sequencing system (ABI PRISM 377, Applied Biosystem, Foster City, California).

Results

Mutations

Lamin A/C gene mutations were identified in the probands and related affected relatives of the seven families investigated. Of the seven mutations, two are

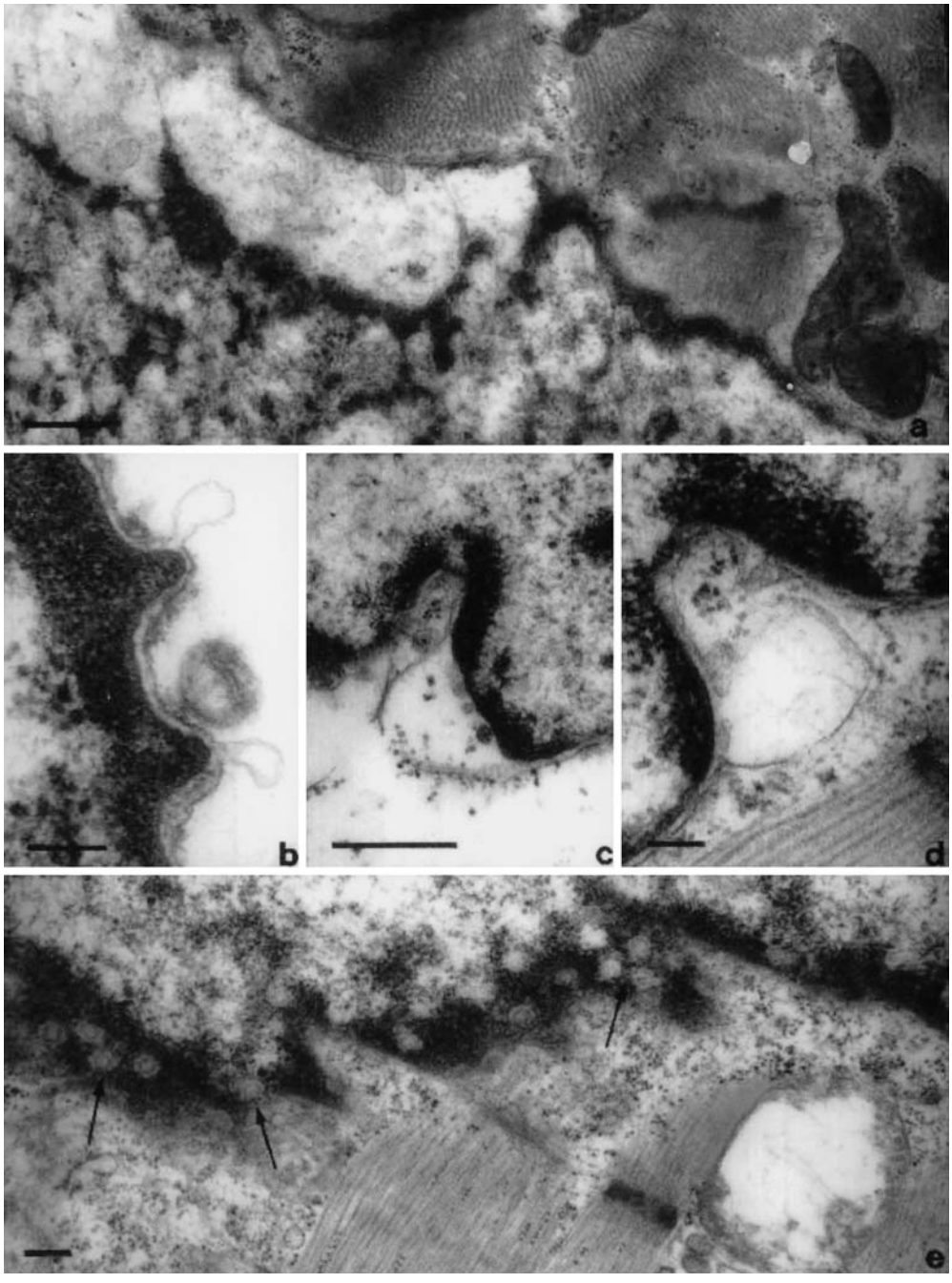

Fig. 1 Conventional electron microscopy. Cardiac myocyte nuclei of patients with dilated cardiomyopathy due to *LMNA* gene mutations. Delamination of the nuclear membrane (**a**). Blebs of the nuclear envelope sprouting into the cytoplasm (**b**). Blebs and disruption of the nuclear envelope (**c, d**). Clustering of nuclear pores (**e**). *Arrows*: nuclear pores. Uranyl acetate and lead citrate. *Magnification* **a** ×32,000, **b** ×64,000, **c** ×39,000, **d** ×57,000, **e** ×26,000. *Scale bars* **a**, **c** and **e** 0.6 μm; **b** and **d** 0.4 μm

novel (165delC, Arg89Leu), while five are known [2]. The 165delC predicts a 105 aminoacid truncated protein.

Conventional electron microscopy

The nuclei of the cardiac myocytes of patients with *LMNA* mutations were irregular in shape, sometimes lobulated, with condensed chromatin and evident nucleoli. Chromatin extrusion through the disrupted nuclear membrane was detected in a number of myocyte nuclei of patients with cardiomyopathy causally linked to *LMNA* gene mutations. The ultrastructural findings of nuclear membrane damage consisted of: (a) the loss of integrity of the nuclear envelope, (b) blebs and "delamination" of the nuclear membrane and (c) nuclear pore clustering.

All of the above changes had a focal distribution in the same or different myocytes (Fig. 1); in particular, the formation of blebs in the nuclear envelope was clear, as was the clustering of nuclear pores, although to a lesser extent. Conventional electron microscopy samples embedded in Epon-Araldite resin are the only appropriate means of identifying nuclear membrane changes.

The ultrastructural examination of non-nuclear components revealed interstitial fibrosis, loss of contractile

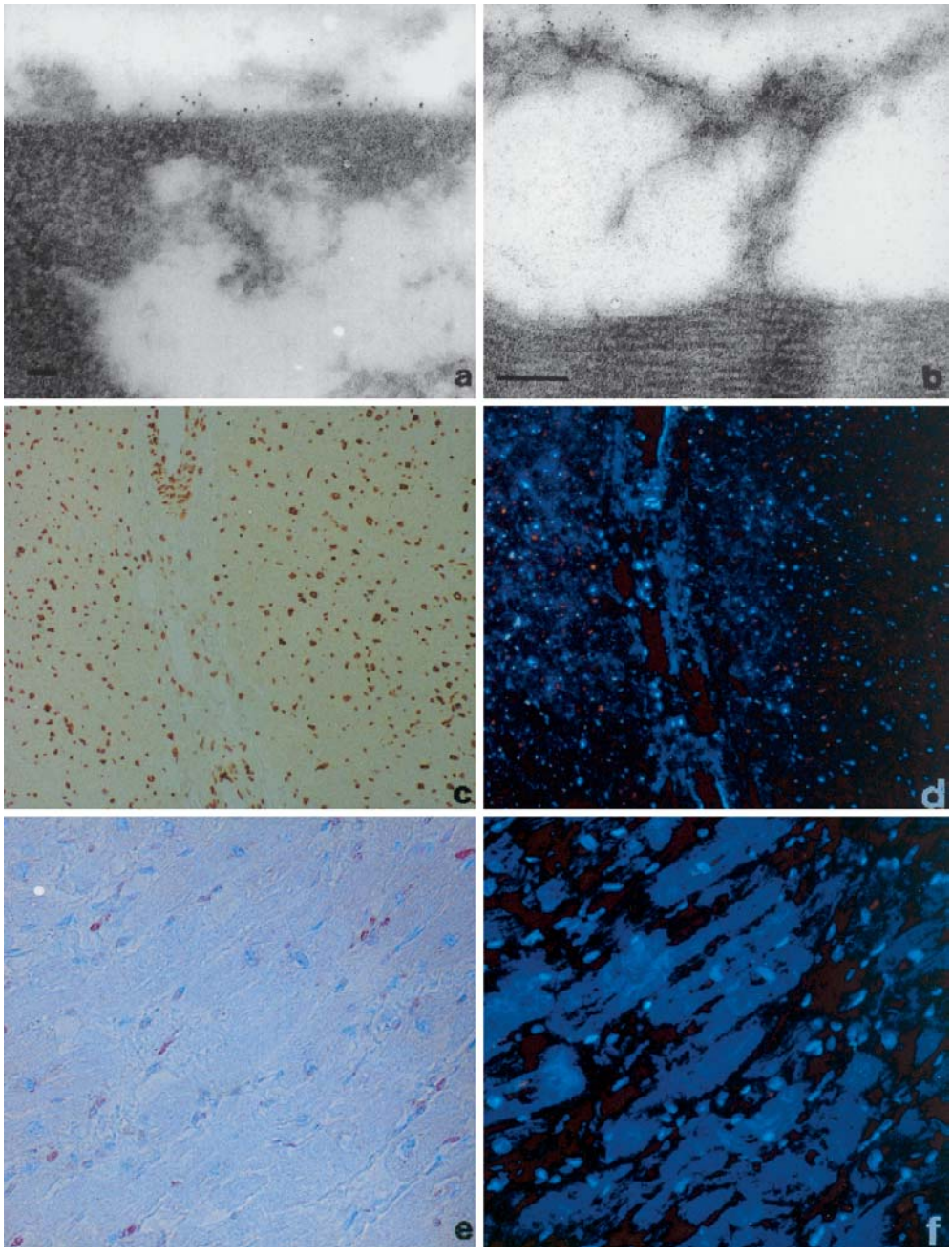

Fig. 2 a, b Immuno-electron microscopy. Cardiac myocyte nuclei of controls without *LMNA* mutations immunostained with anti-lamin A/C antibody. Pre-embedding technique: the nuclear envelope is roughly visible (**a**). Post-embedding in London Resin White plus silver enhancement: immunostaining is specific, but the morphological details are lost (**b**). Uranyl acetate and lead citrate. *Magnification* **a** ×130,000, **b** ×67,000. *Scale bars* **a** 0.5 μm, **b** 0.4 μm. **c–f** Light microscopy immunostain with anti-lamin A/C (**c**, **e**) and corresponding DAPI (4,6 diamidino-2-phenylindole) nuclear stain (**d**, **f**). Endomyocardial biopsy of a donor before transplantation: both myocyte and interstitial-vascular nuclei are immunostained (**c**). In the heart of a patient with DCM due to *LMNA* gene mutation, immunostaining is lost in part of the myocyte nuclei, while interstitial and vascular cell nuclei are still positive (**e**). Avidin-Biotin Complex, DAPI nuclear stain. *Magnification* **c**, **d** ×10, **e**, **f** ×40

fibrils and non-specific degenerative features of cardiac myocytes.

Light microscopy immunostain

The light microscopy immunostain showed regular stain of nuclear membranes of myocytes and of interstitial and vascular cells of hearts of patients with DCM not caused by *LMNA* gene defects and of donors (Fig. 2c), while immunostaining was lost in several myocyte nuclei of patients with DCM due to *LMNA* gene mutations (Fig. 2e).

Immuno-electron microscopy

The pre-embedding method allowed good preservation of tissue antigenicity, but the morphological detail of the nuclear envelope was poor (Fig. 2a). The post-embedding technique applied to specimens embedded in Epon-Araldite resin gave sub-optimal results (not shown). For this reason, we optimised the post-embedding method to combine morphology (although not as good as that obtained using embedding in Epon-Araldite resin) and antigen preservation. This was achieved by embedding in LRW and subsequent post-embedding processing of the sections (Fig. 3a, d). Silver enhancement of the immunolabelled sections revealed well-preserved antigenicity and

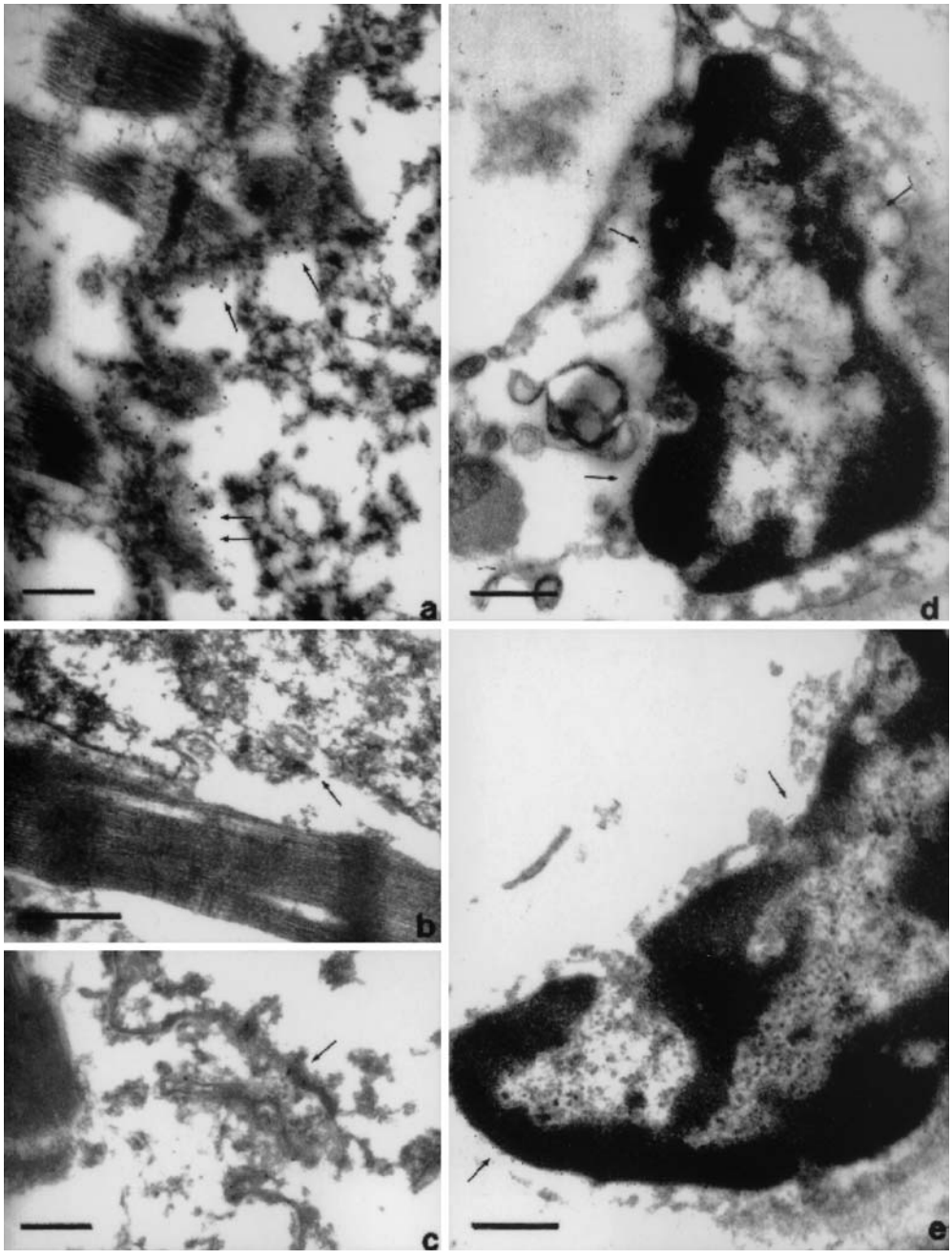

Fig. 3 Immunostaining with anti-lamin A/C antibody. Cardiac myocyte of control patient without *LMNA* gene mutation, post-embedding in London Resin White (**a**). The inner nuclear membrane is intensely and specifically stained (*arrows*). Cardiac myocytes of patients with dilated cardiomyopathy due to *LMNA* gene mutations; post-embedding in London Resin White (**b, c**) The immuno-labelling of the nuclear envelope is almost completely lost (*arrow*). Endothelial cells of a control (**d**) and a patient with *LMNA* gene mutation (**e**): pre-embedding technique. The immunostaining of the nuclear envelope is intense and specific (*arrows*). Uranyl acetate and lead citrate. *Magnification* **a** ×28,000, **b** ×29,000, **c** ×28,000, **d** ×33,000, **e** ×24,000. *Scale bars* **a–e** 0.6 μm

subsequent intense immuno-labelling of the myocyte nuclear envelope, but the morphological detail remained sub-optimal (Fig. 2b).

In the control samples of DCM cases not due to *LMNA* gene defects and normal donor hearts before cardiac transplantation, the immunoreaction with anti-lamin A/C antibody intensely and specifically stained the nuclear envelope of cardiac myocytes (Fig. 3a) and interstitial and vascular cells (Fig. 3d). In the myocardial samples taken from patients with DCM due to *LMNA* gene mutations, the nuclear envelopes of all the cardiac myocytes almost completely lost their immuno-labelling (Fig. 3b, c), whereas the vascular and interstitial cell nuclei retained specific immunostaining (Fig. 3e), although to a lesser extent than that observed in the hearts of control patients (i.e. the immuno-labelling was only a little less intense).

Genotype–immunophenotype correlations

The loss of immuno-labelling was similar in all heart samples of the nine patients carrying the seven different mutations of the *LMNA* gene. The severity of loss of lamin A/C expression did not vary according to the different gene defects.

Discussion

Our findings document first the defective expression of lamin A/C revealed by immuno-electron microscopy in the nuclear envelopes of cardiac myocytes of patients with lamin A/C defects causing DCM and associated with AVB. The only technique that combined both immuno-labelling and useful morphological preservation was the post-embedding staining of LRW sections. The procedure is time consuming but documents the precise localisation of protein on the inner side of the nuclear envelope. Patients carrying *LMNA* gene mutations concordantly show a loss or severe decrease in the immunostaining of the nuclear membranes of cardiac myocytes, regardless of the position and type of *LMNA* gene mutation.

The spectrum of nuclear membrane damage seen in the myocytes of patients with *LMNA* defect-related DCM includes three features shared by experimental models and other human disorders causally linked to *LMNA* gene defects:

1. Nuclear membrane disruption: the integrity of the nuclear envelope is lost, and the nuclear material may spread out of the nucleus itself. Similar features have been reported in the skeletal muscle cells of patients with EDMD [11, 16] and in embryonic fibroblasts and hepatocytes of *LMNA*-null mice [26].
2. Nuclear membrane blebs: the loss of lamin A/C, which connects the membrane to lamin B and emerin, may make the nuclear envelope unstable, thus leading to a reduction in the load-bearing properties of the lamina and finally to the death of cardiac myocytes [16].
3. Nuclear pore clustering has been described in the *Drosophila* lamin Dm0 mutant [18]; according to the authors, this is due to the existence of a direct interaction between the nuclear pore proteins and the lamins [15] and a consequently disturbed assembly process in lamin-deficient flies [18]. As previously shown [2], the phenomenon is characterised by the apparently random concentration of nuclear pores along tracts of the membrane.

Electron microscopy may contribute towards arousing the suspicion of an *LMNA* gene defect when the details are of a high quality, as in the case of conventional ultrastructural studies. Apart from the clinical and genetic data that play a diagnostic role, and light immunohistochemical microscopy showing the loss of myocyte nuclei immuno-labelling in mutated patients, the major contribution of electron microscopy is the precise characterisation of the nuclear damage and the confirmation of a selective loss of lamin A/C in the nuclear lamina of cardiac myocytes.

The selective loss of lamin A/C on the nuclear membranes of cardiac myocytes and the preservation of protein expression in the non-myocyte nuclei support our preliminary hypothesis that non-actively cycling cells are the elective candidates for protein depletion in mutated subjects [2]. The degradation of lamin A/C and the failure to replace degraded protein may constitute the molecular basis of the loss of lamin A/C observed in the nuclei of the non-cycling myocytes. In cycling cells, such as fibroblasts and endothelial cells, *LMNA* mRNA levels remain high, likely enough to guarantee a sufficient amount of protein [21]. An alternative hypothesis suggested for patients with X-linked EDMD is that, in the presence of mutated protein, the nuclear lamina becomes more fragile and less effective as a load-bearing structure, particularly in myocytes [9].

Overall, the loss of lamin A/C expression and nuclear membrane damage selectively affecting part of the myocyte nuclei confirm an organ-specific effect that depends on the functional status of the *LMNA* gene in non-cycling cells such as cardiac myocytes [5, 23]. The different types of mutation (missense, nonsense and insertion) do not seem to change the spectrum of nuclear membrane damage or the loss of protein expression. Similarly, it is unknown why different *LMNA* mutations produce analogous morphological defects; loss of myocyte nuclei immuno-labelling and ultrastructural alterations were present in all heart samples of patients carrying the different mutations of the *LMNA* gene. These issues, common in many other disorders with genetic heterogeneity, are beyond the aim of this study.

In conclusion, immuno-electron microscopy of lamin A/C expression in patients diagnosed with DCM plus AVB caused by *LMNA* gene mutations confirms that all types of gene defect are associated with a loss of protein expression in the selective compartment of non-cycling myocyte nuclei.

Acknowledgements Supported by grants RF 2000, Progetto Strategico Congestive Heart Failure (TL); subprojects: Familial Cardiomyopathies (AE), I.R.C.C.S. Policlinico San Matteo, Pavia, Italy, and by grant Eurogene-Heart Failure, Leducq Foundation, France.

References

1. Arbustini E, Morbini P, Verga L, Concardi M, Porcu E, Pilotto A, Zorzoli I, Garini P, Anesi E, Merlini G (1997) Light and electron microscopy immunohistochemical characterization of amyloid deposits. Amyloid: Int J Exp Clin Invest 4:157–170
2. Arbustini E, Pilotto A, Repetto A, Grasso M, Negri A, Diegoli M, Campana C, Scelsi L, Baldini E, Gavazzi A, Tavazzi L (2002) Autosomal dominant dilated cardiomyopathy with atrioventricular block: a lamin A/C defect-related disease. J Am Coll Cardiol 39:981–990
3. Bonne G, Merceni E, Muchir A, Urtizberea A, Becane HM, Recan D, Merlini L, Wehnert M, Boor R, Reuner U, Vorgerd M, Wicklein EM, Eymard B, Duboc D, Penisson-besnier I, Cuisset JM, Ferrer X, Desguerre I, Lacombe D, Bushby K, Pollitt C, Toniolo D, Fardeau M, Schwartz K, Muntoni F (2000) Clinical and molecular genetic spectrum of autosomal dominant Emery-Dreifuss muscular dystrophy due to mutation of the lamina A/C gene. Ann Neurol 48:170–180
4. Brodsky GL, Muntoni F, Miocic S, Sinagra G, Sewry C, Mestroni L (2000) Lamin A/C gene mutation associated with dilated cardiomyopathy with variable skeletal muscle involvement. Circulation 101:473–476

5. Burke B, Mounkes LC, Stewart CL (2001) The nuclear envelope in muscular dystrophy and cardiovascular diseases. Traffic 2:675–683
6. Cao H, Hegele RA (2000) Nuclear lamin A/C R482Q mutation in Canadian kindreds with Dunningan-type familial partial lipodystrophy. Hum Mol Genet 9:109–112
7. Caux F, Dubosclard E, Lascols O, Buendia B, Chazouilleres O, Cohen A, Courvalin JC, Laroche L, Capeau J, Vigouroux C, Christin-maitre S (2003) A new clinical condition linked to a novel mutation in lamins A and C with generalized lipoatrophy, insulin-resistant diabetes, disseminated leukomelanodermic papules, liver steatosis and cardiomyopathy. J Clin Endocrinol Metab 88:1006–1013
8. De Sandre-Giovannoli A, Chaouch M, Kozlov S, Vallat JM, Tazir M, Kassouri N, Szepetowsky P, Hammadouche T, Vandenberghe A, Stewart CL, Grid D, Levy N (2002) Homozygous defects in LMNA, encoding lamin A/C nuclear-envelope proteins, cause autosomal recessive axonal neuropathy in human (Charcot-Marie-Tooth disorder type 2) and mouse. Am J Hum Genet 70:726–736
9. Fairley EA, Riddell A, Ellis JA, Kendrick-Jones J (2002) The cell cycle dependent mislocalisation of emerin may contribute to the Emery-Dreifuss muscular dystrophy phenotype. J Cell Sci 115:341–354
10. Fatkin D, MacRae C, Sasaki T, Wolff MR, Porcu M, Frenneaux M, Atherton J, Vidaillet HJ Jr, Spudich S, De Girolami U, Seideman C, Muntoni F, Muehle G, Johnson W, McDonough B (1999) Missense mutations in the rod domain of the lamin A/C gene as causes of dilated cardiomyopathy and conduction-system disease. N Engl J Med 341:1715–1724
11. Fidzianska A, Toniolo D, Hausmanowa-Petrusewicz I (1998) Ultrastructural abnormality of sarcolemmal nuclei in Emery-Dreifuss muscular dystrophy (EDMD). J Neurol Sci 15:88–93
12. Garg A, Speckman RA, Bowcock AM (2002) Multisystem dystrophy syndrome due to novel missense mutations in the amino-terminal head and alpha-helical rod domains of the lamin A/C gene. Am J Med 112:549–555
13. Gavazzi A, Repetto A, Scelsi L, Inserra C, Laudisa ML, Campana C, Specchia C, Dal Bello B, Diegoli M, Tavazzi L, Arbustini E (2001) Evidence-based diagnosis of familial non-X-linked dilated cardiomyopathy. Prevalence, inheritance and characteristics. Eur Heart J 22:73–81
14. Genschel J, Schmidt HH (2000) Mutations in the LMNA gene encoding lamin A/C. Hum Mutat 16:451–459
15. Goldberg MW, Allen TD (1992) High resolution scanning electron microscopy of the nuclear envelope: the baskets of the nucleoplasmic face of the nuclear pores. J Cell Biol 119:1429–1440
16. Hutchison CJ, Alvarez-Reyes M, Vaughan OA (2001) Lamins in disease: why do ubiquitously expressed nuclear envelope proteins give rise to tissue-specific disease phenotypes? J Cell Sci 114:9–19
17. Krohne G, Benvente R (1986) The nuclear lamins: a multigene family of proteins in evolution and differentiation. Exp Cell Res 162:1–10
18. Lenz-Bohme B, Wismar J, Fuchs S, Reifegerste R, Buchner E, Betz H, Schmitt B (1997) Insertional mutation of the *Drosophila* nuclear lamin Dm0 gene results in defective nuclear envelopes, clustering of nuclear pore complexes, and accumulation of annulate lamellae. J Cell Biol 137:1001–1016
19. Muchir A, Bonne G, van der Kooi AJ, van Meegen M, Baas F, Bolhuis PA, de Visser M, Schwartz K (2000) Identification of mutations in the gene encoding lamins A/C in autosomal dominant limb girdle muscular dystrophy with atrioventricular conduction disturbances (LGMD1B). Hum Mol Genet 9:1453–1459
20. Novelli G, Muchir A, Sangiuolo F, Helbling-Leclerc A, D'Apice MR, Massart C, Capon F, Sbraccia P, Federici M, Lauro R, Tudisco C, Pallotta R, Scarano G, Dallapiccola B, Merlini L, Bonne G (2002) Mandibuloacral dysplasia is caused by a mutation in LMNA-encoding lamin A/C. Am J Hum Genet 71:426–431
21. Pugh GE, Coates PJ, Lane EB, Raymond Y, Quinlan RA (1997) Distinct nuclear assembly pathways for lamins A and C lead to their increase during quiescence in Swiss 3T3 cells. J Cell Sci 110:2483–2493
22. Raharjo WH, Enarson P, Sullivan T, Stewart CL, Burke B (2001) Nuclear envelope defects associated with LMNA mutations cause dilated cardiomyopathy and Emery-Dreifuss muscular dystrophy. J Cell Sci 114:4447–4457
23. Salina D, Bodoor K, Enarson P, Raharjo WH, Burke B (2001) Nuclear envelope dynamics. Biochem Cell Biol 79:533–542
24. Shackleton S, Lloyd DJ, Jackson SN, Evans R, Niermeijer MF, Singh BM, Schmidt H, Brabant G, Kumar S, Durrington PN, Gregory S, O'Rahilly S, Trembath RC (2000) LMNA, encoding lamin A/C, is mutated in partial lipodystrophy. Nat Genet 24:153–156
25. Speckman RA, Garg A, Du F, Bennett L, Veile R, Arioglu E, Taylor SI, Lovett M, Bowcock AM (2000) Mutational and haplotype analyses of families with familial partial lipodystrophy (Dunningan variety) reveal recurrent missense mutations in the globular C-terminal domain of lamin A/C. Am J Hum Genet 66:1192–1198
26. Sullivan T, Escalante-Alcalde D, Bhatt H, Anverc M, Bhat N, Nagashima K, Stewart CL, Burke B (1999) Loss of A-type lamin expression compromises nuclear envelope integrity leading to muscular dystrophy. J Cell Biol 147:913–920
27. Vigouroux C, Auclair M, Dubosclard E, Pouchelet M, Capeau J, Courvalin JC, Buendia B (2001) Nuclear envelope disorganization in fibroblasts from lipodystrophic patients with heterozygous R482Q/W mutations in the lamin A/C gene. J Cell Sci 114:4459–4468

Virchows Arch (2003) 443:672–677
DOI 10.1007/s00428-003-0866-3

ORIGINAL ARTICLE

Ritsuto Fujiwaki · Kohji Iida · Kentaro Nakayama · Haruhiko Kanasaki · Tomoya Ozaki · Kohkichi Hata · Eiichi Sakai · Kohji Miyazaki

Dihydropyrimidine dehydrogenase in normal and malignant endometrium: relationship with cell proliferation and thymidine phosphorylase

Received: 28 April 2003 / Accepted: 19 June 2003 / Published online: 9 August 2003
© Springer-Verlag 2003

Abstract Dihydropyrimidine dehydrogenase (DPD) is a pyrimidine salvage enzyme responsible for degradation of thymine, which is produced from thymidine by thymidine phosphorylase (TP). Our purpose was to determine the relationship between DPD, cell proliferation and TP expression in human endometrium. We examined DPD gene expression using reverse transcription-polymerase chain reaction, DPD protein levels using enzyme-linked immunosorbent assay, and DPD protein localization using immunohistochemistry in 58 normal endometria and 28 endometrial cancers. DPD gene expression was then related to the proliferating cell nuclear antigen index and to TP gene expression. DPD gene expression, which was correlated with DPD protein level, was relatively stable throughout various menstrual phases but was significantly elevated in postmenopausal status. It was significantly lower in endometrial cancer than in normal endometrium. Localization analysis revealed that DPD protein was located primarily in epithelial cells, but was also present in stromal cells. DPD gene expression correlated inversely with the PCNA index. TP gene expression pattern contrasted with that of DPD in postmenopausal and malignant endometrium. A high ratio of TP to DPD gene expression was significantly more frequent in endometrial cancer than in normal endometrium in any menstrual phase. DPD may act cooperatively with TP to affect cell function by maintaining the pyrimidine nucleotide pool balance in normal and malignant endometrium.

R. Fujiwaki (✉) · K. Iida · K. Nakayama · H. Kanasaki · T. Ozaki · K. Hata · K. Miyazaki
Department of Obstetrics and Gynecology,
Shimane Medical University,
693-8501 Izumo, Japan
e-mail: fuji39@shimane-med.ac.jp
Tel.: +81-853-202268
Fax: 81-853-202264

E. Sakai
Nihon Gene Research Lab's Inc.,
Sendai, Japan

Keywords Dihydropyrimidine dehydrogenase · Thymidine phosphorylase · Endometrium · Endometrial cancer · Proliferating cell nuclear antigen.

Introduction

Both thymidine phosphorylase (TP) and dihydropyrimidine dehydrogenase (DPD) are important enzymes in the pyrimidine salvage pathway [1, 2, 4, 12]. TP, which is identical to platelet-derived endothelial cell growth factor, catalyzes the reversible phosphorolysis of thymidine from the extracellular fluid to thymine and 2-deoxy-D-ribose-1 phosphate [1, 12]. TP and the degradation products thymine and 2-deoxy-D-ribose have angiogenic and anti-apoptotic effects [13, 16, 18]. We recently found the correlation between TP expression and increased microvessel counts in endometrial cancer, suggesting that TP plays an important role in angiogenesis in endometrial cancer [6]. In normal human endometria, TP expression varied during the menstrual cycle, demonstrating that it was influenced by sex steroid hormones [5, 23, 28]. Subsequently, thymine is degraded to CO_2 and β-aminoisobutyric acid in three sequential reactions [2, 4]. DPD, the first and rate-limiting enzyme of this chain, is responsible for the conversion of thymine to dihydrothymine. Also, DPD catalyzes the conversion of uracil to dihydrouracil, which is finally catabolized to β-alanine. Previous studies demonstrated that DPD activity varied among organs, with the liver having the highest enzymatic activity. Minimal activity was found in the kidney, spleen, lung, pancreas, and breast [11, 21]. DPD activity correlated inversely with hepatoma growth rate in the rat liver and malignant behavior in murine neuroblastoma cell lines [24, 27]. Additionally, DPD and TP cooperatively affected malignant behaviors and the efficacy of the fluoropyrimidine cytotoxic agent [8, 14]. Although DPD itself and the combination of TP and DPD may be associated with several biological behaviors, DPD ex-

pression and the relationship between TP and DPD have not been determined in human endometria.

In this study, we examined DPD gene expression using reverse transcription-polymerase chain reaction (RT-PCR), DPD protein levels using enzyme-linked immunosorbent assay (ELISA), and DPD protein localization using immunohistochemistry in normal endometria during various menstrual phases and in cancerous endometrium. Additionally, DPD gene expression was then related to the proliferating cell nuclear antigen (PCNA) index and TP gene expression.

Materials and methods

Samples

Normal human endometrial samples (58) and endometrial cancer samples (28) were obtained after hysterectomy performed at Shimane Medical University Hospital, Izumo, Japan, and affiliated hospitals. All research was conducted with informed consent and with the approval of the hospital research ethics board. All normal endometrial tissues were taken from patients who had non-endometrial gynecological disorders (i.e., uterine leiomyoma and early cervical cancer) and who had not taken exogenous hormones before surgery. These included 50 samples from patients with regular menstruation and 8 samples from postmenopausal patients. Endometrial dating was determined from the histology of the endometrium [20] and classified into five phases of the menstrual cycle: menstrual (n=4), early-mid proliferative (n=9), late proliferative (n=12), early secretory (n=4), mid secretory (n=14), and late secretory (n=7). The clinicopathological characteristics of 28 endometrial cancers are as follows: mean patient age, 61 years; FIGO (International Federation of Gynecologists and Obstetricians) stage, stage I, n=20, stage II, n=3, stage III, n=5; histological type, well-differentiated endometrioid adenocarcinoma, n=17, moderately differentiated endometrioid adenocarcinoma, n=7, poorly differentiated endometrioid adenocarcinoma, n=3, clear cell carcinoma, n=1. A block of fresh tissue, which was prepared to eliminate inappropriate components, was snap frozen in liquid nitrogen as close as possible to the time of surgical removal and stored at −80°C until used for assay. A portion of the frozen tissue from each case (tumor and normal) was processed to create formalin-fixed and paraffin-embedded tissue blocks that were matched and oriented relative to the frozen tissue.

Reverse-transcription polymerase chain reaction

Conventional RT-PCR for determination of each gene expression was performed according to a modified method previously described [8]. In brief, the method involved isolation of mRNA from each specimen, preparation of cDNA using reverse transcriptase and random priming and PCR amplification of the specific cDNA of target (DPD or TP) in a range of concentrations that gives rise to a linear curve of the resulting PCR products. An internal control [β2-microglobulin (β2-MG)] the same cDNA solution was PCR-amplified separately. The primers were CTCCATTGCCATCGATACG and CCTTAGCAAGCTCCATCTCC (158-bp PCR product) for the human DPD gene (GenBank accession number U09178)), TGGCTCAGTCGGGACAGCAG and TCCGCTGATCATTGGCACCT (152 bp) for the human TP gene (GenBank accession number M63193), and ACCCCCACTGAAAAAGATGAG and ATCTTCAAACCTCCATGATGC (120 bp) for β2-MG gene (GenBank accession number U00567). PCR conditions were as follows: initial 2 min denaturation at 94°C followed by cycles of 1 min denaturation at 94°C, 1 min annealing at 58°C, and 1 min extension at 72°C, with a final extension at 72°C for 10 min. When quantitative RT-PCR analysis was carried out, the PCR for DPD and TP was 28 cycles and that for β2-MG was 24 cycles. TS gene expression level was described in terms of the relative yield of target gene to that of the β2-MG gene using these cycle numbers

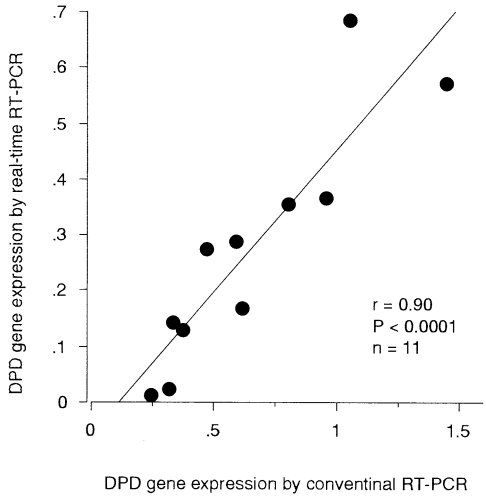

Fig. 1 Scatter diagram of dihydropyrimidine dehydrogenase gene expression measured by conventional reverse transcription-polymerase chain reaction (RT-PCR) and by real-time quantitative RT-PCR in normal and malignant endometrium

In order to determine the accuracy of our conventional RT-PCR methods, DPD gene expression was determined by a real-time quantitative RT-PCR method previously described in 11 tissue specimens [9]. Real-time quantitative PCR was performed by hybridization probe format LightCycler system. The PCR protocol was as follows: 95°C/10 min; PCR cycles: denaturation 95°C/15 s, annealing 60°C/15 s (detection), extension 72°C/7 s (45 cycles); cooling 40°C/30 s. For DPD, the primers used in PCR were forward 5′AAGATGCCATCTTCCAAGGC 3′ and reverse 5′AGATGTTGCACAGTCGAAGG 3′. The hybridization probes were fluoresce in probe 5′CAGTAAAGCAGGAATGTGCGCCT 3′-fluorescein and LC Red640 probe, LC Red640–5′TCACTCTCCATTGCCATCGATACG 3′-phosphorylation. Real-time PCR methods for glyceraldehyde-3-phosphate dehydrogenase (GenBank accession number M33197; GAPDH) have been previously described [9].

We examined the correlation between DPD gene expression measured by conventional RT-PCR and real-time quantitative RT-PCR. There was a strong correlation between these two parameters (r=0.90, P<0.0001; Fig. 1). Therefore, only the results of the conventional RT-PCR methods were analyzed in this study.

ELISA

The DPD protein level was determined by a sandwich ELISA with two monclonal antibodies specific to human DPD (4B9 and 3A5) according to a method previously described in 15 tissue specimens [19]. DPD levels were expressed as units per milligram of protein, and one unit is equivalent to the amount of DPD protein that catabolizes 1 pmol fluorouracil (5-FU) per minute. The DPD protein level measured by this ELISA strongly correlated with DPD activity measured by the enzyme reaction assay [19].

Immunohistochemistry

To examine DPD protein localization, 15 tissue samples of normal endometrium and 9 of those of endometrial cancer were used for immunohistochemistry. For examination of PCNA index, 46 tissue samples were used. Immunohistochemical analysis was performed on 4-μm formalin-fixed, paraffin-embedded tissue sections as previously reported [7]. For antigen retrieval, slides were mi-

crowaved 2×5 min in 0.01 M citrate buffer (pH 6.0) for PCNA. Primary antibodies were a rabbit polyclonal antibody (1:100; Taiho, Hanna, Japan) for DPD and a mouse monoclonal antibody PC 10 (1:50; Dako, Copenhagen, Denmark) for PCNA. The characteristics of the anti-DPD polyclonal antibody have been previously described [22]. The PCNA index was determined by counting at least 1000 epithelial cells, expressed as a percentage of positive nuclear cells. To assess the immunospecificity of each antibody, normal rabbit or mouse serum (negative control) was used instead of primary antibodies.

Statistical analysis

Results are expressed as the mean ± SEM. Student's test (for comparison of two groups) or one-way analysis of variance (ANOVA; for comparison of more than two groups) was used to evaluate numeric data. The chi-square test or Fisher's exact test was used for comparisons of categorical data. The correlation coefficient (r) between different parameters was determined by simple regression analysis. A value of $P<0.05$ was considered statistically significant.

Results

DPD expression in normal and malignant endometria

DPD gene expression correlated significantly with the DPD protein level using ELISA in 15 resected specimens (r=0.73, $P<0.01$; Fig. 2). DPD gene expression in normal endometria during the menstrual cycle and endometrial cancer is shown in Fig. 3. In normal endometria, DPD gene expression was relatively stable in various menstrual phases, but was significantly elevated in postmenopausal status compared with any menstrual phase ($P<0.0001$ to $P<0.05$). It was lower in endometrial cancer than the normal endometrium ($P<0.01$). In endometrial cancer, there was no significant correlation between DPD gene expression and any clinicopathological factor (patient age, FIGO stage, histological type, or histological grade).

The usual pattern of immunohistochemical DPD protein expression was cytoplasmic and diffuse in the endometrial epithelial cells (Fig. 4A). DPD immunoreactivity was also found in stromal and inflammatory cells (Fig. 4B, C). Apparent difference in DPD staining pattern in different menstrual phases or between normal endometrium and endometrial cancer was not found. Because of the small number of samples, we could not determine the relationship between DPD protein expression and clinico-biological factors.

Relationship among DPD gene expression, PCNA index, and TP gene expression

DPD gene expression correlated inversely with the PCNA index in normal and malignant endometria (r=0.32, $P<0.05$; Fig. 5). In the normal endometria, during the menstrual cycle TP gene expression was highest in the mid-secretory phase and gradually decreased in the late proliferative phase (Fig. 6). In contrast to DPD gene expression, TP gene expression was lowest in postmenopausal status, but highest in endometrial cancer. TP gene expression did not correlate with DPD gene expression in the normal and malignant endometria (r=0.06; Fig. 7). For combined analysis of DPD and TP gene status, we calculated a ratio of TP to DPD gene expression (TP/DPD ratio). High-TP/DPD ratio (>2) was significantly more frequent in endometrial cancer (93%) than the normal endometrium in any menstrual phase (20–64%; $P<0.001$ to $P<0.05$) and postmenopausal status (0%; $P<0.0001$; Table 1).

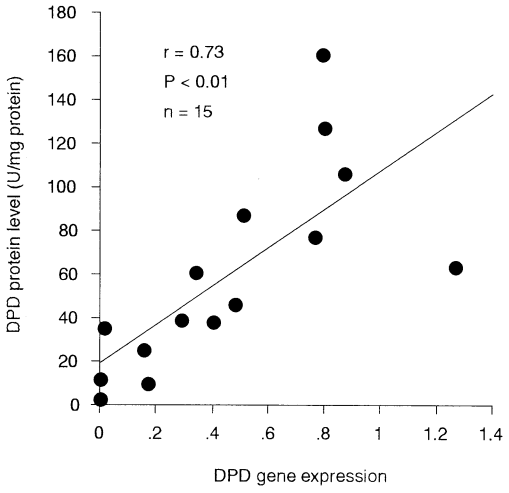

Fig. 2 Scatter diagram of dihydropyrimidine dehydrogenase (DPD) gene expression and DPD protein level in normal and malignant endometrium

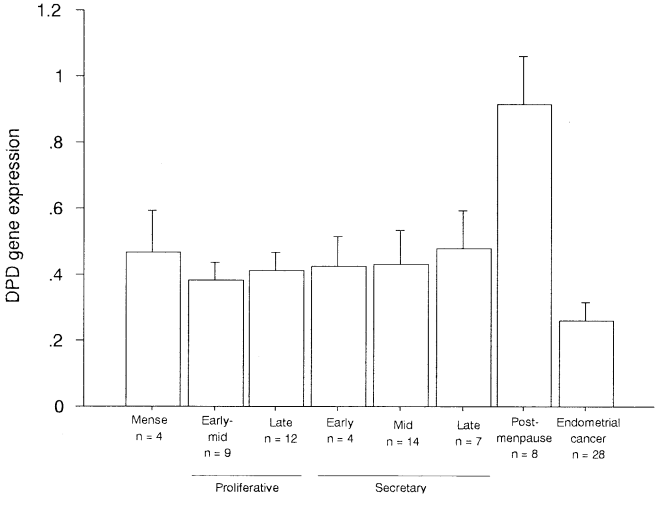

Fig. 3 Distribution of dihydropyrimidine dehydrogenase gene expression in endometrium in various states. *Columns* mean, *bars* SEM. Post-menopause versus mense, $P<0.05$; versus early/mid-proliferative, late-proliferative, and mid-secretory, $P<0.001$; versus early-secretory and mid-secretory, $P<0.01$; versus endometrial cancer, $P<0.0001$

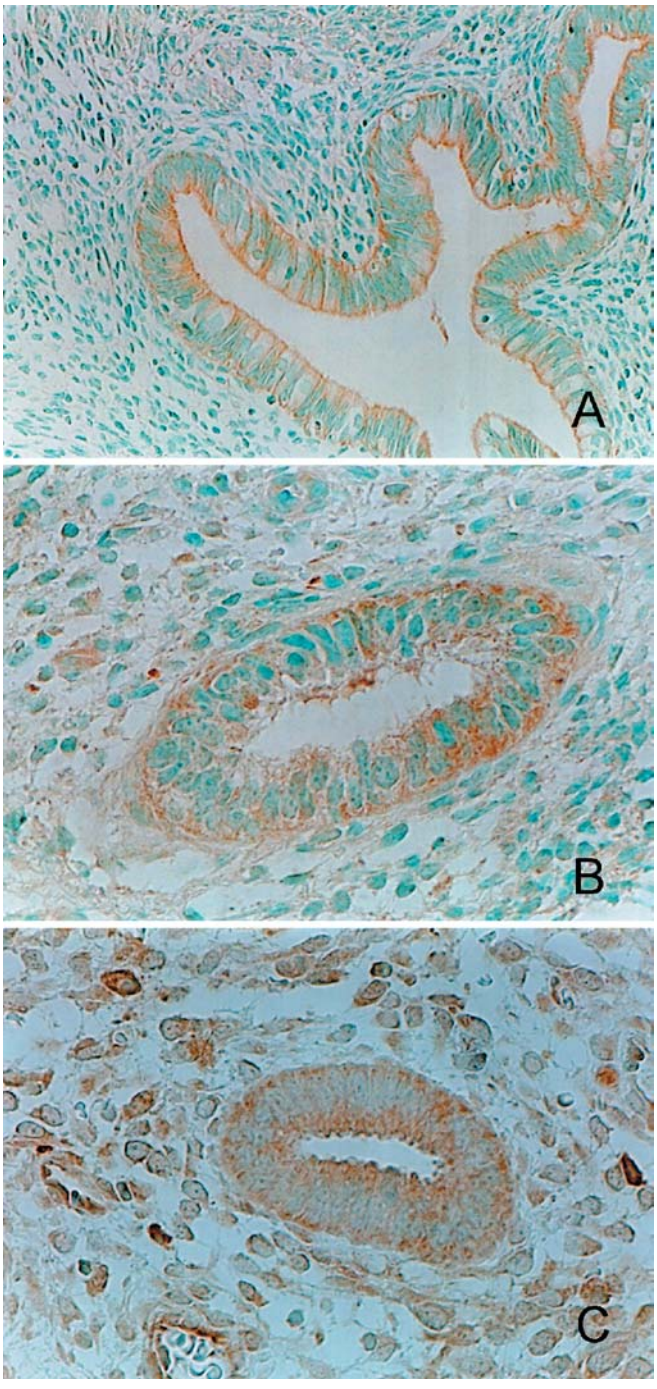

Fig. 4 Endometrium immunohistochemical staining using antibodies to dihydropyrimidine dehydrogenase (DPD). **A** Cytoplasmic DPD immunostaining was found only in endometrial epithelial cells (×50). **B** DPD immunoreactivity was mainly observed in endometrial epithelial cells, but slight immunoreactivity was also found in endometrial stromal cells (×100). **C** Both epithelial and stromal cells had strong DPD expression (×100)

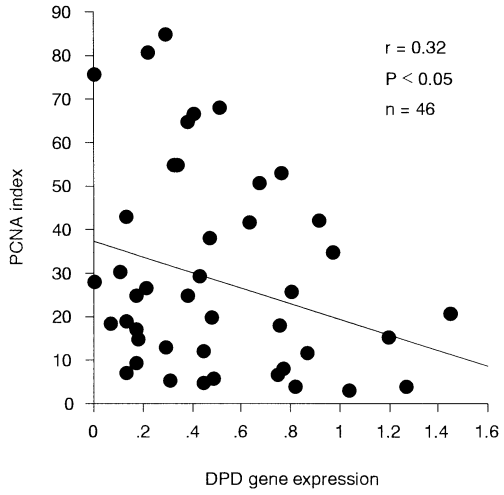

Fig. 5 Scatter diagram of dihydropyrimidine dehydrogenase gene expression and proliferating cell nuclear antigen index in normal and malignant endometrium

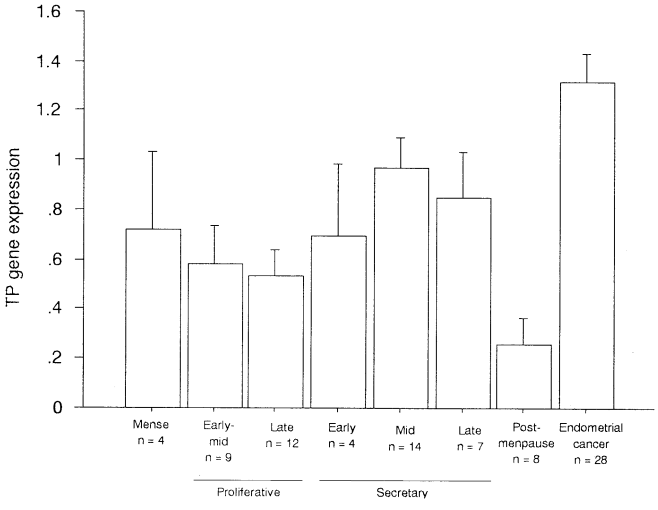

Fig. 6 Distribution of thymidine phosphorylase (TP) gene expression in endometrium in various status. TP gene expression: *Columns* mean, *bars* SEM. Endometrial cancer versus early/mid-proliferative, $P<0.01$; versus late-proliferative, $P<0.001$; versus post-menopause, $P<0.0001$; mid-secretory versus late-proliferative, $P<0.05$; versus post-menopause, $P<0.01$

Discussion

We report the first study of DPD expression in human normal and malignant endometria. Localization analysis revealed that the DPD protein was located primarily in endometrial epithelial cells, but was also present in stromal cells. DPD gene expression, which correlated significantly with DPD protein levels measured using ELISA, was relatively stable throughout various menstrual phases, but was significantly elevated in postmenopausal patients. Reporting results consistent with ours, Queener et al. [24] demonstrated that DPD activity in the rat liver gradually increased with age, and was about 2.5-fold higher in the adult rat liver than in the newborn rat liver. DPD gene expression was significantly lower in endometrial cancer than in normal endometria, which is consistent with assays of colon, hepatocellular, and ovarian cancers [8, 15, 17]. Experimental studies demon-

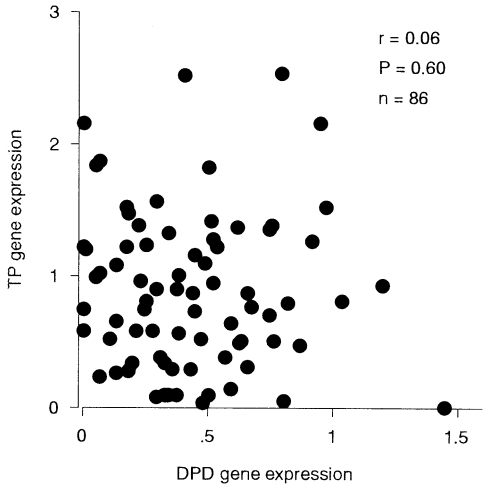

Fig. 7 Scatter diagram of dihydropyrimidine dehydrogenase gene expression and thymidine phosphorylase in normal and malignant endometrium

Table 1 The frequency of high ratio of thymidine phosphorylase to dihydropyrimidine dehydrogenase gene expression (TP/DPD ratio)

	No.	The frequency of high TP/DPD ratio (>2)
Normal endometria		
Menstrual	4	50%
Early-mid proliferative	9	33%[a]
Late proliferative	12	25%[b]
Early secretory	4	25%[c]
Mid secretory	14	64%[d]
Late secretory	7	14%[e]
Post-menopausal	8	0%[f]
Endometrial cancer	28	93%[g]

P<0.001: g versus a, c, e
P<0.0001: g versus b, f
P<0.05: g versus d

strated that the level of DPD activity in malignant murine neuroblastoma cell lines was inversely related to malignant behavior [27]. Although the details of underlying mechanisms remain unclear, increasing age and malignant potential may be associated with the regulation of DPD in human endometria. Investigation of the pyrimidine salvage pathway is important because these enzymes may critically regulate the pyrimidine nucleotide pool concentration required for DNA and RNA biosynthesis during cellular proliferation [27]. In this study, DPD gene expression correlated inversely with the PCNA index (a proliferative marker) in normal and malignant endometrium. Our results are consistent with a study that showed DPD activity decreased in parallel with an increase in rat hepatoma growth rate [24]. DPD downregulation in the normal endometrium at certain phases of the menstrual cycle and in the case of endometrial cancer results in decreased thymine and uracil catabolism. This may create a favorable environment for cyclic cellular proliferation during the menstrual cycle and with endometrial cancerous growth.

The lack of correlation between DPD and TP gene expression in normal and malignant endometrial specimens suggests that DPD and TP genes are controlled by independent mechanisms in these tissues. Previous studies demonstrated that progesterone, some cytokines, and typical microenvironmental characteristics of cancer tissues, such as hypoxia and low pH, resulted in specific upregulation of TP expression [3, 10, 23, 28]. High TP expression, which was found in the normal endometrium in the mid-secretory phase and in endometrial cancer, stimulates angiogenic effects [13, 16, 18]. Combination analysis showed that a high-TP to DPD ratio was significantly more frequent in endometrial cancer than normal endometrium regardless of menstrual status. Because thymine has been shown to prevent hypoxia-induced apoptosis in human KB epidermoid carcinoma cells in vitro [16], an increased thymine level resulting from a high TP/DPD ratio may enhance anti-apoptotic activity and may enhance tumor growth in endometrial cancer. In normal endometrium, high TP/DPD ratio was more frequent in the mid-secretory phase because of increased TP gene expression. However, whether TP expression is increased in the glandular or the stromal component of the endometrium and its biological roles remain unclear.

An imbalance of TP and DPD may influence the effect of prodrugs of 5-FU (capecitabine and 5′-deoxy-5-fluorouridine). These drugs are metabolized by TP to active 5-FU, and subsequently to the inactive dihydrofluorouracil by DPD. Because of this, the efficacy of these drugs has been shown to correlate with a high TP/DPD activity ratio in xenograft models of various human cancer cell lines and in clinical specimens of gastric cancer [14, 25]. The high-TP to DPD ratio that is found frequently in endometrial cancer, compared with normal endometrium, may offer an exploitable opportunity to enable tumor-specific activation of these drugs. DPD may act cooperatively with TP to affect cell function by maintaining the balance of the pyrimidine nucleotide pool in normal and malignant endometrium. Thus, this may present an important opportunity for therapeutic intervention for treatment of endometrial cancer.

Acknowledgements This work was supported by a Grant-in-Aid (No. 13770917) from the Japan Society for the Promotion of Science. We thank Mr. Mikio Koike, Laboratory Medicine and Central Clinical Laboratory, Shimane Medical University, for providing paraffin-embedded tissues and Miss Taeko Yamada, Department of Obstetrics and Gynecology, Shimane Medical University, for her management of medical records.

References

1. Brown NS, Bicknell R (1998) Thymidine phosphorylase, 2-deoxy-D-ribose and angiogenesis. Biochem J 334:1–8
2. Canellakis ES (1956) Pyrimidine metabolism-enzymatic pathways of uracil and thymidine degradation. J Biol Chem 221:315–322

3. Eda H, Fujimoto K, Watanabe S, Ura M, Hino A, Tanaka Y, Wada K, Ishitsuka H (1993) Cytokines induce thymidine phosphorylase expression in tumor cells and make them more susceptible to 5′-deoxy-5-fluorouridine. Cancer Chemother Pharmacol 32:333–338
4. Fink RM, Fink K, Henderson RB (1955) Beta-amino acid formation by tissue slices incubated with pyrimidines. J Biol Chem 201:349–355
5. Fujimoto J, Ichigo S, Sakaguchi H, Hirose R, Tamaya T (1998) Expression of platelet-derived endothelial cell growth factor and its mRNA in uterine endometrium during the menstrual cycle. Mol Hum Reprod 4:509–513
6. Fujiwaki R, Hata K, Iida K, Koike M, Miyazaki K (1998) Immunohistochemical expression of thymidine phosphorylase in human endometrial cancer. Gynecol Oncol 68:247–252
7. Fujiwaki R, Hata K, Iida K, Maede Y, Koike M, Miyazaki K (1999) Thymidine phosphorylase expression in progression of cervical cancer: correlation with microvessel count, proliferating cell nuclear antigen, and apoptosis. J Clin Pathol 52:598–603
8. Fujiwaki R, Hata K, Nakayama K, Fukumoto M, Miyazaki K (2000) Gene expression for dihydropyrimidine dehydrogenase and thymidine phosphorylase influences outcome in epithelial ovarian cancer. J Clin Oncol 18:3946–3951
9. Fujiwaki R, Hata K, Nakayama K, Moriyama M, Iwanari O, Katabuchi H, Okamura H, Sakai E, Miyazaki K (2002) Thymidine kinase in epithelial ovarian cancer: relationship with the other pyrimidine pathway enzymes. Int J Cancer 99:328–335
10. Griffiths L, Dachs GU, Bicknell R, Harris AL, Stratford IJ (1997) The influence of oxygen tension and pH on the expression of platelet-derived endothelial cell growth factor/thymidine phosphorylase in human breast tumor cells grown in vitro and in vivo. Cancer Res 57:570–572
11. Ho DH, Townsend L, Luna MA, Bodey GP (1986) Distribution and inhibition of dihydrouracil dehydrogenase activities in human tissues using 5-fluorouracil as a substrate. Anticancer Res 6:781–784
12. Iltzsch MH, el Kouni MH, Cha S (1985) Kinetic studies of thymidine phosphorylase from mouse liver. Biochemistry 24:6799–6807
13. Ishikawa F, Miyazono K, Hellman U, Drexler H, Wernstedt C, Hagiwara K, Usuki K, Takaku F, Risau W, Heldin CH (1989) Identification of angiogenic activity and the cloning and expression of platelet-derived endothelial cell growth factor. Nature 338:557–562
14. Ishikawa T, Sekiguchi F, Fukase Y, Sawada N, Ishitsuka H (1998) Positive correlation between the efficacy of capecitabine and doxifluridine and the ratio of thymidine phosphorylase to dihydropyrimidine dehydrogenase activities in tumors in human cancer xenografts. Cancer Res 58:685–690
15. Jiang W, Lu Z, He Y, Diasio RB (1997) Dihydropyrimidine dehydrogenase activity in hepatocellular carcinoma: implication in 5-fluorouracil-based chemotherapy. Clin Cancer Res 3:395–399
16. Kitazono M, Takebayashi Y, Ishitsuka K, Takao S, Tani A, Furukawa T, Miyadera K, Yamada Y, Aikou T, Akiyama S (1998) Prevention of hypoxia-induced apoptosis by the angiogenic factor thymidine phosphorylase. Biochem Biophys Res Commun 253:797–803
17. McLeod HL, Sludden J, Murray GI, Keenan RA, Davidson AI, Park K, Koruth M, Cassidy J (1998) Characterization of dihydropyrimidine dehydrogenase in human colorectal tumours. Br J Cancer 77:461–465
18. Moghaddam A, Zhang HT, Fan TP, Hu DE, Lees VC, Turley H, Fox SB, Gatter KC, Harris AL, Bicknell R (1995) Thymidine phosphorylase in angiogenic and promotes tumor growth. Proc Natl Acad U S A 92:998–1002
19. Mori K, Hasegawa M, Nishida M, Toma H, Fukuda M, Kubota T, Nagasue N, Yamana H, Hirakawa-YS Chung K, Ikeda T, Takasaki K, Oka M, Kameyama M, Toi M, Fujii H, Kitamura M, Murai M, Sasaki H, Ozono S, Makuuchi H, Shimada Y, Onishi Y, Aoyagi S, Mizutani K, Ogawa M, Nakao A, Kinoshita H, Tono T, Imamoto H, Nakashima Y, Manabe T (2000) Expression levels of thymidine phosphorylase and dihydropyrimidine dehydrogenase in various human tumor tissues. Int J Oncol 17:33–38
20. Noyes RW, Hertig AT, Rock J (1955) Dating the endometrial biopsy. Fertil Steril 1:3–25
21. Naguib FN, el Kouni MH, Cha S (1985) Enzymes of uracil catabolism in normal and neoplastic human tissues. Cancer Res 45:5405–5412
22. Okabe H, Arakawa K, Takechi S, Fukushima M (2000) Expression of recombinant human dihydropyrimidine dehydrogenase and its application to the preparation of anti-DPD antibodies for immunohistochemical detection. Jpn J Cancer Chemother 27:891–898
23. Osuga Y, Toyoshima H, Mitsuhashi N, Taketani Y (1995) The presence of platelet-derived endothelial cell growth factor in human endometrium and its characteristic expression during the menstrual cycle and early gestational period. Hum Reprod 10:989–993
24. Queener SF, Morris HP, Weber G (1971) Dihydrouracil dehydrogenase activity in normal, differentiating, and regenerating liver and hepatomas. Cancer Res 31:1004–1009
25. Terashima M, Fujiwara H, Takagane A, Abe K, Araya M, Irinoda T, Yonezawa H, Nakaya T, Oyama K, Takahashi M, Saito K (2002) Role of thymidine phosphorylase and dihydropyrimidine dehydrogenase in tumour progression and sensitivity to doxifluridine in gastric cancer patients. Eur J Cancer 38:2375–2381
26. Tuchman M, Ramnaraine ML, O'Dea RF (1985) Effects of uridine and thymidine on the degradation of 5-fluorouracil, uracil, and thymine by rat liver dihydropyrimidine dehydrogenase. Cancer Res 45:5553–5556
27. Tuchman M, O'Dea RF, Ramnaraine ML, Mirkin BL (1988) Pyrimidine base degradation in cultured murine C-1300 neuroblastoma cells and in situ tumors. J Clin Invest 81:425–430
28. Zhang L, Mackenzie IZ, Rees MC, Bicknell R (1997) Regulation of the expression of the angiogenic enzyme platelet-derived endothelial cell growth factor/thymidine phosphorylase in endometrial isolates by ovarian steroids and cytokines. Endocrinology 138:4921–4930

Virchows Arch (2003) 443:678–685
DOI 10.1007/s00428-003-0867-2

ORIGINAL ARTICLE

Sylvia Stadlmann · Ruth Raffeiner · Albert Amberger · Raimund Margreiter · Alain Gustave Zeimet · Burkhardt Abendstein · Patrizia Lucia Moser · Gregor Mikuz · Bernd Klosterhalfen · Felix Albert Offner

Disruption of the integrity of human peritoneal mesothelium by interleukin-1β and tumor necrosis factor-α

Received: 6 May 2003 / Accepted: 24 June 2003 / Published online: 26 July 2003
© Springer-Verlag 2003

Abstract Inflammatory and neoplastic disease processes of the abdominal cavity are frequently associated with disruption of the integrity of the peritoneal mesothelium. In the present study, we analyzed the effects of the pro-inflammatory cytokines interleukin-1β (IL-1β) and tumor necrosis factor-α (TNF-α) on the morphology and expression of adhesion molecules of human peritoneal mesothelial cells (HPMC). Treatment of HPMC with IL-1β and TNF-α resulted in a time- and dose-dependent alteration of the normal cobblestone morphology of the mesothelium with loss of polarization, cellular retraction and exposure of the submesothelial matrix. The effect was already observable after 6 h of treatment and was most pronounced at a dose of 10 ng/ml of IL-1β or TNF-α. These morphological alterations were associated with a significant rearrangement of the expression of mesothelial adhesion molecules as detected by flow cytometry. IL-1β and TNF-α both led to a loss of the expression of the hemidesmosomal integrin subunits α6 (P<0.01 and P<0.001) and β4 (P<0.01) and an increased expression of the integrin subunit α5 (P<0.001 and P<0.01). IL-1β furthermore upregulated the expression of the integrin subunits α1, α2 and the adhesion molecule CD44 while the latter was downregulated by TNF-α. Our data indicate that IL-1β and TNF-α may significantly affect disease processes of the abdominal cavity by their potential to disrupt the mesothelial basal cell-matrix adhesion and, thus, the integrity of the peritoneal mesothelial cell lining.

Keywords Peritoneal mesothelial cells · Integrins · CD44 · Pro-inflammatory cytokines

S. Stadlmann · R. Raffeiner · P. L. Moser · G. Mikuz
Institute of Pathology, University of Innsbruck,
6020 Innsbruck, Austria

A. Amberger
Tyrolean Cancer Research Institute, 6020 Innsbruck, Austria

R. Margreiter
Department of Transplant Surgery,
D. Swarovski Research Laboratory, University Hospital Innsbruck,
6020 Innsbruck, Austria

A. G. Zeimet
Department of Obstetrics and Gynecology,
University of Innsbruck, 6020 Innsbruck, Austria

B. Abendstein
Department of Obstetrics and Gynecology,
Hospital Hall, 6060 Hall in Tirol, Austria

B. Klosterhalfen
Institute of Pathology,
RWTH-Aachen, 52062 Aachen, Germany

F. A. Offner (✉)
Institute of Pathology, Academic Teaching Hospital Feldkirch,
6800 Feldkirch, Austria
e-mail: felix.offner@lkhf.at
Tel.: +43-5522-3033400
Fax: +43-5522-3037521

Introduction

The peritoneal mesothelium is a highly specialized monolayer of polarized flat epithelial cells that covers the entire surface of the abdominal cavity. It serves as a protective anatomical barrier, as a non-adhesive friction-less interface for the movement of abdominal organs and is involved in the formation and turnover of abdominal fluid [7, 27]. The integrity of the mesothelial cell lining is a prerequisite for these functions.

Injury to the abdominal cavity is a common phenomenon. It can be caused by trauma, surgery, infections, or various neoplasms. Both inflammatory and neoplastic disease processes involving the abdominal cavity are associated with marked structural alterations of peritoneal mesothelium, which include loss of polarization, cellular retraction with exposure of the submesothelial extracellular matrix (ECM) and frequently detachment and suspension of mesothelial cells in peritoneal effusions

[7, 27, 39]. The precise pathomechanisms involved in the disruption of the mesothelial integrity are still poorly defined but are likely to involve alterations of the expression of mesothelial adhesion molecules [4, 6, 33].

Mesothelial cells, like other epithelial cells, adhere to the ECM by various adhesion molecules. Of particular importance are integrins, a group of transmembraneous heterodimeric glycoproteins composed of α and β subunits [11, 28]. There are at least 16 α and 8 β subunits with intracellular domains associated with the cytoskeleton and extracellular domains that bind to the ECM. The classical fibronectin receptor ($\alpha5\beta1$), the $\alpha V\beta1$ fibronectin receptor, and the $\alpha6\beta1$ laminin receptor appear to have specific ligands [28]. Other members of the integrin subfamiliy can exhibit different ligand specificities, depending on the cell type by which they are expressed. In addition to their role as adhesion molecules, integrins function as signaling receptors and have been demonstrated to modulate cellular differentiation, growth, and migration as well as cell shape and cytoskeletal organization [5, 11]. An important integrin-independent mechanism of the adhesion of mesothelial cells to the ECM is provided by CD44 [12].

Inflammatory as well as malignant peritoneal effusions contain a variety of cytokines, which may affect and alter the functions and the structure of the peritoneal mesothelial cell lining [16, 20, 26, 34, 41]. Studies from our group and others suggest that the pro-inflammatory cytokines interleukin (IL)-1β and tumor necrosis factor-α (TNF-α) are key regulators of the pathobiological functions of the peritoneal mesothelium. They stimulate human peritoneal mesothelial cells (HPMC) to a markedly increased secretion of various cytokines such as IL-6, IL-8, transforming growth factor-β (TGF-β), basic fibroblast growth factor (bFGF), and vascular endothelial cell growth factor (vEGF) and, thus, seem to induce an "activated" mesothelial cell phenotype [9, 19, 25, 35, 36].

In the present study, we investigated the effects of IL-1β and TNF-α on the morphology, adhesive properties, and expression of adhesion molecules of HPMC.

Materials and methods

Isolation and culture of HPMC

HPMC were obtained from omental tissue of consenting patients undergoing elective abdominal surgery as described previously [25]. In every case small pieces of the omental specimens were fixed in formalin, embedded in paraffin and used to control the morphology of the mesothelium on hematoxylin & eosin-stained sections (Fig. 1E, F). The rest of the omental tissue (approximately 1–3 cm^3) was rinsed in phosphate-buffered saline (PBS, Seromed, Biochrom, Berlin, Germany) at room temperature and incubated in a collagenase I solution (0.88–1.76 mg/ml, 220 U/ml; Seromed) for 1 h at 37°C. Subsequently, the collagenase solution containing the detached mesothelial cells was filtered through a 70 µm cell strainer and centrifuged at 500 g for 10 min. The cell pellet was resuspended in RPMI-1640 medium (Seromed) supplemented with 10% fetal calf serum (Sebak, Suben, Austria), penicillin/streptomycin (200 U/ml, 200 µg/ml; Seromed) and L-glutamine (2 mM; Seromed) and grown to confluence in 25-cm^2 tissue culture flasks (Greiner, Kremsmuenster, Austria) at 37°C in a humidified atmosphere of 5% CO_2 in air. Primary cultures of HPMC were characterized by flow cytometry using monoclonal antibodies (mAbs) against cytokeratin subtypes 8 and 18 (MAb CAM 5.2; Becton Dickinson, Mountain View, CA) and vimentin (MAb V9; Dakopatts, Glostrup, Denmark) and the demonstration of a uniform coexpression of both intermediate filaments. Passage 2 cultures were used for experiments.

Treatment of HPMC with pro-inflammatory cytokines

For experiments, HPMC were detached with trypsine/versene (0.05%/0.02%), washed once in medium and seeded in 12.5-cm^2 falcon flasks in a volume of 2.5 ml. After confluency, the cultures were washed twice with fresh culture medium and then incubated for 0–48 h in the absence or presence of the appropriate cytokines. Recombinant IL-1β and interferon (IFN)-γ were purchased from R&D Systems (Minneapolis, USA). TNF-α was obtained from Sigma (Munich, Germany). Incubation of cells with cytokines did not have any significant effect on cell viability as shown by trypan blue exclusion and a cell analyzer system CASY1 (Schärfe System, Reutlingen, Germany) and did not induce apoptosis as demonstrated by flow cytometry (see below). All experiments were done in duplicate.

Scanning electron microscopy

For scanning electron microscopy, HPMC were grown to confluency on glass slides placed in 12-well culture dishes and treated with the respective cytokines as described above. They were then fixed in 3% glutaraldehyde in 0.1 mol/l (molar) sodium cacodylate, pH 7.5 for 30 min, postfixed in 1% OsO_4, in 0.1 mol/l cacodylate, rinsed in water, and dehydrated through graded ethanol. Thereafter, the specimens were critical-point dried from absolute ethanol in a critical point dryer using CO_2 as transition medium. The dried preparations were coated with 20 nm gold in a sputter coater, and viewed on a Philips SEM 515 scanning electron microscope at 15 kv or 30 kv.

Analysis of adhesion molecule expression by fluorescence activated cell sorting

Analysis of adhesion molecules was conducted in cells that were incubated at the various culture conditions for 48 h. At the end of the incubation period, HPMC were washed in PBS and harvested by gentle treatment with 0.05% versene (Biochrom, Berlin, Germany) as described previously [2]. Cell numbers were determined by a cell counter and analyzer (CASY1). After centrifugation, cells were resuspended in PBS supplemented with 1% BSA. Thereafter, 100,000 cells were incubated with the appropriate monoclonal antibodies in a volume of 100 µl at 4°C for 30 min. Antibodies used were fluorescein-isothiocyanate (FITC)-conjugated mouse anti-human integrin $\alpha1$ (CD49a), integrin $\alpha2$ (CD49b), integrin $\alpha3$ (CD49c), integrin $\alpha4$ (CD49d), integrin $\alpha5$ (CD49e), integrin $\alpha6$ (CD49f), integrin $\beta1$ (CD29) and anti-CD44 from Serotec (Oxford, Great Britain; Table 1). A monoclonal antibody against human $\beta4$ integrin (CD104) was purchased from Calbiochem (Novabiochem, La Jolla, USA; Table 1). After incubation, the cells were washed three times in PBS, suspended in a volume of 200 µl PBS and stored at 4°C until fluorescence activated cell sorting (FACS) analysis. For analysis of integrin $\beta4$, the cells were incubated with anti-mouse rabbit IgG conjugated with FITC (Calbiochem-Novabiochem) at 4°C for 30 min at a dilution of 1:15. Immediately before FACS analysis, cells were stained with propidium iodide (20 µg/ml) to determine cell viability. To rule out apoptosis parallel samples (100,000 cells) for each probe were collected and apoptosis was determined according to Nicoletti et al. [22]. HPMC incubated with mouse anti-human IgG1-HCG as primary antibody and FITC-conjugated F(ab′)2 rabbit anti-mouse

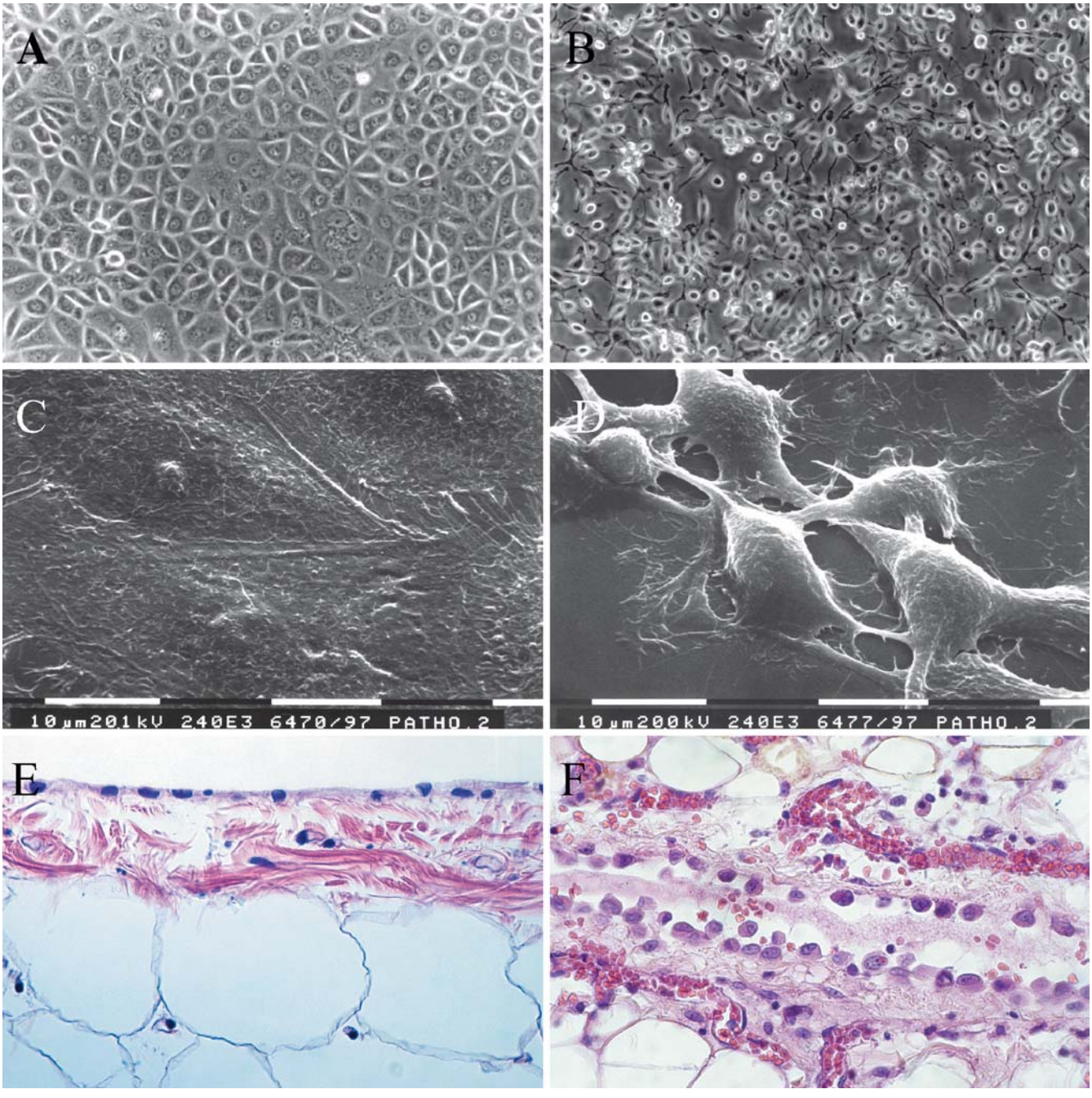

Fig. 1 **A** Confluent human peritoneal mesothelial cells (HPMC) under control conditions. HPMC are organized in monolayers of flat polygonal cells with close cell–cell contacts giving a cobblestone appearance. Phase contrast microscopy ×200. **B** Confluent mesothelial cells after treatment with interleukin (IL)-1β (10 ng/ml) for 48 h. HPMC show retraction of the cytoplasms, loss of cell–cell contacts and extensive exposure of the submesothelial matrix. Phase contrast microscopy ×200. **C** HPMC under control conditions. Cells are flat and connected to each other by fine intercellular bridges. There is almost no exposure of the submesothelium. Scanning electron microscopy; *bar* 10 µm. **D** HPMC treated for 48 h with IL-1β (10 ng/ml). The cells reveal plump cellular processes and show a rounded, cuboidal shape. There is extensive exposure of the submesothelial matrix (*stars*). Scanning electron microscopy; *bar*=10 µm. **E** Omental specimen used for one of the experiments prior to isolation of HPMC. The mesothelium is flat and resting on a layer of submesothelial matrix. Hematoxylin & eosin ×40. **F** Omental specimen with cellular retraction and cuboidalization, presumably due to early inflammation. Note the similarity to the mesothelial changes depicted in **B** and **D**. The cells isolated from this specimen were not used for experiments

Table 1 Antibodies and dilutions used for fluorescence activated cell sorting analysis

Antigen	VLA-subtype	Clone	Isotype	Substrate	Dilution	Source
Integrin α1 (CD49a)	VLA-1	TS2/7	IgG1 (mouse)	Collagen, laminin	1:60	Serotec
Integrin α2 (CD49b)	VLA-2	AK7	IgG1 (mouse)	Collagen, laminin	1:30	Serotec
Integrin α3 (CD49c)	VLA-3	11G5	IgG1 (mouse)	Fibronectin, laminin	1:30	Serotec
Integrin α4 (CD49d)	VLA-4	44H6	IgG1 (mouse)	Fibronectin	1:30	Serotec
Integrin α5 (CD49e)	VLA-5	SAM-1	IgG2b (mouse)	Fibronectin	1:30	Serotec
Integrin α6 (CD49f)	VLA-6	4F10, 450–30A	IgG2b, IgG1 (mouse)	Laminin	1:30	Serotec
Integrin β1 (CD29)	VLA-β1	3S3, 4B7	IgG1 (mouse)	–	1:30	Serotec
Integrin β4 (CD104)	VLA-β4	3E1	IgG1 (mouse)	–	1:1000	Calbiochem
CD44	–	F10–44–2	IgG2a (mouse)	Hyaluronate, fibronectin, collagen	1:30	Serotec

IgG as secondary antibody served as negative controls. Fluorescence intensity was calculated with the CellQuest Software (Becton Dickinson). Overlap of spectral signals when double staining the samples for viability (PI) and integrin/CD44 expression (FITC) was excluded by appropriate compensations. Since the yield of median fluorescence intensities differed between the donors of HPMC, results are expressed as percentage of controls that were set as 100%. Human umbilical vein endothelial cells were used as a control to analyze adhesion molecule expression. They were isolated as described previously [2]. For experiments they were treated in a similar fashion as HPMC.

Statistical analysis

All experiments were performed at least five times in duplicates. Statistical analysis was performed using the Student's *t*-test for paired data with Excel for MS Windows. Fluorescence intensities are presented as median values ± median absolute deviation in relation to controls, which were set as 100% [29]. A P value under 0.05 was considered significant.

Results

Disruption of the mesothelial cell integrity by IL-1β and TNF-α

Under control conditions, confluent HPMC formed a monolayer of flat polygonal, polarized cells exhibiting a typical cobblestone morphology. The cells were connected to each other by tight cell junctions and covered the whole submesothelial matrix without any visible intercellular clefts (Fig. 1A). These observations were also confirmed by scanning electron microscopy that revealed multiple fine cellular processes between the flat mesothelial cells (Fig. 1C).

Treatment of HPMC with the pro-inflammatory cytokines IL-1β or TNF-α resulted in a dramatic change of the morphology of the mesothelium and a disruption of its integrity. The cells revealed a retraction of their cytoplasms with loss of cell–cell contacts and a consecutive exposure of the submesothelial matrix. This phenomenon appeared to occur rapidly and in a time- and dose-dependent fashion. The maximal effect was seen at doses of 10 ng/ml of either IL-1β or TNF-α. At this dose, the first signs of cellular retraction became already evident after only 6 h of treatment. Over time, the morphological alterations developed in a progressive manner with a maximum effect after 24–48 h of incubation. At this time, the mesothelial cell monolayer showed a complete disorganization with loss of cellular polarization (Fig. 1B). The adhesion of the cells to the submesothelial matrix seemed to be only granted by residual thin finger-like cellular processes and there was a denudation of large areas of the submesothelial matrix (Fig. 1D). Similar, but less pronounced effects were already noticed at doses of 0.1 ng/ml of both pro-inflammatory cytokines. Doses of 0.01 ng/ml were, however, not effective in changing the morphology of the mesothelium. The effects induced by IL-1β and TNF-α were consistently observed in independent experiments in HPMC derived from ten different donors, both male and female. Treatment with IFN-γ was not associated with any structural alterations of the mesothelium.

Analyses of mesothelial adhesion molecules

The disruption of the structural integrity of the mesothelium by IL-1β and TNF-α was associated with a significant alteration of the expression of mesothelial adhesion molecules. Under control conditions, the mesothelial cells showed a distinct expression of the integrin subunits α2, β1, β4 and CD44 and a comparably lower expression of integrin subunits α1, α5 and α6. The integrin subunits α3 and α4 were not detectable.

Treatment of HPMC with IL-1β (10 ng/ml) for 48 h resulted in a significant increase of the expression of the integrins α1, α2, and α5 (Fig. 2A). The median fluorescence levels of the subunits α1, α2, and α5 were increased by 35.7±16.3% (P<0.05), 75.7±22.3 (P<0.01), and 28.7±6.5% (P<0.001), respectively. In addition, IL-1β induced a significant upregulation of the CD44 molecule with median fluorescence levels being 40.5±12.5% (P<0.001; Fig. 3) over control values. In contrast, IL-1β induced a loss of the expression of the laminin receptor α6 integrin. The respective median fluorescence intensity showed a significant reduction to 77±8.6% (P<0.01) of the control levels (Fig. 2A). The expression of β4 was also reduced by IL-1β, but this effect did not reach statistical significance. Interestingly, treatment with TNF-α (10 ng/ml) also led to a loss of the α6β4 integrin. Under these conditions, the median fluorescence levels of the α6

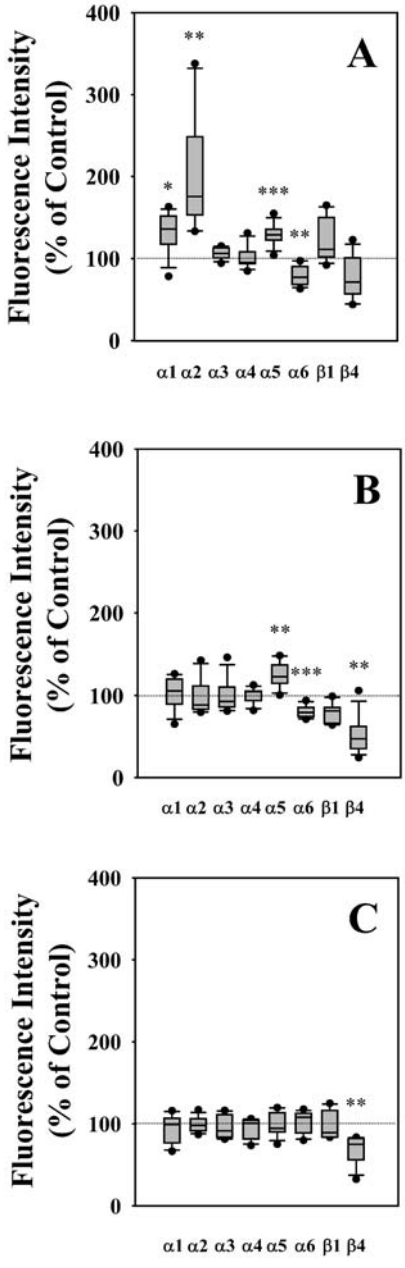

Fig. 2 Regulation of the expression of mesothelial integrins by pro-inflammatory cytokines. The 10th, 25th, 50th (median), 75th and 90th percentiles of the percentage increase/decrease of the expression of α and β integrin subunits after treatment with interleukin (IL)-1 β (A), tumor necrosis factor (TNF)-α (B) or interferon (IFN)-γ (**C**) (each 10 ng/ml) are presented. Untreated controls were set as 100%. Results are derived from duplicate cultures of human peritoneal mesothelial cells isolated from five separate donors. *P<0.05, **P<0.01, ***P<0.001

chain decreased to 79.3±4.8% (P<0.001) and of the β4 chain to 47.2±13.3% (P<0.01) of controls (Fig. 2B). As after IL-1β treatment, the integrin subunit α5 was also upregulated (+22.9±9.6%, P<0.01) after incubation with TNF-α (Fig. 2B). However, in contrast to IL-1β, TNF-α induced a decrease of the expression of the CD44-molecule (−18.1±7.0%, P<0.01; Fig. 3).

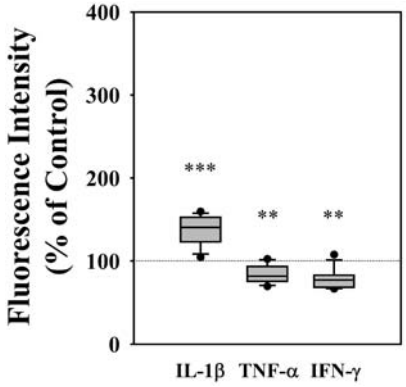

Fig. 3 Regulation of the expression of CD44 by pro-inflammatory cytokines. The 10th, 25th, 50th (median), 75th and 90th percentiles of the percentage increase/decrease of the expression of CD44 after treatment with interleukin (IL)-1β, tumor necrosis factor (TNF)-α and interferon (IFN)-γ are presented. Untreated controls were set as 100%. Results are derived from duplicate cultures of human peritoneal mesothelial cells isolated from five separate donors. **P<0.01, ***P<0.001

IFN-γ treatment of HPMC (10 ng/ml) resulted in a reduced expression of CD44 (−22.7±8.5%, P<0.01; Fig. 3) and a downregulation of the β4 chain (−25.0±8.0%, P<0.01; Fig. 2C). All other investigated mesothelial integrin subunits (α1–6, β1) remained unaffected by IFN-γ.

The downregulation of the α6β4 integrin and disruption of the integrity of the mesothelium by IL-1β and TNF-α was also associated with a marked decline of the adhesive properties of HPMC. Under control conditions, a 10-min incubation with collagenase-I was required to detach the HPMC from the submesothelial matrix. This time span was significantly reduced to 4 min and 6 min in cells pre-treated with IL-1β or TNF-α (data not shown).

Discussion

Disruption of the mesothelial integrity is a characteristic pathological phenomenon almost invariably occurring in disease processes of the abdominal cavity. Various pathogenic factors are thought to be involved. These include trauma and surgery, exposure to air and gases or the action of cytokines and free oxygen radical species released by invading inflammatory cells or tumor cells [3, 14, 21, 31, 38]. The detailed pathomechanisms are, however, still rather poorly understood. Recent studies have identified IL-1β and TNF-α as key regulators in the mesothelial response to peritoneal injury by "activating" mesothelial cells to increase their release of various cytokines [9, 19, 24, 25, 35, 36, 41].

In the present paper, we demonstrated that IL-1β and TNF-α can also cause profound morphological changes of the mesothelium, resulting in the loss of its integrity. The alterations induced by IL-1β and TNF-α were characterized by cellular retraction, loss of cellular polarization and wide-spread exposure of the submesothelial ECM and

closely mimicked the alterations that can be observed in injured mesothelium in vivo (Fig. 1E, F). The morphological alterations were associated with marked alterations of the expression of mesothelial adhesion molecules and a significant reduction of the adhesive properties of the cells.

Our study provides the first analysis of the regulation of integrins and CD44 in HPMC by flow cytometry. In normal HPMC, we observed the expression of the $\beta 1$ integrin subunits $\alpha 1$ and $\alpha 2$ (collagen and laminin receptors), $\alpha 5$ (fibronectin receptor), $\alpha 6$ (laminin receptor), and the integrin subunit $\beta 4$ (laminin receptor). The $\alpha 4$ chain (fibronectin receptor) was not detectable. These data are in agreement with in vitro and in vivo studies recently published on resting peritoneal mesothelial cells [33, 40]. However, in contrast to our results, these studies additionally revealed expression of the integrin subunit $\alpha 3$ (collagen, fibronectin, and laminin receptor) a difference that may be due to different culture conditions or cell preparations used by these investigators.

The most remarkable alteration of the integrin-expression profile induced by IL-1β and TNF-α was the strong downregulation and loss of the laminin receptor subunits $\alpha 6$ and $\beta 4$. The $\alpha 6\beta 4$ integrin is a hemidesmosomal transmembrane molecule that is crucial for the maintenance of the basal cell-matrix adhesion of epithelial cell [1, 5, 10, 11, 28]. Our data thus support the hypothesis that both IL-1β and TNF-α may disrupt the mesothelial integrity by the downregulation of the $\alpha 6\beta 4$ integrin [1, 10]. Molecular defects and/or a functional downregulation of the normal $\alpha 6\beta 4$ expression have been well described in the epidermis and are thought to be responsible for the formation of blistering skin disorders and the epithelial detachment during keratinocyte maturation [5, 11, 28]. In the peritoneum, the downregulation of $\alpha 6\beta 4$ may finally facilitate the mobilization and detachment of mesothelial cell from the submesothelial matrix. Interestingly, similar mechanisms have been suggested to be involved in the detachment of ovarian carcinoma cells that are derived from a modified mesothelium, i.e., the ovarian surface epithelium. Skubitz et al. [30] demonstrated that exfoliated ovarian carcinoma ascites cells show a loss of the $\alpha 6\beta 4$ expression when compared to solid tumors and proposed that the floating tumor cells may be released from the basement membrane due to their deficit of $\alpha 6$ and $\beta 4$ subunits.

The molecular mechanisms of the downregulation of the mesothelial cell $\alpha 6$ and $\beta 4$ subunits are currently unclear but may involve a protein kinase C-dependent mobilization from the basolateral hemidesmosomes as described in other epithelial cells [1, 5, 10]. Detailed studies of the localization and potential redistribution of mesothelial integrins under the influence of IL-1β and TNF-α using confocal and two-photon laser-scanning microscopy would be helpful to further unravel these complex issues [40].

We have previously shown that IL-1β may be an important growth factor for exponentially growing HPMC [24]. Together with its potential exfoliating activity, IL-1β may thus be one of the key regulators of the suspension and proliferation of mesothelial cells in peritoneal effusions. In ascitic fluids, mesothelial cells are frequently found to show cellular clustering. This phenomenon may be enhanced by the concomitant upregulation of the mesothelial $\alpha 5$ fibronectin receptor subunits by IL-1β and TNF-α [8].

The disruption of the mechanical barrier function of the peritoneal mesothelium by IL-1β and TNF-α may be of critical importance for the initiation and progression of inflammatory and neoplastic peritoneal disease processes. The loss of the mesothelial cell junctions may lead to an increased loss of proteins into the peritoneal cavity and subsequently to an increased intraperitoneal oncotic pressure with formation of ascitic fluids [21, 27]. Both, IL-1β and TNF-α may further booster these effects by inducing HPMC to release VEGF and bFGF, which may, in turn, increase the submesothelial capillary permeability [9, 19]. These combined effects on the permeability of peritoneal mesothelial and endothelial cells may also facilitate the transmigration of inflammatory cells into the peritoneal cavity [4, 18, 20]. The loss of the non-adhesive properties of the peritoneal surface in conjunction with an IL-1β-induced secretion of the fibrogenic growth factors bFGF and TGF-β by HPMC may finally be a crucial step in the development of peritoneal adhesions and fibrosis [9, 15, 25].

In malignant peritoneal disease processes, the alterations of the mesothelium may profoundly affect the mechanisms of peritoneal tumor spread. We show that the mesothelial CD44 expression can be upregulated by IL-1β and downregulated by TNF-α and IFN-γ. The interaction of CD44 molecules with hyaluronic acid is supposed to be one of the most important mechanisms of the initial implantation of various cancers, e.g., ovarian cancer, gastric cancer, or pancreatic cancer, to the peritoneal mesothelium. This important step of the peritoneal tumor dissemination may be significantly modified by pro-inflammatory cytokines [13, 17, 23, 37]. However, the loss of the mechanical barrier function of the peritoneal cell lining may be even more important. Tumor cells generally adhere much faster and stronger to the ECM than to the intact mesothelium [17, 32]. The disruption of the mesothelium by IL-1β or TNF-α may thus facilitate the adhesion of floating tumor cells to the submesothelial ECM. In fact, this hypothesis is strongly supported by a recent in vivo model of peritoneal carcinosis in which damage to the mesothelium caused by a pneumoperitoneum resulted in an advanced peritoneal tumor spread and a significant decrease in animal survival [38].

The present data further support the concept that peritoneal mesothelial cells are key players in the regulation of peritoneal diseases. Detailed in situ analyses of the expression of integrins and CD44 in normal peritoneum and various peritoneal diseases will be of great interest.

Acknowledgements The excellent technical assistance of Mrs. I. Jehart is gratefully acknowledged. We would also like to thank Mr. J. Pollheimer for helpful comments on statistics.

References

1. Alt A, Ohba M, Li L, Gartsbein M, Belanger A, Denning MF, Kuroki T, Yuspa SH, Tennenbaum T (2001) Protein kinase C-delta-mediated phosphorylation of alpha6beta4 is associated with reduced integrin localization to the hemidesmosome and decreased keratinocyte attachment. Cancer Res 61:4591–4598
2. Amberger A, Maczek C, Jurgens G, Michaelis D, Schett G, Trieb K, Eberl T, Jindal S, Xu Q, Wick G (1997) Co-expression of ICAM-1, VCAM-1, ELAM-1 and Hsp60 in human arterial and venous endothelial cells in response to cytokines and oxidized low-density lipoproteins. Cell Stress Chaperones 2:94–103
3. Andreoli SP, Mallett C, Williams K, McAteer JA, Rothlein R, Doerschuk CM (1994) Mechanisms of polymorphonuclear leukocyte mediated peritoneal mesothelial cell injury. Kidney Int 46:1100–1109
4. Bittinger F, Schepp C, Brochhausen C, Lehr HA, Otto M, Kohler H, Skarke C, Walgenbach S, Kirkpatrick CJ (1999) Remodeling of peritoneal-like structures by mesothelial cells: its role in peritoneal healing. J Surg Res 82:28–33
5. Borradori L, Sonnenberg A (1999) Structure and function of hemidesmosomes: more than simple adhesion complexes. J Invest Dermatol 112:411–418
6. Cannistra SA, Kansas GS, Niloff J, DeFranzo B, Kim Y, Ottensmeier C (1993) Binding of ovarian cancer cells to peritoneal mesothelium in vitro is partly mediated by CD44. Cancer Res 53:3830–3838
7. Carter D, True L, Otis CN (1997) Serous membranes: histology for pathologists. In: Sternberg SS (ed) Lippincott–Raven, New York, pp 2299–2328
8. Casey RC, Burleson KM, Skubitz KM, Pambuccian SE, Oegema TR Jr, Ruff LE, Skubitz AP (2001) Beta 1-integrins regulate the formation and adhesion of ovarian carcinoma multicellular spheroids. Am J Pathol 159:2071–2080
9. Cronauer MV, Stadlmann S, Klocker H, Abendstein B, Eder IE, Rogatsch H, Zeimet AG, Marth C, Offner FA (1999) Basic fibroblast growth factor synthesis by human peritoneal mesothelial cells. Am J Pathol 155:1977–1984
10. Dowling J, Yu QC, Fuchs E (1996) Beta4 integrin is required for hemidesmosome formation, cell adhesion and cell survival. J Cell Biol 134:559–572
11. Giancotti FG, Ruoslahti E (1999). Integrin signaling. Science 285:1028–1032
12. Goodison S, Urquidi V, Tarin D (1999). CD44 cell adhesion molecules. Mol Pathol 52:189–196
13. Hosono J, Narita T, Kimura N, Sato M, Nakashio T, Kasai Y, Nonami T, Nakao A, Takagi H, Kannagi R (1998) Involvement of adhesion molecules in metastasis of SW1990, human pancreatic cancer cells. J Surg Oncol 67:77–84
14. Ikubo A, Morisaki T, Katano M, Kitsuki H, Anan K, Uchiyama A, Tanaka M, Torisu M (1995) A possible role of TGF-beta in the formation of malignant effusions. Clin Immunol Immunopathol 77:27–32
15. Klaus A, Margreiter R, Pernthaler H, Klima G, Offner FA (2003) Diffuse mesenterial sclerosis: a characteristic feature of chronic small-bowel allograft rejection. Virchows Arch 442:48–55
16. Kutteh WH, Kutteh CC (1992) Quantitation of tumor necrosis factor-alpha, interleukin-1 beta, and interleukin-6 in the effusions of ovarian epithelial neoplasms. Am J Obstet Gynecol 167:1864–1869
17. Lessan K, Aguiar DJ, Oegema T, Siebenson L, Skubitz AP (1999) CD44 and beta1 integrin mediate ovarian carcinoma cell adhesion to peritoneal mesothelial cells. Am J Pathol 154:1525–1537
18. Li FK, Davenport A, Robson RL, Loetscher P, Rothlein R, Williams JD, Topley N (1998) Leukocyte migration across human peritoneal mesothelial cells is dependent on directed chemokine secretion and ICAM-1 expression. Kidney Int 54:2170–2183
19. Mandl-Weber S, Cohen CD, Haslinger B, Kretzler M, Sitter T (2002) Vascular endothelial growth factor production and regulation in human peritoneal mesothelial cells. Kidney Int 61:570–578
20. Margetts PJ, Kolb M, Yu L, Hoff CM, Holmes CJ, Anthony DC, Gauldie J (2002) Inflammatory cytokines, angiogenesis, and fibrosis in the rat peritoneum. Am J Pathol 160:2285–2294
21. Nagy JA, Morgan ES, Herzberg KT, Manseau EJ, Dvorak AM, Dvorak HF (1995) Pathogenesis of ascites tumor growth: angiogenesis, vascular remodeling and stroma formation in the peritoneal lining. Cancer Res 55:376–385
22. Nicoletti I, Migliorati G, Pagliacci MC, Grignani F, Riccardi C (1991) A rapid and simple method for measuring thymocyte apoptosis by propidium iodide staining and flow cytometry. J Immunol Methods 139:271–279
23. Nishimura S, Chung YS, Yashiro M, Inoue T, Sowa M (1996) CD44H plays an important role in peritoneal dissemination of scirrhous gastric cancer cells. Jpn J Cancer Res 87:1235–1244
24. Offner FA, Obrist P, Stadlmann S, Feichtinger H, Klingler P, Herold M, Zwierzina H, Hittmair A, Mikuz G, Abendstein B, Zeimet A, Marth C (1995) IL-6 secretion by human peritoneal mesothelial and ovarian cancer cells. Cytokine 7:542–547
25. Offner FA, Feichtinger H, Stadlmann S, Obrist P, Marth C, Klingler P, Grage B, Schmahl M, Knabbe C (1996) Transforming growth factor-β synthesis by human peritoneal mesothelial cells. Induction by interleukin-1. Am J Pathol 148:1679–1688
26. Propst T, Propst A, Herold M, Schauer G, Judmaier G, Braunsteiner H, Stoffler G, Vogel W (1993) Spontaneous bacterial peritonitis is associated with high levels of interleukin-6 and its secondary mediators in ascitic fluid. Eur J Clin Invest 23:832–836
27. Runyon BA, Hillebrand DJ (1998) Surgical peritonitis and other diseases of the peritoneum, mesentery, momentum, and diaphragm. In: Feldman M, Scharschmidt BF, Sleisenger MH (eds) Gastrointestinal and liver disease. Pathophysiology, diagnosis, management. Saunders, Philadelphia, pp 2035–2046
28. Ruoslahti E, Vaheri A (1997). Cell-to-cell contact and extracellular matrix. Curr Opin Cell Biol 9:605–607
29. Sachs L (1997) Angewandte statistik. In: Sachs L (ed) Anwendung statistischer methoden. Springer, Berlin Heidelberg New York, pp 335–337
30. Skubitz AP, Bast RCJr, Wayner EA, Letourneau PC, Wilke MS (1996) Expression of alpha 6 and beta 4 integrins in serous ovarian carcinoma correlates with expression of the basement membrane protein laminin. Am J Pathol 148:1445–1461
31. Sriram PS, Mohammed KA, Nasreen N, Hardwick J, Van Horn R, Sanders K, Antony VB (2002) Adherence of ovarian cancer cells induces pleural mesothelial cell (PMC) permeability. Oncol Res 13:79–85
32. Strobel T, Cannistra SA (1999) Beta1-integrins partly mediate binding of ovarian cancer cells to peritoneal mesothelium in vitro. Gynecol Oncol 73:362–367
33. Tietze L, Borntraeger J, Klosterhalfen B, Amo-Takyi B, Handt S, Gunther K, Merkelbach-Bruse S (1999) Expression and function of beta(1) and beta(3) integrins of human mesothelial cells in vitro. Exp Mol Pathol 66:131–139
34. Topley N (1995) The cytokine network controlling peritoneal inflammation. Perit Dial Int 15:35–40
35. Topley N, Joerres A, Luttmann W, Petersen MM, Lang J, Thierauch KH, Muller C, Coles GA, Davies M, Williams JD (1993) Human peritoneal mesothelial cells synthesize interleukin-6: induction by IL-1β and TNFα. Kidney Int 43:226–233
36. Topley N, Brown Z, Joerres A, Westwick J, Davies M, Coles GA, Williams JD (1993) Human peritoneal mesothelial cells synthesize interleukin-8: synergistic induction by interleukin-1

beta and tumor necrosis factor-alpha. Am J Pathol 142:1876–1886
37. Van Rossen ME, Hofland LJ, van den Tol MP, van Koetsveld PM, Jeekel J, Marquet RL, van Eijck CH (2001) Effect of inflammatory cytokines and growth factors on tumour cell adhesion to the peritoneum. J Pathol 193:530–537
38. Volz J, Volz-Koster S, Kanis S, Klee D, Ahlert C, Melchert F (2000) Modulation of tumor-induced lethality after pneumoperitoneum in a mouse model. Cancer 89:262–266
39. Whitaker D, Papadimitriou J (1985) Mesothelial healing: morphological and kinetic investigations. J Pathol 145:159–175
40. Witz CA, Montoya-Rodriguez IA, Miller DM, Schneider BG, Schenken RS (1998) Mesothelium expression of integrins in vivo and in vitro. J Soc Gynecol Invest 5:87–93
41. Zeimet AG, Widschwendter M, Knabbe C, Fuchs D, Herold M, Muller-Holzner E, Daxenbichler G, Offner FA, Dapunt O, Marth C (1998) Ascitic interleukin-12 is an independent prognostic factor in ovarian cancer. J Clin Oncol 16:1861–1868

Virchows Arch (2003) 443:686–689
DOI 10.1007/s00428-003-0876-1

CASE REPORT

Fumio Ide · Kenji Mishima · Ichiro Saito

Sarcomatoid salivary duct carcinoma of the oral cavity

Received: 2 April 2003 / Accepted: 9 July 2003 / Published online: 21 August 2003
© Springer-Verlag 2003

Abstract This report recounts a new case of sarcomatoid variant of salivary duct carcinoma in a 45-year-old woman. The 1.5-cm polypoid mass protruded from the retromolar area and focally extended into the pharyngeal wall. The patient was free of disease for 11 years. The tumor showed a biphasic malignancy; nondescript sarcomatous proliferation predominated over ductal carcinoma population, with perceptible blending of the two components. The sarcomatoid areas had no heterologous properties. Discohesive pleomorphic cells were immunopositive for vimentin, epithelial membrane antigen and AE1/AE3 at a significant rate. A dual expression of AE1/AE3 and vimentin was also evident in enmeshed foci of conventional cribriform adenocarcinoma. Thus, the sarcomatoid histology represents a dedifferentiated phenotype of salivary duct carcinoma.

Keywords Carcinosarcoma · Minor salivary gland · Salivary duct carcinoma · Sarcomatoid carcinoma · Spindle cell carcinoma

Introduction

Sarcomatoid salivary gland carcinoma, analogous to spindle cell carcinoma (SpCC) or sarcomatoid carcinoma (SC) of the upper aerodigestive tract mucosa, represents sarcoma-like transformation of the original carcinoma with no evidence of truly divergent differentiation into committed mesenchymal tissues. Its biphasic appearance and nondescript sarcomatous morphology are obvious and fairly readily diagnosed as overtly malignant. Little has been published on this diagnostically challenging lesion [22, 24], but sarcomatoid change has been documented in various distinct types of salivary gland carcinoma, including mucoepidermoid carcinoma [14], acinic cell carcinoma [4], adenoid cystic carcinoma [3], squamous cell carcinoma [9, 13], epithelial–myoepithelial carcinoma [15], undifferentiated carcinoma [2, 7] and salivary duct carcinoma (SDC) [8, 19]. In all likelihood, no particular histological subtype has a predilection for sarcomatoid differentiation.

We describe an intraoral dimorphic tumor in which SDC and pleomorphic sarcoma coexist. Since the sarcomatous phenotype was not adequately characterized, this case was initially diagnosed as carcinosarcoma (CS). Subsequent thorough sampling and rigorous immunohistochemical scrutiny provided compelling evidence of sarcomatoid morphological transformation of dedifferentiated SDC. It is important to be aware of the existence of a rare variant of SDC that histologically mimics sarcoma.

F. Ide (✉) · K. Mishima · I. Saito
Department of Pathology,
Tsurumi University School of Dental Medicine,
2-1-3 Tsurumi, Tsurumi-ku, 350-0283 Yokohama, Japan
e-mail: ide-f@tsurumi-u.ac.jp
Tel.: +81-45-5808360
Fax: +81-45-5722888

Case report

Our patient was a 45-year-old woman with a 2-month history of dysphagia. A non-ulcerated, partially fixed, broad-based polypoid mass, measuring 1.5×1.3×1.2 cm, was excised from the retromolar gingiva of the right mandible. The tumor focally extended into the lateral wall of the pharynx. There was no evidence of bone involvement or nodal metastases. The patient has been disease-free for 11 years.

Despite gross circumscription, the margins of the tumor were infiltrative (Fig. 1A).The polypoid component was two reproducible malignancies: SDC and pleomorphic sarcoma. A volumetrically limited but definite component of SDC was present along the periphery of the tumor (Fig. 1B, C). It was composed of ductal-type cells with abundant eosinophilic cytoplasm and pleomorphic nuclei, often showing apocrine-like features. Typical cystic nodules with central comedonecrosis and characteristic cribriform nests were evident. Diffusely infiltrating, detached carcinoma cells and pleomorphic sarcoma cells blended into each other (Fig. 1D). More than 80% of the lesion, particularly in its central portions, consisted of uncommitted sarcoma (Fig. 1E). Tumor stroma was often hyalinized but there was no area of myxoid, myxochondroid, chondro–osseous, osteoid or myogenic tissue in extensive sampling. Neither dysplastic change in the covering epithelium nor underlying pleomorphic adenoma could be found.

Ductal carcinoma component stained intensely with AE1/AE3 (monoclonal, 1:50; Dako, Glostrup, Denmark; Fig. 2A) and

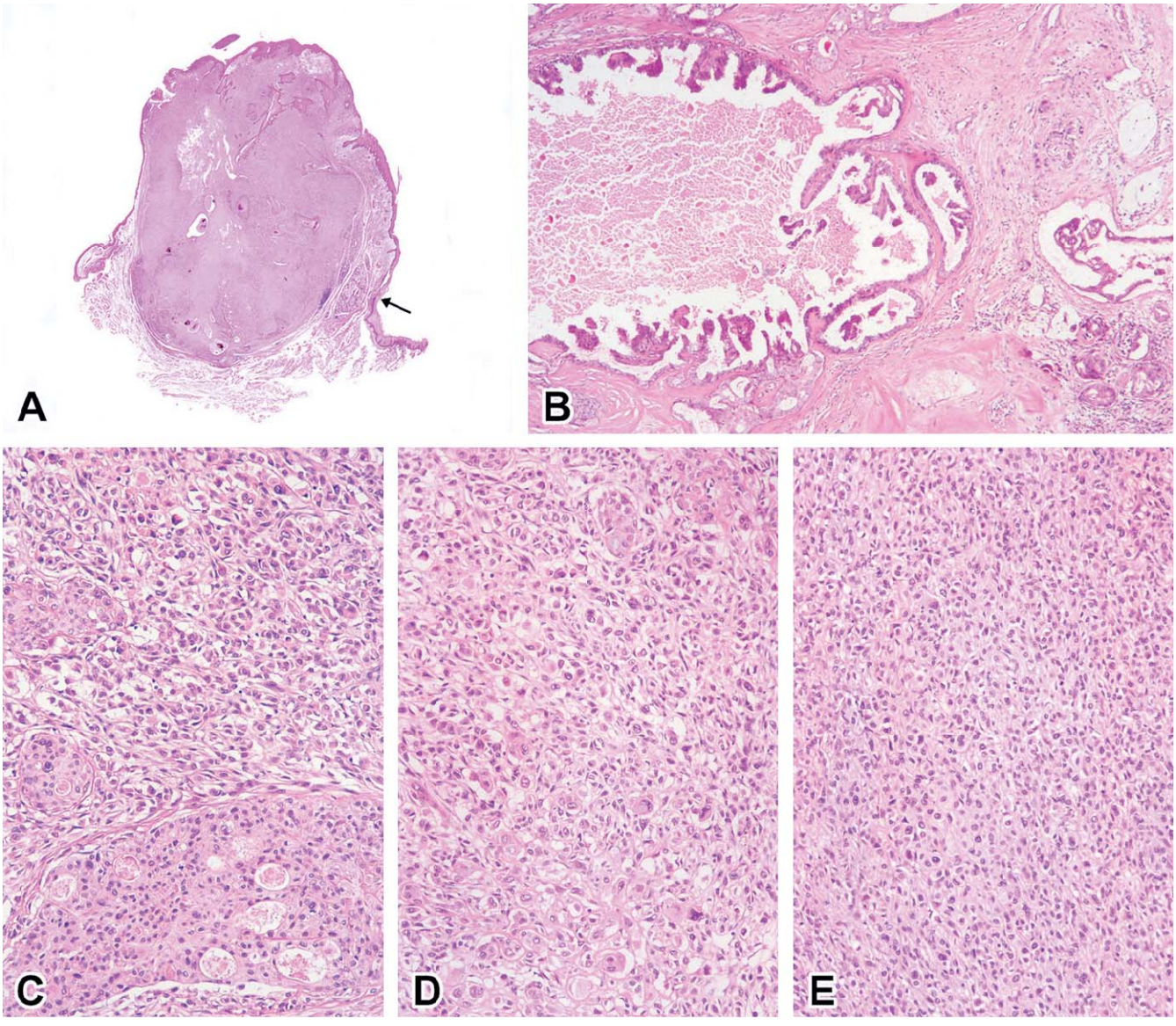

Fig. 1 Well-circumscribed polypoid tumor occupies the submucosa. Salivary glands (*arrow*) are observed (**A**). Cystic nodules of salivary duct carcinoma showing comedonecrosis. In this field, sarcomatous element is not evident but small clusters of carcinoma cells are scattered in the hyalinized stroma (**B**). Cribriform nest and sarcomatoid component (**C**). Diffuse proliferation of discohesive carcinoma cells (**D**). Non-descript sarcomatous area (**E**)

epithelial membrane antigen (E29, 1:200; Dako; Fig. 2B). Expression of vimentin (V9, 1:20; Dako; Fig. 2C) was also pervasive in the overt carcinoma foci, in a diffuse pattern. The sarcoma-appearing element exhibited extensive vimentin (Fig. 2C) and epithelial membrane antigen (Fig. 2B) positivity with focal accentuation of AE1/AE3 (Fig. 2D). The p53 (DO7, 1:100; Dako) staining was approximately evenly distributed (more than 50%) between the two components. Up to 30% of both populations were labeled by Ki67 (MIB-1, 1:200; Dako). α-Smooth muscle actin (1A4, 1:2000; Sigma, St. Louis, Mo., USA), desmin (D33, 1:100; Dako), CD68 (KP-1, 1:200; Dako), S-100 protein (polyclonal, 1:800; Dako) and glial fibrillary acidic protein (6F-2, 1:200; Dako) were negative in tumor cells.

Discussion

There is now growing evidence that SC, SpCC and CS are essentially carcinomas that have undergone differing degrees of mesenchymal metaplasia [23]. Consequently, most authors favor the single unifying term SC, which embraces SpCC and CS, with subdivisions into homologous and heterologous types [1, 11, 22, 23]. Albeit artificial, we prefer to classify these confounding tumors separately, that is, to catalogue salivary gland carcinoma with a homologous sarcomatoid component as SC, whereas those with a large amount of clear-cut heterologous malignant stroma such as chondrosarcoma, osteosarcoma, rhabdomyosarcoma or combinations of these

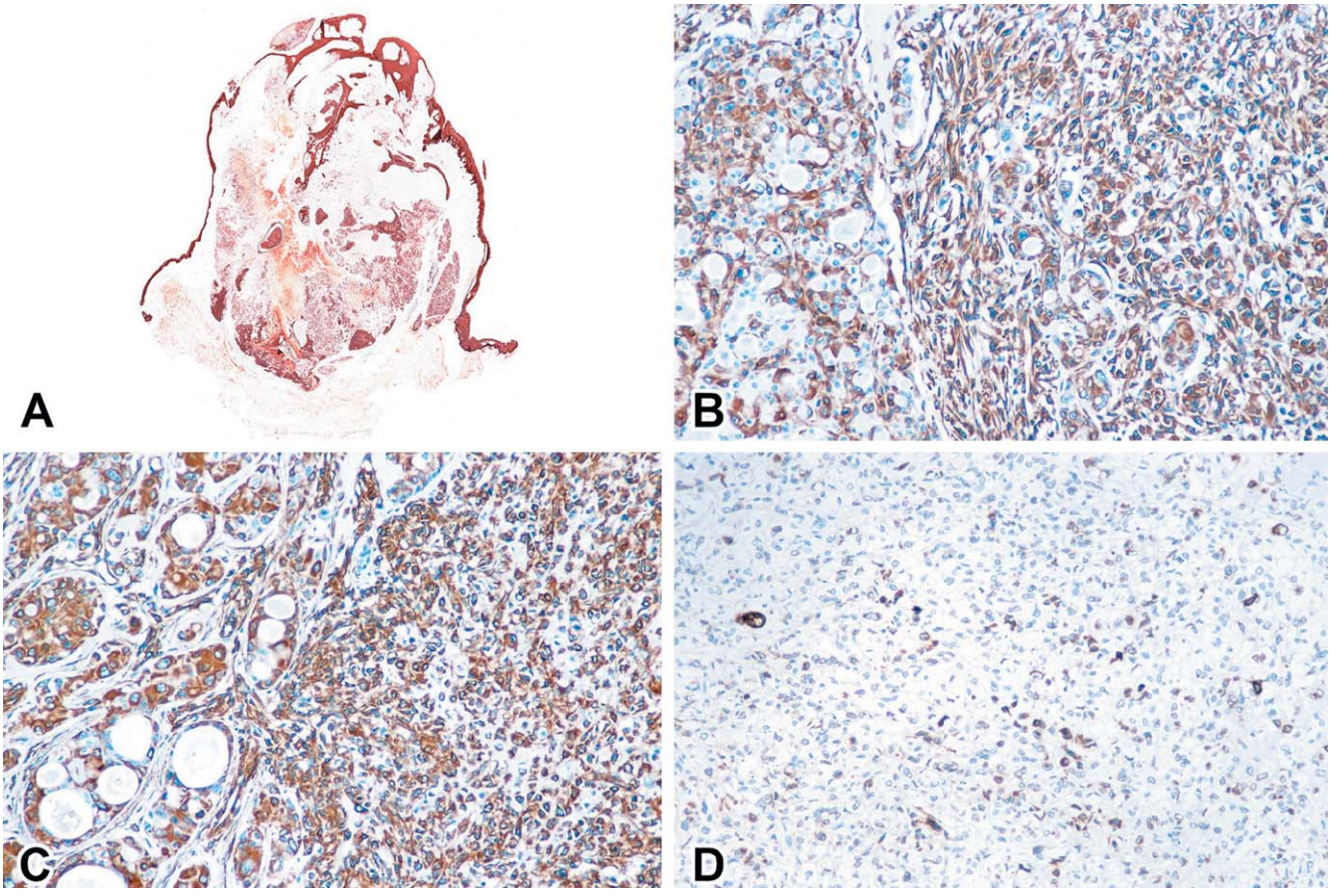

Fig. 2 AE1/AE3 decorates strongly both carcinomatous element and covering epithelium (**A**). Epithelial membrane antigen (**B**) and vimentin (**C**) are diffusely positive in both adenocarcinoma and sarcomatoid components. Sarcomatous population manifests focal weaker positivity for AE1/AE3 (**D**)

elements should be referred to as CS, in order to reserve the outmoded but most popular diagnostic term CS in salivary tumor pathology.

The histogenesis of SC has been the focus of a great deal of discussion over the years [1, 5, 11, 20, 22, 23]. As intuitively expected, there are no significant differences in the p53 expression and Ki67-labeling indices between the carcinomatous and sarcomatoid components in this case, thus confirming that the latter population is unquestionably neoplastic and not just a reactive change. Because of convincing reactivity for cytokeratin and epithelial membrane antigen, sarcoma-appearing cells are frequently found to retain epithelial properties. A noteworthy finding is the diffuse expression of vimentin in the well-formed SDC. Similarly, vimentin positivity is demonstrable in the adenocarcinoma component of CSs of various organs [6, 10, 12, 17, 18]. Recent evidence suggests that vimentin-positive adenocarcinomas progressively changed their epithelial phenotype and showed a sarcomatous proliferation with loss of intercellular cohesion [16, 21]. The co-expression of cytokeratin and vimentin may trigger the detachment and migration of carcinoma cells due to the reverse transformation to embryonic status [1, 5]. Pertinently, the validity of this hypothesis is applicable in the present tumor; namely, the vimentin-positive SDC reliably showing a continuous spectrum of phenotypic conversion into sarcomatoid morphology.

In summary, this is the first case of sarcomatoid SDC in which the minor salivary gland was involved [8, 19]. The distinctly exophytic configuration with a shallow depth of invasion allowed for complete eradication by local resection alone. Like our lesion, if the intraoral tumor appeared as a polypoid mass attached to the mucosa by a stalk and sarcomatous tissue ran up to almost all areas, it is possible to be misdiagnosed as SC of mucosal origin. As easily reproducible diagnostically, mucosal SC lacks the adenocarcinoma component and usually contains the malignant surface epithelium [1, 20, 22]. Particularly in the case of sarcomatous tumor of the salivary gland, a diligent search for an elusive carcinoma is recommended before rendering the unqualified diagnosis of sarcoma.

References

1. Batsakis JG, Suarez P (2000) Sarcomatoid carcinomas of the upper aerodigestive tracts. Adv Anat Pathol 7:282–293
2. Bocklage T, Feddersen R (1995) Unusual mesenchymal and mixed tumors of the salivary gland. An immunohistochemical and flow cytometric analysis of three cases. Arch Pathol Lab Med 119:69–74
3. Cheuk W, Chan JKC, Ngan RKC (1999) Dedifferentiation in adenoid cystic carcinoma of the salivary gland. An uncommon complication associated with an accelerated clinical course. Am J Surg Pathol 23:465–472
4. Ferreiro JA, Kochar AS (1994) Parotid acinic cell carcinoma with undifferentiated spindle cell transformation. J Laryngol Otol 108:902–904
5. Guarino M, Micheli P, Pallotti F, Giordano F (1999) Pathological relevance of epithelial and mesenchymal phenotype plasticity. Pathol Res Pract 195:379–389
6. Hansen LT, Kristensen S, Moesner J (1995) Polypoidal carcinosarcoma of the oropharynx: a clinicopathological and immunohistochemical study. J Laryngol Otol 109:459–465
7. Harada H (2000) Histomorphological investigation regarding to malignant transformation of pleomorphic adenoma (so-called malignant mixed tumor) of the salivary gland origin: special reference to carcinosarcoma. Kurume Med J 47:307–323
8. Henley JD, Seo IS, Dayan D, Gnepp DR (2000) Sarcomatoid salivary duct carcinoma of the parotid gland. Hum Pathol 31:208–213
9. Ishibashi T, Hojo H (1995) Spindle cell carcinoma of the parotid gland. J Laryngol Otol 109:683–686
10. Kamishima T, Fukuda T, Usuda H, Takato H, Iwamoto H, Kaneko H (1997) Carcinosarcoma of the urinary bladder: expression of epithelial markers and different expression of heat shock proteins between epithelial and sarcomatous elements. Pathol Int 47: 166–173
11. Koss MN, Hochholzer L, Frommelt RA (1999) Carcinosarcomas of the lung. A clinicopathologic study of 66 patients. Am J Surg Pathol 23:1514–1526
12. Kwon MY, Gu M (2001) True malignant mixed tumor (carcinosarcoma) of parotid gland with unusual mesenchymal component. A case report and review of the literature. Arch Pathol Lab Med 125:812–815
13. Latkovich P, Johnson RL (1998) Carcinosarcoma of the parotid gland. Report of a case with cytohistologic and immunohistochemical findings. Arch Pathol Lab Med 122:743–746
14. Love GL, Sarma DP (1986) Spindle cell mucoepidermoid carcinoma of submandibular gland. J Surg Oncol 31:66–68
15. Manuel S, Mathews A, Chandramohan K, Pandey M (2002) Carcinosarcoma of the parotid gland with epithelial-myoepithelial carcinoma and pleomorphic sarcoma components. Br J Oral Maxillofac Surg 40:480–483
16. Miyagi J, Tsuhako K, Kinjo T, Iwamasa T, Hashimoto H, Ishikawa S (2000) Rhabdoid tumour of the lung is a dedifferentiated phenotype of pulmonary adenocarcinoma. Histopathology 37:37–44
17. Nakayama Y, Murayama H, Iwasaki H, Iwanaga S, Kikuchi M, Ikeda S, Okada M, Iizuka Y, Iwashita A (1997) Gastric carcinosarcoma (sarcomatoid carcinoma) with rhabdomyoblastic and osteoblastic differentiation. Pathol Int 47:557–563
18. Sreenan JJ, Hart WR (1995) Carcinosarcomas of the female genital tract. A pathologic study of 29 metastatic tumors: further evidence for the dominant role of the epithelial component and the conversion theory of histogenesis. Am J Surg Pathol 19:666–674
19. Talmi YP, Halpern M, Finkelstein Y, Gal R, Zohar Y (1990) True malignant mixed tumour of the parotid gland. J Laryngol Otol 104:360–361
20. Thompson LDR, Wieneke JA, Miettinen M, Heffner DK (2002) Spindle cell (sarcomatoid) carcinomas of the larynx. A clinicopathologic study of 187 cases. Am J Surg Pathol 26:153–170
21. Utsunomiya T, Yao T, Tamiya S, Tsuneyoshi M (2002) Intracellular distribution of intermediate filaments in vimentin-positive gastric carcinomas: confocal laser scanning microscopy using formalin-fixed paraffin-embedded specimens. Pathol Res Pract 198:69–76
22. Weidner N (1987) Sarcomatoid carcinoma of the upper aerodigestive tract. Semin Diagn Pathol 4:157–168
23. Wick MR, Ritter JH, Humphrey PA (1997) Sarcomatoid carcinomas of the lung. A clinicopathologic review. Am J Clin Pathol 108: 40–53
24. Zarbo RJ (2002) Salivary gland neoplasia: a review for the practicing pathologist. Mod Pathol 15:298–323

Virchows Arch (2003) 443:690–692
DOI 10.1007/s00428-003-0868-1

LETTER TO THE EDITOR

Kazuto Yamazaki

Unique follicular carcinoma of the thyroid gland with extracellular deposition of amorphous globular structures mimicking an adenoid cystic pattern

Received: 21 May 2003 / Accepted: 26 June 2003 / Published online: 5 August 2003
© Springer-Verlag 2003

Sir,

I observed that a follicular carcinoma of the thyroid exhibited a unique hyaline globular stromal material mimicking follicular colloid, amyloid deposition, or an adenoid cystic pattern [5, 8]. The features of this tumor made a differential diagnosis of thyroid follicular neoplasm difficult because a diagnosis of medullary carcinoma, insular (poorly differentiated) carcinoma, or even the recently introduced entity of hyalinizing trabecular tumor with focal nodular accumulations of basement membrane difficult to exclude [1, 2, 3, 6, 9].

A 69-year-old Japanese man presented complaining of a thyroid mass. Upon cytological examination, numerous amorphous globular structures with diameters of 20–60 μm were seen among aggregations of hyperchromatic atypical follicular epithelial cells. Under suspicion of epithelial malignancy (either medullary carcinoma with amyloid deposition or follicular epithelial neoplasm), a widened left thyroid lobectomy was performed. The excised, well-encapsulated mass measured approximately 12×7 mm (Fig. 1A).

Conventional histology, immunohistochemistry, and electron microscopy examinations were performed upon the excised tumor. Microscopically, a dense proliferation of cancer cells with a microfollicular pattern and intervening hyaline globular amorphous structures in the stroma were observed (Fig. 1B). The unique extracellular deposition consisted mainly of laminin and type-IV collagen molecules but did not contain thyroglobulin, amyloid, or calcitonin (Fig. 1C, D). The deposition stained positive when treated with periodic acid-methenamine silver. In the surrounding capsule, slight invasion to the capsular stroma and vascular invasion were seen (Fig. 1E). Immunohistochemically positive stains for thyroglobulin were observed in the cavities of the microfollicules and the cytoplasm of some tumor cells (Fig. 1C). Immunohistochemically positive stains for thyroid transcription factor (TTF)-1, keratin (AE1/AE3), epithelial membrane antigen, CD56 (NCAM), and CD57 (Leu 7) were also seen in the tumor cells. Carcinoembryonic antigen, calcitonin, chromogranin, synaptophysin, and neuron-specific enolase were not observed in the tumor cells. Furthermore, muscle actin (HHF-35), S-100 protein, vimentin, secretory component, and p53 were not observed in the tumor cells. Some cells were stained positive by Ki-67 (approximately 2–4% of tumor cells were labeled). The amorphous globular structures stained positive for type-IV collagen and laminin (Fig. 1D). Amyloid A protein, amyloid P component, and calcitonin were not observed in the amorphous globules.

Under the electron microscope, cancer cells that had proliferated with a microfollicular or solid sheet-like pattern were observed admixed with small, hyalinized amorphous nodules; the fibrous thickening of some vessels was also seen (Fig. 2). The small, hyalinized amorphous nodules consisted of extracellular matrix with a sparse distribution of globular or lamellar aggregations of lamina-like matrices of medium electron density. Continuity between the amorphous nodules and the fibrous thickening of hyalinous vessel walls was observed. The lumina of the microfollicules in the tumor cell nests exhibited apical microvillous differentiation. Ultrastructurally, several apical microvilli and several intracytoplasmic lysosomal granules, similar to those seen in follicular epithelial cells, were observed within the microfollicular structures (Fig. 2). In periodic acid methanamine-stained sections, electron-dense positive lamellar substructures were seen within the amorphous globular structures (Fig. 2). Amyloid fibrils were not observed.

The amorphous extracellular material was not amyloid in nature, but consisted of the massive extracellular deposition of basement-like materials [10]. The cancer cells in the present case did not exhibit neuroendocrine cell differentiation or calcitonin immunostaining. However, the cells did stain positive for not only conventional

K. Yamazaki (✉)
Department of Pathology,
Saiseikai Central Hospital,
l-4-17 Mita, Minatoku, 108-0073 Tokyo, Japan
e-mail: KazutoYamazaki@aol.com
Tel.: +81-3-34518211
Fax: +81-3-34516102

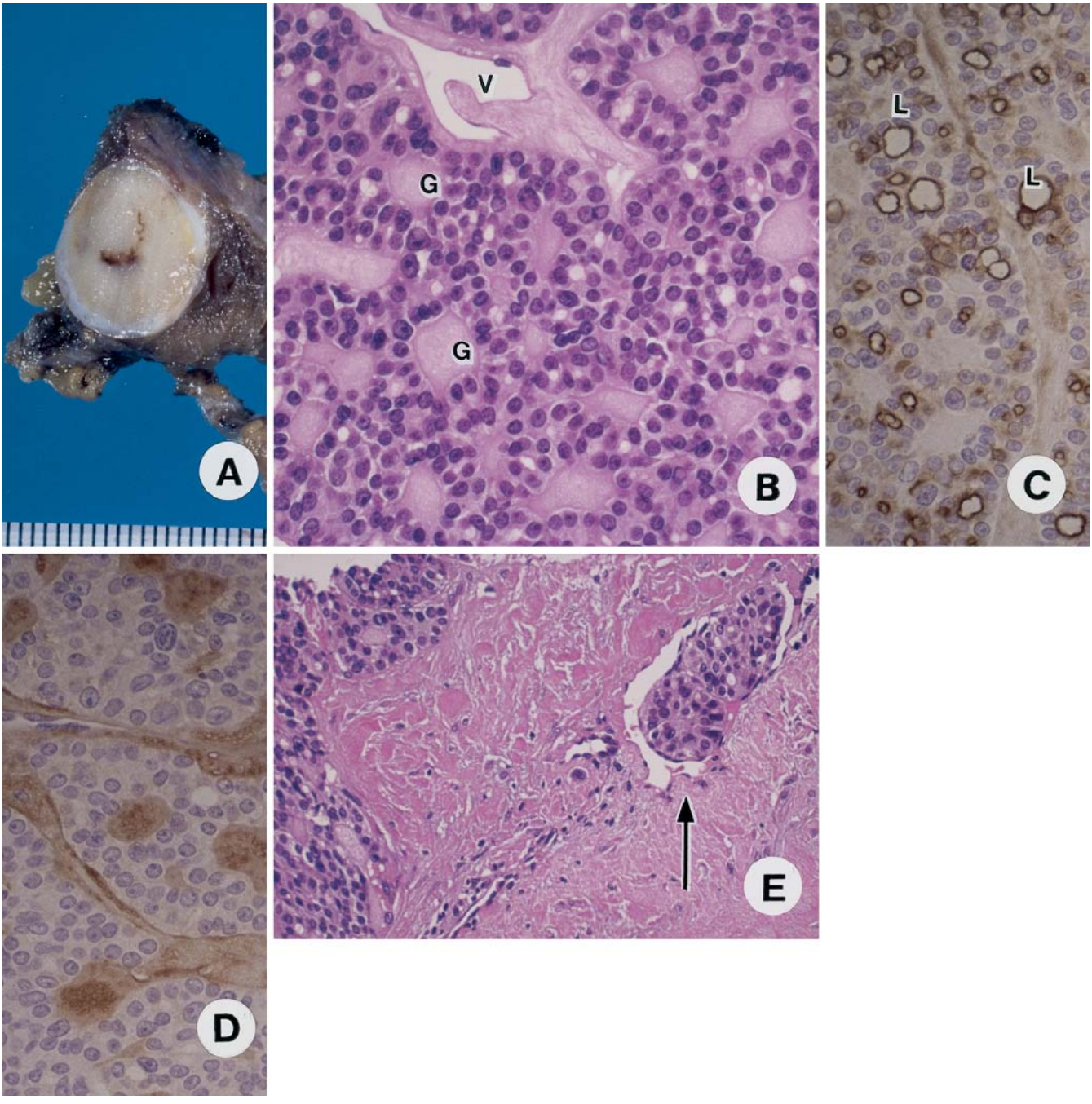

Fig. 1. **A** Macroscopic view of the cut surfaces of the thyroid tumor, showing an encapsulated yellowish-white nodular mass with a small central hemorrhage. The units of the marker are in millimeters. **B** Light microscopy findings showing an adenoid cystic pattern in the thyroid tumor tissue. *G* small, hyalinized amorphous globules, *V* a fibrous thickening of the blood vessels. The small empty spaces in the centers of the microfollicules represent the extraction of colloid materials during tissue preparation [hematoxylin and eosin (H&E) stain, ×380]. **C** Thyroglobulin immunostaining. Positive staining is visible in the lumens of the microfollicules. *L* lumina of microfollicules (light microscopy ×380). **D** Light microscopy findings showing positive staining for laminin in the small, hyalinized amorphous nodules and the fibrous thickening of some vessels (light microscopy, laminin immunostaining, ×380). **E** Light microscopy findings showing capsular and vascular invasion (*arrow*; H&E stain, ×190)

immunohistochemical epithelial markers, but also for TTF-1 and thyroglobulin. Ultrastructurally, the tumor cells sometimes exhibited microfollicular structures with apical microvilli and numerous intracytoplasmic lysosomal granules, similar to follicular epithelial cells lacking typical neurosecretory-type intracytoplasmic small granules. These findings ruled out the possibility of a diagnosis of medullary carcinoma [2, 3, 6, 9, 10]. The cancer cells also lacked the characteristic nuclear features seen in papillary carcinomas [2, 6, 7, 9]. The peculiar histological features of hyalinizing trabecular adenoma and other thyroid carcinomas, including insular (or poorly differen-

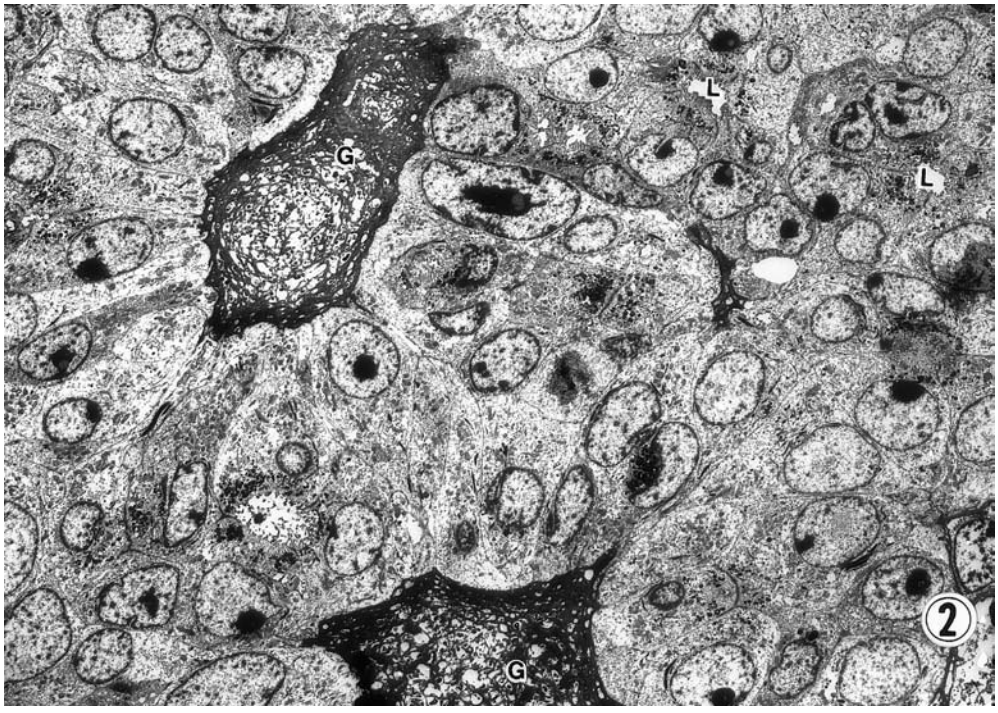

Fig. 2 Electron microscopy findings showing periodic acid methanamine staining of the thyroid tumor tissue (*G* amorphous globule, *L* lumen of microfollicules, ×2100)

tiated) carcinomas, as well as those of synovial sarcoma were also lacking [1, 2, 4, 6, 7, 9]. Thus, the tumor in the present case was diagnosed as a follicular carcinoma of the thyroid gland with a unique extracellular deposition of amorphous globular structures, mimicking an adenoid cystic pattern [8]. A similar case of a "follicular carcinoma with an adenoid cystic pattern" was reported by Nguyen et al. [8]. In their case, the microfollicular pattern was not as clear as it is in the present case.

The formation of the amorphous globules in the present tumor might be related to the stromal hyaline sclerosis that is frequently observed in some thyroid tumors, but which is not as organized as the adenoid cystic pattern observed in the present case [2, 6, 7, 9]. Outside the thyroid gland, the notion of adenoid cystic carcinoma is well known [5]. Myoepithelial cells in tumor tissues are thought be related to the production of globular stromal matrices in conventional adenoid cystic carcinomas [5]. No tumor cells with myoepithelial differentiation were observed in the present case. Li et al. [7] reported that abnormal production or alterations in the secretory pathways of tumor cells seem to occur in some thyroidal papillary carcinomas and hyalinizing trabecular tumors. The peculiar extracellular deposition of amorphous globular structures, mimicking an adenoid cystic pattern, in the presently reported follicular carcinoma of the thyroid gland appears to be quite unique [5, 8]. Nevertheless, recognizing that follicular carcinomas of the thyroid gland may exhibit an adenoid cystic pattern or even amorphous globular structures in aspiration cytology preparations is important for making accurate histopathological and cytopathological diagnoses of thyroid gland masses and not to confuse medullary carcinoma with the appearance of amyloid deposition [2, 3, 6, 8, 9,10].

References

1. Carney J, Ryan J, Goeliner JR (1987) Hyalinizing trabecular adenoma of the thyroid gland. Am J Surg Pathol 11:583–591
2. Chan J (2000) Tumors of the thyroid and parathyroid glands. Diagnostic histopathology of tumors. Churchill Livingstone, London, pp 959–1056
3. Collins B, Cramer HM, Tabatowski K, et al (1995) Fine needle aspiration of medullary carcinoma of the thyroid. Cytomorphology, immunohistochemistry and electron microscopy. Acta Cytol 39:920–930
4. Dharan M, Natchigal D, Rosen G, et al (1998) Basement membrane material (hyaline globules) in synovial sarcoma: a case report with description of a potential pitfall. Acta Cytol 42:791–795
5. Ellis G, Auclair PL (1996) Adenoid cystic carcinoma. 5. Malignant epithelial tumors in tumors of the salivary glands. In: Rosai J, Sobin LH (eds) Atlas of tumor pathology. Armed Forces Institute of Pathology, Washington, DC, pp 203–216
6. Kini S (1998) Thyroid, chapter thirteen. In: Mitchell CW (ed) Color atlas of differentiatial diagnosis in exfolliative and aspiration cytopathology. Williams & Wilkins, Pennsylvania, pp 227–254
7. Li N, Carcangiu ML, Rosai J (1997) Abnormal intracellular and extracellular distribution of basement membrane material in papillary carcinoma and hyalinizing trabecular rumors of the thyroid: implication for deregulation of secretory pathways. Hum Pathol 28:1366–1372
8. Nguyen G-K, Vogelsang PJ, Schumann GB (1993) Follicular carcinoma of the thyroid with an adenoid cystic pattern. Report of a case with aspiration biopsy cytology, immunohistochemistry and electron microscopy. Acta Cytologica 37:740–744
9. Rosai J, Carcangiu ML, Delellis RA (1992) Tumors of the thyroid gland. Atlas of tumor pathology. Armed Forces Institute of Pathology, Washington, DC
10. Valenta L, Michel-Bechet M, Mattson JC, et al (1977) Microfollicular thyroid carcinoma with amyloid rich stroma, resembling the medullary carcinoma of the thyroid (MCT). Cancer 39:1573–1586

Virchows Arch (2003) 443:693–694
DOI 10.1007/s00428-003-0878-z

LETTER TO THE EDITOR

Vincenzo Villanacci · Stefano Maria Giulini

The normal gastric cardia: fact or fiction?

Received: 14 April 2003 / Accepted: 13 June 2003 / Published online: 12 August 2003
© Springer-Verlag 2003

Sir,

With this appropriate title (The normal gastric cardia fact or fiction?) John R. Goldblum [7] and Sony P. Kilgore et al. [8] in recent reviews outlined one of the most great histopathological controversies in recent years: the real existence of the gastric cardia as a normal structure or not.

In *Histology for Pathologists* [9], David A. Owen described the gastric cardia as "a narrow strip of mucosa separating the most distal portion of the esophageal squamous mucosa from the acid-producing fundic mucosa (oxyntocardiac mucosa OCM) histologically composed exclusively by mucus secreting glands".

In recent years, the group of Parakrama T. Chandrasoma at the University of Southern California USC [1, 2, 3, 4, 10] have suggested that the gastric cardia is not a normal structure as previously described and, in reality, is the expression of a metaplasia of esophageal mucosa related to gastro-esophageal reflux. Under normal condition, there is a direct continuity between esophageal mucosa and acid-producing fundic mucosa or oxyntocardiac mucosa (OCM).

This assertion was based on an autopsy study [2] in which Chandrasoma examined 72 patients who had an evaluable section across the squamocolumnar junction. Thirty percent of all cases, including 9 of 11 patients younger than age 20 years, did not have any cardiac mucosa, the squamous epithelium transitioned directly to the oxyntic mucosa of the gastric fundus. In those who had cardiac mucosa, the length of this mucosa was short, being less than 1 cm in all but two cases.

V. Villanacci (✉)
Department of Surgical Pathology,
University of Brescia,
Piazzale Spedali Civili 1, 25124 Brescia, Italy
e-mail: villan@iol.it
Tel.: +39-030-3995479
Fax: +39-030-3995053

S. M. Giulini
Department of Surgery,
University of Brescia,
Brescia, Italy

In contrast, in a series [3] of 71 patients with gastroesophageal reflux disease (GERD) who had multiple biopsies, all 71 patients had cardiac mucosa, and 30% had cardiac mucosal lengths of over 2 cm.

"The results of this comparison strongly suggest that cardiac mucosa is not a normal structure but is an abnormal mucosa that results from the metaplastic transformation of the squamous epithelium damaged by reflux."

In agreement with this observation, there was recently the experience of Young S. Park et al. [11], in which the entire gastroesophageal junction (EGJ) and the proximal part of the stomach from 23 fetal and pediatric autopsies was examined. In 78% of cases, the transitional zone between the EGJ and fundic mucosa was always characterized by some scattered parietal cells in mucous glands. The parietal cells were consistently identified adjacent to the EGJ in all cases. The conclusion was that the cardiac mucosa composed of pure mucous cells does not exist as a normal developmental structure.

In contrast to this evaluation, S.P. Kilgore [8] et al. evaluated the entire EGJ in 30 pediatric autopsies from patients aged 18 years or younger with no known history of GERD or Barret's esophagus.

In all cases, cardiac mucosa was present, always on the gastric side of the EGJ, although it was quite small, ranging from only 1 mm to 4 mm in length.

The results of this study support the concept that the gastric cardiac-type mucosa is present from birth as a normal structure and is not related to GERD or *Helicobacter pylori* infection.

More recently, Derdoy et al. [5] examined the EGJ in 100 pediatric autopsies, and their conclusions were that cardiac-type mucosa on the distal side of the EGJ was present in all 100 pediatric autopsy specimens; therefore, there is a normal, variably narrow developmental zone at the EGJ covered by cardiac mucosa and is present at birth. It does not necessarily represent evidence of a mucosal metaplastic response to GERD.

Similar results were also obtained from J.N. Glickman et al. [6]. These authors examined the mucosal biopsies of the cardia of 74 pediatric patients (age range 0.1–18 years). The results were correlated with the patient's

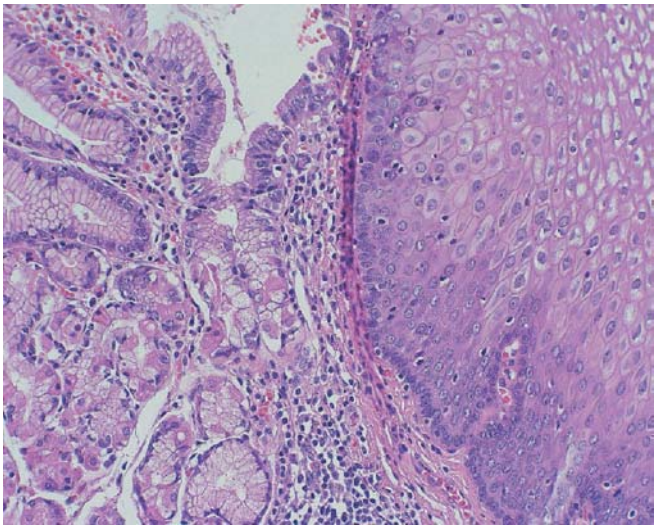

Fig. 1 Gastro–esophageal junction: it is possible to note the absence of signs of reflux disease in the esophageal mucosa and the typical aspects (parietal and chief cells) in gastric oxintic mucosa. Haematoxilin & eosin ×20

clinical symptoms and with other histological features such as esophagitis, gastritis, *Helicobacter pylori* and the presence of goblet cells. The results showed that either pure mucous glands (81%) or mixed mucous/oxyntic glands (19%) were present within 1 mm of the squamous columnar junction in all of the patients (100%).

Both active esophagitis and increased inflammation in the cardia correlated positively with a longer length of pure mucous glands in the EGJ region.

An intermediate position was expressed by Hong Zhou et al. [13]. This group studied the microscopic characteristics of the gastric side of the squamous-columnar junction of 77 autopsied fetuses and of infants, young children and adolescents. The study revealed that a transitional zone with the microscopic characteristics of cardiac mucosa was universally present at the squamous columnar junction. They concluded that the cardiac mucosa was partially if not entirely the result of normal embryonic gastric development. Both mucous and mixed gland constitute normal components of the cardiac mucosa.

On the basis of this short review about the gastric cardia morphology, we have two different positions: on the one hand, the position of Chandrasoma et al. in which a cardiac mucosa with pure mucous glands under the normal condition doesn't exist and, on the other hand, the findings that support a congenital origin of this type of epithelium; in addition, there is an intermediate position of Zhou et al., in which mucous and mixed glands constitute normal components of cardiac mucosa.

In this debate, we have the possibility to support one of the three positions on the basis of a personal observation.

We examined the surgical specimen of an esophagus in a 63-year-old woman in which there was a small cell neoplasia (oat cell) and a squamous carcinoma in situ in the middle part of the esophagus.

In the sections performed at the EGJ, we histologically observed a continuity between squamous epithelium of the esophagus and the oxynto-cardiac mucosa of the stomach (Fig. 1); this picture is in a 63-year-old woman! In the squamous epithelium of the esophagus, there are no signs of reflux in particular, no dilated intercellular spaces (DIS) that, as we have shown, are the more precocious expression of GERD also in routine biopsies [12]. Chandrasoma's theory is confirmed in this case.

It is only one case, but this observation, in our opinion, supports the possibility of OCM in direct continuity with the squamous epithelium of the esophagus in absence of reflux. In the presence of reflux, a metaplastic change of the squamous epithelium, real expression of GERD, is possible. The obvious conclusion is: gastric cardia, as we histologically know, under normal condition, could be in many cases a fiction.

References

1. Chandrasoma P (1999) Non-neoplastic diseases of the esophagus. In: Gastrointestinal pathology. Appleton and Lange, Stamford Connecticut, pp 9–42
2. Chandrasoma PT, Der R, Ma Y, Dalton P, Taira M (2000) Histology of the gastroesophageal junction. An autopsy study. Am J Surg Pathol 24:402–409
3. Chandrasoma PT, Lokuhetty DM, DeMeester TR, Bremner CG, Peters JH, Oberg S, Groshen S (2000) Definition of histopathologic changes in gastroesophageal reflux disease. Am J Surg Pathol 24:344–351
4. Der R, Tsao-Wei DD, DeMeester T, Peters J, Groshen S, Lord RVN, Chandrasoma P (2001) Carditis. A manifestation of gastroesophageal reflux. Am J Surg Pathol 25:245–252
5. Derdoy JJ, Bergwerk A, Cohen H, Kline M, Monforte HL, Thomas DW (2003) The gastric cardia: to be or not to be? Am J Surg Pathol 27:499–504
6. Glickman JN, Fox V, Antonioli DA, Wang HH, Odze R (2002) Morphology of the cardia and significance of carditis in pediatric patients. Am J Surg Pathol 26:1032–1039
7. Goldblum JR (2002) Barret's esophagus and Barret's related dysplasia. New concepts in gastrointestinal pathology long course. International Academy of Pathology, Chicago, pp 16–31
8. Kilgore SP, Ormsby AH, Gramlich TL, Rice TW, Richter JE, Falk GW, Goldblum JR (2000)The gastric cardia. Fact or fiction? Am J Gastroenterol 25:921–924
9. Owen DA (1997) Stomach. In: Sternberg SS (ed) Histology for pathologists, 2nd edn. Raven Press, New York, pp 481–493
10. Oberg S, Peters JH, DeMeester TR, Chandrasoma P, Hagen JA, Ireland AP, Ritter MP, Mason RJ, Crookes P, Bremner CG (1997) Inflammation and specialized intestina metaplasia of cardiac mucosa is a manifestation of gastroesophageal reflux disease. Ann Surg 226:522–532
11. Park YS, Park HJ, Kang GH, Kim CJ, Chi JG (2002) Histology of gastroesophageal junction in fetal and pediatric autopsy. Arch Pathol Lab Med 127:451–455
12. Villanacci V, Grigolato PG, Cestari R, Missale G, Cengia G, Klersy C, Rindi G (2001) Dilated intercellular spaces as markers of reflux disease: histology, semiquantitative score and morphometry upon light microscopy. Digestion 64:1–8
13. Zhou H, Greco A, Daum F, Kahn E (2001) Origin of cardiac mucosa: ontogenic considerations. Pediatr Dev Pathol 4:358–363

Virchows Arch (2003) 443:695–699
DOI 10.1007/s00428-003-0879-y

LETTER TO THE EDITOR

Mattheos Bobos · Prodromos Hytiroglou · Georgios Karkavelas · Christos Papakonstantinou · Constantine S. Papadimitriou

Sialadenoma papilliferum of bronchus

Received: 8 May 2003 / Accepted: 15 July 2003 / Published online: 21 August 2003
© Springer-Verlag 2003

Sir,

Salivary gland-type tumours of the bronchi include a variety of neoplasms with identical histological features to tumours of the major and minor salivary glands [4, 8, 9]. These lesions are uncommon and presumably arise from bronchial glands. Sialadenoma papilliferum (SP) is a rare tumour that has mostly been described in minor salivary glands of the mouth [3, 5]. In an extensive search of the literature, we have not found any mention of this neoplasm in the larynx, trachea or bronchi. We present a case of an endobronchial papillary tumour with histological and immunohistochemical features of SP.

The patient was a 53-year-old man who was found to have a radiopaque lesion in the right lung on a routine X-ray examination. The patient had a 40-year history of heavy smoking (40–60 cigarettes per day). He had noticed deterioration of the morning cough, accompanied by increased sputum production during the 4 months preceding admission. He also complained of dyspnea on exertion and mild weight loss. Chest radiographs showed a radiopaque lesion in the parahilar region of the lower lobe of the right lung (Fig. 1A). The cardiopulmonary index was within normal range. Bronchoscopy showed occlusion of the apical bronchus of the right lower lobe, which contained purulent and necrotic material. Cytological examination of a bronchial wash showed squamous cells without evidence of malignancy. Histological examination of a bronchial biopsy showed findings consistent with a benign papillary lesion. Computed tomography (CT) scan of the chest revealed an area of bronchial thickening and consolidation accompanied by parenchymal changes suggestive of inflammation (Fig. 1B). Brain, abdominal and retroperitoneal CT scans, as well as bone nuclear scan, were normal. Pulmonary function tests included:

- Forced vital capacity (FVC): 2.60 l/s (69% of predicted 3.79 l/s)
- Peak expiratory flow rate: 3.74 l/s (47% of predicted 8.00 l/s)
- Forced expiratory volume after 1 s: 1.38 l/s (45% of predicted 3.07 l/s)
- Forced expiratory flow at 25–75% of FVC: 0.69 l/s (19% of predicted 3.62 l/s)

These findings were consistent with moderate bronchial obstruction.

Laboratory findings on admission included: hematocrit 44.3%, haemoglobin 15.1 g/dl, glucose 84 mg/dl, urea 36 mg/dl (normal 10–50 mg/dl), creatinine 0.74 mg/dl (normal 0.5–1.4 mg/dl), total protein 5.91 g/dl (normal 6.40–8.30 g/dl), albumin 3.60 g/dl (normal 3.40–4.80 g/dl), globulin 2.31 g/dl (normal 3.00–5.00 g/dl), aspartate aminotransferase 18 U/l (normal 0–41 U/l), alanine aminotransferase 20 U/l (normal 0–38 U/l), serum lactate dehydrogenase 260 U/l (normal 0–480 U/l), prothrombin time 10.0/10.6 s, partial thromboplastin time 26.9/30.0 s and erythrocyte sedimentation rate 12 mm (1st hour). The patient underwent resection of the lower lobe of the right lung with dissection of paratracheal, interlobar and paraoesophageal lymph nodes. The patient is well 8 months after the operation, without evidence of recurrent tumour.

The resected right lower pulmonary lobe measured 14×9×5 cm and weighed 190 g. The lumen of the apical bronchus was occluded and moderately dilated by an exophytic papillary yellowish tumour mass, which measured 2.2×1.0×1.0 cm and was located 0.8 cm from the surgical resection margin (Fig. 1C). The surrounding area of pulmonary parenchyma, measuring 4×3 cm, showed marked consolidation. Serial sections through the lobe

M. Bobos · P. Hytiroglou (✉) · G. Karkavelas · C. S. Papadimitriou
Department of Pathology,
Aristotle University Medical School,
540 06 Thessaloniki, Greece
e-mail: phitir@med.auth.gr
Tel.: +30-231-0999218
Fax: +30-231-0999229

C. Papakonstantinou
Department of Cardiothoracic Surgery,
Aristotle University Medical School,
Thessaloniki, Greece

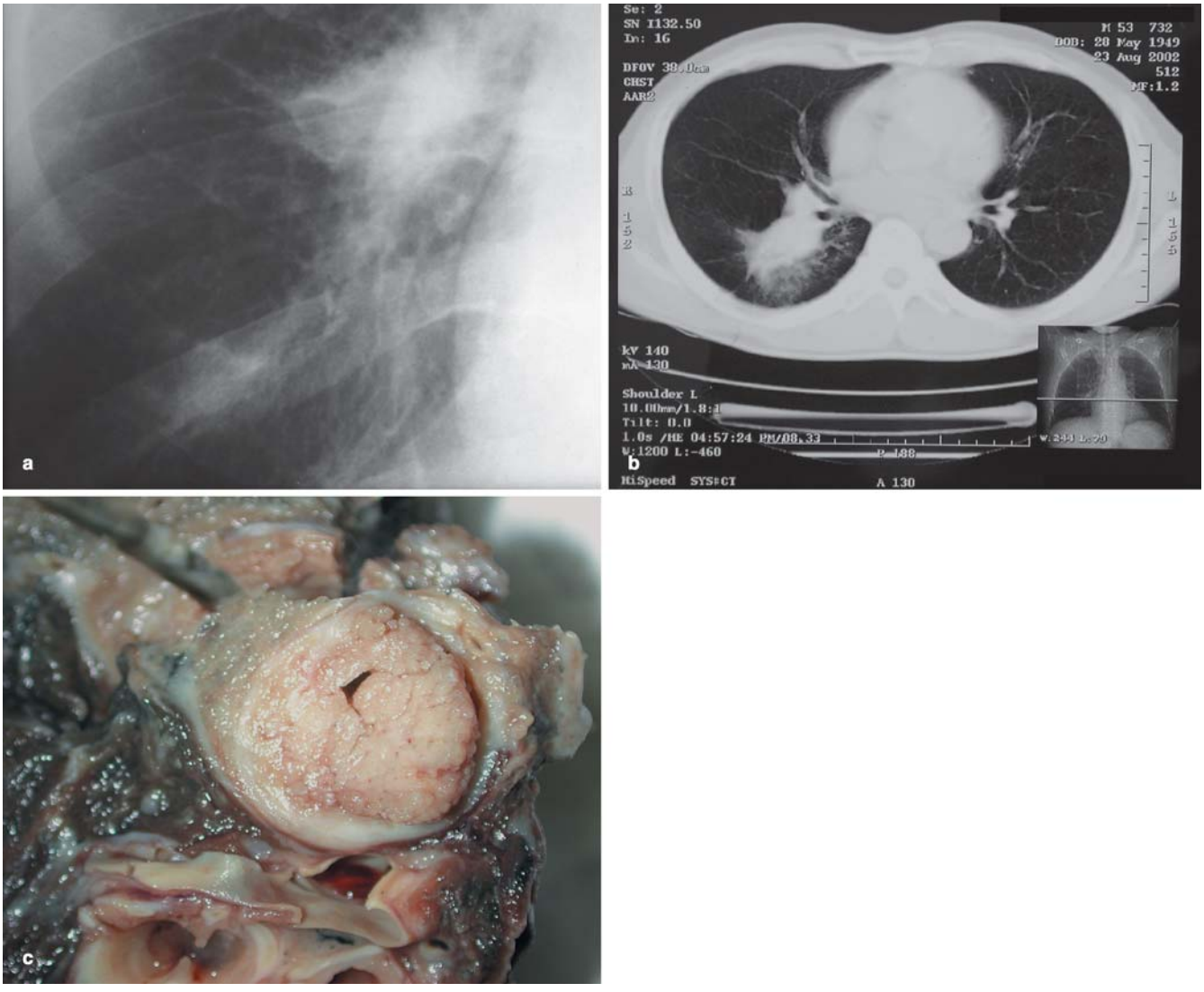

Fig. 1 Radiographic and gross pathological findings. **A** Plain chest X-ray showing a radiopaque lesion in the lower lobe of the right lung. **B** Computed tomography scan of the chest confirming the presence of an area of consolidation. **C** Exophytic papillary lesion protruding at the cut surface of the apical bronchus of the right lower lobe

revealed a second circumscribed roundish tumour nodule located 4.5 cm from the surgical resection margin. This was whitish in colour, firm in consistency and measured 1.8 cm in greatest dimension.

Routinely stained sections of the papillary tumour showed complex papillary structures protruding into the bronchial lumen (Fig. 2A). The papillae were lined by a double row of cells, consisting of a luminal layer of non-ciliated columnar epithelial cells and a basal layer of cuboidal myoepithelial cells (Fig. 2B). The epithelial cell nuclei showed mild pleomorphism without evident mitotic activity. In most areas, the epithelium was one to two cells in thickness; however, in multiple foci, epithelial tufts with thickness of several cells were present. Superficial portions of the papillae were lined by non-keratinizing stratified squamous epithelium (Fig. 2A). Inside the papillae, multiple gland- or duct-

Fig. 2 Histological and immunohistochemical findings. **A** The tumour is composed of complex papillary structures filling the bronchial lumen. Metaplastic squamous epithelium is present in superficial portions of the papillae (*left*; original magnification ×20). **B** The lining of the papillae consists of a double row of epithelial and myoepithelial cells. Focal tufting is present. Lymphoplasmacellular infiltrates are seen in the stroma (original magnification ×200). **C** Gland-like structures containing eosinophilic material are seen inside the complex papillae (original magnification ×100). **D** The deepest portion of the lesion is in continuity with bronchial glands (original magnification ×100). **E** Both epithelial and myoepithelial cells are positive for cytokeratin 7 (*upper left*), whereas only myoepithelial cells are positive for cytokeratin 17 (*upper right*). Myoepithelial cells are positive for α-smooth muscle actin (*lower left*); both epithelial and myoepithelial cells are positive for S-100 protein (*lower right*; original magnification ×200)

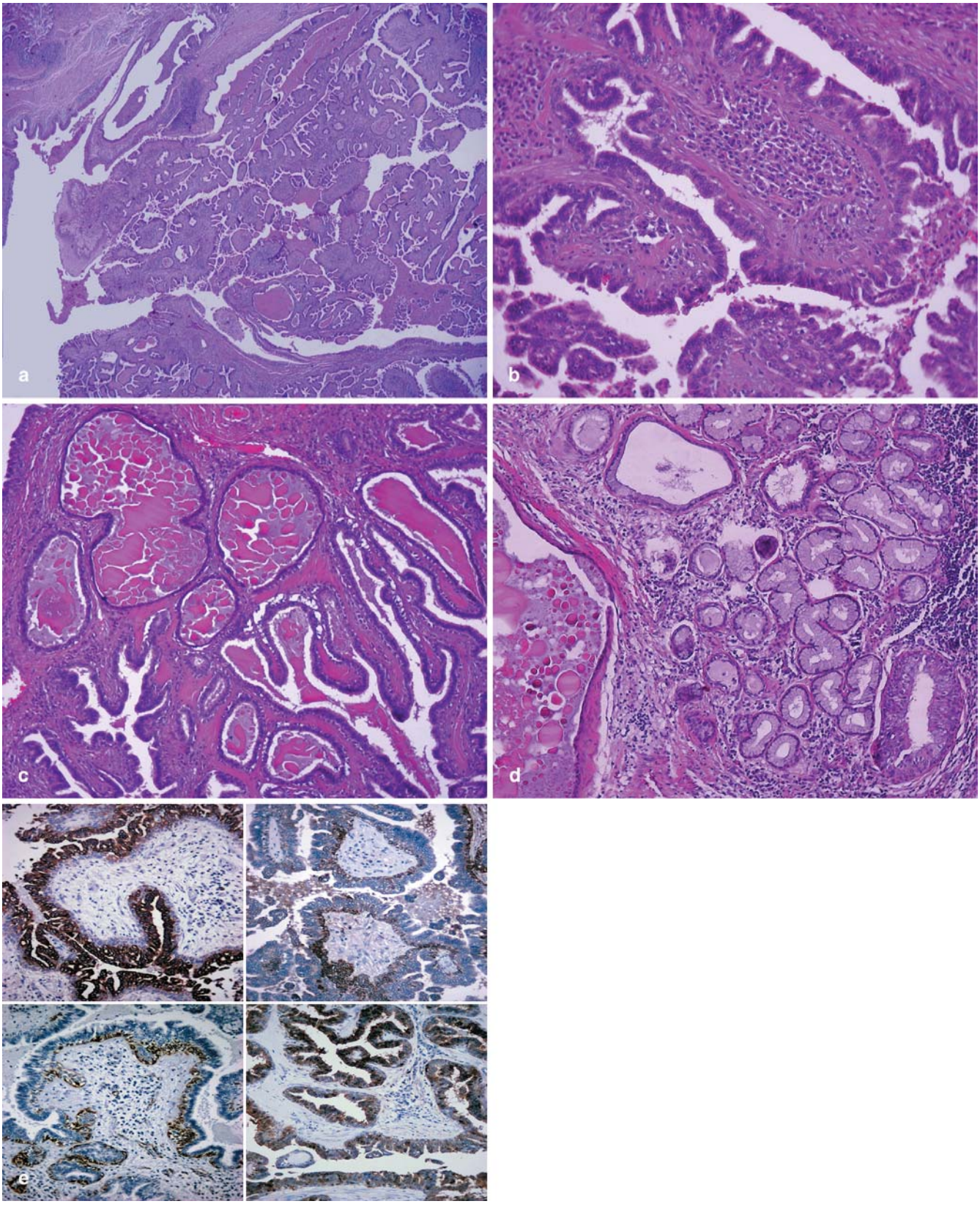
a
b
c
d
e

Table 1 Immunohistochemical findings in sialadenoma papilliferum of bronchus (comparison with bronchial glands and respiratory epithelium)

Immunohistochemical stains	Sialadenoma papilliferum		Bronchial glands		Respiratory epithelium
	Epithelium	Myoepithelium	Epithelium	Myoepithelium	
Cytokeratin cam 5.2	Positive	Rare positive foci	Positive	Focally positive	Positive
Cytokeratin 7	Positive	Focally positive	Positive	Focally positive	Positive
Cytokeratin 17	Rare positive foci	Positive	Negative	Positive	Focally positive in basal cells
Cytokeratin 19	Positive	Positive	Positive	Positive	Positive
Cytokeratin 20	Negative	Negative	Negative	Negative	Negative
EMA	Positive	Negative	Focally positive	Negative	Positive
SMA	Negative	Positive	Negative	Positive	Negative
S-100 protein	Mostly positive	Mostly positive	Focally positive	Positive	Negative
GFAP	Negative	Focally positive	Negative	Negative	Negative

Note: Abbreviations: *EMA* epithelial membrane antigen, *SMA* α-smooth muscle actin, *GFAP* glial fibrillary acidic protein

like structures were present; these were also lined by epithelial and myoepithelial cells. Most of these structures had irregular outlines, due to the presence of epithelial tufts and micropapillae protruding into the lumens (Fig. 2C). Some gland-like structures contained amorphous eosinophilic material. The stroma of the papillae consisted of fibrous tissue with moderate chronic inflammatory infiltrates, predominantly composed of lymphocytes and plasma cells. At the periphery of the lesion, the double-layered epithelium merged smoothly with the respiratory-type epithelium of the dilated bronchus. In one of the sections adjacent to the gland-like structures of the deepest part of the lesion, secretory units of mucinous and serous bronchial glands were present (Fig. 2D). The lung tissue distal to the tumour showed acute and chronic inflammation with fibrosis and alveolar remodelling. Sections of the smaller tumour showed poorly differentiated squamous cell carcinoma. Ten hilar, two paratracheal, two interlobar and five para-oesophageal lymph nodes were negative for metastatic tumour.

Periodic acid-Schiff (PAS) stain of the papillary neoplasm showed focal apical staining in tumour epithelial cells, which was diastase resistant. The eosinophilic material present in gland-like structures was also PAS-positive, diastase resistant. Immunohistochemical stains for various epithelial and myoepithelial markers were performed using the streptavidin-biotin-peroxidase complex method [7], in order to compare the features of the tumour cells with those of the bronchial glands and the respiratory epithelium. All antibodies were purchased from Dako (Glostrup, Denmark) with the exception of cytokeratin cam 5.2, which was obtained from Novocastra (Newcastle, U.K). The immunohistochemical findings are summarised in Table 1 and illustrated in Fig. 2E.

SP has been reported in a variety of locations, including the palate, buccal mucosa, gingiva, tonsillar pillar, mandibular retromolar pad, lip, parotid gland and submandibular gland [2, 3, 5]. The pathological features of this neoplasm have been well described. SP is unique among salivary gland tumours because it manifests as an exophytic papillary excrescence of the mucosa rather than as a submucosal or intraglandular mass. A glandular proliferation is present immediately subjacent to the papillary part of the tumour; this is composed of elongated and ectatic duct-like structures within the lamina propria, some of which may be cystically enlarged. Both ductal and papillary structures are lined by a double row of cells, including columnar epithelial and cuboidal myoepithelial cells. The superficial portions of the papillae are lined by stratified, presumably metaplastic, squamous epithelium [3]. The pathological features of our case were similar to those described in SP of other locations. The exophytic growth of the tumour resulted in obstruction of the bronchial lumen and bronchopneumonia. This clinically significant lesion was treated by lobectomy. The specimen was found to contain an incidental 1.8-cm squamous cell carcinoma, located away from the SP.

Salivary gland-type tumours of the bronchi are uncommon and usually present as polypoid endobronchial lesions [4, 8]. The tumour types thus far reported in the literature include benign (mucus gland adenoma, myoepithelioma, oncocytoma, pleomorphic adenoma) and malignant (acinic cell carcinoma, adenoid cystic carcinoma, adenosquamous carcinoma with amyloid-like stroma, carcinoma ex pleomorphic adenoma, epithelial–myoepithelial carcinoma, mucoepidermoid carcinoma, sebaceous carcinoma) neoplasms [1, 4, 6, 9, 10, 11]. These lesions are believed to arise from bronchial glands and recapitulate the histological features of salivary gland tumours. In our case, the presence of focal continuity between bronchial glands and neoplastic structures strongly suggested such an origin. Furthermore, the immunohistochemical stains (Table 1) disclosed similar phenotypes in the epithelial and myoepithelial cells of the tumour and those of the bronchial glands. These histological and immunohistochemical features were sufficiently distinctive to rule out other salivary gland-type tumours, as well as the relatively common squamous papilloma of the tracheobronchial tree.

In conclusion, we report a case of SP occurring in a large bronchus. Awareness of such rare lesions is important for pathologist and clinician alike, because such lesions may occasionally cause significant morbidity.

References

1. Borczuk CA, Sha KK, Hisler ES, Mann MJ, Hajdu IS (2002) Sebaceous carcinoma of the lung: histologic and immunohistochemical characterization of an unusual pulmonary neoplasm. Report of a case and review of the literature. Am J Surg Pathol 26:795–798
2. Brannon RB, Sciubba JJ, Giulani M (2001) Ductal papillomas of salivary gland origin: a report of 19 cases and a review of the literature. Oral Surg Oral Med Oral Pathol Oral Radiol Endod 92:68–77
3. Cleary KR, Batsakis JG (1990) Sialadenoma papilliferum. Ann Otol Rhinol Laryngol 99:756–758
4. Colby TV, Koss MN, Travis WD (1994) Tumors of the lower respiratory tract. In: Atlas of tumor pathology. Third series. Fascicle 13. Armed Forces Institute of Pathology, Washington, pp 65–89
5. Ellis GL, Auclair PL (1996) Tumors of salivary glands. In: Atlas of tumor pathology. Third series. Fascicle 17. Armed Forces Institute of Pathology, Washington, pp 120–130
6. Fulford LG, Kamata Y, Okudera K, Dawson A, Corrin B, Sheppard MN, Ibrahim NB, Nicholson AG (2001) Epithelial–myoepithelial carcinomas of the bronchus. Am J Surg Pathol 25:1508–1514
7. Hsu SM, Raine L (1984) The use of avidin-biotin-peroxidase complex (ABC) in diagnostic and research pathology. In: DeLellis RA (ed) Advances in immunochemistry. Masson, New York, pp 31–42
8. Moran CA (1995) Primary salivary gland-type tumors of the lung. Semin Diagn Pathol 12:106–122
9. Moran CA, Suster S, Askin FB, Koss MN (1994) Benign and malignant salivary gland-type mixed tumors of the lung. Clinicopathologic and immunohistochemical study of eight cases. Cancer 73:2481–2490
10. Moran CA, Suster S, Koss MN (1994) Primary adenoid cystic carcinoma of the lung. A clinicopathologic and immunohistochemical study of 16 cases. Cancer 73:1390–1397
11. Travis WD, Colby TV, Corrin B, Shimosato Y, Brambilla E (1999) Histological typing of lung and pleural tumours. WHO international histological classification of tumors, 3rd edn. Springer Verlag, Berlin Heidelberg New York

Virchows Arch (2003) 443:700–701
DOI 10.1007/s00428-003-0913-0
© Springer-Verlag 2003

European Society of Pathology (ESP)

EXTRAORDINARY GENERAL ASSEMBLY

Day: Saturday, February 7, 2004,

Time: 15.30h. In the event of the General Assembly not being quorate a second General Assembly based on simple majority will be called for **16.00h**

Duration: about 2 hours.

Place: Palais des Congrès, Porte Maillot 75016, Paris – France

Agenda:

1. Welcome
2. Approval of agenda
3. Approval of the Minutes of the preceding General Assembly (Ljubljana, September 2003)
4. Report of the President
5. Approval of the adaptation to the Belgian law of the Statutes and By-laws already approved in the General Assembly of Berlin 2001
6. Announcement and consequences of the results of the ballot for election of President-elect (2003-2005)
7. Report of the Chairman of the Organizing Committee of the 20th ESP Congress, Paris 2005
8. Any other business

Antonio Cardesa
President

11–15 February 2004
Conference on "Clinical Oncology 2004/2005"

In cooperation with the National Oncology Societies, the Tumorzentrum Düsseldorf (Director: Prof. Dr. med. R. Haas) will be holding a five-day conference. The results will be published in a symposium volume for the conference. More than 800 experts, mainly from the field of oncology, are expected to attend. The workshop will be held in the MNR Clinic, Lecture Hall 13A. The following general topics have been scheduled:

Wednesday:
Pharynx, larynx, CUP syndrome, parotid gland, nasopharynx, skin tumors
Bier, Dummer, Ganzer, Roth, Ruzicka, Schmitt, Schulte, Stadler, Suter

Thursday:
Esophageal carcinoma, gastric carcinoma, colorectal carcinoma
Gabbert, Häussinger, Knöfel, Ramp, Röher, Röhrborn, Wettstein, Willich, Sauer

Friday:
Seminoma, urinary bladder carcinoma, prostatic carcinoma, renal cell carcinoma
Ackermann, Alberti, Alken, Bamberg, Fornara, Hartmann, Rübben, Vögeli, Wirth

Saturday:
NHL, Hodgkin's disease, ALL, AML, CML, multiple myeloma, bronchial carcinoma, thymona
Bentz, Böhner, Gattermann, Germing, Haas, Kobbe, Stilgenbauer, Schmitt

Sunday:
Mammary carcinoma: biology, new treatment standards
Bender, Dall, Gerber, Harbeck, Kaufmann, Mallmann, von Mickwitz, Nitz, Yarnold

Head of the organization team: Prof. Dr. Stephan Roth, Klinik für Strahlentherapie, Moorenstr. 5, Postfach 101007, 40001 Düsseldorf, Germany

The conference fee will be E30 per day.

The symposium volume published for the conference can be purchased for E20.

For further information, please contact:
Head of the organization team:
Prof. Dr. Stephan Roth
Klinik für Strahlentherapie
Heinrich-Heine-Universität
Moorenstr. 5
40225 Düsseldorf
Germany
Tel.: +49 (0)211 811 8989/7990
Fax: +49 (0)211 811 8051
e-mail: roth@med.uni-duesseldorf.de
www.uni-duessdorf.de/tumorzentrum

1–11 June 2004
International course on Laboratory Animal Science
Utrecht, The Netherlands

A two week intensive course on laboratory animal science will be organized at the Department of Laboratory Animal Science – Utrecht, The Netherlands in June 2004. This course is organized once a year since 1993.

The objective of this course is to present basic facts and principles that are essential for the humane use and care of animals and for the quality of research.

The contents of the course are in line with recommendations of the Federation of European Laboratory Animal Science Associations (FELASA) regarding the training of the young scientist whose research involves the use of vertebrate animals.

The course may also be of interest for those who intend to set up a similar course at their location. For this purpose, during the course the acquisition of teaching materials can be discussed with the course committee.

For information and application forms please contact:
Prof. L.F.M. van Zutphen, PhD or
Mr. Stephan van Meulebrouck, MA
Department of Laboratory Animal Science
Faculty of Veterinary Medicine
P.O. Box 80.166
3508 TD Utrecht
The Netherlands
Tel.: ++31-30-2532033
Fax: ++31-30-2537997
E-mail: pdk@las.vet.uu.nl
Internet: http://las.vet.uu.nl (click on "Education and Training")

Virchows Arch (2003) 443:703–717
DOI 10.1007/s00428-003-0918-8

REVIEW ARTICLE

Fabio Facchetti · William Vermi · David Mason · Marco Colonna

The plasmacytoid monocyte/interferon producing cells

Received: 5 September 2003 / Accepted: 15 September 2003 / Published online: 28 October 2003
© Springer-Verlag 2003

Keywords Plasmacytoid · Monocyte · Interferon

Introduction

In 1958 Lennert and Remmele drew attention to a cell type present in the interfollicular areas of human lymph nodes that they described (on the basis of pure morphology) as a "lymphoblast" [79]. This cell type was subsequently recognized by other hematopathologists, but it received little attention until the availability in the 1980s of antibodies to lineage-associated markers that allowed it to be more easily recognized in tissue sections. This led to studies of its phenotype and of its involvement in a number of pathological conditions.

As a result of these studies by hematopathologists, the cell was given a number of different names, including "T-associated plasma cell" [80], "plasmacytoid T cell" [91, 127], "plasmacytoid T-zone cell" [63] and "plasmacytoid monocyte" [34]. However, there were few clues to its functions and its developmental relationship to other hematopoietic cells until, in the late 1990s, several laboratories started to isolate these cells (and their probable circulating equivalent) and maintain them in culture for detailed studies. These efforts revealed for the first time their capacity to produce high levels of interferon alpha (IFN-α) and also indicated that they could differentiate in vitro into dendritic cells.

A cell that started its career as an unremarkable "lymphoblast", recognized only by a few pathologists, thus emerged almost 50 years later as a cell of considerable potential importance in human immunity and in pathological conditions [20, 54, 82, 114]. The following paragraphs will review the most significant aspects of this cellular type. They have been variously referred to in the recent literature as "plasmacytoid monocytes", "interferon producing cells" and "plasmacytoid dendritic cells", but we have chosen, for simplicity, to use PM as acronym of plasmacytoid monocytes in this text.

F. Facchetti (✉) · W. Vermi
Department of Pathology,
University of Brescia,
Brescia, Italy
e-mail: facchett@med.unibs.it
Tel.: +39-030-3995426
Fax: +39-030-3995053

D. Mason
Nuffield Department of Clinical Laboratory Sciences,
University of Oxford,
Oxford, United Kingdom

M. Colonna
Department of Pathology and Immunology,
Washington University School of Medicine,
St Louis, MO, USA

Location of PM in lymphoid tissues

PM can, with experience, be easily recognized in well-processed conventionally stained tissue sections, provided fixation and staining is optimal [35, 127] (Fig. 1A, B). However, they are much more readily recognized following immunostaining, since they have a very distinctive phenotype (Table 1; Fig. 1D, E) [33]. They are typically slightly larger than lymphocytes, with moderately abundant and well-demarcated cytoplasm that is eosinophilic (in hematoxylin/eosin stained sections) or faintly basophilic (following Giemsa staining). The nucleus is round, oval or slightly indented, with finely dispersed chromatin and one or two small nucleoli.

PM are observed both as single scattered elements and as aggregates, and in the latter setting apoptotic bodies and macrophages containing tingible bodies are often present, sometimes mimicking a germinal center. Ultrastructural examination reveals why the term "plasmacytoid" was applied by pathologists to these cells, since they contain abundant rough endoplasmic reticulum, with non-dilated cisternae that lie parallel to the plasma membrane [35] (Fig. 1C).

In peripheral lymph nodes and tonsils, PM are typically found in the extranodular compartment at the periphery of "composite nodules", a dynamic micro-

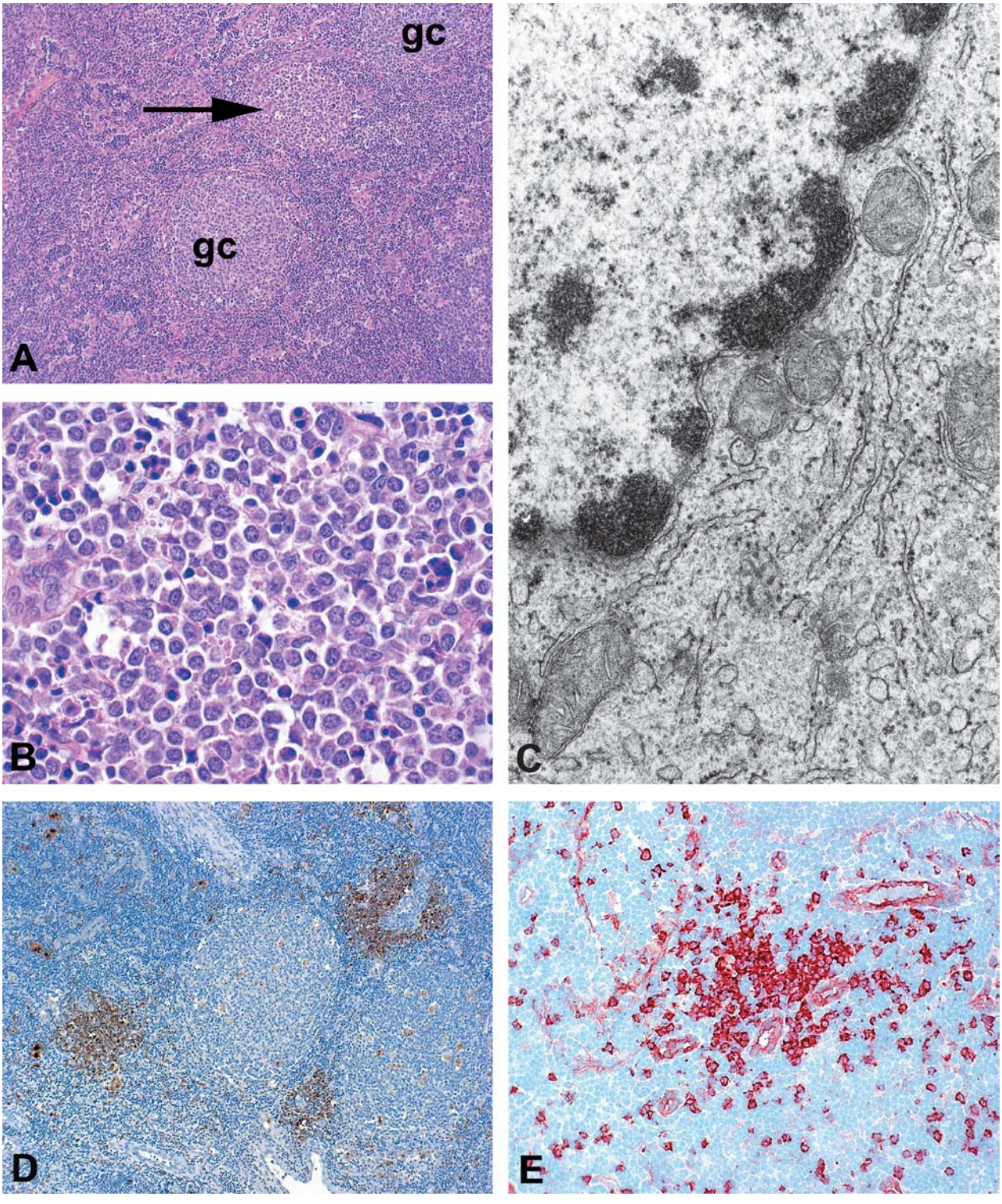

Fig. 1 Histological, electron microscopical and immunohistochemical features of the plasmacytoid monocyte. All pictures were taken form a reactive lymph node. **A** Between two secondary follicles (*gc*), a large cluster of plasmacytoid monocytes (PM) is indicated by the *arrow*; the cytological details of which are illustrated in **B** (note the scattered apoptotic bodies typically found in clusters); the ultrastructural hallmark of the PM, represented by the abundant rough endoplasmic reticulum lamellae, is shown in **C**. The most useful immunohistochemical markers to visualize PM on paraffin and on frozen sections are represented by anti-CD68 (**D**) and anti-CD123 (**E**), respectively. Anti-CD68 identifies three large clusters of PM; anti-CD123 also strongly labels the endothelium of high endothelial venules, which are closely associated with PM

Table 1 Plasmacytoid monocytes (PM) phenotype. Data refer to published studies on in situ immunohistochemistry and on unpublished personal observations. Antigens labeled with °/°° are particularly helpful for PM identification on frozen (°) and paraffin sections (°°). Note: + positive, – negative, –/+ low expression

Cluster of differentiation antigens	
CD1	–
CD2	– (+)[1]
CD3	–
CD4	+
CD5	– (+)[1]
CD7	– (+)[1]
CD8	–
CD10	–
CD11a	+
CD11b	–
CD11c	– (+)[2]
CD13	– (+)[2]
CD14	–
CD15	– (+)[3]
CD16	–
CD19	–
CD20	–
CD21	–
CD23	–
CD25	–
CD27	–
CD28	–
CD30	–
CD31	+
CD32	+[6]
CD33	– (+)[2]
CD34	–
CD35	–
CD36 °	+
CD38	–
CD40	+
CD43	+
CD44	+
CD45RA	+
CD45RB	+
CD45R0	–
CD49e	+[6]
CD56	– (+)[1]
CD57	–
CD62L	+[4]
CD64	–[6]
CD65	–[6]
CD68 °°	+
CD71	+
CD74	+
CD80	–
CD83	–
CD86	–/+
CD95	–/+[6]
CD103	–
CD123 °°	+
CD125	–[6]
CD128	+[6]
CDw150	–[6]
CD161	–[6]
CD162	+[6]
CD206	–[5]
CD207	–[5]
CD208	–[5]
CD209	–[5]
Chemokine receptors	
CXCR1	–[6]
CXCR2	–/+[6]
CXCR3	+[6]
CXCR4	+[6]
CXCR5	–[6]
CCR1	–/+[6]
CCR2	+[6]
CCR3	–[6]
CCR4	–/+[6]
CCR5	+[6]
CCR6	–[6]
CCR7	+[6]
Toll-like receptors	
TLR1	+
TLR2	–
TLR3	–
TLR4	–
TLR5	–
TLR6	–
TLR7	+
TLR8	–
TLR9	+
Miscellanea	
BDCA2 °	+
CLA/Heca452 °°	+
E-cadherin	+[6]
Elastase	–
FceRI	+[6]
Granzyme B °°	+
HLA-ABC	+
HLADR	+
HLADP	+
HLADQ	+
Lysozyme	–
LAT (linker for activation of T cells)	–
Myeloperoxidase	–
Perforin	–
TCL-1	+
TIA-1	–
T-cell receptor AB	–
T-cell receptor GD	–

[1] Positivity found on a fraction (subset?) of circulating PM, not confirmed on tissue sections
[2] Minimal expression, especially upon in vitro differentiation
[3] Positivity after neuraminidase digestion
[4] Membranous on circulating PM, cytoplasmic on tissue PM
[5] CD206, 207, 208 and 209 recognize macrophage mannose receptor, langerin, DCLAMP and DCSIGN
[6] Data from Galibert [54], but not tested in situ; 7: T-cell leukemia-I oncogene

anatomic structure comprising a classical B follicle located at the periphery of a T-cell region [125]. This area is populated by a mixture of B and T cells, macrophages and plasma cells and, typically, PM tend to localize in the vicinity of high endothelial venules (HEV) [35, 39] (Fig. 1B, D, E), which highlight this compartment. PM can be extremely numerous in palatine and pharyngeal tonsils as well as in superficial reactive lymph nodes from young subjects [35]. These lymph nodes (a) affect patients without any significant evidence (clinical, serological and molecular) of known etiological factors; (b) are enlarged in the context of a generalized or localized lymphadenopathy and biopsy is generally recommended due to the long-lasting course of the lymphadenopathy;

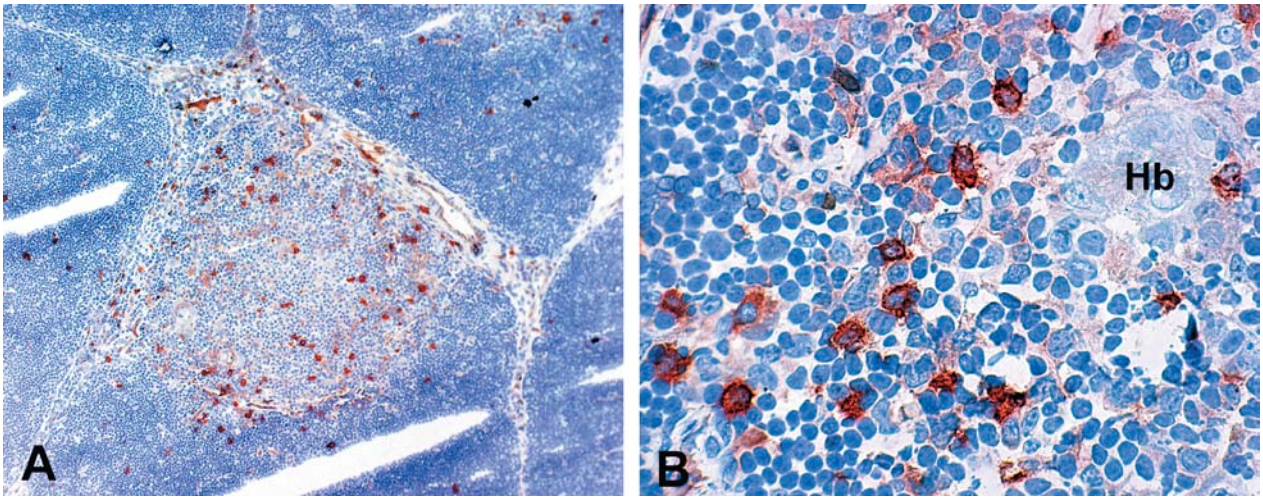

Fig. 2 Thymic distribution of CD123+ plasmacytoid monocytes (PM; frozen sections from human thymus): positive cells are mainly recognizable in the thymic medulla (**A**), scattered among medullary thymocytes and Hassal's bodies (**Hb**; **B**)

and (c) are characterized, on histology, by reactive changes, primarily cortical and/or paracortical hyperplasia, in absence of specific histological features.

PM have also been observed in bone marrow [29, 128] and in the thymus mainly located in the medulla, closely associated with mature interdigitating dendritic cells (Fig. 2A, B) [7]. In the spleen, they are scant and localized in the periarteriolar lymphoid sheets or at the edge of the marginal zone [32]. PM have also been identified in fetal lymph nodes [97] and cord blood [119], and it is of interest that these cells are present in lymph nodes in a variety of different primary immunodeficiency states including X-linked agammaglobulinemia, hyper-IgM syndrome due to mutations in CD40 ligand, non-functional severe combined immunodeficiency, as well as DiGeorge syndrome [42].

PM therefore appear to represent a cell population at the interface between peripheral blood and organized lymphoid tissues, as indicated by their typical localization in the "traffic area" of lymph nodes. Furthermore, their presence in cord blood and fetal lymph nodes and in immunodeficiency states suggests that they can migrate to secondary lymphoid organs even in the absence of an inflammatory response, indicating a patrolling role in "germ-free" conditions.

Migration of PM from peripheral blood to lymphoid tissues.

Cellular traffic between peripheral blood, secondary lymphoid organs and extra-lymphoid tissues is influenced by the expression of surface molecules that interact with ligands on endothelial cells. Circulating PM show intense membrane positivity for L-selectin (CD62L) [16, 97], a critical molecule in the homing of naive T cells to secondary lymphoid organs via HEV. This molecule has been reported to be critical also in the murine system for lymph-node homing of the murine counterpart of PM (mPM) [92]. However, once they enter peripheral lymphoid tissues, PM internalize CD62L.

Peripheral blood PM also express a second category of molecules involved in leukocyte migration, namely the chemokine receptors CCR2, CCR5, CCR7, CXCR3 and CXCR4, although a consistent migratory response has been demonstrated only for CXCR4 ligand [99, 101]. It has been shown that immature PM respond in vivo to "lymphoid or homeostatic chemokines" typical of the lymph-node microenvironment, namely CXCL12/SDF1 (stromal cell-derived factor—a ligand for CXCR4) while they are sensitive to CCL19/ELC and CCL21/SLC (ligands for CCR7) after cell maturation upon CD40 ligation. The role of CXCR3 remains unclear since PM do not respond to its ligands (CXCL9, CXCL10 and CXCL11) in vitro [99]. Recently, however, Krug et al. [78] demonstrated that migration of murine and human PM in response to CXCR3 ligands requires engagement of CXCR4 by CXCL12/SDF1, the latter expressed by HEVs in inflamed lymph nodes and by tumor cells in ovarian cancer [131] and melanoma [126]. This pattern reflects the preferential localization of these cells to secondary lymphoid organs via the HEV and their active recruitment to sites of primary tumors. PM may also actively attract other leukocytes secreting inflammatory chemokines. Penna et al. [100, 101] have reported that blood PM stimulated with CpG oligonucleotides secrete high amounts of CCL3/MIP-1α and CCL4-MIP-1β, two pro-inflammatory chemokines capable to recruit effector Th1-cells to sites of inflammation. These data were recently confirmed and expanded to demonstrate that on activation with influenza virus, CpG or CD40L, PM secrete CCL5, CXCL9 and CXCL10. This means that large numbers of leukocytes including PM can be recruited to lymph nodes on infection by PM-mediated secretion of inflammatory chemokines; this might explain the observed clustering of PM in lymph nodes [35].

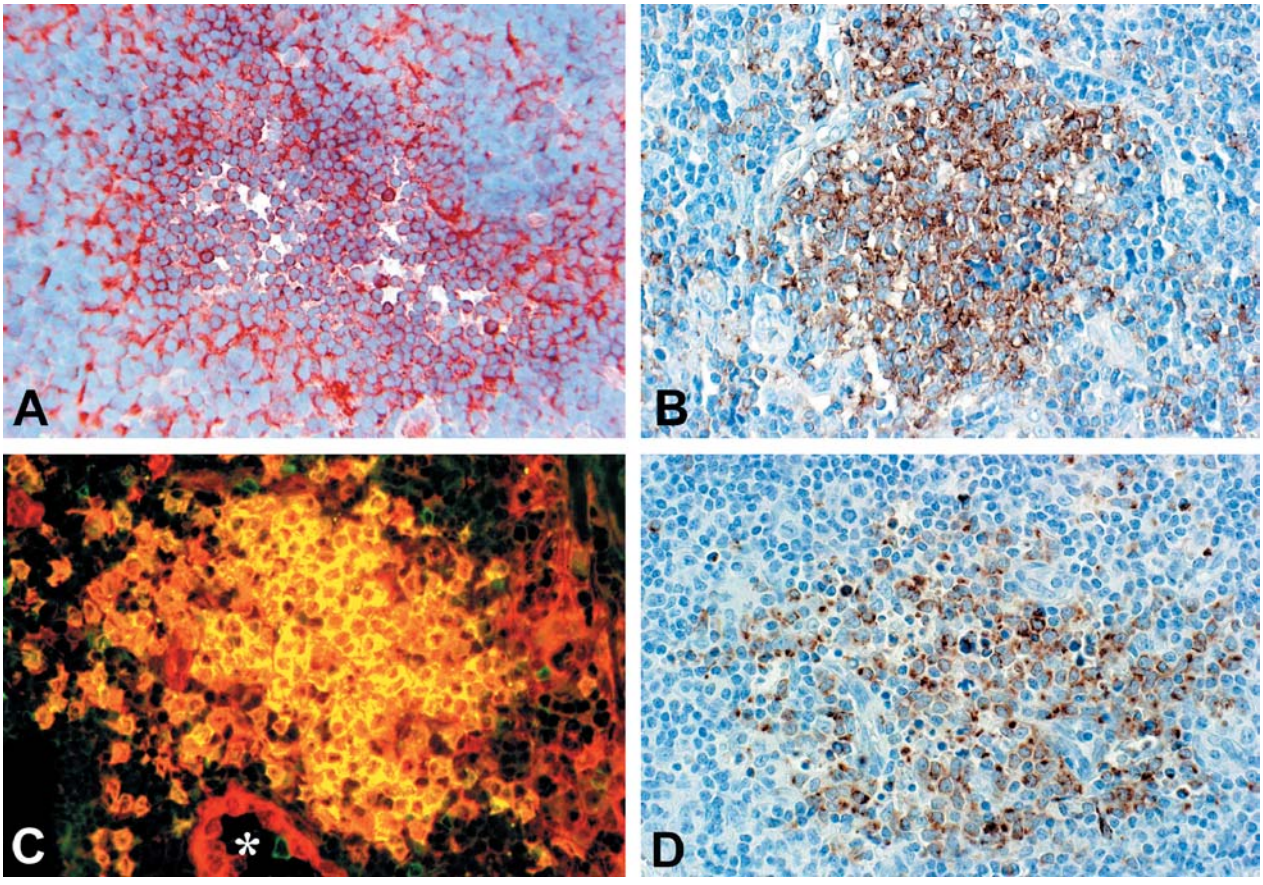

Fig. 3 Secretory products and regulatory molecules of plasmacytoid monocytes (PM). PM strongly reacts with anti-interferon-alpha antibody (**A**) and express MxA, a reliable index of the production of type-I interferons (**B**). Circulating and tissue PM express BDCA2 ("blood dendritic cell antigen 2"), a negative regulator of the secretion of IFN-α; **C** double immunofluorescence where anti-CD123 (*red*) and anti-BDCA2 (*green*) were simultaneously applied: note that the majority of perivascular PM are double-labeled (*yellow*), while the high endothelial venule (*asterisk*) only expresses CD123; rare single BDCA2 positive cells are also noted. Human PM contain high levels not only of granzyme B mRNA, but also of protein, as shown in **D**

Taken together, these data suggest that PM retain migratory machinery able to direct them to lymph nodes and produce Th1-attracting chemokines. However, since PM have been observed at effector sites in inflammatory diseases, it is conceivable that other chemokine receptor/ligand pairs may be utilized in vivo.

The secretory function of PM

The ability to purify PM and maintain them in culture has begun to shed light on the enigma of which proteins are produced in their prominent endoplasmic reticulum, since they have been shown to secrete high levels of IFN-α, and, to a lesser degree, other forms of type-I IFN, such as IFN-β and IFN-ω. The synthesis of IFN-α by PM in vivo is confirmed by their intense cytoplasmic immunoreactivity for this cytokine in tissue sections (Fig. 3A). IFN-α has a number of fundamental roles in innate and adaptive responses to pathogens [60]. During the early phases of viral infection, IFN-α protects cells from cytopathic effects and activates other effector cells such as natural killer cells and macrophages. Its practical importance is attested for by its therapeutic use in eradicating chronic viral infections, e.g., hepatitis [60]. It also influences leukocytes involved in adaptive immunity in mouse and human, such as dendritic cells (differentiation, maturation and cytokine secretion), T cells (survival, Th1-cell switch, proliferation and expansion of CD8 T cells), and B lymphocytes (antibody production). Finally, IFN-α can exert an anti-proliferative effect on various cell types, an effect exploited in the treatment of several neoplasms [60] including the neighboring myeloid DC of the T-cell area of lymph nodes. Finally, we cannot exclude that an autocrine loop due to the basal level of IFN-α produced by PM would also account for their low proliferative index.

Although IFN-α is produced by several leukocyte populations, PM appear to be the major cellular source of this cytokine [16, 17, 74]. Among PBMCs, a small fraction of primary cells producing high levels of IFN-α were recognizable on the basis of their lin-CD4+CD36+HLADR+ phenotype, a cell type whose tissue distribution, morphology and phenotype remained

elusive for a long time [49]. The phenotype of this cell population is identical to that of PM [116], although it is probable that the latter do not account for the entire population of the natural IFN producing cells in human blood [10, 54].

PM also stain strongly in lymph-node sections for MxA, a protein which is considered a reliable index of the production of type-I IFNs, which is not dependent on an external stimulus such as viral infection, since it is seen even in non-specific reactive conditions of human lymph nodes (Fig. 3B). Furthermore, freshly isolated PM show high levels of MxA in vitro. This basal level of MxA expression, either constitutive or induced in autocrine fashion via IFN-α, may have a protective role against viral cytopathic damage [17].

The basal level of IFN-α secretion by PM can be greatly increased by several stimuli, including viruses (herpes simplex viruses, influenza virus and adenovirus) [16, 74, 75, 130], bacteria (e.g., *Staphylococcus aureus*) [123], cytokines [16], hypomethylated bacterial DNA sequences (CpG ODN) [5, 77], and serum from systemic lupus erythematosus patients [124]. The molecular mechanisms involved in regulating IFN-α production by PM remain to be fully explored, but at least one element, namely BDCA2 ("blood dendritic cell antigen 2"), has been identified. This molecule is selectively expressed by circulating and tissue PM [27] (Fig. 3C), and its ligation by monoclonal anti-BDCA2 drastically reduces the secretion of IFN-α induced by various stimuli [28]. This suggests that a ligand of BDCA2 (currently unknown) may act as master player in the regulation of the IFN-α production in vivo.

Circulating and tissue PM express high levels of CD123, the receptor for interleukin (IL)-3 alpha-chain (Fig. 1E and 3C), a cytokine of major importance for the survival, proliferation and differentiation of hematopoietic cells [112]. This is likely to be physiologically relevant since IL-3 rescues PM in vitro from rapid apoptosis, which they undergo once isolated from blood or tissues [59]. Another leading molecule in target-cell apoptosis that was unexpectedly found to be secreted by human PM is granzyme B. High levels of mRNA are evident on PM freshly isolated from tonsils [107]. Immunohistochemistry confirms that tissue PM regularly and strongly express granzyme B [44](Fig. 3D). Since PM lack perforin, the function of this protein in PM still remains elusive. It is possible that at effector sites in certain pathological conditions where PM are abundantly recruited, they cooperate with cytotoxic lymphocytes, which provide a sufficient amount of perforin to mediate GrB-dependent target cell apoptosis. This hypothesis is consistent with the evidence that highly purified PM are unable to exert cytolytic activity, which is achieved when they are mixed with other cells [12]. The recent evidence that PM express the intracellular granzyme B inhibitor, proteinase inhibitor 9, suggests that, as for professional cytotoxic cells, PM have developed a protective mechanism against misdirected granzyme B (autocrine granule leakage or endocytosed granzyme B) [66].

A new subset of dendritic cells

The concept of the dendritic cell as a key element in the afferent arm of the adaptive immune response (through their uniquely potent ability to present antigen to T cells) dates from Steinman's work in the 1980s [122]. Immature dendritic cells at the site of entry of exogenous antigens (e.g., intraepithelial Langerhans' cells and dermal interstitial dendritic cells) are responsible for antigen capture and processing, exploiting a complex array of uptake mechanisms including phagocytosis, micropinocytosis and receptor-mediated endocytosis [15]. Following antigen capture, these dendritic cells migrate to lymphoid tissues, express co-stimulatory molecules (e.g., HLADR, CD80, CD83, CD86, DC-LAMP/CD208) and the chemokine receptor CCR7, abundantly produce interleukin 12 and acquire potent immunostimulatory activity (e.g., proliferation of quiescent naive and memory T- and B cells and IFN-γ production by CD4+ Th1).

Since it is difficult to extract dendritic cells from tissues, much effort has been devoted to define possible circulating precursors of dendritic cells. CD11c-positive "myeloid dendritic cells" were identified in human peripheral blood [15, 82], and it was found that circulating CD34-positive or CD14-positive precursors could be used to generate cells resembling tissue dendritic cells in vitro [13]. It was then reported by O'Doherty et al. that a subpopulation of peripheral blood leucocytes with PM-like morphology and phenotype differentiate to become dendritic cells [93]. Subsequent confirmatory studies indicated these cells can differentiate into dendritic cells under the influence of stimuli, such as viruses, IL-3, CD40L, and non-methylated bacterial DNA (CpG-ODN) [5, 17, 59, 77]. Dendritic cells generated from putative peripheral blood and tonsillar PM (i.e., from IL-3R/CD123-positive cells) express adhesion and co-stimulatory molecules typical of mature dendritic cells, produce IL-12 and can stimulate naive allogenic T lymphocytes [5, 17, 77].

Further study of these cells, for which the term "plasmacytoid dendritic cell" was coined [17, 59], showed that there are substantial differences between myeloid and plasmacytoid dendritic cells, raising the possibility of different functional roles [82]. These differences include the patterns of surface molecule expression (including the chemokine receptor profile) and the very limited phagocytic capacity of plasmacytoid dendritic cells, partly explained by the lack of receptors such as those for mannose and Fc. There are also dramatic differences in the expression of toll-like receptors, a family of molecules involved primarily in the recognition of microbial products (Table 1). It may be noted that dendritic cells of myeloid origin populate, when immature (e.g., Langerhans' cell or interstitial dendritic cells), areas of entry of exogenous antigens in the peripheral tissues and subsequently migrate to T cell-rich areas to become mature antigen-presenting cells (e.g., interdigitating dendritic cells). In contrast, PM are strategically distributed, irrespective of their activation state, around HEV where

blood-derived antigens and circulating leukocytes enter lymphoid tissues. The capacity of PM to efficiently present antigen to naive T cells, a requisite that is mandatory for the definition of full blown DC, remains to be fully elucidated. However, it has recently been demonstrated that upon influenza virus exposure, PM expand virus-specific CTL and TH1 CD4+ T cells [52]. The differences between various populations of dendritic cells may reflect different immunoregulatory responses to various stimuli and reciprocal roles in fine tuning the immune response [10, 78, 130].

Finally, it may be noted that despite the experimental evidence that circulating and tissue plasmacytoid cells can acquire the morphological and functional features of dendritic cells in vitro, the existence of "plasmacytoid dendritic cells" in vivo is still controversial. In lymphoid organs, it is possible to observe cells with clearly dendritic morphology that co-express CD123 (IL-3R) and BDCA2, but they are much rarer than PM with typical round-oval morphology. Moreover, the co-stimulatory molecules [77] found on plasmacytoid dendritic cells in vitro are present on only a very limited number of tissue PM [17]. However, it remains possible that DC derived from PM lose BDCA2 and CD123 once matured in vivo.

PM in pathological conditions

The number of PM in the peripheral blood of healthy volunteers declines significantly with age in both men and women in association with a fall in IFN-α production [113] and largely parallels the depletion of PM in lymph nodes during aging. In contrast, variability in the number of circulating PM reported in different pathological conditions may reflect, at least partially, tissue recruitment of these cells. In particular, loss of peripheral blood PM has been observed in human immunodeficiency virus (HIV)-infected patients [25], especially in those with active HIV replication [4] and in patients suffering from chronic myeloid leukemia [89]. In contrast, an increased number of circulating PM has been reported in patients with allergic asthma [86].

A marked increase of PM in lymph nodes can be observed in a range of inflammatory states, including reactions to infection (e.g., tuberculosis, toxoplasmosis), non-infectious conditions (e.g., sarcoidosis) [36] and epithelial neoplasms [68], as well as in association with lymphoproliferative processes [37] and myeloproliferative diseases (as discussed below in more detail). Data on the presence of PM in extranodal tissues are limited to cutaneous inflammatory conditions such as pseudolymphomas [30], Jessner's lymphocytic infiltrate [40], lupus erythematosus [45], psoriasis and contact dermatitis [129]. Finally P-DCs accumulate dramatically in nasal mucosa on experimentally induced allergic reaction [72] and were found to infiltrate allergic nasal polyps [118].

In two rare forms of lymphadenopathy such as Kikuchi-Fujimoto disease [104] and the hyaline-vascular subtype of Castleman's disease (HV-CD) [62], the occurrence of large numbers of PM represent an important diagnostic criterion.

Kikuchi-Fujimoto disease is a disorder characterized by fever, cervical lymphadenopathy, leukopenia and transient skin rashes. In most cases, Kikuchi-Fujimoto disease enters spontaneous and permanent remission within a few months, but a small minority of patients can develop full blown systemic lupus erythematosus (SLE) [19]. Laboratory findings are mostly non-specific, and the diagnosis is established by identifying characteristic pathological features in lymph nodes. Large clusters of PM in lymph nodes are the hallmark histological feature of Kikuchi-Fujimoto disease, together with coagulative necrosis, histiocytic reaction and variable immunoblastic proliferation (Fig. 4A, B) [38, 104]; it should be noted that the histological changes seen in lymph nodes from SLE are reminiscent of Kikuchi-Fujimoto disease, suggesting a link between the two disorders (as discussed below).

Castleman's disease (CD) encompasses two clinicopathological variants, the localized type and the multicentric type [53]. Localized CD usually presents with a solitary mass, predominantly involving the mediastinum, in patients who are typically asymptomatic, until the mass compresses organ structures. In contrast, the less frequent multicentric CD is a systemic lymphoproliferative disorder, associated with hepatosplenomegaly, abnormal laboratory findings, constitutional symptoms, and frequently complicated by the development of malignancies. Histologically, a hyaline-vascular type (HV-CD) and a plasmacell type of CD have been described, usually associated with localized CD and multicentric CD, respectively. HV-CD diagnosis relies on abnormal B-follicles, loss of lymph-node sinuses, prominent vascularization and clusters of PM in the interfollicular area [23, 62]. How the accumulation of PM is related to pathogenesis of HV-CD remains unclear.

The pathogenetic role of PM in these very different conditions still remains the subject of speculation, but several mechanisms, outlined in the following paragraphs, have begun to provide a possible interpretative key.

Response to pathogens: the possible role of PM in HIV infection

PM are extremely abundant in adenoidal lymphoid tissue, suggesting a potential role in local anti-viral defense. In unpublished experiments by Brandtzaeg et al., accumulation of PM was found in cutaneous lesions caused by varicella-zoster virus [73]. In addition, it has been demonstrated that PM mature following exposure to influenza virus and are able to expand anti-influenza virus CTL and TH1 CD4+ T cells, suggesting a prominent role in the adaptive anti-viral immune response [52]. Preliminary studies of HIV infection suggest a relevant role for PM in acquired immunodeficiency syndrome (AIDS). PM are severely reduced in number in the peripheral blood of

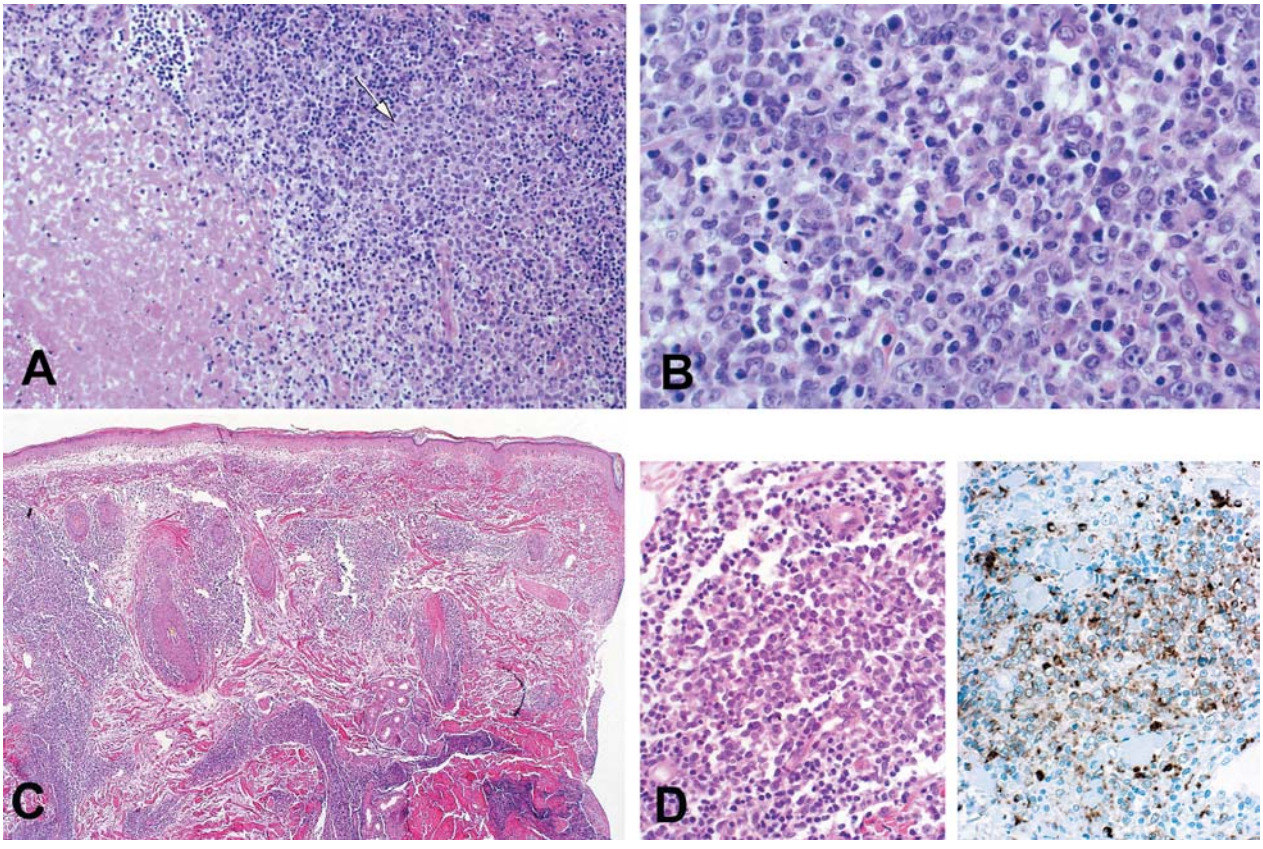

Fig. 4 Plasmacytoid monocytes (PM) in human diseases, namely Kikuchi's lymphadenitis (**A**, **B**) and cutaneous lupus erythematosus (**C**, **D**). Typical zonation in Kikuchi's lymphadenitis, with an eosinophilic necrotic area (*left lower corner*) surrounded by a polymorphic cell area and, more peripherally, by a cluster of PM (*arrow*; **A**). The cell composition of the polymorphic area is illustrated in **B**, where PM, histiocytes, lymphocytes and immunoblasts are found. In a case of systemic lupus erythematosus, the skin biopsy shows perivascular and periadnexal inflammatory infiltrates in the dermis (**C**), which contain numerous PM, identifiable on the basis of both cyto-morphological (**D**, *left*, hematoxylin & eosin) and immunohistochemical (**D**, *right*, anti-CD68/PGM1 immunostain) features

HIV-infected patients [25, 120]. This reduction correlates with (a) a diminished ability of peripheral blood mononuclear cells to generate IFN-α, (b) a high viral load, (c) a decrease in the peripheral CD4-positive T-cell count, and (d) the occurrence of opportunistic infections [115, 117, 120]. A qualitative dysfunction of PM may also be associated since reduction in IFN-α production is observed on HIV infection [46]. Interestingly, high numbers of functional PM with increased function were observed in HIV+ long-term survivors [120]. The issue of restoration of PM number and function after highly active antiretroviral therapy still remains controversial (discussed in [121]).

Taken together, these data suggest that loss of functionally competent circulating PM occur as an early event in the pathogenesis of HIV infection. It is possible that the reduction of peripheral blood PM in HIV infection reflects tissue redistribution, but it is also conceivable that these cells are the direct targets for HIV. PM express known receptors for the virus (e.g., high levels of CD4 along with constitutive expression of CCR5 and CXCR4) and there is evidence that PM are permissive for productive HIV infection [75]. In particular, the virus can (i) replicate efficiently inside PM, (ii) be released as infectious provirus [98], and (iii) efficiently transmit to CD4 T cells [51]. Secondary lymphoid organs still remain the principal site where HIV replicates, and where CD4-positive T cells are infected and become the major tissue reservoir for the virus [61]. It is of note that PM co-exist in the "traffic area" of lymph nodes and tonsils in close proximity to CD4-positive T cells, and to a subpopulation of dendritic cells expressing DC-SIGN, an HIV binding protein thought to be a key molecule in the intercellular transmission of the virus [55] (Fig. 5). Tissue PM may thus represent a reservoir, or at least a transitory carrier [51], of HIV during the process of infection of CD4-positive T lymphocytes. Despite the rapid evolution of this field, many important questions remain to be addressed on the interaction between HIV and PM [121], which may have important implications for the management of AIDS patients.

Recent studies of toll-like receptors (TLRs) on human leucocytes have shed new light on the mechanism of innate immunity and have also suggested that the activity

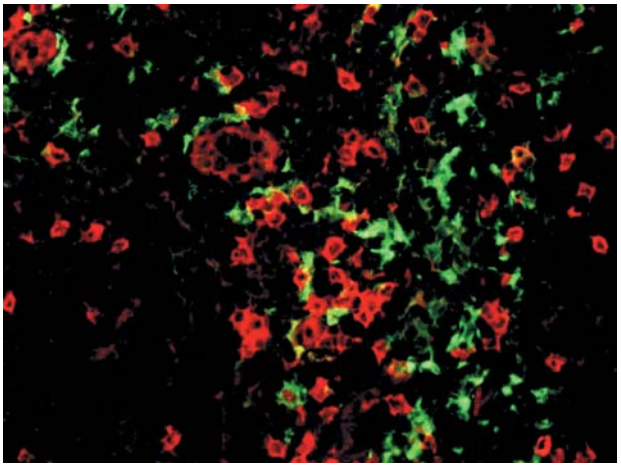

Fig. 5 In the "traffic area" of lymph nodes and tonsils, plasmacytoid monocytes (PM) are closely associated with another subset of dendritic cells, which express the HIV binding protein DC-SIGN, as shown in this double immunofluorescence for CD123 (*red*) and DCSIGN (*green*)

of PM is not directed only against viruses. TLRs comprise a family of membrane receptors recognizing microbial products that play a major role in the early phases of pathogen recognition [1]. In contrast to other dendritic cell subsets, the TLR profile in PM is restricted to TLR7 and TLR9. The first of these is a receptor for imidazoquinolines [64], a group of compounds with anti-viral activity [87]. Some imidazoquinolines are potent inducers of IFN-α production and have been successfully used in the treatment of genital warts and genital herpes virus infections. TLR9 recognizes non-methylated bacterial DNA (CpG-ODN) sequences and binding of its ligand influences several functional features of PM, including survival, phenotypic maturation, secretion of IL-12 and IFN-α and CCR7 expression [70, 71, 109].

These data indicate that both viral and bacterial products can activate PM (either directly or via the generation of endogenous ligands) and this in turn could serve to modulate the immune response to infection. Clarification of these TLR-mediated interactions involving PM may lead to new therapeutic strategies for infectious diseases.

PM and autoimmune diseases

SLE represents the prototype of an abnormal immunological process resulting in autoimmune damage to a range of tissues, and several findings have suggested that PM may play a role in the pathogenesis of this disease [108]. For example, SLE and SLE-like conditions [26] may develop in patients treated long-term with IFN-α. Furthermore, high levels of IFN-α are found in the blood of SLE patients in the active phase of the disease. This is associated with reduced numbers of circulating "natural interferon-producing cells" [14], a paradoxical finding that may be explained by recruitment of PM to sites of tissue damage, as has been reported in cutaneous lesions in SLE [45](Fig. 4C, D). It is also of interest that Jessner's benign lymphocytic infiltrate of the skin, in which clusters of PM are commonly observed [40], is considered by some authors to be a variant of lupus erythematosus. Finally, a soluble factor that stimulates PM to produce high levels of IFN-α has been reported in the blood of patients with active SLE [124].

SLE may have features in common with Kikuchi-Fujimoto disease (see introductory paragraph of the current section); therefore, it is tempting to speculate that SLE and Kikuchi-Fujimoto disease may share a common pathogenetic mechanism that involves tissue accumulation of PM. In Kikuchi-Fujimoto disease, the process may be limited to an initial response in the context of an acute viral infection, as demonstrated for herpes virus 6, by serological and molecular studies in a large cohort of patients recently reported [24]. In contrast, tissue damage occurring in SLE would lead to on-going hyperproduction of IFN-α by PM. This hyperproduction would in turn activate myeloid dendritic cells to stimulate auto-reactive T-cell clones and support B-cell proliferation and differentiation with generation of a high number of plasma cells producing autoantibodies. By global gene expression profiling of peripheral blood mononuclear cells, it has been demonstrated that dysregulated expression of genes in the IFN pathway distinguish most SLE patients from healthy controls. This IFN "signature" identifies a subgroup of patients with more severe disease and can be shut down upon treatment with high-dose glucocorticoids [8]. Altogether, these data strengthen the notion of a role for this cytokine in SLE, and may help to select patients who can benefit from therapies targeting the IFN pathway. It would be of interest to investigate in these diseases the regulation of mechanisms that normally inhibit INF-α production (e.g., via BDCA2 and its ligand).

PM and tumor immunity

In the past few years, many studies of anti-tumor immune responses have focused on mechanisms of antigen recognition and presentation and, in particular, on the possible role of dendritic cells [50]. Improved methods for isolating and manipulating dendritic cells have prompted attempts to develop dendritic cell-based anti-tumor vaccines for human clinical use. Several promising preliminary results have been reported, but high rates of relapse and disease progression indicate that further investigations are needed. In particular, in situ studies of dendritic cell numbers, distribution and phenotype at different stages of tumor progression would be helpful.

The suggestion that PM may play a role in anti-tumor immunity dates from the observation that metastatic lymph nodes draining breast carcinomas contain clusters of PM [68]. More recently, Zou et al. have documented the presence of PM in cases of ovarian carcinoma, and reported that they are recruited to the primary tumor and

to the ascitic fluid [131]. In such a context, PM expressed IFN-α and MxA and were chemotactically attracted by SDF-1 produced by neoplastic cells. SDF-1 was responsible not only for the migration of PM to the tumor sites, but also for their protection from apoptosis induced by interleukin 10 secreted by intratumoral macrophages. Lastly, this study has emphasized a functional defect of PM in the stimulation of T lymphocytes isolated from tumors, suggesting a possible "tumor escape" mechanism acting on PM.

Primary cutaneous melanoma has been widely studied as a model in human anti-tumor immune responses, and histological analysis has demonstrated that PM are present in significant numbers not only in sentinel lymph nodes but also in primary and metastatic cutaneous melanomas [126]. In these samples, PM are located mainly at the periphery of neoplastic cell nests, associated with myeloid dendritic cells with which they share an immature phenotype. The production of IFN-α by these PM appears limited, as indicated by the low number of MxA-positive cells in the vicinity of the tumor. Furthermore, peripheral blood PM can stimulate a population of cytotoxic T lymphocytes specific for melanoma-associated antigens and favor their migration to the effector site [110]. Finally, T lymphocytes within the peri-tumoral infiltrate partially display a naive phenotype (CD45RA+ CD27+), and the production of interleukin 12, a reliable indicator of dendritic cell activation, is very low. Taken together, these findings suggest that the tumor microenvironment may restrict the immune response against melanoma cells and the functional activity of different dendritic cell subsets.

The cellular origin of PM: a continuing controversy

PM appear to arise from FLT3 ligand cultured CD34-positive mononuclear cells [11] and their precursors, CD34+IL-3Ra^{hi} progenitors, were detected by Olweus et al. in fetal bone marrow [97]. In addition, using four-color flow cytometry, the developmental pathway of PM from CD34(+) hematopoietic stem cells has been described [11]. These precursors account for only a negligible fraction (less than 1%) of the bone marrow cells but can be easily mobilized into the peripheral blood by G-CSF and F1t3-ligand [9, 11, 84, 97, 106].

These findings do not however resolve the long-debated question of whether PM belong to the lymphoid or the myelo-monocytic cell lineage [21, 54]. A powerful argument for their derivation from myeloid cells stems from rare cases in which a massive accumulation of PM is seen in lymph nodes and, less commonly, in the bone marrow, spleen, skin and even the peripheral blood in patients affected with myeloproliferative disorders [3, 6, 63, 91, 105]. The latter are heterogeneous, but mainly represented by acute or chronic myelomonocytic or monocytic leukemias, often arising in elderly subjects in whom lymphadenopathy (and hepatosplenomegaly) is present from the onset.

Several explanations have been proposed for the striking expansion of PM in these cases, including (a) an exaggerated response to the myeloid neoplasm and (b) a neoplastic proliferation of PM, either unrelated to the myeloproliferative disease or resulting from divergent differentiation from a common myelomonocytic precursor [3]. The PM observed in these conditions show only minimal morphological atypia and have a low proliferation index; however, their extensive expansion throughout the lymph-node parenchyma, often extending to the extra-nodal tissue, and the presence of some phenotypic aberrations, such as de novo expression of CD2, CD5, CD10, CD14 and CD15, suggest their neoplastic nature. Furthermore, the presence of identical cytogenetic abnormalities in the two cell populations has been observed in cases of myelodysplasia [47, 90] and in one case of acute myeloid leukemia [43], unequivocally arguing both for the neoplastic nature of PM and for a close developmental relationship between the two tumor populations. It is interesting to note that Mohty et al. demonstrated in several cases of myeloid leukemia that "normal" peripheral blood PM (as well as myeloid dendritic cells) share cytogenetic abnormalities with the leukemic cells [88].

Recently, tumor proliferation of PM has been documented in the form of a "hematodermic neoplasm" characterized by an aggressive course, dense massive marrow infiltration, and nodal and extra nodal (primarily skin) neoplastic lesions [102]. These patients are leukemic, with high levels of CD4+CD56+ atypical cells that lack T, B and myeloid markers. On the basis of phenotypic (e.g., IL-3R/CD123 expression), molecular and functional data (e.g., production of IFN-α), these tumor cells seem to represent the neoplastic counterpart of PM [18, 48, 103]. It should be noted that CD56 was never found on PM either in peripheral blood or lymphoid tissues [18, 32]. Very recently, it has been documented that CD4+CD56+ neoplastic cells share many features with a subset of CD4/CD56 positive cells that comprise a proportion (1.6±0.9%) of the circulating CD123+ cells of healthy volunteers treated with Flt3 ligand [21, 103]. These cells have many features in common with PM and are absent or very rare in non-treated donors. It is therefore likely that the CD123+CD4+CD56+ tumors may represent the neoplastic counterpart of CD56-positive activated PM. Curiously, reactivity for CD56 seems to be particularly restricted to a single clone (B159) [21]. Immunostaining of sections from lymph nodes and tonsils demonstrate that the majority of PM are negative for CD56, with very occasional coexpression of B159 on BDCA2+CD123+ cells (personal observation). Very recently, an additional variant of CD4+CD56+ hematodermic neoplasm related to myelomonocytic leukemia has been reported, and tumor cells have been shown to express TCL1, a potent oncogene for B cells. Interestingly, TCL1 was also expressed on PM in reactive lymph nodes [65, 76]. The distinguishing clinical and pathological features of the neoplasms related to PM are reported in Table 2.

Table 2 Clinical and phenotypical features of tumor proliferations of plasmacytoid monocytes (PM). *n.d.* not done

Source	References [18, 48, 102, 103]	References [65, 76]	Reviewed in [33]
Number of patients	37	13 [1]	16
Clinical features			
Median age (years)	67	61	64
Male/female	25/12	6/1	17/5
Associated myeloid leukemia	0	3/7	16 [2]
Prognosis	Poor	Poor	Poor
Site of tumor extension at diagnosis and relapses			
Bone marrow	29/37 (78%)	7/7 (100%)	10/16 (62%)
Lymph nodes	21/37 (57%)	5/7 (71%)	14/16 (87%)
Spleen	9/37 (24%)	1/7 (14%)	1/16 (6%)
Skin	27/37 (73%)	7/7 (100%)	6/16 (37%)
Circulating PM	16/35 (46%) [3]	n.d.	1/16 (6%)
Phenotype			
CD4	+	+	+
CD36	− (+) [4]	n.d.	+
CD56	+	+	− (+) [5]
CD68	+	− (+) [6]	+
CD123	+	+	+ [8]
Granzyme B	− (+)	−	+ [8]
Perforin	n.d. (−)	−	−
CD16, CD57	−	− (+) [7]	−
TCL1	n.d.	+	+ [8, 9]

[1] The clinical and pathological data are reported in detail only by the study of Khoury et al. [76], while phenotypical data are from both studies
[2] The associated myeloid neoplasms were predominantly represented by acute or chronic monocytic or myelo-monocytic leukemia
[3] In the study by Petrella et al. circulating blasts were identified as myeloperoxidase-/esterase-, while in the study by Feuillard et al. they were also demonstrated to be CD4+/CD56+
[4] Data within parentheses are referred to the study by Feuillard et al. [48] and Chaperot et al. [18]
[5] Positivity was found on occasional cells in a case reported by Horny et al. [69] and in a single from five cases personally observed
[6] Two of seven cases positive
[7] Three of seven cases positive for CD16
[8] Nuclear positivity was found in one of five cases, while in the remaining four cases only cytoplasmic reactivity was found
[9] Personal observation, previously unreported data

The significance of these different PM tumor entities has yet to be established. Tumor cells have several features in common, i.e., plasmacytoid morphology and phenotype, extranodal involvement (especially of the skin), and aggressive behavior. However some clinical (e.g., association with myeloid disorders) as well as morpho-phenotypical differences (e.g., in cytological atypia, proliferation index and CD56 and granzyme B expression) suggest that tumor transformation may affect PM at different stages in their differentiation and maturation/activation pathways [44].

The murine counterpart of PM

Searching for a counterpart of human PM, Nakano and colleagues [92] isolated dendritic cells with plasmacytoid morphology from mouse secondary lymphoid organs. These cells, which are typically localized within the T-cell areas of lymph nodes, display an immature phenotype (Lin-negative, CD11c/Gr1/B220-positive). CD11c+Gr1+ B220+ cells are capable of stimulating T-cell proliferation and producing IFN-α after activation by CpG or influenza virus. These features suggest that these cells represent the murine counterpart of human PM.

Subsequent groups have succeeded in the identification of immature mPM in both primary (bone marrow and thymus) and secondary lymphoid organs (spleen), as well as in the peripheral blood [94, 96]. In addition, a constitutive population of mPM has also been observed in non-lymphoid organs such as the liver [81]. Additionally, these studies have documented the ability of these cells to produce high levels of IFN-α and to change their phenotype and functional properties (e.g., IL-12 production) in response to different stimuli [2, 58, 85, 94]. The role of mPM in innate immunity against viruses has been confirmed in vivo in murine cytomegalovirus infection [2, 22]. In addition, it has been demonstrated that mPM from mouse lymphoid organs can differentiate into CD8+CD205- DCs and prime T cells [95] upon microbial stimulation. However, in steady-state conditions, mPM may play a tolerogenic role [85] producing IL-10 and being involved in the generation of T-regulatory cells, as suggested for the human counterpart [56].

Although these data suggest a high degree of similarity between mPM and human PM [67], at least two notable differences exist. First, the putative mPM express variable levels of CD11c, a marker found on human and mouse myeloid dendritic cells, but not on human PM [11, 58]. Second, mPM lack high expression of CD123 [95] and their survival, consequently, does not depend primarily on IL-3. Very recently, differences were also reported for the expression of Toll-like receptors [31].

New insight into the true nature of mPM and their in vivo function should emerge now that large number of these cells can be generated from bone marrow cells cultured in the presence of FLT3-ligand [57] and by exploiting murine models where this cell population is expanded [83] or abrogated [111].

Conclusions and future perspectives

Recent data on PM have shed new light on the physiological responses of peripheral lymphoid tissue. The ability to mobilize tissue PM in vivo or manipulate their circulating counterpart ex vivo could open new avenues for therapy. The identification of the murine counterpart of PM may make it possible to define in more detail the functions of these cells in vivo. Pathologists will continue to play a fundamental role, through careful immuno-

morphogical observation, in evaluating how PM are implicated in different types of human disease.

Acknowledgements The authors wish to thank Amanda Blasius and Anne Krug for their critical comments to the manuscript. The enthusiastic technical support of Silvana Festa, Francesca Gentili, Wilma Pellegrini, Anna Galletti and the secretarial assistance of Gisella Scibè were also greatly appreciated.

References

1. Aderem A, Ulevitch RJ (2000) Toll-like receptors in the induction of the innate immune response. Nature 406:782–787
2. Asselin-Paturel C, Boonstra A, Dalod M, Durand I, Yessaad N, Dezutter-Dambuyant C, Vicari A, O'Garra A, Biron C, Briere F, Trinchieri G (2001) Mouse type I IFN-producing cells are immature APCs with plasmacytoid morphology. Nat Immunol 2:1144–1150
3. Baddoura FK, Hanson C,Chan WC (1992) Plasmacytoid monocyte proliferation associated with myeloproliferative disorders. Cancer 69:1457–1467
4. Barron MA, Blyveis N, Palmer BE, MaWhinney S, Wilson CC (2003) Influence of plasma viremia on defects in number and immunophenotype of blood dendritic cell subsets in human immunodeficiency virus 1-infected individuals. J Infect Dis 187:26–37
5. Bauer M, Redecke V, Ellwart JW, Scherer B, Kremer JP, Wagner H, Lipford GB (2001) Bacterial cpg-DNA triggers activation and maturation of human cd11c(−), cd123(+) dendritic cells. J Immunol 166:5000–5007
6. Beiske K, Langholm R, Godal T, Marton PF (1986) T-zone lymphoma with predominance of 'plasmacytoid T-cells' associated with myelomonocytic leukaemia—a distinct clinicopathological entity. J Pathol 150:247–255
7. Bendriss-Vermare N, Barthelemy C, Durand I, Bruand C, Dezutter-Dambuyant C, Moulian N, Berrih-Aknin S, Caux C, Trinchieri G, Briere F (2001) Human thymus contains IFN-alpha-producing CD11c(−), myeloid CD11c(+), and mature interdigitating dendritic cells. J Clin Invest 107:835–844
8. Bennett L, Palucka AK, Arce E, Cantrell V, Borvak J, Banchereau J, Pascual V (2003) Interferon and granulopoiesis signatures in systemic lupus erythematosus blood. J Exp Med 197:711–723
9. Bjorck P (2001) Isolation and characterization of plasmacytoid dendritic cells from Flt3 ligand and granulocyte-macrophage colony-stimulating factor-treated mice. Blood 98:3520–3526
10. Blanco P, Palucka AK, Gill M, Pascual V, Banchereau J (2001) Induction of dendritic cell differentiation by IFN-alpha in systemic lupus erythematosus. Science 294:1540–1543
11. Blom B, Ho S, Antonenko S, Liu YJ (2000) Generation of interferon alpha-producing predendritic cell (Pre-DC)2 from human CD34(+) hematopoietic stem cells. J Exp Med 192:1785–1796
12. Burg S, Rissoan M-C, Brindon J-M, Dhuen T, D'Agostini M, Bendriss-Vermare N, Brière F (2002) Role of granzyme B in human plasmacytoid dendritic cells (abstract). In: Seventh International Symposium on Dendritic Cells 52:P45
13. Caux C, Vanbervliet B, Massacrier C, Dezutter-Dambuyant C, de Saint-Vis B, Jacquet C, Yoneda K, Imamura S, Schmitt D, Banchereau J (1996) CD34+ hematopoietic progenitors from human cord blood differentiate along two independent dendritic cell pathways in response to GM-CSF+TNF alpha. J Exp Med 184:695–706
14. Cederblad B, Blomberg S, Vallin H, Perers A, Alm GV, Ronnblom L (1998) Patients with systemic lupus erythematosus have reduced numbers of circulating natural interferon-alpha- producing cells. J Autoimmun 11:465–470
15. Cella M, Sallusto F,Lanzavecchia A (1997) Origin, maturation and antigen presenting function of dendritic cells. Curr Opin Immunol 9:10–16
16. Cella M, Jarrossay D, Facchetti F, Alebardi O, Nakajima H, Lanzavecchia A, Colonna M (1999) Plasmacytoid monocytes migrate to inflamed lymph nodes and produce large amounts of type I interferon. Nat Med 5:919–923
17. Cella M, Facchetti F, Lanzavecchia A, Colonna M (2000) Plasmacytoid dendritic cells activated by influenza virus and CD40L drive a potent Th1 polarization. Nat Immunol 1:305–310
18. Chaperot L, Bendriss N, Manches O, Gressin R, Maynadie M, Trimoreau F, Orfeuvre H, Corront B, Feuillard J, Sotto JJ, Bensa JC, Briere F, Plumas J, Jacob MC (2001) Identification of a leukemic counterpart of the plasmacytoid dendritic cells. Blood 97:3210–3217
19. Chen YH, Lan JL (1998) Kikuchi disease in systemic lupus erythematosus: clinical features and literature review. J Microbiol Immunol Infect 31:187–192
20. Colonna M, Krug A, Cella M (2002) Interferon-producing cells: on the front line in immune responses against pathogens. Curr Opin Immunol 14:373–379
21. Comeau MR, Van der Vuurst de Vries AR, Maliszewski CR, Galibert L (2002) CD123 bright plasmacytoid predendritic cells: progenitors undergoing cell fate conversion? J Immunol 169:75–83
22. Dalod M, Salazar-Mather TP, Malmgaard L, Lewis C, Asselin-Paturel C, Briere F, Trinchieri G, Biron CA (2002) Interferon alpha/beta and interleukin 12 responses to viral infections: pathways regulating dendritic cell cytokine expression in vivo. J Exp Med 195:517–528
23. Danon AD, Krishnan J, Frizzera G (1993) Morpho-immunophenotypic diversity of Castleman's disease, hyaline-vascular type: with emphasis on a stroma-rich variant and a new pathogenetic hypothesis. Virchows Arch A Pathol Anat Histopathol 423:369–382
24. Dominguez DC, Torres ML, Antony S (2003) Is human herpesvirus 6 linked to kikuchi-fujimoto disease? The importance of consistent molecular and serologic analysis. South Med J 96:226–233
25. Donaghy H, Pozniak A, Gazzard B, Qazi N, Gilmour J, Gotch F, Patterson S (2001) Loss of blood CD11c(+) myeloid and CD11c(−) plasmacytoid dendritic cells in patients with HIV-1 infection correlates with HIV-1 RNA virus load. Blood 98:2574–2576
26. Dumoulin FL, Leifeld L, Sauerbruch T, Spengler U (1999) Autoimmunity induced by interferon-alpha therapy for chronic viral hepatitis. Biomed Pharmacother 53:242–254
27. Dzionek A, Fuchs A, Schmidt P, Cremer S, Zysk M, Miltenyi S, Buck DW, Schmitz J (2000) BDCA-2, BDCA-3, and BDCA-4: three markers for distinct subsets of dendritic cells in human peripheral blood. J Immunol 165:6037–6046
28. Dzionek A, Sohma J, Nagafune M, Cella M, Colonna M, Facchetti F, Gunther G, Johnston I, Lanzavecchia A, Nagasaka T, Okada T, Vermi W, Winkels G, Yamamoto T, Zysk M, Yamaguchi Y, Schmitz J (2001) BDCA-2, a novel plasmacytoid dendritic cell cell-specific type II C-type lectin, mediates antigen-capture and is a potent inhibitor of interferon-alpha/beta induction. J Exp Med 194:1823–1834
29. Dzionek A, Inagaki Y, Okawa K, Nagafune J, Rock JJ, Sohma Y, Winkels G, Zysk M, Yamaguchi Y, Schmitz JJ (2002) Plasmacytoid dendritic cells: from specific surface markers to specific cellular functions (1). Hum Immunol 63:1133–1148
30. Eckert F, Schmid U (1989) Identification of plasmacytoid T cells in lymphoid hyperplasia of the skin. Arch Dermatol 125:1518–1524
31. Edwards AD, Diebold SS, Slack EM, Tomizawa H, Hemmi H, Kaisho T, Akira S, Sousa CR (2003) Toll-like receptor expression in murine DC subsets: lack of TLR7 expression by CD8alpha+ DC correlates with unresponsiveness to imidazoquinolines. Eur J Immunol 33:827–833
32. Facchetti F, De-Wolf-Peeters C (1991) The plasmacytoid monocyte (the so-called plasmacytoid T-cell). An enigmatic cell of the human lymphoid tissue. Biotest Bulletin 4:225–240

33. Facchetti F, Vermi W (2002) Plasmacytoid monocytes and plasmacytoid dendritic cells. Immune system cells linking innate and acquired immunity. Pathologica 94:163–175
34. Facchetti F, de Wolf-Peeters C, Mason DY, Pulford K, van den Oord JJ, Desmet VJ (1988) Plasmacytoid T cells. Immunohistochemical evidence for their monocyte/macrophage origin. Am J Pathol 133:15–21
35. Facchetti F, De Wolf-Peeters C, van den Oord JJ, De vos R, Desmet VJ (1988) Plasmacytoid T cells: a cell population normally present in the reactive lymph node. An immunohistochemical and electronmicroscopic study. Hum Pathol 19:1085–1092
36. Facchetti F, De Wolf-Peeters C, De Vos R, van den Oord JJ, Pulford KA, Desmet VJ (1989) Plasmacytoid monocytes (so-called plasmacytoid T cells) in granulomatous lymphadenitis. Hum Pathol 20:588–593
37. Facchetti F, De Wolf-Peeters C, van den Oord JJ, Desmet VJ (1989) Plasmacytoid monocytes (so-called plasmacytoid T cells) in Hodgkin's disease. J Pathol 158:57–65
38. Facchetti F, De Wolf Peeters C, Van Den Oord JJ, De Vos R, Desmet VJ (1989) Plasmacytoid monocytes (so-called plasmacytoid T-cells) in Kikuchi's lymphadenitis. An immunohistologic study. Am J Clin Pathol 92:42–50
39. Facchetti F, de Wolf-Peeters C, van den Oord JJ, Meijer CJ, Pals ST, Desmet VJ (1989) Anti-high endothelial venule monoclonal antibody HECA-452 recognizes plasmacytoid T cells and delineates an "extranodular" compartment in the reactive lymph node. Immunol Lett 20:277–281
40. Facchetti F, Boden G, De Wolf Peeters C, Vandaele R, Degreef H, Desmet VJ (1990) Plasmacytoid monocytes in Jessner's lymphocytic infiltration of the skin. Am J Dermatopathol 12:363–369
41. Facchetti F, De Wolf-Peeters C, Kennes C, Rossi G, De Vos R, van den Oord JJ, Desmet VJ (1990) Leukemia-associated lymph node infiltrates of plasmacytoid monocytes (so-called plasmacytoid T-cells). Evidence for two distinct histological and immunophenotypical patterns. Am J Surg Pathol 14:101–112
42. Facchetti F, Blanzuoli L, Ungari M, Alebardi O, Vermi W (1998) Lymph node pathology in primary combined immunodeficiency diseases. Springer Semin Immunopathol 19:459–478
43. Facchetti F, Vergoni F, Rossi E, Ungari M, Vermi W, Grigolato PG, Frizzera G (2002) Neoplastic nature of nodal plasmacytoid monocytes associated with acute myeloid leukemia. Mod Pathol 15:239A
44. Facchetti F, Vermi W, Santoro A, Vergoni F, Chilosi M, Doglioni C (2003) Neoplasms derived from plasmacytoid monocytes/interferon producing cells. Variability of CD56 and Granzyme B expression. Am J Surg Pathol (in press)
45. Farkas L, Beiske K, Lund-Johansen F, Brandtzaeg P, Jahnsen FL (2001) Plasmacytoid dendritic cells (natural interferon-alpha/beta-producing cells) accumulate in cutaneous lupus erythematosus lesions. Am J Pathol 159:237–243
46. Feldman S, Stein D, Amrute S, Denny T, Garcia Z, Kloser P, Sun Y, Megjugorac N, Fitzgerald-Bocarsly P (2001) Decreased interferon-alpha production in HIV-infected patients correlates with numerical and functional deficiencies in circulating type 2 dendritic cell precursors. Clin Immunol 101:201–210
47. Ferry JA, Harris NL (1999) Plasmacytoid monocytes? Am J Clin Pathol 111:569
48. Feuillard J, Jacob MC, Valensi F, Maynadie M, Gressin R, Chaperot L, Arnoulet C, Brignole-Baudouin F, Drenou B, Duchayne E, Falkenrodt A, Garand R, Homolle E, Husson B, Kuhlein E, Le Calvez G, Sainty D, Sotto MF, Trimoreau F, Bene MC (2002) Clinical and biologic features of CD4(+)CD56(+) malignancies. Blood 99:1556–1563
49. Fitzgerald-Bocarsly P (1993) Human natural interferon-alpha producing cells. Pharmacol Ther 60:39–62
50. Fong L, Engleman EG (2000) Dendritic cells in cancer immunotherapy. Annu Rev Immunol 18:245–273
51. Fong L, Mengozzi M, Abbey NW, Herndier BG, Engleman EG (2002) Productive infection of plasmacytoid dendritic cells with human immunodeficiency virus type 1 is triggered by CD40 ligation. J Virol 76:11033–11041
52. Fonteneau JF, Gilliet M, Larsson M, Dasilva I, Munz C, Liu YJ, Bhardwaj N (2003) Activation of influenza virus-specific CD4+ and CD8+ T cells: a new role for plasmacytoid dendritic cells in adaptive immunity. Blood 2:2
53. Frizzera G (1988) Castleman's disease and related disorders. Semin Diagn Pathol 5:346–364
54. Galibert L, Maliszewski CR, Vandenabeele S (2001) Plasmacytoid monocytes/T cells: a dendritic cell lineage? Semin Immunol 13:283–289
55. Geijtenbeek TB, Kwon DS, Torensma R, van Vliet SJ, van Duijnhoven GC, Middel J, Cornelissen IL, Nottet HS, KewalRamani VN, Littman DR, Figdor CG, van Kooyk Y (2000) DC-SIGN, a dendritic cell-specific HIV-1-binding protein that enhances trans-infection of T cells. Cell 100:587–597
56. Gilliet M, Liu YJ (2002) Human plasmacytoid-derived dendritic cells and the induction of T-regulatory cells. Hum Immunol 63:1149–1155
57. Gilliet M, Liu YJ (2002) Generation of human CD8 T regulatory cells by CD40 ligand-activated plasmacytoid dendritic cells. J Exp Med 195:695–704
58. Gilliet M, Boonstra A, Paturel C, Antonenko S, Xu XL, Trinchieri G, O'Garra A, Liu YJ (2002) The development of murine plasmacytoid dendritic cell precursors is differentially regulated by FLT3-ligand and granulocyte/macrophage colony-stimulating factor. J Exp Med 195:953–958
59. Grouard G, Rissoan MC, Filgueira L, Durand I, Banchereau J, Liu YJ (1997) The enigmatic plasmacytoid T cells develop into dendritic cells with interleukin (IL)-3 and CD40-ligand. J Exp Med 185:1101–1111
60. Gutterman JU (1994) Cytokine therapeutics: lessons from interferon alpha. Proc Natl Acad Sci U S A 91:1198–1205
61. Haase AT (1999) Population biology of HIV-1 infection: viral and CD4+ T cell demographics and dynamics in lymphatic tissues. Annu Rev Immunol 17:625–656
62. Harris NL, Bhan AK (1987) "Plasmacytoid T cells" in Castleman's disease. Immunohistologic phenotype. Am J Surg Pathol 11:109–113
63. Harris NL, Demirjian Z (1991) Plasmacytoid T-zone cell proliferation in a patient with chronic myelomonocytic leukemia: histologic and immunohistologic characterization. Am J Surg Pathol 15:87–95
64. Hemmi H, Kaisho T, Takeuchi O, Sato S, Sanjo H, Hoshino K, Horiuchi T, Tomizawa H, Takeda K, Akira S (2002) Small anti-viral compounds activate immune cells via the TLR7 MyD88-dependent signaling pathway. Nat Immunol 3:196–200
65. Herling M, Teitell MA, Shen RR, Medeiros LJ, Jones D (2003) TCL1 expression in plasmacytoid dendritic cells (DC2) and the related CD4+ CD56+ blastic tumors of skin. Blood 6:6
66. Hirst CE, Buzza MS, Bird CH, Warren HS, Cameron PU, Zhang M, Ashton-Rickardt PG, Bird PI (2003) The intracellular granzyme B inhibitor, proteinase inhibitor 9, is upregulated during accessory cell maturation and effector cell degranulation, and its overexpression enhances CTL potency. J Immunol 170:805–815
67. Hochrein H, O'Keeffe M,Wagner H (2002) Human and mouse plasmacytoid dendritic cells. Hum Immunol 63:1103–1110
68. Horny HP, Feller AC, Horst HA, Lennert K (1987) Immunocytology of plasmacytoid T cells: marker analysis indicates a unique phenotype of this enigmatic cell. Hum Pathol 18:28–32
69. Horny HP, Kaiserling E, Handgretinger R, Ruck P, Frank D, Weber R, Jaschonek KG, Waller HD (1995) Evidence for a lymphotropic nature of circulating plasmacytoid monocytes: findings from a case of CD56+ chronic myelomonocytic leukemia. Eur J Haematol 54:209–216

70. Ito T, Amakawa R, Fukuhara S (2002) Roles of toll-like receptors in natural interferon-producing cells as sensors in immune surveillance. Hum Immunol 63:1120–1125
71. Ito T, Amakawa R, Kaisho T, Hemmi H, Tajima K, Uehira K, Ozaki Y, Tomizawa H, Akira S, Fukuhara S (2002) Interferon-alpha and interleukin-12 are induced differentially by Toll-like receptor 7 ligands in human blood dendritic cell subsets. J Exp Med 195:1507–1512
72. Jahnsen FL, Lund-Johansen F, Dunne JF, Farkas L, Haye R, Brandtzaeg P (2000) Experimentally induced recruitment of plasmacytoid (CD123high) dendritic cells in human nasal allergy. J Immunol 165:4062–4068
73. Jahnsen FL, Farkas L, Lund-Johansen F, Brandtzaeg P (2002) Involvement of plasmacytoid dendritic cells in human diseases. Hum Immunol 63:1201–1205
74. Kadowaki N, Antonenko S, Lau JY, Liu YJ (2000) Natural interferon alpha/beta-producing cells link innate and adaptive immunity. J Exp Med 192:219–226
75. Keir ME, Stoddart CA, Linquist-Stepps V, Moreno ME, McCune JM (2002) IFN-alpha secretion by type 2 predendritic cells up-regulates MHC class I in the HIV-1-infected thymus. J Immunol 168:325–331
76. Khoury JD, Medeiros LJ, Manning JT, Sulak LE, Bueso-Ramos C, Jones D (2002) CD56(+) TdT(+) blastic natural killer cell tumor of the skin: a primitive systemic malignancy related to myelomonocytic leukemia. Cancer 94:2401–2408
77. Krug A, Towarowski A, Britsch S, Rothenfusser S, Hornung V, Bals R, Giese T, Engelmann H, Endres S, Krieg AM, Hartmann G (2001) Toll-like receptor expression reveals CpG DNA as a unique microbial stimulus for plasmacytoid dendritic cells which synergizes with CD40 ligand to induce high amounts of IL-12. Eur J Immunol 31:3026–3037
78. Krug A, Uppaluri R, Facchetti F, Dorner BG, Sheehan KC, Schreiber RD, Cella M, Colonna M (2002) IFN-producing cells respond to CXCR3 ligands in the presence of CXCL12 and secrete inflammatory chemokines upon activation. J Immunol 169:6079–6083
79. Lennert K, Remmele W (1958) Karyometrische Untersuchungen an Lymphknotenzellen des Menschen: I. Mitt. Germinoblasten, Lymphoblasten und Lymphozyten. Acta Haematol (Basel) 19:99–113
80. Lennert K, Kaiserling E, Muller-Hermelink HK (1975) T-associated plasma-cells. Lancet 1:1031–1032
81. Lian ZX, Okada T, He XS, Kita H, Liu YJ, Ansari AA, Kikuchi K, Ikehara S, Gershwin ME (2003) Heterogeneity of dendritic cells in the mouse liver: identification and characterization of four distinct populations. J Immunol 170:2323–2330
82. Liu YJ (2001) Dendritic cell subsets and lineages, and their functions in innate and adaptive immunity. Cell 106:259–262
83. Manfra DJ, Chen SC, Jensen KK, Fine JS, Wiekowski MT, Lira SA (2003) Conditional expression of murine flt3 ligand leads to expansion of multiple dendritic cell subsets in peripheral blood and tissues of transgenic mice. J Immunol 170:2843–2852
84. Maraskovsky E, Daro E, Roux E, Teepe M, Maliszewski CR, Hoek J, Caron D, Lebsack ME, McKenna HJ (2000) In vivo generation of human dendritic cell subsets by Flt3 ligand. Blood 96:878–884
85. Martin P, Del Hoyo GM, Anjuere F, Arias CF, Vargas HH, Fernandez LA, Parrillas V, Ardavin C (2002) Characterization of a new subpopulation of mouse CD8alpha+ B220+ dendritic cells endowed with type 1 interferon production capacity and tolerogenic potential. Blood 100:383–390
86. Matsuda H, Suda T, Hashizume H, Yokomura K, Asada K, Suzuki K, Chida K, Nakamura H (2002) Alteration of balance between myeloid dendritic cells and plasmacytoid dendritic cells in peripheral blood of patients with asthma. Am J Respir Crit Care Med 166:1050–1054
87. Miller RL, Gerster JF, Owens ML, Slade HB, Tomai MA (1999) Imiquimod applied topically: a novel immune response modifier and new class of drug. Int J Immunopharmacol 21:1–14
88. Mohty M, Jarrossay D, Lafage-Pochitaloff M, Zandotti C, Briere F, de Lamballeri XN, Isnardon D, Sainty D, Olive D, Gaugler B (2001) Circulating blood dendritic cells from myeloid leukemia patients display quantitative and cytogenetic abnormalities as well as functional impairment. Blood 98:3750–3756
89. Mohty M, Isnardon D, Vey N, Briere F, Blaise D, Olive D, Gaugler B (2002) Low blood dendritic cells in chronic myeloid leukaemia patients correlates with loss of CD34+/CD38- primitive haematopoietic progenitors. Br J Haematol 119:115–118
90. Mongkonsritragoon W, Letendre L, Qian J, Li CY (1998) Nodular lesions of monocytic component in myelodysplastic syndrome. Am J Clin Pathol 110:154–162
91. Müller-Hermelink HK, Steinmann G, Stein H, Lennert K (1983) Malignant lymphoma of plasmacytoid T cells. Morphologic and immunologic studies characterizing a special type of T-cell. Am J Surg Pathol 7:849–862
92. Nakano H, Yanagita M,Gunn MD (2001) CD11c(+)B220(+) Gr-1(+) cells in mouse lymph nodes and spleen display characteristics of plasmacytoid dendritic cells. J Exp Med 194:1171–1178
93. O'Doherty U, Peng M, Gezelter S, Swiggard WJ, Betjes M, Bhardwaj N, Steinman RM (1994) Human blood contains two subsets of dendritic cells, one immunologically mature and the other immature. Immunology 82:487–493
94. Okada T, Lian ZX, Naiki M, Ansari AA, Ikehara S, Gershwin ME (2003) Murine thymic plasmacytoid dendritic cells. Eur J Immunol 33:1012–1019
95. O'Keeffe M, Hochrein H, Vremec D, Caminschi I, Miller JL, Anders EM, Wu L, Lahoud MH, Henri S, Scott B, Hertzog P, Tatarczuch L, Shortman K (2002) Mouse plasmacytoid cells: long-lived cells, heterogeneous in surface phenotype and function, that differentiate into CD8(+) dendritic cells only after microbial stimulus. J Exp Med 196:1307–1319
96. O'Keeffe M, Hochrein H, Vremec D, Scott B, Hertzog P, Tatarczuch L, Shortman K (2002) Dendritic cell precursor populations of mouse blood: identification of the murine homologues of human blood plasmacytoid pre-DC2 and CD11c+ DC1 precursors. Blood 10:10
97. Olweus J, BitMansour A, Warnke R, Thompson PA, Carballido J, Picker LJ, Lund-Johansen F (1997) Dendritic cell ontogeny: a human dendritic cell lineage of myeloid origin. Proc Natl Acad Sci U S A 94:12551–12556
98. Patterson S, Rae A, Hockey N, Gilmour J, Gotch F (2001) Plasmacytoid dendritic cells are highly susceptible to human immunodeficiency virus type 1 infection and release infectious virus. J Virol 75:6710–6713
99. Penna G, Sozzani S, Adorini L (2001) Cutting edge: selective usage of chemokine receptors by plasmacytoid dendritic cells. J Immunol 167:1862–1866
100. Penna G, Vulcano M, Roncari A, Facchetti F, Sozzani S, Adorini L (2002) Cutting edge: differential chemokine production by myeloid and plasmacytoid dendritic cells. J Immunol 169:6673–6676
101. Penna G, Vulcano M, Sozzani S, Adorini L (2002) Differential migration behavior and chemokine production by myeloid and plasmacytoid dendritic cells. Hum Immunol 63:1164–1171
102. Petrella T, Dalac S, Maynadie M, Mugneret F, Thomine E, Courville P, Joly P, Lenormand B, Arnould L, Wechsler J, Bagot M, Rieux C, Bosq J, Avril MF, Bernheim A, Molina T, Devidas A, Delfau-Larue MH, Gaulard P, Lambert D (1999) CD4+ CD56+ cutaneous neoplasms: a distinct hematological entity? Groupe Francais d'Etude des Lymphomes Cutanes (GFELC). Am J Surg Pathol 23:137–146
103. Petrella T, Comeau MR, Maynadie M, Couillault G, De Muret A, Maliszewski CR, Dalac S, Durlach A, Galibert L (2002) 'Agranular CD4+ CD56+ hematodermic neoplasm' (blastic NK-cell lymphoma) originates from a population of CD56+

precursor cells related to plasmacytoid monocytes. Am J Surg Pathol 26:852–862
104. Pileri S, Kikuchi M, Helbron D, Lennert K (1982) Histiocytic necrotizing lymphadenitis without granulocytic infiltration. Virchows Arch A Pathol Anat Histol 395:257–271
105. Prasthofer EF, Prchal JT, Grizzle WE, Grossi CE (1985) Plasmacytoid-T-cell lymphoma associated with chronic myeloproliferative disorder. Am J Surg Pathol 9:380–387
106. Pulendran B, Banchereau J, Burkeholder S, Kraus E, Guinet E, Chalouni C, Caron D, Maliszewski C, Davoust J, Fay J, Palucka K (2000) Flt3-ligand and granulocyte colony-stimulating factor mobilize distinct human dendritic cell subsets in vivo. J Immunol 165:566–572
107. Rissoan MC, Duhen T, Bridon JM, Bendriss-Vermare N, Peronne C, de Saint Vis B, Briere F, Bates EE (2002) Subtractive hybridization reveals the expression of immunoglobulin-like transcript 7, Eph-B1, granzyme B, and 3 novel transcripts in human plasmacytoid dendritic cells. Blood 100:3295–3303
108. Ronnblom L, Alm GV (2001) A pivotal role for the natural interferon alpha-producing cells (plasmacytoid dendritic cells) in the pathogenesis of lupus. J Exp Med 194:F59–F63
109. Rothenfusser S, Tuma E, Endres S, Hartmann G (2002) Plasmacytoid dendritic cells: the key to CpG(1). Hum Immunol 63:1111–1119
110. Salio M, Cella M, Vermi W, Facchetti F, Palmowski MJ, Smith CL, Shepherd D, Colonna M, Cerundolo V (2003) Plasmacytoid dendritic cells prime IFN-gamma-secreting melanoma-specific CD8 lymphocytes and are found in primary melanoma lesions. Eur J Immunol 33:1052–1062
111. Schiavoni G, Mattei F, Sestili P, Borghi P, Venditti M, Morse HC, 3rd, Belardelli F, Gabriele L (2002) ICSBP is essential for the development of mouse type I interferon-producing cells and for the generation and activation of CD8alpha(+) dendritic cells. J Exp Med 196:1415–1425
112. Scrader JW (2003) Interleukin 3. In: Thomas AW, Lotze MT (eds) The cytokine handbook, Academic Press, London, pp 201–225
113. Shodell M, Siegal FP (2002) Circulating, interferon-producing plasmacytoid dendritic cells decline during human ageing. Scand J Immunol 56:518–521
114. Shortman K, Liu YJ (2002) Mouse and human dendritic cell subtypes. Nature Rev Immunol 2:151–161
115. Siegal FP, Lopez C, Fitzgerald PA, Shah K, Baron P, Leiderman IZ, Imperato D, Landesman S (1986) Opportunistic infections in acquired immune deficiency syndrome result from synergistic defects of both the natural and adaptive components of cellular immunity. J Clin Invest 78:115–123
116. Siegal FP, Kadowaki N, Shodell M, Fitzgerald-Bocarsly PA, Shah K, Ho S, Antonenko S, Liu YJ (1999) The nature of the principal type 1 interferon-producing cells in human blood (see comments). Science 284:1835–1837
117. Siegal FP, Fitzgerald-Bocarsly P, Holland BK, Shodell M (2001) Interferon-alpha generation and immune reconstitution during antiretroviral therapy for human immunodeficiency virus infection. Aids 15:1603–1612
118. Soilleux EJ, Morris LS, Leslie G, Chehimi J, Luo Q, Levroney E, Trowsdale J, Montaner LJ, Doms RW, Weissman D, Coleman N, Lee B (2002) Constitutive and induced expression of DC-SIGN on dendritic cell and macrophage subpopulations in situ and in vitro. J Leukoc Biol 71:445–457
119. Sorg RV, Kogler G, Wernet P (1999) Identification of cord blood dendritic cells as an immature CD11c- population. Blood 93:2302–2307
120. Soumelis V, Scott I, Gheyas F, Bouhour D, Cozon G, Cotte L, Huang L, Levy JA, Liu YJ (2001) Depletion of circulating natural type 1 interferon-producing cells in HIV-infected AIDS patients. Blood 98:906–912
121. Soumelis V, Scott I, Liu YJ, Levy J (2002) Natural type 1 interferon producing cells in HIV infection. Hum Immunol 63:1206–1212
122. Steinman RM (1991) The dendritic cell system and its role in immunogenicity. Annu Rev Immunol 9:271–296
123. Svensson H, Cederblad B, Lindahl M, Alm G (1996) Stimulation of natural interferon-alpha/beta-producing cells by Staphylococcus aureus. J Interferon Cytokine Res 16:7–16
124. Vallin H, Blomberg S, Alm GV, Cederblad B, Ronnblom L (1999) Patients with systemic lupus erythematosus (SLE) have a circulating inducer of interferon-alpha (IFN-alpha) production acting on leucocytes resembling immature dendritic cells. Clin Exp Immunol 115:196–202
125. van den Oord JJ, de Wolf-Peeters C,Desmet VJ (1986) The composite nodule. A structural and functional unit of the reactive human lymph node. Am J Pathol 122:83–91
126. Vermi W, Bonecchi R, Facchetti F, Bianchi D, Sozzani S, Festa S, Berenzi A, Cella M, Colonna M (2003) Recruitment of immature plasmacytoid dendritic cells (plasmacytoid monocytes) and myeloid dendritic cells in primary cutaneous melanomas. J Pathol 200:255–268
127. Vollenweider R, Lennert K (1983) Plasmacytoid T-cell clusters in non-specific lymphadenitis. Virchows Arch 44:1–14
128. Waller EK, Rosenthal H, Jones TW, Peel J, Lonial S, Langston A, Redei I, Jurickova I, Boyer MW (2001) Larger numbers of CD4(bright) dendritic cells in donor bone marrow are associated with increased relapse after allogeneic bone marrow transplantation. Blood 97:2948–2956
129. Wollenberg A, Wagner M, Gunther S, Towarowski A, Tuma E, Moderer M, Rothenfusser S, Wetzel S, Endres S, Hartmann G (2002) Plasmacytoid dendritic cells: a new cutaneous dendritic cell subset with distinct role in inflammatory skin diseases. J Invest Dermatol 119:1096–1102
130. Zou W, Borvak J, Wei S, Isaeva T, Curiel DT, Curiel TJ (2001) Reciprocal regulation of plasmacytoid dendritic cells and monocytes during viral infection. Eur J Immunol 31:3833–3839
131. Zou W, Machelon V, Coulomb-L'Hermin A, Borvak J, Nome F, Isaeva T, Wei S, Krzysiek R, Durand-Gasselin I, Gordon A, Pustilnik T, Curiel DT, Galanaud P, Capron F, Emilie D, Curiel TJ (2001) Stromal-derived factor-1 in human tumors recruits and alters the function of plasmacytoid precursor dendritic cells. Nat Med 7:1339–1346

Virchows Arch (2003) 443:718–724
DOI 10.1007/s00428-003-0881-4

ORIGINAL ARTICLE

Tibor Tot

The diffuse type of invasive lobular carcinoma of the breast: morphology and prognosis

Received: 7 March 2003 / Accepted: 16 June 2003 / Published online: 22 August 2003
© Springer-Verlag 2003

Abstract Invasive lobular carcinoma (ILC) of the breast represents a heterogeneous group of tumors, which can be classified according to the histological growth pattern into classic ILC and its variants and according to the cytomorphological characteristics into pleomorphic and non-pleomorphic subgroups. The most established morphological prognostic factors in ILC are the lymph-node status, the tumor size and the presence or absence of pleomorphic cytological features. In the present study, we analyzed the distribution of the lesions in 130 consecutive cases of ILC documented on large histological sections and followed up to, on average, 78 months (range 4–131 months). We found that 39% of the cases were unifocal, 12% multifocal, 28% diffuse and 19% combined (where the term combined represents those cases containing minor areas of diffuse growth of the tumor cells). In three cases, the distribution of the lesions could not be assessed. The diffuse cases were associated with a higher cancer-related death rate (25%) than the average (12%), the unifocal, the multifocal and the combined tumors (6–8%). The diffuse growth pattern represented a significant negative prognostic factor in relation to overall survival, but not in relation to disease-free survival. The only further negative prognostic factors found in this study were: more than three positive lymph nodes, tumor size larger than or equal to 40 mm and presence of pleomorphic cytological features. We propose to delineate the diffuse group of the ILCs as a separate diagnostic category with distinct morphological and radiological features and with unfavorable prognosis.

Keywords Diffuse type · Invasive lobular carcinoma of the breast · Morphology

T. Tot (✉)
Department of Pathology,
Falun Central Hospital,
791 82 Falun, Sweden
e-mail: tibor.tot@ltdalarna.se
Tel.: +46-23-492696
Fax: +46-23-492389

Introduction

Invasive lobular carcinoma (ILC) of the breast is a heterogeneous group of tumors representing 5–10% of breast cancer cases [15, 21] and has steadily increasing incidence rates [5]. On the basis of differences in histological growth pattern, these tumors were classified into classic ILC and its variants (solid, alveolar, and tubulolobular), but cases with a mixture of the different growth patterns are frequent and necessitate the inclusion of a "mixed" category [15]. Most of the tumors are built of small rather uniform cells. ILCs with pleomorphic cytological features have been recognized as a distinct subgroup of lobular carcinomas [11]. Multifocality, multicentricity and bilaterality are frequently occurring characteristics of ILC [3]. Although the majority of the ILCs exhibit a distinct tumor body, which is easily detected both radiologically and macroscopically, a minority of these tumors grows diffusely, representing a palpable induration of the breast tissue without distinct limits [12]. The underlying histological picture in these cases was described as tumor cells growing mainly in dispersed, disorderly foci without producing a discrete mass [20].

A considerable proportion of ILC is mammographically undetectable or easily missed [18]. Many ILCs manifest on a mammogram as asymmetric, ill-defined densities [16]. The size of the tumor and the extent of the disease are frequently underestimated by the radiologist when compared with macroscopic and histological findings in these cases [30]. Difficulties in radiological detection and in the characterization of ILCs have mostly been attributed to the classic histological subtype of the disease [4] and, occasionally, were explained as a consequence of "diffuse growth" of the tumor [6].

The studies on the prognosis in ILC have generated conflicting results. There are reports of a more favorable prognosis in cases of ILCs than in cases of invasive ductal carcinomas of the breast [7, 22, 25], but there are also reports of no significant difference in overall survival, locoregional control or in the frequency of distant

metastasis between these two tumor types [21]. Studies comparing the prognosis of different histological subtypes of ILC are also conflicting; favorable prognosis of classic invasive lobular carcinoma compared with the variants [7, 8] has been reported, as has research showing no significant difference [14]. The most important morphological prognostic factors identified in a multicentric study of ILCs were the tumor size and lymph-node status [17]. The prognostic importance of pleomorphic cytological features in cases of ILCs was repeatedly evidenced [1, 11, 29]. Some observations suggest that the diffuse growth pattern of ILCs may have clinical and prognostic relevance; for example, patients with ILC manifesting as a spiculated mass on the radiogram are less likely to have residual carcinoma in re-excision specimens than those with ill-defined lesions [28].

Although the macroscopic and the microscopic appearance of the diffusely growing lobular carcinomas have been described for a long time, these cases have not been recognized as a special subgroup of ILC. The present study aimed to analyze the distribution of the lesions in ILC (unifocal, multifocal or diffuse growth), to correlate the distribution to other histological parameters and to test its prognostic significance. The study focused on the subgroup of the ILCs with diffuse growth.

Materials and methods

The study group

This study represents a retrospective analysis of 130 consecutive cases of ILC diagnosed at the Department of Pathology and Clinical Cytology of the Central Hospital in Falun, Sweden, between 1991 and 1997. The study material represents 10.5% (130/1088) of all the new breast cancer cases diagnosed in the same period at the Department. All of the patients were women, with the average age of 64 years (range 37–89 years). The majority of the patients (73/130) were surgically treated by mastectomy, 27 of them after initial segmentectomy or open biopsy. In 57 patients, breast-conserving surgery was performed.

Histological features

All the tumors were documented using the large section technique routinely used in our institution. The technical details of the procedure are described elsewhere [26]. All the cases were reviewed by the author and classified on the basis of their growth pattern and cellular characteristics according to criteria summarized elsewhere [9]. Briefly, if at least 90% of the tumor was built up of uniform small cells often containing an intracytoplasmic vacuole and growing in "one-cell files" or in a disperse manner, the tumor was classified as "classic ILC." Tumors composed of solid masses of typical cells were classified as "ILC, solid variant," while tumors consisting of small aggregates of uniform cells were classified as "ILC, alveolar variant." Cases similar to classic ILC, but containing distinct microtubules were classified as "ILC, tubulolobular variant." If the histological picture contained areas of different subtypes with none of them representing 90% of the tumor surface, the tumor was classified as "ILC, mixed." All the cases, irrespective of their growth pattern, were classified as "pleomorphic" if they exhibited significant cellular atypia and "non-pleomorphic" if they did not.

Independently from the classification mentioned, the tumors were also grouped according to the distribution of the lesions in the large histological sections. Tumors forming a single distinct tumor mass were classified as "unifocal." If more than one distinct tumor foci were present and separated by tissue free from tumor cells, the tumor was classified as "multifocal," irrespective of the distance between the foci. An effort was made to reconstruct the relation of the tumor foci by comparing several large sections for the same case to exclude the possibility that extensions of a tumor perceived as isolated foci in a section level would not be recognized as part of the same tumor. Those tumors seen in the large section to be dispersed over an area much like a spider's web with no distinct tumor mass evident were classified as "diffuse." If such a distribution of the lesions was not dominant, but was present in a part of the tumor (comprising less than 50% of it), the tumor was considered to be "combined." Typical cases of unifocal, multifocal and diffuse ILCs are illustrated in Fig. 1, Fig. 2, Fig. 3 and Fig. 4.

The size of the tumor was taken to be the largest diameter of the largest invasive focus on the large histological section. In diffuse

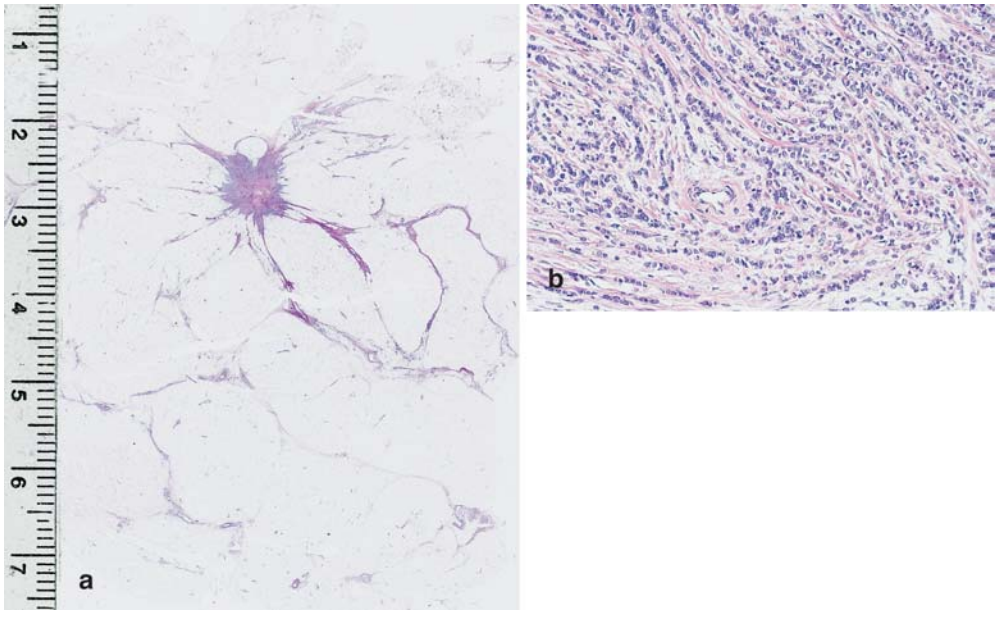

Fig. 1. a Large section histological image of a unifocal invasive lobular carcinoma (ILC). **b** Histological detail of the lesion shown in **a** demonstrating classic ILC

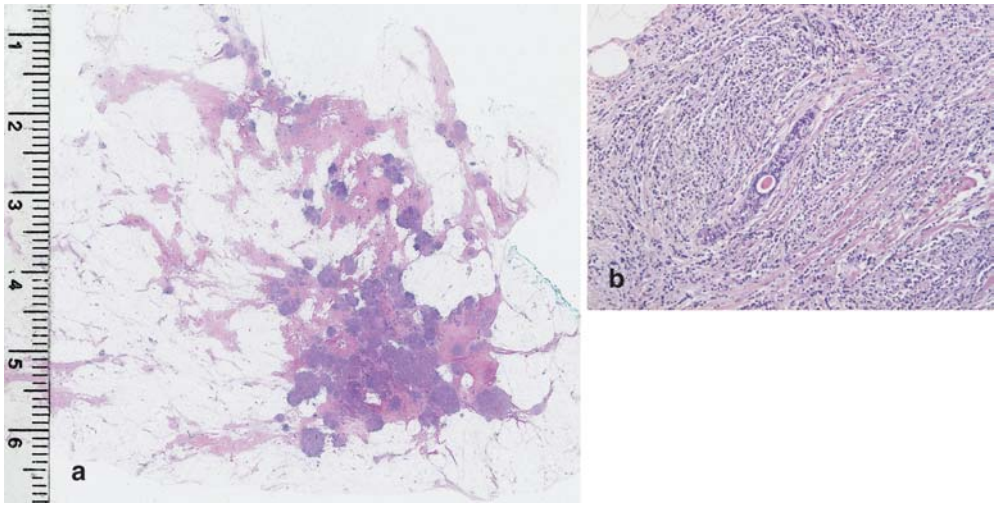

Fig. 2. a Large section histological image of a multifocal invasive lobular carcinoma (ILC): over 50 small invasive foci are evident within the same section. **b** Histological detail of one of the invasive foci demonstrating classic ILC

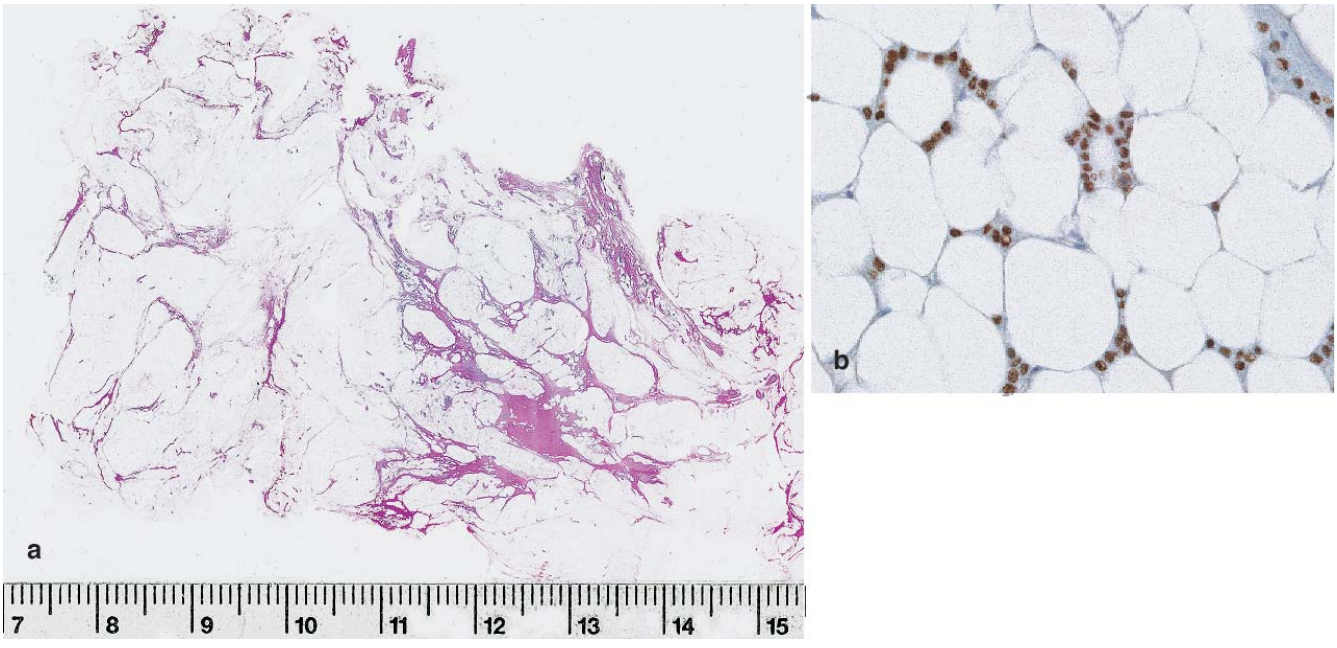

Fig. 3. a Large section histological image of an invasive lobular carcinoma (ILC) exhibiting diffuse growth: the *right half* of the section contains a network of tumor cells resembling a spider's web covering a 45×45-mm area. **b** Histological detail of the previous picture demonstrating estrogen receptors immunohistochemically in the cells of this tumor

tumors, the maximum diameter of the whole area of the histologically verified invasive tumor growth was taken. The three unclassified cases were not measured, as the sections did not include a transsection of the whole tumor. The lymph-node status was determined after a review of the archived histological slides of the nodes stained by the hematoxylin and eosin method. All the nodes with a detectable metastasis revealed using this method were considered as "positive," irrespective of the size of the metastases.

Follow-up data

The follow-up data were taken from the official files of the Regional Cancer Registry for Uppsala–Örebro Region. The time to the follow-up duration was calculated from the date of diagnosis until the date of death or until the end of the follow-up period. The follow-up period was 77.6 months (range 4–131 months). Of patients, 15 had died of breast carcinoma prior to 31 December 2001. Of these patients, 11 had no other cancers registered in their files. One of the patients had had a 15-mm large ductal carcinoma in situ grade I without invasion in her contralateral breast diagnosed 4 years before the diagnosis of ILC was made. Another patient had a grade-III invasive ductal carcinoma measuring 12 mm diagnosed and excised 14 years before the diagnosis of ILC was made in the same breast. In these two patients, we assumed that their deaths were related to their ILCs. Two other patients had bilateral ILCs, one synchronous and the other asynchronous. Most of the patients who died of the disease (13/15) were treated by mastectomy. Autopsy was carried out in only two cases and confirmed widespread metastatic lobular carcinoma.

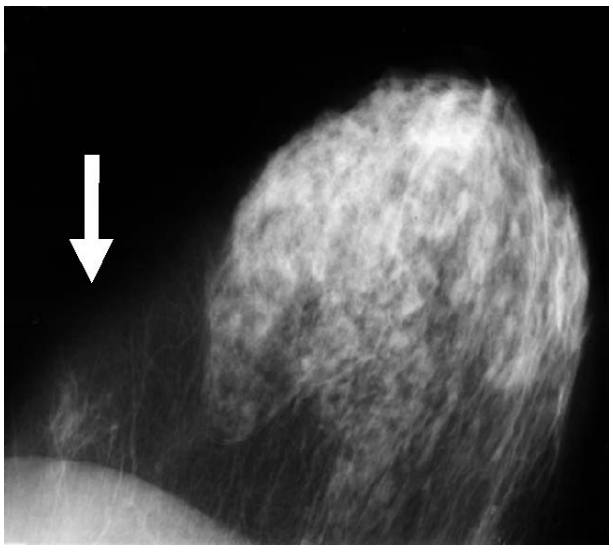

Fig. 4 Radiogram of the patient whose tumor was shown in Fig. 3**A** and **B**: note the ill-defined shadow marked with an *arrow* highlighting the tumor

Statistical methods

For the statistical analysis, the patients were separated into the following groups according to the lymph-node status: node-negative, node-positive with one to three positive nodes, node-positive with more than three positive nodes and a group composed of patients who had not had lymph-node assessments made. The patients were also grouped into two categories, depending on the size of the tumor: those with tumors of less than 40 mm and those with tumors larger than or equal to 40 mm. For statistical analysis, the patients with diffuse tumor growth and the patients with combined tumor growth (i.e., with diffuse growth pattern covering less than 50% of the tumor surface in the large histological section) were grouped together and compared with the patients with tumors without diffuse tumor growth. The overall survival rates and disease-free survival rates were calculated using the Kaplan-Meyer method with a P value of less than 0.05 taken to be significant.

Results

The most important results are presented in Table 1. The diffuse growth pattern was dominant in 28% (36/130) of the tumors. Furthermore, this pattern was evident, but occupied less than 50% of the tumor surface in the large histological section in an additional 25 cases that were classified as combined (unifocal plus diffuse or multifocal plus diffuse). Most of the ILCs, 39% (51/130), were unifocal, but 12% (15/130) were multifocal. In 3 of 130 cases, the growth patterns could not be properly assessed, as only a part of the tumor was included in the large section.

The most frequently encountered histological growth pattern in the diffuse group was the classic one; this was present in 69% of cases. This proportion was higher than in the unifocal (43%) or in the combined group (48%), but was approximately the same as that of the multifocal cases (67%). The diffuse growth pattern was not limited to the cases with classic histological features; tubulolob-

Table 1 The most important results of the present study

Distribution	Number of cases	Histological type			Pleomorphic	Axillary lymph-node metastasis				Average size	Local recurrence	Death
		Classic	Variant	Mixed		Not analyzed	0	1–3	>3			
Unifocal	39% (51/130)	43% (22/51)	33% (17/51)	24% (12/51)	18% (9/51)	21% (11/51)	51% (26/51)	16% (8/51)	12% (6/51)	15.3 mm (5–50)	12% (6/51)	6% (3/51)
Multifocal	12% (15/130)	67% (10/15)	13% (2/15)	20% (3/15)	27% (4/15)	13% (2/15)	40% (6/15)	27% (4/15)	20% (3/15)	19.3 mm (10–60)	7% (1/15)	7% (1/15)
Diffuse	28% (36/130)	69% (25/36)	22% (8/36)	8% (3/36)	22% (8/36)	14% (5/36)	44% (16/36)	19% (7/36)	22% (8/36)	37.6 mm (11–70)	3% (1/36)	25% (9/36)
Combined	19% (25/130)	48% (12/25)	12% (3/25)	40% (10/25)	20% (5/25)	40% (10/25)	38% (8/25)	16% (4/25)	12% (3/25)	30.5 mm (11–60)	4% (1/25)	8% (2/25)
Not classified	2% (3/130)	67% (2/3)	0% (0/3)	33% (1/3)	0% (0/3)	0% (0/3)	100% (3/3)	0% (0/3)	0% (0/3)		0% (0/3)	0% (0/3)
Sum	100% (130/130)	55% (71/130)	23% (30/130)	22% (29/130)	20% (26/130)	22% (28/130)	44% (57/130)	18% (23/130)	16% (20/130)	25.7 mm (5–70)	7% (9/130)	12% (15/130)

ular and alveolar variants of ILC exhibited the diffuse growth pattern in eight cases and mixed ILCs in two cases. Of the 36 diffuse cases, 8 (22%) showed pleomorphic cytological features, which were approximately the same proportion as in the unifocal, in the multifocal and in the combined groups.

The axillary lymph nodes were examined histologically in 78% of the cases. The patients with ILC with a diffuse growth pattern had metastases in 41% of the cases, the patients with multifocal tumors in 47%. This was significantly higher than in unifocal and in combined cases (28% in each). More than half of the node positive diffuse cases had more than three positive nodes.

The diffusely growing ILCs had a significantly larger average tumor size than the other groups. Tumors of less than 40 mm in diameter appeared to have a low death rate, independent of their largest diameter [tumors of 1–9 mm: 7% (1/14), 10–19 mm: 5% (2/38), 20–29 mm: 8% (2/24) and 30–39 mm: 6% (1/18)]. Tumors 40–49 mm had a death rate of 38% (5/13) and tumors larger than 50 mm had a death rate 20% (4/20). Importantly, one has to take into account the methodological differences of assessing the tumor size in the groups with different distributions of the lesions, as discussed below.

The group of the tumors exhibiting a diffuse growth pattern had a significantly higher rate of cancer related death than the other groups (25% compared with 6–8% in unifocal, multifocal and combined cases) and compared with the average death rate of 12% for the study group as a whole. The statistically significant difference in the overall survival between the patients with tumors exhibiting (combined cases included) and not exhibiting a diffuse growth pattern (P=0.0046) is illustrated in Fig. 5. As most of the few local recurrences we observed appeared after surgical excision of unifocal tumors, this significant difference was not maintained when disease-free survival was analyzed (P=0.5695).

The average risk of a cancer-related death for the study group was 12%. A significantly higher risk was evident for those patients with more than three positive lymph nodes (death rate 35%, 7/20), those with tumor size greater or equal to 40 mm (death rate 27%, 9/33), those with a diffuse growth pattern evident in more than 50% of the tumor section surface (death rate 25%, 9/36) and those with pleomorphic cytological features of the tumor (death rate 22%, 6/27). A combination of these negative prognostic factors worsened the prognosis; a diffuse growth pattern combined with pleomorphic cytological features and more than three positive lymph nodes was present in four patients, all of whom died during the follow-up period. A combination of diffuse growth pattern and more than three metastatic lymph nodes gave a risk of cancer-related death within this period of 63% (5/8), a combination of diffuse growth and pleomorphic cytological features a risk of 63% (5/8), and a combination of diffuse growth and tumor size equal or larger than 40 mm a risk of 32% (6/19). The classic type of ILC was associated with only a slightly higher death rate than the average (15%, 11/71). The mixed cases (classic plus variant histological growth pattern) had a death rate of 10% (3/29). None of the patients with a purely solid or alveolar growth pattern died during the follow-up period. Of the 15 patients with tubulolobular carcinoma, 1 is registered as having died of breast carcinoma. Having one to three positive lymph nodes represented only an average risk of a cancer related death (13%, 3/23) in this series.

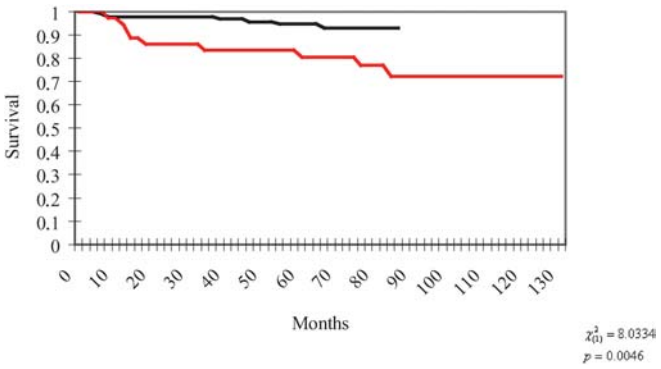

Fig. 5 Kaplan-Meyer curve demonstrating a statistically significant difference in overall survival rate between the group of patients with a diffuse distribution of invasive lobular carcinoma (*red line*) and with a non-diffuse distribution (*black line*)

Discussion

The significance of differences in the distribution of the lesion(s) in cases of invasive breast carcinomas is poorly understood. Radiological methods detect multifocality in many cases of ILC, ultrasound and magnetic resonance examinations being superior to mammography in this aspect [2, 10, 23]. However, the absence of a generally accepted definition for multifocality represents a crucial problem. Defining multifocality by the distance between the tumor foci has the disadvantage of needing a hardly achievable wide consensus on the number of centimeters between the lesions required to call a tumor "multifocal" and, of course, the biological significance of such a distance can easily be questioned. Introducing the term "multicentric" for multiple tumors, which are simultaneously present in different quadrants of the same breast, does not help to clarify multifocality other than to restrict certain "multifocal" cases to a single quadrant. In this study, we used the term "multifocal" to mean the presence of more than one distinct tumor foci separated by tumor-free breast tissue in the same large histological section, irrespective of the distance between the foci. Theoretically, these tumors may develop simultaneously in several distant terminal ductal–lobular units. We assumed that the large sections, up to 9×8 cm in size and often representing a transsection of the whole segmentectomy specimen, are representative of the documented tumor. We found 12% of the cases in the present series to be multifocal, which is a lower proportion in comparison to some other studies [19]. Probably, some diffuse tumors were classified in these studies as multifocal. According to our results,

multifocality itself does not represent a significant prognostic factor.

A diffuse distribution of the lesions in the breast has been defined as tumors simultaneously developing in a large number of neighboring terminal ductal–lobular units and/or exhibiting a non-lobulocentric growth [27]. This results in the tumor having an appearance resembling that of a spider's web in large histological sections. This type of ILC does not form a distinct tumor body and it is difficult to determine the borders of the tumor, even histologically. These tumors appear on the mammogram as a weak shadow and may even be missed. This appearance of the tumor is not restricted to the cases of ILC showing classic histological growth pattern, although it is often associated with such cases. "Diffuse" refers to the distribution of the lesions, while "classic" is a histological type; the distribution of the lesion can be assessed radiologically, macroscopically or by naked eye examination of a large histological section, while the histological type of ILC can only be assessed microscopically. The diffuse distribution of the tumor cells seems to be a powerful negative prognostic factor in patients with ILC associated with cancer-related death in relatively short follow-up time.

Diffuse growth of the tumor cells is probably not restricted to certain ILCs but rather, it seems to be a relatively frequent characteristic in this type of breast tumor. Interestingly, according to our results, the diffuse growth had to dominate the histological picture to affect the prognosis within the period of the study. Adequate sampling, preferably using large histological sections, is needed for proper analysis of the proportions of diffuse and non-diffuse growth pattern within the same tumor. In addition to biological factors, delay in detection and clinical and morphological understaging of the disease may affect the prognosis in these cases.

We only observed nine local recurrences in the study group during the follow-up period. Unexpectedly, six of these cases were originally unifocal, while the others were evenly distributed amongst the other groups. A probable explanation is the influence of surgical therapy, as breast-conserving surgery was more often accepted as a definite surgical intervention in unifocal tumors, while mastectomy was more often performed in the multifocal and diffuse cases.

Assessing the tumor size is relatively easy in cases of unifocal tumors. In multifocal cases, the tumor size is defined as the largest diameter of the largest invasive focus. In multifocal cases, the area including all the invasive and in situ foci is called the extent of the disease. Larger average tumor size in the group of the diffuse tumors may represent a simple explanation for the unfavorable prognosis of these cases. However, as the diffuse tumors lack a distinct tumor body, it is very difficult to correctly measure their size. The results of the measurement in these cases correspond to the extent of the disease rather than to a parameter comparable with the size of unifocal or multifocal tumors. On this ground, the results considering the prognostic importance of the tumor size in cases of ILC may be questioned, as they may represent a comparison of different parameters in diffuse and non-diffuse cases.

The prognostic significance of the lymph-node status in cases of ILC has been repeatedly proven [17, 24] and was confirmed by the results of the present study, as well. However, our finding that only patients with more than three positive nodes had an increased risk of dying of the disease conflicts somewhat with the results of the cited studies and may be explained by the relatively short follow-up period in the present study. We confirmed the prognostic significance of the pleomorphic cytological features in cases of ILC in concordance with a series of other studies [11, 13]. Prognostically, the distribution of the invasive foci in ILCs seems to be a more important morphological parameter than the histological subtypes (classic ILC and the variants), as only 15% of the patients exhibiting a classic histological growth pattern died of the disease within the period of this study, which was only slightly, and not significantly, higher than the average for the whole study group. None of the five patients with solid histological type of ILC in the present series died of the disease (followed up at 75–114 months).

In conclusion, we propose to delineate a separate diagnostic category of invasive lobular carcinomas: ILC exhibiting a diffuse growth pattern. Diffuse lobular carcinomas usually, but not exclusively, show a classic growth pattern on histological examination and may have pleomorphic cellular features. These tumors may be difficult to detect mammographically and to measure on a radiogram, ultrasonogram or by macroscopic examination. Patients with tumors of this type have a much less favorable prognosis than those with the other ILCs.

References

1. Bentz JS, Yassa N, Clayton F (1998) Pleomorphic lobular carcinoma of the breast: clinicopathologic features of 12 cases. Mod Pathol 11:814–822
2. Berg WA, Gilbreath PL (2000) Multicentric and multifocal cancer: whole breast US in preoperative evaluation. Radiology 214:59–66
3. Broet P, de la Rochefordiere A, Scholl SM, Fourquet A, Mosseri V, Durand JC, Puillart P, Asselain B (1995) Contralateral breast cancer: annual incidence and risk parameters. J Clin Oncol 13:1578–1583
4. Butler RS, Venta LA, Wiley EL, Ellis RL, Dempsey PJ, Rubin E (1999) Sonographic evaluation of infiltrating lobular carcinoma. Am J Roentgenol 172:325–330
5. Christopher IL, Anderson BO, Porter P, Holt SK, Daling JR, Moe RE (2000) Changing incidence rate of invasive lobular breast carcinoma among older women. Cancer 88:2561–2569
6. Cornford EJ, Wilson ARM, Athanassiou E (1995) Mammographic features of invasive lobular and invasive ductal carcinoma of the breast: a comparative analysis. Br J Radiol 68:450–453
7. Dixon JM, Anderson TJ, Page DL Lee D, Duffy SW (1982) Infiltrating lobular carcinoma of the breast. Histopathology 6:149–161
8. Du Toit RS, Locker AP, Ellis IO, Elston CW, Nicholson RI, Blamey RW (1989) Invasive lobular carcinoma of the breast—the prognosis of histopathological subtypes. Br J Cancer 60:605–609

9. Elston CW, Ellis IO (1998) The breast. Churchill Livingstone, Edinburgh, pp 291–296
10. Esserman L, Hylton N, Yassa L, Barclay J, Frankel S, Sickles E (1999) Utility of magnetic resonance imaging in the management of breast cancer: evidence for improved preoperative staging. J Clin Oncol 17:110–119
11. Eusebi V, Magalhaes F, Azzopardi JG (1992) Pleomorphic lobular carcinoma of the breast: an aggressive tumor showing apocrine differentiation. Hum Pathol 23:655–662
12. Foot Jr FW, Stewart FW (1946) A histologic classification of carcinoma of the breast. Surgery 19:74–99
13. Frolik D, Caduff R, Varga Z (2001) Pleomorphic lobular carcinoma of the breast: its cell kinetics, expression of oncogenes and tumor suppressor genes compared with invasive ductal carcinomas and classical infiltrating lobular carcinomas. Histopathology 39:503–513
14. Frost AR, Terahata S, Yeh IT, Siegel RS, Overmoyer B, Silverberg SG (1995) An analysis of prognostic features in infiltrating lobular carcinoma of the breast. Mod Pathol 8:830–836
15. Martinez V, Azzopardi JG (1979) Invasive lobular carcinoma of the breast: incidence and variants. Histopathology 3:467–488
16. Mendelson EB, Harris KM, Doshi N, Tobon H (1989) Infiltrating lobular carcinoma: mammographic patterns with pathologic correlation. Am J Radiol 53:265–271
17. Moreno-Elola A, Aguilar R, Roman JM, Hernandez A, Martin M, Diaz Rubio E, Furio V, Fernandez C, De La Fuente P, San Roman JM, Escudero M (1999) Prognostic factors in invasive lobular carcinoma of the breast: a multivariate analysis. A multicentre study after seventeen years follow-up. Ann Chir Gynaecol 88:252–258
18. Porter PL, El-Bastawissi AY, Mendelsohn MT, Lin MG, Khalid N, Watney EA, Cousens L, White D, Taplin S, White E (1999) Breast tumor characteristics as predictors of mammographic detection: comparison of interval and screen-detected cancers. J Natl Cancer Inst 91:2020–2028
19. Ringberg A, Palmer B, Linell F, Rychterova V, Ljungberg O (1991) Bilateral and multifocal breast carcinoma. A clinical and autopsy study with a special emphasis on carcinoma in situ. Eur J Surg Oncol 17:20–29
20. Rosen PP (2001) Rosen's breast pathology, 2nd edn. Lippincott, Williams and Wilkins, PA, p 630
21. Sartre-Garau X, Jouve M, Asselain B, Vincent-Salomon A, Beuzeboc P, Dorval T, Durand JC, Fourquet A, Pouillart P (1996) Infiltrating lobular carcinoma of the breast. Clinicopathologic analysis of 975 cases with reference to data on conservative therapy and metastatic patterns. Cancer 77:113–120
22. Silverstein MJ, Lewinsky BS, Waisman JR Gierson ED, Colburn WJ, Senovsky GM, Gamagami P (1994) Infiltrating lobular carcinoma. Is it different from infiltrating duct carcinoma? Cancer 73:1673–1677
23. Skaane P, Skjorten F (1999) Ultrasonographic evaluation of invasive lobular carcinoma. Acta Radiol 40:369–375
24. Tabár L, Vitak B, Chen HH, Duffy SW, Yen MF, Chiang CF, Krusemo UB, Tot T, Smith R (2000) The Swedish two-county trial twenty years later. Updated mortality results and new insight from long-term follow-up. Radiol Clin N Am 38:625–651
25. Toikkanen S, Pylkkänen L, Joensuu H (1997) Invasive lobular carcinoma of the breast has better short- and long-term survival than invasive ductal carcinoma. Br J Cancer 78:1234–1240
26. Tot T, Tabár L, Dean BP (2002) Practical breast pathology. Thieme, Stuttgart, pp 116–123
27. Tot T, Tabár L, Dean BP (2002) Practical breast pathology. Thieme, Stuttgart, pp 26–33
28. White JR, Gustafson GS, Wimbish K, Ingold JA, Lucas RJ, Levine AJ, Matter RA, Martinez A, Vicini FA (1994) Conservative surgery and radiation therapy for infiltrating lobular carcinoma of the breast: the role of preoperative mammogram in guiding treatment. Cancer 74:640–647
29. Wiedner N, Semple JP (1992) Pleomorphic variant of invasive lobular carcinoma of the breast. Hum Pathol 23:1167–1171
30. Yeatman TJ, Cantor AB, Smith TJ, Smith SK, Reintgen DS, Miller MS, Ku NN, Balkey PA, Cox CE (1995) Tumor biology of infiltrating lobular carcinoma. Implications for management. Ann Surg 22:549–561

Virchows Arch (2003) 443:725–733
DOI 10.1007/s00428-003-0896-x

ORIGINAL ARTICLE

Heike Welkerling · Susanne Kratz · Volker Ewerbeck · Günter Delling

A reproducible and simple grading system for classical chondrosarcomas. Analysis of 35 chondrosarcomas and 16 enchondromas with emphasis on recurrence rate and radiological and clinical data

Received: 17 April 2003 / Accepted: 6 August 2003 / Published online: 25 September 2003
© Springer-Verlag 2003

Abstract In the past, six histological grading systems for classical chondrosarcoma have been published. Due to the inhomogeneity and complexity of these classifications, the comparison of clinical data, survival rates and local failures has to be considered critically. In 1996, the author published a grading system that was simple to use and easily reproduced. This system was based on a few nuclear features [30]. The main intention of the current study was to verify whether the histological grade, which was defined by the author's classification, correlates with the recurrence rate. In a retrospective study, clinical data, X-rays and histological material from 35 patients with classical chondrosarcoma and 16 patients with enchondroma were analysed. Statistical analysis was done using the chi-squared test and the Fisher exact test. Local recurrence occurred in 25.7% of all patients. The difference in recurrence rate among grades 1–3 was statistically significant (P=0.002). The frequency of grades 1–3 varied up to 54%, when published grading systems were compared. No significant difference between the histological grade and features such as double nuclei and mitosis were observed. The frequency of cellularity, double nuclei and mitoses was similar between enchondromas and low-grade chondrosarcomas. Of chondrosarcoma patients, 90.6% of total patients and 87.5% of those with grade-1 lesions reported pain, whereas only 43.8% of the enchondroma patients did. Even in patients with grade-1 chondrosarcomas, radiological findings were much more aggressive in comparison with enchondromas. The histological grade, defined on the basis of the author's simple and reproducible grading system, indicates the risk of local recurrence, especially in cases that are inadequately treated. Grade-3 chondrosarcomas and lesions located in regions where the removal of the tumour would be difficult have to be given special attention.

Keywords Chondrosarcoma · Grading · Enchondroma · Recurrence · Growth pattern

H. Welkerling (✉)
Department of Orthopaedic Surgery,
Karl Franzens University Graz,
Auenbruggerplatz 9, 8036 Graz, Austria
e-mail: heike.welkerling@uni-graz.at
Tel.: +43-31-638581881
Fax: +43-31-63854806

S. Kratz
Institute of Diagnostic Radiology,
Erlangen-Nürnberg University,
Maximiliansplatz 1, 91054 Erlangen, Germany

V. Ewerbeck
Department of Orthopaedic Surgery,
Heidelberg University, Abteilung Orthopädie I,
Schlierbacher Landstrasse 200a, 69118 Heidelberg, Germany

G. Delling
Department of Osteopathology,
Institute of Pathology, Hamburg University,
Martinistrasse 52, 20246 Hamburg, Germany

Introduction

The classical chondrosarcoma is the most common type of chondrosarcoma and should be distinguished from dedifferentiated, mesenchymal and clear cell chondrosarcomas, which are separate entities. Six grading systems have been published to assess the level of malignancy of classical chondrosarcoma [4, 10, 18, 24, 25, 26]. However, these grading systems are controversial because they are not easily comparable. One reason for this is that different numbers of cytological factors are used, and the second main problem is that the pathologists do not agree on the extent or level of cytological factors when assigning grades to the chondrosacomas (Table 1).

In order to easily assess the level of malignancy of classical chondrosarcoma, a practical grading system that is easy to use and gives a high level of inter-observer agreement is needed. In addition to this, it should be easy

Table 1 Comparison of histological chondrosarcoma grading systems in the literature. *n.m.* not mentioned

Features	Grade 1	Grade 2	Grade 3	Author
Cellularity	++	++	+++	Mankin et al. [18]
	+	++	+++	Evans et al. [10]
	n.m.	n.m.	+++	Campanacci [4]
Nuclear size	n.m.	++	n.m.	Mankin et al. [18]
	+	++	>++	Evans et al. [10]
	+/++	++	+ to +++	O'Neal and Ackerman [24]
	>Enchondroma	>+	>++	Sanerkin [26]
	>Enchondroma	++	n.m.	Campanacci [4]
Nuclear polymorphism	+	++	+++	Sanerkin [26]
	+	++	+++	Campanacci [4]
Visible nucleoli	+	n.m.	n.m.	Mankin et al. [18]
	n.m.	+	n.m.	Evans et al. [10]
	(+)	n.m.	n.m.	Sanerkin [26]
Double nuclei	+	++	n.m.	Mankin et al. [18]
	++	n.m.	n.m.	Evans et al. [10]
	++	n.m.	+++	O'Neal and Ackerman [24]
	++	+++	n.m.	Campanacci [4]

to use within the pathologists' daily routines and should allow pathologists with little experience of chondrosarcomas to make a diagnosis. Only when these conditions are met will it be possible to compare different studies, especially with emphasis on clinical behaviour.

In some cases, making a distinction between enchondromas and low-grade chondrosarcomas can be extremely difficult. It is still a widespread belief that enchondromas and chondrosarcomas can be distinguished by their cytological features. Mirras' view [22], a view that has been generally accepted, is that enchondromas and chondrosacomas can only be distinguished by their growth patterns and local invasion. In order to successfully assess the growth patterns and local invasion of enchondromas and chondrosacromas, biopsy material consisting of medullary and cortical bone is required. In addition to this, the X-ray has to be taken into account.

In 1996, Welkerling et al. [30] produced a simple and reproducible grading system that used three nuclear features to assess the grade of the chondrosarcomas. Using this system, three independent investigators reached an inter-observer agreement of 80.7%. The investigators consisted of two pathologists and the author of this study. Included in the study were 74 chondrosarcoma cases. In addition to this, the study found that there was a significant difference in the nuclear size of grade-1 and -2 chondrosarcomas. Low-grade chondrosarcomas had a nuclear size of 5.23 μm, and enchondromas had a nuclear size of 5.16 μm, but the nuclear size of grade-2 chondrosarcomas was 8.57 μm.

The intention of this new study was to determine whether a correlation exists between the grade of chondrosarcoma, according to this study, and recurrence. The secondary aim of the study was to compare the cytological features of enchondromas and low-grade chondrosarcomas. The focus of this aspect of the study is on the histological analysis of enchondromas and chondrosarcomas. Clinical and radiological results have been included but are not so detailed.

Materials and methods

Patients with chondrosarcomas (35) and enchondromas (16), managed at the Department of Orthopaedic Surgery of Heidelberg University over 18 years, were analysed retrospectively. The cases were only included in the study when complete clinical documentation and radiological and histological material were available. Clinical, radiological and histological material was coded. The original intention of the study was to analyse 56 cases. However, histological material was only available for 43 cases and, therefore, 8 cases had to be excluded because the diagnosis was wrong; these were not chondrosarcomas or enchondromas. In addition to this, subtypes of chondrosarcomas, such as dedifferentiated and mesenchymal chondrosarcomas, which contain a second high malignant mesenchymal component, were strictly excluded from this study.

The clinical data used in the study was composed of the patient's age and sex, the location of the tumour, the recurrence rate and the patient's history of pain. Cortical destruction, Lodwick's grade and presence of extraosseous tumours were analysed on each X-ray. Archived paraffin block material and corresponding paraffin sections were collected. The available paraffin sections were observed, and the quality was assessed. Six-μm-thick paraffin sections were prepared and stained using haematoxylin and eosin, toluidine-blue, periodic-acid Schiff and nuclear stain using Weigerts nuclear staining technique. In 5 of the cases, plastic sections were available. In 3 cases, biopsy material was not available and, in 16 cases, biopsy was done externally. Therefore, exclusively operation material was employed for the histological investigations. Enchondromas were distinguished from low-grade chondrosarcomas using the growth patterns published by Mirra [22]. Enchondroma is characterised by islands of tumour cartilage surrounded by trabecular bone and/or osteoid, whereas the tumour cartilage of chondrosarcoma infiltrates marrow spaces by embedding the trabecular bone. Only when these chondrosarcoma patterns were present was diagnosis of the grade-1 chondrosarcoma carried out (Fig. 1 and Fig. 2).

In each case, the histological grade was analysed using the Welkerling et al. grading system [30] and the classifications that were published. Rosenthal's grading system [25] only distinguishes two histological grades, and for this reason, it was not used in this study. This fact has only been mentioned for the sake of clarity.

The results of all grading systems were compared. In addition to the assessment of the nuclear features of the cases, each case was assessed for cellularity, cell polymorphism, double nuclei, giant nuclei, mitoses and the type of matrix. All tumours were classified independently of each other by Welkerling and Prof. Delling (head of the Department of Osteopathology, Hamburg University). The inter-observer agreement between Welkerling and Delling was 80%

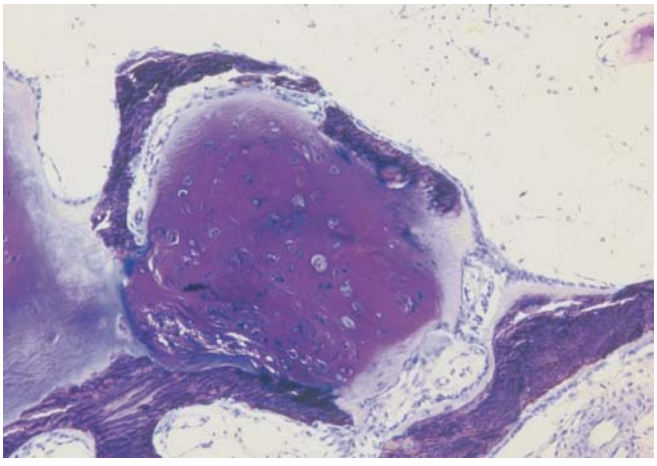

Fig. 1 Classical enchondroma. Islands of tumour cartilage are surrounded by trabecular bone and osteoid (toluidine blue, original magnification ×63)

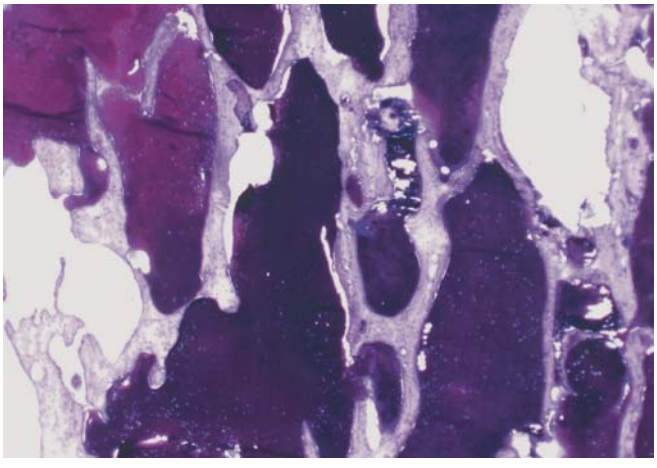

Fig. 2 Classical chondrosarcoma grade 1. Tumour cartilage infiltrates marrow spaces with embedding of trabecular bone (toluidine blue, original magnification ×12)

for the 35 cases to which the method of Welkerling et al. [30] was applied and 79% for the same 35 cases to which the other grading systems were applied [4, 10, 18, 24, 26].

In some cases, especially in the periphery of tumour lobules, some enlarged nuclei were found. These tumours were defined as grade 2 when more than a few scattered enlarged nuclei were found. Statistical analysis was done using the Chi-squared test and Fisher's exact probability test, where the level of significance was set at $P<0.05$.

Basics of chondrosarcoma grading

The grading systems that were published previously are based on the assessment of different numbers of cytological features [4, 10, 18, 24, 25, 26]. Marked differences in the levels defined by the pathologists exist. Therefore, the frequency of grades 1–3 differs up to 50% [30]. The purpose of the authors' study was to select criteria that could be reliably quantified. Assuming that a grading system correlates with malignancy, it is crucial to use features that are atypical of benign lesions. A homogeneous distribution of cytological or growth features within the histological section is crucial for a reproducible and quantitative assessment. The assessment of features has to be independent of the amount of available material.

Welkerling et al. [30] found that nuclear features, such as nuclear size and nuclear polymorphism, were the most reliable criteria. The structure and density of chromatin, as well as the presence of nucleoli, depend on the nuclear size. Three groups of classical chondrosarcomas were separated and a simple grading system was developed with an inter-observer agreement of 80.7% (Table 2). Tumours with small, isomorphic nuclei and with high densities of chromatin were classified as grade 1. The second group (grade 2) was characterised by enlarged nuclei with stippled chromatin and visible nucleoli, but without nuclear polymorphism. Nuclear polymorphism is the most important criterion of grade-3 chondrosarcomas.

Results

Histological investigation of chondrosarcomas

Cellularity was low in 25.7%, moderate in 68.6% and high in 5.7% of the cases. Double nuclei were visible in 94% of all cases. In most cases (67%), the number of double nuclei was low. Giant nuclei were found in 34%, and mitoses in 31% of cases. In these cases, the number of mitotic figures were low. The matrix was hyaline in 77% of the cases, myxoid in 20% and mixed in one case. No predilection for particular histological grades was seen in cases with myxoid matrix formation. Bands of fibrosis, as detailed by Mirra [22], could be found in 90% of the cases. In all cases, lobulated structures were present.

The grading system of Welkerling et al. [30] was compared with the other grading systems. In some cases it was not possible to assign the microscopic findings to a particular grade using the previously published classifications because, for example, nuclear size was moderate and cellularity was high, and these characteristics fell into two separate grades. For this reason, the reliability of each case was assessed and graded as: 1 = definite assignment, 2 = assignment with limitations, 3 = uncertain assignment. The six systems were used to grade the cases. However, the results differed from each other. When

Table 2 Chondrosarcoma grading system by Welkerling et al. [30]

Features	Enchondroma	Chondrosarcoma		
		Grade 1	Grade 2	Grade 3
Cytological				
Nuclear size	+	+	++	+ to +++
Nuclear polymorphism	0	0	+	+++
Stippled chromatin and visible nucleoli	0	0/(+)	+/++	+/++

Table 3 Grading of current 35 cases on the basis of different grading systems

Grade	Welkerling et al. [30]	Evans et al. [10]	Sanerkin [26]	O'Neal and Ackerman [24]	Mankin et al. [18]	Campanacci [4]
Grade 1	51%	24%	74%	56%	65%	73%
Grade 2	31%	70%	16%	32%	29%	17%
Grade 3	17%	6%	10%	12%	6%	10%
Agreement		60%	66%	89%	66%	60%
Assignment impossible		5.7%	11.4%	2.9%	2.9%	14.3%
Definite assignment		60%	63%	43%	46%	29%

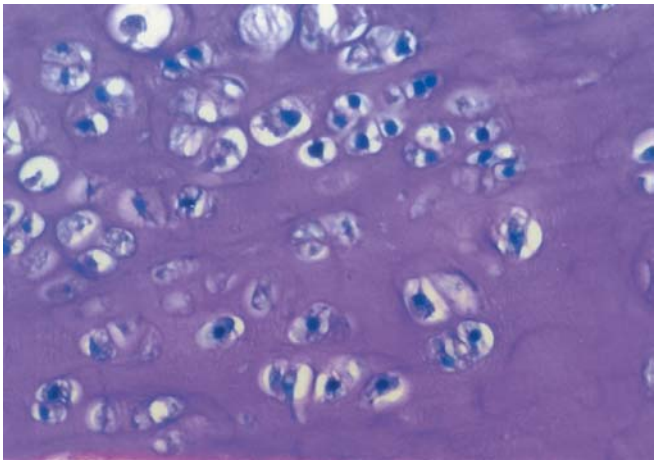

Fig. 3 Grade-1 chondrosarcoma with small, isomorph nuclei (toluidine blue, original magnification ×600)

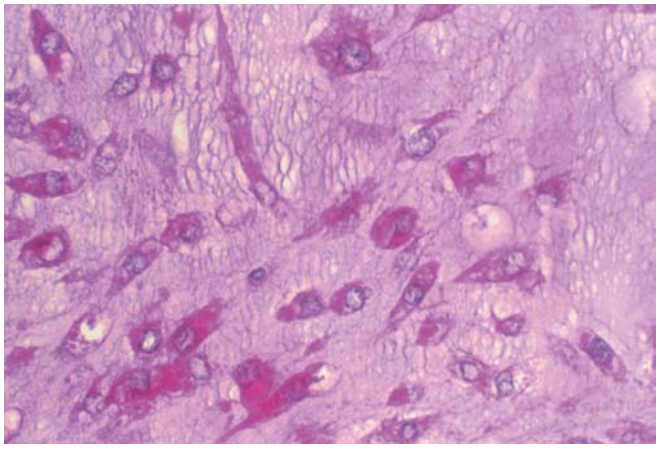

Fig. 4 Grade-2 chondrosarcoma with enlarged, isomorph nuclei, visible nucleoli and stippled chromatin (periodic-acid Schiff, original magnification ×600)

grading the 35 cases into grades 1–3, the results varied up to 54% (Table 3). The closest results were those from the authors' and O'Neal and Ackerman's grading systems [24]. However, O'Neal and Ackerman's grading system [24] only provided a definite assignment in 43% of the cases.

Grading and histological features

According to the results using the authors' grading system, 51% of the cases were grade-1 chondrosarcomas, 31% grade 2, and 17% were classified as grade 3 (Fig. 3, Fig. 4, Fig. 5). Cellularity was seen to increase significantly with histological grade (P=0.011). The assessment of cellularity is not suitable for the differentiation of histological grades, as the distribution is not homogeneous and the quantification is critical for reproducibility. In 61% of the grade-1 chondrosarcoma cases, the cellularity was moderate, and close to 20% of the grade-2 lesions had low cellularity.

In all grade-2 and -3 chondrosarcomas, double nuclei were found, and only in two cases of grade-1 lesions were double nuclei not present (Table 4). There was no significant difference between the histological grades (P=0.9) and the presence or absence of double nuclei. The majority of grade-2 chondrosacomas (73%) had a low

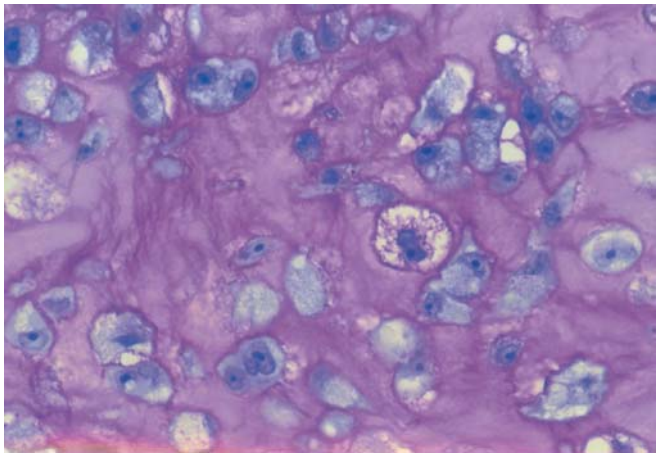

Fig. 5 Grade-3 chondrosarcoma is characterised by nuclear polymorphism (toluidine blue, original magnification ×600)

level of double nuclei, whereas in 33% of grade-1 lesions, many double nuclei were found.

Mitoses were observed in 67% of grade-3 chondrosarcomas, but only in small numbers [$\leq$2 per 10 high power field (HPF)] (Table 4). Mitoses were rare in grade-1 and -2 lesions (17% and 36%). The differences are not statistically significant (P=0.067). Giant nuclei could only be observed in grade-2 and -3 chondrosarcomas (Table 4). Half of the grade-2 and all of the grade-3

Table 4 Frequency of histological features of grades 1–3

Cellularity	Grade 1 (*n*=18)	Grade 2 (*n*=11)	Grade 3 (*n*=6)
Low	7 (39%)	2 (18%)	0
Moderate	11 (61%)	9 (82%)	4 (67%)
High	0	0	2 (33%)
Double nuclei			
Absent	2 (11%)	0	0
Few	10 (56%)	8 (73%)	4 (67%)
Many	6 (33%)	3 (27%)	2 (33%)
Mitoses			
Absent	15 (83%)	7 (64%)	2 (33%)
Few	3 (17%)	4 (36%)	3 (50%)
Many	0	0	1 (17%)
Giant nuclei			
Absent	18 (100%)	5 (45%)	0
Few	0	6 (55%)	5 (83%)
Many	0	0	1 (17%)

lesions had giant nuclei, but the number was limited in each case.

Histological features of enchondromas and low-grade chondrosarcomas

The histological features such as cellularity, mitoses and double nuclei were frequently used to determine the dignity of lesion, and enchondromas and low-grade chondrosarcomas were compared. The number of cases in both groups was similar. The cellularity was moderate in 63% of enchondromas and 61% of the grade-1 chondrosarcomas. The level of cellularity, mitoses and the number of double nuclei in enchondromas and low-grade chondrosarcomas were similar. No significant differences were observed in the levels of cellularity (P=0.531), mitoses (P=0.087) and the number of double nuclei (P=0.367) (Table 5). Double nuclei were found in 88% of enchondromas and 89% of low-grade chondrosarcomas. Mitoses were absent in enchondromas and rare in grade-1 chondrosarcomas (17%). The nuclei were the same size (Fig. 6). The histological distinctions between enchondromas and low-grade chondrosarcomas were made using the growth patterns detailed by Mirra [22].

Table 5 Frequency of histological features of low-grade chondrosarcoma and enchondroma

Cellularity	Grade 1 (*n*=18)	Enchondroma (*n*=16)
Low	7 (39%)	5 (31%)
Moderate	11 (61%)	10 (63%)
High	0	1 (6%)
Double nuclei		
Absent	2 (11%)	2 (12%)
Few	10 (56%)	10 (63%)
Many	6 (33%)	4 (25%)
Mitoses		
Absent	15 (83%)	16 (100%)
Few	3 (17%)	0
Many	0	0

In all enchondroma cases, no infiltration of marrow spaces or embedding of trabecular bone had taken place, and the nuclei were small and isomorphic. In five of the cases, cellularity was low; it was moderate in 63% of the cases. Only in one lesion was high cellularity observed. The cellularity was moderate in all of the peripherally located enchondromas, and giant nuclei and mitoses were not present; all lesions had a lobulated structure. In ten

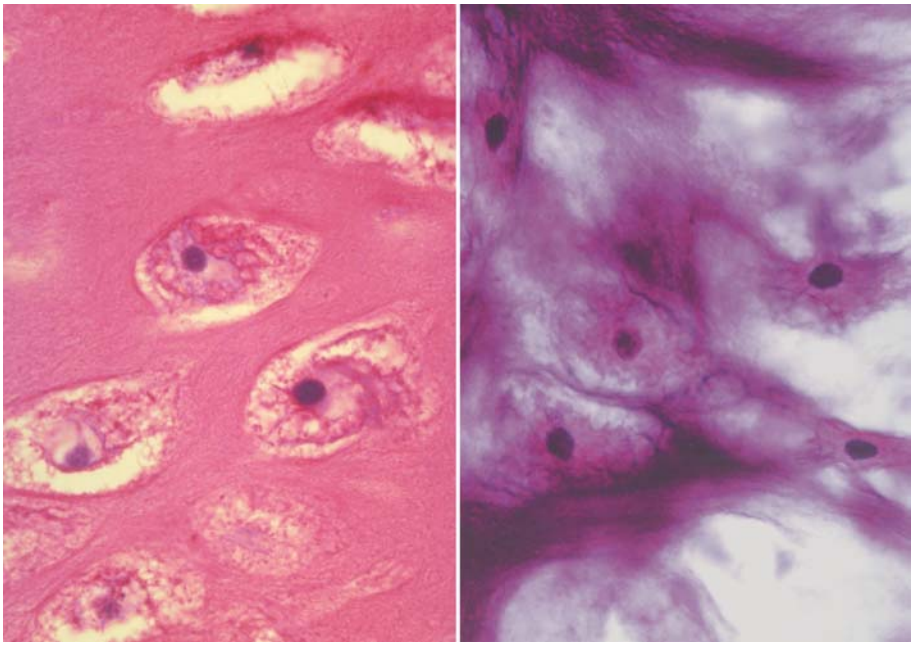

Fig. 6 Enchondroma (*left*) and chondrosarcoma grade 1 (*right*): the nuclei have the same size (toluidine blue, original magnification ×630)

cases, there was a hyaline matrix and, in the remaining cases, there was a hyaline and myxoid matrix. Matrix calcification was found in nine cases.

Clinical and radiological data of enchondromas

The average age of the 16 enchondroma patients was 43.6 years, with a male to female ratio of 5:3. Of the lesions, 50% were located in the periphery (metatarsal bone) and 50% centrally:

- 4× femur (3× distally, 1× proximally)
- 1× tibia (proximally)
- 3× humerus (proximally)

The average follow-up time of all cases was 23 months (range 3–90 months). All patients were treated intralesionally by curettage and bone grafting without local recurrence. Of the enchondroma patients, 43.8% reported pain, compared with 90.6% of all chondrosarcoma patients. Even 87.5% of the patients with grade-1 chondrosarcoma reported pain. This is a significant difference (P=0.009).

In contrast to the chondrosarcoma cases (90.6%), cortical destruction was only seen in three of the enchondroma cases (18.8%) with significant difference (P=0.000). Two of the three cases were located in the hand skeleton. All of the enchondroma cases were Lodwick's grade I, as extraosseous tumours were absent on X-rays. In conclusion, even in grade-1 chondrosarcomas, X-ray findings showed that cortical destruction was much more severe in chondrosarcoma cases than in the enchondroma cases.

Clinical and radiological data of chondrosarcomas

The male to female ratio was 3:2 and the average age at first contact was 50.3 years old with an age range from 5 years to 85 years old. Of lesions, 45.7% were located in the trunk and 45.7% in long bones. Only 8.6% were found in the periphery. The pelvis was affected in 34% and the femur in 29% of the cases. Pelvic tumours, especially, are often difficult to identify in X-ray (Fig. 7, Fig. 8). There was no correlation between the location of the tumours, age and the histological grade. Grade-1 tumours had a tendency to occur earlier than grade-2 and -3 lesions (at 45 years compared with 55 years).

The average follow-up time of the patients with chondrosacomas was 40.5 months. Three patients died after the operation but for reasons that were not related to the chondrosarcoma diagnosis. Therefore, the shortest period was 1 month and the longest follow-up time was 147 months (i.e. 12 years and 3 months).

Local recurrence occurred in nine cases (25.7%) with the shortest disease-free interval being 5 months (grade 3) and the maximum 4 years (grade 1). Most of the patients had only one local recurrence (n=6). One patient with grade-1 chondrosarcoma was treated eight times externally using intra-lesional procedures. After hemipelvectomy, there was no further recurrence.

Fig. 7 X-ray of grade-2 chondrosarcoma in the left side of the sacrum, which is difficult to see

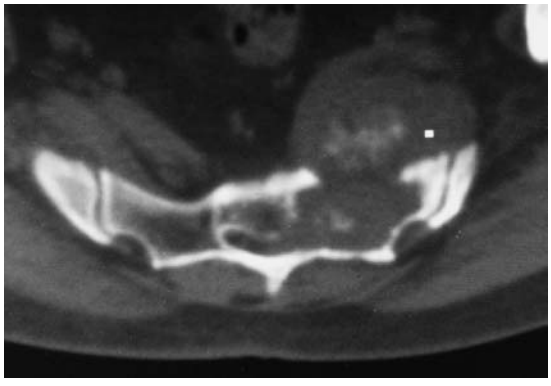

Fig. 8 In computed tomography scan cortical destruction and large extraosseous tumour mass are visible

Five of the nine recurring lesions were grade 3. All but one of the patients with grade-3 tumours experienced local recurrence of the chondrosarcoma. The difference in recurrence rates between histological grades 1–3 were statistically significant (P=0.002). In contrast to grade-1 lesions, patients with grade-3 chondrosarcomas tended to experience local recurrence earlier. With grade-3 lesions, local recurrence occurred after 5–19 months, whereas in grade-1 cases, the tumour recurred after 42–46 months. All patients that experienced local recurrence were treated externally through curettage as intralesional (n=6) procedure or marginal operations (n=3), but without macroscopical tumour remnants. This group could be classified as homogeneous. Seven of the nine patients with local recurrence were cured after further wide resection. The remaining two cases located in the pelvis were resected marginally.

In four of the cases, no local recurrence was observed after marginal or intralesional procedure, but two of these patients died postoperatively (grade 1 and 2) for other reasons. In one case (grade 2) the follow-up time was relatively short (28 months) and one woman with grade-1 chondrosarcoma and marginal resection had no re-growth of the tumour 62 months after the operation.

In 82.4% of all patients, resection with adequate margins could be carried out. This included patients that had not received adequate treatment previously. Limb salvage procedure was possible in 73.5% of all cases. Only one patient had metastasis. The woman with grade-3 chondrosarcoma was still alive 3.5 years after resection of lung metastasis. Although 20% of the patients died, in only four cases was chondrosarcoma the cause. The remaining three patients suffered from emboli or cardiac arrest. Three of the four patients who died from chondrosarcoma had the tumour located in the pelvis and were treated through the *non in sano* procedure. Three lesions were grade 2 and one tumour was grade 3. In one case, wide resection was carried out after the primary intralesional procedure due to a benign biopsy result. After 14 months, multiple implant metastases occurred, and the patient died 2 years after the last operation. The tumour was grade 2. Of the chondrosarcoma patients, 90.6% reported pain independently of the histological grade. Even in 87.5% of grade-1 cases, pain was mentioned.

Cortical destruction could be observed in the X-rays in 90.6% of all chondrosarcomas and even in 94% of grade-1 lesions. No significant difference was found between the histological grade and the presence of cortical destruction or the Lodwick's stage (P=0.512); none of the grade-3 tumours according to Lodwick's grade I. Extraosseous tumour was visible in the X-rays in 55% of all chondrosarcomas and 44% of grade-1 lesions.

Discussion

The classical chondrosarcoma is the most frequent type. Compared with dedifferentiated and mesenchymal chondrosarcomas, as separate entities, the classical form has a much better prognosis [9, 10, 29]. Classical chondrosarcomas are characterised by the synthesis of pure cartilaginous matrix, but with variable differentiation of tumour chondrocytes [29]. Different histological grades can be distinguished. Aside from the histological grade, the prognosis depends on localisation and tumour size, which influence the operability and the extent of surgical therapy.

Six grading systems have been published that attempt to predict the prognosis or malignancy of classical chondrosacroma [4, 10, 18, 24, 25, 26]. The main problem is the inhomogeneity of these classifications, as they are based on a different number of cytological features. The assessment of different cytological criteria is incomplete in many of the reported grading systems, therefore, the frequency of the grades 1–3 differs up to 50% [30]. As a result, the comparisons of clinical data, survival rates and local failures have to be viewed critically. The grading system, previously published by the author, was only based on a few nuclear features [30]. Due to the limited number of features, this histological grading system is easy to use in daily routine with high inter-observer agreement. Atypical nuclei are distinctly visible and usually cannot be found in benign lesions. Several authors [10, 13, 17, 24] are of the opinion that mitotic figures, the presence of double nuclei and cellularity are of great importance for the grading of chondrosarcomas. Furthermore, it has been reported that a cartilage tumour should be considered as evidence of chondrosarcoma when many cells with plump nuclei, more than an occasional cell with two nuclei, giant cartilage cells with large single or multiple nuclei and hypercellularity are present [13, 17]. As Mirra [22] indicates, these features are of limited value for the realisable assessment of malignancy. The average pathologist is confronted with a small number of cartilaginous lesions per year. Diagnostically accurate assessment of plumpness, hypercellularity and more than an occasional double-nucleated chondrocyte would be difficult.

The assessment of these features is complicated by the problem of quantification. In previous studies [22, 30], double nuclei were also found in enchondromas, other benign tumors, articular cartilage and growth plate. The current study confirmed that there was no significant difference among the histological grade and the presence and quantity of binucleated cells. Even between enchondromas and low-grade chondrosarcomas, the proportion of presence (88% compared with 89%) and the number of double nuclei were similar. Mirra [22] also found an overlap in the frequency of binucleated cells in enchondroma with grade-1 chondrosarcoma. Several authors [1, 6, 22, 30] indicated that mitotic figures are extremely rare. The absence of mitoses does not preclude a low-grade chondrosarcoma [22]. In the present study, no significant difference between histological grades and the rate of mitoses was observed. In 83% of grade-1 chondrosarcomas, mitoses were absent. The findings of the study agreed with those of Mirra [22], as found in the enchondromas, and most of the grade-1 chondrosarcomas did not have a single mitosis per 50 HPFs. Dahlin [8] and Mirra [22] stated that the assessment of cellularity is not a useful criterion for distinguishing enchondromas from low-grade chondrosarcomas. The current study confirmed that no significant difference between the cellularity of enchondromas and grade-1 chondrosarcomas existed. Even 63% of the enchondromas had moderate cellularity, and 6% had high cellularity.

Quantification of cellularity remains subjective and the aspect of the histological section that is examined is not necessarily representative of the whole lesion. Criteria, such as hypercellularity and double nuclei, do not prove malignancy of the lesion. Therefore, grading features have to be used, which are untypical in benign lesions, and, furthermore, the number of features has to be limited because the pathologist needs a simple grading system

that is easy to use within the daily routine. The authors' classification is reliable with an inter-observer agreement of 80% and provides an approach to classify chondrosarcomas accurately, even if limited material is available.

In several studies [10, 16] dedifferentiated chondrosarcomas were included in the group of grade-3 classical chondrosarcomas. Due to of the second high malignant mesenchymal component, dedifferentiated chondrosarcomas are separate entities with poor prognosis and were strictly excluded from this study. The mortality rate of patients with dedifferentiated chondrosarcoma varied from 72% to 93% [5, 21], and 87% died within 5 years [20]. Therefore, the inclusion of dedifferentiated chondrosarcomas in the group of grade-3 chondrosarcomas would alter the results of clinical behaviour and prognosis.

Lee et al. [16] distinguished only two types of chondrosarcomas: low-grade and high-grade tumours. However, 53% of the grade-3 chondrosarcomas were dedifferentiated chondrosarcomas and 19% of the grade-1 chondrosarcoma group consisted of atypical enchondromas (grade-0 lesions). When entities with an extremely good or bad prognosis are included in studies, the highly significant differences of recurrence rate, death and rate of metastases documented in these studies have to be interpreted critically. In many studies [1, 2, 14, 16, 31], the definition of distinguishing features of enchondroma and grade-1 chondrosarcoma are lacking or features are overlapping; whereas the distinction Mirra [22]—made using the growth pattern—is a simple and safe method. In addition to this, clinical symptoms and radiological features have to be taken into account. Invasion of marrow spaces by chondrosarcoma mass results in marked radiolucency with hazy calcifications. The biopsy should be taken from this ominous area. It is also crucial to take cortical and medullary bone samples in order to be able to distinguish between enchondromas and low-grade chondrosarcomas on the basis of growth patterns [22].

Pain seems to be a significant clinical symptom. Chondrosarcoma patients usually have a clinical history of pain [3, 11, 19, 23]. In the current study only 43.8% of the enchondroma patients reported pain, whereas 90.6% of all chondrosarcoma patients and 87.5% of grade-1 cases reported pain. This is a significant difference (P=0.009), and these results agree with those of Mirra [22], who reported that about 97% of chondrosarcoma patients suffered pain in contrast with only 44% of the enchondroma cases.

In the present study, the difference in the rate of recurrence between grades 1–3 was statistically significant, but there was also a correlation between recurrence and inadequate therapy. Evans et al. [10] observed a significant difference concerning the rate of metastases and the rate of survival between grade 1 or 2 lesions and grade-3 chondrosarcomas; whereas no difference between the recurrence rate and the histological was found. Larsson et al. [15] showed that the histological grade has little influence on the long-term survival rate, but the surgical therapy has. The histological grade influences the rate of local recurrence, but the important prognostic factor is the adequate surgical treatment.

Local recurrence occurred in 46% of patients with grade-1 and -2 lesions who initially received inadequate treatment, but only in 9.5% of those who received wide resections or amputations [10]. Similar results were noticed by Gitelis et al. [12]. After 10 years, irrespective of the histological grade, 78% of the patients were disease free after adequate resection, whereas only 6% of the group that was treated inadequately remained disease free. An adequate radiological and magnetic resonance image control is important for assessment of local control, especially in pelvis cases where resection margins are often more difficult to perform. The rate of metastasis is low. Bjornsson et al. [3] found metastases in 13.7% of 344 patients, and Dahlin [7] found metastases in 10% of 212 cases. Local control of metastases is crucial for preserving the patient's quality of life. The histological grade and the correlation to the recurrence rate influence the planning of therapy. In this study, local recurrence was observed in 25.7% of the cases. In the literature on the subject, the recurrence rate differs between 19.7% [3] and 58% [27]. The recurrence rate depends on previous surgical procedures or wrong diagnosis [8, 10, 12]. The operability depends on the localisation and size of the tumour [10, 12]. In the current study, in most cases local recurrence occurred only after intralesional or marginal procedures. In addition to this, in cases with multiple recurrences, all the earlier procedures were inadequate. Therefore, adequate surgical therapy seems to be the most important factor for local control.

Bauer et al. [2] recommended intralesional procedures in grade-1 chondrosarcomas, but the authors did not clarify how low-grade chondrosarcomas and enchondromas were distinguished. As a result of recurrences after intralesional or marginal treatment, even in low-grade chondrosarcomas, intralesional procedures in grade-1 chondrosarcomas are not recommended; whereas the care of the curettage and adjuvant therapy seems to be crucial for success. Schreuder et al. [28] did not notice any recurrences after curettage and adjuvant treatment in grade-1 chondrosarcomas, which were distinguished from enchondroma using the growth patterns put forward by Mirra [22]. Grade-1 chondrosarcomas (n=9) were compared with enchondromas (n=14), but the average follow-up time of 26 months was relatively short.

In order to verify the first results of this study, further prospective and randomised studies must be carried out. Based on the current results for chondrosarcoma, grades 1- to 3-wide procedure is recommended. In this study, local recurrence occurred most frequently in cases of grade-3 chondrosarcomas. Only one patient with grade-3 chondrosarcoma did not experience recurrence. As a result of previous inadequate treatment, without macroscopically tumour rests in the recurrent cases, this group could be classified as homogeneous. In contrast to enchondroma, radiographic morphology is much more aggressive in chondrosarcoma, but cortical destruction without extraosseous tumour can be present in enchon-

droma cases located in the periphery. The results of this study are similar to the observations of Murphey et al. [23]. Clinical, radiological and histological findings have to be taken into account in chondrosarcoma diagnosis.

In conclusion, the histological grade, defined on the basis of the authors' grading system, seems to indicate the risk of local recurrence, especially in cases of inadequate treatment. In particular, grade-3 chondrosarcomas and lesions located in the pelvis or other regions where tumour removal would be difficult have to be treated with special attention in order to prevent recurrence.

References

1. Alho A, Connor JF, Mankin HJ, Schiller AL, Campbell CJ (1983) Assessment of malignancy of cartilage tumors using flow cytometry. J Bone Joint Surg Am 65:779–785
2. Bauer HCF, Brosjö O, Kreicbergs A, Lindholm J (1995) Low risk of recurrence of enchondroma and low-grade chondrosarcoma in extremities. 80 patients followed for 2–25 years. Acta Orthop Scand 66:283–288
3. Bjornsson J, Mc Leod RA, Unni KK, Ilstrup DM, Pritchard DJ (1998) Primary chondrosarcoma of long bones and limb girdles. Cancer 83:2105–2119
4. Campanacci M (1976) Giant-cell tumor and chondrosarcoma: grading, treatment and results (studies of 209 and131 cases). Recent Results Cancer Res 54:257–261
5. Capanna R, Bertoni F, Bettelli G, Picca P, Bacchini P. Present D, Giunti A, Campanacci M (1988) Dedifferentiated chondrosarcoma. J Bone Joint Surg Am 70:60–69
6. Cuvelier CA, Roels HJ (1979) Cytophotometric studies of the nuclear DNA content in cartilaginous tumors. Cancer 44:1363–1374
7. Dahlin DC (1956) Chondrosarcoma, a surgical and pathological problem. J Bone Joint Surg Am 38:1025–1038
8. Dahlin DC (ed) (1978) Chondrosarcoma (Primary, secondary, dedifferentiated, and clear cell). In: Bone tumors, 3rd edn. Charles C. Thomas, Springfield, p 201
9. Eriksson AI, Schiller A, Mankin H (1980) The management of chondrosarcoma of bone. Clin Orthop 153:44–66
10. Evans HL, Ayala AG, Romsdahl MM (1977) Prognostic factors of chondrosarcoma of bone. A clinicopathologic analysis with emphasis on histological grading. Cancer 40:818–831
11. Flemming DJ, Murphey MD (2000) Enchondroma and chondrosarcoma. Semin Musculoskelet Radiol 4:59–71
12. Gitelis S, Bertoni F, Picci P, Campanacci M (1981) Chondrosarcoma of bone. The experience at the Istituto Ortopedico Rizzoli. J Bone Joint Surg Am 63:1248–1257
13. Jaffe HL (ed) (1958) Tumors and tumorous conditions of the bones and joints. Lea & Febiger, Philadelphia, p 270, pp 326–328
14. Kreicbergs A, Silvferswärd C, Tribukait B (1984) Flow DNA analysis of primary bone tumors. Relationship between cellular DNA content and histopathologic classification. Cancer 53:129–136
15. Larsson SE, Borssen B, Boquist L (1979) Chondrosarcoma: a multifactorial clinical and histopathological study with particular regard to therapy and survival. Int Orthop 2:333–341
16. Lee FY, Mankin HJ, Fondren G, Gebhardt MC, Springfield DS, Rosenberg AE, Jennings LC (1999) Chondrosarcoma of bone: an assessment of outcome. J Bone Joint Surg Am 81:326–338
17. Lichtenstein L, Jaffe HL (1943) Chondrosarcoma of bone. Am J Pathol 19:553–590
18. Mankin HJ, Cantley KP, Lippiello L, Schiller AL, Campbell CJ (1980) The biology of human chondrosarcoma. I. Description of cases, grading, and biochemical analyses. J Bone Joint Surg Am 62:160–176
19. Marco RA, Gitelis S, Brebach GT, Healey JH (2000) Cartilage tumors: evaluation and treatment. J Am Acad Orthop Surg 8:292–304
20. Mercuri M, Picci P, Campanacci M, Rulli E (1995) Dedifferentiated chondrosarcoma. Skeletal Radiol 24:409–416
21. Mc Carthy EF, Dorfman HD (1982) Chondrosarcoma of bone with dedifferentation: a study of eighteen cases. Hum Pathol 13:36–40
22. Mirra JM, Gold R, Downs J, Eckardt JJ (1985) A new histologic approach to the differentiation of enchondroma and chondrosarcoma of the bones. A clinicopathologic analysis of 51 cases. Clin Orthop 201:214–237
23. Murphey MD, Flemming DJ, Boyea SR, Bojescul JA, Sweet DE, Temple HT (1998) Enchondroma versus chondrosarcoma in the appendicular skeleton: differentiating features. Radiographics 18:1244–1245
24. O'Neal LW, Ackerman LV (1951) Cartilaginous tumors of ribs and sternum. J Thorac Surg 21:71–108
25. Rosenthal DI, Schiller AL, Mankin HJ (1984) Chondrosarcoma: correlation of radiological and histological grade. Radiology 150:21–26
26. Sanerkin NG (1980) The diagnosis and grading of chondrosarcoma of bone. A combined cytologic and histologic approach. Cancer 45:582–594
27. Sanerkin NG, Gallagher P (1979) A review of behaviour of chondrosarcoma of bone. J Bone Joint Surg Br 61:395–400
28. Schreuder HWB, Pruszszynski M, Veth RPH, Lemmens JAM (1998) Treatment of benign and low-grade malignant intramedullary chondroid tumours with curettage and cryosurgery. Eur J Surg Oncol 24:120–126
29. Welkerling H, Dreyer T, Delling G (1991) Morphological typing of chondrosarcoma: a study of 94 cases. Virchows Arch 418:419–425
30. Welkerling H, Werner M, Delling G (1996) Zur histologischen Gradeinteilung der Chondrosarkome. Eine quantitative und qualitative Analyse an 74 Fällen des Hamburger Knochentumorregisters. Pathologe 17:18–25
31. Zeppa P, Zabatta A, Marino G, Boschi R, di Benedetto G, Fazioli F, Vetrani A, De Rosa G, Palombini L (1989) A morphometric approach to the grading of chondroid tumours on fine-needle smears. Pathol Res Pract 185:760–763

Virchows Arch (2003) 443:734–740
DOI 10.1007/s00428-003-0905-0

ORIGINAL ARTICLE

Kutsal Yorukoglu · Burcin Tuna · Emel Dikicioglu · Ender Duzcan · Aydin Isisag · Sait Sen · Ugur Mungan · Ziya Kirkali

Reproducibility of the 1998 World Health Organization/International Society of Urologic Pathology classification of papillary urothelial neoplasms of the urinary bladder

Received: 25 June 2003 / Accepted: 3 September 2003 / Published online: 8 October 2003
© Springer-Verlag 2003

Abstract *Objectives:* This study assessed the diagnostic agreement and intra- and inter-observer reproducibility of the World Health Organization/International Society of Urologic Pathology Consensus Classification of Urothelial Neoplasms (1998 WHO/ISUP classification) and the 1973 WHO classification. *Methods:* A teaching set with 5 slides of each papillary neoplasm of low malignant potential, low-grade papillary carcinoma, high-grade papillary carcinoma, and a guideline, as well as a study set of 30 slides containing ten cases of each category, were sent to participants. Six pathologists expert in urological pathology reviewed the 30 slides of non-invasive papillary urothelial tumors in the study set. Diagnostic accuracy and reproducibility were evaluated using intra- and inter-rater techniques (kappa statistic). *Results:* A moderate to substantial intra- and inter-observer reproducibility was achieved for both the 1998 WHO/ISUP and 1973 WHO classification. The results of the two classification systems were not different statistically ($P>0.05$). Reproducibility was lower in low-grade tumors for both classifications. *Conclusions:* The new proposed classification system for non-invasive urothelial neoplasms does not increase the reproducibility. There is still a need for uniformity in grading in order to compare the different studies and therapies and to provide more accurate information for management.

Keywords Bladder neoplasms · Urothelium · World Health Organization · Classification

K. Yorukoglu (✉) · B. Tuna
School of Medicine, Department of Pathology,
Dokuz Eylul University,
35340 Inciralti Izmir, Turkey
e-mail: kutsal.yorukoglu@deu.edu.tr
Tel.: +90-23-22591190
Fax: +90-23-22777274

E. Dikicioglu
School of Medicine, Department of Pathology,
Adnan Menderes University, Turkey

E. Duzcan
School of Medicine, Department of Pathology,
Pamukkale University, Turkey

A. Isisag
School of Medicine, Department of Pathology,
Celal Bayar University, Turkey

S. Sen
School of Medicine, Department of Pathology,
Ege University, Turkey

U. Mungan · Z. Kirkali
School of Medicine, Department of Urology,
Dokuz Eylul University, Izmir, Turkey

Introduction

There have been several classification and grading systems proposed for non-invasive urothelial neoplasms to create a uniform terminology and allow for comparison of the results of different studies. Of these, the most commonly used has been the 1973 World Health Organization (WHO) classification [24].

In 1998, a new terminology for neoplastic urothelial lesions was suggested. The main aim was to standardize the classification and grading of urothelial neoplasms and create a uniform terminology that could be used universally by pathologists, urologists, and oncologists. A consensus report was published in 1998 as "The World Health Organization/International Society of Urologic Pathology Consensus Classification of Urothelial Neoplasms" (1998 WHO/ISUP classification), and noninvasive papillary neoplasms were classified as papilloma, inverted papilloma, papillary neoplasm of low malignant potential (PUNLMP), low-grade papillary carcinoma (LGPC), and high-grade papillary carcinoma (HGPC) [15]. In 1999, the WHO "blue book" was published, with a little modification in collaboration with pathologists in ten countries [25].

There have been substantial efforts to analyze the prognostic impact of 1998 WHO/ISUP classification. It is well appreciated that there is inter- and intra-observer

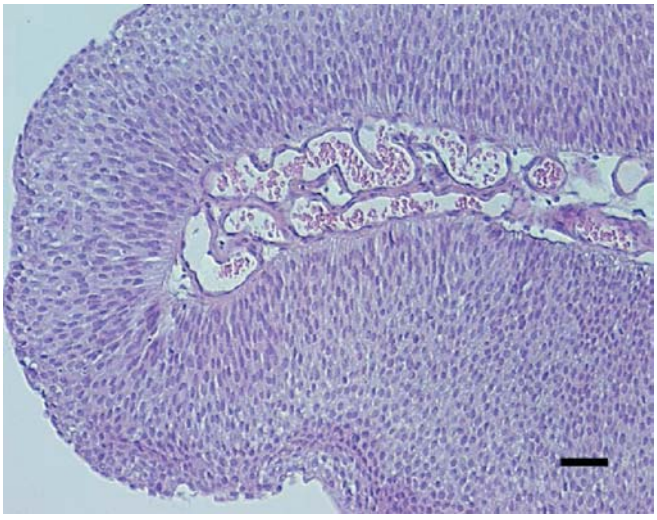

Fig. 1 Urothelial neoplasm of low malignant potential. There is minimal architecture distortion and nuclear enlargement (*magnification* ×100, *bar* 50 μm)

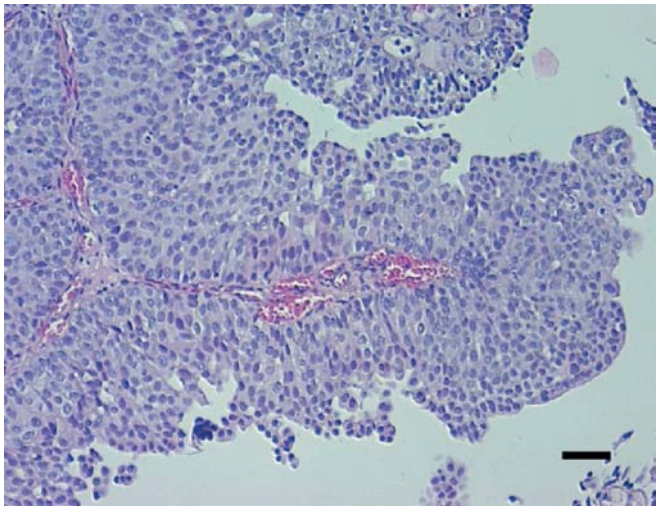

Fig. 2 Low-grade papillary urothelial carcinoma. The normal architecture is disrupted. Nuclei are hyperchromatic and enlarged with moderate pleomorphism (*magnification* ×100, *bar* 50 μm)

variation in assessing tumor differentiation and grade for both urothelial and other tumors [1, 2, 29, 35].

We aimed to determine the inter- and intra-observer reproducibility of the 1998 WHO/ISUP classification and compare the results with the reproducibility of the 1973 WHO classification.

Materials and methods

Two of the authors (KY and BT) reevaluated the archival material of the Dokuz Eylul University School of Medicine, Pathology Department and collected 45 hematoxylin and eosin stained glass slides of noninvasive urothelial tumor (15 PUNLMP, 15 LGPC, and 15 HGPC cases) (Fig. 1, Fig. 2, Fig. 3) considered to represent classic examples of each category. For each category, 5 slides were selected randomly, and these 15 slides constituted the teaching set. A written guideline was prepared from the original reference [15] and attached to the teaching set. The other 30 slides, considered to contain 10 cases of each category, constituted the study set. All cases were considered for inclusion in the study or teaching set only if the sections were of high technical quality and free of artifacts. Each case was relabeled with a random number. Six sets of slides and guidelines for the total material were prepared, and one set was given to each of the six authors.

The authors were asked to review the teaching set, interpret the study set, and classify the cases according to both the 1998 WHO/ISUP and 1973 WHO classification systems (Table 1). After the first review, the results and the study sets were collected, and the labels were changed and given to the authors for second interpretation. The time interval between the two interpretations was at least 4 weeks. The participants were aware that the second circulation comprised repeat slides, but the identification codes had been changed.

Reproducibility was expressed either by the crude rate of agreement or by the kappa (κ) statistics [16]. Statistical comparisons in agreement between classifications were made using a paired *t*-test of differences in κ statistics. All analyses were performed using Scientific Package for Social Sciences software.

The level of agreement for various κ values was as follows: 0.0–0.2, slight; 0.21–0.4, fair; 0.41–0.6, moderate; 0.61–0.8, substantial; 0.81–1.0, almost perfect [38].

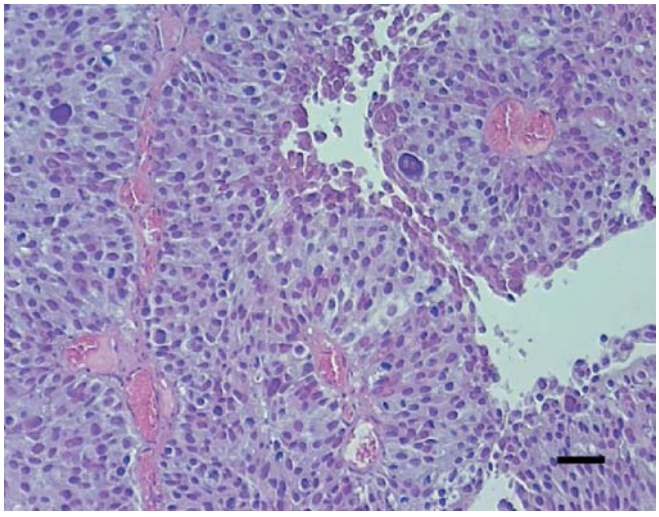

Fig. 3 High-grade papillary urothelial carcinoma. The architecture is disorganized. There is marked nuclear pleomorphism and hyperchromasia (*magnification* ×100, *bar* 50 μm)

Results

The six participants were from five different University Hospital Medical Faculties and were responsible for urological pathology in their pathology departments. Three of the participants were using the 1973 WHO classification system, two were using both the 1998 WHO/ISUP and the 1973 WHO classification systems, and one was using a modified Bergkvist grading system in daily routine practice. The classification categories of the six pathologists for each of the 30 study cases are presented in Table 2.

Table 1 Histological features of urothelial papillary tumors. *PUNLMP* papillary neoplasm of low malignant potential, *LGPC* low-grade papillary carcinoma, *HGPC* high-grade papillary carcinoma. *WHO* World Health Organization, *ISUP* International Society of Urologic Pathology

WHO 1973 classification grade-1 tumors
Urothelium more than seven cell layers thick, minimal to slight nuclear enlargement, normal or slightly distorted architecture, rare or absent mitotic figures
WHO 1973 classification grade-2 tumors
Greater nuclear pleomorphism than grade-1 tumors, coarsely clumped nuclear chromatin, minimal loss of polarity WHO 1973 classification grade-1 tumors
Increased cellularity and nuclear crowding, disturbance of cellular polarity, nuclear pleomorphism, high mitotic activity WHO/ISUP 1998 classification, PUNLMP
Orderly arrangement of cells within papillae, minimal to slight nuclear enlargement, normal or slightly distorted architecture, rare or absent mitotic figures
WHO/ISUP 1998 classification, LGPC
Greater nuclear pleomorphism than PUNLMP, coarsely clumped nuclear chromatin, disruption of the normal architecture, infrequent mitotic figures
WHO/ISUP 1998 classification, HGPC
Loss of normal architecture and cell polarity, increased cellularity and nuclear crowding, variation in nuclear shape and chromatin pattern, increased number of mitotic figures

Table 2 Classification and grading in 30 non-invasive urothelial tumor evaluated by six pathologists. (1998 World Health Organization (WHO)/ International Society of Urologic Pathology Consensus Classification of Urothelial Neoplasms/1973 WHO grade).- *PUNLMP* papillary neoplasm of low malignant potential, *LGPC* low-grade papillary carcinoma, *HGPC* high-grade papillary carcinoma

Case no.	Pathologist					
	A	B	C	D	E	F
1	HGPC/3	HGPC/3	HGPC/3	HGPC/3	HGPC/3	LGPC/2
2	PUNLMP/1	LGPC/2	PUNLMP/1	PUNLMP/1	LGPC/1	PUNLMP/1
3	LGPC/2	LGPC/2	LGPC/2	LGPC/2	LGPC/1	LGPC/2
4	PUNLMP/1	LGPC/2	LGPC/2	PUNLMP/1	PUNLMP/1	PUNLMP/1
5	LGPC/2	LGPC/2	PUNLMP/2	LGPC/2	LGPC/2	PUNLMP/1
6	PUNLMP/1	LGPC/2	PUNLMP/1	LGPC/1	PUNLMP/1	PUNLMP/1
7	HGPC/3	HGPC/3	HGPC/3	HGPC/3	HGPC/2	HGPC/3
8	PUNLMP/1	LGPC/2	PUNLMP/1	PUNLMP/1	LGPC/1	PUNLMP/1
9	PUNLMP/1	LGPC/2	LGPC/2	LGPC/2	LGPC/1	LGPC/2
10	LGPC/2	PUNLMP/1	LGPC/2	LGPC/2	LGPC/2	PUNLMP/1
11	HGPC/3	LGPC/2	LGPC/2	LGPC/2	HGPC/2	HGPC/3
12	HGPC/3	HGPC/3	HGPC/3	HGPC/3	HGPC/3	LGPC/2
13	HGPC/3	HGPC/3	HGPC/3	HGPC/3	HGPC/3	HGPC/3
14	LGPC/2	LGPC/2	LGPC/2	LGPC/2	LGPC/1	LGPC/2
15	HGPC/3	HGPC/3	HGPC/2	HGPC/3	HGPC/2	HGPC/3
16	HGPC/2	LGPC/2	LGPC/2	LGPC/2	LGPC/2	LGPC/2
17	LGPC/1	LGPC/2	LGPC/2	PUNLMP/1	PUNLMP/1	PUNLMP/1
18	HGPC/2	LGPC/2	LGPC/2	LGPC/2	PUNLMP/1	LGPC/2
19	HGPC/2	HGPC/3	HGPC/3	HGPC/3	HGPC/2	HGPC/3
20	LGPC/2	LGPC/2	LGPC/2	PUNLMP/1	LGPC/1	LGPC/2
21	HGPC/2	PUNLMP/1	LGPC/2	PUNLMP/1	PUNLMP/1	LGPC/2
22	PUNLMP/1	PUNLMP/1	PUNLMP/1	PUNLMP/2	PUNLMP/1	PUNLMP/1
23	PUNLMP/1	PUNLMP/1	PUNLMP/1	PUNLMP/1	PUNLMP/1	PUNLMP/1
24	HGPC/3	LGPC/2	HGPC/3	HGPC/3	HGPC/3	HGPC/3
25	LGPC/2	LGPC/2	LGPC/2	PUNLMP/1	LGPC/1	LGPC/2
26	PUNLMP/1	LGPC/2	LGPC/2	LGPC/2	LGPC/2	LGPC/2
27	HGPC/3	HGPC/3	HGPC/3	HGPC/3	HGPC/3	HGPC/3
28	HGPC/3	HGPC/3	HGPC/3	HGPC/3	HGPC/3	HGPC/3
29	PUNLMP/1	PUNLMP/1	LGPC/2	PUNLMP/1	PUNLMP/1	PUNLMP/1
30	HGPC/3	HGPC/3	HGPC/3	HGPC/3	HGPC/3	HGPC/3

1998 WHO/ISUP classification

General intraobserver reproducibility was studied by comparing classes on primary and duplicate slides. Mean observer reproducibility was 78.3% (κ, 0.67), varying from 63.3% to 93.3% (κ, 0.45 to 0.89) for the individual observers (Table 3). The number of duplicates was between 19 and 28.

General inter-observer reproducibility was studied by comparing the three classes given by the six observers to each tumor. Complete agreement among all six observers was seen in 11 of 30 cases (37%). Of these, 2 were PUNLMP cases, 2 were LGUC, and 7 were HGUC cases. Five or more observers arrived at the same class in 20 cases (67%), and four or more rendered the same class in 27 (90%) cases. The overall κ was 0.56, with a range from

Table 3 Intra observer reproducibility in duplicate classification of non-invasive urothelial neoplasms (1998 World Health Organization/International Society of Urologic Pathology Consensus Classification of Urothelial Neoplasms)

Observer	No. of duplicates	Rate of agreement	Kappa
A	26	86.6	0.79
B	23	76.7	0.62
C	28	93.3	0.89
D	19	63.3	0.45
E	20	66.7	0.50
F	25	83.3	0.75
Total	141	78.3	0.67

Table 4 Interobserver reproducibility (Kappa) (1993 World Health Organization/International Society of Urologic Pathology Consensus Classification of Urothelial Neoplasms)

Observer	Observer				
	B	C	D	E	F
A	0.42	0.56	0.5	0.59	0.51
B		0.57	0.6	0.64	0.44
C			0.6	0.54	0.65
D				0.65	0.55
E					0.6

0.42 to 0.65 (Table 4). Rate of agreement was between 60% and 76.7%, with a mean rate of 70.9%. The mean rate of agreement for PUNLMP, LGUC, and HGUC categories were 48, 72.7, and 92%, respectively. When the inter-observer reproducibility figures were calculated only for cases in which the individual pathologists were consistent, the mean interobserver κ was 0.66, with a range from 0.59 to 0.77.

1973 WHO classification

For intra-observer reproducibility figures, the total rate of agreement was 77.8% (κ, 0.66), with individual variations from 63.3% to 93.3% (κ, 0.45 to 0.89) (Table 5). The number of duplicates was between 19 and 28.

For inter-observer reproducibility figures, complete agreement was seen in five cases (17%). Of these five cases, one was grade 1, one was grade 2, and the other three cases were grade 3. Five or more observers arrived at the same grade in 20 cases (67%), and four or more

Table 5 Intraobserver reproducibility in duplicate classification of non-invasive urothelial neoplasms (1973 World Health Organization classification)

Observer	No. of duplicates	Rate of agreement	Kappa
A	24	80	0.7
B	23	76.7	0.62
C	28	93.3	0.89
D	19	63.3	0.45
E	21	70	0.54
F	25	83.3	0.75
Total	140	77.8	0.66

Table 6 Interobserver reproducibility (Kappa) (1973 World Health Organization classification)

Observer	Observer				
	B	C	D	E	F
A	0.4	0.6	0.6	0.45	0.65
B		0.55	0.5	0.19	0.44
C			0.6	0.38	0.54
D				0.55	0.55
E					0.2

rendered the same grade in all but 1 (97%) case. The overall κ was 0.48, with a range from 0.19 to 0.65 (Table 6). Rate of agreement was between 43.3% and 76.7%, with a mean rate of 65.1%. The mean rate of agreement for grade 1, 2, and 3 tumors was 56, 67.3, and 72%, respectively. When the inter-observer reproducibility figures were calculated only for cases in which the individual pathologists were consistent, the mean inter-observer κ was 0.66, with a range from 0.47 to 0.79. The results of the two classification systems were not different statistically (P>0.05).

Discussion

The reproducibility of grading for urothelial tumors has been subject to different studies (Table 7). Using a 1973 WHO or Bergkvist classification systems, 50–87% intra-observer agreement rates were obtained [1, 7, 29]. Inter-observer reproducibility differed in a broad range, and slight to substantial agreement (κ, 0.19 to 0.85) was observed in different analyzes [4, 28, 35, 36, 37]. Kappa

Table 7 Intra- and inter-observer variation in grading of urothelial tumors. *WHO* World Health Organization

First author	Reference no.	Grading system	Intra-observer agreement rate	Inter-observer kappa value
Ooms	4	Bergkvist	50%	
Abel	6	1973 WHO	87%	
Busch	10	Bergkvist	80%	
Robertson	5	1973 WHO		0.19
Sorensen	11	Bergkvist and 1973 WHO		0.51
Olsen	12	Bergkvist		0.50
Blomjous	13	1973 WHO		0.38–0.63
Schapers	14	1973 WHO		0.33–0.77
Schapers	14	Two-tiered		0.71–0.85

value was increased from 0.33–0.77 to 0.71–0.85 by the use of a two-tiered grading system [36]. Inter-observer agreement was improved by the use of a Bayesian Belief Network [23].

In our series, overall agreement rates and κ values were similar for the same pathologists, and a substantial agreement was achieved. The participants were first asked to classify the cases for the 1998 WHO/ISUP classification. Grading for the 1973 WHO classification was performed thereafter. The participants acknowledged that, in general, they translated the 1998 WHO/ISUP classification to the 1973 WHO classification. Therefore, the comparison of our results probably would not reflect the facts. In previous studies, overall agreement for the 1973 WHO classification ranged from 50% to 87% [1, 7, 29]. Our intra-observer agreement results seem to be a little higher (78.3%) between the two classification systems, but not different statistically, and the 1998 WHO/ISUP classification does not seem to be superior for reproducibility.

Inter-observer variability results of this study are more valuable for comparing the two systems and analyzing the reproducibility of the 1998 WHO/ISUP classification. A moderate agreement was achieved for both the 1998 WHO/ISUP and 1973 WHO classification systems (κ=0.56 and κ=0.48, respectively), and the difference was not significant.

In calculating inter-observer variability, the figures should be calculated only on cases in which the individual pathologists were consistent [13]. The corrected κ values of our cases ranged from 0.59 to 0.77, with a mean of 0.66 for the 1998 WHO/ISUP classification, and from 0.47 to 0.79, with a mean of 0.66 for the 1973 WHO classification. There was no difference between the two classification systems. The κ values ranged from 0.33 to 0.77 in a limited number of previous studies [4, 28, 36, 37], and the 1998 WHO/ISUP classification system does not seem to improve the reproducibility.

Grading in the 1973 WHO classification system was based on the degree of anaplasia of tumor cells, but there was not any detailed histological criteria leading to an important intra- and inter-observer variability. The main problem was the indefinite cutoff points for different grades. Therefore, the incidence of grade-2 tumors ranged from 13% to 69% [32].

The main aim of the 1998 WHO/ISUP classification was to develop a universally accepted and reproducible classification system [15]. The histological criteria were explained in detail and the terminology and criteria for flat intraepithelial lesions was standardized. The three- to four-tiered classification of these lesions was changed to a two-tiered classification, as in uterine, cervix, and prostate, which would lead to a rise in reproducibility. However, non-invasive papillary urothelial neoplasms (urothelial carcinomas grades 1, 2, and 3 in the 1973 WHO classification) were classified under three categories with the creation of a new terminology. PUNLMP terminology is the most disputatious point.

As the histological criteria is not defined in detail in the 1973 WHO classification, it is difficult to compare the other grading systems. This can be clearly seen in the interpretations of the 1998 WHO/ISUP classification. Busch and Algaba interpret some of the 1973 WHO grade-1 tumors as PUNLMP and some as LGPC; grade-2 tumors are interpreted as LGPC or HGPC [6]. Bostwick and Mikuz translate the 1973 WHO grade-1, 2, and 3 tumors as PUNLMP, LGPC, and HGPC, respectively [5]. Reuter and Melamed interpret the 1973 WHO grade-1 tumors as PUNLMP, grade-2 tumors as LGPC or HGPC, and grade-3 tumors as HGPC [34]. Notably, all of these authors participated in the consensus committee [15].

The new 1998 WHO/ISUP classification system was found to differentiate the prognostic groups of non-invasive papillary urothelial tumors in different series [3, 11, 14, 18, 33]. The 1998 WHO/ISUP classification system in transurethral resection of bladder (TURB) specimens also predicted the pathological stage in cystectomy specimens [12]. However, the recurrence and progression rates in the literature are conflicting. In some series, the prognostic value of the 1998 WHO/ISUP classification system was found to be limited [10, 17, 18, 32].

Despite the variation in histological grading, tumor grade is found to be one of the independent prognostic factors for urothelial tumors in both of the series, using the 1973 WHO [8, 20, 21, 30] or 1998 WHO/ISUP classification system [6, 11, 18, 19]. The new proposed classification system adds little to non-invasive papillary urothelial neoplasms. Despite the clearly defined histological criteria, the 1998 WHO/ISUP classification system provided a slight but not significant increase in both intra- and inter-observer reproducibility in our study. In only 48% of cases, there was agreement for PUNLMP, and this ratio was 56% for the 1973 WHO grade-1 tumors. Reproducibility was lower in low-grade tumors for both the 1998 WHO/ISUP and 1973 WHO classification systems. Still, there is a need to separate low-grade tumors from intermediate grade tumors or vice versa. If pTa grade-1 tumors are heterogeneous, the patients at risk for recurrence or progression can be identified by a variety of prognostic factors, such as tumor number, tumor dimensions, and associated mucosal abnormalities. In the 1999 WHO classification, a new category is added to the 1973 WHO and 1998 WHO/ISUP classification systems, which means a decrease in reproducibility.

Potential limitations of this study merit consideration. The authors who selected the study cases also participated in the interpretation. The participants from different institutions were asked to evaluate only one slide from each case. All of the slides were prepared at the same institution, and this may influence the potential for tissue sampling, processing, and staining variability.

However, our results show that the new proposed classification system for non-invasive urothelial tumors does not increase the reproducibility. Any three-tiered grading system does not seem to increase reproducibility.

A two-tiered grading system may improve the reproducibility, as shown by Lipponen et al. [22].

In a recent study, Murphy et al. reported inter-observer discrepancy using the 1998 WHO/ISUP classification system. They reported slight to moderate inter-observer agreement for PUNLMP and low-grade tumors (κ, 0.12–0.50). Substantial agreement was achieved for high-grade tumors (κ, 0.75–0.82) [27]. Their cases consisted of a heterogeneous group of both flat papillary and nodular lesions of urothelium. Urothelial neoplasms consisted of both non-invasive and invasive tumors, but did not report the distribution nor analyze them separately. However, a higher discrepancy was reported for low-grade tumors, and the authors are of the same opinion as we are—that a modification of the scheme to create two distinct categories would increase both reproducibility and biological significance without altering patient management.

In the 1998 WHO/ISUP classification, PUNLMP terminology is the main point of discussion. Some authors considering the new terminology claim PUNLMP to be a benign tumor, not cancer, and the progression of these tumors to be negligible [6, 26]. However, others believe that the new terminology adds a complexity to grading and find the term PUNLMP to be cumbersome and confusing [5, 9, 31].

Grading of urothelial tumors has been practiced for a long time. Grading shows a correlation with the stage of the tumor and associates it with biological behavior. However, it suffers from lack of reproducibility, as do most subjective histopathological grading systems. As there have been reported cases of progression and death from tumor, PUNLMP terminology does not reflect its true natural behavior. PUNLMP terminology also does not reflect a biological difference or change the clinical management. There is still a need for uniformity in grading to compare the different studies and therapies and to provide more accurate information to management.

References

1. Abel PD, Henderson D, Bennett MK, Hall RR, Williams G (1988) Differing interpretations by pathologists of the pT category and grade of transitional cell cancer of the bladder. Br J Urol 62:339–342
2. Allsbrook WC, Mangold KA, Jonson MH, Lane RB, Lane CG, Epstein JI (2001) Interobserver reproducibility of Gleason grading of prostatic carcinoma: general pathologists. Hum Pathol 32:81–88
3. Alsheikh A, Mohamedali Z, Jones E, Masterson J, Gilks CB (2001) Comparison of the WHO-ISUP classification and cytokeratin 20 expression predicting the behavior of low grade papillary urothelial tumors. Mod Pathol 14:267–272
4. Blomjous CEM, Smeulders AWM, Baak JPA, Vos W, van Galen EM, Meijer CJLM (1989) A comparative study in morphometric grading of transitional cell carcinoma of the urinary bladder. Anal Quant Cytol Histol 11:426–432
5. Bostwick DG, Mikuz G (2002) Urothelial papillary (exophytic) neoplasms. Virchows Arch 441:109–116
6. Busch C, Algaba F (2002) The WHO/ISUP 1998 and WHO 1999 systems for malignancy grading of bladder cancer. Scientific foundation and translation to one another and previous systems. Virchows Arch 441:105–108
7. Busch C, Engberg A, Norlen BJ, Stenkvist B (1977) Malignancy grading of epithelial bladder tumors. Reproducibility of grading and comparison between forceps biopsy, aspiration biopsy and exfoliative cytology. Scand J Urol Nephrol 11:143–148
8. Carbin B-E, Ekman P, Gustafson H, Christensen NJ, Sandstedt B, Silfversward C (1991) Grading of human urothelial carcinoma based on nuclear atypia and mitotic frequency. I. Histological description. J Urol 145:968–971
9. Cheng L, Bostwick DG (2000) World Health Organization and International Society of Urological Pathology classification and two-number grading system of bladder tumors. Reply. Cancer 88:1513–1516
10. Cheng L, Neumann RM, Bostwick DG (1999) Papillary urothelial neoplasms of low malignant potential. Clinical and biologic implications. Cancer 86:2102–2108
11. Cheng L, Neumann RM, Nehra A, Spotts BE, Weaver AL, Bostwick DG (2000) Cancer heterogeneity and its biologic implications in the grading of urothelial carcinoma. Cancer 88:1663–1670
12. Cheng L, Neumann RM, Weaver AL, Cheville JC, Leibovich BC, Ramnani DM, Schere BG, Nehra A, Zincke H, Bostwick DG (2000) Grading and staging of bladder carcinoma in transurethral resection specimens. Am J Clin Pathol 113:275–279
13. Cramer SF (1988) Methods for evaluating reproducibility in anatomic pathology. Hum Pathol 19:1472–1473
14. Desai S, Lim SD, Jimenez RE, Chun T, Keane TE, McKenney JK, Zavala-Pompa A, Cohen C, Young RH, Amin MB (2000) Relationship of cytokeratin 20 and CD44 protein expression with WHO/ISUP grade in pTa and pT1 papillary urothelial neoplasia. Mod Pathol 13:1315–1323
15. Epstein JI, Amin MB, Reuter VR, Mostofi FK, The Bladder Consensus Conference Committee (1999) The World Health Organization/International Society of Urologic Pathology consensus classification of urothelial (transitional cell) neoplasms of the urinary bladder. Am J Surg Pathol 22:1435–1448
16. Holman CDJ, James IR, Heenan PJ, Matz LR, Blackwell JB, Kelsall GR, Singh A, Seldam RE (1982) An improved method of analysis of observer variation between pathologists. Histopathology 6:581–589
17. Holmang S, Hedelin H, Anderström C, Johansson SL (1995) The relationship among multiple recurrences, progression and prognosis of patients with stages Ta and T1 transitional cell cancer of the bladder followed for at least 20 years. J Urol 153:1823–1827
18. Holmang S, Hedelin H, Anderstrom C, Holmberg E, Busch C, Johansson SL (1999) Recurrence and progression in low grade papillary urothelial tumors. J Urol 162:702–707
19. Holmang S, Andius P, Hedelin H, Wester K, Busch C, Johansson SL (2001) Stage progression in Ta papillary urothelial tumors: relationship to grade, immunohistochemical expression of tumor markers, mitotic frequency and DNA ploidy. J Urol 165:1124–1130
20. Jordan AM, Weingarten J, Murphy WM (1987) Transitional cell neoplasms of the urinary bladder: can biologic potential be predicted from histologic grading? Cancer 60:2766–2774
21. Kakizoe T, Tobisu K, Mizunati T, Tsutsumi M, Tanaka Y, Sakamoto M (1992) Analysis by step sectioning of early invasive bladder cancer with special reference to G3 pT1 disease. Jpn J Cancer Res 83:1354–1358
22. Lipponen P, Simpanen H, Pesonen E, Eskelinen M, Sotarauta M, Collan Y (1989) Potential of morphometry in grading transitional cell carcinoma of the urinary bladder. Path Res Pract 185:617–620
23. Montironi R, Mazzucchelli R, Colanzi P, Streccioni M, Scarpelli M, Thompson D, Bartels PH (2002) Improving inter-observer agreement and certainty level in diagnosing and grading papillary urothelial neoplasms: usefulness of a Bayesian belief network. Eur Urol 41:449–457

24. Mostofi FK, Sobin LH, Torloni H (1973) Histological typing of urinary bladder tumours. Volume 10. Geneva: World Health Organization
25. Mostofi FK, Davis CJ, Seterhenn IA (1999) Histological typing of urinary bladder tumors. World Health Organization international histological classification of tumours, 2nd edn. Springer, Berlin Heidelberg New York
26. Murphy WM (1999) Bladder cancer redefined. Cancer 86:1890–1892
27. Murphy WM, Takezawa K, Maruniak NA (2002) Interobserver discrepancy using the 1998 World Health Organization/International Society of Urologic Pathology classification of urothelial neoplasms: practical choices for patient care. J Urol 168:968–972
28. Olsen LH, Overgaard S, Frederiksen P, Ladefoged C, Ludwigsen E, Petri J, Poulsen JT (1993) The reliability of staging and grading of bladder tumors. Scand J Urol Nephrol 27:349–353
29. Ooms ECM, Anderson WAD, Alons CL, Boon ME, Veldhuizen RW (1983) Analysis of the performance of pathologists in the grading of bladder tumors. Hum Pathol 14:140–143
30. Oosterhuis JWA, Schapers RFM, Janssen-Heijnen MLG, Pauwels RPE, Newling DW, ten Kate F (2002) Histological grading of papillary urothelial carcinoma of the bladder: prognostic value of the 1998 WHO/ISUP classification system and comparison with conventional grading systems. J Clin Pathol 55:900–905
31. Oyasu R (2000) Urological Pathology classification and two-number grading system of bladder tumors. Cancer 88:1509–1512
32. Pauwels RPE, Schapers RFM, Smeets AWGB, Debruyne FMJ, Geraedts JPM (1988) Grading in superficial bladder cancer. (1) Morphological criteria. Br J Urol 61:129–134
33. Pich A, Chiusa L, Formiconi A, Galliano D, Bortolin P, Navone R (2001) Biologic differences between noninvasive papillary urothelial neoplasms of low malignant potential and low-grade (grade 1) papillary carcinomas of the bladder. Am J Surg Pathol 25:1528–1533
34. Reuter VE, Melamed MR (1999) The urothelial tract. In: Sternberg SS (ed) Diagnostic surgical pathology, 3rd edn. Lippincott Williams & Wilkins, Philadelphia, p 1871
35. Robertson AJ, Swanson Beck J, Burnett RA, Howatson SR, Lee FD, Lessells AM, McLaren KM, Moss SM, Simpson JG, Smith GD, Tavadia HB, Walker F (1990) Observer variability in histopathological reporting of transitional cell carcinoma and epithelial dysplasia in bladders. J Clin Pathol 43:17–21
36. Schapers RFM, Pauwels RPE, Wıjnen JThM, Arends JW, Thunnissen FBJM, Coebergh JWW, Smeets AWGB, Bosman FT (1994) A simplified grading method of transitional cell carcinoma of the urinary bladder: reproducibility, clinical significance and comparison with other prognostic parameters. Br J Urol 73:625–631
37. Sorensen FB, Sasaki M, Fukuzawa S, Yamabe H, Olsen S, Yoshida O (1994) Qualitative and quantitative histopathology in transitional cell carcinomas of the urinary bladder. An international investigation of intra- and interobserver reproducibility. Lab Invest 70:242–254
38. Wells WA, Carney PA, Eliassen MS, Grove MR, Tosteson ANA (2000) Pathologists' agreement with experts and reproducibility of breast ductal carcinoma-in-situ classification schemes. Am J Surg Pathol 24:651–659

Virchows Arch (2003) 443:741–744
DOI 10.1007/s00428-003-0883-2

ORIGINAL ARTICLE

Mona Pache · Katharina Glatz · Doris Bösch · Stephan Dirnhofer · Martina Mirlacher · Ronald Simon · Peter Schraml · Alex Rufle · Josef Flammer · Guido Sauter · Peter Meyer

Sequence analysis and high-throughput immunhistochemical profiling of KIT (CD 117) expression in uveal melanoma using tissue microarrays

Received: 11 June 2003 / Accepted: 17 July 2003 / Published online: 26 September 2003
© Springer-Verlag 2003

Abstract We aimed to immunohistochemically examine the expression of KIT (CD 117) in human posterior uveal melanoma and to analyze KIT-positive tumors for gene mutations. Brought into a tissue microarray (TMA) format were 101 formalin-fixed, paraffin-embedded posterior uveal melanomas. Immunhistochemistry was performed using the polyclonal anti-CD117 antibody from Dako (A4502). In ten selected KIT-positive tumors, exons 2, 8, 9, 11, 13 and 17 were sequenced. Of the 101 cases, 89 (88%) could be evaluated on the TMAs. Immunohistochemistry for CD 117 was weakly positive in 5 cases (6%), moderately positive in 10 cases (12%) and strongly positive in 57 cases (69%). No KIT mutations were detected in the analyzed exons. In conclusion, human posterior uveal melanoma frequently expresses CD117 at high levels. Although KIT mutations could not be found, it appears justified to investigate the utility of imatinib mesylate in the treatment of these patients.

Keywords Uveal melanoma · CD 117 · cKIT · Tissue microarray · Sequence analysis

Introduction

Although posterior uveal melanoma is the most common primary intraocular malignancy, the neoplasm is rare, with an overall incidence of 0.1–1.5. Its frequency increases with advanced age. The average age of detection of posterior uveal melanoma ranges between 55 years and 60 years [19]. The tumor has not only the capacity to destroy vision, but can also metastasize and cause death. In recent years, a marked progress in local tumor control was achieved using therapeutic options such as enucleation, radiation, photocoagulation, microsurgical resection or transpupillary thermotherapy [19]. However, none of these treatments can prevent metastases. Therefore, the prognosis of locally treated posterior uveal melanoma has not changed during recent years. The metastatic rate of the malignant uveal melanoma is about 35% at 10 years. Results of systemic treatment for metastatic uveal melanoma are still discouraging.

It is hoped that novel adjuvant cancer drugs targeting specific gene products in cancer cells, such as imatinib mesylate (STI 571; Glivec), will improve the success of systemic therapy in uveal melanoma and other tumor entities. Imatinib mesylate is a small molecule that specifically inhibits several kinases, including ABL, KIT (CD117) and platelet derived growth factor receptor. Imatinib mesylate is of special interest in melanomas because melanocytes are known to express at least one of its molecular targets (KIT). KIT is a transmembrane tyrosine kinase and acts as a type-III receptor for mast cell growth factor or stem cell factor. KIT expression has been described in various tumor entities [1, 7, 12, 14, 23]. Remarkably, metastatic and/or advanced gastrointestinal stroma tumors (GIST), the tumor entities with the highest KIT expression, responded well to imatinib mesylate therapy in initial studies [4, 24]. There is hope that imatinib mesylate might also be effective in other KIT-expressing tumor entities. Several clinical studies are currently investigating the effect of imatinib mesylate on KIT-positive tumors of various sites, such as gliomas, soft tissue sarcomas/bone sarcomas, ovarian cancers, primary peritoneal cancers, pediatric solid tumors and colorectal cancers [16].

As far as melanomas are concerned, only skin melanomas have been analyzed for KIT expression.

M. Pache · D. Bösch · J. Flammer · P. Meyer
University Eye Clinic of Basel,
Basel, Switzerland

K. Glatz · D. Bösch · S. Dirnhofer · M. Mirlacher · R. Simon · P. Schraml · A. Rufle · G. Sauter · P. Meyer
Institute of Pathology,
University of Basel,
Basel, Switzerland

P. Meyer (✉)
University Eye Clinic Basel,
Mittlere Str. 91, 4056 Basel, Switzerland
e-mail: pemeyer@uhbs.ch
Tel.: +41-61-2658643
Fax: +41-61-2658747

These studies have indicated a frequency of KIT expression ranging between 20% and 90% [1, 7, 23]. Uveal melanoma has not been examined for KIT expression up to now. To investigate the importance of KIT as a potential therapeutic target in uveal melanomas, we analyzed KIT expression in a series of 101 uveal melanomas using the tissue microarray (TMA) technique [2, 3]. In addition, we sequenced exons 2, 8, 9, 11, 13 and 17 in a subset of KIT-expressing tumors to identify possible mechanisms of KIT activation in uveal melanoma.

Materials and methods

Tumors, TMA construction

Formalin-fixed, paraffin-embedded tissue material from 101 posterior uveal melanomas from the years 1985–2002 were collected from the archives of the Institute of Ophthalmopathology and Pathology, University of Basel. All cases were classified according to the pTNM classification [UJCC 5th edition, 1997]. The series included 44 males and 57 females. The mean age was 79 years (range 39–98 years). The pT stage was pT1a in 3, pT1b in 1, pT2a in 25, pT2b in 27, pT2c in 6, pT3 in 15 and pT4 in 20 cases. pT stage could not be determined in four cases. Histologically, a spindle cell type was present in 50 cases, an epitheloid type in 13 cases and a mixed type in 38 cases. The construction of TMAs was done exactly as described [2, 3]. In brief, tissue cylinders with a diameter of 0.6 mm were taken from representative tumor areas of each "donor" tissue block using a robotic precision instrument and brought into a recipient paraffin block. Sections 4-μm thick of the resulting TMA blocks were transferred to an adhesive coated slide system (Instrumedics Inc., Hackensack, New Jersey).

Immunohistochemistry

Immunhistochemistry was performed using the polyclonal anti-CD117 antibody A4502 (Dako, Glostrup, Denmark). In a comparison of different commercially available anti-CD117 antibodies, A4502 yielded the highest specificity and the least background (unpublished data). A4502 was applied at a dilution of 1:300 at 4°C for 18 h, after 3 min pressure cooking in 10 mM sodium citrate buffer (pH 6.0) for antigen retrieval. Endogenous peroxidase was blocked using 0.3% hydrogen peroxidase diluted in methanol for 30 min. A standard avidin-biotin complex (ABC) technique (Vector ABC kit) using diaminobenzidine for visualization was used. For specificity control, a preabsorption of the antibody was performed (CD117 peptide stock solution; Neomarkers PP1518). This antigen matches the sequence of the epitope recognized by the polyclonal antibody of Dako. A case of KIT-positive GIST was used for control. The percentage of positive cells was estimated and the staining intensity was semi-quantitatively recorded as 1+, 2+ or 3+. For statistical analyses, the staining results were categorized into four groups. Tumors without any staining were considered negative. Tumors with 1+ staining intensity in less than 60% of cells and 2+ intensity in less than 30% of cells were considered weakly positive. Tumors with 1+ staining intensity in 60% of cells or more, 2+ intensity in 30% or more up to 80% (not inclusive) or 3+ intensity in less than 30% were considered moderately positive. Tumors with 2+ intensity in 80% or more or 3+ intensity in 30% or more of cells were considered strongly positive.

Sequence analysis

Ten melanomas showing intense CD117 staining were selected for KIT mutation analysis. Deparaffinizing of the formalin-fixed tissues and DNA extraction was performed using a commercial DNA extraction kit (Qia Amp DNA minkit, cat. #51304, Qiagen GmbH, Hilden, Germany). Exons 2, 8, 9, 11, 13 and 17 were amplified using a semi-nested polymerase chain reaction approach [10] and were sequenced using the Big Dye Terminators Cycle Sequencing Ready Reaction Kit (Applied Biosystems, Foster City, CA, USA). Sequence products were analyzed on an ABI Prism 310 Genetic Analyzer (Applied Biosystems; Foster City, CA, USA).

Statistical analysis

Statistical analyses were performed using the statistical package StatView 5.0 (Abacus Concepts, Berkley, CA). The chi-square statistic was used for frequency comparisons of nominal categorized variables. In the case of 2×2 contingency tables, significances were calculated using Fisher's exact test.

Results

Immunohistochemistry

Immunohistochemistry was interpretable in 89 of 101 cases (88%). Analysis failures were due to either lack of tissue on the TMA section or a lack of vital tumor cells in the arrayed samples. A positive CD 117 staining was seen in 72 of 83 interpretable tumors (87%). The staining was membranous in all cases (Fig. 1). Positivity was weak in 5 cases (6%), moderate in 10 cases (12%) and strong in 57 cases (69%). Examples of positive and negative staining for CD 117 are shown in Fig. 2. There was no difference in frequency or intensity of KIT staining between males and females or between tumors of different stages or different tumor cell types.

Mutation analysis

Sequence alterations of exons 2, 8, 9, 11, 13 and 17 were not detected in any of the ten analyzed tumors.

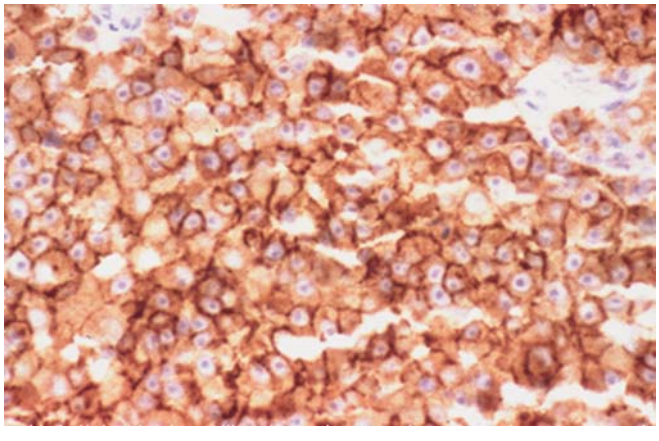

Fig. 1 Example of a CD 117-positive tumor (magnification ×100)

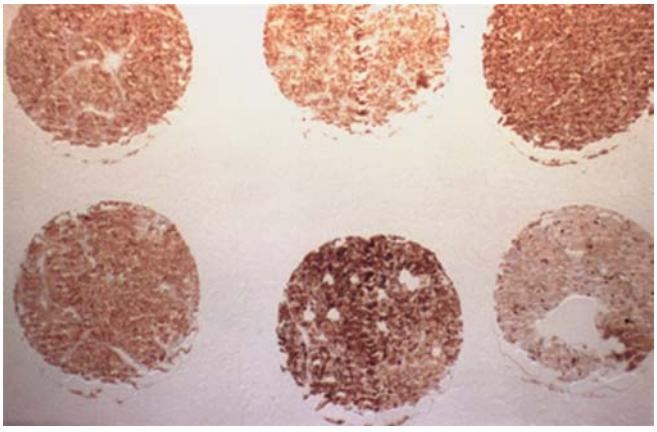

Fig. 2 Examples of positive and negative tumors. Single punches (0.6 mm diameter) of posterior uveal melanoma positive and negative for CD 117, respectively (magnification ×5)

Discussion

A TMA was used to evaluate the expression frequency of KIT in a series of clinically well-documented 101 uveal melanomas. Using this method, minute tissue samples (diameter 0.6 mm) are analyzed on one microscope glass slide. It is likely that focal alterations in gene expression are not always detected in a TMA setting. However, this perceived disadvantage seems to be compensated by a maximal standardization of the analysis (where all samples are processed under identical conditions) and the high number of tumors that can be included in a TMA study. Numerous studies have shown that representative information can be obtained in TMA analyses [9, 17, 20, 21, 22] (Went et al., personal communication). For example, the known frequencies of amplifications of various genes were confirmed in TMA studies in various tumor types [9, 18]. Other TMA projects confirmed the previously established prognostic impact of molecular markers such as the expression of estrogen receptor, progesterone receptor and p53 in breast cancer [22] or of the Ki67-labeling index in bladder cancer [15].

The results of this study show that KIT is frequently expressed in uveal melanoma. More than 81% of our tumors were KIT positive. Although it is difficult to compare immunohistochemical studies if different antibodies, staining conditions and scoring procedures are applied, these data suggest that KIT expression is more frequent in uveal than in skin melanoma. Such a high frequency of KIT expression in uveal melanoma raises the possibility that imatinib mesylate could be a therapeutic option in these tumors. Imatinib mesylate was initially designed to inhibit the bcr/abl fusion protein in chronic myeloid leukemia, for which it was FDA approved in May 2001 [5]. Later it was shown that imatinib mesylate is also effective in KIT-positive GIST [24]. Several studies are now ongoing to assess whether imatinib mesylate has a beneficial effect on other KIT-positive tumors [16].

Our data suggest that uveal melanoma is one of the tumors with the highest frequency of immunohistochemically detectable KIT expression. This could make uveal melanoma a prime candidate for imatinib mesylate therapy. However, c-KIT protein is also expressed in normal melanocytes, and there is evidence that its expression is downregulated or even lost in skin melanoma [13]. It is therefore possible that KIT expression in uveal melanoma does not reflect "overexpression" but rather represents preservation of normal protein expression. The lack of mutations in all ten tumors sequenced for exons 2, 8, 9, 11, 13 and 17 also does not provide evidence for presence of KIT alterations in uveal melanoma. It has recently been shown that the response rate to imatinib mesylate may depend on presence and type of KIT mutation in a tumor [8]. If this is true in general, the likelihood of uveal melanomas responding favorably to imatinib mesylate may be low. However, other authors have reported at least some therapeutic effect in KIT-positive tumors expressing wild-type protein [6, 11].

Taken together, our data show that posterior uveal melanoma is one of the most frequently KIT-positive tumor entities. Although this seems to reflect preservation of "normal level KIT expression" in melanocytes rather than KIT mutations, these data may justify investigating possible beneficial effects of imatinib mesylate in uveal melanoma.

Acknowledgement The authors thank Miriam Vonlanten and Andreas Meyer for their technical assistance.

References

1. Arber DA, Tamayo R, Weiss LM (1998) Paraffin section detection of the c-kit gene product (CD117) in human tissues: value in the diagnosis of mast cell disorders. Hum Pathol 29:498–504
2. Bubendorf L, Kolmer M, Kononen J, Koivisto P, Mousses S, Chen Y, Mahlamaki E, Schraml P, Moch H, Willi N, Elkahloun AG, Pretlow TG, Gasser TC, Mihatsch MJ, Sauter G, Kallioniemi OP (1999) Hormone therapy failure in human prostate cancer: analysis by complementary DNA and tissue microarrays. J Natl Cancer Inst 91:1758–1764
3. Bubendorf L, Kononen J, Koivisto P, Schraml P, Moch H, Gasser TC, Willi N, Mihatsch MJ, Sauter G, Kallioniemi OP (1999) Survey of gene amplifications during prostate cancer progression by high-throughout fluorescence in situ hybridization on tissue microarrays. Cancer Res 59:803–806
4. Demetri GD, von Mehren M, Blanke CD, Van den Abbeele AD, Eisenberg B, Roberts PJ, Heinrich MC, Tuveson DA, Singer S, Janicek M, Fletcher JA, Silverman SG, Silberman SL, Capdeville R, Kiese B, Peng B, Dimitrijevic S, Druker BJ, Corless C, Fletcher CD, Joensuu H (2002) Efficacy and safety of imatinib mesylate in advanced gastrointestinal stromal tumors. N Engl J Med 347:472–480
5. Druker BJ, Sawyers CL, Kantarjian H, Resta DJ, Reese SF, Ford JM, Capdeville R, Talpaz M (2001) Activity of a specific inhibitor of the BCR-ABL tyrosine kinase in the blast crisis of chronic myeloid leukemia and acute lymphoblastic leukemia with the Philadelphia chromosome. N Engl J Med 344:1038–1042
6. Heinrich MC, Griffith DJ, Druker BJ, Wait CL, Ott KA, Zigler AJ (2000) Inhibition of c-kit receptor tyrosine kinase activity by

STI 571, a selective tyrosine kinase inhibitor. Blood 96:925–932
7. Hornick JL, Fletcher CD (2002) Immunohistochemical staining for KIT (CD117) in soft tissue sarcomas is very limited in distribution. Am J Clin Pathol 117:188–193
8. Joensuu H, Fletcher C, Dimitrijevic S, Silberman S, Roberts P, Demetri G (2002) Management of malignant gastrointestinal stromal tumours. Lancet Oncol 3:655–664
9. Kononen J, Bubendorf L, Kallioniemi A, Barlund M, Schraml P, Leighton S, Torhorst J, Mihatsch MJ, Sauter G, Kallioniemi OP (1998) Tissue microarrays for high-throughput molecular profiling of tumor specimens. Nat Med 4:844–847
10. Lasota J, Jasinski M, Sarlomo-Rikala M, Miettinen M (1999) Mutations in exon 11 of c-Kit occur preferentially in malignant versus benign gastrointestinal stromal tumors and do not occur in leiomyomas or leiomyosarcomas. Am J Pathol 154:53–60
11. Ma Y, Zeng S, Metcalfe DD, Akin C, Dimitrijevic S, Butterfield JH, McMahon G, Longley BJ (2002) The c-KIT mutation causing human mastocytosis is resistant to STI571 and other KIT kinase inhibitors; kinases with enzymatic site mutations show different inhibitor sensitivity profiles than wild-type kinases and those with regulatory-type mutations. Blood 99:1741–1744
12. Matsuda R, Takahashi T, Nakamura S, Sekido Y, Nishida K, Seto M, Seito T, Sugiura T, Ariyoshi Y, et al (1993) Expression of the c-kit protein in human solid tumors and in corresponding fetal and adult normal tissues. Am J Pathol 142:339–346
13. Montone KT, van Belle P, Elenitsas R, Elder DE (1997) Proto-oncogene c-kit expression in malignant melanoma: protein loss with tumor progression. Mod Pathol 10:939–944
14. Natali PG, Nicotra MR, Sures I, Santoro E, Bigotti A, Ullrich A (1992) Expression of c-kit receptor in normal and transformed human nonlymphoid tissues. Cancer Res 52:6139–6143
15. Nocito A, Bubendorf L, Maria Tinner E, Suess K, Wagner U, Forster T, Kononen J, Fijan A, Bruderer J, Schmid U, Ackermann D, Maurer R, Alund G, Knonagel H, Rist M, Anabitarte M, Hering F, Hardmeier T, Schoenenberger AJ, Flury R, Jager P, Luc Fehr J, Schraml P, Moch H, Mihatsch MJ, Gasser T, Sauter G (2001) Microarrays of bladder cancer tissue are highly representative of proliferation index and histological grade. J Pathol 194:349–357
16. Radford IR (2002) Imatinib. Novartis. Curr Opin Investig Drugs 3:492–499
17. Richter J, Wagner U, Kononen J, Fijan A, Bruderer J, Schmid U, Ackermann D, Maurer R, Alund G, Knonagel H, Rist M, Wilber K, Anabitarte M, Hering F, Hardmeier T, Schonenberger A, Flury R, Jager P, Fehr JL, Schraml P, Moch H, Mihatsch MJ, Gasser T, Kallioniemi OP, Sauter G (2000) High-throughput tissue microarray analysis of cyclin E gene amplification and overexpression in urinary bladder cancer. Am J Pathol 157:787–794
18. Schraml P, Kononen J, Bubendorf L, Moch H, Bissig H, Nocito A, Mihatsch MJ, Kallioniemi OP, Sauter G (1999) Tissue microarrays for gene amplification surveys in many different tumor types. Clin Cancer Res 5:1966–1975
19. Shields JA, Shields CL, Donoso LA (1991) Management of posterior uveal melanoma. Surv Ophthalmol 36:161–195
20. Simon R, Nocito A, Hubscher T, Bucher C, Torhorst J, Schraml P, Bubendorf L, Mihatsch MM, Moch H, Wilber K, Schotzau A, Kononen J, Sauter G (2001) Patterns of her-2/neu amplification and overexpression in primary and metastatic breast cancer. J Natl Cancer Inst 93:1141–1146
21. Simon R, Richter J, Wagner U, Fijan A, Bruderer J, Schmid U, Ackermann D, Maurer R, Alund G, Knonagel H, Rist M, Wilber K, Anabitarte M, Hering F, Hardmeier T, Schonenberger A, Flury R, Jager P, Fehr JL, Schraml P, Moch H, Mihatsch MJ, Gasser T, Sauter G (2001) High-throughput tissue microarray analysis of 3p25 (RAF1) and 8p12 (FGFR1) copy number alterations in urinary bladder cancer. Cancer Res 61:4514–4519
22. Torhorst J, Bucher C, Kononen J, Haas P, Zuber M, Kochli OR, Mross F, Dieterich H, Moch H, Mihatsch M, Kallioniemi OP, Sauter G (2001) Tissue microarrays for rapid linking of molecular changes to clinical endpoints. Am J Pathol 159:2249–2256
23. Tsuura Y, Hiraki H, Watanabe K, Igarashi S, Shimamura K, Fukuda T, Suzuki T, Seito T (1994) Preferential localization of c-kit product in tissue mast cells, basal cells of skin, epithelial cells of breast, small cell lung carcinoma and seminoma/dysgerminoma in human: immunohistochemical study on formalin-fixed, paraffin-embedded tissues. Virchows Arch 424:135–141
24. van Oosterom AT, Judson I, Verweij J, Stroobants S, Donato di Paola E, Dimitrijevic S, Martens M, Webb A, Sciot R, Van Glabbeke M, Silberman S, Nielsen OS (2001) Safety and efficacy of imatinib (STI571) in metastatic gastrointestinal stromal tumours: a phase I study. Lancet 358:1421–1423

Virchows Arch (2003) 443:745–751
DOI 10.1007/s00428-003-0897-9

ORIGINAL ARTICLE

Daniela Mihic-Probst · Parvin Saremaslani · Paul Komminoth · Philipp U. Heitz

Immunostaining for the tumour suppressor gene p16 product is a useful marker to differentiate melanoma metastasis from lymph-node nevus

Received: 7 August 2003 / Accepted: 7 August 2003 / Published online: 24 October 2003
© Springer-Verlag 2003

Abstract Upon the introduction of extensive sampling protocols of sentinel node biopsies, pathologists are increasingly confronted with small melanoma metastases. Using conventional histology, it proves sometimes difficult or impossible to differentiate small melanoma metastases from lymph-node nevi. Loss of the tumour suppressor gene p16 has been shown to be associated with tumour progression of melanoma. We investigated nevus and melanoma cells for the presence of the product of the gene p16, using immunohistochemistry. All nevus cells, independent of their location (nodal or skin) displayed an extensive nuclear and cytoplasmic staining for p16. In contrast, all cells of melanoma metastases, except one skin metastasis, lacked nuclear staining for p16. These findings indicate that p16 is a reliable marker to distinguish lymph-node nevi from melanoma metastasis.

Keywords Nodal nevus · Metastatic melanoma · Sentinel lymph node · Tumour suppressor gene · p16

Introduction

The reliable differentiation between lymph-node nevus and melanoma metastasis is sometimes difficult. The recommended marker panel for diagnosis of melanoma [S-100 protein, gp100 (HMB45), Melan-A/MART-1 (A103) and Tyrosinase (T311)] is not always useful to reliably discriminate the two lesions [4]. However, this differential diagnosis bears a particular importance in sentinel lymph nodes, as the diagnosis of melanoma metastasis leads to therapeutic lymph-node dissection.

The product of the p16/INK4a/CDKN2/MTS tumour suppressor gene acts as a negative cell cycle regulator by inhibiting G1 cyclin-dependent kinases, which are phosphorylating the retinoblastoma protein [10, 18]. P16 is inactivated or lost in a wide range of human malignancies [15], including familial melanoma [3]. In sporadic melanoma, the results are still not conclusive [7, 8]. Loss or inactivation of the p16 gene has been shown to be associated with the progression of melanoma and other tumours [9, 16].

The goal of this study was to test the p16 as a marker to discriminate nodal nevi from melanoma metastases. We investigated dermal and nodal nevi, melanoma metastases of lymph nodes and other organs for loss of p16 expression, using immunohistochemistry.

D. Mihic-Probst · P. Saremaslani · P. U. Heitz
Department of Pathology, University Hospital, Zürich

P. Komminoth
Institute of Pathology, Cantonal Hospital, Baden, Switzerland

D. Mihic-Probst (✉)
Department of Pathology, University Hospital,
Schmelzbergstrasse 12, 8091 Zürich, Switzerland
e-mail: daniela.mihic@pty.usz.ch
Tel.: +41-1-2552595
Fax: +41-1-2554440

Materials and methods

Tissue samples

Formaldehyde-fixed and paraffin-embedded tissue specimens from the archives of the Department of Pathology, University of Zürich and of the Institute of Pathology, Kantonsspital Aarau (one sample) were investigated. Tested for the presence of p16 product were 18 nodal nevi of 13 patients, 26 sentinel lymph-node metastases of 19 melanoma patients, 10 non-sentinel lymph-node melanoma metastases of 10 patients and 13 organ metastases of melanoma of 12 patients. As lymph-node nevi are relatively uncommon [1, 17], and in this study most of them were from melanoma patients, we additionally tested 15 skin nevi (9 dermal, 5 compound and 1 junctional) of 9 patients. Haematoxylin and eosin-stained sections of all samples were reviewed by one pathologist (D.M.). For clinical data, see Table 1, Table 2 and Table 3.

Immunohistochemistry

A monoclonal primary antibody directed against an epitope of p16 (Neomarkers, Freemont, CA, USA) was used. The epitope of Ab-4 maps among amino acids 1–32 of the p16/INK4a protein.

Two-micron-thick sections of paraffin-embedded tissue were collected onto Superfrost Plus slides (Menzel Gläser, Germany) and dewaxed in graded alcohols. Non-specific peroxidase activity was

Table 1 Lymph-node nevi. *Nuc* nuclear staining, *CS* cytoplasmic without nuclear staining, *NP* no proliferation

Patient no.	Age (years)/sex	Site of node	Primary tumor	Operation	Size (mm)	S-100 P	HMB 45	P16 Nuc	P16 CS	MIB-1
1	49/Female	Axilla	Melanoma	Node dissection	7	4+	0	4+	4+	NP
2	67/Male	Neck	Melanoma	Node dissection	0.5	4+	0	4+	4+	*
3	30/Female	Axilla	Melanoma	Sentinel node	0.4	4+	0	3+	3+	NP
4	57/Female	Inguina	Melanoma	Sentinel node	0.5	4+	0	4+	4+	NP
5	66/Male	Axilla	Melanoma	Sentinel node	2.5	4+	0	3+	3+	<0.2%
6a	61/Male	Inguina	Melanoma	Sentinel node	5	4+	0	3+	3+	<0.3%
b		Inguina		Sentinel node	3	4+	0	4+	4+	<0.3%
c		Inguina		Node dissection	0.5	4+	0	3+	3+	NP
d		Inguina		Node dissection	2	4+	0	3+	3+	<0.3%
7a	63/Male	Axilla	Melanoma	Sentinel node	0.5	4+	0	4+	4+	NP
b		Axilla		Sentinel node	0.3	4+	0	4+	4+	NP
8	67/Female	Inguina	No	Femoral hernia	0.8	4+	0	3+	3+	<0.2%
9a	66/Female	Axilla	Breast cancer	Node dissection	20	4+	0	4+	4+	NP
b		Axilla		Node dissection	2.5	4+	0	4+	4+	NP
10	20/Male	Inguina	Melanoma	Sentinel node	0.1	4+	0	4+	4+	NP
11	50/Female	Axilla	Melanoma	Sentinel node	2.5	4+	0	4+	4+	NP
12	61/Male	Axilla	Melanoma	Sentinel node	0.2	4+	0	4+	4+	NP
13	60/Male	Neck	Melanoma	Sentinel node	0.2	4+	0	4+	4+	NP

* On additional serial sections the lesion was no longer present

Table 2 Sentinel lymph-node metastases. *Nuc* nuclear staining, *CS* cytoplasmic without nuclear staining, *NP* no proliferation

Patient no.	Age (years)/sex	Site of node	Size (mm)	S-100 P	HMB 45	P16 Nuc	P16 CS	MIB-1
1	57/Male	Axilla	2.5	4+	0	0	0	*
2	50/Male	Infraclavicular	0.5	4+	4+	0	0	*
3	62/Male	Ocipital	1	4+	4+	0	0	25–50%
4	68/Male	Axilla	0.7	4+	0	0	0	10–25%
5a	64/Male	Axilla	1.4	4+	1+	0	3+	10–25%
b		Axilla	1.3	4+	2+	0	2+	10–25%
6	61/Male	Ocipital	2.5	4+	2+	0	2+	6%
7	48/Female	Axilla	1	4+	4+	0	0	25–50%
8	59/Male	Inguina	8	4+	4+	0	3+	25–50%
9	58/Male	Inguina	0.6	4+	2+	0	0	10–25%
10a	68/Male	Inguina	0.2	4+	4+	0	0	4%
b		Inguina	1	4+	4+	0	3+	25–50%
11a	64/Male	Ellbow	1	4+	0	0	0	10–25%
b		Axilla	0.6	4+	1+	0	0	10–25%
12a	74/Female	Inguina	0.8	4+	1+	0	0	10–25%
b		Inguina	0.4	4+	0	0	0	3%
13	63/Female	Inguina	2	4+	4+	0	0	10–25%
14	60/Male	Inguina	1	4+	0	0	0	NP
15	22/Female	Inguina	1.2	4+	2+	0	1+	*
16	59/Male	Axilla	3.5	4+	3+	0	0	10–25%
17a	19/Female	Ocipital	0.5	4+	0	0	0	4%
b		Ocipital	0.8	4+	0	0	0	5%
18	61/Male	Inguina	0.7	4+	0	0	0	10–25%
19a	71/Male	Axilla	0.7	4+	1+	0	0	10–25%
b		Axilla	0.2	4+	1+	0	0	10–25%
c		Axilla	0.1	4+	1+	0	0	10–25%

* On additional serial sections the lesion was no longer present

blocked with 3% hydrogen peroxide in phosphate buffer saline for 10 min. Microwave pre-treatment was performed for 10 min in 0.01 mol/l tri-natrium citrate puffer at pH 6.3. The sections were incubated with p16 antibody (Clone 16P04; Neomarkers, Freemont, CA, USA) at an antibody concentration of 40 μg/ml at room temperature for 2 h. P16 detection was performed with "Elite" universal detection kit (Vector, Peterborough, UK) and colour was developed using diaminobenzidine. A dermal nevus, an oligoastrocytoma (G2, World Health Organization) and endocrine cells of the pancreas were used as positive controls. Negative controls were performed by replacing the specific antiserum with pure Tris saline.

We differentiated nuclear and cytoplasmic staining from exclusive cytoplasmic staining. The extent of each staining was recorded according to the following system: 0=no staining; 1+=<25% of cells positive; 2+=25–49% of cells positive; 3+=50–74% of cells positive; 4+=>75% cells positive.

For Ki-67, HMB45 and S-100 protein, immunohistochemistry was performed on paraffin sections of formalin-fixed tissues, using a Ventana Benchmark automated staining system (Ventana Medical Systems, Tucson, Arizona). For antigen retrieval, slides were heated with cell conditioner 1 (mild protocol). Primary antibodies (all from DakoCytomation, Glostrup, Denmark) against the following antigens were applied: Ki-67 proliferation antigen (clone

Table 3 Melanoma metastases: node dissection and organ metastasis. *Nuc* nuclear staining, *CS* cytoplasmic without nuclear staining

Patient no.	Age (years)/sex	Site	S-100 P	HMB 45	P 16 Nuc	P16 CS	MIB-1
1	77/Male	Neck*	4+	0	0	4+	10–25%
2	54/Female	Infraclavicular*	4+	2+	0	0	5%
3	78/Male	Inguinal*	4+	1+	0	0	25–50%
4	40/Male	Neck*	4+	0	0	4+	25–50%
5	59/Female	Neck*	4+	4+	0	0	25–50%
6	75/Male	Axilla*	4+	3+	0	0	10–25%
7	47/Female	Axilla*	4+	3+	0	0	8%
8	73/Male	Axilla*	4+	0	0	3+	25–50%
9	36/Male	Axilla*	4+	1+	0	0	25–50%
10	56/Female	Retroauricular*	4+	2+	0	0	10–25%
11	30/Female	Liver	4+	2+	0	1+	10–25%
12	67/Male	Skin (thorax)	3+	3+	0	0	10–25%
13	47/Male	Subcutis (face)	4+	0	0	0	10–25%
14	59/Male	Small bowel	4+	1+	0	4+	10–25%
15	69/Male	Skin (inguina)	4+	4+	1+	3+	25–50%
16	60/Male	Parotid gland	4+	0	0	0	10–25%
17	59/Male	Soft tissue axilla	4+	1+	0	0	25–50%
18	58/Male	Soft tissue axilla	4+	1+	0	0	10–25%
		Soft tissue axilla	4+	2+	0	0	10–25%
19	56/Male	Skin (thorax)	4+	2+	0	4+	25–50%
20	69/Male	Subcutis (inguina)	4+	4+	0	0	4%
21	47/Female	Soft tissue axilla	4+	4+	0	0	10–25%
22	63/Male	Skin	4+	0	0	0	25–50%

* Node dissection

MIB-1, dilution 1:20), melanosome antigen (clone HMB45, dilution 1:50) and S-100 protein (rabbit affinity purified antibodies, dilution 1:1000). Monoclonal mouse MIB-1 antibodies were detected with the Ventana iVIEW DAB detection kit, yielding a brown reaction product. Monoclonal mouse HMB45 and polyclonal rabbit anti-S-100 antibodies were revealed with the Ventana-Red enhanced detection kit (red reaction product). For HMB45, the signal was enhanced with the Ventana amplification kit. Slides were counterstained with haematoxylin. MIB-1 labelling of lymph-node nevi and melanoma metastases was recorded as the ratio of marked nuclei (cells) of the total number of cells per visual field.

Results

Clinical findings

The clinical findings in 13 patients (20–67 years old) with nodal nevi, 22 patients (30–78 years old) with melanoma metastasis and 19 patients (19–74 years old) with sentinel node melanoma metastasis are listed in Table 1, Table 2 and Table 3. Nine nodal nevi were located in axillary lymph nodes, seven in inguinal nodes and two in neck nodes. Of the patients, 11 had undergone lymph-node biopsies for cutaneous melanoma, 1 patient for breast cancer and 1 for a femoral hernia. In all but one (patient 6) patient with nodal nevi, neither concomitant melanoma metastasis nor clinical signs of metastasis were present (mean clinical follow-up to 2 years). In nine patients (6–68 years old), 9 of 15 skin nevi were dermal, 5 were compound and 1 was junctional.

Histopathology

For a lesion to be accepted as lymph-node nevus, aggregates of cytologically typical melanocytes must be present in the lymph-node capsule and/or fibrous trabeculae. Only three large nodal nevi (patients 6a, b, d) and one small nodal nevus (0.4 mm, patient 3, Fig. 1) did not fulfil these conditions, as they were partially localised within the lymph node and were in direct contact with its parenchyma. The benign nature of these four lesions was confirmed by the presence of cytologically typical melanocytes, a very low (<0.3%) proliferation index in combination with a clear-cut nuclear staining for p16. Patient 6 suffered from an additional sentinel node micrometastasis (registered as patient 18) displaying a different, malignant (atypical) morphology of the melanocytes, a distinctly higher proliferation index (18%) and an absent staining for p16.

The histological findings are illustrated in Fig. 1, Fig. 2, Fig. 3 and Fig. 4 and listed in Table 1, Table 2 and Table 3. The size of nodal nevi (measured as the single greatest dimension) ranged from 0.1 mm to 20 mm with an average of 2.7 mm. Of 18 nodal nevi, 11 were small (maximum 2 mm). The size of melanoma metastasis in sentinel lymph nodes ranged from 0.1 mm to 8 mm with an average of 1.3 mm. The diameter of 21 of 26 sentinel node metastases measured less than 2 mm. Diagnostic difficulties occurred in two lymph-node metastases, as they were partially localised within the capsule and were almost lacking HMB 45 reactivity (patients 5a and 12b). Melanoma micrometastasis in the lymph-node parenchyma displaying an identical morphology and immunohistochemistry confirmed the metastatic origin of these cells (Fig. 2).

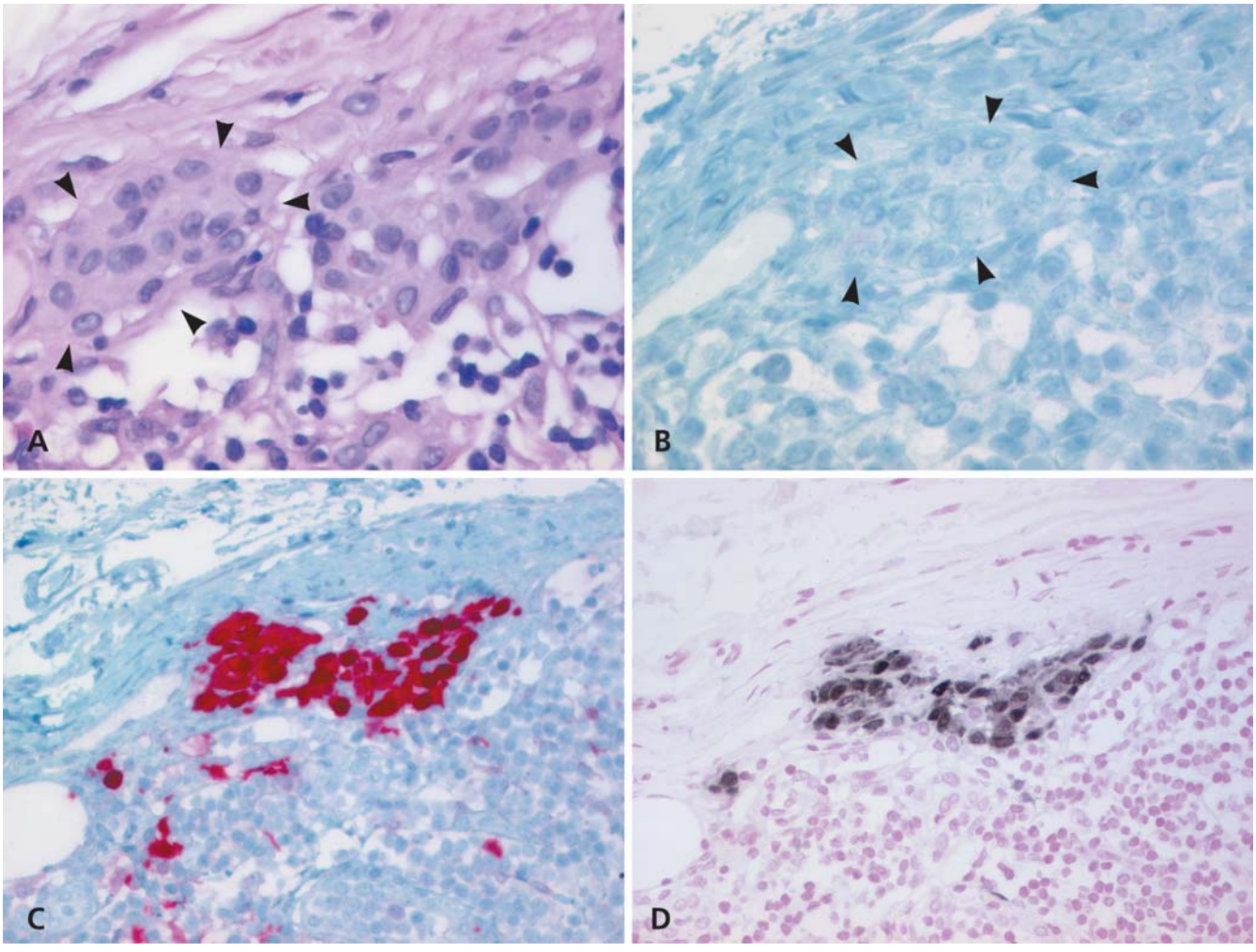

Fig. 1 Nodal nevus (patient 3). **A** Cluster of melanocytes lacking clear-cut atypia but extending into the lymph node parenchyma (haematoxylin-eosin, ×500). **B** Lack of immunostaining for HMB 45 (×500). **C** Immunostaining for S-100 protein (×250). **D** 3+ nuclear and cytoplasmic immunostaining for p16 (×250)

Immunohistochemistry

We found two types of immunoreactions of p16 in melanocytes: nuclear and cytoplasmic staining and diffuse cytoplasmic staining with absence of nuclear staining. All 33 nevi (18 nodal and 15 dermal) displayed an extensive and intense nuclear and cytoplasmic staining, whereas nuclear staining was absent in 48 of 49 melanoma metastases (26 sentinel nodes, 10 non-sentinel nodes and 13 organ metastases) (Fig. 3). Only one inguinal skin metastasis displayed a focal weak (1+) nuclear positivity. In contrast, melanoma metastases in 6 of 26 sentinel nodes, in 3 of 10 non-sentinel nodes and in 4 of 13 organ metastases displayed an exclusive cytoplasmic staining (Fig. 3).

Controls

All positive controls displayed an extensive and intense 4+ positive combined nuclear and cytoplasmic staining. All negative controls lacked cells displaying an immunoreaction. Except for one sentinel node metastasis, all melanoma metastases displayed an elevated proliferative index as shown by MIB-1 staining. Of melanoma metastases, 8 showed an index in less than 10% of melanoma cells; the index was 10–25% in 24 melanoma metastases, and 25–50% in 13 melanoma metastases. Of lymph-node nevi, 12 showed no proliferation while 5 showed a proliferative index of less than 0.3%. Three sentinel-node metastases and one lymph-node nevus could not be stained with Ki-67 because the lesion was not present in additional serial sections. The detailed results of immunohistochemical staining for p16 and Ki-67 are shown in Table 1, Table 2 and Table 3.

Discussion

The differential diagnosis of lymph-node nevus and melanoma metastasis becomes increasingly important in the investigation of sentinel lymph nodes. It is, however,

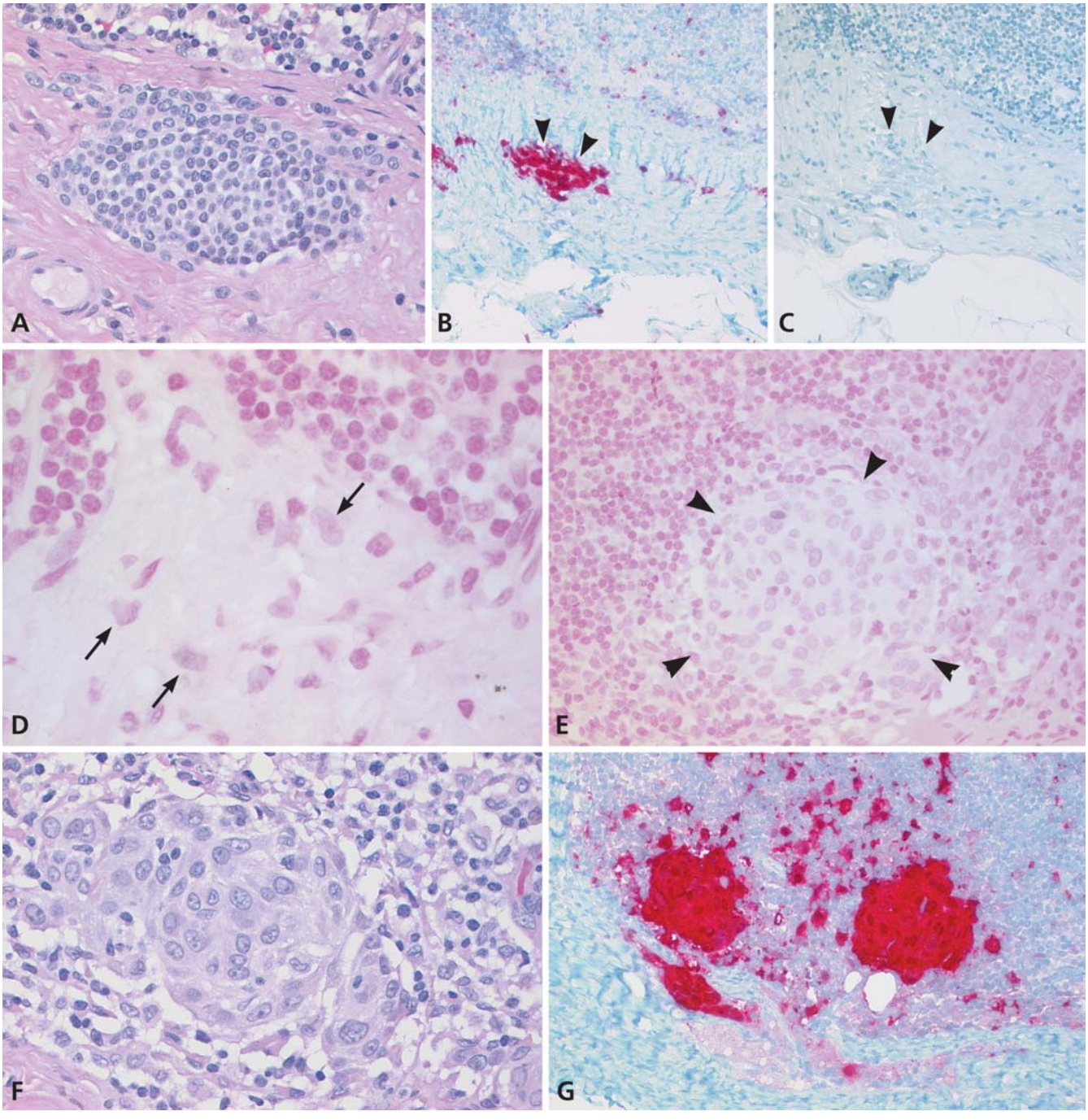

Fig. 2 Melanoma metastasis in a sentinel-node biopsy (patient, 12b). **A** A small number of melanoma cells are confined to the lymphatic space within the capsule and are not markedly atypical (haematoxylin-eosin, ×300). **B** S-100 protein immunostaining (×125). The melanoma cells are negative for HMB 45 (×125; **C**) and p16 (×500; **D**). **E** A micrometastasis with identical morphology in the parenchyma of the same lymph node confirms the diagnosis of the presence of melanoma cells within the capsule. Lack of immunostaining for p16 (×250). **F** Haematoxylin-eosin (×320). **G** Immunostaining for S-100 protein (×150)

difficult to reliably distinguish lymph-node nevi from metastases of melanoma using conventional histology. This difficulty is partly due to the nevoid pattern of some melanoma metastases, which may be devoid of clear-cut atypical cells (Fig. 2) [5, 11, 12, 19, 21]. Even upon comparing the primary with its metastasi(e)s, it is sometimes less than obvious that the lymph-node lesion represents a metastasis. The localisation within the lymph-node capsule is an important diagnostic criterion for the diagnosis of nodal nevi [2, 14]. However, this criterion proves not to be entirely reliable, as melanoma metastases are sometimes confined to the lymphatic space adjacent to the lymph-node capsule (Fig. 2) and nodal nevi may show parenchymal involvement [20]. The demonstration of the expression of HMB 45 may be helpful, although not entirely reliable, as a loss of HMB

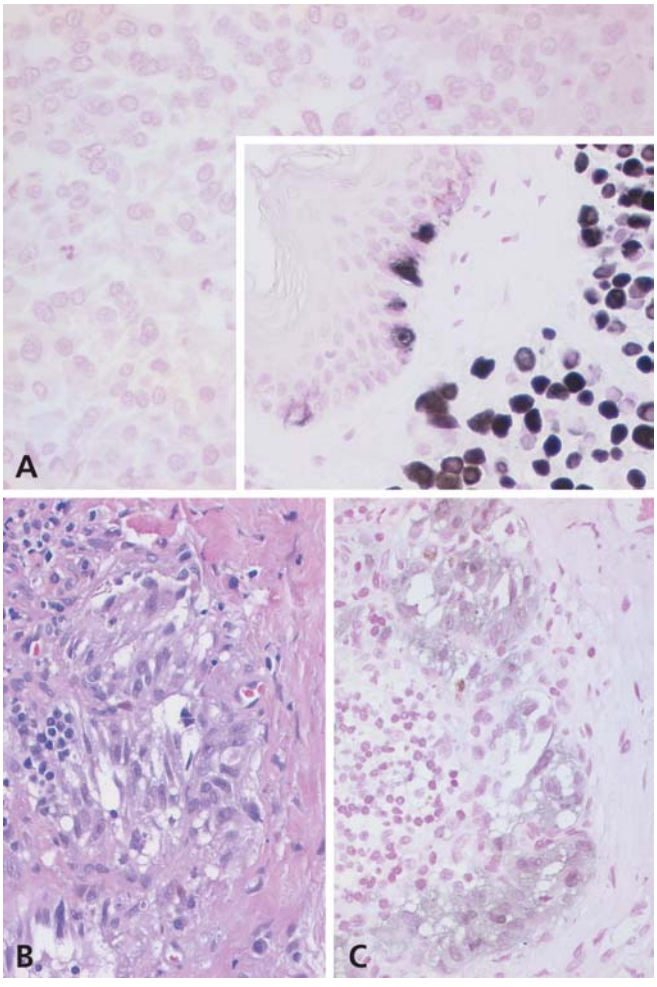

Fig. 3 Soft tissue metastasis of the axilla (patient 17, **A**) and inguinal sentinel lymph-node metastasis (patient 8, **B** and **C**). **A** Lack of immunostaining for p16 (×250). Dermal nevus with 4+ nuclear and cytoplasmic immunostaining for p16 as positive control (*inset*, ×200). **B** Haematoxylin-eosin (×200). **C** Weak cytoplasmic staining in absence of nuclear immunostaining for p16 (×200)

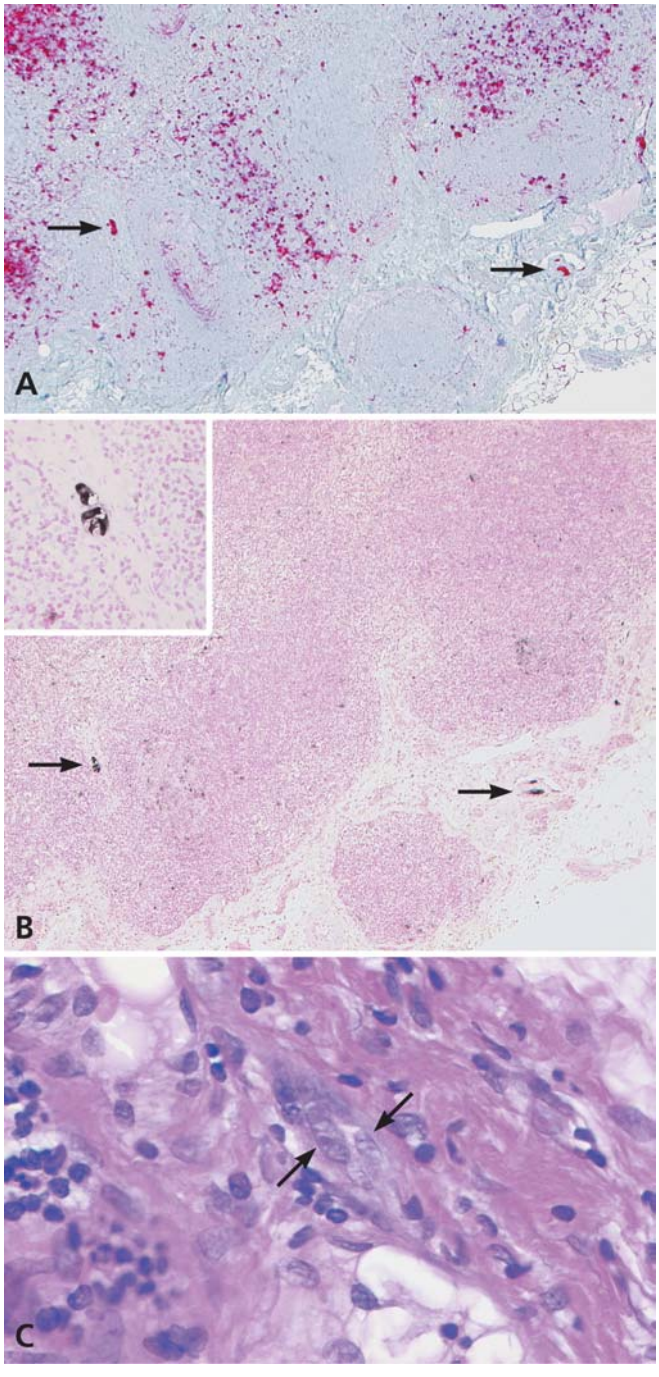

Fig. 4 Histology of a small cluster of intracapsular melanocytes. **A** Melanocytes are masked by S-100 protein-immunostained dendritic cells (×35). **B** Some intracapsular melanocytes detected with 4+ nuclear and cytoplasmic immunostaining for p16, ×35 (*inset*, ×250). **C** Haematoxylin-eosin (×400)

45 expression is reported in at least 20% of melanoma metastases [4].

We demonstrated a clear-cut difference in the staining pattern of p16 between lymph-node nevi and melanoma metastases. Using immunohistochemistry, we found nuclear and cytoplasmic p16 staining in all nevi, independent of their localisation (dermal or lymph node). Furthermore, we have demonstrated the absence of nuclear staining in 48 melanoma metastases, except for 1 skin metastasis, which displayed a weak nuclear immunoreaction. However, a diffuse cytoplasmic staining in the absence of nuclear staining was present in 13 of 49 melanoma metastases.

P16 immunohistochemistry often revealed a larger extent of nodal nevi in comparison with tinctorial staining. Sometimes small melanocyte groups are present within the lymph-node capsule. They may, therefore, be difficult to recognise, even upon using S-100 protein immunohistochemistry, because—depending on the antibody used—they may be masked by dendritic cells (Fig. 4). Nodal nevi were reported to occur from less than 1% of axillary nodes dissected for mammary carcinoma [1, 17] up to 3.9% in sentinel lymph nodes of various localisations of patients suffering from cutaneous melanoma [2]. Due to the aforementioned diagnostic difficul-

Table 4 Immunohistochemical findings in lymph-node nevi and melanoma metastases. + positive, −negative, *(+)* rarely positive, *(−)* rarely negative, *((+))* very rarely positive, *((−))* very rarely negative, *+/−* positive or negative, *Nuc* nuclear staining, *CS* cytoplasmic without nuclear staining, *NP* no proliferation

	P16 Nuc	P16 CS	HMB45	Melan A	Tyrosinasee	S-100 P	MIB-1
Lymph-node nevi	+	+	−/(+)	+/−	+/−	+	NP or <0.3%
Melanoma metastases	−/((+))	−/(+)	+/−	+/−	+/−	+/((−))	10% or more*

* Rarely no proliferation or less than 10%

ties, the real incidence of nodal nevi might be higher than hitherto reported.

In some larger nevi, we found p16-positive cells displaying co-expression of S-100 protein in the lymph-node parenchyma. We, therefore, assume these cells to be melanocytes. This finding adds support to the hypothesis of the embolic origin of lymph-node nevi [2], which was put forward in previous reports in which melanocytes have been demonstrated to occur in the sinus of lymph nodes [20]. A recent study [6] has noted a strong association between nodal and cutaneous nevi.

A recent report showed that lack of MIB-1 staining or a labelling index below 1% strongly favours nevus versus melanoma metastasis [13]. This is consistent with our assessment of the proliferation index in nevi and melanoma metastases. Unfortunately it may prove difficult or impossible to precisely define a labelling index in very small lesions.

We consider immunostaining for p16 an important additional marker to differentiate nodal nevi from melanoma metastases and, therefore, recommend its use (Table 4).

Acknowledgements We thank N. Wey for photographic and computer-assisted reproductions and Dr. W. Jochum, Department of Pathology, University Hospital Zürich, for critical reading of the manuscript.

References

1. Andreola S, Clemente C (1985) Nevus cells in axillary lymphnodes from radical mastectomy specimens. Pathol Res Pract 179:616–618
2. Carson KF, Wen DR, Li PX, Lana AM, Bailly C, Morton DL, Cochran AJ (1996) Nodal nevi and cutaneous melanomas. Am J Surg Pathol 20:834–840
3. Castellano M, Pollock PM, Walters MK, Sparrow LE, Down LM, Gabrielle BG, Parson PG, Hayward NK (1997) CDKN2A/p16 is inactivated in most melanoma cell lines. Cancer Res 57:4868–4875
4. de Vries TJ, Smeets M, de Graaf R, Hou-Jensen K, Brocker EB, Renar N, Eggermont AM, van Muijen GN, Ruiter D (2001) Expression of gp100, MART-1, tyrosinase, and S100 in paraffin-embedded primary melanomas and locoregional, lymph node, and visceral metastases: implications for diagnosis and immunotherapy. A study conducted by the EORTC Melanoma Cooperative Group. J Pathol 193:13–20
5. Fisher CJ, Hill S, Millis RR (1994) Benign lymph node inclusions mimicking metastatic carcinoma. J Clin Pathol 47:245–247
6. Fontaine D, Parkhill W, Greer W, Walsh N (2002) Nevus cells in lymph nodes: an association with congenital cutaneous nevi. Am J Dermatopathol 24:1–5
7. Fujimoto A, Morita R, Hatta N, Takehara K, Takata M (1999) p16INK4a inactivation is not frequent in uncultured sporadic primary cutaneous melanoma. Oncogene 18:2527–2532
8. Funk JO, Schiller PI, Barret MT, Wong DJ, Kind P, Sander CA (1998) p16INK4a expression is frequently decreased and associated with 9p21 loss of heterozygosity in sporadic melanoma. J Cutan Pathol 25:291–296
9. Hilton DA, Penney M, Evans B, Sanders H, Love S (2002) Evaluation of molecular markers in low-grade diffuse astrocytomas: loss of p16 and retinoblastoma protein expression is associated with short survival. Am J Surg Pathol 26:472–478
10. Kamb A, Grius NA, Weaver-Feldhaus J, Liu Q, Harshman K, Tavtigian SV, Stockert E, Day RS 3rd, Johnson BE, Skolnick MH (1994) A cell cycle regulator potentially involved in genesis of many tumor types. Science 264:436–440
11. Kossard S, Wilkinson B (1997) Small cell (naevoid) melanoma: a clinicopathologic study of 131 cases. Australas J Dermatol 38[Suppl 1]:S54–S58
12. Lambert WC, Brodkin RH (1984) Nodal and subcutaneous cellular blue nevi. A pseudometastasizing pseudomelanoma. Arch Dermatol 120:367–370
13. Lohmann CM, Iversen K, Jungbluth AA, Berwick M, Busam KJ (2002) Expression of melanocyte differentiation antigens and ki-67 in nodal nevi and comparison of ki-67 expression with metastatic melanoma. Am J Surg Pathol 26:1351–1357
14. McCarthy SW, Palmer AA, Bale PM, Hirst E (1974) Naevus cells in lymph nodes. Pathology 6:351–358
15. Nobori T, Miura K, Wu DJ, Lois A, Takabayashi K, Carson DA (1994) Deletions of the cyclin-dependent kinase-4 inhibitor gene in multiple human cancers. Nature 368:753–756
16. Reed JA, Loganzo F Jr, Shea CR, Waker GJ, Flores FJ, Glendening JM, Bogdany JK, Shiel MJ, Haluska FG, Fountain JW (1995) Loss of expression of the p16/cyclin-dependent kinase inhibitor 2 tumor suppressor gene in melanocytic lesions correlates with invasive stage of tumor progression. Cancer Res 55:2713–2718
17. Ridolfi RL, Rosen PP, Thaler H (1977) Nevus cell aggregates associated with lymph nodes: estimated frequency and clinical significance. Cancer 39:164–171
18. Serrano M, Hannon GJ, Beach D (1993) A new regulatory motif in cell-cycle control causing specific inhibition of cyclin D/CDK4. Nature 366:704–707
19. Sterchi JM, Muss HB, Weidner N (1987) Cellular blue nevus simulating metastatic melanoma: report of an unusually large lesion associated with nevus-cell aggregates in regional lymph nodes. J Surg Oncol 36:71–75
20. Subramony C, Lewin JR (1985) Nevus cells within lymph nodes. Possible metastases from a benign intradermal nevus. Am J Clin Pathol 84:220–223
21. Zembowicz A, McCusker M, Chiarelli C, Dei Tos AP, Granter SR, Calonje E, McKee PH (2001) Morphological analysis of nevoid melanoma: a study of 20 cases with a review of the literature. Am J Dermatopathol 23:167–175

Virchows Arch (2003) 443:752–760
DOI 10.1007/s00428-003-0899-7

ORIGINAL ARTICLE

Isamu Hayashi · Hitoshi Tsuda · Tadakazu Shimoda · Arafumi Maeshima · Takahiro Kasamatsu · Takuro Yamada · Ryuichiro Tsunematsu

Difference in cytoplasmic localization pattern of neutral mucin among lobular endocervical glandular hyperplasia, adenoma malignum, and common adenocarcinoma of the uterine cervix

Received: 16 June 2003 / Accepted: 26 August 2003 / Published online: 11 October 2003
© Springer-Verlag 2003

Abstract To investigate whether the cytoplasmic localization pattern of neutral mucin differs between lobular endocervical glandular hyperplasia (LEGH) and cervical adenocarcinoma (CxAd), including minimal-deviation adenocarcinoma (MDA), or adenoma malignum, alcian blue (pH 2.5)/periodic acid-Schiff (AB-PAS) staining was performed to formalin-fixed paraffin-embedded tissue sections of 13 lesions of LEGH and 53 tumors of CxAd, including 6 tumors of MDA. The cytoplasmic localization of neutral mucin was classified as a "whole cytoplasmic pattern," in which neutral mucin filled the cytoplasm entirely, or as an "apical pattern," in which neutral mucin was localized in the subsurface area only. Cytoplasmic neutral mucin patterns were detected in all 13 cases of LEGH and in 19 cases (36%) of CxAd, including five cases of MDA. The localization of neutral mucin was always the whole cytoplasmic pattern in 13 cases of LEGH, but was the apical pattern in these 19 cases of CxAd. The other 34 cases of CxAd, including 1 case of MDA, corresponded to the acid mucin pattern stained purple or blue or no staining pattern by AB-PAS. Among the 53 cases of CxAd, the apical neutral mucin pattern was an indicator of poorer patient prognosis by univariate and multivariate analyses. The examination of cytoplasmic localization of neutral mucin might be applicable, not only to differential diagnosis between LEGH and CxAd, including MDA, but also to estimate clinical aggressiveness of CxAd.

Keywords Lobular endocervical glandular hyperplasia · Minimal deviation adenocarcinoma (adenoma malignum) · Adenocarcinoma of uterine cervix · Alcian blue-PAS stain

I. Hayashi · T. Shimoda
Department of Clinical Laboratory,
National Cancer Center Hospital,
5-1-1 Tsukiji, Chuo-ku, 104-0045 Tokyo, Japan

H. Tsuda
Department of Pathology II,
National Defense Medical College,
3-2 Namiki, Tokorozawa, 359-8513 Saitama, Japan

A. Maeshima
Pathology Division, National Cancer Center Research Institute,
5-1-1 Tsukiji, Chuo-ku, 104-0045 Tokyo, Japan

T. Kasamatsu · T. Yamada · R. Tsunematsu
Department of Gynecological Oncology,
National Cancer Center Hospital,
5-1-1 Tsukiji, Chuo-ku, 104-0045 Tokyo, Japan

I. Hayashi (✉)
Pathology Division, Shizuoka Cancer Center,
1007 Shimo-Nagakubo, Nagaizumi-cho, 411–8777 Shizuoka,
Suntou-gun, Japan
e-mail: i.hayashi@scchr.jp

Introduction

It is an important diagnostic issue to differentiate adenocarcinoma of the uterine cervix (CxAd) preoperatively or postoperatively from benign hyperplastic lesions, e.g., lobular endocervical glandular hyperplasia (LEGH) or pyloric metaplasia of the endocervical gland. In particular, minimal deviation adenocarcinoma (MDA) or adenoma malignum, a variant of CxAd, is histologically very similar to normal endocervical glands or LEGH and is frequently difficult to diagnose preoperatively [3, 9, 11, 12, 17]. Using conventional alcian blue (pH 2.5)/periodic acid-Schiff (AB-PAS) staining, we previously found that mucin secreted from normal endocervical glands contains both acid and neutral mucin, but mucin secreted by the cells of MDA is composed primarily of neutral mucin [6]. In addition, cervical glandular cells in the lesions of LEGH are also stained red by AB-PAS [5]. Therefore, at present, it is often very difficult to differentiate lethal MDA from LEGH pre- or postoperatively by clinical and pathological features or by AB-PAS staining.

When we scrutinized the distribution of neutral mucin in tumor cell cytoplasm, different patterns were observed in its cytoplasmic localization among tumors. Neutral

mucin filled the cytoplasm entirely in most of the LEGHs, but tended to be localized in the apical or subsurface areas in some CxAd, including MDA. Under the hypothesis that the localization pattern of neutral mucin might be diagnostically meaningful, we examined whether it was possible to differentiate between LEGH and potentially lethal CxAd, including MDA, by the mucin localization pattern.

Materials and methods

Patients and diagnostic criteria

We selected 13 cases of LEGH and 53 cases of CxAd of the uterine cervix, including 6 cases of MDA, for this study. Of patients, 60 received surgical therapy at the National Cancer Center Hospital, Tokyo, 2 at the Gunma University Hospital, Maebashi, 2 at the Keio University Hospital, Tokyo, and 2 at the Tohoku University Hospital, Sendai, Japan.

LEGH was differentiated from MDA according to cellular atypia and the pattern of local growth; in the cells of LEGH, cellular atypia was absent except for a slight enlargement of nuclear size and nucleoli. The LEGH preserves the lobular structure of endocervical glands, extends to the submucosa or myometrium with a pushing pattern, and is mostly localized around the isthmus and high cervix. If the tumor was composed of LEGH only and lacked the glands of adenocarcinoma, the case was diagnosed as LEGH.

We gave the diagnosis of MDA when the tumor was composed of both the LEGH and adenocarcinoma components and when the LEGH component occupied the significant percentage (>33%) of the tumor area. When the tumor was the composite of LEGH and CxAd and the LEGH component occupied $\leq$33% of the tumor area, we classified the tumor as common CxAd. The division between MDA and common CxAd with the LEGH component was performed arbitrarily, as there is no report defining the ratio of area as criteria for the division.

Six tumors were diagnosed as MDA. In three cases of MDA, most of the glands of the tumor were composed of LEGH, but the tumor sparsely contained the glands of adenocarcinoma (Fig. 1). The component of LEGH-looking glands, mixed with the glands of obvious adenocarcinoma, infiltrated into the smooth muscle layer of cervical wall and extended into the lower cervix and portio vaginalis. Three cases of MDA were composed of two distinct parts, LEGH and CxAd. In these three, LEGH tended to constitute the superficial part of the tumor, whereas the deeper part tended to be composed of adenocarcinoma. Only the deeper adenocarcinoma part infiltrated into the cervical wall.

The other 47 tumors were diagnosed as common CxAd. Histologically, 28 cases and 12 cases were classified as mucinous type (or endocervical type) and endometrioid type, respectively. Other minor histological types comprised clear-cell type (2 cases), poorly differentiated type with neuroendocrine features (2 cases), adenosquamous carcinoma (2 cases), and unknown subtype (1 case). Of cases, 4 were adenocarcinoma in situ, and among the 43 other tumors, the degree of differentiation was well in 31 cases, moderate in 2 cases, poor in 6 cases, and unknown in 4 cases.

Follow-up data were obtained for 10 cases of LEGH and 52 of CxAd, including 5 cases of MDA. These patients were followed up at 1-month intervals for the first year after surgery and every 3–6 months at the outpatient clinic thereafter. All 10 patients with the LEGH are alive without tumor recurrence, whereas 4 patients with MDA had a recurrence; 2 died from tumor spread, and the other died from gastric cancer. Among the 47 patients with common CxAd, 14 had a recurrence, and 9 died from the spread of CxAd. Follow-up data were not available for the 3 patients with LEGH and 1 patient with MDA.

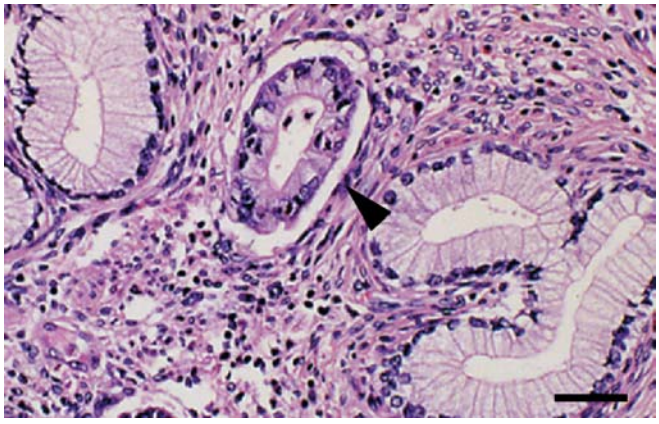

Fig. 1 A typical case of minimal deviation adenocarcinoma, or adenoma malignum. Most of the glands of the tumor were composed of those morphologically identical with lobular endocervical glandular hyperplasia, but the tumor sparsely contained the glands of obvious adenocarcinoma (*arrowheads*). Hematoxylin and eosin staining. *Bar* represents 67 μm

Histochemistry

Routinely processed formalin-fixed paraffin-embedded tissue specimens of these 66 lesions were cut into 2- to 3-μm-thick sections and stained with AB-PAS [14]. AB-PAS stains acid mucin blue by AB and neutral mucin red by PAS. The cases were classified into three groups according to the stain of the mucin in >50% of the tumorous glands: neutral mucin-predominant group stained red, acid mucin-predominant group stained blue or purple, and no staining.

The cytoplasmic localization of neutral mucin was further subclassified as a "whole cytoplasmic pattern," in which neutral mucin filled the cytoplasm entirely, or as an "apical pattern," in which neutral mucin was localized in the subsurface area only. A tumor was classified into the whole cytoplasmic pattern group when 90% or more of the tumorous glands showing a neutral mucin pattern corresponded to the whole cytoplasmic pattern. A tumor was classified into the apical pattern subgroup when 10% or more of the tumorous glands showing the neutral mucin pattern corresponded to the apical neutral mucin pattern, and less than 90% of these glands corresponded to the whole cytoplasmic pattern.

The judgment of AB-PAS stain sections was independently given by two pathologists (HT and AM), and, in cases when there was disagreement, discussions were held as slides were viewed until a consensus was reached.

Immunohistochemistry

The expression of carcinoembryonic antigen (CEA) was examined by means of immunohistochemistry in 33 cases of CxAd, including 5 cases of MDA, and 8 cases of LEGH. Routinely processed formalin-fixed paraffin-embedded tissue specimens were cut into 4-μm-thick sections. The antibody used was monoclonal anti-human-CEA (1:500, Mochida/Takara, Otsu, Japan). Without antigen retrieval, tissue sections were incubated in 0.3% hydrogen peroxide in methanol for 30 min, reacted with the primary antibody overnight at room temperature, incubated for 30 min with biotinylated goat anti-mouse immunoglobulin as a secondary antibody (Vector Laboratories Inc., Burlingame, CA) diluted 1:200, and incubated for 30 min with avidin-biotinyl peroxidase complex using a Vectastain ABC kit (Vector) diluted 1:200. Subsequently, the peroxidase reaction was performed using 3,3′-diaminobenzidine tetrahydrochloride-hydrogen peroxide as a chromogen for 10 min.

The CEA expression level was scored as 1+ if the apical portion of cytoplasm and/or membrane border was weakly to moderately stained and as 2+ if the apical portion of cytoplasm and/or membrane border was strongly stained in 10% or more of the constituent tumorous cells. If no staining was observed, or if staining was observed in less than 10% of constituent tumorous cells, a score of 0 was given. Cases with the score of 1+ or 2+ were judged as CEA positive.

Statistical analysis

The correlation of the mucin localization pattern with a clinical stage, histological type, or differentiation of tumors was examined using the chi-squared test or the Fisher's exact test. Survival curves of patients were drawn with the Kaplan-Meier method [10], and the difference between these curves was analyzed using the log-rank test [16]. Proportional hazards general linear model analysis was performed using a StatView version 5.0 program (SAS Institute Inc., Cary, NC, USA) on a Macintosh personal computer.

Results

In unremarkable cervical glands, the cytoplasm of glandular epithelial cells corresponded to the acid mucin-predominant pattern stained purple by AB-PAS (Fig. 2). In all 13 cases of LEGH, the whole cytoplasmic pattern of neutral mucin localization was observed in the cells of LEGH (Fig. 3 and Fig. 4, Table 1). All ten followed-up patients who had pure LEGH have survived after surgical therapy without recurrence of the lesion.

In the five of six cases of MDA, neutral mucin stained red by PAS showed the apical pattern. In these five, the neutral mucin tended to fill the cytoplasm entirely in the superficial part, but was localized in the apical area in the deeper part of the tumor (Fig. 5). Particularly in the two cases comprising two distinct components of LEGH and adenocarcinoma, the apical pattern of neutral mucin staining was only observed in the adenocarcinoma component. Another case of MDA showed the acid mucin pattern, as the component of LEGH showed the whole cytoplasmic pattern of neutral mucin, but the component of adenocarcinoma (>50% of the tumor area) showed the acid mucin pattern (Table 1). In these six cases, four with the apical neutral mucin pattern had a recurrence, but the one with an acid mucin pattern had no recurrence to the present time.

Of the 47 cases of common CxAd, the neutral mucin pattern stained red was observed in 14 (30%). Of these 14, the neutral mucin localization corresponded to the apical pattern and none to the whole cytoplasmic pattern (Fig. 6).

Of cases of common CxAd, 30 corresponded to the acid mucin-predominant pattern stained blue to purple. Of these, mucin localization had the apical pattern in 16 and a patchy cytoplasmic distribution in 8 cases; in 6 cases, acid mucin was found in the goblet cell component. Three carcinomas showed no AB-PAS staining.

The histological type and the degree of differentiation of common CxAd were significantly correlated with mucin pattern. In 28 cases of mucinous-type adenocarcinoma, 12 (43%) showed the apical neutral mucin pattern, whereas the other 16 (57%) showed the acid mucin pattern. However, other histological types of common CxAd mostly showed the acid mucin pattern or no mucin production: In 12 cases of endometrioid type, only 2 showed the apical neutral mucin pattern, but the other 9 showed the acid mucin pattern, and 1 showed no mucin production. In cases of clear-cell type, 2 revealed the acid mucin pattern, whereas 2 cases of neuroendocrine type showed no mucin production. In common CxAd, cases showing the apical neutral mucin pattern were more frequent in the mucinous type than in the other histological types comprising the endometrioid type, clear-cell type, neuroendocrine type, and others (P=0.034) (Table 1). The common CxAd showing the apical neutral mucin pattern was also more frequent in well-differentiated adenocarcinoma (14 of 31, 45%), excluding adenocarcinoma in situ, than in poorly and moderately differentiated adenocarcinomas (0 of 8, 0%) (P=0.035) (Table 1).

Among the 18 patients with CxAd, including 5 cases of MDA, that showed the apical neutral mucin pattern, 10 (56%) had a recurrence, and 8 (44%) died from cancer spread. However, in 30 patients with CxAd, including 1 case of MDA that showed the acid mucin-predominant

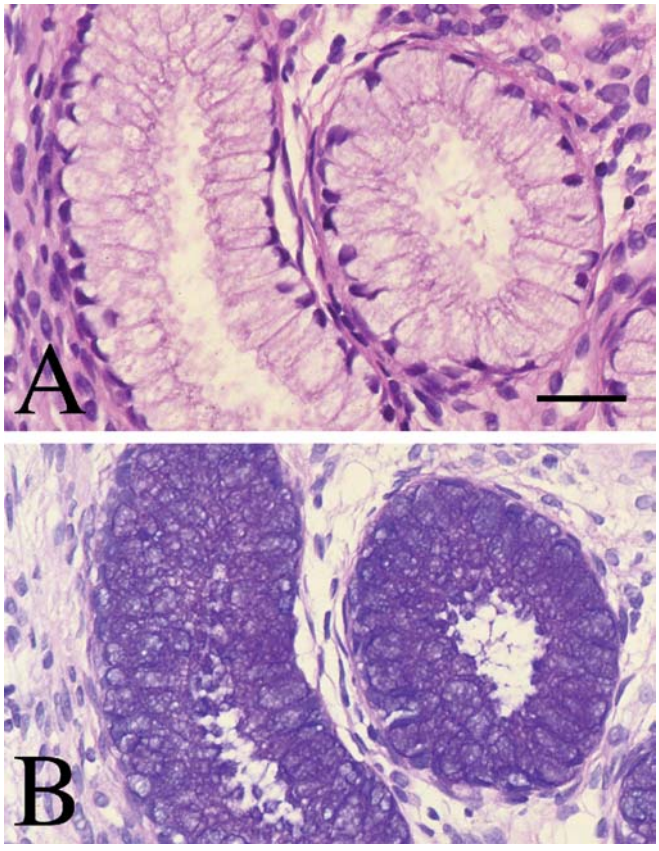

Fig. 2 Unremarkable cervical glands. The cytoplasmic mucin is composed of acid mucin with neutral mucin stained purple. **A** Hematoxylin and eosin staining. **B** Alcian blue/periodic acid-Schiff staining. *Bar* represents 33 μm

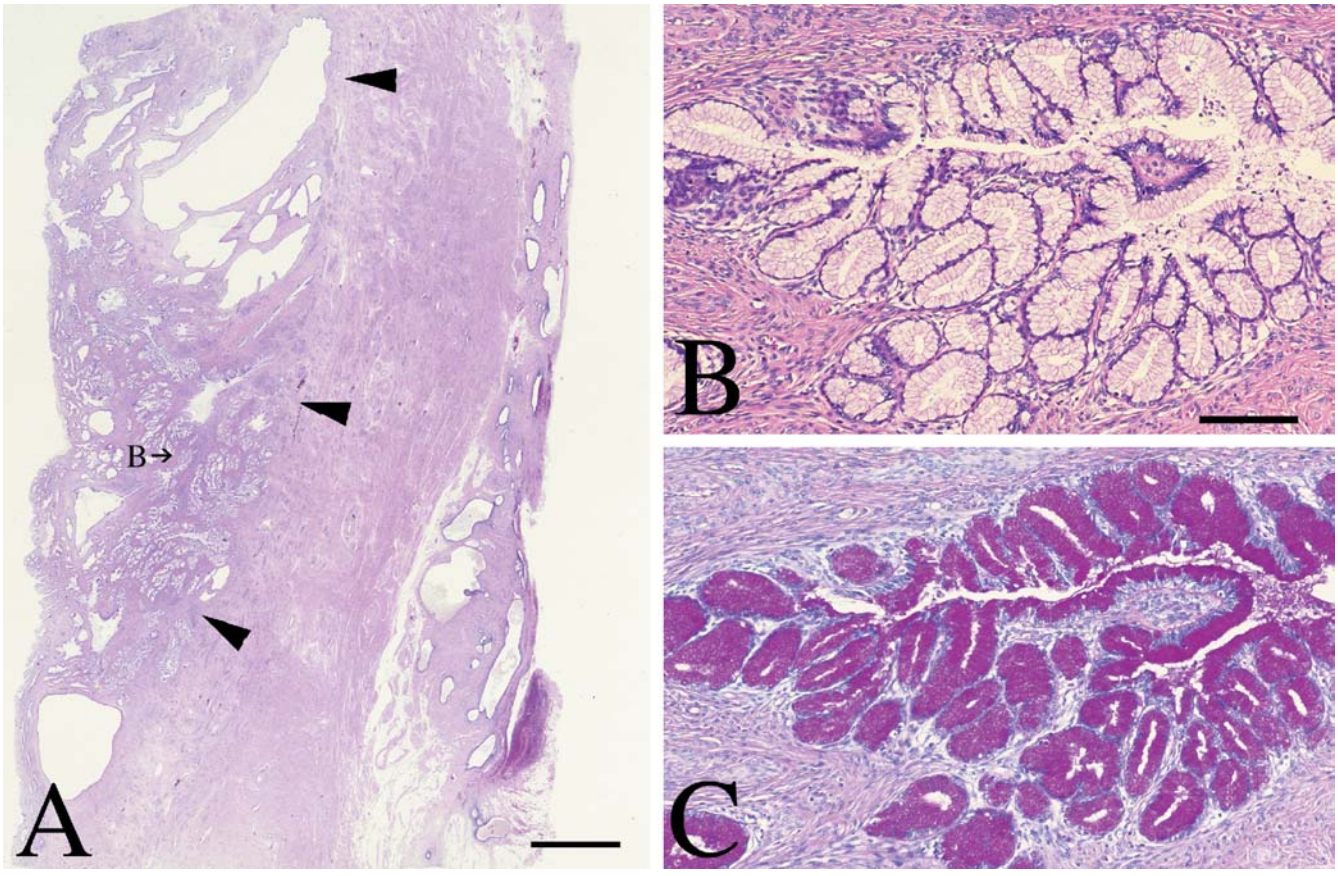

Fig. 3 A case of lobular endocervical glandular hyperplasia. **A** Low magnification view. Tumor cells preserving lobular structure proliferate into the myometrium layer with a pushing pattern. Tumorous tissue is indicated by *arrowheads*. **B**, **C** Higher magnification view. The constituent cells show the whole cytoplasmic pattern of neutral mucin localization. **A**, **B** Hematoxylin and eosin staining. **C** Alcian blue/periodic acid-Schiff staining. *Bar* represents 3.3 mm (**A**) and 133 μm (**B**)

Table 1 The incidence of neutral mucin production and its cytoplasmic localization pattern in lobular endocervical glandular hyperplasia (LEGH), minimal deviation adenocarcinoma (MDA), and common cervical adenocarcinoma

	Number of tumors (%)				
	Total	Neutral mucin pattern		Acid mucin pattern	No mucin
		Apical pattern	Whole cytoplasmic pattern		
I. LEGH	13	0	13	0	0
II. MDA	6	5	0	1	0
III. Common cervical adenocarcinoma	47	14	0	30	3
A. Histological type					
Mucinous	28	12	0	16	0
Endometrioid	12	2	0	9	1
Clear cell	2	0	0	2	0
Neuroendocrine	2	0	0	0	2
Adenosquamous, others	2	0	0	2	0
Unknown	1	0	0	1	0
B. Differentiation					
Well-differentiated	31	14	0	17	0
Moderately differentiated	2	0	0	1	1
Poorly differentiated	6	0	0	5	1
Adenocarcinoma in situ	4	0	0	3	1
Unknown	4	0	0	4	0
Total	66	19	13	31	3

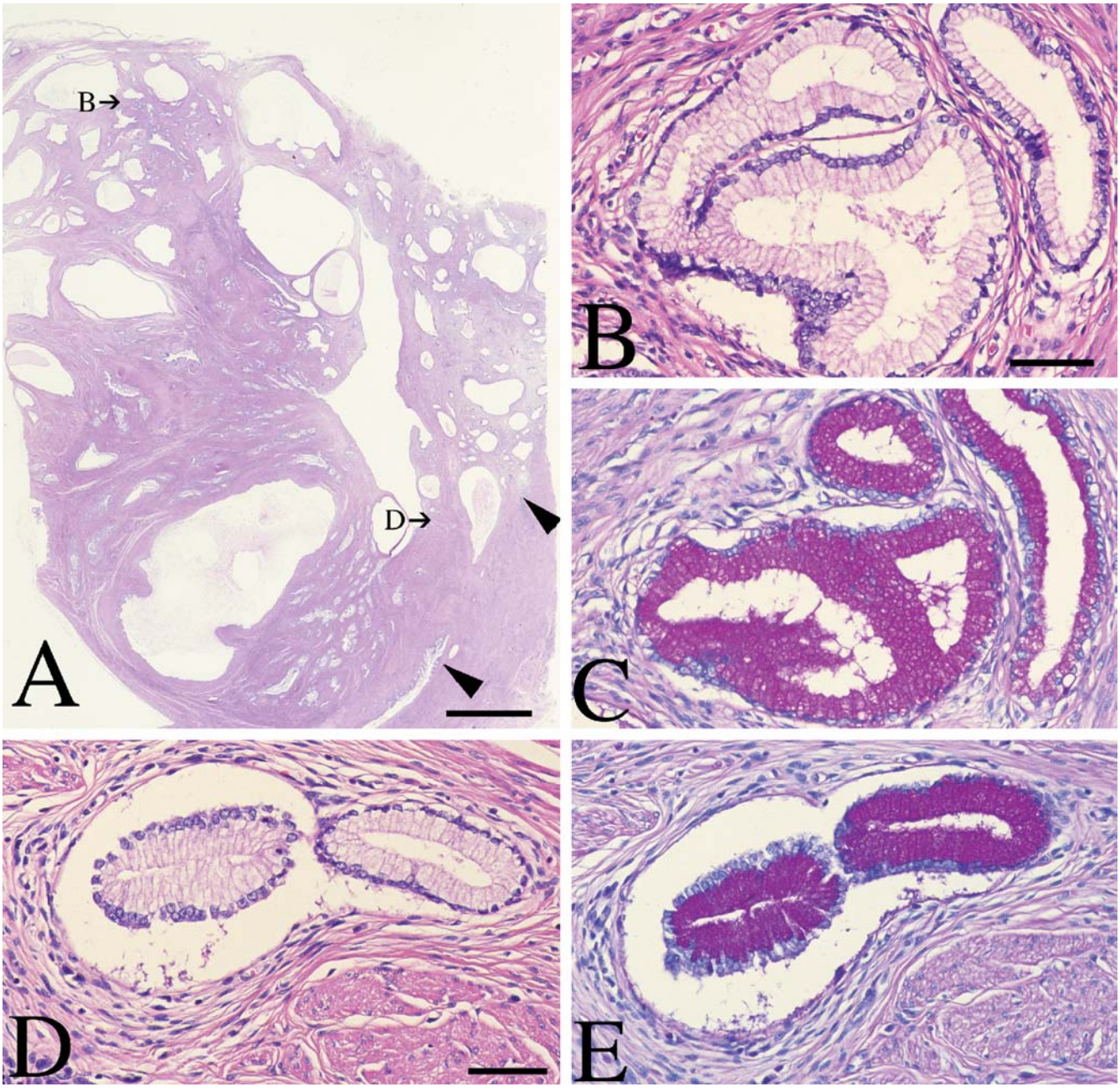

Fig. 4 Another case of lobular endocervical glandular hyperplasia. **A** Low magnification view. Tumorous cells preserving lobular structure proliferate into the myometrial layer with a pushing pattern. Tumor tissue is indicated with arrowheads. **B–E** Higher-magnification view. **B**, **C** In the superficial part, the constituent cells show the whole cytoplasmic pattern of neutral mucin localization. **D**, **E** Deeper part of the tumor showed the same pattern of staining. **A**, **B, D** Hematoxylin and eosin staining. **C**, **E** Alcian blue/periodic acid-Schiff staining. *Bar* represents 3.3 mm (**A**) and 67 μm (**B**, **D**)

pattern or no AB-PAS staining, 6 (20%) had a recurrence, and 3 (10%) died from cancer spread.

Among 52 followed-up cases of CxAd, including MDA, patient prognosis was poorer in the group with the apical neutral mucin pattern (n=18) than in the group with the acid mucin or no-mucin pattern (n=34) for disease-free survival (P=0.0017) and overall survival (P=0.0018) (Fig. 7).

In these cases of CxAd, the proportional hazards general linear model, including cytoplasmic mucin, clinical stage, tumor cell differentiation, the age of patients, and histological type of the tumor disclosed that the former three parameters were independent prognostic factors for disease-free survival of patients (Table 2). No factors showed statistical significance as a prognostic factor for overall survival by the multivariate analysis, probably because of relatively small number of events.

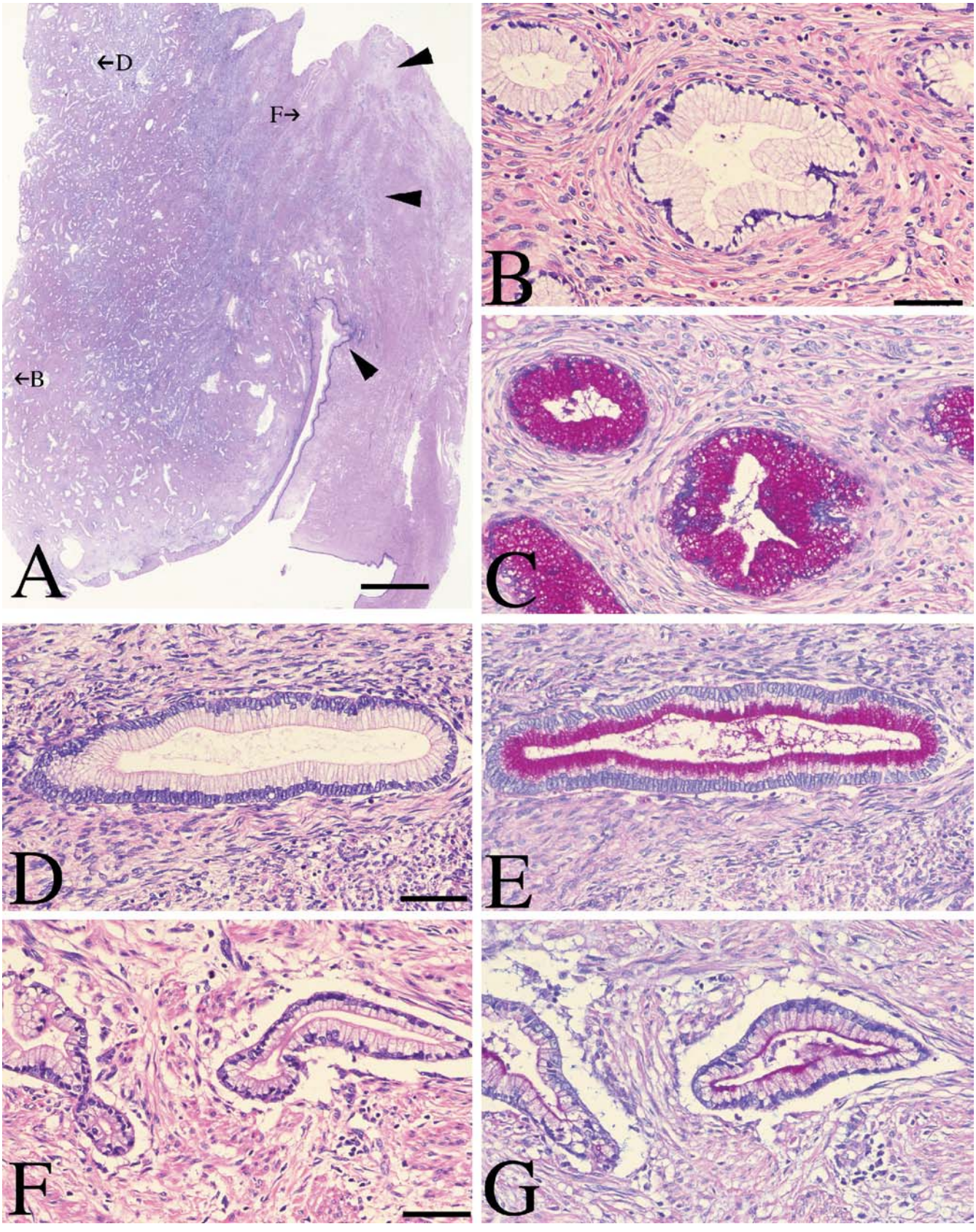

Fig. 5 A case of minimal deviation adenocarcinoma. **A** Low magnification view. Tumor cells diffusely infiltrate into the myometrium layer of the portio vaginalis. Tumor tissue is indicated with arrowheads. Higher-magnification view of superficial part (**B**, **C**), intermediate part (**D**, **E**), and deeper part (**F**, **G**) of the tumor. The tumor cell cytoplasm shows the whole cytoplasmic pattern of neutral mucin localization in the superficial part, whereas neutral mucin is located only in the apical area in the intermediate and deeper parts. **A**, **B**, **D**, **F** Hematoxylin and eosin staining. **C**, **E**, **G**, Alcian blue/periodic acid-Schiff staining. *Bar* represents 3.3 mm (**A**) and 67 μm (**B**, **D**, **F**)

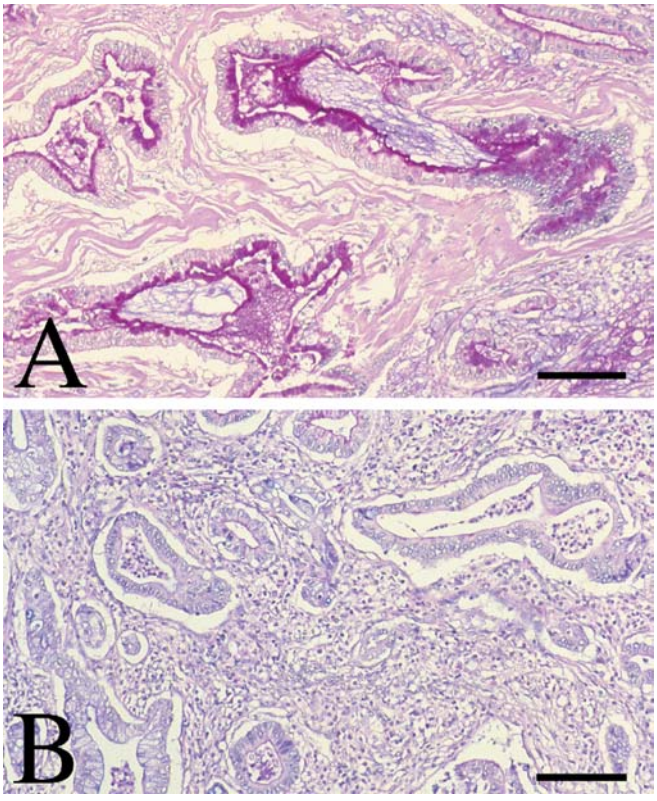

Fig. 6 Sections of two cases of cervical adenocarcinoma of the mucinous (endocervical) type. In both tumors, the cytoplasm shows the apical pattern of neutral mucin localization. **A, B** Alcian blue/periodic acid-Schiff staining. *Bars* represent 133 μm (**A**, **B**)

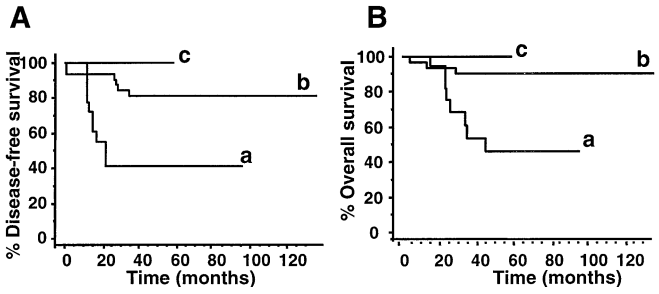

Fig. 7 Survival curves for 52 patients groups with adenocarcinoma of the uterine cervix, including 5 cases of adenoma malignum. Disease-free survival (**A**) and overall survival (**B**). The group with the apical neutral mucin pattern (curve **a**, n=18) shows a poorer clinical outcome than the group with the acid mucin pattern or the no-mucin production pattern (curve **b**, n=34). The group with the apical neutral mucin pattern shows poorer prognosis than other groups for both disease-free survival (P=0.0017) and overall survival (P=0.0018). As reference, a survival curve for 10 patients with lobular endocervical glandular hyperplasia is shown (curve 0)

CEA was judged as negative in all 8 cases of LEGH, although less than 1% of cells showed weak immunostaining of CEA in the membrane border in the 4 cases. CEA was positive in 2 of 5 cases (40%) of MDA and 23 of 28 (82%) cases of common CxAd. In the mucinous type, CEA was positive in all 13 (100%) cases. In the endometrioid type, clear-cell type, and other types, CEA was positive in 100% (8 of 8), 0% (0 of 1), and 0% (0 of 1), respectively. The positive rates of CEA were 91% (20 of 22) in well-differentiated adenocarcinomas except for adenocarcinoma in situ, 0% (0 of 1) of moderately differentiated adenocarcinoma, 100% (1 of 1) of poorly differentiated adenocarcinoma, 100% (2 of 2) cases of adenocarcinoma in situ, and 0% (0 of 2) of unknown cases. CEA was positive in 10 of 13 (77%) CxAd cases that showed the apical neutral mucin pattern, and in 15 of 20 (75%) CxAd cases that showed the acid mucin pattern or no mucin production.

Discussion

Recently, it has been shown that the prognosis for MDA patients as a group is not as poor as previously described [7]. It was also clarified that tumors diagnosed as MDA comprise the component of a benign lesion called LEGH and the component of adenocarcinoma [4, 8, 13, 15]. In the present study, we clarified that LEGH and the component of LEGH in MDA always demonstrated the cytoplasmic neutral mucin. That neutral mucin pattern was also almost always observed in the adenocarcinoma component of MDA and often observed in common CxAd, especially in mucinous-type and/or well-differentiated adenocarcinoma.

Furthermore, the localization pattern of neutral mucin was clearly different between LEGH and the CxAd, including MDA. All of 13 cases of LEGH showed the whole cytoplasmic pattern of neutral mucin localization. However, in five of six cases of MDA, the apical cytoplasmic pattern of neutral mucin was observed in the intermediate and deeper parts of the invasion. Furthermore, in the 14 cases of common CxAd showing the cytoplasmic neutral mucin, its localization pattern was always apical.

Table 2 Proportional hazards general linear model analysis of prognostic factors on disease-free survival of patients with cervical adenocarcinoma, including minimal deviation adenocarcinoma (n=49). *w/d* well differentiated, *m/d* moderately differentiated, *p/d* poorly differentiated, *AIS* adenocarcinoma in situ

Parameter	Hazard ratio (95% confidence interval)	P value
Cytoplasmic mucin pattern (apical neutral versus others)	12.5 (1.4–110.6)	0.02
Differentiation (p/d, m/d, versus w/d, AIS)	9.40 (1.0–86.9)	0.04
Clinical stage (II–IV versus 0–I)	3.03 (0.9–9.5)	0.05
Histological type (mucinous type versus others)	1.44 (0.4–5.9)	0.60
Age of patients ($\leq$60 versus >60)	0.93 (0.2–4.4)	0.92

The present results suggested that the cytoplasmic localization pattern of neutral mucin might be applicable to postoperative differential diagnosis of cervical glandular lesions. Many pathologists would have difficulty in the differential diagnosis of LEGH from MDA. For a preoperative differential diagnosis, a biopsy specimen might only serve to sample a superficial part of the tumor. If tissue specimens were obtained from deeper part of the tumor by multiple sampling or conization, it would be easier to identify the glands that show the apical neutral mucin pattern, and, in MDA, earlier detection of the component of well-differentiated adenocarcinoma might be possible among the glands of LEGH.

The present results also showed that the localization pattern of neutral mucin was correlated with the prognosis of patients with CxAd. In all of ten followed-up cases of LEGH with the whole cytoplasmic neutral mucin pattern, postoperative clinical course was uneventful. Among the patients with CxAd, including MDA, the presence of the apical pattern in a significant part (10% or more of the tumor) indicated poorer prognosis, whereas the acid mucin pattern or no mucin secretion pattern of the tumor indicated better prognosis.

Although the distribution and intensity of mucin staining were suggested to differ between the mucinous (or endocervical) type and the endometrioid type, it is reported that mucin stains were not specific for differentiation between these two types of CxAd [1, 2]. In the present study, we showed that the apical pattern of neutral mucin localization was observed characteristically in well-differentiated adenocarcinoma and the mucinous histological type. By the multivariate analysis, both the apical neutral mucin pattern and lack thereof in tumor cell differentiation, as well as advanced clinical stage, were significant indicators of higher recurrence rate of the tumor.

The cases of MDA were composed of both LEGH and adenocarcinoma components, and it was suggested that the latter component arose from the former. In these cases of MDA, the LEGH component showed the whole cytoplasmic pattern of neutral mucin, but the CxAd component showed the apical pattern of neutral mucin or the acid mucin pattern. The localization of neutral mucin appeared to change in accordance with the progression from LEGH to CxAd. The whole cytoplasmic pattern of neutral mucin might be simply an indicator of metaplastic change, and such a phenotype might be attenuated during tumor progression from a benign phenotype to a malignant phenotype and/or the loss of differentiation. The characteristics of mucin are shown to change largely during the malignant transformation from mucin-producing cells to CxAd of the mucinous type [1]. The alteration of neutral mucin localization from the whole cytoplasmic pattern to the apical pattern would be one of such changes during the malignant progression.

It was shown that the examination of CEA using immunohistochemistry was useful for differential diagnosis between benign cervical glands and MDA/well-differentiated CxAd [18]. We could confirm that CEA was frequently positive in MDA and common CxAd. Even in LEGH, faint staining of CEA in the membrane border was often observed in <1% of constituent cells. The combination of CEA immunostaining and the examination of mucin localization pattern by AB-PAS staining might be helpful for preoperative and postoperative differential diagnosis of the cervical glandular lesions.

Acknowledgments The authors thank Professor Hironobu Sasano (Department of Pathology, Tohoku University Graduate School, Sendai, Miyagi, Japan), Professor Takashi Nakajima (Department of Pathology II, Gunma University School of Medicine, Maebashi, Gunma, Japan), and Professor Makio Mukai (Department of Diagnostic Pathology, Keio University Hospital, Tokyo, Japan) for providing tissue specimens and clinical data.

References

1. Cohen C, Shulman G, Budgeon L (1982) Endocervical and endometrial adenocarcinoma: an immunoperoxidase and histochemical study. Am J Surg Pathol 6:151–157
2. Cooper P, Russel G, Wilson B (1987) Adenocarcinoma of the endocervix—a histochemical study. Histopathology 11:1321–1330
3. Gilks CB, Young RH, Aguirre P, DeLellis RA, Scully RE (1989) Adenoma malignum (minimal deviation adenocarcinoma) of the uterine cervix. Am J Surg Pathol 13:717–729
4. Gilks CB, Young RH, Clement PB, Hart WR, Scully RE (1996) Adenomyomas of the uterine cervix of the endocervical type: a report of ten cases of a benign cervical tumor that may be confused with adenoma malignum (corrected). Mod Pathol 9:220–224
5. Hata S, Mikami Y, Manabe T (2002) Diagnostic significance of endocervical glandular cells with "golden-yellow" mucin on pap smear. Diagn Cytopathol 27:80–84
6. Hayashi I, Tsuda H, Shimoda T (2000) Reappraisal of orthodox histochemistry for the diagnosis of minimal deviation adenocarcinoma of the cervix. Am J Surg Pathol 24:559–562
7. Hirai Y, Takeshima N, Haga A, Arai Y, Akiyama F, Hasumi K (1998) A clinicocytopathologic study of adenoma malignum of the uterine cervix. Gynecol Oncol 70:219–223
8. Jones MA, Young RH, Scully RE (1991) Diffuse laminar endocervical glandular hyperplasia. A benign lesion often confused with adenoma malignum (minimal deviation adenocarcinoma). Am J Surg Pathol 15:1123–1129
9. Kaku T, Enjoji M (1983) An extremely well-differentiated adenocarcinoma ("adenoma malignum") of the cervix. Int J Gynecol Pathol 2:28–41
10. Kaplan EL, Meier P (1958) Nonparametric estimation from incomplete observations. J Am Stat Assoc 53:457–481
11. Kurman RJ, Norris HJ, Wilkinson EJ (1992) Tumors of the cervix, vagina, and vulva. In: Rosai J, Sobin LH (eds) Atlas of tumor pathology. Third series fascicle 4. Armed Forces Institute of Pathology, Washington DC, pp 91–93
12. McKelvey JL, Goodlin RR (1963) Adenoma malignum of the cervix. A cancer of a deceptively innocent histological pattern. Cancer 16:549–557
13. Mikami Y, Hata S, Fujiwara K, Imajo Y, Kohno I, Manabe T (1999) Florid endocervical glandular hyperplasia with intestinal and pyloric gland metaplasia: worrisome benign mimic of "adenoma malignum." Gynecol Oncol 74:504–511
14. Mowry RW (1963) The special value of methods that color both acidic and vicinal hydroxyl groups in the histochemical study of mucins. With revised directions for the colloidal iron stain, the use of alcian blue G8X, and their combinations with the periodic acid-Schiff reaction. Ann N Y Acad Sci 106:402–423

15. Nucci MR, Clement PB, Young RH (1999) Lobular endocervical glandular hyperplasia, not otherwise specified: a clinicopathologic analysis of thirteen cases of a distinctive pseudoneoplastic lesion and comparison with fourteen cases of adenoma malignum. Am J Surg Pathol 23: 886–891
16. Peto P, Pike MC, Armitage P, Breslow NE, Cox DR, Howard SV, Mantel N, McPherson K, Peto J, Smith PG (1977) Design and analysis of randomized clinical trials requiring prolonged observation of each patient. Br J Cancer 35:1–39
17. Silverberg SG, Hurt G (1975) Minimal deviation adenocarcinoma (adenoma malignum) of the cervix: a reappraisal. Am J Obstetr Gynecol 121:971–975
18. Steeper TA, Wick MR (1986) Minimal deviation adenocarcinoma of the uterine cervix (adenoma malignum). An immunohistochemical comparison with microglandular endocervical hyperplasia and conventional endocervical adenocarcinoma. Cancer 58:1131–1138

Virchows Arch (2003) 443:761–767
DOI 10.1007/s00428-003-0887-y

ORIGINAL ARTICLE

Y. Wakayama · T. Jimi · M. Inoue · H. Kojima · S. Yamashita · T. Kumagai · M. Murahashi · H. Hara · S. Shibuya

Altered aquaporin 4 expression in muscles of Fukuyama-type congenital muscular dystrophy

Received: 10 June 2003 / Accepted: 22 July 2003 / Published online: 26 August 2003
© Springer-Verlag 2003

Abstract This study was undertaken to investigate the expression of aquaporin 4 (AQP4) in the muscle plasma membrane of children with Fukuyama-type congenital muscular dystrophy (FCMD) at protein and mRNA levels. The biopsied six muscles with FCMD, six histochemically normal muscles and eight disease control muscles were analyzed by means of immunoblots, immunohistochemistry and reverse-transcription polymerase chain reaction (RT-PCR). Immunoblots showed that the band of FCMD muscle extracts stained with anti-AQP4 antibody was faint in comparison with that of normal muscle extracts. The immunohistochemistry revealed that most of the FCMD myofibers showed negative immunostaining with anti-AQP4 antibody, although the partially positive immunostaining of sporadic FCMD myofibers was noted. The immunoreactivity was positive with anti-dystrophin and anti-β-spectrin antibodies in almost all FCMD myofibers. The quantitative RT-PCR demonstrated that the AQP4 mRNA level of the FCMD muscles was markedly reduced. On the basis of these findings, we conclude that the expression of AQP4 in FCMD myofibers is reduced and the reduced content of AQP4 mRNA in FCMD muscles may be related to the decreased expression of AQP4 at the muscle plasma membrane of FCMD myofibers.

Keywords Fukuyama-type congenital muscular dystrophy · Skeletal muscle aquaporin 4 · Immunoblot · Immunohistochemistry · Aquaporin 4 mRNA

Y. Wakayama · T. Jimi · M. Inoue · H. Kojima · M. Murahashi · H. Hara · S. Shibuya
Department of Neurology,
Showa University Fujigaoka Hospital,
Yokohama, Japan

S. Yamashita
Department of Neurology,
Kanagawa Children's Medical Center,
Yokohama, Japan

T. Kumagai
Department of Pediatric Neurology,
Aichi Prefectural Colony,
Kasugai, Japan

Y. Wakayama (✉)
Department of Neurology,
Showa University Fujigaoka Hospital,
1-30 Fujigaoka, Aoba-Ku, 227-8501 Yokohama, Japan
e-mail: wakayama@showa-university-fujigaoka.gr.jp
Tel.: +81-45-9711151
Fax: +81-45-9742204

Introduction

Fukuyama-type congenital muscular dystrophy (FCMD) is now recognized as an independent subtype of childhood progressive muscular dystrophy characterized by generalized and severe muscle atrophy of extremely early onset, joint contracture at an early stage and mental retardation [6]. The relative prevalence rate of FCMD compared with Duchenne muscular dystrophy (DMD) is 1:2.1 [6]. FCMD is an autosomal recessive disease affecting not only skeletal muscle, but also the central nervous system [6, 15, 32]. The gene locus is on chromosome 9q31 [22]. In 1998, the causative gene was identified and was named as fukutin [12].

Our previous freeze-fracture study of the muscle plasma membranes of children with FCMD [24] showed that the number of the intramembranous particle assembly "orthogonal array" was markedly reduced and its subunit particle number was also decreased [25]. The orthogonal array protein is composed of the aquaporin 4 (AQP4) molecule [4, 8, 16, 19, 33, 34], which is associated with syntrophin in its post-synaptic density-95, Drosophila discs large protein and zona occludens protein 1 (PDZ) domain [1, 3]. The name PDZ comes from the first three proteins found to contain the repeat of this domain [7, 20]. The immunoreactivity of anti-AQP4 antibody is lacking in the skeletal muscle and brain of α1-syntrophin knockout mice [35]. Syntrophin is a member of the dystrophin glycoprotein complex. Using the freeze-fracture technique, we previously showed a decreased number of orthogonal arrays in the muscle plasma membrane of

dystrophin-deficient DMD muscles [17, 23]. We also showed a marked reduction of AQP4 molecules in DMD myofibers, although one of the causes of the reduced expression of AQP4 molecules was a decreased amount of AQP4 mRNA in DMD muscles [30, 31].

In this study we investigated: (1) whether the immunoreactivity of anti-AQP4 antibody is reduced in muscles of children with FCMD caused by mutation of the fukutin gene [12] and (2) whether the AQP4 mRNA level is reduced if the expression of AQP4 is reduced in FCMD muscles.

Materials and methods

Muscle samples

Quadriceps femoris muscles were biopsied under local anesthesia from six affected children with FCMD who had muscle weakness and hypotonia from infancy, delayed motor milestone, myopathic facies, mental retardation, high serum creatine kinase (CK) values and myopathic changes shown in electromyograms [6]. Among the six patients, the parents of one patient agreed to our examining the fukutin gene mutation of that patient, which resulted in our finding that the patient was homozygous for the retroposal insertion into the fukutin gene. The diagnosis of FCMD in the remaining five patients was made by the typical clinical manifestations and laboratory examinations, such as the elevated serum CK values and myopathic electromyograms. For normal control specimens, six histochemically normal biopsy specimens of quadriceps femoris muscles were taken from patients who were thought to have myopathy, but were free of neuromuscular disorders after histochemical and immunological examinations. Muscle samples obtained by biopsy from six patients with myotonic dystrophy, one patient with dermatomyositis and one patient with polymyositis served as disease controls. All muscle samples were taken under informed consent. The procedure of muscle biopsy was approved by the ethics committee of Showa University.

Anti-AQP4 antibody production and immunoblot analysis

General procedures for peptide synthesis and antibody generation of the anti-AQP4 antibody are described elsewhere [13]. Immunoblot analysis of antiserum against AQP4 in the histochemically normal quadriceps femoris muscle samples and those of children with FCMD was done using previously described methods [26] with minor modifications. Sodium dodecyl sulfate polyacrylamide gel electrophoresis was done using a 12.5% homogeneous gel for AQP4 and 3–10% gradient gel for dystrophin and β-spectrin. The protein was transferred from the gel to a clear blot P membrane sheet (ATTO, Tokyo, Japan) using horizontal electrophoresis at 108 mA for 90 min at room temperature. Immunostainings were done with rabbit anti-AQP4 and anti-β-spectrin [27] antisera diluted to 1:500 and 1:200, respectively, and with mouse monoclonal anti-dystrophin (Dys I) antibody (Novocastra Laboratories, Ltd., Newcastle upon Tyne, England) diluted to 1:500.

Immunohistochemistry

The muscle biopsy specimens were immediately frozen in isopentane cooled with liquid nitrogen. Frozen, 6-μm-thick cross sections of the muscles were placed on cover slips and were incubated with primary antiserum for rabbit anti-AQP4 diluted to 1:200. Serial cross sections of muscles were also incubated with primary monoclonal Dys I antibody (Novocastra) diluted to 1:30 and, using rabbit anti-β-spectrin antiserum [27], diluted to 1:200. Indirect immunofluorescent staining was done by the method previously described [26].

Quantitative reverse-transcription polymerase chain reaction

Total RNA was extracted from approximately 30 mg of each FCMD, control or disease control muscle sample with an acid–phenol extraction reagent [TRI zol (code 15596–026); Gibco BRL, Rockville, MD]. The concentration of AQP4 mRNA was estimated by means of reverse-transcription polymerase chain reaction (RT-PCR). The oligonucleotide primers were designed from the human AQP4 sequence [33]: sense strand (AQP4F), 5′ - GGTGCT-CATCTCCCTTTGCTTT-3′; antisense strand (AQP4R), 5′-GTCTTTCCCCTTCTTCTCCTCTC-3′. The synthetic DNA competitor was made by PCR from synthetic DNA templates provided in the kit [Competitive DNA Construction Kit (code PRO17); TaKaRa Co], which included both the upper (AQP4F) and lower (AQP4R) sequences specific for human AQP4. We used a kit [competitive RNA transcription kit (code 6125); TaKaRa Co] to make the synthetic RNA competitor from the synthetic DNA template by transcription with SP6 RNA polymerase. The concentration of purified AQP4 RNA competitor was calculated as a copy number for each microgram of total RNA. Serial dilutions of synthetic AQP4 RNA competitor were prepared. With 200 ng of total RNA and serial dilutions of synthetic AQP4 RNA competitor, several rounds of competitive RT-PCR for each sample were done according to the kit instructions [mRNA Selective PCR Kit (code RR025A); TaKaRa Co]. Both the sample and the competitor RNA were reverse transcribed for 30 min at 50°C followed by 25 cycles of PCR (30 s each at 85°C and 60°C and 1 min at 72°C) with the reaction mixture containing 1×PCR buffer, 2 μM each of primer pair, 5 mM magnesium chloride, 1 mM each of dNTP analogue mixture, 0.8 U/μl ribonuclease inhibitor, 0.1 U/μl reverse transcriptase, and 0.1 U/μl *Taq* polymerase. The competitive RT-PCR products were separated by electrophoresis, and the concentration of AQP4 mRNA in the sample was estimated by image analysis using an image processing system (NIH image 1.61; National Institutes of Health, Bethesda, MD). To compare the concentration of AQP4 mRNA with that of a housekeeping gene, a parallel assay of α-tubulin was done for each sample. For the comparison of the concentration of AQP4 mRNA in three groups of six FCMD muscles, six normal control muscles and eight disease control muscles, the ratio of AQP4 mRNA copies to α-tubulin mRNA copies was calculated. The oligonucleotide primers for α-tubulin [Human α-Tubulin Control Amplimer Set, (Code 9222–1) Clontech Laboratories Inc., Palo Alto, CA] were as follows: sense strand, 5′-CACCCGTCTTCAGGGCTTCTTGGTTT-3′; antisense strand, 5′-CATTTCACCATCTGGTTGGCTGGCTC-3′.

Results

Immunoblot analysis of antibody

Immunoblot analysis showed that the anti-AQP4 antibody reacted with 31-kDa protein extracts of normal muscles, but the reactions of AQP4 markedly decreased in FCMD muscle extracts (Fig. 1A). The reactions of both Dys I (Fig. 1B) and anti-β-spectrin (Fig. 1C) antibodies in FCMD muscle extracts were similar to those in extracts of normal control muscles.

Immunohistochemistry

The immunoreactions of AQP4, dystrophin and β-spectrin with normal human quadriceps femoris muscles were

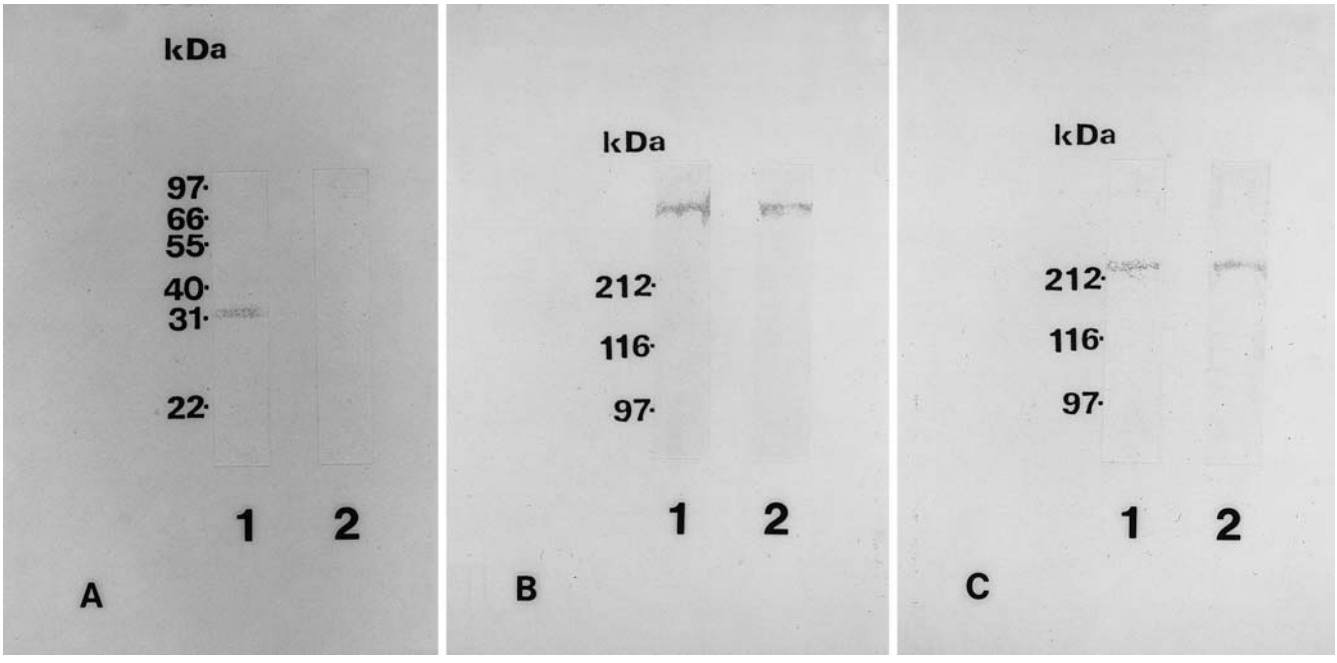

Fig. 1 Immunoblot analysis of aquaporin 4 (AQP4; **A**), dystrophin (**B**), and β-spectrin (**C**) expressions in histochemically normal human quadriceps femoris muscles (*lane 1* of **A**, **B** and **C**, respectively) and in muscles of patients with Fukuyama-type congenital muscular dystrophy (FCMD) (*lane 2* of **A**, **B** and **C**, respectively). Electrophoresis and blotting were done as described in the Materials and methods. In normal human muscle extracts, bands of AQP4, dystrophin and β-spectrin were observed at 31, 427 and 270 kDa, respectively (**A**, **B** and **C**, respectively). The reaction for AQP4 markedly decreased in FCMD muscle extracts (**A**), whereas the reactions in FCMD muscle extracts of dystrophin and β-spectrin were similar to those in normal control muscle extracts (**B** and **C**, respectively). Numbers to the *left* of each figure are the molecular masses of standards

observed at the myofiber surface (Fig. 2A, B, C). The immunostainability of the anti-AQP4 antibody in FCMD muscles was markedly decreased and most FCMD myofibers were not immunostained with scattered partially immunopositive myofibers (Fig. 2D). Some FCMD myofibers had the internal labeling (Fig. 2D), which was related to nonspecific IgG deposition in necrotic myofibers. The immunoreaction with anti-dystrophin and anti-β-spectrin antibodies in FCMD muscles appeared to be normal in this study (Fig. 2E, F). Among disease control muscles, the muscles from patients with myotonic dystrophy showed the slight irregularity of immunoreactivity of anti-AQP4 antibody at the myofiber surface.

Quantitative RT-PCR

Gel electrophoresis of competitive RT-PCR products of AQP4 in normal control muscles (Fig. 3A) and disease control muscles contained two bands of 733 bp and 568 bp that corresponded to the RT-PCR products of total RNA samples extracted from muscle biopsy specimens and AQP4 RNA competitor, respectively. The 733-bp RT-PCR product of AQP4 was not obtained with 200 ng of total RNA from each of six FCMD muscles (Fig. 3B). Gel electrophoresis of competitive RT-PCR products of α-tubulin in FCMD muscles (Fig. 3C), normal muscles (Fig. 3D) and disease control muscles included two bands of 527 bp and 452 bp that corresponded to the RT-PCR products of total RNA samples extracted from muscle biopsy specimens and α-tubulin competitor, respectively. The 527 bp RT-PCR product of α-tubulin appeared to be normal in three of six FCMD muscles compared with that of normal muscles. Since there was no 733-bp RT-PCR product of AQP4 in each of six FCMD muscles, the ratio of AQP4 mRNA copies to α-tubulin mRNA copies could not be calculated in FCMD muscles. The group mean ratio ± standard error of the mean of AQP4 mRNA copies to α-tubulin mRNA copies was 1.70±0.43 and 1.55±0.29 in six normal control muscles and eight disease control muscles, respectively. The difference of these two values was not statistically significant by two-tailed t-test (P>0.1).

Discussion

FCMD is an autosomal recessive disorder caused by the mutation of the fukutin gene that produces the glycoprotein (53.6 kDa molecular weight) of 461 amino acids [12]. Although mRNA of fukutin is ubiquitously expressed, it is even more strongly expressed in the heart, brain, skeletal muscle and pancreas [12]. This agrees with the fact that children with FCMD show micropolygyria, skeletal muscle atrophy and cardiomyopathy [6]. The precise function of fukutin is speculative, but its absence may cause structural alteration of the basal lamina of the central nervous system [15, 32].

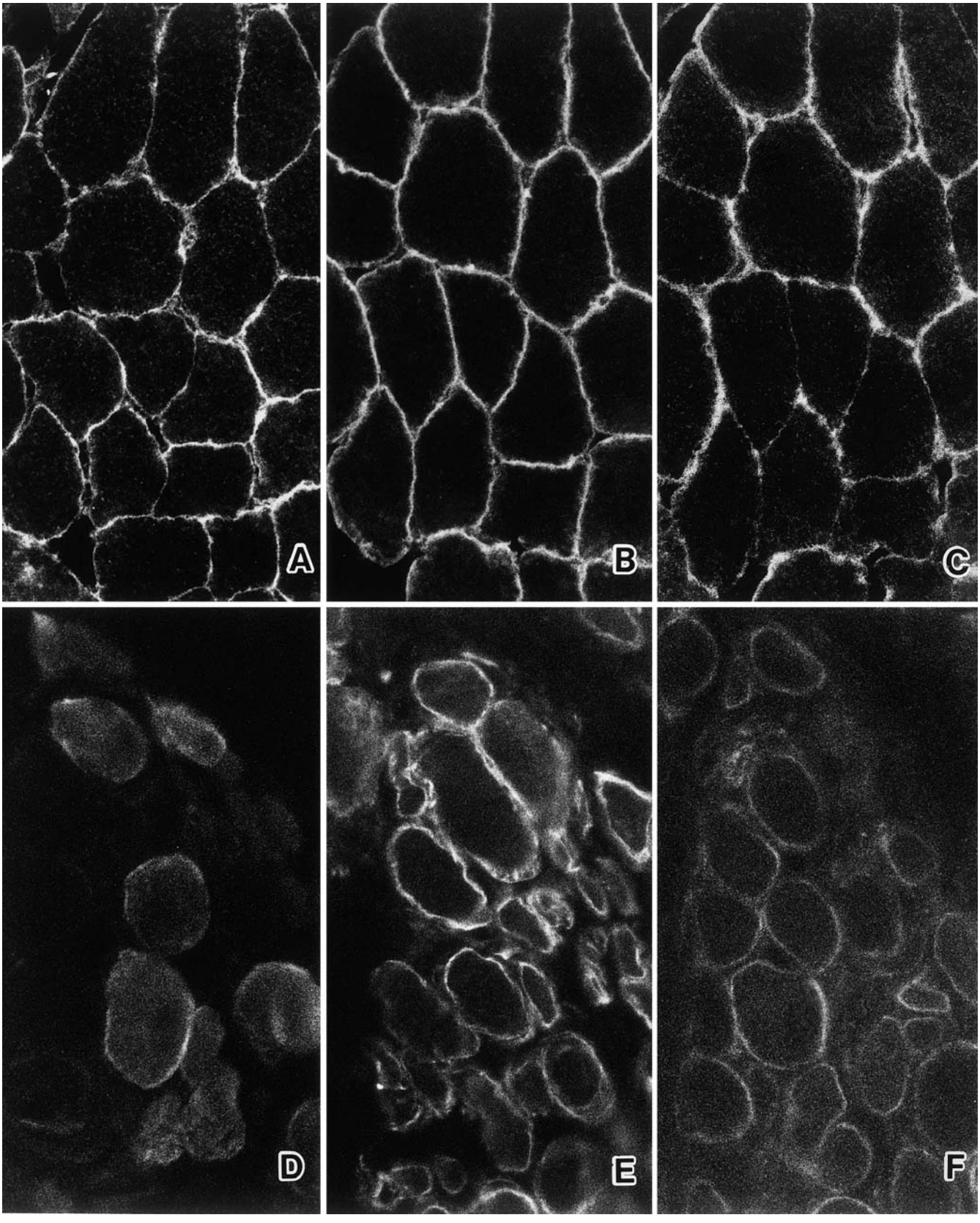

Fig. 2 Immunohistochemical staining of normal muscle (**A–C**) and Fukuyama-type congenital muscular dystrophy (FCMD) muscle (**D–F**) with anti-aquaporin 4 (anti-AQP4) (**A**, **D**), anti-dystrophin (**B**, **E**) and anti-β-spectrin (**C**, **F**) antibodies. The cell surface of each myofiber in normal muscles shows a thin layer of immunofluorescence with these antibodies. In muscle samples from patients with FCMD, immunostaining for AQP4 is markedly reduced, and the pattern of staining of AQP4 in FCMD muscles is strikingly patchy with most fibers being negative and some remaining fibers having normal amounts (**D**). Some FCMD myofibers have the internal labeling (**D**), which is related to nonspecific IgG deposition in necrotic myofibers. Immunoreaction with anti-dystrophin (**E**) and anti-β-spectrin (**F**) antibodies shows positive staining (×350)

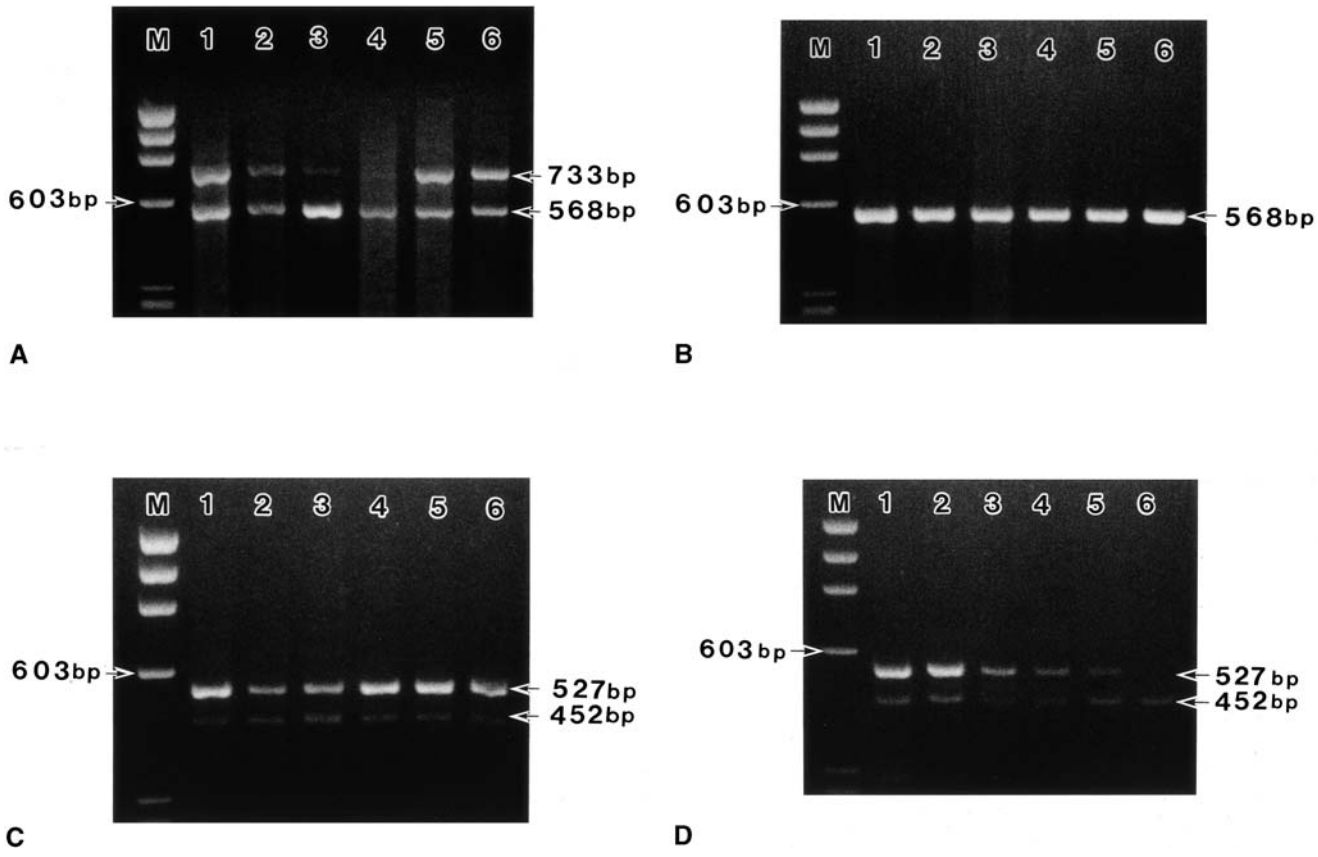

Fig. 3 Competitive reverse-transcription polymerase chain reaction (RT-PCR) products obtained for human aquaporin 4 (AQP4) as described in the Materials and methods. The gel electrophoresis of competitive RT-PCR products of AQP4 in normal muscles (**A**) contained two bands of 733 bp and 568 bp that corresponded to the RT-PCR products of total RNA samples extracted from muscles and AQP4 RNA competitor, respectively. The 733-bp RT-PCR product of AQP4 appeared to be absent with 200 ng of total RNA in each of six FCMD muscles (each *lane*) (**B**) compared with that of normal control muscles (**A**) in which the product appeared to decrease in one muscle (*lane 4* in **A**). Gel electrophoresis of competitive RT-PCR products of α-tubulin in normal muscles (**C**) and FCMD muscles (**D**) included two bands of 527 bp and 452 bp that corresponded to the RT-PCR products of total RNA samples extracted from muscles and α-tubulin RNA competitor, respectively. The 527 bp RT-PCR product of α-tubulin appeared to be normal in three of six FCMD muscles (*lanes 1–3* in **D**) compared with that of normal control muscles (**C**). *Lane M* is the ×174 *Hae*III digest marker. Each of *lanes 1* through *6* represents the result of a normal control muscle (**A**, **C**) or a FCMD muscle (**B**, **D**)

The freeze-fracture technique enables us to see the hydrophobic interior of the biological membrane, as the fracture plane preferentially goes into the hydrophobic interior of the biological membrane. Using this technique for the study of muscle tissue, we previously showed the alteration of molecular architecture of the muscle plasma membrane in patients with FCMD [24, 25]. The orthogonal arrays of the FCMD muscle plasma membrane are scanty and the subunit particles of the remaining orthogonal arrays decrease in number [24, 25]. These results were similar to those of the muscle plasma membrane of boys with DMD [17, 23]. In this study, the results of immunohistochemical staining of FCMD muscles with anti-AQP4 antibody agreed with those of the freeze-fracture study of FCMD muscles. This study showed that the decrease in AQP4 mRNA of FCMD muscles was related to the reduced AQP4 expression of FCMD myofibers. The results of the present study were similar to those for DMD muscles, except for the negative immunostaining for dystrophin in DMD muscles [30, 31]. The reduced AQP4 expression in DMD muscles [5] and mdx mouse muscles [2] has been described by the investigators of two other research groups. In DMD muscles, the serial sections showed that the sporadic AQP4 positive myofibers were not the dystrophin-positive revertant fibers. Thus, the expression of AQP4 was not solely dependent on the presence of α1-syntrophin-dystrophin complex, and other factor(s) may be involved in AQP4 expression [31]. The decreased expression of AQP4 mRNA in DMD muscles may be one of the factor(s). The mechanism of decreased expression of AQP4 in FCMD muscles is thought to be more complicated. Dystrophin is expressed in FCMD muscles, so the decreased expression of AQP4 may be due to the decreased AQP4 mRNA and/or immaturity of FCMD myofibers.

We previously reported the severe reduction and small size of orthogonal arrays in merosin negative muscles of dy/dy mice, which are the model of merosin-negative human congenital muscular dystrophy [18]. Merosin is

localized at the most inner portion of the muscle basal lamina [28] and extracellular matrix abnormalities, such as a deficiency in merosin, can cause alteration of the molecular architecture of the muscle plasma membrane. In the case of the merosin immunoreactivity of FCMD myofibers, decreased immunoreactivity for merosin in the basal lamina of FCMD myofibers has been described [9]. Alterations of the basal lamina of FCMD myofibers at the ultrastructural level have been described [10, 32], as well as the apparently normal ultrastructure of the basal lamina of FCMD myofibers [29].

A 180-kDa extracellular matrix protein is deficient in the skeletal muscles of children with FCMD [21], which is presumed to be caused specifically by primary deficiency of fukutin gene [12]. The fukutin gene shares some homology with fringe-like glycosyltransferases and causes hypoglycosylation in FCMD [14]. Hypoglycosylation of α-dystroglycan directly eliminates the binding activity of α-dystroglycan with the ligands laminin, agrin and neurexin. As loss of α-dystroglycan ligand interactions disrupts the normal extracellular matrix composition and structure at important anchoring sites [14], α-dystroglycan seems to target proteins associated with the dystrophin glycoprotein complex in the neuromuscular synapse. In this context, muscles of patients with FCMD may have faulty motor nerve innervation. The decreased amounts of AQP4 and AQP4 mRNA in FCMD muscles may be due to the dysinnervation of skeletal muscles in FCMD, since lack of AQP4 mRNA after denervation has been reported [11]. Alternatively, many patients with FCMD are very young and their muscle biopsies contain the immature and regenerating myofibers. At present, no data are present with regard to the possible developmental regulation of AQP4 molecule. This may influence the results and, thus, further studies of AQP4 in fatal, neonatal and mature muscles are needed to fully assess our present data.

Reduction in AQP4 expression of FCMD muscles in this study provides important evidence that altered AQP4 expression in skeletal muscles can occur in muscular dystrophy caused by gene mutations other than dystrophin. Further investigations on the mechanism of decrease of AQP4 mRNA in FCMD muscles will shed light on the molecular pathogenesis of FCMD.

References

1. Adams ME, Mueller HA, Froehner SC (2002) In vivo requirement of the alpha-syntrophin PDZ domain for the sarcolemmal localization of nNOS and aquaporin-4. J Cell Biol 155:113–122
2. Crosbie RH, Dovico SA, Flanagan JD, Chamberlain JS, Ownby CL, Campbell KP (2002) Characterization of aquaporin-4 in muscle and muscular dystrophy. FASEB J 16:943–949
3. Fanning AS, Anderson JM (1999) PDZ domains: fundamental building blocks in the organization of protein complexes at the plasma membrane. J Clin Invest 103:767–772
4. Frigeri A, Gropper MA, Umenishi F, Kawashima V, Brown D, Verkman AS (1995) Localization of MIWC and GLIP water channel homologs in neuromuscular, epithelial and glandular tissues. J Cell Sci 108:2993–3002
5. Frigeri A, Nicchia GP, Repetto S, Bado M, Minetti C, Svelto M (2002) Altered aquaporin-4 expression in human muscular dystrophies: a common feature? FASEB J 16:1120–1122
6. Fukuyama Y, Osawa M, Suzuki H (1981) Congenital progressive muscular dystrophy of the Fukuyama type: clinical, genetic and pathologic considerations. Brain Dev 3:1–29
7. Gee SH, Madhavan R, Levinson SR, Caldwell JH, Sealock R, Froehner SC (1998) Interaction of muscle and brain sodium channels with multiple members of the syntrophin family of dystrophin-associated proteins. J Neurosci 18:128–137
8. Hasegawa H, Ma T, Skach W, Matthay MA, Verkman AS (1994) Molecular cloning of a mercurial-insensitive water channel expressed in selected water-transporting tissues. J Biol Chem 269:5497–5500
9. Hayashi YK, Engvall E, Arikawa-Hirasawa E, Goto K, Koga R, Nonaka I, Sugita H, Arahata K (1993) Abnormal localization of laminin subunits in muscular dystrophies. J Neurol Sci 119:53–64
10. Ishii H, Hayashi YK, Nonaka I, Arahata K (1997) Electron microscopic examination of basal lamina in Fukuyama congenital muscular dystrophy. Neuromusc Disord 7:191–197
11. Jimi T, Wakayama Y, Murahashi M, Shibuya S, Inoue M, Hara H, Matsuzaki Y, Uemura N (2000) Aquaporin 4: lack of mRNA expression in the rat regenerating muscle fiber under denervation. Neurosci Lett 291:93–96
12. Kobayashi K, Nakahori Y, Miyake M, Matsumura K, Kondo-Iida E, Nomura Y, Segawa M, Yoshioka M, Saito K, Osawa M, Hamano K, Sakakihara Y, Nonaka I, Nakagome Y, Kanazawa I, Nakamura Y, Tokunaga K, Toda T (1998) An ancient retrotransposal insertion causes Fukuyama-type congenital muscular dystrophy. Nature 394:388–392
13. Liu JW, Wakayama Y, Inoue M, Shibuya S, Kojima H, Jimi T, Oniki H (1999) Immunohistochemical studies of aquaporin 4 in the skeletal muscle of mdx mouse. J Neurol Sci 164:24–28
14. Michele DE, Barresi R, Kanagawa M, Saito F, Cohn RD, Satz JS, Dollar J, Nishino I, Kelley RI, Somer H, Straub V, Mathews KD, Moore SA, Campbell KP (2002) Post-translational disruption of dystroglycan–ligand interactions in congenital muscular dystrophies. Nature 418:417–422
15. Nakano I, Funahashi M, Takada K, Toda T (1996) Are breaches in the glia limitans the primary cause of the micropolygyria in Fukuyama-type congenital muscular dystrophy (FCMD)?—pathological study of the cerebral cortex of an FCMD fetus. Acta Neuropathol (Berl) 91:313–321
16. Rash JE, Yasumura T, Hudson CS, Agre P, Nielsen S (1998) Direct immunogold labelling of aquaporin-4 in square arrays of astrocyte and ependymocyte plasma membranes in rat brain and spinal cord. Proc Natl Acad Sci U S A 95:11981–11986
17. Schotland DL, Bonilla E, Wakayama Y (1981) Freeze fracture studies of muscle plasma membrane in human muscular dystrophy. Acta Neuropathol (Berl) 54:189–197
18. Shibuya S, Wakayama Y, Oniki H, Kojima H, Saito M, Etou T, Nonaka I (1997) A comparative freeze-fracture study of plasma membrane of dystrophic skeletal muscles in dy/dy mice with merosin (laminin 2) deficiency and mdx mice with dystrophin deficiency. Neuropathol Appl Neurobiol 23:123–131
19. Shibuya S, Wakayama Y, Inoue M (1999) Identification of aquaporin 4 molecule in the replica of normal rat sarcolemma: fracture-label immunoelectron microscopin study (abstract). Ann Neurol 46:460
20. Stein V, House DR, Bredt DS, Nicoll RA (2003) Postsynaptic density-95 mimics and occludes hippocampal long-term potentiation and enhances long-term depression. J Neurosci 23:5503–5506
21. Sunada Y, Saito F, Higuchi I, Matsumura K, Shimizu T (2002) Deficiency of a 180-kDa extracellular matrix protein in Fukuyama type congenital muscular dystrophy skeletal muscle. Neuromusc Disord 12:117–120
22. Toda T, Segawa M, Nomura Y, Nonaka I, Masuda K, Ishihara T, Suzuki M, Tomita I, Origuchi Y, Ohno K, Misugi N, Sasaki

Y, Takeda K, Kawai M, Otani K, Murakami T, Saito K, Fukuyama Y, Shimizu T, Kanazawa I, Nakamura Y (1993) Localization of a gene for Fukuyama type congenital muscular dystrophy to chromosome 9q31–33. Nat Genet 5:283–286
23. Wakayama Y, Okayasu H, Shibuya S, Kumagai T (1984) Duchenne dystrophy: reduced density of orthogonal array subunit particles in muscle plasma membrane. Neurology 34:1313–1317
24. Wakayama Y, Kumagai T, Shibuya S (1985) Freeze-fracture studies of muscle plasma membrane in Fukuyama-type congenital muscular dystrophy. Neurology 35:1587–1593
25. Wakayama Y, Kumagai T, Jimi T (1986) Small size of orthogonal array in muscle plasma membrane of Fukuyama type congenital muscular dystrophy. Acta Neuropathol (Berl) 72:130–133
26. Wakayama Y, Jimi T, Takeda A, Misugi N, Kumagai T, Miyake S, Shibuya S (1990) Immunoreactivity of antibodies raised against synthetic peptide fragments predicted from mid portions of dystrophin cDNA. J Neurol Sci 97:241–250
27. Wakayama Y, Shibuya S, Takeda A, Jimi T, Nakamura Y, Oniki H (1995) Ultrastructural localization of the C-terminus of the 43-kd dystrophin-associated glycoprotein and its relation to dystrophin in normal murine skeletal myofiber. Am J Pathol 146:189–196
28. Wakayama Y, Murahashi M, Jimi T, Kojima H, Shibuya S, Oniki H (1997) Immunogold and freeze etch electron microscopic studies of merosin localization in basal lamina of human skeletal muscle fibers. Acta Neuropathol (Berl) 93:34–42
29. Wakayama Y, Shibuya S, Kumagai T, Kobayashi T, Yamashita S, Misugi N, Miyake S, Murahashi M, Jimi T, Oniki H (1997) Ultrastructural alterations of the muscle plasma membrane and related structures in Fukuyama muscular dystrophy: comparative study with other types of muscular dystrophies. In: Fukuyama Y, Osawa M, Saito K (eds) Congenital muscular dystrophies. Elsevier, Amsterdam, pp 213–230
30. Wakayama Y, Jimi T, Inoue M, Kojima H, Murahashi M, Kumagai T, Yamashita S, Hara H, Shibuya S (2000) Analytical studies on the mechanism of the depletion of the aquaporin 4 molecule in the muscle plasma membrane with Duchenne muscular dystrophy (abstract). Ann Neurol 48:471–472
31. Wakayama Y, Jimi T, Inoue M, Kojima H, Murahashi M, Kumagai T, Yamashita S, Hara H, Shibuya S (2002) Reduced aquaporin 4 expression in the muscle plasma membrane of patients with Duchenne muscular dystrophy. Arch Neurol 59:431–437
32. Yamamoto T, Shibata N, Kanazawa M, Kobayashi M, Komori T, Kondo E, Saito K, Osawa M (1997) Early ultrastructural changes in the central nervous system in Fukuyama congenital muscular dystrophy. Ultrastruct Pathol 21:355–360
33. Yang B, Ma T, Verkman AS (1995) cDNA cloning, gene organization, and chromosomal localization of a human mercurial insensitive water channel: evidence for distinct transcriptional units. J Biol Chem 270:22907–22913
34. Yang B, Brown D, Verkman AS (1996) The mercurial insensitive water channel (AQP-4) forms orthogonal arrays in stably transfected Chinese hamster ovary cells. J Biol Chem 271:4577–4580
35. Yokota T, Miyagoe Y, Hosaka Y, Tsukita K, Kameya S, Shibuya S, Matsuda R, Wakayama Y, Takeda S (2000) Aquaporin 4 is absent at the sarcolemma and at perivascular astrocyte endfeet in alpha1-syntrophin knockout mice. Proc Jpn Acad 76(B):22–27

Virchows Arch (2003) 443:768–773
DOI 10.1007/s00428-003-0895-y

ORIGINAL ARTICLE

Janine Wechsler · Laurent Lantieri · Jacques Zeller · Marie-Catherine Voisin · Nadine Martin-Garcia · Pierre Wolkenstein

Aberrant axon neurofilaments in schwannomas associated with phacomatoses

Received: 10 March 2003 / Accepted: 5 August 2003 / Published online: 24 September 2003
© Springer-Verlag 2003

Abstract Neurofibromas and schwannomas express S100 protein, while axon filaments are not commonly found in schwannomas. Histopathological distinction between neurofibromas and schwannomas is usually easy, except for some variants. To assess the reliability of immunohistochemistry results for the differential diagnosis of the latter, 46 neural tumors of the skin were studied: 31 schwannomas [12 schwannomatosis, 7 neurofibromatosis type 2 (NF2)-associated, 12 solitary] and 15 plexiform neurofibromas associated with neurofibromatosis type 1. All tumors were subjected to immunohistochemical-labeling studies with antibodies to S100 protein and axon-specific neurofilament proteins. All tumors were positive with anti-S100 protein antibody. Schwannomas were strongly and diffusely positive while neurofibromas displayed more varied and limited S100 protein reactivity. Axon filaments were detected in 15 of 15 plexiform neurofibromas and 7 of 19 schwannomas associated with NF2/schwannomatosis. None of the 12 solitary schwannomas reacted with anti-axon neurofilament antibodies. Aberrant axons were observed in the schwannomas associated with NF2/schwannomatosis but not in the solitary schwannomas. Therefore, when there are multiple neural tumors, immunohistochemical visualization of axons may be misleading if it is not related to the clinical context and the standard histological features.

J. Wechsler (✉) · M.-C. Voisin · N. Martin-Garcia
Département de Pathologie, Hôpital Henri-Mondor,
AP-HP, Université Paris XII,
51 avenue de-Lattre-de-Tassigny, 94010 Créteil Cedex, France
e-mail: janine.wechsler@hmn.ap-hop-paris.fr
Tel.: +33-14-9812738
Fax: +33-14-9812733

L. Lantieri
Department of Plastic and Reconstructive Surgery,
Hôpital Henri-Mondor, Creteil, France

J. Zeller · P. Wolkenstein
Department of Dermatology, Hôpital Henri-Mondor,
Creteil, France

Keywords Diagnosis · Pathology · Immunohistochemistry · Neurofilament · Axon · S100 protein · Neurofibromatosis · Schwannomatosis · Neurofibroma · Schwannoma · Neural tumor

Introduction

Neurofibromas and schwannomas are the most frequent cutaneous neoplasms with neural differentiation. They can be classified as solitary or multiple. The solitary tumors are incidental findings, which are usually not associated with systemic manifestations [16]. Multiple tumors, however, are observed in patients with neurofibromatosis 1 (NF1), neurofibromatosis 2 (NF2) or schwannomatosis [13]. These diseases are phacomatoses. They may begin with skin disorders, especially neural neoplasms [12, 23]. NF1 and NF2 are two distinct forms of neurofibromatoses, which are well defined by diagnostic criteria [11, 14]. Neurofibromas are the hallmark of NF1 and schwannomas the hallmark of NF2. Like NF2, schwannomatosis is characterized by multiple nonvestibular schwannomas and various neurological deficits. It is still a matter of debate whether or not NF2 and schwannomatosis are the same condition [18, 21]. Neurofibromas and schwannomas differ in terms of location, histological aspect, immunohistochemical labeling pattern, electron microscopic features and potential for malignant transformation.

Histopathology is necessary to diagnose them. Schwannomas are encapsulated nodules, typically composed of dense spindle-cell proliferations. They characteristically have a nuclear palisade arrangement, forming Verocay bodies. Neurofibromas are typically diffuse and made of a loose proliferation of short spindle-shaped cells with wavy nuclei that are either fasciculated or dispersed in a myxoid stroma [16]. Some variants of both tumors may be difficult to diagnose. For example, schwannomas may have poor cellularity and myxoid stroma, i.e., Antoni type-B areas, which may resemble neurofibromas. Conversely, the plexiform variant of neurofibromas, which is

constituted by well-delimited tumors, may be mistaken for schwannomas, and, furthermore, schwannomas can also have plexiform variants [1, 6, 20, 22]. Because schwannomas, unlike neurofibromas, are not usually associated with malignant transformation, it is important to diagnose these neoplasms correctly. In addition to their differing morphologies, schwannomas and neurofibromas classically differ in their involvement of nerve components. The nerve of origin of a schwannoma is usually found at the periphery of the tumor, but not inside the body of the tumor, whereas neurofibromas usually contain axon filaments. Thus, the presence of axons within the tumor or at its periphery should be an additional feature to differentiate neurofibromas from schwannomas. However, it was previously mentioned [5] that NF2-associated schwannomas tended to have original nerves embedded in the tumor substance. Using an antibody to a neurofilament protein component of axons, we conducted a comparative immunohistochemical study of 46 tumors, including NF1-, NF2-, schwannomatosis-associated tumors, and solitary neural tumors histologically diagnosed as neurofibromas or schwannomas.

Materials and methods

We found 46 subcutaneous neural tumors registered in our institution between 1993 and 2000. Patients were classified according to the National Institutes for Health consensus criteria for neurofibromatoses and schwannomatosis diagnostic criteria [11, 14, 21]. We identified 15 patients with NF1, 7 with NF2, 12 with schwannomatosis and 12 with solitary extracranial schwannomas. Applying standard histological criteria [1, 16] to routine tissue preparations, we diagnosed 15 plexiform neurofibromas and 31

Table 1 Main data in 46 patients according to their diagnosis: schwannomatosis, neurofibromatosis type 2 (NF2), neurofibromatosis type 1 (NF1) or solitary schwannoma. *NF staining* + presence of intralesional neurofilament, *NF staining* − absence of intralesional neurofilament

Patient	Age/sex	Site	Clinical context	Microscopy	NF staining
1	36/Male	Cheek	Schwannomatosis	Schwannoma	−
2	29/Male	Back	Schwannomatosis	Schwannoma	−
3	79/Male	Arm	Schwannomatosis	Schwannoma	−
4	49/Male	Thigh	Schwannomatosis	Schwannoma	−
5	44/Male	Arm	Schwannomatosis	Schwannoma	−
6	55/Male	Neck	Schwannomatosis	Schwannoma	−
7	40/Male	Scarpa	Schwannomatosis	Schwannoma	−
8	43/Male	Leg	Schwannomatosis	Schwannoma	−
9	26/Male	Wrist	Schwannomatosis	Schwannoma	+
10	62/Female	Buttock	Schwannomatosis	Schwannoma	+
11	48/Female	Arm	Schwannomatosis	Schwannoma	+
12	69/Male	Back	Schwannomatosis	Schwannoma	+
13	21/Male	VIIIth nerve	NF2	Schwannoma	+
14	63/Male	VIIIth nerve	NF2	Schwannoma	+
15	30/Female	VIIIth nerve	NF2	Schwannoma	+
16	44/Male	VIIIth nerve	NF2	Schwannoma	−
17	29/Female	VIIIth nerve	NF2	Schwannoma	−
18	69/Female	VIIIth nerve	NF2	Schwannoma	−
19	17/Male	VIIIth nerve	NF2	Schwannoma	−
20	37/Male	Cheek	NF1	Plexiform neurofibroma	+
21	38/Female	Back	NF1	Plexiform neurofibroma	+
22	16/Female	Neck	NF1	Plexiform neurofibroma	+
23	22/Male	Face	NF1	Plexiform neurofibroma	+
24	30/Male	Thorax	NF1	Plexiform neurofibroma	+
25	56/Male	Knee	NF1	Plexiform neurofibroma	+
26	20/Female	Face	NF1	Plexiform neurofibroma	+
27	35/Female	Arm	NF1	Plexiform neurofibroma	+
28	34/Male	Face	NF1	Plexiform neurofibroma	+
29	45/Male	Flank	NF1	Plexiform neurofibroma	+
30	26/Female	Neck	NF1	Plexiform neurofibroma	+
31	36/Female	Back	NF1	Plexiform neurofibroma	+
32	21/Female	Neck	NF1	Plexiform neurofibroma	+
33	22/Female	Face	NF1	Plexiform neurofibroma	+
34	24/Female	Foot	NF1	Plexiform neurofibroma	+
35	49/Male	Leg	Solitary schwannoma	Schwannoma	−
36	31/Female	Finger	Solitary schwannoma	Schwannoma	−
37	25/Male	Leg	Solitary schwannoma	Schwannoma	−
38	44/Male	Arm	Solitary schwannoma	Schwannoma	−
39	43/Male	Limb	Solitary schwannoma	Schwannoma	−
40	26/Male	Back	Solitary schwannoma	Schwannoma	−
41	15/Female	Flank	Solitary schwannoma	Schwannoma	−
42	34/Female	Knee	Solitary schwannoma	Schwannoma	−
43	25/Male	Arm	Solitary schwannoma	Schwannoma	−
44	55/Male	Leg	Solitary schwannoma	Schwannoma	−
45	65/Female	Foot	Solitary schwannoma	Schwannoma	−
46	45/Female	Hand	Solitary schwannoma	Schwannoma	−

schwannomas. Immunohistochemical labeling studies were performed on paraffin sections using avidin-biotin or avidin-biotin complex-alkaline phosphatase, depending on the routine technique applied in our laboratory at time of the diagnosis. The antibodies were directed against S100 protein (polyclonal; Dako, Glostrup Denmark, diluted 1:200) or neurofilament protein (monoclonal, 2F11; Dako, diluted 1:300), which is a specific marker for axon filaments. The latter reaction was amplified by microwave pretreatment of the sections. Normal mouse or rabbit IgG was used as the negative control instead of the primary antibodies. Langerhans cells, adipocytes and nerves were positive controls for anti-S100 protein; nerves were also positive controls for the anti-neurofilament protein.

Neurofilament-labeling was considered to be positive only when axons were located inside the tumor, even when only a single axon could be identified. The presence of a small nerve at the periphery of the tumor was not taken into account. All the slides were reviewed by two of us (JW, MCV), who had no knowledge of the clinical data.

Results

Clinical data

Clinical and histological data for the 46 patients are summarized in Table 1. The 34 patients with NF1, NF2, or schwannomatosis had been reported [21]. The remaining 12 patients had solitary extracranial schwannomas.

Histopathological findings

On the basis of the standard histological criteria, we identified 31 schwannomas and 15 plexiform neurofibromas. All the schwannomas presented as nodules circumscribed by a fibrous capsule. They consisted of proliferations of spindle cells. Schwannomas were diagnosed on the basis of the presence of Antoni type-A areas with typical nuclear palisade arrangements forming Verocay bodies (Fig. 1). In most cases, they were admixed with myxoid Antoni type-B areas; hyalinized vessels were always present with frequent hemorrhagic and degenerative changes with microcystic formations. Solitary schwannomas and schwannomas associated with NF2 or with schwannomatosis were histologically similar. One solitary schwannoma showed a plexiform architecture. Microscopically, it was composed of several nodules infiltrating the dermis and subcutis. All NF1-associated neurofibromas contained diffuse and intraneural components. The diagnosis was based on the proliferation of small spindle-shaped cells with wavy nuclei admixed with abundant myxoid stroma. In some areas, cells took on a fascicular pattern. The plexiform component was composed of multiple intraneural neurofibromas (Fig. 2)

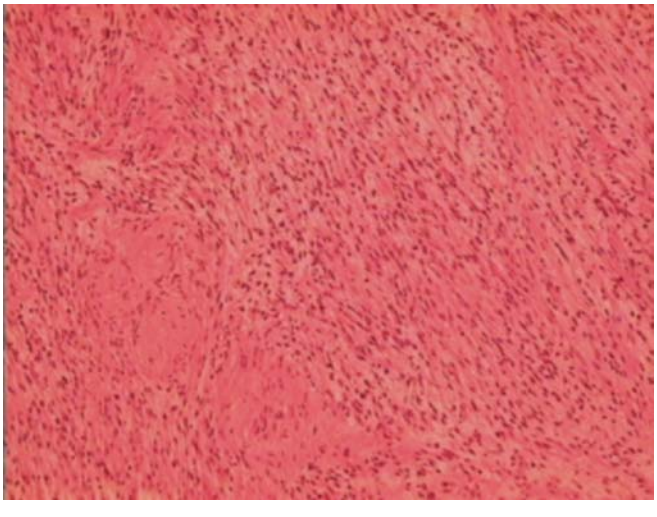

Fig. 1 Typical nuclear palisade arrangement with Verocay bodies in a schwannoma associated with schwannomatosis (original magnification ×160)

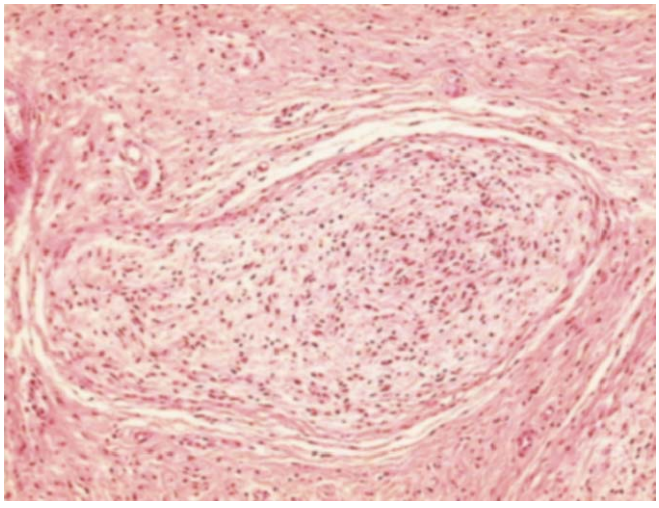

Fig. 2 Intraneural neurofibroma: myxoid proliferation of spindle-shaped cells with wavy nuclei surrounding residual nerve tissue (original magnification ×40)

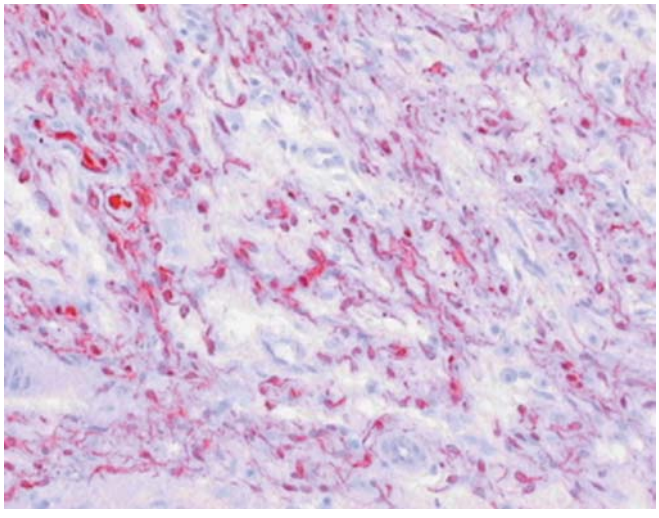

Fig. 3 Heterogeneous S100 protein positivity in neurofibroma (avidin-biotin complex-alkaline phosphatase, original magnification ×250)

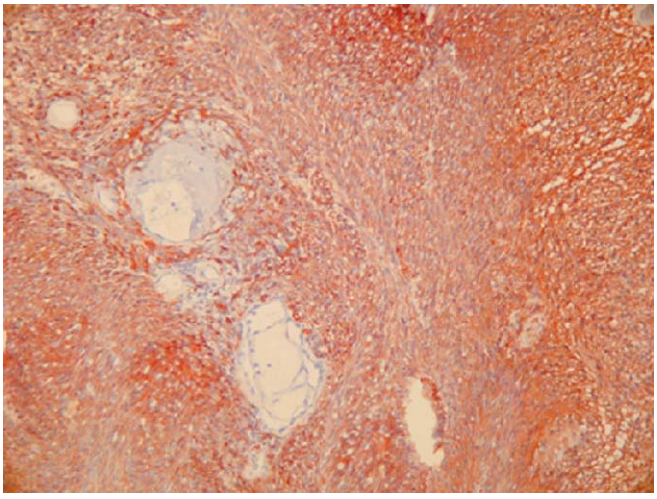

Fig. 4 Strong and homogeneous S100 protein positivity in schwannoma associated with schwannomatosis (avidin-biotin, original magnification ×160)

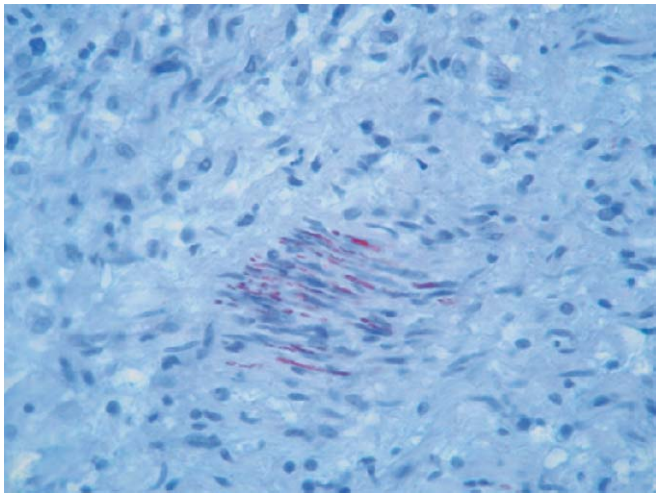

Fig. 5 Plexiform neurofibroma: axon filaments identified in the center of the nodule (avidin-biotin complex-alkaline phosphatase, original magnification ×250)

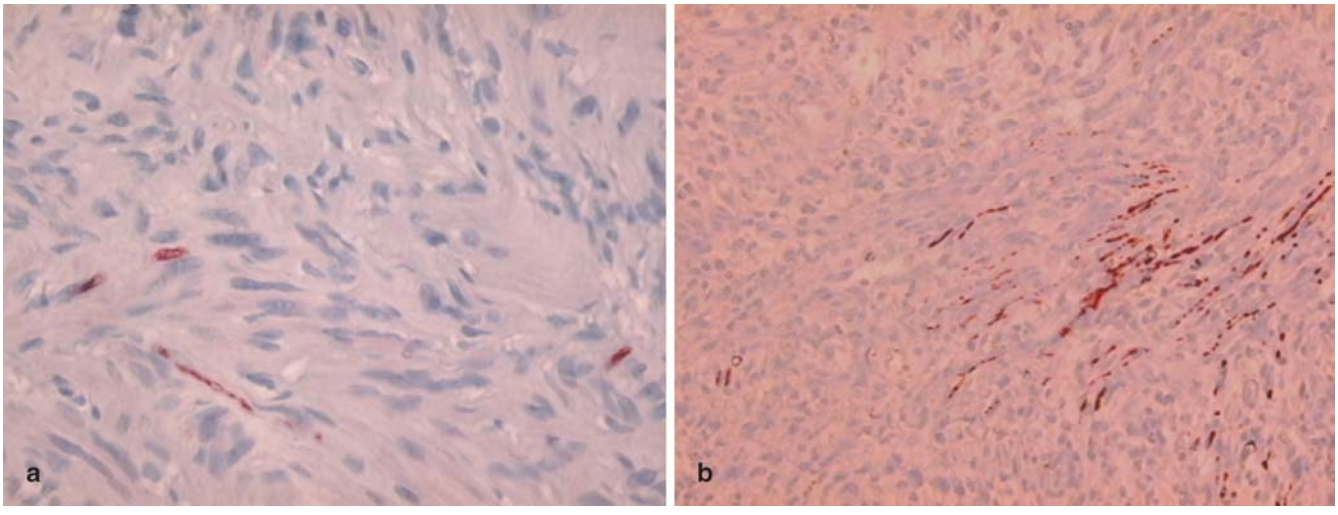

Fig. 6 Axon neurofilaments in two schwannomas associated with NF2: **a** scarce, **b** numerous (avidin-biotin-complex-alkaline phosphatase, original magnification ×400)

surrounded by diffuse neurofibroma. No lesion showed malignant transformation.

Immunohistochemical-labeling findings

All tumors were positively labeled by the anti-S100 protein antibody. In the 15 neurofibromas, S100 protein immunoreactivity was heterogeneously positive (Fig. 3) and sometimes patchy, while it was always strong and more homogeneous in the 31 schwannomas (Fig. 4). Schwannomas with predominant Antoni type-B myxoid areas reacted less intensively, but it was always possible to find more positive Antoni type-A areas.

Neurofilament-labeling was positive in 15of 15 NF1-associated plexiform neurofibromas. Axons were either dispersed or localized in the center of the tumor (Fig. 5). None of the solitary schwannomas contained axon filaments (12/12).

Among the 19 schwannomas associated with NF2/schwannomatosis, 12 were negative and 7 contained axon filaments. Among the latter, 4 were schwannomatosis- and 3 were NF2-associated schwannomas. Axon-neurofilaments were either scarce (Fig. 6a) or abundant (Fig. 6b). They were found in Antoni type-A and type-B areas.

Discussion

Accurate diagnosis of neurofibroma versus schwannoma is important. Indeed, the presence of at least two of these

tumors is included in the diagnostic criteria of NF1, NF2, and schwannomatosis. Misclassification of these tumors would lead to misclassification of the disease with genetic counseling and an inappropriate follow-up strategy.

Molecular studies might help to differentiate neurofibromas from schwannomas. Indeed, the respective involvement of NF1 gene in neurofibroma and NF2 gene in schwannoma has been studied [4, 7]. However, those studies, especially for NF1, are very labor intensive and not yet available for routine use. We undertook this study to assess the reliability of immunohistochemistry labeling patterns in neurofibromas versus schwannomas.

The distinct patterns of S100 protein immunoreactivities in neurofibromas and schwannomas were previously described by Sharma et al. [19], who demonstrated by transmission electron microcopy that, unlike schwannomas, which were predominantly composed of Schwann cells expressing S100-protein, neurofibromas were composed of an admixture of Schwann cells, fibroblast-like cells, and intermediate cells considered to be modified Schwann cells. This heterogeneous composition explains the S100 protein-labeling pattern in neurofibromas.

For 39 of 46 tumors (15 neurofibromas and 24 schwannomas) studied herein, the results were in accordance with the classical distribution of axons in schwannomas and neurofibromas, which is due to the irrespective growth patterns and cellular compositions. Because schwannoma development pushes aside the nerve from which it arises, the axon is displaced to the periphery of the tumor and should not be found therein. In contrast, because neurofibroma grows within the nerve of the origin, the axon filaments are trapped within the tumor [2, 15]. Axon filaments are usually found in the central area of plexiform neurofibromas; whereas, they may be absent or few in number in superficial dermal neurofibromas. Kuhn et al. [10] could not detect the presence of axon filaments in solitary cutaneous neurofibromas. In addition, Kawahara et al. [9] showed that dermal neurofibromas were also negative for glial fibrillary acidic protein, which appeared to be closely associated with neurofilament-positive axons. More difficult to understand is the presence of axons inside 7 of the 31 schwannomas in our series. These axons were located inside the tumors and not at the periphery, as usually described for this kind of nerve sheath tumor. Because these axon filaments were dispersed within the tumor, it was not possible to attribute the image to an inappropriate orientation of the section. Furthermore, none the solitary schwannomas contained neurofilaments; all the neurofilament-positive schwannomas were either schwannomatosis- or NF2-associated tumors. In patients with NF2, all the lesions with axons arose from the VIIIth nerve. Even though the presence of scarce neurofilaments has exceptionally been described in plexiform schwannomas [17], this finding suggests that hamartomatous neoplasms developing in phacomatoses are probably more complex than their solitary counterparts. Many of the previously reported hybrid tumors appeared to arise in plexiform neurofibromas, which are considered the hallmark of NF1. A hybrid tumor may present a diagnostic obstacle, as the schwannomatous part may be misdiagnosed as a malignant transformation of neurofibroma. Because S100-protein positivity is usually weak in malignant peripheral nerve sheath tumor, strong positivity should favor benign schwannomatous differentiation. Feany et al. [3] reported on nine lesions, two dermal, two subcutaneous, and five subfascial, with hybrid microscopic features of neurofibroma and schwannoma. Five lesions had a plexiform pattern and one patient had overt NF1. Occurring during the course of NF2, two hybrid tumors were reported in a patient who also developed two additional classic spinal schwannomas [3]. Furthermore, a unique tumor with divergent differentiation admixing features of astrocytoma, ependymoma, and primitive neuroectodermal tumor has been described in a patient with NF2 [8]. Thus, even though distinct origins of schwannomas and neurofibromas have been generally accepted, various nerve constituents may regroup in an anarchic manner, giving rise to malformed neo-nerves in particular circumstances, like hamartomatous neoplasms occurring in phacomatoses. These malformed hamartomas should be named "hybrid tumors" or "benign nerve-sheath tumors" rather than pure schwannomas or neurofibromas, as they completely or incompletely resemble nerves with a broad spectrum of differentiation. In the present series, the tumors were distinct from so-called hybrid tumors because their histological features looked the same as classic schwannomas, except for the presence of intralesional axons.

From a practical point of view, if axons are found in a schwannoma, then perhaps this is diagnostic of NF2/schwannomatosis. Besides, the possible, even rare, occurrence of such tumors in NF2/schwannomatosis highlights the difficulties of diagnosing these tumors and leads us to assert that the distinction between schwannoma and neurofibroma is probably too simplistic in this context. Therefore, histological findings and immunohistochemical labeling patterns should be carefully compared with clinical and genetic data before classifying this group of tumors.

References

1. Argenyi ZB (1993) Recent developments in cutaneous neural neoplasms. J Cutan Pathol 20:97–108
2. Aso M, Hashimoto K, Hamzavi A (1985) Immunohistochemical studies of selected skin diseases and tumors using monoclonal antibodies to neurofilament and myelin proteins. J Am Acad Dermatol 13:37–42
3. Feany MB, Anthony DC, Fletcher CD (1998) Nerve sheath tumors with hybrid features of neurofibroma and schwannoma: a conceptual challenge. Histopathology 32:405–410
4. Gutmann DH (2001) The neurofibromatoses: when less is more. Hum Mol Genet 10:747–755
5. Hamada Y, Iwaki T, Fukui M, Tateishi J (1997) A comparative study of embedded nerve tissue in six NF2-associated schwannomas and 17 nonassociated NF2 schwannomas. Surg Neurol 48:395–400
6. Ishida T, Kuroda M, Motoi T, Oka T, Imamura T, Machinami R (1998) Phenotypic diversity of neurofibromatosis 2: association with plexiform schwannoma. Histopathology 32:264–270

7. Jacoby LB, Jones D, Davis K, Kronn D, Short MP, Gusella J, MacCollin M (1997) Molecular analysis of the NF2 tumor-suppressor gene in schwannomatosis. Am J Hum Genet 61:1293–1302
8. Jay V, Edwards V, Varela-Stavrinou M, Rutka J (1997) Unique cerebral tumor with divergent differentiation in a patient presenting as NF2: report of a case with features of astrocytoma, ependymoma, and PNET. Ultrastruct Pathol 21:57–61
9. Kawahara E, Oda Y, Ooi A, Katsuda S, Nakanishi I, Umeda S (1988) Expression of glial fibrillary acidic protein (GFAP) in peripheral nerve sheath tumors. A comparative study of immunoreactivity of GFAP, vimentin, S100 protein, and neurofilament in 38 schwannomas and 18 neurofibromas. Am J Surg Pathol 12:115–120
10. Kuhn A, Mahrle G, Steigleder GK (1986) Immunohistochemical studies of paraffin-embedded material of solitary cutaneous neurofibromas. Z Hautkr 61:855–859
11. MacCollin M, Woodfin W, Kronn D, Short MP (1996) Schwannomatosis: a clinical and pathologic study. Neurology 46:1072–1079
12. Mautner VF, Lindenau M, Baser ME, Kluwe L, Gottschalk J (1997) Skin abnormalities in neurofibromatosis 2. Arch Dermatol 133:1539–1543
13. Mautner VF, Schroder S, Pulst SM, Ostertag H, Kluwe L (1998) Neurofibromatosis versus schwannomatosis. Fortschr Neurol Psychiatr 66:271–277
14. NIH Consensus Development Conference Statement Neurofibromatosis (1988) Arch Neurol 45:575–578
15. Reed ML, Jacoby RA (1983) Cutaneous neuroanatomy and neuropathology. Normal nerves, neural-crest derivatives, and benign neural neoplasms in the skin. Am J Dermatopathol 3:335–362
16. Requena L, Sangueza OP (1995) Benign neoplasms with neural differentiation: a review. Am J Dermatopathol 17:75–96
17. Scheithauer BW, Woodruf JM, Erlandson RA (1999) Tumors of the peripheral nervous system. Atlas of Tumor Pathology, Third series, Fascicle 24, AFIP, Washington, p 152
18. Seppala MT, Sainio MA, Haltia MJ, Kinnunen JJ, Setala KH, Jaaskelainen JE (1998) Multiple schwannomas: schwannomatosis or neurofibromatosis type 2? J Neurosurg 89:36–41
19. Sharma S, Sarkar C, Mathur M, Dinda AK, Roy S (1990) Benign nerve sheath tumours: a light microscopic, electron microscopic and immunohistochemical study of 102 cases. Pathology 22:191–195
20. Val-Bernal JF, Figols J, Vazquez-Barquero A (1995) Cutaneous plexiform schwannoma associated with neurofibromatosis type 2. Cancer 76:1181–1186
21. Wolkenstein P, Benchiki H, Zeller J, Wechsler J, Revuz J (1997) Schwannomatosis: a clinical entity distinct from neurofibromatosis type 2. Dermatology 195:228–231
22. Woodruff JM, Funkhouser JW, Marshall ML (1983) Plexiform (multinodular) schwannoma. A tumour simulating the plexiform neurofibroma. Am J Surg Pathol 7:691–697
23. Zvulunov A,Esterly NB (1995) Neurocutaneous syndromes associated with pigmentary skin lesions. J Am Acad Dermatol 32:915–935

Virchows Arch (2003) 443:774–781
DOI 10.1007/s00428-003-0900-5

ORIGINAL ARTICLE

Ben Vainer · Susanne Sørensen · Jakob Seidelin · Ole Haagen Nielsen · Thomas Horn

Expression of ICAM-1 in colon epithelial cells: an ultrastructural study performed on in vivo and in vitro models

Received: 26 August 2003 / Accepted: 26 August 2003 / Published online: 16 October 2003
© Springer-Verlag 2003

Abstract *Background:* Studies have suggested that in ulcerative colitis (UC), intercellular adhesion molecule-1 (ICAM-1) is involved in migration of leukocytes toward the colonic epithelium. A suitable in vitro model of chronic colonic inflammation does not exist, and the role of the epithelium is based on monolayers of cancer cells. Conflicting results exist on epithelial ICAM-1 expression, and the aim of this study was to compare the expression in various models of colonic epithelium. *Materials and methods:* Colonic biopsies from four UC patients and four controls were examined by cryoimmuno-electron microscopy using ICAM-1-antibodies. In four other controls, the epithelium was isolated from colonic biopsies, embedded in collagen, and evaluated similarly. Isolated crypts and cultured cancer cells were stimulated with interferon-γ (IFN-γ) or tumor necrosis factor-α (TNF-α). *Results:* ICAM-1 was not expressed in the biopsies. In contrast, HT29 cells and the collagen-embedded crypts expressed ICAM-1 on the apical membranes proximal to the junctional complexes when stimulated with IFN-γ or TNF-α in a dose-related manner. *Conclusions:* ICAM-1 is not expressed on colonic epithelium in vivo. However, both colonocytes and HT29 cells were capable of expressing ICAM-1 on their apical membranes in response to supraphysiologic cytokine concentrations. These observations question the justification of extrapolating observations from colon cancer cell lines to in vivo inflammatory conditions.

Keywords Colonocytes · Cryotechnique · Electron microscopy · ICAM-1 · Ulcerative colitis

B. Vainer · S. Sørensen · T. Horn
Department of Pathology,
Herlev Hospital, University of Copenhagen,
Denmark

J. Seidelin · O. H. Nielsen
Department of Gastroenterology C,
Herlev Hospital, University of Copenhagen,
Denmark

B. Vainer (✉)
Department of Pathology,
Rigshospitalet,
Blegdamsvej 9, 2100 Copenhagen Ø, Denmark
e-mail: vainer@rh.dk
Tel.: +45-35451389
Fax: +45-35455418

Introduction

Histopathological hallmarks of the chronic inflammatory bowel disease ulcerative colitis (UC) include extravasation of neutrophil granulocytes into the colonic lamina propria and migration toward and across the colonic epithelium, creating the characteristic histological lesions of cryptitis, crypt abscesses, and ulcerations. This locomotion of neutrophils depends on the interaction of specialized membrane glycoproteins, collectively designated cell adhesion molecules.

Intercellular adhesion molecule-1 (ICAM-1) is a member of this cell adhesion molecule receptor family, with the primary function of binding leukocytes firmly to the endothelium and initiating the leukocyte extravasation process through interactions with β_2-integrins (dimers of CD18 and one of either CD11a, CD11b, or CD11c) [13, 27]. ICAM-1 has, in experimental in vitro studies, been reported to be expressed not only on the luminal surface of endothelial cells, but also on epithelial cells [7, 12, 20], indicating that ICAM-1 is involved in phenomena other than neutrophil chemotaxis [30] and leukocyte locomotion across lamina propria [5, 8, 14, 15, 17], such as transepithelial neutrophil migration [1]. This is further substantiated by studies on cultured colon cancer cells, e.g., HT29, showing that transepithelial leukocyte migration is blocked by the use of specific antibodies towards ICAM-1 [5, 20]. However, little is known regarding ICAM-1 expression in vivo, and conflicting results exist [7, 12, 16, 17, 19, 24, 31]. In a recent ultrastructural study, ICAM-1 expression on the endothelium was upregulated in both inflamed and non-inflamed segments of the colon of UC patients compared with colonic tissue from patients with non-inflammatory bowel disorders [32]. ICAM-1

was, in these experiments, not expressed in any of the situations, which does not agree with the results of in vitro assays using monolayers of colon carcinoma cells [3, 5, 7, 10, 12, 20].

ICAM-1 expression is under the influence of pro-inflammatory cytokines, such as interferon-γ (IFN-γ) and tumor necrosis factor-α (TNF-α) [22, 25, 26]. In active UC, blood concentrations of TNF-α (but not IFN-γ) [4] are increased [11, 18], and, in in vitro culture models, TNF-α as well as IFN-γ have been shown to upregulate ICAM-1 expression on both endothelial and epithelial cells [7, 12, 20].

The aim of the present study was to evaluate the ultrastructural localization and expression of ICAM-1 on in vitro models (i.e., HT29 cells and isolated cultured crypts) and in the in vivo condition (biopsies). Furthermore, the effects of stimulation with different concentrations of IFN-γ and TNF-α in the in vitro models were assessed. Since physiological concentrations of IFN-γ in the mucosa of UC patients were unknown, values were measured.

Materials and methods

Patients

Colonic tissue samples were obtained with ordinary biopsy forceps during routine follow-up colonoscopies from four patients with well-established UC and during diagnostic colonoscopies from four patients examined due to continuous diarrhea, but without inflammatory changes of the colon (negative controls). Light microscopy of the samples obtained from the latter subjects subsequently showed the absence of inflammation.

One UC patient (female, age 38 years) had mild disease activity confined to proctosigmoideum recovering from a period of severe left-sided colitis, whereas another UC patient (male, age 42 years) had mild disease activity with macroscopic changes distal to the splenic flexure. The third UC patient (male, age 41 years), from whom only rectal tissue samples could be collected due to endoscopy problems, had mild disease activity confined to the rectum. The fourth UC patient (female, age 36 years) had moderate inflammation in the left side of the colon. The diagnosis of UC had previously been made from internationally recognized guidelines, including clinical, endoscopic, radiological, and histopathological criteria [2]. All patients received long-term treatment with mesalazine (5-aminosalicylic acid) 2.4 g/day, but did not receive any other immunomodulatory agents, including corticosteroids, azathioprine, 5-mercaptopurine, or cyclosporin. From each of the four UC patients, four tissue samples were collected: two from the grossly most inflamed area of the colon/rectum and two from non-inflamed areas. One of each set of specimens was used for immunoelectron microscopic (immuno-EM) evaluation of ICAM-1, whereas the other was processed for light microscopy.

From the four control subjects, two tissue samples were collected from randomly chosen sites of the colon. Histological examination revealed that one of these patients, originally included as a negative control (female, age 65 years), had collagenous colitis. Since the histopathological characteristics of this disorder are significant, i.e., lymphocyte infiltration of the lamina propria and development of a thickened subepithelial collagen band coincident with normal gross appearance at endoscopy, this patient was used as a control of the inflammatory process per se. Normal, non-inflamed colonic tissue was observed in samples from the other three control subjects (one male, age 62 years; two females, ages 22 years and 61 years). None of the control subjects had, for the previous 2 weeks, taken any medication believed to interfere with the inflammatory response, including aspirin and NSAIDs. These samples were used as controls, illustrating ICAM-1 expression in non-inflamed colon from patients without inflammatory disorders: one of each set used for light microscopy and one for immuno-EM.

Additionally, five to seven colonic biopsies were obtained from each of the four patients without UC who underwent colonoscopies for removal of polyps. These samples were used for colonocyte isolation and culturing.

Concentrations of IFN-γ and TNF-α in inflamed colon

To optimize the resemblance with in vivo conditions, snap-freeze fixed biopsies obtained during colonoscopies from 20 patients with active UC (9 female, 11 male; median age 59 years, range 35–79 years) and 10 controls with non-inflammatory bowel disorders (8 female, 2 male; median age 44 years, range 18–70 years) were examined for the content of IFN-γ and TNF-α. Following sonication of the thawed biopsies, the cytokine concentrations were measured using the enzyme-linked immunosorbent assay (ELISA) technique (IFN-γ; R&D Systems, TNF-α; Biotrak Amersham Pharmacia, Buckinghamshire, UK), as previously described [29].

Ethics

The investigation was approved by the Scientific Ethics Committee for Copenhagen County.

Biopsy preparation

One of the two tissue samples collected from each site was fixed in 3.7% buffered formalin and subsequently embedded in paraffin and processed conventionally for histopathological evaluation. Sections were stained with hematoxylin and eosin. Biopsies were evaluated in a blinded manner by two pathologists. Another sample was immediately cut into small pieces (1×1 mm) and fixed for 2 h in 4% paraformaldehyde in 0.1 M cacodylate buffer, pH 7.2, followed by immersion overnight in 20% PVP (polyvinylpyrrolidone; Sigma Chemicals, St. Louis, MO, USA) in 1.84 M sucrose. The tissue was subsequently mounted on silver pins and snap frozen in liquid N_2 for later immuno-EM processing.

Culture of the carcinoma cell line HT29

The human colonic cancer cell line HT29 (American Tissue Type Culture Collection; Rockville, MD, USA) was cultured in McCoys medium supplemented with 10% fetal calf serum (FCS) and passaged twice weekly. Cells were cultured in 24-well plates (NUNC, Naperville, IL, USA) in Dulbecco's modified Eagles Medium (DMEM) containing 10% FCS, 50 IU/ml penicillin, 50 µg/ml streptomycin, and 0.5 mg/ml gentamycin at 37°C in an atmosphere of 5% CO_2 with 90% relative humidity. All cell culture materials were purchased from Invitrogen, Taastrup, Denmark. After 24 h, cell cultures were exposed to 10^{-12}, 10^{-10} or 10^{-8} M human recombinant IFN-γ or TNF-α (both from Sigma-Aldrich) for 24 h.

Cultured HT29 cells were harvested with a cell scraper and fixed for 30 min in 4% paraformaldehyde supplemented with 0.1 M phosphate buffer, pH 7.2. The cells were transferred to an Eppendorf tube and incubated in 15% gelatine (Sigma Chemicals) for 10 min at 37°C. Following centrifugation, the gelatine-cell mixture was left cold overnight for setting, and the tip of the tube containing the cells was cut off and immersed in 20% PVP and 1.84 M sucrose in phosphate-buffered saline (PBS) for 2 h. The gelatine was then cut into small pieces, mounted on silver pins, and snap frozen in liquid N_2 for later immuno-EM processing.

Isolation of fresh colonocytes

Colonocytes were isolated as described by Whitehead et al. [33]. Five to seven endoscopically obtained biopsies were washed three times in ice cold PBS without Mg^{2+} or Ca^{2+}, containing 50 IU/ml penicillin, 50 µg/ml streptomycin, and 0.5 mg/ml gentamycin. The biopsies were subsequently incubated in 1 mM ethylenediaminetetraacetic acid and 1 mM ethylene glycol-bis(β-aminoethyl ether)-N,N,N′,N′-tetraacetic acid in PBS without Mg^{2+} or Ca^{2+} at 21°C for 75 min. The chelating buffer was replaced by ice cold PBS, and crypts and surface epithelium were detached from the biopsies by shaking. Crypts and surface epithelium in suspension were transferred to a new tube and centrifuged at 45×*g* for 2 min. This method yields a highly pure fraction of isolated crypts without significant elements of connective tissue and low levels of stromal cells [28]. However, small fragments of lamina propria connective tissue containing capillaries can be present occasionally. To minimize cell death induced by detachment from the underlying basement membrane [28], crypts were embedded in a collagen type I gel, consisting of rat tail collagen (collagen type I) at final 0.6 mg/ml in DMEM supplemented with 15% FCS and adjusted to neutral pH with the addition of NaOH (all materials from Invitrogen). The gels were incubated on 0.2-µm pore size Anopore inserts (Nunc, Roskilde, Denmark) for 24 h at 37°C in an atmosphere of 5% CO_2 at 90% relative humidity. The further procedure for the initial fixation prior to immuno-EM was as outlined above.

Stimulation with pro-inflammatory cytokines

Based on the measurements described in the previous section, the cultured HT29 cells were stimulated with 10^{-12}, 10^{-10}, and 10^{-8} M of either IFN-γ or TNF-α for 24 h by adding the cytokines to the culture medium [5, 20]. For the isolated crypts, the cytokines were mixed into the collagen gel before jellification and admixture of the cells (for procedure, see previous section).

As a chronic inflammatory disease, the colonic epithelial cells in UC are presumably exposed to pro-inflammatory cytokines for a longer period of time. Since this might influence the interpretation of the observations comparing HT29 cells or freshly isolated colonocytes with biopsies obtained from UC patients, HT29 cells were stimulated for a period of 7 days with 10^{-10} M IFN-γ or 10^{-10} M TNF-α, in the same conditions as mentioned in the above section. Controls consisted of unstimulated cells. Subsequently, the cells were harvested and processed for immuno-EM as described.

Effects of mesalazine

To assess the influence of mesalazine treatment on the colonic ICAM-1 expression, HT29 cells were incubated with 1, 10, or 100 nM mesalazine [6, 21, 30], either with or without simultaneous stimulation with 10^{-10} M IFN-γ and subsequently processed for immuno-EM as described below.

Immunogold-labeling with silver enhancement

For immunogold-labeling, 100 nm sections were cut on a Leica EM FCS cryostat (Vienna, Austria) at 115°C and placed on Formvar/carbon Nickel 200 mesh grids (Electron Microscopy Sciences, Fort Washington, PA, USA) using 2.3 M sucrose and 2% methyl cellulose (1:1) for mounting. Grids with sections were stored in PBS (pH 7.4) until labeling.

Sections were incubated with 0.02 M glycine (10 min), blocked with 10% goat serum (Dako, Roskilde, Denmark) and 1% bovine serum albumin (15 min), and incubated overnight at 4°C with primary antibodies to ICAM-1, diluted 1:50 from stock solution (clone BBIG-I1(11C81); R&D Systems Europe, Oxon, UK). On the following day, sections were washed three times and incubated for 2 h with immunoglobulins conjugated with 1-nm diameter gold particles (1:300) (Gam IgG, Ultra Small; Aurion AA, Wageningen, The Netherlands), washed, and post-fixed in 2% glutaraldehyde in PBS for 10 min. Silver enhancement was performed by incubation with Aurion R-GENT SE-EM (Aurion) for 10 min. Finally, sections were incubated with 2% neutral uranylacetate for 5 min and subsequently with a mixture of 2% methyl cellulose and 4% uranylacetate (9:1) for 5 min. Two sets of negative control sections were made by omitting the primary antibody and by adsorption of the antibodies to recombinant human ICAM-1 (R&D Systems) in saturating concentrations.

The labeled sections were examined using a Philips EM208 electron microscope (Philips, Eindhoven, The Netherlands). Photomicrographs at a ×16,000 magnification were taken (five to eight per specimen), and the number of gold particles per micrometer of the surface membrane was determined in each photograph. Thicker sections from the same specimens were mounted on glass slides, stained with toluidine blue, and examined using ordinary light microscopy in order to evaluate the quality of the fixation and the localization of the observed structures.

Statistics

Non-parametric statistics (the Mann-Whitney rank sum test) were applied for comparison of the density of ICAM-1 labeling (counted as gold particles per micrometer surface length). Data are given as medians and ranges.

Results

Normal

Light microscopy of colonic samples from control patients showed normal crypt architecture and no inflammation, except in one patient with collagenous colitis (see Materials and methods).

Electron microscopic examination on biopsies obtained from these patients revealed a sparse ICAM-1 expression on the luminal aspects of endothelial cells and no expression of ICAM-1 on colonic epithelial cells (data not shown). Non-specific staining (evaluated as the presence of gold particles in the nuclei) was minimal. Tissue from the patient with collagenous colitis had ICAM-1 expression identical to the non-inflamed control samples, i.e., no epithelial and only little endothelial expression.

UC colon

Light microscopy revealed the absence of active inflammation as well as an intact epithelial surface without crypt distortion in the samples taken from endoscopically non-inflamed areas of the colon. Samples from macroscopically inflamed areas contained significant amounts of granulocytes and mononuclear cells, with the presence of cryptitis and crypt abscesses in all specimens.

Ultrastructurally, ICAM-1 expression was not detected on the luminal, the lateral, or basal parts of the cell membranes of colonocytes (Fig. 1b). In contrast, significantly increased endothelial expression was observed (as would be expected from previously published studies) [26] (Fig. 1a). There were no differences between inflamed and non-inflamed areas.

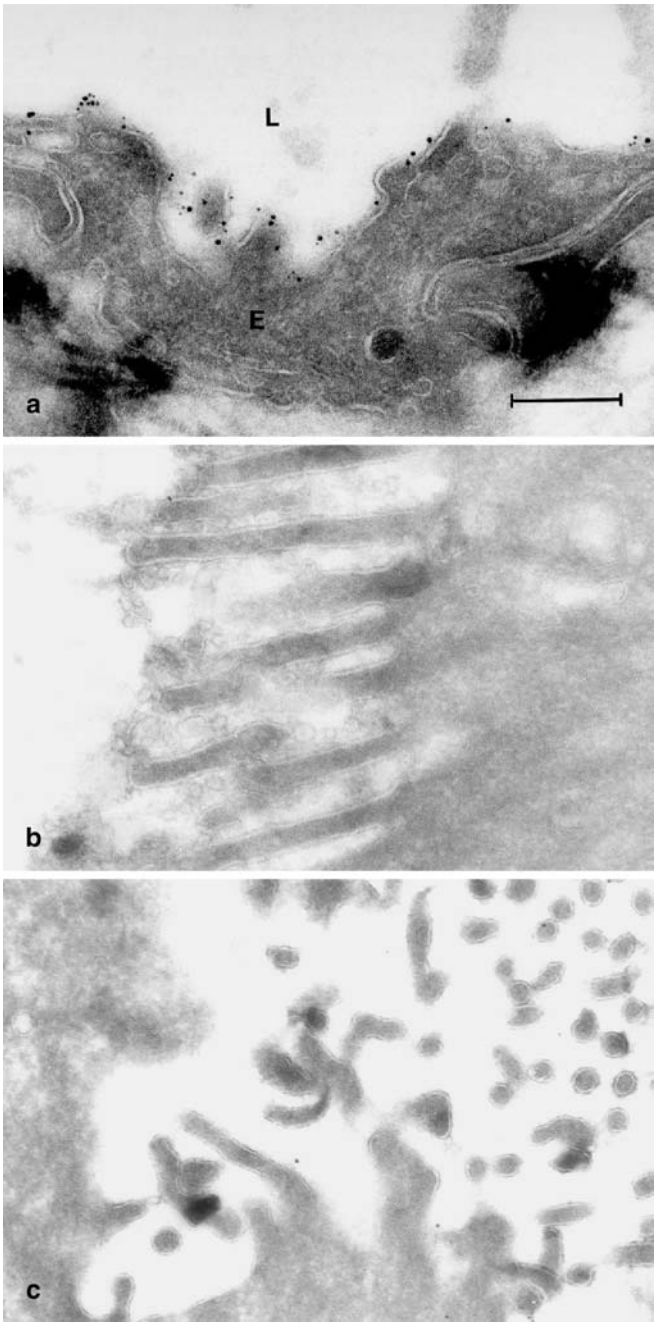

Fig. 1 Photomicrograph of a colonic biopsy from a patient with ulcerative colitis (UC) (**a**, **b**) and from unstimulated HT29 cells (**c**). **a** Luminal expression of intercellular adhesion molecule-1 (ICAM-1) on the luminal surface membrane of an endothelial cell, where the lumen and the supporting layer of collagen are clearly visualized. **b** The apical part of the epithelium with presence of glycocalyx bodies (attached to the microvilli) and terminal web with filaments. In contrast to the colonocytes in vivo, a small amount of ICAM-1 was expressed on HT29 cells (**c**). The apparently detached rounded structures are tips of microvilli. *Original magnification* ×16,000

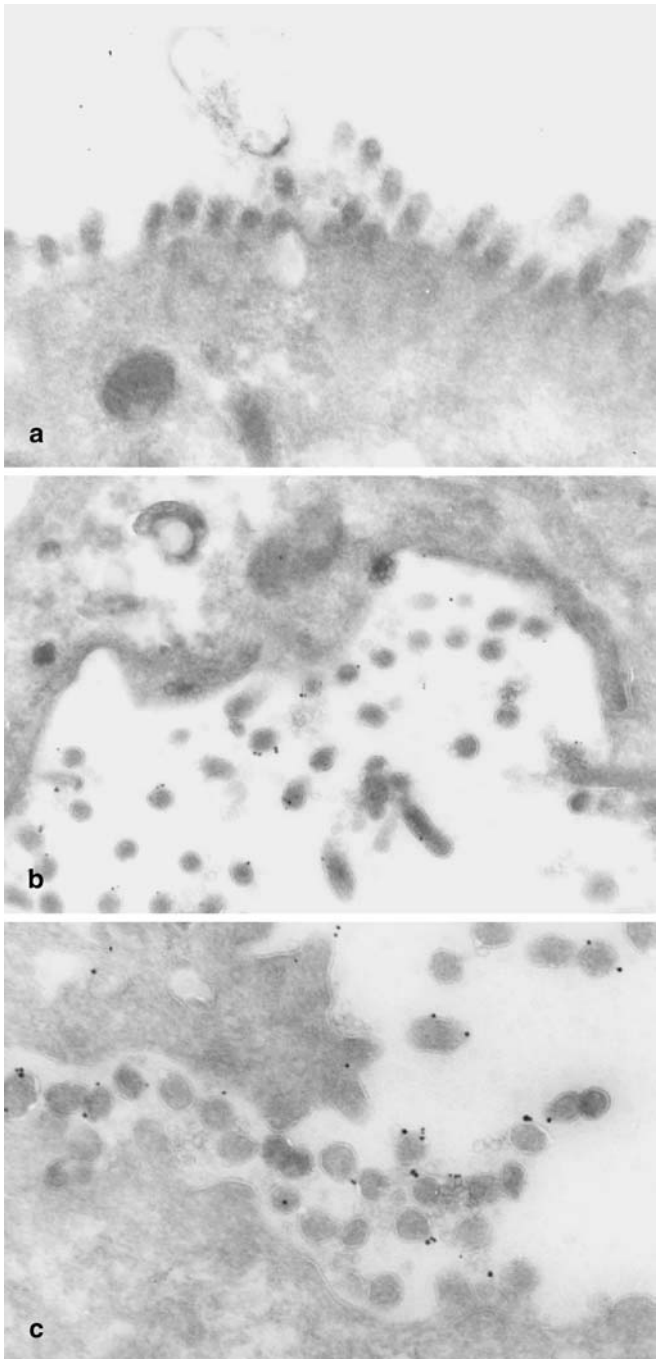

Fig. 2 Photomicrographs of freshly isolated and collagen gel-embedded colonocytes (crypts and surface epithelium), stimulated for 24 h with interferon gamma (IFN-γ): 10^{-12} M IFN-γ (**a**); 10^{-10} M IFN-γ (**b**); 10^{-8} M IFN-γ (**c**). Unstimulated colonocytes did not express intercellular adhesion molecule-1 (not shown). *Original magnification* ×16,000

Concentrations of INF-γ and TNF-α

The ELISA measurements revealed colonic tissue concentrations of median 0.03×10^{-12} M (range 0.00–0.52×10^{-12} M) for IFN-γ and median 0.032×10^{-12} M (range 0.006–0.148×10^{-12} M) for TNF-α, with no corre-

Table 1 Density of intercellular adhesion molecule-1 on the surface membrane of cultured colonic cancer cells (HT29) and isolated and cultured colon crypts upon stimulation with interferon-γ (IFN-γ), evaluated by immuno-electron microscopy. Results are given as the number of gold particles per micrometer surface membrane (medians and ranges). *NS* non-significant

	Unstimulated	IFN-γ		
		10^{-12} M	10^{-10} M	10^{-8} M
HT29 cells	1.33 (0.63–2.57)	0.38 (0.00–0.53) P=0.039[1]	5.72 (0.00–12.67) NS[1]	10.09 (3.91–33.24) P=0.034[1], P=0.046[2]
Colonocytes	0.00 (0.00–0.00)	0.58 (0.00–0.71) NS[1]	9.86 (3.91–22.27) P=0.025[1]	12.36 (6.22–14.14) P=0.001[1], P=0.046[2]

[1] Comparison with unstimulated cells
[2] Comparison with 10^{-10} M IFN-γ stimulation

lation to diagnosis or disease activity. Based on these results, cultured colon cancer cells and cultured freshly isolated colonocytes were stimulated with 10^{-12} M IFN-γ and TNF-α as a physiological equivalent and with the supraphysiological concentrations 10^{-10} M and 10^{-8} M of either cytokine. The effects on ICAM-1 expression were identical to the two cytokines, and, accordingly, only the data for IFN-γ are presented.

Isolated colonocytes

In unstimulated crypts, no ICAM-1 was detected, except from very few scattered gold particles on the surface projections (Table 1). In contrast, stimulation with 10^{-10} M (Fig. 2b) and 10^{-8} M (Fig. 2c) IFN-γ resulted in expression of ICAM-1 with the same localization as on HT29 cells. The upregulation was, however, not as dose dependent as for HT29 cells, and the expression in crypts stimulated with the two highest cytokine concentrations was identical (Table 1). Only minimal expression was observed after stimulation with 10^{-12} M IFN-γ (Fig. 2a). Exactly the same pattern of expression was observed when stimulating with TNF-α (data not shown).

As an internal control, the endothelial cells adjacent to the crypts in some specimens expressed ICAM-1 in the same pattern as previously reported [26], and the expression was increased after application of the higher IFN-α concentrations (not shown).

All the included UC patients received continuous treatment with mesalazine, and in order to assess the effect of mesalazine on the surface expression of ICAM-1, HT29 cells were simultaneously incubated with pharmacological concentrations of the drug (1, 10, and 100 nM) [4, 11, 20] and either 10^{-8} M or 10^{-12} M IFN-γ. The ICAM-1 expression in this setting was not altered, relative to incubation with IFN-γ alone.

Colon cancer cell

Electron microscopic examination revealed a minimal and dispersed expression of ICAM-1 on the luminal surface of unstimulated HT29 cells (Fig. 1a) with large areas entirely devoid of ICAM-1 labeling (for ICAM-1 density see Table 1). Stimulation with IFN-γ showed a marked dose-related increase in the surface expression of ICAM-1: physiological concentrations of IFN-γ or TNF-α (10^{-12} M) did not result in upregulation of ICAM-1, and only sparse labeling was observed at 10^{-10} M. In contrast, significant expression of ICAM-1, mainly on the surface projections, was observed after stimulation with 10^{-8} M IFN-γ (Fig. 3a, b, c, Table 1). ICAM-1 was mainly expressed on membranes of the microvilli. No ICAM-1 was detected in the epithelial junctional complexes, on the lateral and basal membrane parts, or in intracellular compartments. Identical expression was revealed with the application of IFN-α (data not shown).

Long-term stimulation of colon cancer cells

Compared with HT29 cells stimulated for 24 h, ICAM-1 remained upregulated after 7 days of 10^{-10} M IFN-γ stimulation (median 8.01 μm^{-1}, range 4.12–9.60 μm^{-1}; P>0.05; Table 1) (Fig. 4a), whereas the ICAM-1 expression decreased significantly upon long-term TNF-α stimulation (median 1.21 μm^{-1}, range 0.27–1.64 μm^{-1}; P=0.04) (Fig. 4b). The ICAM-1 expression after 1 day of stimulation in these series of experiments did not differ from that observed in the short-term stimulation assays described above.

The control assays, in which the primary antibody was omitted or the anti-ICAM-1 antibodies were pre-adsorbed to recombinant human ICAM-1 antigen, resulted in total absence of labeling, both for colonocytes and for HT29 cancer cells. Regardless of presence or absence of IFN-γ stimulation, incubation with mesalazine did not alter the ICAM-1 expression (data not shown).

Discussion

This is the first report on the ultrastructural expression of ICAM-1 in colonic epithelial cells. ICAM-1 was not expressed on colonocytes under normal or chronic inflammatory conditions, although colonocytes appear to possess the capability of expressing ICAM-1 during adequate stimulation with the pro-inflammatory cytokines IFN-γ and TNF-α. Thus, ICAM-1 was significantly upregulated in a dose-dependent manner both in freshly isolated colonocytes, embedded and incubated in a

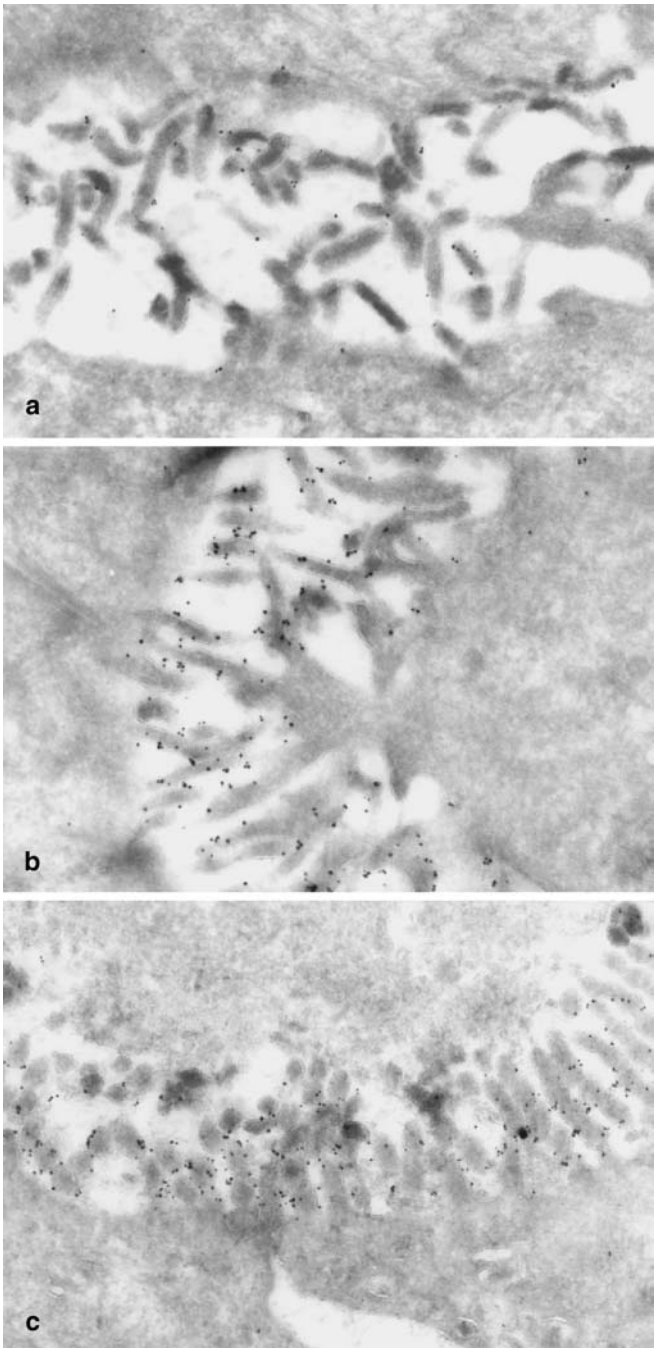

Fig. 3 Immuno-electron microscopy of the intercellular adhesion molecule-1 expression on the colon cancer cell line HT29 after 24 h of incubation with 10^{-12} M (**a**), 10^{-10} M (**b**), and 10^{-8} M (**c**) of interferon gamma. *Original magnification* ×16,000

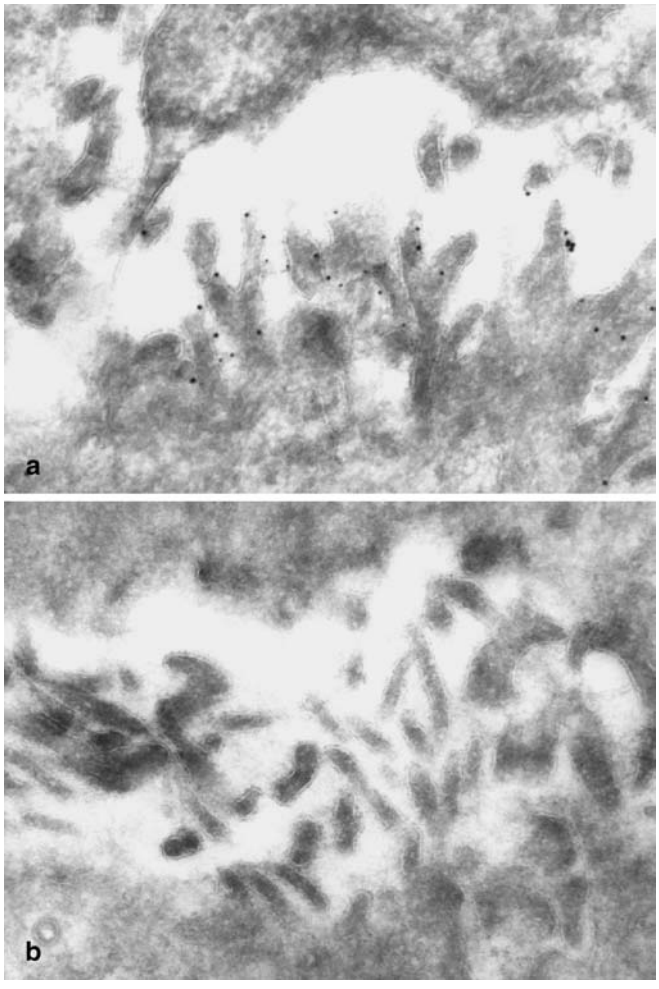

Fig. 4 Intercellular adhesion molecule-1 expression on HT29 cells stimulated with 10^{-10} M interferon gamma (IFN-γ) (**a**) or tumor necrosis factor-α (TNF-α) (**b**) for 7 days. Compare these photomicrographs with the short-term stimulated cells in Fig. 3c. *Original magnification* ×16,000

collagen gel, and in cultured HT29 colon cancer cells, when stimulated with high concentrations of either IFN-γ or TNF-α (Table 1). The expression was limited to the luminal cell membrane of colonocytes only, in particular membranes on the microvilli. In contrast, low levels of these cytokines did not result in detectable expression of ICAM-1. It was further shown that continuous stimulation with IFN-γ or TNF-α affects the ICAM-1 synthesis and expression in colonic epithelial cells differently, as long-term stimulation with IFN-γ did not alter the ICAM-1 expression observed after 1 day, whereas the ICAM-1 was downregulated to the basic level upon stimulation for 7 days with TNF-α. Finally, mesalazine does not appear to affect ICAM-1 regulation.

Cryotechniques in processing tissue for immuno-EM are necessary in order to preserve antibody-binding sites on membrane-bound protein structures, such as ICAM-1, since these antigens are destroyed by the conventional use of glutaraldehyde for EM. The fixation and labeling procedures were evaluated by omitting the primary antibody or by pre-adsorption of the primary antibody with ICAM-1 antigen, both resulting in total absence of ICAM-1 labeling, and by verifying the presence of ICAM-1 on endothelial cells in the biopsy specimens [9, 17, 23, 31].

The differences in expression of ICAM-1 in the in vitro models (HT29 cells and cultured crypts) and in vivo

(biopsies) are highly interesting and may question the usefulness of studying inflammatory mechanisms on cancer cell lines [3, 4, 7, 10, 12]. In contrast to cultured HT29 cells, colon crypts in culture did not reveal genuine expression of ICAM-1 (Table 1). When stimulated with IFN-γ or TNF-α, colon crypts demonstrated ICAM-1 on the surface of epithelial cells, showing that colonocytes, at least in culture, are able to express ICAM-1. However, ICAM-1 expression on colonocytes in cultured crypts was only minimal when using physiological concentrations of IFN-γ and TNF-α. Whereas mucosal concentration of TNF-α has been determined in UC patients [18] and was similar to those measured in the present study, concentrations of IFN-γ have never previously been assessed. In the present study, only low (picomolar) concentrations of IFN-γ and TNF-α in colonic tissue were demonstrated, with identical levels in active UC colon and in colonic tissue from control subjects.

The absence of ICAM-1 in isolated colonic crypts shows that the isolation procedures per se do not induce upregulation of surface ICAM-1 on colonocytes. Hence, the expression on unstimulated HT29 cells must have another genesis, which might be due to phenotypical or genetic (mutational) changes in cancer cells. Whether this change is only present in the cultured cancer cell lines (e.g., HT29) or is a general feature of colon cancer cells is currently being explored.

As an in vitro model for the continuous cytokine exposure of colonocytes, the long-term stimulated HT29 cells in the present study might reflect the in vitro situation. As such, the downregulation of ICAM-1 upon long-term TNF-α stimulation is especially interesting. Other studies have suggested that TNF-α loses some of its cytotoxic effects on colonic epithelial cells over time, as the apoptosis rate decreases to basic levels after 7 days of stimulation following a significant increase observed at days 1–3 [9]. The present observations indicate, however, that the mechanism includes development of "resistance" of colonocytes to the pro-inflammatory effects of TNF-α. This form of cellular adaptation does obviously not seem to be involved in the effect of the other ubiquitous pro-inflammatory cytokine IFN-γ.

It is important to address the question of why isolated colonocytes express a small amount of ICAM-1 when colonocytes in vivo are totally devoid of ICAM-1. Technical conditions cannot be ruled out, although the expression on unstimulated cells in vitro and on the colonic epithelial cells in vivo were identical. Theoretically, concentrations of the cytokines at the epithelium could be higher than in a suspension of sonicated tissue, but since the molecules in vivo diffuse in the tissue centrifugally from the infiltrating leukocytes, it is not conceivable that the levels at the bases of the epithelial cells are of such magnitudes. In the applied technique, it was not possible to adjust for tissue edema and, hence, potential dilution of the cytokines.

In conclusion, the in vitro assays do not reflect ICAM-1 expression and inductability in vivo, even though the results do not unequivocally deny that colonic epithelial cells are able to express ICAM-1 in vivo. The results clearly demonstrate that cultured colon cancer cells are not optimal for studying inflammatory reactions and that caution should be observed when extrapolating data from in vitro assays to in vivo conditions. The observations emphasize the importance of developing and optimizing a culture technique using non-neoplastic cells for the research of the inflammatory process in UC and other inflammatory conditions in the colon.

Acknowledgements The authors wish to thank Ms. Hanne Kruse for invaluable technical assistance as well as Jakob Hendel, MD, and Anders Perner, MD, PhD, for assistance in obtaining biopsies. Mesalazine was kindly donated by Søren Halskov, Ferring Pharmaceuticals, Copenhagen, Denmark. The study was supported by a grant from Else and Mogens Wedell-Wedellsborg's Foundation, Denmark.

References

1. Agace WW, Patarroyo M, Svensson M, Carlemalm E, Svanborg C (1995) Escherichia coli induces transuroepithelial neutrophil migration by an intercellular adhesion molecule-1-dependent mechanism. Infect Immun 63:4054–4062
2. Allan RN, Rhodes JM, Hanauer SB, Keighley MRB, Alexander-Williams J, Fazio VW (1997) Inflammatory bowel diseases, 3rd edn. Churchill Livingstone, New York
3. Bloom S, Simmons D, Jewell DP (1995) Adhesion molecules intercellular adhesion molecule-1 (ICAM-1), ICAM-3 and B7 are not expressed by epithelium in normal or inflamed colon. Clin Exp Immunol 101:157–163
4. Capobianchi MR, Fais S, Di Paolo MC, Agostini D, Paoluzi P, Pallone F, et al (1992) Absence of circulating interferon in patients with inflammatory bowel disease. Suggestion against an autoimmune etiology. Clin Exp Immunol 90:85–87
5. Colgan SP, Parkos CA, Delp C, Arnaout MA, Madara JL (1993) Neutrophil migration across cultured intestinal epithelial monolayers is modulated by epithelial exposure to IFN-gamma in a highly polarized fashion. J Cell Biol 120:785–798
6. De Vos M, Verdievel H, Schoonjans R, Praet M, Bogaert M, Barbier F (1992) Concentrations of 5-ASA and Ac-5-ASA in human ileocolonic biopsy homogenates after oral 5-ASA preparations. Gut 33:1338–1342
7. Dippold W, Wittig B, Schwaeble W, Mayet W, Meyer zum Büschenfelde K-H (1993) Expression of intercellular adhesion molecule 1 (ICAM-1, CD54) on colonic epithelial cells. Gut 34:1593–1597
8. Gao J-X, Wilkins J, Issekutz AC (1995) Migration of human polymorphonuclear leukocytes through a synovial fibroblast barrier is mediated by both β_2 (CD11/CD18) integrins and the β_1 (CD29) integrins VLA-5 and VLA-6. Cell Immunol 163:178–186
9. Jones SC, Banks RE, Haidar A (1995) Adhesion molecules in inflammatory bowel disease. Gut 36:724–730
10. Kaiserlian D, Rigal D, Abello J, Revillard JP (1991) Expression, function and regulation of the intercellular adhesion molecule-1 (ICAM-1) on human epithelial cell lines. Eur J Immunol 21:2415–2421
11. Komatsu M, Kobayashi D, Saito K, Furuya D, Yagihashi A, Araake H, et al (2001) Tumor necrosis factor-α in serum of patients with inflammatory bowel disease ad measured by a highly sensitive immuno-PCR. Clin Chem 47:1297–1301
12. Kvale D, Krajci P, Brandtzaeg P (1992) Expression and regulation of adhesion molecules ICAM-1 (CD54) and LFA-3 (CD58) in human intestinal epithelial cell lines. Scand J Immunol 35:669–686
13. Larson RS, Springer TA (1990) Structure and function of leukocyte integrins. Immunol Rev 114:181–217

14. Malizia G, Calabrese A, Cottone M, Raimondo M, Trejdosiewicz LK, Smart CJ, et al (1991) Expression of leukocyte adhesion molecules by mucosal mononuclear phagocytes in inflammatory bowel disease. Gastroenterology 100:150–159
15. Mishra L, Mishra BB, Harris M, Bayless TM, Muchmore AV (1994) In vitro cell aggregation and cell adhesion molecules in Crohn's disease. Clin Exp Immunol 96:432–436
16. Morise K, Yamaguchi T, Kuroiwa A (1994) Expression of adhesion molecules and HLA-DR by macrophages and dendritic cells in aphtoid lesions in Crohn's disease: an immunocytochemical study. J Gastroenterol 29:257–264
17. Nakamura S, Ohtani H, Watanabe Y, Fukushima K, Matsumoto T, Kitano A, et al (1993) In situ expression of the cell adhesion molecules in inflammatory bowel disease: evidence of immunologic activation of vascular endothelial cells. Lab Invest 69:77–85
18. Nielsen OH, Brynskov J, Bendtzen K (1993) Circulating and mucosal concentrations of tumour necrosis factor and inhibitor(s) in chronic inflammatory bowel disease. Dan Med Bull 40:247–249
19. Oshitani N, Campbell A, Bloom S, Kitano A, Kobayashi K, Jewell DP (1995) Adhesion molecule expression on vascular endothelium and nitroblue titrazolium reducing activity in human colonic mucosa. Scand J Gastroenterol 30:915–920
20. Parkos CA, Colgan SP, Diamond MS, Nusrat A, Liang TW, Springer TA, et al (1996) Expression and polarization of intercellular adhesion molecule-1 on human intestinal epithelia: consequences for CD11b/CD18-mediated interactions with neutrophils. Mol Med 2:489–505
21. Pimpo MT, Frieri G, Palumbo G, Pantaleoni GC, Viscido A, Caprilli R, et al (1997) Postoperative recurrence of Crohn's disease and 5-ASA mucosal concentration. A GISC study. Gastroenterology 112:A1061
22. Pober JS, Gimbrone MA, Lapierre LA, Mendrick DL, Fiers W, Rothlein R, et al (1986) Overlapping patterns of activation of human endothelial cells by interleukin-1, tumor necrosis factor and immune interferon. J Immunol 137:1893–1896
23. Pooley N, Ghosh L, Sharon P (1995) Up-regulation of E-selectin and intercellular adhesion molecule-1 differs between Crohn's disease and ulcerative colitis. Dig Dis Sci 40:219–225
24. Schürmann GM, Aber-Bishop AE, Facer P, Lee JC, Rampton DS, Doré CJ, et al (1993) Altered expression of cell adhesion molecules in uninvolved gut in inflammatory bowel disease. Clin Exp Immunol 94:341–347
25. Seidelin JB, Jäättelä M, Nielsen OH (2003) Continuous interferon-γ or tumor necrosis factor-α stimulation of colonocytes increase cell proliferation and decrease apoptosis. Am J Gastroenterol (in press)
26. Simmons D, Makgoba MW, Seed B (1988) ICAM, and adhesion ligand of LFA-1, is homologous to the neural cell adhesion molecule NCAM. Nature 331:624–627
27. Springer TA (1994) Traffic signals for lymphocyte recirculation and leukocyte migration: the multistep paradigm. Cell 76:301–314
28. Sträter J, Wedding U, Barth TFE, Koretz K, Elsing C, Möller P (1996) Rapid onset of apoptosis in vitro follows disruption of β_1-integrin/matrix interactions in human colonic crypt cells. Gastroenterology 110:1776–1784
29. Vainer B, Nielsen OH (2000) Changed colonic profile of P-selectin, PECAM-1, ICAM-1, ICAM-2, and ICAM-3 in inflammatory bowel disease. Clin Exp Immunol 121:242–247
30. Vainer B, Nielsen OH (2000) Chemotactic properties of ICAM-1 and PECAM-1 on neutrophil granulocytes in ulcerative colitis: effects of prednisolone and mesalazine. Aliment Pharmacol Ther 14:1023–1032
31. Vainer B, Nielsen OH, Horn T (2000) Comparative studies on the colonic in situ expression of intercellular adhesion molecules (ICAM-1, -2, and 3), β_2 integrins (LFA-1, Mac-1, and p150,95), and PECAM-1 in ulcerative colitis and Crohn's disease. Am J Surg Pathol 24:1115–1124
32. Vainer B, Sørensen S, Nielsen OH, Horn T (2002) Subcellular localization of intercellular adhesion molecule-1 in colonic mucosa in ulcerative colitis. Ultrastruct Pathol 26:113–121
33. Whitehead RH, Brown A, Bhathal PS (1987) A method for the isolation and culture of human colonic crypts in collagen gels. In Vitro 3:436–442

Virchows Arch (2003) 443:782–786
DOI 10.1007/s00428-003-0910-3

ORIGINAL ARTICLE

Filippo Fraggetta · Giuseppe Pelosi · Alessia Cafici · Paolo Scollo · Paolo Nuciforo · Giuseppe Viale

CDX2 immunoreactivity in primary and metastatic ovarian mucinous tumours

Received: 16 June 2003 / Accepted: 9 September 2003 / Published online: 24 October 2003
© Springer-Verlag 2003

Abstract The caudal-related homeobox transcription factor CDX2 regulates the differentiation of intestinal epithelial cells. Recent studies have suggested that CDX-2 immunoreactivity is strictly confined to benign and malignant intestinal epithelium. In the present study, we evaluated the prevalence of CDX2 immunoreactivity in a series of benign, borderline and malignant primary ovarian mucinous neoplasms. We tested 62 mucinous tumours of the ovary, including 28 benign cystadenomas, 18 borderline tumours, 16 adenocarcinomas, 35 serous and endometrioid ovarian lesions and 10 ovarian metastases of colonic adenocarcinoma. Overall, the CDX2 prevalence in primary mucinous tumours was 79%, including 20 of 28 (71.5%) cystadenomas, 14 of 18 (77.7%) borderline tumours and 15 of 16 (93.5%) adenocarcinomas. Immunoreactivity usually correlated with intestinal differentiation of tumour cells, although wide heterogeneity in the distribution of immunolabelled cells was noted. No immunoreactivity was observed in serous lesions; whereas, 1 of 13 (7.7%) endometrioid adenocarcinomas and all of the 10 metastatic colonic adenocarcinomas were immunostained. These results indicate that CDX2 is detectable in the majority of benign, borderline and malignant ovarian mucinous tumours and, therefore, makes this marker unsuitable when distinguishing primary from metastatic ovarian mucinous adenocarcinomas. However, CDX2 immunoreactivity could be useful in the distinction between endocervical and intestinal-type mucinous tumours of the ovary, which may have clinical relevance.

Keywords CDX2 · Ovary · Mucinous tumours · Primary · Metastases

F. Fraggetta
Department of Pathology,
Cannizzaro Hospital,
Via Messina 829, 95126 Catania, Italy

G. Pelosi (✉) · G. Viale
Departments of Pathology and Laboratory Medicine,
and University of Milan, School of Medicine,
European Institute of Oncology,
Via G. Ripamonti 435, 20141 Milan, Italy
e-mail: giuseppe.pelosi@ieo.it
Tel.: +39-02-57489414
Fax: +39-02-57489417

A. Cafici
Departments of Experimental and Clinical Pharmacology,
University of Catania School of Medicine,
Viale Doria 6, 95125 Catania, Italy

P. Scollo
Departments of Obstetric and Gynecology,
Cannizzaro Hospital,
Via Messina 829, 95126 Catania, Italy

P. Nuciforo
Molecular Pathology Unit,
FIRC Institute of Molecular Oncology,
Via Adamello 16, 20139 Milan, Italy

Introduction

The caudal-related homeobox transcription factor, CDX2, regulates the differentiation of intestinal epithelial cells [12, 17] by controlling the expression of molecules involved in cell–cell and cell–substratum interaction and by promoting the complete differentiation of intestinal cells [9]. It has been suggested that CDX2 plays a role in directing early processes in intestinal cell morphogenesis and in the maintenance of the differentiated phenotype by supporting the transcription of differentiated gene products [17].

A growing body of literature has recently dealt with CDX2 immunoreactivity in benign and malignant lesions of the gastrointestinal tract, such as intestinal metaplasia of the stomach, intestinal-type gastric cancer and primary and metastatic intestinal adenocarcinomas [1, 2, 5, 11, 14, 15, 19]. Due to the restricted expression in normal and neoplastic intestinal epithelial cells, it has been suggested that CDX2 immunostaining could be useful in assessing the intestinal origin of metastases in the lung [2, 19]. Although CDX2 immunoreactivity has been

occasionally reported in extra-intestinal sites, including the ovary [2, 19], little is known about the prevalence of CDX2 immunoreactivity in mucinous tumours of the ovary and its diagnostic role in distinguishing ovarian mucinous primaries from metastases of intestinal adenocarcinomas.

Materials and methods

Formalin-fixed and paraffin-embedded primary mucinous tumours of the ovary (n=62), primary serous and endometrioid ovarian benign and malignant lesions (n=35) and ovarian metastases from colonic adenocarcinoma (n=10) were retrieved and tested for CDX2 immunoreactivity. Distinction between primary and metastatic mucinous carcinomas was based on well-refined clinicopathological criteria [7, 8].

Among the 62 primary ovarian mucinous lesions, 28 were classified as benign cystadenomas, 18 as borderline tumours and 16 as primary adenocarcinomas [13]. According to well-refined histopatological criteria, all but one of the cystadenomas were classified as endocervical type; 13 of 18 borderline tumours and all of the adenocarcinomas were classified as intestinal type [13].

The serous tumours included 3 benign cystadenomas, 2 borderline tumours and 15 serous adenocarcinomas; whereas, the endometrioid lesions included 2 endometrioid cysts and 13 endometrioid adenocarcinomas. For CDX2 immunohistochemistry, after blocking endogenous peroxidase activity with 5% hydrogen peroxide for 12 min and microwave antigen retrieval at 750 W for 20 min in ethylene diamine tetraacetic acid buffer, pH 8, de-waxed sections were reacted with an anti-CDX2 monoclonal antibody (Clone CDX2–88; Biogenex) for 30 min at room temperature using an automatic immunostainer (DakoAutostainer; Dako, Glostrup, Denmark) and then incubated with a high sensitivity detection kit (Dako EnVision Plus-HRP; Dako) according to the manufacturer's instructions. Peroxidase activity was developed with 3–3′-diaminobenzidine-copper sulphate (Sigma Chemical Co, St Louis, MO, USA) to obtain a brown-black end product. The specificity of all immunoreactions was double checked by substituting the primary antibody with an unrelated isotypic mouse immunoglobulin at a comparable dilution and with normal serum alone [4]. Samples of normal colonic mucosa were immunostained as an external positive control.

Immunoreactivity was recorded both as the percentage (labelling index) of immunoreative cells (by scoring a minimum of 1000 cells in the representative fields of immunostaining) and according to an arbitrary five-tiered scale from negative to 4+. Briefly, tumours were considered negative if staining was completely absent, 1+ if staining was present in 1–5% neoplastic cells, 2+ if present in 6–25% neoplastic cells, 3+ if present in 26–50% neoplastic cells and 4+ if present in 51–100% neoplastic cells. Only immunoreactivity confined to the nuclei of tumour cells was taken into account.

Continuous data was expressed using median values and contrasted employing the Wilcoxon signed-rank test or the Kruskal-Wallis test if medians were analysed between two or more groups, respectively. Categorical associations were evaluated by Fisher's exact t-test or chi-square test. Any statistical test was considered significant if the corresponding P value was ≤ 0.05.

Results

CDX2 immunoreactivity was highlighted by a fine granular to diffuse pattern of staining confined to the nuclei, which was independent of the labelling intensity. Control experiments showed that most nuclei of the normal intestinal epithelium were strongly reactive with CDX2. In ovarian tumours, CDX2 immunoreactivity was usually confined to neoplastic cells showing intestinal differentiation; whereas, in rare instances, the labelling was related to clusters of cells without definite morphological evidence of intestinal differentiation. Representative features of CDX2 immunoreactivity in primary mucinous tumours of the ovary are depicted in Fig. 1A, B, C, D, E, F, G, H.

The results are summarised in Table 1. Overall, CDX2 immunoreactivity was detected in 49 of 62 (77%) primary ovarian mucinous tumours, 20 of 28 (71.5%) benign mucinous cystadenomas, 14 of 18 (77.7%) borderline tumours, 15 of 16 (93.5%) mucinous carcinomas and 10 of 10 (100%) ovarian metastases from colonic adenocarcinomas. In cystadenomas, CDX2 immunoreactive cells ranged from 0% to 100% (mean±SD: 6.7±18.9; median 1), in borderline tumours from 0% to 100% (mean±SD: 47.3±43.5; median 56), and in primary adenocarcinomas from 0% to 100% (mean±SD: 66.3±35.7; 90) (P<0.0001). In metastases, CDX2 immunoreactive cells ranged from 85% to 95% (mean±SD: 90.2±3.7; median 90). No statistically significant differences were seen between borderline tumours and primary carcinomas, as well as between mucinous primaries and metastatic colonic adenocarcinomas (P=NS). Only 1 of 28 (3.5%) benign cystadenomas was scored 3+ to 4+;

Table 1 CDX2 immunoreactivity in primary and metastatic ovarian tumours. Tumours were considered 3+ if staining was present in 26–50% neoplastic cells and 4+ if present in 51–100% neoplastic cells

Primary	No. positive cases (%)	Percentage of immunoreactive cells		
		Mean±SD	Range (%)	Score 3+/4+
Mucinous (overall)	49/62 (77%)			
Benign	20/28 (71.5%)	6.7±18.9	0–100	1/28 (3.5%)
Borderline	14/18 (77.7%)	47.3±43.5	0–100	10/18 (55.5%)
Malignant	15/16 (93.5%)	66.3±35.7	0–100	13/16 (81.2%)
Serous (overall)	0/20 (0%)			
Benign	0/3 (0%)	-	-	-
Borderline	0/2 (0%)	-	-	-
Malignant	0/15 (0%)	-	-	-
Endometrioid (overall)	1/15 (6.6%)			
Benign	0/2 (0%)	-	-	-
Malignant	1/13 (7.7%)	-	35*	1/13 (7.7%)
	10/10 (100%)	90.2±3.7	85–95	10/10 (100%)

* Only one case showed immunoreactivity for CDX2

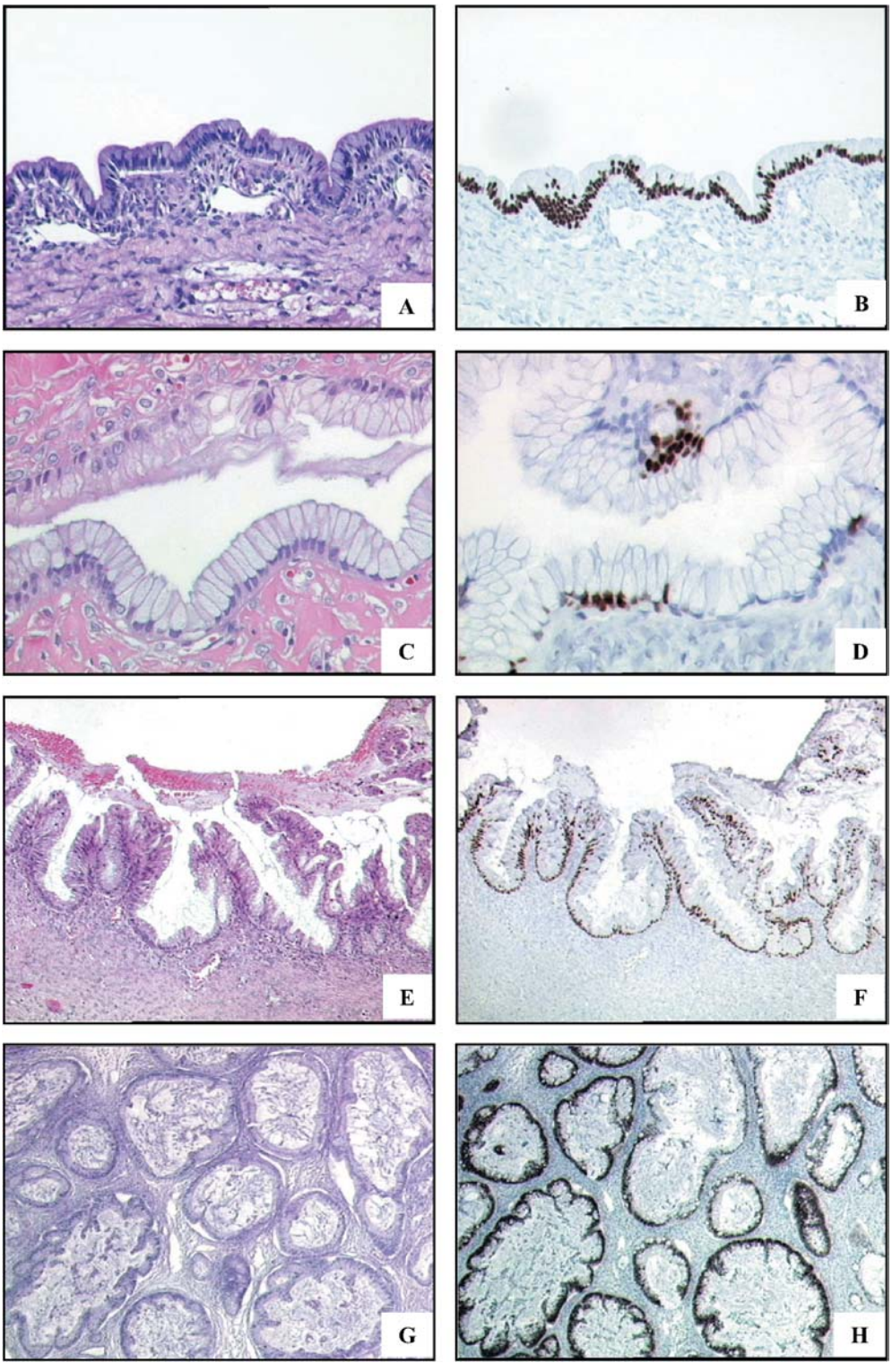

Fig. 1 Representative examples of CDX2 immunoreactivity in primary ovarian tumours: diffuse CDX2 immunostaining in a case of intestinal type cystadenoma (**A**, **B**); CDX2 immunostaining in scattered endocervical-like cells of a benign cystadenoma (**C**, **D**); diffuse CDX2 immunostaining in borderline (**E**, **F**) and malignant (**G**, **H**) primary mucinous tumours of the ovary

whereas, 10 of 18 (55.5%) borderline tumours and 13 of 16 (81.2%) primary mucinous adenocarcinomas attained a 3+ to 4+ score ($P<0.0001$). All cases of metastatic adenocarcinomas belonged to the 4+ score. No cases of serous, either benign or malignant, and benign endometrioid lesions showed CDX2 immunoreactivity, whereas 1 of 13 (7.7%) endometrioid adenocarcinoma exhibited CDX2 immunostaining, with 35% of neoplastic cells labelled in both glandular and squamous cell components (Fig. 2A, B).

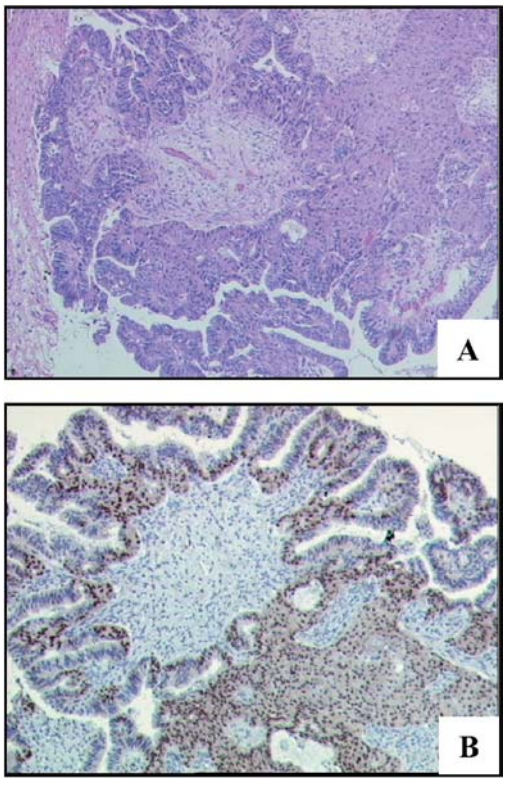

Fig. 2 A case of endometrioid adenocarcinoma with foci of squamous cell differentiation (**A**) showing consistent immunostaining for CDX2 (**B**)

Discussion

Our study first documents that CDX2 immunoreactivity is consistently detectable in benign, borderline and malignant ovarian mucinous tumours; whereas, serous tumours and endometrioid lesions are usually unreactive with this marker. Since CDX2 is commonly expressed in primary mucinous ovarian carcinomas, this marker is unsuitable in assisting the distinction between primary and metastatic mucinous tumours.

Although homeobox gene products, namely CDX2 and TTF-1, are considered to be organ-specific molecules, they may sometimes be detected outside their native organs. For example, extra-intestinal immunoreactivity for CDX2 has been reported in ovarian mucinous lesions, urinary bladder adenocarcinomas, papillary thyroid carcinoma and carcinoid tumours [2, 19]. Another homeobox gene product, namely TTF-1, is frequently expressed by extrapulmonary small cell carcinomas and even expressed in gastric, endometrial and colonic adenocarcinomas, although this is much more rare. In the present series, immunoreactivity for CDX2, either focal or diffuse, was consistently documented in the entire spectrum of primary mucinous tumours of the ovary, including benign, borderline and malignant lesions.

Mucinous tumours, accounting for only 12–15% of all ovarian tumours, still represent a challenge in daily pathological diagnostic practices and in the correct management of the patient [13]. In particular, the distinction between primary and metastatic ovarian mucinous adenocarcinomas must be based on a combination of morphological, immunohistochemical, clinical and surgical findings [3, 7, 8, 18]. More recently, a combination of immunostaining for CDX2 with cytokeratins 7 and 20 has been suggested for differentiating ovarian mucinous primaries from metastatic colonic adenocarcinomas [6].

Herein, we show a high prevalence of CDX2 immunoreactivity within the primary mucinous adenocarcinoma group, with the majority of cases belonging to scores 3–4. Although metastatic mucinous adenocarcinomas showed, by far, the highest prevalence of immunoreactive cells per case, with a more homogenous CDX2 immunostaining pattern, no statistically significant differences were found when compared with the primaries. A high prevalence of CDX2 immunoreactive cells in primary ovarian mucinous adenocarcinoma has also been reported by Werling et al. [19], with figures approaching 65% of cases. Therefore, this marker seems unsuitable for reliably distinguishing primary from secondary mucinous adenocarcinomas of the ovary.

The diagnostic utility of CDX2 needs an additional note of caution in differentiating ovarian endometrioid adenocarcinoma from metastatic colonic adenocarcinomas. Cases of poorly differentiating colonic adenocarcinomas may lack CDX2 immunoreactivity [2] and, as shown in the present study, endometrioid carcinomas may aberrantly express this marker. However, endometrioid adenocarcinomas are cytokeratin 7-positive and cytokeratin 20-negative; whereas, metastatic colorectal adenocarcinomas usually exhibit the opposite immunophenotype [10].

We have shown that CDX2 immunoreactivity is usually restricted to cells recapitulating the morphological appearance of intestinal type epithelium. Therefore, we suggest CDX2 should be considered a cell type-related antigen rather than a site-specific marker. Moreover, the progressive increase in the percentage of CDX2 immunoreactive cells from benign mucinous cystadenomas to borderline tumours and malignant primary mucinous adenocarcinomas is in keeping with the results obtained by Werling et al. [19] and with the increasing prevalence of intestinal differentiation in these neoplasms [13]. In a few instances, CDX2 immunoreactivity was also detected in tumour cells devoid of morphological features of intestinal differentiation. It is worth noting that even tumours morphologically composed of endocervical-like epithelium may express markers of gastrointestinal differentiation [13]. The unexpected finding of CDX2 immunoreactivity in a case of endometrioid adenocarcinoma is particularly intriguing, with foci of squamous cell differentiation showing consistent immunostaining for this marker. CDX2 immunoreactivity has been rarely described outside mucinous epithelium (i.e. gastrointestinal carcinoids and thyroid carcinoma) [19], and this unexpected expression in squamous-appearing tumour cells needs further investigation.

Although it has been suggested that distinguishing endocervical-type from intestinal-type mucinous tumours of the ovary is prognostically relevant [16], it should be noted that this distinction is sometimes difficult on histological grounds only. Therefore, we believe that CDX2 immunoreactivity could help to detect intestinal-type components in ovarian mucinous tumours; whether the percentage of CDX2 immunoreactive cells is relevant to prognosis, however, needs further investigation.

Acknowledgement The authors thank Mr. Steven Lawson for the English revision of the manuscript.

References

1. Bai YQ, Yamamoto H, Akiyama Y, Tanaka H, Takizawa T, Koike M, Kenji Yagi O, Saitoh K, Takeshita K, Iwai T, Yuasa Y (2002) Ectopic expression of homeodomain protein CDX2 in intestinal metaplasia and carcinomas of the stomach. Cancer Lett 176:47–55
2. Barbareschi M, Murer B, Colby TV, Chilosi M, Macri E, Loda M, Doglioni C (2003) CDX-2 homeobox gene expression is a reliable marker of colorectal adenocarcinoma metastases to the lungs. Am J Surg Pathol 27:141–149
3. Berezowski K, Stastny JF, Kornstein MJ (1996) Cytokeratins 7 and 20 and carcinoembryonic antigen in ovarian and colonic carcinoma. Mod Pathol 9:426–429
4. Burry RW (2000) Specificity controls for immunocytochemical methods. J Histochem Cytochem 48:163–166
5. Eda A, Osawa H, Yanaka I, Satoh K, Mutoh H, Kihira K, Sugano K (2002) Expression of homeobox gene CDX2 precedes that of CDX1 during the progression of intestinal metaplasia. J Gastroenterol 37:94–100
6. Groisman GM, Meir A (2003) The intestinal marker CDX2 is useful in differentiating primary ovarian carcinoma from metastatic colonic carcinoma. Mod Pathol 16:190A
7. Lee KR, Scully RE (2000) Mucinous tumors of the ovary: a clinicopathologic study of 196 borderline tumors (of intestinal type) and carcinomas, including an evaluation of 11 cases with pseudomyxoma peritonei. Am J Surg Pathol 24:1447–1464
8. Lee KR, Young RH (2003) The distinction between primary and metastatic mucinous carcinomas of the ovary: gross and histologic findings in 50 cases. Am J Surg Pathol 27:281–292
9. Lorentz O, Duluc I, Arcangelis AD, Simon-Assmann P, Kedinger M, Freund JN (1997) Key role of the Cdx2 homeobox gene in extracellular matrix-mediated intestinal cell differentiation. J Cell Biol 139:1553–1565
10. McCluggage WG (2002) Recent advances in immunohistochemistry in gynecological pathology. Histopathology 40:309–326
11. Mizoshita T, Inada K, Tsukamoto T, Kodera Y, Yamamura Y, Hirai T, Kato T, Joh T, Itoh M, Tatematsu M (2001) Expression of Cdx1 and Cdx2 mRNAs and relevance of this expression to differentiation in human gastrointestinal mucosa—with special emphasis on participation in intestinal metaplasia of the human stomach. Gastric Cancer 4:185–191
12. Qualtrough D, Hinoi T, Fearon E, Paraskeva C (2002) Expression of CDX2 in normal and neoplastic human colon tissue and during differentiation of an in vitro model system. Gut 5:184–190
13. Scully RE, Young RH, Clement PB (1998) Mucinous tumors and pseudomyxoma peritonei. In: J Rosai (ed) Tumors of the ovary, maldeveloped gonads, fallopian tube, and broad ligament. Armed Forces Institute of Pathology, Washington, DC, pp 81–106
14. Seno H, Oshima M, Taniguchi MA, Usami K, Ishikawa TO, Chiba T, Taketo MM (2002) CDX2 expression in the stomach with intestinal metaplasia and intestinal-type cancer: prognostic implications. Int J Oncol 21:769–774
15. Silberg DG, Sullivan J, Kang E, Swain GP, Moffett J, Sund NJ, Sackett SD, Kaestner KH (2002) Cdx2 ectopic expression induces gastric intestinal metaplasia in transgenic mice. Gastroenterology 122:689–696
16. Siriaunkgul S, Robbins KM, McGowan L, Silverberg SG (1995) Ovarian mucinous tumors of low malignant potential: a clinicopathologic study of 54 tumors of intestinal and mullerian type. Int J Gynecol Pathol 14:198–208
17. Suh E, Traber PG (1996) An intestine-specific homeobox gene regulates proliferation and differentiation. Mol Cell Biol 16:619–625
18. Wang N-P, Zee S, Zarbo RJ, Bacchi CE, Gown AM (1995) Coordinate expression of cytokeratins 7 and 20 define unique subsets of carcinoma. Appl Immunohistochem 3:99–107
19. Werling RW, Yaziji H, Bacchi CE, Gown AM (2003) CDX2, a highly sensitive and specific marker of adenocarcinomas of intestinal origin: an immunohistochemical survey of 476 primary and metastatic carcinomas. Am J Surg Pathol 27:303–310

Virchows Arch (2003) 443:787–791
DOI 10.1007/s00428-003-0911-2

CASE REPORT

Mauro G. Mastropasqua · Giancarlo Pruneri · Giuseppe Renne · Ottavio De Cobelli · Giuseppe Viale

Basaloid cell carcinoma of the prostate. Case report and review of the literature

Received: 25 June 2003 / Accepted: 9 September 2003 / Published online: 24 October 2003
© Springer-Verlag 2003

Abstract We report on a case of malignant basal cell carcinoma of the prostate combined with a poorly differentiated conventional adenocarcinoma, infiltrating bilaterally the seminal vesicles and with lymph-node and distant metastases. Basal cell carcinoma represented the prevalent component of the tumour (80%), showed high mitotic activity, extensive perineural infiltration and vascular invasion and was immunoreactive for basal cell related antigens (high molecular weight cytokeratins 34βE12 and p63). Our data confirm previous observations that basal cell carcinoma represents an aggressive tumour with an adverse clinical outcome.

Keywords Adenoid cystic carcinoma · Basaloid cell carcinoma · Prostate

Introduction

Malignant tumours arising from the basal cells of the prostatic glands are exceedingly rare [2, 4, 8, 22, 32], with only 20 cases (11 of which with complete clinicopathological data) reported thus far [1, 3, 5, 10, 11, 14, 15, 16, 17, 18, 19, 26, 28, 31]. These tumours have been classified according to the prevalent pattern of growth as adenoid cystic carcinomas (ACC) or basaloid cell carcinomas (BCC). ACC/BCC may occur in a pure form or, rarely, in combination with conventional adenocarcinoma [17, 25, 31]. ACC/BCC with a prominent adenoid cystic architecture usually behave indolently, while the occurrence of an extensive basaloid pattern has been associated with a more aggressive disease [7].

We report on a case of a malignant basal cell tumour of the prostate with an exclusive basaloid pattern combined with a poorly differentiated conventional adenocarcinoma, infiltrating bilaterally the seminal vesicles and with lymph-node and distant metastases. Our data re-emphasise that ACC/BCC with prominent basaloid features are aggressive tumours, whose correct identification is mandatory for adequately planning clinical staging and treatment of the disease.

M. G. Mastropasqua · G. Pruneri · G. Renne · G. Viale (✉)
Division of Pathology and Laboratory Medicine,
European Institute of Oncology,
Via Ripamonti 435, 20141 Milan, Italy
e-mail: giuseppe.viale@ieo.it
Tel.: +39-08-057489419
Fax: +39-08-057489417

M. G. Mastropasqua · G. Pruneri · G. Renne · G. Viale
School of Medicine, University of Milan, Milan, Italy

O. De Cobelli
Division of Urology, European Institute of Oncology,
Milan, Italy

Clinical history

A 65-year-old Caucasian man suffering from nicturia and hypogastric pain was admitted to a general hospital. Due to a high prostate-specific antigen (PSA) serum level, prostatic biopsies were performed and a histological diagnosis of carcinoma, most probably of a urinary bladder origin, was rendered. Following cystoscopy and random biopsies, which did not reveal any bladder tumour, the patient was referred to the Division of Urology of the European Institute of Oncology for further evaluation. The serum PSA level was 8.5 ng/ml and the prostate was enlarged and firm on digital rectal examination. Additional prostatic biopsies were taken, leading to the diagnosis of basaloid cell carcinoma of the prostate. The patient underwent radical prostatectomy with pelvic lymphadenectomy 1 month later. The histological examination of the resected prostate revealed a basaloid carcinoma combined with a poorly differentiated classical adenocarcinoma without clinically evident metastatic deposits at time of surgery (Gleason's score 4+4=8; pT3bN1M0). A computed tomography scan performed in an outside hospital 8 months later revealed pulmonary and bone metastases, which were not biopsied. The patient is currently alive with disease 12 months after surgery.

Materials and methods

Prostatic biopsies and the resected prostate were fixed in 10% buffered formalin and embedded in paraffin. Sections 3-μm thick were stained with hematoxylin & eosin. Sections representative of the tumour were also stained with periodic acid Schiff (PAS) diastase and Alcian blue. Immunohistochemical reactions were

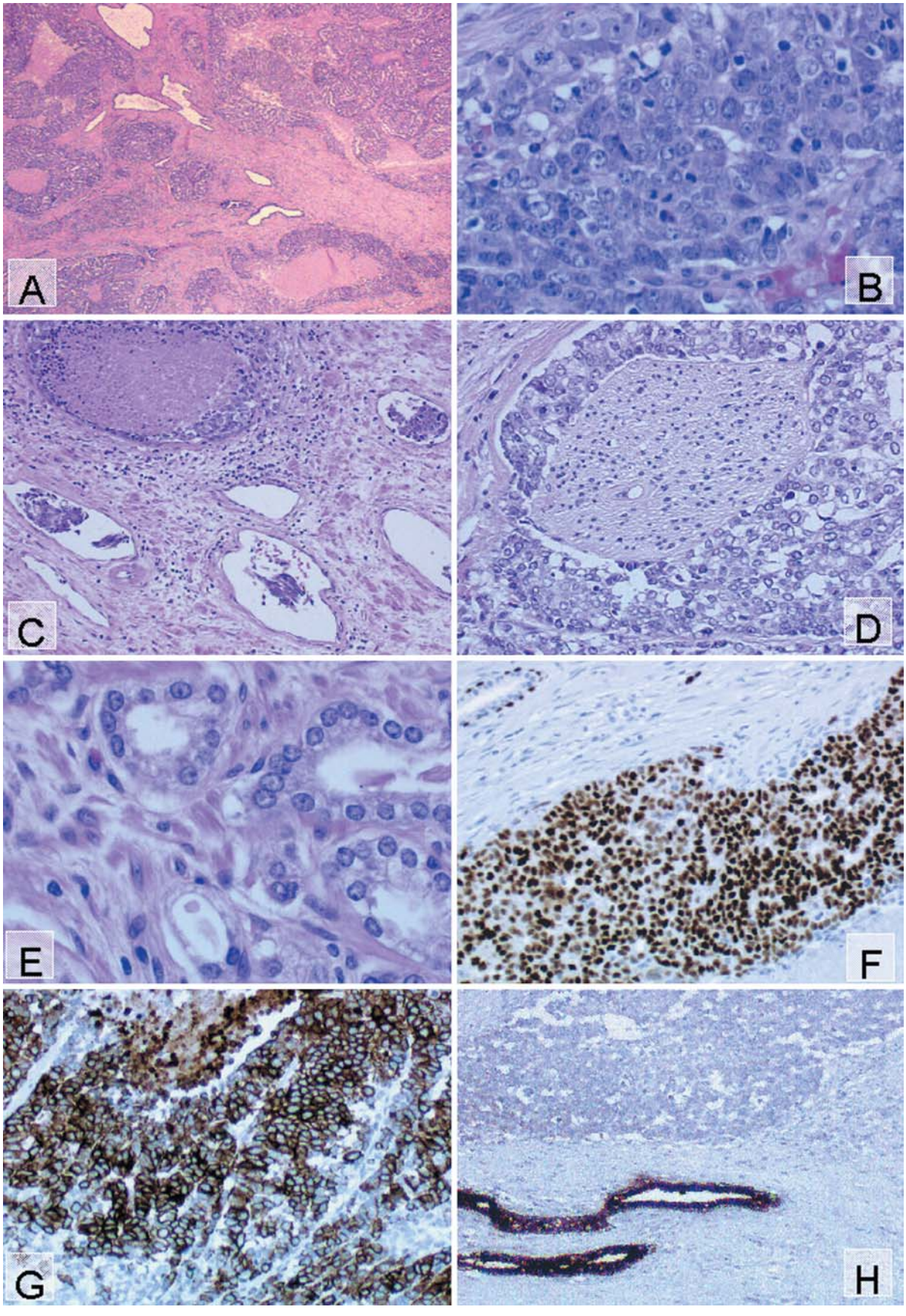
A
B
C
D
E
F
G
H

Table 1 Antibodies, sources and dilution used for immunohistochemistry and immunostaining results in basaloid cell carcinomas

Antibodies	Clone	Source	Dilution	Pre-treatment	Immunoreactivity
High molecular weight cytokeratins	34βE12	Dako	1:50	Citrate	Strongly positive
p63 protein	4A4	Dako	1:100	Ethylene diamine tetraacetic acid	Strongly positive
Prostate-specific antigen	Polyclonal	Dako	1:1200	None	Negative
Prostatic specific acid phosphatase	Polyclonal	Dako	1:2000	None	Negative
Cytokeratin 7	OV-TL12/30	Dako	1:400	Pepsin	Negative
Cytokeratin 20	Ks20.8	Dako	1:80	Pepsin	Negative
Myosin	SMMS-1	Dako	1:50	Citrate	Negative
S-100 protein	Polyclonal	Dako	1:1600	None	Weakly positive
Chromogranin	LK2H10	Ortho	1:40	None	Negative
Synaptophysin	SY38	Dako	1:20	Citrate	Negative

performed using the primary antibodies listed in Table 1 and a commercially available kit (Dako EnVision Plus-HRP; Dako), according to the manufacturer's instructions.

Results

The surgical specimen, including the prostate and bilateral seminal vesicles, measured 4.5×4x4 cm and weighed 144 g. The left seminal vesicle was strictly adherent to the prostate bladder neck. Eight bilateral iliac and otturatory lymph nodes were isolated.

The cut surface of the prostate was grey-pinkish with yellowish areas. Histologically, the tumour was composed of two distinct components. The prevalent component (80% of the tumour area) involved both the peripheral and transitional zone and had an exclusively basaloid growth pattern, with solid tumour nests, peripheral palisading and central necrosis. It consisted of small cells with scant cytoplasm, round nuclei with stipped chromatin and a single small nucleolus and a high mitotic rate (more than 10 mitoses/10 high power fields) (Fig. 1A, B, C). Although there was not a frankly adenoid cystic pattern, cystic spaces filled with PAS diastase and Alcian-blue positive amorphous material were focally detectable. The tumour showed extensive vascular (Fig. 1C) and perineural (Fig. 1D) invasion and widely infiltrated the prostate with bilateral extension to the seminal vesicles. The minor component (20% of the tumour) was a poorly differentiated conventional adenocarcinoma (Gleason 4+4=8) located in the peripheral zone and clearly separated from the BCC component (Fig. 1E) [12, 13]. The non-neoplastic prostatic tissue was characterised by multiple foci of basal cell hyperplasia.

Fig. 1 Basal cell carcinoma (**A–D**, **F–H**) combined with classical poorly differentiated usual adenocarcinoma (**E**). Basal cell carcinoma is characterised by an exclusive basaloid pattern of growth with peripheral palisading (**A**) and central necrosis (**C**). The tumour is composed by small cells with scant cytoplasm, round nuclei with stipped chromatin and a single small nucleolus, showing a high mitotic rate (**B**), extensive vascular invasion (**C**) and perineural infiltration (**D**) and is immunoreactive for the basal cell associated antigens p63 (**F**) and high molecular weight cytokeratins 34βE12 (**G**), but not for prostate-specific antigen (**H**)

The cells of BCC were consistently immunoreactive for p63 (Fig. 1F), high molecular weight cytokeratins 34βE12 (Fig. 1G) and, focally and weakly, for S-100 protein; whereas, they were unreactive for myosin, PSA (Fig. 1H), prostate-specific antigen phosphatase (PSAP) and cytokeratins 7 and 20. The same pattern of immunoreactivity was shared by the foci of basal cell hyperplasia. In contrast, the cells of classical adenocarcinoma were immunoreactive for PSA and PSAP and not reactive for the basal cell markers cytokeratins 34βE12 and p63. One of the eight lymph nodes examined harboured a small (0.5 mm in diameter) metastatic deposit of PSA-positive adenocarcinoma.

Discussion

We report on a case of BCC of the prostate combined with a poorly differentiated conventional adenocarcinoma showing extra-prostatic extension and lymph-node and distant metastases. The differential diagnosis of BCC includes poorly differentiated (Gleason's grade 4 and 5) adenocarcinoma and metastatic tumours. Poorly differentiated adenocarcinomas may grow in solid nests and, similarly to ACC/BCC, are not reactive for PSA. The lack of immunoreactivity for p63 and 34βE12, however, is helpful in recognising conventional adenocarcinomas [27, 28], though it has been recently reported that this tumour may occasionally express p63 [20, 21]. Among the non-prostatic tumours, the most challenging differential diagnosis is with high-grade transitional cell carcinoma (TCC) invading the prostate gland. As a matter of fact, in the present case, a carcinoma, possibly arising in the urinary bladder, was originally diagnosed. Similarly to BCC, TCC may exhibit a solid growth pattern with peripheral palisading and central necrosis and may express high levels of p63 mRNA. Since mRNA overexpression is usually associated with protein overexpression, p63 immunostaining would be of little value in distinguishing TCC from BCC [23, 29]. The immunoreactivity of the neoplastic cells for cytokeratins 34βE12, but not for cytokeratins 7 and 20, and the occurrence of extensive basal cell hyperplasia in the surrounding prostate strongly favour the diagnosis of BCC [6, 9, 24, 30].

Table 2 Characteristics of the 11 cases of ACC/BCC with available clinico-pathological data. *ACC* adenoid cystic carcinoma pattern, *BCC* basal cell carcinoma pattern, *NA* not available, *TUR* trans-urethral resection, *RT* radiotherapy, *RP* radical prostatectomy, *AW* alive and well, *RD* recurrence of disease

Case	Age (years)	Prevalent pattern	Mitotic rate	Spread	Necrosis	Perineural invasion	Adeno-carcinoma	Treatment	Follow-up (months)	Status
1[10]	69	ACC/BCC	No one	NA	No	No	No	TUR	36	AW
2[17]	66	ACC	Scant	NA	No	No	No	TUR+RT	15	AW
3[3]	60	ACC	Scant	NA	No	No	No	TUR	NA	NA
4[11]	76	ACC	NA	NA	NA	NA	No	TUR	8	AW
5[31]	60	ACC/BCC	Rare	No	No	No	Yes	TUR+RP	72	AW
6[31]	68	ACC	Rare	NA	No	No	Yes	TUR+RT	8	AW
7[14]	NA	BCC	NA	NA	NA	Extensive	No	NA	NA	NA
8[1]	38	ACC	No one	Yes*	No	Extensive	No	RP+RT	NA	NA
9[5]	28	BCC	No one	Yes*	No	No	No	TUR+RT/CT	18	AW
10[26]	44	ACC	No one	Yes*	No	No	No	RP+RT	87**	RD
11[18]	43	ACC/BCC	NA	Yes*	NA	NA	No	RP+RT	NA	NA

* Clinico-strumental finding
** Recurrence of disease after 87 months; alive and well 26 months after the recurrence

The clinico-pathological data available in 11 cases of ACC/BCC reported thus far are shown in Table 2. Although this tumour is more common in the elderly (mean age 56.2±15.8 years, median 60 years), as confirmed by the present case (65 years), it is worth noting that 4 of 10 (40%) patients were less than 50 years. Most of the cases (6 of 11, 54.5%) showed a predominant adenoid-cystic pattern, 3 (27%) cases showed a mixed ACC/BCC pattern, and only 2 (18.2%) cases showed an exclusive basaloid pattern. There is some evidence that a predominant basaloid pattern may be associated with an adverse clinical outcome, independent of the presence of a usual adenocarcinoma component. In particular, the occurrence of unfavourable pathological features (high mitotic rate, necrosis, perineural invasion and extra-prostatic spread) has been encountered in more than 60% of the cases. Moreover, although all of the six patients with available follow-up were alive and well, one of them had relapsing tumour 87 months after surgery and radiotherapy. In the remaining five patients, the mean follow-up time was 27.8±27.2 months, but only two patients were followed for more than 2 years (Table 2). Likewise, the current tumour was also characterised by high mitotic rate, necrosis, perineural and vascular invasion and extra-prostatic spread. The lymph-node metastasis was composed by conventional adenocarcinoma, but the pulmonary and bone metastases (which were not histologically evaluated) may well be derived from the BCC component, which showed an extensive vascular invasion. Overall, the currently available data suggest that recognition of a predominant basaloid pattern in ACC/BCC may require a closer follow-up of the patients and a more aggressive therapeutic approach.

References

1. Ahn SK, Kim K, Choi IJ, Lee JM (1991) Adenoid cystic carcinoma of the prostate. Yonsei Med J 32:74–77
2. Bostwick DG (1997) Neoplasms of the prostate. In: Bostwick DG, Eble JN (eds) Urologic surgical pathology. Mosby, St Louis, pp 375–377
3. Chan SS, Walters MN (1984) Adenoid cystic carcinoma of the prostate. Pathology 16:337–338
4. Cohen RJ, Goldberg RD, Verhaart MJ, Cohen M (1993) Adenoid cyst-like carcinoma of the prostate gland. Arch Pathol Lab Med 117:799–801
5. Denholm SW, Webb JN, Howard GC, Chisholm GD (1992) Basaloid carcinoma of the prostate gland: histogenesis and review of the literature. Histopathology 20:151–155
6. Devaraj LT, Bostwick DG (1993) Atypical basal cell hyperplasia of the prostate. Immunophenotypic profile and proposed classification of basal cell proliferations. Am J Surg Pathol 17:645–659
7. Eby LS, Johnson DS, Baker HW (1972) Adenoid cystic carcinoma of the head and neck. Cancer 29:1160–1168
8. Epstein JI (1989) Adenocarcinoma. In: Epstein JI (ed) Prostate biopsy interpretation. Biopsy interpretation series. Raven, New York, pp 120–125
9. Epstein JI, Armas OA (1992) Atypical basal cell hyperplasia of the prostate. Am J Surg Pathol 16:1205–1214
10. Frankel K, Craig JR (1974) Adenoid cystic carcinoma of the prostate. Report of a case. Am J Clin Pathol 62:639–645
11. Gilmour AM, Bell TJ (1986) Adenoid cystic carcinoma of the prostate. Br J Urol 58:105–106
12. Gleason DF (1966) Classification of prostatic carcinomas. Cancer Chemoter 50:125–128
13. Gleason DF (1977) Histologic grading and clinical staging of prostatic carcinoma. In: Tannenbaum M (ed) Urologic pathology: the prostate. Lea & Febiger, Philadelphia, pp 171–197
14. Grignon DJ, Ro JY, Ordonez NG, Ayala AG, Cleary KR (1988) Basal cell hyperplasia, adenoid basal cell tumour, and adenoid cystic carcinoma of the prostate gland: an immunohistochemical study. Hum Pathol 19:1425–1433
15. Hasan N, Dodd S (1996) Basal cell carcinoma of the prostate. Histopathology 28:571
16. Kramer SA, Bredael JJ, Krueger RP (1978) Adenoid cystic carcinoma of the prostate: report of a case. J Urol 120:383–384
17. Kuhajda FP, Mann RB (1984) Adenoid cystic carcinoma of the prostate. A case report with immunoperoxidase staining for prostate-specific acid phosphatase and prostate-specific antigen. Am J Clin Pathol 81:257–260
18. Minei S, Hachiya T, Ishida H, Okada K (2001) Adenoid cystic carcinoma of the prostate: a case report with immunohisto-

chemical and in situ hybridization staining for prostate-specific antigen. Int J Urol 8:S41–S44
19. Mostofi FK, Price EB Jr (1973) Malignant tumours of the prostate. In: Atlas of tumours of the male genital system, 2nd series, fascicle. Armed Forces Institute of Pathology, Washington DC, p 244
20. Oliai BR, Kahane H, Epstein JI (2002) Can basal cells be seen in adenocarcinoma of the prostate?: an immunohistochemical study using high molecular weight cytokeratin (clone 34βE12) antibody. Am J Surg Pathol 26:1151–1160
21. Parson JK, Gage WR, Nelson WG, De Marzo AM (2001) p63 protein expression is rare in prostate adenocarcinoma: implications for cancer diagnosis and carcinogenesis. Urology 58:619–624
22. Petersen RO (1992) Prostate and seminal vesicles. In: Petersen RO (ed) Urologic pathology, 2nd edn. J.B. Lippincott Co, Philadelphia, p 642
23. Pruneri G, Pignataro L, Manzotti M, Carboni N, Ronchetti D, Neri A, Cesana BM, Viale G (2002) p63 in laryngeal squamous cell carcinoma: evidence for a role of TA-p63 down-regulation in tumorigenesis and lack of prognostic implications of p63 immunoreactivity. Lab Invest 82:1327–1234
24. Reed RJ (1984) Consultation case: prostate (prostatectomy)—adenoid basal-cell tumour—multifocal basal-cell hyperplasia. Am J Surg Pathol 8:699–704
25. Ronnett BM, Epstein JI (1989) A case showing sclerosing adenosis and an unusual form of basal cell hyperplasia of the prostate. Am J Surg Pathol 13:866–872
26. Schmid HP, Semjonov A, Eltze E, Wortler K, Hertle L (2002) Late recurrence of adenoid cystic carcinoma of the prostate. Scand J Urol Nephrol 36:158–159
27. Shah RB, Zhou M, Leblanc M, Synder M, Rubin MA (2002) Comparison of the basal cell-specific markers, 34βE12 and p63, in the diagnosis of prostate cancer. Am J Surg Pathol 26:1161–1168
28. Tannenbaum M (1975) Adenoid cystic or "salivary gland" carcinomas of prostate. Urology 6:238–239
29. Urist MJ, Di Como CJ, Lu ML, Charytonowicz E, Verbel D, Crum CP, Ince TA, McKeon FD, Cordon-Cardo C (2002) Loss of p63 expression is associated with tumor progression in bladder cancer. Am J Pathol 161:1199–1206
30. Yang XJ, McEntee M, Epstein JI (1998) Distinction of basaloid carcinoma of the prostate from benign basal cell lesions by using immunohistochemistry for bcl-2 and Ki-67. Hum Pathol 29:1447–1450
31. Young RH, Frierson HF Jr, Mills SE, Kaiser JS, Talbot WH, Bhan AK (1988) Adenoid cystic-like tumour of the prostate gland. A report of two cases and review of the literature on "adenoid cystic carcinoma" of the prostate. Am J Clin Pathol 89:49–56
32. Young RH, Srigley JR, Amin MB, Ulbright TM, Cubilla AL (1998) Variants of prostatic adenocarcinoma, other primary carcinomas of prostate, and secondary carcinomas. In: Atlas of tumours of the prostate gland, seminal vesicles, male urethra, and penis, 3rd series, fascicle 28. Armed Forces Institute of Pathology, Washington DC, pp 230–233

Virchows Arch (2003) 443:792–796
DOI 10.1007/s00428-003-0901-4

CASE REPORT

Yasuyoshi Shikama · Tadaharu Osawa · Nobuo Yagihashi · Hidekachi Kurotaki · Soroku Yagihashi

Neuroendocrine differentiation in hyalinizing trabecular tumor of the thyroid

Received: 7 March 2003 / Accepted: 7 July 2003 / Published online: 2 October 2003
© Springer-Verlag 2003

Abstract The presence of neuroendocrine cells is putative in thyroid hyalinizing trabecular tumor (HTT), although this entity requires a differential diagnosis from paraganglioma or medullary carcinoma of the thyroid, due to similarity of the growth pattern of the cells. Here, we present a case of HTT with a mixture of endocrine cells stained positive for somatostatin, chromogranin A and Grimelius' silver impregnation. The histology and results of other immunostainings were consistent with the features typical for HTT. In the world literature to date, only two cases of HTT with endocrine cells, including the current case, have been reported. Nevertheless, the cases may indicate the diversified differentiation of cells in HTT and may, in part, account for the resemblance of HTT to paraganglioma and medullary carcinoma.

Keywords Thyroid · Hyalinizing trabecular tumor · Neuroendocrine cells · Somatostatin

Introduction

Hyalinizing trabecular tumor (HTT) of the thyroid is a rare tumor, first described by Carney et al. [3], with distinct features of cellular growth pattern and overproduction of matrix proteins [3, 17]. This tumor was initially considered to belong to a benign follicular tumor [3]. Recently, it has been proposed that it is a variant of papillary carcinoma [4] and potentially malignant, based on the evidence that it often shows characteristic nuclear changes with pseudo-inclusion bodies or grooves [4] as well as specific oncogenic expression of RET/PTC [4, 15] or cytokeratin 19 expression [6]. However, the pure histology of HTT mimics the neuroendocrine tumors, such as paraganglioma or medullary carcinoma. In fact, some cases of HTT were even named paraganglioma-like adenoma [1, 11]. Although the original report identified HTT as a tumor without endocrine differentiation [3], Katoh et al. first pointed out the presence of endocrine cells in HTT among one of the three reported cases, implicating a heterogeneity of HTT [10]. It has been still unclear, however, whether the presence of endocrine cells in HTT reflects a combination or collision of HTT with an endocrine tumor or indicates diversified differentiation of the tumor. We recently encountered a case of HTT presenting a typical histology with a mixture of endocrine cells. The endocrine cells exhibited characteristic positive reactions to membrane MIB-1, thyroglobulin and somatostatin. These findings suggest that HTT has a potential to differentiate into an endocrine tumor and may, in part, account for the reason why the growth pattern of HTT mimics paraganglioma or medullary carcinoma.

Clinical history

A 56-year-old female visited our hospital, complaining of a swollen mass in the anterior neck region. She noted the mass 3 months previously, but there was no pain or tenderness. Under ultrasound examination, a well-circumscribed mass measuring 1.9×1.4 cm was detected. With suspicion of a benign follicular tumor, guided aspiration cytology was undertaken. On smears, despite the absence of definite malignant cells, there were some

Y. Shikama
Department of Clinical Laboratory,
Kuroishi City Hospital, Kuroishi, Aomori, Japan

T. Osawa · N. Yagihashi
Department of Surgery, Kuroishi City Hospital,
Kuroishi, Aomori, Japan

Y. Shikama · H. Kurotaki · S. Yagihashi
Department of Pathology,
Hirosaki University School of Medicine, Hirosaki, Japan

S. Yagihashi (✉)
Department of Pathology,
Hirosaki University School of Medicine,
5 Zaifu-cho, 036-8562 Hirosaki, Japan
e-mail: yagihasi@cc.hirosaki-u.ac.jp
Tel.: +81-17-2395025
Fax: +81-17-2395026

atypical cells showing nuclear pseudo-inclusion bodies and grooves as well as slightly thickened nuclear membranes. Hemithyroidectomy of the right lobe was performed under the suspicious diagnosis of papillary carcinoma.

Materials and methods

The mass was clearly demarcated from the intact area, showing solid, yellow-gray color, and measured 1.8×1.6×1.2 cm in size (Fig. 1). The tumor specimen was fixed in 10% formalin, embedded in paraffin and sectioned. The 4-μm-thick sections were stained with hematoxylin and eosin (HE). Special stainings with periodic acid-Schiff (PAS) with or without diastase digestion and Grimelius' silver impregnation were conducted.

For the detection of neuroendocrine cells, streptavidin-biotin immunostainings using antibodies to thyroglobulin (rabbit polyclonal, 1:1000; Dako, Glostrup, Denmark), chromogranin A (rabbit polyclonal, 1:200; Dako), MIB-1 (Ki-67 antigen) (mouse, monoclonal, 1:100; Immunotech, Marceille, France), somatostatin (rabbit polyclonal, 1:20,000; Dako), calcitonin (mouse monoclonal, 1:50; Dako), carcinoembryonic antigen (mouse monoclonal; Dako), vimentin (mouse monoclonal; 1:100, Dako) and S-100 protein (rabbit polyclonal, 1:1000; Dako) were performed on the serially cut sections. Specificity of the stainings was confirmed by omission of the first antibody and by replacement of the first antibody with unimmune rabbit or mouse sera. Positive controls of thyroglobulin, somatostatin and chromogranin A were also stained with respective antibodies on normal human thyroid and pancreatic tissues.

Small pieces of formalin-fixed tissues were used for electron microscopic observations. They were postfixed in 1% osmium tetroxide and embedded in epon. Ultrathin sections stained with uranyl acetate and lead citrate were examined under a Hitachi H600 electron microscope.

Fig. 1 Macroscopic finding of the tumor, which is well circumscribed. The cut surface is solid, with gray-yellow color

Results

Light microscopic findings

The tumor was solid and circumscribed with a thick fibrous capsule. The tumor cells proliferated with a trabecular pattern. Basement membranes were thickened, showing a hyalinous appearance. There were no follicles containing colloid or foci of papillary proliferation of tumor cells. The tumor cells were oval to ellipsoid or spindle-shaped with abundant cytoplasm. In the cytoplasm, there were often yellow bodies. The nuclei had a thickened membrane with pseudo-inclusion bodies and grooves with perinucleolar clearing (Fig. 2A). The hyalinized basement membranes were PAS-positive with

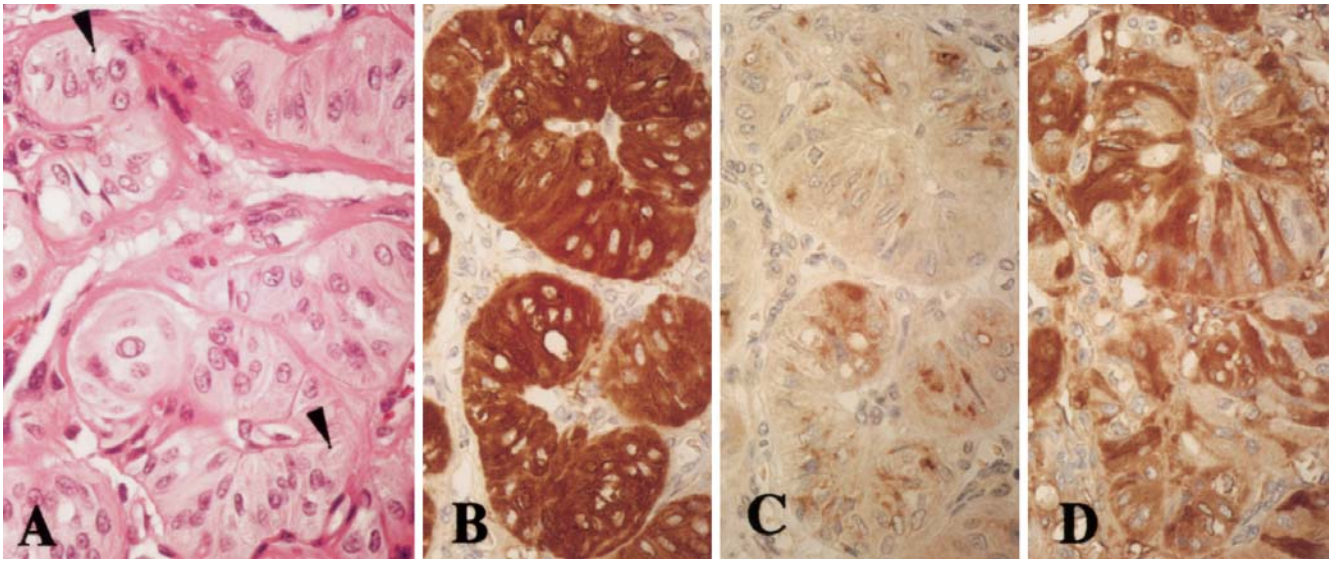

Fig. 2 Light microscopic appearance of the tumor. The tumor shows a characteristic appearance of hyalinizing trabecular tumor of the thyroid, where trabecular or Zellballen pattern is prominent with abundant matrix collagens. Note the presence of yellow bodies (*arrowhead*) (**A**). On the serially stained slides, the tumor cells were positive for thryoglobulin (**B**), chromogranin A (**C**) as well as somatostatin (**D**) (all, ×400)

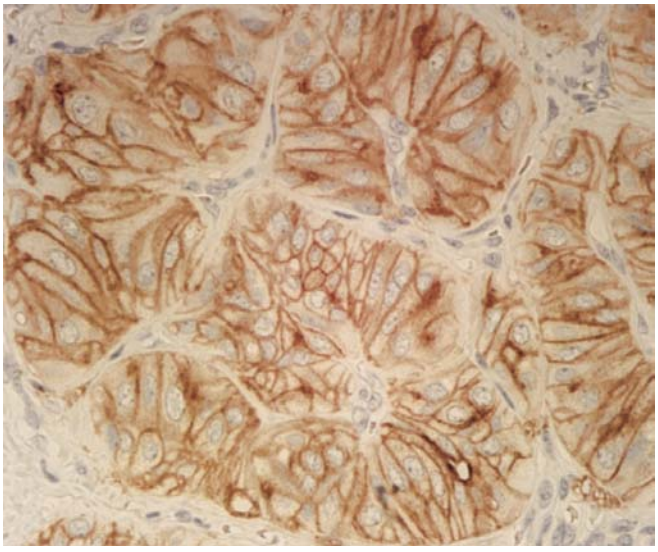

Fig. 3 Immunostaining of the tumor cells with MIB-1. The tumor cells show a characteristic membrane-positive appearance (×400)

diastase-resistance, but negative for Congo-red. With these findings, the tumor was diagnosed as HTT. Staining with Grimelius silver impregnation demonstrated that scattered tumor cells were positive, showing neuroendocrine differentiation.

Immunostainings

The tumor cells were positive for thyroglobulin (Fig. 2B), for vimentin, occasionally for chromogranin A (Fig. 2C) and for somatostatin (Fig. 2D), where the positive reactions were concurrent with Grimelius positivity on the serial sections. Cells positive both for somatostatin and thyroglobulin were distributed widespread within the tumor and occupied about 20% of all the tumor cells. MIB-1 staining was positive for cytoplamic membranes, but not on the nuclei (Fig. 3). Calcitonin, carcinoembryonic antigen and S-100 were all negative in any part of the tumor. Negative control stainings yielded no reactions on the tumor sections, whereas positive controls showed strong reactions in normal thyroid follicular cells for thyroglobulin and, in pancreatic islets, for chromogranin A and somatostain.

Electron microscopic findings

The tumor cells contained aggregates of intermediate filaments in the cytoplasm. There were a few small neuroendocrine-type electron-dense-cored vesicles, predominantly in the periphery of the cytoplasm (Fig. 4A, B).

Discussion

The histological appearance of the current case was typical for HTT, showing a characteristic trabecular

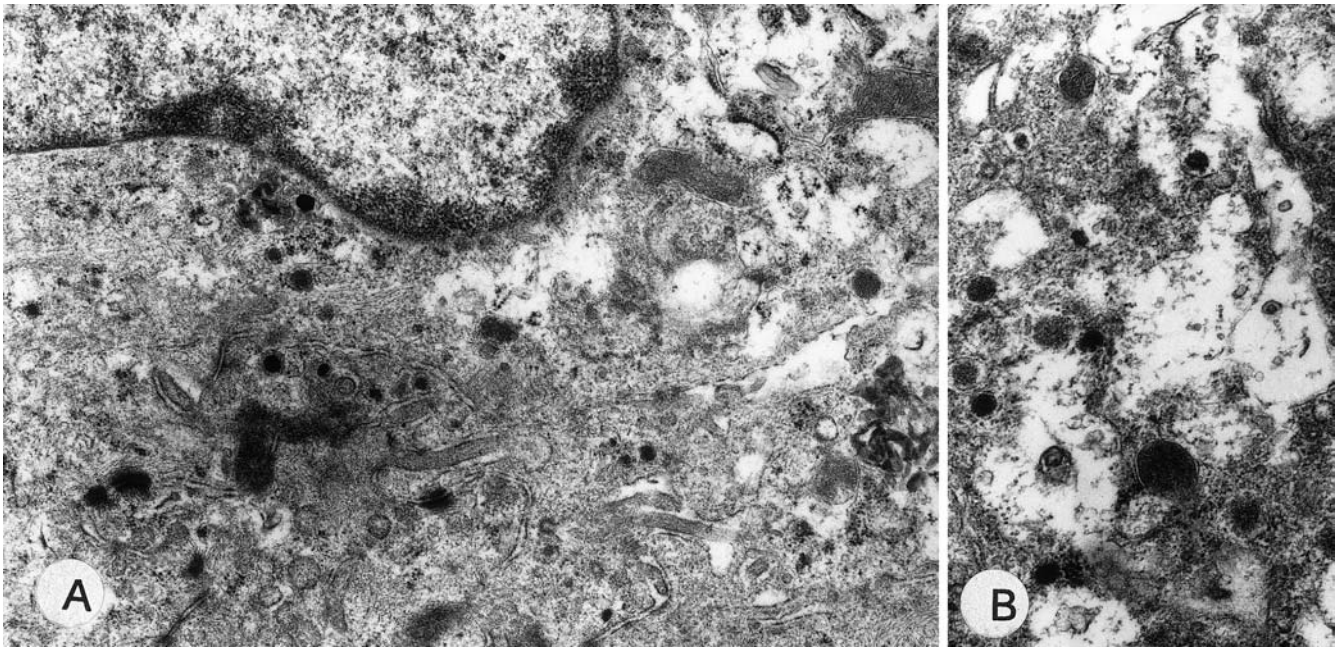

Fig. 4 Electron micrograph of tumor cells. Within the tumor cell cytoplasm, small electron-dense neurosecretory granules were located near the cytoplasmic membranes (**A**, ×7200). At a higher magnification, electron-dense cored vesicles with clear halo, approximately 200–400 nm in size, were visible (**B**, ×18,000)

pattern of the tumor cells, abundant stromal collagen and basement membrane-like materials. Immunohistochemical results were also consistent with HTT with positivity to membrane MIB-1 and cytoplasmic thyroglobulin. These features are unequivocal for the diagnosis of HTT. The unusual finding of the current case was the presence of many endocrine cells showing positive stainings with chromogranin A and somatostatin. The presence of neurosecretory granules was confirmed at ultrastructural levels. These endocrine cells were distributed widely within the tumor, suggesting the diversified differentiation of the tumor, not the pattern of collision or a mixed tumor.

The first description of HTT (the term coined by Carney and originally described as hyalinizing trabecular adenoma) [3] is exemplified by the absence of endocrine cells, thus allowing for differentiation of this tumor from paraganglioma or medullary carcinoma. However, definition of HTT is not necessarily dependent on the differentiation of the cells, but on the pure histological appearance of the tumor stained with HE. Recent studies on the collection of HTT cases revealed that HTT closely resembles papillary carcinoma, due to the characteristic nuclear structures [4], oncogenic expression of RET/PTC [15] or cytokeratin 19 expression [6]. Our case also presented nuclear pseudo-inclusion bodies and nuclear grooves, reminiscent of papillary carcinoma. Nevertheless, the tumor classification and malignant potential of this tumor is still putative [10, 11, 13]; is it follicular or papillary, adenoma or carcinoma? [13]. These controversies may belie on the basis that the RET gene is localized in parafollicular cells [2], and its rearrangement is limited to only 28.6% of HTT cases [15]. In addition, expression of cytokeratin 19 was not limited to HTT, but also detected in follicular tumors [9]. More recent studies on the expression of galectin-3, usually strongly expressed in thyroid carcinomas, showed intermediate reactions in the collection of 58 cases of HTT, again serving as a difficulty for determining the malignancy of this tumor [7].

Our case strongly supports the contention that this tumor, derived from pluripotent primitive cells, can differentiate into both follicular cells and neuroendocrine cells, based on the finding of concurrent positive reactions of tumor cells to somatostatin and thyroglobulin. This result is in keeping with the Katoh report [10], in which they first described a case of HTT containing some endocrine cells. The positive reaction of tumor cells to somatostatin is the same in these two cases, showing a specific direction of cellular differentiation in HTT, not simply indicating proliferation of parafollicular cells. It has been shown that medullar carcinoma is infrequently positive for somatostatin and that cultured tumor cells from medullar carcinoma produces somatostatin [8, 18]. During the early development of parafollicular endocrine cells, growth of somatostatin and calcitonin-positive cells is differently regulated by environmental factors [19]. Recent experimental data identified the transcription factor PAX 8 for the differentiation of follicular cells separated from parafollicular cells [14]. The presence of somatostatin cells in HTT may, therefore, reflect the potential of this tumor into multidirectional differentiation, not simply containing calcitonin-positive parafollicular cells.

There are some cases that have combined areas of medullary carcinoma and papillary carcinoma [12, 16] or a case of medullary carcinoma with exocrine mucus cells (amphicrine carcinoma) [5]. These cases may also illustrate the potential of thyroid tumor cells to differentiate into heterogeneous cells within a single tumor. Since our patient did not show any special symptoms, clinical significance of somatostatin production remains unclear. Our patient has been free of recurrence and there has been no sign of metastasis for 2 years after the operation. The potential for malignancy is unknown and careful follow-up may be required. Accumulation of such cases will give us further information regarding the biological behavior.

Acknowledgment The authors appreciate the excellent technical support of Ms. Kaori Okamoto.

References

1. Bronner MP, LiVolsi VA, Jennings TA (1988) PLAT. Paraganglioma-like adenomas of the thyroid. Surg Pathol 1:383–389
2. Bunone G, Uggeri M, Mondellini P, Pierotti MA, Bongarzone I (2000) RET receptor expression in thyroid follicular epithelial cell-derived tumors. Cancer Res 60:2845–2849
3. Carney JA, Ryan J, Goellner JR (1987) Hyalinizing trabecular adenoma of the thyroid gland. Am J Surg Pathol 11:583–591
4. Cheung CC, Boerner SL, MacMillan CM, Ramyar L, Asa SL (2000) Hyalinizing trabecular tumor of the thyroid: a variant of papillary carcinoma proved by molecular genetics. Am J Surg Pathol 24:1622–1626
5. Dominguez-Malagon H, Macias-Martinez V, Molina-Cardenas H, Suster S (1997) Amphicrine medullary carcinoma of the thyroid with luminal differentiation: report of an immunohistochemical and ultrastructural study. Ultrastruct Pathol 21:569–574
6. Fonseca E, Nesland J, Sobrinho-Simoes M (1997) Expression of stratified epithelial type cytokeratins in hyalinizing trabecular adenoma supports their relationship with papillary carcinoma of the thyroid. Histopathology 31:330–335
7. Gaffney RL, Carney JA, Sebo TJ, Erickson LA, Volante M, Papotti M, Lloyd RV (2003) Galectin-3 expression in hyalinizing trabecular tumors of the thyroid gland. Am J Surg Pathol 27:494–498
8. Gagel RF, Palmer WN, Leonhart K, Chan L, Leong SS (1986) Somatostatin production by a human medullary thyroid carcinoma cell line. Endocrinology 118:1643–1651
9. Hirokawa M, Carney JA, Ohtsuki Y (2000) Hyalinizing trabecular adenoma and papillary carcinoma of the thyroid gland express different cytokeratin patterns. Am J Surg Pathol 24:877–881
10. Katoh R, Jasani B, Williams ED (1989) Hyalinizing trabecular adenoma of the thyroid. A report of three cases with immunohistochemical and ultrastructural studies. Histopathology 15:211–224
11. LaGuette J, Matias-Guiu X, Rosai J (1997) Thyroid paraganglioma: a clinicopathologic and immunohistochemical study of three cases. Am J Surg Pathol 7:748–753
12. Lax SF, Beham A, Kronberger-Schonecker D, Langsteger W, Denk H (1994) Coexistence of papillary and medullary carcinoma of the thyroid gland-mixed or collision tumour?

Clinicopathological analysis of three cases. Virchows Arch 424:441–447
13. LiVolsi VA (2000) Hyalinizing trabecular tumor of the thyroid: adenoma, carcinoma, or neoplasm of uncertain malignant potential? Am J Surg Pathol 24:1683–1684
14. Mansouri A, Chowdhury K, Gruss P (1998) Follicular cells of the thyroid gland require Pax 8 gene function. Nature Genet 19:87–90
15. Papotti M, Volante M, Giuliano A, Fassina A, Fusco A, Bussolati G, Santoro M, Chiappetta G (2000) RET/PTC activation in hyalinizing trabecular tumors of the thyroid. Am J Surg Pathol 24:1615–1621
16. Pastolero GC, Coire CI, Asa SL (1996) Concurrent medullary and papillary carcinomas of thyroid with lymph node metastases. A collision phenomenon. Am J Surg Pathol 20:245–250
17. Rosai JA, Carcangiu ML, DeLellis RA (1992) Atlas of tumor pathology, Tumors of thyroid gland. 3rd AFIP Series No. 5, Washington DC, pp 31–34
18. Tamir H, Liu KP, Payette RF, Hsiung SC, Adlersberg M, Nunez EA, Gershon MD (1989) Human medullary thyroid carcinoma: characterization of the serotonergic and neuronal properties of a neuroectodermally derived cell line. J Neurosci 9:1199–1212
19. Zabel M, Surdyk J, Biela-Jacek I (1987) Immunocytochemical studies on thyroid parafollicular cells in postnatal development of the rat. Acta Anat (Basel) 130:251–256

Virchows Arch (2003) 443:797–800
DOI 10.1007/s00428-003-0912-1

CASE REPORT

Gudrun Ratzinger · Bettina Zelger · Walter Höbling · Gregor Mikuz · Bernhard W. Zelger

Sinus histiocytosis with massive lymphadenopathy Rosai-Dorfman: three unusual manifestations

Received: 9 May 2003 / Accepted: 9 September 2003 / Published online: 24 October 2003
© Springer-Verlag 2003

Abstract We report on three exceptional courses of sinus histiocytosis Rosai-Dorfman. Patient one developed regional lymph-node disease subsequent to two independent malignancies in the right head and neck region. Patient two suffered from extensive extranodal disease with more than 100 mucocutaneous lesions over 17 years, which spontaneously resolved. Patient three showed exclusively extranodal disease, including bilateral conjunctival/scleral lesions, before he developed lung cancer. Our cases are unique for three reasons: the association of the disease with solid malignancies in two cases, the extent and persistence of exclusively extranodal disease in one patient and the appearance of thus far undescribed conjunctival/scleral lesions.

Keywords Cutaneous sinus histiocytosis · Mucosal sinus histiocytosis · Sinus histiocytosis and malignancy · Sinus histiocytosis Rosai-Dorfman

Introduction

Sinus histiocytosis with massive lymphadenopathy (SHML) was first described by Destombes in 1965 [6] and recognized as a distinct clinicopathological entity by Rosai and Dorfman in 1969 [12, 13]. It typically appears with cervical lymphadenopathy accompanied by unspecific signs of immunoactivation. Other lymph-node groups also may be involved. In approximately 40%, extranodal lesions, especially in skin, respiratory tract, eyes and soft tissue, can be found [9, 15]. Extranodal manifestations can also be the predominant finding or, rarely, even be exclusive.

Skin is the most common site of extranodal involvement, but exclusively cutaneous disease is rare [14]; approximately 50 cases have been reported to date [2, 4]. The course of disease is benign and tends to spontaneous remission, although fatal outcomes due to infiltration of vital organs are described. In addition, aggressive courses can be due to immunological abnormalities. The cause of the disease still remains unknown, although it probably comprises a disease of immune dysregulation [8]. An association with hematological malignancies has been described in a few cases [1].

G. Ratzinger (✉) · B. W. Zelger
Department of Dermatology and Venerology,
University of Innsbruck, Anichstrasse 35, 6020 Innsbruck, Austria
e-mail: gudrun.ratzinger@uibk.ac.at
Tel.: +43-512-5042971
Fax: +43-512-5042990

B. Zelger · G. Mikuz
Department of Pathology, University of Innsbruck,
Müllerstrasse 44, 6020 Innsbruck, Austria

W. Höbling
General Public Hospital, Institute of Pathology,
Grieskirchnerstrasse 42, 4600 Wels, Austria

Clinical history

Patient one

In 1990, a 60-year-old woman presented to the ENT Department of our University Hospital with a swelling of the right glandula submandibularis. The tumor was excised and histopathological examination revealed an adenoid cystic carcinoma of the salivary gland. No secondary lesions could be found. Local irradiation therapy was performed (60 Gray). In 1993, 3 years later, the patient presented to the Department of Dermatology of our University Hospital with a melanoma, Clark level III, tumor thickness 1.2 mm, on her right cheek. Extensive examinations did not show any metastases. In 1995, 2 years later, our patient noticed a swelling at the right angulus mandibulae. Sonography showed reactive lymph nodes without signs of malignancy. Because of the history of two malignant diseases in the same body region, we still recommended the excision of the swollen lymph nodes. Histological examination revealed typical features of SHML Rosai-Dorfman (Fig. 1). In spring 1996, 5 months later, the patient showed again a single swollen lymph node in the right cervical region, which was removed and showed identical histopathological features. Up to now, the patient has remained free of neoplastic disease and SHML.

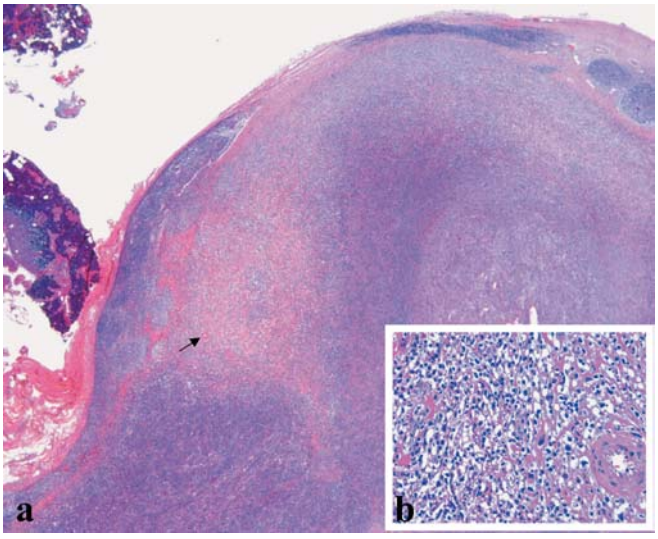

Fig. 1 **a** Retromandibular lymph node with destruction of normal architecture. Note sheets of faint to slightly eosinophilic macrophages which, on higher magnification (indicated by *arrow*), reveal prominent emperipolesis (**b**)

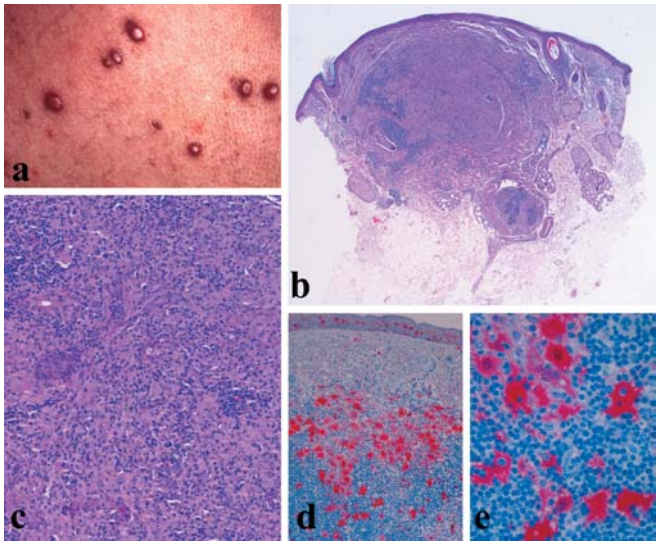

Fig. 2 **a** Cherry-pit-sized reddish-brown papules of sinus histiocytosis with massive lymphadenopathy on the body. **b** Nodular to diffuse infiltrate of macrophages with clusters of lymphocytes and plasma cells. **c** The faintly eosinophilic cytoplasm of macrophages again shows emperipolesis. **d** Another lesion with numerous lymphocytes (**e**) within the cytoplasm of S100 protein positive macrophages

Patient two

In 1985, a 56-year-old man presented to the ENT Department of a peripheral hospital with a nodular lesion at the nasal mucosa. Histological examination of a biopsy showed granulomatous features and led to the diagnosis of Mb. Wegener. An overall examination did not reveal any other manifestations. A therapy with prednisone and cyclophosphamide succeeded in complete remission of the lesions. In 1988, 3 years later, the patient presented with recurring lesions at the nasal mucosa extending into the left sinus maxillaris to the same hospital. He also noticed cherry-pit-sized reddish-brown papules all over the body (Fig. 2). Histological examination again led to the diagnosis of Mb. Wegener and was followed by a therapy with prednisone and cyclophosphamide, this time with modest response. In 1992, the patient showed progressive disease with numerous cutaneous and mucosal lesions. Biopsies, at this time sent to the Dermatohistopathologic Laboratory of our University Hospital for a second opinion, led to the diagnosis of cutaneous SHML. Reexamination of the previous biopsies confirmed this diagnosis. In the following 10 years, our patient kept developing new cutaneous lesions; therapy was performed with liquid nitrogen, external steroids and excision. In February 2002, he presented with anemia and a bone-marrow biopsy showed features of SHML. The anemia was successfully treated with erythropoietin; no specific treatment was performed. In the meantime, all cutaneous and mucosal lesions as well as the bone-marrow infiltration resolved, and the patient is free of disease.

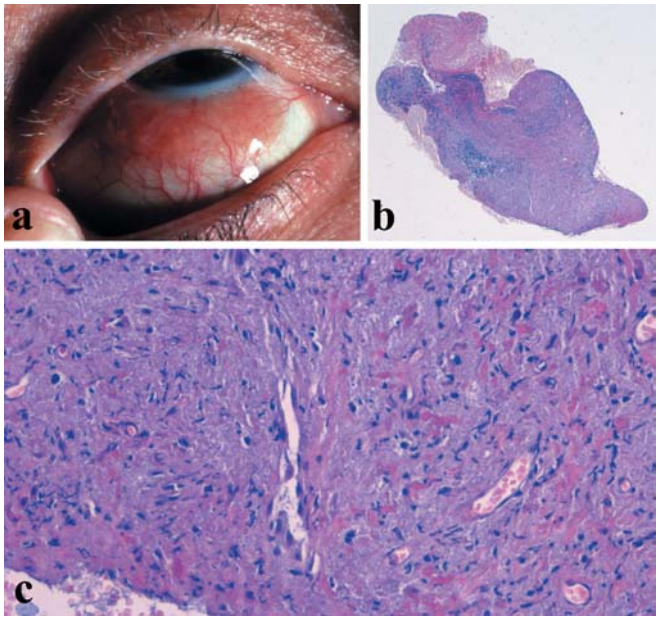

Fig. 3 **a** Yellowish infiltrate of sinus histiocytosis with massive lymphadenopathy in the conjunctiva/sclera. **b** Scanning magnification of conjunctival and scleral fragment which, on a higher magnification, reveals sheets of faintly stained macrophages (damaged by crash artifacts), some vessels and remnants of collagen (**c**)

Patient three

In 1984, a 42-year-old man suffered from nasal obstruction. Examination at a peripheral hospital revealed a polypoid lesion at the nasal mucosa; a biopsy showed a lymphoplasmacytic infiltrate without any signs of malignancy. In 1998, 15 years later, the patient developed a recurrent lesion at the nasal mucosa and, additionally, multiple bluish indolent subcutaneous nodules at the right upper arm as well as extremely bothersome infiltrates at the conjunctival mucosa and sclera of both eyes (Fig. 3), for which he was referred to our University Hospital. Histopathology displayed characteristics of SHML, and the reevaluation of the biopsy taken 15 years earlier showed identical features. Overall examination revealed a 1.5-cm lesion in the lung and swollen axillary lymph nodes; biopsies showed small cell lung cancer. The patient was treated with polychemotherapy, which resolved all Rosai-Dorfman lesions, while the lung cancer did not respond to treatment. The patient died from metastatic disease in the brain about 1 year after the diagnosis of lung cancer.

Table 1 Immunohistochemically, these macrophages typically stain positive for S100 protein and with Ki-M1p, but are negative for CD1a

Marker	Dilution	Source	Main reactivity
S100 protein*	1:100	Dako**	Langerhans cells (LC), nerves, melanocytes, naevus cells
CD1a	Straight	Immunotech***	Dendritic cells including LC
Ki-M1p	1:5 (supernatant)	Professor Parwaresch	Macrophages

*Polyclonal, others monoclonal
**Dakopath, Glostrup, Denmark
***Immunotech, Marseille, France

Light microscopy and immunohistochemistry

Lymph node

In the lymph node of patient one (Fig. 1), instead of normal lymph-node architecture, there are sheets of faintly stained macrophages with round to oval nuclei and prominent eosinophilic nucleoli as well as multinucleate macrophages reminiscent of Reed-Sternberg cells. Lymphocytes are seen within the cytoplasm of macrophages, so-called emperipolesis. Prominent vascularity, extravasation of erythrocytes and hemosiderin deposits are additional findings. Immunohistochemically (Table 1), these macrophages typically stain positive for S100 protein and with Ki-M1p, but are negative for CD1a.

Skin and mucosa

In the skin and mucosa of patients two and three (Fig. 2 and Fig. 3) there is a diffuse, sheet-like infiltrate of macrophages intermingled with lymphocytes and plasma cells. Some lesions are well demarcated, thereby imitating lymph nodes (except the lack of sinus); others are more ill defined. The cytoplasm of the macrophages is pale to slightly eosinophilic and, again, emperipolesis can be found. Some of the lesions show focal fibrosis. Immunohistochemically, macrophages are positive for S100 protein and with Ki-M1p, but are negative for CD1a.

Discussion

We report on three patients with unusual courses of SHML for several reasons. First, 80% of patients described in the literature primarily present with painless bilateral cervical lymphadenopathy [12, 13]. None of our patients showed this feature at any time of disease. Second, about 40% of patients show extranodal disease in combination with nodal disease; exclusively extranodal involvement is rare [14]. The second patient developed multiple lesions in skin and mucosa as well as bone marrow infiltration. Also, the extent of disease, with more than 100 lesions over 17 years, was remarkable. The third patient showed mucosal and cutaneous lesions only. Third, rare cases of patients have been reported who were previously affected or subsequently developed a malignant disorder; but, to our knowledge, mainly hematological malignancies have been described [1]. Two of our patients suffered from solid tumors in combination with SHML. The first patient had been treated for an adenoid cystic carcinoma of the salivary gland and for a melanoma before the diagnosis of SHML. The third patient subsequently developed small cell lung cancer 15 years after the first lesion of SHML. Finally, head and neck are preferred localizations for the occurrence of SHML [7]. However, to the best of our knowledge, bilateral SHML at the conjunctiva/sclera, as in the third patient, has not been reported before.

Irrespective of the site of occurrence, the histopathological appearance of SHML is essentially similar [5]. The histopathological hallmarks are sheets of pale to slightly eosinophilic macrophages with engulfment of lymphocytes, erythrocytes or other cellular debris within their cytoplasm—so-called emperipolesis. This feature is common in nodal SHML, but less frequently and reliably seen in extranodal disease. In contrast, fibrosis is more common in an extranodal location [7, 16]. Immunohistochemistry of macrophages reveals reactivity for S100 protein and with macrophage markers such as Ki-M1p or KP1 (CD68), but is negative for CD1a [3]. Due to the coexpression of S100 protein—a labeling regularly found in Langerhans cell disease—and macrophage markers, SHML are sometimes listed among the group of indeterminate cell disorders.

The clinical appearance of SHML leads to a substantial number of differential diagnoses [4, 11, 17]. For nodal SHML, a tremendous number of inflammatory and neoplastic causes of cervical or multilocular lymphadenopathy has to be evaluated [10]. In particular, Hodgkin's disease is important. Multinucleate macrophages found in nodal SHML can be reminiscent of Reed-Sternberg cells. Immunohistochemistry reveals reactivity for CD30 in the absence of reactivity for S100 protein, CD1a and with Ki-M1p. For SHML of skin and soft tissue, the family of xanthogranulomas has to be considered first [17]. Histology reveals a variable mixture of mononuclear and multinucleate macrophages, including vacuolated, xanthomatized, scalloped, oncocytic and spindle-shaped cells as well as Touton, ground glass and foreign body giant cells, respectively. All lesions express according to their monocyte/macrophage differentiation Ki-M1p, KP1 (CD68) or HAM56 and are negative for Langerhans cell markers. A clinicopathological presentation very similar to the various types of xanthogranuloma is seen in indeterminate cell histiocytosis. Yet, these lesions are positive for S100 protein, with Ki-M1p and showing variable expression of CD1a. Cutaneous Langerhans cell

disease reveals typical kidney-shaped cells positive for S100 protein and CD1a, negative for macrophage markers and ultrastructurally with Birbeck granules. In rare cases, myelomonocytic and monocytic leukemias show skin involvement. One finds a diffuse dermal infiltrate of atypical monocytes, characteristically with Indian filing and numerous mitoses. Immunohistochemically, these lesions are positive with Ki-M1p and are positive histochemically for cholinacetate esterase, but negative for S100 protein and CD1a. Furthermore, granulomatous infections, i.e., tuberculosis or cat scratch disease, can appear with a clinical similarity to cutaneous SHML, but history, symptoms, histopathology and bacteriological tests reveal the microbial background of the lesions.

The course of disease is usually benign and, thus, surgical excision of mutilating lesions provides sufficient treatment. In rare cases of aggressive disease, chemotherapy and irradiation have been performed with modest success [11]. Careful evaluation of disease, especially the distinction from malignant disorders, is of greatest importance to avoid unnecessary treatment.

Acknowledgement We thank Prof. Parwaresch, Department of Pathology, University of Kiel, Germany, for kindly providing us with the macrophage marker Ki-M1p.

References

1. Allen MR, Ninfo V, Viglio A et al (2001) Sinus histiocytosis with massive lymphadenopathy (Rosai-Dorfman Disease) in a girl previously affected by acute lymphoblastic leukemia. Med Pediatr Oncol 37:150–152
2. Annessi G, Giannetti A (1996) Purely cutaneous Rosai-Dorfman disease. Br J Dermatol 134:749–757
3. Bonetti F, Chilosi M, Menestrina F et al (1978) Immunohistological analysis of Rosai-Dorfman histiocytosis: a disease of S-100+ CD1- histiocytes. Virchows Arch 411:129–135
4. Brenn T, Calonje E, Granter SR et al (2002) Cutaneous Rosai-Dorfman disease is a distinct clinical entity. Am J Dermatopathol 24:385–391
5. Chu P, LeBoit PE (1992) Histologic features of cutaneous sinus histiocytosis (Rosai-Dorfman disease): study of cases both with and without systemic involvement. J Cutan Pathol 19:201–206
6. Destombes P (1965) Adenitis with lipid excess, in children or young adults, seen in the Antilles and in Mali (4 cases). Bull Soc Pathol Exot Filiales 58:1035–1039
7. Foucar E, Rosai J, Dorfman RF (1978) Sinus histiocytosis with massive lymphadenopathy. Ear, nose and throat manifestations. Arch Otolaryngol 104:687–693
8. Foucar E, Rosai J, Dorfman RF (1988) Sinus histiocytosis with massive lymphadenopathy. Current status and future directions. Arch Dermatol 124:1211–1214
9. Foucar E, Rosai J, Dorfman RF (1990) Sinus histiocytosis with massive lymphadenopathy (Rosai-Dorfman Disease). Semin Diagn Pathol 7:83–86
10. Habermann TM, Steensma DP (2000) Lymphadenopathy. Mayo Clin Proc 75:723–732
11. Montgomery EA, Meis JM, Frizzera G (1992) Rosai-Dorfman disease of soft tissue. Am J Surg Pathol 16:122–129
12. Rosai J, Dorfman RF (1969) Sinus histiocytosis with massive lymphadenopathy: a newly recognized benign clinicopathological entity. Arch Pathol 87:63–70
13. Rosai J, Dorfman RF (1972) Sinus histiocytosis with massive lymphadenopathy: a pseudolymphomatous benign disorder. Analysis of 34 cases. Cancer 30:1174–1188
14. Thawerani H, Sanchez RL, Rosai J et al (1978) The cutaneous manifestations of sinus histiocytosis with massive lymphadenopathy. Arch Dermatol 114:191–195
15. Wang E, Anzai Y, Paulino A et al (2001) Rosai-Dorfman disease presenting with isolated bilateral orbital masses. Report of two cases. Am J Neuroradiol 22:1386–1388
16. Wenig BM, Abbondanzo SL, Childers EL et al (1993) Extranodal sinus histiocytosis with massive lymphadenopathy (Rosai-Dorfman Disease) of the head and neck. Human Pathol 24:483–492
17. Zelger B, Burgdorf WHC (2001) The cutaneous histiocytosis. Adv Dermatol 17:77–113

Virchows Arch (2003) 443:801–802
DOI 10.1007/s00428-003-0933-9
© Springer-Verlag 2003

European Society of Pathology (ESP)

EXTRAORDINARY GENERAL ASSEMBLY

Day: Saturday, February 7, 2004,

Time: 15.30h. In the event of the General Assembly not being quorate a second General Assembly based on simple majority will be called for **16.00h**

Duration: about 2 hours.

Place: Palais des Congrès, Porte Maillot 75016, Paris – France

Agenda:

1. Welcome
2. Approval of agenda
3. Approval of the Minutes of the preceding General Assembly (Ljubljana, September 2003)
4. Report of the President
5. Approval of the adaptation to the Belgian law of the Statutes and By-laws already approved in the General Assembly of Berlin 2001
6. Announcement and consequences of the results of the ballot for election of President-elect (2003-2005)
7. Report of the Chairman of the Organizing Committee of the 20th ESP Congress, Paris 2005
8. Any other business

Antonio Cardesa
President

11–15 February 2004
Conference on "Clinical Oncology 2004/2005"

In cooperation with the National Oncology Societies, the Tumorzentrum Düsseldorf (Director: Prof. Dr. med. R. Haas) will be holding a five-day conference. The results will be published in a symposium volume for the conference. More than 800 experts, mainly from the field of oncology, are expected to attend. The workshop will be held in the MNR Clinic, Lecture Hall 13A. The following general topics have been scheduled:

Wednesday:
Pharynx, larynx, CUP syndrome, parotid gland, nasopharynx, skin tumors
Bier, Dummer, Ganzer, Roth, Ruzicka, Schmitt, Schulte, Stadler, Suter

Thursday:
Esophageal carcinoma, gastric carcinoma, colorectal carcinoma
Gabbert, Häussinger, Knöfel, Ramp, Röher, Röhrborn, Wettstein, Willich, Sauer

Friday:
Seminoma, urinary bladder carcinoma, prostatic carcinoma, renal cell carcinoma
Ackermann, Alberti, Alken, Bamberg, Fornara, Hartmann, Rübben, Vögeli, Wirth

Saturday:
NHL, Hodgkin's disease, ALL, AML, CML, multiple myeloma, bronchial carcinoma, thymona
Bentz, Böhner, Gattermann, Germing, Haas, Kobbe, Stilgenbauer, Schmitt

Sunday:
Mammary carcinoma: biology, new treatment standards
Bender, Dall, Gerber, Harbeck, Kaufmann, Mallmann, von Mickwitz, Nitz, Yarnold

Head of the organization team: Prof. Dr. Stephan Roth, Klinik für Strahlentherapie, Moorenstr. 5, Postfach 101007, 40001 Düsseldorf, Germany

The conference fee will be E30 per day.

The symposium volume published for the conference can be purchased for E20.

For further information, please contact:
Head of the organization team:
Prof. Dr. Stephan Roth
Klinik für Strahlentherapie
Heinrich-Heine-Universität
Moorenstr. 5
40225 Düsseldorf
Germany
Tel.: +49 (0)211 811 8989/7990
Fax: +49 (0)211 811 8051
e-mail: roth@med.uni-duesseldorf.de
www.uni-duessdorf.de/tumorzentrum

9–12 May 2004
XIV EUROCELLPATH COURSE: The Impact of Proteomics and Genomics in Pathology
Girona, Spain

The Organising Committee of the next EuroCellPath Course invites you to come to the beautiful city of Girona to enjoy an outstanding program on a very timely topic, addressed by leading authorities in the field, in an inspiring setting. The subjects covered in this course will be the following:

- DNA arrays: Methods and Goals
- Tissue Microarrays: A Tool for Rapid, Efficient Translational Research
- Proteomics: From Genes to Functions
- Tissue Procurement and Handling: Laser Capture Microdissection and Other Techniques
- Bioinformatic Tools for Array Data Mining
- Application of Array Genomics and Proteomics in Pathology
- Molecular Pathology of Genes and Proteins: What to Look For and When.

You may also submit your abstracts on these or other related topics, to be presented either as platform or poster during the Course.

For further information, please contact:
Prof. Josep Lloreta-Trull (local organizer)
Department of Pathology
Hospital del Mar-IMAS-IMIM
Universitat Pumpeu Fabra
Passeig Marítim 25–29, 08003-Barcelona, Spain
Tel.: +34 93 248 30 31
Fax: +34 93 248 31 31
E-mail:jlloreta@imas.imim.es or enter the course website
http://www.tilesa.es/eurocellpath04/

1–11 June 2004
International course on Laboratory Animal Science
Utrecht, The Netherlands

A two week intensive course on laboratory animal science will be organized at the Department of Laboratory Animal Science – Utrecht, The Netherlands in June 2004. This course is organized once a year since 1993.

The objective of this course is to present basic facts and principles that are essential for the humane use and care of animals and for the quality of research.

The contents of the course are in line with recommendations of the Federation of European Laboratory Animal Science Associations (FELASA) regarding the training of the young scientist whose research involves the use of vertebrate animals.

The course may also be of interest for those who intend to set up a similar course at their location. For this purpose, during the course the acquisition of teaching materials can be discussed with the course committee.

For information and application forms please contact:
Prof. L.F.M. van Zutphen, PhD or
Mr. Stephan van Meulebrouck, MA
Department of Laboratory Animal Science
Faculty of Veterinary Medicine
P.O. Box 80.166
3508 TD Utrecht
The Netherlands
Tel.: ++31-30-2532033
Fax: ++31-30-2537997
E-mail: pdk@las.vet.uu.nl
Internet: http://las.vet.uu.nl (click on "Education and Training")

11–16 July 2004
ULTRAPATH XII: Conference on Diagnostic Electron Microscopy with Surgical, Clinical, and Molecular Pathology Correlations
Barcelona, Spain

The scientific program will cover diagnostic Electron Microscopy as well as Diagnostic Pathology – with immunohistochemical and molecular correlations – and translational research. Renowned experts in the field from both sides of the Atlantic will present updated comprehensive reviews of significant areas of Pathology. In addition, a new section of the meeting will be devoted to a Pathology Review Course. Platform and Poster presentations will also be an important part of the program.

For further information, please contact:
Josep Lloreta-Trull, M.D., Ph.D. (chairman)
Department of Pathology, Hospital del Mar-IMAS-IMIM
Universitat Pompeu Fabra
Passeig Maritim 25–29, 08003-Barcelona, Spain
Tel.: +34 93 248 30 31
Fax: +34 93 248 31 31
E-mail: jlloreta@imas.imim.es.
The Application form and Abstract form can be found on the meeting website, http://www.tilesa.es/ultrapath04/